The Pre- and Post-Failure Deformation Behaviour of Soil Slopes

Gavan James Hunter

A thesis submitted in partial fulfilment
of the requirements for the degree of
Doctor of Philosophy

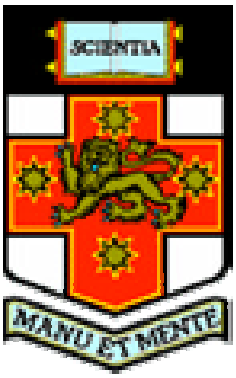

School of Civil and Environmental Engineering

The University of New South Wales

April 2003

Abstract

This thesis examines the pre and post failure deformation behaviour of landslides in cut, fill and natural soil slopes, and of the deformation behaviour of embankment dams. The deformation behaviour of landslides and embankment dams have been analysed from a database of case studies from a number of classes of slope (and dam) and material type. The database included some 450 landslides in cuts, fills and natural slopes, and some 170 embankment dams.

For landslides in soil slopes, methods and guidelines have been developed for use in the analysis, evaluation and prediction of the pre and post failure deformation behaviour. They take into consideration the factors influencing and the mechanics controlling the deformation behaviour for the classes of slope and material types, which are different for pre and post failure. Pre-failure deformations are largely controlled by the effective stress conditions within the slope, changes in the boundary conditions and the response of the soil to those changes in boundary conditions. Whether the soil, under the effective stress conditions imposed within the slope, is contractive (and saturated or near saturated) or dilative on shearing, has a significant influence on the pre failure deformation behaviour. The post failure deformation behaviour is strongly influenced by the mechanics of failure (including whether the soil is contractive or dilative on shearing), the source area slope angle, the downslope geometry, the orientation of the surface of rupture, the material properties and slide volume. Guidelines are presented for prediction of "rapid" and "slow" post failure velocity.

For embankment dams, methods and guidelines have been developed for evaluation and prediction of the deformation behaviour during and post construction for selected embankment types. They take into consideration the influence of material type and placement methods, material strength and compressibility properties, embankment zoning geometry, embankment height, and reservoir operation, amongst other factors. Guidelines have been developed to assist in the identification of "abnormal" deformation behaviour, which can be related to internal deformations or a marginal stability condition and the onset to failure.

Acknowledgements

This project would not have been possible were it not for the vision and enthusiasm of Professor Robin Fell. It is with heartfelt thanks and much appreciation that I acknowledge Robin for his support, guidance and encouragement throughout the project. It has been a most rewarding experience.

The support of the Australian Research Council and the industry sponsors of the project (listed below) are acknowledged. I would like to thank those organizations, in particular the personnel within those organizations, that gave of their time and efforts in providing case study information, and feedback and discussion on aspects of the work.

I would also like to thank the staff of and the services provided by the School of Civil and Environmental Engineering of the University of New South Wales. In particular, I thank Messrs Paul Gwynne and Lindsay O'Keeffe for their efforts in the establishment and the on-going running of the laboratory creep testing facility.

The friendship and support of my colleagues within the School of Civil and Environmental Engineering is acknowledged. In particular I thank Doctor James Glastonbury for his friendship, his listening and his thoughtful discussion. James and I travelled on similar paths within the research project, and it has been a pleasure to have made this journey with James.

Lastly, but by no means least, I would like to thank my friends and family for their patience, encouragement and unquestioning support throughout the project.

Financial sponsors of the project:

- Australian Capital Territory Energy and Water Corporation;
- BC Hydro and Power Authority, Canada;
- Dams Safety Committee of New South Wales;
- DamWatch Services (New Zealand);
- Goulburn Murray Water;
- Gutteridge Haskins and Davey;
- Hydro Tasmania;
- Melbourne Water Corporation;
- Natural Resources and Environment, Victoria;
- New South Wales Department of Land and Water Conservation;
- New South Wales Department of Public Works and Services;

- Pacific Power;
- Pells Sullivan Meynink;
- Queensland Department of Main Roads;
- Roads and Traffic Authority of New South Wales;
- Snowy Mountains Engineering Corporation;
- Snowy Mountains Hydro-Electric Authority;
- South Australian Water Corporation;
- Sun Water (formerly Queensland Department of Natural Resources);
- Sydney Catchment Authority;
- United States Bureau of Reclamation;
- URS Corporation;
- Vattenfall, Sweden;
- Water Corporation of Western Australia.

In kind sponsors of the project:

- Australian Soil Testing;
- Geo-Eng Group;
- Geotechnical Engineering Office, Hong Kong Government;
- Jeffrey and Katauskas;
- River Murray Water;
- Wimmera Mallee Water.

TABLE OF CONTENTS

1.0 INTRODUCTION 1.1

1.1 OBJECTIVES OF THE RESEARCH 1.1

1.1.1 Landslides in Soil Slopes 1.2

1.1.2 Deformation Behaviour of Embankment Dams 1.3

1.2 STRUCTURE OF THE THESIS 1.4

1.3 TERMS AND DEFINITIONS 1.5

1.3.1 General Terms and Definitions 1.5

1.3.2 Terms and Definitions for Landslides 1.5

1.3.3 Terms and Definitions for Embankments 1.9

2.0 LITERATURE REVIEW 2.1

2.1 LANDSLIDES IN SOIL SLOPES 2.1

2.2 DEFORMATION BEHAVIOUR OF EMBANKMENT DAMS 2.7

2.3 WHERE THIS RESEARCH FITS IN 2.9

3.0 "RAPID" LANDSLIDES FROM FAILURES IN SOIL SLOPES 3.1

3.1 OUTLINE OF THIS CHAPTER 3.1

3.2 DATABASE OF CASE STUDIES ANALYSED 3.2

3.2.1 Flow Slides in Coal Mine Waste Spoil Piles and Stockpiled Coal 3.5

3.2.2 Landslides from Failures in Cut, Fill and Natural Slopes, Hong Kong 3.7

3.2.3 Flow Slides from Tailings Dam Failures 3.9

3.2.4 Flow Slides from Failures in Hydraulic Fill Embankment Dams 3.9

3.2.5 Flow Slides from Failures in Sub-Aqueous Constructed Fills 3.9

3.2.6 Flow Slides from Failures in Submarine Slopes 3.12

3.2.7 Flow Slides in Sensitive Clays 3.12

3.3 THE MECHANICS OF SHEARING OF CONTRACTIVE GRANULAR SOILS 3.15

3.3.1 Definitions 3.15

3.3.2 Characteristics of Contractive and Dilative Soils Sheared Under Monotonic Load Conditions 3.16

3.3.3 Field Methods for Evaluation of Flow Liquefaction Potential 3.22

3.3.4 Effects of Non-plastic Fines and Gravels based on Flow Liquefaction Potential *3.30*
3.3.5 Residual Undrained Shear Strength of Flow Liquefied Soils *3.32*
3.4 MECHANICS OF FAILURE OF FLOW SLIDES 3.39
3.4.1 Mechanics of Development of Flow Sliding *3.39*
3.4.2 Flow Slides in Granular Stockpiles *3.43*
3.4.3 Flow Slides from Failures in Sensitive Clays *3.49*
3.4.4 Flow Slides in Loose Silty Sand Fills, Hong Kong *3.54*
3.4.5 Tailings Dams *3.57*
3.4.6 Hydraulic Fill Embankment Dams *3.60*
3.4.7 Submarine Slopes and Slopes in Sub-Aqueous Fills *3.62*
3.5 MECHANICS OF FAILURE IN DILATIVE SOILS LEADING TO "RAPID" SLIDING 3.64
3.5.1 Slope Types of Failures in Dilative Soils Leading to "rapid" Sliding *3.64*
3.5.2 Slides Through Soil Mass – Dilative Failures *3.65*
3.5.3 Defect Controlled Landslides *3.79*
3.6 SUMMARY OF THE CHARACTERISTICS AND MATERIAL TYPES OF "RAPID" LANDSLIDES 3.83
3.6.1 Flow Slides in Contractant Soils Susceptible to Flow Liquefaction *3.83*
3.6.2 Characteristics and Identification of Conditions Under Which Failures in Dilative Soils Result in "Rapid" Landsliding *3.88*
3.7 PRE-FAILURE DEFORMATION BEHAVIOUR 3.89
3.7.1 Flow Slides *3.90*
3.7.2 "Rapid" Landslides from Slope Failures in Dilative Soils *3.97*
3.7.3 Summary of Pre Failure Deformation Behaviour *3.99*
3.8 POST-FAILURE DEFORMATION BEHAVIOUR – REVIEW OF THE LITERATURE 3.102
3.8.1 Factors Affecting Travel Distance and Velocity *3.102*
3.8.2 Velocity of the Slide Mass *3.104*
3.8.3 Empirical Methods for Assessment of Travel Distance *3.107*
3.9 POST-FAILURE DEFORMATION – DEVELOPED METHODS FOR ASSESSMENT OF TRAVEL DISTANCE FROM THE DATABASE 3.112
3.9.1 Travel Distance Versus Slide Volume and Initial Slide Classification *3.113*
3.9.2 Travel Distance Versus Slide Volume, Degree of Confinement of the Travel Path and Initial Slide Classification *3.116*
3.9.3 Travel Distance Versus Volume, Down-slope Angle and Slide Type from Failures in Dilative Soils *3.124*

3.9.4 Travel Distance Versus Volume, Down-slope Angle and Slide Type from Failures in Contractile Soils *3.137*
3.9.5 Summary of Methods for Predicting Travel Distances *3.150*
3.10 POST-FAILURE NUMERICAL MODELLING - METHODS AND RESULTS 3.152
3.10.1 "Rapid" Landsliding in Hong Kong *3.155*
3.10.2 "Rapid" Landslides from Coal Mine Waste Spoil Pile Failures in British Columbia *3.158*
3.10.3 Flow Slides from Tailings Dams Failures *3.160*
3.11 CONCLUSIONS 3.162

4.0 EMBANKMENTS ON SOFT GROUND 4.1

4.1 INTRODUCTION TO THIS CHAPTER 4.1
4.2 LITERATURE REVIEW 4.3
4.2.1 Excess Pore Water Pressure Response *4.5*
4.2.2 Deformation Behaviour *4.15*
4.3 ANALYSIS OF THE BEHAVIOUR OF FAILURE CASE STUDIES 4.22
4.3.1 Case Studies Analysed *4.22*
4.3.2 Excess Pore Water Pressure *4.26*
4.3.3 Pre-Failure Deformation Behaviour and the Effects of Progressive Failure *4.32*
4.3.4 Factor of Safety Versus Relative Embankment Height *4.45*
4.3.5 Post-Failure Deformation Behaviour *4.47*
4.4 POST CONSTRUCTION BEHAVIOUR OF EMBANKMENTS ON SOFT GROUND 4.51
4.4.1 Effect of Effective Stress State on the Post Construction Behaviour *4.52*
4.4.2 Deformation Behaviour and Pore Water Pressure Response in the Initial Period Post Construction *4.52*
4.4.3 Long-Term Post Construction Deformation *4.59*
4.5 DISCUSSION AND CONCLUSIONS 4.61
4.5.1 Indicators of an Impending Failure *4.61*
4.5.2 Guidelines on Monitoring for Identification of an Impending Failure Condition *4.63*
4.5.3 Post Failure Deformation Behaviour *4.64*
4.5.4 Discussion on Failure Mechanism *4.65*

5.0 LANDSLIDES IN EMBANKMENT DAMS AND CUT SLOPES IN HEAVILY OVER-CONSOLIDATED HIGH PLASTICITY CLAYS 5.1

5.1 INTRODUCTION TO THIS CHAPTER 5.1

5.2 LITERATURE REVIEW 5.2

5.2.1 Statistics on Dam Incidents Involving Slope Instability 5.2

5.2.2 Progressive Failure 5.8

5.2.3 Mechanics of Post Failure Deformation 5.11

5.3 DATABASE OF CASE STUDIES ANALYSED 5.12

5.3.1 Case Studies of Failures in Dam Embankments 5.14

5.3.2 Case Studies of Failures in Cut Slopes of High Plasticity Clays 5.15

5.4 MECHANICS OF FAILURE OF CUT SLOPES IN HEAVILY OVER-CONSOLIDATED HIGH PLASTICITY CLAYS 5.18

5.4.1 Progressive Failure 5.18

5.4.2 Trigger to Failure 5.20

5.4.3 Time to Failure 5.22

5.4.4 Effect of Defects Within the Soil Mass 5.23

5.5 MECHANICS OF FAILURE FOR FAILURES IN EMBANKMENT DAMS 5.24

5.5.1 Failures in Embankment Dams During Construction 5.24

5.5.2 Failures in Embankments During Drawdown 5.30

5.5.3 Post Construction Failures in the Downstream Slope of Embankments 5.39

5.6 POST FAILURE DEFORMATION BEHAVIOUR – FAILURES IN EMBANKMENT DAMS 5.44

5.6.1 Factors Affecting the Post Failure Deformation 5.44

5.6.2 Summary of Case Studies of Failures in Embankment Dams 5.45

5.6.3 Failures During Construction - Post Failure Deformation Behaviour 5.46

5.6.4 Failures During Drawdown – Post Failure Deformation Behaviour 5.68

5.6.5 Post Failure Deformation Behaviour of Failures in the Downstream Shoulder After Construction 5.80

5.7 POST FAILURE DEFORMATION BEHAVIOUR - CUT SLOPES IN HEAVILY OVER-CONSOLIDATED CLAYS 5.86

5.7.1 Summary of Factors Affecting the Post Failure Deformation 5.86

5.7.2 Summary of the Post Failure Deformation and Velocity of the Failure Case Studies 5.87

5.7.3 Failures in Cut Slopes – Type 2 Slope Failure Geometry 5.92
5.7.4 Failures in Cut Slopes – Type 1 Slope Failure Geometry 5.94
5.7.5 Failures in Cut Slopes – Type 5 Slope Failure Geometry 5.95
5.8 PREDICTION OF POST-FAILURE TRAVEL DISTANCE 5.97
5.8.1 Khalili et al (1996) Model for Intact Slides 5.97
5.8.2 Empirical Methods for Prediction of Travel Distance of Intact Slides . 5.105
5.9 CONCLUSIONS AND GUIDELINES FOR PREDICTION OF POST-FAILURE DEFORMATION BEHAVIOUR OF INTACT SLIDES IN SOIL SLOPES 5.108
5.9.1 Summary of Findings from the Case Study Analysis 5.108
5.9.2 Guidelines for Prediction of Post-Failure Deformation 5.117

6.0 THE DEFORMATION BEHAVIOUR OF ROCKFILL 6.1

6.1 OUTLINE OF THIS CHAPTER 6.1
6.2 DEFINITIONS AND TERMINOLOGY 6.2
6.2.1 Unconfined Compressive Strength of Rock 6.2
6.2.2 Rockfill Placement and Compaction 6.3
6.2.3 Rockfill Moduli 6.4
6.2.4 Zoning of Main Rockfill in Concrete Face Rockfill Dams 6.7
6.3 LITERATURE REVIEW OF ROCKFILL DEFORMATION 6.9
6.3.1 Historical Summary of Rockfill Usage in Embankment Design 6.9
6.3.2 Deformation Properties of Rockfill 6.9
6.3.3 Predictive Methods for Rockfill Deformation 6.14
6.4 ANALYSIS OF THE DEFORMATION BEHAVIOUR OF ROCKFILL IN CONCRETE FACE ROCKFILL DAMS 6.27
6.4.1 Case Study Database 6.28
6.4.2 Deformation During Construction 6.28
6.4.3 Deformation of the Face Slab of CFRD on First Filling 6.44
6.4.4 Post Construction Crest Settlement 6.53
6.5 DISCUSSION AND RECOMMENDED METHODS FOR PREDICTION 6.71
6.5.1 Guidelines on Deformation Prediction During Construction 6.71
6.5.2 Guidelines on Deformation Prediction During First Filling 6.75
6.5.3 Guidelines on Deformation Prediction Post-Construction 6.76
6.6 CONCLUSIONS 6.77

VOLUME 2

7.0 THE DEFORMATION BEHAVIOUR OF EMBANKMENT DAMS..... 7.1

7.1 INTRODUCTION TO THIS CHAPTER 7.1

7.2 LITERATURE REVIEW 7.2

7.2.1 Failure and Accident Statistics..... 7.2

7.2.2 Historical Development of Embankment Dams as this Affects Deformation Behaviour 7.3

7.2.3 Factors Affecting The Deformation of Embankment Dams 7.5

7.2.4 Predictive Methods of Deformation Behaviour..... 7.9

7.3 DATABASE OF CASE STUDIES 7.17

7.3.1 Earthfill and Zoned Earth and Earth-Rockfill Embankments..... 7.17

7.3.2 Puddle Core Earthfill Embankments..... 7.18

7.4 GENERAL DEFORMATION BEHAVIOUR DURING CONSTRUCTION OF EARTHFILL AND ZONED EARTH AND EARTH-ROCKFILL EMBANKMENTS 7.18

7.4.1 Stresses During Construction..... 7.23

7.4.2 Lateral Deformation of the Core During Construction 7.43

7.4.3 Vertical Deformation of the Core During Construction 7.51

7.5 GENERAL DEFORMATION BEHAVIOUR ON FIRST FILLING OF EARTHFILL AND ZONED EARTH AND EARTH-ROCKFILL EMBANKMENTS 7.69

7.5.1 Effect of Water Load on the Core..... 7.70

7.5.2 Collapse Compression During First Filling 7.73

7.5.3 Lateral Surface Deformation Normal to the Dam Axis During First Filling. 7.84

7.6 GENERAL POST CONSTRUCTION DEFORMATION BEHAVIOUR OF EARTHFILL AND ZONED EARTH AND EARTH-ROCKFILL EMBANKMENTS 7.99

7.6.1 Post Construction Internal Vertical Deformation of the Core..... 7.100

7.6.2 Post Construction Total Deformation of Surface Monitoring Points ... 7.102

7.6.3 Post Construction Crest Settlement Versus Time..... 7.110

7.6.4 Post Construction Horizontal Displacement of the Crest Normal to the Dam Axis. 7.132

7.6.5 Post Construction Deformation of the Mid to Upper Downstream Slope 7.140

7.6.6 Post Construction Deformation of the Upper Upstream Slope and Upstream Crest *7.148*

7.7 GENERAL DEFORMATION BEHAVIOUR OF PUDDLE CORE EARTHFILL EMBANKMENTS 7.158

7.7.1 Deformation During Construction of Puddle Core Earthfill Embankments *7.158*

7.7.2 Deformation During First Filling of Puddle Core Earthfill Embankments *7.159*

7.7.3 Deformation Behaviour Post First Filling of Puddle Core Earthfill Dams *7.166*

7.8 "ABNORMAL" EMBANKMENT DEFORMATION BEHAVIOUR – METHODS OF IDENTIFICATION 7.185

7.9 "ABNORMAL" DEFORMATION BEHAVIOUR DURING CONSTRUCTION OF EARTH AND EARTH-ROCKFILL EMBANKMENTS 7.187

7.9.1 Plastic Deformation of the Core During Construction *7.188*

7.9.2 Collapse Compression of the Central Earthfill Zone *7.191*

7.9.3 Reservoir Filling During Construction *7.192*

7.9.4 Shear Surface Development in the Core During Construction *7.193*

7.10 "ABNORMAL" DEFORMATION BEHAVIOUR POST CONSTRUCTION OF ZONED EARTH AND ROCKFILL EMBANKMENTS 7.196

7.10.1 Rockfill Susceptibility to Collapse Compression *7.197*

7.10.2 Deformation on First Filling in Embankments where Collapse Compression occurs in the Upstream Rockfill Shoulder *7.201*

7.10.3 Development of Shear Surfaces Within the Earthfill Core *7.217*

7.10.4 Post First Filling Acceleration in Deformation that is Not Known to be Shear Related *7.241*

7.10.5 Other Case Studies with Potentially "Abnormal" Deformation Behaviour Post Construction *7.243*

7.11 "ABNORMAL" DEFORMATION BEHAVIOUR POST CONSTRUCTION OF EARTHFILL AND ZONED EMBANKMENTS WITH VERY BROAD CORE WIDTHS 7.252

7.11.1 Collapse Compression of the Earthfill on Wetting *7.252*

7.11.2 "High" Shear Stress or Marginal Stability Conditions Within the Embankment *7.260*

7.11.3 The Effect of the Development of the Phreatic Surface on the Displacement of the Crest and Downstream Shoulder. *7.269*

7.11.4 Other Cases of Potential "Abnormal" Deformation Behaviour *7.270*

7.12 "ABNORMAL" DEFORMATION BEHAVIOUR OF PUDDLE CORE EARTHFILL DAMS 7.274
7.12.1 Comparison with the Deformation Behaviour of Other Puddle Dams . 7.275
7.12.2 General Movement Trends Indicative of Deformation to Failure 7.278
7.12.3 Other Indicators of "Abnormal" Deformation Behaviour 7.279
7.13 SUMMARY OF "ABNORMAL" DEFORMATION BEHAVIOUR 7.280
7.14 SUMMARY AND METHODS FOR PREDICTION OF DEFORMATION OF EMBANKMENT DAMS 7.287
7.14.1 Earthfill, and Zoned Earth and Earth-Rockfill Dams 7.288
7.14.2 Prediction of Deformation Behaviour During Construction for Earthfill and Zoned Earth and Earth-Rockfill Embankments 7.288
7.14.3 Prediction of Deformation Behaviour Post Construction for Earthfill and Zoned Earth and Earth-Rockfill Embankments 7.291
7.14.4 Puddle Core Earthfill Dams 7.300
7.15 CONCLUSIONS 7.302

8.0 CONCLUSIONS AND RECOMMENDATIONS 8.1

8.1 CONCLUSIONS 8.1
8.1.1 Landslides in Soil Slopes 8.1
8.1.2 Deformation Behaviour of Embankment Dams 8.4
8.2 RECOMMENDATIONS FOR FURTHER RESEARCH 8.6

9.0 REFERENCES R1

VOLUME 3

APPENDICES

LIST OF TABLES

Table 1.1: IUGS (1995) velocity classifications for landslides. 1.6

Table 1.2: Classification of unconfined compressive strength of intact rock (AS 1726-1993) 1.13

Table 3.1: Summary of database on "rapid" landslides. 3.3

Table 3.2: Summary of data sources for "rapid" landslides from coal mine waste spoil piles and coal stockpiles 3.5

Table 3.3: Summary of landslide cases analysed from Hong Kong 3.8

Table 3.4: Summary of case studies of "rapid" landslides from tailings dams 3.10

Table 3.5: Summary of failure case studies in hydraulic fill embankment dams 3.11

Table 3.6: Summary of failure case studies in sub-aqueous constructed fill slopes 3.11

Table 3.7: Summary of "rapid" flow slides in natural submarine slopes 3.13

Table 3.8: Summary of flow slides in sensitive clays 3.14

Table 3.9: SPT blow count ($(N_1)_{60}$) yield strength and residual strength correction factors for fines content (Seed et al 1985; Seed 1987) 3.35

Table 3.10: Features of flow slides in loose fill from Hong Kong 3.56

Table 3.11: Summary of properties of liquefaction susceptible materials from flow slides in hydraulic fill embankments 3.61

Table 3.12: Summary of material types of dilative slides of debris in natural slopes that developed in "rapid" debris slides and debris flows. 3.75

Table 3.13: Source area slope angle (a_1) of dilative slides in natural slopes that developed into "rapid" debris flows and debris slides 3.77

Table 3.14: Failures through the soil mass in dilative soils that developed into "rapid" landslides, from Hong Kong 3.78

Table 3.15: Features of defect controlled compound slides that developed into "rapid" landslides from Hong Kong 3.82

Table 3.16: Features of defect controlled translational slides that developed into "rapid" landslides from Hong Kong 3.82

Table 3.17: Summary of pre-failure observations in coarse-grained loose fills 3.92

Table 3.18: Measured slope deformations adjacent to failures in the Ottawa area (Mitchell and Eden 1972) 3.95

Table 3.19: Summary of characteristics of pre-failure deformation of slope failures that developed into "rapid" landslides 3.100

Table 3.20: Velocity of the slide mass for "rapid" landslides from failures in soil slopes (mostly from case studies analysed).....3.105

Table 3.21: Velocity of slide mass for debris slides and debris flows.....3.106

Table 3.22: Regression analysis of *H/L* (Equation 3.11) versus landslide volume (Corominas 1996a).....3.111

Table 3.23: Summary of empirical correlation coefficients (Equation 3.11) for debris flows by Corominas (1996a).....3.114

Table 3.24: Empirical correlation coefficients for power law fit of travel distance angle to slide volume (Equation 3.11, $H/L = AV^B$) for unconfined "rapid" landslides.....3.122

Table 3.25: Empirical correlation coefficients for power law fit of travel distance angle to slide volume (Equation 3.11, $H/L = AV^B$) for confined and partly confined "rapid" landslides.....3.124

Table 3.26: Summary of empirical correlations for flow slides in coal waste spoil piles in British Columbia.....3.139

Table 3.27: Statistical summary of *H/L* to tan a_2 correlation for flow slides in coarse-grained coal mine waste spoil piles.....3.143

Table 3.28: Summary of slide properties of flow slides in hydraulic fill embankments.....3.149

Table 3.29: Mean and standard deviation of *H/L* for several types of slopes giving "rapid" landslides.....3.153

Table 3.30: Summary of recommended methods for prediction of H/L (tangent of the travel distance angle).....3.154

Table 3.31: Summary of "rapid" landslides from Hong Kong analysed by Hungr Geotechnical Research (1998) and Ayotte and Hungr (1998).....3.156

Table 3.32: Summary of results of numerical modelling using DAN for "rapid" landslides in Hong Kong (Hungr Geotechnical Research 1998; Ayotte and Hungr 1998).....3.157

Table 4.1: Summary of failure case studies of embankments on soft ground. 4.24

Table 4.2: Excess pore water pressure observations for the failure case studies.....4.26

Table 4.3: Summary of exceptions to general observations of excess pore water pressure response. 4.31

Table 4.4: Summary of case studies that are exceptions or have other explanations to deformation as an indicator of impending failure.....4.44

Table 4.5: Results of the post-failure deformation analysis.....4.50

Table 5.1: Incidence of slope instability in embankment dams (Foster 1999) 5.3
Table 5.2: Factors influencing downstream slides - accident and failure incidents (Foster 1999) 5.4
Table 5.3: Factors influencing upstream slides - accident and failure incidents (Foster 1999) 5.5
Table 5.4: Failures involving slope instability, excluding sloughing cases (Foster 1999) 5.9
Table 5.5: Summary of case study database of slope failures 5.13
Table 5.6: Summary of embankment dam slope stability incidents by failure slope geometry 5.15
Table 5.7: Slope instability case studies in embankment dams by embankment type 5.16
Table 5.8: Mechanics of failure for failures in embankment dams during construction. 5.24
Table 5.9: Material types through which the surface of rupture passed of post construction failures in the downstream shoulder. 5.40
Table 5.10: Timing of the failure for post construction slides in the downstream shoulder. 5.42
Table 5.11: Distribution of slide volume for slides in embankment dams. 5.46
Table 5.12: Summary of failure case studies in embankment dams during construction – failures within the embankment only 5.47
Table 5.13: Summary of failure case studies in embankment dams during construction – failure within the embankment and foundation 5.48
Table 5.14: Summary of the case studies of slides in the upstream shoulder of embankment dams triggered by drawdown 5.69
Table 5.15: Post failure deformation behaviour and slope/material properties of slides in embankment dams during drawdown. 5.72
Table 5.16: Summary of the case studies of slides in the downstream shoulder of embankment dams that occurred post construction. 5.82
Table 5.17: Cut slope failures in London clay. 5.88
Table 5.18: Cut slope failures in Upper Lias clay. 5.89
Table 5.19: Results of the post-failure deformation analysis using the Khalili et al (1996) method. 5.102
Table 5.20: Characteristics of the case study groupings from the post failure deformation analysis (Figure 5.52) 5.104
Table 5.21: Factors affecting the peak post-failure velocity for slides in embankment dams during drawdown. 5.116

Table 5.22: Guidelines for post-failure deformation prediction using the Khalili et al (1996) models.....5.118

Table 6.1: Classification of unconfined compressive strength or rock (AS 1726-1993) 6.2
Table 6.2: Historical summary of rockfill usage in embankment design (Galloway 1939; Cooke 1984; Cooke 1993). 6.10
Table 6.3: Parameters for deformation prediction (Soydemir and Kjærnsli 1979).....6.25
Table 6.4: Rates of post-construction crest settlement of dumped and compacted rockfills in CFRDs (Sherard and Cooke 1987) 6.26
Table 6.5: Summary of embankment and rockfill properties for CFRD case studies.....6.29
Table 6.6: Assessment of cross-valley influence on arching for case studies analysed.....6.38
Table 6.7: Stress conditions representative of the data sets from Figure 6.21.....6.43
Table 6.8: Summary of crest settlement during the period of first filling.....6.62
Table 6.9: Values of the coefficient, *m*, in the strain rate – time power function (Equation 6.5).....6.63
Table 6.10: Estimates of long-term crest settlement rates for dumped rockfills.....6.67
Table 6.11: Location of internal post-construction vertical settlement in CFRD 6.70
Table 6.12: Approximate stress reduction factors to account for valley shape.....6.73

Table 7.1: Mechanisms affecting the long-term deformation behaviour of old puddle core earthfill embankments (Tedd et al 1997a).....7.8
Table 7.2: Vertical compression of rolled, well-compacted earthfills measured during construction (adapted from Sherard et al 1963).....7.12
Table 7.3: Published ranges of post construction deformation of embankment dams 7.14
Table 7.4: Central core earth and rockfill embankments in the database 7.19
Table 7.5: Zoned earth and rockfill embankment case studies 7.20
Table 7.6: Zoned earthfill embankment case studies 7.21
Table 7.7: Earthfill embankment case studies.....7.21
Table 7.8: Puddle core earthfill embankment case studies 7.22
Table 7.9: Multiplying coefficients for the calculation of the total vertical stress at the embankment centreline at end of construction (Equation 7.3).....7.26
Table 7.10: Properties of central core used in finite difference analyses.....7.29

Table 7.11: Lateral deformations of the central core at end of construction for central core earth and rockfill embankments. 7.44

Table 7.12: Summary of embankment and earthfill properties for cases used in the analysis of lateral core deformation during construction. 7.46

Table 7.13: Confined secant moduli during construction for well-compacted, dry placed earthfills. 7.57

Table 7.14: Equations of best fit for core settlement versus embankment height during construction 7.68

Table 7.15: Equations of best fit for core settlement (as a percentage of embankment height) versus embankment height during construction 7.68

Table 7.16: Properties of central core used in finite difference analyses 7.80

Table 7.17: Lateral displacement of the crest (centre to downstream edge) on first filling. 7.89

Table 7.18: Thirteen cases with largest downstream crest displacement on first filling 7.92

Table 7.19: Typical range of post construction crest settlement. 7.104

Table 7.20: Typical range of post construction settlement of the upstream and downstream shoulders. 7.109

Table 7.21: Summary of long-term crest settlement rates (% per log cycle of time). 7.122

Table 7.22: Range of long-term settlement rate of the downstream shoulder. 7.141

Table 7.23: Range of long-term settlement rate of the upper upstream slope and upstream crest region. 7.151

Table 7.24: Summary of the post construction surface deformations of the puddle core earthfill dam case studies. 7.168

Table 7.25: Embankments for which collapse compression caused moderate to large settlements. 7.199

Table 7.26: Figure references for post construction crest deformation 7.292

Table 7.27: Figure references for post construction deformation of the embankment shoulders 7.293

Table 7.28: References to post construction settlement magnitude tables and plots . 7.295

Table 7.29: Embankment crest region, typical range of post construction settlement and long-term settlement rate 7.295

Table 7.30: Embankment shoulder regions, typical range of post construction settlement and long-term settlement rate 7.296

Table 7.31: References to tables and figures of long-term settlement rate 7.296

Table 7.32: Predictive methods of long-term crest settlement and displacement under normal reservoir operating conditions for puddle core earthfill embankments 7.301

LIST OF FIGURES

Figure 1.1: Landslide classification system and main slide types.....1.7

Figure 1.2: Definition of travel distance, travel distance angle, and slope geometry. 1.8

Figure 1.3: Slope failure geometries *(a)* Type 1 - failure at the top of the cut or fill slope, *(b)* Type 2 – the toe of failure is coincident with the toe of the slope, and *(c)* Type 5 – the surface of rupture extends below and daylights beyond the toe of the slope. 1.8

Figure 1.4: Classification of slope failure geometries *(a)* Type 3 –travel on relatively uniform or gradually decreasing slope angles, and *(b)* Type 4 – travel on changing slope angles from steep to shallow.....1.9

Figure 1.5: Embankment zoning classification system (Foster 1999) 1.11

Figure 1.6: Dam zoning categories of embankment types (Foster et al 2000).....1.11

Figure 2.1: Schematic of the system for geotechnical characterisation of slope movement (Leroueil et al 1996).....2.3

Figure 2.2: The stages of slope movement (Leroueil et al 1996).....2.4

Figure 2.3: Concept of the creep model under constant deviatoric stress conditions. 2.6

Figure 2.4: Monitored deformation behaviour at retained cut slope failure in London clay at Kensal Green (Skempton 1964) 2.7

Figure 3.1: Typical coal waste spoil pile profile in British Columbia (Hungr et al 1998) 3.6

Figure 3.2: Steady state line of Toyoura sand (Ishihara 1993) 3.16

Figure 3.3: Undrained behaviour of states on the contractive side of the steady state line (Ishihara 1993).....3.17

Figure 3.4: Undrained behaviour from states close to steady state and on dilative side (a) stress-strain plot and (b) effective stress paths (Ishihara 1993) 3.17

Figure 3.5: Schematic diagram showing different types of behaviour for undrained stress paths of samples at the same void ratio and different initial confining pressures (Yamamuro and Lade 1998).....3.18

Figure 3.6: Definition of the state parameter (Been and Jefferies 1985). 3.20

Figure 3.7: Collapse surface concept, defined by the locus of the peak deviator stress from undrained triaxial samples tested at the same void ratio and different initial effective mean normal stress (Sladen et al 1985a).....3.20

Figure 3.8: Correlation for cyclic resistance ratio (CRR) based on corrected SPT blow count, $(N_1)_{60}$, for clean sands under level ground conditions (Robertson and Wride 1997)..... 3.23

Figure 3.9: Corrected SPT blow count, $(N_1)_{60}$, versus vertical effective over-burden pressure (s'_{vo}) for saturated non-gravelly silty sand deposits that have experienced large deformations and were triggered by earthquake (Baziar and Dobry 1995) 3.24

Figure 3.10: Flow liquefaction and no-flow bounds in terms of *(a)* field measured SPT blow count and *(b)* CPT q_c value from flow liquefaction case histories (static and earthquake triggered) and laboratory undrained testing (Ishihara 1993). 3.25

Figure 3.11: Influence of void ratio range on flow potential of sandy soils for *(a)* round-grained sands and *(b)* angular grains (Cubrinovski and Ishihara 2000)..... 3.26

Figure 3.12: Relationship between relative density, D_{ro}, at the threshold void ratio, e_o, and void ratio range ($e_{max} - e_{min}$) for sandy soils (Cubrinovski and Ishihara 2000). 3.27

Figure 3.13: Relationship between the slope of the steady state line, l , and void ratio range for *(a)* round-grained sands and *(b)* angular grained sands (Cubrinovski and Ishihara 2000)..... 3.28

Figure 3.14: Correlation between $N_1 / D_r^{\,2}$ (N_1 = SPT blow count corrected for over-burden pressure, D_r = relative density) and void ratio range for cohesionless soils (Cubrinovski and Ishihara 2000). 3.28

Figure 3.15: Field measured SPT blow count boundaries differentiating flow liquefaction no-flow conditions for void ratio range of 0.3 to 0.6 for *(a)* round-grained sands and *(b)* angular sands (Cubrinovski and Ishihara 2000)..... 3.29

Figure 3.16: Flow characterisation of sand based on field measured SPT blow count showing liquefaction flow no-flow boundary, and region of flow at zero residual undrained strength (Cubrinovski and Ishihara 2000) 3.30

Figure 3.17: Increase in liquefaction potential (as measured by relative density) with increasing content of non-plastic fines (Lade and Yamamuro 1997) 3.31

Figure 3.18: Fording sandy gravel sample *(a)* undrained triaxial compression test results and *(b)* consolidation and steady states (Dawson et al 1998)..... 3.32

Figure 3.19: Relationship between equivalent clean sand SPT blow count, $(N_1)_{60\text{-}CS}$, and residual undrained strength from field case studies (Seed and Harder 1990) 3.34

Figure 3.20: Relationship between undrained critical strength ratio and equivalent clean sand SPT blow count, $(N_1)_{60\text{-}CS}$ (Stark and Mesri 1992)..... 3.35

Figure 3.21: Residual undrained shear strength, S_r, to vertical effective over-burden pressure for silty sand deposits (≥ 10% fines), triggered by earthquake, that have experienced large deformation (Baziar and Dobry 1995) .. 3.36

Figure 3.22: Flow chart for assessment of residual undrained shear strength of liquefied soil (NSF 1998) 3.38

Figure 3.23: Idealised mechanism for initiation of flow slides 3.40

Figure 3.24: Definition of undrained brittleness index, I_B, in strain weakening soil. .. 3.41

Figure 3.25: Effective stress states on some planes (submarine slopes) located within the region of potentially instability (Lade 1992). 3.42

Figure 3.26: Collapse model for mine waste dumps (Dawson et al 1998) 3.43

Figure 3.27: Particle size distribution of coal mine waste and coking coal susceptible to static liquefaction 3.44

Figure 3.28: Particle size distribution of sensitive clays 3.50

Figure 3.29: Frequency distribution of landslides in Quebec (Tavenas 1984) 3.52

Figure 3.30: Slope height versus slope inclination for unstable slopes in eastern Canada (Tavenas 1984) 3.52

Figure 3.31: Retrogressive landslide in sensitive clay (Leroueil et al 1996) 3.54

Figure 3.32: Peak shear strength from undrained triaxial compression tests of contractive fill samples (HKIE 1998) 3.57

Figure 3.33: Effect of partial saturation on steady state line in void ratio – mean effective stress space (HKIE 1998) 3.58

Figure 3.34: Particle size distribution of tailings from flow slide case studies 3.59

Figure 3.35: Particle size distributions of hydraulic fills from flow slide case studies 3.61

Figure 3.36: Particle size distributions of soil types from submarine slopes and sub-aqueous fills susceptible to liquefaction and flow sliding. 3.62

Figure 3.37: Hypothetical model for transformation of dilative materials from rigid to fluid behaviour, path D_i to D_f (Fleming et al 1989) 3.68

Figure 3.38: Relationship between peak hourly rainfall, landsliding and severity of consequence for Hong Kong (Brand et al 1984) 3.70

Figure 3.39: Relationship between severity of landsliding and rainfall intensity for Hong Kong (Brand 1985b) 3.70

Figure 3.40: Source area particle size distributions of dilative slides of debris in natural slopes 3.73

Figure 3.41: Distribution of head slope angle (source area slope angle) for slides of debris in natural terrain that developed into “rapid” landslides, Hong Kong (Evans et al 1997) 3.79

Figure 3.42: Cross section through the failure and "rapid" landslide at Fei Tsui Road, Hong Kong (GEO 1996a) 3.81

Figure 3.43: Particle size distributions of material types susceptible to liquefaction and flow sliding. 3.84

Figure 3.44: Comparison of flow liquefaction no-flow boundaries (in terms of SPT $(N_1)_{60}$) for sands and silty sands from monotonic laboratory undrained tests and earthquake triggered field cases (after Cubrinovski and Ishihara 2000). 3.87

Figure 3.45: Pre-failure deformation of two separate failures at the Clode waste dump, Fording Coal, British Columbia (Campbell and Shaw 1978). 3.93

Figure 3.46: Measured deformations in a natural slope, Ottawa River (Mitchell and Eden 1972) 3.94

Figure 3.47: Deformation and pore pressure ratio of an induced slope failure (Mitchell and Williams 1981) 3.96

Figure 3.48: Sliding block model showing kinetic energy lines for different rheological models (Golder Assoc. 1995) 3.106

Figure 3.49: Schematic profile of a slope failure showing travel distance and travel distance angle 3.108

Figure 3.50: Travel distance from the toe of the cut, R, versus cut slope height, H_s, for failures in cut slopes from Lantau Island, Hong Kong (Wong and Ho 1996) 3.109

Figure 3.51: Landslide volume versus tangent of the travel distance angle for 204 landslides (Corominas 1996a) 3.110

Figure 3.52: Ratio *H/L* versus volume for landslides that break-up on sliding (Finlay et al 1999) 3.111

Figure 3.53: Ratio *H/L* versus volume for all slides from database. 3.114

Figure 3.54: *H/L* ratio versus volume relationships for Corominas (1996a) data on unconfined debris flows. 3.115

Figure 3.55: *H/L* ratio versus volume relationships for Corominas (1996a) data on confined debris flows. 3.115

Figure 3.56: Travel distance beyond source area versus volume for unconfined travel paths. 3.117

Figure 3.57: Travel distance beyond source area versus volume for confined and partly confined travel paths. 3.117

Figure 3.58: Comparison of trendlines of *H/L* versus slide volume differentiated on travel path confinement for "rapid" landslides from failures in dilative soils, from Hong Kong. 3.118

Figure 3.59: *H/L* versus volume for "rapid" landslides with unconfined travel paths. 3.120
Figure 3.60: *H/L* ratio versus volume for "rapid" landslides from failures in dilative soils with unconfined travel paths. 3.120
Figure 3.61: *H/L* ratio versus volume for "rapid" landslides from failures in contractive soils (flow slides) with unconfined travel paths. 3.121
Figure 3.62: *H/L* versus volume for "rapid" landslides with confined travel paths. .. 3.123
Figure 3.63: *H/L* versus volume for "rapid" landslides with partly confined travel paths. 3.123
Figure 3.64: *H/L* versus slide volume for cut slope cases studies from Hong Kong . 3.126
Figure 3.65: *H/L* normalised against tangent of the cut slope angle versus volume for cut slopes in Hong Kong failing onto a near horizontal slope at the toe. 3.127
Figure 3.66: Idealised effect of volume on travel distance for cut slope failures of *(a)* small volume compared with *(b)* significantly larger volumes. 3.127
Figure 3.67: Classification of slope categories *(a)* Type 1 – failure at top of cut slope, and *(b)* Type 2 – failure encompassing the full cut height. 3.128
Figure 3.68: Definition of down-slope angle below source area, a_2 ..... 3.132
Figure 3.69: *H/L* versus tangent of the down-slope angle, a_2, for unconfined travel paths, failures in natural slopes from Hong Kong. 3.133
Figure 3.70: *H/L* versus tangent of the down-slope angle, a_2, for partly confined travel paths, failures in natural slopes from Hong Kong. 3.134
Figure 3.71: *H/L* versus tangent of the down-slope angle, a_2, for confined travel paths, failures in natural slopes from Hong Kong. 3.134
Figure 3.72: Natural slopes (Hong Kong). Trendlines for *H/L* versus tangent of the down-slope angle, a_2, for all types of travel path. 3.135
Figure 3.73: *H/L* versus slide volume for flow slides in loose silty sand to sandy silt fills 3.137
Figure 3.74: *H/L* versus slide volume for flow slides in coarse-grained coal mine waste spoil piles. 3.142
Figure 3.75: *H/L* versus the tangent of the down-slope angle below the toe of the spoil pile, a_2; flow slides in coarse-grained coal mine waste spoil piles. 3.142
Figure 3.76: *H/L* versus volume for retrogressive "rapid" slides 3.146
Figure 3.77: Distance of retrogression versus liquidity index for slides in sensitive clays 3.148
Figure 3.78: Distance of retrogression based on stability number for landslides in sensitive clays (Mitchell and Markell 1974) 3.148
Figure 3.79: Ratio of retrogression distance to slide depth versus stability number . 3.149

Figure 3.80: DAN results of frictional back-analysis models of “rapid” landslides from Hong Kong (data from Hungr GR (1998) and Ayotte and Hungr (1998)) 3.158

Figure 3.81: Back calculated bulk friction angle from DAN analysis of flow slides from coal mine waste spoil pile failures in British Columbia (Golder Assoc. 1995) 3.159

Figure 3.82: Simple sliding block model for analysis of tailings strength (Blight 1997) 3.160

Figure 3.83: Variation of shear strength with moisture content for gold tailings (Blight 1997) 3.161

Figure 3.84: Model for flow of liquefied tailings (Jeyapalan et al 1983a)..... 3.162

Figure 4.1: Computed factor of safety for field failures (Tavenas and Leroueil 1980) 4.2

Figure 4.2: Effective vertical stress profile and pre-consolidation stress profile prior to construction, and the effective vertical stress profile at end of construction of the Saint Alban B test embankment (Tavenas and Leroueil 1980). 4.8

Figure 4.3: Field observations of excess pore water pressures in clay foundations during the initial period of embankment construction (Tavenas and Leroueil 1980). 4.8

Figure 4.4: Total (*OPFR*) and effective (*O¢P¢F¢R¢*) stress paths under the centre of embankments (Tavenas and Leroueil 1980) 4.9

Figure 4.5: Relationship between the excess pore water pressure and the applied vertical stress (Tavenas and Leroueil 1980)..... 4.9

Figure 4.6: Dimensionless variations of changes in total stresses under the centreline of an infinite strip load on an elastic half space (Poulos and Davis 1974) 4.10

Figure 4.7: Effective stress paths for varying $\overline{B}$ values and total stress ratios (Folkes and Crooks 1985). 4.11

Figure 4.8: Effective stress paths and pore water pressure generation associated with different types of yield conditions (Leroueil and Tavenas 1986). 4.11

Figure 4.9: Element of soil at depth z beneath on centreline of uniform circular load (Muir Wood 1990) 4.13

Figure 4.10: Total stresses on centreline beneath uniform circular load on elastic half space (Muir Wood 1990). 4.14

Figure 4.11: Total (*BCDE*) and effective (*B¢C¢D¢E¢*) stress paths for a soil element on the centreline beneath a circular load (Muir Wood 1990). 4.14

Figure 4.12: Variation of pore water pressure with applied surface load for element on centreline beneath circular load (Muir Wood 1990). 4.15

Figure 4.13: Variation of the dimensional factor *R* (proportional to the horizontal surface displacement at the toe) with factor of safety (Marche and Chapuis 1974) 4.17

Figure 4.14: Definition of the geometry and deformation parameters (Tavenas et al 1979)..... 4.18

Figure 4.15: Average correlation between the maximum lateral movement at the toe, y_m, and settlement under the centre of the embankment, *s*, during construction (Tavenas and Leroueil 1980)..... 4.18

Figure 4.16: Effective stress and lateral displacement profiles at the end of construction under *(a)* Cubzac-les-Ponts A and *(b)* Saint Alban B test fills (Tavenas et al 1979)..... 4.19

Figure 4.17: Comparison of horizontal movement (on berm beyond embankment toe) during loading and for 24 hour period for the Thames test embankment (Marsland and Powell 1977)..... 4.20

Figure 4.18: Observations of lateral displacement at the base of the embankment with increasing embankment thickness at the Rio test embankment (Ramalho-Ortigao et al 1983a)..... 4.21

Figure 4.19: Contours of normalised shear-stress ratios at 4 m fill thickness from finite element modelling at Muar-F test embankment, Malaysia (Indraratna et al 1992)..... 4.22

Figure 4.20: Idealised section of embankment indicating the types of monitored observations..... 4.23

Figure 4.21: *(a)* and *(b)* Excess pore water pressure under centre of embankment versus applied embankment load. 4.27

Figure 4.22: Settlement under the centre of the embankment versus relative embankment height (H/H_f). 4.34

Figure 4.23: Vertical displacement at the embankment toe versus relative embankment height. 4.35

Figure 4.24: Vertical displacement beyond the embankment toe versus relative embankment height. 4.36

Figure 4.25: Lateral surface displacement at the embankment toe versus relative embankment height. 4.38

Figure 4.26: Incremental vertical inclination angle (from inclinometer observations at the embankment toe) with fill height (and time) for *(a)* Thames and *(b)* King's Lynn. 4.39

Figure 4.27: Vertical inclination angle on the surface of rupture from inclinometer observations at the embankment toe versus relative embankment height. 4.40

Figure 4.28: Maximum lateral displacement at the embankment toe versus settlement under the centre of the embankment. 4.43

Figure 4.29: Factor of safety versus relative embankment height 4.46

Figure 4.30: Failure model for post-failure deformation (Khalili et al 1996)..... 4.49

Figure 4.31: Effective stress paths post construction (Leroueil and Tavenas 1986).... 4.53

Figure 4.32: Excess pore water pressure response with time for several piezometers at the Muar-EC test embankment. 4.55

Figure 4.33: Excess pore water pressure response at Piezometer C1 with time at the St. Alban-A test embankment. 4.56

Figure 4.34: Schematic behaviour of strain rate effects on limit state surface with decreasing strain rate in undrained creep tests (adapted from Leroueil and Marques 1996) 4.58

Figure 4.35: Relationship between the maximum lateral displacement at the toe, y_m, and settlement at the centre, s, at the end of construction (Tavenas et al 1979). 4.60

Figure 4.36: Relationship between maximum lateral displacement (toe) and settlement (centre) at the end of construction for different embankment geometries and stability conditions (Tavenas et al 1979). 4.61

Figure 5.1: Comparison of population to slope stability incidents for earthfill, rockfill and hydraulic fill embankments (excluding sloughing and unknown embankment zonings). 5.6

Figure 5.2: Sloughing type failure (Foster 1999)..... 5.7

Figure 5.3: Sliding block model showing kinetic energy lines for different rheological models (Golder Assoc. 1995)..... 5.11

Figure 5.4: Redistribution of the potential energy after failure (D'Elia et al 1998) 5.12

Figure 5.5: Contours of accumulated deviatoric plastic strain, $e_D{}^P$, from finite element analysis of an excavation: 3H to 1V slope, 10 m cut slope height, K_o = 1.5, surface suction = 10 kPa (Potts et al 1997)..... 5.19

Figure 5.6: Distribution of water content near the slip place from failures in cut slopes in London clay (Skempton 1964)..... 5.20

Figure 5.7: Moisture content migration to the shear zone and decreasing shear strength with time to failure from consolidated undrained tests on brown London clay (Skempton and La Rochelle 1965)..... 5.20

Figure 5.8: Annual records of cut slope failures in heavily over-consolidated clays in the UK (James 1970).....5.21

Figure 5.9: Gradual reduction in the factor of safety with time due to soil weakening and oscillations due to climatic effects (Picarelli et al 2000) 5.22

Figure 5.10: Variation of the pore water pressure coefficient, r_u, with time in cuttings in Brown London clay (Skempton 1977). 5.23

Figure 5.11: Time to first time failure versus cut slope angle for Type 1 and Type 2 slope failure geometries in London clay. 5.23

Figure 5.12: Idealised development of surface of rupture during construction for embankments with wet placed fill layer/s.....5.26

Figure 5.13: Compound type surface of rupture for failures during construction at *(a)* Scout Reservation dam (Mann and Snow 1992), and *(b)* Waco dam (Stroman et al 1984).....5.26

Figure 5.14: Carsington dam, section through the region of the initial failure at chainage 725 m (Skempton and Vaughan 1993). 5.27

Figure 5.15: Carsington dam; drained strength properties of intact "yellow clay" and solifluction shears (Skempton and Vaughan 1993).....5.28

Figure 5.16: Contours of deviatoric strain predicted by finite element analysis at chainage 725 m prior to the failure of Carsington dam (Potts et al 1990). 5.29

Figure 5.17: Section through the failure in the upstream shoulder at San Luis dam (courtesy of U.S. Bureau of Reclamation). 5.35

Figure 5.18: Drawdown causing failure and prior large drawdowns for *(a)* Dam FD2, *(b)* Dam FD3, and *(c)* San Luis dam. 5.36

Figure 5.19: Composite shear strength envelope (Duncan et al 1990). 5.38

Figure 5.20: Effect of moisture migration on the undrained strength within the shear band using idealised strength parameters. 5.38

Figure 5.21: Type 1 failure slope geometries with different surface of rupture orientations.....5.45

Figure 5.22: Total post-failure deformation for slides in embankment dams during construction. 5.49

Figure 5.23: Maximum post failure velocity of slides in embankment dams during construction. 5.50

Figure 5.24: Residual drained strength from field case studies in clay soils in the UK and ring shear tests on sand, kaolin and bentonite (Skempton 1985). 5.51

Figure 5.25: Ring shear tests on normally consolidated sand-bentonite mixtures (Skempton 1985, after Lupini et al 1981). 5.52

Figure 5.26: Section through Punchina cofferdam (adapted from Villegas 1982). 5.54

Figure 5.27: Punchina cofferdam, *(a)* deformation and *(b)* velocity of the downstream slope during construction (adapted from Villegas (1982)).....5.54

Figure 5.28: Section through the failed region of Muirhead dam (Banks 1948).....5.55

Figure 5.29: Muirhead dam, post failure deformation and velocity of the failure in the upstream shoulder during construction. 5.55

Figure 5.30: Crest settlement monitoring of the slide at Waco dam (adapted from Stroman et al 1984). 5.59

Figure 5.31: Carsington dam, deformation monitoring of upstream shoulder *(a)* leading up to failure, *(b)* during failure (Skempton and Vaughan 1993), and *(c)* the velocity of the slide mass. 5.61

Figure 5.32: Section through failed region of Acu dam (Penman 1986) 5.62

Figure 5.33: Cross section of the slide during construction at Chingford dam (Cooling and Golder 1942) 5.63

Figure 5.34: Deformation and velocity of the slide at Lake Shelbyville dam (adapted from Humphrey and Leonards (1986, 1988)).....5.67

Figure 5.35: Post failure deformation and velocity of slide at Scout Reservation dam (adapted from Mann and Snow (1992)). 5.67

Figure 5.36: Slides in embankment dams during drawdown; post failure *(a)* deformation and *(b)* estimated velocity. 5.73

Figure 5.37: San Luis dam; the latter stages of post failure *(a)* deformation and *(b)* velocity of the first time slide following the 1981 drawdown (data courtesy of U.S. Bureau of Reclamation). 5.76

Figure 5.38: Section through the slide at Dam FD2. .....5.77

Figure 5.39: Deformation behaviour of the slide at Dam FD2 on reactivation during the 1994 drawdown; *(a)* deformation and *(b)* velocity. 5.78

Figure 5.40: Upstream slope angle versus total post failure deformation for slides in embankment dams during drawdown. 5.79

Figure 5.41: Post construction slides in the downstream shoulder; post failure *(a)* deformation, and *(b)* estimated peak velocity. 5.84

Figure 5.42: Slide in the cut slope in London clay at Northolt in 1955 (Skempton 1964) 5.87

Figure 5.43: Post-failure slide deformation for cut slopes in London clays. 5.90

Figure 5.44: Estimated peak post failure velocity of slides in cut slopes in London clays.....5.90

Figure 5.45: Cut slope angle versus post-failure deformation at the slide toe for cut slopes in heavily over-consolidated clays of Type 1 and Type 2 slope failure geometry. 5.91

Figure 5.46: Cut slope angle versus estimated post-failure slide velocity for cut slopes in heavily over-consolidated clays. 5.91
Figure 5.47: Failure in the cut slope in London clay at New Cross in 1841 (Skempton 1977) 5.94
Figure 5.48: Failure in the retained cut slope in London clay at Wembley Hill (Skempton 1977) 5.95
Figure 5.49: Failure in the retained cut slope in London clay at Uxbridge in 1954 (adapted from Henkel 1956) 5.97
Figure 5.50: Monitored post-failure deformation of the slide in the retained cut in London clay at Uxbridge in 1954 (adapted from Watson 1956) 5.97
Figure 5.51: Failure model for post-failure deformation (Khalili et al 1996) 5.98
Figure 5.52: Observed deformation versus the calculated residual factor of safety. . 5.103
Figure 5.53: Schematic profile of slope failure showing travel distance and travel distance angle 5.106
Figure 5.54: *H/L* versus the slide volume for embankment dams and cut slopes of moderate to rapid post-failure velocity. 5.107
Figure 5.55: *H/L* versus the tangent of the fill or cut slope angle for embankment dams and cut slopes of moderate to rapid post-failure velocity. 5.108

Figure 6.1: Determination of rockfill moduli, *(a)* modulus during construction, E_{rc}, and *(b)* modulus during reservoir filling, E_{rf} (Fitzpatrick et al 1985) 6.5
Figure 6.2: Typical design of dumped rockfill CFRD (adapted from ICOLD (1989b)) 6.7
Figure 6.3: Typical zoning of main rockfill in current CFRD design practice for construction with sound quarried rockfill (adapted from Cooke (1997); zoning designators after Fell et al (1992)) 6.8
Figure 6.4: Compression curves for dry and wet states, and collapse compression from dry to wet state for Pyramid gravel in laboratory oedometer test (Nobari and Duncan 1972a) 6.13
Figure 6.5: Settlement versus time curves for laboratory oedometer tests on rockfill (Sowers et al 1965) 6.14
Figure 6.6: Typical stress-strain relationship of rockfill from a triaxial compression test (Mori and Pinto 1988) 6.17
Figure 6.7: Finite element analysis of Foz do Areia CFRD (Saboya and Byrne 1993), *(a)* model and *(b)* stress paths during construction and first filling. 6.18
Figure 6.8: Deformation modulus during construction (E_{rc}) versus void ratio (Pinto and Marques Filho 1998) 6.20

Figure 6.9: Ratio of deformation modulus on first filling to during construction (E_{rf}/E_{rc}) versus valley shape factor (Pinto and Marques Filho 1998)..... 6.20

Figure 6.10: Deformation modulus during construction (E_{rc}) for Hydro Tasmania CFRDs (Giudici et al 2000)..... 6.21

Figure 6.11: Results of 3-dimensional finite element analysis of CFRD, to give vertical displacement during construction versus valley shape (Giudici et al 2000)..... 6.22

Figure 6.12: Settlement rate analysis of Cedar Creek dam; *(a)* determination of time t_o and *(b)* settlement rate versus time (Parkin 1977)..... 6.24

Figure 6.13: Post-construction crest settlement of membrane faced compacted rockfill dams (Clements 1984)..... 6.26

Figure 6.14: Settlement index versus time for well-compacted rockfills (adapted from Public Works Department NSW 1990)..... 6.27

Figure 6.15: Stress-strain relationship for rockfills observed during construction..... 6.33

Figure 6.16: Secant modulus versus vertical stress from monitoring during construction..... 6.33

Figure 6.17: Tangent modulus versus vertical stress from monitoring during construction..... 6.35

Figure 6.18: Idealised model for two-dimensional finite difference analysis of cross-valley influence..... 6.36

Figure 6.19: Results of two-dimensional finite difference analysis of the effect of cross-valley shape on vertical stresses in the dam. *(a)*, *(c)* and *(e)* represent construction in 5 m lifts (to 100 m) and *(b)*, *(d)* and *(f)* construction in a single 100 m lift..... 6.38

Figure 6.20: Indicators of cross valley arching effects from variations in the secant modulus with vertical stress..... 6.39

Figure 6.21: Representative secant modulus (mostly Zone 3A rockfill) at end of construction (E_{rc}) versus D_{80} from average grading of the rockfill..... 6.42

Figure 6.22: E_{rf}/ E_{rc} ratio versus embankment height..... 6.45

Figure 6.23: Stress paths during construction and first filling for nominal 100 m embankment with 1.3H to 1V upstream slope angle; *(a)* monitoring point locations, *(b)* stress paths for points normal to face slab at 30% of the embankment height..... 6.49

Figure 6.24: Stress paths during construction and first filling for nominal 100 m embankment with 1.55H to 1V upstream slope angle; *(a)* monitoring point locations, *(b)* stress paths for points normal to face slab at 30% of the embankment height..... 6.49

Figure 6.25: Face slab deflection during first filling (4/2/71 to 25/4/71) of Cethana dam (Fitzpatrick et al 1973). 6.50
Figure 6.26: Face slab deformation during first filling of Aguamilpa dam (Mori 1999) 6.51
Figure 6.27: Face slab deformation during first filling of Ita dam (Sobrinho et al 2000) 6.51
Figure 6.28: Scotts Peak dam; embankment zoning and location of face cracks (courtesy of Hydro Tasmania)..... 6.52
Figure 6.29: Mackintosh dam *(a)* embankment section (courtesy of Hydro Tasmania) and *(b)* face slab deformation on first filling (Knoop and Lack 1985) 6.52
Figure 6.30: Examples of derivation of zero time for post-construction settlement 6.56
Figure 6.31: Post-construction crest settlement versus time for dumped rockfill CFRD, t_o at end of main rockfill construction. 6.57
Figure 6.32: *(a)* and *(b)* Post-construction crest settlement versus time for CFRD constructed of compacted rockfills of medium to high intact strength, t_o at end of main rockfill construction. 6.58
Figure 6.33: *(a)* and *(b)* Post-construction crest settlement versus time for CFRDs constructed of well-compacted rockfills of very high intact strength and of well-compacted gravels, t_o at end of main rockfill construction. 6.59
Figure 6.34: Post-construction crest settlement versus time for dumped rockfill CFRD, t_o at end of first filling. 6.60
Figure 6.35: Post-construction crest settlement versus time for CFRD constructed of compacted rockfills of medium to high intact strength, t_o at end of first filling. 6.60
Figure 6.36: Post-construction crest settlement versus time for CFRDs constructed of well-compacted rockfills of very high intact strength and of well-compacted gravels, t_o at end of first filling. 6.61
Figure 6.37: Post construction crest settlement of Bastyan dam..... 6.65
Figure 6.38: Long-term crest settlement rate (as a percentage of embankment height per log cycle of time) versus embankment height for compacted rockfills 6.66
Figure 6.39: Crest settlement attributable to first filling (excluding time dependent effects)..... 6.68

Figure 7.1: Embankment construction indicating *(a)* broad layer width to embankment depth ratio in the early stages of construction and *(b)* narrow layer width to embankment depth ratio in the latter stages of construction. 7.24

Figure 7.2: *(a)* Total vertical stress ($s_{z,EOC}$) contours at end of construction for 1.8H to 1V embankment slopes, and *(b)* vertical stress ratio, Z_1, versus *h/H* under the embankment axis for various embankment slopes..... 7.26

Figure 7.3: Embankment model for finite difference analysis during construction. 7.29

Figure 7.4: Total vertical stress, total lateral stress, and lateral (horizontal) displacement distributions at end of construction for zoned earthfill finite difference analysis. 7.30

Figure 7.5: Finite difference modelling results; *(a)* total vertical stress on the dam centreline at end of construction, *(b)* settlement profile at dam axis at end of construction, and *(c)* lateral deformation at Point a (Figure 7.3) during construction. 7.32

Figure 7.6: Finite element analysis of zoned embankments highlighting arching of core zone from *(a)* Beliche dam at about mid-height, elevation 22.5 m (Naylor et al 1997), and *(b)* a puddle core embankment (Dounias et al 1996)..... 7.33

Figure 7.7: Estimated versus measured (from pressure cells) total vertical stresses during construction. 7.34

Figure 7.8: Total vertical stress profiles from the numerical analysis of construction for zoned embankments with different core slopes; *(a)* 0.2H to 1V case, *(b)* 0.5H to 1V case, and *(c)* total vertical stress at *h/H* = 0.70 with increasing embankment height. 7.36

Figure 7.9: Idealised types of pore water pressure response in the core during construction. 7.38

Figure 7.10: Pore water pressure response during construction in the core zone of clayey earthfills placed at close to or wet of Standard optimum moisture content. 7.39

Figure 7.11: Triaxial isotropic compression tests with staged undrained loading and partial drainage on a partially saturated silty sand (Bishop 1957). 7.41

Figure 7.12: Estimated lateral displacement ratio of the core at end of construction. 7.45

Figure 7.13: Estimated lateral displacement ratio of the core versus fill height above gauge during construction. 7.45

Figure 7.14: Lateral displacement ratio and pore water pressure versus fill height or measured total vertical stress at *(a)* Dartmouth dam; *(b)* Blowering dam; *(c)* Talbingo dam and *(d)* Thomson dam. 7.50

Figure 7.15: Vertical stress versus strain of the core during construction for selected cross-arm intervals of selected case studies; *(a)* dry placed clay cores, and *(b)* dry placed dominantly sandy and gravelly cores with plastic fines. 7.54

Figure 7.16: Confined secant moduli of the core versus vertical stress during construction for selected cross-arm intervals of selected case studies, *(a)* dry placed clay cores, and *(b)* dry placed dominantly sandy and gravelly cores with plastic fines. 7.55

Figure 7.17: Seating settlements at low stresses suspected as cause of low moduli estimates at low stresses..... 7.56

Figure 7.18: Vertical strain versus effective vertical stress in the core at end of construction for *(a)* dry placed clay earthfills and *(b)* dry placed dominantly sandy and gravelly earthfills. 7.58

Figure 7.19: Confined secant moduli versus effective vertical stress in the core at end of construction for *(a)* dry placed clay earthfills and *(b)* dry placed dominantly sandy and gravelly earthfills. 7.59

Figure 7.20: Vertical strain in the core versus fill height during construction at selected cross-arm intervals in selected case studies of earthfills placed close to or wet of Standard optimum, for *(a)* thin core (combined slopes less than 0.5H to 1V), and *(b)* medium cores (combined slope ≥ 0.5H to 1V and < 1H to 1V). 7.62

Figure 7.21: Vertical strain in the core versus fill height at end of construction for dominantly sandy and gravelly earthfills with plastic fines placed close to or wet of Standard optimum, for *(a)* thin cores (combined slopes less than 0.5H to 1V), and *(b)* medium to thick cores (combined slope ≥ 0.5H to 1V). 7.63

Figure 7.22: Vertical strain of the core versus fill height at end of construction for clay earthfills placed close to or wet of Standard optimum moisture content, for *(a)* thin core (combined slopes less than 0.5H to 1V), and *(b)* medium to thick cores (combined slope ≥ 0.5H to 1V). 7.64

Figure 7.23: Core settlement during construction of earth and earth-rockfill embankments *(a)* including Nurek dam, and *(b)* excluding Nurek dam. 7.67

Figure 7.24: Effect of reservoir filling on a zoned embankment (Nobari and Duncan 1972b) 7.70

Figure 7.25: Water load acting on a homogeneous earthfill dam. 7.71

Figure 7.26: Lateral stress distribution at *(a)* end of construction, and *(b)* reservoir full condition, for central core earth and rockfill embankment with core of similar compressibility properties to the rockfill. 7.72

Figure 7.27: Lateral stress distribution at *(a)* end of construction, and *(b)* reservoir full condition, for a central core earth and rockfill embankment with wet placed core of low undrained strength. 7.73

Figure 7.28: Compression curves for dry and wet states and collapse compression from the dry to wet state for Pyramid gravel in the laboratory oedometer test (Nobari and Duncan 1972a). 7.75

Figure 7.29: Idealised effect of matric suction on collapse compression of earthfills (Khalili 2002)..... 7.75

Figure 7.30: Cracking caused by post construction differential settlement between the core and the dumped rockfill shoulders (Sherard et al 1963)..... 7.77

Figure 7.31: Embankment model for finite difference analysis during first filling. 7.78

Figure 7.32: Model of the stress-strain relationship of the upstream rockfill incorporating collapse compression (in one-dimensional vertical compression). 7.80

Figure 7.33: Case 8 – "dry" placed, very stiff core modelling collapse compression in the upstream rockfill; numerical results of *(a)* vertical and *(b)* lateral displacement on first filling. 7.82

Figure 7.34: Case 9 – "dry" placed, very stiff core without collapse compression; numerical results of *(a)* vertical and *(b)* lateral displacement on first filling. 7.82

Figure 7.35: Case 10 – "wet" placed clay core of low undrained strength modelling collapse compression in the upstream rockfill. Numerical results of vertical and lateral deformation on first filling; *(a)* and *(b)* for reservoir at 40% of embankment height, *(c)* and *(d)* for reservoir at 98% of embankment height. 7.83

Figure 7.36: Case 11 – "wet" placed clay core without collapse compression; numerical results of *(a)* vertical and *(b)* lateral displacement on first filling. 7.84

Figure 7.37: Regional division of the embankment for analysis of post construction surface deformation. 7.85

Figure 7.38: Lateral displacement of the crest (centre or downstream region) on first filling versus embankment height (displacement is after the end of embankment construction). 7.88

Figure 7.39: Lateral displacement of the downstream slope (mid to upper region) on first filling versus embankment height (displacement is after the end of embankment construction). 7.95

Figure 7.40: Lateral displacement at the upper upstream slope of upstream crest region on first filling versus embankment height (displacement after the end of embankment construction). 7.97

Figure 7.41: Lateral displacement of the crest (centre to downstream region) on first filling versus downstream slope. 7.98

Figure 7.42: Lateral displacement of the downstream slope (mid to upper region) on first filling versus downstream slope. 7.98

Figure 7.43: Post construction internal settlement of the core at Talbingo dam (IVM ES1 at the main section). 7.101

Figure 7.44: Post construction internal settlement of the core at Copeton dam (IVM B, 9 m downstream of dam axis at main section). 7.101

Figure 7.45: Post construction internal settlement of the core at Bellfield dam. 7.102

Figure 7.46: Post construction crest settlement at 3 years after end of construction, *(a)* all data, *(b)* data excluding Ataturk. 7.105

Figure 7.47: Post construction crest settlement at 10 years after end of construction. 7.105

Figure 7.48: Post construction crest settlement at 20 to 25 years after end of construction. 7.106

Figure 7.49: Post construction settlement of the downstream slope (mid to upper region) at 3 years after end of construction. 7.107

Figure 7.50: Post construction settlement of the downstream slope (mid to upper region) at 10 years after end of construction. 7.107

Figure 7.51: Post construction settlement of the upper upstream slope and upstream crest region at 3 years after end of construction. 7.108

Figure 7.52: Post construction settlement of the upper upstream slope and upstream crest region at 10 years after end of construction. 7.108

Figure 7.53: Crest settlement versus time for zoned embankments with thin to medium width central core zones of dry placed clayey earthfills; *(a)* all data, *(b)* data excluding Ataturk. 7.113

Figure 7.54: Crest settlement versus time for zoned embankments with thin to medium width central core zones of wet placed clayey earthfills 7.114

Figure 7.55: Crest settlement versus time for zoned embankments with thin to medium width central core zones of dry placed clayey sand to clayey gravel (SC to GC) earthfills. 7.114

Figure 7.56: Crest settlement versus time for zoned embankments with thin to medium width central core zones of wet placed clayey sand to clayey gravel (SC to GC) earthfills. 7.115

Figure 7.57: Crest settlement versus time for zoned embankments with thin to medium width central core zones of silty sand to silty gravel (SM to GM) earthfills 7.116

Figure 7.58: Crest settlement versus time for zoned embankments with central core zones of clayey earthfills of thick width (1 to 2.5H to 1V combined width). 7.116

Figure 7.59: Crest settlement versus time for zoned embankments with central core zones of silty to clayey gravel and sand (SC, GC, SM, GM) earthfills of thick width (1 to 2.5H to 1V combined width). 7.117

Figure 7.60: Crest settlement versus time for embankments with very broad core widths (> 2.5H to 1V combined width) and limited foundation influence. 7.118

Figure 7.61: Crest settlement versus time for embankments with very broad core widths (> 2.5H to 1V combined width) and potentially significant foundation influence. 7.118

Figure 7.62: Long-term post construction crest settlement rate for zoned earthfill and earth-rockfill embankments of thin to thick core widths, *(a)* all data, and *(b)* data excluding Ataturk. 7.120

Figure 7.63: Long-term post construction crest settlement rate for embankments of very broad core width, (a) all data, and (b) data excluding Belle Fourche, Roxo and Rector Creek. 7.121

Figure 7.64: Crest settlement versus time for central core earth and rockfill embankments with central core zones of clayey earthfills and steady post first filling reservoir operation. 7.127

Figure 7.65: Crest settlement versus time for central core earth and rockfill embankments with thin to thick central core zones of clayey earthfills subjected to seasonal reservoir fluctuation. 7.127

Figure 7.66: Post construction settlement and reservoir operation at Enders dam (data courtesy of USBR). 7.131

Figure 7.67: Post construction settlement at main section and reservoir operation at San Luis dam (data courtesy of USBR). 7.132

Figure 7.68: Crest displacement versus time for zoned embankments with thin to medium width central core zones of dry placed clayey earthfills. 7.133

Figure 7.69: Crest displacement versus time for zoned embankments with thin to medium width central core zones of wet placed clayey earthfills 7.134

Figure 7.70: Crest displacement versus time for zoned embankments with thin to medium width central core zones of dry placed clayey sand and clayey gravel (SC/GC) earthfills. 7.134

Figure 7.71: Crest displacement versus time for zoned embankments with thin to medium width central core zones of wet placed clayey sand and clayey gravel (SC/GC) earthfills. 7.135

Figure 7.72: Crest displacement versus time for zoned embankments with thin to medium width central core zones of silty sand and silty gravel (SM/GM) earthfills..... 7.135

Figure 7.73: Crest displacement versus time for zoned embankments with central core zones of clayey earthfills of thick width (1 to 2.5H to 1V combined width). 7.136

Figure 7.74: Crest displacement versus time for zoned embankments with central core zones of silty to clayey sand and gravel earthfills of thick width. 7.136

Figure 7.75: Crest displacement versus time for embankments with very broad core zones (> 2.5H to 1V width) and with limited foundation influence..... 7.137

Figure 7.76: Crest displacement versus time for embankments with very broad core zones (> 2.5H to 1V width) and with potentially significant foundation influence on the embankment deformation. 7.137

Figure 7.77: Crest displacement normal to dam axis post first filling..... 7.139

Figure 7.78: Long-term settlement rates for the downstream slope (mid to upper region) versus embankment height; *(a)* all data, and *(b)* data excluding Belle Fourche..... 7.143

Figure 7.79: Post construction settlement of the downstream shoulder (mid to upper region) for selected case studies..... 7.144

Figure 7.80: Post construction displacement of the downstream shoulder (mid to upper region) for selected case studies of embankments with very broad core widths. 7.145

Figure 7.81: Post construction displacement of the downstream shoulder (mid to upper region) for selected case studies of central core earth and rockfill embankments..... 7.147

Figure 7.82: Post construction displacement of the downstream shoulder (mid to upper region) for embankments with compacted earthfills and gravels in the downstream shoulder. 7.148

Figure 7.83: Long-term settlement rates of the upper upstream slope to upstream crest region of earthfill and earth-rockfill embankments. 7.152

Figure 7.84: Post construction settlement of the upper upstream slope to upstream crest region for embankments with poorly compacted rockfill in the upstream slope. 7.153

Figure 7.85: Post construction settlement of the upper upstream slope to upstream crest region for selected case studies (excluding poorly compacted rockfills)... 7.153

Figure 7.86: Post construction lateral displacement of the upper upstream slope and upstream crest region for selected case studies of embankments with rockfill in the upstream shoulder..... 7.156

Figure 7.87: Post construction lateral displacement of the upper upstream slope to upstream crest region for selected case studies of embankment with earthfills and gravels in the upstream shoulder. 7.157

Figure 7.88: Selset Dam internal settlements during construction (data from Bishop and Vaughan 1962) 7.159

Figure 7.89: "Idealised" model of collapse compression of poorly compacted shoulder fill of puddle core earthfill dam on first filling. 7.164

Figure 7.90: "Idealised" model of yielding of poorly compacted shoulder fill and puddle core on first drawdown of a puddle core earthfill dam. 7.164

Figure 7.91: "Idealised" model of collapse compression on wetting of poorly compacted earthfill in the downstream shoulder of a puddle core earthfill dam. 7.165

Figure 7.92: Post construction crest settlement versus log time of puddle core earthfill dams. 7.167

Figure 7.93: Definitions of "steady state" conditions during normal reservoir operating conditions. 7.172

Figure 7.94: Fluctuation of pore water pressures adjacent to and upstream of the puddle core with fluctuations in reservoir level. 7.174

Figure 7.95: Ramsden Dam, internal horizontal deformation of the puddle core, 1988 to 1990 (Holton 1992). 7.176

Figure 7.96: Ramsden Dam, internal vertical strains measured in the puddle core from 1988 to 1990 (data from Tedd et al 1997b and Kovacevic et al 1997). 7.177

Figure 7.97: Vertical strain (or settlement) at the crest versus drawdown depth for specific drawdown and refilling cycles (Tedd et al 1997b). 7.179

Figure 7.98: Permanent vertical crest strains during cyclic drawdown (in normal operating range) for puddle core dams with permeable upstream filling (after Tedd et al 1997b). 7.179

Figure 7.99: Ramsden Dam, settlement of SMPs versus time from 1988 to 1990 (data from Tedd et al 1990). 7.180

Figure 7.100: Ogden Dam, crest settlement versus time (Tedd et al 1997a). 7.181

Figure 7.101: Idealised model of deformation during historically large drawdown. . 7.182

Figure 7.102: Walshaw Dean (Lower) dam, crest settlement versus time (Tedd et al 1997a) 7.183

Figure 7.103: Cross section through Beliche dam at the main section (Maranha das Neves et al 1994) 7.189

Figure 7.104: Cross section of Chicoasen dam at the main section (Moreno and Alberro 1982) 7.189

Figure 7.105: Section at Hirakud dam (Rao and Wadhwa 1958) 7.192
Figure 7.106: Cumulative settlement during construction at Hirakud dam (adapted from Rao 1957) 7.192
Figure 7.107: Cross section of Nurek dam (adapted from Borovoi et al 1982)..... 7.193
Figure 7.108: Carsington dam, section at chainage 825 m after failure (adapted from Skempton and Vaughan 1993). 7.194
Figure 7.109: Carsington dam, vertical strain profiles from IVM during construction, *(a)* IVM C at chainage 850 m, and *(b)* IVM B at chainage 705 m (adapted from Rowe 1991)..... 7.195
Figure 7.110: Carsington dam, variation of the maximum vertical strain in the core with bank level (Rowe 1991). 7.195
Figure 7.111: Maximum section at El Infiernillo dam (Marsal and Ramirez de Arellano 1967). 7.203
Figure 7.112: El Infiernillo dam, deformation instrumentation on station 0+135 at the lower left abutment (Marsal and Ramirez de Arellano 1967)..... 7.204
Figure 7.113: El Infiernillo dam, internal settlements during first filling at Station 0+135..... 7.205
Figure 7.114: Main section at Chicoasen dam (Moreno and Alberro 1982)..... 7.206
Figure 7.115: Chicoasen dam, inclinometer and cross-arm locations at the main section (Moreno and Alberro 1982)..... 7.206
Figure 7.116: Internal settlement profiles during first filling at Chicoasen dam (adapted from Moreno and Alberro 1982). 7.207
Figure 7.117: Beliche Dam, cross section (Maranha das Neves et al 1994)..... 7.209
Figure 7.118: Beliche dam, post construction internal vertical settlement profile within the embankment for the period from end of construction to 2.75 years post construction. 7.209
Figure 7.119: Typical section of Canales dam (Bravo 1979). 7.210
Figure 7.120: Canales dam, *(a)* cracking and differential settlement at the crest, and *(b)* post construction settlement at the crest (Giron 1997) 7.211
Figure 7.121: Main section at Djatiluhur dam (Sowers et al 1993)..... 7.212
Figure 7.122: Djatiluhur dam; *(a)* location of crack observed during construction, January 1965; and *(b)* deformation of monuments at elevation 103 m, January to April 1965 (Sherard 1973). 7.214
Figure 7.123: Eppalock dam, post construction settlement of SMPs on the crest and slopes for the first five years after construction. 7.215
Figure 7.124: Main section at Blowering dam (courtesy of NSW Department of Public Works and Services, Dams and Civil Section). 7.218

Figure 7.125: Blowering dam, vertical strain during construction for selected cross-arms intervals in the core. 7.220
Figure 7.126: Blowering dam, post construction internal settlement of the core from IVM A during first filling. 7.221
Figure 7.127: Cross section of Ataturk dam (Cetin et al 2000) 7.221
Figure 7.128: Post construction settlement of the crest and downstream shoulder at Ataturk dam. 7.223
Figure 7.129: LG-2 dam; crack in crest and possible shear plane in core (Paré 1984) 7.224
Figure 7.130: Main section at Copeton dam (courtesy of New South Wales Department of Land and Water Conservation) 7.225
Figure 7.131: Copeton dam, post construction internal settlement profile in the core at IVM A. 7.227
Figure 7.132: Copeton dam, post construction settlement between cross-arms versus time. 7.228
Figure 7.133: Eppalock dam, original design at maximum section (Woodward Clyde 1999) 7.230
Figure 7.134: Eppalock dam, post construction settlement at main section and CS1. ..... 7.231
Figure 7.135: Eppalock dam, post construction horizontal displacement at the main section. 7.233
Figure 7.136: Djatiluhur dam, post construction crest settlement. 7.234
Figure 7.137: Bellfield dam, main section at chainage 701 m (courtesy of Wimmera Mallee Water) 7.235
Figure 7.138: El Infiernillo dam, internal *(a)* settlement and *(b)* displacement in the core from 1966 to 1972 (Marsal and Ramirez de Arellano 1972) 7.236
Figure 7.139: El Infiernillo dam, post construction *(a)* settlement and *(b)* displacement of surface markers. 7.237
Figure 7.140: Main section at Eildon dam (courtesy of Goulburn Murray Water). 7.239
Figure 7.141: Eildon dam, post construction settlement of SMPs at chainage 685 m. 7.240
Figure 7.142: Eildon dam, internal settlement profiles in core from IVM records for the period 1981 to 1998. ..... 7.240
Figure 7.143: Main section at Svartevann dam (Kjœrnsli et al 1982). 7.243
Figure 7.144: Svartevann dam, post construction *(a)* settlement and *(b)* displacement. 7.246
Figure 7.145: Cross section at Cougar dam (Cooke and Strassburger 1988). 7.247

Figure 7.146: Cougar dam; post construction *(a)* settlement and *(b)* displacement normal to dam axis of the crest at the maximum section (adapted from Pope 1967). 7.248

Figure 7.147: Cougar dam; differential settlement and cracks on crest (Pope 1967) 7.249

Figure 7.148: Wyangala dam, post construction internal settlement in IVM B located 9 m upstream of dam axis. 7.250

Figure 7.149: Section at Wyangala dam (courtesy of New South Wales Department of Land and Water Conservation). 7.251

Figure 7.150: Rector Creek dam main section (Sherard 1953)..... 7.254

Figure 7.151: Rector Creek dam; post construction settlement and displacement versus log time (adapted from Sherard et al 1963). 7.254

Figure 7.152: Roxo dam, settlement versus log time (adapted from De Melo and Direito 1982). 7.255

Figure 7.153: Main section at Mita Hills dam (Legge 1970)..... 7.256

Figure 7.154: Main section at Dixon Canyon dam (courtesy of U.S. Bureau of Reclamation). 7.258

Figure 7.155: Post construction *(a)* settlement and *(b)* displacement of SMPs on the upper upstream slope at the Horsetooth Reservoir embankments. 7.259

Figure 7.156: Belle Fourche dam; main section as constructed in 1911 (courtesy of U.S. Bureau of Reclamation). 7.260

Figure 7.157: Belle Fourche dam; post construction crest settlement over the period 1911 to 1928 (to 17 years post construction). 7.264

Figure 7.158: Belle Fourche dam closure section; post construction *(a)* settlement and *(b)* displacement normal to dam axis of the crest and slopes over the period 1985 to 2000 (73 to 89 years post construction). 7.265

Figure 7.159: San Luis dam, section of the slide in the upstream slope in 1981 at Station 135+00 (courtesy of United States Bureau of Reclamation). 7.266

Figure 7.160: San Luis dam, difference between actual and predicted settlement (Von Thun 1988)..... 7.268

Figure 7.161: San Luis dam, comparison of settlement between SMPs at 13 m upstream of dam axis and SMPs at 6.5 m downstream. 7.268

Figure 7.162: San Luis dam, post construction settlement of SMPs in the vicinity of the slide area. 7.269

Figure 7.163: Main section at Horsetooth dam (courtesy of the United States Bureau of Reclamation). 7.271

Figure 7.164: Horsetooth dam, post construction displacement of SMPs near to the main section. 7.272

Figure 7.165: Pueblo dam; cross section of left abutment embankment at Station 75.....7.273
Figure 7.166: Pueblo dam, post construction settlement of the left embankment near Station 75.....7.274
Figure 7.167: Yan Yean dam; settlement rate versus time of SMPs at Chainage 150 and 750 m. 7.279

TABLE OF CONTENTS

1.0 INTRODUCTION 1.1

1.1 OBJECTIVES OF THE RESEARCH 1.1

1.1.1 Landslides in Soil Slopes 1.2

1.1.2 Deformation Behaviour of Embankment Dams 1.3

1.2 STRUCTURE OF THE THESIS 1.4

1.3 TERMS AND DEFINITIONS 1.5

1.3.1 General Terms and Definitions 1.5

1.3.2 Terms and Definitions for Landslides 1.5

1.3.3 Terms and Definitions for Embankments 1.9

LIST OF TABLES

Table 1.1: IUGS (1995) velocity classifications for landslides. 1.6

Table 1.2: Classification of unconfined compressive strength of intact rock (AS 1726-1993) 1.13

LIST OF FIGURES

Figure 1.1: Landslide classification system and main slide types 1.7

Figure 1.2: Definition of travel distance, travel distance angle, and slope geometry. 1.8

Figure 1.3: Slope failure geometries *(a)* Type 1 - failure at the top of the cut or fill slope, *(b)* Type 2 – the toe of failure is coincident with the toe of the slope, and *(c)* Type 5 – the surface of rupture extends below and daylights beyond the toe of the slope. 1.8

Figure 1.4: Classification of slope failure geometries *(a)* Type 3 –travel on relatively uniform or gradually decreasing slope angles, and *(b)* Type 4 – travel on changing slope angles from steep to shallow 1.9

Figure 1.5: Embankment zoning classification system (Foster 1999) 1.10

Figure 1.6: Dam zoning categories of embankment types (Foster et al 2000) 1.10

1.0 INTRODUCTION

1.1 OBJECTIVES OF THE RESEARCH

This thesis is a study of the pre and post failure deformation behaviour of landslides in cut, fill and natural soil slopes, and of the deformation behaviour of embankment dams.

The need for the research on the deformation behaviour of landslides stems from recognition of the deficiency of quantitative information databases for risk assessment methods in evaluation of landsliding in soil slopes. The fundamental objective of the research was to address these deficiencies for a number of slope conditions and material types. No risk assessment of itself has been undertaken.

The main objectives of the research on the deformation behaviour of landslides in soil slopes were, for selected classes of slope and soil characteristics, to:

i) Develop methods or guidelines for assessment/evaluation of the pre-failure deformation behaviour leading up to landsliding;
ii) Identify the slope conditions and soil characteristics that will result in "slow" or "rapid" landsliding; and
iii) Develop methods for prediction of the post failure deformation behaviour.

For embankment dams, those who are responsible for interpreting the deformation behaviour do not have clear criteria to assess their data and often have to rely on their judgement and personal experience. Whilst numerical modelling methods make for useful tools in modelling embankment dam behaviour, few reported Type A predictions have been able to accurately model the deformation behaviour during construction and on first filling. Methods based on comparison to historical records of similar embankments are still heavily relied upon and, particularly for the assessment of post construction deformation behaviour, provide the responsible personnel with the best guide to assessment of embankment performance.

The main objectives of the research on the deformation behaviour of embankment dams were, from the historical performance records of case studies of selected embankment types, to:

i) Broadly define "normal" deformation behaviour and from this platform to then identify "abnormal" deformation behaviour;

ii) Define trends in the deformation behaviour that are potentially indicative of a marginally stable or unstable slope condition, and are precursors to potential slope instability; and

iii) Provide owners and their consultants with methods that allow comparison of the deformation behaviour of their structures to similar embankment types during and post construction.

The method of research was case study driven. Outcomes were developed from analysis of the database in consideration of the mechanism/s influencing the deformation behaviour. The database of landslides included some 450 case studies and of embankment dams some 170 case studies.

1.1.1 LANDSLIDES IN SOIL SLOPES

For the landslides in constructed and natural soil slopes, information for each case study was collected on:

- Slope geometry, both in the source area and the downslope travel path;
- Geology;
- Hydrogeology;
- Geotechnical properties of the soils within which the landslide occurred, and on the downslope path for slides that travelled large distances beyond the toe of the slide area;
- Slope history;
- Characteristics of the surface of rupture;
- Mechanism and trigger of the slope failure, and mechanism of the post failure travel; and
- Deformation behaviour pre, at and post failure, both actual records and anecdotal information.

Most of the case study data was from the published literature, but for a minority of cases it was obtained or enhanced from unpublished reports from sponsors or in-kind sponsors of the project.

Monitored records of pre-failure deformation were available for a limited number of cases only. These were generally from well-instrumented cut or fill slopes constructed

to failure, but also from several of the failures in embankment dams during construction and failures in active waste spoil piles. Anecdotal information from eyewitness accounts was also available for several of the case studies.

For the post failure deformation behaviour of landslides case studies with actual monitoring records were also limited. In most cases the data is limited to the travel distance and areal extent of the failed slide mass. Some data is available on the actual slide velocity from measurement points on "slow" moving slides, but is mostly from estimates based on eyewitness accounts or the super-elevation on bends in the travel path of fast moving confined debris flows or flow slides. Delineation in the travel velocity of the slide mass is therefore often as either "slow" or "rapid".

The slope classes, soil and slide types considered in the research were for landslides in:

- Soil types that are potentially contractile on shearing under the stress conditions imposed, including loose placed granular fills, mine waste stockpiles, hydraulic fills, submarine slopes and sensitive clays.
- Cut slopes in residual soils, colluvium and weathered rock;
- Cut slopes in high plasticity, heavily over-consolidated clays;
- "Slides of debris";
- Fill embankments constructed on soft ground; and
- Embankment dams, including failures during construction, on drawdown and post construction in the downstream shoulder.

For several of the slope classes (e.g. landslides in sensitive clays) the current literature on deformation behaviour has been well researched. Inclusion of these slide types is mainly for comparative purposes to other slide groups.

1.1.2 DEFORMATION BEHAVIOUR OF EMBANKMENT DAMS

The analysis of embankment dams was on the following embankment types:

- Earthfill, zoned earthfill and zoned earth and rockfill embankments of rolled earthfill construction;
- Puddle core earthfill embankments;
- Concrete face rockfill dams.

The deformation behaviour during construction, on first filling and post first filling was analysed for the above embankment types.

About 40 to 50% of the case studies were from Australian dam authorities / owners and the United States Bureau of Reclamation for which detailed information was made available on material types, construction procedures and instrumentation records. This was supplemented with case studies from the published literature for which the available information was of variable quality.

1.2 STRUCTURE OF THE THESIS

The thesis structure is as follows:

- A brief review of the literature pertaining to the broader concepts of landslides in soil slopes and deformation behaviour of embankment dams (Chapter 2). A more detailed literature review is presented at the beginning of each of Chapters 3 through 7.
- Landslides in soil slopes of "rapid" post failure velocity (Chapter 3). From analysis of the database, review of the literature and in consideration of the mechanics of failure, guidelines are developed for slope geometrical conditions, soil characteristics and the pre-failure deformation behaviour for the classes of "rapid" landslides considered. Methods are developed for estimation of the post failure travel distance that incorporate the quantifiable factors thought to significantly affect the post failure travel for a specific slide class.
- Failures in fill embankments constructed on soft ground (Chapter 4). From analysis of the pre-failure deformation behaviour guidelines are developed for identification of an impending failure condition. Guidelines are presented in Chapter 5 for prediction of the post failure deformation.
- Landslides in cut slopes of heavily over-consolidated high plasticity clays, and failures in embankment dams (Chapter 5). The analysis concentrates on the mechanics of failure and post failure deformation behaviour. Guidelines are presented for prediction of the post failure deformation.
- The deformation behaviour of rockfill (Chapter 6). Guidelines are developed for estimation of the moduli of rockfill during construction and prediction of deformation behaviour during and post construction developed from the deformation records of mostly concrete face rockfill dams.

- The deformation behaviour of embankment dams (Chapter 7). From a large database of case studies, methods are developed and existing methods enhanced for evaluation and prediction of the deformation behaviour of an embankment during and post construction. Guidelines are presented for identification of potentially "abnormal" deformation behaviour, and the potential indicators of a marginally stable slope condition.

Each of Chapters 3 through 7 were published as individual reports through the School of Civil and Environmental Engineering at The University of New South Wales (Hunter et al (2000); Hunter and Fell (2001, 2002a, 2002b, 2003)).

1.3 TERMS AND DEFINITIONS

1.3.1 GENERAL TERMS AND DEFINITIONS

The classification of soils is in accordance with the Australian soil classification system (Australian Standard AS 1726-1993 - Geotechnical Site Investigations). This classification system is similar to the Unified Soil Classification System (USBR Earth Manual and ASTM D2487-69) except that the particle size limits for the sand and gravel sizes are in metric units and at slightly different sizes.

1.3.2 TERMS AND DEFINITIONS FOR LANDSLIDES

Following is a summary of definitions of terms. Details are given in Appendix A.

Landslide Velocity. The post failure velocity of the slide mass is classified according to the system proposed by the International Union of Geological Sciences (IUGS 1995), as presented in Table 1.1.

"Rapid Landslide" – a landslide that has a post failure travel velocity in the rapid, very rapid or extremely rapid class as defined by IUGS (1995). Most of what are termed "rapid" landslides would classify as very rapid or extremely rapid, having post failure velocities greater than 3 metres/minute and generally in the order of metres/sec.

"Slow Landslide" – a landslide that has a post failure travel velocity in the moderate, slow or very slow class as defined by IUGS (1995), in the range from centimetres/year to less than 1.8 metres/hour.

Table 1.1: IUGS (1995) velocity classifications for landslides.

Velocity Classification	**Description of Velocity**	**Velocity limits**	**Value in mm/sec**
7	Extremely rapid	> 5 m/sec	$> 5x10^{3}$
6	Very rapid	3 m/min to 5 m/sec	50 to $5x10^{3}$
5	Rapid	1.8 m/hour to 3 m/min	0.5 to 50
4	Moderate	13 m/month to 1.8 m/hour	$5x10^{-3}$ to 0.5
3	Slow	1.6 m/year to 13 m/month	$50x10^{-6}$ to $5x10^{-3}$
2	Very slow	16 mm/year to 1.6 m/year	$0.5x10^{-6}$ to $50x10^{-6}$
1	Extremely slow	≤ 16 mm/year	$\leq 0.5x10^{-6}$

Landslide Classification is according to Hutchinson (1988). For "rapid" landslides a dual classification is used to describe the initiating landslide in the source area and the subsequent slide movement in the travel region. The main terms used to describe the movement of a landslide are shown in Figure 1.1 and described below.

Dilative and Contractile Slides – description of the initial tendency of the soil on the surface of rupture to increase (dilate) or decrease (contract) in volume under drained shear, or to develop negative or positive pore water pressures in undrained shear when in a saturated (or near saturated) condition.

Flow Slide is used to describe the initiating slide in saturated (or near saturated) contractile soils, where the failure or rapid acceleration of the slide mass occurs as a result of a large loss in undrained strength due to static liquefaction on shearing. *Flow slide* is also used as a travel classification descriptor to describe landslides where the main volume of the slide mass is bodily carried on a liquefied basal zone, but is only applicable to landslides initially classified as flow slides (Figure 1.1).

Defect Controlled Slide is used to describe landslides that are dominantly controlled by defects in the soil or weathered rock mass.

"Slide of Debris" is a general term that is used to describe landslides in colluvium, talus or other slope mantling debris.

Debris Flow is used to describe turbulent post failure slide movements of a combination of water, air and debris. The slide mass is a broken up mass of material that no longer retains its original structure or fabric.

Debris Slide is used to describe sliding on a defined basal surface where the slide mass retains its structure and fabric during travel. *Debris Slide* is generally used as a descriptor for slides that travel beyond the source area, and *intact slide* for slides where the post failure deformation is largely confined to the source area.

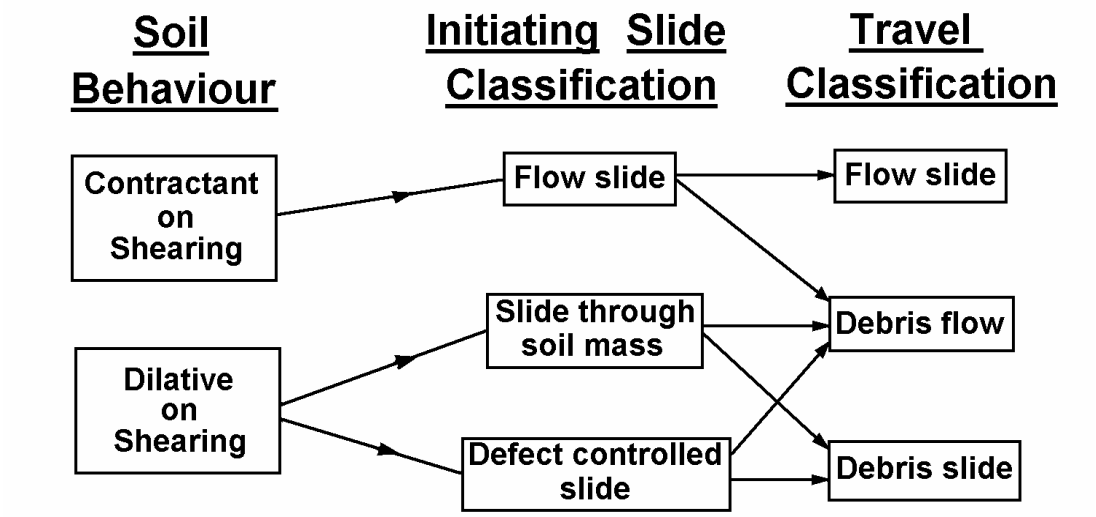

Figure 1.1: Landslide classification system and main slide types.

Travel distance, L, landslide height, H, and travel distance angle, a, defined in Figure 1.2, are used to describe the overall longitudinal geometry of the slide mass from the crest of the source area to the distal toe of the travel.

Source area slope angle (a_1), rupture surface inclination (a_{base}), initial downslope angle (a_2) and distal downslope angle (a_3), defined in Figure 1.2, and *cut (a_{cut}) or fill slope angle (a_{fill}),* are used to describe the longitudinal slope geometry. Note that a_3 is undefined for several failure slope geometries (see below).

Slope failure geometry or *failure type* is a classification of the position of the initial failure within the slope and the longitudinal shape of the downslope geometry. Five types have been defined. Types 1, 2 and 5 are defined in Figure 1.3, and Types 3 and 4 in Figure 1.4. For Types 1 and 2 the slope below the cut of fill slope is near horizontal. For "rapid" landslides with relatively long travel paths Types 1, 2 and 4 are characterised by sharp changes in slope angle whilst Type 3 is characterised by relatively smooth changes. Further details are given in Appendix A.

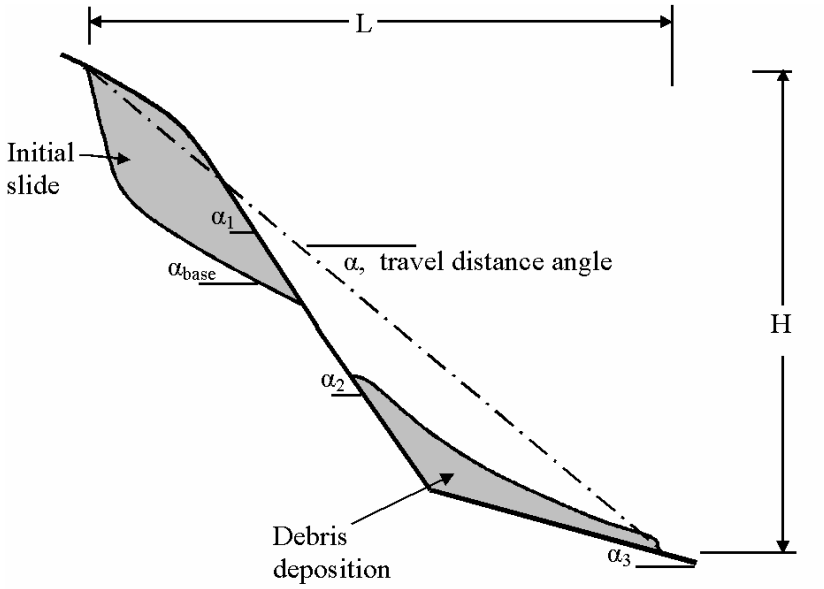

Figure 1.2: Definition of travel distance, travel distance angle, and slope geometry.

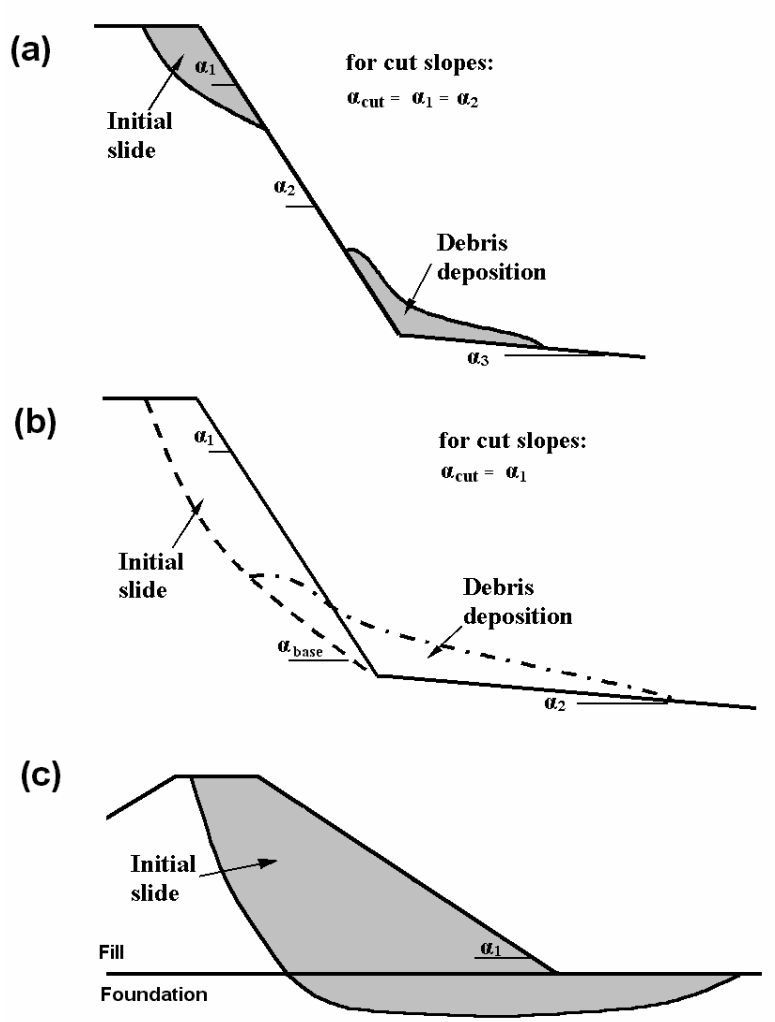

Figure 1.3: Slope failure geometries *(a)* Type 1 - failure at the top of the cut or fill slope, *(b)* Type 2 – the toe of failure is coincident with the toe of the slope, and *(c)* Type 5 – the surface of rupture extends below and daylights beyond the toe of the slope.

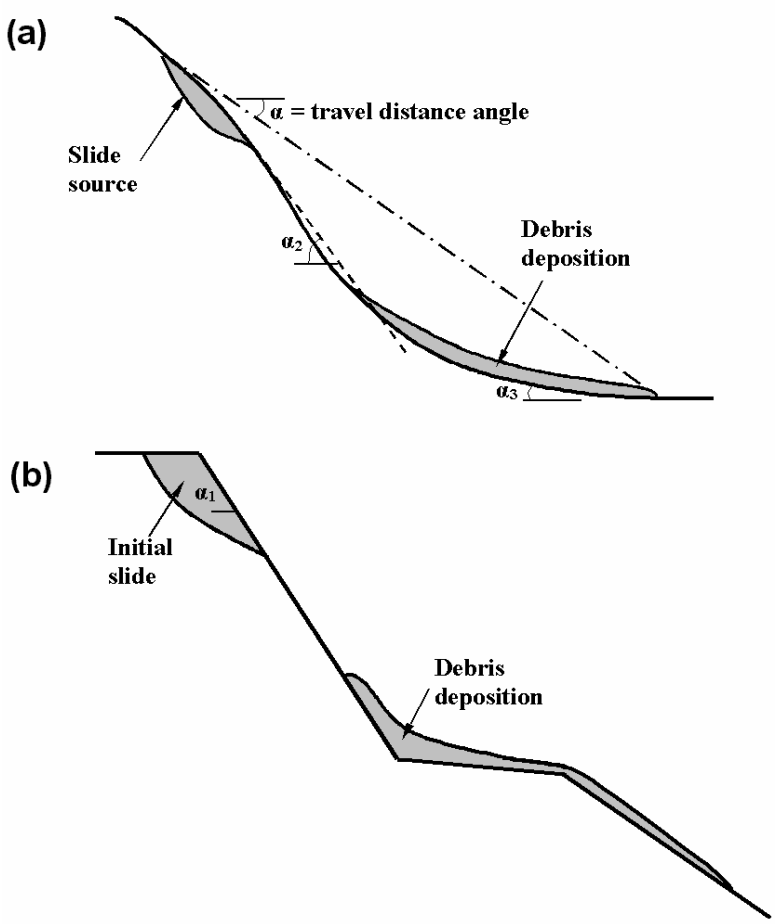

Figure 1.4: Classification of slope failure geometries *(a)* Type 3 –travel on relatively uniform or gradually decreasing slope angles, and *(b)* Type 4 – travel on changing slope angles from steep to shallow.

Degree of confinement of the travel path - the terms used (after Golder Assoc. 1995) are; c*onfined* – the travel path is constrained by the relatively steep side-slopes of a gully or small valley; *unconfined* – the travel path is on open slopes; and *partly confined* – the travel path is not sharply defined by a topographic depression. Further details are given in Appendix A.

1.3.3 TERMS AND DEFINITIONS FOR EMBANKMENTS

(a) Embankment Dam Zoning Classification

The embankment dam zoning classification system used is essentially the system developed by Foster (1999). The system incorporates three components to describe the general zoning of the embankment; embankment type, embankment filters and

foundation filters, and consists of a three number system (Figure 1.5). The codes to the numbering used for the embankment zoning category are given in Figure 1.6.

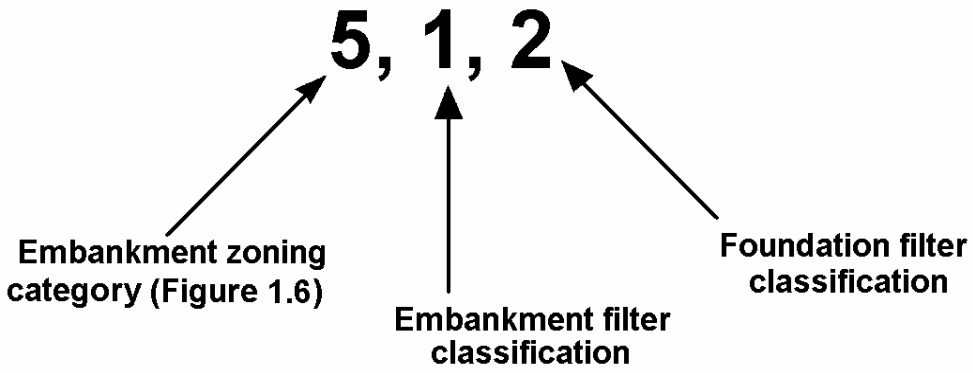

Figure 1.5: Embankment zoning classification system (Foster 1999; Foster et al 2000)

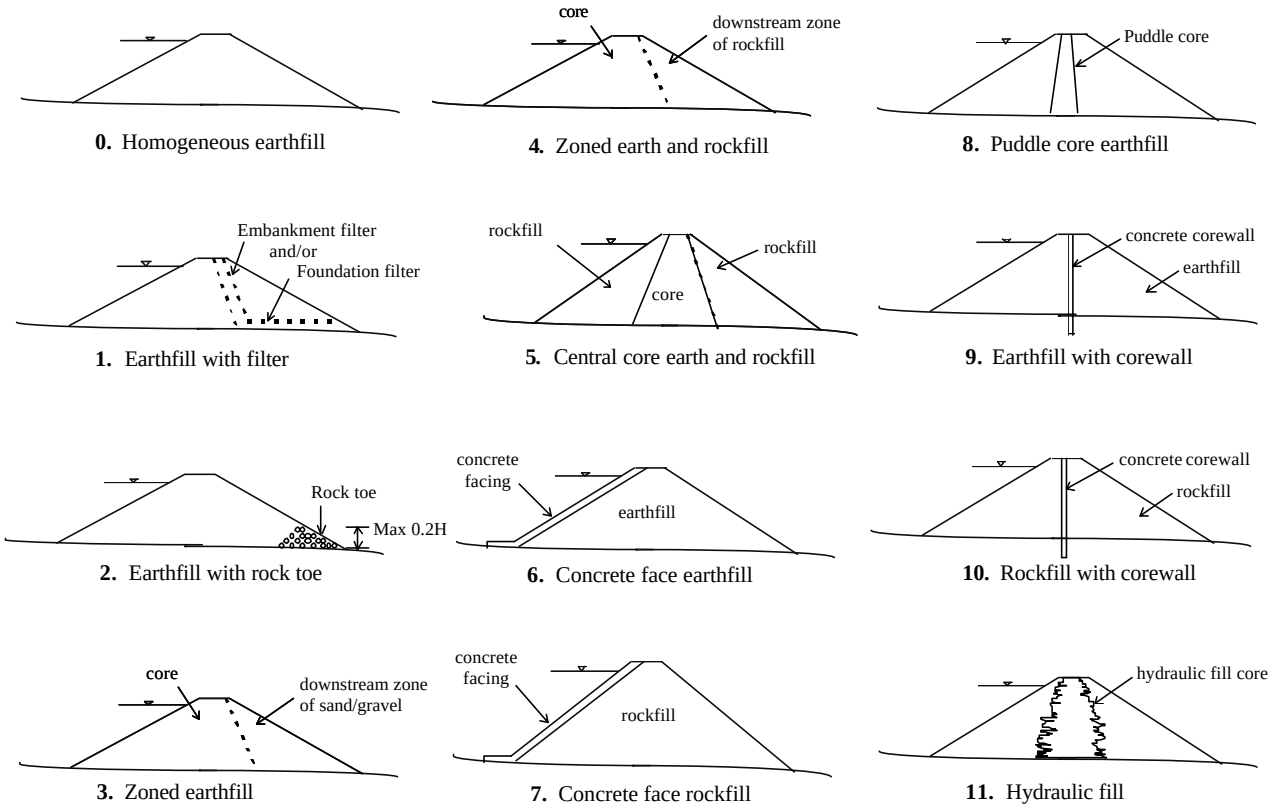

Figure 1.6: Dam zoning categories of embankment types (Foster 1999)

For the filter classification the numbering code system used for both the embankment and foundation filters is as follows:

0 - No filter drains present

1 - One filter present

2 - Two (or more) filter zones present

X - Unknown

A sub-classification system has been developed to describe the thickness or width of the core. It was developed mainly to distinguish between zoned earthfill or earth and rockfill embankments with thin central cores from those with thick central cores. It was then broadened to encompass all earthfill and zoned earth-rockfill embankments. The core width classification is:

- Thin earthfill core – symbol *c-tn*. Core width increasing at less than or equal to 0.5 times the vertical distance below the crest; i.e. slopes less than or equal to 0.25H to 1V for central cores (H to V = horizontal to vertical).
- Medium thickness earth core – symbol *c-tm.* Core width increase in the range 0.5 to 1.0 times the vertical distance below the crest. For central cores it includes cores with slopes greater than 0.25H to 1V and less than or equal to 0.5 H to 1V.
- Thick earthfill core – symbol *c-tk*. Core width increase in the range 1.0 to 2.5 times the vertical distance below the crest. For central cores it includes cores with slopes greater than 0.5H to 1V and less than 1.25 H to 1V.
- Very broad earthfill core - symbol *c-vb*. This classification includes all homogeneous earthfill embankments and earthfill embankments with filters as well as zoned earthfill and zoned earth and rockfill embankments where the main earthfill water barrier zone has an average width equal to or greater than the width at the crest plus 2.5 times the depth below the crest.

For zoned earthfill embankments the core width classification only considers the width of the main water barrier zone, from its upstream edge to the downstream edge of the filter or permeable transition zones. Therefore, zoned embankments with filters separating the core from similar type earthfills in the downstream shoulder may not be classified as “very broad”, although, earthfill embankments with chimney filters are classified as “very broad”. This is somewhat contradictory but the database only includes one earthfill embankment with a chimney filter (Mita Hills) classified as “very broad” that would fail the zoned embankment criteria for the “very broad” classification.

(b) Classification of Rockfill Placement

The method of placement of rockfill has a significant influence on its compressibility during construction and its deformation behaviour post construction. The definitions by Cooke (1993, 1984) for dumped and compacted rockfill have been used as a basis for categorisation of the method of placement. The definitions used are:

- Compacted Rockfill – rockfill placed in layers up to 2 m thickness (generally 0.9 to 2.0 m thick) and compacted by smooth drum vibrating roller (SDVR). Accepted practice is typically 4 to 6 passes of a minimum 10 tonne (possibly up to 15 tonne) deadweight vibrating roller, with variation in layer thickness, added water and number of passes depending on the quality and type of the rockfill, amount of fines and location within the embankment. Three classifications for compacted rockfill have been used:
  - Well-compacted – layer thickness typically less than about 1.0 m (depending on the compressive strength of the intact rock) and compacted with a minimum of four passes of a 10 to 15 tonne deadweight SDVR.
  - Reasonable Compaction – layer thickness typically 1.5 to 2.0 m and compacted with typically four passes of a 10 tonne SDVR.
  - Reasonably to Well Compacted - layer thickness typically 1.2 to 1.6 m (depending on the compressive strength of the intact rock) and compacted with typically 4 to 6 passes of a 10 to 15 tonne SDVR.
- Rockfill not formally compacted or "poorly compacted". Several methods of rockfill placement have been included under the definition "poorly compacted", these include:
  - Dumped rockfill – rockfill placed in lifts ranging from several to tens of metres thickness, with or without sluicing, and without formal compaction.
  - Rockfill placed in lifts less than about 2 to 3 m thickness and not formally compacted (i.e. without the use of rollers for compaction). Specified track rolling by bulldozer or other plant, or rockfill indicated as being trafficking by trucks or other haulage equipment has been classified under "not formally compacted".
  - Rockfill placed in lifts greater than 2 to 3 m and formally compacted. For these rockfills the lift thickness is considered too great for compaction to have any significant influence at depth.

Watering is an important component for placement of rockfills, particularly in cases where the compressive strength of the rock used in the rockfill is susceptible to reduction on wetting, breaks down under the action of the roller, or if the rockfill contains large quantities of fines. Cooke (1993) comments that watering is not overly important for compaction of very high strength rockfills that are not susceptible to weakening on wetting. However, these rockfills can still show collapse type settlements on wetting.

For dumped rockfills, sluicing had a significant influence on the deformation behaviour of the rockfill as evidenced by the large collapse deformations of dry dumped or poorly sluiced rockfills when wetted (Cogswell dam (Baumann 1958), Strawberry and Dix River dams (Howson 1939)).

(c) Unconfined Compressive Strength of Rock

The classification system from Australian Standard AS 1726-1993 is used to define the unconfined compressive strength (UCS) of intact rock used in rockfill. The descriptors and the UCS range they represent are given in Table 1.2.

Table 1.2: Classification of unconfined compressive strength of intact rock (AS 1726-1993)

Strength Descriptor	**UCS Range (MPa)**
Extremely High	> 240
Very High	70 to 240
High	20 to 70
Medium	6 to 20

TABLE OF CONTENTS

2.0 LITERATURE REVIEW 2.1

2.1 LANDSLIDES IN SOIL SLOPES 2.1

2.2 DEFORMATION BEHAVIOUR OF EMBANKMENT DAMS 2.7

2.3 WHERE THIS RESEARCH FITS IN 2.9

LIST OF FIGURES

Figure 2.1: Schematic of the system for geotechnical characterisation of slope movement (Leroueil et al 1996) 2.3

Figure 2.2: The stages of slope movement (Leroueil et al 1996) 2.4

Figure 2.3: Concept of the creep model under constant deviatoric stress conditions. 2.6

Figure 2.4: Monitored deformation behaviour at retained cut slope failure in London clay at Kensal Green (Skempton 1964) 2.7

2.0 LITERATURE REVIEW

The following literature review is a summary of the broader concepts related to the deformation behaviour of landslides and embankment dams. A more detailed review of the literature oriented toward the chapter subject is presented at the beginning of each of Chapters 3 through to 7.

2.1 LANDSLIDES IN SOIL SLOPES

The slope movement classification systems of Varnes (1978) and Hutchinson (1988) are primarily based on geomorphological classification of the type of slope movement with lesser considerations of the mechanism/s of slope movement, material types, stages of movement and rates of movement. The system of Varnes (1978) characterises the type of movement into falls, topples, slides, spreads and flows, and material types into bedrock, debris (coarse grained soils) and earth (fine grained soils). Hutchinson (1988) expanded on aspects of the Varnes system to incorporate information on aspects of the post failure behaviour of several classes of landslides including the relationship between sediment concentration and flow type, material gradation, rate of movement and post failure travel distance.

With the gradual shift toward risk based methods of assessment of landslides it became evident that the geomorphologically based classification systems available at the time, which are fundamental to any slope movement classification system, were not sufficient in their current form. Leroueil (2001) comments that he and his colleagues started working toward an expert system on slope stability in the late 1980's, the outcome of which is the geotechnical characterisation system described by Leroueil et al (1996) (after Vaunet et al. 1994). Before briefly commenting on the geotechnical characterisation of slope movement system, the comments by Leroueil (2001) in relation to the problem at hand and the state of the published literature at the time (in the mid to late 1980's) are interesting; he states that:

> "… w*e rapidly realised that the problem involves a large variety of geomaterials and many types of slope movement under a variety of climatic conditions, that the problem is complex and controlled by laws and parameters that vary with the stage of movement, and the type of*

> *geomaterial, that the relevant information was extremely scattered in the literature, and that solutions to problems related to slopes have often been developed on a local or regional basis*."

Another important point to acknowledge that has been raised in a number of keynote papers / lectures is the need for integration between geo-disciplines in the study of landslides. Fell et al (2000), when commenting on the priority areas of research and development associated with landsliding, emphasise the "*overwhelming need to integrate geology, geomorphology and geotechnical engineering in these studies*". Leroueil (2001) in his Rankine lecture states:

> "*… slope movements as such are mechanical responses of soil or rock to changes in geometry, boundary conditions, pore pressures or strength parameters with time. They have thus also to be examined from a mechanical or geotechnical viewpoint. In fact, good understanding of slope movements can be obtained only from a joint effort from geologists, geomorphologists and geotechnical engineers. As water is a major factor in slope behaviour, the contribution of hydrologists and hydrogeologists is also important. Slope movements must thus be seen as a multidisciplinary domain in which the role of the geotechnical engineer is to improve our understanding of soil behaviour in this specific context and to try and minimize the economic and social impacts of slope movements*."

The system for geotechnical characterisation of slope movement as described by Leroueil et al (1996) is the integration of movement types, material types and movement stages into a 3-dimensional matrix, as shown in Figure 2.1. The movement stages (Figure 2.2) are:

- Pre-failure – representing the slope deformation behaviour for first time slides prior to the slope failure;
- At failure or the onset of failure – "*characterised by the formation of a continuous shear band or surface through the entire soil mass*" (Leroueil et al 1996);
- Post failure – representing the movement of the slide mass from the failure condition until it essentially stops; and
- Reactivation – renewal of movement of a quiescent landslide mass along one or more pre-existing shear surfaces. Picarelli (2000) comments that this stage may include a pre and post failure stage of movement.

The earlier described geomorphological classification systems form the movement type categories. Leroueil et al (1996) considered it necessary to expand the material type categories used in the earlier systems to "*take into account the mechanical characteristics of soils and rocks*" known to influence the deformation behaviour under the boundary conditions imposed (e.g. the influence of over-consolidation, soil structure and discontinuities on the deformation behaviour of natural and cut slopes in clays).

For each "active" element within the matrix there is a characterisation sheet (Figure 2.1) that contains information on the factors affecting or controlling the slope movement, the potential evidentiary signs of movement and the possible consequences of the movement. The basis of the characterisation for each element is an understanding of the mechanisms involved and the mechanics of the deformation.

From a risk assessment point of view, the characterisation system provides a framework within which the components (e.g. the hazard, its probability of failure and the consequences of that failure) can be analysed and evaluated. It allows for informed judgements to be made related to the potential for and consequences of landsliding including the type and location of monitoring instrumentation, warning systems and possible slope remedial measures. It also identifies deficiencies in the current state of knowledge that can be targeted for research investment.

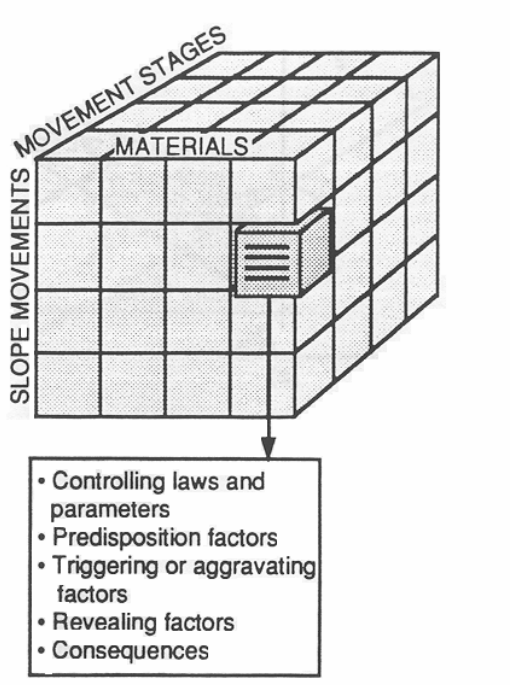

Figure 2.1: Schematic of the system for geotechnical characterisation of slope movement (Leroueil et al 1996)

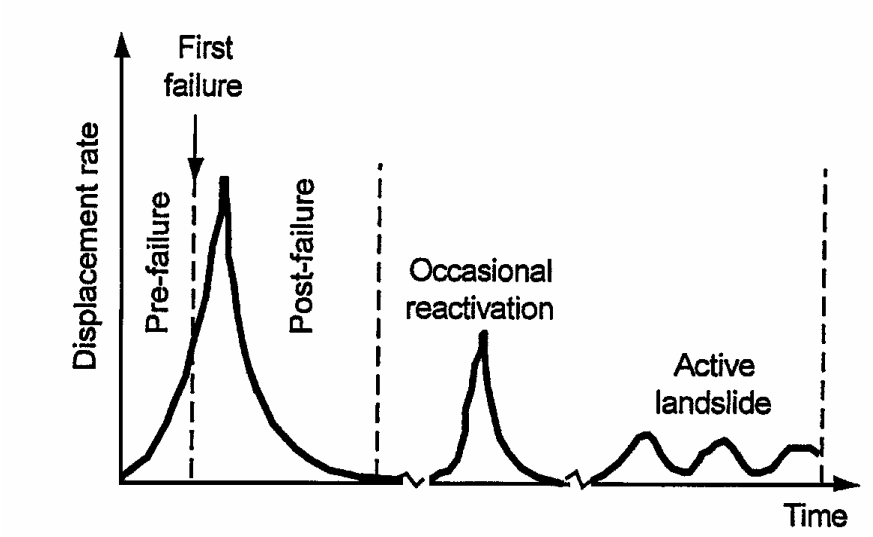

Figure 2.2: The stages of slope movement (Leroueil et al 1996)

The outcomes of the risk assessment framework of analysing landsliding is evident in the structure of a number of keynote papers of recent years, for example Fell et al (2000), Picarelli (2000) and Leroueil (2001). These papers are aimed at bringing together the knowledge published in the public domain relating to a specific topic and structuring it into a framework consistent with thinking from a risk assessment point of view.

D'Elia et al (1998) present a very useful example of the application of the geotechnical characterisation system of slope movements for structurally complex clay soils and stiff jointed clays of the Italian Apennine for the various stages of movement from pre-failure through to reactivation. From the Italian (research by Picarelli, Esu, their colleagues and others) and UK perspective (research by Skempton, Chandler, Potts, their colleagues and others), the bringing together of research on stiff fissured or jointed clays, clay shales and indurated fine grained soils, such as by Picarelli (2000), provides for a broader understanding of slope movements and the mechanisms of slope movement in these clay soil types. What is evident for both regions is the wealth of research invested over many 10's of years in areas related to landsliding that has been required in developing the state of knowledge to its present level of understanding. Within this framework it is recognised that there may be regionally, or even locally or geologically, specific influences. Overall though, the developed concepts and research findings are useful for the broader application in other areas where the research is not as well developed, notwithstanding the need for recognition of regional differences.

Another example is the Hong Kong experience of landslides in cuts in deeply weathered soils, loose fills and natural slopes triggered by prolonged or intense rainfall. The establishment of the Geotechnical Engineering Office by the Hong Kong Government in 1977 to address the regional issues of landsliding following the catastrophic consequences of several relatively small volume slides, has seen a wealth of information gathered and knowledge developed relating to landslides over 10's of years (Brand et al 1984; Brand 1985b; Wong and Ho 1996; for example) for use in quantitative risk assessment (Wong et al (1997) for example). Some of the outcomes of this research include priority ranking of slopes for remediation, focus on landslide types of high risk and high consequence (e.g. flow liquefaction of loose fills (HKIE 1998; Sun 1999)) and development of rainfall related landslide warning systems.

The post failure deformation behaviour of "rapid" landslides such as flow slides and debris flows in a range of material types from soil through to rock has been an active area of research for the last 20 to 30 years. Research by eminent researchers such as Cruden, Sassa, Hungr, Iverson and Hutchinson (Sassa 1988; Hutchinson 1986, 1988; Hungr 1995; Smith and Hungr 1992; Iverson et al 1997; Corominas 1996a; van Gassen and Cruden 1989) amongst others has contributed to the state of knowledge on post failure deformation of these slide types.

The concept of creep is a useful macroscopic model for evaluation of the pre-failure deformation behaviour of first time slides. The term creep is somewhat misleading in the context as used above. The mechanical meaning of creep, as described by Picarelli (2000), "*implies viscous movements of a soil mass subjected to a constant effective stress field characterised by local values of stress smaller than soil strength*". But, as used above it implies more than this and encapsulates the overall pre-failure deformation leading up to failure including creep itself (in the true sense of the word) and deformations due to the progressive development of the shear surface for slopes where the effective stress field does not change.

Mitchell (1964) developed the concept of creep from rate process theory. The various phases of creep under constant deviatoric stress conditions (Figure 2.3) as described by Singh and Mitchell (1968) are:

- Primary creep – deformation at a decreasing rate of strain with time. This is essentially the mechanical meaning defined by Picarelli (2000);
- Tertiary creep – deformation at an accelerating rate of strain with time (under constant effective stress conditions) culminating in creep rupture or failure. This

incorporates deformations related to the formation of a shear surface that are outside of the mechanical meaning of creep; and

- Secondary creep – deformation at a constant rate with time. Varnes (1982) considered secondary creep as the concurrent processes of primary and tertiary creep.

An example of the use of the creep model to describe the stages of pre-failure deformation behaviour is shown in Figure 2.4 for the failure in the retained cut slope in London Clay at Kensal Green (Skempton 1964). The creep concept is also useful for analysis of the post construction deformation behaviour of embankments.

Another application of the strain rate concepts is the prediction of the time to failure for first time slides in soil and rock slopes based on the minimum strain rate in the pre-failure period (Saito 1965). The method is applicable where the overall effective stress conditions within the slope are near constant.

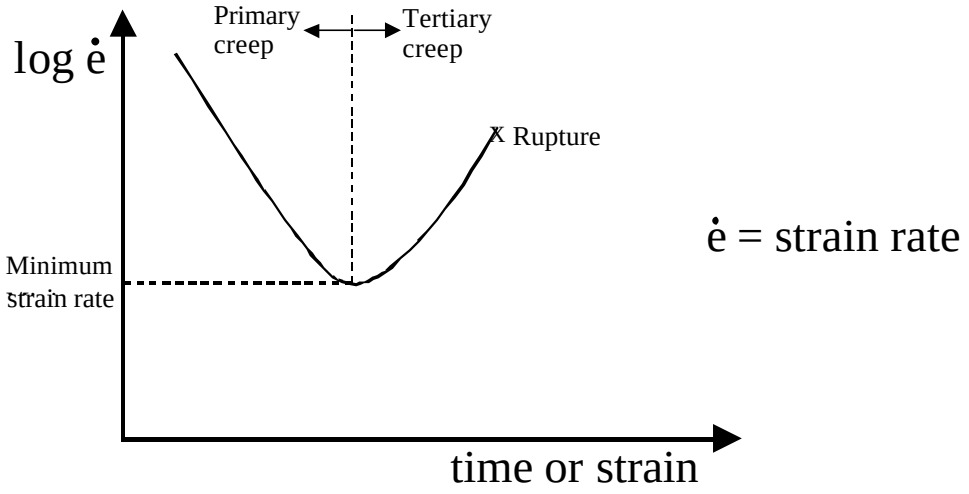

Figure 2.3: Concept of the creep model under constant deviatoric stress conditions.

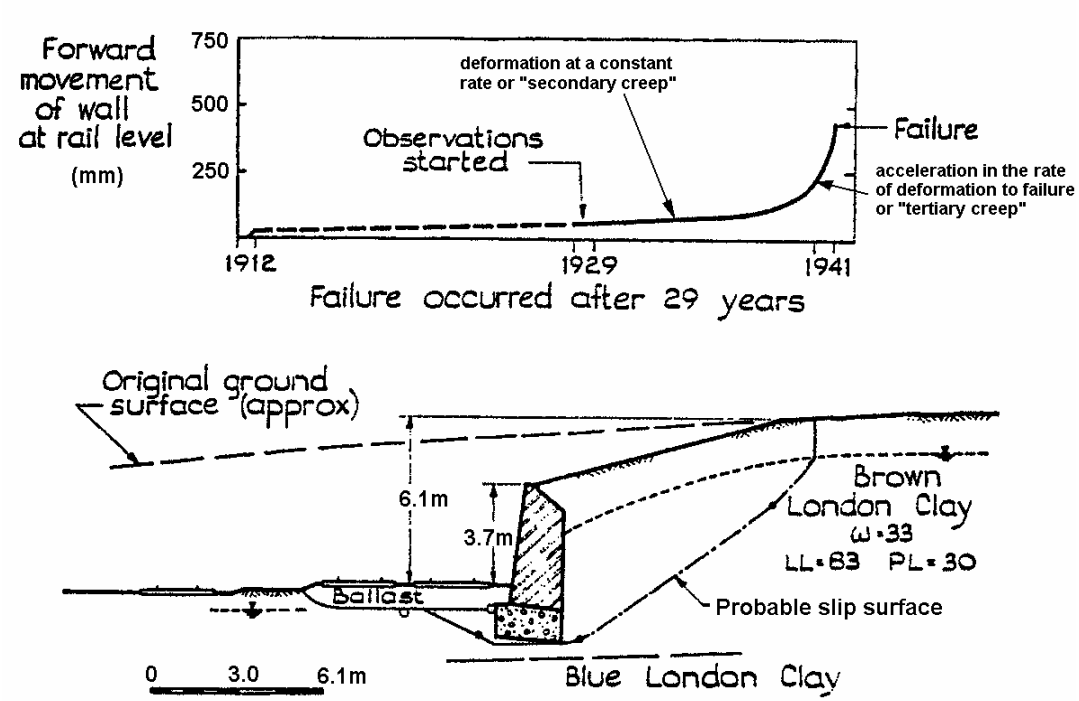

Figure 2.4: Monitored deformation behaviour at retained cut slope failure in London clay at Kensal Green (Skempton 1964)

2.2 DEFORMATION BEHAVIOUR OF EMBANKMENT DAMS

The embankment types considered in this thesis consist of earthfill, rockfill (concrete face rockfill dams), and zoned earth and earth-rockfill dams. The earthfills, apart from the core of puddle dams, are rolled and well compacted in most cases, particularly the zone acting as the main water barrier element. The placement of the rockfill zones covers a broad range from well compacted to dumped in high lifts.

The general features of the stress-strain relationship of rolled earthfills are well described in textbooks on soil mechanics and are applicable to describe the deformation behaviour of rolled earthfills. Factors such as the degree of over-consolidation, permeability, soil structure, matric suction and the rate, magnitude and direction of loading affect the strength and compressibility properties of an earthfill. Some of these factors are affected by:

- The soil type, including its mineralogy, gradation and plasticity;
- The degree of compaction; and
- The moisture content at placement relative to Standard optimum moisture content.

For rockfills, field observations (Mori and Pinto 1988; and others) and the results of large scale laboratory tests (Marsal 1973; Marachi et al 1969; and others) indicate the compressibility properties of rockfill are affected by:

- Degree of compaction of the rockfill;
- Applied stress conditions and stress path;
- Particle shape and particle size distribution; and
- Intact strength of the rock used as rockfill.

An important aspect in the evaluation of the deformation behaviour of rockfill in embankment dams is its susceptibility to collapse compression on wetting (Nobari and Duncan 1972a; Marsal 1973; Justo 1991; Alonso and Oldecop 2000). Collapse compression of earthfills is equally important, but in rolled earthfills its occurrence is much less frequent.

For embankment dams, the components of deformation are those that occur as a result of changes in effective stress conditions (during construction, on impoundment and due to reservoir fluctuation), changes in total stress (for wet placed earthfill cores in zoned embankments), on saturation or wetting (e.g. collapse compression) and the on-going time dependent or creep type deformations. Predictive methods are typically divided into the three components of deformation during construction, on first filling and long-term post construction (or post first filling).

Most predictive methods cover the deformation behaviour of one or two of these components. Finite element analyses have been used (Saboya and Byrne 1993; Kovacevic 1994; Naylor et al 1997; Dounias et al 1996, amongst others) for analysis of deformation due to changes in stress conditions, mostly for deformation during construction and first filling, but also for deformation under large drawdown. Empirical predictive methods, which are usually based on historical performance of embankments, are more generally available for assessment of post construction deformation (Sowers et al 1965; Clements 1984; Dascal 1987; Charles 1986; Soydemir and Kjœrnsli 1975; amongst others) some of which incorporate the deformation on first filling, although methods are available to assist with the assessment / prediction of deformation during construction (Poulos et al 1972; Penman et al 1971; Gould 1953; Pinto and Marques Filho 1998; Giudici et al 2000).

2.3 WHERE THIS RESEARCH FITS IN

The main focus of this thesis is toward improving the understanding and prediction of the deformation behaviour of landslides and embankment dams for the classes of slope and material types considered. Within the context of the geotechnical characterisation system of slope movements, this thesis concentrates on the deformation related aspects within the framework rather than providing a comprehensive consideration of all components for certain slope types. The outcomes are in the form of guidelines and/or methods for prediction or for evaluation of the deformation behaviour: pre and post failure deformation behaviour for landslides, and more generally the deformation behaviour of embankment dams. They are geared toward practical usage by consulting geotechnical engineers, geologists and engineering geologists within an overall risk assessment framework.

For embankment dams the database represents one of the largest put together for the types of embankments considered. The outcomes are geared toward providing dam owners and their consultants with a framework (developed from analysis of the database) within which they are able to evaluate and/or predict the deformation behaviour of their structure.

TABLE OF CONTENTS

3.0 "RAPID" LANDSLIDES FROM FAILURES IN SOIL SLOPES 3.1

3.1 OUTLINE OF THIS CHAPTER 3.1

3.2 DATABASE OF CASE STUDIES ANALYSED 3.2

3.2.1 Flow Slides in Coal Mine Waste Spoil Piles and Stockpiled Coal 3.5

3.2.2 Landslides from Failures in Cut, Fill and Natural Slopes, Hong Kong 3.7

3.2.3 Flow Slides from Tailings Dam Failures 3.9

3.2.4 Flow Slides from Failures in Hydraulic Fill Embankment Dams 3.9

3.2.5 Flow Slides from Failures in Sub-Aqueous Constructed Fills 3.9

3.2.6 Flow Slides from Failures in Submarine Slopes 3.12

3.2.7 Flow Slides in Sensitive Clays 3.12

3.3 THE MECHANICS OF SHEARING OF CONTRACTIVE GRANULAR SOILS 3.15

3.3.1 Definitions 3.15

3.3.2 Characteristics of Contractive and Dilative Soils Sheared Under Monotonic Load Conditions 3.16

3.3.3 Field Methods for Evaluation of Flow Liquefaction Potential 3.22

3.3.4 Effects of Non-plastic Fines and Gravels based on Flow Liquefaction Potential 3.30

3.3.5 Residual Undrained Shear Strength of Flow Liquefied Soils 3.32

3.4 MECHANICS OF FAILURE OF FLOW SLIDES 3.39

3.4.1 Mechanics of Development of Flow Sliding 3.39

3.4.2 Flow Slides in Granular Stockpiles 3.43

3.4.3 Flow Slides from Failures in Sensitive Clays 3.49

3.4.4 Flow Slides in Loose Silty Sand Fills, Hong Kong 3.54

3.4.5 Tailings Dams 3.57

3.4.6 Hydraulic Fill Embankment Dams 3.60

3.4.7 Submarine Slopes and Slopes in Sub-Aqueous Fills 3.62

3.5 MECHANICS OF FAILURE IN DILATIVE SOILS LEADING TO "RAPID" SLIDING 3.64

3.5.1 Slope Types of Failures in Dilative Soils Leading to "rapid" Sliding 3.64

3.5.2 Slides Through Soil Mass – Dilative Failures 3.65

3.5.3 Defect Controlled Landslides 3.79

3.6 SUMMARY OF THE CHARACTERISTICS AND MATERIAL TYPES OF "RAPID" LANDSLIDES 3.83
3.6.1 Flow Slides in Contractant Soils Susceptible to Flow Liquefaction 3.83
3.6.2 Characteristics and Identification of Conditions Under Which Failures in Dilative Soils Result in "Rapid" Landsliding 3.88
3.7 PRE-FAILURE DEFORMATION BEHAVIOUR 3.89
3.7.1 Flow Slides 3.90
3.7.2 "Rapid" Landslides from Slope Failures in Dilative Soils 3.97
3.7.3 Summary of Pre Failure Deformation Behaviour 3.99
3.8 POST-FAILURE DEFORMATION BEHAVIOUR – REVIEW OF THE LITERATURE 3.102
3.8.1 Factors Affecting Travel Distance and Velocity 3.102
3.8.2 Velocity of the Slide Mass 3.104
3.8.3 Empirical Methods for Assessment of Travel Distance 3.107
3.9 POST-FAILURE DEFORMATION – DEVELOPED METHODS FOR ASSESSMENT OF TRAVEL DISTANCE FROM THE DATABASE 3.112
3.9.1 Travel Distance Versus Slide Volume and Initial Slide Classification . 3.113
3.9.2 Travel Distance Versus Slide Volume, Degree of Confinement of the Travel Path and Initial Slide Classification 3.116
3.9.3 Travel Distance Versus Volume, Down-slope Angle and Slide Type from Failures in Dilative Soils 3.124
3.9.4 Travel Distance Versus Volume, Down-slope Angle and Slide Type from Failures in Contractile Soils 3.137
3.9.5 Summary of Methods for Predicting Travel Distances 3.150
3.10 POST-FAILURE NUMERICAL MODELLING - METHODS AND RESULTS 3.152
3.10.1 "Rapid" Landsliding in Hong Kong 3.155
3.10.2 "Rapid" Landslides from Coal Mine Waste Spoil Pile Failures in British Columbia 3.158
3.10.3 Flow Slides from Tailings Dams Failures 3.160
3.11 CONCLUSIONS 3.162

LIST OF TABLES

Table 3.1: Summary of database on "rapid" landslides. 3.3

Table 3.2: Summary of data sources for "rapid" landslides from coal mine waste spoil piles and coal stockpiles 3.5

Table 3.3: Summary of landslide cases analysed from Hong Kong 3.8

Table 3.4: Summary of case studies of "rapid" landslides from tailings dams 3.10

Table 3.5: Summary of failure case studies in hydraulic fill embankment dams 3.11

Table 3.6: Summary of failure case studies in sub-aqueous constructed fill slopes 3.11

Table 3.7: Summary of "rapid" flow slides in natural submarine slopes..... 3.13

Table 3.8: Summary of flow slides in sensitive clays 3.14

Table 3.9: SPT blow count ($(N_1)_{60}$) yield strength and residual strength correction factors for fines content (Seed et al 1985; Seed 1987)..... 3.35

Table 3.10: Features of flow slides in loose fill from Hong Kong..... 3.56

Table 3.11: Summary of properties of liquefaction susceptible materials from flow slides in hydraulic fill embankments 3.61

Table 3.12: Summary of material types of dilative slides of debris in natural slopes that developed in "rapid" debris slides and debris flows. 3.75

Table 3.13: Source area slope angle (a_1) of dilative slides in natural slopes that developed into "rapid" debris flows and debris slides..... 3.77

Table 3.14: Failures through the soil mass in dilative soils that developed into "rapid" landslides, from Hong Kong..... 3.78

Table 3.15: Features of defect controlled compound slides that developed into "rapid" landslides from Hong Kong..... 3.82

Table 3.16: Features of defect controlled translational slides that developed into "rapid" landslides from Hong Kong..... 3.82

Table 3.17: Summary of pre-failure observations in coarse-grained loose fills 3.92

Table 3.18: Measured slope deformations adjacent to failures in the Ottawa area (Mitchell and Eden 1972)..... 3.95

Table 3.19: Summary of characteristics of pre-failure deformation of slope failures that developed into "rapid" landslides 3.100

Table 3.20: Velocity of the slide mass for "rapid" landslides from failures in soil slopes (mostly from case studies analysed)..... 3.105

Table 3.21: Velocity of slide mass for debris slides and debris flows..... 3.106

Table 3.22: Regression analysis of *H/L* (Equation 3.11) versus landslide volume (Corominas 1996a)..... 3.111

Table 3.23: Summary of empirical correlation coefficients (Equation 3.11) for debris flows by Corominas (1996a)..... 3.114

Table 3.24: Empirical correlation coefficients for power law fit of travel distance angle to slide volume (Equation 3.11, $H/L = AV^B$) for unconfined "rapid" landslides..... 3.122

Table 3.25: Empirical correlation coefficients for power law fit of travel distance angle to slide volume (Equation 3.11, $H/L = AV^B$) for confined and partly confined "rapid" landslides..... 3.124

Table 3.26: Summary of empirical correlations for flow slides in coal waste spoil piles in British Columbia..... 3.139

Table 3.27: Statistical summary of *H/L* to tan a_2 correlation for flow slides in coarse-grained coal mine waste spoil piles..... 3.143

Table 3.28: Summary of slide properties of flow slides in hydraulic fill embankments..... 3.149

Table 3.29: Mean and standard deviation of *H/L* for several types of slopes giving "rapid" landslides..... 3.153

Table 3.30: Summary of recommended methods for prediction of H/L (tangent of the travel distance angle)..... 3.154

Table 3.31: Summary of "rapid" landslides from Hong Kong analysed by Hungr Geotechnical Research (1998) and Ayotte and Hungr (1998)..... 3.156

Table 3.32: Summary of results of numerical modelling using DAN for "rapid" landslides in Hong Kong (Hungr Geotechnical Research 1998; Ayotte and Hungr 1998)..... 3.157

LIST OF FIGURES

Figure 3.1: Typical coal waste spoil pile profile in British Columbia (Hungr et al 1998) 3.6

Figure 3.2: Steady state line of Toyoura sand (Ishihara 1993) 3.16

Figure 3.3: Undrained behaviour of states on the contractive side of the steady state line (Ishihara 1993) 3.17

Figure 3.4: Undrained behaviour from states close to steady state and on dilative side (a) stress-strain plot and (b) effective stress paths (Ishihara 1993) 3.17

Figure 3.5: Schematic diagram showing different types of behaviour for undrained stress paths of samples at the same void ratio and different initial confining pressures (Yamamuro and Lade 1998) 3.18

Figure 3.6: Definition of the state parameter (Been and Jefferies 1985). 3.20

Figure 3.7: Collapse surface concept, defined by the locus of the peak deviator stress from undrained triaxial samples tested at the same void ratio and different initial effective mean normal stress (Sladen et al 1985a) 3.20

Figure 3.8: Correlation for cyclic resistance ratio (CRR) based on corrected SPT blow count, $(N_1)_{60}$, for clean sands under level ground conditions (Robertson and Wride 1997) 3.23

Figure 3.9: Corrected SPT blow count, $(N_1)_{60}$, versus vertical effective over-burden pressure (s'_{vo}) for saturated non-gravelly silty sand deposits that have experienced large deformations and were triggered by earthquake (Baziar and Dobry 1995) 3.24

Figure 3.10: Flow liquefaction and no-flow bounds in terms of *(a)* field measured SPT blow count and *(b)* CPT q_c value from flow liquefaction case histories (static and earthquake triggered) and laboratory undrained testing (Ishihara 1993). 3.25

Figure 3.11: Influence of void ratio range on flow potential of sandy soils for *(a)* round-grained sands and *(b)* angular grains (Cubrinovski and Ishihara 2000) 3.26

Figure 3.12: Relationship between relative density, D_{ro}, at the threshold void ratio, e_o, and void ratio range ($e_{max} - e_{min}$) for sandy soils (Cubrinovski and Ishihara 2000). 3.27

Figure 3.13: Relationship between the slope of the steady state line, l, and void ratio range for *(a)* round-grained sands and *(b)* angular grained sands (Cubrinovski and Ishihara 2000). 3.28

Figure 3.14: Correlation between N_1/D_r^2 (N_1 = SPT blow count corrected for over-burden pressure, D_r = relative density) and void ratio range for cohesionless soils (Cubrinovski and Ishihara 2000). 3.28

Figure 3.15: Field measured SPT blow count boundaries differentiating flow liquefaction no-flow conditions for void ratio range of 0.3 to 0.6 for *(a)* round-grained sands and *(b)* angular sands (Cubrinovski and Ishihara 2000)..... 3.29

Figure 3.16: Flow characterisation of sand based on field measured SPT blow count showing liquefaction flow no-flow boundary, and region of flow at zero residual undrained strength (Cubrinovski and Ishihara 2000) 3.30

Figure 3.17: Increase in liquefaction potential (as measured by relative density) with increasing content of non-plastic fines (Lade and Yamamuro 1997) 3.31

Figure 3.18: Fording sandy gravel sample *(a)* undrained triaxial compression test results and *(b)* consolidation and steady states (Dawson et al 1998). 3.32

Figure 3.19: Relationship between equivalent clean sand SPT blow count, $(N_1)_{60\text{-}CS}$, and residual undrained strength from field case studies (Seed and Harder 1990) 3.34

Figure 3.20: Relationship between undrained critical strength ratio and equivalent clean sand SPT blow count, $(N_1)_{60\text{-}CS}$ (Stark and Mesri 1992)..... 3.35

Figure 3.21: Residual undrained shear strength, S_r, to vertical effective over-burden pressure for silty sand deposits (≥ 10% fines), triggered by earthquake, that have experienced large deformation (Baziar and Dobry 1995).. 3.36

Figure 3.22: Flow chart for assessment of residual undrained shear strength of liquefied soil (NSF 1998)..... 3.38

Figure 3.23: Idealised mechanism for initiation of flow slides..... 3.40

Figure 3.24: Definition of undrained brittleness index, I_B, in strain weakening soil. .. 3.41

Figure 3.25: Effective stress states on some planes (submarine slopes) located within the region of potentially instability (Lade 1992). 3.42

Figure 3.26: Collapse model for mine waste dumps (Dawson et al 1998) 3.43

Figure 3.27: Particle size distribution of coal mine waste and coking coal susceptible to static liquefaction 3.44

Figure 3.28: Particle size distribution of sensitive clays 3.50

Figure 3.29: Frequency distribution of landslides in Quebec (Tavenas 1984) 3.52

Figure 3.30: Slope height versus slope inclination for unstable slopes in eastern Canada (Tavenas 1984)..... 3.52

Figure 3.31: Retrogressive landslide in sensitive clay (Leroueil et al 1996)..... 3.54

Figure 3.32: Peak shear strength from undrained triaxial compression tests of contractive fill samples (HKIE 1998) 3.57

Figure 3.33: Effect of partial saturation on steady state line in void ratio – mean effective stress space (HKIE 1998) 3.58

Figure 3.34: Particle size distribution of tailings from flow slide case studies..... 3.59

Figure 3.35: Particle size distributions of hydraulic fills from flow slide case studies..... 3.61

Figure 3.36: Particle size distributions of soil types from submarine slopes and sub-aqueous fills susceptible to liquefaction and flow sliding. 3.62

Figure 3.37: Hypothetical model for transformation of dilative materials from rigid to fluid behaviour, path D_i to D_f (Fleming et al 1989)..... 3.68

Figure 3.38: Relationship between peak hourly rainfall, landsliding and severity of consequence for Hong Kong (Brand et al 1984)..... 3.70

Figure 3.39: Relationship between severity of landsliding and rainfall intensity for Hong Kong (Brand 1985b)..... 3.70

Figure 3.40: Source area particle size distributions of dilative slides of debris in natural slopes..... 3.73

Figure 3.41: Distribution of head slope angle (source area slope angle) for slides of debris in natural terrain that developed into "rapid" landslides, Hong Kong (Evans et al 1997)..... 3.79

Figure 3.42: Cross section through the failure and "rapid" landslide at Fei Tsui Road, Hong Kong (GEO 1996a) 3.81

Figure 3.43: Particle size distributions of material types susceptible to liquefaction and flow sliding. 3.84

Figure 3.44: Comparison of flow liquefaction no-flow boundaries (in terms of SPT $(N_1)_{60}$) for sands and silty sands from monotonic laboratory undrained tests and earthquake triggered field cases (after Cubrinovski and Ishihara 2000). 3.87

Figure 3.45: Pre-failure deformation of two separate failures at the Clode waste dump, Fording Coal, British Columbia (Campbell and Shaw 1978). 3.93

Figure 3.46: Measured deformations in a natural slope, Ottawa River (Mitchell and Eden 1972) 3.94

Figure 3.47: Deformation and pore pressure ratio of an induced slope failure (Mitchell and Williams 1981) 3.96

Figure 3.48: Sliding block model showing kinetic energy lines for different rheological models (Golder Assoc. 1995)..... 3.106

Figure 3.49: Schematic profile of a slope failure showing travel distance and travel distance angle 3.108

Figure 3.50: Travel distance from the toe of the cut, *R*, versus cut slope height, H_s, for failures in cut slopes from Lantau Island, Hong Kong (Wong and Ho 1996) 3.109

Figure 3.51: Landslide volume versus tangent of the travel distance angle for 204 landslides (Corominas 1996a) 3.110

Figure 3.52: Ratio *H/L* versus volume for landslides that break-up on sliding (Finlay et al 1999) 3.111

Figure 3.53: Ratio *H/L* versus volume for all slides from database. 3.114

Figure 3.54: *H/L* ratio versus volume relationships for Corominas (1996a) data on unconfined debris flows. 3.115

Figure 3.55: *H/L* ratio versus volume relationships for Corominas (1996a) data on confined debris flows. 3.115

Figure 3.56: Travel distance beyond source area versus volume for unconfined travel paths. 3.117

Figure 3.57: Travel distance beyond source area versus volume for confined and partly confined travel paths. 3.117

Figure 3.58: Comparison of trendlines of *H/L* versus slide volume differentiated on travel path confinement for "rapid" landslides from failures in dilative soils, from Hong Kong. 3.118

Figure 3.59: *H/L* versus volume for "rapid" landslides with unconfined travel paths. 3.120

Figure 3.60: *H/L* ratio versus volume for "rapid" landslides from failures in dilative soils with unconfined travel paths. 3.120

Figure 3.61: *H/L* ratio versus volume for "rapid" landslides from failures in contractive soils (flow slides) with unconfined travel paths. 3.121

Figure 3.62: *H/L* versus volume for "rapid" landslides with confined travel paths. .. 3.123

Figure 3.63: *H/L* versus volume for "rapid" landslides with partly confined travel paths. 3.123

Figure 3.64: *H/L* versus slide volume for cut slope cases studies from Hong Kong . 3.126

Figure 3.65: *H/L* normalised against tangent of the cut slope angle versus volume for cut slopes in Hong Kong failing onto a near horizontal slope at the toe. 3.127

Figure 3.66: Idealised effect of volume on travel distance for cut slope failures of *(a)* small volume compared with *(b)* significantly larger volumes. 3.127

Figure 3.67: Classification of slope categories *(a)* Type 1 – failure at top of cut slope, and *(b)* Type 2 – failure encompassing the full cut height. 3.128

Figure 3.68: Definition of down-slope angle below source area, a_2 ..... 3.132

Figure 3.69: *H/L* versus tangent of the down-slope angle, a_2, for unconfined travel paths, failures in natural slopes from Hong Kong. 3.133

Figure 3.70: *H/L* versus tangent of the down-slope angle, a_2, for partly confined travel paths, failures in natural slopes from Hong Kong. 3.134

Figure 3.71: *H/L* versus tangent of the down-slope angle, a_2, for confined travel paths, failures in natural slopes from Hong Kong. 3.134

Figure 3.72: Natural slopes (Hong Kong). Trendlines for *H/L* versus tangent of the down-slope angle, a_2, for all types of travel path. 3.135

Figure 3.73: *H/L* versus slide volume for flow slides in loose silty sand to sandy silt fills 3.137

Figure 3.74: *H/L* versus slide volume for flow slides in coarse-grained coal mine waste spoil piles. 3.142

Figure 3.75: *H/L* versus the tangent of the down-slope angle below the toe of the spoil pile, a_2; flow slides in coarse-grained coal mine waste spoil piles. 3.142

Figure 3.76: *H/L* versus volume for retrogressive "rapid" slides 3.146

Figure 3.77: Distance of retrogression versus liquidity index for slides in sensitive clays 3.148

Figure 3.78: Distance of retrogression based on stability number for landslides in sensitive clays (Mitchell and Markell 1974) 3.148

Figure 3.79: Ratio of retrogression distance to slide depth versus stability number . 3.149

Figure 3.80: DAN results of frictional back-analysis models of "rapid" landslides from Hong Kong (data from Hungr GR (1998) and Ayotte and Hungr (1998)) 3.158

Figure 3.81: Back calculated bulk friction angle from DAN analysis of flow slides from coal mine waste spoil pile failures in British Columbia (Golder Assoc. 1995) 3.159

Figure 3.82: Simple sliding block model for analysis of tailings strength (Blight 1997) 3.160

Figure 3.83: Variation of shear strength with moisture content for gold tailings (Blight 1997) 3.161

Figure 3.84: Model for flow of liquefied tailings (Jeyapalan et al 1983a) 3.162

3.0 "RAPID" LANDSLIDES FROM FAILURES IN SOIL SLOPES

3.1 OUTLINE OF THIS CHAPTER

"Rapid" landslides from failures in soil slopes have mass destructive capabilities; resulting in loss of life, destruction of property and damage to the natural environment. Examples are Aberfan, South Wales in 1966 (failure of coal waste stockpile resulting in 144 deaths); Stava, Italy in 1985 (failure of tailings dam resulting in some 268 deaths); earthquake triggered failures in loessic soils in Gansu Province, China in 1920 (killed some 100,000 people); loss of life from relatively small volume landslides in Hong Kong; and the relatively small volume landslide at Thredbo Village, Australia in 1997 resulting in 18 deaths.

Most of this chapter is dedicated to presenting the results from analysis of a database of some 350 "rapid" landslides. The case studies, in most cases, are of landslides that post-failure have reached travel velocities within the rapid, very rapid and extremely rapid IUGS (1995) velocity categories (Table 1.1). This is as opposed to debris flows that have evolved through channel erosion, which are not considered here. In most cases the initial landslide has been "statically" triggered as opposed to "dynamically" triggered (e.g. by blasting or earthquake), but several dynamically triggered landslides are included in the database. The chapter also draws on the published literature on failures in soil slopes that developed into "rapid" landslides, including areas of the literature on cyclic liquefaction of granular soils.

The main objectives of this chapter are centred on:

- The characteristics of soils and slope conditions within which "rapid" landslides develop, including the identification of soils susceptible to liquefaction and potential flow behaviour;
- Identification of the triggers and failure mechanism/s of slides in soil slopes that develop into "rapid" landslides post failure;
- Review and refinement of empirical methods for prediction of travel distance;
- Review of numerical models to predict travel of the landslide, what models are available and under what conditions are they applicable.

The database of "rapid" landslides from failures in soil slopes assembled for this study is briefly summarised (Section 3.2). This is followed by a review of the literature on the mechanics of shearing of contractive granular soils (Section 3.3), which leads into a discussion on the mechanics of failure for the slope and material classes considered; Section 3.4 for flow slides in soils that are potentially contractile on shearing and Section 3.5 for landslides in soils that are dilative on shearing (Section 3.6 is a summary). The analysis of the pre-failure (Section 3.7) and post-failure deformation behaviour (Sections 3.8 to 3.10) is then presented, which includes methods developed for travel distance estimation for several classes of slope types considered.

3.2 DATABASE OF CASE STUDIES ANALYSED

The database comprises some 350 "rapid" landslides from failures in predominantly soil slopes from published sources. Table 3.1 presents a summary of material types of the landslides sorted in terms of the initial landslide type, either initially in contractive or dilative soil types. For some 100 individual cases, reasonably detailed data was available from either reports or published conference and journal papers. The remainder of the data was gathered from other sources including Corominas (1996a), Golder Assoc. (1995), Siddle et al (1996), Hutchinson (1988), Wong and Ho (1996), Sun (1999) and Edgars and Karlsrud (1983). Tabulated information on almost 200 of the "rapid" landslides from failures in soil slopes is presented in Section 1 of Appendix B.

The travel classification of most of the "rapid" landslides is debris flow or flow slide. There are only several that would be classified as debris slides because most slides that initiate in dilative soils tend to break-up and flow rather than move as a relatively intact slide mass on a defined basal sliding plane.

The database of debris flows from Corominas (1996a) incorporates a number of slides initially within rock that developed into debris flows. The sub-groups chalk cliffs and sturztroms are also slides initially within rock that developed into flow slides and debris flows. The purpose of including these events is for comparison with debris flows initiated in soil slopes.

Table 3.1: Summary of database on "rapid" landslides.

Initial Landslide Type	Material Type	Sub-group	No.	Volume Range (m^3)	Material Description	References
Slides in Contractile Soils	Loose Fills	Road and building fills, Hong Kong	16	50 to 10,500	Loose dumped silty sands to sandy silts with low clay content.	Wong and Ho (1996), Sun (1999), GEO reports
		Coal waste spoil piles	56	3000 to $8x10^6$	Loose dumped sandy gravels (British Columbia and South Wales)	Refer Appendix B, Section 1.
		Coking coal stockpiles	9	850 to 16,000	Sandy gravels to gravelly sands, low specific gravity (Hay Point)	Refer Appendix B, Section 1.
		Hydraulic fill embankment dams*[2]	5	16,000 to $8x10^6$	Hydraulically placed silty and sandy soils, stratified (1 case is of loose dumped sand).	Refer Appendix B, Section 1.
		Tailings dams	9	20,000 to $3x10^6$	Hydraulically placed sand to clay sized soils, stratified.	Refer Appendix B, Section 1.
		Sub-aqueous hydraulic and dumped fills	4	4,000 to 150,000	Hydraulically placed and dumped sands and silty sands.	Refer Appendix B, Section 1.
	Natural Soils Slopes	Sensitive clays	12	100,000 to $55x10^6$	Leached marine deposits, highly sensitive, clayey silts to silty clays.	Refer Appendix B, Section 1.
		Submarine slopes	22	6,000 to $1x10^{12}$	Mainly in sands and silts.	Edgars and Karlsrud (1983).

*[1] Inclusive of defect controlled slides, slides of debris and slides through the soil mass

*[2] Includes 4 flow slides in hydraulic fill embankment dams and 1 flow slide in a loose dumped sand fill embankment dam

GEO = Geotechnical Engineering Office, Hong Kong Government

Table 3.1 (cont.): Summary of database on "rapid" landslides (sheet 2 of 2)

Initial Landslide Type	Material Type	Sub-group	No.	Volume Range (m^3)	Material Description	References
Slides in Dilative Soils*[1]	Cut Slopes	Road and building cuts, Hong Kong	61	4 to 52,000	Colluvium, residual soils and saprolite. Silty sands to sandy silts with gravel to boulders, low clay content.	Wong and Ho (1996), Ayotte and Hungr (1998), GEO reports
	Fill Slopes (dilative)	Road and building fills, Hong Kong	10	40 to 500	Mainly silty sands to sandy silts, low clay content.	Sun (1999), GEO reports
		Washouts of road fills, Hong Kong	19	40 to 4000	Silty sands to sandy silts with gravel to boulders, low clay content.	Wong and Ho (1996), Sun (1999)
	Natural Soil and Rock Slopes	Natural slopes in granitic and volcanic terrain, Hong Kong	27	20 to 26,000	Mostly in colluvium, some in residual soils and saprolite. Silty sands to sandy silts with gravel to boulders, low clay content.	Refer Appendix B, Section 1.
		Chalk talus	4	1,200 to 14,000	-	Hutchinson (1988)
		Chalk cliffs	13	25,000 to $1.3x10^6$	Rock slope failures in chalk cliffs of UK.	Hutchinson (1988), Golder Assoc. (1995)
		Kaolinised granite	1	6000	Failure in kaolinised granite	Hutchinson (1988)
	Debris flows in Soil and Rock	Soil and rock slopes	70	36 to $1.2x10^{10}$	Debris flows emanating from initial slides in soil and rock.	Corominas (1996a)
		Sturzstroms	9	10^6 to $1.5x10^9$	Essentially from initial slides in rock.	Hutchinson (1988)

*[1] Inclusive of defect controlled slides, slides of debris and slides through the soil mass

*[2] Includes 4 flow slides in hydraulic fill embankment dams and 1 flow slide in a loose dumped sand fill embankment dam

GEO = Geotechnical Engineering Office, Hong Kong Government

3.2.1 FLOW SLIDES IN COAL MINE WASTE SPOIL PILES AND STOCKPILED COAL

"Rapid" flow slides from failures in coal mine waste spoil piles and coal stockpiles have been reported by a number of published sources. Data for some 67 flow slides has been analysed from three geographic regions as summarised in Table 3.2, all of associated with the coal industry. Flow slides in granular stockpiles have been reported in other geographic regions and from other than the coal industry (Bishop 1973), however these three regions represent the better sources of available published information particularly with respect to general information on material properties, topography and climate.

For most of the case studies within the database only limited data was obtained from the literature. Detailed information was available for several case studies including the Aberfan tip failure (Tip 7) in 1966, several other flow slides from South Wales and several flow slides from British Columbia. Information on the individual slides is given in Section 1 of Appendix B.

Table 3.2: Summary of data sources for "rapid" landslides from coal mine waste spoil piles and coal stockpiles

Geographic Region	**Material Description *[1]**	**No. of Slides**	**Data Sources**
British Columbia, Canada	Coal waste - loose end dumped spoil piles of sandy gravels to boulder size	40	Data sourced mainly from Golder Assoc. (1995). Detailed information on 3 failures (Dawson 1994; Dawson et al 1998).
South Wales, UK	Coal waste - dumped, mainly sandy gravels with trace to some silt sized fines	18	Limited data on most case studies from Siddle et al (1996), data for some slides from Knox (1927) and Bishop (1973). Detailed information and data on Aberfan and several other failures from HMSO (1967) and associated technical reports.
Hay Point, Australia	Loose stockpiled coking coal, low specific gravity, typically gravelly sands to sandy gravels with trace to some silt fines.	9	Limited data for field case studies from Eckersley (1985, 1986, 1990). Detailed laboratory data and laboratory scale tests from Eckersley (1986, 1990).

Note: *[1] "trace" is less than 5% by weight, and "some" is more than 5% and less than 12% by weight.

Dumping operations and material properties vary between the three geographic regions. In British Columbia the coal waste is placed by end dumping from haul trucks at the

edge of the tipping face creating a flat platform at the crest and steep tipping face with average slopes of 36 to 38 degrees (Figure 3.1). The waste is tipped onto relatively steep foundation slopes, typically from 10 up to 35 degrees. The waste itself varies widely from cobble to boulder size strong sandstone rock fragments to finer fractions (sandy gravels) derived from weaker mudstones and re-handle (materials handled or moved more than once) with silt contents of less than 5 percent. The stockpile profile (Figure 3.1) generally comprises layers of the finer waste parallel to the tipping face within the coarser sandstone waste and a basal zone of coarse waste formed by segregation during tipping.

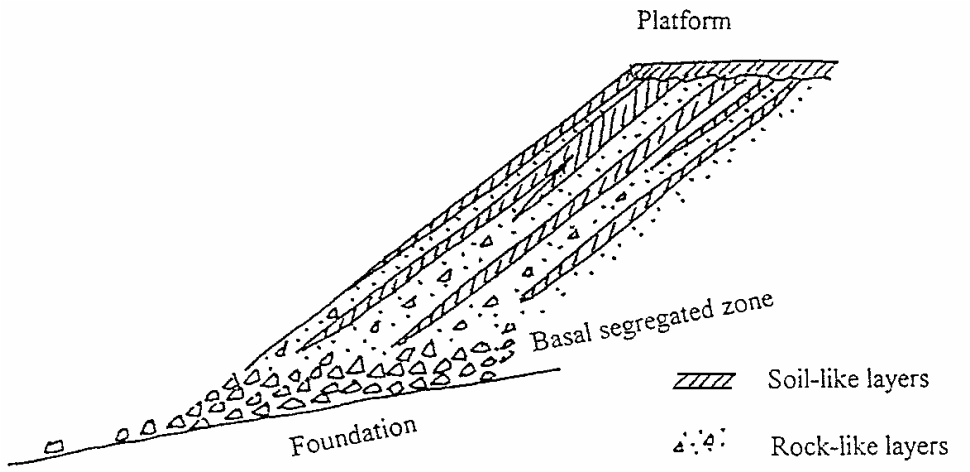

Figure 3.1: Typical coal waste spoil pile profile in British Columbia (Hungr et al 1998)

Most of the "rapid" landslides from failures in the coal mine waste spoil piles of South Wales, as described by Siddle et al (1996), were located within the central to eastern portion of the coalfield where the hills are capped by the massive Pennant Sandstone formation and the topography is characterised by greater relief and steeper hill-slopes than the western part of the coalfield. The method of disposal of the spoil involved deposition onto the active steep face of the stockpile using methods including tipping from trams, aerial ropeways and various tippler mechanisms. The waste itself is predominantly derived from shale with some coal and finer coal washery waste (post 1930's).

Hay Point, Australia is a shipping port for coking coal. Stockpiles of the coking coal are typical formed by rail-mounted stackers to a maximum height of about 14 m onto a flat platform area (Eckersley 1985). Bulldozers are sometimes used to extend the stockpiles beyond the reach of the stackers. The coking coal itself has a low specific

gravity (approximately 1.35 t/m^3) and classifies as a sandy gravel to gravelly sand with trace to some silt sized fines.

3.2.2 LANDSLIDES FROM FAILURES IN CUT, FILL AND NATURAL SLOPES, HONG KONG

Hong Kong is particularly susceptible to the development of "rapid" landslides from slope failures. Its steep topography, tropical climate, geology and intense development are considered to be the dominant factors for the prevalence of "rapid" landslides. Debris slides and debris flows in natural slopes are numerically the predominant type of "rapid" landslide, but "rapid" slides developed from failures in loose fill slopes and steep cut slopes are economically and from a loss of life viewpoint the most important. Most failures are typically of shallow depth and are triggered during seasonal heavy rainfall as a result of a reduction in suction due to infiltration and/or development of transient high ground water pressures.

As part of this study on "rapid" landslides, forty-three landslides from Hong Kong have been analysed in detail, the main source of information being specific reports on the slide by the Geotechnical Engineering Office (GEO), its consultants or the Hong Kong Government (prior to 1977) supplemented with additional information from other sources (Hungr Geotechnical Research 1998; Morgenstern 2000; Irfan and Woods (1998); Irfan (1997); Ayotte and Hungr 1998). Table 3.3 summaries the types of slope failures analysed that developed into "rapid" landslides. Further details on each case study are given in Section 1 of Appendix B. A slide volume of 20 m^3 was established as a minimum for detailed analysis.

The term "flow slide" has only been applied to fill slope failures where the failure mechanism was considered most likely due to shear induced flow liquefaction of the near saturated soil structure. The assessment of the flow liquefaction potential of a fill was based firstly on measured density results (if available) and then on the type of placement and age of the fill. In general, failures in dumped fills of decomposed granite or volcanics with densities less than 80 to 85% of Standard Maximum Dry Density (SMDD) have been deemed flow slides based on previous studies of these materials (HKIE 1998; Gov't of Hong Kong 1977).

Other studies on "rapid" landslides from Hong Kong have been incorporated into the overall analysis undertaken. Sources of this information are summarised as follows:

- Wong and Ho (1996) analysed forty-two landslides, predominantly from failures in cut slopes, on Lantau Island following the severe rainstorm of 5 November 1993. They looked at the factors affecting travel distance including; down-slope geometry, slide volume, mechanism of failure and mode of debris movement.
- Finlay et al (1999), from a database of 1100 landslides in Hong Kong between 1984 and 1993, undertook statistical analysis to assess the correlation of various slope factors to travel distance for cut slopes, fill slopes, retained fills and boulder falls.
- GEO reports on failures in natural slopes (Wong et al 1996; Franks 1996; Evans et al 1997). Evans et al (1997) used a regression analysis developed from landslides in the Tung Chang area of Lantau Island to predict the travel distance angle of landslides from failures in natural slopes from the south Lantau area reported by Wong et al (1996).
- Ayotte and Hungr (1998) and Hungr Geotechnical Research (1998) numerically analysed the travel of some 26 "rapid" landslides from Hong Kong using the DAN computer program. The cases analysed were mostly failures in natural slopes with several failures in cut and fill slopes. Their findings are discussed in Section 3.10.1.

Table 3.3: Summary of landslide cases analysed from Hong Kong

Slope Type	**No. Cases**	**Failure Mechanism**	**Data Sources (from GEO*[1], *[2])**	**Additional Cases *[3]**
Fill Slopes	10	6 flow slides in loose fill 1 dilatant slide through the soil mass 3 retained slopes, one possibly a flow slide	GEO Report Nos. 52, 88, 89, LSR 6/99 Gov't HK (1977)	-
Cut Slopes	21	8 strongly defect-controlled slides (translational and compound). 12 slides in dilatant residual soils, colluvium and saprolite, some with limited defect control. 1 retained cut slope	GEO Report Nos. 52, 88, 90, 91, 92, LSR 5/99, LSR 7/99, LSR 8/99, ADR 1/95, GR 1/95 Halcrow (1998a, 1998b), GEO (1994, 1996a), Vail (1972), Knill (1996a), Morgenstern (1994).	1 with limited information
Natural Slopes (and quasi-natural or modified)	12	11 slides of debris, mostly in colluvium, of which 8 developed into confined debris flows. 1 defect-controlled compound slide	GEO Report Nos. 88, 89, 90, 91, SPR 6/96, SPR 10/96, LSR 7/99, DN 2/97 GEO (1996b), Knill (1996b),	14 with limited information. All developed into debris flows; 3 into confined debris flows.

Notes: *[1] GEO = Geotechnical Engineering Office of Hong Kong Government

*[2] A full list of references of the slide specific GEO Reports are given in Appendix B

*[2] Additional cases from Ayotte and Hungr (1998)

3.2.3 FLOW SLIDES FROM TAILINGS DAM FAILURES

A total of nine case studies of landslides from tailings dam have been collected from the literature (Table 3.4). Details of the individual case studies are given in Section 1 of Appendix B.

Information on earthquake triggered flow slides from tailings dams was also collected from the published literature (refer Appendix B). However, very little information was found on the post-failure behaviour of these case studies and they have therefore not been considered in detail.

3.2.4 FLOW SLIDES FROM FAILURES IN HYDRAULIC FILL EMBANKMENT DAMS

Five case studies of "rapid" landslides from failures in embankment dams constructed of hydraulically placed or loose dumped sands and silty sands have been analysed (Table 3.5). Details are given in Section 1 of Appendix B. For the hydraulic fill embankments, failure was associated with liquefaction of either the hydraulic placed fill or the foundation. It was evident that the outer denser materials and non-saturated zones remained virtually intact during sliding, and were carried forward on a liquefied zone of the looser and saturated materials. An important characteristic of these failures is the stratified nature of the hydraulically placed materials.

In the case of Wachusett Dam the failure occurred in the upstream shoulder of loose dumped sand fill during first filling and Olson et al (2000) consider it to have involved static liquefaction and flow of the loose dumped sand fill.

3.2.5 FLOW SLIDES FROM FAILURES IN SUB-AQUEOUS CONSTRUCTED FILLS

Four case studies of failures that developed into "rapid" flow slides in sub-aqueous constructed fills have been included in the database (Table 3.6) and all are suspected as being retrogressive. Details for each case study are given in Section 1 of Appendix B. All failures were in loose to very loose sands with some to trace silt fines (density index estimated at 15 to 30%).

Table 3.4: Summary of case studies of "rapid" landslides from tailings dams

Name and Country	Mine / Tailings Type	Embankment		Operating State at Time of Failure	Material Description of Tailings	Data Sources
		Type of Construction	Materials			
Stava, Italy	Flourite	Centreline then upstream, cycloned	Silty sands (SM)	In operation	Interlayered silty clays (CL) and silty sands (SM)	Blight (1997) Chandler and Tosatti (1995) Morgenstern (2000), Berti et al (1988)
Bafokeng, South Africa	Platinum	Upstream, mechanical	Silty sands (SM) with slimes layers	In operation	Clayey silts (ML)	Fourie (2000), Blight (1997) Jennings (1979), Rudd (1979) Midgley (1979)
Merriespruitt, South Africa	Gold	Upstream (?)	Sandy soils	In operation	Sandy silts (ML)	Fourie (2000), Blight (1997) Wagener et al (1998)
Saaiplass, South Africa (3 slides)	Gold	Upstream (?)	-	In operation	-	Blight (1997)
Arcturus, Zimbabwe	Gold	Upstream (?)	-	In operation	-	Blight (1997)
Texas, USA	Phosphate, gypsum tailings	Upstream, mechanical	Sandier beached tailings	In operation	Sandy silts (ML)	Kleiner (1976) Jeyapalan et al (1983a, 1983b)
Buffalo Creek, USA	Coal	Coarse coal waste dumped over existing dammed slimes		In operation	Sandy silts and sandy clays (ML/CL)	Wahler and Assoc. (1973) Johnson (1980)

Table 3.5: Summary of failure case studies in hydraulic fill embankment dams

Name	Year of Failure	Embankment Construction	Material Type/s	Location and Timing of Failure	Data Sources
Sheffield Dam, USA	1925	Hydraulic	Silty sands to sandy silts	Downstream shoulder, during earthquake	Seed et al (1969), Seed (1987)
Lower San Fernando, USA	1971	Hydraulic	Silty sands to sandy silts	Upstream shoulder, during earthquake	Seed et al (1975), Castro et al (1985, 1992) Gu et al (1993), Baziar and Dobry (1995)
Calaveras Dam, USA	1918	Hydraulic	Sandstone, soft, sluiced	Upstream shoulder, during construction	Hazen (1918), Hazen and Metcalf (1918) Seed (1987)
Fort Peck Dam, USA	1938	Hydraulic	Sands	Upstream shoulder, during construction	ENR (1939a), Middlebrooks (1940) Casagrande (1965), Seed (1987)
Wachusett Dam, USA	1907	Loose dumped	Sands	Upstream shoulder, during first filling	Olson et al (2000)

Table 3.6: Summary of failure case studies in sub-aqueous constructed fill slopes

Name	Date of Failure	Method of Construction	Material Description *[1]	Timing/Cause of Failure	Data Sources
Nerlerk Sea Berm, Canada (3 slides)	1982	Hydraulically placed sand fill	Sand with trace to some silt, loose (D_R = 25 to 35%)	Failure during construction due to localised over-steepening	Sladen et al (1985b) Sladen and Hewitt (1989) Rogers et al (1990)
Willamette River Terminal, USA	18/1/67	Bulldozed sand fill over hydraulically placed sand fill	Sand, medium to coarse grained, very loose (D_R = 15%) bulldozed fill to loose to medium dense (D_R = 20 to 60%).	Failure induced by excavation at the toe of the slope. Flow slide in the very loose bulldozed fill.	Cornforth et al (1974)

Note: *[1] D_R = relative density or density index

3.2.6 FLOW SLIDES FROM FAILURES IN SUBMARINE SLOPES

"Rapid" flow slides from failures in natural submarine slopes were included in the database for comparative purposes with other flow slides. The twenty-two case studies used in the post-failure analysis were from Edgars and Karlsrud (1983). Table 3.7 is a summary of the case studies and further details are given in Section 1 of Appendix B. The landslides were predominantly of large volume (up to 8 x 10^{11} m^3) and mostly ancient slides in mainly sandy and silty soils.

Published literature on research of submarine slopes from the Zeeland Province of The Netherlands provides more detailed information on the mechanics of failure for these type of flow slides (Silvas and de Groot 1995; de Groot and Stoutjesdijk 1997; Stoutjesdijk et al 1998; Koppejan et al 1948). However, the literature from these sources is limited on specific cases and therefore none of these were included in the database. The submarine flow slides from Zeeland were generally within loose, uniformly graded sands and were commonly retrogressive.

3.2.7 FLOW SLIDES IN SENSITIVE CLAYS

The work on "rapid" flow slides from slope failures in sensitive clays is a summary of the findings from the literature. The focus of much of the research has been on initiation of landsliding, material properties and the distance of retrogression. Recent published papers include Locat and Leroueil (1997), Trak and Lacasse (1996), Leroueil et al (1996), Lefebvre (1996) and Torrence (1996), and earlier publications including Tavenas (1984), Mitchell and Markell (1974), Bentley and Smalley (1984) and Bjerrum et al (1969) amongst others. The properties of 15 slides in sensitive clays and data sources are given in Table 3.8. Further details are given in Section 1 of Appendix B.

The sensitivity, S_t, of a soil is defined as the ratio of the undisturbed to remoulded unconfined compressive strength (Equation 3.1). It is often evaluated by comparison of the undisturbed and remoulded shearing strengths as measured in the field by vane shear tests. Soils with a sensitivity of greater than about 16 are known as quick clays.

$$\text{Sensitivity, } S_t = \frac{\text{Undisturbed unconfined compressive strength}}{\text{Remoulded unconfined compressive strength}} \qquad (3.1)$$

Table 3.7: Summary of "rapid" flow slides in natural submarine slopes

Site	Failure Date	Material Description	Trigger	Data Sources
Orkdalsfjord, Norway	2/5/30	Glacial - loose sand, silt and clay deposits.	Exceptional low tide	Karlsrud & Edgars (1982), Edgars and Karlsrud (1983), Terzaghi (1956)
Bassien	Ancient	-	Earthquake or rapid sedimentation	Edgars and Karlsrud (1983)
Storegga	Ancient	-	Earthquake (?)	Edgars and Karlsrud (1983)
Grand Banks	1929	Sand / silt	Earthquake	Edgars and Karlsrud (1983)
Spanish Sahara	Ancient	Gravelly clayey sand	rapid sedimentation	Edgars and Karlsrud (1983)
Walvis Bay (SW Africa)	Ancient	-	-	Edgars and Karlsrud (1983)
Icy Bay / Malaspina	Ancient	Clayey silt	Earthquake	Edgars and Karlsrud (1983)
Copper River	Ancient	Silt / sand	rapid sedimentation	Edgars and Karlsrud (1983)
Ranger	Ancient	Clayey and sandy silt	rapid sedimentation (earthquake)	Edgars and Karlsrud (1983)
Mid Alb. Bank	Ancient	silty clay	earthquake / rapid sedimentation	Edgars and Karlsrud (1983)
Wil. Canyon	Ancient	silty clay and silt	rapid sedimentation	Edgars and Karlsrud (1983)
Kidnappers	Ancient	sandy silt, clay	Earthquake (?)	Edgars and Karlsrud (1983)
Kayak Trough	Ancient	clayey silt	rapid sedimentation / earthquake	Edgars and Karlsrud (1983)
Paoanui	Ancient	silt / sand	Earthquake (?)	Edgars and Karlsrud (1983)
Mid. Atl. Cont. Slope	Ancient	silty clay	rapid sedimentation	Edgars and Karlsrud (1983)
Magdalena R.	1935	-	rapid sedimentation	Edgars and Karlsrud (1983)
California	Ancient	clayey and sandy silt	Earthquake (?)	Edgars and Karlsrud (1983)
Suva, Fiji	1953	sand	Earthquake	Edgars and Karlsrud (1983)
Valdez	1964	gravelly silty sand	Earthquake	Edgars and Karlsrud (1983)
Sokkelvik, Norway	1959	quick clay (?) and sand	-	Edgars and Karlsrud (1983)
Sandnessjoen, Norway	1967	-	Blasting, man made fill	Edgars and Karlsrud (1983)
Helsinki Harbour, Norway	1936	sand / silt	Man made fill	Edgars and Karlsrud (1983)

Table 3.8: Summary of flow slides in sensitive clays

Site	Initial Slide Classification	Material Description (Liquefied Material on the Surface of Rupture)		Data Sources
		Description *[1]	S_t *[2]	
Lemieuse, Ottawa	Retrogressive flow slide	Clay (CH), high plasticity, firm	10 to 100	Lawrence et al (1996)
South Nation River, Canada	Retrogressive flow slide	Clay (CH), high plasticity, firm, $I_L = 1$	10 to 100	Lawrence et al (1996) Eden et al (1971)
St. Jean Vianney, Quebec	Retrogressive flow slide	Silty Clay (CL), low plasticity, cemented, soft to firm, $I_L = 1.8$	> 200	Edgars and Karlsrud (1983), Tavenas et al (1971), Trak and Lacasse (1996), Bentley and Smalley (1984)
La Grande River, Quebec	Retrogressive flow slide	Clayey Silt (CL), low plasticity, stiff, $I_L = 1.8$	-	Lefebvre et al (1991)
Baastad, Norway	Translational flow slide	Clayey Silt (ML), low plasticity, firm, $I_L = 1.6$	50 to 100	Edgars and Karlsrud (1983) Trak and Lacasse (1996) Gregerson & Loken (1979)
Rissa, Norway	Translational flow slide, some retrogression	Clay (CL), low plasticity, very soft, $I_L = 2.3$	100	Edgars and Karlsrud (1983), Trak and Lacasse (1996), Gregersen (1981).
Furre, Norway	Translational flow slide (some retrogression)	Silty Clay (CL), low plasticity, firm, $I_L = 2.1$	> 70	Hutchinson (1961)
Vibstad, Norway	Translational flow slide	Clayey Silt (ML), low plasticity, firm, $I_L = 1.3$	-	Hutchinson (1965)
Bekkelaget, Norway	Translational flow slide	Silty Clay / Clayey Silt (CL/ML), low plasticity, very soft, $I_L = 2.4$	80	Eide and Bjerrum (1956)
Tuve, Sweden	Retrogressive flow slide	Silty Clay (CH), high plasticity, soft, $I_L = 1.3$	15 to 40	Duncan et al (1980)
Borgen	Retrogressive (?) flow slide	Clay (CL), low plasticity, soft, $I_L = 1.4$	20 to 100	Edgars and Karlsrud (1983) Trak and Lacasse (1996)
Hekseberg	Retrogressive (?) flow slide	Clay, soft to firm	50 to 150	
Skjelstadmarken	Retrogressive (?) flow slide	Clay (CL), low plasticity, firm, $I_L = 1.3$	-	
Verdal	Retrogressive (?) flow slide	Clay (CL), low plasticity, soft to firm, $I_L = 2.5$	20 to 200	
Selnes	Retrogressive (?) flow slide	Clay (CL), low plasticity, soft, $I_L = 1.9$	> 100	

*[1] I_L = liquidity index

*[2] S_t = sensitivity, refer Equation 3.1

3.3 THE MECHANICS OF SHEARING OF CONTRACTIVE GRANULAR SOILS

Many "rapid" landslides are the result of a loss of strength of the soil at failure as it shears in undrained loading under static (monotonic) and cyclic (earthquake) conditions. This usually occurs in granular soils, which in drained loading would be contractive.

The behaviour of granular soils on shearing in undrained loading is quite complex and dependent on a number of factors including the material properties, stress conditions and stress path. This section discusses:

- The general behaviour of granular soils in undrained shear from laboratory testing;
- The identification of soils susceptible to contraction on shearing and development of liquefaction based on field in-situ tests, particle size distribution and other characteristics;
- The large strain (residual) undrained strength.

Several aspects of the literature review on soils susceptible to liquefaction and potential flow are discussed further in Section 2 of Appendix B.

3.3.1 DEFINITIONS

The definition of several key terms used is as follows:

- Liquefaction (or flow liquefaction) – Undrained strain weakening in contractant soils where, as a result of some disturbance, part (or all) of the load supported by the soil structure is transferred onto the pore fluid.
- Temporary liquefaction – where a liquefaction condition is only temporarily developed within a soil mass. The soil mass that displays temporary liquefaction behaviour is usually contractant on initial shearing (thus liquefaction occurs) but then dilative as shearing continues (or strain hardening in undrained loading).
- Static liquefaction – the disturbance causing liquefaction is by monotonic loading and not associated with dynamic events such as earthquake or blasting. Often the cause of static liquefaction is a change in effective stress conditions such as change in groundwater level, excavation or rapid sedimentation.
- Cyclic or dynamic liquefaction – liquefaction developed through undrained cyclic loading in laboratory testing or by earthquake.

3.3.2 CHARACTERISTICS OF CONTRACTIVE AND DILATIVE SOILS SHEARED UNDER MONOTONIC LOAD CONDITIONS

The observations from monotonic, consolidated undrained triaxial compression tests on clean sands (Ishihara 1993) indicate that the steady state condition in undrained loading (Figure 3.2) is dependent on the void ratio alone. For sands at an initial state in *e log p'* space (*e* = void ratio, *p'* = mean normal effective stress) to the right of the steady state line, on shearing in drained conditions the sand will contract toward the steady state line. In undrained loading conditions the tendency for contraction is suppressed and post peak strain weakening is observed (Figure 3.3) as load is transferred to the pore fluid and the effective stress path moves to the left (at constant void ratio) toward steady state.

For sands at an initial state on the left side of the steady state line, when sheared in drained loading conditions will dilate. In undrained loading conditions the dilation is suppressed and strain hardening is observed (Figure 3.4) as pore water pressures reduce and load is transferred onto the soil structure. A "quasi steady state" condition in undrained loading (where strain hardening follows post-peak strain weakening) is observed for some initial states as shown in Figure 3.4. It is generally observed where the initial state is slightly above or slightly below the steady state. Ishihara (1993) showed the quasi steady state to be dependent on void ratio, initial effective confining stress and the fabric of the sample, and is therefore not a fundamental state parameter for sands. The change from strain weakening to strain hardening is termed the phase transformation.

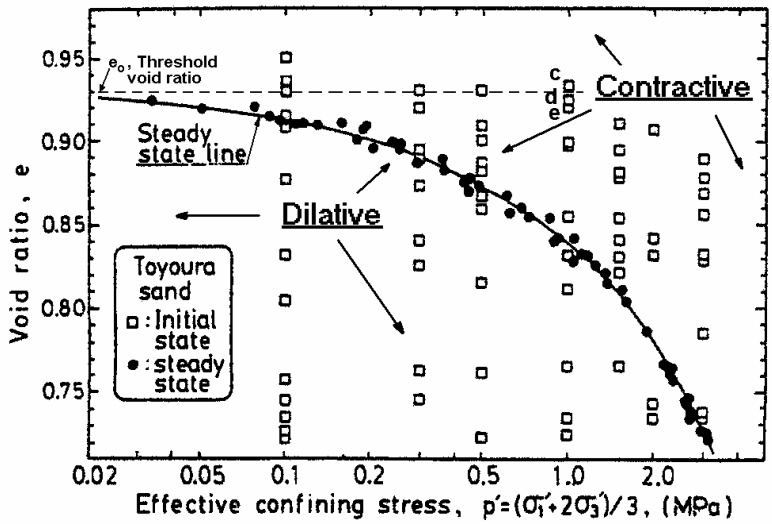

Figure 3.2: Steady state line of Toyoura sand (Ishihara 1993)

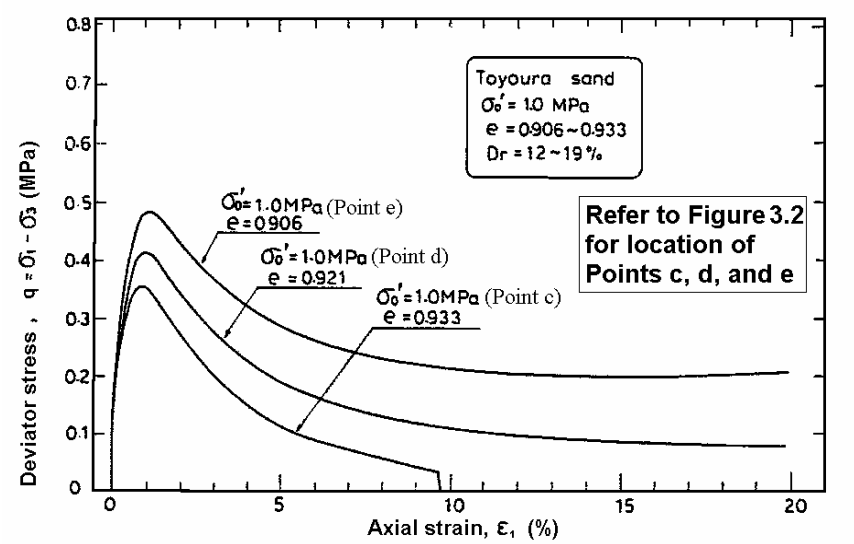

Figure 3.3: Undrained behaviour of states on the contractive side of the steady state line (Ishihara 1993)

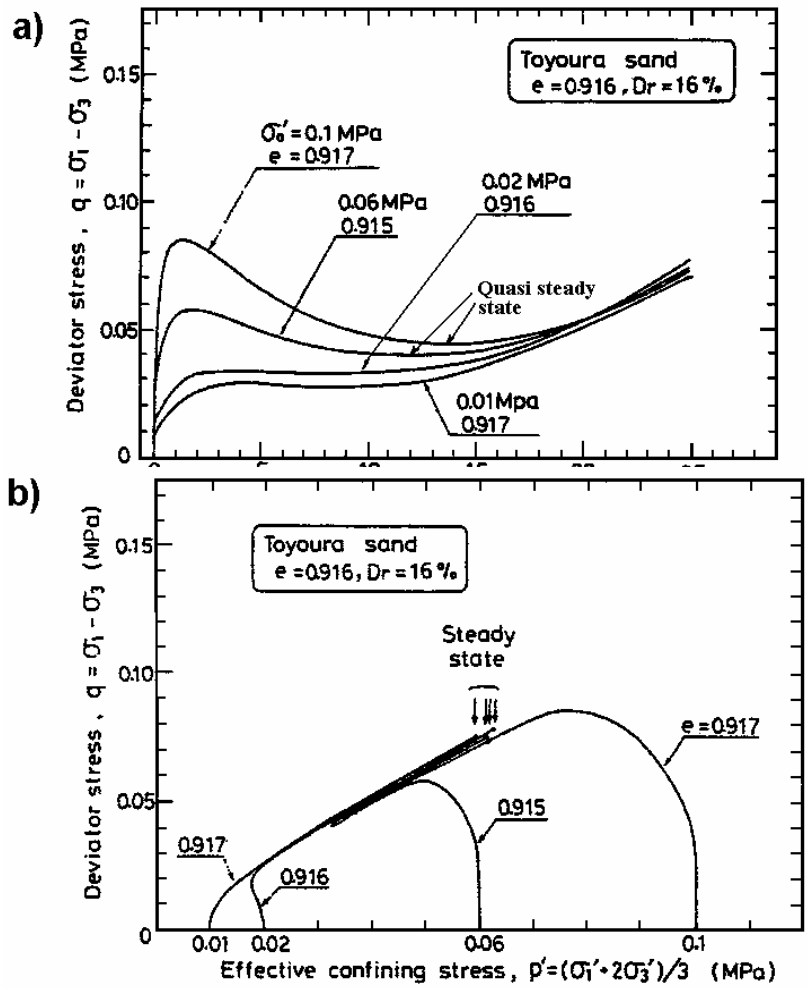

Figure 3.4: Undrained behaviour from states close to steady state and on dilative side (a) stress-strain plot and (b) effective stress paths (Ishihara 1993)

When clean sands are tested in undrained conditions from the same initial void ratio and different initial effective stress conditions the steady state strength reached for all samples is similar (Figure 3.5). Yamamuro and Lade (1998) defined three "normal" states of behaviour for clean sands:

- Stable behaviour, where the undrained stress path is strain hardening. This is similar to the behaviour observed for clean sands sheared from initial states well to the left of the steady state line that are strongly dilative and representative of sands with large negative state parameter, j (see below).
- Temporary instability, where phase transformation or a quasi steady state condition occurs post the initial peak undrained strength. Decreasing stability is observed with increasing confining pressure in this region.
- Instability (liquefaction), indicative of the contractive tendency resulting in the development of positive pore pressures to a steady state condition. Once the effective stress path exceeds the peak deviatoric stress the sand, in undrained conditions, becomes unstable and failure occurs. This corresponds to states to the right of the steady state line (Figure 3.2). Yamamuro and Lade (1998) comment that this behaviour is observed at relatively high confining pressures, the high confining pressure suppressing the tendency for dilation.

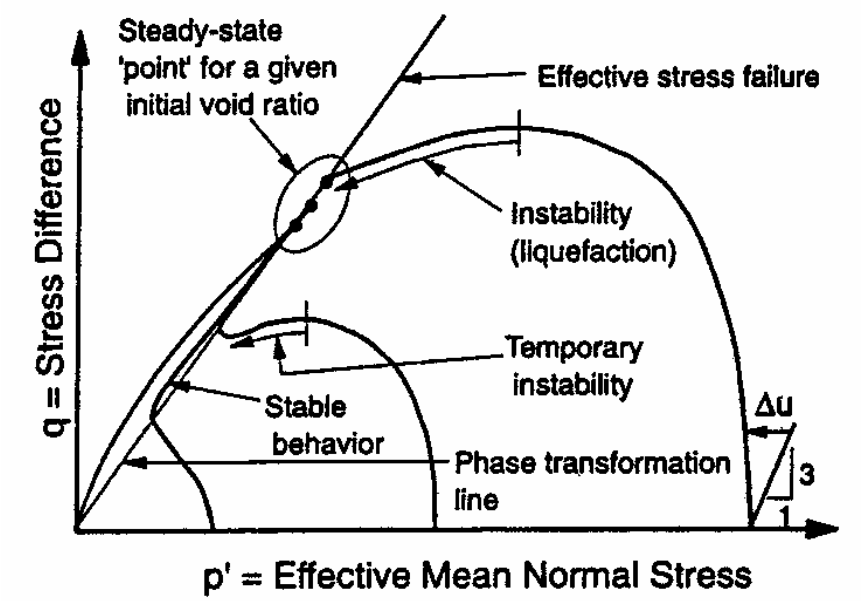

Figure 3.5: Schematic diagram showing different types of behaviour for undrained stress paths of samples at the same void ratio and different initial confining pressures (Yamamuro and Lade 1998).

If we now consider a series of samples tested undrained under monotonic load conditions from the same initial effective confining stress and different initial void ratios, the findings from the literature (Ishihara 1993; and others) indicate:

- At very high void ratios, corresponding to sands in a very loose condition, complete static liquefaction (i.e., zero residual undrained strength) is observed, as typified by Point c in Figure 3.3. Ishihara (1993) defined the threshold void ratio, e_o (refer Figure 3.2), as the void ratio at or above which samples exhibit zero residual strength. It corresponds to the void ratio at steady state for zero effective stress.
- At a void ratio slightly less than the threshold void ratio (Points d and e in Figure 3.2) static liquefaction is observed with low residual undrained strength (Figure 3.3). This corresponds to contractive states located above the steady state line.
- At initial states close to the steady state line temporary instability is observed.
- Stable or strain hardening behaviour is observed at low void ratios, corresponding to strongly dilative states located well below the steady state line (Figure 3.2).

Two important concepts have been developed to characterise the behaviour of sands. Been and Jefferies (1985) defined the "state parameter", j , to uniquely characterise the state of a sand (Figure 3.6). The state parameter is defined as the difference between the initial void ratio, e_1 , and the void ratio at steady state corresponding to the initial mean normal effective stress, e_{ss} ($j = e_1 - e_{ss}$). The concept of the state parameter is that it characterises the effective stress path and normalised steady state strength of samples with identical values of the state parameter, regardless of the initial mean normal effective stress.

Sladen et al (1985a) proposed the concept of the collapse surface (or instability line) for evaluation of the liquefaction potential of very loose sands located on the contractive side of the steady state line. They defined the collapse surface as the locus of the peak deviatoric stress of undrained triaxial compression tests (Figure 3.7) of samples tested at the same initial void ratio (but different initial mean normal stress). For liquefaction to occur the effective stress state of very loose sands must reach the collapse surface in undrained loading, thereafter in stress controlled tests a static liquefaction condition develops rapidly. The instability line (or collapse surface) is located at effective stress states below the steady state. As shown in Figure 3.7, the position of the instability line and the steady state deviatoric strength for potentially liquefiable sands will vary

depending on the initial void ratio. It is important to note that under static loading conditions and in undrained conditions samples are stable at effective stress states below the instability line.

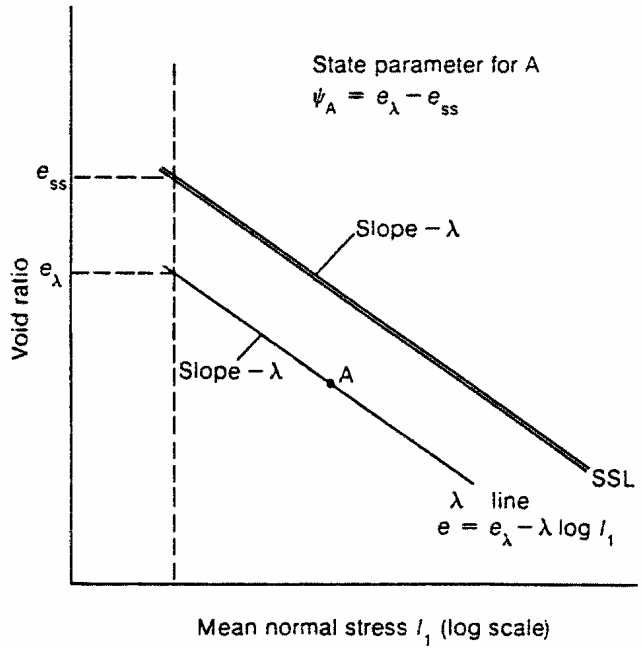

Figure 3.6: Definition of the state parameter (Been and Jefferies 1985).

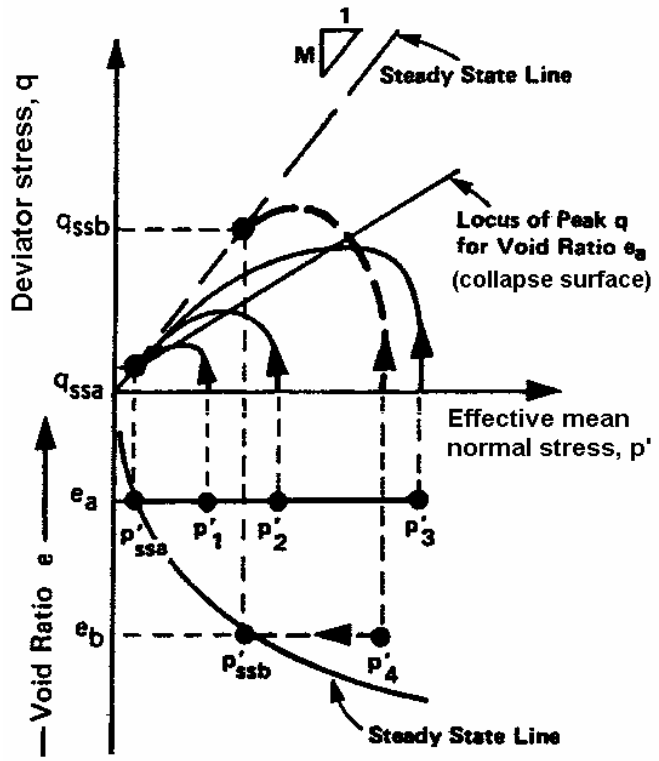

Figure 3.7: Collapse surface concept, defined by the locus of the peak deviator stress from undrained triaxial samples tested at the same void ratio and different initial effective mean normal stress (Sladen et al 1985a).

The above summary describes the characteristics of sand based on the concept that the steady state line is a unique parameter for clean sand and that, in undrained loading, the steady state strength can be determined from void ratio alone. The findings have been based predominantly on isotropically consolidated, undrained triaxial compressive tests on clean sands. However, this concept of uniqueness of the steady state line is queried by the results of research, in particular from work using stress paths other than drained and undrained compressive testing and also from testing of sands with fines (Uthayakumar and Vaid 1998; Yamamuro and Lade 1998). This is summarily discussed below with several aspects discussed further in Section 2 of Appendix B.

For silty sands Lade and Yamamuro (1997) and Yamamuro and Lade (1998) found that liquefaction was observed at low confining stresses in undrained conditions and termed this behaviour as "reverse" behaviour to that of clean sands. They considered that particle re-arrangement of the unstable and highly compressive particle structure formed due to deposition under very low energy environments as the mechanism for liquefaction and temporary liquefaction. Under increasing confining pressures the "normal" states defined for clean sands are observed for silty sands.

Vaid, and his co-workers (Uthayakumar and Vaid 1998; Sivathayalan and Vaid 1998; Vaid and Eliadorani 1998) have shown that the undrained response of loose sand is highly dependent on the load direction, i.e. whether in triaxial compression or triaxial extension or simple shear. They showed that samples tested in triaxial extension are more brittle and mobilize at lower peak strength (i.e. the collapse surface is lower and the peak undrained strength is lower) than those tested in triaxial compression.

This indicates that the use of triaxial compression tests may not be conservative. Soils that are dilative under triaxial compression may be contractive under triaxial extension. Vaid and his co-workers concluded that the ultimate strength is not uniquely related to void ratio alone, but on the direction of the principal stresses, the effective mean normal stress prior to shearing, and the magnitude of the intermediate principal stress.

Imam et al (2002), in researching the yield surface for sands, attributed the dependency of the undrained response of loose sand on load direction to the inherent anisotropy associated with deposition of the sand, which existed prior to consolidation. Higher yielding stresses are observed where the major principal stress is in the direction of soil deposition. Therefore, for a sand sample formed by vertical deposition the highest yielding stress in undrained loading is observed for a standard undrained triaxial

compression test, and the minimum yielding stress for a standard undrained triaxial extension test.

3.3.3 FIELD METHODS FOR EVALUATION OF FLOW LIQUEFACTION POTENTIAL

Methods for evaluation of liquefaction potential have been developed from the results of laboratory testing and empirically from field case studies. Most of these methods are related to cyclically induced liquefaction (i.e., from earthquakes), but it is considered that much can be learnt from this relative to static liquefaction.

The early work of Harry Bolton Seed pioneered much of the development of empirical methods from case study analysis for evaluation of liquefaction potential based on cyclic resistance of the soil under dynamic loading. Robertson and Wride (1997) discuss the importance of distinguishing between deformations that occur during cyclic loading (termed cyclic liquefaction) and deformations from flow liquefaction that usually occurs under the static load after the triggering mechanism (i.e., after an earthquake). Empirical methods for evaluation of large deformation potential have been developed for; the Standard Penetration Test (SPT), Cone Penetration Test (CPT), shear wave velocity from seismic refraction, and the Becker Penetration Test (BPT), applicable to gravelly soils where the SPT is not appropriate. Empirical correlations to SPT and CPT are the most widely used given the larger field database of information.

Seed (1979) developed a correlation between the cyclic stress ratio to cause cyclic liquefaction and the N value of the SPT test based on field data of sand deposits for essentially level ground condition subject to strong shaking from earthquakes. Seed et al (1985), recognising that the amount of shear strain observed was dependent on the relative density of the sand, further developed the correlation to provide guidelines on the level of shear strain (Figure 3.8) with respect to SPT and cyclic resistance ratio for clean sands. Robertson and Wride (1997) comment that much larger shear strains can be expected for loose sands ($(N_1)_{60}$ < 15), where effective stresses may reduce to zero under dynamic loading, than for denser sands ($(N_1)_{60}$ > 15) where large pore pressures may develop but effective stresses may not fully reduce to zero. The line on Figure 3.8 for shear strains of 20% could be considered as representing a boundary of flow liquefaction conditions.

Baziar and Dobry (1995) provide an indication of flow liquefaction potential for silty sands and sandy silts (≥ 10% fines) based on case histories of flow failure and large

ground deformation all triggered by earthquakes corresponding to a moment magnitude less than or equal to 8. They hypothesise that the right boundary in Figure 3.9 is the boundary between flow liquefaction and no-flow conditions (no-flow for $(N_1)_{60}$ to the right of this boundary).

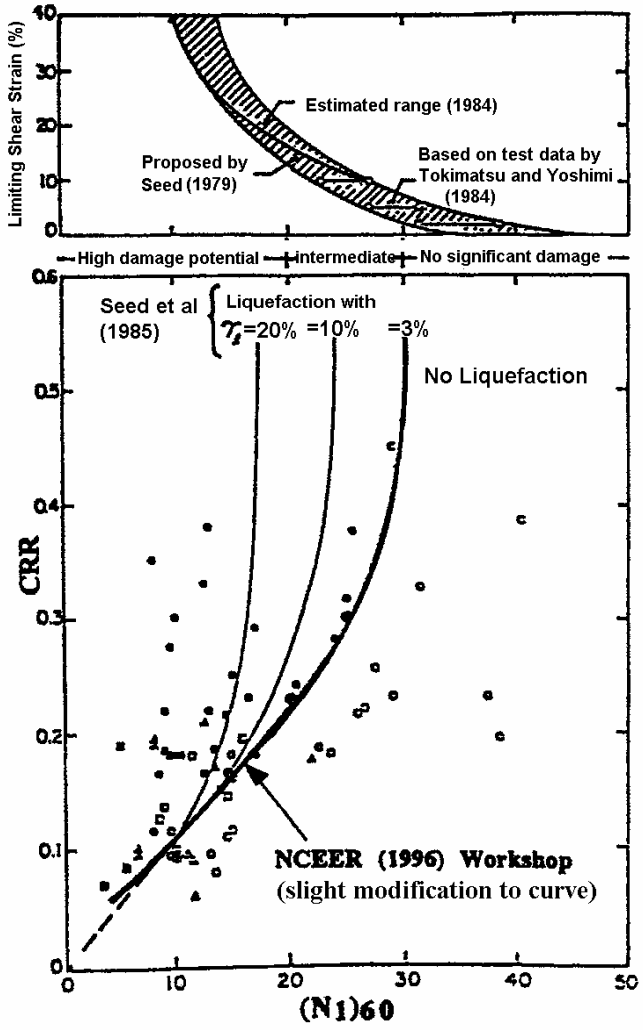

NCEER = National Centre for Earthquake Engineering Research

Figure 3.8: Correlation for cyclic resistance ratio (CRR) based on corrected SPT blow count, $(N_1)_{60}$, for clean sands under level ground conditions (Robertson and Wride 1997)

Ishihara (1993) compared the threshold flow liquefaction boundary determined from laboratory undrained monotonic compression tests on clean sands and silty sands (separate comparison for sands and silty sands) to known cases of field flow liquefaction triggered by earthquake (Niigata in 1964 and Nihonkai-Chuba in 1983) where SPT *N* value data was known prior to the earthquake. The laboratory sand and silty sand samples were not from the field sites, but were considered by Ishihara as

typical of the liquefied sands. The flow liquefaction boundary for the laboratory samples was defined from the quasi-steady state for water sedimented samples. This boundary was converted into a plot of SPT *N* value as a function of effective overburden stress, using an empirical correlation derived from the correlation between density ratio and *N* value (Equation 3.2) suggested by Skempton (1986). Ishihara (1993) found the flow liquefaction no-flow boundaries (in SPT *N* value versus effective over-burden pressure space) of the laboratory samples to be relatively diverse between samples and commented on the marked difference in density ratio at which the quasi-steady state occurs for clean sands. However, the SPT *N* values were in the same range as the field values from actual sites of flow failure.

$$\frac{N_1}{(D_r/100)^2} = a + b \tag{3.2}$$

where N_1 is the SPT *N* value corrected for over-burden pressure, D_r the relative density of the sand, and *a* and *b* constants based on the fines content and mean particle diameter of sand particles.

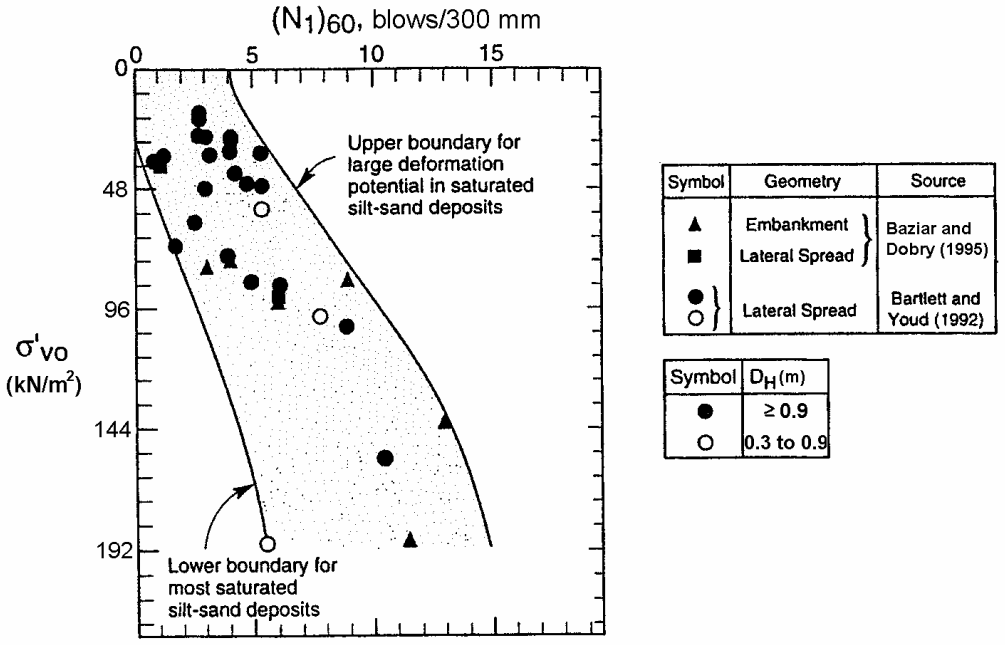

Figure 3.9: Corrected SPT blow count, $(N_1)_{60}$, versus vertical effective over-burden pressure (s'_{vo}) for saturated non-gravelly silty sand deposits that have experienced large deformations and were triggered by earthquake (Baziar and Dobry 1995)

Figure 3.10a presents the boundary between flow liquefaction and no-flow, and the boundary between cyclic liquefaction and no-liquefaction estimated by Ishihara (1993) for sands with fines contents up to 30%. The flow liquefaction no-flow boundary represents the two boundary curves (one from clean sands and one from silty sands) giving the maximum possible N value determined from the comparisons between laboratory testing and field values from actual sites of flow failure, and can therefore be considered conservative. Figure 3.10b is the boundary between flow liquefaction and no-flow in terms of q_c, the CPT tip resistance, determined by conversion of the SPT N value boundary using a correlation between q_c and N. This boundary is compared to the boundaries proposed by Sladen and Hewitt (1989) and Robertson et al (1992).

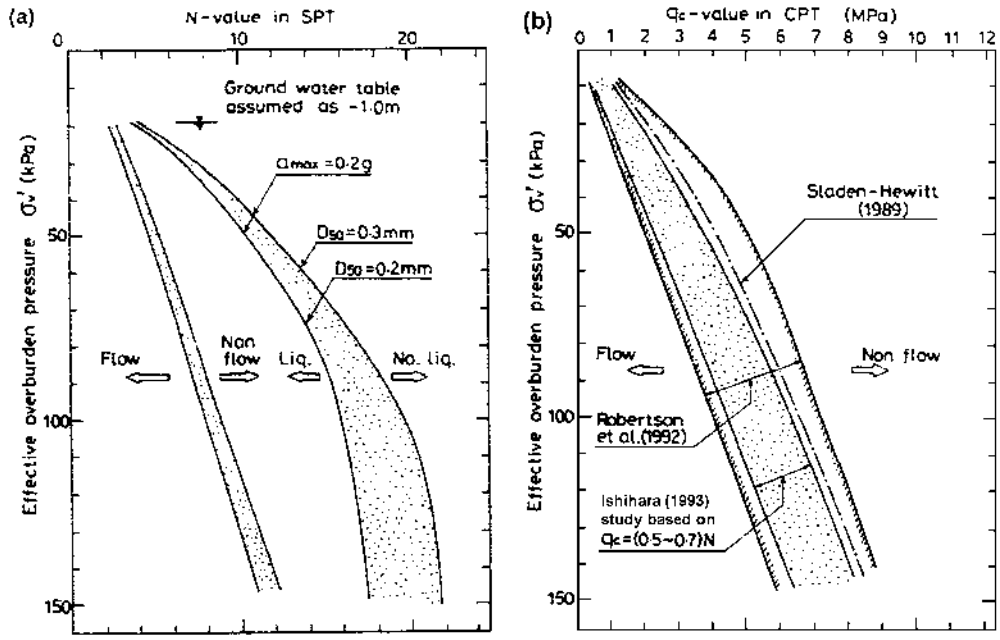

Figure 3.10: Flow liquefaction and no-flow bounds in terms of *(a)* field measured SPT blow count and *(b)* CPT q_c value from flow liquefaction case histories (static and earthquake triggered) and laboratory undrained testing (Ishihara 1993).

More recently, Cubrinovski and Ishihara (2000) have researched the effects of particle size distribution, fines content and particle shape on the flow liquefaction potential of sands and silty sands (with up to 30% non-plastic fines content). From analysis of published laboratory results for some 52 sandy soils they found that the flow liquefaction potential (and steady state line) could be defined based on the value of void ratio range ($e_{max} - e_{min}$) and consideration of particle shape. They found that at a given effective mean normal stress the relative density (or density index) defining the flow

liquefaction no flow boundary increased with increasing void ratio range. Figure 3.11 presents the comparison of flow liquefaction potential (Cubrinovski and Ishihara 2000) for the void ratio ranges 0.35 and 0.60 for both round-grained sands and angular grains. The shaded area above the line (in density ratio to mean normal stress space) defines the zone of flow liquefaction potential. For a void ratio range of 0.60 the relative density, at a given mean normal stress, below which the sand is susceptible to flow liquefaction is much greater than for a sand with a void ratio range of 0.35.

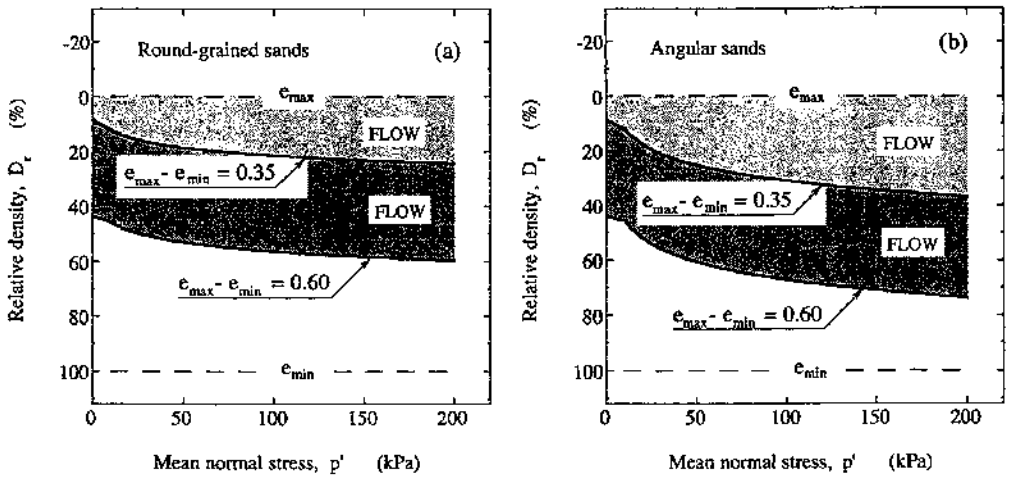

Figure 3.11: Influence of void ratio range on flow potential of sandy soils for *(a)* round-grained sands and *(b)* angular grains (Cubrinovski and Ishihara 2000)

Typical values of void ratio range ($e_{max} - e_{min}$) from their data set ranged from 0.25 to 0.65 for sands with up to 30% non-plastic fines content. For a given grain shape, the factors affecting void ratio range were fines content (the greater the fines content the greater the void ratio range) and mean grain size, D_{50} (the greater D_{50} the lower the void ratio range). Therefore, the findings indicate that finer sands and silty sands are more susceptible to flow liquefaction than coarser and cleaner sands.

Cubrinovski and Ishihara (2000), from their database, derived empirical correlations of relative density (at the threshold void ratio) and slope of the steady state line, l, with respect to the void ratio range. As shown in Figure 3.12 and Figure 3.13, whilst the data correlate reasonably well with the trendlines, there is a significant scatter. Cubrinovski and Ishihara (2000) then, using their derived correlation of relative density to SPT N value corrected for over-burden pressure, N_1, (Figure 3.14), derived empirical relationships to define the flow liquefaction no-flow boundary in terms of field measured SPT blow count. These equations (Equation 3.3 for round-grained sands and

Equation 3.4 for angular sands), by Cubrinovski and Ishihara (2000), define the field measured SPT N value corresponding to the flow liquefaction no-flow boundary, N_s, in terms of effective overburden stress, s'_v, void ratio range ($e_{max} - e_{min}$) and mean normal stress, p'.

$$N_s = \frac{9}{(e_{max} - e_{min})^{1.7}} \left(\frac{\sigma'_v}{98} \right)^{0.5} \left\{ -0.4 + 1.4(e_{max} - e_{min}) + \frac{0.01 - (1 - \log p')\{-0.01 + 0.125(e_{max} - e_{min})\}}{(e_{max} - e_{min})} \right\}^2 \quad (3.3)$$

$$N_s = \frac{9}{(e_{max} - e_{min})^{1.7}} \left(\frac{\sigma'_v}{98} \right)^{0.5} \left\{ -0.4 + 1.4(e_{max} - e_{min}) + \frac{0.01 - (1 - \log p')\{-0.02 + 0.25(e_{max} - e_{min})\}}{(e_{max} - e_{min})} \right\}^2 \quad (3.4)$$

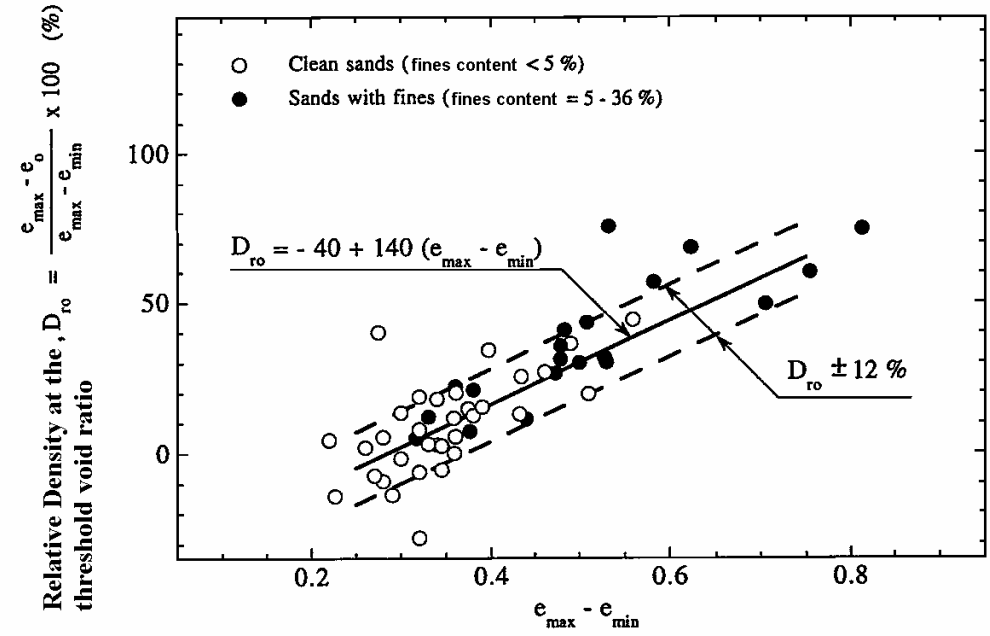

Figure 3.12: Relationship between relative density, D_{ro}, at the threshold void ratio, e_o, and void ratio range ($e_{max} - e_{min}$) for sandy soils (Cubrinovski and Ishihara 2000).

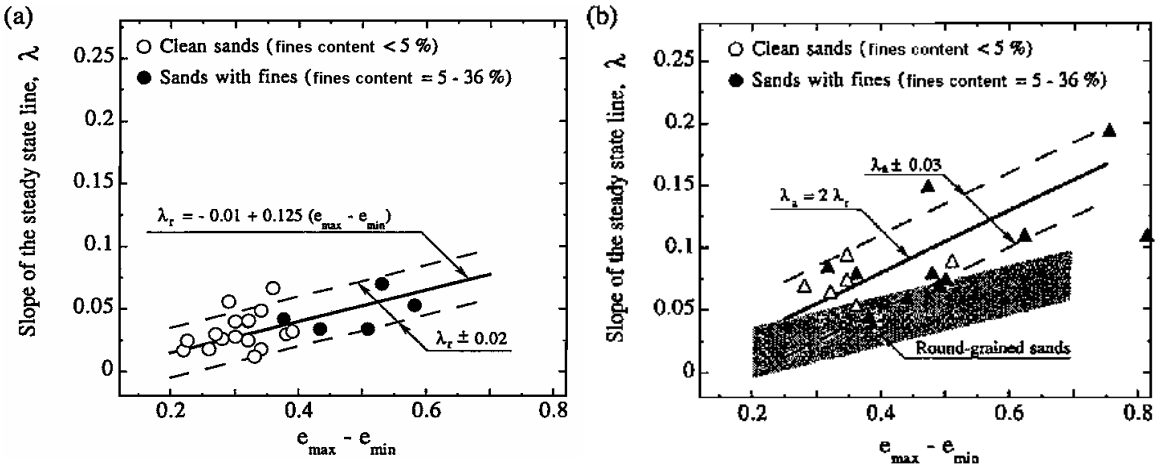

Figure 3.13: Relationship between the slope of the steady state line, l , and void ratio range for *(a)* round-grained sands and *(b)* angular grained sands (Cubrinovski and Ishihara 2000).

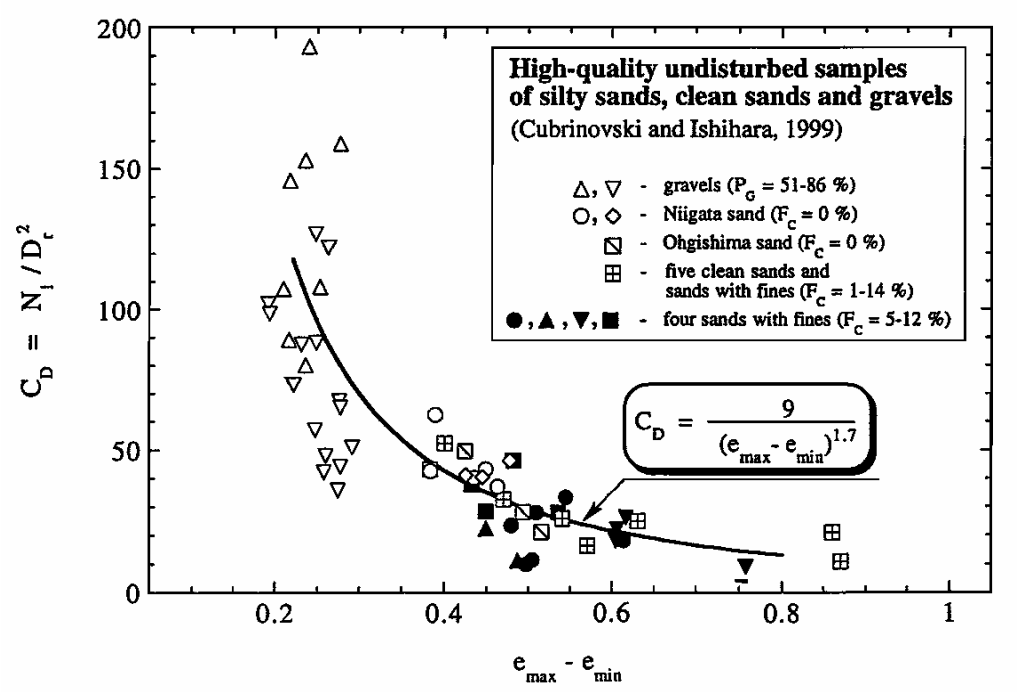

Figure 3.14: Correlation between N_1/D_r^2 (N_1 = SPT blow count corrected for over-burden pressure, D_r = relative density) and void ratio range for cohesionless soils (Cubrinovski and Ishihara 2000).

Graphical representations of the flow liquefaction no-flow boundary for both round-grained and angular sands according to Equations 3.3 and 3.4 are shown in Figure 3.15 for void ratio range from 0.3 to 0.6 and lateral stress ratios, K_o, of 0.5 and 1.0.

It is important to note that the National Standards for determining the minimum void ratio are not consistent between countries and this will therefore affect the void ratio range and relative density (density index). The Australian Standard is likely to result in a lower minimum void ratio than the Japanese Standards referred to by Cubrinovski and Ishihara (2000). In addition, the scatter associated with derivation of the empirical correlations should also be considered when applying these relationships.

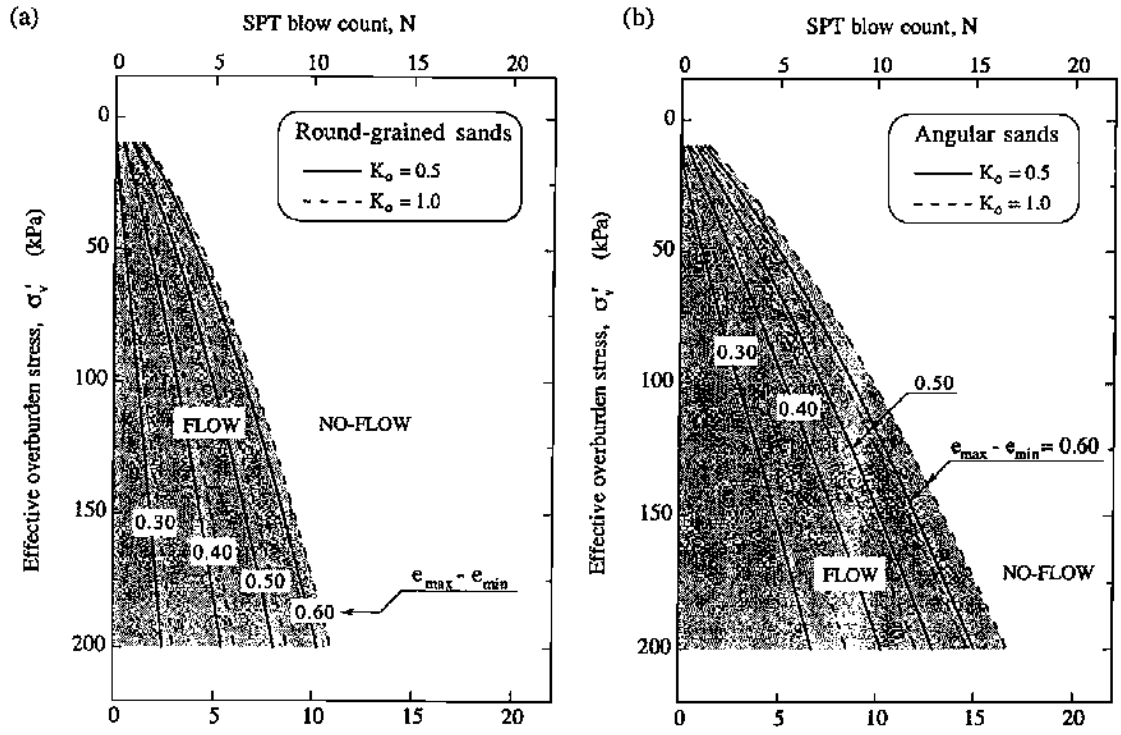

Figure 3.15: Field measured SPT blow count boundaries differentiating flow liquefaction no-flow conditions for void ratio range of 0.3 to 0.6 for *(a)* round-grained sands and *(b)* angular sands (Cubrinovski and Ishihara 2000)

Cubrinovski and Ishihara (2000) also defined the region of flow liquefaction at zero residual undrained strength (i.e., for void ratios at or above the threshold void ratio, defined in Section 3.3.2) in terms of SPT N value, using Equations 3.3 and 3.4. From Figure 3.11 the region of flow liquefaction at zero residual undrained strength is at relative densities less than at the intercept of the liquefaction flow no-flow boundary; i.e., at zero effective mean normal stress. For example, from Figure 3.11a flow liquefaction at zero residual strength would be at relative densities less than about 10% for a void ratio range of 0.35 and less than about 43% for a void ratio range of 0.6 (both for round-grained sands). Figure 3.16 is an example showing the liquefaction flow no-

flow boundary and the region of flow liquefaction at zero residual undrained strength in terms of SPT N value and effective over-burden pressure.

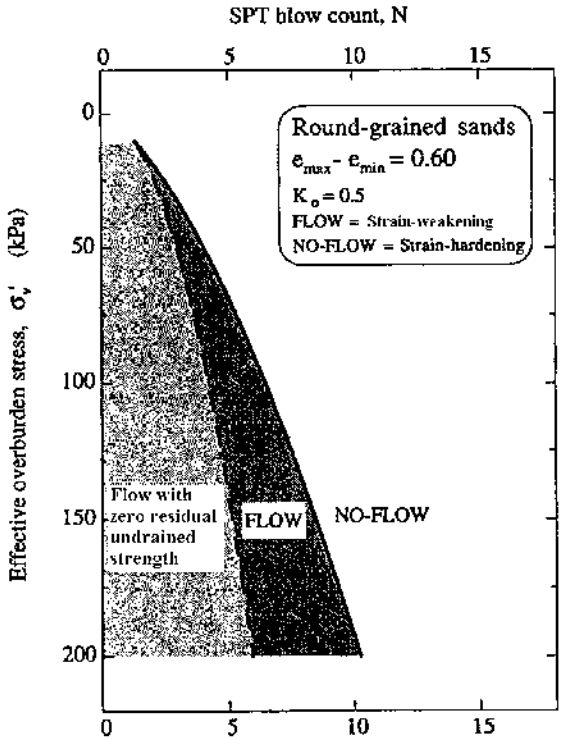

Figure 3.16: Flow characterisation of sand based on field measured SPT blow count showing liquefaction flow no-flow boundary, and region of flow at zero residual undrained strength (Cubrinovski and Ishihara 2000)

3.3.4 EFFECTS OF NON-PLASTIC FINES AND GRAVELS BASED ON FLOW LIQUEFACTION POTENTIAL

Byrne and Beaty (1998) considered the question of whether fines in sands were an instigator or inhibitor of liquefaction potential, and commented that the structure of the soil had a significant influence on the characteristics of sands with fines. Robertson and Wride (1997) commented that from field case studies it was not clear what effect fines had, whether the cyclic liquefaction resistance of the soil is increased or whether the $(N_1)_{60}$ value of the soil decreases as a consequence of the increase in compressibility and decrease in permeability associated with increasing fines content.

The results from undrained monotonic laboratory testing on silty sands with non-plastic fines (Cubrinovski and Ishihara 2000; Lade and Yamamuro 1997) indicate that, in terms of relative density, the fines content significantly increases the flow

liquefaction potential of sands as indicated by Figure 3.11 and Figure 3.17. Lade and Yamamuro (1997) comment that the fines have a significant role in the particle structure, resulting in highly compressible soils with increased liquefaction potential. They also recognised the findings of field-testing correlations with actual earthquake induced liquefaction events that indicated sands with significant fines content were more resistant to cyclic liquefaction. Lade and Yamamuro (1997) considered that the effects of stress history and aging (creep or cementation) are likely to increase the field resistance of silty sands. However, for newly constructed hydraulic fills and very recent natural deposits they considered that fines content would decrease the liquefaction resistance.

Field evidence (Eckersley 1985; Dawson et al 1998; Bishop 1973; Siddle et al 1996) indicates that sandy gravels, typically with low fines content, are susceptible to static liquefaction and flow sliding. This is supported by observations of static liquefaction in laboratory undrained monotonic tests on materials similar to those for which flow liquefaction occurred in the field (Dawson et at 1998; Dawson 1994; Eckersley 1986). The results from Dawson (1994) on the Fording mine over-burden dump sandy gravel material are presented in Figure 3.18 and show that at low confining pressures the sample was strain-weakening on shearing in undrained loading.

Cubrinovski and Ishihara (2000) comment that coarse sands and gravels are practically safe against flow liquefaction due to the typically narrow void ratio range of these soil types.

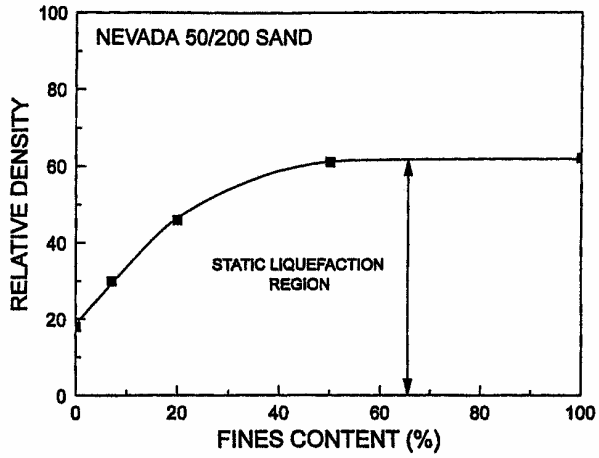

Figure 3.17: Increase in liquefaction potential (as measured by relative density) with increasing content of non-plastic fines (Lade and Yamamuro 1997)

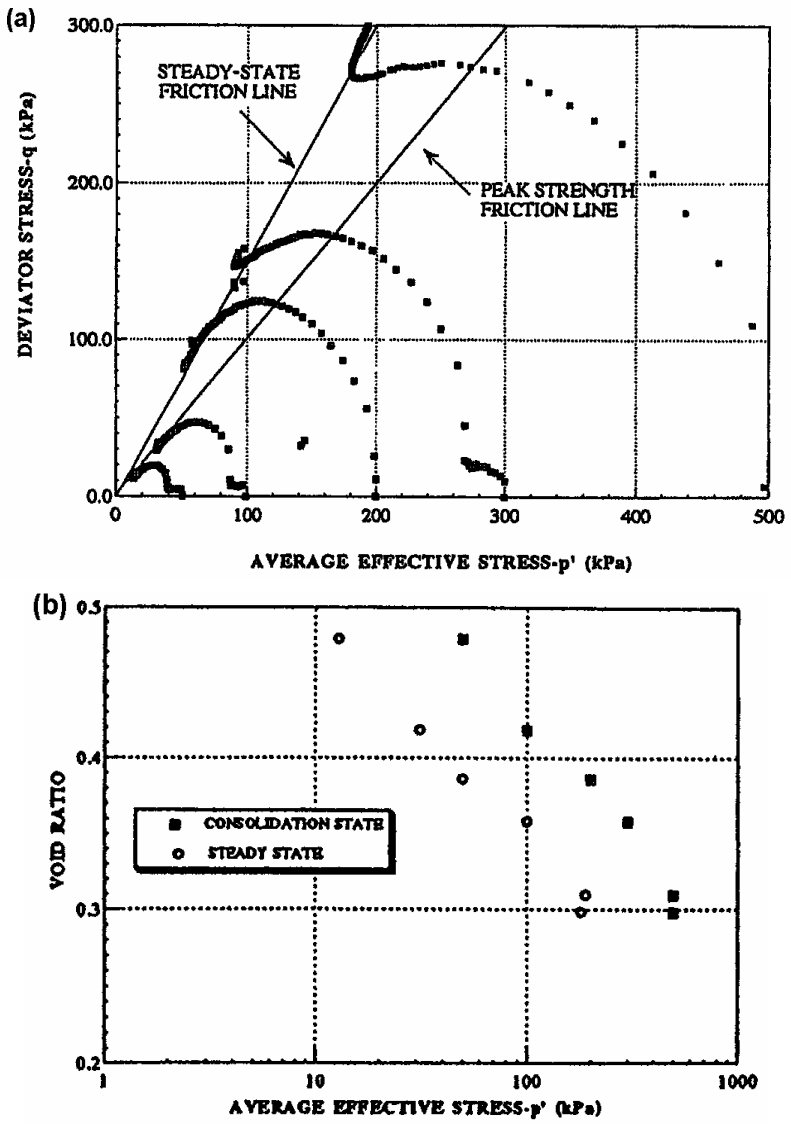

Figure 3.18: Fording sandy gravel sample *(a)* undrained triaxial compression test results and *(b)* consolidation and steady states (Dawson et al 1998).

3.3.5 RESIDUAL UNDRAINED SHEAR STRENGTH OF FLOW LIQUEFIED SOILS

Methods developed for assessment of the residual undrained shear strength of flow liquefied soils include empirical correlations based on back analysis of mostly earthquake induced liquefaction flow failures (Stark and Mesri 1992; Seed 1987; Seed and Harder 1990; Baziar and Dobry 1995), and estimation from laboratory test results. Whilst undrained conditions can be guaranteed in the laboratory and the term residual undrained strength is appropriate at large strains, in the field cases some drainage may occur. However, the term residual undrained strength is used here for both the laboratory and field cases.

Prediction of the residual undrained shear strength from laboratory test results would appear to be a relatively straightforward process. As shown in Figure 3.7, the residual undrained shear strength can be estimated from knowledge of the field void ratio and the steady state line. However, it is not this simple. Seed (1987) reported that experience with the laboratory method seemed to give values of residual undrained shear strength much greater than those determined by back analysis of field case studies. Seed queried the use of laboratory methods to field situations with respect to the effects of water re-distribution and the assumption of constant void ratio, particularly for stratified soil deposits and for liquefaction triggered by earthquake. At the National Science Foundation workshop on the shear strength of liquefied soils (NSF 1998) the significant debate amongst eminent researchers in this field over aspects of the theoretical fundamentals is indicative of the limitations of knowledge in this area.

As discussed in Section 3.3.2, it is the void ratio and effective mean normal stress that determine the behaviour of cohesionless sands and silts (and gravels to some extent) in undrained conditions. At void ratios less than the threshold void ratio, the residual undrained shear strength (for contractant samples) is determined from the void ratio (Figure 3.2 or Figure 3.7) and will increase with decreasing void ratio. At void ratios greater than or equal to the threshold void ratio (Figure 3.2) the laboratory residual undrained shear strength is zero. The recent research by Cubrinovski and Ishihara (2000) indicates that the relative density defining the threshold void ratio is greatly dependent on the void ratio range (Figure 3.11). For silty sands (typically broad void ratio range) zero residual undrained shear strength is observed in laboratory undrained triaxial tests at relative densities as high as 40 to 50%. For clean, medium to coarse grained sands (typically narrow void ratio range) zero residual undrained shear strength is generally observed at much lower relative densities, typically less than about 10%.

Seed (1987) back analysed some 12 case studies of flow sliding (or large deformation) and developed a correlation of residual undrained strength to the equivalent clean sand SPT blow count, $(N_1)_{60\text{-}CS}$. He commented that this would provide a useful guide to estimation of the residual undrained strength of flow liquefied soils. Figure 3.19 presents the correlation from Seed and Harder (1990) whom added to the Seed (1987) case studies and also considered dynamic effects in the travel of the flow slide. They recommended use of the lower bound relationship for estimation of the residual undrained strength.

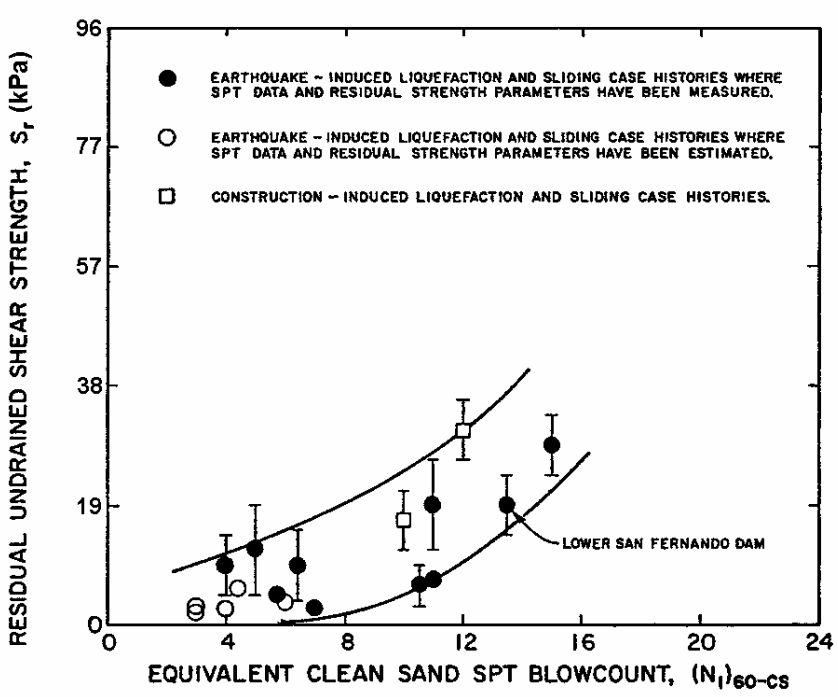

Figure 3.19: Relationship between equivalent clean sand SPT blow count, $(N_1)_{60\text{-}CS}$, and residual undrained strength from field case studies (Seed and Harder 1990)

Stark and Mesri (1992) proposed a correlation (Equation 3.5) between the residual undrained shear strength ($S_{u(crit)}$), "normalised" with respect to the initial effective over-burden pressure (s'_{vo}), and the equivalent clean sand SPT blow count, $(N_1)_{60\text{-}CS}$. They used the yield strength correction factor for fines content (Table 3.9) whilst Seed (1987) and Seed and Harder (1990) used the residual strength correction factor. Equation 3.5 represents a lower bound through the laboratory-undrained test data used to establish the correlation and is shown in Figure 3.20. Flow slides in silty sands and sandy silts plot close to the correlation and Stark and Mesri comment that this indicates limited drainage during flow. The case studies in sands and gravelly sands with limited fines contents plot well above the line indicating significant drainage during flow.

$$S_{u(crit)} / s'_{vo} = 0.0055 \times (N_1)_{60-CS} \tag{3.5}$$

Baziar and Dobry (1995) further analysed the case histories used by Seed and Harder (1990) and Stark and Mesri (1992). They considered those case histories of flow slides and large lateral spreads in silty sand deposits (greater than 10% fines) triggered by earthquake and concluded that the residual undrained shear strength (S_r) from back

analysis was related to the initial effective over-burden pressure, with the limits of S_r / s'_{vo} in the range 0.04 to 0.2 (Figure 3.21).

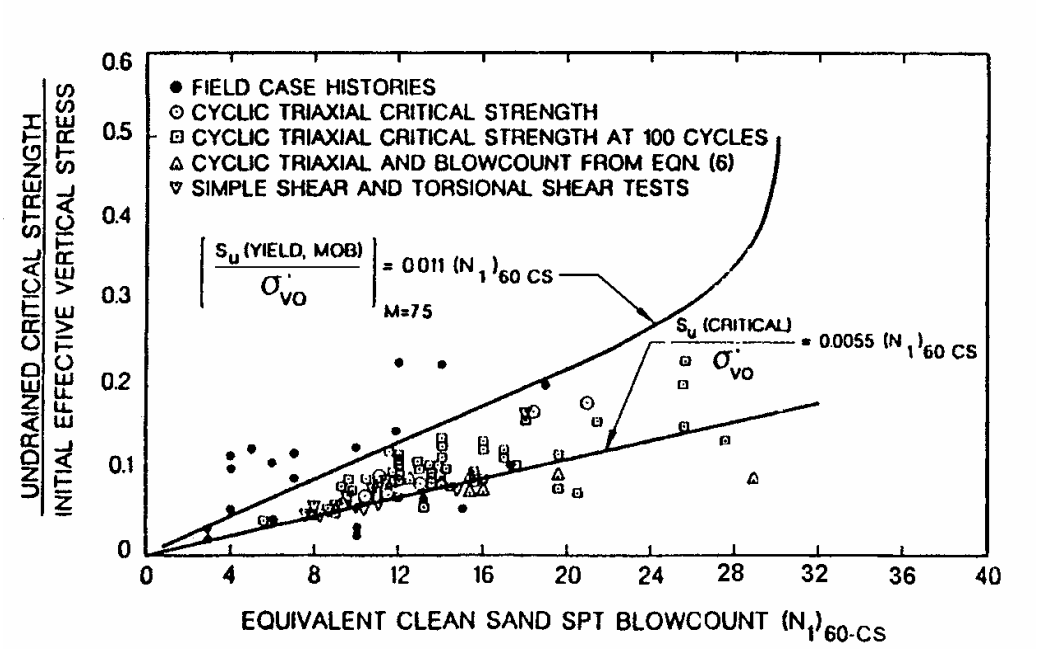

Figure 3.20: Relationship between undrained critical strength ratio and equivalent clean sand SPT blow count, $(N_1)_{60\text{-}CS}$ (Stark and Mesri 1992)

Table 3.9: SPT blow count ($(N_1)_{60}$) yield strength and residual strength correction factors for fines content (Seed et al 1985; Seed 1987)

Fines Content (%)	**$(N_1)_{60}$ Correction Factor for Yield Strength**	**$(N_1)_{60}$ Correction Factor for Residual Strength**
10	2.5	1
15	4	-
20	5	-
25	6	2
30	6.5	-
35	7	-
50	7	4
75	7	5

Riemer (1998) comments that there is little theoretical basis for correlation of the residual undrained shear strength to effective vertical stress. Poulos (1998) comments, and the observations of undrained laboratory tests indicate, that the residual undrained shear strength is a function of void ratio only. Poulos (1998) and Martin (1998) indicate that some correlation of residual undrained strength to the initial effective over-burden

pressure may be observed due to consolidation effects and increased relative density under increasing vertical stress; however, the ratio would not be constant and would vary for different soil types.

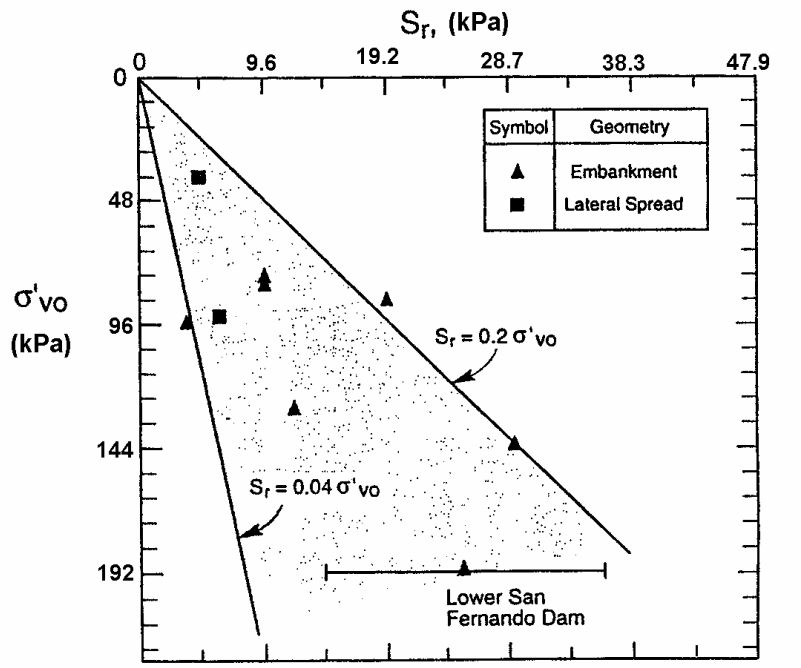

Figure 3.21: Residual undrained shear strength, S_r, to vertical effective over-burden pressure for silty sand deposits (≥ 10% fines), triggered by earthquake, that have experienced large deformation (Baziar and Dobry 1995)

In concluding, it is considered that there is significant uncertainty associated with estimation of the residual undrained shear strength, both from laboratory testing methods and from correlations with case histories, and any method should be used with caution.

With respect to laboratory testing, there is an element of uncertainty with respect to fundamental theoretical issues and these issues significantly affect determination of the residual shear strength of the liquefied soil. Although the methodology for assessment based on laboratory testing is relatively straight forward, application of theoretical concepts from laboratory testing have proven difficult to apply to site conditions, the difficulty being associated with obtaining "undisturbed" samples of cohesionless soils, the sensitivity of the soil behaviour to small changes in void ratio, complexity of factors such as in-situ stratification and the actual test results themselves. No consensus was reached at the National Science Foundation Workshop on the shear strength of liquefied

soils (NSF 1998) regarding sample preparation, the type of laboratory testing to be undertaken, and the evaluation of the residual undrained strength from the results.

Most of the empirical methods derived from back analysis of historical case studies have been from flow slides and large deformations triggered by earthquake; although, the manner in which flow liquefaction is triggered (either static or cyclic) will not affect the large strain residual undrained strength. One of the difficulties with using empirical correlations based on SPT blow count data is considered to be that it does not (and cannot) incorporate all the material properties that affect flow liquefaction behaviour.

Of the available empirical methods, it is considered that the lower limit of the Seed and Harder (1990) correlation (Figure 3.19) provides a reasonable estimate of the residual undrained shear strength. The shape of the relationship is similar to that which would be obtained between residual undrained strength and relative density (or void ratio) from laboratory results, with close to zero residual undrained strength at low relative densities, and increasing relatively rapidly with increasing relative density. The Stark and Mesri (1992) correlation is also considered to provide reasonable estimates of residual undrained strength. Direct correlations of residual undrained strength with effective over-burden stress, such as by Baziar and Dobry (1995), are considered questionable as they do not consider the fundamental relationship between residual undrained shear strength and void ratio. The results of back-analysis indicate that drainage during flow sliding is an important aspect in travel behaviour and the potential for drainage during flow must be considered (Stark and Mesri 1992; Castro 1998). For the materials of lower permeability (e.g., silty sands) back-analysis results indicate that little drainage during flow sliding occurs compared to the cleaner sands.

Figure 3.22 presents guidelines for assessment of the residual undrained shear strength of liquefied soil that came out of the 1997 National Science Foundation Workshop on the shear strength of liquefied soil (NSF 1998). The working group recommended the effort and complexity of field and laboratory testing for site assessment be dependent upon project risk. They devised three risk categories; low, moderate and high, for which they recommended assessment comprise:

- For "Low Risk" projects, site investigation consisting of cone penetration testing (CPT) or piezocone testing (CPTU) in combination with limited SPT testing, followed by limited classification type laboratory testing. Estimation of residual undrained shear strength using existing empirical correlations based on historical cases.

- For "Medium Risk" projects - inclusion of additional in-situ testing, such as geophysical methods, and inclusion of laboratory testing on reconstituted samples for assessment of the critical state line. Estimation of residual undrained shear strength using existing empirical correlations and observations of soil behaviour from the laboratory testing.
- For "High Risk" projects a two-phase investigation is recommended. Identification of potential critical areas from the initial phase based on predicted behaviour using estimates from empirical correlations. Detailed second phase investigation aimed at reducing uncertainty from the preliminary phase. Laboratory testing on undisturbed samples (taken using ground freezing techniques) in the detailed stage that could include triaxial compression/extension, simple shear, and/or torsional ring shear tests. Estimation of residual undrained shear strength from results of the detailed laboratory testing program.

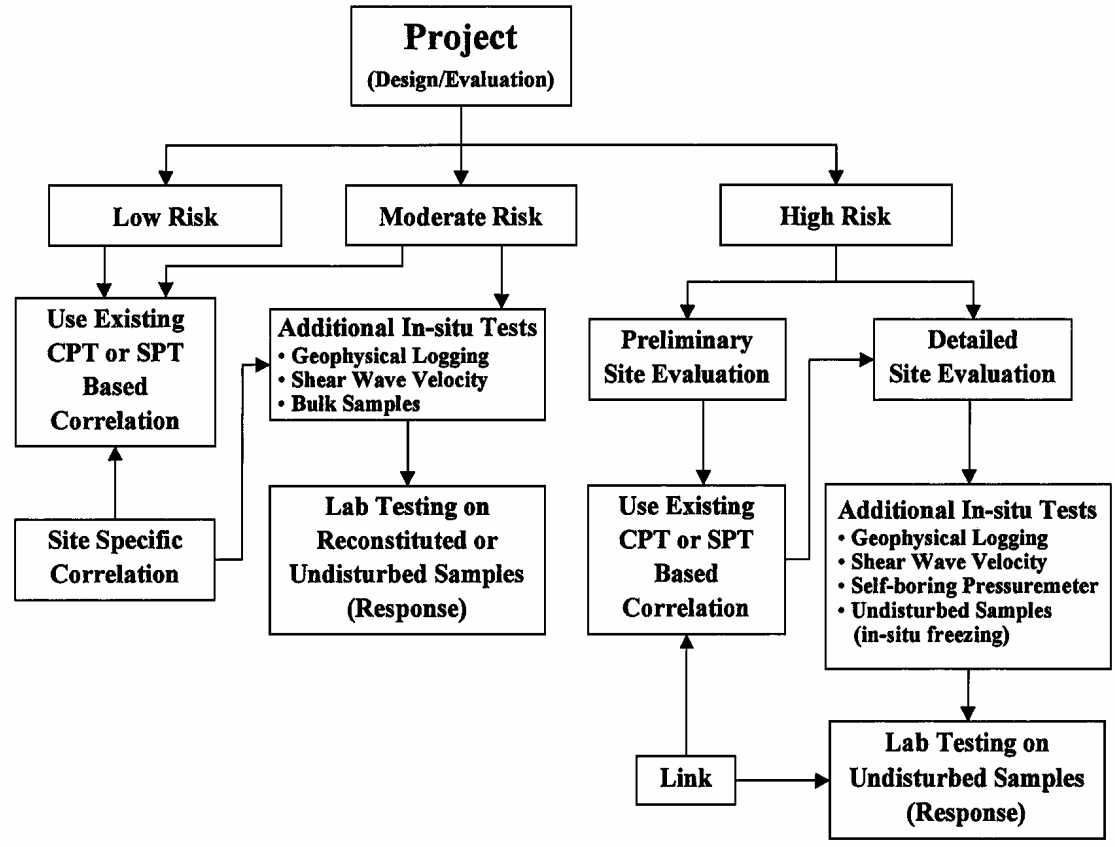

Figure 3.22: Flow chart for assessment of residual undrained shear strength of liquefied soil (NSF 1998)

3.4 MECHANICS OF FAILURE OF FLOW SLIDES

This section discusses the mechanics of failure of flow slides in contractile soils. Within each slide sub-group the properties of the slide material and factors influencing the triggering of and development of slope failure are drawn from the literature and case study data.

It is important to distinguish between the trigger mechanism/s for the processes leading up to slope instability and the occurrence of "rapid" sliding. Once an unstable slope condition is reached the progression to "rapid" sliding is dependent on the slope geometry and material properties within the unstable slope. For example, if a static liquefaction condition is triggered in part of a slope a "rapid" flow slide event is not necessarily the outcome.

3.4.1 MECHANICS OF DEVELOPMENT OF FLOW SLIDING

The characteristic common to all soils susceptible to static liquefaction is that the soil structure is prone to contract in drained shear. In undrained loading, a loss in undrained strength occurs as a portion of the load once supported by the soil structure is transferred onto the pore fluid. In most cases the soil is in a saturated condition, but laboratory testing (Vaid and Eliadorani 1998) indicates that liquefaction can be triggered in near saturated states.

The mechanism of initiation of flow sliding under static conditions is summarised as follows:

- The effective stress state of the saturated (or near saturated) soil within which liquefaction is initially triggered is at or above the instability line or collapse surface (Figure 3.23). It is possible for soils to exist in drained conditions above the instability line even though they are contractive on shearing in drained conditions under these stress conditions (see below).
- A change in effective stress conditions is required to trigger liquefaction for effective stress states existing above the instability line (i.e. within highly stressed regions of the slope). For effective stress states below the instability line a change in effective stress conditions is required to move the effective stress state to the instability line at which point a liquefaction condition can be triggered.
- Deformation occurs as a result of the change in effective stress conditions.

- At effective stress states at or above the instability line the soil structure is contractile on shearing and it is within these highly stressed regions of the slope that a localised static liquefaction condition is initially developed. As a result of this propensity for contraction on shearing, load once supported by the soil structure is transferred onto the pore fluid. Undrained conditions will persist if the resulting pore water pressures cannot be dissipated.
- Once liquefaction has initiated the load once supported by the soil in the localised liquefied zone is transferred onto the soil structure in the immediate vicinity. Progression of the zone of liquefaction will occur if the adjacent soil structure cannot support the additional stresses imposed. The rate of progression is dependent on the loss in undrained strength of the soil on liquefaction and the additional load capacity of the adjacent soils. The undrained brittleness index (Figure 3.24), I_B, is a measure of the loss in undrained strength. The higher the value of I_B the more likely the faster the rate of progression of the liquefied zone will be.
- Failure of the slope will occur if or when it has reached an unstable condition.
- The kinetic energy of the failed mass is, to some extent, dependent on the undrained brittleness index. High kinetic energy is associated with high undrained brittleness index.

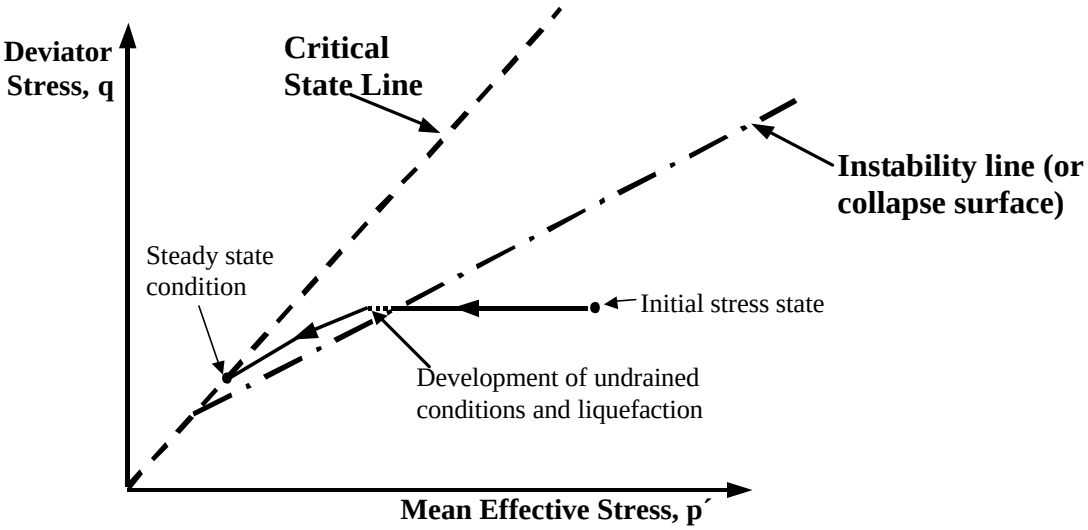

Figure 3.23: Idealised mechanism for initiation of flow slides.

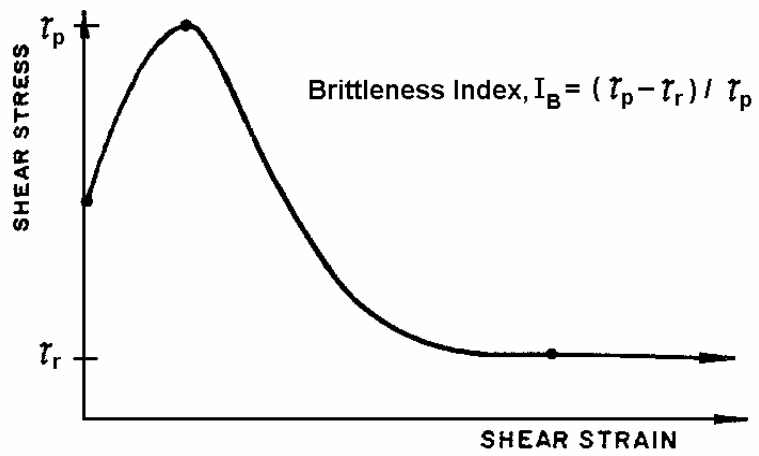

Figure 3.24: Definition of undrained brittleness index, I_B, in strain weakening soil.

As discussed above, a change in the effective stress state is the trigger for static liquefaction and potential flow sliding. The forms of trigger and effective stress changes are considered to include:

- Triggering of static liquefaction at effective stress states at or above the instability line. Lade (1992) considered that the states of stress on some planes in the soil mass within the slope are in the region of potential instability, i.e., above the instability line (Figure 3.25 as an example of a submarine slope). In drained conditions the slope is in a stable condition; however, Lade (1992) considers that a small disturbance, in soils that have a relatively low permeability will trigger static liquefaction that could result in development of a flow slide. Flow slides in submarine slopes triggered by large tidal changes are an example. This mechanism could also be appropriate to the initial failure for flow slides in tailing dams and sensitive clays.
- Rising groundwater levels that move the effective stress state to the instability line. Dawson (1994) proposed this mechanism (Figure 3.26) for flow slides in loose dumped coal mine waste spoil piles in British Columbia, Canada. On reaching the instability line static liquefaction occurs within critically stressed regions of the slope resulting in the development of an unstable slope and triggering a flow slide.
- Reduction in soil suction of partially saturated soils due to water infiltration and wetting up of the soil mass. Flow slides in loose fills in Hong Kong are considered to fail by this mechanism. The effect of decreasing soil suction is to push the effective stress state toward the instability line.

- Excavation, erosion and rapid sedimentation resulting in over-steepening and heightening of slopes are considered to move the effective stress state toward the instability line. Leroueil et al (1996) consider these factors to be predominantly aggravating factors, but they can also trigger a slope failure.
- Layering in the soil profile is considered to have an important influence. Differences in soil stiffness due to layering will result in concentration of shear strain at the interface and can trigger liquefaction in this region. Examples of this are evident from the analysis of failures of embankments on soft ground (Chapter 4) and it is considered a significant factor for a number of failures across the broad spectrum of flow slides considered here.

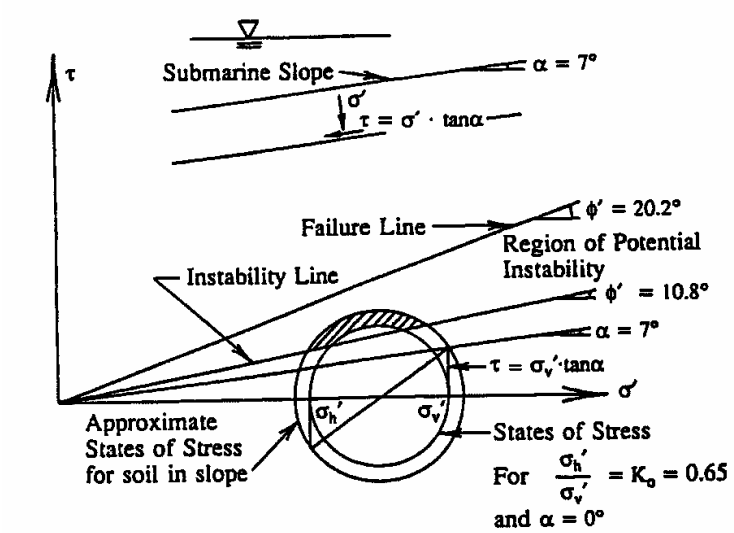

Figure 3.25: Effective stress states on some planes (submarine slopes) located within the region of potentially instability (Lade 1992).

A static liquefaction condition will only be triggered where pore water pressures developed due to contraction on shearing cannot be dissipated. The factors, some of them inter-related, that are considered to influence the development of undrained conditions and therefore flow sliding in contractive soil structures include; soil permeability, the rate of shearing, amount of potential volume contraction, effective stress level and the undrained brittleness index. The effect of soil permeability and rate of shearing are considered to be as follows:

- For fine-grained soils (clays, silts, sandy silts, etc.) of low permeability, low rates of shear strain are required to trigger static liquefaction. This is evident from the

limited pre-failure deformation behaviour observed for flow slides in these soil types.

- For the coarser grained, more permeable soil types, such as sandy gravels and gravelly sands, relatively high strain rates are required to trigger static liquefaction. This is evident from the pre-collapse strain rates of up to 15 to 50 m/day and deformations of at least several metres for flow slides in coal waste spoil piles in Canada and South Wales (refer Section 3.7.1.1).

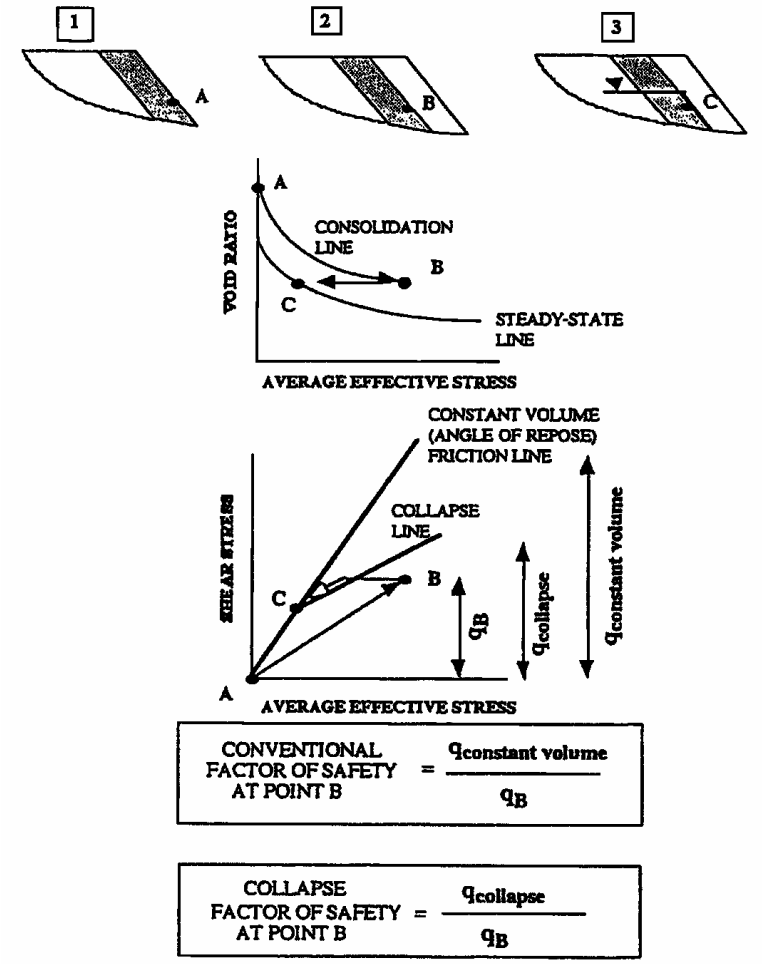

Figure 3.26: Collapse model for mine waste dumps (Dawson et al 1998)

3.4.2 FLOW SLIDES IN GRANULAR STOCKPILES

(a) Material Properties

The particle size distribution and relative density of the stockpiled granular material are considered the two most significant material properties influencing the likelihood or otherwise of susceptibility to static liquefaction.

Figure 3.27 presents the approximate particle size distributions for coal waste and coking coal susceptible to static liquefaction and within which flow slides have developed in British Columbia, South Wales and Hay Point. The materials classify as sandy gravels with some to a trace of silt sized fines (1.5 to 12% finer than 75 micron).

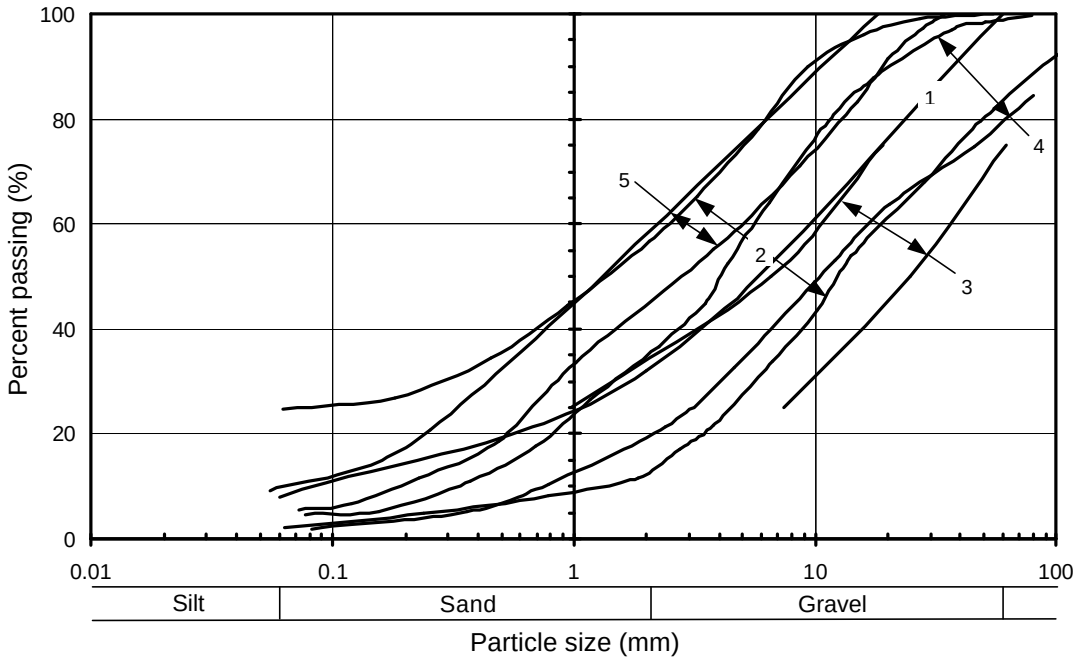

1 - Aberfan, Tip 7 (Bishop et al 1969)
2 - Aberfan, Tip 7 (Hutchinson 1986)
3 - Coal mine waste spoil piles, South Wales. One standard deviation around the mean (Taylor 1984).
4 - Coal mine waste spoil piles, British Columbia - materials susceptible to liquefaction (Dawson et al 1998)
5 - Coking coal stockpiles, Hay Point (Eckersley 1990)

Figure 3.27: Particle size distribution of coal mine waste and coking coal susceptible to static liquefaction

It is considered from the available case studies that the coarser side of the grading curves in Figure 3.27 are close to representative of the upper bound of materials within which liquefaction and flow sliding can occur. Particle size distributions coarser than this, particularly at the finer end of the grading curve, have sufficient permeability that pore water pressures developed due to contraction of the structure on shearing can be dissipated. Flow slides have not developed in coarser materials such as the coarser sections of the spoil piles in British Columbia or within dumped dirty rockfills used in construction of dam embankments that have undergone significant settlements on first filling and drawdown.

Density is a significant factor in susceptibility of a material to static liquefaction. Laboratory undrained tests on coal waste and coking coal (Section 3.3.4) indicate that at void ratios greater than 0.3 the sandy gravels typical of the stockpiles in British Columbia and Hay Point are susceptible to static liquefaction, and that the undrained brittleness increases is with increasing void ratio above 0.3. Field testing indicates that void ratios in excess of 0.3 are obtained for these materials in a loose dumped condition, but it is dependent on the method of placement and to some extent moisture content at placement. For the flow slides at Hay Point (Eckersley 1985, 1986) most failures occurred within bulldozed stockpiles, for which Eckersley (1985) comments is a result of the low dry densities achieved for this method of placement (compared to placement from the aerial stackers). The density profile of the stockpiled coal waste of Tip 7 at Aberfan (from Bishop et al (1969) data) indicates densities as low as 82% to 91% of the Standard Proctor Maximum Dry Density at depths up to 15 m to 20 m (equivalent to void ratios greater than about 0.43), indicative of the loose state of the coal waste placed by tippler.

For the coal mine waste spoil piles at British Columbia and South Wales tipping is (or was) from a low height onto the active portion of the tip. It is notable from the literature that no "rapid" flow slides are reported to have developed from failures in coal mine waste spoil piles formed by dumping from draglines. The findings would indicate that the stockpiling technique affects the material density such that likelihood of flow sliding is negligible in coal waste placed by dragline and much less likely in coal placed by stackers.

Flow slides have been reported in stockpiles of other than coal waste and coking coal. Su and Miller (1995) report flow slides, from China, in waste spoil piles from the mining of iron ore, copper, coal and non-ferrous metals. They indicate that the spoil piles contain a proportion of fine granular material derived mainly from weathered rock and/or overburden soils and that the materials are loosely placed by dumping at the crest of the advancing face of the spoil pile. Bishop (1973) reports on flow slides in loose spoil piles of well graded sands (from China clay mining) and flyash.

(b) Factors Influencing Flow Sliding in Granular Stockpiles

From analysis of the case studies and review of published literature it is evident that there are several key factors that influence the likelihood of a flow slide occurring:

- Particle size distribution and material density (or placement technique) as discussed above.
- Rainfall and snow/ice melt. Analysis of the case studies indicates that rainfall is a significant triggering factor for flow slides in South Wales and Hay Point, and both rainfall and snow or ice melt are significant factors for flow slides in British Columbia. Su and Millar (1995) indicate that heavy rainfall is a significant factor for the triggering of flow slides in waste spoil piles in China. The case study data indicates:
  - For British Columbia more than 60% of flow slides occurred in spring and early summer, the time of snowmelt. The other significant period for flow sliding in autumn, generally the wettest period.
  - For South Wales all flow slides (where the date of the landslide is known) occurred between October and February, the wettest months in South Wales. A significant, although not severe, period of rainfall (typically 1 in 2 to 1 in 5 year event) usually preceded flow sliding.
  - For Hay Point flow sliding was associated with significantly wet periods.
- Foundation slope angle for slides in coal waste spoil piles. For British Columbia Dawson et al (1998) report that flow slides tended to occur where foundation slope angles exceeded 15 degrees. Golder Assoc. (1994) report the average foundation slope of 46 flow slide events in British Columbia to be 25.4 degrees (standard deviation of 6.4 degrees). For South Wales the foundation slope angles of flow slide events ranged from 8 to 27 degrees (average of 17.2 degrees and standard deviation of 5 degrees). For the flow slides in spoil piles in China, although not directly discussed by Su and Millar (1995), they imply steep foundation slopes were present in a number of the failures. The China clay spoil piles were constructed on foundations sloping at 6 and 7 degrees and the flyash failure in Jupille on a hillside (Bishop 1973).
- Active dumping is usually in progress leading up to the failure (but not always).
- Springs, streams or high pore pressures in the foundation. In 55% of the case studies from South Wales the toe of the spoil pile encroached over an existing spring or stream. A significant number of the tips in South Wales were constructed over the Pennant Sandstone formation (massive sandstone with high permeability along discontinuities) and the springs were generally associated with the outcrop of inter-bedded argillaceous seams, coal seams or surficial glacial boulder clay deposits.

- Construction of the tip over pre-existing earthflows (specific to South Wales). Almost 44% of the flow slide case studies from South Wales were within tips known to have been constructed over pre-existing earthflows.

Siddle et al (1996) observed that within the United Kingdom the coal waste spoil piles at South Wales are the only geographic region (in the UK) where flow sliding of these materials is observed, the reasons being the significantly wetter climate and steeper topography. From Taylor (1984) it is evident that for the South Wales spoil piles the material grading was generally on the coarser side of average for coal spoil piles in the UK, whilst the method of placement (in the early to mid 1900's) did not vary significantly, indicating that grading and placement method are not significant factors for the confinement of flow sliding in the UK to South Wales.

The foundation conditions and hydrogeology are also considered significant factors in the occurrence of flow slides at South Wales. At Aberfan, piezometers installed into the Pennant Sandstone foundation indicated a significant rise in pore pressure following heavy rainfall (Bishop et al 1969) and an increase in the foundation pore pressures in the toe region of the tip, and this may have been the trigger for initial instability in the toe region of the spoil pile which encroached over an existing spring.

Saturation or near saturation of the coal waste or coking coal (or other liquefaction susceptible loose stockpiles granular material) is a requisite for static liquefaction. It is possible that melting of ice and snow within the coal waste spoil piles at British Columbia is sufficient to saturate the finer sandy gravel sized mine spoil within which static liquefaction can occur. At South Wales and Hay Point saturation of the lower portion of the waste is likely following heavy rainfall due to the lower permeability of the foundation. At Aberfan, piezometers located close to the base of the tip recorded excess pore pressures of up to 3 m following heavy rainfall and maintained this level for the subsequent 1 to 2 days (Bishop et al 1969).

High rates of shearing seem to be a requisite for triggering of undrained conditions and therefore potential flow sliding in these coarse grained materials as indicated by the pre-failure deformation observations (refer Section 3.7.1.1). In addition, the pre-collapse shearing may also be creating the critical stress and void ratio conditions needed for development of static liquefaction.

(c) Failure Mechanism for Flow Sliding in Granular Stockpiles

The specific mechanics of failure for flow slides in granular stockpiles from analysis of the case studies and published literature is not clear. The possible mechanisms discussed in Section 3.4.1 are the collapse model proposed by Dawson (1994) and Dawson et al (1998) for mine waste failures in British Columbia (Figure 3.26) and the model proposed by Lade (1992), Figure 3.25.

The Lade (1992) model is considered to have merit given the likely high stress conditions present within the steep spoil and stockpiles. Together with the low density of the materials, the stress conditions under which contractile conditions on shearing are prevalent is considered likely. Shearing along interfaces that are located within the instability region (e.g. between the spoil and foundation or between the fine and coarse zones for British Columbian waste stockpiles) as a result of changes in effective stress conditions (loading for active tips or changes in pore pressure conditions) could then trigger static liquefaction and result in failure and flow sliding. High stress conditions are also considered to develop in the toe region of the spoil piles due to stress re-distribution from deformation of the spoil pile and changes in foundation slope.

Whilst this mechanism may not be solely responsible for triggering of static liquefaction, leading to slope instability and flow sliding, it is considered significant in the overall mechanism. Bulging observed in the lower portion of the spoil pile prior to failure and the results of numerical modelling (Dawson 1994) are considered to support the likelihood of high stress conditions in the toe region. In addition, the influence of foundation slope for flow slides in British Columbia and South Wales would tend to support the potential for development of shear strains in saturated to near-saturated regions of the slope where contractile conditions are prevalent.

Hungr and Kent (1995), commenting on the findings by Golder Assoc. (1994), indicate that static liquefaction could be triggered within the foundation of the spoil pile failures in British Columbia. They consider that the upper zone of the foundation could potentially be susceptible to static liquefaction due to weakening from frost heave processes. Dawson et al (1998) also comment that other processes can act as a collapse trigger such as shearing in the toe region, creep and weathering, although they consider the collapse model discussed above to be the more likely mechanism.

It is not clear on the timing for development of liquefaction and its progression in relation to the stability of the slope during pre-collapse deformation and that at collapse, particularly for the flow slides in British Columbia. At South Wales it is considered

that the slope (or part of the slope) is in a meta-stable condition resulting in the observed pre-collapse deformation, and it is this deformation that is the trigger for liquefaction leading to collapse of the slope.

It is considered likely that a combination of the above mechanisms has a significant role in the development of liquefaction and flow sliding, with the dominant mechanism differing on a case by case basis. The collapse model in association with high stress conditions in the toe region is considered the most likely for the failures in coal waste spoil piles in British Columbia.

3.4.3 FLOW SLIDES FROM FAILURES IN SENSITIVE CLAYS

The following discussion on flow slides in sensitive clays covers the material properties of sensitive clays and the mechanics of failure. Two aspects of the mechanics of failure are discussed; the initial failure (general to landslides in sensitive soft clay environments) and factors associated with those failures that develop into "rapid" retrogressive flow slides.

(a) Material Properties

Highly sensitive or quick clays are predominantly confined to Canada, Alaska and the Scandinavian countries. They are fine-grained sediments of glacial origin deposited in a marine environment. Post glacial uplift of the land mass has raised these soft marine deposits above sea level and fresh water leaching has removed the salt ions within the pore water. The soil structure of these leached fine-grained soils is described as "flocculated" or open structured, and unstable, i.e., susceptible to contraction and flow liquefaction on disturbance potentially leading to flow sliding. Torrence (1996) comments that the sensitivity of some of these soils is enhanced by cementation, for example the Champlain clays of eastern Canada.

Particle size distributions of sensitive clays in general and from flow slides are shown in Figure 3.28. Fines fractions (minus 60 micron) typically range from 85 to 100% and clay fractions (minus 2 micron) from 15 to 70%.

The material and pore water properties of sensitive clays that make them susceptible to flow sliding (Tavenas 1984; Leroueil et al 1996; Lefebvre 1996; Trak and Lacasse 1996; and Torrence 1996) are:

- The clay fraction comprises a significant content of non-clay minerals (quartz and feldspar) derived from the grinding action of glaciers, resulting in the low activity and generally low plasticity of sensitive clays.
- Low pore water salinity. Tavenas (1984) suggests that flow sliding occurs in sensitive clays with salinity levels of less than 3 g/litre salts.
- A high undrained brittleness index (Figure 3.24) and very low residual undrained strength, c_{ur} (determined from vane testing), is required for flow. Leroueil et al (1996) suggest that for flow sliding to occur $c_{ur\ (vane)}$ is less than 1 kPa or the liquidity index, I_L, is greater than 1.2. Leroueil et al (1983) proposed an empirical relationship (Equation 3.6) relating the residual undrained strength (determined from vane testing), c_{ur}, to the liquidity index.

$$c_{ur(vane)}(kPa) = (I_L - 0.21)^{-2} \tag{3.6}$$

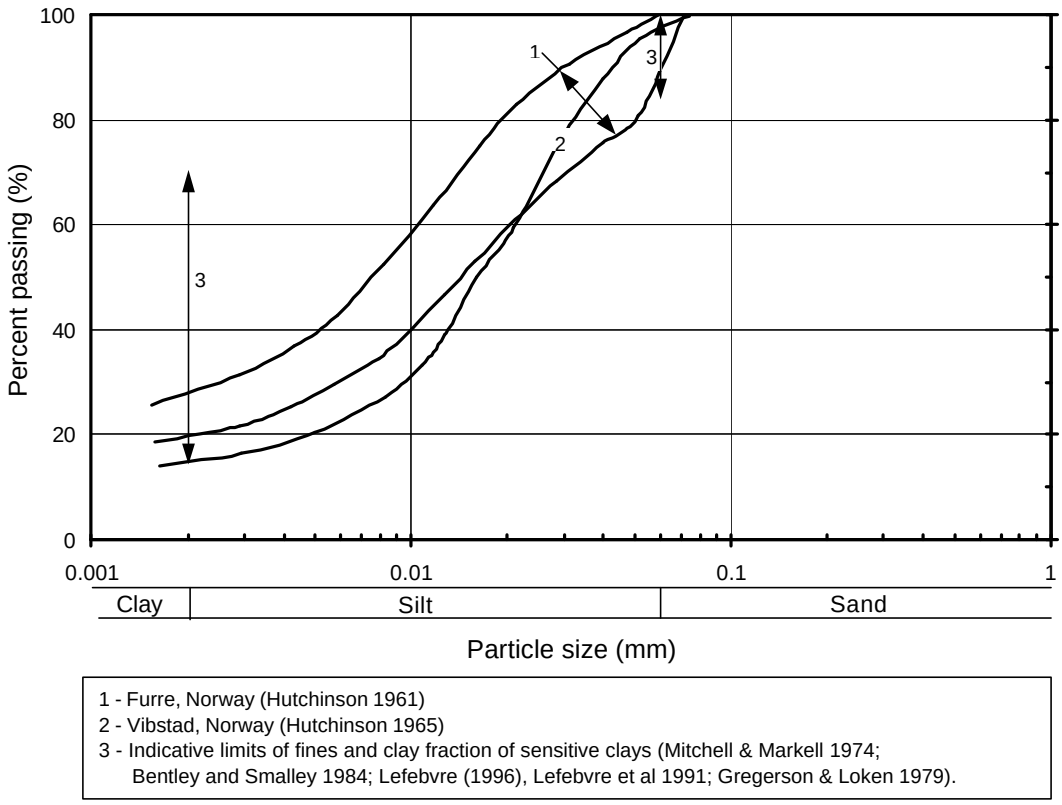

Figure 3.28: Particle size distribution of sensitive clays

Leroueil et al (1996) point out that the remoulded strength determined by vane shear can be much lower than that determined by laboratory testing and suggest the reasons for

this are strain and strain rate effects, which in laboratory tests are not sufficient to allow for complete remoulding of the clay. An additional reason may be that in the vane shear test the remoulded strength may be affected by load transfer of the remoulded region onto the surrounded intact soil and therefore the test is undertaken within an isolated remoulded region of very low confining pressure.

A summary of the plasticity, undrained strength, liquidity index and sensitivity of the liquefied soil on the surface of rupture for each of the case studies is given in Table 3.8 (Section 3.2.7). The sensitive clays are typically of low plasticity ($I_P \leq 12\%$ in most cases), of very soft to firm strength consistency and moderate to high sensitivity (S_t of 10 to 200) with liquidity index generally greater than 1.3.

(b) Initial Failure

It is evident from the literature that flow slides in sensitive soils develop from an initial relatively small failure (Leroueil et al 1996; Lefebvre 1996) usually located within a steep river or stream bank subject to active erosion.

The mechanism of the initial failure is considered by a number of authors (Leroueil et al 1996; Lefebvre 1996) to occur as a drained failure of a slope triggered by a small change in effective stress conditions, usually associated with rising groundwater. Laboratory undrained triaxial compression test results (Aas 1981) indicate that sensitive clays may be susceptible to static liquefaction at stress levels less than steady state (i.e. comply with the collapse surface concept, Figure 3.7, as per contractant cohesionless soils). Therefore, the trigger and mechanism of initial failure is potentially similar to that for cohesionless soi1s that are contractive on shearing as idealised in Figure 3.23.

The triggering and aggravating factors for initial landsliding in sensitive clays are:

- Increasing pore pressure conditions due to snowmelt and rainfall (observed in 8 of 10 cases analysed in which the trigger was known). Tavenas and Leroueil (1981a) present statistical data strongly correlating the frequency of landsliding in Canada, Norway and Sweden to the months of snowmelt and climatic wet periods. For Quebec, Tavenas (1984) indicates that the frequency of landsliding is significantly greater in April to June, the period associated with snowmelt and high rainfall (Figure 3.29).
- Stream erosion. Tavenas (1984) comments that landslide activity is strongly associated with the active erosion processes of streams and rivers and along lakeshores due to the formation of steep and high slopes of marginal stability. Locat

and Leroueil (1997) consider erosion to be an aggravating factor for initial landsliding rather than the trigger. The forms of active erosion include vertical erosion (down-cutting) and lateral erosion. Tavenas (1984) comments that flow velocities in excess of 1 m/sec are sufficient to cause lateral erosion and that transported ice blocks enhance the erosive power of streams and rivers. In the case of the flow slide at Furre, Norway (Hutchinson 1961) an ice jam in the river resulted in a period of very active erosion.

- Human influences such as excavation and filling.

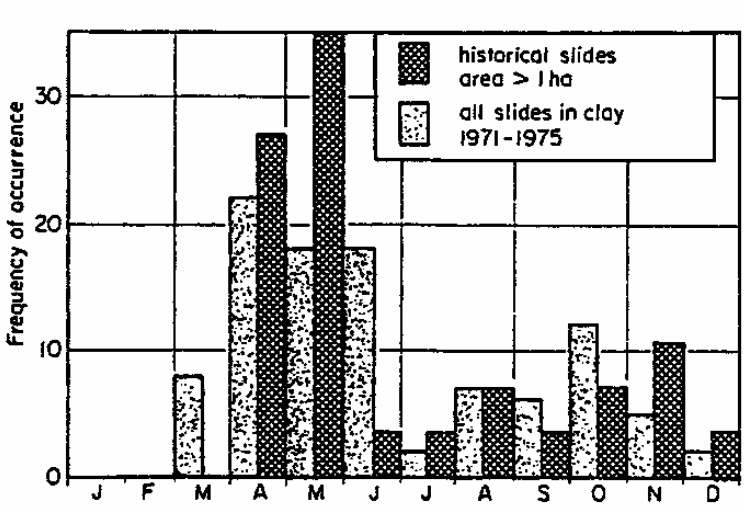

Figure 3.29: Frequency distribution of landslides in Quebec (Tavenas 1984)

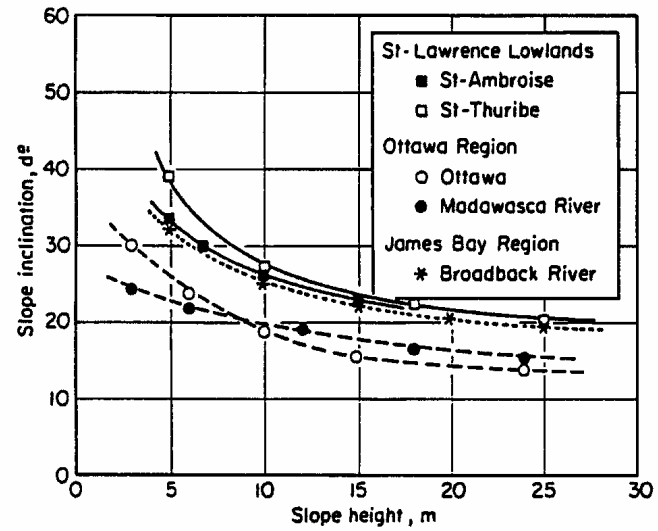

Figure 3.30: Slope height versus slope inclination for unstable slopes in eastern Canada (Tavenas 1984)

Morphological relationships of actual failures from eastern Canada are presented in Figure 3.30. For slopes in the Scandinavian countries (Bjerrum et al 1969) field observations indicate that at less than 20 to 21 degrees slopes are stable regardless of height. This type of information is considered useful as a guide to the stability of natural slopes given the complexity associated with assessment of strength properties, hydro-geological conditions and progressive failure.

(c) Retrogressive Flow Sliding

Two types of "rapid" flow slides are observed in sensitive clays; retrogressive sliding that occurs as a series of rotational slides or slumps of limited size (Tavenas 1984) as shown in Figure 3.31, and translational slides (or "flake" slides) along a liquefied surface of rupture. Cases of translational slides from the literature (Rissa, Bekkelaget, Furre, Vibstad as examples) appear to be confined to the Scandinavian countries. This is considered, in some cases, to be due to sediment layering (at Furre and Vibstad the quick clays were overlain by up to 20 m of low sensitivity materials (Hutchinson 1961 and 1965)).

The criteria that predispose a slope in soft sensitive clay to retrogressive failure (Tavenas 1984; Leroueil et al 1996; Lefebvre 1996; Trak and Lacasse 1996) are:

- There must be an initial slope failure.
- The back-scarp must be unstable in undrained loading for retrogression to occur. From analysis of retrogressive flow slides (Mitchell and Markell 1974), Leroueil et al (1996) suggest a stability number, N_c ($N_c = gH/c_u$ where H = height of the back-scarp, c_u = undrained strength and g = saturated unit weight), of greater than 4 for back-scarp instability if the plasticity index, I_P, is less than 10%, and N_c greater than 8 if I_P is approximately 40%.
- The slide debris must have the ability to become remoulded during the failure and flow out of the slide crater when remoulded to leave the subsequent back-scarp exposed to maximum height. Leroueil et al (1996) comment that the energy required for remoulding is dependent not only on c_u but also on the plasticity index, with clays of lower plasticity requiring less energy for remoulding.

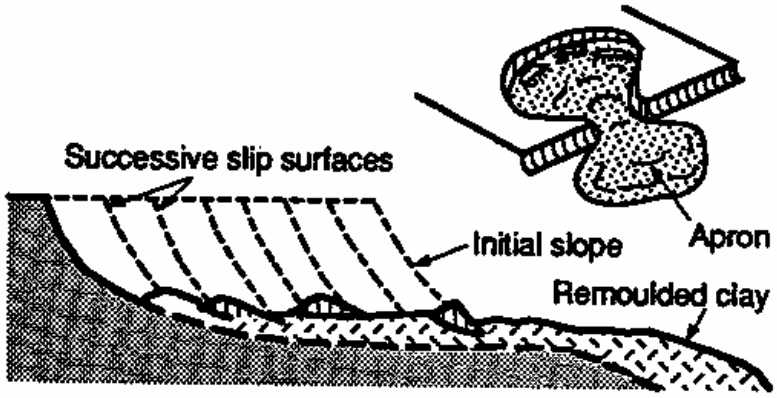

Figure 3.31: Retrogressive landslide in sensitive clay (Leroueil et al 1996)

3.4.4 FLOW SLIDES IN LOOSE SILTY SAND FILLS, HONG KONG

(a) Material Properties

HKIE (1998) undertook a detailed study of the properties of fills (from Hong Kong) susceptible to liquefaction and flow sliding, and their findings are summarised as follows:

- The materials classify as silty sands with fines contents (% passing 75 micron) of 10 to 50% and clay contents typically less than 10%. Most fills in Hong Kong are sourced from completely decomposed granite.
- The fines are generally of medium to high plasticity. Liquid limits typically range from 35 to 70% and plasticity index from 20 to 30%.
- The dry density of fills placed by end dumping is generally in the range 70 to 85% of Standard Maximum Dry Density (SMDD), indicative of their loose condition. The dumped fills tend to show layering parallel to the face slope.
- Laboratory triaxial tests indicate the loose placed fill (derived from completely decomposed granite) is contractive at densities less than about 85 to 90% of SMDD.

Seven of the case studies analysed from Hong Kong were considered to be flow slides in loose fill, one of which is a retained loose fill that possibly liquefied once the initial failure had de-stabilised the retaining wall. A summary of the material properties and slope geometry features of these landslides is given in Table 3.10 along with those from an additional five flow slides in loose fill reported by HKIE (1998). The available information on material type and density for these cases is in agreement with the findings from HKIE (1998).

(b) Factors Influencing Flow Sliding in Loose Silty Sand Fills

From analysis of the case studies and review of published literature it is evident that there are several key factors that influence the likelihood of a flow slide occurring:

- Material type and material density as previously discussed.
- Rainfall. The trigger for most flow slides in loose fill slopes in Hong Kong is rainfall. Further details on the relationship between rainfall and landsliding in Hong Kong are given in Section 3.5.2.2.
- Fill slope angle. The fill slope angle for the flow slide case studies (Table 3.10) is greater than or equal to 34 degrees.

(c) Failure Mechanism for Flow Sliding in Loose Silty Sand Fills

Laboratory undrained triaxial compression tests on loose silty sand fill samples of completely decomposed granite (HKIE 1998) indicate that these soil types display undrained strength characteristics similar to liquefaction susceptible loose sands and silty sands (Section 3.3.2). For samples prepared at a dry density ratio of 85% of SMDD or less and tested at low confining pressures, the peak undrained strength defining an instability line (or collapse surface) was observed at $c' = 3$ kPa and $f' = 26$ degrees (Figure 3.32), which is below the range of the steady state strength of 36 to 40 degrees. Therefore, the loose silty sand fills are susceptible to contraction on shearing when in a saturated or near saturated condition at effective stress states at or above the instability line.

HKIE (1998) indicate that the fills in the field are in a partially saturated condition, with the degree of saturation typically ranging from 30 to 100%. In the upper several metres of the fill slope significant changes in soil suction are measured due to climatic influences, with near fully saturated conditions observed in the wet season due to infiltration from rainfall. Wetting up of the soil mass and reduction in soil suction results in a leftward shift of the effective stress state toward the instability line (Figure 3.23) within the relatively steep fill slopes, resulting in conditions under which the fill is susceptible to liquefaction. The shallow depth of the surface of rupture (1.5 to 4 m) for the flow slide case studies (Table 3.10) reflects the shallow depth affected by seasonal changes in degree of saturation.

Table 3.10: Features of flow slides in loose fill from Hong Kong

Slide Name	Date of Failure	Material, Placement Method, Dry Density Ratio	Slope Height (m)	Fill Slope Angle (°)	Slide Depth (m)	Base Angle of Slide (°)	Slide Volume (m^3)	Travel Distance Angle (°)
Sau Mau Ping	25/8/76	CDG, 75 – 90% SMDD	32	34	2 to 4	34 to 40	2500	< 22
Kennedy Road	8/5/92	Silty sand (SM), CDG, placed in 1940s.	15	35	2	34	500	31
Sha Tin Heights (A)	4/6/97	Silty sand (SM)	10	34 to 49	1.5	34	150	25
Kau Wa Keng San Tseun (D)	4/6/97	CDG, end tipped	8	36 to 40	3 to 4	20	500	23
Kau Wa Keng San Tseun (C)	4/6/97	Silty gravelly sand (SM), loose to very loose	2.5	90 (retained)	2.5	33 to 51	60	26
Chung Shan Terrace	4/6/97	Silty sand (SM), avg 75% SMDD	14	37	3	30	450	18
Au Ta Village	9/6/98	Silty gravelly sand (SM) 70% SMDD	7	35	2	23	170	24
Kwun Tong*[1]	1964	No details	-	-	-	-	10000	17
Victoria Height*[1]	1966	No details	-	-	-	-	4000	19
Sau Mau Ping*[1]	1972	No details	40	35	-	-	6000	16
Princess Margaret Road *[1]	1989	No details	11	40	-	-	200	26
Kowloon Wah Yan College*[1]	1989	No details	12	40	-	-	50	24

*[1] flow slides in loose fill from HKIE (1998) SMDD =Standard Maximum Dry Density CDG = completely decomposed granite

Further laboratory test results on loose silty sand fill samples published by HKIE (1998) demonstrate the effect of soil suction (Figure 3.33). Increasing soil suction results in an upward shift of the steady state line in void ratio versus mean effective stress space. At a void ratio and mean effective stress defined by Point B a sample is susceptible to contraction when in a saturated condition but dilative in a partially saturated condition defined by the upper curve.

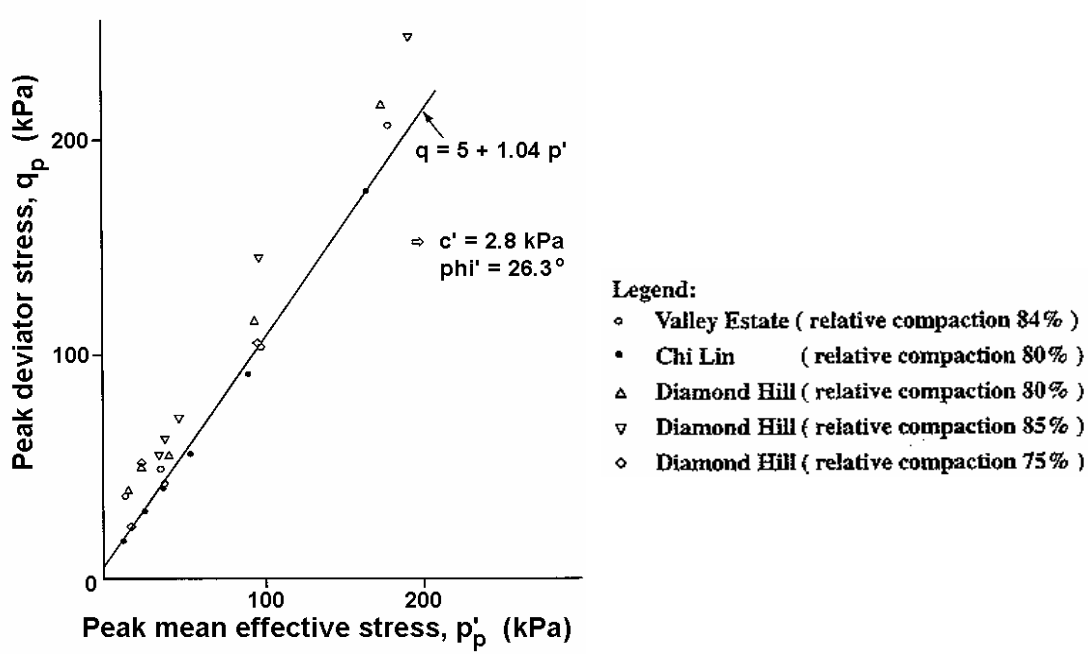

Figure 3.32: Peak shear strength from undrained triaxial compression tests of contractive fill samples (HKIE 1998)

3.4.5 TAILINGS DAMS

The particle size distribution of tailings susceptible to liquefaction and flow from the case studies analysed are shown in Figure 3.34. The mine tailings cover a broad range of soil types from silty clays to clayey silts to silty sands to medium grained sands. In most cases the tailings were derived from the crushing of ore and the finer clay and silt sized fractions are predominantly finely ground rock particles rather than clay minerals. Therefore, the finer particle size distributions, representative of the middle beach region, generally classify as silts of low plasticity (plasticity index generally less than about 5 to 10%).

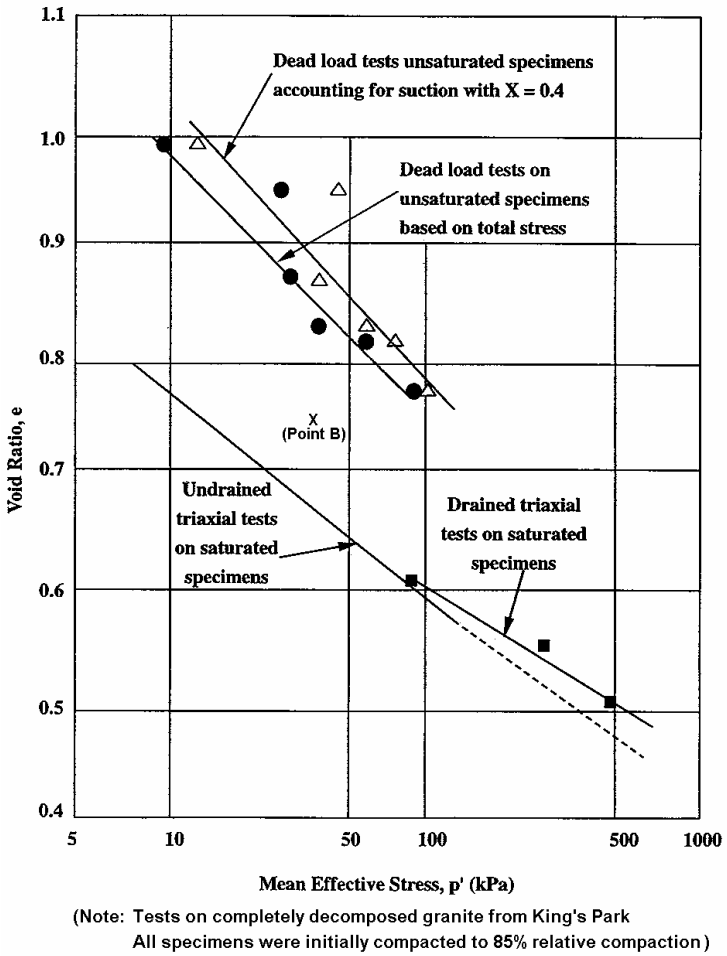

Figure 3.33: Effect of partial saturation on steady state line in void ratio – mean effective stress space (HKIE 1998)

To say the finer grained tailings are liquefaction susceptible is somewhat misleading given that these materials often exist in a virtually liquid state during (and for some time after) operation of the tailings dam, and therefore if exposed by breach will flow. The more critical range of liquefaction susceptible soils is the silty and sandy soil types with likely low clay contents that settle out relatively rapidly and have measurable strength properties. The particle size distributions of the tailings are similar for the earthquake triggered and statically triggered flow slide events.

Apart from earthquake triggered flow slides in tailings dams, the majority of the case studies analysed (Table 3.4) were triggered by drained instability of the retaining embankment (6 or 7 of the 9 cases). Piping was the trigger in 2 cases and over-topping in 1 case. Once a breach in the embankment had occurred and exposed the stored tailings, "rapid" retrogressive landsliding ensued in 8 of the 9 cases. The mechanism of retrogression is considered to be similar to that for sensitive clays (Section 3.4.3) with

continued back-scarp instability and evacuation of liquefied tailings out of the initial breach. Several characteristics associated with flow slides in tailings dams are:

- The tailings dam was in operation (or recent operation) at the time of failure.
- Most retaining embankments were constructed by upstream methods or a combination of upstream and centreline methods.
- The shape of the stable back-scarp within the impoundment after failure generally consisted of a series of near horizontal terraces with relatively low height vertical steps separating the terrace sections. This is considered indicative of the layering within the impoundment.
- Stratification within each layer of deposited tailings is considered to have a significant effect on susceptibility to liquefaction. From the literature review on liquefaction it is evident that silty sands are more susceptible to liquefaction at a given density index and similar effective stress conditions. However, it may also relate to water tables perched on the silty layers so the coarse tailings are not saturated.

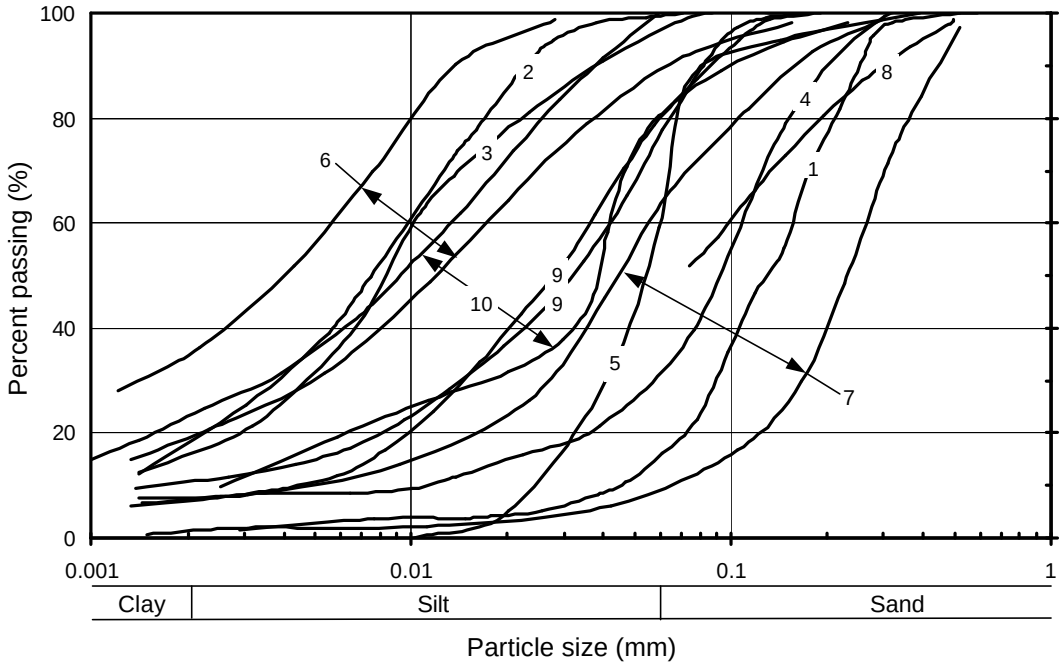

1 - Bafokeng, near discharge (Blight et al 1981)
2 - Bafokeng, from centre (Blight et al 1981)
3 - Merriespruit, fine limit (Fourie 2000)
4 - Merriespruit, coarse limit (Fourie 2000)
5 - East Texas, gypsum tailings (Kleiner 1976)
6 - Stava, silty tailings (Chandler & Tosatti 1995)
7 - Stava, sandy tailings (Chandler & Tosatti 1995)
8 - El Cobre, earthquake triggered (Dobry & Alvarez 1967)
9 - Mochikoshi, earthquake triggered (Marcuson et al 1979)
10 - Tailings slimes, low resistance to liquefaction (Ishihara 1985)

Figure 3.34: Particle size distribution of tailings from flow slide case studies.

The failure at Buffalo Creek, West Virginia, USA is considered to be different to the other failures in that it is not clear if flow sliding of the impounded slimes occurred. The slimes may have been eroded and then transported by the large quantity of water impounded by the dams.

3.4.6 HYDRAULIC FILL EMBANKMENT DAMS

The particle size distribution of hydraulically placed fill in embankment construction covers a broad range of depositional soil types from silty clays to sandy gravels, dependent on the particle size distribution of the materials used for fill and the distance from the point of discharge. The particle size distributions for Fort Peck and Lower San Fernando dams (Figure 3.35) partly reflect this broad range of soil types. For the case studies analysed (Table 3.11) the liquefied zone of the hydraulic fill generally consisted of sandy silts to silty sands to fine grained sands.

The likely mechanics of failure for the case studies is summarised as follows:

- For Lower San Fernando (LSFD) and Sheffield dams the flow slides were triggered by earthquake. Under the stress conditions imposed by the earthquake the hydraulically placed silty sands to sandy silts in a loose to medium dense condition and similar foundations soils (Sheffield dam) liquefied. Castro et al (1992) considered stratification to have had a significant effect on susceptibility to liquefaction at LSFD.
- At Fort Peck and Calaveras dams, both flow slides during construction, abnormally large deformations occurred prior to the flow slide event, an indication of the meta-stable condition of the slope. At Fort Peck a significant factor in the pre failure deformation was the basal shear deformations along pre-sheared bentonitic clay seams in the foundation. It is suspected in both cases that these deformations were significant in the triggering of liquefaction within the hydraulic fill and resultant "rapid" flow slide that developed.
- Wachusett dam is somewhat different to the other cases. A flow slide developed in the loose dumped sand fill forming the upstream shoulder of the embankment during first filling. The very loose to loose dumped sand fill was most likely to have been susceptible to contraction on wetting, and it is suspected that these strains associated with wetting up of the fill were a significant factor in the triggering of the flow slide.

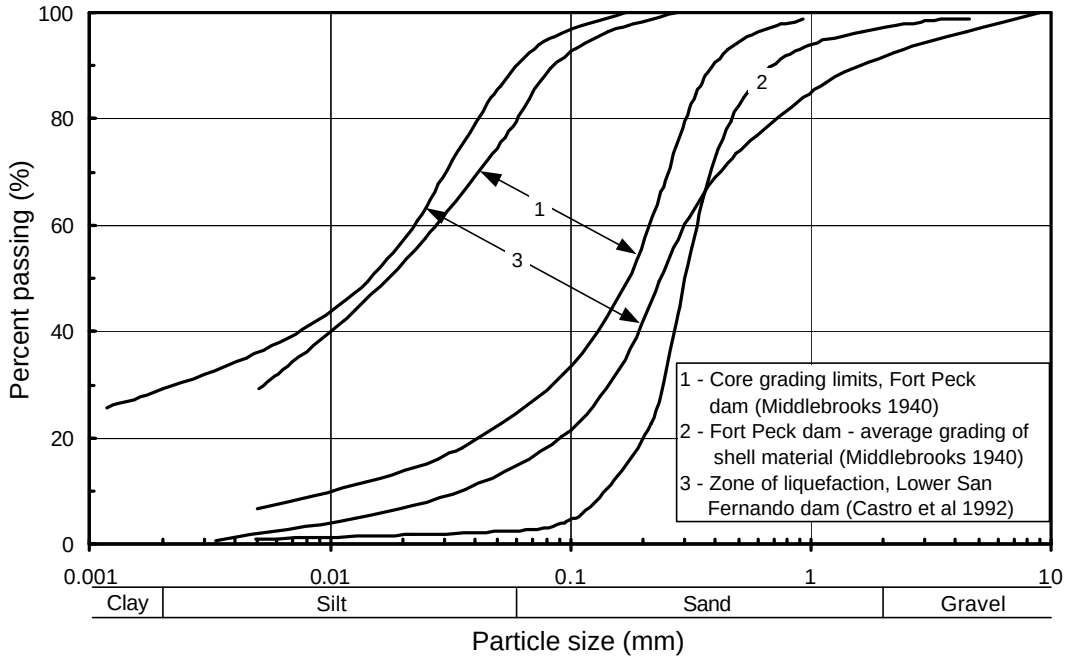

Figure 3.35: Particle size distributions of hydraulic fills from flow slide case studies

Table 3.11: Summary of properties of liquefaction susceptible materials from flow slides in hydraulic fill embankments

Name	**Material Properties (Liquefiable Zone)**	**Embankment**		**Comments on Trigger and Slide Location**
		Height (m)	**Slope (°)**	
Sheffield Dam	Silty sands to sandy silts in a loose to medium dense condition (D_R = 35 to 50%).	7.6	22	Slide in downstream shoulder triggered by earthquake. Liquefaction of either the lower portion of the embankment or the foundation.
Lower San Fernando Dam	Silty sands to sandy silts in a medium dense condition (D_R = 50 to 55%), highly stratified.	35	21.8	Slide in upstream shoulder triggered by earthquake some 46 years after construction.
Calaveras Dam	Highly variable depositional PSD from sandy gravels to silty sands to silty clays in the pool area.	56	18	Slide in upstream shoulder during construction. Hydraulic fill from colluvial soils and soft sandstones. Likely that siltier and sandier soil types liquefied.
Fort Peck Dam	Fine to medium sand, stratified	58	12.6	Slide in upstream shoulder during construction. The likely trigger of liquefaction was deformation along bentonitic seams at depth in the shale foundation.
Wachusett Dam *[1]	Fine sand to silty sand in a loose to very loose condition. Placed by dumping.	24.4	22	Slide in upstream shoulder during first filling. Liquefaction of loose dumped fine sands, most likely due to strains on saturation.

*[1] Constructed of loose dumped sand

D_R = relative density PSD = particle size distribution

3.4.7 SUBMARINE SLOPES AND SLOPES IN SUB-AQUEOUS FILLS

The particle size distributions from flow slide events in coastal sub-aqueous slopes and sub-aqueous fill slopes (Figure 3.36) indicate that fine to medium grained sands with low fines contents (less than 10%) are susceptible to static liquefaction (as opposed to earthquake or other dynamic trigger) and flow sliding. The spectrum of particle size distribution in these environments is broader than shown in Figure 3.36 most likely ranging from soils with relatively high silt contents (Karlsrud and Edgars 1982) to sandy gravels (Howe Sound, Terzaghi (1956)).

For flow slides covering the broader spectrum of submarine slopes and including earthquake triggered flow slides Edgars and Karlsrud (1983) indicate flow slides, whilst predominantly in silts and fine sands, have been observed in more clayey and more gravely soils.

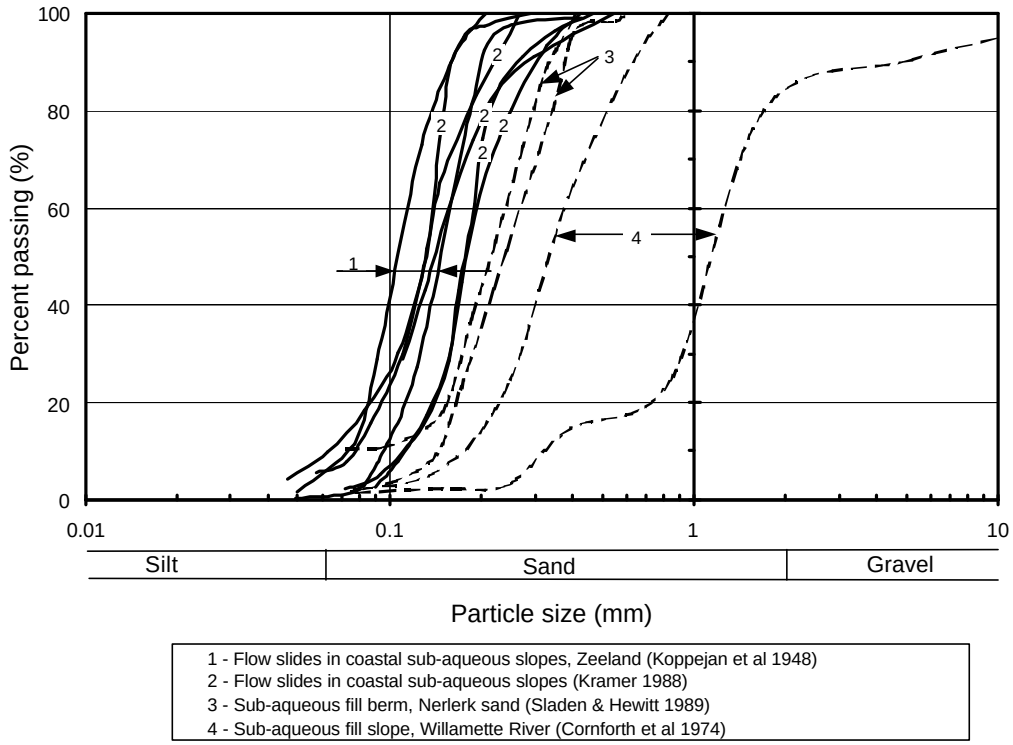

Figure 3.36: Particle size distributions of soil types from submarine slopes and sub-aqueous fills susceptible to liquefaction and flow sliding.

Relative density is also a significant material property of sub-aqueously deposited soils that are susceptible to liquefaction. As discussed in Section 3.3.3 the relative density defining the liquefaction boundary is dependent on material type and effective stress conditions. For the case studies in sub-aqueous fill slopes (Table 3.6) flow sliding

occurred in very loose, medium to coarse sands (Willamette River) and very loose to loose, fine to medium grained sands (Nerlerk Berm), both with low silty fines contents.

For flow slides in coastal sub-aqueous deposits a common element of the failures is that they occur in geologically recent deposits generally placed under rapid sedimentation conditions. In Norway post glacial deposits near river mouths are susceptible (Karlsrud and Edgars 1982) and in the Zeeland province of The Netherlands tidal channel fills and rapidly deposited fluvial channel fills of sand are identified as the most susceptible to flow sliding (Silvas and de Groot 1995). Silvas and de Groot (1995), as a broad guide to assessment of susceptibility to liquefaction (for Zeeland province), consider loose sands from CPT testing or sands with a relative density of less than 30% to be susceptible to liquefaction and flow sliding, and sands with a relative density of greater than 60% as not susceptible.

The mechanism associated with initial failure and retrogression is similar to that for sensitive clays. Silvas and de Groot (1995) consider that three conditions are necessary to trigger flow sliding:

- The soil must be susceptible to liquefaction;
- The slope must be relatively steep and relatively high for the initial failure to be triggered. From empirical data (for Zeeland province) they suggest a steep section within the overall slope greater than 5 m in height and steeper than 18.4 degrees, but consider this to be conservative due to the simplistic qualitative evaluation; and
- An initiation or triggering mechanism must be present. Identified triggers have included changes in water pressure due to waves, increased outflow of groundwater during extremely low spring tides, dredging activities, erosion at the toe (causing localised over-steepening) or vibration.

Edgars and Karlsrud (1983) considered either earthquake and/or rapid sedimentation to be the trigger in most cases they analysed.

In effect, therefore, the slope conditions provide the effective stress conditions under which the soil is susceptible to liquefaction (i.e. at or above the instability line, Figure 3.23). The static trigger to flow sliding is then a change in effective stress conditions (Section 3.4.1).

3.5 MECHANICS OF FAILURE IN DILATIVE SOILS LEADING TO "RAPID" SLIDING

This section discusses the mechanics of failure for failures of slopes in dilative soils that developed into "rapid" landslides. Within each landslide sub-group the properties of the slide material and factors influencing the triggering of and development of slope failure are drawn from the literature and case study data.

3.5.1 SLOPE TYPES OF FAILURES IN DILATIVE SOILS LEADING TO "RAPID" SLIDING

"Rapid" landslides from slope failures in dilative soils occur in steep cuts in residual soils, completely weathered rock and colluvium, in natural slopes of mostly colluvium, and steep compacted fill slopes. Retained soil slopes are another class of slope within which failures develop into "rapid" landslides, but they have not been considered in detail here.

From the case study data, the slides in dilative soils are mostly either translational or have significant translational components. For slides in colluvium and compacted fills the surface of rupture is generally through the soil mass and is, in a number of cases, coincident with soil interfaces either between the colluvium and underlying weathered rock or between differing soil units in the colluvium. For slides in residual soils and weathered rocks the surface of rupture (or part thereof) may preferentially be located along defects within the slide mass that are adversely oriented to the face slope and the strength along which is significantly lower than that of the soil mass. In the following discussion defect controlled slides are considered separately to slides through the soil mass in dilative soils. Only those slope failures where there is evidence of strong defect-control are grouped under the defect-controlled class of dilative slide; all others are included under the slides through soil mass class (including the dilative fill slope failures).

To be consistent with the landslide classification system (Figure 1.1) and avoid confusion with terminology, the term "slide of debris" is used to describe the initial landslide in preference to the terms "debris slide" and "debris flow" used by some of the referenced authors, which are more appropriate to the post failure travel of the slide mass.

3.5.2 SLIDES THROUGH SOIL MASS – DILATIVE FAILURES

The literature on slides of debris presented in this chapter is sourced from published research from Hong Kong as well as that from the international community. The strong emphasis on the research from Hong Kong is because of the availability of detailed reports on individual landslides and studies into rainfall and topography associated with slides of debris.

Also included within this section are slides through the soil mass, where the soil is initially dilative on shearing, for failures in cut slopes in residual soils and deeply weathered rocks, and compacted fills where the post-failure travel was "rapid". The case study information on these failure types is from Hong Kong.

3.5.2.1 *Mechanics of Development of Dilative Slides Through the Soil Mass*

Debris slides and debris flows in natural slopes initiate from either landslides (slides of debris) or as slurry that evolves into a debris flow through channel erosion (Johnson and Rodine 1984). Only those "rapid" debris slides or debris flows initiated from a landslide are considered here.

The typical geometric features of slides of debris in natural slopes (Hutchinson 1988; Corominas 1996b) are shallow failure depth, low depth to length ratios (often < 0.05) and high length to breadth ratios (typically 5 to 10 or greater).

An important aspect of landslides from slides of debris (and other slide types) is the distinction between the initial development of the failure itself and the transformation of the slide mass into a "rapid" debris flow or debris slide. Initiation of the failure occurs when a critical equilibrium condition is reached within the slope along a defined surface of rupture. Triggering of an unstable slope condition is dependent on material strength, slope geometry and the hydro-geological conditions within the slope. Often it is changes in hydro-geological conditions due to rainfall or snowmelt and their effect on material strength properties due to changes in soil suction that trigger the initial slide. Most authors are in general agreement with the fundamentals of this process (Johnson and Rodine 1984; Brand et al 1984; Corominas 1996b; Iverson et al 1997; Fannin and Rollerson 1992; amongst others).

The subsequent models to explain the mechanics associated with transformation of the slide mass from a "slide of debris" into a "rapid" debris flow or debris slide is largely based on observation of actual flow slides or large-scale experimental work

within a soil mechanics framework. Broadly speaking there are two main models; one is associated with contractile behaviour on shearing and subsequent liquefaction related flow sliding, and the other associated with dilative behaviour of the soil mass. In this section the dilative response is of interest, but the observations of liquefaction flow slides in natural slopes of colluvium (i.e. slides of debris) will be briefly discussed.

Large-scale experimental studies reported by Iverson et al (1997) indicate that in contractile soils the progression from initial failure to "rapid" flow occurs very abruptly and without warning. In the field a similar observation of very abrupt transformation of a slide of debris (in soils that are contractive on shearing) to a flow condition is observed, particularly for very shallow slides in the surficial colluvium (Ellen et al 1988). From the previous discussion on flow slides in Section 3.4.1 (within which these slides in contractile colluvium would be classified), the progression of the liquefied zone along the surface of rupture is considered to occur very rapidly once initiated and therefore transformation to a "rapid" flow is very abrupt.

For slides of debris in soils that are initially dilative on shearing, the mechanics associated with transformation of the slide mass into a "rapid" debris flow or debris slide is considered by several authors (Johnson and Rodine 1984; Fleming et al 1989; Corominas et al 1996) to involve dilation and remoulding of the slide mass on shearing. Johnson and Rodine (1984) idealise the transformation process once a failure condition has been reached as:

- Progressive failure starts from the base of the slide area where deformation, dilation, tensile cracking and incorporation of water occur, leading to sliding of the mass.
- Landsliding and remoulding progress, whilst the debris continues to soften due to dilation, water ingress and remoulding.
- The slide mass loses coherency and begins to slide (or flow).

The observations of development of slides of debris (Johnson and Rodine 1984) indicate that the transformation of the slide of debris into a "rapid" debris slide or debris flow occurs over distances of 1 to 3 m (sometimes in a matter of seconds), with a rapid change in velocity initially from very slow to "rapid". They comment that the strain softening during transformation is critical to the development of "rapid" movement of the slide mass.

Corominas et al (1996), whilst generally agreeing with the initiating mechanism described by Johnson and Rodine (1984), comment that it is uncertain. They believe

liquefaction may develop within the base of the slide mass (post the initial failure), giving rise to the rapid increase in velocity observed.

Iverson et al (1997) observed, from field experimentation, that for failure in a dilative soil the slide mass did not take on the appearance of a liquefied soil mass until it had evacuated the source area and was descending the 50 degree run-out ramp. Interestingly, the soil moisture content at failure and during flow was similar between the slides in the contractile and dilatant soils in their experiments (both soils were of the same type). Iverson et al (1997) concluded that for the dilative soils, at some point in the travel of the landslide mass beyond the source area excess pore pressures are developed due to conversion of energy within the slide mass leading to transformation into "rapid" debris flow. Another important observation by Iverson et al (1997) was that additional ingress of water was not required for remoulding.

Fleming et al (1989) investigated the Salmon Creek slide of debris (Marin County, California) and concluded that the initial slide, predominantly within a dilative clayey silty sand colluvium, transformed into a debris flow. They observed a basal surface of rupture of about 10 cm thickness, located within the colluvium directly above the weathered sandstone, that comprised a series of softened shear surfaces. Density measurements within the basal shear zone indicated that the material had dilated about 5% in volume compared with similar material outside the failure area, and that the mass above the basal shear zone had also dilated. Fleming et al (1989) considered that the slide of debris within the initially dilative colluvium had transformed into a contractive material (Figure 3.37) through dilation of the slide mass leading up to the development of the eventual debris flow.

The mechanism proposed by Fleming et al (1989) is considered a reasonable mechanism for slides in dilative soils on natural slopes.

For slides through the soil mass in cut slopes, the loss of strength from peak as the slide displaces is sufficient to explain the acceleration of the slide mass. If the cut slope is steep, then the post failure movement of the slide mass is generally "rapid".

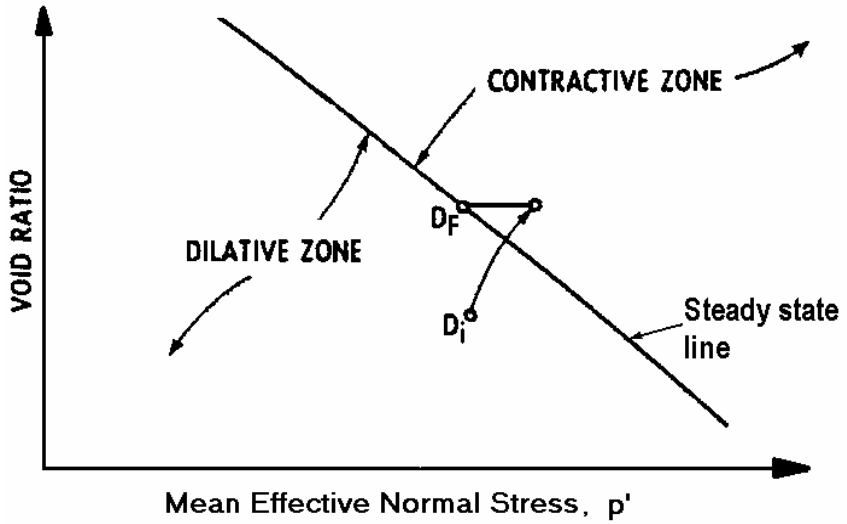

Figure 3.37: Hypothetical model for transformation of dilative materials from rigid to fluid behaviour, path D_i to D_f (Fleming et al 1989)

3.5.2.2 Correlation of Rainfall to Triggering of Slides of Debris

Rainfall is considered by most authors (Johnson and Rodine 1984; Hutchinson 1988; Ellen et al 1988; Brand 1989; Kim et al 1991; Wong et al 1996; Corominas 1996b; Iverson et al 1997; amongst others) to be the trigger for initiation of most slides of debris, but other sources include snowmelt and springs.

In areas where a high incidence of rainfall triggered landsliding occur with the potential to cause loss of life and damage to property, studies are generally undertaken in an attempt to correlate rainfall and landsliding for the purpose of providing warning systems. A common finding by authors researching this relationship (Caine 1980; Wieczorek 1987; Cannon and Ellen 1988; Kim et al 1991; Church and Miles 1987; amongst others) is that both antecedent rainfall and short term rainfall intensity are important factors. In the San Francisco Bay region for example, Wieczorek (1987) found that sufficient antecedent rainfall was required before landslides that developed into debris flows could be triggered, and Cannon and Ellen (1988) concluded that once antecedent rainfall conditions were sufficient to near saturate the surficial soil profile intense rainfall will lead to debris flow activity. Corominas et al (1996) commented that the general form of the failure threshold concept proposed by Caine (1980), Equation 3.7, was a useful correlation that incorporated the need to consider soil saturation.

$$I = 14.82 \cdot D^{-0.39} \tag{3.7}$$

where I is the rainfall intensity in mm/hour and D is the rainfall intensity in hours.

Johnson and Rodine (1984) considered it ridiculous to relate landsliding or debris flow initiation to a single parameter such as slope geometry or rainfall intensity.

In Hong Kong, the trigger for most landslides (including slides of debris, cut slope failures, flow slides and defect–controlled slides) has been identified as rainfall (Brand 1989, 1995). Of the slides of debris in natural terrain (Wong et al 1996; Evans et al 1997; Franks 1996) and the failures in cut slopes on Lantau Island (Wong and Ho 1996) the trigger was identified as intense rainfall. Brand concluded that:

- Localised short duration rainfalls of high intensity induce the large majority of landslides, and that these landslides take place at about the same time as peak hourly rainfall.
- Antecedent rainfall is not a major influence on landslide occurrence, except in some cases of minor landslide events.
- A rainfall intensity of about 70 mm/hour is about the threshold value at which landsliding occurs (Figure 3.38), with the number of landslides and severity of consequences increasing as the peak hourly rate of rainfall intensity increases above the threshold of 70 mm/hour. Figure 3.39 shows the relationship between severity of landslides and rainfall intensity. Note that these landslides are predominantly from constructed fills, cuts and retained slopes, not natural slopes; and the casualty rate is historic and unlikely to be the current situation as Hong Kong has, and is continuing to, expend large sums in slope remedial works.

The landslide warning issued by the Hong Kong Government (obtained from the Hong Kong Government web site) is when the 1-hour intensity exceeds 70 mm/hour and the 24-hour intensity exceeds 175 mm. Both these warning criteria are closely coincident with the change from minor to severe landslide events (Figure 3.39).

Brand (1989) considers that the high correlation of landsliding and short duration rainfall is related to the relatively high permeability of the colluvial and saprolitic soils mantling the steeper slopes in Hong Kong and the dominance of short-term rainfall intensity is related to the rapid rise in piezometric pressures (Brand 1995). He considers the increases in piezometric pressures observed are largely the result of rapid rises in transient perched water and groundwater fed mainly by natural erosion pipes and

tunnels caused by sub-surface erosion observed in the soil profile at many landslides. Franks (1996) reported that erosion pipes were observed in 65% of the failure scarps inspected with most of the soil piping observed in residual soils and colluvium, and Irfan (1997) observed erosion pipes in a number of saprolitic soil slopes. Brand (1989) suspects that similar correlations to rainfall intensity would be appropriate for soils with relatively high permeability in tropical areas. For soils of lower permeability he expects antecedent rainfall to become increasingly important.

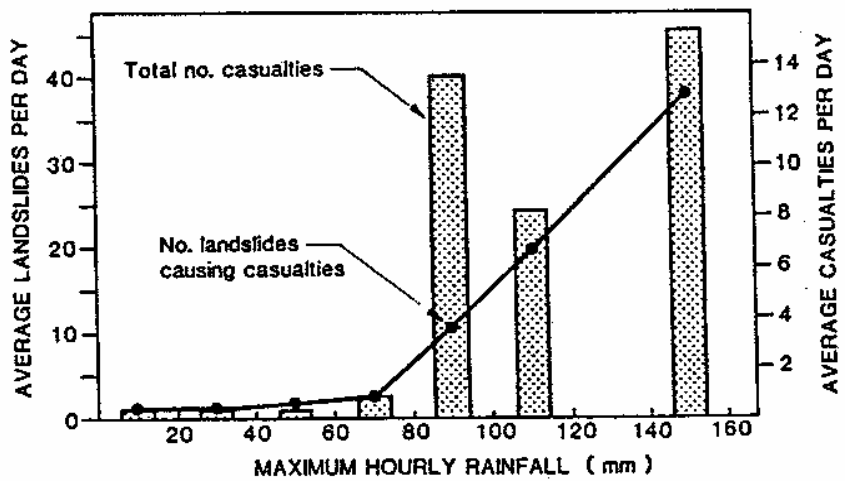

Figure 3.38: Relationship between peak hourly rainfall, landsliding and severity of consequence for Hong Kong (Brand et al 1984)

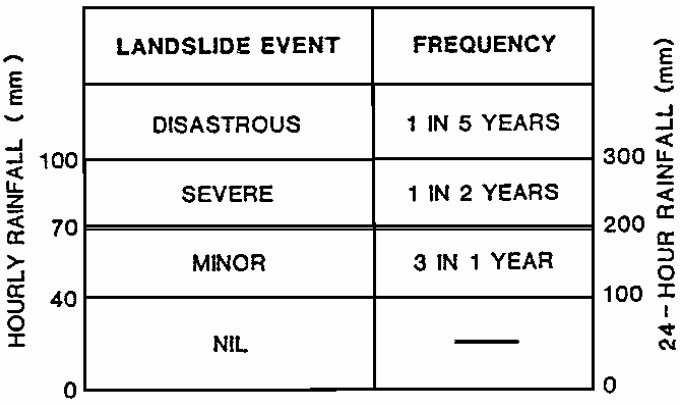

Where:

Minor = localised damage, with less than 10 failures in one day

Severe = widespread damage, with between 10 and 50 failures in one day

Disastrous = Territory wide damage, with more than 50 individual failures recorded in one day

Figure 3.39: Relationship between severity of landsliding and rainfall intensity for Hong Kong (Brand 1985b)

It should be noted that Finlay et al (1997), using detailed rainfall and landslide data for Hong Kong Island that allowed better correlation of rainfall and sliding than the Territory wide data Brand (1989, 1995), demonstrated that antecedent rainfall did have some influence. This is also evident for the case studies analysed from Hong Kong where the depth to sliding is greater than about 5 to 7 metres and the slide volume is greater than about 1500 to 5000 m^3.

Of the forty-three landslides analysed from Hong Kong (refer Section 1 of Appendix B) the trigger in forty-two cases was rainfall, with one case (Kwun Lung Lau on 23 July 1994) triggered by a leaking service pipe. From analysis of these case studies the following tentative conclusions are drawn:

- For the most part, the significant rainfall triggering landsliding was rainfall intensities over periods ranging from less than 1 hour up to 4 hours. This is particularly significant for landslides of shallow (= 3 m depth) to medium depth (> 3 m to = 7 m depth).
- Longer term antecedent rainfall in conjunction with heavy rainfall at the time of sliding appears to be significant for some of the deeper and larger volume compound and translational defect controlled slides (Po Shan Road, Fei Tsui Road, Ten Thousand Buddhas Monastery, Ma On Shan Road and Shum Wan). The 15 to 31 day rainfall events were significant for these landslides with reported annual probabilities of 1 in 40 years to 1 in 1000 years.
- Delay between heavy rainfall and landsliding was noted in three cases (Castle Peak Road - Milestone 14.5, Lido Beach and Allway Gardens). In all three cases the GEO reports considered that rising groundwater levels triggered landsliding (as opposed to development of transient perched water in most cases).

Vegetation affects the frequency of debris slides and debris flows in several ways. Positive effects of vegetation in reducing the frequency of landsliding include; reduction in the amount of precipitation reaching the ground surface, reduction in soil moisture content through transpiration, and the root system may strengthen the upper soil profile. However, vegetal cover does increase infiltration compared with barren soil because it retards surface water flow and the root system makes the soil more pervious. Hutchinson (1988), Corominas et al (1996) and Johnson and Rodine (1984) consider that the destruction of fire to be significant in increasing the probability of debris slides and debris flows. From a study in North Lantau, Hong Kong, Franks

(1996) commented that sparsely vegetated slopes appeared to be the most susceptible to landsliding. Evans et al (1997) found it difficult to draw any conclusions with respect to slope vegetation.

It is possible that the implicit assumption drawn from the above discussion is that debris slides and debris flows are only associated with intense and/or antecedent rainfall. This is not correct. Rather it is rainfall that initiates sliding, then the soil and slope characteristics that determine whether the movement of failed slide mass is "rapid" or will transform into a "rapid" debris slide or debris flow.

3.5.2.3 Material Properties

Indicative particle size distributions and material properties of the source area of slides of debris in natural slopes that developed into "rapid" debris slides and debris flows from published literature are presented in Figure 3.40 and Table 3.12. Several of the particle size distributions have been estimated from material descriptions given by the referenced author/s. The source area material types in natural slopes susceptible to development of "rapid" sliding cover a wide range from high plasticity silts to low to medium plasticity clays and clayey sands to coarse grained granular soils (predominantly cobble to boulder size) with low fines contents. The broad range is considered to reflect the significant influence of slope geometry.

Two modes of post failure deformation and slide mass behaviour are evident for the slides in dilative soils:

- Slides of debris that remain relatively intact during travel (i.e. debris slides). For the slides in the San Francisco Bay region Ellen et al (1988) comment that the higher clay content soil types (high plasticity silts and low to medium plasticity sandy clays and clayey sands) generally remain relatively intact during travel and reach maximum slide velocities of metres per second (rapid to low end of very rapid category). The slides at La Honda (Figure 3.40 and Table 3.12) are an example.
- Slides of debris that undergo significant break up and remoulding, transforming into debris flows. Material types typically range from clayey silty sands to coarse grained granular soils (predominantly cobble to boulder size) with low fines contents. Travel velocities are much higher than for the debris slides in finer grained and more plastic soils, and typically in the range very rapid to extremely rapid. For the slides in the San Francisco Bay region Ellen et al (1988) comment

that the higher velocity slides are observed in soil types with an upper clay content of 25%. The published data (Ellen et al 1988) also indicates that these soils have low plasticity index (0 to approximately 10 to 15%).

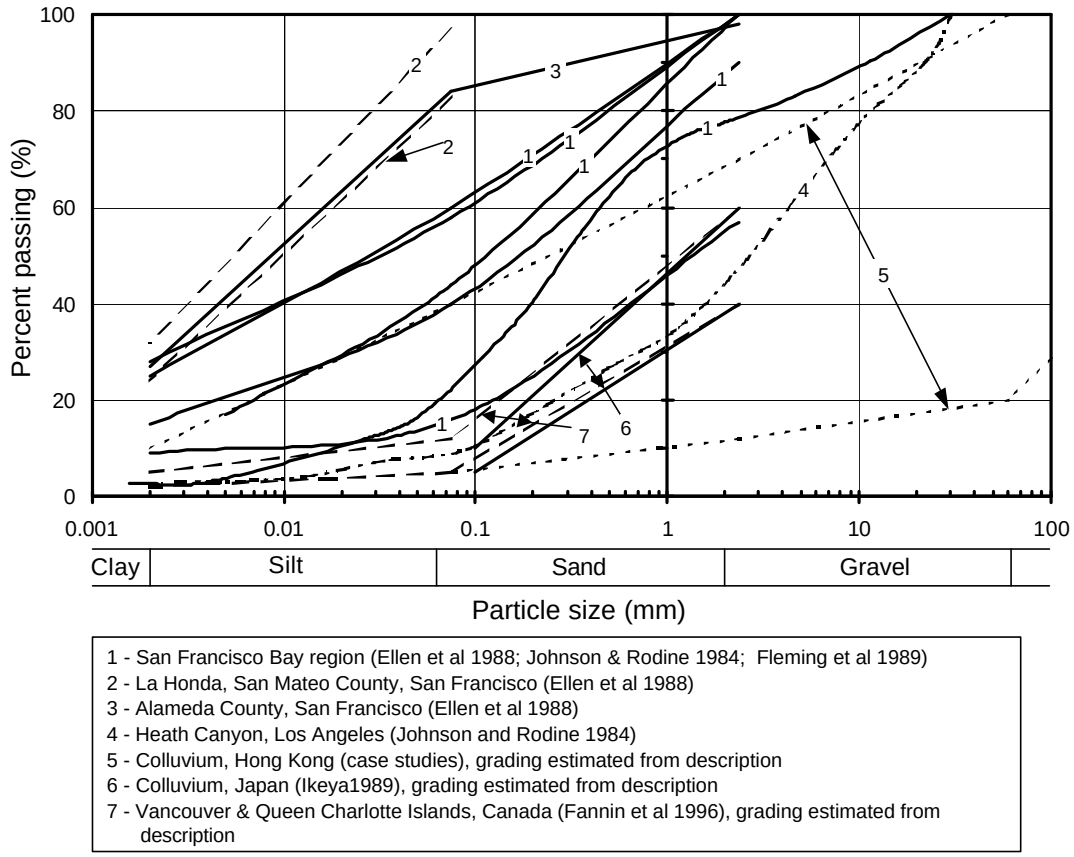

Figure 3.40: Source area particle size distributions of dilative slides of debris in natural slopes.

For slides of debris in natural terrain from Hong Kong the colluvial soil types (in the source area) ranged from silty sands to predominantly cobble to boulder size materials with clay to gravel contents as low as 15 to 25%. Failures in natural slopes (from Hong Kong) have also been reported to incorporate residual and saprolitic soils of granitic and volcanic origin classifying as silty sands to clayey silty sands to sandy silts with varying gravel to boulder size content.

Rodine (1974) considered that the reason why the transformation into debris flows were uncommon in clay-rich materials was because of the difficulty of introducing enough water into soils of relatively low permeability to reduce the strength sufficiently to form a debris flow. Johnson and Rodine (1984) add that debris flows can develop in clay-rich soils when the soil has a high degree of saturation (and low strength) and

requires only a small increase in moisture content for instability and sufficient softening to allow a slide or flow to develop.

Johnson and Rodine (1984) comment that slides of debris that transform into "rapid" debris slides and debris flows are significantly more prevalent in cohesionless or low cohesion soils as they are more permeable and require much smaller changes in soil moisture for strength reduction and remoulding. They add that in general, debris flows (as opposed to debris slides) comprise only minor amount of clay with the larger clasts typically carried (or suspended) on or within the debris flow. Corominas et al (1996) describe the debris flow material type as typically well graded with clay contents of less than 5%.

Material permeability is also a significant material property affecting the development of slope instability and the transformation from landslide into debris flows. Numerous authors (Johnson and Rodine 1984; Brand 1989; Brand 1995; Franks 1996; Iverson et al 1997; amongst others) comment that soil permeability affects the rate and depth to which water infiltrates the ground, and that defects within the soil mass (erosion pipes, root holes, etc.) and differential material permeability enhance slope failure by development of locally elevated pore pressure conditions or transient perched water.

The range of particle size distribution for slides of debris that develop into "rapid" debris slides and debris flows is very broad. The grading limits in Figure 3.40 and material properties in Table 3.12 and the above discussion are considered useful as a guide in conjunction with assessment of slope geometry and other factors affecting the transformation from slides of debris in "rapid" debris slides and debris flows.

3.5.2.4 *Slope Geometry*

A summary of the source area slope angle (a_1 in Figure 1.2) of dilative slides that developed into "rapid" debris slides and debris flows from this study and published sources is given in Table 3.13. Table 3.14 summaries the source area and initial down-slope slope geometry for the case studies (from Hong Kong) considered in this study.

Table 3.12: Summary of material types of dilative slides of debris in natural slopes that developed in "rapid" debris slides and debris flows.

Location/Region	Material Properties		Slide Description	References
	Classification	Properties		
Marin County, San Francisco	SM/ML - clayey silty sands to sandy silts, colluvium	Low plasticity, W_L = 18 to 24%, I_P = 0 to 4%	Slides of debris that developed in "rapid" debris flows. Very to extremely rapid.	Fleming et al (1989) Ellen et al (1988)
La Honda, San Mateo County, San Francisco	MH	High plasticity	Travelled as relatively intact debris slides. "Rapid" velocities in metres/minute.	Ellen et al (1988)
Pacifica, San Mateo County, San Francisco	SC/CL – sandy clays and silts, and clayey sands	Low plasticity, W_L = 18 to 42%, I_P = 3 to 20%	Slides of debris that developed into debris flows. Rapid to extremely rapid.	Ellen et al (1988) Howard et al (1988)
Heath Canyon, Los Angeles	Sandy gravel to gravelly sand	Low fines content (< 10%)	Slide of debris that developed into debris flow	Johnson and Rodine (1984)
Vancouver and Queen Charlotte Islands, Canada	Colluvium. Gravelly sands to sandy gravels.	Some to little silt and trace clay	Slides of debris that developed into debris flows.	Fannin et al (1996)
Queen Charlotte Islands, Canada	Colluvium. Silty sands to sandy silts.	Some to little silt and trace clay	Slides of debris that developed into debris flows.	Fannin and Rollerson (1992)
Taeback Mountains, Korea	Residual soils (and colluvium?) derived from gneiss, schist and granitic rock types.		Developed into debris flows.	Kim et al (1991)
Eastern Alps, Austria	Moraine. From boulder to clay size, loose.		Developed into debris flows. Very to extremely rapid.	Aulitzky (1989)
Japan	Sandy gravels to gravelly sands with boulders and low fines content (< 10% passing 0.1 mm)		Developed into very rapid to extremely rapid debris flows.	Ikeya (1989)
Campanian Apennines, Italy	Colluvium derived from pyroclastic soils. Sandy gravels to clayey sandy silts. Low plasticity (W_L = 25 to 34%, I_P close to 0%).		Slides of debris that developed into confined debris flows.	Guadagno (1991)

W_L = liquid limit I_P = plasticity index

For slides of debris in natural slopes Hutchinson (1988), Corominas et al (1996) and Corominas (1996b) consider that slope angles in which slides of debris are transformed into "rapid" debris slides and debris flows typically range from 25 to 45 degrees, although they can take place on slope angles as low as 18 degrees and as steep as 50 degrees. The findings from other studies (Table 3.13) concur with these findings.

Evans et al (1997) report the findings from more than 26,000 debris slides and debris flows in natural terrain from Hong Kong. The study included some 18,000 relict landslides (pre 1945) and almost 9000 recent landslides (1945 to 1994). The distribution of head slope angle (or source area slope angle, a_1) for both the relict and recent landslides from this study is given in Figure 3.41. As an indication of the lower limit of slope angles in which debris slides occur in Hong Kong, Irfan and Woods (1998) report slow moving landslides of colluvium (sliding on weathered rock interface) on slopes of 15 to 18 degrees and in weathered saprolite soils of 21 degrees.

The locality of the initial slide is reported by the referenced authors (Table 3.13) to be dominantly on either open slopes or the head region of the watershed. Ellen et al (1988) commented, for the initial slides in the San Francisco Bay region during the intense rainstorm of January 1982, that the initial slide occurred in areas conducive to concentration of water such as concavities, breaks in the slope or geological contacts, but also occurred in areas without these features (i.e. open slopes).

From Table 3.13 it can be concluded that development of "rapid" debris slides and debris flows derived from slides of debris in natural slopes predominantly occur where the source and immediate down-slope angle is greater than about 25 degrees, but can occur on slopes down to about 18 to 20 degrees. The broad regional spread would suggest that these slope angles are typical in most regions of high landslide intensity around the world.

For the cut slope case studies from Hong Kong (Table 3.14) "rapid" slides from failures in dilative soil types (and not defect controlled) occur in slopes greater than about 34 degrees. This is likely to be regionally specific considering the limited geological environment of the case studies, but is considered applicable to cut slopes in similar soil and weathered rock types (silty sands to sandy silts with low clay contents and decomposed granitic and volcanic rock types). Studies on cut slopes in high plasticity clays (James (1970) and Chapter 5) indicates "rapid" sliding occurred for failures in cut slopes steeper than about 27 to 30 degrees, with some dependency on the location of the slide within the slope.

Table 3.13: Source area slope angle (a_1) of dilative slides in natural slopes that developed into "rapid" debris flows and debris slides

Reference / Location	**Locality and/or Spread**	**Source area slope angle, a_1 (°)**
This study (Hong Kong) – natural slopes	In colluvium In saprolite	31 to 44 33 to 52
Evans et al (1997) – Natural slopes in Hong Kong	Total range 95% of slides Most landslides (75%)	11 to >45 >27 30 to 45
Irfan and Woods (1998), natural slopes in Hong Kong	Approximate minimum	15 to 21
Corominas (1996b), slides of debris	Total range Majority	18 to 50 25 to 45
Hutchinson (1988) –slides of debris	Typical range	25 to 45
Johnson and Rodine (1984), natural slopes in USA	Typical range southern California Virginia, USA Hawaii western USA	25 to 40 >39 >17 42 to 48 >30
Ellen and Fleming (1987), Ellen et al (1988) – natural slopes in San Francisco Bay Region	Typical range Approximate minimum	25 to 40 18 to 20 (possibly as low as 14)
Fannin and Rollerson (1992) – Vancouver and Queen Charlotte Islands	Total range Majority of slides	> 22 to 43 28 to 40
Kim et al (1991) - Taeback Mountains, Korea	Typical range	30 to 35 (some on shallower slopes)
Guadagno (1991) - Campanian Apennines, Italy	Typical Approximate minimum	> 25 as low as 18
Rapp and Nyberg (1981), Rapp (1986) *[1]	-	25 to 40
Zimmermann (1990) *[1]	-	25 to 40
Lewin and Warburton (1994) *[1]	-	15 to 39
Campbell (1975) *[1]	-	22 to 45
Johnson and Rahn (1970)*[1]	-	25 to 40

*[1] Sourced from Corominas et al (1996)

Table 3.14: Failures through the soil mass in dilative soils that developed into "rapid" landslides, from Hong Kong

Slide Name	Slope Type	Source Slide Material	Initiating Slide Description	Geometrical *[1] Slopes (degrees)			Vol. (m^3)	TDA, a *[1] (°)
				a_1	a_{base}	a_2		
Keng Hau Rd-B	Cut	Residual (G)	Non-circular, int	53	29	40	210	26
Cheung Shan Estate	Cut	Colluvium	Slide of debris, translational, int	51	36.5	51	35	36
Lai Cho Road	Cut	Colluvium & saprolite (G)	Non-circular, int	34	34	34	33	32
St. Joseph's	Cut	Saprolite (G)	Non-circular	65	65	0	25	44
Yue Sun Garden-B	Cut	Saprolite (V)	Compound, trans	52	50	2	1100	29
Castle Peak Rd (M 14.5)	Cut	Saprolite (G)	Rotational	46	-	0	300	28
Yue Sun Garden-A	Cut	Saprolite (V)	Non-circular	56	-	56	200	36
Bayview Gardens	Cut	Saprolite (V)	Rotational	66	-	0	70	47
Ha Wo Che Shatin	Cut	Saprolite (G)	Non-circular	55	-	0	60	34
Keng Hau Rd-A	Cut	Residual & saprolite (G)	Compound	64	31	26	150	19
Chung Shan Terrace-B	Cut	Saprolite (G)	Non-circular	52	35	0	85	41
Hong Tseun Road	Cut	Saprolite (V)	Non-circular	36	-	43	250	25
Tao Fung Shan Cemetery-A	Nat	Residual (G)	Translational, int	50	30	40	900	30
GP Christian Centre	Nat	Residual (G)	Compound, trans, int	33	0	32.5	20	28
Lui Pok School	Nat	Colluvium	Slide of debris, compound, trans, int	31	31	29	450	19
Tsing Shan	Nat	Colluvium	Slide of debris, compound, int	40	40	33	13000	23
Lantau Island – C1	Nat	Colluvium	Slide of debris, compound, trans, int	33	30	23	1000	21
Wonderland Villas	Nat	Residual (G)	Compound, trans, int	40	37	34	80	29
Sha Tin Height – Slide B	Nat	Colluvium	Slide of debris, translational, int	37	40	13	170	18
Ma On Shan Rd	Nat	Colluvium & saprolite (G)	Compound	34	32 to 45	7	3000	22
Outward Bound School	Nat	Colluvium & saprolite (V)	Non-circular	44	-	33.5	900	27
Ka Tin Court, Shatin	Nat	Saprolite (G)	Compound, trans	52	36	37.5	150	29
Lido Beach	Nat	Residual & saprolite (G)	Non-circular	52	-	17	750	21
Tuen Mun Road	Fill	Silty sand	Compound, trans	34	29	0	200	27

***[1]** refer Figure 1.2 for the definitions of slope geometry terms, a_1 = source slope angle, a_{base} = rupture surface inclination angle, a_2 = initial down-slope angle and TDA (or a) = travel distance angle.

Nat = natural (G) = granitic origin (V) = volcanic origin int = sliding on interface

trans = significant translational component Vol. = slide volume

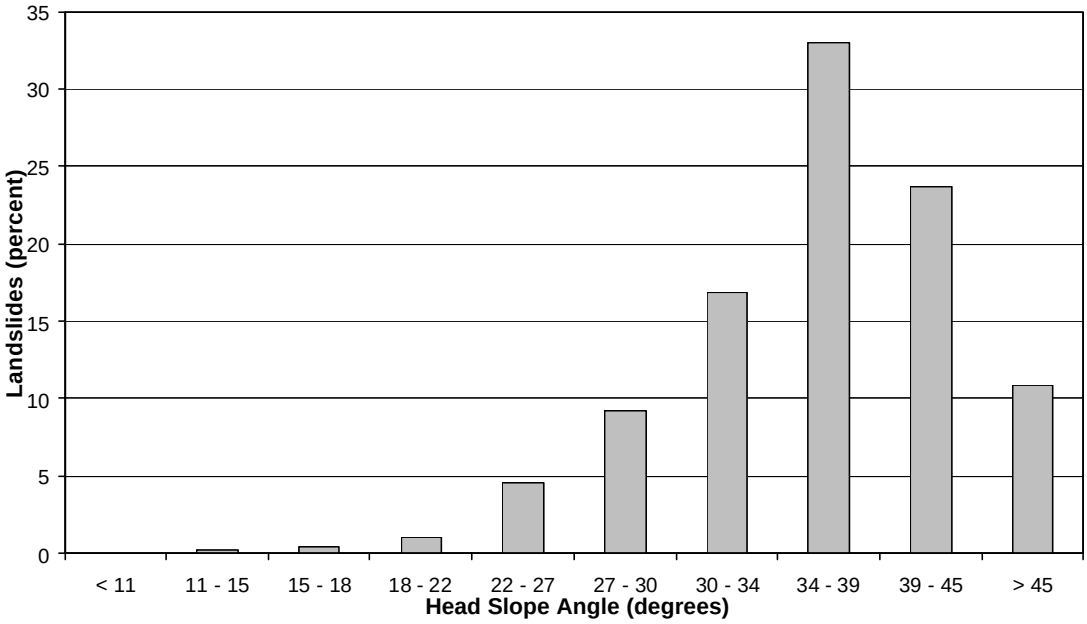

Figure 3.41: Distribution of head slope angle (source area slope angle) for slides of debris in natural terrain that developed into "rapid" landslides, Hong Kong (Evans et al 1997)

3.5.3 DEFECT CONTROLLED LANDSLIDES

The nine case studies of defect-controlled landslides analysed are from Hong Kong.

Glastonbury and Fell (2000) in their analysis of large (mostly greater than 1 million m^3) "rapid" failures in rock slopes, found that for compound rupture surfaces, brittle rock mass failure is required to cause "rapid" movement. For toe buttress compound slides rupture of the rock mass at the toe is required, for bi-planar and curved compound rupture surfaces brittle internal deformation is required. For translational planar surfaces of rupture, brittleness associated with either the basal rupture surface or lateral rupture surfaces is required for "rapid" sliding. They compared the rupture surface inclination angle to the basic friction angle of the controlling defect for compound and translational failures, and found that:

- For compound rock slides that develop into "rapid" landslides the rupture surface inclination angle is typically 10 to 30 degrees greater than the basic friction angle, indicating the significance of the rock mass restraint on "rapid" sliding.
- For translational rock slides that develop into "rapid" landslides the difference between the rupture surface inclinational angle and the basic friction angle is significantly less, generally in the order of 0 to 10 degrees, suggesting therefore that dilation angles are of the order 0 to 10 degrees.

Whilst the defect-controlled failures that developed into "rapid" landslides from Hong Kong are of significantly smaller volume and the intact strength of the saprolitic soils significantly less than for the rock slides analysed by Glastonbury and Fell (2000), it is considered that similar principals are applicable for the development of "rapid" post-failure movement for this slide group. Table 3.15 summarises the features of defect controlled compound slides and Table 3.16 defect controlled translational slides case studies that developed into "rapid" landslides post failure. Estimates of basic friction angle and residual friction angle on the controlling defect are based on laboratory shear strength test results where available from the site or else approximated from published strength test results (Irfan and Woods (1998); Irfan (1997)) on discontinuities within similar rock types with similar infilling. No estimate of the asperity roughness (dilation angle) has been made.

Saprolitic soils derived from weathering of volcanics and granite in Hong Kong typically classify as silty sands with varying gravel to boulder content depending on the degree of decomposition (weathering) and generally have low clay contents (typically less than about 10%). The thickness of these weathered rocks is variable; Irfan (1997) reports thicknesses of up to 60 m in granitic rocks and typically less than 15 m in volcanic rocks. Weathering is concentrated on structural and lithological discontinuities in the original rock mass (Irfan and Woods (1998)) leaving relict discontinuities in the saprolitic soil mass. These relict discontinuities often contain a thin veneer of silty clay to clay with kaolinite often the dominant mineral. The surfaces can be rough, polished or in some cases slickensided. These relict discontinuities are typically of significantly lower strength than the intact saprolitic soils and strength results of shear testing of discontinuities are given in Tables B1.1 and B1.2 of Appendix B (after Irfan and Woods, and Irfan). The presence of relict discontinuities affects both the hydrogeology (discontinuities typically of lower permeability) and slope stability, depending on their orientation in relation to the slope.

For the compound slides (Table 3.15), the inclination of the surface of rupture is 5 to 20 degrees greater than the basic friction angle. This is slightly less than the difference obtained by Glastonbury and Fell (2000) and is possibly due to a combination of the weaker strength of saprolitic soil mass (than intact rock strength), relatively low stresses within the failure mass and intense hydro-geological conditions of Hong Kong.

For the translational slides the difference ranges from 5 degrees less than the basic friction angle (Fei Tsui Road) to 15 degrees greater (Fung Wong Reservoir). For Fung

Wong Reservoir part of the rupture surface was through intact saprolitic soils and is possibly the reason for the relatively high difference. Fei Tsui Road on the other hand (Figure 3.42) presents an interesting example of a translational slide that developed into a "rapid" debris slide. On first impression it is unlikely to consider that the slide could develop into a "rapid" slide post failure given the low angle of the surface of rupture and strong defect control on the lateral margins. It is considered that the brittleness for this "rapid" landslide is likely to be associated with the dilation required on the irregular surface of rupture and possibly some brittleness on the lateral margins. It is also considered possible that altered tuff layer may have been pre-sheared to some extent and the basic friction angle lower than given in Table 3.16. The hydro-geological conditions present at the time of the landslide must have been sufficient to overcome the dilation effects to result in failure of the slope.

The limited number of slides and the limited breadth of the geological environment of the cases make it impossible to give general conclusions with any degree of confidence. However, the principle that basal slide surfaces need to be steeper than the residual friction angle for defect controlled slope failures to developed into "rapid" landslides is logical, and the findings presented can be used as a guide for translational and compound defect-controlled slides.

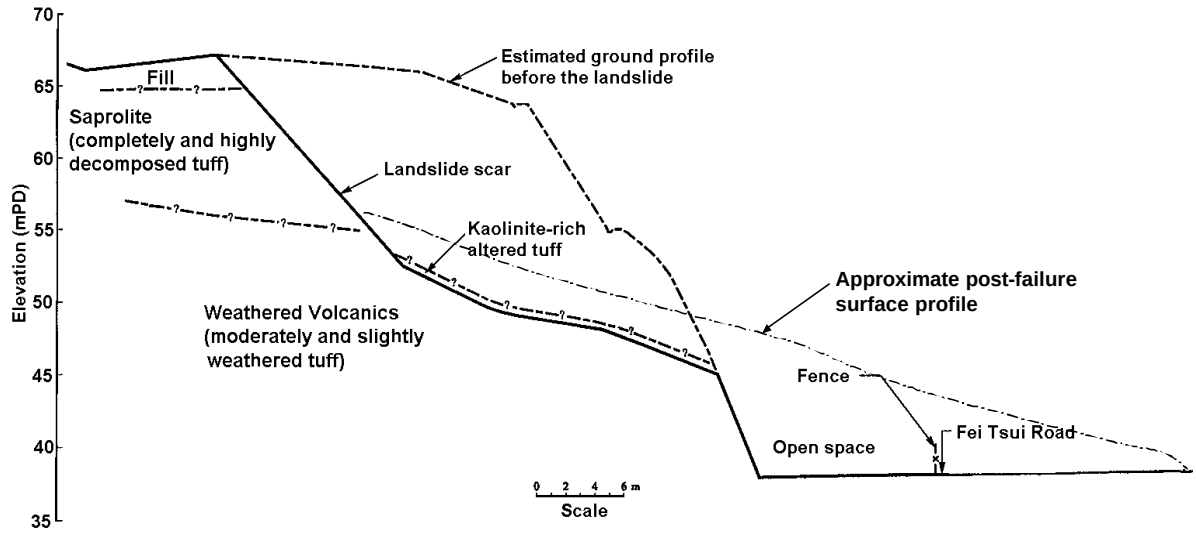

Figure 3.42: Cross section through the failure and "rapid" landslide at Fei Tsui Road, Hong Kong (GEO 1996a)

Table 3.15: Features of defect controlled compound slides that developed into "rapid" landslides from Hong Kong

Slide Name	Description	Slope Angle (º)	a_{base} (º)	Estimated f_b (º)	Estimated f_r' (º)	Approx $f_b - a_{base}$	Rupture Surface Description
Ching Cheong Road (1997)	Cut slope in granitic saprolite	48	40 to 50	26 to 34	18 to 22	-15 ± 5	Infilled kaolinitic joint, persistent
Allway Gardens (1993)	Cut slope in volcanic saprolite and PW rock	41	23 to 47	22 to 30	22	-10 ± 5	10 mm thick clay infilled relict joints
10000 Buddhas Monastery (1997)	Cut slope in granitic saprolite and PW rock	52	30 to 52	35 ± 2	31	-5 ± 2	Rough, silt infilled joints
Po Shan Road (1972)	Cut slope in volcanic saprolite	57	43	26 ± 4	18 to 22	-20 ± 5	Persistent relict joint
Shum Wan Road (1995)	Quasi-natural slope of volcanic saprolite	31	10 to 51	26 to 30	21	-5 ± 2	Clay seam of 100 to 350 mm thickness.

a_{base} = rupture surface inclination f_b = estimated basic friction angle f_r' = estimated residual friction angle PW = partially weathered

Table 3.16: Features of defect controlled translational slides that developed into "rapid" landslides from Hong Kong

Slide Name	Description	Slope Angle (º)	a_{base} (º)	Estimated f_b (º)	Estimated f_r' (º)	Approx $f_b - a_{base}$	Rupture Surface Description
Kau Wa Keng San Tseun, A (1997)	Cut slope in granitic saprolite and PW rock	45 to 70	45	35 ± 2	22 to 30	-10 ± 5	Along relict discontinuities parallel to the slope
Fung Wong Reservoir (1998)	Cut slope in granitic saprolite	52	45 to 60	26 (defect) 40 to 42 (intact)	20 to 25	-15 ± 10	Kaolin infilled relict discontinuity (failure partly through intact soil)
Fei Tsui Road (1995)	Cut slope in volcanic saprolite and PW rock	60 to 65	19 (10 to 25)	24 ± 2	18 ± 4	+5 ± 2	Altered tuff layer, 0.6 m thickness, completely decomposed, kaolin veins.
Ka Wa Keng Upper Village (1997)	Cut slope in granitic saprolite	60	30	25 to 30	20 to 25	-3 ± 2	Persistent 20 mm thick relict joint, kaolin and maganiferous deposits.

a_{base} = rupture surface inclination f_b = estimated basic friction angle f_r' = estimated residual friction angle PW = partially weathered

3.6 SUMMARY OF THE CHARACTERISTICS AND MATERIAL TYPES OF "RAPID" LANDSLIDES

As previously discussed, it is important to distinguish between the trigger mechanism/s for the processes leading up to slope instability and the occurrence of "rapid" landsliding post failure. Once an unstable slope condition is reached the progression to "rapid" sliding is dependent on the slope geometry and material properties within the unstable slope. Whilst rainfall and hydro-geological conditions may be a significant factor in the development of an unstable slope condition in a number of slide classes considered, it does necessitate that the post failure movement will be "rapid". In fact the material properties and slope geometry are far more significant influences on the likelihood or otherwise of "rapid" sliding.

3.6.1 FLOW SLIDES IN CONTRACTANT SOILS SUSCEPTIBLE TO FLOW LIQUEFACTION

A wide variety of soil types covering a broad spectrum of particle size distribution (Figure 3.43) are susceptible to contraction on shearing and development of flow sliding. For cohesionless soils Fell et al (2000) consider the material types susceptible to liquefaction and flow sliding include submarine and sub-aqueous slopes, mine tailings, dredged and hydraulically placed fills, dumped mine wastes, uncompacted or poorly compacted fills, loose dumped rockfills and loose colluvium on hill slopes. Sensitive clays derived from leached marine deposits are also susceptible to liquefaction and flow sliding. Nearly all of these cases could be considered as dumped or loosely placed man made fills or recent natural deposits. Being contractant in drained conditions, slopes in these soil types are potentially susceptible to liquefaction and flow sliding.

General guidelines on relative density of cohesionless soils susceptible to flow liquefaction based on analysis of the literature are as follows:

- Clean sands are susceptible to flow liquefaction at a density index less than about 15 to 30%, but this is likely to vary depending on the shape of the grading curve and particle size (i.e., coarse sands are likely to be less susceptible than fine sands). A complete liquefaction condition (zero residual undrained strength) is observed in the laboratory for very loose sands (relative density less than about 10%, but this will also vary).

- Silty sands are more susceptible to flow liquefaction than clean sands (in terms of relative density) with flow liquefaction possible at relative densities up to 45 to 60%.
- Sandy gravels are less susceptible to flow liquefaction than sands. Laboratory and field tests on coal waste and coking coal indicate these materials are susceptible to liquefaction at void ratios greater than about 0.3. Moisture content at placement (dumping) has a significant effect on the initial void ratio of these materials. Field case studies indicate that flow slides in mine waste spoil piles generally occur when the spoil pile is located on a hillside and has been placed by tipping onto the crest of the active dump.
- Silty sands (typically with clay contents less than about 10%) are susceptible to liquefaction at densities below 85 to 90% of Standard Maximum Dry Density (from laboratory tests on decomposed granite in Hong Kong). Flow slides in these materials are typically of shallow depth (up to 3 m) and therefore effective stresses are low.

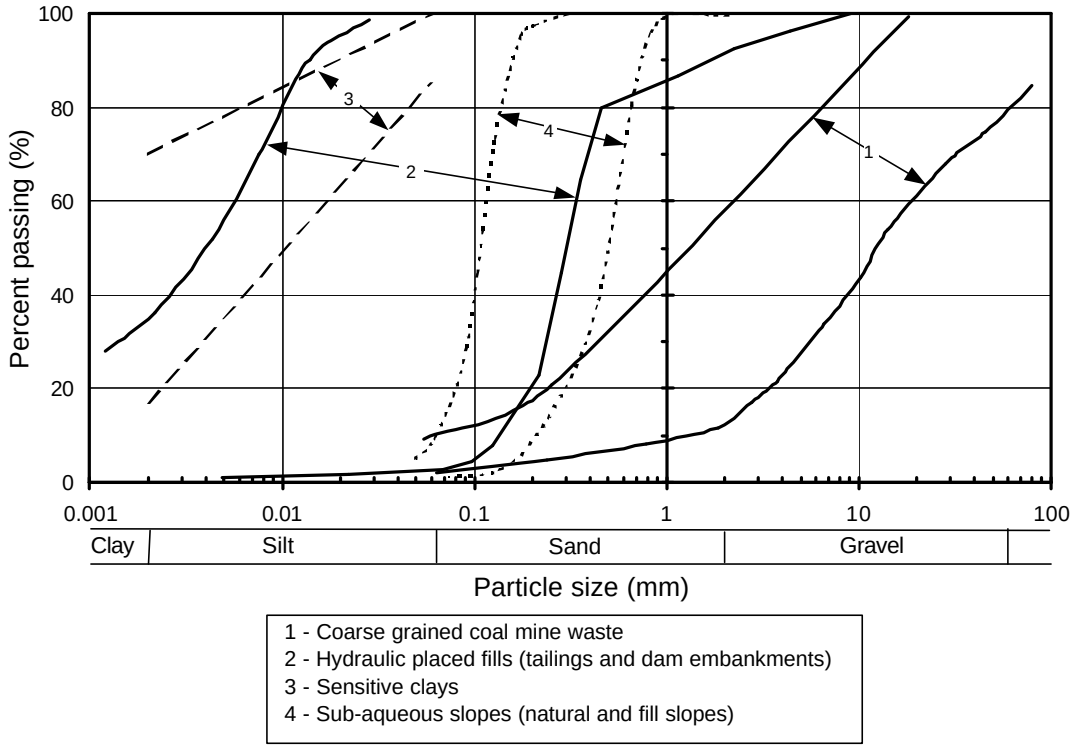

Figure 3.43: Particle size distributions of material types susceptible to liquefaction and flow sliding.

These guidelines and particle size distributions are general and should be used with caution as soil types outside these limits may liquefy and conversely soil types within these limits may not.

Whether or not liquefaction and subsequent flow sliding will occur is dependent on the material properties, degree of saturation and the effective stress conditions. The mechanism for initiation of flow sliding under static conditions requires:

- The soil to be in a saturated or near saturated state.
- The effective stress state within the slope to be at or above the instability line (or collapse surface) (Figure 3.23), under which conditions the soil is contractive on shearing in drained loading. It should be recognised that under these stress conditions the potentially contractile soils can exist in a stable state in drained conditions.
- The trigger to liquefaction and flow sliding is a change in effective stress conditions, and most likely the shear deformations that occur as a result of the change in stress conditions.

The slope geometry, conditions under which liquefaction is triggered and factors affecting the development of flow slides within the various soil types considered is discussed in Sections 3.4.1 to 3.4.7.

The general guidelines (and discussion in Sections 3.4.1 to 3.4.7) provide an indication of the potential soil types and conditions under which flow slides have developed. They should be used with caution and as a general indicator of potential for flow sliding. Other methods (laboratory and field based) are available and should be used for further evaluation of liquefaction and flow slide potential.

3.6.1.1 *Laboratory Based Methods*

The instability line or collapse surface concept (Figure 3.7) is a useful theoretical model, appropriate to liquefaction susceptible soils, for estimating the stress conditions at the onset of strain weakening (and therefore liquefaction) in undrained conditions. Soils with a positive state parameter (as determined by their void ratio) are strain weakening in undrained loading and may be susceptible to flow liquefaction. Several studies have attempted to define parameters for the instability line; however, its location will vary depending on the sample void ratio.

Current research queries the uniqueness of the steady state line. Recent work by Cubrinovski and Ishihara (2000) indicates that the steady state line in void ratio versus log effective normal stress space is not linear below effective normal stresses of 10 kPa (Figure 3.6).

The methodology for assessment based on laboratory testing is relatively straight forward, however, the application of theoretical concepts from laboratory testing to site conditions have proven difficult. Most of the difficulty is associated with obtaining "undisturbed" samples of soils, the sensitivity of the soil behaviour to small changes in void ratio, complexity of factors such as in-situ stratification and the actual test results themselves. If laboratory testing is to be used to assess the potential for flow liquefaction, care must be taken to model the void ratio, fabric and initial stress conditions of the in-situ soil, and the likely stress path to failure.

3.6.1.2 *Field Testing*

For assessment of flow liquefaction potential of sandy soils several useful in-situ methods have been developed, some derived purely on an empirical basis from case study analysis and some from a combination of theoretical and empirical analysis. Cubrinovski and Ishihara (2000), Baziar and Dobry (1995), Ishihara (1993), Robertson et al (1992) and Sladen and Hewitt (1989) have developed useful guidelines for assessment of the boundary between flow and no-flow conditions of sands and silty sands under earthquake and static loading, and in terms of SPT N value and/or CPT q_c. The most useful for static liquefaction is considered to be the recent research by Cubrinovski and Ishihara (2000) where the flow potential takes into consideration particle size distribution, fines content and particle angularity (Figure 3.11 and Figure 3.15), and is applicable for sands and silty sands with up to 30% fines content.

Figure 3.44 presents a comparison of the liquefaction flow no-flow boundaries in terms of SPT $(N_1)_{60}$ value derived from field cases of earthquake induced flow liquefaction (Baziar and Dobry 1995; Ishihara 1993) and derived from (with some exceptions) laboratory undrained monotonic triaxial compression tests in sands and silty sands (Ishihara 1993; Cubrinovski and Ishihara 2000). The upper bounds of Ishihara (1993) and the bounds by Cubrinovski and Ishihara (2000) have been converted from SPT N value to $(N_1)_{60}$ correcting for over-burden pressure and energy ratio (assuming 78% rod energy for the SPT results from Japan). The liquefaction flow no-flow

boundaries of Baziar and Dobry (1995) and Ishihara (1993) compare reasonably well with those of Cubrinovski and Ishihara (2000) in consideration of the materials they represent (Ishihara (1993) upper bound for clean sands and silty sands (up to 30% fines), Baziar and Dobry (1995) sands with at least 10% silt).

Based on the comparisons between field and laboratory, and between static and cyclic trigger (Figure 3.44 for SPT and Figure 3.10b for CPT), it is concluded that the flow liquefaction no-flow boundary is dependent primarily on the properties of the material and is independent of the triggering mechanism; i.e., cyclic (earthquake) or static. Therefore, importantly, the methodology of Cubrinovski and Ishihara (2000) can be applied to the assessment of flow liquefaction potential for clean sands and silty sands (up to 30% fines) for static and dynamic triggered events.

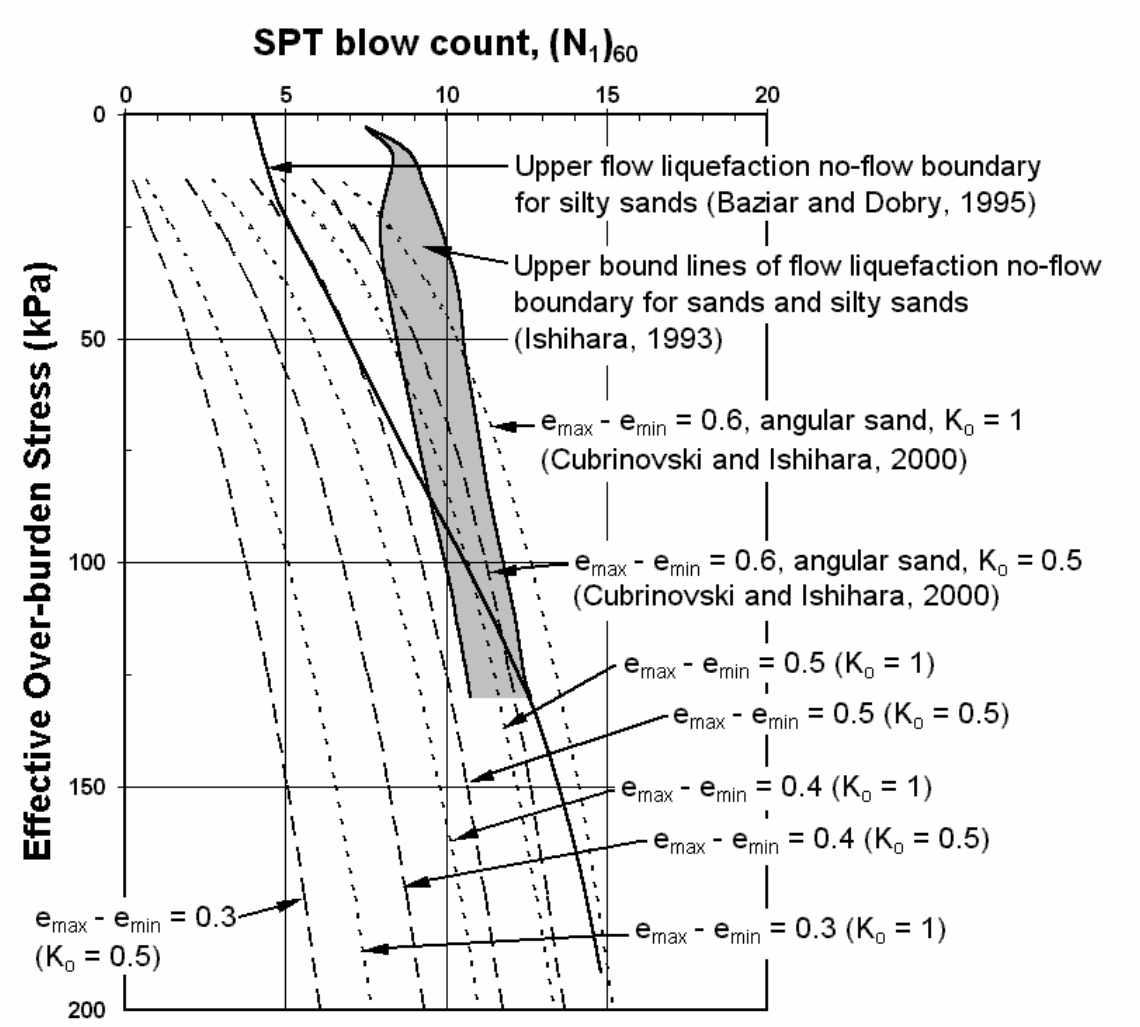

Figure 3.44: Comparison of flow liquefaction no-flow boundaries (in terms of SPT $(N_1)_{60}$) for sands and silty sands from monotonic laboratory undrained tests and earthquake triggered field cases (after Cubrinovski and Ishihara 2000).

3.6.2 CHARACTERISTICS AND IDENTIFICATION OF CONDITIONS UNDER WHICH FAILURES IN DILATIVE SOILS RESULT IN "RAPID" LANDSLIDING

The "rapid" landslides developed from failures in dilative soils were divided into two categories, those where the surface of rupture passed through the soil mass, and those where it is preferentially located along defects within the slide mass, termed defect controlled slides. A greater weighting was given to the slides through the soil mass due to the greater weighting of case study information. An important aspect of landslides from dilative soils is the distinction between the initial development of the failure itself and the transformation of the slide mass into a "rapid" debris flow or debris slide. Initiation of the failure occurs when a critical equilibrium condition is reached within the slope along a defined surface of rupture and is dependent on material strength, slope geometry and the hydro-geological conditions within the slope.

For slides through the soil mass in natural slopes the significant factors affecting initiation of the slide itself and its transformation into a "rapid" debris slide or debris flow are:

- Rainfall is often the trigger for initiation of the slide. Correlations of rainfall to landsliding, while useful, are not straightforward due to the influence of the hydrogeology, material properties and slope geometry on slope stability.
- Material properties and particle size distribution. The range of particle size distribution and material properties is very broad, ranging from high plasticity silts to low plasticity sandy clays and clayey silty sands to dominantly coarse granular soils with low fines contents (less than about 10 percent). Figure 3.40 and Table 3.12 provide guidelines on material properties.
- Slope geometry. Landsliding predominantly occurs where the source and immediate down-slope angle is greater than about 25 degrees, but can occur on slopes down to about 18 to 20 degrees. The slides occurred on open slopes as well as in areas conducive to concentration of water (concavities, breaks in the slope or geological contacts).

Two modes of post failure deformation and slide mass behaviour are evident for slides through the soil mass in natural slopes:

- Slides of debris that remain relatively intact during travel (i.e. debris slides). The higher clay content soil types (high plasticity silts and low to medium plasticity

sandy clays and clayey sands) generally remain relatively intact during travel and reach maximum slide velocities in the rapid to low end of very rapid category.

- Slides of debris that undergo significant break up and remoulding, transforming into debris flows. Material types typically range from clayey silty sands to coarse grained granular soils (predominantly cobble to boulder size) with low fines contents. Travel velocities are much higher and typically in the range very rapid to extremely rapid.

For slides through the soil mass in cut slopes the case studies are from one region (Hong Kong) and occurred in colluvium, residual soils and decomposed rock types derived from granitic and volcanic rocks. Material types were generally silty sands to sandy silts with low clay contents containing varying quantities of gravel to boulder sized material. In Hong Kong, "rapid" landslides developed from failures in cut slopes that were greater than about 34 degrees. Studies in other soil types suggest sliding can occur in cut slopes as low as 27 to 30 degrees, but is dependent on the strength properties of the soil and the location of the slide within the slope.

For the defect controlled slides in dilative soils only a limited number of slides were analysed and they were all from a similar geological environment, making it impossible to give general conclusions with any degree of confidence. However, the analysis indicated that "rapid" sliding occurred where the inclination of surface of rupture is:

- 5 to 20 degrees greater than the basic friction angle for compound slides.
- Equal to or greater than the basic friction angle for translational slides.

The principle that basal slide surface need to be steeper than the residual friction angle for "rapid" sliding to occur post failure is a logical one, and the findings can be used as a guide for translational and compound defect-controlled slides.

3.7 PRE-FAILURE DEFORMATION BEHAVIOUR

The pre failure deformation behaviour can give warning of an impending failure, and allow evacuation of persons, closure of roads, etc., so mitigating risks. The following summarises the observations of pre failure deformation made for each class of slope.

3.7.1 FLOW SLIDES

Monitoring records of pre-failure deformation of flow slides has been obtained for a limited number of case studies. Most of these are from coal waste stockpiles in British Colombia where monitoring of deformations at the crest of the tip is used as a control measure in an attempt to avoid a potential failure by halting of waste deposition and also as a measure to reduce the risk to loss of life and property. Monitoring of deformation was also recorded for the two flow slides in embankments during construction (Fort Peck Dam and Calaveras Dam). For the remainder, records of pre-failure deformation are observational. In most cases no formal monitoring is (or was) undertaken.

Discussion and actual records of pre-failure monitoring for the various sub-groups of flow slides is given in Sections 3.7.1.1 to 3.7.1.4.

3.7.1.1 Coarse-Grained Coal Mine Waste Spoil Piles on Hillsides and Coking Coal Stockpiles

Pre-failure deformation was measured or observed at a number of the failures in coarse-grained dumped fills at British Columbia, South Wales and Hay Point. The records and observations are summarised in Table 3.17. Recorded measurements of crest displacement leading up to failure at two waste dumps in British Columbia are shown in Figure 3.45.

Where recorded or closely observed, the rate of displacement leading up to an impending failure increased significantly in the days and sometimes weeks prior to the failure reaching, maximum rates of 2.5 to 50 m/day in the last 1 to 2 hours prior to failure and "rapid" movement of the slide mass. This observation of increasing rate of deformation prior to failure is quite common in monitored failures in soil and rock slopes.

Hungr and Kent (1995) comment that most of the coal mines in British Columbia have criteria for closure of dumping operations based on the rate of deformation. Monitoring of the coal waste spoil piles (in British Columbia) indicates that deformations during active tipping, even if of large magnitude, and tension cracking do not necessarily indicate an impending failure condition. The deformation behaviour of the coal mine waste spoil piles (in British Columbia) that was considered as "normal" behaviour are:

- Rates of deformation during active tipping up to 1 to 1.5 m/day are not uncommon and do not necessarily indicate an impending failure condition (Hungr and Kent 1995; Campbell and Shaw 1978).
- Total crest displacements in excess of 9.1 m have occurred that did not lead to a slope failure (Campbell and Shaw 1978).
- Tension cracking at the crest is also a common feature of the coal waste dumps and is not an indication of impending instability (Nichols 1982).
- Foundation slope has a significant effect on the rate of deformation whilst precipitation has a negligible effect (Nichols 1982; Campbell and Shaw 1978). Monitored rates of deformation at one mine decreased significantly as the toe of the waste pile advanced onto a flatter slope (reduction in rate from average of about 0.7 m/day to less than 0.2 m/day as the toe advanced over a 27 degree slope to a 14 degree slope).

Deformation monitoring of coal mine waste spoil piles in South Wales and coking coal stockpiles at Hay Point, Australia is (or was) not undertaken. However, observations of failures indicate that "abnormally" large deformations and high deformation rates preceded the failure. The observations from South Wales, although similar in some ways to British Columbia, comment on the development of a distinctive "boot" shape or bulge at the toe of the spoil pile of failed slopes.

3.7.1.2 *Hydraulic Fill Embankment Dams*

Pre-failure deformation was observed at Fort Peck and Calaveras Dam. In both cases the failure occurred during construction. At Calaveras Dam, horizontal deformations had been recorded for some nine months prior to the failure and totalled some 1100 mm up to the day prior to failure. On 18 June 1917, some 600 mm of deformation occurred in 1.5 days and sluicing operations were shutdown for a period of time. After this date, further deformations occurred during periods of sluicing in the nine months leading up to the flow slide on 24 March 1918.

At Fort Peck Dam initial deformations were a result of shear displacements on slickensided bentonitic seams within the Bearpaw Shale formation underlying the alluvial, predominantly sand, embankment foundation. Over-night the upstream bank of the core pool had settled some 450 to 600 mm and continued up to the time of failure

and flow sliding at 1:15 pm that same day. Eyewitness reports (ENR 1939a) indicate the core pool began to settle slowly at first, and then at an increasing rate.

In both cases large deformations at an increasing rate of deformation were observed prior to the failure.

Table 3.17: Summary of pre-failure observations in coarse-grained loose fills

Case Study	Rate (m/day)	Observation / Comment	Reference
British Columbia (B.C.), general	30 (max) 3.5 (1 day prior)	Total cumulative displacements exceeding 10s of metres and rates up to 1 m/day do not indicate failure. Impending failure indicated by acceleration of crest displacement to rates of 1 to 5 m/day (up to 1 m/hour prior to failure).	Hungr and Kent (1995)
Fording, B.C. (22/6/72)	15 (hour prior) 1 (day prior)	Total displacement of about 8.5 m over period of 3 weeks (refer Figure 3.45).	Campbell and Shaw (1978)
Fording, B.C. (2/7/72)	2.5 (hour prior)	Total displacement of about 8.2 m over period of 6 days (refer Figure 3.45).	Campbell and Shaw (1978)
Fording, B.C.	-	Recorded rates up to 1.5 m/day and total crest displacements in excess of 9 m have not resulted in failure.	Campbell and Shaw (1978)
Quintette 1660, B.C. (9/9/85)	-	Large cracks several hours prior to failure. Major cracking and bulging not evident until just before failure.	Dawson et al (1998)
Greenhills Cougar 7, B.C. (11/5/92)	-	Cracks observed in dump face	Dawson et al (1998)
Fording South, B.C. (29/10/89)	25 to 30 (immed. prior) 2.4 (day prior)	Dump closed due to high rates of deformation on 24/10/89, 5 days prior to failure.	Dawson et al (1998)
Aberfan, Tip 7, Sth Wales (21/10/66)	30 to 50 (immed. prior)	Approx. 6 m crest settlement in 12 hours prior to the failure, 3 m in the last 1.5 to 2 hours. Deformations observed 3 to 6 months prior to failure.	Bishop et al (1969)
Aberfan, Tip 4, Sth Wales (21/11/44)	-	Bulging observed in months prior to failure. Some minor sliding before final failure.	Bishop et al (1969)
Cilfynydd, Sth Wales (5/12/39)	-	Deformation observed on day prior to failure. Survey suggests toe bulging well before failure.	Bishop et al (1969)
South Wales	-	Toe bulging a common observation of failed spoil piles. Pre-failure deformation observed at Maerdy (1911), Mynydd Corrwg Fechan (1963) and Pentre (1909).	Siddle et al (1996)
Peak Downs, Hay Pt., Aust. (3/2/77)	-	Longitudinal cracking observed on face of stockpile prior to failure.	Eckersley (1985)

B.C. = British Columbia, Canada

Hay Pt., Aust. = Hay Point, Australia

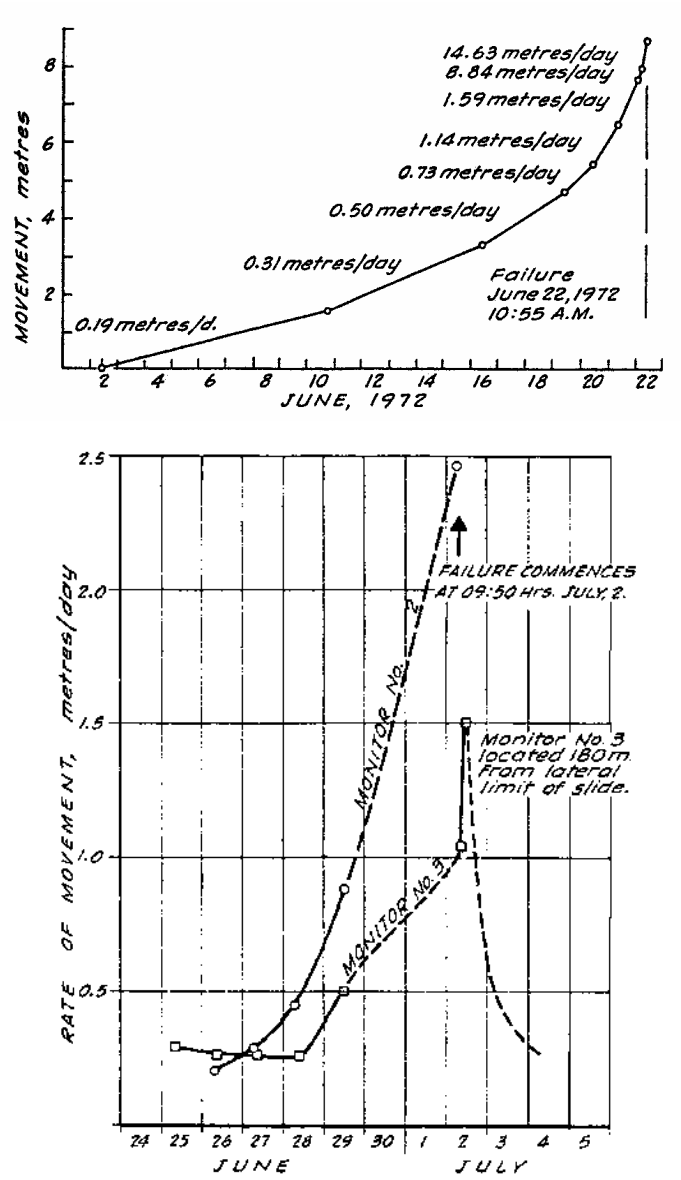

Figure 3.45: Pre-failure deformation of two separate failures at the Clode waste dump, Fording Coal, British Columbia (Campbell and Shaw 1978).

3.7.1.3 *Sensitive Clays*

As discussed in Section 3.4.3 retrogressive flow slides in sensitive clays generally develop from an initial failure, usually within a steep river or stream bank subject to active erosion. The pre failure deformation behaviour of interest is therefore associated with this initial slope failure.

Pre-failure deformation has been recorded for a small number of natural and man-made slopes in Canada (Mitchell and Eden 1972; Eden 1977; Mitchell and Williams 1981). The measured rates of deformation from six slopes adjacent to slopes that failed

are presented in Table 3.18. The deformation behaviour from these slopes is considered to be representative of deformation rates of the initial slide in similar slopes (and soil types) that can develop into large-scale retrogressive landslides. Tavenas (1984) comments that the increased rates of deformation observed in spring are associated with higher groundwater conditions following snowmelt and seasonal rainfall and therefore at effective stress states closer to a failure condition (i.e. at a reduced factor of safety).

The typical deformation profile within an instrumented slope (Figure 3.46) indicates the pre-failure deformation has developed within the soil mass rather than along a distinct shear band and also shows some rotation of the inclinometer tube. The analysis of failures in embankments on soft ground (Chapter 4) shows that a similar deformation profile is observed whilst embankment construction is in progress, and, for sensitive clay foundations, it is not until shortly prior to slope failure that shearing within a localised shear band is observed.

The recorded slope deformations (Figure 3.47) from an instrumented natural slope brought to failure by raising groundwater levels through recharge wells (Mitchell and Williams 1981) indicates that the rate of deformation is affected by the stress state within the slope. The onset to failure occurs several days prior to slope failure when the pore pressure ratio is increased from 0.43 to 0.47 and the rate of deformation increases markedly.

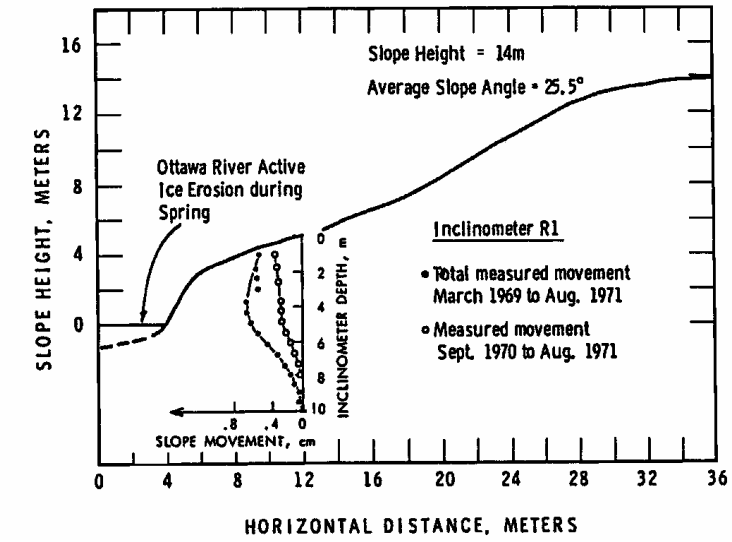

Figure 3.46: Measured deformations in a natural slope, Ottawa River (Mitchell and Eden 1972)

Table 3.18: Measured slope deformations adjacent to failures in the Ottawa area (Mitchell and Eden 1972)

Site of Inclinometer Monitoring							**Site of Recent Landslide**		
Location	**Description**	**Slope *[1]**		**Rate of Deformation (mm/year)**		**Time of Maximum Deformation**	**Description of failure**	**Slope *[1]**	
		Height (m)	**Angle (deg.)**	**3 year Average**	**Maximum Rate**			**Height (m)**	**Angle (deg.)**
Rockcliffe, R1	Natural slope (typical for bank)	14	26	2.5	25	Spring	6000 m^3, retrogressive, 1969	13	28
Green Creek, G1	Natural slope (typical), no toe erosion	19	28	1.1	35	Spring	6000 m^3, retrogressive, 1971	20	26
Breckenridge, B1	Natural slope, toe loading from recent landslide	29	27	Not known	70	Spring	23000 m^3, retrogressive, 1963	28	25
Rockcliffe, R2	Graded natural slope	13	20	13	700	After slope grading	23000 m^3, retrogressive, 1967	13	28
Green Creek, G2	Steep natural slope	15	35	2.7	25	Spring	1500 m^3, 1969 (monolithic?)	19	26
Breckenridge, B2	Natural slope, subject to rapid erosion. The slope failed.	28.5	22	-	500	Autumn	23000 m^3, retrogressive, 1963	28	25

Note: *[1] Slope angles are an average over the height of the slope.

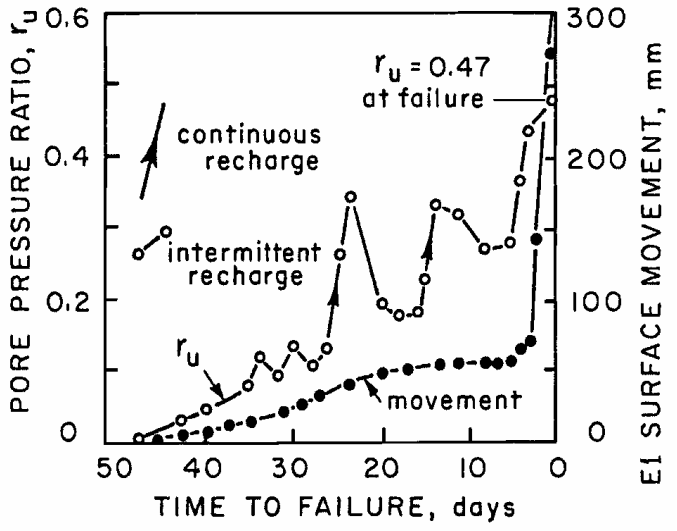

Figure 3.47: Deformation and pore pressure ratio of an induced slope failure (Mitchell and Williams 1981)

3.7.1.4 *Flow Slides in Other Soil Types*

No published records of pre-failure deformation prior to "rapid" landsliding could be found for flow slides in loose sandy and fine-grained fills (tailings dams, loose fills from Hong Kong) or natural slopes (submarine slopes, loessic soils and other colluvial soils). Based on the pre-failure deformation and failure mechanism from flow slides in other soil types, it is considered that:

- For flow slides that develop from an initial, essentially drained type failure within a slope of limiting stability, pre-failure deformation would be observable if monitored. This would apply to several failures in tailings dams and failures in submarine slopes where the initial failure occurred in the steep outer slope and was triggered by changes in effective stress. The initial failures of the tailings dams at Stava, Arturus, Saaiplass and Buffalo Creek were considered to be drained type failures of the outer slope triggered by high perched or groundwater conditions. Previous slope failure (Buffalo Creek) and toe sloughing (Merriespruit) confirmed the limiting stability of these slopes.
- For flow slides triggered by intense or heavy rainfall (loose fills in Hong Kong, and loessic and other colluvial soils) some, but very limited, pre-failure deformation would be expected due to changes in effective stress conditions during the rainfall period. During the rainfall event, leading up to failure, the stability of a slope would be expected to reduce to one of meta-stability due to the reduction in matrix suction

of the partially saturated soil and the development of perched water tables in these hydro-geologically complex slope profiles.

Laboratory undrained triaxial compression tests on loose fill materials derived from completely decomposed granite (HKIE 1998) indicates peak strengths were reached at small axial strains (1 to 2%) prior to the rapid onset of static liquefaction. This would indicate that limited pre-failure deformation occurs prior to failure in these loose fills. However, it is recognised that the effective stress path in these laboratory tests is not representative of the actual effective stress path that would be observed in the field.

3.7.2 "RAPID" LANDSLIDES FROM SLOPE FAILURES IN DILATIVE SOILS

3.7.2.1 *Slides Through Soil Mass – Dilative Failures*

No published records of pre-failure deformation prior to slope failure could be found for "rapid" landslides that developed from failures in dilative soil types; including the slides in natural and cut slopes in colluvial and residual soil profiles.

These slides are often triggered by intense or heavy rainfall. During the rainfall event the stability of a slope would be expected to reduce to one of meta-stability due to the reduction in matrix suction of the partially saturated soil and the development of perched water tables in these hydro-geologically complex slope profiles. Pre failure deformation would be expected to occur for these shallow dilatant failures due to changes in effective stress conditions; however, the amount of deformation is likely to be small.

These slides, particularly the shallow slides, generally occur during the period of rainfall. Rainfall based systems are used to warn of the potential for landslides in populated regions where the climate and topography make them susceptible to these types of failures (such as Hong Kong and Rio de Janiero). Due to high incidence and the wide spread occurrence of rainfall triggered landslides in these regions such systems are more appropriate than methods to monitor deformation.

3.7.2.2 *Defect Controlled Slides*

The case studies of defect-controlled slides (all from Hong Kong) occurred in saprolitic soils derived from the weathering of granite and volcanics (typically tuff). No formal deformation instrumentation was installed for monitoring of pre failure deformation behaviour. However, observations at several sites provide some indication that pre-failure deformation did occur. The observations were:

- Previous landsliding within or nearby to the reported failure in the months leading up to the reported landslide. This was observed in 3 of the 9 cases (Po Shan Road, 1972; Ching Cheong Road, 1997; Ka Wa Keng San Tseun (Slide A), 1997).
- Evidence of open joints or cracking that existed prior to the reported failure. This was observed in four cases (Po Shan Road 1972, Ching Cheong Road 1997, Ten Thousand Buddas Monastery 1997 and Allway Gardens 1993). All four were defect-controlled compound type landslides.
- Deformation and cracking in the days and weeks leading up to failure and "rapid" movement of the failed slide mass. This was observed at one site only (Po Shan Road, 1972) of the cases analysed. Pre-failure deformation was also observed at Cut CC2 at Ching Cheong Road in 1972 (50000 m^3 defect controlled compound slide).

The Po Shan Road landslide of 1972 (Vail 1972) comprised the failure of a cut slope in volcanic saprolite and a significant portion of the natural slope above the cut. The estimated volume of the landslide was 40000 m^3. It was a relatively deep failure for Hong Kong (6 to 16 m depth) and the surface of rupture indicates a compound slide consisting of a significant defect-controlled translational component with buttressing at the toe. The collapse of the slope was preceded by observations of deformation (cracking and sliding) in the nine months prior to the failure. In the days leading up to the failure cracking and deformations were observed on and above the cut slope. Although the deformation records are somewhat haphazard, it is considered that they indicate an increase in the rate of deformation leading up to the slope failure.

Glastonbury and Fell (2000) concluded that the defect-controlled translational and compound failures in rock slopes, that developed into "rapid" landslides, generally showed precursory warning of the impending collapse, mainly in the form of cracking, localised failures and increased noise, with greater warning for the compound slides. Pre failure deformation monitoring records were limited but indicated an increasing rate

of deformation generally over a period of days to months prior to collapse. They found a general trend of increasing pre collapse deformation with increasing failure volume.

The observational data for the defect-controlled slides in saprolitic soils are similar to those observed for the rock slides, even though the slide volumes are several orders of magnitude less. This is to be expected given the similar mechanism/s associated with failure. The findings also indicate that the warning signs are more prevalent for the compound slides.

3.7.3 SUMMARY OF PRE FAILURE DEFORMATION BEHAVIOUR

Pre failure deformation monitoring records of slope failures is limited to a handful of case studies of "rapid" post failure movement. Observational records of deformation and other pre failure warning signs are available for a larger group of the landslides.

Overall, pre failure deformation is considered to occur for all slides prior to failure in the form of acceleration in the rate of deformation. For a number of slide groups appropriately located deformation instrumentation is likely to provide sufficient warning of an impending failure. However, for a number of slide groups the total deformation associated with the onset to failure is likely to be small and the increase in rate of deformation obscured by deformation rate changes associated with changes in effective stress conditions. The characteristics of pre-failure deformation of slope failures that developed into "rapid" landslides are summarised in Table 3.19, and in summary:

- Slides through the soil mass triggered by intense rainfall were mostly of small volume and/or shallow slides. Pre-failure deformation is limited and likely to occur within the rainfall period. Rainfall based warning systems are useful in regions where these slide types occur.
- For compound type defect controlled slides of slide volumes greater than about 1000 to 2000 m^3, observational warning signs should be evident. Deformation monitoring should provide adequate warning of the impending failure.
- For translational type defect controlled slides, limited observational signs of the failure case studies suggests deformation monitoring may not provide adequate warning of the impending failure. However, there were only four case studies in the database (ranging in volume from 80 to 14000 m^3).

Table 3.19: Summary of characteristics of pre-failure deformation of slope failures that developed into "rapid" landslides

Initial Slide Classification	Slide Sub-Group	Total Deformation	Deformation Rates	Comments
Flow Slides in Contractile soils	Coarse-grained stockpiles	Large, in the order of metres for large volume slides	High (2.5 to 30 m/day)	For larger volume slides significant warning in terms of days to failure. Limited information on smaller volume slides from Hay Point.
	Hydraulic fill embankment dams (static trigger)	Large, up to 1 m	Medium	At least 0.5 to 1 day period of "abnormal" deformation prior to failure. Sudden and rapid increase in the rate of deformation at failure.
	Sensitive clays	Small	Very low (up to 1m/year ?)	Initial drained failure shows typical pre-failure increase in rate of deformation to failure. Small deformations and very low rates of deformation.
	Tailings dams	Not known	Not known	No records. Observations at failure were of piping induced failures.
	Loose sandy fills (sub-aerial)	Suspect very limited	Suspect very low	Hong Kong failures triggered by loss of suction and/or transient pore pressures during intense rainstorms. No observations, suspect very limited deformation.
Slides in Dilative soils	Slides through the soil mass	Suspect limited	Suspect low	Typically shallow slides in colluvial and residual soils, and predominantly in natural and cut slopes. Triggered by reduction in matrix suction and/or transient pore pressures due to rainfall, snowmelt. No observations, suspect limited deformation. Rainfall based systems provide better warning.
	Defect controlled slides	Not known. Suspect moderate to large (up to metres ?) Dependency on slide volume and slide type.	Not known	Compound slides show greater warning signs than translational slides. For compound slides the typical warning signs are cracking, opening of joints, previous sliding and acceleration in deformation in the days and weeks leading up to failure.

For flow slides in contractile soils it is concluded that:

- Pre-failure deformation is a pre-cursor to flow sliding in most cases where the trigger is due to static changes in effective stress (as opposed to dynamic trigger such as earthquake or blasting). The exceptions to this would be piping or over-topping induced failures of tailings dam embankments.

- The on-set to failure is evidenced by an increase in the rate of pre-failure deformation above that which could normally be expected due to increasing load (from active placement or construction) or from other changes in effective stress conditions such as increased pore water pressures.
- The rate of shear straining (and total deformation) required to induce undrained conditions, and therefore static liquefaction and flow sliding in undrained strain weakening soils, is strongly dependent on the permeability of the potentially liquefiable soil. Soils of higher permeability requiring greater rates of shear strain to induce undrained conditions (i.e., sandy gravel compared to a sensitive clay or silty sand).
- The undrained brittleness index, amount of potential volume contraction on shearing, size and complexity of the landslide will also affect the pre-failure rate of shear strain and total deformation.

With respect to the last point, the undrained brittleness index affects the rate of progression of the liquefied zone once liquefaction has been initiated along a portion of the surface of rupture. If the undrained brittleness index is small then the rate of progression of the liquefied zone will be slower. Complexity of the slide is the consideration of factors such as internal shearing for kinematic admissibility of the slide, three-dimensional effects, layering effects and variation in soil properties. The complexity of the slide mass is considered likely to increase with increasing volume, and the amount of pre-failure deformation increases with complexity (e.g., failure of Fort Peck Dam compared to Wachusett Dam, and Hay Point failures compared to say Aberfan). The amount of potential volume contraction (related to the relative density and undrained brittleness index) will affect the volume of pore fluid to be dissipated if drained conditions, and stability, are to be maintained. Soils with high volume contraction on shearing generate a greater volume of fluid to dissipate, which can lead to very rapid progression of a liquefaction condition on the surface of rupture.

For flow slides therefore, pre failure deformation and other warning signs of impending failure are more evident for the coarser material types within which liquefaction occurs (e.g. sandy gravels of the coal mine waste spoil piles) and the larger volume slides (excluding the retrogressive slides).

3.8 POST-FAILURE DEFORMATION BEHAVIOUR – REVIEW OF THE LITERATURE

3.8.1 FACTORS AFFECTING TRAVEL DISTANCE AND VELOCITY

The mechanics at failure of flow slides and defect-controlled landslides can give the sliding mass significant kinetic energy on failure and these slides can therefore develop high velocities in short distances from the slide source. As indicated by Hutchinson (1988), the degree of brittleness associated with the failure is a significant controlling factor in the generally high velocity of post failure movement of flow slides.

Locat and Leroueil (1997) comment that a logical approach to post failure behaviour would be to consider the energy balance in the post-failure stage, the basis of which is used in numerical models such as those developed by Hungr (1995). The components of the energy equation, as stated by Locat and Leroueil (1997), are:

$$E_p = E_f + E_d + E_v + E_k \tag{3.8}$$

where E_p, E_f, E_d, E_v and E_k are the potential, friction, disaggregation or fragmentation, viscous and kinetic energy respectively. However, it is difficult to estimate all these. For flow slides in strongly strain-weakening soils (i.e. with high undrained brittleness index) the frictional energy on the surface of rupture is significantly reduced once liquefaction has occurred leaving the failing mass with significant kinetic energy to quickly accelerate to very high velocities and therefore have the potential to reach very large travel distances.

Observations of the initiation of debris slides and debris flows on steep slopes indicate that these landslides also develop significant kinetic energy in the early stages of deformation and therefore quickly accelerate to reach relatively high velocities. In these cases the initial landslide is transformed into a "rapid" debris slide or debris flow due to strength reduction associated with incorporation of water, dilation, loss of cementing and remoulding, or due to a second phase of contractive shear of the loosened slide mass. For soil types where the strength is sensitive to small changes in moisture content (cohesionless and low cohesion materials) and it is possible for water to become readily entrained in the dilating soil mass, the transformation to a "rapid" debris slide or debris flow is generally observed to occur rapidly.

Once the landslide (or part thereof) has failed, the factors affecting travel distance and velocity of the slide mass are:

- Down-slope geometry, including the down-slope angle, changes in down-slope angle and degree of confinement. It will be shown, particularly for cut slopes (Section 3.9.3), sharp changes in down-slope angle (from steep to flat) dissipate the energy of the sliding mass thereby decreasing the velocity and travel distance, although scale effects are important.
- Confined debris flows tend to develop greater travel distance than those on unconfined or open slopes at a similar down-slope angle (Corominas 1996a; Golder Assoc. 1995).
- The presence of water. Water within the travel path will generally become entrained in the slide mass resulting in overall reduction in strength and greater travel distance. For mine tailings dams (Section 3.9.4.3 and 3.10.3) the presence of water can alter the flow behaviour.
- Volume of slide mass. Analysis of "rapid" slides (Corominas 1996a; Hutchinson 1988) indicates that the greater the slide volume the greater the travel distance (by virtue of the decrease in travel distance angle with increase slide volume).
- Material type of the slide mass. Cohesionless (or low cohesion) materials are more prone than cohesive materials to strength loss on entrainment of water (Johnson and Rodine 1984). Conversely, the rate of dissipation of pore pressures developed during flow or on initiation (flow slides) would be significantly lower in soils with high fines contents (finer than 75 micron), such as for sensitive clays compared to sandy gravels.
- Material mantling the down-slope. Dawson et al (1998) and Golder Assoc. (1995) comment that the travel distance of flow slides from coal waste stockpiles increased when the foundation soils were susceptible to strength loss on rapid loading from the slide mass. The soil types susceptible (Golder Assoc. 1995) were saturated (or near saturated), loose, finer grained soil deposits, particularly those with a high proportion of organic matter; i.e., those soils of relatively low permeability within which high pore water pressures can develop due to contraction on rapid (and high impact) loading. This excluded soils with a low degree of saturation (high pore pressures cannot be generated), high relative density (dilative under high impact loading) and coarse granular grading (i.e. free draining).

- Obstructions to the slide mass dissipate energy thereby decreasing the velocity and travel distance (Corominas 1996a).

For any specific group of "rapid" landslides (e.g. from dilatant slides in cut slopes, from flow slides in mine tailings dams, etc.), the dominant factors influencing the travel distance and velocity will vary. For flow slides in Canadian mine waste spoil piles Golder Assoc. (1995) concluded that the dominant influences on travel distance were the degree of confinement of the slide mass and the presence of potentially liquefiable materials mantling the down-slope. For flow slides in mine tailings dams the down-slope angle and presence of free water have a dominant influence. Where the down-slope angle is relatively flat (for flow slides in mine tailings), the flow is typically laminar; however, for down-slope angles steeper than about 5 to 7 degrees the flow behaviour of fluid tailings will become turbulent. Laboratory results (Blight 1997) indicate that the shear strength of the tailings is strongly dependent on the moisture content (Figure 3.83) and if water is present on the down-slope the basal portion of the flow (for laminar flow on relatively flat down-slope) will entrain the free water thereby reducing the shear strength and result in much greater travel distance.

There is also significant co-dependence between the factors affecting travel distance. For the post-failure behaviour of Canadian waste spoil piles Golder Assoc. (1995) the potentially liquefiable materials were generally located in confined valleys and therefore the very long travel distance events with low travel distance angle were for a group of confined flow slides where liquefiable materials were present in the gully region.

3.8.2 VELOCITY OF THE SLIDE MASS

Reported velocities of the slide mass for debris slides, debris flows and flow slides in soil slopes are summarised in Table 3.20, for the case studies analysed, and Table 3.21, for debris slides and debris flows from Corominas et al (1996) and Corominas (1996b). All rates of deformation are within the extremely rapid and very rapid classifications for landslides (IUGS 1995, refer Table 1.1).

Table 3.20: Velocity of the slide mass for "rapid" landslides from failures in soil slopes (mostly from case studies analysed).

Location	**Type of Slide (travel classification)**	**Velocity *[1] (m/sec)**	**Down-Slope Angle (degrees)**	**Comments**
Debris slides and debris flows (generally)		0.3 to 30	various	Refer Table 3.21 for sources.
Hong Kong	Flow slides in loose fill Debris flows Confined debris flows	5 to 15 8 to 15 9 to 24	18 to 30	DAN model (Hungr GR*[2] 1998; Ayotte and Hungr 1998)
Coal waste spoil piles - British Columbia	Flow slide - Confined - Unconfined	 30 to 60 (D), 4 to 27 (A) 20 to 40 (D)	typically 15 to 25 (initially)	various sources
Coal waste spoil piles - South Wales	Flow slide	3 to 10	10 to 13	Bishop (1973), Siddle et al (1996), Bishop et al (1969)
Hydraulic Fill Embankment dams	Flow slide	0.6 to 9	-2 to 2	Various sources
Tailings dams	Flow slide	2 to 25	0 to 8	Various sources
Quick clays	Flow slide	0.2 to 15	Not known	Various sources
Submarine slopes	Flow slide	0.8 to 8	Not known	Average rates. Edgars and Karlsrud (1983) and other sources.

Notes: Refer to summary tables in Section 1 of Appendix B for sources of information on specific slides

*[1] D = DAN model (Golder Associates 1995), A = actual

*[2] Hungr GR (1998) = Hungr Geotechnical Research (1998)

Two methods are available for prediction of velocity; they are prediction from simple sliding block models and from numerical continuum models.

The sliding block models, summarised by Fell et al (2000), analyse the sliding mass as a dimensionless lumped mass moving from the centre of gravity of the pre-failure position to the centre of gravity of the post slide position (Figure 3.48). The line connecting these two centres of gravity represents the kinetic energy head and its alignment is dependent on the type of rheological model used to model the movement of the sliding mass (Figure 3.48). The kinetic energy of the lumped mass at any point is represented by the vertical elevation of the kinetic energy head line above the slide path.

Assuming the resistance to motion is purely frictional (therefore the line joining the pre-failure and post slide centre of gravities will be a straight line) the kinetic energy of the slide mass equals $v^2 / 2g$, where v is the velocity of the centre of the slide mass, and

the velocity can be estimated. This method presents a relatively simple means of estimating the velocity, which does not properly model the loss of strength on disaggregation of the slide mass or the deposition/accumulation on the travel path. Simple sliding block models, tends to predict velocities higher than the actual estimated velocity.

Table 3.21: Velocity of slide mass for debris slides and debris flows

Reference	Slide Type	Velocity (m/s)	Comments
San Francisco Bay region – Ellen et al (1988), Wieczorek et al (1988), Howard et al (1988)	Debris flows in sandy soils Debris slides in clayey soils	8 to 22 metres/min	High velocities in granular soil types. Much lower velocities for medium to high plasticity silts, sandy clays and clayey sands
Hutchinson (1988)	Debris flows and flow slides	Max. 30	Velocity increases with increasing slope angle and decreases with increasing clay content
Johnson and Rodine (1984)	Debris flows	3.5 to 11	Source area slope angle 20 to 45 degrees
Pierson and Costa (1987)	Dry and wet debris flows	0.1 to 35	
Terzaghi (1950) *[1]	Debris flows	3 to 4.5	
Curry (1966) *[1]	Debris flows	< 16	
Johnson and Hampton (1969)*[1]	Debris flows	3.5 to 12	
Morton (1971) *[1]	Debris flows	0.5 to 3.5	
Campbell (1975) *[1]	Debris flows	0.3 to 12	Source area slope angle 22 to 45 degrees
Sauret (1987) *[1]	Debris flows	0.5 to 15	
Bovis (1993) *[1]	Debris flows	5 to 10	
Lowe (1993) *[1]	Debris flows	0.3 to 12	
Corominas (1996b)	Debris slides and debris flows	< 16	Initiating from "slides of debris"

Note: *[1] sourced from Corominas et al (1996), mostly confined debris flows

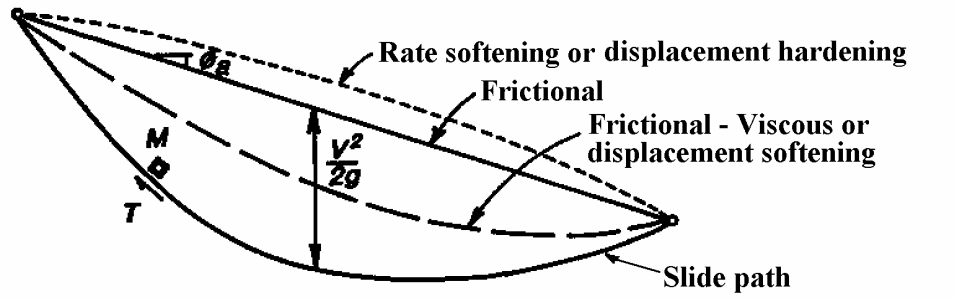

Figure 3.48: Sliding block model showing kinetic energy lines for different rheological models (Golder Assoc. 1995).

Better methods of prediction of velocity use numerical continuum models that have been calibrated against historical events of "rapid" sliding in similar soil types with similar morphological, topographical and climatic conditions within a consistent rheological framework that can then be applied to prediction of identified potential landslides.

The results of numerical continuum modelling (by Hungr in association with others) using the DAN program for "rapid" landslides from slope failures in Hong Kong and coal mine waste spoil piles in British Columbia are discussed in Section 3.10. They found that:

- The frictional model gives reasonable predictions of velocity for slide masses travelling on open and partly confined travel paths.
- For confined travel paths the frictional model predicts much higher velocities than estimated velocities of the actual slide. The Voellmy model (frictional – turbulent model) provides better predictions of velocity for confined travel paths.

3.8.3 EMPIRICAL METHODS FOR ASSESSMENT OF TRAVEL DISTANCE

The available empirical methods for assessment of travel distance originated from work on very large landslides by Heim (1932), Scheidegger (1973) and Abele (1974) who recognised that the travel distance angle of the slide debris reduced with increasing volume. Empirical equations of the form of Equation 3.11, derived from historic events, could be used to predict the travel distance angle (Figure 3.49) of a potential landslide based on estimation of the slide volume. The travel distance could then be predicted by application of the travel distance angle to the slope geometry (Figure 3.49) and the velocity could then be assessed from the kinetic energy of the slide mass (Figure 3.48). Hsü (1975), Sassa (1988), Van Gassen and Cruden (1989), Hutchinson (1986), Koerner (1977), amongst others, further developed the understanding of travel behaviour of the slide mass.

Empirical correlations (Equation 3.9) have also been developed for depositional area to slide volume for rock avalanches (Li-Tianchi 1983; Hungr 1990; Smith and Hungr 1992). Hungr (1990) used this approach, with the assumption of a simplified bi-linear travel profile (after Hsü 1975), for prediction of the excess travel distance, L_e (Figure 3.49), in the form of Equation 3.10. A review of these area to volume concepts shows

they seem to present no advantages over other methods (discussed further in Section 3.9.4.2).

$$A = cV^{n} \tag{3.9}$$

$$L_e = \left(R * c * V^{n}\right)^{0.5} \tag{3.10}$$

where A = depositional area (in square metres), V = slide volume (in cubic metres), c and n are constants, and R, the spreading ratio, is a measure of the degree of lateral spreading of the deposit.

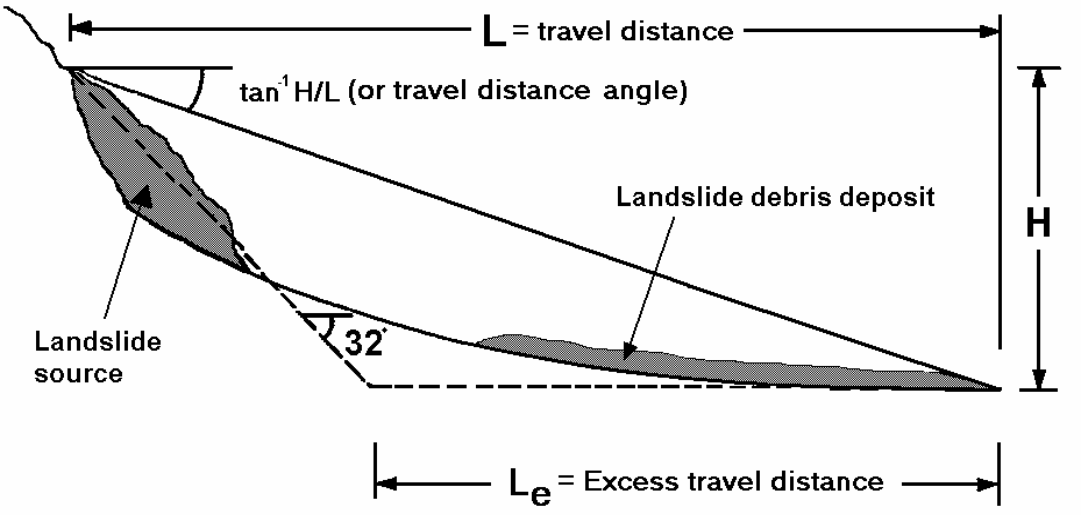

Figure 3.49: Schematic profile of a slope failure showing travel distance and travel distance angle

For this review though, of interest is the research relevant to smaller volume slides more typical of landslides in soil slopes.

Wong and Ho (1996) analysed the post-failure movement of forty-two landslides in cut slopes on Lantau Island (Hong Kong) following the severe rainstorm of November 1993. They compared the travel distance beyond the toe of the cut slope, R, to the height of the slope, H_s, (Figure 3.50) and concluded that:

- For shallow landslides in cut slopes with a relatively flat ground slope at the toe of the cut, the travel distance (R) ranges from 0.33 to 1 H_s (average of 0.7 H_s).
- If the landslide incorporates a substantial portion of the slope uphill of the cut, R can increase to up to 1.5 H_s.

- For slopes below the toe of the cut slope greater than about 15 degrees, R exceeding 2 H_s is likely.

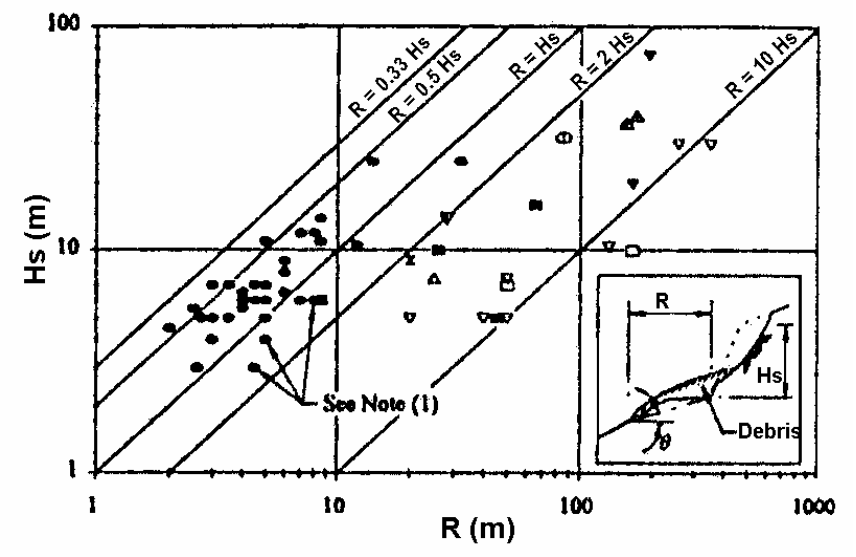

Legend :

Mechanism of Failure	θ				
	< 5°	5° - 15°	16° - 25°	26° - 35°	> 35°
Typical rain-induced landslide	●		▼	■	x
Liquefaction of loose fill	⊙	▲	▼		
Wash-out by convergent water flow		△	▽	□	

Notes : (1) Landslides involing failure of a substantial portion of the slope uphill of the cut face.
(2) This is a natural slope failure involving channelised debris flow.
(3) Unbulked landslide volume is used.

Figure 3.50: Travel distance from the toe of the cut, R, versus cut slope height, H_s, for failures in cut slopes from Lantau Island, Hong Kong (Wong and Ho 1996)

Corominas (1996a), from a database of 204 landslides in soil and rock and covering a volume range from small (less than 10 m^3) to very large, considered the mechanism of slide initiation and topographical constraints (including confinement of the slide mass and obstructions to the mass movement) as a means of prediction of the travel distance angle. His data (all 204 slides) is shown in Figure 3.51 and the results of statistical analysis are presented in Table 3.22 for a power law fit of the ratio H/L to volume (Equation 3.11) for various landslide groups. The results indicate there is significant scatter even within the various landslide groups and sub-groups.

$$H/L = AV^{B} \tag{3.11}$$

where H and L (in metres) are defined in Figure 3.49, V is the volume of the landslide mass (in cubic metres), and A and B are constants.

The degree of scatter, particularly for small volume landslides, is emphasised from the results of Finlay et al (1999) shown in Figure 3.52 for landslides that break-up on sliding. The range of travel distance angle is very large at the small volume end of the scale and reflects the significantly greater influence of factors other than volume on travel distance angle. Fell et al (2000) comment that the large range of travel distance angle for the smaller volume landslides (from Hong Kong) reflect the different mechanisms of failure and the degree of obstruction. The very low travel distance angles for some fills being associated with liquefaction and flow sliding or wash-out (surface water flow over the fill), and the high values representing cases of dilatant failure or falls from very steep cut slopes.

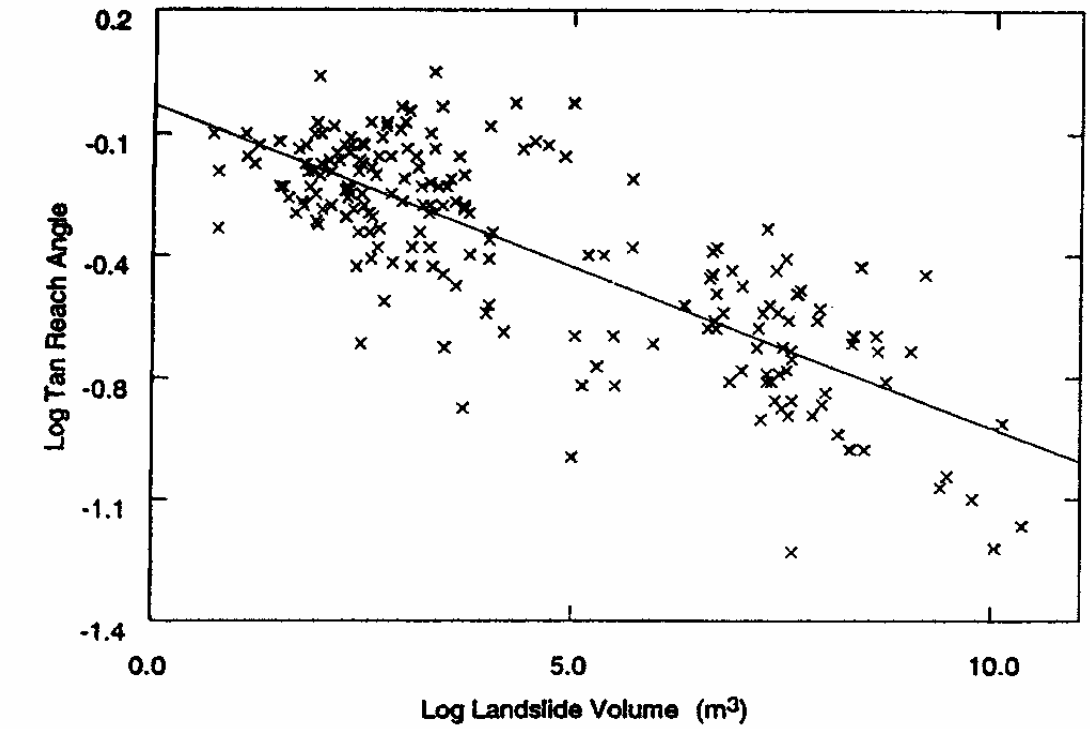

Figure 3.51: Landslide volume versus tangent of the travel distance angle for 204 landslides (Corominas 1996a)

Table 3.22: Regression analysis of *H/L* (Equation 3.11) versus landslide volume (Corominas 1996a)

Landslide Type	Number of Slides	Path Type	A	B	R^{2} (*1)	Standard Error *2
All landslides	204	All	0.897	-0.085	0.625	0.161
Rockfalls	47	All	1.622	-0.109	0.759	0.123
	16	Unobstructed	1.469	-0.119	0.924	0.073
Translational slides	69	All	0.693	-0.068	0.670	0.137
	42	Unobstructed	0.719	-0.080	0.796	0.115
Debris flows	71	All	0.972	-0.105	0.763	0.137
	19	Confined	0.838	-0.109	0.690	0.171
	18	Unobstructed	0.931	-0.102	0.868	0.093
Earthflows and mudslides	17	All	0.611	-0.070	0.648	0.131
	8	Unobstructed	0.603	-0.138	0.908	0.074

*1 R^2 is the regression coefficient of the statistical correlation between *H/L* and slide volume

*2 The standard error applies to log *H/L* and not *H/L*.

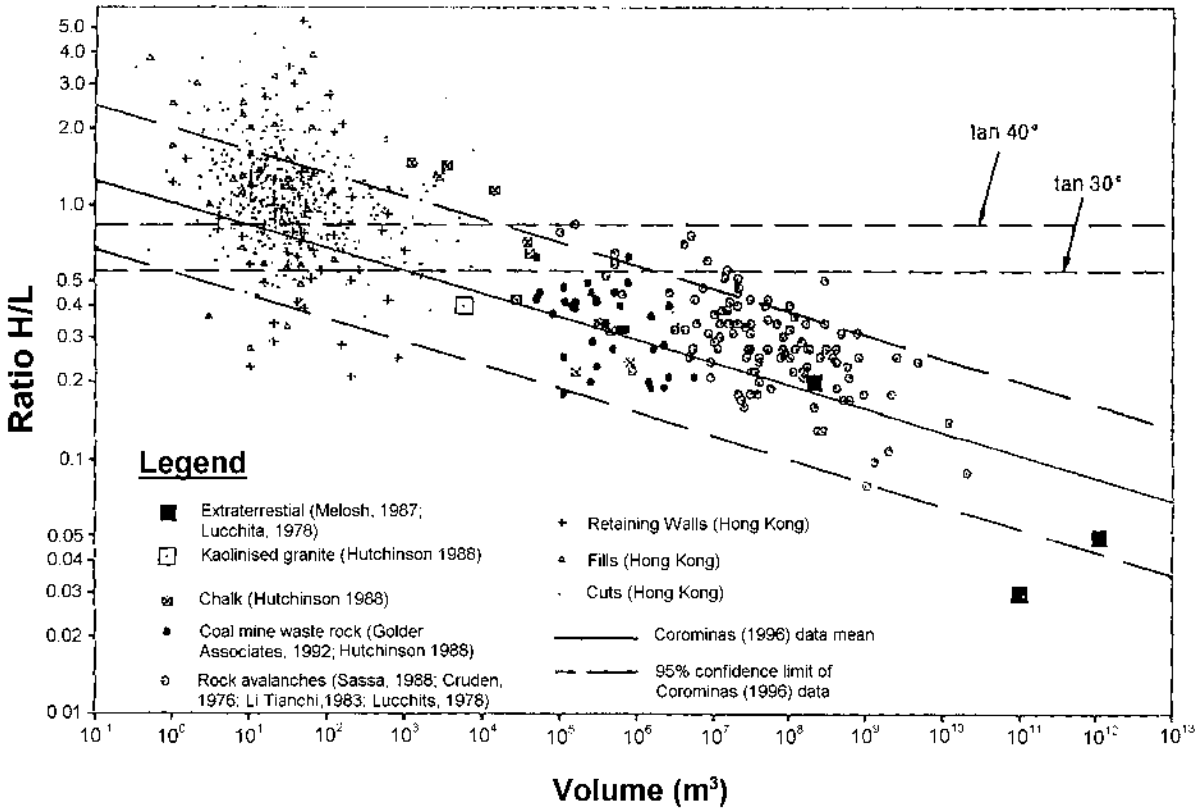

Figure 3.52: Ratio *H/L* versus volume for landslides that break-up on sliding (Finlay et al 1999)

3.9 POST-FAILURE DEFORMATION – DEVELOPED METHODS FOR ASSESSMENT OF TRAVEL DISTANCE FROM THE DATABASE

In the following sections the results of empirical analyses from the database are presented, with the purpose of providing empirical correlations for prediction of travel distance angle that are useful of "rapid" landslides. The analyses concentrate on the smaller volume (less than 10^6 to 10^7 m^3) sub-aerial landslides, as these slides are of greater concern to engineers and engineering geologists dealing with soil slopes, within the following material and slope types:

- "Rapid" landslides from failures in dilative soils in cut slopes.
- "Rapid" landslides from failures in dilative soils in natural slopes.
- "Rapid" landslides from failures in contractive soils (flow slides) in loose silty sand to sandy silt materials.
- "Rapid" landslides from failures in contractive soils (flow slides) in loose dumped sandy gravels.
- "Rapid" landslides from failures in contractive soils (flow slides) from tailings dams, in sensitive clays and in hydraulic fill embankment dams.

As will be shown, useful empirical predictive methods require consideration of the factors influencing the travel, as outlined in Section 3.8.1; in particular the failure mechanism, material type, mechanism of post-failure movement, degree of confinement and down-slope geometry. Within each sub-group of "rapid" landslides it is considered that the dominant factors affecting travel distance vary, and these are discussed in the following sub-sections.

For larger volume (volumes greater than 10^6 m^3) "rapid" landslides in rock slopes Glastonbury et al (2002) discuss the dominant factors influencing travel distance and provide guidelines for prediction of travel distance angle (and travel distance).

The statistical analyses undertaken on any set of data initially comprised a test of significance to determine if the null hypothesis was acceptable (i.e. no correlation exists) or could be rejected (i.e. accept the correlation exists) using a 95% confidence interval for the null hypothesis. If the null hypothesis was rejected the goodness of fit of the correlation can then assessed by the regression coefficient (R^2), the higher the value of R^2 the better the correlation, although the number of data points within the data

set does have a significant influence on R^2. The following general terms have been adopted to describe the significance of correlation between factors based on R^2 values:

- $R^2 < 0.3$ Poor correlation
- $R^2 = 0.3 – 0.5$ Minor correlation
- $R^2 = 0.5 – 0.65$ Moderate correlation
- $R^2 = 0.65 – 0.80$ Good correlation
- $R^2 > 0.80$ Excellent correlation

3.9.1 TRAVEL DISTANCE VERSUS SLIDE VOLUME AND INITIAL SLIDE CLASSIFICATION

Figure 3.53 presents the ratio of *H/L* (tangent travel distance angle) versus volume for all slides from the database. It includes the approximate limits of the data from Finlay et al (1999) for small volume landslides in Hong Kong and the mean and 95% confidence limits for all slides by Corominas (1996a). The slides analysed as part of this study have been grouped based on the initial landslide type (i.e. flow slides in contractile soils and the remaining groups as dilative soils) and then sub-grouped based on factors considered to dominantly influence the travel distance angle. It is evident from Figure 3.53 that, whilst a general trend of reducing *H/L* with increase in volume is evident there is considerable scatter in the data.

Significant departure outside the Corominas (1996a) confidence limits occurs for the small volume landslides from Hong Kong (Finlay et al (1999) data) and for the strongly retrogressive landslides (hydraulic fills, sensitive clays and sub-aqueous slopes). Some sub-groups generally plot below the Corominas mean (flows slides in loose fills from Hong Kong, flow slides in coking coal stockpiles and confined debris flows) and some sub-groups above (cut slopes). The confidence limits and data for the smaller slide volumes in the range most appropriate to engineers and engineering geologists (less than about 10^6 m^3) cover a broad range of travel distance angle, thereby limiting their usefulness.

Corominas (1996a) presented data for small and large volume landslides combined, which had high regression coefficients indicating a good to excellent correlation between *H/L* and slide volume. However, further analysis of the Corominas (1996a) data for debris flows shows (Table 3.23, Figure 3.54 and Figure 3.55) that when the small volume landslides (less than 10^6 m^3) are analysed separately the regression

coefficients are significant lower and statistically the correlation is a lot weaker. No correlation was evident for the confined debris flows.

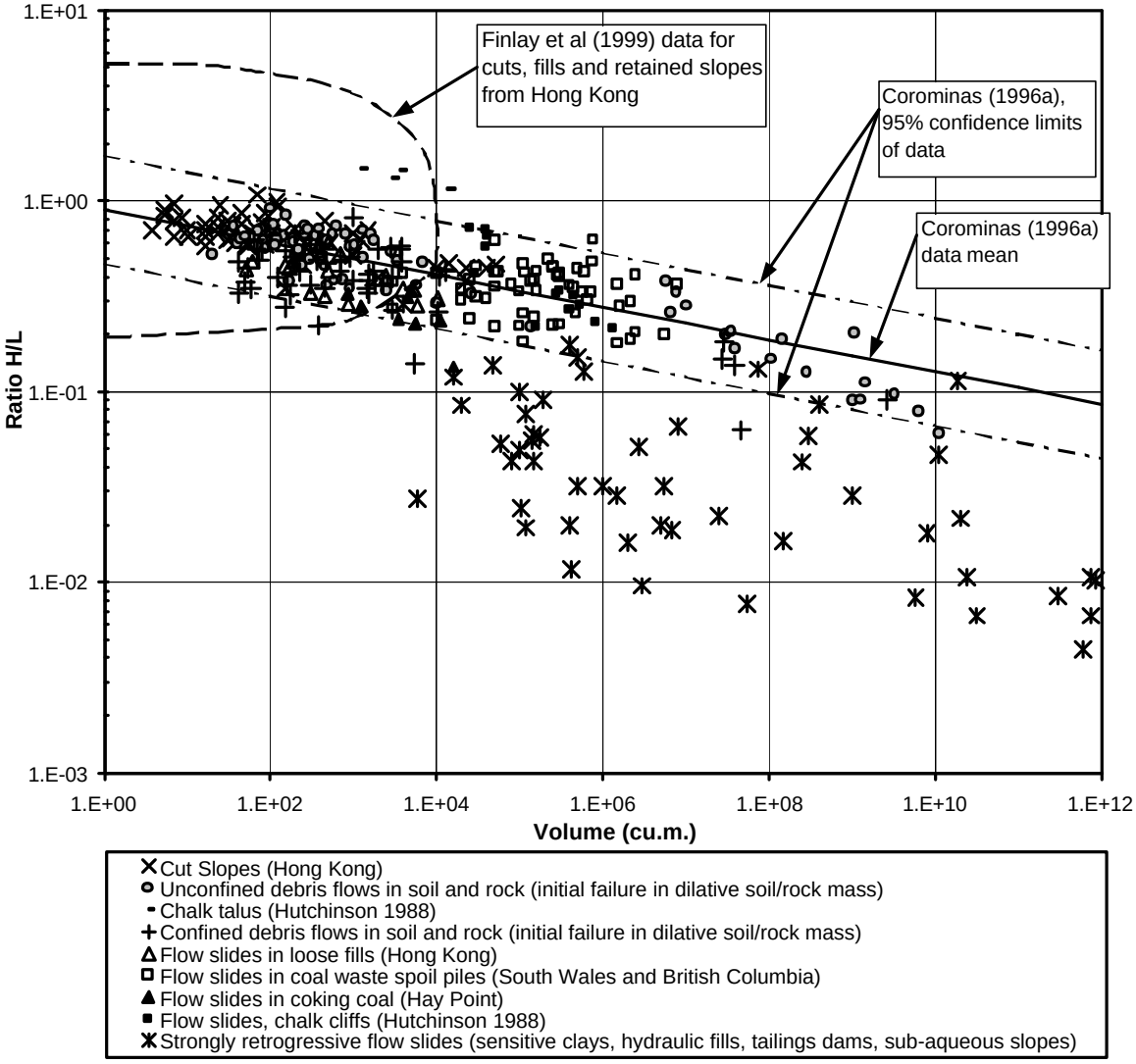

Figure 3.53: Ratio *H/L* versus volume for all slides from database.

Table 3.23: Summary of empirical correlation coefficients (Equation 3.11) for debris flows by Corominas (1996a)

Travel Classification	Volume Range (m^3)	Number of Slides	A	B	R^2	Std. *[1] Error	Comments
All Debris Flows	$< 1.2x10^{10}$	70	1.005	-0.1056	0.76	0.137	Good correlation
	$< 10^6$	56	1.155	-0.1289	0.37	0.122	Minor correlation
Unconfined Debris Flows	$< 1.2x10^{10}$	51	1.028	-0.1002	0.82	0.110	Excellent correlation
	$< 10^6$	42	1.158	-0.1219	0.46	0.094	Minor correlation
Confined Debris Flows	$< 3x10^9$	19	0.866	-1.095	0.69	0.171	Good correlation
	$< 10^5$	14	0.774	-0.0933	0.13	-	No correlation

Note: *[1] The standard error applies to log *H/L* and not *H/L*.

In Figure 3.54 and Figure 3.55 the *H/L* axis is presented in normal scale to highlight the broad scatter around the trendline at small volumes compared to the lesser degree of scatter at larger volumes. It is evident therefore; using correlations of this type for prediction of the travel distance angle for small volume landslides can lead to significant errors.

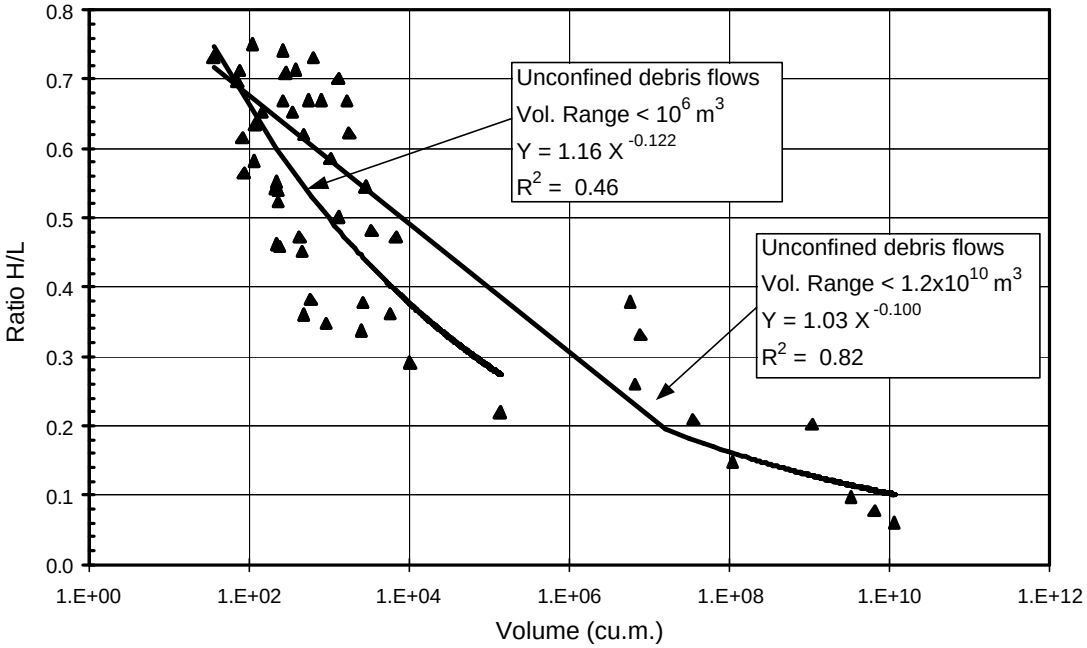

Figure 3.54: *H/L* ratio versus volume relationships for Corominas (1996a) data on unconfined debris flows.

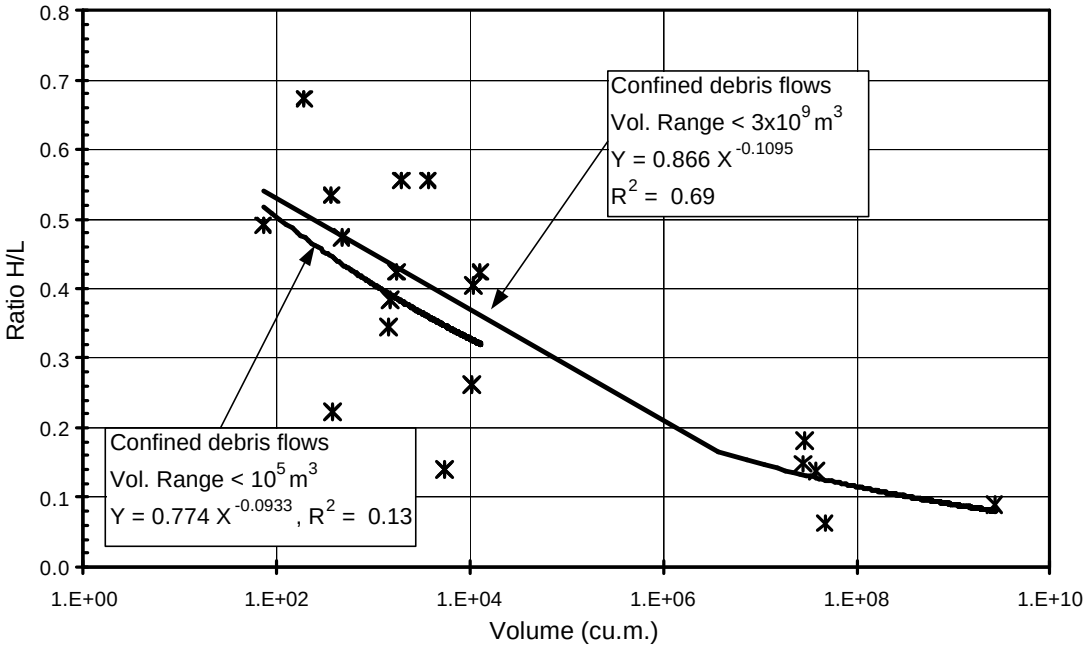

Figure 3.55: *H/L* ratio versus volume relationships for Corominas (1996a) data on confined debris flows.

3.9.2 TRAVEL DISTANCE VERSUS SLIDE VOLUME, DEGREE OF CONFINEMENT OF THE TRAVEL PATH AND INITIAL SLIDE CLASSIFICATION

3.9.2.1 Travel Distance Beyond the Toe of the Source Area Versus Degree of Confinement

Prior to presenting the results of the analysis in terms of the ratio *H/L*, the effect of degree of confinement on the horizontal distance of travel beyond the toe the source area is discussed; the purpose being to provide an indication of the actual distance of travel of the slide mass. For unconfined travel paths the case study data is presented in Figure 3.56 and for confined and partly confined travel paths in Figure 3.57. Strongly retrogressive slide types have been excluded.

The findings indicate that the horizontal distance of travel beyond the toe of the source area increases with increasing slide volume. The distance of travel for confined travel paths is greater than for unconfined travel paths of similar volume, in the order of 3.5 to 4.5 times for slide volumes in the range 10^3 m^3 to 10^6 m^3. For most unconfined travel paths the horizontal distance of travel beyond the toe of the source area is less than 100 m for slide volumes up to 10,000 m^3.

The trendlines in Figure 3.56 and Figure 3.57 are not intended for use in prediction of the travel distance as they do not consider many of the factors known to influence the travel of the slide mass. The data serves merely to indicate that, in general, confined travel paths result in greater distances of travel beyond the source area. The overall trend with slide volume is to be expected, however, when considering a specific slide type the correlation is quite poor in most cases. The better correlations are obtained where the slide is within a particular material type, and the slope of the travel path and height of the source area is similar, e.g. the flow slides in stockpiled coking coal at Hay Point.

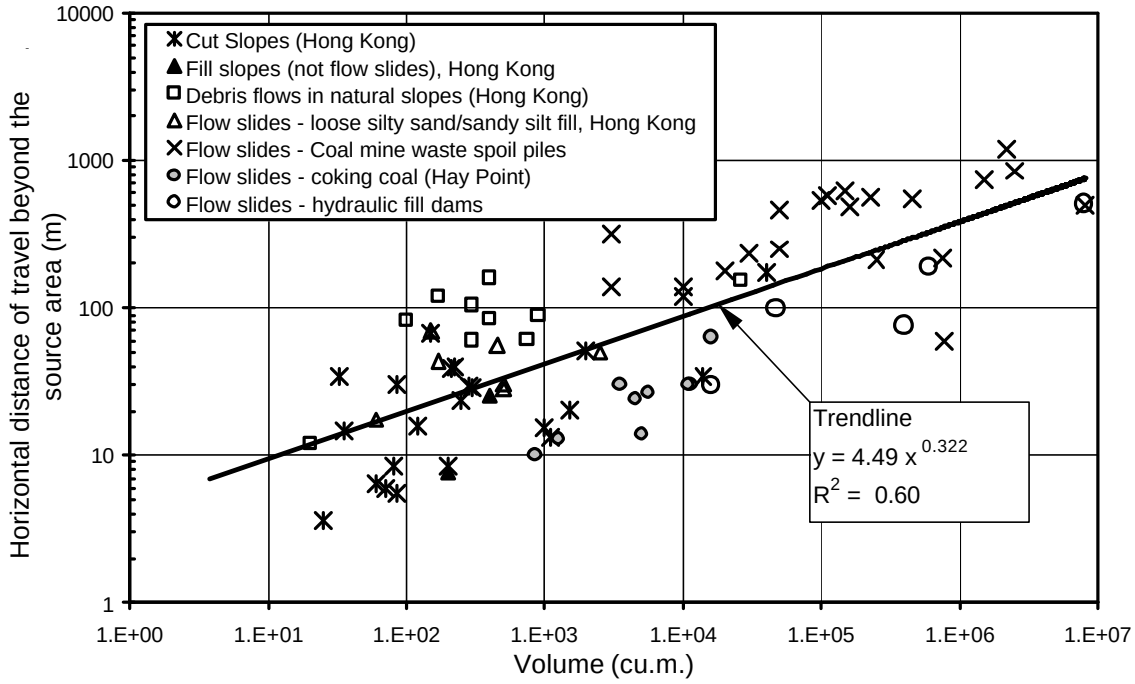

Figure 3.56: Travel distance beyond source area versus volume for unconfined travel paths.

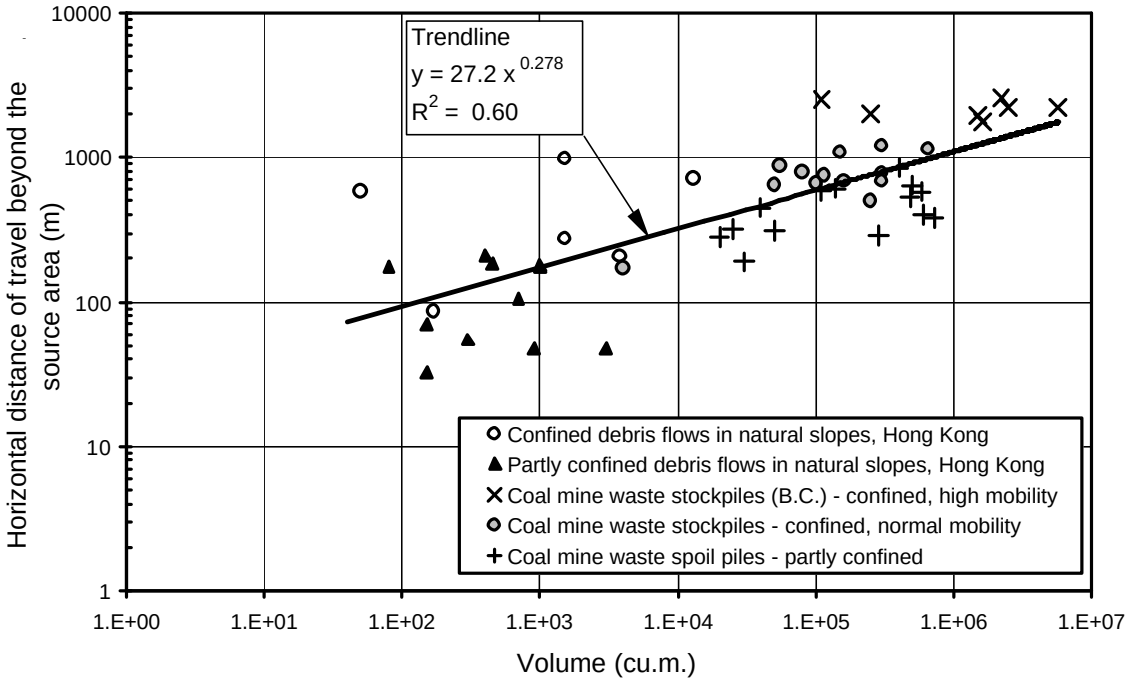

Figure 3.57: Travel distance beyond source area versus volume for confined and partly confined travel paths.

3.9.2.2 Travel Distance Versus Degree of Confinement of the Travel Path

Within this section, the data has been analysed to assess the influence of the degree of confinement of the slide mass in the travel path (in combination with slide volume) on the travel distance angle. Travel paths have been sub-divided into confined, partly confined and unconfined. Excluded from this analysis are the strongly retrogressive landslides (tailings dams, sensitive clays and sub-aqueous slides), hydraulic fill embankment dams, sturzstroms, chalk talus and Corominas (1996a) debris flows greater than 10^6 m^3 in volume. The flow slides from chalk cliffs and in coking coal stockpiles have been included but are considered as special groups.

Plots of the data are presented in the format *H/L* (normal scale) versus slide volume (log scale). The purpose of presenting the plots in this format is so that the variation around the trendline is more clearly evident than log-log plots.

The trendlines of travel distance angle versus slide volume and degree of travel path confinement (Figure 3.58) for "rapid" landslides from failures in dilative soils from Hong Kong (trendlines from Figure 3.59 to Figure 3.63) indicate that, in general, the greater the degree of confinement the lower the travel distance angle for a given slide volume. This finding is in agreement with the data for other landslide specific groups (e.g. flow slides in coal waste spoil piles from British Columbia) and the research findings of others (Corominas 1996a; Golder Assoc. 1995; Wong and Ho 1996; Evans et al 1997).

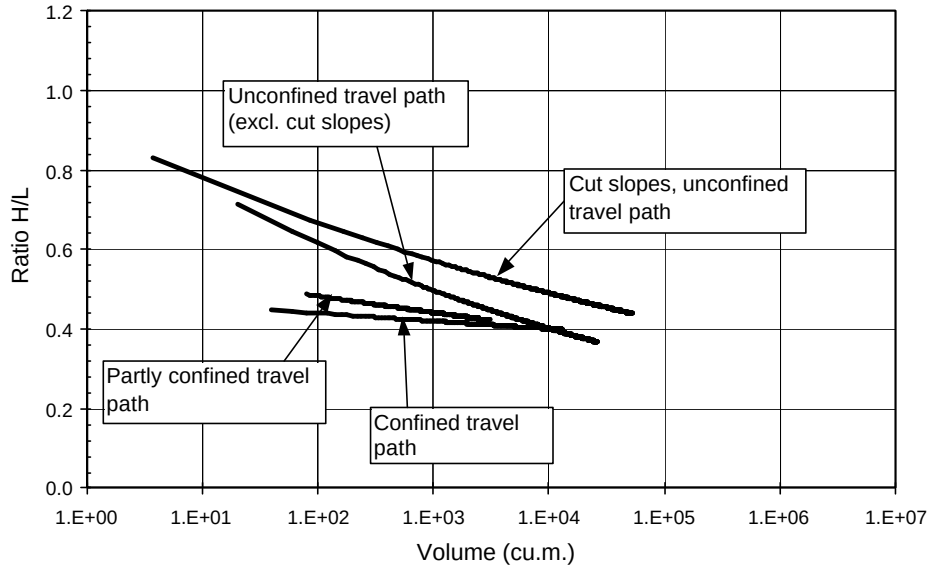

Figure 3.58: Comparison of trendlines of *H/L* versus slide volume differentiated on travel path confinement for "rapid" landslides from failures in dilative soils, from Hong Kong.

Figure 3.59 to Figure 3.61 present the *H/L* ratio versus slide volume for unconfined travel paths (or travel on open slopes) of "rapid" landslides from failures in soil slopes. Table 3.24 presents a summary of the empirical analyses for a power law fit between travel distance angle and slide volume (in the form of Equation 3.11) for various data groupings based on degree of confinement of the travel path, mechanism of failure, slope type and material type.

The results indicate that for unconfined "rapid" landslides from sub-aerial slopes there is a general trend of decreasing travel distance angle with slide volume. However, within any individual sub-group the slope type, failure mechanism and material type have a strong influence on the travel distance angle. The correlations between *H/L* and volume (Table 3.24) generally range from no correlation to minor. For the larger data sets the regression coefficients are generally higher, however, there is generally a large degree of scatter around the trendline.

The flow slides in loose contractive fills have significantly lower travel distance angles than dilatant failures in fill and also cut slopes (Figure 3.59), even though the soils are from similar origins (all cases from Hong Kong). The potentially high degree of brittleness at failure and therefore initially high kinetic energy of the slide mass, and travel on a low undrained strength liquefied basal layer for these flow slides in fine grained contractive soils is the likely explanation for the lower travel distance angles. Flow slides in the coarser soil types (sandy gravels to gravelly sands in coal mine waste spoil piles) appear to have a travel distance angle to volume correlation more in line with those of the dilative soil types (Figure 3.59), although there is little overlap in the volume range of these slide groups to confirm this. Explanation for this observation could be that for these failures (flow slides in coarser materials) the undrained brittleness index could be lower than for the finer silty sands (as indicated by the laboratory results of Dawson (1994) and Eckersley (1986)) and that these materials have a much higher permeability and therefore have greater potential for dissipation of pore pressures during flow.

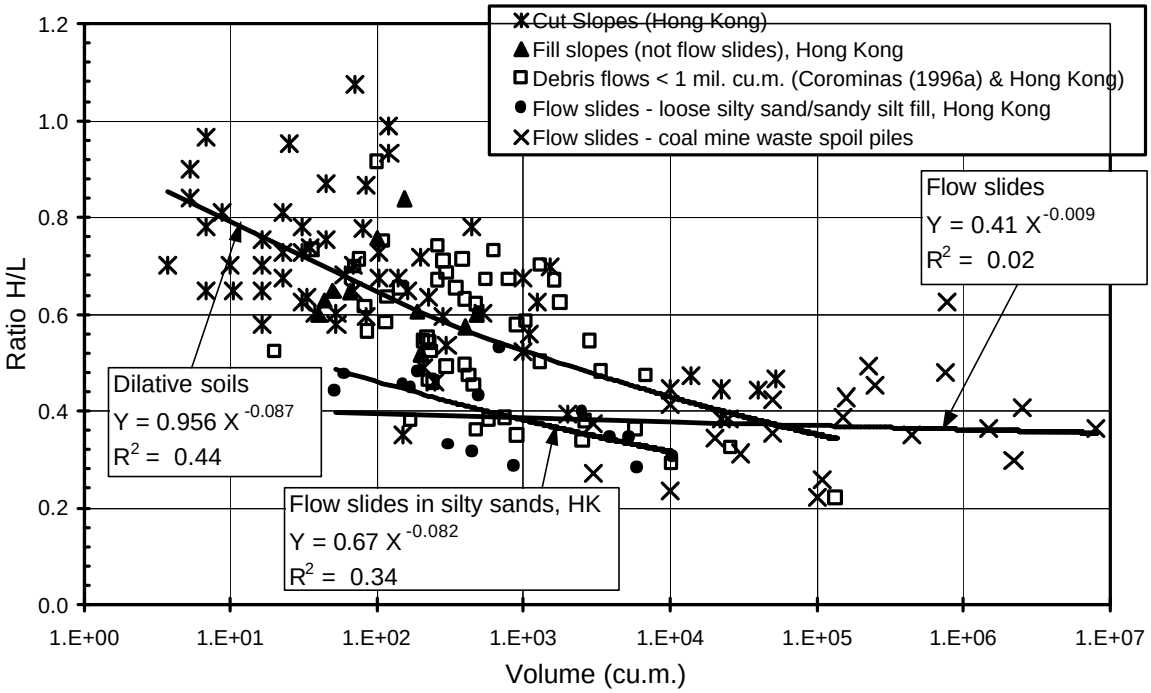

Figure 3.59: *H/L* versus volume for "rapid" landslides with unconfined travel paths.

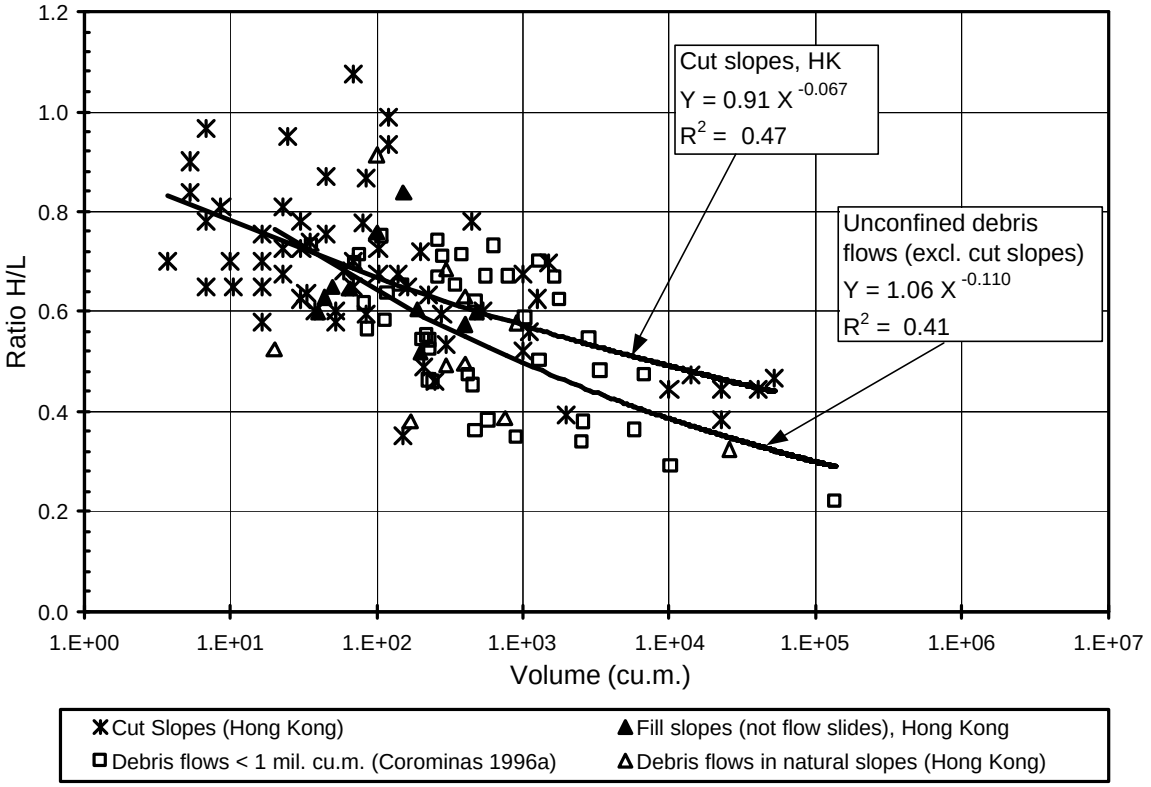

Figure 3.60: *H/L* ratio versus volume for "rapid" landslides from failures in dilative soils with unconfined travel paths.

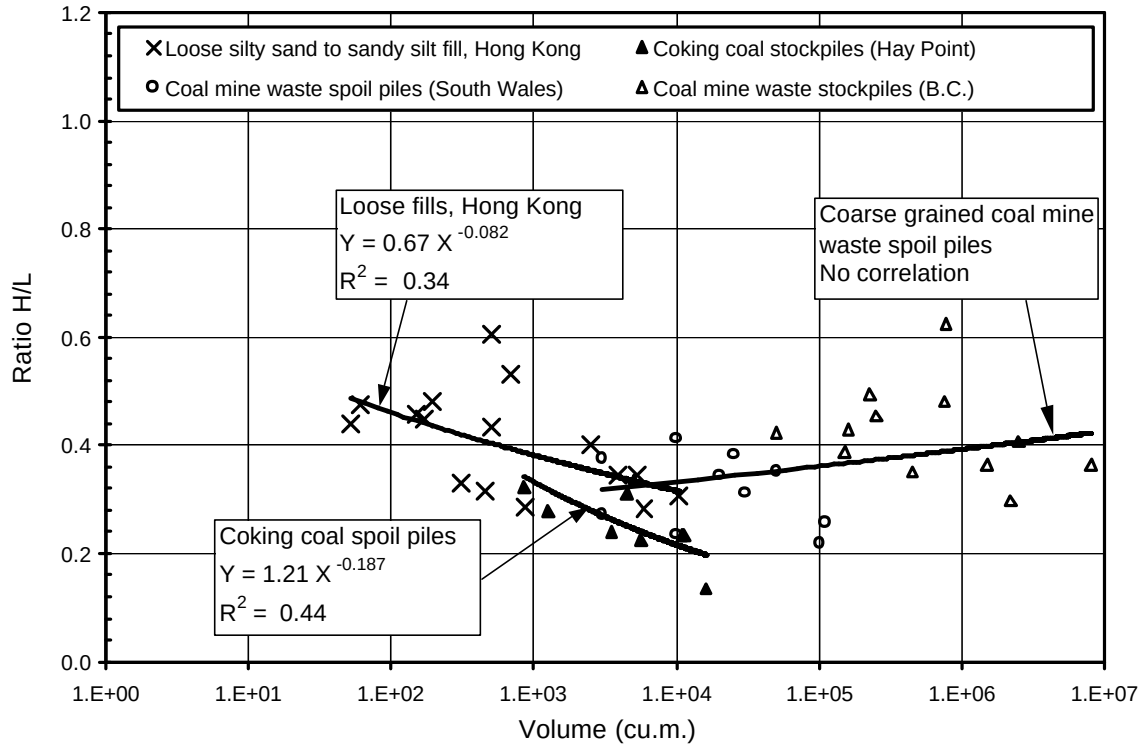

Figure 3.61: *H/L* ratio versus volume for "rapid" landslides from failures in contractive soils (flow slides) with unconfined travel paths.

Table 3.24: Empirical correlation coefficients for power law fit of travel distance angle to slide volume (Equation 3.11, $H/L = AV^B$) for unconfined "rapid" landslides.

Initial Landslide Type	Sub-group	Volume Range (m^3)	No.	A	B	R^2	Std. *[2] Error	Comments
All Unconfined Travel Paths	All (excl. coking coal & chalk cliffs)	< $8x10^6$	161	0.848	-0.072	0.47	0.108	Minor to moderate correlation (but large scatter)
Slides in Contractile Soils (Flow Slides)	Silty sand fill and coal mine waste	50 to $8x10^6$	38	0.412	-0.009	0.02	-	No correlation
	Loose silty sand fill (Hong Kong)	50 to 10,500	16	0.671	-0.082	0.34	0.085	Minor correlation
	Coal mine waste	3000 to $8x10^6$	22	0.238	0.036	0	-	No correlation
	Coking Coal	850 to 16,000	9	1.209	-0.187	0.44	0.096	Minor correlation
Slides in Dilative Soils*[1]	All	< 136,000	123	0.956	-0.087	0.44	0.090	Minor correlation
	All (excl cut slopes)	20 to 136,000	62	1.063	-0.110	0.41	0.093	Minor correlation
	Cut slopes (Hong Kong)	4 to 52,000	61	0.908	-0.067	0.47	0.081	Minor to moderate correlation
	Fill slopes (Hong Kong)	40 to 500	10	0.748	-0.034	0.05	-	No correlation
	Natural slopes (Hong Kong)	20 to 26000	10	0.877	-0.088	0.27	-	No correlation
	Corominas (1996a)	36 to 136,000	42	1.158	-0.122	0.46	0.094	Minor to moderate correlation
Failures in Chalk Cliffs (Hutchinson 1988; Golder Assoc. 1995)		25,000 to $1.3x10^6$	13	10.98	-0.203	0.76	0.101	Good correlation

Note: No. = number of case studies

*[1] Inclusive of defect controlled slides, slides of debris and slides through the soil mass.

*[2] The standard error applies to log H/L.

Figure 3.62 and Figure 3.63 present *H/L* versus slide volume for confined and partly confined travel paths respectively of "rapid" landslides from failures in soil slopes. Table 3.25 presents a summary of the empirical analyses for a power law fit between travel distance angle and slide volume (in the form of Equation 3.11) for the confined and partly confined travel paths.

The results show a general trend of decreasing travel distance angle with slide volume for both the confined and partly confined travel paths; however, the correlations are poor to minor. The no to poor correlation between travel distance angle and slide volume for individual sub-group (Table 3.25), which indicates that factors other than or in addition to volume have a significant influence on the travel distance angle for confined and partly confined travel paths.

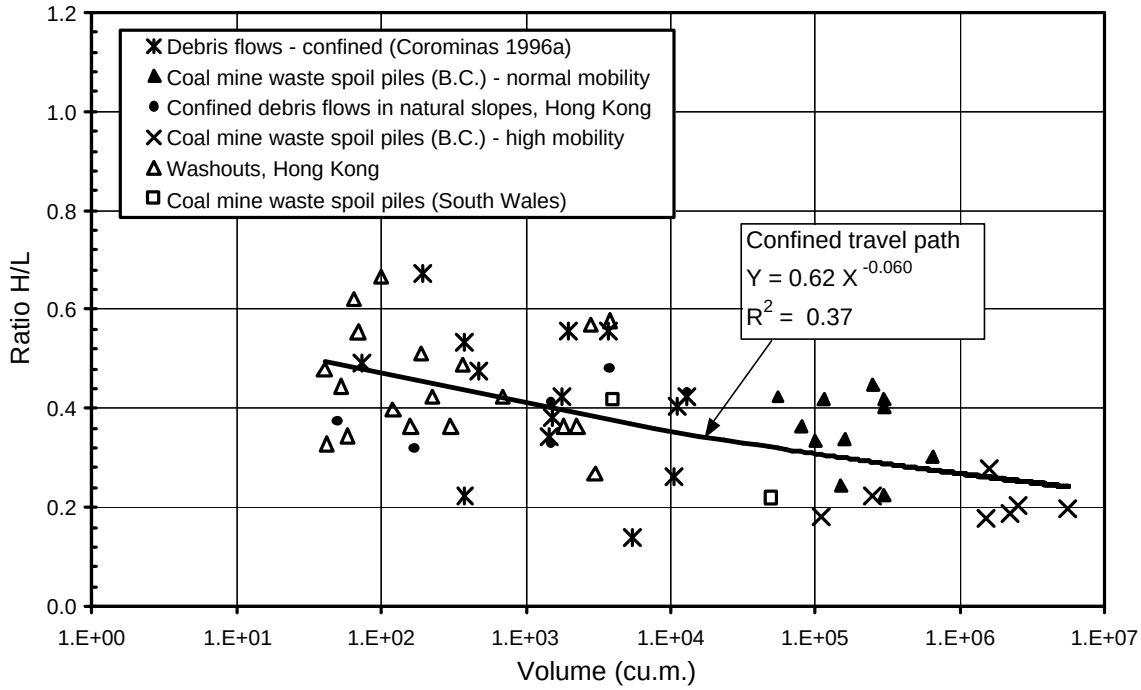

Figure 3.62: *H/L* versus volume for "rapid" landslides with confined travel paths.

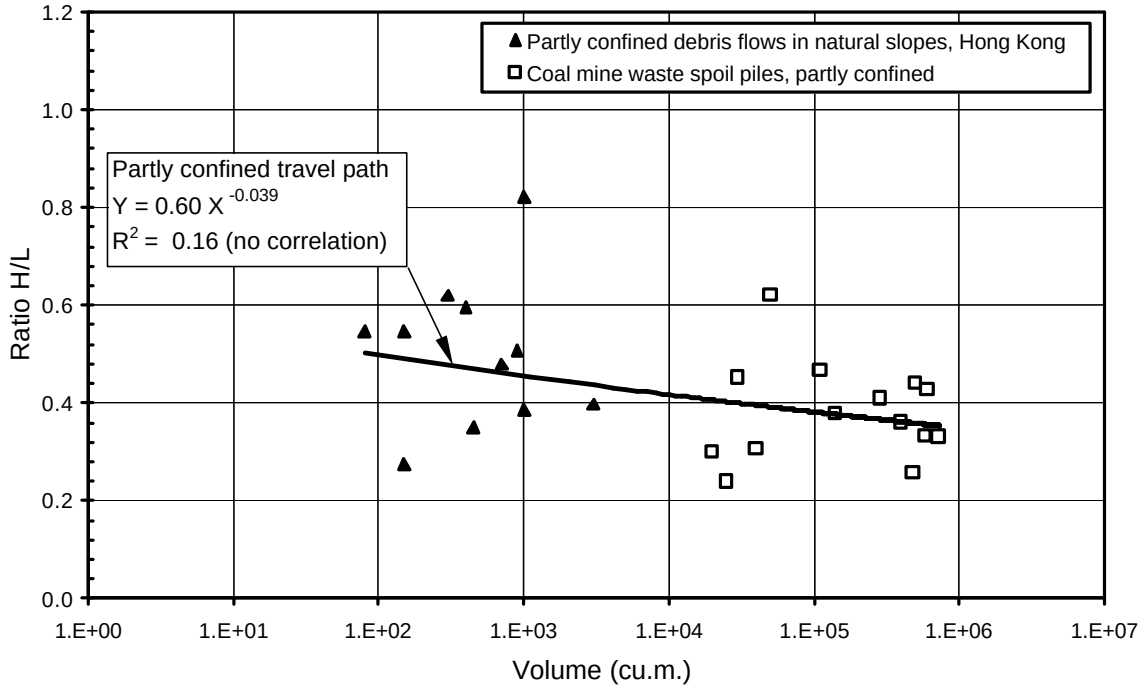

Figure 3.63: *H/L* versus volume for "rapid" landslides with partly confined travel paths.

Table 3.25: Empirical correlation coefficients for power law fit of travel distance angle to slide volume (Equation 3.11, $H/L = AV^B$) for confined and partly confined "rapid" landslides.

Degree of Travel Path Confinement	Sub-group	Volume Range (m^3)	No.	A	B	R^2	Std *[1] Error	Comments
Partly confined and confined	All	40 to $6x10^6$	84	0.602	-0.0517	0.27	0.124	Poor correlation
Partly confined	All	80 to 720,000	25	0.600	-0.0386	0.16	0.124	Poor correlation
	Natural slopes (Hong Kong), dilative	80 to 3,000	11	0.579	-0.0391	0.03	-	No correlation
	Coal mine waste (flow slides)	20,000 to $6x10^6$	14	0.333	0.0085	0	-	No correlation
Confined	All	40 to $6x10^6$	59	0.617	-0.0602	0.37	0.118	Minor correlation
	Dilative Soils	40 to						
	- All	13,000	39	0.484	-0.0203	0.02	-	No correlation
	- Natural slopes, HK		6	0.281	0.0469	0	-	No correlation
	- Washouts, HK		19	0.495	-0.0221	0.02	-	No correlation
	- Corminas (1996a)		14	0.774	-0.0933	0.13	-	No correlation
	Contractile Soils							
	- Coal mine waste	40000 to $6x10^6$	20	1.071	-0.106	0.29	0.125	Poor to minor correlation

Note: No. = number of case studies

*[1] The standard error applies to log *H/L*.

From the above analysis of travel distance angle to slide volume and degree of confinement it is evident that whilst there is general trend of decreasing travel distance angle with increasing slide volume, other factors such as failure mechanism, slide type, failure geometry type and material properties have a significant influence on the travel distance angle.

3.9.3 TRAVEL DISTANCE VERSUS VOLUME, DOWN-SLOPE ANGLE AND SLIDE TYPE FROM FAILURES IN DILATIVE SOILS

The following sections (and Section 3.9.4) discuss the use of slide volume, down-slope angle (a_2), slide type and material properties to predict travel distance angle.

3.9.3.1 *Cut Slopes*

The Hong Kong case studies of "rapid" landslides from failures in cut slopes have been analysed in detail. The failures includes:

- Slides through the soil mass within residual soils and weathered rock (saprolite).
- Strongly defect-controlled slides within the weathered rock slope (saprolite).
- Slides of debris in colluvial soils from the upper portion of the cut slope.
- Slides through soil mass within fill slopes of typically silty gravelly sands and clayey silty sands. This group of failures are not flow slides, but considered to be within initially dilative soils. Only two case studies of this type of failure have been included.

A significant portion of the empirical analyses on travel distance angle and travel distance for landslides in Hong Kong has been centred on cut slopes, for which Finlay et al (1999) and Wong and Ho (1996) have developed useful correlations. The research by Finlay et al (1999) found that the travel distance, L, was strongly correlated (R^2 = 0.85) to the landslide height, H, and cut slope angle, a_{cut}, (Equation 3.12) for cut slopes where the slope below the cut is near horizontal. The correlation developed by Finlay et al (1999) was based on 515 cut slope failures with mean volume of 138 m^3 (5^{th} percentile of 3 m^3 and 95^{th} percentile of 446 m^3) and mean cut slope angle of 62 degrees (5^{th} percentile of 45º and 95^{th} percentile of 80º). Given that the power function of H in Equation 3.12 is very close to 1 the equation can be more simply presented in the form of H/L (Equation 3.13) without introducing significant error (error of 1 to 5% for cut slope angles of 30 to 75 degrees and heights of 5 to 50 metres).

$$L = 1.2853 * H^{1.010} * \left(\tan a_{cut}\right)^{-0.506}, R^2 = 0.85 \quad (3.12)$$

$$H / L = 0.78 * (\tan a_{cut})^{0.5} \quad (3.13)$$

The case study data for all cut slopes and those for which detailed slope geometry and travel distance is available from Hong Kong is presented in Figure 3.64. The subset is seen to be representative of the overall data set. But, the correlation of travel distance angle to slide volume alone is minor, as indicated by the significant scatter around the trendline.

Figure 3.65 presents the same set of data (excluding several case studies where the run-out was not onto a near horizontal slope at the toe of the cut) with the *H/L* ratio normalised against the tangent of the cut slope angle to the power 0.42 (best fit determined by multiple regression analysis). This shows a moderate to good correlation, with regression coefficient of 0.62.

This finding is not unexpected when the mechanics of sliding are considered. The sharp change in slope angle from a steep cut slope angle to a flat slope at the toe is a significant obstruction to the post-failure travel and would result in a significant loss of energy of the slide mass. A reduction in the difference in this angle (either by a flattening of the cut slope angle or steepening of the slope below the cut) would reduce the loss in energy of the impact at the change in slope and result in increased travel distance and decreased travel distance angle.

As the volume of the slide mass increases it is considered that the energy lost on impact per unit volume is reduced. As idealised in Figure 3.66, the initial material deposited at the toe of the cut reduces the sharp change to a more gradual change in slope angle, and the debris following would lose less energy in the transition of movement direction. Finlay et al (1999) did not find that volume was a significant factor for the travel distance angle from cut slope failures, and it is considered the reason is the heavy weighting to small volumes in their database, whilst this database has a wider spread.

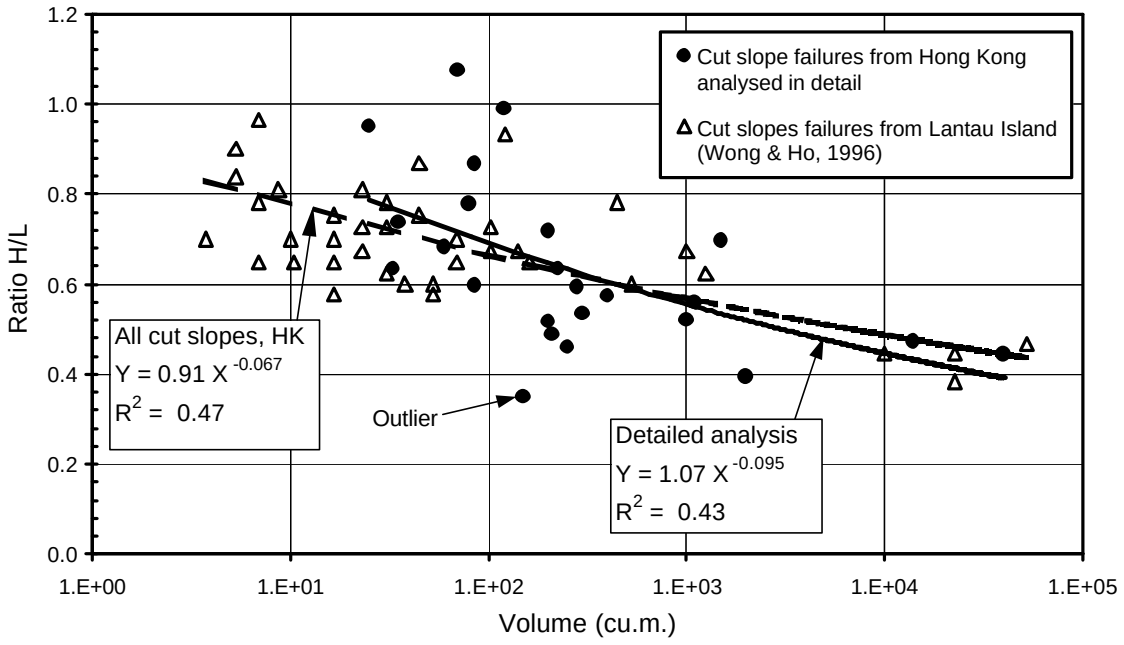

Figure 3.64: *H/L* versus slide volume for cut slope cases studies from Hong Kong

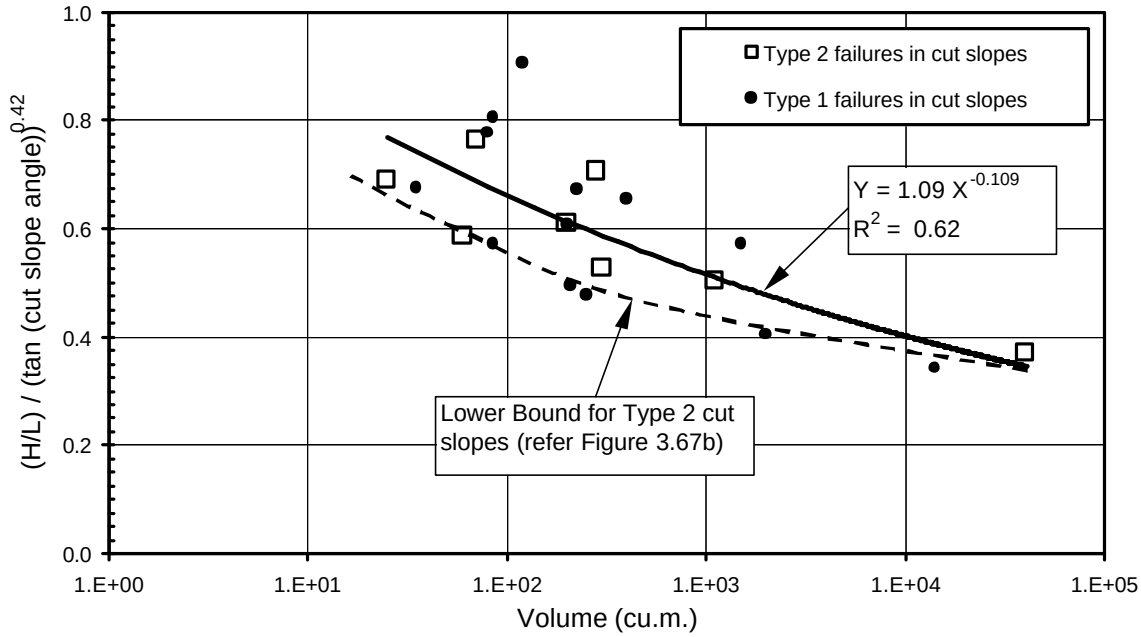

Figure 3.65: *H/L* normalised against tangent of the cut slope angle versus volume for cut slopes in Hong Kong failing onto a near horizontal slope at the toe.

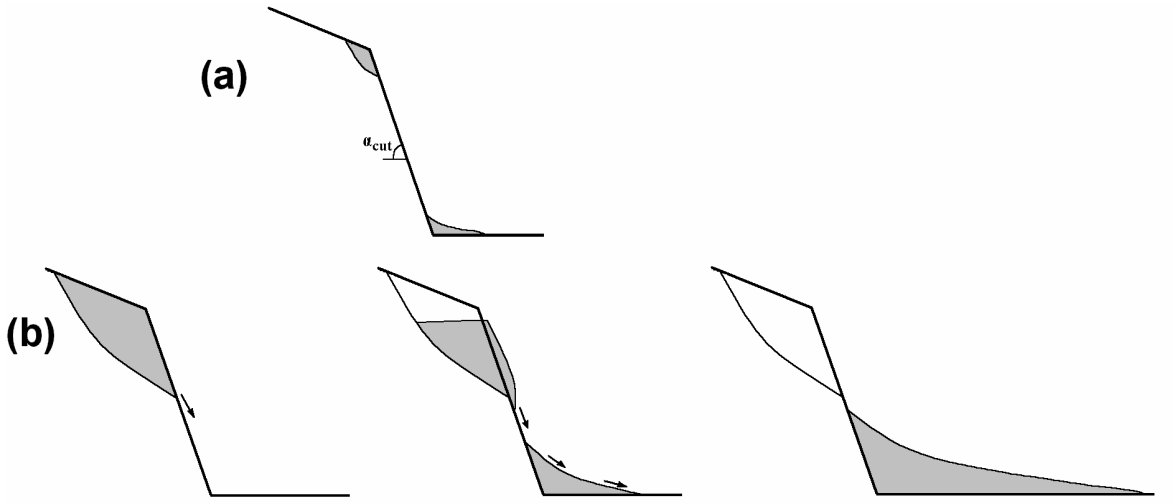

Figure 3.66: Idealised effect of volume on travel distance for cut slope failures of *(a)* small volume compared with *(b)* significantly larger volumes.

For the cut slope case studies analysed in detail the relationship between travel distance, R, and cut slope height, H_s, is generally in agreement with the findings from Wong and Ho (1996). However, the scatter of results is significant and regression analysis indicates a very weak correlation compared with the correlation of travel distance angle to cut slope angle and volume shown in Figure 3.65.

Further analysis of the cut slope case studies indicates that other factors have an influence, but to a lesser degree than volume and cut slope angle, on the travel distance angle, they are:

- The location of the slide in the cut slope; Type 1, at the top of the cut slope, or Type 2, encompassing virtually the full height of the cut slope (Figure 3.67). In Figure 3.65 the Type 2 cut slope failures plot in the range slightly above to well below the trendline shown indicating a lower travel distance angle. This finding is to be expected given that the basal sliding surface of the Type 2 slope category results in a lower difference in the angle with the slope at the toe of the cut (Figure 3.67b) and would therefore reduce the loss in energy of the impact.
- Obstructions to the travel of the slide mass, such as buildings. The obstructed slides result in a loss of energy on impact with the obstruction and therefore it would be expected that the travel distance angle would be increased due to obstructions. In Figure 3.65 the obstructed slides generally plot above the trendline, although in several cases, mainly Type 2 slides they plot below it. Scale effects also require consideration for obstructions as small volume slides can be obstructed by relatively small obstructions, which for a larger volume slide are not significant. For example, the wall in front of a house that obstructed the 85 m^3 slide at Chung Shan Terrace (Slide B) would have had little significance for the 40,000 m^3 Po Shan slide of 1972.
- The initial failure mechanism (defect-controlled or slide through soil mass), geological origin and material type do not show an observable trend in Figure 3.65. They would therefore appear to have a minor effect on the travel distance angle. Finlay et al (1999) also found that geological origin and material type had no discernable influence on the slide mobility.

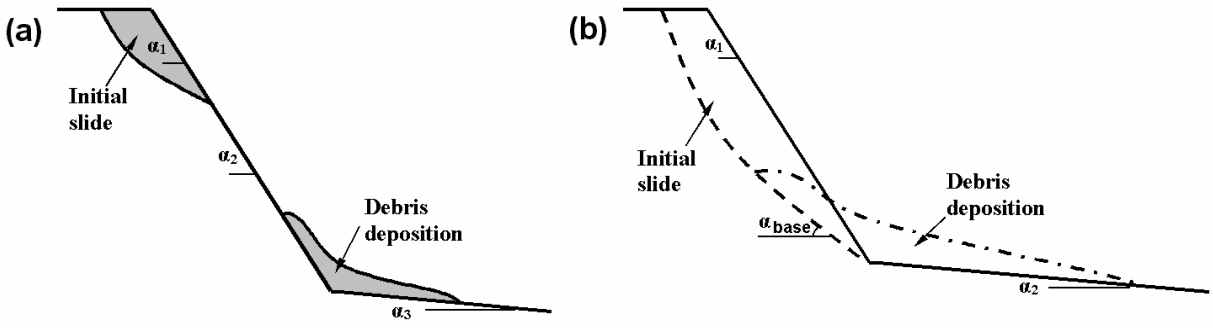

Figure 3.67: Classification of slope categories *(a)* Type 1 – failure at top of cut slope, and *(b)* Type 2 – failure encompassing the full cut height.

In summary, the dominant factors considered to affect the travel distance angle for "rapid" landslides from cut slopes failures (from Hong Kong) are the cut slope angle and volume of the slide mass. The slope angle below the cut also has an influence and to a lesser extent so does the location of the slide within the cut slope (i.e. Type 1 or Type 2), and obstructions in the travel path. Flatter cut slope angles, increased volume, steeper slope angles below the cut and Type 2 cut slopes (encompassing the full height of the cut) result in a reduced travel distance angle and potentially greater travel distances. Steeper cut slope angles, smaller volumes, Type 1 cut slopes (above the toe of the cut) and obstructions in the travel path result in an increased travel distance angle and potentially reduced travel distances.

Figure 3.65 and Equation 3.14 presents a useful guide to prediction of the travel distance angle for cut slopes of Type 1 failure geometry (see Figure 3.67) and near horizontal slopes below the cut, for slide volume in the range 25 to 20,000 m^3. For slide volumes less than 25 m^3 the approximation of the corrected Finlay et al (1999) correlation (Equation 3.13) is recommended. For Type 2 cut slopes the lower bound line in Figure 3.65 is recommended for predictive purposes.

$$H / L = 1.09 * (\tan a_{cut})^{0.42} * V^{-0.11} \quad \text{for slide volumes of 25 to 20,000 m}^3 \quad (3.14)$$

where a_{cut} is the cut slope angle and V is the estimated slide volume (in cubic metres).

Based on energy principles, where the slope below toe of the cut is not near horizontal, Figure 3.65 and Equation 3.14 can be used provided that the difference in slope angle between the cut slope and slope below the toe of the cut is used in Equation 3.14 in place of the cut slope angle (i.e. $a_{cut} - a_3$ for Type 1 failure geometries and $a_{cut} - a_2$ for Type 2 failure geometries, instead of a_{cut}, refer Figure 3.67).

Limitations to the above guidelines include:

- Material type and geological origin. The information presented is considered suitable for prediction of travel distance angle for colluvium, residual soils and weathered rocks of granitic and volcanic origin. It is likely to be a reasonable predictor for slopes in soils of silty sands, clayey silty sands and sandy clays of low plasticity, and more unreliable for more plastic soils. Extension of its use for cut slopes in other soils and their parent rocks should be done so with caution, and by verification against a number of failures in slopes similar to that being considered.

- Slide volume. The case studies on which the analysis is based are limited to volumes up to 40,000 m^3, with only two slides above 10,000 m^3. It is considered that the volume limitation is in the order of 10,000 to 20,000 m^3.
- The cut slope angle. From the case studies analysed, the guidelines are considered appropriate to cut slopes steeper than 33 degrees and flatter than 70 degrees (and similar differences in slope angle for slopes below the cut that are not near horizontal).
- Type 2 failures (Figure 3.67b) where the basal angle of the surface of rupture (a_{base}, see Figure 3.67) is more than 15 to 20 degrees steeper than the angle of the slope below the cut (a_2 for Type 2 failure geometries). The case study identified as an outlier on Figure 3.64 was a Type 2 cut slope failure with the basal angle of the surface of rupture almost coincident with the angle of the slope below the cut, and for these cases there is limited loss in energy due to the slope angle transition. While there is only one case study data point, the use of the correlations derived from natural slopes (Section 3.9.3.2) would be more appropriate for prediction of travel distance angle for these cases.

3.9.3.2 *Natural Slopes in Dilative Soils*

The analysis of travel distance angle in terms of slide volume (Section 3.9.2) for "rapid" landslides from natural slopes (in Hong Kong) found a negligible to very weak correlation, even when the data is sorted based on degree of confinement of the travel path. Prior to discussing improved methods for prediction of travel distance angle, the characteristics of the slide mass movement are considered. The characteristics of the travel and deposition of the slide mass, from the case study data, indicate:

- The distance of travel beyond the toe of the source area for confined travel paths is significantly greater than for unconfined and partly confined travel paths.
- The smaller volume (less than about 500 m^3) "rapid" landslides with unconfined travel paths generally deposit slide debris along the entire travel path regardless of the down-slope angle (up to 43 degree slopes) and will terminate on these steep slopes. Where the travel path extends on to flatter slopes (less than about 10 to 15 degrees) the slide mass will quickly come to rest.

- For the larger volume "rapid" landslides along unconfined travel paths deposition occurs on slopes as steep as 30 degrees and the slide will flow for significant distances on slopes less than 10 to 15 degrees before eventually coming to rest.
- "Rapid" landslides along partly confined travel paths generally show similar characteristics to those on unconfined travel paths. In one case (Lui Pok School, slide volume 450 m^3) some of the characteristics were more like a confined debris flow with minimal deposition and minor accumulation on slopes of 15 to 30 degrees. The slide mass eventual came to rest after travelling about 40 m on the flat slopes of the school playground.
- For "rapid" landslides along confined travel paths the length of travel beyond the toe of the source area can be very long regardless of the slide volume, possibly reflecting entrainment of water within the flow. In general, these slides accumulated slide debris on slopes steeper than 15 to 20 degrees, continued to flow on slopes steeper than about 10 to 15 degrees and travelled for long distances on slopes of less than 10 degrees. These slides usually terminated either on unconfined relatively flat slopes in a fan type deposition or were obstructed at the toe of the confined travel path (e.g. an embankment, reservoir of water or building).

These observations are similar to those of other researchers (Franks 1996; Finlay et al 1999) who analysed "rapid" landslides from natural terrain from Hong Kong. Franks (1996) found that for unconfined travel paths deposition starts at an average slope angle of 27 degrees, with a standard deviation of 6 degrees. For confined debris flows Franks (1996) comments that deposition will occur on slopes of less than 20 degrees and Finlay et al (1999) comment that where the confined debris flow accumulates mass (without deposition) flow will continue on slopes down to 14 degrees.

Analysis of the data on "rapid" landslides from natural slopes found that the down-slope angle below the source area, a_2, and degree of confinement of the travel path have a significant influence on the travel distance angle. This is not unexpected in light of the characteristics of the slide mass movement discussed above. The down-slope angle below the source area, a_2, is defined in Figure 3.68 and is the average angle of the portion of the down-slope from below the landslide source area to the point where the slope begins to flatten out. This definition is somewhat subjective; however, for the case studies analysed it typically represents at least 50% of the length of travel distance beyond the toe of the source area (for confined travel paths) and in a number of cases up

to 100% of this length (for a number of unconfined and partly confined travel paths). Thus, a_2 incorporates short steeper and flatter sections (e.g., terraces) on the upper portion of the travel path.

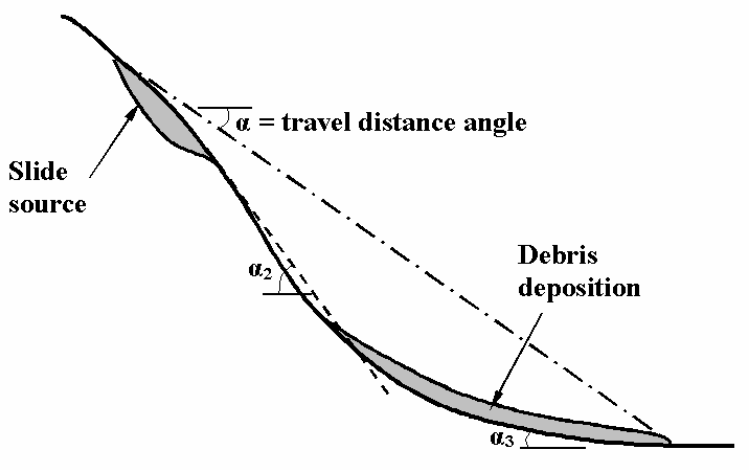

Figure 3.68: Definition of down-slope angle below source area, a_2.

Figure 3.69 to Figure 3.71 present plots of the travel distance angle to down-slope angle, and trendline of best fit for unconfined, partly confined and confined travel paths respectively for the Hong Kong case studies. Also shown in these figures is a 1 to 1 trendline between *H/L* and tangent of the down-slope angle, a_2. No published information on the down-slope angle was available for the Corominas (1996a) "rapid" debris flows to incorporate them into the analysis.

The plots (Figure 3.69 to Figure 3.71) indicate a moderate to excellent correlation of the travel distance angle to down-slope angle, with the travel distance angle increasing with increasing down-slope angle. The poorer correlation for the partly confined travel paths is associated with the different types of travel path within the partly confined group; for example, some slide mass movements are located entirely within relatively broad gullies and others have short sections of the travel path in a relatively confined gully.

Comparison of the trendlines based on the degree of confinement of the travel path (Figure 3.72) shows that they are relatively closely grouped. However, for a specific down-slope angle below the source area, a_2, the *H/L* ratio is highest for the unconfined travel path and lowest for the confined travel path. This relatively small difference in *H/L* ratio can translate into a relatively large difference in travel distance for the down-slope topography represented by the case studies. It is therefore important to consider

the degree of confinement in travel distance angle predictions. The likely availability of water in confined travel paths, which can become entrained in the slide mass and result in greater mobility, is considered the dominant reason for lower frictional losses apparent for confined travel paths.

The trendlines for the different travel paths are almost coincident with each other and the 1 to 1 trendline at down-slope angles (a_2) in the range 15 to 22 degrees. These slope angles are considered to be close to the lower limit of slope angles at which "rapid" landslides will develop and continue to slide or flow (refer Section 3.5.2.4). With steeper slopes the kinetic energy of the slide mass is increasing during travel, so the slide mass has greater kinetic energy to run-out further distances on the lower flatter slopes below.

The increase in travel distance angle with increasing down-slope angle (a_2) is likely to be a result of the increasing energy loss in travel of the slide mass. With increasing down-slope angle the velocity of the slide mass is likely to be greater, resulting in greater energy loses due to disaggregation of the slide mass.

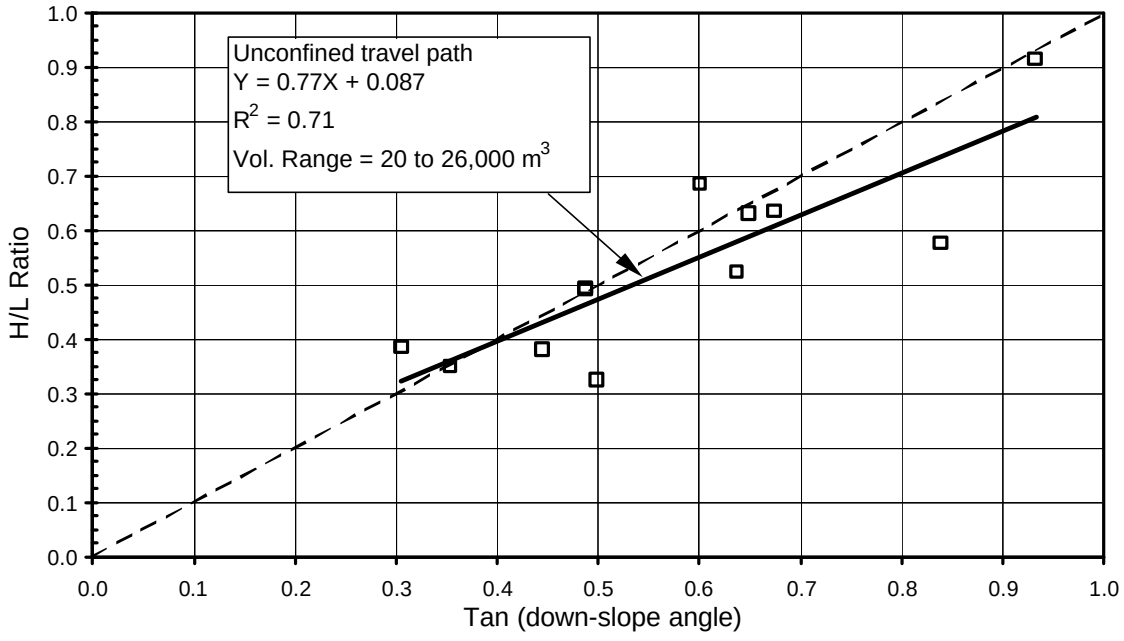

Figure 3.69: *H/L* versus tangent of the down-slope angle, a_2, for unconfined travel paths, failures in natural slopes from Hong Kong.

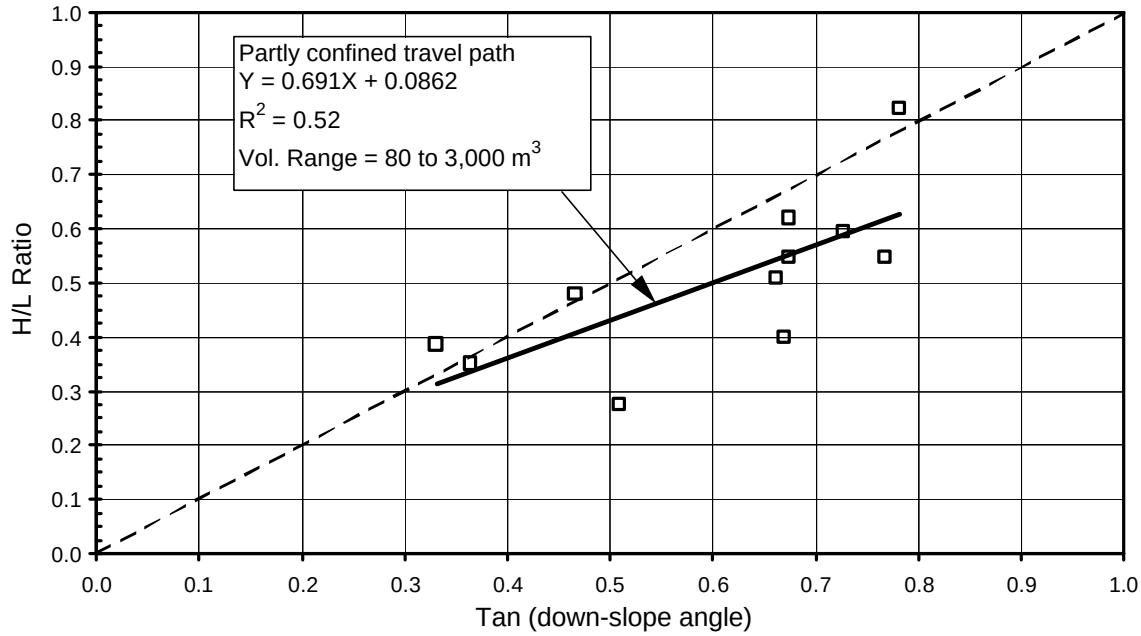

Figure 3.70: *H/L* versus tangent of the down-slope angle, a_2, for partly confined travel paths, failures in natural slopes from Hong Kong.

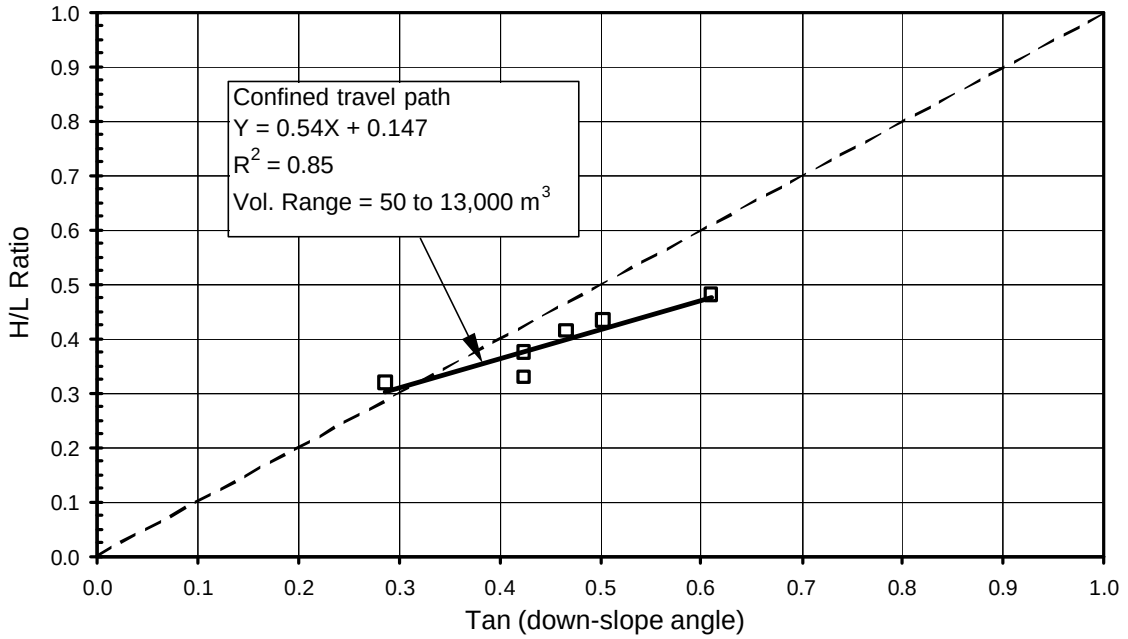

Figure 3.71: *H/L* versus tangent of the down-slope angle, a_2, for confined travel paths, failures in natural slopes from Hong Kong.

The scatter around the trendlines in Figure 3.69 to Figure 3.71 is not necessarily associated with slide volume. Only for the unconfined travel path events did the larger volume slides plot below the trendline; for partly confined and confined travel paths no trend with slide volume was evident. No trend was evident for major obstructions to the

slide mass either. The reasons for the scatter are considered to be associated with relatively small obstructions to the slide mass particularly for the smaller volume slides, the flow behaviour, the potential availability of water that can become entrained in the slide mass and differences in material properties (geological origin had no influence).

Multiple regression analyses of *H/L* with slide volume and down-slope angle below the source area, a_2, were also carried out; however, no correlation was found for the partly confined and confined travel paths, and only a poor correlation was obtained for the unconfined travel path.

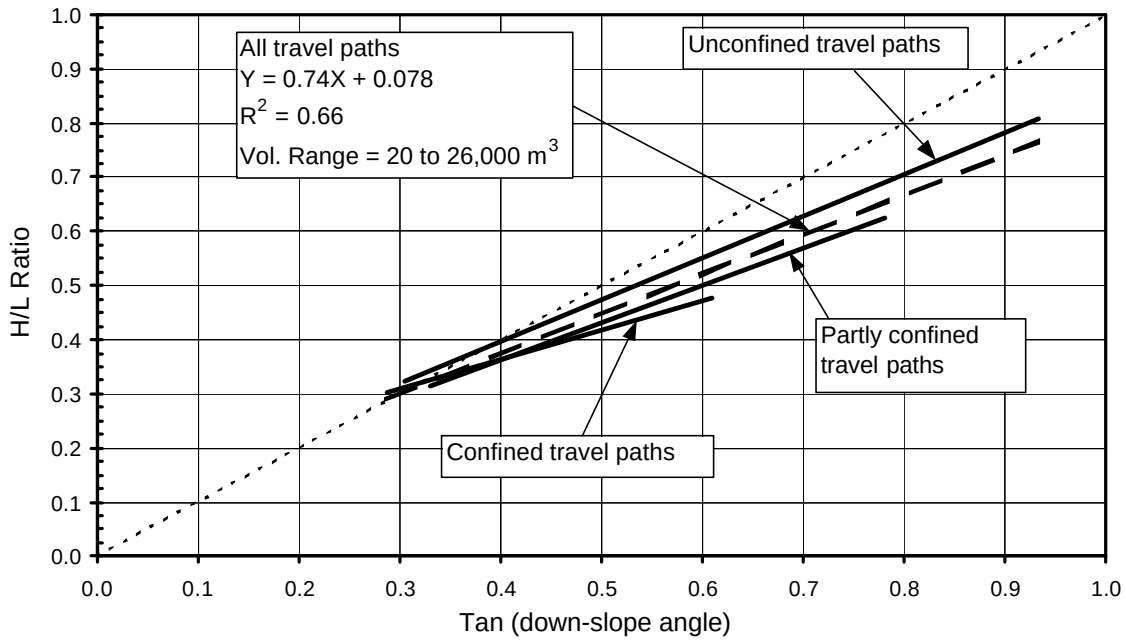

Figure 3.72: Natural slopes (Hong Kong). Trendlines for *H/L* versus tangent of the down-slope angle, a_2, for all types of travel path.

From the study it is apparent that the down-slope angle below the source area, a_2, presents a useful method for prediction of the travel distance angle for "rapid" landslides from natural slopes. Equations 3.15, 3.16 and 3.17 represent the trendlines for unconfined, partly confined and confined travel paths respectively from Figure 3.69 to Figure 3.71.

Unconfined $H / L = 0.77 * (\tan a_2) + 0.087$ Std. Error = 0.095 (3.15)

Partly confined $H / L = 0.69 * (\tan a_2) + 0.086$ Std. Error = 0.110 (3.16)

Confined $H / L = 0.54 * (\tan \alpha_2) + 0.147$ Std. Error = 0.027 (3.17)

where α_2 is the down-slope angle below the source area (Figure 3.68).

These equations are also applicable to Type 2 cut slope failures (Figure 3.67b) where the basal angle of the surface of rupture is less than about 10 degrees (and possibly up to 15 to 20 degrees) steeper than the angle of the slope below the cut. The analysis for unconfined travel paths incorporated two case studies of cut slopes that complied with this criterion.

For prediction of the travel distance angle the following steps are recommended:

- Approximate estimation of the travel distance angle based on the statistical mean of the travel distance angle from slides in similar soil types with similar degree of confinement of the travel path (refer Table 3.29).
- Transposing of the travel distance angle onto a long section of the potential slide and travel path.
- Estimation of the down-slope angle below the landslide source area, α_2, from this section. The length over which the estimate is made should represents at least 50% of the length of travel beyond the toe of the source area.
- Prediction of the travel distance angle based on assessment of the degree of confinement of the travel path from either Equations 3.15 to 3.17 or Figure 3.69 to Figure 3.71.

Limitations to the above guidelines are:

- Slide volume. The case studies on which the analyses are based is limited to volumes up to 26,000 m^3 and a limitation of 25,000 m^3 is considered appropriate at this stage until further verification is undertaken for larger volume slides.
- Material type and geological origin. The guidelines are considered appropriate to similar soil types to that analysed, i.e., colluvial and residual soils derived predominantly from granitic and volcanic (rhyolite and fine to coarse ash tuffs) rocks. The colluvial soil types cover a broad range of soil types from dominantly finer grained silty sands to dominantly gravel to boulder size, both with low clay contents (less than 10%). The number of case studies within residual soils is limited, and the material types were typically silty sands to clayey silty sands to sandy silts). The method should be applicable to similar soils but of different geological origin, but not to more plastic or high clay content soils.

3.9.4 TRAVEL DISTANCE VERSUS VOLUME, DOWN-SLOPE ANGLE AND SLIDE TYPE FROM FAILURES IN CONTRACTILE SOILS

3.9.4.1 Fills Constructed of Loose Silty Sands

The analysis of flow slides in loose fill slopes of silty sands to sandy silts with low clay content (from Hong Kong), Section 3.9.2, indicated that a minor correlation exists between travel distance angle and slide volume (Figure 3.73). Further analysis of the smaller data set, for which detailed information was available, indicated some correlation exists between the travel distance angle and down-slope angle below the source area, a_2. However, given the relatively low regression coefficient (R^2 of 0.50) for the limited number of case studies (7) the correlation was statistically unacceptable.

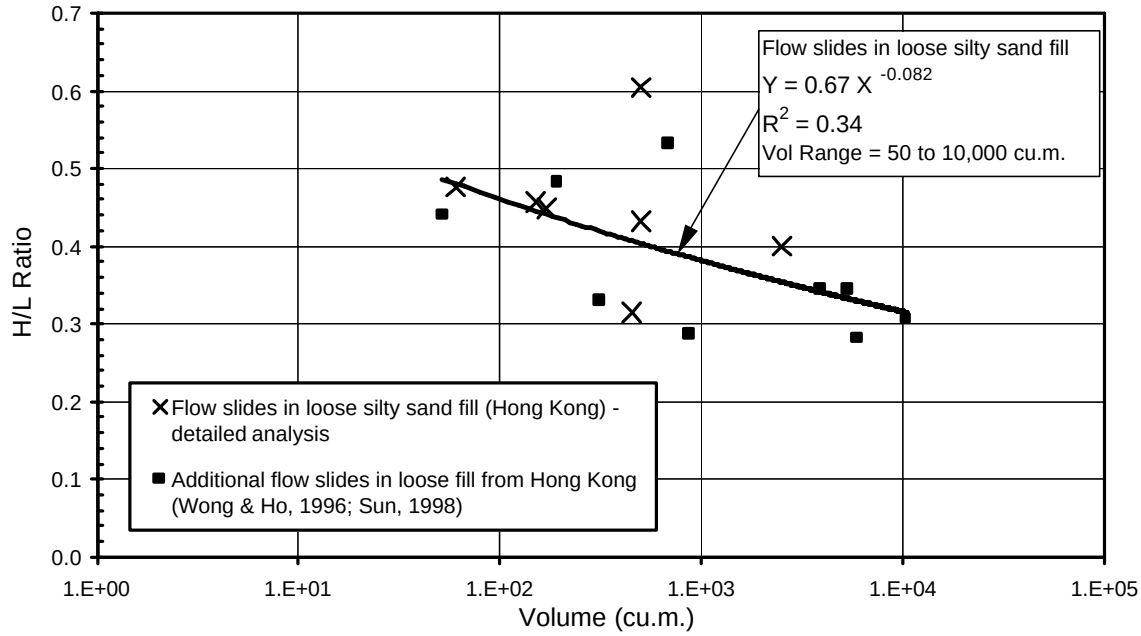

Figure 3.73: *H/L* versus slide volume for flow slides in loose silty sand to sandy silt fills.

Factors other than slide volume influencing the travel distance angle are the relative density of the fill, obstructions along the travel path and presence of water. The effect of these factors on the potential travel of the slide mass are:

- Relative density. The lower the relative density of the fill, in comparison to similar fill types, the lower will be the residual undrained strength on liquefaction and higher the undrained brittleness index. Therefore, at failure the slide mass will have a higher kinetic energy than for comparative fills of higher relative density that are

still susceptible to liquefaction. Thus, the lower the relative density the lower the expected travel distance angle.

- Obstructions to the travel of the slide mass will reduce its kinetic energy and therefore reduce the travel distance and increase the travel distance angle.
- Free water, if available, can become entrained in the slide mass and for low cohesion materials will reduce the strength of the slide mass and potentially lead to increased travel distance and decreased travel distance angle.

For prediction of the travel distance angle of flow slides in loose silty sand to sandy silt fills with low clay content (less than 10%) two methods should be used:

(a) For slide volumes between 50 m^3 and 500 m^3 use the mean and standard deviation from Table 3.29;

(b) For slide volumes between 500 m^3 and 10000 m^3 use Figure 3.73 and Equation 3.18.

In each case an appropriate degree of conservatism should be used.

$$H / L = 0.67 * V^{-0.082} \quad \text{(standard error of log } H/L = 0.085) \qquad (3.18)$$

Limitations to the above guidelines are:

- Slide volume. The case studies on which the analyses are based are limited to volumes up to 10,000 m^3.
- Material type and geological origin. The guidelines are considered appropriate to similar soil types to that analysed; i.e., silty sands to sandy silts with fines contents of 10 to 50% and clay contents less than 10% derived from completely to highly decomposed granitic and volcanic rocks. They should apply other silty sandy soils, e.g. those from alluvium, colluvium or derived from sandstone.
- Density and/or placement method. The compaction limit for static liquefaction in these soils is 85% of Standard Maximum Dry Density (HKIE 1998), and the fills were generally placed by end dumping without any formal compaction.

3.9.4.2 *Coarse-grained Mine Waste Spoil Piles on Hillsides*

Golder Assoc. (1995) analysed the post failure travel of 40 "rapid" flow slides from coal mine waste spoil piles in British Columbia, for which the scatter of the travel distance

angle was large with respect to slide volume (Figure 3.74). They derived the relationship between the excess travel distance, L_e, and slide volume (Equation 3.10) that incorporates a spreading ratio, R (where $R = L_e / B$, B is the breadth of the deposit), based on the actual case studies and taking into account the degree of confinement of the travel path. Their analysis was based on the assumption of a correlation between depositional area and volume (Equation 3.9) and the assumption that L_e approximated the length of the deposit.

Golder Assoc. (1995) identified a group of highly mobile events where the travel path was confined and the slide debris over-rode suspected liquefiable organic materials mantling the lower slopes and gullies of the confining channels. This group of slides was separate from the "normal" mobility events. Golder Assoc. (1995) derived expressions for L_e in terms of slide volume for each group (Table 3.26) and found a standard deviation of 30% between the actual L_e and calculated L_e (excess travel distance) from the correlations given in Table 3.26.

As part of this study, further analysis of the Golder Assoc. (1995) case studies was undertaken to convert their predictions of the excess travel distance, L_e, into predictions of the *H/L* ratio for comparison against analyses using other methods. The percentage differences of the mean and standard deviation for the *H/L* ratio between the actual and predicted ratios and the standard error are given in Table 3.26.

Table 3.26: Summary of empirical correlations for flow slides in coal waste spoil piles in British Columbia

Slide Mobility	**Equations of Best Fit (Golder Assoc. 1995)**	**Difference Between Actual and Predicted H/L Ratio**		
		Mean	**Std. Dev.**	**Standard Error of H/L prediction**
High mobility	$A = 22.8 * V^{0.662}$ $L_e = \left(22.8 * R * V^{0.662}\right)^{0.5}$	5%	11%	0.015
Normal mobility	$A = 74.5 * V^{0.5}$ $L_e = \left(74.5 * R * V^{0.5}\right)^{0.5}$	-2%	12%	0.042

Note: Std. Dev. = standard deviation

The difficulty with analyses of this type is that in order to predict the travel distance angle of a potential landslide, estimation of the spreading ratio is required. For the flow

slides in coal waste spoil piles from British Columbia analysed by Golder Assoc. (1995) the variation in spreading ratio ranged from 0.5 to 100, although there is much less variability within the morphological sub-groups. The inaccuracy associated with estimation of the spreading ratio for a potential landslide detracts from using such correlations and other methods (discussed below) are preferable.

With a view to developing improved methods for prediction of travel distance further analyses were undertaken of flow slides in coal mine spoil piles incorporating the case studies from British Columbia and South Wales. It is considered that given the similarity of the particle size distribution of the liquefaction susceptible materials, the loose nature resulting from the two methods of placement and that both are on hill slopes, that methods of prediction of travel distance angle should be applicable to both sets of case studies. The coking coal stockpile case studies from Hay Point were excluded due to the low specific gravity (S_G approximately 1.35 t/m^3) of coking coal even though their particle size distribution was similar to that of the coal mine spoil pile case studies.

The long section profile of the travel paths for the flow slides in South Wales was generally different to that for the flow slides in British Columbia. At South Wales the hill slope angles (8 to 27 degrees for the case studies) generally maintained a relatively constant slope, only flattening off toward the toe. In a number of cases (slightly less than half) the travel of the flow slide terminated on the hill slope. For the remaining cases the flow reached the toe of the hill slope, but did not generally travel a great distance beyond the toe, it either came to rest on the flatter slopes or else was obstructed by embankments or channels in the toe region.

In contrast, the topography in the region of the British Columbian coal mines consists of glacially over-steepened valleys with typically very steep upper slopes (up to 35 to 50 degrees) that decrease gradually to relatively flat slopes in the toe region of these valleys, giving the down-slope a markedly curved shape. The travel path for these slides varied dependent on the position of the toe of the spoil pile in relation to the toe of the valley, varying from initially relatively steep in some cases to relatively flat in other cases. In a significant number of cases the flow slide travelled for long distances (more than 1000 m in several cases) on relatively flat slopes of 0 to 10 degrees. The high kinetic energy of the slide mass as a result of the steep topography and large height of the spoil piles (100 to 400 vertical metres) and the potentially liquefiable foundation soils are dominant factors for the long travel distances on relatively flat slopes for

several of these slides. In contrast, the vertical height of the spoil piles for the South Wales case studies typically ranged from 30 to 70 m.

The case study data is presented in Figure 3.74 in the form of *H/L* versus slide volume. The two case studies with *H/L* ratios exceeding 0.6 were considered as outliers to the group and therefore omitted from the analysis. Fforchman was also omitted as it was considered not to have initiated as a flow slide. Whilst it does not appear as an outlier on Figure 3.74 it does so when plotted in the form of *H/L* versus down-slope angle below the toe of the spoil pile. The earlier analysis based on degree of confinement of the travel path (Section 3.9.2) indicated that a poor correlation existed between the travel distance angle and volume for confined travel paths and no correlation (with volume) for unconfined and partly confined travel paths.

Further analyses were undertaken of *H/L* ratio versus the down-slope angle below the toe of the spoil pile, a_2. The analysis showed (Table 3.27 and Figure 3.75) a general trend of decreasing *H/L* ratio (and travel distance angle) with decreasing down-slope angle below the toe of the spoil pile (a_2) where the angle, a_2, is taken as the average slope from the toe of the spoil pile for a distance of at least 30 to 40% of the total distance travelled beyond the toe. The regression coefficients indicate minor correlations with down-slope angle for confined and unconfined travel paths. No correlation was statistically evident for the partly confined travel paths. Comparing the correlations for confined travel paths, the correlation based on down-slope angle is stronger than for slide volume.

Multiple regression analyses of the tangent of the travel distance angle were undertaken with respect to a combination of slide volume, down-slope angle below the toe of the spoil pile and height of the spoil pile. However, no correlations were evident. It was thought that the height of the spoil pile might have had some discernable effect on the travel distance angle due to kinematic effects.

The case studies were also analysed by assuming no correlation with volume or down-slope angle. Table 3.29 (in Section 3.9.5) presents the mean and standard deviation of the data, and the estimated confidence interval of the standard deviation of the population. The findings indicate, as shown in Figure 3.74, that the confined, high mobility flow slides have a lower mean *H/L* ratio than the remainder of the cases. For the cases other than confined, high mobility (i.e. partly confined and unconfined travel path, and normal mobility confined travel path) the mean and standard deviation were similar.

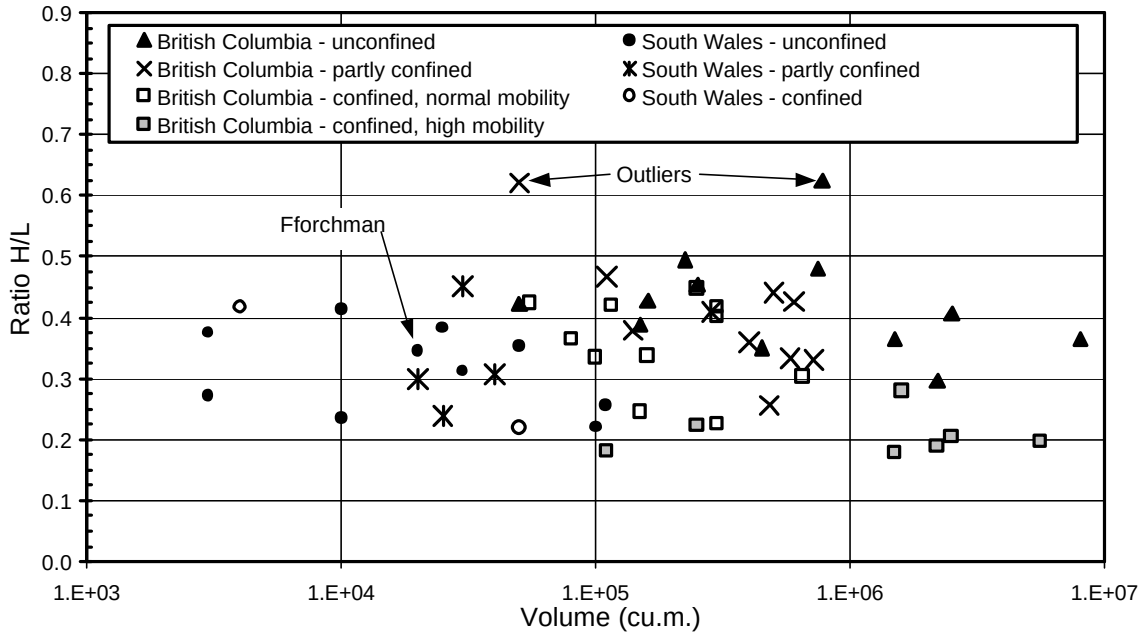

Figure 3.74: *H/L* versus slide volume for flow slides in coarse-grained coal mine waste spoil piles.

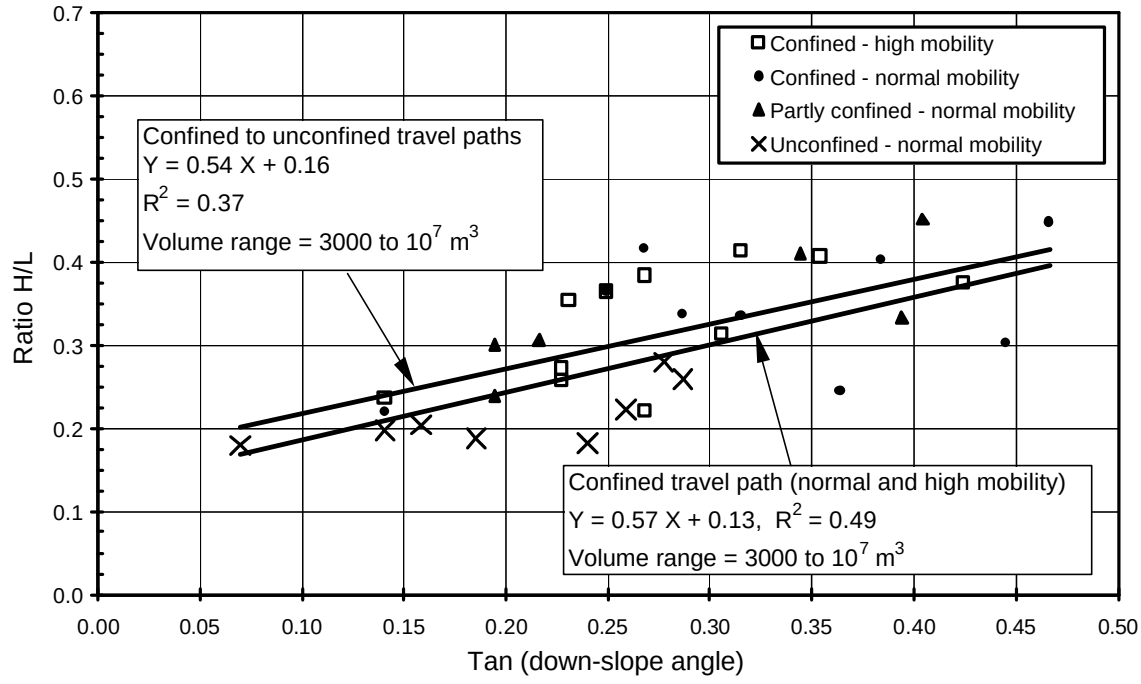

Figure 3.75: *H/L* versus the tangent of the down-slope angle below the toe of the spoil pile, a_2; flow slides in coarse-grained coal mine waste spoil piles.

Table 3.27: Statistical summary of *H/L* to tan a_2 correlation for flow slides in coarse-grained coal mine waste spoil piles.

Landslide Group / Sub-group	Correlation	No. Cases	R^2	Std. Error	z *[1]	Comment
All cases	$H/L = 0.53 \tan a_2 + 0.13$	35	0.37	0.068	4.0	Minor correlation
Confined travel path - all	$H/L = 0.57 \tan a_2 + 0.13$	17	0.49	0.065	3.2	Minor correlation
Confined travel path – high mobility	$H/L = 0.35 \tan a_2 + 0.14$	8	0.53	0.027	2.1	Moderate correlation. The z test indicates the correlation is very weak.
Unconfined travel path	$H/L = 0.59 \tan a_2 + 0.17$	11	0.39	0.058	2.1	Minor correlation

Note: Std. Error = Standard error R^2 = regression coefficient

*[1] z is the statistic for test of null hypothesis (accept correlation for z > 1.96 or z < -1.96)

The factors affecting the travel distance angle for flow slides in loose, coarse grained coal mine waste spoil piles are:

- The materials mantling the down-slope travel path. Saturated or near-saturated soils susceptible to liquefaction on rapid loading can significantly reduce the travel distance angle. For the flow slides in British Columbia liquefaction susceptible materials were suspected for the high mobility (> 1 km distance of travel beyond the spoil pile toe) of a number of flow slides in confined valleys.
- Longitudinal down-slope section. The steeper the initial down-slope angle generally the larger the travel distance angle.
- Degree of confinement, height of the spoil pile and slide volume are considered to affect the travel distance angle, although their influence appears to be over-shadowed by other factors.
- Relative density and undrained brittleness index of the loose dumped waste material are considered to have an affect on the travel distance angle, but cannot be quantified.

For prediction of the travel distance angle of flow slides in coarse grained dumped mine waste deposits on hillsides it is recommended that:

- For longitudinally curved down-slopes, where estimation of the angle a_2 can be difficult, use the mean and standard deviations from Table 3.29. Take into

consideration the potential for liquefaction of the material mantling the travel path where the travel path is likely to be confined. Otherwise use the values for normal mobility events disregarding the degree of confinement of the travel path.

- Where the down-slope angle is relatively consistent below the toe of the spoil pile use the down-slope angle correlations given in Figure 3.75.

Limitations to the above guidelines are:

- Slide volume. The case studies on which the analyses are based cover a broad range of volume from 3000 to 8 x 10^6 m^3.
- Material type. The guidelines are considered appropriate to similar material types to that analysed; i.e., spoil piles of sedimentary rock types composed entirely or partly of sandy gravels with low silty fines content (less than 3 to 5%) dominantly from argillaceous rock types. It should apply to materials of similar grading derived from other rock types.
- Material density/placement method. Density is a very significant factor in susceptibility of the material to static liquefaction. The guidelines are considered appropriate to spoil piles formed by end dumping from low height at the crest or peak of the spoil pile. Spoil piles formed by dumping from height, such as by dragline, are not likely to be susceptible to flow slide.
- Hillside topography. The formation of the spoil pile on hillsides is a feature of all case studies. Further details are given in Section 3.4.2.

3.9.4.3 *Retrogressive "Rapid" Landslides*

The soil types or sub-groups within which slide retrogression is a dominant mechanism include sensitive clays, tailings dams, submarine slopes and very loose sub-aqueous fill deposits. The significant feature for retrogression of these slides is continued back-scarp instability as discussed for sensitive clays in Section 3.4.3.

As shown in Figure 3.53 (and Figure 3.76 for retrogressive slides only) the travel distance angle for these slide groups is very small compared with "rapid" landslides in other soils. The dominant factors contributing to this are considered to be:

- The retrogressive nature of the slide. Retrogression distances of several hundred metres are typical for sensitive clays (up to 6 km has been recorded, Mitchell and Markell (1974)) and tailings dams. The distance of retrogression, in a number of

cases, represents a significant percentage of the total slide length, L (15 to 70% for tailings dams, 10 to 50% for sensitive clays). Therefore, its influence on reducing the calculated travel distance angle can be significant.

- The significant loss of strength on liquefaction and remoulding (particularly for sensitive clays) and the high volume of water entrained in the soil structure. These factors contribute to the fluid like characteristics of the remoulded soil and potentially large travel distances. In addition, the greater the flow potential of the remoulded soil the greater the likelihood of continued back-scarp instability due to exposure of the full back-scarp height (Leroueil et al 1996).
- The relatively low permeability of tailings and quick clays and therefore the likely low rate of dissipation of pore pressures during flow.
- The post-failure flow behaviour. For the sub-aerial slope failures (tailings and sensitive clays) the liquefied material has fluid like characteristics and the flow behaviour is reported (Jeyapalan et al 1983a; Blight 1997) to be laminar on relatively flat slopes and turbulent for the more "rapid" flows on steeper slopes. For laminar flow conditions a Bingham plastic fluid model is reported to give a reasonable approximation of the flow (Jeyapalan et al 1983a; Blight 1997).
- Entrainment of free water into the slide mass will significantly alter the flow properties of the fluid. For sub-aerial laminar type flows entrainment of water into the lower portion of the flow can significantly reduce the yield strength at the base of sliding resulting in much greater travel distances. In several cases confinement of the flow into running streams and rivers resulted in development of hyper-concentrated stream flows that travelled for distances in excess of 20 km on relatively flat slopes; the failures at Bafokeng, South Africa in 1974 and Stava, Italy in 1985 are examples.

Several case studies of "rapid" flow slides from tailings dams and sensitive clays have been particularly destructive, resulting in significant loss of life and extensive damage to property. These two groups of retrogressive landslides therefore deserve further discussion on the factors influencing their post-failure travel behaviour.

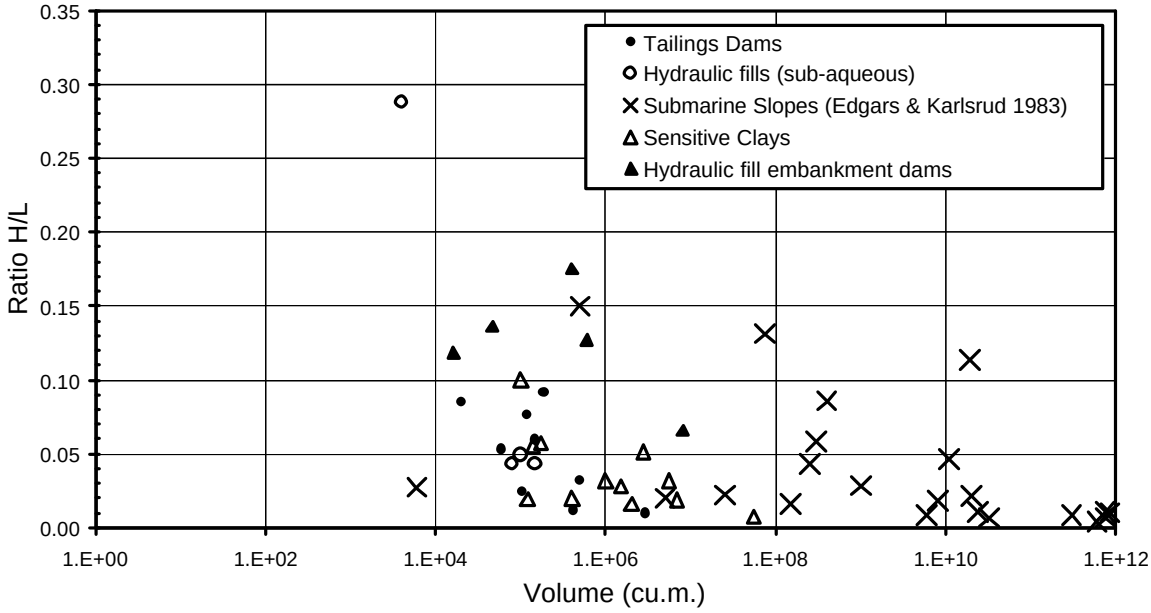

Figure 3.76: *H/L* versus volume for retrogressive "rapid" slides

(a) Flow Slides from Tailings Dams

For tailings dams the risk to life and property is down-slope of the failure. The properties and factors of those flow slides from tailings dams that were particularly destructive or had the potential to be particularly destructive are:

- The amount of water stored within the impoundment at the time of failure. Large volumes of water were reportedly stored within the impoundments of Stava, Bafokeng, Merriespruit and Buffalo Creek at the time of failure. This free water is available for entrainment into the flowing tailings and will significantly influence the flow properties leading to greater travel distances.
- The state of operation. All case studies of statically triggered "rapid" flow slides from tailings dams were active at the time of failure. Whilst this is not a significant factor leading to destructive (or potentially destructive) landslides in tailings dams triggered by static liquefaction, freshly deposited tailings do have a greater potential for flow. The state of operation is also a significant factor for earthquake triggered landslides in tailings dams (Tronsoco 1988, 2000).
- Presence of water or wet foundation on the travel path (as discussed above).
- Confinement or partial confinement of the flow. This is particularly significant where the tailings enter an actively flowing watercourse. For Stava, Buffalo Creek and Bafokeng (all with travel distances in excess of 20 km) it is considered that the

flow transformed into a turbulent stream-flow as a result confinement into a flowing watercourse.

- Down-slope angle. For most of the case studies analysed the gradient of the down-slope was less than 1.5 degrees. In the case of Stava the down-slope angle averaged 4.5 to 7.6 degrees and the velocity of the flowing mass increased from an average of 8 m/sec over the first 4 km up to 12 to 25 m/sec for the subsequent 20 plus kilometres. For earthquake-triggered failures it is suspected (from the available information) that the large travel distances recorded (5 to 12 km in a number of cases) were associated with down-slope angles that were as shallow as 3 to 5 degrees.

Travel distance angle predictions based on empirical correlations are not recommended for flow slides in tailings dams. Predictions based on numerical modelling are considered more appropriate (Section 3.10.3).

(b) Flow Slides from Landslides in Sensitive Clays

For retrogressive landslides in sensitive clays the greatest destructive potential is to persons and property up-slope within the area encompassed by the retrogression of the landslide. Leroueil et al (1996) comment that the distance of retrogression is very difficult to predict, but that it has a tendency to increase with increasing liquidity index. Figure 3.77 shows a broad degree of variation in the distance of retrogression relative to the liquidity index for the case study data from Mitchell and Markell (1974) and other published case studies included as part of this study.

Mitchell and Markell (1974) indicate some correlation of retrogressive distance with the stability number, N_s (N_s = $?H/c_u$, where H = slide depth, c_u = undrained shear strength and $?$ = bulk unit weight), as shown in Figure 3.78. Trak and Lacasse (1996), for eight flow slides in sensitive clays, showed some correlation between the ratio of retrogressive distance to slide depth and stability number (slightly different to the stability number used by Mitchell and Markell). However, addition of a number of flow slides in sensitive clays from Mitchell and Markell (1974) and from the published literature show this to provide a poor correlation (Figure 3.79).

In conclusion, the existing empirical based methods for prediction of the retrogression distance of "rapid" flow slides in sensitive clays, based on liquidity index and stability number, are relatively inaccurate and should be used cautiously. No

improvement to the current empirically based methods is suggested from analysis of the case study data.

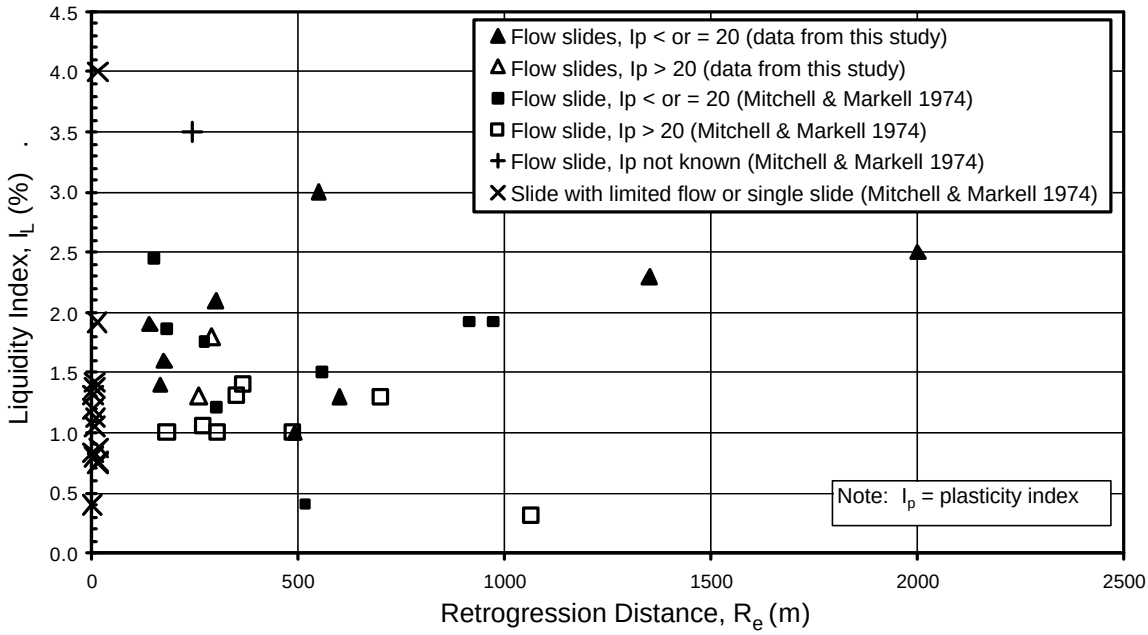

Figure 3.77: Distance of retrogression versus liquidity index for slides in sensitive clays

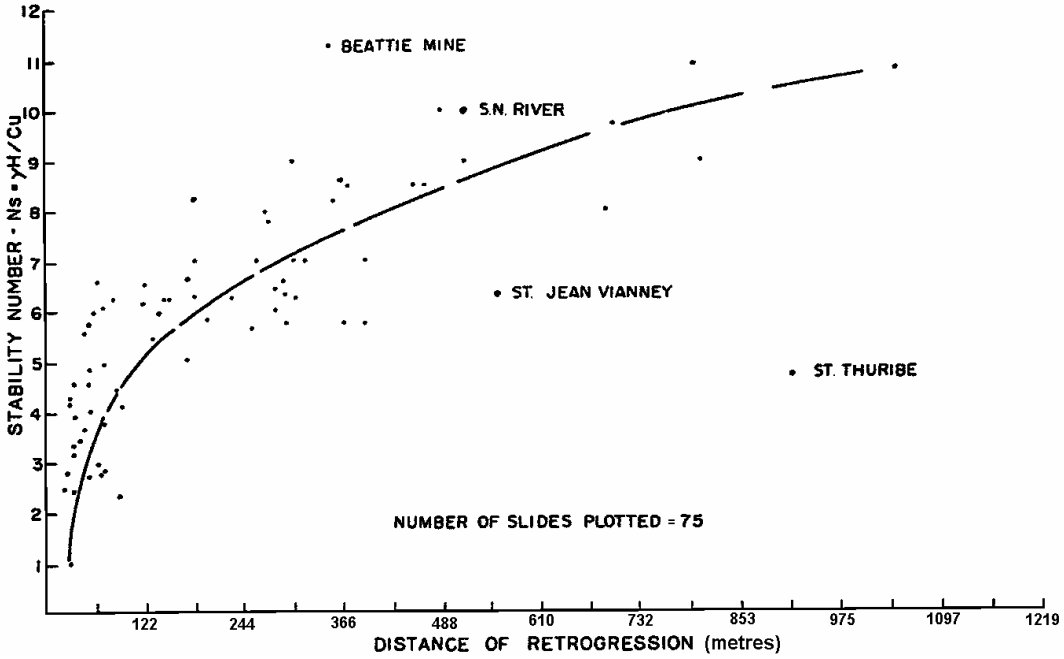

Figure 3.78: Distance of retrogression based on stability number for landslides in sensitive clays (Mitchell and Markell 1974)

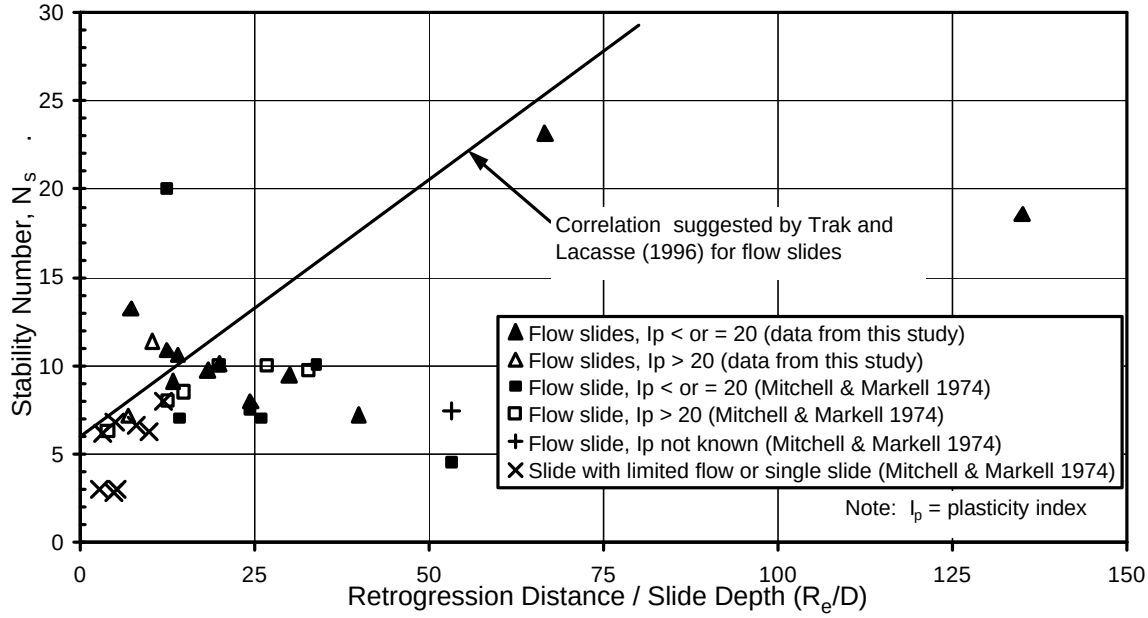

Figure 3.79: Ratio of retrogression distance to slide depth versus stability number

3.9.4.4 Hydraulic Fill Embankment Dams

The post failure analysis of the "rapid" flow slides from failures in hydraulic fill embankment dams included the failure of Wachusett dam in loose dumped sands due to similarities in material type, the failure mechanism (flow liquefaction) and the post-failure deformation behaviour. A summary of the slide properties for the 5 case studies is given in Table 3.28.

Table 3.28: Summary of slide properties of flow slides in hydraulic fill embankments

Name *[1]	**Material Type (Liquefiable Zone)**	**Embankment**			**Slide Volume (m^3)**	**TDA (°)** *[2]
		Slide Location (shoulder)	**Height (m)**	**Slope (°)**		
Sheffield Dam	Silty sands to sandy silts	downstream	7.6	22	16×10^3	6.8
Lower San Fernando Dam	Silty sands to sandy silts	upstream	35	21.8	400×10^3	9.9
Calaveras Dam	Not clear what part of embankment liquefied, possibly the siltier and sandier fractions	upstream	56	18	600×10^3	7.3
Fort Peck Dam	Fine sand	upstream	58	12.6	8000×10^3	3.8
Wachusett Dam *[3]	Fine sand to silty sand	upstream	24.4	22	47×10^3	7.9

Note: *[1] For all slides the travel path was unconfined and on near horizontal slopes

*[2] TDA = travel distance angle, a

*[3] Constructed of loose dumped sand

The limited number of case studies makes empirical methods of analysis based on historic events difficult to quantify statistically. Whilst regression coefficients may be relatively high, statistically the correlation may not be acceptable, or only just acceptable.

The distance of travel beyond the toe of the source area shows an excellent correlation with slide volume (Figure 3.56) and also with embankment height. The goodness of fit of these correlations is probably somewhat fortuitous given the small data set, however, in all cases the failure geometry is similar (all are Type 2 geometry) and the travel path is unconfined and on near horizontal slopes, and therefore some correlation to embankment height and slide volume would be expected. The slide volume has a positive correlation with embankment height (Table 3.28).

When the data is plotted in the form *H/L* to slide volume the data points plot at and below the lower 95% confidence interval of Corominas (1996a). This is generally lower than for most sub-aerial "rapid" landslide groups except for the retrogressive flow slides in sensitive clays and tailings dams. Figure 3.76 presents the case studies plotted with the retrogressive flow slides and shows the low *H/L* ratio of these events (0.07 to 0.18) and the lack of correlation of travel distance angle to slide volume.

Due to the significance of these structures and the potential catastrophic consequences in the event of an embankment breach, numerical analysis of the post-failure travel is recommended. Laboratory testing of high quality samples should be undertaken to assess the potential for liquefaction and provide estimates of residual undrained strengths. Earthquake is considered to be the most likely trigger of a potential flow slide event in hydraulic fill embankment dams given that these construction methods are no longer used in dam construction. However, the guidelines for post failure analysis are considered applicable to embankments on liquefaction susceptible foundations and also other hydraulic fill structures.

3.9.5 SUMMARY OF METHODS FOR PREDICTING TRAVEL DISTANCES

Previous researchers have combined the smaller volume slides typical of soil slopes with the significantly larger volume slides observed in rock slopes and derived correlations based on slide volume for prediction of the travel distance angle. It has been found that correlations of this type give poor predictions for the smaller volume slides.

The analysis of travel distance angle with volume, failure mechanism and degree of confinement of the travel path found relatively weak statistical correlations (Section 3.9.2). Improvement in the accuracy of predictive methods was obtained when the data was divided further to take into consideration slope type (cut, fill or natural slope), material type, initial failure mechanism, down-slope angle below the source area, a_2, the cut slope angle (for cut slopes), travel path confinement or slide volume, or a combination of these. The main sub-groupings of "rapid" landslides considered were from:

- Cut slopes (Section 3.9.3.1) in saprolitic, residual soils and some colluvial soils consisting typically of gravel to boulder sized weathered rock fragments in a silty sand matrix, with low clay content.
- Natural slopes (Section 3.9.3.2) mainly in cohesionless to low cohesion colluvial soils. These cases studies were further separated based on degree of confinement of the travel path.
- Flow slides in fills constructed of loose silty sand with low clay content (Section 3.9.4.1).
- Flow slides in coarse-grained (sandy gravels) loose dumped mine waste fills (Section 3.9.4.2). These case studies were of the coal mine waste spoil pile failures in British Columbia and South Wales, and were further divided based on degree of confinement of the travel path and materials mantling the down-slope travel path.

Guidelines on predictive methods for the travel distance angle for each of the above sub-groups are given in the referenced chapter sections and are summarised in Table 3.30. Table 3.30 briefly summarises the method of prediction and references the relevant figures, tables and equations where the correlations can be found, and the volume range over which the correlation is considered applicable. Limitations on the application of the correlation are discussed at the end of the chapter sub-sections referenced above.

For a number of sub-groups of landslides analysed in Sections 3.9.3 and 3.9.4 no or poor correlations were obtained for the travel distance angle with respect to either slide volume or the down-slope angle, a_2. For these slide groups it has been recommended to use the mean and standard deviation of the *H/L* data specific to that group for prediction of the travel distance angle. Table 3.29 presents the results of statistical analysis of these slide groups and includes ranges for slide volume and *H/L* ratio of the case studies

analysed. Also included are the data for "rapid" landslides from natural slopes for preliminary predictive estimates of travel distance angle.

Although not discussed separately in Section 3.9, statistical results from analysis of the slide groups flow slides in coking coal, dilative failures in fills constructed of silty sands with low clay content and washout failures of silty sand fills are included in Table 3.29. Further data on the post failure travel of "rapid" landslides in these sub-groups are given in Table 3.24, Table 3.25, and Figure 3.59 to Figure 3.63. The mean and standard deviations given in Table 3.29 for these slide groups are a basis for prediction of the travel distance angle.

Retrogressive flow slides in tailings dams and sensitive clays (Section 3.9.4.3), and flow slides in hydraulic fill embankment dams (Section 3.9.4.4) have been considered separately. For flow slides in tailings dams and hydraulic fill embankment dams empirical methods of predictions are considered not appropriate and numerical methods of analysis are recommended.

3.10 POST-FAILURE NUMERICAL MODELLING - METHODS AND RESULTS

The following sub-sections summarise the results of numerical modelling applied to the post failure travel of groups of "rapid" landslides from Hong Kong, coal waste spoil piles in British Columbia and tailings dams. Fell et al (2000) present a summary on the background and available methods for numerical modelling of the post-failure behaviour of "rapid" slides. The method that shows the most promise at this time is the DAN model (Hungr 1995).

The DAN model is a universal continuum model based on the Lagrangian approach, where the solution is based on moving frame of reference attached to the elements of the moving mass (Hungr 1995). It is described as universal in that a broad range of rheological models can be used within the program. The DAN program can also take into consideration three-dimensional effects, such as for a confined flow, from estimation of the slide width from the slope topography, and various rheological models can be incorporated into the one travel path. Hungr (1995) gives a more detailed discussion of the DAN program and its capabilities, and Fell et al (2000) and Hungr (1995) give discussions on the various rheological models that are incorporated within DAN.

Table 3.29: Mean and standard deviation of *H/L* for several types of slopes giving "rapid" landslides.

Initial Slide Classification	Material Type / Slope Type	Degree of Confinement of Travel Path	No. Cases	Volume Range (cu.m.)	H/L Range	H/L Mean	H/L Std. Dev.	Range of *[3] Std. Dev. of Population	Comments
Flow Slides in Contractive Soils	Coal mine waste spoil piles (sandy gravels) *[2]	Confined, high mobility	7	110,000 to 5.6×10^6	0.18 to 0.28	0.208	0.035	0.023 to 0.077	High mobility associated with liquefaction susceptible materials mantling the down-slope.
		No confinement condition, normal mobility	47	3,000 to 8×10^6	0.22 to 0.49	0.359	0.076	0.063 to 0.095	Similar mean and std. dev. for all travel path types.
	Loose silty sand fills (Hong Kong)	All unconfined	16	50 to 10,400	0.28 to 0.60	0.405	0.094	0.070 to 0.146	
	Coking coal stockpiles	All unconfined	9	850 to 16,000	0.14 to 0.34	0.257	0.0625	0.042 to 0.120	Limited number of cases for analysis. Low specific gravity
Failures in Dilative Soils*[1]	Natural Slopes (incl. Corominas debris flow data)	Confined	19	50 to 13,000	0.22 to 0.67	0.426	0.110	0.083 to 0.162	For preliminary estimate of travel distance angle
		Partly confined	10	80 to 3,000	0.28 to 0.62	0.470	0.114	0.078 to 0.207	
		Unconfined	52	20 to 140,000	0.22 to 0.75	0.547	0.137	0.115 to 0.170	
	Washout failures of silty sand fills (Hong Kong)	Confined (assumed)	19	40 to 4,000	0.18 to 0.67	0.450	0.109	0.083 to 0.162	Silty sands of low clay content.
	Fills of silty sands (Hong Kong)	Unconfined	10	40 to 500	0.52 to 0.84	0.641	0.093	0.064 to 0.170	Silty sands of low clay content.

*[1] Inclusive of defect controlled slides, slides of debris and slides through the soil mass.

*[2] High mobility events associated with confined travel path and liquefaction susceptible materials mantling down-slope travel path.

*[3] Statistical estimate of 95% confidence intervals of population based on case studies representing a sample of the population.

Std. Dev. = standard deviation.

Table 3.30: Summary of recommended methods for prediction of H/L (tangent of the travel distance angle)

Initial Slide Classification	Slope / Material Type	Material Properties	Volume Range (cu.m.)	Degree of Confinement	Method of Prediction of Travel Distance Angle	Reference Table / Figure / Equation	Comments
Flow Slides in Contractile Soils	Coal mine waste spoil piles on hillsides.	Sandy gravels with low fines content	Up to 5×10^6	Confined –high mobility	For curved down-slope angle use mean and standard deviation. If relatively constant use Down-slope angle, a_2	Table 3.29, Table 3.27	Consider confined high mobility separately*[1]. For normal mobility disregard degree of confinement when using tables and figure.
				Confined to unconfined		Table 3.29, Table 3.27, Figure 3.75	
	Fill Slopes	Silty sands with 10 to 50% fines and low clay content (< 10%). Dry density < 85% SMDD.	50 to 500	Unconfined	Mean and standard deviation	Table 3.29	Case studies from flow slide failures in loose fill slopes, Hong Kong
			500 to 10,000	Unconfined	Mean and standard deviation, or slide volume	Table 3.29, Figure 3.73, Equation 3.18	
Failures in Dilative Soils*[1]	Cut Slopes	Silty sands to sandy silts, low clay content, varying gravel content (residual soils, saprolite and colluvium)	Up to 100 to 500	Unconfined	Cut slope angle, a_{cut}	Equation 3.13	Derived from case studies of cut slope failures with run-out onto near horizontal slopes at the toe. Lower bound in Figure 3.65 for Type 2 cut slopes. Use natural slope correlations if the difference between the cut slope and slope below is < 10 to 20 degrees.
			Up to 20,000	Unconfined	Cut slope angle, a_{cut}, and slide volume	Figure 3.65, Equation 3.14	
	Natural Slopes	Colluvial and some residual soils. Silty sands to gravelly and cobbly soils. Low clay content.	Up to 10,000	Confined	Down-slope angle, a_2	Figure 3.71, Equation 3.17	Use mean and standard deviation for preliminary estimate of travel distance angle to establish a_2 (from Table 3.29) Then use Figure 3.69 to Figure 3.71 (or Equations 3.15 to 3.17) for more accurate prediction.
				Partly confined	Down-slope angle, a_2	Figure 3.70, Equation 3.16	
				Unconfined	Down-slope angle, a_2	Figure 3.69, Equation 3.15	

*[1] High mobility flow slides associated with suspected liquefaction of materials mantling the confined travel path. Normal mobility is not associated with the liquefaction of materials mantling the travel path.

3.10.1 "RAPID" LANDSLIDING IN HONG KONG

Ayotte and Hungr (1998) and Hungr Geotechnical Research (1998) undertook numerical modelling of some twenty-six reported "rapid" slides from Hong Kong using the DAN program. The case studies analysed (Table 3.31) included 21 dilatant slides in natural (and some quasi-natural) slopes, 4 failures in cut slopes (3 defect-controlled) and 1 flow slide failure in a loose fill slope. The debris flow travel classification would be appropriate to all failures in natural terrain and cut slopes.

The purpose of the modelling was to attempt to match the actual debris deposition, travel distance and velocity of the slide mass (where estimation was possible) using a consistent rheological framework that could then be applied to similar potential landslides within a risk assessment framework. The models used were the friction model for unconfined and partly confined travel paths and dominantly translational sliding type debris flows (e.g. Fei Tsui Road), and the Voellmy model for confined debris flows. A combination of models was used for several landslides where the initial travel path was on open or partly confined slope (using the frictional model) and the distal part confined within a gully (using the Voellmy model).

The frictional model incorporates a frictional resistance component at the base of the sliding mass (bulk friction angle, f_b) estimated from the normal effective friction (f') of the loose debris and an estimated pore pressure coefficient, r_u, according to Equation 3.19.

$$tan f_b = (1 - r_u) tan f' \qquad (3.19)$$

where $r_u = u / s_n$, the ratio of the excess pore pressure, u, to the total normal stress, s_n.

The Voellmy model is a combination of frictional sliding and turbulent flow.

The findings of the analysis are summarised in Table 3.32. Based on the results, Ayotte and Hungr (1998) concluded that:

- Good results were achieved with respect to matching the debris deposition profile, travel distance and velocity (where available) of the back-analysis to the actual event.
- For confined debris flows the Voellmy model, using a bulk friction angle of 5.7 to 11.3 degrees and turbulent friction coefficient of 500 m/sec^2 resulted in a good prediction of the slide mass travel. For predictive purposes, Ayotte and Hungr

(1998) suggest using a bulk friction angle of 11.3 degrees and turbulent friction coefficient of 500 m/sec^2 for the confined portion of debris flows (in Hong Kong).

- For unconfined and partly confined debris flows in natural slopes a broad variation in the bulk friction angle resulted from the back-analysis (Figure 3.80), particularly for small volume slides. Ayotte and Hungr (1998) considered the reasons for this to be small obstructions in the flow path such as trees and boulders that affect the flow behaviour of small magnitude slides, but not the larger magnitude slides. A reasonable correlation is evident between the bulk friction angle of the travel path and slide volume (Figure 3.80). They recommend the use of this correlation for estimation of the bulk friction angle in the prediction of travel behaviour for open slope failures of similar type and magnitude.
- For the larger volume events (greater than about 1000 m^3) on open or partly confined slopes the bulk friction angle is in the range 19 to 23 degrees. The findings indicate that the travel of these larger volume mostly debris flows is independent of the initiating mechanism (i.e. whether it is a flow slides, defect-controlled failure or slide of debris) and slope type (cut, fill or natural slope). Although, it is difficult to draw any definitive conclusions from the small number of slides analysed larger than about 1000 m^3.

Table 3.31: Summary of "rapid" landslides from Hong Kong analysed by Hungr Geotechnical Research (1998) and Ayotte and Hungr (1998)

Slide Type	**No. Cases**	**Volume Range (m^3)**	**Initial Slide Classification**	**Source Area Material Description**	**Travel Classification**
Cut	4	85 to 40000 (3 greater than 2000 m^3)	3 defect-controlled 1 dilatant slide through saprolitic soil mass.	3 in volcanic saprolite, 1 in granitic saprolite	4 debris flows. Rear portion of Po Shan (1972) possibly a debris slide.
Fill	1	2500	Flow slide in loose, end dumped fill	Silty sand (decomposed granite)	Flow slide
Natural	21 (2 quasi natural)	50 to 26000 (most less than 1000)	17 slides of debris 1 defect-controlled 3 dilatant slides through saprolite or residual soil mass.	Slides of debris in colluvium mantling the slope. Of the 4 remaining slides, 1 was in residual volcanic, 2 were in volcanic saprolite, and 1 was in granitic saprolite.	4 confined debris flows. 9 partly confined debris flows. 8 debris flows (unconfined), 1 of which is a debris slide / debris flow.

Ayotte and Hungr (1998) encountered difficulties modelling several slides within the framework of using a consistent rheologic approach. Three of the partly confined debris flows were modelled using the Voellmy model. In addition, they had difficulties getting the debris to initially slide out of the source area and overcame this problem by using a lower bulk friction angle for the source area.

The back-analysis results (Table 3.32 and Figure 3.80) present useful guidelines for selection of model type and material parameters for use in modelling the travel of slides in similar soil types based on slide type, volume and degree of confinement of the travel path. It is interesting that for the larger volume unconfined and partly confined events the mechanism of failure (flow slide, slide of debris or defect-control) has a limited influence on the estimated bulk friction angle. The limited number of case studies of each failure mechanism type makes it difficult to draw any firm conclusions as to the reason for this finding; however, it is considered possible that it reflects the large degree of break-up and flow type behaviour of the slide mass. Fei Tsui Road stands out as an outlier and this possibly reflects the lesser degree of break-up and suspected significant basal sliding component of the slide mass. For the small volume slides small obstructions to the flow are a dominant factor in the debris travel behaviour (as concluded from the empirical analysis) that is difficult to take into consideration and significant uncertainty is prevalent in predictive modelling.

Table 3.32: Summary of results of numerical modelling using DAN for "rapid" landslides in Hong Kong (Hungr Geotechnical Research 1998; Ayotte and Hungr 1998)

Slide Type	**Source Volume Range (m^3)**	**No. Cases**	**Frictional Model**		**Voellmy Model**	
			f_b source (º)	**f_b path (º)**	**f (º)**	**Turbulent Coeff^t**
Natural Slopes – unconfined and partly confined using frictional model.	<200 200 to 500 500 to 26000	4 6 5	14 to 30 23 to 34 20 to 25	24 to 43 25 to 34 20 to 25	-	-
Natural Slopes – partly confined using Voellmy model	150 to 450	3			11 to 22	500
Natural Slopes - confined	50 to 13000	4	-	-	5.7 to 11	500
Cut Slopes – defect controlled	85 to 40000	4	14 to 24	20, 23, 26 & 36	-	-
Flow Slide in loose fill	2500	1	20	20	-	-

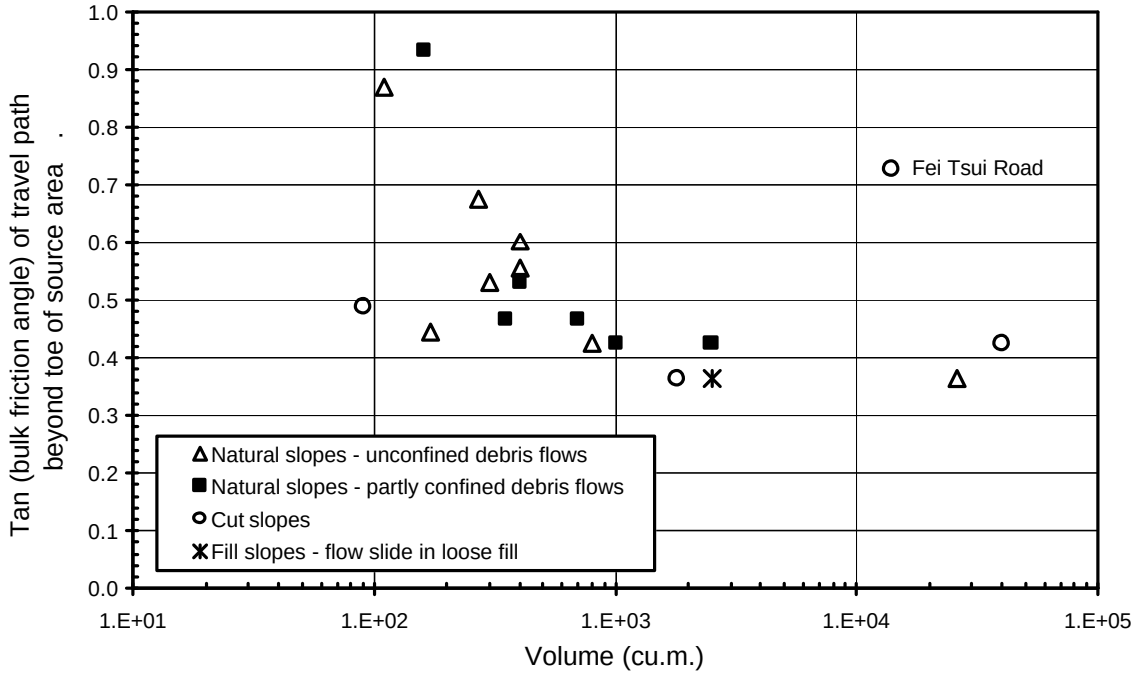

Figure 3.80: DAN results of frictional back-analysis models of "rapid" landslides from Hong Kong (data from Hungr GR (1998) and Ayotte and Hungr (1998))

3.10.2 "RAPID" LANDSLIDES FROM COAL MINE WASTE SPOIL PILE FAILURES IN BRITISH COLUMBIA

Golder Assoc. (1995) undertook numerical modelling of some forty-one case studies of "rapid" flow slides from failures in coal mine waste spoil piles from British Columbia using the DAN program. The purpose of the modelling (as for Hong Kong) was to attempt to match the actual debris deposition, travel distance and slide mass velocity (where estimation was possible) using a consistent rheological framework that could then be applied to similar potential landslides within a risk assessment framework. The models used were the frictional model for unconfined and partly confined travel paths (generally less than 1 km travel distance) and the Voellmy model for confined flow slides. A combination of models was used for several "rapid" landslides where the initial travel path was unconfined (using frictional model) and the distal portion confined within a gully (using Voellmy model).

Based on the findings of the numerical analyses, Golder Assoc. (1995) concluded that:

- A good simulation of the observed velocities, debris deposition profile and travel distance was achieved for the partly confined and unconfined flow slides with travel

distances less than 1 km using the frictional model with bulk friction angles of 18 to 24 degrees (Figure 3.81). For an estimated dynamic friction angle of 30 degrees for the debris, this equates to pore pressure coefficients in the range 0.23 to 0.44.

- The frictional model was less suitable for the confined flows with travel distances in excess of 1 km. Quite low bulk friction angles (10 to 18 degrees) were required to match the travel distance and the modelled velocities were up to three times greater than field estimates.
- Using the Voellmy model for the portion of the confined travel path for the large travel distance cases provided a reasonable simulation of the debris deposition and velocities when matching the travel distance. The parameters used for the Voellmy model were a bulk friction angle of 3 to 6 degrees and turbulent friction coefficient of 200 to 300 m/sec^2.

Based on the results from Golder Assoc. (1995), it is concluded that for predictive modelling purposes it is necessary to calibrate against known failures in similar materials, with similar degree of confinement and foundation conditions along the travel path. Otherwise it is necessary to accept large uncertainty in the use of numerical models.

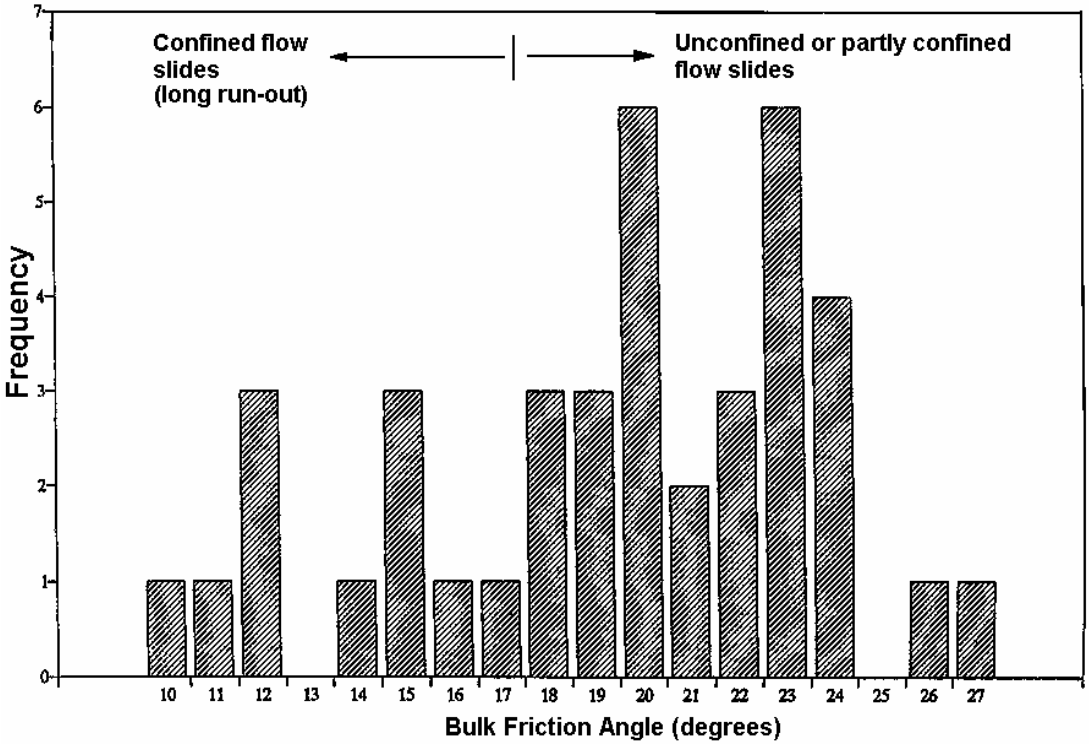

Figure 3.81: Back calculated bulk friction angle from DAN analysis of flow slides from coal mine waste spoil pile failures in British Columbia (Golder Assoc. 1995)

3.10.3 FLOW SLIDES FROM TAILINGS DAMS FAILURES

Numerical analysis has been undertaken for flow slides from tailings dam failures by Jeyapalan et al (1983b) and Blight (1997).

Blight (1997) undertook a simple sliding block model analysis (Figure 3.82) assuming hydrostatic pore pressures within the flowing tailings and shear resistance to flow along the interface between the down-slope foundation and flowing tailings. He used the model to estimate the shear resistance along the interface (Equation 3.20) from the known characteristics of the slide.

$$t = \frac{(P_1 - P_2)\cos i + W \sin i}{L / \cos i} \tag{3.20}$$

From analysis of 8 case studies Blight (1997) concluded that the undrained residual strength of the liquefied tailings ranged from 1 to 4 kPa and that the shear strength was sensitive to the availability of free water down-slope of the failure. For the cases that flowed onto a wet down-slope (from recent rainfall) the shear resistance along the interface ranged from 1.0 to 2.6 kPa. Where the tailings flowed onto a dry down-slope the shear resistance along the interface ranged from 3.4 to 5.2 kPa. From laboratory testing (Figure 3.83) it is evident that the shear strength of liquefied tailings (derived from the crushing of ore) decreases rapidly with increasing moisture content. Therefore, any free water entrained within the base of a laminar type flow of tailings can significantly reduce the shear strength.

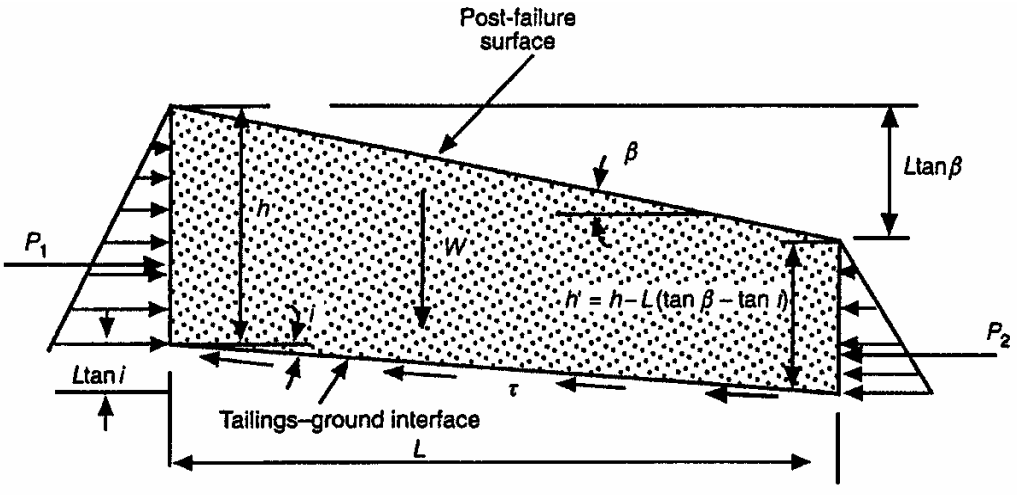

Figure 3.82: Simple sliding block model for analysis of tailings strength (Blight 1997)

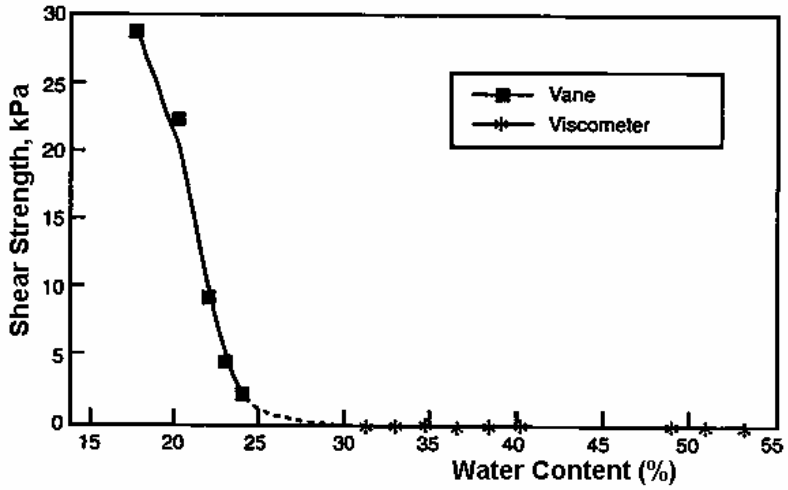

Figure 3.83: Variation of shear strength with moisture content for gold tailings (Blight 1997)

Jeyapalan et al (1983a) and Blight (1997) comment that the Bingham plastic rheologic model is a good approximation to the flow of liquefied tailings where the flow is laminar. For turbulent flow of tailings, i.e. a hyper-concentrated stream-flow, Jeyapalan et al (1983a) recommend the use of flood routing computer programs to model the flow.

Jeyapalan et al (1983a) developed solutions using the Bingham plastic rheological model to a dam break type analysis (Figure 3.84) for flow on horizontal sloping planes (one-dimensional model) and for flows within prismatic valleys. They developed graphical solutions for the horizontal sloping plane analysis based on the strength and viscous parameters of the flow for down-slope angles ranging from 0 to 14 degrees.

Jeyapalan et al (1983b) tested the model against flume tests using viscous oil and found good agreement between the model and the test. They then applied the model to two actual failures (Aberfan in 1966, which is not a tailings dam failure, and the gypsum tailings dam failure in Texas in 1966) and reported reasonable agreement even though the model is limited to one-dimension and therefore cannot take into consideration spreading of the flow. Golder Assoc. (1995) found that the Bingham plastic rheologic model was not suitable for flow slides in the coal waste spoil piles of British Columbia.

The degree of agreement between the case study and the numerical model for the Bingham plastic rheologic model is very strongly dependent on the estimated value of viscosity and yield strength. Given the potential broad variation in shear strength of tailings (Figure 3.83) use of the model for predictive purposes should be undertaken

cautiously and factors such as potential entrainment of water in the slide mass should be considered. Its use is likely to be more applicable to laminar type flow conditions of fine grained tailings flows as the findings by Jeyapalan et al (1983b) and Golder Assoc. (1995) suggest.

Jeyapalan et al (1983b) also applied a turbulent flow model (using a flood routing program) to the catastrophic failure at Buffalo Creek. They reported comparable results between the model and the actual flow. This type of flow behaviour (hyper-concentrated stream flow) is not uncommon within tailings dam failures. Other cases of turbulent or hyper-concentrated stream flows are considered to include the confined flow portions of the tailings dam failures at Stava, Italy (in 1985), Bafokeng, South Africa (in 1974) and a number of the earthquake induced failures that flowed for many kilometres.

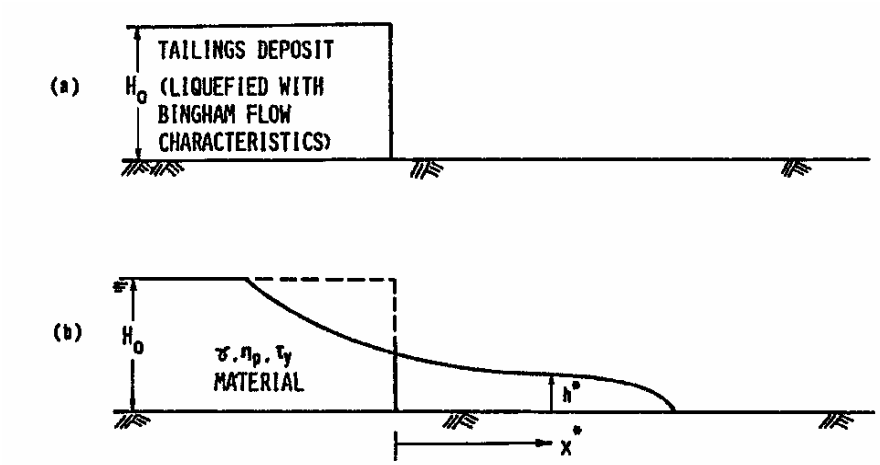

Figure 3.84: Model for flow of liquefied tailings (Jeyapalan et al 1983a)

3.11 CONCLUSIONS

"Rapid" landslides from failures in soil slopes have the potential to cause mass destruction, resulting in loss of life, destruction to property and damage to the natural environment. It is important therefore that geotechnical engineers, engineering geologists and geologists understand the soil characteristics, slope conditions and failure mechanics that can result in "rapid" sliding, and are alert to the pre-failure warning signs prevalent for several classes of slope failure that develop into "rapid" landslides post failure. An important part of any risk assessment of potential slope instability is prediction of the post-failure deformation behaviour for evaluation of the risk to life, property and the environment down-slope (or up-slope in the case of retrogressive

failures) of the potential failure. An understanding of the soil characteristics (both the slide mass and slope mantling materials), failure mechanics, down-slope conditions and travel behaviour is important in making informed predictions of travel distance.

The mechanics of failure of landslides that develop into "rapid" slides has been divided into two broad classifications; flow slides in contractive soils and landslides in dilative soils. Several classes of landslide have been identified and analysed within each classification, they are:

- For flow slides in contractile soils:
  - Flow slides (sub-aerial) in loose dumped fills of soil types ranging from silty sands to hillside mine waste spoil piles of sandy gravels.
  - Flow slides in hydraulically placed fills (including tailings dams, hydraulic fill embankment dams and sub-aqueous fills).
  - Flow slides in natural soils (including sensitive clays and submarine slopes)
- For landslides in dilative soils, failures within steep cut, fill and natural slopes have been analysed. Two dominant failure types have been identified:
  - Strongly defect-controlled slope failures in weathered soil slopes (residual soil and weathered rock masses) along discontinuities adversely orientated to the face slope.
  - Slope failures within the soil mass (with no defect control) including; slides of debris in colluvium and failures through the soil mass in residual soils, weathered rock masses and compacted fills.

An important component of the research was the literature review on the mechanics of shearing of contractive, granular soils. The characteristics of soils susceptible to static liquefaction and potential flow sliding, and methods of assessment of flow-liquefaction potential are summarised in Section 3.6. Section 3.3.5 summarises the available methods for assessment of the residual undrained strength of flow-liquefied soils. Section 3.4 provides additional information on the soil properties, triggering and failure mechanics of flow slides for the categories of flow slide considered.

For failures in dilative soils, Section 3.6 summarises the material properties and slope characteristics within which the failure has developed into a "rapid" debris flow or debris slide post failure. Additional information is provided in Section 3.5, for both

failures through the soil mass (Section 3.5.2) and strongly defect-controlled failures (Section 3.5.3).

Travel distance angle, and therefore travel distance, of the failed slide mass can be predicted empirically using correlations with slide volume, down-slope angle and other factors. Section 3.9.5 summarises the analysis on methods of travel distance angle prediction and Table 3.30 (within Section 3.9.5) summarises the recommended methods for prediction of the travel distance angle for various slope and material types. These methods are, in most cases, improvements on current methods. Details of the analysis, findings and limitations of the predictive methods for the various slope and material types analysed in detail are given in Sections 3.9.3 and 3.9.4.

There is inherently a large uncertainty associated with predictions of post-failure deformation analysis, for both empirical and numerical analyses. For important projects it is recommended that empirical methods and numerical models be calibrated using local, similar type failures to reduce some of the uncertainty. Risk analysis methods can also be incorporated into the analysis by assessment of the mean and range of outcomes.

TABLE OF CONTENTS

4.0 EMBANKMENTS ON SOFT GROUND..... 4.1

4.1 INTRODUCTION TO THIS CHAPTER 4.1

4.2 LITERATURE REVIEW 4.3

4.2.1 Excess Pore Water Pressure Response 4.5

4.2.2 Deformation Behaviour 4.15

4.3 ANALYSIS OF THE BEHAVIOUR OF FAILURE CASE STUDIES 4.22

4.3.1 Case Studies Analysed 4.22

4.3.2 Excess Pore Water Pressure 4.26

4.3.3 Pre-Failure Deformation Behaviour and the Effects of Progressive Failure 4.32

4.3.4 Factor of Safety Versus Relative Embankment Height 4.45

4.3.5 Post-Failure Deformation Behaviour 4.47

4.4 POST CONSTRUCTION BEHAVIOUR OF EMBANKMENTS ON SOFT GROUND 4.51

4.4.1 Effect of Effective Stress State on the Post Construction Behaviour 4.52

4.4.2 Deformation Behaviour and Pore Water Pressure Response in the Initial Period Post Construction 4.52

4.4.3 Long-Term Post Construction Deformation 4.59

4.5 DISCUSSION AND CONCLUSIONS 4.61

4.5.1 Indicators of an Impending Failure 4.61

4.5.2 Guidelines on Monitoring for Identification of an Impending Failure Condition 4.63

4.5.3 Post Failure Deformation Behaviour 4.64

4.5.4 Discussion on Failure Mechanism 4.65

LIST OF TABLES

Table 4.1: Summary of failure case studies of embankments on soft ground. 4.24

Table 4.2: Excess pore water pressure observations for the failure case studies 4.26

Table 4.3: Summary of exceptions to general observations of excess pore water pressure response. 4.31

Table 4.4: Summary of case studies that are exceptions or have other explanations to deformation as an indicator of impending failure. 4.44

Table 4.5: Results of the post-failure deformation analysis 4.50

LIST OF FIGURES

Figure 4.1: Computed factor of safety for field failures (Tavenas and Leroueil 1980) 4.2

Figure 4.2: Effective vertical stress profile and pre-consolidation stress profile prior to construction, and the effective vertical stress profile at end of construction of the Saint Alban B test embankment (Tavenas and Leroueil 1980). 4.8

Figure 4.3: Field observations of excess pore water pressures in clay foundations during the initial period of embankment construction (Tavenas and Leroueil 1980). 4.8

Figure 4.4: Total (*OPFR*) and effective (*O¢P¢F¢R¢*) stress paths under the centre of embankments (Tavenas and Leroueil 1980) 4.9

Figure 4.5: Relationship between the excess pore water pressure and the applied vertical stress (Tavenas and Leroueil 1980) 4.9

Figure 4.6: Dimensionless variations of changes in total stresses under the centreline of an infinite strip load on an elastic half space (Poulos and Davis 1974) 4.10

Figure 4.7: Effective stress paths for varying $\overline{B}$ values and total stress ratios (Folkes and Crooks 1985). 4.11

Figure 4.8: Effective stress paths and pore water pressure generation associated with different types of yield conditions (Leroueil and Tavenas 1986). 4.11

Figure 4.9: Element of soil at depth z beneath on centreline of uniform circular load (Muir Wood 1990) 4.13

Figure 4.10: Total stresses on centreline beneath uniform circular load on elastic half space (Muir Wood 1990). 4.14

Figure 4.11: Total (*BCDE*) and effective (*B′C′D′E′*) stress paths for a soil element on the centreline beneath a circular load (Muir Wood 1990). 4.14

Figure 4.12: Variation of pore water pressure with applied surface load for element on centreline beneath circular load (Muir Wood 1990). 4.15

Figure 4.13: Variation of the dimensional factor *R* (proportional to the horizontal surface displacement at the toe) with factor of safety (Marche and Chapuis 1974) 4.17

Figure 4.14: Definition of the geometry and deformation parameters (Tavenas et al 1979)..... 4.18

Figure 4.15: Average correlation between the maximum lateral movement at the toe, y_m, and settlement under the centre of the embankment, *s*, during construction (Tavenas and Leroueil 1980)..... 4.18

Figure 4.16: Effective stress and lateral displacement profiles at the end of construction under *(a)* Cubzac-les-Ponts A and *(b)* Saint Alban B test fills (Tavenas et al 1979) 4.19

Figure 4.17: Comparison of horizontal movement (on berm beyond embankment toe) during loading and for 24 hour period for the Thames test embankment (Marsland and Powell 1977) 4.20

Figure 4.18: Observations of lateral displacement at the base of the embankment with increasing embankment thickness at the Rio test embankment (Ramalho-Ortigao et al 1983a)..... 4.21

Figure 4.19: Contours of normalised shear-stress ratios at 4 m fill thickness from finite element modelling at Muar-F test embankment, Malaysia (Indraratna et al 1992)..... 4.22

Figure 4.20: Idealised section of embankment indicating the types of monitored observations..... 4.23

Figure 4.21: *(a)* and *(b)* Excess pore water pressure under centre of embankment versus applied embankment load. 4.27

Figure 4.22: Settlement under the centre of the embankment versus relative embankment height (H/H_f). 4.34

Figure 4.23: Vertical displacement at the embankment toe versus relative embankment height. 4.35

Figure 4.24: Vertical displacement beyond the embankment toe versus relative embankment height. 4.36

Figure 4.25: Lateral surface displacement at the embankment toe versus relative embankment height. 4.38

Figure 4.26: Incremental vertical inclination angle (from inclinometer observations at the embankment toe) with fill height (and time) for *(a)* Thames and *(b)* King's Lynn. 4.39

Figure 4.27: Vertical inclination angle on the surface of rupture from inclinometer observations at the embankment toe versus relative embankment height. 4.40

Figure 4.28: Maximum lateral displacement at the embankment toe versus settlement under the centre of the embankment. 4.43

Figure 4.29: Factor of safety versus relative embankment height 4.46

Figure 4.30: Failure model for post-failure deformation (Khalili et al 1996)..... 4.49

Figure 4.31: Effective stress paths post construction (Leroueil and Tavenas 1986).... 4.53

Figure 4.32: Excess pore water pressure response with time for several piezometers at the Muar-EC test embankment. 4.55

Figure 4.33: Excess pore water pressure response at Piezometer C1 with time at the St. Alban-A test embankment. 4.56

Figure 4.34: Schematic behaviour of strain rate effects on limit state surface with decreasing strain rate in undrained creep tests (adapted from Leroueil and Marques 1996) 4.58

Figure 4.35: Relationship between the maximum lateral displacement at the toe, y_m, and settlement at the centre, s, at the end of construction (Tavenas et al 1979). 4.60

Figure 4.36: Relationship between maximum lateral displacement (toe) and settlement (centre) at the end of construction for different embankment geometries and stability conditions (Tavenas et al 1979). 4.61

4.0 EMBANKMENTS ON SOFT GROUND

4.1 INTRODUCTION TO THIS CHAPTER

The results of stability analysis of failure case studies of embankments on soft ground (Bjerrum 1972; Pilot 1972; Aas et al 1986) indicate conventional total stress stability analysis is unreliable in prediction of the failure height, with failure generally occurring at factors of safety of greater than unity. The uncertainty in the assessment of the stability of embankments on soft ground is due to the difficulty in predicting the undrained shear strength of the soils in the foundation, given the inherent variability of the soil strata and the uncertainty in the methods of measuring the strength; modelling the strength of the upper over-consolidated, often fissured, desiccated crust; the potential for fissuring in the lightly over-consolidated soils below the crust; and the potential for cracking in the embankment.

To account for this uncertainty various guidelines have been developed for stability analysis of embankments on soft ground and methods of interpretation of field data. Bjerrum (1972) proposed a correction factor based on the plasticity of the soft clay foundation to account for the discrepancy between the vane strength and the mobilised strength at failure. The predominant factors attributing to the strength discrepancy were considered by Bjerrum (1972, 1973) to be the difference in the rate of loading between the vane and actual embankment construction, strength anisotropy and progressive failure. As shown in Figure 4.1 there is significant uncertainty surrounding this correction factor. Other guidelines included; correction factors for specific soil types, such as leached, sensitive marine deposits (Dascal and Tournier 1975); methods of assigning strength properties to fissured soils, particularly the crust (La Rochelle et al 1974; Ferkh and Fell 1994); the effect of plant matter and shells on the vane strength (La Rochelle et al 1974; Ferkh and Fell 1994; Marsland and Powell 1977); and treatment of the strength of the embankment.

However, even with the methods of interpretation and analysis available, the Type A predictions for the Muar test embankment (Brand and Premchitt 1989) highlight the uncertainty that is still prevalent in limit equilibrium analysis of embankments on soft ground. Of thirty-one predictions, the predictions of fill height at failure ranged from 2.8 m to 9.5 m (mean = 4.7 m, standard deviation = 1.5 m, actual = 5.4 m) and the predictions of the depth of the failure surface ranged from 2.5 m to 13 m depth (mean =

6.3 m, standard deviation = 2.2 m, actual = 8 m). Most of this variation may relate to those involved not being directly responsible for the project, and failure to differentiate between designing a safe embankment and predicting a failure height, but there is a significant element of uncertainty inherent at this time.

El-Ramley (2001) showed that for the soft ground case studies he studied, a factor of safety of 1.5 corresponded to a probability of unsatisfactory performance (failure) of about 1 in 50. This reflected the large uncertainty in estimating the undrained strength.

The uncertainty surrounding the estimation of factor of safety (and settlement behaviour) for embankments on soft ground has led to the construction of full-scale test embankments, particularly for large projects. In a number of cases these test embankments (which were generally well-monitored) were constructed to failure to determine appropriate design and construction procedures of the actual embankment.

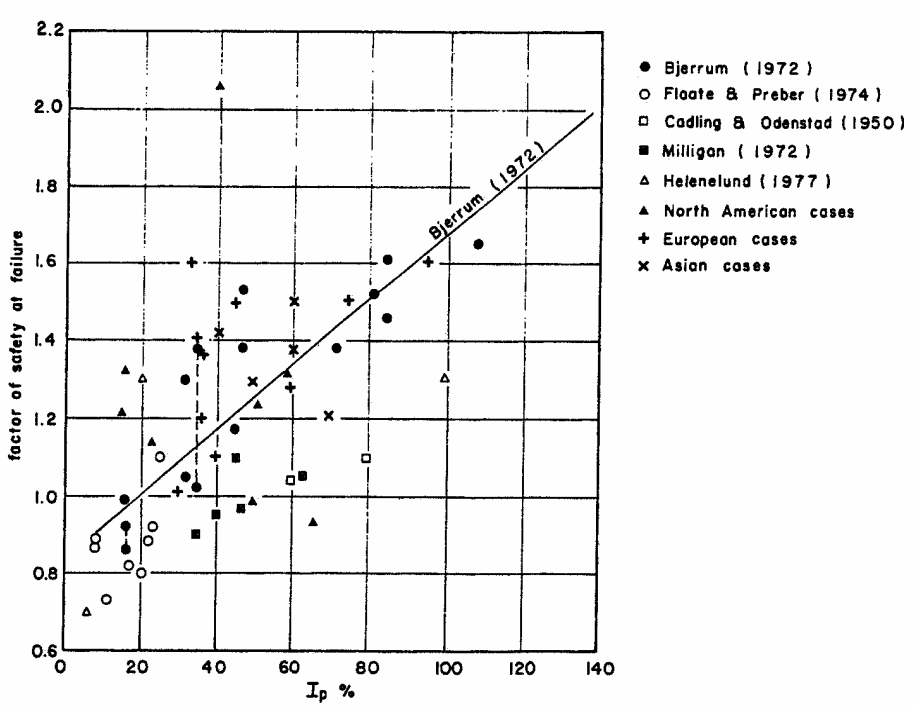

Figure 4.1: Computed factor of safety for field failures (Tavenas and Leroueil 1980)

The main purpose of the research on embankments on soft ground was to evaluate the pre-failure deformation behaviour and pore water pressure response from well-monitored case studies constructed to failure, and to identify field indicators of an impending failure condition. This will provide designers and construction supervisors with guidelines on interpretation of monitoring allowing early identification of an impending failure condition, which would allow appropriate measures to be undertaken

to avert failure (eg. stopping construction to allow pore water pressures induced by the embankment construction to dissipate, and the foundation to gain strength).

A secondary objective of the research was to develop further the understanding of post failure deformation and evaluate the applicability of existing models to predict the post failure deformation behaviour.

Initially, a summary is given of the literature in the context of the factors and findings affecting the deformation behaviour of embankments on soft ground (Section 4.2). It is by no means exhaustive, but focuses on observations, models and proposed methods related to the mechanics controlling the deformation, and causing changes in the deformation behaviour during loading, and the indicators of deformation behaviour leading up to a failure condition. Thirteen case studies of well-documented and monitored embankments on soft ground that were constructed to failure are then analysed (Section 4.3). Guidelines are developed for identification of an impending failure condition taking into consideration the mechanics of failure and the soil properties (Section 4.5). The general trend of the deformation behaviour and pore water pressure response is described within this framework.

The analysis of the post failure deformation behaviour of four of the embankment on soft ground case studies was undertaken using the Khalili et al (1996) method for intact sliding (Section 4.3.5.2). General guidelines on the applicability and use of this type of model are given in Section 4.5 and are discussed in Chapter 5 together with the findings from analysis of failures in embankments dams and cut slopes in high plasticity heavily over-consolidated clays (Sections 5.8.1 and 5.9.2).

4.2 LITERATURE REVIEW

This literature review concentrates on developing an understanding of the mechanics of the deformation behaviour during construction and leading up to failure. Predictive methods from the literature and further discussion of the factors affecting the deformation behaviour are presented with the findings of the case study analyses in Section 4.3. Related issues such as stability and consolidation behaviour are not discussed in any detail, but are implicit in the analysis of the data.

Bjerrum (1972, 1973), in his review of settlement behaviour of embankments on soft ground, recognised (as had Höeg et al 1969; and D'Appolonia et al 1971a) that the

in-situ over-consolidated state of the soft clay foundation had a significant influence on the pore water pressure response and settlement behaviour. Bjerrum commented that:

- At stress levels less than the pre-consolidation pressure, settlements are small and dissipation of pore water pressure is rapid. He described this as being due to the over-consolidated clays having high coefficients of consolidation, c_v, as a consequence of their low compressibility (related to the recompression index, C_s) and relatively small amount of pore water required to flow out of the soil structure.
- At stress levels in excess of the pre-consolidation pressure (normally consolidated condition) total settlements (during and post construction) are relatively large due to the high compressibility of the clay. The initial excess pore water pressures are high and dissipate relatively slowly due a much lower coefficient of consolidation, c_v, of the normally consolidated clay. The "immediate" settlement during loading occurs as a result of lateral straining associated with plastic yielding of the normally consolidated foundation.

The one-dimensional relationship between the soil stiffness (C_c, compression index) and coefficient of consolidation, c_v, proposed by Terzaghi is:

$$c_v = \frac{k}{g_w m_v} = \frac{k s_v' (1+e)}{0.434 g_w C_c} \tag{4.1}$$

where k is the hydraulic conductivity, e the void ratio, g_w the unit weight of water, s_v' the effective vertical stress and m_v the coefficient of volume change. Lambe and Whitman (1979) report ratios of the compression index, C_c, for clays in a normally consolidated condition compared to similar clays in an over-consolidated condition in the range 3 to 50, indicating the significant effect on c_v of compressibility between stress levels below and above the pre-consolidation pressure.

Höeg et al (1969) described the change between the two states as a critical value of applied stress at which settlements increased rapidly and a pronounced increase in rate of pore water pressure build up occurred with additional loading. D'Appolonia et al (1971a) also observed a similar increase in rate of pore water pressure development per unit increase in load in the MIT test embankment and attributed this increase to local yielding and contained plastic flow.

4.2.1 EXCESS PORE WATER PRESSURE RESPONSE

The Geotechnical Section at Université Laval, Quebec and the Research Group on Compressible Soils at the Laboratoire Central des Ponts et Chaussées, Paris undertook a joint research effort in the 1970's to develop further the understanding of deformation behaviour in soft clays under embankments. The following is a summary of the pertinent findings of their research related to field observation of excess pore water pressure response within the foundation during embankment construction. Discussion on the findings of their research on the deformation behaviour of embankments on soft ground is given in Section 4.2.2.

Leroueil et al (1978a) analysed the pore water pressure response observed under the centre of 30 embankments on soft clay from case studies covering a wide variety of clays in the Americas, Europe and Asia. The observed behaviour was interpreted using the YLIGHT model of clay behaviour (Cam Clay model incorporating strength anisotropy) proposed by Tavenas and Leroueil (1977). They recognised that all clays had developed some pre-consolidation (Figure 4.2), by aging, past loading, and other mechanisms such as desiccation by surface drying or evapo-transpiration of plants, and fluctuations in the ground water levels. For lightly over-consolidated clay (OCR < 2.5, OCR = over-consolidation ratio) the observed behaviour and stress path interpretation is summarised as follows:

i) In the early stages of loading (at effective stress levels less than the pre-consolidation pressure, s'_p) the excess pore water pressures generated (Δu) are influenced by the process of consolidation, i.e. dissipation of pore water pressure occurs during loading due to the relatively high coefficient of consolidation, c_v. Maximum excess pore water pressures developed in the central portion of the clay layer corresponded to $\overline{B}$ (Equation 4.2) values of 0.38 to 0.75, and the pore water pressure profile with depth was similar to that of a consolidation isochrone (Figure 4.3). The observed excess pore water pressure response was significantly below that corresponding to an undrained condition. In this stage of loading the over-consolidated clay foundation is characterised by relatively high stiffness (i.e. low compressibility) and high c_v, and dissipation of excess pore water pressures therefore occurs during construction. Path $O'P'$ (Figure 4.4) is idealised as the effective stress path for this stage of loading.

$$\overline{B} = \frac{Du}{Ds_1} = B\left[1-(1-A)\left(1-\frac{Ds_3}{Ds_1}\right)\right] \quad (4.2)$$

ii) At some stage in the construction process, the excess pore water pressure generated (at a specific piezometer) is observed to increase to an incremental $\overline{B}$ value of approximately 1 (Figure 4.5). Leroueil et al (1978a) interpreted this to be at Point *P¢* (Figure 4.4), where the effective vertical stress at the piezometer is equivalent to the pre-consolidation pressure, i.e. the limit state surface defining the normally consolidated state. The location is termed the "critical embankment load", $s'_{1,crit}$, or the "threshold embankment height", H_{nc}.

iii) With further loading, the excess pore water pressure response is typically at an incremental $\overline{B}$ value of approximately 1 ($\overline{B}_2$ in Figure 4.5), i.e. an undrained condition with the clay in a normally consolidated condition. In this stage of the loading the clay is characterised by high compressibility and low c_v resulting in low rates of excess pore water pressure dissipation. In most of the cases analysed by Leroueil et al (1978a), the rate of construction was sufficiently high that negligible excess pore water pressure dissipation occurred. In terms of the interpreted stress path (Figure 4.4) the effective stress path for this stage of loading is *P'F'*.

iv) With further loading, the effective stress path reaches the critical state surface (Point *F´* in Figure 4.4) and the soil reaches a localised failure condition. A localised failure is generally initiated in the foundation below the shoulder of the embankment where shear stresses are greatest. For:

- Strain weakening soils, further straining of a soil at Point *F´* results in a reduction in shear strength or deviator stress (along path *F´R´*) and therefore generation of excess pore water pressures within the localised failure zone of greater than the applied load ($\overline{B}_f > 1$, Figure 4.5). The total stress path shifts to the right with a reducing deviatoric stress (path *FR* in Figure 4.4). Tavenas and Leroueil (1980) consider that the initial structure of the soil is partly destroyed during deformation in a normally consolidated condition, resulting in a change in mechanical properties and modification of the shape of the limit state surface from that originally represented by *F´Y*$_o$ to *F´R´* (Figure 4.4).
- Soils that are not strain weakening, the effective stress state does not change from Point F´. As discussed by Muir Wood (1990), application of additional

load results in a sideways shift in the total stress path (Figure 4.11), with pore water pressure increases that are equal to the change in total vertical stress (Figure 4.12), and plastic deformation occurs.

v) Complete failure of the embankment does not necessarily occur once a localised failure condition is reached. The localised failure zone is supported by the surrounding unfailed soil.

Equations 4.3 and 4.4 (Tavenas and Leroueil 1980) define the excess pore water pressure generated up to the threshold height (Equation 4.3) and beyond the threshold height (Equation 4.4), as shown in Figure 4.5.

$$\Delta u = \overline{B}_1 IgH \tag{4.3}$$

$$\Delta u = \overline{B}_2 I\Delta gH \quad \text{where } \overline{B}_2 = 1 \tag{4.4}$$

where Δu is the excess pore water pressure, I is the stress influence factor from elastic solutions, gH is the applied load of the embankment and ΔgH is the change in the applied load above the threshold height, H_{nc}. $\overline{B}_1$ and $\overline{B}_2$ are defined in Figure 4.5. The threshold height is defined in Equation 4.5.

$$H_{nc} = \frac{\left(s'_p - s'_{vo}\right)}{gI\left(1-\overline{B}_1\right)} \tag{4.5}$$

It is important to note that the threshold height varies with depth. From Equation 4.5, the threshold height at any location is dependent on the difference between the pre-consolidation pressure and initial effective stress ($s'_p - s'_{vo}$), the pore water pressure response ($\overline{B}_1$) and the stress influence factor; i.e. the shape of the effective vertical stress profile and how this relates to the pre-consolidation stress profile. Figure 4.2 shows the zone of normally consolidated soft clay for an effective stress profile, s'_v, determined from the applied total stress and pore water pressure response. With increasing applied load the zone of normally consolidated clay will also increase. The effect of this on the deformation behaviour is discussed in Section 4.2.2.

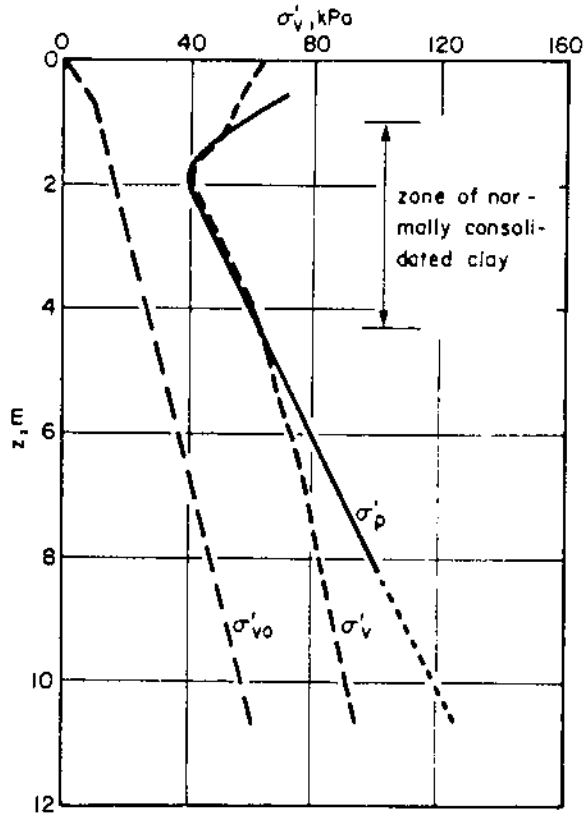

Where:
z = depth below ground surface
s'_{vo} = initial effective vertical stress
s'_{p} = pre-consolidation stress
s'_{v} = effective vertical stress at end of construction

Figure 4.2: Effective vertical stress profile and pre-consolidation stress profile prior to construction, and the effective vertical stress profile at end of construction of the Saint Alban B test embankment (Tavenas and Leroueil 1980).

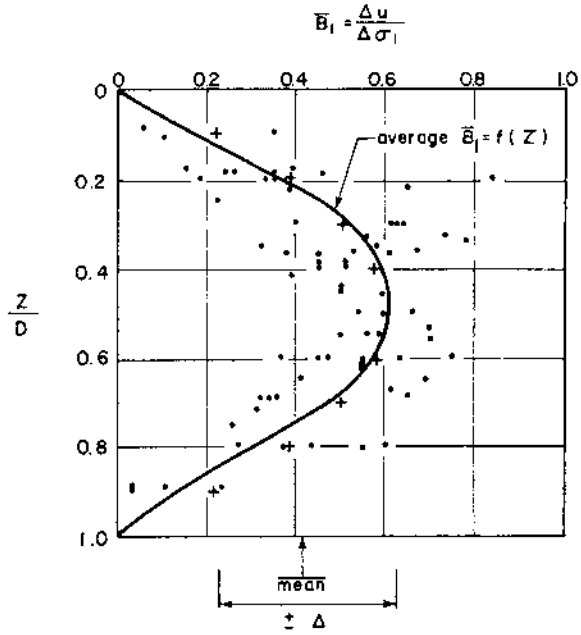

Where:
Z/D is the normalised depth with respect to the depth of the soft clay (measured from ground surface level).
$\overline{B}_1 = \overline{B}$ measured at effective stress levels less than the pre-consolidation pressure.

Figure 4.3: Field observations of excess pore water pressures in clay foundations during the initial period of embankment construction (Tavenas and Leroueil 1980).

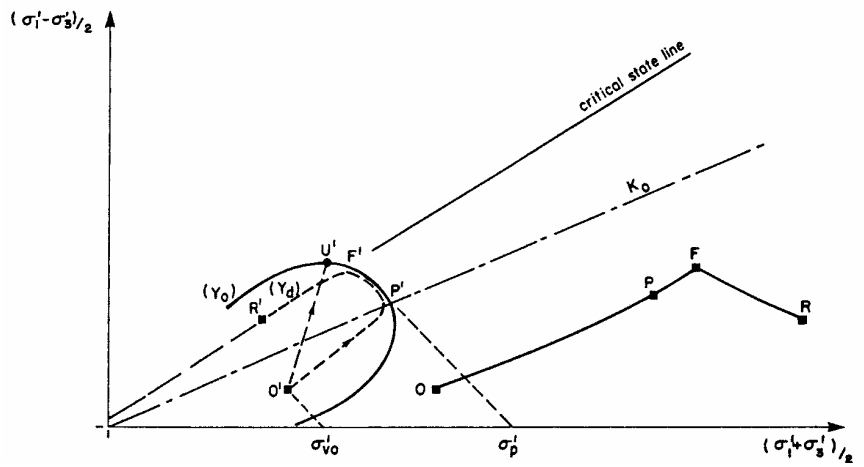

Figure 4.4: Total (*OPFR*) and effective (*O′P′F′R′*) stress paths under the centre of embankments (Tavenas and Leroueil 1980)

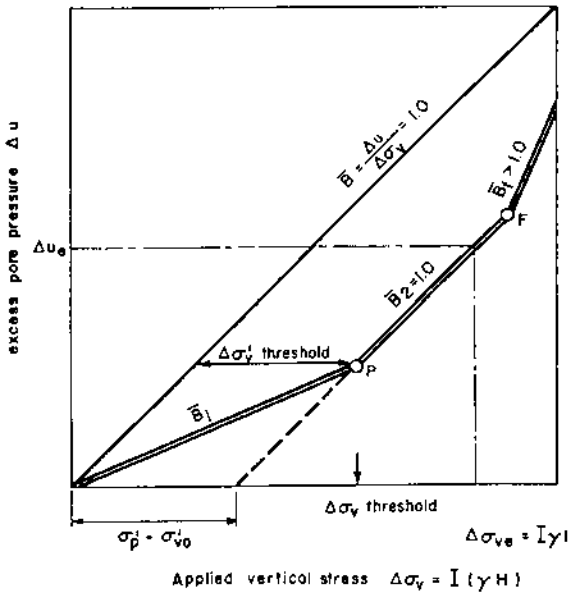

Figure 4.5: Relationship between the excess pore water pressure and the applied vertical stress (Tavenas and Leroueil 1980)

Whilst more recent publications concur with the pore water pressure response described by Tavenas and Leroueil (1980), there is conjecture on the effective stress path, particularly in the over-consolidated region. Folkes and Crooks (1985) comment that $\bar{B}$ does not provide a satisfactory description of the effective stress path direction since it is a function of the total stress ratio, $\Delta s_3 / \Delta s_1$, (Equation 4.2) and the total stress ratio varies with depth (Figure 4.6). As Figure 4.7 indicates, $\bar{B}$ does not provide an indication of the direction of the effective stress path. Folkes and Crooks (1985)

recommend that more emphasis be placed on the actual effective stress path rather than the value of $\overline{B}$.

Leroueil and Tavenas (1986) agree that $\overline{B}$ does not provide a satisfactory description of the effective stress path, but still contend that partial drainage does occur during the initial stages of embankment construction. Figure 4.8 presents a summary of effective stress paths and pore water pressure response associated with different types of yield conditions for embankments constructed to failure (Leroueil and Tavenas 1986). In the context of the discussion to date on pore water pressure response Figure 4.8b is the relevant effective stress path and is considered to be generally representative of the effective stress path for most of the failure case studies analysed in Section 4.3. Figure 4.8a relates to case studies where limited drainage occurred during construction whilst the effective stress state was below the pre-consolidation pressure (i.e. in an over-consolidated state). Examples and discussion of this behaviour are given in Appendix C (Section 3).

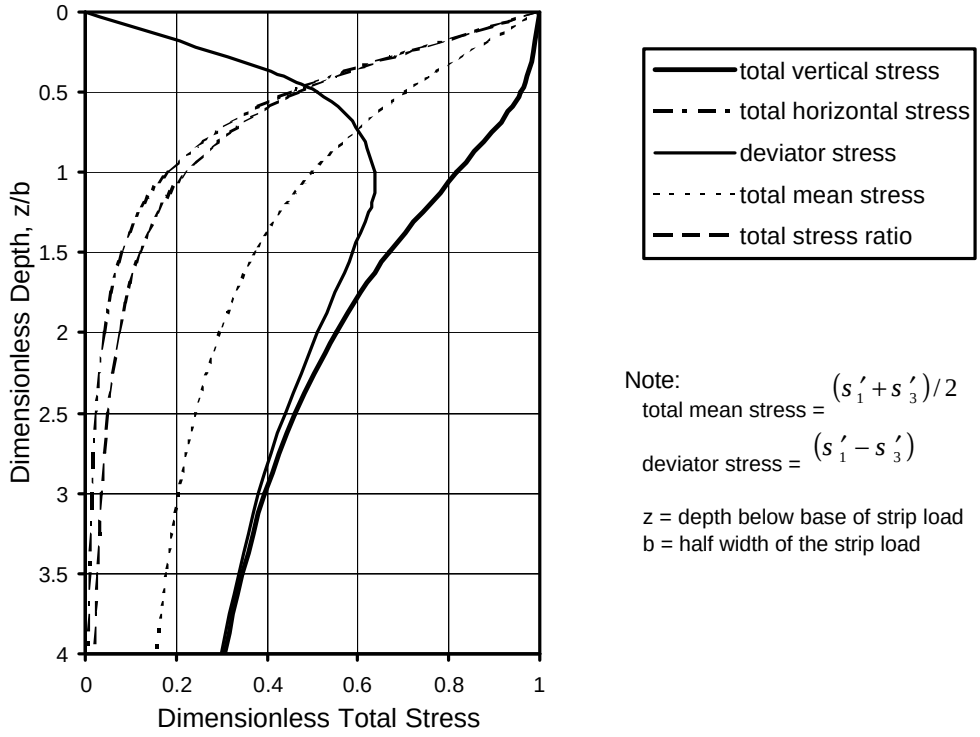

Figure 4.6: Dimensionless variations of changes in total stresses under the centreline of an infinite strip load on an elastic half space (Poulos and Davis 1974)

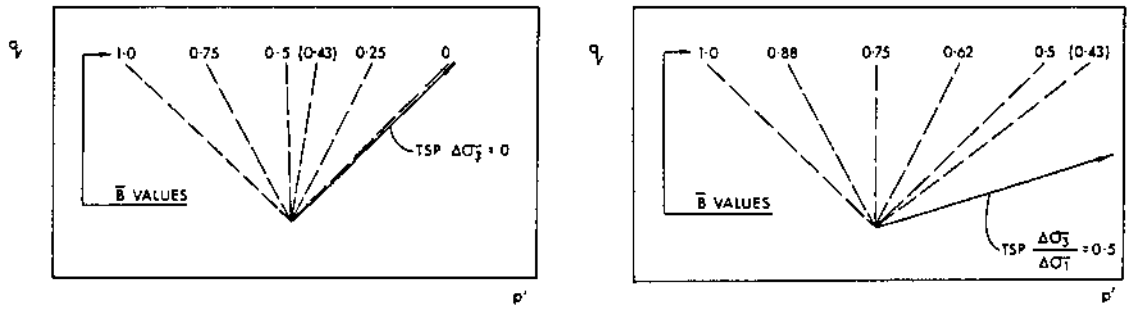

Note: $p' = (s'_1 + s'_3)/2$ (= mean effective normal stress)

$q = (s'_1 - s'_3)/2$ (= deviatoric stress/2)

TSP = total stress path

Figure 4.7: Effective stress paths for varying $\overline{B}$ values and total stress ratios (Folkes and Crooks 1985).

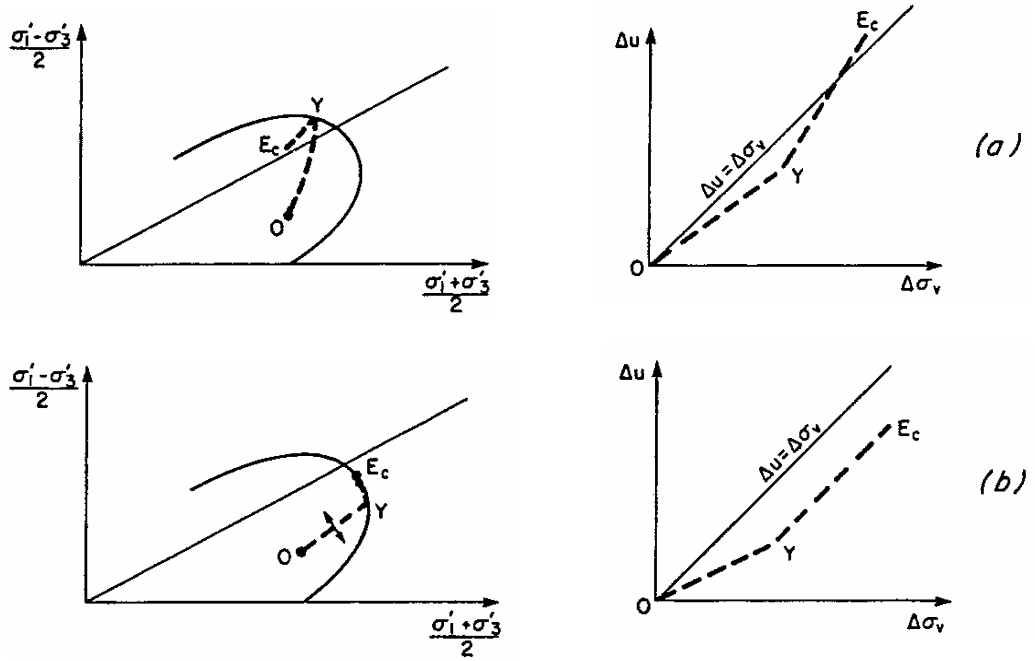

Note: E_c = end of construction

Figure 4.8: Effective stress paths and pore water pressure generation associated with different types of yield conditions (Leroueil and Tavenas 1986).

Muir Wood (1990) considered the undrained response of a soil element beneath the centre of a circular load on a lightly over-consolidated, soft clay foundation (Figure 4.9). He described the soft clay using the Cam Clay model, assuming the soil to behave isotropically and elastically prior to yield. A summary of the behaviour of the foundation under the applied load as described by Muir Wood is as follows:

- The total stress path is dependent on the total stress ratio and can be determined from elastic analysis (Figure 4.10 for circular load).
- The effective stress changes (undrained response) are fixed by the stress-strain behaviour of the soil and are largely independent of the total stress changes. Prior to yield, the effective stress path shows no change in mean effective stress until the yield locus is reached at Point C' (Figure 4.11).
- Once the soil has yielded at Point C', the effective stress path turns toward the critical state at D' and an increase in the rate of pore water pressure response occurs.
- The effective stress path $B'C'D'$ (Figure 4.11) is the undrained effective stress path that is followed whatever the total stress path, provided it involves an increase in the deviator stress, q.
- The total stress changes can be deduced from elastic analysis up to the point of yield at C'. Once yielding has occurred the elastic analysis is no longer strictly valid because the yielding elements of soil have a lower stiffness for continual increase in shear stress, but it will provide a reasonable estimate so long as only a small proportion of the total soil has reached yield.
- The initial excess pore water pressure response in undrained loading (Figure 4.12) up to the point of yield arises entirely from the change in total mean stress that has developed at that depth (Figure 4.10). Thus, for a soil element at depth $z/a = 0.48$, $\Delta u = 0.567\Delta z$ (where Δz is the change in applied load) up to the point at yield at C'.
- Once yielded, the excess pore response is made up of two parts; one due to the applied change in total mean stress and the other due to the change in effective mean stress as a consequence of yielding. The total stress path may or may not have been affected by the occurrence of yield, and therefore it is not possible to make precise statements about the excess pore water pressure response from C to D (Figure 4.12).
- Local failure is reached at Point D' on the critical state line. At this point the soil is unable to support any further stress, however, the local failure is contained and supported by the surrounding unfailed soil. Assuming the soil is not strain weakening, the effective stress path stops at Point D', no further change in deviator stress can occur and deformation continues without further change in effective stress. This implies that the pore water pressure changes at Point D' are equal to the change in total mean stress and hence to the change in total vertical stress (Figure 4.10). The total stress path moves sideways at constant q (path DE in Figure 4.11).

With respect to the pore water pressure response on loading, the idealistic example given by Muir Wood (1990) summarised above assumes an undrained response of the soft clay foundation. As discussed, the effective stress path up to the yield locus (path *B´C´* on Figure 4.11) is independent of the total stress path and the pore water pressure response arises entirely from the change in total stress in undrained loading. Based on field observation, Leroueil et al (1978a) indicated that the typical pore water pressure response (Figure 4.3) observed during the initial stages of loading of an embankment on soft ground (whilst the foundation is in an over-consolidated state) is significantly different to that predicted by an undrained response because of consolidation and partial drainage during loading whilst the foundation is in an over-consolidated condition. Leroueil and Tavenas (1986) indicated that the amount of consolidation varies from case to case, depending on the coefficient of consolidation of the over-consolidated clay, drainage path length, and rate of loading. Jardine and Hight (1987) concur that the field observation of pore water pressure response during the initial stages of loading (whilst the foundation is in an over-consolidated condition) are indicative of consolidation and therefore partial drainage. Folkes and Crooks (1986) comment that consolidation due to partial drainage can occur during the initial stages of embankment construction, but they consider that the incidence of near undrained conditions is prevalent in a relatively large number of cases (approximately 35%).

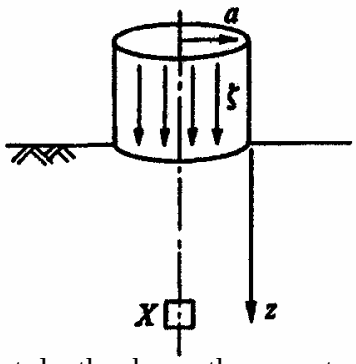

Figure 4.9: Element of soil at depth z beneath on centreline of uniform circular load (Muir Wood 1990)

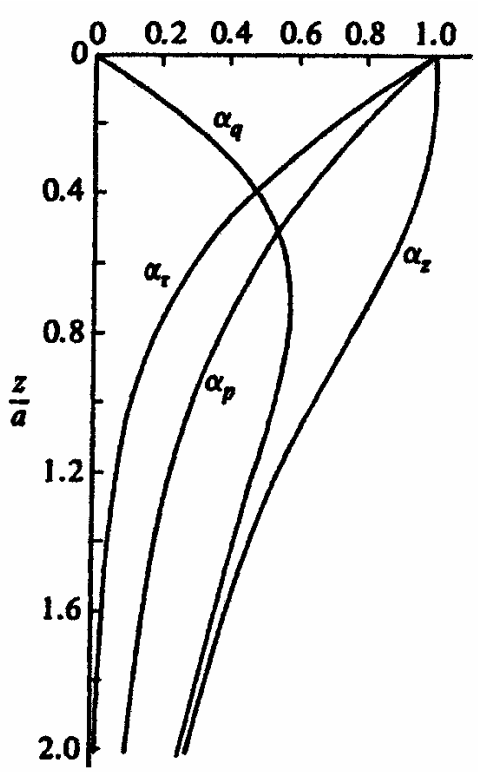

Note:
Total stresses are dimensionless.

a_z = vertical stress

a_r = horizontal stress

a_p = mean stress

a_q = deviator stress

Figure 4.10: Total stresses on centreline beneath uniform circular load on elastic half space (Muir Wood 1990).

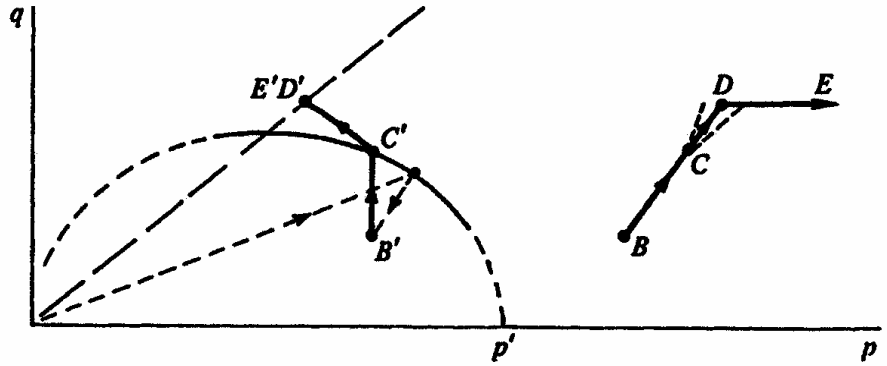

Note: p and p' are the mean total and mean effective stresses of the form $(s'_1 + 2s'_3)/3$
q is the deviatoric stress defined as $(s'_1 - s'_3)$.

Figure 4.11: Total (*BCDE*) and effective (*B¢C¢D¢E¢*) stress paths for a soil element on the centreline beneath a circular load (Muir Wood 1990).

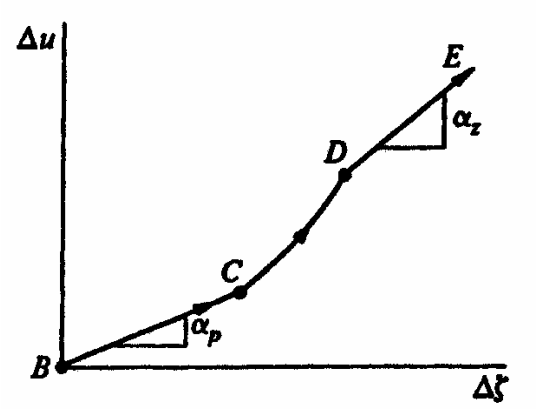

Note:

a_p is the dimensionless total mean stress defined as $\Delta p / \Delta z$

a_z the dimensionless vertical stress defined as $\Delta s_v / \Delta z$

Δz is the change in applied load

Points *BCDE* relate to total stress states *BCDE* in Figure 4.11

Figure 4.12: Variation of pore water pressure with applied surface load for element on centreline beneath circular load (Muir Wood 1990).

In summary, the published literature on field case studies of embankments constructed on lightly over-consolidated (OCR < 2.5) soft foundations indicates that in the majority of cases partial drainage does occur in the initial stages of embankment construction whilst the foundation is in an over-consolidated condition. However, in a number of case studies the pore water pressure response of individual or a group of piezometers during initial construction was close to that of an undrained response. Based on published information and analysis of the 16 cases as part of this study (Appendix C, Section 1) it is concluded that it is difficult to predict the pore water pressure response during the over-consolidated stage of loading with any degree of accuracy. However, it is important to closely monitor the excess pore water pressure response for assessment of the effective stress state of the foundation for prediction of the likely deformation behaviour. To do this it is necessary to monitor:

- The effective stress path, as recommended by Folkes and Crooks (1985), to assess at what location it is likely to intersect the limit state surface (either below or above the critical state line, Figure 4.7)
- The rate of pore water pressure generation ($\overline{B}_1$ as recommended by Tavenas and Leroueil (1980)) to assess the change in state of the foundation from an over-consolidated to a normally consolidated condition.

4.2.2 DEFORMATION BEHAVIOUR

Marche and Chapuis (1974) analysed the horizontal displacements at the toe of eight embankments as a function of the factor of safety during construction (Figure 4.13).

They concluded that when the factor of safety falls below 1.4 the horizontal deformation behaviour changes significantly indicating the approach of failure, and can therefore be used to monitor the stability of embankments. Tavenas et al (1979) analysed the horizontal deformation behaviour at the toe of some 21 embankments and concluded that the change in deformation behaviour identified by Marche and Chapuis (1974) was related to the change associated with going from a partially drained, over-consolidated condition to a normally consolidated, undrained condition as previously discussed in Section 4.2.1.

Tavenas et al (1979) proposed an empirical correlation, based on their case study analysis, between the settlement under the centre of the embankment and the maximum lateral displacement measured at the toe (from inclinometer observations). The definition of parameters is shown in Figure 4.14 and the empirical correlation presented in Figure 4.15. In the context of limit state theory, Tavenas et al (1979) and Tavenas and Leroueil (1980) describe the deformation behaviour as follows:

- During the early stages of construction of an embankment on soft clay (whilst the foundation is in an over-consolidated condition) deformations are small and partial drainage is observed due to the relatively high modulus and high coefficient of consolidation of the foundation. Lateral deformations at the toe are relatively small in comparison to the settlement under the centre of the embankment due to the effects of partial drainage, with $y_m \sim 0.18s$ (standard deviation = 0.09), where y_m is the maximum lateral displacement at the toe and s is the settlement under the centre of the embankment measured at any point in time (Figure 4.14 and Figure 4.15). They indicated that the lateral displacement during this stage could probably be predicted by the theory of elasticity adopting drained parameters for the clay foundation and a Poisson's ratio of about 0.3.
- A significant change in the deformation behaviour occurs once the effective stress path intersects with the limit state surface (Point P' on Figure 4.4) and the threshold height, H_{nc}, is reached. As the threshold height is reached the behaviour of the foundation changes from over-consolidated, partially drained conditions to normally consolidated, undrained conditions. The effective stress path for increased loading beyond Point P' follows the path $P'F'$ of the now normally consolidated clay. Undrained shear deformations occur under constant effective stress and the stress-strain behaviour corresponds to plastic flow of the undrained normally consolidated

clay. Deformations are much larger and both settlement and lateral displacements increase at about the same rate ($\Delta y_m \approx 0.91\Delta s$) as shown on Figure 4.15.

Tavenas et al (1979) comment that the ratio $\Delta y_m / \Delta s$ is dependent on a variety of parameters including the factor of safety and the angle of the embankment slope. Plotting the ratio $\Delta y_m / \Delta s$ with time (Figure 4.15) is useful as a guide to the change from over-consolidated conditions to normally consolidated, undrained conditions (i.e. the onset of yielding of the foundation).

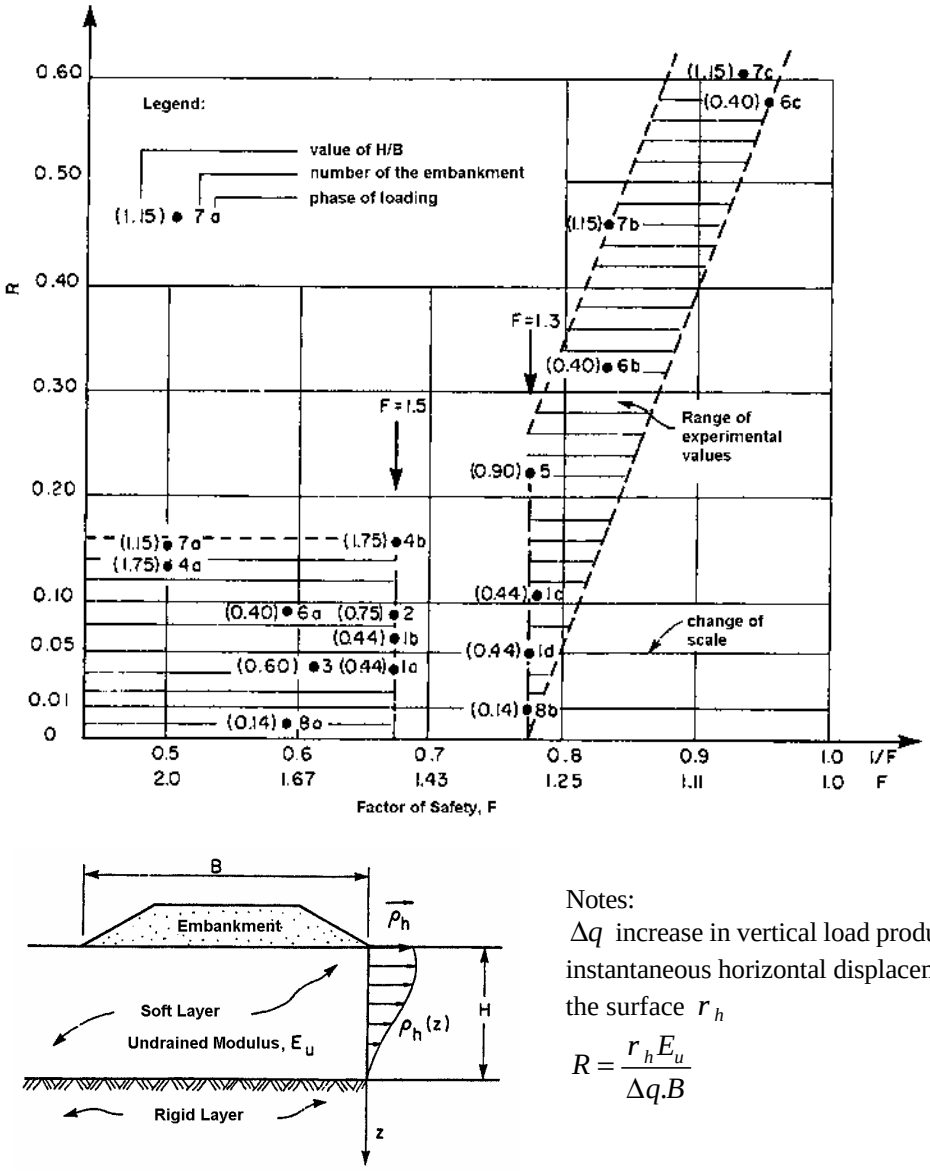

Notes:
Δq increase in vertical load producing instantaneous horizontal displacement at the surface r_h

$$R = \frac{r_h E_u}{\Delta q . B}$$

Figure 4.13: Variation of the dimensional factor *R* (proportional to the horizontal surface displacement at the toe) with factor of safety (Marche and Chapuis 1974)

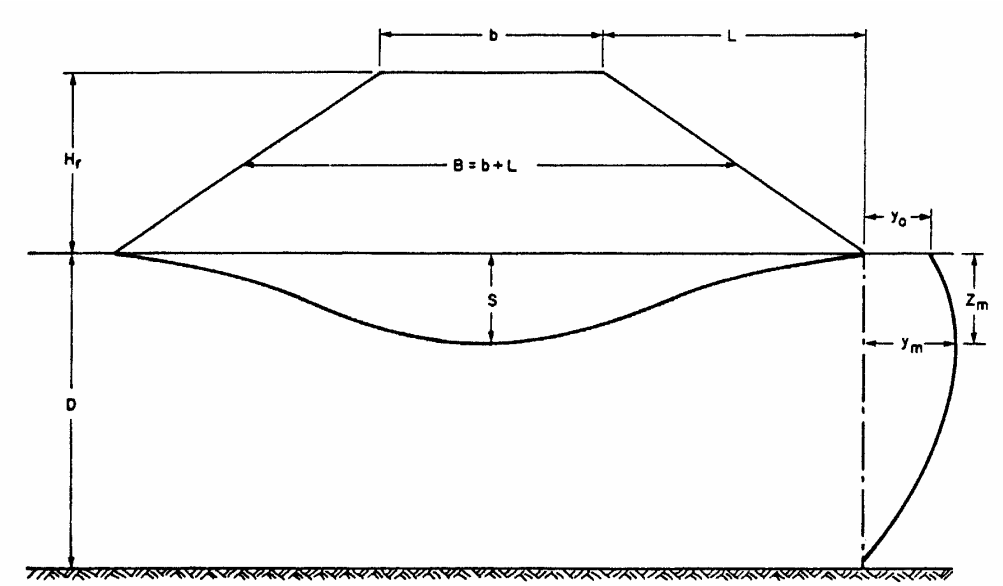

Figure 4.14: Definition of the geometry and deformation parameters (Tavenas et al 1979)

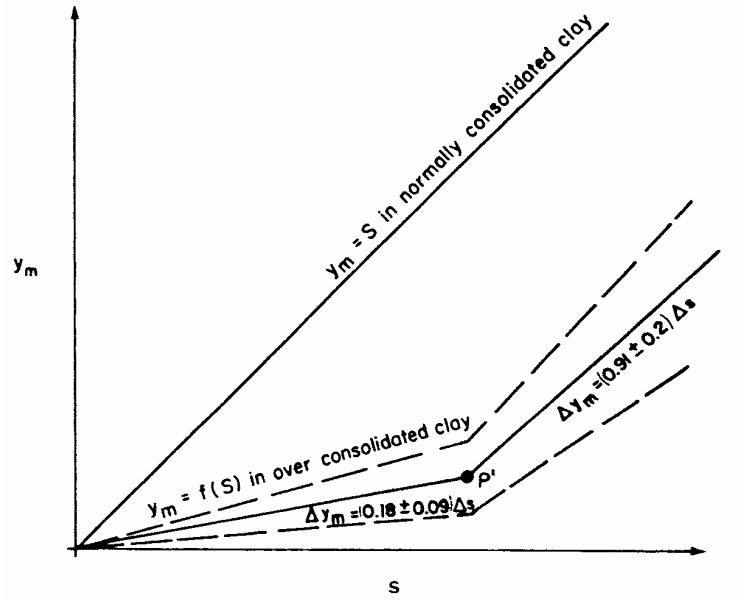

Figure 4.15: Average correlation between the maximum lateral movement at the toe, y_m, and settlement under the centre of the embankment, s, during construction (Tavenas and Leroueil 1980)

Tavenas et al (1979) also comment that the lateral displacement profile at the embankment toe from inclinometer records is related to the thickness of the normally consolidated clay layer at any stage during and post embankment construction (noting that it increases as the load is applied). Figure 4.16 presents the observed effective stress and lateral displacements profiles for a case where the full thickness of the soft clay foundation is normally consolidated (Cubzac-A) and where only a part of the soft

clay foundation is normally consolidated (St. Alban-B). For St. Alban-B, greater lateral movements are observed within the zone of normally consolidated clay and are associated with yielding (or plastic flow).

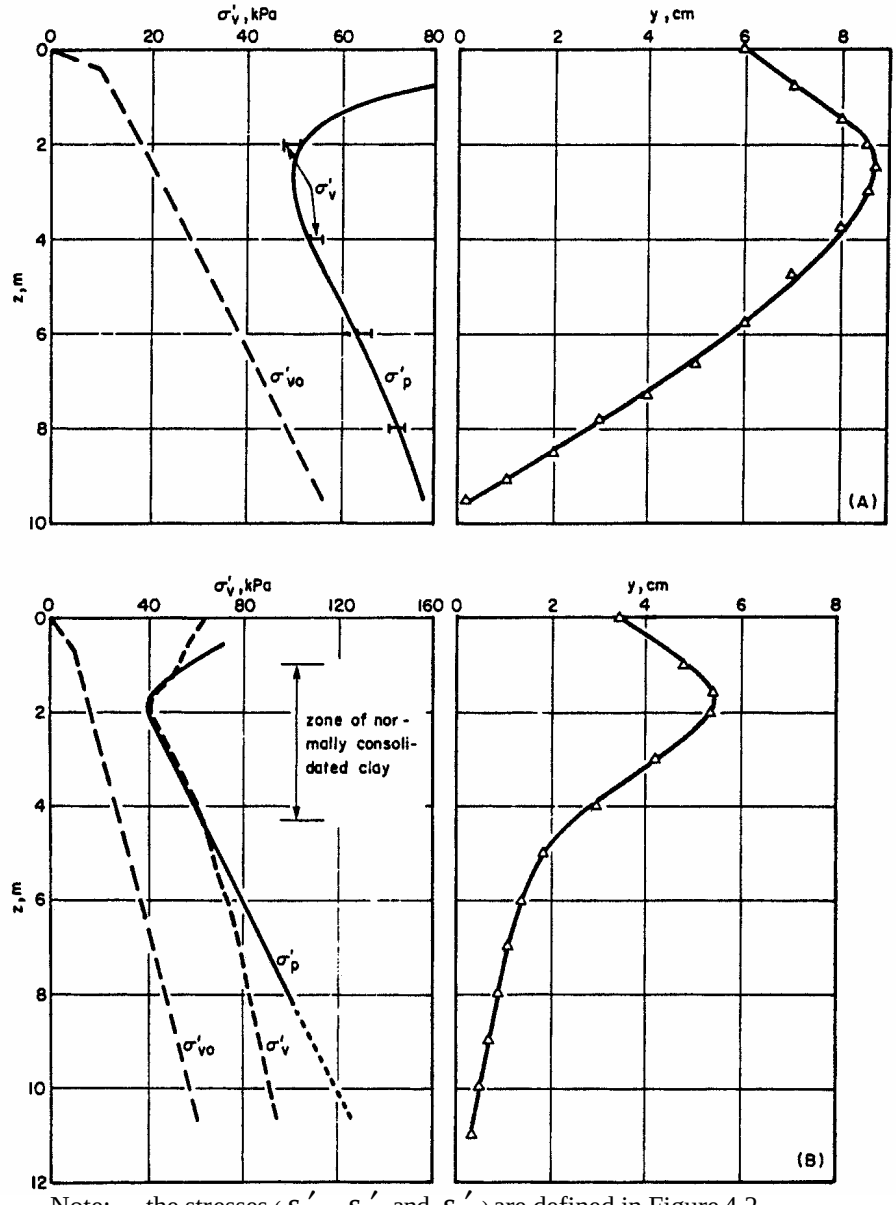

Note: the stresses (s'_{vo}, s'_{v}, and s'_{p}) are defined in Figure 4.2
y is lateral displacement at the embankment toe
z is the depth below ground surface

Figure 4.16: Effective stress and lateral displacement profiles at the end of construction under *(a)* Cubzac-les-Ponts A and *(b)* Saint Alban B test fills (Tavenas et al 1979)

Marsland and Powell (1977) considered that, for the Thames test embankment, the most sensitive means of predicting the onset of failure was to monitor the ratio of the total horizontal movement (at the toe of the embankment) to that occurring during actual

application of the load. Figure 4.17 presents their data comparing the movement during placement of one lift on the embankment (typical 5 hour placement time) with the movement over a 24 hour period (including movement during loading) as the embankment height is increased. This approach requires placement of lifts in uniform layer thicknesses and in the case of Thames, at a rate of one lift per day. This method incorporates the observations of; increase in lateral deformation as the effective stress state moves from over-consolidated to normally consolidated (discussed above); increase in lateral deformation as the zone of normally consolidated foundation increases with increasing embankment height; and the theory of creep type movements where the rate of creep type deformation increases with increasing levels of shear stress.

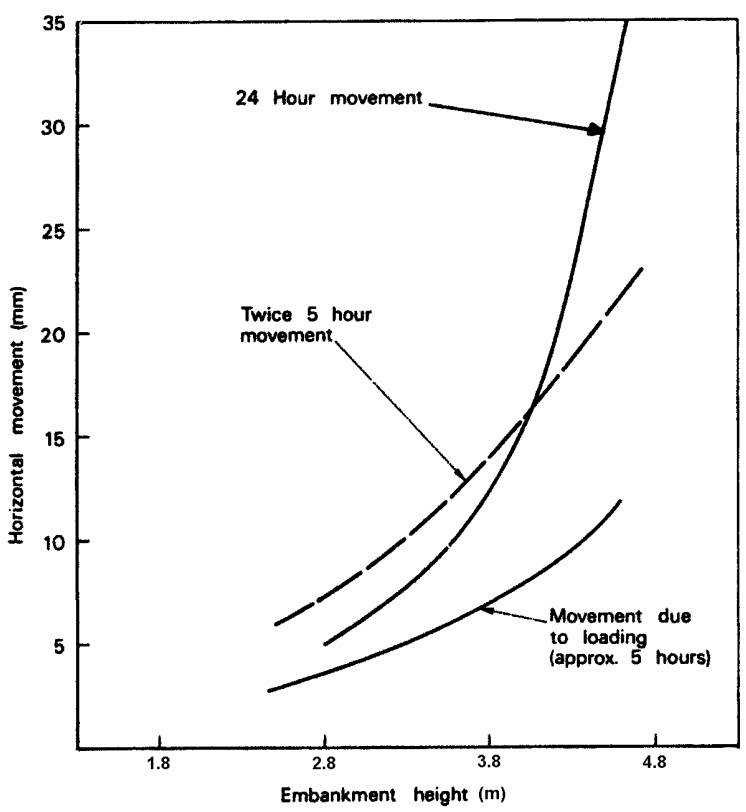

Figure 4.17: Comparison of horizontal movement (on berm beyond embankment toe) during loading and for 24 hour period for the Thames test embankment (Marsland and Powell 1977)

Ramalho-Ortigao et al (1983a) measured the horizontal displacements at the base of the embankment of the Rio test embankment. The observed displacements (Figure 4.18) indicate that the greatest displacement occurs under the slope of the embankment. This is possibly a reflection of the concentration of the shear strain at depth under the

embankment slope; however, this effect could be masked by stiffness variations between the soft clay and upper, weathered and heavily over-consolidated crust, and between the crust and embankment.

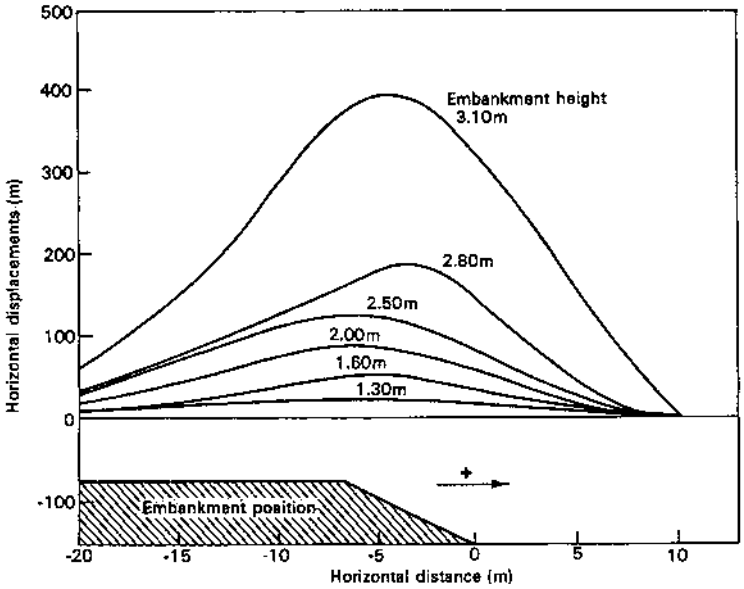

Figure 4.18: Observations of lateral displacement at the base of the embankment with increasing embankment thickness at the Rio test embankment (Ramalho-Ortigao et al 1983a)

Finite element modelling of numerous case studies of embankments on soft ground is reported in the literature. Whilst the predicted results of deformation behaviour, particularly lateral deformation, are in general relatively poor, what the results collectively indicate is the development of high concentrations of shear stress at depth below the slope of the embankment (Figure 4.19). Relatively high shear stress concentrations are modelled at embankment thicknesses significantly below the reported failure thickness; in the case of the Muar-F test embankment the stresses in Figure 4.19 are at a fill thickness of 74% of the eventual failure thickness (Indraratna et al 1992). Associated with this concentration of shear stress is a concentration of shear strain. The implications of this concentration of shear stresses and strains in relation to the observed lateral deformation profile in inclinometers at the toe of the embankment are discussed in Section 4.3.

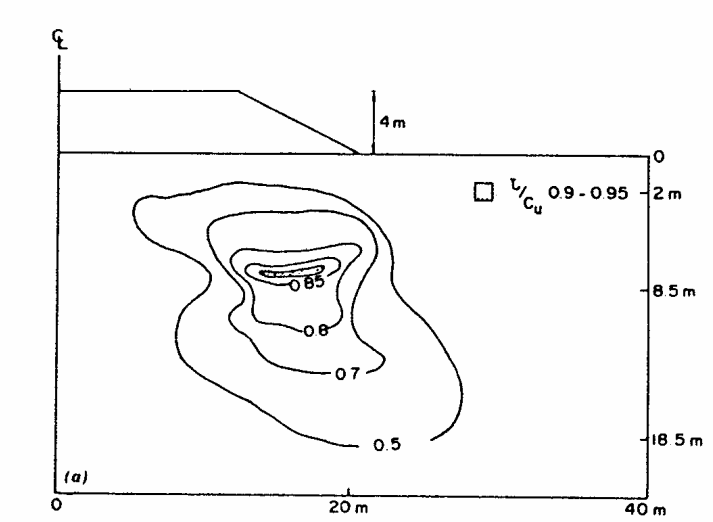

Figure 4.19: Contours of normalised shear-stress ratios at 4 m fill thickness from finite element modelling at Muar-F test embankment, Malaysia (Indraratna et al 1992)

4.3 ANALYSIS OF THE BEHAVIOUR OF FAILURE CASE STUDIES

4.3.1 CASE STUDIES ANALYSED

The deformation behaviour and excess pore water pressure response of thirteen case studies of well-monitored embankments on soft ground that were constructed to failure have been analysed. Selection of suitable case studies was based on the level of available information on the properties of the foundation and embankment filling, and the amount, type, location and available published results of instrumentation. A summary of each case study is given in Table 4.1.

Except for Mastemyr, which is a circular embankment, all the embankments are rectangular in shape. In the case of Sackville the embankment is geotextile reinforced. The embankment failure height at Sackville was assessed to have occurred when the foundation failed, as the embankment did not fail until several additional metres of filling had been placed. Two embankments have been included from the Muar test embankments, Malaysia; Muar-F was purposely constructed to failure at a constant rate of construction (Brand and Premchitt 1989), and Muar-EC was one of a series of thirteen trial embankments constructed to assess various methods of ground improvement (Malaysian Highway Authority 1989a). Prior to construction, the foundation for the Muar-EC embankment was electro-chemically injected with Condor-SS, a sulphonated petroleum based ion exchanger, to a depth of 7.6 m with hole

spacings at 2 m centres. The main purpose of the Condor-SS chemical was to "*reduce the bound water in order to subsequently eliminate cavities and reduce the swell capacity of the individual soil particles*" (Malaysian Highway Authority 1989a). Details of the Muar series of trial embankments are given in Appendix C (Section 2).

The foundations at the Kalix, St. Alban, James Bay, Portsmouth and Mastemyr embankment sites are of sensitive clays with high undrained brittleness. For the remainder of the case studies the foundations are of low sensitivity clays with limited strain weakening in undrained loading.

In the context of identifying indicators of an impending failure condition, the monitored observations analysed (Figure 4.20) are as follows:

- Excess pore water pressures under the centre and under the toe of the embankment;
- Settlement under the centre of the embankment (Point 1);
- Vertical deformation at the toe of the embankment (Point 2) and at a point beyond the toe (Point 3), but within the zone of the eventual failure;
- Lateral deformation at the toe of the embankment (Point 2);
- Lateral deformation with depth (from inclinometer records) at the toe of the embankment. Both the vertical inclination angle in the vicinity of the surface of rupture (as an assessment of shear strain) and the maximum lateral deformation have been analysed.

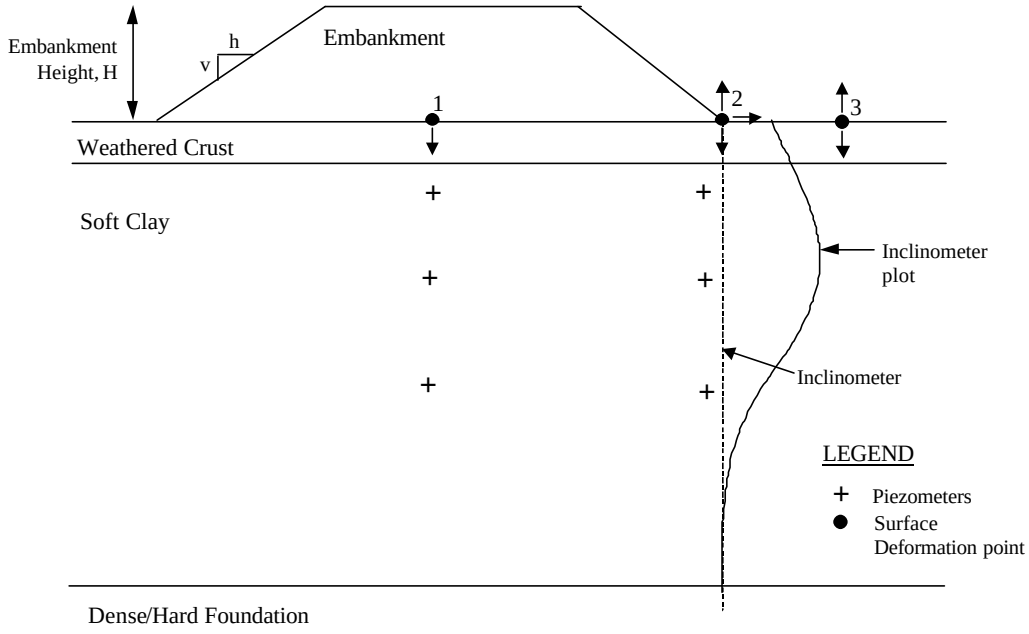

Figure 4.20: Idealised section of embankment indicating the types of monitored observations.

Table 4.1: Summary of failure case studies of embankments on soft ground.

Name	Failure Height , H (m)	Slope (H to V)	Rate of Construction (m/day)	Material Properties *[1]			Analysis of Excess Pore Pressure Response		
				Embankment	Foundation		Threshold Height, H_{nc}	B_1 (refer Figure 4.5)	B_2 (refer Figure 4.5)
					Crust	Soft Clay			
Narbonne, France	9.6	3.7 to 1	1.9	Gravelly material	3m thick, CL clay, I_L < 1	9m thick, CL/ML, soft, layered, I_L = 1.1 - 1.5	Est ~ 5.5 m	na	na
Rio de Janiero, Brazil	2.8	2 to 1	0.10	Silty sand, loosely placed, some cohesion	2.4 m thick, CH clay, fissured, I_L > 1 below 1.2 m	8.8 m thick, CH clay, very soft, marine deposition, relatively homogeneous, low sensitivity, ductile, I_L = 1.2 - 1.3	1 m - (1.5 to 4.5 m depth) > 2.8 m - (from 4.5 m)	0.25 - 0.35 (1.5 to 4.5 m depth) 0.6 - 0.75 (> 4.5 m)	0.8 (1.25 to 2.25 for H > 2.8 m)
Kings Lynn, UK	6.7	1.4 to 1	0.67	Weathered sandstone, compacted	1.2 m thick, CH silty clay, I_L < 1	5.1 m CH clay, soft, tidal marine deposition, layered (peat layers), I_L = 1.0 - 1.5	1.9 to 2.1 m	0.1 - 0.4	0.85 (upper clay), 1.15 (Peat and lower clay)
Kalix, Sweden	4.1 (incl 1 m cut at toe)	1.4 to 1	0.35	Crushed rock, loosely placed	2 m thick, CH/MH silty clay, fissured	16 m thick, MH/OH silt overlying CH clay, soft to very soft, marine deposition, homogeneous, fissured, sensitive, brittle, I_L = 0.6 - 1.0	2.2 to 2.9 m	0.47 to 0.75	1.4 to 1.7 at P2 on the surface of rupture, B_2 = 11 for H > 2.82 m
Thames, UK	6.3 (incl 1 m cut at toe)	2.6 to 1	0.10	Sandy gravel, loosely placed	3 m thick, CH organic silty clay, with 0.5 m layer of organic growth	9 m thick, CL/ML, soft to very soft, tidal marine deposition, layered (peat layers). ML/SC below 7.3 m, firm	1.0 to 1.6 m	0.18 - 0.4	0.8 to 1.0
St. Alban-A, Quebec, Canada	4.02	1.5 to 1	0.45	Uniform sand, compacted	1.5 m thick, CL/CH clay, I_L = 0.5 to 1.4	12.2 m thick, CL/ML, soft to very soft, leached marine deposition (Champlain Sea Clay), cemented, sensitive, brittle, I_L = 2 to 3	2.0 m at depth of 1.5 m, NC zone increases with fill height.	0.07 to 0.65	0.5 (base of crust) to 0.92
Cubzac-A, France	4.5	1.5 to 1	0.26 - 0.75	cohesionless ?	1.8 m thick, CH clay, I_L = 0.3 to 1.0	7.2 m thick, CH clay, soft to very soft, I_L = 1 to 5.5	1.5 to 2.5	0.4 to 0.7	0.7 to 1.7
James Bay, Canada	7.6	2 to 1	0.15	Granular material (sand to cobbles), loosely compacted	5.5 m thick, 0.9 m organic CL/OL silt overlying weathered CL clay, I_L = 1.0 1.1, fissured, very sensitive.	9.5 m thick, CL/ML marine clay, soft, leached, very sensitive, brittle, I_L = 1.3 to 3, contains shells.	3.9 to 4.8 m	0.3 - 0.65	0.85 to 1.1
Portsmouth, USA, New Hampshire	6.55	4 to 1	0.19 - 0.42	Clean sand	2.4 m thick, 0.3 m dense swamp overlying CL/CH silty clay, I_L = 0.5 - 1.3, fissured.	11 m thick, CL marine clay, soft to very soft, leached, sensitive, brittle, I_L = 1.3 to 2.3. Contains occassional shells. Underlain by SM/ML and soft clay.	2 to 3 in upper clay and SM/ML	0.45 - 0.65	0.95 - 1.0
Mastemyr, Norway	2.84	1 to 1	0.19	Sand, some compaction	2.5 m thick, MH/OH fibrous peat, I_L = 0.35 - 1.0, very soft.	15 m thick, CL/ML marine clay, very soft, leached, very sensitive (quick), brittle, fissured, I_L = 2 to 4.	2 m (?)	0.75 - 1	1 - 1.7
Sackville, Canada, New Brunswick	5.7	1 to 1	0.14 - 1.6	Gravelly silty sand with some clay, loosely placed	1.2 m thick, organic clayey silt (ML), matrix of fibrous material, I_L = 0.6 - 0.8.	8.8 m thick, ML-MH clayey silt, soft to firm, intertidal salt marsh deposit, layered, I_L = 2 to 2.5 (to 6 m depth), OCR ~ 3.6 to 1.2.	1.5 to 2.4 m	0.6 - 0.75	1
Muar-F, Malaysia	5.4	2 to 1	0.054	Decomposed Granite, CH/SC, compacted	2 m thick, weathered CH marine clay, I_L < 1, fissured.	16 m thick, CH marine clay. Upper clay layer (6 m thick) very soft, lower clay layer soft, I_L = 1 to 1.5, some shells, ductile, low sensitivity	1 m in upper clay >3m in lower clay	0.15 (upper clay) 0.8 (lower clay)	1.0 - 1.2
Muar-EC, Malaysia (Electro-chemical injection)	4.68	2 to 1	0.017	Decomposed Granite, CH/SC, compacted	2 m thick, weathered CH marine clay, I_L < 1, fissured.	15 m thick, CH marine clay. Upper clay layer (6 m thick) very soft, lower clay layer soft, I_L = 1.25 to 2, some shells, ductile, low sensitivity	1.5 to 1.9	0.4 - 0.6	0.7 - 1.6

Note: *[1] Soils classified to the Australian Soil Classificastion System (Australian Standard AS1726 - 1993: Geotechnical Site Investigations)

I_L is the liquidity index = $(w_{FMC} - w_P)/(w_L - w_P)$, where w_{FMC} = field moisture content, w_L = liquid limit and w_P = plastic limit

na indicates data or information not available

Table 4.1 (cont.): Summary of failure case studies of embankments on soft ground (Sheet 2 of 2).

Name	Pre Failure Deformation		Observations Leading up to Failure	Post-Failure Deformation	Geometry of Surface of Rupture	References
	Settlement (centre), mm	Lateral Displacement (toe), mm				
Narbonne, France	700	na	No cracking prior to failure.	na	Rotational	Pilot (1972)
Rio de Janiero, Brazil	295	155	Embankment cracked at H = 2.5 m. Raised to 2.8 m and severe cracking but no failure. Failure during placement of lift above 3.1 m.	Suspect slow to moderate rate of movement at failure, displaced ~ 700 mm.	Rotational	Ramalho-Ortigao et al (1983a & 1983b) Costa-Filho et al (1977) Alameida & Ramalho-Ortigao (1982)
Kings Lynn, UK	460	> 125	Embankment cracking observed on day before failure (H = 6.15 m). Failure morning after construction to final height.	Suspect possibly rapid rate of movement. Crest settled ~ 1.25 m and toe heaved ~ 1.5 m.	Complex - Rotational and Translational	Wilkes (1972) Wroth & Simpson (1972)
Kalix, Sweden	755	> 105	No embankment cracking prior to failure. Significant heave and settlement on placement of last layer, failure 3 hours later.	Moderate rate of movement (max. rate ~1100 mm/day). Total movement at failure ~700 mm	Rotational	Holtz & Holm (1979) Stille et al (1976)
Thames, UK	na	450	Possible embankment cracking prior to failure. Appreciable movement on placement of final layers, failure soon after completion of final layer.	Moderate rate of movement (max. rate ~700 mm/day). Total movement at failure ~2200 mm. Full slip developed over 10 hours.	Complex - Rotational and Translational	Marsland & Powell (1977)
St. Alban-A, Quebec, Canada	150	> 40	No embankment cracking prior to failure. At failure, most of movement occurred in 1 min followed by slow creep for next 10 mins.	Rapid rate of movement (~ 900 mm/min). Total movement at failure ~ 1150 mm at crest and toe heave of 1200 mm.	Rotational	La Rochelle et al (1974)
Cubzac-A, France	170	130	No indication of embankment cracking prior to failure.	Total movement on surface of rupture ~ 1.4 m.	Rotational	Magnan et al (1982) Blondeau et al (1977) Josseaume et al (1977)
James Bay, Canada	120	> 35	No embankment cracking observed prior to failure. Rise in water level in IN tube at toe observed prior to failure. Failure occurred morning after construction to H = 7.6 m.	Rapid failure at maximum rate of ~1800 mm/min. Total movement ~2.5 - 3 m crest settlement and 1.5 - 1.8 m toe heave.	Rotational	Dascal & Tournier (1975)
Portsmouth, USA, New Hampshire	160	> 30	No embankment cracking observed prior to failure. Failure occurred during the night, after construction to 7.6 m.	Suspect likely rapid failure, but no observations. Total movement of 3 m crest settlement and similar toe heave.	Rotational	Ladd (1972)
Mastemyr, Norway	700	215	Circular embankment so not plane strain conditions. Failure occurred over-night.	na	na	Clausen (1972)
Sackville, Canada, New Brunswick	520	> 410	Cracking observed in morning following construction to 5.7 m, also large increase in strain gauges on geotextile and shearing of INs.	na	Rotational	Rowe et al (1995) Rowe et al (1996)
Muar-F, Malaysia	640	370 (at 4.5 m depth)	Raised to 5.4 m, cracking observed following morning with slow increase in width over day. Next day raised to 5.6 m with failure on layer completion.	Rapid failure (~3 mins) at estimated maximum rate of ~1000 mm/min. Total movement ~ 1.4 m crest settlement.	Rotational	Brand & Premchitt (1989) Poulos et al (1990) Indraratna et al (1992)
Muar-EC, Malaysia (Electro-chemical injection)	720	200	Embankment cracking observed 11 days after construction to 4.68 m. Further cracking developed with failure 31 days after construction.	Suspect moderate rate of failure. Initial 340 mm movement followed by slow continued movement for many days.	Rotational	Malaysian Highway Authority (1989a)

4.3.2 EXCESS PORE WATER PRESSURE

The observed excess pore water pressures in selected piezometers under the centre of the embankment during embankment construction (of the analysed case studies) are presented in Figure 4.21, and includes the excess pore water pressure response for $\overline{B} = 1$ for comparative purposes. The critical effective vertical stress ($s'_{1.crit}$), describing the change from an over-consolidated to a normally consolidated condition, assessed from the excess pore water pressure response, is indicated on Figure 4.21 and is summarised in Table 4.2 for the piezometers plotted.

Table 4.2: Excess pore water pressure observations for the failure case studies

Name	**Piezometer (depth)**	s'_{vo} **(kPa)**	**Rate of Construction (m/day)**	$\overline{B}_1$	$\overline{B}_2$	$s'_{1.crit}$ **(kPa)**	s'_p **(lab) (kPa)**	H_{nc} **(m)**
Muar-F	P2 (5 m)	27	0.054	0.23	1.0	44	44	1.1
King's Lynn	P215 (4.7 m)	37	0.67	0.1	1.15	68	-	1.9
Muar-EC	P4 (4.6 m)	31	0.017*[1]	0.37 to 0.5	1.0 to 1.5	51	44	1.5
Portsmouth	V5 (5.8 m)	55	0.19 – 0.42	0.6	0.98	62	69	2.0
Thames	C1 (2.3 m)	11.6	0.10	0.18	0.98	27	24	1.0
Sackville	P15 (2 m)	18	0.14 – 1.6	0.66	0.97	28	43	1.5
James Bay	A3 (7.6 m)	62	0.15	0.66	1.1	88	125	3.9
Kalix	P1 (2.5 m)	17	0.35	0.4 to 0.8	1.0 to 1.7	35	38	2.2
	P5 (5 m)	24		0.4 to 0.65	1.2 to 11	36	42	2.4
Rio	P2B (3 m)	9.6	0.10	0.27	0.80	23	22.5	1.0
Mastemyr	P1 (3.5 m)	16	0.19	0.5 to 1.0	1.0 to 2.0	20	24	1.3
St. Alban-A	C1 (3 m)	26	0.45	0.2 to 0.4	0.92	39	45	1.7
Cubzac-A	P112 (4 m)	32	0.26 – 0.75	0.4	1.0 to 1.7	53	51	1.8

Nore: *[1] Muar-EC was constructed in stages at an overall average rate of 0.017 m/day.

s'_{vo} = initial vertical effective stress (at the piezometer)

$\overline{B}_1$ and $\overline{B}_2$ are defined in Figure 4.5

$s'_{1.crit}$ = effective vertical stress at the threshold height (at the piezometer)

s'_p = pre-consolidation pressure (at the piezometer)

H_{nc} = threshold height at the piezometer (defined in Equation 4.5)

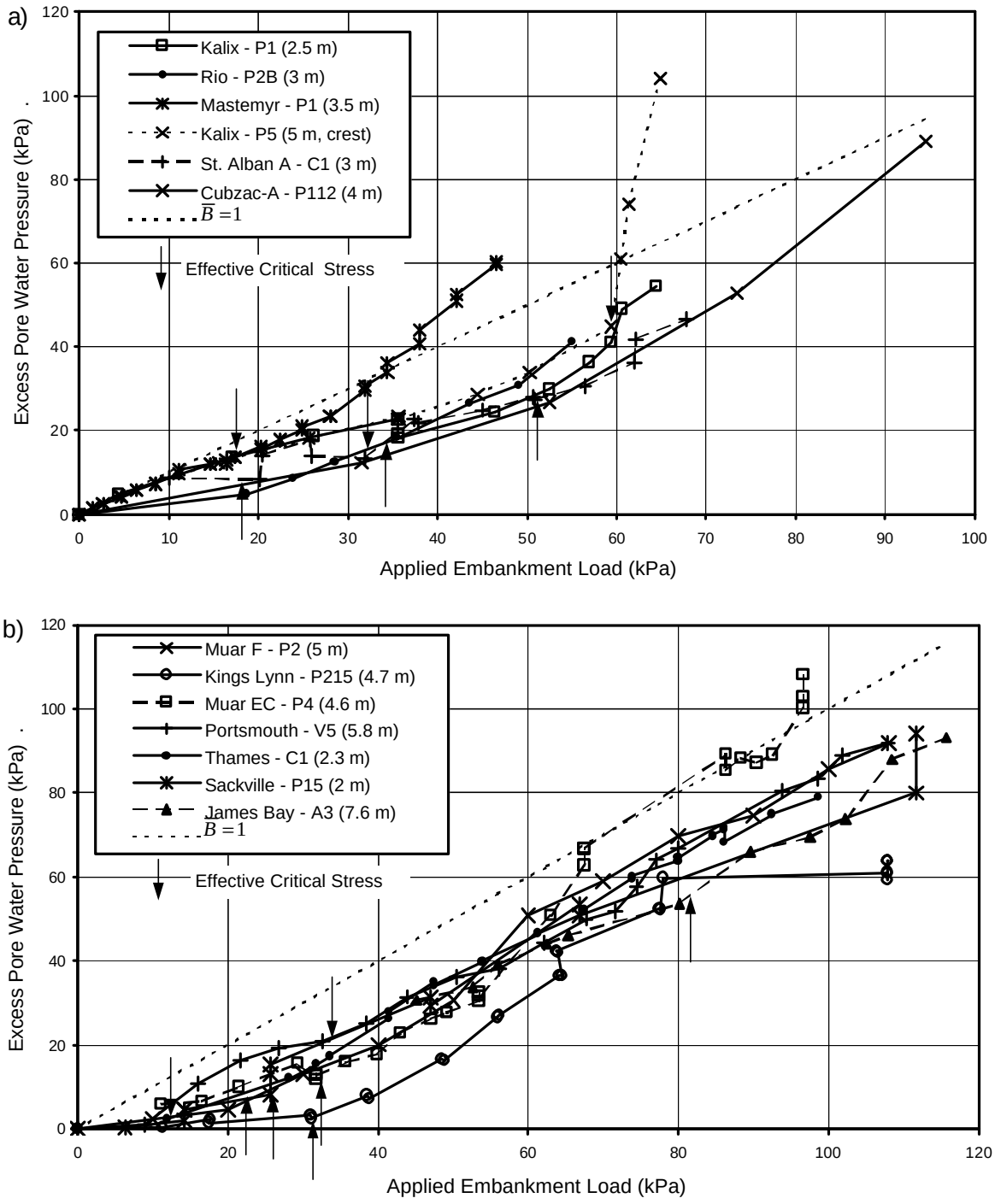

Figure 4.21: *(a)* and *(b)* Excess pore water pressure under centre of embankment versus applied embankment load.

In general, the excess pore water pressure response during embankment construction is in accordance with the limit state interpretation by Leroueil et al (1978a) with an initial partially drained response followed by an undrained response ($\overline{B}_2 \approx 1$) as discussed in Section 4.2.1 and shown on Figure 4.5. Only Piezometer P5 at Kalix (Figure 4.21a) is considered to represent the pore water pressure response at the onset of failure; i.e.

$\overline{B}_f > 1$ (Figure 4.5). This is because the piezometer is considered to be located close to the eventual surface of rupture and within the initial localised failure zone. At an applied load of 64 kPa the total pore water pressure at Piezometer P5 equates to approximately the total effective vertical stress and is considered to represent static liquefaction on the surface of rupture prior to the eventual embankment failure.

From Table 4.2 it is evident that the estimated effective critical stress ($s'_{1,crit}$) from the excess pore water pressure response, in most cases, reasonably approximates the laboratory estimated pre-consolidation pressure, s'_p, taking into consideration the accuracy of the estimation of the critical stress, sampling disturbance and accuracy of the laboratory procedures. Therefore, the excess pore water pressure response under the embankment centreline is a good indicator of the change from partially drained over-consolidated to undrained normally consolidated conditions for lightly over-consolidated clay foundations (OCR < 2.5). The exception, Piezometer A3 at James Bay (refer Table 4.3), is discussed further in Appendix C (Section 3).

The values of $\overline{B}_1$ are quite variable as indicated in Table 4.2. Leroueil and Tavenas (1986) commented that the degree of consolidation during the initial construction period (whilst the foundation is in an over-consolidated condition) varies from case to case, depending on the coefficient of consolidation, c_v, of the over-consolidated clay, the length of the drainage path and the rate of loading. Crooks (1987) considers that the clay stiffness and permeability, rate of loading and drainage boundary conditions affect the degree of consolidation during initial loading. He comments that clay foundations with high stiffness (in an over-consolidated condition) would be expected to generate only moderate excess pore water pressure response during initial loading whilst clays of lower stiffness would be expected to develop significant excess pore water pressure response. However, most of these assertions (except for drainage path length, Leroueil et al (1978a)) are intuitive and little case study evidence is given in support.

With respect to rate of construction, Leroueil et al (1978b) provide field evidence from the St. Alban test site that shows the initial rate of pore water pressure generation ($\overline{B}_1$) for embankment A (constructed at approximately twice the rate of other embankments) was greater than that for embankments B, C and D (Appendix C, Section 1). Leroueil et al (1978b) attributed this to the reduced consolidation associated with a faster rate of construction.

To evaluate the influence of the properties of the foundation and rate of loading on the rate of pore water pressure generation during the initial stages of construction prior to yielding of the foundation, the field observations from 16 case studies (54 piezometers) were analysed. The excess pore water pressure profiles from each case were compared against each other as well as to an undrained response assuming an infinite strip load on elastic half space. The results of the analysis are given in Appendix C (Section 1) and the findings are summarised as follows:

- Virtually all cases indicate significant drainage occurs in the upper soil profile. The excess pore water pressure profile (in comparison to the undrained profile for an infinite strip on elastic half space) for most case studies is typical of a consolidation isochrone for upward drainage only. Several case studies (Portsmouth, James Bay and St. Alban A and B) are typical of a consolidation isochrone for drainage boundaries at the surface and at depth. All four of these case studies have foundations comprising low plasticity, sensitive, leached marine clays.
- There is a high degree of variability in the pore water pressure profile from case to case with no clear correlation evident with respect to rate of loading (between different sites), material type (sensitive, low plasticity clays compared to high plasticity clays of low sensitivity) or likely material stiffness. For sites analysed with more than one test embankment, the St. Alban test embankments (Leroueil et al 1978a) do indicate a correlation with respect to rate of loading as discussed above, however, no correlation is evident between the Muar test embankments.
- Permeability is considered to being a key factor in controlling the variation of coefficient of consolidation, c_v, between case studies at different sites. In the case of the Muar test embankments a significant variation in $\overline{B}_1$ was observed between the upper and lower clay layers, with lower $\overline{B}_1$ values obtained in the more permeable upper clay and much higher $\overline{B}_1$ values in the less permeable lower clay. A similar pore water pressure profile to the Muar embankments was observed at the Rio test embankment.
- In 7 of the 16 case studies analysed the rate of pore water pressure generation at a depth below 4 to 6 m exceeded 80% of the pore water pressure profile assuming undrained conditions. This indicates that near undrained conditions are observed at depth in a significant proportion of cases during the initial stages of construction whilst the foundation is in an over-consolidated condition.

- The Mastemyr test embankment stands out as having a very high rate of pore water pressure generation during the initial stages of construction, greater than that estimated assuming undrained conditions. This observation may be due to the assumptions of the foundation as a half space and that the foundation behaves elastically prior to yielding for the undrained case considered.

For the piezometric response during normally consolidated conditions the analysed case studies (Figure 4.21) indicate most of the excess pore water pressure observations maintain a $\overline{B}_2$ of approximately 1, with several exceptions (refer Table 4.3). As previously discussed, only in the case of Kalix is it considered that the excess pore water pressure response is indicative of the onset to failure (i.e. $\overline{B}_f > 1$, Figure 4.5). The reason for the observation of constant $\overline{B}_2$ leading up to a failure condition for most piezometers is that the piezometers are not located within the localised failure zone. To observe an onset to failure condition ($\overline{B}_f > 1$), as is the case for Kalix, the piezometer must be located within the localised failure zone of a strain weakening soil. In most cases the zone of localised failure is relatively small, and coincident with the eventual surface of rupture, and therefore it would generally be unlikely for a piezometer to be located in this zone. Elsewhere in the foundation (away from the developed localised failure zone), at the time of failure the effective stress conditions have not yet reached a localised failure condition (Point *F´* on Figure 4.4), and no change is therefore observed for $\overline{B}_2$ up to failure.

It is concluded that whilst the excess pore water pressure response is a good indicator of the onset of undrained, normally consolidated conditions, it is not a reliable indicator of an impending failure condition. This is because only piezometers located within the relatively thin localised failure zone of strain weakening soils will the onset of failure be observed (i.e. $\overline{B}_f > 1$).

It is important to note that the analysis of excess pore water pressure is generally for piezometers under the centre of the embankment for which it can be assumed that the equations for excess pore water pressure development apply (Equations 4.2, 4.3 and 4.4). The more general solution (proposed by Henkel (1961)) applicable to all stress states is of the form:

$$Du = bDs_{oct} + 3aDt_{oct} \quad (4.5)$$

where Ds_{oct} is the octahedral normal stress, Dt_{oct} the octahedral shear stress, and a and ß are coefficients related to the soil behaviour.

The response of excess pore water pressure with time during periods of no construction is also an important aspect in the assessment of stability and deformation behaviour of embankments on soft ground. The excess pore water pressure response in some piezometers increased during periods on no construction leading up to the failure at Muar-EC, St. Alban-A and King's Lynn embankments. A delayed failure was also reported at Kalix, James Bay, Portsmouth and Mastemyr, where the failure occurred less than 24 hours after the final fill layer had been placed. The observations and mechanisms associated with increasing pore water pressure response during no construction periods are discussed in Section 4.4.2.

Table 4.3: Summary of exceptions to general observations of excess pore water pressure response.

Case Study	Exception	Comments / Reasons *[1]
James Bay	$s'_p > s'_{1,crit}$ (Table 4.2)	Effective critical stress significantly lower than the pre-consolidation pressure determined by laboratory testing. This is thought to be due the to relatively high over-consolidation ratio for the foundation (OCR > 2.5) and effective stress path for this condition.
Mastemyr	$\overline{B}_2 >> 1$ (Table 4.2)	Effective stress path possibly as per path OYE_c in Figure 4.8a. High $\overline{B}_2$ observed in piezometers down to 6 m depth. Possibly a result of strain weakening and indicative of partial breakdown in the soil structure.
Kalix	$\overline{B}_2 >> 1$ (Table 4.2)	Effective stress path possibly as per path OYE_c in Figure 4.8a. High $\overline{B}_2$ observed in piezometers down to 7.5 m depth. Possibly a result of strain weakening and indicative of partial breakdown in the soil structure.
Muar-EC	$\overline{B}_2 >> 1$ (Table 4.2)	Only Piezometer P4 gave high $\overline{B}_2$. Uncertain as to the cause of this observation.
Cubzac-A	$\overline{B}_2 >> 1$ (Table 4.2)	Piezometer P112 shows $\overline{B}_2$ in excess of 1.0. Only limited information is available and it is uncertain as to the cause of the observation.

Note: *[1] The exceptions are discussed further in Appendix C (Section 3).

4.3.3 PRE-FAILURE DEFORMATION BEHAVIOUR AND THE EFFECTS OF PROGRESSIVE FAILURE

This sub-section discusses the pre-failure deformation behaviour of embankments on soft ground leading up to a failure condition, and includes consideration of the mechanism/s of failure, such as progressive failure.

As discussed in Section 4.2.2, the deformation behaviour of embankments on soft ground is significantly affected by the effective stress state of the foundation in relation to its limit state. At effective stress states within the limit state (i.e. an over-consolidated condition) deformations will be small and partial drainage is observed due to the low compressibility of the over-consolidated clay (and resultant high coefficient of consolidation, c_v) and small amount of pore fluid that flows from the soil. On reaching the limit state surface (normally consolidated condition) deformations are much larger due to yielding of the foundation and negligible pore water pressure dissipation occurs (i.e. undrained conditions) due to the much lower c_v value associated with greater compressibility of the foundation.

Discussing the deformation behaviour of embankments on soft ground with respect to the type of movement for brittle, sensitive clays as opposed to ductile clays Ladd (1991) commented that:

- Brittle, sensitive soils show small undrained shear deformations during loading with little warning prior to a well-defined failure. Post-failure the displacements are very abrupt and large due to large strength reduction along a distinct surface of rupture, and large pore water pressure increases occur along the rupture surface.
- Ductile soils show large undrained shear deformations during loading, especially at low factors of safety, and provide ample warning prior to an ill-defined failure. At and post failure, deformations are relatively small and occur within a zone rather than along a distinct surface of rupture, with small pore water pressure changes.

Numerous authors (Ladd 1991; Rowe et al 1995; Marsland and Powell 1977; Fell et al 1987; Marche and Chapuis 1974) consider the horizontal movement at the toe of the embankment to be a good indicator of an impending failure condition. Ladd (1991) remarked that for ductile, soft clay foundations of low sensitivity the horizontal movement at the toe provides the clearest evidence of an impending failure condition because it is less affected by consolidation than settlement data and therefore reflects more clearly the deformation caused by undrained shear.

In the following sub-sections the deformation behaviour of the case study analysis of failures of embankments on soft ground is discussed in the context of the pre-failure deformation behaviour.

4.3.3.1 Vertical Displacement under the Centre of the Embankment

The settlement under the centre of the embankment versus relative embankment height (H/H_f, where H is the embankment height and H_f is the embankment failure height) of the analysed case studies is shown in Figure 4.22. The general behaviour, as expected, indicates an increase in the rate of the settlement (with relative embankment height) at embankment heights exceeding the threshold height, H_{nc}.

From the results it is considered that settlement under the centre of the embankment does not provide an indication of an impending failure condition. The reason for this is considered to be that in most cases the settlement monitoring point under the centre of the embankment is not located within the failure zone.

4.3.3.2 Vertical Deformation At and Beyond the Embankment Toe

The vertical deformation at the toe of the embankment versus relative embankment height for the analysed case studies is shown in Figure 4.23. Figure 4.24 presents the vertical deformation behaviour beyond the embankment toe (approximately 5 m distance beyond the toe). In all cases the monitoring point beyond the toe was located within the eventual failure zone.

It is considered that the vertical displacement at and beyond the toe of the embankment is a good indicator of an impending failure condition, particularly for monitoring points located beyond the embankment toe (and within the eventual failure zone). A measurable change in rate or direction of vertical displacement is observable in most of the case studies beyond the threshold height and within the range 70 to 95% of the eventual failure height.

For the monitoring points beyond the embankment toe (Figure 4.24), in most cases negligible vertical deformations were observed during the initial period of embankment construction, and the impending failure condition was identifiable by heave movements or large increases in the rate of heave movement with increasing embankment height. The observations therefore indicate that deformations at (and more significantly

beyond) the toe are not significantly affected by the immediate settlement associated with the embankment load, but are indicative of movements associated with instability of the embankment.

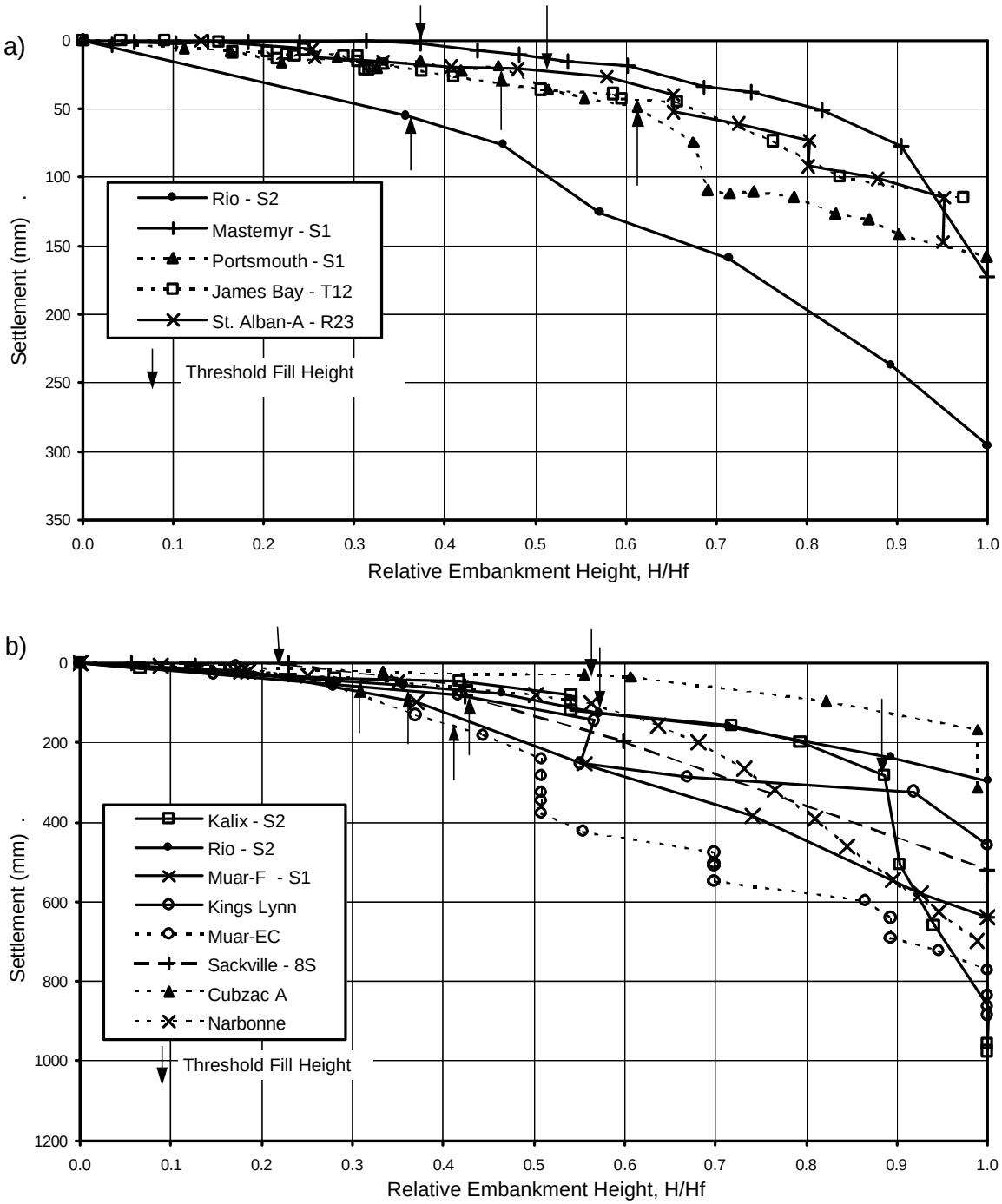

Figure 4.22: Settlement under the centre of the embankment versus relative embankment height (H/H_f).

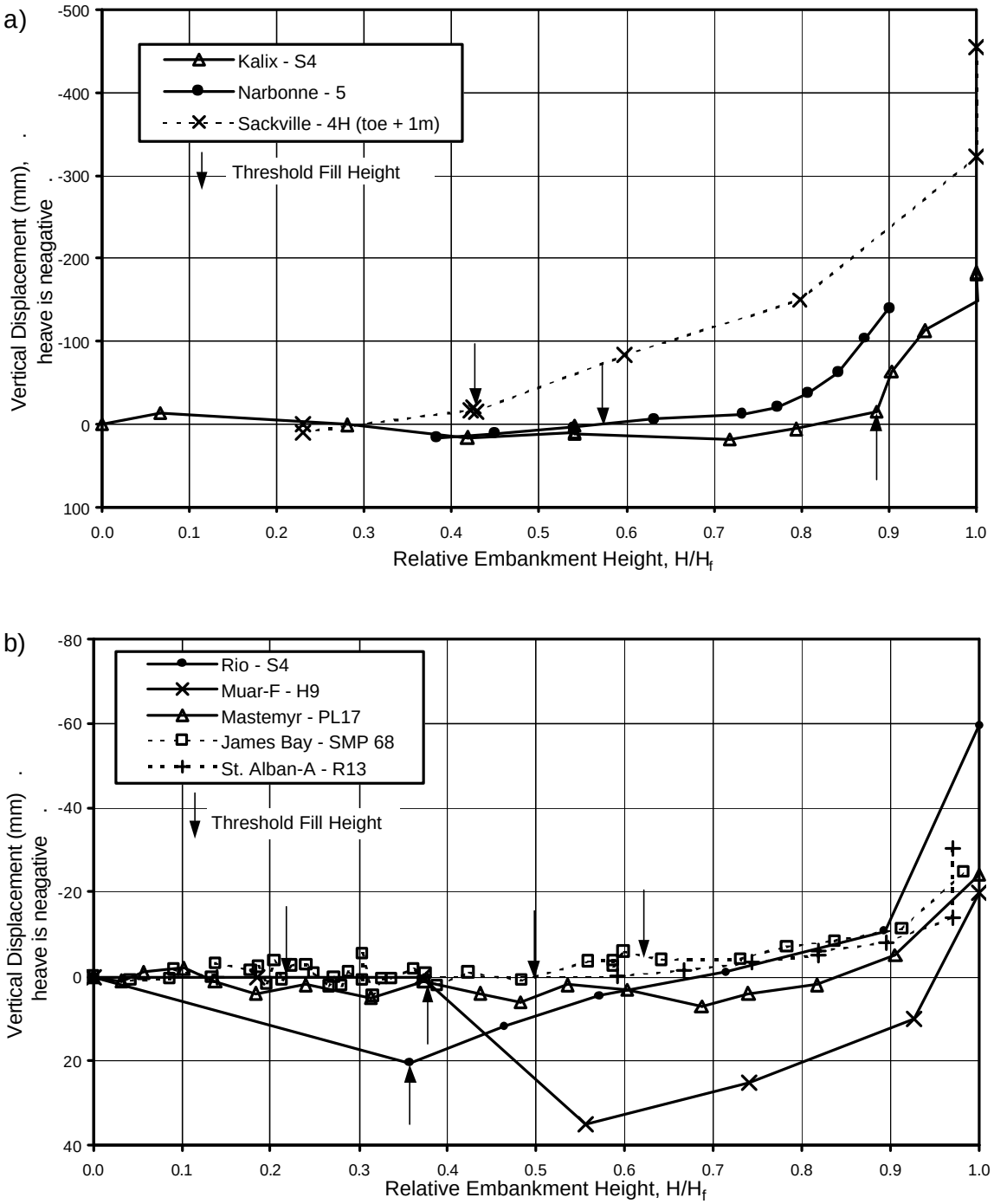

Figure 4.23: Vertical displacement at the embankment toe versus relative embankment height.

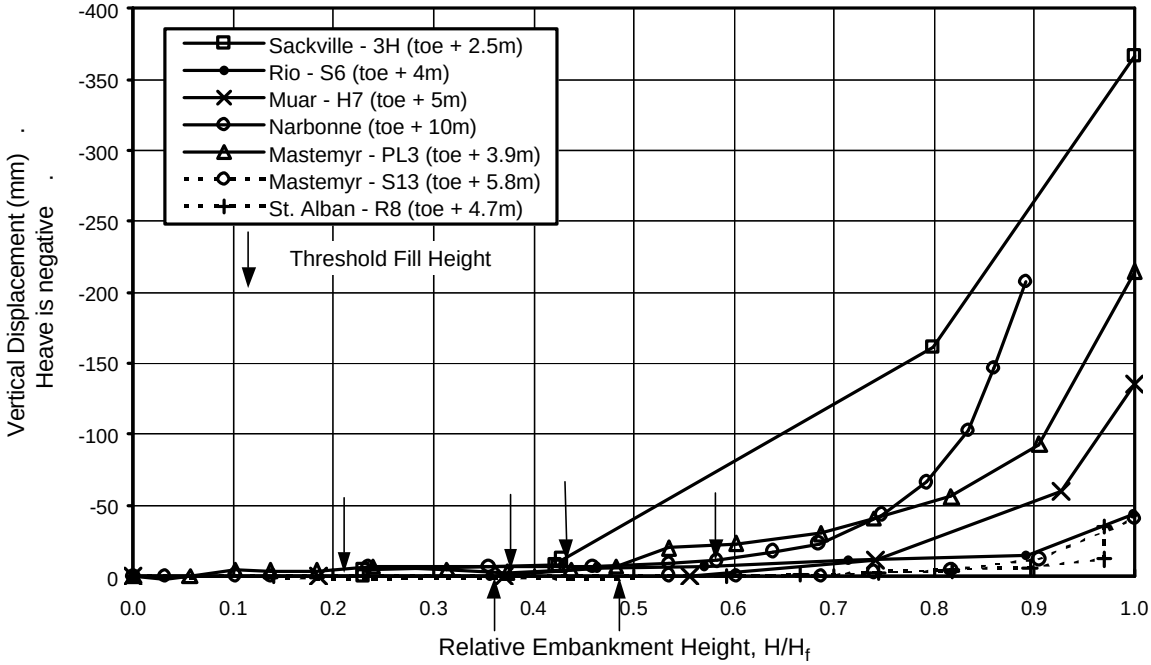

Figure 4.24: Vertical displacement beyond the embankment toe versus relative embankment height.

The cases where the vertical deformation at and beyond the toe is a good indicator of an impending failure condition cover a wide variety of soil types from high plasticity clays of low sensitivity to highly sensitive, low plasticity clays and silts, making it a good indicator for embankments on all types of soft ground conditions.

For the embankments on highly sensitive, low plasticity clay foundations (St. Alban and James Bay) the amount of vertical movement is relatively small (up to 10 to 15 mm) for up to approximately 90% of the eventual embankment failure height. However, in recognising this, the vertical deformation at and beyond the toe is still considered a good indicator for these types of foundation conditions as the purpose of the monitoring would be to identify these small but measurable heave movements.

The vertical displacement at and beyond the toe of the Kalix and Rio test embankments is considered as a reasonable to good indicator of an impending failure condition, however, the deformation behaviour is not explainable only by being close to the failure height (refer Table 4.4). For St. Alban-A the vertical deformation behaviour at the toe is considered to be a reasonable indicator of an impending failure condition. The heave movements start at about 60% of the failure height, however, the movements are small (less than 10 mm up to 90% fill height) and a change in rate in not clearly perceptible over the later stages of construction.

4.3.3.3 Lateral Surface Displacements at the Embankment Toe

The lateral displacement at the toe of the embankment for the failure case studies has been presented as the lateral surface displacement versus relative embankment height (Figure 4.25).

From Figure 4.25 it is concluded that:

- In most cases an increase in the rate of lateral displacement relative to the embankment height occurs at about the threshold height, H_{nc}, determined from the pore water pressure response, which is in agreement with the interpretation of the behaviour of embankments on soft ground to limit state theory.
- A further increase in the rate of lateral surface displacement occurs in most of case studies analysed at relative embankment heights of 70 to 90%. It is considered that this behaviour is an indication of an impending failure condition.
- For 11 of the 12 cases analysed, the lateral surface displacement is a good indicator of impending failure. These cases cover a broad range of soil types from low to high sensitivity and low to high plasticity, making it a good indicator for embankments on all types of soft ground conditions.

The lateral surface displacement versus embankment height plots for Thames (increase in rate beyond 75 to 80%), Muar-F (increase in rate beyond 75 to 80%), Mastemyr (beyond 80%), Cubzac A (beyond 80%), Muar-EC (beyond 85%), St. Alban-A (beyond 75%) and Portsmouth (beyond 80 to 85%) all show an increase in the rate of displacement beyond the threshold height. For James Bay, Kalix and Sackville there are insufficient data points beyond the threshold height to draw any firm conclusions, however, the trend of the plots for these cases indicate the lateral surface displacement at the toe is a good indicator.

For Kalix and Rio the change in deformation behaviour is not explainable only by being close to the failure height, and at King's Lynn the impending failure is not clearly identifiable (refer Table 4.4).

The results indicate that the rate of embankment construction affects the amount of lateral surface displacement measured, particularly for the case studies with high plasticity, low sensitivity foundations. For embankment constructed at relatively slow rates (Muar-F and Muar-EC constructed at rates of 0.02 to 0.055 m/day) the lateral surface displacement was a good indicator of the impending failure, and for the embankments constructed at more rapid rates (Rio at 0.1 m/day and King's Lynn at 0.67

m/day) the lateral surface displacement was not such a good indicator of the impending failure. For Muar-EC it was evident that a significant proportion of the lateral displacement occurred during rest periods in the later stages of construction, whilst the rate during construction periods did not increase significantly. During these rest periods at Muar-EC when the embankment height was above 50% of the eventual failure height, the excess pore water pressure was either steady or else increased.

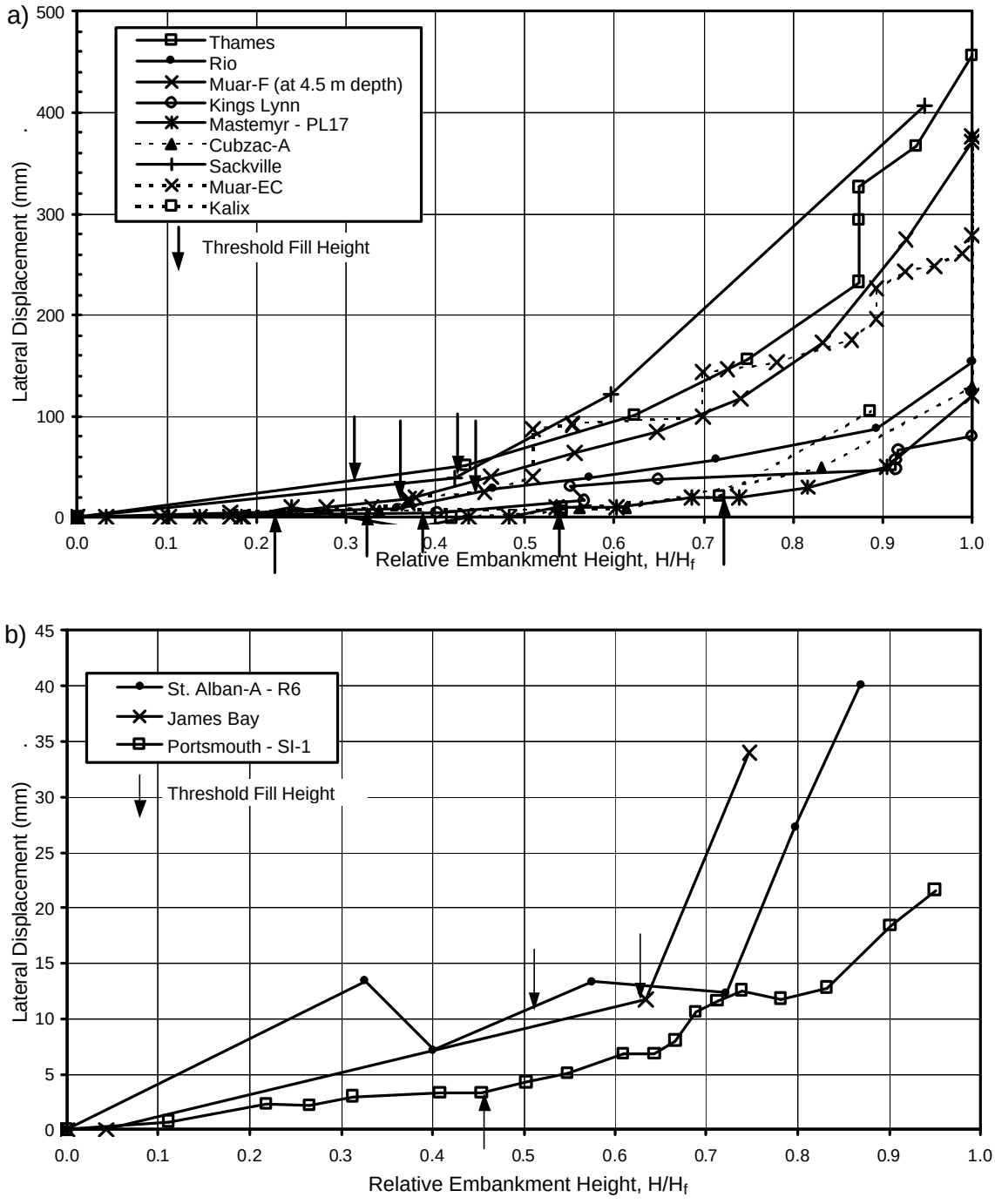

Figure 4.25: Lateral surface displacement at the embankment toe versus relative embankment height.

4.3.3.4 Lateral Displacement with Depth at the Embankment Toe

The data on lateral displacement with depth at the embankment toe, from inclinometer observations, is presented in the form of the vertical inclination angle at the eventual surface of rupture versus relative embankment height (Figure 4.27). It is recognised that during construction the eventual surface of rupture is not known. However, by monitoring the incremental vertical inclination angle (Figure 4.26) the zone of localised failure, particularly for foundations of low sensitivity, will become evident prior to the eventual failure. Once the localised failure zone becomes evident then the data from this zone can be plotted in the form of Figure 4.27.

Figure 4.26 clearly shows the development of the localised failure zone with increasing fill height and time for the Thames and King's Lynn case studies. Ramalho-Ortigao et al (1983a, 1983b) presented similar type plots for the Rio test embankment. From Figure 4.26 it is evident that the eventual surface of rupture is located within the localised failure zone.

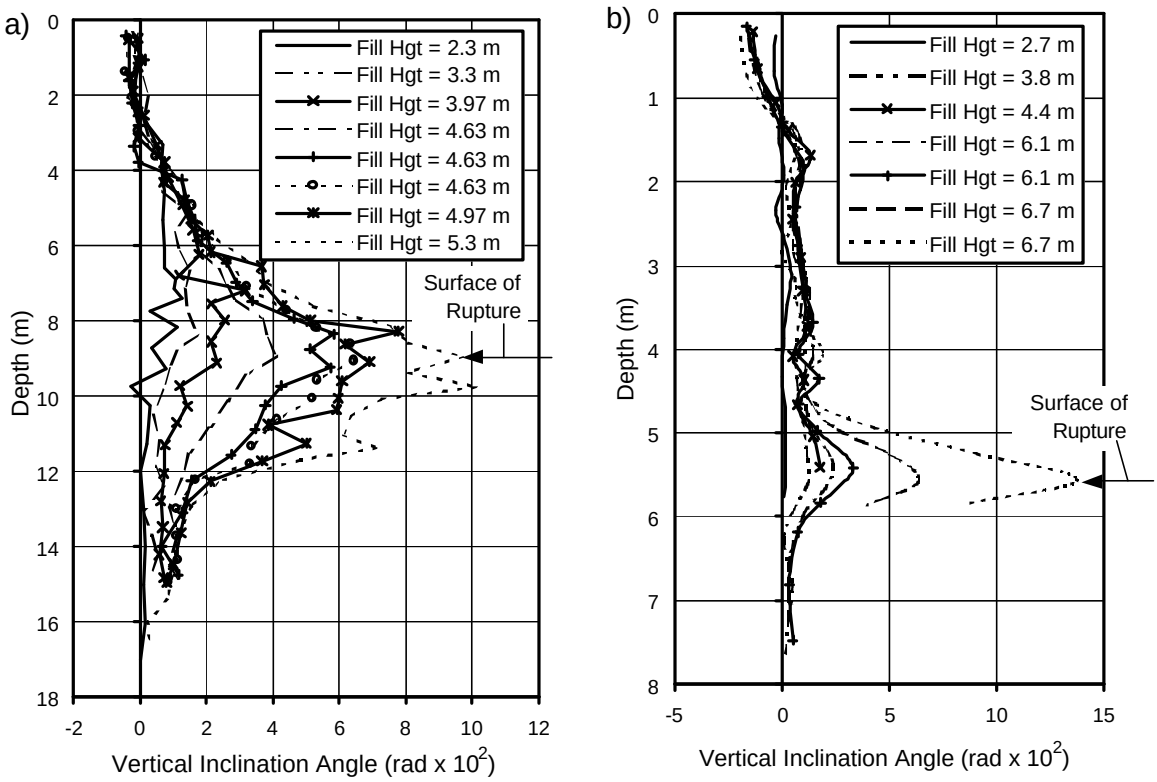

Figure 4.26: Incremental vertical inclination angle (from inclinometer observations at the embankment toe) with fill height (and time) for *(a)* Thames and *(b)* King's Lynn.

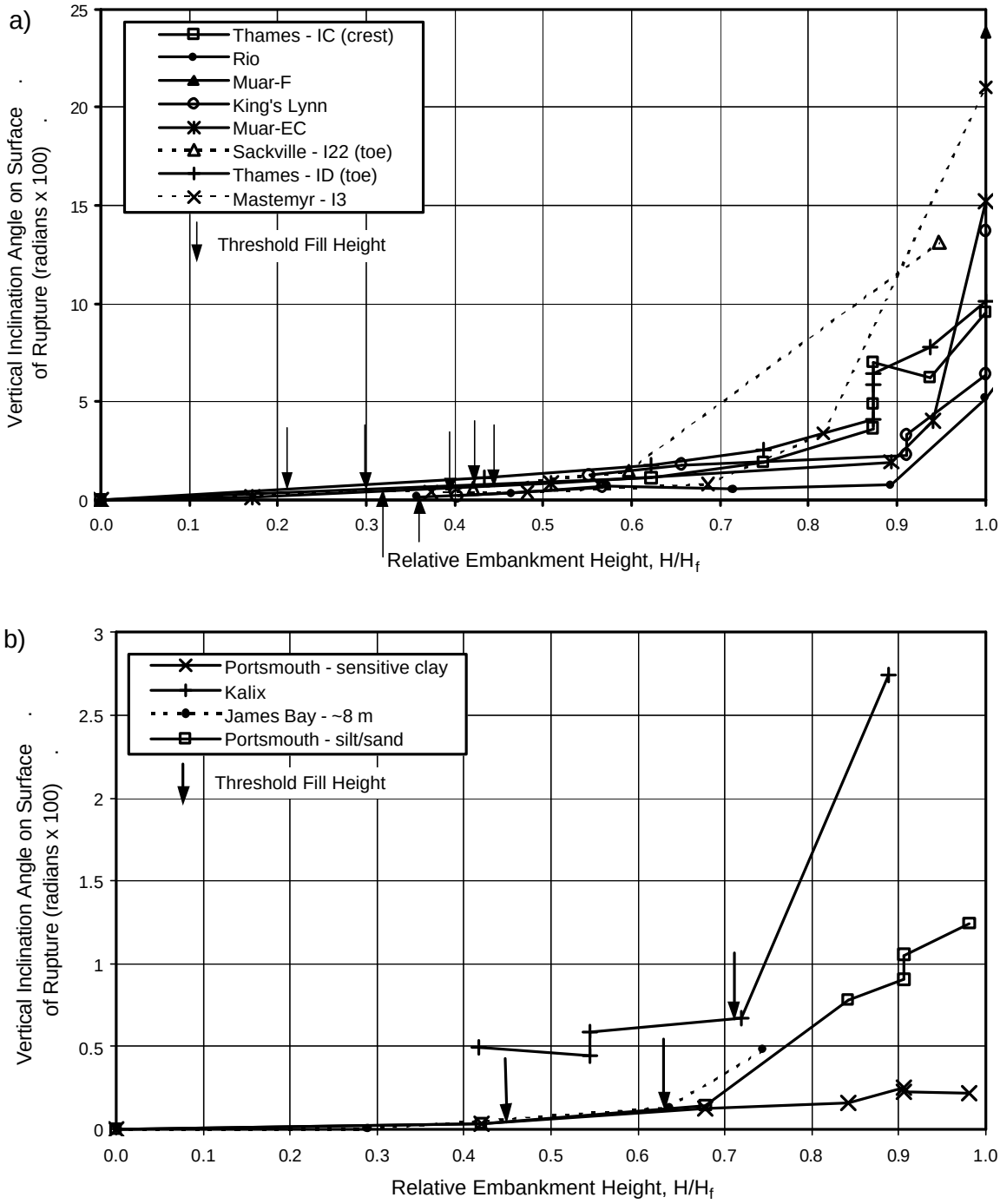

Figure 4.27: Vertical inclination angle on the surface of rupture from inclinometer observations at the embankment toe versus relative embankment height.

Figure 4.27a is of predominantly low sensitivity clays (except for Mastemyr) and shows that in all cases (except Rio and to a lesser extent King's Lynn) significant increases in the vertical inclination angle on the eventual surface of rupture occur at embankment heights of 70 to 90% of the failure height. The increases in shear strain within the localised failure zone and on the eventual surface of rupture occur well beyond the

threshold height (Figure 4.27a) and are considered to represent a localised failure condition within which large shear strains as a result of plastic deformation develop (Figure 4.26). At the onset of localised failure the effective stress state within the localised failure zone is considered to be at or close to the point of failure on the effective stress path (Point *F´* in Figure 4.4).

For embankments constructed on sensitive, brittle foundations (Portsmouth, Kalix and James Bay in Figure 4.27b and Mastemyr in Figure 4.27a) the plot of maximum vertical inclination angle versus relative embankment height as an indicator of an impending failure is considered to vary from poor to good. Although the plots from Figure 4.27 would indicate that it is a reasonable indicator of an impending failure condition for these soil types, there are other explanations for the observed behaviour.

The development of the localised failure zone is considered to initiate within the highly stressed zone of the foundation located under the shoulder of embankment shoulder (as discussed in Section 4.2.2). At this point the soil in the localised failure zone is unable to support any further stress, however, the local failure is contained and supported by the surrounding unfailed soil (Muir Wood 1990). This is the start of a progressive failure mechanism. With additional loading the size of the localised failure zone increases and with increased straining the strength within the localised failure zone decreases due to strain weakening. At some point the driving forces exceed the resisting forces and failure occurs, and the mobilised strength at failure for strain weakening soils will be less than peak strength.

It would be expected, and the results indicate, that the development of the localised failure zone is more clearly developed for foundations of low sensitivity due to their significantly lower undrained brittleness index (or lower amount of post peak strain weakening). Once a localised failure zone has developed the amount of load transferred to the surrounding soil is much less for the low sensitivity soils, due to their relatively low undrained brittleness. In addition, relatively large post-peak strains are required for strain weakening, and therefore a progressive failure mechanism develops relatively slowly.

In the case of sensitive clay foundations, particularly those of low plasticity, a progressive failure mechanism also occurs; however, it develops much more quickly and possibly not until the embankment has been constructed to its failure height. For these soils, peak strengths are reached at relatively small strains and at failure (of the soil) a large reduction in the undrained strength occurs with relatively small strain. The

large loss in undrained strength of these sensitive soils is associated with contraction of the soil structure on shearing and transfer of load onto the pore fluid resulting in the development of high excess pore water pressures; i.e. a static liquefaction condition. Therefore, once a failure condition is reached progressive failure develops rapidly and failure of the embankment quickly ensues. The observation of the deformation behaviour within the inclinometer at the toe of the embankment at Portsmouth and James Bay tend to confirm this rapid progression to failure.

For Portsmouth no significant increase in vertical inclination angle is evident in the region of the eventual surface of rupture up to 98% of the embankment failure height (Figure 4.27b). This indicates that the localised failure zone at Portsmouth is not likely to have developed until some time after the end of construction. The embankment failure occurred at some stage during the night (Ladd 1972), less than 12 to 18 hours after construction to the eventual failure height. Within the sandy silt layer below about 10.4 m depth an increase in the vertical inclination angle (VIA) is evident from 68% of the embankment failure height (Figure 4.27b).

The description leading up to failure of the James Bay embankment (Dascal and Tournier 1975) strongly supports the rapid development of progressive failure as discussed above. They state that:

> "*The failure started during the inclinometer readings by the field crew. At the thirteenth measurement, they started to notice that that the order of magnitude of the readings was quite different from the previous ones. At the fifteenth measurement, the variation was such that the reading scale had to be changed. At the twentieth measurement the probe became stuck and could neither be lowered nor extracted. At the same moment, water started to rise in the tube. Simultaneously they observed the rising of the natural ground at the toe of the slope by about 0.3 m in approximately 10 sec, during which the fill was ruptured.*"

These observations would indicate the rapid development of shearing in the region of the surface of rupture leading up to the failure and that significant shearing did not take place until shortly prior to the failure. The observation of water rise in the inclinometer tube would be consistent with static liquefaction on the surface of rupture due to collapse of clay structure followed by the rapid failure of the embankment.

In the case of Kalix and Mastemyr it is considered that the partial breakdown in the soil structure has reduced the undrained brittleness of the foundation and therefore

progressive failure is more clearly evident than for the other case studies with sensitive clay foundations.

4.3.3.5 Settlement Versus Lateral Displacement

Figure 4.28 presents the plot of settlement under the centre of the embankment versus maximum lateral displacement at the embankment toe for ten of the thirteen failure case studies analysed. The results indicate that an increase in the ratio of settlement to maximum lateral displacement ($\Delta y_m / \Delta s$) occurs above the threshold height and that the ratio above the threshold height is quite variable. For those embankments that cracked prior to failure (Rio, King's Lynn, Muar-F and Muar-EC) an increase in the $\Delta y_m / \Delta s$ ratio occurs after cracking. No indication of the onset of failure is apparent from the plot nor was it expected. Tavenas et al (1979) and Tavenas and Leroueil (1980) used this type of plot as confirmation of the change in deformation behaviour that occurs at the change from over-consolidated to normally consolidated conditions and as field evidence to indicate that partial drainage does occur whilst the foundation is in an over-consolidated condition.

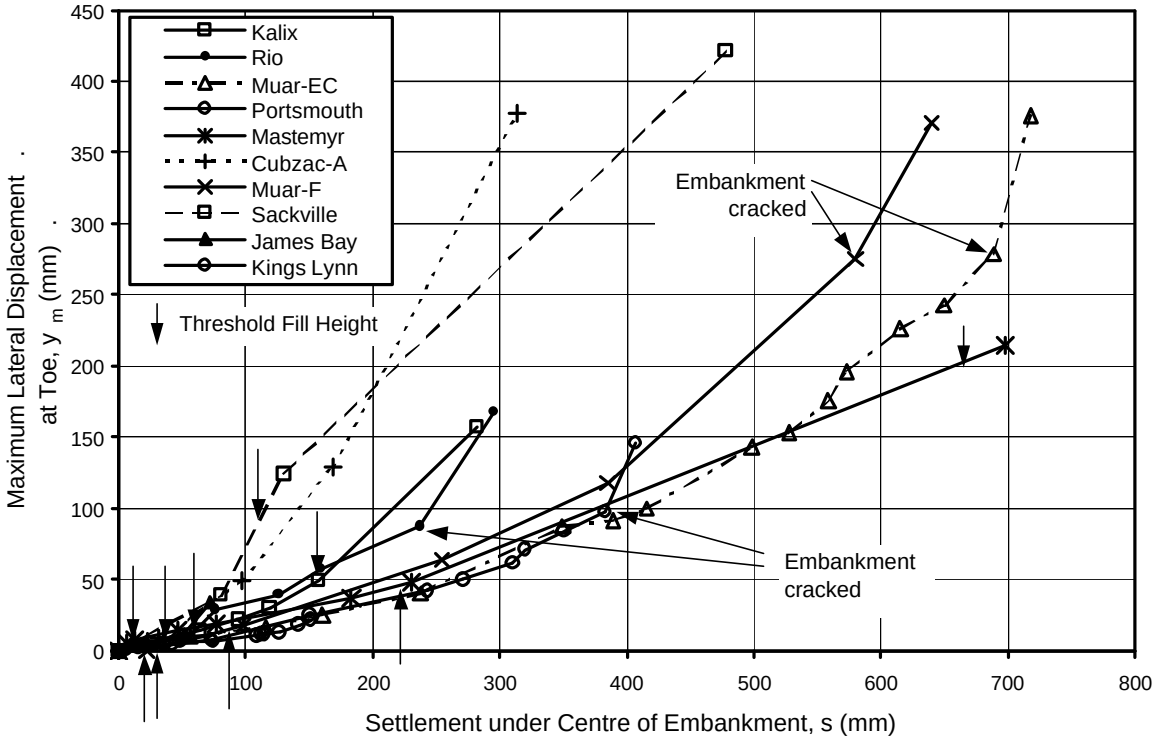

Figure 4.28: Maximum lateral displacement at the embankment toe versus settlement under the centre of the embankment.

4.3.3.6 Case Study Exceptions to Deformation as an Indicator of Impending Failure

The case studies for which deformation was a poor indicator of an impending failure condition or the change in deformation behaviour has alternative explanations are summarised in Table 4.4. Only those deformation indicators that provided a good indication of an impending failure condition for most case studies have been considered; vertical deformation at and beyond the embankment toe, lateral surface displacement at the embankment toe and lateral displacement at depth at the embankment toe.

Table 4.4: Summary of case studies that are exceptions or have other explanations to deformation as an indicator of impending failure.

Case Study	Indicator	Comments / Reasons *[1]
Rio	Vertical deformation at and beyond the toe (Section 4.3.3.2); lateral surface displacement at the embankment toe (Section 4.3.3.3)	Reasonable to good indicators. Alternative explanation is that the large increase in rate is associated with cracking of embankment.
	Lateral displacement at depth at the embankment toe (Section 4.3.3.4)	Poor indicator. Localised failure zone may not have developed until the embankment had cracked. Possibly influenced by the small embankments constructed at the toe of the main embankment.
St. Alban-A	Vertical deformation at and beyond the toe (Section 4.3.3.2)	Reasonable indicator, however, heave movements are small (< 10 mm) and a change in rate is not clearly perceptible.
Kalix	All indicators *[2]	Good indicator, but alternative explanation is that the change in deformation behaviour is coincident with the threshold fill height. Also, limitation on number of measurement points taken beyond the threshold height.
King's Lynn	Lateral surface displacement at the embankment toe (Section 4.3.3.3)	Not a good indicator. An impending failure condition is not clearly identifiable
Low plasticity, sensitive clay foundations	Lateral displacement at depth at the embankment toe (Section 4.3.3.4)	Incorporates the Portsmouth, James Bay and St. Alban-A test embankments. Poor indicator due to late development of localised failure zone and rapid progressive failure mechanism (refer Section 4.3.3.4 for further discussion).

Note: *[1] Most of the exceptions are discussed further in Appendix C (Section 3).

*[2] All indicators includes vertical deformation at and beyond the toe (Section 4.3.3.2), lateral surface displacement at the embankment toe (Section 4.3.3.3) and maximum lateral displacement at depth at the embankment toe (Section 4.3.3.4).

In the case of the Rio test embankment, the increase in rate of displacement at the toe (both vertical and lateral), which occurred at about 90% of the eventual embankment failure height, is coincident with cracking observed in the embankment. The cracking of the embankment is considered to have had an effect on the increased rates of displacement observed due to changes in the effective stress conditions in the foundation. However, the lateral displacement probably caused the cracking.

4.3.4 FACTOR OF SAFETY VERSUS RELATIVE EMBANKMENT HEIGHT

The purpose of this section is to assess the relationship between embankment height and the factor of safety for embankments on soft ground. The results (Figure 4.29) are given in the form of factor of safety versus relative embankment height, as most of the previously presented deformation plots are in this form.

From the database of failure case studies, the factor of safety with increasing embankment height was taken as published for Thames (Marsland and Powell 1977), Cubzac-A (Blondeau et al 1977) and Narbonne (Pilot 1972), and was calculated for Rio, Muar-F, St. Alban-A and Portsmouth test embankments. The computer program SLOPE-W was used to calculate the factor of safety of the four case studies analysed adopting the following methodology:

- Total stress analysis using undrained strengths determined by the vane (Portsmouth, St. Alban and Rio) or laboratory triaxial testing (Muar-F). No correction was applied to the vane readings.
- A strength anisotropy function was used for the soft clay foundation where sufficient data was available from the published information (Portsmouth).
- Shear strength for the crust using the median strength analysis approach proposed by Ferkh and Fell (1994) to account for loss of strength of the crust associated with the presence of pre-existing fissures and the cracking that occurs under the settlement of the embankment. The crust strength is determined from assessment the profile of liquidity index (I_L) and the median of the measured vane strengths. Where the liquidity index is greater than 1.0 the median of the vane strength is used. Above the level where the liquidity index equals 1.0 (i.e. where $I_L < 1$) a constant strength equivalent to the median vane strength at the base of the layer (i.e. where $I_L = 1$) is adopted. The results for Portsmouth do not include this crust strength correction because the analysis using the correction gives a factor of safety at failure of 0.9.

This observation is possibly due to using an un-conservative function for the strength anisotropy.

- Embankment strength as reported and modelling of cracking (at the location reported) if this was observed prior to failure.
- The model was, as far as practical, allowed to determine the surface of rupture corresponding to the minimum factor of safety. In most cases the surface of rupture modelled was reasonably close to that observed. For the Muar-F and Rio test embankments, difficulties were encountered in matching the observed large radius of the surface of rupture and it was considered that this was due to the likelihood of progressive failure at Muar-F and possibly a complex translational – rotational surface of rupture at Rio.
- Once a factor of safety of close to one was calculated for the failure condition and a reasonable match of the observed surface of rupture obtained, the modelling was continued for lower embankment heights.

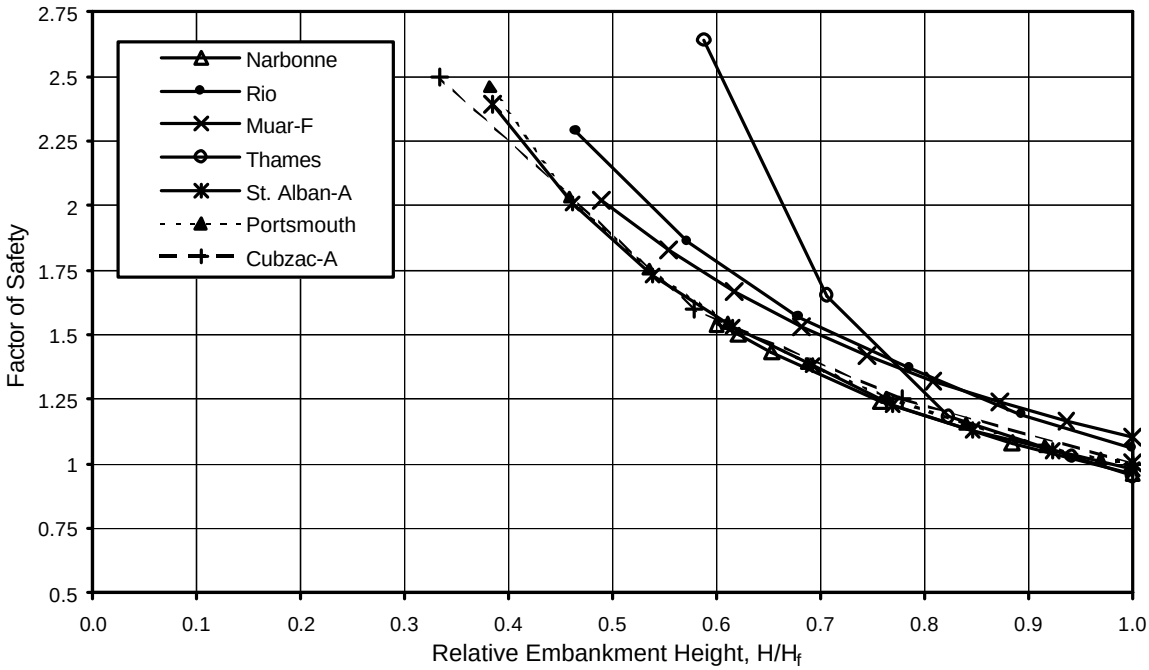

Figure 4.29: Factor of safety versus relative embankment height

The conclusion from the analysis is that the calculated factor of safety approaching a failure condition is quite low, as the observed deformation behaviour at monitoring points located within the eventual failure zone indicates. The calculated factors of safety (Figure 4.29) fall below 1.5 at relative embankment heights of 60 to 70% of the

failure height in most cases, and below 1.25 at 75 to 85% of the failure height. The vertical and lateral displacements at and beyond the embankment toe (Figure 4.23 to Figure 4.25) indicate, for all types of foundation conditions, an increase in the rate of displacement with increasing embankment height typically in the range 60 to 90% of the eventual failure height.

As shown in Figure 4.29, there is a close correlation of the plots of factor of safety versus relative embankment height for the rotational failures despite the varying soil types (low to high sensitivity and low to high plasticity) and embankment geometry between the case studies. For the Thames embankment, the surface of rupture is complex translational-rotational.

4.3.5 POST-FAILURE DEFORMATION BEHAVIOUR

4.3.5.1 Post Failure Rates of Movement

The post failure rates of movement from the case studies analysed, classified in accordance with the velocity categories of IUGS (1995) (refer Table 1.1), are summarised as follows:

- For St. Alban-A and James Bay (both sensitive clay foundations) the failure occurred in minutes, with maximum rates of movement estimated at 0.9 and 1.8 m/min. Both classify at the upper end of the rapid category.
- For the Muar-F embankment, the failure also occurred in minutes at an estimated maximum rate of 1 m/min, also classifying at the upper end of the rapid category. A "fairly loud noise" (Brand and Premchitt 1989) was heard at the time of the failure possibly indicating internal brittleness in the slide mechanism.
- For Thames and Kalix the maximum rates of movement are estimated at 30 and 45 mm/hour respectively, classifying in the moderate range. For Thames the full slip developed over some 10 hours.
- For the Muar-EC embankment, continued movement for many days followed the initial post failure movement of 340 mm. Ramalho-Ortigao et al (1983b) reported the failure at Rio as "a general slip slowly occurred". In both cases the maximum rate of movement would probably classify within the moderate range.

For the remaining case studies insufficient information was available with which to estimate the maximum velocity of the slide mass post failure. The amount of deformation and estimated velocity of the slide mass post failure for the case studies is summarised in Table 4.1.

Where reasonable estimates of the post failure velocity are possible from the published literature, they indicate that:

- For embankments on low plasticity, sensitive clay foundations the post failure velocity is likely to be in the range of metres per minute (rapid category).
- For embankments on foundations of low to high plasticity clays of low sensitivity, the post failure velocity is likely to be in the slow to moderate velocity category (centimetres per hour, possibly up to metres/hour).

However, there are exceptions. In the case of Muar-F (a high plasticity clay foundation of low sensitivity) the failure was at a rapid velocity, but the mechanics of failure were thought to possibly incorporate some internal brittleness at failure (as indicated by the large noise at failure), which contributed to the high velocity. In the case of Kalix the post failure velocity was quite low for a sensitive clay foundation.

4.3.5.2 *Analysis of the Post-Failure Deformation Behaviour*

Khalili et al (1996) have proposed a simplified method for estimating the post-failure deformation of intact sliding along a rotational surface of rupture. They applied the method to six case studies, five were embankments on soft ground (that remained basically intact on sliding) and one was an embankment dam subject to liquefaction (Lower San Fernando dam).

The Khalili et al (1996) model considers two modes of failure defining the upper and lower bounds of post-failure deformation:

- A “rapid model” based on the principle of conservation of energy where the potential energy of the slide mass is resisted by the frictional forces along the surface of rupture approximated using the residual shear strength. This is essentially a simplified lumped mass model.
- A “slow model” based on equations of equilibrium between the driving force of the slide mass and resisting forces along the surface of rupture approximated using the

residual shear strength, i.e. assuming the rate of movement would be so slow that the effect of inertia forces of the sliding mass are negligible.

The failure model is shown in Figure 4.30 and is based on the assumptions of a circular slide surface, the failure is plane strain, the failed slide mass moves as a rigid body and energy losses during failure are only due to the frictional forces acting along the slip surface. Approximate solutions for the rapid model are calculated using Equation 4.6 and for the slow model using Equation 4.7, where $FS_{residual}$ is the factor of safety calculated using residual strengths along the surface of rupture, and $?_i$ and $?_f$ are the initial and final positions of the centre of gravity as defined in Figure 4.30.

Rapid Model: $$q_f = 2q_i(FS_{residual} - 0.5) \quad (4.6)$$

Slow Model: $$\sin q_f = FS_{residual} \sin q_i \quad (4.7)$$

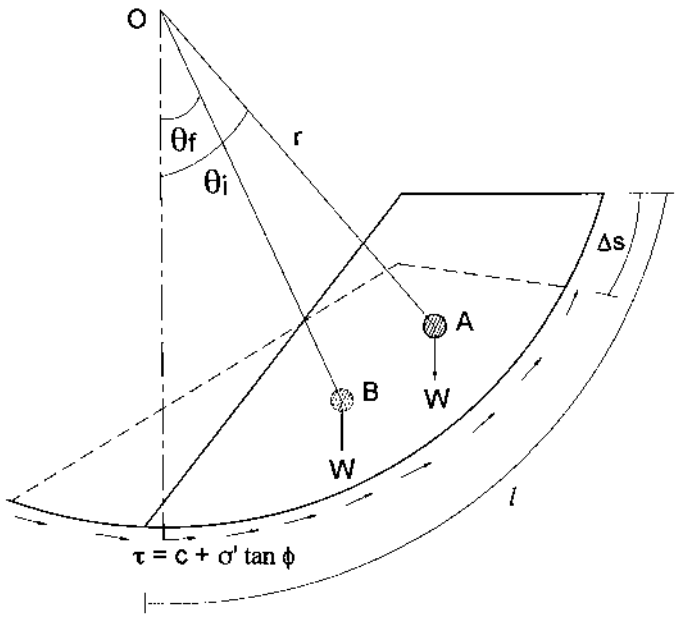

Figure 4.30: Failure model for post-failure deformation (Khalili et al 1996)

Note that the terms “rapid” model and “slow” model defined and used by Khalili et al (1996) are different to the definitions of “rapid” slides and “slow” slides used throughout the thesis and the definitions of rapid and slow post failure velocity defined by IUGS (1995).

Analysis of the post-failure deformation using the Khalili et al (1996) method has been undertaken on four of the failure case studies of embankments on soft ground (Rio,

St. Alban-A, Portsmouth and Muar-F). The results of the analysis are summarised in Table 4.5. Details of the post failure deformation for each case study and the analysis undertaken are given in Appendix C (Section 4).

Table 4.5: Results of the post-failure deformation analysis

Case Study	$?_i$ (°)	$FS_{residual}$	$?_i - ?_f$ **Calculated** (°)		$?_i - ?_f$ **Observed** (°)	**Calculated Crest Settlement (m)**		**Observed Crest Settlement (m)**
			Slow	**Rapid**		**Slow**	**Rapid**	
Rio	8.5	0.43 (vane)*[1] 0.70 (f'_r)*[2]	4.9 2.55	9.8 5.1	3.0	1.1 0.59	2.1 1.14	0.68
Muar-F	5.1	0.40 (vane) 0.71 (f'_r)	3.1 1.5	6.1 2.9	5.6	0.78 0.38	1.53 0.75	1.4
St. Alban-A	21.5	0.26 (vane) 0.75 (lab)*[3]	16.1 5.6	32 10.8	8.1	2.3 0.79	4.6 1.53	1.15
Portsmouth	14.5	0.27 (vane)	10.6	21.2	10.4	3.4	6.45	3.3 – 3.4

Note: *[1] vane = vane remoulded shear strength

*[2] f'_r = large strain undrained shear strength calculated from the estimated drained residual shear strength (see below).

*[3] Lab = large strain laboratory undrained shear strength

For the Rio and Muar-F test embankments, both constructed on high plasticity, low sensitivity clay foundations, the large strain undrained shear strength was obtained by estimating a residual friction angle (f'_r) based on the clay fines content and plasticity of the soft clay, and then calculating the large strain undrained shear strength (S_{ur}) profile from Equation 4.8. Estimation by this method is considered suitable only for soils that are not contractive on shearing.

$$S_{ur} = s'_p \tan f'_r \qquad (4.8)$$

where s'_p is the pre-consolidation pressure of the soft clay.

The predictions based on the estimates of the residual undrained strength profile from laboratory test results (St. Alban-A) and estimated residual friction angle (Rio and Muar-F) are much closer to the observed post-failure deformation behaviour (Table 4.5), than the predictions using the estimates from vane testing.

For the Rio test embankment, the failure occurred relatively slowly and therefore the observed behaviour would be expected to be closer to the slow method prediction as is the case. For St. Alban-A the failure occurred rapidly and therefore the observed behaviour would be expected to be closer to the rapid method prediction, it is located about mid way between the slow and the rapid model.

In the case of the Muar-F embankment, the observed settlement is significantly greater than the prediction based on the large strain undrained shear strength obtained by the estimate of the residual friction angle method. It is considered that the actual surface of rupture may have incorporated a significant translational component and the assumption therefore of rotational, intact sliding by the Khalili et al (1996) model may invalidate its use for this embankment.

General guidelines on the use of this type of model are discussed in Chapter 5 together with the findings from analysis of failures in embankments dams and cut slopes in high plasticity heavily over-consolidated clays (Sections 5.8.1 and 5.9.2).

4.4 POST CONSTRUCTION BEHAVIOUR OF EMBANKMENTS ON SOFT GROUND

The study of the post construction behaviour of embankments on soft ground (i.e. of embankments that do not fail during construction) is limited to the following aspects:

- A discussion on the effect of the effective stress state on the post construction deformation behaviour and excess pore water pressure response.
- The pore water pressure response and deformation behaviour in the period following the end of construction. For a number of reported case studies it is observed that at the end of construction excess pore water pressures continue to rise and relatively large deformations occur. The observations from five case studies are discussed in the context of the mechanics. This aspect of the behaviour of embankments on soft ground is of fundamental importance, because failure may occur many days after the end of construction as was observed at the Muar-EC test embankment which failed some 30 days after construction.
- Estimates of long-term deformation behaviour in the form of lateral displacement at the toe versus settlement at the centre. This is essentially a summary of the work by Tavenas et al (1979).

4.4.1 EFFECT OF EFFECTIVE STRESS STATE ON THE POST CONSTRUCTION BEHAVIOUR

The post construction excess pore water pressure response and deformation behaviour of a soft clay foundation at the end of construction is significantly affected by its effective stress state in relation to the limit state surface. The two most common effective stress states for lightly over-consolidated, soft clay foundations at the end of construction are at a point on the yield surface below the critical state line (Figure 4.31a) and therefore in a normally consolidated condition, or else within the limit state surface (Figure 4.31b) and therefore in an over-consolidated condition.

Assuming that the effective stress state at a point under the foundation at the end of construction is in an over-consolidated condition (defined by point E_c in Figure 4.31b), as drainage takes place the effective stress path will move to the right. The initial rate of pore water pressure dissipation will be relatively rapid and the settlement relatively small whilst the effective stress state is within the limit state surface (i.e. in an over-consolidated condition). Once the effective stress path reaches the yield surface (Point Y in Figure 4.31b) the foundation will be in a normally consolidated condition. The change in the soil characteristics (increase in compressibility and decrease in coefficient of consolidation) will result in a marked decrease in the rate of pore water pressure dissipation and marked increase in settlement per unit increase in effective vertical stress.

The behaviour observed under the centre of the embankment at Kars Bridge (Folkes and Crooks 1985) presents a good example of the significant effect of effective stress state on the post construction pore water pressure response and settlement behaviour.

4.4.2 DEFORMATION BEHAVIOUR AND PORE WATER PRESSURE RESPONSE IN THE INITIAL PERIOD POST CONSTRUCTION

The observation of increasing pore water pressure during periods of no construction and at the end of construction within the soft foundation of embankments constructed on soft ground is not uncommon. Crooks et al (1984) and Becker et al (1984) reported pore water pressure increases in 11 of 31 case studies. Of the failure case studies analysed as part of this research, in 4 of 13 cases the pore water pressure was observed to increase in at least one piezometer during periods of no construction or at the end of

construction prior to failure. Of the remaining 9 case studies there was insufficient information to state if pore water pressures increased during periods of no construction.

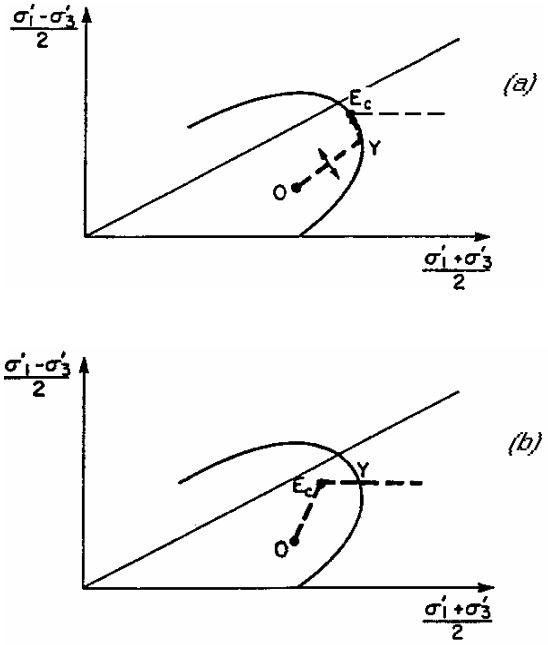

Note:
Ec = end of construction
O defines the initial effective stress state prior to construction.
Y denotes the limit state or state boundary surface

Figure 4.31: Effective stress paths post construction (Leroueil and Tavenas 1986).

In 6 of the failure case studies analysed, deformations (mainly lateral displacement at the toe) were observed to increase at relatively steady rates at the end of construction leading up to a failure condition. Significant deformations were also observed during periods of no construction for a number of the case studies, particularly in the later stages of construction.

The observations from five test embankments are presented (two of which failed) and the findings from these case studies are discussed in the context of the probable mechanics involved. For the Muar-EC, Muar-3C, Olga-C and Queensborough test embankments details of the embankment, foundation, pore water pressure response and deformation behaviour are given in Appendix C (Section 2). A summary of the observations is as follows:

- The Muar-EC test embankment (constructed over soft Malaysian marine clays of high plasticity) failed 30 days after the end of construction at an embankment height of 4.68 m (Malaysian Highway Authority 1989a). Figure 4.32 shows that at Piezometer P2 (located at 9 m depth below the embankment toe) the excess pore water pressure response continued to increase after the end of construction and up to the time of failure. The pore water pressure also increased in the non-construction

period after the embankment had been constructed to 3.9 m height (97 kPa applied load).

- At the Muar-3C test embankment (same site as Muar-EC, but the embankment did not fail) pore water pressures in several piezometers were observed to increase for periods of 110 to 120 days after the end of construction. During this period, significant settlements under the centre of the embankment and lateral displacements at the embankment toe were measured.
- The St. Alban-A test embankment (constructed over low plasticity, leached marine clays of high sensitivity) failed some 12 to 18 hours after placement of the final fill lift (La Rochelle et al 1974). The pore water pressure in Piezometer C1 (located at 3 m depth below the embankment slope) increased some 23 kPa over this period up to failure (Figure 4.33).
- At the Olga-C test embankment (Lavallée et al 1992), constructed over soft varved clays of high plasticity, pore water pressures in several piezometers were observed to increase for periods of 50 to 70 days after the end of construction. During this period significant vertical strains were observed in the region of the foundation under the embankment centreline where increasing pore water pressure were observed.
- At the Queensborough test embankment (Jardine and Hight 1987), constructed over soft marine alluvial clays, cracking of the embankment halted construction. Concern over potential failure of the embankment (due to rising pore water pressures in several piezometers and continuing large deformations) led to the reduction of the embankment height and placement of several berms at the embankment toe.

Possible explanations of why this behaviour (rising pore water pressures and continuing deformation at the end of construction) occurs are as follows:

- Mitchell (1986) considered it was due to structural breakdown as a result of stress levels exceeding the pre-consolidation pressure of the soft clay, thereby leading to greater compressibility accompanied by large decreases in permeability.
- Schiffman et al (1984) showed that large strain and self weight effects may retard the rate of pore water pressure dissipation.
- Mesri and Choi (1979) attributed the behaviour to secondary compression effects.

- Brand (1985a) referred to the unreliability of pore water pressure data usually caused by the slow response times of piezometer systems.
- Crooks (1987) attributed the continued rise in pore water pressure to the time dependent increase of total horizontal stress, therefore suggesting that the total stress path changes with time. He further commented that a rising pore water pressure condition is indicative of critical stressing of significant portions of the foundation, but that it does not necessarily indicate an impending failure condition.

Tavenas and Leroueil (1977) considered that the limit state surface has a strain rate or time dependency (Figure 4.34). With decreasing rates of strain in laboratory triaxial tests they showed that the limit state surface (for Champlain Clays from the St. Alban test site) was strain rate dependent. Other authors (Graham et al 1983; Soga and Mitchell 1996; Vaid and Campanella 1977) have also commented on the strain rate dependence of undrained shear strength and the limit state surface. Tavenas et al (1978) used the YLIGHT model and concept of limit state isotaches (time dependent limit state surfaces) to describe the creep to failure (under constant stress) behaviour of drained and undrained triaxial samples at effective stress states above the critical state line and below the outer limit state surface.

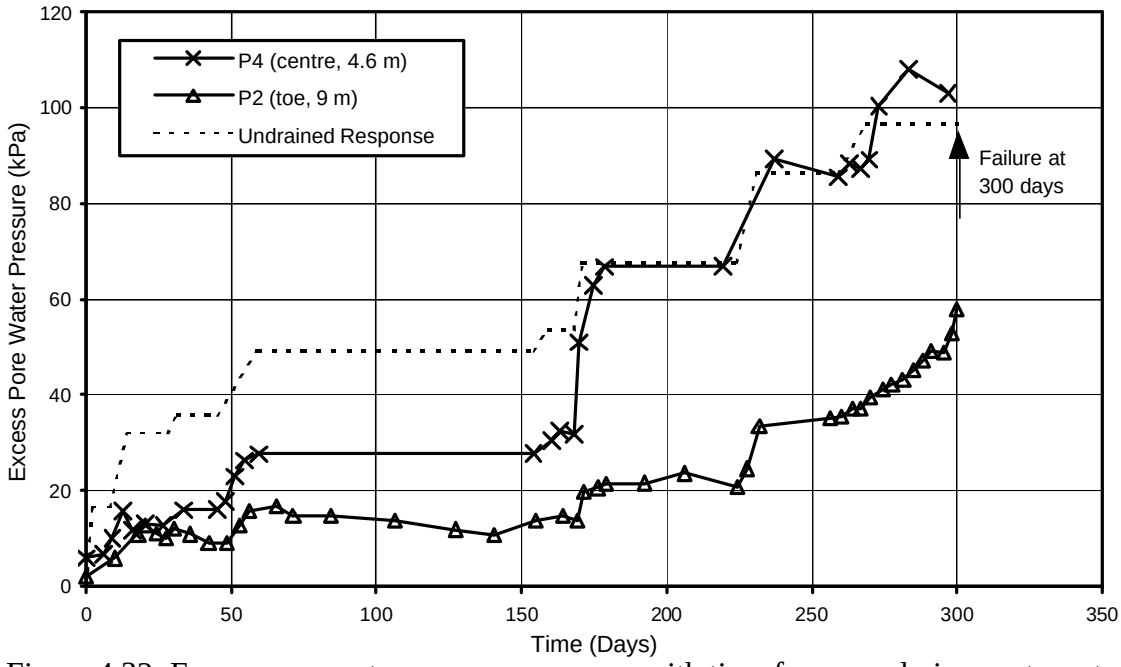

Figure 4.32: Excess pore water pressure response with time for several piezometers at the Muar-EC test embankment.

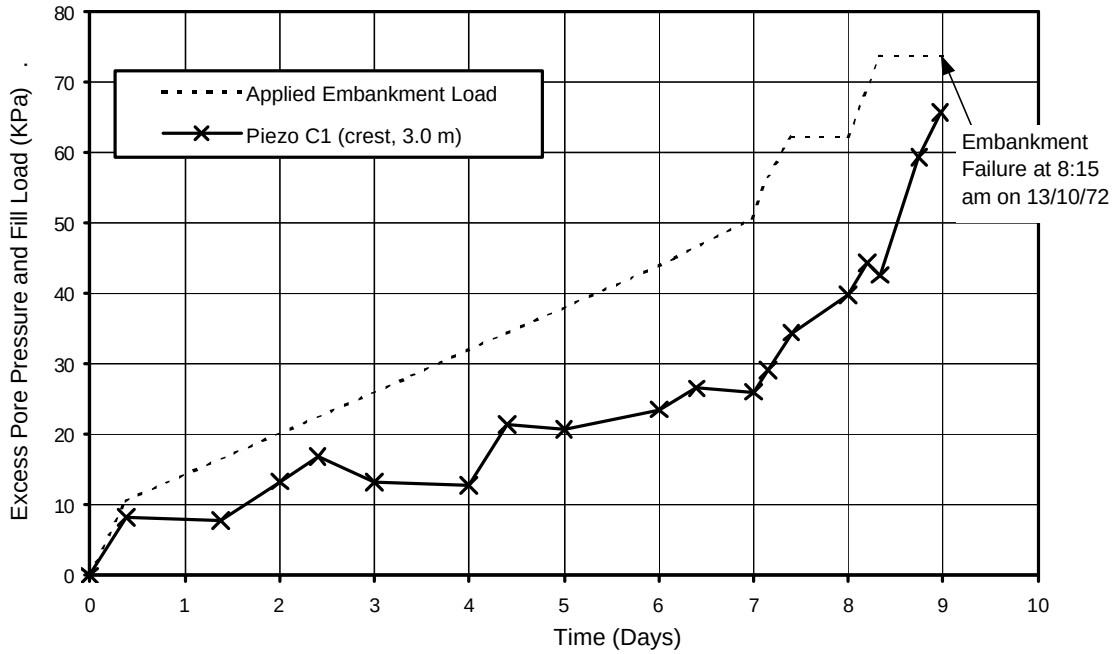

Figure 4.33: Excess pore water pressure response at Piezometer C1 with time at the St. Alban-A test embankment.

In an attempt to understand the observation of increasing pore water pressure during no construction periods, and particularly the delayed time to failure shown by a number of the case studies, it is considered that the concept of time or strain rate dependent limit state isotaches would predict an increase in pore water pressure with time. For foundations in a normally consolidated condition (i.e. effective stress state coincident with the yield surface below the critical state line) the pore water pressure would increase with time due to contraction of the limit state surface and the requirement that the effective stress state must be bounded by the limit state surface.

Three hypothetical situations have been considered to further explain the observations of increased pore water pressure and delay to failure. The three hypothetical situations are represented by effective stress states A_i, B_i and C_i (Figure 4.34), for which the outer limit state surface is representative of the end of construction condition, the inner limit state surface representative of some time, t_f, after construction and the intermediate limit state surface representative of some intermediate time. Assume for the moment that consolidation does not take place (i.e. the effective stress state and limit state surface will not move to the right). The likely pore water pressure response with time, for each hypothetical case, based on critical state soil mechanics would be:

- For stress state A_i at the end of construction, pore water pressures will increase with time as the limit state surface contracts. This is because the effective stress state must contract (i.e. move to the left) with the limit state surface, as states outside the limit state do not exist. As no consolidation is assumed to occur the total stress state will remain fixed and deformation will occur as a result of yielding. At some point the effective stress state intersects with the critical state surface (Figure 4.34) and with time the effective stress path follows the critical state line as is bounded by the limit state and critical state surfaces. Therefore, strain weakening develops in the soil described by the initial stress state A_i to the stress state A_f at some time t_f. Deformations during strain weakening would occur as plastic flow and pore water pressures would be expected to rise significantly as the total stress path is forced downward. This behaviour (or similar type behaviour) is considered to have occurred within the highly stressed regions of St. Alban-A and Muar-EC (amongst other cases) where localised failure occurs and significant plastic flow develops on the surface of rupture leading up to a failure condition.
- For stress state B_i at the end of construction, pore water pressures will increase with time as the limit state surface contracts because, as for case A_i, the effective stress state must contract (i.e. move to the left) with the limit state surface. As no consolidation is assumed to occur the total stress state is assumed to remain fixed and deformations occur as a result of yielding.
- For stress state C_i at the end of construction, the effective stress state is within the limit state surface and therefore describes an over-consolidated condition. However, at some intermediate time (assuming no consolidation) the effective stress state is coincident with the limit state surface and the soil is now in a normally consolidated condition. With further time, pore water pressures will increase as the limit state surface contracts and the effective stress state moves to the left to position C_f at some time t_f. Deformations occur as a result of yielding from the intermediate stress state to the stress state at time t_f.

It is important to note that for the hypothetical case "A" strain weakening can occur in essentially ductile clays due to the effects of strain rate on the limit state surface.

In reality it is accepted that consolidation will occur with time from the end of construction. Therefore, it is concluded that the processes of deformation due to consolidation and deformation due to undrained creep (as described by the hypothetical

examples) occur at the same time. Leroueil (1996) used the observations of pore water pressure response and settlement of the Olga-C test embankment to draw similar conclusions.

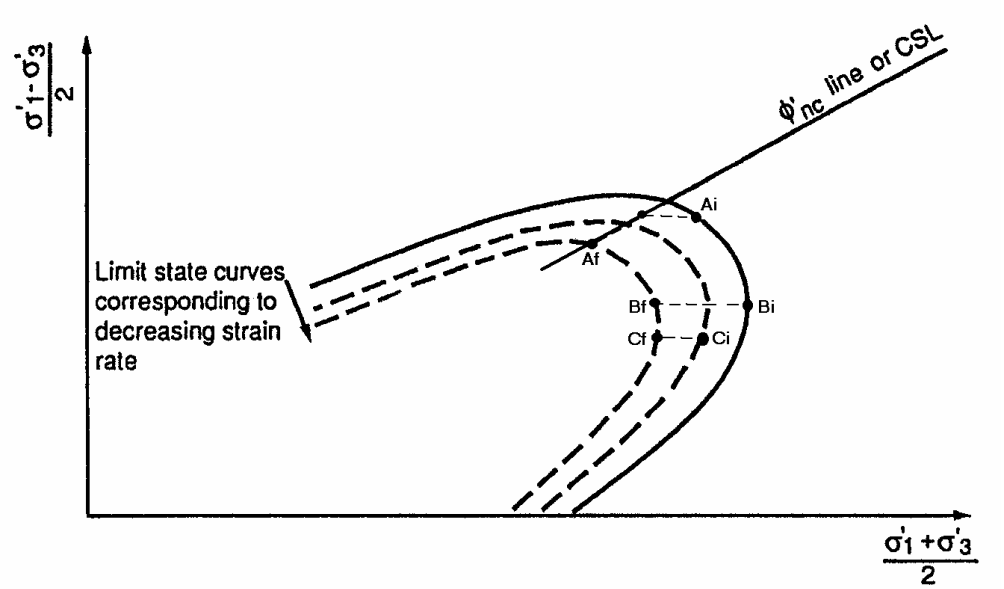

Figure 4.34: Schematic behaviour of strain rate effects on limit state surface with decreasing strain rate in undrained creep tests (adapted from Leroueil and Marques 1996)

Comparing the case studies of Muar-EC and Muar-3C (described in Appendix C, Section 2), the rate of increase in pore water pressure response in Piezometer 2, located close to the surface of rupture at Muar-EC, was significantly greater at Muar-EC. In addition, the plots of vertical inclination angle from an inclinometer at the toe of the embankment (given in Appendix C) indicate that a localised failure condition developed at Muar-EC (between 8 m and 9.5 m depth) whilst no localised failure condition developed at Muar-3C. It is concluded that for Muar-EC embankment, the effective stress path within the localised failure zone could be described by the hypothetical case A_i to A_f, and for Muar-3C at location Piezometer P2 it is more closely described by hypothetical case B_i to B_f.

For a number of case studies analysed a significant period of time delay was observed between end of construction and embankment failure (up to 30 days for Muar-EC). The properties of the soil are considered to have a significant effect on the time length of the delay. At Muar-EC the foundation is a high plasticity clay of low sensitivity whilst at St. Alban-A and James Bay (12 to 18 hour delay in each case) the

foundation is highly sensitive and brittle with significant strain weakening occurring over relatively small strains in undrained loading. Once a localised failure condition does occur in foundations of brittle, sensitive clays, it will progress relatively quickly due to significant strain weakening as loads within the localised failure zone are transferred onto the pore fluid. For clays of low sensitivity in undrained loading (i.e. which do not contract on shearing) strain weakening and progressive failure will develop more slowly. Therefore, due to the potentially slow development of strain weakening and progressive failure for these foundations, the delay to failure can take longer, as observed at the Muar-EC test embankment.

Several other issues that are important in the context of this discussion are:

- It would appear that the higher the level of shear stresses on a soil in a normally consolidated condition the more rapid the rate and prolonged the period of pore water pressure increase. It is considered that this is due to the greater strain rates expected at stress states closer to the critical state line. Therefore, the limit state surface described for higher levels of shear stress is larger than that at lower levels of shear stress.
- Another implications of these observations at the Muar-EC and St. Alban-A test embankments is that the factor of safety is not a minimum at the end of construction, but is at a minimum at some time after the end of construction. Whilst for embankments on sensitive, brittle foundations the findings indicate that this time period is relatively short (typically a matter of hours), for clays of low sensitivity the delay to failure (and a minimum factor of safety) may be several months.

4.4.3 LONG-TERM POST CONSTRUCTION DEFORMATION

The purpose of this section is to provide some guidelines on the lateral deformation that occurs post construction. Methods are available for estimation of settlements under the centre of the embankment post construction; however, estimation of the lateral deformation is somewhat more difficult.

Tavenas et al (1979), based on analysis of some 13 case studies, proposed that the post construction maximum lateral displacement at the embankment toe increases linearly with the settlement under the centre of the embankment. The relationship during the initial period of consolidation (about 5 years) is on average $\Delta y_m = 0.16\Delta s$ (refer Figure 4.14 for definition of terms), with a standard deviation of 0.09, and this

rate may be reduced for longer periods of consolidation as observed at Skå Edeby (Figure 4.35). They commented that the ratio $\Delta y_m / \Delta s$ is dependent on a number of parameters including the factor of safety and the inclination of the embankment slope. Figure 4.35 presents the findings from 7 case studies analysed by Tavenas et al (1979). Figure 4.36 presents their findings for different slope geometries and stability conditions indicating the ratio $\Delta y_m / \Delta s$ reduces with increasing factor of safety.

In the context of the discussion in Section 4.4.2, it would be expected that the post construction ratio $\Delta y_m / \Delta s$ is also dependent on whether or not yielding and possibly plastic flow is occurring at some depth within the foundation. The results from Muar-EC, Muar-3C and Queensborough (Appendix C, Section 2) indicate the ratio can be as high as 1 in the initial post construction period.

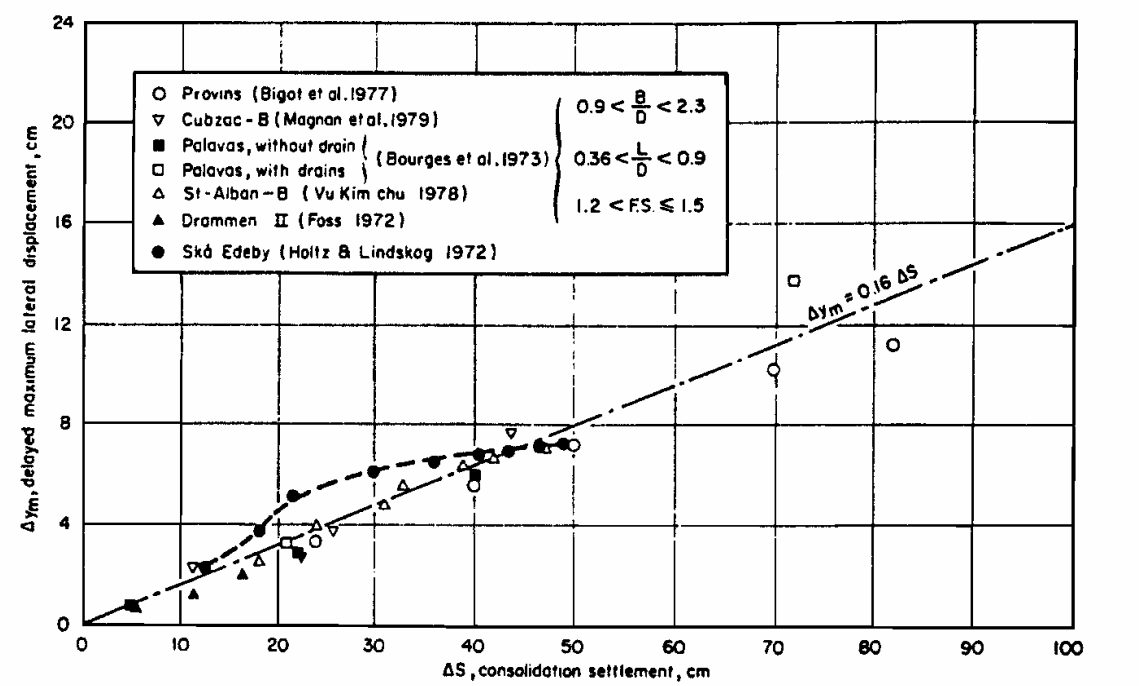

Figure 4.35: Relationship between the maximum lateral displacement at the toe, y_m, and settlement at the centre, s, at the end of construction (Tavenas et al 1979).

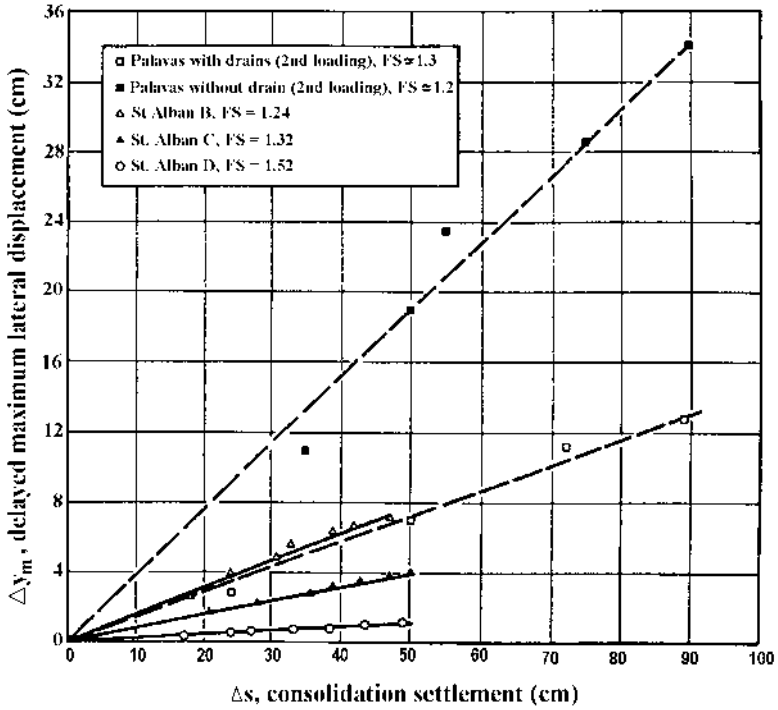

Figure 4.36: Relationship between maximum lateral displacement (toe) and settlement (centre) at the end of construction for different embankment geometries and stability conditions (Tavenas et al 1979).

4.5 DISCUSSION AND CONCLUSIONS

4.5.1 INDICATORS OF AN IMPENDING FAILURE

The research on the deformation behaviour of embankments on soft ground comprised the detailed analysis of 13 well-monitored and documented case studies from the literature that failed during construction and an additional 4 case studies that did not fail after construction.

The findings of the analysis of the 13 failure case studies indicates that appropriately located deformation monitoring instrumentation can be used to identify an impending failure condition during construction. As a general guide, for embankments constructed on a wide variety of soft foundation conditions (clay and silts of low to high sensitivity and low to high plasticity) the following deformation monitoring instrumentation provides a good indication of an impending failure condition:

- Lateral surface displacement at the embankment toe. In virtually all cases analysed the rate of lateral displacement increased significantly as a failure condition was

approached, typically at embankment heights within the range 70 to 90% of the eventual failure height.

- Vertical deformation at and beyond the toe of the embankment. The monitoring point beyond the embankment toe must be located within the eventual failure zone. In all cases studied it was from 2 m to 10 m beyond the embankment toe (from 0.4 to 1.5 times the eventual embankment failure height). Monitoring vertical deformation at these locations (at and beyond the embankment toe) is not significantly affected by settlement under the embankment load and heave, particularly beyond the toe, can identify an impending failure condition. Heave is generally observed at embankment heights of 60 to 90% of the eventual failure height, with significant increases in the rate of heave movement (relative to the fill height) at 70 to 95% of the eventual failure height.

The changes in rate and/or direction of movement described above occurs, in most cases, beyond the threshold height of the embankment (the height at which the effective stress state within the foundation goes from an over-consolidated to normally consolidated condition) indicating that the observed changes in deformation behaviour leading up to failure are not associated with changes that occur at the threshold height.

From limit equilibrium analysis it is evident that the factor of safety is typically less than about 1.25 at embankment heights of 75 to 85% of the failure height. Therefore, stress levels within the foundation are relatively high beyond about 75% of the eventual failure height and are coincident with the changes in undrained deformation behaviour observed.

Other good indicators of an impending failure condition, but which are more specific to certain foundation conditions, are:

- Inclinometer observations at the toe of the embankment. For foundations of low sensitivity (or ductile) clays an impending failure condition can be identified by large plastic shear strains that occur within a localised failure zone prior to failure. Increases in the maximum vertical inclination angle versus relative fill height are observed at 70 to 90% of the eventual failure height.
- Cracking of the embankment is a useful guide for foundations of low sensitivity (or ductile) clays.
- The deformation and pore water pressure response during periods of no construction. In several case studies the pore water pressure in some piezometers

was observed to increase and deformations were ongoing (i.e. creep type movements) during periods of no construction. With increasing embankment height (i.e. increased level of shear stress) the rate of pore water pressure increase was more rapid and for a more prolonged period of time, and the rate and amount of creep type deformation increased. These observations are best identified within the foundation under the embankment slope or toe.

4.5.2 GUIDELINES ON MONITORING FOR IDENTIFICATION OF AN IMPENDING FAILURE CONDITION

In analysing the deformation behaviour of an embankment on soft ground for identification of an impending failure, it is considered necessary to supplement the monitoring that identifies an impending failure condition with additional instrumentation to better understand the mechanism of movement and therefore improve the prediction of a failure condition. Suggested guidelines for monitoring are as follows:

- Vertical displacement at and beyond the toe of the embankment, recommended for identification of an impending failure;
- Lateral surface displacement at the toe of the embankment, recommended for identification of an impending failure;
- Inclinometer installed in the embankment slope or at the toe. For all soil types the inclinometer observations will assist in identification of the change from partially drained over-consolidated conditions to normally consolidated undrained conditions, as well the depth of foundation over which this change has occurred. For foundations of low sensitivity clays the inclinometer observations will show the development of the localised failure zone leading up to a failure condition;
- Settlement under the centre of the embankment. Whilst this is considered optional, it is usually installed for the purposes of monitoring the amount of settlement during construction and ongoing settlement post construction;
- Piezometers under the centreline of the embankment are considered fundamental to the understanding of the mechanism associated with the deformation for all foundation types. The pore water pressure response will:
  - Provide an indication of the degree of consolidation whilst the foundation is in an over-consolidated condition.

  - Allow estimation of the initial direction of the effective stress path and its likely intersection point with the limit state surface, which has significant implications for the deformation behaviour as discussed in Section 4.5.4.
  - Indicate the change from partially drained over-consolidated conditions to normally consolidated undrained conditions (i.e. when the effective stress path intersects with the limit state surface).
- Piezometers under the embankment slope are considered optional. In several case studies they have been located within the localised failure zone and the rate of pore water pressure generation observed has exceeded the rate of applied loading. However, given the generally narrow band of the localised failure zone particularly for the sensitive foundation case studies, it is probably good fortune that a piezometer is located within the localised failure zone.

Two additional factors that are important in the context of identification of an impending failure condition are:

- Construction should proceed slowly in order for an impending failure condition to be more clearly identified from the deformation monitoring. If construction proceeds too quickly it can mask the indicators of the onset to failure. Of those case studies for which an impending failure was clearly identified, construction rates were less than 0.15 to 0.2 m/day. For the Muar test embankments the embankments were constructed in stages (large lifts initially followed by lifts of lesser height) with each stage followed by a period of no construction.
- In at least six of the failure case studies analysed, the base of the surface of rupture was coincident (or very close to) an interface between layers in the sub-surface profile. Possible reasons for this are considered to be due to a concentration of shear strains at the interface of two layers with a stiffness or permeability variation, or the presence of discontinuities at the interface.

4.5.3 POST FAILURE DEFORMATION BEHAVIOUR

It is considered that the Khalili et al (1996) model for intact sliding provides reasonable estimates of the post failure deformation provided that the peak and residual undrained strengths are properly estimated by laboratory triaxial tests. The “slow model” is considered more appropriate for foundations of low sensitivity (or ductile) clays and the

"rapid model" for prediction of the post-failure deformation for foundations of sensitive, brittle cohesive soils.

The analysis undertaken was limited by the number of cases analysed and available data for estimation of the large strain residual undrained shear strength. The analysis is considered appropriate for rotational failures (as Khalili et al (1996) indicate). In addition, the vane remoulded strength is considered to under estimate the actual large strain undrained shear strength and will therefore over predict the post-failure deformation.

4.5.4 DISCUSSION ON FAILURE MECHANISM

From analysis of the thirteen failure case studies of embankments on soft ground, it is apparent that the case studies can be divided into three general groups:

- Sensitive, brittle clays that fail rapidly on a well-defined surface of rupture (St. Alban, Portsmouth and James Bay).
- Sensitive clays that show a breakdown in the structure of the clay over a large zone of the foundation prior to failure, and post failure movements are relatively slow (Kalix and Mastemyr).
- Foundations of low sensitivity that develop significant plastic flow within a defined zone prior to failure. In these cases progressive failure is evident at embankment heights less than the failure height.

4.5.4.1 Sensitive Clay Foundations – Rapid Onset of Failure

The case studies St. Alban-A, Portsmouth and James Bay are considered representative of embankments on sensitive, brittle, highly strain weakening foundations that, once a localised failure condition is initiated, rapidly progress to a failure condition on a well-defined surface of rupture. In all three cases the foundation comprised low plasticity, soft to very soft, leached marine deposits.

From observations of the inclinometer at the toe of the embankment, it is apparent that for these cases significant plastic flow does not occur until the embankment is at or very close to its failure height. The mechanics at failure are summarised as follows:

- Once the embankment has been constructed to its failure height, creep type undrained plastic deformations occur and excess pore water pressures increase,

particularly within the zone/s of relatively high shear stress, located under the slope of the embankment.

- In the regions of relatively high shear stress, reduction in the limit state surface due to strain rate effects results in the effective stress state reaching the critical state line. Once this occurs a localised failure condition is reached and with further straining strain weakening begins to develop. These brittle materials are generally contractive on shearing post-peak and further straining beyond the peak results in contraction of the soil structure and transfer of load onto the pore fluid resulting in the development of high excess pore water pressures; i.e. a static liquefaction condition.
- Due to the significant loss of strength within the localised failure zone, the size of the failure zone expands rapidly as load is transferred onto the surrounding soil. Thus, progressive failure develops quickly once a localised failure condition is reached.
- The factor of safety reduces to values significantly below 1 over relatively small shear strains giving the sliding mass significant kinetic energy at failure to reach post failure travel velocities of metres/minute (rapid to very rapid velocity categories).

The observations at failure of the James Bay case study (Section 4.3.3.4) confirm the rapid development of shearing in the region of the surface of rupture leading up to the failure and that significant shearing did not take place until shortly prior to the failure. The observation of water rise in the inclinometer tube would be consistent with static liquefaction on the surface of rupture due to collapse of the soil structure followed by the rapid post failure movement of the failed embankment.

In terms of identifying an impending failure condition at embankment heights less than the failure height, these sensitive, brittle clays are considered the most difficult to identify due to the relatively small deformations observed and the rapid development to a failure condition. However, it is considered that deformation monitoring at the following locations provides a good indication of an impending failure condition:

- Vertical deformation behaviour at and beyond the toe of the embankment, in the form of heave type movements and increases in the rate of heave movement with increasing embankment height. Heave movements occur at St. Alban-A at about 60 to 70% of the failure height and for James Bay an increase in the rate of heave occurs at about 75% and then again beyond 90% of the failure height (Figure 4.23

and Figure 4.24). The heave movements are small, less than 15 mm up to 90 to 95% of the failure height, but perceptible.

- Lateral surface displacement at the toe of the embankment, in the form of increasing rates of lateral displacement with increasing embankment height. For Portsmouth and St. Alban-A a significant increase in the rate of lateral displacement with increasing embankment height is observed at 80 to 85% and 70 to 75% respectively of the eventual failure height.

4.5.4.2 Sensitive Clay Foundations – "Slow" Post Failure Movement

For Kalix and Mastemyr, both highly sensitive foundations, it is considered that a partial breakdown in the soil structure of a significant proportion of the foundation occurred prior to reaching a failure condition. The reason for this occurrence, and therefore the difference between this classification and the rapid onset of failure classification for sensitive clay foundations, is considered to be related to the effective stress path crossing the critical state line whilst still in an over-consolidated condition (i.e. represented by path OYE_c in Figure 4.8a). Given the expected significant reduction in strength associated with the partial breakdown of the soil structure, it is not clear why a static liquefaction and flow condition did not occur at this point. At Kalix it may be related to the high plasticity of the sensitive clay foundation.

The occurrence of these type failures is the subject of some conjecture. Leroueil and Tavenas (1986) consider this type of behaviour having only occurred at 2 of 45 failure case studies (including Mastemyr). Folkes and Crooks (1985) consider this type of failure condition to be more prevalent than this.

Given that Mastemyr is a circular embankment and Kalix a rectangular embankment, and the limited number of case studies within this group, it is difficult to draw any firm conclusions on the prediction of the onset of an impending failure condition. However, the indicators of an impending failure condition for case studies where partial breakdown of the soil structure occurs are considered to include:

- Lateral surface displacement at the embankment toe;
- Vertical deformation at and beyond the toe of the embankment; and
- The development of excess pore water pressures, in piezometers under the centre of the embankment, significantly greater than the applied vertical stress. At Kalix this

was observed at embankment heights above 70 to 80% of the failure height, and at Mastemyr above 70% of the embankment failure height.

Post failure, the rate of movement at Kalix occurred relatively slowly (45 mm/day) in comparison to the much higher post failure velocities of St. Alban and James Bay (1 to 2 m/min).

4.5.4.3 Foundations of Low Sensitivity Clay

Eight of the thirteen failure case studies analysed (Muar-F, Muar-EC, King's Lynn, Narbonne, Sackville, Thames, Cubzac-A and Rio) are considered to be representative of embankments on foundations of low sensitivity (or ductile) clays.

For foundations of low sensitivity the inclinometer observations indicate that, in most cases, a localised failure condition initially develops at embankment heights less than the failure height. The localised failure zone is considered to initially develop at depth below the slope of the embankment coincident with the zone of high shear stress. The eventual surface of rupture for these case studies was located within this localised failure zone. It is considered that the observations of localised failure are indicative of a progressive failure mechanism that, in general, starts at embankment heights of 70 to 90% of the eventual failure height.

The onset to failure does not occur rapidly, as for the case of sensitive, brittle soft clay foundations (Section 4.5.4.1), for two reasons; the loss of strength from strain-weakening is significantly less than that for the brittle, sensitive clays; and the strain-weakening develops slowly over large strains as opposed to the rapid development over small strains for brittle, sensitive clays. Clearly, these are typical properties that define clays of low sensitivity.

Failure occurs when the mobilised strength on the surface of rupture is less than the driving force. The observation of delayed failure for some of these cases is considered to be due to undrained creep effects and the strain rate dependency of the limit state surface. The indications of this are in the inclinometer observations and also in the excess pore water pressure readings, which tend to increase during rest periods. The deformation and pore water pressure observations leading up to the failure of the Muar-EC embankment being a case in point.

For the case studies of embankments on clay foundations of low sensitivity the indicators of an impending failure condition are generally clearly identifiable. The better indicators are considered to be:

- The maximum positive vertical inclination angle (Figure 4.27) from the inclinometer at the embankment toe is a good indicator of an impending failure condition. A significant increase in the vertical inclination angle was observed at 60 to 90% of the failure height for most of these case studies. Also, monitoring of the vertical inclination angle with depth (Figure 4.26) will clearly identify the development of the localised failure zone.
- The lateral surface displacement at the toe of the embankment (Figure 4.25) is a good indicator for most case studies. The rate of lateral displacement increased significantly as a failure condition is approached, typically at embankment heights within the range 70 to 90% of the eventual failure height.
- The vertical deformation behaviour at and beyond the toe of the embankment. The onset of heave displacements and the increase in rate of heave movements with respect to increasing embankment height are a good indicator of an impending failure condition.
- Cracking of the embankment was observed in four cases and is a good indicator that the embankment is very close to failure. In the case of Muar-EC the embankment failed some 30 days after end of construction and cracking was observed some 20 days prior to the failure.

The impending failure condition at the Rio and King's Lynn embankments was more difficult to identify. The above indicators were only prevalent at embankment heights of greater than 90% of the failure height. In both cases cracks were observed in the embankment before the deformation behaviour at the toe of the embankment indicated an impending failure condition.

TABLE OF CONTENTS

5.0 LANDSLIDES IN EMBANKMENT DAMS AND CUT SLOPES IN HEAVILY OVER-CONSOLIDATED HIGH PLASTICITY CLAYS 5.1

5.1 INTRODUCTION TO THIS CHAPTER 5.1

5.2 LITERATURE REVIEW 5.2

5.2.1 Statistics on Dam Incidents Involving Slope Instability 5.2

5.2.2 Progressive Failure 5.8

5.2.3 Mechanics of Post Failure Deformation 5.11

5.3 DATABASE OF CASE STUDIES ANALYSED 5.12

5.3.1 Case Studies of Failures in Dam Embankments 5.14

5.3.2 Case Studies of Failures in Cut Slopes of High Plasticity Clays 5.15

5.4 MECHANICS OF FAILURE OF CUT SLOPES IN HEAVILY OVER-CONSOLIDATED HIGH PLASTICITY CLAYS 5.18

5.4.1 Progressive Failure 5.18

5.4.2 Trigger to Failure 5.20

5.4.3 Time to Failure 5.22

5.4.4 Effect of Defects Within the Soil Mass 5.23

5.5 MECHANICS OF FAILURE FOR FAILURES IN EMBANKMENT DAMS 5.24

5.5.1 Failures in Embankment Dams During Construction 5.24

5.5.2 Failures in Embankments During Drawdown 5.30

5.5.3 Post Construction Failures in the Downstream Slope of Embankments 5.39

5.6 POST FAILURE DEFORMATION BEHAVIOUR – FAILURES IN EMBANKMENT DAMS 5.44

5.6.1 Factors Affecting the Post Failure Deformation 5.44

5.6.2 Summary of Case Studies of Failures in Embankment Dams 5.45

5.6.3 Failures During Construction - Post Failure Deformation Behaviour 5.46

5.6.4 Failures During Drawdown – Post Failure Deformation Behaviour 5.68

5.6.5 Post Failure Deformation Behaviour of Failures in the Downstream Shoulder After Construction 5.80

5.7 POST FAILURE DEFORMATION BEHAVIOUR - CUT SLOPES IN HEAVILY OVER-CONSOLIDATED CLAYS 5.86

5.7.1 Summary of Factors Affecting the Post Failure Deformation 5.86
5.7.2 Summary of the Post Failure Deformation and Velocity of the Failure Case Studies 5.87
5.7.3 Failures in Cut Slopes – Type 2 Slope Failure Geometry 5.92
5.7.4 Failures in Cut Slopes – Type 1 Slope Failure Geometry 5.94
5.7.5 Failures in Cut Slopes – Type 5 Slope Failure Geometry 5.95
5.8 PREDICTION OF POST-FAILURE TRAVEL DISTANCE 5.97
5.8.1 Khalili et al (1996) Model for Intact Slides 5.97
5.8.2 Empirical Methods for Prediction of Travel Distance of Intact Slides. 5.105
5.9 CONCLUSIONS AND GUIDELINES FOR PREDICTION OF POST-FAILURE DEFORMATION BEHAVIOUR OF INTACT SLIDES IN SOIL SLOPES 5.108
5.9.1 Summary of Findings from the Case Study Analysis 5.108
5.9.2 Guidelines for Prediction of Post-Failure Deformation 5.117

LIST OF TABLES

Table 5.1: Incidence of slope instability in embankment dams (Foster 1999) 5.3

Table 5.2: Factors influencing downstream slides - accident and failure incidents (Foster 1999) 5.4

Table 5.3: Factors influencing upstream slides - accident and failure incidents (Foster 1999) 5.5

Table 5.4: Failures involving slope instability, excluding sloughing cases (Foster 1999) 5.9

Table 5.5: Summary of case study database of slope failures 5.13

Table 5.6: Summary of embankment dam slope stability incidents by failure slope geometry 5.15

Table 5.7: Slope instability case studies in embankment dams by embankment type 5.16

Table 5.8: Mechanics of failure for failures in embankment dams during construction. 5.24

Table 5.9: Material types through which the surface of rupture passed of post construction failures in the downstream shoulder. 5.40

Table 5.10: Timing of the failure for post construction slides in the downstream shoulder. 5.42

Table 5.11: Distribution of slide volume for slides in embankment dams. 5.46

Table 5.12: Summary of failure case studies in embankment dams during construction – failures within the embankment only 5.47

Table 5.13: Summary of failure case studies in embankment dams during construction – failure within the embankment and foundation 5.48

Table 5.14: Summary of the case studies of slides in the upstream shoulder of embankment dams triggered by drawdown 5.69

Table 5.15: Post failure deformation behaviour and slope/material properties of slides in embankment dams during drawdown. 5.72

Table 5.16: Summary of the case studies of slides in the downstream shoulder of embankment dams that occurred post construction. 5.82

Table 5.17: Cut slope failures in London clay. 5.88

Table 5.18: Cut slope failures in Upper Lias clay. 5.89

Table 5.19: Results of the post-failure deformation analysis using the Khalili et al (1996) method. 5.102

Table 5.20: Characteristics of the case study groupings from the post failure deformation analysis (Figure 5.52) 5.104

Table 5.21: Factors affecting the peak post-failure velocity for slides in embankment dams during drawdown. 5.116

Table 5.22: Guidelines for post-failure deformation prediction using the Khalili et al (1996) models..... 5.118

LIST OF FIGURES

Figure 5.1: Comparison of population to slope stability incidents for earthfill, rockfill and hydraulic fill embankments (excluding sloughing and unknown embankment zonings). 5.6

Figure 5.2: Sloughing type failure (Foster 1999) 5.7

Figure 5.3: Sliding block model showing kinetic energy lines for different rheological models (Golder Assoc. 1995) 5.11

Figure 5.4: Redistribution of the potential energy after failure (D'Elia et al 1998) 5.12

Figure 5.5: Contours of accumulated deviatoric plastic strain, e_D^P, from finite element analysis of an excavation: 3H to 1V slope, 10 m cut slope height, K_o = 1.5, surface suction = 10 kPa (Potts et al 1997). 5.19

Figure 5.6: Distribution of water content near the slip place from failures in cut slopes in London clay (Skempton 1964) 5.20

Figure 5.7: Moisture content migration to the shear zone and decreasing shear strength with time to failure from consolidated undrained tests on brown London clay (Skempton and La Rochelle 1965) 5.20

Figure 5.8: Annual records of cut slope failures in heavily over-consolidated clays in the UK (James 1970) 5.21

Figure 5.9: Gradual reduction in the factor of safety with time due to soil weakening and oscillations due to climatic effects (Picarelli et al 2000) 5.22

Figure 5.10: Variation of the pore water pressure coefficient, r_u, with time in cuttings in Brown London clay (Skempton 1977). 5.23

Figure 5.11: Time to first time failure versus cut slope angle for Type 1 and Type 2 slope failure geometries in London clay. 5.23

Figure 5.12: Idealised development of surface of rupture during construction for embankments with wet placed fill layer/s. 5.26

Figure 5.13: Compound type surface of rupture for failures during construction at *(a)* Scout Reservation dam (Mann and Snow 1992), and *(b)* Waco dam (Stroman et al 1984). 5.26

Figure 5.14: Carsington dam, section through the region of the initial failure at chainage 725 m (Skempton and Vaughan 1993). 5.27

Figure 5.15: Carsington dam; drained strength properties of intact "yellow clay" and solifluction shears (Skempton and Vaughan 1993) 5.28

Figure 5.16: Contours of deviatoric strain predicted by finite element analysis at chainage 725 m prior to the failure of Carsington dam (Potts et al 1990). 5.29

Figure 5.17: Section through the failure in the upstream shoulder at San Luis dam (courtesy of U.S. Bureau of Reclamation). 5.35
Figure 5.18: Drawdown causing failure and prior large drawdowns for *(a)* Dam FD2, *(b)* Dam FD3, and *(c)* San Luis dam. 5.36
Figure 5.19: Composite shear strength envelope (Duncan et al 1990). 5.38
Figure 5.20: Effect of moisture migration on the undrained strength within the shear band using idealised strength parameters. 5.38
Figure 5.21: Type 1 failure slope geometries with different surface of rupture orientations. 5.45
Figure 5.22: Total post-failure deformation for slides in embankment dams during construction. 5.49
Figure 5.23: Maximum post failure velocity of slides in embankment dams during construction. 5.50
Figure 5.24: Residual drained strength from field case studies in clay soils in the UK and ring shear tests on sand, kaolin and bentonite (Skempton 1985). 5.51
Figure 5.25: Ring shear tests on normally consolidated sand-bentonite mixtures (Skempton 1985, after Lupini et al 1981). 5.52
Figure 5.26: Section through Punchina cofferdam (adapted from Villegas 1982). 5.54
Figure 5.27: Punchina cofferdam, *(a)* deformation and *(b)* velocity of the downstream slope during construction (adapted from Villegas (1982)) 5.54
Figure 5.28: Section through the failed region of Muirhead dam (Banks 1948) 5.55
Figure 5.29: Muirhead dam, post failure deformation and velocity of the failure in the upstream shoulder during construction. 5.55
Figure 5.30: Crest settlement monitoring of the slide at Waco dam (adapted from Stroman et al 1984). 5.59
Figure 5.31: Carsington dam, deformation monitoring of upstream shoulder *(a)* leading up to failure, *(b)* during failure (Skempton and Vaughan 1993), and *(c)* the velocity of the slide mass. 5.61
Figure 5.32: Section through failed region of Acu dam (Penman 1986) 5.62
Figure 5.33: Cross section of the slide during construction at Chingford dam (Cooling and Golder 1942) 5.63
Figure 5.34: Deformation and velocity of the slide at Lake Shelbyville dam (adapted from Humphrey and Leonards (1986, 1988)) 5.67
Figure 5.35: Post failure deformation and velocity of slide at Scout Reservation dam (adapted from Mann and Snow (1992)). 5.67
Figure 5.36: Slides in embankment dams during drawdown; post failure *(a)* deformation and *(b)* estimated velocity. 5.73

Figure 5.37: San Luis dam; the latter stages of post failure *(a)* deformation and *(b)* velocity of the first time slide following the 1981 drawdown (data courtesy of U.S. Bureau of Reclamation). 5.76

Figure 5.38: Section through the slide at Dam FD2. ..... 5.77

Figure 5.39: Deformation behaviour of the slide at Dam FD2 on reactivation during the 1994 drawdown; *(a)* deformation and *(b)* velocity. 5.78

Figure 5.40: Upstream slope angle versus total post failure deformation for slides in embankment dams during drawdown. 5.79

Figure 5.41: Post construction slides in the downstream shoulder; post failure *(a)* deformation, and *(b)* estimated peak velocity. 5.84

Figure 5.42: Slide in the cut slope in London clay at Northolt in 1955 (Skempton 1964) 5.87

Figure 5.43: Post-failure slide deformation for cut slopes in London clays. 5.90

Figure 5.44: Estimated peak post failure velocity of slides in cut slopes in London clays..... 5.90

Figure 5.45: Cut slope angle versus post-failure deformation at the slide toe for cut slopes in heavily over-consolidated clays of Type 1 and Type 2 slope failure geometry. 5.91

Figure 5.46: Cut slope angle versus estimated post-failure slide velocity for cut slopes in heavily over-consolidated clays. 5.91

Figure 5.47: Failure in the cut slope in London clay at New Cross in 1841 (Skempton 1977) 5.94

Figure 5.48: Failure in the retained cut slope in London clay at Wembley Hill (Skempton 1977) 5.95

Figure 5.49: Failure in the retained cut slope in London clay at Uxbridge in 1954 (adapted from Henkel 1956) 5.97

Figure 5.50: Monitored post-failure deformation of the slide in the retained cut in London clay at Uxbridge in 1954 (adapted from Watson 1956)..... 5.97

Figure 5.51: Failure model for post-failure deformation (Khalili et al 1996)..... 5.98

Figure 5.52: Observed deformation versus the calculated residual factor of safety. . 5.103

Figure 5.53: Schematic profile of slope failure showing travel distance and travel distance angle 5.106

Figure 5.54: *H/L* versus the slide volume for embankment dams and cut slopes of moderate to rapid post-failure velocity. 5.107

Figure 5.55: *H/L* versus the tangent of the fill or cut slope angle for embankment dams and cut slopes of moderate to rapid post-failure velocity. 5.108

5.0 LANDSLIDES IN EMBANKMENT DAMS AND CUT SLOPES IN HEAVILY OVER-CONSOLIDATED HIGH PLASTICITY CLAYS

5.1 INTRODUCTION TO THIS CHAPTER

This chapter primarily analyses the post-failure deformation behaviour of landslides in embankment dams (excluding hydraulic fill embankment dams) and cut slopes in heavily over-consolidated high plasticity clays. The concentration of research on slow moving slides in these two slope types is due to the amount of published case study data, the level of investigation undertaken on the failures and research into areas related to landsliding in these slope types. The factors affecting the failure mechanics and post failure deformation behaviour of slow moving landslides from this study can be considered for the broader application to other slope types.

For the most part, landslides in embankment dams, cut slopes in high plasticity clays and fills on soft ground remain relatively intact during failure and reach post failure velocities ranging from very slow to rapid according to the IUGS (1995) classification (Table 1.1 of Section 1.3), i.e. velocities from centimetres per day to several metres per hour. These predominantly "slow" slides do not possess the mass destructive capabilities of "rapid" slides due to their generally limited amount of post-failure deformation and their "slow" velocity. Often, the post-failure velocity is sufficiently "slow" that the path of the slide can be avoided or remedial measures undertaken to halt the progress of the slide and prevent potential catastrophic consequences such as the breach of an embankment dam. However, such slides can cause extensive property damage on or just below the slide that can be costly to repair and result in a significant loss of amenity, as well as the potential for litigation claims and associated indirect loses for designers and owners.

The main objectives of the research on the post failure deformation behaviour of embankment dams and cut slopes in heavily over-consolidated high plasticity clays are:

- Assessment of the mechanics of and trigger for failure of landslides that post failure generally remain intact and travel at "slow" velocities;
- Assessment of the material properties and slope conditions of typically "slow" and intact landslides;

- Assessment of the mechanics of post failure deformation behaviour affecting the travel distance, mechanics of deformation and post failure velocity; i.e. how does the slope failure geometry, slope angle, material properties and other factors affect the travel of the slide mass;
- Evaluation of methods and development of new methods or guidelines (where appropriate) for prediction of the post-failure deformation behaviour.

The chapter is structured such that the statistics on dam incidents involving slope instability and a summary of the literature on progressive failure and the mechanics of post failure deformation (Section 5.2) provide a background, and is followed by the analysis of the case study database (Sections 5.3 to 5.8). The analysis is presented in three main components: Sections 5.4 and 5.5 on the mechanics of failure; Sections 5.6 and 5.7 on the post failure deformation behaviour; and Section 5.8 on the prediction on post failure travel distance. The prediction of post failure deformation (Section 5.8) includes the analysis of 22 cases using the methods developed by Khalili et al (1996) for intact sliding, and includes three failure case studies of embankments on soft ground (from Chapter 4) and one road embankment fill slope failure. Section 5.9 presents a summary of the research findings and guidelines for prediction of the post failure deformation behaviour.

5.2 LITERATURE REVIEW

5.2.1 STATISTICS ON DAM INCIDENTS INVOLVING SLOPE INSTABILITY

Foster (1999) and Foster et al (2000) present statistical data on dam failure and accident incidents (definitions of the International Commission on Large Dams (ICOLD)). Their database comprises some 11192 large embankment dams constructed up to 1986 (large as defined by ICOLD). The database excludes all dams constructed in China and those in Japan constructed prior to 1930.

Foster et al (2000) reported 124 slope instability incidents, which they categorised into upstream and downstream incidents, and the type or location of the slide (Table 5.1). Of these 124 incidents, 12 were failures that involved a breach and uncontrolled release of water from the reservoir. The remaining 112 were accidents.

Table 5.1: Incidence of slope instability in embankment dams (Foster 1999)

Type / Location of Slide	**No. of Incidents**	**Downstream Slope Incidents**		**Upstream Slope Incidents**	
		Failure	**Accident**	**Failure**	**Accident**
Sloughing	15	4	10	0	1
Within embankment only	60	1	33	0	26
Through embankment and foundation	35	1	17	0	17
Unknown	4	5	2	1	2
Total	**124**	**11**	**66**	**1**	**46**

Foster (1999) and Foster et al (2000) concluded that the major factors influencing the likelihood of downstream (Table 5.2) and upstream (Table 5.3) slope instability were:

- Slope instability is more likely in earthfill embankments than earth and rockfill embankments. Homogeneous and hydraulic fill dam embankments are statistically the most susceptible to slope instability.
- Slope instability is more likely for dam embankments on soil foundations than for dam embankments on rock foundations. Of the slides passing through the embankment and foundation, the incidence of slope instability is much greater in foundations of high plasticity clays.
- Slope instability is much more likely in dam embankments constructed of high plasticity clays and silts, particularly for slides in the downstream slope. Dam embankments constructed of sands and gravels have a significantly lower incidence of slope instability.
- Compaction, or lack there of, of the earthfill materials is also a significant factor. The incidence of slope instability is much more likely for earthfill constructed by placement with no formal compaction, and the least likely for rolled, well compacted earthfill.

Table 5.2: Factors influencing downstream slides - accident and failure incidents (Foster 1999)

FACTOR	GENERAL FACTORS INFLUENCING LIKELIHOOD OF INITIATION OF DOWNSTREAM SLIDES				
	MUCH MORE LIKELY	**MORE LIKELY**	**NEUTRAL**	**LESS LIKELY**	**MUCH LESS LIKELY**
ZONING	Homogeneous earthfill, earthfill with corewall, hydraulic earthfill	Earthfill with rock toe	Earthfill with filter	Concrete face earthfill, puddle core earthfill	Zoned earthfill, zoned earth and rockfill, central core earth and rockfill, concrete face rockfill, rockfill with corewall
FOUNDATION TYPE	Soil foundations			Rock foundations	
GEOLOGY TYPES *[1]	High plasticity clays in foundation (i.e. marine, lacustrine)	Residual soils of sedimentary origin and 'soft' sedimentary rocks	All other geology types (due to low number of foundation slide cases)		
CORE GEOLOGICAL ORIGIN	Lacustrine		Residual, alluvial, colluvial, volcanic	Glacial, aeolian	
CORE SOIL TYPE	High plasticity clays and silts (for rotational slides)	Low plasticity silts and clays (ML, CL)	Clayey sands (SC)	Clayey gravels (GC)	Silty sands and gravels (SM, GM)
CORE COMPACTION	No formal compaction	Rolled, modest control	Puddle, hydraulic fill (accounted for by zoning)	Rolled, well compacted (for foundation slides)	Rolled, well compacted (particularly for embankment slides and sloughing)

Note: *[1] For slides that incorporate the foundation

Table 5.3: Factors influencing upstream slides - accident and failure incidents (Foster 1999)

FACTOR	GENERAL FACTORS INFLUENCING LIKELIHOOD OF INITIATION OF UPSTREAM SLIDES				
	MUCH MORE LIKELY	**MORE LIKELY**	**NEUTRAL**	**LESS LIKELY**	**MUCH LESS LIKELY**
ZONING	Homogeneous earthfill, Hydraulic fill	Concrete face earthfill, Puddle core earthfill, Earthfill with corewall	Earthfill with rock toe Rockfill with corewall	Earthfill with filter, Zoned earthfill	Zoned earth and rockfill, Central core earth and rockfill Concrete face rockfill
FOUNDATION TYPE	Soil foundations			Rock foundations	
GEOLOGY TYPES *[1]	High plasticity clays in foundation (i.e. marine, lacustrine)	Residual soils of sedimentary origin and 'soft' sedimentary rocks	All other geology types (due to low no. of foundation slide cases)		
CORE GEOLOGICAL ORIGIN	Glacial, Lacustrine	Alluvial	Residual, Marine, Volcanic	Aeolian, Colluvial	Glacial
CORE SOIL TYPE		Low plasticity silts and clays (ML, CL)	High plasticity clays (CH)	Clayey sands and gravels (SC, GC)	Silty sands and gravels (SM, GM)
CORE COMPACTION	No formal compaction	Rolled, modest control	Puddle, hydraulic fill (accounted for by zoning)	Rolled, well compacted (for foundation slides)	Rolled, well compacted (for embankment slides and sloughing)

Note: *[1] For slides that incorporate the foundation

Further analysis was undertaken on slope stability incidents from the Foster database, excluding the sloughing type failures (Figure 5.2) and cases of unknown embankment zoning. Figure 5.1 presents a comparison of the incidence of slope instability and dam population for various embankment types and confirms the strong weighting toward failures in earthfill embankments, in particular homogeneous earthfill embankments, and low incidence of instability for rockfill and zoned earthfill embankments compared to their population. The term "rockfill" in Figure 5.1 includes zoned earth and rockfill, and central core earth and rockfill embankment types.

The analysis also found that:

- Sliding often extends into the foundation for incidents during construction (75%, excluding hydraulic fill dams), and for incidents in zoned earthfill embankments (60% of incidents) and rockfill embankments (80% or 4 of 5 incidents).
- Incidents involving the embankment only (i.e. the surface of rupture is located within the embankment only) occur mostly for failures during first filling (65% of incidents) and in the downstream slope post construction (74% of incidents). They also mostly occur in homogeneous embankments (70% of incidents), concrete corewall earthfill embankments (100% of incidents) and earthfill with rock toe embankments (70% of incidents).

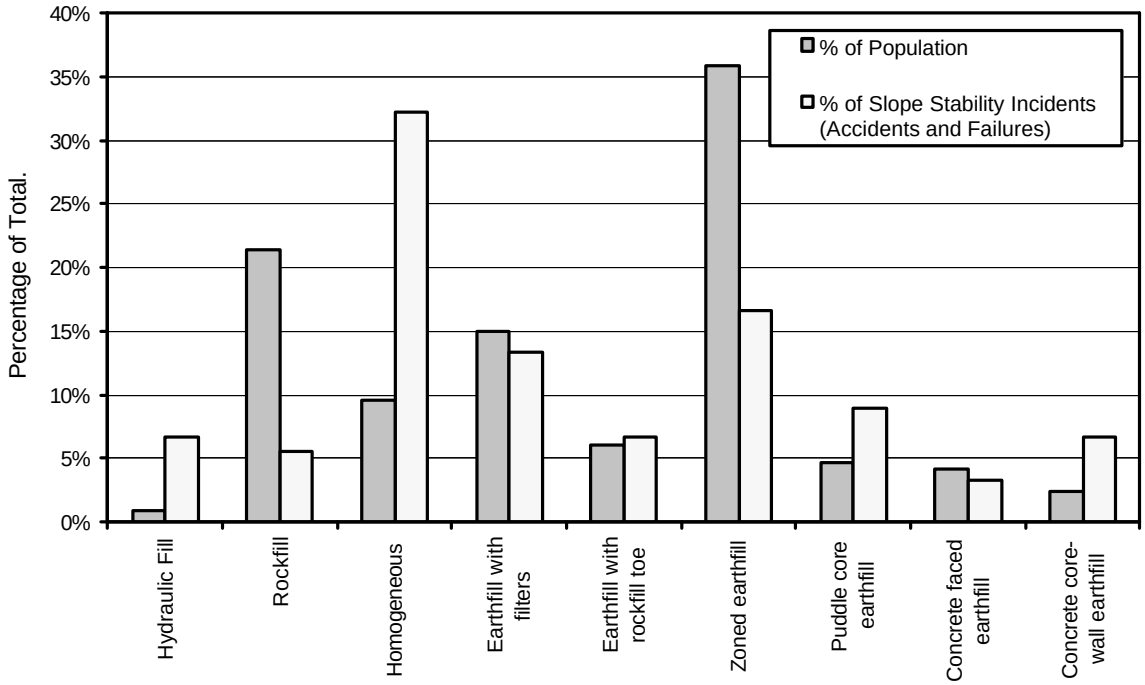

Figure 5.1: Comparison of population to slope stability incidents for earthfill, rockfill and hydraulic fill embankments (excluding sloughing and unknown embankment zonings).

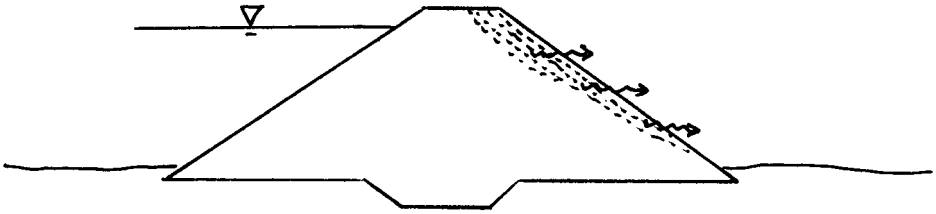

Figure 5.2: Sloughing type failure (Foster 1999)

Excluding sloughing type failures, the overall incidence of slope instability for large embankment dams reported by Foster (1999) is 106 incidents in 300,400 dam years up to 1986. It is important to recognise that a small number of poorly performing embankments have contributed significantly to the incident statistics, with 46 incidents coming from 13 embankments.

Of the 12 slope instability related failures (i.e. incidents involving breach) reported by Foster (1999) four were sloughing type failures (progressive sliding of the downstream slope due to seepage through the embankment, Figure 5.2). Of the remaining 8 failures (Table 5.4), slope instability is not directly attributable as the sole cause of the failure incident. In two cases (Fruitgrowers Dam and Utica Dam) slope instability was known to be the initiator of the failure incident; however, the eventual failure was by intentional breach in the case of Fruitgrowers Dam[1] and by piping in the case of Utica Dam. In five of the eight cases slope instability was thought to be only one of the probable causes of failure. In the case of Kaila Dam slope instability resulted in the breach, but was preceded by excessive seepage from a leaking conduit and piping.

Therefore, slope instability on its own has not been identified as being responsible for a failure incident. In the case of Fruitgrowers Dam it could well have occurred; however, had the slide not damaged the outlet works it may have been possible to draw down the reservoir in a controlled, albeit rapid, manner and averted the failure.

[1] Fruitgrowers Dam (Sherard 1953) was initially constructed in 1898 and then raised in 1905, 1910 and 1935. In 1937, when the reservoir was at its highest historical level, a failure in the downstream slope occurred which extended back to the crest of the embankment. The outlet works were inoperable as a result of the slide and the reservoir could not be drawn down. Due to concerns over potential uncontrolled breach as a result of back-scarp instability (the slide continued to move intermittently and seepage was observed emanating from a high level on the downstream slope) the embankment was intentionally breached near to the abutment.

In several accidents a failure (i.e. breach) was narrowly averted; at Great Western Dam[2] the reservoir was drawn down to avoid a breach and at Lower San Fernando Dam[3] it was fortunate that the reservoir level was relatively low at the time of failure. Foster (1999) comment that slides in dam embankments usually occur slowly thereby providing warning of the slope stability incident and allowing time for remedial action to avoid a breach. It is also notable that no modern dams have failed by slope instability.

5.2.2 PROGRESSIVE FAILURE

Progressive failure is the process whereby a localised failure condition, initially developed in part of a slope, progressively spreads through the slope culminating in eventual slope failure. At collapse (or slope failure), the mobilised shear stress and amount of shear strain along the surface of rupture is not uniform and overall the average shear stress is less than the peak shear strength of the soil mass (inclusive of defects). The degree of significance of progressive failure is related to the overall amount of strain weakening below the peak strength of the soil mass.

Progressive failure is a significant factor associated with the mechanics of failure of slopes in soils that show post peak strain weakening in drained or undrained loading, including heavily over-consolidated high plasticity clays and sensitive soils (Terzaghi and Peck 1948; Skempton 1948, 1964; Bjerrum 1967; Bishop 1967; Potts et al 1997; D'Elia et al 1998; Picarelli 2000; Leroueil 2001).

---

[2] At Great Western dam (Sherard et al 1963) the slide extended back into the upstream face of the embankment. Drawing down the reservoir level and stabilising the toe region of the slow moving slide narrowly avoided a breach. At one stage the rate of drawdown equalled the rate of vertical crest settlement (300 mm/day) at which point the freeboard (between the crest level in the slide area and the reservoir level) reached a minimum of 0.9 m.

[3] At Lower San Fernando dam, failure of the upstream slope occurred due to liquefaction and flow sliding following an earthquake. At the time of the earthquake the reservoir level was relatively low. The slide extended back into the downstream slope such that the minimum remaining freeboard was in the order of 1 m.

Table 5.4: Failures involving slope instability, excluding sloughing cases (Foster 1999)

Dam Name	Year Constr[d]	Year Failed	Embankment Details			Slope	Slide Type	Description of Materials and Placement	Description of Failure Incident
			Type	Class[n]	Height (m)				
Jackson's Bluff	1930	1957	homog	0,0,0	9	down-stream	Unk	Silty sands (SM) placed by dumping (no formal compaction)	Not observed. Assumed downstream slope instability following wet period.
Kelly Barnes	1899	1977	other	12,x,x	6	down-stream	Unk	Earthfill placed over rock crib dam.	Attributed to failure of 1H to 1V downstream slope. Associated with piping and/or localised breach.
Wheatland No. 1	1893 (raised 1959)	1969	homog	0,0,0	13	down-stream	Unk	Unknown. Originally built in 1893, raised in 1935 and 1959.	Cause of failure not known. Attributed to sliding of downstream slope and/or piping along conduit.
Fruitgrowers	1898 (raised 1905, 1910 & 1935)	1937	homog	0,0,0	11	down-stream	Emb & fndn	Medium plasticity clays (CL) derived from residual shales. Original dam placed with no formal compaction.	Slide in downstream slope when reservoir at highest level. Outlet works inoperable due to slide. Embankment intentionally breached.
Ema	1932	1940	unknown	13,x,x	18	down-stream	Unk	Unknown	Slide in downstream slope. Due to piping.
Snake Ravine	1898	1898	hydraulic fill	11,0,0	19	down-stream	Unk	Central core zone of low plasticity silts and clays. Hydraulically placed.	Slide in downstream slope, possibly associated with piping.
Utica	1873	1902	unknown	13,x,x	21	down-stream	Emb	Unknown	Slides in downstream slope. Breach associated with piping following slides.
Kaila	1955	1959	concrete core-wall earthfill	9,0,x	26	upstream	Unk	Modest control of earthfill.	Slide in upstream slope. Slide preceded by excessive seepage around leaking conduit and piping.

Note: Year Constr[d] = year when construction was completed Class[n] = dam zoning classification (refer Section 1.3.3)
homog = homogeneous embankment unk = unknown Emb = failure through the embankment only
Emb & fndn = failure through the embankment and foundation

Failures in cut slopes of heavily over-consolidated high plasticity clays, where progressive failure is significant, are prevalent in the published literature due to the engineering significance of the structures and the delay of many years to failure after excavation, such as cuts in London clay (Skempton 1964; James 1970) and in the Culebra clays of the Panama Canal (Banks et al 1975). Progressive failure was also significant for several embankment dam failures, namely Carsington dam (Skempton and Vaughan 1993) and San Luis dam (Stark and Duncan 1991), failures in riverbank slopes of sensitive clays (Leroueil 2001), and failures in embankments on soft ground (Chapter 4).

The mechanics of progressive failure and the formation of a shear zone and eventual surface of rupture are discussed in recent papers by Leroueil (2001), Picarelli (2000), Potts et al (1997), Fell et al (2000) and Cooper et al (1998b). Several general aspects related to progressive failure are:

- Once a localised failure condition has been reached in part of a slope, progression to a slope failure condition does not necessarily occur. In fact, the numerical analysis by Potts et al (1997) and research by Leroueil (2001) would indicate that in a high proportion of slopes in brittle soils a localised failure condition has been reached in some part of the slope.
- The progression from initiation of a localised failure condition to slope failure (or collapse) generally requires a change in material strength properties and/or boundary conditions (i.e. a change in stress conditions such as due erosion at the toe of the slope). Processes leading to a reduction in material strength properties include; the stress relief process of dilation and softening (Potts et al 1997; Bjerrum 1967), creep under constant effective stress conditions (Tavenas and Leroueil 1977; Mitchell 1993; Leroueil 2001; Fell et al 2000), fatigue due to cyclic loading (Leroueil 2001; Stark and Duncan 1991), weathering, and changes in pore water chemistry (Picarelli 2000).
- In cases where progressive failure is significant, the concept of the factor of safety of a slope is not clearly defined (Terzaghi 1950; Picarelli 2000; Leroueil 2001; Potts et al 1997), it changes with time due to strain weakening in the slope.

Further aspects of progressive failure particular to the mechanics of failure in cut slopes in heavily over-consolidated high plasticity clays and embankment dams are discussed in Sections 5.4 and 5.5.

5.2.3 MECHANICS OF POST FAILURE DEFORMATION

Models developed for post failure deformation analysis of landslides, such as sliding block or "lumped mass" models (e.g. Banks and Strohm 1974; Koerner 1977) and numerical continuum models (e.g. Hungr 1995; Norem et al 1990), are based on energy principles. The kinetic energy of the slide mass in these models is dependent on the rheological model used to define material properties and mechanics of movement (e.g. Figure 5.3 as an example of sliding block models), and the geometrical constraints that define the potential energy of the slide mass at failure. Locat and Leroueil (1997) comment that the energy balance from initial failure to travel of the slide mass is complex and not well known, and that available models are simplistic approximations of this behaviour.

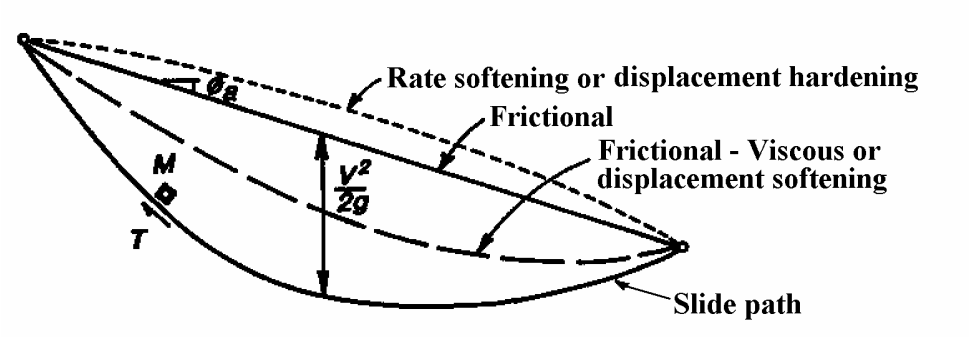

Figure 5.3: Sliding block model showing kinetic energy lines for different rheological models (Golder Assoc. 1995).

D'Elia et al (1998) comment that for first time slides the potential energy of the slide mass at failure dissipates with movement into the major components of frictional energy between the sliding mass and surface over which it slides, energy used in internal deformation (i.e. destructuration, disaggregation and remoulding of the slide mass) and kinetic energy (Figure 5.4). They comment, and as idealised in Figure 5.4, that the amount of potential energy dissipated as frictional energy may vary with strain or displacement due to strain weakening on shearing from the shear strength at the point of failure, i.e. it is dependent on the brittleness of the material.

For soils that are not strain weakening on shearing (i.e. zero brittleness), D'Elia et al (1998) comment that the velocity of the slide mass remains small as the potential energy is essentially consumed in friction. For soils that are strain weakening (i.e. brittleness is large) then the frictional energy decreases with strain and a greater part of the potential

energy is transformed into kinetic energy for movement and acceleration of the slide mass. Picarelli (2000) also points out that the mechanics of failure are significant in the post failure deformation behaviour.

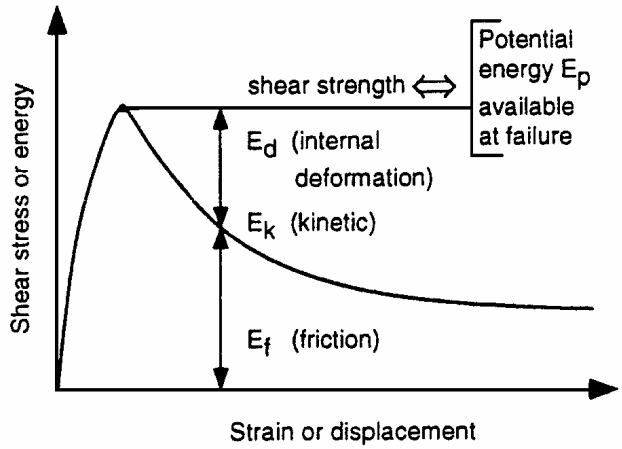

Figure 5.4: Redistribution of the potential energy after failure (D'Elia et al 1998)

Leroueil et al (1996) and Leroueil (2001) comment that the frictional energy component may not be easily evaluated due to the variability of the stress strain characteristics of the material (due to variation in stress path and strength anisotropy, and variation in effective stress conditions) and the type and development of the surface of rupture (e.g. deformation along a well defined surface of rupture or plastic deformation within a shear band). Leroueil (2001) comments that for structured soils the energy required for disaggregation and remoulding of the material can have an important influence on the post failure deformation behaviour, citing examples of failures in sensitive clays and chalk cliffs, but that overall the literature is limited in this field.

5.3 DATABASE OF CASE STUDIES ANALYSED

The database of failures in embankment dams and cut slopes in high plasticity clays comprises some 91 case studies sourced mostly from published literature. For several of the embankment dams, the data was sourced from unpublished reports obtained from the owners or surveillance authority, and alternate names have been used for these dams (e.g. Dam FD2).

Table 5.5 presents a summary of the case study database. The failures in fills on soft ground (analysed in Chapter 4) have been included in Table 5.5 as several of these case studies were included in the post failure deformation analysis (Section 5.8).

For most of the case studies, the failed slide mass remained relatively intact during sliding. Post failure deformations were generally limited to less than 2 to 5 m, but were up to 20 to 30 m. Post failure velocities were estimated to be in the slow to moderate classes for most cases, but several were in the rapid class.

Table 5.5: Summary of case study database of slope failures

Group / Material Type	**Sub-grouping**	**No.**	**Volume Range (m^3)**	**Comments *[2]**	**Main References**
Embankment Dams (excluding hydraulic fill dams)	During construction	22	13,000 to $1.2x10^6$	Slope failure geometry of Types 1, 2 and 5.	Various references. Refer to Appendix D (Section 1) for the individual case study references.
	Drawdown induced, upstream slope	19	7000 to $1x10^6$	Mostly Type 2 slope failure geometries, but several of Type 1.	
	Downstream slope, post construction	13	300 to 100,000	Mostly Type 2 slope failure geometries. Significant number of cases in earthfill embankments without embankment filters.	
Cut Slopes in High Plasticity Clays	Type 1 *[2]	7	600 to 40,000 *[3]	Case studies from cuts in London clays (25 cases) and Upper Lias clays (12 cases).	London clays – James (1970), Skempton (1964, 1977) Upper Lias clays – Chandler (1972, 1974), James (1970)
	Type 2 *[2]	25			
	Type 5 *[2], retained cuts	5			
Fills on Soft Ground *[1]	Sensitive clay foundations	5	-	Mainly from Canada and Scandinavian countries. Clayey silts to silty clays of high sensitivity and high undrained brittleness.	Refer to Chapter 4 (Section 4.3.1) for case study references
	Low sensitivity (or ductile) clay foundations	8	-	Very soft to firm clays of low undrained brittleness.	

Note: *[1] all fill on soft ground case studies are of Type 5 failure geometry

*[2] The slope failure geometries Types 1,2 and 5 are defined in Figure 1.3 in Section 1.3 of Chapter 1.

*[3] volume unknown or could not be estimated for a large number of cases

5.3.1 CASE STUDIES OF FAILURES[4] IN DAM EMBANKMENTS

Some 54 case studies of slope instability incidents in dam embankments have been analysed. Hydraulic fill embankment dams were excluded from this chapter as the failures involved liquefaction and flow sliding, resulting in rapid to very rapid post failure velocities (they have been included in the analysis of "rapid" landslides in Chapter 3).

The case studies of dam embankment slope stability incidents have been classified into three categories (Table 5.6); slides during construction, post construction slides in the upstream slope on drawdown, and post construction slides in the downstream slope. The weighting toward slides during construction, in comparison to their statistical weighting in slope stability incidents in large dams (refer Section 5.2.1), is because of the availability of slope deformation monitoring records for these slides. For the post-construction slides, monitoring records were scarce and in most cases no records were available.

The slope failure geometry types are given in Table 5.6. In a number of cases the location of the surface of rupture was not precisely known.

Information on the individual case studies analysed is presented in Appendix D (Section 1). Summary details are given in a number of tables in this chapter (refer Table 5.6). The information presented in Appendix D includes; general details on the dam; description of materials used in construction; description of the foundation conditions; details of the failure (location, dimensions, post failure deformation behaviour); comments on the hydro-geological conditions, and comments on the trigger and mechanism of the failure.

Table 5.7 presents the classification of the slope instability case studies with respect to embankment type. In summary:

- Earthfill embankments (homogeneous earthfill, earthfill with filters and earthfill with rock toe) comprise 36 (67%) of the case studies analysed and make up 80% (24 of 30) of the failures through the embankment only.
- Five of the case studies were in rockfill embankments. In four of these, the surface of rupture did not pass through the rockfill zones.

[4] The term 'failure' here means the formation of and sliding along a distinct surface of rupture through the soil mass. It does not mean that the dam was breached. This meaning of the term 'failure' is used extensively in Sections 5.4 to 5.9.

Table 5.6: Summary of embankment dam slope stability incidents by failure slope geometry

Failure Category	No. Case Studies	Location of Surface of Rupture *[1]			Slope Failure Geometry *[2]			Location of Tabulated Data on Individual Case Studies
		Emb Only	Emb & Fndn	Unk *[3]	Type 1	Type 2	Type 5	
During Construction	22 (41%)	11	11	-	7 poss. 9	5 poss. 7	8	Table 5.12, Table 5.13, Table D1.1 (Appendix D)
Drawdown Induced, Upstream Slope	19 (35%)	16	3	-	5 poss. 9	8 poss. 13	0	Table 5.14 Table D1.2 (Appendix D)
Downstream Slope, Post-construction	13 (24%)	3	6	4	1*[4] poss 4	5 poss. 10	2 poss. 3	Table 5.16 Table D1.3 (Appendix D)

Notes: *[1] Emb = embankment only; Emb & Fndn = embankment and foundation; Unk = unknown

*[2] The slope failure geometries Types 1,2 and 5 are defined in Figure 1.3 in Section 1.3 of Chapter 1.

*[3] unsure if the surface of rupture passed through the foundation

*[4] failure in the downstream slope above the rockfill toe of an earthfill with rock toe embankment dam.

5.3.2 CASE STUDIES OF FAILURES IN CUT SLOPES OF HIGH PLASTICITY CLAYS

Good quality information on the post-failure deformation behaviour of "slow" slides in cut slopes from the literature, particularly for first time slides, is limited. What information is available is generally anecdotal and qualitative, such as '*x*' amount of displacement in '*t*' time, with very few cases having quantitative surface or sub-surface monitoring. The approach taken for the analysis of the post-failure deformation of "slow" slides in cut slopes has therefore been to restrict the research to soil formations with reasonably uniform (and well published) properties, and for which the published literature contains numerous cases of slope instability with some information on post-failure deformation.

Table 5.7: Slope instability case studies in embankment dams by embankment type

Failure Category	**Failure Type *[1]**	**No. Cases**	**Homogeneous Earthfill *[2]**	**Earthfill with filters *[3]**	**Earthfill with rock toe**	**Puddle core earthfill**	**Zoned earthfill**	**Zoned earth and rockfill**	**Concrete core - wall earth and rockfill**
Construction	Emb	11	1	6 (1)	1	1	-	2*[4]	-
	Emb & fndn	11	-	3 (1)	1	2	5	-	-
Drawdown	Emb	16	8	2 (1)	3	1	2	-	-
	Emb & fndn	3	1	-	-	-	-	1*[4]	1
Downstream Slope, post-construction	Emb	3	1	1 (1)	1	-	-	-	-
	Emb & fndn	6	3	1 (1)	-	-	1	1*[4]	-
	Unk	4	3	-	-	1	-	-	-
TOTAL	**-**	**54**	**17**	**13 (5)**	**6**	**5**	**8**	**4**	**1**

Notes: *[1] Emb = failure within the embankment only; Emb & fndn = failure through the embankment and foundation; Unk = the location of the surface of rupture is not known

*[2] In 5 (of the 17) cases classified as homogeneous earthfill embankments it was unknown or not sure if filters were present.

*[3] The number in brackets refers to the number of cases with foundation filters only; e.g. 6 (1) indicates six cases of failures in earthfill embankments with filters and in one of these cases the embankment only had foundation filters.

*[4] Zoned earth and rockfill dams with either thin outer rockfill zone/s (horizontal thickness less than or equal to $0.5H$, where H = the height below the dam crest) or where the surface of rupture did not pass through the rockfill zone/s (it preferentially passed through the foundation).

The cut slope failure case studies come from two geological formations, London clay and the weathered portion of the Upper Lias clay. Both formations are located in the UK and are derived from marine clay deposition; during the Eocene period (early Tertiary) for the London clay, and the Jurassic period for the Upper Lias clay-shale. Uplifting and subsequent erosion has resulted in heavy over-consolidation of both formations. Other similarities between the London clay and weathered Upper Lias clay are that they are both of high plasticity, typically of stiff to very stiff undrained strength consistency and are strain weakening on shearing in both drained and undrained loading. Further details on the material properties are given in Appendix D (Section 2).

The exposed profile of the London clay formation (Skempton 1977) typically comprises an upper weathered zone, referred to as "brown" London clay, of 5 to 15 m thickness overlying the unweathered "blue" London clay. The formation is heavily fissured with no preferred orientation (Skempton et al 1969), but concentrated in the sub-horizontal plane. Other defects (Skempton et al 1969) comprise near horizontal bedding and jointing. The permeability of the soil mass is very low.

Chandler (1972) identifies two surface profiles within the Upper Lias clay formation, a brecciated profile and a fissured profile. He indicated that the brecciated profile resulted from disturbance due to permafrost during the Pleistocene age. The depth of brecciation is about 10 m and is typified by a lack of fissuring and permeability one to two orders of magnitude greater than for the fissured profile. The fissured profile (Chandler 1972) of the weathered Upper Lias clay is observed where the zone of brecciation has been eroded. Fissuring is prevalent within the upper weathered profile and does not extend into the underlying un-weathered profile. Other defects include near horizontal bedding. Slickensiding is observed on fissures in the more weathered materials.

A summary of the failure case studies for cuts in London clay (25 case studies) are given Table 5.17 and for the Upper Lias clay (12 case studies) in Table 5.18. Further details are given in the tables in Section 2 of Appendix D. Of the failure case studies:

- Cut slope height ranged from 5 to 17 m.
- Cut slope angle ranged from as low as 13.5 degrees to as steep as 56 degrees.
- Most failures are of Type 2 slope failure geometry.
- Seven are of Type 1 failure geometry where, in most cases, the basal plane is likely to be controlled by dominant sub-horizontal defects (bedding or jointing).

- Five are of Type 5 failure geometry (all in London clay), all of which involve a deep-seated surface of rupture passing below the lower retained portion of the cut slope.
- Of the failures in the Upper Lias clay, eight were in the fissured profile and four in the brecciated profile.

5.4 MECHANICS OF FAILURE OF CUT SLOPES IN HEAVILY OVER-CONSOLIDATED HIGH PLASTICITY CLAYS

5.4.1 PROGRESSIVE FAILURE

Progressive failure is significant in the mechanics of failure of cut slopes in heavily over-consolidated clays. The numerical analysis of cuts in London clay by Potts et al (1997) shows that the process of stress relief occurs concurrently with the process of progressive failure. The process of stress relief results in time dependent dilation (or swelling) and softening of the soil mass and changes in effective stress conditions as excavation induced pore water pressure dissipate. The process of progressive failure is, to a large extent, contingent on the changes in effective stress conditions and material strength properties associated with stress relief, and results in shear induced dilation and strain weakening of the soil mass initiating in highly shear stressed regions of the slope.

The factors affecting the effective stress conditions within the slope, and therefore the regions of high shear stress, are the slope geometry, pore water pressure conditions and the coefficient of earth pressure at rest, K_o (Bishop 1967; Duncan and Dunlop 1969). For a cut slope of given geometry, increasing concentration of shear stress is observed at the toe of the cut slope with increasing K_o. Potts et al (1997) showed, by numerical analysis using an elasto-plastic model incorporating a softening function, that localised failure initiates in the highly shear stressed toe region of a cut slope in heavily over-consolidated clays and then gradually spreads from the toe region into the slope (Figure 5.5). They modelled the material properties on those of Brown London clay, with the softening function related to the deviatoric plastic strain invariant.

The process of progressive failure involves the development of reduced pore water pressures in the highly shear stressed region/s of the slope due to the dilative response of the over-consolidated clay under shear. This establishes differential pore water pressure conditions within the slope. Moisture migrates toward these regions of

reduced pore water pressure, resulting in localised dilation and softening. Evidence of moisture migration has been reported from field investigation of cut slopes in London clay (Figure 5.6) and laboratory undrained triaxial testing (Figure 5.7).

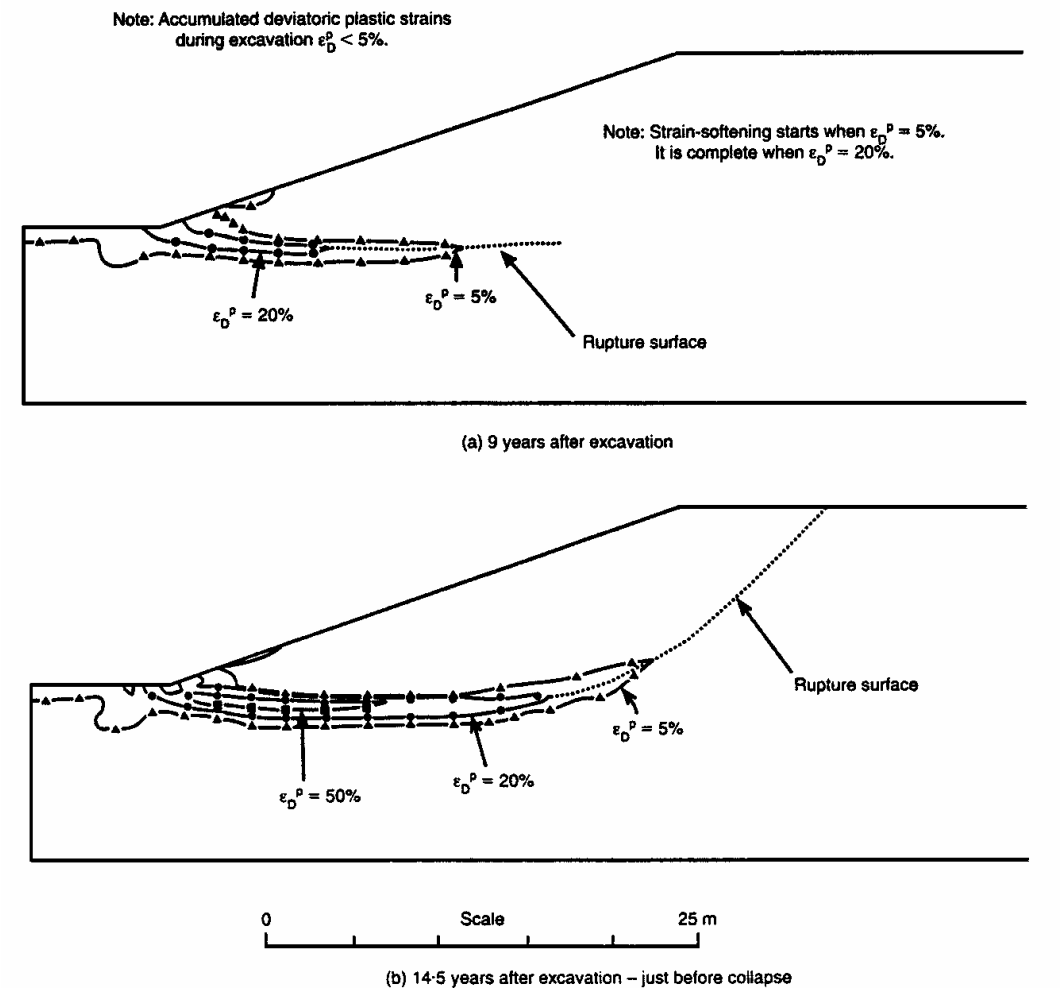

Figure 5.5: Contours of accumulated deviatoric plastic strain, $e_D{}^P$, from finite element analysis of an excavation: 3H to 1V slope, 10 m cut slope height, K_o = 1.5, surface suction = 10 kPa (Potts et al 1997).

Progressive failure is significant in the mechanics of failure for cut slopes of 18 to 30 degrees in heavily over-consolidated high plasticity clays. For first time failures in cut slopes in London clay, this is evidenced by the large time to delay to failure after excavation, which has been reported to occur up to 50 to 100 years after excavation (James 1970; Skempton 1977). It is also a factor, although not as significant, in the mechanics of failure in steeper cut slopes (steeper than about 35 degrees). Failures in steeper cut slopes in London clays are reported to have occurred within days to years after excavation (Skempton and La Rochelle 1965; James 1970).

Several other aspects of cut slope failures in heavily over-consolidated high plasticity clays of note are the trigger for failure, time to failure and the influence of defects. These are discussed in the following sections.

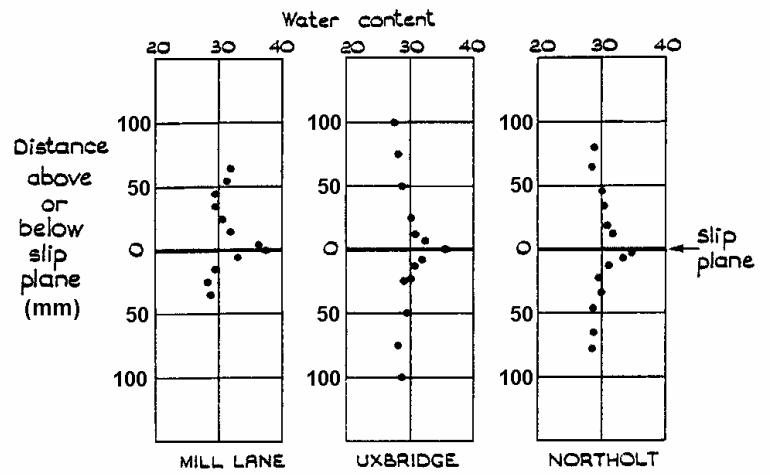

Figure 5.6: Distribution of water content near the slip place from failures in cut slopes in London clay (Skempton 1964)

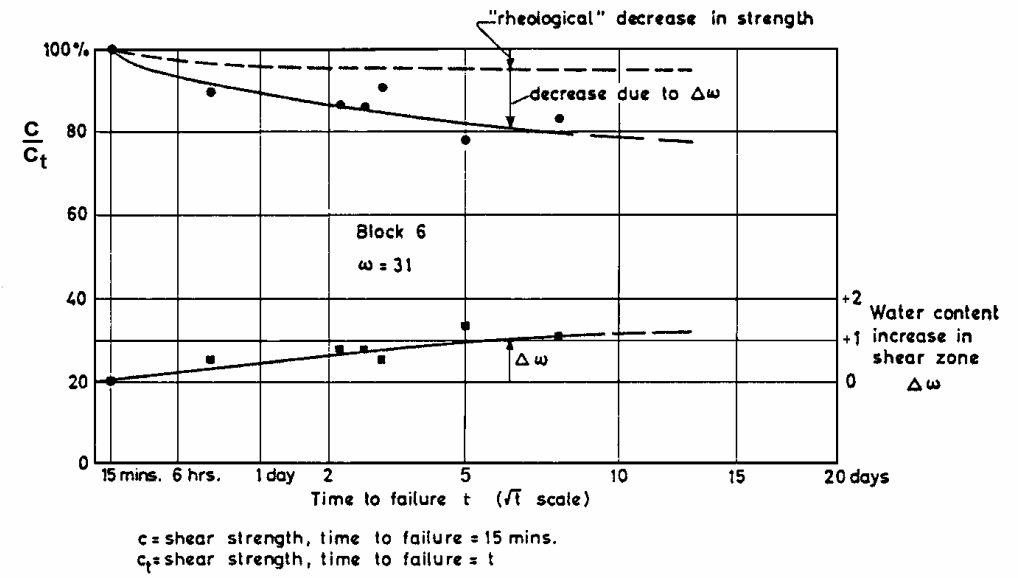

Figure 5.7: Moisture content migration to the shear zone and decreasing shear strength with time to failure from consolidated undrained tests on brown London clay (Skempton and La Rochelle 1965)

5.4.2 TRIGGER TO FAILURE

James (1970) commented that cut slope failures in heavily over-consolidated clays in the UK typically occurred in the period from October to February, the cooler and wetter

months, and that the annual number of recorded slides (Figure 5.8) was greater during years where the seasonal winter rainfall was above average. Potts et al (1997) commented that the incidence of cut slope failures in the seasonally wetter months is indicative of the importance of the slope hydrogeology in controlling the eventual failure of the slope.

Chandler (1974), from observation of pore water pressure response in cut slopes in Upper Lias clays, indicated that the seasonal fluctuation in piezometric levels was substantial at shallow depths in the over-consolidated clay, but was very small at depths below about 2 m. It is this fluctuation at shallow depth that is significant in the trigger for slope failure of a large number of first time failures.

Picarelli et al (2000) comment that climate is the trigger for landsliding in slopes of stiff clays and clay shales (Figure 5.9). They describe the factors associated with progressive soil weakening that result in a decrease in the factor of safety of the slope with time, as aggravating factors.

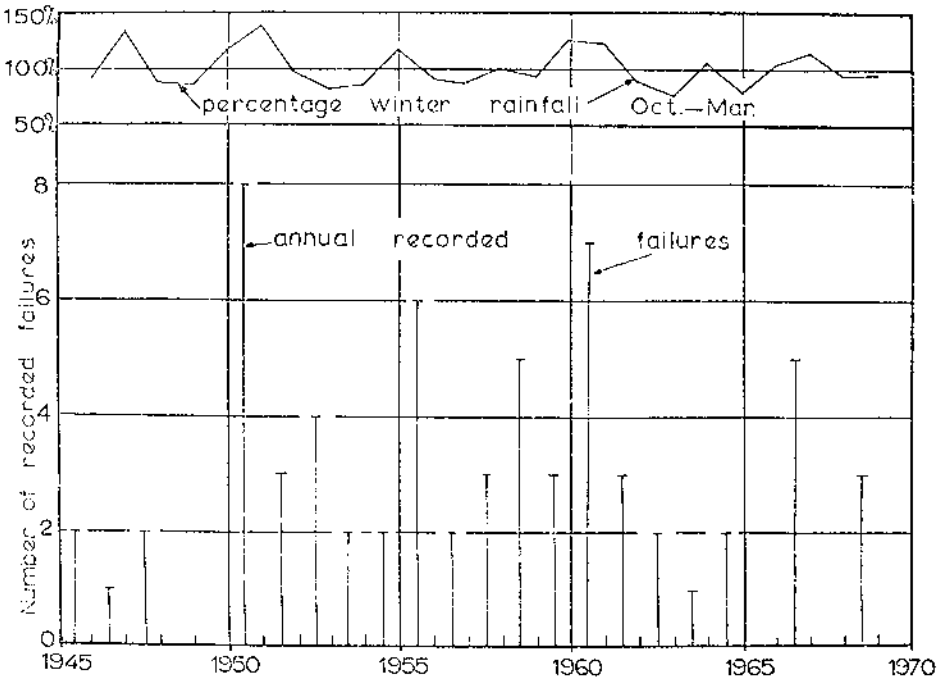

Figure 5.8: Annual records of cut slope failures in heavily over-consolidated clays in the UK (James 1970).

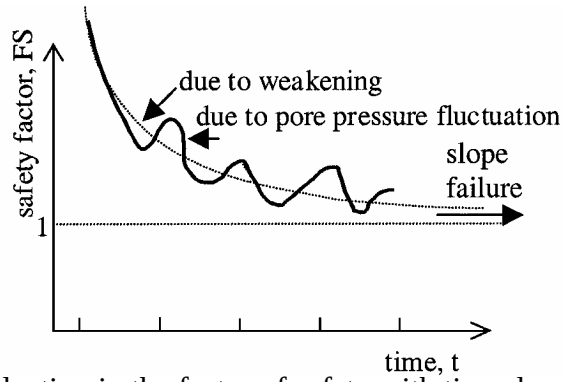

Figure 5.9: Gradual reduction in the factor of safety with time due to soil weakening and oscillations due to climatic effects (Picarelli et al 2000)

5.4.3 TIME TO FAILURE

The time for equilibration of pore water pressures post excavation is considered by Skempton (1977) to be the major reason for delay in failure of cuts in heavily over-consolidated brown London clay. Chandler (1984a) comments that the lengthy time for equilibration of pore water pressures is due to the very low permeability of these materials. He adds that uniform deposition conditions over a lengthy time period, omission of pervious horizons in the deposition sequence and high density associated with heavy over-consolidation contribute to the low permeability.

Skempton (1977) indicates that the time to reach pore water pressure equilibrium could take up to 50 years for cuts in London clays (Figure 5.10) and Chandler (1974) estimates up to 60 years for cuts in the weathered, fissured Upper Lias clays. James (1970) also reports a similar time frame for cuts in Oxford clay (heavily over-consolidated marine clay). However, for cuts in the brecciated Upper Lias clays Chandler (1974) estimates equilibrium is reached in less than 10 years due to the higher permeability of the brecciated soil profile.

These findings indicate the significance of permeability of the soil mass on the time for pore water pressure equilibration, and therefore the rate of development of progressive failure and the time to failure.

Slope geometry is also a factor in the time to failure. Figure 5.11, for cut slopes in London clay of Type 1 and Type 2 slope failure geometry, shows that the time to failure after excavation increases with decreasing cut slope angle.

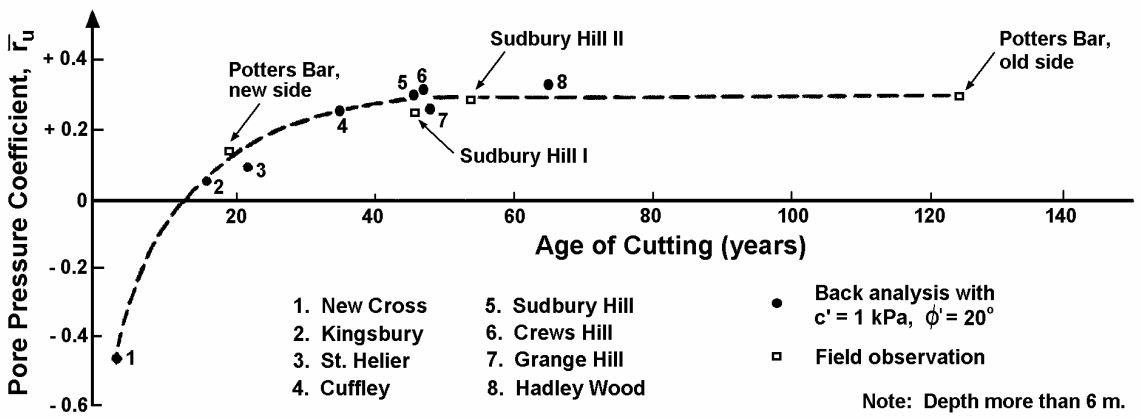

Figure 5.10: Variation of the pore water pressure coefficient, r_u, with time in cuttings in Brown London clay (Skempton 1977).

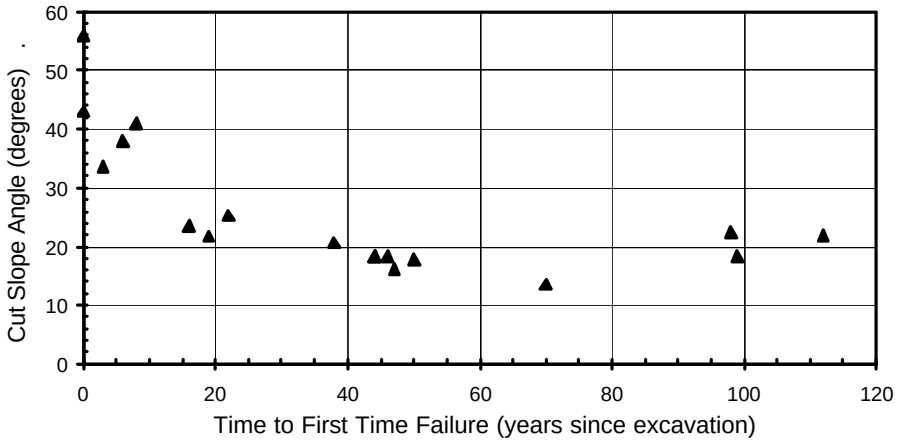

Figure 5.11: Time to first time failure versus cut slope angle for Type 1 and Type 2 slope failure geometries in London clay.

5.4.4 EFFECT OF DEFECTS WITHIN THE SOIL MASS

The presence of fissuring is generally synonymous with high plasticity clays formed due to weathering processes and that are heavily over-consolidated as a result of erosion of significant depths of overburden (typical of the marine clays in the UK). However, the presence of defects such as fissures is not a necessary requirement for progressive failure in cut slopes in these soil types as indicated from the numerical analysis by Potts et al (1997).

The presence of defects though can have an effect on progressive failure depending on the strength properties of the defect in comparison to that of the intact soil and their orientation with respect to the orientation of the cut slope. For most defects, such as

fissuring, bedding or jointing, the modulus and strength properties are usually less than that of the intact soil. Under the stress conditions imposed on excavation of the slope, shear strains will therefore concentrate along these defects.

Preferential deformation along defects in the highly stressed toe region of the cut during the early stages of progressive failure was observed at the Saxon Pit excavation in Oxford clay (Burland et al 1977), the Selbourne cut in Gault clay (Cooper et al 1998b), and cuts in the jointed Santa Barbara clay (D'Elia et al 1998; Bertuccioli et al 1996).

D'Elia et al (1998) discuss further the effect of defects, their type and orientation, on the shape of the surface of rupture and observed pre-failure deformation behaviour for slopes in stiff jointed clays and structurally complex clays.

5.5 MECHANICS OF FAILURE FOR FAILURES IN EMBANKMENT DAMS

5.5.1 FAILURES IN EMBANKMENT DAMS DURING CONSTRUCTION

Four main types of failure mechanics have been identified (Table 5.8) for failures in embankment dams during construction.

Table 5.8: Mechanics of failure for failures in embankment dams during construction.

Failure Type	No. Cases	Comments
Embankment only – undrained failure in wet placed fill	5	Mainly homogeneous earthfill embankments with materials placed well wet of OMC (average greater than 4% wet, but material dependent).
Embankment only – undrained failure controlled by wet layers in fill	6	Undrained instability within wet, low undrained strength layers in the embankment. Mainly homogeneous earthfill embankments.
Embankment and Foundation – undrained failure in low strength foundation layer	10	Failure controlled by weak layers in foundation. Either pre-sheared seams at residual strength or low undrained strength layers.
Embankment and Foundation – progressive failure of foundation and undrained failure in the embankment.	1	Only one case, Carsington. Progressive failure within the over-consolidated clay foundation layer (with solifluction shears) and undrained failure within the embankment.

5.5.1.1 *Wet Placed Fills*

The mechanics of failure in wet placed fills is simply undrained failure of an unstable slope. In all five cases the earthfill within the embankment was placed well wet of the optimum moisture content for Standard compaction, at least 4% wet. The characteristics of the wet placed earthfill are low undrained shear strength, low pre-consolidation pressure at compaction and development of high pore water pressures. Even at low confining pressures these materials are near normally consolidated.

5.5.1.2 *Wet Placed Layers of Fill or Low Undrained Strength Foundations*

These case studies are more complex than for the failure case studies in wet placed fills. The wet placed earthfill layers or layers of low undrained strength in the foundation typically form the basal plane of the surface of rupture. The overall slide mechanism is generally characterised by the development of a back-scarp and lateral shear surfaces through partially saturated soils. Failures involving the foundations are also characterised by the persistence of the weak foundation stratum.

The mechanism for development of a surface of rupture and kinematically admissible slide for these failure case studies is considered to be controlled by the wet placed earthfill layer or weak foundation layer, and to incorporate the following process:

- Once the shear stresses imposed by the embankment exceed the undrained shear capacity of the weak layer then plastic deformations will occur (Figure 5.12).
- With increase in the applied stresses due to embankment raising, the weak zone cannot support the additional stresses once its stress capacity has been reached. Therefore, the additional stresses are transferred from these highly stressed areas to areas where the shear capacity of the soil has not yet been exceeded. This will typically be onto the lateral margins or in the central region of the embankment immediately above the wet placed layers (Figure 5.12), thereby concentrating stresses in these regions.
- The third stage involves the development of a full surface of rupture as shearing progresses into the partially saturated soils of significantly greater undrained strength capacity and which are potentially dilative on shearing.

- Once a failure surface has formed deformations are then dependent on brittleness of the slide mechanism and materials along the surface of rupture (discussed in Section 5.6.3).

Once developed, the surface of rupture is typically a compound type rupture surface with translational basal plane in the weak layer and a rotational back-scarp as shown in Figure 5.13.

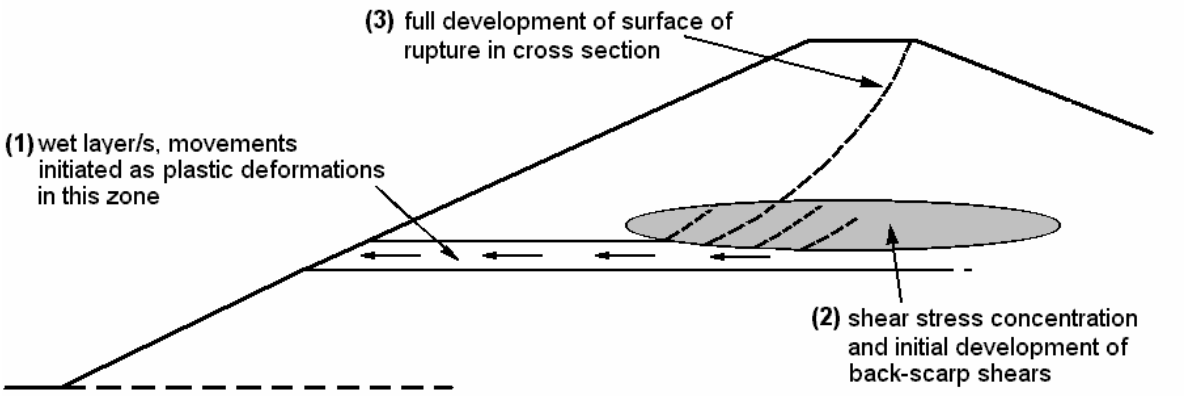

Figure 5.12: Idealised development of surface of rupture during construction for embankments with wet placed fill layer/s.

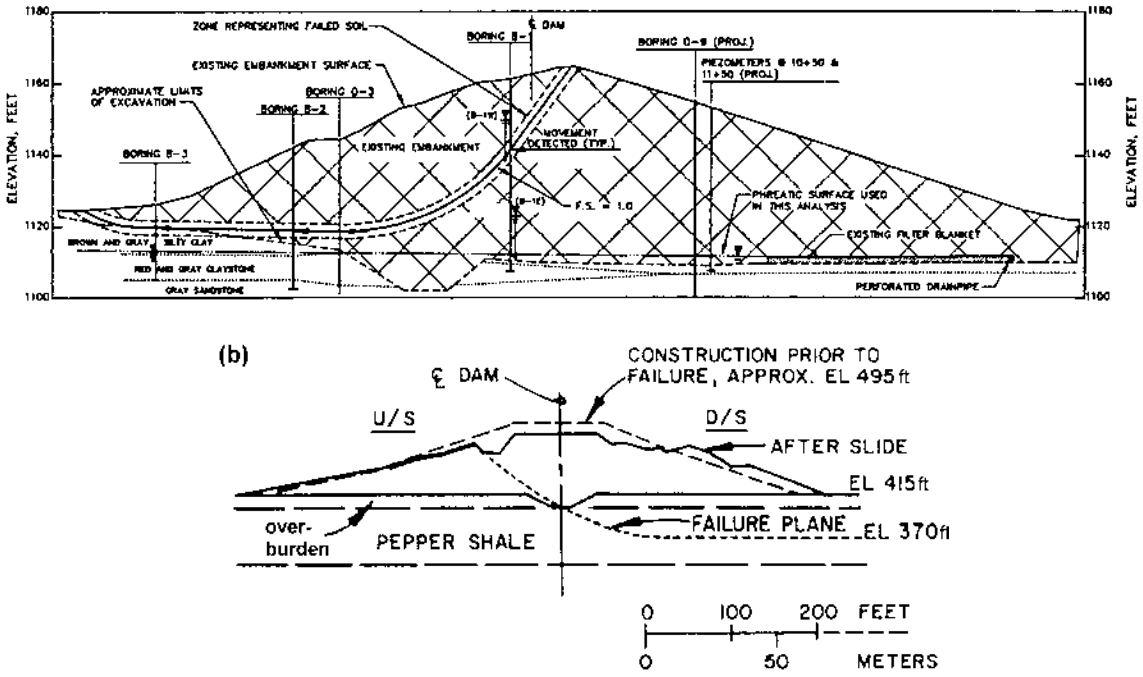

Figure 5.13: Compound type surface of rupture for failures during construction at *(a)* Scout Reservation dam (Mann and Snow 1992), and *(b)* Waco dam (Stroman et al 1984).

5.5.1.3 Carsington Dam

Skempton and Vaughan (1993), amongst others, concluded that progressive failure was a significant factor in the mechanics of failure of Carsington dam, which failed during construction.

The central core of Carsington dam, including its unusual "boot" structure on the upstream side (Figure 5.14), comprised high plasticity clays that were placed well wet of Standard optimum moisture content and heavily rolled. Potts et al (1990) report the peak undrained strength of the core as 42 kPa taking into consideration strain rate effects, the presence of shears from trafficking and plane strain conditions, and undrained residual strength of about 30 kPa. The pre-consolidation pressure of the core material, estimated at about 140 to 150 kPa, is relatively low. This estimate is based on the development of positive pore water pressures (of very high incremental pore water pressure coefficient) at applied loads of approximately 8 m head of fill (Skempton and Vaughan 1993) as being indicative of normally consolidated conditions.

The outer earthfill zones (Zones I and II) were of weathered mudstone placed in thin layers and well compacted (average density ratio of 101.1% of Standard Maximum Dry Density).

The "yellow clay" foundation, a moderately to heavily over-consolidated layer of glacially deposited high plasticity clay, was strongly strain weakening in drained loading beyond its peak intact strength (Figure 5.15). It contained numerous solifluction shears formed due to glacial disturbance, the strength of which were significantly below the peak strength of the intact clay (Figure 5.15) and along which only small displacements were required to reach residual strength.

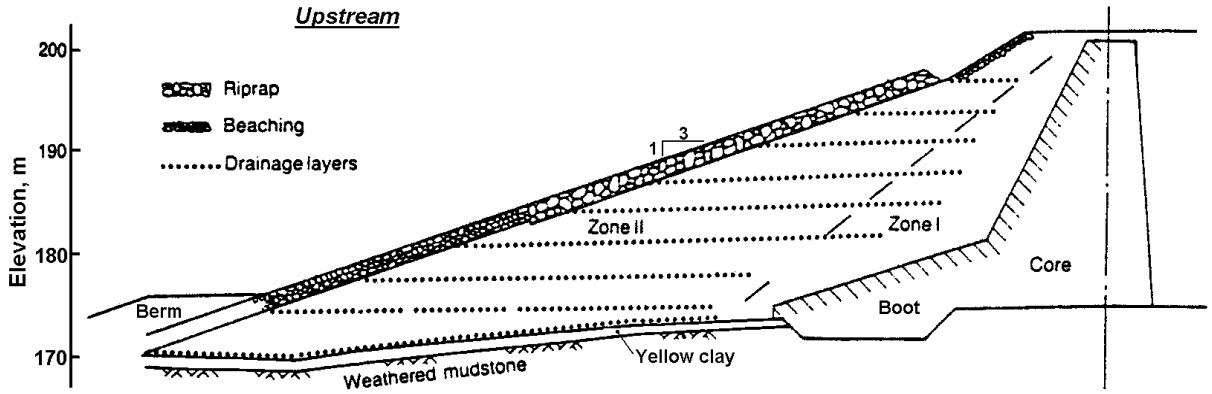

Figure 5.14: Carsington dam, section through the region of the initial failure at chainage 725 m (Skempton and Vaughan 1993).

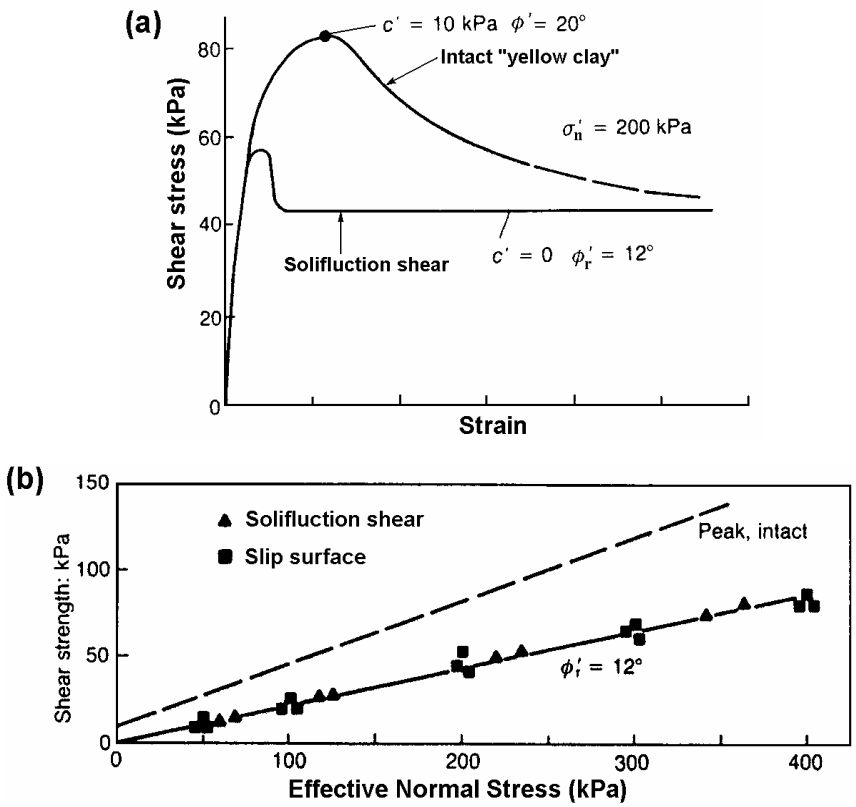

Figure 5.15: Carsington dam; drained strength properties of intact "yellow clay" and solifluction shears (Skempton and Vaughan 1993)

Potts et al (1990) undertook finite element analysis of the section at which the failure first occurred (chainage 725 m) using a non-linear elastic model with a Mohr-Coulomb yield criterion and incorporating strain softening as a function of the deviatoric plastic strain. The modelling showed that progressive failure was a significant factor in the mechanics of failure. A localised failure condition was initiated in the highly stressed lower portion of the wet placed core and boot structure when the embankment was about 5 m below its height at failure. With further raising of the embankment the localised failure zone propagated into the "yellow clay" foundation immediately upstream of the core boot structure. At failure (Figure 5.16) the shear strains along the eventual surface of rupture were not uniform. The strength conditions (Potts et al 1990) varied from:

- In the region incorporating the lower core and boot, and section of "yellow clay" upstream of the boot structure, the soils in the zone of high shear strain had been sheared beyond their peak strength and strain weakened to a strength between residual and peak.

- In the head and toe regions the stress states had not yet reached failure and therefore strengths were less than peak strength. In these regions a surface of rupture had not yet formed when the overall embankment had reached an unstable condition.

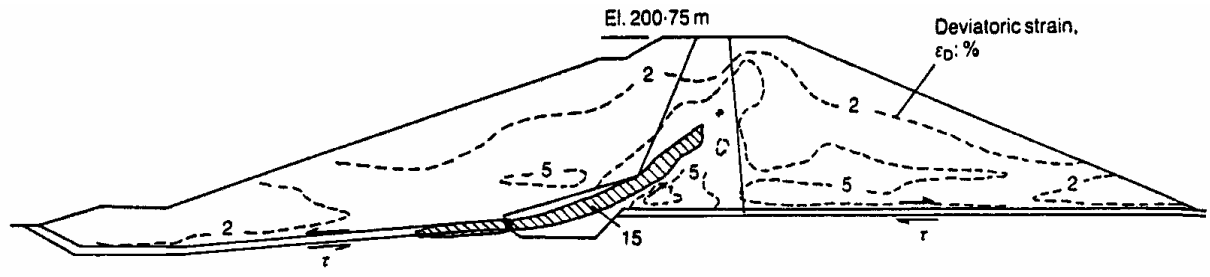

Figure 5.16: Contours of deviatoric strain predicted by finite element analysis at chainage 725 m prior to the failure of Carsington dam (Potts et al 1990).

Skempton and Vaughan (1993) commented that the solifluction shears within the "yellow clay" played a significant role in the progressive failure. Under the stress condition imposed on the foundation in the vicinity of the "boot" structure prior to failure, the reduced strength of the solifluction shears would mean that the stress capacity of the existing shears would be reached well before that of the intact clay. The existing shears could not support the increasing shear stresses due to embankment raising once their stress capacity had been reached, which would then be distributed to the edges of the defect and supported by the intact soil. The concentration of and increasing shear stresses at the margins of the defect as the embankment is raised will result in localised failure of the intact soil around the defect and extension of the defect into the intact soil. Whilst the orientation of the solifluction shears were not aligned with the eventual surface of rupture, the overall process would have led to progressive softening of the soil mass.

For the Carsington case study several issues are important in the context of the failure:

- Only limited deformations were observed in the toe region of the slide prior to failure. This is expected given that the effective stress state of the foundation in the toe region had not yet reached the failure surface and strengths were still less than peak strength.
- The failure was initiated in the highly stressed region of the embankment incorporating the lower portion of the wet core, boot and "yellow clay" foundation immediately upstream of the "boot", as the results of the finite element analyses

indicate. This is supported by the observation of plastic deformations in the lower portion of the core in the deepest section of the embankment from the internal vertical settlement gauges (Skempton and Vaughan 1993).

- Restraint on the lateral margins, due the lack of persistence of the "yellow clay" foundation and also due to changes in the topography, had a significant effect in supporting the unstable portion of the embankment and probably in suppressing the amount of deformation of the unstable portion of the slope prior to the actual failure and also in the post failure stage. Once the shear capacity on the lateral margins was reached, due to shedding of load from the failed region and also strain weakening on the margins, the velocity of the slide mass increased and the width of the slide increased significantly (refer Section 5.6.3.3 for discussion of the post failure deformation behaviour at Carsington dam).

5.5.2 FAILURES IN EMBANKMENTS DURING DRAWDOWN

The failure of embankments during drawdown is complex. It is complicated by: the embankment zoning geometry; variation in strength properties of materials under the stress conditions imposed; permeability variation within (horizontal to vertical permeability) and between different embankment zones; the response of the phreatic surface under the drawdown; the drawdown itself; and progressive failure. The effects of partial saturation and changes in degree of saturation as the wetting front progresses within the embankment adds further complexity to some of these aspects.

5.5.2.1 *Case Studies of Failures in Embankments During Drawdown*

For the case studies of failure during drawdown analysed, the categories of drawdown causing failure were:

- Failure on first drawdown, within 1 to 2 years after completion of construction (5 cases).
- Failure during the historically quickest and largest drawdown in the embankments history (4, possibly 5 cases).
- Failure during large drawdown, but historically not the largest drawdown (5, possibly 6 cases).
- Failure during a routine operational drawdown (4 cases).

Other notable aspects of the failure case studies were:

- All but one failure occurred within 35 years of construction or raising of the embankment, with most (16 of 19 cases) occurring within 20 years.
- Medium to high plasticity clays were the dominant material type within which the surface of rupture was located (10 of 15 cases).
- Failures occurred in upstream slopes ranging from as steep as 1.5H to 1V (horizontal to vertical) to flatter than 3H to 1V. The upstream slope angle was governed to some extent by material type in the outer upstream slope.

5.5.2.2 *Mechanics of Failure of Embankments During Drawdown*

The mechanics of failure of embankments during drawdown is, in a number of cases, simply a case of undrained instability of the upstream slope for the slope geometry, material strength properties and pore water pressure conditions as a result of the drawdown. Most of these failures are observed during the first drawdown or during the historically largest and/or fastest drawdown. Several features of these failures are worth highlighting:

- Failure occurred in at least two embankments (Lake Shelbyville and Old Eildon dams) where water was impounded during the period of construction. In both cases the slide existed prior to first drawdown, but the drawdown resulted in acceleration of the slide mass due to removal of the water load support.
- Failures during drawdown in sandy and gravelly soils occurred during very to extremely rapid drawdown; 2300 mm/hour over 2 hours at Forsythe dam, and > 500 mm/day at Pilarcitos dam.
- High construction pore water pressures in the outer upstream earthfill zones (discussed below) were significant for at least three failures that occurred within 1 to 2 years of completion of construction.

A number of failures from the case studies analysed did not occur during historically the largest and most rapid drawdown. Contributing factors to these failures include:

- Softening of over-consolidated embankment materials due to progressive strain weakening in undrained loading (discussed below).

- Softening due to saturation of partially saturated soils. An increase in saturation with time would effectively result in a decrease of the undrained strength due to reduction in matrix suction.
- Softening from deformation of the embankment during and post construction, e.g. crest spreading and crest cracking on first filling and under fluctuating reservoir operation.
- Increase in pore water pressures with time within the earthfill as the wetting front advances under high reservoir conditions (discussed below).
- Reservoir operation in the years prior to the failure. Pore water pressures are likely to be greater where the reservoir level has been maintained at a high level in the years preceding a large drawdown than in the case of large seasonal drawdowns or periods of low reservoir level in the preceding years. For most of the case studies no information on prior operation of the reservoir is available.
- Possible breakdown of rockfill in the outer zones. This is considered to have had a small influence in the failure case studies analysed but it may not be possible to ignore its influence.

(a) Influence of construction pore water pressures and reservoir support

The critical period of stability for embankments constructed of wet placed earthfills or on foundations of low undrained strength is during and shortly after construction. The high proportion of failure case studies that occur during construction involving wet placed earthfills or earthfill layers and weak foundations are evidence of this.

The failures in the upstream slope at Mondely, Lake Shelbyville and Dam FC10 are considered to be cases of undrained instability due to the low undrained shear strength of wet placed earthfill zones or wet placed earthfill layers. At Lake Shelbyville and Dam FC10 the failure was evident during or shortly after the end of construction. In both these cases water was impounded during the latter stages of construction and acceleration of the slide was thought to be associated with drawdown (the acceleration occurred within 1.5 years of the end of construction). At Mondely dam it is possible that the drawdown triggered the slide, but it is not evident if water was impounded during the latter stages of construction. It is possible that in all three cases the water load on the upstream face supported the slope during the latter stages of construction, and on drawdown this support was removed resulting in either acceleration of the existing slide or the slide itself.

The wet placed earthfills or earthfill layers in each case study were of medium to high plasticity and were reasonably well to heavily compacted. In the case of Mondely dam, dissipation of construction pore water pressures was very slow and they were still evident more than 10 years after construction. This very slow dissipation of construction pore water pressures is typical in these well compacted, medium to high plasticity clayey soils.

The slide at Old Eildon dam also involved accelerated of the existing slide on removal of the water load support.

(b) Time to establish equilibrium phreatic surface

The pore water pressure conditions within the embankment at the time of drawdown are an important factor in stability under drawdown. For partially saturated soils, advancement of the wetting front within the embankment affects the effective stress conditions as a result of the change in pore water pressure conditions, the reduction in undrained strength of the materials as matric suction is reduced and possibly softening due to swelling on saturation. Therefore, the time to reach an equilibrium phreatic surface can be a factor in the timing of instability under drawdown for embankments; particularly for partially saturated earthfills of low permeability placed in the upstream shoulder.

Sampna Tank, a zoned earthfill embankment with an upstream earthfill zone of medium to high plasticity clays and upstream slope of 2H to 1V, is considered one such example. Failures in the upstream slope occurred under drawdown 4 and 7 years after the end of construction.

The records of pore water pressure monitoring in the upstream slope of several embankments allow for estimation of the time to reach equilibrium conditions for embankments constructed of low permeability fills in the upstream slope. Fell (2002) comments that, based on his experience, a steady state condition may not be reached for 20 to 30 years after construction for large dams.

Of the failure case studies analysed, the maximum vertical depth to the surface of rupture, where measurable, ranged from 5 to 12 m in most cases. The deep-seated failures at San Luis dam and Old Eildon dam, both of which involved the foundation, are exceptions. Therefore, in the majority of cases, the significant issue is the time for development of near steady state conditions for distances of penetration (measured

perpendicular to the embankment face) up to about 10 m into the upstream face. The results of piezometric records for three embankments analysed indicates:

- For Dam FD2 (earthfill embankment constructed of medium plasticity clays) observation well records, although difficult to interpret, indicate relatively steady levels in the outer earthfill (outer 10 m) within 10 to 15 years. In the central to upstream section of the embankment significant longer time periods were required to reach steady conditions, much greater than 20 years.
- For Dam FD3 (earthfill embankment constructed of low plasticity clays in the failure section) pore water pressures in the outer section of the earthfill (outer 10 m) were relatively steady some 10 years after construction. Further toward the central embankment section pore water pressures were relatively steady some 15 to 30 years after construction.
- For San Luis dam (zoned earth and rockfill embankment with core of well compacted, medium plasticity sandy clays) piezometer records indicate the pore water pressures in the outer section of the broad central core (outer 10 to 20 m) were relatively steady some 15 years after construction. Further toward the central core section pore water pressures were relatively steady some 15 to 25 years after construction.

Clearly three cases is not sufficient on which to base assumptions regarding pore water pressures in the outer upstream zone of low permeability clayey earthfills. However, all three cases do indicate that pore water pressures in the outer 10 m zone (the zone of interest for most cases of upstream slope instability on drawdown) reach virtually steady conditions within 10 to 15 years for clays of low to medium plasticity.

It could be tentatively concluded that the influence of rising pore water pressures due to the advance of the wetting front have a negligible effect on the case studies constructed of low permeability earthfills in the upstream shoulder that failed after more than 10 years of operation.

(c) Progressive Strain Weakening in Undrained Loading

Stark and Duncan (1987, 1991) undertook back-analysis of the failure during drawdown at San Luis dam (Figure 5.17). Their analysis incorporated a rigorous analysis of pore water pressure response under drawdown. To achieve a calculated unstable slope condition, drained strength properties below fully softened for the fissured foundation

(fissured due to desiccation but not slickensided) and close to (but above) fully softened strength for the embankment materials were required. They considered that progressive failure was a significant factor in the failure, particularly within the high plasticity slopewash foundation, where strain weakening occurred under the higher stress conditions imposed under large drawdown events that preceded the failure.

The drawdown resulting in failure of San Luis dam and prior large drawdowns are shown in Figure 5.18, along with the drawdowns of Dams FD2 and FD 3. The failure at Dam FD2 (Figure 5.18a) clearly occurred during the largest and most rapid drawdown event in the history of the reservoir operation. At San Luis dam, the drawdown during which failure occurred in 1981 was historically the largest and fastest, but was preceded by a significant drawdown in 1976.

For Dam FD3, failure occurred during a relatively large drawdown in 1931 but was preceded by drawdowns both faster in rate of drawdown and larger in depth of drawdown. Cracking of the crest was observed in Dam FD3 following the large drawdown in 1928, indicating that the upstream shoulder was of marginal stability under large drawdown. No significant rainfall was recorded in the months leading up to the slide and no rainfall was recorded in the days prior to the slide, so pressures due to water infilled cracks did not contribute to the failure.

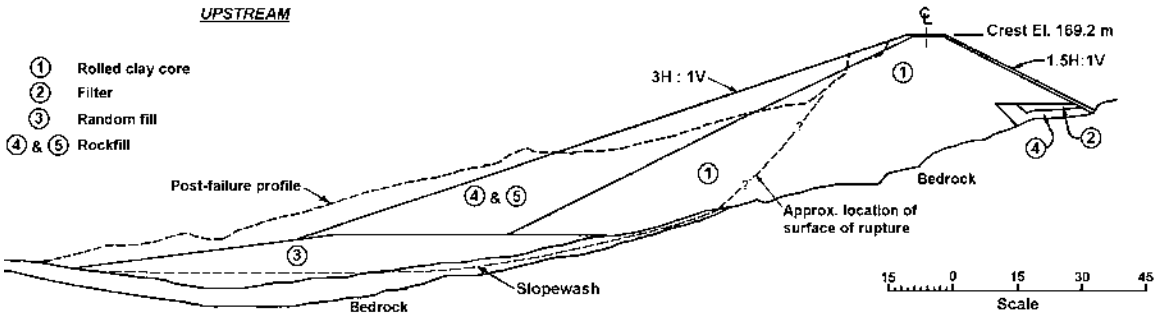

Figure 5.17: Section through the failure in the upstream shoulder at San Luis dam (courtesy of U.S. Bureau of Reclamation).

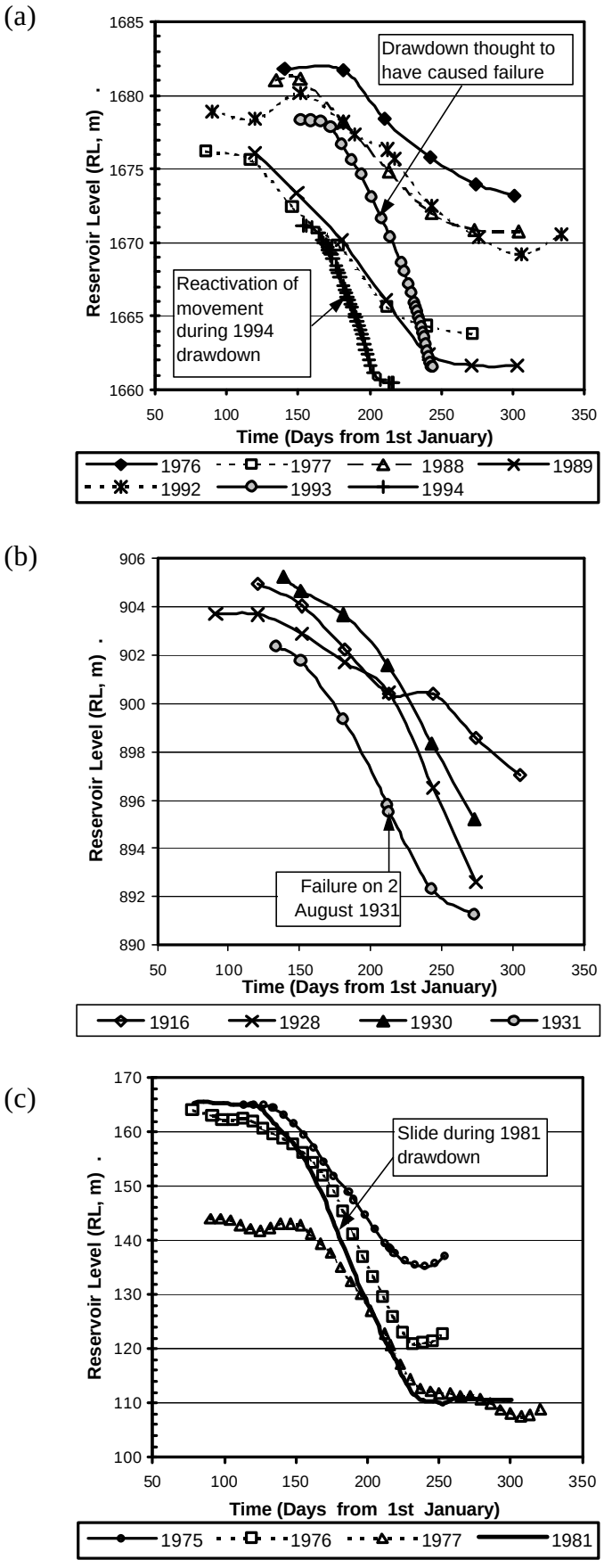

Figure 5.18: Drawdown causing failure and prior large drawdowns for *(a)* Dam FD2, *(b)* Dam FD3, and *(c)* San Luis dam.

It is considered that progressive strain weakening in undrained loading is significant in the failures during drawdown of embankments constructed with upstream shoulders or broad central cores of over-consolidated clay earthfills. The stress conditions imposed under large drawdown events (preceding the failure) are considered to cause shear stress induced reduction of pore water pressures in highly stressed regions in the embankment, resulting in the development of differential pore water pressure conditions in the shoulder. Migration of moisture to these regions of shear stress induced low pore water pressure will lead to dilation and softening in undrained strength.

This progressive failure mechanism could explain why in a number of failure case studies that failure occurred on large, but historically not the largest or most rapid drawdown as well as the relatively low drained strengths (less than peak strength) for earthfill obtained by back analysis of cases such as San Luis dam.

5.5.2.3 *Limit Equilibrium Analysis of Slope Stability Under Rapid Drawdown*

Duncan et al (1990), recognising the significance of progressive strain weakening in undrained loading under cyclic reservoir operation, recommended the use of a composite drained and undrained strength envelope (Figure 5.19) for assessment of the strength properties for limit equilibrium analysis under drawdown for embankments zones that are partly or non free draining. At low stress levels, where on shearing in undrained loading a reduction in pore water pressures will develop, Duncan et al recommend using the drained strength envelope, and at higher stress level, where positive pore water pressures may develop on shearing, they recommend using the undrained strength envelope. For the zones above the normal maximum reservoir operating level, Duncan et al (1990) recommend using undrained strengths allowing for the effects of softening and cracking.

As an example, consider that a compacted clay earthfill (in a homogeneous embankment) has peak drained strength properties of c′ = 10 kPa and f' = 30 degrees and undrained strength properties (assuming saturated) approximated by S_u = 75 kPa and f_u = 6 degrees (note that the undrained strength properties will vary dependent upon the variation in K_o and A_f with confining stress). The composite strength envelope is as shown in Figure 5.20. The effective normal stress at which the envelopes intersect is about 140 kPa. Assuming K_o = 0.7 at this effective stress, this relates to an effective

vertical stress of close to 160 kPa or roughly 16 m assuming a saturated unit weight of 20 kPa (based on effective stresses).

In this example, which is not atypical say for a well compacted rolled clay earthfill, the zone of the upstream slope within which most slope failures occur (i.e. 5 to 12 m) is within this over-consolidated zone of the earthfill. Thus, undrained strain weakening, according to the concept discussed in Section 5.5.2.2, could occur under the stress conditions associated with drawdown in the outer over-consolidated upstream slope. The effect of this reduction in undrained strength within the developing shear band is shown on Figure 5.20.

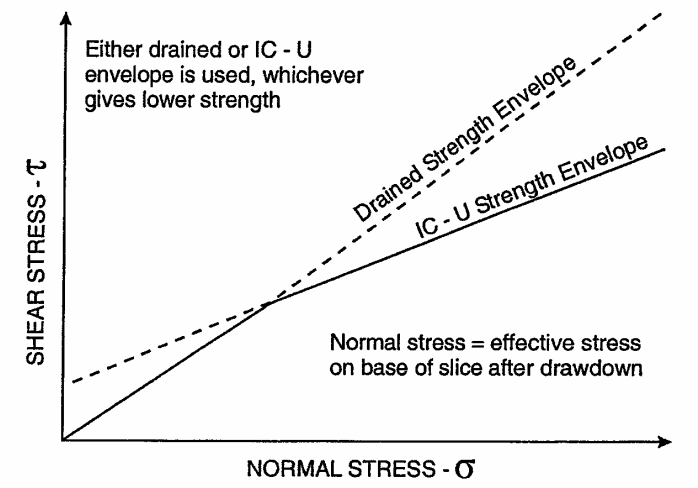

Figure 5.19: Composite shear strength envelope (Duncan et al 1990).

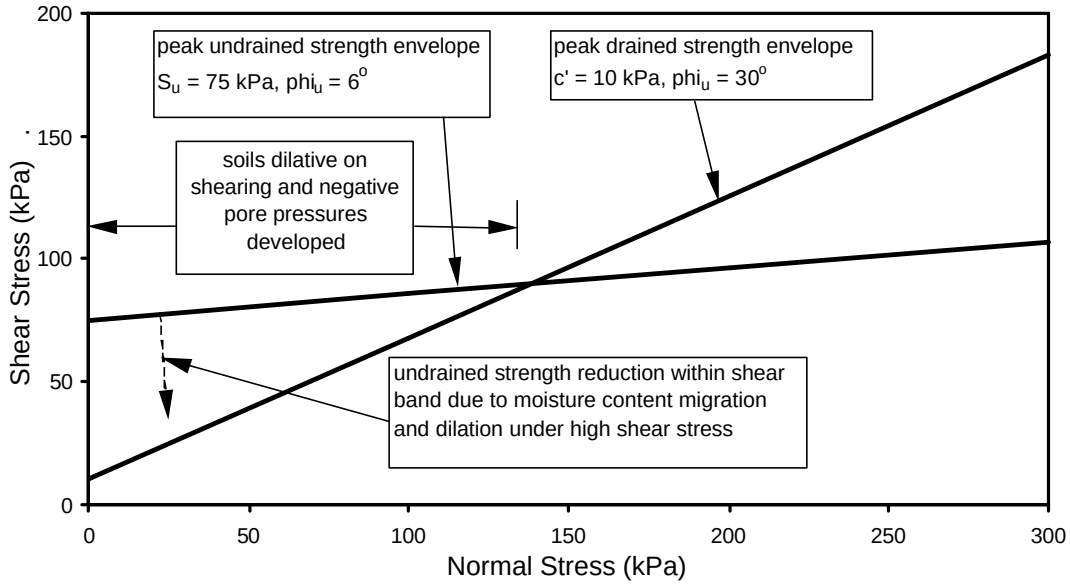

Figure 5.20: Effect of moisture migration on the undrained strength within the shear band using idealised strength parameters.

5.5.3 POST CONSTRUCTION FAILURES IN THE DOWNSTREAM SLOPE OF EMBANKMENTS

Most failures in embankment dams that occur in the downstream shoulder post construction are considered to be related to changes in effective stress conditions and material strength properties due to changes in pore water pressure conditions, and seepage pressures in development of the phreatic surface under the impounded reservoir (discussed below). Consideration should also be given to the potential for progressive failure in heavily over-consolidated earthfill and foundation materials.

5.5.3.1 Embankment Zoning, Material Type and Slope Geometry

For most of the down-slope post construction failure case studies information on the actual slide and material properties is limited. The following discussion therefore concentrates on the embankment types, material types and slope geometry within which the failures occurred.

(a) Embankment type

For post construction failures in the downstream slope, the dominant embankment type (Table 5.7) consisted of homogeneous earthfill embankments (5 possibly 7 of 13 cases). But, the most notable observation from the failure case studies is the absence of embankment filters or downstream more permeable zones in the embankment design and zoning. The high proportion of failures in the downstream shoulder post construction in these embankments types is most likely related to the high phreatic surfaces developed within the embankment and uncontrolled seepage conditions.

(b) Location of the surface of rupture and material type

Of the thirteen failure case studies, three were known to be located within the embankment only, six through the embankment and foundation, and in four cases it was not known if the surface of rupture passed through the foundation. In both the zoned earthfill and zoned earth and rockfill cases, the surface of rupture passed though the central core and foundation.

The embankment and foundation material types through which the surface of rupture passed were dominantly clay soils (Table 5.9). In at least eight of the thirteen cases the embankment materials were of medium to high plasticity clays. For the slides

that were known to pass through the foundation, the foundation comprised medium to high plasticity clays in at least four of the six cases.

The high proportion of post construction failures in the downstream shoulder that incorporate medium to high plasticity clays is considered to be associated with the greater loss in strength on wetting from a partially saturated condition. But, it may simply reflect that these soils are commonly used in dam construction.

Table 5.9: Material types through which the surface of rupture passed of post construction failures in the downstream shoulder.

Material Type **(within which the surface of rupture passed)**	**Embankment Type**	**Foundation** **(where surface of rupture known or possibly passed through the foundation)**
High plasticity clays	4 cases (2 homogeneous earthfill, 1 zoned earthfill and 1 zoned earth and rockfill)	3 cases, all failures known to be through the foundation.
Medium plasticity clays	4 cases (3 homogeneous earthfill and one puddle core earthfill).	1 case, known to be through the foundation.
Low plasticity clays	1 case (homogeneous earthfill)	1 case, known to be through the foundation.
Clays, plasticity not known	2 cases (both homogeneous earthfill)	4 cases, 1 known to be through the foundation, 3 possibly through the foundation.
Clayey sands	1 case (homogeneous earthfill)	1 case, possibly through the foundation
Gravelly Soils (GP/GW)	1 case (homogeneous earthfill)	None.

(c) Downstream slope angle

The steepness of the downstream shoulder is considered to be a significant factor in the incidence of sliding, although it is difficult to quantify due to the combined influence and variability of material strength properties and pore water pressures. For most of the case studies of post construction instability in the downstream slope, the down-slope was equal to or steeper than 2H to 1V (26.6 degrees).

In the case of Arroyito dam the slope was 2.5H to 1V, however, it is considered likely the failure was a sloughing type failure in sandy gravels with fines content of up to 10%. In the case of the Seven Sisters dyke (zoned earth and rockfill) and Aran dam (zoned earthfill) the failures were of Type 5 slope failure geometry through the high

plasticity clay foundation (i.e. deep seated failures where the surface of rupture extended below and beyond the toe of the embankment). Therefore the downslope angle was not as significant for the Type 1 and Type 2 slope failure geometries (failures within the shoulder or possibly along the embankment / foundation interface; refer to Figure 1.3 in Section 1.3 of Chapter 1 for definitions of slope failure geometry).

5.5.3.2 Seepage Related Failures

In nine of the thirteen case studies (Arroyito, Barton, Woodrat Knob, Fruitgrowers, Santa Ana, Siburua, Great Western, Aran and Lake Yosemite dams), post construction instability of the downstream slope was considered to be directly related to a high phreatic surface and or uncontrolled seepage in the embankment or foundation. Importantly, in at least seven of these cases the slide occurred at a time when the reservoir level was at close to full supply level and in at least six cases seepage was observed on the downstream slope. The likely intra and inter layer permeability variation of the embankment materials ($k_h > k_v$, where k_h = horizontal permeability and k_v = vertical permeability), and absence of embankment filters or downstream more permeable zones to intercept lateral seepage is likely to have been a significant factor for a number of these failure cases.

The timing of these failures (Table 5.10) was generally within 25 years of initial construction or within 2 years of raising of the embankment. The slide at Lake Yosemite dam (60 years after construction) is the exception in terms of timing. The strong coincidence between the timing of the slide and high reservoir level most probably indicates that the trigger for the slide, in most cases, is increasing pore water pressures within the embankment and/or foundation.

5.5.3.3 Failures not Directly Attributable to Seepage

Sliding in four of the case studies (Seven Sisters, Yuba, Park Reservoir and Harrogate dams) was considered not directly attributable to seepage and high phreatic conditions associated with seepage of impounded water from the reservoir. The mechanics of and trigger for failure in these cases was considered to be:

- Failure in undrained loading. At Seven Sisters dyke (Peterson et al 1957), a zoned earth and rockfill embankment, 13 failures were recorded over a period of seven

years from the end of construction. The surface of rupture passed through the high plasticity, wet placed core and high plasticity firm to stiff clay foundation. The mechanism of failure is considered to be in undrained loading, and probably influenced by the wetting up and softening of the upper fissured foundation due to advance of the wetting front.

Table 5.10: Timing of the failure for post construction slides in the downstream shoulder.

Timing of Slide (years after construction)	**No. Cases**	**Comments**
Within 1 year	2	Seven Sisters – surface of rupture through wet placed CH core and soft CH foundation. Aran dam - surface of rupture through CH core and weak CH foundation. The slide occurred when the reservoir was at its highest historical level.
Within 2 years (of recent embankment raise)	3	At Great Western and Fruitgrowers dams the slide occurred when the reservoir was at an historical high level after the recent embankment raise. Seepage on the downstream face was observed at Yuba and Fruitgrowers. At Yuba the failure was triggered by earthquake.
Within 5 to 10 years	3	At Woodrat Knob and Arroyito dams seepage was observed on the downstream shoulder. At Arroyito and Siburua dams the slide occurred (or was initiated) when the reservoir was close to full supply level.
Within 10 to 25 years	2	The slide at Santa Ana and Barton dams occurred when the reservoir was close to full supply level. In both cases seepage was observed on the downstream shoulder.
More than 50 years	3	The failure at Harrogate was triggered by rainfall. At Yosemite dam seepage occurred through the foundation.

Note: CH = high plasticity clay

- Earthquake trigger. The slide at Yuba dam (homogeneous earthfill constructed of medium plasticity sandy clays) was triggered by earthquake. It is considered that the relatively steep downstream shoulder (slope of 1.75H to 1V) was possibly of marginal stability prior to the earthquake, and the earthquake was sufficient to trigger the failure. Seepage was observed to emanate from the downstream slope prior to the raise in 1949.

- Rainfall trigger. The slide at Harrogate dam (puddle core earthfill embankment) and possibly Park Reservoir dam (homogeneous earthfill constructed of clayey sands) were triggered by rainfall. At Harrogate dam the slide occurred during winter following the wettest monthly (and yearly) rainfall period on record since embankment construction. The deep shrinkage cracks in the medium plasticity downstream shoulder fill (Davies 1953) contributed to the instability by allowing ready access of water to the earthfill. At Park Reservoir the slide occurred in the upper portion of the downstream slope above the rockfill toe, and seepage and possibly rainfall may have affected the stability of the steep (1.5H to 1V) downstream slope.

Degree of compaction of earthfill materials is also an important factor for consideration in the stability of the downstream slope. Saturation of poorly compacted earthfills initially placed in a partially saturated condition will result in a large loss in undrained strength. The deformation behaviour at the Hume Dam No. 1 embankment (Cooper et al 1997) is an example of the effect of saturation of poorly compacted earthfill. The earthfill shoulders of the concrete corewall embankment, constructed from 1921 to 1936, were of low to medium plasticity sandy clays and clays, and were poorly compacted by horses hooves and cartwheels. Investigations of the downstream slope in the 1990's, undertaken due to concern over the large observed deformations, indicated that saturation of the lower portion of the downstream earthfill had reduced the undrained strength consistency from an initially very stiff condition when partially saturated to much lower strengths consistent with normally consolidated behaviour.

Cooper et al (1997) considered that the saturation occurred due to seepage and leakage following construction. Their analysis showed that the embankment deformations observed and low factor of safety of the downstream slope at periods of high reservoir level were due to saturation and the resultant strength reduction in the lower portion of the downstream earthfill. Undrained strain weakening on shearing in the saturated earthfill layer was used in their numerical model to explain the observed deformation behaviour. When residual strength was used within this saturated layer in the downstream shoulder, their limit equilibrium analysis showed the factor of safety of the approached unity under full supply conditions.

5.6 POST FAILURE DEFORMATION BEHAVIOUR – FAILURES IN EMBANKMENT DAMS

This section presents the post failure deformation behaviour for the case studies of failures in embankment dams. Data on travel distance and travel velocity of the case studies is presented, and the factors affecting the deformation behaviour of the slide mass are discussed. Greater detail is given for several case studies to highlight some of the factors affecting the post failure deformation behaviour.

5.6.1 FACTORS AFFECTING THE POST FAILURE DEFORMATION

As a prelude to presentation of the case study data, several important factors affecting the post failure deformation of the case studies (both embankment dams and cuts in heavily over-consolidated high plasticity clays) are summarily introduced. Further discussion on their influence is given in the following sections and in Section 5.7 for cuts in heavily over-consolidated high plasticity clays. The factors are:

(i) The potential for strain weakening of the soil on shearing post failure, as discussed in Section 5.2.3.

(ii) Slope failure geometry. The slope failure geometry directly affects the potential energy of the slide mass. Type 1 geometries have greater potential energy than Type 2 geometries and in turn Type 5 geometries (refer Figure 1.3 in Section 1.3 of Chapter 1 for slope failure geometry definitions).

(iii) Orientation of the surface of rupture. For a given material and given slope failure geometry the orientation of the surface of rupture has a significant effect on the post failure deformation behaviour. For example, a Type 1 geometry with steep basal angle of the surface of rupture (Figure 5.21a) has the potential for greater travel distance at higher velocity than for a surface of rupture with near horizontal basal angle (Figure 5.21b). In the former case the slide has the potential to realise its potential energy, and in doing so a significant amount of the potential energy may be dissipated as kinetic energy resulting in acceleration of the slide mass and relatively large travel distance. In the latter case the slide may not realise its potential energy and most, if not all, of the slide mass may remain in the source area and only travel a short distance.

(iv) Brittleness associated with the slide mechanism (e.g. internal brittleness or toe buttressing) and release of the slide on the lateral margins. Some of the potential energy that becomes available from these sources will be redistributed to kinetic energy resulting in acceleration of the slide mass.

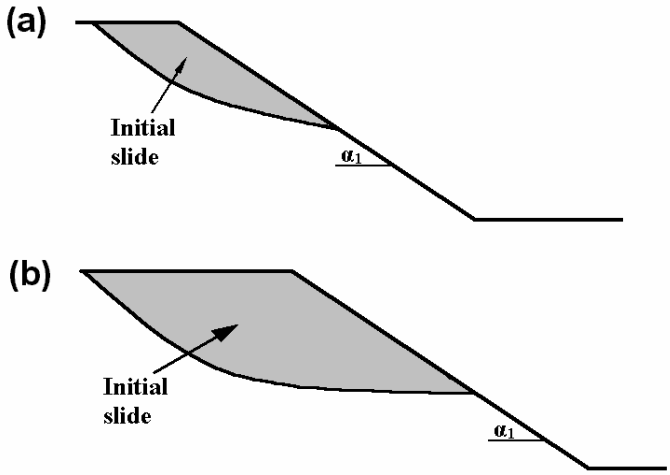

Figure 5.21: Type 1 failure slope geometries with different surface of rupture orientations.

5.6.2 SUMMARY OF CASE STUDIES OF FAILURES IN EMBANKMENT DAMS

Of the fifty-four embankment dam case studies, the failures during construction generally have better quality and more detailed information on material properties and deformation behaviour. This is due mainly to the early detection of the failure from observation of warning signs (e.g. cracking) or monitoring, and then further close observation and monitoring as the slide progressed, as well as the level of investigation generally undertaken post failure. Therefore, discussion of the post failure deformation behaviour and on the factors influencing the deformation is more substantial for the failures during construction than for the failures during drawdown and post construction in the downstream shoulder.

Table 5.11 presents a distribution of slide volume for the case studies. The failures during construction are generally of greater volume and the post construction slides in the downstream slope generally of the smallest volume. This is reflected in the typically greater slide depth and width of the failures during construction.

Table 5.11: Distribution of slide volume for slides in embankment dams.

Timing of Slide	**No of Cases**	**Slide Volume (where known or possible to estimate)**			
		= 5,000 m^3	**> 5,000 and = 50,000 m^3**	**> 50,000 and = 500,000 m^3**	**> 500,000 m^3**
During construction	22	none 0%	5 (of 15) 33%	5 (of 15) 33%	5 (of 15) 33%
Post-construction, on drawdown	19	none 0%	6 (of 9) 67%	2 (of 9) 22%	1 (of 9) 11%
Post-construction, downstream slope	13	9 (of 12) 75%	1 (of 12) 8%	2 (of 12) 17%	none 0%

5.6.3 FAILURES DURING CONSTRUCTION - POST FAILURE DEFORMATION BEHAVIOUR

Table 5.12 and Table 5.13 present a summary of the embankment geometry, material properties and deformation behaviour of the twenty-two case studies of slope instability in embankment dams during construction; Table 5.12 for failures within the embankment only and Table 5.13 for failures through the embankment and foundation. Of the failure case studies, nineteen were observed during the placement of fill materials and the other three cases were not observed or recognised until shortly after construction had been completed (Lake Shelbyville, Dam FC10 and Scout Reservation dams). In addition, three of the case studies (Otter Brook, Skiatook and Truscott dams) were not considered as failures and have been classified as cases of lateral bulging due to the low moduli of wet placed earthfills.

The post failure deformation and estimated maximum velocity of the slide mass for the failures during construction are presented in Figure 5.22 and Figure 5.23 respectively. Where possible the velocities have been determined from reported deformation monitoring results, but in a number of cases has been estimated based on the amount of deformation and qualitative information on the times over which the deformation occurred. In general, these latter estimates are broad range as indicated by the range given in Figure 5.23.

Table 5.12: Summary of failure case studies in embankment dams during construction – failures within the embankment only

Name of Dam	Year of Failure	Slope Failure Geometry	Embankment Geometry (at failure)			Const n Rate, (mm/day)	Material Properties (in zone of the surface of rupture)			Summary of Post Failure Deformation			Comments
			Emb Type	Hgt (m)	Slope (°) *5		ASCS *1 Class n	Comp n Rat g *2	Moisture (%) *3	Deform n (m)	Velocity *4 (mm/day)	Category	
Punchina	1980	Type 1	E'fill – rock toe (2,0,0)	45	26.6 (d)	570 to 1500	SM – silty sand	2	4.1% wet	1.57	250 to 350	slow	Lateral bulging of downstream shoulder during construction.
Troneras	1962	Type 1	E'fill - filters (1,1,1)	31.5	18.4 (d)	360 to 1330	ML –sandy silt, med. plasticity	2	4.0% wet	unk	600 (high ?)	Slow to moderate	Lateral bulging of downstream shoulder during construction.
Muirhead	1941	Type 1	Puddle E'fill (8,0,1)	21.3	21.8 (u)	85 at failure	CL – med. plasticity sandy clay core and CL/SC shoulders.	1	well wet of OMC	2.1	40 to 115	Slow	Failure of upstream shoulder incorporating core and upstream earthfill.
Waghad	1884	Type 2 (?)	Homog (0,0,0)	32	26.6 (u)	240	CH/MH – high plasticity	1	6% wet	15.2	unk	Moderate	Failure in upstream shoulder during reconstruction of gorge section.
Dam FC10	1937	Type 1	Zoned E&R (4,0,0)	19.5	22 avg (u)	60	CH earthfill, SC/SM random fill and outer rockfill.	2	4.5% wet	2.8	unk	Slow to moderate	Failure in upstream shoulder shortly after end of construction. Affected by reservoir level fluctuation.
Otter Brook	1957	Type 1	E'fill - filters (1,1,1)	40.5	21.8 (u)	470 (max.)	SC – clayey fine sand	3	0.6% dry (20% > 1% wet)	0.88	40	slow	Lateral bulging of upstream shoulder during construction.
Truscott	1981	Type 1	E'fill - filters (1,1,1)	30	18.4 (d)	360 (max.)	C? – clayey, plasticity unk.	unk (3 ?)	Spec ± 2%	0.84	20	Slow	Lateral bulging of downstream shoulder during construction.
Skiatook	1982	Type 1	E'fill - filters (1,1,1)	33.8	16 (d)	230	C? – clayey, plasticity unk.	unk (3 ?)	Spec ± 2%	0.79	23	Slow	Lateral bulging of downstream shoulder during construction.
Lake Shelbyville	1970	Type 1	E'fill - filters (1,1,1)	33	21.8 (u)	100	CL – sandy clay, med. plasticity	3	0.1% wet	0.39	24	Slow to very slow	Failure in upstream shoulder after the end of construction. Affected by reservoir level fluctuation.
Scout Reservation	1984	Type 2	E'fill - filters (1,0,1)	13.7	26.6 (u)	30 (?)	CL – silty clay, low to med. plasticity	unk (3 ?)	unk	1.8	10	Slow	Failure in upstream shoulder after the end of construction. Latter part of deformation affected by infiltration of rainfall into cracks.
Acu	1981	Type 2	Zoned E&R (4,1,1)	34.8	21.8 (u)	unk	CH (?) earthfill in core and under upstream rockfill.	unk (3 ?)	Lower wet, then ± OMC	25	1.2×10^6	Rapid	Failure in upstream zoned earthfill shoulder. Passed through wet clay fill zone under upstream shoulder.

Note: Notes to Table 5.12 follow Table 5.13.

Table 5.13: Summary of failure case studies in embankment dams during construction – failure within the embankment and foundation

Name of Dam	Year of Failure	Slope Failure Geometry	Embankment Geometry (at failure)			Earthfill Properties (in zone of surface of rupture)		Foundation Properties (through which surface of rupture passed)	Summary of Post Failure Deformation			Comments
			Emb Type	Hgt (m)	Slope (^{o}) *5	Description *1, *3	Comp n Rat g *2		Deform n (m)	Velocity *4 (mm/day)	Category	
Waco	1961	Type 5	E'fill - filters (1,1,1)	25.9	19.7 (d)	CL (?) – sandy and shaly clays.	3	CH - bentonitic clay bedding defect, pre-sheared	1.57	250 to 350	slow	Deep seated compound slide in the downstream shoulder.
Dam FC21	1969	Type 5	Zoned E'fill (3,1,1)	43	18.4	SC/GC – clayey sands and gravels, 0.2% dry OMC	3	CH - bentonitic shear zones, pre-sheared.	0.9	unk	Slow to very slow	Lateral spreading of foundation, no surface expression of deformation.
West Branch	1964	Type 5	E'fill - filters (1,0,1)	21.5	14 (u)	CL (?) – "impervious fill"	unk (3 ?)	CL – silty clays of low to medium plasticity, soft to stiff.	0.76	21	Slow	Deep seated failure in upstream shoulder, limited to closure section.
North Ridge	1953	Type 5	E'fill - filters (1,1,1)	18.3	12.5 (d)	CL – low plasticity clays, 0.1% dry OMC	3	CH – high plasticity clays, firm to stiff.	1.37	unk	Moderate (?)	Deep seated compound failure in downstream shoulder.
Marshall Creek	1930	Type 5	E'fill – rock toe (2,0,0)	24.4	20.5 (d)	CL (?) – "impervious fill"	unk (2 or 3 ?)	CL/CH (?) – silty clays, variable consistency, soft to firm (?)	15	1.5×10^6	Rapid	Deep seated compound failure in downstream shoulder. Possible flow liquefaction of loessic soils in foundation.
Chingford	1937	Type 2	Puddle E'fill (8,0,1)	7.9	21.8 (d)	CH clays for core and shoulder fill.	Puddle (1 outer)	CH – high plasticity, soft to very soft.	4.3	unk	moderate	Compound failure in downstream shoulder.
Hollowell	1937	Type 5	Puddle E'fill (8,1,1)	11.4	14 (d)	CH for core, sandy soils in shoulder.	Puddle (1? outer)	CL/CH (?) – soft to very soft clay layer in foundation.	0.49	unk	Slow	Deep seated compound failure in downstream shoulder.
Lafayette	1928	Type 5	Zoned E'fill (3,0,0)	35.5	20 (d)	CL/CH (?) – clayey soils placed dry of OMC	2 to 3	CH – high plasticity sandy clays	10	2000	Moderate	Deep seated compound failure in downstream shoulder.
Galisteo	1970	Type 5	Zoned E'fill (3,1,1)	38.5	17.5 (u)	CL – low to medium plasticity sandy clays, placed ± OMC	3	CL/CH (?) – clay stratum, firm to stiff.	2	50	Slow	Deep seated compound failure in upstream shoulder.
Park Reservoir	1981	Type 2 (?)	Zoned E'fill (3,1,1)	21.3	19.7 (u)	CL (?) – lacustrine clays, shoulder is of sandy moraine	unk	CL (?) – lacustrine varved clays and silts.	0.9	unk	Slow to moderate	Compound failure in upstream shoulder.
Carsington	1984	Type 2	Zoned E'fill (3,0,1)	28	18.4 (u)	CH core zone (8% wet of OMC) with shoulders of weathered mudstone (SC/CL)	3	CH – high plasticity clays, heavily over-consolidated, solifluction shears.	18.1	17000 to 24000	Moderate	Compound failure in upstream shoulder. Passed through wet central core and clay foundation.

Note: See next page for notes to Table 5.13.

Notes for Table 5.12 and Table 5.13:

Emb = embankment Hgt = height Class [n] = classification
Const [n] = construction Comp [n] – Rat [g] = compaction rating (see *[2])
Homog = homogeneous earthfill embankment
E'fill – filters = earthfill embankment with filters
E'fill – rock toe = earthfill embankment with rock toe
Puddle E'fill = puddle core earthfill embankment
Zoned E'fill = zoned earthfill embankment
Zoned E&R = zoned earth and rockfill embankment
OMC = Standard optimum moisture content
*[1] Soil classification to the Australian soil classification system (AS 1726-1993)
*[2] Compaction Rating, 1 = no formal compaction, 2 = rolled moderate compaction, 3 = rolled well compacted.
*[3] = moisture contents of earthfill are relative to Standard optimum moisture content (OMC).
*[4] = IUGS (1995) velocity class, refer Table 1.1 in Section 1.3 of Chapter 1.
*[5] (d) = downstream slope, and (u) = upstream slope.

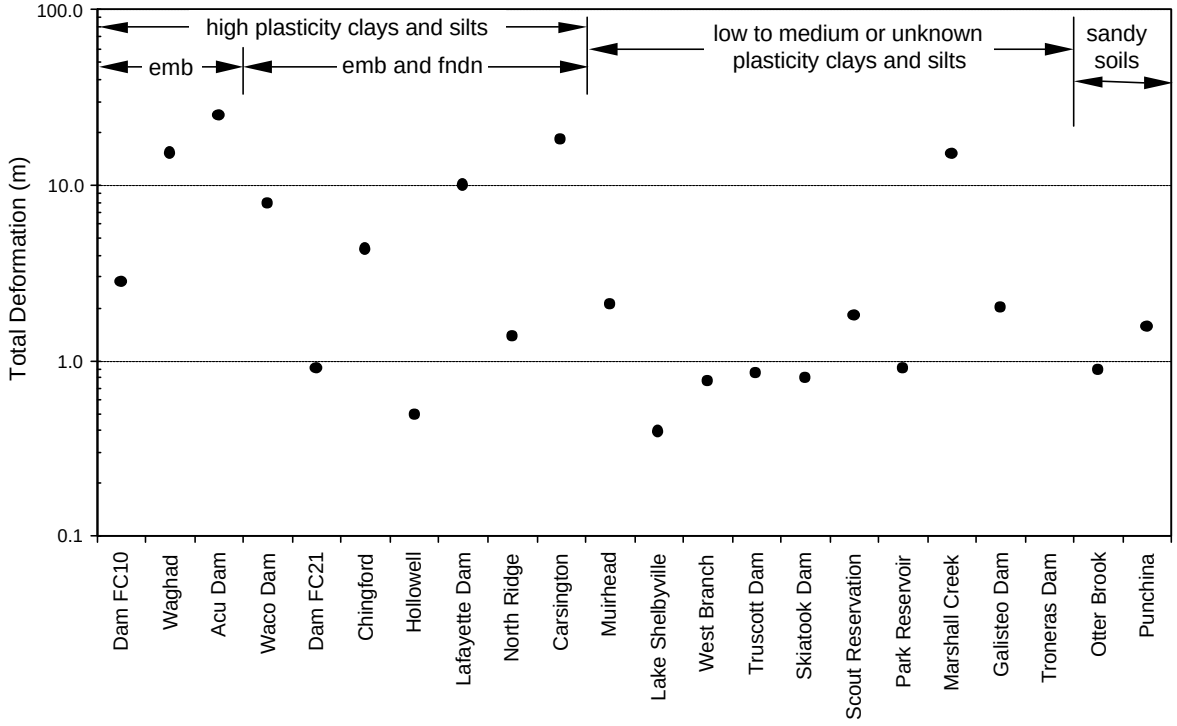

Figure 5.22: Total post-failure deformation for slides in embankment dams during construction.

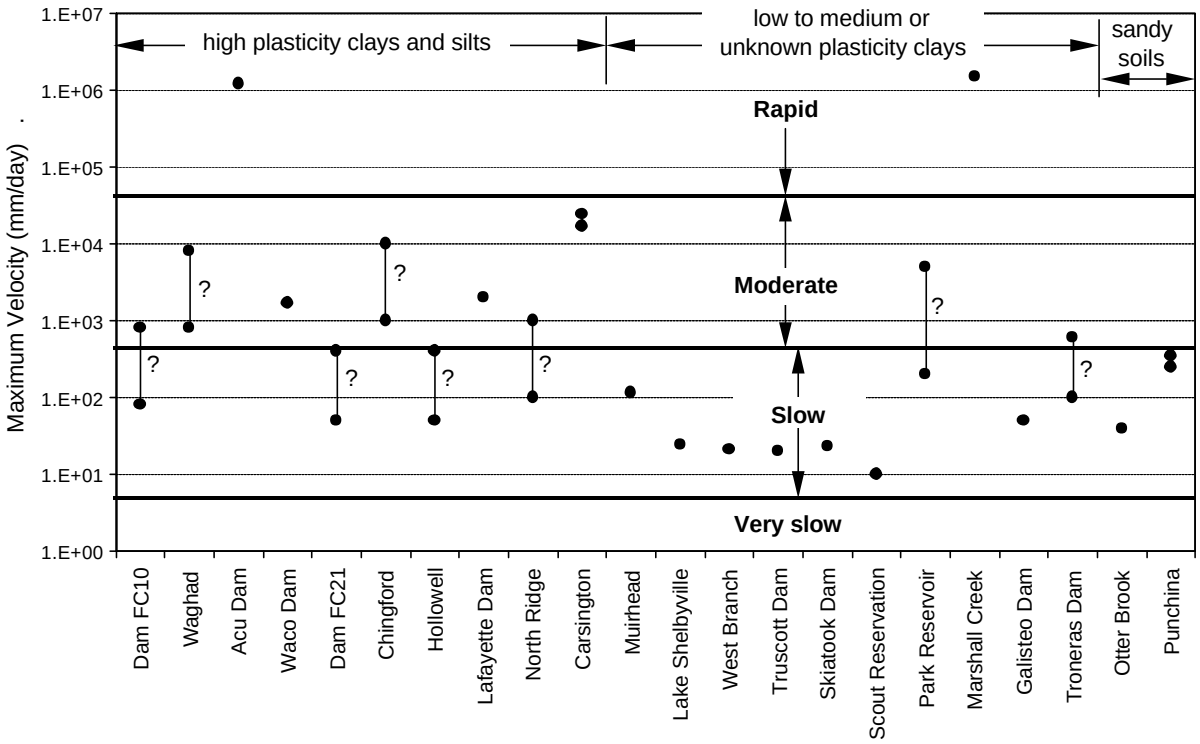

Figure 5.23: Maximum post failure velocity of slides in embankment dams during construction.

5.6.3.1 Slope Failure Geometry and Orientation of the Surface of Rupture

Slope failure geometry was found not to be a significant factor in the post failure deformation behaviour for the failures in embankment dams during construction. This was considered to be due to the typical compound orientation of the surface of rupture of most slides during construction for the Types 1, 2 and 5 slope failure geometries, influenced by either weak layers in the foundation or wet, low undrained strength layers within the earthfill. These weak or wet layers formed a near horizontal translational basal component of the surface of rupture typified by Scout Reservation dam (Figure 5.13a), Waco dam (Figure 5.13b) and Carsington dam (Figure 5.14).

For some of the failures in wet placed earthfills, such as Punchina, Troneras, Waghad and Dam FC10, the surface of rupture was considered likely to be closer to rotational than compound. The failures at Punchina and Troneras, within wet placed silty sands and sandy silts, were relatively shallow. In contrast, the failures in high plasticity clays (Waghad and Dam FC10) were relatively deep-seated rotational slides.

5.6.3.2 Material Type

Material type can have a significant affect on the post failure deformation behaviour. Figure 5.22 and Figure 5.23 show that, with exceptions, greater deformations and higher velocities were generally observed for failures where the surface of rupture passed through high plasticity clays. For the low to medium plasticity clays and silts, and sandy soil types deformations were of lesser magnitude, generally limited to less than 2 to 2.5 m, and post failure velocities were generally in the slow class.

For most of the case studies of failure during construction the mechanics of failure (Section 5.5.1) involved shearing through low undrained strength, and likely near normally consolidated layers, in either the foundation or earthfill. For these near normally consolidated non-structured soils, strain weakening on shearing is affected by the potential for strain weakening from fully softened to residual strength associated with particle orientation.

Skempton (1985), amongst others, showed that clay content (percent finer than 2 micron) and plasticity index influence the potential for strain weakening due to particle orientation (Figure 5.24 and Figure 5.25). Their findings indicate that strain weakening due to particle orientation is significant for high clay content and high plasticity soils, and is not significant for sandy soils and low to medium plasticity fine-grained soils (clays and silts). These figures are presented merely to highlight the effects of clay content and plasticity index, and if used should be done so with caution in consideration of other factors affecting the residual strength of clay soils including; effective stress, mineralogy, soil structure, pore water chemistry and rate of displacement, as summarised by Fell et al (2000).

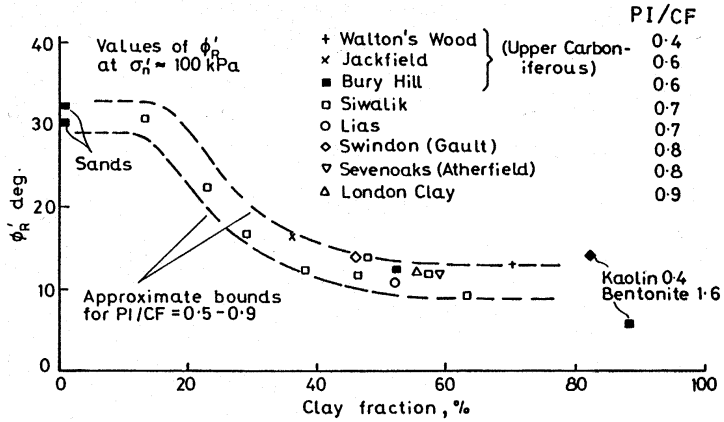

Figure 5.24: Residual drained strength from field case studies in clay soils in the UK and ring shear tests on sand, kaolin and bentonite (Skempton 1985).

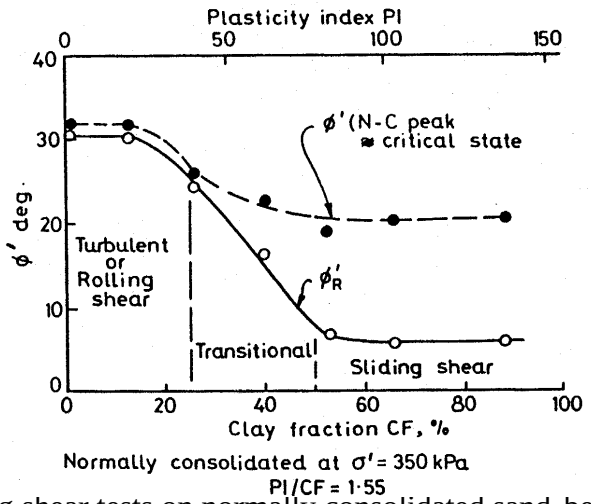

Figure 5.25: Ring shear tests on normally consolidated sand-bentonite mixtures (Skempton 1985, after Lupini et al 1981).

The post failure deformation behaviour of the case studies of undrained failure during construction within wet placed earthfills provide a good example of the effect of material type and potential for strain weakening due to particle orientation on the post failure deformation behaviour. In the case studies considered the earthfill zones within which failure occurred were placed well wet of optimum moisture content, and the earthfill is characterised by low undrained shear strength, near normally consolidated conditions under small effective normal stresses and being non-structured. The deformation behaviour of these case studies is summarised as follows:

- Punchina cofferdam (Figure 5.26), an earthfill embankment, was constructed of silty sands derived from deeply weathered quartz diorite placed on average 4.1% wet of Standard optimum. The earthfill was considered as not strain weakening on shearing due to particle orientation. The deformation of the downstream shoulder (Figure 5.27a), during the latter stages of construction, only occurred whilst construction was in progress and stopped shortly after cessation of construction. This would indicate that the deformation of the unstable slope was controlled by fill placement. Villegas (1982), by limit equilibrium analysis, demonstrated that the factor of safety of the downstream shoulder was close to unity during the latter stages of construction when construction rates were high (greater than 0.5 to 1 m/day). The slide also deformed as a relatively intact unit as indicated by the reasonably uniform velocity at the different surface monitoring points (Figure 5.27b). A similar pattern of deformation behaviour was observed at Troneras dam, an earthfill embankment constructed of wet placed medium plasticity sandy silts.

- The failure during construction of Waghad dam in 1884 contrasts that at Punchina dam. The homogeneous embankment was constructed of high plasticity, high fines content (63 to 93% finer than 75 micron) "black cotton" soils placed without formal compaction and at moisture contents well wet of Standard optimum (Nagarkar et al 1981). Post failure, the failed slope deformed a total distance of approximately 15 m at a velocity estimated to be in the moderate range. It is considered that strain weakening in undrained loading contributed significantly to the amount and velocity of the post failure deformation due to a likely large reduction in strength between fully softened and residual strength.
- The failure during construction of Muirhead dam in 1941 (Figure 5.28) falls somewhere between that of Punchina and Waghad dams. The puddle core earthfill embankment was constructed of medium plasticity clays for the core and a mix of medium plasticity clays, gravels and sands (Boulder clay) placed on the wet side of Standard optimum for the shoulder fill. The post failure deformation behaviour (Figure 5.29) showed continuing deformations at a decreasing velocity for some 10 to 20 days after suspension of fill placement. Placement of an additional earthfill layer in early November 1941 resulted in an immediate resumption of deformation that eventually totalled more than 60% of the thickness of the placed layer. The total estimated lateral displacement of the upstream slope was in the order of 2.1 m. It is considered that the deformation is essentially driven by fill placement as indicated by the decreasing rate of velocity on cessation of filling, but undrained strain weakening of the medium plasticity clays may have been a factor given the length of time over which the deformation occurred after cessation of filling.

In the case of Waco dam and Dam FC21 failure through the foundation was along pre-sheared high plasticity bentonite seams, the strength of which would have been at or close to the residual strength. For these cases therefore, strain weakening due to particle orientation was not a factor in the post failure deformation behaviour.

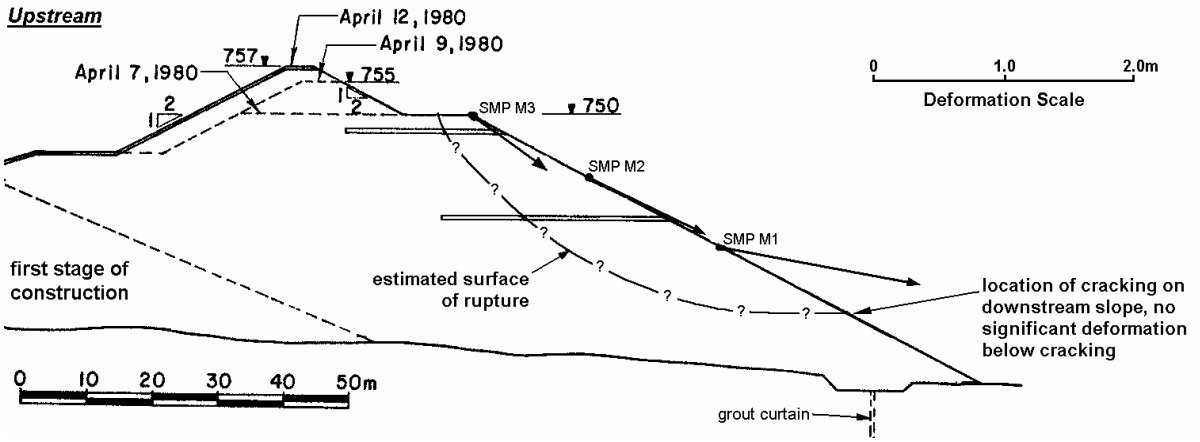

Figure 5.26: Section through Punchina cofferdam (adapted from Villegas 1982).

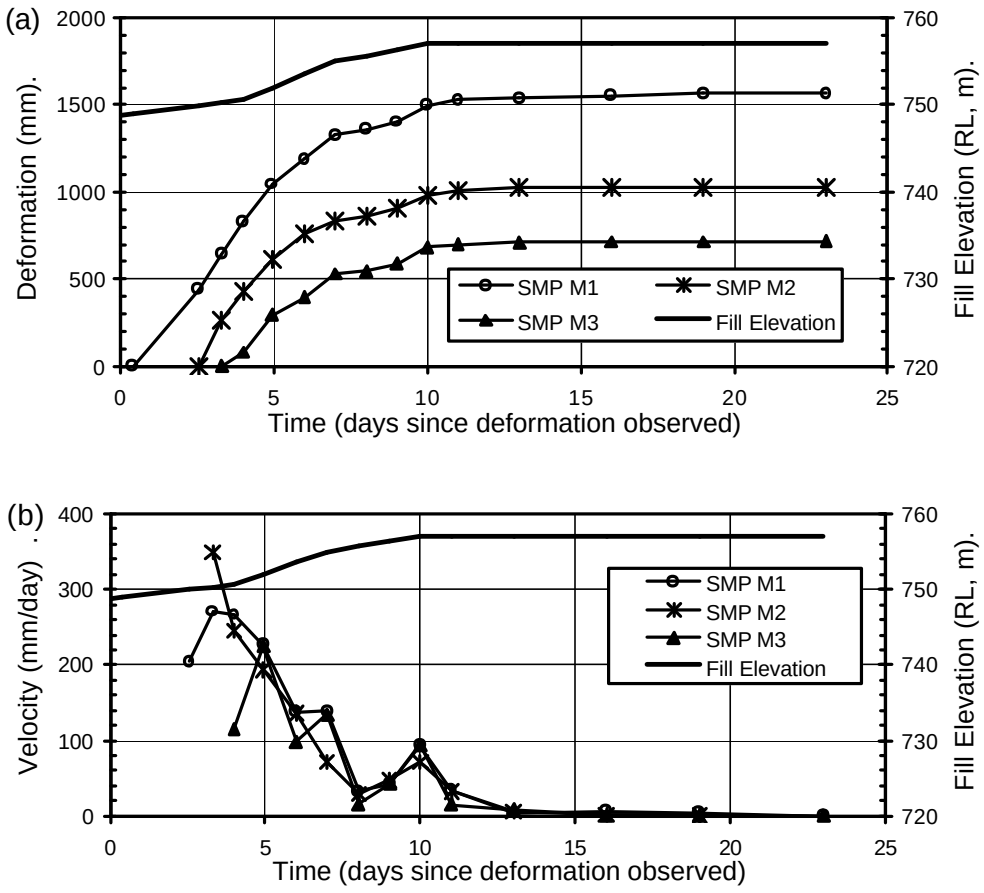

Note: The SMP locations are shown in Figure 5.26.

Figure 5.27: Punchina cofferdam, *(a)* deformation and *(b)* velocity of the downstream slope during construction (adapted from Villegas (1982)).

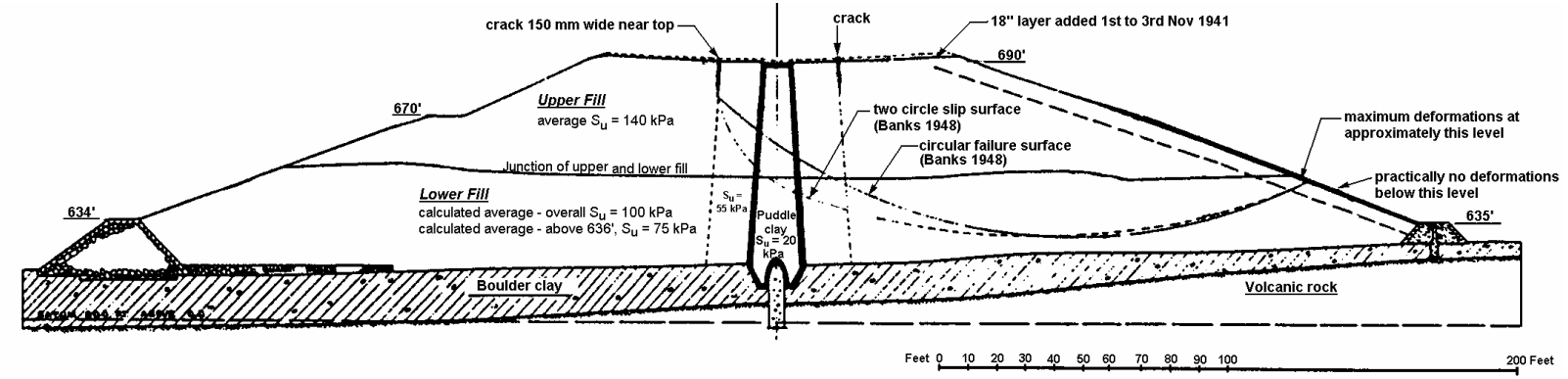

Figure 5.28: Section through the failed region of Muirhead dam (Banks 1948)

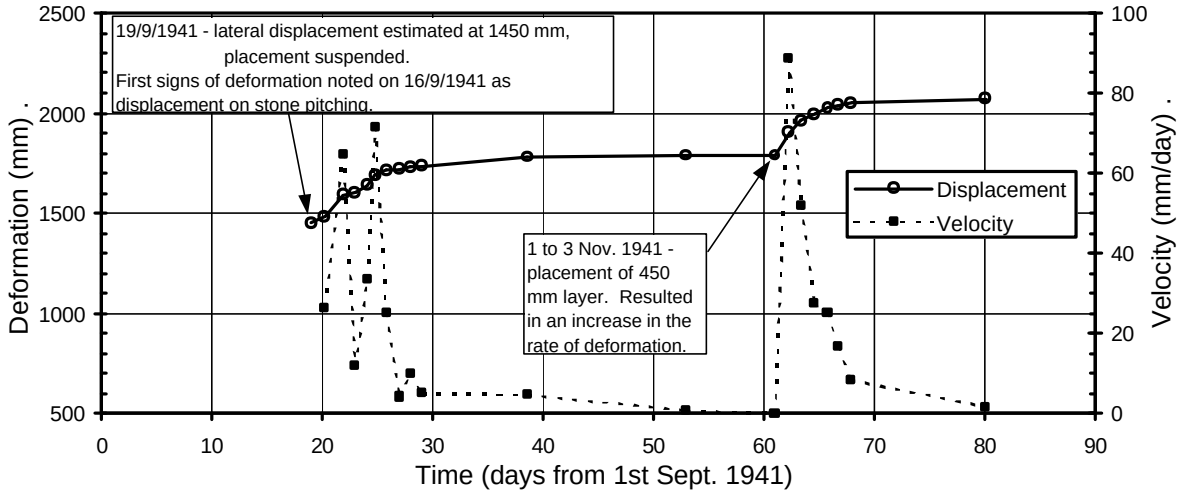

Figure 5.29: Muirhead dam, post failure deformation and velocity of the failure in the upstream shoulder during construction.

5.6.3.3 Failures Where Progressive Strain Weakening is Significant

The definition of significant progressive strain weakening is where on suspension of fill placement the deformation continues to accelerate to a failure or collapse condition. The mechanism of post failure deformation therefore involves brittleness of the slide mass, which could be associated with strain weakening of the materials along the surface of rupture, internal brittleness in the slide mechanics (e.g. internal shearing in formation of a graben type failure or toe buttressing) or release from restraint on the lateral margins (e.g. formation of a rupture surface on the margins through higher strength earthfill zones). These types of failures are considered separately from those where progressive strain weakening is not considered significant, i.e. cases where the out of balance driving forces and deformation of the slide mass are largely controlled by additional placement of fill, and on suspension of filling the deformation of the slide mass decelerates.

Of the twenty-two case studies of failure during construction, progressive strain weakening is considered significant in eight; Waghad, Acu, Waco, Carsington, Marshall Creek, Chingford, Lafayette and possibly North Ridge dams. In these eight cases the deformation behaviour either indicated acceleration of the slide mass after cessation of filling or this was inferred from description of the failure or from the post failure travel distance of the slide mass. The total post failure deformation of the slide mass (Figure 5.22) and the peak post failure velocity (Figure 5.23) for these cases was generally greater than for the slides where progressive strain weakening was considered not to be significant.

The deformation behaviour for several of the case studies is discussed in greater detail below, but several general observations are worth highlighting:

- The slides remained virtually intact on sliding. Some break up of the slide mass was observed at the back scarp and toe regions, as well as some break up in the mid region of the slide. In most cases the compound shaped surface of rupture contributed to the observed break up in the mid slope to head regions of the slide. In several cases formation of multiple back scarps and possibly retrogressive instability of the back scarp contributed to the break up.
- Total post failure deformations (Figure 5.22) ranged from 1.5 m (North Ridge dam) to 25 m (Acu dam). The travel distance for most of these slides was generally greater than 5 to 10 m.

- Peak post failure velocities (Figure 5.23) were generally in the moderate range. At Acu and Marshall Creek dams the peak post failure velocity was in the rapid range, reflecting a high degree of brittleness in the post failure mechanics and greater kinetic energy of the slide mass.
- Acceleration of the slide mass to peak velocity, once the failure was recognised, ranged from about 0.5 hour (Acu dam) to 35 days (Waco dam). At Acu and Marshall Creek dams peak velocities were reached within several hours indicating relatively rapid development of brittleness of the slide mass. At Waco dam (Figure 5.30) and Carsington dam (Figure 5.31c) the slide mass accelerated relatively slowly for a number days to weeks followed by a relatively abrupt increase in velocity, possibly due to release on the lateral margins.

Of the eight cases, the factors attributed to progressive strain weakening of the slide mass were:

- Strain weakening due to particle orientation of high plasticity, near normally consolidated clays in either the earthfill or foundation (6 of 8 cases; exclusions are Marshall Creek and Waco dam). At Waco the high plasticity bentonite seams in the foundation were pre-sheared and therefore, close to the residual strength with limited likelihood of further strain weakening. At Carsington dam (refer Section 5.5.1.3) progressive failure due to strain weakening in the over-consolidated foundation was of greater significance than that due to particle orientation in the wet placed core.
- Strain weakening and progressive failure within over-consolidated high plasticity clays (Carsington dam).
- Strain weakening due to contraction on shear and static liquefaction. At Marshall Creek dam (refer below) the rapid development of a failure condition was possibly associated with static liquefaction within the low to high plasticity loessic clays in the foundation.
- Internal brittleness in the slide mechanics. This was considered a factor in the failure of Acu dam (see below) due to the embankment zoning geometry, and at Waco dam due to passive resistance in the toe region of the slide (see below).
- Strain weakening due to release or reduction of restraining forces on the lateral margins. Two factors are considered significant: the lateral persistence of weak layers in either the foundation or earthfill (Carsington and possibly Lafayette dam);

and the formation of a surface of rupture on the margins through embankment zones of higher strength (Acu, Waco and Carsington dams). In either case, strength reduction due to strain weakening is significant. Either strain weakening within the weaker section of the embankment occurs and increases the stresses on the margins such that failure occurs, or else strain weakening on the lateral margins occurs. In all eight cases progressive strain weakening within the weaker section of the embankment was considered a factor resulting in increased shear stresses to be supported on the lateral margins.

Further details on the failure and deformation behaviour at Waco, Carsington, Acu, Marshall Creek and Chingford dams are discussed below.

(a) Waco Dam

The failure at Waco dam (Beene 1967; Stroman et al 1984) occurred in 1961. The zoned earthfill embankment (Figure 5.13b) consisted of a central core zone of rolled, well-compacted clayey soils and shoulders of well-compacted earthfills. The surface of rupture within the foundation was along a pre-sheared bentonitic clay seam in the Pepper Shale formation, bounded at the margins by near vertical fault zones. Along both the basal and lateral slide planes (in the foundation) the strength at failure was at residual strength due to pre-shearing, and therefore strain weakening on shearing at the time of the slide did not occur. The near vertical fault zones were oriented slightly offset from perpendicular to the embankment centreline and to each other (the width between the fault zones increased in the downstream direction), which was a significant factor in the downstream direction of failure.

The slide was first noticed on 4 October 1961 when cracks were observed on the downstream slope. The cracks consisted of a longitudinal crack (parallel to the embankment centreline) about one third of the distance down the slope from the centreline, and small diagonal cracks at the downstream toe located approximately above the two fault zones at the margins of the eventual slide. Beene (1967) thought that the failure may have initiated some two weeks prior and was obscured from earlier observation by embankment construction and the presence of riprap on the upstream slope.

The monitored deformation of the crest after 4 October 1961, Figure 5.30, shows the slow development of the slide. The velocity of deformation increased relatively quickly

after about 33 days (from when the slide was thought to have initiated) and reached a maximum at about 36 days before slowing significantly.

The significant factors affecting the slide deformation are thought to include:

- Passive resistance at the toe of the slide. The toe of the slide was located some 140 m downstream from the downstream toe of the embankment, and the basal surface of rupture some 14 m below ground surface level.
- No strain weakening along the basal surface of rupture.
- Overall strain weakening of the slide mass, as evidenced by the gradually increasing velocity of deformation, was considered to be associated with strain weakening on the margins and back-scarp in the earthfill, and weakening in the toe region.
- The large increase in velocity of deformation from Day 33 is thought to be associated with release on the lateral margins and reduction in passive resistance in the toe region. The pulling away of the slide mass from the north fault is also likely to have been a contributing factor.

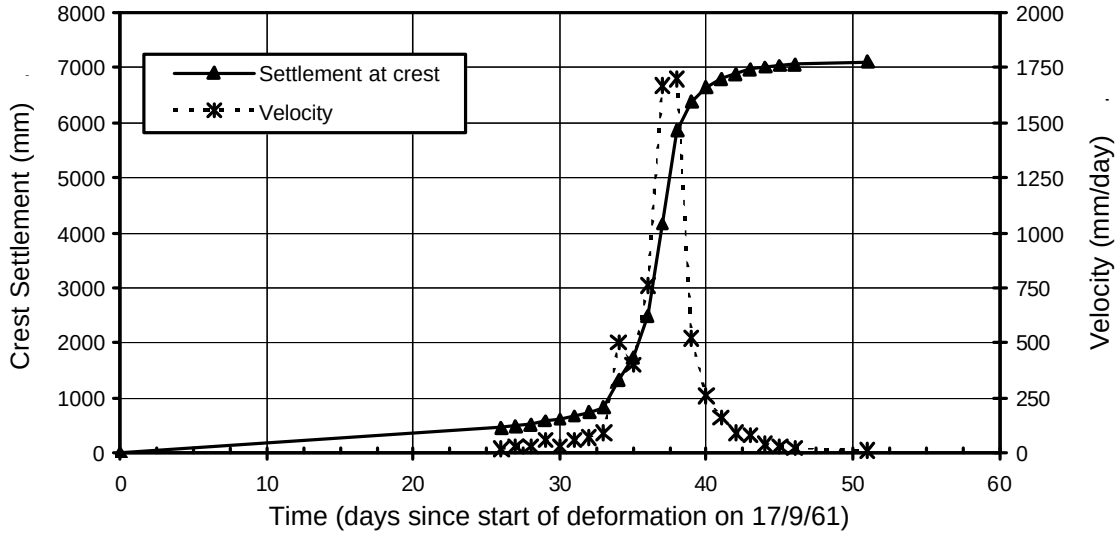

Figure 5.30: Crest settlement monitoring of the slide at Waco dam (adapted from Stroman et al 1984).

(b) Carsington Dam

Section 5.5.1.3 briefly discusses the earthfill materials and placement methods used, and the mechanics of progressive failure leading up to the failure in the upstream shoulder at Carsington dam. The slide occurred over a period of about 5 to 6 days.

The surface monitoring at the upstream toe, when analysed in hindsight, indicated a small (49 mm) but significant increase in the lateral displacement over the period from

30th May to 1st June 1984 (at chainages 675 and 750 m only) in the last stages of fill placement prior to the failure (Figure 5.31a). Following a weekend of wet weather it was noted on Monday 4th June that an additional 75 mm of displacement had occurred in the toe region and a tension crack was observed on the embankment crest between chainages 670 and 790 m. Over the next 30 hours the width and velocity of the slide increased significantly (Figure 5.31c) culminating in a large deformation (10.4 m) overnight on the 5th June (Figure 5.31b). By the 7th June the deformation had virtually ceased.

There are several important observations associated with the pre and post failure deformation of the slide and the slide mechanics, they are:

- During the winter shutdown period starting in October of 1983, the IVM (internal vertical settlement gauge) within the core at chainage 850 m indicated an increase in vertical compression of the fill from 7 to 9% before it became blocked. This location was coincident with the eventual surface of rupture.
- Over the period 24th May to 4th June 1984 the IVM within the core at chainage 705 m showed a large (2.5 to 5%) increase in vertical compression over the depth range 10 to 15 m. This equates to a vertical deformation in this zone of some 225 mm for placement of less than 1 m thickness of fill.
- The surface monitoring on the lower upstream slope (Figure 5.31a) gave little warning of the impending failure, only some 2 to 3 days. This is not unexpected given the mechanics of failure (Section 5.5.1.3) and findings from the Potts et al (1990) analysis indicating the surface of rupture had not formed in the toe region prior to the failure.
- Over the course of the slide the width of the failed section increased from about 120 m on the 4th June to 500 m by the 6th June.

Skempton and Vaughan (1993) commented that significant restraining forces were exerted by the as yet unfailed portions of the embankment on either side of the failed portion of the embankment (approximately from chainage 660 to 800 m). Toward the gully region significant restraint was afforded due to the lack of lateral persistence of the "yellow clay" foundation (from chainages 800 to greater than 900 m the foundation was on weathered mudstone). The effect of the lateral restraint is likely to have been significant in suppressing the amount of deformation within the unstable portion of the slope prior to and in the early stages of failure.

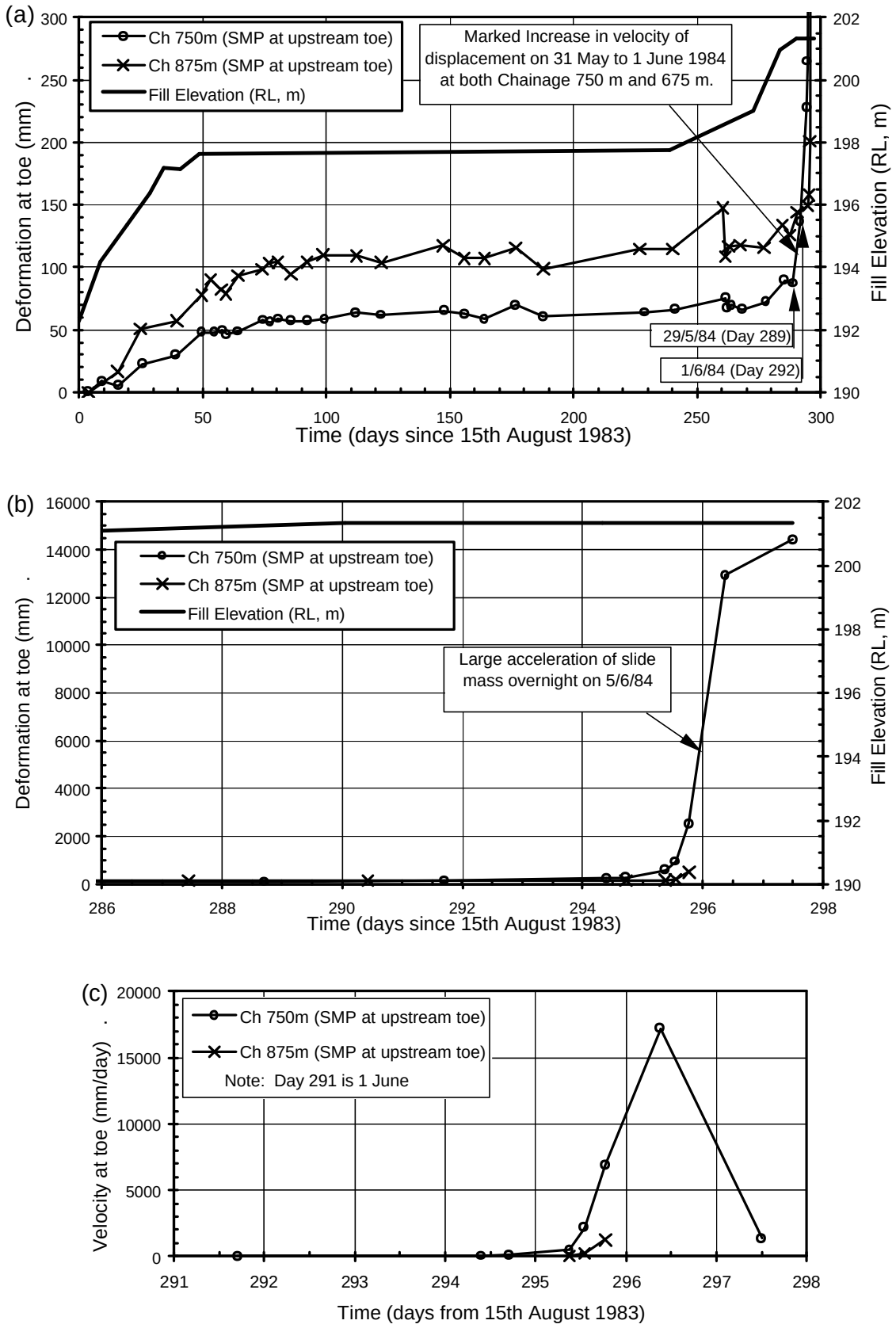

Figure 5.31: Carsington dam, deformation monitoring of upstream shoulder *(a)* leading up to failure, *(b)* during failure (Skempton and Vaughan 1993), and *(c)* the velocity of the slide mass.

A significant factor in the observed increase in velocity of the slide mass (Figure 5.31c) over time was strain weakening on shearing within the failed portion of the embankment, thereby increasing the shear stresses on the lateral margins. Once the shear capacity of the lateral margins was reached the slide mass accelerated at a much faster rate and the width of the failure spread from about 120 m to 500 m.

(c) Acu Dam

In the case of Acu Dam (Figure 5.32) the surface of rupture passed through a wet placed, high plasticity clay layer at the base of the upstream shoulder and extended back through the central high plasticity clay core (initially placed wet of optimum then adjusted to close to optimum in the mid to upper portion of the core). The failure, as described by Penman (1985), was initially observed as a tension crack at crest level on the downstream edge of the core zone. This was followed by sinking of the core and upstream shoulder, and a massive pushing outward of the lower section some 25 m in distance over a width of some 600 m. The deformation at and post failure took place over a period of about 30 minutes (average velocity of 50 m/hour or 1.2 x 10^6 mm/day) putting the failure into the rapid velocity category (Figure 5.23).

The large post failure travel distance of 25 m and rapid velocity of the slide mass are indicative of a relatively high degree of brittleness of the overall slide mechanism. Contributing factors to the high degree of brittleness are considered to include; a buttressing effect of the sandy and gravelly earthfill in the toe region of the slide, internal shearing in development of the compound slide mechanism, undrained strain weakening of the high plasticity wet clays and development of the back-scarp through partially saturated earthfill. The extensive lateral persistence of the layer of clay earthfill under the upstream slope and the high shear strength of the shoulder fill (compacted clayey sands and gravels) are considered to have contributed to the broad width (600 m) of the slide.

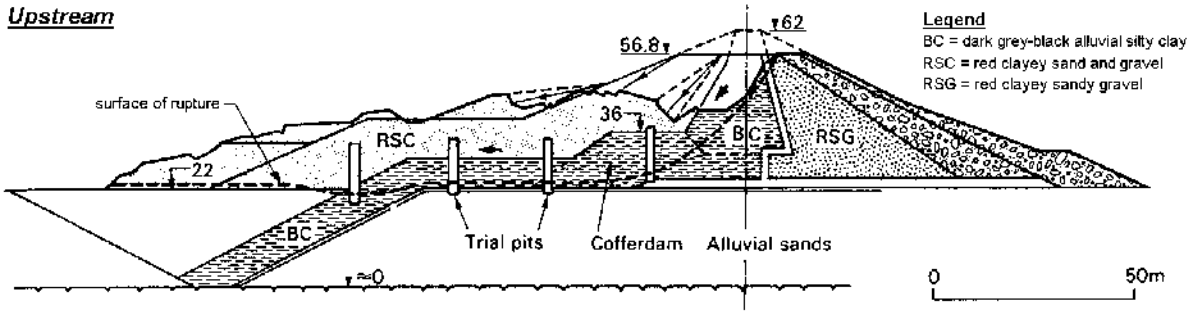

Figure 5.32: Section through failed region of Acu dam (Penman 1986)

(d) Marshall Creek Dam

The slide at Marshall Creek dam (Sherard et al 1963; ENR 1937a, 1937c, 1938a and 1938b) was located within the relatively broad gully region of the foundation. The failure occurred within several hours of the observation of cracking on the embankment crest. The majority of the post failure deformation (about 15 m) occurred at a rapid velocity over a period of 15 to 20 minutes. The relatively large post failure travel distance and rapid velocity of the slide mass are indicative of a relatively high degree of brittleness of the overall slide mechanism. Significant strain weakening associated with static flow liquefaction of the saturated loess foundation is possibly the reason for the high degree of brittleness.

(e) Chingford Dam

The failure of Chingford dam (Cooling and Golder 1942) consisted of a compound type failure (Figure 5.33) with basal translational component within the very soft, highly plastic clay foundation and rotational back-scarp through the soft to very soft, highly plastic core and select earthfill zones. The relatively high rate of construction (approximately 100 mm/day) of this relatively low height (7.9 m height at failure) puddle core earthfill dam was considered to be a significant factor in the undrained slope failure.

Breakage of a water pipe at the toe of the slope several days prior to the slide was an indication of the impending slide. The slide travelled a distance of 4.3 m at the toe at an estimated peak post failure velocity in the moderate range. Undrained strain weakening of the near normally consolidated highly plastic clay foundation and embankment materials is considered to have been the major factor contributing to strain weakening of the slide mass.

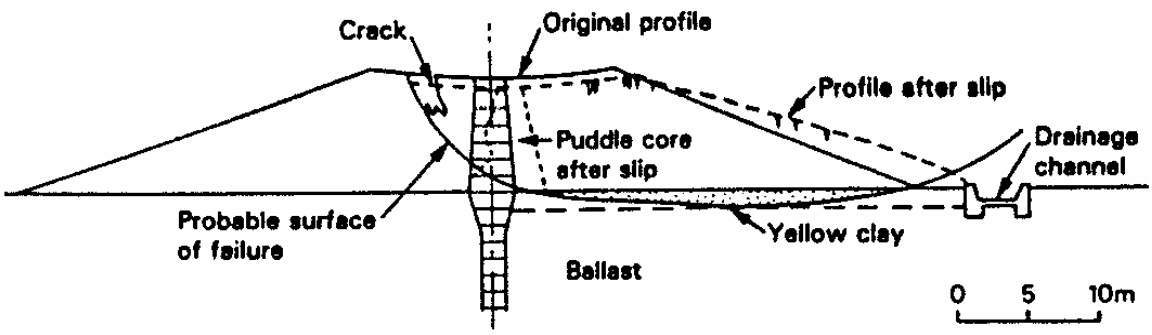

Figure 5.33: Cross section of the slide during construction at Chingford dam (Cooling and Golder 1942)

5.6.3.4 *Failures Where Progressive Strain Weakening was Not Significant*

For failures where progressive strain weakening is not considered significant, the deformation of the slide mass is largely controlled by the placement of fill, which provides the out of balance driving forces for the deformation to occur. Deceleration of the slide mass is generally observed for these cases on suspension of filling, such as observed at Muirhead dam (Figure 5.29) and Punchina cofferdam (Figure 5.27).

In at least ten of the twenty-two case studies of failure during construction, progressive strain weakening of the slide mass was considered as not significant (Otter Brook, Truscott, Skiatook, Troneras, Punchina, West Branch, Dam FC21, Muirhead, Hollowell and Galisteo dams). The failures at Lake Shelbyville and Scout Reservation dams were considered marginal (discussed below) and for Park Reservoir insufficient information was available on the deformation behaviour and material types for evaluation of the influence of progressive strain weakening of the slide mass. The material types of these case studies included:

- Wet placed silty sand and low to medium plasticity sandy silt earthfills (Punchina cofferdam and Troneras dam).
- Wet placed earthfill layers or non-structured low strength foundations consisting of low to medium plasticity clays (Otter Brook, Truscott, Skiatook, West Branch, Muirhead and Galisteo dams). For these cases the materials within which the basal portion of the surface of rupture was located were considered to be near normally consolidated.
- Deformation along pre-sheared high plasticity bentonitic seams in the foundation (Dam FC21).

The failure at Hollowell dam (Kennard 1955), a puddle core earthfill embankment, is an exception to the general material types. The basal portion of the surface of rupture was located within medium to high plasticity clays of soft to very soft strength consistency in the foundation, with a back-scarp through the puddle and select high plasticity core zone of the embankment. Progressive strain weakening was considered as not significant for the overall slide even though strain weakening on shearing of the high plasticity soils was likely to have occurred. This is because of the limited lateral extent of the weak foundation (30 to 40 m width) and the capacity of the lateral margins to accommodate the increased shear stresses associated with the strain weakening in the narrow failure section. The deformation of the slide was limited to less than 500 mm

and was estimated to have occurred at a slow velocity. The overall width of the embankment affected by the slide was about 200 m, but the bulk of the deformation was confined to the embankment section over the soft to very soft clay foundation layer.

For the case studies where progressive strain weakening was not considered significant, total deformations of the slide mass were limited to 0.5 m to 2 m (Figure 5.22) and peak velocities generally to the slow class (Figure 5.23). Several aspects of the deformation behaviour for these case studies is important in the context of identifying potential instability and undertaking remedial measures, they are:

- For the case studies controlled by wet placed earthfill layers or low undrained strength foundation conditions, the failures (including the cases where progressive strain weakening was considered significant) were usually recognised by cracking on the embankment crest or slopes, and in some cases by cracking in the toe region of the slide, movement of the outer slope or spreading in conduits. For these cases the deformation of the outer slopes was significant when the slide was first recognised. This was considered to be because the critically stressed weak layer formed the basal portion of the surface of rupture within which plastic deformations had occurred. Therefore, deformation monitoring for identification of potential instability in these case studies is best undertaken in the region from the toe to the mid slope of the embankment.
- The lengthy time for development of the surface of rupture. On recognition of a potentially unstable slope condition remedial measures can be (and were) undertaken to improve the factor of safety of the embankment slope. The remedial measures generally took the form of addition of stabilising berms or changes in the embankment design, or in some cases adjustment in the construction program to allow construction pore water pressures to dissipate.

Further details on the failure and deformation behaviour of several of the marginal case studies (Lake Shelbyville, Scout Reservation and Dam FC10) are discussed in the following sections.

(a) Lake Shelbyville dam

In the case of Lake Shelbyville dam, an earthfill embankment constructed using sandy clays of low to medium plasticity, a slide occurred in the closure section. The slide was not recognised until after the end of construction. Wet placed earthfill layers formed the

basal surface of rupture. The inclinometer records and development of back-scarps at the embankment crest confirmed the full development of the surface of rupture in cross section, but the slide may not have fully developed on the lateral margins.

The published deformation records (Figure 5.34) show the "slow" velocity of post failure deformation (generally less than 0.5 mm/day) that persisted over a period of up to 2 years after the end of construction. During this time construction pore water pressures were still present.

Prior to completion of embankment construction the reservoir impounded water, and it was on drawdown, prior to proposed remedial works, that acceleration of the slide mass was observed. This suggests that the water load on the upstream slope acted as support for the unstable portion of the upstream slope. The persistence of deformation for several years after the end of construction, during which time pore water pressures are likely to have dissipated to some degree, is considered to probably reflect some degree of strain weakening of the overall slide mechanism.

(b) Scout Reservation dam

The slide at Scout Reservation dam (Figure 5.13a), an earthfill embankment constructed using sandy clays of low to medium plasticity, was not recognised until after the end of construction. Inclinometer records and development of back-scarps at the embankment crest indicated that a surface of rupture had fully developed in cross section.

The published deformation records (Figure 5.35) show the "slow" post failure velocity of the slide mass (less than 10 mm/day) that persisted over a period of up to 2 years after the end of construction, during which time construction pore water pressures were still present. This persistence of deformation over several years, during which time pore water pressures are likely to have dissipated to some degree, is considered to reflect strain weakening of the overall slide mechanism. Deformations that occurred more than 2 years after the end of construction were triggered by rainfall, most likely due to water infilled cracks at the crest of the embankment.

(c) Dam FC10

Dam FC10 is a zoned earth and rockfill embankment with broad central clay core of high plasticity and high clay content (35% passing 2 micron) supported by thin outer random fill and rockfill zones on the upstream shoulder. Monitoring during

construction indicated the deformation behaviour of the upstream shoulder was "abnormal", and the slope to potentially be at a limiting stability condition.

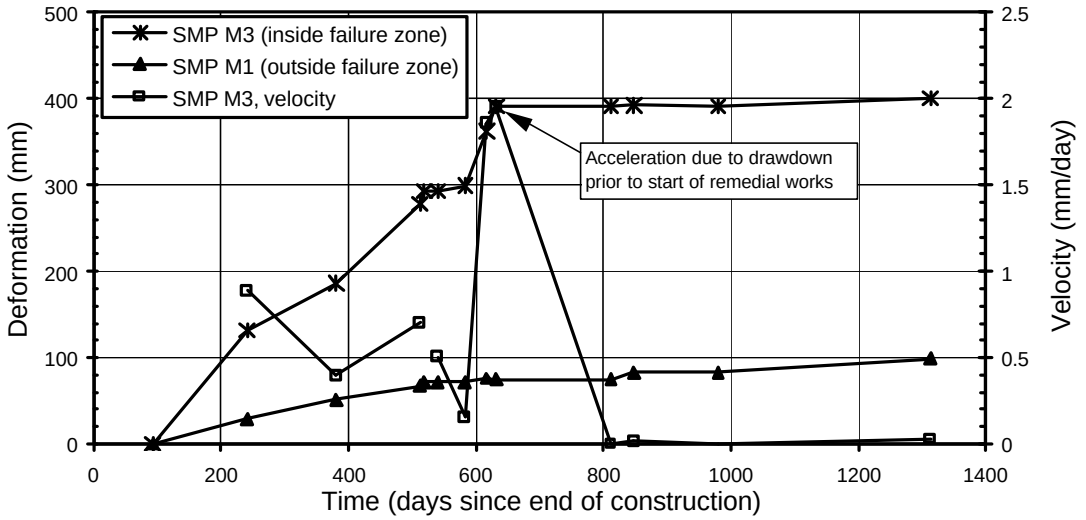

Figure 5.34: Deformation and velocity of the slide at Lake Shelbyville dam (adapted from Humphrey and Leonards (1986, 1988)).

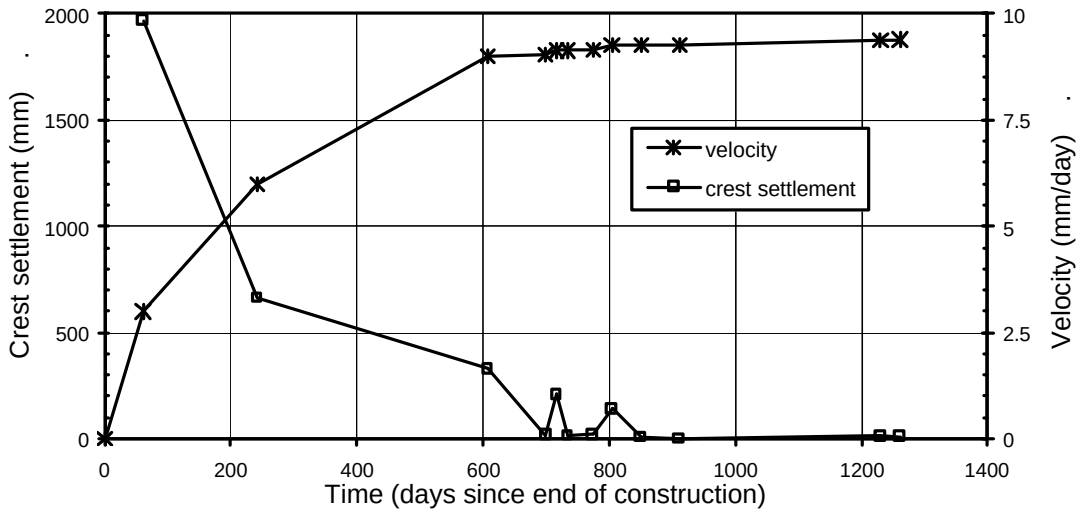

Figure 5.35: Post failure deformation and velocity of slide at Scout Reservation dam (adapted from Mann and Snow (1992)).

The total measured lateral displacement of the upstream slope during construction was 390 mm, which was significantly greater than for the downstream slope. Of this, some 230 to 260 mm occurred during placement of the final 2.5 m (13% of the total height). Shortly after the end of construction the deformations were observed to accelerate

reaching a total of some 2.8 m over a period of many days. This acceleration may have been triggered by a reduction in the reservoir level.

Strain weakening of the wet placed, near normally consolidated high plasticity broad core zone at Dam FC10 is likely to have occurred. But, the overall effect of the strain weakening was not greatly significant, as indicated by the deformation behaviour of the slide. The zoned earth and rockfill geometry is likely to have been significant in the limited total deformation of 2.8 m measured. Cases such as Dam FC10 are considered marginal in that strain weakening on shearing is a factor in the mechanics of post failure deformation and under different design circumstances post failure strain weakening may have been significant.

5.6.4 FAILURES DURING DRAWDOWN – POST FAILURE DEFORMATION BEHAVIOUR

Of the nineteen failures in embankment dams that occurred during drawdown, sixteen were within the embankment only and the remaining three through the embankment and foundation. The embankment types (Table 5.7) consisted predominantly of earthfill embankments; homogeneous earthfill (6 possibly 9 cases), earthfill with filters (2 cases), and earthfill with rock toe (3 cases). For the two failures in embankments with upstream rockfill zones, the surface of rupture preferentially passed through the foundation and not the outer rockfill zones.

Table 5.14 presents a summary of the timing of the failure, embankment type and geometry, material properties, drawdown causing failure and comments on the slide itself. Further details are given in Section 1 of Appendix D. Table 5.15 presents a summary of the post failure deformation behaviour (total deformation and estimated peak velocity), slope failure geometry and material properties. Plots of the estimated total post-failure deformation and estimated peak post failure velocity are presented in Figure 5.36.

The deformation records of the case studies are limited. In most cases information was only available on the total deformation and in some cases this was estimated off sections provided in the literature. The peak velocities have been estimated from the monitoring data where possible (4 cases) or a velocity range has been estimated based on the amount of deformation and reference to times over which the deformation occurred. These estimates are broad range.

Table 5.14: Summary of the case studies of slides in the upstream shoulder of embankment dams triggered by drawdown

Name	Year of Failure/s	Years since Const [d]	Embankment Details			Material Properties (through which surface of rupture passed)		Drawdown (causing failure)	Comments
			Type	Hgt (m)	Slope (^{o})	Embankment *[1]	Foundation *[1]		
Old Eildon	1927 & 1929	2 to 4	Conc. C-wall R'fill (10,0,0)	29	36	Puddle clay zone (CL – medium plasticity) upstream of corewall. Dumped rockfill shoulder.	CL to CH – alluvial clays of firm to stiff strength consistency	First two drawdowns. 1927 - 32.5 m at 200 mm/day (increasing to 500), and 1929 - 15.5 m at 100 mm/day (increasing to 230).	Deep seated compound slide passing through the puddle core and foundation. Back-scarp at corewall (centre of crest). Crest settled 14 m 1929.
Wassy	1883	1	Homog (0,0,0)	16.5	33.7	CL –silty clays, medium plasticity. No formal compaction	(failure through embankment only)	First drawdown, very rapid (10 m drawdown at 400 to 500 mm/day)	Rotational slide through the outer earthfill zone of the steep upstream shoulder. Back-scarp at upstream edge of crest. Brick facing on upstream slope.
Mondely	1981	1	E'fill - filters (1,1,1)	24	18.4	CL – low to medium plasticity clays placed wet of OMC. Rolled, well compacted.	(failure through embankment only)	First drawdown. Re-activation of deformation on second drawdown.	Relatively shallow rotational slide in the upper part of the upstream slope. Limited deformation. High pore water pressures from construction still present in the earthfill.
Malko Sharkovo	unk	1	Zoned E'fill (3,0,1)	41	unk	CL (?) – sandy clay in outer earthfill upstream shoulder.	(failure through embankment only)	First drawdown.	No information on the slide.
Forsythe	1921	1	Homog (0,0,0)	19.8	26.6	SM/ML – silty sands and sandy silts of low plasticity. No formal compaction.	(failure through embankment only)	First drawdown, very rapid (4.6 m drawdown in several hours, rate ˜ 2.3 m/hour)	Rotational slide through the outer earthfill zone of the steep upstream slope. Back-scarp at the centre of the crest.
San Luis	1981	14	Zoned E&R (4,2,2)	56	15.8	CL – sandy clays, medium plasticity. Rolled, well compacted. Broad central core.	CH – colluvial sandy clays, low permeability, fissured.	Largest and quickest drawdown in embankment history in 1981 (55 m at max. 50 day rate of 625 mm/day)	Deep seated compound slide through the broad central core, foundation and random fill zones. The slide travelled some 17 m.

Table 5.14 (cont.): Summary of the case studies of slides in the upstream shoulder of embankment dams triggered by drawdown (Sheet 2 of 3).

Name	Year of Failure/s	Years since Const [d]	Embankment Details			Material Properties (through which surface of rupture passed)		Drawdown (causing failure)	Comments
			Type	Hgt (m)	Slope (^{o})	Embankment *[1]	Foundation *[1]		
Charmes	1909	3	Homog (0,0,0)	16.8	33.7	CL – silty sandy clays of medium plasticity. Rolled, limited compaction.	(failure through embankment only)	Largest drawdown in embankment history.	Rotational slide through the outer earthfill zone of the steep upstream slope. Back-scarp at centre of crest. Slow post failure deformation.
Enista	1982	13	E'fill - filters (1,0,1)	32.2	18.4	CL/CH (?) – alluvial silty clays. Rolled, well compacted.	(failure through embankment only)	Drawdown to lowest historical level.	Incipient slide. 400 mm wide cracks in upstream slope, no vertical displacement across cracks.
Dam FD2	1993	32	Homog (0,0,0)	28.7	26.6	CL – sandy clays, low plasticity. Rolled, well compacted.	(failure through embankment only)	Likely failure during 1993 drawdown, largest and quickest in history of operation (16.7 m at 335 to 400 mm/day).	Relatively shallow (5.5 m depth) compound slide. Reactivation of deformation during 1994 drawdown.
Mount Pisgah	1928	18	Homog (0,0,0)	23.2	33.7	ML – sandy silts. Poor construction practice.	(failure through embankment only)	13.4 m drawdown over several months (average 220 mm/day). Drawdown very rapid over several days prior to failure.	Rotational slide in the steep upstream slope. Back-scarp at downstream edge of crest. Rapid deformation. Concrete facing on upstream slope.
Pilarcitos	1969	103	Puddle E'fill (8,0,0)	29	21.8	GC – clayey sandy gravel of low plasticity (upstream shoulder zone). No formal compaction.	(failure through embankment only)	Very rapid drawdown (7.6 m at 540 mm/day), possibly the most rapid historical drawdown.	Rotational slide in the upstream slope. Limited deformation (˜ 1 m)
Sampna Tank	1961 & 1964	4 and 7	Zoned E'fill (3,0,0)	17.8	26.6	CL/CH (?) – clayey earthfill used in embankment shoulders.	(failure through embankment only)	1964 drawdown to lowest historical level. Drawn down 9.1 m over 8 months (average 30 to 60 mm/day)	Rotational slide in outer earthfill zone of the embankment. Back-scarp at upstream edge of crest. Rapid post failure deformation.
Waghad	1919	34	E'fill – rock toe (2,0,0)	26.9	14	CH/MH – alluvial clays and silts of high plasticity. Placed well wet of OMC, no formal compaction.	(failure through embankment only)	Large drawdown (up to 14 m), no indication of rate or if abnormally large.	Deep seated rotational slide that extended back to the downstream edge of the crest. Large post failure deformation of the slide mass.

Table 5.14 (cont.): Summary of the case studies of slides in the upstream shoulder of embankment dams triggered by drawdown (Sheet 3 of 3).

Name	Year of Failure/s	Years since Const [d]	Embankment Details			Material Properties (through which surface of rupture passed)		Drawdown (causing failure)	Comments
			Type	Hgt (m)	Slope (^{o})	Embankment *[1]	Foundation *[1]		
Dam FD3	1931	20	E'fill – rock toe (2,0,0)	27.4	26.6	CL/CH – silty clays of medium to high plasticity. Rolled, limited compaction.	(failure through embankment only)	Large but not unprecedented drawdown (10.3 m drawdown at 110 mm/day)	Shallow rotational slide in the steep upstream slope. Possible rapid post failure deformation at the toe of the slide. Concrete faced upstream shoulder.
Bear Gulch	1936, 1942 & 1944	40 to 48 (6 to 14 after raising)	Homog (0,0,0) ?	19.4	18.4	CL – sandy clays of medium plasticity. No formal compaction.	Soft and wet clay layer in foundation (interbedded sandstones and clay shales)	Similar drawdowns in 1936, 1942 and 1944 causing deformation (8 m drawdown at average 90 mm/day)	Compound slide in the upstream slope through the embankment and foundation. Limited post failure deformation.
Mechka	1981	11	Homog (unk) ?	32	18.4 (?)	CL (?) – sandy silty clays	(failure through embankment only)	Routine drawdown.	No indication of location or size of slide, or amount of deformation.
Sushitsa	1981	11	Homog (unk) ?	32.5	18.4 (?)	CL (?) – sandy silty clays	(failure through embankment only)	Routine drawdown.	No indication of location or size of slide, or amount of deformation.
Telish	1982	14	Homog (0,0,0) ?	29.5	18.4	CL (?) – sandy silty clays	(failure through embankment only)	Routine drawdown.	Rotational slide in the upstream shoulder. Limited post failure deformation.
Drenovets	1984	16	E'fill – rock toe (2,0,0)	29	18.4	CL (?) – sandy silty clays	(failure through embankment only)	Routine drawdown.	No indication of location or size of the slide, or amount of post failure deformation.

Notes: Hgt = height Const [d] = construction unk = unknown OMC = Standard optimum moisture content Homog = homogeneous earthfill embankment
E'fill – filters = earthfill embankment with filters E'fill – rock toe = earthfill embankment with rock toe Zoned E'fill = zoned earthfill embankment
Puddle E'fill = puddle core earthfill embankment Zoned E&R = zoned earth and rockfill embankment
Conc. C-wall R'fill = concrete core-wall rockfill embankment
*[1] Soil classification to the Australian soil classification system (AS 1726-1993)

Table 5.15: Post failure deformation behaviour and slope/material properties of slides in embankment dams during drawdown.

Dam Name	**Slide Deformation (m)**	**Estimated Peak Velocity (mm/day)**	**Slope Failure Geometry*[1]**	**Upstream Slope Angle (degrees)**	**ASCS Class[n] (*[2])**
San Luis dam	15 (crest), 17 (toe)	1000 to 2000	Type 2	15.8	CI (emb), CH (fndn)
Waghad	4.8 (crest), 10 (toe)	4000 to 40000 (est.)	Type 2	18.4	CH/MH
Sampna Tank	11.9 (crest)	50000 to 200000 (est.)	Type 1 (?)	26.6	CI (upstream earthfill)
Dam FD3	1.7 (crest), 6 to 9 (toe)	50000 to 500000 (est.)	Type 1	26.6	CI
Old Eildon	14 (crest), 17 (toe)	5000	Type 2	36	CI (puddle core and fndn)
Mount Pisgah	7 (crest), 9 (toe)	10000 to 400000 (est.)	Type 2 (?)	33.7	ML
Forsythe	4 (crest), 22 ? (toe)	100000 to 1000000 (est.)	Type 1 (?)	26.6	ML/SM
Bear Gulch	0.32 (crest)	10 to 200 (est.)	Type 2	18.4	CI
Mondely	0.4 (crest)	10 to 30	Type 2 (?)	18.4	CI
Enista	0.4 (crest)	50 to 400	Type 2 (?)	18.4	CL/CH (?)
Dam FD2	0.42	27	Type 2	26.6	CL
Telish	1 (crest)	100 to 500 (est.)	Type 2 (?)	18.4	CL (?)
Pilarcitos	1 est. (crest)	200 to 500 (est.)	?	21.8	GC

Notes: crest = crest of back-scarp toe = toe of slide est. = estimated
emb = embankment fndn = foundation
*[1] refers to the location of the slide in the slope, see Section 1.3 for definitions.
*[2] = Australian soil classification system, CI refers to clays of medium plasticity

From analysis of the deformation data, the significant factors influencing the post failure deformation behaviour of slides in embankment dams triggered by drawdown (and discussed further in the following sub-sections) include:

- The material type of the earthfill and foundation materials within which the surface of rupture is located.
- The slope failure geometry.
- The slope angle of the upstream slope.
- Factors that add brittleness to the mechanics of failure and sliding at and post failure, such as slope facing materials (e.g. concrete facing).

- Factors contributing to restraint on the lateral margins including lateral persistence of weak layers, shearing through higher strength outer earth or rockfill zones, and changes in foundation topography.

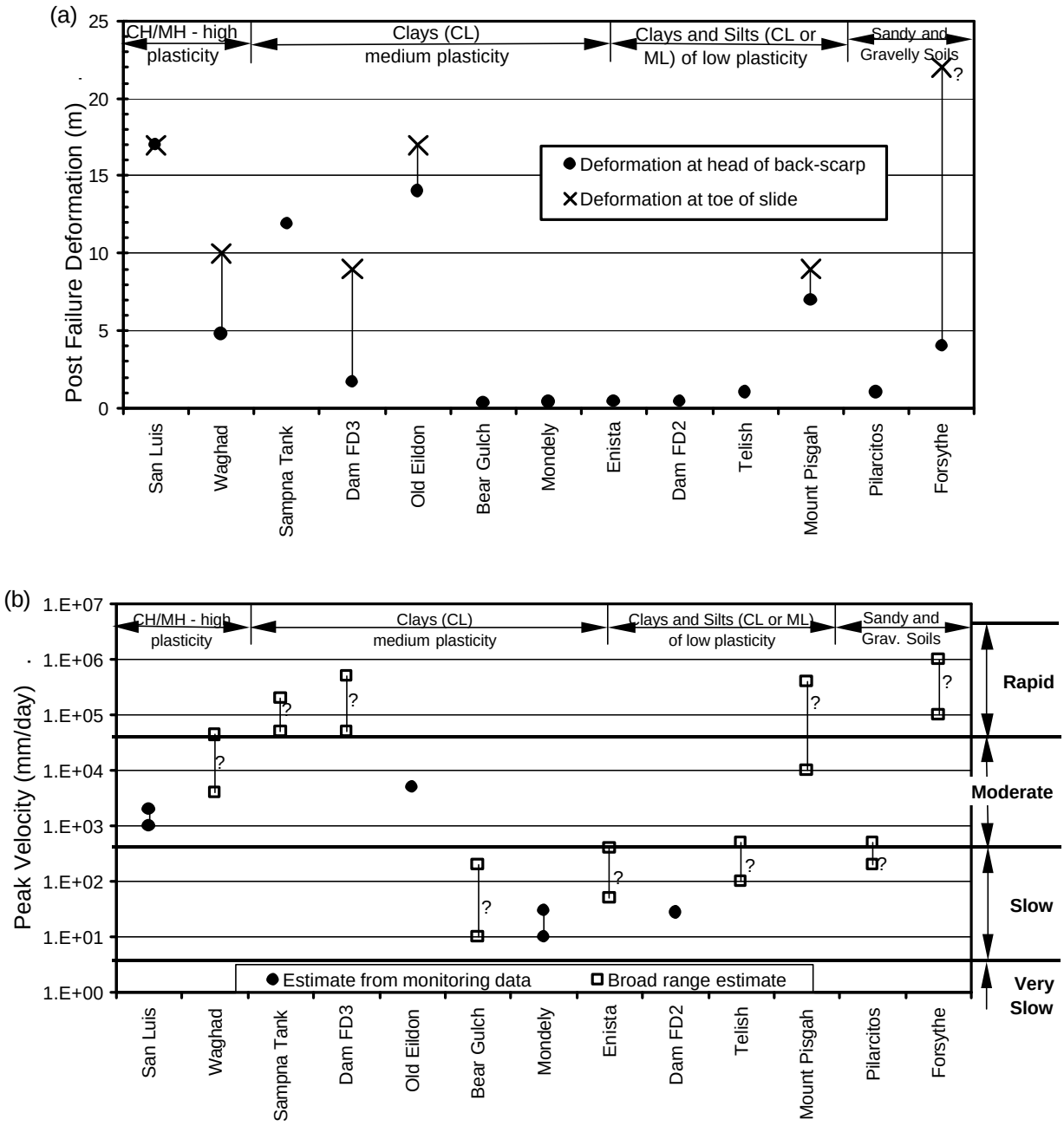

Figure 5.36: Slides in embankment dams during drawdown; post failure *(a)* deformation and *(b)* estimated velocity.

5.6.4.1 *Material Type and Strain Weakening Potential*

Material type has a significant effect on the potential for strain weakening on shearing, leading to potentially large deformations at failure. As discussed for the failures during construction (Sections 5.6.3.2 and 5.6.3.3), material types with high strain weakening potential include:

- Near normally consolidated high plasticity clays or silts with a high clay fraction, which have significant strain weakening potential due to particle orientation.
- Soil types, in a saturated or near saturated condition, that are potentially contractile on shearing.
- Progressive failure in over-consolidated soil types (refer Section 5.2.2).

Of the case studies of failure during drawdown, material strain weakening from the failure condition was considered significant at Waghad, San Luis, and possibly Sampna Tank, Dam FD3 and Old Eildon dams. In these cases the surface of rupture passed through medium to high plasticity soil types. At Waghad dam (wet placed near normally consolidated earthfill) strain weakening due to particle orientation in the high plasticity earthfill was considered significant. At Sampna Tank strain weakening due to particle orientation and possibly progressive failure (mainly due to strength loss on shearing in partially saturated soils) in the medium to high plasticity outer earthfill were considered significant factors in the large post failure travel distance of 12 m for this slide. At San Luis (refer below) strain weakening due to progressive failure and particle orientation were considered significant factors in the relatively large post failure travel distance of 15 to 17 m.

Of the remaining cases material strain weakening on shearing was not considered greatly significant in the mechanics of post failure deformation. For several of these cases relatively large deformations were observed at failure due to factors other than material strain weakening, but in most cases post failure deformations were less than about 1 m and peak post failure velocities estimated to be in the slow class for failures in low to medium plasticity clays and silts, and in sandy and gravelly soil types.

In the discussion on the mechanics of failure (Section 5.5.2), progressive strain weakening in undrained loading of over-consolidated earthfills was considered significant in the mechanics of failure for a number of these cases. Athough, the limited post failure deformation would suggest it was not significant in the mechanics of post failure deformation. It is possible that a reduction of pore water pressures on shearing

within the shear band or along the surface of rupture retarded the post failure deformation in several of these cases, such as at Dam FD2 (discussed below).

(a) San Luis dam

The drawdown failure at San Luis dam (Figure 5.17) consisted of a deep-seated failure through the high plasticity slope wash foundation, broad central medium plasticity clay core and outer random earthfill zone. As discussed in Section 5.5.2.2, progressive failure was considered a significant factor in the mechanics of failure and would also have been significant for the mechanics of post failure deformation.

The slide itself was not observed until 14th September 1981 when the back-scarp was at a height of about 8 m. Photographic evidence indicated that limited deformations had occurred by the 4th September, but they were obscured by the riprap facing on the upstream slope. It is possible that the slide initiated in early to mid August toward the end of the very large drawdown.

The deformation monitoring only picked up the deceleration component of the slide movement (Figure 5.37). The records show that the post failure deformations were ongoing for some 100 days after the end of drawdown (about 28th August) and that the slide velocity gradually decreased over a period of 50 to 60 days. The likely period of peak velocity is estimated to have been between the 10th to 12th September and is broadly estimated at 1000 to 2000 mm/day. The velocity profile of the slide is therefore likely to be similar to that at Waco dam (Figure 5.30) and Carsington dam (Figure 5.31c), where the velocity increased slowly for several to many days prior to rapid acceleration to peak velocity followed by a period of deceleration. This type of deformation behaviour is indicative of progressive strain weakening during post failure deformation.

Factors contributing to the brittleness of the slide are likely to include; material strain weakening, due to both particle orientation in high plasticity clays and strain weakening in undrained loading of over-consolidated earthfills (Stark and Duncan 1991), and restraint on the lateral margins due to the variation in foundation topography (Von Thun 1988).

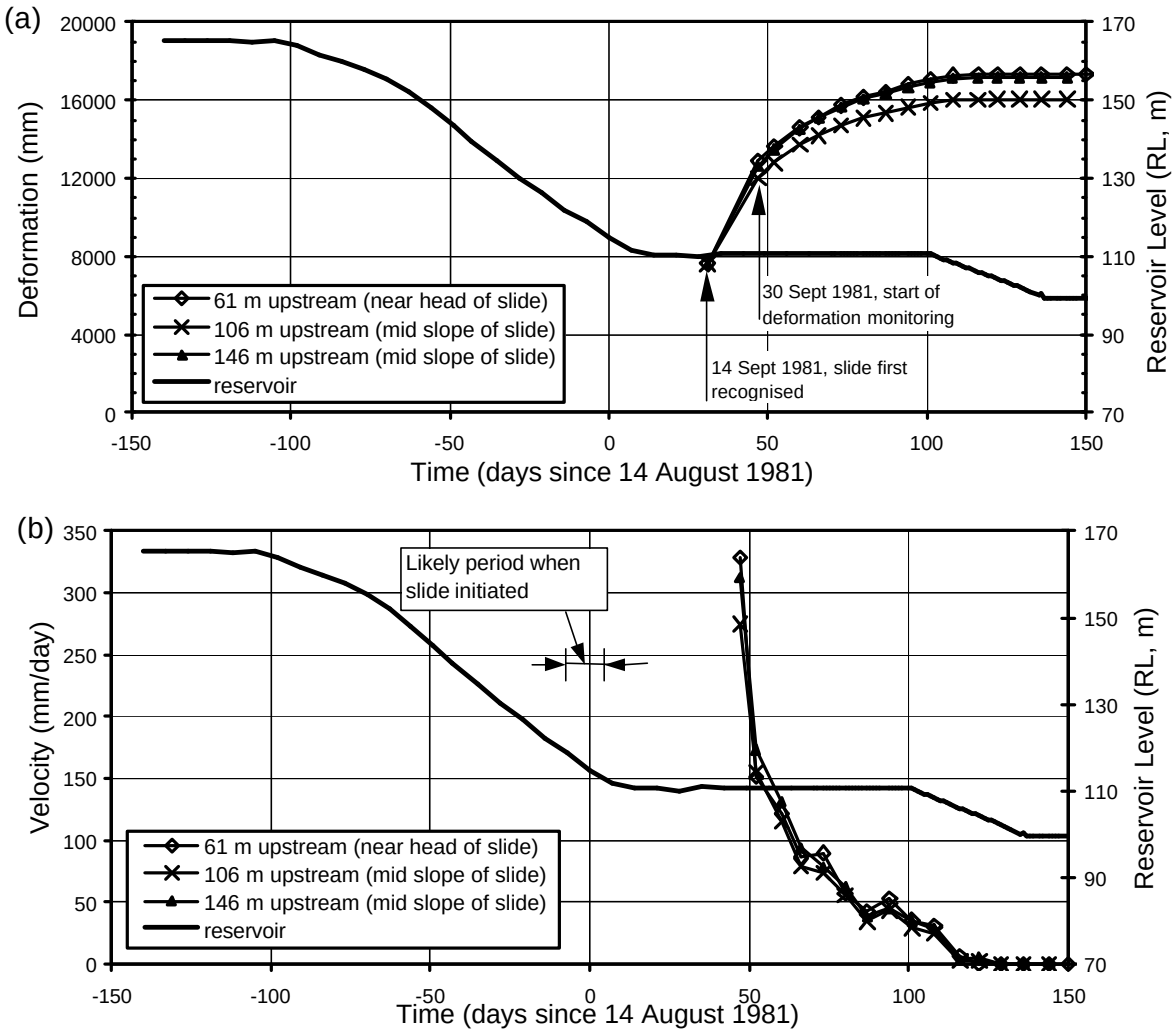

Figure 5.37: San Luis dam; the latter stages of post failure *(a)* deformation and *(b)* velocity of the first time slide following the 1981 drawdown (data courtesy of U.S. Bureau of Reclamation).

(b) Dam FD2

The deformation behaviour of the reactivated slide at Dam FD2 contrasts that of the first time slide at San Luis dam. The failure at Dam FD2 (Figure 5.38) occurred in the homogeneous left abutment section of the embankment in earthfills comprising well-compacted low plasticity sandy clays. The slide was thought to have initially occurred during the historically large and rapid 1993 drawdown (Figure 5.18a). The monitored deformation behaviour (Figure 5.39) is from reactivation of the slide during the subsequent 1994 drawdown.

Deformation of the slide was reactivated when the reservoir level was approximately coincident with the centre of mass of the slide. The interesting aspects of the deformation behaviour are that the slide moved as an intact unit and the velocity was

relatively constant whilst the drawdown rate was constant. Once the rate of drawdown slowed the velocity of the slide mass also decreased (Figure 5.39b), and continued for some 10 to 15 days after the drawdown rate was significantly reduced. Therefore, the out of balance forces due to the pore water pressure conditions in the upstream slope and reducing support of the reservoir water load on the upstream face were driving the deformation during reactivation of the slide. Progressive strain weakening is not significant during the reactivation as indicated by the constant velocity under constant drawdown rate and deceleration on decrease in the drawdown rate.

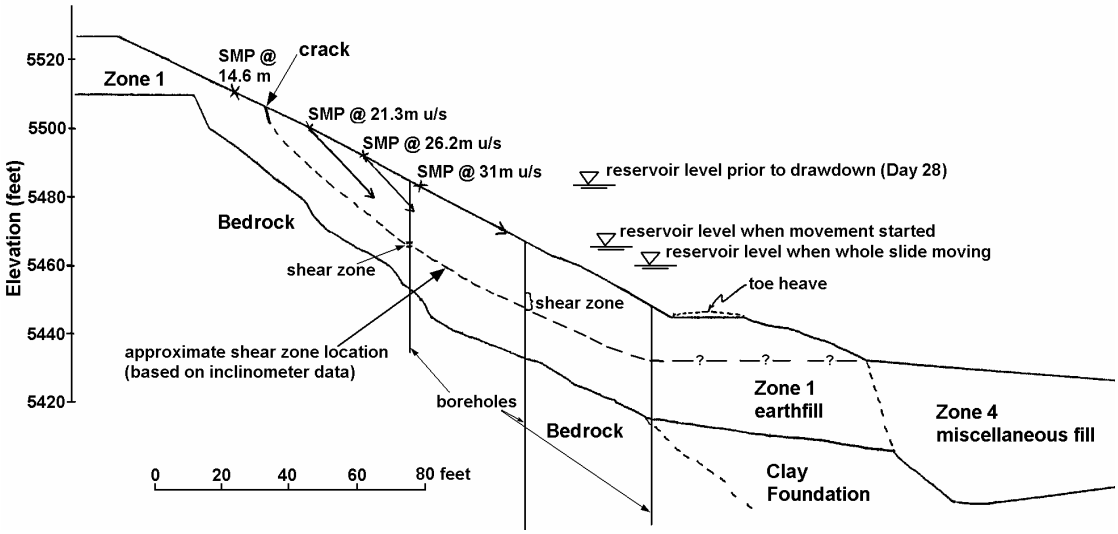

Figure 5.38: Section through the slide at Dam FD2.

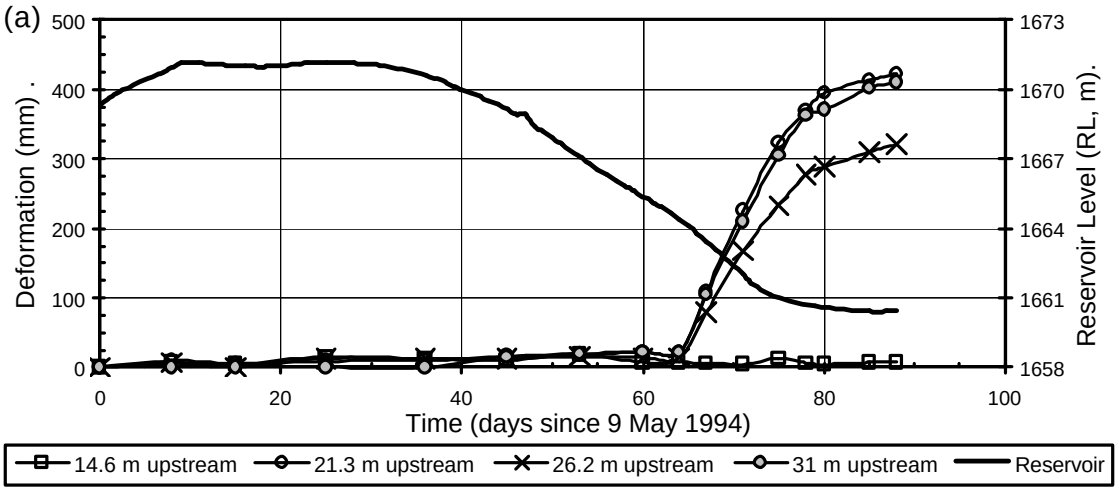

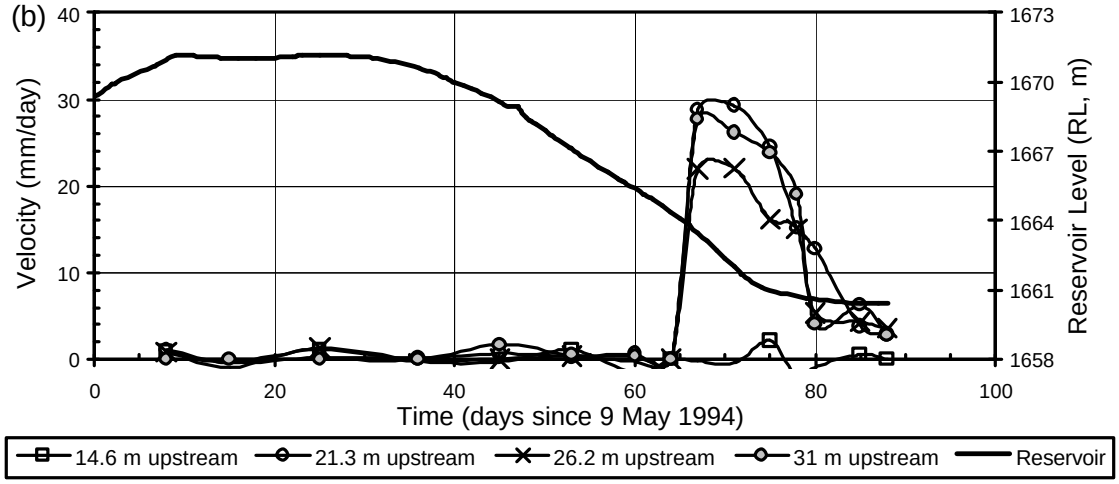

Figure 5.39: Deformation behaviour of the slide at Dam FD2 on reactivation during the 1994 drawdown; *(a)* deformation and *(b)* velocity.

5.6.4.2 Slope Failure Geometry and Upstream Slope Angle

The slope failure geometry (definitions given in Section 1.3 of Chapter 1) and upstream slope angle are significant factors in the post failure deformation behaviour of the slides during drawdown.

The failures at Dam FD3 and Forsythe dam were of Type 1 slope failure geometry. In these cases the toe of slide mass broke up and travelled "rapidly" for relatively large distances (Figure 5.36) down the face of the upstream slope whilst the bulk of the slide mass was retained in the source area and travelled only limited distance (1.7 m and 4 m respectively) at a likely much slower velocity. At Dam FD3 the toe of the slide mass travelled up to 6 to 9 m distance down the 2H to 1V slope and onto the upstream bench. At Forsythe dam the toe of the slide mass possibly travelled as much as 22 m down the 1.5H to 1V upstream slope to the upstream toe of the embankment.

The slope angle of the upstream slope is significant for the failures during drawdown. For Type 1 slope failure geometries, break up of the toe region and "rapid" travel of this broken up mass down the face of the upstream slope is likely for upstream slope angles greater than or equal to 2H to 1V (or about 27 degrees). For the Type 1 and Type 2 slope failure geometries, analysis indicates that a correlation exists between travel distance at the head of the slide and upstream slope angle for slides in medium plasticity clays (Figure 5.40). However, there is not a lot of case data with which to support the trend.

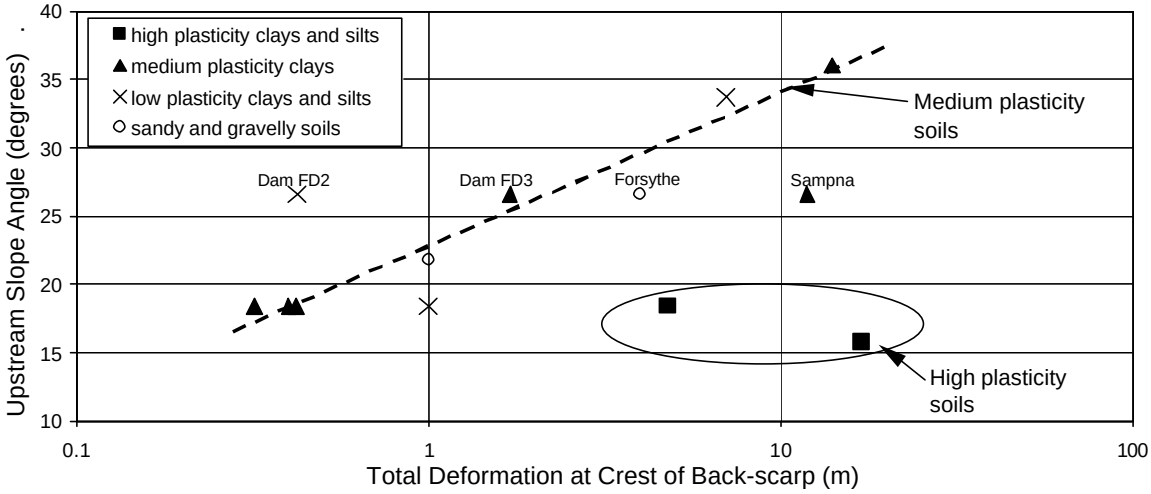

Figure 5.40: Upstream slope angle versus total post failure deformation for slides in embankment dams during drawdown.

5.6.4.3 Other Factors Affecting the Post Failure Deformation Behaviour of Drawdown Triggered Slides in Embankment Dams

For the failures at Mount Pisgah, Dam FD3 and Old Eildon dam, factors other than or in addition to material strain weakening on shearing and slope failure geometry were considered significant in the post failure deformation behaviour. At Dam FD3 and Mount Pisgah dam the presence of a concrete facing on the steep upstream slope (2H to 1V or steeper) was considered to contribute to the brittleness of the slide.

At Old Eildon dam, a concrete core-wall rockfill embankment with puddle clay zone on the upstream side of the core-wall, the loss of support from the water load on the upstream slope was considered to have contributed to the post failure deformation behaviour. The initial failure was thought to have occurred during the drawdown of 1927 (prior to completion of construction). Additional rockfill was placed on the upstream slope in 1928 whilst the reservoir was at close to full supply level, and during this period it was noted that continued placement of rockfill was required in the slide area due to ongoing subsidence (Knight 1938). On drawdown in 1929 a crest settlement of 7 m occurred, followed by subsequent deformations during the later remedial works. The post failure deformation on drawdown in 1929 was considered to have been a reactivation due to the reduction of the water load on the upstream face and the change in slope conditions from additional rockfill placement. Prior to the slide in 1929 deformations at the crest from previous slide movement were estimated at about 9 m.

5.6.5 POST FAILURE DEFORMATION BEHAVIOUR OF FAILURES IN THE DOWNSTREAM SHOULDER AFTER CONSTRUCTION

Of the thirteen case studies of slides in the downstream shoulder of embankment dams that occurred post construction, the dominant embankment types (Table 5.7) consisted of earthfill embankments (8 possibly 10 of 13 cases), in particular homogeneous earthfill embankments (5 possibly 7 cases). For the zoned earthfill and zoned earth and rockfill cases (1 case of each) the surface of rupture passed though the central core and foundation. Table 5.16 provides a summary of the timing of the failure, embankment type and geometry, material properties, drawdown causing failure and comments on the slide itself. Further details are given in the tables in Section 1 of Appendix D.

Information on the materials types and properties, location of the surface of rupture and post failure deformation records for these case studies is limited.

The post failure deformation and estimated peak velocity for the case studies is presented in Figure 5.41. Of the deformation records, only in one case (Siburua dam) are there records of deformation with time. For a further nine cases estimates of the total deformations were available mainly from sections provided in the published literature. Maximum post failure velocity ranges have been estimated for a number of the cases based on the amount of deformation and reference to times over which the deformation occurred. In general these estimates are very broad range and limited to the IUGS (1995) velocity categories.

As for the slides in embankment dams during construction and during drawdown, progressive strain weakening on shearing has the potential to result in post failure acceleration and relatively large travel distance of the slide mass. This is particularly important for slides in the downstream shoulder post construction due to the potential for breach and uncontrolled release of the water storage of slides with large and relatively rapid post failure deformation.

Assessment of factors that are significant in the deformation behaviour for slides in the downstream shoulder post construction is somewhat subjective because of the limited information on material properties and post failure deformation behaviour. Factors that were found to be significant in the post failure deformation behaviour of the case studies are:

- The potential for strain weakening due to particle orientation for near normally consolidated high plasticity clays (Seven Sisters and Santa Ana Acaxochitlan dam).

- Progressive failure. Progressive failure within the fissured clay foundation was possibly a significant factor in the relatively high degree of brittleness of the failure at Aran dam (as indicated by the large travel distance and high post failure velocity, refer Figure 5.41).
- Slope failure geometry. The slope failure geometry and orientation of the surface of rupture will affect the potential energy of the slide mass.
- Seepage into the deforming and dilating slide mass resulting in softening and strength reduction (see below). Apart from Yuba dam, greater post failure deformations and higher peak velocities were evident for the case studies where seepage was considered significant in triggering the slide (Barton, Santa Ana, Woodrat Knob, Fruitgrowers, Siburua, Great Western and Aran dams).
- Earthquake triggered liquefaction condition. For the slide at Yuba dam, triggered by earthquake, liquefaction in either the foundation or poorly compacted earthfill may have been a significant factor in the large and "rapid" post failure deformation behaviour observed.

For the case studies where instability was considered to be directly related to seepage and high pore water pressures (refer Section 5.5.3), the amount of post-failure deformation was generally greater, from as small as 1.5 to 2 m up to 9 to 11 m. The maximum post-failure velocity was estimated to range from slow (Great Western) to rapid, with most cases estimated to be in the moderate category. The failures at Santa Ana, Aran and Fruitgrowers dams were estimated to be in the moderate to rapid and rapid category. Dilation on shearing and softening due to infiltration of free water into the slide mass may have been significant for these failures.

For the case studies where, apart from Yuba dam, instability was considered not directly related to seepage and high pore water pressures (Harrogate, Seven Sisters and possibly Park Reservoir dams), the post failure deformation of the slide mass was less than 2 m and peak post-failure velocities were estimated to be in the slow or slow to low end of moderate categories.

Table 5.16: Summary of the case studies of slides in the downstream shoulder of embankment dams that occurred post construction.

Name of Dam	Year of Failure	Years since Const [d]	Slope *[1] Failure Geometry	Embankment Details			Material Properties (in zone of surface of rupture)		Location of Back-scarp	Comments
				Type	Hgt (m)	Slope (^{o})	Embankment *[2]	Foundation *[2]		
Park Reservoir	1969	60	Type 1	E'fill – rock toe (2,0,0)	24.4	33.7	SC – clayey sand. No formal compaction (?).	(failure through embankment only)	Crest, centre	Rotational slide in the upper part of the steep downstream slope (above the rockfill toe).
Arroyito	1984	6	Type 2	E'fill - filters (1,0,2)	20	21.8	GP/GW – well compacted sandy gravels, < 10% fines	(failure through embankment only)	Downstream slope	Shallow rotational slide, possibly a sloughing failure. Seepage out of the slope.
Barton	1922	12	Type 1/2 (?)	Homog (0,0,0)	12.2	33.7	CH – silty clays. No formal compaction.	(failure through embankment only)	Crest, downstream edge	Rotational slide in the steep downstream slope. Seepage on the downstream face.
Harrogate	1951	81	Type 2	Puddle E'fill (8,0,0)	8.8	27.8	CL – Boulder clay of medium plasticity. No formal compaction.	Deep clay profile, stiff to very stiff. Surface soil not removed.	Crest, downstream edge	Slow rotational slide. May have extended into foundation. Triggered by rainfall. Deep shrinkage cracks in the embankment.
Woodrat Knob	1961	5	unk	Homog (0,0,0 ?)	26	29.7	unk (suspect clayey and low permeability)	unk (possibly through fndn)	Downstream slope	No details. 9 m of post failure deformation at moderate rate. Steep downstream slope.
Fruit-growers	1937	39 (2 since raise)	Type 1/2 (?)	Homog (0,0,0)	11	26.6	CL – silty clay (residual shales) of medium plasticity. No formal compaction.	SC - clayey sands, alluvial (possibly through fndn)	Crest, centre	Likely rapid rotational slide. Occurred when reservoir was at its highest historical level. Seepage observed prior to the downstream raise in 1935.
Santa Ana	1952	21	Type 2	Homog (0,0,0)	12	26.6	CH – silty clays.	CH/OH – organic clay layer over soft clays. No fndn clean up.	Upstream slope	Deep seated compound (?) slide in the downstream slope that extended back to the upstream slope. Moisture observed on downstream slope in month prior to failure.
Siburua	1964	7	Type 5	E'fill - filters (1,0,1)	14.4	26.6	CL – shaly clays of medium plasticity. Rolled, well compacted	CL – shaly clays of medium plasticity. Possible favourable relict bedding.	Downstream slope	Shallow compound slide through the embankment and foundation in the lower downstream slope. Slide initiated when the reservoir was at full supply level.

Table 5.16: Summary of the case studies of slides in the downstream shoulder of embankment dams that occurred post construction (Sheet 2).

Name of Dam	Year of Failure	Years since Const [d]	Slope *[1] Failure Geometry	Embankment Details			Material Properties (in zone of surface of rupture)		Location of Back-scarp	Comments
				Type	Hgt (m)	Slope (^{o})	Embankment *[2]	Foundation *[2]		
Seven Sisters	1949 to 1956	0.3 to 13	Type 5	Zoned E & R	7.3	21.8	CH – clay, placed well wet of OMC. Rolled.	CH – clay, firm to stiff. Fissured to 2.1 m.	Crest, upstream edge	Deep seated (for low embankment height) rotational slide through the soft clay foundation.
Great Western	1958	51 (1 since raise)	Type 2	Homog (0,0,0 ?)	18.6	unk (≈ 26 ?)	Rolled earthfill	Alluvial clays	Upstream slope	Deep seated compound (?) slide that extended back to the upstream embankment slope. Close to highest reservoir level in embankment history at the time of failure.
Aran	1978	1	Type 2/5 (?)	Zoned E'fill	30.3	23	CH – clay, rolled	CH – alluvial fissured clays.	Crest, downstream edge	Deep seated compound (?) slide through the fissured clay foundation. Rapid post failure deformation.
Lake Yosemite	1943	60	Type 2	Homog (0,0,0)	16.2	26.6	CL/SC – low plasticity gravelly sandy clays and clayey sands. No formal compaction.	CL/SC – as per embankment material. Referred to as cemented.	Downstream slope	Shallow rotational (?) slide that passed through upper foundation. Possibly triggered by rainfall.
Yuba	1951	41 (2 since raise)	Type 2	Homog (0,0,0)	7.6	29.7	CL – sandy clays of medium plasticity. No formal compaction.	Alluvial clays	Crest, centre	Compound (?) slide triggered by earthquake. Seepage on the downstream slope. Likely rapid post failure deformation.

Notes: Hgt = height Const [d] = construction unk = unknown OMC = Standard optimum moisture content

Homog = homogeneous earthfill embankment E'fill – filters = earthfill embankment with filters

E'fill – rock toe = earthfill embankment with rock toe Zoned E'fill = zoned earthfill embankment

Puddle E'fill = puddle core earthfill embankment Zoned E&R = zoned earth and rockfill embankment

*[1] Slope failure geometries defined in Figure 1.3 in Section 1.3 of Chapter 1.

*[2] Soil classification to the Australian soil classification system (AS 1726-1993)

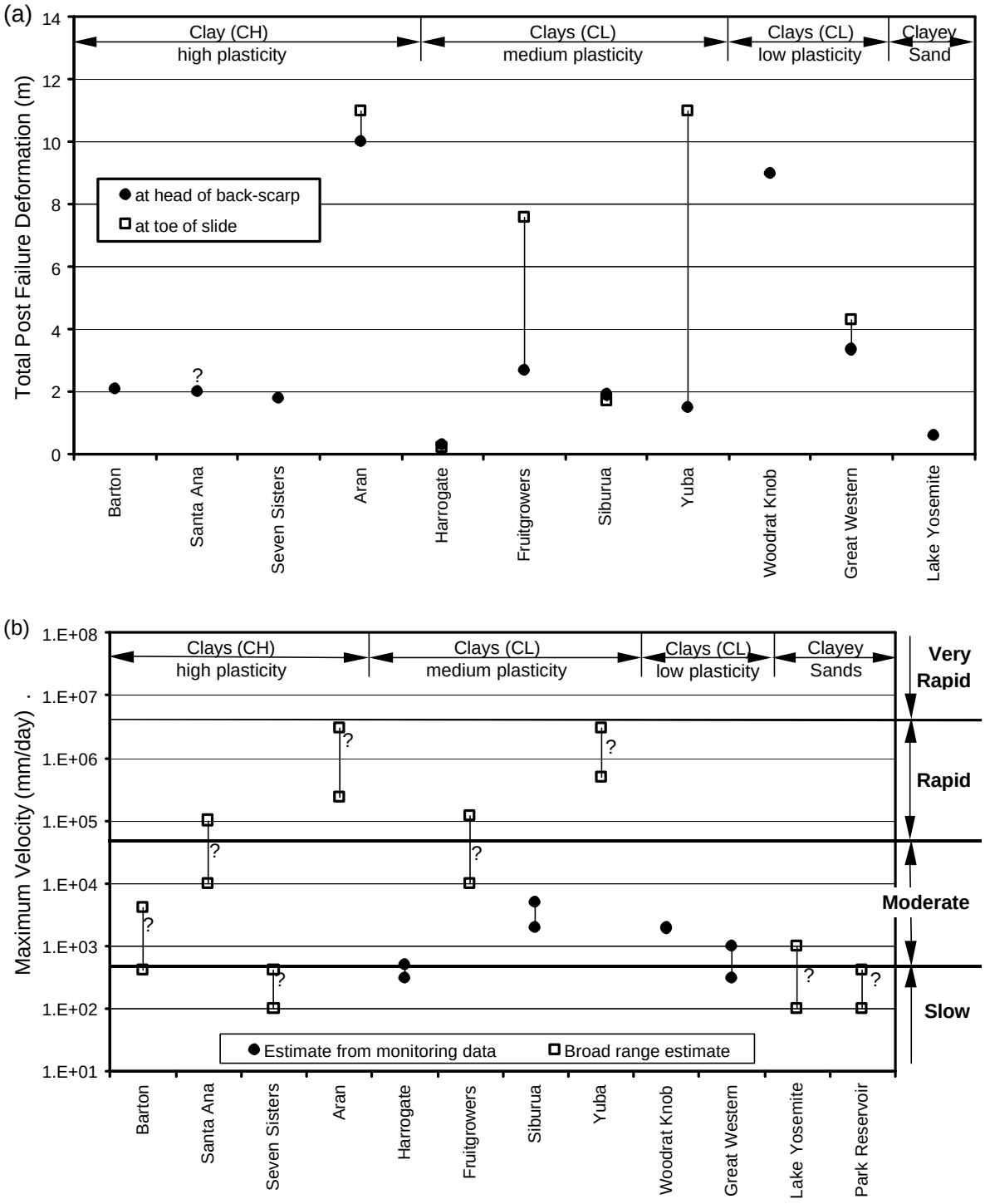

Figure 5.41: Post construction slides in the downstream shoulder; post failure *(a)* deformation, and *(b)* estimated peak velocity.

5.6.5.1 Potential for Dam Breach due to Instability of the Downstream Slope

An important aspect of post construction slides in the downstream shoulder is the potential for large deformation on sliding that could potentially result in a breach and uncontrolled release of water from the reservoir. The slide at Santa Ana dam resulted in

breach of the embankment, at Fruitgrowers dam it was a significant factor in the eventual breach (refer Section 5.2.1) and at Great Western dam a breach was only narrowly averted. Importantly, the reservoir was at or close to full supply level at the time of the failure in these three cases and a number of the other cases where instability was triggered by seepage and high pore water pressures.

The case studies of failures during construction (Section 5.6.3) indicates that there is a greater likelihood for extension of the back-scarp to incorporate the opposite slope where the surface of rupture involves the foundation. In eight of the ten cases involving the foundation the back-scarp extended back to between the central region of the crest and the opposite slope. This compares to three of seven cases involving the embankment only (excluding the cases of lateral bulging). The strength of the foundation in comparison to the strength of the embankment material/s is significant in the likelihood of involvement of the foundation in the failure.

For the post construction slides in the downstream shoulder the case study evidence is not as clear as for the failures during construction. In three of the six cases where the slide back-scarp extended to or upstream of the embankment centreline (refer Table 5.16), the surface of rupture passed through the foundation (Santa Ana, Great Western and Seven Sisters dams). In two cases it was unsure if the foundation was involved in the failure (Fruitgrowers and Yuba dam) and at Park Reservoir dam the surface of rupture was through the embankment only (the small slide was confined to the upper part of the steep down-slope). Of the three slides known to incorporate the foundation, in two cases (Santa Ana and Seven Sisters dams) the foundation was of high plasticity clays, and in the case of Santa Ana dam the back-scarp extended back to a level below that of the reservoir and a breach subsequently occurred. At Great Western dam the foundation was of alluvial clays of unknown plasticity, and although the back-scarp extended back to a level below that of the reservoir on the upstream slope of the crest, a breach was averted by drawing down the reservoir and stabilising the downstream toe of the embankment.

Therefore, embankments founded on weak or high plasticity clay foundations are potentially susceptible to deep-seated failures that could potentially lead to an uncontrolled breach from the reservoir. Higher post failure velocities are likely with increased brittleness of either the materials and/or the slide mechanics, and where the trigger for failure is seepage related.

5.7 POST FAILURE DEFORMATION BEHAVIOUR - CUT SLOPES IN HEAVILY OVER-CONSOLIDATED CLAYS

This section presents the post failure deformation behaviour for the case studies of failures in cut slopes in heavily over-consolidated high plasticity clays. Data on travel distance and travel velocity of the case studies is presented, and the factors affecting the deformation behaviour of the slide mass are discussed, with greater detail given for several case studies to highlight some of the factors affecting deformation behaviour.

5.7.1 SUMMARY OF FACTORS AFFECTING THE POST FAILURE DEFORMATION

Progressive failure is a significant factor in the mechanics of failure of cuts in high plasticity heavily over-consolidated clays as discussed in Section 5.4.1. It is also significant in the mechanics of post failure deformation. The brittleness of the slide post failure is dependent, amongst other factors, on the strength loss on shearing from the shear strength at failure. Therefore, if at failure the strength of the soil mass is close to peak strength (i.e. progressive failure was not greatly significant in the mechanics of failure), such as undrained failure of a very steep cut, then the failed slide mass has a high potential brittleness due to the large strength difference between at failure and residual strength. Conversely, if the average shear strength along the surface of rupture at failure is close to the steady state strength (i.e. progressive failure was significant in the mechanics of failure) then the potential brittleness of the failed slide mass is much lower and due to the smaller difference in strength between at failure and residual strength.

Other factors contributing to the brittleness of the slide mass at failure and the post failure deformation behaviour of cuts in heavily over-consolidated high plasticity clays are:

- Internal brittleness in the slide mechanics.
- Brittleness due to three-dimensional effects and release of the slide on the lateral margins, such as formation of shear surfaces through retaining walls.
- Orientation of the surface of rupture. For most Type 1 and Type 2 slope failure geometries the surface of rupture was of compound shape with basal translational component and rotational back-scarp, such as the failure in London clay at Northolt in 1955 (Figure 5.42).
- Slope failure geometry.

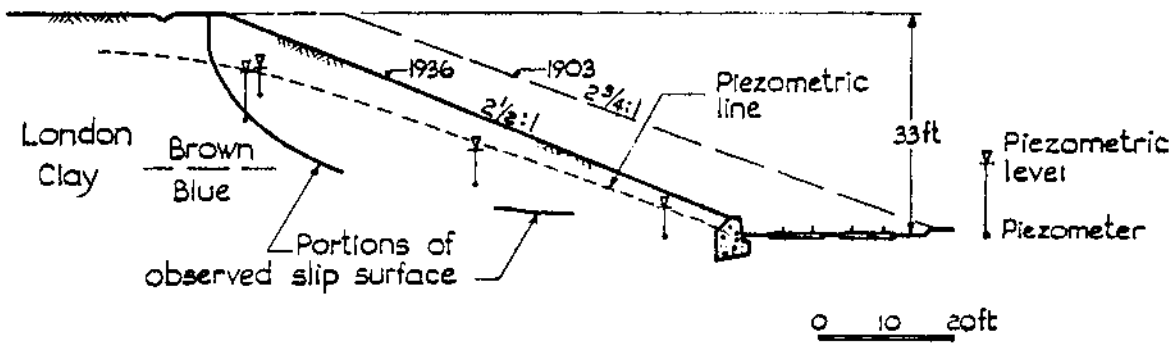

Figure 5.42: Slide in the cut slope in London clay at Northolt in 1955 (Skempton 1964)

5.7.2 SUMMARY OF THE POST FAILURE DEFORMATION AND VELOCITY OF THE FAILURE CASE STUDIES

Table 5.17 and Table 5.18 present a summary of the slope geometry and post-failure travel distance and velocity of the failure case studies within cut slopes in London clay and Upper Lias clay respectively. Further details on the individual cases are given in Section 2 of Appendix D.

The post failure deformation records for most of the case studies analysed is limited. Monitored deformation records were only available for several cases. For most cases the deformation was estimated from pre and post failure sections of the slides. Post failure velocities were estimated from the total deformation and qualitative information on the time over which the deformation occurred. These velocity estimates are broad range and have generally been restricted to the IUGS (1995) velocity categories unless sufficiently detailed information was available for more precise estimation.

Figure 5.43 and Figure 5.44 present plots of the post failure deformation (deformation plotted as a percentage of the slide length measured as the straight line distance from the head to the toe of the slide) and estimated peak post failure velocity for the case studies of cuts in London clay. For the Type 1 and Type 2 slope failure geometries the post failure deformation and velocity typically increased with increasing cut slope angle. But, the figures also show that a significant change in deformation behaviour (for both deformation and velocity) is evident for the Type 1 and Type 2 slope failure geometry. This trend is more clearly evident in Figure 5.45 and Figure 5.46 where the post failure deformation and velocity are plotted against cut slope angle. The group of slides of rapid post failure velocity and greater deformation occur in the steeper cut slopes when the slides are separated on slope failure geometry.

Table 5.17: Cut slope failures in London clay.

Name	Age (yrs)	Slope Geometry		SFG *[1]	Post-failure Deformation		Comment
		Hgt (m)	Slope (°)		Deformation (m)	Velocity*[2] Category	
Hadley Wood	70	13.6	13.5	1	0.9 (c), 1.8 (t)	Slow	Possible reactivation of deformation.
Grange Hill	50	17.4	17.8		2 (c & t)	Slow	Occurred in winter, suspect slow.
West Acton A	44	4.7	18.4		0.36 (c), 1.5 (t)	Slow	Limited deformation, suspect slow
Northolt	19	10.1	21.8		1.2 (c), 0.8 (t)	Slow to moderate	Compound slide in slope above retained section.
Grove Park	98	9.4	22.5		3.3 (c), 10.8 (t)	Rapid	At toe slide travelled 10.8 m on 22.5 degree slope.
New Cross	3	23	33.7		10 (c), 31 (t)	Rapid	Rapid compound failure in steep cut.
Crews Hill	47	5.3	16.2	2	1.2 (c), 1.5 (t)	Slow	Possibly a reactivated translational slide
West Acton B	44	4.8	18.4		0.41 (c), 2.5 (t)	Slow	Limited deformation, suspect slow.
Whitstable	99	11.4	18.4		1.5 (c), 2 (t)	Slow	Deformation occurred over a period of several weeks to months.
Sudbury Hill	46	7	18.4		2.2 (c), 1.6 (t)	Slow	Deformation in winter over several years.
Fareham	59	9.5	19.5		1.5 (c), 4 (t)	Slow	Deformation over several years, reactivated in 1967.
Althorne	60	8.8	20.5		2 (c), 3 (t)	Slow	Suspected reactivation.
Cuffley	38	12	20.7		2.8 (c), 3.5 (t)	Slow	Seasonal winter deformations over at least 6 years.
Dedham	112	10.2	22		2.1 (c), 5 (t)	Moderate	Continued slow deformation when toe of slide cut back.
Kingsbury S1	16	6.2	23.5		0.5 (c), 1.0 (t)	Slow	Limited deformation, suspect slow.
St. Helier	22	7.3	25.3		2.3 (c), 2.5 (t)	Slow to moderate	Deformation over at least 4 years.
Isle of Sheppey A	6	12	38		12.5 (t)	Rapid (?)	Steep cut slope, suspect rapid velocity of deformation.
Isle of Sheppey B	8	10	41		9 (t)	Rapid (?)	Steep cut slope, suspect rapid velocity of deformation.
Uxbridge 1937	37	9	43		5 (t)	Rapid	Failure of temporary vertical excavation, suspect rapid.
Bradwell	5 days	14.8	56		unk	Rapid	Steep cut, rapid deformation.
Upper Holloway	81	5.3	25	5 (retained cuts)	1.3 (c) to 0.7 (t)	Slow	Initial deformation in 1951. Reactivation of slide (new retaining wall) in 1953-55.
Wembley Hill	13	17	26		6 (c & t)	Rapid	6 m deformation over 0.5 hour period, only slight deformation thereafter.
Wood Green	55	11.3	28		0.9 (t)	Slow	Limited slow deformation.
Kensal Green	29	6.1	29.7		0.3 (t)	Slow	Limited slow deformation.
Uxbridge 1954	54	10.2	32		0.7 (t)	Slow	Deep-seated failure.

Age = age of cut slope at failure Hgt = cut slope height Slope = cut slope angle
(c) = crest deformation (t) = deformation at toe unk = unknown
*[1] SFG = Slope failure geometry. Refer Section 1.3 for definitions.
*[2] IUGS (1995) velocity category (refer Table 1.1 in Section 1.3).

Table 5.18: Cut slope failures in Upper Lias clay.

Name	Age (yrs)	Slope Geometry		SFG *[1]	Post-failure Deformation		Comment
		Hgt (m)	Slope (°)		Deformation (m)	Velocity*[2] Category	
Ardley	52	15	22	1	0.5 (c), 0.8 (t)	-	Slide in slope above retaining wall following heavy storms.
Wothorpe B	5	6.1	18.5	2	3.5 (c), 2 (t)	slow	Deformation initiated in winter of 1964/65 and continued over several years.
Seaton	67	9.3	20.8		2.0 (c), 2.2 (t)	-	Translational slide in brecciated clays.
Stowehill B	122	8.2	23		0.6 (c), 1.4 (t)	-	Rotational slide that partly encompassed earlier slide (56 years earlier).
Heyford	125	9.1	24		2.0 (c), 2.3 (t)	-	Slide in winter following very heavy December 1960 rainfall.
Hunsbury Hill Tunnel (1954)	77	16.4	24.5		7.6 (c), 1 (t)	-	Reactivated slide deformations over many years. Large crest deformation as a result of continued trimming back of toe.
Stowehill A	66	10.2	24.8		2 (c), 1 (t)	-	Initial Stowehill slide in 1901.
Culworth A	61	8	26.5		2 (c & t)	-	Slide occurred in the winter of 1957/58 following a very wet summer.
Culworth B	61	8	26.5		2 (c), 1.6 (t)	-	Slide occurred in the winter of 1957/58 following a very wet summer.
Charwelton	40	9.6	27.2		1.4 (c), 1.3 (t)	slow	Slide active for more than 1 week, therefore slow.
Barrowden	83	4.3	28.8		0.55 (c), 0.5 (t)	-	Deep-seated rotational slide.
Wellingborough Station	105	10	31		unk	-	Limited information on slide.

Age = age of cut slope at failure Hgt = cut slope height Slope = cut slope angle
(c) = crest deformation (t) = deformation at toe unk = unknown
*[1] SFG = Slope failure geometry. Refer Section 1.3 for definitions.
*[2] IUGS (1995) velocity category (refer Table 1.1 in Section 1.3).

No such correlation is evident for the slides in cut slopes of London clay of Type 5 slope failure geometry, indicating that cut slope angle is not greatly significant for these failures.

For the cut slopes in Upper Lias clays, estimates of the post failure velocity were possible for only two cases. Both were estimated to be in the slow IUGS category. The limited post failure deformation of all of the cut slope failures (Table 5.18) suggests it is likely that the post failure velocity is within the slow to lower end of the moderate range for them all. In addition, no travel distance correlation is evident with respect to cut slope angle. This is likely to be partly due to the limited range of cut slope angles for the case studies, which ranged from 18 to 31 degrees.

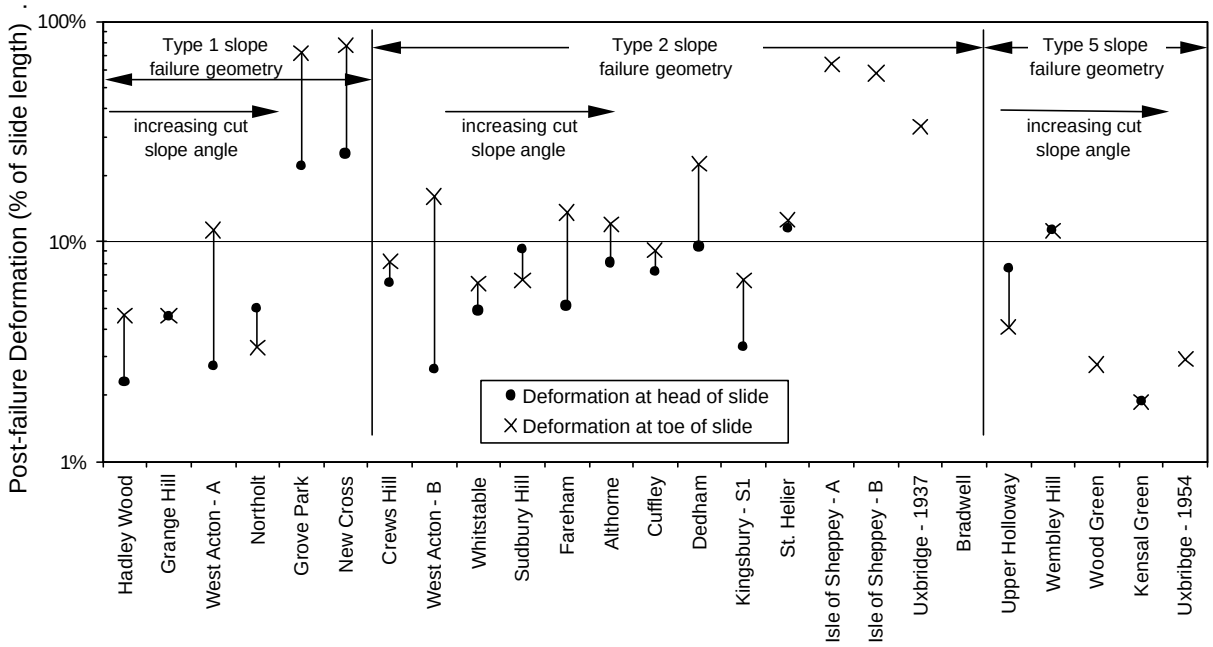

Figure 5.43: Post-failure slide deformation for cut slopes in London clays.

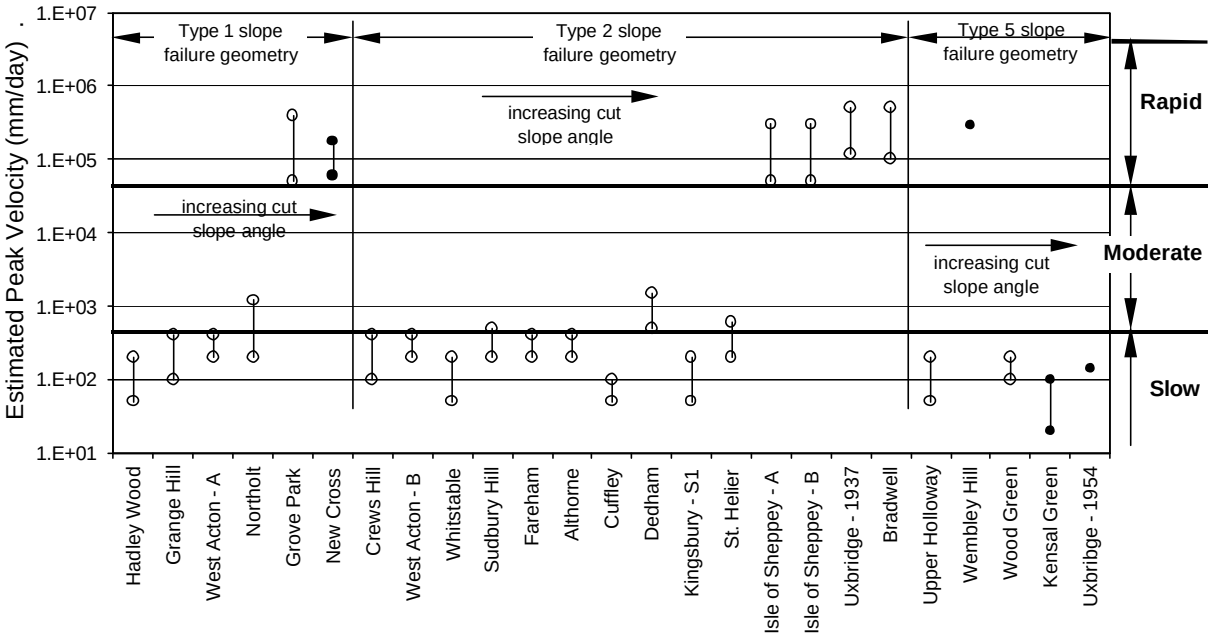

Figure 5.44: Estimated peak post failure velocity of slides in cut slopes in London clays.

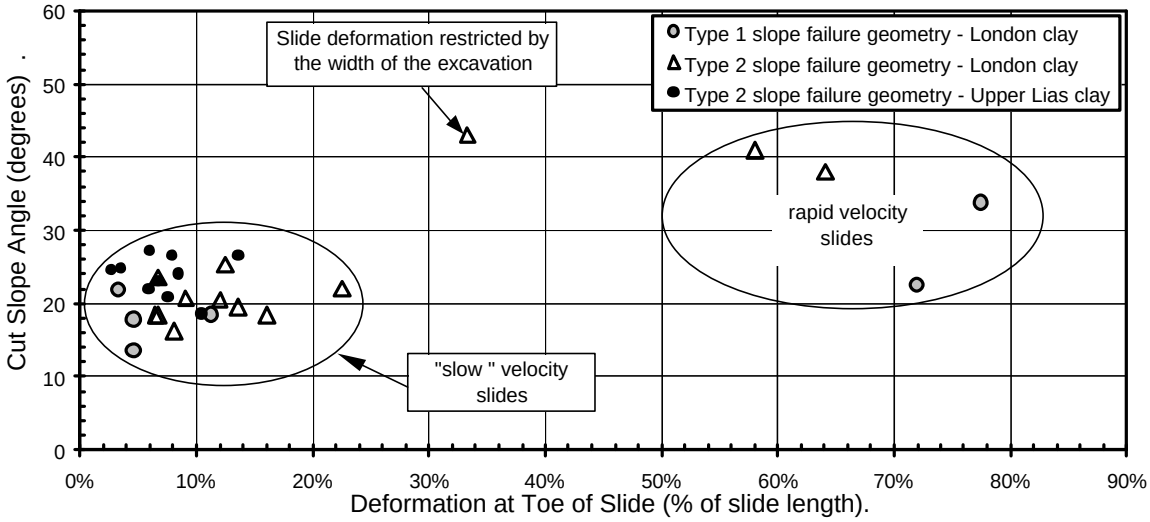

Figure 5.45: Cut slope angle versus post-failure deformation at the slide toe for cut slopes in heavily over-consolidated clays of Type 1 and Type 2 slope failure geometry.

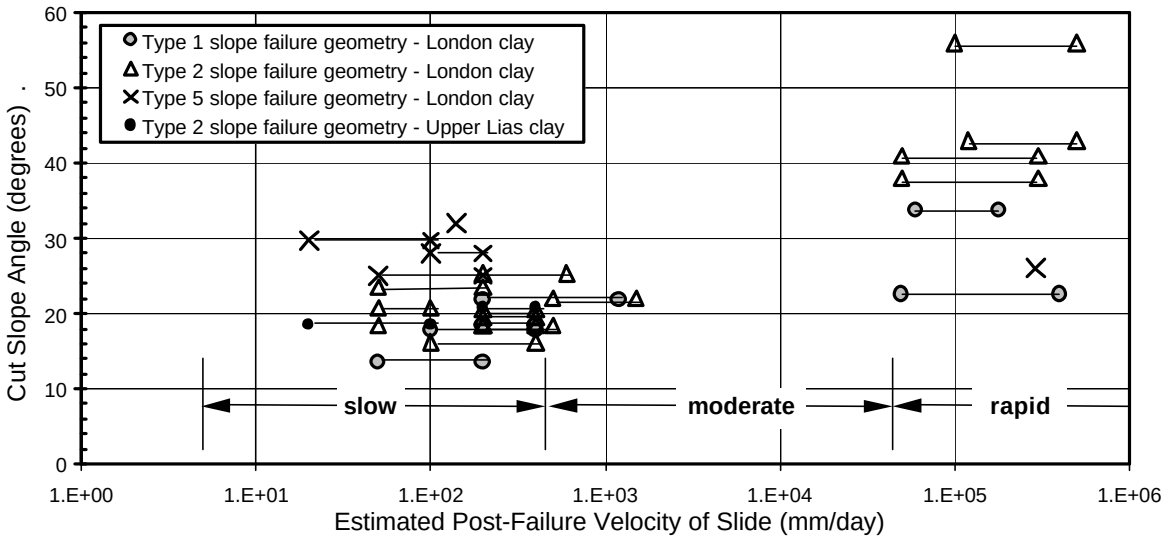

Figure 5.46: Cut slope angle versus estimated post-failure slide velocity for cut slopes in heavily over-consolidated clays.

The deformation behaviour within the three types of slope failure geometry (Type 1, Type 2 and Type 5) is discussed in the following sections. Factors influencing the post failure deformation behaviour are discussed in greater detail under the section on Type 2 slope failure geometry, the most dominant category for the failure case studies in cut slopes.

5.7.3 FAILURES IN CUT SLOPES – TYPE 2 SLOPE FAILURE GEOMETRY

For the Type 2 slope failure geometries the post failure deformation behaviour, from analysis of the case studies, indicates:

- At cut slopes less than about 28 to 35 degrees the slide mass remains virtually intact and within the source area on sliding. Post failure deformation of the slide mass is generally limited to less than 2 to 4 m, and the peak velocity is likely to be in the slow to lower end of the moderate range. Post failure deformations generally occur over a period of days to weeks and are readily reactivated during adverse weather conditions.
- At cut slopes greater than about 30 to 35 degrees, the post failure travel distance of the toe region of the slide is generally much greater (50 to 70% of the slide length, Figure 5.45) and post failure velocities typically in the rapid range (Figure 5.46). The post-failure deformation generally occurs over a short time period (minutes to hours in most cases depending on the steepness of the cut slope). Continued deformations after the initial event are likely to be very limited.

For the Type 2 cut slope failures in London clays in slopes less than 28 to 30 degrees (i.e. the "slow" slides), the age of the slope at failure ranged from 16 to more than 100 years after excavation. For these failures progressive failure is likely to have been a significant factor in the mechanics of failure.

For these "slow" slides of Type 2 slope failure geometry (and also Type 1) the post-failure deformation at initial (or first time) failure occurred "slowly" over many days. Deformations of the slide mass were reactivated during subsequent wet winters or seasonally wet periods in the years following the initial failure (James 1970), and generally at lower velocities than at the initial failure. This seasonal reactivation indicates that the failed slope is of marginal stability and triggered by seasonally high pore water pressure conditions in the slope.

Two-dimensional limit equilibrium analysis of some of these "slow" slides (Table 5.19 in Section 5.8.1) indicated that the residual factor of safety was relatively low (0.55 to 0.8). This would suggest that the initial slide has a potentially high degree of brittleness post failure. However, the mechanics of post failure deformation as observed would suggest that the kinetic energy of the slide mass at any time is relatively small (i.e. most of the available potential energy is consumed as frictional energy or by other means).

The factors restricting these "slow" slides from reaching higher velocities at initial failure (and therefore greater travel distances) are thought to include:

- Restraint on the lateral margins in the form of resistance to development of a shear surface, including three-dimensional effects such as changes in slope geometry.
- Strain hardening on shearing in these over-consolidated clays and development of a reduction in pore water pressure due to dilation. The effect of strain hardening on the deformation behaviour would be to retard the deformation of the slide mass.
- Change in geometrical shape with deformation of the slide mass, i.e. the slide deforms to a more stable configuration for a given set of strength parameters.
- Visco-plastic properties of these high plasticity soils.

All explanations are considered to have some merit in the overall mechanics of post failure deformation for these "slow" slides. The strain hardening response is considered to have greater merit in terms of being able to explain the subsequent reactivation of deformation under climatic conditions less adverse than what triggered the initial slide. Reduced pore water pressures are developed in the region of the surface of rupture due to the propensity of the soil to dilate on shearing. Moisture will then migrate to these regions of low pore water pressure due to pore water pressure variation set up in the slope post the failure, and with time, result in softening and dilation in the region of the surface of rupture. The consequent reduction in the shear strength properties means that the slope is of limiting equilibrium during subsequent seasonally wet periods and deformation is reactivation. Equilibration of pore water pressure variations in the slope are likely to occur slowly in these high plasticity clays due to their low permeability.

The cut slope failures in slopes greater than 30 to 35 degrees in London clays generally occurred in a matter of days to years after excavation (upper limit of 8 years for the case studies). The rapid post failure velocity and greater deformation of the slide mass for these slides is indicative of a greater conversion of available potential energy to kinetic energy than for the "slow" slides. These "rapid" slides tended to break up to a greater degree post failure indicating a greater amount of energy was used in disaggregation of the slide mass.

5.7.4 FAILURES IN CUT SLOPES – TYPE 1 SLOPE FAILURE GEOMETRY

For the Type 1 slope failure geometries the post failure deformation behaviour, from analysis of the case studies, indicates:

- At cut slopes less than about 22 degrees, the slide mass remains virtually intact on sliding within the slide source area. Limited post failure deformation (less than about 1 to 2 m) at a velocity in the slow to lower end of the moderate range is generally observed. Deformations generally occur over a period of days to weeks and are readily reactivated during adverse weather conditions.
- At cut slopes greater than about 22 degrees, the toe region of the slide will potentially break up and travel at a moderate to rapid velocity and travel for relatively large distances (over a short time period) on the lower portion of the cut slope. The portion of the slide that does not exit the failure bowl remains virtually intact and, as observed, the travel distance is much lower than at the toe of the slide. Further deformations after the initial event are likely given the potential for additional material to move out of the failure bowl and onto the cut slope below.
- With increasing cut slope angle above about 22 degrees, the volume of material likely to evacuate the source area and travel "rapidly" down the cut slope below is likely to increase. At Grove Park (cut slope of 22.5 degrees) only a small volume of the slide mass evacuated the source area compared with the much larger volume at New Cross (Figure 5.47) where the cut slope angle was much steeper at 34 degrees.

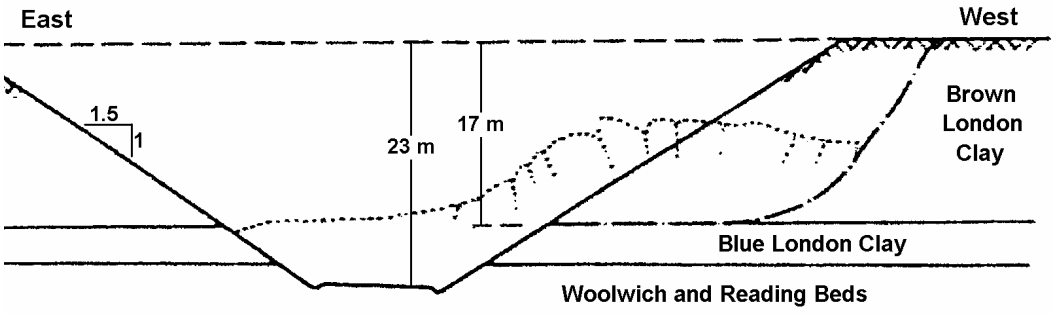

Figure 5.47: Failure in the cut slope in London clay at New Cross in 1841 (Skempton 1977)

The brittleness of the slide mass at failure is considered a significant factor in the relative volume of material that evacuates the source area. For the failure at New Cross, which occurred three years after excavation, the average available shear capacity along the surface of rupture at failure and therefore potential for post failure strain weakening

on shearing was likely to have been significantly greater than at Grove Park where failure occurred 98 years after initial excavation.

5.7.5 FAILURES IN CUT SLOPES – TYPE 5 SLOPE FAILURE GEOMETRY

For the failure case studies of Type 5 slope failure geometry (all retained cut slopes in London clays), the cut slope angle is not a significant factor in the post failure deformation behaviour (Figure 5.46). In four of the five case studies the post-failure deformation was less than 1.5 m and post failure velocity was estimated to be in the slow category (Table 5.17). In contrast, the slide at Wembley Hill (Figure 5.48) travelled a distance of 6 m, most of this within a 30 minute period, and therefore at a rapid velocity.

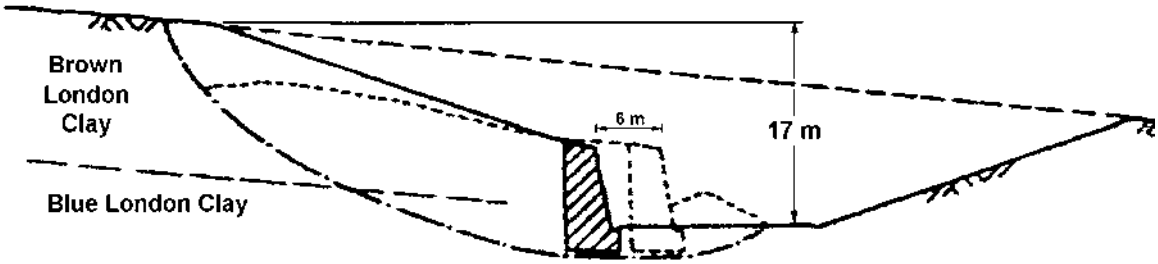

Figure 5.48: Failure in the retained cut slope in London clay at Wembley Hill (Skempton 1977)

The factors controlling the mechanics of post failure deformation behaviour are as previously discussed for the Type 2 slope failure geometries (Section 5.7.3). Conditions resulting in increasing kinetic energy of the slide mass will result in acceleration to higher velocities and greater travel distances.

For the slide at Wembley Hill factors influencing the post failure deformation behaviour potentially include:

- Greater inertia of the slide mass. The volume and cross sectional area of the Wembley Hill slide (volume estimated at 70000 m^3) were significantly greater than for the other four Type 5 slides.
- Brittleness associated with release on the lateral margins. At Wembley Hill loud reports were heard at the time of failure, most likely associated with failure through the retaining wall on the margins. Of the other four Type 5 case studies, cracking in the retaining wall was reported at Uxbridge and it is suspected that similar limited

damage to the retaining wall was likely at the other retained cut slope sites given the limited deformation observed.

- Timing of the initial recognition of the slide to the stage of failure and whether or not any remedial works were undertaken to ameliorate the stability of the slope.

Deformation behaviour at Uxbridge in 1954

The slide at Uxbridge in 1954 (Figure 5.49) is considered to be typical of the "slow" post failure deformation behaviour of slides of Type 5 slope failure geometry in retained cut slopes. The post failure deformation of the slide developed slowly over many days before accelerating as shown in Figure 5.50. The first signs of instability (Watson 1956) were observed in late September of 1954, some 60 days prior to the monitoring shown, in the form of cracking in the pavement above the cut slope. By the 10th of November 1954 further deformation was observed in the head region of the slide as well as deformation in the toe region (a crack in the retaining wall was observed to have been getting worse and the track drain beyond the retaining wall was not functioning properly). By the 22nd of November the railway officials were unable to maintain the super-elevation of the track in the vicinity of the slide indicating heave deformations in this area. Monitoring points were then established on the retaining wall in the toe region of the slide. The records show an increase in the post failure velocity of the slide over a period of several days (from < 10 mm/day to about 150 mm/day).

Restraint on the lateral margins (mainly from the retaining wall, but also from the changing slope topography) and passive resistance at the toe of the retaining wall are thought to have been influential in the "slow" post failure velocity of the slide. Given the length time over which the slide developed (a six to eight week period), it was possible for remedial measures to be undertaken to slow down and stop the deformation of the slide as was observed (Figure 5.50). These measures included excavation works at the head of the slide, filling works at the toe of the retaining wall and strutting of the retaining wall (Watson 1956).

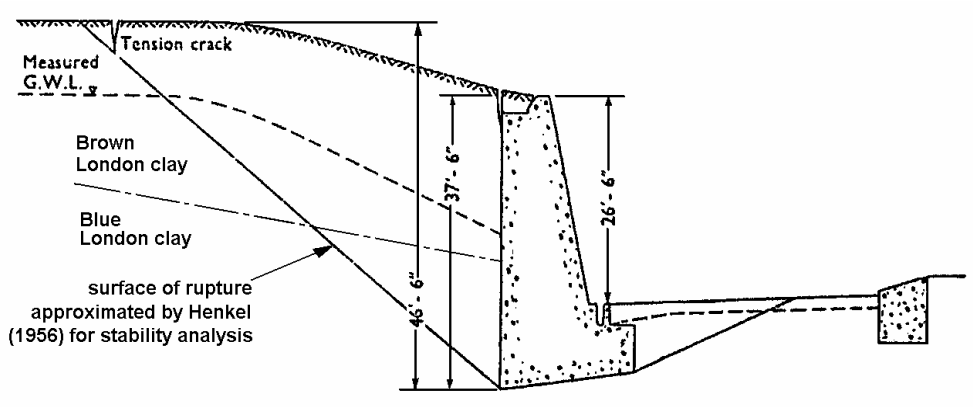

Figure 5.49: Failure in the retained cut slope in London clay at Uxbridge in 1954 (adapted from Henkel 1956)

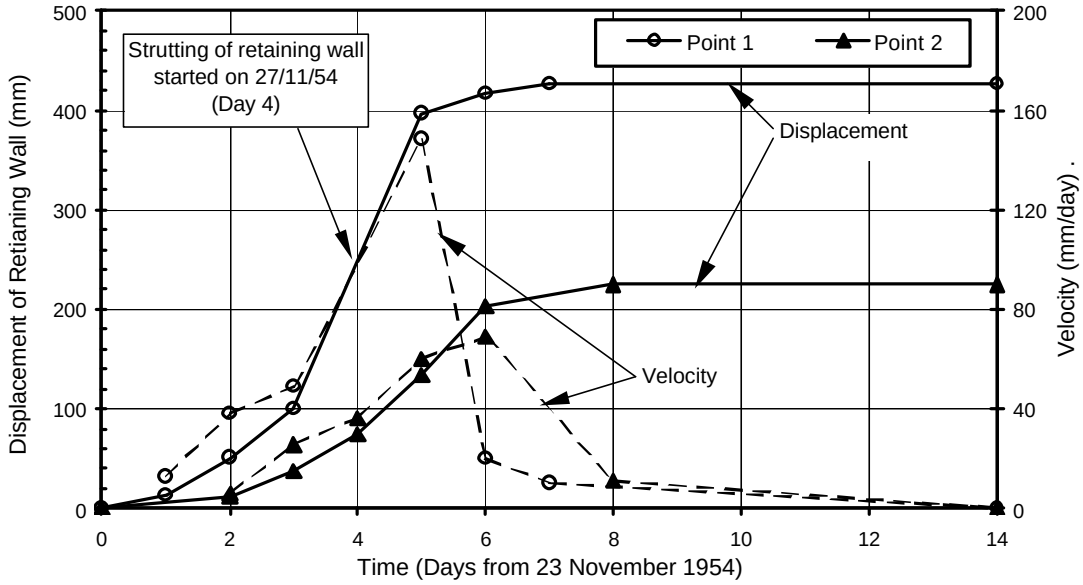

Figure 5.50: Monitored post-failure deformation of the slide in the retained cut in London clay at Uxbridge in 1954 (adapted from Watson 1956).

5.8 PREDICTION OF POST-FAILURE TRAVEL DISTANCE

5.8.1 KHALILI ET AL (1996) MODEL FOR INTACT SLIDES

The Khalili et al (1996) model for estimating the post-failure deformation of intact slides has been used to analyse the post failure deformation behaviour of a number of the failure case studies in embankment dams and cut slopes in heavily over-consolidated high plasticity clays. The model is described in Section 4.3.5.2 of Chapter 4. In summary, the model considers two modes of failure; a "rapid" model based on the principle of conservation of energy (i.e. a simplified lumped mass model), and a "slow"

model based on equations of equilibrium between the driving and resisting forces of the slide.

The failure model is shown in Figure 5.51. $?_i$ and $?_f$ are the initial and final positions of the centre of gravity of the slide mass. Note that the terms "rapid" model and "slow" model defined and used by Khalili et al (1996) are different to the definitions of "rapid" slides and "slow" slides used here (refer Section 1.3 for definitions) and the definitions of rapid and slow post failure velocity defined by IUGS (1995).

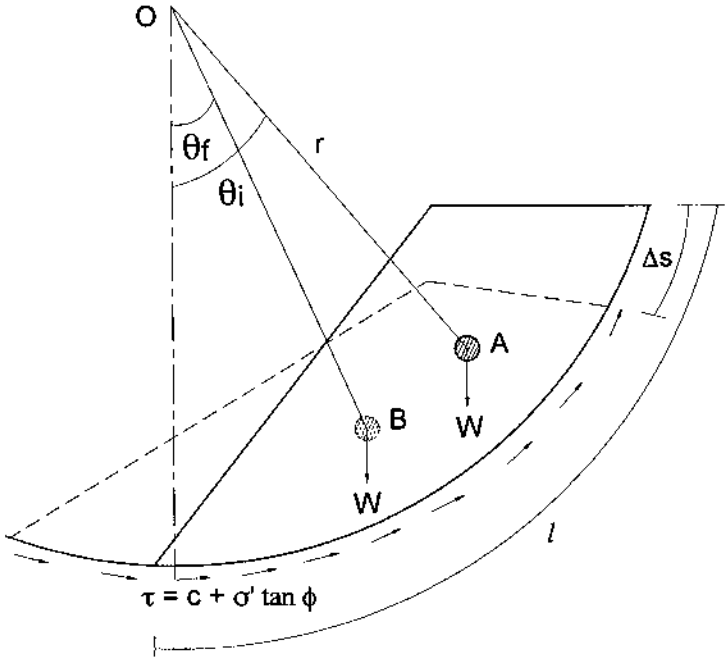

Figure 5.51: Failure model for post-failure deformation (Khalili et al 1996)

Analysis of the post-failure deformation using the Khalili et al (1996) method has been undertaken on twenty-two case studies. In most cases the slide mass remained virtually intact during sliding. A summary of the cases analysed is given in Table 5.19 and included:

- Four cut slopes in heavily over-consolidated, high plasticity Upper Lias clays (all of Type 2 slope failure geometry). The slope height of the four cases ranged from 4 to 10 m and the cut slope angle from 18.4 to 28.8 degrees.
- Nine cut slopes in heavily over-consolidated, highly plasticity London clays. The cut slope height ranged from 5 to 17 m and cut slope angle from 18.4 to 38 degrees. Seven of the cases analysed were of Type 2 slope failure geometry and one each of Type 1 (Northolt) and Type 5 (Wembley Hill).

- Five cases of slope instability within embankment dams. These cases included one failure during construction (Carsington dam), three failures on drawdown (Dam FD2, San Luis and Old Eildon dams) and one post construction slide in the downstream slope (Siburua dam).
- Three cases of slope instability of embankments on soft clay foundations. In two cases (St Alban A and Portsmouth) the foundation comprised low plasticity sensitive clays and in the remaining case (Rio) the foundation comprised high plasticity clays of low sensitivity. Details on the analysis of these three case studies are given in Section 4.3.5.2 (of Chapter 4).
- One case of slope instability in a part fill part quasi-natural road embankment (Case RF1) of 15 m height and average slope angle of 25 degrees. The initial failure occurred shortly after completion of road widening and was triggered by a heavy and prolonged period of rainfall. Subsequent reactivation occurred during wet periods over the following 4 years. The compound slide had a basal translational surface of rupture along a pre-sheared surface in the foundation, possibly associated with part of the toe region of an ancient slide, and rotational back-scarp through compacted filling.

Further details of the individual embankment dam and cut slope case studies analysed are given in Sections 5.4 to 5.7 and in the tables in the Appendix D. Case studies of Type 1 slope failure geometry where break up and "rapid" travel of the toe of the slide mass occurred were not analysed using the Khalili et al (1996) model because is not appropriate for slides where separation of the slide mass occurs.

The methodology used for analysis of the case studies was as follows:

(i) Limit equilibrium analysis (using the computer program SLOPE-W) to estimate the centre of rotation of the slide and therefore the radius, r, and initial position of the centre of gravity, $?_i$. This was done by approximating the circular slide surface to the known surface of rupture of the actual slide. Materials parameters and pore water pressure conditions used for this part of the analysis were those giving close to a factor of safety of unity.

(ii) Limit equilibrium analysis to determine the factor of safety at residual strength ($FS_{residual}$). This was carried out using the known surface of rupture and Morgenstern Price force equilibrium method for cases with a non-circular surface of rupture.

(iii) Estimation of $?_f$ from the post failure deformation of the slide mass and approximated circular surface of rupture (determined in step i), and calculation of $q_i - q_f$ and $1 - q_f / q_i$.

In most cases the actual surface of rupture was classified as compound (i.e. non-circular) as opposed to rotational upon which the methodology is based. In a number of non-circular cases the fitted circular analysis was compared to a non-fitted circular analyses. The results indicated that, in most cases, there was no significant effect on the initial angle of the centre of gravity ($?_i$); however, the fitted analysis did tend to result in a significantly greater radius for the slip circle (r in Figure 5.51).

Residual strength parameters were assessed from available laboratory test results. For the embankment dam and fill on soft ground cases this was usually from site specific laboratory tests. For the cut slopes in London and Upper Lias clays it was from published representative parameters of residual strength (Skempton et al 1969; Chandler 1976; Skempton 1977; Chandler 1984b). Drained residual strength parameters were used for heavily over-consolidated soils such as rolled, well-compacted earthfills and the over-consolidated natural soils. For normally and near normally consolidated soils residual undrained strength parameters were used. These included the wet placed core materials of Carsington and Old Eildon dams, and the soft foundations of the fill on soft ground case studies (Rio, St. Alban A and Portsmouth).

The use of undrained strength parameters for the normally and near normally consolidated soils obviated the need for assessment of pore water pressures. However, for the soil types analysed in terms of drained strength it was necessary to determine pore water pressures. For these cases the results of the analysis were sensitive to the pore water pressure parameters/profiles used, and there was the added uncertainty associated with shear induced pore water pressures. Where possible, piezometric records were used for assessment of the pore water pressure conditions and these were generally available for most of the case studies analysed. In cases where no piezometric records were available (Wembley Hill, Dedham, Althorne, Kingsbury S1, St. Helier, West Acton B and Isle of Sheppey A) a pore water pressure coefficient, r_u, was estimated based on the age of the cut slope from correlations given by Skempton (1977) (Figure 5.10).

The results of the deformation analysis are presented in Figure 5.52 and summarised in Table 5.19. For two cases, 21 (Portsmouth) and 17 (Dam FD2), the actual location of the plotted point in Figure 5.52 was thought to differ from that calculated. In the case of Portsmouth the residual factor of safety was estimated based on residual undrained shear strengths determined by field shear vane. The remoulded vane strength was considered to significantly under-estimate the large strain undrained shear strength and therefore result in low predictions of the residual factor of safety (refer Section 4.3.5.2). The actual location of Portsmouth on Figure 5.52 is considered to be located toward the mid range between the "slow" and "rapid" model estimates as shown.

In the case of Dam FD2 the post failure deformation records used in the analysis were only those recorded during the 1994 drawdown, which amounted to 430 mm. The deformation that occurred during the initial slide event, thought to be during the 1993 drawdown, was not included as no indication of the amount of deformation was given. The actual location of point No. 17 is therefore likely to be further to the right toward the "slow" model as indicated by the arrow in Figure 5.52.

In theory all results should plot between the lines shown for "slow" model (no inertia forces) and "rapid" model (inertia forces considered). It is evident from Figure 5.52 that this is in fact not the case as a significant number of cases plot below the "slow" model. Table 5.20 summarises the characteristics of the case studies and their post failure deformation behaviour in relation to where they plot in Figure 5.52.

For the case studies that plot from about mid range between the "slow" and "rapid" model up to the "rapid" model generally include cases where strain weakening at or post the initial failure was considered significant and post failure velocities were in the higher end of moderate to rapid range. The Khalili et al (1996) "rapid" model is considered a reasonable upper bound for these cases. It is an upper bound because of the assumption that the potential energy of the slide mass is consumed entirely as frictional energy along the surface of rupture in the model (based on the residual strength). In reality, a portion of the potential energy will be consumed in disaggregation of the slide mass, and in the initial stages of failure the frictional energy consumed will be greater than that assumed using residual strength parameters.

Table 5.19: Results of the post-failure deformation analysis using the Khalili et al (1996) method.

Slope Type	Case	$?_i$ *1 (°)	FS_{res} *2	$?_i - ?_f$ *1 Observed (°)	Deform-ation (m) *3	Velocity Category *4	Comment
Cut Slopes in Upper Lias Clay	Wothorpe B	18.2	0.53 – 0.62	4.2 – 7.6	2 to 3.5	slow	Deformation over 3 year period, translational slide
	Barrowden	18.8	0.65 – 0.75	1.0 – 1.1	0.5 to 0.55	slow	Rotational slide
	Heyford	22.7	0.53 – 0.61	3.8 – 4.4	2 to 2.3	suspect slow	Compound slide
	Seaton	20.1	0.58 – 0.67	2.6 – 2.9	2 to 2.2	suspect slow	Translational slide
Cut Slopes in London Clay	Wembley Hill	22.5	0.56 – 0.63	7.9	6	rapid	Retained cut, Type 5
	Northolt	22.3	0.60 – 0.69	2.4 – 3.6	0.8 to 1.2	slow	Type 1, 22 degree cut.
	Sudbury Hill	20.0	0.66 – 0.85	4.1 – 5.7	1.6 to 2.2	slow to moderate	
	St. Helier	20.3	0.52 – 0.66	5.8 – 6.3	2 to 2.3	slow to moderate	
	West Acton B	18.1	0.64 – 0.79	1.5 – 9.1	0.41 to 2.5	slow	Limited deformation at crest of slope.
	Althorne	21.3	0.54 – 0.65	4.5 – 6.7	2 to 3	slow	
	Kingsbury S1	22.7	0.59 – 0.65	1.7 – 3.5	0.5 to 1.05	slow	
	Dedham	23.5	0.57 – 0.65	6.1 – 14.7	2.1 to 5 (toe)	moderate	Large deformation at toe of slide.
	Isle of Sheppey - A	35.6	0.21 – 0.28	38	12.5 (toe)	rapid (?)	Steep cut slope of 38 degrees.
Embankment Dams	Carsington	19.1	0.70 – 0.81	8.3 – 9.4	14.3 to 18.1	moderate	Slide during construction
	San Luis	17.9	0.70 – 0.87	5.2 – 5.6	16 to 17.3	moderate	Slide during drawdown
	Siburua	26.9	0.65 – 0.73	8.5 – 9.4	1.7 to 1.9	moderate	Slide post construction
	Dam FD2 (1994 drawdown)	23.0	0.80 – 0.83	0.4	0.43	slow	Reactivation during drawdown
	Old Eildon (1929 drawdown)	22.7	0.64 – 0.78	16.2	13.5	moderate	Slide during drawdown
Fill on Soft Ground *5	Rio	8.5	0.70	3.0	0.68	slow to moderate	Ductile CH clay foundation
	St. Alban-A	21.5	0.75	8.1	1.15	rapid	Sensitive clay foundation.
	Portsmouth	14.5	0.27	10.4	3.3 to 3.4	rapid (?)	Sensitive clay foundation.
Road Fill Embankment	Case RF1	23.5	0.57 – 0.64	7 to 8	3.5 to 4.3	slow	Pre-sheared basal plane. Slope = 25° (avg.)

*1 $?_i$ and $?_f$ are the initial and final positions of the centre of gravity (refer Figure 5.51).

*2 FS_{res} is the factor of safety calculated using residual strengths along the surface of rupture.

*3 Deformations are the actual post failure deformations along the surface of rupture.

*4 Velocity categories are to the IUGS (1995) classification system (refer Table 1.1 in Section 1.3).

*5 for the fill on soft ground case studies the post failure deformations given are crest settlements.

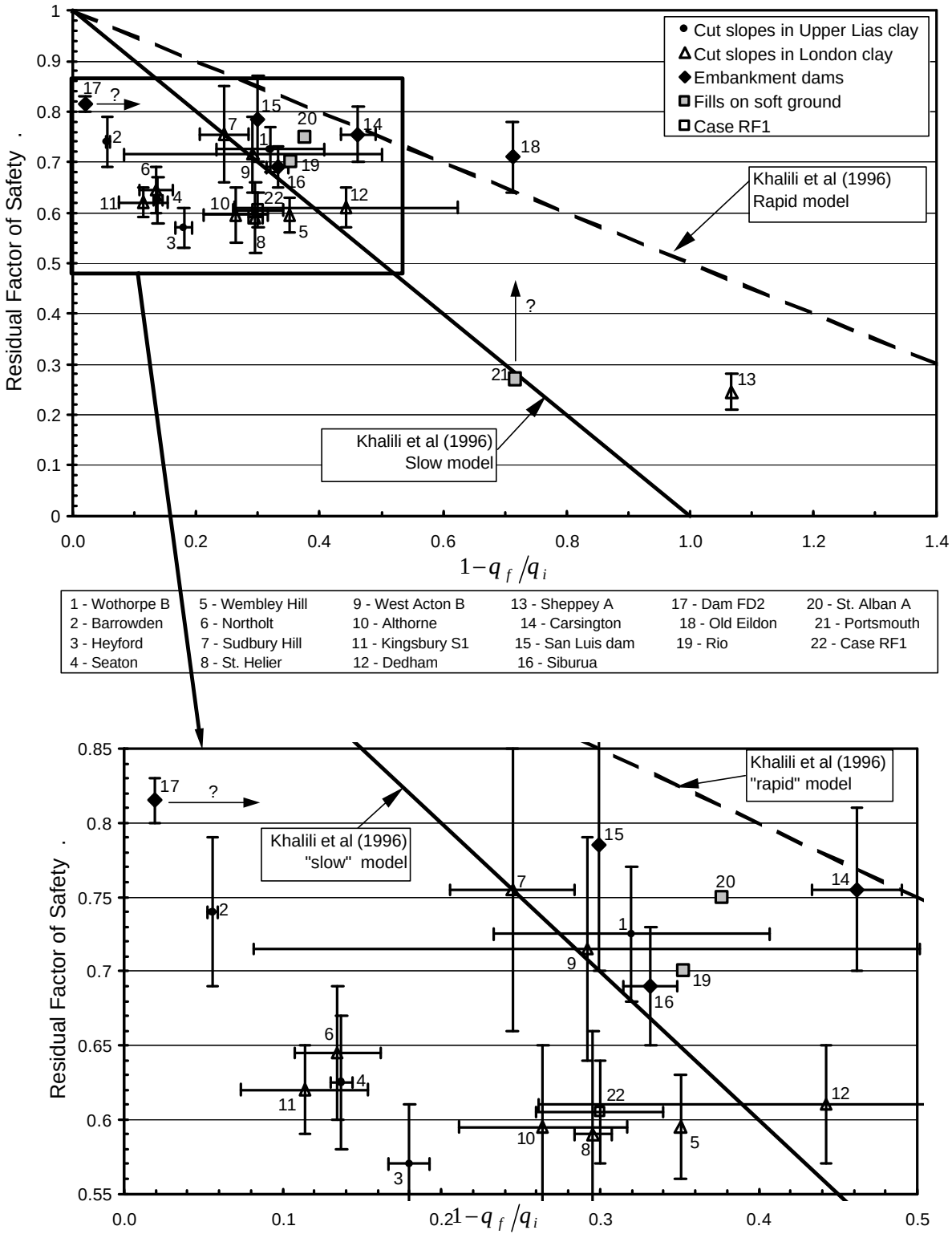

Figure 5.52: Observed deformation versus the calculated residual factor of safety.

Table 5.20: Characteristics of the case study groupings from the post failure deformation analysis (Figure 5.52)

Case Study Grouping	**Case Nos.**	**Characteristics *[1]**
Cases that plot well below the "slow" model.	2, 3, 4, 6, 11	Cuts in heavily over-consolidated clays of Type 1 and Type 2 slope failure geometry with cut slope angle typically less than 20 to 25 degrees. Post failure velocity in the slow to low end of moderate category and limited post failure deformation, less than 1.5 to 2.5 m.
Cases that plot close to the "slow" model.	1, 5, 7, 8, 9, 10, 12, 16, 17, 19, 22	Cuts in heavily over-consolidated clays of Type 1 and Type 2 slope failure geometry with cut slope angle typically less than 20 to 25 degrees. Post failure velocity in the slow to low end of moderate category. Slides in embankment dams of relatively small volume, and of slow to moderate post failure velocity and limited deformation (less than 2 m). Limited post failure brittleness of slide mass and mechanism. Fills on high plasticity soft clay foundations of low sensitivity. Slow to moderate post failure velocity. Road embankment case study (slope = 25 degrees (avg) and Type 2 slope failure geometry) and Type 5 retained cut slope in London clay (Wembley Hill).
Cases that plot from mid range up to the "rapid" model.	13, 14, 15, 18, 20, 21	Significant post failure brittleness of slide mass and mechanism for most slides, and includes: • Slides in embankment dams of relatively large volume (> 300,000 m^3). Post failure slide velocity in the moderate to rapid range. • Steep angled Type 2 cuts in heavily over-consolidated high plasticity clays, with post failure velocity in the rapid range. • Fills on brittle, highly sensitive, soft clay foundations with peak post failure velocity in the rapid range.

*[1] References to post failure velocity are to the IUGS (1995) classification system.
The embankment dam case studies analysed remained virtually intact on sliding and reached a peak velocity no greater than the moderate category.

The five case studies that plot well below the "slow" model are all slides in cut slopes of heavily over-consolidated high plasticity clays of slow post failure velocity and post failure deformations less than about 1.5 to 2.5 m. In all cases the surface of rupture was fully formed in cross section as indicated by the development of a back-scarp and displacement in the toe region of the slide. The reason why these slides plot well below the "slow" model is likely to be related to insufficient displacement along the surface of rupture for residual strengths to have been reached and to strain hardening on post failure shearing for these over-consolidated clays. The typical deformation behaviour for these "slow" slides in relatively flat cut slopes is for deformation to occur as an initial failure followed by subsequent reactivations over a period of several years (refer

Section 5.7.3). If the monitored deformation only captures the initial post failure deformation of the slide then it will plot below the "slow" model in Figure 5.52.

Of the cut slope case studies that plot close to the "slow" model, the information from the published literature indicates that the deformation of the slide mass, in most cases, has accumulated over a period of at least 3 years and is representative of several reactivations of slide movement. Therefore, the assumption of residual strength on the surface of rupture is probably a reasonable one for these cases. Case RF1 is also representative of initial sliding and a number of subsequent reactivations of movement. It too plots close to the "slow" model.

It is notable that the slide at Wembley Hill (Type 5 slope failure geometry in a retained cut slope), which travelled at a rapid post failure velocity, plotted close to the "slow" model. The reason for this may be associated with energy losses and effects on the lateral margins where shearing occurred through the existing retaining wall.

For the embankment dam case studies, the slides of smaller volume (Siburua and Dam FD2) and/or slow post-failure velocity (Dam FD2) plotted close to the "slow" model. The slides of relatively large volume (greater than about 100,000 m^3) and of moderate post-failure velocity (Old Eildon, San Luis and Carsington dams) plotted from midway between the "slow" and "rapid" model up to "rapid" model. The results for the embankment dam analyses would suggest the greater inertia of the larger volume slides, for a given slide velocity, is significant in the type of model used for prediction of travel distance, but the data is insufficient to confirm this.

For the fill on soft ground case studies, the failures in low plasticity sensitive clay foundations reached post failure velocities in the rapid range due to the highly strain weakening properties of the sensitive clays at failure (refer Section 4.3.5.2 for further details). For these cases the "rapid" model provides a reasonable upper bound for travel distance prediction.

5.8.2 EMPIRICAL METHODS FOR PREDICTION OF TRAVEL DISTANCE OF INTACT SLIDES

Empirical analysis has been undertaken on the slides in embankment dams and cut slopes in heavily over-consolidated soils that were considered to have reached post-failure velocities greater than about the mid moderate range (greater than about 2000 to 5000 mm/day) and that travelled distances in excess of about 5 m. Case studies where

the post-failure velocity was in the slow to low end of moderate range were excluded from the analysis given the limited travel distance of these slides. The slides with Type 5 slope failure geometry were also excluded because of the limited significance of slope angle on the post failure deformation behaviour.

From the analysis of the post failure deformation behaviour of "rapid" landslides in soil slopes (Section 3.9 of Chapter 3), reasonable correlations were found for the travel distance angle with respect to slope angle (both cut slope angle and downslope angle), slide volume and degree of confinement. Definitions of the terminology are given in Section 1.3. Figure 5.53 defines the travel distance angle, *a*, travel distance, *L*, and landslide height, *H*.

For the embankment dam case studies the empirical analysis indicates that statistically no correlation exists between the ratio *H/L* (tangent of the travel distance angle) and slide volume (Figure 5.54). With respect to the tangent of the cut or fill slope angle (Figure 5.55), statistically a correlation does exist with the ratio *H/L* although it is relatively weak given the limited number of cases ($R^2 = 0.62$ for 14 cases). For the cut slopes in heavily over-consolidated clays the number of cases is insufficient to undertake a statistical analysis. Combining the two sets of case studies does not improve the statistical correlation.

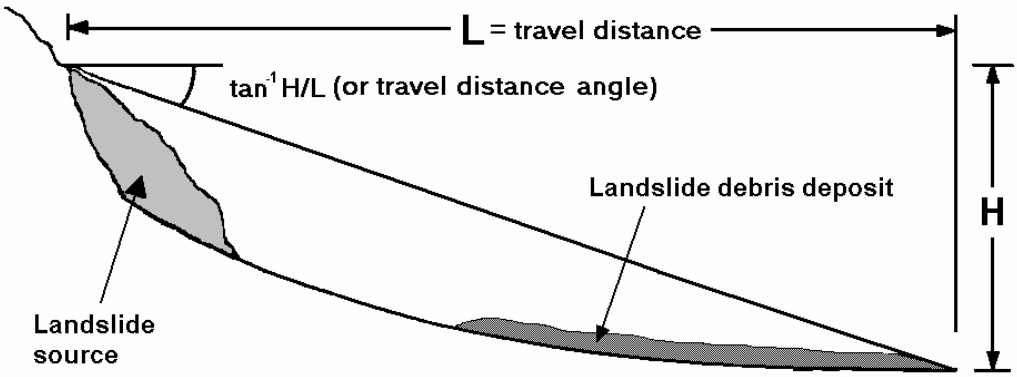

Figure 5.53: Schematic profile of slope failure showing travel distance and travel distance angle

The lack of correlation of *H/L* with slide volume is to be expected given the significant effect of the material strength properties (strength at failure and strain weakening on shearing), slide mechanism and slide geometry on the post failure distance of travel. The statistical correlation with respect to slope angle is also to be expected due to the limited distance of travel beyond the initial toe of the slide (5 m up to a maximum of 15

to 20 m) for the moderate to rapid post-failure slide velocity cases and the co-dependence between slope angle and kinetic energy of the slide mass for slides in similar soils, such as for the cut slope failures of Type 2 slope failure geometry in London clays. This is partly reflected in Figure 5.55 as a trend of increasing distance of separation with increasing cut slope angle between the point representing the case study and the line representing *H/L* = slope angle.

The range of cut slopes angles over which limited deformations at slow post failure velocity were observed in London clays is also shown in Figure 5.55. For cut slope angles less than about 25 to 30 degrees limited post failure deformations were generally observed indicating that at these slopes the travel distance angle would be closely coincident with the cut slope angle.

For the embankment dam case studies a similar correlation is likely to exist; however, it is complicated by variation in material properties, zoning geometry and slide mechanism.

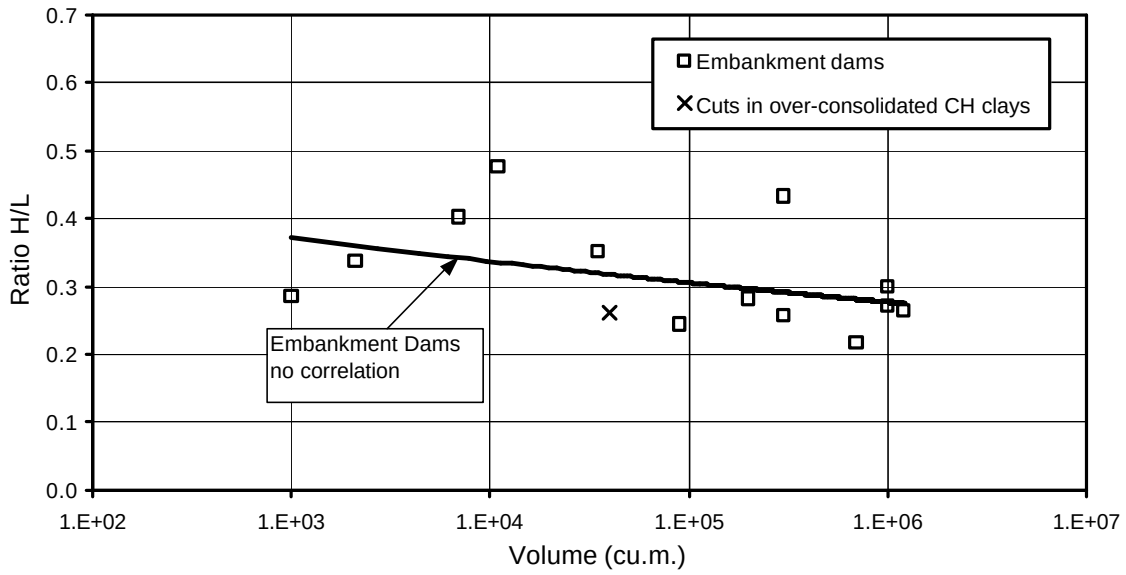

Figure 5.54: *H/L* versus the slide volume for embankment dams and cut slopes of moderate to rapid post-failure velocity.

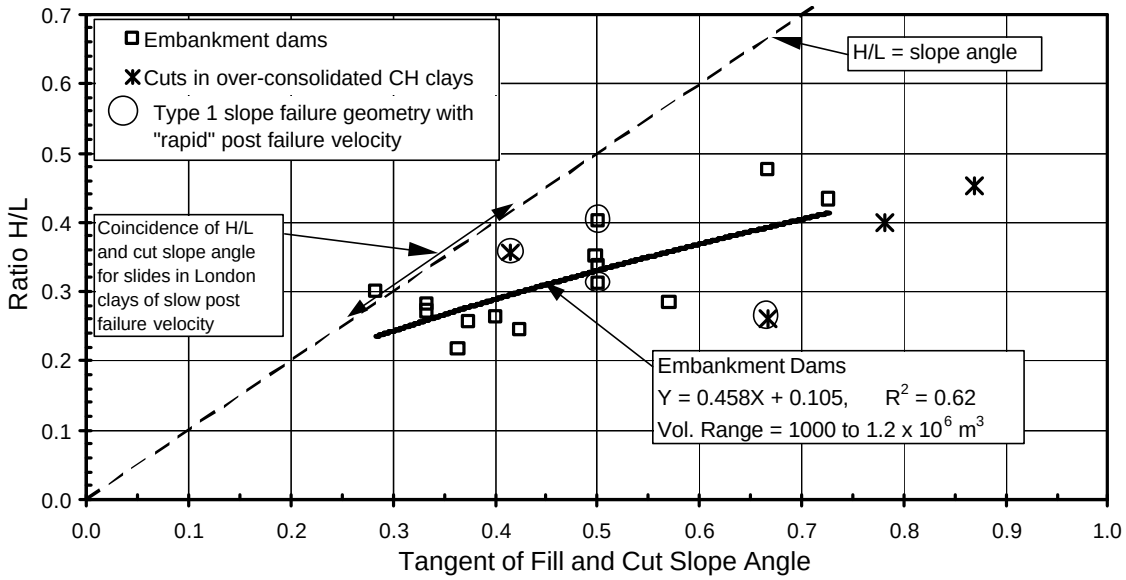

Figure 5.55: *H/L* versus the tangent of the fill or cut slope angle for embankment dams and cut slopes of moderate to rapid post-failure velocity.

5.9 CONCLUSIONS AND GUIDELINES FOR PREDICTION OF POST-FAILURE DEFORMATION BEHAVIOUR OF INTACT SLIDES IN SOIL SLOPES

The findings from the case study analysis of the mechanics of failure and mechanics of post failure deformation behaviour of slides in embankment dams (excluding hydraulic fills) and in cut slopes in heavily over-consolidated high plasticity clays are summarised in Section 5.9.1. Guidelines for the prediction of post-failure travel distance of slides in these slope and material types are presented in Section 5.9.2.

5.9.1 SUMMARY OF FINDINGS FROM THE CASE STUDY ANALYSIS

5.9.1.1 Case Studies

Fifty-four case studies for failures in embankment dams (excluding hydraulic fill dams) have been analysed. They have been sub-divided into failures during construction, failures that occur on drawdown and failures that occur post construction in the downstream shoulder.

In most cases the slide mass remained relatively intact during sliding. Post failure travel distances ranged from less than 1 m up to about 30 m, and in most cases was less

than 5 to 10 m. Post failure velocities were generally in the slow to moderate IUGS (1995) categories (i.e. centimetres per day to metres per hour) with a limited number in the rapid category. Slide volumes ranged from about 5000 cubic metres up to more than 1 million cubic metres.

Of the failures in cut slopes in heavily over-consolidated high plasticity clays, thirty-seven case studies were analysed, all from cuts in London clay and Upper Lias clay in the UK.

5.9.1.2 Embankment Types Susceptible to Slope Instability

The findings of the statistical analysis by Foster (1999) of slope instability incidents in large dam embankments and further analysis of the Foster database (refer Section 5.2.1) as well as the case study analysis, indicates that:

- Overall, slope instability is:
  - Much more likely in homogeneous earthfill, puddle core and concrete core-wall earthfill embankments;
  - Much less likely in rockfill and zoned earthfill embankments;
  - Much more likely in embankments constructed of medium to high plasticity clays and silts;
  - Where the foundation is involved in the slide, slope instability is much more likely in embankments founded on medium to high plasticity fine-grained soils (mainly clays), and much less likely in embankments founded on bedrock or sandy and gravelly soils;
  - Where the slide is through the embankment only, slope instability is much less likely in zoned or core-wall embankments with dominantly sandy or gravelly materials or rockfill in the outer zones, provided the outer zone is of substantial thickness;
- For failures during construction, the foundation is involved in a high proportion of slope instability incidents, about 75%;
- For failures post construction, either during drawdown or in the downstream shoulder:
  - A high proportion of incidents occur in homogeneous embankments (94% of incidents in homogeneous embankments occur post construction);

– A high proportion of failures in the downstream shoulder occur within earthfill embankments (homogeneous, earthfill with filters and earthfill with rock toe), mainly in embankments without embankment filters or more permeable zones in the downstream shoulder.

These findings point to the dominance of material type, predominantly medium to high plasticity clays, in the likelihood of slope instability in embankment dams, and this could be more generally extended to encompass fills. This is exclusive of fills susceptible to flow liquefaction, such as the failures in hydraulically placed sandy fills (refer Chapter 3).

5.9.1.3 Mechanics of Failure

The stress conditions within the slope and the material strength properties are the two important factors controlling failure in soil slopes. The stress conditions within the slope are affected by the slope geometry, pore water pressure conditions and coefficient of earth pressure at rest, K_o.

The effect of defects (bedding, jointing, fissuring, etc.) and layering/zoning on the strength of the soil mass is dependent on the strength of the defect (or layer) in relation to that if the intact soil. Under the stress conditions within a slope the shear stresses (as a percentage of shear stress capacity of the soil or defect) will be higher where the strength of the defect (or of a weak layer) is lower than that of the intact soil. The orientation of defects (and weak layers) is an important factor in the stability of the slope and in the mechanics of failure.

(a) Cut Slopes in Heavily Over-Consolidated High Plasticity Clays

Progressive failure is significant in the mechanics of failure of slides in cut slopes in heavily over-consolidated high plasticity clays. Localised failure initiates in regions of high shear stress, typically in the toe region of the cut, and progressively spreads into the slope (Potts et al 1997). The stress relief process (as shown by Potts et al) is important in the continuation of progressive failure in these slopes due to the gradual change in effective stress condition as pore water pressures equilibrate, and dilation and softening of the soil mass occurs. The permeability of the soil mass is an important

factor in the stress relief process as it directly affects the time for equilibration of pore water pressures.

Stress relief and progressive failure, amongst other factors, results in a gradual decrease in the overall stability of slope with time (Picarelli 2000). The trigger for failures in cut slopes in heavily over-consolidated high plasticity clays is often rainfall or seasonal wetter periods. But, for steeper slopes it can be the processes of stress relief and progressive failure.

(b) Embankment Dams

For failures in embankment dams during construction, the trigger is often increasing stress conditions due to embankment raising. The mechanics of failure can, and in a number of cases is, simply undrained failure under the stress conditions imposed.

Most of the cases of failure during construction involve low undrained strength layers in either the foundation or the earthfill (wet placed zones or wet placed layers within a zone). The very high percentage of clay soils involved in failures during construction is often related to their low undrained strength, high construction pore water pressures and slow dissipation of pore water pressures in these low permeability soil types. Progressive failure can be significant in the mechanics of failure for slides during construction, as was the case in the slide at Carsington dam.

For failures during drawdown, it is the drawdown itself that triggers the slide due to the change in stress conditions within the slope and reduction in support of the water load on the upstream face. Embankments with clayey soils in the upstream shoulder predominate in slides during drawdown due to their low permeability and high pore water pressures retained in the slope under the drawdown condition. Other factors though are significant in failures during drawdown:

- The change in effective stress conditions within the slope due to wetting up and saturation of partially saturated soils.
- The change in material strength properties, mainly clay soils, due to swelling on saturation.

An important observation of the slides during drawdown is that failure is often not triggered by the largest and/or fastest drawdown in the history of reservoir operation. This is due in part to the above factors, but more significantly due to progressive strain

weakening in undrained loading of over-consolidated low permeability soils, mainly fine-grained clayey soils.

For failures in the downstream shoulder that occur post construction, seepage and saturation within the embankment from the impounded water storage is the trigger for failure in most cases. Changes in effective stress conditions within the slope occur as a result of saturation of partially saturated soils, rising pore water pressures and seepage pressures. Material strength properties are also affected by the change in moisture content and swelling. These failures dominantly occur in fine-grained soils, and once again material permeability is a significant issue. Rainfall and earthquake have also triggered slides in the downstream shoulder post construction.

An important issue with the seepage triggered slides is the potential for a breach condition. Most of these failures (i.e. seepage triggered slides) initiated when the reservoir was close to full supply level or had reached its historically highest level.

5.9.1.4 *Mechanics of Post Failure Deformation Behaviour*

The mechanics of post failure deformation is complex. It is complicated by, amongst other factors, strain and stress dependent material strength properties, time dependent material properties, slope geometry, orientation of the surface of rupture and the mechanics of failure. Therefore, simple empirical criteria for assessment of travel distance and slide velocity in these slopes, such as cut or fill slope angle, are inadequate.

For most failures in embankment dams (excluding hydraulic fill dams) and cuts in heavily over-consolidated high plasticity clays, the slide remained virtually intact during sliding. Travel distances were generally relatively limited, less than 5 to 10 m in most cases but can be up to 25 to 30 m, and post failure velocities typically ranged from the slow to rapid IUGS (1995) velocity categories, or from metres/year to metres/minute.

The potential energy of the slide mass at failure is defined by geometrical constraints including the slope geometry and orientation of the surface of rupture. The amount of this potential energy (if fully realised by the slide) that is consumed as frictional energy, and the remainder that is available for kinetic energy and energy for disaggregation of the slide mass is dependent on the material properties and slide mechanism. Materials that are significantly strain weakening from their strength at failure and slide mechanisms that incorporate brittleness on slide release, have the potential for conversion of a significant proportion of the potential energy into kinetic

energy for acceleration of the slide mass and achievement of greater travel distances at higher velocities.

In summary, the factors affecting the post failure deformation behaviour of slides in embankment dams and in cuts in heavily over-consolidated high plasticity clays were:

- Potential for material strain weakening. Significant strain weakening at or post the initial failure was observed for:
  - Near normally consolidated high plasticity clays due to particle orientation and pore water pressure generation on shearing in undrained loading;
  - Over-consolidated mainly clay type soils where progressive strain weakening on shearing after initial failure (at strengths between peak and critical state) occurred in either drained or undrained loading;
  - Structured soils that are susceptible to large loss in undrained strength on shearing and consequent increase in pore water pressure as load is transferred onto the pore fluid (i.e. static liquefaction);
- Brittleness associated with the slide mechanics, such as due to internal brittleness or toe buttressing;
- Brittleness associated with slide release or reduction of restraining forces on the lateral margins;
- Slope failure geometry. The slide mass for slides of Type 1 slope failure geometry generally has greater potential energy than for Type 2 and in turn Type 5 slope failure geometries;
- Orientation of the surface of rupture. This will influence the potential energy realised by the slide mass (e.g. for a slide of Type 1 slope failure geometry, where the slide remains intact in the source area, has not realised its potential energy compared to a slide that fully evacuates the source area) and to some extent the distribution of the potential energy to frictional energy.

The analysis of post failure deformation behaviour of the case studies (Sections 5.6 and 5.7), particularly for the failures in embankment dams, attempted to differentiate those slides where post failure brittleness of the slide mechanics was significant from those where brittleness was not greatly significant. The assessment of significance of brittleness was based on the likelihood of acceleration of the slide mass due to strain weakening of the slide mechanism or materials as discussed above. Where it was not significant, post failure deformations were likely to be limited and at slow post failure

velocity. Where it (brittleness of the slide mechanics) was significant, post failure travel distances were generally greater and the post failure velocity of the slide mass higher, typically of moderate to rapid velocities (i.e. metres/hour to metres/minute or faster).

The following sub-section summarise the findings from the case study analysis on factors, both general and more specific, that influenced the post failure deformation behaviour of the various sub-groups of slides analysed. General guidelines for estimation of slide velocity are based on the analysis and are given for the purpose of allowing slide velocity estimation for improved prediction of the post failure travel distance (Sections 5.8.1 and 5.9.2) and for other risk assessment purposes. They should be used with caution.

5.9.1.5 *Post Failure Deformation Behaviour of Slides in Embankment Dams*

The general guidelines for estimation of post failure slide velocity in embankment dams are divided into the three groups; failures during construction, failures during drawdown and post construction failures in the downstream shoulder. The factors summarised below are for landslides where the post failure velocity was in the moderate to rapid IUGS (1995) classes or faster (i.e. metres/hour to metres/minute or faster).

(a) Failures during construction

For most landslides in embankment dams during construction the post failure deformation of the slide was driven by out of balance forces as a result of fill placement. In most cases the slide decelerated on cessation of fill placement and the travel distance was of limited extent and generally at a slow post failure velocity.

Of importance though is the group of landslides that accelerated after cessation of filling due to progressive strain weakening of the slide mass. For a number of these slides, material strain weakening of near normally high plasticity clays in the foundation or earthfill due to particle orientation was sufficiently significant for acceleration of the slide mass for these relatively large volume failures. Progressive failure in the over-consolidated high plasticity clays was significant in the failure at Carsington dam and static liquefaction due to contraction on shearing of structured soils was likely to have been significant in the rapid failure at Marshall Creek dam.

For several of these slides of higher post failure velocity, brittleness of the slide mechanism due to release or weakening on the margins, passive toe resistance and/or internal shearing was significant. In these cases the persistence of the weak zone in the foundation or earthfill was typically of broad extent both in cross section and in long section. Therefore, even though the resistance on the lateral margins was significant, strain weakening on the surface of rupture is likely to have resulted in high shear stresses on the margins sufficient to cause either formation of a shear surface on the margins or large lateral extension of the slide, and result in moderate to rapid slide velocities and relatively large travel distances.

(b) Failures in the upstream slope during drawdown

The material type, slope failure geometry, upstream slope angle and the drawdown itself were significant influences on the post failure deformation behaviour of slides in the upstream shoulder triggered by drawdown. Table 5.21 provides a summary of the how these factors affect the post failure velocity. For about half of the failure case studies, post failure travel distances were of limited extent and estimated peak velocities were in the slow to low end of moderate category.

Significant factors in the moderate to rapid failures during drawdown were:

- Progressive failure in over-consolidated medium to high plasticity clay earthfills and high plasticity foundations, where strain weakening occurred on shearing after the initial slope failure occurred;
- Brittleness in the slide mechanics at and post failure, such as from concrete facing elements; and
- The slope failure geometry and upstream slope angle. For slides of Type 1 slope failure geometry, the toe of the slide mass broke up and travelled at a "rapid" velocity down the face of the upstream slope where the upstream slope was equal to or greater than 2H to 1V (about 27 degrees).

(c) Failures in the downstream slope post construction

The slide volumes of failures in the downstream shoulder post construction were much smaller than for the failures during construction and during drawdown (Table 5.11). The factors contributing to higher post failure velocity of the slide mass (i.e. post failure velocities generally in the mid moderate to rapid range) were:

- Material type. Slides involving high plasticity clays tended to show higher post failure velocity, more so for slides of Type 2 slope failure geometry than Type 5;
- Progressive failure. Where progressive failure was significant in the mechanics of failure and post failure deformation, velocities were likely to be higher;
- Trigger to failure is seepage related. Those failures where pore water pressure and seepage were considered to trigger the failure tended to travel at higher post failure velocities, most probably due to softening of the slide mass from seepage infiltrating the dilating slide mass during post failure deformation.

Table 5.21: Factors affecting the peak post-failure velocity for slides in embankment dams during drawdown.

Material Type/s (along the surface of rupture)	**IUGS (1995) Velocity Categories**		
	Slow	**Moderate**	**Rapid**
High plasticity silts and clays	-	Slopes less than or equal to 3H to 1V	-
Low to medium plasticity silts and clays	Slopes of 2 - 3H to 1V	Slopes of about 2H to 1V up to about 1.5H to 1V.	Type 1 failure and/or brittleness to slide mechanism (e.g. concrete facing). Slopes greater than or equal to 2H to 1V.
Sandy and Gravelly soils with significant fines content	Slopes of 2 - 3H to 1V. Very rapid sustained drawdown to trigger failure (> 500 mm/day).	-	Extremely rapid drawdown, Type 1 failure, Slope steeper than or equal to 2H to 1V.

5.9.1.6 Post Failure Deformation Behaviour of Slides in Cut Slopes in Heavily Over-Consolidated High Plasticity Clays

The potential for progressive strain weakening of the material once failure had occurred, slope geometry and slope failure geometry were significant factors in the post failure travel distance and velocity of slides from failures in cut slopes of heavily over-consolidated high plasticity clays.

For the failures in cut slopes in London clay, a rapid post failure velocity was observed, in most cases, where the timing of the failure occurred within days to less than ten years after excavation for slides of Type 1 and Type 2 slope failure geometry,

and within 15 years for Type 5 slope failure geometry (based on a limited number of case studies). For these slides this relatively early time of failure (for cuts in London clay) may reflect a higher average shear strength at failure on the surface of rupture and greater potential for strain weakening to residual strength post failure. Therefore, greater slide velocity is generally observed where there is greater potential for material strain weakening from initial failure.

The post failure deformation behaviour for the cuts slopes showed a distinctive change in behaviour with increasing cut slope angle for slides of Type 1 and Type 2 slope failure geometry (Figure 5.45 and Figure 5.46). In summary, rapid post failure velocity is likely for:

- Slides of Type 1 slope failure geometry in cut slopes steeper than about 22 degrees. For these cases the toe region of the slide mass will potentially break up and travel at a moderate to rapid velocity for relatively large distances on the lower portion of the cut slope. With increasing cut slope angle above about 22 degrees the volume of material likely to evacuate the source area is likely to increase.
- Slides of Type 2 slope failure geometry in cut slopes steeper than about 30 to 35 degrees.

5.9.2 GUIDELINES FOR PREDICTION OF POST-FAILURE DEFORMATION

The post-failure deformation analysis undertaken (Section 5.8) included simplistic empirical type analyses and limit equilibrium related analyses based on the Khalili et al (1996) method for intact sliding.

The results of the empirical analyses, related to slide volume and cut (or fill) slope angle, are presented in Section 5.8.2. No correlation was found with respect to slide volume. The analyses with respect to cut or fill slope angle indicated that a statistical correlation does exist, however, it is relatively weak (Figure 5.55). Better correlations were obtained with respect to slope angle where the case studies in the analysed group consisted of similar material type, slope failure geometry and/or mechanism (e.g. Figure 5.40 for drawdown related failures). Overall, the empirical methods are considered to be of limited use, and useful only for a broad based estimate of travel distance. It is better to rely simply on the general performance (Section 5.9.1).

The limit equilibrium modelling and Khalili et al (1996) method proved to be a useful method for prediction of post-failure travel distance. The results of the analysis

are presented in Figure 5.52 (in Section 5.8.1). Guidelines for deformation analysis using the Khalili et al (1996) model are summarised in Table 5.22. The guidelines are mainly for those slides that remain basically intact or coherent on sliding and are not susceptible to static liquefaction or other phenomenon that can lead to "rapid" sliding. Excluded from the Khalili et al (1996) analysis were slides in hydraulic fill embankment dams and slides of Type 1 slope failure geometry in relatively steep slopes where the toe region of the slide mass broke up and travelled "rapidly" down the cut or fill slope were.

For the embankment dam case studies, reference in Table 5.22 is made to slide volume and potential peak post-failure slide velocity. The volume categories are somewhat arbitrary given the limited number of cases analysed, although the modelling did indicate the larger volume slides of moderate velocity approached the "rapid" model compared with smaller volume slides of similar post-failure velocity. General guidelines for estimation of peak post-failure velocity are summarised in Section 5.9.1.4.

Table 5.22: Guidelines for post-failure deformation prediction using the Khalili et al (1996) models.

Slope Type	**Khalili et al (1996) "Slow" Model**	**Khalili et al (1996) "Rapid" Model**
Cut slopes in heavily over-consolidated clays	Type 1 slope failure geometry at cut slopes less than about 22 degrees. Type 2 slope failure geometry at cut slopes less than about 25 to 30 degrees. Type 5 retained cut slopes.	Type 2 slope failure geometry at cut slopes greater than about 25 to 30 degrees.
Fills on Soft Ground	Fills on soft clay foundations of low sensitivity.	Fills on brittle, highly sensitive clay foundations.
Embankment Dams (excluding hydraulic fills)	Large volume (> 100,000 m^3) slides with potential peak velocities in the slow range. Smaller volume (< 100,000 m^3) with potential for peak velocities in the slow to moderate range.	Large volume (> 100,000 m^3) slides with potential peak velocities in the moderate to rapid range. Smaller volume (< 100,000 m^3) with potential for peak velocities in the rapid range.

The Khalili et al (1996) "slow" model often over-estimates the amount of initial deformation for the materials and slope conditions identified in Table 5.22 (refer Figure 5.52 in Section 5.8.1), and it can therefore be regarded as a reasonable upper bound. The reason for the over-estimation by the "slow" model for the cut slope case studies analysed was considered to be related to the mode of post failure deformation of these slides (generally deformation on initial failure followed by reactivation in subsequent wet periods), and the likelihood that residual strength is not reached following the initial failure. Only the slide in the retained cut slope in London clay at Wembley Hill appeared to contradict this general trend. A similar post failure mode of deformation was observed for several slides in embankment dams triggered by drawdown (e.g. Dam FD2 and Bear Gulch dam) and the road fill embankment failure (Case RF1).

For those case studies under the Khalili et al (1996) "rapid" model, post failure deformations generally occurred within a single event (i.e. no subsequent reactivation). For the smaller volume slides (including cut slopes and fills on soft ground) the post failure deformation of the slide usually occurred within a matter of minutes to hours at a rapid post failure velocity. For the larger volume embankment dam case studies, the post failure deformation of the slide took from days to months, but typically involved a phase of large acceleration.

These slides (under the "rapid" model) tended to plot below the post failure deformation estimated by the "rapid" model. The reason for this is considered to be in the formulation of the "rapid" model, which assumes that all available potential energy of the slide mass is resisted by frictional forces along the surface of rupture approximated by the residual soil strength. The model does not take into consideration energy losses associated with disaggregation of the slide mass, internal shearing or energy used in deformation to reach residual strength conditions. Therefore, the "rapid" model can be considered as an upper bound estimate of the post failure deformation of the intact slides for the slide categories in Table 5.22.

TABLE OF CONTENTS

6.0 THE DEFORMATION BEHAVIOUR OF ROCKFILL 6.1

6.1 OUTLINE OF THIS CHAPTER 6.1

6.2 DEFINITIONS AND TERMINOLOGY 6.2

6.2.1 Unconfined Compressive Strength of Rock 6.2

6.2.2 Rockfill Placement and Compaction 6.3

6.2.3 Rockfill Moduli 6.4

6.2.4 Zoning of Main Rockfill in Concrete Face Rockfill Dams 6.7

6.3 LITERATURE REVIEW OF ROCKFILL DEFORMATION 6.9

6.3.1 Historical Summary of Rockfill Usage in Embankment Design 6.9

6.3.2 Deformation Properties of Rockfill 6.9

6.3.3 Predictive Methods for Rockfill Deformation 6.14

6.4 ANALYSIS OF THE DEFORMATION BEHAVIOUR OF ROCKFILL IN CONCRETE FACE ROCKFILL DAMS 6.27

6.4.1 Case Study Database 6.28

6.4.2 Deformation During Construction 6.28

6.4.3 Deformation of the Face Slab of CFRD on First Filling 6.44

6.4.4 Post Construction Crest Settlement 6.53

6.5 DISCUSSION AND RECOMMENDED METHODS FOR PREDICTION 6.71

6.5.1 Guidelines on Deformation Prediction During Construction 6.71

6.5.2 Guidelines on Deformation Prediction During First Filling 6.75

6.5.3 Guidelines on Deformation Prediction Post-Construction 6.76

6.6 CONCLUSIONS 6.77

LIST OF TABLES

Table 6.1: Classification of unconfined compressive strength or rock (AS 1726-1993) 6.2

Table 6.2: Historical summary of rockfill usage in embankment design (Galloway 1939; Cooke 1984; Cooke 1993). 6.10

Table 6.3: Parameters for deformation prediction (Soydemir and Kjærnsli 1979) 6.25

Table 6.4: Rates of post-construction crest settlement of dumped and compacted rockfills in CFRDs (Sherard and Cooke 1987) 6.26

Table 6.5: Summary of embankment and rockfill properties for CFRD case studies 6.29

Table 6.6: Assessment of cross-valley influence on arching for case studies analysed 6.38

Table 6.7: Stress conditions representative of the data sets from Figure 6.21 ..... 6.43

Table 6.8: Summary of crest settlement during the period of first filling 6.62

Table 6.9: Values of the coefficient, *m*, in the strain rate – time power function (Equation 6.5). 6.63

Table 6.10: Estimates of long-term crest settlement rates for dumped rockfills 6.67

Table 6.11: Location of internal post-construction vertical settlement in CFRD 6.70

Table 6.12: Approximate stress reduction factors to account for valley shape 6.73

LIST OF FIGURES

Figure 6.1: Determination of rockfill moduli, *(a)* modulus during construction, E_{rc}, and *(b)* modulus during reservoir filling, E_{rf} (Fitzpatrick et al 1985) 6.5

Figure 6.2: Typical design of dumped rockfill CFRD (adapted from ICOLD (1989b)) 6.7

Figure 6.3: Typical zoning of main rockfill in current CFRD design practice for construction with sound quarried rockfill (adapted from Cooke (1997); zoning designators after Fell et al (1992)) 6.8

Figure 6.4: Compression curves for dry and wet states, and collapse compression from dry to wet state for Pyramid gravel in laboratory oedometer test (Nobari and Duncan 1972a) 6.13

Figure 6.5: Settlement versus time curves for laboratory oedometer tests on rockfill (Sowers et al 1965) 6.14

Figure 6.6: Typical stress-strain relationship of rockfill from a triaxial compression test (Mori and Pinto 1988) 6.17

Figure 6.7: Finite element analysis of Foz do Areia CFRD (Saboya and Byrne 1993), *(a)* model and *(b)* stress paths during construction and first filling. 6.18

Figure 6.8: Deformation modulus during construction (E_{rc}) versus void ratio (Pinto and Marques Filho 1998) 6.20

Figure 6.9: Ratio of deformation modulus on first filling to during construction (E_{rf}/E_{rc}) versus valley shape factor (Pinto and Marques Filho 1998) 6.20

Figure 6.10: Deformation modulus during construction (E_{rc}) for Hydro Tasmania CFRDs (Giudici et al 2000) 6.21

Figure 6.11: Results of 3-dimensional finite element analysis of CFRD, to give vertical displacement during construction versus valley shape (Giudici et al 2000) 6.22

Figure 6.12: Settlement rate analysis of Cedar Creek dam; *(a)* determination of time t_o and *(b)* settlement rate versus time (Parkin 1977) 6.24

Figure 6.13: Post-construction crest settlement of membrane faced compacted rockfill dams (Clements 1984). 6.26

Figure 6.14: Settlement index versus time for well-compacted rockfills (adapted from Public Works Department NSW 1990) 6.27

Figure 6.15: Stress-strain relationship for rockfills observed during construction 6.33

Figure 6.16: Secant modulus versus vertical stress from monitoring during construction 6.33

Figure 6.17: Tangent modulus versus vertical stress from monitoring during construction 6.35

Figure 6.18: Idealised model for two-dimensional finite difference analysis of cross-valley influence 6.36

Figure 6.19: Results of two-dimensional finite difference analysis of the effect of cross-valley shape on vertical stresses in the dam. *(a)*, *(c)* and *(e)* represent construction in 5 m lifts (to 100 m) and *(b)*, *(d)* and *(f)* construction in a single 100 m lift. 6.38

Figure 6.20: Indicators of cross valley arching effects from variations in the secant modulus with vertical stress. 6.39

Figure 6.21: Representative secant modulus (mostly Zone 3A rockfill) at end of construction (E_{rc}) versus D_{80} from average grading of the rockfill 6.42

Figure 6.22: E_{rf}/ E_{rc} ratio versus embankment height 6.45

Figure 6.23: Stress paths during construction and first filling for nominal 100 m embankment with 1.3H to 1V upstream slope angle; *(a)* monitoring point locations, *(b)* stress paths for points normal to face slab at 30% of the embankment height. 6.49

Figure 6.24: Stress paths during construction and first filling for nominal 100 m embankment with 1.55H to 1V upstream slope angle; *(a)* monitoring point locations, *(b)* stress paths for points normal to face slab at 30% of the embankment height. 6.49

Figure 6.25: Face slab deflection during first filling (4/2/71 to 25/4/71) of Cethana dam (Fitzpatrick et al 1973). 6.50

Figure 6.26: Face slab deformation during first filling of Aguamilpa dam (Mori 1999) 6.51

Figure 6.27: Face slab deformation during first filling of Ita dam (Sobrinho et al 2000) 6.51

Figure 6.28: Scotts Peak dam; embankment zoning and location of face cracks (courtesy of Hydro Tasmania)..... 6.52

Figure 6.29: Mackintosh dam *(a)* embankment section (courtesy of Hydro Tasmania) and *(b)* face slab deformation on first filling (Knoop and Lack 1985) 6.52

Figure 6.30: Examples of derivation of zero time for post-construction settlement 6.56

Figure 6.31: Post-construction crest settlement versus time for dumped rockfill CFRD, t_o at end of main rockfill construction. 6.57

Figure 6.32: *(a)* and *(b)* Post-construction crest settlement versus time for CFRD constructed of compacted rockfills of medium to high intact strength, t_o at end of main rockfill construction. 6.58

Figure 6.33: *(a)* and *(b)* Post-construction crest settlement versus time for CFRDs constructed of well-compacted rockfills of very high intact strength and of well-compacted gravels, t_o at end of main rockfill construction. 6.59

Figure 6.34: Post-construction crest settlement versus time for dumped rockfill CFRD, t_o at end of first filling. 6.60

Figure 6.35: Post-construction crest settlement versus time for CFRD constructed of compacted rockfills of medium to high intact strength, t_o at end of first filling. 6.60

Figure 6.36: Post-construction crest settlement versus time for CFRDs constructed of well-compacted rockfills of very high intact strength and of well-compacted gravels, t_o at end of first filling. 6.61

Figure 6.37: Post construction crest settlement of Bastyan dam..... 6.65

Figure 6.38: Long-term crest settlement rate (as a percentage of embankment height per log cycle of time) versus embankment height for compacted rockfills 6.66

Figure 6.39: Crest settlement attributable to first filling (excluding time dependent effects)..... 6.68

6.0 THE DEFORMATION BEHAVIOUR OF ROCKFILL

6.1 OUTLINE OF THIS CHAPTER

Rockfill, including other coarse granular materials such as gravels and granular colluvium, have since the late 19th century been an integral part of embankment dam construction. Recent and current dam projects incorporating rockfill as a key component in embankment design include concrete faced rockfill dams (CFRD) now reaching heights in excess of 200 m and earth and rockfill dams (mostly central core earth and rockfill dams) reaching heights of 250 to 300 m. The key attributes of rockfill are its high shear strength, allowing for stable embankment slopes up to 1.3 to 1.4H to 1V (horizontal to vertical), and its low compressibility when placed in a well-compacted condition.

The stability of rockfill embankments is evidenced by the lack of historical records of slope instability associated with embankments incorporating rockfill zones. The statistical data on slope instability incidents in large dams (Foster et al. 2000), summarised in Section 5.2.1, indicates that of 124 incidents in embankment dams only 7 cases incorporated rockfill zoning. Of the failure case studies of embankment dams analysed in Chapter 5, rockfill was incorporated in the embankment design in 5 of the 54 case studies. Only in 1 of these 5 cases did slope instability involve shear through the outer rockfill (it was a zoned earth and rockfill dam with very thin outer rockfill shoulders); in the other four cases the surface of rupture preferentially passed through the foundation.

This chapter presents the results of the research on the deformation properties of rockfill. Section 6.3 presents an historical summary of the usage of rockfill in embankment design, and review of the literature on the properties of rockfill affecting its deformation behaviour and methods for prediction of rockfill deformation (during and post construction). Analysis of the deformation behaviour of 36 well-monitored rockfill dams (mostly concrete face rockfill dams (CFRD)) is presented in Section 6.4. The analysis is sub-divided into; the deformation of rockfill during construction, the face slab deformation of CFRD on first filling, and the post construction crest settlement of CFRD.

Guidelines on methods for prediction of the deformation behaviour of rockfill are presented in Section 6.5 based on the findings from the analysis in Section 6.4.

Methods based on the historical performance of case studies are developed for estimation of the rockfill modulus and the post construction crest settlement of CFRD.

6.2 DEFINITIONS AND TERMINOLOGY

Section 1.3 includes a summary of the terminology used to describe the classification of rockfill placement and the unconfined compressive strength of intact rock. Additional discussion is presented on these two areas as well as rockfill moduli and embankment zoning in CFRD in the following sub-sections

6.2.1 UNCONFINED COMPRESSIVE STRENGTH OF ROCK

The classification system from Australian Standard AS 1726-1993 is used to classify the unconfined compressive strength (UCS) of intact rock used for rockfill. The descriptors and the UCS range they represent are given in Table 6.1.

Table 6.1: Classification of unconfined compressive strength or rock (AS 1726-1993)

Strength Descriptor	UCS Range (MPa)
Extremely High	> 240
Very High	70 to 240
High	20 to 70
Medium	6 to 20

For the purposes of the deformation analysis of rockfill, the strength of intact rock has been simplified into two classes, very high strength and medium to high strength. It is recognised that the medium to high strength grouping (UCS of 6MPa to 70 MPa) is very broad, but they have been grouped together for several reasons:

- The database consists of very few cases of medium strength rockfills and the analysis indicated they could be grouped with the high strength rockfills without introducing significant uncertainty into the statistical correlations presented;
- On handling, placement and compaction of rockfills sourced from medium to high UCS rock, particle size distributions generally show that significant breakdown occurs as reflected in the high percent passing 19 mm and the generally high C_u (coefficient of uniformity, D_{60}/D_{10}). It is recognised that there is likely to be "grey

zone" rather than a division based only on UCS strength, as the amount of breakdown will be affected by the rock type, type and weight of roller, compaction procedure and strength of cementing of the rock.

Extremely high strength rock has been used as rockfill in embankment construction for a few case studies and these have been included with those of very high strength.

6.2.2 ROCKFILL PLACEMENT AND COMPACTION

The method of placement of rockfill has a significant influence on its compressibility during construction and its deformation behaviour post construction. The definitions by Cooke (1984, 1993) for dumped and compacted rockfill have been used as a basis for categorisation of the method of placement. The definitions used are:

- Compacted Rockfill – rockfill placed in layers up to 2 m thickness (generally 0.9 to 2.0 m thick) and compacted by smooth drum vibrating roller (SDVR). Accepted practice is typically 4 to 6 passes of a minimum 10 tonne (possibly up to 15 tonne) deadweight vibrating roller, with variation in layer thickness, added water and number of passes depending on the quality and type of the rockfill, amount of fines and location within the embankment. Three classifications for compacted rockfill have been used:
  - Well-compacted – layer thickness typically less than about 1.0 m (depending on the compressive strength of the intact rock) and compacted with a minimum of four passes of a 10 to 15 tonne deadweight SDVR.
  - Reasonable Compaction – layer thickness typically 1.5 to 2.0 m and compacted with typically four passes of a 10 tonne SDVR.
  - Reasonably to Well Compacted - layer thickness typically 1.2 to 1.6 m (depending on the compressive strength of the intact rock) and compacted with typically 4 to 6 passes of a 10 to 15 tonne SDVR.
- Rockfill not formally compacted or "poorly compacted". Several methods of rockfill placement have been included under the definition "poorly compacted", these include:
  - Dumped rockfill – rockfill placed in lifts ranging from several to tens of metres thickness, with or without sluicing, and without formal compaction.

- Rockfill placed in lifts less than about 2 to 3 m thickness and not formally compacted (i.e. without the use of rollers for compaction). Specified track rolling by bulldozer or other plant, or rockfill indicated as being trafficking by trucks or other haulage equipment has been classified under "not formally compacted".
- Rockfill placed in lifts greater than 2 to 3 m and formally compacted. For these rockfills the lift thickness is considered too great for compaction to have any significant influence at depth.

Watering is an important component for placement of rockfills, particularly in cases where the compressive strength of the rock used in the rockfill is susceptible to reduction on wetting, breaks down under the action of the roller, or if the rockfill contains large quantities of fines. Cooke (1993) comments that watering is not overly important for compaction of very high strength rockfills that are not susceptible to weakening on wetting. However, these rockfills can still show collapse type settlements on wetting.

For dumped rockfills, sluicing had a significant influence on the deformation behaviour of the rockfill as evidenced by the large collapse deformations of dry dumped or poorly sluiced rockfills when wetted (Cogswell dam (Baumann 1958), Strawberry and Dix River dams (Howson 1939)). Terminology used to define the level of sluicing of dumped rockfill has been broadly defined into three classes; dry dumped, poorly sluiced and well sluiced. A well-sluiced rockfill is described (Steele and Cooke 1958) as rockfill sluiced at a water ratio of 2 - 3 to 1 (water to embankment fill volume) using high-pressure jets that are directed on the tipped material.

6.2.3 ROCKFILL MODULI

Fitzpatrick et al (1985) defined two moduli for assessment of the deformation behaviour of rockfill (Figure 6.1), the rockfill modulus during construction, E_{rc}, and the rockfill modulus on first filling, E_{rf}, calculated from Equations 6.1 and 6.2. Both moduli are used extensively throughout this chapter.

$$E_{rc} = g\ H\ d_1 / d_s \tag{6.1}$$

$$E_{rf} = g_w h d_2 / d_n \quad (6.2)$$

where E_{rc} and E_{rf} are in MPa, *?* = unit weight of the rockfill in kN/m^3, ?$_w$ = unit weight of water in kN/m^3, d_s = settlement of layer of thickness d_1 due to the construction of the dam to a thickness H above that layer; d_n = face slab deflection at depth h from the reservoir surface, and d_2 is measured normal to the face slab as shown. H, h, d_1 and d_2 are all measured in meters, and d_s and d_n are measured in millimeters.

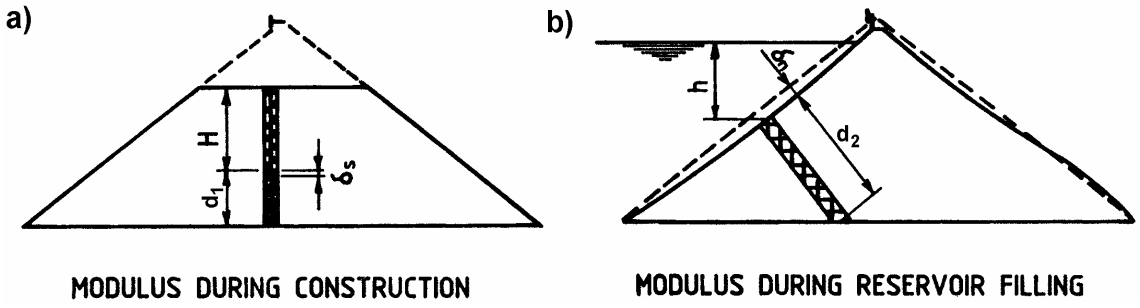

Figure 6.1: Determination of rockfill moduli, *(a)* modulus during construction, E_{rc}, and *(b)* modulus during reservoir filling, E_{rf} (Fitzpatrick et al 1985)

E_{rc} is determined from the settlement of hydrostatic settlement gauges (HSG) installed during construction, generally from under the embankment centreline. The modulus is a secant modulus and, for HSGs under the embankment centreline, very closely approximates the confined modulus. The method by Fitzpatrick et al (1985), shown in Figure 6.1a, does not take into consideration the stress distribution effect of embankment shape.

Where possible the calculation of E_{rc} for the case studies analysed has taken into account the distribution in applied vertical stress with depth due to embankment shape. For case studies where detailed data was available on internal settlements (from HSGs) as construction proceeds it has been possible to calculate the rockfill modulus (both secant and tangent modulus) with increasing vertical stress, allowing for the effects of embankment shape. The effect of embankment shape has been allowed for by using the stress intensity factors for elastic solutions by Poulos et al (1972) and vertical stresses calculated from finite element analysis. In summary, the method used to calculate the vertical stress and the rockfill moduli between say two HSGs or between a HSG and the foundation, was:

- Take the mid point between the HSGs as representative of the vertical stress of the layer of rockfill (the HSGs were usually a vertical distance of 10 to 20 m apart).
- On placement of the upper HSG, estimate the initial vertical stress at the mid point of the layer from elastic solutions. This is the stress at the zero settlement reading of the upper HSG.
- For subsequent fill heights above the upper HSG determine the vertical stress (at the layer mid-point) appropriate to each fill height from elastic solutions.
- The secant modulus (or E_{rc}) at each fill height can then be determined by dividing the change in vertical stress (from the initial vertical stress) by the vertical strain in the rockfill zone of interest (i.e. the settlement between the HSGs) appropriate to the change in vertical stress.

The elastic solutions by Poulos et al (1972) are for an embankment with slopes of 30 degrees (1.75H to 1V, horizontal to vertical) constructed of materials with a Poisson's Ratio of 0.3 on a rigid foundation. From finite difference analysis it was found that these solutions reasonably approximated the vertical stresses for embankments with slopes as steep as 1.3H to 1V without introducing significant errors. For HSGs located off centreline, the effect of the offset was taken into consideration in the estimation of vertical stress. Only HSGs from within the central half of the embankment (in most cases on or very close to the embankment centreline) and in the lower 40 to 60% of the embankment were used for estimation of the rockfill moduli during construction. A Poisson's Ratio of 0.3 is considered a reasonable estimate for rockfill.

In comparison to the vertical stresses under the embankment centreline estimated by the Fitzpatrick et al (1985) method, equivalent stresses are obtained up to 60 to 70 percent of the embankment height. For construction above this height (i.e. on construction of the upper 30 to 40%) the embankment shape influences the vertical stresses and the Fitzpatrick et al 1985 method will over-estimate the actual stresses and under-estimate the rockfill moduli.

E_{rf} is calculated from the deformation of the face slab normal to the upstream face on first filling as shown in Figure 6.1b. Fitzpatrick et al (1985) comment that the modulus calculated is only an indicative value of the modulus of the rockfill on first filling, but that the face slab deformations calculated using this method reasonably (and simply) approximate those from finite element analysis. The method is used very broadly throughout the concrete face rockfill dam (CFRD) community. In reality, E_{rf} is

not a true modulus of the rockfill, rather it is an artefact of the method of calculation and an index of performance useful for the estimation of face slab deflection. It should only be used for this purpose. This is discussed further in Section 6.4.3.

6.2.4 ZONING OF MAIN ROCKFILL IN CONCRETE FACE ROCKFILL DAMS

Zoning descriptors used for the main rockfill zones varies widely throughout the CFRD community. A uniform system of classification of the main rockfill zones has been applied to the CFRD case studies analysed. It broadly follows the classification systems of Cooke and Sherard (1987), ICOLD (1989b) and Fell et al (1992).

For CFRDs of dumped rockfill construction (typical of the CFRD design of the 1920's to 1960's) the typical embankment design incorporates the main body of dumped rockfill (designated Zone 3) and an upstream zone of derrick placed rockfill supporting the facing membrane (Figure 6.2).

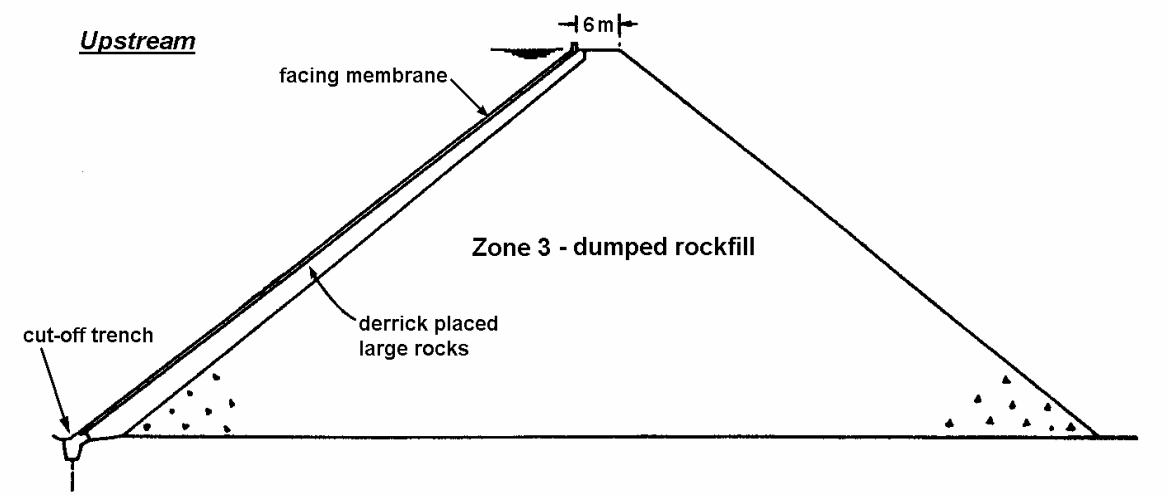

Figure 6.2: Typical design of dumped rockfill CFRD (adapted from ICOLD (1989b))

Following the resurgence of CFRD usage in dam design with the change to compaction of rockfill from about the mid to late 1960's, current design practice is dependent on a number of factors including the minimisation of deformation of the face slab on first filling and control of any leaks which may occur through the face slab or seepage through the foundation. For rockfills sourced from quarried sound rock the design of the main rockfill (Figure 6.3) typically incorporates two zones; Zone 3A and Zone 3B. Zone 3A, the main support zone for the upstream face, is typically placed in 1 m layers and well compacted to achieve a high modulus for minimisation of face slab

deformation. For Zone 3B, the downstream rockfill zone, a high modulus is not as critical as for Zone 3A and the rockfill is typically coarser and placed (and compacted) in 1.5 to 2 m thick layers.

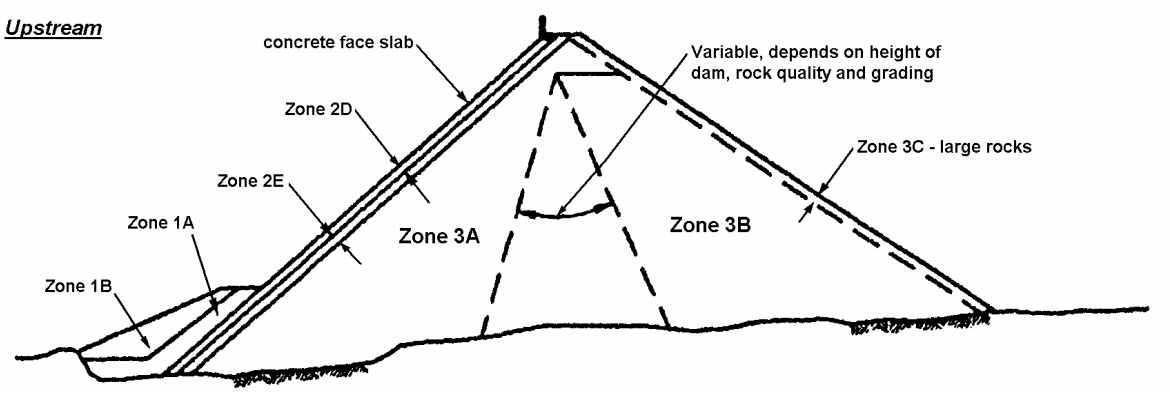

Figure 6.3: Typical zoning of main rockfill in current CFRD design practice for construction with sound quarried rockfill (adapted from Cooke (1997); zoning designators after Fell et al (1992))

The central variable zone in Figure 6.3 represents variations in the sizing of Zones 3A and 3B in current design practice around the world. Hydro Tasmania (formerly Hydro-Electric Commission, Tasmania) typically design with a dominant Zone 3A forming 75 to 100% of the main rockfill (i.e. Zone 3B is only present in the outer portion of the downstream shoulder). The typical design of large CFRDs in Brazil (of sound quarried rockfill) consists of Zone 3A comprising the upstream third of the main rockfill and Zone 3B the downstream two thirds.

Design of the main rockfill zones becomes more complex when the rockfill is to consist of potentially low permeability materials, such as dirty gravels or medium to high strength quarried rockfills that breakdown significantly on compaction. Drainage zones behind the face slab and above the foundation are generally incorporated into the design for control of seepage. The zoning classification of the main rockfill used for designs other than typical is based on similar principles as for the typical design, with Zone 3A designated the main upstream zone and Zone 3B, if used, the main downstream zone. To be designated Zone 3A the rockfill zone must comprise at least 25% of the main rockfill.

In the case of Aguamilpa dam (refer Figure 6.26 in Section 6.4.3) the main rockfill incorporated three zones designated Zone 3A for the upstream zone of compacted

gravels, Zone 3T for the central/downstream rockfill zone and Zone 3B for the outer downstream rockfill zone.

For details on current design features for the concrete face slab, plinth slab, jointing details, upstream facing zones, upstream toe zoning and non-typical CFRD designs for low strength and low permeability rockfills refer to Cooke and Sherard (1987), ICOLD (1989b), Fell et al (1992), Cooke (1999) and Marulanda and Pinto (2000).

6.3 LITERATURE REVIEW OF ROCKFILL DEFORMATION

6.3.1 HISTORICAL SUMMARY OF ROCKFILL USAGE IN EMBANKMENT DESIGN

An historical summary of the use of rockfill in embankment design and construction (Galloway 1939; Cooke 1984; Cooke 1993) is given in Table 6.2.

From the 1930's to the mid 1960's the height of construction of CFRDs was limited to about 80 to 100 m due to extensive face slab cracking and high leakage rates as a result of excessive deformation of the dumped and sluiced rockfill. In terms of stability though (Cooke 1984) the embankment performance was excellent. The transition from dumped and sluiced to compacted rockfill in embankment design (Cooke 1984, 1993) occurred in the late 1950's to 1960's and resulted in proliferation in the use of CFRD from the late 1960's.

6.3.2 DEFORMATION PROPERTIES OF ROCKFILL

From the mid 1930's (Galloway 1939; Morris 1939) it was recognised that a significant component of rockfill deformation was associated with particle breakage at point contacts under increasing loads during construction and on reservoir filling. Peterson (1939) commented on the *"critical importance"* of sluicing in obtaining settlements during the construction period. Terzaghi (1960) surmised that the particle breakage that occurred under increasing stress conditions resulted in the rearrangement in the granular structure to a more stable position, giving the large deformations during construction and impounding and the subsequent significant reduction in the rate of deformation post initial impounding.

Table 6.2: Historical summary of rockfill usage in embankment design (Galloway 1939; Cooke 1984; Cooke 1993).

Approximate Time Period	**Method of Placement and Characteristics of Rockfill**	**Comments**
Concrete Face Rockfill Dams		
Mid to late 1800's to early 1900's	Dumped rockfill with timber facing	Early embankments constructed with timber facing. Typically of very steep slopes (up to 0.5 to 0.75H to 1V). First usage of concrete facing in the 1890's. Height limited to about 25 m.
1920's to 1930's	Main rockfill zone dumped in high lifts (up to 20 to 50 m) and sluiced, although the sluicing was relatively ineffective. A hand or derrick placed rockfill zone was used upstream.	Rockfill typically sound and not subject to disintegration. Dam heights reaching 80 to 100 m. For high dams, cracking of the facing slab and joint openings resulted in high leakage rates (2700 l/sec Dix River, 3600 l/sec Cogswell, 570 l/sec Salt Springs).
Late 1930's to 1960's	High pressure sluicing used for the main rockfill zone. Rockfill still very coarse.	Cracking of face slab, particularly at the perimeter joint, and high leakage rates a significant issue with higher dams (3100 l/sec at Wishon, 1300 l/sec at Courtright).
From late 1960's	Rockfill placed in 1 to 2 m lifts, watered and compacted. Reduction in particle size. Usage of gravels and lower strength rock.	Significant reduction in post-construction deformations due to low compressibility of compacted rockfill. Significant reduction in leakage rates; maximum rates typically less than 50 to 100 l/sec. Continued improvement in plinth design and facing details to reduce cracking and leakage.
Earth and Rockfill Dams		
1900 to 1930	Dumped rockfill	Use of concrete cores with dumped rockfill shoulders at angle of repose. Limited use of earth cores. Dam heights up to 50 to 70m.
1930's to 1960's	Earth core (sloping and central) with dumped rockfill shoulders.	Use of earth cores significant from the 1940's due to the difficulties with leakage of CFRD. Increasing dam heights up to 150 m.
From 1960's	Use of compacted rockfill. Typically placed in 1 to 2 m lifts, watered and compacted with rollers.	Improvements in compaction techniques. Early dams compacted in relatively thick layers with small rollers. Gradual increase in roller size and reduction in layer thickness reduced the compressibility of the rockfill. Significant increase in dam heights in the mid to late 1970's, up to 250 to 300 m.

With the increased usage of rockfill in embankment construction of high dams from the 1960's came the use of large scale laboratory testing (mainly oedometer, and triaxial and plane strain shear testing) to better understand the strength and deformation

properties of rockfill. The testing confirmed the significance of particle breakage on the deformation behaviour of rockfill under increasing applied stresses and on saturation. In summary, it was found that the deformation (and modulus) of rockfill was predominantly affected by:

- The compactive effort in placement of the rockfill. Increased modulus was observed with increased compactive effort (Marsal 1973).
- The applied stress level. Increased particle breakage and decreasing modulus were observed with increasing deviatoric stress levels in triaxial compression tests (Marsal 1973; Marachi et al 1969). In oedometer tests relatively high moduli were observed for compacted rockfill samples up to normal stresses in the order of 800 to 1000 kPa, thereafter the modulus was observed to decrease with increasing normal stress (Marsal 1973).
- The stress path. Significantly higher modulus was observed on un-loading and re-loading at stress levels less than previously experienced by the rockfill as shown in Figure 6.6 (Mori and Pinto 1988).
- The particle shape and grading of the rockfill. Greater deformation (and lower modulus) was observed for angular (in comparison to rounded), more uniformly graded (i.e. lower coefficient of uniformity, C_u) and coarser rockfills (of similar C_u but higher maximum particle size) (Marachi et al 1969; Marsal 1973; Bowling 1981).
- Intact rock strength. Reduced modulus, greater deformation and reduced strength were observed for weaker strength rockfills (Marsal 1973).

A significant aspect of rockfill deformation behaviour is its propensity to collapse on wetting. Probably the most infamous case of collapse settlement was observed during the construction of Cogswell dam (CFRD) in 1933 (Baumann 1958). The rockfill was dumped in high lifts, up to 46 m, without sluicing. Following a very heavy rainstorm in December 1933 the embankment crest was observed to settle up to 4.6 m (or 5.4%) and bulging on the mid to lower slopes caused significant damage to the facing. High pressure sluicing after the rainstorm resulted in further crest settlements of up to 1.7 m. Similar, but not as dramatic, collapse deformations during construction on flooding of poorly sluiced rockfills were observed at Strawberry and Dix River dams (Howson 1939). Terzaghi (1960) attributed the deformation on saturation to a loss in

strength of the rockfill, mainly in the outer surface of the particles and commented that it was more likely to occur in weathered rockfills.

The results of laboratory testing investigating the collapse deformation behaviour of rockfill indicate:

- The stress-strain curve of rockfill in a dry state is of lower compressibility than for similar rockfill (similar grading and density) in a saturated state (Figure 6.4).
- Collapse deformation on wetting occurs for dry rockfill when the stress state (in stress-strain space) is above the normal compression line for wetted or saturated rockfill (Alonso and Oldecop 2000).
- On wetting, the collapse strain is equivalent to the difference in strain (at a given confining stress) between the dry and wetted states (Figure 6.4) (Nobari and Duncan 1972a; Alonso and Oldecop 2000).
- The initial water content at placement has a significant influence on the amount of collapse deformation on wetting (Nobari and Duncan 1972a), the higher the moisture content at placement the lesser the collapse deformation on wetting.
- There is a time delay between flooding of the sample and collapse deformation (Marsal 1973; Alonso and Oldecop 2000). Martin (1970), as reported by Justo (1991), using water and organic liquids for sample flooding, found that the amount of collapse deformation and time for collapse deformation to occur was dependent on the liquid used for saturation of the sample.
- Collapse deformations of similar magnitude to that occurring on flooding were obtained by imposing 100% relative humidity on the rockfill sample (Alonso and Oldecop 2000), indicating that flooding or wetting of the voids between the rock particles was not required for collapse deformation.

Alonso and Oldecop (2000) concluded that the collapse deformation occurred within the individual rock particles, and that the amount of deformation was controlled by the imposed stresses and initial moisture content within the outer exposed voids or pores of the individual rock particles. They hypothesised that the collapse mechanism was associated with crack propagation of the rock pores, and that the rate of propagation was significantly affected by the total suction in the rock pores. They further concluded that *"any situation leading to a change in moisture content in the rock pores is enough to cause collapse deformation"*, which is consistent with the observation of collapse deformations induced by flooding, such as on reservoir filling, or rainfall.

This assessment seems to assume that the reduction in compressive strength on saturation observed for many rocks, which leads to failure at the highly stressed point contacts in an angular rockfill mass, is entirely dependent on suction effects in the outer pores of the rock pieces at the highly stressed point contacts. This seems unlikely.

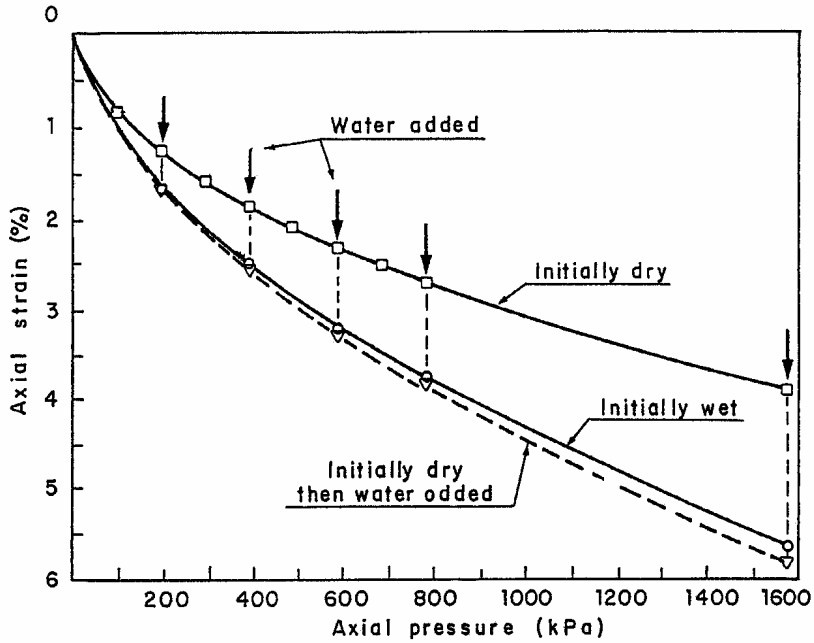

Figure 6.4: Compression curves for dry and wet states, and collapse compression from dry to wet state for Pyramid gravel in laboratory oedometer test (Nobari and Duncan 1972a)

From laboratory oedometer tests on rockfill (Sowers et al 1965; Marsal 1973; Alonso and Oldecop 2000) it is observed that the deformation on application of an increase in applied stress occurred as a large, almost instantaneous component followed by a much smaller time-dependent strain component. Sowers et al (1965) commented that this secondary time-dependent component of strain approximated a straight line when plotted against the log of time (Figure 6.5). They further commented that the log rate of strain increased with increasing applied stress for dry rockfill samples and on saturation (post the collapse deformation). Alonso and Oldecop (2000) observed similar findings and hypothesised that this time dependent strain was due to the on-going process of crack propagation and particle breakage.

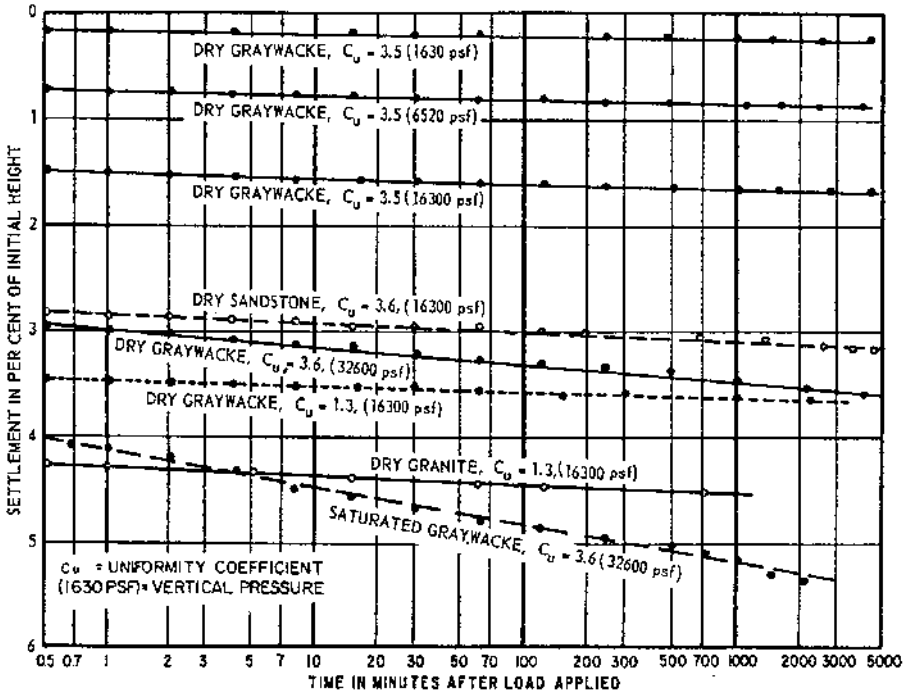

Figure 6.5: Settlement versus time curves for laboratory oedometer tests on rockfill (Sowers et al 1965)

6.3.3 PREDICTIVE METHODS FOR ROCKFILL DEFORMATION

For CFRD and the rockfill zones of earth and rockfill dams the components of rockfill deformation are deformations that occur due to load application (during construction and impoundment), on saturation or wetting and on-going time dependent or creep type deformations. Predictive methods are typically divided into the three components deformation during construction, on first filling and long-term post construction (or post first filling).

Most predictive methods cover the deformation behaviour of one or two of these components. Finite element analyses have been used (Saboya and Byrne 1993; Kovacevic 1994; amongst others) for analysis of rockfill deformation during construction and on first filling treating the events sequentially, and depending on the embankment type, consider the deformation on saturation only during first filling. Empirical methods, usually based on historical performance of embankments, are typically available for prediction of deformation during construction and post-construction. The deformation on first filling and on wetting or saturation is implicitly incorporated in the post-construction deformation component for these methods. In the case of CFRD, methods are available that specifically consider face slab deformation

during first filling, and in these cases, the rockfill is assumed to remain un-wetted or unsaturated on impoundment.

From field observations the significant factors affecting the deformation behaviour of rockfill in embankment dams (mainly from CFRD) are reported to include:

- Degree of compaction of the rockfill;
- Applied stress conditions and stress path (Mori and Pinto 1988);
- Particle shape and size distribution;
- Intact strength of the rock used as rockfill;
- Wetting or saturation of the rockfill causing collapse deformation;
- Time dependent or creep type deformations.

Pinto and Marques Filho (1998) and Giudici et al (2000) consider that the geometric shape of the valley has a significant influence on the deformation behaviour due to cross valley arching, resulting in a reduction in vertical stresses within the embankment. Deformation moduli calculated using Equation 6.1, which ignores the three-dimensional effect of valley shape on vertical stress, will over-estimate the vertical stress and therefore over-estimate the moduli.

Available predictive methods incorporate several of these factors as discussed in the following sub-sections. Finite element analyses may incorporate most of these factors in the stress-strain relationships on which the constitutive models are based, but are generally not used to model the time-dependent deformations.

6.3.3.1 *Finite Element Analyses*

Duncan (1996) and Kovacevic (1994) are recent references covering the state of the art in finite element analyses applicable to the deformation behaviour of embankments (mainly zoned earth and rockfill dams) during construction and on first filling. They discuss the methods of analysis, their limitations, available constitutive models of the stress-strain relationship and areas of uncertainty. As Duncan points out, most analyses from the literature are Class C1 (Lambe 1973), i.e. after the event, which may account for the generally good agreement between predicted and observed deformation behaviour.

Duncan (1996) comments that the choice of stress-strain constitutive model used in the analysis is a balance between simplicity and accuracy, and that the choice of

constitutive model will depend on the purpose of the modelling. He commented that if the purpose of the analysis is to analyse stresses and/or the trend of deformations then more simplistic models could be suitable, depending on the relative stiffness between different embankment materials. More accurate modelling of deformations requires a more complex stress-strain model that more realistically approximates the real behaviour of the rockfill and earthfill.

Several other important aspects of finite element analysis with respect to modelling dam embankments (more specifically toward embankments constructed of rockfill) raised by Duncan (1996) and Kovacevic (1994) include:

- The importance of modelling the construction as a series of incremental layers
- The type of stress-strain relationship used for modelling materials. Linear elastic models are not suitable for accurate modelling of deformation behaviour due to the non-linear stress-strain relationship of rockfill (Figure 6.6). Hyperbolic or multi-linear elastic models (determined from laboratory oedometer tests) can reasonably model deformations during construction given that the stress paths in oedometer testing are similar to the stress paths under the centreline of the embankment and that plastic deformations under the shear stress conditions are generally not significant for rockfill embankments.
- A limitation of hyperbolic and multi-linear elastic models is that the model parameters are typically derived from triaxial compression or oedometer laboratory tests and are therefore limited by the narrow range of stress paths covered in comparison to the broader range of stress paths imposed in the field. Kovacevic (1994) highlighted the limitations of multi-linear elastic models to accurately model the deformation of the face slab of concrete face rockfill dams (CFRD) on reservoir impoundment. This would also apply to zones in other embankment types (e.g. the downstream shoulder in central core earth and rockfill dams) where the stress path on impoundment is markedly different to that in the triaxial compression or oedometer test.
- Kovacevic (1994) found that elasto-plastic models that model pre-peak plasticity were more suited for modelling the deformation behaviour of the upstream face of CFRD during reservoir impoundment due to the ability of these constitutive models to more realistically account for the rockfill deformation under the stress path conditions imposed (Figure 6.7).

- A significant factor of uncertainty associated with Class A type predictions based on laboratory testing is the difference in material properties between the laboratory test results and those in the field due to limitations on the maximum particle size that can be tested and variations in stiffness due to differences in material strength, compacted density and moisture content.

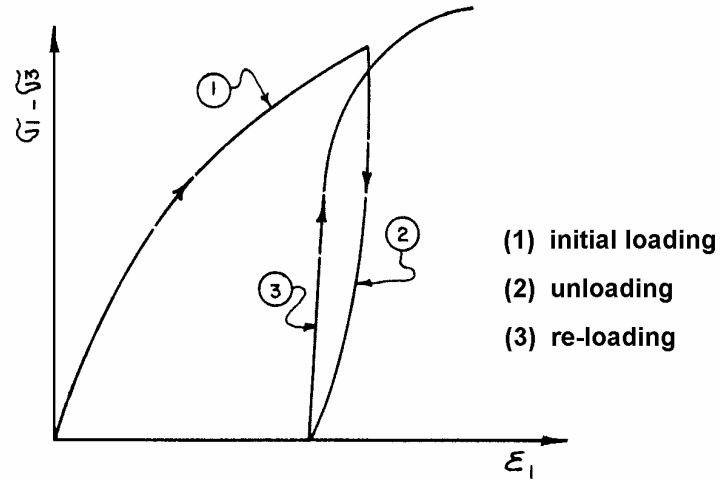

Figure 6.6: Typical stress-strain relationship of rockfill from a triaxial compression test (Mori and Pinto 1988)

A further problem with laboratory test results is the limitation of representing the layering and segregation that occurs within any single layer of rockfill. The upper part of the layer is broken down to a greater degree under the action of the roller than the lower part of the layer and segregation occurs during placement. As a result of the field compaction process this layering effect results in density, modulus and grading variations within a single layer.

An important component of the modelling of embankment dams is the consideration of collapse compression of susceptible rockfills and earthfills on wetting. The effects of collapse compression are most noted for the upstream shoulder on initial impoundment, but collapse compression has also been observed in the downstream shoulder following wetting due to rainfall, leakage or tail-water impoundment. Incorporating collapse compression into constitutive models adds further complexity and greater uncertainty in the estimation of material parameters between laboratory and field conditions due to the dependency of collapse compression on compaction moisture content, compacted density, applied stress conditions and material properties. Justo (1991) and Naylor et al (1989) propose methods for incorporation of collapse compression of rockfill into

constitutive models. The analysis of Beliche Dam, a central core earth and rockfill dam, by Naylor et al (1997) is an example where collapse compression of the upstream rockfill was considered in the modelling.

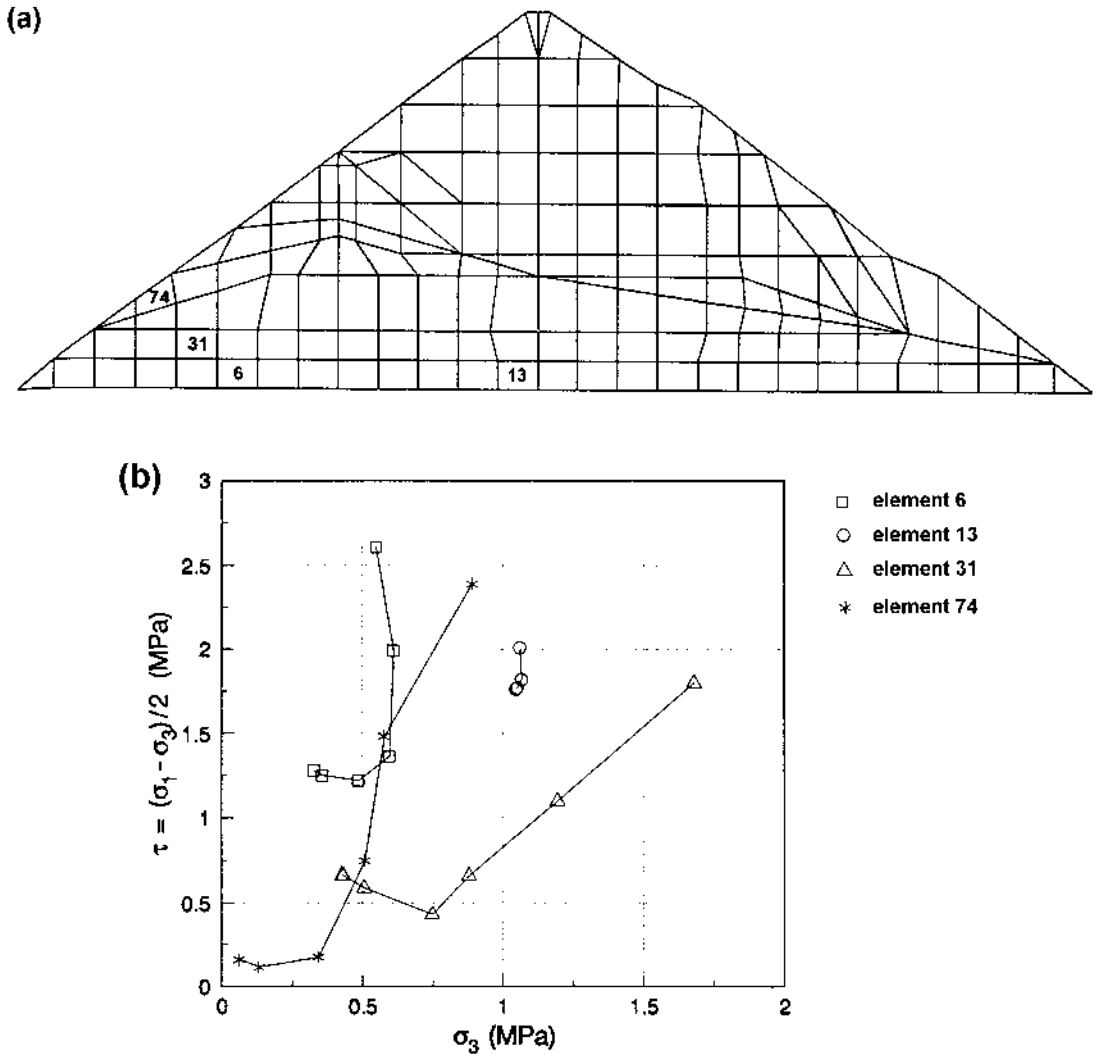

Figure 6.7: Finite element analysis of Foz do Areia CFRD (Saboya and Byrne 1993), *(a)* model and *(b)* stress paths during construction and first filling.

6.3.3.2 Empirical Predictive Methods of Deformation Behaviour During Construction and on First Filling

As previously discussed, Class A predictions of deformation behaviour of rockfill embankments during construction and first filling using finite element analysis are often based on stress-strain relationships of rockfills from laboratory testing or from empirically derived properties. Laboratory testing requires specialist laboratory equipment, particularly for rockfill, to accommodate particle size distributions that are

at least somewhat representative, although still scaled down, of the placed rockfill. Available facilities to undertake this testing are also limited and the testing is expensive. Depending on the proposed embankment design, construction materials and compaction specifications justification for laboratory testing of rockfill may not be warranted.

Several methods are available for estimation of the rockfill modulus from historical records of performance of CFRD for well-compacted rockfills. Poulos et al (1972) provide a simplistic procedure, based on linear elastic analysis, for estimation of the deformation during construction from non-dimensional factors.

Most of the methods based on historical performance serve to highlight the significant factors associated with the field deformation behaviour, although, Pinto and Marques Filho (1998) proposed a simple method to provide a *"rough estimate"* of the modulus for estimation of the face slab deflection of CFRD. From historical records of the performance of CFRDs constructed typically of well-compacted angular rockfills they conclude that void ratio and valley shape (Figure 6.8) are the dominant influences on the calculated two-dimensional deformation modulus during construction for narrow valleys (note that valley shape affects the vertical stress, and will therefore affect the calculated E_{rc} using the method by Fitzpatrick et al (1985), refer Equation 6.1 and Figure 6.1a). They define a narrow valley as having a valley shape factor (*SF*) of less than 3.5 ($SF = A/H^2$, where A = area of the upstream face slab measured normal with the upstream face in square metres and H = embankment height in metres).

For wide valleys (shape factor, *SF*, greater than 4), Pinto and Marques Filho (1998) comment that the effect of the valley shape can be disregarded and the deformation modulus (ranging from 30 to 60 MPa) is dependent on the void ratio. For well-compacted rockfills they comment that the void ratio is dependent on the rockfill gradation, with higher void ratios representative of poorly graded rockfills and lower void ratios of well-graded rockfills. For CFRD constructed of rounded gravels Pinto and Marques Filho (1998) indicate that the deformation modulus during construction is very high, in the order of 200 MPa.

Pinto and Marques Filho (1998) recommended that the maximum face slab deformation, *D*, on first filling be estimated from Equation 6.3, based on empirical correlation of the ratio of the deformation modulus on reservoir filling (E_{rf}) to during construction (E_{rc}) with the valley shape factor (Figure 6.9).

$$D = \left(\frac{0.003}{e^{0.21\left(1+A/H^2\right)}} \right) \cdot \left(\frac{H^2}{E_{rc}} \right) \tag{6.3}$$

where D = face slab deflection in metres, A = area of the upstream face slab in m^2, H = embankment height in metres and E_{rc} = deformation modulus during construction in MPa. Pinto and Marques Filho (1998) comment that the deformation estimate is a rough estimate, but that it is sufficient for design of CFRDs.

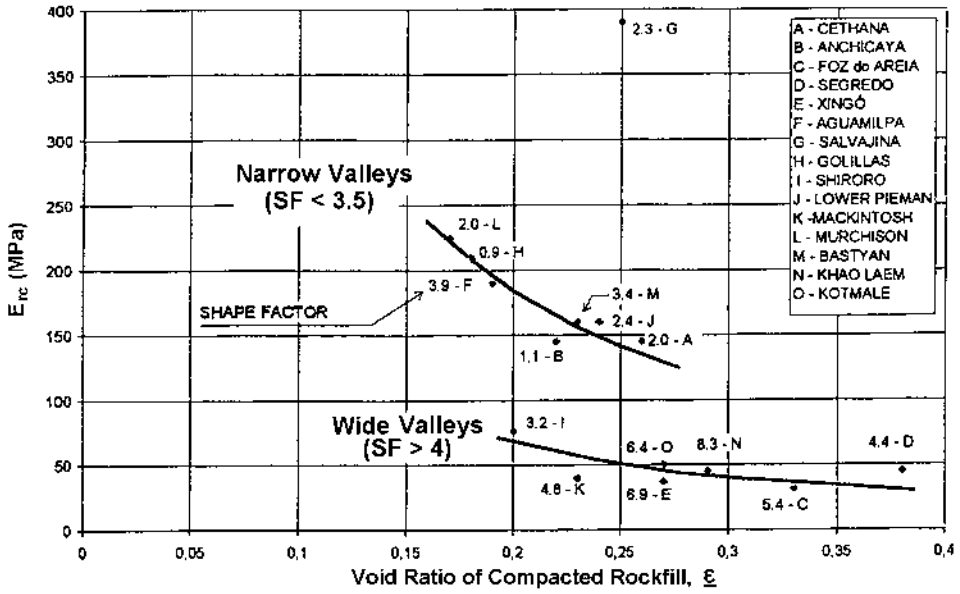

Figure 6.8: Deformation modulus during construction (E_{rc}) versus void ratio (Pinto and Marques Filho 1998)

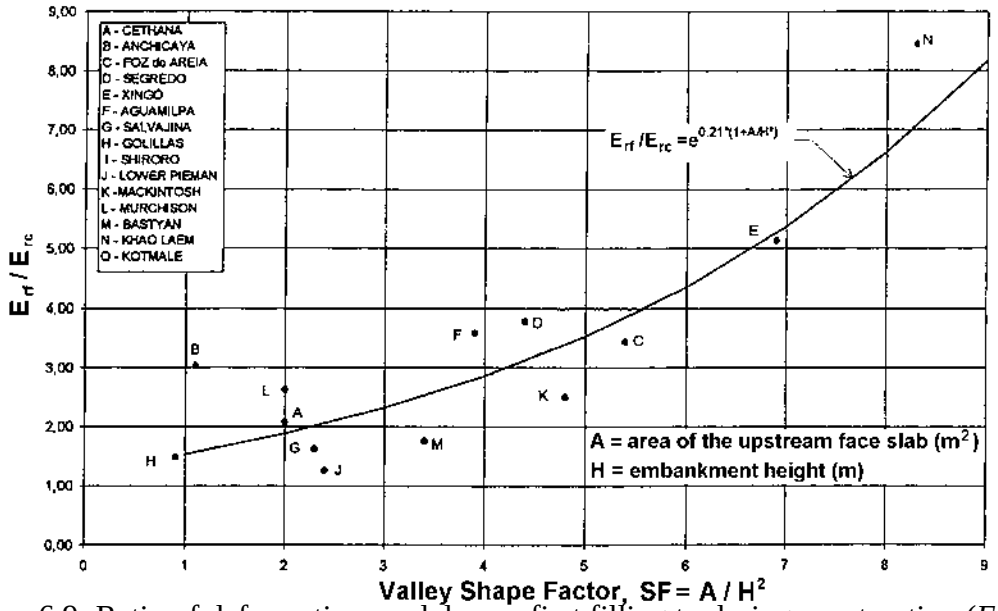

Figure 6.9: Ratio of deformation modulus on first filling to during construction (E_{rf}/E_{rc}) versus valley shape factor (Pinto and Marques Filho 1998)

Guidici et al (2000), based on field observations of well-compacted rockfill from Hydro Tasmania CFRDs, also considered that valley shape had a significant effect on vertical stress and therefore the deformation moduli calculated during construction from Equation 6.1 (Figure 6.10), and on that calculated on first filling, E_{rf}, from Equation 6.2 (refer Figure 6.1b). Higher deformation moduli during construction (E_{rc}) were generally calculated for narrower valleys (as expected given that the vertical stresses will be over-estimated by ignoring the 3-dimensional effect of valley shape). They commented that the scatter is associated with other factors affecting the deformation moduli including intact rock strength and stress levels (as a function of embankment height). Guidici et al (2000) further investigated the effects of valley shape by undertaking 3-dimensional finite element analysis of an idealised CFRD and commented that the results confirm the influence of valley shape on deformation behaviour during construction (Figure 6.11) and on first filling due to arching effects.

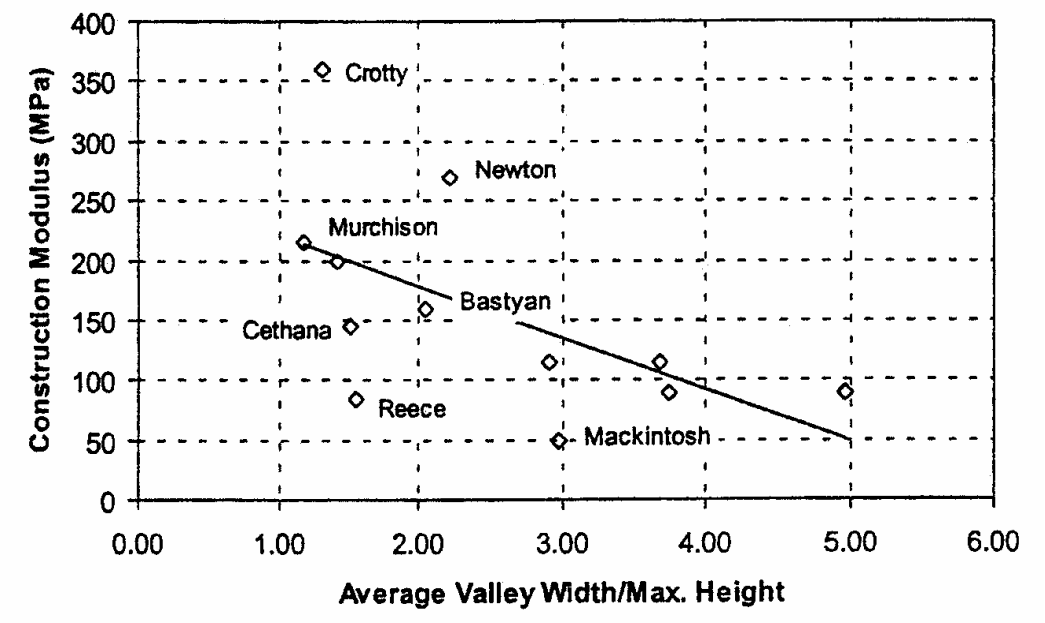

Figure 6.10: Deformation modulus during construction (E_{rc}) for Hydro Tasmania CFRDs (Giudici et al 2000)

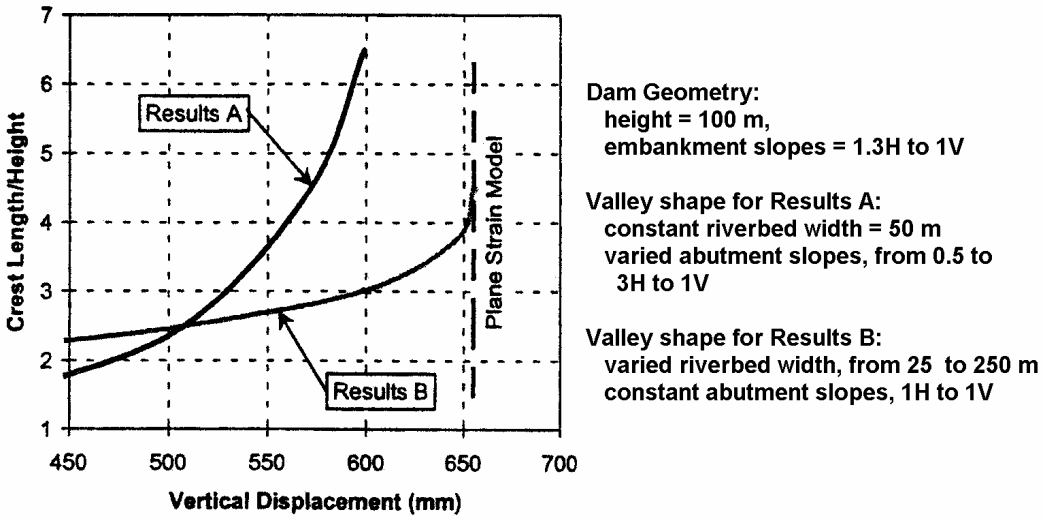

Figure 6.11: Results of 3-dimensional finite element analysis of CFRD, to give vertical displacement during construction versus valley shape (Giudici et al 2000)

6.3.3.3 Predictive Methods for Deformation Behaviour Post Construction

For CFRD and other rockfill embankments, post-construction time dependent deformations are observed for more than 30 years after construction (Sherard and Cooke 1987), typically at a gradually reducing strain rate with time. Empirical predictive methods of the post-construction deformation from the literature are typically based on historical deformation curves for similar embankment types or empirical relationships derived from historical performance of deformation behaviour. Several of the methods incorporate the deformation during first filling whilst others only consider the prediction of deformation post first filling.

Sowers et al (1965) proposed a logarithmic relationship between crest settlement and time (Equation 6.4) to describe the post construction crest settlement for "rockfill" dams. It was derived from a database of 14 rockfill dams (mix of concrete face rockfill, central core earth and rockfill, and sloping core rockfill dams) with rockfill ranging from sluiced and compacted to dumped and poorly sluiced. Sowers et al found that the coefficient a was dependent on the method of placement of rockfill and ranged from 0.2 %/log cycle of time for compacted and well sluiced rockfills up to 0.7 %/log cycle of time. They commented that a straight line could not be used to approximate the post construction settlement at Dix River dam where the rockfill was dumped and poorly sluiced. It should be noted that at the time of publication of this paper rockfill placement procedures were in the transitional phase from dumped to compacted and

therefore the level of compaction was dissimilar to what would currently be considered well-compacted.

$$DH = a(\log t_2 - \log t_1) \tag{6.4}$$

where DH = crest settlement as a percentage of dam height, t_1 and t_2 are time in months from the date when construction was half completed, and a = slope of the crest settlement-time curve (in units of settlement as a percentage of dam height per log cycle of time, time in months).

Parkin (1977) commented that a rate analysis, based on the power law relationship derived from rate process theory (Equation 6.5), allows for more accurate prediction of post construction settlement of rockfill and is a more powerful tool for evaluation of performance because it encapsulates the fundamentals of creep deformation. For a power coefficient of -1 (i.e. m = 1), integration of Equation 6.5 converts to the logarithmic form of Equation 6.4, and Parkin comments that for many purposes this approximation may be adequate for predictive purposes. He further indicates that problems with interpretation or prediction of settlement versus time records using Equation 6.4 is in the incorrect establishment of the initial time (t_o) or where m is not equal to 1 from the rate process equation, which will result in curvature in the settlement versus log time plot. Figure 6.12a shows the estimation of time t_o (from the plot of the inverse of settlement rate versus time) and Figure 6.12b the settlement rate versus time ($t - t_o$) plot with slope of m for Cedar Creek dam.

$$\dot{e} = a(t - t_o)^{-m} \tag{6.5}$$

where $\dot{e}$ = settlement rate in percent/month, a = constant, t_o = initial or origin of time, t = time in months after t_o and m = slope of the settlement rate versus time plot (Figure 6.12b).

Soydemir and Kjærnsli (1979) analysed the post construction deformation behaviour of 23 membrane faced rockfill dams (mostly CFRD), and proposed an empirical correlation (Equation 6.6) for prediction of deformation with respect to embankment height. Table 6.3 presents the coefficient values ($ß$ and d) for maximum crest settlement, crest horizontal displacement and deflection of the membrane normal to the

upstream slope for dumped and compacted rockfill on initial impounding and after 10 years service.

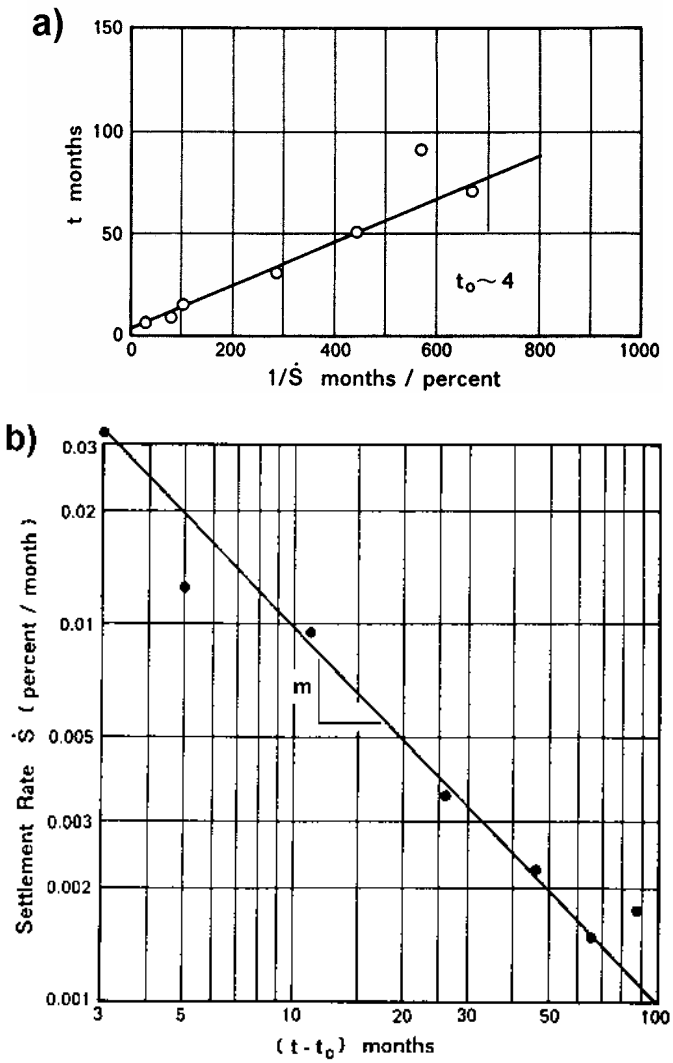

Figure 6.12: Settlement rate analysis of Cedar Creek dam; *(a)* determination of time t_o and *(b)* settlement rate versus time (Parkin 1977)

$$s = bH^d \tag{6.6}$$

where s = deformation in metres, H = embankment height in metres, and *ß* and d are constants.

Clements (1984) studied the post-construction deformation behaviour of 68 rockfill dams, comprising membrane faced (dumped and compacted), sloping core and central core embankments. Clements proposed upper and lower bound limits of crest settlement and crest displacement for each type of dam differentiating between dumped

and compacted rockfill. The individual deformation curves and bounding limits for the crest settlement of compacted rockfill for the membrane-faced dams are presented in Figure 6.13. In comparing the predicted deformations of Soydemir and Kjærnsli (1979) with the data for the case studies he analysed, Clements concluded that the errors were too large (correlation coefficients of 0.274 to 0.897) to make any reasonable predictions using their method. He recommended the use of deformation curves of existing dams (e.g. Figure 6.13) of similar design and construction methods for prediction of deformation behaviour. The zero time has been taken as the time of the initial measurement after the end of construction.

Table 6.3: Parameters for deformation prediction (Soydemir and Kjærnsli 1979)

	Coefficients for *b* and *d* (Equation 6.6)			
	Membrane Faced Dumped Rockfill		**Membrane Faced Compacted Rockfill**	
	b	*d*	*b*	*d*
Maximum crest settlement, s_V:				
- Initial inpounding	0.0005	1.5	0.0001	1.5
- 10 years service	0.001	1.5	0.0003	1.5
Maximum crest horizontal displacement, s_H:				
- Initial inpounding	0.00035	1.5	0.00005	1.5
- 10 years service	0.0006	1.5	0.00015	1.5
Maximum deflection normal to upstream face, s_N:				
- Initial inpounding	0.01	2	0.002	2

Pinto and Marques Filho (1985) commented that the methods of historical comparison proposed by Clements (1984) are useful, however, their application is not so straightforward as the deformation behaviour is strongly dependent on the initial time of measurement in relation to the end of construction (they suggested that comparisons could be based on the time from start of first filling). And, as pointed out by Parkin (1977), the shape of the deformation versus time curve will vary depending on the established zero time.

Sherard and Cooke (1987) compared the post-construction crest settlement from nine CFRDs of dumped and compacted rockfills. They observed that the crest settlement of dumped rockfill is 5 to 8 times greater than for compacted rockfill and the

rate of crest settlement (Table 6.4) for dumped rockfill 10 to 20 times that of compacted rockfill.

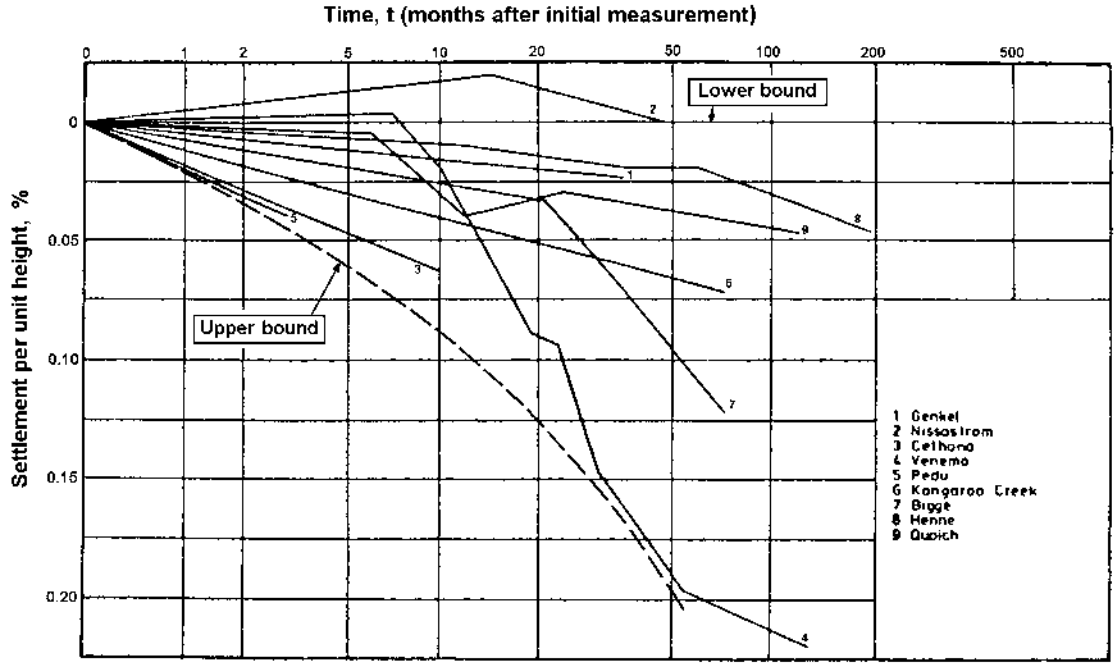

Figure 6.13: Post-construction crest settlement of membrane faced compacted rockfill dams (Clements 1984).

Table 6.4: Rates of post-construction crest settlement of dumped and compacted rockfills in CFRDs (Sherard and Cooke 1987)

	Approximate Rate of Crest Settlement for 100 m High CFRD (mm/yr)		
Type	**After 5 yrs**	**After 10 yrs**	**After 30 yrs**
Compacted Rockfill	3.5	1.5	0.6
Dumped Rockfill	45	30	10

Public Works Department NSW (1990) presented a plot of settlement index (Equation 6.7) versus time (Figure 6.14) for well-compacted CFRDs, defining bounds for low compressive strength and high compressive strength rockfill. The initial time is established after the end of construction. The data points have been updated where data records have been available, several data points have been added and the rockfill has been categorised with respect to intact UCS strength and coefficient of uniformity (C_u). Further discussion on these aspects is discussed in Section 6.4.4.

$$\text{Settlement Index} = \text{Crest Settlement} / (\text{Dam Height}/100)^2 \qquad (6.7)$$

where crest settlement is measured in millimetres from initial monitoring after the end of construction and dam height is in metres.

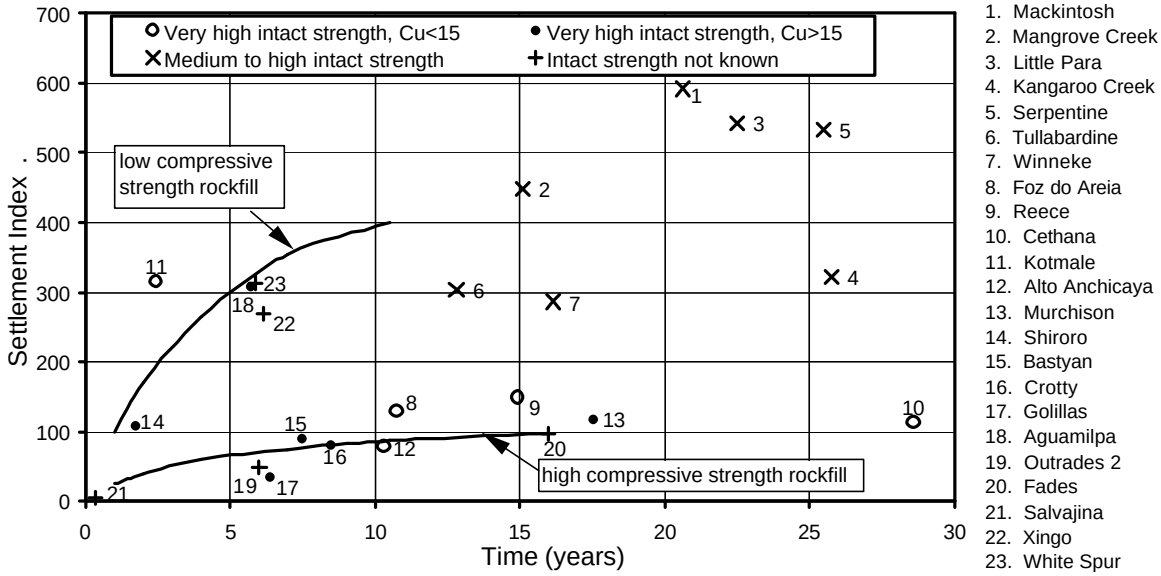

Figure 6.14: Settlement index versus time for well-compacted rockfills (adapted from Public Works Department NSW 1990)

6.4 ANALYSIS OF THE DEFORMATION BEHAVIOUR OF ROCKFILL IN CONCRETE FACE ROCKFILL DAMS

CRFDs are recognised for their stability, so one can be confident that measured deformations are not linked to instability. Conventional limit equilibrium analyses are generally not undertaken for CFRD (Sherard and Cooke 1987) unless potential stability problems associated with the foundation are identified, such as shear along a weak bedding seam in the foundation.

The deformation behaviour of rockfill during construction, on first filling and long-term post-construction (post first filling) has been analysed from the case study database of thirty-six mainly CFRD. The factors likely to affect the deformation behaviour of rockfill that have been considered in the analysis include placement methods, UCS of the rock used as rockfill, particle size distribution (grading and size), particle angularity, wetting or saturation, embankment geometry and valley geometry.

As part of the analysis, current methods (mainly empirical methods) for prediction of deformation are evaluated and, where appropriate, what are considered improved methods have been developed.

6.4.1 CASE STUDY DATABASE

The database of case studies (Table 6.5) includes thirty-five CFRDs and one central core earth and rockfill embankment (El Infiernillo dam). A summary of the embankment details and rockfill properties of the case studies is presented in Table 6.5 with further details given in Appendix E.

Selection of case studies was limited, as far as practicable, to CFRDs on rock foundation or those with a limited depth/area of alluvial gravels in the foundation, with good quality monitoring records and adequate information on the properties of the rock used in the rockfill. Case studies were targeted so as to assess the potential factors affecting deformation behaviour, including dumped versus compacted rockfill, and very high strength versus medium to high strength rockfill. The deformation during construction at El Infiernillo dam has been included because of the quality of published internal deformation records of dry placed and poorly compacted rockfill, for which little information was found in the literature for dumped rockfills in CFRDs.

6.4.2 DEFORMATION DURING CONSTRUCTION

The analysis of rockfill deformation behaviour during construction has been based on the observed deformation behaviour from the monitoring of internal settlements mostly from hydrostatic settlement gauges. This is the most frequently used method of deformation monitoring in CFRDs. For the most part deformations from gauges installed under the embankment centreline have been used. Unless otherwise stated, the data is for Zone 3A rockfill or the equivalent zone/s. Internal horizontal movements are generally monitored less frequently in CFRD and are not considered here.

Table 6.5: Summary of embankment and rockfill properties for CFRD case studies

Dam Name	Embankment Dimensions			Material Parameters / Properties of Rockfill													E_{rf} (MPa)	Time For First Filling (from end of main rockfill construction)
	Hgt, H (m)	L/H	Upstream Slope	Zone *[4] Class	Zone *[4] Auth	Rockfill Source*[1]	Strength*[2] Class[n] UCS (MPa)	Particle Shape	C_u	d_{max} (mm)	% finer 19 mm	Dry Density (t/m^3)	Void Ratio, e	Layer Thickness (m)	Placement	Level of Compaction	E_{rc} (MPa), average	
Aguamilpa (Zone 3A)	185.5	2.6	1.5 to 1	3A	3B	dredged alluvium	(Very High)	rounded	85	600	34	2.22	0.18	0.6	4p 10t SDVR, in moist condition	Good	305 (250 to 330)	770	0.48 to 1.83 years
Crotty	83	2.9	1.3 to 1	3A	3A	Gravels (Pleitocene)	(Very High)	rounded	70	200	48	2.54	0.20	0.6	8-12p 6-10t SDVR, watered	Good	375 (113 to 636)	470	0.87 to 2.0 years
Golillas	125	0.9	1.6 to 1	3A	2	gravels, unprocessed	(Very High)	rounded	125	350	40	2.135	0.24	0.6	4p 10t SDVR, water added	Good	155 (145 to 165), arching likely	250	4 to 5.17 years (June 82 to Aug 83)
Salvajina (Zone 3A)	148	2.4	1.5 to 1	3A	2	gravels, unprocessed	(Very High)	rounded	9.2	400	32	2.24	0.25	0.6	4p 10t SDVR, water added	Good	205 (175 to 260) - arching likely	500	0.33 to >0.75 years (1985)
Aguamilpa (Zone 3T)	185.5	2.6	1.5 to 1	3T	T	ignimbrite	UCS = 180 Very High	angular	30	500	28	2.04	0.24	0.6	4p 10t SDVR	Good	104	-	-
Alto Anchicaya	140	1.9	1.4 to 1	3A	D	hornfels	(Very High)	angular	18	600	22	2.28	0.294	0.6	4p 10t SDVR, 20% water	Good	138 (100 to 170), likely arching	375 (@ 30 to 40% height)	0.18 to 0.2 (Oct 74)
Bastyan	75	5.7	1.3 to 1	3A	3A	Rhyolite, SW to FR	(Very High)	angular	42	600	25	2.20	0.23	1.0	8p (10t ?) SDVR, 20% water	Good	130 (120 to 140)	290	0.86 to 1.05 years
Cethana	110	1.9	1.3 to 1	3A	3A	Quartzite	(Very High)	angular	23	900	21	2.07	(0.27)	0.9	4p 10t SDVR, 15% water	Good	160 (120 to 210) 105 (85 to 120) likely arching	300	0.26 to 0.48 years (1971)
Chengbing	74.6	4.4	1.3 to 1	3A	3B/3C	Tuff lava	UCS = 80 Very High	angular	10.4	1000	-	2.06	0.277	1.0	6p 10t SDVR, 25% water	Good	43	110	-0.5 to 4 years (12/88 to 1993).
Foz Do Areia *[3] (Zone 3A)	160	5.2	1.4 to 1	3A	1B	basalt (max 25% basaltic breccia)	UCS = 235 Very High	angular	6	600	10	2.12	0.33	0.8	4p 10t SDVR, 25% water	Good	47 (38 to 56)	80 (65 to 92)	0.5 to 0.9 years (Apr to Aug 80)
Ita (Zone 3A) *[3]	125	7.0	1.3 to 1	3A	E1/E3'	basalt	(Very High)	angular	11	700	12	2.179	0.308	0.8	6p 9t SDVR, 10% water	Good	48	87 (83 to 91)	0.7 to 0.9 years
Kangaroo Creek	60	3.0	1.3 to 1	3A	3	schist	UCS = 25 Medium to High	angular to subangular	310	600	44	2.34	0.201	0.9 to 1.8	4p 10t SDVR, 100% water	Good	-	140	0 to 1.95 yrs (Sept 69 to Aug 71)
Khao Laem (Zone 3A)	130	7.7	1.4 to 1	3A	3A	limestone	UCS < 190 Very High	angular	-	900	-	-	-	1.0	4p 10t SDVR, 15% water lower in 70 m	Good	59 (43 to 79)	130 to 240	0.6 to 1.9 years (June 84 to Nov 85)
Kotmale	90	6.2	1.4 to 1	3A	3A	charnockitic / gneissic	(High to Very High)	angular	-	700	-	2.20	-	1.0	4p 15t SDVR, 30% water	Good	61 (47 to 87)	145 (135 to 155)	0.54 to 1.04 years (Nov 84 to Aug 85)
Little Para	53	4.2	1.3 to 1	3A	3A	dolomitic siltstone	UCS = 8 - 14 Medium	angular, elongated ?	110	1000	35	2.15	0.223	1.0	4p 9t SDVR, no water lower half	Good	21.5 (19.5 to 23.5)	-	0.58 to 2.83 years (Aug 77 to Nov 79)
Mackintosh	75	6.2	1.3 to 1	3A	3A	Greywacke, some slate	UCS = 45 High	angular, elongated	52	1000	38	2.20	0.24	1.0	8p 10t SDVR, 10% water	Good	45 (35 to 60)	63	1.92 to 2.93 years
Mangrove Creek (Zone 3A)	80	4.8	1.5 to 1	3A	1B	fresh siltstone & sandstone	UCS = 45 - 64 High	angular to subangular	310	400	27	2.24	0.18	0.45 to 0.6	4p 10t SDVR, 7.5% water	Good	55 to 60	-	0.6 to > 15 years (not reached FSL by 1996)
Mangrove Creek (Zone 3B)	80	4.8	1.5 to 1	3B	4	weathered to fresh siltstone & sandstone	UCS = 26 - 64 High	angular to subangular	330	450	32	2.06	0.26	0.45	4p 10t SDVR, dry of OMC	Good	46 (36 to 56)	-	-
Murchison	94	2.1	1.3 to 1	3A	3A	Rhyolite (SW to FR)	UCS = 148 Very High	angular	19	600	22	2.27	0.234	1.0	8p 10t SDVR, 20% water	Good	190 (170 to 205)	560 (485 to 640)	1.04 to 1.09 years

Table 6.5 (cont.): Summary of embankment and rockfill properties for CFRD case studies (sheet 2 of 3)

Dam Name	Embankment Dimensions			Material Parameters / Properties of Rockfill														E_{rf} (MPa)	Time For First Filling (from end of main rockfill construction)
	Hgt, H (m)	L/H	Upstream Slope	Zone *[4]		Rockfill Source*[1]	Strength*[2] Class[n] UCS (MPa)	Particle Shape	C_u	d_{max} (mm)	% finer 19 mm	Dry Density (t/m^3)	Void Ratio, e	Layer Thickness (m)	Placement	Level of Compaction	E_{rc} (MPa), average		
				Class	Auth														
Reece	122	3.1	1.3 to 1	3A	3A	Dolerite	UCS = 80 - 370 Very High	angular	10	1000	11	2.287	0.29	1.0	4p 10t SDVR, 5 to 10% water	Good	86 (57 to 115)	190 (175 to 205)	1.32 to 1.46 yrs (Apr to June 1986)
Salvajina (Zone 3B)	148	2.4	1.5 to 1	3B	4	weak sandstone and siltstone	(Medium ?)	angular ?	45	600	32	2.26	0.21	0.9	6p 10t SDVR, water added	Good	62 (likely arching)	-	-
Scotts Peak	43	24.8	1.7 to 1	3A	3A	argillite	UCS = 22 Medium to High	angular ?	380	914	38	2.095	0.266	0.915	4-6p 10t SDVR, no water	Good	20.5 (18.5 to 23.5)	59 (Zone 3A) 420 (Zone 2B)	0.42 to 2.58 years (June 72 to Aug 74)
Segredo *[3] (Zone 3A)	145	5.0	1.3 to 1	3A	1B	basalt (<5% basaltic breccia)	UCS = 235 Very High	angular	7.4	-	-	2.13	0.37	0.8	6p 9t SDVR, 25% water	Good	55 (arching likely)	175	Approx. 0.6 years
Serpentine	38	3.5	1.5 to 1	3A	3A	Ripped quartz schist	(Medium to High)	angular to subangular	210	152	69	2.10	0.262	0.6 to 0.9	4p 9t SDVR, not sure if water added	Good	92 (46 to 142)	97 (94 to 100)	0.24 to 2.94 years (Dec 71 to Aug 74)
Shiroro	125	4.5	1.3 to 1	3A	2	granite	(Very High)	angular	32	500	22	2.226	0.20	1.0	6p 15t SDVR, 15% water	Good	66 (61 to 71)	-	1.44 to >1.8 years (from 5/84)
Tianshengqiao - 1 (Zone 3A)	178	6.6	1.4 to 1	3A	3B	Limestone, SW to FR	UCS = 70 - 90 Very High	angular	15 to 20	800	-	2.19	0.23	0.8	6p 16t SDVR, 20% water	Good	49 (40 to 57)	-	-1.5 to >0.8 years
Tianshengqiao - 1 (Zone 3B)	178	6.6	1.4 to 1	3B	3C	Mudstone	UCS = 16 - 20 Medium	angular	40	600	20 to 35	2.23	0.21	0.8	6p 16t SDVR, 20% water	Good	37 (32 to 42)	-	-
Tullabardine	25	8.6	1.3 to 1	3A	3A	Greywacke, some slate	UCS = 45 High	angular, elongated	28	400	30.5	2.22	0.23	0.9 to 1.0	4p 10t SDVR, > 10% water	Good	74	170	2.05 to 2.35 years (5/81 to 8/81)
White Spur	43	3.4	1.3 to 1	3A	3A	Tuff - SW to FR	(High to Very High ?)	angular	-	1000	-	2.30	0.18 to 0.25	1.0	(4p 10t ?) SDVR, > 10% water	Good	180 (160 to 200)	340	0.18 to 0.24 years (June to July 1989).
Winneke	85	12.4	1.5 to 1	3A	3	SW to FR Siltstone	UCS = 66 High	angular	33	800	28	2.07	0.302	0.9	4-6p 10t SDVR, 15% water	Good	55 (50 to 59)	104	1.62 to 5.04 years (6/80 to 11/83)
Xibeikou	95	2.3	1.4 to 1	3A	1	Limestone - FR	UCS = 240 Very High	angular	-	600	-	2.18	0.284	0.8	8p 12t SDVR, 25 to 50% water	Good	80 (60 to 100)	260	-1.5 to 6 years (June 1995)
Xingo (Zone 3A)	140	6.1	1.4 to 1	3A	3	granite gneiss	(High to Very High ?)	angular	18	650	4 to 33	2.15	0.28	1.0	4p 10t SDVR, 15% water	Good	34 (30 to 39)	76 (73 to 80)	1.02 to 1.46 (mid to late 1994) years
Foz Do Areia *[3] (Zone 3B)	160	5.2	1.4 to 1	3B	1C & 1D	mix basalt & basaltic breccia	UCS = 235, High to Very High	angular	14.2	-	-	1.98	0.27	0.8 for 1D 1.6 for 1C	4p 10t SDVR, 25% water	Good to Reasonable	32 (29 to 38)	-	-
Aguamilpa (Zone 3B)	185.5	2.6	1.5 to 1	3B	3C	ignimbrite	UCS = 180 Very High	angular	22	700	-	-	-	1.2	4p 10t SDVR	Good to reasonable	36 (25 to 45)	-	-
Ita (Zone 3B) *[3]	125	7.0	1.3 to 1	3B	E3	Breccia and Basalt	(High to Very High)	angular	13.3	750	15	2.066	(0.33 to 0.39)	1.6	4p 9t SDVR, no water	Reasonable	24 (14 to 46)	-	-
Khao Laem (Zone 3B)	130	7.7	1.4 to 1	3B	3B	limestone	UCS < 190 Very High	angular	-	1500	-	-	-	2.0	4p 10t SDVR, 15% water lower in 70 m	Reasonable	30	-	-
Segredo *[3] (Zone 3B)	145	5.0	1.3 to 1	3B	1C & 1D	basalt (<5% basaltic breccia)	UCS = 235, High to Very High	angular	10.2	-	-	2.01	0.43	1D - 0.8 1C - 1.6	4p 9t SDVR, no water	Reasonable	28 (25 to 33), likely arching	-	-

Table 6.5 (cont.): Summary of embankment and rockfill properties for CFRD case studies (sheet 3 of 3)

Dam Name	Embankment Dimensions			Material Parameters / Properties of Rockfill													E_{rf} (MPa)	Time For First Filling (from end of main rockfill construction)
	Hgt, H (m)	L/H	Upstream Slope	Zone *4 Class	Zone *4 Auth	Rockfill Source*1	Strength*2 Class^n UCS (MPa)	Particle Shape	C_u	d_{max} (mm)	% finer 19 mm	Dry Density (t/m^3)	Void Ratio, e	Layer Thickness (m)	Placement	Level of Compaction	E_{rc} (MPa), average	
Xingo (Zone 3B)	140	6.1	1.4 to 1	3B	4	Sound and weathered granite gneiss	(Medium to Very High ?)	angular	80	750	15 to 60	2.1	0.31	2	6p 10t SDVR, no water	Reasonable	13 (12 to 14)	-	-
Courtright	97	2.8	1.15 to 1	3	3	granite	(Very High)	angular	(<7)	1750	-	(1.8)	0.47	8 to 52	dumped and well sluiced	Poor	-	-	0 to 9 years (from 1959)
El-Infiernillo (Zone 3B)	148	2.3	1.75 to 1	3B	3B	diorite & silicified conglomerate	UCS = 125 Very High	angular	13	600	22	1.85	0.47	0.6 to 1.0	4p D8 dozer, no water	Poor	39 (27 to 48)	-	-
Lower Bear No. 1	75	3.9	1.3 to 1	3	3	granodiorite	UCS = 100 - 140, very High	angular	8 to 10	2000 to 3000	low	-	-	max 65	dumped and well sluiced	Poor	-	21	0.07 to 0.58 years (Dec 52 to June 53)
Lower Bear No. 2	46	5.7	1 to 1	3	3	granodiorite	UCS = 100 - 140, very High	angular	8 to 10	2000 to 3000	low	-	-	max 36.5	dumped and well sluiced	Poor	-	40	0.07 to 0.58 years (Dec 52 to June 53)
Wishon	90	11.3	1.15 to 1	3	3	granite	(Very High)	angular	(<7)	1500 to 2000	-	1.80	0.47	8 to 52 (variable)	dumped and well sluiced	Poor	-	-	0.4 to 0.45 years (May 1958)
Dix River	84	3.7	1.1 to 1	3	3	Limestone & Shale (?)	(Very High)	angular ?	low	-	-	-	-	21	dumped and poorly sluiced	Poor to Very Poor	-	-	Started in 1925
Salt Springs	100	4.0	1.3 to 1	3	3	granite	UCS = 100 - 130, Very High	angular, blocky	low (<10)	2000 to 3000	low	(1.88)	0.41	5 to 52	dumped and poorly sluiced	Poor to Very Poor	-	20	0 to 1.48 years (1931/32)
Cogswell	85.3	2.1	1.3 to 1	3	3	Granitic Gneiss	UCS = 45 High	angular	7	1300	5	2.05	0.37	7.6 (46 m max)	dumped dry (no water)	Very Poor	-	44	2.6 years. Filled in 71 hours (Mar 1938)
El-Infiernillo (Zone 3C)	148	2.3	1.75 to 1	3C	3C	diorite & silicified conglomerate	UCS = 125 Very High	angular	<13	>600	-	1.76	0.54	2.0 to 2.5	Dumped and spread, no water	Very Poor	22 (17 to 27)	-	-

Legend:

H = dam height

L = crest length

C_u = uniformity coefficient (d_{60}/d_{10})

d_{max} = average maximum particle size

E_{rf} = deformation modulus during first filling

- indicates unknown

E_{rc} = secant modulus during construction (average)

4p 10t SDVR = 4 passes of 10 tonne smooth drum vibrating roller

% water = % by volume

(…) in strength classification, Cu, dry density and void ratio columns indicate estimation

*1 FR = fresh, SW = slightly weathered

*2 rock strength classification to AS 1726-1993

*3 Brazilian CFRDs constructed with a mix of very high strength basalt, vesicular basalt and high strength basalt breccia.

*4 Class = For the classification system used (refer Section 6.2.4);
Auth = rockfill zoning used by author/s of referenced paper

6.4.2.1 *Base Plots of Data*

Figure 6.15 and Figure 6.16 present the stress-strain and secant modulus-stress relationships from the internal settlement monitoring records of eleven embankments (10 CFRDs and El Infiernillo dam). For the ten CFRDs the monitoring records are from HSGs installed under the embankment centreline and in the lower third to half of the embankment. For El Infiernillo the monitoring records are from internal vertical settlement gauges (IVM) in the rockfill shoulders, and include monitoring records within the dry placed and poorly compacted rockfill zones (Zones 3B and 3C).

Vertical stresses have been estimated from the elastic solutions for embankments by Poulos et al (1972) and assume that the embankment has been constructed in horizontal layers across the full embankment width. Use of these solutions takes into consideration the effect of embankment shape on vertical stress (refer Section 6.2.3).

Note that in Figure 6.15 and Figure 6.16 zero strain is equivalent to the vertical stress at the mid point of the layer analysed when the upper HSG was placed. Therefore, in Figure 6.15 the stress-strain curve will not intersect the origin. It will intersect the vertical stress axis at stresses in the range 30 to 150 kPa. The assumption of zero strain at a small but finite value of vertical stress introduces a slight error in the secant moduli calculations.

6.4.2.2 *Effect of Compaction/Placement Method*

The stress-strain relationships (Figure 6.15) indicate that the degree of compaction has a significant influence on rockfill modulus, confirming the results of large scale laboratory tests on rockfill (Section 6.3.2). The dry placed and poorly rockfills of El Infiernillo dam have lower modulus than for the well-compacted rockfills. The results also indicate:

- The very high modulus of well-compacted gravels (Crotty dam) in comparison to well-compacted quarried (or angular) rockfills, although the smaller size and well-graded particle size distribution of the Crotty gravel fill may also have influenced the modulus.
- The intact strength (UCS) of the rock used as rockfill has an influence on the modulus for well-compacted quarried rockfills. The very high strength rockfills

(Cethana, Murchison and Reece dams in particular) have greater moduli than the medium to high strength rockfills used at Tullabardine and Mackintosh dams.

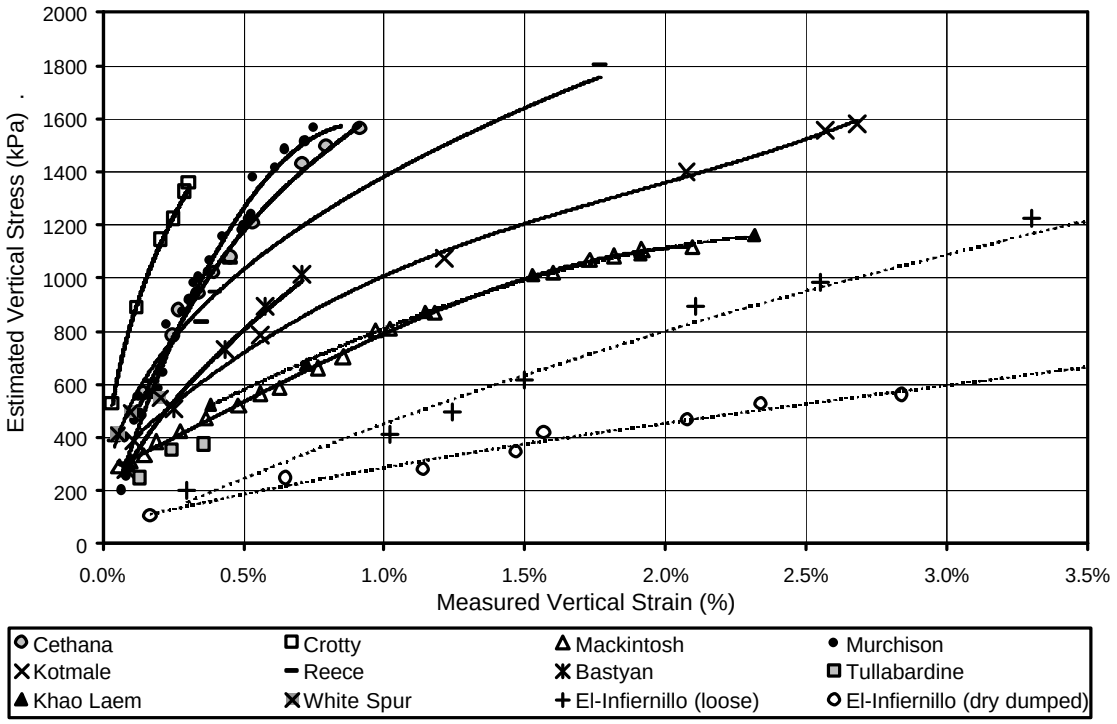

Figure 6.15: Stress-strain relationship for rockfills observed during construction

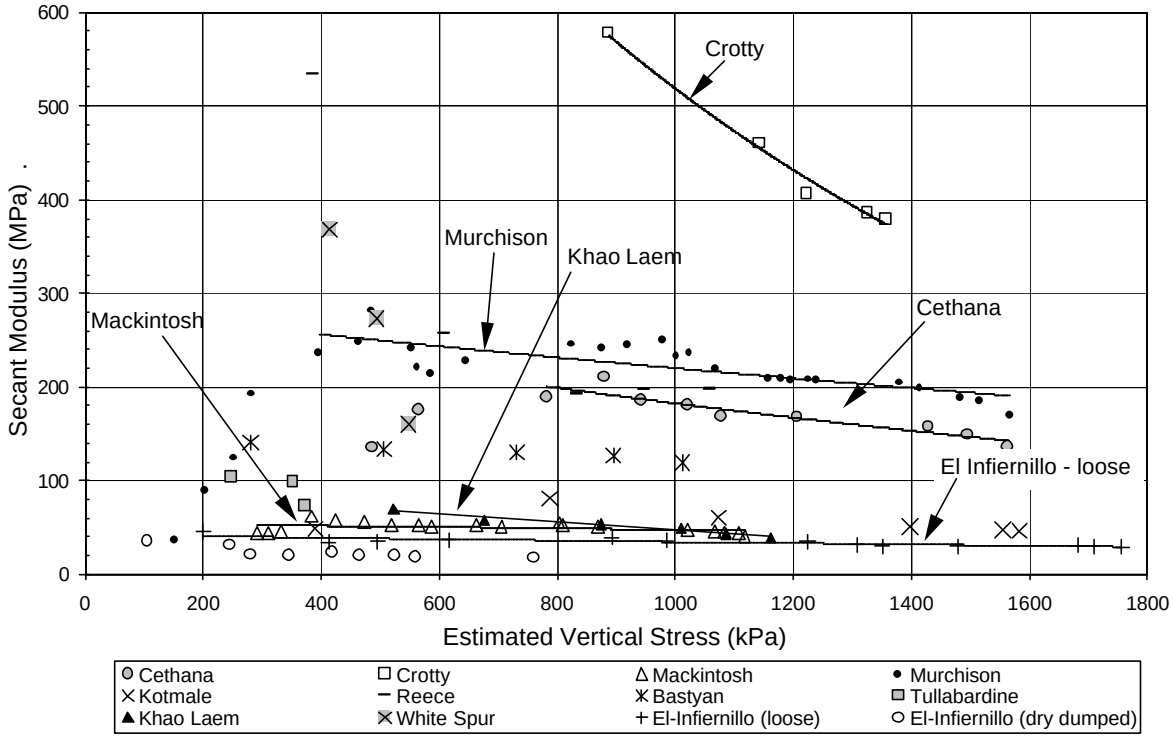

Figure 6.16: Secant modulus versus vertical stress from monitoring during construction

Particle size distribution and valley shape also influence the stress-strain relationship of the rockfill shown in Figure 6.15, although they are not readily apparent from the small number of case studies represented. The effect of these factors is addressed later. Note that for valley shape, the error in estimation of the vertical stress by ignoring valley shape effects is then introduced into the stress-strain relationship plotted (i.e. the valley shape influences the vertical stress in the embankment, and not the vertical stress-strain relationship of the rockfill).

6.4.2.3 *Effect of Confining Stress*

An important aspect of rockfill deformation behaviour identified from laboratory testing is the effect of increasing applied stress. The non-linear stress-strain relationship of rockfill, indicative of decreasing modulus with increasing applied stress (either deviatoric, confining or mean normal stress), evident from laboratory oedometer and triaxial compression testing is clearly evident in the field observations (Figure 6.16 and Figure 6.17). The initial behaviour of increasing secant modulus at low stress levels (less than 400 to 600 kPa) for several dams in Figure 6.16 (Murchison and Cethana dams for example) is considered to be due to seating of the HSG as a result of initial incompatibility between the filling placed around the instrument and the predominant rockfill.

Plotting the field data against deviatoric, confining or mean normal stress has not been attempted due to the introduction of errors in confining stress estimation associated with estimation of Poisson's ratio and the observation that Poisson's ratio is also stress dependent (Duncan 1996). It is also noted that the stress path represented by the field observations under the centreline of the embankment closely approximates that of the oedometer laboratory test (Kovacevic 1994) and the moduli (secant and tangent) would therefore approximate the confined modulus.

The plot of tangent modulus (Figure 6.17) shows a greater variation in modulus than for secant modulus plot due to the incremental calculation of tangent modulus. However, the trend of decreasing modulus with increasing vertical stress is clearly evident. Over the vertical stress range 500 to 1000 kPa, reductions in the tangent modulus of approximately 40 to 50% are observed for the well-compacted rockfills.

The variation in modulus (both secant and tangent) for an individual case study is affected by the accuracy of settlement measurements, the time-dependent or creep

deformation of rockfill and therefore the rate of construction, and the variation in rockfill height across the width and length of the embankment during construction.

6.4.2.4 *Effect of Valley Shape*

The influence of valley shape is identified (Pinto and Marques Filho 1998; Giudici et al 2000) as a significant factor affecting the vertical stress and therefore the calculated deformation modulus during construction (from 1 or 2-dimensional analysis), particularly for embankments constructed in narrow valleys with relatively steep abutment slopes, because of arching across the abutment slopes. To check these hypotheses finite difference analysis (FDA), using the FLAC program, was undertaken.

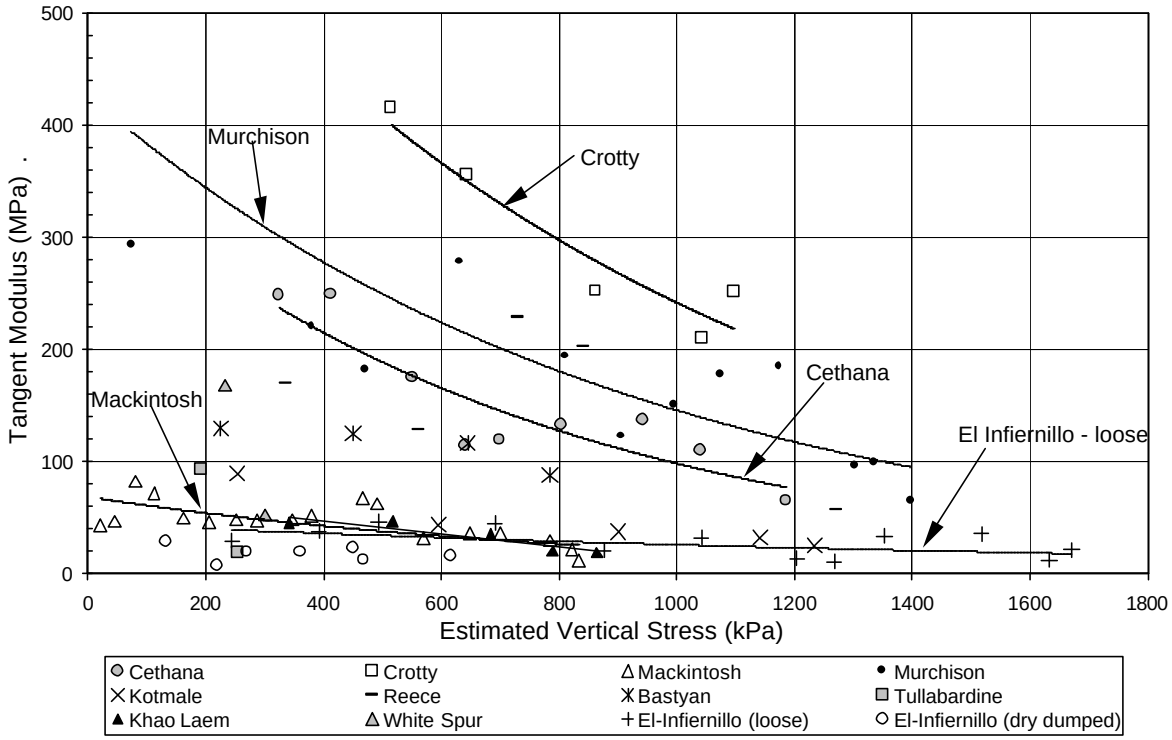

Figure 6.17: Tangent modulus versus vertical stress from monitoring during construction

A two-dimensional FDA was undertaken assuming an idealised rockfill embankment of 100 m height constructed in valleys with river widths of 20, 50 and 100 m, and uniform abutment slopes of 0, 26.5, 45 and 70 degrees. The rockfill was modelled as a linear elastic material with Young's modulus of 100 MPa and Poisson's ratio (ν) of 0.27, and the foundation with Young's modulus of 50 GPa (Figure 6.18). After establishing

initial stresses in the foundation, the embankment construction was modelled in 5 m lifts and stresses (major and minor principal stresses, vertical stress and horizontal stress) monitored at seven locations (a to g in Figure 6.18) in the centre of the gully. Grid element sizes of 1.25 m height and 1.25 to 2.5 m width were used. The analysis was then repeated by construction of the embankment in a single 100 m lift (as was done in the analysis by Giudici et al. (2000)).

It is recognised that the analysis has several deficiencies, however, for the purpose of assessment of arching effects on stresses within the embankment the results are considered reasonably representative. The greatest deficiency in the two-dimensional analysis is not taking into consideration the significant three-dimensional effect of embankment shape, which will therefore result in over-estimation of stresses in the latter stages of construction.

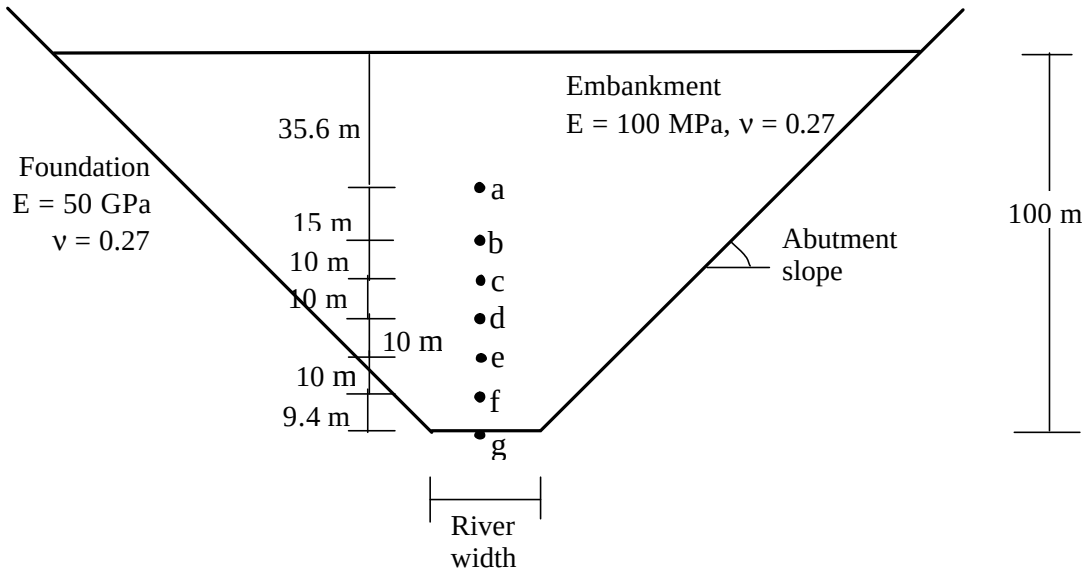

Figure 6.18: Idealised model for two-dimensional finite difference analysis of cross-valley influence

The results of the analysis are presented in Figure 6.19. Vertical stresses at the end of construction have been normalised against those for the case with zero abutment slopes (i.e. no cross-valley arching effect) and plotted against the abutment slope angle. Points a to g correspond to the locations shown in Figure 6.18.

The results of the analysis indicate:

- Cross-valley arching is only significant (greater than 20% reduction in vertical stress) for narrow valleys (river width less than 30 to 40% of the dam height) with

steep abutment slopes (greater than about 50 degrees, but also dependent on river width), and then only in the lower third to half of the embankment.

- Where the river width is approximately equal to half the embankment height, cross-valley arching has some effect (10 to 20% reduction in vertical stress) for abutment slopes steeper than about 45 degrees, and then only in the lower third to half of the embankment.
- Negligible arching is observed for river widths equal to about the embankment height regardless of the abutment slope.
- Modelling embankments in single or very large lifts is likely to result in significant under-estimation of stresses within the embankment, particularly for river widths less than about half the embankment height.

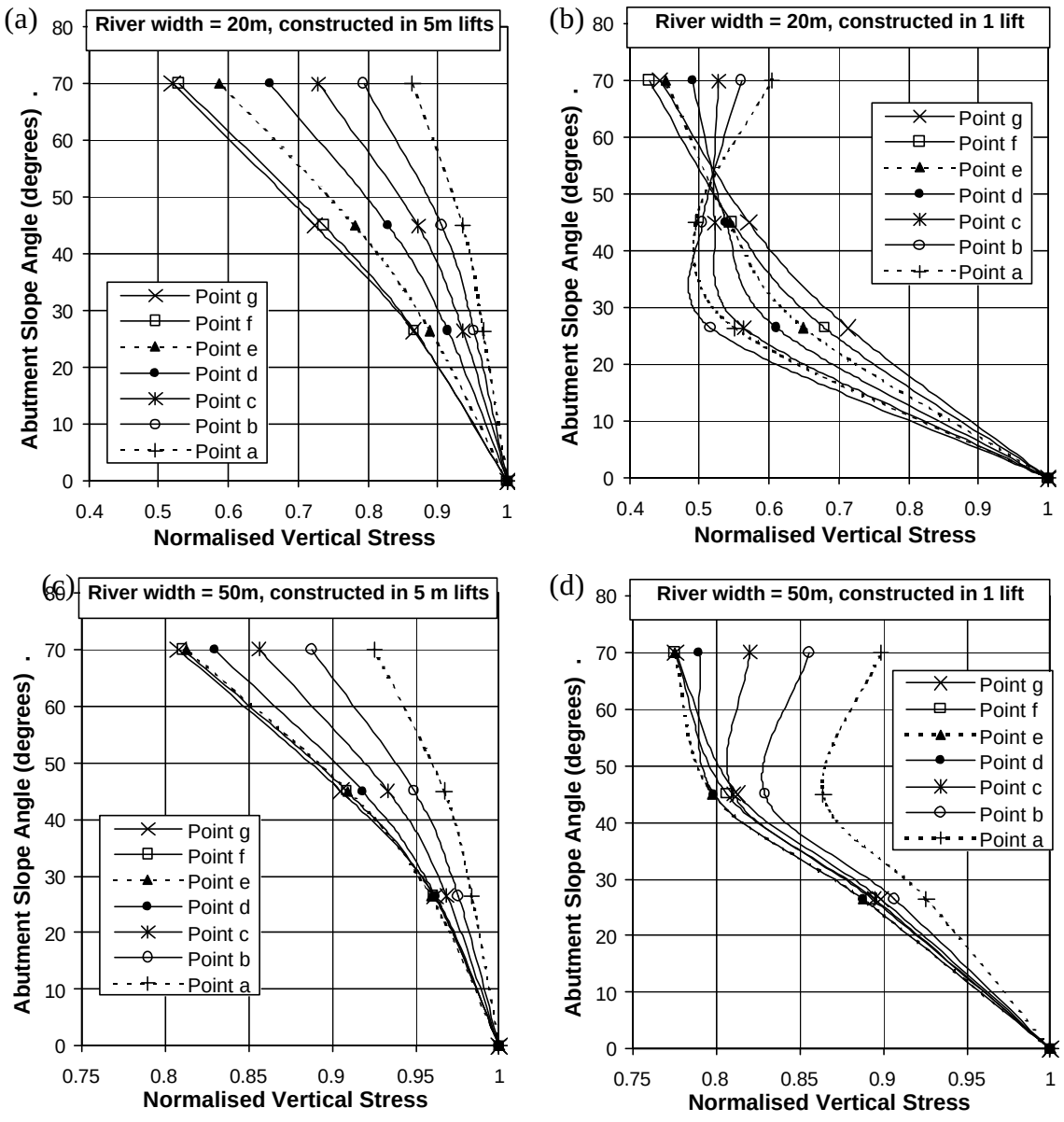

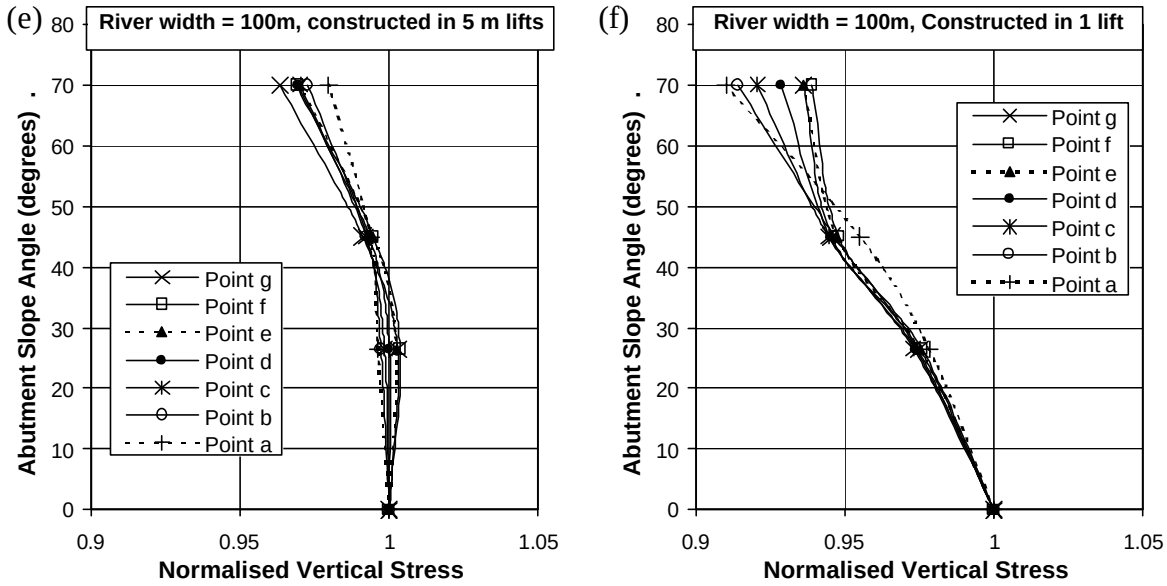

Note: The normalised vertical stress is the vertical stress at the end of construction normalised against the vertical stress obtained for the flat abutment slope analysis.

Figure 6.19: Results of two-dimensional finite difference analysis of the effect of cross-valley shape on vertical stresses in the dam. *(a)*, *(c)* and *(e)* represent construction in 5 m lifts (to 100 m) and *(b)*, *(d)* and *(f)* construction in a single 100 m lift.

Table 6.6 presents an assessment of the effects of cross-valley arching on the embankments studied as part of this analysis. Significant arching (greater than 20% reduction in vertical stress) is likely in the lower 25 to 50% portion of the narrow, steep valley embankment sections of Segredo, Salvajina, Murchison, Cethana and Alto Anchicaya dams. For Golillas cross valley arching is a significant factor given the narrow and very steep sided valley in which the embankment has been constructed.

Table 6.6: Assessment of cross-valley influence on arching for case studies analysed

Influence of Cross-Valley Arching		
Significant (> 20% reduction in Vertical Stress)	Some (10 to 20% reduction in Vertical Stress)	Limited to Negligible (< 10% reduction in Vertical Stress
Segredo (narrow gully section, lower 15%)	White Spur (lower quarter)	Wishon, Xingo, Xibeikou,
Salvajina (lower half in narrow gully)	Shiroro (lower third)	Winneke, Tullabardine,
Murchison (lower quarter)	Lower Bear No. 1 (lower quarter)	Tianshengqiao, Serpentine,
Golillas	Little Para (lower 15%)	Scotts Peak, Salt Springs,
Cogswell (lower quarter)	Kangaroo Creek (lower third)	Reece, Mangrove Creek,
Cethana (lower quarter in steep gully)	Courtright (lower third)	Mackintosh, Lower Bear No.2,
Alto Anchicaya (lower half in steep gully)	Bastyan (lower third)	Kotmale, Khao Laem, Ita, Foz do Areia, Dix River, Crotty,
	El Infiernillo (lower third)	Aguamilpa,

The secant modulus versus vertical stress plot during embankment construction should be able to provide an indication of cross-valley arching (for cases where the estimated vertical stresses have ignored the cross valley influence). The typical plot, assuming no arching effects, is for a small reduction in the secant modulus with increasing vertical stress (Figure 6.16). An increase in the calculated secant modulus with increasing vertical stress is considered to provide an indication of cross-valley arching. The deformation behaviour for HSG 1 to foundation (lower 10 m or 15%) at Bastyan dam (Figure 6.20) is indicative of this behaviour. The plot for HSG 1 to 2 (located 50 to 65 m below crest level) is more typical of the normal response. Another indicator could also be a relatively high calculated secant modulus in the lowest section of the embankment compared with the section above such as indicated by the monitoring results at Cethana dam (Figure 6.20). However, this may be affected by variations in the rockfill properties or placement techniques.

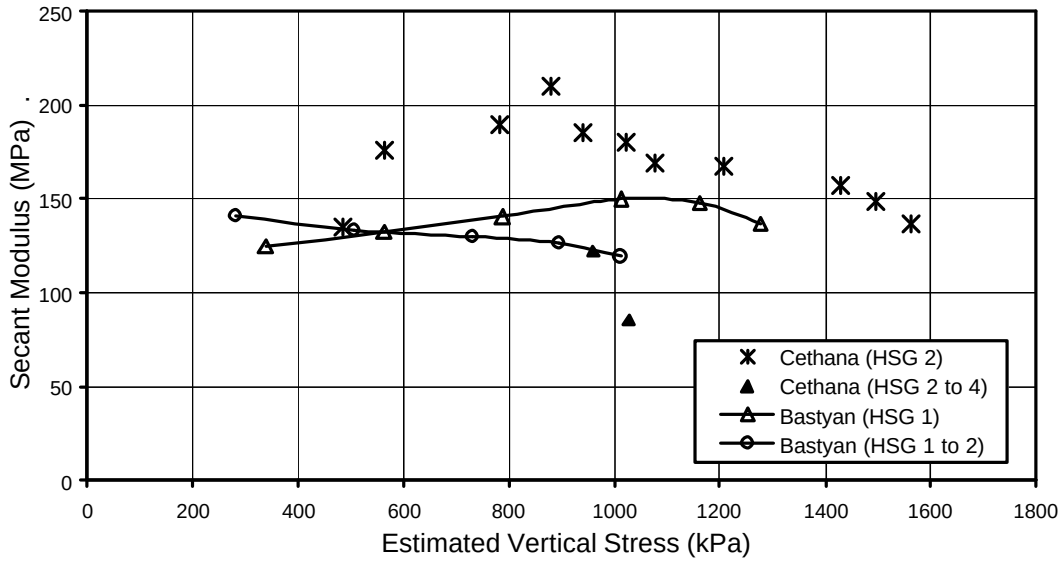

Figure 6.20: Indicators of cross valley arching effects from variations in the secant modulus with vertical stress.

The analysis shows that valley shape is not as significant as indicated from the empirical analyses of Pinto and Marques Filho (1998) and Giudici et al (2000), Figure 6.8 and Figure 6.10 respectively, and the finite element analyses by Giudici et al (2000), Figure 6.11. The differences in calculated deformation moduli for the well-compacted rockfills must be due to other factors in addition to valley arching, including the rockfill particle size grading, strength of the rock and type of fill. The analysis also shows that

significant errors are introduced into the vertical stress profiles, particularly for embankments constructed in narrow valleys, by construction of the embankment in a single stage rather than "building" the embankment in layers.

The method used to calculate the rockfill modulus during construction is also an important consideration for the empirical analyses. Pinto and Marques Filho (1998) and Giudici et al (2000) (Figure 6.8 and Figure 6.10) used, as far as the writer is aware, the simplifying assumption of Figure 6.1a, which would over-estimate the vertical stresses and therefore over-estimate the calculated moduli.

6.4.2.5 *Effect of Particle Size Distribution*

The effect of particle size distribution (PSD) on the secant modulus was investigated by grouping the data into sets with similar degree of compaction, type of fill (rockfill or gravel) and intact rock strength.

For each rockfill zone (mostly Zone 3A) of each case study the procedure to estimate a representative secant modulus at the end of construction was:

- Estimation of the vertical stress and secant modulus at the end of construction for each pairing of HSGs within the rockfill zone allowing for the effect of embankment shape (refer Section 6.2.3). The secant moduli were, in general, determined from internal monitoring points in the region bounded by the lower 60% of the embankment and within the central half of the dam cross section.
- For case studies where valley shape was considered to having had some to significant influence (Table 6.6) the secant moduli was adjusted by multiplication with an appropriate stress reduction factor determined from Figure 6.19. Secant moduli values considered as being greatly affected by valley arching were omitted.
- A representative secant modulus for each rockfill zone was then calculated by averaging the estimates of secant moduli from that rockfill zone corrected for valley shape.

The results of laboratory testing on rockfills (Section 6.3.2) indicated that the shape of the particle size distribution curve (measured by the uniformity coefficient, $C_u = D_{60}/D_{10}$) and particle size itself affected the deformation behaviour. To take into consideration both of these factors various combinations of particle size (e.g. D_{50}, D_{60}, D_{80}, etc.) and different definitions of uniformity coefficient (D_{60}/D_{10}, D_{80}/D_{30}, etc.) from

the average particle size distribution (PSD) for each rockfill zone were statistically analysed (using single and multiple variable methods) against the representative secant modulus at end of construction, determined as outlined above. Further statistical analyses were undertaken incorporating embankment height as a variable in an attempt to normalise the data against vertical stress.

The analysis indicated that the best predictors of the secant modulus at the end of construction (E_{rc}) were:

- D_{80} (diameter for 80% passing from average grading curve) for the very high strength well compacted quarried rockfill data set (Figure 6.21) with a regression coefficient of 0.83 for the power function shown.
- D_{90} (diameter for 90% passing from average grading curve) for the medium to high strength rockfills with a regression coefficient of 0.70 for the exponential function given as Equation 6.8. The fit to D_{80} provided a reasonable correlation with coefficient of regression of 0.44 (Figure 6.21) for the exponential function shown. In comparing of the two methods, the difference in calculated moduli in most instances is less than 5 MPa, or statistically, a standard deviation of less than 7%. Higher moduli are obtained using the D_{90} method for PSD with a steep coarse part of the curve (i.e. above D_{70}) and higher moduli for the D_{80} method for PSD with a relatively flat coarse part of the PSD curve typical of gravels. Either approach is suggested for estimation of E_{rc} for medium to high strength rockfills. For simplicity D_{80} has been selected for predictive methods.

$$E_{rc} = 153 \cdot e^{(-0.0045 D_{90})} \tag{6.8}$$

where E_{rc} = secant modulus during construction in MPa, D_{90} = diameter for 90% passing from average grading curve in millimetres. Equation 6.8 is for medium to high strength well-compacted rockfills.

From Figure 6.21 it is evident that the secant moduli of the medium to high strength rockfills shows less variation with increasing D_{80} than for the very high strength rockfills. This is considered to reflect the broad, well-graded shape of the particle size distribution of the medium to high strength rockfills as indicated by the high uniformity coefficients (C_u values from 45 to 300) in comparison to steeper shape of the very high strength rockfills (C_u values from 6 to 42).

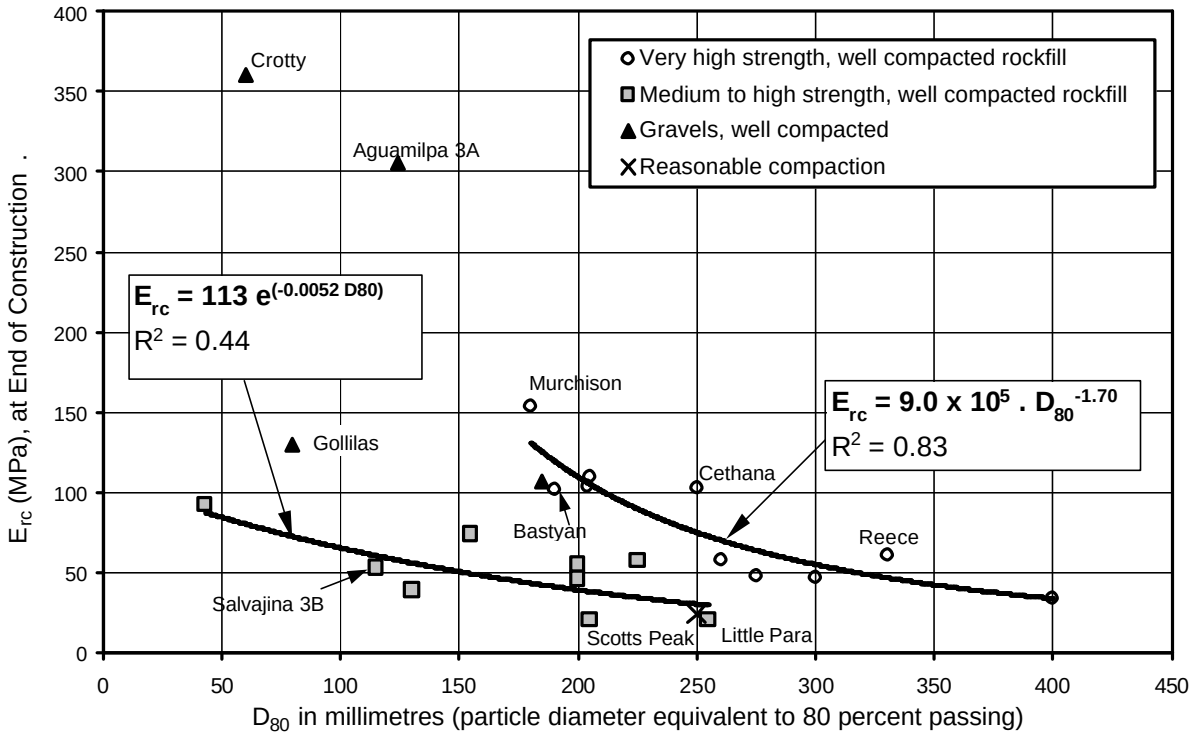

Figure 6.21: Representative secant modulus (mostly Zone 3A rockfill) at end of construction (E_{rc}) versus D_{80} from average grading of the rockfill.

Other points to note are:

- The medium strength rockfills of the medium to high strength data set (Little Para, Scotts Peak and Salvajina Zone 3B) plot below the trendline for the medium to high strength case studies.
- For the well-compacted gravels there is not enough data to establish a relationship between D_{80} and E_{rc}.
- D_{80}, and D_{90} in the case of medium to high strength rockfills, is a better predictor of E_{rc} than uniformity coefficient, C_u.
- The predictions are not improved by adding C_u to the equation. This is possibly related to the partial inter-dependence of C_u and D_{80}, with decreasing C_u generally observed with increasing D_{80}, particularly for the very high strength rockfills.
- For the very high strength rockfills embankment height (and hence stress level) appears to have some influence. Apart from Bastyan dam (75 m height) the cases with embankment heights less than about 120 m plot above the trendline and embankment heights greater than about 130 m below the trendline. This finding is not unexpected given the influence of stress level on the secant modulus (Figure 6.16).

- No similar correlation with height is evident for the medium to high strength quarried rockfill data set.

The E_{rc} values in Figure 6.21 for each individual rockfill zone are representative of the applied vertical stress range of the internal points considered in the estimation of E_{rc}. The representative mean vertical stress for each data set in Figure 6.21 is given in Table 6.7.

Table 6.7: Stress conditions representative of the data sets from Figure 6.21

Data Set	**No. Cases**	**Vertical Stress Characteristics of Data Points**		
		Range (kPa)	**Mean (kPa)**	**Comment**
Very high strength, well-compacted quarried rockfill	9	900 to 2200	1400	5 of 9 points with mean from 1300 to 1550 kPa
Medium to high strength, well-compacted quarried rockfill	9	400 to 1300	800	Even spread of data points across the stress range
Well-compacted gravels	4	950 to 2200	1500	Spread of data points across the stress range

6.4.2.6 *Moduli During Construction of Dumped Rockfill*

For dumped rockfill, the limited internal deformation data during construction is insufficient for analysis and assessment of predictive methods for estimation of the moduli during construction. The available data records for dumped or poorly compacted rockfills are:

- At El Infiernillo very high strength diorite and silicified conglomerate were used for the rockfill. The deformation records indicate E_{rc} values (Figure 6.16) of:
  - For the Zone 3B rockfill, placed dry in 0.6 to 1.0 m layers and compacted by bulldozer, E_{rc} at end of construction ranged from 25 to 49 MPa (average 39 MPa) at vertical stress levels in the range 550 to 1800 kPa.
  - For the Zone 3C rockfill, dumped dry and spread in 2 m thick layers, E_{rc} at end of construction ranged from 17 to 27 MPa (average 22 MPa) at vertical stress levels in the range 400 to 800 kPa.

- At Ita dam (Figure 6.27), the base 10 m thickness of rockfill in the river section was dumped, presumably through water. E_{rc} at end of construction for the dumped rockfill (very high strength basalt) was estimated at 15 to 19 MPa at vertical stress levels in the range 1400 to 2100 kPa.

The tangent moduli for the rockfill at El-Infiernillo (Figure 6.17) approached values as low as 15 to 20 MPa for the Zone 3B rockfill and 10 to 15 MPa for the Zone 3C rockfill. Based on back-analysis of the deformations of central core earth and rockfill dams (Fell et al 2000; Woodward Clyde 1999) the tangent moduli is likely to be lower for dirty or weathered dumped rockfills, possibly down to as low as 5 MPa at stress levels exceeding those previously experienced by the rockfill.

6.4.3 DEFORMATION OF THE FACE SLAB OF CFRD ON FIRST FILLING

6.4.3.1 Simplified Methods of Estimation of Maximum Face Slab Deformation

Fitzpatrick et al (1985) and Pinto and Marques Filho (1998) suggest that simple empirical methods are sufficient to estimate face slab deformations. The most simple empirical estimates are based on ratios of the modulus on first filling, E_{rf}, to the deformation modulus during construction, E_{rc}, calculated according to Equation 6.1 (refer Figure 6.1a). Cooke (1993) indicates that the ratio of moduli on first filling to moduli during construction (E_{rf}/ E_{rc}) is typically in the range 1.3 to 3, a range generally confirmed by most authors discussing the variation.

The calculation of E_{rf} (Fitzpatrick et al 1985) from Equation 6.2 (refer Figure 6.1b) does not take into consideration the stress path or stress distribution within the upstream rockfill due to first filling. It is based on the assumption of a uniform stress change, equivalent to the applied stress from the water load on the concrete face, acting over the distance normal to the face slab between it and the foundation (Figure 6.1b). Fitzpatrick et al (1985) recognised that these assumptions were incorrect; but commented that the method provides a simple and reasonable approximation of the rockfill modulus and face slab deformation. They indicate that the method is applicable for estimation of E_{rf} (and therefore prediction of face slab deformation) over the range from 20% to about 60% of the embankment height.

Analysis of the data set was undertaken in an attempt to improve on the method of prediction of the E_{rf}/E_{rc} ratio. Valley shape effects were not specifically taken into consideration given that valley shape is potentially likely to affect both the secant moduli at end of construction and modulus during first filling. In the analysis therefore, the representative secant moduli at end of construction for the Zone 3A rockfill of each case study are not corrected for valley shape.

The results of the analysis show (Figure 6.22) that there is a reasonable correlation between E_{rf}/E_{rc} and embankment height taking into consideration the upstream slope angle. A reasonable estimation of E_{rf}/E_{rc} is possible for upstream slope angles of 1.3 to 1.4H to 1V. For flatter upstream slopes a lower ratio is considered appropriate, however, there are insufficient data points for estimation of a correlation, although a very approximate estimation of the trendline is presented in Figure 6.22.

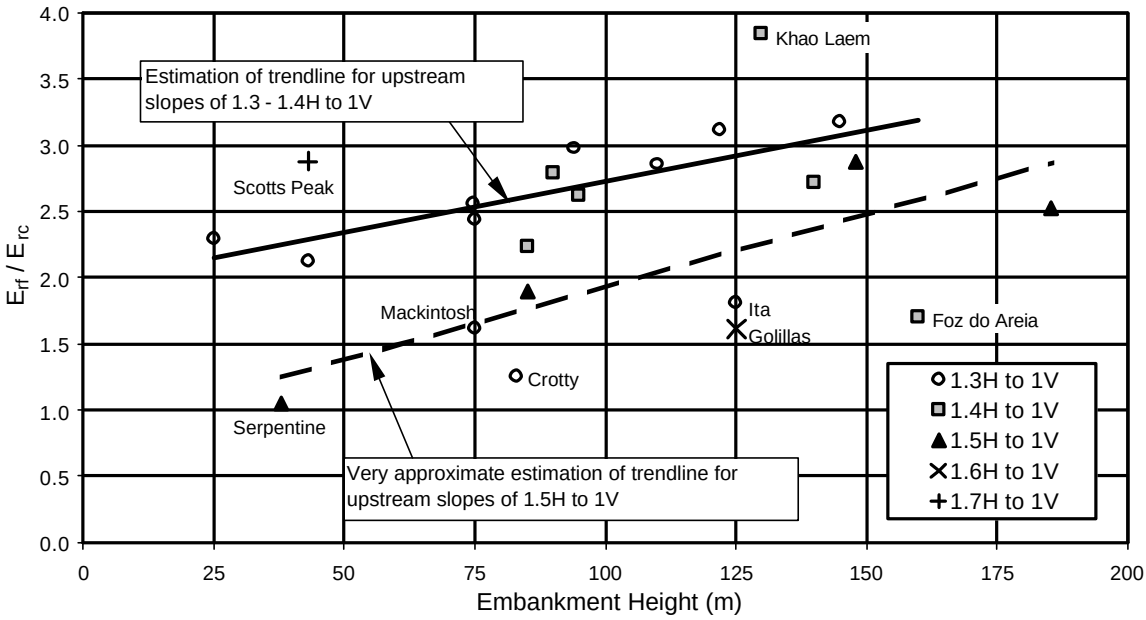

Figure 6.22: E_{rf}/E_{rc} ratio versus embankment height

A number of cases plot away from the trendline for the 1.3 –1.4H to 1V data set or are not in accordance with the general trend of decreasing E_{rf}/E_{rc} ratio with flattening of the upstream slope. The reasons for these observations are:

- For Mackintosh and Foz do Areia the face slab deflection profiles are different to the typical profile (refer Section 6.4.3.2) with maximum deflection measured at 15 to 20% of the dam height above the toe; i.e. lower than normal.

- For Ita dam the dumped rockfill in the river section (Figure 6.27), which is of low secant modulus in comparison to the Zone 3A compacted rockfill, is considered to have influenced the face slab deflection.
- At Crotty, the facing zone between the main gravel rockfill and the concrete face comprised quarried rockfill. The likely lower modulus of this facing zone is considered to have had an effect of the deformation behaviour of the face slab resulting in the relatively low value of the E_{rf}/ E_{rc} ratio.
- At Scotts Peak the embankment zoning (Figure 6.28) is considered to have affected the calculation of E_{rf}, which was based on the measured settlement in the HSGs adjacent to the upstream face slab.
- Serpentine dam plots at quite a low ratio. The reason for this is uncertain.
- At Khao Laem the high value of E_{rf}, and hence the high E_{rf}/ E_{rc} ratio, was considered by Watakeekul et al (1985) to possibly be due to arching effects at the maximum section within a localised deep zone confined to upstream of the embankment centreline. Therefore, arching effects influenced E_{rf} and not the secant modulus at the end of construction, E_{rc} (i.e. they influenced one but not both moduli, which is unusual).

Other factors considered to affect the E_{rf}/ E_{rc} ratio are:

- Fitzpatrick et al (1985) considered the time to completion of first filling a factor, the shorter the time of first filling the greater the likely ratio due to time dependent strain effects.
- Cooke (1984) suggested that the compacted rockfill might be substantially stiffer in the horizontal direction, due to the greater compaction of the upper compared to the lower sections of a compacted layer. A two-dimensional finite difference analysis, using the computer program FLAC, was undertaken on Reece dam to further evaluate the effect of intra-layer differential moduli (differential in the both vertical and horizontal directions) on the face slab deformation behaviour. The embankment was modelled in 1 m layers with a 3 to 1 ratio in moduli between the upper 0.5 m and lower 0.5 m of each layer calculated such that the overall vertical modulus of any layer was equivalent to that measured from actual observations during construction. The modelling indicated that the deformations on first filling were similar, less than 5% variation, with or without consideration of variable inter-layer modulus. In addition, finite element analysis by Kovacevic (1994), using and an

elasto-plastic constitutive model (modelling pre-peak plasticity), obtained reasonable predictions of face slab deformation on first filling by for Winscar and Roadford dams (refer Section 6.3.3.1). It is concluded, therefore, that the effect of intra-layer differential moduli has a negligible effect on the face slab deformation behaviour during first filling.

- Valley shape may influence the E_{rf}/E_{rc} ratio to a small extent. For the 1.3H to 1V cases, the CFRDs constructed in narrow valley (L/H < 3.2, the ratio of crest length, L, to the embankment height, H) tend to plot above the trendline whilst for the broader valleys tend to plot below the trendline, although there are exceptions. For the 1.4H to 1V cases the trend with respect to valley shape is not as evident.

Two-dimensional finite difference analysis was undertaken to evaluate the stress paths of the rockfill in the upstream zone of the embankment for different upstream slopes. Analyses were undertaken on a nominal 100 m high embankment with upstream slopes of 1.3H to 1V and 1.55H to 1V. The embankment was constructed in 5 m lifts and the reservoir impoundment in 6 stages to a maximum height of 96 m (i.e. assuming 4 m of freeboard). Given that the interest was in the stresses within the embankment, the rockfill was modelled as a linear elastic material with Young's modulus of 100 MPa and Poisson's ratio of 0.27. The concrete face slab was not modelled and the upstream facing zone was modelled with similar modulus parameters to the main rockfill. It is recognised that the assumption of linear elastic properties would lead to some errors in the stress distribution, however, the purpose of the analysis was for comparison and errors were likely to be relatively minimal.

Stresses were calculated at 16 locations in the upstream zone and under the embankment centreline (Figure 6.23 and Figure 6.24). The stress paths for the points normal to the face slab at a height 30% above the embankment toe are presented in Figure 6.23 for the 1.3H to 1V upstream slope angle case and Figure 6.24 for the 1.55H to 1V upstream slope angle case. The results indicate that:

- The stress paths during construction (Figure 6.23b and Figure 6.24b) show a similar trend, with some variation, for both the 1.3H to 1V and 1.55H to 1V upstream slope angle. The general trend of the stress path up to the end of construction is for increasing deviatoric and mean normal stress.
- In the early stages of first filling the deviatoric stress decreases whilst the mean normal stress continues to increase. In the mid to latter stages of filling the

deviatoric stress starts to increase again reaching stress levels in excess of those at the end of construction.

- The overall increase in deviator stress from the end of construction to the end of first filling is greater (at all comparison points in the upstream shoulder) for the 1.55H to 1V upstream slope case, whilst the overall increases in mean normal stress are relatively uniform.
- The difference in stress path from the end of construction to the end of first filling is likely to result in greater strains in the 1.55H to 1V case on first filling and therefore a reduced deformation modulus on first filling (E_{rf}). Given that the secant modulus at the end of construction (E_{rc}) will be similar between the cases, the ratio E_{rf}/ E_{rc} is likely to be smaller for the 1.55H to 1V upstream slope. Estimation of E_{rf} from the deformation of the upstream face during first filling modelling confirms this.

The finite difference analysis confirms the findings from field observations (Figure 6.22) that the upstream slope angle is likely to affect the E_{rf}/ E_{rc} ratio. Flatter upstream slope angles will result in a reduced E_{rf}/ E_{rc} ratio all other factors being equal.

It is important to recognise that E_{rf} is not a proper simulation of the rockfill modulus during first filling rather it is an artefact of the method of calculation (refer Figure 6.1b). This method uses simplifying assumptions in regard to the geometry of the section analysed, and the assumed stress increase due to the water is not properly modelling the stresses, as seen in Figure 6.23b and Figure 6.24b. E_{rf} should only be used to calculate face slab deflections.

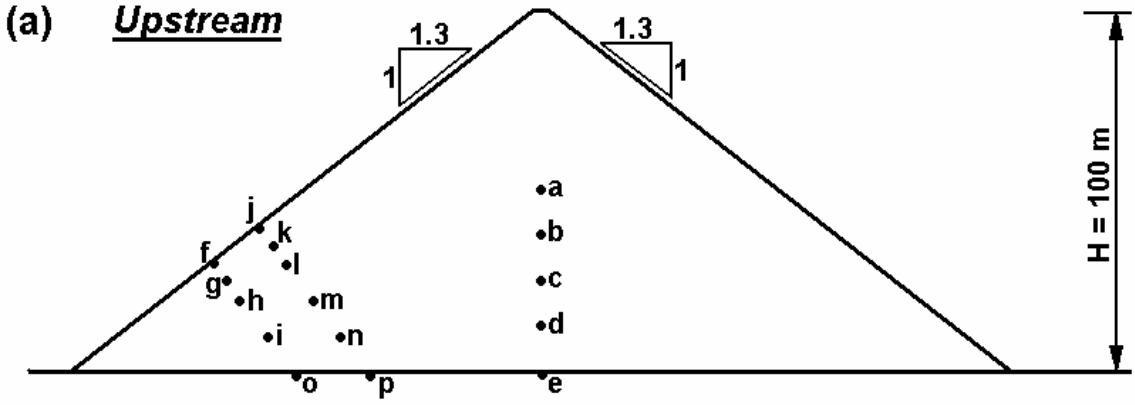

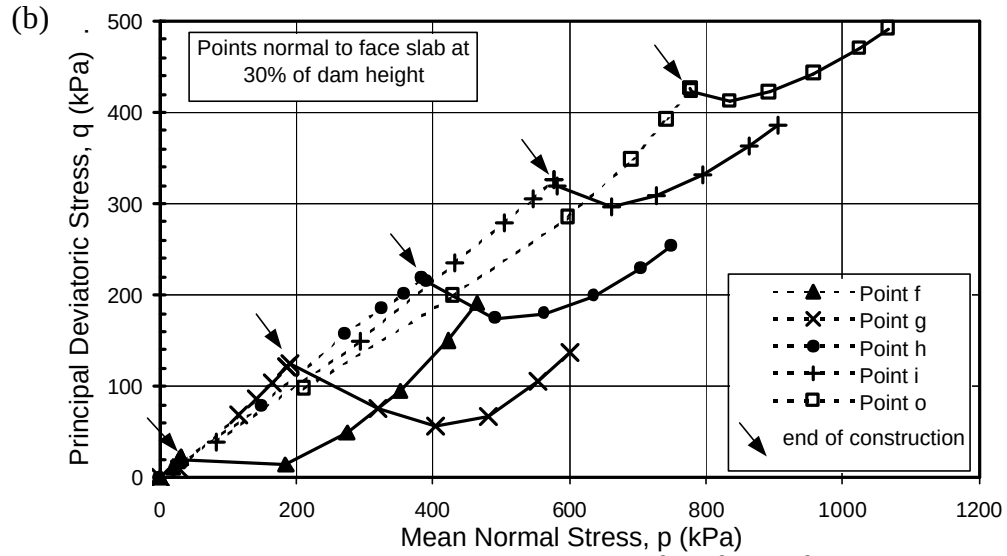

Figure 6.23: Stress paths during construction and first filling for nominal 100 m embankment with 1.3H to 1V upstream slope angle; *(a)* monitoring point locations, *(b)* stress paths for points normal to face slab at 30% of the embankment height.

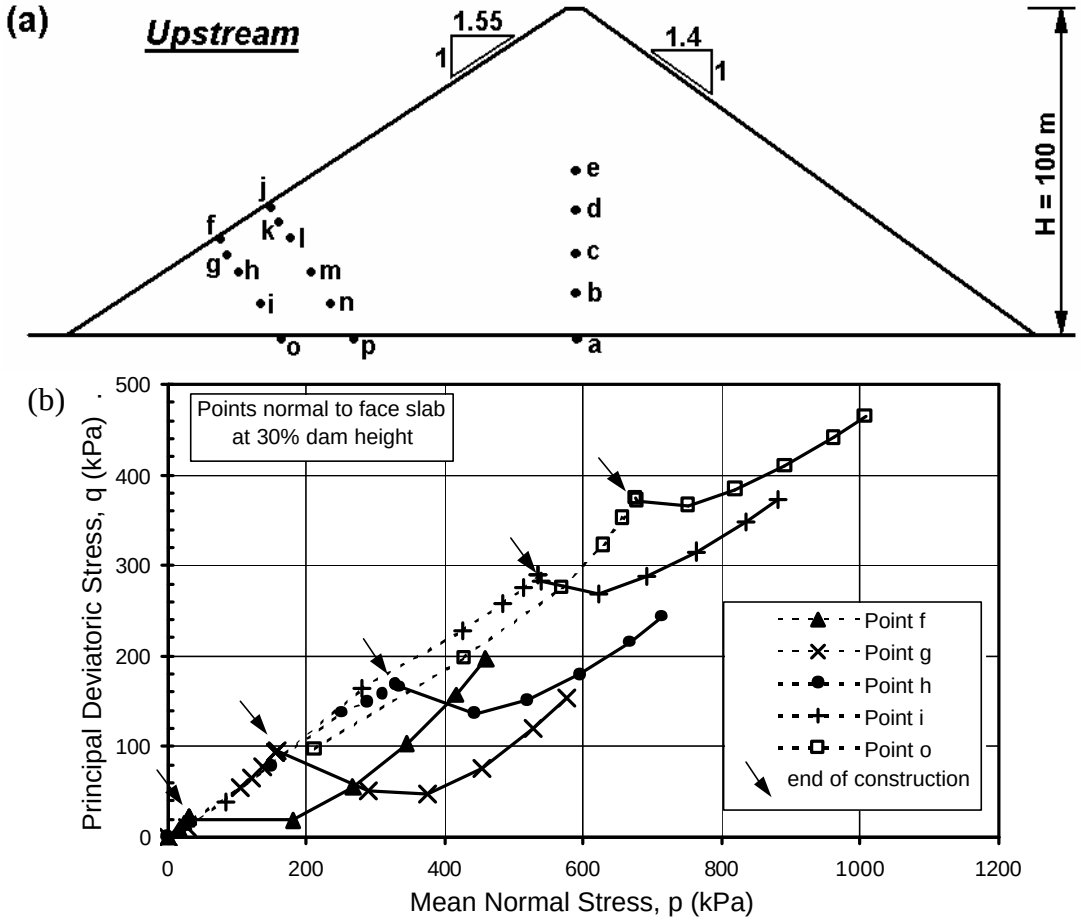

Figure 6.24: Stress paths during construction and first filling for nominal 100 m embankment with 1.55H to 1V upstream slope angle; *(a)* monitoring point locations, *(b)* stress paths for points normal to face slab at 30% of the embankment height.

6.4.3.2 Shape of the Face Slab Displacement

The deformed shape of the concrete face on first filling is strongly dependent on the zoning of rockfill in the body of the embankment. For embankments constructed almost entirely of a single rockfill zone (Figure 6.25) the typical pattern of deformation is for maximum deflection at about 30 to 50% of the embankment height reducing to zero at the toe and with constant to gradual reduction in deformation toward the crest.

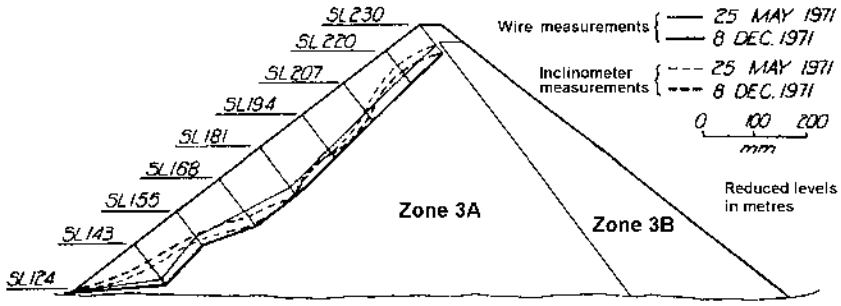

Figure 6.25: Face slab deflection during first filling (4/2/71 to 25/4/71) of Cethana dam (Fitzpatrick et al 1973).

Where the embankment zoning comprises rockfill zones of differing modulus the deflected shape of the face slab can reflect the modulus variations. In cases where large differences in rockfill modulus occur, such as the use of gravels of very high modulus with quarried rockfills of significantly lower modulus, problems with cracking of the face slab due to development of tensile stresses can occur resulting in leakage. Several examples of the effect of rockfill modulus variation on face slab deflection are:

- Aguamilpa dam (Mori 1999), Figure 6.26. The face slab deflection (Figure 6.26) was significantly affected by the modulus variation between the upstream gravel zone and downstream zone of quarried rockfill. The maximum deflection was measured near to the embankment crest. And the resultant deformation profile was considered by Mori (1999) to have caused cracking in the upper section of the face slab.
- The typical design detail for several large Brazilian CFRDs (Ita dam Figure 6.27) incorporates the better quality quarried rockfill placed in relatively thin layers in the upstream third of the embankment and the poorer quality rockfill placed in larger lifts in the central and downstream regions resulting in a modulus variation. Ita dam incorporated a zone of dumped rockfill in the river section resulting in larger deflections where the zone of influence incorporated these weaker rockfill zones.

- A similar pattern of face slab deflection was observed at Mangrove Creek dam due to modulus variation between the fresh sedimentary rockfill used close to the upstream face and the main body of weathered sedimentary rockfill.
- At Scotts Peak dam (Figure 6.28) the use of rockfill zones with significantly different moduli contributed to cracking of the asphaltic concrete membrane face. The embankment design incorporated a zone of well-compacted gravels at the upstream toe and main body of argillite rockfill of medium to high intact rock strength. On first filling, large differential deflections caused tensile cracking of the upstream face near to the contact between the gravel and argillite rockfill zones resulting in leakage flows in the order of 100 litres/sec.

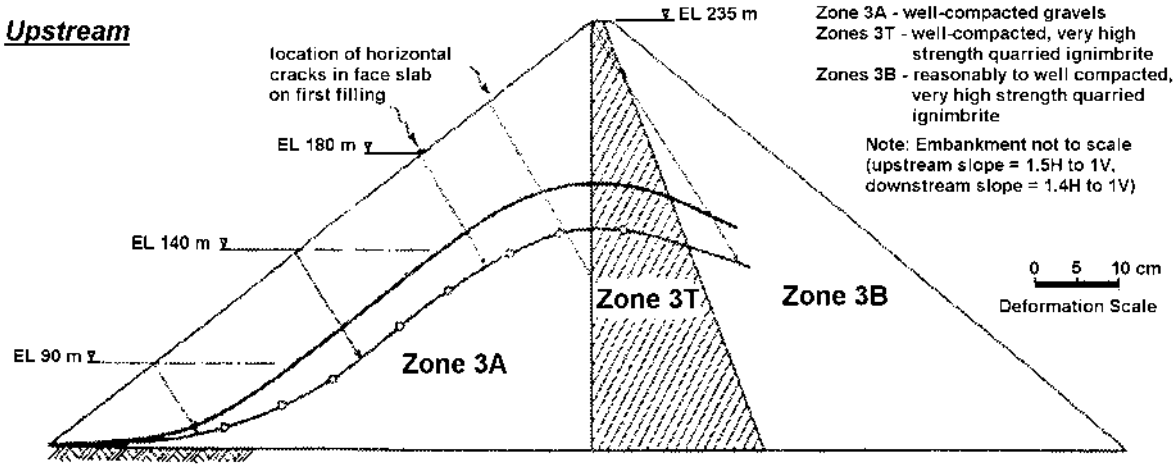

Figure 6.26: Face slab deformation during first filling of Aguamilpa dam (Mori 1999)

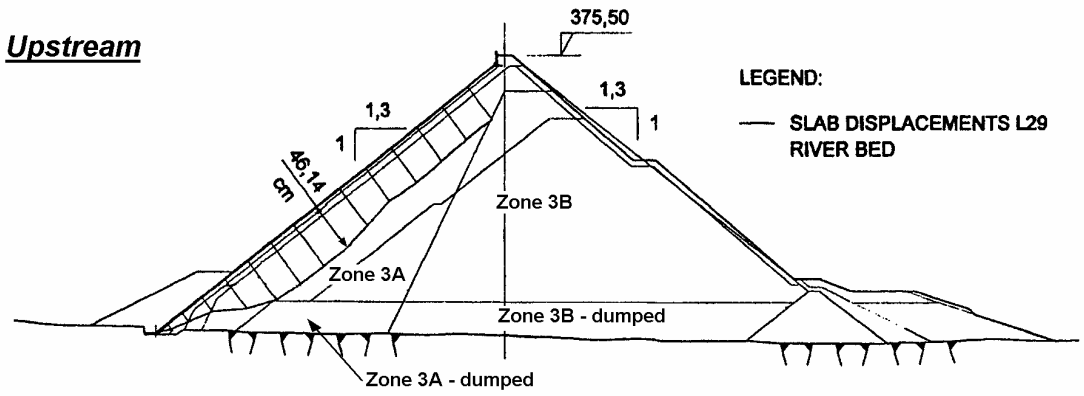

Figure 6.27: Face slab deformation during first filling of Ita dam (Sobrinho et al 2000)

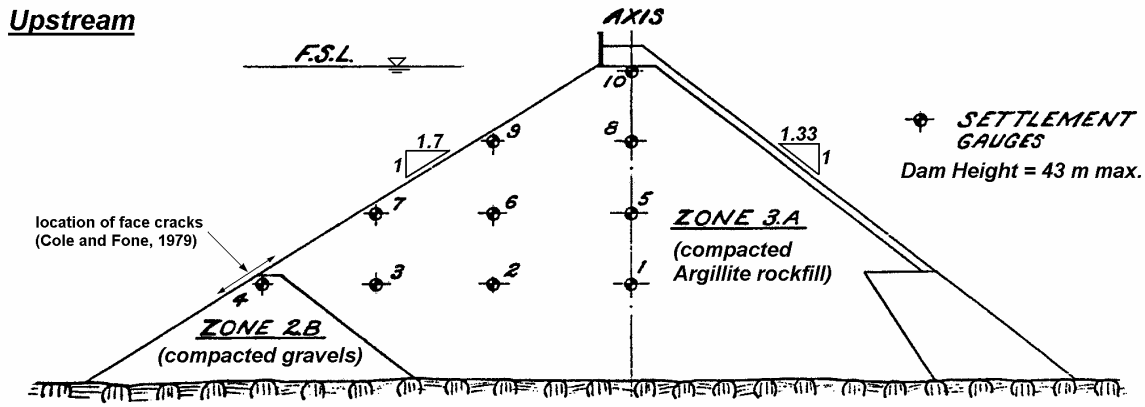

Figure 6.28: Scotts Peak dam; embankment zoning and location of face cracks (courtesy of Hydro Tasmania)

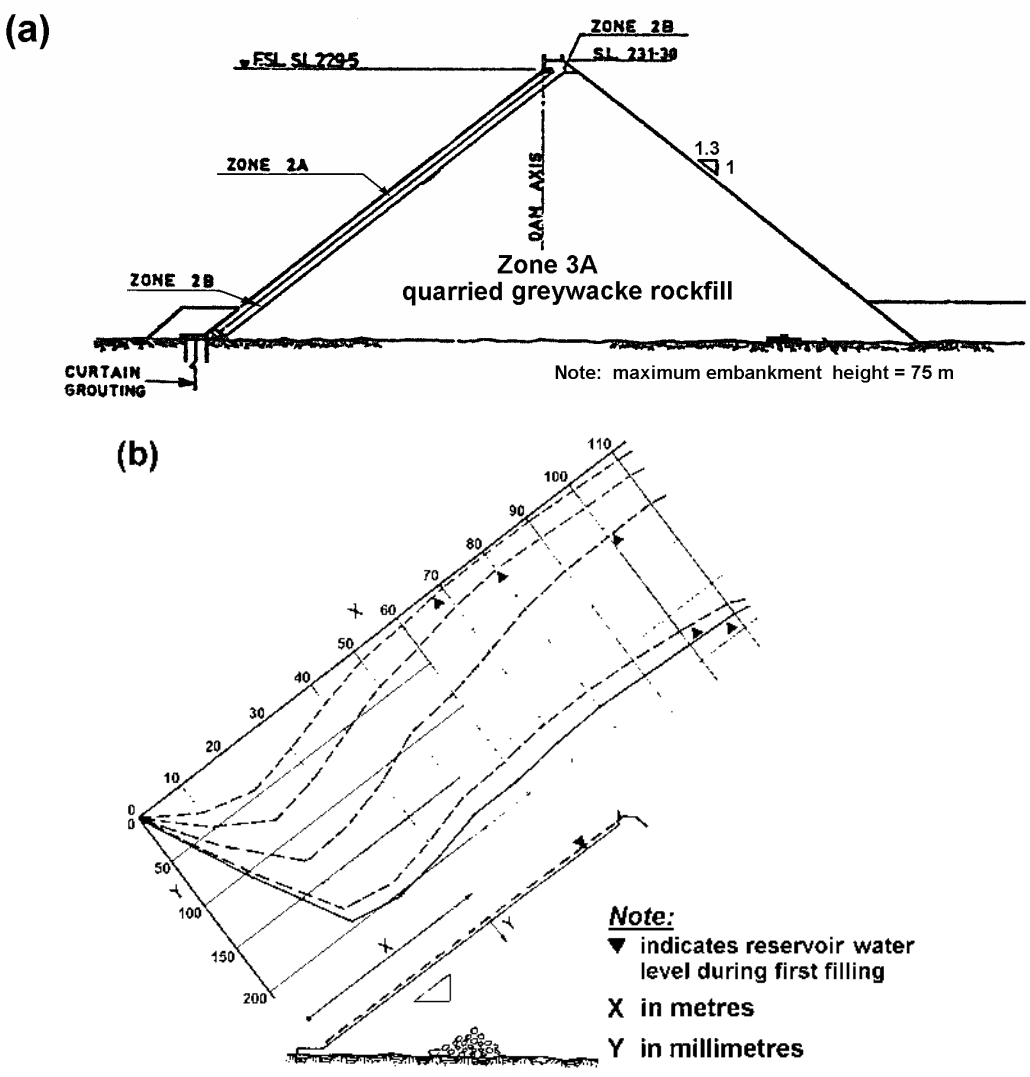

Figure 6.29: Mackintosh dam *(a)* embankment section (courtesy of Hydro Tasmania) and *(b)* face slab deformation on first filling (Knoop and Lack 1985)

Face slab deflection profiles different to the typical profile (Figure 6.25) were also observed at Mackintosh (Figure 6.29) and Foz do Areia dams. In both cases the maximum deflection during first filling was measured at 15 to 20% of the dam height above the toe, a much lower level than typically observed. The reasons for this observation are not clear, however, it is suspected that it is likely to be related to the rockfill modulus. Potentially lower modulus zones may have been present in lower portion of these embankments due to the initial production of rockfill of weaker intact rock strength or poorer gradation (low C_u or larger particle size), or placement at a lower relative density.

6.4.3.3 Prediction of Face Slab Deflection on First Filling

For the more typical CFRD geometries (Figure 6.25) or where large variations in rockfill moduli are not likely between rockfill zones, simple empirical correlations are considered sufficient for prediction of face slab deflection on first filling, using E_{rf} values estimated from Figure 6.22. Details on the suggested procedure for empirical estimation of deformations are discussed in Section 6.5.2.

Mori (1999) considers that a more rigorous method of determination of the face slab deformation than the method by Pinto and Marques Filho (1998) is required. He states that it should take into consideration the geometry of the structure, the stress path on impounding and the strength and deformation of the various rockfill zones within the embankment.

For prediction of face slab deformation behaviour during first filling for complex rockfill zoning geometries and/or with large moduli variations between the rockfill zones, finite element analyses should be considered. The detailed analysis would be justified considering the potential for face slab cracking as a result of possible development of tensile stresses.

6.4.4 POST CONSTRUCTION CREST SETTLEMENT

Available methods for prediction of post-construction crest settlement of rockfill embankments (see Section 6.3.3.2) are empirical and are generally based on historical records of similar embankment types and similar methods of construction.

An important aspect of the post construction deformation behaviour of rockfill related to its stress-strain characteristics is that relatively large deformations occur on application of stresses above those not previously experienced by the rockfill, such as on first filling or embankment raising. On un-loading or re-loading to stress states less than those previously experienced (such as due to fluctuations in the reservoir level) the rockfill moduli is very high and the resultant deformation therefore likely to be minimal. Collapse deformation on initial wetting can also result in relatively large deformations. The following discussion will consider post-construction deformation behaviour of rockfill (predominantly crest settlements) in CFRD due to:

- Events where stresses are likely to exceed those previously experienced, most notably first filling;
- Ongoing, time-dependent (or creep) deformation of rockfill; and
- Deformations due to wetting from rainfall or leakage.

Two significant factors in using empirical methods for prediction of the crest settlement post construction are the base time of deformation, and consideration of the timing of events such as first filling. If near full impoundment occurs before completion of construction or before monitoring points are established, then a significant component of the deformation is likely to have occurred and will not be captured by the post-construction monitoring. It is important that this be considered in comparison between case studies and the forward prediction of future deformations. It is also important that the base time of deformation is clearly defined in the predictive method being used and that the same definition is used when forward predicting future deformations.

6.4.4.1 *Case Study Records of Post-Construction Crest Settlement*

The typical post-construction crest settlement pattern, ignoring first filling effects, is for crest settlement to occur at a decreasing rate with time. Most equation based empirical methods for prediction of post-construction deformation model this behaviour by logarithmic relationships of strain versus log time (Sowers et al 1965) or power type relationships of strain (Soydemir and Kjaernsli 1979) or strain rate (Parkin 1977) versus time.

Total post-construction crest settlements will be dependent on when the base reading of monitoring points is established after the end of construction. Differences in terms of even months to establish base readings after the end of construction are significant as strain rates are greatest immediately after construction.

6.4.4.1.1 Zero Time, t_o, for Post Construction Crest Settlement

The method proposed by Parkin (1971) (refer Figure 6.12 in Section 6.3.3.3) was used for evaluation of the initial or zero time, t_o, for start of post-construction crest deformation for each case study. The basis of Parkin's method, derived from rate process theory, is the assumption that strain rate versus time is a power law relationship and therefore a plot of log strain rate versus log time (Figure 6.12b) will be linear provided t_o is correctly established.

Figure 6.30 shows examples of the time versus inverse strain rate plots for four dams, showing that for three cases t_o at the end of the main rockfill construction is the best fit of the data, and in one case (Crotty dam) t_o at the end of first filling the best fit. It was found that the best fit to each case study was for a t_o at either the end of the main rockfill construction or at close to the completion of first filling. In summary, the analysis indicated that:

- For CFRD constructed of dumped rockfill (excluding Salt Springs dam) and for well-compacted CFRD generally less than 100 m in height (excluding Crotty dam) the best fit for t_o was at the end of construction.
- For well-compacted CFRD generally greater than 100 m in height as well as Salt Springs dam (dumped rockfill CFRD of 100 m height) and Crotty dam (83 m high well-compacted CFRD constructed of river gravels), the best fit for t_o was at the end of first filling.

The end of main rockfill construction is defined as the time of completion of the main rockfill zones (Zones 3A and 3B). In some cases this may be a significant time (up to 1 to 2 years) before actual completion of the concrete face and crest detail works.

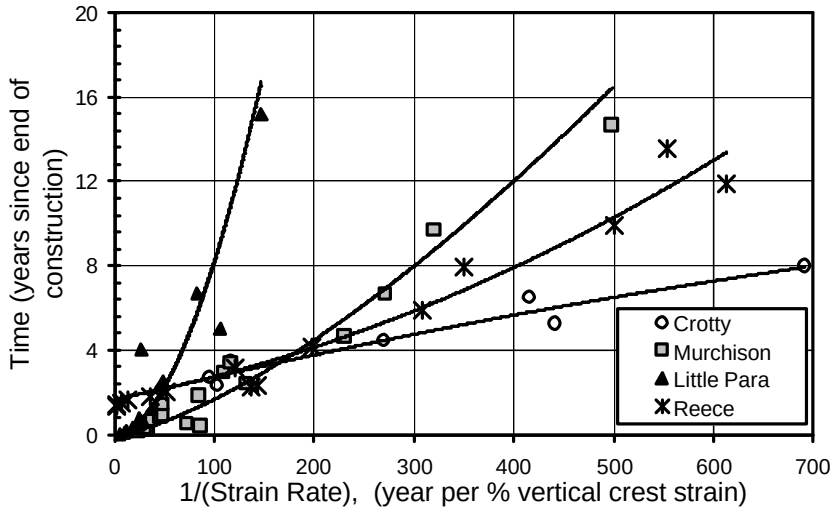

Figure 6.30: Examples of derivation of zero time for post-construction settlement

For consistency it is considered necessary for the initial or zero time, t_o, to be at either the end of main rockfill construction or at the completion of first filling. For zero time at the end of main rockfill construction (Figure 6.31 to Figure 6.33), the power function of the slope of the log strain rate versus time log plot (Equation 6.5 and Figure 6.12b) was closer to 1, and therefore the long-term slope of the vertical crest strain versus log time was close to linear (with some exceptions) allowing for easier prediction of future deformation. However, visual interpretation for comparative purposes is difficult due of the variation in time between end of construction and start of monitoring for the cases and the deformations during first filling.

For zero time, t_o, at the end of first filling (Figure 6.34 to Figure 6.36) visually the comparison between case studies is much clearer and upper and lower bounds for a specific set of historical monitoring records more readily identified, allowing for easier evaluation of "abnormal" deformation behaviour. However, future predictions are visually more difficult given the curved nature of the deformation behaviour in the plots of crest settlement versus log time. This curvature is due to the power function, m, in Equation 6.5 being less than 1 for most case studies.

6.4.4.1.2 Shape of the Vertical Crest Settlement Plots

For the vertical crest settlement versus log time plots for zero time at the end of the main rockfill construction (Figure 6.31 to Figure 6.33) two features are readily observed; the 'S' shape behaviour for a number of the case studies, and the effect of the

time difference between the end of rockfill construction and the initial crest settlement reading. The 'S' shaped curve is a feature of those cases where first filling was commenced more than about 0.3 to 0.5 years after the end of the main rockfill construction and the embankment height was greater than about 50 m. The steep portions of the curve are associated with crest settlement during first filling due to the increase in stress levels in the body of the rockfill beyond levels previously experienced. Steeper sections of the slope are generally observed for those case studies where the rate of filling was relatively rapid and where first filling started at least several years after construction. At the end of first filling the strain rate remains at a relatively high rate (on log time scale) due to time dependent effects and then decreases to a strain rate typical of the long-term deformation rate (on a log scale).

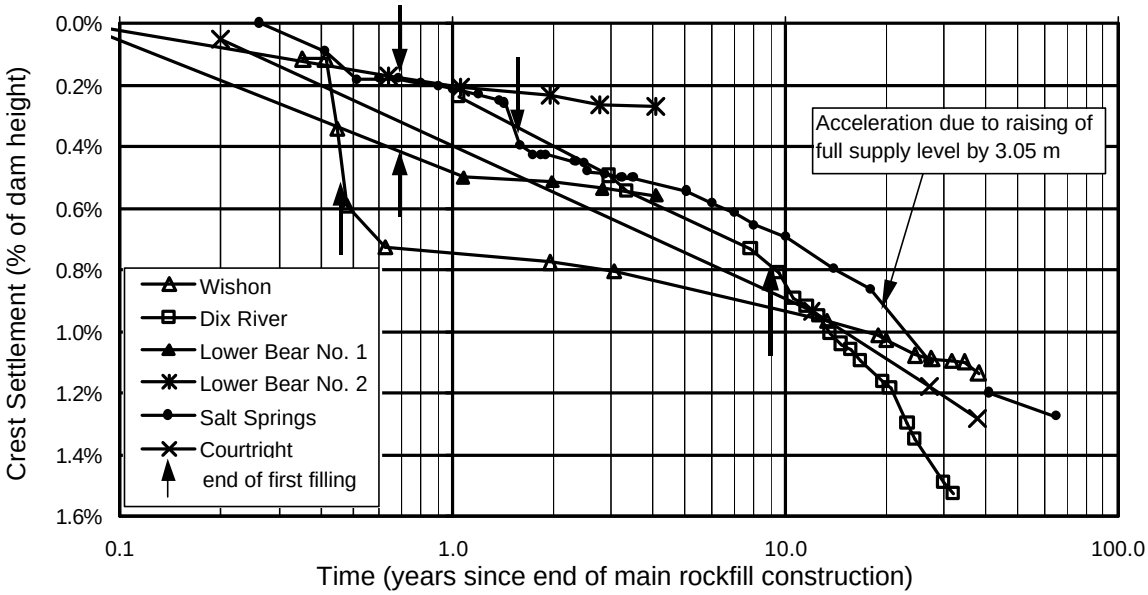

Figure 6.31: Post-construction crest settlement versus time for dumped rockfill CFRD, t_o at end of main rockfill construction.

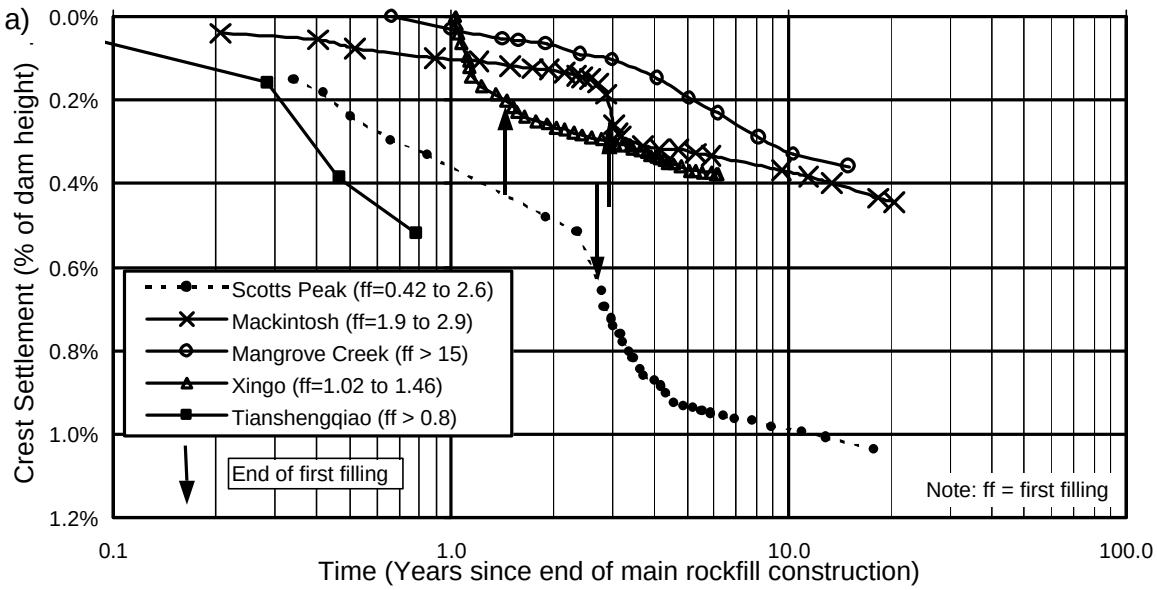

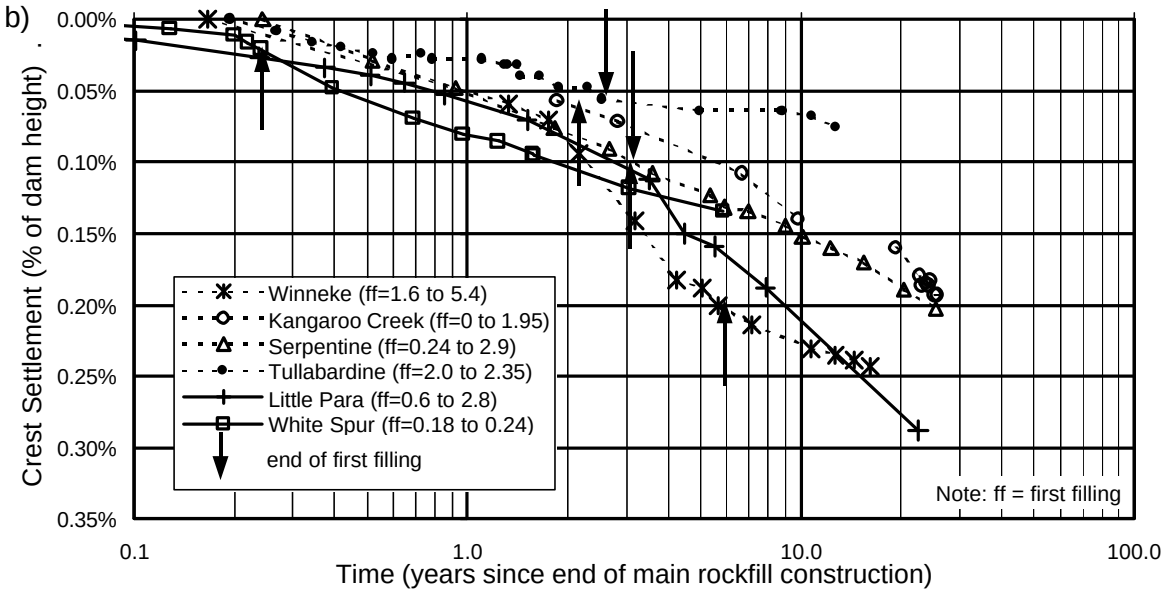

Figure 6.32: *(a)* and *(b)* Post-construction crest settlement versus time for CFRD constructed of compacted rockfills of medium to high intact strength, t_o at end of main rockfill construction.

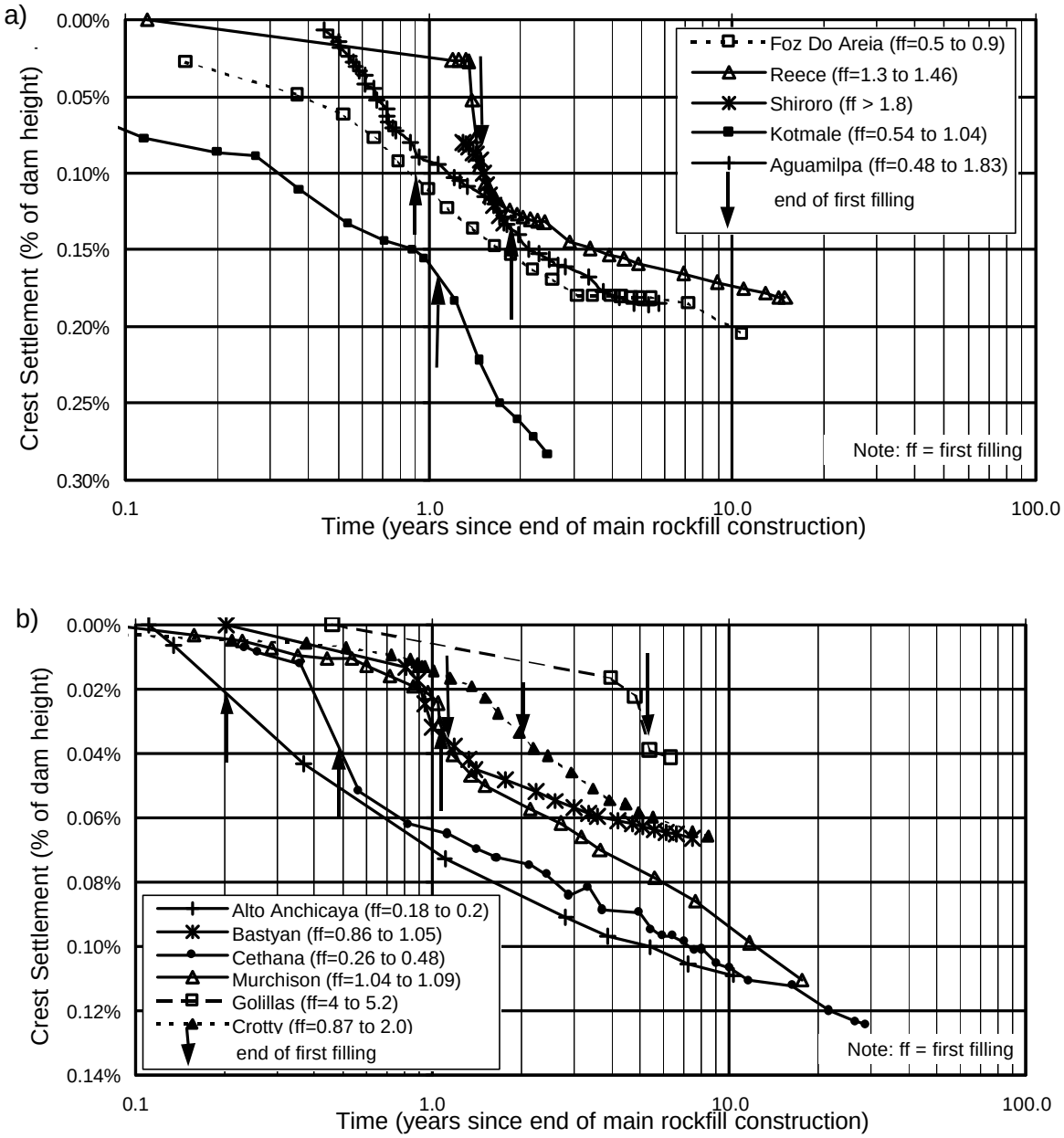

Figure 6.33: *(a)* and *(b)* Post-construction crest settlement versus time for CFRDs constructed of well-compacted rockfills of very high intact strength and of well-compacted gravels, t_o at end of main rockfill construction.

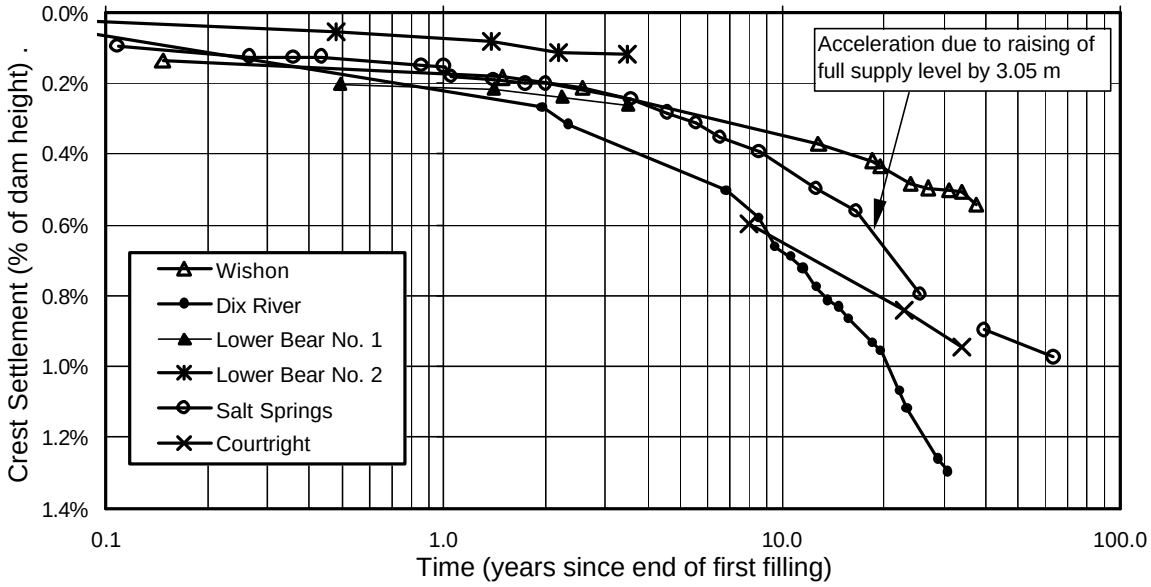

Figure 6.34: Post-construction crest settlement versus time for dumped rockfill CFRD, t_o at end of first filling.

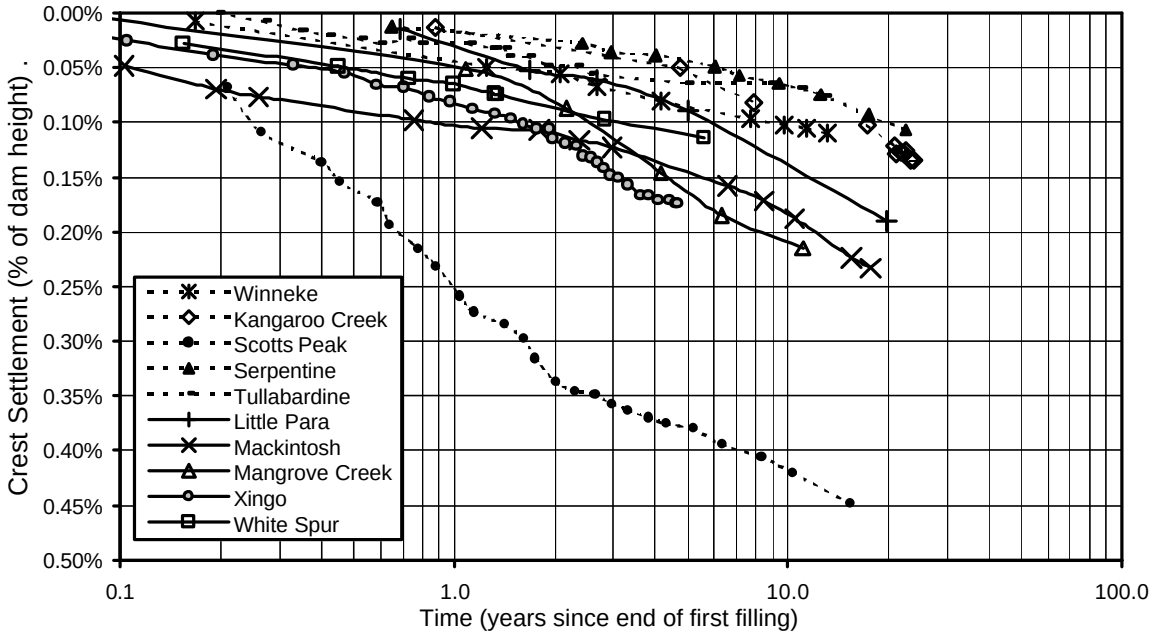

Figure 6.35: Post-construction crest settlement versus time for CFRD constructed of compacted rockfills of medium to high intact strength, t_o at end of first filling.

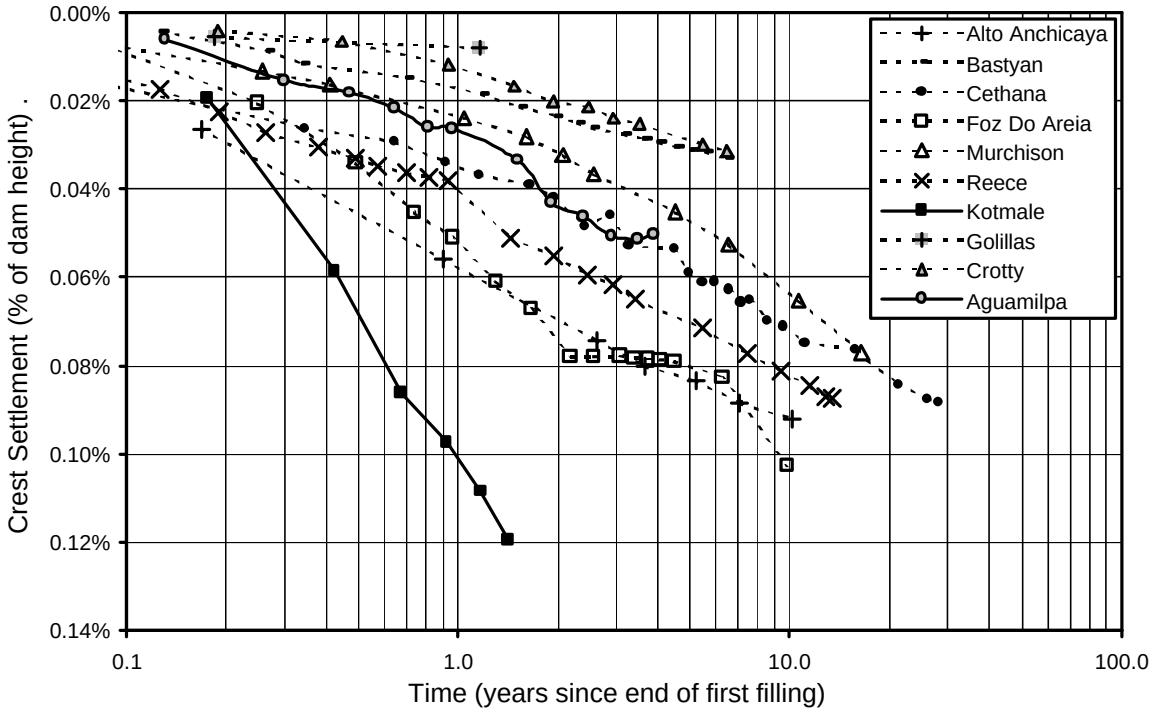

Figure 6.36: Post-construction crest settlement versus time for CFRDs constructed of well-compacted rockfills of very high intact strength and of well-compacted gravels, t_o at end of first filling.

From analysis of the deformation during first filling it was observed that the amount of crest settlement during the period of first filling was dependent on a number of factors (Table 6.8). The settlement (as a percentage of embankment height) was found to increase with/for:

- Increasing time of first filling;
- Increasing embankment height;
- Dumped compared to compacted rockfills;
- Decreasing intact rockfill strength for compacted quarried rockfills. For embankments constructed predominantly of gravels the crest settlements (as a percentage of embankment height) were similar to those of the very high strength rockfills; and
- The closer the start of first filling to the end of the main rockfill construction. This was considered to be due to the concurrent process of time dependent deformation, the rate for which decreases with time after the end of construction.

Table 6.8: Summary of crest settlement during the period of first filling

Rockfill Placement Method and Intact Rock Strength	**No. of Cases**	**Time of First Filling (years)**	**Embankment Height Range (m)**	**Range of Crest Settlement (% of embankment height)**
Dumped rockfill	6	Up to 1 year > 1 year	43 to 100	0.15 to 0.48 0.23 to 0.34
Compacted gravels	2	1.13 to 1.2	83 and 125	0.017 to 0.024
Compacted very high strength rockfill	10	< 0.1 yrs	43 to 140	0.010 to 0.014
		0.1 to < 0.5 year	75 to 110 m > 110 m	0.020 to 0.027 0.053 to 0.20
		> 0.5 year	90 and 166	0.030 to 0.13
Compacted medium to high strength rockfill	7	< 0.5 year	25	0.008
		> 1 year	38 to 53 60 to 85	0.058 to 0.096 0.058 to 0.129

The time between the end of rockfill construction and the initial crest settlement reading has a significant influence on the measured crest settlement. Relatively large magnitude total crest settlements (as a percentage of embankment height)are observed when initial readings are taken shortly after the end of construction (Tianshengqiao in Figure 6.32a and Kotmale in Figure 6.33a). Where the time delay to monitoring is relatively large (more than about four to six months after the end of rockfill construction), the magnitude of total crest settlement is smaller than for similar type CFRD (e.g. Gollilas in Figure 6.33b and Mangrove Creek in Figure 6.32a). As previously discussed, this effect makes for difficulties when attempting to compare the deformation behaviour of CFRD.

These effects are not as evident for the crest settlement plots for zero time at the end of first filling (Figure 6.34 to Figure 6.36) for which upper and lower bounds of deformation are clearer and can be more meaningfully defined.

The values of the coefficient, *m*, in the strain rate versus time power function (Equation 6.5) was investigated for both t_o at the end of the main rockfill construction and at the end of first filling. Results are given in Table 6.9. The value of *m* represents the slope of the log strain rate versus log time linear relationship.

The findings indicated some dependence of *m* on the method of placement and intact rockfill strength with lower values for the poorly sluiced dumped rockfill.

Overall the degree of variability within any data set was quite large and no readily identifiable correlation was apparent for prediction of *m*.

Table 6.9: Values of the coefficient, *m*, in the strain rate – time power function (Equation 6.5).

Rockfill Placement Method and Intact Strength	**Power Coefficient, *m***		**Comments**
	t_o at end of rockfill construction	**t_o at end of first filling**	
Dumped and poorly sluiced	0.61 and 0.88	0.50 and 0.57	Limited number of cases (6), only two poorly sluiced.
Dumped and well sluiced	1.21 to 1.84	0.78 to 0.97	
Compacted medium to high strength quarried rockfill	0.49 to 1.44	0.29 to 0.69	More consistent values for t_o at end of first filling; 6 of 7 cases in the range 0.42 to 0.69. Greater spread for t_o at end of rockfill construction.
Compacted very high strength quarried rockfill	0.92 to 1.84	0.62 to 1.04	Broad spread of values for t_o at end of rockfill construction. Better consistency for t_o at end of first filling; 7 of 8 cases in the range 0.82 to 1.09.
Compacted gravels	1.77 and 1.86	0.96 (both)	Only two cases, but reasonably consistent values.

6.4.4.1.3 Summary of the Factors Affecting the Post Construction Crest Settlement Behaviour

In summary, the most dominant factors influencing the post-construction crest settlement (as a percentage of the embankment height) are:

- The method of placement (dumped versus compacted). Significantly greater crest settlements are evident for the dumped and sluiced rockfills compared with compacted rockfills. The rates of crest settlement (on a log scale) post first filling are also significantly greater for the dumped rockfills.
- Intact rockfill strength for compacted rockfills. For embankments constructed of medium to high intact strength rockfill, the total magnitude of settlement at 10 years is on average approximately twice that of very high strength rockfills. The long-term, post first filling rates of crest settlement (on a log scale) are also significantly

higher for the medium to high strength rockfills, 2 to 10 times that of the very high strength rockfills.

- Use of gravels as opposed to rockfill. For embankments constructed of predominantly well-compacted gravels (Crotty and Golillas) the total post-construction settlement is less than that for the well-compacted, very high strength rockfills. This is likely to be due to several reasons, but is considered to be mainly a result of the rounded shape of the gravels. The point area of contact between particles of rounded gravel will be significantly greater than that of angular quarried rockfill. Hence, the contact stresses will be significantly less resulting is less particle breakage.
- Embankment height. The long-term rate of crest settlement (on a log scale) is lower for the smaller embankments within each data set; e.g. Lower Bear No. 2 of the dumped rockfill cases; Tullarbardine, Serpentine and Little Para dams of the compacted medium to high strength rockfill cases; and Bastyan and Murchison dams of the compacted very high strength rockfill cases. The effect of embankment height is probably not as significant for the compacted very high strength rockfill cases.

Other factors that appear to affect the post construction crest settlement are:

- The poorly sluiced dumped rockfills (Salt Springs and Dix River dams) tend to have greater rates of long-term crest settlement (on a log scale) than for well-sluiced dumped rockfills. The values of the power coefficient *m* are also lower for the poorly sluiced dumped rockfills.
- Particle size and uniformity coefficient are thought to have some influence on post-construction crest settlement behaviour. Greater long-term crest settlement rates (on a log scale) are likely for dams with coarser rockfills. However, no statistical correlation is evident from the data indicating that its influence is relatively minor in relation to other factors.
- Embankment zoning geometry of the main rockfill. Given that the Zone 3B rockfill is generally of lesser quality compaction (and sometimes lesser quality rockfill materials) for typical CFRD designs, greater crest settlement rates (per log cycle of time) would be expected for increasing size of the Zone 3B.

- Amount of fluctuation in reservoir level. It is suspected, although the data does not indicate, that the greater cyclic stress changes associated with larger fluctuations in reservoir level could result in greater overall settlements.
- Climate. In higher rainfall areas greater amounts of water infiltration into the rockfill would be expected, potentially resulting in greater settlements.

6.4.4.1.4 Prediction of Post Construction Crest Settlement

Prediction of the post-construction crest settlement is relatively difficult given the variable influence of first filling and the significant effect of timing on the initial base reading. However, reasonable predictions are possible.

The proposed method is to consider separately the time dependent deformation and the settlement due to first filling, as shown in Figure 6.37 for Bastyan dam for example. During (and shortly after) the period of first filling, the time dependent deformations are assumed to occur concurrently with the crest settlements due to increase in vertical stresses from the water load. Estimation of the settlement at some time after the end of main rockfill construction is therefore by summation of the time dependent and first filling related components.

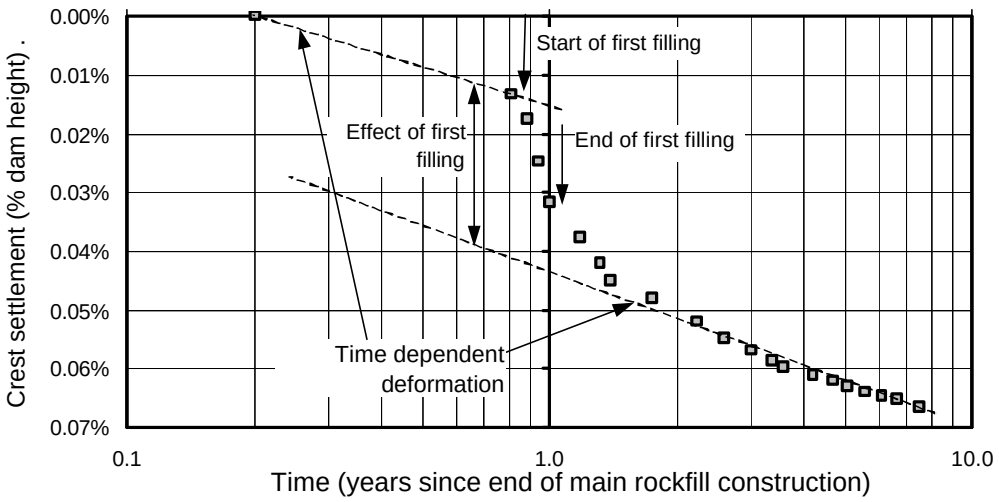

Figure 6.37: Post construction crest settlement of Bastyan dam

(a) Time dependent crest settlement

Figure 6.38 presents the data for long-term post first filling crest settlement rate (percent per log cycle of time) for the compacted rockfill embankments, for t_o at the end of main

rockfill construction. Trendlines with reasonable to good regression coefficients have been derived for compacted high strength rockfills and for compacted very high strength rockfills and gravels. The intact strength classification is that of the dominant rockfill zone under the dam axis, which in most cases is the Zone 3A rockfill, but in several cases is the Zone 3B rockfill. A tentative trendline is also given for the medium strength rockfills.

Kotmale and Mangrove Creek dams stand out as outliers to the general trend. For Mangrove Creek dam this is thought to be due to the fact that first filling to full supply level has yet to be reached after 15 years, and for which the long-term settlement rate was estimated from the settlement data more than 3 years after the end of construction (refer Figure 6.32a). For Kotmale dam the reason is not clear, although the available crest settlement data is limited to about 1 year after first filling, and it is possible that the rate (per log cycle of time) may have since reduced.

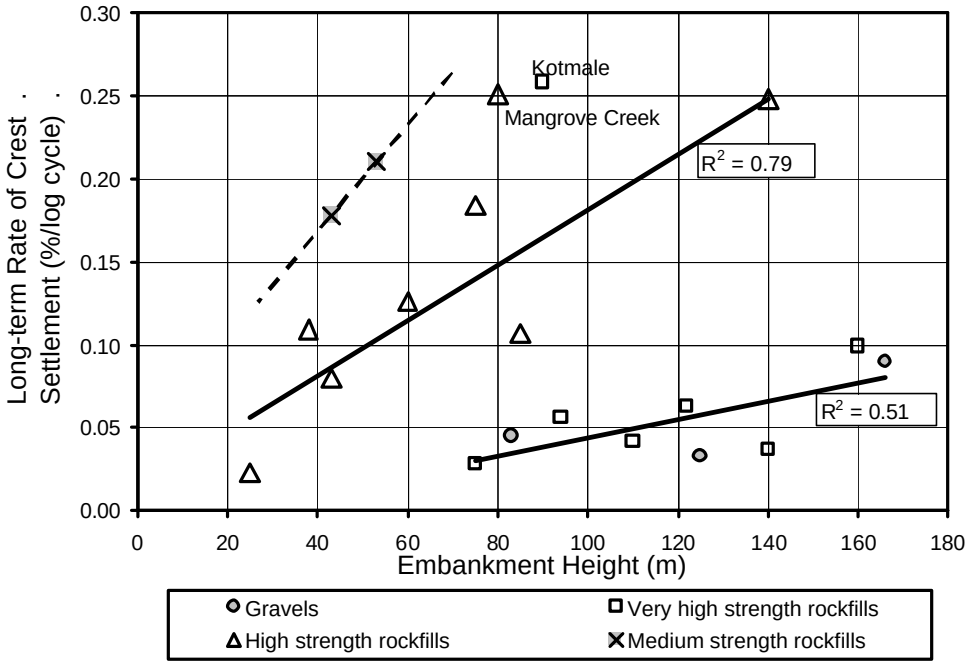

Figure 6.38: Long-term crest settlement rate (as a percentage of embankment height per log cycle of time) versus embankment height for compacted rockfills

For the dumped rockfill CFRD the data (Figure 6.31) indicates an increasing rate of vertical crest strain (per log cycle of time) with time. Estimates of the long-term vertical crest strain (per log cycle of time) can be derived from either Figure 6.31 or Table 6.10 based on the time period after the end of main rockfill construction.

Table 6.10: Estimates of long-term crest settlement rates for dumped rockfills

Time Period (from end of main rockfill construction)	**Post First Filling Crest Settlement Rate (settlement as a % of embankment height per log cycle of time)**	
	Range	Mean
0.5 to 5 years	0.10 to 0.58	0.27
5 to 20 years	0.25 to 1.14	0.66
20 years plus	0.33 to 1.44	0.85

(b) Crest settlement under increased stresses from first filling

Whilst a reasonable estimate of the crest settlement rate per log cycle of time (as a percentage of embankment height) can be made for the time dependent component of crest settlement from Figure 6.38 and Table 6.10, estimates of crest settlement during first filling are more difficult. Two alternatives methods are proposed:

(i) Estimation of the crest settlement attributable to first filling which covers the period of first filling and the short time thereafter as shown in Figure 6.37. Figure 6.39 summarises the crest settlement (as a percentage of embankment height) attributable to first filling and can be used for predictive purposes based on the intact strength of the rockfill, placement method (either dumped or compacted) and embankment height. The relatively broad variation for some groups, in particular for dumped rockfill, reflects the high degree of variability from the case studies (refer Section 6.4.4.1.2). Trendlines are provided for the compacted gravels and rockfill.

(ii) Estimation of the crest settlement during first filling from Table 6.8. The estimates from Table 6.8 are different to those from Figure 6.39 in that they are inclusive of the time dependent settlement component and only cover the period during first filling (i.e. they do not consider the higher rate of crest settlement observed that occurs for some CFRDs after the end of first filling). When using Table 6.8 the time dependent settlement component during the period of first filling should not be added to that from the Table 6.8.

There is a high degree of variability in using either method, particularly for the dumped rockfill case studies. Interpretation of crest settlement attributable to first filling in Figure 6.39 (from Figure 6.31 to Figure 6.33) was imprecise for a number of

case studies, particularly those where first filling occurred soon after the end of construction. For the dumped rockfill case studies the large variation may be attributable to high rates of leakage and possible collapse settlement of the rockfill during first filling amongst other factors. The high rate of settlement after the end of first filling for some case studies is an indication that the response of the rockfill under changes in stress is not elastic. In addition, higher time dependent settlement rates are likely under the higher stress conditions imposed at full supply level.

Method (i) is the considered the preferable method to use for prediction of crest settlements attributable to first filling.

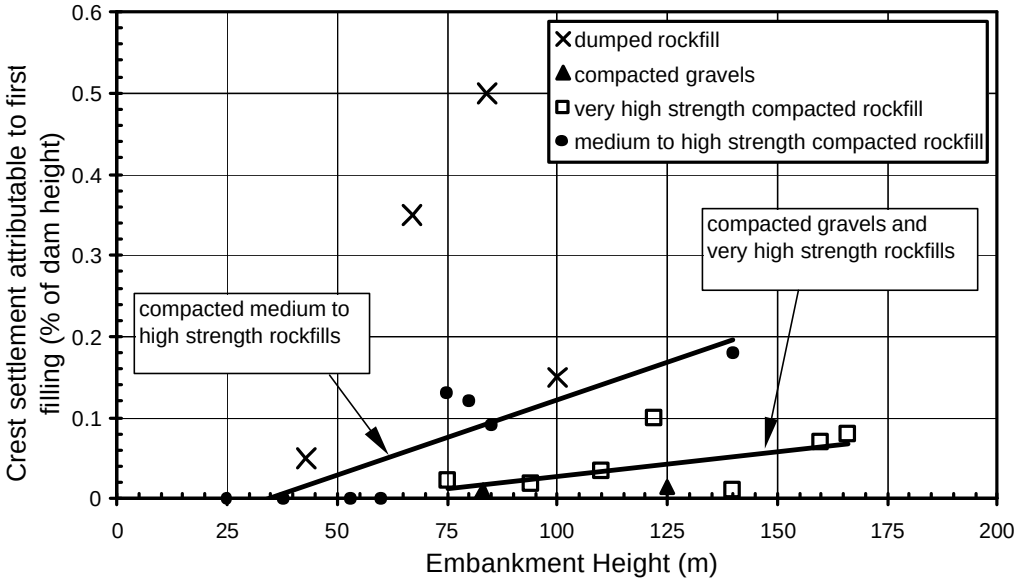

Figure 6.39: Crest settlement attributable to first filling (excluding time dependent effects)

(c) Identification of "abnormal" crest settlement behaviour post construction

Figure 6.31 to Figure 6.36 are useful in providing upper and lower bounds of deformation behaviour and identification of potential "abnormal" deformation behaviour. In the case of Scotts Peak dam (Figure 6.35) the post first filling deformation behaviour is distinctly different from the typical behaviour. In this case significant leakage occurred during the latter stages of first filling due to cracking of the asphaltic concrete membrane face (Figure 6.28) resulting in wetting and saturation of the rockfill. Collapse type settlements occurred on wetting of the medium strength argillite rockfill, which was prone to strength loss on saturation.

6.4.4.2 Post-Construction Internal Settlement

Post-construction internal settlements (under the embankment crest) were analysed for thirteen of the compacted CFRD case studies, most of which are Australian CFRD. The settlements were determined from the records of crest monitoring points and internal settlement gauges and divided into roughly four zones; the upper 25%, the central upper 25%, the central lower 25% and the bottom 25%. The settlements were analysed from both the start of monitoring (or first filling) and also from the end of first filling. The findings are summarised in Table 6.11 and indicate:

- For very high strength compacted rockfills and compacted gravels, a very high percentage of the total settlement from initial monitoring occurs in the bottom 25% of the embankment and a negligible amount within the upper 25 to 50%.
- For the medium to high strength rockfills this trend is evident for some case studies, whilst for others the distribution is more evenly spread.
- After the end of first filling the percentage settlement in the bottom 25% of the embankment decreases (compared to the percent settlement measured from the start of first filling), typically in the order of 10 to 20%.

The reason for the observed distributions of small settlements in the upper part and very high settlements in the lower part of the embankment can be explained by a combination of several factors:

- On first filling the increase in stress levels (above those previously experienced) will be greatest at the base of the embankment and lowest at the crest.
- The non-linear stress-strain relationship of rockfill, which has a general tendency of decreasing tangent modulus with increasing vertical stress (Figure 6.17). Therefore, combined with stress changes from first filling, greater settlements would be expected in the lower portion of the embankment.
- The tendency for time dependent strain rates to be dependent on stress level. Greater time dependent strains would therefore be anticipated in the deeper sections of the embankment.

In Table 6.11 the medium to high strength rockfills have, in most cases, been sourced from sedimentary rock types, and the very high strength rockfills from igneous or metamorphic rock types. The sedimentary rock types typically show a greater loss in

strength on wetting and therefore, may account for the greater percent of total settlement in the upper portion of the embankment for several cases due to rainfall infiltration.

Zoning of the embankment will also have an affect as the results for Mangrove Creek dam indicate. A high proportion of the post-construction crest settlement under the embankment centreline for Mangrove Creek is from within the random fill zone (Zone 3B - weathered to fresh sedimentary rockfill) rather than in the better quality Zone 3A rockfill (fresh siltstones and sandstones).

Table 6.11: Location of internal post-construction vertical settlement in CFRD

CFRD Name	Intact *[2] Rock Strength	Height (m)	Start of Time Period *[1]	No of Years Data	Percent of Total Crest Settlement			
					Top 25%	25 to 50%	50 to 75%	Bottom 25%
Crotty	Gravel	83	Start M	2.2	4	6	6	84
Bastyan	VH	75	Start FF	6.75	4		18	78
Cethana	VH	110	Start ff	14.5	0		51	49
			End FF	13.5	(heave)		64	36
Kotmale	VH	90	Start M	1.5	(heave)	25	12	63
Murchison	VH	94	Start M	11.5	(heave)	27	37	36
			End FF	9.25	14	40	30	15
Reece	VH	122	Start M	8	4		40	79
			End FF	6.25	(heave)		21	49
White Spur	H to VH	43	Start M	5.75	40	8	18	33
			End FF	4.5	42	4	29	24
Tullabardine	H	25	Start M	5	8	52	40	
Winneke	H	85	Start M	15.5	11			89
			End FF	10.5	20			80
Mangrove Creek *[3]	H	80	Start M	8.3	5	43	26	26
Mackintosh	M to H	75	Start M	7.5	(heave)	23	31	46
			End FF	6	(heave)	23	32	45
Serpentine	M to H	38	Start M	8	25	42	16	17
			End FF	4	15	51	13	21
Scotts Peak	M	43	Start M	17	15	7	29	49
			End FF	14	37	9	15	39

Notes: *[1] M = monitoring; FF = first filling

*[2] VH, H and M refer to very high, high and medium intact strength respectively

*[3] For Mangrove Creek the central region (25 to 75%) is representative of the random fill zone (Zone 3B).

6.5 DISCUSSION AND RECOMMENDED METHODS FOR PREDICTION

Data on the deformation behaviour of 36 mostly CFRD (35 CFRD and 1 central core earth and rockfill embankment) has been collected and analysed. The following discussion provides guidelines for prediction of internal deformations during construction, face slab deformations during first filling and post-construction crest settlements of CFRD based on the findings of the analyses undertaken. The proposed methods are then compared to other existing methods.

6.5.1 GUIDELINES ON DEFORMATION PREDICTION DURING CONSTRUCTION

Empirical methods based on historical performance are useful for prediction of the deformation of rockfill in CFRD. For relatively standard CFRD designs to be constructed with quarried rockfills the empirical methods are considered to provide reasonable estimates of deformation, at least comparable, and possibly superior, to those based on the results of triaxial and oedometer laboratory tests given the difficulties and limitations associated with particle size, particle size distribution and sample preparation of laboratory samples.

Prediction of rockfill deformation (both numerical and empirical) is based on the quality of representation of the non-linear stress-strain relationship of the rockfill, which is strongly dependent on the rockfill properties, in particular its intact strength, method of placement and particle size distribution after compaction. The embankment height is a significant factor as this predicates the level of applied stress within the embankment. Valley shape is a significant factor for embankments constructed in narrow valleys due to the effects of cross-valley arching and resultant reduction in applied stresses. Typical stress-strain relationships of rockfill from field measurements during construction (Figure 6.15) show that the relationship is non-linear and has a general trend of decreasing secant (and tangent) modulus with increasing applied stress.

The proposed method of prediction of a stress-strain relationship for the rockfill is to firstly derive a representative secant modulus at the end of construction, E_{rc}, from Figure 6.21 and then apply correction factors for layer thickness, stress level and valley shape. The representative secant modulus at the end of construction, E_{rc}, is for Zone 3A rockfill, placed in layers 0.9 to 1.2 m thick, compacted with 4 to 6 passes of a 10 tonne smooth drum vibratory roller and water added, and applies to average vertical stresses of (Table 6.7):

- 1400 kPa for the very high strength, well-compacted rockfills;
- 800 kPa for the medium to high strength, well-compacted rockfills; and
- 1500 kPa for the well-compacted gravels.

To estimate the secant modulus at the end of construction:

- For the proposed rockfill source, estimate the UCS within the broad ranges of Table 6.1 and the rockfill particle size distribution, most likely from compaction trials. For existing dams (or those in the process of construction) use the actual average particle size distribution.
- Estimate the representative E_{rc} from the equations shown on Figure 6.21 using the estimated D_{80} value and the appropriate equation for intact strength (either very high strength or medium to high strength).
- For medium strength well-compacted rockfills apply a correction factor of 0.7 to the E_{rc} value determined from the equation for medium to high strength rockfills.
- For Zone 3B or other thicker layer rockfills comprising similar rock type (and UCS range) to Zone 3A, apply a correction factor of 0.5 to obtain a representative E_{rc} for rockfill placed in 1.5 to 2.0 m layers. This correction factor is based on the ratio of E_{rc} (of Zone 3A to Zone 3B) from six field cases.
- To account for the non-linearity of the stress-strain relationship for rockfill, estimates of E_{rc} at stress levels less than or greater than that representative for the corrected E_{rc} can be estimated from historical records (Figure 6.16). Although the relationship is likely to be exponential, the data (Figure 6.16) indicates a linear approximation is reasonable over a defined vertical stress range. The following corrections are suggested:
  - For very high strength rockfills apply a linear correction of ±7.5% per 200 kPa to the E_{rc} estimated from Figure 6.21 from a vertical stress of 1400 kPa (applicable range is 400 to 1600 kPa). Apply positive corrections for decreasing stresses and negative corrections for increasing stresses.
  - For medium to high strength rockfills apply a linear correction of ±6 % per 200 kPa to the E_{rc} estimated from Figure 6.21 from a vertical stress of 800 kPa (applicable range is 200 to 1200 kPa).
- For one-dimensional analyses appropriate correction factors for stress reduction due to the shape of the embankment should be considered. These can be estimated from equations and charts such as those published by Poulos et al (1972).

- To correct for valley shape either:
  - Model the valley and the dam using 3-dimensional numerical analysis, and a stress-strain relationship for the rockfill based on the E_{rc} versus vertical stress relationship derived above; or
  - For simplified one-dimensional analyses, to estimate the maximum settlement under the centreline in the centre of the valley correct the vertical stress profile for embankment shape (refer Section 6.2.3) and then correct for valley shape using the appropriate stress reduction factors given in Table 6.12.

Table 6.12: Approximate stress reduction factors to account for valley shape

W_r/H Ratio (river width to height)	**Average Abutment Slope Angle (degrees)**	**Stress Reduction Factor (embankment location)**			
		Base (0 to 20%)	Mid to Low (20 to 40%)	Mid (40 to 65%)	Upper (65% to crest)
0.2	10 to 20	0.93	0.95	0.97	1.0
	20 to 30	0.88	0.92	0.96	0.98
	30 to 40	0.82	0.88	0.94	0.97
	40 to 50	0.74	0.83	0.91	0.96
	50 to 60	0.66	0.76	0.86	0.94
	60 to 70	0.57	0.69	0.82	0.92
0.5	< 25	1.0	1.0	1.0	1.0
	25 to 40	0.93	0.95	0.97	1.0
	40 to 50	0.91	0.92	0.95	0.95 – 1.0
	50 to 60	0.87	0.88	0.93	0.95 – 1.0
	60 to 70	0.83	0.85	0.90	0.95 – 1.0
1.0	All slopes	0.95 - 1.0	0.95 - 1.0	1.0	1.0

Note: W_r = river width H = embankment height

Other relevant issues relating to the estimation of secant modulus and derivation of the correlation between secant modulus and D_{80} (Figure 6.21) are:

- C_u, the uniformity coefficient for the particle size distribution curve, is implicitly allowed for in the D_{80} value. Generally, decreasing C_u is observed for increasing D_{80}.
- For materials placed with larger rollers (i.e. 13 to 15 tonne deadweight vibrating rollers) the data does not indicate an increase in moduli for the greater compactive effort. This may be due to greater material breakdown under the heavier rollers, and a resultant reduction of $D_{80,}$ which can then be accounted for directly in Figure 6.21.

- For weathered rockfills intact strength will be lower than for fresh rock, which will result in a decrease in secant moduli, but the greater breakdown will give an increase in moduli associated with a reduction in D_{80}.
- The E_{rc} values in Figure 6.21 for each data point have been determined from published internal deformation records, and generally from the lower 60% of the embankment and within the central portion of this lower section. The E_{rc} values have also been corrected for cross-valley arching effects using the normalised vertical stress charts (Figure 6.19). It is recognised that these may not be a true representation of the actual stresses due to assumptions made in the modelling process (refer Section 6.4.2). However, errors associated with the assumptions in modelling are minimised by applying the same assumptions for prediction as is proposed in the above.
- If testing on the proposed rock source for rockfill indicates a significant reduction in UCS on wetting is likely and only limited water has been, or is proposed to be, used in construction, then this strength reduction should be taken into consideration. There is not sufficient data to advise on how this should be done; however, the rockfill is likely to be more susceptible to collapse settlements on wetting due to rainfall and flooding.

Limitations of the data and application of the proposed methodology include:

- For well-compacted gravels only a limited number of cases were available, insufficient to undertake analysis. These materials generally have significantly greater secant moduli at any given stress level in comparison to quarried, very high strength rockfill. Where the rockfill is of finer size (e.g. Crotty Zone 3A) the use of large scale laboratory test that virtually encompass the field particle size distribution would provide suitable estimates of moduli provided the layering and density in the field are reflected in the laboratory testing.
- For the data presented in Figure 6.15 (vertical stress versus vertical strain), the stress-strain curves do not pass through the origin. This is because zero strain is assumed at a vertical stress equivalent to the mid-height between hydrostatic settlement gauges (HSGs). Zero strain is generally at vertical stresses in the range 50 to 200 kPa (depending on the vertical distance between HSGs).
- During the actual embankment construction, monitoring should be undertaken as a check on the pre-construction estimation of deformation. Deformation estimates

can be reassessed, if required, as construction proceeds using the stress-strain relationship/s extrapolated from the actual field records.

For estimating deformations due to embankment raising, it is recommended that the modulus be obtained from monitoring during the earlier construction phase if that is available. If not, the methods outlined above can be used to estimate the secant modulus versus vertical stress relationship. Simplistic estimates of deformation could be obtained by modelling the embankment in a series of layers of varying tangent moduli (estimated from the secant moduli vertical stress relationship). For a more rigorous analysis numerical modelling would be appropriate.

For dumped rockfill there is not sufficient data from which to give guidelines on moduli during construction. The data records from the limited number of cases is summarised in Section 6.4.2.6.

6.5.2 GUIDELINES ON DEFORMATION PREDICTION DURING FIRST FILLING

As discussed in Section 6.4.3, the modulus on first filling, E_{rf}, estimated using the method by Fitzpatrick et al (1985) is an artefact of the method used to calculate it and is not a true modulus of the rockfill, as Fitzpatrick et al (1985) recognised. The high values of E_{rf} compared to E_{rc} are to be expected given the stress paths on first filling in the upstream slope (Figure 6.23b and Figure 6.24b). The stress paths show an unloading then reloading of deviatoric stress whilst compressive stresses continue to increase with increasing reservoir level.

The predictive method of face slab deformation comprises estimation of the ratio E_{rf}/ E_{rc} from Figure 6.22. Given that E_{rc} is already known or estimated, E_{rf} can be estimated. The face slab deflection can then be predicted using Equation 6.2 after Fitzgerald et al (1985) (refer Figure 6.1b). The method is considered applicable to the region of the face slab between 20% and 60% of the embankment height, the region of maximum face slab deflection on first filling in most cases.

Guidelines for use of Figure 6.22 for estimation of E_{rf} are:

- Estimate the ratio E_{rf}/ E_{rc} based on the embankment height and upstream slope angle. Trendlines are given for upstream slopes of 1.3 – 1.4H to 1V, and 1.5H to 1V, which cover most CFRD designs.

- Estimate E_{rc}, the representative secant moduli at end of construction, of the Zone 3A rockfill from the methods outlined in Section 6.5.1. The E_{rc} value should be adjusted for vertical stress such that it is representative of the lower 50% of the rockfill in the central region of the embankment. The E_{rc} values used in the derivation of Figure 6.22 were not corrected for arching effects due to valley shape because valley shape is potentially likely to affect both E_{rc} and E_{rf}, and would therefore be taken into consideration in the E_{rf}/E_{rc} ratio. Hence, E_{rc} estimates derived from Figure 6.21 (corrected for valley shape effects) must be un-corrected.
- E_{rf} can then be estimated by multiplication of the E_{rf}/E_{rc} ratio by E_{rc} (not corrected for valley shape).

In using Figure 6.22 for estimating the E_{rf}/E_{rc} ratio, consideration should be given to the qualifications to this figure as discussed in Section 6.4.3. The trendline for upstream slope angles of 1.5H to 1V is based on a limited number of cases and it should therefore be recognised that the estimated E_{rf}/E_{rc} ratio will be very approximate.

The zoning geometry of the embankment has a significant effect on the deformation behaviour of the face slab on first filling (Section 6.4.3) and the method of prediction of the face slab deformation is dependent on this geometry and consideration of the differential moduli between the main rockfill zones. The empirical predictive method developed (based on Figure 6.22) is appropriate for CFRD with relatively simple zoning geometries comprising a significant Zone 3A (at least 50 to 60% of the main rockfill) and/or where large variations in rockfill moduli are not likely between rockfill zones. For embankments with complex geometries (particularly in the upstream half of the embankment) and/or large moduli variations between the rockfill zones, finite element analyses should be considered. The detailed analysis would be justified considering the potential for face slab cracking as a result of possible development of tensile stresses.

6.5.3 GUIDELINES ON DEFORMATION PREDICTION POST-CONSTRUCTION

Guidelines for the prediction of post-construction crest settlements are given in Section 6.4.4.1.4. The methods proposed are considered to provide an improvement on current available methods of crest settlement prediction for CFRD.

The method of prediction comprises separate estimation of the time dependent deformation component and the crest settlement attributable to first filling, and then summation to estimate the total post construction settlement. In summary:

- The time dependent crest settlement rate (as a percentage of the embankment height per log cycle of time) for compacted rockfill can be estimated from Figure 6.38. The estimate is based on the embankment height and intact strength of the compacted rockfill under the embankment centreline. The zero time, t_o, has been taken at the end of the main rockfill construction.
- For dumped rockfills, estimates of the long-term crest settlement rate (as a percentage of the embankment height per log cycle of time) can be derived from either Figure 6.31 or Table 6.10 based on the time period after the end of main rockfill construction.
- Two methods are provided for prediction of the crest settlement during or attributable to first filling. Method (i) or Figure 6.39, the preferred method, is an estimation of the crest settlement attributable to first filling based on the embankment height, intact rock strength and placement method. The degree of variability is relatively large, particularly for the dumped rockfill cases, due to the number of factors influencing the deformation behaviour.
- The time dependent deformations and deformations on first filling occur concurrently.

The plots of the historical records of case studies (Figure 6.31 to Figure 6.36) are useful in providing upper and lower bounds of deformation behaviour and identification of potential "abnormal" deformation behaviour based on the method of placement and intact strength of compacted rockfill. As discussed in Section 6.4.4.1 the plots for settlements after the end of main rockfill construction (Figure 6.31 to Figure 6.33) should be used with caution due to the influences of first filling and initial time of reading.

6.6 CONCLUSIONS

The proposed empirical predictive methods for estimation of the deformation of rockfill (summarised in Section 6.5), specifically targeted at the deformation of CFRD, are considered to provide improvements over currently available empirical predictive

methods because of the larger good quality data set available, and consideration of significant factors which influence the deformation behaviour. The methods are based on historical records of embankment performance and allow for estimation/prediction of the vertical deformation during construction, deformation of the face slab and post-construction crest settlement. Where possible the significant factors affecting the deformation behaviour of rockfill, evaluated from the analysis of historical records, were incorporated into the empirical predictive methods.

The results of the historical data presented on the stress-strain behaviour of rockfill measured in the field is considered to have advantages over rockfill properties estimated by laboratory test methods. Laboratory testing of rockfill has the disadvantages of limitation on particle size and placement methods, both of which are shown to have a significant effect on the prediction of the rockfill modulus. Methods, although relatively crude, are proposed for estimation of the stress-strain relationship of a compacted rockfill sample and could therefore be used as a basis for the constitutive model in finite element analyses.

The proposed empirical predictive methods of deformation are generally applicable to the more typical CFRD designs. For relatively complex geometries, particularly those that incorporate high differential moduli between rockfill zones (e.g. compacted gravels and rockfills such as Aguamilpa dam) numerical methods are considered more appropriate. They are considered particularly appropriate for modelling potential tensile stress development in the concrete face that could result in cracking.

TABLE OF CONTENTS

7.0 THE DEFORMATION BEHAVIOUR OF EMBANKMENT DAMS..... 7.1

7.1 INTRODUCTION TO THIS CHAPTER 7.1

7.2 LITERATURE REVIEW 7.2

7.2.1 Failure and Accident Statistics..... 7.2

7.2.2 Historical Development of Embankment Dams as this Affects Deformation Behaviour..... 7.3

7.2.3 Factors Affecting The Deformation of Embankment Dams 7.5

7.2.4 Predictive Methods of Deformation Behaviour..... 7.9

7.3 DATABASE OF CASE STUDIES 7.17

7.3.1 Earthfill and Zoned Earth and Earth-Rockfill Embankments..... 7.17

7.3.2 Puddle Core Earthfill Embankments..... 7.18

7.4 GENERAL DEFORMATION BEHAVIOUR DURING CONSTRUCTION OF EARTHFILL AND ZONED EARTH AND EARTH-ROCKFILL EMBANKMENTS 7.18

7.4.1 Stresses During Construction..... 7.23

7.4.2 Lateral Deformation of the Core During Construction..... 7.43

7.4.3 Vertical Deformation of the Core During Construction..... 7.51

7.5 GENERAL DEFORMATION BEHAVIOUR ON FIRST FILLING OF EARTHFILL AND ZONED EARTH AND EARTH-ROCKFILL EMBANKMENTS..... 7.69

7.5.1 Effect of Water Load on the Core..... 7.70

7.5.2 Collapse Compression During First Filling..... 7.73

7.5.3 Lateral Surface Deformation Normal to the Dam Axis During First Filling. 7.84

7.6 GENERAL POST CONSTRUCTION DEFORMATION BEHAVIOUR OF EARTHFILL AND ZONED EARTH AND EARTH-ROCKFILL EMBANKMENTS 7.99

7.6.1 Post Construction Internal Vertical Deformation of the Core..... 7.100

7.6.2 Post Construction Total Deformation of Surface Monitoring Points... 7.102

7.6.3 Post Construction Crest Settlement Versus Time..... 7.110

7.6.4 Post Construction Horizontal Displacement of the Crest Normal to the Dam Axis. 7.132

7.6.5 Post Construction Deformation of the Mid to Upper Downstream Slope..... 7.140

7.6.6 Post Construction Deformation of the Upper Upstream Slope and Upstream Crest *7.148*

7.7 GENERAL DEFORMATION BEHAVIOUR OF PUDDLE CORE EARTHFILL EMBANKMENTS 7.158

7.7.1 Deformation During Construction of Puddle Core Earthfill Embankments *7.158*

7.7.2 Deformation During First Filling of Puddle Core Earthfill Embankments *7.159*

7.7.3 Deformation Behaviour Post First Filling of Puddle Core Earthfill Dams *7.166*

7.8 "ABNORMAL" EMBANKMENT DEFORMATION BEHAVIOUR – METHODS OF IDENTIFICATION 7.185

7.9 "ABNORMAL" DEFORMATION BEHAVIOUR DURING CONSTRUCTION OF EARTH AND EARTH-ROCKFILL EMBANKMENTS 7.187

7.9.1 Plastic Deformation of the Core During Construction *7.188*

7.9.2 Collapse Compression of the Central Earthfill Zone *7.191*

7.9.3 Reservoir Filling During Construction *7.192*

7.9.4 Shear Surface Development in the Core During Construction *7.193*

7.10 "ABNORMAL" DEFORMATION BEHAVIOUR POST CONSTRUCTION OF ZONED EARTH AND ROCKFILL EMBANKMENTS 7.196

7.10.1 Rockfill Susceptibility to Collapse Compression *7.197*

7.10.2 Deformation on First Filling in Embankments where Collapse Compression occurs in the Upstream Rockfill Shoulder *7.201*

7.10.3 Development of Shear Surfaces Within the Earthfill Core *7.217*

7.10.4 Post First Filling Acceleration in Deformation that is Not Known to be Shear Related *7.241*

7.10.5 Other Case Studies with Potentially "Abnormal" Deformation Behaviour Post Construction *7.243*

7.11 "ABNORMAL" DEFORMATION BEHAVIOUR POST CONSTRUCTION OF EARTHFILL AND ZONED EMBANKMENTS WITH VERY BROAD CORE WIDTHS 7.252

7.11.1 Collapse Compression of the Earthfill on Wetting *7.252*

7.11.2 "High" Shear Stress or Marginal Stability Conditions Within the Embankment *7.260*

7.11.3 The Effect of the Development of the Phreatic Surface on the Displacement of the Crest and Downstream Shoulder. *7.269*

7.11.4 Other Cases of Potential "Abnormal" Deformation Behaviour *7.270*

7.12 "ABNORMAL" DEFORMATION BEHAVIOUR OF PUDDLE CORE EARTHFILL DAMS 7.274
7.12.1 Comparison with the Deformation Behaviour of Other Puddle Dams 7.275
7.12.2 General Movement Trends Indicative of Deformation to Failure 7.278
7.12.3 Other Indicators of "Abnormal" Deformation Behaviour 7.279
7.13 SUMMARY OF "ABNORMAL" DEFORMATION BEHAVIOUR 7.280
7.14 SUMMARY AND METHODS FOR PREDICTION OF DEFORMATION OF EMBANKMENT DAMS 7.287
7.14.1 Earthfill, and Zoned Earth and Earth-Rockfill Dams 7.288
7.14.2 Prediction of Deformation Behaviour During Construction for Earthfill and Zoned Earth and Earth-Rockfill Embankments 7.288
7.14.3 Prediction of Deformation Behaviour Post Construction for Earthfill and Zoned Earth and Earth-Rockfill Embankments 7.291
7.14.4 Puddle Core Earthfill Dams 7.300
7.15 CONCLUSIONS 7.302

LIST OF TABLES

Table 7.1: Mechanisms affecting the long-term deformation behaviour of old puddle core earthfill embankments (Tedd et al 1997a). 7.8

Table 7.2: Vertical compression of rolled, well-compacted earthfills measured during construction (adapted from Sherard et al 1963). 7.12

Table 7.3: Published ranges of post construction deformation of embankment dams 7.14

Table 7.4: Central core earth and rockfill embankments in the database 7.19

Table 7.5: Zoned earth and rockfill embankment case studies 7.20

Table 7.6: Zoned earthfill embankment case studies 7.21

Table 7.7: Earthfill embankment case studies 7.21

Table 7.8: Puddle core earthfill embankment case studies 7.22

Table 7.9: Multiplying coefficients for the calculation of the total vertical stress at the embankment centreline at end of construction (Equation 7.3) 7.26

Table 7.10: Properties of central core used in finite difference analyses 7.29

Table 7.11: Lateral deformations of the central core at end of construction for central core earth and rockfill embankments. 7.44

Table 7.12: Summary of embankment and earthfill properties for cases used in the analysis of lateral core deformation during construction. 7.46

Table 7.13: Confined secant moduli during construction for well-compacted, dry placed earthfills. 7.57

Table 7.14: Equations of best fit for core settlement versus embankment height during construction 7.68

Table 7.15: Equations of best fit for core settlement (as a percentage of embankment height) versus embankment height during construction 7.68

Table 7.16: Properties of central core used in finite difference analyses 7.80

Table 7.17: Lateral displacement of the crest (centre to downstream edge) on first filling. 7.89

Table 7.18: Thirteen cases with largest downstream crest displacement on first filling 7.92

Table 7.19: Typical range of post construction crest settlement. 7.104

Table 7.20: Typical range of post construction settlement of the upstream and downstream shoulders. 7.109

Table 7.21: Summary of long-term crest settlement rates (% per log cycle of time). 7.122

Table 7.22: Range of long-term settlement rate of the downstream shoulder. 7.141

Table 7.23: Range of long-term settlement rate of the upper upstream slope and upstream crest region. 7.151

Table 7.24: Summary of the post construction surface deformations of the puddle core earthfill dam case studies. 7.168

Table 7.25: Embankments for which collapse compression caused moderate to large settlements. 7.199

Table 7.26: Figure references for post construction crest deformation 7.292

Table 7.27: Figure references for post construction deformation of the embankment shoulders 7.293

Table 7.28: References to post construction settlement magnitude tables and plots . 7.295

Table 7.29: Embankment crest region, typical range of post construction settlement and long-term settlement rate 7.295

Table 7.30: Embankment shoulder regions, typical range of post construction settlement and long-term settlement rate 7.296

Table 7.31: References to tables and figures of long-term settlement rate 7.296

Table 7.32: Predictive methods of long-term crest settlement and displacement under normal reservoir operating conditions for puddle core earthfill embankments 7.301

LIST OF FIGURES

Figure 7.1: Embankment construction indicating *(a)* broad layer width to embankment depth ratio in the early stages of construction and *(b)* narrow layer width to embankment depth ratio in the latter stages of construction. 7.24

Figure 7.2: *(a)* Total vertical stress ($s_{z,EOC}$) contours at end of construction for 1.8H to 1V embankment slopes, and *(b)* vertical stress ratio, Z_1, versus *h/H* under the embankment axis for various embankment slopes..... 7.26

Figure 7.3: Embankment model for finite difference analysis during construction. 7.29

Figure 7.4: Total vertical stress, total lateral stress, and lateral (horizontal) displacement distributions at end of construction for zoned earthfill finite difference analysis. 7.30

Figure 7.5: Finite difference modelling results; *(a)* total vertical stress on the dam centreline at end of construction, *(b)* settlement profile at dam axis at end of construction, and *(c)* lateral deformation at Point a (Figure 7.3) during construction. 7.32

Figure 7.6: Finite element analysis of zoned embankments highlighting arching of core zone from *(a)* Beliche dam at about mid-height, elevation 22.5 m (Naylor et al 1997), and *(b)* a puddle core embankment (Dounias et al 1996). 7.33

Figure 7.7: Estimated versus measured (from pressure cells) total vertical stresses during construction. 7.34

Figure 7.8: Total vertical stress profiles from the numerical analysis of construction for zoned embankments with different core slopes; *(a)* 0.2H to 1V case, *(b)* 0.5H to 1V case, and *(c)* total vertical stress at *h/H* = 0.70 with increasing embankment height. 7.36

Figure 7.9: Idealised types of pore water pressure response in the core during construction. 7.38

Figure 7.10: Pore water pressure response during construction in the core zone of clayey earthfills placed at close to or wet of Standard optimum moisture content. 7.39

Figure 7.11: Triaxial isotropic compression tests with staged undrained loading and partial drainage on a partially saturated silty sand (Bishop 1957). 7.41

Figure 7.12: Estimated lateral displacement ratio of the core at end of construction. 7.45

Figure 7.13: Estimated lateral displacement ratio of the core versus fill height above gauge during construction. 7.45

Figure 7.14: Lateral displacement ratio and pore water pressure versus fill height or measured total vertical stress at *(a)* Dartmouth dam; *(b)* Blowering dam; *(c)* Talbingo dam and *(d)* Thomson dam. 7.50

Figure 7.15: Vertical stress versus strain of the core during construction for selected cross-arm intervals of selected case studies; *(a)* dry placed clay cores, and *(b)* dry placed dominantly sandy and gravelly cores with plastic fines. 7.54

Figure 7.16: Confined secant moduli of the core versus vertical stress during construction for selected cross-arm intervals of selected case studies, *(a)* dry placed clay cores, and *(b)* dry placed dominantly sandy and gravelly cores with plastic fines. 7.55

Figure 7.17: Seating settlements at low stresses suspected as cause of low moduli estimates at low stresses 7.56

Figure 7.18: Vertical strain versus effective vertical stress in the core at end of construction for *(a)* dry placed clay earthfills and *(b)* dry placed dominantly sandy and gravelly earthfills. 7.58

Figure 7.19: Confined secant moduli versus effective vertical stress in the core at end of construction for *(a)* dry placed clay earthfills and *(b)* dry placed dominantly sandy and gravelly earthfills. 7.59

Figure 7.20: Vertical strain in the core versus fill height during construction at selected cross-arm intervals in selected case studies of earthfills placed close to or wet of Standard optimum, for *(a)* thin core (combined slopes less than 0.5H to 1V), and *(b)* medium cores (combined slope ≥ 0.5H to 1V and < 1H to 1V). 7.62

Figure 7.21: Vertical strain in the core versus fill height at end of construction for dominantly sandy and gravelly earthfills with plastic fines placed close to or wet of Standard optimum, for *(a)* thin cores (combined slopes less than 0.5H to 1V), and *(b)* medium to thick cores (combined slope ≥ 0.5H to 1V). 7.63

Figure 7.22: Vertical strain of the core versus fill height at end of construction for clay earthfills placed close to or wet of Standard optimum moisture content, for *(a)* thin core (combined slopes less than 0.5H to 1V), and *(b)* medium to thick cores (combined slope ≥ 0.5H to 1V). 7.64

Figure 7.23: Core settlement during construction of earth and earth-rockfill embankments *(a)* including Nurek dam, and *(b)* excluding Nurek dam. 7.67

Figure 7.24: Effect of reservoir filling on a zoned embankment (Nobari and Duncan 1972b) 7.70

Figure 7.25: Water load acting on a homogeneous earthfill dam. 7.71

Figure 7.26: Lateral stress distribution at *(a)* end of construction, and *(b)* reservoir full condition, for central core earth and rockfill embankment with core of similar compressibility properties to the rockfill. 7.72

Figure 7.27: Lateral stress distribution at *(a)* end of construction, and *(b)* reservoir full condition, for a central core earth and rockfill embankment with wet placed core of low undrained strength. 7.73

Figure 7.28: Compression curves for dry and wet states and collapse compression from the dry to wet state for Pyramid gravel in the laboratory oedometer test (Nobari and Duncan 1972a). 7.75

Figure 7.29: Idealised effect of matric suction on collapse compression of earthfills (Khalili 2002)..... 7.75

Figure 7.30: Cracking caused by post construction differential settlement between the core and the dumped rockfill shoulders (Sherard et al 1963)..... 7.77

Figure 7.31: Embankment model for finite difference analysis during first filling. 7.78

Figure 7.32: Model of the stress-strain relationship of the upstream rockfill incorporating collapse compression (in one-dimensional vertical compression). 7.80

Figure 7.33: Case 8 – "dry" placed, very stiff core modelling collapse compression in the upstream rockfill; numerical results of *(a)* vertical and *(b)* lateral displacement on first filling. 7.82

Figure 7.34: Case 9 – "dry" placed, very stiff core without collapse compression; numerical results of *(a)* vertical and *(b)* lateral displacement on first filling. 7.82

Figure 7.35: Case 10 – "wet" placed clay core of low undrained strength modelling collapse compression in the upstream rockfill. Numerical results of vertical and lateral deformation on first filling; *(a)* and *(b)* for reservoir at 40% of embankment height, *(c)* and *(d)* for reservoir at 98% of embankment height. 7.83

Figure 7.36: Case 11 – "wet" placed clay core without collapse compression; numerical results of *(a)* vertical and *(b)* lateral displacement on first filling. 7.84

Figure 7.37: Regional division of the embankment for analysis of post construction surface deformation. 7.85

Figure 7.38: Lateral displacement of the crest (centre or downstream region) on first filling versus embankment height (displacement is after the end of embankment construction). 7.88

Figure 7.39: Lateral displacement of the downstream slope (mid to upper region) on first filling versus embankment height (displacement is after the end of embankment construction). 7.95

Figure 7.40: Lateral displacement at the upper upstream slope of upstream crest region on first filling versus embankment height (displacement after the end of embankment construction). 7.97

Figure 7.41: Lateral displacement of the crest (centre to downstream region) on first filling versus downstream slope. 7.98

Figure 7.42: Lateral displacement of the downstream slope (mid to upper region) on first filling versus downstream slope. 7.98

Figure 7.43: Post construction internal settlement of the core at Talbingo dam (IVM ES1 at the main section). 7.101

Figure 7.44: Post construction internal settlement of the core at Copeton dam (IVM B, 9 m downstream of dam axis at main section). 7.101

Figure 7.45: Post construction internal settlement of the core at Bellfield dam. 7.102

Figure 7.46: Post construction crest settlement at 3 years after end of construction, *(a)* all data, *(b)* data excluding Ataturk. 7.105

Figure 7.47: Post construction crest settlement at 10 years after end of construction. 7.105

Figure 7.48: Post construction crest settlement at 20 to 25 years after end of construction. 7.106

Figure 7.49: Post construction settlement of the downstream slope (mid to upper region) at 3 years after end of construction. 7.107

Figure 7.50: Post construction settlement of the downstream slope (mid to upper region) at 10 years after end of construction. 7.107

Figure 7.51: Post construction settlement of the upper upstream slope and upstream crest region at 3 years after end of construction. 7.108

Figure 7.52: Post construction settlement of the upper upstream slope and upstream crest region at 10 years after end of construction. 7.108

Figure 7.53: Crest settlement versus time for zoned embankments with thin to medium width central core zones of dry placed clayey earthfills; *(a)* all data, *(b)* data excluding Ataturk. 7.113

Figure 7.54: Crest settlement versus time for zoned embankments with thin to medium width central core zones of wet placed clayey earthfills. 7.114

Figure 7.55: Crest settlement versus time for zoned embankments with thin to medium width central core zones of dry placed clayey sand to clayey gravel (SC to GC) earthfills. 7.114

Figure 7.56: Crest settlement versus time for zoned embankments with thin to medium width central core zones of wet placed clayey sand to clayey gravel (SC to GC) earthfills. 7.115

Figure 7.57: Crest settlement versus time for zoned embankments with thin to medium width central core zones of silty sand to silty gravel (SM to GM) earthfills..... 7.116

Figure 7.58: Crest settlement versus time for zoned embankments with central core zones of clayey earthfills of thick width (1 to 2.5H to 1V combined width). 7.116

Figure 7.59: Crest settlement versus time for zoned embankments with central core zones of silty to clayey gravel and sand (SC, GC, SM, GM) earthfills of thick width (1 to 2.5H to 1V combined width). 7.117

Figure 7.60: Crest settlement versus time for embankments with very broad core widths (> 2.5H to 1V combined width) and limited foundation influence. 7.118

Figure 7.61: Crest settlement versus time for embankments with very broad core widths (> 2.5H to 1V combined width) and potentially significant foundation influence. 7.118

Figure 7.62: Long-term post construction crest settlement rate for zoned earthfill and earth-rockfill embankments of thin to thick core widths, *(a)* all data, and *(b)* data excluding Ataturk. 7.120

Figure 7.63: Long-term post construction crest settlement rate for embankments of very broad core width, (a) all data, and (b) data excluding Belle Fourche, Roxo and Rector Creek. 7.121

Figure 7.64: Crest settlement versus time for central core earth and rockfill embankments with central core zones of clayey earthfills and steady post first filling reservoir operation. 7.127

Figure 7.65: Crest settlement versus time for central core earth and rockfill embankments with thin to thick central core zones of clayey earthfills subjected to seasonal reservoir fluctuation. 7.127

Figure 7.66: Post construction settlement and reservoir operation at Enders dam (data courtesy of USBR). 7.131

Figure 7.67: Post construction settlement at main section and reservoir operation at San Luis dam (data courtesy of USBR). 7.132

Figure 7.68: Crest displacement versus time for zoned embankments with thin to medium width central core zones of dry placed clayey earthfills. 7.133

Figure 7.69: Crest displacement versus time for zoned embankments with thin to medium width central core zones of wet placed clayey earthfills..... 7.134

Figure 7.70: Crest displacement versus time for zoned embankments with thin to medium width central core zones of dry placed clayey sand and clayey gravel (SC/GC) earthfills. 7.134

Figure 7.71: Crest displacement versus time for zoned embankments with thin to medium width central core zones of wet placed clayey sand and clayey gravel (SC/GC) earthfills. 7.135

Figure 7.72: Crest displacement versus time for zoned embankments with thin to medium width central core zones of silty sand and silty gravel (SM/GM) earthfills..... 7.135

Figure 7.73: Crest displacement versus time for zoned embankments with central core zones of clayey earthfills of thick width (1 to 2.5H to 1V combined width). 7.136

Figure 7.74: Crest displacement versus time for zoned embankments with central core zones of silty to clayey sand and gravel earthfills of thick width. 7.136

Figure 7.75: Crest displacement versus time for embankments with very broad core zones (> 2.5H to 1V width) and with limited foundation influence..... 7.137

Figure 7.76: Crest displacement versus time for embankments with very broad core zones (> 2.5H to 1V width) and with potentially significant foundation influence on the embankment deformation. 7.137

Figure 7.77: Crest displacement normal to dam axis post first filling..... 7.139

Figure 7.78: Long-term settlement rates for the downstream slope (mid to upper region) versus embankment height; *(a)* all data, and *(b)* data excluding Belle Fourche..... 7.143

Figure 7.79: Post construction settlement of the downstream shoulder (mid to upper region) for selected case studies..... 7.144

Figure 7.80: Post construction displacement of the downstream shoulder (mid to upper region) for selected case studies of embankments with very broad core widths. 7.145

Figure 7.81: Post construction displacement of the downstream shoulder (mid to upper region) for selected case studies of central core earth and rockfill embankments..... 7.147

Figure 7.82: Post construction displacement of the downstream shoulder (mid to upper region) for embankments with compacted earthfills and gravels in the downstream shoulder. 7.148

Figure 7.83: Long-term settlement rates of the upper upstream slope to upstream crest region of earthfill and earth-rockfill embankments. 7.152

Figure 7.84: Post construction settlement of the upper upstream slope to upstream crest region for embankments with poorly compacted rockfill in the upstream slope. 7.153

Figure 7.85: Post construction settlement of the upper upstream slope to upstream crest region for selected case studies (excluding poorly compacted rockfills)... 7.153

Figure 7.86: Post construction lateral displacement of the upper upstream slope and upstream crest region for selected case studies of embankments with rockfill in the upstream shoulder..... 7.156

Figure 7.87: Post construction lateral displacement of the upper upstream slope to upstream crest region for selected case studies of embankment with earthfills and gravels in the upstream shoulder..... 7.157

Figure 7.88: Selset Dam internal settlements during construction (data from Bishop and Vaughan 1962)..... 7.159

Figure 7.89: "Idealised" model of collapse compression of poorly compacted shoulder fill of puddle core earthfill dam on first filling..... 7.164

Figure 7.90: "Idealised" model of yielding of poorly compacted shoulder fill and puddle core on first drawdown of a puddle core earthfill dam. 7.164

Figure 7.91: "Idealised" model of collapse compression on wetting of poorly compacted earthfill in the downstream shoulder of a puddle core earthfill dam. 7.165

Figure 7.92: Post construction crest settlement versus log time of puddle core earthfill dams..... 7.167

Figure 7.93: Definitions of "steady state" conditions during normal reservoir operating conditions..... 7.172

Figure 7.94: Fluctuation of pore water pressures adjacent to and upstream of the puddle core with fluctuations in reservoir level..... 7.174

Figure 7.95: Ramsden Dam, internal horizontal deformation of the puddle core, 1988 to 1990 (Holton 1992)..... 7.176

Figure 7.96: Ramsden Dam, internal vertical strains measured in the puddle core from 1988 to 1990 (data from Tedd et al 1997b and Kovacevic et al 1997)..... 7.177

Figure 7.97: Vertical strain (or settlement) at the crest versus drawdown depth for specific drawdown and refilling cycles (Tedd et al 1997b)..... 7.179

Figure 7.98: Permanent vertical crest strains during cyclic drawdown (in normal operating range) for puddle core dams with permeable upstream filling (after Tedd et al 1997b). 7.179

Figure 7.99: Ramsden Dam, settlement of SMPs versus time from 1988 to 1990 (data from Tedd et al 1990)..... 7.180

Figure 7.100: Ogden Dam, crest settlement versus time (Tedd et al 1997a)..... 7.181

Figure 7.101: Idealised model of deformation during historically large drawdown.. 7.182

Figure 7.102: Walshaw Dean (Lower) dam, crest settlement versus time (Tedd et al 1997a)..... 7.183

Figure 7.103: Cross section through Beliche dam at the main section (Maranha das Neves et al 1994) 7.189
Figure 7.104: Cross section of Chicoasen dam at the main section (Moreno and Alberro 1982) 7.189
Figure 7.105: Section at Hirakud dam (Rao and Wadhwa 1958) 7.192
Figure 7.106: Cumulative settlement during construction at Hirakud dam (adapted from Rao 1957) 7.192
Figure 7.107: Cross section of Nurek dam (adapted from Borovoi et al 1982) 7.193
Figure 7.108: Carsington dam, section at chainage 825 m after failure (adapted from Skempton and Vaughan 1993). 7.194
Figure 7.109: Carsington dam, vertical strain profiles from IVM during construction, *(a)* IVM C at chainage 850 m, and *(b)* IVM B at chainage 705 m (adapted from Rowe 1991) 7.195
Figure 7.110: Carsington dam, variation of the maximum vertical strain in the core with bank level (Rowe 1991). 7.195
Figure 7.111: Maximum section at El Infiernillo dam (Marsal and Ramirez de Arellano 1967). 7.203
Figure 7.112: El Infiernillo dam, deformation instrumentation on station 0+135 at the lower left abutment (Marsal and Ramirez de Arellano 1967). 7.204
Figure 7.113: El Infiernillo dam, internal settlements during first filling at Station 0+135 ..... 7.205
Figure 7.114: Main section at Chicoasen dam (Moreno and Alberro 1982) 7.206
Figure 7.115: Chicoasen dam, inclinometer and cross-arm locations at the main section (Moreno and Alberro 1982). 7.206
Figure 7.116: Internal settlement profiles during first filling at Chicoasen dam (adapted from Moreno and Alberro 1982). 7.207
Figure 7.117: Beliche Dam, cross section (Maranha das Neves et al 1994) 7.209
Figure 7.118: Beliche dam, post construction internal vertical settlement profile within the embankment for the period from end of construction to 2.75 years post construction. 7.209
Figure 7.119: Typical section of Canales dam (Bravo 1979). 7.210
Figure 7.120: Canales dam, *(a)* cracking and differential settlement at the crest, and *(b)* post construction settlement at the crest (Giron 1997) 7.211
Figure 7.121: Main section at Djatiluhur dam (Sowers et al 1993) 7.212
Figure 7.122: Djatiluhur dam; *(a)* location of crack observed during construction, January 1965; and *(b)* deformation of monuments at elevation 103 m, January to April 1965 (Sherard 1973). 7.214

Figure 7.123: Eppalock dam, post construction settlement of SMPs on the crest and slopes for the first five years after construction. 7.215

Figure 7.124: Main section at Blowering dam (courtesy of NSW Department of Public Works and Services, Dams and Civil Section). 7.218

Figure 7.125: Blowering dam, vertical strain during construction for selected cross-arms intervals in the core. 7.220

Figure 7.126: Blowering dam, post construction internal settlement of the core from IVM A during first filling. 7.221

Figure 7.127: Cross section of Ataturk dam (Cetin et al 2000) 7.221

Figure 7.128: Post construction settlement of the crest and downstream shoulder at Ataturk dam. 7.223

Figure 7.129: LG-2 dam; crack in crest and possible shear plane in core (Paré 1984) 7.224

Figure 7.130: Main section at Copeton dam (courtesy of New South Wales Department of Land and Water Conservation) 7.225

Figure 7.131: Copeton dam, post construction internal settlement profile in the core at IVM A. 7.227

Figure 7.132: Copeton dam, post construction settlement between cross-arms versus time. 7.228

Figure 7.133: Eppalock dam, original design at maximum section (Woodward Clyde 1999) 7.230

Figure 7.134: Eppalock dam, post construction settlement at main section and CS1. ..... 7.231

Figure 7.135: Eppalock dam, post construction horizontal displacement at the main section. 7.233

Figure 7.136: Djatiluhur dam, post construction crest settlement. 7.234

Figure 7.137: Bellfield dam, main section at chainage 701 m (courtesy of Wimmera Mallee Water) 7.235

Figure 7.138: El Infiernillo dam, internal *(a)* settlement and *(b)* displacement in the core from 1966 to 1972 (Marsal and Ramirez de Arellano 1972) 7.236

Figure 7.139: El Infiernillo dam, post construction *(a)* settlement and *(b)* displacement of surface markers. 7.237

Figure 7.140: Main section at Eildon dam (courtesy of Goulburn Murray Water). .. 7.239

Figure 7.141: Eildon dam, post construction settlement of SMPs at chainage 685 m. 7.240

Figure 7.142: Eildon dam, internal settlement profiles in core from IVM records for the period 1981 to 1998. ..... 7.240

Figure 7.143: Main section at Svartevann dam (Kjœrnsli et al 1982). 7.243
Figure 7.144: Svartevann dam, post construction *(a)* settlement and *(b)* displacement. 7.246
Figure 7.145: Cross section at Cougar dam (Cooke and Strassburger 1988). 7.247
Figure 7.146: Cougar dam; post construction *(a)* settlement and *(b)* displacement normal to dam axis of the crest at the maximum section (adapted from Pope 1967). 7.248
Figure 7.147: Cougar dam; differential settlement and cracks on crest (Pope 1967) 7.249
Figure 7.148: Wyangala dam, post construction internal settlement in IVM B located 9 m upstream of dam axis. 7.250
Figure 7.149: Section at Wyangala dam (courtesy of New South Wales Department of Land and Water Conservation). 7.251
Figure 7.150: Rector Creek dam main section (Sherard 1953)..... 7.254
Figure 7.151: Rector Creek dam; post construction settlement and displacement versus log time (adapted from Sherard et al 1963). 7.254
Figure 7.152: Roxo dam, settlement versus log time (adapted from De Melo and Direito 1982). 7.255
Figure 7.153: Main section at Mita Hills dam (Legge 1970)..... 7.256
Figure 7.154: Main section at Dixon Canyon dam (courtesy of U.S. Bureau of Reclamation). 7.258
Figure 7.155: Post construction *(a)* settlement and *(b)* displacement of SMPs on the upper upstream slope at the Horsetooth Reservoir embankments. 7.259
Figure 7.156: Belle Fourche dam; main section as constructed in 1911 (courtesy of U.S. Bureau of Reclamation). 7.260
Figure 7.157: Belle Fourche dam; post construction crest settlement over the period 1911 to 1928 (to 17 years post construction). 7.264
Figure 7.158: Belle Fourche dam closure section; post construction *(a)* settlement and *(b)* displacement normal to dam axis of the crest and slopes over the period 1985 to 2000 (73 to 89 years post construction). 7.265
Figure 7.159: San Luis dam, section of the slide in the upstream slope in 1981 at Station 135+00 (courtesy of United States Bureau of Reclamation). 7.266
Figure 7.160: San Luis dam, difference between actual and predicted settlement (Von Thun 1988)..... 7.268
Figure 7.161: San Luis dam, comparison of settlement between SMPs at 13 m upstream of dam axis and SMPs at 6.5 m downstream. 7.268
Figure 7.162: San Luis dam, post construction settlement of SMPs in the vicinity of the slide area. 7.269

Figure 7.163: Main section at Horsetooth dam (courtesy of the United States Bureau of Reclamation). 7.271

Figure 7.164: Horsetooth dam, post construction displacement of SMPs near to the main section. 7.272

Figure 7.165: Pueblo dam; cross section of left abutment embankment at Station 75 ..... 7.273

Figure 7.166: Pueblo dam, post construction settlement of the left embankment near Station 75. ..... 7.274

Figure 7.167: Yan Yean dam; settlement rate versus time of SMPs at Chainage 150 and 750 m. 7.279

7.0 THE DEFORMATION BEHAVIOUR OF EMBANKMENT DAMS

7.1 INTRODUCTION TO THIS CHAPTER

Failures by slope instability constitute about 6% of failures and 37% of incidents of embankment dams (Foster 1999). A number of these incidents were prevented from becoming failures by early detection of the impending failure from visual inspection or from deformation monitoring, and remedial action is taken by lowering the reservoir and/or construction of stabilization works.

Those who are responsible for interpreting the monitoring data do not have clear criteria to assess their data and have to rely on their judgement and personal experience. Currently available numerical modelling packages and the sophistication of the constitutive models on which they are based are improving making for useful tools in modelling embankment dam behaviour. However, few reported Type A predictions have been able to accurately model the deformation behaviour during construction and on first filling. Methods based on comparison to historical records of similar embankments are still heavily relied upon and, particularly for the assessment of post construction deformation behaviour, provide the responsible personnel with the best guide to assessment of embankment performance.

Overall, the purpose of the presented data is, from a broad database of well-instrumented earth and earth-rockfill embankments, to provide dam owners and their consultants with methods that:

- Allow comparison of their structures to similar embankment types in terms of the deformation behaviour during construction, on first filling and post first filling.
- Broadly define “normal” deformation behaviour and from this platform to then identify potentially “abnormal” deformation behaviour, either in terms of magnitude, rate or trend.
- Provide some guidance on the trends in deformation behaviour that are potentially indicative of a marginally stable to unstable slope condition, and precursors to slope instability.

The embankment types considered in this chapter include earthfill, zoned earthfill, zoned earth and rockfill (mainly central core earth and rockfill) and puddle core earthfill

embankments. A brief summary of the literature related to slope instability statistics and prediction of deformation behaviour is presented in Section 7.2. The database of case studies is summarised in Section 7.3. Sections 7.4 to 7.7 present the general deformation behaviour for the embankment types considered, and Sections 7.8 to 7.12 the methods for identification of "abnormal" deformation behaviour with reference to case studies.

Section 7.13 presents a summary of the methods of identification of "abnormal" deformation behaviour and highlights important aspects evident from the case study analysis. Guidelines are also presented on trends in the deformation behaviour that are potentially indicative of a marginal stability condition. Section 7.14 presents a summary of the outcomes from the analysis for use in prediction of, or comparison of the deformation behaviour of an embankment during and post construction.

7.2 LITERATURE REVIEW

7.2.1 FAILURE AND ACCIDENT STATISTICS

This review of slope instability incidents in embankment dams is a summary of that presented in Section 5.2.1 of Chapter 5 as part of the post-failure deformation analysis of instability incidents in embankment dams. Most of the data and findings on slope stability incidents is a summary of the work by Foster (1999) and Foster et al (2000) on dam failure and accident incidents, derived from a database of some 11192 large embankment dams from around the world constructed up to 1986.

Foster (1999) reported 124 incidents of slope instability. Of these, 12 were failures that involved a breach and uncontrolled release of water from the reservoir and the remaining 112 were accidents (no breach). They concluded that the major factors influencing the likelihood of slope instability in embankment dams were:

- Slope instability is more likely in earthfill embankments than earth and rockfill embankments. Homogeneous dam embankments (without filters) and hydraulic fill dam embankments are statistically the most susceptible to slope instability.
- Slope instability is more likely for dam embankments on soil foundations than for dam embankments on rock foundations. Of the slides passing through the embankment and foundation, the incidence of slope instability is much greater in foundations of high plasticity clays.

- Slope instability is much more likely in dam embankments constructed of high plasticity clays and silts, particularly for slides in the downstream slope. Dam embankments constructed of sands and gravels have a significantly lower incidence of slope instability.
- Compaction, or lack there of, of the earthfill materials is also a significant factor. The incidence of slope instability is much more likely for earthfills constructed by placement with no formal compaction, and the least likely for rolled, well compacted earthfills.

Further analysis as part of this research project (refer Section 5.2.1) found that:

- Earthfill embankments (homogeneous earthfill, earthfill with filters and earthfill with rock toe) made up a very high percentage (80%) of the slope stability incidents that passed through the embankment only.
- For embankments that incorporate rockfill zones, it is very to extremely unlikely that the surface of rupture will pass through the rockfill zone itself, it will preferentially pass through the foundation.

7.2.2 HISTORICAL DEVELOPMENT OF EMBANKMENT DAMS AS THIS AFFECTS DEFORMATION BEHAVIOUR

7.2.2.1 Earth and Earth-Rockfill Dams

An historical summary of the use of rockfill in embankment design and construction (Galloway 1939; Cooke 1984; Cooke 1993) is given in Table 6.2 in Section 6.3.1 (of Chapter 6).

For earthfills, the significant changes affecting deformation behaviour were developments in placement methods. The use of rollers from about the 1850's was significant, although their usage was more widespread from about the late 1890's into the early 20th century. But, the most significant development was after the 1930's with the application of soil mechanics principles (Wilson and Squier 1969; Penman 1986) and consideration of moisture content control, compacted layer thickness and level of compaction. Consideration of these principles was evident in embankment construction earlier in the 20th century (Schuyler 1912), such as at Belle Fourche dam in California.

7.2.2.2 Puddle Core Earthfill Dams

Skempton (1990) referred to the puddle core earthfill dam as the preferred method of dam construction in the United Kingdom (UK) in the 19th and first half of the 20th century. It was also the preferred method of construction in India and Australia up to the 1930's.

The significant historical events in the design and construction of puddle dams in the UK (Skempton 1990; Foster 1999) are summarised as follows:

- The first puddle dams were constructed in the late 18th century.
- Puddle Core - improvements in preparation procedures resulting in greater uniformity of the core material
  - Late 18th century to mid 19th century the puddle core was watered on the embankment, allowed to soak and then heeled (by foot) or rammed (using hand held rammers) in 150 to 200 mm layers.
  - In the second half of the 19th century the clays for core material were generally wetted up in the borrow area before being brought onto the embankment.
  - 20th century, preparation of core materials in pugmills and placement in 100 to 150 mm layers.
- Shoulder Fill - significant improvements in design and method of placement
  - Initially, no zoning in shoulder fill and no formal compaction. Compaction was typically using loaded wagons and carts in relatively thick layers (generally less than 1 m but up to 1.5 - 2 m).
  - From the 1850's/60's, following the failures of Bilberry Dam in 1852 (by internal erosion) and Dale Dyke in 1864 (by a combination of internal erosion and over-topping), embankment designs generally included a select zone of the more cohesive earthfills adjacent to the core.
  - From the 1900's improved compaction of shoulder fill using thinner layers and steam driven rollers.
  - From the 1940's further improvements in compaction procedures following improvements in earth-moving plant and the application of soil mechanics.
- The use of rolled clay cores took over from puddle clay cores in the UK in the 1960's.

In Australia and India the use of rolled clay cores took over from puddle clay cores in the 1930's. The last large puddle dam constructed in Australia was in the 1930's. Improvements in the preparation of puddle cores and alteration in design and placement methods of the shoulder fill occurred in Australia at relatively similar time periods to those in the UK. There is evidence of the use of horse or bullock drawn sheepsfoot rollers (up to 3.5 tonne dead-weight) for compaction of the shoulders and bullocks for compaction of the puddle core in Australia from the 1870's.

7.2.3 FACTORS AFFECTING THE DEFORMATION OF EMBANKMENT DAMS

7.2.3.1 Deformation Properties of Rockfill

An assessment of the factors affecting the compressibility of rockfill is presented in Section 6.3.2 of Chapter 6. In summary, field observations (Mori and Pinto 1988; and others) and the results of large scale laboratory tests (Marsal 1973; Marachi et al 1969; and others) indicate the compressibility properties of rockfill are affected by:

- Degree of compaction of the rockfill;
- Applied stress conditions and stress path;
- Particle shape and particle size distribution; and
- Intact strength of the rock used as rockfill.

An important aspect in the evaluation of the deformation behaviour of rockfill in embankment dams is its susceptibility to collapse compression on wetting. This is discussed in Sections 7.5.2 and 7.10.1.

The time dependent or creep type deformation of rockfill is an important aspect for evaluation of the post construction deformation behaviour in embankment dams. Guidelines based on case study analysis of field records of concrete face rockfill dams are given in Sections 6.4.4 and 6.5.3.

7.2.3.2 Deformation Properties of Earthfill

The general features of the stress-strain relationship of soils are well described in textbooks on soil mechanics and are applicable to describe the deformation behaviour of rolled earthfills. Factors such as the degree of over-consolidation, permeability, soil structure, matric suction and the rate, magnitude and direction of loading affect the

strength and compressibility properties of an earthfill. Some of these factors are affected by:

- The soil type, including its mineralogy, gradation and plasticity;
- The degree of compaction; and
- The moisture content at placement relative to Standard optimum.

Gould (1953,1954) found that a reasonable prediction of the drained compressibility of a well compacted, rolled earthfill could be estimated from its classification and plasticity of the fines fraction. For more plastic soil types, he found that the moisture content relative to the Standard Proctor optimum influenced the shape and magnitude of the compressibility curve. Most of Gould's data was of earthfills placed on the dry side of Standard Proctor optimum.

The compacted earthfill is a partially saturated soil with an amount of over-consolidation that is related to the compactive effort of the roller and the pore water suction. The pore water suction is dependent on the moisture content at placement, the degree of saturation of the compacted earthfill and the material type. For a dry placed, well-compacted earthfill, the amount of settlement increases with the increase in effective stress as the embankment is constructed. The settlement occurs due to compression of pore air in the partially saturated soil and is a relatively rapid process, as demonstrated by the fact that most of the earthfill's settlement occurs during construction. As the pore air is compressed the degree of saturation increases and pore water suction decreases. At some point, positive pore water pressures may be developed. Laboratory data presented by Fredlund and Rahardjo (1993) and Holtz and Kovacs (1981) indicate that the value of the pore water pressure parameter, *B*, is low for degree of saturation up to 85 to 90% and possibly higher.

In compacted earthfills placed close to or wet of Standard optimum moisture content, the degree of saturation is relatively high at compaction (generally greater than 85 to 90%) and the matric suction relatively low compared with dry placed earthfills. Positive pore water pressures are generally developed at low levels of confining stress and the pore water pressure parameter, *B*, approaches high values, from about 0.6 to almost 1.0. Assuming the earthfill to be of low permeability, conditions during conditions will be close to undrained. For these earthfill types deformations largely occur as plastic type deformations due to yielding in undrained loading.

On filling, seepage through the earthfill begins. It may take many years to reach a steady seepage condition, depending on the permeability of the partially saturated and/or saturated earthfill (refer Section 7.6.3, item f). As the degree of saturation of the partially saturated earthfill increases on saturation, deformations will occur. Deformations due to collapse compression on wetting can occur if the rolled earthfill is placed well dry of Standard optimum (even if heavily compacted) or dry placed and poorly compacted (refer Sections 7.5.2 and 7.13). In the long term, there will be a small time dependent creep component to the deformation behaviour. This is generally greater for poorly compacted soils than for well-compacted soils.

7.2.3.3 Summary of Research on Puddle Core Earthfill Dams

Building Research Establishment (BRE) and Imperial College have, since the 1980s, published the findings of research into the performance of puddle core earthfill dams. In the area of deformation behaviour the research has been mainly targeted at the long-term performance of these embankments more than 50 to 100 years after construction. Instrumentation installed in a number of puddle core embankments from about the late 1970's/early 1980's comprised monitoring of:

- Pore water pressures, horizontal stresses and internal deformations (both vertical and horizontal) in the puddle core and in some cases in the puddle clay cut-off.
- Pore water pressures in the downstream fill.
- Surface deformations of the crest, upper part of the upstream slope and downstream slope.

A set of puddle dams owned by Yorkshire Water, including Ramsden, Walshaw Dean Lower, Ogden and Holmestyes dams, have been reasonably well monitored and analysed by BRE and Imperial College in conjunction with the owners. Imperial College has undertaken finite element analysis of these and other puddle core earthfill embankments (Tedd et al 1997b; Dounias et al 1996; Kovacevic et al 1997).

Table 7.1 summarises the mechanisms identified by Tedd et al (1997a) affecting the long-term deformation behaviour of puddle core earthfill embankment dams. They comment that an understanding of the likely deformation behaviour due to processes not detrimental to dam safety allows for easier identification of deformations that may be indicative of a "hazardous" situation.

Tedd et al (1997a) defined the factors affecting the magnitude and/or direction of "normal" long-term deformation behaviour of puddle core earthfill dams as:

- The age of the dam;
- The height of the dam;
- The position of the element controlling the phreatic surface within the dam. For most puddle dams the central puddle core itself is the element controlling the phreatic surface within the dam, but there are several embankments where an upstream lining is the controlling element (e.g. Holmestyes Dam).
- The compressibility properties of the various embankment zones and foundation;
- The permeability of the earthfill/s in the upstream shoulder; and
- The reservoir operation, in particular the past history of operation, the reservoir level at the time of measurement and the duration and depth of drawdown.

Table 7.1: Mechanisms affecting the long-term deformation behaviour of old puddle core earthfill embankments (Tedd et al 1997a).

Mechanisms Causing "Normal" Deformation Behaviour	**Deleterious Mechanisms / Processes**
Shrink-swell related deformations due to seasonal fluctuations in moisture content. Secondary consolidation of the core and creep of the shoulder fill under "steady state" conditions. Deformations due to stress changes associated with the fluctuation in reservoir level during normal operation. Consolidation of the foundation.	Slope instability Internal erosion processes

The case study data and some of the findings from the published literature by BRE and Imperial College relating to the deformation behaviour of puddle core earthfill dams is included with the analysis and discussion in this chapter (refer Sections 7.7, 7.12, 7.13 and 7.14.4). Some of the findings of the research by BRE, other than from the monitored field deformation behaviour, are:

- Laboratory oedometer tests on samples of the core and upstream fill (Holton 1992; Tedd et al 1994; Tedd et al 1997b) showed:
  - Measured $c_{a,}$ coefficient of secondary compression, were in the range 0.0001 to 0.0032. The general trend was for c_a to increase with increasing effective vertical stress.

  - Non-linear stress-strain behaviour on repeated unloading and reloading on remoulded samples (at stress levels below the initially applied stress). The stress-strain behaviour followed hysteresis loops, with the constrained modulus value decreasing as the number of reload cycles increased, and each load cycle resulted in a non-recovered strain, the magnitude of which was dependent on the magnitude of the load.

- Where the shoulder fill has been sourced from weathered sedimentary deposits it is relatively permeable, although the permeability is quite variable (Tedd et al 1993). These fills generally comprised a mixture of silty and sandy clays with varying proportions of gravel to boulder size fragments of mudstone, siltstone and sandstone. Tedd and Holton (1987) report the permeability from constant head tests to vary from 2×10^{-5} m/s to 10^{-7} m/s in the downstream shoulder fill at Ramsden Dam. For Cwnwernderi Dam, Charles and Watt (1987) reported a relatively rapid response in horizontal earth pressure on reservoir filling indicating the upstream filling to be quite permeable.
- Charles and Watt (1987) found that the horizontal stresses in the core of puddle dams some 100 years post construction were relatively low, significantly lower than nominal stresses for a homogeneous type embankment, and Charles and Tedd (1991) comment that measured vertical stresses were not significantly greater than the horizontal stresses. These findings confirm the low stresses in the core present at the end of construction due to arching are still present some 100 years after construction.

7.2.4 PREDICTIVE METHODS OF DEFORMATION BEHAVIOUR

For embankment dams, the components of deformation are those that occur as a result of changes in effective stress conditions (during construction, on impoundment and due to reservoir fluctuation), changes in total stress (for wet placed earthfill cores in zoned embankments), on saturation or wetting (e.g. collapse compression) and the on-going time dependent or creep type deformations. Predictive methods are typically divided into the three components of deformation during construction, on first filling and long-term post construction (or post first filling).

Most predictive methods cover the deformation behaviour of one or two of these components. Finite element analyses have been used (Saboya and Byrne 1993;

Kovacevic 1994; Naylor et al 1997; Dounias et al 1996, amongst others) for analysis of deformation due to changes in stress conditions, mostly for deformation during construction and first filling, but also for deformation under large drawdown. Empirical predictive methods, usually based on historical performance of embankments, are more generally available for post construction deformation some of which incorporate the deformation on first filling, although methods are available for deformation during construction.

7.2.4.1 Empirical Predictive Methods

(a) Predictive Methods of Deformation During Construction

There are methods available for prediction of deformations during construction, but they are limited in number. Development of these methods has probably been curtailed by the availability of finite element methods in the last 30 to 40 years, their relative ease of use to model embankment construction and improvements in constitutive relationships to model the material compressibility and deformation behaviour. In addition, the complexity of stress and deformation behaviour during construction, particularly for zoned embankments, makes assessment by simple empirical methods difficult. Several of the methods developed are:

- Poulos et al (1972) developed charts for estimation of stresses and vertical and horizontal deformations during construction based on elastic solutions for a homogeneous embankment on a rigid foundation. The methods provide a quick and simple means of estimating deformations, which the authors comment are suitable as a preliminary estimate.
- Penman et al (1971) developed a method for estimation of the settlement during construction under the dam axis based on elastic solutions, but that allows for material stress-strain non-linearity by using an equivalent compressibility. It is based on the assumption of confined conditions (i.e. zero lateral strain) under the dam axis and is therefore suitable where this assumption is reasonable (e.g. homogeneous embankment).
- ICOLD (1993) derived a general equation for the vertical strain of rockfill in terms of vertical stress, rockfill modulus and creep strain parameters (Equation 7.1) based on the assumption of a linear relationship between stress and strain of coarse rockfill and non-linear relationship between strain and time. Derivations are given (refer

ICOLD 1993) for the settlement at a specific elevation and period of time after start of construction, settlement at end of construction and settlement post construction.

- Several other methods have been developed for prediction of the lateral deformation of the shoulder during construction, including:
  - Resendiz and Romo (1972) and Walker and Duncan (1984) for earthfill or essentially homogenous dams.
  - Penman (1986) provides guidelines for assessment of "acceptable" and "excessive" rates of horizontal displacement, mainly as guide for evaluation of a possible impending failure condition. It is based on a limited number of case studies of differing embankment type and should be used with caution.

$$e = \frac{s}{E_M} + s\,\frac{t}{q + l\,t} \tag{7.1}$$

where e = relative strain, s = vertical stress (in MPa), E_M = modulus of instantaneous strain of the rockfill (in MPa), t = time (in years), and q and l are the empirical parameters describing creep strain (in MPa/year and MPa respectively).

One of the major issues with deformation during construction relates to material compressibility properties under the imposed stresses from the stress path during construction. The stress path and stress conditions from field instrumentation (Charles 1976) and finite element analysis (Saboya and Byrne 1993; Kovacevic 1994; Charles 1976; and implicit in the analysis by others) are shown to vary depending on the embankment zoning geometry, material properties and location within the embankment. Hence, the dependency on finite element analyses to model the stress path, stress conditions and deformation behaviour in all but the simplest problems. The assumption of confined conditions under the central embankment region for homogeneous embankments or embankments with broad central zones is shown by field instrumentation and finite element analysis to be a reasonable assumption. For these conditions published data is available for estimation of material moduli of earthfills from Gould (1953, 1954).

Gould (1953, 1954) analysed the compressibility characteristics of rolled earthfill from the internal deformation records of some 22 rolled earthfill and earth-rockfill embankments. All case studies were USBR embankments and predominantly of embankments with thick to very broad and well compacted rolled earthfill cores. Gould

found that the classification of the earthfill and plasticity of the fines fraction provided a reasonable prediction of compressibility. For the more plastic soil types, he found moisture content relative to the Standard Proctor optimum influenced the shape and magnitude of the compressibility curve. Table 7.2 presents a summary of Gould's data (adapted from Sherard et al 1963).

Giudici et al (2000) and Pinto and Marques Filho (1998) provide methods for estimation of the rockfill moduli during construction from the deformation behaviour of concrete face rockfill dams. These methods are summarised in Section 6.3.3.2 of Chapter 6. What is considered an improved method for prediction of rockfill moduli is presented in Sections 6.4.2 and 6.5.1.

(b) Predictive Methods of Deformation Behaviour Post Construction

Empirical predictive methods of the post-construction deformation from the literature are typically based on historical deformation curves for similar embankment types or empirical relationships derived from historical deformation performance. Several of the methods incorporate the deformation during first filling whilst others only consider the prediction of deformation post first filling.

Table 7.2: Vertical compression of rolled, well-compacted earthfills measured during construction (adapted from Sherard et al 1963)

Embankment Soil Type	**Approximate Range of Measured Vertical Compression (%) *[1]**	
	At 10 psi (approx. 70 kPa) *[2]	At 100 psi (approx. 700 kPa) *[2]
Silty gravels and coarse silty sands (GM and SM).	0.2 to 0.3	0.9 to 1.4
Fine silty sands and silts of low plasticity (SM/ML).	0.2 to 0.5	1.2 to 2.1
Clayey sands and gravels (GC and SC).	0.3 to 0.8 *[3]	1.9 to 3.3
Clays of low to medium plasticity (CL and CL/ML).	0.2 to 1.1 *[3]	2.8 to 4.6 *[4]

*[1] vertical compression measured from internal settlement gauges within the embankment

*[2] pressures are vertical effective stresses

*[3] variation directly with placement moisture content relative to Standard Proctor optimum, low value for soils placed well dry of optimum and high value for soils placed wet of optimum (Gould 1954).

*[4] spread influenced by moisture content at placement and plasticity of the fines fraction (Gould 1954).

Table 7.3 provides a summary the range of post construction deformations of earthfill and earth and rockfill dams from the published literature. The data indicates that the

post construction settlements and displacements are generally relatively small for well-compacted earthfills and rockfills, and are much greater for embankments incorporating dumped rockfill.

Sowers et al (1965), Soydemir and Kjærnsli (1975), Clements (1984), Dascal (1987), ICOLD (1993) and Charles (1986), amongst others, have proposed predictive methods of post construction deformation behaviour. All have been derived from the historical performance of a database of embankments, in most cases from dams predominantly of rockfill (concrete or membrane face, and sloping and central core earth and rockfill dams). The method proposed by Charles (1986) is for puddle core earthfill embankments.

The methods by Clements (1984), Dascal (1987) and the data summarised in Table 7.3, provide a range or bounds of likely deformation behaviour, with Clements having the largest database of case studies. Both Dascal and Clements assume zero time is the time of the first deformation reading after construction. Clements (1984) suggested the bounds be used to provide an expected range of deformation, and for better prediction he suggested estimating from the deformation curves of dams with similar characteristics. Pinto and Marques Filho (1985) commented that these methods are useful, however, their application is not so straightforward as the deformation behaviour is strongly dependent on the initial time of measurement in relation to the end of construction. And, as pointed out by Parkin (1977), the shape of the deformation versus time curve will vary depending on the established zero time.

The other methods have developed empirical relationships for estimation of settlement and/or displacement. The methods by Sowers et al (1965) and Soydemir and Kjærnsli (1979), and comments by Parkin (1977) on strain rate analysis are summarised in Section 6.3.3.2 of Chapter 6. The Russian method referenced by ICOLD (1993) and Charles (1986) are summarised below. Most of the proposed equations are simple logarithmic or power type relationships based on one or two variables.

The Russian method for estimation of settlement (referenced in ICOLD (1993)), which is based on time after the end of construction, stress level and the creep strain empirical parameters, is quite complex in comparison to other proposed relationships. Equation 7.1 gives the basic form of the equation. ICOLD (1993) provides further details on this method.

Table 7.3: Published ranges of post construction deformation of embankment dams

Reference	Dam Type/s	Deformation Parameter	Range of Deformation (% of dam height) *[1]	Comments
ICOLD (1993)	"rockfill" *[2]	crest settlement	0.2 to 1.0%	Crest displacement up to 50% of the crest settlement.
		crest displacement	0.1 to 0.5%	
		shoulder settlement	0.1 to 0.2%	
Sowers et al (1965)	"rockfill" *[2]	crest settlement	0.25 to 1.0% (upper range for dumped RF)	14 dams, settlements up to 10 years after construction.
Clements (1984)	CFRD	crest settlement	Up to 2.5% (dumped RF) 0 to 0.25% (compacted RF)	Database of 68 dams.
		crest displacement	0 to 2.5%	
	CCER	crest settlement	0.05 to 1.25%	
		crest displacement	-0.75% to 0.5%	
	Sloping core	crest settlement	0.06 to 1.1%	
		crest displacement	0 to 0.6%	
Bernell (1958)	CCER with moraine core	crest settlement (during first filling)	0 to 0.2% (silty and sandy moraines) 0.05 to 0.3% (clayey moraines)	6 dams with moraine cores placed using the wet compaction method. Fine fractions less than 20%.
Dascal (1987)	"rockfill" dams (*2) with moraine cores	crest settlement	< 0.35% (compacted RF) 0.3 to 0.55% (dumped RF)	15 Hydro Quebec dams and dikes on rock foundations
		crest displacement	≥ crest settlement for compacted RF < crest settlement for dumped RF	
		downstream shoulder settlement	up to 0.7 to 0.8%	
Sherard et al (1963)	"rockfill" *[2]	crest settlement	0.1 to 0.4% (for well constructed wetted RF)	Greater settlement for dumped RF.
	well constructed dams	crest displacement on first filling	< 25 to 50 mm	Greater displacements for dams with dumped RF.
Gould (1954)	rolled earthfill dams	crest settlement	< 0.2% in first 3 years <0.4% up to 14 years	Typical range of settlement for USBR dams.

*[1] displacement is horizontal deformation, downstream displacement is positive and upstream is negative.

*[2] "rockfill" dams including membrane face rockfill dams, and central and sloping earth core rockfill dams

CFRD = concrete face rockfill dam CCER = central core earth and rockfill dam RF = rockfill USBR = United States Bureau of Reclamation

Charles (1986) proposed a settlement index, S_I, for assessment of the long-term crest settlement behaviour of puddle core earthfill embankments (Equation 7.2). Charles and Tedd (1991) point out that the settlement index is analogous to the coefficient of secondary consolidation for a clay soil. They provide values of the settlement index for a number of puddle core embankments during the period of normal reservoir operation. Tedd et al (1997b) suggest that values of settlement index *"greater than 0.02 could indicate some mechanism other than creep was causing the settlement and that the situation should be seriously examined"*.

$$S_I = \frac{s}{1000 \cdot H \cdot \log(t_2/t_1)} \tag{7.2}$$

where s is the crest settlement in millimetres measured between times t_2 and t_1 after the completion of embankment construction, and H is the height of the dam in metres. The equation is of the same form as that proposed by Sowers et al (1965).

7.2.4.2 *Numerical Methods*

Duncan (1996) and Kovacevic (1994) are recent references on the state of the art in finite element analyses applicable to the deformation behaviour of embankments, mainly zoned earth and rockfill dams. They discuss the methods of analysis, their limitations, available constitutive models of the stress-strain relationship and areas of uncertainty.

Duncan (1996) comments that the choice of stress-strain constitutive model used in the analysis is a balance between simplicity and accuracy, and that the choice of constitutive model will depend on the purpose of the modelling. He commented that if the purpose of the analysis is to analyse stresses and/or the trend of deformations then more simplistic models could be suitable, depending on the relative stiffness between different embankment materials. More accurate modelling of deformations requires a more complex stress-strain model that more realistically approximates the real behaviour of the rockfill and earthfill.

Aspects of finite element analysis (after Duncan (1996) and Kovacevic (1994)) as they relate to modelling rockfill are summarised in Section 6.3.3.1 of Chapter 6. Important aspects raised by Duncan (1996) and Kovacevic (1994) related to modelling in general and for earthfills more specifically are:

- The importance of modelling the construction as a series incremental layers
- The type of stress-strain relationship used for modelling materials. Duncan (1996) comments that elastic stress-strain models (e.g. linear elastic, multi-linear elastic or hyperbolic models) are appropriate where the soils are not stressed to failure, but, that these models are not suitable for modelling undrained behaviour or problems where local failure occurs. He recommends the use of models that incorporate plasticity theory for these situations (e.g. for wet placed earthfill cores of thin to medium width in zoned embankments).
- For situations where the earthfills are not stressed to failure, linear elastic models are generally not suitable for accurate modelling of deformation behaviour due to the non-linear stress-strain relationship of earthfill and rockfill. For these situations, the use hyperbolic or multi-linear elastic models provide improved predictions of deformation and have been successfully used, particularly for deformation prediction during embankment construction.
- A limitation of hyperbolic and multi-linear elastic models is that the model parameters are typically derived from triaxial compression or oedometer laboratory tests and are therefore limited by the narrow range of stress paths covered in comparison to the broader range of stress paths imposed in the field (Kovacevic 1994).

An important component of the modelling of embankment dams is the consideration of collapse compression of susceptible rockfills and earthfills on wetting. This is discussed further in Section 6.3.3.1 of Chapter 6.

The effect of pore water pressure dissipation in earthfills during construction has been considered by a number of authors including Eisenstein and Law (1977), in modelling Mica dam, and by Cavounidis and Höeg (1977), amongst others. For these cases, the incremental embankment construction was modelled as a two stage process, the first stage modelling the new layer construction using undrained properties for the core and the second stage modelling pore water pressure dissipation.

In most cases though, pore water pressure development in the core is ignored. For wet placed earthfills, where high pore water pressures are developed during construction, the core is often modelled using undrained strength and compressibility parameters, and the permeability is assumed as sufficiently low such that pore water pressures will not dissipate during the period of construction. For dry placed earthfills,

the earthfills are often modelled using elastic models (e.g. multi-linear elastic or hyperbolic elastic). In some cases, the earthfill is analysed in terms of effective stresses and using elasto-plastic models with pore water pressures input into the model; e.g. Naylor et al (1997) for the core of Beliche dam. In this case, the analysis was undertaken after the embankment had been constructed and actual pore water pressures were used to derive the input to the model.

7.3 DATABASE OF CASE STUDIES

The case study database comprises some 134 embankments; 63 central core earth and rockfill dams, 21 zoned earth and rockfill dams, 23 zoned earthfill dams, 10 earthfill dams and 17 puddle core earthfill embankments. A summary of the case studies in the database is presented in Table 7.4 to Table 7.8.

7.3.1 EARTHFILL AND ZONED EARTH AND EARTH-ROCKFILL EMBANKMENTS

The type of rolled earthfill and zoned earth and earth-rockfill embankments (Figure 1.6 in Section 1.3.3 of Chapter 1) in the case study database include:

- Central core earth and rockfill embankments (Table 7.4), this is the dominant embankment type;
- Zoned earth and rockfill embankments (Table 7.5);
- Zoned earthfill embankments (Table 7.6); and
- Earthfill embankments (Table 7.7), including homogeneous earthfill, earthfill with filters and earthfill with rock toe.

Embankments with unusual design or of design with limited numbers of case studies available from the literature were excluded. Sloping core zoned earth and rockfill embankments have not been considered.

Further details on most of the case studies are given in the tables in Section 1 of Appendix F, including a summary of the embankment details, material types and their method of placement, reservoir operation, hydrogeology, monitoring (during and post construction) and references for each dam. In most embankments the main earthfill zone acting as the water barrier has generally been placed in thin layers and well compacted using rollers suitable for the earthfill type.

Approximately half of the earthfill and zoned earth and earth-rockfill case studies are embankments owned or supervised by sponsors and in-kind sponsors of the research project. For most of these embankments the deformation records are of good quality. These case studies have been supplemented by case studies from the published literature for which the deformation records were of reasonably to good quality, and a reasonable level of detail was available on the embankment design, material types and construction methods.

7.3.2 PUDDLE CORE EARTHFILL EMBANKMENTS

A database of seventeen case studies of puddle core earthfill dams (3 from Australian and 14 from the UK) has been gathered for analysis of deformation behaviour (Table 7.8). Further details on the case studies are given in Section 1 of Appendix F, including a summary of the embankment details, reservoir operation, hydrogeology and monitoring for each dam.

Most of the available deformation records are from surface measurement points (SMP) established many years after construction, in the 1970's to 1980's for a number of the case studies. Some monitoring data and anecdotal information is available on the early performance of several embankments. Compared to the rolled earthfill and zoned earth and earth-rockfill embankment case studies, the monitoring records for the puddle core earthfill dam data set is fairly limited, but to be expected given the age of most of the dams.

7.4 GENERAL DEFORMATION BEHAVIOUR DURING CONSTRUCTION OF EARTHFILL AND ZONED EARTH AND EARTH-ROCKFILL EMBANKMENTS

For virtually all of the embankments considered the main earthfill zone/s have generally been placed in thin layers and well compacted in line with modern practice. In some of the older embankments the moisture content control of the earthfill was possibly not as stringent as it would have been with modern practice, but this has not necessarily been detrimental to the embankment performance.

Table 7.4: Central core earth and rockfill embankments in the database

Dam Name	Country *[1]	Height H (m)	Embankment Class[n]			Rockfill	
			Class[n]	Core Size	Core Type	Source	Compaction Rating
Agigawa	Japan	102	5,1,1	c-tm	CL	-	good (?)
Ajuare	Sweden	46	5,2,2	c-tn	SM	schists & gneisses	poor
Ataturk	Turkey	184	5,2,0	c-tm	CH	basalt & limestone	reasonable (?)
Bath County Upper Dam	USA, Virginia	134	5,2,0	c-tm	SC (?)	siltstone & sandstone	good (?)
Beliche	Portugal	55	5,2,2	c-tn	GC	schists & greywacke	poor (?)
Bellfield	Australia, Vic.	40	5,2,0	c-tm	CL/SC	sandstone	poor, dry placed
Bjelki-Peterson	Australia, Qld	41.5	5,2,1	c-tn	CL	phyllite	good
Blowering	Australia, NSW	112	5,2,0	c-tm	SC - CL	quartzite & phyllite	good
Chaffey	Australia, NSW	54	5,2,0	c-tm	CH/GC	jasper	reasonable to good
Cherry Valley	USA, San Francisco	100	5,2,0	c-tk	SM/ML	granite & granodiorite	dumped and sluiced
Chicoasen	Mexico	261	5,2,0	c-tn	GC	limestone	good
Copeton	Australia, NSW	113	5,2,0	c-tm	SC	granite	reasonable to good, dry placed
Corin	Australia, ACT	74	5,2,0	c-tm	SM	quartzite, sandstone & siltstone	good
Cougar	USA, Oregon	159	5,2,0	c-tn (u)	GM	basalt and andesite	good (downstream), reasonable (upstream)
Dalesice	Checkoslovakia	90	5,2,0	c-tn (u)	CL	-	good
Dartmouth	Australia, Vic.	180	5,2,0	c-tm	SC/SM	granitic gneiss	good, dry placed
Djatiluhur	Indonesia	105	5,2,0	c-tm (u)	CH	andesite	poor
Eildon	Australia, Vic.	79	5,1,0	c-tk	CL	quartzitic sandstone	poor, dry placed (?)
El Infiernillo	Mexico	148	5,2,0	c-tn	CL-CH	diorite & silicified conglomerate	poor to reasonable, dry placed
Eppalock	Australia, Vic.	47	5,2,0	c-tk	CL	basalt	poor, dry placed
Frauenau	Germany	80	5,2,0	c-tn	SM	-	-
Fukada	Japan	55.5	4,1,2	c-tm	GC (?)	sandstone & granite.	good (?)
Geehi	Australia, NSW	91	5,2,0	c-tn	SM	granitic gneiss	reasonable to good (inner), poor (outer)
Gepatsch	Austria	153	5,2,0	c-tn	GM/GC	gneiss	reasonable, dry placed
Glenbawn Saddle A	Australia, NSW	35	5,2,0	c-tm	-	limestone & sandstone	good (?)
Glenbawn - main dam (original, prior to raising)	Australia, NSW	76.5	5,1,0	c-tk	CL	limestone	poor, dry placed
Googong (before raising)	Australia, ACT	62	5,2,0	c-tm	SC	dacite & granite	good, dry placed
Kisenyama	Japan	88	5,2,0	c-tm	-	slate, chert & sandstone	good (?)
Kurokawa	Japan	98	5,2,0	c-tn (u)	-	-	good (?)
La Grande 2 (LG-2)	Canada, James Bay	160	5,2,0	c-tn (u)	SM	granite ?	reasonable to good, dry placed
Maroon	Australia, Qld	52	5,2,2	c-tk	SC/CL	porphery	reasonable to good
Matahina	New Zealand	85	5,1,0	c-tm	CL/ML	ignimbrite	poor, dry placed
Mud Mountain	USA, Washington	128	5,1,0	c-tm	SM/GM	andesite & tuff	dumped and sluiced
Naramata	Japan	158	5,1,0	c-tn	GM/GC	rhyolite & granite	good
Netzahualcoyotl	Mexico	132	5,2,0	c-tn	MH	conglomerate	poor to reasonable.
Nillahcootie	Australia, Vic.	35	5,2,0	c-tm	CL	sandstone & mudstone	poor (?)
Nottely	USA, Tennessee	56	5,1,1	c-tk	CL	quartzite & mica schist	dumped and sluiced
Parangana	Australia, Tas.	53	5,2,2	c-tm	SM	quartzite & schist	reasonable to good, dry placed
Peter Faust	Australia, Qld	51	5,2,0	c-tn	CL	hornfelsed andesite & andesitic tuff	reasonable to good
Round Butte	USA, Oregon	134	5,2,0	c-tn (u)	SM	basalt	reasonable to good, dry placed
Rowallan	Australia, Tas.	43	5,1,0	c-tn	GM	quartzite	reasonable to good, dry placed
Sagae	Japan	112	5,2,0	c-tn	-	-	good (?)
Seto	Japan	102	5,1,0	c-tn	-	-	good (?)
Shimokotori	Japan	119	5,1,0	c-tn	-	-	good (?)
Split Yard Creek	Australia, Qld.	76	5,2,1	c-tm	CL	brecciated quartzites & greenstone	reasonable
South Holson	USA, Tennessee	87	5,2,1	c-tk	CL	sandstone, some shale	dumped and sluiced
Srinagarind	Thailand	140	5,2,0	c-tn	GC/SC	limestone	good
Svartevann	Norway	129	5,2,0	c-tn (u)	GM	granitic gneiss	reasonable, dry placed
Taisetsu	Japan, Hokkaido	86.5	5,1,0	c-tn	-	-	good (?)
Talbingo	Australia, NSW	162	5,2,0	c-tm (u)	CL	rhyolite & porphyry	good
Tedorigawa	Japan, Honshu Island	153	5,2,0	c-tn	GM/GC	-	good (?)

Table 7.4: Central core earth and rockfill embankments in the database (continued)

Dam Name	Country *[1]	Height H (m)	Embankment Class[n]			Rockfill	
			Class[n]	Core Size	Core Type	Source	Compaction Rating
Terauchi	Japan, Fukuada	83	5,2,0	c-tm	SC/SM	lutaceous schist	good
Thomson	Australia, Vic.	166	5,2,0	c-tm	SC	sandstone & siltstone	good, dry placed
Tokachi	Japan, Hokkaido	84.3	5,1,0	c-tm	GC	keratophyre, 30% slate	good (?)
Upper Dam	Korea	88.5	5,2,0	c-tn	GC	tuff & rhyolite	poor (?)
Upper Yarra	Australia, Vic.	90	5,0,0	c-tk	CL	sandstone & siltstone	poor, dry placed
Vatnedalsvatn	Norway	121	5,2,0	c-tn	SM	quartz, granite & gneiss	reasonable, dry placed
Waipapa	New Zealand	36	5,1,1	c-tk	CH/SC	ignimbrite	poor
Watuaga	USA, Tennessee	94	5,2,1	c-tk	CL/SC	quartzite	dumped and sluiced
William Hovell	Australia, Vic.	34	5,2,0	c-tm	ML	rhyodacite	reasonable to good
Windemere	Australia, NSW	67	5,2,1	c-tm	CL	andesite	reasonable to good (inner), reasonable (outer)
Wivenhoe	Australia, Qld	59	5,2,1	c-tn	CL	sandstone	good
Wyangala	Australia, NSW	86	5,2,0	c-tm	SC-SM	porphyritic gneiss	reasonable to good (inner), reasonable (outer), dry placed

Note: Class[n] = classification

*[1] For Australian dams; Qld = Queensland, NSW = New South Wales, Vic. = Victoria Tas. = Tasmania, ACT = Australian Capital Territory

Table 7.5: Zoned earth and rockfill embankment case studies

Dam Name	Country *[1]	Height H (m)	Embankment Class[n]			Comment
			Class[n]	Core Size	Core Type	
Andong	Korea	83	4,1,1	c-tn	SM	Rockfill used in outer shoulders
Bradbury	USA, California	85	4,1,1	c-tk	SC/GC	Weathered shale in downstream shoulder
Burrendong	Australia, NSW	76	4,2,1	c-tk	CL	Rockfill in up and downstream shoulder, poorly compacted.
Canales	Spain	156	4,1,0	c-tn	CH	Limestone rockfill in up and downstream shoulder
Cardinia	Australia, Vic.	86	4,2,1	c-tm (u)	SC/CL	granodiorite in upstream shoulder
Dixon Canyon	USA, Colorado	74	4,1,0	c-vb	CL	thin outer rockfill zones. Virtually homogeneous.
Eucembene	Australia, NSW	116	4,1,0	c-vb	SC	Quartzite rockfill as thin outer zones.
Greenvale	Australia, Vic.	52	4,2,2	c-tk	SM	granodiorite rockfill in upstream shoulder
Jackson Gulch	USA, Colorado	56	4,0,1	c-tm (u)	CL	Broad GC earthfill zones up and downstream of the core, and thin outer rockfill shoulders
La Agnostura	Mexico	146	4,0,0	c-tn	CL	poor quality limestone used in up and downstream shoulders
La Grande - LG4	Canada	125	4,1,0	c-tm	SM	granite and gneiss used in up and downstream shoulders
Long Lake	USA	39	4,0,0	c-tk	CL/ML	Broad earthfill zones up and downstream of core and thin outer rockfill zones.
Nurek	Russia	289	4,2,0	c-tn	GC/GM	thin outer rockfill zone
Peublo (right abutment)	USA, Colorado	51	4,0,1	c-vb	CL	limited use of rockfill
Rector Creek	USA, California	61	4,0,0	c-vb	SC/SM	limited rockfill used, outer shoulders. Close to homogeneous classification.
San Justo	USA, California	41	4,2,2	c-tk	CL	limestone rockfill used upstream shoulder
San Luis - Main Dam	USA, California	116	4,2,1	c-vb	CL	limited rockfill used, outer shoulders
San Luis - Slide Area	USA, California	30 to 45	4,1,1	c-vb	CL	limited rockfill used, outer shoulders
Soyang	Korea	123	4,1,0	c-tm	GC	poor ly compacted rockfill used in outer shoulders
Spring Canyon	USA, Colorado	68	4,1,0	c-vb	CL	limited rockfill used, outer shoulders
Tooma	Australia, NSW	67	4,1,2	c-tk	SM	dumped and sluiced granite rockfill in upstream shoulder
Tullaroop	Australia, Vic.	41	4,1,0	c-tk	CL	limited rockfill used, at up and downstream toe regions. Could also classify as 2,1,0.

Note: Class[n] = classification

*[1] For Australian dams; NSW = New South Wales, Vic = Victoria

Table 7.6: Zoned earthfill embankment case studies

Dam Name	Country	Height H (m)	Embankment Class[n]			Comment
			Class[n]	Core Size	Core Type	
Benmore	New Zealand	110	3,2,1	c-tk	GM/GC	thick core with compacted gravel shoulders
Cairn Curran	Australia, Vic.	44	3,0,0	c-vb	CL/ML	embankment with very broad core
Carsington	England	36	3,0,1	c-tm	CH	wet placed core supported by shoulders of well-compacted weathered mudstones. Failed during construction.
Cobb	New Zealand	35	3,0,1	c-tk	GM/GP	thick core with gravel upstream shoulder and talus downstream shoulder
Davis	USA, Arizona	60	3,0,1	c-tm (u)	CL	upstream sloping medium width core supported by broad silty sand to silty gravel earthfill zones.
Deer Creek	USA, Utah	71	3,0,0	c-tk	CL-GC	central core of thick width with earthfill shoulders
Granby	USA, Colorado	88	3,0,0	c-vb	SC-GC	embankment with very broad core
Hirakud	India	59	3,0,1	c-vb	SC-GC	embankment with very broad core
Horsetooth	USA, Colorado	48	3,0,0	c-vb	CL	embankment with very broad core
Kastraki	Greece	95	3,1,0	c-tn	CL	thin clay core with well compacted gravel shoulders
Khancoban	Australia, NSW	18	3,0,2	c-vb	SM	embankment with very broad core, upstream gravel shoulder.
Kremasta	Greece	165	3,1,0	c-tn	CL	thin clay core with well compacted gravel shoulders
Mammoth Pool	USA, California	113	3,2,2	c-tk	SM	thick core with compacted earthfill shoulders
Medicine Creek	USA, Nebraska	48	3,0,0	c-vb	CL	embankment with very broad core
Meeks Cabin	USA, Wyoming	57.5	3,1,1	c-tk	CL	thick core with gravel shoulders
Navajo	USA, New Mexico	123	3,1,1	c-tk	CL	thick core with compacted gravel and earthfill shoulders
O'Sullivan	USA, Washington	64	3,1,0	c-tk	SM	central core of thick width with filter / transition zones up and downstream of the core
Pukaki	New Zealand	76	3,2,1	c-tk	GM	thick core with compacted gravel shoulders
Rosshaupten	Germany	41	3,1,1	c-tm	GM/ML	medium width core with compacted gravel shoulders
Ruataniwha	New Zealand	50	3,2,1	c-tk	GM	thick core with well compacted gravel shoulders
Soldier Canyon	USA, Colorado	70	3,0,0	c-vb	CL	embankment with very broad core
Steinaker	USA, Utah	49	3,0,0	c-vb	CL	embankment with very broad core
Trinity	USA, California	164	3,0,0	c-tk	SM/GM	thick core with gravel shoulders

Note: Class[n] = classification

*[1] For Australian dams; NSW = New South Wales, Vic = Victoria

Table 7.7: Earthfill embankment case studies

Name	Country	Height H (m)	Embankment Classification			Comment
			Dam Type	Class[n]	Core Type	
Belle Fourche	USA, South Dakota	35	Homogeneous Earthfill	0,0,0	CL-CH	concrete facing on upstream slope
Biet Netufa	Israel	11	Earthfill with rock toe	2,0,0	CH	
Bonny	USA, Colorado	44	Earthfill with foundation filter	1,0,1	ML-SM	Foundation filter under downstream shoulder
Enders	USA, Nebraska	31.5	Earthfill with thin rockfill shell	2,0,0	SM/ML	virtually a homogeneous embankment
Fresno	USA, Montana	24	Earthfill with rock toe	2,0,0	ML-CL	
Heart Butte	USA, North Dakota	42	Earthfill with rock/gravel toe	2,0,0	SC-SM	
Mita Hills	Africa, Zambia	49	Earthfill with filters	1,2,1	CL-ML (?)	upstream sloping dual chimney filter
Peublo (left abutment embankment)	USA, Colorado	37	Earthfill, rockfill toe	1,0,1 (or 3,0,1)	CL	thin downstream outer shoulder zone of gravels. Stability berm on downstream shoulder, placed 1981.
Roxo Dam	Portugal	34	Earthfill, rockfill toe	2,0,0	CL/SC	Part earthfill part concrete gravity & buttress dam.
Sasumua	Kenya	35	Earthfill with filters	1,2,0	MH	central chimney filter (dual filters) and large rockfill zones at up and downstream toe.

Table 7.8: Puddle core earthfill embankment case studies

Name	Country	Year Comp.	Height H (m)	Core Dimensions		Puddle Material		Select Zone Yes/No	General Earthfill
				Top Width (m)	Core Slope (H to V)	Source	Class[n]		
Burnhope	UK	1935	41	nk	nk	Boulder Clay	CL	Yes	hard mudstone - 450 mm layers, compacted by steam rollers
Challocombe	UK	1944	15	1.2	1 to 15	nk	ML	Yes	nk
Cwnwernderi	UK	1901	22	1.5	1 to 10	nk	CL	No ?	nk
Dean Head	UK	1840	19	nk	nk	nk	nk	nk	nk
Happy Valley	Aust.	1896	25	2.44	1 to 8.25	residual	CL	Yes	Residual clays (CL) - 150 mm layers compacted by wagons, carts and grooved rollers
Hollowell	UK	1937	13.1	2	1 to 10	Upper Lias blue clay	nk	Yes	Sand and sand-rock, placed in thin layers by dozer
Holmestyes	UK	1840	25	2	1 to 20	Boulder Clay	nk	No	Weathered mudstones & sandstones, mix sandy silty clay with gravel to boulder size fragments
Hope Valley	Aust.	1872	21	1.8	1 to 12	alluvial / fluvial	CH	Yes	alluvial / fluvial (downstream only), SC/SM, placed in 1200 mm layers compacted by 3.5t sheepsfoot roller
Ladybower	UK	1945	43	nk	nk	nk	nk	nk	nk
Langsett	UK	1904	33	nk	nk	nk	Clay	Yes	Not sure, possibly weathered shale, placed in 900 mm lifts and compacted by slewing of the rails
Ogden	UK	1858	25	2	1 to 10	Boulder Clay	CH	No	Weathered mudstones & sandstones, mix sandy silty clay with gravel to boulder size fragments
Ramsden	UK	1883	25	3	1 to 12	Boulder Clay	ML/MH	Yes	Weathered mudstones & sandstones, mix sandy silty clay with gravel to boulder size fragments
Selset	UK	1959	39	1.5	1 to 20	Boulder Clay	CL	Yes	Boulder Clay (CL) sandy clay, placed in 225 mm layers by dozers and 13.6 t rollers
Walshaw Dean	UK	1907	22	2.6	1 to 12	Boulder Clay	CL	No	Weathered mudstones & sandstones, mix sandy silty clay with gravel to boulder size fragments
Widdop	UK	1878	20	nk	nk	nk	nk	No	nk
Yan Yean	Aust.	1857	9.6	3.05	1 to 3.3	alluvium	CL/CH	No	alluvium, CL/CH clays upstream and ML/CL sandy silts and silty clays downstream, placed in 600 to 1200 mm lifts
Yateholme	UK	1872	17	nk	nk	Boulder Clay	CL	No	Weathered mudstones & sandstones, mix sandy silty clay with gravel to boulder size fragments

Note: Class[n] = classification Year Comp. = year of completion of construction
nk = not known
*[1] For Australian dams; NSW = New South Wales, Vic = Victoria

The deformation behaviour has been sub-grouped into deformation during construction (this section, Section 7.4) and deformation post construction (Sections 7.5 and 7.6). The deformation behaviour during first filling is discussed as a separate section (Section 7.5) but the plotted deformation behaviour has, in most cases, been incorporated into plots of the post construction deformation behaviour presented in Section 7.6.

The analysis of the deformation behaviour during construction of earthfill and earth-rockfill embankments is mostly concentrated on the central earthfill core zone of the embankment because this is where instruments are located. Most of the deformation data collected and analysed is vertical deformations, usually from internal vertical settlement gauges (IVM) installed in the core as construction proceeds. Data on

horizontal deformations, usually from internal horizontal movement gauges (IHM) or inclinometers, is less frequently monitored, but has been collected and analysed for a number of embankments.

Analysis of deformation requires consideration of the stress conditions imposed during construction and the stress-strain relationship of the materials used in embankment construction. In zoned embankment construction it is also important to consider both the total and effective stress conditions, and the interaction between the different material zones in the analysis. While finite element analysis can be used for individual dams, this was impracticable for this study due to the number of case studies analysed. Therefore, simplified approaches have been used with reference to finite difference or finite element analysis to indicate the generalised stress conditions and deformation behaviour.

7.4.1 STRESSES DURING CONSTRUCTION

7.4.1.1 Stresses in a Homogeneous Embankment on a Rigid Foundation

For the simplified case of a homogeneous embankment on a rigid foundation and assuming elastic behaviour, the vertical and lateral stresses within the embankment are dependent on the slope geometry, and the total unit weight and Poisson's ratio of the earthfill.

During the initial stages of embankment construction the embankment width is much greater than the height of earthfill. Under these conditions, assuming plane strain conditions along the dam axis, the stresses below the dam axis can be modelled assuming zero lateral strain normal to the dam axis (Figure 7.1a). The elastic stress-strain relationships for a soil element under the embankment axis following placement of an incremental layer of distributed load p kPa are approximated as:

$$e_x = e_y = 0$$

$$\Delta s_z = p; \qquad \Delta s_x = \Delta s_y = \frac{n\,\Delta s_z}{(1-n)}$$

constrained tangent modulus, $DD = \Delta s_z / \Delta e_z$

$$\text{Young's tangent modulus, } DE = \frac{DD\,(1+n)(1-2n)}{(1-n)}$$

where e = strain, s = stress, x, y and z are axis co-ordinates, n is Poisson's ratio and Δ represents the incremental or tangential component of the parameter.

Because of geometry effects, this approximation is not sufficiently accurate for estimating the change in stresses in a soil element low in the dam in the latter stages of construction where the layer width is small compared to the constructed embankment height (Figure 7.1b).

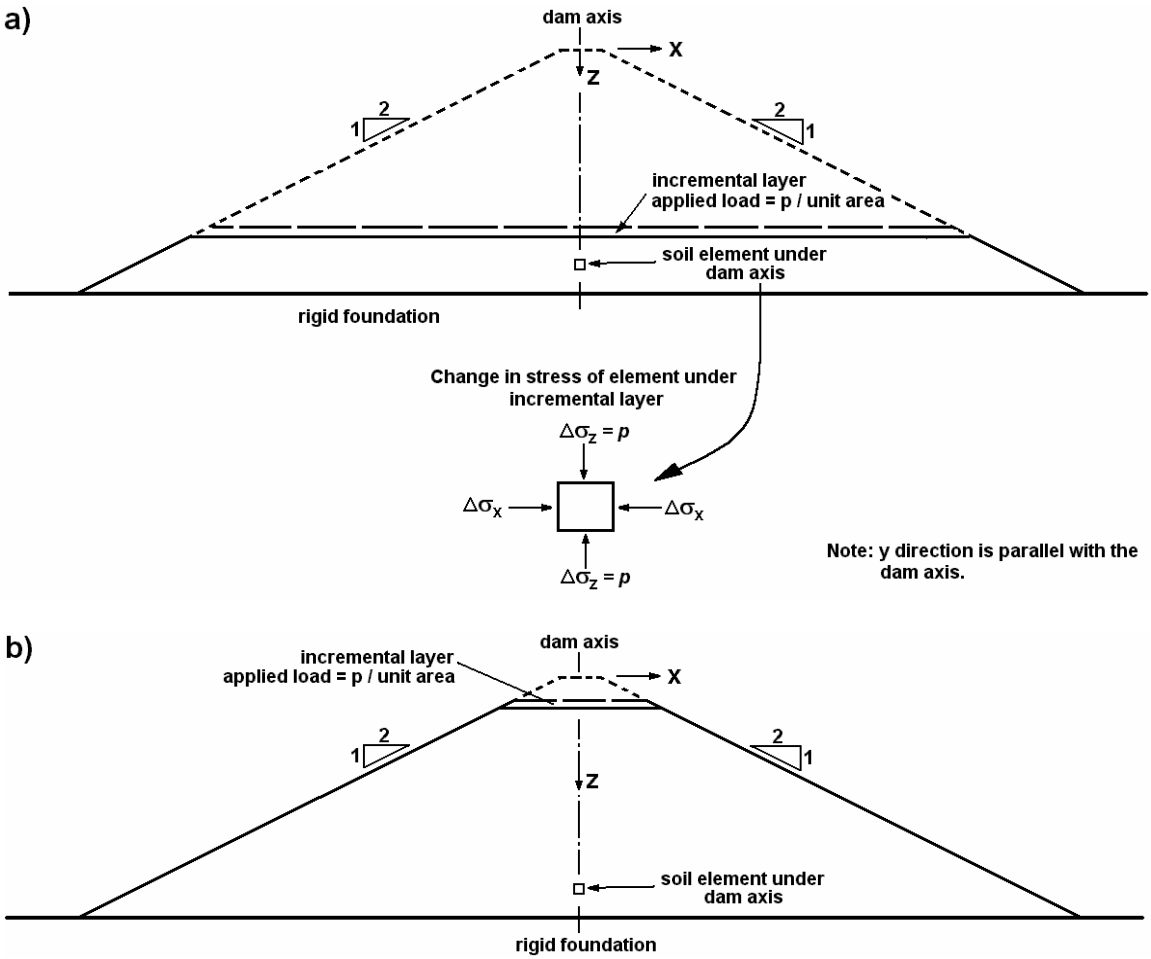

Figure 7.1: Embankment construction indicating *(a)* broad layer width to embankment depth ratio in the early stages of construction and *(b)* narrow layer width to embankment depth ratio in the latter stages of construction.

To facilitate analysis of the data, total vertical stress profiles during and at the end of construction were estimated for a variety of symmetrical embankment shapes by elastic finite difference analysis. Figure 7.2a presents a typical total vertical stress profile at

end of construction for an embankment with slopes of 1.8H to 1V and Figure 7.2b the ratio of total vertical stress at the end of construction for various embankment slopes compared to the total vertical stress calculated simply by the depth below the ground surface and the unit weight (i.e. *gH*). Lines of best fit were obtained using a second order polynomial equation according to Equation 7.3. Values of the coefficients A_1 and A_2 for the various embankment slopes analysed are given in Table 7.9.

$$\begin{aligned} s_{z,EOC} &= g \cdot H \left(A_1 (h/H)^2 + A_2 (h/H) \right) \\ &= Z_1 \cdot g \cdot H \end{aligned} \tag{7.3}$$

where $s_{z,EOC}$ = total vertical stress at end of construction (at depth *h/H*), *?* = bulk density, *H* = embankment height, *h* = depth below crest, A_1 and A_2 are coefficients and Z_1 is the vertical stress ratio.

For estimation of stresses within the embankment during construction finite element or finite difference methods can be used. Alternatively, published charts such as those by Clough and Woodward (1967) or Poulos et al (1972) can be used.

7.4.1.2 *Stresses in Zoned Embankments*

Zoned embankments present a greater degree of complexity for analysis than the homogeneous embankment case because of the potential for stress transfer or shedding of stresses from the core to the shoulder or vice versa. Simplification to a homogeneous analysis is only acceptable where arching has a negligible influence on the vertical stress profile. As will be demonstrated in Section 7.4.1.3 this is a reasonable assumption for:

- Zoned embankments with broad central earthfill zones, e.g. for central core widths with a combined core slope (upstream and downstream core slope combined) greater than about 1.5 to 2H to 1V. It may also be a reasonable simplification for combined central core widths down to 1H to 1V where the well-compacted core has been placed on the dry side of Standard optimum moisture content, giving a core of high undrained strength, so that the stress conditions in the core are maintained in the elastic region.
- Zoned embankments where the compressibility properties of the central earthfill zone and gravelly or rockfill shoulders are similar; i.e. compacted sandy and

gravelly soils with non-plastic fines or low (less than about 20% finer than 75 micron) plastic fines contents, with shoulders of compacted gravels or rockfill. This is on the proviso that pore water pressures generated in the core during construction are small and potential plastic type core deformations due to lateral spreading of the core are therefore negligible.

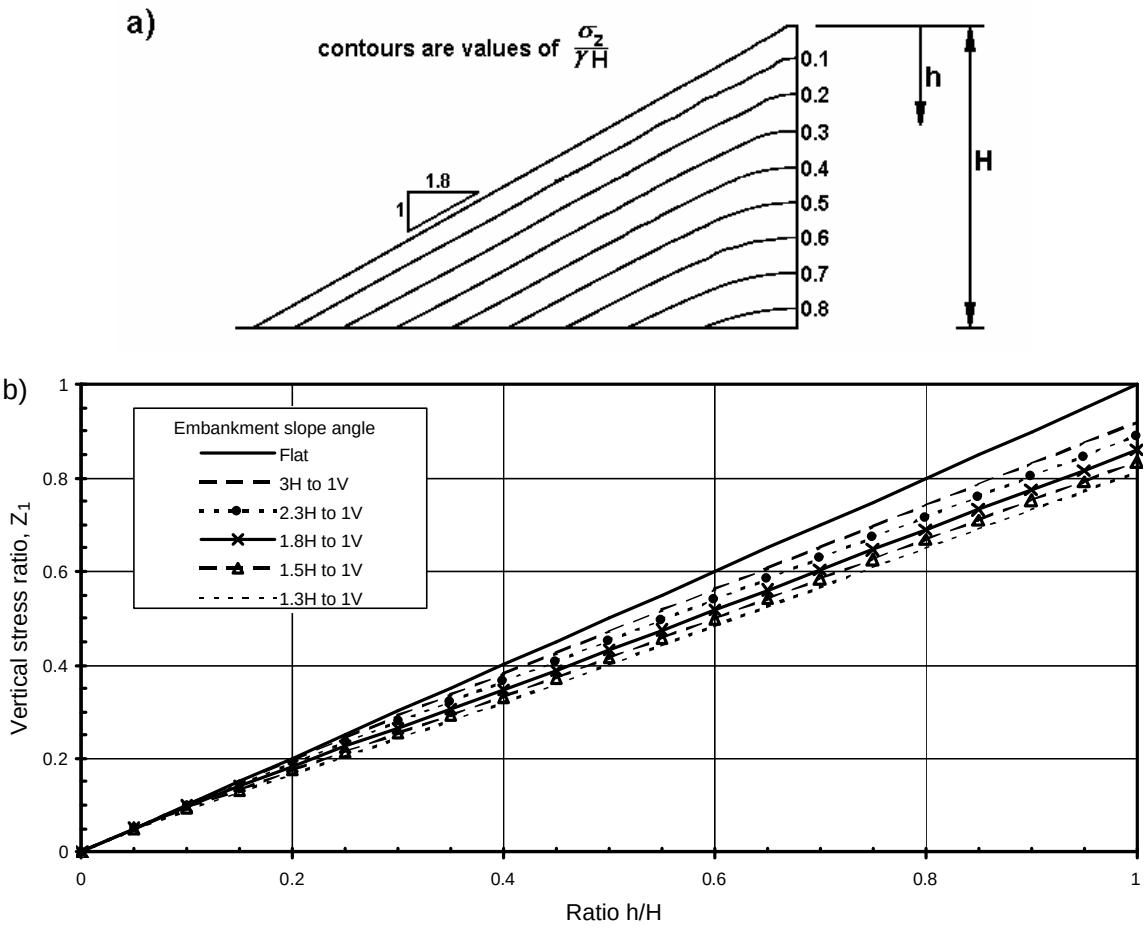

Figure 7.2: *(a)* Total vertical stress ($s_{z,EOC}$) contours at end of construction for 1.8H to 1V embankment slopes, and *(b)* vertical stress ratio, Z_1, versus *h/H* under the embankment axis for various embankment slopes.

Table 7.9: Multiplying coefficients for the calculation of the total vertical stress at the embankment centreline at end of construction (Equation 7.3)

Embankment Slope Angle	**A_1**	**A_2**
1.3H to 1V	0.0084	0.803
1.5H to 1V	-0.0098	0.843
1.8H to 1V	-0.029	0.886
2.3H to 1V	-0.044	0.931
3.0H to 1V	-0.062	0.978

Where the core is of thin to medium width and the compressibility properties of the core and shoulders are dissimilar it is not possible to use the simple methods described in Section 7.4.1.1 to analyse the deformation of the core. The problem is no longer one-dimensional because the vertical strain of the core under the embankment centreline comprises two components, one due to the vertical strain under the imposed vertical stress and a second component due to the lateral strain of the core. In addition, stress transfer effects cannot be ignored. Meaningful analysis of stresses and strains during construction can only be undertaken using finite element modelling based on constitutive models that reasonably approximate the as placed properties of the various materials used in construction.

However, to facilitate the analysis of the case study deformation data, the analysis of a simple plane strain finite difference model of a zoned embankment was undertaken to assess the general stress conditions and trend of deformation behaviour during construction. The modelled embankment (Figure 7.3) consisted of a 100 m high central core earth and rockfill dam, of thin core width, on a rigid foundation. Construction was modelled in ten lifts each of 10 m height. A Mohr-Coulomb linear-elastic perfectly plastic model was used for both the central core and rockfill. Three analyses were carried out each using the same properties for the rockfill (Figure 7.3) and varying the properties of the core material (Table 7.10) as follows:

- Case 1 – core with similar shear strength properties to the rockfill. Poisson's ratio was assumed to be the same for the core and rockfill shoulders. This case is considered typical of a well-compacted silty gravel core with non-plastic fines.
- Case 2 – A very stiff core with Poisson's ratio much greater than that of the rockfill (0.40 compared to 0.22) and strength indicative of the undrained strength envelope.
- Case 3 – A wet placed core. The core is assumed to behave nearly fully undrained with a Poisson's ratio of 0.48 and a small equivalent undrained friction angle of 5 degrees.

The same modulus has been used for the core (100 MPa) and the rockfill (80 MPa) in all three cases to minimise where possible the number of variants. A friction angle of 45 degrees is used to model the rockfill.

The results, shown in Figure 7.4 and Figure 7.5, highlight the influence of the difference in shear strength and Poisson's ratio of the core on the stresses within the embankment and on the deformation behaviour. Where the properties of the core are

similar to those of the rockfill (Case 1) the lateral stress distribution is similar to the homogeneous case and lateral displacements in the core and rockfill are small (Figure 7.4 and Figure 7.5c). The vertical stress distribution on the embankment centreline for this case (Case 1) is similar to the homogeneous case, except that the higher modulus core attracts higher stresses during construction. The assumption of homogeneous conditions reasonably models the lateral stresses but will under-estimate the vertical stresses in the core where the core is less compressible than the rockfill, and vice versa if the core is more compressible than the rockfill. For broader core widths the vertical stress profile on the centreline approaches the homogeneous case (refer Section 7.4.1.3).

Where the stress-strain properties of the core are different to those of the rockfill, such as for Cases 2 and 3, the stress profiles (Figure 7.4) differ significantly from the homogeneous case. Higher lateral stresses are developed during construction as well as arching across the core, as shown. Outward lateral displacements of the core and rockfill are observed that are much larger than for Case 1 or for the homogeneous case (Figure 7.4 and Figure 7.5c). The displacements are caused by the differential lateral stress conditions that develop between the core and shoulders. For Case 3, yield conditions are reached in a large portion of the core and in this case the rockfill is in effect acting as support for the core.

The results also show:

- Lateral stresses and strains increase with increasing Poisson's ratio of the core, reflecting yielding and plastic deformation of the core, particularly for Case 3.
- Maximum lateral strains are observed at a depth below the crest of approximately 65% of the embankment height ($h/H = 0.65$).
- The lateral strains, which occur largely as plastic deformation of the core, contribute significantly to the vertical strain observed in the core.
- Arching occurs in the narrow core as a result of the large differential vertical deformation between the core and the shoulders. Figure 7.5a shows the vertical stress profile at end of construction for Case 3 is much less than for the homogeneous condition, and Cases 1 and 2.

The finite difference analysis was based on the assumption of plane strain conditions. This assumption is valid for embankments that are long compared to their height because strains in the direction parallel to the dam axis (i.e. y-direction in Figure 7.1) are negligible compared to those measured vertically and perpendicular to the dam

axis. Consideration should be given to the potential for cross-valley arching and its effect on the stresses within the embankment for embankments constructed in steep valleys with narrow river sections.

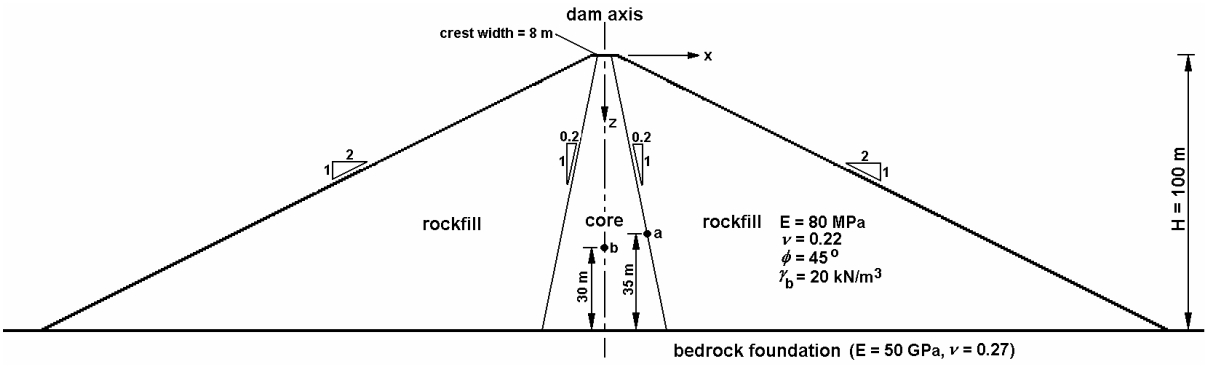

Figure 7.3: Embankment model for finite difference analysis during construction.

Table 7.10: Properties of central core used in finite difference analyses

Analysed Case	**Modulus, *E*** **(MPa)**	**Poisson's ratio, *n***	**Bulk Unit Weight, *g*** **(kN/m^3)**	**Cohesion, *c*** **(kPa)**	**Angle of Internal Friction, *f*** **(degrees)**
Case 1 – zoned embankment with core similar to rockfill	100	0.22	20	0	45
Case 2 – zoned embankment with very stiff core	100	0.4	20	75	20
Case 3 - zoned embankment with stiff, wet core	100	0.48	20	30	5
Homogeneous (same as rockfill)	80	0.22	20	0	45
Cases 4 to 7 – zoned embankment, core slope 0.2H to 1V to 0.75H to 1V (refer Section 7.4.1.3)	40	0.33	20	2	32

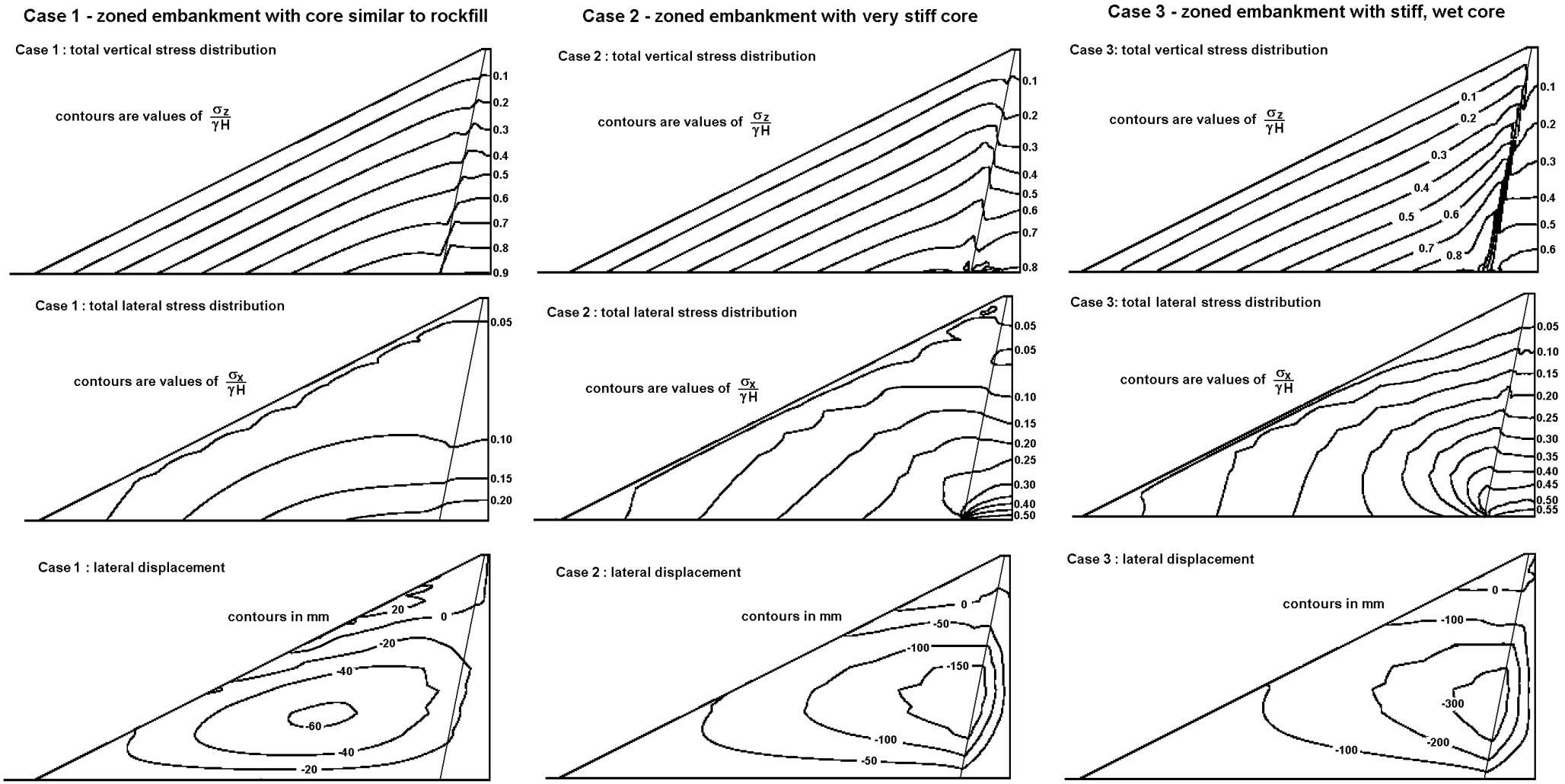

Figure 7.4: Total vertical stress, total lateral stress, and lateral (horizontal) displacement distributions at end of construction for zoned earthfill finite difference analysis.

a)

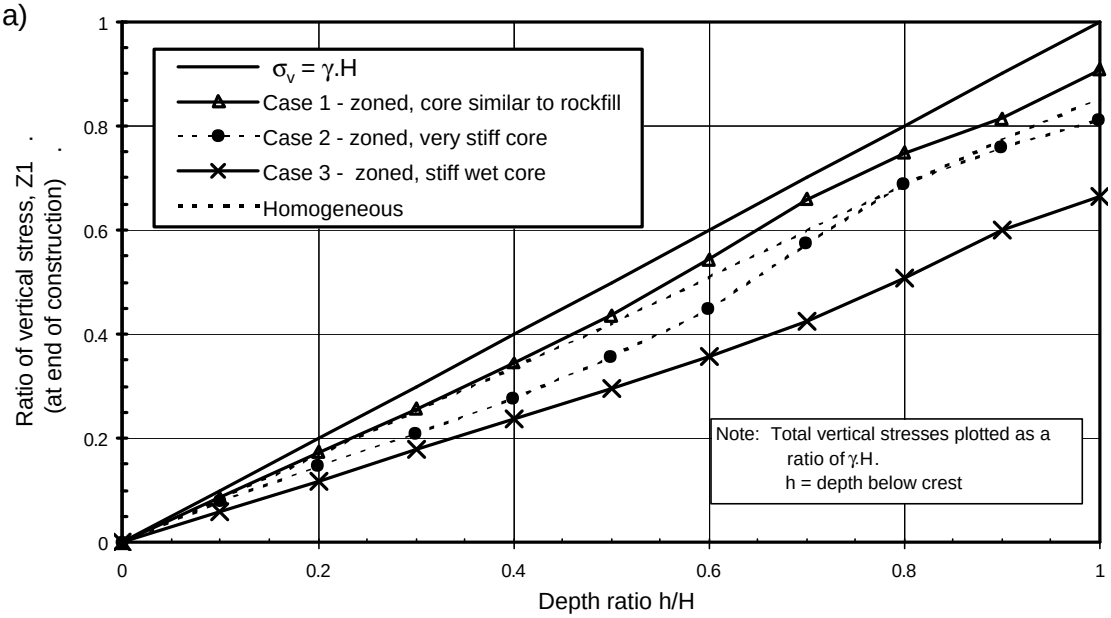
σv = γ.H
Case 1 - zoned, core similar to rockfill
Case 2 - zoned, very stiff core
Case 3 - zoned, stiff wet core
Homogeneous
Note: Total vertical stresses plotted as a ratio of γ.H.
h = depth below crest
Ratio of vertical stress, Z1 . . (at end of construction)
Depth ratio h/H
0
0.2
0.4
0.6
0.8
1

b)

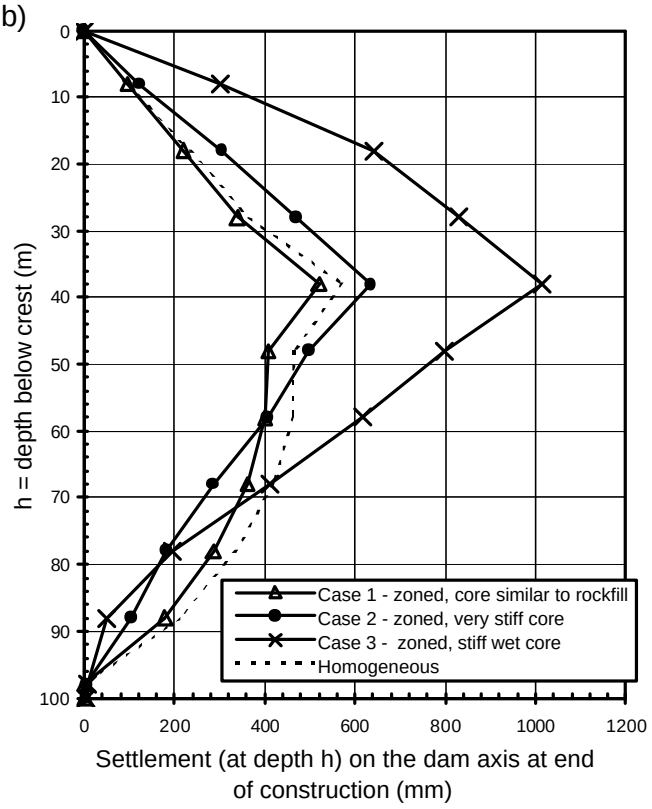
h = depth below crest (m)
Settlement (at depth h) on the dam axis at end of construction (mm)
Case 1 - zoned, core similar to rockfill
Case 2 - zoned, very stiff core
Case 3 - zoned, stiff wet core
Homogeneous
0
10
20
30
40
50
60
70
80
90
100
0
200
400
600
800
1000
1200

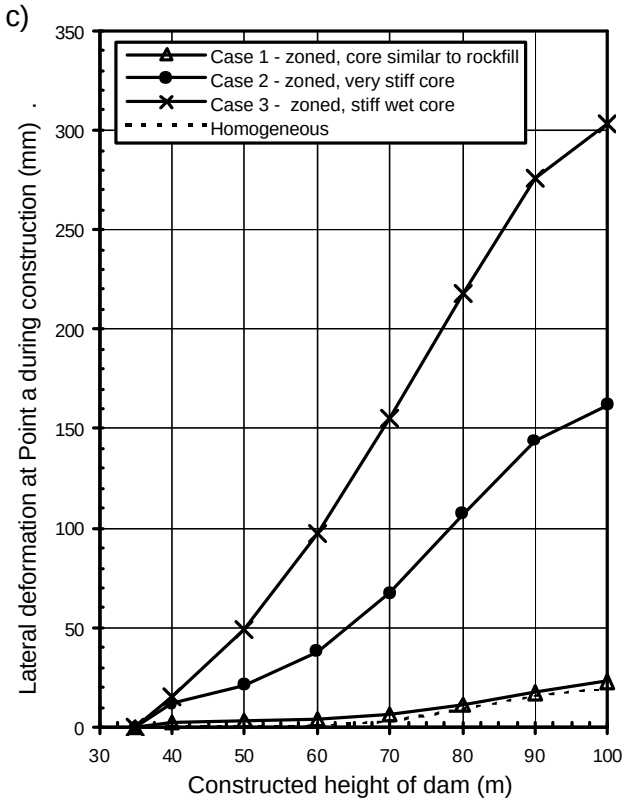

Figure 7.5: Finite difference modelling results; *(a)* total vertical stress on the dam centreline at end of construction, *(b)* settlement profile at dam axis at end of construction, and *(c)* lateral deformation at Point a (Figure 7.3) during construction.

7.4.1.3 Arching or Stress Transfer in Zoned Embankments

Arching across the core of zoned embankments, including puddle core earthfill embankments, has important implications on the deformation behaviour of the core during construction as well as the potential for hydraulic fracture post construction due to the reduced stresses in the core. Bishop (1952), for undrained conditions in puddled core dams, and Nonveiller and Anagnosti (1961), for fully drained conditions in zoned embankments, have developed methods for assessment of arching for embankments with narrow cores. The progression to finite element analysis and improvements in constitutive models to more accurately model the stress-strain relationship of materials allows for realistic assessment of arching in zoned embankments, as shown by the analysis of Beliche dam (Naylor et al 1997) (Figure 7.6a) and the modelling of puddle core earthfill dams by Dounias et al (1996) (Figure 7.6b).

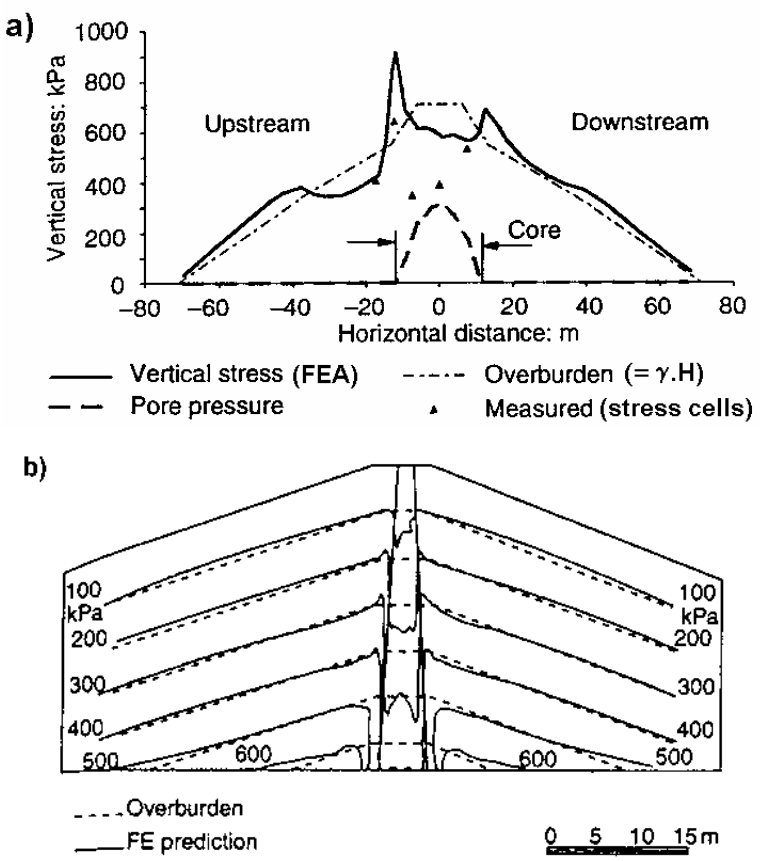

Figure 7.6: Finite element analysis of zoned embankments highlighting arching of core zone from *(a)* Beliche dam at about mid-height, elevation 22.5 m (Naylor et al 1997), and *(b)* a puddle core embankment (Dounias et al 1996).

As the published analyses and those from Section 7.4.1.2 show, arching is developed in zoned embankments with narrow cores not only due to the core being more compressible than the supporting shoulders but also due to lateral spreading of the core. Bishop and Vaughan (1962) comment that for the Selset puddle core earthfill embankment the vertical deformations of the core were largely a result of plastic deformations due to lateral spreading and not consolidation type settlements due to pore water pressure dissipation.

Factors contributing to the potential for arching are the difference in strength and compressibility properties between the core, filter/transition and outer earth or rockfill zones, the stress path and the embankment geometry (particularly the width of the core).

Some examples of total vertical pressures measured during construction in the core of zoned embankments using pressure cells are shown in Figure 7.7, and are compared to the total vertical stress estimated for a homogeneous embankment allowing for the embankment shape. The core width to depth ratio is 0.4 to 0.5 for most of the cases (i.e.

thin cores) and is 0.7 for Talbingo dam. The near symmetrical thin cores comprised sandy clays to clayey sands and clayey gravels placed close to or on the wet side of Standard optimum moisture content and were supported by reasonably to well compacted filters, and gravel or rockfill shoulders.

For Kastraki, Thomson, Beliche and Chicoasen dams the measured vertical stresses are less than the homogeneous case. All four cases are considered to represent arching across the core. At the higher stress levels associated with the latter stages of construction the measured stresses tend toward the horizontal (i.e. minimal measured increase in total stress with increasing embankment height) at Kastraki, Thomson and Beliche dams. At Chicoasen dam (Alberro and Moreno 1982) the pressure cell measurements do not show the curvature in the latter stages of construction as do the other three cases.

For Talbingo dam the pressure cells in the mid region of the slightly upstream oriented core show a linear stress response with the stresses plotting close to the homogeneous case indicating arching is not a factor. However, the pore water pressure response in the core and settlement during construction (refer Appendix G, Section 1.14) indicate that arching occurred in the vicinity of the near vertical downstream core / filter interface but not in the central region or the upstream region next to the core / filter interface sloped at 0.9H to 1V.

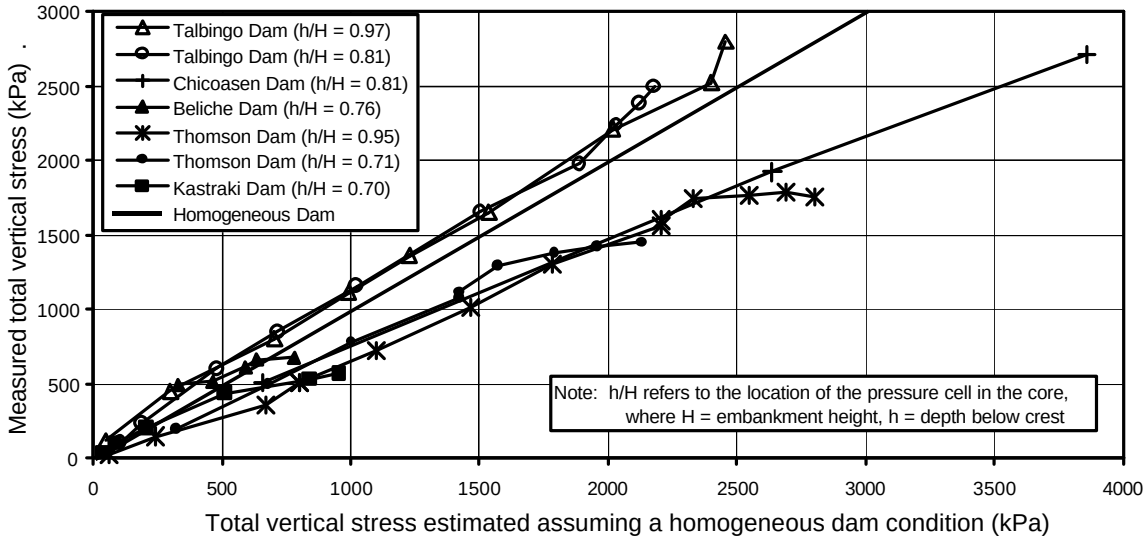

Figure 7.7: Estimated versus measured (from pressure cells) total vertical stresses during construction.

Further numerical analysis was undertaken to analyse the effect of core width (in zoned embankments) on the stresses during construction. The same procedure and embankment geometry was used as described in Section 7.4.1.2 analysed with symmetrical core slopes of 0.2H, 0.3H, 0.5H and 0.75H to 1V (Cases 4 to 7 respectively). Properties for the core are given in Table 7.10 and those for the rockfill were as per the earlier analysis (Figure 7.3). For these cases the core was modelled with a Young's modulus of 40 MPa, half that of the rockfill. The results are presented in Figure 7.8.

The total vertical stresses on the embankment centreline at Point *b* (Figure 7.3, *h/H* = 0.70) for each stage of construction are presented in Figure 7.8c, and include those from Cases 2 and 3. The total vertical stress for the zoned cases initially approximates that for the homogeneous case at low stress levels and then curves away at higher stress levels, similar to that observed for the thin core case studies (Figure 7.7) and is indicative of arching of the core.

The results of the analysis also show that at end of construction the total vertical stresses on the embankment axis increase with increasing core width, and for this example, approached stresses close to the homogeneous case for core slopes greater than about 0.5H to 1V (i.e. thick cores). However, there is still a significant differential in stress at the interface between the core and rockfill as can be seen in Figure 7.8b.

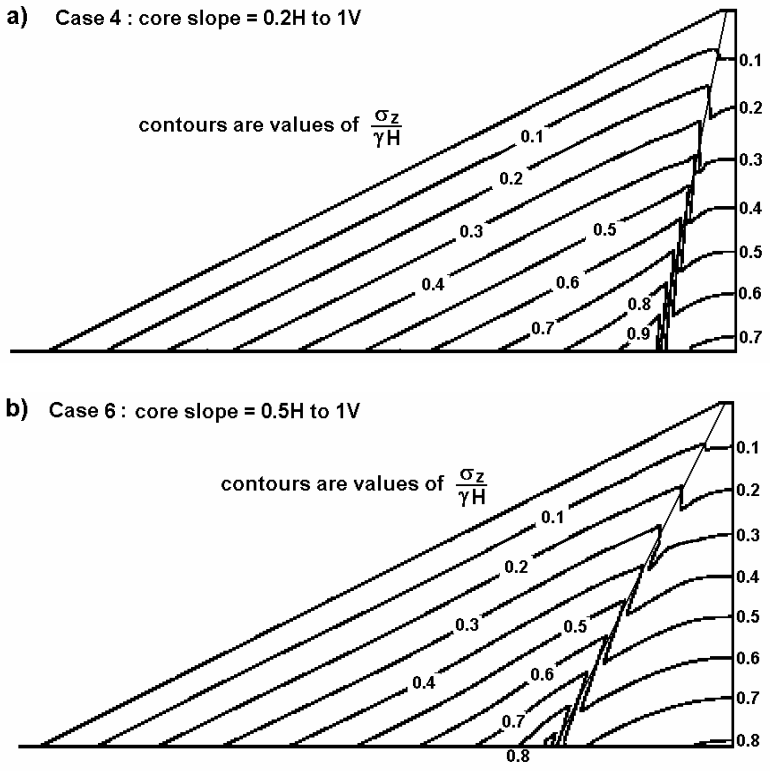

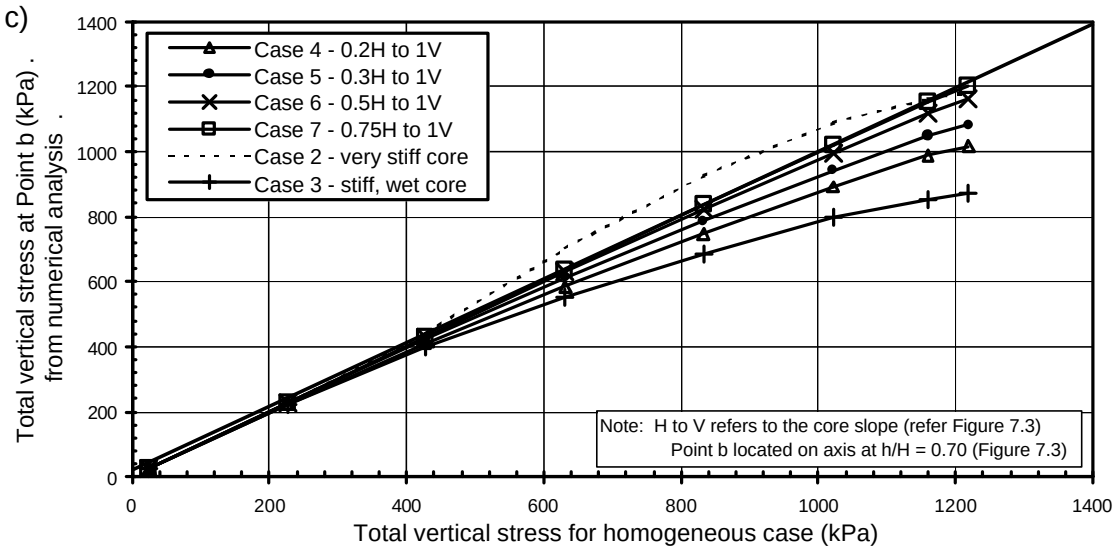

Figure 7.8: Total vertical stress profiles from the numerical analysis of construction for zoned embankments with different core slopes; *(a)* 0.2H to 1V case, *(b)* 0.5H to 1V case, and *(c)* total vertical stress at $h/H = 0.70$ with increasing embankment height.

7.4.1.4 Pore Water Pressures Developed During Construction

So far the discussion on stresses during construction has been on total stresses. However, for a more complete assessment of the deformation behaviour it is important to consider effective stresses and the effective stress paths during construction. For permeable embankment materials such as clean or free draining rockfills, gravels and sands the assumption of drained conditions during construction is valid. Therefore effective stresses and the effective stress state in these materials are readily assessable from the total stress conditions and consideration of partial impoundment, if this occurs during construction.

For low permeability embankment materials effective stresses are more difficult to predict prior to construction, but their assessment can be critical in terms of embankment stability. Therefore, instrumentation is often installed and monitored during construction in the form of piezometers, pressure cells, and internal and external deformation monitoring gauges. However, due to the unreliability of pressure cells, total stresses are generally assessed from finite element analysis, which can also be unreliable.

At placement, earthfill materials are partially saturated, with the degree of saturation dependent on the moisture content, material type, and the method and degree of compaction of the earthfill. The pore water pressures that are developed in the earthfill

during construction, assuming it is well-compacted, are dependent on a number of factors including the initial degree of saturation, material compressibility properties, permeability, time of construction and applied stress levels. It is convenient to consider the positive pore water pressures in terms of r_u, the pore water pressure coefficient, as defined in Equation 7.4.

$$r_u = u/s_z \text{ or } Dr_u = Du/Ds_z \tag{7.4}$$

where r_u = pore water pressure coefficient, u = pore water pressure, s_z = total vertical stress and Δ represents the incremental or tangential component of the parameter. The term r_u is used for the pore water pressure coefficient determined from case study data rather than $\overline{B}$, as defined in Equation 7.5 (on page 7.40), because the lateral stresses (s_x and s_y) parallel and perpendicular to the dam axis may not be equal.

Three main types of pore water pressure response are generally observed (Figure 7.9):

- Negligible or limited positive pore water pressure response (r_u generally less than 0.1 to 0.2). Gould (1953, 1954) observed and the case study data indicates that for earthfills placed drier than about 0.5% to 1% of Standard optimum limited positive pore water pressures are developed during construction for most soil types.
- Moderate to very high sustained positive pore water pressure response (Δr_u greater than 0.5) with negligible to very limited drainage. This type of response is generally observed for clayey sands, clayey gravels and dominantly clayey earthfill types placed wetter than about 0.2 to 0.5% dry of Standard optimum (i.e. close to or above Standard optimum). Often the positive pore water pressure response is preceded by a period of negative pore water pressure response at low stress levels (Figure 7.9).
- Drainage during construction is significant. This is generally observed for earthfills of silty sands to silty gravels placed close to or wet of Standard optimum (i.e. wetter than about 0.2 to 0.5% dry of Standard optimum), but in some cases it is also observed for clayey sands and clayey gravels with low plasticity and possibly low content fines (less than about 15 to 25% finer than 75 micron). The typical pore water pressure response for these earthfills when placed wet of optimum is for an initially high pore water pressure coefficient, which then decreases with increasing embankment height above the piezometer. Partial drainage during shutdown is also evident.

There are case studies that fall outside or between these general types of pore water pressure response.

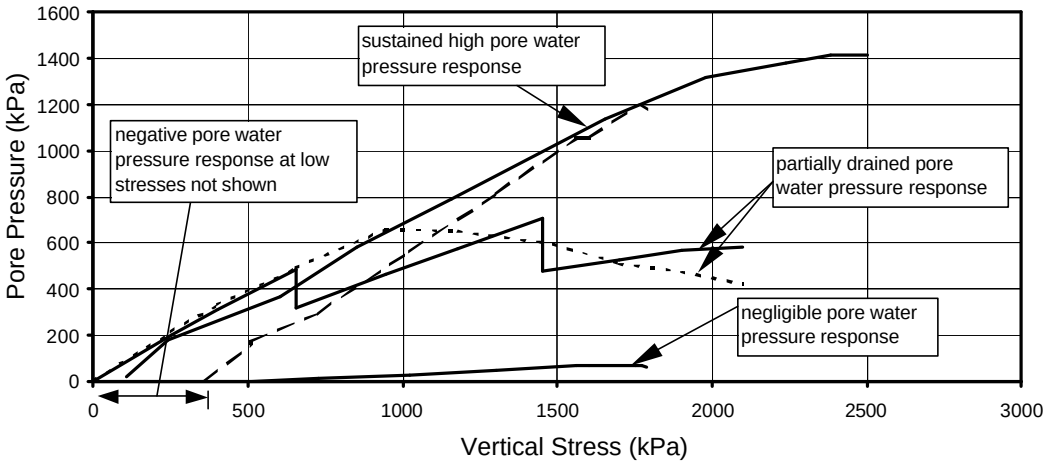

Figure 7.9: Idealised types of pore water pressure response in the core during construction.

Hilf (1948) provides a method for prediction of the pore water pressure response for partially saturated soils derived from one-dimensional consolidation theory and applied to field prediction using oedometer tests on laboratory samples prepared at proposed field placement specifications. The method assumes undrained conditions, and field compression is one-dimensional (i.e. zero lateral strain) and due to compression of the air voids. The method gives predictions indicating that the rate of pore water pressure increase becomes very rapid as the air voids volume approaches zero and a saturated condition is reached. Once saturated the pore water pressure increase is assumed to be equal to the increase in total vertical stress (i.e. no change in effective stress). Fredlund and Rahardjo (1993) comment that whilst the Hilf method provides a reasonable estimate of pore water pressure, it will over-estimate it because the derivation assumes matric suction equals zero (i.e. the pore water pressure equals the pore air pressure).

Khalili (2002) comments that for partially saturated soils of very low permeability (i.e. where undrained conditions may be a reasonable assumption) the rate of pore water pressure increase in confined compression will always be less than the rate of vertical stress increase due to the presence of a small volume of air voids that remain under the magnitude of effective stresses likely in embankment dams. The field data for clayey earthfills of very low permeability placed close to or above Standard optimum moisture content tend to support this (Figure 7.10), with maximum rates of pore water pressure

increase equivalent to 60 to 90% of the change in total vertical stress (i.e. Δr_u = 0.6 to 0.9).

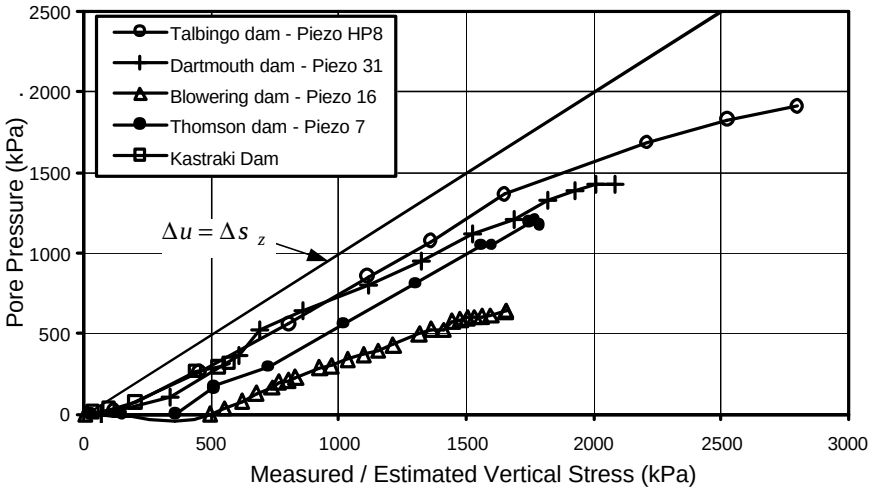

Figure 7.10: Pore water pressure response during construction in the core zone of clayey earthfills placed at close to or wet of Standard optimum moisture content.

It is noticeable from Figure 7.10 that the pore water pressure coefficient, Δr_u, may decrease toward the end of construction. The reason for this is possibly partly due to pore water pressure dissipation. A more likely explanation is that for piezometers in the mid to lower region of the core the total stress ratio (Ds_3 / Ds_1) in Skempton's equation for pore water pressure (Equation 7.5) is not constant but decreases in the latter stages of construction where the layer width is small compared to the height above the gauge (Figure 7.1b). Assuming the coefficients *A* and *B* are constant, the effect of a reduction in total stress ratio would be for a reduction in the ratio Du / Ds_1.

In contrast, the pore water pressure observations in the narrow, medium to high plasticity wet placed clay core at Yonki dam indicated that the pore water pressure actually increased during non-construction periods (Fell et al 1992). This behaviour is possibly due to yielding as a result of the strain rate dependency of the limit state surface. Whilst not common, an increasing pore water pressure response during non-construction periods has been observed in the soft foundations of fills constructed on soft ground, several examples of which are referred to in Section 4.4.2 of Chapter 4.

For wet placed earthfills of permeability and construction staging such that partial drainage during construction occurs, the pore water pressure response displays an interesting feature that is replicated in laboratory testing. Triaxial isotropic compression

tests on wet placed silty sands and silty gravels (Bishop 1957; Bernell 1982) undertaken in stages of undrained loading with a period of drainage between loading stages (Figure 7.11) show a reduction in Skempton's pore water pressure parameter, $\overline{B}$ (Equation 7.5), during subsequent stages of undrained loading.

A similar pore water pressure response is observed in wet placed dominantly sandy and gravelly soils (silty sands and gravels, and some clayey sands and gravels) where partial dissipation of pore water pressures occurred in shutdown periods during construction (Bishop 1957; Eisenstein and Law 1977; Nakagawa et al 1985). Bishop (1957) considers the response is due to a decrease in the compressibility of the earthfill under increased effective stress conditions that result from partial drainage.

A decrease in the degree of saturation during dissipation of pore water pressures at shutdown periods could also influence the pore water pressure response afterward. The relatively high degree of saturation at placement is likely to result in the migration of water rather than air from the soil structure during the drainage stage, and as pressures dissipate previously dissolved air in water is likely to return to the air phase. The net effect could result in an overall decrease in the degree of saturation below that at initial placement.

$$\frac{\Delta u}{\Delta \sigma_1} = \overline{B} = B\left[1-(1-A)\left(1-\frac{\Delta \sigma_3}{\Delta \sigma_1}\right)\right] \tag{7.5}$$

where u = pore water pressure, σ_1 = major principal stress, σ_3 = minor principal stress, Δ represents incremental or tangential component of the parameter, and $\overline{B}$, B and A are pore water pressure parameters defined by Skempton (1954).

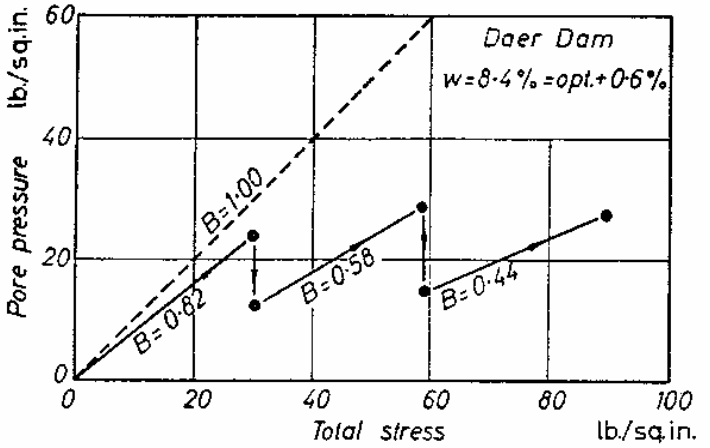

Figure 7.11: Triaxial isotropic compression tests with staged undrained loading and partial drainage on a partially saturated silty sand (Bishop 1957).

7.4.1.5 *Summary of Stress Conditions During Construction*

The total and effective stress conditions established in an embankment during construction are shown to be dependent on the embankment geometry, the embankment zoning geometry, and the strength and compressibility properties of the embankment materials.

For the simplest case of a homogeneous embankment on a rigid foundation, elastic solutions show that under the embankment centreline the vertical stress profile is dependent on the embankment geometry and the lateral stresses are dependent on the Poisson's ratio of the earthfill and embankment geometry. During the initial stages of construction when the embankment width is large in comparison to its height the assumption that the increase in stress equals the depth of soil times its weight is reasonable in the central region of the embankment. However, in the latter stages of construction this assumption is no longer valid due to the decreasing layer width in relation to the embankment height.

The homogeneous model is also a reasonable assumption for the stress conditions under the embankment axis for:

- Zoned embankments with broad central earthfill zones where the earthfill has been well compacted and placed drier than about 0.5% of Standard optimum moisture content. Under these placement conditions the core has a high undrained strength and the stress conditions in the core are likely to be maintained in the elastic range. Analysis and the case study data suggests central core widths with a combined core

slope (i.e. upstream and downstream core slope combined) greater than about 1.5 to 2H to 1V are sufficiently broad, but it may also be a reasonable simplification for combined central core widths down to 1H to 1V.

and,

- Zoned embankments where the compressibility properties of the central earthfill zone and gravelly or rockfill shoulders are similar; i.e. compacted sandy and gravelly soils with non-plastic fines or low (less than about 20% finer than 75 micron) plastic fines contents, with shoulders of compacted gravels or rockfill. This is on the proviso that pore water pressures generated in the core during construction are small and potential plastic type core deformations due to lateral spreading of the core are therefore negligible.

For zoned embankments the stress conditions during construction become more complex and are affected by the differential strength and compressibility properties of the embankment materials and the embankment zoning geometry. Total vertical stresses are affected by stress transfer or arching not only from differential compressibility but also from differential lateral stresses and the resulting lateral deformations to reach equilibrium stress conditions. Lateral stresses are affected by differences in Young's modulus and Poisson's ratio between the core and shoulders.

Finite element analysis is required for analysis of stresses and deformations in zoned earthfill embankments due to the complexity of the problem. Whilst finite element analysis is a standard tool for assessment of stresses and deformations during construction of embankment dams there is often a trade off between accuracy and simplicity (Duncan 1996) due to the complexity of the constitutive model to accurately model the strength and compressibility properties of partially saturated earthfills and the free draining gravel and rockfill zones.

For assessment of the effective stress conditions it is necessary to consider the pore water pressure response in the partially saturated embankment materials that are not free draining. Advances in the theory of partially saturated soils have developed constitutive models and methods that allow better estimation of pore water pressures than the simplistic Hilf (1948) method, but they have not been studied in detail here. Partial drainage during construction should also be considered.

7.4.2 LATERAL DEFORMATION OF THE CORE DURING CONSTRUCTION

Table 7.11 summarises the lateral deformation of the core for 12 central core earth and rockfill embankments. In all cases the central, well-compacted core is of thin to medium width and is supported by filters/transition zones and shoulders of rockfill and/or gravels. Further information on the material and geometrical properties of the core, filter / transition zones and outer shoulders is given in Table 7.12 and the tables in Section 1 of Appendix F. No data is given for Beliche dam, but Naylor et al (1997) comment that the deformations during construction distorted the inclinometer tubes such that lateral deformation measurements could not be taken, indicating the lateral deformation of the core was likely to have been quite large.

Lateral deformations were, in most cases, measured by internal horizontal movement gauge (IHM) installed in the filter and rockfill zones downstream of the core, and in some cases upstream of the core. The displacements quoted in Table 7.11 are from the IHM gauge closest to the core, usually from within the downstream filter or transition zone. The "lateral displacement ratio" is defined as the lateral displacement divided by the core width. Where only deformations on the downstream side of the core were available the "lateral displacement ratio" of the core has been estimated by dividing the displacement by the half width of the core and it is assumed that this displacement ratio is representative of the core at this location.

Figure 7.12 presents the estimated lateral displacement ratio versus fill height above the measuring gauge at the end of embankment construction. Figure 7.13 presents the estimated lateral displacement ratio versus fill height above the measuring gauge during embankment construction. It would be preferable to present these plots of the lateral displacement ratio versus vertical stress, but for several of the cases no pressure cell records were available and the likelihood of arching meant that vertical stresses could not be accurately estimated.

The data shows that the lateral displacement ratios during construction are significant for zoned embankments with thin to medium width cores. Estimated lateral displacement ratios range from less than 0.5% up to more than 3% from the case study data.

Table 7.11: Lateral deformations of the central core at end of construction for central core earth and rockfill embankments.

Dam Name	**Height (m)**	**Core Summary (refer Table 7.12 for more details)**		**Displacement Details**			
		Material Type / Placement	**Width (H to V)**	**Depth (m) *[1]**	**h/H**	**Displacement (mm) *[2]**	**LDR *[3] (%)**
Copeton	113	SC – medium plasticity fines, spec. = 1% dry to 1% wet of OMC (likely dry of OMC)	0.8H to 1V	40 59 89	0.35 0.52 0.79	140 150 285	-0.77 -0.58 -0.76
Wyangala	86	SC/SM – 1% dry of OMC	0.8H to 1V	51 66	0.59 0.77	67 158	-0.24 -0.70
Fukada	56	GC – no details on moisture spec., suspect dry of OMC.	0.6H to 1V	18.5 36.5	0.33 0.65	-6 42	0 -0.31
Dartmouth	180	SC/SM – medium plasticity fines, spec. 0.5% dry to 2% wet.	0.65H to 1V (average)	64 124	0.36 0.69	385 (dn), -450 (up) 1220 (dn)	-1.71 -2.69
Beliche	55	GC – low plasticity fines, spec. ± OMC	0.44H to 1V	-	-	-	large
La Grande, LG4	125	SM - non-plastic fines, spec. 1% dry to 2% wet	0.5H to 1V	70	0.56	300 (dn), -200 (up)	-1.3
Nurek	289	GC/GM – no details on moisture spec., suspect at or above OMC given high PWP.	0.46H to 1V	145	0.50	425	-0.7 to -1.2
Thomson	166	SC – medium plasticity fines, 2% wet of OMC	0.5H to 1V	88 118	0.53 0.71	770 (dn), -750 (up) 445	-3.3 -1.45
Gepatsch	153	GM/GC – 0.5 to 2% wet of OMC	0.25H to 1V	82 122	0.54 0.80	300 to 400 (dn - up) 750 (dn - up)	-1.25 to -1.7 -2.2
Talbingo	162	CL – medium plasticity, at OMC	0.7H to 1V	95	0.59	410 (dn), -1310 (up)	-2.80
Blowering	112	CL/SC – medium plasticity fines, 0.3% dry to 0.3% wet	0.9H to 1V	73	0.65	735	-2.26
El Infiernillo	148	CL/CH - medium to high plasticity, 3.7% wet of OMC	0.18H to 1V	74	0.59	-	-1.60

*[1] Depth = depth below crest.

*[2] Lateral displacements mainly from IHM gauges and from the gauge closest to the core (usually within the downstream filter/transition zone). Downstream (dn) is the default. Denoted (up) if from upstream of the core.

*[3] LDR = lateral displacement ratio and is calculated from the measured lateral core displacement divided by the core width. Values are negative in accordance with the convention that compressive strains are positive.

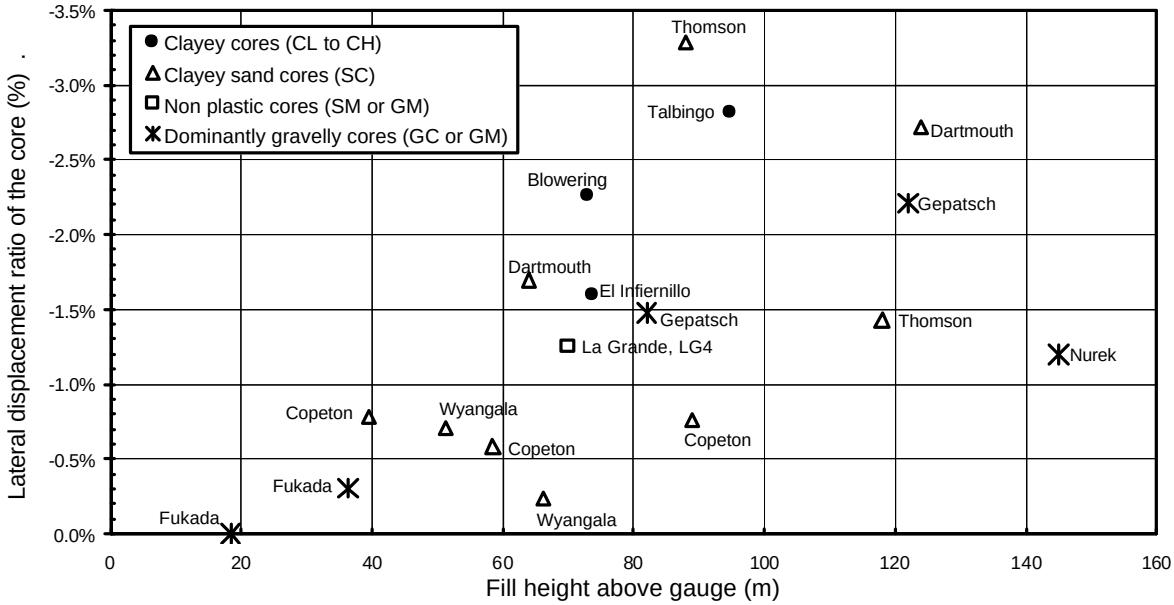

Figure 7.12: Estimated lateral displacement ratio of the core at end of construction.

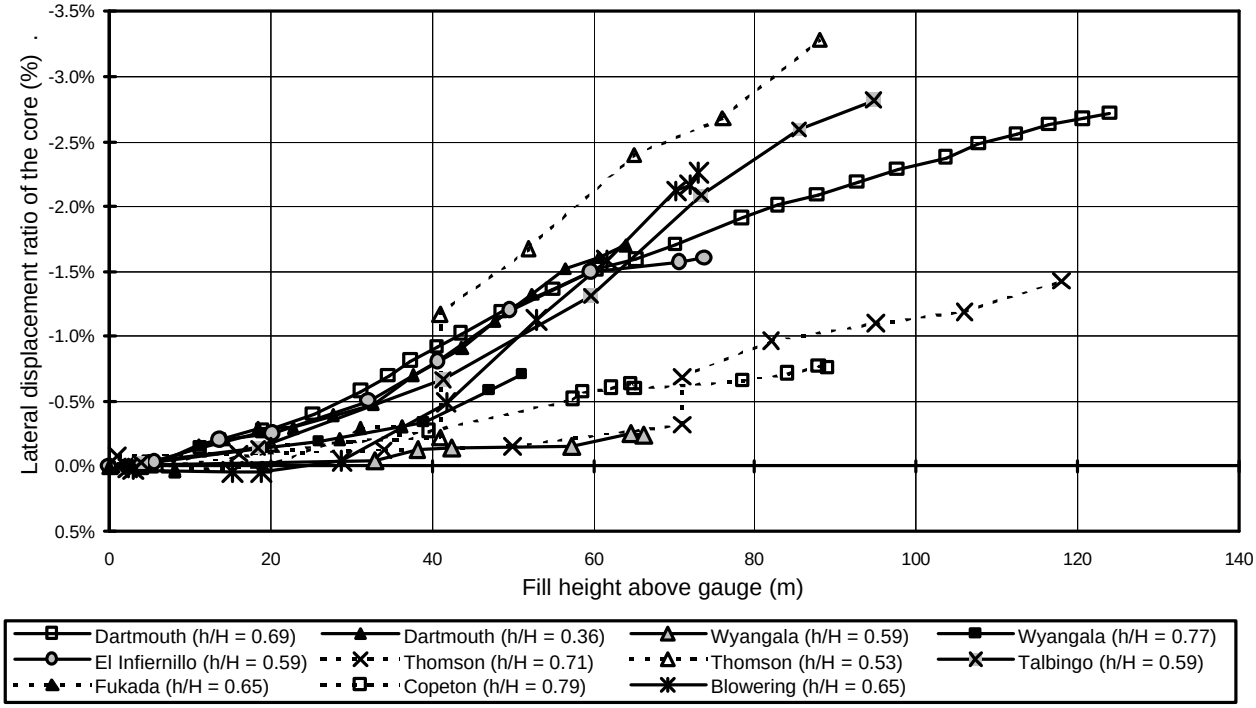

Figure 7.13: Estimated lateral displacement ratio of the core versus fill height above gauge during construction.

Table 7.12: Summary of embankment and earthfill properties for cases used in the analysis of lateral core deformation during construction.

Dam Name	Height (m)	Zoning Class*1	Core Details						Filters / Transition			Shoulders		Comment
			Width *2 (H to V)	ASCS *3	Fines *4 (%)	Plasticity *4	FMC to OMC *5	Pore *6 Pressure	Material	Width *7	Compaction Rating *8	Material	Compaction Rating *9	
Fukada	56	5,1,2 c-tm	0.6 to 1	GC (?)	-	-	No details	-	-	thin	good (?)	weathered sandstone & granite "dirty"	good (?)	relatively high moduli for weathered rockfill
La Grande, LG4	125	4,1,0 c-tm	0.5 to 1	SM	30	non-plastic	1% dry to 2% wet, suspect avg. is wet.	negl to low	sandy gravels	mod to thin	good	gravels	good (inner)	outer rockfill shoulders (granite & gneiss), reasonable to good
Nurek	289	4,2,0 c-tn	0.46 to 1	GC/GM	-	-	No details	med to high	sands & gravels	mod to thin	good	gravels	good	Suspect core placed close to OMC given high PWP response.
Copeton	113	5,2,0 c-tm	0.8 to 1	SC	25 to 60	medium	Spec. 1% dry to 1% wet	negl to low	crushed rock	thin	good	granite (very high strength)	reasonable to good	Likely dry core placement given low PWP.
Wyangala	86	5,2,0 c-tm	0.8 to 1	SC-SM	-	-	1% dry	negligible	sands & crushed rock	mod to thin	good	porphyritic gneiss (high to very high strength)	reasonable to good (inner)	outer rockfill of reasonable to poor compaction.
Thomson	166	5,2,0 c-tm	0.5 to 1	SC	44	medium	2% wet	med to high	crushed sandstone	thin	reasonable	sandstone and siltstone	good (inner)	High to very high strength rock. Outer rockfill of lesser quality.
Gepatsch	153	5,2,0 c-tn	0.25 to 1	GM/GC	30	-	0.5 to 2% wet	low to high (rapid dissipation)	gravels	broad	reasonable to good	gneiss	reasonable	clean to "dirty" coarse rockfill.
Beliche	55	5,2,2 c-tn	0.44 to 1	GC	20 to 36	low	Spec. ± OMC	med to high	sandy gravels	thin	reasonable (?)	rockfill (med to high strength)	poor to reasonable	inner rockfill high fines and low moduli
Dartmouth	180	5,2,0 c-tm	0.6-0.7 to 1	SC/SM	24	medium	Spec. 0.5% dry to 2% wet	high to very high	crushed rock	thin	good	granitic gneiss	good (inner)	reasonable compaction of outer rockfill
Talbingo	162	5,2,0 c-tm (u)	0.7 to 1	CL	18 to 70	medium	OMC	very high	crushed rock	broad	good	rhyolite & porphry	good (inner)	reasonable compaction of outer rockfill
Blowering	112	5,2,0 c-tm	0.9 to 1	CL/SC	30 to 80	medium	0.3% dry to 0.3% wet	med to high	sandy gravels	thin	good	quartzite & phyllite	good (inner), reasonable (outer)	relatively low moduli of rockfill
El Infiernillo	148	5,2,0 c-tn	0.18 to 1	CL/CH	54 to 70	med to high	3.7% wet	suspect very high	sands & gravels	moderate	good	diorite & silicified conglomerate	reasonable (inner) to poor (outer)	very narrow core.

Note: The notes to Table 7.12 are on the next page

Notes to Table 7.12:

*[1] Zoning classification system defined in Figure 1.5 in Section 1.3.3 of Chapter 1.

*[2] core width refers to the width of the core compared to the height (H = horizontal, V = vertical)

*[3] ASCS = Australian Soil Classification System.

*[4] Fines = % finer than 75 micron, Plasticity: low = low plasticity, med = medium plasticity, high = high plasticity

*[5] FMC to OMC = field or placement moisture content relative to Standard optimum moisture content

*[6] Pore water pressures during construction; negl = negligible (r_u < 0.1), low = r_u of 0.1 to 0.25, med = medium (r_u = 0.25 to 0.5), high = r_u of 0.5 to 0.75, very high = r_u of > 0.75.

*[7] Qualitative assessment of width of filters / transition zone; thin = 3 to 6 m width, broad = more than about 20 m but dependent on dam height

*[8] Compaction rating for filters / transition based on placement methods, layer thickness and relative density.

*[9] Compaction rating for rockfill summarised in Section 1.3.3 of Chapter 1.

The earlier finite difference analyses of zoned embankments on a rigid foundation (Section 7.4.1.2, Figure 7.4 and Figure 7.5) showed that the lateral deformation of the core was dependent on the development of differential lateral stress conditions between the core and supporting shoulder zones. The greater the stress difference the greater the lateral deformation of the shoulders to equilibrate the greater lateral stresses in the core. The rigid foundation also influenced the lateral stress and displacement profiles, the maximum lateral displacement being observed at approximately one third of the dam height above foundation level.

In the analyses the compressibility properties of the supporting rockfill zone were the same for each case. But, the compressibility properties of the supporting rockfill zone will also influence the amount of lateral deformation. Under similar differential stress conditions greater deformations will occur for more compressible supporting shoulders. The case study data tends to support this as discussed below.

Several trends are evident from the lateral displacement case study data:

- Placement moisture content of the core relative to Standard optimum moisture content is significant. Low lateral displacement ratios (< 1% at fill heights of 35 to 90 m) are observed for earthfills placed on the dry side of Standard optimum (Wyangala, Copeton and probably Fukada dams). Higher lateral displacement ratios (1.0 to 2.2% at 60 m fill height) are generally observed for earthfills placed at or on the wet side of Standard optimum.
- Low lateral displacement ratios are observed for embankments with broad well-compacted gravelly zones of likely very high moduli adjacent to the central core

(Nurek, La Grande LG4 and Gepatsch dams). For these cases the cores are silty to clayey sands and gravels placed at or wet of Standard optimum.

- Large lateral displacement ratios are observed for clayey earthfills placed at or wet of Standard optimum supported by shoulders of relatively highly compressible rockfills (Beliche and Blowering dams). At Beliche dam, Naylor et al (1997) describe the inner rockfill zone of weathered, medium strength schists and greywackes as "*relatively lightly compacted*" and of "*relatively high compressibility*". At Blowering dam the rockfill, although wetted and reasonably (outer Zone 3B) to well compacted (inner Zone 3A), the vertical secant moduli of the rockfill was calculated from hydrostatic gauges to be relatively low (20 to 40 MPa for Zone 3A placed in 0.9 m lifts and 10 to 20 MPa for the outer Zone 3B). Further details on the material properties at Blowering dam are given in Section 6 of Appendix G.
- Arching effects in the very thin wet placed clay core at El Infiernillo dam are possibly significant in the relatively low lateral strain measured.
- At Talbingo dam the lateral deformation was significantly greater on the upstream side of the core (1310 mm) compared to the downstream side (410 mm) at elevation 457 m (h/H = 0.59). Possible reasons for this are the slight upstream orientation of the core and the much broader width of the filter and transition zones (of well-compacted finer sized rockfill) on the downstream side.

For a number of case studies the lateral displacement ratio versus fill height plot (Figure 7.13) shows a marked increase in the rate of lateral displacement ratio at fill heights in the range 20 to 50 m above the gauge. The cases that display this behaviour are typically clayey earthfills placed at or wet of Standard optimum. It is possible that this response may be due to yielding or may reflect an increase in the undrained Poisson's ratio as the initially over-consolidated earthfill approaches or becomes normally consolidated.

For several case studies the lateral displacement ratio of the core was compared to the pore water pressure response at similar elevations to ascertain if the incremental increase in lateral displacement ratio observed correlated to a change in the pore water pressure response (Figure 7.14). The results indicate:

- At Thomson dam (h/H = 0.53) and Talbingo dam (h/H = 0.59) the data indicates that the increase in incremental lateral displacement ratio occurs at about the same level

of total vertical stress level as an incremental increase in the pore water pressure response.

- At Dartmouth dam (Figure 7.14a) there is some indication of an incremental increase in the lateral displacement ratio and the pore water pressure response at 20 to 25 m fill height, although it is not clearly evident for the lateral displacement ratio.
- At Blowering dam the pore water pressure response at Piezometer 16, at a lower elevation than the deformation gauge, shows a similar response at 22 m fill height, but the piezometer at the same elevation (Piezometer 23) shows no incremental increase in the pore water pressure response.

Overall, there is some data, although it is not conclusive, that the observed incremental increase in lateral displacement ratio for several of the wet placed clayey earthfill case studies occurs concurrently with an incremental increase in the pore water pressure response.

Several case studies show a flattening in the curve of lateral displacement ratio versus fill height near the end of construction (Figure 7.13). This is potentially due to arching (El Infiernillo) and the effect of embankment shape on the distribution of vertical and lateral stresses, which is not properly allowed for by considering depth of fill as the variable.

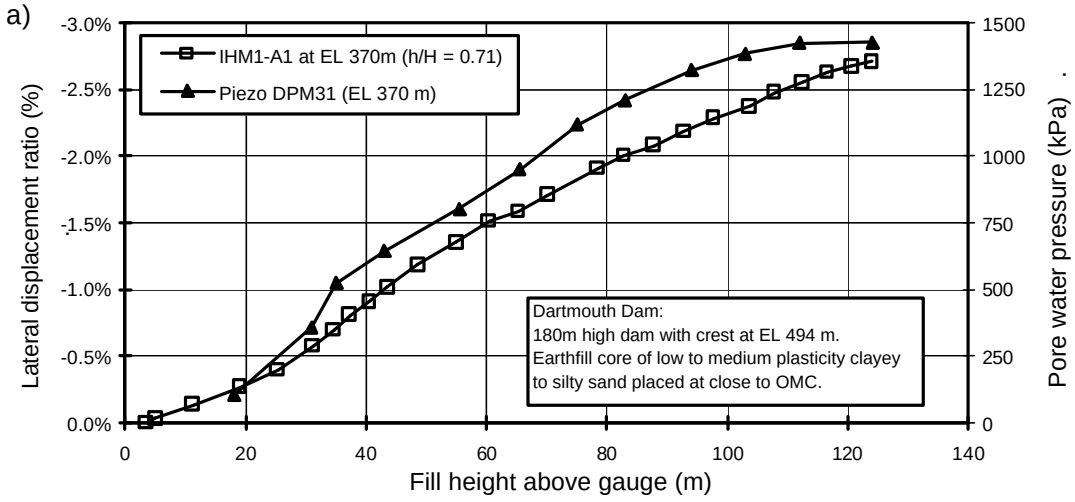

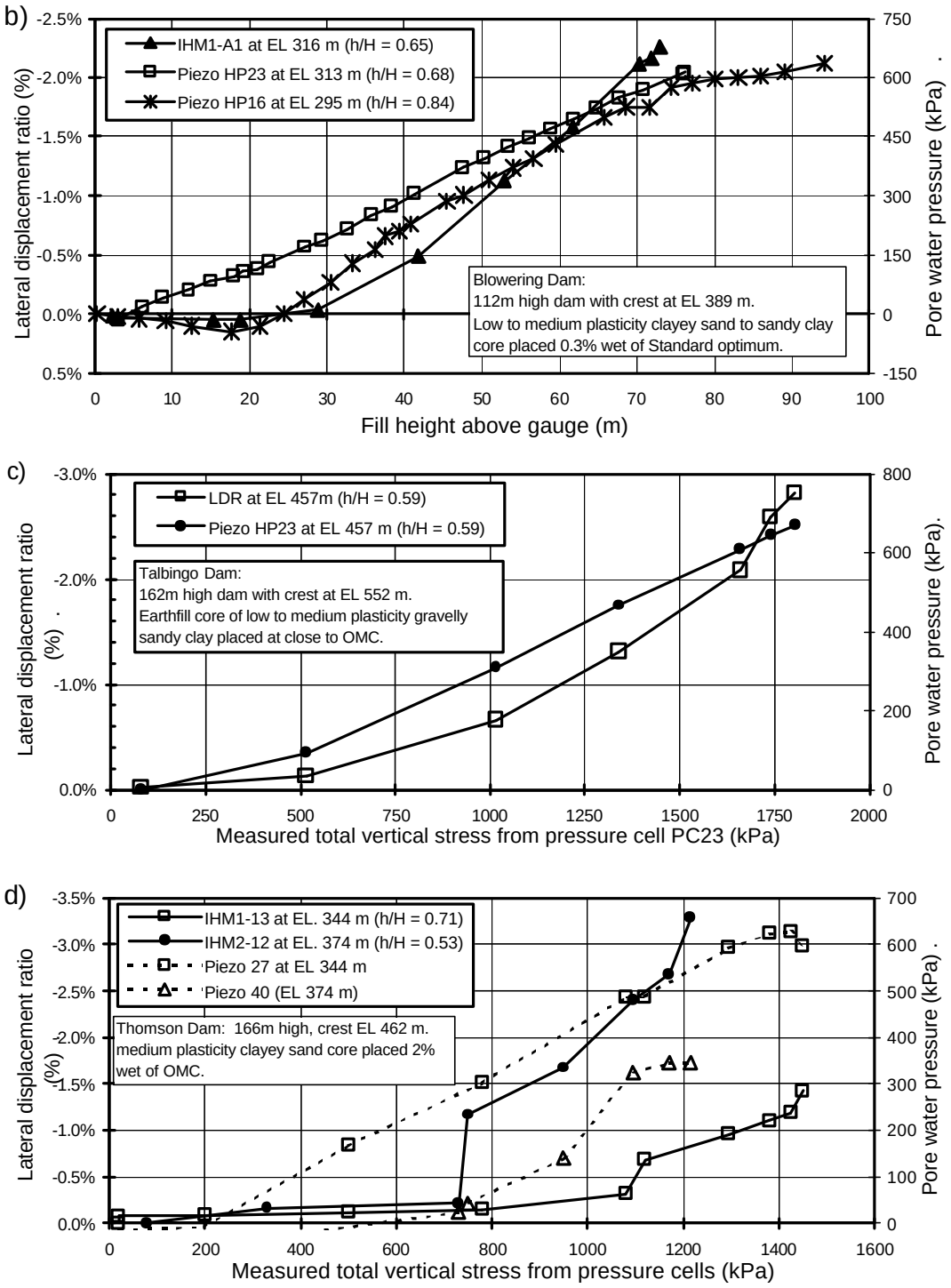

Figure 7.14: Lateral displacement ratio and pore water pressure versus fill height or measured total vertical stress at *(a)* Dartmouth dam; *(b)* Blowering dam; *(c)* Talbingo dam and *(d)* Thomson dam.

7.4.3 VERTICAL DEFORMATION OF THE CORE DURING CONSTRUCTION

Internal settlements during construction were collected for 57 embankments of earthfill, zoned earthfill and zoned earth and rockfill types. The settlement records were mostly from internal vertical settlement gauges (IVMs) installed in the central core of the earthfill (near the dam axis) as construction proceeded.

The purpose of the analysis is to define "normal" deformation behaviour so case studies showing "abnormal" deformation can be identified and then further analysed. The data is grouped into those case studies where a "homogeneous" type analysis (i.e. small lateral core strain) is appropriate, and those where lateral deformations are likely to be significant.

The vertical deformation in the core under the embankment axis (or within close proximity to the axis) is presented in the following formats:

- Vertical strain versus effective vertical stress (and secant modulus versus effective vertical stress) for those case studies where a "homogeneous" type analysis is appropriate.
- Vertical strain versus fill height above the cross-arm for case studies where lateral deformations are likely to be significant.
- Total vertical settlement (in millimetres) of the core during the period of construction versus embankment height. The total vertical settlements are estimated from the cumulative settlement between the cross-arm gauges.

Vertical strains in the core are calculated between the individual cross-arm intervals of the IVM by dividing the measured settlement (between the cross-arm interval) by the original distance between the cross-arms. The vertical stresses or fill heights are representative of the midpoint between the nominated cross-arm intervals. Corrections have been made to the strain readings so that the zero strain reading is equivalent to zero stress (or zero fill height). The corrections are based on the strain measurements at low stress levels.

The vertical strain (and secant modulus) plots are presented in two forms; *(i)* vertical strain at the end of construction, and *(ii)* vertical strain during construction. For the plots at the end of construction the vertical strains (or secant moduli) are calculated and plotted at cross-arm intervals over the full depth of the IVM gauge from near to crest level to foundation level. These plots, which include all the case studies, are referred to as the "*vertical strain profile at end of construction*" and they broadly define the range

of the data. The deformations in the upper 10 to 20% of the embankment have generally been excluded because of narrowing of the embankment and reduction in the lateral confinement, which often gives relatively large vertical strains resulting in low estimates of apparent moduli.

The vertical strain (and secant modulus) plots during construction (as opposed to the plots at the end of construction) only present data from selected cross-arm intervals from selected representative case studies. For these cases the cross-arm interval and its *h/H* ratio are identified in the legend. The purpose of these plots is to highlight the change in vertical strain (or secant modulus) with increasing vertical stress (or fill height), which is more clearly evident in these plot types.

7.4.3.1 *Vertical Deformation for Dry Placed Earthfills and Other Cases with Small Lateral Core Displacement*

The types of case studies analysed in this section are those for which simplification to an essentially one-dimensional analysis of the earthfill core is considered a suitable approximation of the deformation behaviour, and they are:

- Embankments with relatively broad core widths and dry placed earthfill cores, typically those placed at moistures contents drier than about 0.5 to 1% dry of Standard optimum. The limitation on core width is for case studies with thick cores (combined slope greater than 1H to 1V), but several case studies with broader medium width cores have been included.
- Embankments with cores of dominantly sandy to gravelly soil types with low plasticity silty fines or with low plasticity clayey fines of low fines content, and within which positive pore water pressures during construction were relatively low. The limitation on pore water pressure development generally restricts these cases to medium to thick core widths that are generally placed on the dry side of Standard optimum moisture content.
- Zoned embankments with thin cores where the compressibility properties of the core are similar to the shoulders. Two cases have been included Naramata and Frauenau, both dominantly sandy and gravelly cores with silty fines placed on the dry side of optimum.

Figure 7.15 presents vertical strain versus vertical effective stress as the embankment is raised for selected cross-arm intervals of selected case studies. The data is from the lower third of the core (i.e. $h/H > 0.66$). Effective vertical stresses at the midpoint between the nominated cross-arms have been estimated from total stresses estimated as described in Section 7.4.1.1 with positive pore water pressures then deducted. Note that negative pore water pressures at low stresses have been ignored and therefore the actual effective stresses at these low stress levels will be higher than indicated in the Figure 7.15 and other figures in this section.

The plots (Figure 7.15) show an apparent pre-consolidation pressure beyond which the incremental vertical strain (in terms of the log of stress) is greater. From the intersection of the two parts of the curves, these apparent pre-consolidation pressures range from 700 to 1000 kPa for the silty gravel, silty sand and clayey sand (with low content fines) earthfills, to 200 to 400 kPa for the clayey earthfills. The influence of negative pore water pressures, which has been ignored, will steepen the stress-strain relationship at low stress levels in these partially saturated earthfills.

Figure 7.16 presents the secant modulus versus vertical effective stress as the embankment is raised for selected cross-arm intervals of selected case studies; the modulus calculated by dividing the estimated vertical effective stress by the vertical strain. The modulus has been termed a "confined secant modulus" based on the assumption of negligible lateral strain. Figure 7.16 shows a relatively broad variation in confined secant modulus at a given stress level, more so for the dominantly sandy and gravelly core types probably because of the effect of variation in fines content and fines plasticity as well as compaction conditions.

For most cases shown in Figure 7.16 the confined secant modulus generally increases with increasing effective vertical stress, but with a large variation in the incremental change in modulus over a given stress level. Other cases show the confined secant modulus to remain relatively steady with increasing stress whilst some even show it to decrease. A gradual increase in the confined secant modulus with increasing stress, for the stress range of the data, is considered the typical response indicating the earthfill becomes less compressible as the voids ratio decreases.

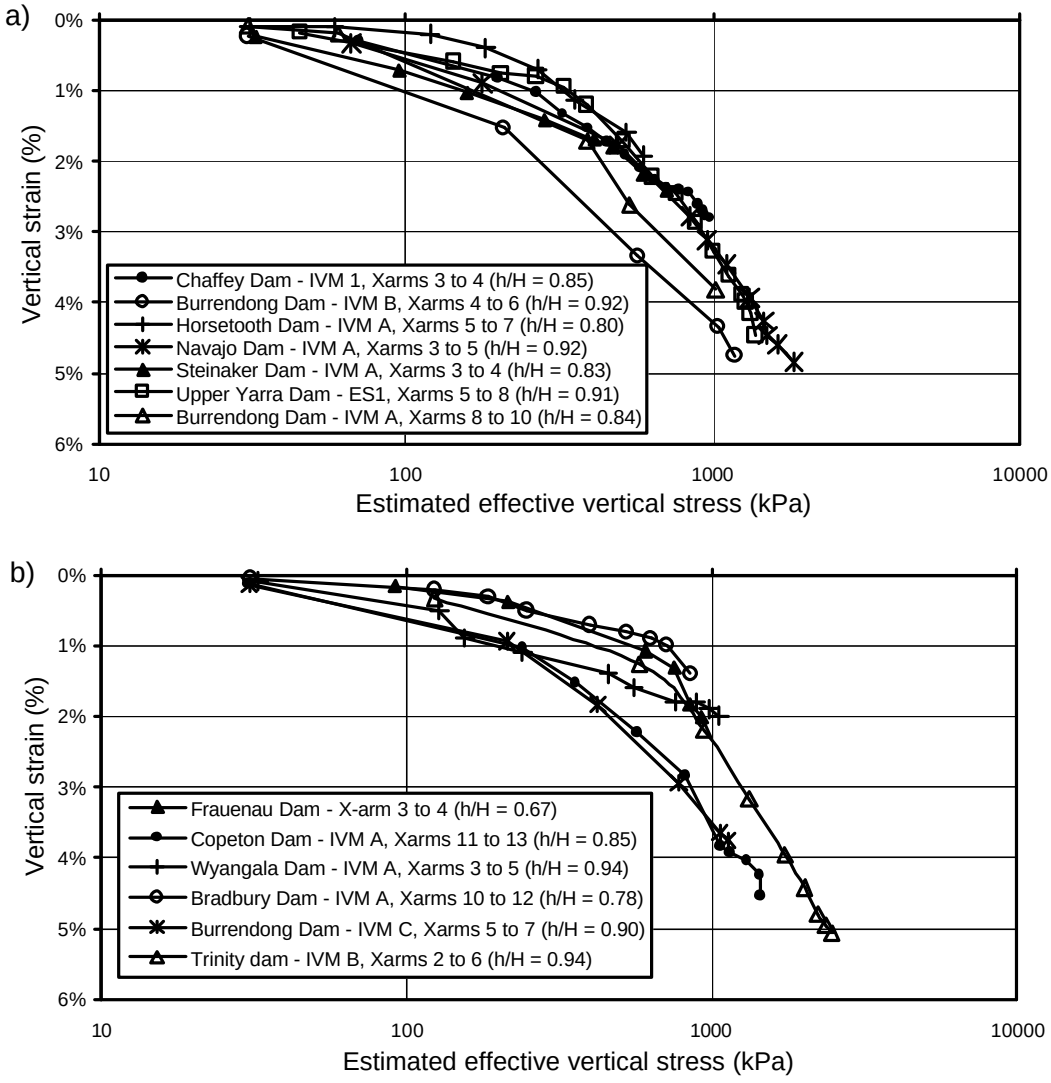

Figure 7.15: Vertical stress versus strain of the core during construction for selected cross-arm intervals of selected case studies; *(a)* dry placed clay cores, and *(b)* dry placed dominantly sandy and gravelly cores with plastic fines.

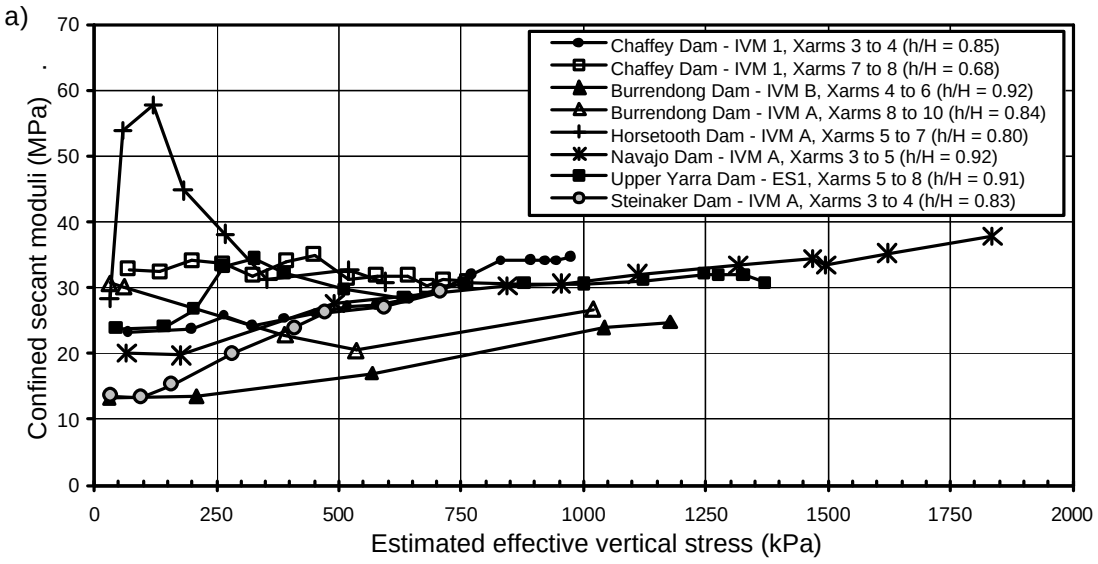

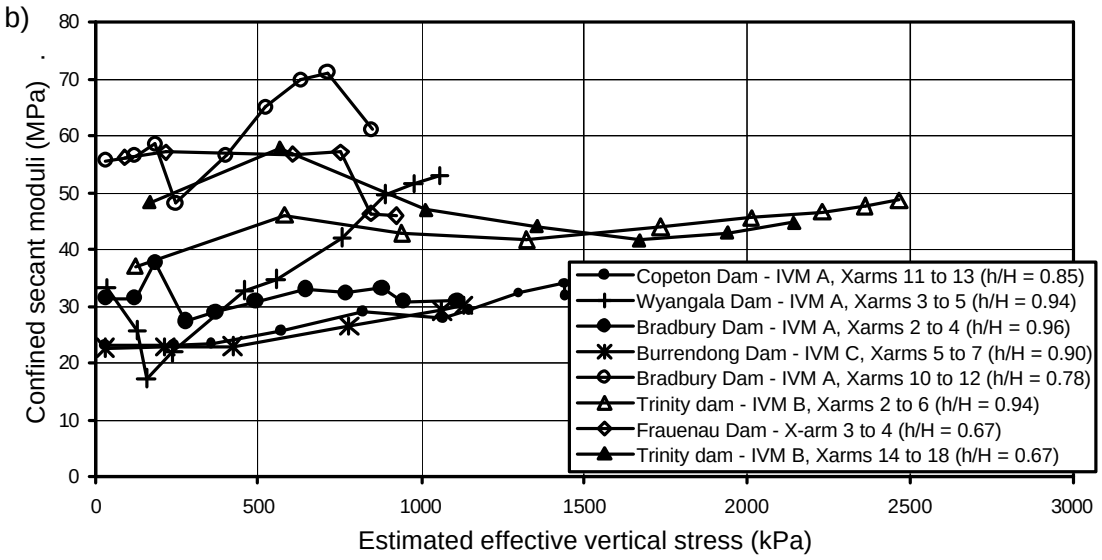

Figure 7.16: Confined secant moduli of the core versus vertical stress during construction for selected cross-arm intervals of selected case studies, *(a)* dry placed clay cores, and *(b)* dry placed dominantly sandy and gravelly cores with plastic fines.

Of the case studies that show an increase in the confined secant modulus with increasing stress, the secant modulus at low stress levels is sometimes quite low; for example, the cross-arm intervals shown for Burrendong, Navajo and Steinaker dams. Evaluation of the stress-strain relationship for several of these cases (Figure 7.17) shows that the tangent confined moduli at low stresses is much lower than that at stress levels in excess of 200 to 300 kPa, and is near constant at the higher stress levels. Given that the earthfill core for these embankments has been placed at moisture contents on the dry side of Standard optimum and well-compacted in thin lifts, this type of stress-strain behaviour is unlikely. It would be expected that the tangent confined moduli at low stresses would be at least similar to that observed at stresses up to 500 to 1000 kPa.

The most likely cause of this observation is suspected to be settlement on seating of the cross-arm after installation possibly due to a slightly uneven bedding surface or loose nature of the bedding material on which the cross-arm sits. Settlements of 20 to 30 mm due to seating can make a large difference in the calculated tangent and confined secant moduli at low stresses.

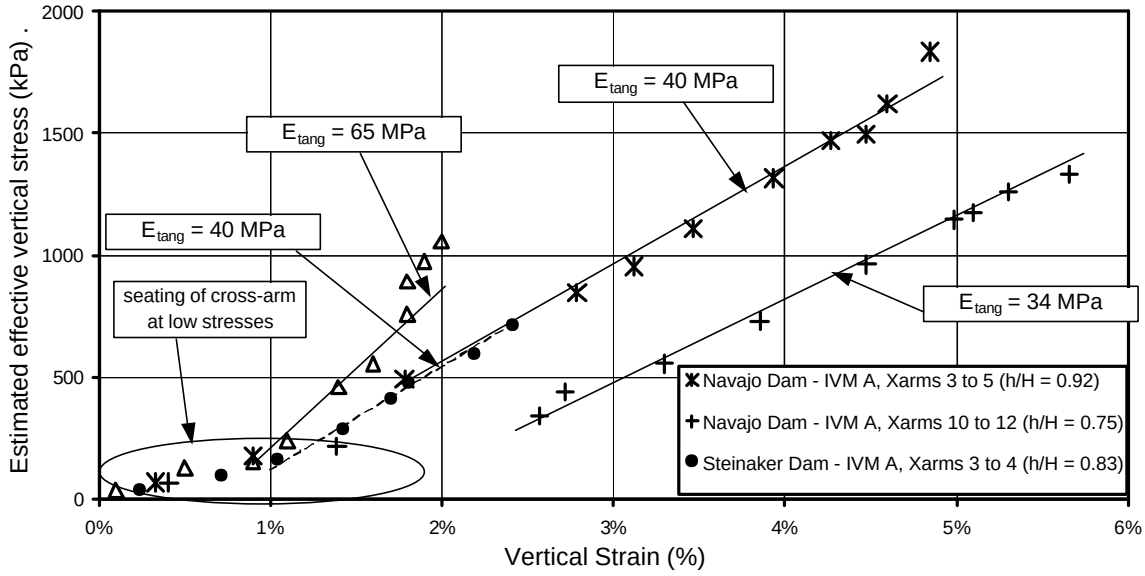

Figure 7.17: Seating settlements at low stresses suspected as cause of low moduli estimates at low stresses.

Table 7.13 presents a summary of the range and average of the confined secant moduli at various effective vertical stress levels from the case studies for well-compacted dry placed central core zones. It includes:

- Data from the case studies represented in Figure 7.15, including values from analyses of other cross-arm intervals in these embankments that are not shown.
- Data from case studies where the vertical strain was also analysed for specific cross-arm intervals but not shown in Figure 7.15.
- Data from the end of construction vertical strain profiles (Figure 7.18 and Figure 7.19).
- Data from Gould (1953, 1954) for a number of USBR dams of dry placed earthfills mainly from embankments with very broad earthfill zones. Gould presented his data in terms of vertical strain versus effective vertical stress. It has been converted here to values of secant moduli.

Seating effects have only been considered in the confined secant modulus values for those cases where the stress-strain relationship indicated this to have had a clearly identifiable influence on the deformation behaviour. For most of the cases represented in Table 7.13 the data was not available from which to make an assessment of seating. Therefore, the real lower limits and averages, particularly at the lower vertical stress levels, are possibly slightly higher than indicated. Categorisation based on material type

is justified from the findings by Gould (1954) and from analysis of the case study data collected for this study.

Table 7.13: Confined secant moduli during construction for well-compacted, dry placed earthfills.

Core Material Type	**No. Cases**	**Confined Secant Modulus (MPa)*[1]**		
		Effective Vertical Stress Range (kPa)		
		500 to 700*[2]	**1000**	**1500 to 2000**
Clayey soil types (CL) – sandy clays and gravelly clays	20	15 to 45 (27)	15 to 50 (30)	25 to 42
Silty soils (ML), data from Gould.	3	30 to 60	-	-
Clayey Sands to Clayey Gravels (SC/GC), plastic fines, > 20% fines	11	20 to 65 (33)	30 to 65 (40)	25 to 65
Silty Sands to Silty Gravels (SM/GM), plastic fines, > 20% fines	9	35 to 65 (46)	45 to 65 (50)	35 to 65
Sandy and Gravelly soils - non-plastic fines or < 20% plastic fines	6	35 to 80 (60)	35 to 90 (60)	40 to 90

Notes *[1] Values represent range of confined secant moduli, values in brackets represent average
*[2] Includes Gould (1953, 1954) data.

The range of confined secant moduli within any core material type is relatively broad, up to 0.5 to 2 times the mean. Part of this variation is likely explainable by variations in material properties (particle size distribution, plasticity, etc.), variations in compacted density ratio and inaccuracies in the IVM measurement readings. Correlation between the compacted density ratio at placement (and dry density) and confined secant moduli for a given earthfill type did not identify any clear trend, however, the database was limited.

Figure 7.18 and Figure 7.19 present the vertical strain and confined secant moduli versus effective vertical stress at end of construction for all case studies of dry placed earthfills. As discussed earlier, they differ from Figure 7.15 and Figure 7.16, which are for selected cross-arm intervals of selected case studies during construction. Essentially there is no difference between the plots, but Figure 7.18 and Figure 7.19 present the data for all case studies representative of dry placed earthfills and show a broader range of variation of vertical strain and modulus.

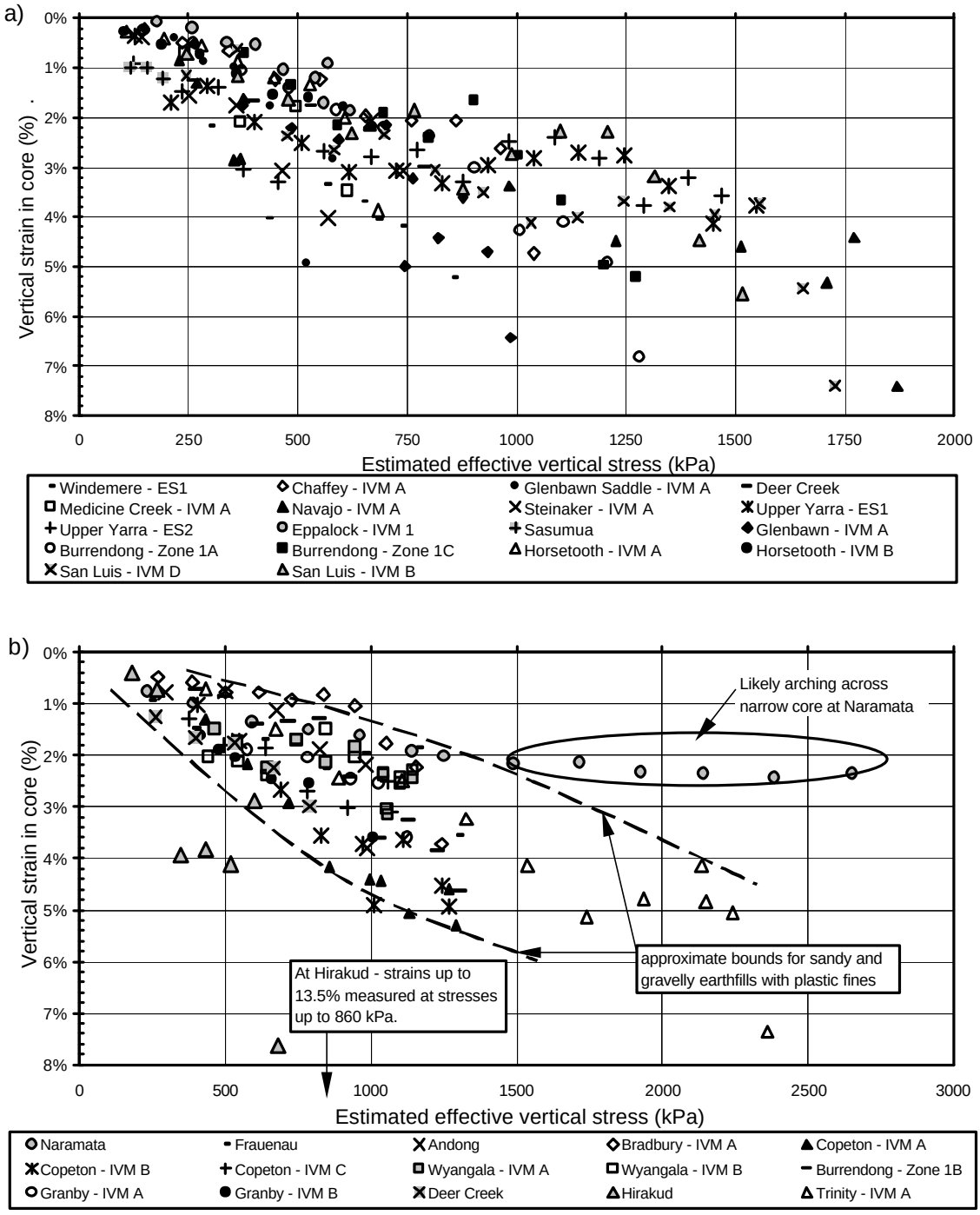

Figure 7.18: Vertical strain versus effective vertical stress in the core at end of construction for *(a)* dry placed clay earthfills and *(b)* dry placed dominantly sandy and gravelly earthfills.

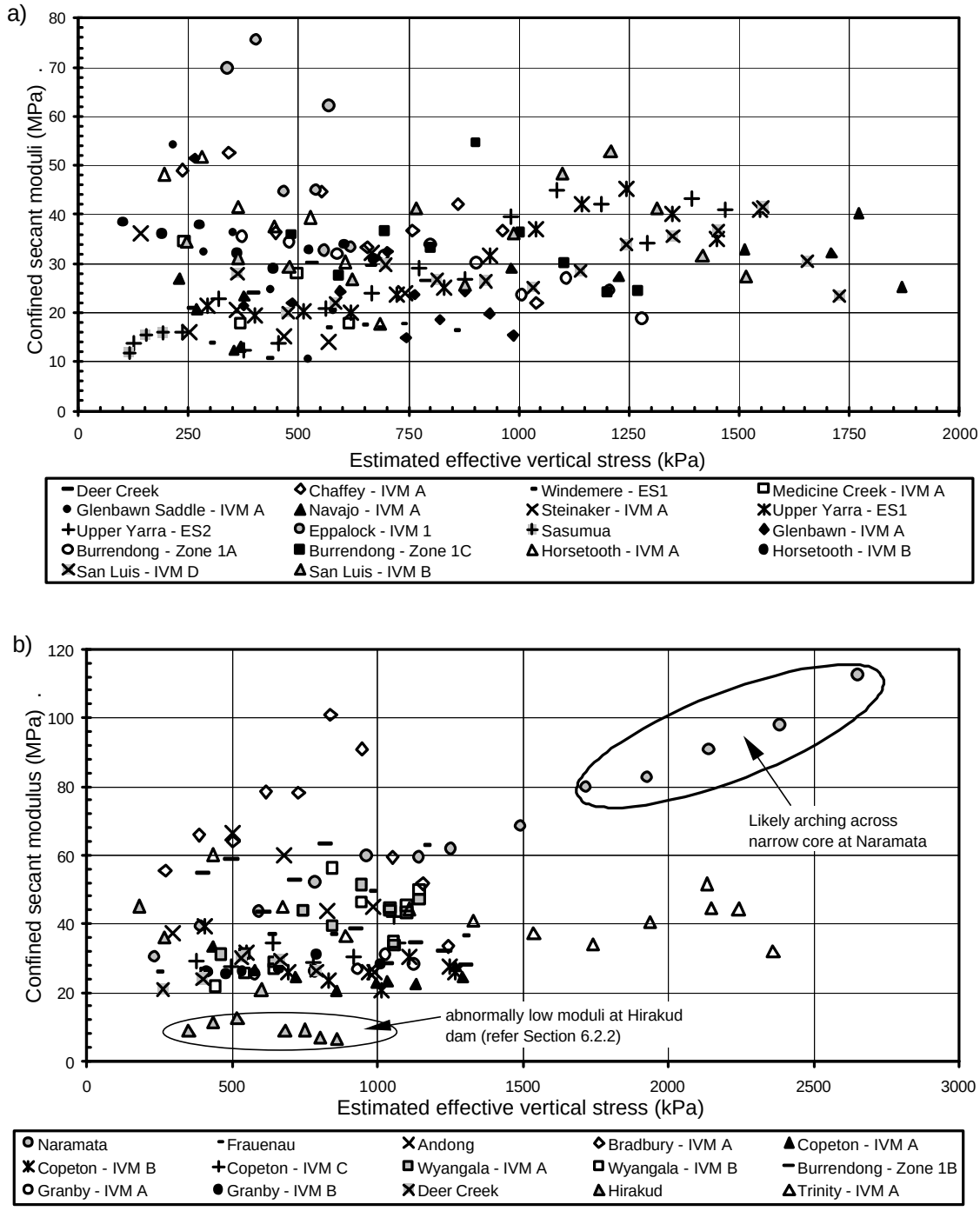

Figure 7.19: Confined secant moduli versus effective vertical stress in the core at end of construction for *(a)* dry placed clay earthfills and *(b)* dry placed dominantly sandy and gravelly earthfills.

For the dominantly sandy and gravelly earthfill types the data (Figure 7.18b and Figure 7.19b) show:

- Higher confined secant moduli for silty sand and silty gravel type earthfills with non-plastic fines, or with low plastic fines content (Bradbury, Naramata, Andong and Frauenau dams).
- On average, lower confined secant moduli in the clayey sand and clayey gravel type earthfills (Copeton, Granby, Deer Creek and Burrendong (Zone 1B) dams).
- Likely arching effects in the narrow, dry placed earthfill core at Naramata.

For the clay earthfills the plots (Figure 7.18a and Figure 7.19a) show a reasonable degree of consistency between case studies. Several of the points that show high strains at a given vertical stress are within wetter placed earthfills near to the interface with the foundation. In general, relatively high vertical strains are observed at this interface region, most probably due to plastic type deformations of the wet placed earthfill in the foundation contact zone.

7.4.3.2 *Vertical Deformation for Wet Placed Earthfills and Other Cases with Large Lateral Core Displacement*

The types of case studies analysed in this section are zoned embankments where the deformation of the earthfill core cannot be adequately modelled by simplification to a one-dimensional analysis. For these case studies the lateral displacement of the core during construction is generally large and has a significant influence on the vertical deformation behaviour of the core. Analysis of the deformation behaviour of the core should be undertaken on a case-by-case basis using finite element methods to model the embankment construction. Notwithstanding this, there is some merit in comparative analysis of the case studies as a general guide to possible identification of "abnormal" deformation behaviour.

The figures in this section are presented versus fill height. It would have been preferable to use total vertical stress, but the data includes a number of case studies where arching was significant and no information of total stresses from pressure cells was available. Rather than attempt to estimate the total vertical stress the fill height was used for all case studies. The case study data on the vertical strain in the core has been sorted based on core width and is presented in the following figures:

- Figure 7.20 – incremental vertical strain versus fill height for selected cross-arm intervals from selected case studies.

- Figure 7.21 and Figure 7.22 – vertical strain profile of the core (i.e. versus fill height) at end of construction. Figure 7.21 is of dominantly sandy and gravelly earthfill cores and Figure 7.22 is of clay cores.

The difference between the plot types, as previously discussed, is that the incremental vertical strain plots highlight the change in vertical strain with increasing fill height, and the vertical strain profiles at end of construction include all the case studies and highlight the degree of variation from the data.

From Figure 7.20, the general trend for thin cores is for an apparent decrease in the incremental vertical strain with increase in fill height. The medium width cores show a similar trend but it is not as evident as it is for the thin cores. Arching across the core is likely to be a significant factor influencing this behaviour, particularly for the thin cores. If measured total vertical stress were used as the x-axis this trend would probably not be evident for most of the case studies because the influence of arching would be included in the total vertical stress. The analysis of the core deformation during construction at Blowering dam shows this to be the case (refer Section 6 of Appendix G).

Figure 7.21 and Figure 7.22 highlight the very high vertical strains measured within some regions of the core of several zoned embankments including Blowering, Beliche, Tedorigawa and Chicoasen dams. High lateral strains and plastic deformation of the wet placed earthfill core are likely to be the reason for the large vertical strains observed in most, but not all cases. Further discussion on several of these cases is presented in Section 7.9.

In Figure 7.21 and Figure 7.22 the bounds shown on several of the figures are an interpretation, based on evaluation of the data, of the general limits of “normal” type deformation during construction in wet placed earthfills. However, assessment of whether or not a point or series of points located outside the bounds shown is potentially “abnormal” requires further evaluation, and this is the main purpose of the indicative bounds. In general, for those cases where a series of points plot below the lower bound (such as for Beliche dam in Figure 7.21a) or one or two points plot well below the lower bound it is likely that the deformation behaviour is an outlier to the general trend.

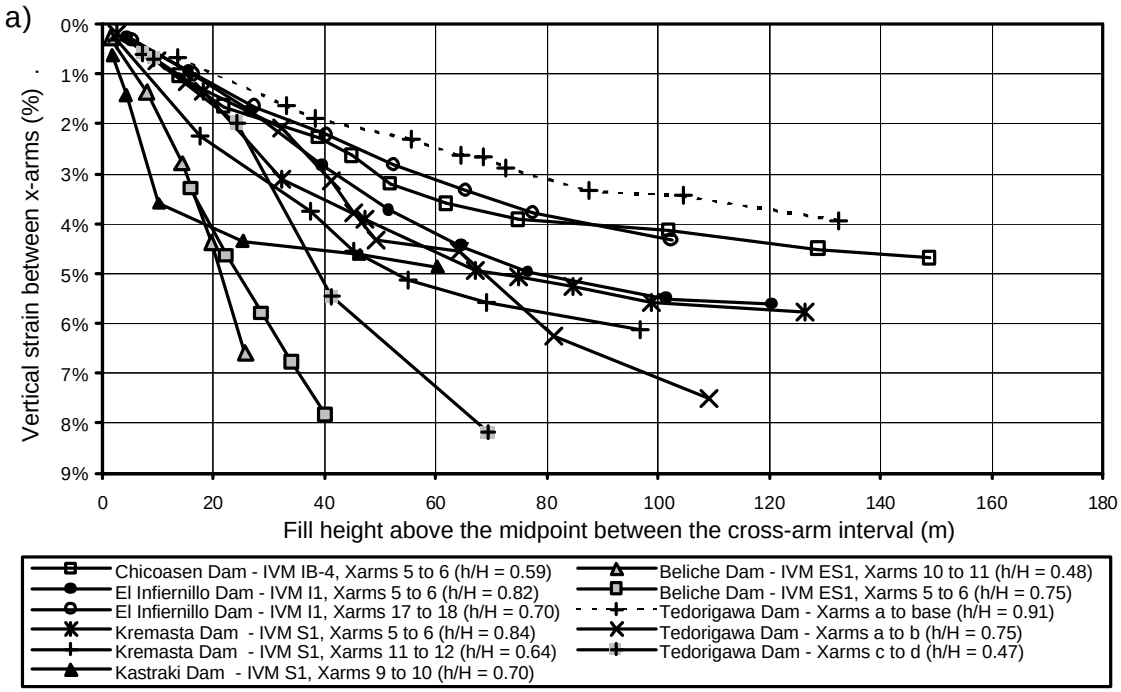

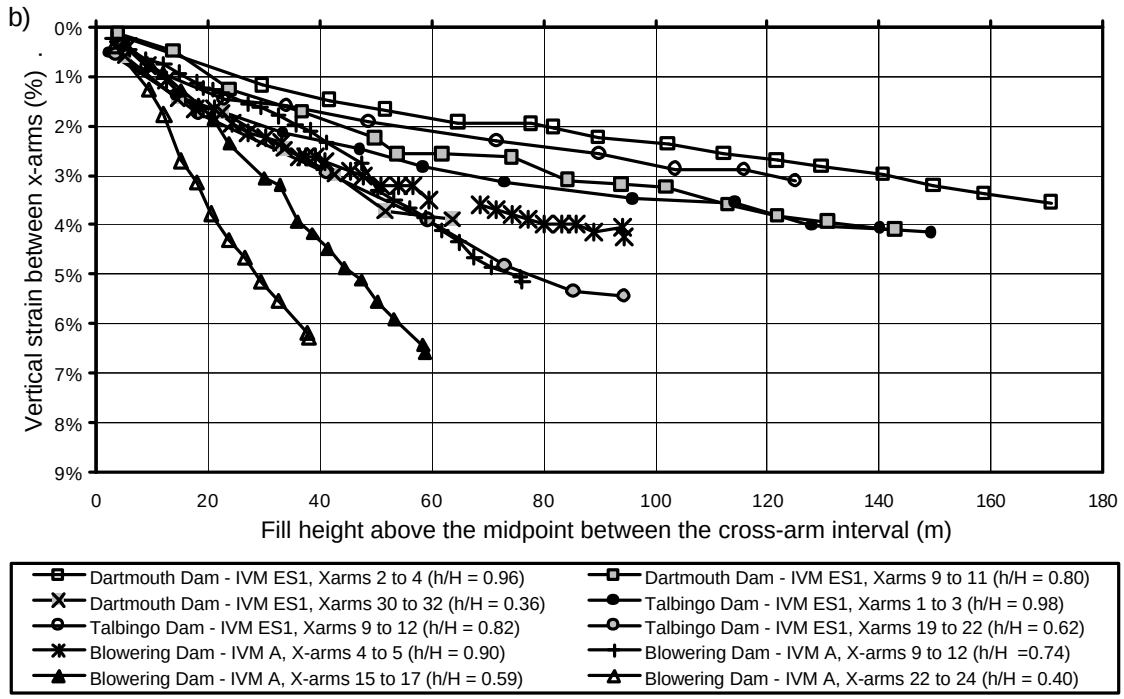

Figure 7.20: Vertical strain in the core versus fill height during construction at selected cross-arm intervals in selected case studies of earthfills placed close to or wet of Standard optimum, for *(a)* thin core (combined slopes less than 0.5H to 1V), and *(b)* medium cores (combined slope ≥ 0.5H to 1V and < 1H to 1V).

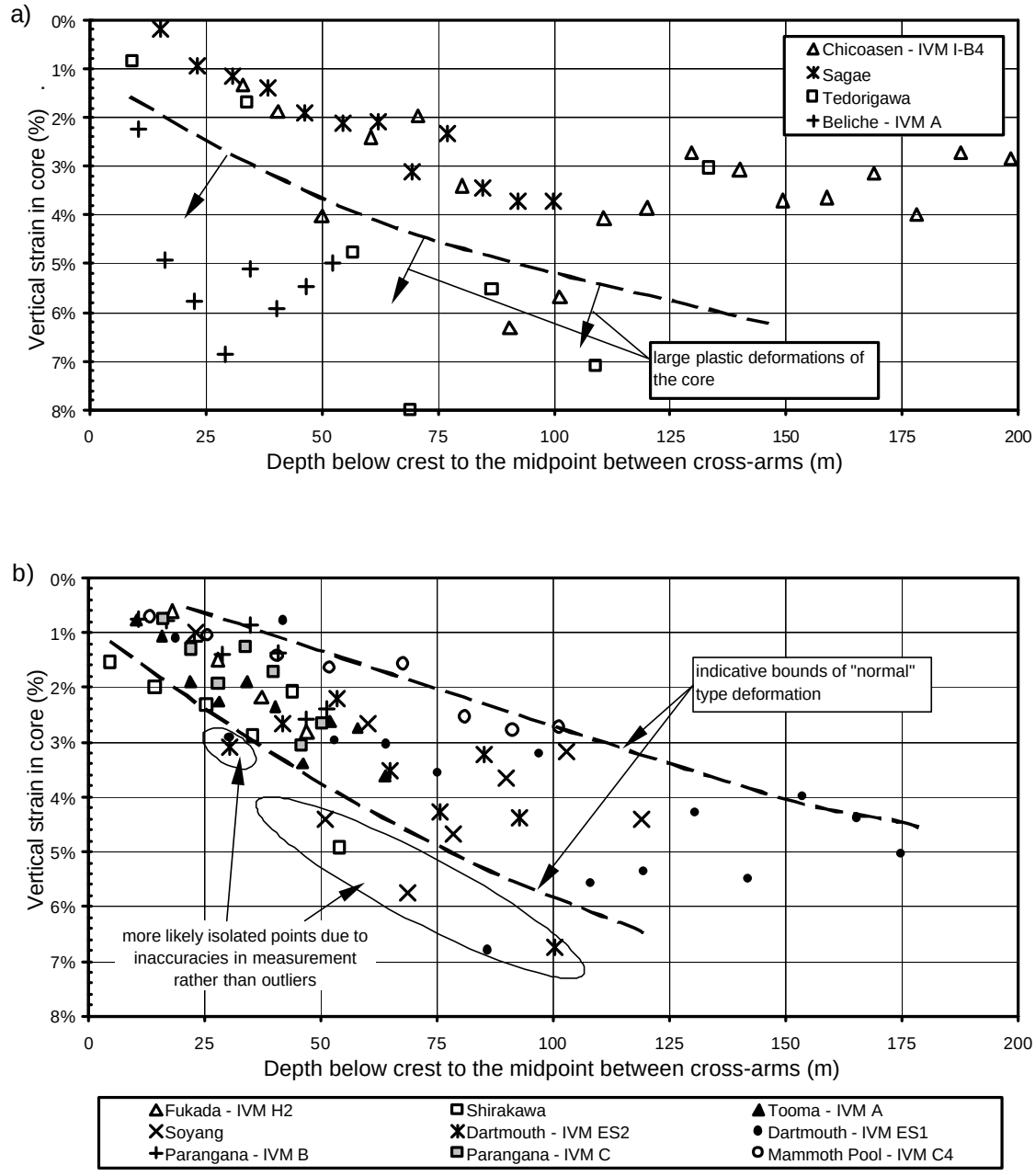

Figure 7.21: Vertical strain in the core versus fill height at end of construction for dominantly sandy and gravelly earthfills with plastic fines placed close to or wet of Standard optimum, for *(a)* thin cores (combined slopes less than 0.5H to 1V), and *(b)* medium to thick cores (combined slope ≥ 0.5H to 1V).

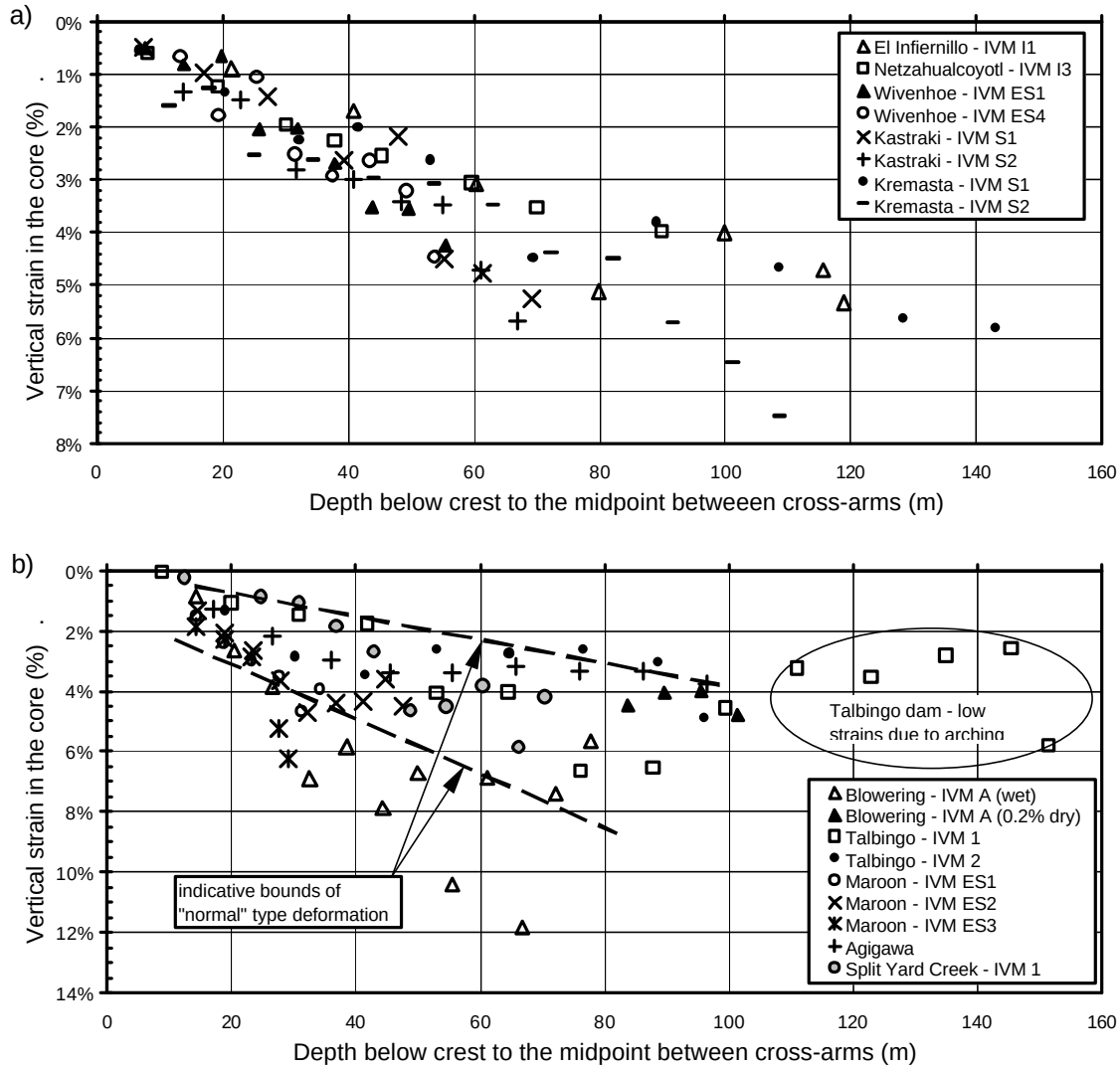

Figure 7.22: Vertical strain of the core versus fill height at end of construction for clay earthfills placed close to or wet of Standard optimum moisture content, for *(a)* thin core (combined slopes less than 0.5H to 1V), and *(b)* medium to thick cores (combined slope ≥ 0.5H to 1V).

For several case studies the point or points that plot outside the bounds are not necessarily indicative of an outlier or potentially "abnormal" deformation behaviour. Several case studies show a large degree of variation in vertical strain between consecutive cross-arm or depth intervals, showing an almost zigzag type pattern (e.g. IVM ES1 at Dartmouth in Figure 7.21b). This type of effect is, in some cases, due to the inaccuracies or errors of measurement in the IVM gauge and does not necessarily represent a large localised region of vertical strain. These points are not likely to be outliers.

Conversely, it should also be recognised that a case study that shows potentially "abnormal" type deformation behaviour in the core during construction may not necessarily be identified as such in plots such as Figure 7.21 and Figure 7.22. Although, of the case studies represented in the plots those within the bounds are all considered to be indicative of "normal" type deformation behaviour.

7.4.3.3 Total Settlement of the Core During the Construction Period

Another type of plot considered useful in the identification of potential "abnormal" deformation behaviour of the core during construction is the total settlement of the core that occurs during the period of embankment construction. Figure 7.23 presents the total settlement of the earthfill core or central earthfill zone during the period of construction versus embankment height for the case studies. The results show a general trend of increasing settlement (as a percentage of the embankment height) with increasing embankment height. At embankment heights of less than 50 m, total settlements were generally in the order of less than 1% up to 2.5%, and for embankment heights greater than 150 m, in the order of 2 to 5%.

Several sub-groups of material type and core width with a similar total settlement versus embankment height relationship are identifiable (Figure 7.23b), they are:

- Dominantly fine grained earthfills, mainly clays but includes some dominantly silty soils, covering thin to very broad cores and dry to wet placement conditions. These cases generally plot on the higher side with settlements in the order of 3 to 3.5% for embankment heights greater than about 100 m.
- Dominantly sandy and gravelly earthfills with plastic fines (i.e. clayey and silty sands and gravels), dry to wet placement conditions and medium width to very broad core sizes. The total settlement for this sub-group is similar to that for the clay earthfills, reaching settlements in the order of 3 to 4% for embankment heights greater than about 100 m.
- Dominantly sandy and gravelly earthfills with non-plastic fines or with low content plastic fines (typically less than 10 to 20%) for thin to thick core widths. The total settlement for these core types is at the low end for embankment dams, approximately half that of the clayey earthfill types at a given embankment height. The low settlement reflects the low compressibility of these earthfills when well

compacted. Settlements are typically in the range 1 to 2% for embankment heights up to 150 m.

- Dominantly sandy and gravelly earthfills with thin width cores. The total settlement for these core types is in between that of the clayey earthfills and non-plastic sandy and gravelly earthfills, reaching maximum settlements in the range 1.5 to 3% for embankment heights greater than about 100 m.

The data within each material / core width sub-group shows a reasonable fit as indicated by the high regression coefficients of the trendlines (Figure 7.23b). The trendlines are quadratic equations and are given in Table 7.14 along with the standard errors and regression coefficients. Outliers to the general trend (Beliche, Hirakud, Blowering, Tedorigawa and Nurek dams) were excluded from the correlations. These cases are discussed further in Section 7.9.

The settlement to embankment height curves from Figure 7.23b are useful as a guideline for estimation of the total core settlement during construction and identification of potentially "abnormal" deformation behaviour for embankment heights up to 100 to 125 m. Above about 125 m only one or two points define the shape of the relationships and therefore settlement estimates will be less reliable.

Correlations between the settlement as a percentage of the embankment height and embankment height in the form of a power function are summarised in Table 7.15. The regression coefficients indicate a good correlation exists for the sub groups and the range in standard error is relatively low, from 0.24 to 0.47%.

The correlation shown for several of the sub groups, in particular for the clayey earthfills, is somewhat coincidental. The clay earthfill sub-group includes dry to wet placement conditions and core widths from thin to very broad. It is evident from previously presented data that the deformation behaviour of a wet placed, thin to medium width clayey core is significantly different to that of a dry placed, very broad clayey earthfill core. Therefore, for these two different material placement conditions and core width geometries to be included in the same sub group is somewhat coincidental.

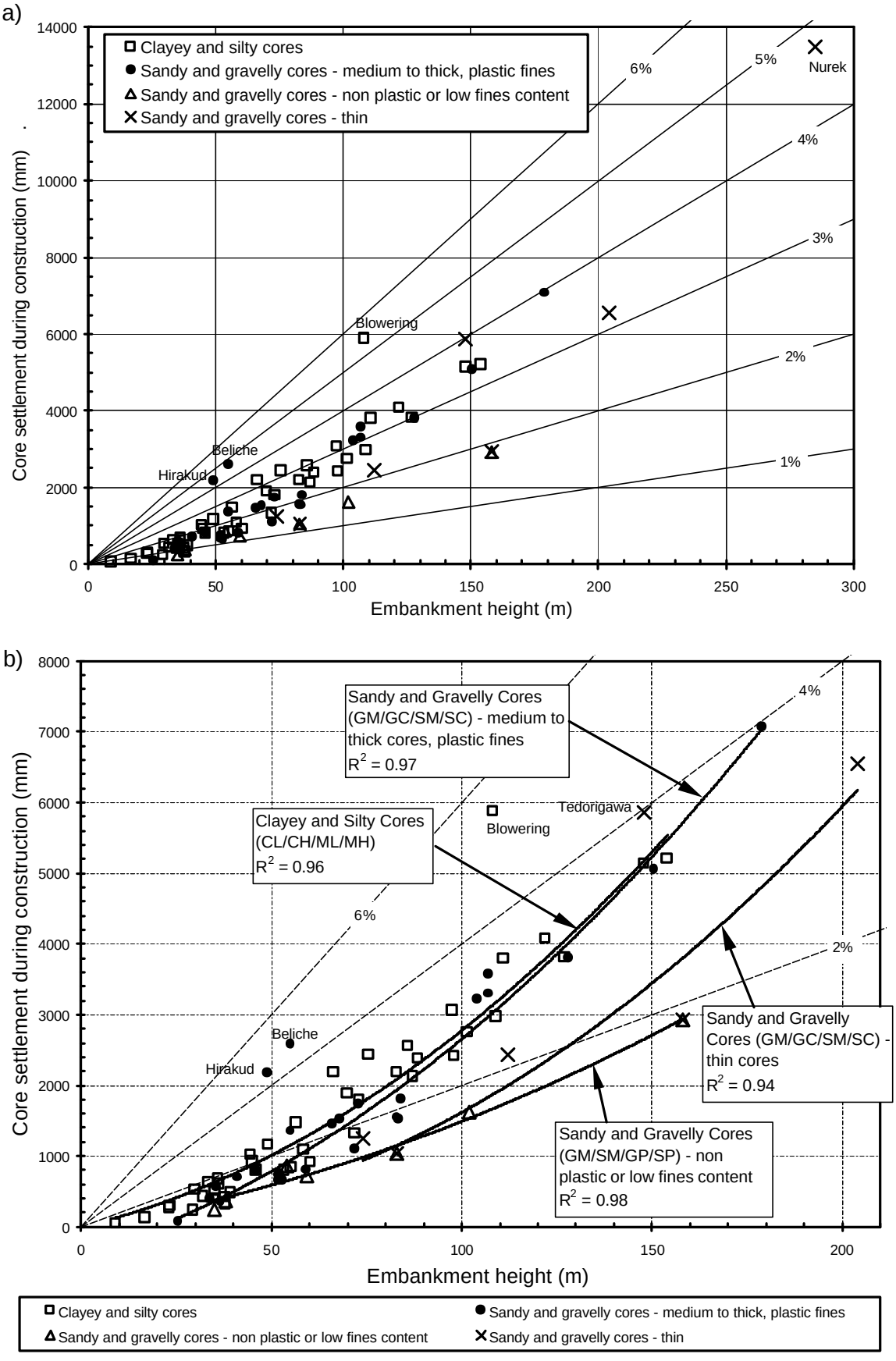

Figure 7.23: Core settlement during construction of earth and earth-rockfill embankments *(a)* including Nurek dam, and *(b)* excluding Nurek dam.

Table 7.14: Equations of best fit for core settlement versus embankment height during construction

Core Material / Shape Type	**No. Cases**	**Equation for Core Settlement*[1]**	**R^2 *[2]**	**Std. Err. (mm) *[3]**
Clay cores – all sizes	42	$Settlement = H(0.152H + 12.60)$	0.96	275
Sandy and gravelly cores:				
- medium to thick, plastic	25	$Settlement = H(0.183H + 7.461)$	0.97	290
- thin	5	$Settlement = H(0.136H + 2.620)$	0.94	635
- non-plastic	7	$Settlement = H(0.063H + 8.57)$	0.98	130

Note: *[1] settlement in millimetres, embankment height H in metres.
*[2] R^2 = regression coefficient
*[3] Std. Err. = standard error of the settlement

Table 7.15: Equations of best fit for core settlement (as a percentage of embankment height) versus embankment height during construction

Core Material / Shape Type	**No. Cases**	**Equation for Core Settlement*[1]**	**R^2 *[2]**	**Std. Err. (%) *[3]**
Clay cores – all sizes	42	$Settlement(\%) = 0.179\,H^{0.60}$	0.77	0.41
Sandy and gravelly cores:				
- medium to thick, plastic	25	$Settlement(\%) = 0.079\,H^{0.76}$	0.81	0.39
- thin	5	$Settlement(\%) = 0.063\,H^{0.72}$	0.70	0.47
- non-plastic	7	$Settlement(\%) = 0.187\,H^{0.46}$	0.71	0.24

Note: *[1] settlement as a percentage of the embankment height, embankment height H in metres.
*[2] R^2 = regression coefficient
*[3] Std. Err. = standard error of the settlement (as a percent of embankment height)

7.5 GENERAL DEFORMATION BEHAVIOUR ON FIRST FILLING OF EARTHFILL AND ZONED EARTH AND EARTH-ROCKFILL EMBANKMENTS

The following discussion summarises the factors affecting the deformation behaviour of earthfill and earth – rockfill embankments during first filling of the reservoir, drawing on relevant information from the published literature. The discussion does not go into case study specific details, but some of the issues raised are discussed in greater detail in the individual case study analysis in Sections 7.9 to 7.11.

Analyses of first filling generally consider the main water barrier element to be impermeable during first filling and the water load to act on the upstream face of this zone. Permeable earth and rockfill zones upstream of the main earthfill zone will become saturated during first filling. Therefore, the factors affecting the deformation behaviour of embankments during reservoir filling are primarily the water load, the compressibility properties of the earthfill core and downstream shoulder, and the susceptibility to collapse compression on wetting of the permeable earth and rockfill zones upstream of the core. Other factors that can affect the embankment deformation during first filling include time dependent deformations, such as creep and earthfill consolidation, and differential settlement of the foundation, neither of which is considered in detail in this section.

Nobari and Duncan (1972b), Sherard (1973) and others, describe the effect of the water load (Figure 7.24) as threefold:

(i) Applied water load on the upstream side of the core or earthfill forming the water barrier, resulting in a net increase in the total stresses within and downstream of this zone. The resultant deformation is downstream and downward.

(ii) Applied water load on the upstream foundation. Sherard (1973) comments that the foundation has an important influence on the embankment deformation if it is compressible or susceptible to collapse compression on wetting. Differential foundation settlements can arise due to differential loading conditions from the reservoir and in cases where the foundation differs under the embankment, such as in the case of a cut-off trench to bedrock under the central core.

(iii) Decrease of effective stresses in the permeable earth and rockfill zones upstream of the core. Deformations will be upward and upstream due to the unloading of

effective stresses, but are likely to be small due to the high tangent modulus on unloading and reloading of gravels and rockfills compared to their modulus during loading.

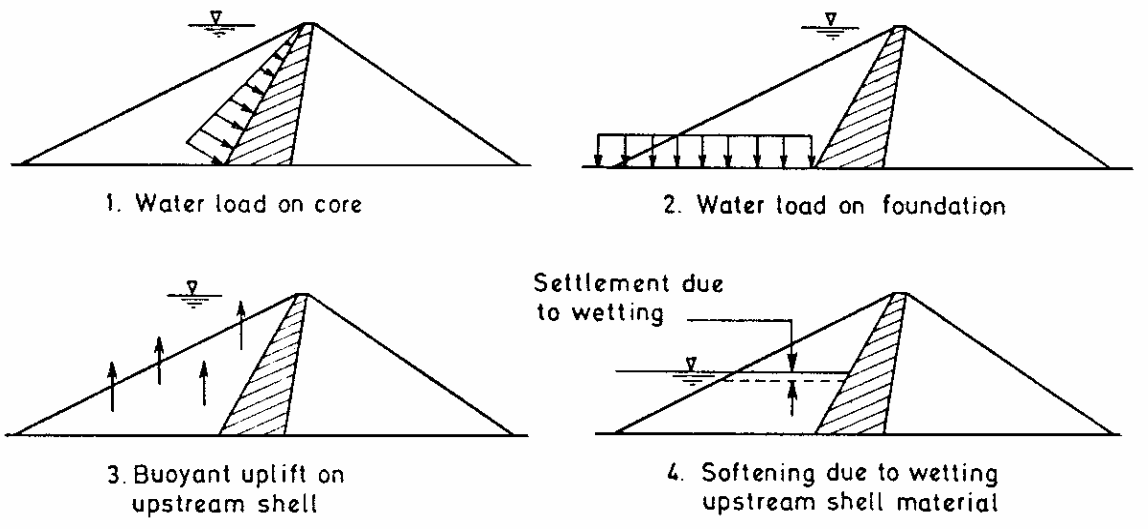

Figure 7.24: Effect of reservoir filling on a zoned embankment (Nobari and Duncan 1972b)

7.5.1 EFFECT OF WATER LOAD ON THE CORE

Assuming the central earthfill zone of the embankment behaves in undrained conditions during first filling, the effect of reservoir filling will be for a net increase in total stress acting on the upstream face of the core zone. The changes in total stress within the central earthfill zone and downstream shoulder zones due to first filling will depend on:

- The magnitude of the change in total stress acting on the upstream face of the core due to first filling, its location and the direction in which it acts as controlled by the orientation of the upstream face of the earthfill zone.
- The existing stresses within the embankment at end of construction.

The magnitude of the total stress difference is greatest where the load acts on the upstream slope of the embankment, as in the case of a homogeneous embankment or embankments with facing elements designed as the main water barrier element (e.g. concrete or asphalt faced rockfill dams). For typical slopes of homogeneous earthfill embankments of greater than 2 - 3H to 1V, the applied direction of the water load is dominantly vertical (Figure 7.25) and stress changes within the embankment will

mainly occur in the upstream slope. Resultant deformations of the crest or under the embankment axis will therefore generally be small.

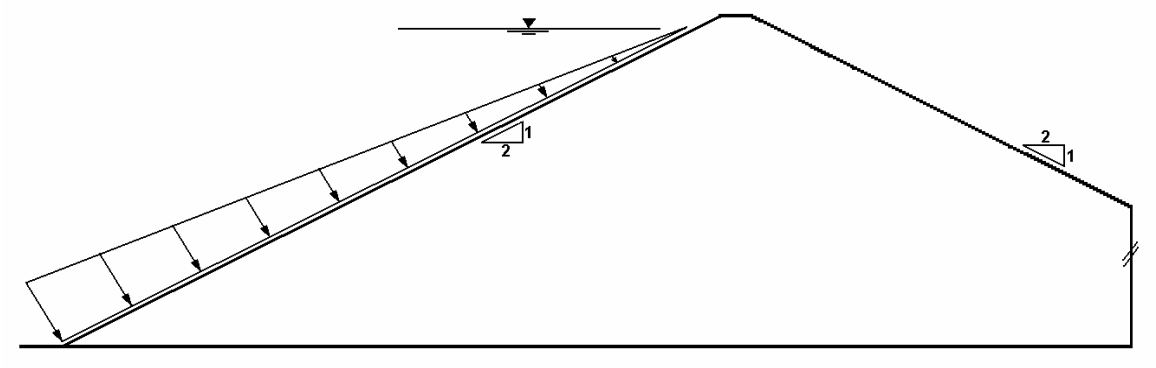

Figure 7.25: Water load acting on a homogeneous earthfill dam.

For zoned earthfill embankments with near vertical narrow cores and free draining gravels or rockfill in the upstream shoulder, the direction of the applied water load is near horizontal (Figure 7.24, Part 1). The magnitude of the difference in applied stress on the upstream face from end of construction to reservoir full will be much less than for water loads acting on the outer upstream face. It will be dependent on the existing stress conditions within the embankment at end of construction, the hydrostatic stress from the water and the reduction in effective stresses in the upstream rockfill on reservoir filling.

The earlier finite difference analysis (Section 7.4.1.2, Figure 7.4) has been extended to compare the lateral stress distributions at end of construction and end of first filling for two cases:

- The central earthfill zone having the same compressibility properties as the rockfill
- A wet placed core of low undrained strength (Case 3 from the earlier analysis).

Given that a linear elastic perfectly plastic Mohr-Coulomb model has been used for the embankment materials, the stress distributions will not necessarily be accurate at the end of first filling but they will be indicative of the general trend.

Where the core has similar compressibility properties to the shoulder the lateral stresses at end of construction are relatively low (Figure 7.26a) compared to the core of low undrained strength (Figure 7.27a), as previously discussed in Section 7.4.1.2. Assuming the core to behave undrained during reservoir filling, the change in total lateral stress in the core and downstream shoulder on reservoir filling is shown to be

greater for the core with similar compressibility properties to the rockfill (Figure 7.26b). For the low undrained strength core, lateral stress changes in the core and downstream rockfill on reservoir filling are smaller in comparison (Figure 7.27b) because of the already high lateral stresses present at the end of construction.

For both cases the lateral stress conditions in the core and downstream rockfill increase so resultant lateral deformations will be in a downstream direction. The high horizontal component of the applied stress vector from the water load acting on the upstream face of the core, compared to its vertical component, results in greater changes in lateral than vertical stress in the core and downstream shoulder. Therefore, deformations will be dominantly horizontal. In reality settlements are observed on the crest and downstream shoulder during first filling, most likely due to a combination of time dependent creep and consolidation, and potentially due to collapse compression in the downstream shoulder.

The magnitude of the deformation will depend on the changes in stress conditions, the compressibility properties of the core and downstream rockfill and the embankment geometry. For the downstream rockfill shoulder the existing lateral stress conditions are shown to be important, but also important is the effective stress path on first filling, which is for a net decrease in deviatoric stress and net increase in bulk stress.

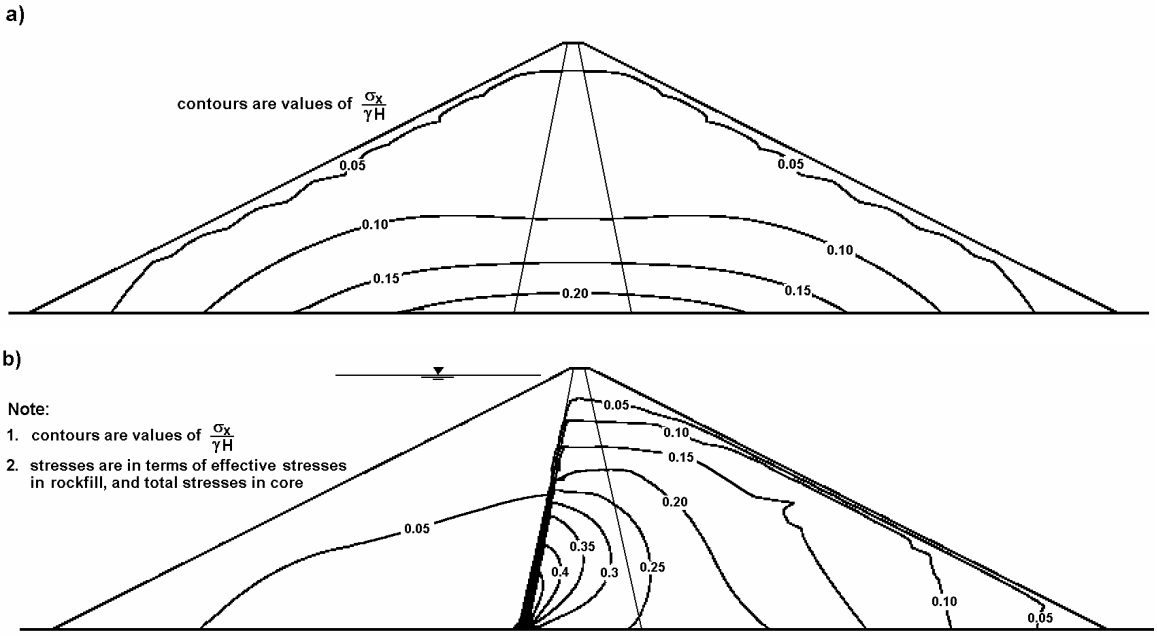

Figure 7.26: Lateral stress distribution at *(a)* end of construction, and *(b)* reservoir full condition, for central core earth and rockfill embankment with core of similar compressibility properties to the rockfill.

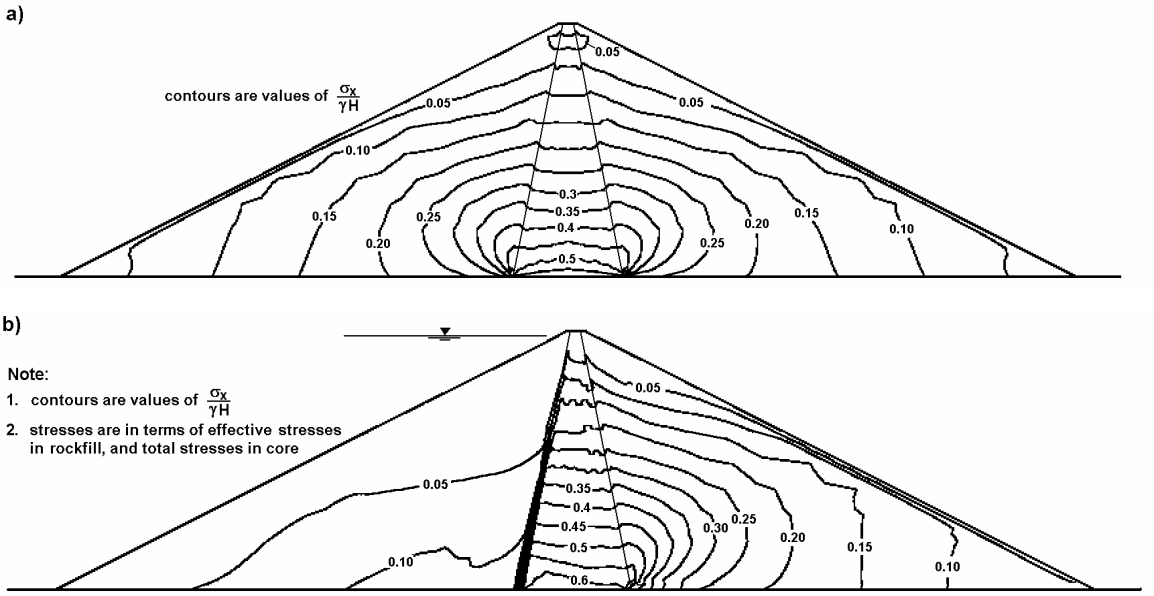

Figure 7.27: Lateral stress distribution at *(a)* end of construction, and *(b)* reservoir full condition, for a central core earth and rockfill embankment with wet placed core of low undrained strength.

7.5.2 COLLAPSE COMPRESSION DURING FIRST FILLING

Collapse compression or collapse settlement on wetting of embankment materials is an important factor in the deformation behaviour during first filling for a large number of embankments. In most cases collapse compression is associated with wetting of the upstream rockfill shoulder during first filling and numerous central core earth and rockfill embankments exhibit this effect including El Infiernillo dam (Marsal and Ramirez de Arellano 1967), Cougar dam (Pope 1967), Round Butte dam (Patrick 1967) and Beliche dam (Naylor et al 1997) amongst many others. Collapse compression can also occur in the downstream rockfill or gravel zones following heavy rainfall or due to inundation of the downstream toe, and earthfills are also potentially susceptible.

Evidence of collapse compression during first filling at the main section includes differential settlement across the crest with greater settlement of the upstream shoulder, crest spreading and longitudinal crest cracking in some case studies.

The susceptibility of a rockfill to collapse compression is dependent on a number of factors including; the rock substance unconfined compressive strength and its reduction on saturation, moisture condition at placement (dry placed, water added or sluiced), degree of compaction, particle size distribution (coarser rockfills are potentially more susceptible) and applied stress levels prior to saturation. Case study and laboratory test

data (Nobari and Duncan 1972a; Marsal 1973; Alonso and Oldecop 2000) indicates the potential for or magnitude of collapse compression is; greater for dry placed rockfills, decreases with increasing compactive effort, and increases with increasing stress level (refer Section 6.3.2 of Chapter 6). Dry dumped and poorly sluiced rockfills are particularly susceptible to collapse compression as evidenced by the very large deformations observed at Cogswell dam in 1933 following a very heavy rainstorm (Baumann 1958) and the deformations observed at Strawberry and Dix River dams (Howson 1939) on flooding during construction. Terzaghi (1960) attributed the deformation to a reduction in compressive strength of the rockfill on saturation, mainly in the outer surface of the particles, leading to failure at the highly stressed point contacts in an angular rockfill mass.

Rock types that are generally more susceptible to collapse compression due to greater strength reduction of the substance strength on saturation include sedimentary rock types from sandstones down to mudrocks (mudrocks are potentially more susceptible), limestones, and metamorphic rocks from sedimentary parent rocks. Igneous rocks tend to be less susceptible.

Laboratory compression curves for a rockfill sample in dry and wet states (Nobari and Duncan 1972a) are shown in Figure 7.28. Collapse compression on wetting occurs for the dry rockfill when the stress state is above the normal compression line for wetted or saturated rockfill, and the collapse strain is equivalent to the difference in strain between the dry and wetted states at a given confining stress.

Earthfills are also susceptible to collapse compression but its occurrence is not as frequently observed in modern embankment dams. This is mainly due to the high compactive effort used and placement at moisture contents close to Standard optimum moisture content.

If we consider the idealised results of a series of constant suction oedometer tests on a compacted cohesive earthfill (Figure 7.29), collapse compression on wetting occurs for a partially saturated soil when at a state, in void ratio – stress space, above that for the saturated soil. At low stress levels heave will occur on saturation. A more typical void ratio – stress relationship for a dry placed well-compacted cohesive earthfill (placed within 1 to 2% dry of Standard optimum) is for a reduction in matric suction with increasing stress (as shown) due to the compression of air voids in the soil structure and increase in the degree of saturation. This is verified by the pore water pressure response in piezometers during construction (Section 7.4.1.4). Therefore, this

reduction in matric suction reduces the susceptibility of the earthfill to collapse compression on wetting compared to the constant suction condition.

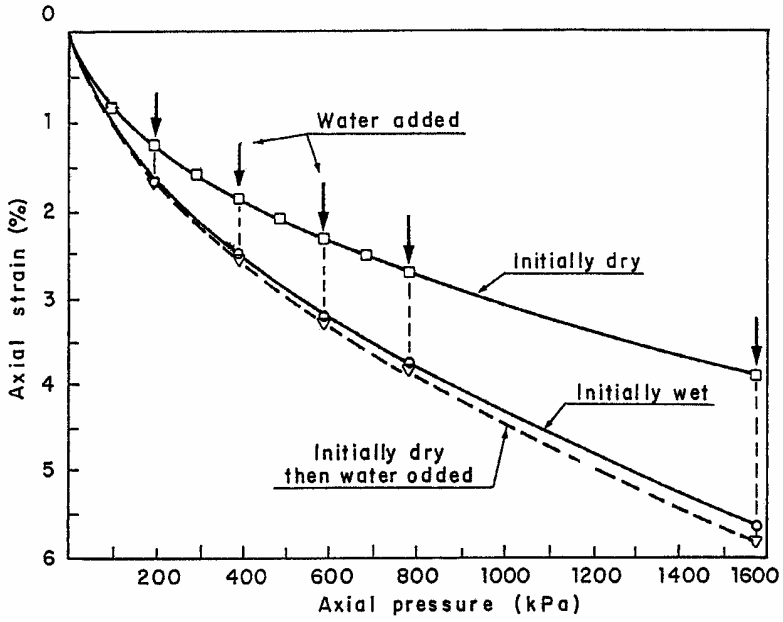

Figure 7.28: Compression curves for dry and wet states and collapse compression from the dry to wet state for Pyramid gravel in the laboratory oedometer test (Nobari and Duncan 1972a).

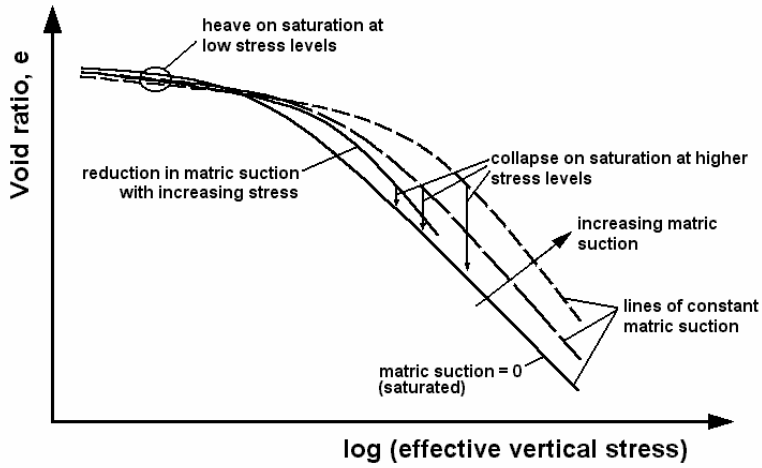

Figure 7.29: Idealised effect of matric suction on collapse compression of earthfills (Khalili 2002).

Another important aspect for well-compacted cohesive earthfills placed within 1 to 2% dry of Standard optimum is that the air voids retained in the soil structure are not readily removed on wetting to give complete saturation as they are for dry placed free draining

rockfills, sands or gravels. Therefore, on wetting the reduction in matric suction will not be significant as a result of the retained air voids in the soil structure and collapse compression, if any, will be limited. Sampling of the "moist placed" medium plasticity compacted clay from below the phreatic surface at Belle Fourche dam (Sherard 1973) more than 25 years after placement indicated the soil structure still retained an air voids content of about 8%.

Factors that will affect the susceptibility of an earthfill to collapse compression are:

- Placement moisture content relative to Standard optimum. The drier soils are placed the more susceptible they are to collapse compression on wetting.
- Compacted density. For a dry placed earthfill, the lower the density ratio of a given soil type the more susceptible it is to collapse compression. The variation in density within a compacted layer is also important. The lower portion of thick placed layers, where the density is often lower, is more susceptible to collapse compression than would be the upper, more heavily compacted part of the layer.
- Earthfill material type. For similarly dry placed earthfills, say at 3% dry of Standard optimum, cohesionless and low cohesion earthfills appear, from the case study data, to be more susceptible to collapse compression than cohesive earthfills.

A number of factors, other than those mentioned above, are likely to influence the susceptibility to collapse compression including particle size distribution, soil plasticity, degree of saturation and the ability of the partially saturated soil to retain air voids in the soil structure on saturation.

Examples of collapse compression of earthfills are much more limited than for rockfills in embankment dams. The database includes several suspected examples that are discussed in Sections 7.9.2 and 7.11.1. The material types involved are mainly silty to clayey sands and gravels that were placed well dry of Standard optimum moisture content.

The effect of collapse compression of the upstream rockfill or gravel zone on the embankment deformation behaviour during first filling is dependent on a number of factors including the strain induced by collapse compression, the embankment zoning and geometry, the strength and compressibility of the embankment materials and the stress conditions at end of construction.

For earthfill cores of relatively low drained compressibility, typified by dry placed well-compacted earthfills, collapse compression of the upstream rockfill on first filling

will result in greater settlement of the rockfill relative to the core (Figure 7.30). The deformation at Cherry Valley dam (Lloyd et al 1958) is an example of this type of deformation where the settlement of the upstream rockfill was more than four times that of the central core and longitudinal cracks on the crest were observed at the upstream core / rockfill interface. Shear stresses, acting as down drag on the upstream face of the core, are developed at the upstream core / rockfill interface due to the differential settlement (Squier 1970).

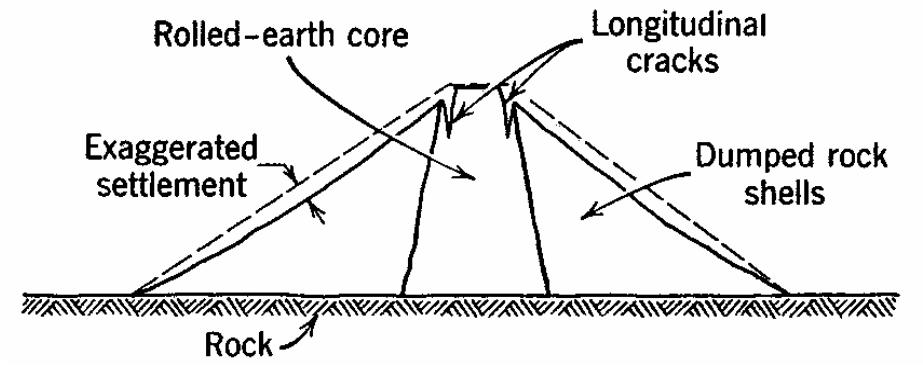

Figure 7.30: Cracking caused by post construction differential settlement between the core and the dumped rockfill shoulders (Sherard et al 1963).

For zoned earth and rockfill embankments with wet placed cohesive earthfill cores the deformation behaviour of the core during first filling is significantly different to that for dry placed earthfills. On collapse compression of the upstream rockfill, the core is not able to support the load that could be transferred to it as a result of differential settlement (because of its low undrained strength). In effect the core is reliant on the shoulders for support. Therefore, if the upstream shoulder settles due to collapse compression on wetting then the core must deform with the upstream rockfill, largely as plastic type deformations, and limited differential settlements occur at the upstream interface.

The deformation behaviour of the wet placed clay core of El Infiernillo dam during first filling (Marsal and Ramirez de Arellano 1967; Squier 1970; Nobari and Duncan 1972b) is an example of this type of deformation behaviour. Collapse compression of the dry placed upstream rockfill occurred during first filling. The measured vertical strains in the core were similar in magnitude and elevation to those in the upstream rockfill, indicating that the core essentially deformed with the upstream shoulder. The actual deformation behaviour at El Infiernillo dam is more complex than summarised

due to the influence of the upstream filters and effect of lateral spreading of the core. The deformation behaviour at El Infiernillo dam is discussed further in Section 7.10 and in Section 1.9 of Appendix G.

Two-dimensional finite difference analysis was undertaken to further assess the effects of collapse compression of the upstream rockfill and the shear strength properties of the core on the embankment deformation behaviour during first filling. The modelled embankment (Figure 7.31) consisted a 100 m high central core earth and rockfill dam with narrow core on a rigid bedrock foundation. Filters and zoning of the rockfill shoulders were omitted for simplicity. Two different core types were modelled; a very stiff dry placed core of low drained compressibility and high undrained strength, and a wet placed core of low undrained shear strength that behaves undrained during construction and on first filling. For each core type the upstream rockfill was modelled with and without collapse compression. Similar properties were used for the downstream rockfill in each case. The shear strength and compressibility properties of the core and rockfill are given in Table 7.16 for the following four analysed cases:

- Case 8 – "dry" placed clay core of very stiff strength consistency and relatively low drained compressibility with collapse compression in the upstream rockfill.
- Case 9 – "dry" placed clay core (as per Case 8), but without collapse compression in the upstream rockfill.
- Case 10 – "wet" placed clay core of low undrained strength with collapse compression in the upstream rockfill.
- Case 11 – "wet" placed clay core (as per Case 10), but without collapse compression in the upstream rockfill.

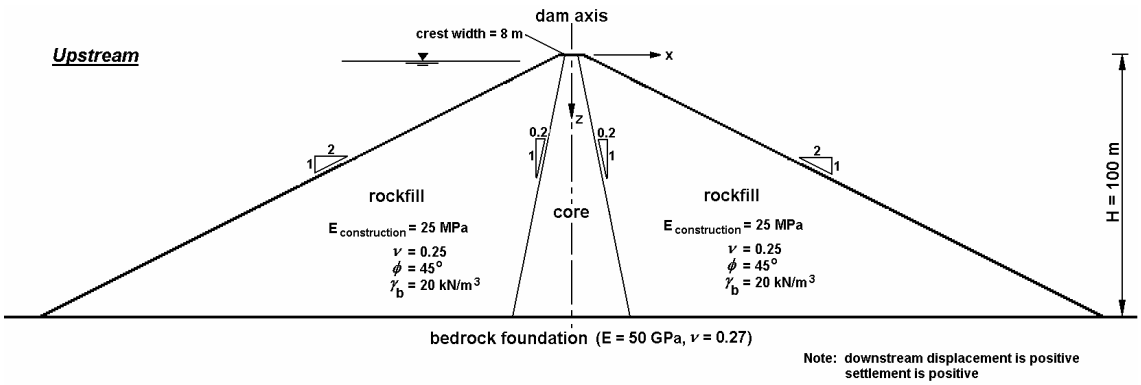

Figure 7.31: Embankment model for finite difference analysis during first filling.

Embankment construction was modelled in ten stages each of ten metres thickness. A Mohr-Coulomb linear-elastic perfectly plastic model was used for both the core and rockfill during construction. The rockfill was modelled using the loading or "construction" compressibility properties. At end of construction the deformations were initialised to zero.

First filling was modelled assuming rapid filling of the reservoir such that the permeable upstream rockfill was saturated and the core was effectively impermeable. A load was applied to the upstream face of the core equivalent to the hydrostatic water load and buoyant unit weights were used in the saturated portion of the upstream rockfill. A reservoir full condition was at a height of 98 m above the foundation.

First filling was modelled differently depending on whether or not collapse compression of the upstream rockfill was to be incorporated into the analysis. For the cases where collapse compression was not included (Cases 9 and 11) first filling was modelled in one stage. Changes to the material properties on first filling were:

- Upstream rockfill - buoyant unit weight and unloading compressibility properties of the saturated portion.
- Downstream rockfill – increased shear modulus (the bulk modulus remained the same) to reflect the effective stress path in the downstream shoulder, which shows an increase in bulk stress and decrease in deviatoric stress on first filling.

For the cases incorporating collapse compression of the upstream rockfill (Cases 8 and 10) first filling was modelled in a series of 10 stages; the first 9 stages in 10 m increments of rising reservoir level and the last stage as an 8 m increment to full supply level. Collapse compression was modelled as per the method by Justo (1991), which involved:

- For the newly saturated layer of each stage, collapse compression was modelled by:
  - Reduction of the effective stresses within the newly saturated layer of the filling stage. The reduction factor is equivalent to the compressibility ratio between the "wetted" and "dry" states of the rockfill (Figure 7.32). In this case a ratio of 0.7, or a 30% reduction, was used.
  - Reduction of the Young's Modulus of this layer to those for the "wetted" rockfill in loading.
- For previously wetted layers, the unloading / reloading moduli were used for the saturated upstream rockfill.

The downstream rockfill for Cases 8 and 10 was also modelled with an increased shear modulus as per the modelling for Cases 9 and 11. In addition, the "dry" placed, very stiff core for the model incorporating collapse compression of the upstream rockfill (Case 8) was also modelled with an increased shear modulus. The ratio of the loading to unloading moduli used was a factor of 10 for the rockfill and a factor of 5 for the earthfill core.

Table 7.16: Properties of central core used in finite difference analyses

Embankment Zone and Properties	**"Dry Placed" Core**		**"Wet Placed" Core**	
	Case 8 (collapse)	**Case 9 (no collapse)**	**Case 10 (collapse)**	**Case 11 (no collapse)**
Earthfill core:				
- modulus, E (MPa)*[1]	30	30	20	20
- Poisson's ratio, n	0.33	0.33	0.48	0.48
- cohesion, c' or c_u (kPa)	5	5	50	50
- friction angle, f' or f_u (degrees)	32	32	2	2
- bulk unit weight, g (kN/m^3)	20	20	20	20
Rockfill:				
- Poisson's ratio, n	0.25	0.25	0.25	0.25
- Cohesion, c' (kPa)	0	0	0	0
- Friction angle, f' (degrees)	45	45	45	45
- Bulk unit weight, g_{bulk} (kN/m^3)	20	20	20	20
- Saturated unit weight, g_{sat} (kN/m^3)	22.3	22.3	22.3	22.3
- Young's Modulus, E (MPa)				
- loading (construction)	25	25	25	25
- "wet" modulus (on collapse)	17.5	na	17.5	na
- unloading / reloading for non-collapse.	250	250	250	250
- unloading / reloading post collapse.	175	175	175	175

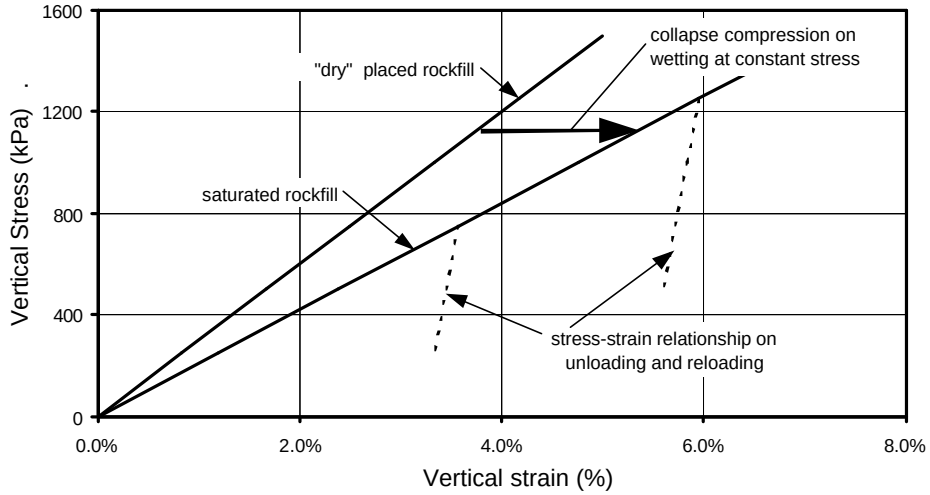

Figure 7.32: Model of the stress-strain relationship of the upstream rockfill incorporating collapse compression (in one-dimensional vertical compression).

The deformation results on first filling from the finite difference modelling are shown in Figure 7.33 to Figure 7.36 for Cases 8 to 11 respectively. The settlement and displacement of the embankment at the end of first filling are presented for all cases, and for the reservoir at 40% of the embankment height for Case 10 only (wet placed core modelling collapse compression of the upstream rockfill). It should be noted that the deformations are not (and are not intended to be) an accurate representation of actual deformation due to the use of simplistic models for the strength and compressibility of the embankment materials. Importantly, though, the general trends of the deformation behaviour are considered to be a reasonable representation of those in reality.

For the cases where collapse compression of the upstream rockfill was not modelled (Cases 9 and 11) the results show:

- Settlements in the upstream rockfill and core are comparatively very much smaller than those for the cases incorporating collapse settlement of the upstream rockfill.
- Upward vertical displacements are observed in the mid to lower upstream shoulder due to decreases in the effective vertical stress on first filling. These are obscured in the collapse compression analyses (Cases 8 and 10) due to the collapse compression.
- Displacements are downstream in the core and shoulders.

For the cases where collapse compression of the upstream rockfill was modelled (Cases 8 and 10) the results show that whilst the settlements in the upstream shoulder are similar for the different core types, the settlements within the core show markedly different patterns of behaviour. For the "dry" placed core model (Case 8), the settlement trend shows (Figure 7.33a) a large differential settlement at the upstream interface of the core. This pattern of settlement is similar to that observed from the case studies, except that the differential settlement in the crest region is often more pronounced in the case studies. This is partly a result of the relatively large shear type deformation that has developed within the core in the model. By adopting higher shear strength parameters for the core, greater differential settlement occur at the upstream core / rockfill interface and smaller settlements within the core.

In contrast, the numerical model for the "wet" core of low undrained shear strength shows virtually no differential settlement at the upstream core interface (Figure 7.35a and c), indicating the core is deforming with the upstream rockfill shoulder as observed in case studies with wet placed clay cores such as El Infiernillo and Canales dams (Giron 1997, refer Section 2.1 of Appendix G). Instead, the modelling shows a

concentration of vertical settlement in the lower part of the core and a large differential settlement at the downstream interface of the core. The concentration of deformation at the downstream interface of the core is clearly demonstrated at Canales dam.

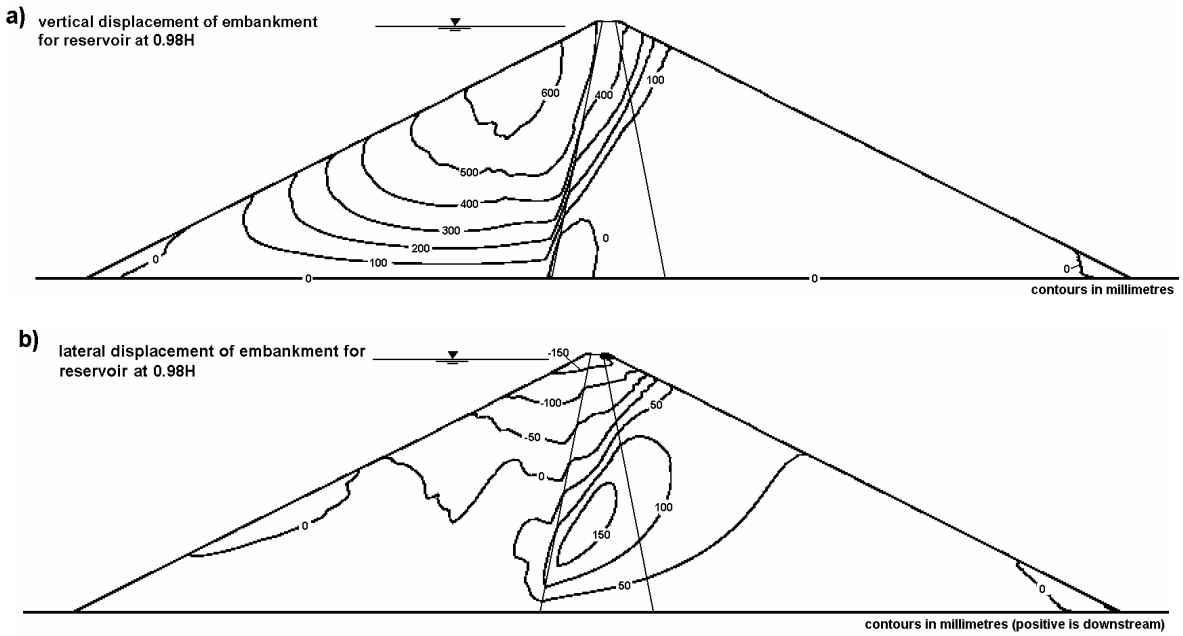

Figure 7.33: Case 8 – "dry" placed, very stiff core modelling collapse compression in the upstream rockfill; numerical results of *(a)* vertical and *(b)* lateral displacement on first filling.

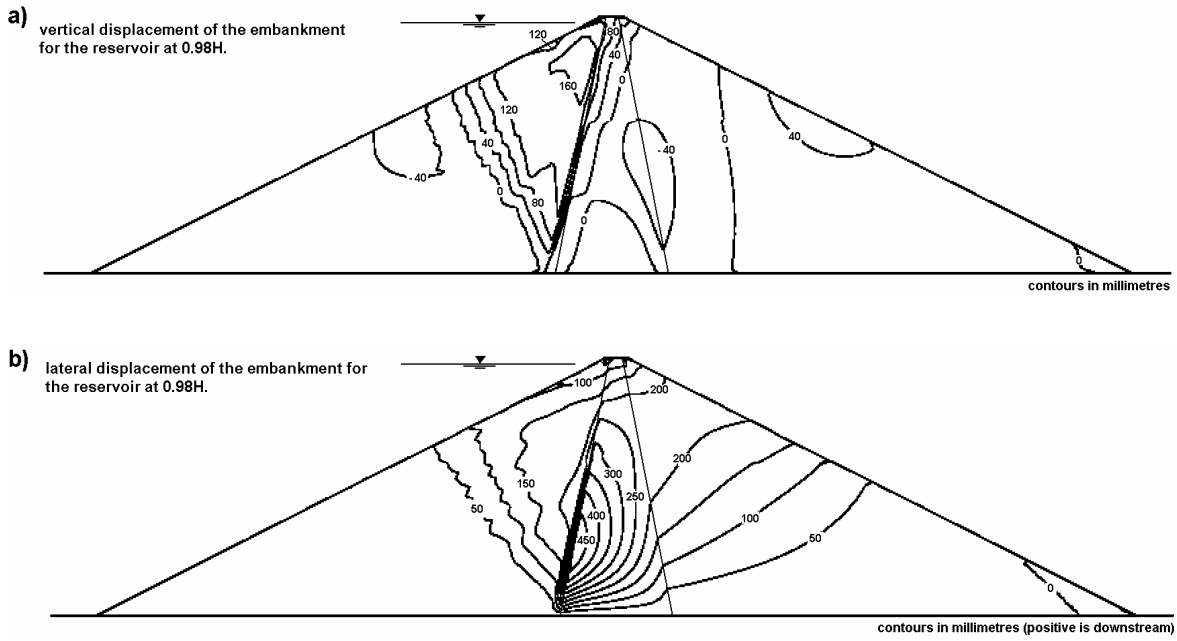

Figure 7.34: Case 9 – "dry" placed, very stiff core without collapse compression; numerical results of *(a)* vertical and *(b)* lateral displacement on first filling.

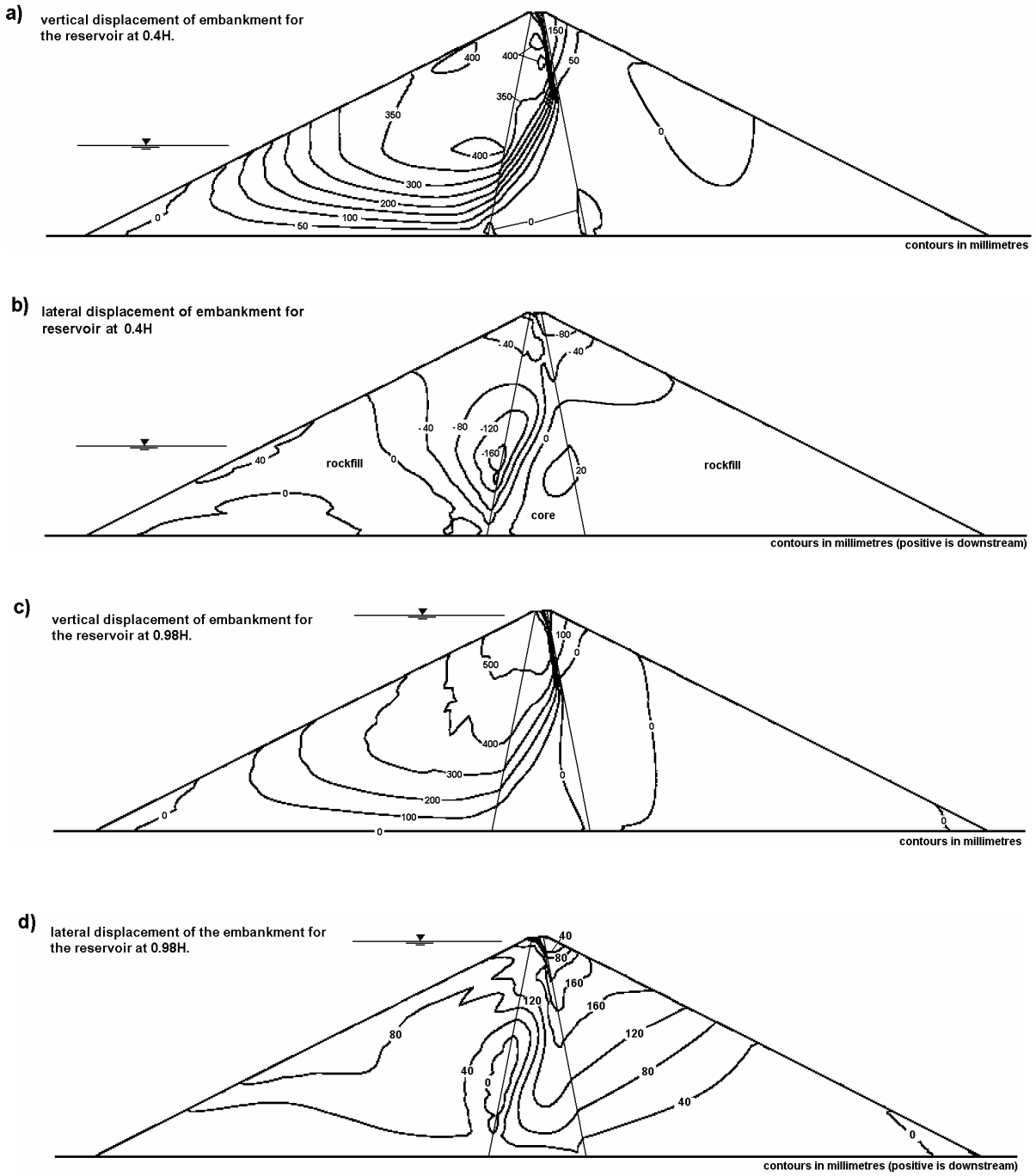

Figure 7.35: Case 10 – "wet" placed clay core of low undrained strength modelling collapse compression in the upstream rockfill. Numerical results of vertical and lateral deformation on first filling; *(a)* and *(b)* for reservoir at 40% of embankment height, *(c)* and *(d)* for reservoir at 98% of embankment height.

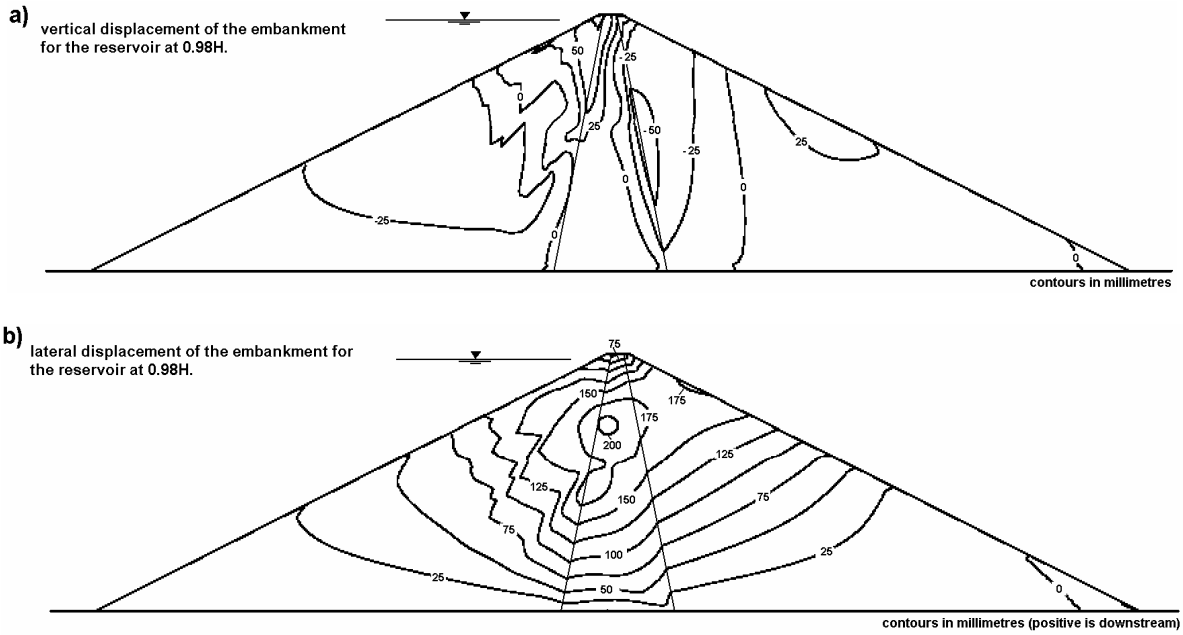

Figure 7.36: Case 11 – "wet" placed clay core without collapse compression; numerical results of *(a)* vertical and *(b)* lateral displacement on first filling.

The lateral displacement of the core on first filling shows a similar "bow" shaped pattern for all four cases, with the region of maximum downstream displacement on the dam axis occurring in the mid region of the core. The displacement for the cases incorporating collapse compression show a tendency for regions of the core and upstream shoulder to displace upstream. For the "wet" placed core (Case 10) the lateral deformation of the core was largely upstream for the reservoir at 40% of the embankment height (Figure 7.35b) and then largely downstream at the end of first filling (Figure 7.35d), still retaining its bow shape. This upstream then downstream deformation pattern of the crest is not uncommon in zoned embankments with narrow, near vertical central cohesive cores placed wet of Standard optimum; it was observed at El Infiernillo, Thomson, Gepatsch and Nurek dams.

7.5.3 LATERAL SURFACE DEFORMATION NORMAL TO THE DAM AXIS DURING FIRST FILLING.

As discussed in Section 7.5.1, a significant portion of the post construction lateral displacement occurs during first filling, particularly for embankments with thin to medium width central cores and permeable upstream fill (mainly central core earth and rockfill dams). The lateral surface displacements during first filling for the case studies

of earthfill and zoned earth-rockfill embankments are presented in the following figures and tables.

For analysis of the post construction surface deformation, the embankment has been divided into three regions (Figure 7.37); the mid to downstream region of the crest, the mid to upper region of the downstream slope and the upper upstream slope to upstream crest region. The regional division was primarily established to separate the deformation of the core of zoned embankments from that of the upstream and downstream shoulders due to the sometimes large difference in observed deformation behaviour, particularly where poorly compacted rockfill was used in the shoulders. It is recognised that because the deformation of the shoulders affects that of the core, any assessment of the embankment deformation requires consideration of the embankment as a whole, but given the large number of case studies within the database it is impractical to do so for all dams. In the discussion on individual embankments in Sections 7.10 and 7.11, and in Appendix G the deformation of the embankment as a whole is discussed for selected case studies.

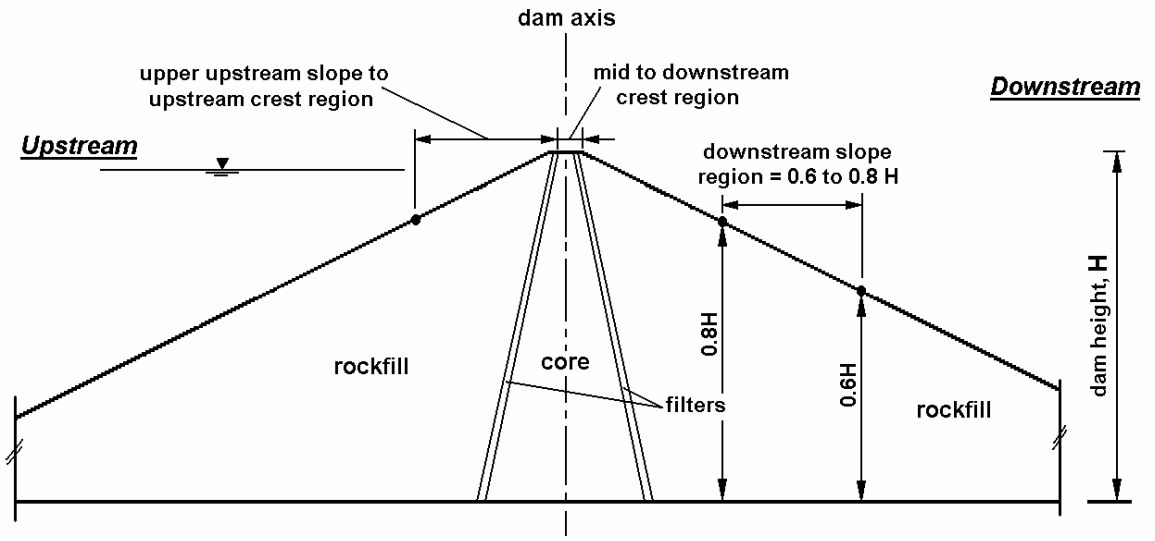

Figure 7.37: Regional division of the embankment for analysis of post construction surface deformation.

Representative surface monitoring points (SMP) for an embankment were generally taken from near to the maximum section, unless otherwise identified. Other selection criteria for SMPs are:

- For the downstream slope SMPs were selected from the slope region in the range 0.6 to 0.8 times the embankment height, which is often where the greatest

displacements were measured. Embankments were not excluded if the only SMPs on the downstream slope were outside this region.

- For zoned embankments with thin to medium width cores SMPs representing the upper upstream shoulder to upstream crest region were preferentially selected from the upstream edge of the crest provided the SMP was located over the upstream shoulder zone.
- For embankments with very broad earthfill zones (including earthfill embankments) the crest region was considered as a whole; i.e. from the upstream edge to the downstream edge. For these embankments SMPs from only the upper upstream slope region were included with the analysis of the upper upstream slope to upstream crest region.

Figure 7.38 to Figure 7.40 present the case study results for the lateral surface displacements during first filling:

- Figure 7.38 for the mid to downstream region of the crest. The data has been sorted based on the width of the central core, and the material type and compaction of the downstream shoulder.
- Figure 7.39 for the mid to upper region of the downstream slope, sorted based on the material type and compaction of the downstream shoulder.
- Figure 7.40 for the upper upstream slope and upstream crest region, sorted based on material type and compaction of the upstream shoulder.

The terms "well-compacted", "reasonably to well-compacted", "reasonably compacted" and "poorly compacted" used to describe the compaction of the rockfill in the embankment shoulders are defined in Section 1.3.3. The term "gravels" refers to free draining coarse grained gravelly and bouldery soils with very low fines content (less than about 5 to 8% passing 75 micron). The term "earthfill" covers a broad range of material types from clays to silty gravels to weak rockfills that breakdown significantly on compaction.

Zero time for measurement of displacement, t_0, is established at the end of embankment construction. In most cases the displacement for each case study captures a large portion of the period of first filling, however, for several cases where the embankment impounded water to relatively high levels during construction some of the displacement due to first filling would have been missed (e.g. Vatnedalsvatn dam). No

differentiation with respect to time of first filling is taken into consideration in the figures. In some cases the reservoir was filled within a matter of days to weeks whilst for others first filling took many years, more than 10 years for several cases.

Highlighted in the figures are those embankments where the rockfill was known to have been placed without the addition of water. These cases are highlighted because of the susceptibility of dry placed rockfill, particularly if not well compacted or if weathered, to collapse compression on wetting. It is recognised that for several of these highlighted embankments the rockfill was likely to have been wetted from rainfall in regions where the climate is very wet, but they have been included rather than to make this judgement.

The figures present information on the general trend and magnitude of the lateral displacement on first filling, and highlight case studies with "abnormally" large deformation or with trends different to the broader group. A more detailed analysis of the overall post construction lateral deformation behaviour is presented in Section 7.6 and the discussion on individual embankments in Sections 7.10 and 7.11.

(a) Crest displacement on first filling

For the displacement of the crest (Figure 7.38) the material forming the downstream shoulder and the width of the core region do have some influence (refer below) but generally speaking it is difficult to establish bounds of deformation other than a general range. Reasons for this are considered to include factors such as the time of first filling, the stress conditions within the downstream shoulder prior to first filling (refer Section 7.5.1), the effect of collapse settlement of the upstream rockfill and resultant core deformation (refer Section 7.5.2), positioning of the SMP on the crest, valley shape, and the curvature of the embankment axis amongst other factors. Attempts to further differentiate the data for one or more of these aspects often resulted in too great a dilution of the database to draw any significant conclusions.

Table 7.17 presents a summary of the lateral crest displacement on first filling. The displacement range for most case studies is from 50 mm upstream to 300 mm downstream (Figure 7.38). For most groups in Table 7.17 the range is less than about 100 to 200 mm, or less than 0.1 to 0.2% of the embankment height. Greater displacements are observed for dams with reasonably to poorly compacted rockfill in the downstream shoulder or embankments with cores of silty sands to silty gravels and of thin to medium width.

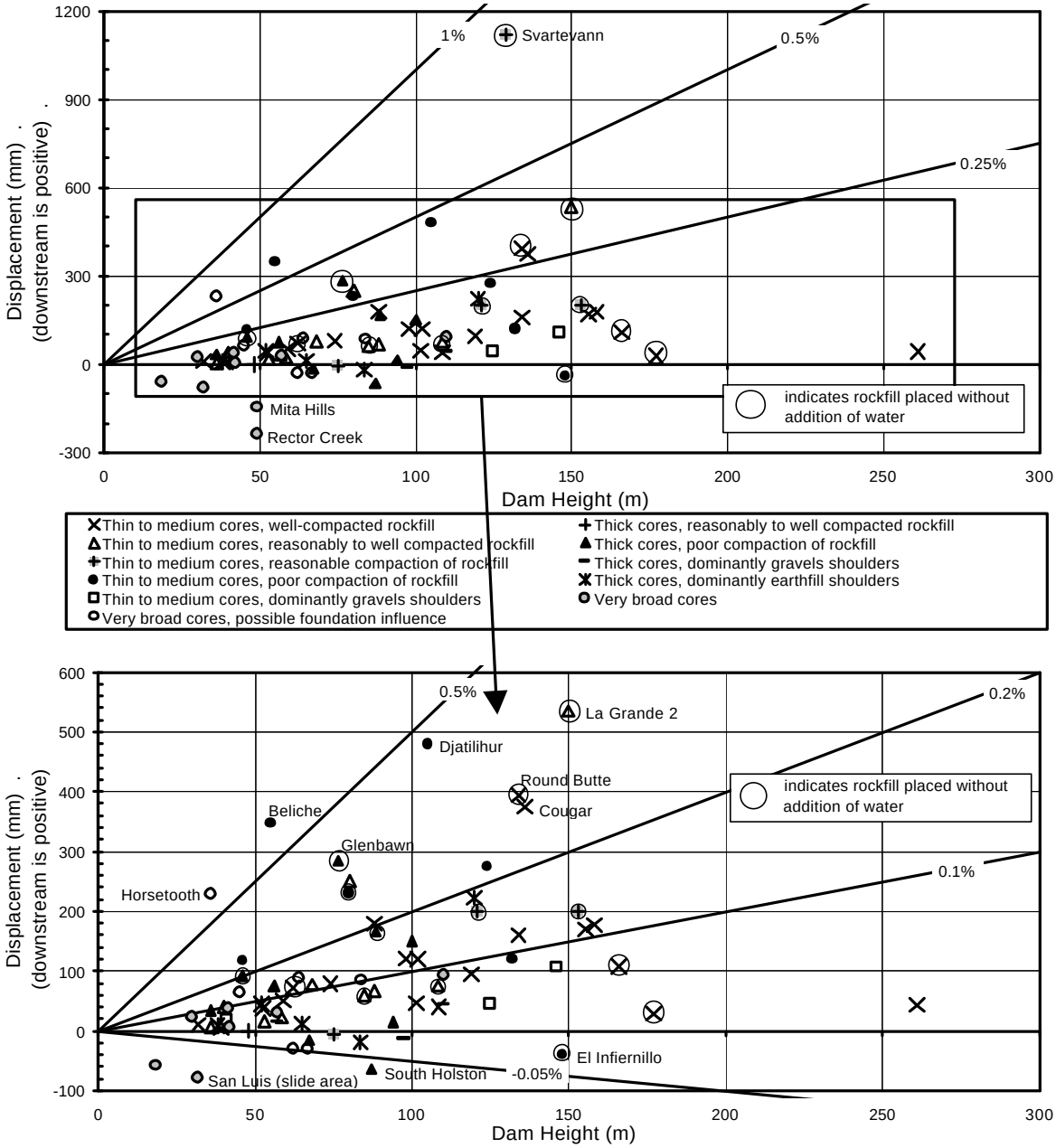

Figure 7.38: Lateral displacement of the crest (centre or downstream region) on first filling versus embankment height (displacement is after the end of embankment construction).

Table 7.17: Lateral displacement of the crest (centre to downstream edge) on first filling.

Core Width	Downstream Shoulder		Core *[2] Classification	No. Cases	Displacement Range		Comments
	Material	Rating *[1]			(mm)	% of *H* *[3]	
Thin to medium	Rockfill	Well-comp	CL/CH/GC/SC, wet	13	29 to 180	0.0 to 0.12	
			CL/SC/GC, dry	5	5 to 80	0.0 to 0.12	
			SM/GM – dry and wet	3	177 to 394	0.10 to 0.30	Naramata (177 mm), Cougar (375 mm), Round Butte (394 mm)
		Reas to well	CL/CH/SC/GC	5	6 to 78	0.0 to 0.11	
			SM/GM	5	6 to 535	0.03 to 0.36	LG2 (535 mm), Frauenau (250 mm)
		Reas	All types	4	-6 to 1120 (most < 200)	-0.01 to 0.17	Svartevann = 1120 mm (SM core)
		Poor	All types	7	-39 to 480	0.09 to 0.63	No correlation to core soil type, Beliche = 347 mm (0.63%), Djatiluhur = 480 mm (0.46%)
	Gravels	-	All types	3	18 to 107	0.04 to 0.07	
Thick	All cases with thick cores			19	-64 to 285 (most –19 to 222)	-0.02 to 0.20	
	Rockfill	Reas to well	All types	1	0	-	Maroon dam
		Poor	All types	9	-64 to 285 (most –15 to 165)	-0.02 to 0.19	Sth Holston = -64 mm (-0.07%), Glenbawn = 285 mm (0.37%)
	Gravels	-	All types	4	-13 to 44	-0.01 to 0.04	
	Earthfill	-	All types	5	-19 to 222 (most –19 to 45)	-0.02 to 0.19 (-0.02 to 0.09)	Navajo = 222 mm, rest < 45 mm
Very Broad			All types	15	-236 to 229 (most –58 to 94)	-0.02 to 0.14	Rector Creek = -236mm, Mita Hills = -146mm, San Luis (slide area) = -79 mm, Horsetooth = 229 mm

*[1] compaction rating of rockfill; well-comp = "well-compacted", reas to well = "reasonably to well compacted", reas = "reasonable compaction", poor = "poorly compacted".

*[2] Soil classification to Australian Standard AS 1726-1993, "wet" = placed at or on the wet side of OMC, "dry" = placed on the dry side of OMC (OMC = Standard optimum moisture content).

*[3] range of displacement as a percentage of dam height (*H*) excludes possible outliers (Svartevann, South Holston, Glenbawn, Rector Creek, Mita Hills, San Luis (slide area) and Horsetooth dams).

Isolated cases of large displacement also occur within the other groupings. For the embankments with cores of very broad width, the relatively large upstream displacement for Rector Creek and Mita Hills is possibly due to collapse compression of dry placed dominantly sandy earthfills, for the slide area at San Luis dam due to the upstream trending hill slope on which this section of the embankment was constructed, and for Horsetooth dam the foundation is thought to have had a significant influence on the displacement. These cases are discussed further in Section 7.11. South Holston would also appear to be an outlier in its sub-grouping with an upstream displacement of 64 mm (-64 mm) on first filling. At Glenbawn dam the crest SMP is located at the downstream edge over the poorly compacted rockfill zone, which would account for the large displacement measured.

Further details on the embankments comprising the 13 largest downstream displacements on first filling (excluding the very broad earthfill case studies) are summarised in Table 7.18. All have a lateral displacement equal to or greater than 200 mm downstream on first filling. These case studies highlight several factors associated with high lateral displacements:

- The case studies are predominantly of central core earth and rockfill dams with thin cores.
- The predominant core type is silty sands to silty gravels, particularly for the larger deformations (4 of the top 5).
- For most cases (8 of 13) the downstream rockfill is of poor to reasonable compaction.
- In 7 cases the downstream rockfill was known to have been placed without the addition of water. Of these, 2 of the 3 well or reasonably to well compacted cases were placed without water, all the reasonable compaction cases were placed without water and 3 of the 4 poorly compacted cases were placed without the addition of water.

The data indicates that potentially important factors leading to relatively large downstream displacement on first filling are:

- Collapse settlement of dry placed or poorly compacted rockfills in the downstream shoulder, possibly as a result of post construction wetting from heavy rainfall.
- Relatively high increases in stress level in the downstream rockfill from the applied water load. The earlier finite difference analysis for zoned embankments (Section

7.4.1.2, Figure 7.4 and Section 7.5.1, Figure 7.26) showed that where the compressibility properties of the core are similar to that of the shoulders the lateral stresses are relatively low at end of construction, and that on first filling the magnitude of increase in lateral stress in the core and downstream shoulder is relatively high. Following on from this, it is reasonable to consider that potentially larger downstream displacements occur for earth and rockfill embankments with thin to medium width earthfill cores of well-compacted silty sands to silty gravels. Although not conclusive, it may be a factor leading to large displacement on first filling.

(b) Displacement of the downstream shoulder on first filling

A similar pattern of behaviour as the crest is observed for the lateral displacement of the mid to upper region of the downstream slope on first filling (Figure 7.39). The data shows that:

- For embankments with very broad earthfill zones or earthfills in the downstream shoulder, displacements are typically less than 100 mm downstream (or less than 0.1% to 0.15% of the embankment height). The much greater displacement at Horsetooth dam is due to the influence of the compressible foundation.
- For embankments with gravels in the downstream shoulder, displacements are typically less than 100 to 150 mm (or less than 0.11% of the embankment height). The higher displacement at Trinity dam (175 mm, 0.11%) may reflect the use of dozer track rolling and the limited amount of water used in compaction of the gravels.
- For embankments where wetted rockfills are used in the downstream shoulder, displacements are typically less than 100 to 200 mm (or less than 0.12 to 0.18% of the embankment height). The displacements at Ataturk and Beliche dams are clear outliers to the general trend, and Blowering and Windemere are slightly above the general trend. At Beliche, Blowering and Ataturk dams the higher displacements are possibly due to the use of weathered materials and/or rockfills susceptible to strength loss on wetting. At Windemere placement in 2 m layers and possibly without the addition of water in the outer downstream slope may be a factor.

Table 7.18: Thirteen cases with largest downstream crest displacement on first filling

Dam Name	Height (m) *[1]	Downstream Slope *[2] (H to 1V)	Core *[3]			Downstream Shoulder			Lateral Displacement (mm)	Time to First Filling (years) *[6]	% of First Filling *[7]
			Width	Class[n]	Moisture Content	Material	Rating *[4]	Placement *[5]			
Svartevann	129	1.43H	Thin (u)	SM/GM	0.4% wet	Rockfill – granite & gneiss	reas	2m lifts, no water, 8p 13t SDVR	1120	2.23	30%
La Grande 2	150	1.6H	Thin (u)	SM	(1% dry to 2% wet), wet ?	Rockfill – granite	reas to well	0.9 to 1.8m lifts, no water, 10t SDVR	535	1.2	100%
Djatiluhur	105	1.3H (upper)	Thin	CH	2.2% wet	Rockfill – andesite	poor	1 to 2 m lifts, dumped, watered	480	2.25	30%
Round Butte	134	1.7H	Thin	SM	dry ?	Rockfill – basalt	well	0.6m lifts, no water, 4p 9t SDVR	395	0.6	18%
Cougar	136	1.6H	Thin (u)	GM	1.0% wet	Rockfill – basalt & andesite	well	0.6m lifts, 4p 10t SDVR	375	0.67	most
Beliche	55	1.95H	Thin	GC	(± OMC), wet ?	Rockfill – schists & greywacke	poor	1m lifts, light compaction	345	4.1	50%
Glenbawn	76.5	2.5H	Thick	CL	2% dry	Rockfill – limestone	poor	1.8m lifts, dumped, no water	285	4.7	100%
Mud Mountain	124	1.75H	Medium	SM/GM	dry ?	Rockfill – andesite & tuff	poor	12m lifts, dumped & sluiced	275	>17	most
Frauenau	80	1.6H	Thin	SM	dry ?	Rockfill	-	No information	250	-	most
Matahina	80	2.3H	Medium	CL	1 to 1.5% dry	Rockfill – ignimbrite	poor	1.0m lifts, no water, dumped	230	0.24	100%
Navajo	120	2.5H	Thick	CL/ML	0.8% dry	Earthfill	-		220	11	most
Gepatsch	153	1.5H	Thin	GM/GC	0.5 to 2% wet	Rockfill - gneiss	reas	2.0m lifts, no water, 4p 9t SDVR	200	1.92	30%
Vatnedalsvatn	121	1.5H	Thin	SM	0.5% wet	Rockfill – quartz, granite & gneiss	reas	Reas (1.5m lifts, no water, 6p 11t SDVR)	200	0.2	10%

Notes to Table 7.18 on next page

Notes to Table 7.18:

*[1] dam height at SMP (surface measuring point)

*[2] downstream slope angle, horizontal to vertical. Values given are to 1V.

*[3] (u) indicates core oriented slightly upstream. Placement moisture content relative to Standard optimum. Values in brackets are specification, ? indicates not sure but likely from pore water pressure response.

*[4] compaction rating of rockfill; well-comp = "well-compacted", reas to well = "reasonably to well compacted", reas = "reasonable compaction", poor = "poorly compacted".

*[5] shoulder placement. 8p 13t SDVR = 8 passes of a 13 tonne smooth drum vibrating roller.

*[6] time to first filling after the end of embankment construction.

*[7] percent of first filling is a reference to the reservoir level prior to the end of construction. 30% means the reservoir was filled to within 0.3H (H = dam height) of the reservoir full condition. Therefore low percentages indicate the reservoir was or had been close to full supply level prior to the end of construction and high percentages or "most" indicates little water was impounded during construction.

- For embankments where dry placed rockfills are used in the downstream shoulder, displacements are typically in the order of 150 to 900 mm, or in the range 0.10 to 0.85% of the embankment height. Collapse compression on wetting due to rainwater infiltration is possibly a significant factor in the large displacements observed. Notably, greater displacements are observed for the dry placed and reasonably to poorly compacted rockfills (greater than 0.2 to 0.25%), which will be more susceptible to collapse compression on wetting. For the dry placed, well and reasonably to well compacted rockfills displacements are generally less than 0.25 to 0.30% of the embankment height.

Case studies with large downstream displacement of the crest also had large downstream displacement of the downstream slope. The exception is Navajo dam (crest displacement = 222 mm or 0.19%, downstream slope displacement = 90 mm or 0.07%) where earthfill was placed in the downstream shoulder. Other notable cases with large downstream displacement include:

- Eppalock dam, a 47 m high central core earth and rockfill dam with a medium plasticity sandy clay core of thick width placed on the dry side of Standard optimum (refer Section 1.10 of Appendix G). The shoulders were of dry placed and poorly compacted rockfill (placed in 2 to 4 m thick layers and spread by tractor) derived from basalt, but was weathered and contained a high fraction of finer sized rockfill. The displacement of the downstream slope on first filling (290 mm or 0.63% of the dam height) was much greater than for the crest (90 mm or 0.2% of the dam height).

- Eildon dam, an 80 m high central core earth and rockfill dam with a well-compacted medium plasticity sandy to gravelly clay core of thick width placed on the dry side of Standard optimum (refer Section 1.8 of Appendix G). The shoulders were of dry placed and poorly compacted rockfill (placed in 2 m thick layers with no formal compaction) sourced predominantly from quartzitic sandstone. The outer downstream random rockfill shoulder consisted of "unsuitable" rock that was poorly graded and contained a high fraction of finer sized rockfill. The displacement of the downstream slope on first filling was very large at 660 mm (or 0.83% of the dam height). The crest displacement was not monitored during first filling.
- El Infiernillo, Dartmouth, Thomson and Blowering dams also show much greater displacement of the downstream slope than the crest. All comprise wet placed clayey sand to sandy clay cores of thin to medium width. For these embankments the core is likely to be strongly reliant on the shoulders for support due to its likely low undrained strength and thin to medium width. Therefore, plastic deformation is likely to be a significant factor in the deformation behaviour of the core during first filling of these embankments affected by collapse settlement of the upstream rockfill shoulder on wetting, as described for El Infiernillo dam (after Nobari and Duncan 1972b) in Section 7.5.2. Thomson and Dartmouth dams show an upstream then downstream displacement during first filling similar to that at El Infiernillo dam.

At Eildon and Eppalock dams, embankments with thick cores of high undrained strength and relatively low drained compressibility, the displacement records suggest that the displacement of the dry placed, poorly compacted downstream rockfill shoulder is not likely to be greatly influenced by first filling. The large displacement of the downstream slope for these cases is more likely due to the large differential settlement between the well-compacted core and downstream rockfill, and the influence of the downstream slope of the core on the vector of deformation. Collapse compression in the downstream rockfill due to wetting from rainfall would contribute to the large deformations of the downstream slope observed during first filling. Similar reasoning would also explain the differential displacement at Copeton dam (crest displacement = 75 mm, downstream slope = 360 mm) where the medium width clayey sand core was dry placed and no water used during placement of the rockfill.

The deformation behaviour of several of these embankments, including Ataturk dam, are discussed in more detail in Section 7.10 and in Appendix G.

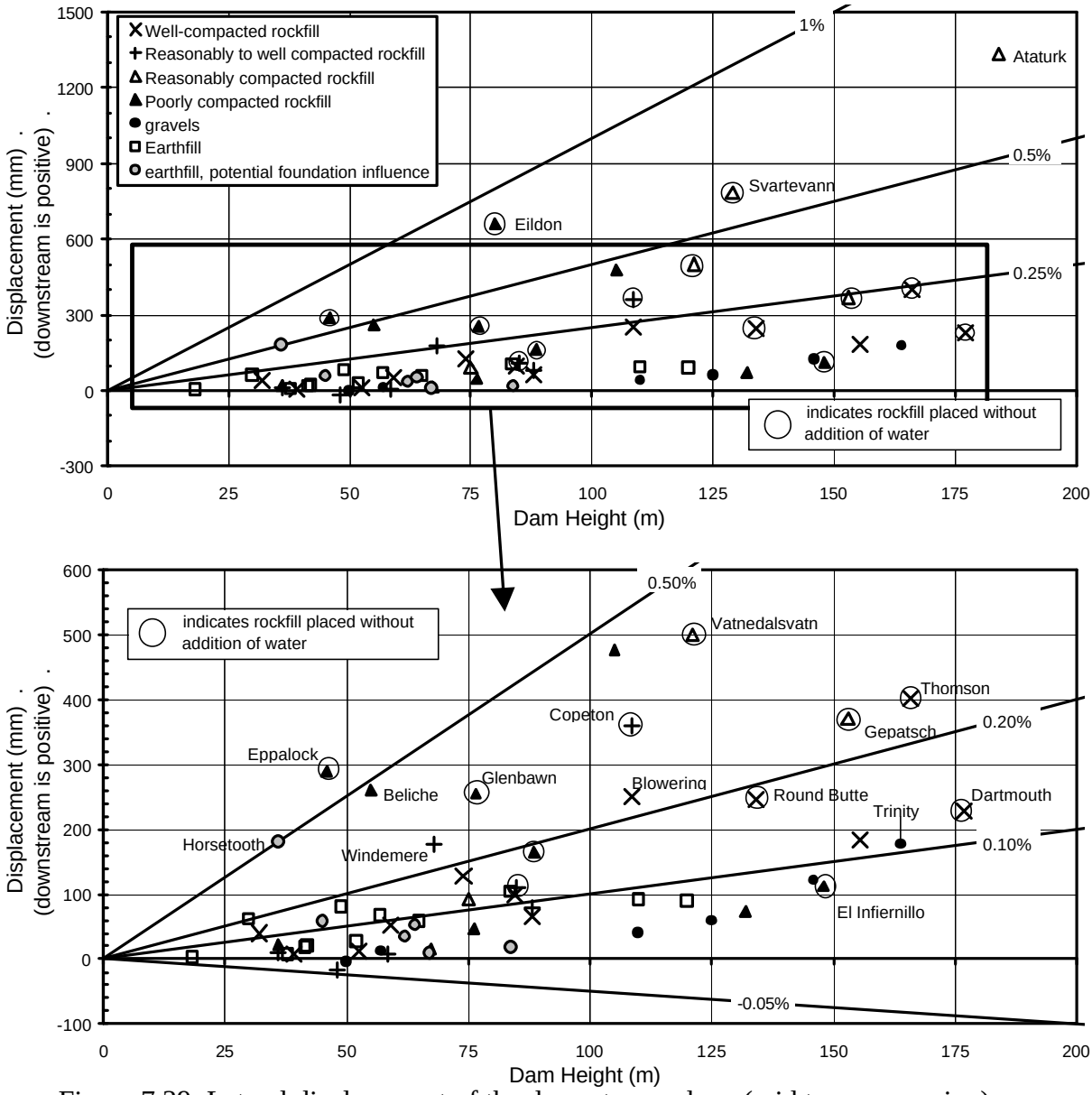

Figure 7.39: Lateral displacement of the downstream slope (mid to upper region) on first filling versus embankment height (displacement is after the end of embankment construction).

(c) Displacement of the upstream shoulder on first filling

The displacement of the upper upstream slope or upstream crest region during first filling (Figure 7.40) highlights Svartevann and Gepatsch dams as outliers to the general displacement trend. For most cases studies the displacement is in the range 200 to 300 mm upstream (-200 to -300 mm) to 300 mm downstream.

(d) General trends of displacement on first filling

The displacement on first filling of the crest and downstream slope were also plotted against the downstream slope (Figure 7.41 and Figure 7.42). The plots indicate a general trend of decreasing magnitude of displacement with flattening of the downstream slope, with some outliers of cases with dry placed rockfill in the downstream shoulder. However, this trend is only evident at the upper bound of lateral displacement as a large number of case studies with relatively steep downstream slope angles show limited deformation on first filling.

The general trends of lateral displacement on first filling are:

- For the crest (centre to downstream region), displacements typically range from 50 mm upstream (-50 mm) to 200 mm downstream, or from -0.02% to 0.20% of the embankment height.
- For the downstream slope (mid to upper region), displacements are typically downstream in the range from 0 up to 200 to 250 mm (or less than 0.2% of the embankment height).
- In the upper upstream slope and upstream crest region, displacements typically range from 200 mm upstream (-200 mm) to 200 mm downstream. The mean is located closer to zero in this region than for the mid to downstream region of the crest.

Much larger downstream displacements on first filling are observed:

- In the crest region for zoned earth and rockfill embankments with thin cores and dry placed or poorly compacted rockfill in the downstream shoulder. In these cases displacements can reach up to 0.3 to 0.65% of the embankment height (up to 600 mm), and in one case 1100 mm or (0.87%) was measured.
- In the mid to upper region of the downstream slope for zoned embankments with dry placed or poorly compacted rockfill in the downstream shoulder. For these cases displacements range from 150 mm to 900 mm (or from 0.10 to 0.85% of the embankment height).

Overall the plots provide useful information on likely bounds of lateral displacement on first filling. They are also useful for identification of embankments that display excessively large displacements on first filling and therefore potentially "abnormal" deformation behaviour. Several of the outliers are discussed further in Sections 7.9 to 7.11, and in Appendix G.

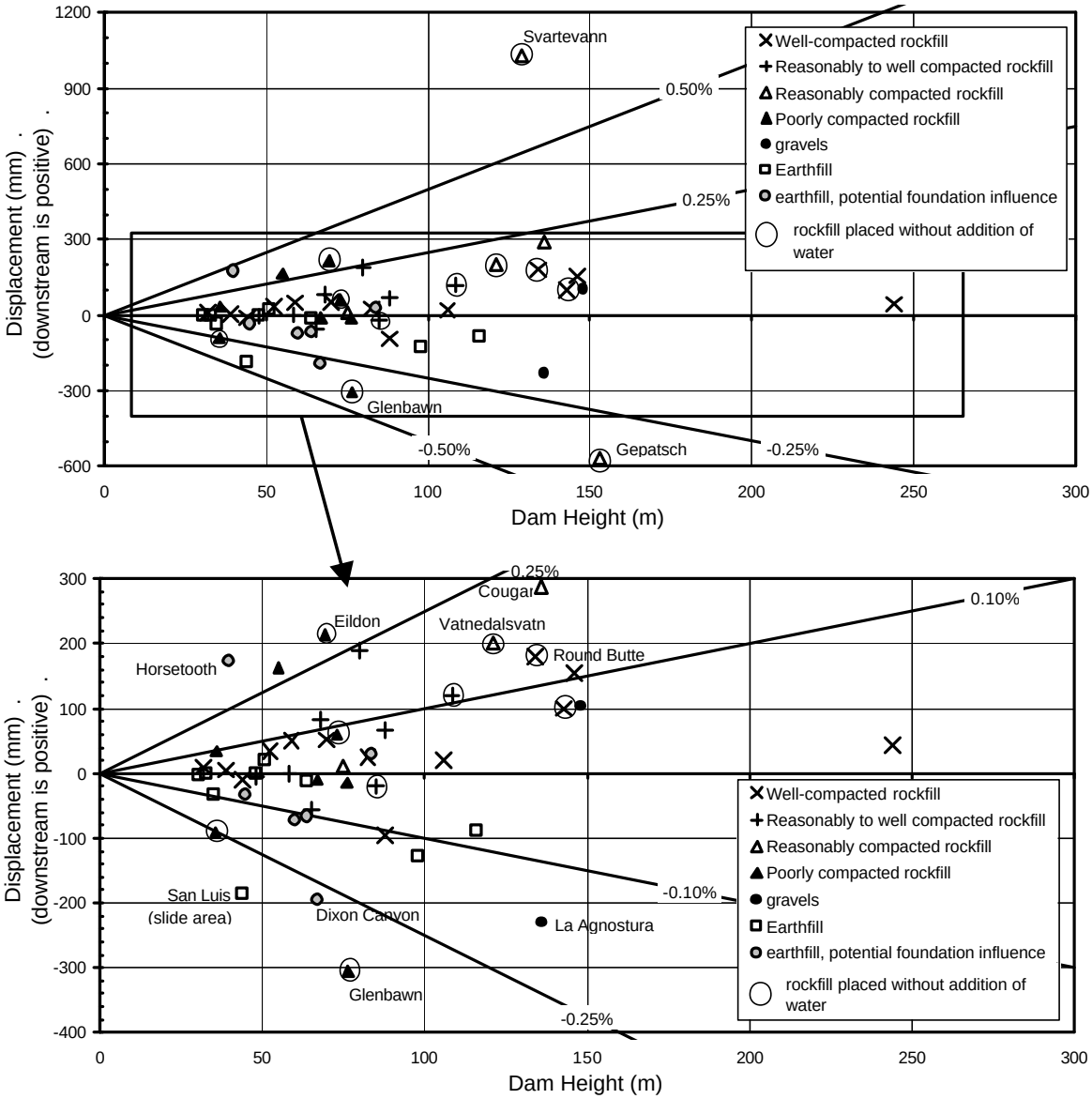

Figure 7.40: Lateral displacement at the upper upstream slope of upstream crest region on first filling versus embankment height (displacement after the end of embankment construction).

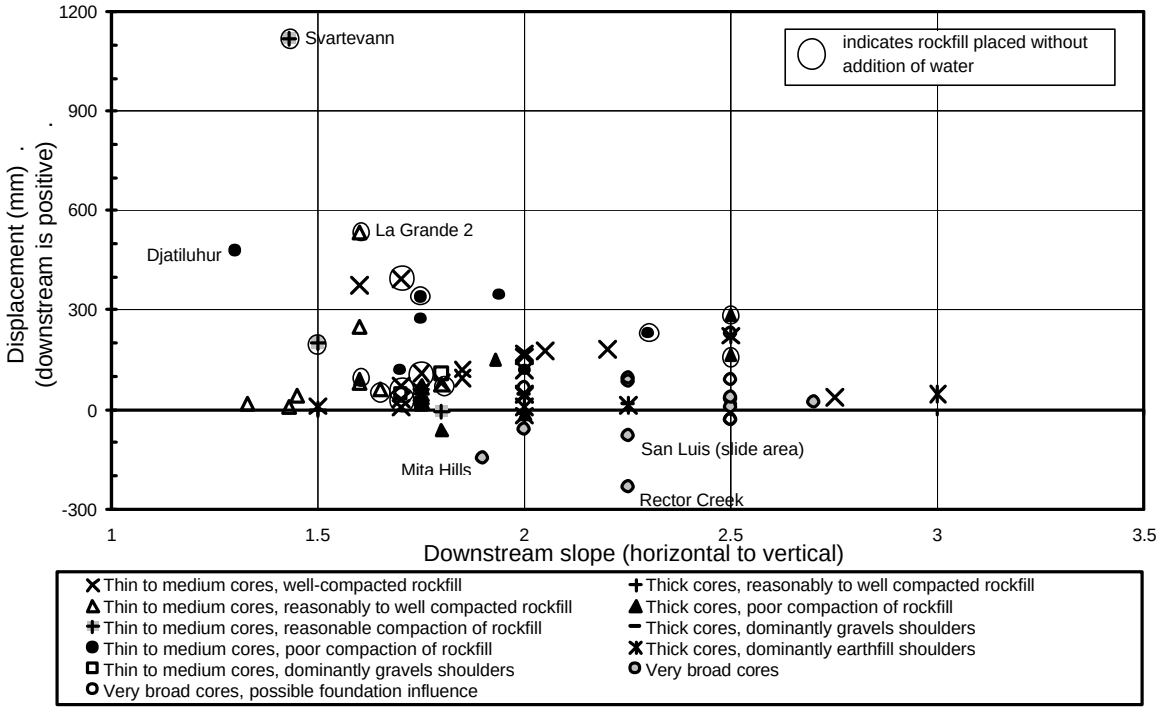

Figure 7.41: Lateral displacement of the crest (centre to downstream region) on first filling versus downstream slope.

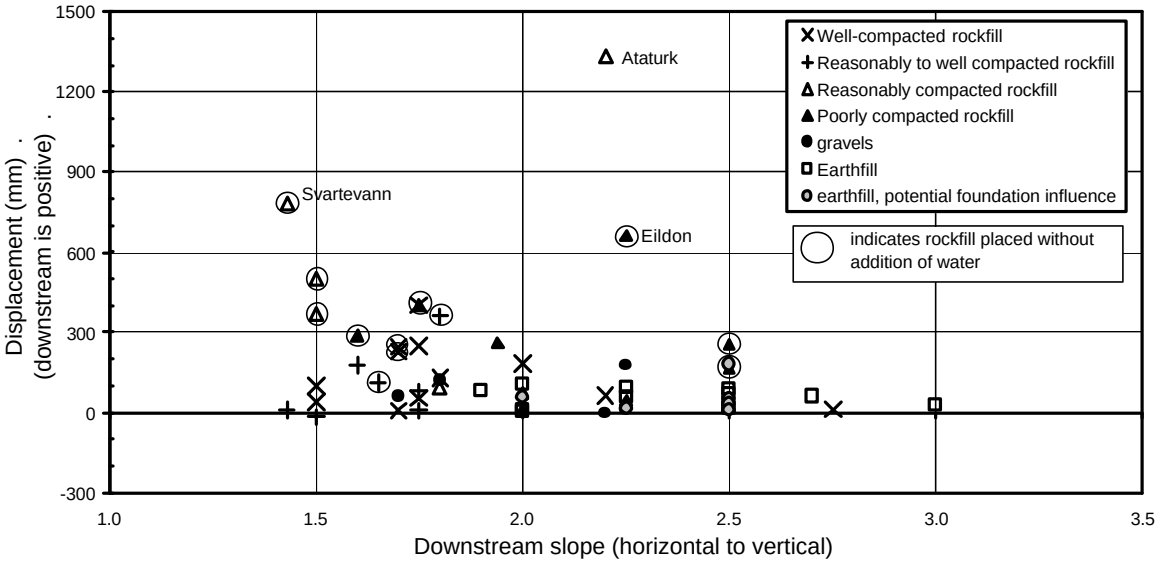

Figure 7.42: Lateral displacement of the downstream slope (mid to upper region) on first filling versus downstream slope.

7.6 GENERAL POST CONSTRUCTION DEFORMATION BEHAVIOUR OF EARTHFILL AND ZONED EARTH AND EARTH-ROCKFILL EMBANKMENTS

The post construction deformation data collected and presented for earthfill and earth-rockfill embankments includes:

- Surface monitoring point (SMP) data on the crest and slopes of the embankment. Both the vertical and horizontal deformation (in the plane normal to the dam axis) is presented.
- Internal vertical deformation data, mainly from IVM gauges, in the central core region of the embankment.

The data presented is usually for the maximum section of the embankment.

Zero time, t_0, is established at the end of embankment construction to provide a consistent basis point for comparison. The unit of time used for all data is years.

Where possible the deformation records used are the actual records. This has been possible for a large number of the Australian dams and most of the United States Bureau of Reclamation (USBR) dams. For a number of case studies however the data has been digitised from published plots in the literature, and for these cases the deformation as plotted is only a representation of the actual measured data as opposed to the actual data records.

The data is presented mostly in graphical format with data or case studies sorted into what are considered appropriate groupings. The number of plots presented is numerous, particularly for the deformation versus time plots, due to the large number of cases and number of groupings used. Total deformation plots incorporating a large number of case studies are also presented at selected time intervals and these visually provide a broad representation of the database.

The data for analysis of the post construction surface deformation behaviour is divided into the three regions of the embankment as previously identified in Section 7.5.3 (Figure 7.37). They are; the mid to downstream region of the crest, the mid to upper region of the downstream slope, and the upper upstream slope to upstream crest region.

7.6.1 POST CONSTRUCTION INTERNAL VERTICAL DEFORMATION OF THE CORE

Analysis of the post construction internal vertical deformation of the core was undertaken for those embankments for which detailed results of the internal deformation monitoring were made available. This was generally limited to a number of Australian and USBR dams, but includes several dams published in the literature.

The post construction IVM records were analysed by plotting the cumulative post construction settlement or vertical strain between the individual cross-arms. Assessment of the behaviour was based on the shape of the cumulative settlement or vertical strain profile at a specific time interval after construction and over time.

Typical plots of cumulative settlement are presented in Figure 7.43 and Figure 7.44 for Talbingo (IVM ES1) and Copeton (IVM B) dams respectively. They are considered representative of "normal" type deformation behaviour.

For Talbingo dam the much higher post construction vertical strains in the lower 40 to 50 m of the 160 m high dam (average of 0.7% at 24 years post construction) are considered to be related to consolidation due to dissipation of high pore water pressures. On first filling, pore water pressures increased by some 200 to 400 kPa above the already high construction pore water pressures. Over the next 20 plus years the pore water pressures slowly dissipated, reducing by as much as 600 to 1100 kPa below the levels at end of first filling. In the mid region of the core the change in pore water pressure due to dissipation was much less than in the lower section and is reflected in the lower vertical strains (average of 0.3% at 24 years post construction). The localised zone of high settlement between 55 and 58 m below crest level is potentially indicative of "abnormal" behaviour. From the data it is evident that the differential settlement between these IVM gauges occurred in the period between 0 and 0.15 years post construction and prior to first filling, and since then has increased only marginally. The reason for the behaviour is not known, but given its timing in relation to end of construction and first filling it is not likely to be "abnormal".

The behaviour of IVM B at the 110 m high Copeton dam is similar to that at Talbingo dam. Higher vertical strains (average of 1.1% at 26 years post construction) were observed in the lower 10 m of the core where pore water pressure dissipation post first filling was in the order of 450 kPa. In the mid to upper regions of the core pore water pressures were negligible at end of construction and slowly rose post first filling. Vertical strains in this region of the core were on average 0.43% at 26 years post construction, much less than in the lower 10 m of the core.

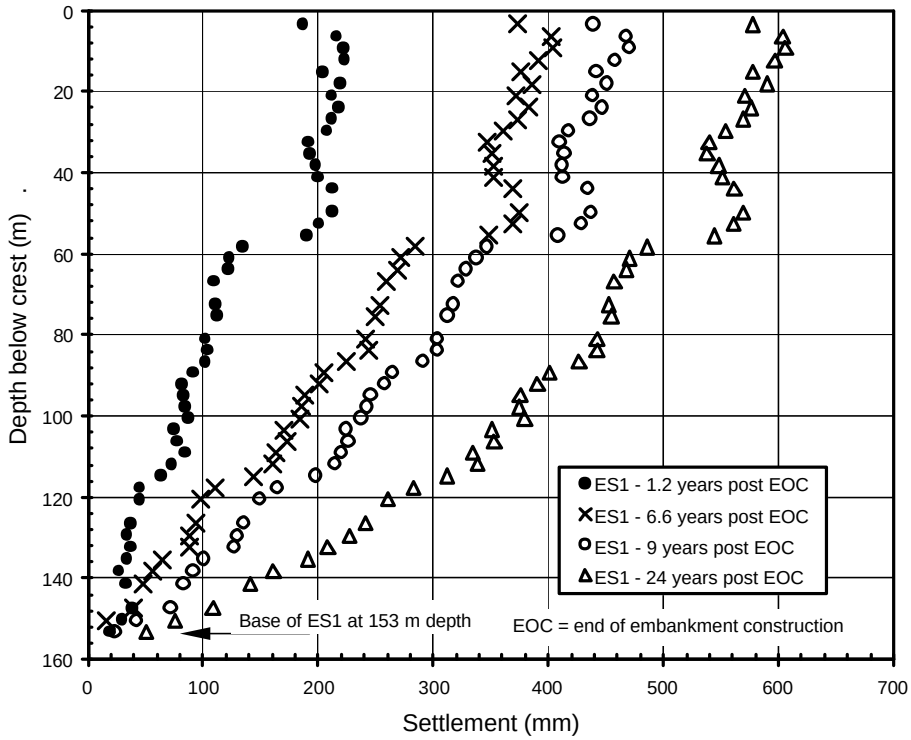

Figure 7.43: Post construction internal settlement of the core at Talbingo dam (IVM ES1 at the main section).

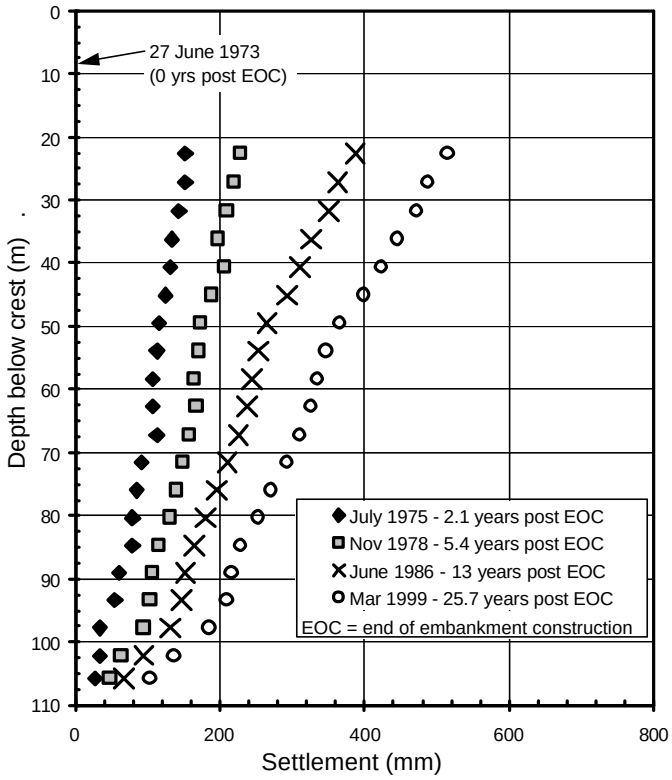

Figure 7.44: Post construction internal settlement of the core at Copeton dam (IVM B, 9 m downstream of dam axis at main section).

In contrast, the behaviour of IVM A at the 55 m high Bellfield dam (Figure 7.45), located in the thick central clay core, is different. The IVM records from end of construction to February 1987 indicate two potential zone of high localised vertical strain. The records from February 1987 to November 1997 (Figure 7.45b) show a localised zone of higher vertical strain developing at 28 to 30 m below crest level, inconsistent with the localised zones of high strain prior to 1987. The narrow rockfill shoulders at Bellfield were dry placed and poorly compacted, and based on the post construction behaviour of Eppalock dam (of similar design and construction to Bellfield), the "abnormal" behaviour may represent local yielding of the core. Bellfield dam is discussed further in Section 7.10 and in Section 1.2 of Appendix G.

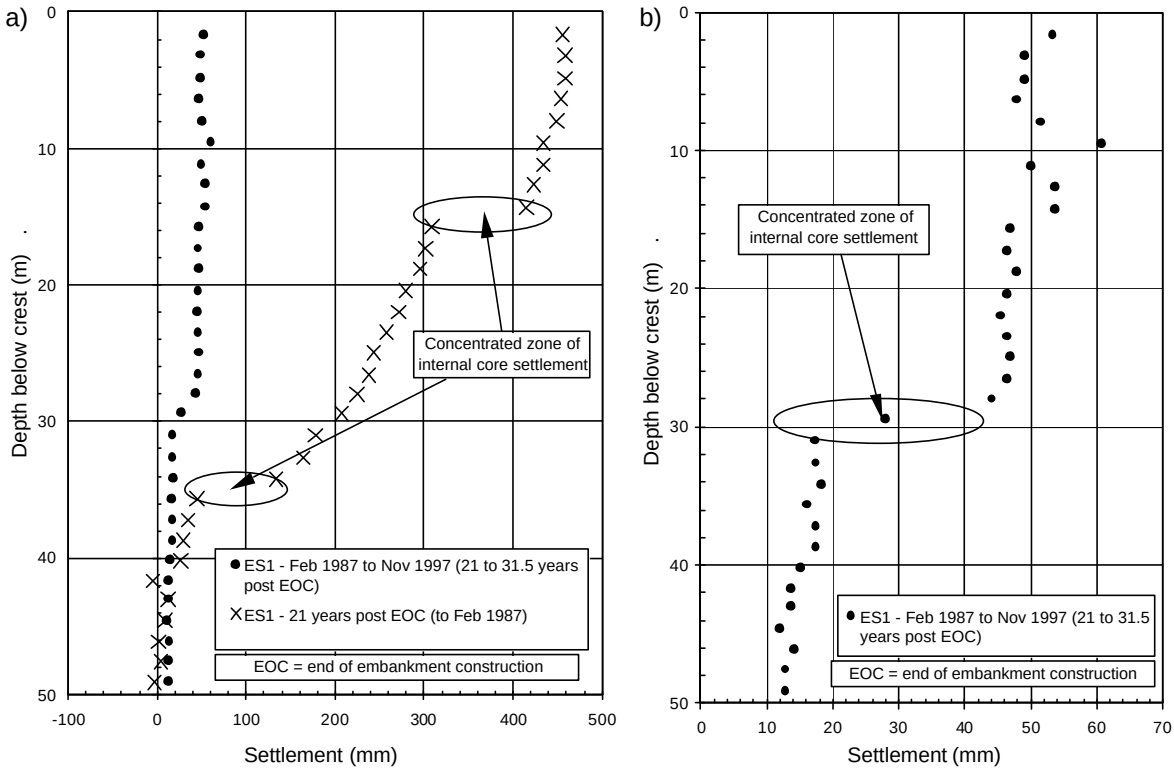

Figure 7.45: Post construction internal settlement of the core at Bellfield dam.

7.6.2 POST CONSTRUCTION TOTAL DEFORMATION OF SURFACE MONITORING POINTS

The total post construction surface deformations are presented as plots of settlement versus dam height at selected times after the end of embankment construction. Plots of the post construction lateral displacement during first filling are presented in Section 7.5.3. No additional lateral displacement plots are presented in this section.

Data is presented for the three embankment surface regions; the mid to downstream crest, the mid to upper downstream slope, and the upper upstream to upstream crest region (refer Figure 7.37). Base readings for the data are generally in the range from 0 to 0.5 years after the end of construction, most within 0.2 years, and include the period of first filling for most dams.

The data are mainly for embankments on rock foundations. Several embankments on soil/rock or soil foundations have been included where the foundation is considered to have a limited influence on the dam settlement, or where it can be excluded by deducting foundation settlement from base plate or base cross-arm readings from IVM gauges.

The settlement data is presented in the following figures:

- Mid to downstream crest region - Figure 7.46 for 3 years, Figure 7.47 for 10 years and Figure 7.48 for 20 to 25 years after the end of construction.
- Mid to upper downstream slope - Figure 7.49 for 3 years and Figure 7.50 for 10 years after the end of construction.
- Upper upstream slope to upstream crest region - Figure 7.51 for 3 years and Figure 7.52 for 10 years after the end of construction.

Plots for 20 to 25 years after the end of construction for the upstream and downstream slope regions are presented in Section 2.1 of Appendix F.

(a) Mid to Downstream Crest Region

The data for the crest region is sorted based on core width, core material type and placement moisture content. It can be seen from the figures that:

- The post construction crest settlements are generally much smaller than the core settlement during construction (refer Figure 7.23).
- Nearly all dams experience less than 1% crest settlement post construction for periods up to 20 to 25 years and longer after construction.
- Most experience less than 0.5% in the first 3 years and less than 0.75% after 20 to 25 years.

Table 7.19 summarises the typical range of crest settlement for various groupings of core width, material type and placement moisture content. Embankments that are clearly outliers (Ataturk, Djatiluhur, Beliche, Mita Hills, Roxo (near buttress), Rector

Creek dams) and potential outliers (Svartevann, Belle Fourche and Dixon Canyon dams) have been excluded from this table. Smaller crest settlements (as a percentage of the embankment height) are observed for dry placed clayey sands to clayey gravels regardless of core width and dry to wet placed silty sands to silty gravels. A broader range of crest settlement is shown for clay cores, wet placed clayey sand to clayey gravel cores, and embankments with very broad core widths, most of which are dry placed clays to sandy clays to clayey sands. For zoned earth and rockfill dams, poor compaction of the rockfill is over-represented at the larger end of the range of crest settlement.

Table 7.19: Typical range of post construction crest settlement.

Core Width	Core Properties		No. Cases	Crest Settlement (% of dam height) *[1]		
	Class[n]	Moisture content		3 years	10 years	20 to 25 years
Thin to medium	CL/CH	Dry	9	0.05 to 0.55	0.10 to 0.65	0.20 to 0.95
		Wet	11	0.04 to 0.75	0.08 to 0.95	0.20 to 1.10
	SC/GC	Dry	5	0.10 to 0.25	0.10 to 0.40	< 0.5
		Wet	18	0.15 to 0.80	0.20 to 1.10	< 1.1
Thin to Thick	SM/GM	All	16	0.06 to 0.30	0.10 to 0.65	< 0.5 to 0.7
Thick	CL/CH	all (most dry)	12	0.02 to 0.75	0.10 to 1.0	0.5 to 1.0
	SC/GC	all (most dry)	5	0.05 to 0.20	0.10 to 0.35	0.10 to 0.45
Very Broad	all	all (most dry)	18	0.0 to 0.60	0.0 to 0.80	0.05 to 0.76

Note: *[1] excludes possible outliers.

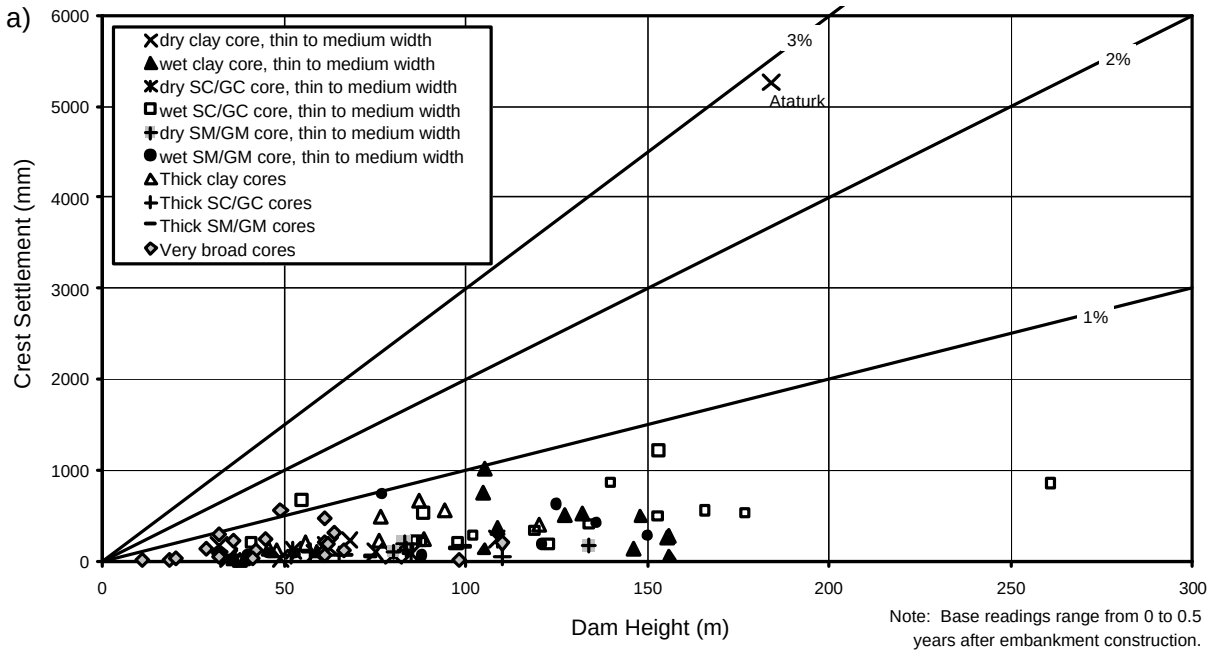

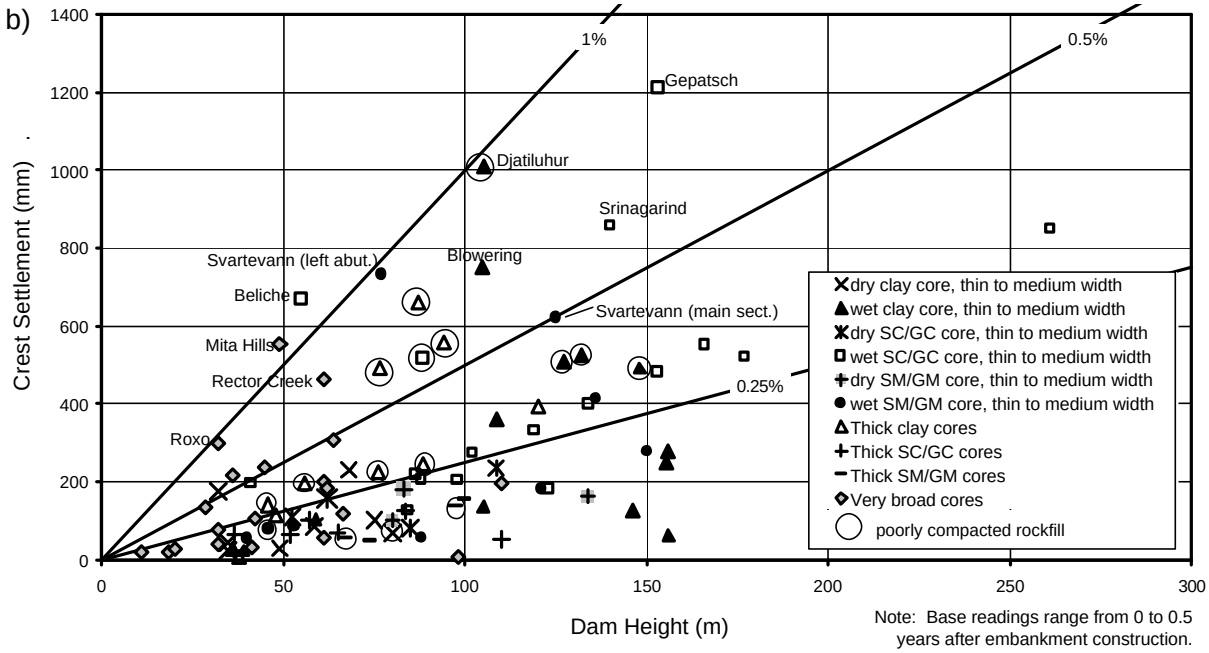

Figure 7.46: Post construction crest settlement at 3 years after end of construction, *(a)* all data, *(b)* data excluding Ataturk.

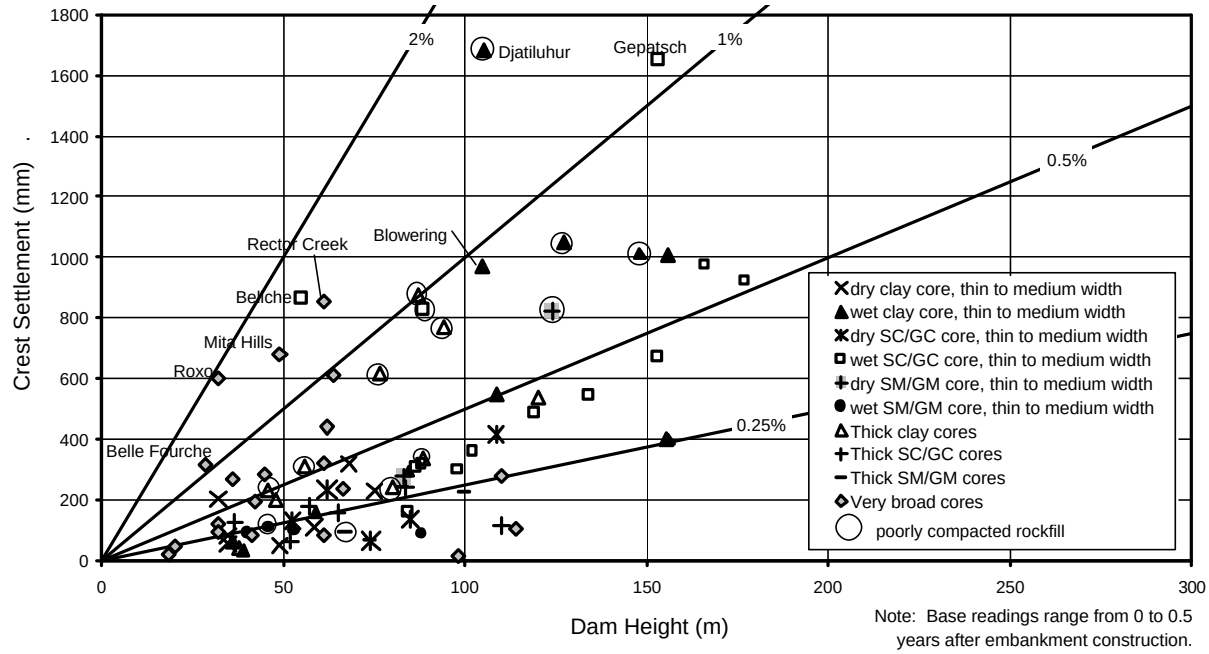

Figure 7.47: Post construction crest settlement at 10 years after end of construction.

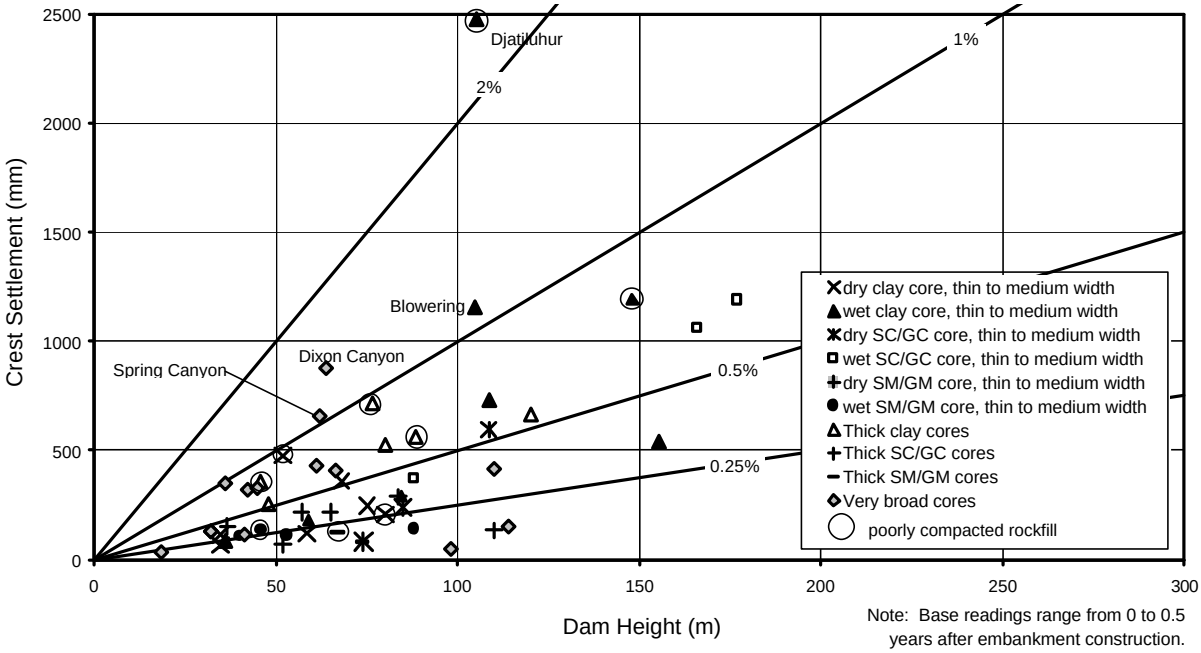

Figure 7.48: Post construction crest settlement at 20 to 25 years after end of construction.

(b) Mid to Upper Downstream Slope Region

For the mid to upper downstream slope region the data has been sorted based on material type of the downstream shoulder fill. The embankments with rockfill shoulders have been further divided into compaction rating of the rockfill. Embankments with dry placed and poorly compacted rockfills have been highlighted.

The height designated for each case study is the height from the SMP to foundation level.

(c) Upper Upstream Slope and Upstream Crest Region

For the upper upstream slope and upstream crest region the data has been sorted based on material type of the upstream shoulder fill. The embankments with rockfill shoulders have been further divided into compaction rating of the rockfill. Embankments with dry, poorly compacted rockfills in the upstream shoulder have been highlighted.

The height designated for each case study is the height from the SMP to foundation level.

Several zoned earthfill embankments with very broad cores where the foundation potentially has had an influence on the settlement have been included in the plots for the upstream and downstream slope. For these cases the height used is that from the SMP

to bedrock foundation. Excluded though were cases where the foundation contributed significantly to the settlement such as at Fresno dam and the downstream slope of Horsetooth dam.

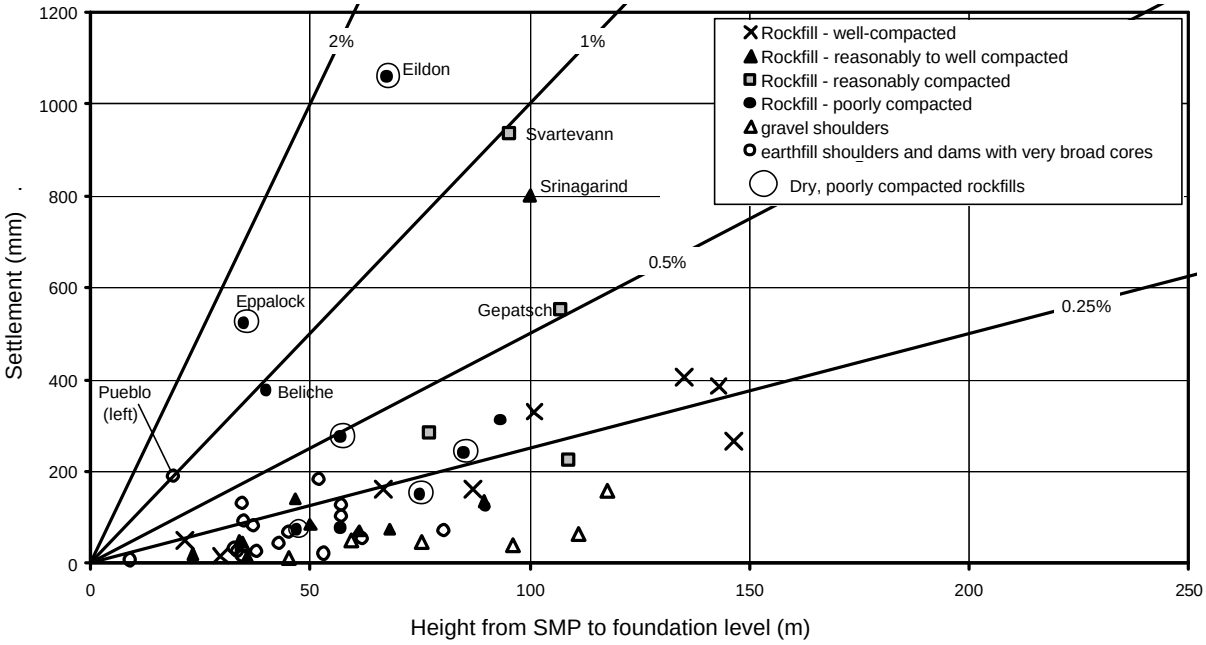

Figure 7.49: Post construction settlement of the downstream slope (mid to upper region) at 3 years after end of construction.

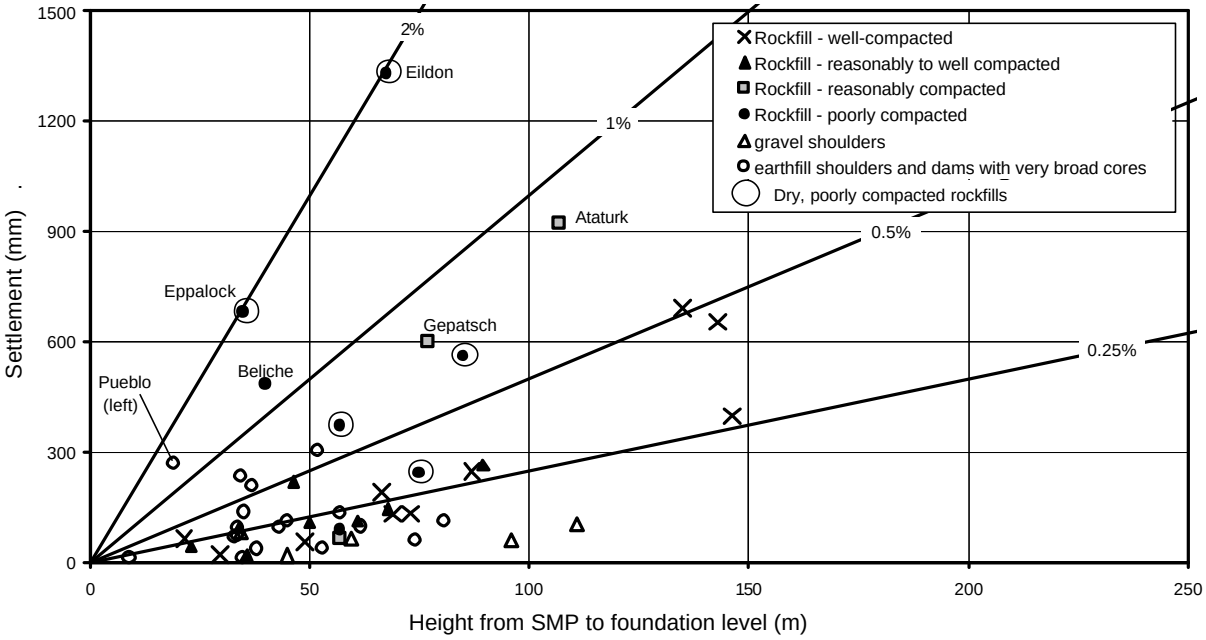

Figure 7.50: Post construction settlement of the downstream slope (mid to upper region) at 10 years after end of construction.

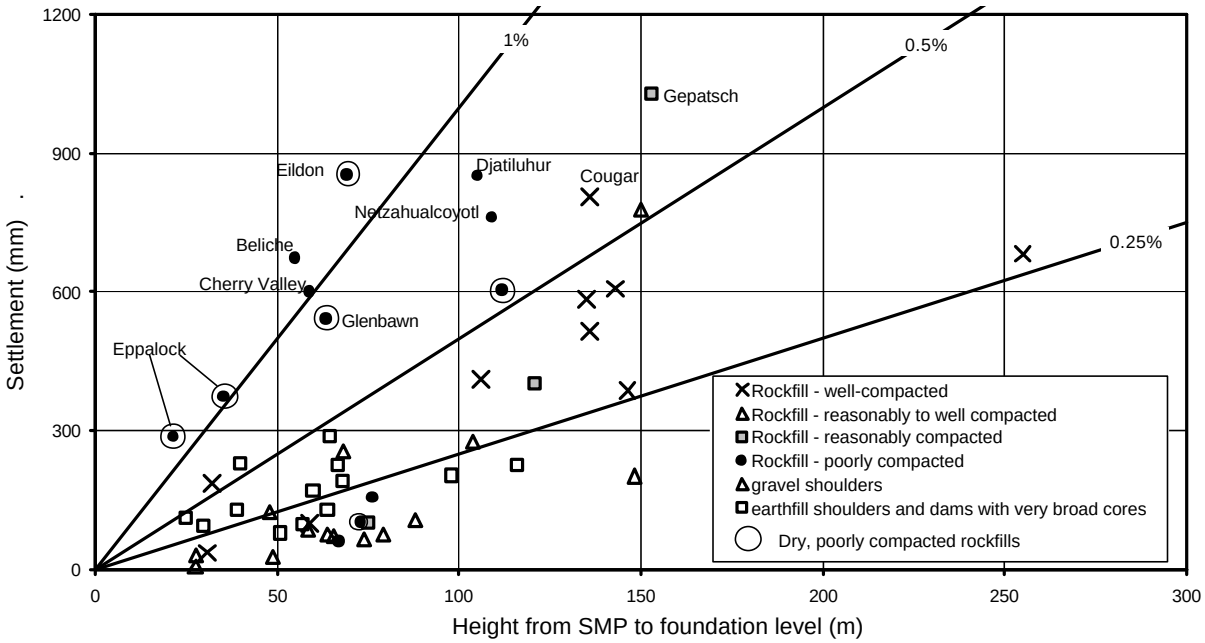

Figure 7.51: Post construction settlement of the upper upstream slope and upstream crest region at 3 years after end of construction.

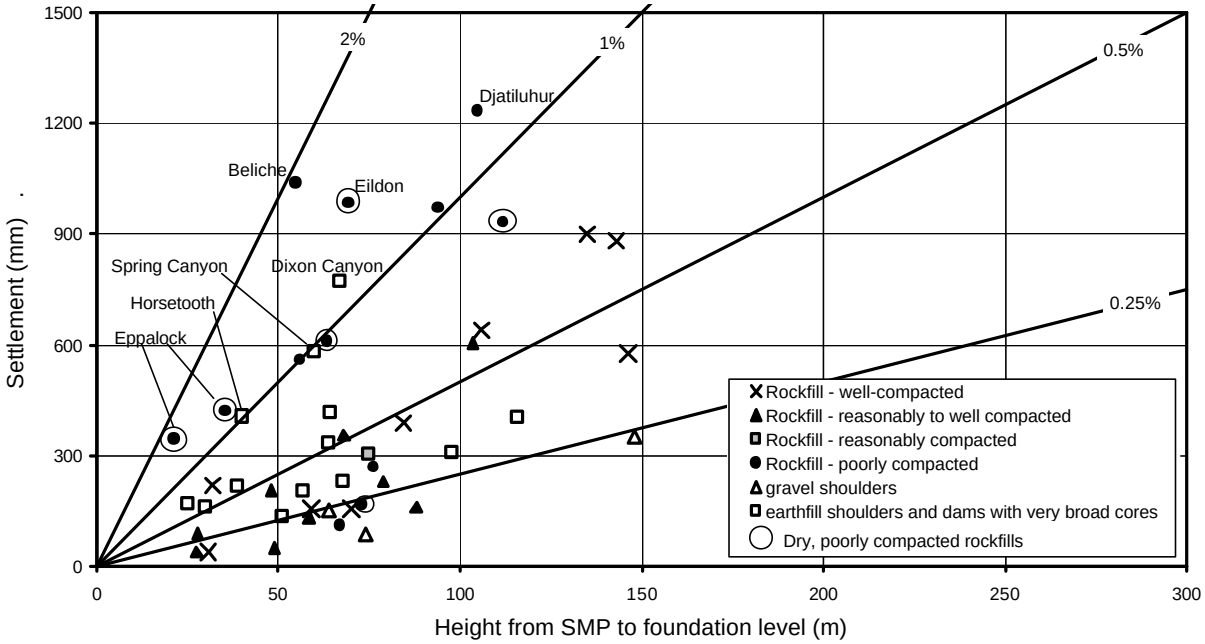

Figure 7.52: Post construction settlement of the upper upstream slope and upstream crest region at 10 years after end of construction.

Table 7.20: Typical range of post construction settlement of the upstream and downstream shoulders.

Material Type	**Compaction Rating**	**Downstream Shoulder *[1], *[2] Settlement (% *H* from SMP to fndn)**			**Upstream Shoulder *[1], *[2] Settlement (% *H* from SMP to fndn)**		
		No.	3 years	10 years	No.	3 years	10 years
Rockfill	well	11	0.05 to 0.35	0.05 to 0.55	12	0.10 to 0.60	0.10 to 0.70
	reas to well	9	< 0.30	< 0.50	11	0 to 0.55	0.10 to 0.60
	reas	5	0.20 to 1.0	0.10 to 1.0	3	< 0.70	- *[4]
	poor	4	0.10 to ? *[4]	0.15 to ? *[4]	8	0.10 to 1.05	0.15 to 1.20
	poor – dry *[3]	7	0.15 to 1.60	0.30 to 2.00	5	0.15 to 1.35	0.20 to 1.6
Gravels	-	7	< 0.15	< 0.25	3	< 0.15	< 0.25
Earthfills	-	20	0.0 to 0.40	0.0 to 0.70	14	0.05 to 0.60	0.10 to 0.70

Note: *[1] Excludes possible outliers.

*[2] Settlements quoted are a percentage of the height from the SMP to foundation level.

*[3] For the dry placed poorly compacted rockfills, settlements at Upper Yarra, Matahina and El Infiernillo are much less than for the other cases, for which settlements are close to or greater than 1% of the height.

*[4] insufficient data.

From the figures and as summarised in Table 7.20 it can be seen that for the embankment shoulders:

- Settlements of up 1 to 2% are observed for poorly compacted rockfills, both in the upstream and downstream shoulder. Greater settlements are observed for the dry placed, poorly compacted rockfills.
- For reasonably compacted rockfills the range of settlement is quite broad, from 0.1% up to 1.0%, for a limited number of cases. At Svartevann and Gepatsch dams the greater settlements are attributable to large collapse type settlement of dry placed rockfills, and at Ataturk dam to collapse settlement of weathered rockfills.
- Much lower settlements, generally less than 0.5 to 0.7% at ten years after construction, are observed for well and reasonably to well compacted rockfills, and for embankments with compacted earthfill in the shoulder.
- Very low settlements (less than 0.25% at 10 years) are observed for embankments with gravel shoulders.

Possible outliers include Svartevann, Horsetooth (upstream slope), Dixon Canyon, Spring Canyon, Srinagarind and the downstream slope of the left abutment embankment

at Pueblo dam. Several of these cases are discussed further in Section 7.10 and 7.11, and in Appendix G.

7.6.3 POST CONSTRUCTION CREST SETTLEMENT VERSUS TIME

The post construction crest settlement versus time for the case studies are presented in Figure 7.53 to Figure 7.61 in the form of settlement as a percentage of the embankment height versus time (in years since end of construction) on a log scale. The case studies have been sorted based on core width, core material type and placement moisture content into the following figures:

- Figure 7.53 – thin to medium core widths, dry placed clay cores;
- Figure 7.54 – thin to medium core widths, wet placed clay cores;
- Figure 7.55 – thin to medium core widths, dry placed dayey sand to clayey gravel cores;
- Figure 7.56 – thin to medium core widths, wet placed clayey sand to clayey gravel cores;
- Figure 7.57 – thin to medium core widths, silty sand to silty gravel cores both dry and wet placed;
- Figure 7.58 – clay cores of thick core width;
- Figure 7.59 – silty and clayey sand and gravel cores of thick core width;
- Figure 7.60 – very broad cores where the foundation has limited influence on settlement; and
- Figure 7.61 – very broad cores where the foundation has or potentially has a significant influence on settlement. This figure is plotted with the total settlement in millimetres.

The foundation influence has been evaluated from IVM or foundation base plate records where available. However, this was not possible at Pueblo, Dixon Canyon and Spring Canyon dams because foundation settlements were not measured post construction. For Horsetooth and Steinaker dams, the embankment only settlement from IVM records is included in Figure 7.60 and the combined embankment and foundation settlement from SMP records is included in Figure 7.61.

In most cases the base survey reading was within 0.5 years of end of embankment construction, but for a number of cases it was after this time. In several cases first

filling had been completed prior to the start of monitoring, these cases included but are not limited to, Nillahcootie, Peter Faust and Eildon dams.

The size of each figure has been set to the same margins for each plot area and the time interval standardised to cover from 0.1 to 100 years to allow for visual comparison between the figures. In most cases a standard vertical axis of 0 to 1.2% settlement has been used, but for several plots where settlements were larger a broader vertical axis has been adopted. If the case studies represented in a particular plot include an outlier/s (such as Ataturk in Figure 7.53a) a secondary plot excluding the outlier/s is presented as figure b.

Several other points to note from the figures are:

- Where the data does not extend to the y-axis it is because the base reading is or has assumed to be at the end of construction; i.e. zero time.
- The end of first filling has been indicated in the figures by an arrow for each case study. There are several reasons why first filling is not indicated for a number of cases studies:
  - First filling was not completed in the period of deformation shown (e.g. Ataturk and La Angostura dams).
  - First filling was completed prior to the base survey reading (e.g. Nillahcootie, Peter Faust and Eildon dams).
  - For cases with the base reading at time = 0 years, first filling occurred in the time period up to the first reading point after the base survey (e.g. Talbingo and Bellfield dams).
  - The time of the end of first filling is not known (e.g. Tooma dam).

The assessment of "wet" or "dry" placement has been based on the average moisture content at placement in relation to Standard optimum moisture content and/or the pore water response during construction from piezometers installed in the core. The following criteria were used:

- "Wet" placement for cores placed from slightly dry (0.2 to 0.3% dry) to wet of Standard optimum moisture content and/or where the pore water pressure response indicated positive pore water pressure coefficients that exceeded about 0.1 to 0.2 at end of construction. As previously discussed (Section 7.4.1.4) earthfills placed wetter than about 0.5% dry of Standard optimum tend to develop positive pore water

pressures during construction, although this is material type and stress level dependent.

- "Dry" placement for cores placed on average drier than about 0.5% dry of Standard optimum moisture content or where positive pore water pressures developed during construction indicated a pore water pressure coefficient less than about 0.1 to 0.2.

For a number of cases no details were available on the moisture content at placement or the pore water pressure data during construction if piezometers had been installed. For these cases a judgement was made as to whether the core was likely to have been placed "dry" or "wet". Some of the judgements made were:

- For the Japanese dams Seto, Kurokawa, Shimokotori, Taisetsu and Kisenyama dams, all central core earth and rockfill dams with thin to medium core widths, limited information was available on the core materials. Most of these dams were constructed in the 1970's and were assumed to be predominantly clayey gravels and wet placed given material availability and typical procedures used in Japan for embankment construction at the time (Takahashi and Nakayama 1973; Shiraiwa and Takahashi 1985; Kanbayashi et al 1979).
- For embankments with silty sand or silty gravel cores no distinction was made with respect to "wet" or "dry" placement for the post construction deformation. Where no information was available it was assumed that construction pore water pressures, if developed, had been dissipated to small values a short time period after end of construction. Embankments with limited or no data on placement moisture condition or pore water pressure response included Mud Mountain, Round Butte, Cherry Valley and Mammoth Pool dams.
- For the Tennessee Valley Authority dams Nottely, Watuaga and South Holston, wet placement of the clay cores was assumed as implied by Leonard and Raine (1958) and Blee and Riegel (1951).
- For Googong, Spilt Yard Creek, Peter Faust, Bjelke Peterson, Corin and Benmore dams the classification is likely to be borderline between "wet" and "dry" as placement was or was likely to have been within about 0.5% of Standard optimum moisture content. All were classified as "dry" placed.
- Cairn Curran, a zoned earthfill embankment with very broad earthfill core, "dry" placement was assumed.

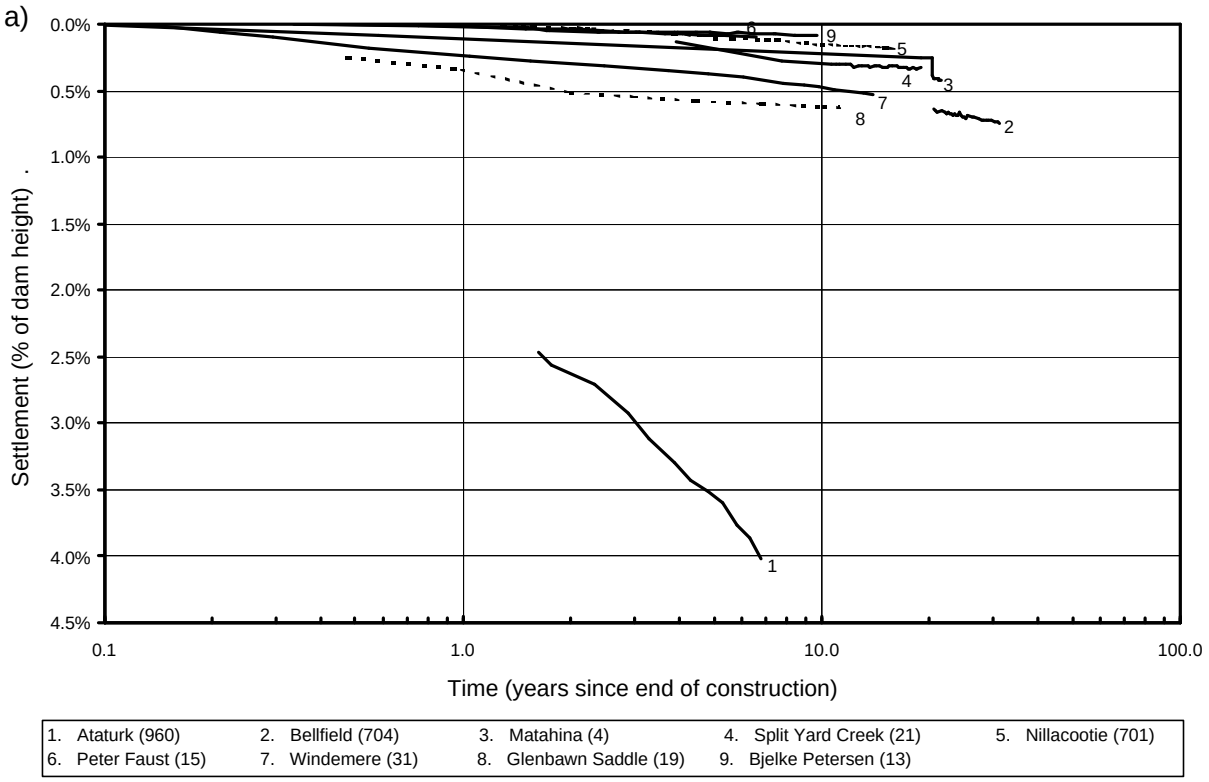

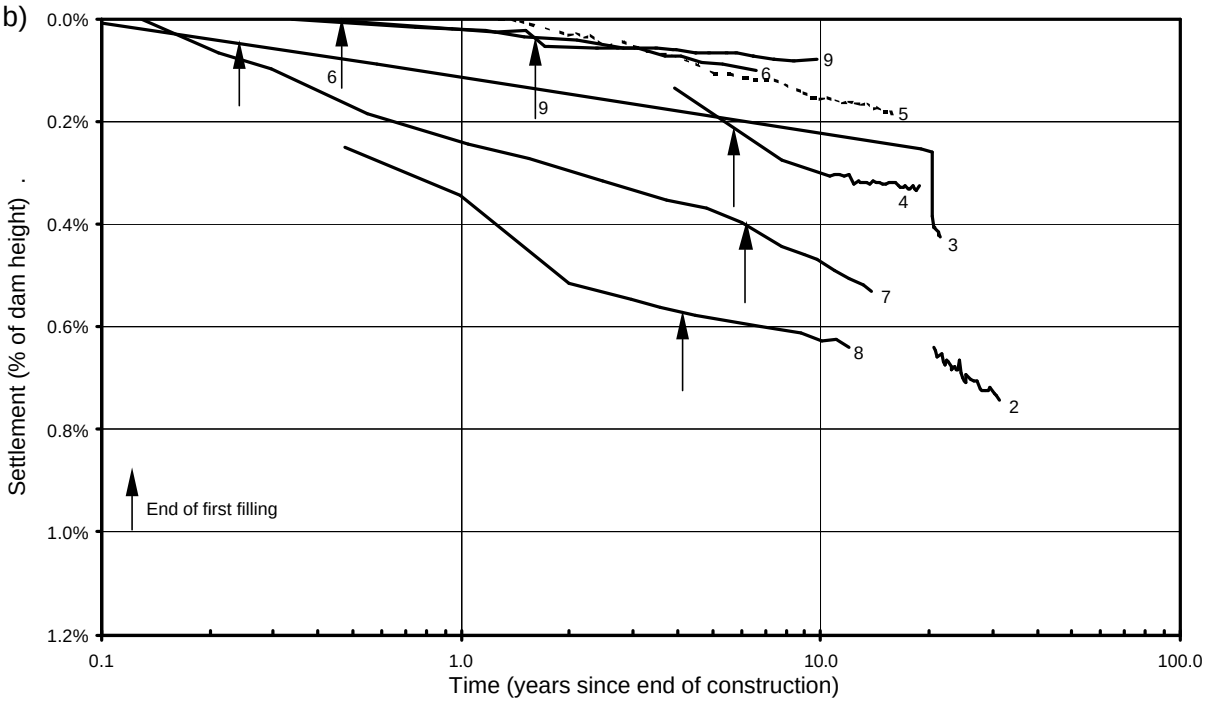

Figure 7.53: Crest settlement versus time for zoned embankments with thin to medium width central core zones of dry placed clayey earthfills; *(a)* all data, *(b)* data excluding Ataturk.

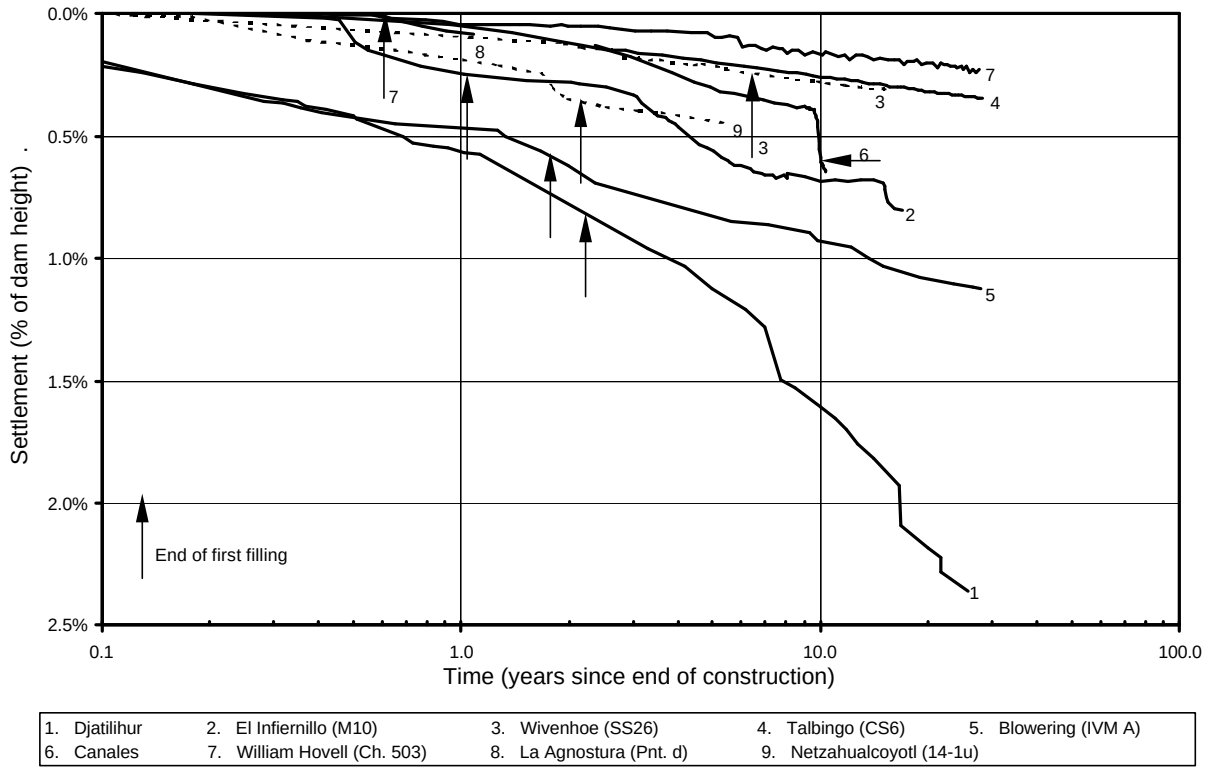

Figure 7.54: Crest settlement versus time for zoned embankments with thin to medium width central core zones of wet placed clayey earthfills.

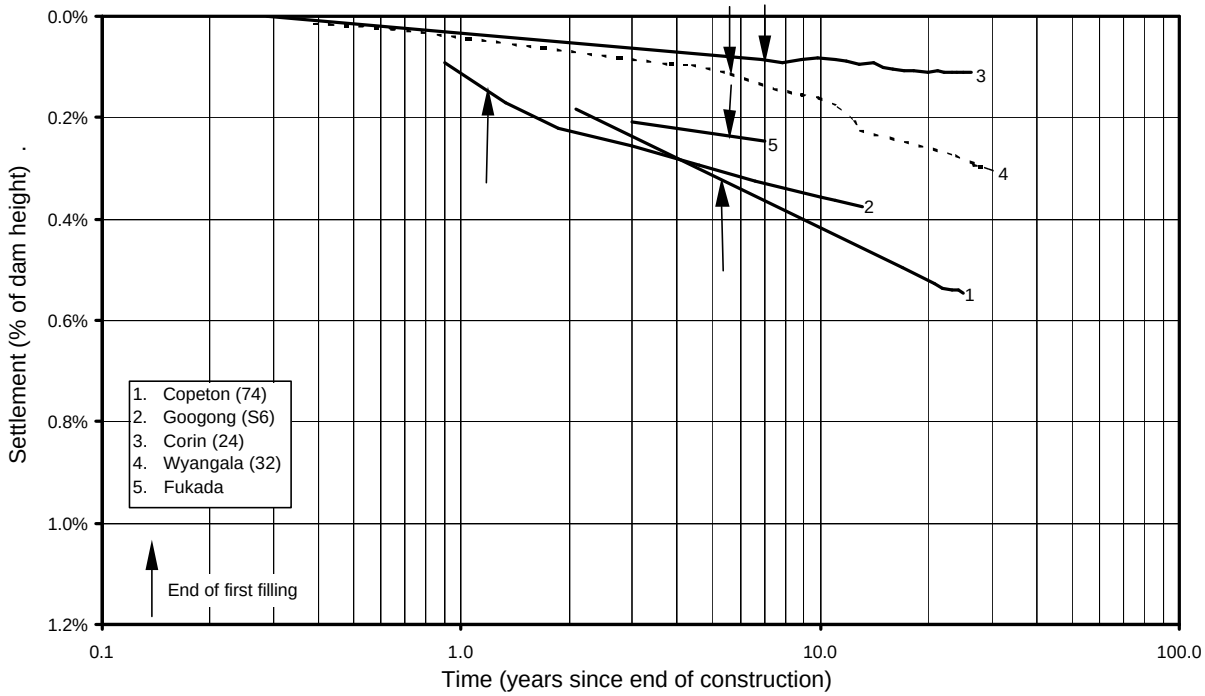

Figure 7.55: Crest settlement versus time for zoned embankments with thin to medium width central core zones of dry placed clayey sand to clayey gravel (SC to GC) earthfills.

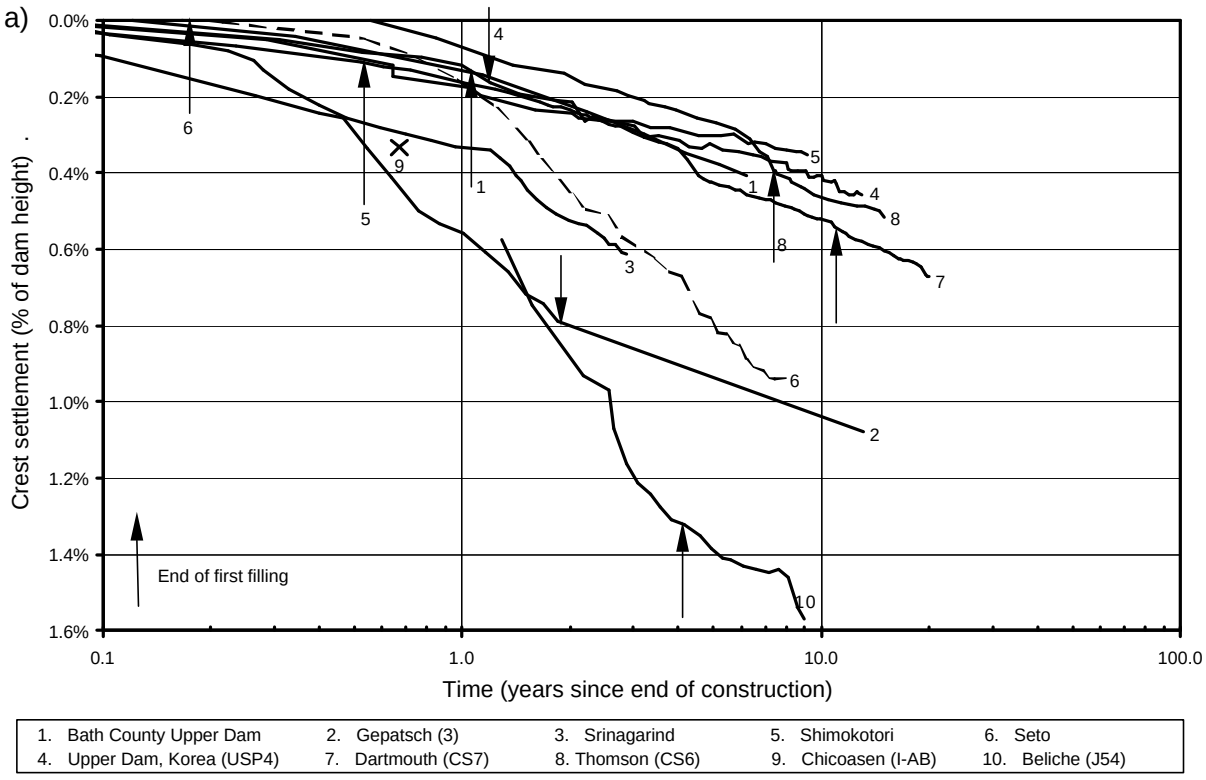

1. Bath County Upper Dam	2. Gepatsch (3)	3. Srinagarind	5. Shimokotori	6. Seto
4. Upper Dam, Korea (USP4)	7. Dartmouth (CS7)	8. Thomson (CS6)	9. Chicoasen (I-AB)	10. Beliche (J54)

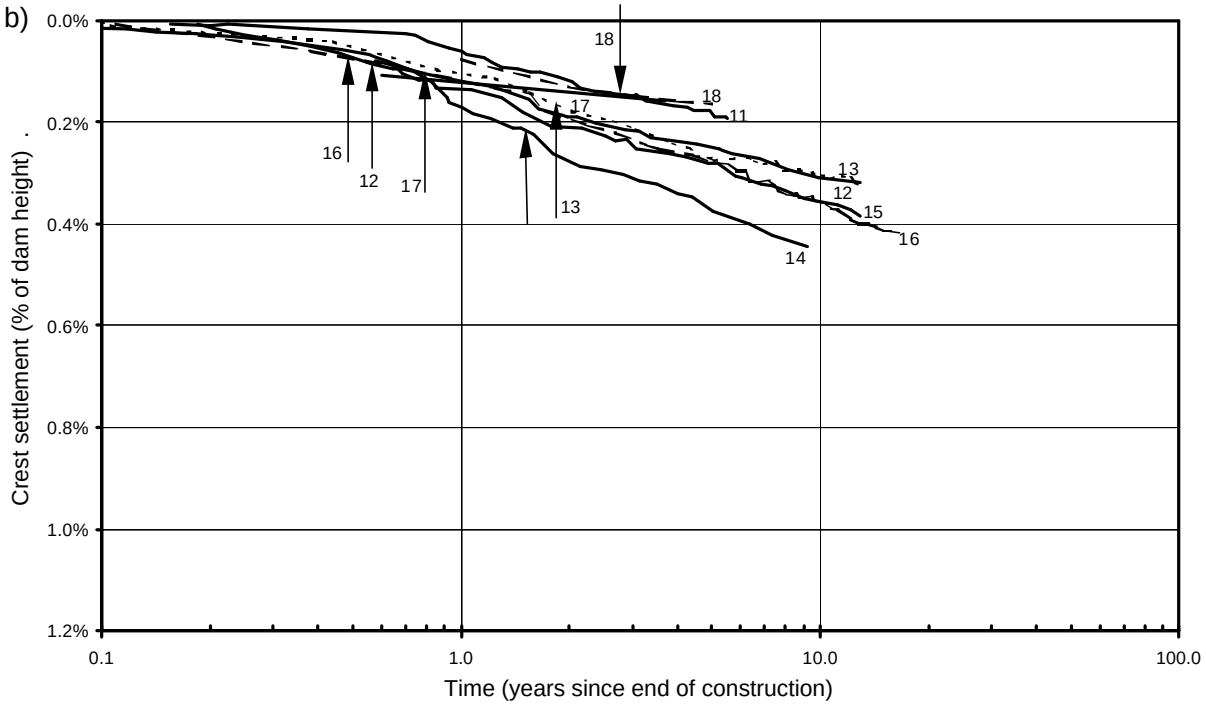

11. Tokachi	12. Terauchi	13. Kurokawa	14. Tedorigawa
15. Taisetsu	16. Kisenyama	17. Rosshaupten	18. Soyang (SP6)

Figure 7.56: Crest settlement versus time for zoned embankments with thin to medium width central core zones of wet placed clayey sand to clayey gravel (SC to GC) earthfills.

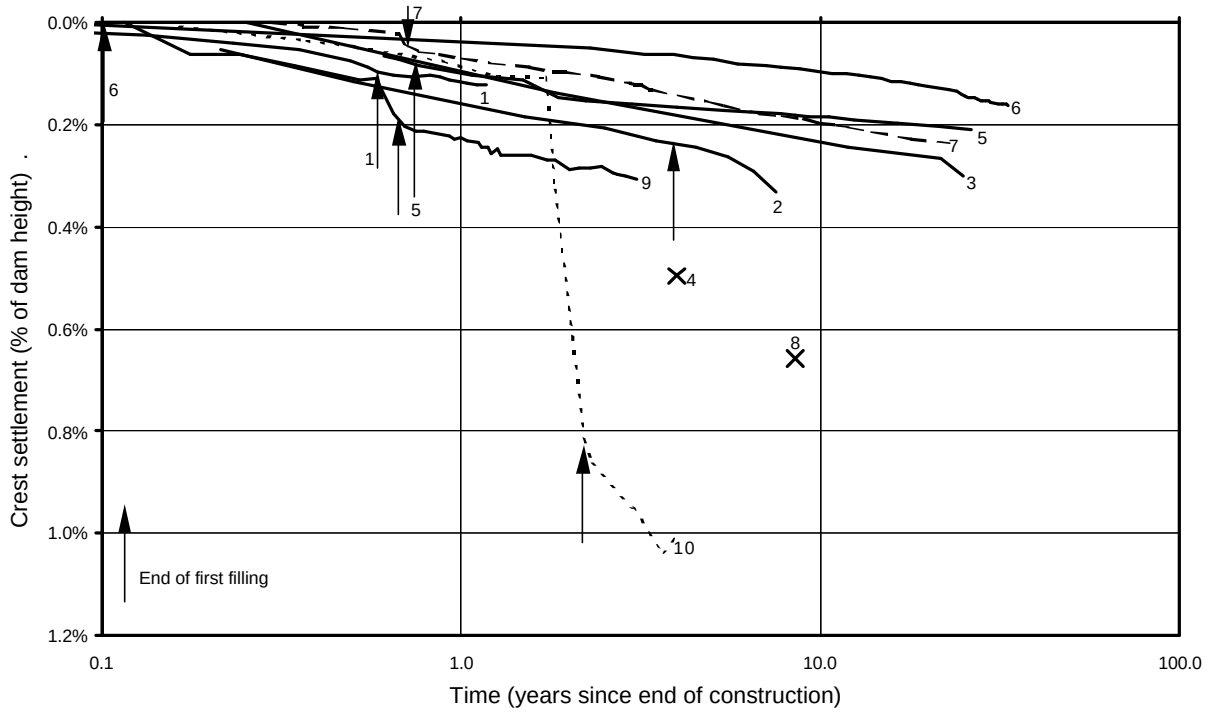

1. Round Butte (19)	2. Andong (CS7)	3. Ajuare	4. Svartevann (main section)	5. Parangana (Ch. 400)
6. Geehi (5)	7. Rowallan (Ch. 1500)	8. Mud Mountain	9. Cougar (TD-11)	10. Svartevann (left abut.)

Figure 7.57: Crest settlement versus time for zoned embankments with thin to medium width central core zones of silty sand to silty gravel (SM to GM) earthfills.

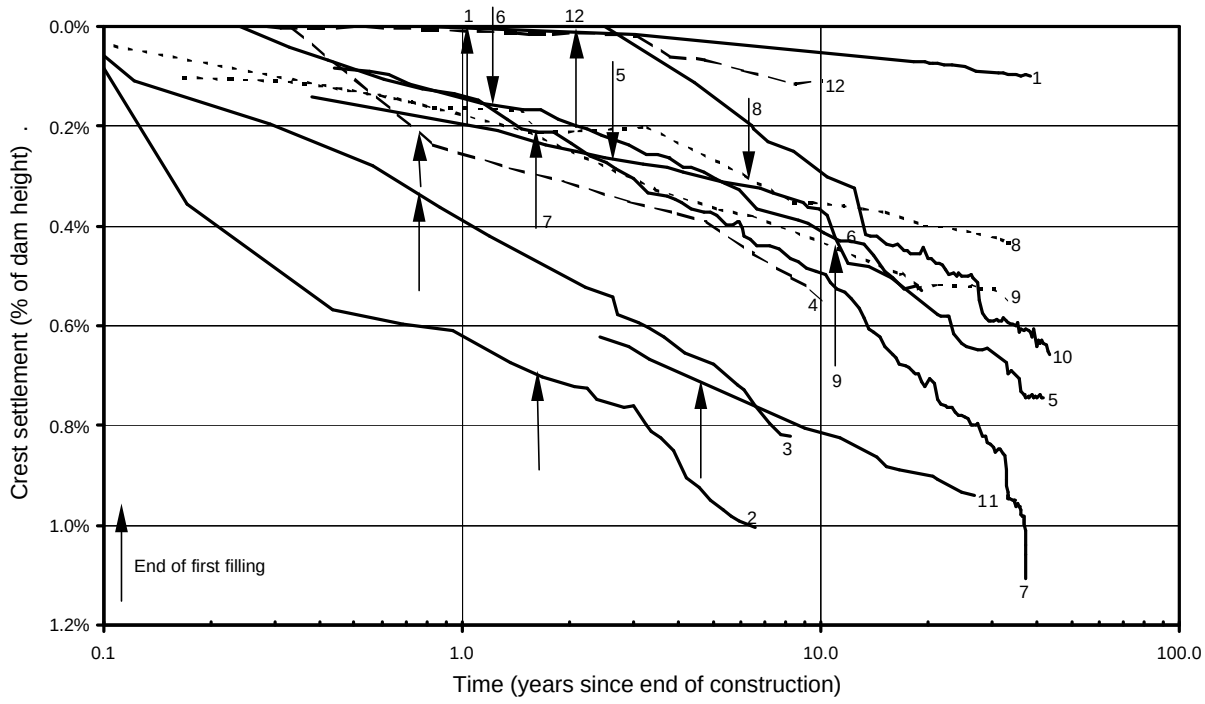

1. Waipapa (DM16)	2. South Holston	3. Watuaga	4. Nottely	5. Upper Yarra (M5)	6. Maroon (25)
7. Eppalock (CS2)	8. Burrendong (73)	9. Navajo (Stn 38)	10. Eildon (CS7)	11. Glenbawn (G2H)	12. San Justo (Stn 3.3)

Figure 7.58: Crest settlement versus time for zoned embankments with central core zones of clayey earthfills of thick width (1 to 2.5H to 1V combined width).

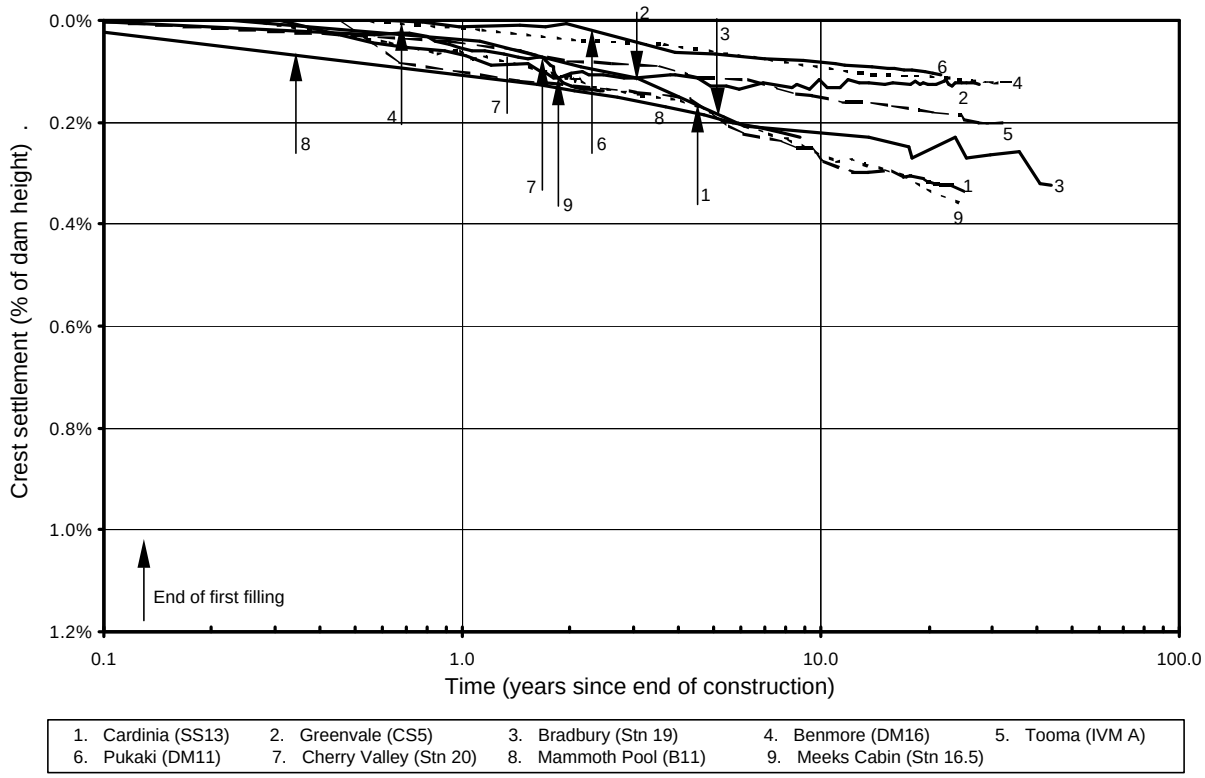

1. Cardinia (SS13) 2. Greenvale (CS5) 3. Bradbury (Stn 19) 4. Benmore (DM16) 5. Tooma (IVM A)
6. Pukaki (DM11) 7. Cherry Valley (Stn 20) 8. Mammoth Pool (B11) 9. Meeks Cabin (Stn 16.5)

Figure 7.59: Crest settlement versus time for zoned embankments with central core zones of silty to clayey gravel and sand (SC, GC, SM, GM) earthfills of thick width (1 to 2.5H to 1V combined width).

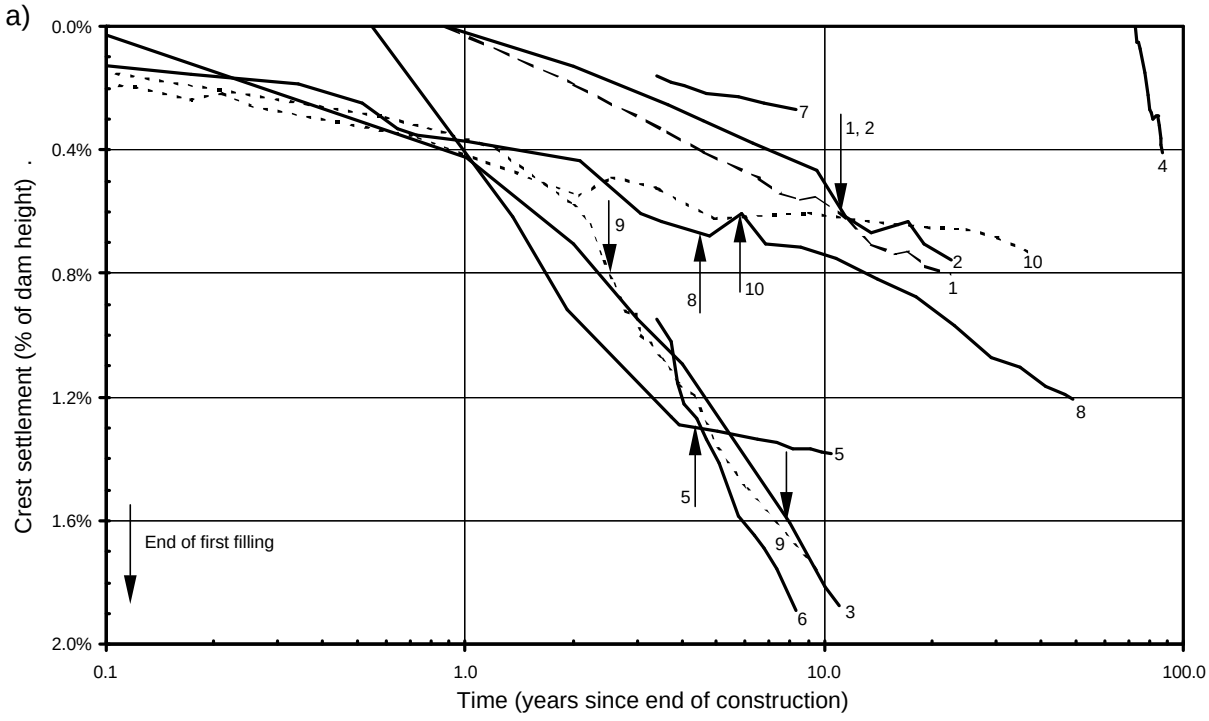

1. Pueblo, right emb. (Stn 46) 2. Pueblo, left emb. (Stn 77.5) 3. Belle Fourche (Stn 31) 4. Belle Fourche (MP10) 5. Mita Hills (A4)
6. Roxo (20m from buttress) 7. Roxo (95m from buttress) 8. Horsetooth (IVM A) 9. Rector Creek (Stn 16) 10. Steinaker (IVM A)

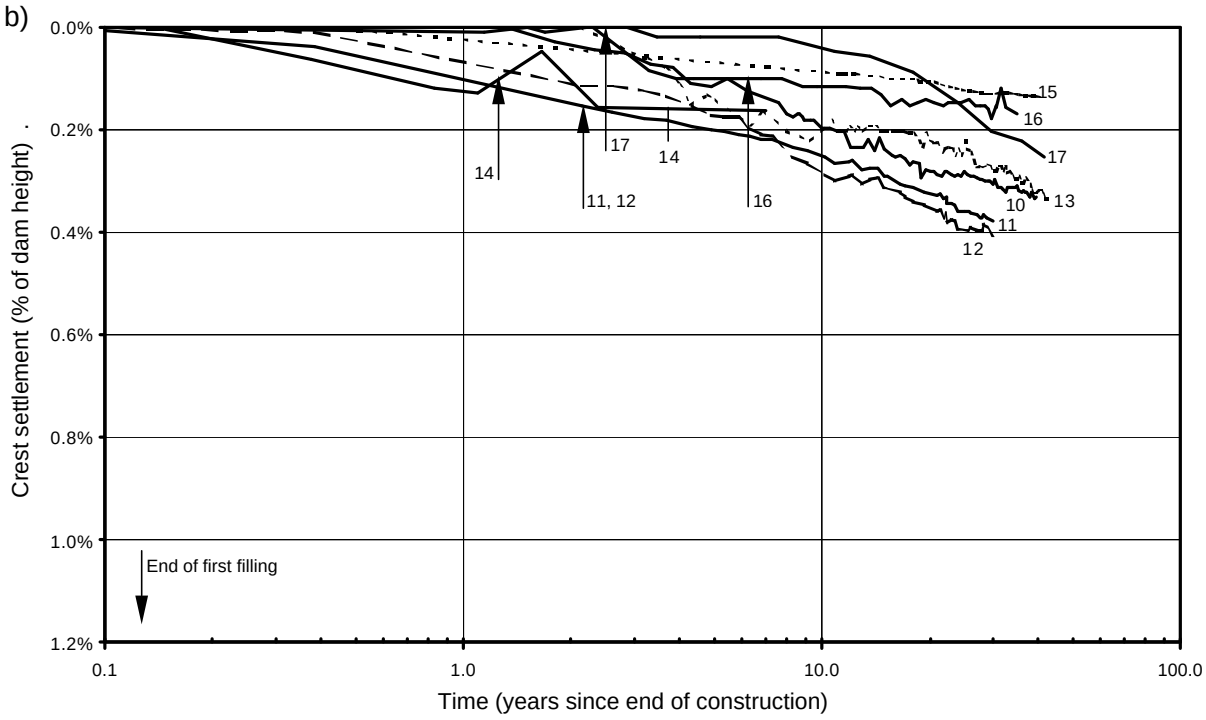

10. Tullaroop (CS2)	11. San Luis (Stn 110)	12. San Luis, slide area (Stn 138)	13. Cairn Curran (C3)
14. Biet Netufa (IVM)	15. Eucembene (15)	16. Khancoban (12/13)	17. Enders (Stn 48.4)

Figure 7.60: Crest settlement versus time for embankments with very broad core widths (> 2.5H to 1V combined width) and limited foundation influence.

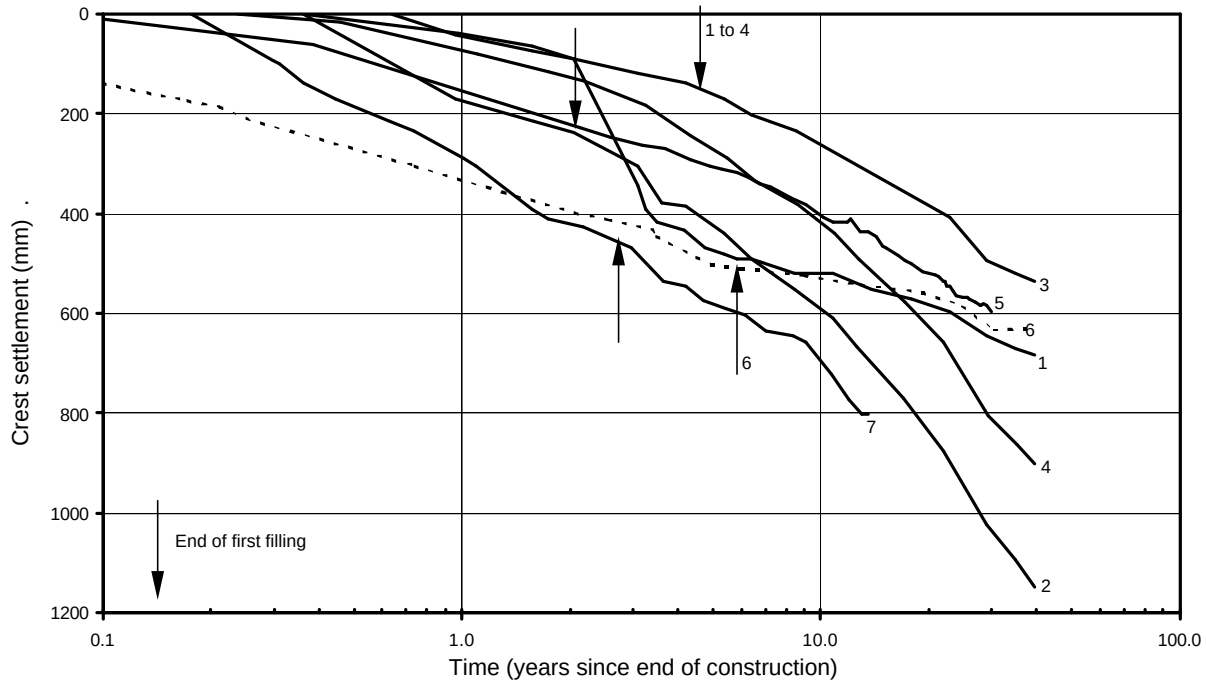

1. Horsetooth (Stn 10)	2. Dixon Canyon (Stn 9)	3. Soldier Canyon (Stn 11)	4. Spring Canyon (Stn 5)
5. San Luis (Stn 86)	6. Steinaker (Stn 14.6)	7. Fresno (Stn 21)	

Figure 7.61: Crest settlement versus time for embankments with very broad core widths (> 2.5H to 1V combined width) and potentially significant foundation influence.

The typical trend of post construction crest settlement versus log time is for a near linear relationship for most case studies, particularly after the end of first filling. Although, a gradual increase in the crest settlement rate (rate per log cycle of time) with time, or in-fact a decrease in rate with time is not unusual.

Before getting into a detailed discussion on the post construction crest settlement behaviour, the data on the long-term or post first filling crest settlement rate (rate per log cycle of time) is presented. Figure 7.62 presents the long-term crest settlement rate versus embankment height for zoned earthfill and earth-rockfill embankments with cores of thin to thick widths, and Figure 7.63 for earthfill and zoned embankments with very broad core widths. The data has been sorted based on reservoir operation. For the embankments of thin to thick core width the data has also been sorted based on core material type and those embankments with poorly compacted upstream rockfill zones have been highlighted. Table 7.21 presents a summary of the typical range of crest settlement rate for various sub-groupings of the case study data.

The assessment of reservoir operation post first filling is:

- "Fluctuating" reservoir where the reservoir is subject to a seasonal (usually annual) or regular (more than once per year) drawdown that is typically greater than about 0.1 to 0.15 times the height of the embankment at its maximum section.
- "Steady" or "slow" reservoir operation for embankments where the reservoir remains steady over time, is subject to fluctuations that occur slowly over time (i.e. slow drawdown over several years) or where the seasonal or regular fluctuation is less than 0.1 to 0.15 times the height of the embankment at its maximum section.

The crest settlement rate for each case study has been determined from the settlement versus log time plots in the above figures from the portion of the curve after the end of first filling. Where the settlement rate increases with time, such as for Enders dam in Figure 7.60b, the longer term rate has been used. For case studies where the settlement post first filling includes short periods of rapid acceleration, such as at Eppalock, Eildon and Djatiluhur dams, the representative rate for these embankments excludes the periods of rapid acceleration.

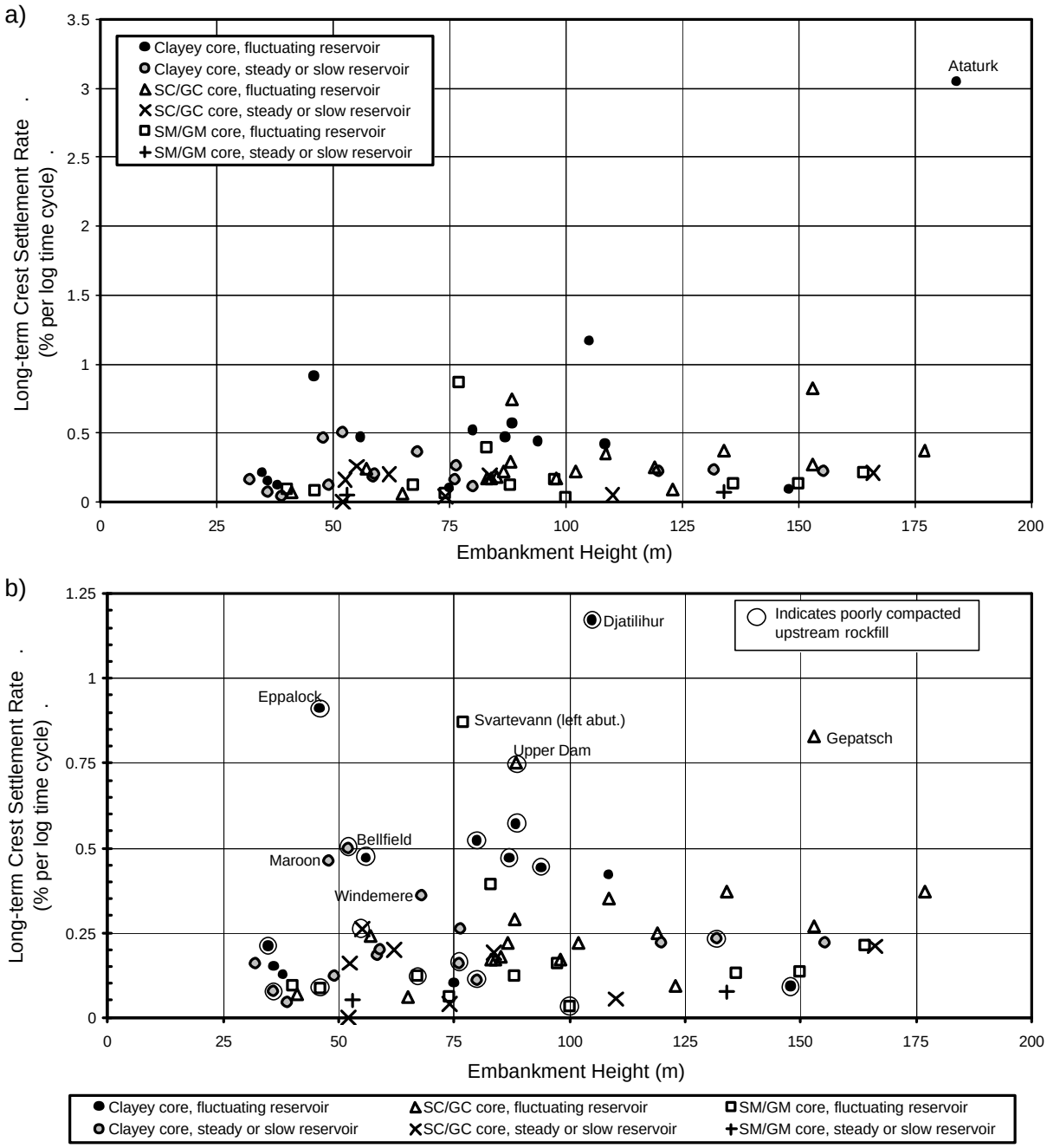

Figure 7.62: Long-term post construction crest settlement rate for zoned earthfill and earth-rockfill embankments of thin to thick core widths, *(a)* all data, and *(b)* data excluding Ataturk.

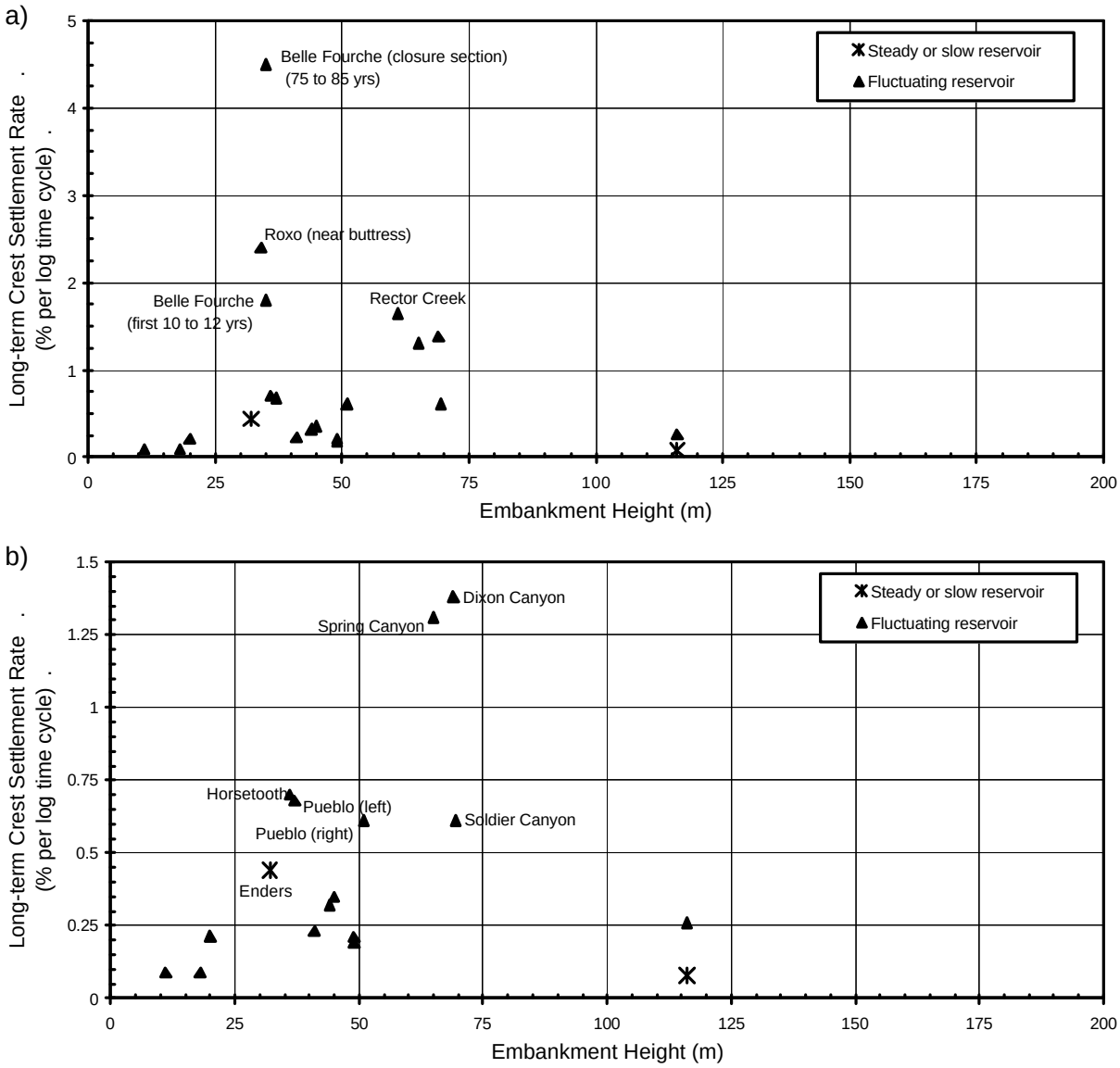

Figure 7.63: Long-term post construction crest settlement rate for embankments of very broad core width, (a) all data, and (b) data excluding Belle Fourche, Roxo and Rector Creek.

As a whole the total settlement, settlement versus time and settlement rate plots provide a comprehensive summary of the post construction crest settlement behaviour for earthfill and earth-rockfill embankments. The data allows for comparisons of magnitude and rate based on core width, core material type and moisture content at placement as well as consideration of reservoir operation post first filling and the use of poorly compacted rockfills in the upstream shoulder. Table 7.19 and Table 7.21 provide typical ranges of total crest settlement and long-term crest settlement rate sorted for most of these factors.

Clear and possible outliers to the general trend of post construction crest settlement are generally evident in at least two of the plot types, usually the settlement versus time plot and then either or both of the total settlement and settlement rate plots. The settlement versus time plots are the most comprehensive for assessment of potential outliers. In addition to highlighting large total settlement or high settlement rates, other trends that are potentially indicative of "abnormal" deformation behaviour are evident, such as acceleration in settlement over short time periods. Embankments indicating this type of behaviour include Djatiluhur, Canales, El Infiernillo, Beliche, Eppalock, Eildon, Upper Yarra, Svartevann, Matahina and possibly Blowering and Wyangala dams. A number of these case studies are discussed in Section 7.10. Often, but not always, these accelerations in settlement rate are associated with drawdown (refer to point d below).

It is important to note that use of the term "abnormal" in relation to the deformation behaviour of an embankment does not necessarily equate with potential instability. In nearly all cases identified as "abnormal" or potentially "abnormal" the overall stability of the embankment is not in question.

Table 7.21: Summary of long-term crest settlement rates (% per log cycle of time).

Core Width	Core Class[n]	Reservoir Operation	No. Cases	Long-term *[1] Settlement Rate	Comments
Thin to thick	CL/CH	Fluctuating	14	0.09 to 0.57	Higher rates at Djatiluhur (1.17%) and Eppalock (0.91%).
		Steady or slow	15	0.04 to 0.50 (most < 0.26)	Very high at Ataturk (3.1%). Higher rates at Maroon (0.46%), Windemere (0.36%) and Bellfield (0.50%).
	SC/GC	Fluctuating	18	0.06 to 0.37	Higher rates at Upper Dam (0.75%) and Gepatsch (0.83%).
		Steady or slow	8	0 to 0.26	
	SM/GM	Fluctuating	12	0.03 to 0.21	Higher rates at Svartevann (0.87%) and Andong (0.39%).
		Steady or slow	2	< 0.10	Only two cases, Round Butte & Parangana
Very broad	All types (most CL)	Fluctuating	17	0.07 to 0.70 (most < 0.35)	Very high rates (> 1.8%) at Belle Fourche & Roxo (near buttress). High rates at Rector Creek (1.65%), Dixon Canyon (1.38%) and Spring Canyon (1.31%).
		Steady or slow	2	0.08 and 0.44	Only two cases, Eucembene (0.08%) and Enders (0.44%).

*[1] Long-term settlement rate in units of settlement as a percentage of the embankment height per log cycle of time.

The factors affecting the post construction settlement of the mid to downstream region of the crest are:

(a) Influence of core material type and core width on the post construction crest settlement

Core material type has an influence on the post construction crest settlement. In general:

- Earthfill cores of silty sands to silty gravels typically show lower total crest settlements (Table 7.19) and lower long-term settlement rates (Table 7.21).
- Clay earthfill cores, on average, tend to have high long-term crest settlement rates (Figure 7.62 and Table 7.21) with clayey sand to clayey gravel cores showing intermediate rates.

Core width also influences the post construction crest settlement behaviour, but its influence is only evident for the crest settlement during and shortly after first filling. During first filling, crest settlements for most of the case studies with very broad earthfill cores (Figure 7.60 and Figure 7.61) and thick earthfill cores (Figure 7.58 and Figure 7.59) are limited, while those for thin to medium width cores are larger. This is likely to be due to several factors:

- The direction of the water load on first filling acting on the upstream face of the core and its distance from the dam axis.
- For embankments with thick cores, the core is generally not reliant on the shoulders zones for support and consequently not significantly influenced if collapse settlement on first filling occurs in the upstream shoulder. Conversely, embankments of thin to medium core width are more reliant on the shoulders for support and therefore can be significantly influenced by collapse settlements in the upstream shoulder on first filling.

The core width appears to have no recognisable influence on the long-term post first filling crest settlement rate (Table 7.21, Figure 7.62 and Figure 7.63). For embankments with very broad core width the long-term crest settlement rates (Figure 7.63) are highly variable and are discussed further in (f) below.

(b) Influence of compaction moisture content on the post construction crest settlement

For embankments with cores of thin to medium width it is evident that, after excluding the case studies likely affected by collapse settlement of the upstream rockfill, the range of crest settlement at any given time for cores placed wet are comparable to those for dry placed cores. For example, for the cases where monitoring started close to zero time the crest settlement at 10 years after end of construction are in the range:

- 0.2 to 0.65% for dry placed clay earthfills (Figure 7.53).
- 0.15 to 0.7% for wet placed clay earthfills (Figure 7.54).
- 0.1 to 0.4% for dry placed clayey sand to clayey gravel earthfills (Figure 7.55).
- 0.2 to 0.5% for wet placed clayey sand to clayey gravel earthfills (Figure 7.56).

This is not to say that compaction moisture content has a negligible influence on the post construction settlement behaviour, but that other factors have a greater influence and over-shadow that of compaction moisture content such as reservoir operation and collapse settlement of the upstream rockfill for wet placed cores.

The effect of compaction moisture content on the post construction internal vertical strain is clearly evident at Talbingo dam. In the lower region of the wet placed core at Talbingo dam reductions in pore water pressure post first filling were very large, up to 600 to 1100 kPa, and post construction vertical strains were up to 2.5 times greater than in the mid to upper region where the core was placed drier and reductions in pore water pressures were consequently much smaller (Figure 7.43 in Section 7.6.1). This reduction in pore water pressure in the core at Talbingo dam was much greater than that at Blowering, Thomson and Dartmouth dams (dams all greater than 100 m height) yet the post construction crest settlement at Talbingo is less than for these other embankments.

The limited influence of compaction moisture content on post construction crest settlement can also be attributable to the usually small reduction in pore water pressure from end of construction to close to equilibrium conditions for wet placed clay cores. In some cases, such as at Talbingo dam, where the reduction in pore water pressure is large (more than 200 to 500 kPa) it is usually confined to small regions of the core. Therefore, the net influence of consolidation due to dissipation of pore water pressures on the overall crest settlement will be relatively small.

Table 7.19 does indicate that a higher range of crest settlement is observed for wet placed clay and clayey sand to gravel cores of thin to medium width. However, the range of settlement for most of these case studies with wet placed cores is similar in magnitude to that of dry placed cores, as shown in Figure 7.53 to Figure 7.56. The reason for the higher range of settlement is that the data for wet placed cores does includes several case studies where the crest settlement was thought to be strongly influenced by collapse compression in the upstream rockfill.

(c) Influence of rockfill placement procedures for zoned embankments with rockfill in the upstream shoulder

The data for zoned earth and rockfill embankments shows that case studies with poorly compacted rockfill in the upstream shoulder are over-represented at the higher end of the total settlement plots (Figure 7.46 to Figure 7.48) and the higher end of long-term settlement rate plot (Figure 7.62). A more correct conclusion from the data would be that embankments where the rockfill in the upstream shoulder is susceptible to large magnitude deformations due to collapse compression on wetting represent a very large portion of the data at the higher end of these plots.

Earlier findings (Section 7.5.2) indicate that the magnitude of deformation on collapse compression is related to a number of factors other than degree of compaction, including placement moisture content, rock substance unconfined compressive strength and its reduction on saturation, stress level and particle size distribution. Assuming the magnitude of deformation of the upstream rockfill due to collapse compression is large on first filling, the shear strength properties of the core strongly influence the magnitude of crest settlement, with wet placed cores of low undrained strength shown to be susceptible to large crest settlements on first filling. The post construction settlement data tends to confirm this, although large settlements are not just confined to wet placed cores, they are also observed for dry placed cores. This is discussed further in Section 7.10.

From Figure 7.46, the plot of total settlement at 3 years after construction, crest settlements greater than 0.35 to 0.4% of the embankment height occur in embankments where the magnitude of settlement of the upstream rockfill due to collapse settlement on wetting was significant, including:

- A number of embankments with poorly compacted rockfill in the upstream shoulder.

- Embankments with dry placed and reasonably compacted (compacted in 2 m lifts) rockfill in the upstream shoulder (Gepatsch and Svartevann dams).
- Embankments with wetted and reasonably compacted weathered rockfill in the upstream shoulder (Ataturk and Beliche dams).
- Blowering dam, where the well-compacted rockfill was susceptible to large loss in strength on wetting.

The greater total settlement in these embankments is also reflected in the plots at 10 years and 20 to 25 years after construction.

The long-term crest settlement rate data (Figure 7.62) shows that for almost all cases where the settlement rate is greater than about 0.4% per log cycle of time the upstream rockfill (and usually the downstream rockfill as well) was poorly compacted and/or susceptible to large magnitude deformations due to collapse compression. This is an important observation because the influence of rockfills susceptible to collapse compression on the embankment deformation behaviour is generally only related to the embankment performance during and shortly after first filling. But the high long-term settlement rates for these embankments suggests that they are more susceptible to softening effects and degradation long-term as a consequence of factors including poor lateral support of the core, lateral spreading, internal cracking and softening in undrained strength. This is discussed further in Section 7.10 referencing the deformation behaviour from selected case studies.

(d) Influence of reservoir operation on the long-term crest settlement rate

The reservoir operation has a significant influence on the long-term post first filling crest settlement rate for zoned embankments as shown in Figure 7.62 and summarised in Table 7.21. Most of the periods of rapid acceleration of the crest settlement after first filling are associated with drawdown events. Exceptions to this are the earthquake influence at El Infiernillo and Matahina dams.

The difference in crest settlement behaviour due to reservoir operation is highlighted in Figure 7.64 and Figure 7.65. Both figures are of central core earth and rockfill embankments with clay cores of thin to thick width, Figure 7.64 for embankments where the reservoir is relatively steady and Figure 7.65 for embankments where the reservoir undergoes seasonal (often annual) drawdown.

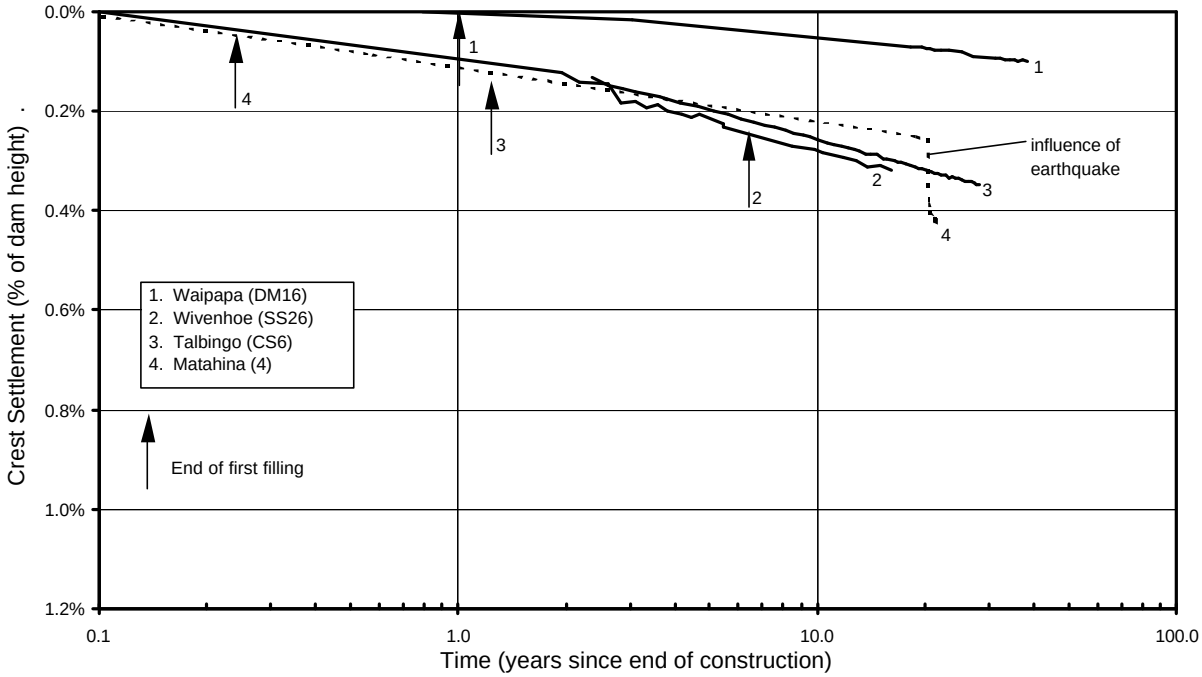

Figure 7.64: Crest settlement versus time for central core earth and rockfill embankments with central core zones of clayey earthfills and steady post first filling reservoir operation.

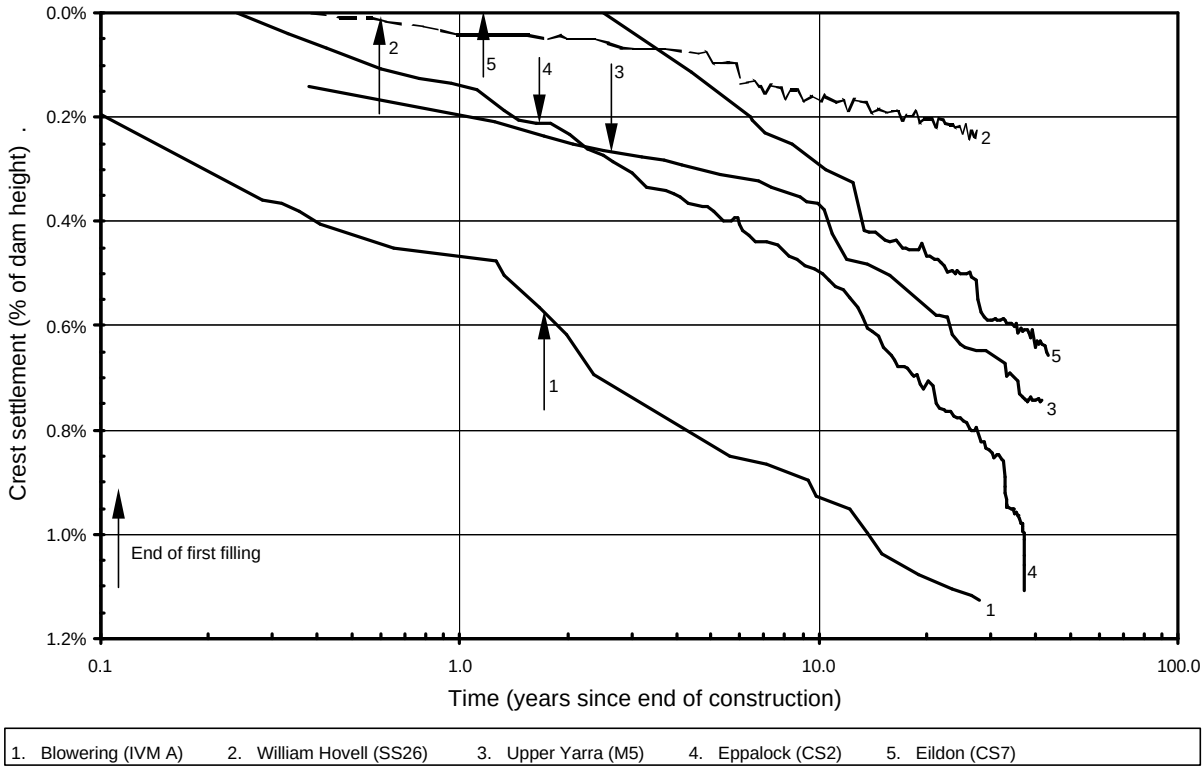

Figure 7.65: Crest settlement versus time for central core earth and rockfill embankments with thin to thick central core zones of clayey earthfills subjected to seasonal reservoir fluctuation.

For the seasonal drawdown case studies the rockfill placement consisted of:

- Placed dry in 1.5 to 2 m layers and spread with dozer tracking for Eildon and Eppalock, and possibly Upper Yarra dams.
- Wetted and well-compacted for Blowering dam, but the rockfill is susceptible to large strength loss on wetting.
- Reasonably to well compacted for William Hovell.

For Eildon, Eppalock, Upper Yarra and Blowering dams the periods of acceleration of the crest settlement post construction (Figure 7.65) are associated with large drawdown events. Other case studies where acceleration in crest settlement occurs on drawdown include Djatiluhur, Beliche and Wyangala dams. These cases are discussed further in Section 7.10 and in Appendix G.

(e) Crest settlement during first filling

Higher rates of crest settlement (per log cycle of time) during first filling are generally observed for zoned embankments of thin to medium core width, but only some of these embankments show this behaviour (Figure 7.53 to Figure 7.57). Dams with higher rates of settlement during first filling include:

- Split Yard Creek and Glenbawn Saddle dams, both of dry placed clay cores of thin to medium width.
- Blowering, Canales and Netzahualcoyotl dams, all wet placed clay cores of thin to medium width.
- Googong dam, a dry placed clayey sand core of medium width.
- Thomson, Beliche, Gepatsch and Dartmouth dams, all wet placed clayey sand to clayey gravel cores of thin to medium width.
- Svartevann, Cougar and Rowallan dams, all wet placed silty sand to silty gravel cores of thin to medium width.
- Nottely and South Holston dams, both clay cores of thick width and possibly wet placed.
- Mita Hills and Horsetooth dams, embankments with very broad earthfill zones.

Apart from Mita Hills and Horsetooth dams, all embankments are central core earth and rockfill embankments.

It is suspected that the mechanism of deformation for most of the case studies includes collapse settlement of the upstream rockfill on first filling and resultant plastic deformation with potential development of localised shearing within the core. This mechanism was discussed in Section 7.5.2 with the aid of finite difference modelling and is discussed in more detail for selected case studies in Section 7.10 and Appendix G.

(f) Influence of very broad core width

For earthfill embankments or zoned embankments with very broad cores, notable aspects of the post construction crest settlement behaviour are:

- For a number of case studies the settlement versus time plots (Figure 7.60 and Figure 7.61) show an increasing rate of settlement after first filling. This trend is clearly evident for Enders dam and the Horsetooth Reservoir dams (Horsetooth, Dixon Canyon, Spring Canyon and Soldier Canyon dams), and to a lesser degree for San Luis dam and several other embankments.
- The long-term settlement rate of these embankments shows a high degree of variability (Figure 7.63), ranging from 0.07% to 4.5% within the closure section at Belle Fourche dam many years after construction.

With respect to the long-term settlement rate, the very high rates (> 1.6% per log time cycle) at Belle Fourche (within the closure section), Rector Creek, Mita Hills and Roxo dam (adjacent to the buttress) are considered "abnormally" high. Within the closure section at Belle Fourche dam it is notable that the settlement rate at 75 to 85 years after construction is almost 3 times what is was at 10 to 12 years after construction. The high rates at Dixon Canyon (1.38%) and Spring Canyon (1.31%) dams are also considered to be "abnormally" high. For these two dams there is a query over the influence of the foundation on the long-term crest settlement, but from review of the data records (refer Section 3.3 of Appendix G) this influence is considered to be limited and most of the long-term crest settlement is attributable to deformation within the earthfill.

The remaining embankments are considered to represent "normal" long-term settlement rates with values ranging from 0.07% to 0.7% per log time cycle. Embankment height appears to have little influence on the settlement rate as indicated by the low rates for the two largest embankments, Eucembene and San Luis (main

section) dams, compared to some of the other case studies of much lower embankment height.

For these embankments with very broad earthfill zones the development of the phreatic surface and the influence of reservoir fluctuation on piezometric levels within the embankment are considered to influence the post construction deformation behaviour. For most of the case studies the earthfill zones are dominantly clayey and of low permeability, and an important consideration for the deformation behaviour of these embankments is the effect of the gradual development of the phreatic surface and associated changes in effective stress conditions within the embankment. For a number of the case studies (of dominantly clayey earthfills) piezometric records indicate the phreatic surface took tens of years to reach steady levels in the central core region of the broad earthfill core, whilst for more permeable earthfills steady levels were reached within several years. Some examples of this are:

- At Belle Fourche dam (35 m high), constructed of medium plasticity clays placed on the dry side of Standard optimum, borehole "well" records indicate it took more than 10 to 15 years to establish steady levels in the upstream earthfill zone and more than 20 years in the central embankment region.
- At Fresno dam (24 m high), constructed of low plasticity sandy clays placed at an average of 0.2% dry of Standard optimum, pore water pressures reached close to equilibrium conditions more than 4 years but less than 15 years after end of construction (Daehn 1955).
- At Steinaker dam (49 m high), central earthfill zone of medium plasticity clays placed on the dry side of Standard optimum, piezometer records indicate it took 15 to 30 years to establish steady levels in the central embankment region.
- At San Luis dam (115 m high), central earthfill zone of low to medium plasticity clays placed on the dry side of Standard optimum, piezometer records indicate it took 15 to 30 years to establish steady levels in the central embankment region.
- At the Horsetooth Reservoir embankments (Horsetooth, Dixon Canyon, Spring Canyon and Soldier Canyon dams of 48 to 74 m height), constructed of predominantly sandy clays placed on the dry side of Standard optimum, USBR (1997) referred to the piezometer levels still rising more than 50 years after end of construction.
- At Khancoban dam, earthfill zone of silty sands, reasonably steady levels were established within 2 to 5 years after end of construction.

For those embankments with cores of low permeability, reservoir fluctuation would not be expected to greatly influence the crest settlement rate due to the likely limited effect it would have on pore water pressures in the central region of the embankment. However, for more permeable earthfills the reservoir operation may have a more substantial influence on the post construction crest deformation behaviour. At Enders dams the increased rate in settlement 8 to 10 years after the end of construction (Figure 7.60b) is coincident with the increased magnitude of fluctuation of the reservoir. In the first 8 to 10 years of operation annual fluctuations were limited to less than about 3 m, but after this period increased to 5 to 8 m (Figure 7.66). Piezometric records indicate that pore water pressures within the central embankment region also fluctuated with reservoir level but at reduced amplitude.

In comparison, the post construction settlement at the main section at San Luis dam (Figure 7.60b) showed no significant change in rate of settlement beyond about 8 years when the seasonal reservoir fluctuation increased substantially (Figure 7.67). Piezometers in the central region of the main earthfill zone (of mostly low to medium plasticity sandy clays) showed a negligible to very limited response to drawdown.

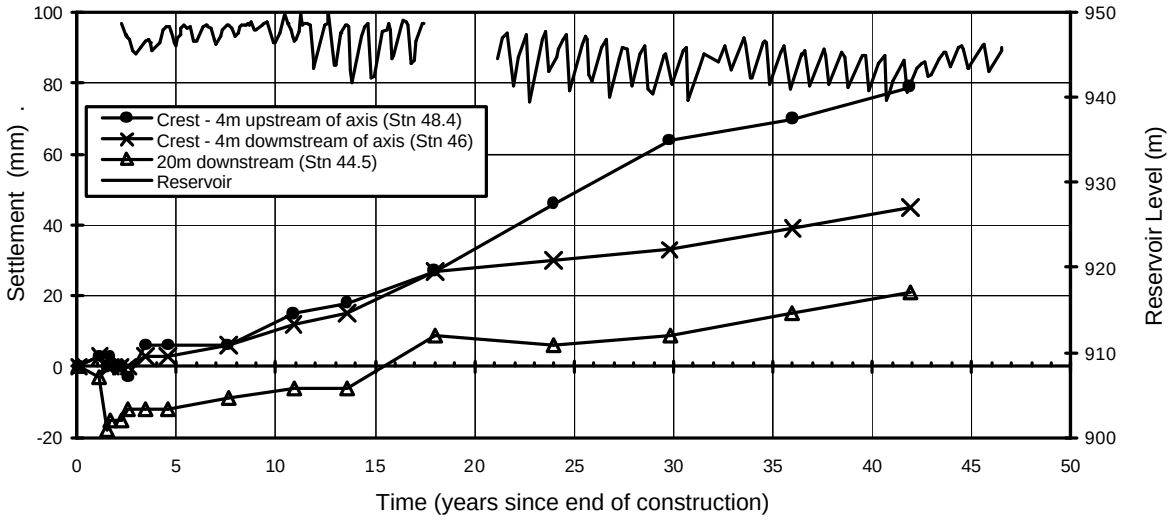

Figure 7.66: Post construction settlement and reservoir operation at Enders dam (data courtesy of USBR).

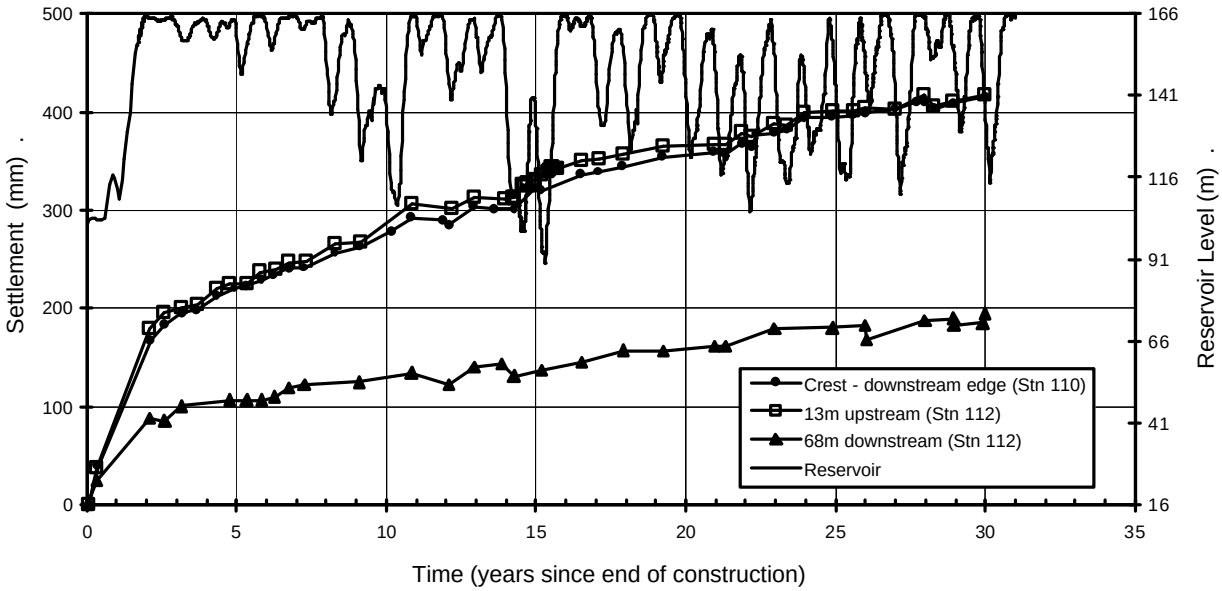

Figure 7.67: Post construction settlement at main section and reservoir operation at San Luis dam (data courtesy of USBR).

7.6.4 POST CONSTRUCTION HORIZONTAL DISPLACEMENT OF THE CREST NORMAL TO THE DAM AXIS.

The post construction horizontal displacements of the crest are presented in Figure 7.68 to Figure 7.76 in the form of total displacement in millimetres versus time (in years since end of construction) on a log scale. The case studies have been sorted based on core width, core material type and placement moisture content into the following figures:

- Figure 7.68 – thin to medium core widths, dry placed clay cores;
- Figure 7.69 – thin to medium core widths, wet placed clay cores;
- Figure 7.70 – thin to medium core widths, dry placed clayey sand to clayey gravel cores;
- Figure 7.71 – thin to medium core widths, wet placed clayey sand to clayey gravel cores;
- Figure 7.72 – thin to medium core widths, silty sand to silty gravel cores both dry and wet placed;
- Figure 7.73 – clay cores of thick core width;
- Figure 7.74 – silty and clayey sand and gravel cores of thick core width;
- Figure 7.75 – very broad cores where the foundation has limited influence on deformation; and

- Figure 7.76 – very broad cores where the foundation has or potentially has a significant influence on settlement.

For most case studies the displacement includes the period of first filling, or at least a substantial portion of it. For several embankments though first filling had been (or was virtually) completed prior to the start of monitoring and includes, but is not limited to, Nillahcootie, Eildon, Belle Fourche and Peter Faust dams.

For several of the embankments with very broad earthfill cores the distinction of foundation influence could not be readily evaluated, as no data on the foundation deformation was available. These cases include Pueblo, Dixon Canyon and Spring Canyon dams.

The size of each figure has been set to the same margins for each plot area and the time interval standardised to cover from 0.1 to 100 years to allow for visual comparison between the figures. In most cases a standard vertical axis of 100 mm upstream (-100 mm) to 300 mm downstream (+300 mm) displacement has been used. For several plots where larger displacements were recorded a broader vertical axis has been adopted. Other points to note about the figures are explained in the preamble for the crest settlement versus time plots (Section 7.6.3).

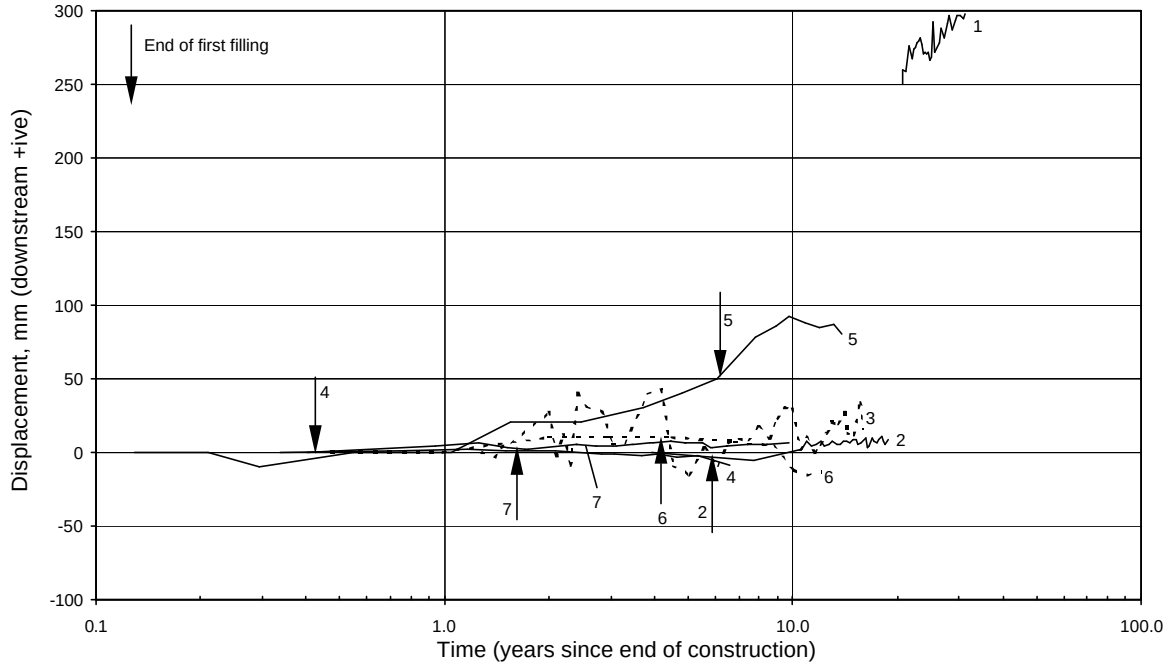

Figure 7.68: Crest displacement versus time for zoned embankments with thin to medium width central core zones of dry placed clayey earthfills.

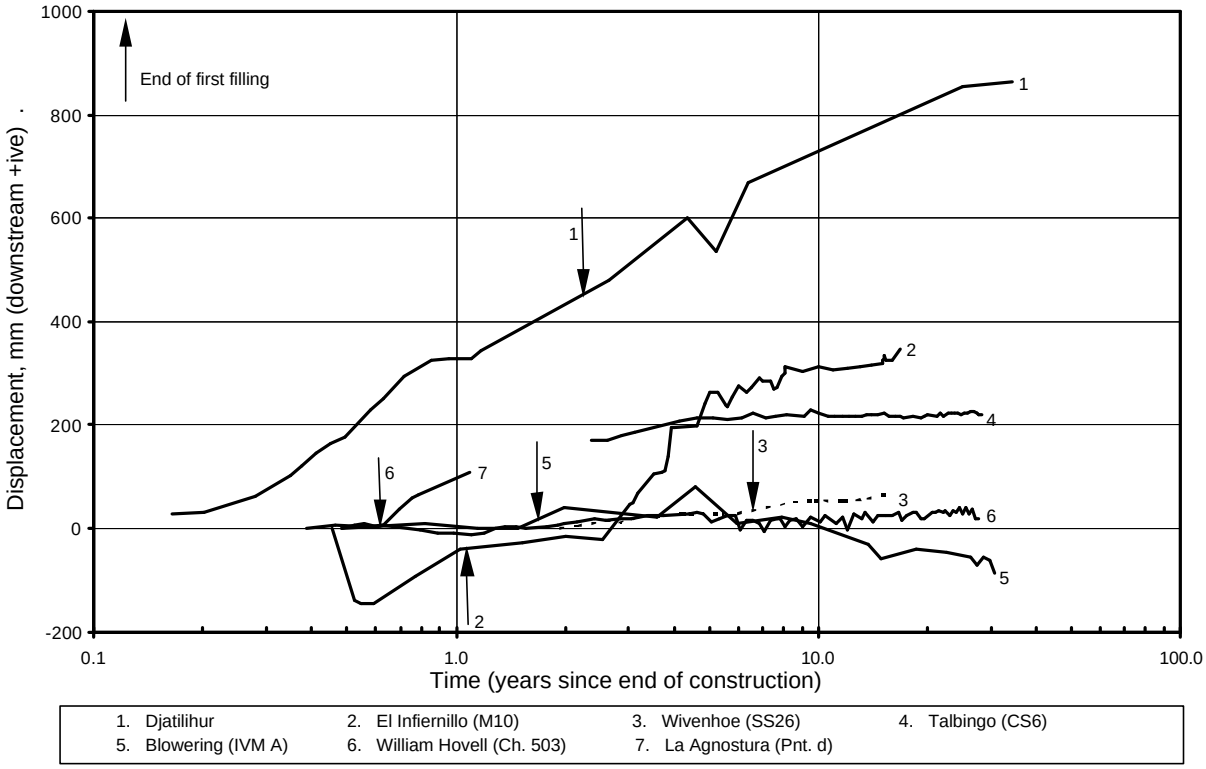

Figure 7.69: Crest displacement versus time for zoned embankments with thin to medium width central core zones of wet placed clayey earthfills.

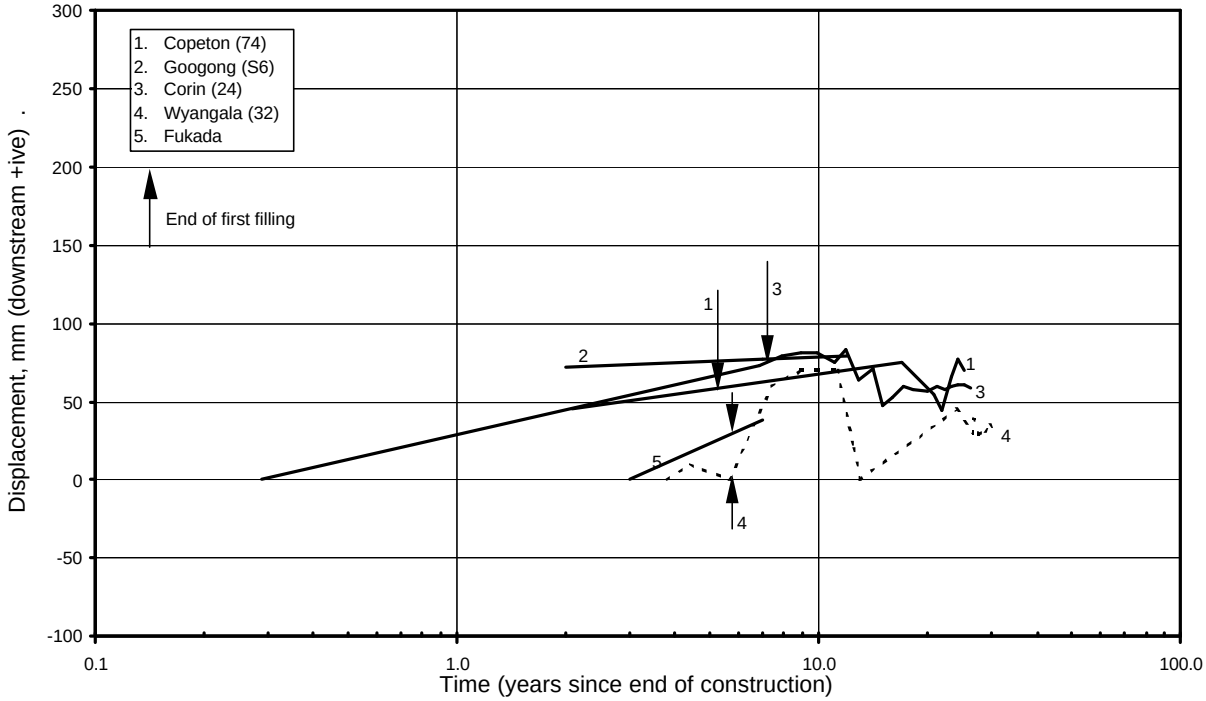

Figure 7.70: Crest displacement versus time for zoned embankments with thin to medium width central core zones of dry placed clayey sand and clayey gravel (SC/GC) earthfills.

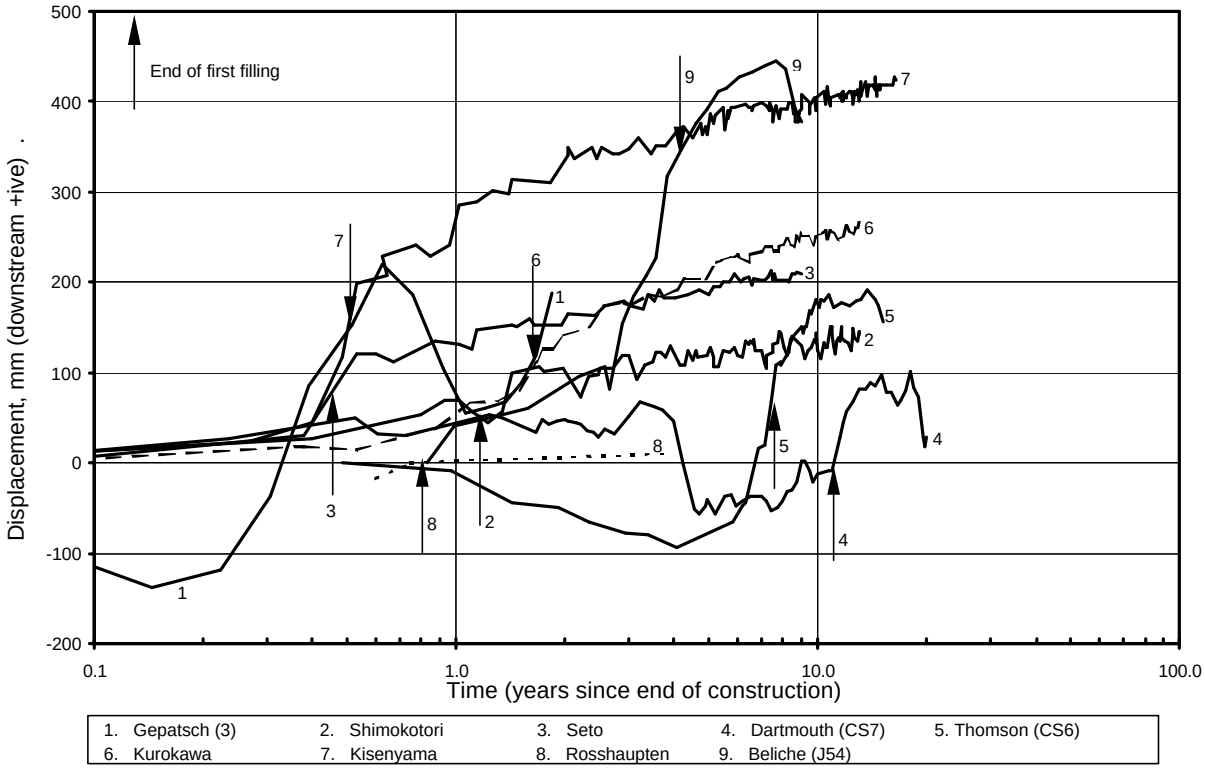

1. Gepatsch (3) 2. Shimokotori 3. Seto 4. Dartmouth (CS7) 5. Thomson (CS6)
6. Kurokawa 7. Kisenyama 8. Rosshaupten 9. Beliche (J54)

Figure 7.71: Crest displacement versus time for zoned embankments with thin to medium width central core zones of wet placed clayey sand and clayey gravel (SC/GC) earthfills.

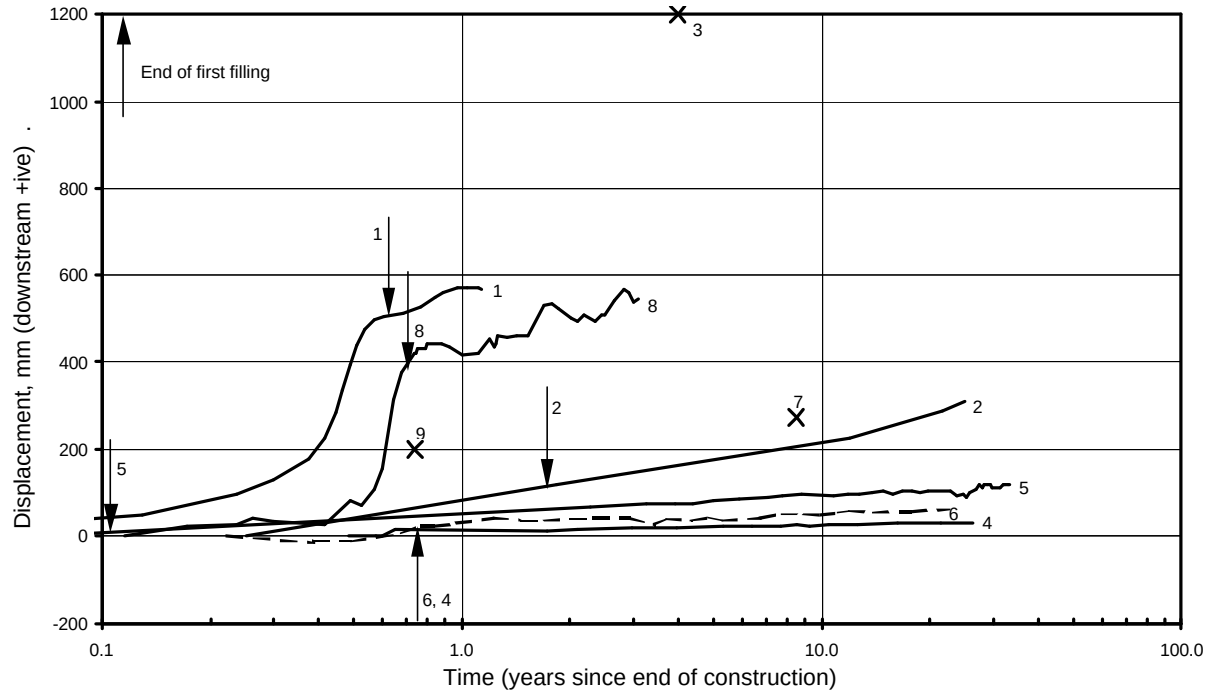

1. Round Butte (19) 2. Ajuare 3. Svartevann (main section) 4. Parangana (Ch. 400) 5. Geehi (5)
6. Rowallan (Ch. 1500) 7. Mud Mountain 8. Cougar (TD-11) 9. Vatnedalsvatn

Figure 7.72: Crest displacement versus time for zoned embankments with thin to medium width central core zones of silty sand and silty gravel (SM/GM) earthfills.

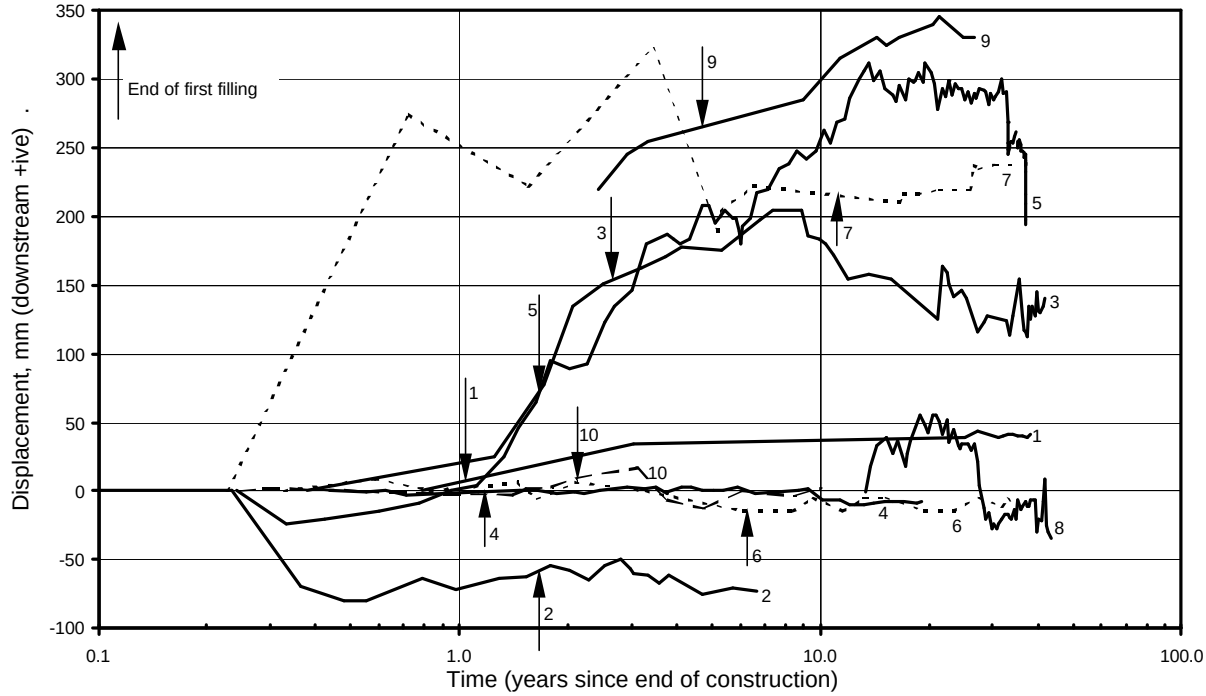

1. Waipapa (DM16) 2. South Holston 3. Upper Yarra (M5) 4. Maroon (25) 5. Eppalock (CS2)
6. Burrendong (73) 7. Navajo (Stn 38) 8. Eildon (CS7) 9. Glenbawn (G2H) 10. San Justo (Stn 3.3)

Figure 7.73: Crest displacement versus time for zoned embankments with central core zones of clayey earthfills of thick width (1 to 2.5H to 1V combined width).

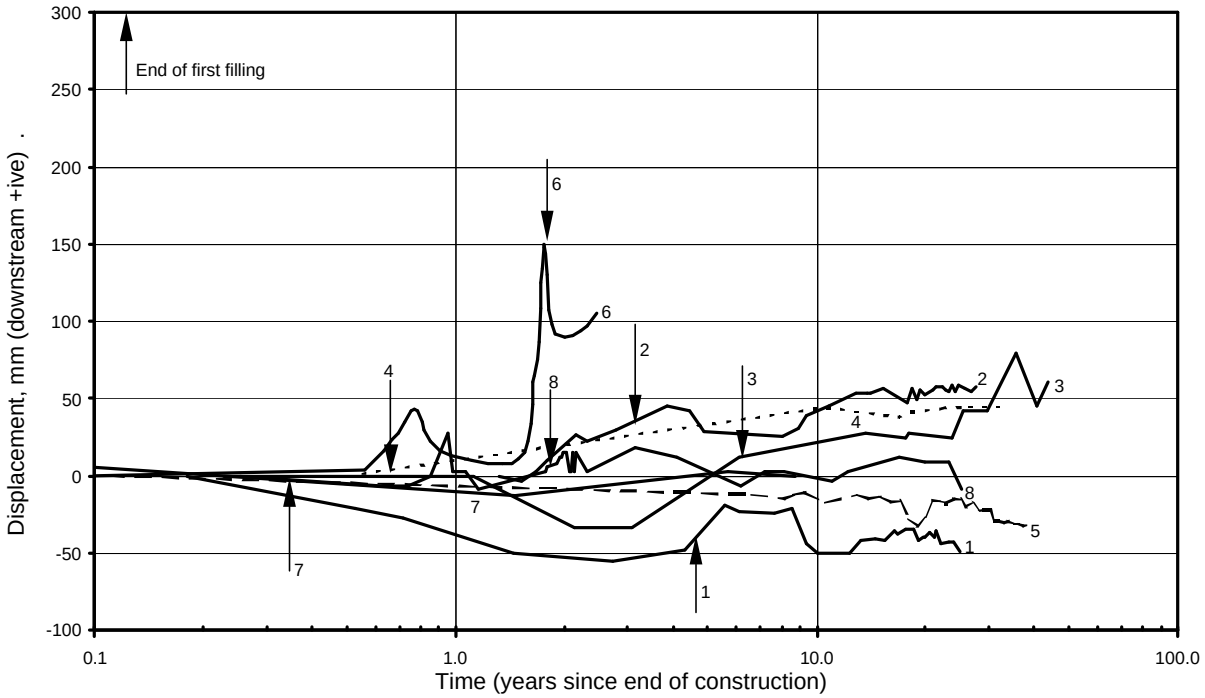

1. Cardinia (SS13) 2. Greenvale (CS5) 3. Bradbury (Stn 19) 4. Benmore (DM16) 5. Tooma (IVM A)
6. Cherry Valley (Stn 20) 7. Mammoth Pool (B11) 8. Meeks Cabin (Stn 16.5)

Figure 7.74: Crest displacement versus time for zoned embankments with central core zones of silty to clayey sand and gravel earthfills of thick width.

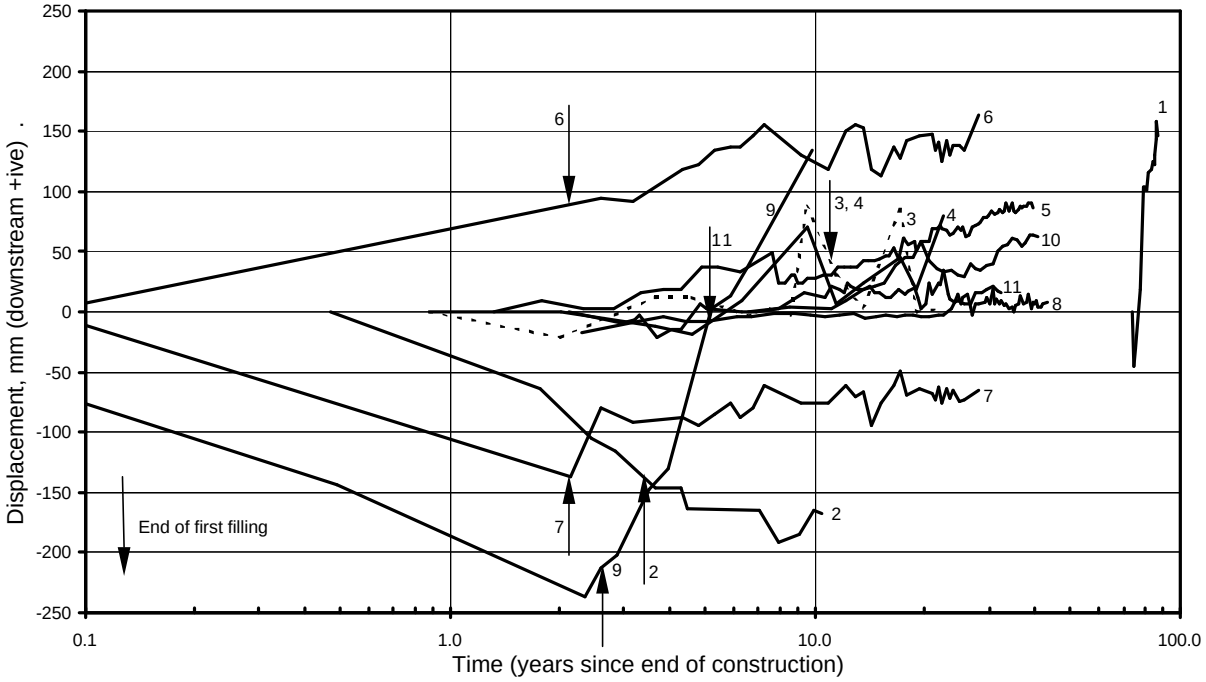

1. Belle Fourche (MP10) 2. Mita Hills (A4) 3. Pueblo, right emb. (Stn 46) 4. Pueblo, left emb. (Stn 77.5)
5. Tullaroop (CS2) 6. San Luis (Stn 110) 7. San Luis, slide area (Stn 138) 8. Cairn Curran (C3)
9. Rector Creek (Stn 16) 10. Eucembene (15) 11. Khancoban (12/13)

Figure 7.75: Crest displacement versus time for embankments with very broad core zones (> 2.5H to 1V width) and with limited foundation influence.

1. Horsetooth (Stn 10) 2. Dixon Canyon (Stn 9) 3. Soldier Canyon (Stn 11) 4. Spring Canyon (Stn 5)
5. San Luis (Stn 86) 6. Steinaker (Stn 15)

Figure 7.76: Crest displacement versus time for embankments with very broad core zones (> 2.5H to 1V width) and with potentially significant foundation influence on the embankment deformation.

A typical pattern of crest displacement behaviour is difficult to define, however, for a large number of the case studies:

- A large portion of the crest displacement occurs during first filling, in most cases the displacement being downstream.
- Post first filling, most cases show a slight to steady downstream trend, approaching very small to near zero displacement rates in the long-term (after 10 to 20 years).
- Fluctuations about the general trend occur due to reservoir fluctuation, with upstream displacement on drawdown and downstream displacement on first filling.

Plots of crest displacement versus reservoir level presented for a number of embankments in the literature highlight this general trend.

(a) Displacement during first filling

The lateral displacement at end of first filling was discussed in Section 7.5.3. Plots of the displacement at end of first filling versus embankment height were presented for the crest (Figure 7.38) as well as the upstream and downstream slopes. Typical ranges of the crest displacement at end of first filling are given in Table 7.17 sorted on core width, core properties (material type and moisture content at placement) and the material type and placement method of the downstream shoulder.

For most cases the crest displacement is dominantly downstream reaching a maximum at the end of first filling.

As discussed in Section 7.5.2, central core earth and rockfill embankments with wet placed cores of low undrained strength and upstream rockfill susceptible to collapse settlement on saturation had the potential to deform upstream during the early stages of reservoir filling followed by downstream displacement as the reservoir approached full supply level. Nobari and Duncan (1972b) proposed this concept to explain the crest displacement behaviour at El Infiernillo dam. From the crest displacement versus time plots it is apparent that this behaviour also occurred at Gepatsch and Thomson dams, and possibly also at Blowering and Dartmouth dams; all of which are central core earth and rockfill embankments with thin to medium width cores of wet placed clays, clayey sands or clayey gravels.

(b) Displacement Post First Filling

Post first filling the general trend for crest displacement, as indicated in the figures, is for a steady or gradual downstream displacement with time approaching low or near zero displacement rates long-term.

Figure 7.77 presents the lateral displacement post first filling versus embankment height. The displacement data is for at least five years after first filling (up to 30 years or more for some cases). Where possible the long-term data point has been taken for the reservoir at close to full supply level. For Belle Fourche dam the data is only for monitoring from the period 75 to 85 years post construction from the closure section, and the actual post first filling displacement is likely to be much greater than shown for this region of the embankment. For Matahina dam the post first filling crest displacement is prior to the earthquake in 1987.

The data shows that for most cases the displacement post first filling is generally in the range 35 mm upstream (-35 mm) to 100 to 150 mm downstream, indicating that post first filling crest displacements are generally small and are not dependent on dam height. Displacements outside this range may be indicative of "abnormal" deformation behaviour. Several of these case studies are discussed further in Sections 7.10 and 7.11.

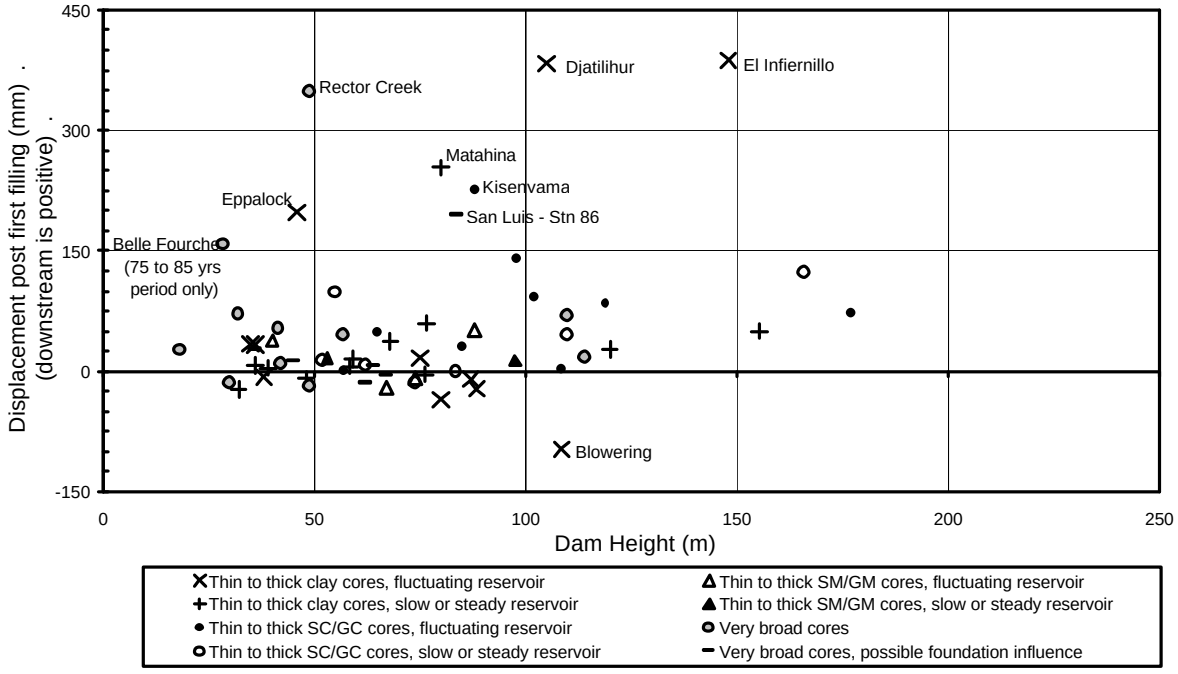

Figure 7.77: Crest displacement normal to dam axis post first filling

7.6.5 POST CONSTRUCTION DEFORMATION OF THE MID TO UPPER DOWNSTREAM SLOPE

Post construction deformation data for the mid to upper region of the downstream slope has been presented in previous sections, including:

- Lateral displacement normal to the dam axis at the end of first filling in Section 7.5.3. Figure 7.39 presents the lateral displacement at end of first filling versus embankment height and Figure 7.42 versus the downstream slope angle.
- Total settlement plots at 3 years (Figure 7.49) and 10 years (Figure 7.50) after the end of embankment construction in Section 7.6.2. Table 7.20 summarises the typical range of settlement sorted based on material type and placement method of the downstream shoulder material. The data was plotted against the height from the SMP to foundation level.

Additional data on the post construction deformation of the mid to upper downstream slope presented below includes:

- Figure 7.78 – Long-term settlement rate (% per log cycle of time) versus the height from the SMP to foundation level;
- Table 7.22, summarising the long-term settlement rate data;
- Figure 7.79 – Settlement, as a percentage of the height from the SMP to foundation level, versus log time for selected case studies; and
- Figure 7.80 to Figure 7.82 – Lateral displacement versus log time for selected case studies.

A full compliment of the total settlement (at 3, 10 and 20 to 25 years after construction), settlement versus time and displacement versus time plots for the mid to upper region of the downstream shoulder are presented in Section 2.1 of Appendix F.

For all plots the data has been sorted based on material type forming the downstream shoulder; rockfill, gravels or earthfill. Embankments with rockfill in the downstream shoulder have been further sorted based on compaction rating. For the total deformation and settlement rate plots, case studies where the rockfill was placed without the addition of water have been highlighted.

Table 7.22: Range of long-term settlement rate of the downstream shoulder.

Material Type	**Compaction Rating *[3]**	**No. Cases**	**Long-term Settlement Rate *[1], *[2] (% per log cycle of time)**	**Comments**
Rockfill	well	10	0.0 to 0.33	
	reas to well	9	0.04 to 0.31 (most = 0.15)	
	reas	4	0.10 and 0.31	Ataturk = 0.96%, Gepatsch = 0.99%
	poor	7	0.10 to 0.25	
	poor – dry	6	0.20 to 0.75	
Gravels	-	6	0.02 to 0.065	0.24% at Meeks Cabin
Earthfills	-	19	0.0 to 0.40	Refer Figure 7.78 for outliers.

Note: *[1] Excludes possible outliers.

*[2] Settlement as a percentage of the height from the SMP to foundation level.

*[3] compaction rating of rockfill; well = well-compacted, reas to well = reasonably to well compacted, reas = reasonable compaction, poor = poorly compacted, poor – dry = dry placed and poorly compacted. Refer Section 1.3.3 for definitions of the terms.

Most of the essential features of the post construction deformation behaviour of the downstream slope are captured in the plots and tables of total deformation and long-term settlement rate.

The typical trend for post construction settlement is for near constant or slightly increasing rate of settlement with the log of time. Periods of higher settlement rate are observed for some of the embankments with poorly and reasonably compacted rockfill in the downstream shoulder. Notable features of the post construction settlement are:

- In terms of total settlement:
  - Settlements in the order of 1 to 2% are observed for poorly compacted rockfills. Greater settlements are observed for the dry placed, poorly compacted rockfills.
  - For reasonably compacted rockfills the range of settlement is quite broad, from 0.1% up to 1.0%, but the number of cases is limited. Settlements toward the upper range are observed for dry placed and/or weathered rockfills, where settlements due to collapse compression are likely to be significant.
  - Much lower settlements, generally less than 0.5 to 0.7% at ten years after construction, are observed for well and reasonably to well compacted rockfills, and compacted earthfills.

  - Very low settlements (less than 0.25% at 10 years) are observed for embankments with gravel shoulders.
- In terms of the long-term settlement rate:
  - For most cases the long-term settlement rate is less than 0.4% per log cycle of time.
  - Higher settlement rates are observed for a number of earthfill embankments. At Belle Fourche dam (within the closure section) the very high rate (close to 4% per log cycle) is a clear outlier and indicative of "abnormal" behaviour.
  - Higher settlement rates apply for poorly compacted rockfills, ranging from 0.2% to 0.75% per log cycle of time, with the dry placed cases generally at the higher end of the range.
  - Higher settlement rates also apply for reasonably compacted rockfills that are susceptible to significant settlements due to collapse compression from wetting (dry placed and/or weathered rockfills). For both Ataturk and Gepatsch dams the indicated rates may be an over-estimate because they have been derived from data inclusive of the first few years after construction.
  - Very low settlement rates apply for embankments with gravel downstream shoulders (< 0.10% per log cycle of time).
  - Reservoir operation post first filling has a limited effect on the settlement rate.

As indicated, the post construction settlement behaviour of the downstream slope within the closure section at Belle Fourche dam is a clear outlier and indicative of "abnormal" behaviour. Other case studies where the magnitude of settlement or long-term settlement rate is possibly indicative of "abnormal" behaviour includes Svartevann, Horsetooth, Dixon Canyon, Spring Canyon, Srinagarind, Pueblo (both the left and right embankments), Ataturk and possibly Gepatsch dams. A number of these cases are discussed further in Sections 7.10 and 7.11, and in Appendix G.

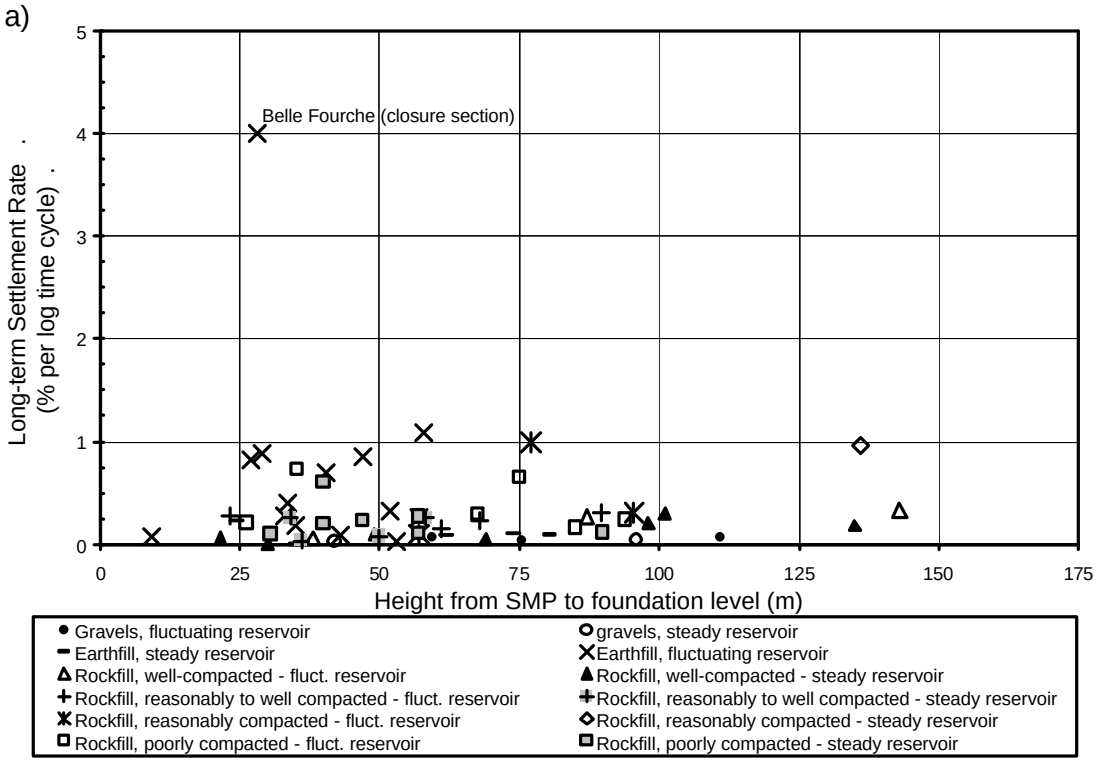

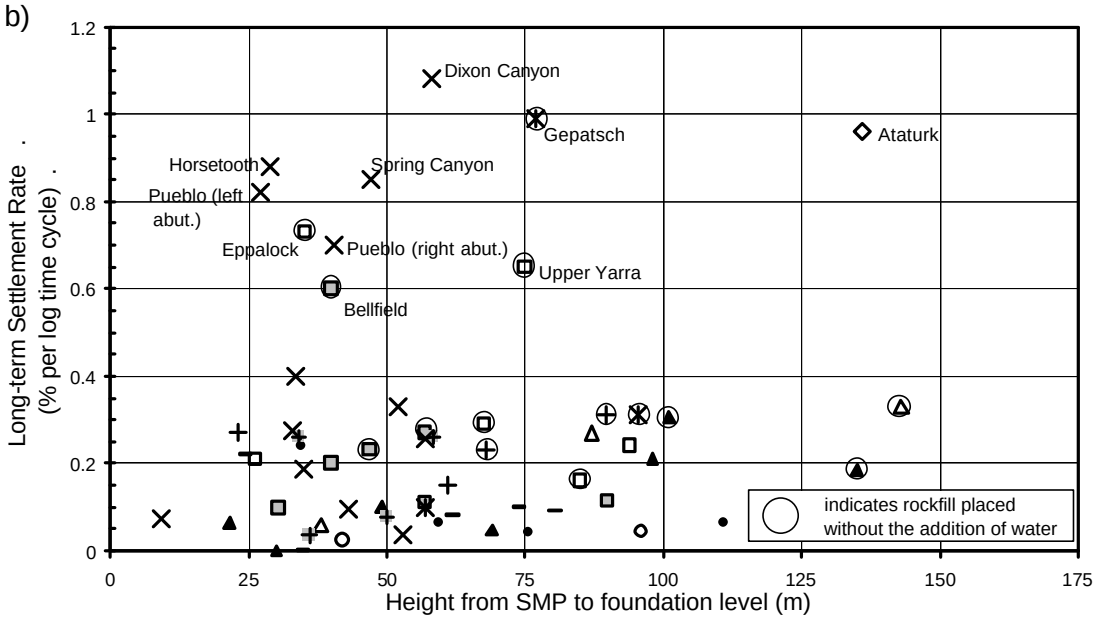

Note: refer to (a) above for legend.

Figure 7.78: Long-term settlement rates for the downstream slope (mid to upper region) versus embankment height; *(a)* all data, and *(b)* data excluding Belle Fourche.

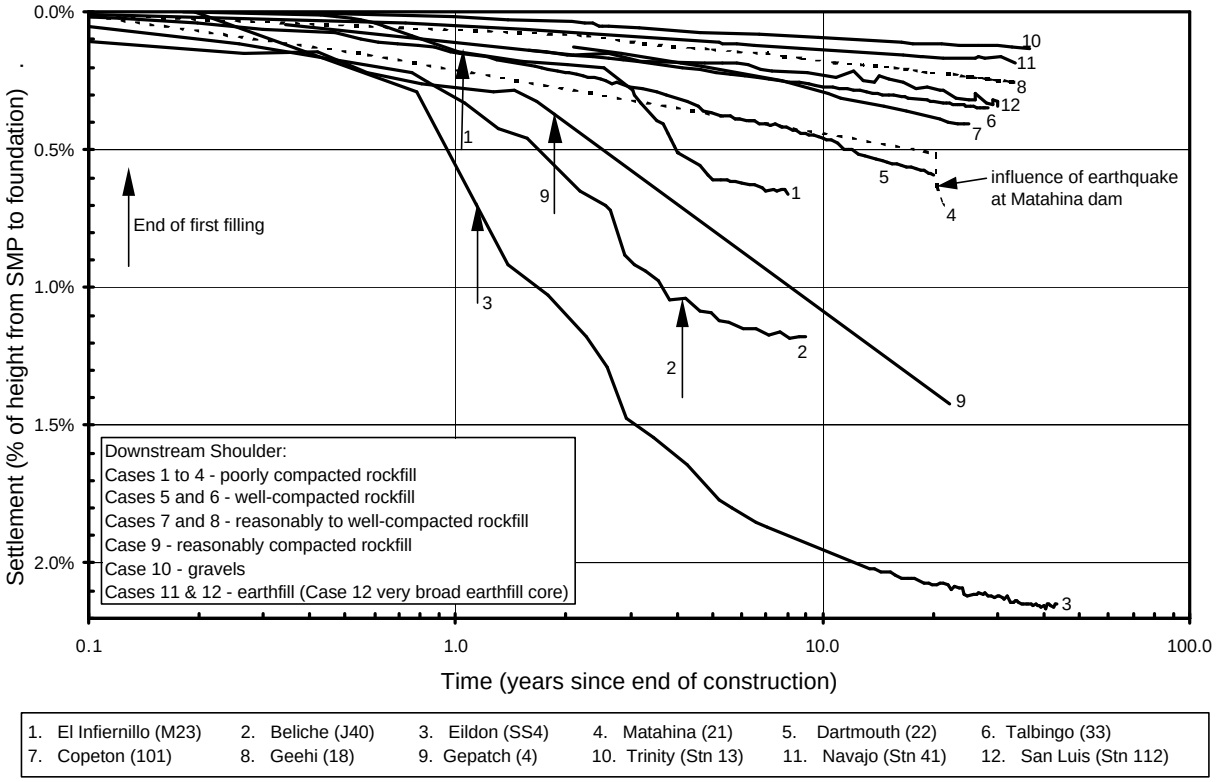

Figure 7.79: Post construction settlement of the downstream shoulder (mid to upper region) for selected case studies.

The displacement versus log time for selected case studies are presented in Figure 7.80 to Figure 7.82, and for all case studies in Figures F2.12 to F2.19 in Section 2.1 of Appendix F. As for the crest displacement, a typical pattern of behaviour for the horizontal displacement of the downstream slope is difficult to define. The general trend is for downstream displacement on first filling and continued downstream displacement long-term, although for several case studies the displacement is slightly upstream. Several trends that are evident are:

(a) Earthfill and zoned embankments with very broad core widths

For embankments of very broad core width the displacement (Figure 7.80) shows a steady downstream rate of displacement with log time, the rate long-term usually being higher than in the early years after construction. First filling generally has little influence on the deformation behaviour, except at Horsetooth dam where the displacement was influenced by the orientation of the cut-off trench and the large deformation of the foundation.

The limited of influence of first filling is largely due to the location and orientation of the applied water load on the upstream face of the very broad earthfill zone. The gradual development of the phreatic surface within the embankment over many years (refer Section 7.6.3, point f) is considered a factor in the observation of higher rates of displacement post first filling (rate per log time).

The magnitude of post construction displacement of the downstream slope is small for earthfill embankments and embankments with very broad core widths. Displacements at 25 to 45 years after construction range from 10 mm to 200 mm downstream, or 0.05% to 0.30% of the embankment height (excludes Horsetooth and Dixon Canyon dams). The displacement at Dixon Canyon dam is much larger at almost 300 mm (0.46% of the embankment height), and at Horsetooth dam is 260 mm, 180 mm of this occurring on first filling due mainly to foundation influence. At Belle Fourche dam the very high rate of displacement of the downstream slope in the closure section (Figure 7.80), where 90 mm was measured over the period 75 to 85 years after construction, is considered to be "abnormally" high.

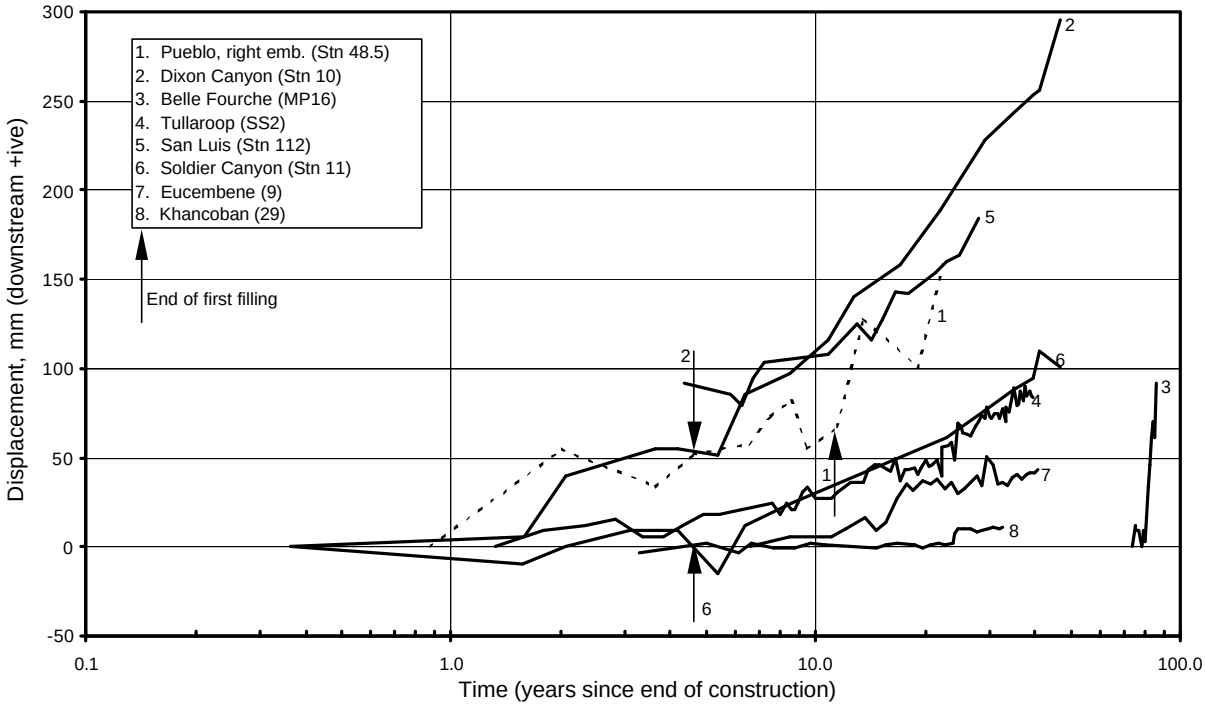

Figure 7.80: Post construction displacement of the downstream shoulder (mid to upper region) for selected case studies of embankments with very broad core widths.

(b) Central core earth and rockfill embankments

For central core earth and rockfill embankments the general trend of displacement of the downstream slope is for higher rates of downstream displacement (rate per log time) during the first few years after end of construction decreasing to much lower rates long-term (Figure 7.81). Two explanations for this are; firstly, for thin to medium central cores the water load has a high horizontal component and is applied close to the centre of the embankment resulting in an increase in lateral stress in the downstream shoulder on first filling and downstream displacement of the downstream shoulder. Secondly, wetting of the downstream rockfill from rainfall infiltration or tail water inundation causing large deformations in those rockfills that are susceptible to large deformations due to collapse compression. Rockfills most susceptible, as previously identified, are those that are dry placed and reasonably to poorly compacted, or where the rock substance strength is susceptible to large loss of strength on wetting.

The magnitudes of displacement of the downstream shoulder is generally in the range:

- For well and reasonably to well compacted rockfills, displacements long-term (more than 10 to 20 years after construction) are typically less than 0.20% of the embankment height, or less than about 100 to 300 mm. Larger displacements, up to 0.25% to 0.40% of the embankment height, can occur where the rockfill has been placed dry, the rock substance strength is susceptible to large strength loss on wetting and/or the outer zone of the rockfill has been placed in thicker layers (i.e. reasonably compacted).
- For reasonably and poorly compacted rockfills, displacements can reach values up to 1.0% to 1.6% of the embankment height long-term. Those most susceptible to the larger displacements are rockfills that have been dry placed and poorly compacted. Post construction displacements close to and in excess of 1 m have been measured at Ataturk (184 m high), Eildon (80 m high), Gepatsch (153 m high) and Svartevann (129 m high) dams. As a percentage of the embankment height the highest displacements have been measured at the 80 m high Eildon dam (1.52% of the embankment height) and the 46 m high Eppalock dam (1.63% of the embankment height). For both these dams the rockfill was dry placed and poorly compacted.

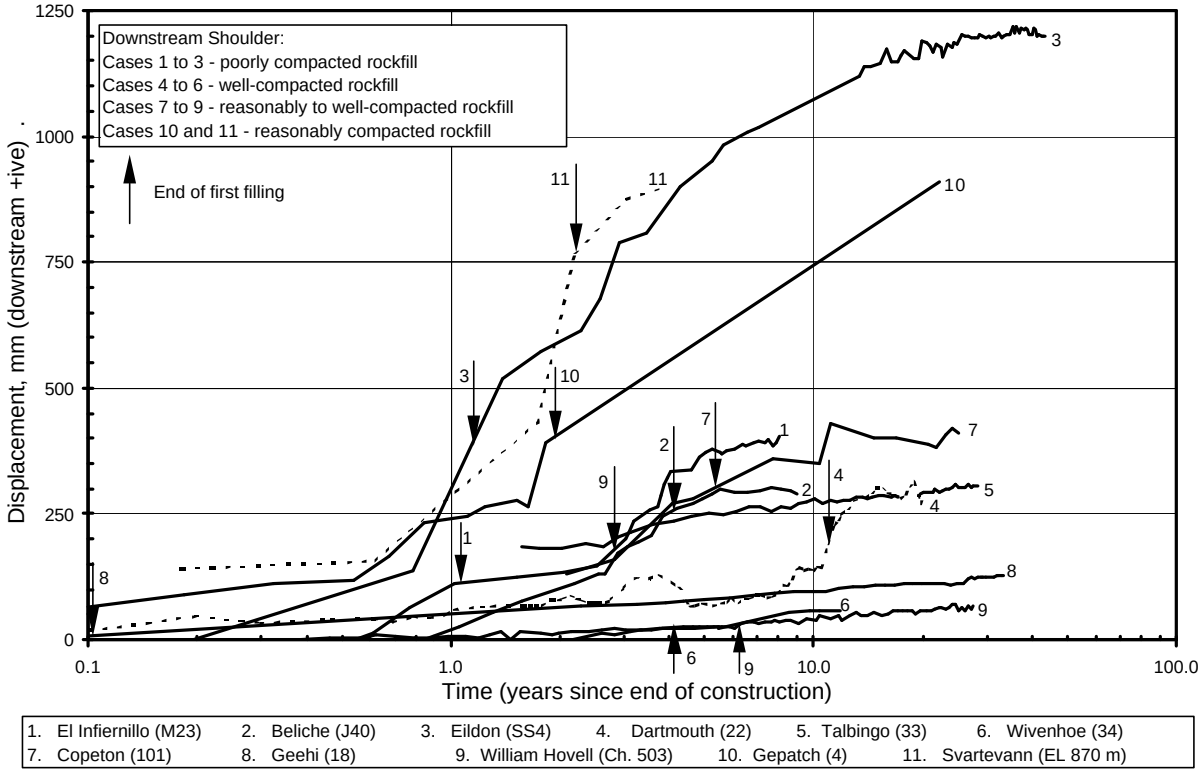

Figure 7.81: Post construction displacement of the downstream shoulder (mid to upper region) for selected case studies of central core earth and rockfill embankments.

(c) Zoned embankments with compacted earthfill and gravels in the downstream shoulder

For zoned embankments with compacted earthfills and gravels in the downstream shoulder, the post construction displacement (Figure 7.82) is relatively small at less than about 150 to 250 mm (less than 0.15 to 0.20% of the embankment height) some 20 to 30 years after construction. For most of the case studies the displacement rate (per log cycle of time) decreases with time approaching near zero or very low values long-term. In general, first filling has a limited to negligible influence on the displacement, except at La Angostura dam, where the embankment comprised a thin clay core, and possibly Trinity dam.

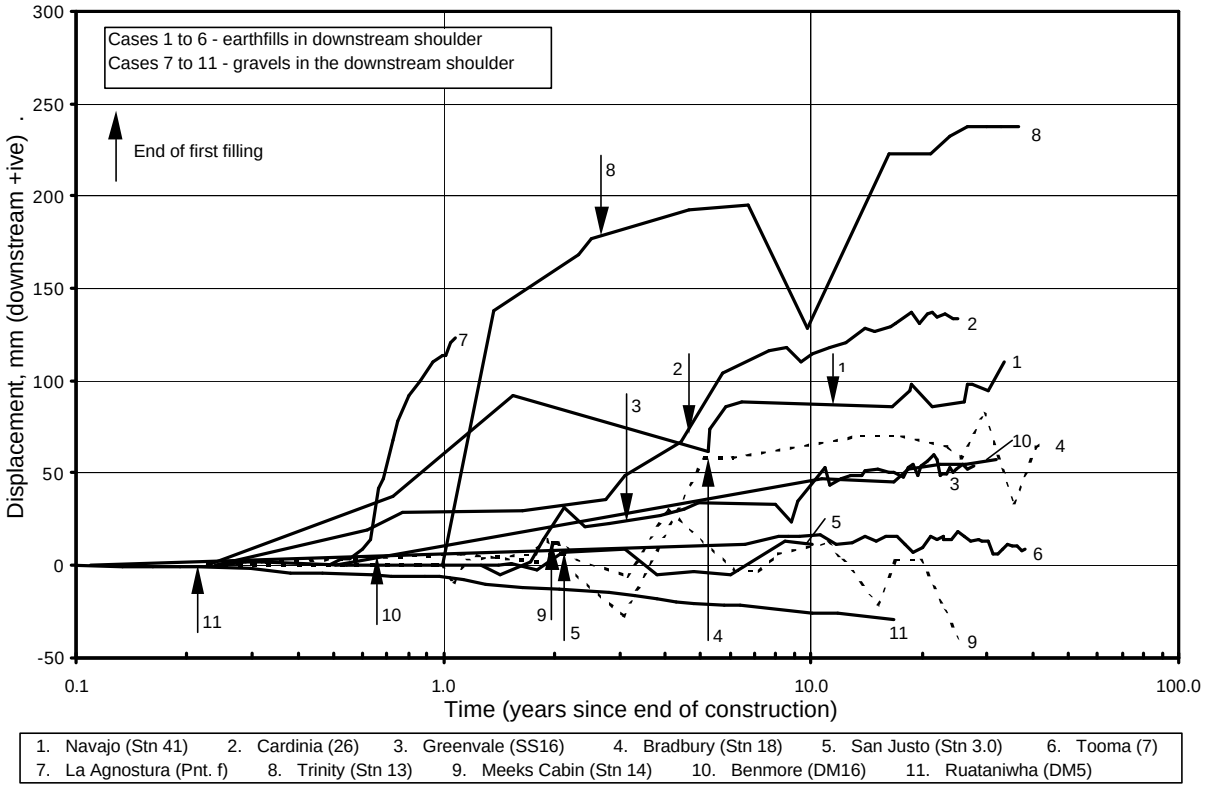

Figure 7.82: Post construction displacement of the downstream shoulder (mid to upper region) for embankments with compacted earthfills and gravels in the downstream shoulder.

7.6.6 POST CONSTRUCTION DEFORMATION OF THE UPPER UPSTREAM SLOPE AND UPSTREAM CREST

Post construction deformation data of the upper upstream slope and upstream crest region has been presented in previous sections, including:

- Lateral displacement normal to the dam axis at the end of first filling in Section 7.5.3. Figure 7.40 presents the lateral displacement at end of first filling versus embankment height.
- Total settlement plots at 3 years (Figure 7.51) and 10 years (Figure 7.52) after the end of embankment construction in Section 7.6.2. Table 7.20 summarises the typical range of settlement sorted based on material type and placement method of the upstream shoulder material. The data was plotted against the height from the SMP to foundation level.

Additional data on the post construction deformation of the upper upstream slope and upstream crest region presented below includes:

- Figure 7.83 – Long-term settlement rate (% per log cycle of time) versus embankment height. The calculated rate excludes short periods of increased settlement rate post first filling shown for some of the embankments, such as on drawdown at 17 years for Djatiluhur dam (Figure 7.84);
- Table 7.23, summarising the long-term settlement rate data;
- Figure 7.84 and Figure 7.85 – Settlement (% of height from SMP to foundation) versus log time for poorly compacted rockfills and selected other case studies respectively; and
- Figure 7.86 and Figure 7.87 – Lateral displacement versus log time for selected case studies.

A full compliment of the total settlement (at 3, 10 and 20 to 25 years after construction), settlement versus time and displacement versus time plots are presented in Section 2.2 of Appendix F.

For all plots the data has been sorted based on material type forming the upstream shoulder; rockfill, gravels or earthfill. Embankments with rockfill in the downstream shoulder have been further sorted based on compaction rating, and for the total deformation and settlement rate plots case studies where the rockfill was placed without the addition of water have been highlighted.

Several trends are apparent for the post construction settlement for the upper upstream shoulder and upstream crest region. For most case studies the usual trend is for near constant or slightly increasing rate of settlement with the log of time. In some cases a decrease or increase in settlement rate is observed post first filling or the settlement versus time curve shows a slight curvature of increasing rate with log time, but the transition is generally smooth. This type of settlement time is generally observed for:

- Zoned embankments with permeable earthfills or gravels in the upstream shoulder.
- Embankments with very broad earthfill cores. Horsetooth is an exception, but this may be due to foundation influence.
- Well-compacted and reasonably to well compacted rockfills in the upstream shoulder. Exceptions are La Angostura (possibly affected by the outer dumped rockfill zone), Dartmouth, Blowering, Wyangala and La Grande 2 dams.

- A limited number of case studies with reasonably and poorly compacted rockfills in the upstream shoulder, e.g., Tooma and Burrendong dams, both of which comprised dumped and sluiced rockfills placed in 1.8 to 3 m lifts.

For a number of the poorly and reasonably compacted rockfills higher settlement rates or periods of higher settlement rate during first filling followed by a relatively steady, reduced settlement rate post first filling are observed. Relatively large collapse settlement of the upstream rockfill on first filling is likely to be the cause of this settlement trend.

A limited number of the case studies show periods of higher settlement rate post first filling, generally occurring on drawdown. These cases include Dartmouth, Blowering, Wyangala, Cougar, Djatiluhur, Beliche, Eildon and Eppalock dams, most of which are represented in Figure 7.84 or Figure 7.85. This type of settlement trend is potentially indicative of "abnormal" deformation behaviour. Assuming the rockfill is of high permeability, close to the highest vertical stress levels are reached in the wetted rockfill during first filling. On drawdown the vertical stresses in the upstream rockfill will increase, but it is essentially in re-loading. Effective stress levels greater than previously experienced by the wetted rockfill can potentially occur in the lateral direction, normal to the dam axis, as the water load acting on the core is reduced and therefore transferred onto the upstream rockfill. Another possible mechanism is localised instability of the core on drawdown due to the reduction in lateral stresses acting on the core on drawdown. These mechanisms, along with a number of the cases studies, are discussed further in Section 7.10.

Table 7.20, Figure 7.51 and Figure 7.52 provide information on the general range of settlement of the upper upstream slope and upstream crest region sorted based on material type and placement method of the upstream shoulder material. In summary, the general ranges of settlement as a percentage of the height from the SMP to foundation level are:

- In the order of 1 to 2% for poorly compacted rockfills. Greater settlements are observed for the dry placed, poorly compacted rockfills. As shown in Figure 7.84 a large portion of the settlement occurs on first filling as collapse type settlement.
- For several embankments with reasonably compacted rockfill in the upstream shoulder, notably Gepatsch and Cougar dams, greater settlements are observed and

are probably due to large collapse type settlements in the dry placed rockfill at Gepatsch dam and the weathered rockfill at Cougar dam.

- Less than 0.5% to 0.7% settlement at 10 years for the well and reasonably well compacted rockfills, and for embankments with earthfill zones in the upstream shoulder, including earthfill embankments.
- Less than 0.25% settlement at 10 years for embankments with gravel shoulders, but there are only three cases with deformation data from the database.

The long-term settlement rate data (Figure 7.83 and Table 7.23) indicates:

- For most cases the long-term settlement rate is less than 0.4 % per log cycle of time.
- Higher rates, up to 0.8% per log cycle of time, are observed for a number of embankments. There is no apparent consistency in material type and reservoir operation for these cases.
- Embankment height, reservoir operation, material type and compaction rating do not appear to have a significant influence. Gravels possibly have a lower settlement rate, but there are only two cases.

Table 7.23: Range of long-term settlement rate of the upper upstream slope and upstream crest region.

Material Type	**Compaction Rating *[3]**	**No. Cases**	**Long-term Settlement Rate *[1] *[2] (% per log cycle of time)**	**Comments**
Rockfill	well	8	0.05 to 0.70 (most < 0.50)	Dartmouth = 0.67%, Glenbawn Saddle = 0.675%
	reas to well	9	0.10 to 0.56 (most < 0.50)	
	reas	3	< 0.55	
	poor	7	0.10 to 0.82 (most < 0.60)	Djatiluhur = 0.82%
Gravels	-	2	< 0.21	
Earthfills	-	18	0.1 to 0.60	Belle Fourche (closure section) = 2%, Dixon Canyon = 1.38%

Note: *[1] Excludes possible outliers.

*[2] Settlement as a percentage of the height from the SMP to foundation level.

*[3] compaction rating of rockfill; well = well-compacted, reas to well = reasonably to well compacted, reas = reasonable compaction, poor = poorly compacted, poor – dry = dry placed and poorly compacted. Refer Section 1.3.3 for definitions of the terms.

Potential outliers in terms of magnitude of settlement of the upstream shoulder include Dixon Canyon, Spring Canyon and Horsetooth dams. Belle Fourche dam (within the closure section) is a clear outlier in terms of long-term settlement rate as is probably Dixon Canyon dam. The settlement rates are on the high side at Glenbawn Saddle and Dartmouth dams compared to other well-compacted rockfills. Several of these cases are discussed further in Section 7.10 and 7.11.

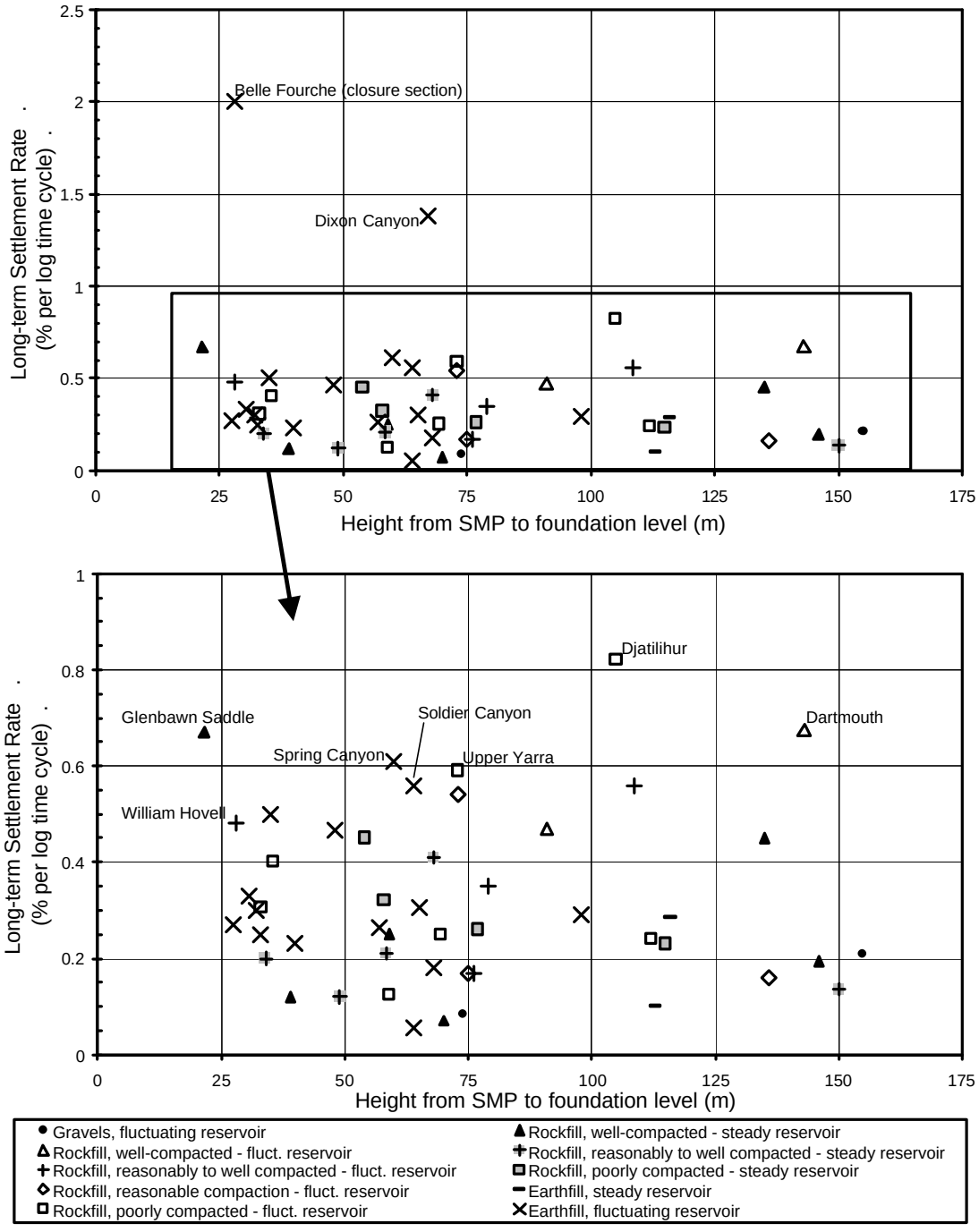

Figure 7.83: Long-term settlement rates of the upper upstream slope to upstream crest region of earthfill and earth-rockfill embankments.

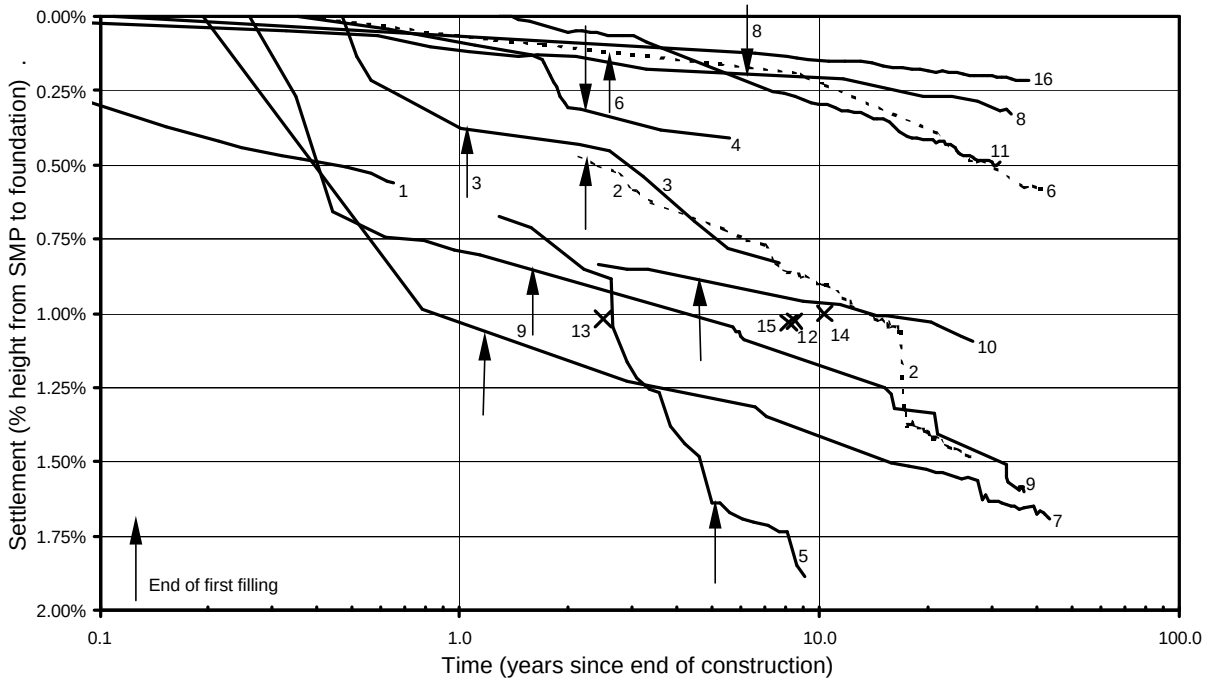

1. Djatilihur 2. Djatilihur (C9) 3. El Infiernillo (IVM D1) 4. Netzahualcoyotl (14-2u) 5. Beliche (M54) 6. Upper Yarra (1U)
7. Eildon (SS10) 8. Burrendong (103) 9. Eppalock (SS2) 10. Glenbawn (L3M) 11. Nillacootie (6U) 12. Mud Mountain
13. Cherry Valley 14. Nottely 15. Watuaga 16. Tooma (25)

Figure 7.84: Post construction settlement of the upper upstream slope to upstream crest region for embankments with poorly compacted rockfill in the upstream slope.

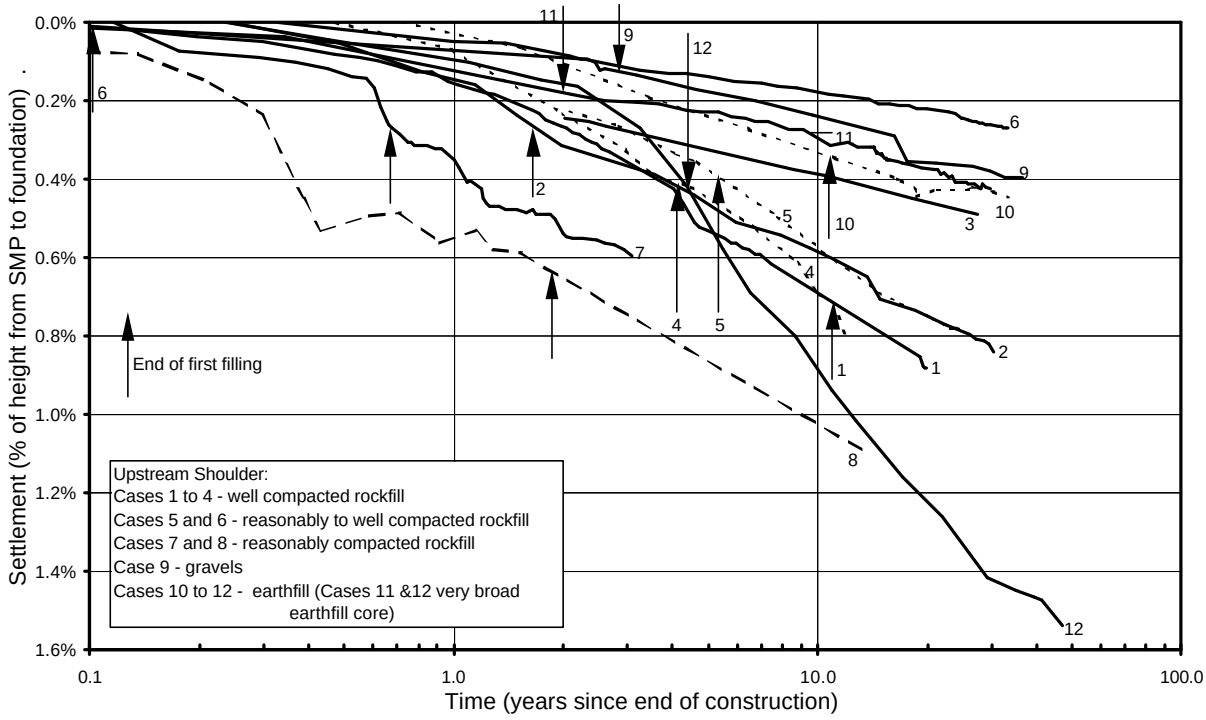

1. Dartmouth (32) 2. Blowering (17) 3. Talbingo (14) 4. Glenbawn Saddle (12) 5. Copeton (54) 6. Geehi (32)
7. Cougar (TD-12) 8. Gepatsch (1) 9. Trinity (Stn 12) 10. Navajo (Stn 41) 11. San Luis (Stn 112) 12. Spring Canyon (Stn 5)

Figure 7.85: Post construction settlement of the upper upstream slope to upstream crest region for selected case studies (excluding poorly compacted rockfills).

The horizontal displacement versus time of the upper upstream slope and upstream crest region for selected case studies is presented in Figure 7.86 and Figure 7.87. The data for all case studies is presented in Figures F2.30 to F2.36 in Section 2.2 of Appendix A. As shown, there is a large variation in the magnitude and direction of the measured displacements. The data presented below has been sub-divided into two groups, those embankments with rockfills in the upstream shoulder, and those with earthfills, including gravels, in the upstream shoulder.

(a) Horizontal displacement of embankments with rockfill upstream shoulders

Figure 7.86 presents the horizontal displacement of the upper upstream slope and upstream crest region of selected case studies with rockfill in the upstream shoulder. The case studies have been selected covering the range of rockfill compaction rating from well compacted through to poorly compacted.

For rockfills that are well and reasonably to well compacted, displacements of the upstream shoulder during and after first filling are generally relatively small. For some case studies a large portion of the displacement occurs on first filling (e.g. for Talbingo dam), whilst for others first filling has a limited influence. Post first filling displacements are small in magnitude and long-term the displacement rate (per log cycle of time) approaches a small to near zero value, with variations about the trend due to reservoir fluctuation. The typical range of displacement for these case studies is:

- At more than 10 to 20 years after construction, displacements range from -0.10% to 0.15% of the embankment height (or -75 mm to 200 mm).
- Additional displacement post first filling ranges from -0.05% to 0.05% of the embankment height (-50 to 50 mm).

For rockfills that are reasonably to poorly compacted, displacements can be much larger reaching magnitudes of close to 1 metre, or close to 1% of the embankment height. The case studies with large displacements tend to be dry placed and reasonably to poorly compacted rockfills. A large portion of the displacement occurs on first filling and long-term the displacement rate (per log cycle of time) approaches a small to near zero value, with variations about the trend due to reservoir fluctuation. The typical range of displacement for these case studies is:

- At more than 10 to 20 years after construction, displacements range from -0.70% to 0.80% of the embankment height (-600 mm to 1000 mm for the case studies). For

most of the case studies the long-term total displacement is less than about 0.2% to 0.3% of the embankment height, either upstream or downstream. Large displacements were measured at Eppalock, Gepatsch, Svartevann and Glenbawn dams, all dry placed rockfills.

- Displacements post first filling generally range from -0.15% to 0.05% of the embankment height.

Factors affecting the magnitude of displacement of the upstream slope are likely to include:

- The magnitude of differential deformation between the upstream shoulder and the core or upstream transition zone of the embankment. For rockfills susceptible to large deformations on collapse compression, differential deformations on first filling can be large, and the vector of deformation of the upstream shoulder will be affected by the internal zoning geometry of the embankment.
- Zoning of the rockfill in the upstream shoulder. Where placement methods, rock types or the degree of weathering differs for different rockfill zones in the upstream slope then differential deformations can develop between these rockfill zones and therefore influence the magnitude and direction of the displacement.
- The deformation of the core and downstream shoulder of the embankment. The closer the SMP on the upstream slope is located to the crest the greater the influence the displacement of the core and downstream shoulder will be. In the case of Svartevann and La Grande 2 dams, large downstream displacement of SMPs on the crest (both the upstream and downstream edge) and downstream shoulder occurred on first filling.
- The slope of the upstream shoulder will have some influence.

For a number of embankments the long-term trend of displacement shows several trends that are potentially indicative of "abnormal" behaviour. These include, continuing high or increasing rates of displacement (rate per log of time), and non-recoverable displacements (usually upstream) on drawdown. Examples of this behaviour include Blowering, Eppalock and possibly Eildon dams as shown in Figure 7.86. Other examples of this type of behaviour are observed at Copeton and Wyangala dams. A number of these cases are discussed further in Section 7.10 and in Appendix G.

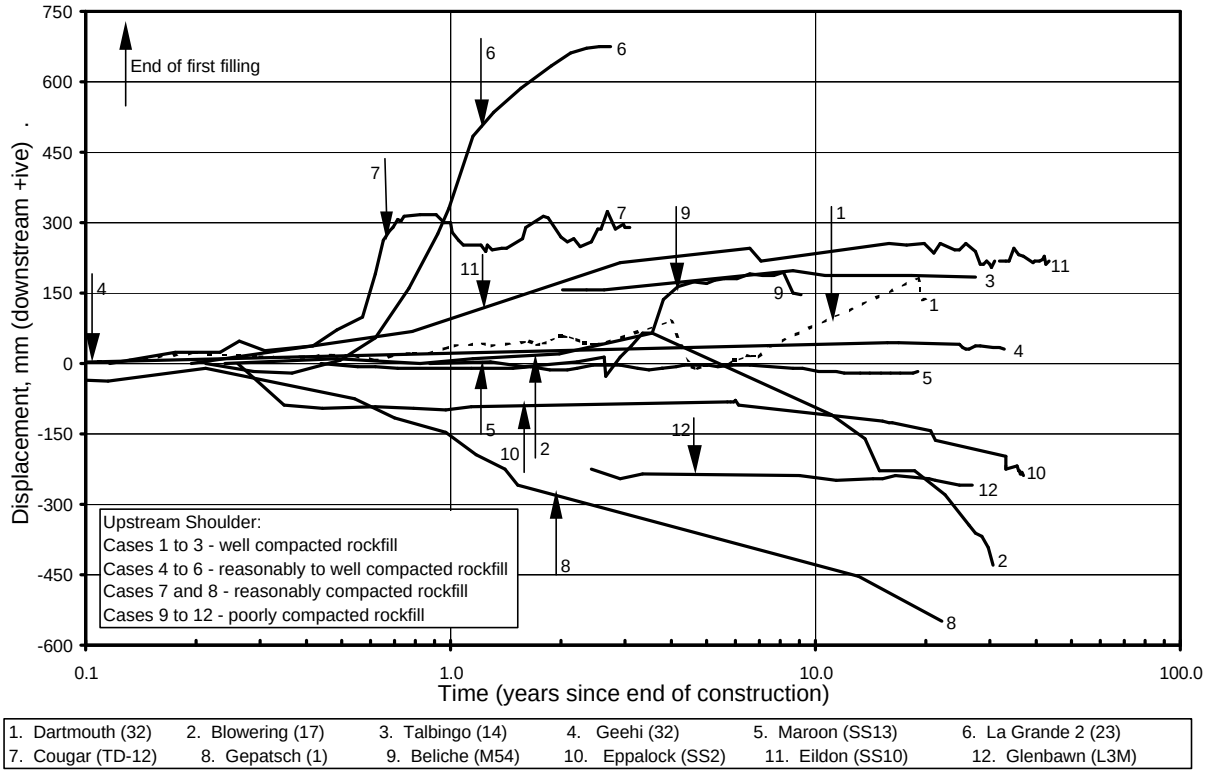

Figure 7.86: Post construction lateral displacement of the upper upstream slope and upstream crest region for selected case studies of embankments with rockfill in the upstream shoulder.

(b) Horizontal displacement of embankments with earthfills and gravels in the upstream shoulder

Embankments included in this sub-group include earthfill embankments, embankments with very broad core width, and zoned embankments of thin to thick core width with earthfills or gravels in the upstream shoulder. The displacement versus time for selected case studies is shown in Figure 7.87.

For most case studies the magnitude of post construction displacement is relatively small, and is either in an upstream direction or downstream direction. Long-term the displacement rate (per log cycle of time) approaches very small (either up or downstream) to near zero average values with fluctuation due to operation of the reservoir. At more than 20 to 30 years after construction, the magnitude of displacement is generally in the range -0.10% to 0.12% of the embankment height, or from 100 mm upstream (-100 mm) to 200 mm downstream.

The influence of the compressible foundation is evident at Horsetooth dam where a large downstream displacement occurred on first filling. The deformation of the

compressible foundation has possible also influenced the displacement of the section of San Luis dam over the broad alluvial plain (San Luis – Stn 80 in Figure 7.87), as well as Steinaker dam. For these two dams the displacements post first filling were larger than at other dams.

A number of case studies show the initial displacement on and after first filling to be upstream, and then long-term changes to downstream. These case studies include; Navajo, Dixon Canyon, San Luis (main section and slide area), Spring Canyon, Soldier Canyon and the right abutment embankment at Pueblo dam. This effect may be due to development of the phreatic surface or possibly softening within the embankment.

The high rate of displacement of the upstream shoulder within the closure section at Belle Fourche dam many years after construction is likely to be indicative of "abnormal" behaviour. The deformation behaviour at Dixon Canyon dam, showing a large upstream displacement on and after first filling followed by downstream displacement, is also potentially "abnormal" when compared to that at similar embankments.

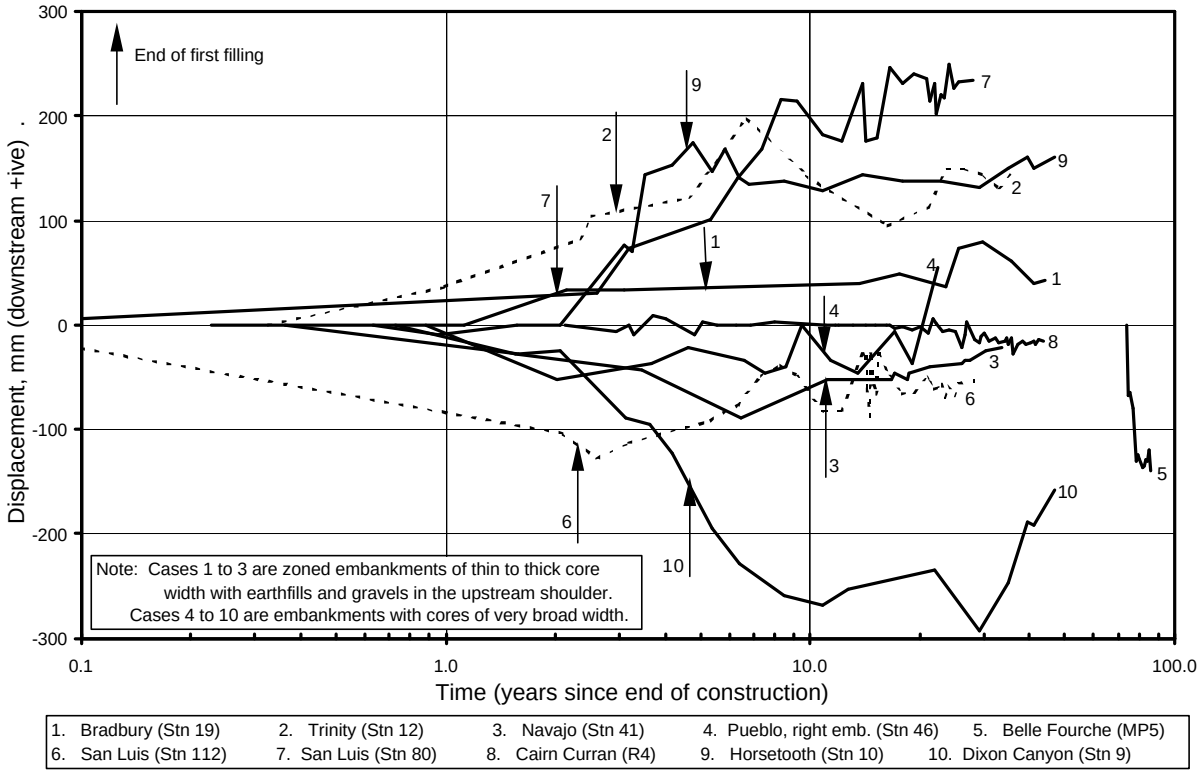

Figure 7.87: Post construction lateral displacement of the upper upstream slope to upstream crest region for selected case studies of embankment with earthfills and gravels in the upstream shoulder.

7.7 GENERAL DEFORMATION BEHAVIOUR OF PUDDLE CORE EARTHFILL EMBANKMENTS

7.7.1 DEFORMATION DURING CONSTRUCTION OF PUDDLE CORE EARTHFILL EMBANKMENTS

Selset Dam (Section 5.6 of Appendix G) is the only puddle dam for which deformation behaviour during construction has been found in the published literature. It was constructed in the late 1950's using relatively modern compaction techniques compared to the remainder of the data set. Therefore, the deformation behaviour of Selset Dam is not likely to be typical of most puddle dams. However, the deformation behaviour and pore water pressure response during construction at Selset dam does highlight several important aspects raised by Bishop and Vaughan (1962) fundamental to puddle cores:

- Arching develops across the core resulting in significant reductions in the total vertical stresses within the core.
- The deformation of the core occurs predominantly as yielding in undrained loading conditions, and the large observed settlements are primarily due to lateral deformation of the narrow puddle core.
- Consolidation type settlements during construction are not significant.
- Relatively high pore water pressures are developed in the puddle core during construction and are still present at the end of construction.
- The internal settlement of the puddle core during construction at Selset Dam (Figure 7.88) is well in excess of that observed in wet placed, rolled clayey earthfills in zoned embankments. The vertical strains in Selset dam reached as high as 5 to 7% at 10 m depth below crest level. In comparison, vertical strains at a similar depth below crest were less than about 2% in zoned embankments with narrow rolled earthfill cores (Figure 7.22).

The issue of arching in embankments with narrow cores is discussed in Section 7.4.1.3 with reference to the literature on puddle core earthfill embankments.

The rate of dissipation of pore water pressures in the puddle core is likely to be affected by the permeability and width of the core, as well as the permeability of the adjacent shoulder earthfill if it is similar to that of the puddle core.

The amount of lateral deformation of the puddle core will primarily be influenced by the differential lateral stress conditions between the puddle core and supporting shoulders and the compressibility of the supporting shoulder earthfill. The lateral stresses that develop within the puddle core will depend on its shear strength and compressibility properties, as well as the stress reducing influence of arching of the core.

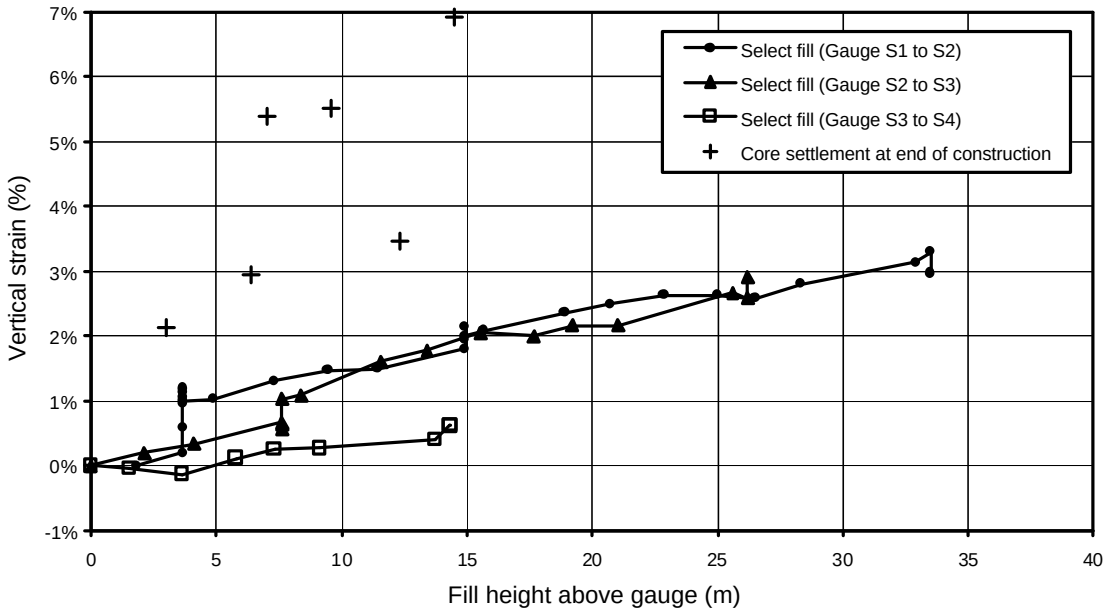

Figure 7.88: Selset Dam internal settlements during construction (data from Bishop and Vaughan 1962)

7.7.2 DEFORMATION DURING FIRST FILLING OF PUDDLE CORE EARTHFILL EMBANKMENTS

Charles (1998) identifies the poorly compacted upstream shoulder of the older puddle dams (presumably those embankments constructed prior to the 1900's without formal compaction) as prone to collapse compression on impounding.

Information on the susceptibility of earthfills to collapse compression from the case study data on rolled earthfills is discussed in Section 7.5.2. In the context of puddle dams, the susceptibility of materials to collapse compression and its effect on the deformation behaviour of the embankment is summarised as follows:

- For puddle dams constructed prior to 1900, typically without any formal compaction of the shoulder earthfill, collapse compression on inundation of the shoulders is likely to be significant.

- For dams constructed without a select zone adjacent to the core, which was typical before 1860, collapse compression is likely to be significant. From the available literature it is apparent that the select zone adjacent to the core was placed in thinner layers, thereby possibly reducing the amount of collapse compression adjacent to the puddle core.
- For puddle core earthfill dams constructed after the late 1930s, when soil mechanics principles were applied to embankment construction, moisture conditioning and good compaction of the shoulder fill could be expected (e.g. Selset Dam). As a result, collapse compression of the upstream shoulder earthfill on inundation is not likely to have occurred.

The puddle core itself is not susceptible to collapse compression. However, because of its very low undrained strength its post construction deformation behaviour is highly dependent (or largely controlled by) the deformation behaviour of the supporting shoulders. If the upstream (or downstream) shoulder region adjacent to the core settles due to collapse compression on wetting, then the puddle core will settle with the upstream shoulder. Therefore, the magnitude of crest settlement of the puddle core embankment on first filling will depend on the embankment zoning geometry and the susceptibility of the upstream shoulder earthfill zones to collapse compression on wetting. The mechanism of deformation of the puddle core on first filling is similar to that of zoned embankments with wet placed cores of low undrained strength and thin to medium width (Section 7.5.2, Figure 7.35).

For puddle dams with well-compacted earthfills either side of the puddle core that are not susceptible to collapse compression, crest settlements will be limited during first filling as observed at Selset and Burnhope dams (Figure 7.92). In the case of Burnhope dam (constructed in 1935) the upstream filling was placed in 450 mm layers and compacted by 10 to 17 tonne steamrollers. In the first four years after construction the settlement of the upstream slope was 104 mm (or 0.4% of the dam height) and 468 mm (or 1.2%) at the crest. For Selset dam, where the shoulder filling was well compacted with moisture content control, the crest settled 177 mm (0.45% of the dam height) on first filling. As shown in Figure 7.92 the magnitude of crest settlement for these dams is relatively small compared to other puddle core dams and the settlement versus time curve shows virtually no influence due to first filling.

Where the shoulder fill adjacent to the puddle core is dry placed and poorly compacted, and therefore susceptible to large magnitude collapse settlements on wetting, crest settlements will be large on first filling as observed at Hope Valley dam (Figure 7.92). The mechanics of the deformation behaviour for this condition are discussed in more detail in Section 7.7.2.1.

7.7.2.1 *Collapse Compression of Poorly Compacted Filling*

The mechanism of deformation considered to be involved during first filling and first drawdown of an old puddle dam with no formal compaction of the shoulder filling is summarised as follows:

- On first filling:
  - Wetting of the poorly compacted upstream filling results in collapse of the soil structure and therefore large settlement of the upstream fill (Figure 7.89a to c). The strength and compressibility properties of the wetted earthfill will be significantly different to those of the "as placed" earthfill; its compressibility and undrained strength will be significantly reduced.
  - The effect of first filling on the deformation of the upstream shoulder is for large settlement as a result of the collapse of the soil structure on wetting.
  - At the upstream (and downstream) interface between the puddle core and shoulder, the core must settle with the shoulder. This is because the puddle core does not have the shear strength to support any significant levels of stress that would be transferred to it by differential settlement.
  - The total horizontal stress acting on the upstream face of the puddle core must at least equal the lateral stresses within the puddle core for equilibrium. Hydrostatic pressures acting on the upstream face of the puddle core increase with the rise in reservoir level, but the lateral stresses within the upstream shoulder decrease due to the substantial loss in strength and compressibility on collapse due to wetting (Figure 7.89d). The deformation of the upstream face of the core / shoulder interface is dependent on the net lateral stress acting. If the net lateral stress at any point increases then the interface at that point will deform downstream and horizontal stresses will increase in the puddle core and downstream shoulder. If the net lateral stress decreases then the interface will deform upstream until equilibrium conditions are re-established as lateral

stresses increase in the upstream shoulder. It is possible that the interface can initially deform upstream at low water levels and then deform downstream as the reservoir approaches full supply level.

- If upstream displacement of the core / shoulder interface occurs then lateral spreading of the core results. The deformation of the puddle core occurs as undrained plastic yielding and is therefore associated with vertical strain to maintain volumetric consistency. Further arching across the core is also likely where lateral spreading occurs, thereby decreasing the lateral stress required for equilibrium.
- Once full supply level is reached, whether or not equilibrium pore water pressure conditions in the upstream shoulder have been reached is dependent on its permeability and the time for first filling. Free draining earthfills will effectively reach equilibrium conditions as the reservoir is filled. For the case studies analysed, in most cases the earthfill comprises a mix of clay to gravel (and larger) sized particles and its permeability is quite variable due to layering as well as material and density variations within and between layers. Therefore, it is likely that for most cases equilibrium pore water pressure conditions are not reached in the upstream shoulder when full supply level is reached (Figure 7.89b). As a result, the upstream shoulder will continue to wet up after first filling is completed and settlements can continue to occur post first filling within the shoulder and possibly the puddle core.

- On first drawdown:
  - Further compression of the upstream shoulder occurs as effective stresses increase under the falling reservoir level. Because the upstream earthfill was not fully saturated at end of first filling, its drained compressibility will have continued to decrease as further softening occurred on wetting post first filling. Therefore, poorly compacted earthfills susceptible to collapse compression and softening on wetting are likely to be close to normally consolidated after the end of first filling, and increases in effective stresses on drawdown will result in large deformations due to yielding. The upstream shoulder can therefore experience large settlements on drawdown (Figure 7.90).
  - The puddle core will also undergo significant settlement and displacement on initial drawdown (Figure 7.90). As the hydrostatic pressures acting on the

upstream face of the puddle core decrease, total stresses in the puddle core and downstream shoulder initially decrease and the embankment deforms upstream. At some point, the lateral stresses in the upstream shoulder must increase to maintain equilibrium with those within the puddle core. Because of the large reduction in compressibility of the poorly compacted upstream shoulder earthfill on wetting, lateral spreading of the puddle core will occur as the upstream shoulder deforms under the increased lateral stresses imposed on it as hydrostatic pressures continue to decrease on drawdown. The deformation of the puddle core occurs as undrained plastic deformation (i.e. yielding) and the lateral spreading is associated with vertical strains to maintain volumetric consistency, and therefore crest settlements are potentially large.

In summary, deformation of the upstream shoulder earthfill (where it is poorly compacted) will be significant on initial filling due to collapse compression. The settlement of the puddle core will also be large on first filling as it deforms with the adjacent upstream zone of the shoulder. On first drawdown large deformations can occur in the upstream shoulder due to drained yielding as effective stresses increase in the near normally consolidated water softened earthfill. Deformations of the puddle core will be large on first drawdown mainly due to lateral spreading as the now softened adjacent shoulder deforms under the increased lateral stresses applied as hydrostatic pressures decrease. Subsequent drawdowns that result in increases in effective stresses in the upstream shoulder above those previously experienced post first filling will also result in large deformations of the upstream shoulder and puddle core (this is discussed in Section 7.7.3.5).

In the case of wetting of part of the downstream earthfill shoulder (Figure 7.91), such as due to seepage through the foundation, or hydraulic fracture through the puddle core due in part to arching of the narrow core, the wetted zone of the filling would undergo collapse compression assuming it to be in a poorly compacted and dry condition. Consequently, deformations of the downstream shoulder and crest region are likely to be large.

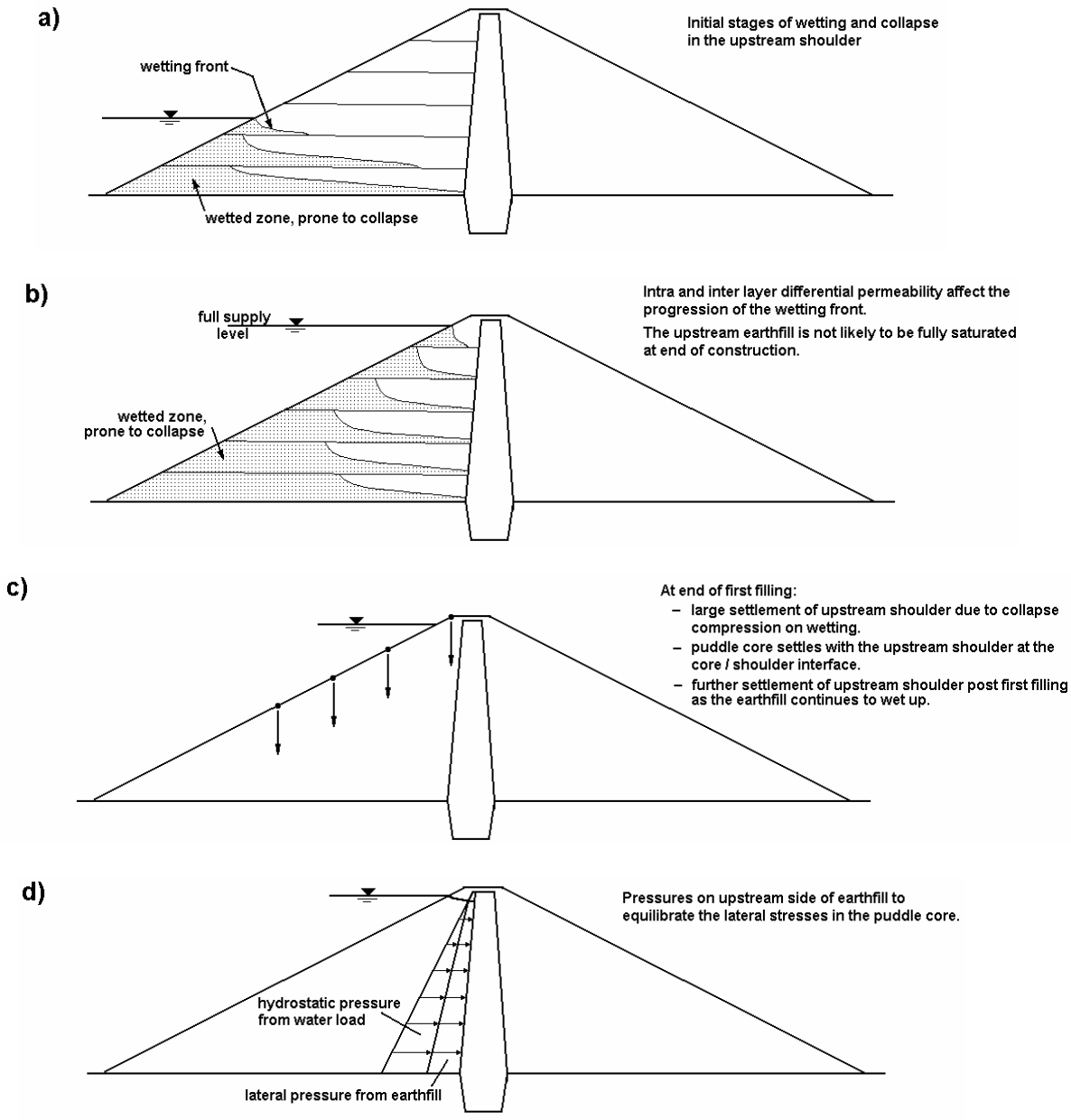

Figure 7.89: "Idealised" model of collapse compression of poorly compacted shoulder fill of puddle core earthfill dam on first filling.

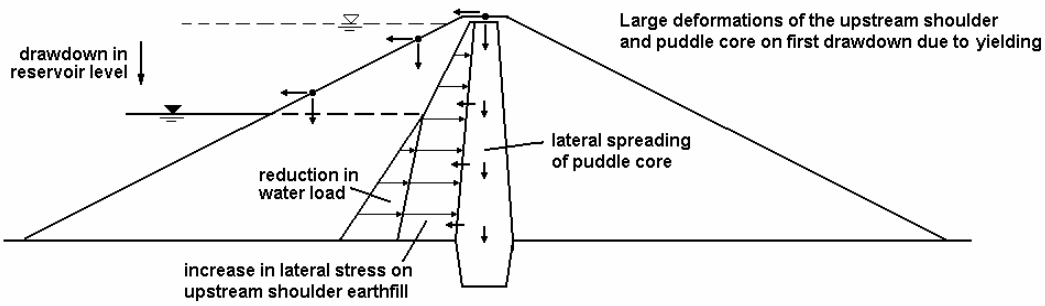

Figure 7.90: "Idealised" model of yielding of poorly compacted shoulder fill and puddle core on first drawdown of a puddle core earthfill dam.

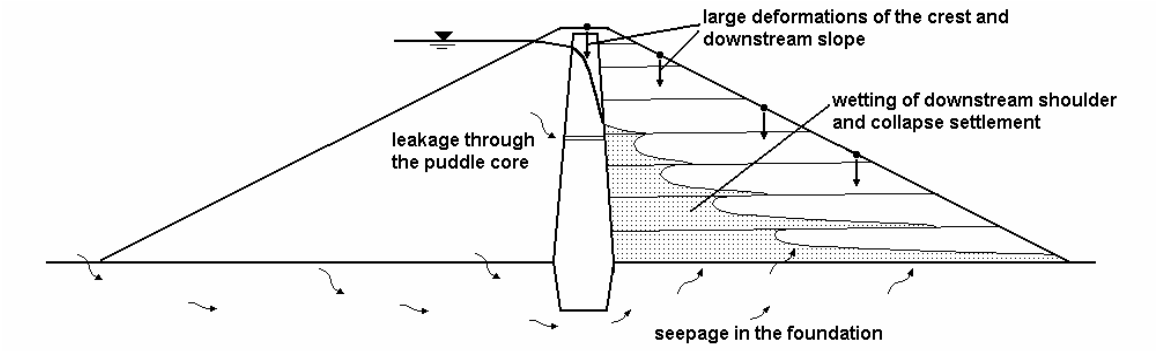

Figure 7.91: "Idealised" model of collapse compression on wetting of poorly compacted earthfill in the downstream shoulder of a puddle core earthfill dam.

In the case of Hope Valley dam (refer Section 5.3 of Appendix G), wetting of the downstream fill was observed shortly after the start of initial filling. This was probably mainly due to seepage in the Tertiary alluvial soils in the foundation. From Figure 7.92 it is evident that significant crest settlement (1250 mm or 5.5% of the embankment height) occurred in the period up to 11 years after construction. Collapse compression on wetting of both the upstream and downstream earthfill shoulders were likely to be significant contributing factors to the large crest settlement, in addition to the deformations due to yielding on drawdown. What influence wetting and collapse compression of the downstream shoulder earthfill had on the magnitude of crest settlement is not known, and the data in Figure 7.92 does not include many comparable dams. But, in comparison to the anecdotal information of the crest settlement for several old UK puddle dams the magnitude of crest settlement of Hope Valley dam is relatively high, possibly suggesting its influence was significant.

In the case of the Dale Dyke dam failure in 1864, Charles (1998) suspected that collapse compression on wetting of the earthfill in the downstream shoulder might have contributed to the loss of freeboard. Although, Binnie (1978) surmises that the large settlement was localised to a small portion of the crest and due to loss of material from piping, a view supported by Foster (1999) and Foster et al (2000). Instability of the downstream slope prior to overtopping as a result of strength loss within the downstream earthfill shoulder could also have been a factor.

It is notable that longitudinal cracking between the core and upstream filling has not been reported on any puddle dams as a result of collapse compression, as has been the case for a number of central core earth and rockfill dams. It is considered that this is due to the low undrained strength and plastic nature of the puddle clay core. Rather

than a crack appearing, the core deforms with the upstream shoulder and may result in the ridge or bulge developed on the upstream face near to crest level that it evident on several puddle dams, or a narrow wedge of upstream zone adjacent to the core dropping to form a "reverse" scarp as is the case for Happy Valley dam.

7.7.3 DEFORMATION BEHAVIOUR POST FIRST FILLING OF PUDDLE CORE EARTHFILL DAMS

Section 7.2.3.3 summarises the research by BRE and Imperial College in terms of the factors they consider to affect the long-term deformation behaviour and the mechanism/s affecting the deformation behaviour of puddle core earthfill embankments.

The following sub-sections present an analysis of the deformation behaviour of the puddle core earthfill dam case studies in the context of defining "normal" deformation behaviour, and the various mechanisms associated with the observed deformation behaviour are discussed. Section 7.12 discusses the methods of identification of "abnormal" deformation behaviour of puddle core earthfill embankments and summarises several case studies considered to indicate "abnormal" deformation behaviour.

7.7.3.1 Available Deformation Records

The database comprises seventeen case studies of puddle core earthfill dams. The embankment details, reservoir operation, hydrogeology and monitoring for each case study are summarised in Table F1.5 in Section 1 of Appendix F. Table 7.24 presents a summary of the post construction surface deformation behaviour of the crest and slopes for each case study. Figure 7.92 presents the post construction crest settlement versus log time for those embankments with records available from end of construction (time is in years and zero time is the end of construction).

Figure 7.92 shows that the post construction crest settlement of puddle core earthfill embankments is significant, ranging from 1% up to 8 to 14% of the dam height after more than 100 years. It is generally the older (pre 1900) embankments that show the greater post construction deformations. The more recent puddle core earthfill embankments constructed in the 1930's to 1950's generally show significantly lower crest settlement (less than 1 to 4% at 10 to 50 years after construction) as expected

given the differences in placement methods of earthfill and compaction equipment between the two periods.

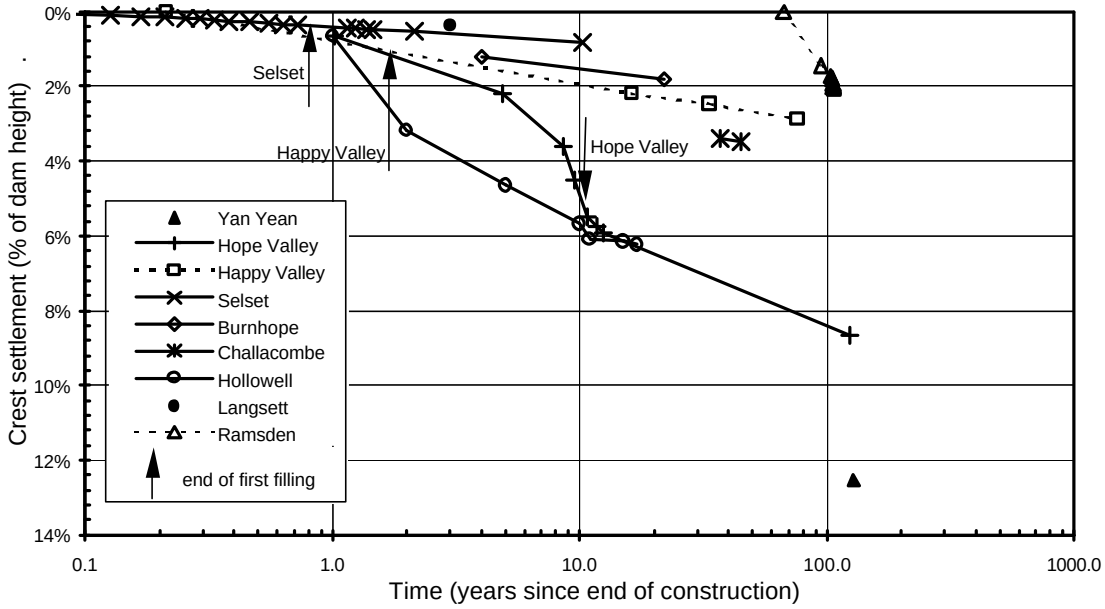

Figure 7.92: Post construction crest settlement versus log time of puddle core earthfill dams.

The understanding of "normal" long-term deformation behaviour is mainly aimed at three situations:

- Deformations during "steady state" conditions. This is basically deformation behaviour assuming the reservoir level is maintained at a constant level, and therefore the components of long-term deformation are foundation settlement, shrink-swell movements, and primary creep type movements under constant stress conditions. Clearly, the data set would be fairly limited given fluctuations in reservoir level occur in most dams, however, as will be discussed later, it is appropriate not only to dams with little fluctuation in reservoir level, but also to cases where the embankment design incorporates a relatively impermeable zone upstream of the core that effectively acts as a water barrier thereby limiting the changes in the phreatic surface in the central portion of the dam.
- Deformations during the normal cyclic operation of the reservoir for puddle core earthfill dams with permeable upstream earthfill.
- Deformations during a historically large drawdown event.

Table 7.24: Summary of the post construction surface deformations of the puddle core earthfill dam case studies.

Name	Year Completed	Height, H (m)	Reservoir Operation	Response to Drawdown Upstream of Puddle Core	Period of Monitoring	Deformation of Embankment Crest				Upstream Slope			Downstream Slope		Downstream Toe	
						Settlement since EOC		Long-term Deformation		Settlement		Displacement Rate (mm/yr)	Long-term Settlement	Long-term Displacement	Long-term Settlement	Long-term Displacement
						mm	% of H	S_{LT}	Displacement Rate (mm/yr)	S_{LT}	Monitored					
Burnhope	1935	41	assume fluctuating	assume minor	EOC to 1957	702 (22 yrs)	1.8	0.80	-	0.14	130 mm in 22 yrs since EOC	-	-	-	-	-
Challocombe	1944	15	Steady	assume minor	EOC to 1981	520 (45 yrs)	3.45	0.80	-	-	-	-	-	-	-	-
Cwnwernderi	1901	22	Steady	assume full	1977 to 1989	-	-	0.90	negligible when at FSL (> 70 yrs after EOC)	-	-	-	-	-	-	-
Dean Head	1840	19	assume fluctuating	assume full	1977 to 1984	-	-	7.4	-	-	-	-	-	-	-	-
Happy Valley	1896	25	Fluctuating (15 to 30% of H)	minor	EOC to 1973 1982 to 1998	770 (76 yrs)	3.1	1.0	-	2.3 to 0.7 (varies with magnitude of drawdown)	29 mm (85 to 102 yrs after EOC)	up to 2.5 mm/yr (85 to 102 yrs after EOC), rate is dependent on magnitude of d'down.	11 mm in 10 yrs (92 to 102 yrs after EOC), SLT = 1.0%	1 mm/yr over 10 yrs (92 to 102 yrs after EOC)	5 mm over 10 yrs (92 to 102 yrs after EOC)	0.6 mm/yr (92 to 102 yrs after EOC)
Hollowell	1937	13.1	assume fluctuating	assume minor	EOC to 1954	817 (17 yrs)	6.2	0.70	-	-	-	-	-	-	-	-
Holmestyes	1840	25	assume fluctuating	negligible	1990 to 1991	-	-	2.3 (only 18 months data)	negligible (150 yrs after EOC)	-	-	-	-	-	-	-
Hope Valley	1872	21	Fluctuating (15 to 25% of H)	variable (minor to full)	EOC to 1983 1988 to 1999	1820 (125 yrs)	8.7	2.6	5 mm/yr at 118 to 128 yrs after EOC (downstream edge of crest)	-	-	-	negligible on mid slope (118 to 128 yrs after EOC)	0.5 mm/yr (118 to 128 yrs after EOC)	-	-
Ladybower	1945	43	assume fluctuating	assume minor	1950 to 1984	-	-	2.0	-	-	-	-	-	-	-	-
Langsett	1904	33	assume fluctuating	nk	EOC to 1907	124 (3 yrs)	3.8	-	-	-	-	-	-	-	-	-
Ogden	1858	25	assume fluctuating	assume full	1989 to 1993	-	-	10 (1 normal drawdown cycle only)	-	-	7 mm on 10 m d'down cycle in 1992/93	-	4 mm on 10 m d'down cycle in 1992/93	-	-	-
Ramsden	1883	25	assume fluctuating	assume full	1949 to 1985 1988 to 1990	(450 mm from 1949 to 1985)	-	6.6 (normal operating conditions)	3 mm/yr (1977 to 1985)	-	12 mm in 2 yrs (1988 to 1990), includes abnormally large d'down	-8 mm in 2 yrs (1988 to 1990)	8 mm in 2 yrs (incl. Extreme d'down)	-2 mm in 2 yrs (incl. Extreme d'down)	2 mm in 2 yrs (1988 to 1990)	negligible (1988 to 1990)
Selset	1959	39	assume fluctuating	minor	EOC to 1970	313 (10 yrs)	0.80	0.4	-	-	-	-	-	-	-	-
Walshaw Dean	1907	22	Fluctuating (50 to 60% of H)	assume full	some early data, 1990 to 1995	-	-	4.5 (1915 to 1943) to 6.7 (1988/90)	3 mm/yr (85 years after EOC)	1.7	2 mm on 13 m d'down in 1988 to 1990.	< 1 mm (1988 to 1990)	5 to 6 mm on 13 m d'down cycle in 1988/90	1 to 2 mm (1988 to 1990)	-	-
Widdop	1878	20	assume fluctuating	assume full	1988 to 1990	-	-	-	-	-	-	-	-	-	-	-
Yan Yean	1857	9.6	Fluctuating (15 to 25% of H)	minor	1986 to 1999	1205 (128 yrs)	12.5	0.5 (upstream edge of the crest) 11 (downstream edge of the crest)	negligible rate at upstream edge of crest. Up to 4.5 to 5.5 mm/yr (increasing rate) on downstream crest and slope -	2.0	4 mm in 6 yrs (> 135 yrs after EOC)	negligible (135 to 141 yrs after EOC)	max 8 - 10 mm/yr, increasing rate with time (> 128 years after EOC)	2 to 3 mm/yr (more than 128 years after EOC)	negligible (more than 130 yrs after EOC)	15 to 20 mm in 13 yrs (more than 130 yrs after EOC), stick - slip type displacement
Yateholme	1872	17	Fluctuating	assume full	1989 to 1992	-	-	5.4 (120 yrs after EOC)	-	-	-	-	-	-	-	-

Notes to Table 7.24:

S_{LT} = long-term settlement index in unit of settlement (as a percentage of dam height) per log cycle of time (refer Equation 7.6 in Section 7.7.3.2).
EOC = end of construction FSL = full supply level
Displacement is the deformation in the horizontal direction normal to the dam axis, positive is downstream and negative is upstream.
d'down = drawdown

In Table 7.24 the reservoir operation for each case study is categorised as either fluctuating or steady, and the level of fluctuation, where it can be estimated, is given as a percentage of the embankment height. For those case studies where the reservoir operation is not known, it has been assumed as fluctuating. Also presented in Table 7.24 is an estimate of the response of the phreatic surface in the zone upstream of the puddle core to changes in reservoir level (more details are given in the Table F1.5 in Section 1 of Appendix F). The assessment is based on piezometer records where available, but in their absence has been assessed from the presence or otherwise of a select earthfill zone upstream of the core. The purpose of categorising the response of the phreatic surface in the zone upstream of the puddle core is because it has important implications on the deformation behaviour (as discussed in Sections 7.7.3.2 to 7.7.3.6). Three categories of response have been used:

- Full or large pore water pressure response to reservoir fluctuation, indicating the earthfill in the upstream shoulder to be permeable.
- Minor response, indicating the earthfill zone upstream of the puddle core is of low permeability such that the change in pore water pressure recorded is a small percentage of the change in reservoir level.
- Negligible response, indicating virtually no change in pore water pressure in the earthfill zone upstream of the puddle core due to the reservoir operation. Only Holmestyes dam is in this category because it has an effective puddle clay blanket on the upstream face of the dam.

It should be noted that the categorisation of the response of the phreatic surface upstream of the puddle core to changes in reservoir level is based on a limited knowledge of the reservoir operation and assumptions regarding the permeability of earthfill zones in the upstream shoulder. For embankments constructed after 1930 it has been assumed that the select filling is well compacted and of low permeability. For Ramsden, Walshaw Dean (Lower), Ogden and Yateholme dams (all Yorkshire Water

dams) the shoulder earthfill comprised weathered Millstone Grit and has been assumed as permeable based on the results of constant head tests at Ramsden dam (permeability varying from 2×10^{-5} m/sec to 10^{-7} m/sec). For the Australian dams Yan Yean, Hope Valley and Happy Valley the classification has been based on the pore water response from piezometers installed in the upstream shoulder.

It is recognised that the compressibility of the zones supporting the puddle core have a significant influence on the deformation behaviour of the core (and settlement of the crest) under cyclic reservoir conditions. The compressibility of the earthfill shoulders will generally be lower and not as susceptible to softening on wetting where it has been well compacted (i.e. post 1930) compared to poorly compacted earthfills. Material type will also influence the material compressibility.

7.7.3.2 Long-term Settlement Rate Index

The long-term settlement rate index, S_{LT}, is used as a guide for prediction of settlements (mainly crest settlement) of puddle core earthfill dams post first filling and as a comparative measure to assess the performance of a specific dam. The settlement rate index, S_{LT}, is calculated using Equation 7.6. It is the same equation as the settlement index proposed by Charles (1986) except that the settlement rate is expressed in units of settlement (as a percentage of dam height) per log cycle of time. The same form of equation has been used to calculate the post first filling long-term settlement rate for the crest and shoulders of rolled earth and earth-rockfill embankments.

$$S_{LT} = s * 100 / [1000 * H * \log(t_2 / t_1)] \tag{7.6}$$

where s is the crest settlement in millimetres measured between times t_2 and t_1 (in years) after the end of embankment construction, and H is the height of the dam in metres.

S_{LT} values for the puddle core earthfill dam case studies are given in Table 7.24 and have been calculated mainly for the crest of the embankments. Some values are given for the upper regions of the upstream and downstream shoulders. The quoted S_{LT} values are for periods of measurement during normal operation conditions (i.e. excluding abnormally large drawdown events) and are generally from deformations observed tens of years after construction.

The long-term settlement rate, S_{LT}, basically encompasses all of the mechanisms involved in the long-term deformation behaviour (summarised in Section 7.2.3.3) into

one factor appropriate to analysis of crest settlement for periods of normal reservoir operating conditions. Analysis of the data indicates that a correlation exists between S_{LT} for crest settlement, the reservoir operation (under normal conditions) and the pore water pressure response of the earthfill zone upstream of the puddle core to changes in reservoir level (i.e. full, minor or negligible as discussed in Section 7.7.3.1). The correlation is summarised as follows:

- For conditions where the change in pore water pressure in the earthfill zone upstream of the puddle core is a small fraction of the change in reservoir level on drawdown or where the reservoir remains steady, S_{LT} generally ranges from 0.4% to 1% settlement per log cycle of time (settlement as a percentage of the embankment height).
- For fluctuating reservoir conditions and where the change in pore water pressure in the earthfill zone upstream of the puddle core closely follows the reservoir level, S_{LT} ranges from 2.6% to 7.4% settlement per log cycle of time.

7.7.3.3 "Normal" Deformation Under "Steady State" Conditions

The results of long-term post construction monitoring indicate the reservoir operation and the pore water pressure response of the earthfill zone upstream of the puddle core to changes in reservoir level have a significant influence on the long-term deformation behaviour. Case studies of "normal" deformation behaviour under "steady state" conditions (Figure 7.93) are consider to comprise those cases where the reservoir level is essentially maintained at a steady level (Cwnwerderi and Challocombe dams), or the pore water pressure response of the earthfill zone upstream of the puddle core is either negligible (Holmestyes) or minor (Burnhope, Hollowell, Ladybower, Selset, Yan Yean and Happy Valley dams) to changes in the reservoir level.

For these nine case studies the long-term crest settlement rate, S_{LT}, typically ranges from 0.4% to 1% settlement per log cycle of time.

Of these embankments both Ladybower and Holmestyes dams exceed an S_{LT} of 1%. For Holmestyes (S_{LT} of 2.3%) the period of monitoring of 1.5 years at 150 years after construction is considered too small to obtain a reasonable estimate, as only 3 mm of crest settlement occurred during this period. Ladybower dam (S_{LT} of 2.0%) was classified as "minor" response to reservoir level fluctuation based on the year of completion of construction (1945) and assumption that a zone of select earthfill of low

permeability was used up and downstream of the puddle core, as was the general design practice used at the time. However, the embankment design details, the construction materials used and their method of placement were not known, and it is therefore possible that these assumptions are not correct for Ladybower dam.

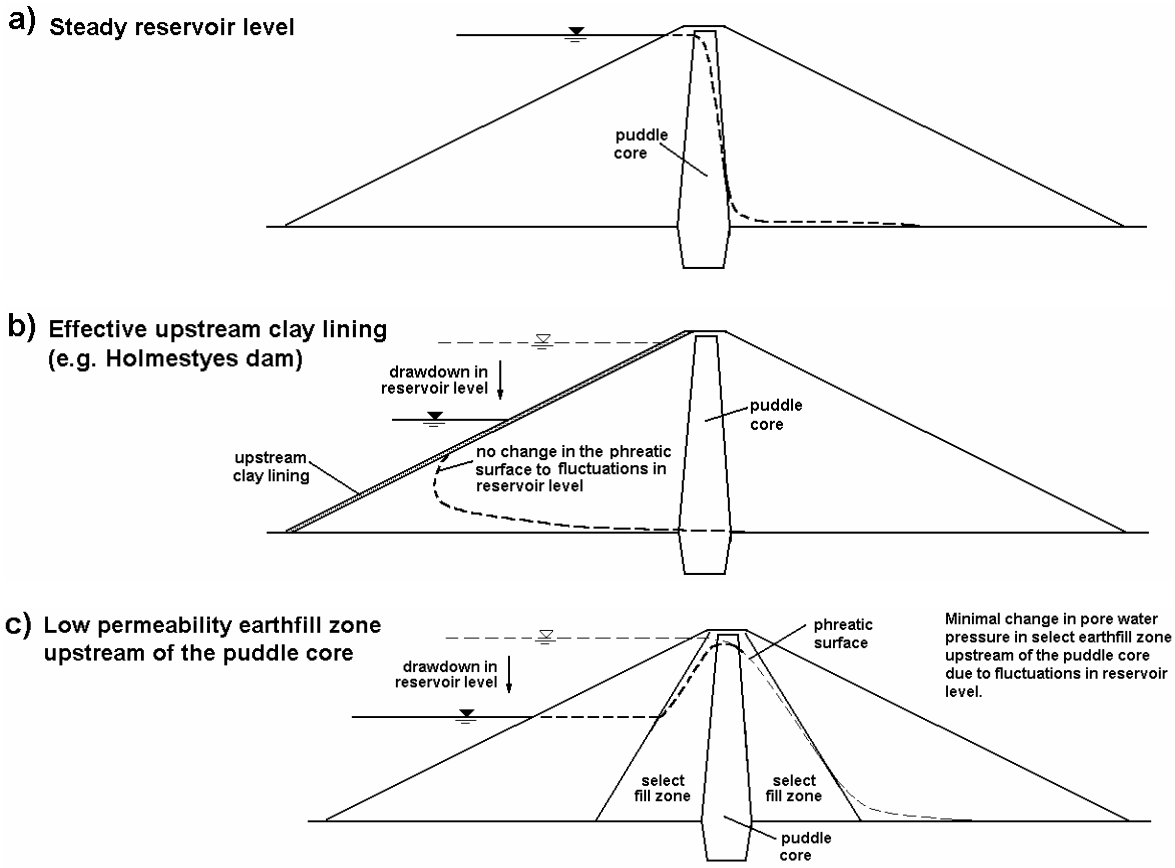

Figure 7.93: Definitions of "steady state" conditions during normal reservoir operating conditions.

Of the remaining seven cases considered as "steady state" conditions there is no clear correlation of the long-term crest settlement rate, S_{LT}, with embankment height or age. However, S_{LT} is be expected to be affected by:

- The age of the embankment, mainly due the difference in design and compaction techniques adopted at the time of construction. The S_{LT} of the older puddle dams would be expected to be greater than for newer dams constructed after the 1930's.
- The height of the embankment. It is not clear what effect the embankment height has because its influence appears to be relative minor and over-shadowed by other factors, as is the case with the earth and earth-rockfill embankments (Figure 7.62

and Figure 7.63). It would be expected that S_{LT} would be greater for dams of greater height.

- Pore water pressure changes in the embankment. Even though steady state conditions have been assumed, the pore water pressures in the puddle core and the zone immediately upstream would be expected to change with time. The available data does indicate some change, albeit minor, with reservoir level.
- The material type and placement method of the various zones within the embankment, and their effect on the time dependent creep coefficients. The data for rolled earthfill and earth-rockfill embankments (Section 7.6.3) indicates clayey earthfills generally have higher long-term settlement rates than dominantly sandy earthfills, and dams with poorly compacted rockfill shoulders higher long-term settlement rates than well-compacted rockfills.

In summary, it is considered based on the available records of the case studies analysed that under "steady state" conditions (or near steady state conditions) the expected long-term crest settlement rate, S_{LT}, for "normal" deformation of puddle core earthfill dams is less than about 1% settlement per log cycle of time. The mechanisms involved are considered to be time dependent primary creep and deformations associated with the small changes in effective stress following the small changes in pore water pressure in the puddle core and upstream shoulder.

Holmestyes Dam (constructed 1840) presents a slightly different case to most puddle core earthfill embankments classified as "steady state" conditions. A layer of puddle clay was placed on the upstream face of the dam in 1857 (some 17 years after construction) due to the observations of leakage (Tedd et al 1993). Installation of piezometers downstream of the upstream blanket indicated the phreatic surface in the upstream shoulder and core to be well below the reservoir level, and on drawdown only minimal responses in piezometric level were recorded. On a large drawdown of approximately 10 m, minor heave movements of the crest and upstream shoulder were observed (Tedd et al 1993).

7.7.3.4 "Normal" Deformation Under Normal Reservoir Operation and Fluctuating Phreatic Surface in the Upstream Shoulder

This section looks at case studies where large changes in pore water pressure occur in the upstream shoulder (adjacent to the core) with fluctuations in reservoir level (Figure 7.94). In these cases cyclic changes in effective stress occur in the upstream shoulder. Cyclic changes in total stress acting on the upstream face of the puddle core also occur as hydrostatic pressure change with fluctuations in reservoir level. Long-term settlement rates of the crest and upstream slope for these cases are generally significantly greater than for "steady state" conditions as described in Section 7.7.3.3.

The case studies include Dean Head, Ramsden, Yateholme and Walshaw Dean dams where the long-term crest settlement rates, S_{LT}, under normal operating conditions range from 4.5 to 7.4 % per log cycle of time (Table 7.24). The rate of crest settlement of these dams is typically 5 to 10 times that under "steady state" conditions and confirms the significant influence of the permeability of the earthfill zone upstream of the puddle core under fluctuating reservoir conditions on the long-term crest settlement rate. Figure 7.92 graphically presents the difference in the long-term crest settlement rate between Ramsden dam and several "steady state" dams.

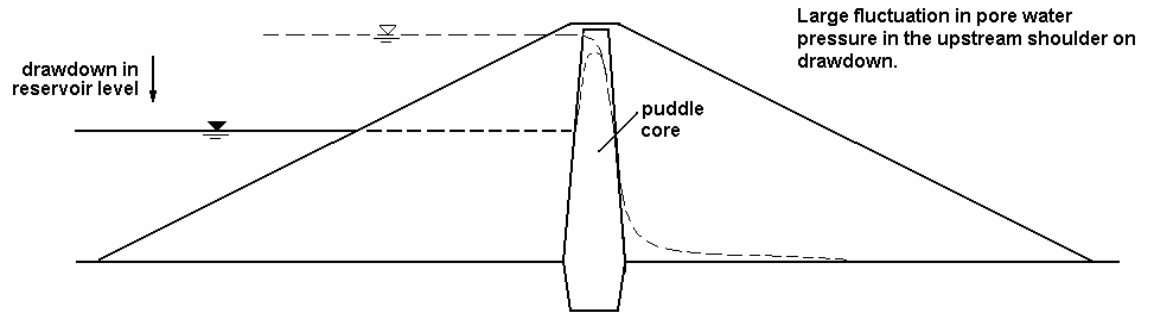

Figure 7.94: Fluctuation of pore water pressures adjacent to and upstream of the puddle core with fluctuations in reservoir level.

For Hope Valley dam (S_{LT} of 2.6%) the pore water pressure response in the earthfill zone upstream of the puddle core is variable, ranging from 25% to 100% of the change in reservoir level. It has been included with this group of case studies even though it possibly lies somewhere between these case studies where large changes in pore water pressure upstream of the puddle core are observed and the "steady state" case studies. The reported long-term crest settlement rate for Hope Valley dam is from SMPs on the

downstream edge of the crest, and the crest settlement rate above the puddle core is therefore possibly higher than 2.6% per log cycle time.

Ladybower dam possibly also falls into this category, however, no information was available on the pore water pressure response under drawdown or the reservoir operation to confirm or deny this.

The mechanism of deformation during the normal cyclic operation of the reservoir for embankments with permeable upstream earthfill is:

- On drawdown:
  - Increasing effective vertical stresses in the upstream shoulder occur as pore water pressures dissipate relatively quickly in the permeable earthfill, resulting in settlement. Settlements are not expected to be overly high because the stress path is in the unloading / reloading range and the earthfill's compressibility will therefore be relatively low.
  - The reduction in hydrostatic pressure acting on the upstream face of the puddle core results in a reduction in the total horizontal stresses within the puddle core and downstream shoulder, and upstream displacement occurs. This upstream displacement was observed for SMPs on the crest, upstream slope and upper downstream slope of Walshaw Dean and Ramsden dams (refer Section 5 of Appendix G) and the internal displacement of the centre of the puddle core at Ramsden dam (Figure 7.95) during drawdowns within the normal operating range for the reservoir.
  - Some of the reduction in hydrostatic pressure acting on the upstream face of the puddle core is transferred onto the upstream shoulder in order to maintain equilibrium with the lateral stresses of the puddle core. This increase in horizontal stress in the upstream shoulder will result in a net upstream displacement of the upstream interface of puddle core and lateral spreading of the puddle core. Deformations within the puddle core occur primarily as undrained plastic yielding and therefore lateral spreading is accompanied by vertical strain to maintain volumetric consistency, and therefore settlement of the crest. Internal vertical strains measured in the puddle core during normal operating drawdown at Ramsden (Figure 7.96) and Walshaw Dean dams confirm this pattern of behaviour (refer Sections 5.4 and 5.5 of Appendix G).

– Vertical strains in the puddle core can also occur due to increases in effective vertical stress as a result of pore water pressure dissipation. The amount of pore water pressure dissipation will depend on the permeability of the puddle core and the time the reservoir is in a drawn down condition.

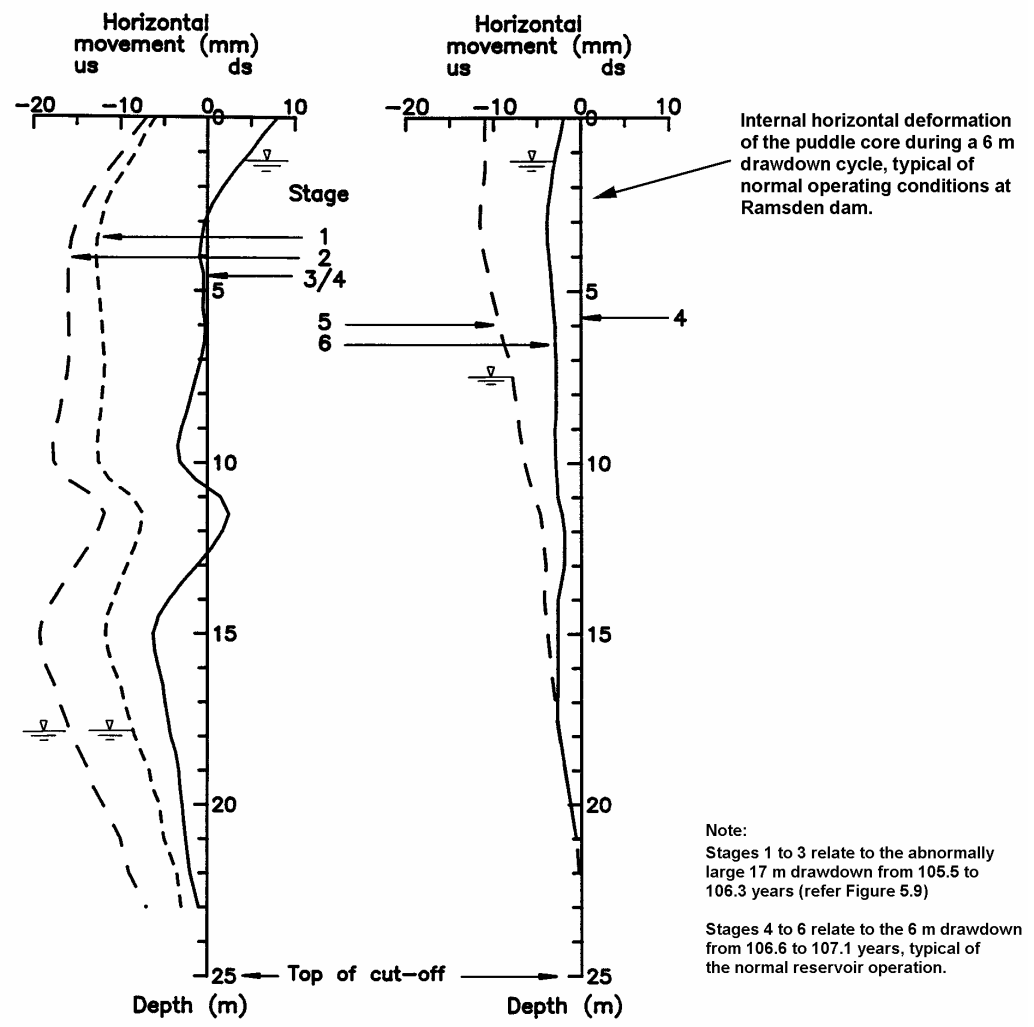

Figure 7.95: Ramsden Dam, internal horizontal deformation of the puddle core, 1988 to 1990 (Holton 1992).

- On re-filling the stress paths are reversed and:
  - Decreases in effective vertical stresses in the upstream shoulder result in heave type deformations.
  - Increase in the horizontal stresses acting on the upstream face of the puddle core results in downstream displacement of the core, upstream slope and downstream slope.

– Within the puddle core heave type internal strains and heave of the crest are observed (Figure 7.96). The mechanism causing this will be a combination of reduction in lateral width of the core under the increased total stress acting (i.e. a plastic type response on re-filling) and heave due reduction in effective vertical stresses as pore water pressures increase. Deformations due to pore water pressure increase will show a time delay due to the low permeability of the core.

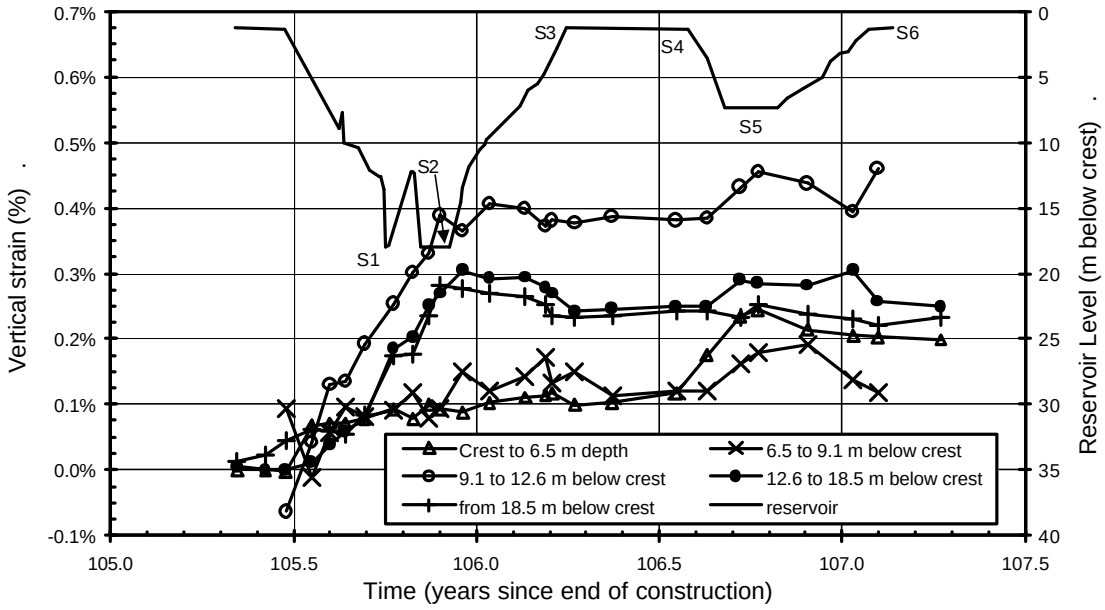

Note: S1 to S6 refer to the stages of reservoir level

Figure 7.96: Ramsden Dam, internal vertical strains measured in the puddle core from 1988 to 1990 (data from Tedd et al 1997b and Kovacevic et al 1997).

The net permanent vertical deformations following a reservoir cycle of normal magnitude are typically settlement of the crest, upstream slope and upper portion of the downstream slope. The magnitude of settlement is generally greatest for the crest. Net permanent crest displacements are generally small and in a downstream direction, but data records are limited. Tedd et al (1997a) attribute the net permanent settlement of the upstream shoulder to the difference in compressibility properties between unloading (lower compressibility on re-filling) and re-loading (higher compressibility on drawdown) as observed in cyclic laboratory oedometer testing (Holton 1992; Tedd et al 1997a). Kovacevic et al (1997) obtained good agreement between measured and predicted settlements (from finite element analysis) under normal reservoir drawdown cycle for several puddle core earthfill embankments when incorporating the differential compressibility between unloading and re-loading in their analysis.

The net internal deformation of the puddle core at Ramsden dam shows upstream displacement (Figure 7.95) and permanent vertical strains (Figure 7.96) over the full height of the core. At Walshaw Dean dam the internal vertical strain shows a permanent increase in strain over the full height of the core (refer Section 5.5 in Appendix G). These permanent core deformations are most likely primarily due to undrained plastic deformations on drawdown.

The net permanent crest settlements (Figure 7.97) are typically 50 to 70% of the maximum settlement at drawdown, for drawdowns within the range of normal reservoir operation. Permanent settlements of greater magnitude are observed for abnormally large drawdowns, and are discussed in Section 7.7.3.5. The data in Figure 7.97 is mainly from puddle dams in Yorkshire, England where the shoulder earthfill is relatively permeable.

The permanent crest settlement on drawdown for puddle core earthfill dams with permeable earthfill in the upstream shoulder is likely to be affected by the magnitude of the drawdown, the length of time of the drawdown and the compressibility of the upstream filling. Ignoring the events associated with abnormally large drawdown events, Figure 7.97 shows some correlation of permanent crest settlement with drawdown height. It should be noted that the data set is relatively small and comprises UK puddle dams of similar height and constructed using similar materials for the shoulders. Therefore, the following preliminary predictive methods, which are based on the data presented by Tedd et al (1997b), should be used with caution:

- Estimation based on the S_{LT} rates of the reported cases within the data set, ranging from 4.5 to 7.4% vertical strain per log cycle of time.
- Estimation based on the plot of permanent crest settlement versus depth of drawdown (as a percentage of the embankment height) as shown in Figure 7.98. This plot is based on the data from Tedd et al (1997b) omitting those points associated with abnormally large drawdown events and normalising the drawdown height with respect to embankment height.

Where the pore water pressure response of the earthfill zone upstream of the core is in-between that of “permeable” and low permeability, such as at Hope Valley dam (and possibly Ladybower dam) the long-term settlement rate is also between that of the two categories. However, there is not sufficient data with which to provide a possible range of long-term crest settlement rate.

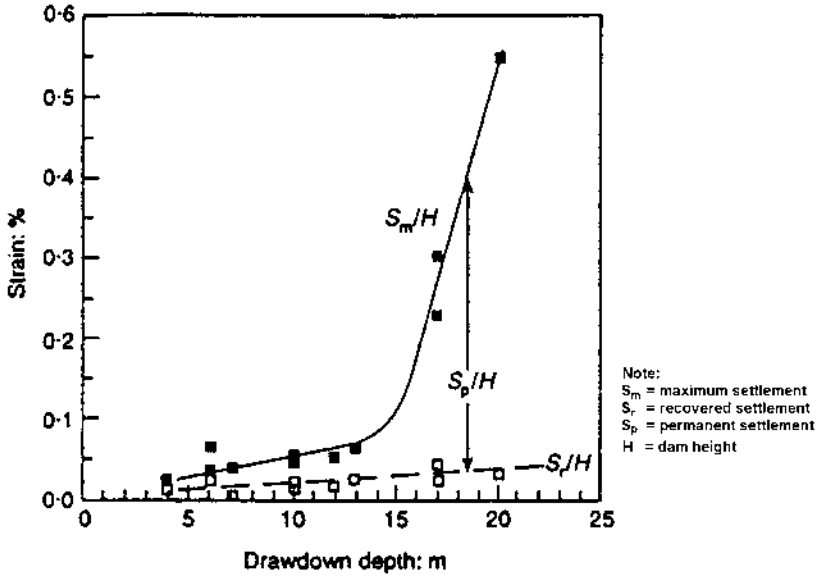

Figure 7.97: Vertical strain (or settlement) at the crest versus drawdown depth for specific drawdown and refilling cycles (Tedd et al 1997b).

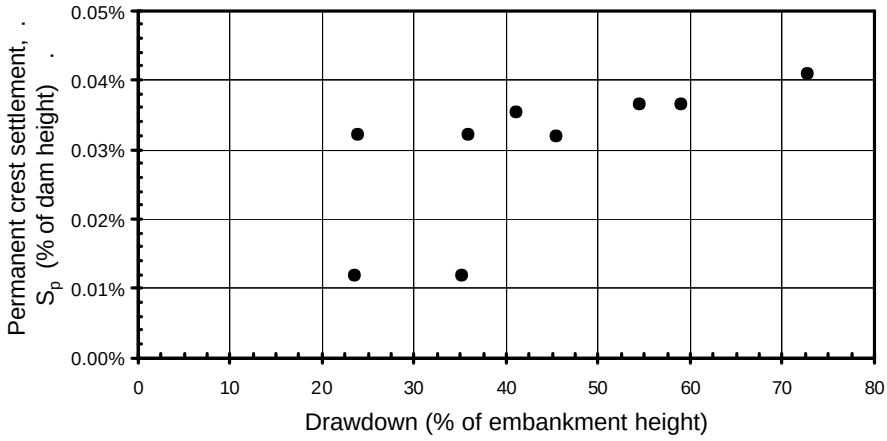

Figure 7.98: Permanent vertical crest strains during cyclic drawdown (in normal operating range) for puddle core dams with permeable upstream filling (after Tedd et al 1997b).

7.7.3.5 Deformation During Abnormally Large Drawdown Events

Tedd et al (1997b) report the deformation behaviour during historically large drawdown events for several UK puddle core dams, including Ramsden, Ogden and Widdop dams. Permanent crest settlements under abnormally large drawdown for these three dams were:

- 51 mm at Ramsden dam (Figure 7.99), or 0.20% of the embankment height, as a result of the abnormally large drawdown cycle of 17 m at 106 years after construction. Further details are given in Section 5.4 of Appendix G.
- 130 mm at Ogden dam (Figure 7.100), or 0.52% of the embankment height, during the abnormally large 20 m drawdown event in 1990 to 1992.
- 52 mm at Widdop dam, or 0.26% of the embankment height, during the abnormally large drawdown cycle of 17 m at 110 years after construction.

The data records indicate large permanent crest settlements occur under abnormally or historically large drawdown events. At Ramsden dam a smaller magnitude, but still relatively large, permanent settlement was measured for the SMP on the upstream slope.

The initial deformation pattern on drawdown to a level commensurate with the normal operating conditions would result in the deformations as described in Section 7.7.3.4. On drawdown to abnormally or historically low levels, drained yielding in the upstream shoulder and undrained yielding in the puddle core are considered to be the dominant mechanisms resulting in the large magnitudes of deformation observed.

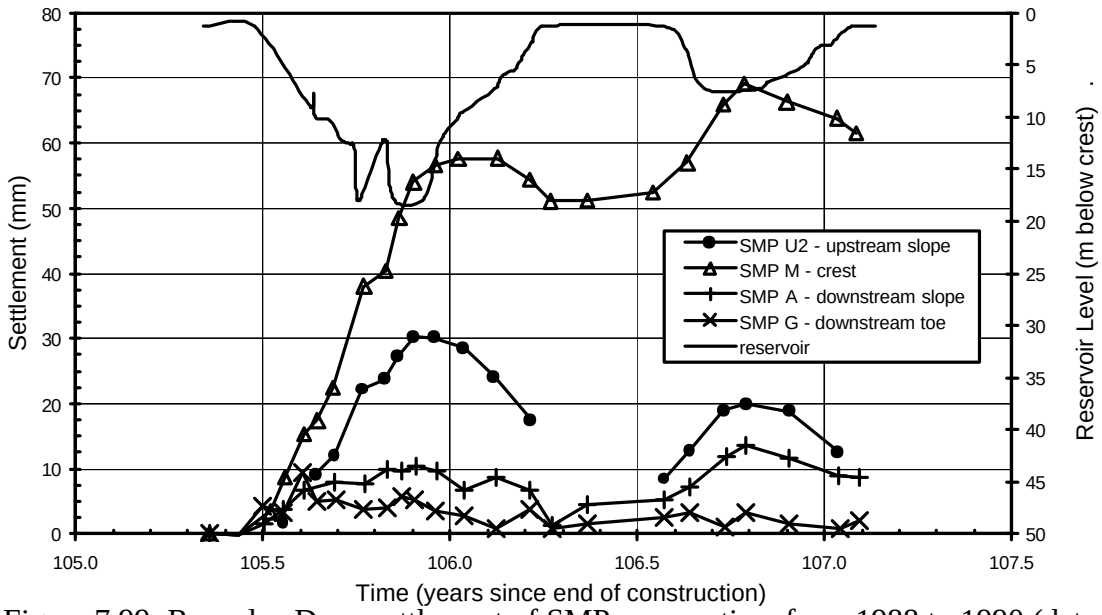

Figure 7.99: Ramsden Dam, settlement of SMPs versus time from 1988 to 1990 (data from Tedd et al 1990).

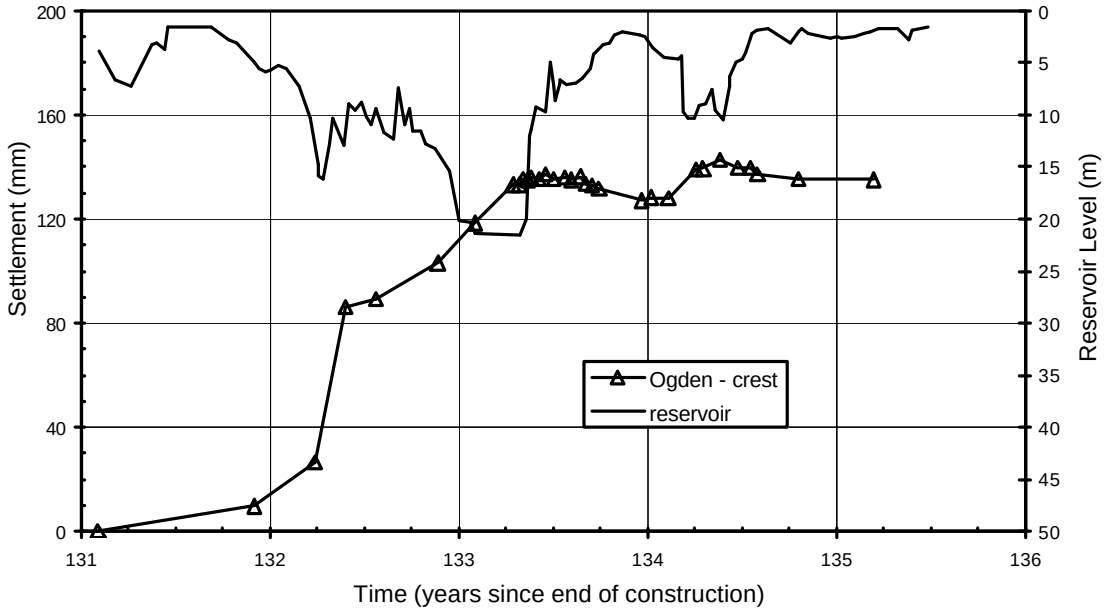

Figure 7.100: Ogden Dam, crest settlement versus time (Tedd et al 1997a).

In Section 7.7.2.1 it was considered that poorly compacted earthfills in the upstream shoulder, susceptible to collapse compression on wetting, were close to normally consolidated after the end of first filling due to the softening effects of collapse and wetting. Increases in effective stresses on drawdown post first filling were considered to result in large deformations due to yielding as vertical stress levels exceeded the pre-consolidation pressure in the near normally consolidated upstream earthfill. On subsequently larger drawdowns where the effective stresses in the upstream shoulder exceeded those previously experienced post first filling, further large deformation of the upstream shoulder due to yielding in drained conditions was also likely. It is on these abnormally or historically large drawdown many years after the end of construction that effective vertical stresses in the permeable upstream shoulder are considered to increase to levels greater than previously experienced. The new high effective vertical stress levels will be experienced in the lower elevations of the upstream shoulder (Figure 7.101) and drained yielding will be confined to this region as stress levels exceed the pre-consolidation pressure and the earthfill's compressibility increases significantly above that for the re-compression range of loading. In the mid to upper regions of the upstream shoulder it is likely that effective stress levels will equal those previously experienced and therefore yielding will not occur; smaller settlements are likely under the re-compression compressibility properties of the earthfill.

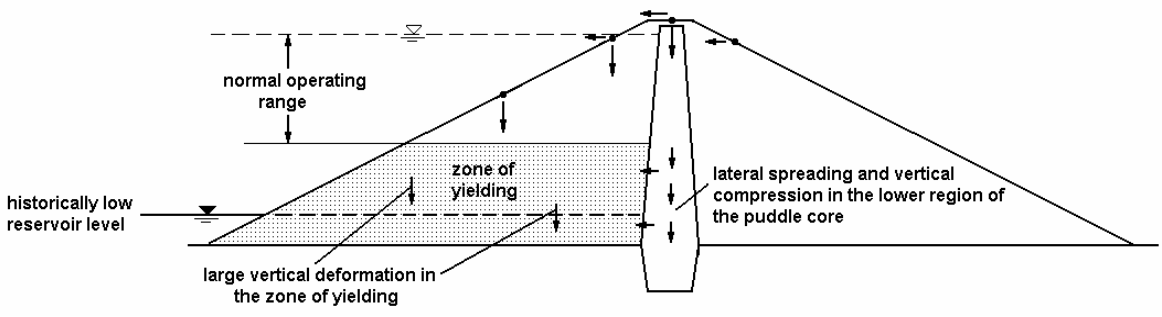

Figure 7.101: Idealised model of deformation during historically large drawdown.

For the puddle core, the hydrostatic pressures acting on the upstream face of the puddle core will be reduced to levels not previously experienced. Therefore, the horizontal stress levels in the upstream shoulder required to equilibrate the lateral stress from the puddle core will exceed those levels previously experienced since first filling. The new high lateral stress levels will be in the lower region of the embankment where a net upstream displacement of the core / upstream shoulder will occur. Deformations in the puddle core will largely occur as undrained plastic lateral spreading and vertical compression (Figure 7.101). This pattern of deformation behaviour of the puddle core was observed at Ramsden dam where vertical strains in the mid to lower region were much greater than in the upper region (Figure 7.96) and the bulk of the lateral deformation was below about 15 m (Figure 7.95).

After the initial plastic deformation, consolidation type settlements within the puddle core may occur as pore water pressures dissipate. For Ramsden dam, Figure 7.95 and Figure 7.96 show significant lag in the deformation of the lower portion of the core. It is suspected that this may not only due to pore water pressure dissipation in the puddle core, but may also due to a lag in pore water pressure dissipation in the upstream shoulder.

On-refilling after the historically large drawdown at Ramsden dam, a large amount of the lateral displacement of the core was recovered (Figure 7.95) as the hydrostatic pressures and horizontal stresses acting on the upstream face of the puddle core increased. However, only a limited amount of the vertical strain was recovered on re-filling (Figure 7.96). At Ogden dam (Figure 7.100) only a small proportion of the maximum crest settlement (approximately 6%) was recovered on re-filling. The reasons for this are considered to be due to the large undrained plastic type deformation of the core and drained yielding in the lower upstream shoulder that is not recovered on re-filling.

Comparison of the crest settlement of Ramsden (Figure 7.99) and Ogden (Figure 7.100) dams with Walshaw Dean Dam (Figure 7.102) during a full drawdown provides some degree of verification of the mechanism discussed. As indicated, for both Ramsden and Ogden dams the magnitude of crest settlement was large on full drawdown, 51 mm and 130 mm respectively. In contrast, the full drawdown of Walshaw Dean dam over the period 86 to 88 years after construction resulted in a permanent crest settlement of only 9 mm, which is in line with the general settlement trend from the earlier drawdowns. The reason for the deformation behaviour at Walshaw Dean is considered to be because the normal reservoir operation is for very large seasonal drawdown, as shown in Figure 7.102, and the maximum effective stresses on full drawdown within the upstream earthfill have previously been experienced. Therefore, the changes in stress are within the re-compression zone for which the compressibility of the earthfill is significantly lower.

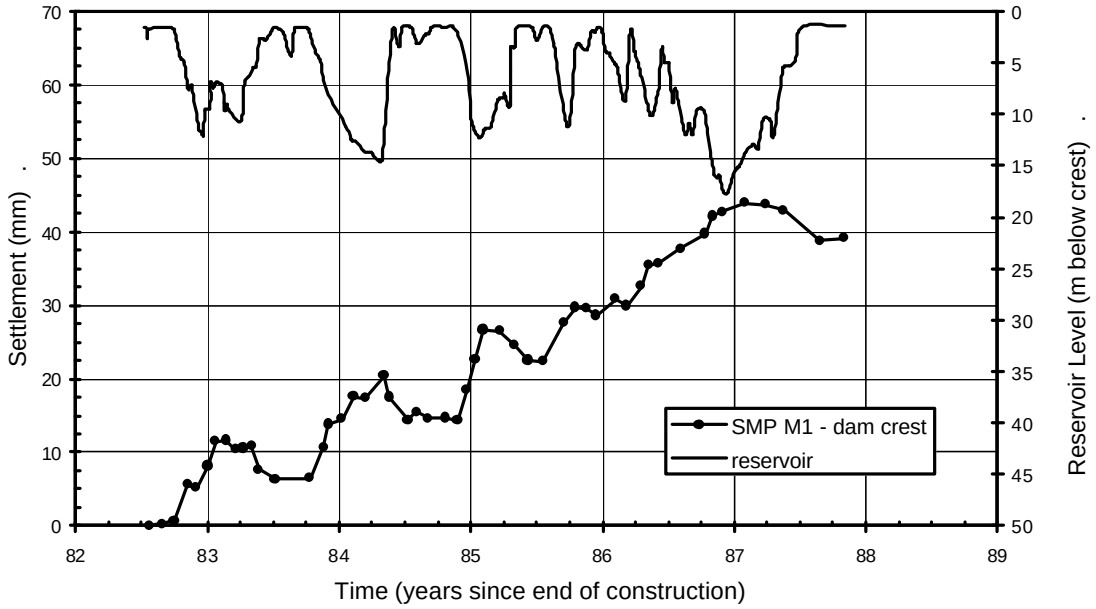

Figure 7.102: Walshaw Dean (Lower) dam, crest settlement versus time (Tedd et al 1997a).

In terms of prediction of deformation during abnormal drawdown events, the only available method would seem to be fully coupled finite element modelling (FEM) due to the complexity of the processes and interaction between the different elements within the embankment. Kovacevic et al (1997) attempted to model the deformation of Ramsden dam during the large drawdown event using finite element methods, but were unable to model the deformation with any accuracy. It is considered that they may not

have been able to model the yielding that occurred in the core and upstream zone when the reservoir was drawn down to an all time low level. Therefore, undertaking FEM is not a simple procedure and to add to the complexity is the lack of known information on material properties and required assumptions necessary in the modelling.

7.7.3.6 Factors Affecting the Long-term Deformation Behaviour of Puddle Core Dams

In summary, from the above analysis and discussion on the "normal" deformation behaviour of puddle dams, the factors affecting the long-term deformation behaviour are considered to be:

- Under normal reservoir operating conditions the permeability of the earthfill zone upstream of the puddle core has a significant effect on the long-term deformation behaviour of puddle core earthfill embankments. Long-term crest settlement rates, S_{LT}, under "steady state" conditions (or near steady state conditions) are typically less than about 1 % per log cycle of time (settlement as a percentage of the embankment height). For embankments where the earthfill upstream of the puddle core is permeable and the seasonal reservoir fluctuation is large, the S_{LT} rates are significantly higher (2.6 to 7.5 % per log cycle of time).
- The historical operation of the reservoir also has a significant effect on the deformation behaviour. Historically large drawdown events result in large, permanent undrained plastic deformations of the puddle core, and yielding (and possibly undrained plastic deformation) of the lower portion of the upstream filling. This type of deformation behaviour could be classified as "abnormal".
- The method of placement and moisture content control of the shoulder filling, particularly, the upstream shoulder. The poorer the quality of compaction and drier the moisture content at placement, the greater the potential for collapse compression on saturation. The shoulder earthfill in the older (pre 1900) puddle core earthfill embankments were likely to be particularly susceptible to collapse compression given their generally poor compaction.
- Primary creep (or creep under constant stress), secondary consolidation and foundation compression are encapsulated in the long-term settlement rate. Given the age of most puddle core earthfill embankments these effects are considered to be relatively minor compared with the effect of cyclic changes in stress in the upstream

earthfill zone and on the upstream face of the puddle core in embankments with permeable upstream earthfill shoulders.

- Shrink-swell movements are likely to influence those sites for which plastic clays are present and seasonal moisture content changes occur.
- Seasonal creep movements of the outer downstream slope. This is creep of the outer surface of the downstream slope due to seasonal factors such as moisture content profile changes. It is dependent on the plasticity of the soil and potential for shrink-swell related movements, the steepness of the slope and the soil strength. The effect of seasonal creep movements is usually offset in the method of installation of surface measurement points on the slopes of the embankment.

7.8 "ABNORMAL" EMBANKMENT DEFORMATION BEHAVIOUR – METHODS OF IDENTIFICATION

"Abnormal" deformation behaviour of embankment dams is deformation that cannot readily be explained as being due to "normal" mechanisms. The purpose of attempting to identify abnormalities in the deformation behaviour is for the early detection of potential problems such as instability or internal erosion. Identification of "abnormal" deformation behaviour is basically from outliers to the "normal" deformations trends from similar embankment types taking into consideration the embankment zoning geometry, material types, placement methods and foundation conditions. Outliers are identified from magnitude of deformations as well as trends in the direction and rate of deformation. Often what may initially be termed "abnormal" may later be proven by investigation, analysis and additional monitoring to in-fact be "normal".

During construction, identification of "abnormal" deformation is from outliers to the total settlement and vertical strain profiles in the core of earthfill and zoned earth and earth-rockfill embankments (Section 7.4.3). The data on lateral core deformations in zoned earthfill embankments with thin to medium core widths (Section 7.4.2) from the case studies is limited and therefore not sufficient for assessment of "abnormal" deformation unless measured core deformations are larger than or the trend different to the case study data presented.

Deformation of SMPs on the shoulders of embankments during construction is available for some embankments in the literature, but it has not been considered here due to inconsistencies in timing and variation in embankment type for which the data is

available. Penman (1986) provides some guidelines for the magnitude of lateral displacement, but the data is from a variety of embankment types and should be used with caution.

Identification of "abnormal" deformation post construction for earthfill and zoned earth and earth-rockfill embankments is from outliers in terms of magnitude and rate of deformation of surface monitoring points on the crest and slopes of the embankment taking into consideration the zoning geometry and material properties of the core and shoulders. "Abnormal" trends in the deformation behaviour, such as increased rates of deformation on first filling, and internal localised zones of high strain in the core are other means of identification of potentially "abnormal" deformation behaviour. For puddle core earthfill dams outliers are more readily evaluated from the rate and trend of the long-term deformation behaviour given the age and period of monitoring of these structures.

It is important to note that for embankments where the deformation is considered to be "abnormal" may be, and in most instances is, explainable on consideration of the type and placement method of the earth or rockfill, or the reservoir operation. For example, embankments with high vertical core strains during construction may be related to plastic core deformations due to low undrained strength of the core and corresponding large lateral strains of the supporting poorly compacted rockfill shoulders. Whilst the core strain may be large in comparison to similar embankments and therefore identified as "abnormal", it may in-fact be "normal" given the reasons for the behaviour.

It is emphasised that the identification of a dam as exhibiting "abnormal" deformation behaviour in no way indicates there is any issue of dam safety with that dam.

In the following sections (Sections 7.9 to 7.12) various methods of identification of "abnormal" deformation behaviour are discussed with reference to and specific discussion on those case studies within which the "abnormal" deformation was observed.

The "abnormal" deformation behaviour may be specific to one part of the embankment whilst the overall stability of the embankment is not in question. For example, movement along a shear plane in the core on a large drawdown event for a zoned earth and rockfill dam would be considered as "abnormal" behaviour of the core, but the upstream rockfill zone provides adequate overall stability of the embankment.

Where failures due to slope instability have occurred in embankment dams there is often limited, if any, information of the deformation behaviour leading up to failure. Of the embankments considered in this chapter only at Carsington, Belle Fourche, San Luis and Steinaker dams did a slope failure occur, and only at Carsington was there any formal monitoring from within the failed region prior to the failure.

Chapter 5 presents information on the characteristics of pre and post failure deformation behaviour from analysis of some 54 case studies of slope failure in embankment dams with discussion on the mechanism causing the deformation behaviour. Most of the data presented relates to the post failure deformation behaviour, but there is some useful information on deformation behaviour leading up to failure that is supplementary to the several case studies discussed within this chapter.

More generally, the basic concept of the creep model under constant deviatoric stress conditions (Singh and Mitchell 1968; Mitchell 1993) is useful for assessment of the deformation behaviour leading up to a failure condition. Primary creep, or deformation at a decreasing rate with time under constant stress conditions, is applicable to "normal" type deformation behaviour. Tertiary creep, or deformation at an increasing rate with time, under constant deviatoric stress conditions is indicative of the onset to failure.

7.9 "ABNORMAL" DEFORMATION BEHAVIOUR DURING CONSTRUCTION OF EARTH AND EARTH-ROCKFILL EMBANKMENTS

From Section 7.4, the embankments highlighted as outliers to the general deformation trend of the core showed up in both the plots of vertical strain profile and of total settlement. All cases are from zoned embankments and mostly of thin to medium core widths (combined core width less than 1H to 1V) with the core placed close to or wet of Standard optimum moisture content.

The outliers to total core settlement at the end of construction (Figure 7.23 of Section 7.4.3.3) include Hirakud, Beliche, Blowering, Nurek and Tedorigawa dams. For Hirakud, Beliche, Blowering and Tedorigawa dams the difference in total settlement from the trendline representative of the core type and width (Table 7.14) was 3 to 10 times the standard error and clearly very much greater than the estimated mean for "normal" behaviour. For Nurek dam the difference above the mean was 2.7 times

the standard error, however, at a height of 290 m Nurek is the highest dam in the data set and therefore the settlement estimate based on the trendline is not accurate.

The outliers to vertical strain profile (Figure 7.18, Figure 7.21 and Figure 7.22) include Hirakud, Beliche, Blowering, Tedorigawa, Chicoasen and possibly Maroon dams. For these embankments the vertical strain at end of construction for portions of the core zone are greater than for the majority of case studies taking into consideration core material type, moisture content at placement and core width.

7.9.1 PLASTIC DEFORMATION OF THE CORE DURING CONSTRUCTION

For Beliche, Tedorigawa, Chicoasen and Maroon dams large plastic deformation of the wet placed core is considered to be the main reason for high vertical strains and/or high total settlement at end of construction. At Nurek and Blowering dams plastic deformation of the wet placed core is also considered to be a significant factor, but other factors are also potentially significant. Beliche, Tedorigawa, Chicoasen and Nurek dams are all zoned earth and rockfill dams with thin cores of clayey gravels placed at about Standard optimum or wetter.

At Beliche dam (Figure 7.103) high vertical strains at end of construction, in the range 5 to 7%, were measured for a large portion of the core from 16 m depth below crest to foundation level at 55 m depth (Figure 7.21a). The vertical strains are well in excess of those measured in similar thin, wet placed clayey sand to clayey gravel cores, as well as those within thin, wet placed clay cores (Figure 7.22a) over a similar depth range. Large lateral displacements of the core, as indicated by distortion of the inclinometer tubes up and downstream of the core (Naylor et al 1997), are considered to be a significant factor in large vertical strains measured. The high compressibility of the lightly compacted, highly weathered schists and greywackes used as the inner rockfill zone is likely to have been a contributing factor to the large lateral displacements of the thin core. Another contributing factor to the potentially large lateral displacement could have been collapse compression of the upstream rockfill on saturation following partial impoundment of the reservoir to elevation 29 m (i.e. above the crest level of the upstream cofferdam) following heavy rainfalls in January 1985 prior to completion of construction. However, no significant acceleration was recorded in the vertical strain rate for the cross-arms represented in Figure 7.20a. Further details of the deformation behaviour at Beliche dam are given in Section 1.3 of Appendix G.

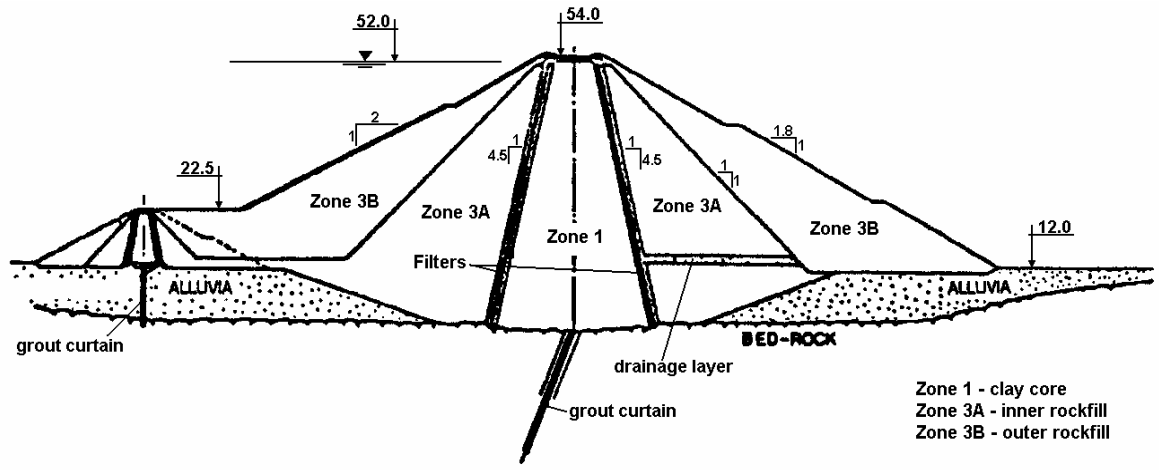

Figure 7.103: Cross section through Beliche dam at the main section (Maranha das Neves et al 1994)

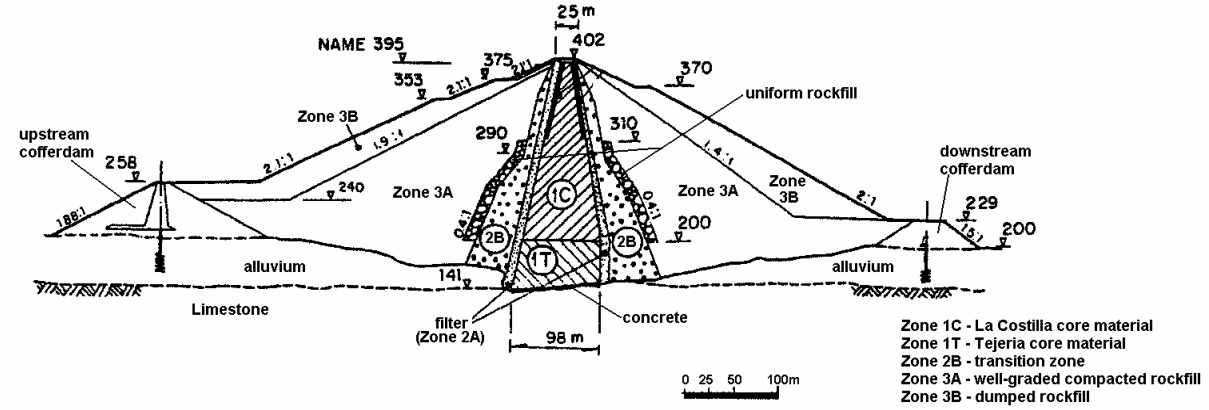

Figure 7.104: Cross section of Chicoasen dam at the main section (Moreno and Alberro 1982)

At Chicoasen dam (Figure 7.104), a 260 m high central core earth and rockfill dam constructed in a broad gully with near vertical abutment slopes, high vertical strains within the core at IVM I-B4 of 5.5 to 6.5% were recorded over the depth range 85 to 105 m depth below crest level (Figure 7.21a). This region of the core is located within the plastic region identified by Moreno and Alberro (1982). In comparison to Beliche and Tedorigawa dams the vertical strains at Chicoasen dam are not overly high and are isolated to a small region of the core. This is possibly reflective of smaller lateral displacements of the core due to the likely low compressibility of the well-compacted, moderately wide to wide gravelly filter / transition zones and well-compacted inner rockfill shoulders. It is notable that the region of high vertical strain in IVM I-B4 at 85 to 105 m depth below crest level (elevation 295 to 315 m) is coincident with the base of

the core region where the filter / transition width is relatively thin (Figure 7.104). Further details are given in Section 1.4 of Appendix G.

For Tedorigawa dam (Kawashima and Kanazawa 1982), a 148 m high zoned earth and rockfill dam, limited information was available from the cited references on the properties and placement methods of earth and rockfill materials. The high vertical strains at end of construction (5 to 8%) over a large section of the core (from 50 to 125 m depth below crest level) as shown in Figure 7.21a are considered indicative of plastic deformation of the core.

At Maroon dam, a central core earth and rockfill dam of 52 m height with thick core of medium plasticity sandy clays to clayey sands placed on the wet side of Standard optimum, relatively high vertical strains of 4.5 to 6.5% were measured in the depth range 26 to 33 m below crest level at end of construction (Figure 7.22b) in all three IVMs (ES1, 2 and 3). Given it is one of very few case studies in the database of zoned embankments with wet placed thick clay cores (combined core width greater than 1H to 1V) and is only marginally outside a nominal limit established from five zoned embankments with wet placed clay cores, it is difficult to really classify the vertical strain as "abnormally" high.

At Blowering dam (Figure 7.124), a 112 m high central core earth and rockfill dam with medium sized core of sandy clays placed on average from 0.2% dry to 0.3% wet of Standard optimum, vertical strains in the core at end of construction ranged from 6 to 12% (Figure 7.22b) in the depth range 32 to 76 m below crest level. This region of the core coincides with core placement on the wet side of Standard optimum. The lateral displacement ratio at 73 m depth below the crest (Figure 7.12) was estimated at 2.3% at end of construction. At the corresponding depth the vertical strain at end of construction was almost 7% indicating the lateral displacement contributed to about 33% of the measured vertical strain at this depth. The relatively low modulus of the supporting rockfill (estimated from HSG records in the rockfill) is thought to be significant in the relatively high vertical strains measured in the core. Blowering dam is discussed further in Section 7.10.3 and Section 6 of Appendix G.

In summary, embankments with high vertical strains within the core where plastic deformations associated with lateral spreading are considered to be significant contributing factor, have the following properties:

- Cores generally comprise clays, clayey sands and clayey gravels placed at moisture contents at or wet of Standard optimum.

- The region of high vertical strain is generally observed over a large portion of the core (e.g. Beliche, Tedorigawa and Blowering). Changes in the embankment zoning geometry or moisture placement conditions of the core may restrict the region of the core where high vertical strains are measured.
- Zoned embankments with relatively compressible rockfill shoulders, such as observed at Beliche and Blowering dams.

7.9.2 COLLAPSE COMPRESSION OF THE CENTRAL EARTHFILL ZONE

The vertical deformation behaviour of the core of Hirakud dam stands out as an outlier in terms of total settlement (Figure 7.23) and vertical strain in the mid to lower portion of the core (Figure 7.18b).

The very broad central earthfill zone at Hirakud dam (Figure 7.105) comprised mostly low to medium plasticity clayey gravels to clayey sands placed 1% to 3% dry of Standard optimum. Vertical strains in the central earthfill zone at IVM C at end of construction, installed in the deeper gully section of the embankment, reached values in the range 7.5% to 13.5% in the lower 15 m of the core (35 to 49 m) as shown in Figure 7.18b. These values are well in excess of the typical vertical strains recorded at end of construction for similar dry placed earthfills.

During the shutdown period of the 1952 monsoon season high water levels were impounded in the reservoir and backwaters engulfed the embankment section within the gully region (about 12 to 13 m height at this time) from July to December 1952 (Rao 1957). The large settlement during the 1952 shutdown period (Figure 7.106) is likely due to collapse settlement of the dry placed earthfill on saturation during inundation. Subsequent large settlements during the following two construction periods in 1953 and 1954 were predominantly within the lower 15 m of the core and likely due to the low moduli of the wetted earthfill. At end of construction the total settlement was in the order of 2170 mm, 1430 mm (or 66%) of which occurred within the lower 15 m or lower 30% of the embankment. Investigations at end of construction (Rao 1957) encountered "*soft soil patches*" in the lower 21 m where moisture contents were as high as 10% above Standard optimum. Further details are given in Section 3.2 of Appendix G.

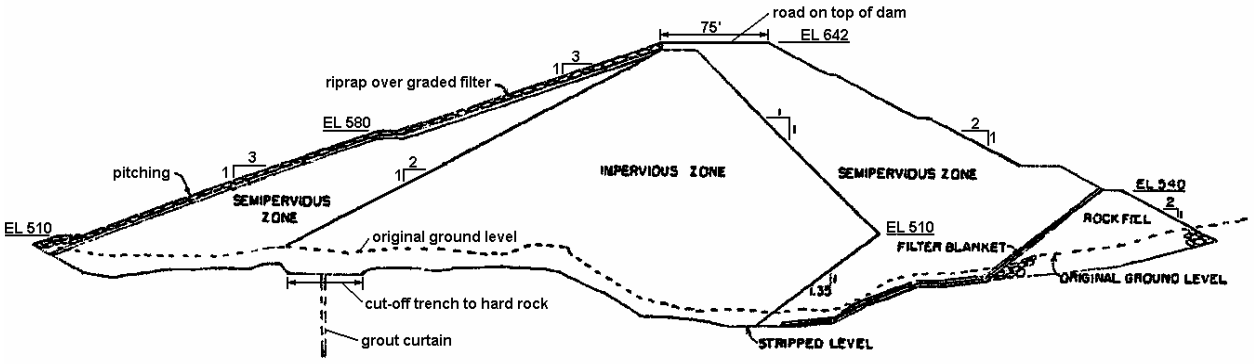

Figure 7.105: Section at Hirakud dam (Rao and Wadhwa 1958)

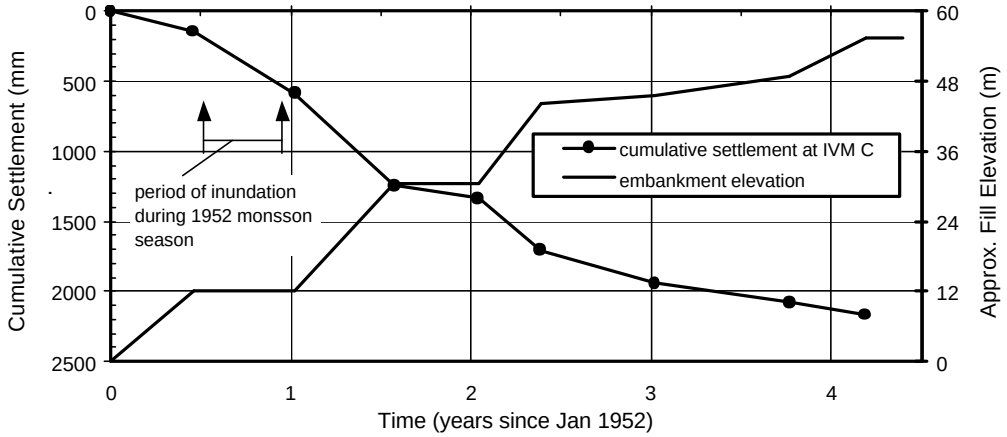

Figure 7.106: Cumulative settlement during construction at Hirakud dam (adapted from Rao 1957)

7.9.3 RESERVOIR FILLING DURING CONSTRUCTION

Partial impoundment during construction can affect the vertical strains and total settlement of the core for zoned embankments with free draining upstream shoulders that are susceptible to collapse compression on wetting. As the monitoring records at several dams (Section 7.10.2) and results of the finite difference modelling (Section 7.5.2) indicate, embankments with wet placed cohesive earthfill cores of low undrained shear strength are susceptible to high vertical strains in the core resulting from collapse compression of the upstream rockfill on first filling.

At Nurek dam (Figure 7.107), a 290 m high zoned earth and rockfill dam with thin central core zone, the total settlement of the core during construction is considered to have been affected by the reservoir impoundment during construction. The thin, sandy clayey gravel core was likely to have been placed close to or wet of Standard optimum given the high pore water pressures developed (Sokolov et al 1985). Reservoir filling

was undertaken at construction proceeded. Sokolov et al (1985) report total settlements at end of construction of 13.7 m for the core, 11.9 m for the upstream shoulder and 4 to 6.5 m for the downstream shoulder. They comment that collapse compression on wetting in the gravel to bouldery upstream shoulder fill contributed to its large settlement relative to the downstream shoulder.

The large settlement of the thin, wet placed sandy clayey gravel core is likely to have been affected by the collapse compression within the upstream shoulder. As discussed in Section 7.5.2 (Figure 7.35), collapse compression in the upstream shoulder can result in plastic deformation from lateral spreading in cores of low undrained shear strength with subsequent large vertical strains in the core.

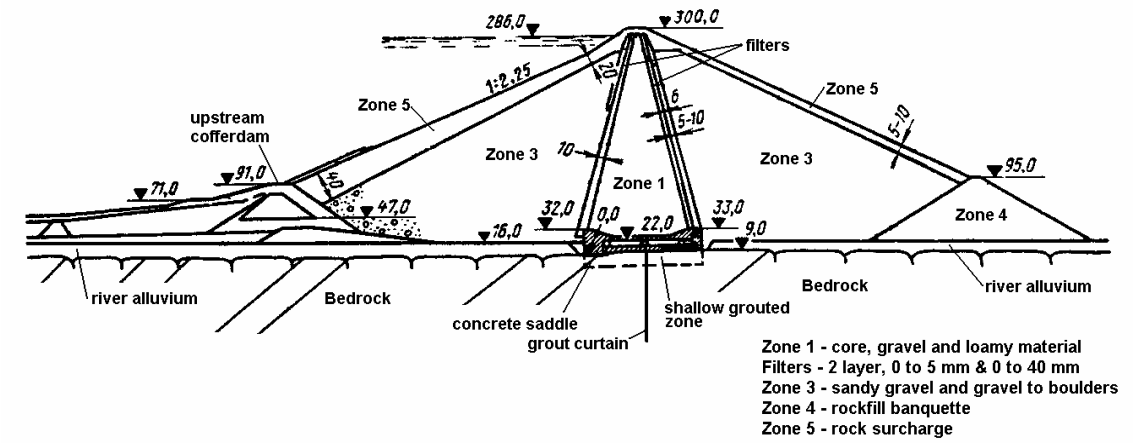

Figure 7.107: Cross section of Nurek dam (adapted from Borovoi et al 1982)

7.9.4 SHEAR SURFACE DEVELOPMENT IN THE CORE DURING CONSTRUCTION

High localised vertical strains in the core can be an indicator of possible development of a shear surface. The clearest example of this in the literature is probably the failure at Carsington dam (Skempton and Vaughan 1993; Rowe 1991; Potts et al 1990).

Carsington dam, a zoned earthfill embankment of 36 m maximum height, failed during construction in early June of 1984. The central core, including its unusual "boot" structure on the upstream side, comprised high plasticity clays that were placed well wet of Standard optimum moisture content and heavily rolled. The outer earthfill zones were of weathered mudstone placed in thin layers and well compacted.

The deformation records from IVM gauges installed in the central core highlighted the development of the shear surface in the core prior to the failure. At IVM C, located 4 m upstream of the axis at chainage 850 m, the vertical strain profile (Figure 7.109a)

shows an increase from 7 to 9% at about elevation 180 m from early to late October 1983 during the early stages of the winter shutdown. After this date, and during the shutdown period, the tube at IVM C became constricted and then blocked at this elevation indicating the continuance of shear type deformation. This zone of high vertical strain, at about elevation 180 m, is coincident with the surface of rupture through the clay core (Figure 7.108) determined from investigation after the failure.

At IVM B, located 4 m upstream of the axis at chainage 705 m, the vertical strain profile (Figure 7.109b) shows a large increase in vertical strain between elevations 185 and 192 m in the days immediately prior to and during the development of the failure.

Figure 7.110 (from Rowe 1991) highlights the large shear strain development in IVMs B and C leading up to the failure. This type of plot of vertical strain versus bank level or height above the gauge is useful in identification of potential shear development as it highlights the development of large localised strains that are not necessarily attributable to increasing total vertical stress or to consolidation type settlements. This behaviour contrasts that for a number of the case studies from the database (Figure 7.20), which typically show a constant or decreasing rate of vertical strain with increasing fill height above the gauge.

Further details on the deformation behaviour from IVM gauges leading up to the failure at Carsington dam are given in Section 3.1 of Appendix G.

At Blowering dam the vertical strain deformation behaviour in the core during construction possibly also shows the development of a shear surface. The deformation behaviour of Blowering dam is discussed in Section 7.10.3.1 and Section 6 of Appendix G.

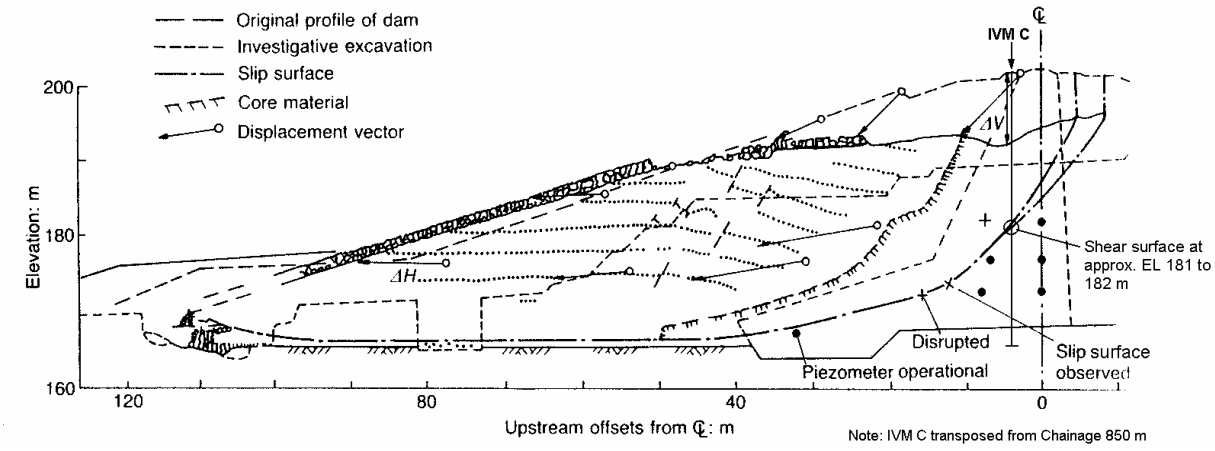

Figure 7.108: Carsington dam, section at chainage 825 m after failure (adapted from Skempton and Vaughan 1993).

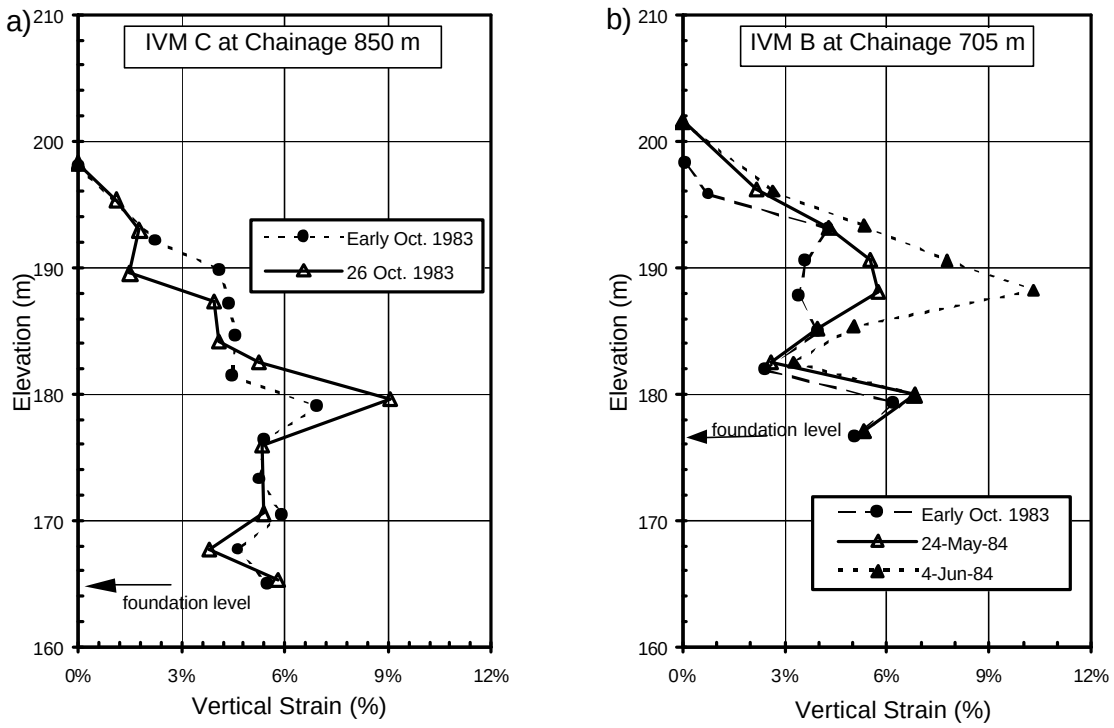

Figure 7.109: Carsington dam, vertical strain profiles from IVM during construction, *(a)* IVM C at chainage 850 m, and *(b)* IVM B at chainage 705 m (adapted from Rowe 1991).

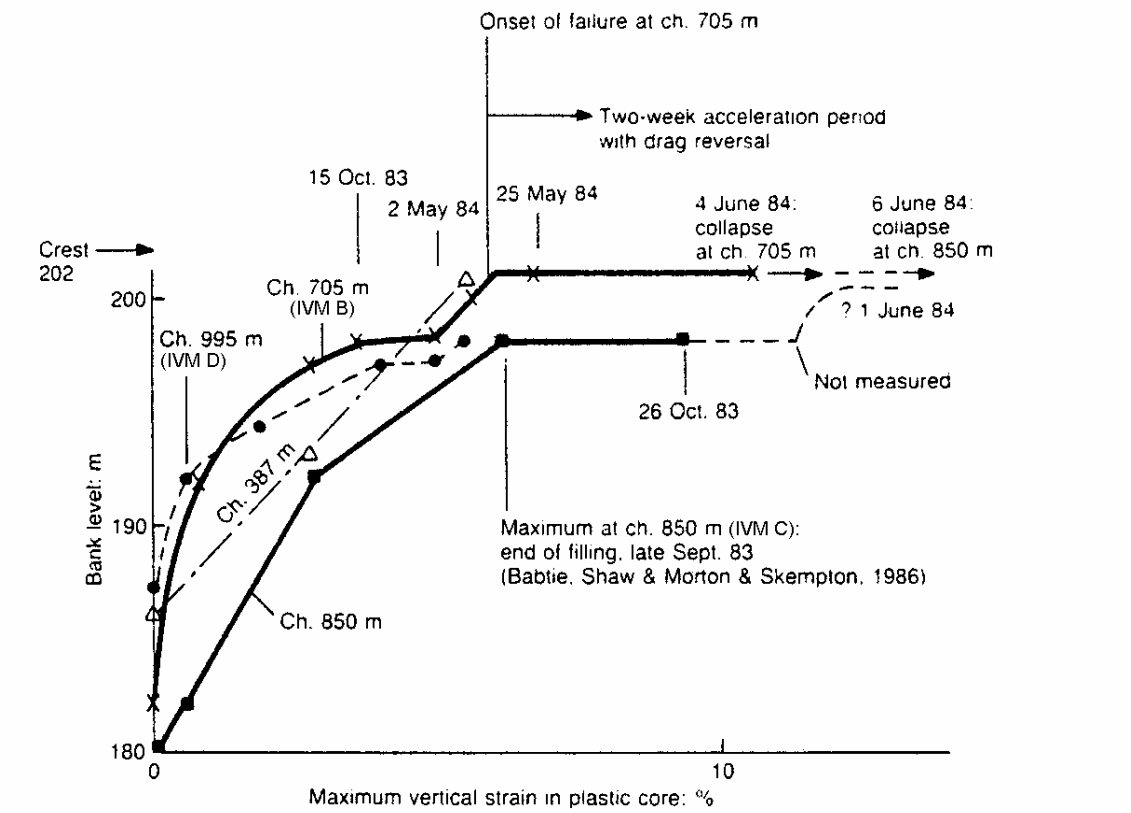

Figure 7.110: Carsington dam, variation of the maximum vertical strain in the core with bank level (Rowe 1991).

7.10 "ABNORMAL" DEFORMATION BEHAVIOUR POST CONSTRUCTION OF ZONED EARTH AND ROCKFILL EMBANKMENTS

In Sections 7.5.3 and 7.6 aspects of the post construction deformation behaviour of a large number of case studies of zoned earth and rockfill dams, mainly central core earth and rockfill dams, were labelled as "abnormal" or possibly "abnormal". Of these, the deformation at several embankments was clearly an outlier to the general trend including Ataturk, Beliche, Svartevann, Eppalock and Djatiluhur dams. At Eppalock and Djatiluhur dams consultants to the owners (Woodward Clyde 1999; Sowers et al 1993) indicated that the upstream slope under a drawn down reservoir condition was approaching a marginal stability condition.

The other case studies where one or more aspects of the deformation behaviour were labelled as possibly "abnormal" included Gepatsch, South Holston, Glenbawn, Srinagarind, Canales, El Infiernillo, Eildon, Upper Yarra, Matahina, Blowering, Wyangala, Bellfield and Cougar dams. Others named for unusual internal deformation behaviour in the core include Copeton and La Grande 2 dams. In total this is approximately 20 of 75 zoned earth and rockfill embankments with thin to thick core widths, most of which are central core earth and rockfill dams. For virtually all but Eppalock dam (which has been remediated with upstream fill to improve stability) and Djatiluhur dam the overall stability of the embankment is not in question. The potentially "abnormal" deformation trends include:

- Accelerations in settlement rate over short periods of time of SMPs on the crest and sometimes the upstream slope, often, but not always, post first filling on drawdown. This is an attribute of quite a number of the case studies, including Eppalock and Djatiluhur dams and therefore potentially indicative of marginal stability conditions (refer also to San Luis and Belle Fourche dams discussed in Section 7.11.2).
- Non-recoverable displacements over short time periods post first filling (usually upstream on drawdown), a change in the direction of the displacement trend, and high rates of displacement long-term. Once again some of these trends are evident in the case studies approaching marginal stability.
- Large magnitudes of settlement or displacement compared to similar types of embankments. The direction of displacement is also a factor.
- High long-term settlement rates.

Of the case studies named, a large number incorporate rockfills that are susceptible to large deformations due to collapse compression on wetting and/or the rockfill is of high compressibility. These include rockfills that are poorly compacted, dry placed and poorly to reasonably compacted, dumped and sluiced rockfills, weathered rockfills, and rockfills of rock type susceptible to large loss in unconfined compressive strength on wetting. The implication is that the rockfills susceptible to large deformations after the end of construction can and do have a significant influence on the post construction deformation behaviour of the overall embankment. Conversely, the data indicates that, in most cases, sound rockfills that are wetted and well and reasonably to well compacted are not susceptible to large collapse compression on first filling and the overall post construction deformation behaviour of the embankment is "normal" and generally of limited magnitude.

7.10.1 ROCKFILL SUSCEPTIBILITY TO COLLAPSE COMPRESSION

Most rockfills in the upstream shoulder undergo some collapse compression on wetting during first filling. In most cases the amount of collapse compression and its effect on the overall deformation behaviour of the embankment is limited to negligible. As previously discussed (Section 7.5.2), the factors affecting the susceptibility of a rockfill to collapse compression include the method of placement (layer thickness, roller type, number of passes), moisture content at placement, effective stress level, particle size distribution, particle shape (angular versus rounded), degree of weathering of the rock, and the rock type itself (its loss in unconfined compressive strength on wetting).

Table 7.25 presents a list of embankments for which collapse compression of the rockfill resulted in moderate to large settlements of the upstream shoulder on first filling. From the data, and other information from the published literature, it is evident that:

- Dry dumped rockfills are susceptible to very large settlements due to collapse compression when wetted. At Cogswell dam the dry dumped rockfill settled up to 6% due to wetting from heavy rainfall and later sluicing (Baumann 1958).
- Dry dumped and poorly sluiced rockfills are also susceptible to large settlements when wetted. Howson (1939) describes the large settlements that occurred at Strawberry and Dix River dams on partial flooding of the dumped and poorly sluiced rockfill. At Dix River dam the settlement amounted to 0.2 to 0.3% of the

height of rockfill, but was more likely closer to 1% in the flooded portion of the rockfill.

- Dry placed and poorly to reasonably compacted rockfills are susceptible to very large settlements due to collapse compression when wetted. Settlements of the upstream shoulder at Eppalock, Eildon and Gepatsch dams, and the downstream shoulder at Svartevann dam were all close to or greater than 1% on first filling. At Eildon and Eppalock dams settlements much greater than the measured 1.23% and 0.90% respectively were likely to have occurred because the monitoring missed about the first half of reservoir filling. Internal vertical strains in the rockfill at Svartevann dam were as much as 1.4 to 2.1% at four years after construction.
- Dumped and sluiced rockfills are susceptible to large settlements due to collapse compression when wetted. At Cherry Valley and Mud Mountain dams measured settlements of the upstream slope were close to 1%. At Watuaga, Nottely and South Holston large settlements of the upstream rockfill also occurred on first filling.
- Some weathered compacted rockfills are susceptible to very large settlements due to collapse compression when wetted, presumably if they are placed with limited quantities of water. At Beliche dam, vertical strains of up to 2.1% were measured on first filling within the "*lightly compacted*" rockfill of weathered schists and greywackes. At Ataturk dam the settlement of the upstream weathered rockfill was potentially very large as indicated by the very large post construction settlement of the crest (4% at almost 7 years after construction).

The use of watering during placement of rockfill reduces the susceptibility of the rockfill to collapse compression as implied in the above summary. Rock type does not appear to stand out as a significant factor, being over-shadowed by placement method and variability in the data. However, the large settlements attributed to collapse compression in the weathered rockfills at Ataturk and Beliche dams tends to indicate that reduction in the rock substance strength due to wetting is a significant influence on susceptibility to collapse compression.

Table 7.25: Embankments for which collapse compression caused moderate to large settlements.

Dam Name	Height (m)	Settlement on First Filling (%) *[1]	Maximum Internal Strain (%) *[2]	Rockfill - Upstream Shoulder			Comment
				Type	Comp[n] Rating *[3]	Water at Placement	
Ataturk	184	very high		weathered basalt & limestone	reas (?)	2 to 6%	suspect very high because of very large settlement of the crest
Beliche	55	1.15	2.1	weathered schists & greywacke	poor	unknown	very high strains in weathered rockfill
Blowering	112	> 0.32 *[4]		quartzite & phyllite	well (3A) reas (3B)	yes	monitoring missed first 50 m of filling
Canales	156	0.64		limestone	unknown	unknown	settlement of upstream edge of crest
Cherry Valley	100	1.05		granite & granodiorite	poor (dumped)	sluiced	
Copeton	113	> 0.5 *[4]		granite	reas to well (3B) poor (3C)	dry	greater because cofferdam was overtopped prior to end of construction
Eildon	79	> 1.23 *[4]		quartzitic sandstone	poor	dry ?	greater because reservoir within 33 m of FSL before monitoring started.
El Infiernillo	148	0.38	0.7	diorite & silicified conglomerate	poor to reas	dry	lower 50 to 75m saturated prior to end of construction.
Eppalock	47	> 0.90 *[4]		basalt	poor	dry	monitoring missed filling of first 20 m.
Gepatsch	153	0.8 to 1.0		gneiss	reas	dry	some influence of the alluvial foundation
Glenbawn (main dam)	76.5	0.83		limestone	poor	dry	large collapse settlement on first filling
Mud Mountain	128	1.05		andesite & tuff	poor (dumped)	sluiced	
Svartevann	129	1.0 (downstream)	1.4 to 2.1 (downstream)	granitic gneiss	reas	dry	settlement in downstream shoulder in first 4 years after construction.
Vatnedalsvatn	121	> 0.37 *[4]		quartz, granite & gneiss	reas	dry	suspect large, missed filling to within 10 m of FSL

Notes: *[1] settlement of upstream shoulder on first filling unless stated

*[2] internal vertical strains measured in the upstream rockfill during first filling unless stated

*[3] Comp[n] Rating = compaction rating of rockfill; "well" = well-compacted, "reas to well" = reasonably to well compacted, "reas" = reasonable compaction, "poor" = poorly compacted. Refer Section 1.3.3 for definitions of the terms.

*[4] ">" indicates settlement likely to be greater than that stated because part of part of the settlement on first filling was not measured.

For well and reasonably to well compacted rockfills collapse compression, in most cases, has a limited to negligible influence on the settlement of the upstream shoulder on first filling, particularly for rockfills sourced from sound rock types and watered during placement. But, for several embankments collapse compression was considered to have had some influence on the settlement of the upstream shoulder on first filling, as indicated by either the relatively large magnitude of settlement (greater than about 0.3% on first filling) and/or a small but significant differential settlement between the up and downstream shoulder (great than about 0.1% difference to upstream). Examples from the database include:

- Several dams with dry placed (and well or reasonably to well compacted) rockfill sourced from sound rock types, including LG-2, Round Butte and possibly Dartmouth and Thomson dams. These embankments are all greater than 130 m in height. Rock types varied from granitic gneiss to basalt to sedimentary sandstones and siltstones.
- Several dams with lesser quality rockfills (including rockfills sourced from weathered rocks or rock types of medium to high unconfined compressive strength, or rockfills with high fines content), including:
  - The 146 m high La Angostura zoned earth and rockfill dam. Much greater settlements were measured for the upstream shoulder on first filling (0.38% compared to 0.10 to 0.18% for the downstream shoulder). The embankment zoning geometry may have partly contributed to the greater settlement, but collapse compression in the well compacted but poor quality (as described by Benassini et al (1976)) limestone rockfill is likely to be the main reason. Benassini et al (1976) indicate the rock used as rockfill was highly contaminated and susceptible to particle breakage on trafficking, and the rockfill as compacted was of high compressibility and low shear resistance.
  - The 90 m high Dalesice dam where much greater settlements were measured for the upstream shoulder than the downstream shoulder (0.39% compared to 0.12 to 0.18%) in the first 15 years after construction. Brousek (1976) indicates that on opening the quarry a considerable proportion of the rock material was of worse quality that originally presupposed, and might have been a factor in the greater settlement of the reasonably to well compacted upstream rockfill shoulder. The rock type and whether or not water was added during placement are not known.
  - The 112 m high Blowering dam where greater settlements on first filling were measured for the upstream than downstream shoulder (0.32% compared to 0.13%). Settlement of the upstream shoulder is likely to have been greater as post construction monitoring did not commence until the reservoir was more than 50% filled. Collapse compression within the reasonably compacted outer Zone 3B and possibly well compacted inner Zone 3A rockfill due to large loss in rock strength on saturation was considered to contribute to the greater settlement of the upstream shoulder, even though large volumes of water were used during placement. The source rock, particularly the phyllite rock used in the Zone 3B

rockfill, was susceptible to large strength loss on wetting, up to 60% of its dry strength.

- At the 35 m high Glenbawn saddle dam (Saddle Dam A) relatively large settlement of both shoulders occurred during first filling, but the settlement of the upstream shoulder was greater (0.40% compared to 0.28%). Possible reasons for the likely collapse compression are not known as only limited details were gathered on the material type and placement methods of the rockfill.

7.10.2 DEFORMATION ON FIRST FILLING IN EMBANKMENTS WHERE COLLAPSE COMPRESSION OCCURS IN THE UPSTREAM ROCKFILL SHOULDER

The influence of collapse compression on wetting of the upstream rockfill shoulder during first filling on the deformation behaviour within zoned earth and rockfill embankments was discussed in Section 7.5.2. Two bounds of behaviour were defined:

(i) Embankments where the core is of high undrained strength and relatively low drained compressibility, such as a partially saturated clayey core of very stiff to hard strength consistency or well compacted sandy to gravelly core. On first filling the upstream rockfill settles relative to the core and the down drag due to differential settlement results in the development of high shear stresses at the upstream core / shoulder interface as described by Squier (1970).

(ii) Embankments with wet placed clayey cores of low undrained strength. On collapse compression in the upstream shoulder the core settles with the upstream shoulder and large differential settlements occur at the downstream core / shoulder interface (Figure 7.35). Deformations within the core are largely plastic.

The actual deformation behaviour is much more complex than the idealised simplified models, but these two bounds of behaviour are observed in a number of the case studies where collapse compression of the upstream rockfill is significant during first filling. Examples from the database are discussed below.

An important aspect of the deformation behaviour on first filling shown in the monitoring records at the well instrumented El Infiernillo dam (refer Section 7.10.2.1 below) and Chicoasen dam (refer Section 1.4 of Appendix G) is the deformation behaviour of the upstream filter zones when collapse compression occurs within the upstream rockfill. For both embankments localised regions of high vertical strain

developed within the upstream filters indicating the formation of shear surfaces. The mechanism for development of the shear surfaces is considered to be due to the high shear stresses that develop within the filter as a result of the differential settlement associated with collapse compression of the upstream rockfill shoulder and shedding of load onto the relatively high modulus filters.

7.10.2.1 Collapse Compression on First Filling and its Influence on the Deformation Behaviour of Wet Placed Clayey Cores.

The following discussion presents a summary of case study evidence of wet placed clayey cores where significant collapse compression occurred within the upstream rockfill shoulder on wetting and the core largely deformed with the upstream shoulder. In several of the cases there is evidence that differential settlements were concentrated at the downstream interface of the core, and at others the internal deformation records indicate large differences in settlement between the core and downstream rockfill shoulder suggesting likely concentration at the downstream interface. The case studies discussed below include El Infiernillo, Djatiluhur, Canales and Beliche dams. A similar mechanism is considered to have occurred at La Angostura and Netzahuacoyotl dams, but data records found in the published literature were limited.

The deformation behaviour at Chicoasen dam, also discussed below, indicates that this behaviour can occur where settlements due to collapse compression of the upstream rockfill are relatively small.

(a) Deformation Behaviour at El Infiernillo Dam During First Filling.

Marsal and Ramirez de Arellano (1967), Squier (1970) and Nobari and Duncan (1972b) discuss the deformation behaviour on first filling at El Infiernillo dam. In the following summary only the vertical deformation behaviour measured from internal deformation gauges and the interaction between various zones in the embankment is discussed. Further details are presented in Section 1.9 of Appendix G.

El Infiernillo dam (Figure 7.111), constructed in the early 1960's, is a central core earth and rockfill dam of 148 m maximum height located in a narrow valley with steep abutment slopes. Well-compacted filter / transition zones are located either side of the wet placed, high plasticity sandy clay core. Rockfill, of quarried diorite and silicified

conglomerate, was placed dry and track rolled by bulldozer; Zone 3A in 0.6 to 1.0 m lifts and Zone 3B in 2.0 to 2.5 m lifts.

The section of the upstream rockfill zone between the embankment and the upstream cofferdam was flooded during construction to reduce the impact of collapse compression on first filling.

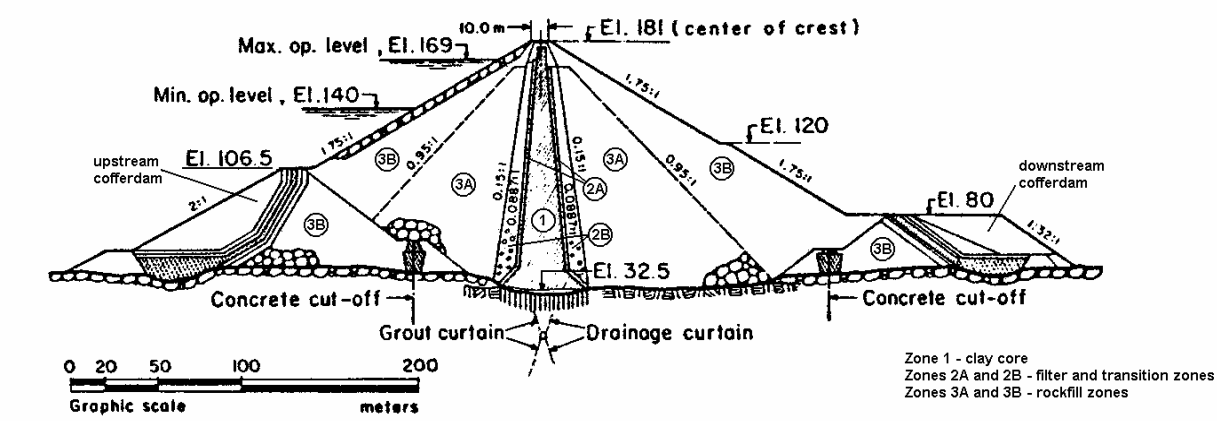

Figure 7.111: Maximum section at El Infiernillo dam (Marsal and Ramirez de Arellano 1967).

The measured internal settlements of the rockfill, filters and core at Station 0+135 at selected time intervals over the period of first filling are presented in Figure 7.113 (instrument locations are shown in Figure 7.112). The plots highlight several important aspects of the deformation behaviour:

- The settlement profiles of the core, upstream filter and upstream rockfill are similar, and are different to that of the downstream rockfill.
- At end of first filling, large and uniform vertical strains were measured in the upstream rockfill between elevation 80 and 125 to 130 m. Similarly, large vertical strains were measured in the core, but at a higher elevation, from 105 to 150 m.
- In the upstream filter (IVM I4) localised zones of high vertical strain were measured at about elevation 102 m and 132 m.
- Low vertical strains were measured below about elevation 80 m in the upstream rockfill. This is likely to be because due to the pre-saturation during construction and therefore this region is not susceptible to collapse settlement post construction.

The settlement of the core and upstream filter / transition on first filling is largely controlled by the collapse compression in the upstream rockfill. Differential settlements

between the upstream rockfill and filters will occur above about elevation 80 m and, as a result of the down-drag effect, high shear stresses are developed on the upstream side of the upstream filter zone. The deformation response within the upstream filter / transition zone to these high shear stresses is the development of shear surfaces, as evidenced by the localised regions of high vertical strain within gauge D1 at elevations 102 m and 132 m.

The vertical strain in the core between elevation 105 and 150 m is almost three times the strain below elevation 105 m (average of 0.66% compared to 0.24% in February 1966). It is considered that the greater vertical strain in the mid region of the core is largely due to plastic type deformations in undrained loading as the core deforms with the upstream shoulder. The strains in the core are not localised as they are in the upstream filter because of the low undrained strength and plastic nature of the wet placed clay core.

The vertical strain profile in the downstream rockfill contrasts that of the core, upstream filter and upstream rockfill. Differential settlements between the core and downstream filter above elevation 105 m are large at more than 200 mm, and indicate a likely concentration at the downstream interface of the core.

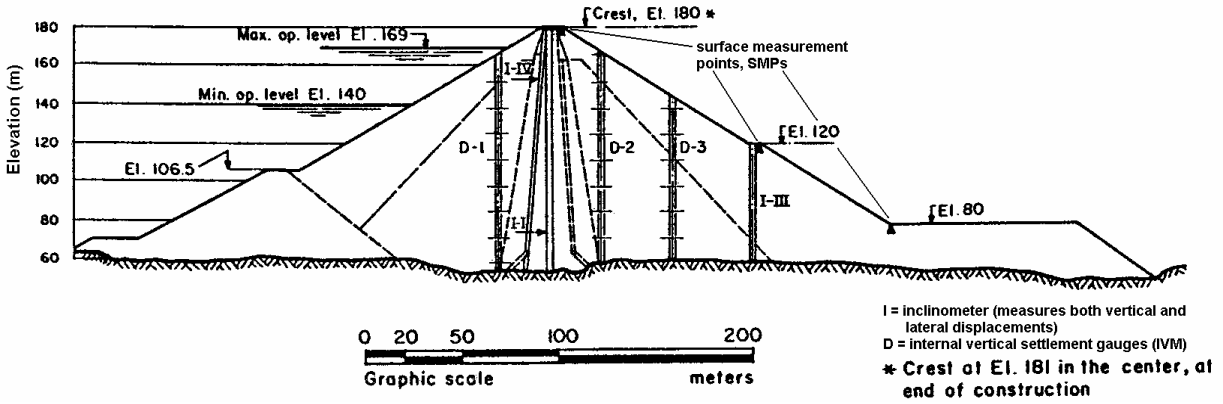

Figure 7.112: El Infiernillo dam, deformation instrumentation on station 0+135 at the lower left abutment (Marsal and Ramirez de Arellano 1967).

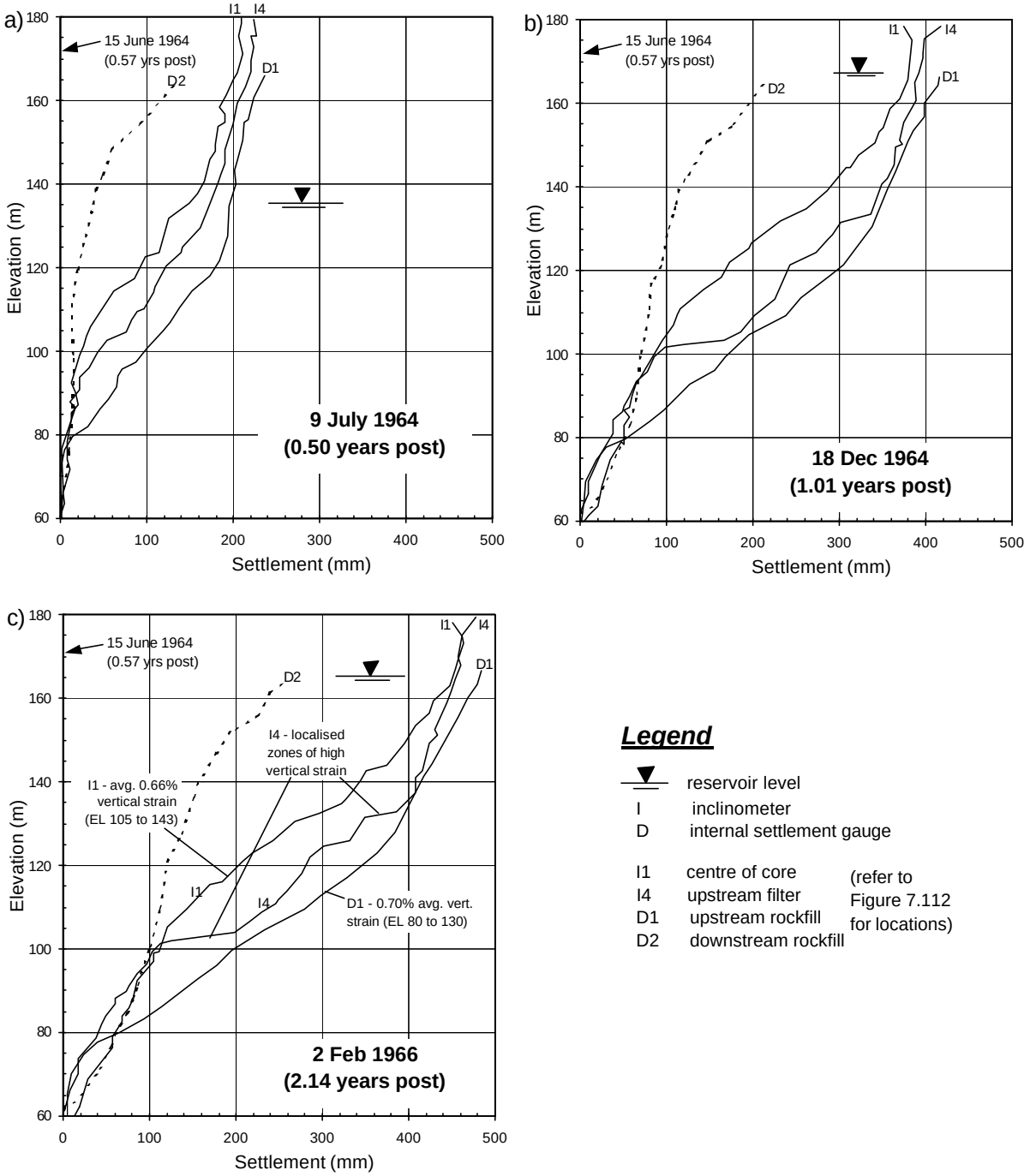

Figure 7.113: El Infiernillo dam, internal settlements during first filling at Station 0+135.

(b) Deformation Behaviour at Chicoasen Dam During First Filling (Section 1.4 of Appendix G).

Chicoasen dam (Figure 7.114), constructed in the late 1970's, is a central core earth and rockfill dam of 261 m maximum height located in a narrow valley with near vertical abutment slopes. The core comprises well-compacted clayey gravels placed at close to Standard optimum moisture content. Filter / transition zones of well-compacted gravels

are located either side of the narrow core and the main rockfill zone (Zone 3A) consists of well-compacted quarried limestone.

The embankment was well instrumented at the main section (Figure 7.115) with numerous inclinometers and cross-arms installed in the core, filters and rockfill zones. Moreno and Alberro (1982) present a selection of the instrumented deformation behaviour on first filling and a summary of the vertical deformation is presented below.

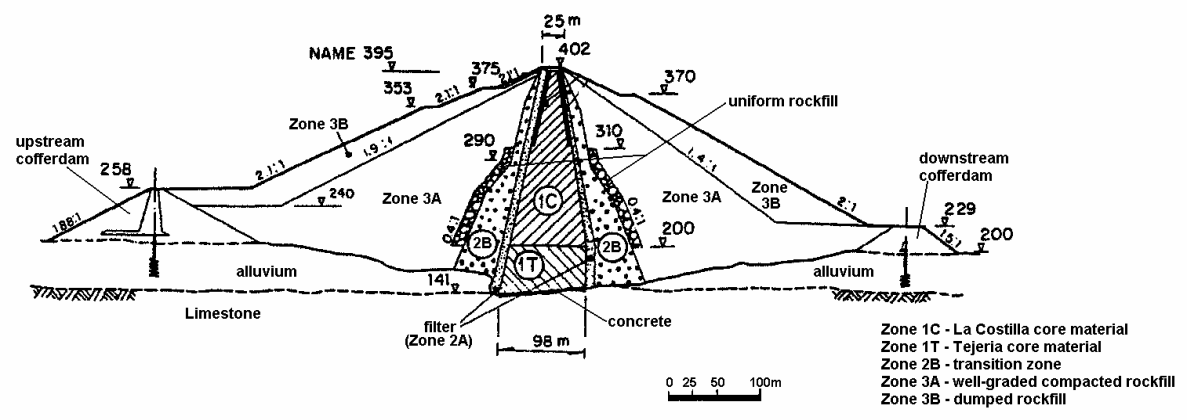

Figure 7.114: Main section at Chicoasen dam (Moreno and Alberro 1982).

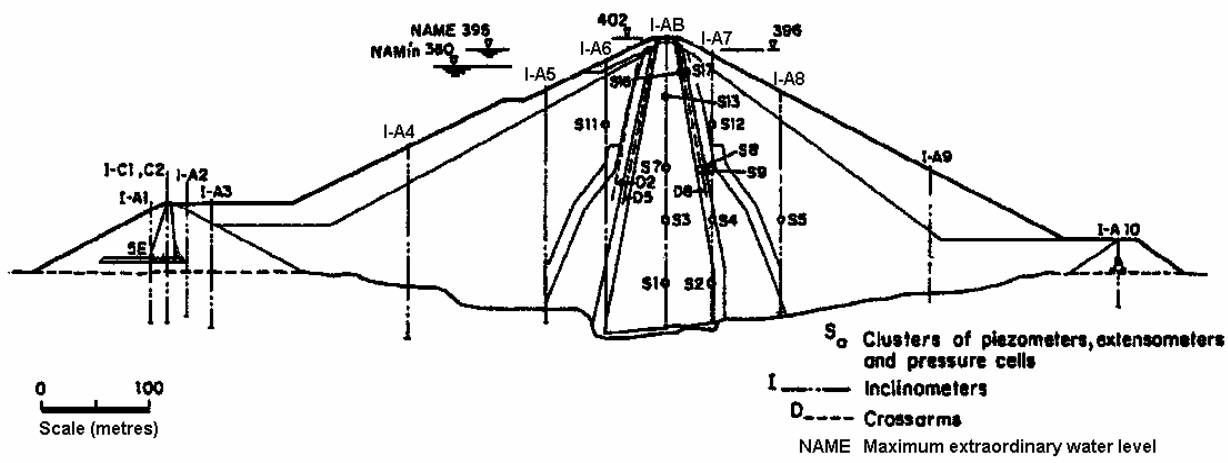

Figure 7.115: Chicoasen dam, inclinometer and cross-arm locations at the main section (Moreno and Alberro 1982).

The internal vertical settlement profiles for the period of first filling are presented Figure 7.116. Note that the dates of the monitoring period are different between gauges, but cover most of the period of first filling from 1 May 1980 to late July 1980. As shown, a region of high vertical strain developed in the upstream rockfill between elevations 260 m and 300 m (strains of 0.4 to 0.5% in IVM I-A5 and I-A6), possibly

due to collapse compression on wetting in the well-compacted limestone rockfill, although Moreno and Alberro (1982) comment that it may be due to plastic type behaviour on reduction in effective horizontal stresses.

Vertical strains in the upstream filter zones are much greater above elevation 270 m and are most likely in response to the higher stresses developed within the filter as a result of differential settlement following collapse compression in the upstream rockfill. In the Zone 2A filter (IVM D5) localised concentrated zones of vertical deformation were evident at elevations 285 m and 317 m, and are likely to be due to shear type deformations. The vertical settlement profile in the core shows that vertical strains are much greater above about elevation 290 m (0.5% to 0.75% compared to 0.3% below elevation 290 m), which is above the base elevation of high strains in the upstream rockfill and upstream filters. The broad zone over which high vertical strains developed in the core suggests it is largely due to plastic type deformations.

The deformation behaviour suggests that the collapse type deformation of the upstream rockfill has a controlling influence on the deformation in the upstream filter / transition zones and core.

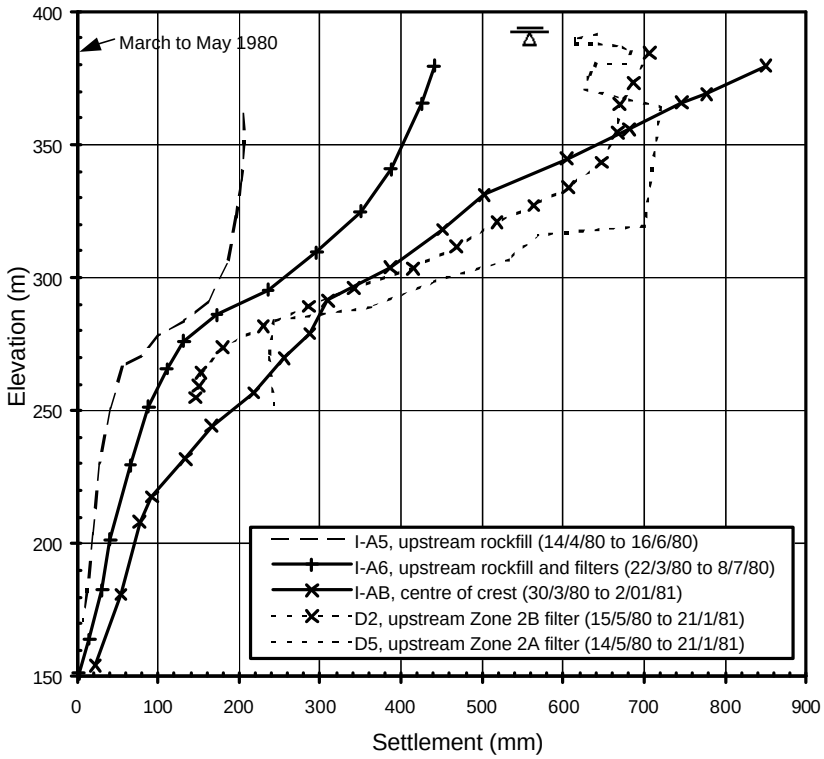

Figure 7.116: Internal settlement profiles during first filling at Chicoasen dam (adapted from Moreno and Alberro 1982).

Moreno and Alberro (1982) comment that no concentration of deformation was measured in the downstream rockfill and it is assumed that the deformations would have been relatively small. Given the high vertical strains in the core it is likely that differential settlements were concentrated between the core and downstream shoulder, but Moreno and Alberro (1982) give no indication that cracking or differential vertical displacements were evident at the crest.

(c) Deformation During First Filling at Beliche Dam (Section 1.3 of Appendix G)

Beliche dam (Figure 7.117), Portugal is a central core earth and rockfill embankment of 55 m maximum height that was completed in 1986. The compacted earthfill core of clayey sandy gravels was placed at moisture contents close to Standard optimum moisture content. Naylor et al (1997) indicate that the inner rockfill zone (Zone 3A) of highly weathered and fractured schists and greywackes was placed in 1.0 m layers, "*relatively lightly compacted*" and comprised a "*significant proportion*" of fines. The outer rockfill zone (Zone 3B) was of "*good quality*" greywackes placed in 1.0 m layers and also "*relatively lightly compacted*". Water is indicated as being added to the rockfill, but in what proportion or to which zones is not clear.

During construction the reservoir level exceeded the height of the upstream cofferdam and saturated the upstream rockfill to elevation 29 m.

The internal vertical settlement profiles of the core and up and downstream rockfill shoulders during the period of first filling after construction are shown in Figure 7.118. Very large vertical strains (average of 2.1%) were measured on first filling above elevation 27 m in the inner upstream rockfill zone of poorly compacted weathered rock, largely due to collapse compression on wetting. Large vertical strains were not measured below about elevation 27 m because the upstream rockfill was saturated to this elevation during construction. The vertical settlement profile in the core is similar to that of the inner upstream rockfill shoulder. Relatively low vertical strains (average 0.7%) were measured below about elevation 29 m and very large vertical strains above elevation 29 m, particularly in the upper 10 to 12 m of the core where they averaged 3.2%. The deformation of the wet placed clayey gravel core is considered to be largely due to undrained plastic type deformation, and to be largely controlled by collapse compression in the upstream rockfill.

Relatively large settlements also occurred in the downstream rockfill shoulder over the monitored period, possibly due to rainfall induced collapse compression.

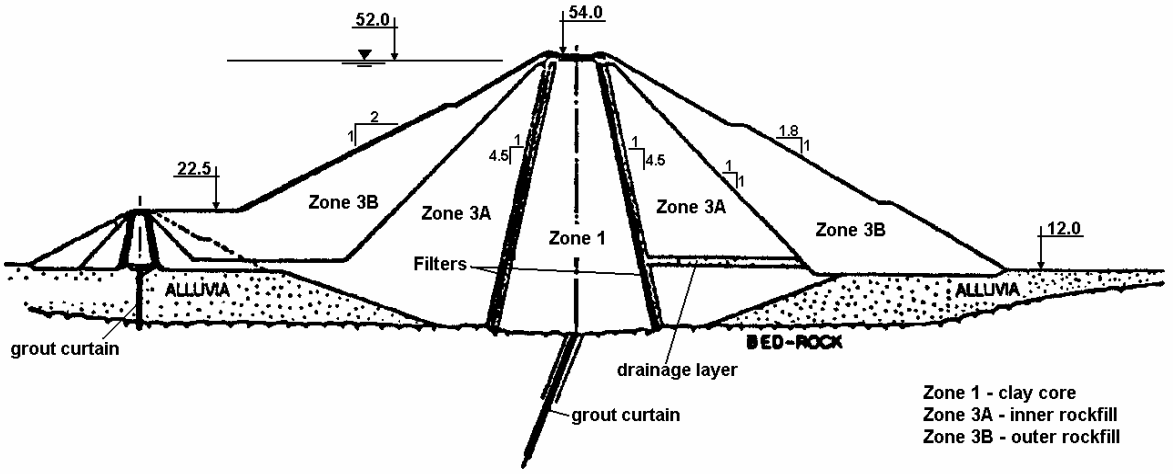

Figure 7.117: Beliche Dam, cross section (Maranha das Neves et al 1994)

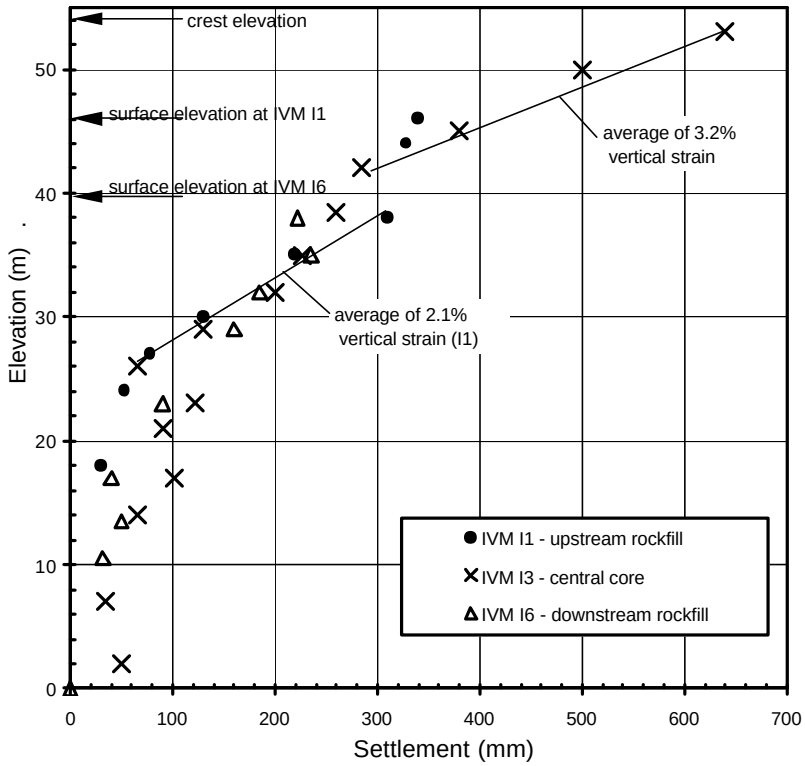

Figure 7.118: Beliche dam, post construction internal vertical settlement profile within the embankment for the period from end of construction to 2.75 years post construction.

(d) Deformation During First Filling at Canales Dam (Section 2.1 of Appendix G)

The deformation behaviour on first filling at Canales dam is a clear example of the development of differential settlement at the downstream interface of the core. Canales dam (Figure 7.119) in southern Spain is a zoned earth and rockfill embankment constructed in a narrow, steep sided valley. The embankment is of 156 m maximum

height and was constructed in two stages; the first stage of 100 m (to elevation 910 m) from 1979 to 1981, and the second stage to crest level from 1985 to 1986.

The thin core (Bravo 1979) consisted of high plasticity silty clays placed at moisture contents on the wet side of Standard optimum (from OMC to 2% wet of OMC). Very broad transition zones of clayey to silty gravelly sand are located either side of the core and the rockfill shoulders are of quarried limestone. Bravo (1979) indicates the embankment materials were compacted to "*the highest possible density*", but it is not known what layer thickness was used or if water was added during placement.

During the period of first filling a substantial longitudinal crack developed in the crest between the core and downstream transition (Figure 7.120a). Giron (1997) indicates that the crack was first observed in 1989 (2 years after end of construction) when the recorded differential settlement of the crest was about 200 mm (Figure 7.120b). On reservoir raising to elevation 930 m at 3.8 years post construction a vertical slump had clearly developed across the downstream core / shoulder interface with a differential settlement of 405 mm. On reservoir raising to full supply level (elevation 958 m) for the first time, the rate of settlement of the mid to upstream portion of the crest increased significantly and differential settlement across the crack increased to about 1000 mm. Giron (1997) and Bravo et al (1994) attribute the crest settlement behaviour to collapse settlement of the upstream shoulder fill on saturation.

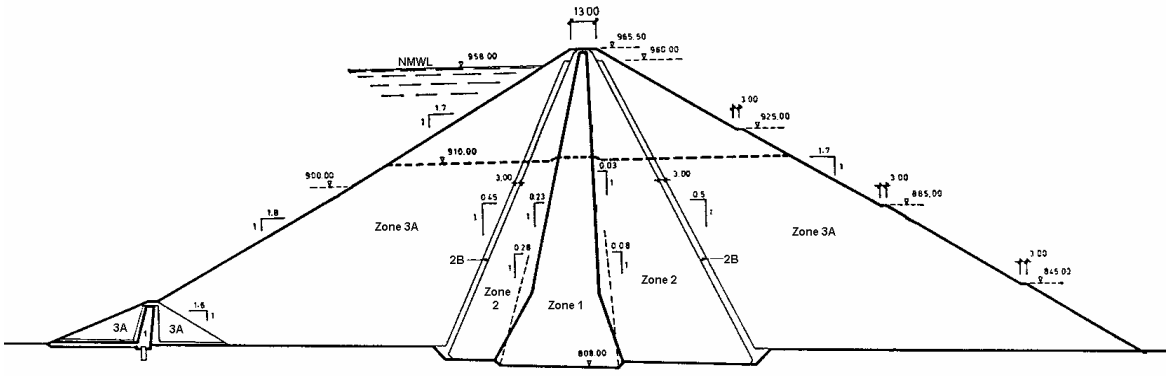

Figure 7.119: Typical section of Canales dam (Bravo 1979).

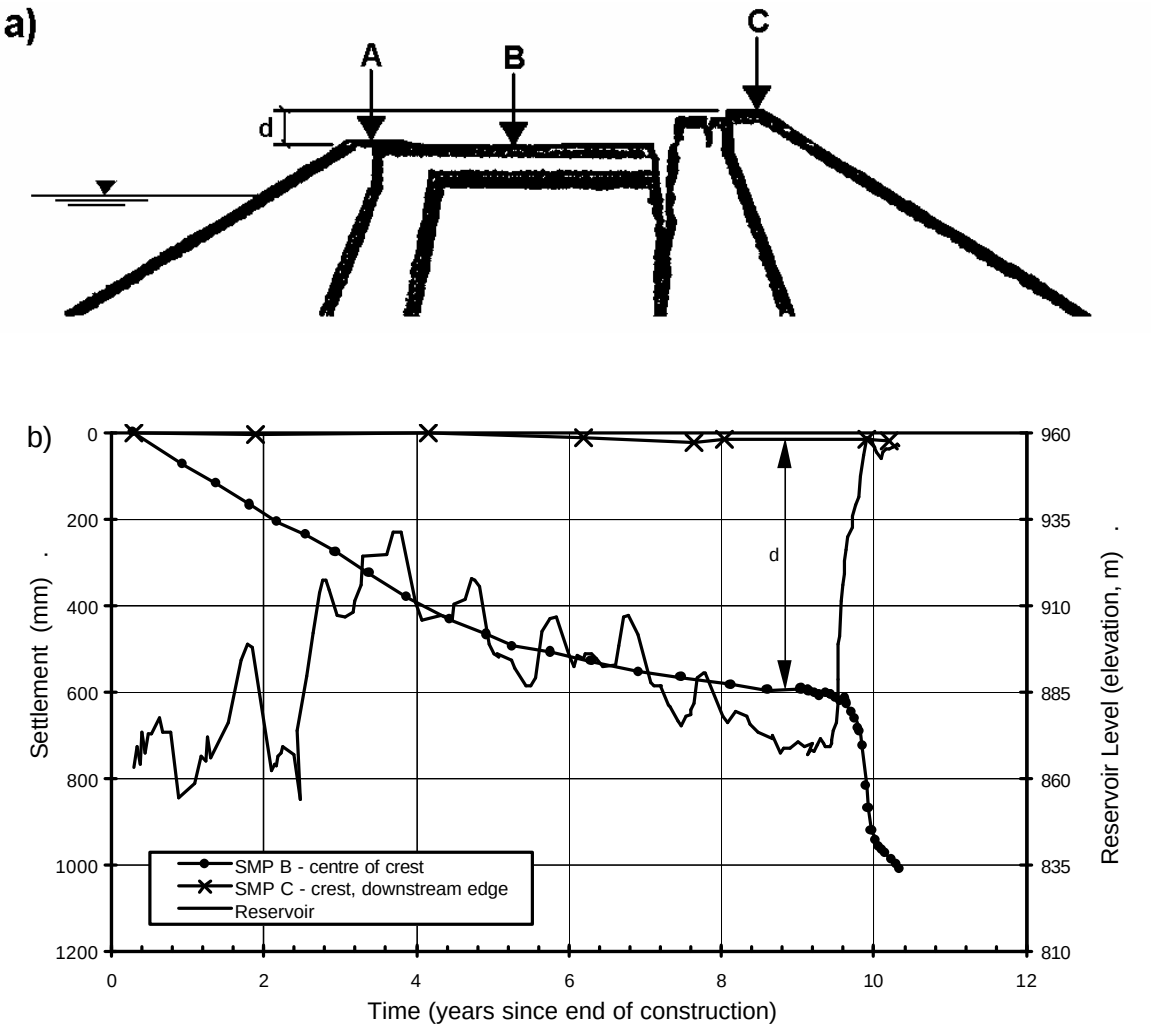

Figure 7.120: Canales dam, *(a)* cracking and differential settlement at the crest, and *(b)* post construction settlement at the crest (Giron 1997)

Several possibilities could explain the observed deformation behaviour:

- The low undrained strength of the wet placed, high plasticity clay core and consequent plastic deformation as the core deforms with the upstream shoulder as it settles due to collapse compression.
- A shear type movement in the core, along a defined plane of shearing with backscarp at the downstream core / transition interface.
- A combination of the above.

The first explanation is considered more feasible than the second mainly because the period of rapid crest settlement (after 9.6 years) occurs when the collapse settlement of the upstream rockfill is localised to the upper 20 to 30 m of the upstream shoulder, and when the reservoir level is close to full supply level where it would provide a high level

of support to the upstream face of the core. For this reason, shear type movements on a pre-existing shear surface in the core seem less likely than plastic deformation of a wet placed high plasticity clay core. However, a combination of both is considered possible.

(e) Deformation at Djatiluhur Dam (Section 1.7 of Appendix G)

Aspects of the deformation behaviour and observations during and after construction at Djatiluhur dam in Indonesia indicate that the core largely deforms with the upstream shoulder and large differential settlements occur at the downstream interface of the core.

Djatiluhur dam (Figure 7.121) is a central core earth and rockfill dam of 105 m maximum height constructed in the early to mid 1960's. The thin core was of high plasticity clays derived from weathered claystone, placed at moisture contents on the wet side of Standard optimum. Investigations after construction indicated the core to be of low undrained strength, particularly above elevation 65 m (Sowers et al 1993). Details on the placement methods of the rockfill, sourced from quarried andesite, are not precisely known but are thought to include both roller compaction and placement without formal compaction in layer thicknesses ranging from 0.5 m up to 2 m (Farhi and Hamon 1967; Sherard 1973; Sowers et al 1993). Farhi and Hamon (1967) comment that most of the rockfill in the mid to lower elevation was well sluiced (300% water by volume), and in the upper section the rockfill was placed in 1 to 2 m lifts, 30% by volume water added and trafficked by trucks and bulldozer.

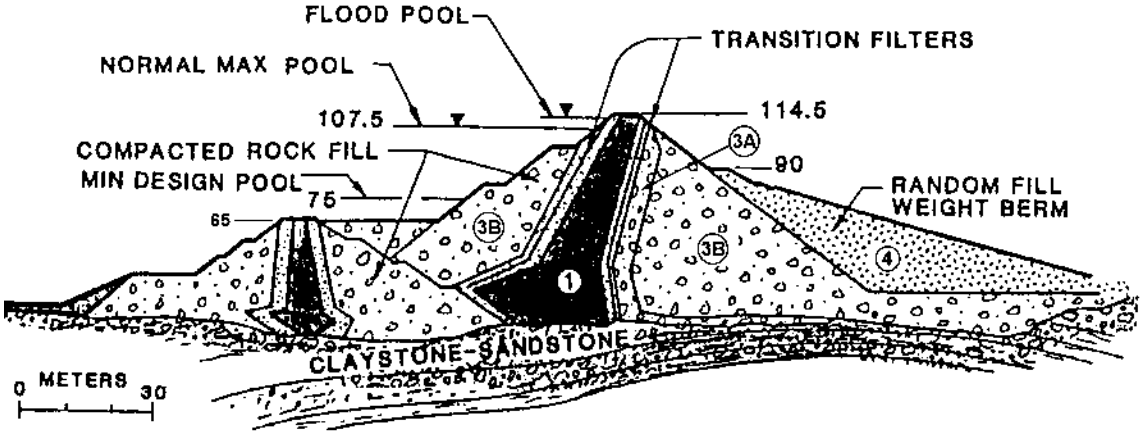

Figure 7.121: Main section at Djatiluhur dam (Sowers et al 1993)

Because first filling largely occurred during the period of construction it is difficult to gauge the magnitude of influence of collapse compression on the settlement of the upstream rockfill. But, important aspects of the deformation behaviour were revealed

from monitoring during a shutdown period in construction and from test pits excavated after construction as described by Sherard (1973).

In early January 1965 construction was halted when the embankment had reached elevation 103 m. As described by Sherard (1973), shortly after construction was stopped a longitudinal crack appeared at the boundary between the core and downstream filter (Figure 7.122a), reaching a total length of some 500 m. Monitoring points were then established at elevation 103 m and the measured deformation records (Figure 7.122b) showed much larger settlements of the core compared to the rockfill shoulders, and limited settlement of the downstream shoulder. Differential displacements indicated lateral spreading of the core amounted to some 400 mm over the period January to July 1965. On raising the embankment to design level in August 1965 the core settlement at elevation 103 m totalled some 800 mm, well in excess of that measured on the downstream slope at a similar elevation, and relatively large settlements were also recorded on the upstream slope at elevation 100 m of about 400 mm over this period.

The very large settlements of the core relative to the shoulders, particularly the downstream shoulder, are considered to be largely due to undrained plastic type deformations from lateral spreading of the core. The large differential settlements between the core and both the upstream and downstream shoulder indicates that arching or stress transfer from the core to the shoulders would have occurred. The low vertical stresses within the core were confirmed by water pressure testing after construction (Sherard 1973), which showed that under relatively low water pressures the horizontal cracks present in the upper region of the core would opened up resulting in high rates of water leakage.

Soon after embankment construction was completed a longitudinal crack (300 m in length and 25 to 40 mm in width) developed on the crest. Several deep test pits were excavated within the core to investigate the cracking, and Sherard (1973) describes the findings. An important observation was that the no cracks were visibly evident in the pit excavated within the upstream portion of the core, yet numerous horizontal cracks were exposed in the pit excavated in the downstream portion of the core. The greater number of horizontal cracks observed in the downstream portion of the core is considered to indicate that differential settlements at the downstream interface of the core were large. This suggests that, whilst lateral spreading is contributing to the greater settlement of the core, the deformation of the core is also controlled to some

extent by the settlement of the upstream shoulder. The upstream orientation of the core would also contribute to the large differential settlement with the downstream shoulder.

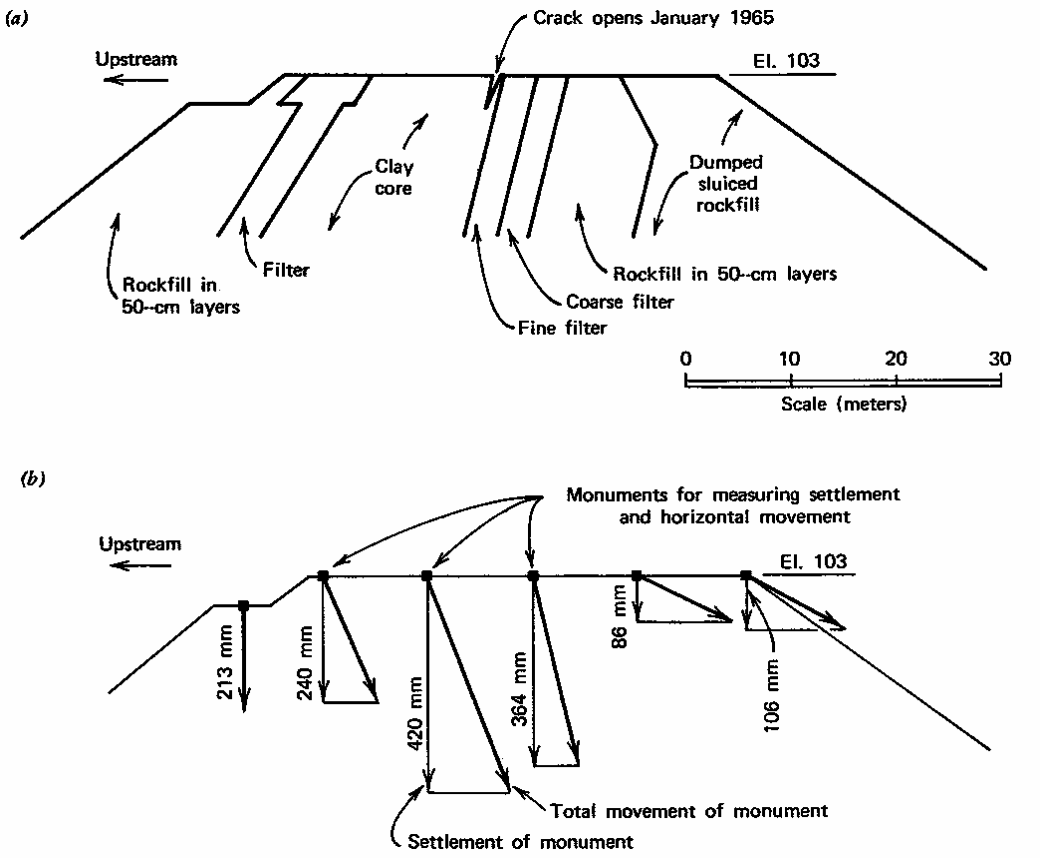

Figure 7.122: Djatiluhur dam; *(a)* location of crack observed during construction, January 1965; and *(b)* deformation of monuments at elevation 103 m, January to April 1965 (Sherard 1973).

7.10.2.2 *Collapse Compression on First Filling and its Influence on the Deformation Behaviour of Cores of High Undrained Strength and Low Compressibility.*

The deformation behaviour during first filling where the settlement of the upstream shoulder (due largely to collapse compression) is much greater than that of the core is observed for a number of case studies within the database. The core types for these embankments include:

- Dry placed and well-compacted clay cores of medium to thick width. Examples include Eppalock and Eildon dams. At Eppalock dam very large settlements of the upstream slope occurred on first filling compared to much smaller settlements of the

crest (Figure 7.123), close to five times smaller when compared on a percentage height basis.

- Embankments with well-compacted silty sand to silty gravel cores. Examples include Cherry Valley, Cougar, Round Butte, Mud Mountain and LG-2 dams, which range in core width from thin to thick.
- Embankments with well-compacted clayey cores of thick width placed at close to Standard optimum moisture content. This would include the series of dams owned by the Tennessee Valley Authority including South Holston, Watuaga and Nottely dams (Leonard and Raine 1958).

For the silty sand to silty gravel cores, the magnitude of crest settlements (as a percentage of dam height) on first filling generally decreased with increasing core width. For the clayey cores, the magnitude of crest settlement was greater for the core placed close to Standard optimum than for cores placed dry of Standard optimum, possibly reflecting the likely lower undrained strength of the wetter placed cores and a larger component of plastic type deformation.

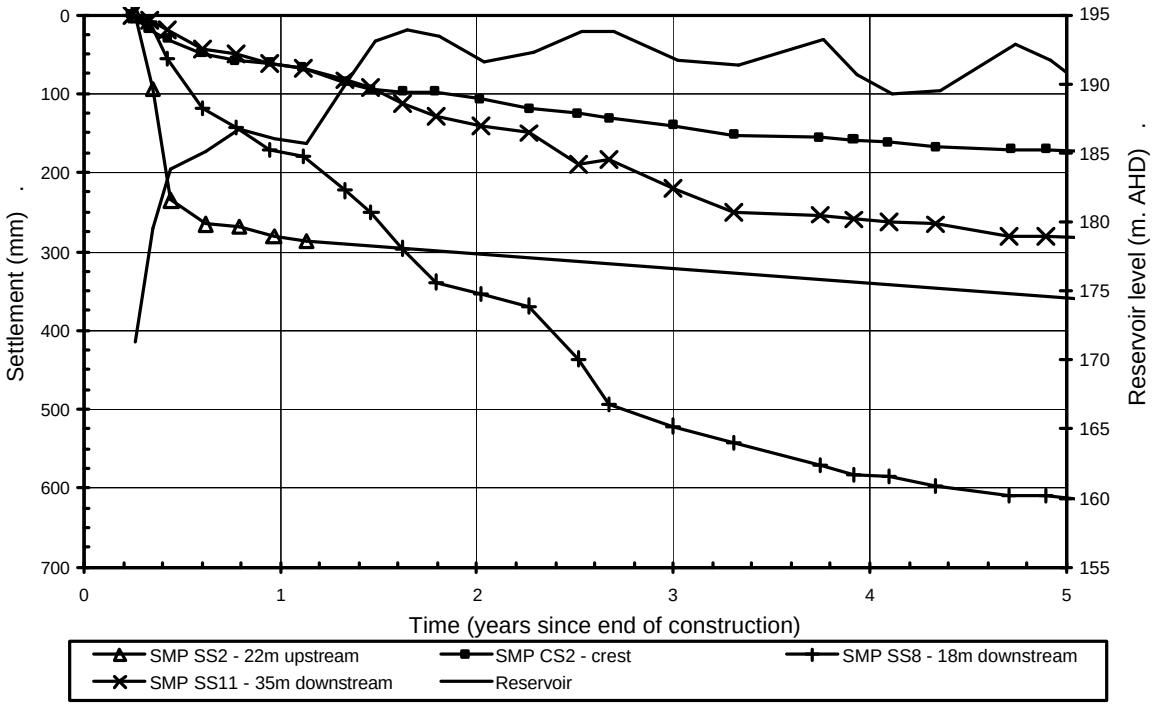

Figure 7.123: Eppalock dam, post construction settlement of SMPs on the crest and slopes for the first five years after construction.

The differential settlement between the upstream shoulder, due to collapse compression on wetting, and the core usually results in the observation of longitudinal cracking on the crest and visibly greater settlement of the upstream edge of the crest. But, this is dependent to some extent on the embankment zoning geometry. In some embankments the surface expression of the differential settlement may be masked within the riprap zone on the upper upstream slope. Examples of the surface expression of differential settlement on first filling are:

- At the 100 m high Cherry Valley dam (Lloyd et al 1958) longitudinal cracking with differential settlement across the crack was observed along the crest at the junction between the core and transition at both the upstream and downstream edges, as idealised in Figure 7.30. On first filling the amount of cracking was greater on the upstream edge of the crest.
- On first filling at the 159 m high Cougar dam (Pope 1967) longitudinal cracks with vertical offset along the crack were located at the upstream and downstream edges of the core. For both crack locations, the vertical settlement on the upstream side of the crack was greater, possibly indicating some localised shear development in the narrow core (refer Section 7.10.5, item b).
- At the 160 m high La Grande No. 2 dam (Paré 1984) longitudinal cracking over a length of 350 m was observed along the upstream edge and centre of the crest. Visibly greater settlements up to 300 mm were evident along the upstream edge of the crest. The differential settlement to upstream across the crack in the centre of the core reached a maximum of 500 mm and Paré (1984) indicates the crack to be associated with a shear surface developed within the core.
- At the 128 m high Mud Mountain dam longitudinal cracking was observed along the crest. Cary (1958) comments that the cracking was associated with the differential settlement between the dumped and sluiced rockfill and the well-compacted core.
- On first filling at the 134 m high Round Butte dam longitudinal crest cracking developed in the centre of the crest above the core to a maximum length of 150 m and width of 15 mm (Patrick 1967). There was also some indication of differential movement between the core and upstream transition due to differential settlement and lateral spreading.
- At the 97 m high Watuaga dam longitudinal cracking was observed on the edge of the crest coincident with the upstream and downstream edges of the core due to the

greater settlement of the rockfill than the core, approximately 150 to 200 mm greater (Leonard and Raine 1958).

- At the 56 m high Nottely dam Leonard and Raine (1958) describe the longitudinal cracking on the upstream side of the crest coincident with the upstream edge of the core as severe. The vertical difference in settlement at the crest was greater than 250 mm.

Much of the observed longitudinal crest cracking on first filling occurs along the upstream edge of the crest, or along both edges indicating both the upstream and downstream shoulders settle relative to the core. In several cases, particularly at LG-2, the crack development was indicative of shear type deformation in the core. This is discussed further in Section 7.10.3.

7.10.3 DEVELOPMENT OF SHEAR SURFACES WITHIN THE EARTHFILL CORE

Included in the database are a number of zoned earth and rockfill embankments for which shear surfaces (at least one, possibly multiple) are known to or thought to have developed in the earthfill core. The timing of the initial shear surface development can be during construction (refer Section 7.9.4), on first filling (e.g. LG-2 dam) or post first filling. Case studies where shear deformation was evident or considered to have most likely occurred are discussed in the following sub-sections. The summary is generally brief and further details are given in Appendix G for most case studies.

For a number of these embankments, it is "abnormal" trends in the deformation behaviour post first filling for which the a case study has often been identified as clearly "abnormal" or potentially "abnormal" compared to other case studies, and in a number of cases has involved shear type deformations in the core. These trends are summarised in the case study discussions.

7.10.3.1 Shear Surface Development in the Core on First Filling

The deformation behaviour on first filling at LG-2, Ataturk and Copeton dams is considered to be indicative of shear type development in the core of the embankment during first filling. At Blowering dam a shear surface is thought to have initially

developed in the core during the latter stages of construction, with further movements along the shear surface on first filling.

(a) Blowering dam (Section 6 of Appendix G)

A detailed analysis of the deformation behaviour at Blowering dam, including finite difference analysis of the embankment construction, is presented in Section 6 of Appendix G. A summary of the findings is presented here.

Blowering dam (Figure 7.124) is a 112 m high central core earth and rockfill embankment that was constructed in the mid to late 1960's. The medium width core was of well-compacted medium plasticity clayey sands to sandy clays placed at moisture contents ranging from slightly dry to slightly wet of Standard optimum (see below). Either side of the core the filter / transition zones were of well-compacted gravels. The rockfill comprised slightly weathered to fresh quarried phyllite, meta-siltstone and quartzite. Placement of the weaker phyllites was limited to the outer Zone 3B. The rock types were susceptible to large loss in unconfined compressive strength when wetted (35 to 62% reduction) and as a consequence high volumes of water were used during placement to offset as far as practicable collapse type settlements post construction. The Zone 3A rockfill was placed in 0.9 layers and the Zone 3B in 1.8 m layers, and compacted by 4 passes of an 8.1 tonne smooth drum vibratory roller.

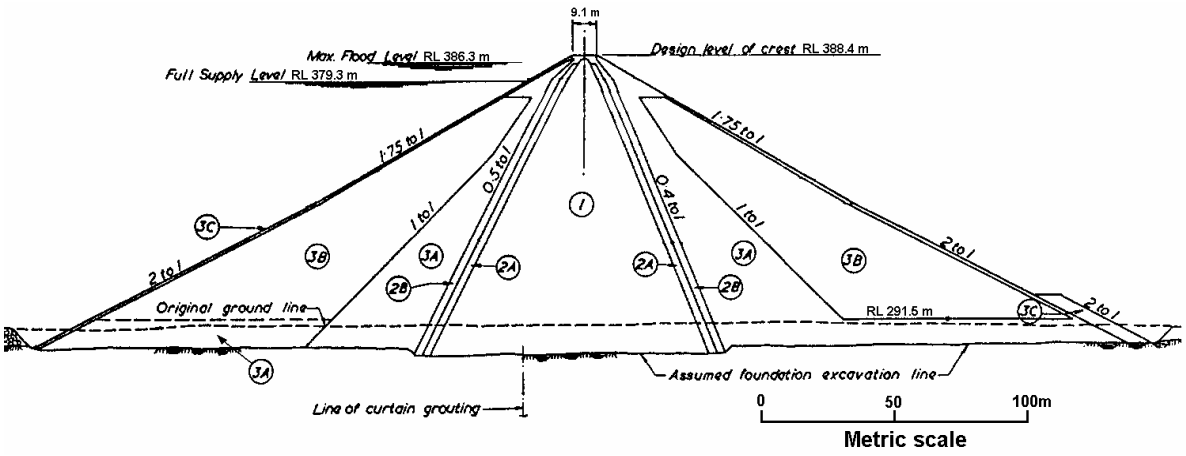

Figure 7.124: Main section at Blowering dam (courtesy of NSW Department of Public Works and Services, Dams and Civil Section).

The moisture content specification for the core was adjusted at various stages during construction as follows:

- Initially the specification was for placement in the range 1.3% dry to 0.7% wet of Standard optimum moisture content (OMC), and averaged 0.3% dry.
- When the embankment height was about 33 to 37 m the specification was adjusted to 0.7% dry to 1.3% wet of OMC, and averaged 0.3% wet.
- When at about 67 to 74 m the specification was adjusted to 1.0% dry to 1.0% wet of OMC, and averaged 0.1% wet.

During the latter stages of construction very high vertical strains were measured within the core at 60 to 71 m depth below crest level (between cross-arms 13 and 14 in IVM A) as shown in Figure 7.125. During construction of the last 17.5 m to crest level the vertical strain at this depth range increased from 4.3% to 11.9%, which was far in excess of the magnitude of strain at other cross-arm intervals in the wet placed region of the core. In addition, the stress-strain trend for this cross-arm interval is "abnormal" when compared to that observed in other embankments (Figure 7.20). Development of a shear surface within the core was considered a possible explanation for the deformation behaviour.

In the early stages of first filling shortly after the end of construction very high vertical strains were concentrated between cross-arms 13 and 15 (Figure 7.126). A constriction or kink in the inclinometer tube developed below cross-arm 14 shortly after construction and several months after the start of first filling, when the reservoir level was still 30 to 35 m below full supply level, the measuring torpedo became blocked between cross-arms 13 and 14. The deformation behaviour was considered to indicate further movement on the shear surface in the core. Collapse compression of the upstream rockfill on first filling was thought to trigger the addition deformation, either due to development of high shear stresses at the upstream interface between the filters and rockfill as a result of differential settlement, or due to reduction in the lateral stresses acting on the upstream face of the core.

In 1982/83 (14 to 15 years after construction) the reservoir was subjected to a large drawdown of 57 m to an elevation more than 70 m below full supply level. This was the largest drawdown in the dam's history. On drawdown, acceleration in the rate of settlement of SMPs on the upstream shoulder and crest was measured, with a crest settlement for the period of about 60 to 80 mm. The internal vertical settlement of the core either side of the drawdown (only the upper 17 cross-arm intervals could be measured due to the earlier constriction) indicated that the upper 55 m of the

embankment virtually settled as a block (i.e. only 3 mm cumulative settlement in the upper 55 m), indicating most of the settlement on drawdown occurred in the lower 50 to 55 m of the core. It is possible that most of this settlement represents shear type deformation on the existing shear surface reactivated on large drawdown. The trigger for the movement was possibly the reduction in lateral stress acting on the upstream face of the core on drawdown.

Further acceleration in the rate of settlement of SMPs on the upstream slope occurred during the next large drawdown of 53 m in 1997/98 (29 to 30 years after construction).

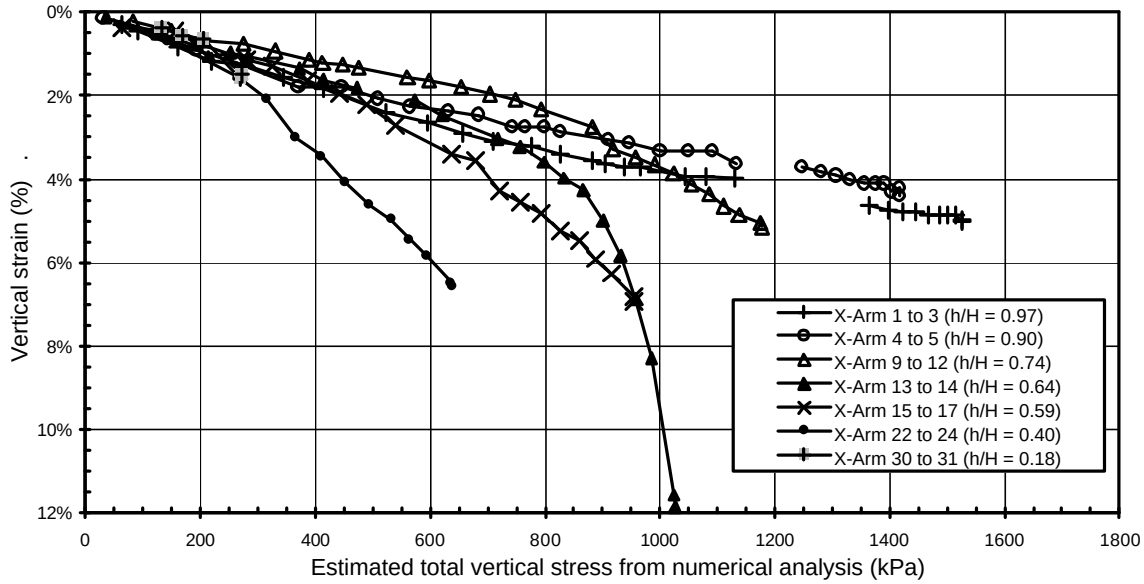

Figure 7.125: Blowering dam, vertical strain during construction for selected cross-arms intervals in the core.

(b) Ataturk dam (Section 1.1 of Appendix G)

Ataturk dam, Turkey (Figure 7.127) is a 184 m high central core earth and rockfill dam constructed in the late 1980's. The medium width central core is of high plasticity, reasonably to well compacted clays to sandy clays placed at moisture contents on average 1.5% dry of Standard optimum. Rockfill was placed in 0.6 m to 1.5 m layers and compacted by vibratory rollers (Cetin 2002), but no specific details are available for each zone. Moisture contents at placement were in the range 2 to 6%. The inner upstream rockfill consisted of weathered, vesicular basalt and outer upstream rockfill of sound basalt. The downstream shoulder consisted of sound basalt and an encapsulated zone of pliacated limestone having a sand to clay sized fraction of 50%. Poor quality

materials were therefore used for the inner rockfill zones up and downstream of the core.

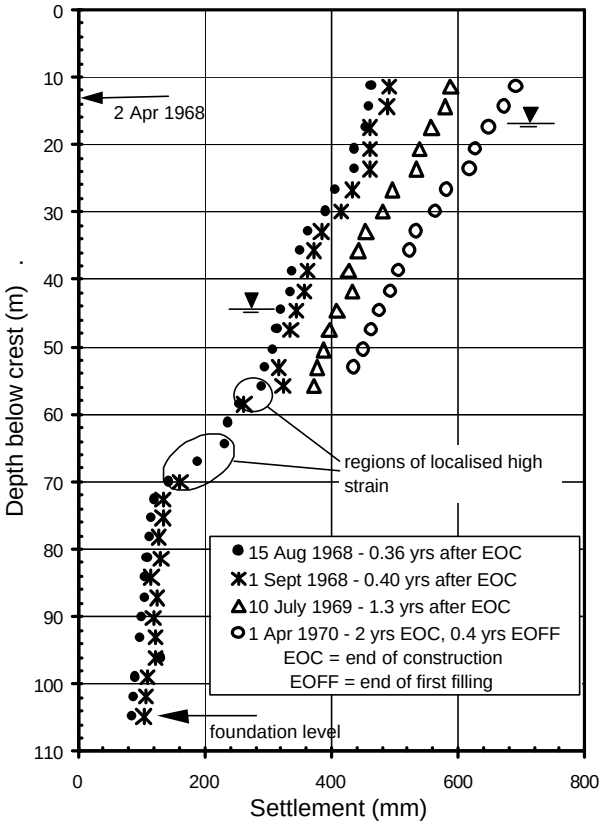

Figure 7.126: Blowering dam, post construction internal settlement of the core from IVM A during first filling.

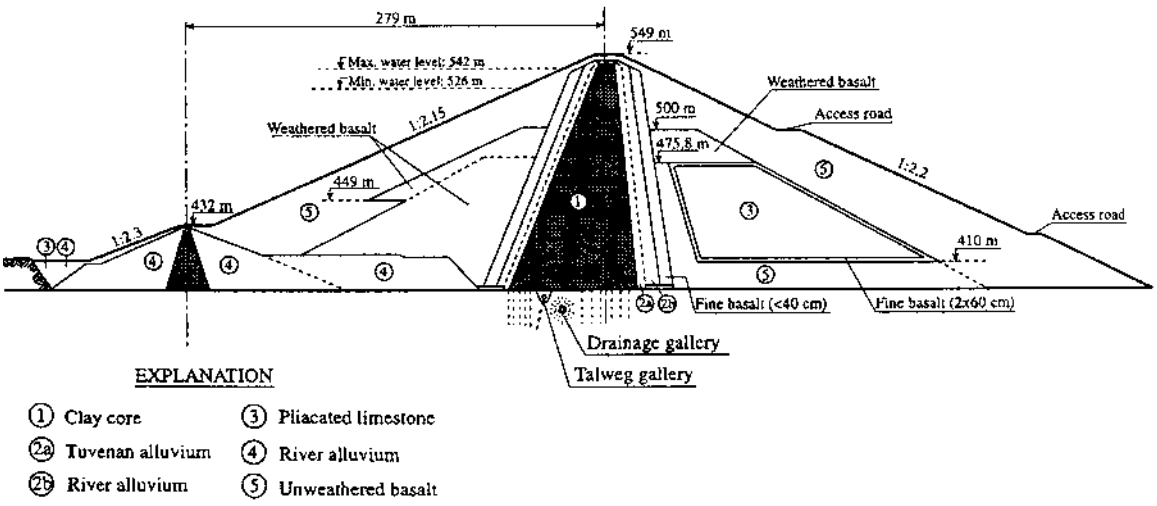

Figure 7.127: Cross section of Ataturk dam (Cetin et al 2000)

The post construction crest settlement at Ataturk dam was of very large magnitude. More than 7 metres settlement was measured in less than 7 years (close to 4% of the dam height) and clearly stands out as "abnormal" in comparison to similar type embankments (Figure 7.46a and Figure 7.53a).

Cetin et al (2000) indicate that large settlements occurred in June to December 1990 and again in early 1992 (1.5 to 2 years post construction) during periods of relatively rapid rise in reservoir level to new high levels. In the early stages of reservoir filling in June 1990, several months before the end of construction, a number of internal monitoring gauges in the lower elevations were lost. Cetin et al (2000) also refers to "*landslides*" occurring in the upstream slope in May 1992. It is possible that they are referring to the surface expression of differential settlement between the upstream shoulder and core. During reconstruction of the upper 6 to 7 m of the crest in 1997 slickensided surfaces were observed in the core at close to the interface between the core and downstream filters.

Cetin et al (2000) considered slaking of the vesicular basalt in the upstream shoulder and poor placement of the core to be significant factors in the very large settlement of the crest post construction. Degradation of the basalt has since been discounted as a possible cause of the large deformation (Riemer 2001).

It is difficult to surmise the potential cause/s and mechanics controlling the deformation behaviour of the embankment given the limited information available. Notwithstanding this, it is suspected that collapse compression of the upstream rockfill on wetting is likely to be a significant factor. On first filling it is suspected that very large settlements occurred in the upstream shoulder due to collapse compression on wetting, the weathered basalt rockfill possibly being particularly susceptible. The observations of differential settlement between the upstream shoulder and core, and the very large magnitude of settlement of the crest tend to confirm this.

The most likely explanation for the very large settlement of the crest, large differential settlement between the crest and downstream shoulder (Figure 7.128), and observation of slickensided surfaces in the core at close to its downstream interface is considered to be the development of a shear surface and shear deformations in the core toward upstream. The available information would suggest that a shear surface (or surfaces) formed within the core during a rising reservoir condition in the early stages of first filling and prior to the end of construction, and that further shear type deformations occurred during the early part of 1992 on a rising reservoir. It is possible that localised

instability developed in the core due to high shear stresses at the upstream interface as a result of the collapse compression of the upstream rockfill on wetting.

How extensive the surface of rupture might be is not known, but the loss of internal instruments in the lower elevations of the embankment may be related to shear displacements, indicating the shear surface (or surfaces) is at depth.

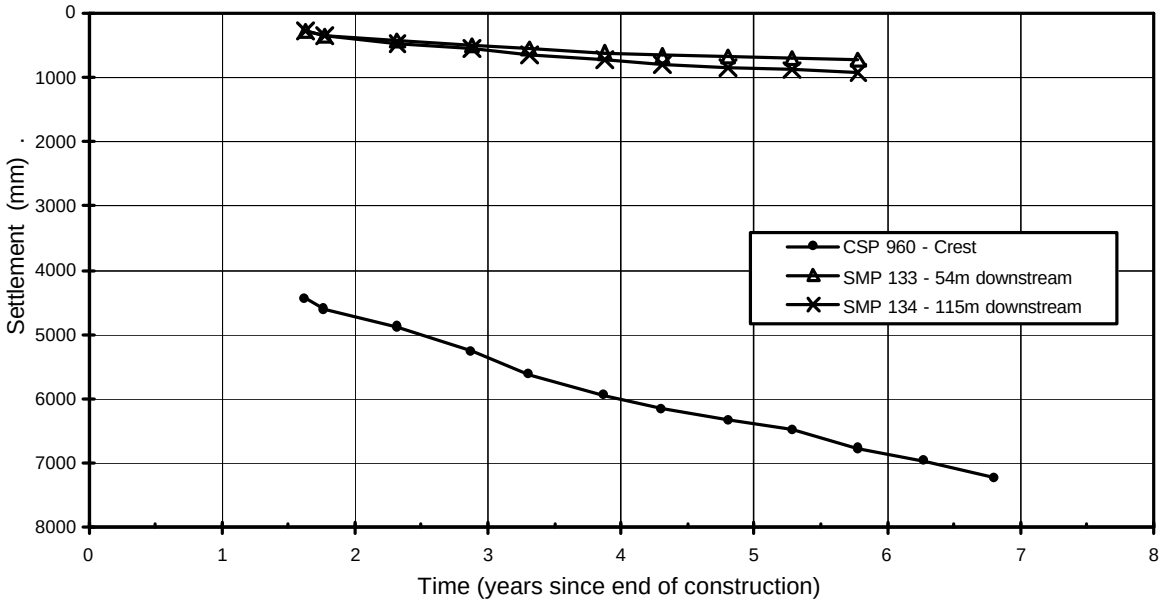

Figure 7.128: Post construction settlement of the crest and downstream shoulder at Ataturk dam.

(c) La Grande No. 2 dam (Section 1.12 of Appendix G)

The LG-2 dam in Quebec is a 160 m high central core earth and rockfill dam, with the core slightly inclined to upstream, that was completed in October 1978. The thin core is of well-compacted non-plastic gravelly silty sand moraine deposits and supported by moderately wide and well-compacted filter / transition zones of gravelly sands to sandy gravels. The rockfill shoulders are of quarried granitic gneiss dry placed in 0.9 to 1.8 m thick layers and compacted with 4 passes of a 9 tonne smooth drum vibratory roller.

The reservoir was filled to close to maximum water level over the period October 1978 to December 1979 (0.1 to 1.2 years after construction). Since first filling the reservoir operation is not known.

Extensive cracking of the crest, described by Paré (1984), occurred during the latter stages of first filling. One of the longitudinal cracks was located close to the centreline of the crest, across which differential settlement to upstream was about 500 mm after first filling (Figure 7.129). Investigation undertaken after first filling found that this

crack was near vertical and in the order of 150 to 200 mm wide decreasing to 50 mm wide at 3.5 m depth. Paré (1984) also refers to a "*sharp tilt*" that developed in September 1980 within an inclinometer located in the upstream portion of the core (Figure 7.129), which became blocked at about 18 m depth in November 1980. The timing of these observations is 1.9 to 2.2 years after end of construction, almost 1 year after completion of first filling.

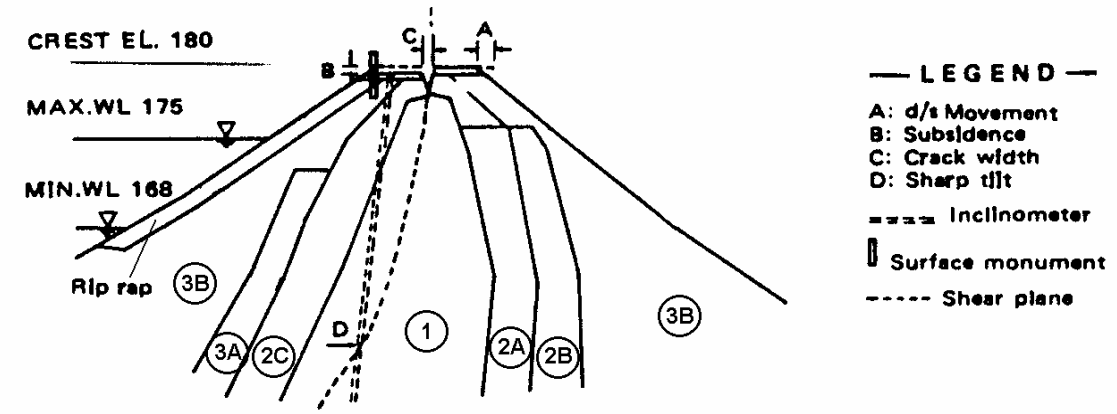

Figure 7.129: LG-2 dam; crack in crest and possible shear plane in core (Paré 1984)

Paré (1984) considered the localised straining in the inclinometer as development of a shear plane in the core. He attributes the longitudinal cracking and shear formation to a combination of the large downstream displacement of the core on first filling and collapse settlement of the upstream rockfill on wetting.

An interesting aspect of the deformation behaviour is the timing of the "*sharp tilt*" and blockage in the inclinometer. Paré (1984) indicates that this occurred almost 1 year after completion of first filling. But, the shear surface in the core developed during the latter stages of first filling as indicated by the timing of the crack and the large settlement (close to 600 mm) of the upstream edge of the crest on first filling. It would have been expected that some indication of the shear formation would have been identified in the deformation of the inclinometer during first filling, however, there is no indication from Paré (1984) that any tilt was recorded during first filling. Maybe the inclinometer was not installed until after first filling when a potential slip surface was identified.

The likely mechanism of the initial shear formation in the core is considered to be a result of high shear stresses on the upstream interface of the core that developed due to the differential settlement between the core and the upstream rockfill shoulder. The

observation of further shear deformation from September to November 1980 is possibly drawdown related and due to the reduction in lateral support on the upstream face of the core as the reservoir level was lowered. This reduction in lateral support possibly led to a locally unstable condition of the already sheared upstream wedge of core, which then deformed to upstream until adequate lateral support was provided by the upstream shoulder.

(d) Copeton dam (Section 1.5 of Appendix G)

The 113 m high Copeton dam in New South Wales, Australia (Figure 7.130) is a central core earth and rockfill dam that was constructed in the early 1970's. The medium width core is of well-compacted clayey sands of medium plasticity placed at moisture contents in the specified range of 1% dry to 1% wet of Standard optimum. The low pore water pressures that were developed during construction suggest the core was placed on the dry side of Standard optimum. The rockfill shoulders are of quarried granite placed in 1.2 m (Zone 3B) to 3.7 m (Zone 3C) thick layers and compacted with 4 passes of a 9 tonne smooth drum vibratory roller. No water was added during construction.

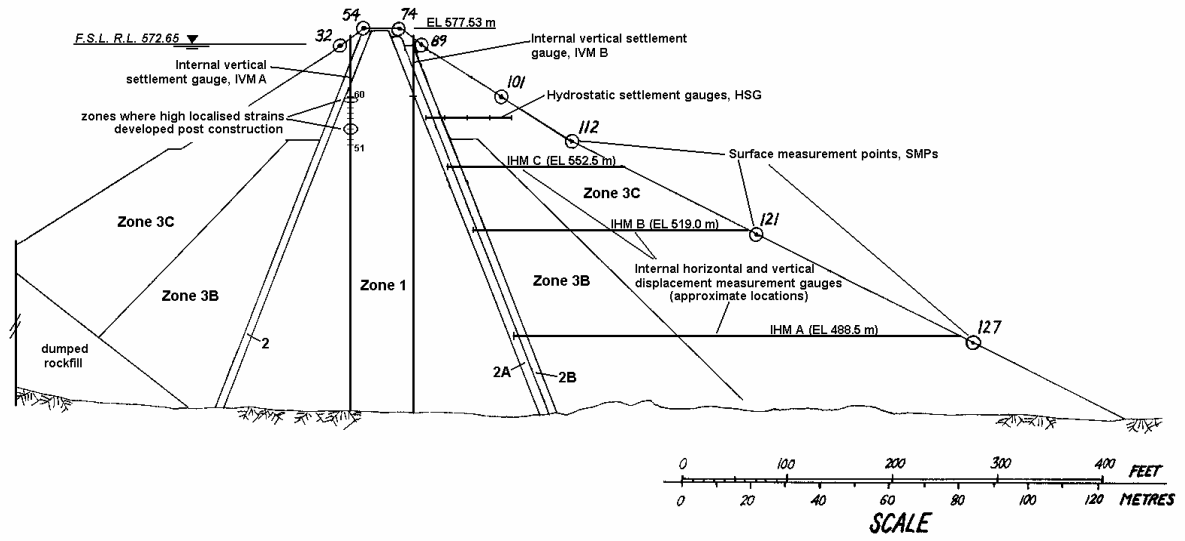

Figure 7.130: Main section at Copeton dam (courtesy of New South Wales Department of Land and Water Conservation)

The post construction deformation behaviour of the SMPs on the crest and slopes of the embankment was "normal" in comparison to similar type embankments. However, the internal core settlement within the internal settlement gauges located slightly upstream of dam axis (IVM A and IVM C) indicated the development of a possible shear zone in

the core at close to its upstream interface. The internal deformation of the core during construction in these IVMs was considered "normal" indicating the shear surface did not develop until first filling.

Figure 7.131 shows the development of localised zones of high strain in IVM A, located upstream of the dam axis, at depths of 20 to 30 m below crest level. Similar localised zones of high strain were measured in IVM C at 20 m depth below crest level. In both IVMs the highest region of strain is between the two top cross-arms and close to the upstream interface of the core with the upstream filter as shown in Figure 7.130. The regions of high shear strain are at elevations where the Zone 3C rockfill (dry placed in 3.7 m lifts) is located immediately upstream of the Zone 2 filter. By March 1999 post construction vertical strains between the upper cross-arms was 6.3% in IVM A (cross-arms 59 to 60) and 8.5% in IVM C (cross-arms 43 to 44), or 95 and 129 mm respectively. In contrast the settlement profile at IVM B, located downstream of the dam axis, shows no localised region of high strain.

The settlement versus time plot of the upper cross-arms intervals in IVMs A and C (Figure 7.132) shows that increases in settlement between the cross-arms occur at similar time periods; during first filling, sometime between 9 and 13 years, and sometime between 20 and 26 years. The localised settlement in the latter periods possibly occurs during rising reservoir level. This is confirmed from the settlement records of SMPs on the upstream edge of the crest which show a small but perceptible increase in the rate of settlement between 10.35 to 11.2 years post construction coincident with the rise in reservoir level to full supply level.

The possible cause and mechanism associated with the development of the localised regions of high strain can only be surmised from the data. It is reasonable to conclude that localised straining between the upper cross-arms in IVMs A and C is concentrated during periods of rising reservoir level, most likely when raised above the elevation of these regions of high strain at 545 to 560 m. A likely explanation is that a shear zone developed within the upstream region of the core on first filling due to high stresses at the upstream core / filter / rockfill interface developed from differential settlement associated with collapse compression on wetting of the Zone 3C dry placed and poorly compacted rockfill. It is notable that the regions of localised high strain in the core are located 5 to 15 m above the elevation where the Zone 3C rockfill was placed immediately upstream of the upstream filter.

The subsequent shear displacements during rising reservoir at about 10.5 to 11 years, and then again at 22 or 25 years, are most likely due to further differential settlement at the upstream interface as indicated by the SMP and IVM data records. A possible explanation for the differential settlement post first filling is softening or degradation of the upstream rockfill over time.

The presence of transverse and longitudinal cracking in the bitumen seal on the crest (first observed in June 1977, 4 years after construction), and the "*visually evident*" greater settlement of the upstream side of crest noted in surveillance reports (Land and Water Conservation NSW 1995a) give further support to the mechanism of shear development.

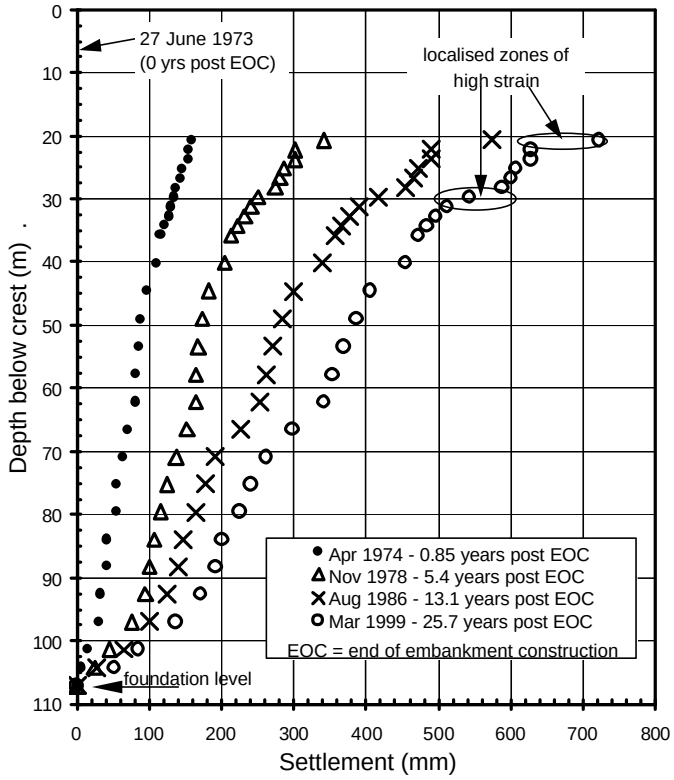

Figure 7.131: Copeton dam, post construction internal settlement profile in the core at IVM A.

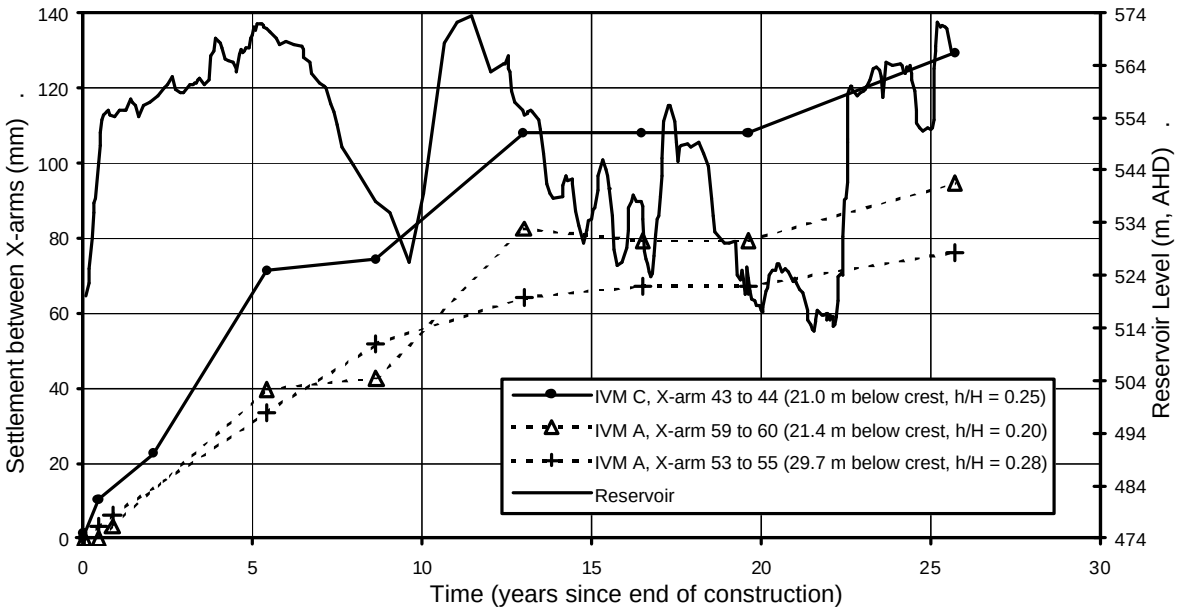

Figure 7.132: Copeton dam, post construction settlement between cross-arms versus time.

7.10.3.2 Shear Surface Development in the Core Post Filling

There are a number of case studies for which a shear surface has or is thought to have developed in the core post first filling. At Eppalock and El Infiernillo dams internal monitoring records indicate that a shear developed in the core, at Djatiluhur dam it is most likely and for Eildon, Bellfield, Cougar and several other dams possibly developed. Details for each of these case studies are presented in Appendix G referencing the sources of data, and they are summarised below (except for Cougar dam which is summarised in Section 7.10.5).

As previously indicated, for virtually all but Eppalock and Djatiluhur dams the overall stability of the embankment is not in question. Therefore these two cases will be dealt with first and in more detail.

(a) Eppalock Dam (Section 1.10 of Appendix G)

The 47 m high Eppalock dam (Figure 7.123), located in central Victoria, Australia is a central core earth and rockfill embankment that was constructed in the early 1960's. The central core of medium plasticity sandy clays were placed in 380 mm loose thickness layers and compacted by sheepsfoot rollers at moisture contents on average 0.8% dry of Standard optimum. The Zone 2A gravel filters were lightly roller and the

crushed basalt rock Zone 2B filter zone was end dumped in high lifts. Rockfill was of quarried basalt was dry placed in 2 to 4 m lifts (and one 10 m lift) and spread by tractor.

The reservoir was first filled over the period from May 1962 to November 1963 (0.2 to 1.65 years after construction) and since then is subjected to a seasonal drawdown of typically 3 to 5 m. Larger drawdowns of 7 to 10 m occurred at 5 to 6 years (1967/68), 14 to 16 years (1976/78), 20 to 21 years (1982/83), 32 to 33 years (1994/95) and 36 to 38 years (1997/99) after construction.

On first filling large settlement of the upstream shoulder occurred due to collapse compression on wetting of the dry placed and poorly compacted rockfill. Similar large settlements also occurred for the downstream shoulder in the first 3 to 4 years after construction. Comparatively, the magnitude of crest settlement was much smaller (Figure 7.134). Internal settlements within the core (measured in the internal settlement gauge) over this period were "normal".

During the larger drawdowns several "abnormal" trends were evident in the deformation behaviour, including:

- Accelerations in the settlement rate of SMPs on the crest, in particular during the drawdowns at 20 to 21 years (SMP CS1 only), 32 to 33 years and 35 to 38 years after end of construction (Figure 7.133). It is notable that the influence of the first large drawdown in 1967/68 (5 to 6 years) on the crest settlement is negligible, but then much larger settlements occurred during the drawdown at 20 to 21 years and increasing settlement magnitude during later large drawdowns. This deformation pattern suggests softening of material strength parameters with time.
- The non-recoverable upstream crest displacement on large drawdown at 32 to 33 years and 37 years (Figure 7.135).
- Acceleration of settlement and non-recoverable upstream displacement of SMP SS2 on the upstream shoulder.

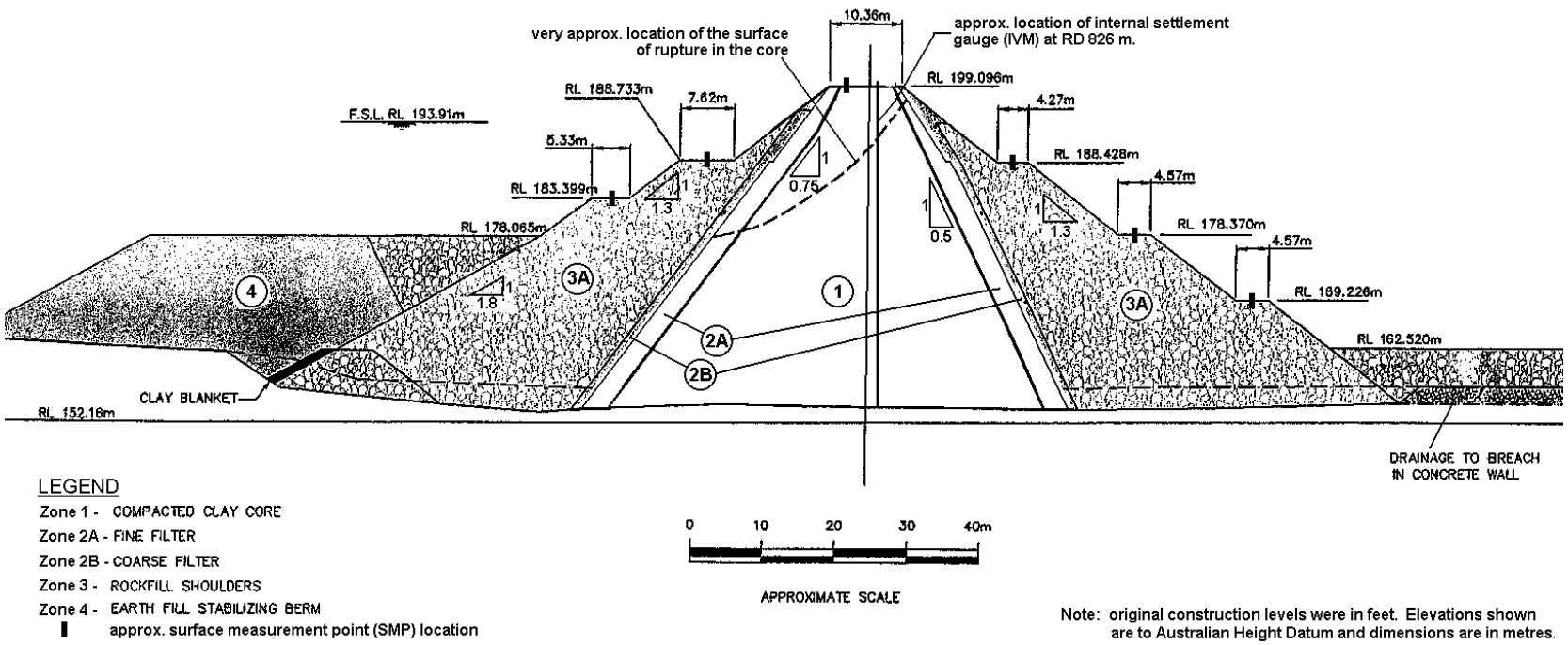

Figure 7.133: Eppalock dam, original design at maximum section (Woodward Clyde 1999)

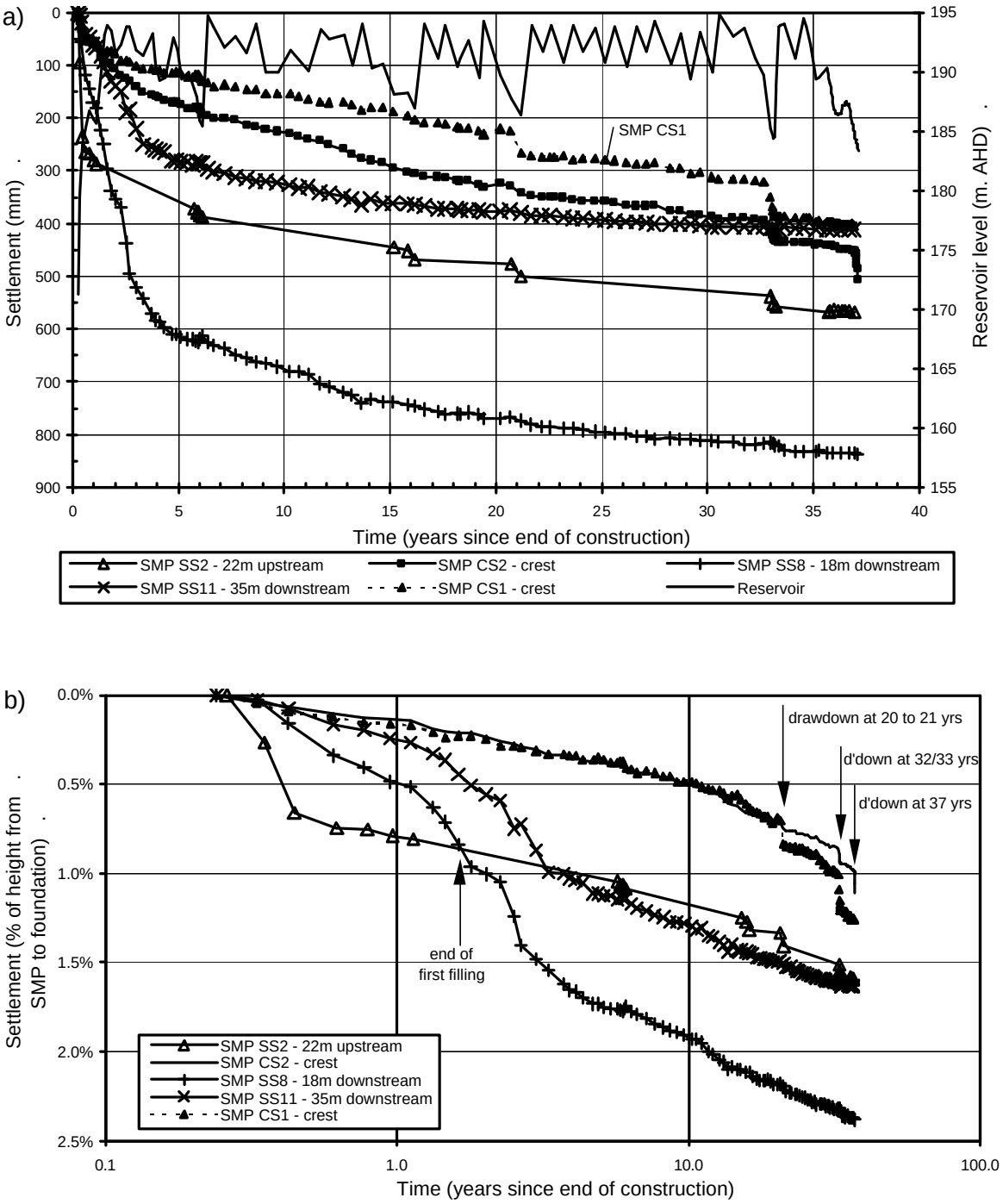

Figure 7.134: Eppalock dam, post construction settlement at main section and CS1.

Inclinometers were installed in the crest of the embankment in 1997. On drawdown in 1998 (35 to 36 years) a localised shear type displacement of 1 to 2 mm was observed at 11 m depth below crest level in the inclinometer located next to SMP CS1. The localised displacement occurred between mid March and mid April 1998 when the reservoir was drawn down below 186.8 m AHD to a low at 186.4 m AHD. Further localised shear type displacement at this depth and also at 4 m depth were detected

during (and following) placement of additional rockfill on the upper berm of the upstream slope at the time of the remedial works in 1999. Davidson et al (2001) refer to observation of shear type deformations along existing longitudinal cracks in the core and to the surface expression of the shear type deformation on the downstream batter of the exposed core during the remedial works.

These observations are clear evidence of the presence of a surface of rupture within the core oriented to upstream. The surface of rupture has formed because of a lack of support of the relatively stiff core by the rockfill and is not indicative of an overall low factor of safety, which was about 1.4. The accelerations in deformation of SMPs on the crest and upstream slope during large drawdown at 20 years (1982/83) are possibly the first indication of shear development in the core. Significant shear type deformations are unlikely to have occurred before this because they are not evident in the larger drawdown at 5 to 6 years (1967/68) and nor are they evident in the internal deformation of the core (IVM 1) during construction and the first three years after construction. The increasing magnitude of crest settlement and lateral spread of the shear zone in the core on subsequent large drawdown at 33 years and 37 years is considered to be indicative of a gradual softening and possible reduction in factor of safety with time. In comparison to other embankments this trend of increasing magnitude of deformation on subsequent similar sized drawdowns is unusual.

It is notable that no indication of shear development was observed in the first 3 to 4 years after construction when the settlement of the rockfill shoulders was very much greater than the core. After this period the settlement of the core has been of similar magnitude to that of the rockfill shoulders. The longitudinal cracking on the crest observed from 1973 (11 years after construction) is therefore unlikely to be caused by the differential settlement between the shoulders and core alone, although it is a contributing factor that led to the initial crack development, softening of the core and subsequent shear type deformations within the core. The initial cause of the cracking is not precisely known, but the ongoing cracking is considered to be reflective of differential deformation between the upstream and downstream portions of the core, and not just as shear type deformations. There are not the monitoring records to confirm such behaviour, but the change in displacement trend of SMP CS2, which started in about November 1975 (13.65 years), from being similar to that of the downstream slope to being similar to that of the upstream slope provides some indication of the differential deformation behaviour of the core. The timing of the change is shortly after the initial

observation of longitudinal cracking in 1973 suggesting that development of significant cracking in the core initially occurred from about 1973 to late 1975, and preceded the shear deformation in the early 1980's.

Another significant observation at Eppalock dam is the softening that has developed in the core, particularly the upper 5 to 6 m, confirmed from piezocone testing and pressuremeter testing in boreholes. Test pits and boreholes have revealed a series of softened zones at angles of 45 degrees to near vertical extending beyond 4 m depth to about the full supply level.

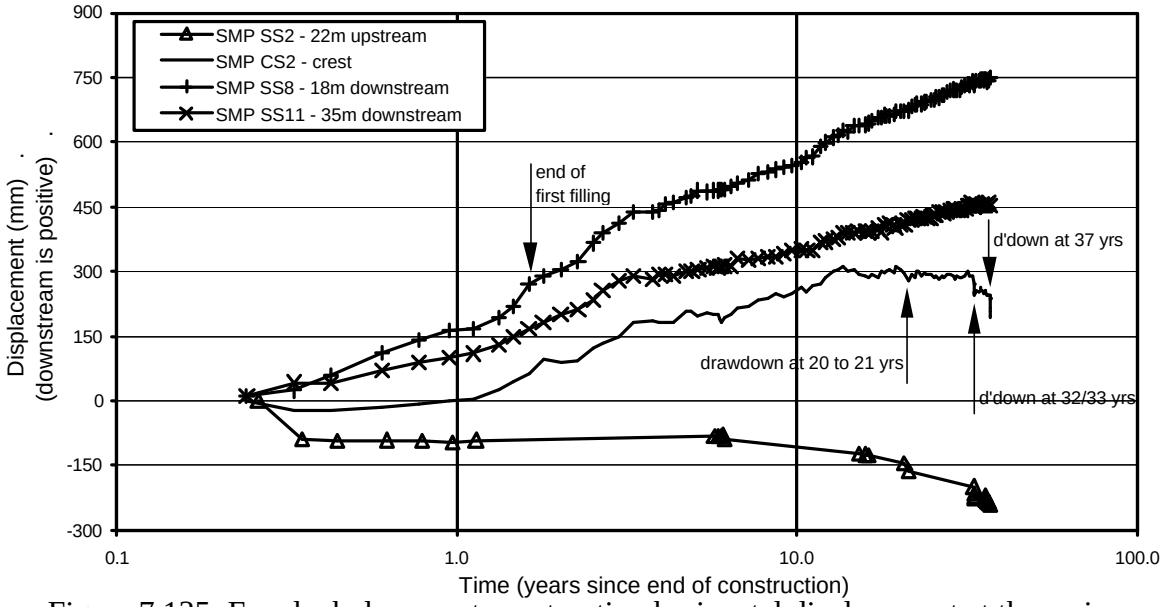

Figure 7.135: Eppalock dam, post construction horizontal displacement at the main section.

(b) Djatiluhur dam (Section 1.7 of Appendix G).

The materials and placement methods of the 105 m high Djatiluhur dam (Figure 7.121) and the surface and internal cracking in the core that developed from the latter stages of construction were previously discussed in Section 7.10.2.1, item e.

The post construction settlement of the crest (Figure 7.136) shows acceleration in the settlement rate of the core and upstream edge of the crest occur post first filling on large drawdown to below about elevation 80 m. In comparison to other embankments that show acceleration in the settlement rate on large drawdown, the magnitude of settlement during drawdown at Djatiluhur dam is large (in the order of 120 to more than 300 mm). In addition, the magnitude of settlement of the core between the drawdowns in 1972 (7 years) and 1982 (17 years) is similar, which is an unusual observation and

has only been observed at Djatiluhur and Eppalock dams. The general trend is for either negligible or reduced magnitude settlement on a second large drawdown of similar magnitude, or a larger magnitude second drawdown is required for an increase in the settlement rate.

Sowers et al (1993) comment that the continuing deformation of the central and upstream region of the crest is reflective of the "highly" stressed state of the upstream slope as indicated by its marginal factor of safety under static loading. They add that the accelerations in settlement on large drawdown are potentially indicative of shear type displacements.

The writer agrees with Sowers et al (1993). The settlement data on drawdown also indicates a softening in the material strength properties over time. This would suggest that the development of a shear surface and strength loss due to shearing on this surface of rupture, at least in the core.

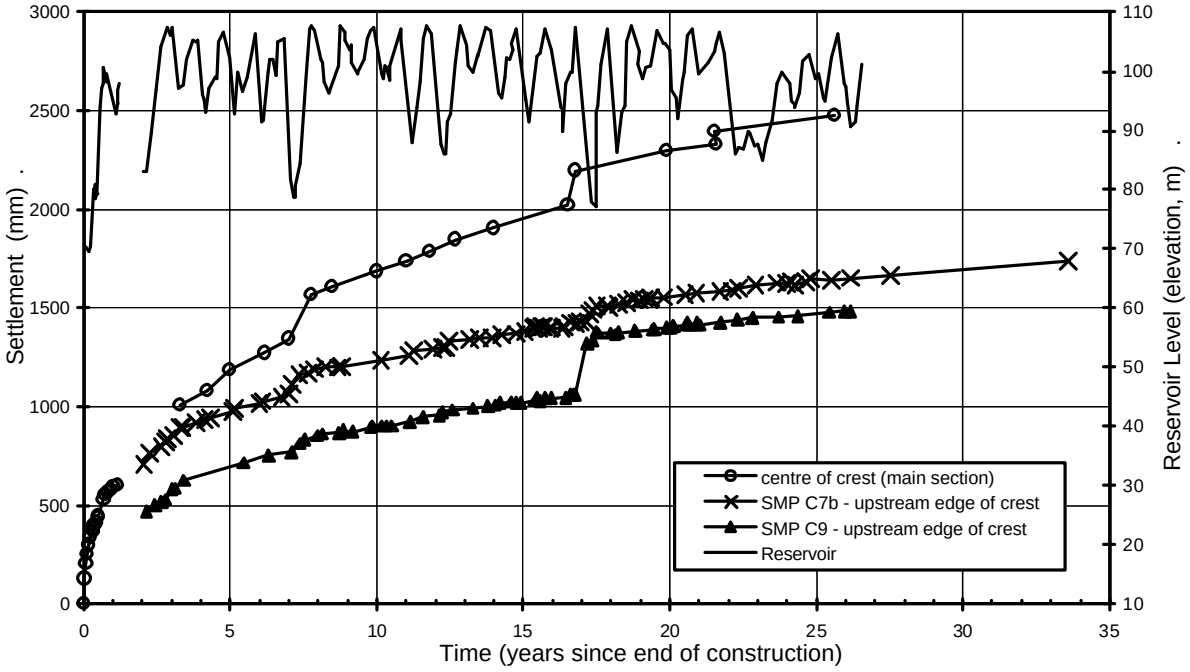

Figure 7.136: Djatiluhur dam, post construction crest settlement.

(c) Bellfield Dam, Victoria, Australia (Section 1.2 of Appendix G).

Bellfield dam is a 55 m high central core earth and rockfill dam constructed in the mid 1960's. The medium width core of sandy clays to clayey sands was compacted in 380 mm layers (loose thickness) at a specified moisture content range from 1.5% dry to 1.5% wet of standard optimum. The thin filter zones were compacted with steel flat

drum rollers and the rockfill shoulders dry placed/dumped in 1.2 to 9.1 m lifts sloped at the angle of repose. The rockfill was sourced from mostly quarried sandstones but with some siltstones and mudstones.

The design and construction methods are very similar to those at Eppalock dam.

The data records obtained (Snowy Mountains Engineering Corp. 1998a) for the SMPs and IVM in the core only cover the post construction period from 1987 to 1997 (21 to 31 years after construction). The IVM records from end of construction to February 1987 (Figure 7.45a) show two regions of high localised vertical strain within the core, one at 14 to 15 m below crest level and the other at 35 m depth. The timing and cause of the concentrated settlement is not known. It may represent local yielding or possible localised shear type displacements in the core.

The records from February 1987 to November 1997 (Figure 7.45b) show a localised zone of higher vertical strain developing at 28 to 30 m below crest level, inconsistent in elevation with those developed prior to 1987.

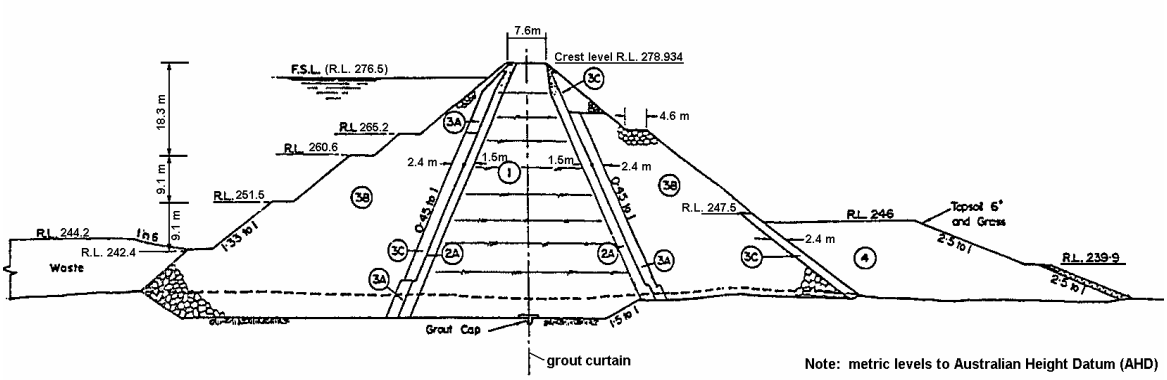

Figure 7.137: Bellfield dam, main section at chainage 701 m (courtesy of Wimmera Mallee Water)

(d) El Infiernillo Dam, Mexico (Section 1.9 of Appendix G).

The materials and placement methods of the 148 m high El Infiernillo dam (Figure 7.111) and the internal vertical deformation behaviour during first filling were previously discussed in Section 7.10.2.1, item a. The post first filling internal settlement records in the core over the period mid 1966 to 1972 (Marsal and Ramirez de Arellano 1972), 2.6 to 8 years after construction, indicate a region of high vertical strain developed in the core at about 45 m depth below crest level (Figure 7.138). The region of high strain is evident in October 1967 and continued to progressively develop into the early 1970s. Over the corresponding period the displacement shows a block type

deformation to downstream above elevation 135 m, and possibly a small reverse displacement to upstream between elevations 130 and 135 m.

At the time of the formation of the localised region of high strain a sustained period of accelerated settlement of the crest and downstream shoulder, and downstream displacement was occurring (Figure 7.139). Marsal and Ramirez de Arellano (1972) comment that the increased rate of deformation was coincident with the flooding of the lower portion of the downstream rockfill due to high tail water levels in October 1966 (2.8 years), January 1967 (3.1 years) and September 1967 (3.8 years) and periods of heavy rainfall. Collapse compression in the downstream rockfill due to wetting from inundation and rainfall is suspected as the cause of the increased rate of settlement and downstream displacement from late 1966 to 1968 of the crest and downstream shoulder.

Interpretation of the deformation behaviour and mechanism leading to development of the localised region of high vertical strain is not clear. It may be related to the deformation of the downstream shoulder, but it could be related to localised instability of the core under the larger drawdowns from 1968 onward. The internal core displacement to upstream at the location of high strain may indicate it is drawdown related.

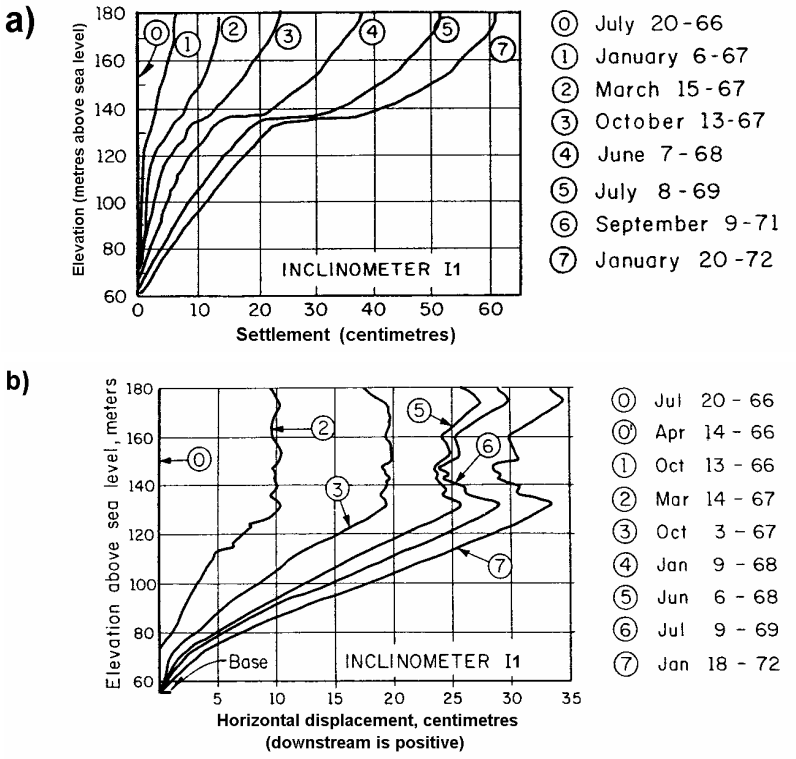

Figure 7.138: El Infiernillo dam, internal *(a)* settlement and *(b)* displacement in the core from 1966 to 1972 (Marsal and Ramirez de Arellano 1972)

Marsal and Ramirez de Arellano (1972) comment that the "abnormalities" in the post construction deformation behaviour are largely controlled by collapse type deformations of the dry and poorly placed rockfill, and due to incompatibility of the stress-strain characteristics between the materials used in the embankment. They add that the deformation of the core is very sensitive to interactions with the surrounding granular mass.

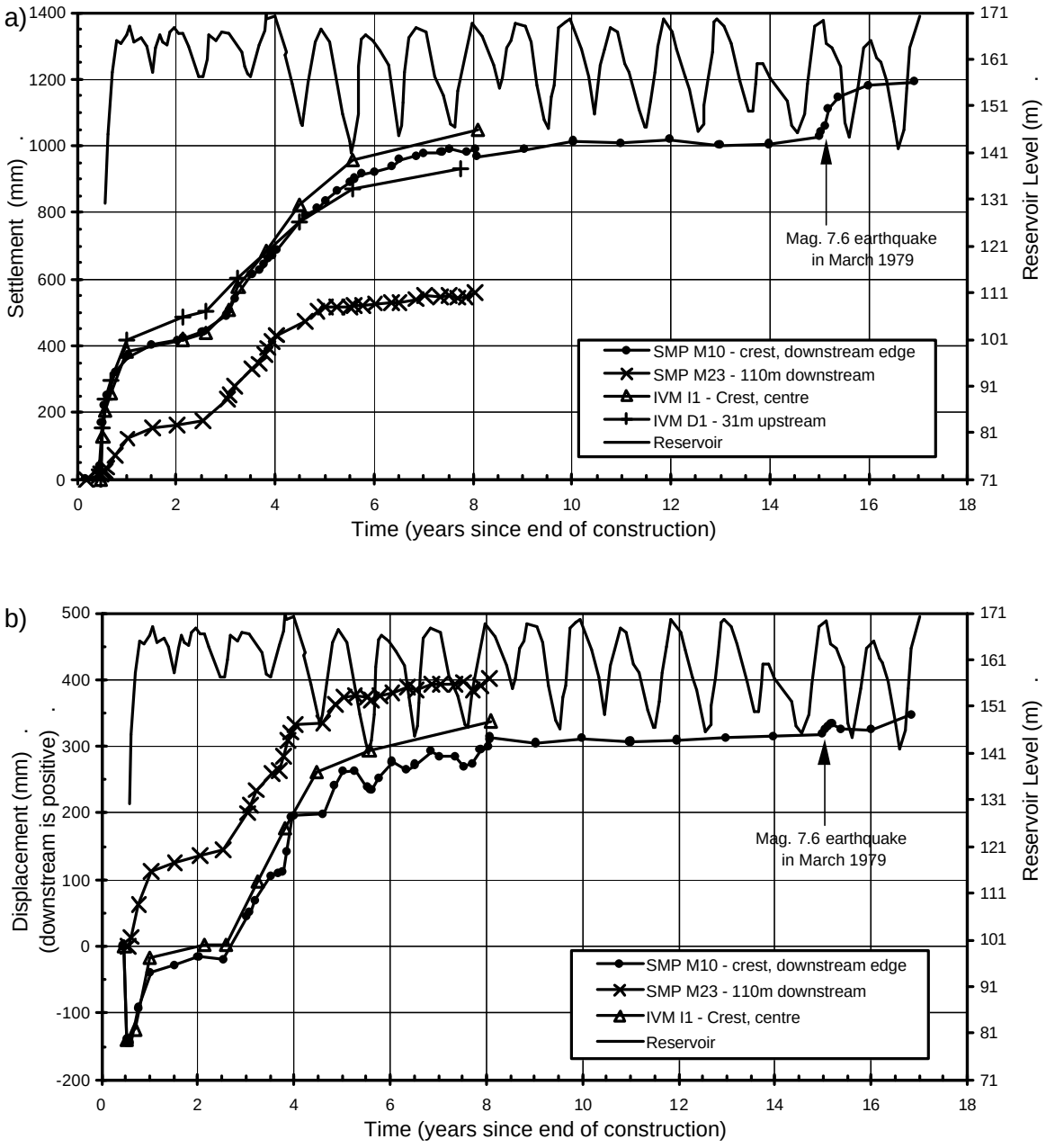

Figure 7.139: El Infiernillo dam, post construction *(a)* settlement and *(b)* displacement of surface markers.

(e) Eildon Dam, Victoria, Australia (Section 1.8 of Appendix G)

Eildon dam (Figure 7.140) is a central core earth and rockfill embankment of 80 m maximum height that was constructed in the early to mid 1950's. The central core consisted of an inner zone (Zone 1A) of medium plasticity silty to sandy and gravelly clays and outer zone (Zone 1B) of clayey sands to silty sands. Both zones were placed on the dry side of Standard optimum and well compacted. The sandy gravel filter / transition zone was generally placed by end dumping without compaction, and the rockfill shoulders were placed in at least 2 m thick layers, probably without the addition of water and not formally compacted. The rockfill was sourced from quartzitic sandstone for Zones 3A and 3B, and the random rockfill zone (Zone 3C) consisted of unsuitable rock that was poorly graded and contained a high fraction of finer sized rockfill.

Aspects of the post construction deformation indicate the possibility that a shear formed within the core sometime after the end of construction and that deformations on the shear surface occur during periods of large drawdown. They are:

- The settlement records from the internal vertical measurement gauges (IVM) installed in the core (Figure 7.142). The records for the period from 26 years after end of construction show localised zones of high vertical strain (IVM ES2 and ES3) at 17 to 20 m depth below crest level, a large portion of which occurred during the latter stages of the large drawdown in 1982/83 at 27 years. These zones are located in Zone 1A within 1 to 2 m of the upstream interface with Zone 1B. At IVM ES3 a blockage or constriction in the tube has limited measurements to the upper 20 m of the gauge.
- SMPs on the crest and upstream slope show an increase in settlement rate on large drawdown at 13 years (1968) and 27 years (1982/83) (Figure 7.141), and also show a non-recoverable upstream displacement at 27 years. Most of the other SMPs on the crest and upstream slope (Snowy Mountains Engineering Corp. 1999a) displayed a similar increase in settlement rate and non-recovered upstream displacement during these drawdowns.

The cause of the possible shear within the core at Eildon dam is not known. It could be due to poor support from the rockfill shoulders as in the case of Eppalock dam or due to differential settlement between the upstream Zone 1B outer sandy loam core and the inner Zone 1A clay core.

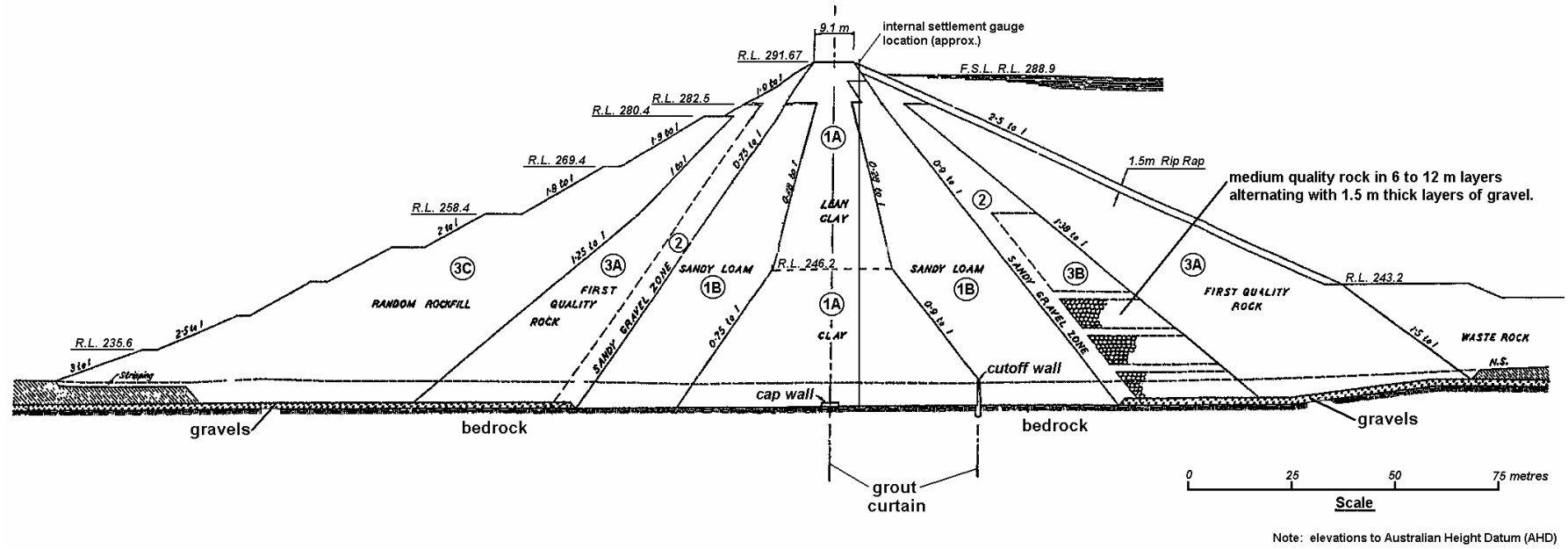

Figure 7.140: Main section at Eildon dam (courtesy of Goulburn Murray Water).

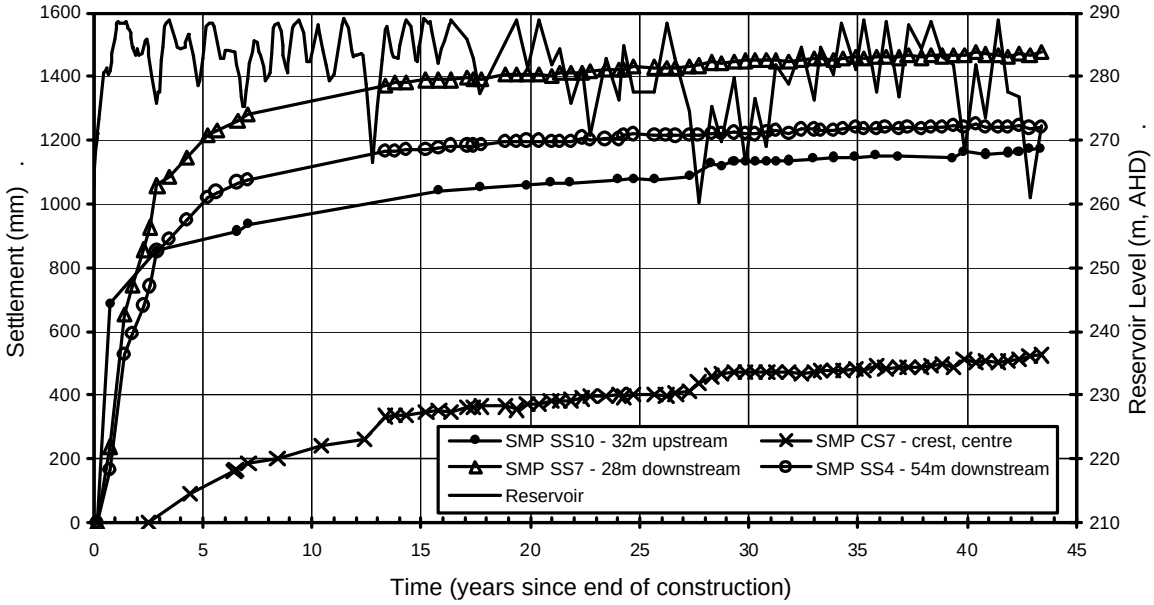

Figure 7.141: Eildon dam, post construction settlement of SMPs at chainage 685 m.

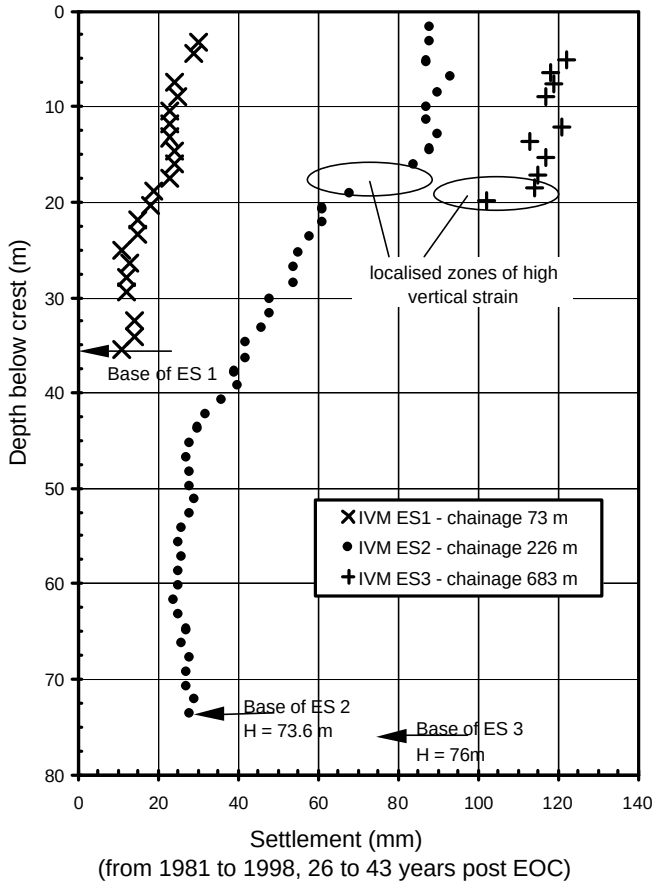

Figure 7.142: Eildon dam, internal settlement profiles in core from IVM records for the period 1981 to 1998.

7.10.4 POST FIRST FILLING ACCELERATION IN DEFORMATION THAT IS NOT KNOWN TO BE SHEAR RELATED

A number of central core earth and rockfill dams show periods of acceleration in the deformation rate post first filling that may not be related to shear deformation in the core. Some of these have already been discussed, including the influence of earthquake such as at Matahina dam (Figure 7.64) and El Infiernillo dam (Figure 7.139a), and the influence of tail water impoundment of the lower downstream shoulder or heavy rainfall, such as at El Infiernillo dam (Figure 7.139a).

In a number of other dams a short period of acceleration and small settlement of SMPs on the crest or upstream shoulder is observed during the first and occasionally the second drawdown. Case studies include, but are not limited to Beliche, Dartmouth, Geehi, Parangana, Cherry Valley, Cougar, Wyangala and Gepatsch dams. The case studies include dams where collapse compression of the upstream rockfill on wetting is potentially significant, and others where it is less significant such as for well and reasonably to well compacted dry placed rockfills (e.g. Dartmouth and Wyangala dams). The deformation behaviour is not considered related to shear type deformation within the core since there are no localised zones of high strain in the IVM data. Although not well understood, several possible explanations for the deformation behaviour have been considered most of which relate to softening of the strength and/or compressibility properties of the materials on wetting.

For rockfills susceptible to collapse compression on wetting, the greatest effective vertical stress acting on the saturated rockfill occurs immediately on wetting. Once the reservoir level is raised slightly the vertical and lateral effective stresses in the upstream rockfill will decrease. If the reservoir is then lowered, the maximum vertical effective stress will increase, but will not exceed the previous maximum level at initial saturation assuming the rockfill is free draining. With respect to the deformation behaviour after saturation and collapse compression, the expectation is that a slight heave may occur on decreasing effective vertical stress and a slight settlement may occur on increasing effective stress as the stress path oscillates along an unloading / reloading path for which the rockfill modulus would be high. A large increase in settlement on increasing vertical stress would therefore be unexpected.

At Gepatsch dam, Schober (1967) attributed the acceleration in settlement of the SMP on the upstream shoulder on drawdown to increased effective vertical stresses in the upstream shoulder due to completion of the embankment construction at high

reservoir levels (refer Section 1.11 of Appendix G). This is a reasonable argument for this case study. At Dartmouth dam this reasoning would partly explain the settlement of the upstream shoulder on drawdown, but part of the settlement occurred before the reservoir had been drawn down to below the reservoir level at end of construction. At Geehi dam, where first filling did not start until after the end of construction, the acceleration in settlement of the upstream shoulder on large drawdown cannot be explained by this reasoning. Nor can it explain the acceleration in deformation at Copeton and Wyangala dams.

Settlements of the crest of these dams are probably more readily explainable by softening of the shear strength and compressibility of the earthfill. Equilibrium pore water pressure conditions after construction can take many years to develop in the core. It is conceivable therefore that on drawdown effective vertical stresses for the near saturated earthfill may exceed those previously experienced on first filling and acceleration in settlement may occur under the "softened" compressibility properties of the earthfill. This may explain the observed increase in settlement rate on first drawdown for the more permeable silty earthfills such as at Cherry Valley and Parangana dams.

For the wet placed clayey earthfills (e.g. at Beliche and Dartmouth dams) softening of the strength and compressibility properties of the earthfill is not a valid explanation for the acceleration in deformation because the earthfills are already close to saturation. In these cases it is likely that the reduction in hydrostatic pressures acting on the upstream face of the core as the water level is drawn down influences the deformation behaviour of the core. On drawdown, the reduction in hydrostatic stress will initially cause the embankment crest to deflect upstream as total stresses are reduced in the core and downstream shoulder. At some point though, lateral stresses must increase in the upstream shoulder to equilibrate the lateral stresses in the wet placed core. For rockfills where collapse compression and reduction of the compressibility occurred during first filling, it is conceivable that this increase in lateral stress will be associated with a net upstream displacement of the core / upstream shoulder interface, resulting in lateral spreading of the core. For wet placed cores of low undrained strength, the lateral spreading is likely to largely occur as undrained plastic deformation and will be associated with vertical compression to maintain volumetric consistency, and hence settlement of the crest.

7.10.5 OTHER CASE STUDIES WITH POTENTIALLY "ABNORMAL" DEFORMATION BEHAVIOUR POST CONSTRUCTION

Further discussion on potentially "abnormal" aspects of the deformation behaviour at Svartevann, Cougar and Wyangala dams is presented due to their informative nature. The deformation behaviour relates to:

- The very large magnitude settlement and displacement of the crest and downstream shoulder at Svartevann dam in the first four years after construction.
- The timing of the large deformation and longitudinal crest cracking at Cougar dam.
- The internal settlement of the earthfill core at close to its upstream interface at Wyangala dam.

A summary of each case study is presented below. Additional details are provided in Appendix G and in the references.

(a) Svartevann dam, Norway (Section 1.13 of Appendix G)

The 129 m high Svartevann dam (Figure 7.143) is a central core earth and rockfill dam with a thin, slightly upstream sloping core. It was constructed in the seasonally warmer months between 1973 and 1976 and stored water during construction. The core of silty sand to silty gravel moraine deposits was placed at an average moisture content of 0.4% wet of Standard optimum and well compacted by heavy vibrating rollers. The filter / transition zones of gravels and crushed rock were sluiced and well compacted. Rockfill of quarried granitic gneiss was dry placed and reasonably compacted (2 metre lifts compacted with 8 passes of a 13 tonne smooth drum vibrating roller).

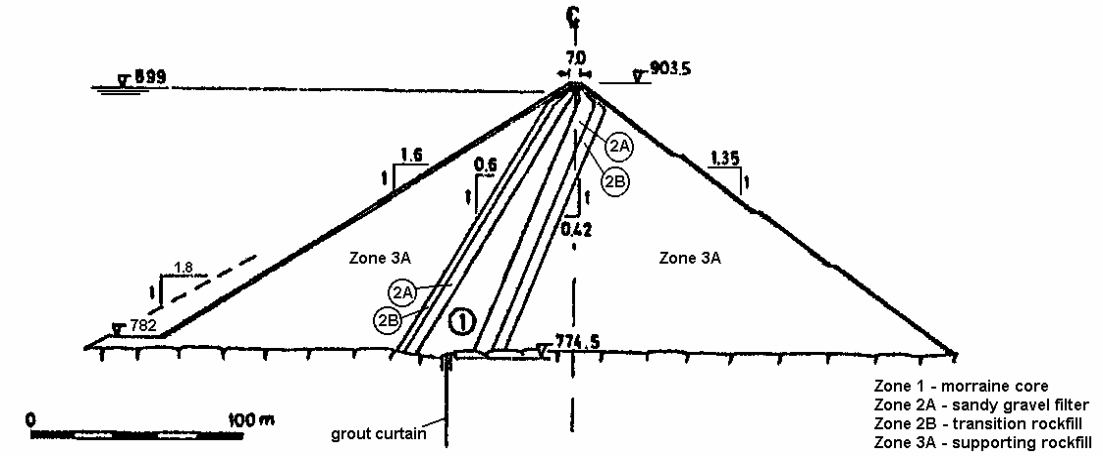

Figure 7.143: Main section at Svartevann dam (Kjærnsli et al 1982).

The post construction deformations at Svartevann dam, particularly during the period of first filling, were relatively high. The magnitude of the crest displacement on first filling at 1100 mm was a clear outlier to other case studies (Figure 7.38 and Figure 7.72) and the crest settlement and deformation of the downstream shoulder very high, but possibly not "abnormally" so. Compared to the case study data for zoned earth and rockfill dams with moraine cores (Dascal 1987) the crest deformation at Svartevann is clearly very large.

As shown in Figure 7.144, a large portion of the surface deformation at the crest and downstream slope occurred during the final 20 m raising of the reservoir to full supply level, although significant settlements were also measured for the upper downstream slope shortly after the end of construction. Finite element analysis by Dibiagio et al (1982) was unable to accurately model the deformation behaviour within the downstream shoulder, it significantly over-predicted the horizontal displacements and significantly under-predicted the settlements.

The post construction internal deformation of the downstream shoulder (Kjœrnsli et al 1982) shows that large settlements and displacements occurred in the mid to upper region of the shoulder in the first 4 years after end of construction. Vertical strains were estimated at 1.4 to 2.2% in the mid to upper region of the downstream rockfill for this post construction period, with much lower vertical strains, 0.5 to 1.0%, estimated for the lower 45 to 50 m (below elevation 820 m). The deformation time plots show that very large settlements and downstream displacements of the mid to upper slopes occurred during the latter stages of first filling, but not on the lower downstream slope.

The large crest deformations on first filling observed at Svartevann dam appear to be related to the deformation of the downstream shoulder. In effect, the core deforms with the downstream shoulder.

The inability of the finite element analysis (Dibiagio et al 1982) to model the deformation behaviour on first filling, particularly the vertical component, suggests that the application of the water load and the associated changes in stress conditions on its own does not account for the actual deformation behaviour. In addition, time dependent or creep related deformations would not account for the vertical deformation because the magnitudes are too large.

It is considered that the large deformations of the mid to upper region of the downstream shoulder are due to collapse compression in the dry placed and reasonably compacted rockfill. The trigger for the collapse type settlement must be moisture

related, so possibly either heavy rainfall or snowmelt is the source of water and the timing during the latter stages of first filling is somewhat coincidental. It is notable that the accelerations in deformation rate of SMPs on the mid to upper downstream slope in the first 2 years post construction occur at the same time period each year, from 0.0 to 0.2, 0.8 to 1.2 and 1.8 to 2.2 years corresponding to the period from June to September, or summer. This is the seasonally wettest and warmest period for the western coast of Norway. Therefore, heavy rainfall together with snowmelt may sufficiently wet the downstream rockfill for collapse settlement to occur. Possibly 1978 was a relatively wet summer or the winter one of high snowfall.

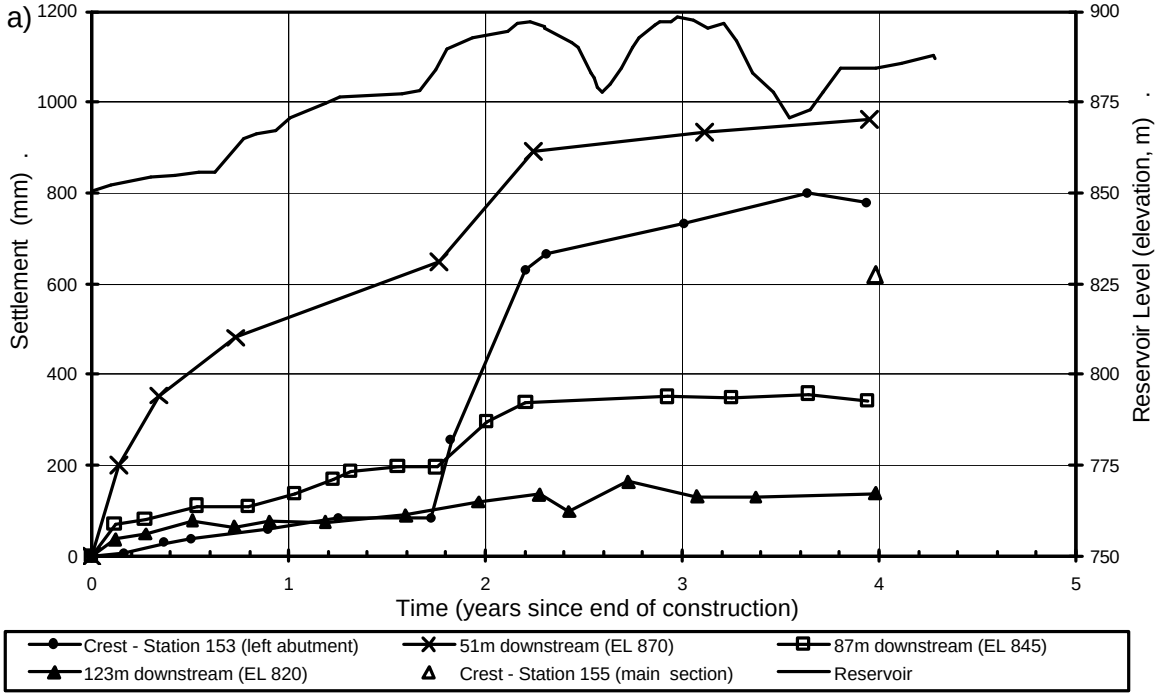

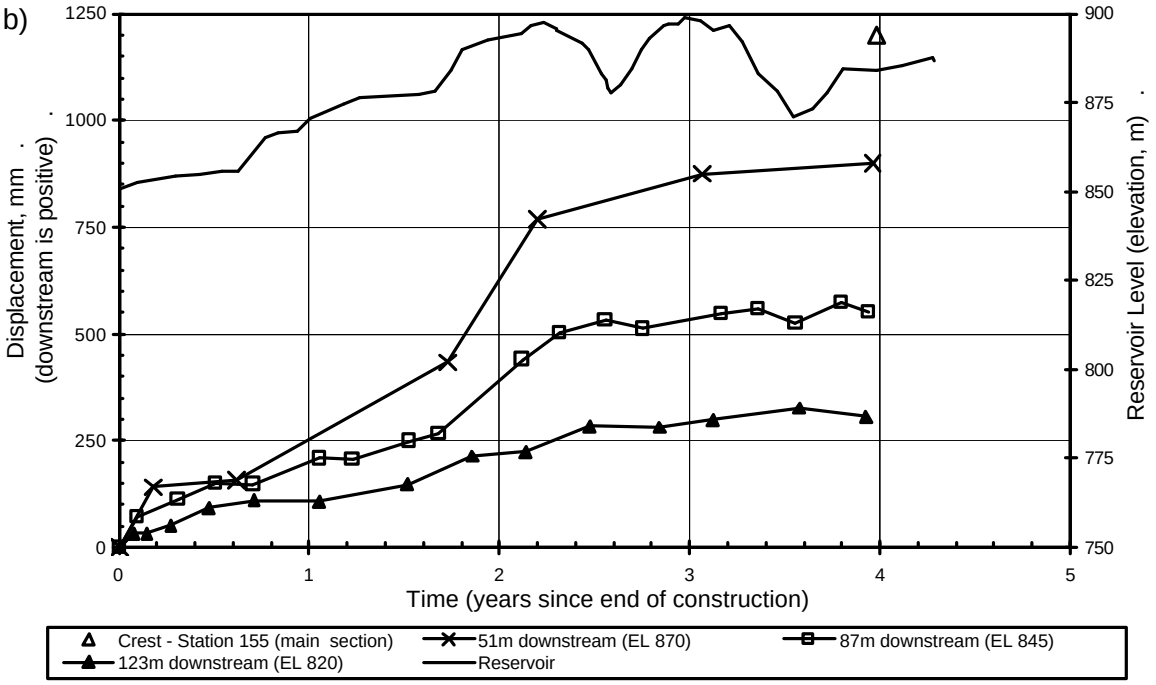

Figure 7.144: Svartevann dam, post construction *(a)* settlement and *(b)* displacement.

(b) Cougar Dam, Oregon, USA (Section 1.6 of Appendix G)

The 159 m high Cougar dam (Figure 7.145) is a central core earth and rockfill embankment that was constructed in the early 1960's (Pope 1967). The slightly upstream sloping narrow core of silty gravels was placed at an average moisture content of 1% wet of Standard optimum and well compacted. The filter / transition zones were also well compacted. Rockfill of quarried basalt and andesite was used. Zone 3A consisted of well-compacted sound rock, Zone 3B of sound rock placed in 900 mm layers and tracked by 2 passes of a D8 bulldozer, and Zone 3C was of lesser quality rock comprising up to 25% weathered rock placed in 600 mm layers and tracked by D8 bulldozer.

On first filling the post construction crest deformations at about the maximum section, Figure 7.146, show that during the last 20 m to full supply level the settlement and downstream displacement of the crest increased significantly in magnitude. This latter part of the deformation was not uniform; settlements were greater at the upstream edge of the crest and displacements greater at the downstream edge of the crest. On the first and second drawdowns acceleration in the settlement rate of the SMP on the upstream edge of the crest occurred, resulting in a marked increase in the magnitude of settlement. At 3 years after construction the differential settlement of the crest had increased to about 400 mm and the lateral spreading to about 250 mm.

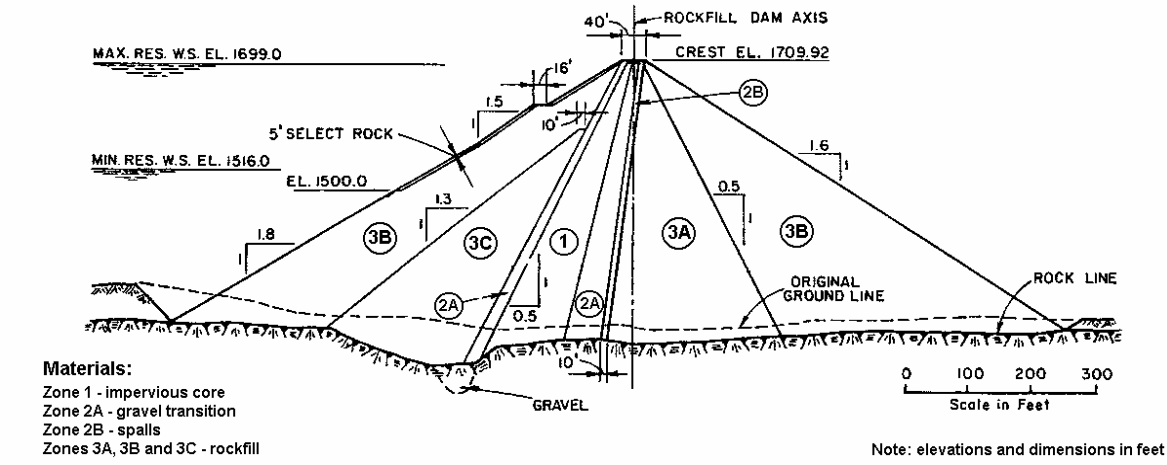

Figure 7.145: Cross section at Cougar dam (Cooke and Strassburger 1988).

Cracking of the embankment was a consequence of the differential deformation between the upstream and downstream edges of the crest. As described by Pope (1967), longitudinal cracking of the crest was observed at the end of first filling and within several days had extended over a length of almost 300 metres. The cracking was mostly near the downstream core / transition interface. The cracking re-appeared in January 1965, shortly after the end of the first drawdown, located at the up and downstream core / filter interfaces and the downstream Zone 2A / Zone 2B interface (Figure 7.147). Cracks widths were up to 150 mm and differential vertical displacement (to upstream) across the crack occurred at the up and downstream edges of the core of 300 mm and 150 mm respectively.

Pope (1967) considered collapse type settlement of the upstream rockfill on wetting, particularly within the lesser quality track rolled Zone 3C rockfill, to be a significant factor in the observed deformation behaviour and cracking. But, what is interesting with the deformation at Cougar dam is that a large proportion of the differential deformation at the crest occurred during drawdown and not on first filling. This would suggest that collapse settlement of the upstream rockfill on initial saturation, whilst significant, is not the major cause of the differential deformation. A possible reason for the large differential settlements post first filling is that the lesser quality Zone 3C rockfill lost additional strength whilst saturated, and then under the increasing effective stress conditions on drawdown further settlement of the upstream rockfill occurred. The second drawdown was to a lower level than the first resulting in higher effective stress conditions in the upstream rockfill than at the end of the first drawdown, which may explain the further increase in settlement on the second drawdown.

The vertical offset at the downstream core / filter interface could indicate a potential shear development in the silty gravel core caused largely as a result of the high shear stresses at the upstream core / filter interface due to differential settlement between the upstream shoulder and the core. The fact that no cracking was observed at the upstream filter / rockfill interface is interesting because these materials probably have the greatest difference in compressibility properties. It is possible that a shear surface has developed in the upstream gravel filter at some point and as a result the upper part of the gravel filter deforms with the upstream rockfill.

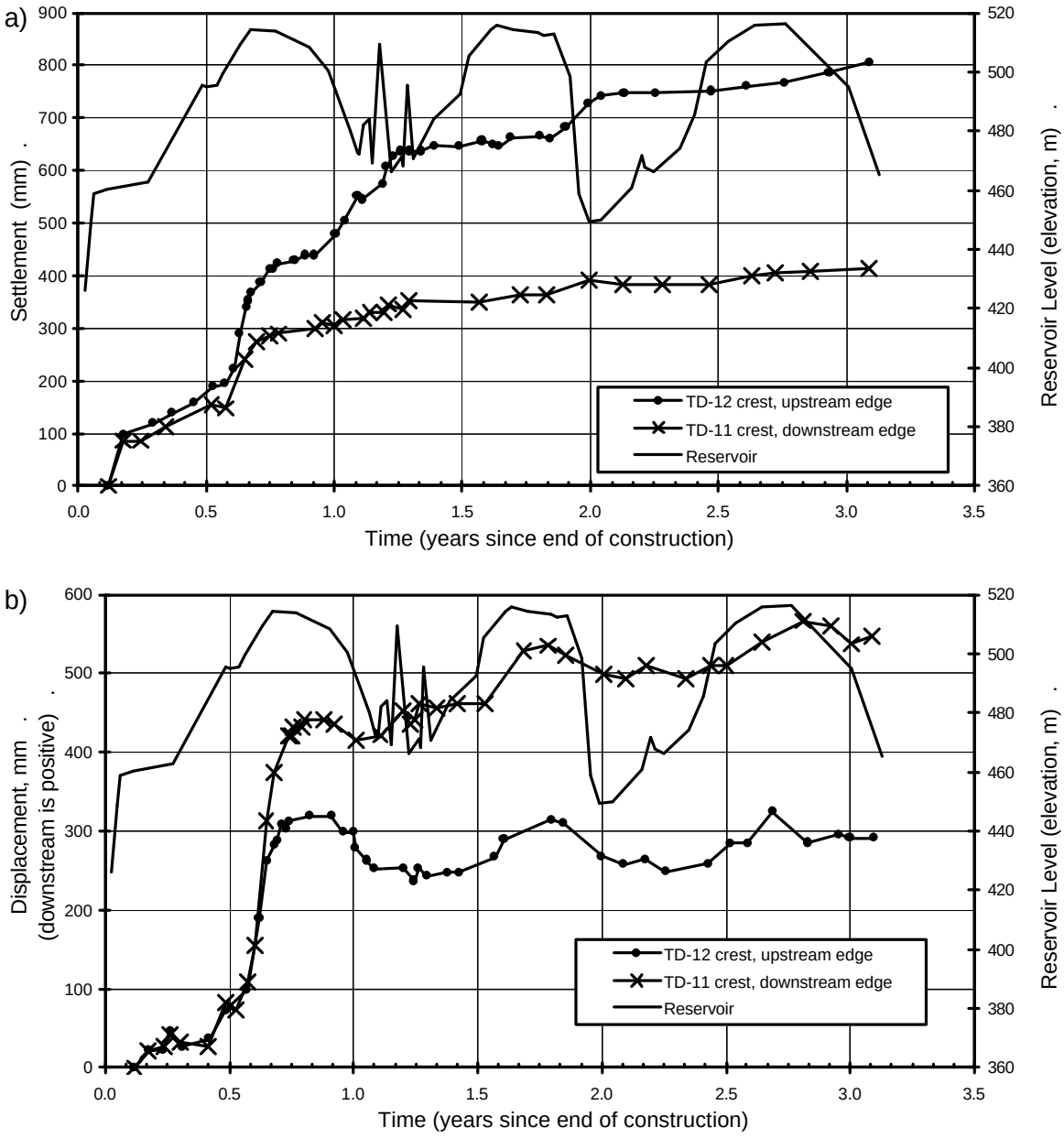

Figure 7.146: Cougar dam; post construction *(a)* settlement and *(b)* displacement normal to dam axis of the crest at the maximum section (adapted from Pope 1967).

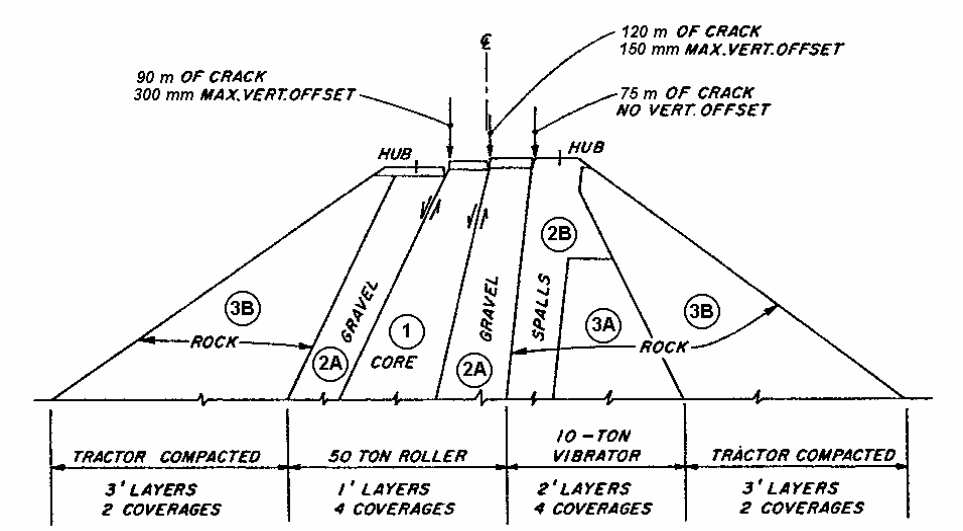

Figure 7.147: Cougar dam; differential settlement and cracks on crest (Pope 1967)

(c) Wyangala dam, New South Wales, Australia (Section 1.16 of Appendix G).

Wyangala dam (Figure 7.149) is a central core earth and rockfill dam of 85 m maximum height constructed in the 1960's. In the deeper valley section the old concrete dam forms the upstream toe of the earth and rockfill dam. The core (Zone 1) of silty to clayey sands was placed at an average moisture content of 1% dry of Standard optimum and well compacted. The filters were also well compacted. Quarried porphyritic gneiss was the main source of rockfill and for the most part was placed without the addition of water. Zone 3A was well-compacted in 0.9 m lifts, Zone 3B reasonably to well compacted in 1.2 m lifts and Zone 3C reasonably compacted in 2.4 m lifts.

During construction, the deformation behaviour of Wyangala dam was considered "normal" in comparison to other similar dams.

Post construction, the deformation behaviour of Wyangala dam was, for the most part, considered "normal". An interesting aspect of the deformation behaviour is the very high vertical strains developed in the core at IVM B (Figure 7.148) between 23 and 32 m depth below crest level (1.85% at 21 years after end of construction). IVM B is located slightly upstream of the dam axis (Figure 7.149) and the region of high vertical strain is located near to the upstream core interface. The vertical strains in this region are very much higher than the average vertical strain of 0.48% in IVM A at a similar depth (located downstream of the dam axis) and in the mid to lower core region at IVM B (average less than 0.15%). The localised high vertical strains developed steadily over the first 11.5 years (1.2% vertical strain at 11.5 years), but increased in rate in the period

from 11.5 to 17 years (0.5% vertical strain over this period for a total of 1.7% to 17 years).

The magnitude of settlement between the cross-arms over the region of high strain totals 155 mm in 17 years, which is approximately equivalent to the differential settlement between the up and downstream edges of the crest (about 100 to 120 mm) over this period plus the "normal" settlement over the depth range (estimated at 20 to 30 mm from IVM A). This would indicate that the region of high strain relates to differential settlement between the core and upstream shoulder. Whilst this is a shear type movement in itself, a single distinct shear surface does not appear to have developed as indicated by the broad width of the region of high strain. It is possible that a series of shears may have developed or that general softening of the earthfill may be a factor within the zone of high strain.

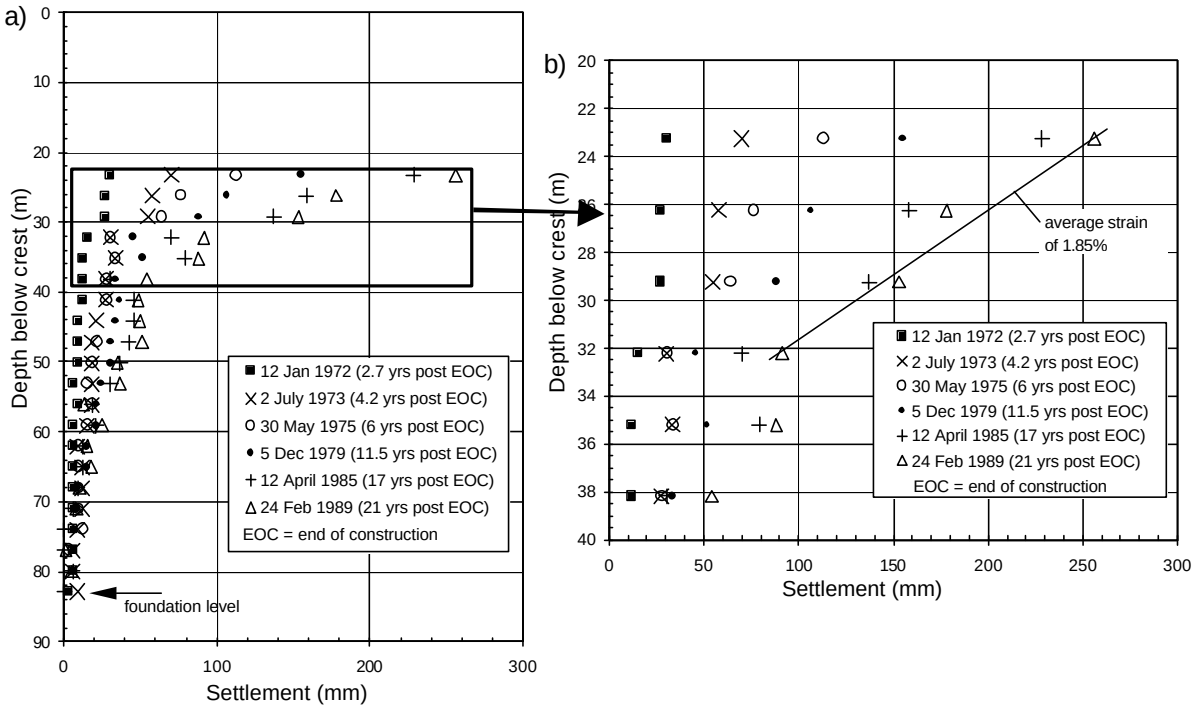

Figure 7.148: Wyangala dam, post construction internal settlement in IVM B located 9 m upstream of dam axis.

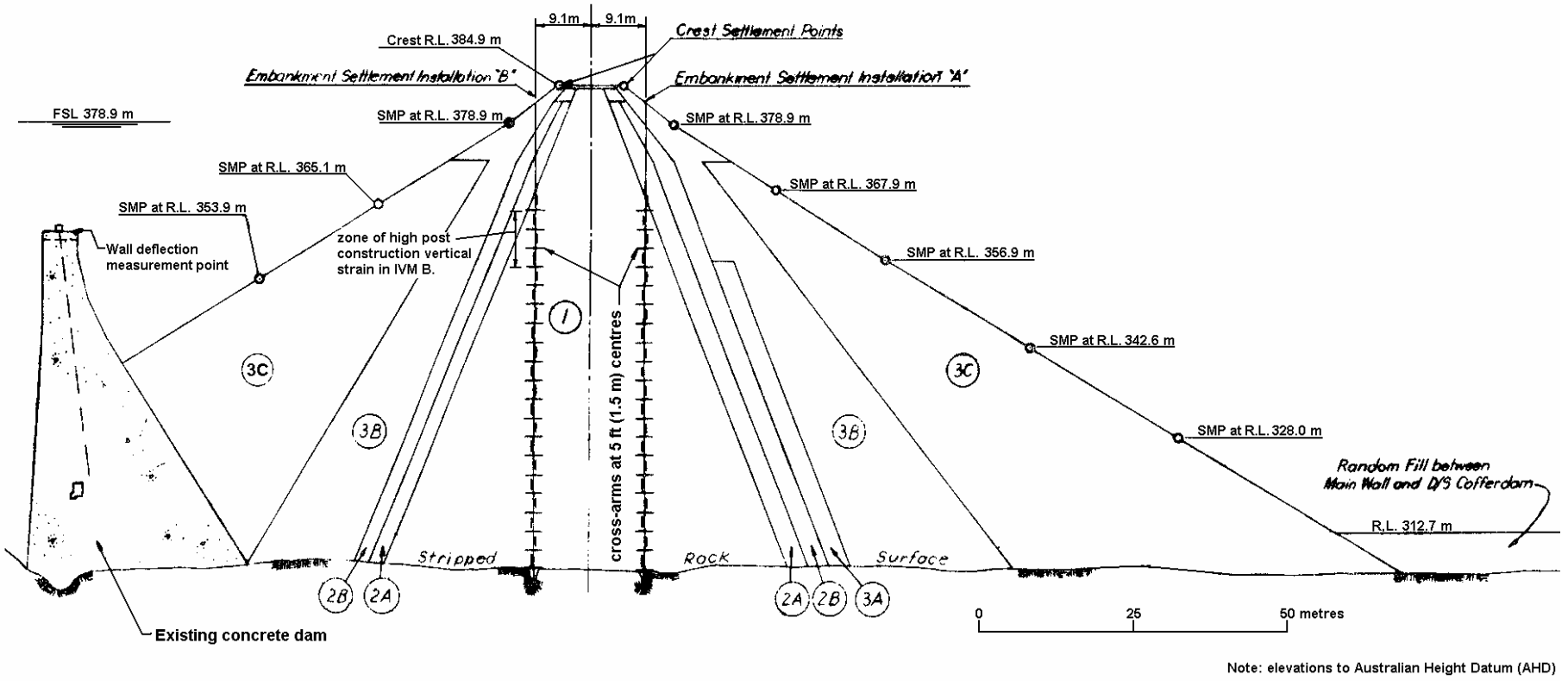

Figure 7.149: Section at Wyangala dam (courtesy of New South Wales Department of Land and Water Conservation).

7.11 "ABNORMAL" DEFORMATION BEHAVIOUR POST CONSTRUCTION OF EARTHFILL AND ZONED EMBANKMENTS WITH VERY BROAD CORE WIDTHS

In Sections 7.5.3 and 7.6 the post construction deformation behaviour of a number of rolled earthfill embankments and zoned embankments with very broad earthfill cores were identified as "abnormal" or possibly "abnormal". In the following sub-sections the possible mechanisms explaining the deformation behaviour are discussed with reference to the case study data. The association of a case study to a particular mechanism has, in some cases, previously been identified by the owner, their consultants or other authors, and in other cases has been considered appropriate based on assessment of the deformation behaviour. For some cases the association is speculative. Further details on the embankment and its deformation behaviour for most of the case studies discussed in this section are presented in Appendix G.

7.11.1 COLLAPSE COMPRESSION OF THE EARTHFILL ON WETTING

At Hirakud dam the large settlements in the lower portion of the embankment that occurred during construction were attributed to the effects of collapse compression of the earthfill on wetting (refer Section 7.9.2). Two factors were significant in the deformation behaviour; the deformation that occurred on initial wetting of the dry placed clayey sand to clayey gravel earthfill under the stress conditions existing at the time, and the large deformations as the embankment was constructed to design level after the shutdown period when the wetting occurred. The large deformations during the subsequent construction were indicative of the low shear strength and compressibility properties of the "collapsed" and softened earthfill. The influence of change in material strength and compressibility properties after wetting for embankments that are initially saturated on first filling after construction is important and its possible influence is discussed further for some of the case studies.

Rector Creek, Mita Hills and Roxo dams are considered examples of collapse compression of dry placed earthfills that occurred due to wetting after construction. Collapse compression possibly also occurred in the upstream shoulder to central region of Dixon Canyon, Spring Canyon and Horsetooth dams. All these cases are discussed further in Appendix G.

"Abnormal" deformation behaviour due to collapse compression on wetting is generally identified by excessive settlements that largely occur on wetting. This is particularly evident at Rector Creek, Mita Hills and Roxo dams. Another pattern sometimes observed is an "abnormally" large upstream displacement of the crest on first filling and later downstream displacement as the wetting front progressively develops through the embankment.

The deformation behaviour at Rector Creek dam (Sherard et al 1963; Sherard 1973; ICOLD 1974) presents probably the clearest example of collapse compression. The embankment (Figure 7.150) is a 61 m high zoned earthfill embankment that was completed in January 1947. The central earthfill region (Zones 1 and 2) was of silty to clayey sands with low plasticity fines, the finer materials being used in the central core region (Zone 1) and the coarser earthfills in the outer Zone 2 region. Compaction was in 150 mm layers by heavy sheepsfoot roller and moisture contents at placement were 2 to 4% dry of Standard optimum.

The post construction deformation of SMPs on the crest near to the main section (Figure 7.151) shows the large magnitude of crest settlement (almost 1.8% at 10 years after construction) and the large upstream then downstream displacement of the crest. In comparison to similar embankments the magnitude of settlement and long-term settlement rate of the crest are "abnormally" high (Figure 7.46, Figure 7.60a and Figure 7.63), and the magnitude and direction of the crest displacement during and post first filling clear outliers to the general behaviour (Figure 7.38, Figure 7.75 and Figure 7.77). ICOLD (1974) consider that collapse settlement on wetting of the dry placed earthfill and the gradual development of the phreatic surface within the embankment contributed to the observed crest settlement and displacement behaviour, and to the observed cracking. Initial wetting and collapse settlement of the upstream shoulder resulted in the upstream displacement of the crest, and subsequent wetting and collapse settlement in the central to downstream portion of the embankment resulted in the change in direction of displacement to downstream some 2 to 2.3 years after construction. The high long-term settlement rate of about 1.65% per log cycle of time maintained for at least 10 years after construction is possibly reflective of the large reduction in material strength and compressibility properties after wetting.

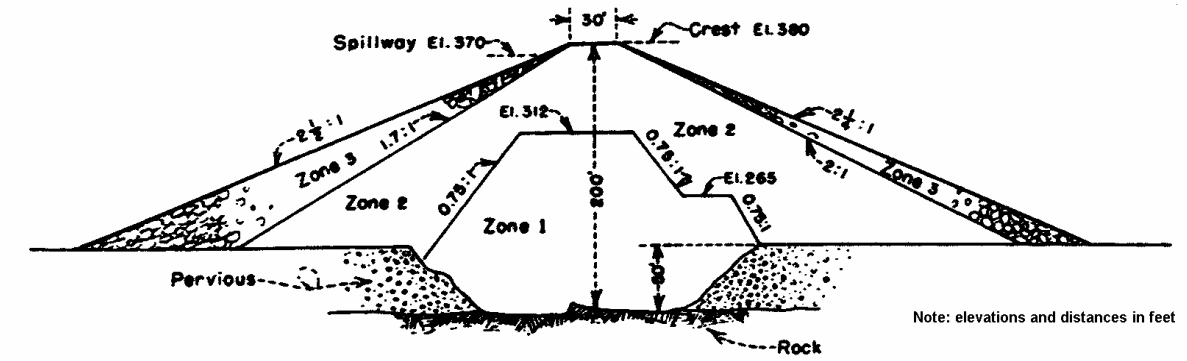

Figure 7.150: Rector Creek dam main section (Sherard 1953).

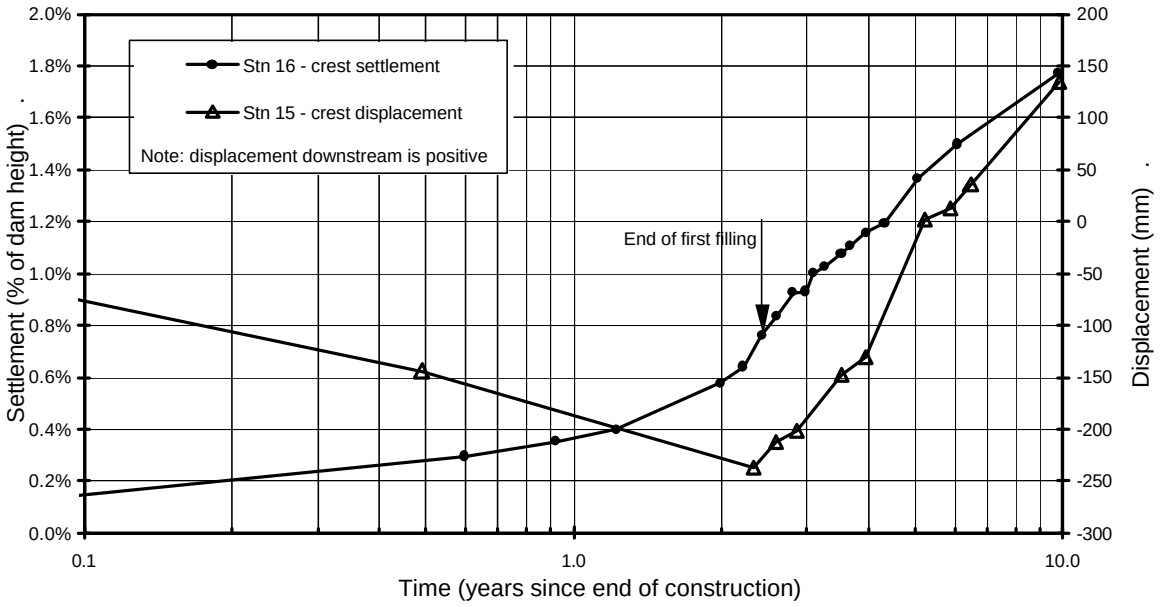

Figure 7.151: Rector Creek dam; post construction settlement and displacement versus log time (adapted from Sherard et al 1963).

Collapse compression is considered a significant factor for the large crest settlements measured at Roxo dam. The dam, constructed in the 1960's, is part concrete and part earthfill embankment. The earthfill embankment is of 27 to 32 m maximum height and is constructed of medium plasticity clayey sands to sandy clays derived from weathered schists placed at moisture contents in the range 2% dry of OMC to OMC (OMC = Standard optimum moisture content). Large post construction crest settlements, up to almost 2% of the embankment height at 8 years (Figure 7.152), were measured over a large portion of the 80 to 100 metre long closure section of the earthfill embankment located at the interface between the two structures. In comparison to similar embankments, the magnitude and rate of the crest settlement is "abnormally" high

(Figure 7.46, Figure 7.60a and Figure 7.63). At 95 metres from the interface the post construction crest settlement is more typical of "normal" type behaviour.

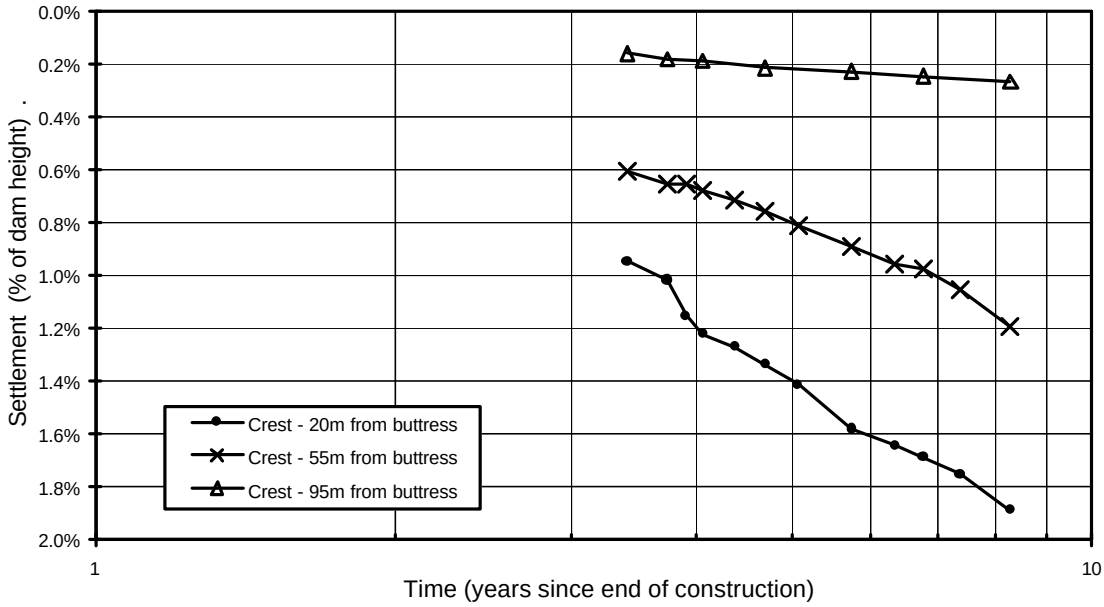

Figure 7.152: Roxo dam, settlement versus log time (adapted from De Melo and Direito 1982).

The cause of the large settlement is considered to be possibly due to collapse type settlements on wetting of dry placed and potentially poorly compacted earthfill in the closure section. Investigations and excavation (De Melo and Direito 1982) showed the presence of wetted and softened layers close to those in the as placed condition, but it is not clear to what extent these layers were observed.

De Melo and Direito (1982) do not consider collapse compression as a cause of the large settlements. Instead, they consider it due to a combination of factors including arching across changes in foundation geometry near to the abutment and the formation of horizontal cracks due to differential settlement and stress transfer between the earthfill and concrete structures. But these factors alone would only influence the deformation in the vicinity of the interface, and, as the settlement records show, the "abnormally" large settlements were measured more than 50 to 60 metres from the interface. Hence, collapse compression on wetting is considered a potentially significant factor.

Large reductions in the shear strength and compressibility properties of the earthfill may be contributing to the "abnormally" high long-term rate of crest settlement.

At Mita Hills dam collapse compression on wetting of the outer upstream earthfill zone (Zone 3) is considered a potentially significant factor in the "abnormally" large magnitude of crest settlement and the upstream crest displacement on first filling reported by Legge (1970). The embankment, constructed in the late 1950's, is of 49 m maximum height (Figure 7.153). The earthfill was placed in 150 mm layers and compacted by heavy sheepsfoot rollers. The specified range in moisture content for the outer earthfill zones was 2% dry of OMC to OMC (OMC = Standard optimum moisture content) and 1% dry to 1% wet of OMC for the internal Zone 2 upstream of the chimney filters.

As shown in Figure 7.60a and Figure 7.46 the magnitude of crest settlement at Mita Hills dam of more than 1% is "abnormally" high, and the magnitude of upstream displacement (Figure 7.75 and Figure 7.38) possibly "abnormal" in comparison to similar type embankments. Most of the deformation occurred on first filling. Post first filling the crest deformation has been "normal" in comparison with that of other embankments. In addition, very high magnitude settlements were measured on the mid abutment slopes (up to 2.3% of the embankment height at these locations) and the deformation of SMPs on the downstream shoulder were very small (settlement of 0.27% of the height from the SMP to foundation level at the main section) in comparison to those on the crest.

The possibility that the deformation is related to marginal stability of the upstream slope has been considered, however, an instability mechanism seems unlikely as no acceleration in settlement rate or further upstream displacement is observed on drawdown (refer Section 4.2 of Appendix G).

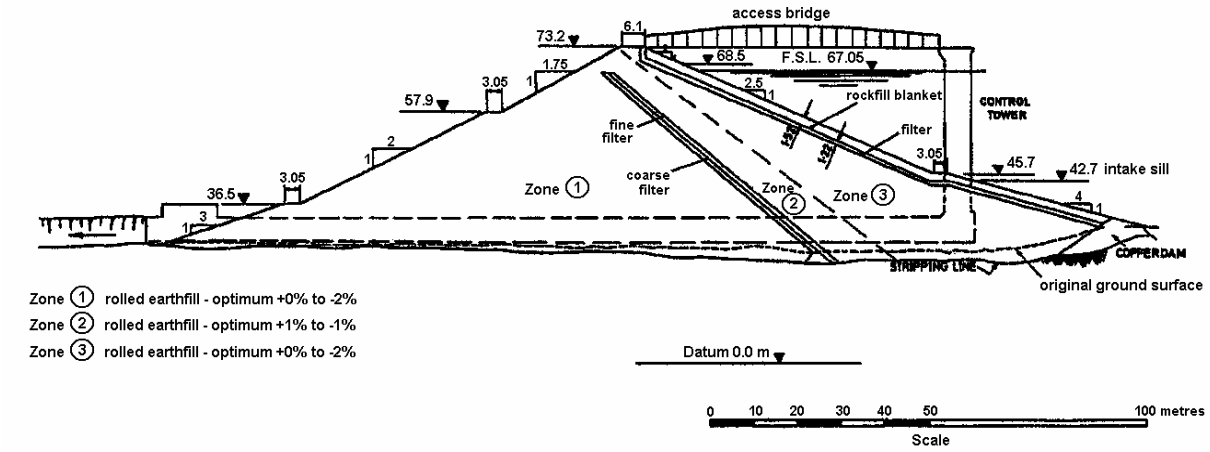

Figure 7.153: Main section at Mita Hills dam (Legge 1970)

For the Horsetooth Reservoir embankments Dixon Canyon, Spring Canyon and Horsetooth dams, collapse compression is considered a possible cause of the large magnitude of settlement of SMPs on the upper upstream slope and crest. The Horsetooth Reservoir embankments were constructed in late 1940's to maximum heights of 48 to 74 m. A similar design was adopted for all of the main embankments (Figure 7.154 is of Dixon Canyon dam) consisting of a very broad central earthfill zone with thin outer zones of gravelly earthfill or rockfill. In the valley sections a cut-off was excavated through the over-burden soils to bedrock with most of the embankment founded on the over-burden soils. The cut-off design was similar for all embankments except Horsetooth dam, where it was located upstream of the dam centreline.

The earthfill zone was constructed of mainly low plasticity sandy clays to clayey sands and clayey gravels of alluvial origin. Finer materials were placed in the central region of the core and coarser materials toward the outer slopes. The earthfill was placed in 150 mm layers and compacted by tamping rollers. Moisture contents were well dry of Standard Proctor optimum, on average 2.2% to 2.9% dry.

The post construction deformation behaviour of SMPs on the upper upstream slope near to the main section for the Horsetooth Reservoir embankments is shown in Figure 7.155. Possible "abnormal" aspects of the deformation behaviour in comparison to similar embankments are:

- The large magnitude of settlement of the upstream slope for Horsetooth, Dixon Canyon and Spring Canyon dams where settlements were in the range 1.35 to 2.0% (Figure 7.52 and Figure F2.28 of Appendix F).
- The high rate of long-term settlement of the upstream slope for Dixon Canyon dam of 1.38% per log cycle of time (Figure 7.83). At Spring Canyon dam the settlement rate was high over the period from 8 to 30 years, but has since reduced in the period from 30 to 45 years.
- For Dixon Canyon dam, the large upstream displacement on and after first filling followed by the change to downstream displacement after 30 years for the upstream slope (Figure 7.87). The trend of displacement at Spring and Soldier Canyon dams is similar, but at a much reduced magnitude and rate of displacement (rate per log time).
- The crest settlement behaviour of Dixon Canyon and Spring Canyon dams is also potentially "abnormal" in terms of the large magnitude (Figure 7.48 and Figure 7.61) and high long-term settlement rate (Figure 7.63).

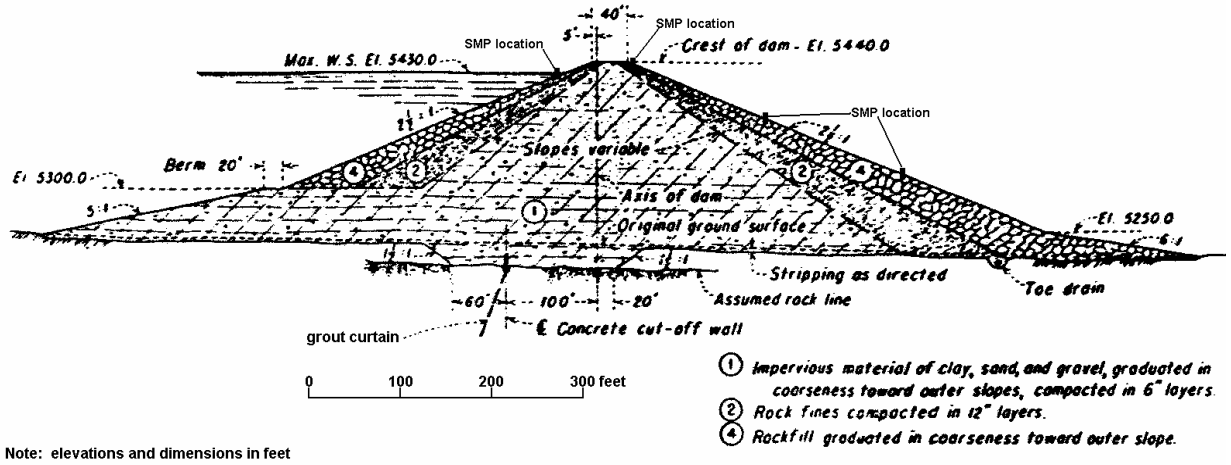

Figure 7.154: Main section at Dixon Canyon dam (courtesy of U.S. Bureau of Reclamation).

The influence of the foundation on the settlement and displacement of the crest at Horsetooth was significant (refer Section 3.3 of Appendix G). It is also likely to have influenced the deformation of the upper upstream slope, but to a lesser degree, as this SMP overlies the downstream edge of the cut-off trench to bedrock. The downstream displacement and large settlement on first filling of the SMP on the upstream slope at Horsetooth dam (Figure 7.155) are likely due to the foundation influence.

At Dixon Canyon and Spring Canyon dams the foundation is considered to have a limited influence on the post construction deformation behaviour and most of the measured deformation occurs within the embankment. This is based on the comparison of the trend of deformation at these embankments to that at Horsetooth dam where the influence of the foundation was very significant during first filling, but much less so post first filling. In addition, the SMPs on the upstream slope at Dixon Canyon and Spring Canyon dams directly overlay the cut-off trench and therefore the foundation influence will be very limited.

Collapse compression of the dry placed earthfill, particularly in the coarser soil types likely to be present in the upstream portion of the main earthfill zone, is considered to be a possible explanation for the observed potentially "abnormal" deformation behaviour of the upstream shoulder of Horsetooth, Spring Canyon and Dixon Canyon dams, and the crest at Spring and Dixon Canyon dams. The effect of softening of the shear strength and reduction in compressibility on wetting is likely to have some influence on the on-going very high settlement rates (rate per log time).

The similarity between the case studies considered to be susceptible to collapse compression, including Hirakud dam, is that the materials were placed well dry of Standard optimum moisture content, and were of low plasticity clayey sands to clayey gravels to sandy clays. In all cases the earthfills were reportedly placed in thin layers (150 mm) and well-compacted by rollers.

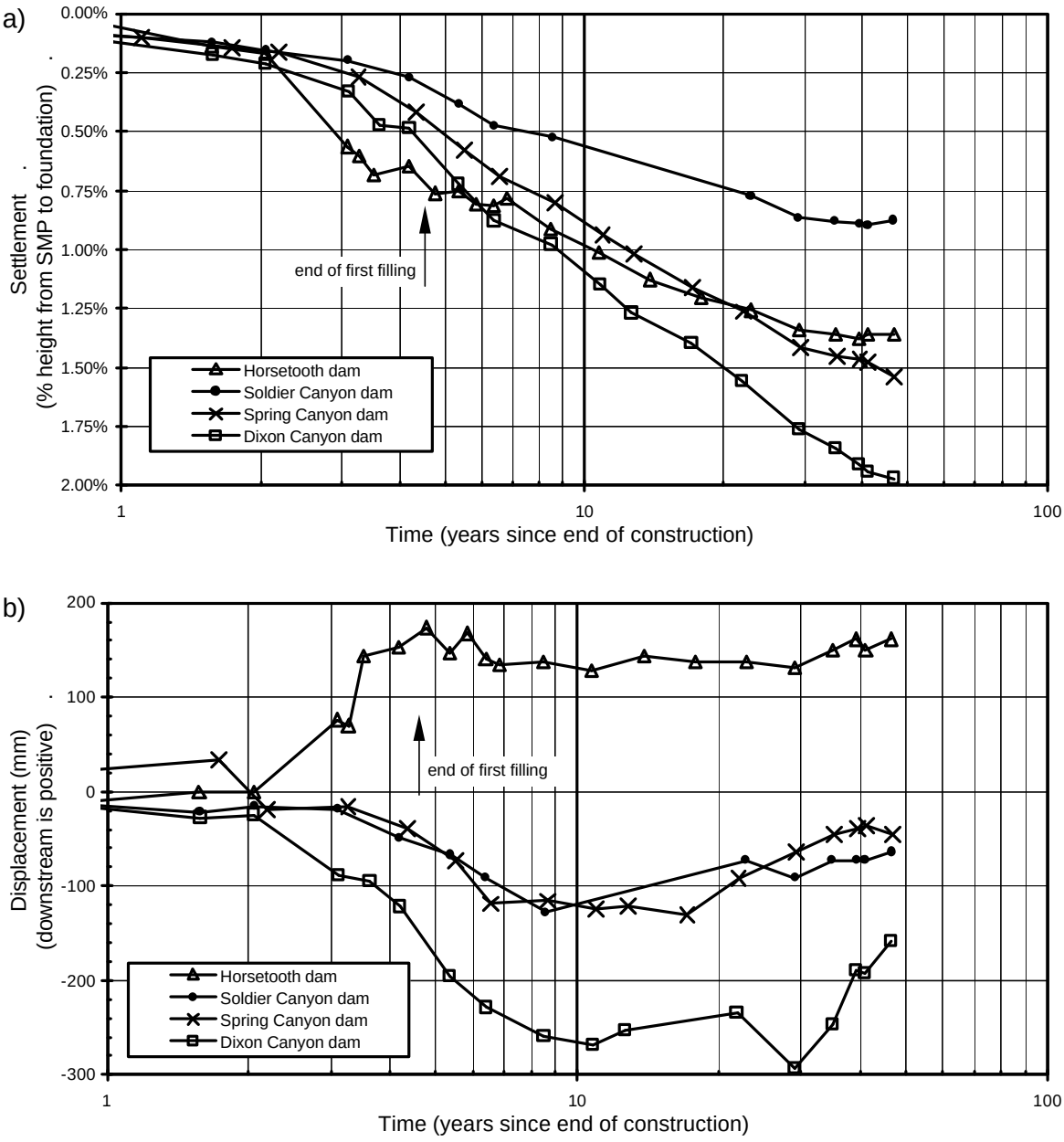

Figure 7.155: Post construction *(a)* settlement and *(b)* displacement of SMPs on the upper upstream slope at the Horsetooth Reservoir embankments.

7.11.2 "HIGH" SHEAR STRESS OR MARGINAL STABILITY CONDITIONS WITHIN THE EMBANKMENT

Three of the case studies within the database of embankment with very broad core zones suffered failures in the upstream slope during large drawdown, these were Belle Fourche, San Luis (Von Thun 1988; Stark and Duncan 1987, 1991) and Steinaker (Cyganiewicz and Dise 1997) dams. The failures are clearly indicative of marginal stability conditions of the embankments under drawdown. The possible mechanism/s of the failures are discussed in Chapter 5.

The following discussion is on the monitored deformation behaviour of Belle Fourche and San Luis dams, concentrating on "abnormal" or potentially "abnormal" trends that may be potential indicators of an upstream failure condition on drawdown. At both these embankments no SMPs or other monitoring instrumentation was located within the actual failed section of the embankment. At Steinaker dam the failure was in a section of the embankment that was not monitored and was different in design to the main section, so is not discussed further. The mechanism and failure itself at each embankment are not discussed in any detail here.

7.11.2.1 Belle Fourche dam (Section 4.1 of Appendix G)

Belle Fourche dam (Figure 7.156) is an earthfill embankment of 35 m maximum height and about 1850 m crest length that was constructed over the period 1905 to 1911. Foundations for the embankment consist of medium plasticity alluvial adobe clay overlying a thin sand and gravel layer and in-turn shale bedrock. The earthfill materials used in construction were the medium plasticity adobe clays placed in 150 mm layers, "*sprinkled*" with water and compacted using heavy rollers with diagonal lugs.

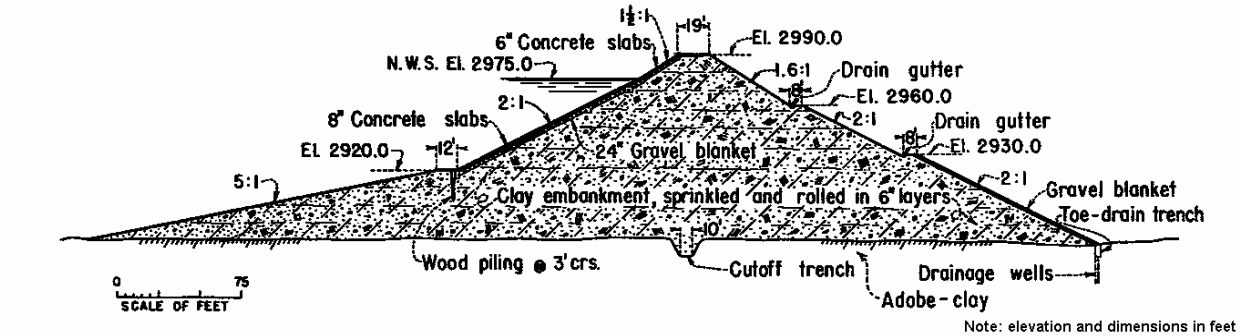

Figure 7.156: Belle Fourche dam; main section as constructed in 1911 (courtesy of U.S. Bureau of Reclamation).

The embankment design incorporated steep upstream and downstream slopes for the type of construction materials used. The steep portion of the upstream slope was faced with concrete slabs placed on a 0.6 m layer of gravel and supported at the toe (elevation 2920 feet) on a concrete footing and driven wooden piles. The closure section at Owl Creek, the highest section of the embankment between stations 40+50 and 42+50, was constructed last and was built very rapidly.

The reservoir was first filled over the period from March 1911 to September 1915 (4.2 years after construction) and is subjected to a seasonal drawdown, usually over the late spring to early autumn period, generally in the range of 4 to 8 metres (Figure 7.158) with occasional larger event of greater than 9 m.

The embankment has performed relatively poorly during the larger drawdown events (Sherard 1953; USBR 1996). In 1928 (17 years after construction) longitudinal cracking on the downstream edge of the crest (Sherard 1953) was observed in November after the drawdown had been completed. A total of 5 cracks, each 5 to 50 m in length, 12 to 50 mm in width and 1 to 3.5 m deep, were observed along the higher embankment sections, including the closure section. In 1931 (19 years after construction) a slide in the upstream slope occurred during drawdown on 2nd August. The slide was approximately 110 m in width and 3 to 5 m in depth located within the steeper upstream slope between Stations 43 and 46+50. The head of the backscarp was about 7 m below crest level. The slide mass was excavated and the upstream slope rebuilt to its original configuration in 1931.

Remedial works of the steep upstream slope were undertaken in 1939 (following the failure of the upstream slope on rapid drawdown in 1931) and again in 1977 to address concerns over embankment stability under drawdown. In 1939 a gravel stabilising berm was added to the lower upstream slope below elevation 2950 feet, and in 1977 the upper portion of the upstream slope was flattened to a slope of 2.33H to 1V, the crest widened 1.4 m to upstream and the crest re-surfaced (refer to Section 4.1 of Appendix G for a cross section of the remediated embankment).

On large drawdown in 1985 (74 years after construction) longitudinal cracking was observed on the crest between Stations 39 and 46, located 1.2 m from the upstream edge of the crest. The crack, which was centred on the Owl Creek closure section, was about 200 m in length and up to 75 to 100 mm in width. A vertical displacement to upstream of 50 mm was measured across the crack. Investigation found that the crack was coincident with the upstream edge of the original structure, located directly above the

buried concrete kerb. On drawdown in 1988 and 1989 (77 and 78 years after construction) the 1985 crack re-opened and the differential settlement to upstream across the crack increased.

During piezometer installations in 1982 softened and very wet zones were encountered within the earthfill and foundation (Hickox and Murray 1983).

Instrumentation for monitoring deformation behaviour at Belle Fourche dam is by surface measurement points (SMP). At end of construction a series of SMPs were installed along the crest in 1911 and were monitored for vertical deformation over a period of about 17 years to 1928 (Figure 7.157), so no monitoring records are available for the large drawdowns in 1928 and 1931. In 1985, some 74 years after construction, SMPs were installed on the crest and slopes between Stations 26 and 46 and the deformation records of the SMPs installed at Station 40 to 42 (within the Owl Creek closure section) are shown in Figure 7.158.

When compared to similar embankments, a number of aspects of the post construction deformation behaviour at Belle Fourche dam are clear outliers and considered as indicative of "abnormal" behaviour. These include:

- The large magnitude of crest settlement in the first 17 years of operation, reaching more than 2% of the embankment height (Figure 7.48 and Figure 7.60).
- The very high crest settlement rate (Figure 7.63a). At 10 to 12 years after construction the rate was about 1.8% per log cycle of time, and increased to about 4.5% per log cycle of time at 75 to 85 years after construction.
- The very high rates of settlement of SMPs on both the upstream (Figure 7.83) and downstream (Figure 7.78a) shoulders within the closure section.
- The very high rate of downstream displacement of the downstream slope (Figure 7.80) and upstream displacement of the upstream slope (Figure 7.87) within the closure section at 75 to 85 years after construction.

Of the SMPs installed on the crest and slopes of the embankment after 1985, the deformations between Stations 40 and 42 (within the Owl Creek closure section) were up to 1.5 to 2 times greater than those measured elsewhere on the embankment, and were very much larger at MP5 (located at Station 42+00) on the upstream slope. During large drawdown at 74 years (1985) and again at 77 years (1988) acceleration in settlement and non-recoverable upstream displacement is observed at MP5 on the upstream slope. This is coincident with the observation of cracking and greater

settlement of the upstream edge of the crest. At 86 years further non-recoverable upstream displacement was observed for MP5.

The embankment performance during large drawdown is indicative of the marginal stability of the upstream slope on drawdown, as evidenced by the failure in the upstream slope during the 1931 drawdown.

USBR (1996) attributes the observed cracking and monitored "abnormal" deformation behaviour of the upstream slope to upstream crest region during the drawdowns in 1985, 1988 and 1989 to settlement / consolidation of the original earthfill under the added weight of the granular filling in the upstream shoulder berm placed in 1977. However, they do not discount the potential for deep-seated movements. A notable aspect of the deformation behaviour of the upstream slope during large drawdown is that only at MP5 (located within the Owl Creek closure section) is the acceleration in settlement and displacement observed, no such behaviour is observed at other SMPs on the upstream slope also located on the newly placed granular filling.

The deformation records after 75 years show relatively similar behaviour for the crest and downstream slope, with average settlement rates of 6 to 10 mm/year and downstream displacement rates of 6 to 13 mm/year. An increase in displacement rate of SMPs on the crest and downstream slope is observed after 82 years, and is approximately coincident with a period of higher average reservoir level. The increase in settlement rate of the downstream edge of the crest and downstream slope after year 85 (1996) may reflect a change in effective stress conditions due to a rising phreatic surface under the high average reservoir level.

Overall, the long-term deformation behaviour at Belle Fourche dam is "abnormal" in comparison to similar embankments. The "abnormal" deformation of the crest and slopes, particularly in the vicinity of the Owl Creek closure section (Stations 40 to 42), possibly reflects the "highly stressed" conditions within the embankment due to the steepness of the embankment slopes for an earthfill embankment constructed of medium plasticity clays. An important aspect of the deformation behaviour is the much higher crest settlement rates (per log cycle of time) from recent monitoring compared to those at 10 to 12 years after construction. This possibly reflects softening of the undrained strength properties of the earthfill due to wetting of the earthfill, strain weakening under the high stress conditions imposed during large drawdown, lateral spreading in the crest region and cracking in the upper portion of the embankment.

The USBR comment that the Owl Creek closure section, which was constructed very rapidly, is a definite discontinuity along the dam embankment and that the deformation behaviour within this closure section is somewhat unique to the rest of the embankment. This is indicated by the greater magnitudes of deformation measured for the SMPs on the crest and slopes of the embankment installed more than 75 years after the end of construction.

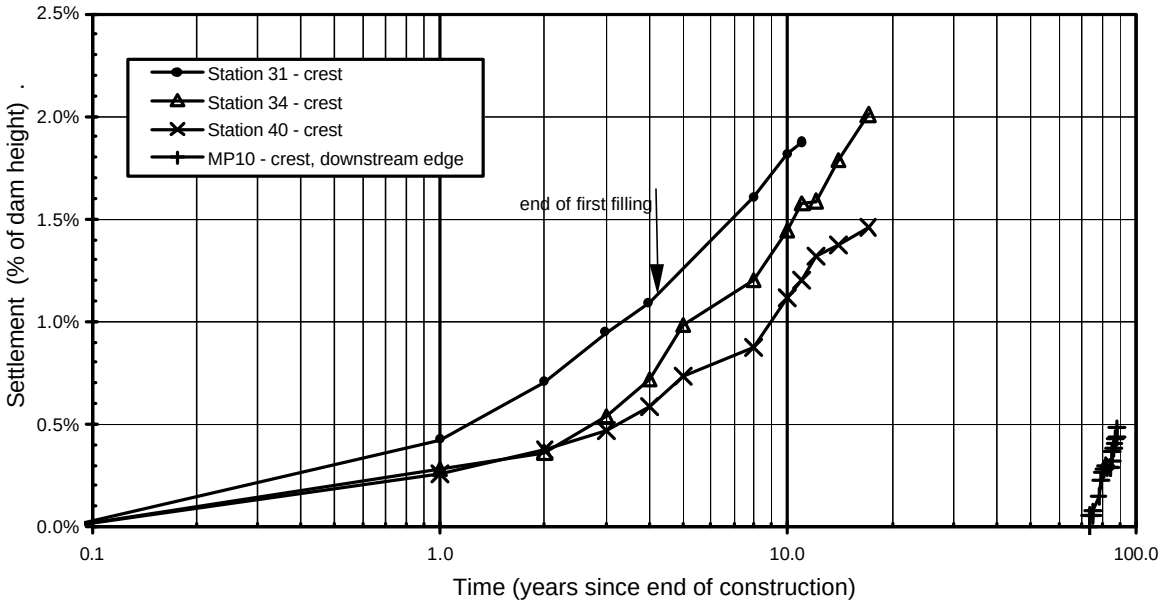

Figure 7.157: Belle Fourche dam; post construction crest settlement over the period 1911 to 1928 (to 17 years post construction).

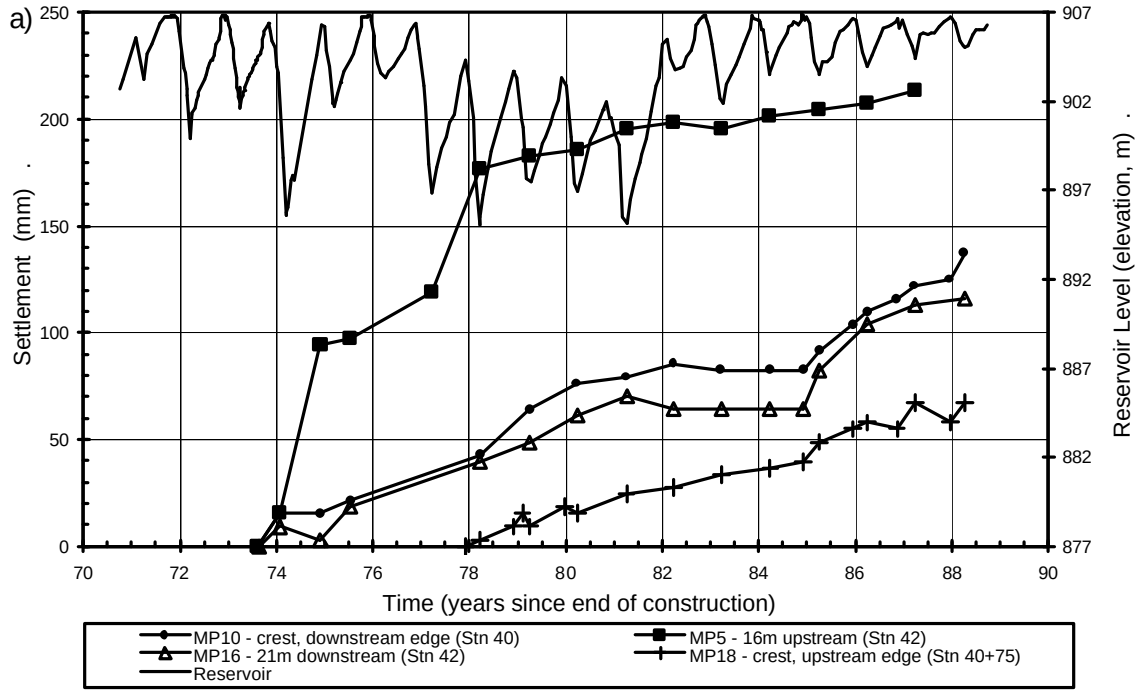

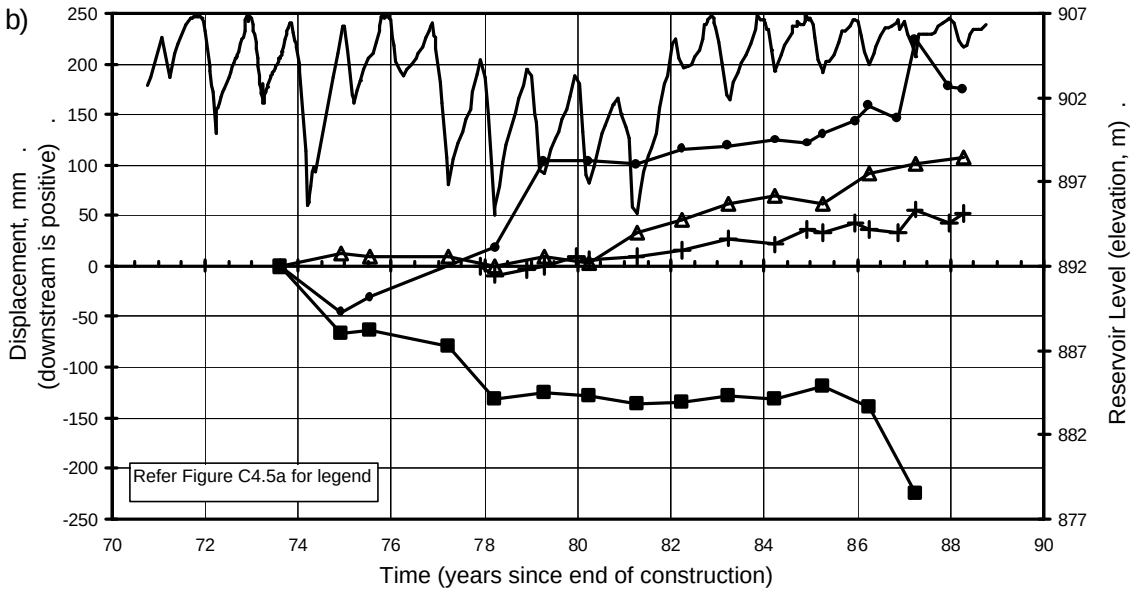

Figure 7.158: Belle Fourche dam closure section; post construction *(a)* settlement and *(b)* displacement normal to dam axis of the crest and slopes over the period 1985 to 2000 (73 to 89 years post construction).

7.11.2.2 *San Luis dam (Section 2.2 of Appendix G)*

San Luis dam is a zoned earth and rockfill embankment with very broad central earthfill zone constructed in the 1960's. The embankment is of 116 m maximum height and 5650 m crest length. Foundation conditions vary along the length of the embankment, from deep alluvial deposits in the floodplain area to bedrock at shallow depth on hillslopes. Changes to the embankment design were made according to the foundation conditions (refer Section 2.2 of Appendix G). A section at the slide area is shown in Figure 7.159.

The very broad central earthfill core was constructed using mainly low to medium plasticity sandy clays, sourced from alluvial terrace and floodplain deposits, compacted by tamping rollers in 150 mm layers to high density ratio at moisture contents on average 1.2% dry of Standard optimum. The miscellaneous fill zone (Zone 3) in the outer downstream shoulder and upstream toe regions comprised materials ranging from Zone 1 type earthfills to weathered rock, and were placed and compacted in 300 mm layers.

Full supply level was reached in July 1969, 2.1 years after construction, and post first filling the reservoir has been subjected to a seasonal drawdown ranging in magnitude from 5 to about 65 m (Figure 7.162a).

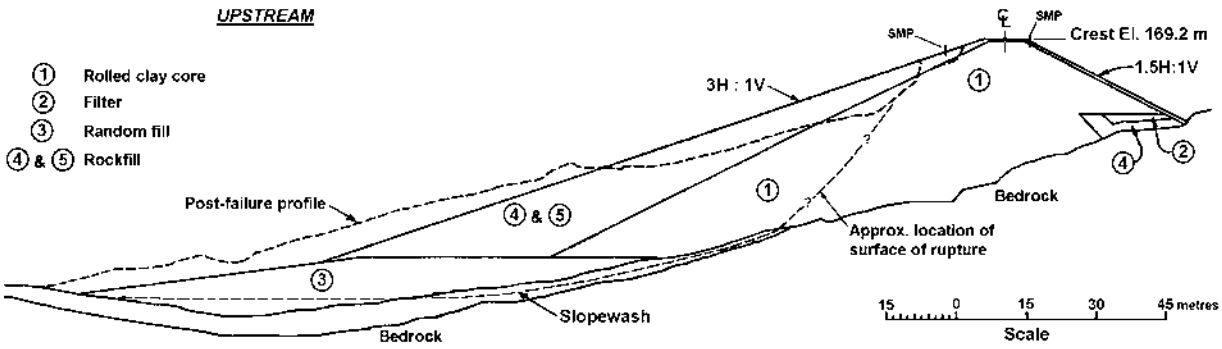

Figure 7.159: San Luis dam, section of the slide in the upstream slope in 1981 at Station 135+00 (courtesy of United States Bureau of Reclamation).

In September 1981, some 14 years after construction, a slide occurred in the upstream slope during large drawdown (Von Thun 1988; Stark and Duncan 1987, 1991). The deep-seated slide (Figure 7.159) was located on the left abutment in a region where the original ground surface under the embankment sloped in an upstream direction at about 10 to 15 degrees. It was approximately 460 metres in width (from Station 122 to 137), 1 million cubic metres in volume, and slid a distance of about 20 m.

Von Thun (1988) considered that the persistent, but minor, longitudinal crest cracking over the 14 years up to the slide and settlement behaviour of SMPs on the upstream at Stations 136 and 138 as indicators of "abnormal" deformation behaviour prior to the slide and precursory warning signs of potential instability. Although, he added that, actual prediction of the timing of the slide was not possible from the monitored deformation.

Von Thun (1988) suggests that in the area of the slide the crest cracking "*was associated with the saturation and progressive straining of the slopewash on the hillsides*". But, the longitudinal crest cracking was not confined to the region of the slide, it was more of a general occurrence along the length of the embankment. This is confirmed by comparison of the displacements along the line of SMPs upstream of the dam axis with those downstream of the dam axis, which showed that leading up to the slide lateral spreading of 50 to 150 mm occurred along most of the embankment length. In addition, most of the differential displacement in the region of the slide occurred during first filling (refer Section 2.2 of Appendix G). However, there is some query over the "original zero" and the accuracy of the lateral displacement measurements in the 1960's and 1970's.

For the overall embankment it could be said that the longitudinal crest cracking is likely to be associated with differential deformations due to progressive development of the phreatic surface in the dry placed and brittle earthfill, and the stress conditions developed in the earthfill. Therefore, it is difficult to consider the crest cracking as an indicator of "abnormal" deformation behaviour and a precursor to slope instability in this case, unless persistence of the cracking was confined to the vicinity of the slide.

With respect to the settlement behaviour of SMPs on the upstream slope, Von Thun (1988) comments that the very large differential between the actual and predicted post construction settlements at Stations 136 and 138 (Figure 7.160) was a clear indicator of the "*anomalous*" behaviour in the region of the slide prior to the failure. The SMPs on the upstream slope at Stations 136 and 138 are located several metres above and therefore outside of the initial slide area as shown in Figure 7.159.

Figure 7.161 presents the actual post construction settlements measured to the date of the last reading prior to the slide for SMPs at 13 m upstream and those at 6.5 downstream of the dam axis. The figure shows that at most locations the measured settlements up and downstream of the crest are similar, however, a differential is notable for the SMPs from Station 130 to 140, in particular at about Station 136 where the slide initiated. In addition, the settlement versus time plot of SMPs in the region of the slide (Figure 7.162) shows that during the first large drawdown period from 8 to 10 years after construction an acceleration in settlement rate was measured for the SMPs on the upstream slope. When the settlement is normalised with respect to the height from the SMP to foundation level (Figure 7.162b) the magnitude of the settlement during drawdown was greater for the SMP at Station 136. This trend in the settlement behaviour might be considered "abnormal" in comparison to other SMPs on the upstream slope at San Luis dam both in the slide vicinity and elsewhere along the embankment.

In summary, the settlement behaviour of the SMP on the upstream slope at Station 136, located in the region of but not within the slide area, during the first large drawdown appears "abnormal" compared to similar embankments and more importantly to other SMPs on the upstream slope at San Luis dam. During the next large drawdown in 1981, at 14 years after construction, the slide in the upstream slope occurred. In hindsight, the settlement behaviour of this SMP could be considered as a precursory sign of the failure, although, it would be almost impossible to predict the occurrence of the slide based on the deformation records as concluded by Von Thun (1988).

The longitudinal crest cracking at San Luis dam is not considered as a reliable indicator of "abnormal" deformation behaviour and precursory sign of slope instability in this case because of its widespread occurrence along the embankment.

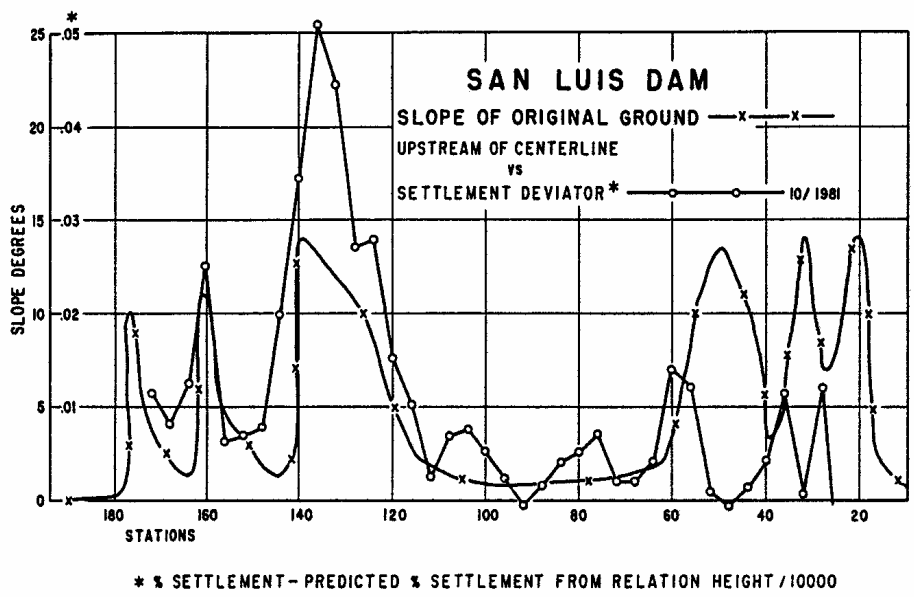

Figure 7.160: San Luis dam, difference between actual and predicted settlement (Von Thun 1988)

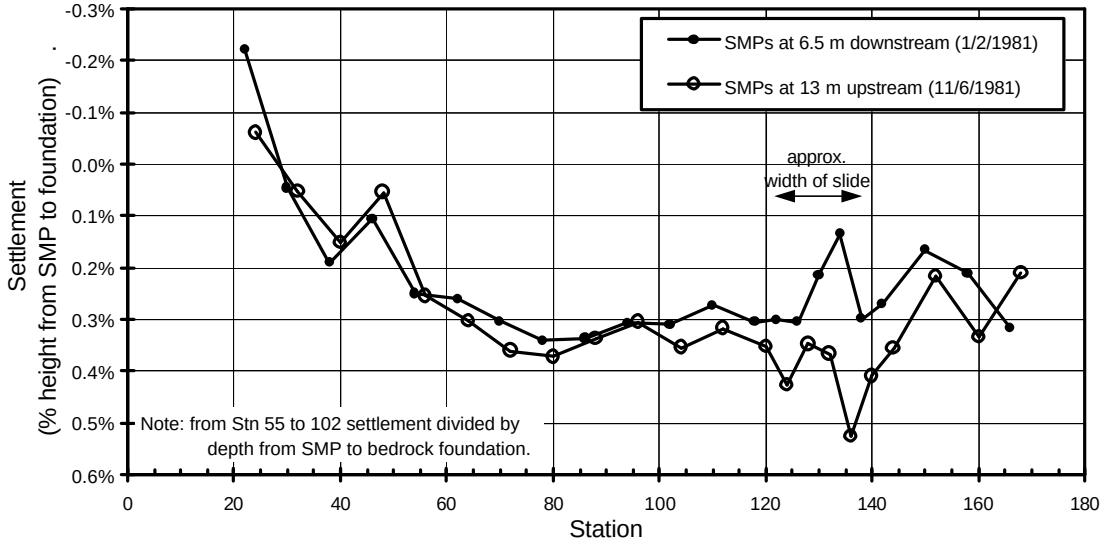

Figure 7.161: San Luis dam, comparison of settlement between SMPs at 13 m upstream of dam axis and SMPs at 6.5 m downstream.

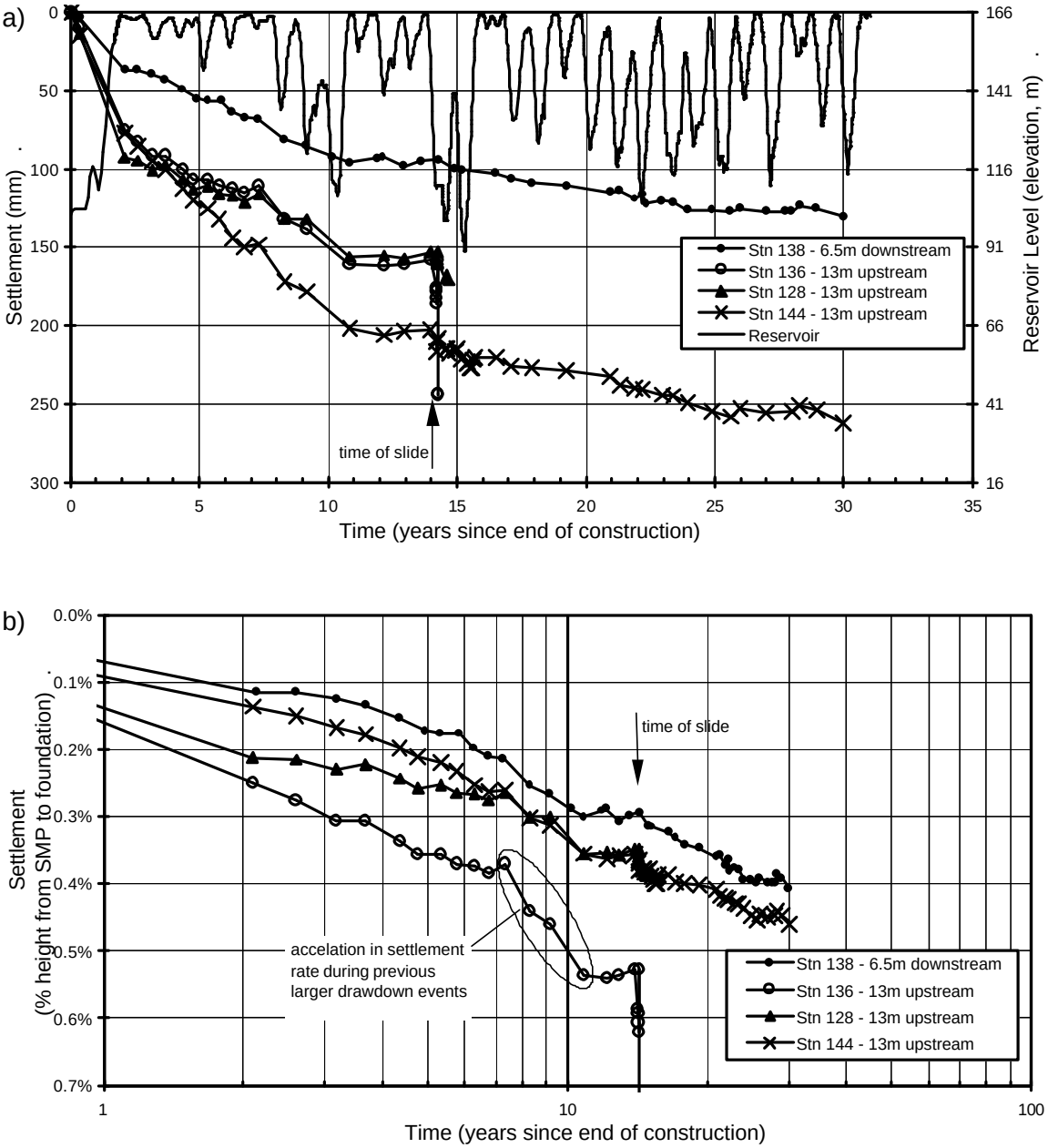

Figure 7.162: San Luis dam, post construction settlement of SMPs in the vicinity of the slide area.

7.11.3 THE EFFECT OF THE DEVELOPMENT OF THE PHREATIC SURFACE ON THE DISPLACEMENT OF THE CREST AND DOWNSTREAM SHOULDER.

For a number of the earthfill embankments or zoned embankments with very broad core width the displacement of the crest and/or downstream shoulder shows an increase in the rate of displacement long-term (Figure 7.76 for the crest, and Figure 7.80 for the downstream shoulder). The affected case studies include Horsetooth, Soldier Canyon,

Spring Canyon, Dixon Canyon, Pueblo (both left and right abutment embankments), San Luis and Belle Fourche dams.

For a number of embankments of very broad core width constructed of low permeability earthfills, the phreatic surface developed gradually within the embankment over tens of years (refer Section 7.6.3 item f). Changes in the reservoir operation are also likely to influence the phreatic surface. Maintaining the reservoir at higher elevations for longer periods that previously experienced will result in a gradual rise in the phreatic surface. The effect of a slow increase in the phreatic surface will cause a gradual change in the effective stress conditions within the embankment and softening of the material strength properties as the degree of saturation increases, particularly if the core is yielded or dilated. These changes are likely to influence the deformation behaviour and are considered a factor in the unusual observation of higher rates of displacement post first filling.

At Belle Fourche dam the increase in displacement rate of SMPs on the crest and downstream slope is observed after 82 years, and is approximately coincident with a period of higher average reservoir level (Figure 7.158). In addition, the increase in settlement rate of the downstream edge of the crest and downstream slope after year 85 may also reflect a change in effective stress conditions due to a rising phreatic surface under the high average reservoir level.

At all the Horsetooth Reservoir embankments (refer Section 3.3 in Appendix G), an increase in displacement rate to downstream was measured many years after the end of first filling for SMPs on the crest and downstream slope. USBR (1997) indicate that the pore water pressures within the earthfill zones of all embankments were still rising more than 50 years after construction. The increase in pore water pressures suggests that equilibrium conditions are yet to be reached, indicating that progressive wetting up is still occurring.

7.11.4 OTHER CASES OF POTENTIAL "ABNORMAL" DEFORMATION BEHAVIOUR

7.11.4.1 Horsetooth dam

As previously discussed, the foundation had a significant influence on the post construction deformation behaviour at Horsetooth dam. The embankment design over the broad gully region (Figure 7.163) was such that the bulk of the embankment was

founded on the over-burden soils and the cut-off trench to bedrock was located upstream of the dam axis. The depth of over-burden soils in the broad gully region was up to 10 to 20 m.

Settlements in the foundation under the centreline of the embankment were very large, estimated at almost 15% of the depth of the over-burden (500 to 1000 mm at the IVM locations). Post construction, the settlement of the foundation was also very large (325 mm at IVM A or up to 5% of the depth of the over-burden over nearly 50 years), most of which (about 70%) occurred on first filling. The post construction vertical strains in the foundation were very much larger than in the earthfill, where they average 1.05% at 45 years after construction.

The large differential settlement between the foundation and earthfill in the cut-off had the effect of causing a downstream rotation of the embankment downstream of the cut-off trench. As shown in Figure 7.164, the upper upstream shoulder to downstream shoulder displaced downstream during the period of first filling from 2 to 4.5 years after construction.

Compared to similar embankments the displacement at Horsetooth dam on first filling is an outlier (Figure 7.38 to Figure 7.40), but not "abnormal" because of the influence of the compressible foundation.

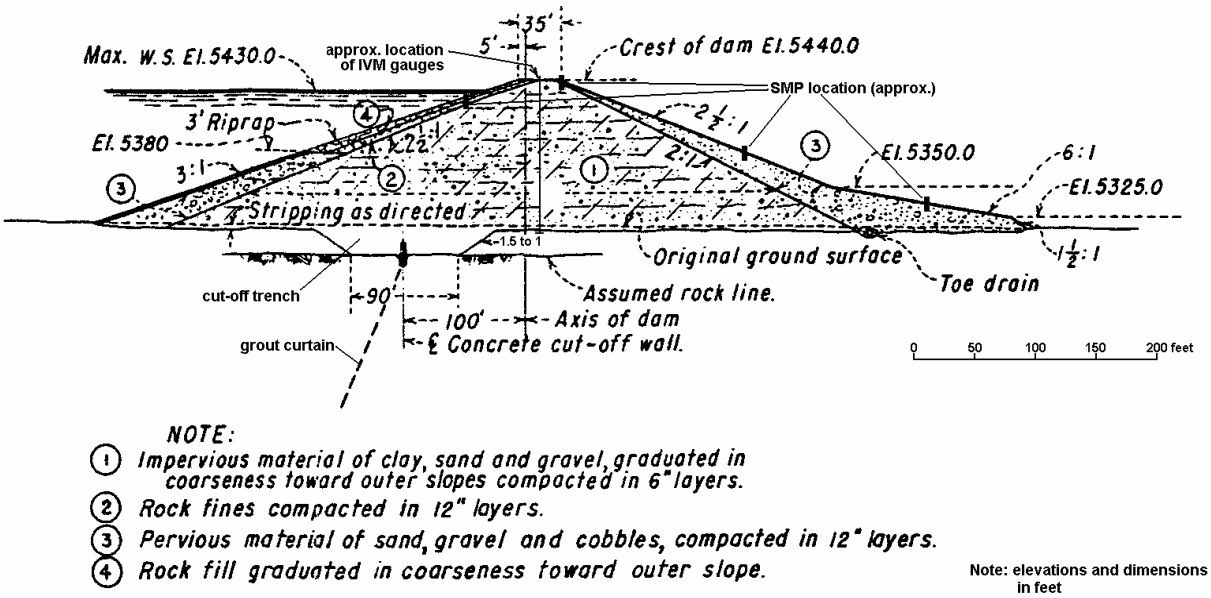

Figure 7.163: Main section at Horsetooth dam (courtesy of the United States Bureau of Reclamation).

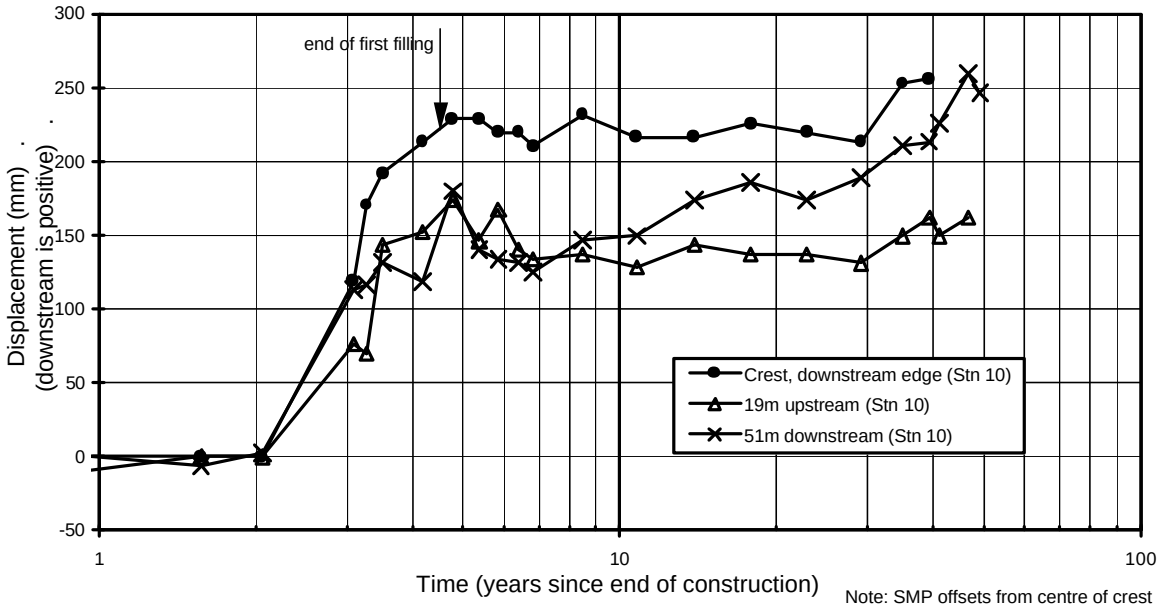

Figure 7.164: Horsetooth dam, post construction displacement of SMPs near to the main section.

7.11.4.2 Pueblo dam, left abutment embankment (Section 3.4 of Appendix G)

The left embankment at Pueblo dam (Figure 7.165) is of 37 m maximum height and about 1100 m crest length. The main earthfill zone consisted of clay to gravel size alluvium placed in 150 mm layers and compacted by tamping rollers. The moisture specification called for the mean moisture content to be in the range 0.5% dry to 1.5% dry of Standard Proctor optimum moisture content. Coarser and more permeable soils were used in the outer up and downstream regions of the main earthfill zone.

During construction (in the early to mid 1970's) shear type deformations were measured in the downstream toe region of the left embankment when the embankment was within about 7 m of design crest level. Inclinometers showed that the deformations were concentrated along weak bentonitic clay seams in the foundation. By end of construction total shear type displacements were estimated (by the USBR) at more than 150 mm at the downstream toe of the left embankment. The shear deformations virtually ceased shortly after the end of construction. In the early 1980's a stability berm was constructed along the downstream toe of the left abutment embankment due to concerns over the potential limiting stability of the downstream slope.

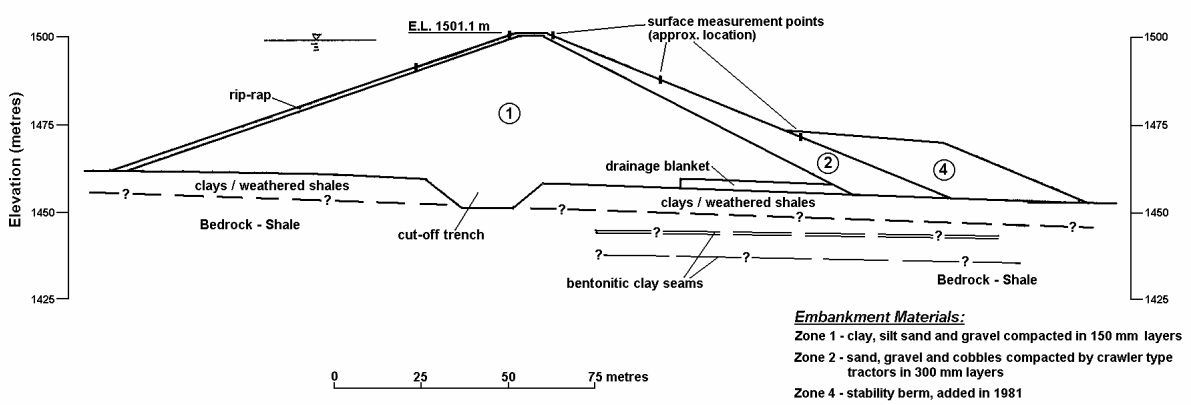

Figure 7.165: Pueblo dam; cross section of left abutment embankment at Station 75

Post construction settlements of the downstream shoulder of the left abutment embankment at Pueblo dam were large (Figure 7.166), and in comparison to similar type embankments the magnitude is "abnormally" high (Figure 7.50 and Figure F2.10a of Appendix F). The long-term settlement rate of the downstream shoulder is on the high side, but not "abnormally" so (Figure 7.78).

In the vicinity of Station 75 borehole records indicate the soils are mainly weathered shales, for which the post construction deformation is likely to be limited and therefore not greatly influence the deformation behaviour of the embankment. In addition, the shear type deformations observed in the foundation during construction had virtually ceased at the end of construction, and therefore would not influence the post construction deformation behaviour of the downstream shoulder with the stability berm added.

As Figure 7.166 shows, the first settlement reading after the base survey of the SMP on the downstream slope is very high (0.75% or almost 150 mm) and contributes significantly to the large post construction settlement (42% of the total settlement measured over 23 years). After this first reading the settlement behaviour is similar in magnitude to other SMPs on the embankment crest and upstream slope, although the settlement rate is slightly higher. Other SMPs along the downstream slope of the left embankment abutment show similar settlement behaviour to that at Station 75.

It is not clear what the cause of this observed settlement behaviour for the downstream slope is. The influence of construction of the stability berm is not the cause because construction started in 1980 some 5 to 5.5 years after end of construction, after the period of large settlement. It is possible that it could be survey error. Apart from the settlement of the downstream shoulder, the post construction deformation behaviour

at the left abutment embankment of Pueblo dam is "normal". Further details on the deformation behaviour at Pueblo dam are discussed in Section 3.4 of Appendix G.

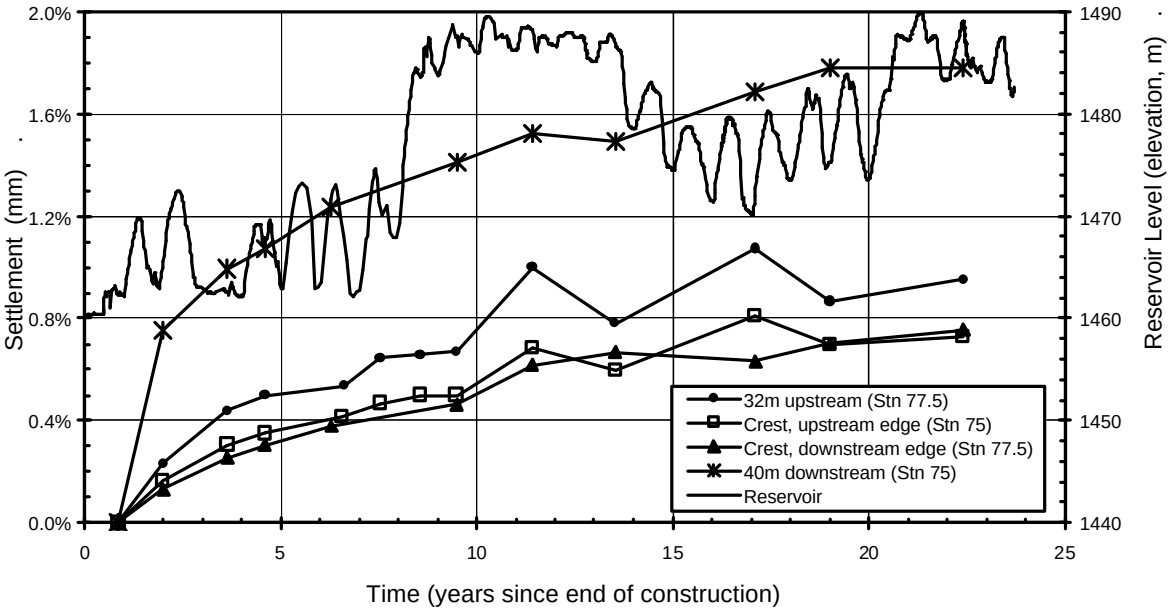

Figure 7.166: Pueblo dam, post construction settlement of the left embankment near Station 75.

7.12 "ABNORMAL" DEFORMATION BEHAVIOUR OF PUDDLE CORE EARTHFILL DAMS

For puddle core earthfill dams, trends of "abnormal" deformation behaviour are specific to the long-term deformation behaviour given the period of construction of these embankment types. Identification of "abnormal" deformation behaviour is from comparison with the deformation behaviour of other puddle dams, mainly in terms of rates of deformation, as well as the deformation trend in relation to the creep model under constant stress conditions. The limited number of records from the end of construction does not allow for comparison based on the magnitude of deformation.

As previously discussed, what may initially be termed "abnormal" may later be proven by investigation and additional monitoring to in-fact be "normal". In the case of puddle core earthfill embankments, the large deformations observed during historically large drawdown events (Section 7.7.3.5) could well be considered as "abnormal" when compared to the deformation trends under normal reservoir operating conditions.

7.12.1 COMPARISON WITH THE DEFORMATION BEHAVIOUR OF OTHER PUDDLE DAMS

Most of the available data to assess the long-term deformation behaviour of a puddle core earthfill embankment relates to crest settlement (Table 7.24, and Table F1.5 in Section 1 of Appendix F). There is some, but limited, data on settlement of the shoulders and at the downstream toe, and on horizontal displacement.

In terms of crest settlement, comparisons can be made as follows:

- Total settlement from the end of construction (Figure 7.92). Although, only limited data is available for comparison. The age of the embankment, embankment height, compaction methods and moisture control affect the total settlement. From Figure 7.92:
  - For dams constructed after about 1900, and particularly after about 1930, the total settlement at about 30 to 50 years is less than 4% of the total height of the embankment. In comparison, the total crest settlement of Hollowell Dam (completed in 1937) stands out as being "abnormal" and is discussed later.
  - For older puddle dams, there is insufficient information to make a judgement on what could be expected as "normal" total settlement. Yan Yean and Hope Valley dams show total vertical settlements of 8 to 13% of the embankment height at more than 100 years.
- The long-term crest settlement rate, S_{LT}, under normal reservoir operating conditions. As discussed in Section 7.7.3, long-term rates of crest settlement depend on a number of factors, in particular the level of fluctuation of the reservoir and the pore water pressure response in the earthfill zone upstream of the puddle core.
  - For "steady state" conditions S_{LT} is typically less than 1% per log cycle of time (settlement as a percentage of the embankment height). "Steady state" conditions are defined as virtually steady reservoir operating levels or, in the case of fluctuating reservoir level, negligible to minor changes in pore water pressure in the earthfill zone upstream of the puddle core to fluctuations in the reservoir level.
  - For embankments subject to reservoir fluctuation and in which the upstream earthfill is permeable (i.e. the changes in pore water pressure in the earthfill zone upstream of the puddle core approximate the fluctuations in reservoir level), S_{LT} rates of 2.6% to 7.4% per log cycle of time have been measured, and are considered to be "normal".

– Figure 7.98 presents data on crest settlement versus drawdown height for dams subject to reservoir fluctuations greater than 20% of the dam height and in which the earthfill zone upstream of the puddle core is permeable. The data has been adapted from Tedd et al (1997b). This figure shows some correlation between height of drawdown and permanent crest settlement, and could be used as preliminary tool for assessment of "abnormal" deformation. However, the use of Figure 7.98 is limited given that the data set comprises older UK dams (pre 1910) of similar height and dimensions, and constructed using similar materials.

Other than for crest settlement, the deformation data on puddle core earthfill dams is limited due to the limited data available. Comparisons based on settlement of the embankment shoulders are not possible. However, assessment of the horizontal displacement of the crest and downstream slope is possible.

The post construction deformation behaviour of earthfill and earth-rockfill dams indicates that the general displacement trend of the crest and downstream shoulder is for downstream displacement at a decreasing rate (on log time scale) with time, eventually reaching a point where the net displacement is negligible with some fluctuation about the general trend due to fluctuations in reservoir level. A similar analogy is possible for puddle dams. The limited amount of available data tentatively suggests:

- Negligible long-term rates of downstream displacement of the crest and downstream slope for case studies at "steady state" conditions.
- Long-term displacement rates of the downstream crest and slope of up to 3 to 5 mm/year downstream for embankments where the upstream shoulder is relatively permeable and the reservoir is subject to relatively large drawdowns (more than about 20% of the embankment height) and the fluctuation is within the range of normal reservoir operation.

The deformation behaviour of the following case studies is considered to be "abnormal" based on comparison with other puddle dams:

(a) Hollowell dam

The crest settlement of Hollowell dam in the period shortly after embankment construction. The magnitude of total crest settlement of Hollowell dam in comparison to puddle dams of similar age is significantly greater (Figure 7.92). At 10 years after

the end of construction crest settlement at Hollowell dam was more than 6% compared to less than 2% for Selset and Burnhope dams.

Kennard (1955) indicates the large deformations at Hollowell dam were due to the marginal factor of safety of the downstream slope at the end of construction as a result of the high pore water pressures in the foundation. Localised shear type deformations occurred during construction and measures were undertaken to improve the factor of safety. The long-term settlement rate for Hollowell dam more than 10 years after the end of construction is about 0.7% per log cycle of time, which is comparable to dams of similar characteristics.

(b) Yan Yean dam (Section 5.2 of Appendix G)

The high long-term rate of settlement of the downstream edge of the crest at Yan Yean dam measured more than 130 years after the end of construction is considered "abnormal".

Yan Yean dam has been categorised in the class of "steady state" embankments based on the minor pore water pressure response in the earthfill zone upstream of the puddle core compared to the change in reservoir level. S_{LT} rates for the crest would be expected to be less than about 1% per log cycle of time, which is the case for the upstream edge of the crest.

However, for the downstream edge of the crest S_{LT} is a maximum of 11% over a period of 14 years from 128 to 142 years after construction, much greater than would be expected of "normal" type behaviour. High rates of settlement and displacement of the downstream crest and slope were also observed over this period of monitoring (up to 8 to 10 mm/year settlement, and up to 4.5 - 5.5 mm/year downstream crest displacement). These high rates are also considered indicative of "abnormal" deformation behaviour. The increasing rate of deformation with time of several SMPs (refer Section 5.2 of Appendix G) is also a strong indicator of "abnormal" deformation behaviour.

The deformation behaviour of the downstream slope is considered to be independent of the reservoir level operation and possibly indicative of a tertiary creep (or creep to failure) phase of movement (refer Section 7.12.2). Investigations showed fissured clays in the foundation were contributing to a marginal stability condition, and a berm has now been constructed to improve stability under normal operating conditions and earthquake, and internal erosion and piping control.

(c) Hope Valley dam (Section 5.3 of Appendix G)

For Hope Valley dam the rate of downstream displacement of the upper downstream slope of 5 mm/year over the monitoring period from 118 to 128 years after construction maybe on the high side, but would not be classified as "abnormal" from the available data. But, the deformation behaviour could be indicative of marginal stability condition of the downstream slope. Hope Valley dam has since been remediated and a downstream stabilising berm added (Gosden et al 2002).

7.12.2 GENERAL MOVEMENT TRENDS INDICATIVE OF DEFORMATION TO FAILURE

From the basic creep model of time dependent deformation under constant deviatoric stress conditions (Singh and Mitchell 1968; Mitchell 1993), an increasing rate of deformation under constant stress is indicative of a deformation to a failure condition (i.e. a tertiary creep phase of deformation). A localised trend of increasing rate of deformation at one SMP may indicate shallow surficial deformations or a faulty SMP, and not a marginal stability condition and potential failure condition. It is therefore important that a similar deformation trend is evidenced by other SMPs on the embankment in the close proximity to each other and that a vector plot of the deformation at a section is indicative of a potential deep-seated movement.

The deformation trends of several SMPs on the downstream crest and slope of Yan Yean dam (Figure 7.167) show an increasing rate of deformation, indicating a potential tertiary creep mode of deformation, that is considered to be independent of reservoir level fluctuation. The possible mechanisms involved in the deformation behaviour of the downstream slope are considered to be a combination of stress changes at the top of the slope due to moisture infiltration into cracks when the reservoir is in a drawdown condition and to progressive failure of the foundation or saturated base of the embankment. It would appear that stick-slip type deformation behaviour of the downstream toe at several locations indicates that the movements are being driven from the top of the slope resulting in build up of stresses in the foundation (or saturated base of the embankment). Continued movements of this type within the over-consolidated foundation could result in strain weakening and a progressive failure. As previously mentioned a downstream berm has now been constructed to improve stability.

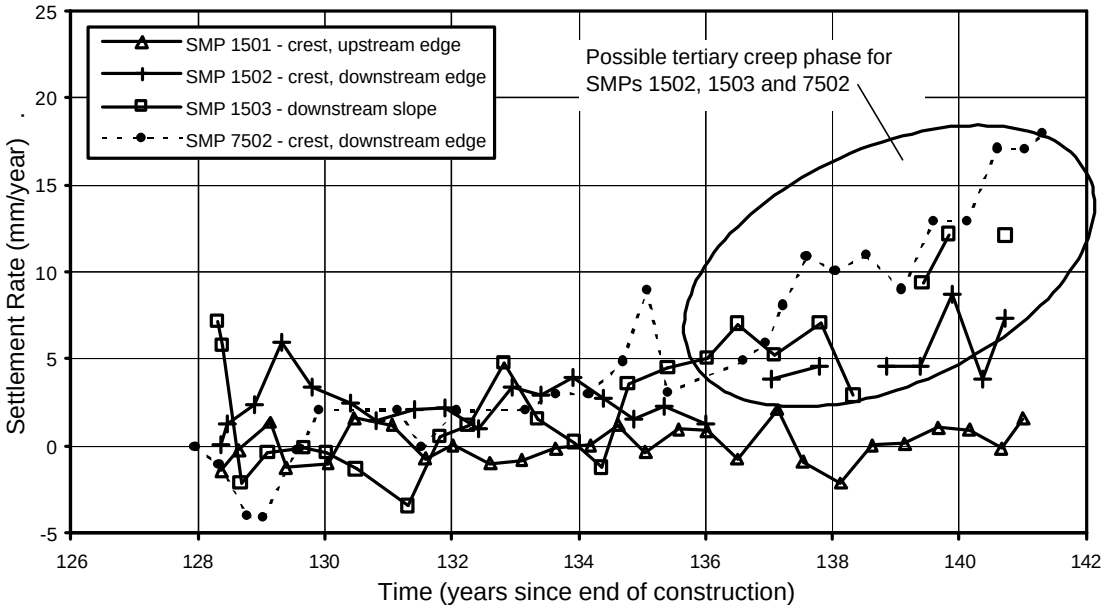

Figure 7.167: Yan Yean dam; settlement rate versus time of SMPs at Chainage 150 and 750 m.

7.12.3 OTHER INDICATORS OF "ABNORMAL" DEFORMATION BEHAVIOUR

Several other examples from the long-term monitoring trends of puddle core earthfill embankment case studies are considered to be indicative of possible "abnormal" deformation behaviour. These were observed at Ramsden and Hope Valley dams, both of which are discussed further in Section 5 of Appendix G.

For Ramsden Dam, the abnormal deformation behaviour is related to the internal deformation of the puddle core on the abnormally large drawdown in 1988 to 1989. It is considered possible that shearing occurred in the puddle core between 10 m and 11 m depth below the crest as indicated by the localised high vertical strain and possible upstream shear displacement at this depth. This is associated with a permanent settlement of 51 mm at the crest, smaller permanent settlements of the upstream slope (2 to 10 mm) and 7 mm permanent upstream displacement of the crest.

For Hope Valley dam (Appendix G, Section 5.3) the displacement rate of the upper downstream slope (5mm/year) is considered to be relatively high in comparison to other puddle dams. The rate is similar to that of Yan Yean dam, although the rate at Hope Valley dam was virtually constant and not increasing. In comparison to the crest of Walshaw Dean and Ramsden, which also shows a steady downstream displacement rate, the rate is higher at Hope Valley dam, however this may be due to type of material

used as shoulder filling and possibly a lower factor of safety of the downstream shoulder.

Based on the available deformation records for Hope Valley dam and in comparison with other puddle dams, it is considered that a significant proportion of the movement of the downstream slope can be attributed to long-term creep and cyclic stress changes associated with reservoir level fluctuations. However, it is not possible to conclude that these are solely the explanation for the movement without considering the possibility that the downstream shoulder is in a marginal stability condition. The discerning factor is the high and constant rate of downstream displacement. As previously mentioned a downstream berm has now been constructed to improve stability.

7.13 SUMMARY OF "ABNORMAL" DEFORMATION BEHAVIOUR

The purpose of identification of "abnormal" deformation behaviour of embankment dams is for the early detection of potential problems, mainly with respect to slope instability. But, it may also have implications with respect to internal erosion and piping because the deformations may lead to cracking and softening. Following identification of "abnormal" deformation behaviour it is necessary to understand the mechanism/s causing the observed behaviour, which may incorporate investigation and analysis, and may eventually lead to some form remedial works. In most cases "abnormal" deformation behaviour does not equate with stability issues for the embankment, but in a number of cases it has.

The methods of identification of "abnormal" deformation behaviour from the case study analysis are mainly as outliers to the "normal" deformation behaviour of similar embankment types in terms of magnitude, rate and trends. In summary, the methods are:

- During construction (for earthfill and zoned earth and earth-rockfill embankments), outliers in terms of:
  - Total core settlement during construction (Figure 7.23, Table 7.14 and Table 7.15).
  - Magnitude of vertical strain within the core at a given depth or effective vertical stress level (Figure 7.18, Figure 7.20 and Figure 7.21).
- Post construction, outliers in terms of:
  - Magnitude of settlement or displacement.

  - Settlement rate (rate in terms of log time) including:
    - Magnitude of the settlement rate
    - Acceleration in rate over short periods of time, often, but not always, post first filling on drawdown.
  - Displacement:
    - Direction of displacement
    - Magnitude of the long-term displacement rate (rate in terms of log time)
    - Change in direction of the underlying general trend, i.e. the trend outside of that due to reservoir fluctuation.
    - Short periods of non-recoverable displacement post first filling, such as a permanent upstream displacement on large drawdown.
- Development of localised regions of high strain (during or post construction) indicative of the formation of a shear surface, and the ongoing deformation within these regions. The case study analysis concentrated on vertical strains in the core region of the embankment, but this would be equally applicable to concentration of lateral strain in the core or foundation measured in inclinometers.
- The tertiary creep analogy from the model of creep under constant stress conditions. Tertiary creep (or creep to failure) is creep at an increasing rate (rate in terms of normal time) with time and is an indication of the onset of failure. Primary creep, or creep at a decreasing rate (rate in terms of normal time) with time is indicative of "normal" type behaviour.

Several important aspects on the deformation behaviour should be noted:

- For zoned earth and rockfill dams, "abnormal" or potentially "abnormal" deformation behaviour was much more likely in embankments where the rockfill was susceptible to large settlements due to collapse compression on wetting or was of high compressibility. These include rockfills that are poorly compacted, dry placed and poorly to reasonably compacted, dumped and sluiced rockfills, weathered rockfills, and rockfills of rock type susceptible to large loss in unconfined compressive strength on wetting. Conversely, sound rockfills that are wetted and well and reasonably to well compacted are, in most cases, not susceptible to large collapse compression on first filling and the overall post construction deformation behaviour of the embankment is "normal" and generally of limited magnitude.

- The development of a shear zone in the earthfill core does not equate with a marginal factor of safety, although it may. The shear zone may be a result of differential settlement between the core and shoulder or a lack of support from the shoulders. The core types within which shear surfaces developed (and the timing of the shear development) included:
  - Compacted silty sands to silty gravels. Shear surfaces in the core generally developed during first filling or with further movements shortly thereafter (often drawdown related). High shear stresses at the interface between the core and upstream rockfill shoulder (that developed due to the greater settlement of the upstream shoulder as it collapse compressed on wetting) were considered the mechanism in most cases for the shear development.
  - Dry placed clayey sand earthfills. Shear surfaces in the core generally developed during first filling with further deformations associated with reservoir operation.
  - Dry placed sandy clay and clay earthfills. Shear surface developed on first filling (e.g. Ataturk dam) or many years post first filling, usually on large drawdown (see below).
  - Wet placed clayey earthfills. Examples of shear surface development during construction and on first filling, as well as post first filling.
- Longitudinal cracking does not equate with a marginal factor of safety. In most cases it may simply be due to differential deformation between the zones in the embankment and may only occur during the period of and shortly after first filling. However, persistent longitudinal cracking may be indicative of a marginal stability condition (refer below).
- Acceleration of the deformation of the crest and upstream slope on large drawdown and resultant permanent deformations do not equate with marginal stability, but they may. These type of deformations are not uncommon on historically large drawdowns where yielding may occur under effective stress levels not previously experienced (such as observed in several puddle dams). Persistent observations of acceleration of the deformation on large drawdown may be indicative of a marginal stability condition (refer below).
- For several central core earth and rockfill embankments with dry placed clay cores and dry placed and/or poorly compacted rockfills, shear surfaces developed (or were

thought to have potentially developed) in the central region of the core many years after the end of construction. In the case of Eppalock dam it was considered that significant cracking in the core preceded the shear development as indicated by observed cracking and/or the change in displacement trend of SMPs on the crest. The cracking prior to shear development was considered a significant factor in the development of the shear surface, which was first identified during a large drawdown (not necessarily the first large drawdown). This type of shear surface development was considered to have possibly developed at several other similar type embankments (i.e. dry placed clayey core with rockfill shoulders susceptible to collapse compression on wetting).

The issue of potential instability or marginal stability of the embankment is the foremost aspect of any deformation monitoring that is undertaken given the potentially catastrophic consequences of a slope failure condition in an embankment dam. Some guidelines from the analysis of those case studies where failure occurred or where the embankment was considered to be in a marginal stability condition are:

- Instability during construction:
  - Deformation behaviour during shutdown periods. Large and ongoing deformations during shutdown or acceleration in the rate of deformation (rate in terms of normal time) may indicate marginal stability or an impending failure condition.
  - The incremental magnitude of deformation with increasing dam height or stress level (refer Penman 1986). High or increasing (e.g. Carsington dam) incremental magnitudes of deformation may be indicative of a marginal stability condition or the onset to a failure condition.
  - Localised regions of “abnormally” high strain as measured in internal settlement gauges or inclinometers may be an indicator of internal shear and potentially a progressive failure mechanism. Increases in the incremental magnitude of localised strain may be indicative of the onset to a failure condition.
- Post construction on drawdown:
  - Persistent development of cracking on large drawdown
  - Persistent acceleration in settlement and/or displacement of SMPs on the crest and/or upstream shoulder on large drawdown.

  - A similar or increasing magnitude of non-recoverable deformation on consecutive large drawdowns of similar magnitude (consecutive meaning 1, 5, 10 or more years between drawdowns of similar magnitude interspersed with smaller magnitude drawdowns).
  - Acceleration in settlement or displacement that is confined to one region of the embankment, such as observed at San Luis dam in the region of the slide in the large drawdown preceding the one that triggered the slide (refer Section 7.11.2.2).
  - Localised regions of high magnitude deformation compared to similar locations elsewhere on the embankment or compared to predicted deformations (Von Thun (1988), for San Luis dam).
- Post construction, downstream shoulder:
  - Tertiary creep phase of deformation (e.g. Yan Yean dam).

From the study of failures in embankment dams (excludes failures in hydraulic fill dams) in Chapter 5, the conversion of a significant portion of the potential energy into kinetic energy at or post failure is required for acceleration of the slide mass and large post failure deformation. Factors contributing to this conversion in energy for the case studies of slides in embankment dams included:

- Potential for material strain weakening on shearing at or after failure in drained or undrained loading conditions (including static liquefaction of structured soils in undrained loading).
- Brittleness in the slide mechanics, such as due to internal brittleness or toe buttressing, and/or brittleness on the lateral margins.
- The slope failure geometry and orientation of the surface of rupture.

The deformation behaviour has important implications on the embankment performance related to the potential for internal erosion and piping, as well as the long-term stability of the embankment. With respect to internal erosion and piping a number of aspects are considered to increase the potential for formation of a seepage path through the core of a zoned embankment, including:

- Cracking. The influence of cracks across the core is readily apparent. The possible causes of cracking associated with deformation behaviour are discussed by others

(Sherard 1973; amongst others). In addition to these mechanisms of crack formation, localised large deformations are likely to give 3D cracking that may persist through the core. Also, further differential deformations post construction, such as between the core and shoulders or core and foundation, can open up or widen existing cracks.

- Further differential deformations post construction, such as between the core and shoulders or core and foundation, can result in further arching and reduction in the stress conditions within the core, thereby increasing the potential for hydraulic fracture.
- Shear or softened zones that persists across the width of the core are also potential seepage paths.

It is evident from the deformation behaviour at a number of embankments that the softening process in ongoing and can lead to deterioration of the embankment over time, and potentially a gradual reduction in the factor of safety of the embankment's stability. The clearest example is evidenced by the timing of upstream slope instability on drawdown in rolled earthfill embankments (e.g. Belle Fourche and San Luis dams) where the embankment was subjected to several large drawdown events before the failure occurred. Part of the mechanism associated with these and other upstream slope failures is considered to be progressive strain weakening in undrained loading under cyclic reservoir operation within the well-compacted over-consolidated rolled earthfill shoulder. This mechanism was recognised by Stark and Duncan (1987, 1991) as significant in the failure at San Luis dam and is reflected in the composite shear strength concept recommended by Duncan et al (1990) for limit equilibrium analysis under drawdown. Other softening processes associated with the deformation behaviour of embankment dams are:

- Lateral spreading and/or cracking of the core. Lateral spreading (and therefore cracking) in central core earth and rockfill dams is more significant where the rockfill is susceptible to large settlements from collapse compression on wetting. Part of the reason for this is considered to be due to the transfer in stress to the core associated with the greater settlement of the shoulders, and due to the reduction in support that is provided by shoulders that have suffered large deformations.
- In earthfills susceptible to collapse compression on wetting, the reduction in shear strength and compressibility properties is significant. These earthfills are virtually

normally consolidated on softening due to wetting or post collapse. In the case of Hume dam (Cooper et al 1997) a significant factor in the marginal stability of the downstream shoulder of the concrete core-wall earthfill embankment at near full supply level was the low undrained shear strength of the near normally consolidated saturated earthfill in the lower portion of the downstream slope.

In limit equilibrium analysis therefore, consideration should be given to the potential for softening and the influence of the embankment deformation behaviour on the shear strength properties of the embankment materials. Some guidelines are:

- Use the method by Duncan et al (1990) for analysis of the upstream shoulder under drawdown. It takes into consideration the effects of progressive strain weakening of over-consolidated earthfills under cyclic reservoir operation.
- For zoned earth and rockfill embankments where the shoulders are susceptible to large settlements associated with collapse compression on wetting, the use of fully softened c' and f' parameters is wise for over-consolidated earthfill cores because of the potential for softening from lateral spreading and cracking (in addition to the softening on wetting from reservoir seepage).
- For earthfills susceptible to collapse compression (refer below) the collapsed earthfill is likely to be near normally consolidated. The potential for development of shear induced positive pore water pressures should be considered in the stability analysis and this may require the use of undrained strength rather than a conventional c', f' analysis.
- Where a concentrated shear is developed residual strength parameters are appropriate. Concentrated shears have developed within the core zone in a variety of core types from silty sands/silty gravels to high plasticity clays, and in both over-consolidated dry placed clays and wet placed clay cores of low undrained strength. Consideration should also be given to the potential for strain localisation near to the interface between zones (e.g. in the core near to interface with the shoulder, such as observed at Ataturk dam (Cetin et al 2000)) and the use of residual strength parameters for these shear zones.

It is widely recognised that poorly compacted and dry placed earthfills are susceptible to collapse compression on wetting leading to large deformations (Gould 1954; Bernell 1958; Penman 1986; Charles 1997; amongst others). The susceptibility

of an earthfill to collapse compression is dependent on its material type, density and moisture content at placement, and the level of stress within the embankment. The case study evidence of earthfills suspected of collapse compression indicates:

- Dry placed and poorly compacted earthfills are susceptible to collapse compression on wetting (e.g. outer earthfill zone in old puddle embankments (pre 1900/1920)). There is no information from the database to suggest how dry poorly compacted earthfills need to be placed for them to be susceptible to collapse compression.
- Formally compacted earthfills susceptible to collapse compression include:
  - Earthfills placed on the dry side of optimum. Clayey earthfills placed drier than about 2% dry of Standard optimum are susceptible. But, this will vary depending on the material type, fines content, fines plasticity and compacted density ratio. Silty sands and gravels and clayey earthfills with low fines content or low plasticity fines may be susceptible when placed only 1% dry of Standard optimum. Charles (1998) suggests the air voids be reduced to less than 5% in clay earthfills to ensure the earthfill is not susceptible to collapse compression.
  - Material types including silty sands and gravels, clayey sands and gravels and sandy clays generally of low plasticity. Medium to high and high plasticity clays do not appear to be susceptible to collapse compression (when well compacted).
  - Layer thickness and the variation in density within the layer are also important considerations. The lower portion of thick placed layers, where the density is often lower, is more susceptible to collapse compression than the upper, more heavily compacted part of the layer.

7.14 SUMMARY AND METHODS FOR PREDICTION OF DEFORMATION OF EMBANKMENT DAMS

This section presents a summary of the outcomes from analysis of the deformation behaviour of earthfill, zoned earth and earth-rockfill, and puddle core earthfill embankments from Sections 7.4 to 7.7 for use in prediction of, or comparison of the deformation behaviour of an embankment. The methods for evaluation of the "normal" deformation behaviour were developed to identify potentially "abnormal" behaviour,

and the figures and tabulated data provide a means for prediction or comparison to similar embankment types.

In part, the summary is a pointer to figures and tables in this chapter relating to specific aspects of embankment deformation behaviour. It also briefly summarises the factors affecting the deformation behaviour as determined from the analysis as well as bringing together some of the data within this chapter for ease of use.

7.14.1 EARTHFILL, AND ZONED EARTH AND EARTH-ROCKFILL DAMS

The methods for prediction of deformation behaviour of earthfill and zoned earth and earth-rockfill dams are divided into two subsections, deformation during construction and deformation post construction.

7.14.2 PREDICTION OF DEFORMATION BEHAVIOUR DURING CONSTRUCTION FOR EARTHFILL AND ZONED EARTH AND EARTH-ROCKFILL EMBANKMENTS

Prediction of the deformations during construction of earthfill and zoned earth and earth-rockfill dams are best undertaken by finite element methods. The difficulty with these methods is in selection of properties and the constitutive model to represent the various material zones, as well as consideration of the use of coupled models and dealing with partial saturation of earthfills and the change in matric suction with stress level.

The total and effective stress conditions established in an embankment during construction are dependent on the embankment geometry, the embankment zoning geometry, and the strength and compressibility properties of the embankment materials. The simplest case to analyse is the elastic analysis of a homogeneous embankment on a rigid foundation where non-linearity of material properties is taken into account in the model used to represent the compressibility properties of the earthfill. Results show that under the embankment centreline lateral strains are negligible and deformation is predominantly in the vertical direction. The homogeneous model is shown to be a reasonable assumption for the stress conditions under the embankment axis for:

- Zoned embankments with broad central earthfill zones for rolled earthfill placed dry of Standard optimum (more than about 0.5% to 1% dry), where only limited to negligible positive pore water pressures are developed during construction.

Analysis and the case study data suggests it is a reasonable assumption for embankments with central core widths having a combined core slope (i.e. upstream and downstream core slope combined) greater than about 1.5 to 2H to 1V, but it may also be a reasonable simplification for combined central core widths down to 1H to 1V.

- Zoned embankments where the compressibility properties of the central earthfill zone and gravelly or rockfill shoulders are similar; i.e., compacted sandy and gravelly soils with non-plastic fines or low (less than about 20% finer than 75 micron) plastic fines contents, with shoulders of compacted gravels or rockfill. This is on the proviso that pore water pressures generated in the core during construction are small and potential plastic type core deformations due to lateral spreading of the core are negligible.

Case study analysis shows that for dry placed earthfills the confined secant modulus shows a gradual increase with increasing effective vertical stress (ignoring matric suction). Therefore, reasonable numerical deformation solutions can be obtained without consideration of pore water pressures provided the model used reasonably approximates the compressibility of the earthfill. Values of confined secant modulus of dry placed earthfills estimated from field data is presented in Table 7.13 and Figure 7.19 sorted based on material type. For dominantly sandy and gravelly earthfills the data is further sorted based on fines plasticity and fines content. The data provides useful bounds for comparison with laboratory test data on proposed core materials and assistance in selection of the confined moduli for use in analysis.

At the other end of the spectrum is wet placed earthfill cores of low undrained shear strength used in zoned earth and earth-rockfill embankments. Numerical analysis modelling the core in undrained conditions is considered to provide a reasonable approximation of the deformation behaviour for earthfills of low permeability, where the deformation of the core occurs largely as undrained plastic type deformations. The amount of lateral spreading of the core, which is influenced by the lateral stresses developed in the core and the compressibility of the supporting shoulder zones, has a significant influence the deformation of the core.

Modelling becomes more complex where:

- Pore water pressure dissipation in the core occurs during construction and the use of a coupled model is desirable.

- Over the period of construction the initial deformation of the core is largely due to compression of air voids, but in the latter stages largely occurs as plastic type deformations in undrained conditions.

For rockfill and gravel earthfill zones, Chapter 6 provides information for use in selection of the confined modulus properties based on intact rock strength, placement method and particle size distribution.

Several methods have been developed for evaluation of the deformation behaviour of embankment dams during construction that are useful for comparative purposes. They are:

- Total core settlement for the period of construction. Estimation of the total core settlement is based on embankment height, core material type and core width (Figure 7.23, Table 7.14 and Table 7.15). This method was effectively used to identify "abnormally" large deformations during construction for several embankments.
- Vertical strain profile in the core at end of construction; Figure 7.18 for dry placed earthfill cores, Figure 7.21 for wet placed dominantly sandy and gravelly cores (SC/GC/SM/GM cores), and Figure 7.22 for wet placed clay cores. The figures provide approximate bounds for "normal" type deformation behaviour. They can also be used for evaluation of core deformation as construction proceeds. The figures are useful for identification of regions of the core in embankments where vertical strains were excessively large. Plots of vertical strain versus effective vertical stress or height above the cross-arm interval (e.g. Figure 7.15 or Figure 7.20) for regions of high strain can then be used to assess the incremental vertical strain and evaluate the possibility of shear type deformation.
- Lateral deformation of the core for central core earth and rockfill dams of thin to medium core width (Section 7.4.2). The estimated lateral displacement ratio (LDR) of the core at selected depths in a limited number of case studies is presented in Figure 7.12 and Figure 7.13. The data indicates:
  - LDR is influenced by the lateral stress developed in the core and so will be greater for wet placed than dry placed cores, and earthfills of low permeability (i.e. limited dissipation of pore water pressures during construction).
  - The compressibility of the supporting shoulder zones has a significant influence on LDR. LDR increases with increasing compressibility of the shoulders.

- The location of measurement affects LDR. Finite element analysis of a dam on a rigid foundation showed LDR at end of construction to be a maximum at about 50 to 70% of the depth below crest level.

7.14.3 PREDICTION OF DEFORMATION BEHAVIOUR POST CONSTRUCTION FOR EARTHFILL AND ZONED EARTH AND EARTH-ROCKFILL EMBANKMENTS

A number of figures and tables have been developed for evaluation and/or prediction of the deformation behaviour post construction of SMPs on the crest and slopes of the embankment. In summary they include:

- Settlement (based on zero time at the end of embankment construction):
  - Magnitude of settlement for the crest and shoulders at 3, 10 and 20-25 years after construction
  - Settlement versus time plots for the crest and shoulders
  - Settlement rate (rate in terms of log time)
- Lateral displacement:
  - Of the crest, upstream shoulder and downstream shoulder on first filling (Section 7.5.3)
  - Of the crest post first filling
  - Lateral displacement versus time plots for the crest and shoulders (based on zero time at the end of embankment construction)

(a) Deformation versus time plots

A large number of figures have been produced of deformation (i.e. settlement or displacement) versus time, with zero time established at the end of embankment construction. Table 7.26 and Table 7.27 are a pointer to the plots of settlement and displacement versus time for the crest and shoulders respectively. Note that for zoned earth and earth-rockfill dams with thin to thick core widths, the upstream edge of the crest is included in the upstream shoulder region and the crest region is from the central to downstream edge of the crest (refer Figure 7.37).

The case studies for crest deformations were sorted based on core width, core material type and moisture content at placement. For embankments with very broad earthfill cores the influence of the foundation was taken into consideration. For the

deformation versus time for the shoulders, the case studies have been sorted based on the material type in the shoulder, and for rockfills its compaction rating.

The general trend of the deformation versus log time plots is:

- For settlement, near linear to slightly increasing rate with time (rate in terms of log time) is the general trend. But, it is not unusual to have a slightly decreasing settlement rate long-term for the crest. In some cases magnitudes of settlement are large on first filling for the crest and upstream slope, particularly where the upstream shoulder is susceptible to collapse settlement.
- For horizontal displacement a general trend is more difficult to define because of the broader range in behaviour, but:
  - A large percentage of the displacement generally occurs on first filling. For the crest and downstream slope, this displacement is generally in a downstream direction.
  - Long-term, the trend of the displacement rate (rate per log time) approaches low to near zero values, with fluctuations about the trend due to reservoir fluctuation.

Table 7.26: Figure references for post construction crest deformation

Core Width *[1]	**Core *[2] Classification**	**Moisture Content *[3]**	**Figure Reference**	
			Settlement	**Displacement**
Thin to Medium	CL/CH	Dry placed	Figure 7.53	Figure 7.68
		Wet placed	Figure 7.54	Figure 7.69
	SC/GC	Dry placed	Figure 7.55	Figure 7.70
		Wet placed	Figure 7.56	Figure 7.71
	SM/GM	Dry and wet placed	Figure 7.57	Figure 7.72
Thick	CL/CH	Mostly dry placed	Figure 7.58	Figure 7.73
	SC/GC/SM/GM	Mostly dry placed	Figure 7.59	Figure 7.74
Very Broad	Limited/negligible foundation influence		Figure 7.60	Figure 7.75
	Potentially significant foundation influence		Figure 7.61	Figure 7.76

Note: *[1] The terms used for core width classification are defined in Section 1.3.3.

*[2] The core classification is to the Australian Soil Classification System.

*[3] Dry placed defines cores where limited to negligible pore water pressures were developed during construction and is generally applicable to placement more than 0.5% to 1% dry of Standard optimum. Wet placed refers to cores where significant pore water pressures were developed during construction. Refer to Section 7.4.1.4 for further discussion and definition of the qualitative terms used.

Table 7.27: Figure references for post construction deformation of the embankment shoulders

Shoulder Material Type	Compaction Rating *1	Downstream Shoulder *2		Upstream Shoulder *2	
		Settlement	Displacement	Settlement	Displacement
Rockfill	Well compacted	Figure F2.4	Figure F2.12	Figure F2.23	Figure F2.30
	Reasonably to well compacted	Figure F2.5	Figure F2.13	Figure F2.24	Figure F2.31
	Reasonably compacted	Figure F2.6	Figure F2.14	Figure F2.25	Figure F2.32
	Poorly compacted	Figure F2.7	Figure F2.15	Figure F2.26	Figure F2.33
Gravels	-	Figure F2.8	Figure F2.16	Figure F2.27	Figure F2.34
Earthfills	-	Figure F2.9	Figure F2.17		
Very broad core width (earthfill)	No foundation influence	Figure F2.10	Figure F2.18	Figure F2.28	Figure F2.35
	Foundation influence	Figure F2.11	Figure F2.19	Figure F2.29	Figure F2.36

Note: *1 Refer to Section 1.3.3 for definitions of the compaction rating terms used.
*2 Figures are in Section 2 of Appendix F.

(b) Magnitude of post construction settlement

The magnitude of post construction settlements for the crest and shoulder regions are presented at 3, 10 and 20 to 25 years after the end of embankment construction. Table 7.28 is a pointer to tables and figures within the chapter. Table 7.29 and Table 7.30 summarise the typical range of "normal" settlement magnitude for the crest and shoulders respectively.

For the crest region, the data has been sorted based on core width, core material type and placement moisture content, and indicates that:

- The post construction crest settlements are generally much smaller than the core settlement during construction.
- Nearly all dams experience less than 1% crest settlement post construction for periods up to 20 to 25 years and longer after construction.
- Most experience less than 0.5% in the first 3 years and less than 0.75% after 20 to 25 years.
- Smaller magnitude settlements are observed for dry placed clayey sands to clayey gravels and dry to wet placed silty sands to silty gravels.

- A broader range of settlement magnitude is shown for clay cores, wet placed clayey sand to clayey gravel cores, and embankments with very broad core widths.
- For zoned earth and rockfill dams, poor compaction of the rockfill is over-represented for case studies at the larger end of the range of crest settlement.

The data for the shoulder regions indicates:

- Settlements in the order of 1 to 2% are observed for poorly compacted rockfills. Greater settlements are observed for the dry placed, poorly compacted rockfills.
- For reasonably compacted rockfills the range of settlement is quite broad, from 0.1% up to 1.0%, but the number of cases is limited. Settlements toward the upper range are observed for dry placed and/or weathered rockfills, where settlements due to collapse compression are likely to be significant.
- Much lower settlements, generally less than 0.5 to 0.7% at ten years after construction, are observed for well and reasonably to well compacted rockfills, and compacted earthfills.
- Very low settlements (less than 0.25% at 10 years) are observed for embankments with gravel shoulders.

(c) Long-term settlement rate

As previously discussed, post first filling the settlement rate (rate in terms of log time) of SMPs on the crest and slopes is generally close to linear. For a number of case studies the rate may increase slightly with time and for some case studies it may decrease slightly with time. The long-term settlement rate for the case studies was estimated assuming a linear relationship between settlement and log time, and over periods of time representing "normal" reservoir operating conditions. For case studies where the rate increased (or decreased) with time after first filling the estimate was generally based on the later period of measurement. Table 7.31 is a pointer to tables and figures related to long-term settlement rate within the chapter, and Table 7.29 and Table 7.30 provide the typical range of long-term settlement rate for the crest and shoulders respectively excluding possible outliers. The units of settlement rate are percent settlement per log cycle of time (settlement as a percentage of the height from the SMP to foundation level). The same units are used for the puddle core earthfill embankments.

Table 7.28: References to post construction settlement magnitude tables and plots

Embankment Region	**Table Reference**	**Time After End of Construction (years) *[1]**		
		3 years	**10 years**	**20 to 25 years**
Crest	Table 7.19	Figure 7.46	Figure 7.47	Figure 7.48
Downstream shoulder	Table 7.20	Figure 7.49 (Figure F2.1)	Figure 7.50 (Figure F2.2)	Figure F2.3
Upstream shoulder	Table 7.20	Figure 7.51 (Figure F2.20)	Figure 7.52 (Figure F2.21)	Figure F2.22

Note: *[1] Figures numbers with an 'F' prefix are in Section 2 of Appendix F.

Table 7.29: Embankment crest region, typical range of post construction settlement and long-term settlement rate

Core Properties			**Crest Settlement (%) *[1, *2]**			**Long-term Settlement Rate *[1, *3]**	
Class[n]	**Core Width**	**Moisture content**	**3 years**	**10 years**	**20 to 25 years**	**Steady/Slow Reservoir**	**Fluctuating Reservoir**
CL/CH	Thin to medium	dry	0.05 to 0.55	0.10 to 0.65	0.20 to 0.95	0.04 to 0.50 (most < 0.26)	0.09 to 0.57
		wet	0.04 to 0.75	0.08 to 0.95	0.20 to 1.10		
	Thick	all (most dry)	0.02 to 0.75	0.10 to 1.0	0.5 to 1.0		
SC/GC	Thin to medium	dry	0.10 to 0.25	0.10 to 0.40	< 0.5	0 to 0.26	0.06 to 0.37
		wet	0.15 to 0.80	0.20 to 1.10	< 1.1		
	Thick	all (most dry)	0.05 to 0.20	0.10 to 0.35	0.10 to 0.45		
SM/GM	Thin to thick	all	0.06 to 0.30	0.10 to 0.65	< 0.5 to 0.7	< 0.10	0.03 to 0.21
Very Broad Earthfill Cores - most CL and dry placed			0.0 to 0.60	0.0 to 0.80	0.05 to 0.76	0.08 & 0.44	0.07 to 0.70 (most < 0.35)

Note: Class[n] = classification to Australian Soil Classification System

*[1] excludes possible outliers.

*[2] crest settlement as a percentage of the embankment height

*[3] long-term settlement rate in units of % settlement per log cycle of time (settlement as a percentage of dam height).

Table 7.30: Embankment shoulder regions, typical range of post construction settlement and long-term settlement rate

Material Type	Compaction Rating	Downstream Shoulder *1			Upstream Shoulder *1		
		Settlement (%) *2		Settlement Rate *3	Settlement *2		Settlement Rate *3
		3 years	10 years		3 years	10 years	
Rockfill	well	0.05 to 0.35	0.05 to 0.55	0.0 to 0.33	0.10 to 0.60	0.10 to 0.70	0.05 to 0.70 (most < 0.50)
	reasonably to well	< 0.30	< 0.50	0.04 to 0.31 (most > 0.15)	0 to 0.55	0.10 to 0.60	0.10 to 0.56 (most < 0.50)
	reasonable	0.20 to 1.0	0.10 to 1.0	0.10 to 1.0	< 0.70	- *5	< 0.55
	poor	0.10 to ? *5	0.15 to ? *5	0.10 to 0.25	0.10 to 1.05	0.15 to 1.20	0.10 to 0.82 (most < 0.60)
	poor – dry *4	0.15 to 1.60	0.30 to 2.00	0.20 to 0.75	0.15 to 1.35	0.20 to 1.6	
Gravels	-	< 0.15	< 0.25	0.02 to 0.065	< 0.15	< 0.25	< 0.21
Earthfills	-	0.0 to 0.40	0.0 to 0.70	0.0 to 0.40	0.05 to 0.60	0.10 to 0.70	0.10 to 0.60

Note: *1 Excludes possible outliers.

*2 Settlements quoted are a percentage of the height from the SMP to foundation level.

*3 The long-term settlement rates are in units of % settlement per log cycle of time (settlement as a percentage of the height from the SMP to foundation level).

*4 For the dry placed and poorly compacted rockfills, a large range in settlements is observed. For rockfills placed in dry climatic regions settlements are likely to be toward the upper end of the range.

*5 insufficient data.

Table 7.31: References to tables and figures of long-term settlement rate

Embankment Region	Table Reference	Figure Reference	Comment
Crest	Table 7.21	Figure 7.62 and Figure 7.63	Figure 7.62 is for zoned embankments with thin to thick core widths, and Figure 7.63 is for embankments with very broad core widths.
Downstream shoulder	Table 7.22	Figure 7.78	
Upstream shoulder	Table 7.23	Figure 7.83	

Reservoir fluctuation was found to influence the long-term settlement rate for the crest, particularly for the zoned embankments of thin to thick core width with permeable upstream shoulder fill (i.e. rockfill or gravels). Generally, greater long-term settlement rates were measured for case studies with fluctuating reservoir levels. The influence of

reservoir fluctuation on the upstream shoulder could not be clearly identified from the available data and it had limited to negligible influence on the downstream shoulder. Two qualitative categories were used for reservoir operation, "fluctuating" for reservoirs subject to a seasonal (usually annual) or regular (more than once per year) drawdown typically greater than about 10 to 15% of the maximum height of the embankment, and "steady" or "slow".

Apart from the influence of reservoir operation, the data for the crest indicated:

- For zoned embankments with thin to thick core widths:
  - Core material type has an influence on the long-term crest settlement rate. In general, earthfill cores of silty sands to silty gravels tend to have low long-term settlement rates and clay earthfill cores, on average, tend to have high long-term crest settlement rates. Clayey sand to clayey gravel cores show intermediate rates.
  - The core width and compaction moisture content appear to have little to no recognisable influence on the long-term crest settlement rate. Their influence is probably over-shadowed by other factors.
  - Embankments with rockfills susceptible to large deformations due to collapse compression have high long-term settlement rates, generally greater than 0.4% per log cycle of time, indicating these embankments are more susceptible to softening and long-term degradation.
- For embankments with very broad width earthfill, zones the long-term settlement rate shows a broad variation in range. Reservoir fluctuation does influence the long-term settlement rate for those embankments with more permeable earthfills.

The data for the embankment shoulders indicates:

- The long-term settlement rate of both the up and downstream shoulder is generally less than about 0.4% per log cycle of time for most cases.
- Higher rates are observed for zoned earth and rockfill dams with rockfills susceptible to large deformations due to collapse compression, particularly in the downstream shoulder.
- Very low rates for zoned embankments with gravel shoulders.

(d) Post construction horizontal displacement

As previously indicated, a large portion of the horizontal displacement generally occurs on first filling, particularly for zoned earthfill and earth-rockfill dams with permeable fills in the upstream shoulder. Additional data (other than the displacement versus time plots) is presented for horizontal displacement, including:

- Lateral displacement on first filling:
  - Table 7.17 and Figure 7.38 for displacement of the crest region;
  - Figure 7.39 for the downstream shoulder region; and
  - Figure 7.40 for the upstream shoulder region
- Lateral displacement of the crest post first filling (Figure 7.77).

The case study records on crest displacement during first filling show that the typical range for most case studies is from 50 mm upstream to 300 mm downstream. A number of trends were evident sorting the data based on core width, core material type and the material type and compaction rating of the downstream shoulder. They were:

- For most groups, the displacement on first filling was downstream and less than 0.1 to 0.2% of the embankment height (less than 100 to 200 mm).
- Greater displacements (from 0.2% to 0.6% and up to almost 1% of the embankment height) were observed for central core earth and rockfill dams of thin to medium core width with:
  - Rockfills susceptible to large deformations due to collapse compression in the downstream shoulder.
  - Silty sand to silty gravel earthfill cores.

These findings suggest that large deformations in the downstream shoulder, possible due to collapse compression on wetting from rainfall, significantly influence the crest displacement for embankments of thin to medium core width. This was confirmed by the observation that those embankments with large crest displacements on first filling also experienced large downstream displacements of the downstream shoulder. The correlation to silty sand and silty gravel cores is possibly indicative of greater magnitude increases of lateral stress in the downstream shoulder on first filling for these embankment types.

The displacement of the downstream shoulder on first filling had many similarities to the crest behaviour on first filling:

- Displacements of the downstream shoulder were less than 0.1 to 0.2% of the embankment height for embankments with very broad earthfill cores, zoned embankments with compacted gravels or earthfills in the downstream shoulder, and zoned embankments with wetted (and generally compacted) rockfills in the downstream shoulder.
- Greater magnitude displacements were generally observed for zoned earth and rockfill dams with dry placed rockfills in the downstream shoulder:
  - Up to 0.25 to 0.30% of the dam height for dry placed and well and reasonably to well compacted rockfills
  - More than 0.2 to 0.25% and up to 0.85% of the dam height for dry placed and poor and reasonably compacted rockfills.

For the upstream shoulder region, displacements on first filling ranged from 200 to 300 mm upstream to 300 mm downstream.

Crest displacements for the period from post first filling to 10's of years after construction are generally of smaller magnitude than the displacement on first filling, particularly for zoned earth and earth-rockfill embankments with thin to medium core widths. Regardless of the embankment type though, the general range of displacement post first filling (for at least 5 years post first filling and up to 40 to 50 years) is quite small, ranging from 35 mm upstream to 100 to 150 mm downstream.

The displacement of the downstream slope post first filling is more erratic than for the crest, even though for a large number of the case studies the displacement post first filling displacement is of small magnitude. In terms of the total magnitude of displacement in a downstream direction since end of construction:

- For embankments with very broad core widths, total displacements generally range from 0.05 to 0.30% of the embankment height at 25 to 45 years after end of construction.
- For zoned earthfill embankments, total displacements are up to 0.15 to 0.20% of the embankment height at 20 to 30 years after end of construction.
- For central core earth and rockfill dams:
  - For well and reasonably to well compacted rockfills, displacements of up to 0.20% are measured at 10 to 20 years after end of construction. Where the

rockfill has been dry placed or is of relatively high compressibility, displacements can be greater; up to 0.25 to 0.40 % of the embankment height.

– For reasonably and poor compacted rockfills, displacements up to 1.0 to 1.6% of the embankment height can occur long-term, particularly for dry placed rockfills susceptible to large deformations due to collapse compression.

7.14.4 PUDDLE CORE EARTHFILL DAMS

The predictive methods for puddle core earthfill dams are appropriate to the long-term deformation behaviour of the embankment, many tens of years after construction. The following presents a summary of the analysis and discussion from Section 7.7.3, of which Section 7.7.3.6 provides a useful summary of the factors affecting the long-term deformation behaviour of puddle core earthfill dams.

The records show that the post construction crest settlement of puddle core earthfill embankments is significant, ranging from 1% up to 8% to 14% of the dam height after more than 100 years. The older (pre 1900) embankments generally show the greater magnitude post construction crest settlement and the more recent embankments (constructed in the 1930's to 1950's) generally show crest settlements of lesser magnitude. A large proportion of the settlement in the older embankments occurred during and shortly after the period of first filling due mainly to collapse compression on wetting of the poorly compacted earthfill supporting the puddle core and yielding on drawdown.

The long-term settlement rate (S_{LT}) of the embankment crest (under normal reservoir operating conditions) was significantly affected by the magnitude of reservoir fluctuation and the permeability of the earthfill zone upstream of the puddle core. Table 7.32 provides guidelines for estimation of the long-term crest settlement under normal reservoir operating conditions. The influence of reservoir fluctuation and earthfill permeability over-shadowed other factors that probably influence the long-term crest settlement including dam height, age and earthfill material type. For several dams the long-term crest settlement rate was intermediate to the ranges given. For Hope Valley dam, part of the reason was thought to be the variable pore water pressure response (ranging from 25 to 100%) in piezometers in the earthfill zone upstream of the puddle core to fluctuations in reservoir level.

Table 7.32: Predictive methods of long-term crest settlement and displacement under normal reservoir operating conditions for puddle core earthfill embankments

Reservoir Operation *[1]	**Response to Drawdown of the Earthfill Zone Upstream of the Puddle Core** *[2]	**No. Cases**	**Crest Settlement Prediction**	**Crest Displacement** *[3]
Steady	("steady state")	7	S_{LT} = 0.4 to 1.0 % *[4]	negligible
Fluctuating	negligible to minor (or "steady state")			
	near full response (i.e. permeable earthfill)	4	S_{LT} = 4.5 to 7.4 % Figure 7.98 for estimation of permanent settlement based on the magnitude of the drawdown	3 to 5 mm/year (downstream)

Notes: *[1] Fluctuating defined as reservoir subject to annual drawdowns generally greater than 10 to 20% of the embankment height
*[2] Refer Figure 7.93 for definitions of "steady state" conditions.
*[3] crest displacement records only available for very few case studies.
*[4] S_{LT} is the long-term crest settlement rate in units of settlement as percentage of embankment height per log cycle of time. Individual values for the case studies are given in Table 7.24.

The methods based on historical performance of similar dams are very approximate because of the limited number of case studies from which they have been derived and the assumptions made regarding the reservoir operation and permeability of earthfill zones upstream of the core. The methods should only be as a general guide in consideration of these factors.

For several embankments, large permanent crest settlements (0.20 to 0.52% of the embankment height) were measured during abnormally or historically large drawdown events (Tedd et al 1997b). In terms of prediction of deformation during these abnormal events, the only available method would seem to be fully coupled finite element modelling (FEM) due to the complexity of the processes and interaction between the different elements within the embankment. But, this is not without difficulties due to the lack of known information on material properties as well as the need to consider stress history.

Available records on the long-term deformation of the shoulders and displacement of the crest are limited. Some preliminary guidance on possible magnitudes of long-term deformation under normal reservoir operating conditions is:

- For displacement of the crest and downstream slope:

  - Under "steady state" conditions long-term rates of displacement are negligible.
  - For fluctuating reservoir conditions and permeable upstream earthfill zones, long-term rates of displacement of up to 3 to 5 mm/years in a downstream direction have been recorded.
- The long-term settlement rate for the shoulders is:
  - Of similar magnitude to the crest for "steady state" conditions (refer Table 7.32).
  - Of lesser magnitude than the crest for fluctuating reservoir conditions and permeable upstream earthfill zones.

7.15 CONCLUSIONS

The main objective of this chapter was to develop methods for identification of potentially "abnormal" deformation behaviour of embankment dams from field monitoring records. The methods were predominantly developed from initially defining what is "normal" deformation behaviour for a particular embankment type in consideration of the imposed stress conditions, and the strength properties and stress-strain relationship of the materials. Potentially "abnormal" deformation behaviour was then broadly identified where the rate, magnitude or trend of the deformation behaviour differed from that of the "norm". Implicit in the methods are concepts such as consolidation, creep under stress conditions and collapse compression on wetting. Once the deformation behaviour for a case study was identified as potentially "abnormal", further analysis was undertaken (where records were available) for evaluation of the possible mechanism/s causing the observed deformation behaviour. Sections 7.8 to 7.12 of the chapter deal with the identification and evaluation of "abnormal" deformation behaviour from the case study data, Section 7.13 providing a summary.

The database comprises some 134 embankments and included the following embankment types:

- Zoned earth and rockfill embankments, most of which were central core earth and rockfill embankments.
- Zoned earthfill embankments
- Rolled earthfill embankments, including homogeneous earthfill, earthfill with filters and earthfill with rock toe.
- Puddle core earthfill embankments.

The deformation monitoring records analysed included:

- During construction – mainly internal vertical deformation of the core, but also the lateral core deformation of zoned earth and rockfill dams with thin to medium core widths.
- Post construction – SMPs on the crest and slopes of the embankment, and the internal vertical deformation of the earthfill core.

From such a broad database of embankment dams it has been possible to develop methods for prediction and evaluation of the deformation behaviour during and post construction from the main types of deformation monitoring records analysed. Section 7.14 provides a summary of these methods with reference to pertinent tables and figures within the chapter.

The methods are considered to be an improvement on currently available methods for the embankment types considered. The influence of material type and placement methods, embankment zoning geometry, embankment height, reservoir operation amongst other factors have been considered.

TABLE OF CONTENTS

8.0 CONCLUSIONS AND RECOMMENDATIONS 8.1

8.1 CONCLUSIONS 8.1

8.1.1 Landslides in Soil Slopes 8.1

8.1.2 Deformation Behaviour of Embankment Dams 8.4

8.2 RECOMMENDATIONS FOR FURTHER RESEARCH 8.6

8.0 CONCLUSIONS AND RECOMMENDATIONS

8.1 CONCLUSIONS

This thesis is a study of the pre and post failure deformation behaviour of landslides in cut, fill and natural soil slopes, and of the deformation behaviour of embankment dams. The primary objective of the research has been to further develop the understanding of the deformation behaviour of landslides and embankment dams, and then to improve predictive methods for use in quantitative risk assessment of landslides, and the evaluation and prediction of the deformation of embankment dams.

The research has been undertaken within the general framework of the geotechnical characterisation system of slope movements (as described by Leroueil et al. 1996), mainly concentrating on deformation related aspects.

8.1.1 Landslides in Soil Slopes

From the study of the deformation behaviour of landslides in soil slopes, it has been possible to identify the factors contributing to the pre and post failure behaviour of the landslide groups studied.

The progression of the initial slope failure to a "rapid" debris flow or "slow" intact slide post failure (for example) is primarily dependent on the mechanics of the failure, slope geometry, geometry of the surface of rupture and material properties of the slide mass. It is not usually controlled by the trigger mechanism/s for the processes leading up to slope instability.

(a) Pre-failure deformation behaviour

The mechanics of failure are significant in controlling the pre-failure deformation behaviour of a landslide. A progressive failure mechanism is present in a large number of slope failures in soil slopes. For soils that are highly strain weakening on shearing, progressive failure may develop very rapidly from a localised failure condition in the slope (e.g. in the case of flow liquefaction) and show little observable pre-failure deformation. In other cases the progressive strain weakening in the slope may develop much more slowly, and for these cases appropriately located and monitored deformation

instrumentation would, with proper interpretation, allow identification of the impending failure.

Other factors also influence the pre-failure deformation behaviour, and these vary from one slide group to the next. For example, the permeability (and therefore particle size) is thought to affect the pre-failure deformation behaviour of slides in contractive soils. For other slide groups, the requirement for internal shearing to form a kinematically admissible slide mechanism (e.g. in defect controlled compound slides in completely weathered rock masses or stiff jointed clays) and brittleness on the slide margins can affect pre-failure deformation. For other cases again, it may not be worthwhile attempting to monitor pre-failure deformation because the trigger of failure is related to climatic conditions, and the slope in question may undergo a reduction in stability from adequate to limiting over a period of hours.

Appropriately located and interpreted deformation monitoring instrumentation would (in most cases) identify the impending failure for slides in embankments of soft ground, larger cut slopes in heavily over-consolidated high plasticity and other clays, embankment dams, flow slides in granular waste spoil piles, and defect controlled slides in weathered rock masses, but for these, mainly for compound slides.

(b) Post failure deformation behaviour

Post failure, the potential for strain weakening strongly influences the deformation behaviour of the failed slide mass. The concept of conservation of energy, and the consideration of the potential for strain weakening of the slide mass within this framework, is a useful method for qualitative assessment of the post failure deformation behaviour. For landslides in soils that are distinctively strain weakening on shearing on the surface of rupture or have a high degree of internal brittleness associated with the slide release mechanism (e.g. toe buttressing), a significant amount of the potential energy of the slide can be available for kinetic energy and dis-aggregation of the slide mass. This would lead to acceleration of the slide mass to “rapid” post failure velocities resulting in potentially large travel distances. At the other end of the scale, slope failures that are triggered by applied load, such as in the case of embankment construction, and for which the soils are not significantly strain weakening on shearing, post failure velocities will generally be slow, the travel distance of limited extent and the slide mass will remain virtually intact during travel.

From the case study analysis, the factors that strongly influenced the post failure deformation behaviour of the slide mass were; the mechanics of failure, the source area slope angle, the down-slope geometry, the slope failure geometry (including the orientation of the surface of rupture) and the stress-strain properties of the soil type. "Rapid" post failure velocity of the slide mass is generally developed where one or more of the following is present:

- Failure was within saturated granular soils that are contractive on shearing and within which a flow liquefaction condition occurred;
- A high degree of brittleness is associated with the slide mechanics or release on the margins;
- Steep source area slope (for all soil types); and
- Steep slopes immediately downslope of the initial slide.

For these slides, often the slide mass disaggregates and develops into a debris flow. Post failure travel distances are generally large and at velocities in the order of metres to 10's of metres per second. For slides in steep natural slopes in dilative soils, the soil type was a significant factor in the ability of the slide mass to transform into a "rapid" debris flow, with low plasticity or non-cohesive silty to sandy and gravelly soils being the most susceptible.

"Slow" slides that generally remain intact on sliding are generally characterised by a relatively flat basal slide plane or a rotational surface of rupture that passes through the horizontal. Post failure travel distances tend to be of limited extent and at "slow" post failure velocities.

Methods for assessment of the post failure travel distance have been developed for landslides of both "rapid" and "slow" post failure velocity.

For landslides of "rapid" post failure velocity it is apparent that the use of slide volume alone does not allow reliable predictions of the travel distance angle (and travel distance). Improvements in predictions for a number of slide groups have been developed from consideration of a combination of material type, mechanics of failure, slope geometry, travel path confinement and/or slide volume. An appropriate degree of caution should be used in application of the methods due to the uncertainty in the methods, and they should be applied to conditions similar in which they have been derived. In all cases, it is best to calibrate the models with case studies for the area under study so that local geological conditions and climatic factors can be allowed for.

For landslides that generally remain intact and are of "slow" post failure velocity, it is demonstrated that the Khalili et al (1996) methods provides a reasonable means for estimation of the post failure deformation of the slide mass. The methods have been developed for rotational slides, but can be applied to slides of compound geometry. They may not be suitable for analysis of slides where internal brittleness in the slide mechanics is significant.

8.1.2 Deformation Behaviour of Embankment Dams

(a) Methods for Prediction of "Normal" Deformation Behaviour

Improved methods for prediction and/or evaluation of the deformation behaviour of an embankment dam (during and post construction) have been developed from an extensive database of case studies. The methods take into consideration the influence of material type and placement methods, embankment zoning geometry, embankment height, and reservoir operation, amongst other factors.

From the case study data during embankment construction, methods for predicting the modulus of compacted rockfill have been developed that take into account the intact rock strength and the particle size distribution of the rockfill, correcting the vertical stress for embankment shape and cross valley influence. Guidelines have also been developed for estimation of the stress-strain relationship of compacted rockfills for use deformation prediction during construction.

The deformation behaviour during construction of compacted earthfills is dependent on the soil type, its moisture content at placement (relative to Standard optimum moisture content), the embankment type, and the material type and compressibility properties of the supporting shoulders. For "dry" placed earthfill cores (placed drier than about 0.5% dry of Standard optimum) of thick to very broad width, it is demonstrated that the assumption of one-dimensional compression and use of elastic solutions are reasonable for prediction of the deformation behaviour under the embankment centreline. Guidelines on the apparent secant moduli of these compacted earthfill types from the case study data have been developed.

For "wet" placed earthfill cores (placed wetter than about 0.5% dry of Standard optimum) of thin to medium width, a significant proportion of the deformation during construction is due to undrained plastic type deformations. For these embankments, the compressibility properties of the supporting shoulders significantly influence the

deformation of the core, with strains of large magnitude observed for shoulders of high compressibility (e.g. poorly compacted rockfills or compacted weathered rockfills).

Post construction, methods have been developed for evaluation / prediction of the crest settlement and face slab deformation of concrete face rockfill dams. The method for crest settlement is by summation of the settlement due to first filling and the time dependent deformation components. The time dependent component for compacted rockfills takes into consideration material type (i.e. rockfills from quarried rock or use of gravels), the intact strength of rock (for quarried rockfills) and embankment height.

Methods for evaluation / prediction of the post construction deformation of embankment dams (both settlement and lateral displacement) have been developed for the crest and shoulder regions. The data is presented in several formats; as deformation versus log time, as snap shots in time at 3, 10 and 20 to 25 years after the end of construction (end of first filling for horizontal displacement), and long-term settlement rate. The factors that influence the deformation behaviour vary for each region of the embankment, and also vary for the component of deformation (i.e. settlement or displacement). The factors considered in the methods include: the material type, placement moisture condition and width of the main earthfill zone; the material type and placement method of the shoulders; the embankment height; the reservoir operation and the foundation influence. Central core earth and rockfill embankments with rockfill shoulders that are susceptible to large deformations due to collapse compression are often over-represented at the high end of the rate or magnitude of deformation.

For all case studies analysed, zero time for the analysis of the post failure deformation has been established at the end of construction. For concrete face rockfill dams this was defined as the end of main rockfill construction.

(b) Methods for Identification of "Abnormal" Deformation Behaviour

Existing general methods or guidelines for identification of "abnormal" deformation behaviour of embankment dams are limited. In general, practitioners rely on their experience, limit equilibrium analysis and simplified numerical methods.

Improvements in this area have been made from the case study analysis and consideration of the mechanics controlling the "abnormal" deformation behaviour. Guidelines have been developed to assist in the identification of potentially "abnormal" deformation behaviour, both during and post construction. The methods of assessment are based on the identification of outliers to the general trend of deformation behaviour

for a given embankment type and consideration of such factors as the core material type, its moisture content at placement, its width, the type and placement method of the supporting shoulders (for zoned embankments) and reservoir operation.

It has been demonstrated that many cases of larger than "normal" deformation behaviour are related to lack of support of the dam core from poorly compacted or dumped rockfill shoulders that, in general, are susceptible to large deformations due to collapse compression on wetting. It has been shown for some of these dams that, over time, spreading, cracking and softening of the core has progressively developed. In some these cases (as well as for other case studies), shear surfaces have developed in the core despite the overall factor of safety being adequate. Large or historic reservoir drawdowns have been shown to trigger further shear movement along the existing shear surface in the core in a number of case studies.

There are however case studies where "abnormal" deformation behaviour is related to marginal stability of the whole or parts of the embankment, as is the case for Eppalock, Djatiluhur and the closure section at Belle Fourche dams. Guidelines for identification of a marginal stability condition have been developed. The considerations include: evidence of shear development; "abnormally" large incremental deformations as layers are placed (during construction); the persistence of longitudinal and diagonal cracking in the core; continued acceleration of the deformation on successive large drawdowns of the reservoir; and the tertiary creep deformations under constant stress conditions.

A critical component of any deformation monitoring program is the foresight to envisage the potential modes of marginal stability, install appropriate monitoring equipment to detect the condition and take measurements within a timing framework that encapsulates the envisaged period of likely minimal stability (i.e. the upstream slope during drawdown or the downstream slope during a reservoir full condition). The deformation behaviour can then be linked to analysis of stability using limit equilibrium and/or finite element methods.

8.2 RECOMMENDATIONS FOR FURTHER RESEARCH

The overall analysis of the pre and post failure deformation of landslides in soil slopes, and of the deformation behaviour of embankment dams in this thesis is case study driven. What has been achieved here has been limited by the quantity and quality of the

case study data despite an extensive search in Australia, Europe, USA/Canada and Hong Kong. There is a particular lack of pre failure deformation data for landslides in cuts, fills and natural slopes. Only for embankment dams is there extensive data, but most of this is not related to the deformation behaviour leading up to slope instability. Post failure data is often of poor quality, although for several of the slide types studied good quality data was available for a number of case studies, particularly the data from Hong Kong.

In the area of post failure deformation behaviour of landslides, it is considered that the slide groups that would most readily benefit from further case study analysis (mainly because of the prevalence of case study records available in the international community) is "rapid" landslides from failures in steep natural slopes and steep cut slopes. "Rapid" debris flows from failures in steep natural slopes occur in regions all over the world and are widely reported in the literature. They were not analysed here because only limited details on the individual case studies were reported in the published literature.

Other areas from the study of the deformation behaviour of landslides in soil slopes for which further research would be beneficial include:

- Further verification of the post failure analysis of intact landslides using the Khalili et al (1996) model and/or other lumped mass models. The guidelines established are based on a limited number of case studies.
- Dynamic analysis of the post failure deformation behaviour of "rapid" landslides. This has been done for several classes of slope including flow slides in waste spoil piles in British Columbia (Golder Associates 1995) and "rapid" landslides in Hong Kong (Hungr Geotechnical Research 1998; Ayotte and Hungr 1998). This could be extended to "rapid" landslides in other areas and the profession would benefit greatly from having a reliably calibrated commercially available program to model flows.
- Pre-failure deformation of cuts and fills to develop further the guidelines for identification of an impending failure condition would be valuable.

For embankment dams, the most significant area of further research is considered to be in the systematic numerical modelling of individual case studies using constitutive models that realistically describe the stress-strain behaviour of earthfills and rockfills. Some of the concepts raised in this thesis rely on simplified modelling using a Mohr-

Coulomb linear-elastic perfectly plastic model. Verification of these concepts by more rigorous numerical modelling would be of great benefit. This should include the use of coupled models, and constitutive models that consider the effects of partial saturation on the stress-strain relationship of fine-grained earthfills, as well as the non-linearity of the strength and compressibility of earth and rockfills, and stress path dependency.

APPENDIX A

Terminology and Definitions for Landslides

TABLE OF CONTENTS

1.0 TERMS AND DEFINITIONS FOR LANDSLIDES A1

1.1 Velocity Classification of Landslides..... A1

1.2 Landslide Classification..... A1

1.3 Definition of Symbols Used for Slope and Travel Geometry..... A5

1.4 Slope Failure Geometry..... A6

1.5 Degree of Confinement..... A12

1.0 TERMS AND DEFINITIONS FOR LANDSLIDES

1.1 VELOCITY CLASSIFICATION OF LANDSLIDES

The post failure velocity of the slide mass is classified according to the system proposed by the International Union of Geological Sciences (IUGS 1995), as presented in Table A1.1. Two broad descriptors to define the post failure velocity of landslides are used throughout the thesis:

i) *"Slow Landslide"*. The classification of "slow" landslides relates to those landslides of very slow, slow and moderate post failure velocities as defined by IUGS (1995), and having an upper velocity limit of 1.8 m/hour.

ii) *"Rapid Landslide"*. The classification of "rapid" landslides relates to those landslides of rapid, very rapid and extremely rapid post failure velocity as defined by IUGS (1995), having a lower velocity limit of 1.8 m/hour. Most of what are termed "rapid" landslides would classify as very rapid or extremely rapid, having post failure velocities greater than 3 metres/minute and generally in the order of metres/sec.

Table A1.1: IUGS (1995) velocity classifications for landslides.

Velocity Classification	**Description of Velocity**	**Velocity limits**	**Velocity in mm/sec**
7	Extremely rapid	> 5 m/sec	$> 5x10^{3}$
6	Very rapid	3 m/min to 5 m/sec	50 to $5x10^{3}$
5	Rapid	1.8 m/hour to 3 m/min	0.5 to 50
4	Moderate	13 m/month to 1.8 m/hour	$5x10^{-3}$ to 0.5
3	Slow	1.6 m/year to 13 m/month	$50x10^{-6}$ to $5x10^{-3}$
2	Very slow	16 mm/year to 1.6 m/year	$0.5x10^{-6}$ to $50x10^{-6}$
1	Extremely slow	≤ 16 mm/year	$\leq 0.5x10^{-6}$

1.2 LANDSLIDE CLASSIFICATION

The method of classification of a landslide is according to Hutchinson (1988). However, for landslides where a large portion of the slide mass evacuates the source

area post failure, a dual system of classification is used to describe the initiating landslide in the source area (termed initial slide classification), and to describe the subsequent movement of the slide in the travel region (termed travel classification). The main terms used to define the initiating landslide and post failure travel of the slide are shown in Figure A1.1.

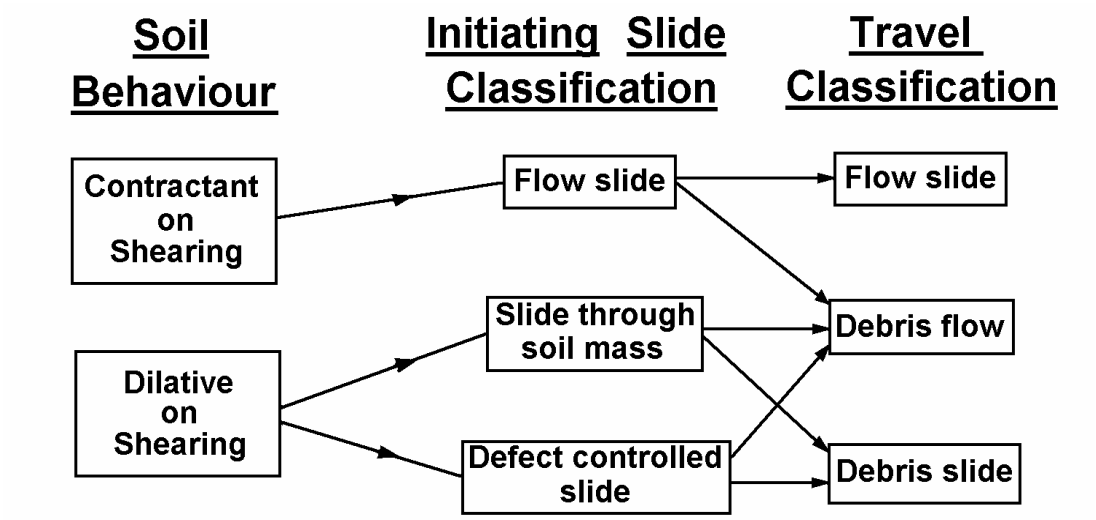

Figure A1.1: Landslide classification system and main slide types.

For classification of the initial landslide, the main classification term (or terms) is indicative of the failure mechanics of the landslide (either in soils that are dilative or contractive on shearing) and is generally followed by a description of the surface of rupture within the general categories of rotational, translational and compound. Dilative or contractive describes the initial tendency of the soil on the surface of rupture to increase (dilate) or decrease (contract) in volume under drained shear, or to develop negative or positive pore water pressures in undrained shear when in a saturated (or near saturated) condition. The main classification terms for the initial slide classification and there definitions are:

- *Flow slide* is used to describe landslides in saturated (or near saturated) soils that are contractive on shearing, where the failure or rapid acceleration of the slide mass occurs as a result of a large loss in undrained strength due to static liquefaction on shearing.
- "*Slide of debris*" for description of landslides in colluvium, talus and other slope mantling debris.

- *Slide through the soil mass* is used to describe failures in dilative soils where the surface of rupture is located through the soil mass.
- *Defect Controlled Slide.* The term defect controlled slide is used as an initiating slide classification to describe landslides that are dominantly controlled by defects in the soil or weathered rock mass.

For the subsequent travel of the landslide, the "travel classification" can be difficult due to the complex and potentially changing behaviour of the moving slide mass. The main purpose of the travel classification is to describe the mode of movement of the slide mass, whether it is dominantly by sliding along a basal surface, in which case the material carried remains relatively intact, or the movement is more as a turbulent flow. The travel classification terms used are as follows:

- *Flow slide* – where the main volume of the slide mass is bodily carried on a liquefied basal zone. The flow slide travel classification is only applicable to landslides initially classified as flow slides.
- *Debris flow* – travel classification to describe turbulent post failure slide movements of a combination of water, air and debris. The slide mass is a broken up mass of material that no longer retains its original structure or fabric. The resistance to flow of a debris flow is a combination of friction (both sliding and internal) and viscous forces. The term "debris" as used here is a generic term. Several terms are used that come under the general *debris flow* classification, they are:
  - *Debris flow* - where used on its own infers that the moving mass is near saturated. In most cases the pressure of the pore fluid in the debris mass is greater than hydrostatic because of partial liquefaction due to remoulding and breakdown during the flow.
  - *Dry debris flow* - where the flowing mass is generally in a dry condition.
  - *Hyper-concentrated stream-flow* is a term used by Pierson and Costa (1987) to describe a flowing mixture of water and sediment that possesses measurable yield strength but still appears to flow like a liquid.
- *Debris slide* – used as a travel classification where the movement occurs essentially as sliding on a defined basal surface and the slide mass remains relatively intact (still retains its structure and fabric) during travel. *Debris Slide* is generally used as a descriptor for slides that travel beyond the source area, and *intact slide* for slides where the post failure deformation is largely confined to the source area.

For a number of slides the mode of movement will change with distance from the source area. Initially a translational slide in a weathered rock mass may occur as basal sliding on a defect and the slide mass may initially move as a virtually intact body. As the moving mass is displaced beyond the toe it is likely to break up to some degree. It may totally disintegrate into a mass of soil and rock pieces and flow down the slope until it comes to rest. In addition, part of the slide mass may remain within the failure scarp in a virtually intact condition and part may have exited the failure bowl and totally disintegrated as it flowed down-slope. Thus the travel stage is complex and difficult to classify as one particular type of movement.

Given the complexity associated with the travel of some landslides, the predominant mechanism of movement has been used to classify the travel stage in most cases. However, in some cases a dual classification system has been used; i.e. debris slide / debris flow or flow slide / confined debris flow.

Several of the terms used in the adopted system are slightly different to their interpretation by Hutchinson (1988) and this has been because of the difficulty of using a dual classification system within the Hutchinson classification system. The terms *debris slide* and *debris flow* cause particular difficulties with their interpretation. Hutchinson (1988) defines *debris slides* as predominantly translational "slides of debris" mantling a slope where the slide material is typically of low cohesion and undergoes significant break-up during travel. He then differentiates *debris flows* from *debris slides* as flow type movements of essentially wet debris. Johnson and Rodine (1984) encompass the term *debris slide* under the general heading of *debris flow*. Pierson and Costa (1987) propose a rheologic classification system for sediment-water flows (Figure A1.2) that would appear to incorporate both *debris slides* and *debris flows* as described above under the "flow" classification system. From the Hutchinson description of *debris slide* the Pierson and Costa system would describe them as "grain flows" under the sub-group of granular flows (flow movements of material in an essentially dry or with limited water condition).

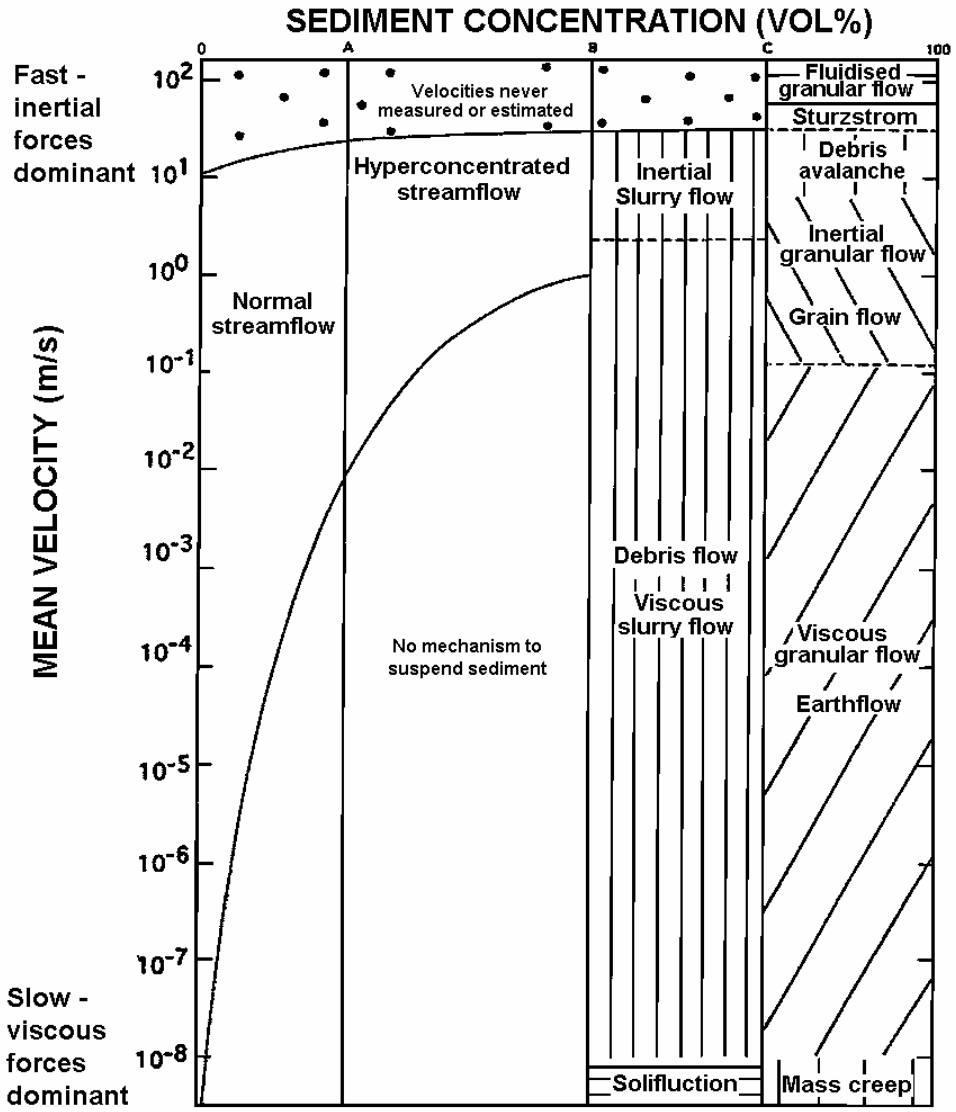

Fluid Type	Newtonian	Non-Newtonian	
Interstitial Fluid	Water	Water - Fines	Water - Air +Fines
Flow Category	Streamflow	Slurry Flow	Granular Flow
Flow behaviour	Liquid	Plastic	

Figure A1.2 : Rheologic classification system for sediment-water flows (Pierson and Costa 1987)

1.3 DEFINITION OF SYMBOLS USED FOR SLOPE AND TRAVEL GEOMETRY

The definitions of the terms used to describe the geometry of the landslide (Figure A1.3) are:

- Slope height, H_s – overall height of the slope, mainly used in relation to cut and fill slopes;

- Slide height, H – height from crest of back-scarp to distal toe of the post-slide debris deposition;
- Travel distance, L – horizontal distance from crest of back-scarp to distal toe of the post-slide debris deposition;
- Travel distance angle, a - the angle between the crest of the back-scarp and the distal toe of the post-slide debris deposition;
- L_{toe} – horizontal distance of travel beyond the toe of the initial failure to the distal toe of the post-slide debris deposition;
- Failure depth, D – vertical depth of the initial failure in the source area, measured from the ground surface to the surface of rupture. It is generally representative of close to the maximum depth to the surface of rupture;
- Sources area slope angle, a_1 - slope angle in the slide source area. For cut slopes it is the cut slope angle (a_{cut}) in the region of the initial slide, and for fill slopes it is the fill slope angle (a_{fill}) in the region of the initial slide;
- a_2 - down-slope angle immediately down-slope of the failure zone;
- a_3 - down-slope angle over the distal portion of the travel path. For landslides of Type 2 slope failure geometry and some Type 3, a_3 is undefined where the downslope angle is relatively constant for the full travel length beyond the source area;
- a_4 - applicable to failures in fill slopes only. It is the slope of the natural ground underlying the fill as defined in Figure A1.4;
- a_{base} – the inclination angle of the surface of rupture. It is generally measured in the central to toe region of the slide, as shown in Figure A1.5.

The terms cut slope angle (a_{cut}) and fill slope angle (a_{fill}) are used to avoid ambiguity between a_1 and a_2 for failures in cut (and fill) slopes where the source area of the failure is either within part of the slope or encompasses the full slope.

1.4 SLOPE FAILURE GEOMETRY

The slope failure geometry is a classification of the overall longitudinal geometry of the landslide. The classification includes an assessment of the location of the initial failure within the overall slope and the longitudinal shape of the down-slope travel path (mainly for slides where the post failure travel distance is largely beyond the source area

of the initial failure). Five slope failure geometry classifications (Type 1 to Type 5) have been used and are defined in Figure A1.4 to Figure A1.8 respectively.

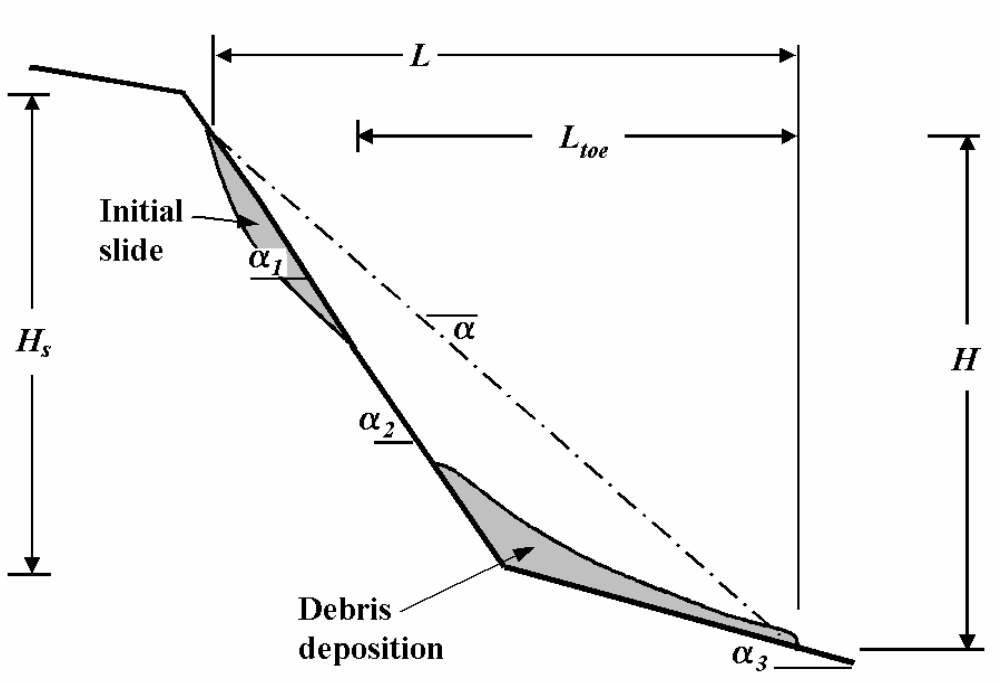

Figure A1.3: Symbol definitions of slope geometry

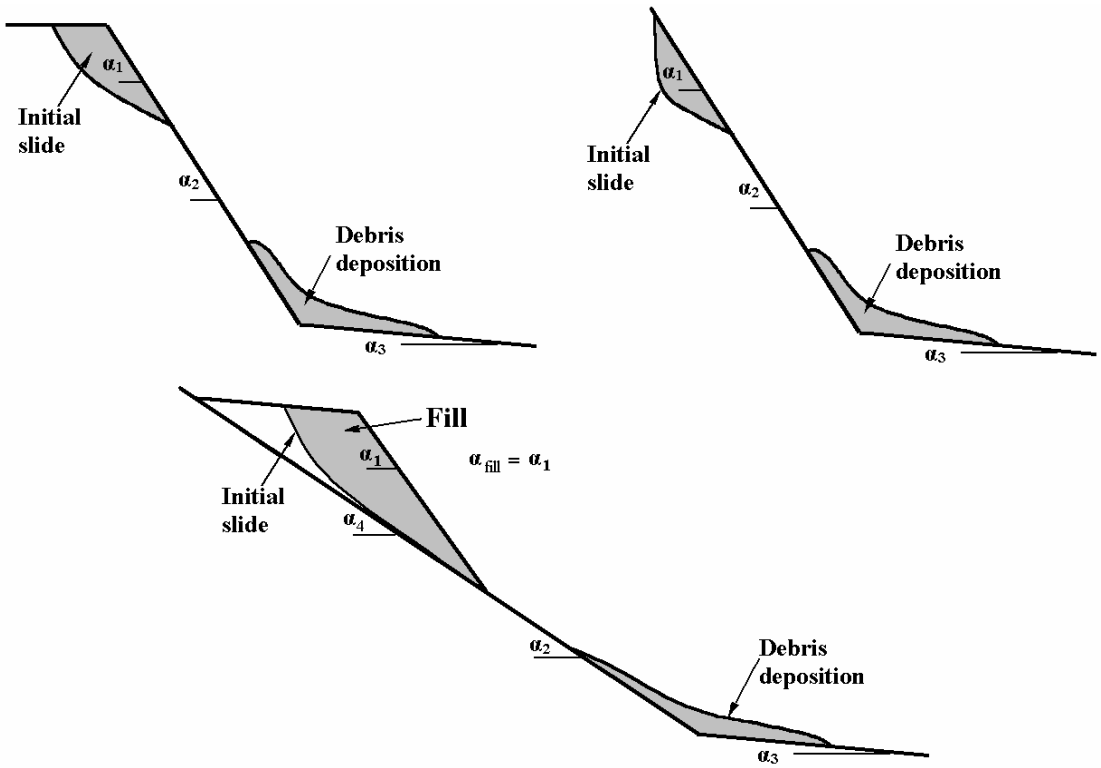

Figure A1.4: Type 1 slope geometry - initial failure above the toe of a cut or fill slope. For "rapid" landslides the deposition is predominantly on relatively flat slope (less than about 5 degrees) at the toe of the slope.

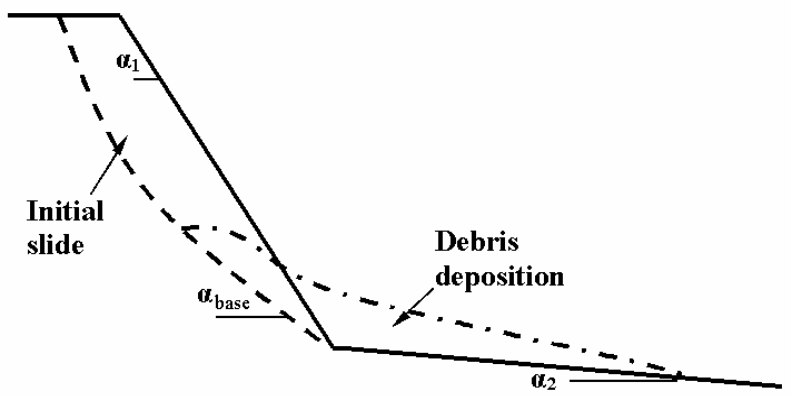

Figure A1.5: Type 2 slope geometry - initial failure coincident with toe of slope (e.g. cut slope) and large decrease in slope angle from a_1 to a_2. Mostly for cut and fill slopes for which a_2 is near horizontal.

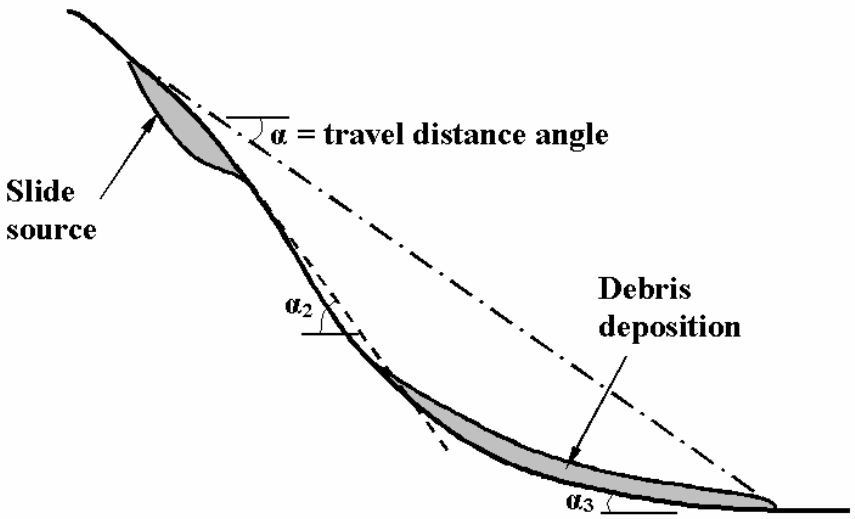

Figure A1.6: Type 3 slope geometry. Initial failure and post failure travel on relatively uniform or gradually decreasing slope angles.

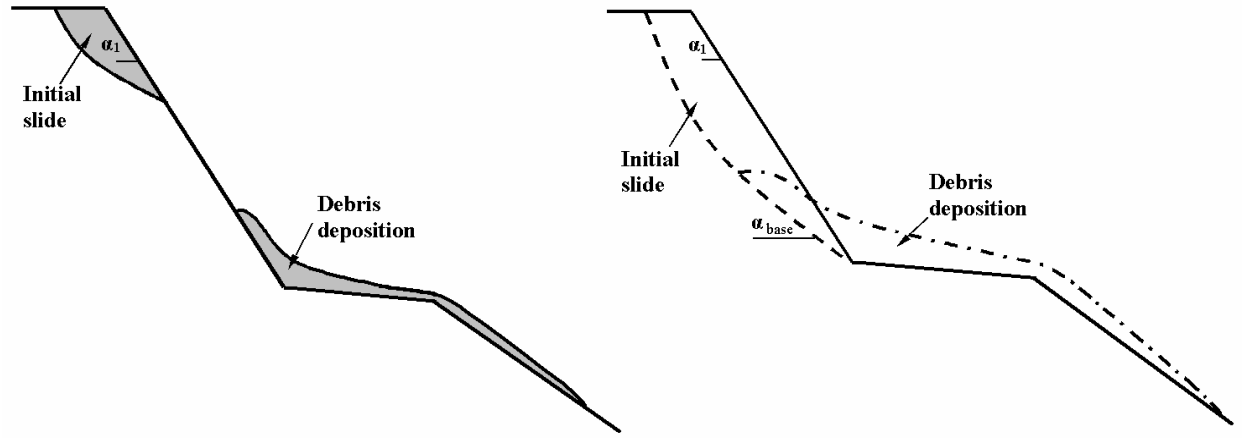

Figure A1.7: Type 4 slope geometry - post failure travel on changing slope angles from steep to shallow.

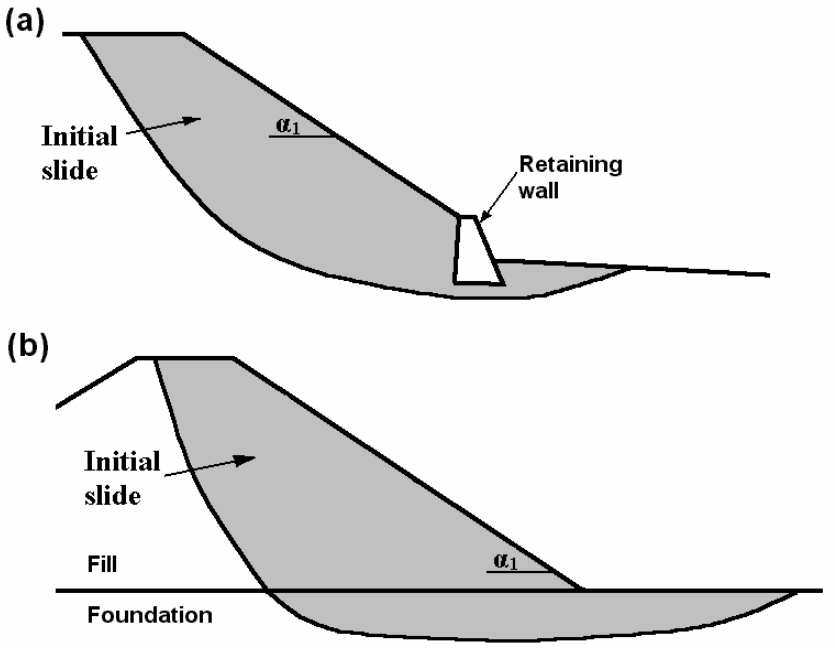

Figure A1.8: Type 5 slope failure geometry. The surface of rupture extends below and daylights beyond the toe of the slope; *(a)* retained cut or fill slope or *(b)* deep seated failure through the foundation of a fill embankment.

The purpose in differentiating between the slope failure geometry is because it can (and does) have a significant effect on the post failure travel distance and velocity of the landslide. For example, for Type 1 failures in steep embankment or cut slopes, the toe of the slide mass can travel relatively large distances at high velocities down the cut or fill slope.

For landslides where the post failure travel is largely beyond the source area of the initial failure, slope failure geometries of Types 1 to 4 are appropriate. These cases are generally landslides of "rapid" post failure velocity. The slope failure geometry classifications relate to:

- *Type 1* – for failures in cut and fill slopes where the slide source area is above the toe of slope, and the slide mass travels down the cut or fill slope depositing predominantly on relatively flat slopes (less than about 5 degrees) at the toe of the slope.
- *Type 2* – for failures in cut or fill slopes where the toe of the slide source is coincident with toe of slope and the slide mass is predominantly deposited on relatively flat slopes at the toe of the slope (i.e. a_2 is near horizontal).
- *Type 3* – for failures where the source area and travel of the slide mass are on relatively uniform or gradually decreasing slope angles. Type 3 geometries are

generally slides in natural slopes, but the term is also used for slides in cut of fill slopes where the slide mass is deposited on the cut or fill slope.

- *Type 4* – for failures where the travel path of the slide mass is characterised by sharp changes in slope angle and does not classify as Type 1.

Slope Failure Geometries of Type 1, 2 and 4 are characterised by sharp changes in slope angle that are likely to absorb a significant amount of the energy of the "rapid" landslide. The slide volume will have an affect on the classification adopted. For example, small volume failures in road cuttings would classify as either Type 1 or Type 2; however, a larger volume may classify as Type 4 if the travel extends beyond the fill edge of road; and a very large volume may classify as Type 3 where the scale of the road cutting is very small in relation to the travel path.

For landslides where the post failure travel is of limited distance beyond the initial failure geometry and most of the slide mass is retained in the source area (i.e. predominantly "slow" and intact slides), slope failure geometries of Type 1, 2 and 5 are appropriate. The slope failure geometry classifications for these slides relate to:

- *Type 1* – where the toe of the landslide is located above the toe of the cut or fill slope, defined in Figure A1.9. Typical examples of Type 1 failures would include:
  - Cut slope failures where the failure is located within the weaker upper portion of the slope or the basal plane of the failure is along a defect that outcrops in the face of the cut slope;
  - Failures in embankment dams with rockfill toe zones, where the failure is located above the rockfill zone;
  - Failures in embankment dams where the basal plane of the failure is coincident with a weak layer in the embankment, for example a wet layer with low undrained strength or a more plastic layer;
- *Type 2* – where the toe of the landslide is coincident with the toe of the slope (Figure A1.10). In the case of benched cut or fill slopes this would also include failures where the toe of the landslide is coincident with the toe of the bench. Case studies where the toe of the landslide may be only slightly beyond the toe of the slope have been included in the Type 2 category, and would include failures in embankment dams or other fills where the failure incorporates the upper portion of the foundation as shown in Figure A1.10b.

- *Type 5* – where the toe of the landslide extends below and beyond the toe of the slope (Figure A1.8). Typical examples of Type 5 failure geometries would include:
  - Failures in retained cut slopes where the failure extends below the base of the retaining wall (Figure A1.8a); and
  - Deep seated failures in embankment dams that extend well into the foundation and daylight well beyond the toe of the slope (Figure A1.8b).

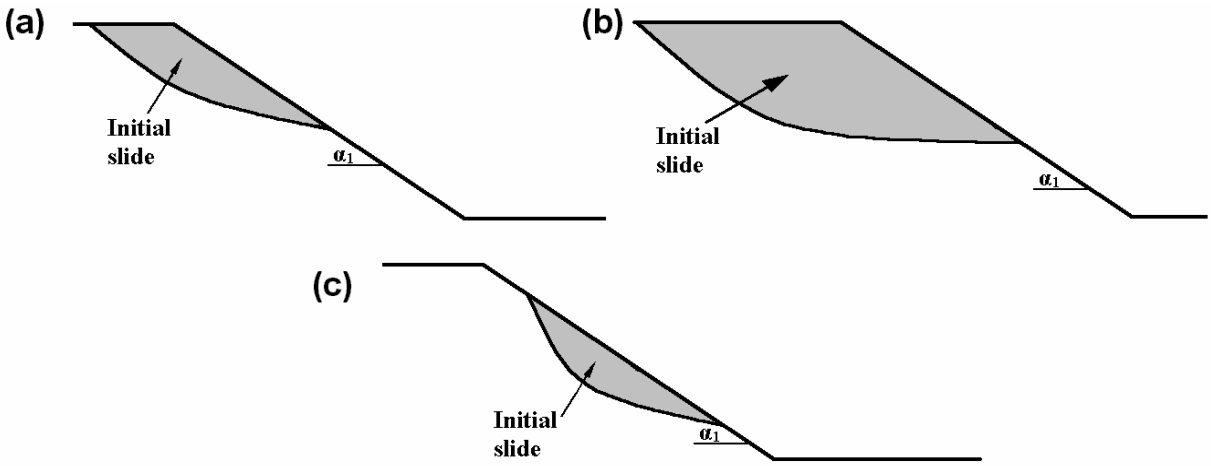

Figure A1.9: Type 1 failure slope geometries. The initial failure is located above the toe of the slope.

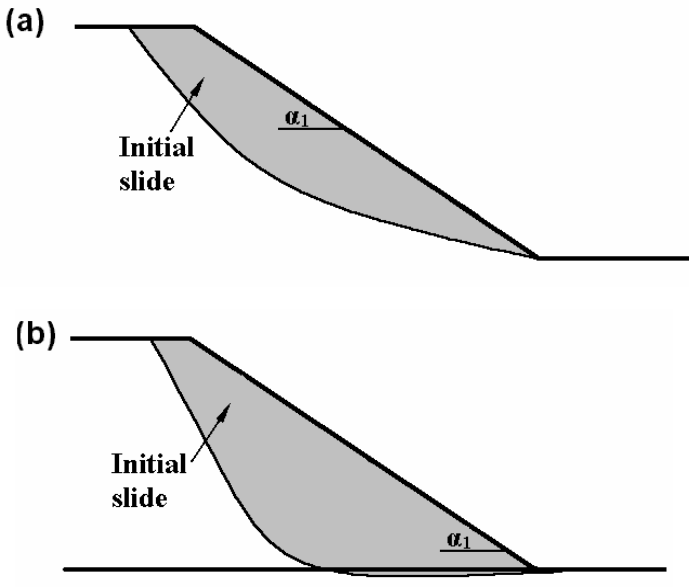

Figure A1.10: Type 2 failure slope geometries. The initial failure is coincident with the toe of the slope.

1.5 DEGREE OF CONFINEMENT

For classification of the degree of confinement of the travel path of the slide mass, two general categories have been considered; confined and unconfined travel paths (Figure A1.11). For several groups of slides the term partly confined travel path has also been used. The definitions for each type of travel path (after Golder Assoc. 1995) are as follows:

- *Confined* – the travel path is constrained by the relatively steep side-slopes of a gully or small valley;
- *Partly confined* – the travel path is not sharply defined by a topographic depression. This includes; movement of the slide mass down relatively broad (relative to the slide mass volume) topographic depressions, movements down relatively small topographic depressions where only a portion the slide mass is confined but the depression controls the direction of movement to a large extent, or events where only a minor (but potentially significant) portion of travel path is confined; and
- *Unconfined* – the travel path is on open slopes.

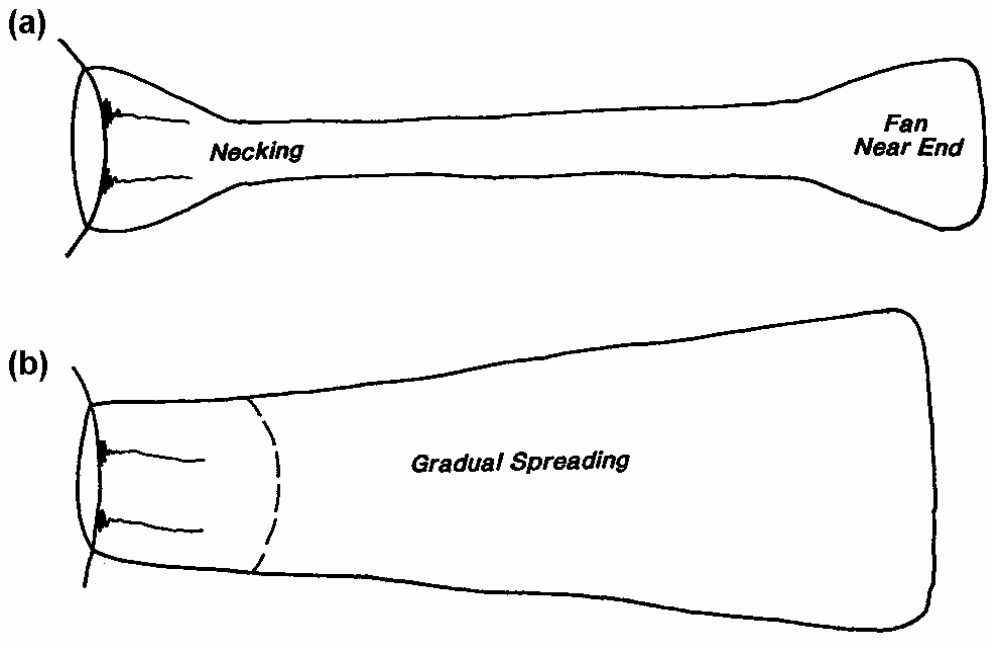

Figure A1.11: Typical plan views of the slide travel for *(a)* confined travel paths and *(b)* unconfined or open slope travel paths (Golder Assoc. 1995).

APPENDIX B

“Rapid” Landslides in Soil Slopes

TABLE OF CONTENTS

1.0 CASE STUDIES OF LANDSLIDES IN SOIL SLOPES OF "RAPID" POST FAILURE VELOCITY..... B1

1.1 "Rapid" Landslides from Failures in Cut, Fill and Natural Slopes, Hong Kong B1

1.2 "Rapid" Landslides from Failures in Granular Fills B5

1.3 Strongly Retrogressive Landslides..... B7

1.4 "Rapid" Landslides from Failures in Hydraulic Fill Embankment Dams B7

2.0 MECHANICS OF SHEARING OF CONTRACTIVE GRANULAR SOILS B27

2.1 Introduction..... B27

2.2 Empirical Field Methods for Evaluation of Liquefaction and Flow Liquefaction Potential B27

2.3 Problems with Laboratory Test Methods For Evaluation of Flow Liquefaction Potential B32

2.4 Characteristics of Contractive and Dilative Soils Sheared Under Monotonic Load Conditions..... B35

2.5 Residual Undrained Shear Strength of Flow Liquefied Soils B50

LIST OF TABLES

Table B1.1: Shear strength of mineral infillings commonly found in weathered rocks (Irfan and Woods 1998; Irfan 1997)..... B1

Table B1.2: Shear strength on relict discontinuities in weathered rocks in Hong Kong (Irfan and Woods 1998; Irfan 1997)..... B2

Table B1.3: Landslide case studies from Hong Kong..... B9

Table B1.4: Landslide case studies from Hong Kong (Ayotte and Hungr 1998) B13

Table B1.5: Case studies of "rapid" landslides in coarse, granular stockpiles B14

Table B1.6: Flow slides from tailings impoundments – cases initiated by static liquefaction. B20

Table B1.7: Flow slides from tailings impoundments – cases initiated by dynamic liquefaction. B22

Table B1.8: Case studies of flow slides in sensitive clays B23

Table B1.9: "Rapid" landslides in submarine slopes (Edgars and Karlsrud 1983)..... B24

Table B1.10: Failure case studies of hydraulic fill embankment dams, sub-aqueous fills and Wachusett Dam. B25

1.0 CASE STUDIES OF LANDSLIDES IN SOIL SLOPES OF "RAPID" POST FAILURE VELOCITY

1.1 "RAPID" LANDSLIDES FROM FAILURES IN CUT, FILL AND NATURAL SLOPES, HONG KONG

Table B1.1 and Table B1.2 present the shear strength properties of mineral infillings and along relict discontinuities in weathered rocks in Hong Kong published by Irfan (1997) and Irfan and Woods (1998).

The case study data for failures in cut, fill and natural slopes from Hong Kong that developed into landslides of "rapid" post failure velocity are presented in Table B1.3 and Table B1.4.

Table B1.1: Shear strength of mineral infillings commonly found in weathered rocks (Irfan and Woods 1998; Irfan 1997)

Mineral and Nature	Strength Parameters
Kaolinite – remoulded	$f¢_r$ = 12 to 22 degrees
Kaolinite	$f¢_{sat}$ = 0.4 to 0.6 f_{dry}
Kaolinite – intact, precut surface	$f¢_r$ = 12 degrees
Illite – remoulded	$f¢_r$ = 6.5 to 11 degrees
Montmorillonite	$f¢_r$ = 4 to 11 degrees
Muscovite	$f¢_r$ = 17 to 24 degrees
Hydrous mica	$f¢_r$ = 16 to 26 degrees
Quartz-dune sand	$f¢_r$ = 30 degrees
Crushed sand	$f¢_r$ = 35 degrees

Table B1.2: Shear strength on relict discontinuities in weathered rocks in Hong Kong (Irfan and Woods 1998; Irfan 1997)

Type	Nature	Strength Parameters	Method of Determination	Remarks
Discontinuity Surface	Completely decomposed planar joint	$f' = 37^\circ$	Direct shear	
	Completely decomposed planar joint with MnO_2 and FeO_2 coating	$f' = 32^\circ$	Direct shear	
	Highly decomposed rough joint in granitic saprolite	$f' = 45$ to 57°	Not known	Peak (?)
	Highly decomposed clean joint in granitic saprolite	$f' = 38^\circ$ $c' = 30$ kPa	Direct shear	Portable shear box
	Highly decomposed joints in granite	$f' = 40$ to 42°	Direct shear	Basic frictional strengths from lab tests.
	Granitic saprolite - clay coated joint - clean joint	 $f' = 25^\circ \pm 2^\circ$ $f' = 35^\circ \pm 2^\circ$	Not known	Compiled laboratory results by Lumb (1971)
	Completely decomposed joint in volcanic saprolite	$f' = 29^\circ$ $c' = 22$ kPa	Direct shear	Failed slope, Pun Shan Tsuen.
	Stained or clean joint in volcanic saprolite	$f' = 23$ to 42°	Multi-stage direct shear	
	Highly weathered volcanic rock	$f' = 38^\circ$ $c' = 5$ kPa	CU triaxial	Failed slope at Shum Wan Road.
	Completely decomposed tuff, intact	$f' = 37^\circ$ $c' = 8$ kPa	CD triaxial, multi-stage and direct shear	
	Completely decomposed rough foliation plane in meta-sandstone with phyllite	$f' = 29^\circ$ (intact material $f' = 34^\circ$, $c' = 3.5$kPa)	Multi-stage direct shear	
	Rhyolitic saprolite - clay coated joint - clean joint	 $f' = 22.5^\circ \pm 2^\circ$ $f' = 30^\circ \pm 2^\circ$	Not known	Compiled laboratory results by Lumb (1971)
Discontinuity with Infilling	Completely decomposed discontinuity with kaolin infill	$f' = 34^\circ$	Direct shear	Failed slope at Sui Sai Wan (kaolin infill may not be fully saturated; alignment problems in shear box)
	Completely decomposed discontinuity in granitic saprolite	$f' = 36^\circ$	CU Triaxial	Lower failure surface, Tsuen Wan
	Completely decomposed discontinuity in granitic saprolite	$f' = 31.5^\circ$	CU Triaxial	Upper failure surface, Tsuen Wan
	Joint filled with stiff brown clay in granite	$f' = 31^\circ$ $c' = 30$ kPa	Direct shear	Portable shear box
	Kaolin-filled joint in granite	$f' = 26^\circ$	Direct shear	Portable shear box
	Joint with 20 mm thick kaolin-infill along rough discontinuity in highly to completely weathered granite	$f' = 27.5^\circ$, $c' = 31$kPa (kaolin infill: $f' = 24.5^\circ$, $c' = 243$kPa)	Back analysis (direct shear)	Failed slope at Junk Bay Road. (full saturation of kaolin may not been achieved)
	Clay filled joint in volcanic saprolite	$f' = 22^\circ$	Multi-stage direct shear	

Table B1.2 (continued): Shear strength on relict discontinuities in weathered rocks in Hong Kong (Irfan and Woods 1998; Irfan 1997)

Type	Nature	Strength Parameters	Method of Determination	Remarks
Discontinuity with Infilling	Manganese coated joint in meta-volcanic saprolite (Intact completely decomposed meta-volcanic)	$f\phi$ = 14 to 26° (20° average) ($f\phi$ = 32°, $c\phi$ = 6 kPa)	Direct shear CU triaxial	For slickensided and non-slickensided.
	Slickensided joint in with smectite infill in migmatic saprolite	$f\phi_r$ = 16°	Direct shear	Failed slope in Brazil
	Joint with black seam in a gneissic saprolite (Slickensided)	$f\phi$ = 14.5°, $c\phi$ = 10 kPa $f\phi_r$ = 10.5° (Intact, $f\phi$ = 18.5°)	CU Triaxial	
Shear Zone	0.7 m thick fault zone (mixture fractured rock with kaolin infilled joints in moderate to highly decomposed volcanic)	$f\phi$ = 32 to 39° $c\phi$ = 0 to 14 kPa	CD triaxial, multi-stage and direct shear	
	Slickensided, pre-existing shear surface between volcanic saprolite and colluvium	$f\phi$ = 18°	CD direct shear	Failed slope sat Borrow Area A, Tuen Mun (possible difficulties with aligning shear surface)
	Pre-existing shear surface with up to 30 mm thick iron rich clay seam between creeping and insitu volcanic saprolite	$f\phi$ = 34°, $c\phi$ = 3.5 kPa (intact completely decomposed tuff, $f\phi$ = 30 to 33° $c\phi$ = 12 to 22 kPa) (Creeping layer, $f\phi$ = 30°, $c\phi$ = 6 kPa)	Direct shear	Failed slope at Island Road Government School
	0.6 m thick, completely decomposed, altered tuff with kaolin clay veins/infilling between less weathered rock (altered bedding shear surface)	$f\phi$ = 29° ($f\phi$ = 22° lower bound) (intact kaolinised material, $f\phi$ = 22°)	Direct shear	Failed slope at Fei Tsui Road
	Clay infilled joints in highly weathered volcanic rock	Clay seam, $f\phi$ = 26°, $c\phi$ = 8 kPa Slickensided, $f\phi$ = 21°	CU triaxial Direct shear	Failed slope at Shum Wan Road
Jointed Saprolite (Mass)	Completely weathered meta-volcanic saprolite	$f\phi$ = 30° $c\phi$ = 5 kPa	Probabilistic analysis	Failed slope at Area 19, Tuen Mun
	Highly weathered volcanic saprolite	$f\phi$ = 11 to 12° $c\phi$ = 32 to 36 kPa	Back analysis	Failed slope at Chai Wan (absence of accurate groundwater data)
	Completely weathered volcanic tuff saprolite with multiple shear surfaces	$f\phi$ = 34°, $c\phi$ = 2 kPa (failed mass, $f\phi$ =28.5°)	Back analysis	Failed slope at Sui Sai Wan

An explanation of some of the terminology used in Table B1.3 and Table B1.4 is as follows:

- Slope Type; 'Cut' for cut slope, 'Fill' for fill slope and 'Nat' for natural slope. Retained slopes are identified with an R following the type of slope retained; e.g. Fill-R refers to a retained fill slope.
- The definitions for slope failure geometry are given in Section 1.4 of Appendix A. 1 = Type 1; 2 = Type 2; 3 = Type 3 and 4 = Type 4.
- Initial slide classification. Several additional terms used that are not defined in Section 1.2 of Appendix A are:
  - Interface - the surface of rupture is coincident with an interface between different material types, such as colluvium and saprolite or fill and natural ground.
  - Defect control – defects have a strong influence on the location of the surface of rupture.
- Travel classification. Classification of the post-failure movement of the landslide. Refer to Section 1.2 of Appendix A for definitions of the terms used.
- Obstructed. Consideration has been given to whether or not the travel of the slide mass has been obstructed. For example, in the case of Sau Mau Ping (1976) the travel distance of the slide was clearly obstructed by the building at the toe of the fill slope.
- Landslide Geometry. The terms used are defined in Section 1.3 of Appendix A.
- The remainder of the terminology used is self explanatory; however, some terms or acronyms have been used that require further explanation:
  - CW – completely weathered rock
  - PW – partially weathered rock
  - SM, ML, MI, CL, CI, CH – soil classification symbols of the Australian soil classification system (Australian Standard AS 1726-1993 "Geotechnical Site Investigations").
  - SMDD – Standard Maximum Dry Density as determined by the Standard compaction test (Australian Standard AS1289.5.1.1.).
  - SPT – Standard penetration test
  - DAN – numerical computer program DAN
  - phiB – bulk friction angle used for frictional model analysis in DAN.

For the flow slide failures in loose fill slopes in Hong Kong, assessment of the potential for the fill material to be contractive on shearing has been based firstly on measured density results (if available) and then on the type of placement and age of the fill.

1.2 "RAPID" LANDSLIDES FROM FAILURES IN GRANULAR FILLS

Virtually all of the landslides in mine waste spoil piles and stockpiled coking coal within the database are classified as flow slides of "rapid" post failure velocity. The granular fills within which the failures occurred are classified as predominantly sandy gravels and gravely sands with trace to some silt fines (up to 12% silt fines). Data for some 67 "rapid" landslides in loose, granular stockpiles of coal mine waste and coking coal have been collected and analysed. They come from three geographic regions, all associated with the coal industry, summarised as follows:

- Landslides in loose, stockpiled coal mine waste from South Wales (18 cases);
- Landslides in loose, stockpiled coal mine waste from British Columbia, Canada (40 cases); and
- Landslides in loose, stockpiled coking coal from Hay Point, Australia (9 cases).

A summary of the collected information of each case study is given in Table B1.5. The regional designation of case study is identified by the prefix to the case study number; SW for South Wales, BC for British Columbia, and HP for Hay Point.

For most case studies only limited information has been collected. For the British Columbian cases the information for most case studies has been obtained from Golder Assoc (1995) supplemented with more detailed information on three cases from Dawson (1994) and Dawson et al (1998). For South Wales most of the case study information has been sourced from Siddle et al (1996) supplemented with additional information on the Aberfan (1944, 1963 and 1966 events) and Cilfynydd (1939) flow slides from the Aberfan tribunal report (H.M.S.O. 1967) and associated technical reports (Bishop et al 1969; Bleasdale 1969; Woodlands 1969). For the Hay Point case studies the available information on the flow slides in coking coal stockpiles at the loading facility in North Queensland were sourced from Eckersley (1985, 1986).

In most cases the landslides have been classified as flow slides, where the failure mechanism and rapid acceleration of the failed mass is associated with contraction and

liquefaction of the loose, stockpiled material (in a saturated or near saturated condition) on shearing. The travel of the slide mass, in most cases, has been classified as a flow slide. In a number of the observed failures non-liquefiable material has been carried forward on a basal liquefied layer (non-liquefiable because of the degree of saturation or high permeability, as in the case of the coarser sandstone waste in the British Columbia spoil piles). In some cases it is possible that the flow slide develops into a turbulent debris flow.

Comments on specific issues relating to each sub-group of flow slides in coarse, granular materials are as follows:

- For South Wales, the initial slide classification in most cases, as described by Siddle et al (1996), is rotational. It is considered likely; however, that each slide has a basal translational component along the fill / foundation interface and an arcuate back-scarp through the spoil pile material. Apart from several slides, the volume of the initial slide that developed into a flow slide is relatively low (less than about 50%) with a significant portion of the initial slide volume retained in the failure bowl. Estimates of both the initial slide volume and the volume involved in the flow slide are given in Table B1.5. For the failure of Tip 7 at Aberfan in October 1966, Bishop et al (1969) considered it likely that the failure occurred as several retrogressive components in rapid succession, that initiated from a localised failure in the toe region (partly along a pre-existing shear surface) triggered by high foundation pore water pressures in this region. It is possible that a similar slide mechanism occurred at a number of the other failures given the number of landslides in tips in South Wales located over pre-existing earthflows and spring or stream lines.
- For the coalfields in British Columbia, Golder Assoc (1995) indicates that the initial landslide is dominantly translational. They describe the typical slide as having a bi-linear profile with a basal component close to the fill / foundation contact and a steep back-scarp (45 to 55 degrees). The parallel layering of the liquefaction susceptible finer zones of sandy gravel within the very coarse cobbly and bouldery sandstone waste material would also be expected to influence the shape of the surface of rupture.
- At Hay Point, the initial landslide classification is considered to have a significant translational component along the fill / platform interface. Observation of an actual event (Eckersley 1986) and the large scale laboratory tests performed by Eckersley

(1986) indicate it is likely that these flow slides develop as a series of retrogressive failures initiated in the toe region of the stockpile. Eckersley indicates that the bulk of the material in the slide mass is carried forward on a liquefied basal layer of the saturated coking coal.

The slide volumes for the most of land slides from South Wales and Hay Point were estimated based on the geometric details provided for each slide. For the South Wales slides the volume of the initial failure that transformed into a flow slide, where it was not reported in the published literature, was based on estimation from the information provided. For a number of cases the estimate is very rough.

1.3 STRONGLY RETROGRESSIVE LANDSLIDES

The groups of case studies considered as strongly retrogressive include flow slides from failures tailings dams, sensitive clays, submarine slopes and sub-aqueous hydraulic fills. The details of the case studies used in the analysis from these slide groups are summarised in the following tables:

- Table B1.6, flow slides from tailings impoundments initiated by static liquefaction;
- Table B1.7 flow slides from tailings impoundments initiated by dynamic liquefaction; i.e. earthquake triggered flow slides;
- Table B1.8 flow slides in sensitive clays; and
- Table B1.9 landslides in submarine slopes.

The case studies of sub-aqueous fills are given in Table B1.10 with the hydraulic fill embankment dam case studies.

1.4 "RAPID" LANDSLIDES FROM FAILURES IN HYDRAULIC FILL EMBANKMENT DAMS

The five case studies of flow slides include four failures in hydraulic fill embankment dams (Fort Peck, Calaveras, Lower San Fernando and Sheffield dams) and one failure (Wachusett dam) in the upstream shoulder of a loose dumped sand fill embankment that failed during first filling. Olson et al (2000) considered the failure of Wachusett Dam to

have involved static liquefaction and flow of the loose sand fill. The details for each case study are summarised in Table B1.10.

Of the four hydraulic fill embankment dams, the initial failure was associated with liquefaction of either the hydraulically placed fill or the foundation. Two of these failures (Fort Peck and Calaveras dams) occurred during construction and the other two (Lower San Fernando and Sheffield dams) shortly following an earthquake. An important characteristic of these failures is the stratified nature of the hydraulically placed materials. A noted observation of the post failure travel from the published literature it that it was evident that the outer denser materials and non-saturated zones remained virtually intact, being carried forward on a liquefied zone of the looser and saturated materials.

Table B1.3: Landslide case studies from Hong Kong

No.	Site	Date of Failure	Slope Type	Slope Failure Geometry	Initial Slide Classification	Travel Classification	Obstr-ucted	Confined (Yes/No)	Landslide Geometry									Travel Distance Angle (^{o})	Ratio H/L	Volume (m^3)	Width (m)		Geology	Material Description (Slide Source)	Hydro-geological Features	Morphological Features
									Slope Height, H_s (m)	Slide Height, H (m)	Slide Length, L (m)	Length, L_{toe} (m)	Failure Depth, D (m)	Alpha 1 (deg.)	Alpha 2 (deg.)	Alpha 3 (deg.)	Alpha 4 (deg.)				Initial Slide	Runout				
HK1	Cheung Shan Estate	16/6/93	Cut	1	Slide of debris, translational on interface	debris flow	Yes	No	> 25	17.7	24	14.6	1.4	51	51	0	na	36.4	0.74	35	9	8	Granodiorite	Colluvium - loose, permeable.	Underlying weathered rock less permeable than colluvium. Infiltration resulted in saturation of colluvium and transient perched water table at colluvium / PW granodiorite interface.	Steep cut (51 degrees) in colluvium and PW granodiorite. Natural slope above cut of 36.5 degrees.
HK2	Allway Gardens	9/27/93	Cut	1	Compound - defect control	debris flow	No	No	54	35	55.2	40.2	2.3	41	41	0	na	32.4	0.63	225	12	12 to 15	Volcanics	Residual, saprolitic soils and PW rock. Relict joints coated with 10 mm layer of soft to firm clay observed in landslip scar.	Evidence of surface seepage on slope 1986 & 1987. Seepage observed flowing out of failure scar (high or perched groundwater). Suspect rapid variation in groundwater following rainfall and rain filled tension cracks. Catch drain upslope of failure (at top of cut).	Chunam covered cut slope (41 degrees) in residual soil, saprolite and PW volcanic rock. Steep natural slope above cut.
HK3	Kau Wa Keng San Tseun - Slide A	4/6/97	Cut	1	Compound - significant translational component, defect control	debris slide / debris flow	Yes	No	80	9.8	12.6	8.4	2 to 3	70	45	0	(30 slope above cut)	37.9	0.78	80	8.5	9	Granite	Residual soil (loose to medium dense, clayey silty gravelly sand) over saprolite over PW granite. Slide exposed closely spaced discontiuities parallel to to slope.	Springline upslope of failure. Infiltration of seepage and rainfall. Development of transient perched water table above weathered rock. Several erosion pipe holes observed in scarp.	Very steep cut slope (up to 70 degrees) in residual soils and saprolite. Chunam covered cut slope with weepholes.
HK4	Keng Hau Road Slide B	2/6/97	Cut	1	Compound - non circular, retrogressive	debris flow	No	No	31.5	31.5	64.5	39	5	53	40	6	na	26.0	0.49	210	16	14 to 7	Granite	Residual soil - clayey silty sand overlain by shallow fill (granular and porous).	Infiltration of surface water during heavy rain saturating slope, possible development perched water above saprolitic soils.	Steep cut slope (53 degrees) in residual soil and saprolite.
HK5	Hong Tseun Road	3/7/97	Cut	1	Compound - non circular	debris flow	No	No	15.3	15.3	33.3	23.3	2.5	36	42.5	0	na	24.7	0.46	250	25	18 to 8	Volcanics - Tuff	Saprolite - moist to wet silty and sandy clay, high plasticity and soft to stiff (SPT < 3). Underlain by stiff to very stiff silty sandy clays, significant gravel to boulders. Jointing, not adverse to failure.	Possible development of high perched groundwater pressures above stiff clays due to infiltration from rainfall. Seepage observed coming out of scarp.	Cut slope (36 to 42.5 degrees) in saprolitic soils.
HK6	Chung Shan Terrace - Slide B	4/6/97	Cut	1	Compound - non circular	debris slide ? / debris flow ?	Yes	No	18.5	12.4	14.3	5.6	3	52	50 (0 to 90)	0	na	40.9	0.87	85	16	14	Granite	Saprolitic soil - medium dense silty fine to coarse sand. No indication of unusually weak materials or adverse discontinuities.	Groundwater table well below failure. Cut off drains at top and toe of cut slope. Possible build up of perched water ollowing infiltration.	Steep cut slope (52 degrees) in saprolitic soils. Unprotected. Steep, sparsely vegetated natural slope above cut.
HK7	Fei Tsui Road	13/8/95	Cut	1	Translational - defect control	debris flow, dry	No	No	27	34	72	34	15	65	65	-2	na	25.3	0.47	14000	40 to 70	95	Volcanic - Tuff	Saprolite (weathered tuff in matrix of clayey silty sand / sandy silt) of 4 to 11 m depth overlying PW rock. Persistent relict jointing in saprolite and altered tuff layer (ML/MI).	Infiltration of rainfall into slope. Development of perched water table on altered tuff (evidenced by seepage). Surface drains at crest of cut and on slope suspected of being blocked.	Steep cut (60 to 65 degrees) in saprolite and PW rock. Upper part of cut chunam covered. 12 degree natural slope above cut with reservoir some 30 m back from cut.
HK8	Ten Thousand Buddha's Monastery	2/7/97	Cut	1	Compound - defect control	debris slide / debris flow	Yes	No	18	27.6	39.6	20.1	5.5	52	62 (56 to 75)	0	na	34.9	0.70	1500	25	42	Granite	Saprolite (slightly clayey sand) over PW rock. Persistent sheeting joint in conjunction with other joint sets were adverse to stability of the cut. Overlain by shallow layer of permeable colluvium.	Groundwater below base of failure. Blocked surface drains at crest. Rapid infiltration through open joints and erosion pipes in saprolite resulted in development of perched water table above PW rock. Seepage observed in scarp post slide.	Steep cut slope (52 to 75 degrees) covered with deteriorated chunam (severely cracked and detached in places). Densely vegetated natural slope (36 degrees) above cut.
HK9	Ching Cheung Road	3/8/97	Cut	1	Compound - defect control	debris flow	No	No	27.4	31.9	81	51	2 to 4	48	38	0	na	21.5	0.39	2000	35	32 to 43	Granite	Saprolite - gravelly silty and clayey sand. Indications of possible adverse jointing. Overlain by shallow layer of colluvium.	Subsurface transient groundwater controlled by a system of natural pipes and basalt dyke aquitards. Raking drains in lower two batters. Seepage in scarp observed post failure.	Cut slope (48 degrees) of 27 m height in 4 benches. Surface drains installed. Slope mostly vegetated, some shotcreting. Natural slope above cut approx 31 degrees.
HK10	Fung Wong Service Reservoir	9/6/98	Cut	1	Translational - wedge type, defect control	debris flow, dry	Yes	No	26.5	29	29.3	15.7	2 to 2.5	52	51	0	na	44.7	0.99	120	8.5	5 to 9	Granite	Saprolite - gravelly silty sand. Adverse, partly kaolin infilled relict joints (10 to 20 mm thickness) in soil mass.	Development of transient perched water table in soil mass above relict discontinuities. No control of surface water from above (blocked drain at crest), therefore exaserbating infiltration.	Steep cut slope (52 degrees) in decomposed granite. Shotcrete and chunam covered. Natural slope of about 36 degrees above cut.
HK11	Yue Sun Garden - Slide A	9/6/98	Cut	1	Compound - non circular	Debris flow	No	No	9.2	10.2	14.2	8.5	1.2	56	56	9.5	na	35.7	0.72	200	13.5	13.5	Volcanics - Tuff	Saprolite - moist, medium dense slightly clayey sandy silt with some gravel (scarp description).	Inadequate surface water drains. Erosion pipes in soil mass provided preferential sub-surface flow paths. No seepage observed 2 days after slide.	Steep cut slope (50 to 60 degrees), old and over-steep, with no slope protection. Natural slope above cut 16 to 20 degrees (densely vegetated).
HK12	Keng Hau Road - Slide A	4/6/97	Cut	2	Compound	debris flow	No	No	11	29	83	66.5	5	64	19.5	6	na	19.3	0.35	150	10 to 12	10 to 12	Granite	Residual soil - clayey silty sand overlain by shallow fill (porous granular fill) of 0.7 m thickness.	Infiltration of surface water during heavy rain saturating slope, possible development of perched water above saprolitic soils.	Steep cut slope (64 degrees) in residual soil.
HK13	Ha Wo Che, Shatin	3/7/97	Cut	2	Compound - non circular (some defect control)	debris slide	Yes	No	9.3	8.8	12.9	6.4	2.5	55	0	-	na	34.3	0.68	60	10	14	Granite	Saprolitic soil - closely spaced discontinuities oriented sub-parallel to slope.	Concentration of surface and sub-surface water flow directed toward landslip site. Possible build up of pore pressures in slope.	Benched cut slope, average 55 degrees, covered with chunam. Natural slope of 25 to 40 degrees above cut.
HK14	St Joseph's, Ngau Tau Kok	3/8/97	Cut	2	Compound - non circular (some defect control)	debris flow, dry	Yes	No	8.6	7.8	8.2	3.6	1	65	0	-	na	43.6	0.95	25	3 to 5.5	8.2	Granite	Weathered granite (saprolite ?)	Groundwater table below base of failure. Likely water ingress due to overflow from blocked drain at crest. Possible delay between rainfall and failure.	Rubble facing on steep cut slope (65 degrees) in weathered granite.
HK15	Bayview Gardens	2/7/97	Cut	2	Rotational	debris flow	No	No	14.5	13	12.1	6	1 to 2	66	0	-	na	47.1	1.07	70	11	11	Volcanics - Tuff	Saprolitic soil - silty fine to medium sand.	Likely water infiltration at crest of cut slope and development of perched water behind rubble wall (blocked weep holes). Seepage observed from failure scar.	Stone facing on steep cut slope (66 degrees) in volcanic saprolitic soils. Densely vegetated 5 degree slope above cut.
HK16	Yue Sun Garden - Slide B	9/6/98	Cut	2	Compound - significant translational component	debris slide / debris flow	No	No	14.1	15.5	27.7	13.2	3.5	52 (50 to 60)	2	-	na	29.2	0.56	1100	36	28 to 17	Volcanics - Tuff	Saprolite - firm to stiff sandy clayey silt (scarp description). Relict joints.	Inadequate surface water drains. Erosion pipes in soil mass provided preferential sub-surface flow paths. No seepage observed 2 days after slide.	Cut slope (50 to 60 degrees), old and over-steep, no slope protection. Natural slope above cut 16 to 20 degrees (densely vegetated).
HK17	Lai Cho Road, Kwai Chung	4/6/97	Cut	3	Slide of debris, compound - non circular (on interface ?)	debris flow	No	No	54	28.2	44.4	34.4	1	34	34	-	na	32.4	0.64	33	6	6 to 7	Granite	Colluvium (loose fine to coarse grained sand with some boulders). Underlain by saprolitic soils (exposed in landslide scar).	Groundwater below base of slide. Surface drainage on cut slope and catch drain at crest. No seepage observed. Direct infiltration of rainfall on slope and potential development of perched water table.	Shallow cut (34 degrees) in colluvium and saprolitic soils. Flat slope above cut.
HK18	Castle Peak Road (Milestone 14.5)	7/8/94	Cut	4	Rotational	debris flow, dry	No	No	9.1	24.5	45.8	28.9	5.5	46	0	30	(23 natural slope above cut)	28.1	0.53	300	30	22	Granite. Intruded by a number of sub-vertical basalt dykes (CW).	Saprolitic soils - gravelly silty sand with cobbles and boulders. Near vertical basalt dykes (CW).	Blocked drain above slide, overflowed onto cut slope. Basalt dykes controlled groundwater regime (dammed groundwater flow and raised groundwater level) within slope. Water seepage within landslide scar uphill of dykes.	After initial failure (July 1994) cut slope cut back from 60 to 46 degrees.
HK19	Po Shan Road	18/6/72	Cut	4	Compound - defect control	debris slide / debris flow	No	No	14.5	120	270	175	6 to 16	57	0	17 (24 reducing to 13)	na	24.0	0.44	40000	25 to 40	60 to 70	Volcanics	Saprolitic soils (clayey silty sand with gravel) to 10 to 30 m. Overlain by colluvium (silty clay to clayey silty sand) of approx 3 m depth.	Infiltration from rainfall and surface water. Development of perched water tables (possible rise in groundwater ?). Seepage from toe of cut and upslope of cut (spring).	14.5 m high cut (57 degrees) at toe of steep (30 to 40 degrees) natural hill slope.
HK20	Kau Wa Keng Upper Village	4/6/97	Cut	4	Translational - defect control	debris flow	No	No	4.4	29	48.8	29.8	1 to 5	60 (31 above cut)	33.5 (some 9 and 65)	0	na	30.7	0.59	280	14	8 to 18	Granite	Saprolite (granitic). Persistent 20 mm thick joint formed surface of rupture. Overlain by shallow layer of permeable colluvium (1 m depth).	Transient perched groundwater developed in weathered granite on discontinuities following heavy rainfall. Infiltration through open discontinuities. Seepage observed from main scarp above discontinuity, which reduced with time after cessation of rainfall.	Low height (4.5 m), steep cut (60 degrees) on natural slope (31 to 33.5 deg). Run-out predominantly on natural slope (below cut) with some flatter and steeper slopes associated with benching.
HK21	Kwun Lung Lau	23/7/94	Cut - R	2	Compound (retained slope)	debris flow	No	No	9.2	12.3	23.6	15.3	3 to 6	75	3.5 (0 to 90)	-	na	27.5	0.52	1000	28	33 to 38	Volcanics - Tuff	Saprolite - sandy silt to silty fine sand, completely to highly weathered tuff, very wet. Overlain by loose fill, placed 1964 to 1969.	Leakage from defective stormwater and sewer services saturated retained soil. Small contribution from rainfall.	Thin masonry block retaining wall (at 75 deg slope) supporting cut in saprolitic soils. Fill placed above retaining wall, chunam covered.

Table B1.3: Landslide case studies from Hong Kong (Sheet 2 of 4)

No.	Site	Slope Type	Rainfall	Pre-Failure Observations	Trigger	Mechanism	Initial Slide Description	Post-Failure Observations	Post-Failure Characteristics (Obstructions, deposition, channelisation)	Velocity (m/s)	Comments	References
HK1	Cheung Shan Estate	Cut	Wet period for 15 to 20 days prior to slide. Heavy rain in 1.5 hrs leading up to slide, peak 79 mm/hr (1 in 10 year event).	na	Rainfall (saturation of colluvium and development of perched water table).	Instability due to rise in groundwater leading to translational debris slide on colluvium / weathered rock interface.	Slide of debris from top of cut slope. Translational - on interface between colluvium and PW granodiorite.	Very quick flow. Rapidity due to angle of cut slope (51 deg).	Bus and bus shelter obstructed slide at toe. No channelisation. No deposition on 51 deg slope, deposition on flat slope at toe.		Failure entirely within colluvium. One person killed.	Chan et al (1996)
HK2	Allway Gardens	Cut	Sept 93 generally dry except for 2 periods of rain - 125 mm (13 to 18/9/93) and 390 mm (23 to 27/9/93). 1 in 5 yr event for 25 & 26/9/93. Little rainfall on 27/9/93 prior to slide.	New chunam placed in 1984 at approx. location of the slide, therefore possibly some minor problems at this time. No prior signs of failure leading up to slide. Pre-existing tension cracks on upper part of failure scar, up to 2 m depth.	Rainfall (likely rise in groundwater level in slope).	Instability due to groundwater and water filled tension cracks. Consider also time effects of softening of relict joints and strain weakening.	Defect controlled compound slide in partially weathered rock.	Loud noise followed by release of debris (soil and rock).	No channelisation. Minor obstruction (edge of building on cut slope). No deposition on steep cut slope (41 deg), deposition on flat slope at toe (max 3m)	na	Cut slope covered with chunam in 1984. Constructed between 1976 to 1978.	Chan et al (1996)
HK3	Kau Wa Keng San Tseun - Slide A	Cut	24 hr - 263 mm, 12 hr - 252.5 mm, max intensity 128.5 mm/hr (1 in 40 yr event).	Minor landslide in base of cut slope on 8/5/97 during heavy rain (one month prior to this failure).	Rainfall (infiltration into soil and development of perched water table).	Instability due to reduced strength of saturated soil and perched groundwater weathered rock.	Defect controlled compound slide in residual and saprolitic soils. Significant translational component along discontinuities parallel to face.	Part of slide mass retained in failure bowl in relatively intact condition. Debris that exited source area came to rest against rear wall of house. No influence of washout.	Obstructed by house. No channelisation. Deposition influenced by house.	na	Constructed before 1954. No washout effects.	Halcrow (1999a)
HK4	Keng Hau Road Slide B	Cut	Heavy rainfall for 4 hours prior to slide (max. 1 hour = 97.5 mm/hr). 1 in 34 year event for 2 hr rainfall.	Large failure preceeded by a smaller failure. Possibly only short time period between failures.	Rainfall (infiltration through platform above cut slope).	Instability due to loss of strength on saturation and possible perched water.	Compound (non-circular) slide through residual soil mass, possibly translational at toe on saprolite interface. Retrogressive.	Two distinct failures. Initial small failure that was highly mobile followed by a second larger failure of lesser mobility.	Deposition on full length of slope - 2 to 4 m deep at toe of cut slope, much shallower at distal end.	na	Loss of lateral support from Slide A possibly a significant factor.	Halcrow (1999e)
HK5	Hong Tseun Road	Cut	Heavy and prolonged rainfall. 31 day - 1193 mm (1 in 40 yr event).	na	Rainfall (infiltration and development of perched groundwater table).	Instability associated with saturation of soils and perched water.	Slide (compound, non-circular) through soil mass in saprolitic soil. Within zone of soft to stiff clay, base close to boundary with very stiff clay.	na	No obstruction or channelisation. Most of deposition on flat slope at toe of cut (2 to 0.5 m), remainder above first berm. No deposition on 42.5 deg slope.	na	Construction completed 1978. Travel down road due to washout. Fully vegetated by 1997.	Halcrow (1999d)
HK6	Chung Shan Terrace - Slide B	Cut	Heavy rainfall - 4 hr event 1 in 50 years.	na	Rainfall (infiltration and development of perched groundwater table).	Instability associated with saturation of soils and possible perched water.	Failure through saprolitic soil mass, compound (non-circular). Shallow.	na	No channelisation. Obstruction from wall in front of slide. Deposition on lower portion of scarp and flat slope at toe (2 to 3 m depth).	na	Slope upgraded in 1990. History of minor failures. Slope vegetated with small shrubs and grass.	Halcrow (1999d)
HK7	Fei Tsui Road	Cut	Heavy prolonged rainfall. 31 day rainfall - 1303 mm (1 in 95 year event), peak 94.5 mm/hr in hours prior to failure.	na	Rainfall (infiltration leading to rise in perched water table above altered tuff layer).	Instability due to rising perched water table from prolonged and heavy rainfall. Likely slide brittleness associated with strain weakening along controlling defects and lateral margins.	Translational defect controlled failure in saprolitic soil mass. Altered tuff layer formed base of slide, persistent joints formed backscarp.	Main failure preceeded by small failure in upper cut slope. Rapid movement of main slide (slid down in a couple of seconds). Large degree of break up of slide mass.	No channelisation or obstruction. Deposition in bowl of failure (4 m deep on 15 deg slope) and on flat slope at toe (10 m max at toe of cut).	10 to 13 (DAN)	DAN model - good representation of deposition using phiB = 24 deg on rupture surface and 36 deg on distal path. GEO consider low travel angle possibly due to angle of trajectory of failed mass.	Hungr GR (1998) Irfan (1997) Irfan & Woods (1998) GEO (1996a) Knill (1996a)
HK8	Ten Thousand Buddha's Monastery	Cut	Heavy rainfall on morning prior to slide. 1 in 25 year for 1 hour prior to slide (118.5 mm/hr).	Open joints evidence of past movement.	Rainfall (infiltration and development of perched groundwater table).	Instability due to high perched water table from heavy rainfall. Brittleness associated with strain weakening along controlling defects and internal slide brittleness.	Defect controlled compound slide in saprolite. Persistent sheet joint in central portion and discontinuous clay joint in lower part. Steeply curved backscarp.	Failure occurred suddenly during torrential rain. Fast moving (quickly buried annex of building). Significant degree of break up at toe, lesser back in scarp.	No channelisation. Obstructed by building at toe of cut slope. Deposition - 4 m deep in failure bowl on 20 deg slope), up to 9 m deep on flat slope.	na	Defect controlled failure in saprolitic soils and weathered rock.	Halcrow (1998b)
HK9	Ching Cheung Road	Cut	Failure on 7/7/97 occurred 2 days after heavy and prolonged rainfall (31 day 1 in 500 yr event). Failure on 3/8/97 preceeded by 278 mm in 3 days (1in 2 year event), 31 day event 1 in 49 years.	History of failures in this slope. Failure on 3/8/97 (this failure) preceeded by two failure in July 1997. Extensive area of cracking and displacement at top of slope (large perimeter crack 2.5 m vert settlement, 1 m horiz) observed prior to failure.	Rainfall (infiltration and development of perched groundwater table).	Instability due to development of perched water table and gradual weakening of slope from progressive movements. Suspect brittleness associated with internal slide mechanism.	Defect controlled compound slide in saprolitic soil.	Run out distance suggests the slide was quite mobile.	No channelisation or obstruction. Deposition on flat slope at toe (1 to 2.5 m depth). Mobility of slide possibly enhanced from ponded water on enclosed section of Ching Cheung Road.	na	Defect controlled landslide in granitic saprolite soils. Cut formed in 1967. History of numerous failures. Possible weakening of slide mass in period up to slide on 3/8/97.	Halcrow (1998a)
HK10	Fung Wong Service Reservoir	Cut	Heavy rainfall in 4 hours prior to failure, 2 hour rainfall 1 in 8 year event.	na	Rainfall	Instability associated with build up of perched water. Partly controlled by persistent relict discontinuity.	Defect controlled translational wedge type failure in saprolite along persistent discontinuity. Shallow. Part failure through soil mass.	Sinlge phase rapid event. Some debris flowed into reservoir. Loose silty sand material with gravel, dry at time of inspection.	Obstructed by fence around edge of reservoir. Partial channelisation. Deposition mainly on flat surface at toe, some spilled into the reservoir.	na	Cut slope formed before 1963. Debris observed to be dry.	Fugro (1999a)
HK11	Yue Sun Garden - Slide A	Cut	Heavy rainfall. 2 to 12 hour events, 1 in 5 to 6 year return period. Peak hourly rate = 60.5 mm/hr.	History of small failures in this slope.	Rainfall (infiltration and development of seepage pressures along preferential flow paths).	Instability associated with infiltration leading to wetting up and seepage pressures. Progressive weakening with time of old cut slope also a contributing factor.	Compound (non-circular) failure through saprolitic soil mass. Shallow spoon shaped surficial slip.	na	No channelisation or obstruction. Deposition on flat slopes below toe of cut, 3 m max at toe of cut.	na	Cut slope formed 1961.	Fugro (1999d)
HK12	Keng Hau Road - Slide A	Cut	Heavy rainfall for 9 hours prior to slide, > 305 mm (max. 1 hour = 81.5 mm/hr). 1 in 22 year event for 4 hr rainfall.	na	Rainfall (infiltration through platform above cut slope).	Instability due to loss of strength on saturation and possible perched water.	Compound slide through residual soil mass.	Highly mobile slide, possibly due to stormwater discharge on to slope from drainage channel near toe of scarp.	Deposition on full length of slope, 0.7 m near rupture and 0.1 to 0.3 m at distal end.	na	Poor condition of slope surfacing. High mobility of slide mass.	Halcrow (1999e)
HK13	Ha Wo Che, Shatin	Cut	2/7/97 - heay rain preceeded slide (1 in 40 yr for 1 to 4 hr duration) 3/7/97 - heavy prolonged rainfall (1 in 120 yr event for 1 to 31 day)	Preceeded by small failure (5m^3) on previous day	Rainfall	Instability associated with wetting up and possible perched water.	Compound (non-circular) failure through saprolitic soil mass, some control by discontinuities.	Evidence of displacement along discontinuities.	No channelisation. Slide obstructed by building at toe. Slide only moved some 2 m at head of scarp, most of deposition remained within failure bowl.	na	Constructed in early 1980s. Evidence of displacement along discontinuities.	Halcrow (1999e)
HK14	St Joseph's, Ngau Tau Kok	Cut	Landslide followed 2 periods of wet weather in July. Prior to slide, rainfall 1 in 1 to 3 for all return periods.	na	Rainfall (infiltration at crest and open joints in facing blocks).	Instability associated with saturation and build up of water pressures behind rubble facing.	Compound (non-circular) shallow slide in weathered granitic saprolite. Slide scarp oriented to one of the major joint sets.	na	Obstruction by building at toe of slide. No channelisation. Deposition at toe, max 2 m depth.	na	Significant obstruction. Slope has a history of past failures. Heavier rainfall in past, deterioration of facing likely to have had an influence.	Halcrow (1999c)
HK15	Bayview Gardens	Cut	Heavy rainfall for 8 hours prior to slide. 31 day rainfall 879.5 mm. Peak hourly = 72.5 mm/hr (1 in 6 yr event).	na	Rainfall	Instability associated with saturation and build up of water pressures behind rubble facing.	Rotational - shallow.	Loud noise heard at time of slide. Some washing out of debris by post failure surface water flow.	No obstruction. No channelisation. Deposition at toe of slope, max 2 m depth.	na	Cut - pre 1977. Rainstorm not particularly severe therefore deterioration of slope and blockage of weep holes probably had an effect on stability.	Halcrow (1999c)
HK16	Yue Sun Garden - Slide B	Cut	Heavy rainfall - 12 to 24 hour events, 1 in 30 to 32 year return period. Peak hourly rate = 62 mm/hr.	History of small failures in this slope.	Rainfall (infiltration and development of seepage pressures along preferential flow paths).	Instability associated with infiltration leading to wetting up and seepage pressures. Progressive weakening with time of old cut slope also a contributing factor.	Compound - significant translational component	Debris in slide remained relatively intact, relatively quick movement.	No channelisation or obstruction. Deposition on flat slopes below toe of cut, 3 m max at toe of cut.	na	Cut slope formed 1961. Slide debris remained relatively intact.	Fugro (1999d)
HK17	Lai Cho Road, Kwai Chung	Cut	Slide during 10 hours of heavy rainfall (364 mm), max hourly rainfall of 128.5 mm. 1 in 50 yr event for rolling 4 hr rain.	Previous sliding in vicinity of this failure.	Rainfall (infiltration into soil, possible development of perched water in colluvium).	Instability due to reduced strength of saturated soil and perched groundwater in colluvium.	Slide of debris (compound - non-circular). Shallow. Sliding partly along colluvium / saprolitic soil interface.	Debris travelled over surface, flattening vegetation, local erosion of surface slope and local deposition of debris on margins.	No obstruction or channelisation. Minor deposition on 34 deg slope (lateral margins), most deposited at top of cut slope in rock, probably stopped by cut-off trench.	na	Initial construction in 1976. Shallow cut back in 1988 and installation of surface drains. No washout effects.	Halcrow (1999a)
HK18	Castle Peak Road (Milestone 14.5)	Cut	July & Aug 1994 generally wet. Heavy rain on 22/7/94 (317 mm) and 23/7/94 (43 mm). Heavy rain on 6/8/94 (287 mm) and 7/8/94 very heavy (peak hourly 42 mm/hr). Little rain 1 hr prior to 23/7/94 slide.	Previous slide in 1982 and further slides in July 1994 (one month prior to this failure).	Rainfall (rising groundwater levels following prolonged rainfall).	Instability due to rising groundwater levels. Brittleness probably from internal brittleness of slide.	Rotational slide in saprolitic soil, large number of defects in weathered rock.	Debris moved swiftly down the slope. Bus hit and tumbled down embankment. 5 to 6 subsequent minor slips over next 1 to 2 hours.	Small bus caused minor obstruction. No channelisation. Depostion mostly on flat slope at toe of cut (4 m max) with some extending down slope below road (thinly deposited on flatter portion of steep slope)	na	Slide on 7/8/94 one of series of three slides. Two earlier failures on 23/7/94. One man killed on 7/8/94 when slide hit light bus and pushed it off the road. Original cut slope formed before 1954.	Chan et al (1996), Franks (1995), Pun and Yeo (1995)
HK19	Po Shan Road	Cut	Heavy rainfall for 3 days prior to slide. Prolonged rainfall for approx 40 days.	1971 - number of slips in cut face and movement above cut. 15 to 18/6/72 - large settlement above cut (> 4.5 m) increasing with time up to failure and movement at toe of cut. Several slips preceeded the large slide.	Rainfall (also contribution from excavation at toe of natural slope).	Instability due to loss of strength on saturation, perched water tables and strain weakening due to movement.	Decfect controlled compound slide in saprolite. Buttress effect at toe. Significant translational component of rupture surface.	Catastrophic failure at 9:00 pm on 18/6/72. Suspect rapid movement. Limited disturbance of material at rear of deposited mass.	No channelisation and limited obstructions given size of failure. Limited deposition in failure scar (except at front), mostly in flat area at toe of cut (up to 12.5 m depth) reducing towards toe of slipped mass.	10 (DAN model).	Suspect increase in mobility due to presence of surface water below toe of cut (particularly on flat cut surface). Material at rear of slipped mass remained relatively intact.	Hungr GR (1998) Vail (1972) Irfan and Woods (1998)
HK20	Kau Wa Keng Upper Village	Cut	Heavy rainfall on morning of failure, 280 mm in 6 hours, peak 129 mm/hr.	na	Rainfall (infiltration and development of perched groundwater table on discontinuities).	Instability due to development of perched water table on persistent discontinuity (discontinuity exposed in face of excavation).	Defect controlled translational slide along slightly undulating discontinuity in saprolite. Subvertical joints acted as release surfaces.	Trees at toe of cut slope fell immediately prior to failure. Landslide was sudden and debris ran out rapidly. Second, smaller slide occurred some 1.5 hours after initial slide.	No channelisation, no obstruction. Most of debris deposited in base of slide scar (29 deg) and platform at toe of cut (1 to 2 m depth). Some material continued down slope below platform and flowed down to Castle Peak Road.	na	Defect controlled landslide in granitic saprolite soils. Cut formed between 1954 and 1959. Suggests possible weakening and opening of joints in period up to slide. 1 fatality.	Halcrow (1998c)
HK21	Kwun Lung Lau	Cut - R	Heavy rainfall for 2 days preceeding slide (1 in 28 year event). Only 29 mm rain in 10 hours up to failure.	Muddy water observed out of weep holes for 2 days prior to failure. 2.5 hours prior to slide greater rate of seepage through weepholes and joints.	Service leakage (saturation of supported soil, possible perched water).	Masonry block retaining wall unable to support saturated saprolite.	Compound (possibly rotational behind retaining wall) failure in retained saprolitic soil slope.	Dislodgement of some masonry stones then wall "burst" out at about mid height. Collapsed instantaneously. Upper portion of failed wall remained relatively intact at toe of failed mass.	No obstruction of channelisation. Deposition on flat slope, maximum 6 m depth at original toe of wall.	na	Collapse of retained cut slope (built before 1904). 5 people killed.	GEO (1994), Morgenstern (1994, 2000)

Table B1.3: Landslide case studies from Hong Kong (Sheet 3 of 4)

No.	Site	Date of Failure	Slope Type	Slope Failure Geometry	Initial Slide Classification	Travel Classification	Obstr-ucted	Confined (Yes/No)	Landslide Geometry									Travel Distance Angle (^{o})	Ratio H/L	Volume (m^3)	Width (m)		Geology	Material Description (Slide Source)	Hydro-geological Features	Morphological Features
									Slope Height, H_s (m)	Slide Height, H (m)	Slide Length, L (m)	Length, L_{toe} (m)	Failure Depth, D (m)	Alpha 1 (deg.)	Alpha 2 (deg.)	Alpha 3 (deg.)	Alpha 4 (deg.)				Initial Slide	Runout				
HK22	Sau Mau Ping	25/8/76	Fill	1	Flow slide Compound - significant translational component	flow slide	Yes	No	32	32	80	50	2 to 4	34	30	0	na	21.8	0.40	2500	42	42	Granite	Loose fill - end dumped decomposed granite (SM - silty sand ?). 10 years old. 75 to 90% SMDD.	Significant stream course at failure location prior to filling. Estimated depth of wetting from rainfall infiltration of 2 to 6 m.	Deep fill (up to 25 m) at slope of 34 degrees over natural ground. Slope and downslope entirely of loose fill. Vegetated.
HK23	Kennedy Road	8/5/92	Fill	1	Flow slide, compound - significant translational component	flow slide / debris flow	No	No	31.1	26.6	44	28	2	35	45	0	24	31.2	0.60	500	9 to 13	6 to 12	Granite.	Fill - wet silty sand (SM) with pieces of brick and stone. 50 years old.	Undistubed fill remaining post slide was wet. Infiltration from rainfall caused wetting.	Fill placed in old valley. Maximum depth approx. 5 m at slope of 42.5 to 55 degrees.
HK24	Sha Tin Heights Road - Slide A	4/6/97	Fill	1	Flow slide (part) Compound - significant translational basal component	flow slide / confined debris flow (for part that flowed) debris slide for intact portions.	Yes	Yes (for flow)	47.5	39.5	86.5	70	1.5	34 (25 to 50)	27.5	0	27.5	24.5	0.46	150	15	9.5	Granite	Fill - loose silty coarse sand (underlain by colluvium)	Infiltration from rainfall and also from prolonged leakage of drainage pipes. Likely perched water table between fill and natural.	Steep (34 up to 49 degrees) shallow fill slope on 25 to 35 degree natural slope.
HK25	Kau Wa Keng San Tseun - Slide D	4/6/97	Fill	1	Flow slide Compound (?), possibly rotational, retrogressive	flow slide	No	No	20	22.5	52	30	3 to 4	36 to 40	32	0	19.5	23.4	0.43	500	11	11 to 12	Granite	Fill - loose, moist to wet clayey silty gravelly sand (decomposed granite). End tipped fill.	Located along line of ephemeral stream. Infiltration of rainfall and water from stream flow into fill, with possible development of perched water table in fill.	1000 m^3 of granitic fill (unretained) dumped on natural slope. Near level fill platform and steep side slopes (36 degrees).
HK26	Chung Shan Terrace, Lai King Hill Rd	4/6/97	Fill	1	Flow slide Compound - significant translational component	flow slide	No	No	23.5	23	73	56	3	37	30	2	30 (21 to 37)	17.5	0.32	450	18	20 to 13	Granite	Fill - sandy silt to clayey sandy silt with gravel. Avg 75% SMDD indicating loose condition.	Infiltration of water into fill and leakage from stormwater system above slope. Buried retaining walls potentially dammed the flow of water resulting in elevated perched water table. Seepage observed from base of main scarp and base of masonry wall.	Steep loose fill slope (37 degrees). Buried retaining walls in fill.
HK27	Tuen Mun Road	2/7/97	Fill	2	Compound - significant translational component	debris slide / debris flow	No	No	11.5	11.5	22.2	7.7	1.2	30 (50 at toe)	0	-	34	27.4	0.52	200	25	25 to 28	Granite	Fill - clayey silty sand (loose to med dense) and clayey sandy silt (soft to firm). 86 to 94% SMDD for general fill. Probes - uniformly low density to 5 m depth.	Herringbone drainage on fill surface, cut off drain at top of slope. Landslide located immediately below blocked drainage channel. Infiltration from rainfall and run-on from upslope. No seepage observed in main scarp.	Benched fill slope. Failure within upper bench at slope of 34 degrees.
HK28	Au Tau Village Road	9/6/98	Fill	3	Flow slide Translational (on interface), retrogressive ?	flow slide	No	No	>80	25.8	57.5	43.5	2	35	23	16.5	23	24.2	0.45	170	15	24	Volcanic - tuff	Fill - silty and gravelly sand (SM), end dumped, loose, 70% SMDD with pieces of building rubble. Underlain by colluvium (firm to stiff clay).	Infiltration from rainfall and run-on from upslope. Leaking drainage pipe.	Shallow illegally dumped fill at slope of 35 degree. Dumped on natural slope of 23 degrees.
HK29	Baguio	8/5/92	Fill - R	1	Compound or Rotational, retrogressive	confined debris flow	Yes	Yes	109	109	227	207	7.5	80	31.4	0	16	25.6	0.48	3800	35	11 to 15	na	Fill - soil with building debris, loose, retained. Traced back to before 1924.	No surface drainage above retaining wall. Run off over-topped retaining wall. Infiltration from rainfall. Possible perched groundwater table within fill.	Retained fill with relatively flat slope above wall. Natural gully below retaining wall.
HK30	Kau Wa Keng San Tseun - Slide C	4/6/97	Fill - R	1	Rotational, possible flow slide	flow slide / debris flow	Yes	No	80	10	21	17.5	2.5	90 (ret wall)	33	0	33	25.5	0.48	60	7	6 to 9	Granite	Fill - loose to very loose, wet, silty gravelly sand with cobbles, boulders, brick and concrete. Numerous voids.	Surface water from upslope flowing onto concrete fill platform. Springs flowing out of exposed rock face above fill. Saturation of fill and possible development of perched groundwater.	Series of fill terraces supported by retaining walls on 33 deg slope. Failed retaining wall had concrete covering in poor condition.
HK31	Tao Fung Shan Cemetery - Slide B	2/7/97	Fill - R	1	Compound - non circular	debris flow	No	No	32.5	21.5	37.5	25.5	2.6	40 (28 to 90)	36 (34 to 46)	0	36	29.8	0.57	400	27	20	Granite	Fill - firm to soft gravelly clayey sandy silt, overlying residual soil (firm gravelly clayey sandy silt).	No drainage at top of slope. No drainage behind retaining wall, some weep holes in face. Substantial run-off from up-slope observed, likely to have ponded behind retaining wall and infiltrated retained fill.	Series of retaining walls on average slope of 40 degrees.
HK32	Sha Tin Heights Road - Slide B	4/6/97	Natural	1	Slide of debris, translational on interface, retrogressive	confined debris flow	No	Yes	44	33.5	105	86	1.5	37 (32 to 42)	16 (13 to 22)	0	na	17.7	0.32	170	12	7 to 12 (in gully), up to 20 m on flatter slopes	Granite	Colluvium - silty fine to coarse sand. Minor filling.	Possibly affected by discharge from upslope (erosion pipes observed in scarp). Infiltration from discharge and rainfall. Perched water table developed in colluvium (above saprolite). Erosion pipes possibly from upslope discharge.	Steep natural slope (up to 42 degrees) above flatter slopes of 13 to 22 degrees.
HK33	Wonderland Villas, Kwai Chung	5/8/97	Natural	1	Compound - significant translational component on interface	debris flow, lower part confined	Yes	Partly	107	104	190	177	1.0 to 1.5	40	34	0	na	28.7	0.55	80	8	6 to 8	Granite	Residual soils - completely decomposed granite.	Groundwater at depth, no evidence of seepage. Possibly run-on from upslope, report of flooding in development at slope crest. Rainfall infiltration and development of perched groundwater table in residual soil.	Detachment scar located within a locally steepened (40 degree slope) topographical depression at the head of a poorly developed drainage line.
HK34	Ka Tin Court, Shatin	2/7/97	Natural	1	Compound - translational basal component (defect control ?)	debris flow, partly confined	Yes	Yes	26.6	23.5	43	32.6	2.5	52	37.5	0	na	28.7	0.55	150	14	8.5	Granite	Saprolitic soils - completely decomposed granite. Overlain by shallow fill (loose, end dumped silty fine sand).	No surface drainage at top of slope. Depression at top of crest allowed ponding of water. Infiltration promoted by shallow loose fill on crest and upper slope. Groundwater at depth.	Located within natural depression at head of gully. Failure in over-steepened slope of 52 degrees.
HK35	Shum Wan	13/8/95	Natural	1	Compound - non circular (defect control)	debris flow	No	No	71	71	219	154	12.5	31	26.5	0	na	18.0	0.32	26000	50	60 to 90	Volcanics - Tuff	Saprolite - sandy silty clay (CI/CH) with weak CH clay seams. Overlain by fill (loose sandy silty clay CL/ML, 71 - 81% SMDD) and colluvium (silt/clay of 1 m depth).	Infiltration and seepage resulting in high perched water table in main slide area, exasperbated by run-on from road at crest following small fill failure. High groundwater table in lower planar slide area.	Natural slope at average angle of 31 degrees. Cut to fill at crest of failure (Nam Long Shan Road, fill 5 m deep). Slope densely vegetated.
HK36	Ma On Shan Road	2- 3/7/97	Natural	2	Compound - some defect control, retrogressive	debris flow, upper part confined	No	Yes, partly	> 45	42.4	106.5	47.5	2.5 to 5	33.8	5	-	na	21.7	0.40	3000	12 to 30	12	Granite	Saprolite - medium dense silty coarse sand with gravel. Persistent planar discontinuity in saprolitic soils.	Concentration of surface and sub-surface water flow within gully.	Natural slope at average of 34 degrees. Minor cutting and filling on lower slopes within gully. Failure located within gully with previous history of landsliding.
HK37	Tsing Shan	11/9/90	Natural	3	Slide of debris, Compound	confined debris flow	No	Yes	480	379	875	715	4	37 (28 to 50)	26.7 (16 to 40)	12.9 (6 to 17)	na	23.4	0.43	13000	25 to 30 (and gully)	50 to 95 (deposition zone)	Granite, Sedimentary and Volcanics	Colluvium - Cobbles and boulders in a matrix (15 to 25%) of gravel to clay size. Less boulders and more finer material in lower valley channel.	Ephemeral stream. Flows strongly during and just after rainfall with some low flow (springs). Infiltration and possible saturation of colluvium.	Initial slide area on steep mountain slope (50 degrees). Narrow V-shaped gully to Ch 500 m (avg 27 to 37 deg). Broad fan area on lower hillslopes below Ch 500 m (17 reducing to 6 degrees).
HK38	Outward Bound School	9/6/98	Natural	3	Compound - non circular (some defect control ?)	debris flow, partly confined / debris slide	No	Partly	60	32	63	48	3 to 5	44	33.5	19	na	26.9	0.51	900	21	16 to 8	Sedimentary and Volcanics - tuffaceous mudstone, siltstone and breccia.	Saprolite (completely decomposed tuff) and residual soil - stiff clayey sandy silt. Overlain by shallow layer of colluvium.	Infiltration through open jointed rock and development of water pressures in joints and/or elevated water pressures in soil mass. Erosion pipes promoted sub-surface flow.	Natural slope (densely vegetated) with steep upper slope (44 degrees) at head of gully. Slopes in gully below slide decrease from 33.5 to 19 degrees.
HK39	Lantau Island - Slide C1	4 and 5/11/93	Natural	3	Slide of debris, Compound - significant translational component on interface	debris flow, partly confined	No	Yes, partly	>100	84	218	181	3	33	18.3 (14 to 23)	-	na	21.1	0.39	1000	10 to 15	10 to 15	Volcanics	Colluvium - 30% cobbles.	No information. Likely infiltration from rainfall resulting in saturation of colluvium.	Natural slope of 14 to 33 degrees. Steeper slope (30 degrees) in failure area (colluvial accumulation). Debris flow within broad and not well formed gully.
HK40	Tao Fung Shan Cemetery - Slide A	2/7/97	Natural / Fill	1	Translational	debris flow	No	No	63	60	104	89	3 to 3.5	50	40	6 (11 to 0)	40	30.0	0.58	900	52 (two backscarps)	50 to 65	Granite	Residual soil - loose to med dense gravelly clayey silty sand. Overlain by fill (tipped, loose to very loose, gravelly silty clayey sand of 1 to 2 m thickness) with topsoil layer below fill.	No drainage at top of slope. Deep groundwater. Erosion pipes (in fill) exposed in backscarp. Spring approx. 30 m below scarp. Infiltration from rainfall, possibly exacerbated by presence of fill.	Natural slope at average angle of 40 degrees. Steep slope (50 degrees) in shallow fill on top of natural slope.
HK41	Glorious Praise Christian Centre	8/5/97	Natural / Fill	1	Compound - translational basal component on interface	debris flow	No	No	8.7	9	17.2	12	1.5	32.5	32.5	1	0 (?)	27.6	0.52	20	4.9	5 to 6	Granite	Residual soil - loose to med dense sand overlain by fill (loose sandy silt / silty sand, 1 m thick).	Infiltration of water into slope. Surface depression at top of slope ponded water which overflowed onto slope. Erosion holes observed in fill in scarp (no seepage). Possible perched water table between residual and weathered rock.	Average slope of 30 degrees. Shallow fill on relatively flat ground at top of slope.
HK42	Lido Beach	2/7/97	Natural / Fill	4	Compound - non circular	debris flow	No	No	48	32	83	60.5	3	52 to 25	17	-	na	21.1	0.39	750	24	14 to 27	Granite	Residual soil (silty sand) overlying saprolitic soils (silty sand). Shallow layer of fill (silty fine sand).	Infiltration of rain water into slope. Ponded water upslope of scarp. Increase in groundwater level within slope. Seepage from base of rupture surface indicative of high groundwater table.	Natural slope (25 to 50 degrees) with series of small terraces down the slope (minor cuts and fills). Modified natural slope.
HK43	Lui Pok School	26/9/93	Natural	1	Slide of debris, Compound - significant translational component on interface	debris flow, partly confined	Yes	Yes, partly	180	77	220	186	2	31	20 (29 to 15)	9.6 (0 to 10)	na	19.3	0.35	450	29	8 to 10 (gully), 34 terminal.	Sedimentary - Sandstone	Colluvium - silty sand with large content of gravel and cobbles.	Infiltration from rainfall and run-on from upslope. Flow in topographic depression possible during heavy rain. Seepage observed in scarp from erosion pipes and bedding discontinuities.	Natural gully - slopes decreasing gradually from 31 degrees at scarp area to 10 degrees above school.

Table B1.3: Landslide case studies from Hong Kong (Sheet 4 of 4)

No.	Site	Slope Type	Rainfall	Pre-Failure Observations	Trigger	Mechanism	Initial Slide Description	Post-Failure Observations	Post-Failure Characteristics (Obstructions, deposition, channelisation)	Velocity (m/s)	Comments	References
HK22	Sau Mau Ping	Fill	Heavy rain on 24 - 25/11/76, 15 to 35 mm/hr.	Some erosion and small periperal slides during 1972 heavy rainfall event.	Rainfall (infiltration into outer zones of loose fill).	Instability due to loss of strength on saturation. Likely collapse of loose fill structure resulting in static liquefaction.	Flow slide in loose fill. Compound with significant translational component. Shallow, entirely within loose fill.	Upper part of slope moved as a whole. No water observed to drain from slipped debris.	Obstructed by building. Deposition only on flat slope (none on 30 deg slope), max depth 1.8 m.	10 to 15 (DAN)	DAN frictional model, phiB = 20. 18 people killed	Hungr GR (1998) HKIE (1998) Morgenstern (2000) Gov't HK (1977)
HK23	Kennedy Road	Fill	163.5 mm in 2 hours leading up to slide (1 in 20 yr event)	na	Rainfall (infiltration into outer zones of loose fill).	Instability due to loss of strength on saturation. Likely collapse of loose fill structure resulting in static liquefaction.	Flow slide in loose fill. Compound with significant translational component.	Debris wet.	Slight obstruction by car. Depostion on steep slope (< 1m depth) possibly due to batters in cut slope. Greatest deposition on flat slope below cut.	5 to 10 (est)	Slide preceeded by collapse of "big" tree.	HKIE (1998), Chan et al (1996)
HK24	Sha Tin Heights Road - Slide A	Fill	Heavy rainfall on 4/6/97 - 296 mm prior to slide, with max hourly 81.5 mm/hr. 4 hr incident 1 in 22 year event.	na	Rainfall (infiltration into fill).	Instability due to loss of strength on saturation. Likely collapse of loose fill structure resulting in static liquefaction.	Possible flow slide in loose fill. Compound with significant translational component along interface between loose fill and natural.	Part of slide flowed down confined travel path. Part remained intact and moved only short distance.	Flow portion of slide mass was confined. Some obstruction from heavily vegetated gully. Stripped vegetation in gully. Most of material deposited on flat slopes at toe (No deposition on 25 to 35 deg slopes).	na	Additional mobility from surface water flowing in gully. Query flow slide classification, possibly dilatant failure of fill on steep hillslope.	Halcrow (1999a)
HK25	Kau Wa Keng San Tseun - Slide D	Fill	24 hr - 263 mm, 12 hr - 252.5 mm, max intensity 128.5 mm/hr (1 in 40 yr).	Initial small slide at front of fill body.	Rainfall (infiltration and possible development of perched water in fill).	Instability due to loss of strength on saturation and perched groundwater in fill. Likely collapse of loose fill structure resulting in static liquefaction.	Flow slide in loose fill. Compound (?), possibly rotational, retrogressive	Possibly two phases of failure - initial failure in steep slope followed by washout failure caused by flow in ephereral stream. 4 m deep channel cut in run-out path.	No obstruction or confinement of flow. Deposition on 32 deg slope and flatter.	na	Fill placed about 1961. Part of fill located on relict landslide debris. Possible extension of slide mass due to washout (initial travel angle possibly 30 deg).	Halcrow (1999a)
HK26	Chung Shan Terrace, Lai King Hill Rd	Fill	Heavy rainfall in 2 hours preceeding slide, peak intensity of 128.5 mm/hr (1 in 41 year event).	na	Rainfall (infiltration and saturation of loose fill, possible perched water table).	Instability due to loss of strength on saturation. Likely collapse of loose fill structure resulting in static liquefaction.	Flow slide in loose fill. Compound with significant translational component.	Landslide sudden and fast moving, liquefaction likely. Following slide, surface water flow eroded some material and resulted in washout for considerable distance.	Some scouring of downslope fill. No obstruction or channelisation. Deposition predominantly on flat slopes at toe.	na	1949 - terraced natural slope evident. 1949 to 1963 - placement of filling.	Halcrow (1999b)
HK27	Tuen Mun Road	Fill	24 hr - 186 mm, 12 hr - 178 mm, 1 in 6 year for rolling 15 min rainfall intensity. 665 mm in 31 days prior to slide.	na	Rainfall	Not liquefaction of fill. Failure due to wetting of the fill from infiltration of rainfall and run-on due to blocked drain. Small cut at toe probably ontributed to instability.	Dilatant failure through soil mass. Compound with significant translational component. Shallow, not particularly mobile.	Photos indicate only partial break up of sliding mass, thus debris slide / debris flow.	Majority of debris remained in source area.	na	Failure and travel completely on fill slope. Fill slopes constructed 1972 to 1975. Cut at toe of fill slope in 1996. Slope vegetated with grass. Compare with cut slopes.	Halcrow (1999a)
HK28	Au Tau Village Road	Fill	Most severe event since mid 1980s for 2 to 24 hour rainfall. 12 hr rainfall 323 mm (18 year event), intensity 30 to 60 mm/hr at peak.	na	Rainfall (infiltration).	Instability due to loss of strength on saturation. Likely collapse of loose fill structure resulting in static liquefaction.	Flow slide in loose fill. Shallow translational slide on interface between fill and natural, retrogressive (?)	Some secondary outwash followed initial debris run-out.	No obstructions or channelisation, width almost doubled, therefore flow spread. Deposition - Less than 0.5 m thick on 23 degree slope, > 1m thick on 16.5 degree slope at distal end slide.	na	Crossfall of road altered in months preceeding slide resulting in ponding above fill slope and run-on onto fill slope.	Fugro (1999b)
HK29	Baguio	Fill - R	Heavy rain on day of failure 350 mm. Short periods of very heavy rainfall, 1 in 60 yr for 5 min rainfall prior to slide.	na	Rainfall.	Initial wall failure due to either erosion at toe (from over-topping) and/or perched water table in retained fill.	Possibly dilatant failure in retained fill slope. Compound or rotational, retrogressive.	Failure occurred as a series of retrogressive failures of 200 to 1000 m^3 over a period of 5 to 6 hours. Flow in natural gully contributed to mobility of the flow.	Building obstructed flow at toe. Confined within natural gully. Accumulation (1500 m^3) in gully. Deposition on flat slopes on and below Victoria Rd .	na	Fluidisation of debris by water flowing in natural gully.	Chan et al (1996)
HK30	Kau Wa Keng San Tseun - Slide C	Fill - R	24 hr - 263 mm, 12 hr - 252.5 mm, max intensity 128.5 mm/hr (1 in 40 yr).	na	Rainfall (infiltration and development of perched water above saprolite).	Instability due to reduced strength of saturated soil and perched groundwater above weathered rock.	Rotational failure of retained fill. Possible development of flow slide once rataining wall had failed.	Single rapid movement followed by secondary washout scarp 6 m back into slope and 2m deep in runout path.	Obstructed by house. No channelisation. Most of deposition on flatter slope (max 2 m depth), minimal on terraced slope (avg 33 degrees).	na	In 1996 no seepage nor distress of slope were observed. No comment on extension of debris due to washout. Possible flow slide once retaining wall failed.	Halcrow (1999a)
HK31	Tao Fung Shan Cemetery - Slide B	Fill - R	971 mm in 31 days prior to slide. Heavy rain prior to slide, peak 1 hour intensity of 124 mm (1 in 32 year event)	1996 - Retaining walls 1 and 2 reported as being unstable. Vertical cracking evident.	Rainfall (infiltration into retained fill).	Instability associated with ingress of water into fill. Water table development due to absense of effective drainage.	Compound - non-circular	Likely rapid movement once retaining walls failed. Possible liquefaction of fill. Secondary outwash (water mainly from run-on from upslope) of fines significant.	No channelisation. 150 m^3 debris picked up by slide. Minimal deposition on steep slopes (34 to 46 deg), most deposited on flat slope at toe.	na	1986 - 1990 retaining walls constructed. Some secondary outwash, 1 m deep erosion through residual soil and channelised outwash 30 m further downslope.	Halcrow (1999b)
HK32	Sha Tin Heights Road - Slide B	Natural	Heavy rainfall on 4/6/97 - 240 mm prior to slide, with max hourly 81.5 mm/hr. 2 hr incident 1 in 9 yrs.	na	Rainfall (infiltration).	Instability due to reduced strength of saturated colluvium and perched groundwater on colluvium / residual soil interface.	Translational slide of debris along interface between colluvium and residual soil. Retrogressive - first stage of 130 m3 followed by two smaller intact movements.	May have occurred in 3 stages. Initial failure (130 m^3) flowed and 2 subsequent intact translational movements of short distance. Travel distance and velocity of first stage probably influenced by surface water flow.	Confined in gully. Minor obstruction. Deposition on slopes flatter than 13 degress in gully. Below gully approx 0.1 m thick deposition on flat slope. Possibly affected by washout to some degree.	na	Additional mobility from surface water flowing in gully. Failure associated with ongoing processes of gully development. Greater mobility than Slide A possibly due to greater catchment area and failure during more intense period of rainfall. Washout likely to have extended slide mass.	Halcrow (1999a)
HK33	Wonderland Villas, Kwai Chung	Natural	8/5/97 - 160 to 200 mm starting 6 hrs prior to failure, intensity peaking at time of slide (I hr rainfall 1 in 12 yr event).	Relict landslides within nearby drainage lines. No evidence of previous instability within this drainage line.	Rainfall (infiltration and development of a perched water table).	Instability due to reduced strength of saturated colluvium and perched groundwater on residual / weathered rock interface.	Compound with significant translational component along weathered rock surface.	Initial failure at 8:00 am, fully developed at 10:00 am. Two phases of movement. Slide mass over-rode channel stripping vegetation and some surface soils, then entered a drainage line and washed down onto road below.	Deposition on outer margins of flow (minimal) most in pipeline and road below (Not on 33 to 35 deg slopes). Lower part of flow confined in drainage line. Obstruction was constriction of flow into drainage pipe.	na	Travel angle = 34 degrees to drainage pipe, 29 degrees to toe of slope. Possible washout effect.	Halcrow (1999a)
HK34	Ka Tin Court, Shatin	Natural	Heavy rainfall. 31 day - 1108 mm. 12 hr - 255.5 mm. 1 in 20 to 1 in 45 yr return period for 1 to 4 hr events.	na	Rainfall	Instability due to loss of strength on saturation. Exaserbated by surficial fill.	Compound failure (translational with steep rotational backscarp) through saprolitic soil mass, possibly some defect control.	Slide debris stripped surface soils from downslope path in gully and partly blocked river. Washout of debris blocked draining cascade.	Partly confined in short gully section. Obstructed by river at toe of slide. Most of debris deposited at toe of slope within water (max 4 m depth). Stripped surface soils in gully on 37 deg slope.	na	Surface fill on slide area end tipped 1978 to 1980. Cut at toe of slope 1980 to 1984. Water flow in gully may have increased the mobility of the slide. Densely vegetated slope.	Halcrow (1999d)
HK35	Shum Wan	Natural	Heavy and prolonged rainfall. 31 day - 1 in 75 yr event. 4 hour - 159 mm (peak 48 mm/hr).	Observation of muddy water on hillslope days prior to failure.	Rainfall (infiltration into fill caused initial small fill failure. Main failure - Surface flow, infiltration and perched water).	Initial small fill failure due to infiltration, which resulted in surface water flow over slope. This (with infiltration) resulted in high perched water table that caused main slide. Planar slide caused by weight of debris from main slide.	Main slide - partly defect controlled compound slide in saprolitic soil. Lower slide - translational planar slide on kaolinite seams in PW tuff.	Main slide - not rapid but continuous, significant degree of break up. The lower planar slide remained relatively intact. Followed by several retrogressive slides which took out Nam Long Shan Road. Surface water likely to have contributed to mobility.	No channelisation or obstruction. Deposition - planar slide material on flat slope (2 to 3 m depth), main slide deposited mostly on hillslope (27 degrees) and in base of main scarp (3 to 5 m depth).	19 (DAN) maybe bit high.	Surface water probably contributed to mobility. Significant control of discontinuities in main failure and also planar failure. 2 people killed. DAN model - OK with phiB = 20 deg, Voellmy model better representation.	Hungr GR (1998) Irfan (1997) Irfan and Woods (1998) GEO (1996b) Knill (1996b)
HK36	Ma On Shan Road	Natural	Heavy rainfall. 1 and 2 day events very severe (1 in 1000 yr return period). Max. hourly = 94.5 mm/hr and daily = 796 mm/day.	na	Rainfall	Instability of main failure possibly caused by smaller failures in cut and fill slopes at toe. Some defect control.	Slide through saprolitic soil mass, some defect control (slide partly along persistent planar discontinuity). Compound and retrogressive.	Initial failure possibly on lower cut and fill slopes due to surface water concentration in gully and subsurface water flow. Triggered further regressive landsliding. Possibly fast moving.	No obstruction. Mid to upper part confined. Deposition on lower slopes (minimal on steeper slopes of 30 to 55 degrees) of 2 to 2.5 m depth.	na	Gully with history of landsliding. Densely vegetated slopes and grassed lower flat slopes. Considerable erosion of debris and washout.	Halcrow (1999c)
HK37	Tsing Shan	Natural	Heavy rainfall, but not exceptional. 138 mm in 5 hrs (< 1in 2.5 yrs event for all storms < 5 hr duration).	na	Rainfall	Initial slide triggered by rainfall. Main slide triggered by flow of initial slide on to it. Possible liquefaction in coarse colluvium given open void structure.	Slide of debris in colluvium mantling slope. Possible signs of being retrogressive.	Loud noise heard for period of 5 to 30 mins. Channelised debris flow to Ch 500m which accumulated colluvium in gully (approx 9000 m^3). Deposition beyond Ch 500 m on slopes of 17 decreasing to 6 degrees.	No obstruction. Channelisation to Ch 500 m. Minor deposition within gully. Most of deposition on 17 decreasing to 6 degrees slopes, and where width of flow widened to 50 to 95 m.	16.5 to 11.5 (15 to 25 frict. model, < 20 using Voellmy model)	Channelised debris flow in colluvium on steep hillside. Interesting that triggered by low return period rainfall.	Hungr GR (1998), King (1996)
HK38	Outward Bound School	Natural	Very heavy rainfall over 12 to 24 hour period prior to failure (1 in 30 to 70 year events)	na	Rainfall (infiltration and development of perched water).	Instability due to adverse water table conditions. Slope already in meta-stable condition. Possible adversely orientated faulting.	Compound (non-circular) failure through residual and saprolitic soil mass. Possible influence of discontinuities.	Relatively intact rafts of material remained within landslide scar, most material developed into debris flow. Initial slide followed by washout further down gully of sandy silt.	Minor obstruction by dense vegetation. Lower portion of slide partly confined in gully. Deposition in failure bowl and on all slopes downslope of failure (33.5 to 19 degree slopes).	na	Would expect surface water flow in gully to have increased the mobility of the slide mass.	Fugro (1999c)
HK39	Lantau Island - Slide C1	Natural	Severe rainfall for 2 days.	na	Rainfall	Instability due to saturation and over-steepening of colluvium.	Slide of debris in colluvium mantling slope. Compound, with significant translational component partly along interface with saprolite.	Considered by GEO as a "gravitational" debris slide. Partly confined within hillslope topographic depression. Eroded channel (< 1 m depth) to Ch 150 m.	Eroded channel to Ch. 150 m. Deposition from failure bowl to distal toe of debris on slopes of 14 to 23 degrees. Most of finer debris deposited to Ch 150 m, thereafter boulder trail.	11 @ ch. 115 (16 to 8 from DAN)	Large runout distance for suspected"gravitational" debris slide (GEO). Classified as partly confined debris flow. DAN model, successful with phiB = 23 degrees, good velocity correlation.	Hungr GR (1998), Wong et al (1996)
HK40	Tao Fung Shan Cemetery - Slide A	Natural / Fill	970 mm in 31 days prior to slide. Heavy rain prior to slide, peak 1 hour intensity of 124 mm (1 in 32 year event)	na	Rainfall (infiltration).	Instability associated with fill surcharge, saturation of fill from infiltration (both rain and run-on). Possible liquefaction and flow of loose fill.	Translational - single event, base of slide in residual soil.	Diverged into two debris trails. Outwash followed initial slide (from surface runoff only ?).	300 m^3 debris accumulated. Deposition on lower slopes at less then 11 degrees (No deposition on 40 degree slopes). No channelisation. Dense vegetation probably obstructed flow to some degree.	na	1988 to 1996 - Loose fill placed at crest of slope. Densely vegetated slope. Some outwash.	Halcrow (1999b)
HK41	Glorious Praise Christian Centre	Natural / Fill	Heavy rainfall prior to slide - 90 mm/hr max hourly fall. (2 hr event 1 in 8 year).	na	Rainfall (infiltration and saturation, possible perched water).	Instability due to saturation from rainfall.	Compound slide in residual soil with significant basal translational component along interface with weathered rock.	Rapid slide. Flowed down 32.5 deg slope to broad channel. Flow down shallow slope of channel probably secondary outwash post initial slide.	No obstruction. No channelisation. Deposition on 30 degree slope and on shallow slope in broad channel.	na	Not sure why low travel angle, because only small volume. Maybe some of secondary outwash included in calculation (several metres would make a significant difference for this small slide).	Halcrow (1999b)
HK42	Lido Beach	Natural / Fill	31 day rainfall - 492.5 mm. 24 hr - 186 mm. 12 hr - 181.5 mm.	Previous small slides in area in 1982.	Rainfall (rising groundwater following rainfall, 2.5 hr lag between heavy rainfall and failure).	Instability due to loss of strength on saturation and rising groundwater level.	Compound (non-circular) slide through residual soil mass.	Two phases of movement. Quick moving.	No significant obstruction or channelisation. Deposition on most of length of runout path.	na	High mobility possibly related presence of surface water on travel path and possibly internal brittleness in slope. Slope heavily vegetated. Developed 1954 to 1969. Filling in area of slip placed in 1980s.	Halcrow (1999b)
HK43	Lui Pok School	Natural	Heavy rainfall - 240 to 250 mm on 26/9/93.	na	Rainfall	Instability, possibly due to development of perched water and saturation of colluvium.	Slide of debris in colluvium mantling slope. Compound with significant translational component along interface with weathered bedrock.	Likely to be fast moving. Entrained water in hillside topographic depression likely to have increased the mobility of the slide. Partly confined.	Obstructed by building at toe. Partly confined in hillside topographic depression. Erosion and accumulation in topo depression. Deposition on lateral margins on hill slopes of 10 to 20 degrees. Most material deposited on flat slopes at toe.	na	Travel angle may be slightly over-estimated, the runout length may include some post failure washout.	King (1997)

Table B1.4: Landslide case studies from Hong Kong (Ayotte and Hungr 1998)

No.	Site	Slope Type	Slope Failure Geometry	Initial Slide Classification	Travel Classification	Confined (Yes/No)	Landslide Geometry						Travel Distance Angle (^{o})	Ratio H/L	Volume (m^3)	Width (m)	
							Height, H (m)	Length, L (m)	Length, L_{toe} (m)	Alpha 1 (deg.)	Alpha 2 (deg.)	Alpha 3 (deg.)				Initial Slide	Runout
HK44	TC - 6A/1, Tung Chung	Natural	3	Slide of debris (?)	Debris flow	No	85	93	83	39	43	-	42.4	0.91	100	9	9
HK45	TC - 5A/10, Tung Chung	Natural	3	Slide of debris (?)	Debris flow	No	50	73	60	44	31 (35 to 29)	-	34.4	0.68	300	12	25
HK46	TC - 5A/13, Tung Chung	Natural	3	Slide of debris (?)	Debris flow (confined along part of travel path)	No	58.5	122	105	31	25	-	25.6	0.48	700	17	9
HK47	Lantau Island - Slide A6	Natural	3	Slide of debris (?)	Debris flow	No	89	180	160	30	26 (28 to 23)	-	26.3	0.49	400	16	7
HK48	JK 419, New Territories	Natural	3	Slide of debris (?)	Debris flow, partly confined.	No	157	191	175	39	38 (39 to 32)	-	39.4	0.82	1000	7	10
HK49	JK 515, New Territories	Natural	3	Slide of debris (?)	Debris flow	No	59	120	105	27	26 (28 to 20)	-	26.2	0.49	300	19	19
HK50	JK 529, New Territories	Natural	3	Slide of debris (?)	Debris flow (confined along part of travel path)	No	135	227	210	34	36 (38 to 34)	-	30.7	0.59	400	12	12
HK51	JK 410, New Territories	Natural	3	Slide of debris (?)	Debris flow	No	63	100	85	28	33	-	32.2	0.63	400	10	15
HK52	Luk Keng	Natural	3	Slide of debris (?)	Debris flow	No	57	150	120	30	24	0	20.8	0.38	170	10	6
HK53	Pak Sha Wan	Natural	3	Slide of debris (?)	Debris flow, partly confined.	No	22	80	70	22	27	-	15.4	0.28	150	9	8
HK54	Pat Sing Leng 1	Natural	3	Slide of debris (?)	Debris flow, partly confined.	No	62	100	55	34	34	-	31.8	0.62	300	14	12
HK55	Fo Tan Station	Cut / Quasi Natural ?	1	Compound, part defect-control	Debris flow	No	22.3	37.5	30	40	48	7 to 0	30.7	0.59	85	9	9
HK56	TC - 5A/2, Tung Chung	Natural	3	Slide of debris (?)	Channelised debris flow	Yes	129	312	275	32	25 (29 to 23)	13	22.5	0.41	1500	30	7
HK57	Sha Tau Kok	Natural	3	Slide of debris (?)	Channelised debris flow	Yes	331	1005	980	42	23 (36 to 13)	5 (6 to 2)	18.2	0.33	1500	27	10
HK58	Pat Sing Leng 2	Natural	3	Slide of debris (?)	Channelised debris flow (poss. hyperconcentrated stream flow)	Yes	225	600	580	36	23 (29 to 19)	13 (16 to 10)	20.6	0.38	50	9	5

Table B1.5: Case studies of "rapid" landslides in coarse, granular stockpiles

No.	Site / Stockpile	Date of Failure	Initial Slide Classification	Travel Classification		Slope and Travel Geometry										Estimated Volume (cu.m.)		Width (m)		Area (sq.m.)	
				Classification	Cross-section Geometry / Plan Shape	Height, H (m)	S/pile Height, H_s (m)	Length, L (m)	Length, L_{toe} (m)	Travel Distance Angle (^{o})	H/L	Alpha 1 (deg.)	Alpha 2 (deg.)	Alpha 3 (deg.)	Alpha 4 (deg.)	Initial Slide	Flow	Initial / Failure	Run-out	Slide Area	Deposit Area
SW1	National, South Wales	3 Nov 1898	rotational ?, part flow slide	flow slide / confined debris flow (?)	Confined, linear, obstructed at toe	125	60	300	170	22.6	0.42	36	15	0	17 to 25	15000 to 20000	< 5000	40	5 to 10	-	-
SW2	Fforchaman, South Wales	22 Feb 1935	rotational ?	debris slide ?	Unconfined, linear, obstructed at toe by river (?)	100	75	290	180	19.0	0.34	36	27	10	27	40000	20000	90	100	-	-
SW3	Abergorchi, South Wales	4 Nov 1931	rotational, part flow slide ?	debris slide / confined debris flow	Confined, curved	162	70	740	640	12.3	0.22	36	8	-	18	100000	< 50000	90	20 to 30	-	-
SW4	Craig-y-Duffryn, South Wales	16 Dec 1910	rotational, part flow slide ?	flow slide ?	Unconfined, linear, obstructed	na	29	190 (?)	60	na	na	36	15	-	15 +	na	na	90	120	-	-
SW5	Cilfynydd (Abercynon), South Wales	5 Dec 1939	rotational, flow slide	flow slide	Unconfined, linear	130	46	590	530	12.4	0.22	36	15 (19 to 11)	4.5	19	100000 to 130000	100000 (?)	115	90 to 140	-	-
SW6	Nantewlaeth, South Wales	1947-60 (?)	(rotational ?), part flow slide	flow slide	Unconfined	40	27	170	120	13.2	0.24	36	8	-	8	< 20000	10000	40	50 to 20	-	-
SW7	Maerdy, South Wales	18 Nov 1911	rotational, flow slide	flow slide	Partly confined, linear (obstructed ?)	105	60	440	320	13.4	0.24	36	11	-	0 (?)	60000 to 80000	20000 to 30000	90	100 to 50	-	-
SW8	Aberfan - Tip 7, South Wales	21 Oct 1966	rotational (some retrogression), flow slide	flow slide	Unconfined, linear	177	71	690	580	14.4	0.26	36	12.8	8 to 8.5	12.8 (11.5 to 14.8)	150000 (?)	110000	80	100 to 220	-	-
SW9	Aberfan - Tip 7, South Wales	Nov 1963	rotational, part flow slide	flow slide	Unconfined, linear	106	68	390	315	15.2	0.27	35	12.8	-	12.8 (11.5 to 14.8)	10000	3000	75	80 to 40	-	-
SW10	Glenrhondda, South Wales	1943	(rotational ?), part flow slide	flow slide	Partly confined, linear, deflected at toe.	108	52	360	280	16.7	0.30	36	11 (5 to 20)	0 (?)	17	30000 to 40000	15000 to 20000	65	70 to 20	-	-
SW11	Aberfan - Tip 4, South Wales	21 Nov 1944	rotational, part flow slide	flow slide	Partly confined, linear	184	85	600	450	17.0	0.31	31 (27 to 33)	12.2 (11 to 18)	-	16 (9 to 18)	170000	30000 to 50000 (?)	115	140 to 35	-	-
SW12	Mynydd Corrwg Fechan, South Wales	17 Oct 1963	(translational basal component ?), flow slide	flow slide	Unconfined, obstructed (?)	100	40	320	235	17.3	0.31	36	17	-	17 to 30	30000 to 50000	20000 to 40000	100	110	-	-
SW13	Bedwelty, South Wales	12 Nov 1926	(rotational ?), part flow slide	flow slide	Unconfined	120	65	340	250	19.4	0.35	36	13	-	13	80000 to 100000	50000	100	110 to 50	-	-
SW14	Rhondda Main, South Wales	16 Feb 1928	rotational, flow slide	flow slide	Unconfined, linear, (obstructed ?)	75	36	200	140	20.5	0.38	36	23	-	23	6000	2000 to 4000	30	15 to 30	-	-
SW15	Pentre, South Wales	4 Feb 1909	(rotational ?), flow slide	flow slide	Unconfined, linear	115	44	300	na	20.9	0.38	36	15	-	20	40000 to 60000	20000 to 30000	70	120 to 30	-	-
SW16	Cefn Glas, South Wales	3 Jan 1925	flow slide	flow slide	Partly confined, linear, obstructed (?)	140	60	310	190	24.2	0.45	36	22	-	22	40000 to 50000	30000	90	50	-	-
SW17	Parc, South Wales	1965	rotational ?, possibly out-burst, flow slide ?	debris flow ? / flow slide ?	Unconfined	88	32	213	140	22.4	0.41	36	12 to 23	-	15 to 19	10000	10000	45	45 to 90	-	-
SW18	Fernhill, South Wales	4 Dec 1960	rotational ?, possibly out-burst, flow slide ?	flow slide ? / debris flow (poss. Hyper-concentrated streamflow)	Unconfined, deflected	na	42	na	na	na	na	36	15	0 (shallow)	15 (?)	<10000	<10000	50	na	-	-
BC1	Brownie (FCL), British Columbia	11/6/83	Flow slide, translational	flow slide	Partly confined, curved	420	235	900	590	25.0	0.47	38	na	15	25	110000	-	60	65	18612	-
BC3	Brownie (FCL), British Columbia	21/9/84	Flow slide, translational	flow slide	Partly confined, linear	408	210	925	640	23.8	0.44	38	na	14	27	500000	-	170	250	47124	-

Table B1.5: Case studies of “rapid” landslides in coarse, granular stockpiles (Sheet 2 of 6)

No.	Site / Stockpile	Date of Failure	Hydro-geological Features	Rainfall / Snowmelt	Morphological Features	Pre-Failure Deformation Behaviour	Post-Failure Observations	Comments	References
SW1	National, South Wales	3 Nov 1898	Overtipping onto streambeds. Spring lines associated with Birthdir coalseam. Slide confined to region of tip located over streambeds.	1 to 5 year antecedent event for 1 to 25 days prior to slide.	na	Indications of active landsliding.	Relatively rapid. Temporarily stopped by retaining wall that eventually gave way resulting in rapid debris flow.	Channelised runout of 5 to 10 m width confined to stream bed. Obstructed by retaining wall. Most of material deposited at toe (?).	Siddle et al (1996)
SW2	Fforchaman, South Wales	22 Feb 1935	na	75 mm in 2 days prior to slide. Before this only minimal rainfall.	na	na	Relatively slow moving, 0.4 m/min reducing to 0.1 m/min after some 6 hours. Decribed as "like sliding lava". Terminated at river at toe of slope (?)	Slide also in 1928. Both slides relatively slow moving. Periodic tipping on this stockpile at time of failure.	Siddle et al (1996)
SW3	Abergorchi, South Wales	4 Nov 1931	Tip covered parts of stream beds. Failure confined to stream bed areas.	130 mm on day prior to slide and 160 - 170 mm for 2 day total prior to slide. Prior to this virtually no rainfall for 23 days.	na	na	Relatively slow moving debris flow (0.5 m/min) within narrow stream channel on 8 degree slope.	Debris slide (poss. flow slide) that developed into debris flow within narrow stream channel. Not clear if tipping active in area at time of failure.	Siddle et al (1996)
SW4	Craig-y-Duffryn, South Wales	16 Dec 1910	Artesian pressures in underlying argillaceous beds. Failure occurred during period of stormy weather.	150 mm in 5 days prior to slide. 1 to 5 year antecedent event over 1 to 25 days prior to failure.	Tip possibly located on pre-existing landslide. Shallow landsliding observed on adjacent hill slopes	na	Relatively rapid flow. Flowed down slope and into the canal and onto the railway line at the base of slope (obstructed).	Obstructed by existing canal and railway line. Possibly triggered by movement of pre-existing landslide following period of heavy rainfall. Tip active at time of failure.	Siddle et al (1996)
SW5	Cilfynydd (Abercynon), South Wales	5 Dec 1939	Tip covered two spring lines, one associated with Daran-ddu coal seam and lower spring associated with Boulder clay mantling slope. Runoff observed to enter fissures (due to subsidence) in sandstone above tip.	Limited rainfall (70 mm) in 9 days prior to slide. Prior to this (Days 10 and 11), 2 day rainfall of 90 mm (1 in 3 year) and 155 mm in 5 days.	Upper part of tip founded on permeable scree. Lower toe underlain by Boulder clay.	"ominous move" on tip on day before failure as observed by coal pickers. Prior to failure a huge bulge developed in the lower half of the tip. Survey suggests toe had bulged prior to failure.	Described as a flowing in a sheet of 90 to 140 m width. Rate of movement approx 3 to 4.5 m/sec. Up to 12 m thick deposition on flatter slopes at toe.	Suspect failure triggered by localised toe instability of that part of tip that had encroached onto Boulder clay foundation. Tip active at time of failure.	Bishop et al (1969), Bleasdale (1969), Woodland (1969), H.M.S.O. (1967), Bishop (1973), Siddle et al (1996)
SW6	Nantewlaeth, South Wales	1947-60 (?)	na	na	na	na	Small volume flow slide that ran-out on slopes of 8 degrees. Small flows in gullies as distal end.	Tipped material included washery waste in addition to normal overburden waste	Siddle et al (1996)
SW7	Maerdy, South Wales	18 Nov 1911	Tip overlies spring line. Active movement of tip associated with heavy rain.	80 mm on day prior to failure Antecedent railfall equivalent to 5 to 20 year event over 25 days prior to slide	Suggestion that lower portion of tip located over pre-existing landslide.	Active movement of crest of tip in month prior to failure following heavy rains (crane tippers to be withdrawn from crest). Suspected similarity leading up to reported failure.	Run-out flowed down hill slopes and crossed colliery sidings. Terminated at Rhondda Fach River where landslide debris dammed river.	Possible pre-failure movements associated with movement of pre-existing landslide following heavy rainfall. Foundation comprised thick deposits of colluvium and glacial till. Active tipping at time of failure.	Siddle et al (1996)
SW8	Aberfan - Tip 7, South Wales	21 Oct 1966	Tip covered stream and spring line. Pennant Sandstone highly permeable. Springs associated with Boulder clay mantling slope. Fluctuating pore pressure conditions at toe associated with rainfall.	Not unusual. 1 in 0.5 year event in days preceeding slide (82 mm in 3 days). No rainfall on day prior to slide.	Boulder clay at toe firm to stiff. Suspect down-slope conditions wet and boggy at time of failure.	Approx. 6 m settlement behind crest in less than 12 hours prior to slide. Scarps behind crest developing 3 - 4 months prior to failure, increasing in rate leading up to failure. Indication of previous failure in toe area as well as back sapping. Toe bulging.	Rapid transformation into flow slide that travelled quickly (rate 4.5 to 9 m/s) down slope. Dominant mechanism of movement as flow sliding on a liquefied basal component. Run-out spread as travelled down-slope and split into two separate components. Out-burst of ground water followed flow slide. Deposition on 12.8 deg slope (approx 1 m thick) and at toe (up to 6 to 7 m deep).	Active tipping at time of failure. Initial failure in toe region on pre-existing basal shear surface followed by several retrogressive larger slide components. Of estimated 150,000 cu.m. in initial failure approx. 110,000 cu.m. involved in flow slide.	Bishop et al (1969), Bleasdale (1969), Woodland (1969), H.M.S.O. (1967), Bishop (1973), Siddle et al (1996) Johnson (1980)
SW9	Aberfan - Tip 7, South Wales	Nov 1963	Tip covered stream and spring line. Foundation groundwater levels and pore pressures at toe of slide suspected to have been significantly affected by rainfall.	Approx 395 mm in month of Nov.	Boulder clay at toe firm to stiff.	Indication of previous failure in toe area as well as back sapping.	Approx 3000 cu.m. of estimated 10,000 cu.m. in failure developed into flow slide.	Active tipping at time of failure. Possibly triggered by heavy rainfall in Nov 1963 and localised instability in toe region. Wet and boggy down-slope conditions.	Bishop et al (1969), Bleasdale (1969), Woodland (1969), H.M.S.O. (1967), Bishop (1973), Siddle et al (1996)
SW10	Glenrhondda, South Wales	1943	na	na	tip located on pre-existing landslide	na	Run-out flowed down hill slopes to Nant Selsig River where it was deflected and flowed downstream.	Active tipping at time of failure. Movement of pre-existing existing landslide may have destabilised toe.	Siddle et al (1996)
SW11	Aberfan - Tip 4, South Wales	21 Nov 1944	Constructed over stream. Possible perched water table above mudstone seam. Large fluctuations in water level in Pennant Sandstone.	None for 2 days prior to slide, 160 mm in 4 days prior to that (equivalent to approx 5 to 10 year antecedent event).	na	Some sliding of tip prior to failure. Jan 1944 - one or two large movements of the tip occurred. Toe bulging for many months prior to failure.	Bulk of failed material remained within bowl of slide, only thin tongue travelled a long distance (approx 40,000 of 170,000 cu.m.). Depth of deposition 11 to 2 m.	Active tipping at time of failure. Initial slide volume approx 170,000 cu.m., 40,000 cu.m. of this travelled a long distance.	Bishop et al (1969), Bleasdale (1969), Woodland (1969), H.M.S.O. (1967), Bishop (1973), Siddle et al (1996)
SW12	Mynydd Corrwg Fechan, South Wales	17 Oct 1963	na	30 mm 3 days prior to failure. Overall, significantly below 1 year antecedent rainfall for period of 25 days prior to slide.	Failure incorporated argillaceous bedrock foundation.	Reference to displacement of natural ground at toe prior to failure.	Flowed down to stream at toe of hillslope and blocked it (obstructed).	Failure incorporated foundation of argillaceous bedrock.	Siddle et al (1996)
SW13	Bedwelty, South Wales	12 Nov 1926	Tip straddled spring associated with Birthdir Seam. Rainfall contributed to tip instability.	None in 2 days prior to slide. Prior to this, rainfall approx. between 1 to 5 year antecedent rainfall over Days 8 to 18.	Tip located on pre-existing "Pochin" landslide.	"Boot" evident at toe of spoil heap adjacent to area of slide.	Halted by impact against wall at rear of school.	Evidence of movement at toe. Movement of pre-existing existing landslide may have destabilised toe. Majority of spoil heap affected by pre-existing landslide. Suspect active tipping in this area at time of failure.	Siddle et al (1996)
SW14	Rhondda Main, South Wales	16 Feb 1928	na	80 mm day prior, 160 mm in 5 days prior (between 1 to 5 year antecedent event over 25 days).	na	na	Very quick, described as speed "like an avalanche". Run-out travelled down steep slopes, crossed railway line and terminated at Ogwr Fawr river. Damaged railway lines, telegraph poles and stone wall embankment.	Failed four years after completion of tipping.	Siddle et al (1996)
SW15	Pentre, South Wales	4 Feb 1909	Tip located over spring associated with outcrop of coal seam in sandstone.	None for 17 days prior to slide	Lower portion of tip located on pre-existing landslide.	Displacement of 3.5 m observed evening prior to failure, some 5 hours later failure occurred. Prior to this, "sliding and giving way" observed during active tipping.	Large noise. Movement described as "speed of an avalanche". No confinefinement and minimal obstruction. Deposition depth 3 to 4 m at toe.	Failure occured 1 year after abandonment of tip. Suggestion of movement of pre-existing landslide caused observed movement on evening prior to flowslide.	Siddle et al (1996), Knox (1927)
SW16	Cefn Glas, South Wales	3 Jan 1925	Suspect high foundation pore pressures following period of heavy rain.	None for 2 days prior to slide, 80 mm on Day 3. Day 3 to Day 17 heavy rainfall, approx 20 to 50 year antecedent rainfall event.	Tip located over pre-existing landslide.	Bulge or "boot" over 200 m length of toe area suggests slow movement over broad area prior to flowslide over 50 m width.	Movement described as "at terriffic speed". Possibly obstructed by railway embankment on lower slopes.	Instability reported as a problem throughout history of spoil heap. Failures observed within other areas of spoil heap. Active tipping (?) at time of failure.	Siddle et al (1996)
SW17	Parc, South Wales	1965	Possible high foundation pore pressures as indicated by outburst of groundwater.	na	Tip located on pre-existing landslide.	Rear scarp of 1965 failure coincident with larger scarp associated with movement of pre-existing landslide.	Failure bowl almost fully evacuated suggesting substantial outburst of water. Flowed down hillslope and terminated at Nant Cwn Parc River.	Possible movement of pre-existing landslide may have triggered rapid failure. Difficult to evaluate mechanism, potential out-burst, but this may have occurred subsequent to the failure. Tip active at time of failure.	Siddle et al (1996)
SW18	Fernhill, South Wales	4 Dec 1960	Tip covered boggy areas and stream courses. Large issue of water emerged from toe of spoil. Failure occurred in area where tip covered stream and springs.	150 mm on day prior to failure. Equivalent to approx. 50 yr antecedent event over 1 to 25 days prior to slide.	na	na	Flowed 50 m down-slope to river where deflected, then flowed as debris flow or hyper-concentrated streamflow downstream. Eventually blocked culvert. No spoil remained in failure bowl.	Failure confined to tip area that covered stream and springs. Difficult to evaluate mechanism, potential out-burst, but this may have occurred subsequent to the failure. Tip active at time of failure.	Siddle et al (1996)
BC1	Brownie (FCL), British Columbia	11/6/83	na	na	na	Near 10 days of 0.9 m/day displacement	Normal mobility event. Small sturzstrom.	na	Golder Assoc (1995)
BC3	Brownie (FCL), British Columbia	21/9/84	na	na	na	na	Normal mobility event. Ran over Event BC1 debris. Distal part spread.	Probable cause steep natural topography, aggravated by precipitation	Golder Assoc (1995)

Table B1.5: Case studies of "rapid" landslides in coarse, granular stockpiles (Sheet 3 of 6)

No.	Site / Stockpile	Date of Failure	Initial Slide Classification	Travel Classification		Slope and Travel Geometry										Estimated Volume (cu.m.)		Width (m)		Area (sq.m.)	
				Classification	Cross-section Geometry / Plan Shape	Height, H (m)	S/pile Height, H_s (m)	Length, L (m)	Length, L_{toe} (m)	Travel Distance Angle (^{o})	H/L	Alpha 1 (deg.)	Alpha 2 (deg.)	Alpha 3 (deg.)	Alpha 4 (deg.)	Initial Slide	Flow	Initial / Failure	Run-out	Slide Area	Deposit Area
BC5	Brownie (FCL), British Columbia	24/7/84	Flow slide, translational	confined flow slide / debris flow	Confined, curved	470	260	1125	780	22.6	0.42	38	na	8	28	300000	-	100	250	34320	-
BC6	Brownie (FCL), British Columbia	16/8/85	Flow slide, translational	flow slide	Partly confined, linear	360	215	950	610	20.7	0.38	38	na	11	24	140000	-	na		na	-
BC7	Brownie (FCL), British Columbia	29/6/85	Flow slide, translational (sliver)	flow slide	Partly confined	360	200	580	310	31.6	0.62	38	na	32	27	50000	-	?		na	-
BC9	2-Spoil (FCL), British Columbia	1/30/84	Flow slide, translational	flow slide			255		60	32.0	0.62	38	na	-	10	775000	-		220	na	-
BC11	Brownie (FCL), British Columbia	19/6/85	Flow slide, translational	flow slide	Unconfined, linear	450	260	910	560	26.2	0.49	38	na	12	25	225000	-	100		34320	-
BC12	13 Seam (FCL), British Columbia	14/8/86	Flow slide, translational	flow slide	Unconfined, linear	250	180	550	210	24.4	0.45	38	na	0	25-45	250000	-	100	150	23760	-
BC13	Brownie (FCL), British Columbia	23/11/86	Flow slide, translational	flow slide			290		500		na	38	na	-	28	45000	-			na	-
BC14	B-stone (FCL), British Columbia	10/5/86	Flow slide, translational	confined flow slide / debris flow	Confined, curved	525	300	1250	750	22.7	0.42	38	na	13	29	115000	-	150	70	59400	18000
BC16	Blackrill (FCL), British Columbia	17/6/85	Flow slide, translational	confined flow slide / debris flow	Confined, deflected	475	140	1120	880	22.9	0.42	38	na	10	33	55000	-	80	90	14784	-
BC19	2-Spoil (FCL), British Columbia	5/5/72	Flow slide, translational	flow slide	Unconfined, linear	275	120	650	460	22.9	0.42	38	na	8	25	50000	-	90	180	14256	-
BC20	2-Spoil (FCL), British columbia	27/5/72	Flow slide, translational	flow slide	Unconfined, linear	270	135	630	480	23.2	0.43	38	na	8	25	160000	-	300	280	53460	-
BC24	2-Spoil (FCL), British columbia	8/11/74	Flow slide, translational	flow slide	Unconfined, linear	270	220	770	550	19.3	0.35	38	na	3	31	450000	-	180	220	52272	-
BC27	2-Spoil (FCL), British columbia	12/11/74	Slump (flow slide ?)	flow slide	Unconfined, linear	250	110	520	220	25.6	0.48	38	na	7	20	750000	-	200	180	29040	55000
BC35	H2 B3 (BLM), British Columbia	18/11/80	Flow slide, translational	flow slide	Unconfined	260	230	450	160	29.9	0.58	38	na	5	35	na	-		75	na	-
BC36	A40-C1 (BLM), British Columbia	29/6/82	Flow slide, translational	confined flow slide / debris flow	Confined, deflected	415	150	1370	1140	16.8	0.30	38	24	12	30	650000	-	200	200	39600	45600
BC38	5975 (BLM), British Columbia	8/2/76	Flow slide, translational	flow slide	Partly confined, deflected	335	260	880	550	20.8	0.38	38	na	7	26	na	-	80	40	27456	25000
BC40	#2 (BLM), British Columbia	24/11/68	Flow slide, translational	flow slide	Unconfined, curved	330	225	850	620	21.2	0.39	38	na	0	32	150000	-		100	na	90000
BC42	A29-N (BLM), British Columbia	5/5/71	Flow slide, translational	confined flow slide / debris flow	Confined, deflected	565	260	3000	2600	10.7	0.19	38	10.5	3	45 to 28	2200000	-	300	150	102960	450000
BC43	H Knob (BLM), British Columbia	13/5/71	Flow slide, translational	confined flow slide / debris flow	Confined, deflected	870	120	3360	3200	14.5	0.26	38	16 (24 to 9)	9	36	na	-	120	120	19008	-
BC44	A29-S (BLM), British Columbia	25/5/73	Flow slide, translational	confined flow slide / debris flow	Confined, deflected	500	120	2750	2500	10.3	0.18	38	13.5 (25 to 8)	3	42	110000	-		160	na	-
BC48	1640 MM (QCL), British Columbia	21/6/86	Flow slide, translational	flow slide	Partly confined, deflected	290	200	680	400	23.1	0.43	38	9.5	-	46	600000	-	100	140	26400	105000
BC49	1705 WN (QCL), British Columbia	30/6/86	Flow slide, translational	confined flow slide / debris flow	Confined, deflected	500	210	1790	1750	15.6	0.28	38	15.5 (20 to 9)	6 (9 to 3)	46 to 20	1600000	-	150	200	41580	91000
BC54	1660 N (QCL), British Columbia	9/9/85	Flow slide, translational (along fill / natural interface)	confined flow slide / debris flow	Confined, curved	515	240	2560	2200	11.4	0.20	38	9 (5 to 15)	4	20 (up to 40)	2500000	-	350	300 to 500	95040	735000
BC62	1966 W (LINE), British Columbia	1/7/82	Flow slide, translational	confined flow slide / debris flow	Confined, deflected	490	136	2200	2000	12.6	0.22	38	14.5 (30 to 10.5)	9 to 5	31	250000	-	90	180	16157	80000
BC75	East (GRH), British Columbia	20/3/83	Flow slide, rotational / translational	flow slide	Partly confined, deflected	360	160	1000	850	19.8	0.36	38	na	run-up	28	400000	-	180	250	38016	-
BC76	East (GRH), British Columbia	11/5/83	Flow slide, rotational	flow slide	Partly confined, linear	225	170	680	380	18.3	0.33	38	na	7	14	720000	-	250	175	56100	68400
BC79	East (GRH), British Columbia	12/7/86	Flow slide, translational	flow slide	Partly confined, linear	200	160	780	530	14.4	0.26	38	na	5	18	480000	-	150	150	31680	24750
BC80	East (GRH), British Columbia	12/2/87	Flow slide, translational	flow slide	Partly confined, linear	250	119	750	580	18.4	0.33	38	21.5	0	50	580000	-	200	200	31416	-
BC81	East (GRH), British Columbia	7/3/87	Flow slide, translational	flow slide	Partly confined, deflected	170	85	415	290	22.2	0.41	38	19	2.5	55 to 19	285000	-	150	150	16830	25000
BC89	North (GRH), British Columbia	1/7/85	Flow slide, translational	confined flow slide / debris flow	Confined, deflected	360	200	1600	1200	12.7	0.23	38	na	6	24	300000	-	350	160	92400	45000

Table B1.5: Case studies of "rapid" landslides in coarse, granular stockpiles (Sheet 4 of 6)

No.	Site / Stockpile	Date of Failure	Hydro-geological Features	Rainfall / Snowmelt	Morphological Features	Pre-Failure Deformation Behaviour	Post-Failure Observations	Comments	References
BC5	Brownie (FCL), British Columbia	24/7/84	Groundwater seen flowing from the toe a few days prior to failure.	na	na	na	Normal mobility event. Toe debris = fine waste and till	Failure did not reach crest.	Golder Assoc (1995)
BC6	Brownie (FCL), British Columbia	16/8/85	na	na	Very steep upper foundation	na	Normal mobility event. Initially gradual, toe crept along creek.	na	Golder Assoc (1995)
BC7	Brownie (FCL), British Columbia	29/6/85	na	na	na	High wireline rates of movement and sliver failures all month	Normal mobility event. Run-out data is estimated	na	Golder Assoc (1995)
BC9	2-Spoil (FCL), British Columbia	1/30/84	Pore water pressures under frozen crust	na	na	na	Normal mobility event.	na	Golder Assoc (1995)
BC11	Brownie (FCL), British Columbia	19/6/85	na	na	na	na	Normal mobility event. Gradual slip over top of existing debris	na	Golder Assoc (1995)
BC12	13 Seam (FCL), British Columbia	14/8/86	Groundwater seepage on face.	na	na	na	Normal mobility event. Failed over 30 mins.	Inactive for 3 months. Toe not involved in failure.	Golder Assoc (1995)
BC13	Brownie (FCL), British Columbia	23/11/86	na	Snow melt.	na	na	Normal mobility event. Very little data.	Crest unaffected. Inactive for 2 weeks. High load rate.	Golder Assoc (1995)
BC14	B-stone (FCL), British Columbia	10/5/86	na	na	na	na	Normal mobility event. 1990 survey shows distal mound.	Failure did not involve toe. Inactive for 4 months. Affected by blasting ?	Golder Assoc (1995)
BC16	Blackrill (FCL), British Columbia	17/6/85	na	na	na	Suspect bulging face.	Normal mobility event. Only 10000 cu.m. moved down channel.	Delayed failure. Rapid.	Golder Assoc (1995)
BC19	2-Spoil (FCL), British Columbia	5/5/72	na	Very heavy snowfall	na	na	Normal mobility event.	Groundwater not felt important.	Golder Assoc (1995)
BC20	2-Spoil (FCL), British columbia	27/5/72	na	Very heavy snowfall	na	na	Normal mobility event. Over-rode haul road embankment.	Groundwater not felt important.	Golder Assoc (1995)
BC24	2-Spoil (FCL), British columbia	8/11/74	na	na	na	na	Normal mobility event.	Rapid failure.	Golder Assoc (1995)
BC27	2-Spoil (FCL), British columbia	12/11/74	na	na	Organic foundation soils. Organic soil displaced ahead.	na	Normal mobility event. Gradual, not dynamic run-out.	na	Golder Assoc (1995)
BC35	H2 B3 (BLM), British Columbia	18/11/80	na	na	na	Abnormal behaviour on 13 Sept, 2 months prior to failure.	Normal mobility event. Probably a slump over old slide debris.	na	Golder Assoc (1995)
BC36	A40-C1 (BLM), British Columbia	29/6/82	na	na	na	na	Normal mobility event. Super-elevated. Good account of run-out.	Rapid failure, run-out well documented.	Golder Assoc (1995)
BC38	5975 (BLM), British Columbia	8/2/76	na	na	na	na	Normal mobility event. Sharp turn.	Limited data available.	Golder Assoc (1995)
BC40	#2 (BLM), British Columbia	24/11/68	na	heavy rain	Steep foundation slope.	na	Normal mobility event. Rapid.	Triggered by heavy rain onto snowpack.	Golder Assoc (1995)
BC42	A29-N (BLM), British Columbia	5/5/71	Pore pressures in foundation.	na	Clay till foundation.	No warning (?reported).	High mobility event. Relatively small volume ran out ?	na	Golder Assoc (1995)
BC43	H Knob (BLM), British Columbia	13/5/71	na	na	na	na	High mobility event. Exposed debris not mud. Distal portion = fan.	Run-out was mudflow following earlier dump slump.	Golder Assoc (1995)
BC44	A29-S (BLM), British Columbia	25/5/73	na	na	Steep toe topography.	na	High mobility event. Unusually large run-out distance. Due to organics?	na	Golder Assoc (1995)
BC48	1640 MM (QCL), British Columbia	21/6/86	Foundation pore pressures?.	na	na	Toe bulge.	Normal mobility event. Not rapid. Fine carbonaceous waste in debris.	High load rate over past 3 months.	Golder Assoc (1995)
BC49	1705 WN (QCL), British Columbia	30/6/86	na	na	na	na	High mobility event. Flowed like water. Explosive failure.	na	Golder Assoc (1995)
BC54	1660 N (QCL), British Columbia	9/9/85	Would expect percolation through dump face to concentrate in gully region. Possible stream at toe given relatively high rainfall. Suspect rainfall trigger to failure.	86 mm in 40 days prior, 30 mm in 6 days prior.	Failed portion of tip located in gully area. Relatively steep slopes to sides of gully. Run-out within confined gully. Organic soils within lower part of run-out.	During dumping - 0.02 to 0.04 m/hour on average, peak rates up to 0.1 m/hour. No monitoring of failure. Large cracks observed several hours prior to failure, dumping stopped at this point. Major cracking and bulging not evident until just before failure.	High mobility, major event. High velocity as indicated by partial super-elevation. Failure contained in broad valley down to RL 1225, thereafter valley narrowed. Coarser waste carried on liquefied layer of finer sandy gravel. Liquefaction of organic foundation below RL 1225 suspected to have led to high mobility.	Active at time of failure. Failed within dump due to wet fines. Suspect rainfall acted as trigger to failure and topography below dump concentrated flow to gully region. Deposition on full length of run-out, indications of flow sliding on gradually depleting layer of finer sandy gravel.	Golder Assoc (1995) Dawson (1994) Dawson et al (1998)
BC62	1966 W (LINE), British Columbia	1/7/82	na	na	Steep toe slope.	na	High mobility event. Wet foundation major cause, not sturzstrom.	na	Golder Assoc (1995)
BC75	East (GRH), British Columbia	20/3/83	na	na	Steep toe slope.	na	Normal mobility event. Run-up on opposite slope. Not sturzstrom.	Poor waste. Over-steep face.	Golder Assoc (1995)
BC76	East (GRH), British Columbia	11/5/83	Excess foundation pore pressures.	na	na	na	Normal mobility event. Not sturzstrom.	Not sturzstrom. Poor waste.	Golder Assoc (1995)
BC79	East (GRH), British Columbia	12/7/86	Foundation seepage.	na	Steep topography.	na	Normal mobility event. Run-out over May 1985 slide debris.	Poor quality debris at toe.	Golder Assoc (1995)
BC80	East (GRH), British Columbia	12/2/87	na	na	Steep terrain.	na	Normal mobility event.	Poor quality debris at toe. Affected by previous slip?.	Golder Assoc (1995)
BC81	East (GRH), British Columbia	7/3/87	na	na	na	na	Normal mobility event. Not a major rapid event.	Poor quality debris at toe. Frozen foundation pushed ahead.	Golder Assoc (1995)
BC89	North (GRH), British Columbia	1/7/85	na	na	Steep foundation.	na	Normal mobility event. Foundation organic soil pushed 350 m ahead.	Sliver failure. Poor rock. High load rate.	Golder Assoc (1995)

Table B1.5: Case studies of "rapid" landslides in coarse, granular stockpiles (Sheet 5 of 6)

No.	Site / Stockpile	Date of Failure	Initial Slide Classification	Travel Classification		Slope and Travel Geometry										Estimated Volume (cu.m.)		Width (m)		Area (sq.m.)	
				Classification	Cross-section Geometry / Plan Shape	Height, H (m)	S/pile Height, H_s (m)	Length, L (m)	Length, L_{toe} (m)	Travel Distance Angle (^{o})	H/L	Alpha 1 (deg.)	Alpha 2 (deg.)	Alpha 3 (deg.)	Alpha 4 (deg.)	Initial Slide	Flow	Initial / Failure	Run-out	Slide Area	Deposit Area
BC112	1690 MT (QCL), British Columbia	17/8/84	Flow slide, translational	flow slide	Unconfined, deflected	390	250	1070	740	20.0	0.36	38	na	9	17?	1500000	-	240	400	79200	135000
BC113	1690 MT (QCL), British Columbia	4/10/85	Flow slide, translational	flow slide	Unconfined, linear	440	250	1480	1180	16.5	0.30	38	na	6	21	2200000	-	250	300	82500	240000
BC149	Blaine (FCL), British Columbia	16/6/86	Flow slide, translational	flow slide	Unconfined, linear	250	230	510	210	26.0	0.49	38	na	11	15	na	-		Full	na	-
BC153	SS STG 2 (FCL), British Columbia	29/5/90	Flow slide, translational	confined flow slide / debris flow	Confined, linear	300	130	670	500	24.1	0.45	38	25	13	35	250000	-	200	50	34320	-
BC154	SS STG 2 (FCL), British Columbia	7/7/90	Flow slide, translational	confined flow slide / debris flow	Confined, curved	350	140	870	690	21.9	0.40	38	21 (25 to 14)	14	49	300000	-	110	70	20328	-
BC155	South (FCL), British Columbia	26/10/89	Flow slide, translational (with rotational back-scarp)	flow slide	Unconfined, linear (flow spread)	490	410	1270	710	21.1	0.39	38	15	-24 (run-up)	33 to 24	3000000	-	230	500 to 600	127512	360000
BC156	North (GRH), British Columbia	22/11/89	Flow slide, translational	confined flow slide / debris flow	Confined, deflected (?)	400	260	2230	1950	10.2	0.18	38	4	-	48 to 4	1500000	-		350	na	190000
BC157	1660 (QCL), British Columbia	7/11/87	Flow slide, translational	confined flow slide / debris flow	Confined, deflected	490	280	2480	2200	11.2	0.20	38	8	5	47 to 8	5600000	-	640	200	236544	450000
BC158	1680 WW (QCL), British Columbia	13/5/88	Flow slide, translational	confined flow slide / debris flow	Confined, deflected	405	240	1110	790	20.0	0.36	38	14	9	36	80000	-	?	100	na	120000
BC162	Brownie (FCL), British Columbia	June 1983	Flow slide, translational	confined flow slide / debris flow	Confined, curved	400	170	1050	870	20.8	0.38	38	(33 to 10 ?)	(33 to 10 ?)	33	na	-		60	na	-
BC163	South (FCL), British Columbia	31/5/93	Flow slide, translational	flow slide	Unconfined, linear	375	385	1030	500	20.0	0.36	38	14	0 to -11.5 (run-up)	24.5	8000000	-	500	500	254100	600000
BC164	Cougar (GRH), British Columbia	11/5/92	Flow slide translational (along fill / natural interface)	confined flow slide / debris flow	Confined, curved	260	95	825	720	17.5	0.32	38	16	8.5	21 (up to 48)	160000	-	150	130 to 70	218381	55000
BC165	2158 (LINE), British Columbia	24/3/90	Flow slide	confined flow slide / debris flow	Confined, curved	308	160	920	660	18.5	0.33	38	17.5 (27 to 14)	9 to 5	31	100000	-	100	100	21120	-
BC166	2158 (LINE), British Columbia	2/5/90	Flow slide	confined flow slide / debris flow	Confined, curved	328	160	1340	1080	13.8	0.24	38	20 (27 to 14)	10	30	150000	-	100	100	21120	-
HP1	Peak Downs, Hay Point	30 Aug 1974	Flow slide, translational on basal interface	flow slide	Unconfined, suspect spreading	11	11	45.7	30	13.5	0.24	35 (approx)	0	-	0	3500	-	55	-	-	-
HP2	Saraji (2 South), Hay Point	2 Aug 1974	Flow slide, translational on basal interface	flow slide	Unconfined, suspect spreading	9	9	26.9	14	18.5	0.34	35 (approx)	0	-	0	5000	-	120	-	-	-
HP3	Saraji (1 South), Hay Point	9 Aug 1976	Flow slide, translational on basal interface	flow slide	Unconfined, suspect spreading	9	9	39.9	27	12.7	0.23	35 (approx)	0	-	0	5600	-	140	-	-	-
HP4	Peak Downs (6 South), Hay Point	3 Feb 1977	Flow slide, translational on basal interface (some retrogression ?)	flow slide	Unconfined, suspect spreading	10.5	10.5	78.0	63	7.7	0.13	35	0	-	0	16000	-	150	170	-	12000
HP5	Goonyella (1 North), Hay Point	9 Mar 1977	Flow slide, translational on basal interface	flow slide	Unconfined, suspect spreading	10.5	10.5	45.0	30	13.1	0.23	35 (approx)	0	-	0	11300	-	200	-	-	-
HP6	Saraji (1 South), Hay Point	9 Mar 1977	Flow slide, translational on basal interface	flow slide	Unconfined, suspect spreading	10.5	10.5	45.0	30	13.1	0.23	35 (approx)	0	-	0	10900	-	200	-	-	-
HP7	Saraji (1 South), Hay Point	9 Oct 1978	Flow slide, translational on basal interface	flow slide	Unconfined, suspect spreading	13.5	13.5	43.3	24	17.3	0.31	35 (approx)	0	-	0	4500	-	60	-	-	-
HP8	Peak Downs (Expt), Hay Point	19 Dec 1974	Flow slide, translational on basal interface	flow slide	Unconfined, suspect spreading	6	6	23.2	13	14.5	0.26	35 (approx)	0	-	0	1250	-	22	-	-	-
HP9	Peak Downs (Expt), Hay Point	19 Dec 1974	Flow slide, translational on basal interface	flow slide	Unconfined, suspect spreading	6	6	20.2	10	16.5	0.30	35 (approx)	0	-	0	850	-	15	-	-	-

Table B1.5: Case studies of "rapid" landslides in coarse, granular stockpiles (Sheet 6 of 6)

No.	Site / Stockpile	Date of Failure	Hydro-geological Features	Rainfall / Snowmelt	Morphological Features	Pre-Failure Deformation Behaviour	Post-Failure Observations	Comments	References
BC112	1690 MT (QCL), British Columbia	17/8/84	na	na	na	na	Normal mobility event. Not a major run-out event.	Regressive with several distinct slumps.	Golder Assoc (1995)
BC113	1690 MT (QCL), British Columbia	4/10/85	na	Heavy precipitation in last 2 months.	na	Previous slip.	Normal mobility event. Toe pushed till slabs ahead (previous event).	Poor rock.	Golder Assoc (1995)
BC149	Blaine (FCL), British Columbia	16/6/86	na	na	na	na	Normal mobility event. Gradual. Stopped against toe berm.	Frozen foundation ? Or strain induced pore pressures.	Golder Assoc (1995)
BC153	SS STG 2 (FCL), British Columbia	29/5/90	Pore pressures in colluvium?	na	Steep foundation.	na	Normal mobility event. Distal portion deflected.	Fines in waste.	Golder Assoc (1995)
BC154	SS STG 2 (FCL), British Columbia	7/7/90	Excess pore pressures in colluvium due to wet weather.	Wet weather	Steep toe.	na	Normal mobility event. Ran over previous debris.	na	Golder Assoc (1995)
BC155	South (FCL), British Columbia	26/10/89	Intermittent stream in Blackwood Gully. Would expect percolation through dump face to concentrate in Blackwood Gully.	Significant in 50 days prior to slide (71 mm), none for 4 days prior.	Failure zone confined to section of spoil pile within Blackwood Gully. Steep, colluvial foundation slopes, up to 27 degrees.	From extensometers: 24/10/89 - 0.1 m/hour 25/10/89 - accel. Rapidly up to 1 to 1.3 m/hour prior to failure	Normal mobility event. Much of flow slide debris crossed creek and ran-up opposite slope. Large spread of material, up to 600 m wide. Very rapid - air blast damage to nearby foliage. Deposition - thin blanket on hill slope, most in base of valley.	Active dumping up until 24/10/89 when stopped due to excessive rates of movement. Finer sandy gravels associated with base of slide. Sharp contact between slide base and underlying foundation.	Golder Assoc (1995) Dawson (1994) Dawson et al (1998)
BC156	North (GRH), British Columbia	22/11/89	Excess pore pressures in organic foundation.	na	na	na	High mobility event. Unusually flat run-out. Thick organic soil.	na	Golder Assoc (1995)
BC157	1660 (QCL), British Columbia	7/11/87	na	na	na	na	High mobility event. Run-out channeled in stream bed over previous failure debris.	na	Golder Assoc (1995)
BC158	1680 WW (QCL), British Columbia	13/5/88	Pore pressure in colluvium.	na	na	na	Normal mobility event. Rapid, fluid like.	Crest steepened to 42 degrees. Dump fines.	Golder Assoc (1995)
BC162	Brownie (FCL), British Columbia	June 1983	na	na	Steep foundation.	na	Normal mobility event.	na	Golder Assoc (1995)
BC163	South (FCL), British Columbia	31/5/93	Pore water pressures in surficial foundation materials.	na	na	na	Normal mobility event. Subsequent debris slump down valley.	na	Golder Assoc (1995)
BC164	Cougar (GRH), British Columbia	11/5/92	Buried snow and ice lenses observed in cuts of unfailed portion of dump. Heavy rains during dumping. Snowmelt possibly triggered failure.	High snowmelt ? - several days of warm weather prior to slide.	Very steep (up to 48 deg) on upper slopes of dump, approx 20.5 deg at toe of dump. Dump located at head of broad gully. Foundation comprised thin layer of sand and gravel colluvium.	Cracks observed in dump face, defined by snowfall. No monitoring prior to failure.	Relatively narrow confined flow event. Suggestion of very rapid movement. Deposition along total length of run-out.	Poor material - pre-dominantly fine materials, surficial soils (till and colluvium) and near surface rock. Fatality. Dump inactive for 13 months prior to failure.	Golder Assoc (1995) Dawson (1994) Dawson et al (1998)
BC165	2158 (LINE), British Columbia	24/3/90	na	na	Steep foundation.	na	Normal mobility event. sharp bend.	Poor waste. 1 m/day crest advance.	Golder Assoc (1995)
BC166	2158 (LINE), British Columbia	2/5/90	na	na	na	na	Normal mobility event. Ran over Event BC165 debris.	na	Golder Assoc (1995)
HP1	Peak Downs, Hay Point	30 Aug 1974	na	Heavy at mine, 3.3 mm at Hay Point	Loose stockpile placed by stacker or dozer on prepared, relatively flat platform.	na	na	Placed very wet (dozer bogging in Layer 2), moisture content = 11 to 16.7%	Eckersley (1986)
HP2	Saraji (2 South), Hay Point	2 Aug 1974	Water level in stockpile 1.5 to 2 m height above base at failure.	11 mm in period 6 to 9 days prior to slide.	Loose, windrowed stockpile placed by dozer on prepared, relatively flat platform.	na	Failure occurred some 2 days after completion of windrowing	Windrows dozed over edge of pile. Placed slightly wetter than usual. Failure occurred some 2 days after completion of windrowing.	Eckersley (1986)
HP3	Saraji (1 South), Hay Point	9 Aug 1976	Water level in stockpile 0.3 to 1 m height above base at failure	na	Loose stockpile placed by stacker and dozer on prepared, relatively flat platform.	na	na	Stacking and dozing windrows at time of failure, windrows dozed over edge of pile. Dry density ~ 0.79 to 0.92 t/m^3 for windrowed coal, 10 to 11.5% mc at Saraji	Eckersley (1986) Eckersley (1985)
HP4	Peak Downs (6 South), Hay Point	3 Feb 1977	Water level in stockpile 1.2 to 1.8 m height above base at failure. Heavy rainfall prior to failure.	272 mm in 5 days prior to slide, most of rainfall within first 30 hours.	Loose stockpile placed by stacker on prepared, relatively flat platform.	Londitudinal cracks observed on face of stockpile prior to flowslide.	Failure initiated near dumping point. Runout obstructed by low height embankment.	Stacking at time of failure. Loose tipped from stacker, mc = 9 - 12 %.	Eckersley (1986) Eckersley (1985)
HP5	Goonyella (1 North), Hay Point	9 Mar 1977	Heavy rainfall prior to failure. Suspect wet coal on placement and possibly high water level in stockpile.	338 mm in 8 days prior to slide, 189 mm on day prior to slide.	Loose stockpile placed by stacker and dozer on prepared, relatively flat platform.	na	na	No stacking or dozing at time of failure. Occurred within 1 - 2 mins of HP6 slide. Failure most likely within windrowed pile dozed over edge.	Eckersley (1986) Eckersley (1985)
HP6	Saraji (1 South), Hay Point	9 Mar 1977	Heavy rainfall prior to failure. Suspect wet coal on placement and possibly high water level in stockpile.	338 mm in 8 days prior to slide, 189 mm on day prior to slide.	Loose stockpile placed by stacker and dozer on prepared, relatively flat platform.	na	na	No stacking or dozing at time of failure. Occurred within 1 - 2 mins of HP5 slide. Failure most likely within windrowed pile dozed over edge.	Eckersley (1986) Eckersley (1985)
HP7	Saraji (1 South), Hay Point	9 Oct 1978	na	6.1 mm, blown onto side of stockpile	Loose, windrowed stockpile placed by dozer on prepared, relatively flat platform.	na	na	No stacking or dozing at time of failure. Windrows dozed over edge of pile.	Eckersley (1986)
HP8	Peak Downs (Expt), Hay Point	19 Dec 1974	Articial injection of water to induce failure. Water level in stockpile 1.75 m max. height above base at failure	Artificial and natural of 113 mm, plus inflow from wells, over 7 days prior to slide.	Loose stockpile dumped from low drop height on prepared, relatively flat platform.	na	na	No stacking or dozing at time of failure. Placed with small drop, no compaction. Average dry density ~ 0.88 t/m3. Moisture at placement 8 to 13% (average 11%).	Eckersley (1986)
HP9	Peak Downs (Expt), Hay Point	19 Dec 1974			Loose stockpile dumped from low drop height on prepared, relatively flat platform.	na	na		

Table B1.6: Flow slides from tailings impoundments – cases initiated by static liquefaction.

Tailings Dam Site	Failure Date	Failure Details								Operating State at Time of Failure	Embankment Properties					Ground Slopes (°)		Other Material Properties		Hydro-geological Features
		Height, H (m)	Length, L (m)	Length, L_{toe} (m)	Distance of Retrogression (m)	Travel Distance Angle (°)	Velocity (m/s)	Volume (10^3 m^3)	Travel Classification		Height (m)	Slope (°)	Type	Construction Method	Material Properties	Under Dam (Alpha 4)	Down-stream (Alpha 2)	Slimes	Foundation	
Bafokeng, South Africa	11/11/74	47 (est to river)	4900 (to river)	4 km to river, 45 km to storage dam	1000	0.55	2.7 to 11 (10 on exiting dam)	3000	slurry flow initially, developed into hyper-concentrated stream flow	in operation	20	33	Ring Dyke, Platinum mine	Upstream, Mechanical	SM - silty fine sand (13% fines) with very thin slimes layers ($k_h >> k_v$)	1.3	1.3 reducing to 0.29	ML - clayey silt (99% fines, 18% CF), strongly contractant	Clay (CH) highly reactive, highly fissured (Black Clay)	Lot of water ponded on dam prior to rainfall.
Stava, Italy	19/7/85	400 (est)	4400	4400 to River Avisio	200 (virtually nothing left)	5.20	8.5 increasing to 12 to 25	190	quickly developed into hyper-concentrated stream flow	in operation (on and off for 23 years)	29.5	34	Sidehill, Fluorite mine	Centreline then upstream, cyclone	SM - silty fine to medium sand (10 to 60% fines)	12 (10 to 18)	4.5 to 7.6	CL/CI interlayered with SM. 85-100% fines (CF 20 - 33%), I_L ~1.2 (0.9 to 1.9).	Recent slope deposits (soft) over glacial deposits	Foundation groundwater levels highest in June - July following snowmelt and heavy rain. Water level in tailings dam reasonably high as water continually on dam. Change in pond operation resulted in high phreatic surface in sand embankment.
Merriespruit, South Africa	22/2/94	74	2330	2000	330	1.83	na	600	slurry flow initially, poss. developed into hyper-concentrated stream flow	in operation (for 16 years)	31	24	Ring dyke, gold mine	Upstream (?)	Layering of tailings, finer layers within coarser more sandy materials ($k_h >> k_v$)	0	1.5	ML - fine sandy silt (60 to 80% fines, CF < 10%), soft to stiff (Su = 34 kPa avg), PI = 1 to 8%.	Aeolian silty sand to 1.5 m deep over clayey sand/silty clay alluvium (soft ?).	Seepage constantly observed at down-stream toe, drains not functioning. Large quantity of water stored in impoundment (no return water dam). Pool located adjacent to embankment that failed, limited freeboard.
Texas, USA	1966	10	410	300	110	1.40	2.5 to 5	105	slurry flow	in operation (for 4 years)	11	26.5	Ring Dyke, Phosphate mine (gypsum tailings)	Upstream, Mechanical, under-drainage.	Sandier portion of tailings from upper beach deposition.	0	0	ML - fine sandy silt (60% fines), non plastic.	Clays and Sandy Clays - stiff, over-consolidated Pleistocene marine clays	High groundwater level in tailings. Seepage exited at toe of slope rather than collected in drains (sand drains did not function).
Arcturus, Zimbabwe	1978	33	390	300	90	4.84	na	20	slurry flow	in operation	25	46	Ring dyke, gold mine	Upstream (?)	na	1.5	1.5	na	na	na
Saaiplass - Slide 1, South Africa	3/18/92	13.5	255	80	175	3.03	na	60	slurry flow	in operation	21.2	21	Ring dyke, gold mine	Upstream (?)	na	-0.5	-0.5 (upslope)	na	na	No water on dam prior to failure.
Saaiplass - Slide 2, South Africa	19/03/92	12.2	160	70	90	4.36	na	120	slurry flow	in operation	18.6	21	Ring dyke, gold mine	Upstream (?)	na	-0.5	-0.5 (upslope)	na	na	No water on dam prior to failure.
Saaiplass - Slide 3, South Africa	22/03/92	31.2	525	300	225	3.40	na	150	slurry flow	in operation	26	23	Ring dyke, gold mine	Upstream (?)	na	1	1	na	na	na
Buffalo Creek	26/2/72	322	27600	27.2 km	- (not flow slide)	0.67	2.8 to 4.6	420	hyper-concentrated stream flow	in operation (for 2 years)	58	4.8 (up to 38)	Dam across valley, coal mine	Dumped coarse coal waste over existing sludge	SM - gravelly silty sand (13 to 20% fines), coarse coal waste.	2.5	0.56 to Man (0.82 reducing to 0.42)	CL/ML - sandy silt (54% fines), discharge from plant	Slimes/Sludge under Dam Nos 2 and 3.	Dam No. 3 stored very large volume of water, almost overtopping prior to failure. High water table through embankment.

Table B1.6: Flow slides from tailings impoundments – cases initiated by static liquefaction (Sheet 2 of 2)

Tailings Dam Site	Failure Date	Rainfall	Failure Mechanics (Trigger and Mechanism)	Pre-Failure Observations	Post-Failure Deformation Behaviour	Post-Failure Characteristics (Channelisation/Obstructions/Deposition)	Comments	References
Bafokeng, South Africa	11/11/74	75 mm on night before failure	Piping caused initial embankment failure. Once breached, tailings exposed and liquefied. Suspect significant amount of erosion due to water volume.	8:45 am - overtopping and breach of diagonal wall. 10:15 am - jet of water from face of embankment. Cracks developed and blocks fell out of wall above water jet. Breach widened rapidly to 100 m.	Spread to width of 800 m a short distance beyond the embankment, then entered broad flat channel and flowed (at quick rate) some 4 km to river. (At river slide reported to be 800 m wide and 10 m deep). Flow continued down river (suspect turbulent, extremely quick flow) for some 40 km to a water storage impoundment.	Channelised flow within broad, flat gully and river. Minimal ground erosion. Flow eventually stopped once entered water storage 45 km downstream from tailings dam. 1×10^6 deposited between dam and river, 2×10^6 flowed to water storage. 10 m depth tailings near river.	Destructive flow slide, some 13 people died. Horseshoe shaped post-failure shape in impoundment with bottle neck through breach.	Fourie (2000) Blight (1997) Jennings (1979) Rudd (1979) Midgley (1979)
Stava, Italy	19/7/85	1985 - wetter than usual, 170 mm in 7 weeks prior to failure.	High phreatic surface within steep sand shell of Upper Basin caused initial drained failure. Exposed tailings liquefied and flowed over-topping Lower Basin.	Jan 1985 (6 months prior) - small slip in Upper Basin and development of sinkhole. Lagoons back in operation 4 days before failure. Lower pond virtually full prior to failure.	Initial movement possibly as laminar flow. Suspect developed reasonably quickly into a turbulent stream flow once entered stream some 50 to 100 m below dam. Thren developed into very rapid and destructive hyperconcentrated stream flow.	Channelised flow for most of length. Broad flow to Stava (200 to 250 m wide) and then narrow width of flow in river channel (50 to 100 m) to River Avisio. Terminated at confluence of Stava tributary and River Avisio. No information on deposition.	Massive catastrophe, some 268 people killed. Greater velocity of slide on flatter angle below Stava suggests increasing fluidity of tailings flow. Very little of tailings dam remained.	Blight (1997) Chandler and Tosatti (1995) Morgenstern (2000) Berti et al (1988)
Merriespruit, South Africa	22/2/94	50 mm in 0.5 hour preceeding failure.	Over-topping, following high rainfall and exaserbated by limited freeboard. Erosion initiated instability resulting in retrogressive failure of the embankment. Exposed tailings liquefied and flowed.	Toe sloughing and excessive seepage during life of dam, toe buttress unsuccessful in preventing sloughing. Slips on lower slope of dam several days prior to failure. Series of bangs heard at time of initial embankment failure.	Suspect as quite a rapid flow.	Flow stopped when entered ornamental lake 2 km from initial breach.	Castasrophic event. Tailings flowed through village of Merriespriut causing destruction, some 17 people died. Series of stepped terraces within impoundment, bulb shaped.	Fourie (2000) Blight (1997) Wagener et al (1998).
Texas, USA	1966	na	Seepage at toe caused softening and minor drained failures (also piping). These developed into a larger drained failure of embankment. Exposed tailings liquefied and flowed.	na	Average velocity estimated from 1 to 2 minute event time. Flow spread broadly on flat slopes beyond breach.	No channelisation or obstruction. Depostion along full runout length (2 m thick some 50 m from the breach).	Flow analysis by Jeyapalan et al (1983b). Reasonable results obtained. Series of stepped terraces within impoundment, bulb shaped.	Kleiner (1976) Jeyapalan et al (1983a) Jeyapalan et al (1983b).
Arcturus, Zimbabwe	1978	Heavy rain preceeded failure.	Initial drained failure of dam, probably due to raised phreatic surface following heavy rain. Exposed tailings liquefied and flowed.	na	na	Flow stopped by low embankment of tailings return water reservoir.	1 person killed.	Blight (1997)
Saaiplass - Slide 1, South Africa	3/18/92	no rain prior to slide	Not clear, possibly just drained failure of downstream slope. Exposed tailings liquefied and flowed.	na	na	Flow obstructed by embankment.	Within impoundment - series of stepped terraces separated by steep low height sections.	Blight (1997)
Saaiplass - Slide 2, South Africa	19/03/92	no rain prior to slide	Not clear, possibly drained failure of downstream slope of embankment. Exposed tailings liquefied and flowed.	na	na	Flow obstructed by embankment.	na	Blight (1997)
Saaiplass - Slide 3, South Africa	22/03/92	19 mm rain prior to slide	Not clear, possibly drained failure of embankment due to high phreatic water table related to rapid rise of tailings level in month preceeding failure. Exposed tailings liquefied and flowed.	na	na	Flow obstructed by embankment of return reservoir.	Within impoundment - series of stepped terraces separated by steep low height sections.	Blight (1997)
Buffalo Creek	26/2/72	89 mm in 2 days leading up to failure, 1 in 2 to 3 year event.	Dam 3 in meta-stable state. High phreatic surface caused initial failure. Subsequent retrogressive failures due to high preatic surface and seepage from high up on face. Last part failed violently releasing stored water.	2 hrs prior - cracks across front of Dam 3, crest had sunk in some places. Just prior to slide - front of had dam broken off, settlement and d/stream displacement of embankment observed. Then large part of central section broke loose.	Turbulent flow at 2.75 to 4.6 m/sec down river. Water volume = 530,000 m3, soilds = 170,000 m3 beyond Dam 1. Most material did not travel far. Of material below Dam 1 - 75000 erosion of refuse bank and 23000 sludge.	Confined flow within narrow valley and narrow gully. Deposition along entire valley to town of Man (27 km downstream), most of deposition within first 5 km beyond Dam 1.	Not a flow slide. Comprised a series of rotational failures followed by breach and large release of water (530,000 cu.m.) that eroded slimes. Classify as turbulent or hyperconcentrated streamflow.	W.A. Wahler & Associates (1973) Johnson (1980).

Table B1.7: Flow slides from tailings impoundments – cases initiated by dynamic liquefaction.

Tailings Dam	Date of Failure	Earthquake Details		Failure Details		Embankment						Foundation Slope (°) (Alpha 4 & Alpha 2)	Properties of Slimes (Source Area)	Pre-Failure Observations	Post-Failure Observations	Failure Scarp Within Impoundment	Comments	References
		Magnitude	Dist. to Epicentre (km)	Length, L_{toe} (km)	Volume (1000 m^3)	Height (m)	Slope (°)	Construction Method	Material Properties	Operating State at Time of Failure	Comments							
Barahona 1, Chile	1/10/28	8.2	95	50	3000	65	27	Upstream, gravitational with separator cones	Silty Sand (SM) - fine to medium sand, 15 to 26% fines	operating (for 11 years)	Rolled earth starter dam to 7m height then upstream construction. 15,500 tonnes/day deposit rate.	8.5 deg. immed. down-slope.	na	Failed 2 to 3 minutes after earthquake.	Turbulent flow down Barahona Creek and Cachapoal Rvr for 50 km. Very fast, wave climbed as high as 60 m on bends. Sand volcanoes on terraces and springs daylighting in scarps post-failure.	Near vertical frontal scarp at breach, series of stepped terraces back into impoundment.	Catastrophic event, 54 persons killed. Crest of dam 17 m above slimes.	Troncoso (2000), Troncoso et al (1993)
El Cobre- Old, Chile	28/03/65	7.5	40	12	1900	35	34	Upstream, gravitational	Silty Sand (SM) - fine to medium sand, 45% fines, non-plastic	emergency storage (operating 35 years)	Since Dec 1963 only used for emergency storage	4	Clayey Silt (ML) - low to medium plasticity, 93% fines, w_L = 19 to 48%, PI = 0 to 19%, I_L = 1.2	na	Dust raised by earthquake. Several chunks of dry crust left on terraces.	Near vertical frontal scarp. Horseshoe shaped shell left. Central depression formed by several almost horizontal terraces.	Catastrophic event, killed more than 200 people.	Troncoso (2000), Dobry & Alvarez (1967)
El Cobre- New, Chile	28/03/65	7.5	40	12	500	19	15	Upstream, cyclones	Silty Sand (SM) - fine to medium sand, 30% fines, non-plastic	operating (for 1.25 years)	Very rapid deposition of tailings, approx. 2000 tonnes/day.	4	Clayey Silt (ML) - low plasticity, 90% fines, w_L = 27%, PI = 4 to 5%, I_L = 1.0 to 1.5	Earthquake liquefied slimes. Waves produced on surface of pond. Erosion or slip in corner of dam.	Tailings flowed through the breach and ran 8 m up the mountain in front, then flowed down the valley.	na	Tailings dam totally destoyed.	Troncoso (2000), Dobry & Alvarez (1967)
Hierro Viejo, Chile	28/03/65	7.5	18	1	1	5	45	Upstream, gravitational	Sandy Silt (ML) - fine sand, 62% fines, non-plastic	operating	Series of 5 dams, 1 in use while others dry out.	1 to 2	Silty Clay (CH) - high plasticity, 100% fines, w_L = 55%, PI = 31%, I_L = 0.83	na	Crust broke into blocks that floated on a mass of liquefied tailings.	Terraced slope within depression left after flow.	Dams located on gentle fluvial terraces of Petorca River (within valley floor). Possibility of some confinement of tailings flow.	Troncoso (2000), Dobry & Alvarez (1967)
Los Maquis No. 3, Chile	28/03/65	7.5	15	5	25	15	30.5	gravitational (upstream)	Silty Sand (SM) - fine sand, 46% fines, non-plastic	operating (for 28 years)	Dam 3 in use at time of earthquake. Production approx. 35 to 45 tonnes/day.	15 to 20	Clayey Silt (ML) - low plasticity, 100% fines, w_L = 35%, PI = 9%, I_L = 1.11	Slimes transformed into liquid mass before the earthquake ended.	Suspect flowed within confined, steep valley.	na	Dam located in narrow valley with 15 to 20 degree slopes. Personnel heard sound like an explosion and then the sound like a waterfall.	Troncoso (2000), Dobry & Alvarez (1967)
La Patagua - New, Chile	28/03/65	7.5	22	5	40	15	35	gravitational (upstream)	Sandy Silt (ML) - fine sand, 55% fines, non-plastic	operating	Production approx. 170 tonnes/day. Lot of water on dam at time of failure.	3 to 5	Silty Clay to Clayey Silt (CL/ML) - medium plasticity, 100% fines, w_L = 43%, PI = 18%, I_L = 0.99	na	na	Semi-circular front slope of 7 to 10 m height. Behind scarp several step-like terraces left.	na	Troncoso (2000), Dobry & Alvarez (1967)
Cerro Negro No. 3, Chile	28/03/65	7.5	38	5	95	20	40	Upstream, gravitational	Sandy Silt (ML) - fine sand, 52% fines, non-plastic	operating (for 4 years)	Production approx. 240 tonnes/day.	20	Silty Clay to Clayey Silt (CL/ML) - medium plasticity, 100% fines, w_L = 47%, Pi = 18%, I_L = 0.99	Slimes transformed into liquid mass. Waves formed on the surface of the pond which eroded the small dyke and tailings poured out of the breach.	na	Low and semi-circular frontal scarp. Within impoundment terraced levels with intermediate small scarps.	na	Troncoso (2000), Dobry & Alvarez (1967)
Bellavista, Chile	28/03/65	7.5	55	0.8	75	20	30.5	gravitational (upstream)	Silty Sand (SM) - fine sand, 43% fines, non-plastic	operating	Production approx. 70 to 75 tonnes/day of tailings.	7	Clayey Silt (ML) - low plasticity, 87% fines, w_L = 26%, Pi = 3 to 4%, I_L = 0.98	Scarps behind crest developing 3 - 4 months prior to failure, increasing in rate leading up to failure. Toe bulging.	Dry upper crust cracked and floated in chunks on liquefied mass. Sands left as lateral ridges.	Vertical horseshoe shaped vertical scarp of 7 to 15 m height. Terraced levels within central depression.	na	Troncoso (2000), Dobry & Alvarez (1967)
Ramayama No. 1, Chile	28/03/65	7.5	85	na	0.15	5	33	gravitational (upstream)	Silty Sand (SM) - fine sand, 25% fines, non-plastic	operating	na	30	Clayey Silt (ML/MH) - medium to high plasticity, 100% fines, w_L = 49%, PI = 18%, I_L = 1.14	na	Material flowed down to the foot of the mountain.	na	Tailings dam built on on mountainside with 30 degree slope.	Troncoso (2000), Dobry & Alvarez (1967)
Mochikoshi Dam No. 1, Japan	14/1/78	7.0	40 (approx.)	30	80	32	15.5	upstream	No information. 3 m high dyke constructed each year.	operating (for 38 years)	Gold mine. 16 m high starter dam then upstream construction (after 1965). 120 tonnes/day deposition rate.	~20 (steep mountainside), then < 0.5 deg to ocean (?)	Sandy Clayey Silt (ML) - low plasticity, 85% fines (CF < 10%), w_L = 20 to 30%, PI = 2 to 13%, I_L = 1.4	na	Flowed down mountainside into a stream and eventually into the ocean. 1 km downstream flow depth approx. 1 to 1.5 m depth.	na	Travel angle approx. 1.2 degrees (H ~ 630 m, L ~ 30 km).	Marcuson et al (1979)
Mochikoshi Dam No. 2, Japan	15/1/78	5.7 (aftershock)	close to dam site (?)		3	22	17.5	upstream	No information. 3 m high dyke constructed each year.	operating (for 38 years)	Gold mine. 8 m high starter dam then upstream construction (after 1965). 120 tonnes/day deposition rate.	~20 (steep mountainside), then < 0.5 deg to ocean (?)	Sandy Clayey Silt (ML) - low plasticity, 85% fines (CF < 10%), w_L = 20 to 30%, PI = 2 to 13%, I_L = 1.5	Failure some 5 hours after aftershock.	na	na	na	Marcuson et al (1979)
Veta del Agua 2, Chile	7/11/81	6.5	85	na	na	20	40	Upstream	na	operating	na	na	na	na	na	na	na	Troncoso (2000)
Veta del Agua 1, Chile	3/3/85	7.8	80	8	na	24	26.5 to 34	Upstream / Centre line	na	operating	na	10	na	Earthquake caused slimes to liquefy. Embankment failes with an "explosive burst" in the central, highest region of the dam.	Breach allowed liquefied tailings to flow. Emptied approx. 40 % of the imponded tailings.	na	No under-drainage within embankment.	Troncoso (2000), Troncoso (1988)
Cerro Negro 4, Chile	3/3/85	7.8	105	10	100	40	22	Upstream / Centre line	Silty sands (SM), non-plastic	operating	Cyclone	na	na	na	After failure - deep gorge within crest of dyke, approx 30 m wide, through which tailings and water flowed.	na	No under-drainage within embankment.	Troncoso (2000), Troncoso (1988)
Almendro, Chile	14/10/97	7.0	100	na	na	18	34	Upstream		operating	na	na	na	na	na	na	na	Troncoso (2000)
Algarrobo, Chile	14/10/97	7.0	80	na	na	20	34	Upstream		operating	na	na	na	na	na	na	na	Troncoso (2000)
Maiten, Chile	14/10/97	7.0	120	na	na	15	34	Upstream		operating / abandoned	na	na	na	na	na	na	na	Troncoso (2000)
La Cocinera, Chile	14/10/97	7.0	80	na	na	30	30.5	Upstream / Centre line		abandoned	na	na	na	na	na	na	na	Troncoso (2000)

Table B1.8: Case studies of flow slides in sensitive clays

Site	Date of Failure	Initial Slide Classification	Slope, Failure and Travel Geometry											Volume (m^3)	Slide Area (ha)	Slide Width (m)	Material Description (Liquefied Material on Surface of Rupture)	Hydro-geological Features	Rainfall	Failure Mechanics	Pre-Failure Deformation Behaviour	Post-Failure Deformation Behaviour	Velocity (m/s)	Comments	References
			Height, H (m)	Slope Height, H_s (m)	Length, L (m)	Distance of Retrogression, Re (m)	Length, L_{toe} (m)	Failure Surface Depth (m)	Travel Distance Angle (^{o})	H/L	Alpha 1 (deg.)	Alpha 2 (deg.)	Basal plane (deg.)												
Hekseberg	na	Flow slide, Retrogressive (?)	40	na	700	160	540	12	3.27	0.057	na	na	na	1.8E+05	na	na	Sensitive clay, soft to firm S_t = 50 to 150	na	na	Initial failure triggered retrogressive sliding	na	na	na		Edgars and Karlsrud (1983) Trak and Lacasse (1996)
Furre, Norway	14/4/59	Flow slide, translational (some retrogression)	18	23	350	300	10 to 150	24	2.94	0.051	24	0 to -5	4 to 6	2.8E+06	18	850	Silty Clay - low plasticity, firm, highly sensitive (quick) PI = 10%, S_t > 70, I_L = 2.1	High groundwater levels (higher than usual in normal winter)	na	Instability of steep river bank due to rising (and high) groundwater. Active erosion an aggravating factor (ice jam in February resulted in rapid erosion at toe of initial slide). Occurred as a translational "flake slide".	na	Blocked Furre Namsen channel. Obstructed by island and passive pressures associated with slide surface location below base of channel.	0.5 to 1.3	Translational slide, limited retrogression. Quick clay overlain by glacial silts and sands of low sensitivity. Suspect translational component due somewhat to soil profile.	Hutchinson (1961)
Verdal	na	Flow slide, Retrogressive (?)	70	na	9100	2000	7100	30	0.44	0.008	na	na	na	5.5E+07	na	na	Sensitive clay, low plasticity, soft to firm, PI = 3 to 5%, S_t = 20 to 200, I_L = 2.5	na	na	Initial failure triggered retrogressive sliding	na	na	10 to 15		Edgars and Karlsrud (1983) Trak and Lacasse (1996)
Selnes	na	Flow slide, Retrogressive (?)	25	na	450	140	310	10	3.18	0.056	na	na	na	1.4E+05	na	na	Sensitive clay, low plasticity, soft, PI = 3 to 9%, S_t > 100, I_L = 1.9	na	na	Initial failure triggered retrogressive sliding	na	na	na		Edgars and Karlsrud (1983) Trak and Lacasse (1996)
Lemieuse (Sth Nation Rvr), Ottawa	20/6/93	Flow slide, Retrogressive	na	na	na	680	na	8 to 23	na	na	na	na	na	2.8E+06	17	na	Clay - high plasticity, firm, PI = 40%, S_t = 10 to 100	Suspect high groundwater level	Above normal snowfall in winter, heavy falls in March and April. Heavy Spring rain.	Initial instability of river bank due to rising groundwater levels from rainfall and snowmelt. Followed by series of retrogressive failures triggered by continued back-scarp instability.	Small slumps observed in week prior to main failure	Flowed down South Nation River.	na		Lawrence et al (1996)
South Nation River	16/5/71	Flow slide, Retrogressive	na	24.5	na	490	na	24.5	na	na	10	na	na	6.0E+06	28	750	Clay - high plasticity, firm, PI = 40%, S_t = 10 to 100, I_L = 1	Suspect high groundwater level following heavy snowmelt.	Wet Spring	Initial instability of river bank due to rising groundwater levels from rainfall and snowmelt. Followed by series of retrogressive failures triggered by continued back-scarp instability.	na	Flowed down South Nation River.	na		Lawrence et al (1996) Eden et al (1971)
Baastad, Norway	5/12/74	Flow slide, translational	34	24	1200	175	1000	24	1.62	0.028	21	1	2	1.5E+06	8	480	Clayey Silt - low plasticity, firm, high sensitivity (quick) PI = 4 to 8%, S_t = 50 to 100, I_L = 1.6	Suspect high groundwater level	Wet Autumn	Instability due to rising groundwater following rainfall. Earthworks was an aggravating factor. Translational slide.	na	Channelised	na	Deep translational slide. Slide within quick clay below approx. 20 m of low sensitivity (IL < 1) silty clay.	Edgars and Karlsrud (1983) Trak and Lacasse (1996) Gregerson and Loken (1979)
Rissa, Norway	29/4/78	Flow slide, translational, some retrogression	35	25	1100	1350	?	10	1.82	0.032	6	na	5	5.5E+06	33	800	Sensitive clay, low plasticity, very soft, PI = 5 to 12%, S_t ~ 100, I_L = 2.3	na	na	Initial instability due to earthworks, which triggered relatively slow, retrogressive sliding due to continued back-scarp instability. Followed by several very large, retrogressive, translational "flake" slides	na	Rapid movement of translational slides.	2.8 to 5.5	Slow retrogressive slide followed by quick translational slide. Initial slide N_b = 7.4 (R/D = 75).	Edgars and Karlsrud (1983) Trak and Lacasse (1996) Gregersen (1981).
Skjelstadmarken	na	Flow slide, Retrogressive (?)	45	na	2800	600	2200	15	0.92	0.016	na	na	na	2.0E+06	na	na	Sensitive clay, low plasticity, firm, PI = 6 to 10%, I_L = 1.3	na	na	Initial failure triggered retrogressive sliding	na	na	0.2		Edgars and Karlsrud (1983) Trak and Lacasse (1996)
Borgen	na	Flow slide, Retrogressive (?)	29	na	1500	165	1350	9	1.11	0.019	na	na	na	1.2E+05	na	na	Sensitive clay, low plasticity, soft, PI = 6 to 8%, S_t = 20 to 100, I_L = 1.4	na	na	Initial failure triggered retrogressive sliding	na	na	na		Edgars and Karlsrud (1983) Trak and Lacasse (1996)
St. Jean Vianney, Quebec	4/5/71	Flow slide, Retrogressive	73	24	3880	550	3330	22.5	1.08	0.019	45	na	na	6.9E+06	26.8	370	Silty Clay - low plasticity, cemented, highly sensitive (quick), soft to firm (Champlain Clay) PI = 7 to 12%, S_t > 200, I_L = 1.8	High groundwater following thaw and snowmelt resulting in partial flooding. First heavy rain after thaw.	na	Initial instability of over-steepened stream bank due to rising groundwater. Active erosion of stream bank an aggravating factor. Followed by series of retrogressive failures due to continued back-scarp instability that progressed quickly in latter stages of slide.	Small failure in bank of Petit Bras 10 days before main slide.	Channelised flow down stream and river for some 3 km.	7.2	Rate of retrogression = 3.75 m/sec (early stages 0.15 m/sec). Occurred in crater of previous slide. Samples indicate clay to be dilatent.	Edgars and Karlsrud (1983) Tavenas et al (1971) Trak and Lacasse (1996) Bentley and Smalley (1984)
La Grande River, Quebec	5/5/87	Flow slide, Retrogressive	na	70	na	290	na	42	na	na	35	na	6	3.5E+06	12	550	Clayey Silt - stiff, low plasticity, sensitive, PI = 8%, I_L = 1.8	Possible high groundwater table following snowmelt and thaw. Strong underdrainage in till.	na	Initial instability in steep river bank due to rising groundwater. Active erosion suspected as an aggravating factor. Followed by series of retrogressive failures due to continued back-scarp instability.	Slide more than four months prior to this failure.	Flowed into La Grande River.	na		Lefebvre et al (1991)
Vibstad, Norway	22/2/59	Flow slide, translational	16.3	28	510	260	250	25	1.83	0.032	22	0 to -3	2 to 9	1.0E+06	7	370	Clayey Silt - low plasticity, firm, sensitive, PI = 8%, I_L = 1.3	High groundwater levels. Mild and very wet February. Ground not frozen and saturated	Wet February (mild)	Instability of river bank due to rising (and high) groundwater levels following wet and mild late Winter. Active erosion an aggravating factor. Occurred as a translational "flake slide".	na	Occurred rapidly. Dammed river. Obstructed by opposite bank of river and also river itself.	na	Translational slide, limited retrogression. Quick clay overlain by glacial silts and sands of low sensitivity. Suspect translational component due somewhat to soil profile.	Hutchinson (1965)
Bekkelaget, Norway	7/10/53	Flow slide, translational, rotational back-scarp	16	12	160	140	20	6	5.71	0.100	2	2	1	1.0E+05	1.6	155	Silty Clay / Clayey Silt - low plasticity, very soft, highly sensitive (quick), PI = 9%, S_t = 80, I_L = 2.4	Hydrostatic groundwater from ground surface	na	Slide triggered by embankment construction works located at the rear of the actual slide. Occurred as single failure with frontal section translational at shallow depth and rotational rear component.	na	Moved 15 to 20 m in 15 to 20 seconds as single failure.	1.0	Single compound slide, no retrogression. Triggered by fill placement at rear slope. Suspect translational front due somewhat to passive failure following failure at rear.	Eide and Bjerrum (1956)
Tuve, Sweden	30/11/77	Flow slide, Retrogressive	17	na	850	320	530	10 to 15	1.15	0.020	na	0.54	na	4.0E+05	28	190	Silty Clay - high plasticity, soft, sensitive, S_t = 15 to 40, I_L = 1.3	Intense rainy period in Autumn (Sept - Nov), probable artesian pressures	na	Initial instability in road embankment with stream at toe possibly triggered by high groundwater levels and/or active stream erosion at toe. Followed by series of rapid retrogressive failures due to continued back-scarp instability.	na	na	na	Rate of retrogression avg 2.5 m/sec	Duncan et al (1980)

Table B1.9: "Rapid" landslides in submarine slopes (Edgars and Karlsrud 1983)

Site	Failure Date	Landslide Geometry					Velocity (m/s)	Volume (m^3)	Material Description	Trigger	Comments	References
		Height, H (m)	Length, L (m)	Length, L_{toe} (km)	Travel Distance Angle (^{o})	H/L						
Orkdalsfjord, Norway	2/5/30	500	22500	> 20 km	1.3	0.022	7.0	2.5E+07	Glacial - loose sand, silt and clay deposits.	Possibly small slide in man-made fill	Initial failure occurred at time of exceptionally low tide. Mechanism - collapse and flow of loose sand and silt sediments. Travel distance and rate determined by broken submarine cables.	Karlsrud & Edgars (1982) Edgars and Karlsrud (1983) Terzaghi (1956)
Bassien	Ancient	2200	215000	200 + km	0.58	0.010	na	8E+11	na	Earthquake or rapid sedimentation		Edgars and Karlsrud (1983)
Storegga	Ancient	1700	160000	160 + km	0.61	0.011	na	8E+11	na	Earthquake (?)		Edgars and Karlsrud (1983)
Grand Banks	1929	5000	750000	750 + km	0.38	0.007	7.7	7.6E+11	Sand / silt	Earthquake		Edgars and Karlsrud (1983)
Spanish Sahara	Ancient	3100	700000	700 km	0.25	0.004	na	6E+11	Gravelly clayey sand	rapid sedimentation		Edgars and Karlsrud (1983)
Walvis Bay (SW Africa)	Ancient	2100	250000	250 km	0.48	0.008	na	3E+11	na	na		Edgars and Karlsrud (1983)
Icy Bay / Malaspina	Ancient	80	12000	12 km	0.38	0.007	na	3.2E+10	Clayey silt	Earthquake		Edgars and Karlsrud (1983)
Copper River	Ancient	85	8000	8 km	0.61	0.011	na	2.4E+10	Silt / sand	rapid sedimentation		Edgars and Karlsrud (1983)
Ranger	Ancient	800	37000	37 km	1.24	0.022	na	2E+10	Clayey and sandy silt	rapid sedimentation (earthquake)		Edgars and Karlsrud (1983)
Mid Alb. Bank	Ancient	600	5300	5.3 km	6.46	0.113	na	1.9E+10	silty clay	earthquake / rapid sedimentation		Edgars and Karlsrud (1983)
Wil. Canyon	Ancient	2800	60000	60 km	2.67	0.047	na	1.1E+10	silty clay and silt	rapid sedimentation		Edgars and Karlsrud (1983)
Kidnappers	Ancient	200	11000	11 km	1.04	0.018	na	8.0E+09	sandy silt, clay	Earthquake (?)		Edgars and Karlsrud (1983)
Kayak Trough	Ancient	150	18000	18 km	0.48	0.008	na	5.9E+09	clayey silt	rapid sedimentation / earthquake		Edgars and Karlsrud (1983)
Paoanui	Ancient	200	7000	7 km	1.64	0.029	na	1.0E+09	silt / sand	Earthquake (?)		Edgars and Karlsrud (1983)
Mid. Atl. Cont. Slope	Ancient	300	3500	3.5 km	4.90	0.086	na	4.0E+08	silty clay	rapid sedimentation		Edgars and Karlsrud (1983)
Magdalena R.	1935	1400	24000	24 km	3.34	0.058	na	3.0E+08	na	rapid sedimentation		Edgars and Karlsrud (1983)
California	Ancient	150	3500	3.5 km	2.45	0.043	na	2.5E+08	clayey and sandy silt	Earthquake (?)		Edgars and Karlsrud (1983)
Suva, Fiji	1953	1800	110000	110 km	0.94	0.016	na	1.5E+08	sand	Earthquake		Edgars and Karlsrud (1983)
Valdez	1964	168	1280	1.28 km	7.48	0.131	na	7.5E+07	gravelly silty sand	Earthquake		Edgars and Karlsrud (1983)
Sokkelvik, Norway	1959	100	5000	5 km	1.15	0.020	na	5.0E+06	quick clay (?) and sand	na		Edgars and Karlsrud (1983)
Sandnessjoen, Norway	1967	180	1200	1.2 km	8.53	0.150	1 to 3	5.0E+05	na	Blasting, Man made fill		Edgars and Karlsrud (1983)
Helsinki Harbour, Norway	1936	11	400	.4 km	1.58	0.028	na	6000	sand / silt	Man made fill		Edgars and Karlsrud (1983)

Table B1.10: Failure case studies of hydraulic fill embankment dams, sub-aqueous fills and Wachusett Dam.

Site	Failure Date	Initial Slide Classification	Travel Classification	Slope and Failure Geometry									Volume (m^3)	Width (m)	Embankment / Fill Description				Foundation Description
				Height, H (m)	Dam/Fill Height, H_s (m)	Length, L (m)	Length, L_{toe} (m)	Travel Distance Angle (^{o})	H/L	Alpha 1 (deg.)	Alpha 2 (deg.)	Alpha 4 (deg.)			State (Age)	Type	Construction	Embankment / Fill Material (Source Area)	
Sheffield Dam, USA	29/6/25	Flow slide, translational basal component	Flow slide	7.6	7.6	64	30	6.8	0.12	22	0	0	16000	90	Completed 1917 (failed 8 years after construction)	Hydraulic Fill Dam	Hydraulic	Silty Sand / Sandy Silt (SM/ML) - D_R = 35 to 50% (75 - 80% SMDD)	Silty Sand / Sandy Silt (SM/ML) - DI = 35 to 40% (upper loose layer)
Lower San Fernando Dam, USA	9/2/71	Flow slide, translational basal component, rotational back-scarp.	Flow slide	31	35	177	76	9.9	0.18	21.8	-2 to -3	-2 to -3	400000	400	Completed 1925 (failed 46 years after construction)	Hydraulic Fill Dam	Hydraulic, rolled upper section.	Silty Sand / Sandy Silt (SM/ML) - Clean sand toward outer part of shoulder, siltier (SM/ML) to centre. Highly stratified. 12 - 85% fines. D_R = 50 to 55%.	Stiff clay with lenses of sand and gravel.
Calaveras Dam, USA	24/3/18	Flow slide, translational basal component, rotational back-scarp.	Flow slide	56	56	440	190	7.3	0.13	18	0	0	600000	215	Failed during construction	Hydraulic Fill Dam	Hydraulic, sluiced soft sandstone	Variable - outer section gravelly grading to Silty Sand/Sandy Silt (SM/ML) to silt/clay in liquid core.	Gravelly alluvium over bedrock
Wachusett Dam, USA	11/4/07	Flow slide, rotational (?), possibly retrogressive.	Flow slide (?)	24.4	24.4	179	100	7.9	0.14	22	0	0	47000	213	Failed during first filling	Zoned Earthfill Embankment	Upstream shoulder comprised dumped fill (no compaction)	Sand - Loose to very loose fine sand with some gravel and silt, some silty sand.	Dense to very dense glacial silts, sands and gravels.
Fort Peck Dam, USA	22/9/38	Flow slide, translational basal component.	Flow slide	58	58	880	510	3.8	0.07	12.6	0	0	8000000	520 to 800	Failed during construction	Hydraulic Fill Dam	Hydraulic sand	Sand (SP) - fine to medium grained, trace silt/clay. (e = 0.67 to 0.75). Stratified.	Alluvium - sands, gravels and clays of 0 to 27 m depth over Bearpaw Shale.
Nerlerk Berm - Slide 1	July to August 1983	Flow slide. Suspect translational basal component and retrogressive.	Flow slide / debris flow (?)	27	27	625	375	2.7	0.04	11	0 to 0.2	0 to 0.2	80000	100	Failed during construction	Hydraulic Sea Berm	Hydraulic, placed using special nozzle to steepen slopes, very loose	Sand (SP) - fine to medium grained, some silt (2 to 15%). D_R = 25 to 35%.	Thin layer of soft to very soft clay (Su = 4 to 7 kPa)
Nerlerk Berm - Slide 2	July to August 1983		Flow slide / debris flow (?)	27	27	550	400	2.6	0.05	11	0 to 0.2	0 to 0.2	100000	110	Failed during construction	Hydraulic Sea Berm			
Nerlerk Berm - Slide 4	July to August 1983		Flow slide / debris flow (?)	27	27	625	400	2.8	0.04	11	0 to 0.2	0 to 0.2	150000	150	Failed during construction	Hydraulic Sea Berm			
Willamette River, Terminal 2	18/1/67	Flow slide. Translational basal component between dozed and hydraulic fill, retrogressive.	Flow slide / debris flow	20.7	20.7	72	38	14.0	0.29	28 (25 to 34)	1	5 (18 between hydraulic and bulldozed fill)	4000	23 to 46	Failed during construction by excavation at toe	River berm	Hydraulic and bulldozed	Sand (SP) - medium to coarse sand, trace silt. Very loose bulldozed (DI < 15%), hydraulic loose to med dense (D_R - 20 to 60%)	Alluvial - thin layer organic clayey silt over sand.

Table B1.10: Failure case studies of hydraulic fill embankment dams, sub-aqueous fills and Wachusett Dam (Sheet 2 of 2)

Site	Failure Date	Hydro-geological Features	Trigger	Mechanism	Pre-Failure Deformation Behaviour	Post Failure Deformation Behaviour	Velocity (m/s)	Comments	References
Sheffield Dam, USA	29/6/25	Low phreatic surface downstream of upstream facing section. Groundwater above foundation.	Earthquake, Mag. 6.3, 11 km from dam.	Liquefaction of saturated, loose to medium dense silty sands to sandy silts close to foundation / embankment interface following earthquake.	na	Flow slide on liquefied, loose silty sand / sandy silt base. Upper partly saturated and outer denser zones carried on liquefied basal zone, only minor break-up of outer zone. Movement hinged about abutment. No channelisation or obstruction. Deposition along full length of travel.	na	Earthquake triggered failure. Failure in downstream slope. Estimated S_{ur} = 2.5 kPa.	Seed et al (1969), Seed (1987)
Lower San Fernando Dam, USA	9/2/71	Reservoir level 11 m below crest at time of failure. Initial rise in piezometers observed in downstream shoulder after earthquake.	Earthquake, Mag. 6.6.	Liquefaction of saturated medium dense silty sands and sandy silts in lower section of hydraulic fill following earthquake. Stratification may have had a significant influence.	na	Flow slide on liqufied layer of SM/ML in base of embankment. Initial large slide followed by several retrogressive slides. Outer zones remained intact (carried on liquefied layer). No channelisation or obstruction. Deposition along full length of travel.	0.6 to 1	Earthquake triggered failure. Failure in upstream slope. Estimated S_{ur} of 19 to 24 kPa from dynamic analysis.	Castro et al (1985), Seed et al (1975), Castro et al (1992), Bazier and Dobry (1995) Gu et al (1993)
Calaveras Dam, USA	24/3/18	Low water level in impoundment. Suspect high pore pressures in liquid core, with phreatic surface in upstream shoulder close to water level in reservoir.	Construction. Long lead up to failure.	Suspect shear strain induced liquefaction of weaker lenses of fill near base of dam. Suspect surface of rupture close to base of embankment.	"Abnormal" movement of upstream section of embankment observed since June 1917 (9 months before failure). Construction induced movement. Approx 1.2 m total horiz movement before failure. Day of failure - initially slow movement then increased in rate.	Whole mass moved forward then broke up as front section moved at greater rate. Steam shovelled fill remained intact (carried on liquefied layer). No channelisation. Deposition along full length of travel, 6 to 25 m deep.	1	Material with greater than 45 to 50% voids flowed, 40% stable. Failure in upstream slope. Estimated Sur of 36 kPa.	Seed (1987), Hazen (1918), Hazen & Metcalf (1918).
Wachusett Dam, USA	11/4/07	Suspect near horizontal phreatic surface in upstream shoulder commensurate with reservoir impoundment level.	Rising water level in reservoir.	Suspect collapse of loose dumped sands on wetting during filling triggered liquefaction.	na	Flow slide. Little information. Possibly retrogressive. No channelisation. Deposition along full length of travel, 0 to 12 m deep.	9 (?)	Failure in upstream slope on first filling. Estimated Sur of 16 kPa based on kinetics (3.8 kPa lower bound). Pre-failure, 38 to 42 kPa.	Olson et al (2000)
Fort Peck Dam, USA	22/9/38	Reservoir level dropped 5.8 m in 2 months prior to slide. High core pool level. Suspect relatively flat phreatic surface in upstream shoulder, commensurate with reservoir level.	Construction. Excess pore pressures in bentonitic seams in foundation. Initial movement on these bentonite seams.	Suspect differential movements triggered liquefaction. Initiated at the upstream toe of the core pool.	Toe bulging of upstream shoulder and "abnormal" subsidence movement of core pool (detected hours prior to failure). Increase in rate of movement. Almost suddenly rapid movements started.	Upper and outer part of embankment remained virtually intact (carried on liquefied layer). Sand boils still issueing 10 days after slide. All over in 10 minutes. No channelisation, inlet channel may have obstructed travel. Deposition 0 to 5 m at toe, 15 to 20 m near dam.	2 to 5	Flow slide carried intact surface blocks. Suspect liquefaction of hydraulic fill, mainly in more silty stratified layers.	Middlebrooks (1940), Casagrande (1965), ENR (1939a), Seed (1987).
Nerlerk Berm - Slide 1	July to August 1983	Saturated (sub-aqueous)	Construction, trigger possibly localised over-steepening of loose to very loose sand.	Suspect collapse and static liquefaction of loose to very loose sand triggered by shear movement due to active fill placement. Shear movements possibly along interface between loose to medium dense fill and foundation. Suspect retrogressive.	na	Collapse and flow down to slopes gradients of 1 to 2 degrees. No channelisation or obstruction.	na	Failure in outer loose hydraulic fill placed using new nozzle to steepen slopes. Suspect failure triggered by differential shear along interface between loose and medium dense sand. Possibly semi-continuous layers of loose sand rather than mass loose sand. Estimated S_{ur} of 0.25 to 1 kPa using Stark and Mesri (1992).	Sladen et al (1985b), Sladen & Hewitt (1989), Rogers et al (1990)
Nerlerk Berm - Slide 2	July to August 1983	Saturated (sub-aqueous)			na	Collapse and flow down to slopes gradients of 1 to 2 degrees. No channelisation or obstruction.	na		
Nerlerk Berm - Slide 4	July to August 1983	Saturated (sub-aqueous)			na	Collapse and flow down to slopes gradients of 1 to 2 degrees. No channelisation or obstruction.	na		
Willamette River, Terminal 2	18/1/67	Near saturated sand (sub-aqueous)	Excavation at toe resulting in over-steepening (approx 34 degrees)	Suspect triggered by shear strains along interface between bulldozed and hydraulic fill as a result of effective stress changes associated with excavation at toe. Retrogressive failure occurred along this interface.	na	Occurred as a series of retrogressive rotational slips on a translational interface between the bulldozed very loose fill and hydraulically placed fill. No channelisation or obstruction.	0.3 to 0.5	Estimated S_{ur} of < 1 kPa using Stark and Mesri (1992).	Cornforth et al (1974)

2.0 MECHANICS OF SHEARING OF CONTRACTIVE GRANULAR SOILS

2.1 INTRODUCTION

This section presents a more detailed review of the literature on several aspects of the mechanics and behaviour of contractive granular soils on shearing that are only summarily covered in Chapter 3 (Section 3.3) of the thesis. These aspects include:

- Empirical field methods for evaluation of liquefaction and flow liquefaction potential from case studies of earthquake induced liquefaction;
- Assessment of the residual (undrained) shear strength of flow liquefied soils from laboratory testing;
- The effect of fines content on liquefaction; and
- Discussion on the merits and pitfalls of laboratory testing.

2.2 EMPIRICAL FIELD METHODS FOR EVALUATION OF LIQUEFACTION AND FLOW LIQUEFACTION POTENTIAL

The purpose of this section is to discuss in more detail the field methods used for evaluation of cyclic liquefaction potential. The methods for evaluation of flow liquefaction potential for statically triggered events are discussed in the thesis (Section 3.3) and not here.

Methods for evaluation of liquefaction potential have been developed from the results of laboratory testing and empirically from field case studies. Most of these methods are related to cyclically induced liquefaction (i.e. from earthquakes).

The early work of Harry Bolton Seed pioneered much of the development of empirical methods for evaluation of liquefaction potential from case study analysis of earthquake-triggered liquefaction. Empirical methods for evaluation of large deformation potential have been developed for; the Standard Penetration Test (SPT), the Cone Penetration Test (CPT), shear wave velocity from seismic refraction, and the Becker Penetration Test (BPT), applicable to gravelly soils where the SPT is not appropriate. Empirical correlations to SPT and CPT are the most widely used given the larger field database of information. There are only a few sites where BPTs were carried out and where liquefaction occurred (Youd et al 1997; Harder 1997), therefore it

cannot be directly correlated with liquefaction resistance and is typically used to estimate an equivalent SPT.

Andrus and Stokoe (1997) present methods for evaluation of liquefaction potential from shear wave velocity results. Youd et al (1997) comment that the limitations of shear wave velocity methods are that the seismic wave velocity measurements are made at small strains compared to the large strain phenomena of liquefaction, and that it requires geotechnical investigation to recover physical samples for classification to aid in liquefaction assessment. However, the latter limitation is also applicable to the CPT, and the use of shear wave velocity in conjunction with SPT would presumably provide a good means of investigation. Also, soils tend to fall into the "it may liquefy zone" rather than the "it will" or "it will not" liquefy, and therefore, at present, shear wave velocity does not provide a good method of separation.

2.2.1 SPT for Evaluation of Liquefaction Potential

Seed (1979) developed a correlation between the cyclic stress ratio to cause liquefaction and the *N* value of the SPT test based on field data of sand deposits subject to strong shaking from earthquakes. The case studies analysed were essentially level ground conditions. The correlation proposed by Seed et al (1985), with minor adjustments proposed by Youd et al (1997), is presented in Figure B2.1. This correlation of liquefaction potential based on cyclic resistance is for large deformation and not necessarily for flow liquefaction.

Seed et al (1983) suggested that a correlation of field performance to the cyclic strain induced by earthquake might improve the basis for liquefaction assessment. Figure B2.2 presents the Seed et al (1985) correlation, with slight modifications from the 1996 NCEER workshop (National Centre for Earthquake Engineering Research), of cyclic resistance ratio for clean sands incorporating consideration of the level of strain associated with liquefaction (Robertson and Wride (1997) provide methods for corrections of the SPT value for overburden pressure, energy ratio and other factors). The line on Figure B2.2 for shear strains of 20% can be considered as representing a boundary of flow liquefaction conditions.

With respect to the effect of fines content (non plastic fines), Seed et al (1985) found that for a given corrected SPT value ($(N_1)_{60}$) the cyclic resistance of the soil increased with increasing fines content. Robertson and Wride (1997) comment that it is not clear

whether the cyclic resistance of the soil is increased because of greater liquefaction resistance or in fact the ($(N_1)_{60}$) value of the soil decreases as a consequence of the increase in compressibility and decrease in permeability associated with increasing fines content.

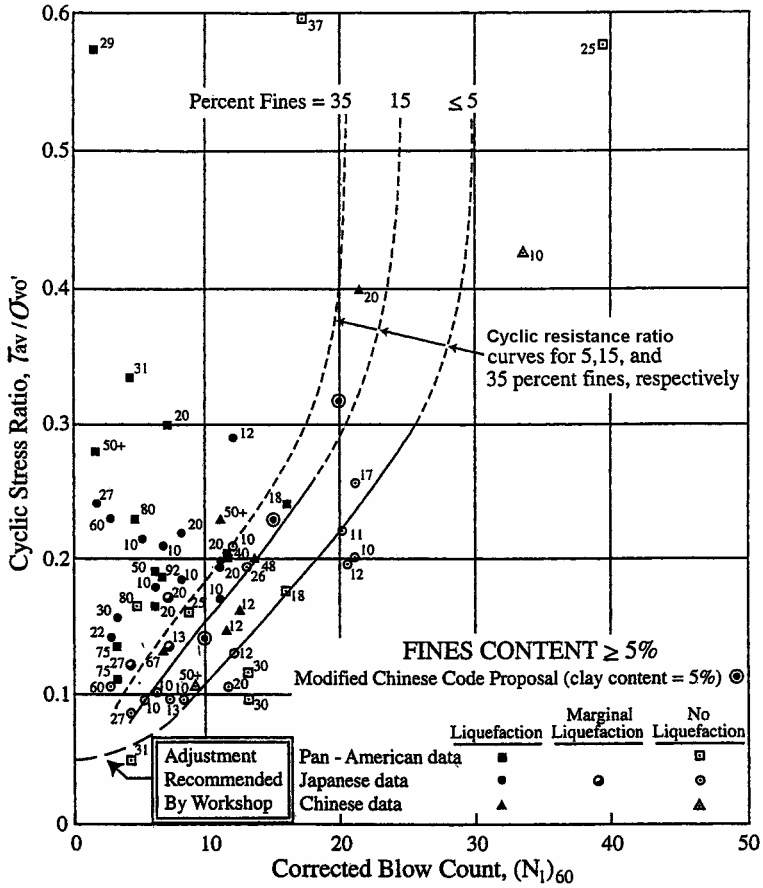

Figure B2.1: Field correlation for cyclic resistance ratio from SPT data (Seed et al (1985) with minor adjustments by Youd et al (1997))

Fear and McRoberts (1995) reviewed the Berkeley data set upon which Seed based his liquefaction assessment. They found that each case record was reduced to a single corrected SPT value ($(N_1)_{60}$) reflecting the state of the cohesionless soil, and this was not the minimum $(N_1)_{60}$ value. The significance of this from a design perspective was that a conservative assessment of liquefaction potential would be obtained if the loosest material on site were evaluated using the Seed criterion. Fear and McRoberts (1995) evaluated the data set (including an additional 25 case records) by selecting the lowest $(N_1)_{60}$ for each case record and developed a lower bound (based on non-liquefied cases) and upper bound (based on liquefied cases) criterion (Figure B2.3). The classification

of cyclic liquefaction, the same as that by Seed for the Berkeley data, was based on observation of surface features including sand boils, cracking, lateral spreading or settlement. They found that the upper bound criterion, i.e. case studies of liquefaction and marginal liquefaction, for clean sands was asymptotic to $(N_1)_{60}$ values in the range 13 to 15, much lower than those of the Seed criterion. The bounds for sand with fines (Fear and McRoberts 1995) are at lower corrected SPT values than for clean sands, indicating that these soils (sands with fines) are more resistant to liquefaction.

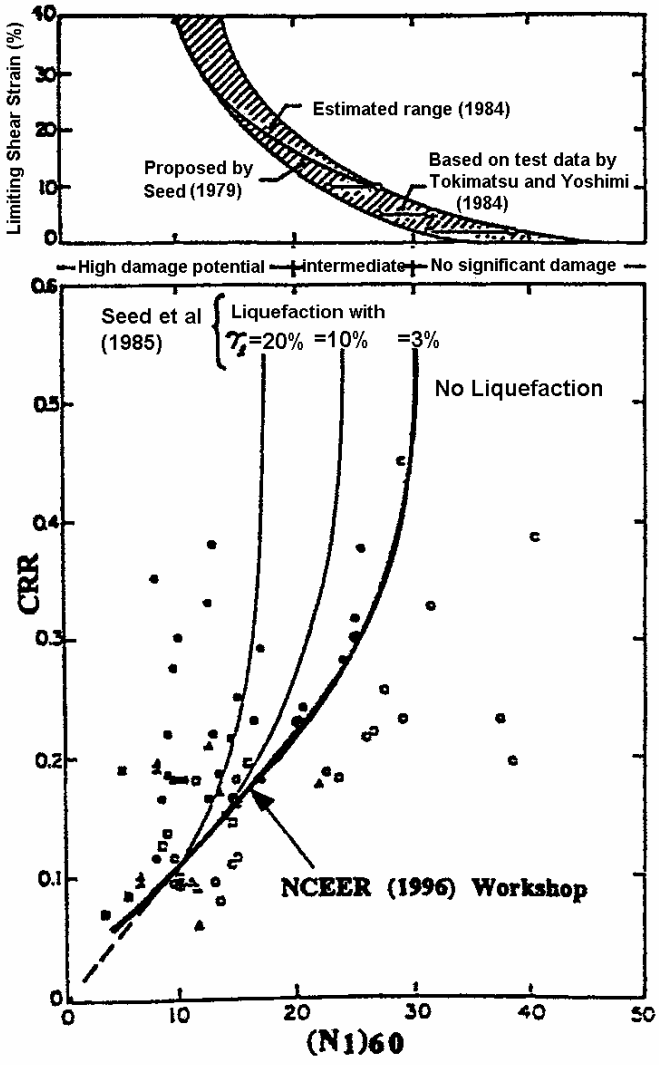

Figure B2.2: Cyclic resistance ratio (CRR) for clean sands under level ground conditions incorporating consideration of potential strain associated with liquefaction (Robertson and Wride 1997)

Fear and McRoberts (1995) commented that the major factors in evaluating the liquefaction potential were the cyclic stress ratio of the earthquake, the corrected SPT

value and fines content. Other factors that influence the potential for liquefaction were the topography and material properties including gravel content, cementation, aging, fabric, layer thickness and drainage characteristics. They commented that the impedance of upward drainage, such as by an upper soil cap of lower permeability, may increase the soils susceptibility to liquefaction.

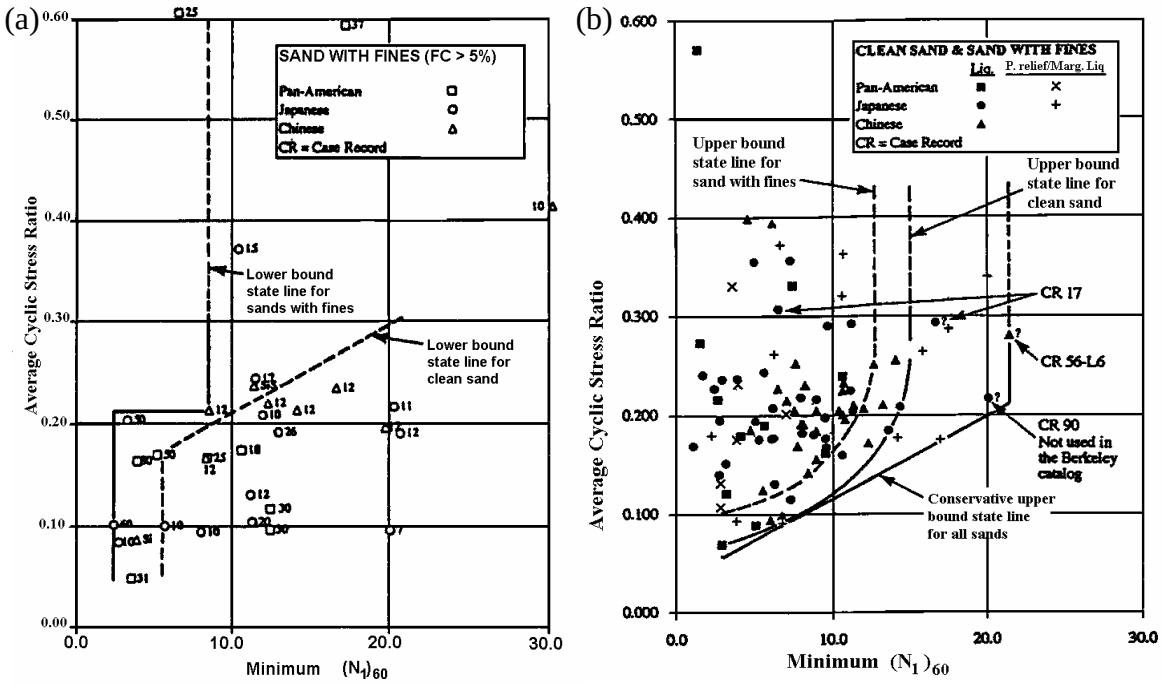

Figure B2.3: Field correlations of cyclic stress ratio versus $(N_1)_{60}$ of *(a)* lower bound from non-liquefied case records and *(b)* upper bound from liquefied and pressure relief case records (Fear & McRoberts 1995).

2.2.2 CPT for Evaluation of Liquefaction Potential

Plots of cyclic liquefaction potential similar to those based on SPT results have been developed for tip resistance from CPT results with similar type correction factors also applicable. The reader is referred to Robertson and Wride (1997) and Olsen (1997) for recent papers discussing correlations of CPT results for assessment of cyclic liquefaction potential.

2.3 PROBLEMS WITH LABORATORY TEST METHODS FOR EVALUATION OF FLOW LIQUEFACTION POTENTIAL

Some of the issues relating to difficulties with laboratory test methods and interpretation are discussed including; the effects of sample disturbance, laboratory assessment of liquefaction, and problems with the use of laboratory prepared samples.

2.3.1 Sample Disturbance

There is significant debate over the merits of laboratory testing as a method of evaluating the flow liquefaction potential of soils in the field. Small changes in void ratio or soil structure due to sample disturbance can significantly affect the laboratory results, and laboratory prepared specimens are not suitable for assessment of field performance due to the effects of stratification and fabric on the results. At the National Science Foundation workshop on the shear strength of liquefied soils (NSF 1998) the working group agreed that high quality "undisturbed" samples are required for laboratory testing if the results are to be used for assessment of field liquefaction evaluation, and the general consensus was for ground freezing as the preferred method of sampling. They recognised that ground freezing may not be suitable for silty sands and sandy silts where the freezing action could cause sample disturbance.

2.3.2 Laboratory Assessment of Liquefaction

Ishihara (1993), for undrained cyclic laboratory tests, considered liquefaction to have occurred when 5% double amplitude strain had been reached in cyclic stress triaxial compressive tests and 3 to 4% in simple shear tests. Robertson and Wride (1997) considered that this definition is conservative and in conflict with field observations, citing the results of Yoshimi et al (1994) as evidence (Figure B2.4). As shown, the results for frozen samples using the 5% double amplitude strain criterion indicate cyclic liquefaction occurs for clean sands with $(N_1)_{60}$ values of up to 40, which is much higher than that from field observations (Figure B2.1 and Figure B2.3) at similar $(N_1)_{60}$ values. Robertson and Wride (1997) comment that for loose sands the strain criterion is applicable as it "*often occurs close to the point at which the effective confining is essentially zero and deformations develop rapidly*". However, they consider that for denser sands the strain criterion may be unduly conservative as "*the 5% double-*

amplitude strain can occur before sufficient pore pressure has developed to take the sample to the state of essentially zero effective stress" and "*deformations may actually be progressing rather slowly*". Poulos (1998) discussed the need to define the term "liquefaction" given their was no distinguishing between its use in field cases of undrained stability failure and its definition as excessive strain in laboratory testing.

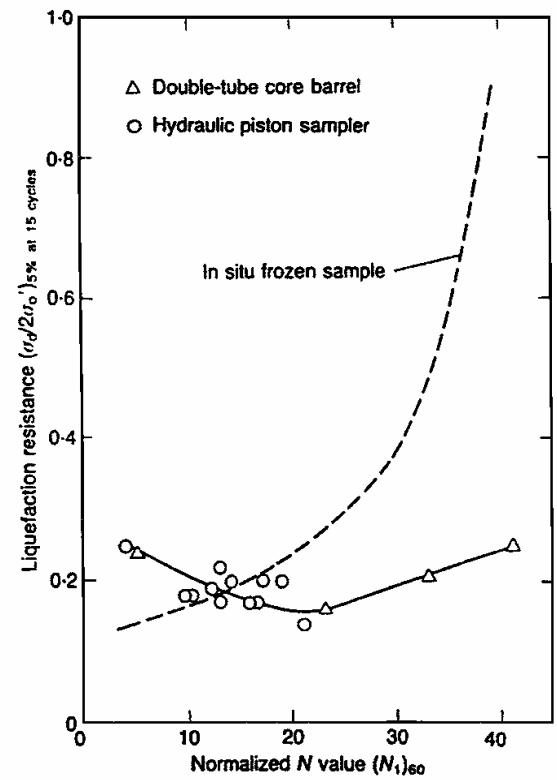

Figure B2.4: Comparison between liquefaction resistance and SPT $(N_1)_{60}$ values from tube samples and undisturbed in-situ frozen samples (Yoshimi et al 1994)

2.3.3 Problems with the Use of Laboratory Prepared Samples For Field Assessment

Ishihara (1993) commented that samples prepared by different methods (moist tamped, water pluviated or dry deposition) show different resistances to flow liquefaction due to the difference in soil structure produced (Figure B2.5). Many authors (including Been et al 1991; Poulos 1998) have discussed the significant effect of soil fabric on liquefaction resistance. In general, they consider laboratory testing using prepared samples only of use for evaluate of field conditions if the sample preparation methods can replicate reasonably the in-situ soil structure, otherwise testing on high quality undisturbed samples is required.

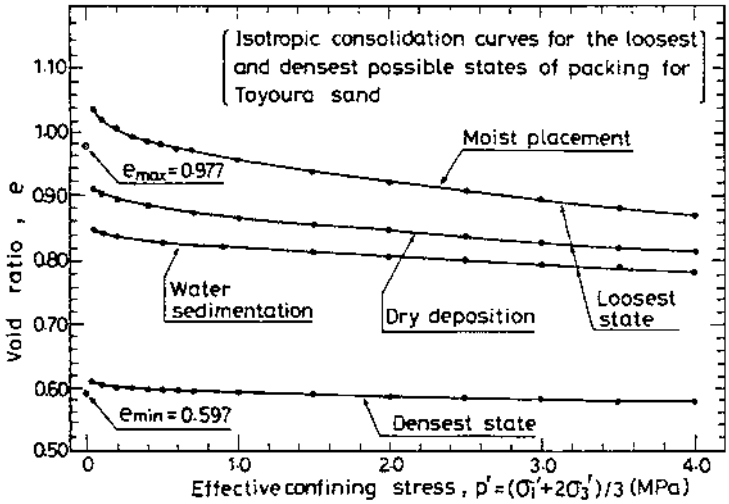

Figure B2.5: Effect of sample preparation method on isotropic consolidation (Ishihara 1993).

The work by Yoshimi et al (1994) compared laboratory test results from both ground freezing and piston undisturbed sampling techniques (Figure B2.4) from a deposit of clean sand. The results from in-situ samples taken after freezing reasonably replicate the shape of the cyclic resistance curve developed from field case analysis. On the other hand, the results from piston type undisturbed samples bear little resemblance. Ishihara (1993) commented that laboratory results indicate piston sampling is useful for recovery of undisturbed samples from loose sand deposits, but sample disturbance effects become increasing pronounced as sand density increases.

Robertson and Wride (1997) and Ishihara (1993) considered the effects of aging and fabric to have a significant effect on the soils liquefaction resistance and that laboratory results from reconstituted samples would not reflect the true behaviour of the in-situ sand. Both authors refer to the cyclic test results after Yoshimi et al (1989) comparing samples from reconstituted freshly deposited sand to in-situ frozen samples (Figure B2.6). The results indicate that the cyclic resistance of reconstituted fresh samples is significantly less than that of the in-situ deposit. Whilst the effect of aging would be difficult to quantify, intuitively it would be expected to have an effect on the results, particularly in silty sands and sandy silts where cementation may occur.

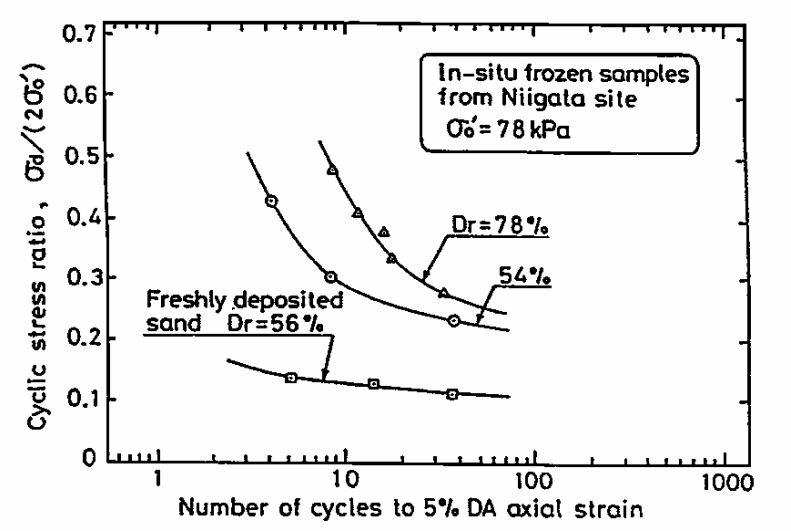

Figure B2.6: Comparison of liquefaction resistance between freshly deposited and in-situ undisturbed samples of sand (Yoshimi et al 1989)

2.4 CHARACTERISTICS OF CONTRACTIVE AND DILATIVE SOILS SHEARED UNDER MONOTONIC LOAD CONDITIONS

2.4.1 Characteristics of Clean Sands

The purpose of this section is to summarise the characteristics of clean sand observed in monotonic laboratory testing and discuss issues such as the uniqueness or otherwise of the steady state line, effects of sample fabric and the effects of stress path based on the published results of research in these areas. Most of the discussion is centred on monotonic stress or strain controlled tests, which would describe more closely the behaviour sands under static liquefaction conditions. The effects of fines content are discussed in Section 2.4.2 and gravelly soils in Section 2.4.3.

Ishihara (1993) presented the results of laboratory undrained triaxial compression tests on Toyoura sand, a fine to medium grained, sub-angular, uniform clean sand, to describe the characteristics of clean sand. The samples were prepared by different preparation techniques (moist placement, dry deposition and water sedimentation), isotropically consolidated, and tested under strain controlled monotonic loading conditions. The results indicate that the steady state condition in undrained loading (Figure B2.7) is dependent on the void ratio alone.

For sands at an initial state in e *log* p' space (e = void ratio, p' = mean normal effective stress) to the right of the steady state line, on shearing in drained conditions the

sand will contract toward the steady state line. In undrained loading conditions the tendency for contraction is suppressed and post peak strain weakening is observed (Figure B2.8) as load is transferred to the pore fluid and the effective stress path moves to the left (at constant void ratio) toward steady state. For sands at an initial state on the left side of the steady state line, when sheared in drained loading conditions will dilate. In undrained loading conditions the dilation is suppressed and strain hardening is observed (Figure B2.9) as pore water pressures reduce and load is transferred onto the soil structure.

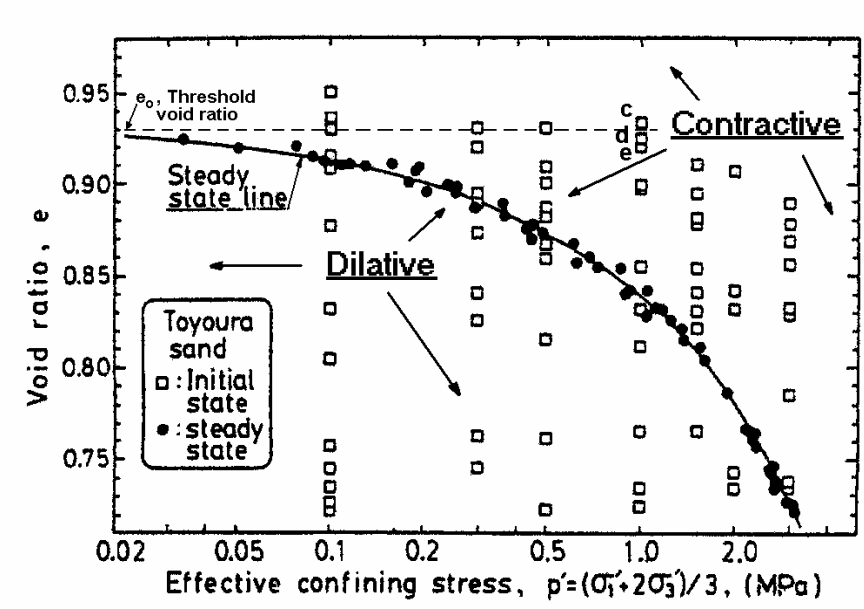

Figure B2.7: Steady state line of Toyoura sand (Ishihara 1993)

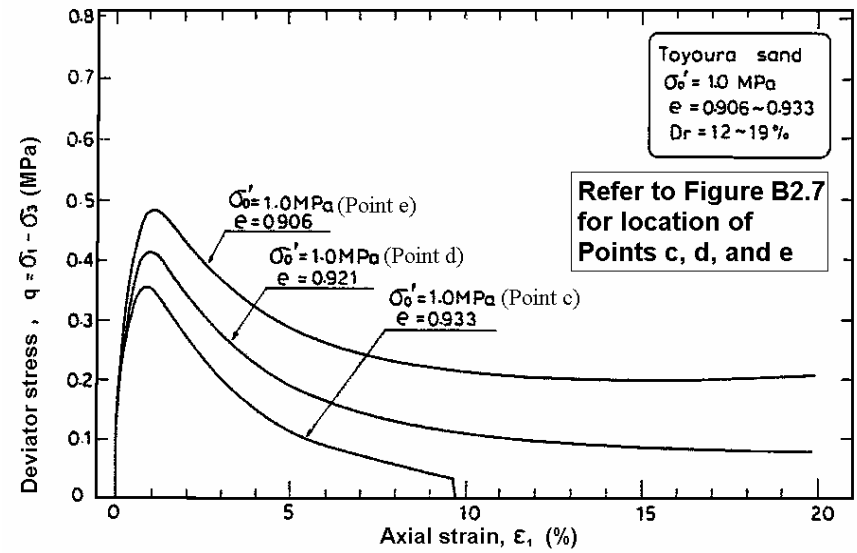

Figure B2.8: Undrained behaviour of states on the contractive side of the steady state line (Ishihara 1993)

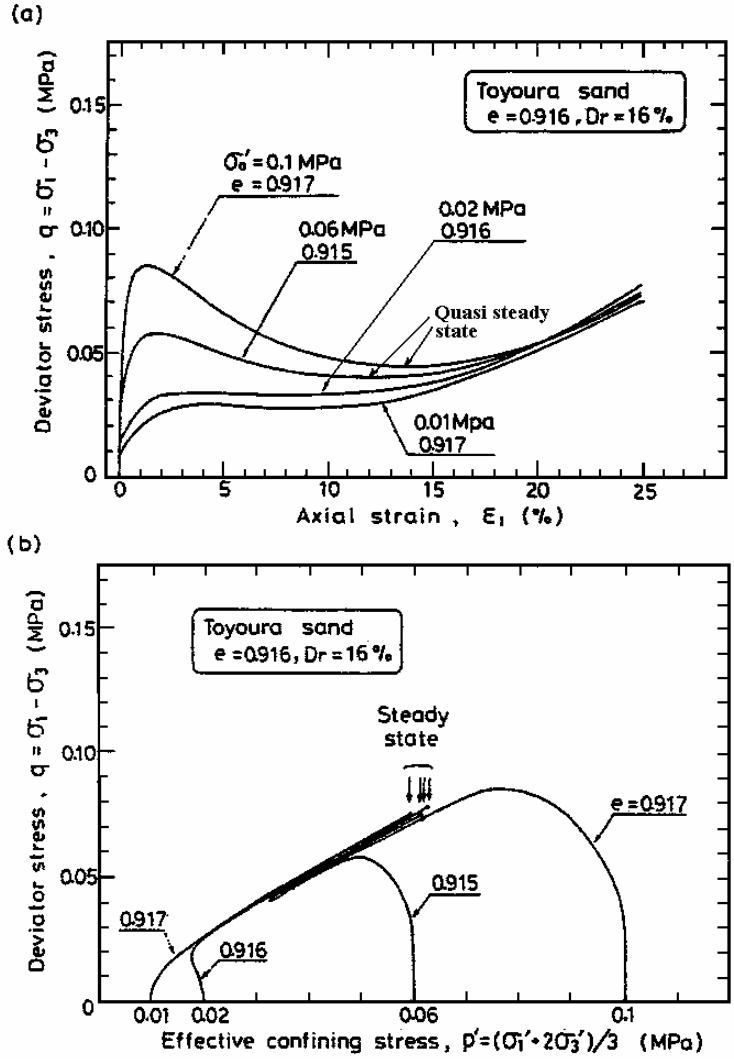

Figure B2.9: Undrained behaviour from states close to and on the dilative side of the steady state line *(a)* stress-strain plot and *(b)* effective stress paths (Ishihara 1993)

A "quasi steady state" condition in undrained loading (where strain hardening follows post-peak strain weakening) is observed for some initial states as shown in Figure B2.9. It is generally observed where the initial state is slightly above or slightly below the steady state. The change from strain weakening to strain hardening is termed the phase transformation. Ishihara (1993) also proposed the concept of the initial dividing line, IDL (Figure B2.10), below which strain hardening is observed and above which stain weakening followed by strain hardening (or quasi behaviour) is observed. The published test results of Figure B2.8 appear to contradict this definition of the IDL because at the states defined by Points c, d, and e (Figure B2.10), all above the IDL, do not show the quasi behaviour. Possibly the IDL is ill defined.

In several very loose samples, prepared by moist preparation, zero residual strength was observed post peak (Figure B2.8). Ishihara (1993) defined the void ratio at or above which samples exhibit zero residual strength as the threshold void ratio, e_o (Figure B2.10).

Ishihara (1993) showed the isotropic compression line, quasi steady state line and initial dividing line are all dependent on the fabric or structure of the sample, void ratio and initial effective confining stress conditions. The quasi steady state condition is not therefore a fundamental state parameter for sands.

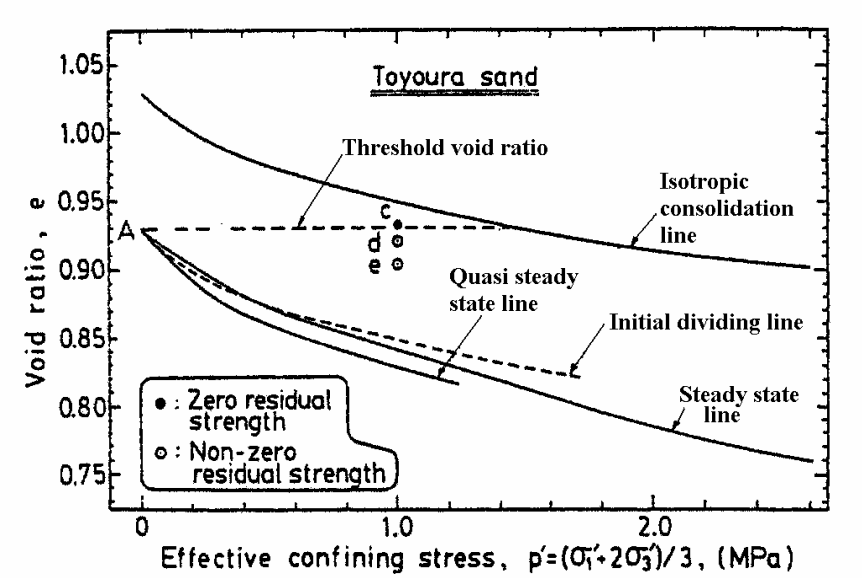

Figure B2.10: Initial states of moist-placed samples from Figure B2.8 and concept of the threshold void ratio (Ishihara 1993)

When clean sands are tested in undrained conditions from the same initial void ratio and different initial effective stress conditions the steady state strength reached for all samples will be the same in accordance with the concept of uniqueness of the steady state line (Figure B2.11).

Sladen et al (1985a) proposed the concept of the collapse surface (or instability line) for evaluation of the liquefaction potential of very loose sands located on the contractive side of the steady state line. They defined the collapse surface as the locus of the peak deviatoric stresses of undrained triaxial compression tests of samples tested at different initial mean normal stress from the same initial void ratio (Figure B2.11). On reaching the collapse surface (in undrained conditions) the soil structure collapses and load is transferred onto the pore fluid. The post collapse effective stress path is downward and

leftward toward the steady state line. The residual undrained strength, defined by the steady state deviatoric stress, q_{ss}, is dependent only on the initial void ratio. An important point here is that the strength defined by the instability line is lower than the critical state strength, which is commonly used in stability analysis.

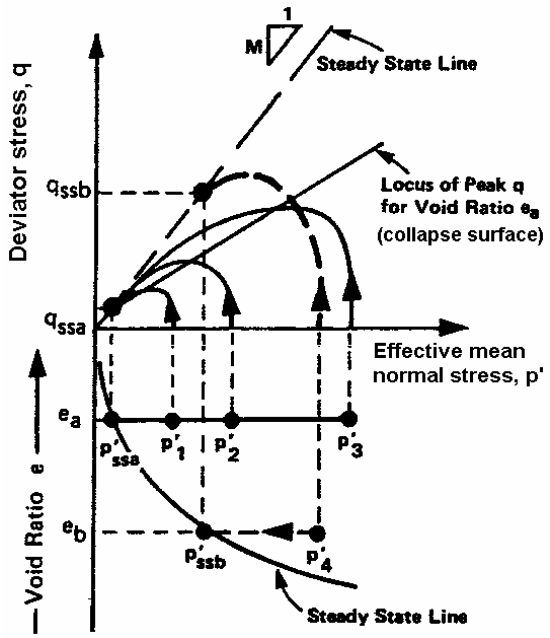

Figure B2.11: Collapse surface concept, locus of peak deviatoric stress of undrained triaxial tests for samples prepared at the same initial voids ratio (Sladen et al 1985a).

Been and Jefferies (1985) defined the concept of the "state parameter", f, to uniquely characterise the state of a sand. Its validity is based on the concept that the steady state line is a unique fundamental parameter, regardless of effective stress path. The state parameter (Figure B2.12) is defined as the difference between the initial void ratio, $e_?$, and the void ratio at steady state corresponding to the initial mean normal effective stress, e_{ss} ($f = e_? - e_{ss}$). The concept of the state parameter is that it characterises the effective stress path and normalised steady state strength of samples with identical values of the state parameter, regardless of the initial mean normal effective stress. It was initially developed for assessment of the characteristics of hydraulic fills, and Been and Jefferies (1985) cautioned its usage for assessment of geologically aged sand deposits.

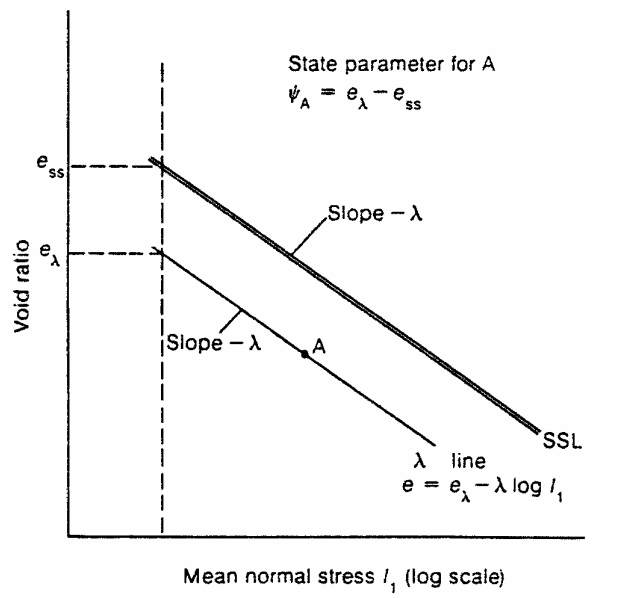

Figure B2.12: Definition of the state parameter (Been and Jefferies 1985).

Yamamuro and Lade (1998) defined three "normal" states of behaviour for clean sands (Figure B2.13) for samples (prepared at the same initial void ratio) tested undrained under monotonic load conditions:

- Stable behaviour, where the undrained stress path is strain hardening. This is similar to the behaviour observed for clean sands sheared from initial states well to the left of the steady state line that are strongly dilative and representative of sands with large negative state parameter, j .
- Temporary instability, where phase transformation or a quasi steady state condition occurs post the initial peak undrained strength. Decreasing stability is observed with increasing confining pressure in this region.
- Instability (liquefaction), indicative of the contractive tendency resulting in the development of positive pore pressures to a steady state condition. Once the effective stress path exceeds the peak deviatoric stress the sand, in undrained conditions, becomes unstable and failure occurs. This corresponds to states to the right of the steady state line (Figure B2.7). Yamamuro and Lade (1998) comment that this behaviour is observed at relatively high confining pressures, the high confining pressure suppressing the tendency for dilation.

The above summary describes the characteristics of sand based on the concept that the steady state line is a unique parameter for clean sand. However, the concept of uniqueness of the steady state line is queried by the results of research, in particular

from research using stress paths other than those for drained and undrained compressive testing and also from testing of sands with fines (Section 2.4.2). The results of research on this aspect of uniqueness (or otherwise) are discussed below.

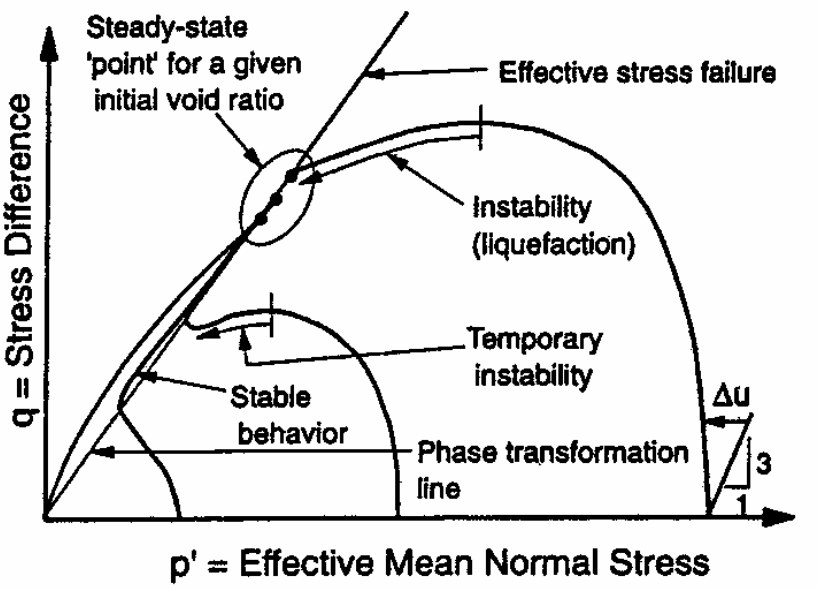

Figure B2.13: Schematic diagram showing different types of behaviour for undrained stress paths of samples at the same void ratio and different initial confining pressures (Yamamuro and Lade 1998).

Yamamuro and Lade (1997) considered that the "normal" behaviour of sand (described above) did not adequately describe their results of laboratory undrained triaxial tests on very loose sands and silty sands (Lade and Yamamuro 1997). They considered that five different states existed for very loose sands and silty sands (Figure B2.14). In addition to the states described earlier, Yamamuro and Lade (1998) consider that for very loose sands (and silty sands) the additional two states are (Figure B2.14):

- Liquefaction region, which occurs at low confining stresses and is characterized by large pore water pressure development resulting in zero effective stresses at low axial strain levels (stress path AO). Increasing confining pressure results in increasing effective stress friction angle at peak undrained strength in this stress region.
- Temporary liquefaction region, characterized by stress path BCDE, which occurs at higher stresses than the static liquefaction region and encompasses a large confining pressure range. The behaviour shows temporary liquefaction from C to D on suppressed contraction, then strain hardening from D to E on suppressed dilation,

which occurs at large axial strains. Increased stability is observed with increasing confining stress in this region.

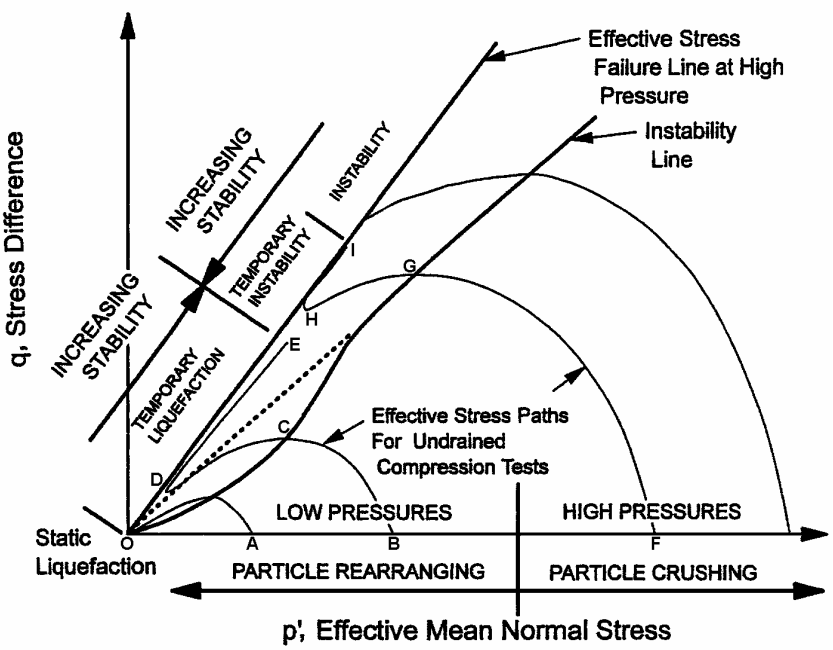

Figure B2.14: General types of undrained effective stress paths for moist placed silty sands sheared from a single isotropic consolidation line (Yamamuro and Lade 1997).

Yamamuro and Lade (1998) refer to the liquefaction and temporary liquefaction regions observed at low confining stresses for very loose silty sands as indicating "reverse" behaviour to that of clean sands. It is reverse in that, at low confining pressures, increasing stability is observed with increasing confining pressure, eventually reaching the earlier described "stable" region where the soil is strain hardening on shearing in undrained loading (Figure B2.14). At confining pressures beyond this point, the "normal" behaviour for sands is observed (i.e. temporary stability and unstable regions).

Yamamuro and Lade (1998) consider particle re-arrangement of the unstable and highly compressive particle structure formed due to deposition under very low energy as the mechanism for liquefaction and temporary liquefaction. At the very high pressures associated with the instability region, they consider particle crushing to be the dominant mechanism (Figure B2.14).

The tests by Yamamuro and Lade (1997, 1998) were undertaken from samples prepared using the same method to the same initial void ratio, then isotropically consolidated to the test confining pressure before undrained testing. The samples (at different confining pressures) were tested from the same isotropic consolidation line

(ICL), but not from the same void ratio. Therefore, Figure B2.14 is dissimilar to Figure B2.11 after Sladen et al (1985a) describing the collapse surface. From Figure B2.15 it is evident that the ICL for the Nevada sand sample crosses the undrained steady state line at two locations. Therefore, with increasing confining pressure the state parameter, f, would go from an initially positive state to a negative state and then back to a positive state. This could partly explain the "reverse" behaviour described by Yamamuro and Lade (1998).

The results of testing by Yamamuro and Lade (1997) on very loose sands with trace to some silt (percent fines less than about 10%) also highlights several other points:

- As the void ratio (or relative density) at preparation is increased, the range of confining pressure under which static liquefaction (to zero residual strength) occurs decreases.
- At higher confining pressures and higher density ratios the compressibility of the sample decreases and better contact between the soil particles increases the samples dilatant tendencies.
- At low confining pressure, the initial portion of the effective stress path for very loose samples is relatively shallow. For these samples in the liquefaction region, the maximum effective stress ratio at liquefaction is significantly less than for the temporary liquefaction region (Figure B2.16).

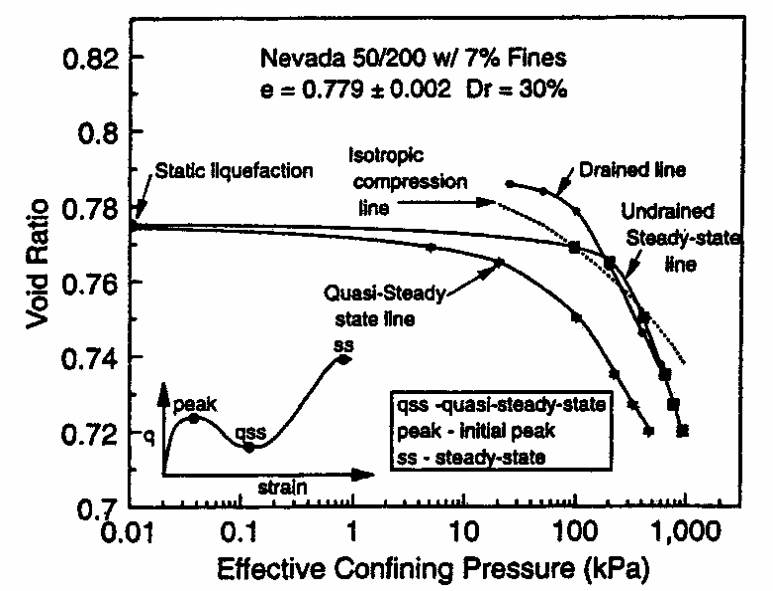

Figure B2.15: Steady state diagram obtained from drained and undrained tests sheared from a single isotropic consolidation line (Yamamuro and Lade 1998)

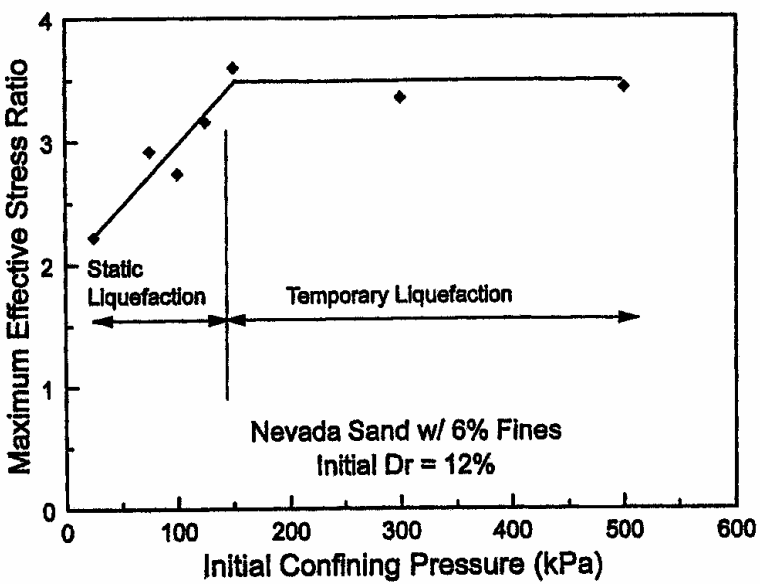

Figure B2.16: Reduced maximum effective stress ratio for very loose sands susceptible to complete static liquefaction at low confining pressures (Yamamuro and Lade 1997)

Been et al (1991), based on the results of drained and undrained triaxial compression on Erksak sand (Figure B2.17a), considered the steady state line to be a unique parameter. For the drained tests on dense samples, Been et al (1991) comment that the samples are generally still dilatant at the end of the test indicating the steady state has not been reached. In addition they comment that strain localisation occurs along the surface of rupture and therefore the void ratio is no longer uniform in the sample. They considered the observed change in direction of the steady state line (Figure B2.17a) to be a result of grain crushing at high confining stresses. For triaxial extension tests on the same sand (Figure B2.17b), Been et al (1991) comment that the samples were still dilating at the end of the test (the arrows indicating the direction of the change in mean effective normal stress at the end of the test). Based on these results, they considered the critical state line to be independent of the stress path.

Uthayakumar and Vaid (1998) considered that the inherent anisotropy of natural sands has a significant effect on the strength and deformation characteristics depending on the principal stress directions in relation to the structure of the sand. Their test results (Figure B2.18) showed that changing the principal stress direction had a significant effect on the stress-strain behaviour and steady state strength. As shown in Figure B2.18, the laboratory results indicate the sample behaviour changed from strain hardening in compression to strain softening in extension. Uthayakumar and Vaid (1998) concluded the steady state condition is not a unique parameter for sands, but that

it is dependent on void ratio, the direction of loading and the intermediate principal stress level.

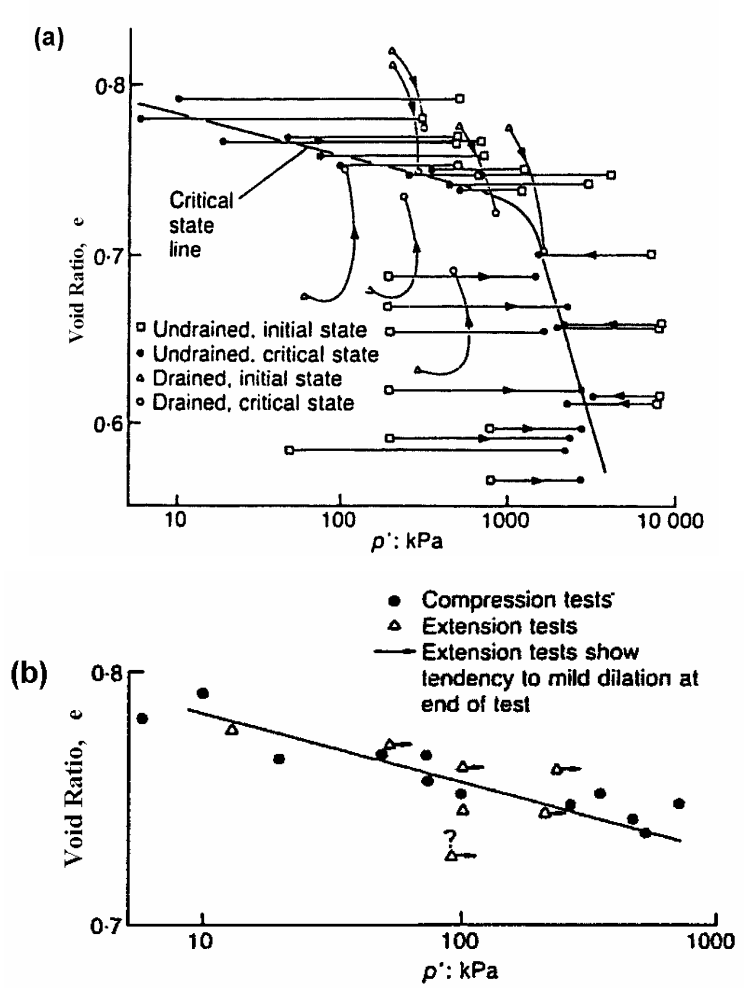

Figure B2.17: Critical or steady state line of *(a)* drained and undrained triaxial compression tests and *(b)* undrained compression and extension tests on Erksak sand (Been et al 1991)

Ayoubian and Robertson (1998), based on the results of monotonic undrained triaxial extension tests on Ottawa sand, concluded that the void ratio at steady state in extension tests was affected by strain localisation. They found that void ratio redistribution was significant from phase transformation and continued up until the failure by necking occurred. Within the zone of necking the void ratio was significantly higher than the average sample void ratio.

Poulos (1998) considered that for triaxial extension tests it is impossible to maintain a uniform void ratio in the sample and that if the void ratio could be measured in the zone of shear that it would correspond to the steady state line for triaxial compression

tests. The results from Ayoubian and Robertson (1998) would tend to support this. Jefferies (1998) considered that much of the non-uniqueness reported comes from an incorrect determination of the steady state condition. Riemer (1998), on the other hand, indicated that the steady state line is not unique, that it is stress path dependent, as published results of triaxial compression compared to triaxial extension, torsional shear and simple shear indicate.

Imam et al (2002), in researching the yield surface for sands, attributed the dependency of the undrained response of loose sand on load direction to the inherent anisotropy associated with deposition of the sand, which existed prior to consolidation. Higher yielding stresses are observed where the major principal stress is in the direction of soil deposition. Therefore, for a sand sample formed by vertical deposition the highest yielding stress in undrained loading is observed for a standard undrained triaxial compression test, and the minimum yielding stress for a standard undrained triaxial extension test.

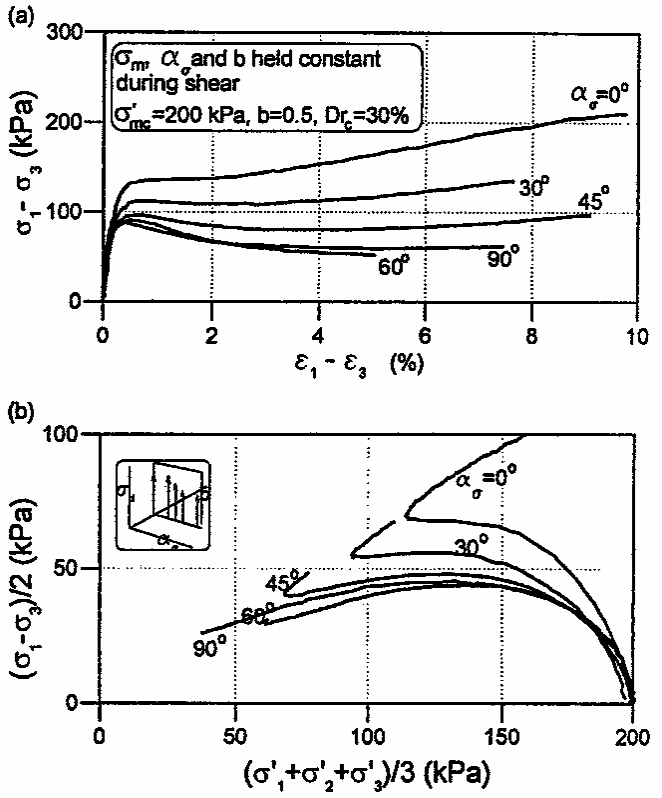

Figure B2.18: Variation in effective stress path and steady state strength due to variation in principal stress direction (Uthayakumar and Vaid 1998).

2.4.2 Characteristics of Sands with Fines

Byrne and Beaty (1998) raised the question of whether fines in sands were an instigator or inhibitor of liquefaction potential. They commented that the structure of the soil had a significant influence on the characteristics of sands with fines. Robertson and Wride (1997) commented that from field case studies it was not clear what effect fines had, whether the cyclic resistance of the soil is increased because of greater liquefaction resistance or in fact the $(N_1)_{60}$ value of the soil decreases as a consequence of the increase in compressibility and decrease in permeability associated with increasing fines content.

Lade and Yamamuro (1997) undertook an extensive study on the effect of non-plastic fines on flow liquefaction potential. They found that the flow liquefaction potential increased with increasing fines content (Figure B2.19) and commented that the fines had a significant role in the particle structure, resulting in highly compressible soils and the increased flow liquefaction potential. For the Nevada 50/200 sand sample (Figure B2.19b) the density index defining the static (or flow) liquefaction / non-liquefaction boundary increased from 20% at zero percent fines to up to 60% at fines contents in excess of 50%. Indicating the presence of fines generated an inherently contractive volume tendency. Lade and Yamamuro (1997) indicate that with increasing confining pressure the void ratio of the silty sand sample reduced due to consolidation. This led to the movement together and better grain-to-grain contact of the larger sand grains, resulting in increased stiffness and an increasingly dilatant tendency of the sample.

Lade and Yamamuro (1997) recognised that the results of other researchers (Kuerbis et al 1988; Pitman et al 1994) found that fines content increased the liquefaction resistance of the soil. They commented that the reason for observations contrary to their findings was due the basis of comparison used, and considered that density ratio should be used as the basis of comparison.

Lade and Yamamuro (1997) also commented that the findings of field testing correlations with actual earthquake induced liquefaction events indicated sands with significant fines content were more resistant to cyclic liquefaction. They considered that the effects of stress history and aging (creep or cementation) are likely to increase the field resistance of silty sands. However, for newly constructed hydraulic fills and very recent natural deposits they considered that fines content could decrease the

liquefaction resistance, depending on the particle structure as a result of the depositional process.

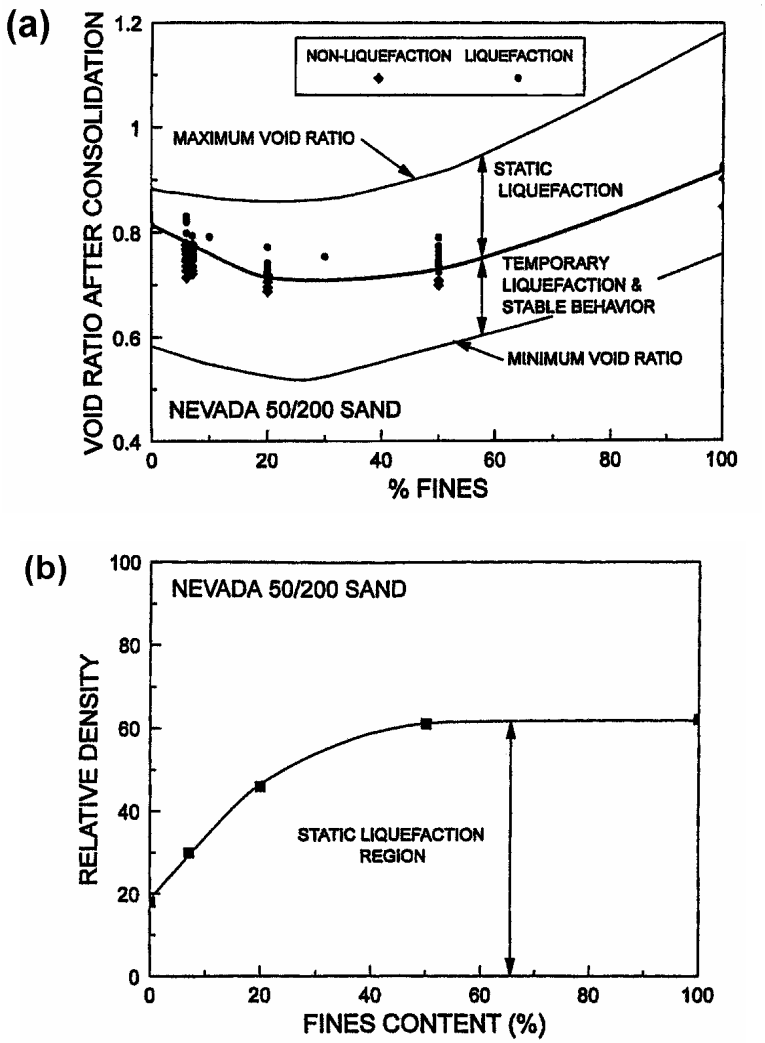

Figure B2.19: Increased liquefaction potential with increasing non-plastic fines content (Lade and Yamamuro 1997)

The question of the steady state being a unique parameter for cohesionless soils has also been raised for silty sands. Yamamuro and Lade (1998) found that the steady state condition was not unique for sands with fines when tested at different density ratios (Figure B2.20) or when tested in drained or undrained conditions from the same density ratio (Figure B2.15). In the latter case the steady state line was coincident above effective confining pressures of 200 kPa, but diverged at lower confining pressures. Yamamuro and Lade (1998) considered the divergence at low confining pressures was due to complete static liquefaction of the undrained tests at these low effective

confining pressures before the tendency for dilation to a steady state condition, as observed at higher confining pressures.

Yamamuro and Lade (1998) also observed a significant change in behaviour as a result of strain rate effects, noting that the soil appeared to be significantly stronger at higher strain rates. They observed that an increase in strain rate resulted in a steepening of the effective stress path to the initial peak and an increase in the steady state strength.

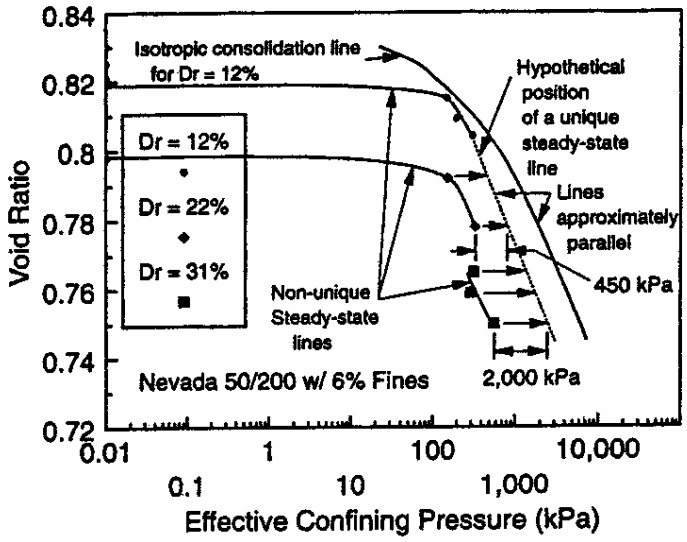

Figure B2.20: Non-unique steady state lines for silty sands tested at different density ratios (Yamamuro and Lade 1998)

2.4.3 Characteristics of Gravels and Sandy Gravels based on Laboratory Testing

Evans and Zhou (1995) carried out cyclic undrained triaxial tests on gap-graded mixtures of medium sand and fine to medium gravel, tested with varying gravel contents. They found that the cyclic liquefaction resistance (based on a 5% double amplitude strain liquefaction criterion) increased with increasing gravel content.

Dawson (1994), as part of his research into liquefaction flow slides of coal mine waste dumps in the Rocky Mountains, undertook a series of undrained triaxial compression tests on well-graded sandy gravels. Samples were prepared by moist placement and then isotropically consolidated to pressures ranging from 50 to 500 kPa. Figure B2.21 presents the results from the Fording sandy gravel sample. Dawson (1994) found that at low confining pressures the samples were unstable and contractive, and therefore in undrained loading the steady state strength was less than the peak strength. At increasing confining pressures he found that the samples became more

stable (i.e. temporary instability condition observed). The consolidation lines were roughly parallel to the steady state line (Figure B2.21b) and the brittleness index, I_b ($I_b = Dq / q_{\max}$ where q is the deviatoric stress), decreased with decreasing void ratio to a brittleness index of 0% at void ratios less than or equal to 0.3.

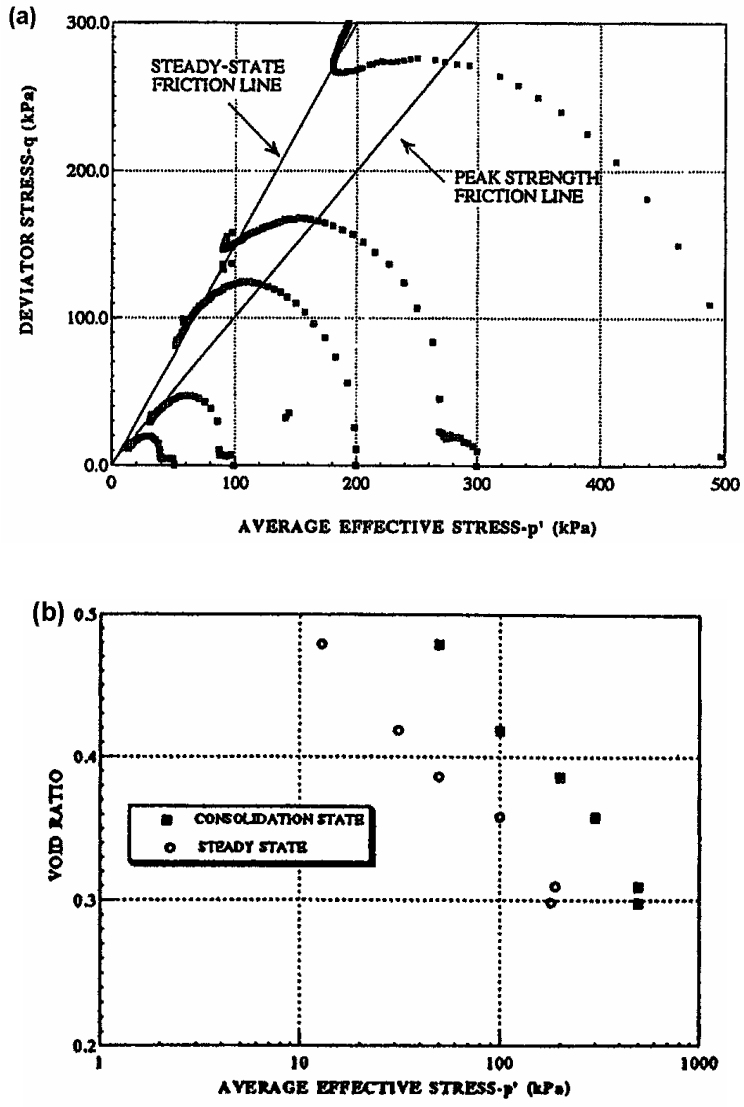

Figure B2.21: Fording sandy gravel sample *(a)* undrained triaxial compression test results and *(b)* consolidation and steady states (Dawson et al 1998)

2.5 RESIDUAL UNDRAINED SHEAR STRENGTH OF FLOW LIQUEFIED SOILS

Methods developed for assessment of the residual undrained shear strength of liquefied soils include:

- Empirical correlation based on back analysis of mostly earthquake induced liquefaction flow failures (Stark and Mesri 1992; Seed 1987; Seed and Harder 1990; Baziar and Dobry 1995). These correlations are presented in Section 3.3.5 of Chapter 3.
- Laboratory test methods, from which theories were developed to explain the observed behaviour of sands (Ishihara (1993) amongst others).

From review of the published literature it is apparent that there is a large uncertainty in the residual undrained strength determined by these methods and that the results from the literature, particularly from laboratory testing, present conflicting results.

Castro (1998) commented that different back-analyses of similar case histories have led to substantially different interpretations. He considered the strong reliance in practice on these empirical correlations from case histories to be unwarranted. Castro (1998) also commented that drainage (of the liquefied soil) affects the strength and therefore travel of the liquefied soil. He recommended that the likelihood or not of drainage should be assessed on a case by case basis taking into account the size of the failure zone, proximity to drainage boundaries, soil permeability and the duration of the post failure movement.

Martin (1998) considered that the undrained, large strain shear strength (residual undrained shear strength) determined from laboratory testing is not necessarily the strength mobilised under field conditions due to issues relating to pore water pressure redistribution, void ratio changes, effective stress path to failure, and the influence of interface conditions associated with stratified silty and sandy soils impacting the residual strength mobilised in the field.

There is significant debate over the merits of laboratory testing as a method of evaluating the undrained residual shear strength of liquefied soils. At the National Science Foundation workshop on the shear strength of liquefied soils (NSF 1998) no consensus could be reached on the type of laboratory testing to be undertaken due to the observed (and sometimes contradictory) behaviour in laboratory tests. The main areas of debate related to; the uniqueness or otherwise of the critical or steady state line (discussed in Sections 2.4.1 and 2.4.2), interpretation of the laboratory results, the effects of strain controlled or load controlled testing, and the limitations of strain in laboratory testing.

A significant number of laboratory triaxial undrained test results show what is referred to as a "quasi steady state", where post peak the deviatoric stress initially decreases to the quasi steady state and then with further straining beyond the quasi steady state increases (Figure B2.9a). The results from Ishihara (1993) indicate that the quasi steady state condition is non-unique in that it is dependent on the initial fabric of the sample tested (refer Section 2.4.1). Kramer (1998) and Gutierrez (1998) comment that given the quasi steady state is not a unique state it cannot be considered a fundamental state on which constitutive models can be based. Jefferies (1998) comments that the strength gain from post peak dilation should not be relied upon and that whilst research into strain localisation continues the quasi steady state should be used as a lower bound estimate of the post liquefaction strength.

Yamamuro and Lade (1998) report that strain rate does have an effect on the steady state condition of silty sands. Conversely, Been et al (1991) and Poulos (1998) comment that strain rate has no effect. Therefore, the results are inconclusive with respect to strain rate effects on the steady state condition.

De Alba (1998) questions the validity of the triaxial test for prediction of post liquefaction behaviour due to the strain limitation of these cells in comparison to the high strains observed in the field. He commented that triaxial samples could not be deformed beyond 20 to 25% axial strain without stress calculations becoming meaningless due to sample distortion. Verdugo et al (1995) commented, from the results of their triaxial testing, that natural non-homogeneous sample structure couldn't be broken down even at large deformations in the triaxial cell.

APPENDIX C

Embankments on Soft Ground

TABLE OF CONTENTS

1.0 ANALYSIS OF EXCESS PORE WATER PRESSURE RESPONSE AND PARTIAL DRAINAGE DURING THE INITIAL STAGES OF EMBANKMENT CONSTRUCTION C1

1.1 Summary of the Literature C1

1.2 Analysis of the Pore Water Pressure Response from the Case Study Data C2

2.0 CASE STUDIES OF POST CONSTRUCTION DEFORMATION BEHAVIOUR C8

2.1 Muar Test Embankments C8

2.2 Olga-C Test Embankment C17

2.3 Queensborough Test Embankment C21

3.0 CASE STUDY EXCEPTIONS TO GOOD INDICATORS OF AN IMPENDING FAILURE C25

3.1 Excess Pore Water Pressure Response C25

3.2 Pre-Failure Deformation Response C28

4.0 POST-FAILURE DEFORMATION ANALYSIS C30

4.1 Rio Test Embankment, Rio de Janiero C31

4.2 Muar-F Test Embankment, Malaysia C33

4.3 St. Alban-A Test Embankment, Quebec, Canada C34

4.4 Portsmouth Test Embankment, New Hampshire, USA C36

LIST OF TABLES

Table C1.1: Field results of pore water pressure response during initial loading..... C4

LIST OF FIGURES

Figure C1.1: Field profiles of the rate of pore water pressure development during initial stages of construction. C3

Figure C1.2: Field profiles of the rate of pore water pressure development during the initial stages of construction. C7

Figure C2.1: Section of the Muar-EC test embankment and interpreted surface of rupture (MHA 1989a) C10

Figure C2.2: Contours of normalised shear-stress ratio at a fill height of 4 m from finite element modelling of the Muar-F test embankment (Indraratna et al 1992) C11

Figure C2.3: Vertical inclination angle profiles with increasing fill height at Inclinometer I1, located at the toe of Muar-EC test embankment. C11

Figure C2.4: Muar-EC, excess pore water pressure response with time for piezometers *(a)* under the centre of the embankment, and *(b)* under the toe of the embankment. C12

Figure C2.5: Muar-EC, settlement and maximum lateral displacement with time. C13

Figure C2.6: Section of the Muar-3C test embankment (MHA 1989b)..... C14

Figure C2.7: Muar-3C, excess pore water pressure response with time for piezometers *(a)* under the centre of the embankment, and *(b)* under the toe of the embankment. C15

Figure C2.8: Vertical inclination angle profiles with increasing fill height at Inclinometer I1, located at the toe of Muar-3C test embankment. C16

Figure C2.9: Muar-3C, settlement with time under the embankment. C16

Figure C2.10: Muar-3C, lateral displacement at the toe of the embankment with time. C17

Figure C2.11: Section A of the Olga-C test embankment with no wick drains (Lavallée et al 1992)..... C18

Figure C2.12: Olga-C, excess pore water pressure response with time at Section A *(a)* below the centre line, *(b)* below the upper slope and *(c)* below the berm. C19

Figure C2.13: Olga-C, vertical inclination angle profiles at various times at Inclinometer INC1, located at about mid berm, at Section A. C20

Figure C2.14: Queensborough test embankment, section of test embankment showing instrumentation (Jardine and Hight 1987). C22

Figure C2.15: Queensborough test embankment, excess pore water pressure response versus *(a)* applied embankment load and *(b)* time. C23

Figure C2.16: Settlement at the centre and maximum lateral displacement at the toe of the Queensborough test embankment. C24

Figure C3.1: Interpretation of effective stress path for heavily over-consolidated clays under embankments (Leroueil et al 1978a)..... C26

Figure C3.2: Effective stress paths and pore water pressure generation associated with different types of yield conditions (Leroueil and Tavenas 1986). C27

Figure C4.1: Pre and post-failure geometry of Rio test embankment (Ramalho-Ortigao et al 1983b) C32

Figure C4.2: Pre and post-failure geometry of Muar-F test embankment (Brand and Premchitt 1989) C33

Figure C4.3: Pre and post-failure geometry of St. Alban-A test embankment (La Rochelle et al 1974) C35

Figure C4.4: Pre and post-failure geometry of Portsmouth test embankment (Ladd 1972) C36

1.0 ANALYSIS OF EXCESS PORE WATER PRESSURE RESPONSE AND PARTIAL DRAINAGE DURING THE INITIAL STAGES OF EMBANKMENT CONSTRUCTION

1.1 SUMMARY OF THE LITERATURE

Based on the results of field observations, Leroueil et al (1978a) and Leroueil and Tavenas (1986) consider that the process of consolidation and therefore partial drainage occurs during the initial stages of embankment construction whilst the clay foundation is in an over-consolidated condition. The assumption of undrained conditions can therefore be erroneous in estimation of pore water pressure response and deformation behaviour.

Leroueil et al (1978a) evaluated the excess pore water pressure response from approximately 95 piezometers located under the embankment centreline of a total of 30 embankments constructed over soft ground. Only the piezometers under the embankment centreline were evaluated because, at this location, the stresses can be estimated with reasonable accuracy and it can be assumed that there is no rotation of the principal stress axes. Leroueil et al (1978a) used Skempton's compounded pore water pressure coefficient, $\overline{B}$ ($\overline{B} = Du/Ds_1$, refer to Equation 4.2 in Section 4.2.1 of Chapter 4 for a full definition), to evaluate the excess pore water pressure response. The results of their analyses (Figure 4.3 in Section 4.2.1 of Chapter 4) indicate that during the initial stages of construction, whilst the clay foundation is in an over-consolidated condition, the shape of the excess pore water pressure profile with depth is similar to that of a consolidation isochrone. The maximum $\overline{B}_1$ value (the subscript 1 referring to the initial stage of loading whilst the clay foundation is in an over-consolidated condition) is located in the central portion of the soft clay layer and reduces to approximately 0 at the drainage boundaries.

Leroueil and Tavenas (1986) considered that a lack of saturation could also result in the observation of pore water pressure generation smaller than expected for undrained conditions. However, the isochronal shape of the pore water pressure profile and the higher excess pore water pressures developed with increasing rate of construction observed at the St. Alban test embankments indicated that consolidation was significant.

Leroueil and Tavenas (1986) commented that the degree of consolidation varies from case to case, depending on the coefficient of consolidation, c_v, of the over-consolidated clay, the length of the drainage path and the rate of loading. Crooks (1987) considers that the stiffness and permeability of the foundation, rate of loading and drainage boundary conditions affect the degree of consolidation during initial loading. He comments that clay foundations with high stiffness (in an over-consolidated condition) would be expected to generate only moderate excess pore water pressures during initial loading, whilst for clays of lower stiffness development of a more significant excess pore water pressure response would be expected. Based on the comments by Crooks (1987) it could be expected therefore that partially cemented, sensitive clay foundations, which have relatively high stiffness on initial loading, would be expected to show a more significant reduction in excess pore water pressure generation than high plasticity clays of low sensitivity, which are typically of significantly lower stiffness.

Tavenas and Leroueil (1980) proposed an equation of best fit (Equation C1.1) to the data from their analysis (Figure 4.3 in Section 4.2.1 of Chapter 4) as a means of predicting the initial rate of pore water pressure development.

$$\overline{B}_1 = 0.6 - 2.4\left(z/D - 0.5\right)^2 \qquad \text{(C1.1)}$$

where z is the depth of the point at which $\overline{B}_1$ is to be estimated and D is the thickness of the soft clay deposit.

1.2 ANALYSIS OF THE PORE WATER PRESSURE RESPONSE FROM THE CASE STUDY DATA

The purpose of this section of Appendix C is to evaluate the influence of the properties of the soft clay foundation and the rate of loading on the pore water pressure response of piezometers located under the embankment centreline during the initial stages of construction prior to yielding.

The excess pore water pressure responses from a total of 55 piezometers, located within the clay foundation under the embankment centreline, from 16 case studies have been analysed. For each piezometer the average $\overline{B}_1$ value has been determined from the pore water pressure response during construction whilst the foundation at that location

has been assessed to be in an over-consolidated condition (i.e. prior to yielding). The results of the analysis are presented in Table C1.1. Plots of the profiles of initial rate of pore water pressure development ($\overline{B}_1$) versus the normalised depth (*z/b*) are presented in Figure C1.1, where *z* is the depth below ground surface level and *b* is the half width of the embankment modelled as a rectangular strip load.

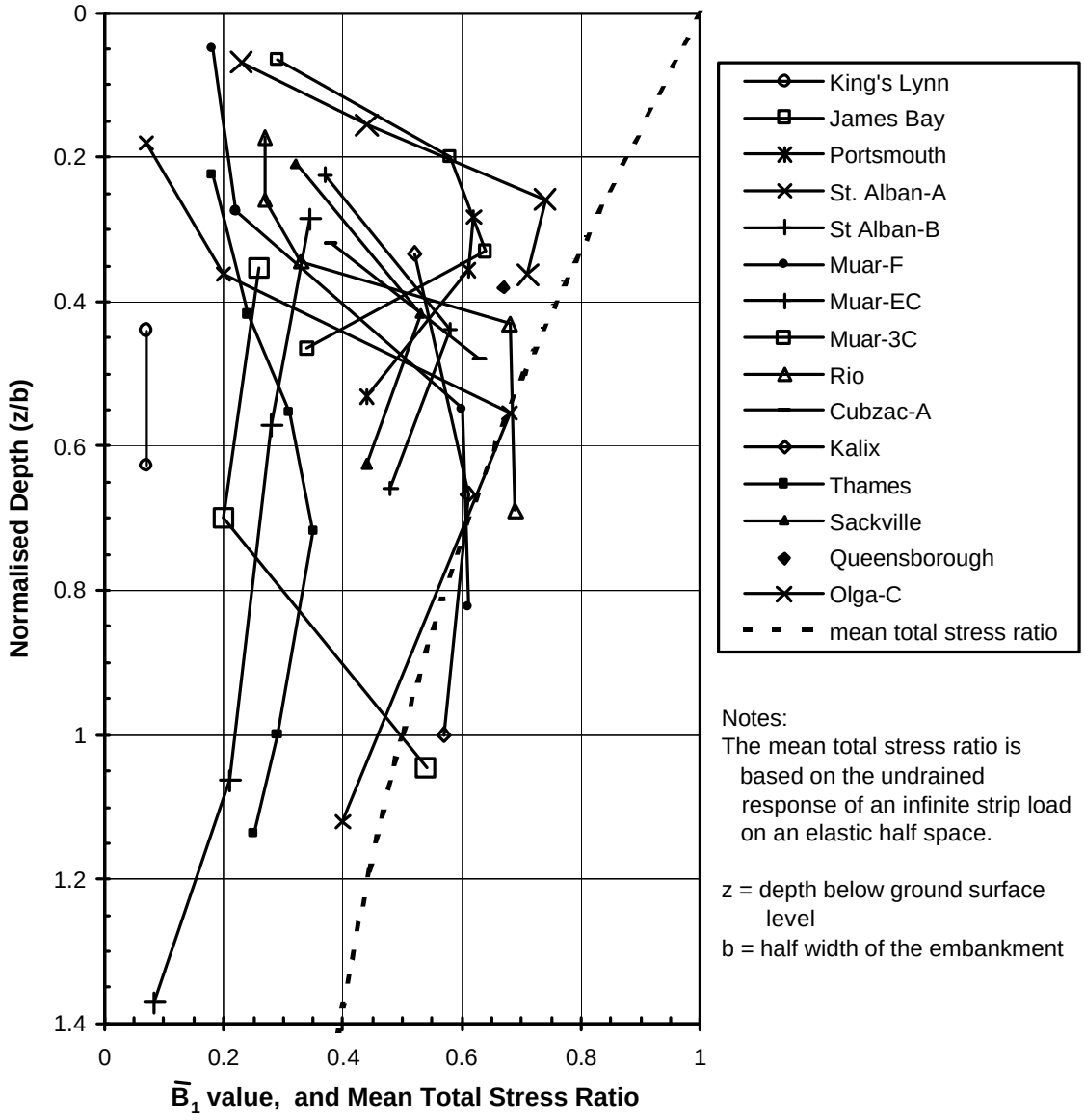

Figure C1.1: Field profiles of the rate of pore water pressure development during initial stages of construction.

Table C1.1: Field results of pore water pressure response during initial loading

Case Study	Piezometer			Rate of Construction (m/day)	$\overline{B}_1 = Du / Ds_v$		OCR	Soil Description
	No.	Depth, z (m)	z/b *[1]		Field	Undrained Response*[2]		
King's Lynn (Wilkes 1972)	214 215	3.3 4.7	0.44 0.63	0.67	0.07 0.07	0.73 0.64	2.1 1.8	CH marine clay with peat layers.
James Bay (Dascal & Tounier 1975)	A-1 A-2 A-3 A-4	1.5 4.6 7.6 10.7	0.07 0.2 0.33 0.47	0.15	0.29 0.58 0.64 0.34	0.96 0.88 0.79 0.72	14 3.3 2.0 1.7	CL/ML leached marine clay, very sensitive, brittle.
Portsmouth (Ladd 1972)	V-5 V-9 V-10	5.8 7.3 10.9	0.28 0.36 0.53	0.19	0.62 0.61 0.44	0.83 0.78 0.69	1.25 1.25 1.2	CL leached marine clay, sensitive, brittle.
Mastemyr*[3] (Clausen 1972)	P1 P2 P3	3.5 6.0 11.0	.41 .70 1.28	0.19	0.87 0.60 0.31	0.63 0.44 0.21	2.5 1.2 1.1	CL/ML leached marine clay, very sensitive, brittle.
St. Alban-A (La Rochelle et al 1974)	D1 D2 D3 C1	1.5 4.6 9.3 3.0	0.18 0.55 1.12 0.36	0.45	0.07 0.68 0.40 0.20	0.89 0.68 0.47 0.78	2.4 1.7 1.6 2.0	CL/ML leached marine clay, cemented, sensitive, brittle.
St. Alban-B (Leroueil et al 1978b)	T1 T2 G3 T4	2.58 5.0 9.3 12.0	0.29 0.57 1.06 1.37	0.19	0.35 0.28 0.21 0.08	0.83 0.67 0.48 0.41	2.1 1.7 1.6	CL/ML leached marine clay, cemented, sensitive, brittle.
Muar-F (Brand & Premchitt 1989)	P1 P2 P3 P4	0.8 4.5 9.0 13.5	.0.5 0.27 0.55 0.82	0.054	0.18 0.22 0.60 0.61	0.97 0.83 0.68 0.56	>10 1.6 1.4 1.25	CH marine clay, low sensitivity, ductile.
Muar-EC (MHA 1989a)	P4 P5 P6	4.6 9.0 13.5	0.22 0.44 0.66	0.017	0.37 0.58 0.48	0.87 0.73 0.63	1.6 1.3 1.3	CH marine clay, low sensitivity, ductile.
Muar-3C (MHA 1989b)	P4 P5 P6	4.6 9.1 13.6	0.35 0.70 1.05	0.05	0.26 0.20 0.54	0.78 0.62 0.49	1.6 1.3 1.3	CH marine clay, low sensitivity, ductile.
Rio de Janiero (Ramalho-Ortigao et al 1983a)	1 2 3 4 5	2.0 3.0 4.0 5.0 8.0	0.17 0.26 0.35 0.43 0.69	0.10	0.27 0.27 0.33 0.68 0.69	0.90 0.84 0.79 0.74 0.62	3.0 2.4 2.0 1.9 1.6	CH marine clay, low sensitivity, ductile.
Cubzac-A (Blondeau et al 1977)	112 132	4.0 6.0	0.32 0.48	0.12 to 0.75	0.38 0.63	0.81 0.72	1.6 1.3	CH clay.
Kalix (Holtz & Holm 1979)	P1 P2 P3	2.5 5.0 7.5	0.33 0.67 1.0	0.35	0.52 0.61 0.57	0.79 0.62 0.50	2.2 1.6 1.4	MH/OH/CH marine silt/clay, sensitive, brittle.
Thames (Marsland & Powell 1977)	C1 C2 C3 C4 C5 C6	2.3 4.3 5.7 7.4 10.3 11.7	0.22 0.42 0.55 0.72 1.0 1.14	0.10	0.18 0.24 0.31 0.35 0.29 0.25	0.87 0.74 0.68 0.61 0.50 0.46	2.3 1.8 1.7 1.4 1.4 1.3	CL/ML marine clay with peat layers.

*[1] *b* is the half width of the embankment modelled as rectangular strip load.

*[2] The undrained response is the estimated pore water pressure response assuming an infinite strip load on an elastic half space.

*[3] Mastemyr is the only circular embankment of the data set. It is not included in Figure C1.1.

Table C1.1: Field results of pore water pressure response during initial loading (continued)

Case Study	Piezometer			Rate of Construction (m/day)	$\overline{B}_1 = Du / Ds_v$		OCR	Soil Description
	No.	Depth, z (m)	z/b *[1]		Field	Undrained Response*[2]		
Sackville (Rowe et al 1995)	15 16 17	2.0 4.0 6.0	0.21 0.42 0.63	0.23	0.32 0.53 0.44	0.87 0.74 0.64	1.6 1.1 1.1	ML/MH intertidal salt marsh deposit.
Queensborough (Jardine & Hight 1987)	P5/2	7.6	0.38	0.07	0.67	0.77	1.1	Alluvial silty clays of Thames estuary, UK (similar to Thames case)
Olga-C (Lavallée et al 1992)	A108 A107 A106 A105	2.0 4.5 7.5 10.5	0.07 0.16 0.26 0.36	0.15	0.23 0.44 0.74 0.71	0.96 0.91 0.84 0.78	12 4.2 2.5 1.8	CH varved clay

Muir Wood (1990) considered that by assuming undrained conditions during loading and that the foundation behaviour is elastic prior to yield (i.e. when in an over-consolidated condition) the excess pore water pressure response could be derived directly from the change in mean total stress. In Table C1.1 comparative values of the estimated rate of pore water pressure development ($\overline{B}_1$) assuming an undrained response of an infinite strip load on elastic half space are given for each piezometer. In Figure C1.1 the plot of mean total stress ratio for undrained conditions is also given for comparative purposes. Figure C1.2 presents the same results with $\overline{B}_1$ normalised with respect to the mean stress ratio, thus giving an estimate of the percent drainage, versus the depth, *z*, below ground surface level.

In comparison to the undrained profile for an infinite strip on elastic half space, the excess pore water pressure profile for most case studies is typical of a consolidation isochrone for upward drainage only (Figure C1.2). The $\overline{B}_1$ profiles of four case studies (Portsmouth, James Bay and St. Alban A and B), all having foundations comprising low plasticity, sensitive, leached marine clays, show signs of drainage toward a second drainage boundary at depth. Therefore, the field observations confirm that the length of the drainage path is a significant factor on the degree of consolidation.

However, apart from this, the results show a high degree of variability from case to case, with no clear correlation with respect to rate of loading between different sites, material type (from very low to high sensitive and low to high plasticity clays) or likely material stiffness. It is considered that these observations reflect that permeability is a key factor in controlling the variation of c_v between case studies and therefore the

degree of consolidation that occurs during the initial stages of loading. The observations that indicate permeability is a significant factor are as follows:

- The pore water pressure profiles for the Muar test embankments (Figure C1.1 and Figure C1.2) indicate a significant increase in the value of $\overline{B}_1$ at greater than about 9 m depth, which is consistent with depth of the interface between the upper and lower clay strata. Brand and Premchitt (1989) indicate that the permeability of the upper clay strata is about 4 times greater than that of the lower layer.
- In the case of King's Lynn it is considered that the relatively high permeability of the peat layer has resulted in the low $\overline{B}_1$ values calculated. Piezometers 214 and 215 are located slightly above and within the extensive peat layer respectively. The permeability of the peat layer is reported by Wilkes (1972) to be 10 to 15 times greater than the permeability of the CH alluvial clays above and below the peat.
- In the case of the Rio test embankment the pore water pressure profile would suggest a lower permeability at depth in the soft clay stratum as indicated by the abrupt increase in $\overline{B}_1$ between Piezometer 3 (4 m depth) and Piezometer 4 (5 m depth).
- The lack of correlation from case to case to the rate of construction.
- No correlation to material stiffness. For near normally consolidated soils, the low plasticity, sensitive, brittle leached marine clays (some of which are cemented) would be expected to have a relatively high stiffness in comparison to high plasticity clays low sensitivity. The pore water pressure profiles show no distinction between these material types.

For sites analysed with more than one test embankment, the St. Alban test embankments (Leroueil et al 1978a) do indicate a correlation with respect to rate of loading. St. Alban A was constructed at a rate approximately 2 to 2.5 times greater than the St. Alban B test embankment and the $\overline{B}_1$ profile for St. Alban A is significantly greater than for St. Alban B, as expected. However, for the Muar tests embankments (Muar-F, Muar-EC and Muar-3C) no correlation is evident with respect to rate of loading.

In 7 of the 16 case studies analysed the rate of pore water pressure generation at a depth below 4 to 6 m (Figure C1.2) exceeded 80% of the pore water pressure profile assuming undrained conditions. This indicates that near undrained conditions are

observed at depth in a significant proportion of cases during the initial stages of construction whilst the foundation is in an over-consolidated condition.

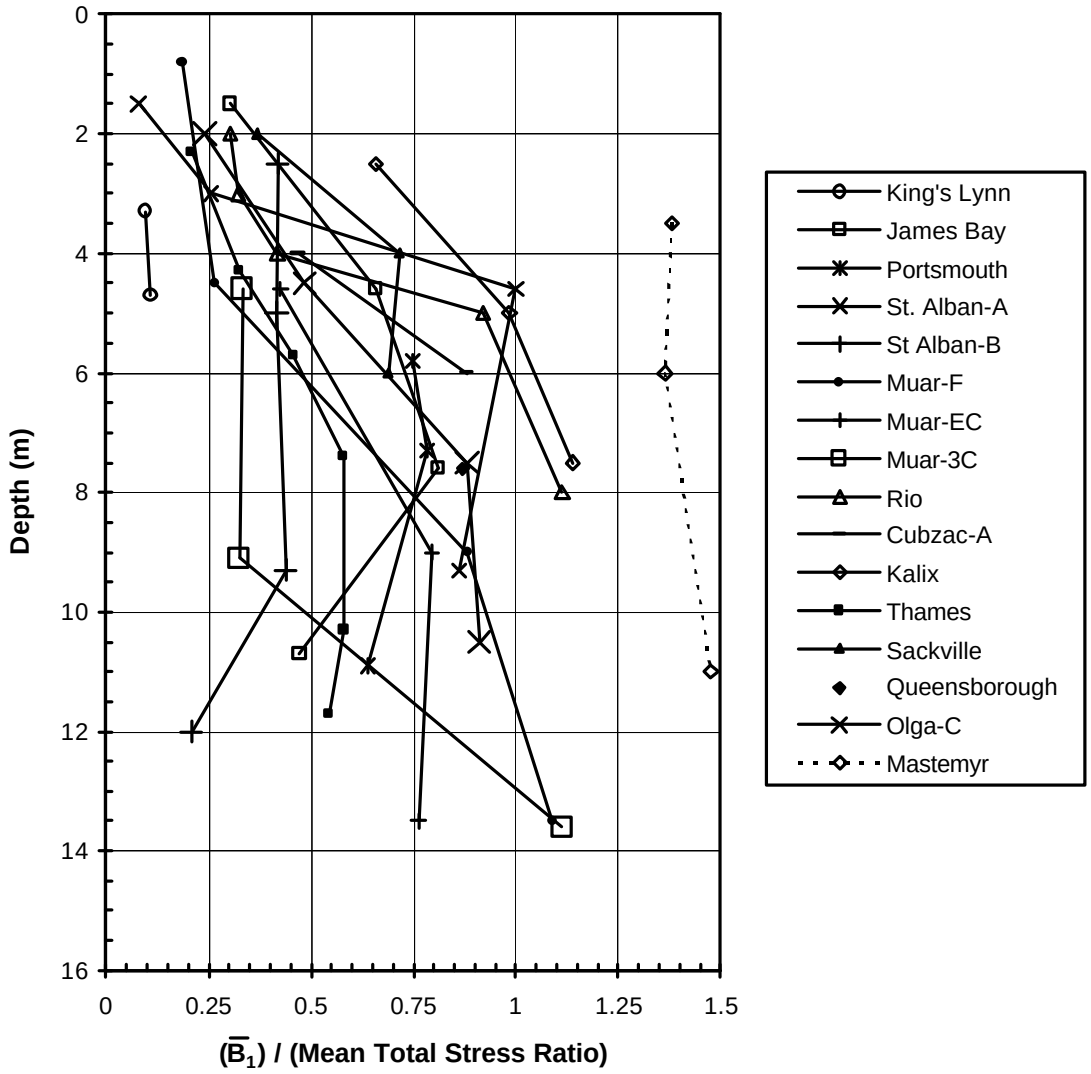

Figure C1.2: Field profiles of the rate of pore water pressure development during the initial stages of construction.

In the case of the Mastemyr test embankment (leached marine deposit of very soft, quick, low plasticity clay) the observed field pore water pressure response stands out as having a very high rate of pore water pressure generation during the initial stages of construction, greater than that estimated assuming undrained conditions. It is not certain of why this behaviour is observed at Mastemyr or why the rate of pore water pressure generation is much greater than at the other test embankment sites. It may possibly be related to a very low permeability of the structured foundation or to its

stress-strain relationship. Leroueil et al (1978b) could not establish the reasons for the pore water pressure response at this site.

The observation of a pore water pressure response greater than the estimate for undrained conditions is likely to be associated with the assumption of the foundation as a half space and that the foundation behaves elastically prior to yielding for the undrained case considered.

2.0 CASE STUDIES OF POST CONSTRUCTION DEFORMATION BEHAVIOUR

2.1 MUAR TEST EMBANKMENTS

The Malaysian Highway Authority (MHA) undertook a major study of embankment construction on soft Malaysian marine clays. The study comprised the construction of 13 well-monitored embankments for assessment of different methods of ground improvement (MHA 1989a) and one embankment constructed to failure (Brand and Premchitt 1989). Three of the embankments have been studied in detail as part of this research project, they are briefly summarised as follows:

- Muar-F – the test embankment constructed to failure (Brand and Premchitt 1989). The fill height at failure was 5.4 m.
- Muar-EC – Scheme 6/1 (MHA 1989a) comprising chemical injection of the foundation to 7.6 m depth prior to embankment construction. The embankment failed at a fill height of 4.68 m.
- Muar-3C – 3 m high control embankment on an untreated foundation. The embankment was constructed to a height of 3.9 m, and no failure occurred.

All three embankments were constructed with slopes of 2H to 1V (horizontal to vertical), but with crest widths ranging from 20 m to 34 m. Highly plastic residual granite was used in all cases as the embankment material. It was placed in thin layers and well compacted using rollers. One noted variation was that the embankment filling for Muar-F appears to have been compacted slightly dry of optimum moisture content compared to slightly wet of optimum for the Muar-EC and Muar-3C embankments. Compacting on the dry side of optimum would be expected to result in a lower compressibility and higher undrained strength of the fill.

The rate of filling also varied between the case studies analysed. Muar-F was filled at a steady rate of 0.054 m/day over a period of 100 days. Muar-3C and Muar-EC were constructed in multiple stages ranging from 0.2 m to 1.8 m stage heights with rest periods of 10 to 100 days between construction periods, with a total construction time of 290 and 270 days respectively. The overall average rate of construction of both these embankments was less than 0.02 m/day.

Details of the subsurface conditions and depositional history of the marine clays at Muar are discussed by MHA (1989a). In summary, the upper 17 to 18 m of the subsurface comprises recent marine clay deposits, with the deposition considered to have occurred in two sequences. A lower sequence of very soft silty clay with considerable shells of approximately 9 m thickness deposited about 5000 years B.P. (before present); and an upper sequence of very soft clay, of approximately 8 m thickness, where deposition commenced some 3000 to 4000 years B.P. A discontinuous layer of sandy silty clay separates the upper and lower clay sequences. A weathered crust of approximately 2 m thickness has since developed in the upper clay profile, largely as a result of the drop in sea level.

The geotechnical properties of the subsurface layers are summarised as follows:

- Weathered crust of heavily over-consolidated (OCR maximum of about 10), fissured, high plasticity clay.
- Upper layer of very soft, high plasticity silty clays (undrained shear strength of 10 to 17.5 kPa measured by vane, liquid limit of 65 to 120 % and plastic limit of 26 to 63 %). The clay is lightly over-consolidated (OCR decreasing from 2.0 to 1.3) and has an average liquidity index of 1.3 to 1.5.
- Lower layer of soft, high plasticity silty clay with considerable shells (undrained shear strength of 19 to 30 kPa measured by vane). The clay is lightly over-consolidated (OCR of 1.2 to 1.3) and has an average liquidity index of 1.25 to 1.5.

Remoulded vane tests indicate a remoulded strength ranging from 2 kPa at 2.6 m depth to 7 kPa at 17 m depth for the soft clays, correlating to an average sensitivity index of 4. Estimation of the permeability from laboratory oedometer tests indicates the upper clay layer to be of higher permeability than the lower clay layer, approximately 4×10^{-9} m/s and 10^{-9} m/s respectively.

The deformation behaviour and excess pore water pressure response for the Muar-EC and Muar-3C embankments, both during and post construction, is discussed in the following sub-sections.

2.1.1 Muar-EC Test Embankment

Figure C2.1 is a section of the Muar-EC test embankment showing the position of instrumentation together with the interpreted surface of rupture and subsurface profile.

Indraratna et al (1992) undertook finite element modelling of the Muar-F test embankment. The analysis showed that a zone of high shear stress concentration developed at a depth of 7.5 to 8 m below the slope of the embankment at embankment heights significantly below the reported failure thickness. Figure C2.2 shows the shear stress concentration for a fill height of 4 m (1.4 m less than the failure height of 5.4 m).

The plot of vertical inclination angle profiles for Inclinometer I1 (Figure C2.3), located at the toe of the Muar-EC embankment, clearly shows the development of a localised failure zone at 8 to 9.5 m depth when the embankment height was at 4.68 m. The eventual surface of rupture was located within this localised failure zone, as was Piezometer P2.

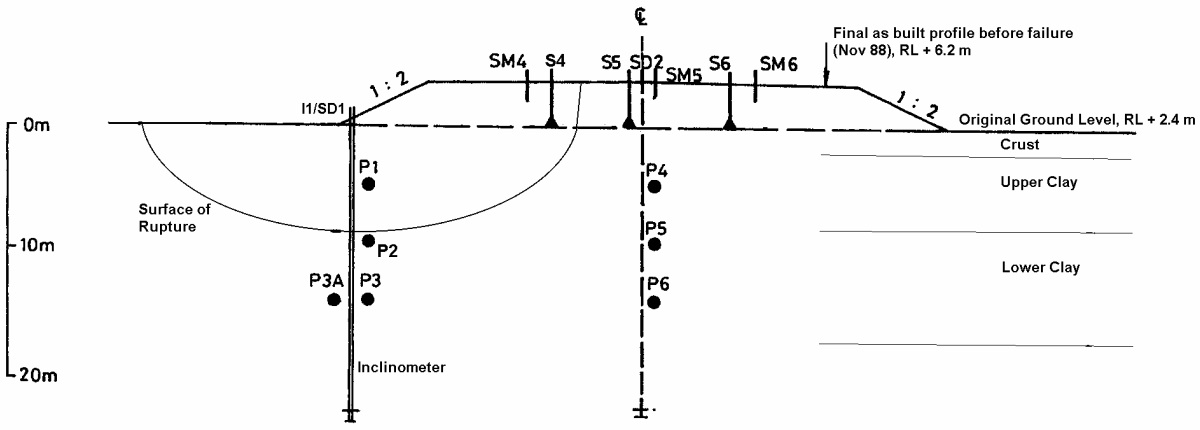

Figure C2.1: Section of the Muar-EC test embankment and interpreted surface of rupture (MHA 1989a)

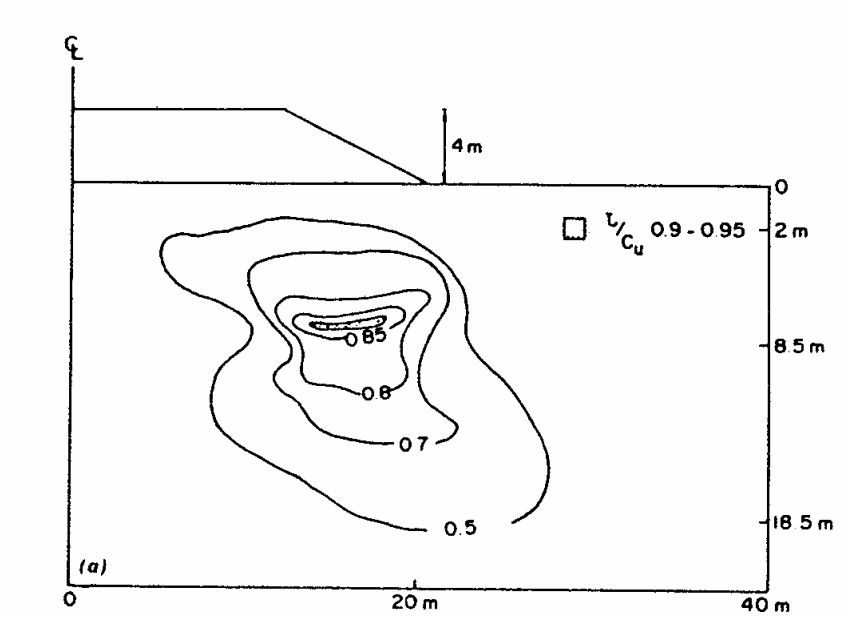

Figure C2.2: Contours of normalised shear-stress ratio at a fill height of 4 m from finite element modelling of the Muar-F test embankment (Indraratna et al 1992)

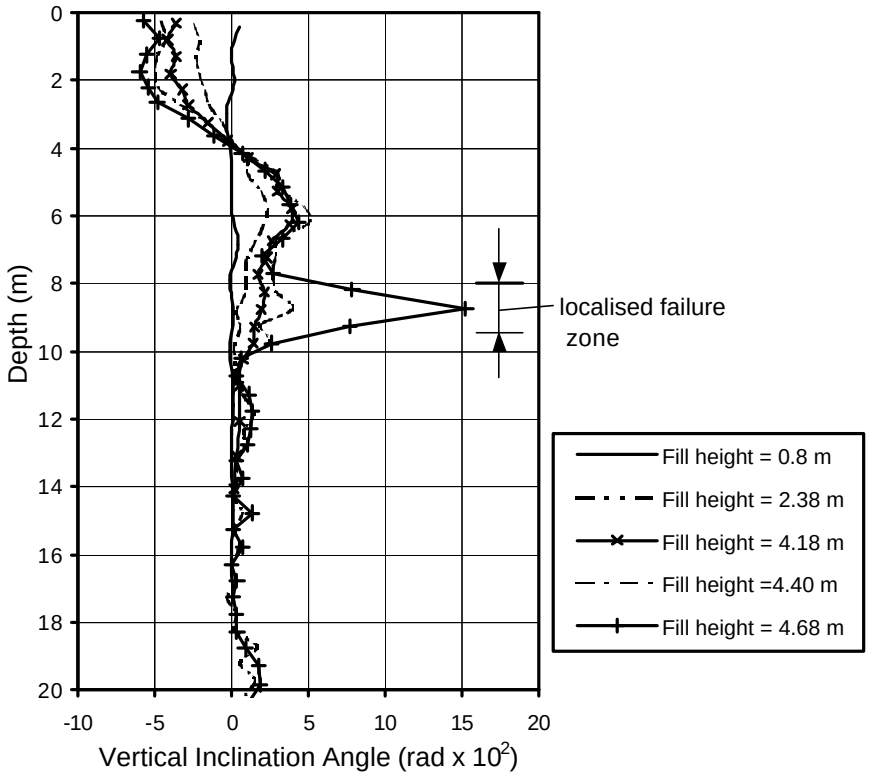

Figure C2.3: Vertical inclination angle profiles with increasing fill height at Inclinometer I1, located at the toe of Muar-EC test embankment.

The excess pore water pressure response with time of Piezometer P2 (Figure C2.4b) shows a significant increase in excess pore water pressure after the end of construction

(Day 269) leading up to the eventual failure condition at Day 300, some 30 days after completion of construction. The response is significantly different to that of the other piezometers under the centre of the embankment and also at 5.3 m and 14.3 m depth below the toe of the embankment, which remain relatively steady in comparison over the same time period. It is considered that the pore water pressure response at P2 is associated with shear induced pore water pressures within the localized failure zone leading up to the embankment failure.

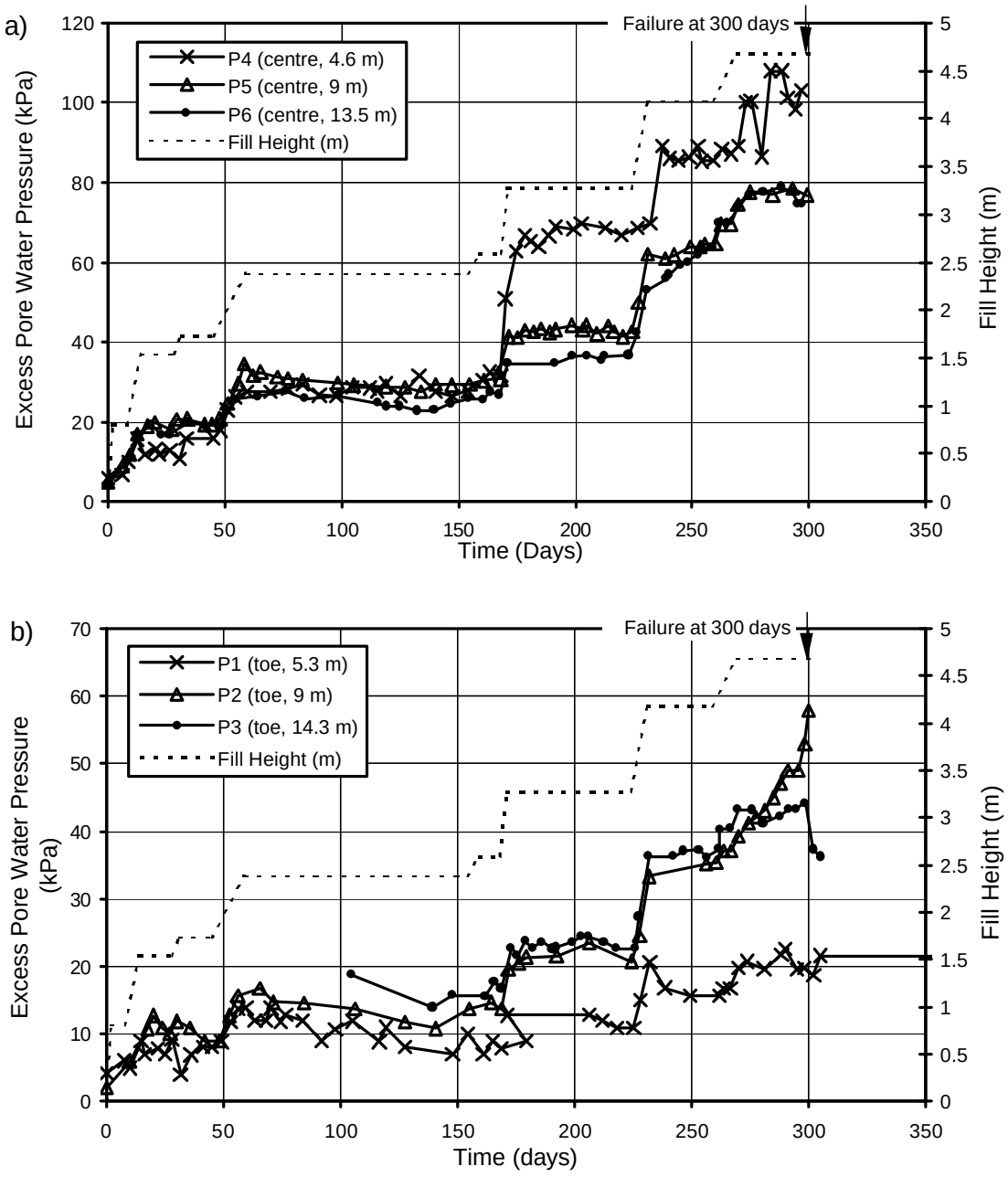

Figure C2.4: Muar-EC, excess pore water pressure response with time for piezometers *(a)* under the centre of the embankment, and *(b)* under the toe of the embankment.

Comparison of the settlement behaviour at Point S4 (within the embankment failure zone) with Point S5 (outside the failure zone) in Figure C2.5 shows the increasing settlement at S4 above that of S5 starting from fill heights greater than about 4.2 m (0.48 m below the failure height) and particularly evident after the end of construction. The maximum lateral displacement in Inclinometer I1 at the embankment toe continued to increase at a relatively steady rate from the end of construction up to the embankment failure (Figure C2.5). It is considered that the lateral displacement at the end of construction is predominantly associated with plastic deformation within the localised failure zone between 8 and 9.5 m depth and is reflected in the increasing settlement observed at S4 above that observed at S5.

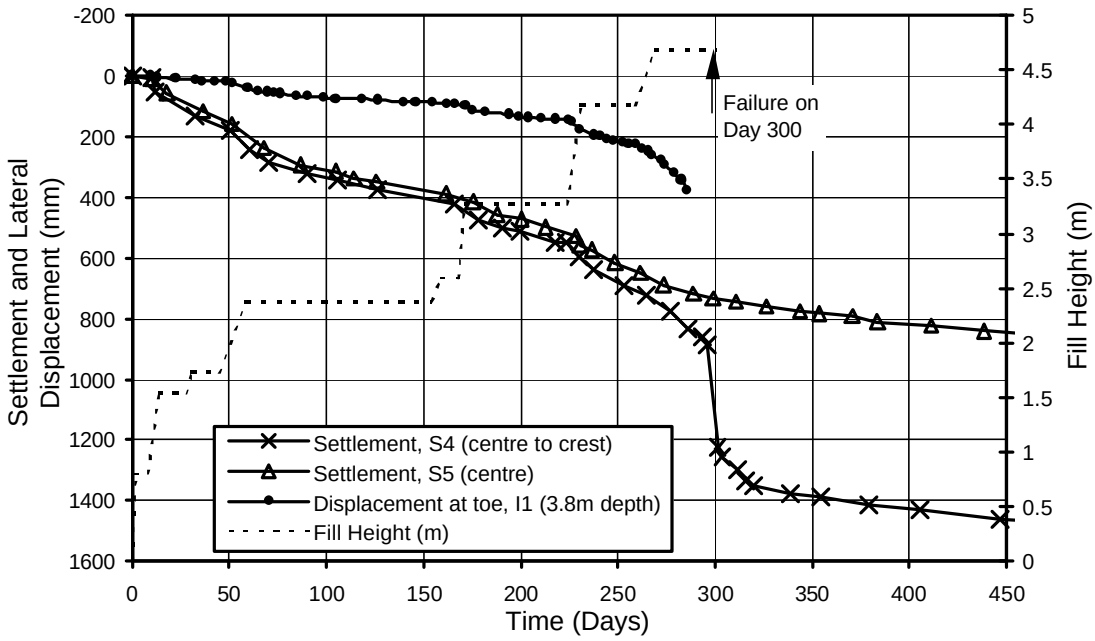

Figure C2.5: Muar-EC, settlement and maximum lateral displacement with time.

2.1.2 Muar-3C Test Embankment

Figure C2.6 is a section of the Muar-3C test embankment showing the position of instrumentation and the interpreted subsurface profile.

The excess pore water pressure response of Piezometer P2, located at 9 m depth below the embankment toe, continues to increase for a period of 110 to 120 days after the end of construction (Figure C2.7). Piezometer P5, located at 9 m depth below the centre of the embankment, shows a similar increase, albeit to a lesser extent, whilst the remainder of the piezometers are relatively steady. It is considered that the increasing

pore water pressure is associated with the relatively high level of shear stress in the vicinity of Piezometer P2.

The rise in excess pore water pressure in Piezometer P2 at Muar-3C is at an average of 0.065 kPa/day for 120 days (Day 290 to 410). In comparison, the rise in excess pore water pressure in Piezometer 2 at the Muar-EC embankment was on average 0.62 kPa/day for the 30 days leading up to the failure, a magnitude of 10 times greater than at Muar-3C.

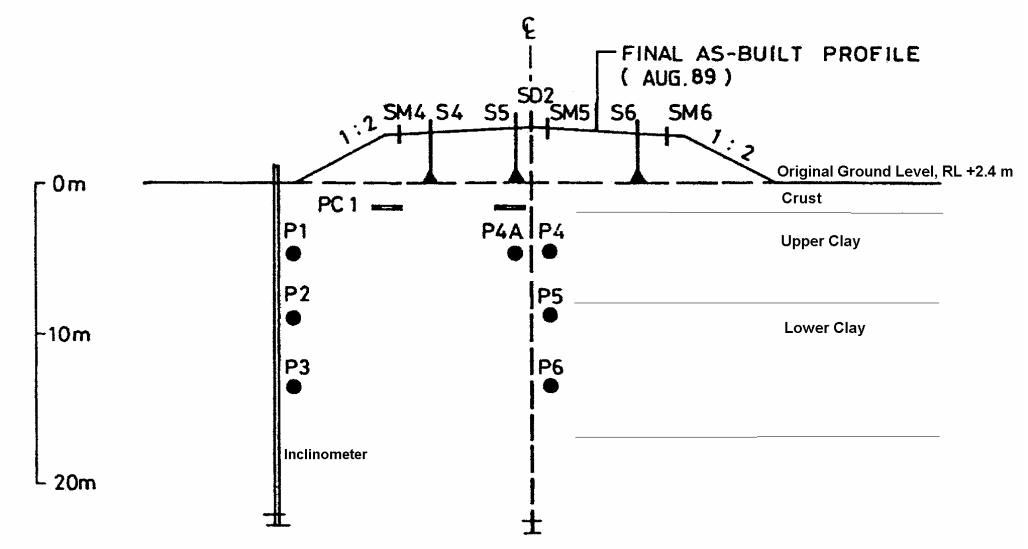

Figure C2.6: Section of the Muar-3C test embankment (MHA 1989b)

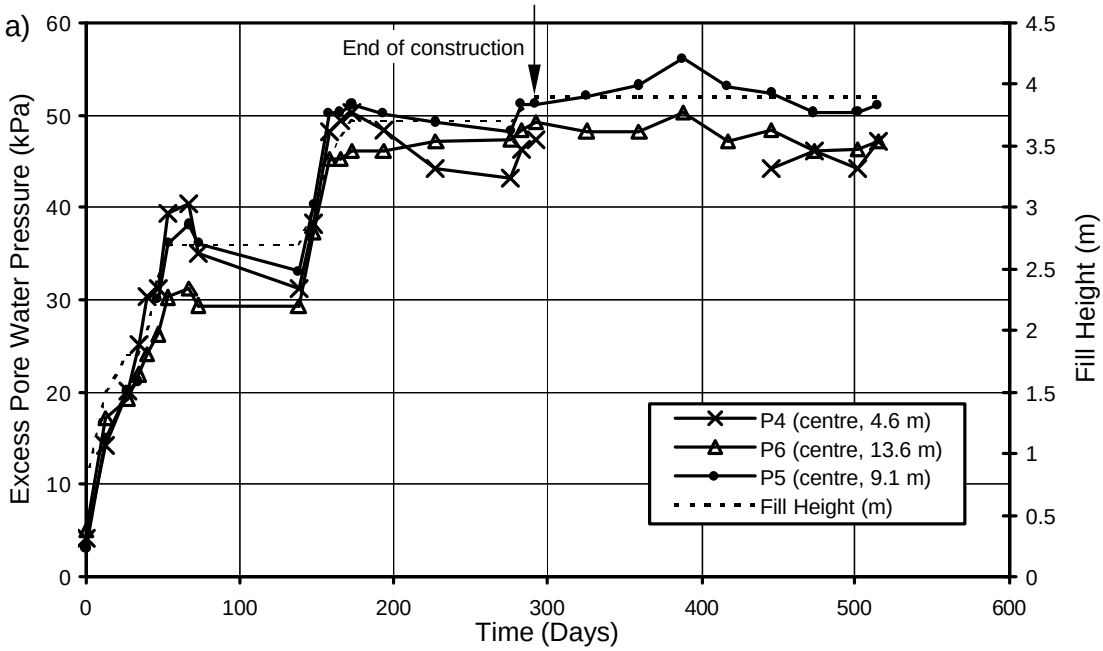

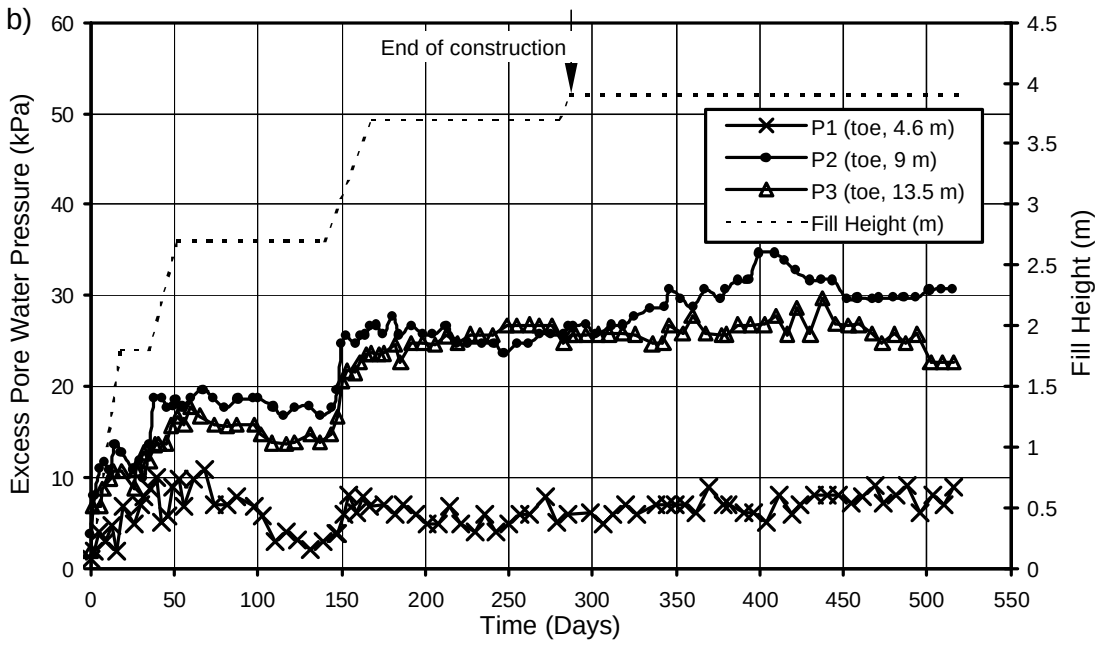

Figure C2.7: Muar-3C, excess pore water pressure response with time for piezometers *(a)* under the centre of the embankment, and *(b)* under the toe of the embankment.

The plot of vertical inclination angle of Inclinometer I1 at the toe of the Muar-3C embankment (Figure C2.8) compared with the Muar-EC embankment (Figure C2.3) indicates that a localised failure condition has not been reached at depth under the toe of the embankment at Muar-3C. It is concluded therefore, that the post construction increase in excess pore water pressure at the Muar-3C embankment is due to yielding of the normally consolidated soft clays and the strain rate dependent reduction in the limit state surface (refer to the discussion in Section 4.4.2 of Chapter 4 and further discussion below).

With respect to the deformation behaviour of Muar-3C it is observed that:

- Large settlements (Figure C2.9) occur during periods of steady or increasing excess pore water pressures under the centreline of the embankment.
- A reduction in the rate of lateral displacement (Figure C2.10) after construction occurs at about Day 420, and is coincident with the time that excess pore water pressures started to decrease in Piezometer P2.

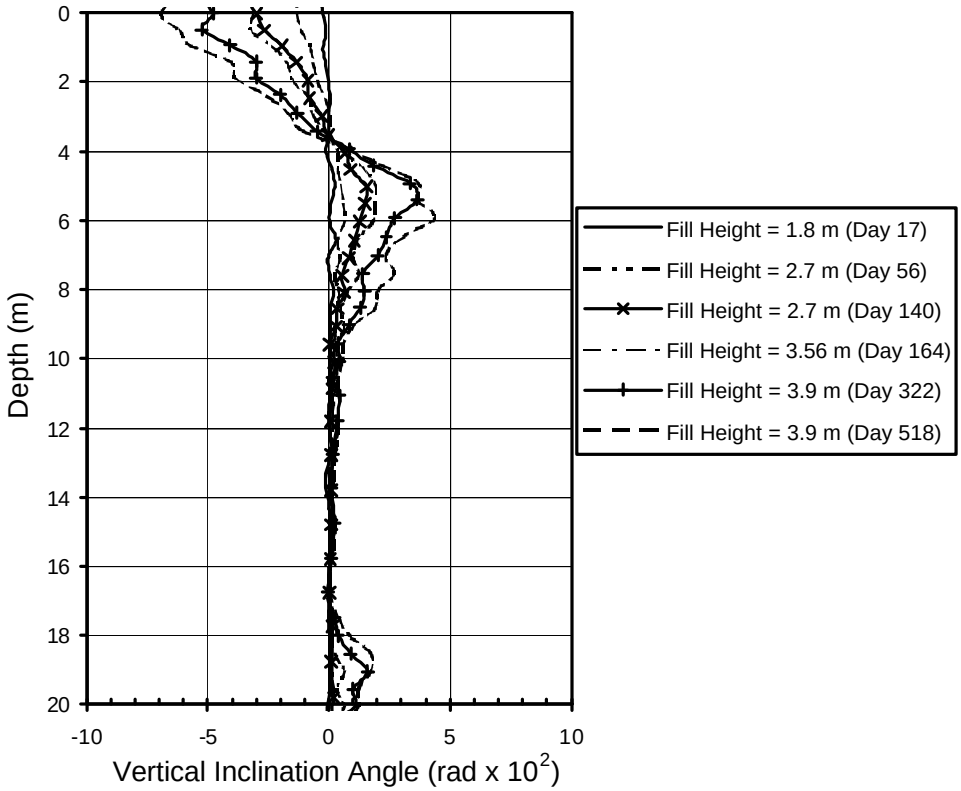

Figure C2.8: Vertical inclination angle profiles with increasing fill height at Inclinometer I1, located at the toe of Muar-3C test embankment.

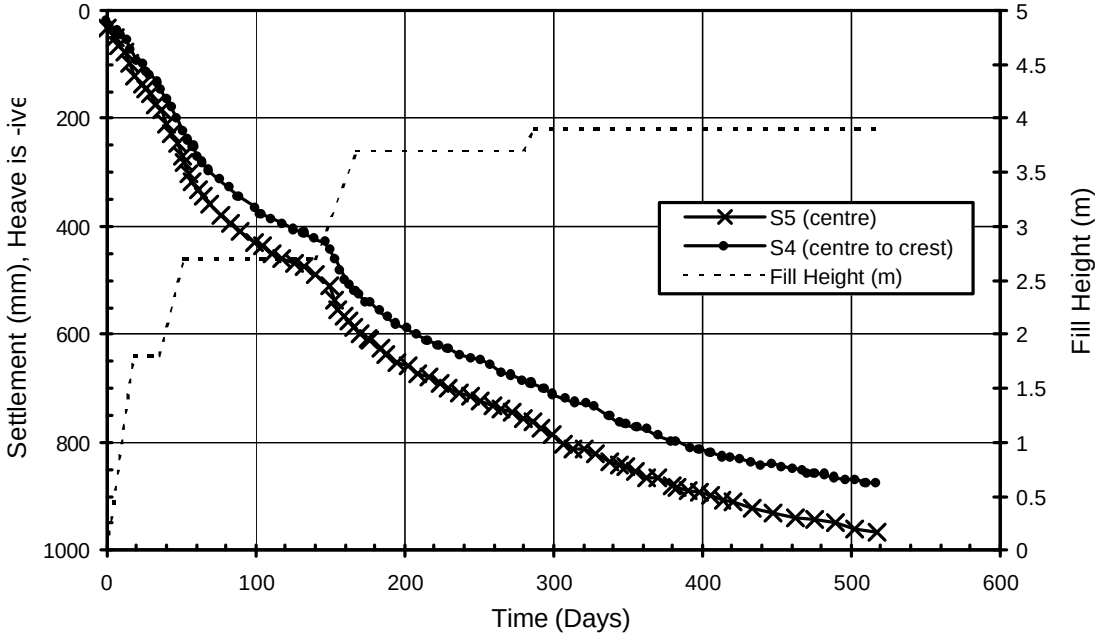

Figure C2.9: Muar-3C, settlement with time under the embankment.

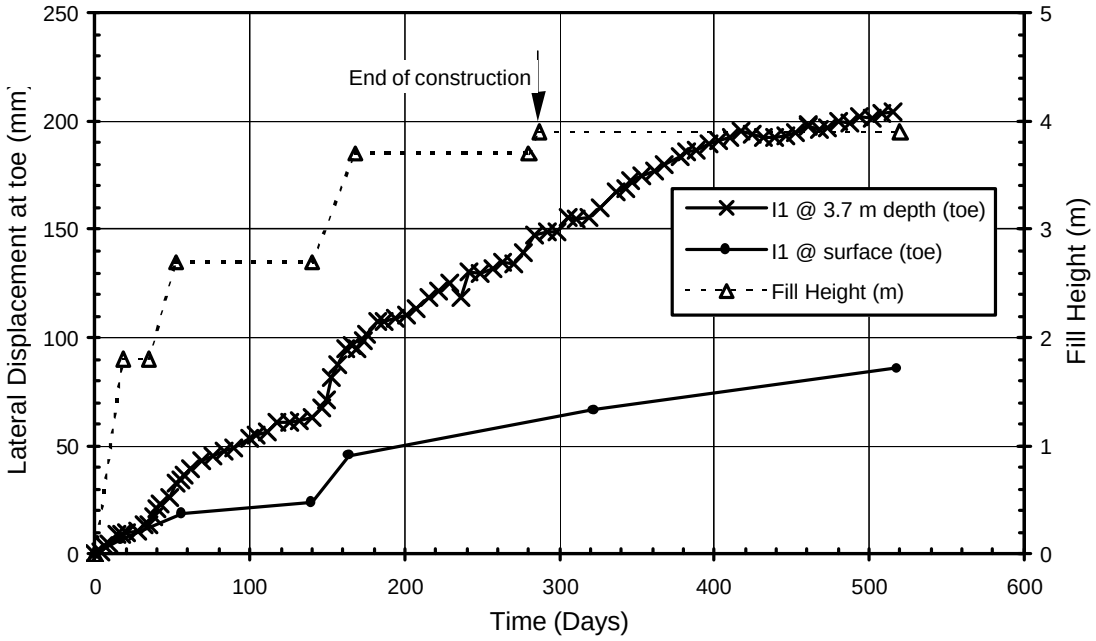

Figure C2.10: Muar-3C, lateral displacement at the toe of the embankment with time.

It is concluded that the pore water pressure response and deformation behaviour indicate that the processes of consolidation and undrained creep (as a result of the strain rate dependence of the limit state surface) are occurring concurrently. Consolidation alone would result in deformations in the soft clay foundation as pore water pressures dissipate. However, the observations of the excess pore water pressure response (Figure C2.7) indicate that the pore water pressure is either relatively steady or else increases over most of the post construction monitoring period (Day 290 to 520), during which period large settlements are measured.

It is considered that the pore water pressure response is due to the strain rate dependency of the limit state surface (refer Section 4.4.2 of Chapter 4). As the limit state surface contracts (assuming for the moment it is not expanding due to pore water dissipation), the effective stress state of the normally consolidated soil on the yield surface must also contract resulting in the increase in pore water pressure. It is in effect an undrained "creep" response.

2.2 OLGA-C TEST EMBANKMENT

The Olga-C test embankment (Figure C2.11) was constructed in 1990 at the NBR Complex site at Matagami, Quebec, Canada. The purpose of the Olga-C test embankment was to assess the performance of wick drains.

The embankment was divided into four sections, three with various wick drain configurations in the foundation and one with no wick drains. The section without wick drains, Section A of the Olga-C test embankment, has been analysed as part of this research.

In the early 1970s the test embankment Olga-A was constructed to failure (located very close to the Olga-C site). The failure occurred at an embankment height of about half that predicted based on a shear strength profile determined from field vane testing.

The subsurface conditions at the Olga C test site (Lavallée et al 1992) comprise varved clay deposits to 13.5 m to 15.3 m depth overlying dense sandy and silty moraine. The varved clay profile comprises a 2 m thick fissured crust overlying soft, high plasticity clays to 10 m depth. Below 10 m depth the clay is of firm to stiff strength consistency (undrained shear strength of 30 to 50 kPa) and the varves are thicker, sandier and siltier. Below the heavily over-consolidated crust the over-consolidation ratio (OCR) decreases from about 12 at 2 m depth to 4 at 4 m depth to less than 2.4 below 8 m depth.

The constructed embankment is of 6 m maximum height with very flat slopes (Figure C2.11). It was constructed in approximately 40 days (Day - 40 to Day 0 in Figure C2.12).

The excess pore water pressure response with time of the piezometers under the centreline, upper slope and mid berm are shown in Figure C2.12.

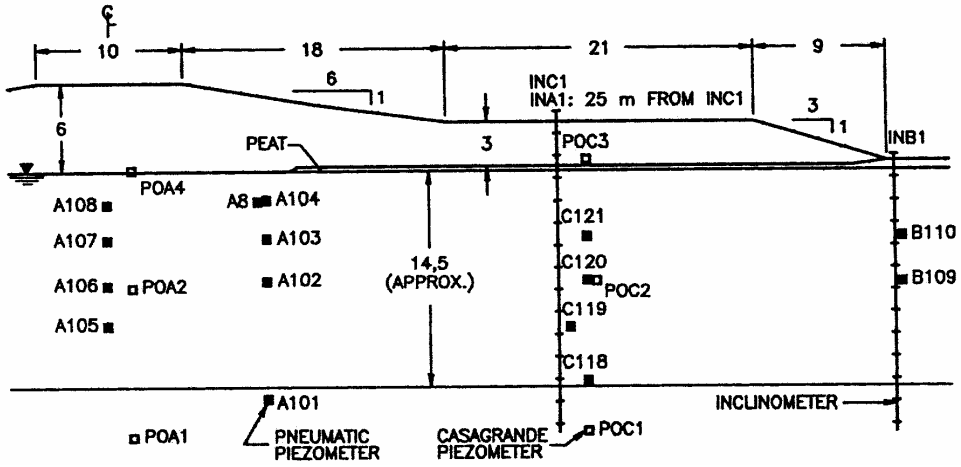

Figure C2.11: Section A of the Olga-C test embankment with no wick drains (Lavallée et al 1992).

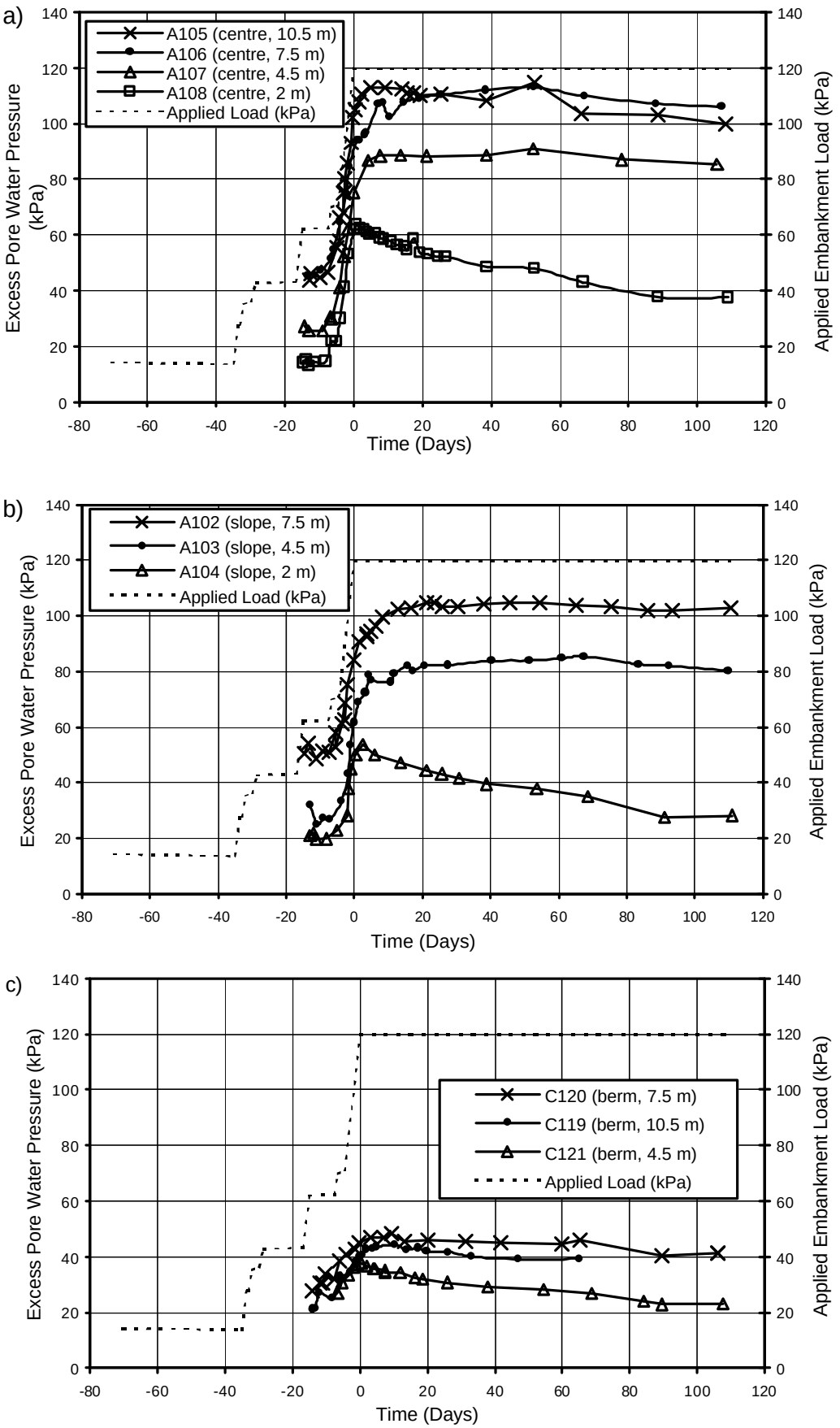

Figure C2.12: Olga-C, excess pore water pressure response with time at Section A *(a)* below the centre line, *(b)* below the upper slope and *(c)* below the berm.

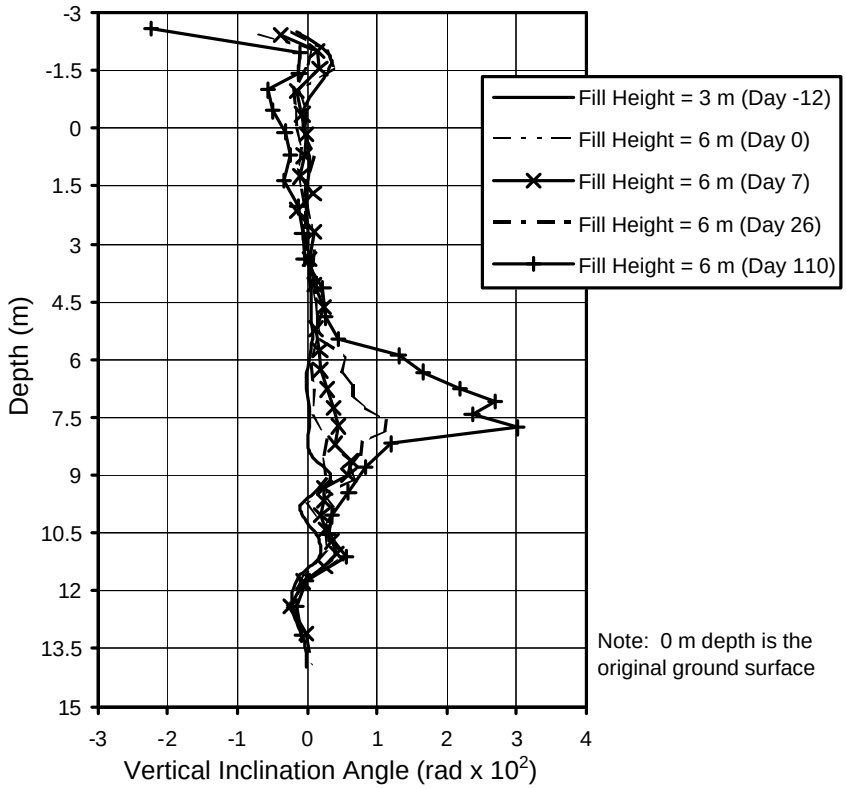

Figure C2.13: Olga-C, vertical inclination angle profiles at various times at Inclinometer INC1, located at about mid berm, at Section A.

Figure C2.13 presents the plot of vertical inclination angle for Inclinometer INC1 positioned at about mid berm (Figure C2.11). It shows the development of what is considerer to be yielding between 5.5 m and 11.5 m depth and possibly the development of localised failure between 6 m and 8.5 m depth.

In the context of this observation, the excess pore water pressure response of the piezometers after the end of construction (at Day 0) is considered to represent:

- Rapid dissipation of excess pore water pressure immediately below the crust (Piezometers A104 and A108) and at 4.5 m depth under the berm (Piezometer C121) of the over-consolidated clay foundation. The dissipation of excess pore water pressures in these piezometers starts shortly after the end of construction at Day 0.
- Piezometers A105 and C119, located in the firm to stiff clays at 10.5 m depth, show a similar response except that the excess pore water pressure increases for about 10 days before decreasing. It is considered that the foundation at this depth is still in an over-consolidated condition.

- The remaining piezometers at depths of 4.5 m and 7.5 m depth under the crest and slope (Piezometers A106, A107, A102 and A103) show a slow increase in excess pore water pressure for 50 to 70 days before decreasing. It is considered that this response represents yielding of the normally consolidated soft clays. The increase in excess pore water pressure is considered to be due to the reduction of the limit state surface (refer Section 4.4.2 of Chapter 4).

Leroueil (1996) report that the vertical strains 300 days after construction were relatively uniform throughout the varved clay, with an average of 6% vertical strain at Section A (5.8% at 7.7 m depth and 8.5% at 10.4 m depth). Leroueil concluded that the post construction settlement behaviour and pore water pressure response at Section A of the Olga-C embankment indicates that the undrained creep and consolidation processes occur simultaneously. In Piezometer A106 (7.5 m depth below the centre) the excess pore water pressure at 300 days after construction was still greater than the pressure on Day 0 at end of construction, yet almost 6% vertical strain has occurred in this region of the foundation.

2.3 QUEENSBOROUGH TEST EMBANKMENT

The Queensborough test embankment (Figure C2.14) is located in North Kent, UK and was constructed in 1976 over soft alluvial soils of the Thames estuary.

The subsurface conditions at the Queensborough test site (Jardine and Hight 1987) consist of a firm, laminated silty clay crust of 0.5 to 2.3 m thickness overlying soft to very soft alluvial silty clays to 8.5 to 10.3 m depth. The soft clays are described as being relatively homogeneous. The OCR ranges from approximately 4 in the crust, to 2.5 below the crust decreasing to 1.1 below 4.5 to 6 m depth. London Clay underlies the soft alluvial clays.

The embankment comprised an initial layer of sand and gravel to act as a drainage medium overlain by chalk filling. The rate of construction was approximately 0.07 m/day. Construction was halted on Day 108 following observation of cracking near the centre of the embankment. The embankment height at this time was a maximum of 2.9 m. Due to concerns over potential failure of the embankment, the fill height was reduced some 150 mm and a toe surcharge was placed in critical areas from about Day 114.

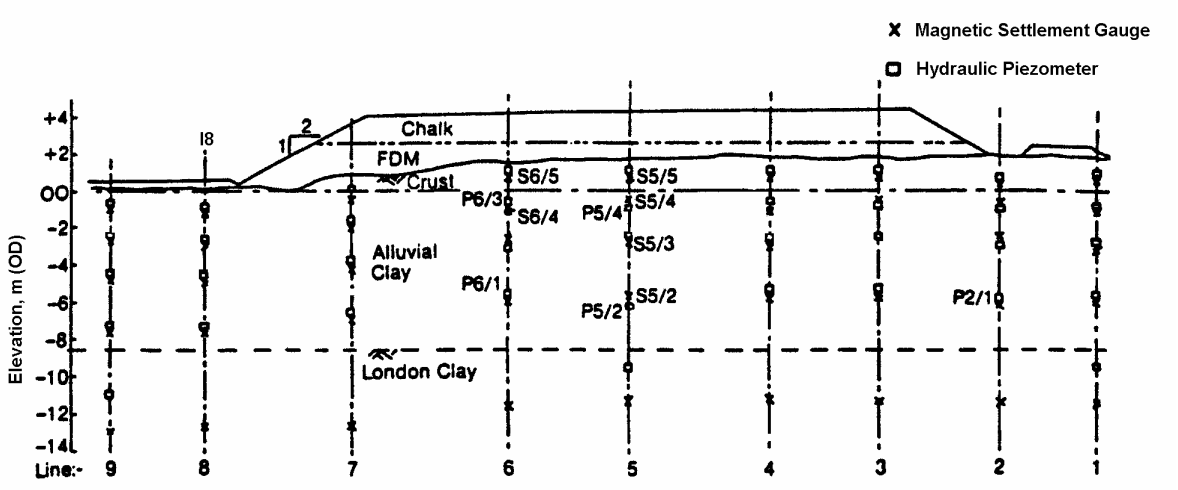

Figure C2.14: Queensborough test embankment, section of test embankment showing instrumentation (Jardine and Hight 1987).

Figure C2.15 presents the excess pore water pressure response (during and post construction) versus time of two piezometers located in lower, very lightly over-consolidated region (OCR approximately 1.1) of the soft clay alluvium. Piezometer P2/1 is located under the toe of the embankment and Piezometer P5/2 is located under the centre of the embankment. Pore water pressures in both these piezometers were observed to rise for the six days following halting of construction (Day 108 to 114). Pore water pressures were observed to decrease after about Day 124.

Figure C2.16 presents the observations of settlement under the centre of the embankment and maximum lateral deflection at the toe of the embankment (from inclinometer I8) during and post construction. It is evident that large lateral displacements at the embankment toe occurred during the later stages of embankment construction and continued after the end of construction. It is considered that these displacements are a result of plastic deformation within a localised failure zone; however, as no records of the inclinometer were published for I8 it was not possible to determine the location of the localised failure zone. A reduction in the rate of lateral displacement was observed after about Day 125, coincident with the time at which the excess pore water pressures started to decrease in Piezometers P2/1 and P5/2 (Figure C2.15).

Jardine and Hight (1987) commented that the ratio of $\Delta y_m / \Delta s = 0.65$ for the first year post construction reducing to about 0.2 thereafter. They considered it to be significantly affected by undrained creep deformations. From Figure C2.16 it is evident that the ratio $\Delta y_m / \Delta s$ post construction is closer to 1 for about the first 40 days after

construction, and by about 90 days after construction (Day 200) had decreased to approximately 0.25.

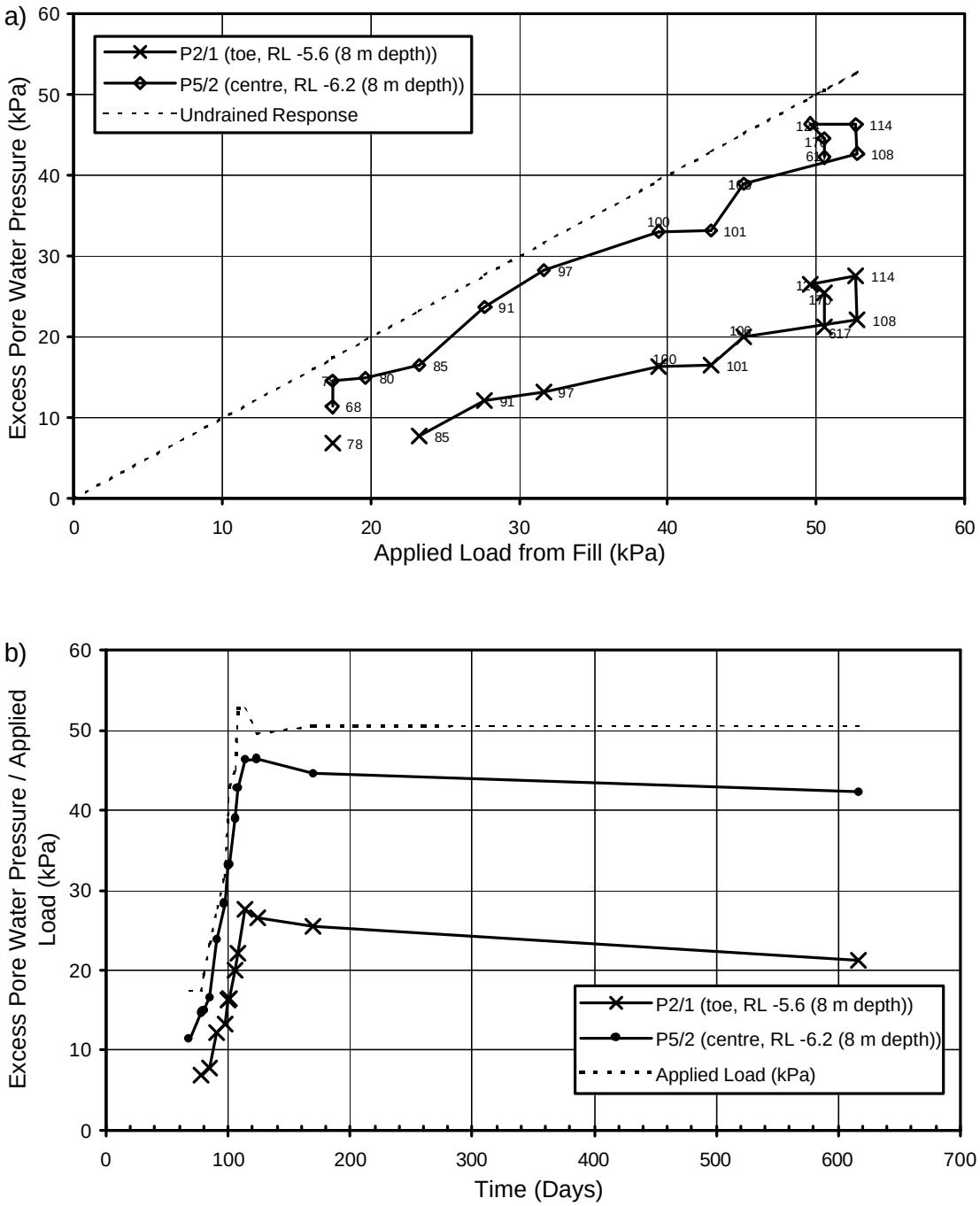

Figure C2.15: Queensborough test embankment, excess pore water pressure response versus *(a)* applied embankment load and *(b)* time.

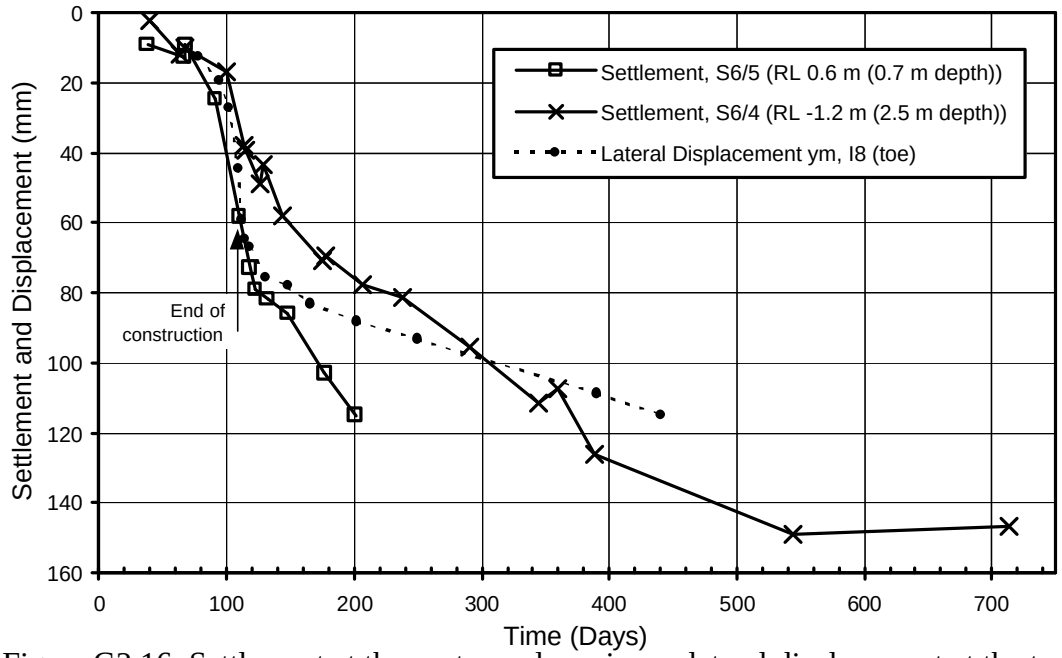

Figure C2.16: Settlement at the centre and maximum lateral displacement at the toe of the Queensborough test embankment.

Several other important observation made by Jardine and Hight (1987) were:

- A yield condition was reached at all depths in the soft clay alluvium below the desiccated crust, with the deeper layers first to yield. From the available information, the threshold height at Piezometer P5/2 was estimated at 0.7 m (equivalent to 14 kPa applied load).
- Settlements during construction were small and were generally concentrated within the upper layers of the soft alluvium.
- The post construction settlements in the lower strata far exceeded those accumulated by pore water pressure dissipation, indicating the significance of plastic deformation in the localised failure zones and undrained creep in the initial post construction period.

3.0 CASE STUDY EXCEPTIONS TO GOOD INDICATORS OF AN IMPENDING FAILURE

This section discusses further those case studies of embankments on soft ground identified in Section 4.3 of Chapter 4 for which:

- The excess pore water pressure response was an exception to the normal trend of most of the failure case studies analysed (refer Table 4.3 of Section 4.3.2).
- Deformation was a poor indicator of an impending failure condition or the change in deformation behaviour had alternative explanations (refer Table 4.4 of Section 4.3.3.6).

3.1 EXCESS PORE WATER PRESSURE RESPONSE

3.1.1 Field Estimation of the Pre-Consolidation Pressure

Piezometer A3 at James Bay (Dounias and Tournier 1975) was identified as an exception with respect to the large difference between the effective critical stress, $s'_{1,crit}$, estimated from the field pore water pressure response and the pre-consolidation pressure estimated by laboratory oedometer testing, s'_p (Table 4.2 of Section 4.3.2 of Chapter 4). The effective critical stress was significantly lower than s'_p.

A similar pattern of behaviour between the effective critical stress and pre-consolidation pressure was observed for Piezometers A1 and A2 (at shallower depth) at this site. At greater depth, Piezometer A4 (10.7 m depth), the effective critical stress was within 1% of the pre-consolidation pressure.

Leroueil et al (1978a) considered that the observation was related to the effective stress path for heavily over-consolidation soils (OCR > 2.5), which intersects the limit state surface at less than the pre-consolidation pressure (Figure C3.1); i.e. at Point P_1. Therefore, for heavily over-consolidated soils the effective critical stress, $s'_{1,crit}$, estimated from the field pore water pressure response would under-estimate the pre-consolidation pressure, P_C, as shown in Figure C3.1.

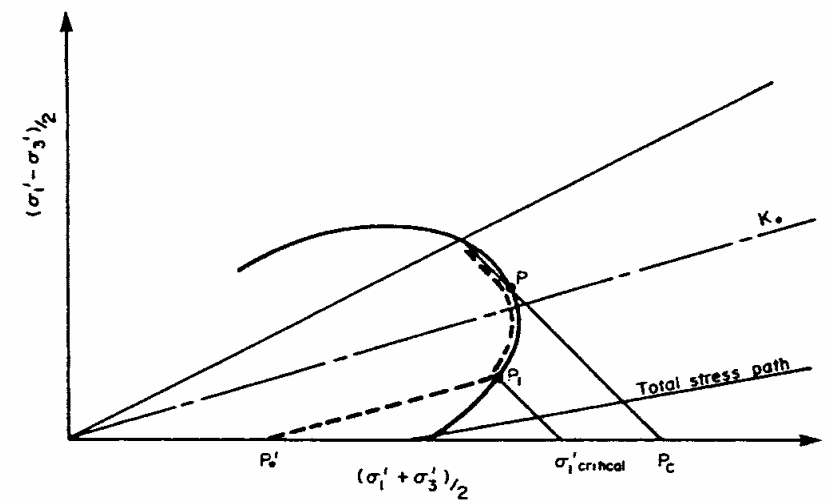

Figure C3.1: Interpretation of effective stress path for heavily over-consolidated clays under embankments (Leroueil et al 1978a)

3.1.2 Excess Pore Water Pressure Response for Normally Consolidated Conditions

For the piezometric response during normally consolidated conditions ($\overline{B}_2$), the analysed case studies indicate that in most cases the excess pore water pressure observations maintain a $\overline{B}_2 \approx 1$ up to the failure height (Table 4.2 in Section 4.3.2 of Chapter 4). Four case studies exhibit excess pore water pressure observations other than $\overline{B}_2 \approx 1$; Kalix, Mastemyr, Muar-EC and Cubzac-A.

For Mastemyr (foundation of very soft, quick, leached marine clay deposit) the initial excess pore water pressure response (Figure 4.21a in Section 4.3.2 of Chapter 4) indicates a $\overline{B}_1$ value of 1.0 reducing to 0.5 up to about 17 kPa applied load. At greater than about 28 kPa applied load, the $\Delta\overline{B}$ response in P1 is then significantly greater than 1. This response is similar for piezometers down to 6 m depth at this site.

Leroueil et al (1978a) consider that the initial effective stress path to be similar to path OYE_c in Figure C3.2a, where it intersects with the limit state surface above the critical state line. They comment that of the 30 case studies they analysed this was the only case for which this behaviour was observed, indicating its unusual occurrence. Leroueil et al could not establish the reasons for this.

The reason that the effective stress path follows this path may possibly be due to the very low permeability of the foundation.

The consistent pore water pressure response of $\Delta\overline{B} > 1$ for all piezometers under the embankment centreline in the upper 6 m depth at applied embankment loads greater

than 28 kPa may be indicative of undrained strain weakening due to partial breakdown of the soil structure throughout at least the upper 6 m of the very soft clay deposit.

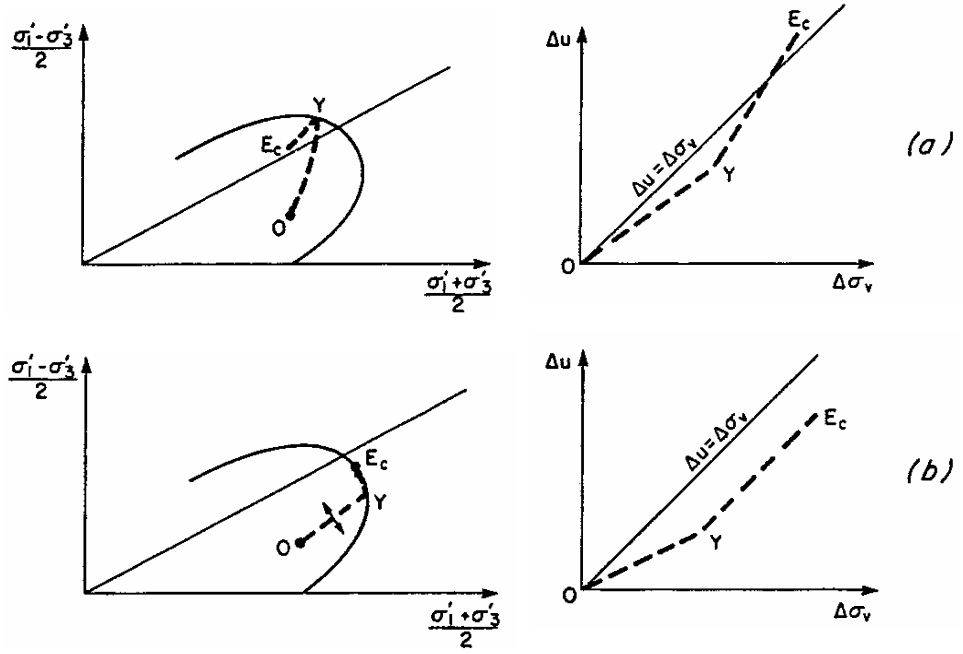

E_c = end of construction

Figure C3.2: Effective stress paths and pore water pressure generation associated with different types of yield conditions (Leroueil and Tavenas 1986).

The piezometers under the embankment centreline at Kalix (foundation of soft to very soft, moderately sensitive, highly plastic, marine deposit of silt/organic clay) showed a similar response to that at Mastemyr for a depth range from the below the crust to a depth of at least 7.5 m. This response may also indicate strain weakening due to partial breakdown of the soil structure over this depth range.

In the case of Mastemyr and Kalix it is considered that the effective stress path is similar to that shown in Figure C3.2a (path OYE_c) where the effective stress path intersects the limit state surface above the critical state line. On reaching the limit state surface (Point *Y*) a localised failure condition is reached and with further increase in applied load, strain weakening occurs resulting in the observation of excess pore water pressures exceeding the increase in total vertical stress (i.e. $D\overline{B}$ greater than 1).

For both Mastemyr and Kalix the excess pore water pressure response equivalent to $\Delta\overline{B}$ greater than 1 was observed in a number of piezometer and is considered to be indicative of a partial breakdown over a significant portion of the foundation. What is not clear is why a general failure did not occur once a significant portion of the

foundation had reached a failure condition. In the case of the Kalix embankment the foundation comprised a highly plastic sensitive clay, and what influence this may have had is uncertain

For the Muar-EC embankment, the excess pore water pressure response of Piezometer P4 (Figure 4.21b in Section 4.3.2 of Chapter 4) was the only piezometer for this case study having a $\overline{B}_2 > 1$. The response of other piezometers under the centre of the embankment, once normally consolidated conditions have been reached, maintain a $\Delta\overline{B}$ value of close to 1. It is uncertain what has caused this observed behaviour at Piezometer P4.

For the Cubzac-A embankment, the observed $\Delta\overline{B}$ response for Piezometer P112 located at 4 m depth under the embankment centreline (Figure 4.21a in Section 4.3.2 of Chapter 4), is greater than 1 above an applied embankment load of 52 kPa. A similar response was measured in the underlying piezometer at 6 m depth. It is uncertain what has caused this observation. It is possible that the response is due to time effects (discussed in Section 4.4.2 of Chapter 4) or else is due to general strain weakening throughout the depth of the soft to very soft, highly plastic clay deposit.

3.2 PRE-FAILURE DEFORMATION RESPONSE

3.2.1 Rio Case Study

For the Rio test embankment (foundation of high plasticity clays of low sensitivity), the vertical displacement at and beyond the toe of the embankment and lateral surface displacement at the embankment toe are considered as reasonable to good indicators of an impending failure condition. However, the abrupt changes in deformation behaviour that occur at a relative embankment height of 89% of the failure height are coincident with the observation of cracking in the embankment. Therefore, the changes in deformation behaviour are not explainable only by being close to the failure height as the cracking of the embankment is considered to have had an effect on the increased rates of displacement observed due to changes in the effective stress conditions in the foundation. It could also be said that the lateral displacement probably caused the cracking.

The lateral displacement (at depth) at the embankment toe, from the inclinometer observations, was considered as a poor indicator of an impending failure for the Rio test

embankment. The plots of vertical inclination angle from the inclinometer did not indicate development of the localised failure zone until the embankment had cracked at an embankment height of 89% of the failure height.

It is not certain why the inclinometer did not indicate the development of the localised failure zone prior to failure. A possible reason is that it was not until the embankment cracked at 2.5 m height that the stresses within the foundation were such that a localised failure condition was reached under the shoulder of the embankment and large plastic deformations occurred. In addition, the soft clay may be typical of a classical ductile clay that is not strain weakening on shearing, however, greater straining in the more highly stressed regions under the embankment slope should still have been evident. Another possible influence is considered to be the influence of the two small embankments constructed at the toe main embankment on the stress conditions within the foundation. The purpose of these small embankments, constructed only 20 m apart, was to contain the failure within the monitored portion of the site.

3.2.2 Kalix Case Study

For the Kalix embankment (foundation of highly plastic, sensitive clays and silts) all indicators provided a reasonable to good indication of the impending failure condition (the vertical deformation at and beyond the embankment toe, and the lateral surface and at depth displacement at the embankment toe). However, the deformation behaviour is not explainable only by being close to the failure height.

A significant change in the deformation behaviour occurred at embankment heights of 70 to 90% of the failure height, and this was coincident with the threshold fill height (heave movements at the embankment toe, large increase in the rate of lateral displacement at the embankment toe, both at the surface and at depth were measured). Whilst the abrupt change is considered a good indicator, it is also explainable by deformation changes associated with reaching the threshold fill height.

As discussed in Section 3.1.2 (of Appendix C), it was considered that the effective stress path for Kalix might have intersected the limit state surface above the critical state line resulting in the abrupt change in $\Delta\overline{B}$ from 0.4 to 1.7. As a consequence, strain weakening due to partial breakdown of the soil structure may have occurred over a significant depth of the upper soft to very soft clay. The change in deformation

behaviour at the embankment toe is generally coincident with this change in pore water pressure response.

3.2.3 King's Lynn Case Study

At the King's Lynn embankment (foundation of soft to very soft, high plasticity marine deposit of low sensitivity), an impending failure condition is not clearly identifiable from the plot of lateral surface displacement at the embankment toe versus relative embankment height (Figure 4.25 in Section 4.3.3.3 of Chapter 4). However, the observations of lateral surface displacement at the toe and cracking of the embankment did provide an indication of the impending failure.

On the morning of the day prior to failure, fine longitudinal cracks were observed on the crest of the embankment (at a relative height of 92% of the eventual failure height) and 10 mm of lateral displacement was recorded overnight. An additional fill lift of 0.55 m thickness was then placed during which time 14 mm of lateral surface displacement was recorded at the toe. In the next 6 to 8 hours of that day a further 45 mm (or 55% of the total lateral surface displacement recorded to completion of fill placement) was recorded, providing a clear indication of the impending failure. Failure occurred at about 8 am the next morning.

The plot of incremental vertical inclination angle (from the inclinometer at the toe of the embankment), Figure 4.26b in Section 4.3.3.4 of Chapter 4, clearly shows the development of the localised failure zone once the embankment had been constructed to its eventual failure height of 6.7 m.

4.0 POST-FAILURE DEFORMATION ANALYSIS

The Khalili et al (1996) method for estimating the post-failure deformation of an intact slide requires the surface of rupture to be known and knowledge of the strength properties at and post failure. For each of the case studies analysed, limit equilibrium analysis was undertaken to calculate a factor of safety of 1 for the initial failure and for the modelled surface of rupture to be a good representation of the actual (refer Section 4.3.4 of Chapter 4 for further details on the modelling). The limit equilibrium analysis was then re-run using the modelled surface of rupture, but with residual strength parameters, to calculate the residual factor of safety, $FS_{residual}$.

In all four cases, use of the remoulded vane strengths resulted in very low residual factors of safety and post-failure movement predictions significantly greater than the observed movement. On evaluation, it was evident that the remoulded vane strengths indicated that the amount of strain weakening to residual strength was much greater than that measured in undrained triaxial tests. Therefore, estimates of the residual strength using the vane were considered to under estimate the actual values.

In the case of Rio and Muar-F the large strain undrained shear strength was also obtained from an estimate of the drained residual friction angle. The post failure deformation predictions based on the estimates of the residual undrained strength profile from laboratory test results (St. Alban-A) and from the residual friction angle (Rio and Muar-F) were much closer to the observed post-failure deformation behaviour.

Further discussion of each case study analysed is presented in the following sub-sections.

4.1 RIO TEST EMBANKMENT, RIO DE JANIERO

The Rio test embankment was constructed over a high plasticity marine clay (Figure C4.1). Field vane tests indicated the remoulded strength to range from 1.5 to 5 kPa and the clay to be of low sensitivity ($S_I \approx 3$, where S_I = sensitivity). Laboratory undrained triaxial testing indicate the soft clay foundation to be highly ductile with deviatoric stress still increasing at axial strains of 8 to 10%.

A weathered, fissured crust of 2.4 m thickness overlies the soft clay foundation. The embankment was constructed of loosely placed silty sand.

During construction, cracking of the embankment was initially observed at an embankment height of 2.5 m. After raising to 2.8 m the next day, severe cracking was observed but no slip failure (2.8 m was deemed to be the failure height). After several days still no slip failure was observed so the embankment was raised to 3.1 m height, which resulted in additional cracking but still no slip failure. The next day, during placement of the next lift on the embankment, a general slip failure “slowly” occurred. The total crest settlement and heave beyond the embankment toe of the slip was approximately 680 mm.

Adopting the remoulded strength profile from the vane tests and modelling the cracked embankment resulted in a residual factor of safety of 0.43 for the reported surface of rupture (Figure C4.1). This gave a crest settlement of 1.1 m for the slow

model and 2.1 m for the rapid model, both of which are well above the actual crest settlement of 680 mm. It is considered that this is due to the under prediction of the residual strength from the remoulded vane test and is typical of all the embankment cases analysed.

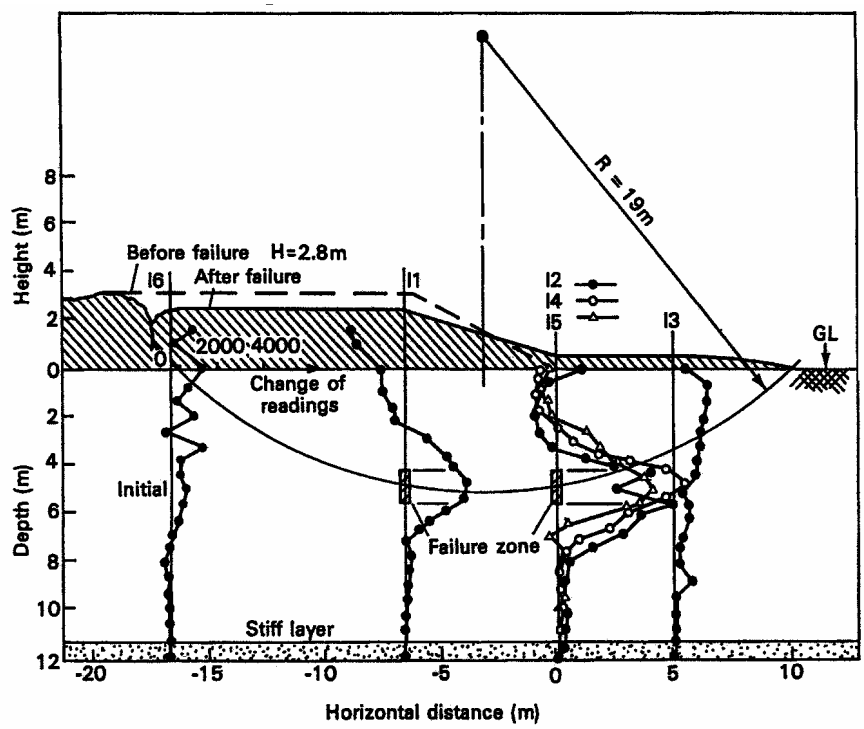

Figure C4.1: Pre and post-failure geometry of Rio test embankment (Ramalho-Ortigao et al 1983b)

The undrained triaxial tests on normally consolidated samples of the soft clay from the Rio site (Almeida 1982) indicate strain-hardening behaviour up to axial strains of 8 to 10%. Therefore, strength reductions to 30% of the peak strength (as indicated from the remoulded vane tests) would appear to be a significant under estimate of the residual strength. A better estimate of the residual strength (S_{ur}) from the laboratory results was considered to be 80% of the peak strength. This was estimated by adopting a residual friction angle (f'_r) of 12 degrees, based on the clay fines content and plasticity of the soft clay (Fell et al 1992), and estimating the undrained strength profile from Equation C4.1 (Equation 4.8 in Section 4.3.5.2 of Chapter 4).

$$S_{ur} = s'_p \tan f'_r \qquad \text{(C4.1)}$$

where s'_p is the pre-consolidation pressure of the soft clay, f'_r the drained residual friction angle and S_{ur} the residual undrained strength.

The residual factor of safety adopting the residual strength profile calculated from Equation C4.1 was 0.70. This resulted in a crest settlement of 590 mm for the slow model and 1140 mm for the rapid model, much closer to the observed crest settlement of 680 mm.

4.2 MUAR-F TEST EMBANKMENT, MALAYSIA

The Muar-F test embankment was constructed over a soft, high plasticity marine clay foundation (Figure C4.2). A weathered crust of 2 m thickness overlies the soft clay foundation and the embankment was constructed of compacted, highly plastic decomposed granite.

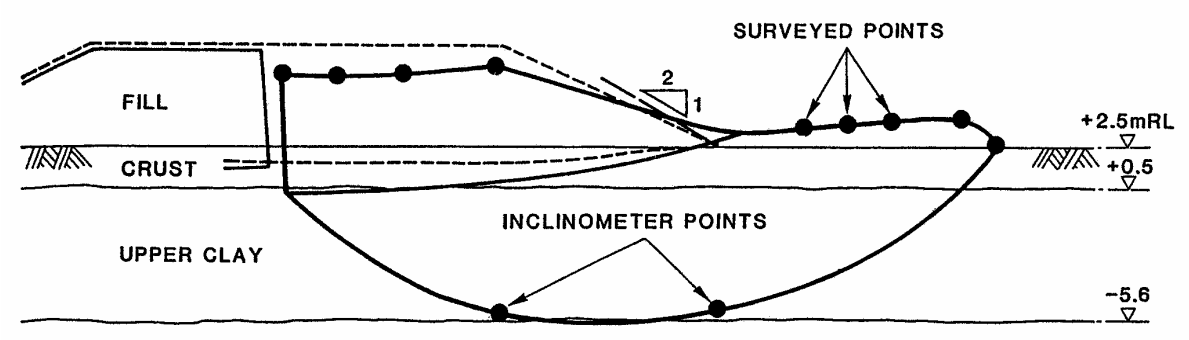

Figure C4.2: Pre and post-failure geometry of Muar-F test embankment (Brand and Premchitt 1989)

Field vane tests indicated the remoulded strength of the soft foundation to range from 2.5 to 7 kPa and the clay to be of low sensitivity ($S_I \approx 4$ where S_I = sensitivity). Effective stress path plots of laboratory undrained triaxial testing (Malaysian Highway Authority 1989a) indicate the soft clay foundation (at close to the in-situ stress conditions) to show little strain weakening and a large strain deviatoric stress of about 90% of the peak deviatoric stress.

During construction, cracking of the embankment was initially observed at an embankment height of 5.4 m with increases in the crack width occurring later that afternoon and over-night. The next day the embankment was raised to 5.6 m height and failure occurred shortly after placement of this layer. The failure occurred rapidly

(within approximately 3 minutes) and the total crest settlement was approximately 1.4 m.

Adopting the remoulded strength profile from the vane tests and modelling the cracked embankment resulted in a residual factor of safety of 0.40 for the reported surface of rupture (Figure C4.2). This resulted in a crest settlement of 0.78 m for the slow model and 1.53 m for the rapid model. The observed crest settlement of 1.4 m is close to the prediction using the rapid model.

However, it is suspected that the reasonable estimate of the rapid model to the observed movement is somewhat fortuitous, as the remoulded strength from the vane would indicate the remoulded strength to be 25% of the peak strength. The results of the laboratory undrained triaxial strength tests do not indicate the remoulded strength to be as low as this.

Adopting a residual friction angle of 12 degrees for the soft clay foundation, based on its clay fraction and plasticity, the residual undrained strengths are estimated to be in the range 7.5 to 13.5 kPa (from Equation C4.1), and the residual factor of safety estimated at 0.71 from limit equilibrium analysis. This resulted in a crest settlement of 0.38 m for the slow model and 0.75 m for the rapid model, significantly lower than the actual movement.

It is suspected that given the large radius (26 m) and relatively shallow depth (8.2 m maximum) of the surface of rupture (Figure C4.2) that the actual surface of rupture may have had a significant translational component. This would result in some internal brittleness of the slide that would explain the "very loud noise" at failure and relatively rapid movement of a soft clay foundation of low sensitivity. In addition, a wedge type settlement of the crest would have occurred for the compound failure surface geometry with rotational back-scarp, and possibly greater crest movements than could be predicted by the Khalili et al (1996) model.

4.3 ST. ALBAN-A TEST EMBANKMENT, QUEBEC, CANADA

The St. Alban-A test embankment was constructed over a soft to very soft, low plasticity leached marine clay/silt (Figure C4.3). A weathered, fissured crust of 1.5 to 1.8 m thickness overlies the soft clay foundation and the embankment was constructed of compacted, uniform sand.

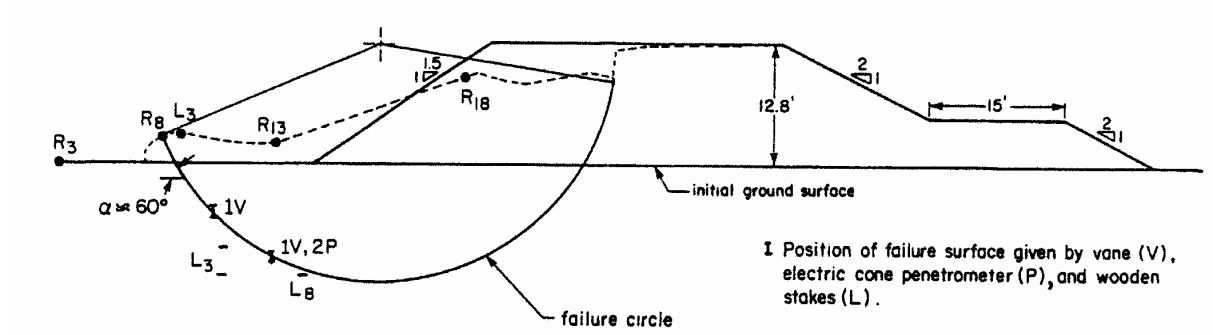

Figure C4.3: Pre and post-failure geometry of St. Alban-A test embankment (La Rochelle et al 1974)

Laboratory triaxial testing indicates the soft foundation to be cemented, sensitive and brittle (La Rochelle et al 1974). The undrained triaxial tests of the soft clay foundation (at close to the in-situ stress conditions) show significant strain weakening with a large strain deviatoric stress of about 75% of the peak deviatoric stress. Field vane tests indicate the remoulded strength to range from 1 to 3 kPa (significantly lower than that from the laboratory undrained triaxial tests) classifying the soft foundation as highly sensitive (S_I of 8 to 22) when compared to the peak vane results.

During construction, no cracking of the embankment was observed prior to failure. The failure occurred rapidly (within approximately 1 minute) at an embankment height of 4 m. The total post failure crest settlement was approximately 1.15 m and toe heave 1.2 m.

Adopting the remoulded strength profile from the vane tests a residual factor of safety of 0.26 was obtained by limit equilibrium analysis for the reported surface of rupture (Figure C4.3). This resulted in a crest settlement of 2.3 m for the slow model and 4.6 m for the rapid model, significantly greater than the observed crest settlement of 1.15 m.

Adopting a residual strength of 75% of the peak strength (equivalent to the reported large strain undrained shear strength from the laboratory undrained triaxial tests) a residual factor of safety of 0.75 is obtained from limit equilibrium analysis. This resulted in a crest settlement of 0.79 m for the slow model and 1.53 m for the rapid model, significantly closer to the observed crest settlement of 1.15 m. It would have been expected that the rapid model would have more closely predicted the observed movement than the results indicate given the rapid post failure velocity of the failed

slide mass. It is considered that the sensitivity of the residual factor of safety to the strength parameters adopted is probably why the prediction was not closer.

4.4 PORTSMOUTH TEST EMBANKMENT, NEW HAMPSHIRE, USA

The Portsmouth test embankment was constructed over a soft, medium plasticity leached marine silty clay (Figure C4.4). A weathered, fissured crust of 2.4 m thickness overlay the soft clay foundation and the embankment was constructed of clean sand.

The remoulded vane test results indicate the soft foundation to be sensitive ($S_t \approx 10$) with remoulded strengths ranging from 1.4 to 7 kPa. Laboratory triaxial undrained testing, as discussed by Ladd (1972), indicates the foundation has significant strength anisotropy. It is suspected that it would also exhibit brittle, and possibly partially cemented, undrained shear strength behaviour with significant post peak strain weakening, although, no stress-strain plots are published by Ladd.

During construction no cracking of the embankment was observed prior to failure at an embankment height of 6.55 m. The failure is suspected to have occurred rapidly. The total crest settlement was approximately 3.3 to 3.4 m with a similar amount of heave movement beyond the embankment toe.

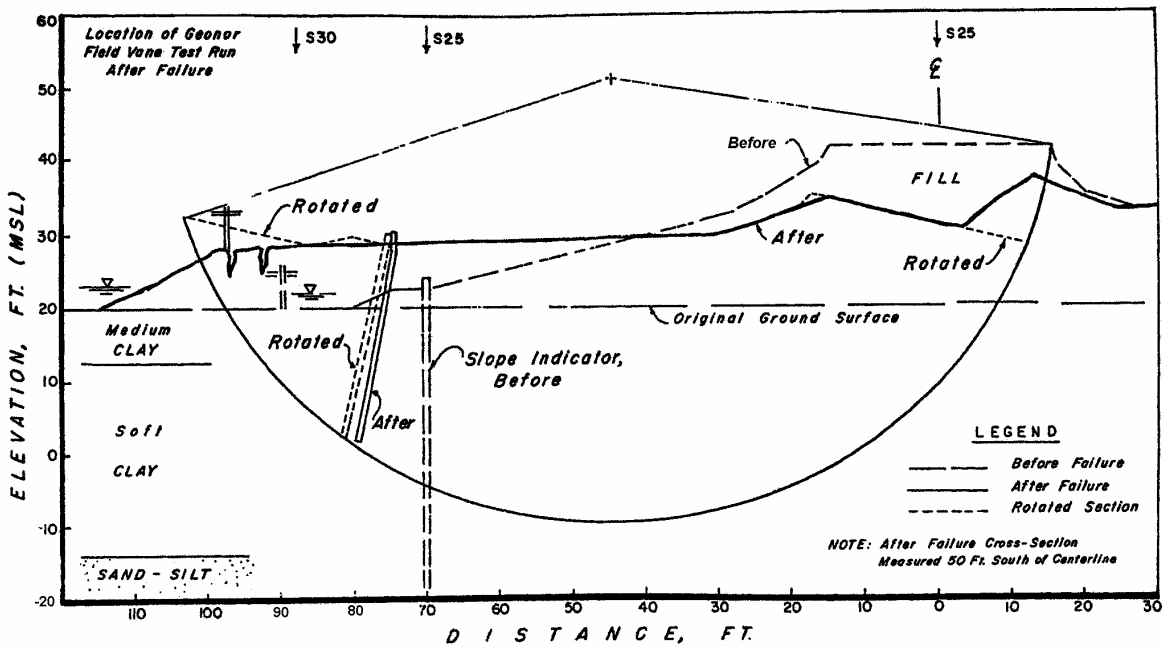

Figure C4.4: Pre and post-failure geometry of Portsmouth test embankment (Ladd 1972)

Adopting the remoulded strength profile from the vane tests a residual factor of safety of 0.27 was obtained by limit equilibrium analysis for the reported surface of rupture

(Figure C4.4). This resulted in a crest settlement of 3.4 m for the slow model and 6.4 m for the rapid model. Given the suspected rapid post-failure movement, the predicted rapid movement is significantly greater than the observed crest settlement of 3.3 to 3.4 m. Once again it is suspected that the remoulded vane strength significantly under estimates the residual strength. However, no laboratory triaxial undrained test data in the form of stress-strain plots were published by Ladd (1972) to allow assessment of the large strain undrained shear strength.

APPENDIX D

Case Studies of Slope Failures in Embankment Dams and in Cut Slopes in Heavily Over-Consolidated High Plasticity Clays

TABLE OF CONTENTS

1.0 CASE STUDY INFORMATION ON LANDSLIDES IN EMBANKMENT DAMS..... D1

2.0 FAILURES IN CUT SLOPES IN HEAVILY OVER-CONSOLIDATED HIGH PLASTICITY CLAYS D22

2.1 Cut Slopes in London Clay D22

2.2 Cut Slopes in Weathered Upper Lias Clay..... D24

2.3 Terminology Used in Tables D26

LIST OF TABLES

Table D1.1: Case studies of slope instability of embankment dams – slides during construction. D3

Table D1.2: Case studies of slope instability of embankment dams – slides in the upstream slope during drawdown. D13

Table D1.3: Case studies of slope instability of embankment dams – post-construction slides in the downstream slope. D18

Table D2.1: Summary of material properties of London clay*[1] D23

Table D2.2: Summary of material properties of weathered Upper Lias clay*[1] D26

Table D2.3: Case studies of failures in cut slopes in London clay D29

Table D2.4: Case studies of failures in cut slopes in weathered Upper Lias clay D31

1.0 CASE STUDY INFORMATION ON LANDSLIDES IN EMBANKMENT DAMS

The case study information for embankment dams is presented in the following tables:

- Table D1.1 for slides in embankment dams during construction;
- Table D1.2 for post-construction slides in the upstream slope of embankment dams during drawdown; and
- Table D1.3 for slides in the downstream slope of embankment dams that occur post-construction.

An explanation of some of the terminology used in these tables is as follows:

- Some general terms or symbols used and their meaning:
  - (?) = unsure of detail, but thought to be likely
  - unk = unknown
  - "-" = not required or not appropriate
  - H to V refers to horizontal to vertical slope angle; i.e. 2H to 1V.
  - S_u = undrained shear strength
  - Spec. = specification.
  - SMP = surface monitoring point.
- Under the section embankment zoning and classification;
  - "Zoning" refers to the embankment zoning classification (refer Figure 1.6 in Section 1.3.3 of Chapter 1)
  - "Classification" refers to the embankment and filter classification (refer Figure 1.5 in Section 1.3.3 of Chapter 1)
  - "Core Width" refers to the thickness classification of the core
  - "Core Type" refers to the classification of the core in accordance with the Australian soil classification system (Australian Standard AS 1726-1993 "Geotechnical Site Investigations").
- Slide location refers to the location of the surface of rupture, being either:
  - Emb = slide through the embankment only
  - Emb & Fndn = slide through the embankment and foundation
- For the material properties:

  - ASCS Class[n] = Australian soil classification system (Australian Standard AS 1726-1993).
  - % fines = percentage finer than 75 micron (i.e. percent silt and clay fraction)
  - CF (%) = percentage of clay fines (i.e. less than 2 micron)
  - PI (%) = plasticity index
  - "Density Ratio" = ratio of the field dry density to Standard maximum dry density (SMDD), in accordance with Australian Standard AS1289.5.1.1 or the Standard Proctor test. Unit weights or densities are quoted where given.
  - Moisture Content = moisture content in relation to Standard optimum moisture content (OMC); dry being dry of OMC, wet being wet of OMC.
- Slide classification refers to the classification of the shape of the surface of rupture (e.g. translational, rotational or compound) using the landslide classification system of Hutchinson (1988).
- For the post-failure deformation behaviour:
  - Velocity category refers to the IUGS (1995) velocity categories.
  - The degree of break-up is a somewhat subjective assessment of the post-failure break up of the slide mass.

Table D1.1: Case studies of slope instability of embankment dams – slides during construction.

Name	Location	Date of Failure	Embankment Zoning and Classification				Slide Location	Geology	CONSTRUCTION								References
									Construction		Embankment Dimensions						
			Type	Class[n]	Core Width	Core Type			Year Started	Rate (mm/day)	Height, H_e (m)	Length, L_e (m)	Ratio L_e/H_e	Upstream Slope	Downstream Slope	Comments	
Otter Brook Dam	USA, New England	Aug-57	Homog	1,1,1	c-vb	SC	Emb	Metamorphic, glaciation	1957	470 (max)	40.5	unk	-	2.5H to 1V	2.5H to 1V	Lateral bulging during construction. Homogeneous earthfill dam with downstream chimney drain and foundation filter	Linell & Shea (1960) Sherard et al (1963) Walker and Duncan (1984)
Truscott Dam	USA, Texas	03-Dec-81	Homog	1,1,1	c-vb	CL/CH (?)	Emb	unk	1980	360 (max), last 6.2 m fill.	30	4720	157.3	2.5 to 3.5H to 1V	3H to 1V	Lateral bulging and cracking observed during latter stages of construction within closure section (6.2 m below design level).	Walker and Duncan (1984)
Skiatook Dam	USA, Oklahoma	Aug-82	Homog	1,1,1	c-vb	CL/CH (?)	Emb	unk	1977	230 (closure section)	33.8	1090	32.2	2.5 to 4H to 1V	3 to 4H to 1V	Lateral bulging and cracking observed during construction within closure section (when 11 m below design level).	Walker and Duncan (1984)
Troneras Dam	Columbia	12-Apr-62	Homog	1,1,1	c-vb	ML	Emb	Quartz diorite - deeply weathered profile.	1960	360 to 1330	31.5	366	11.6	3 to 4H to 1V	2.5 to 3.5H to 1V	Lateral bulging of downstream slope when construction rate in excess of 1 m/day (upper 8 m of embankment).	Villegas (1984) Li (1963) Li (1967)
Punchina Cofferdam	Columbia	3-Apr-80	Homog	2,0,0	c-vb	SM	Emb	Quartz diorite	1980	570 to 1500	45 (35 when movement observed)	350	7.8	3.4H to 1V	2H to 1V	Lateral bulging (incipient failure) of downstream slope. Occurred when constructing downstream section at very rapid rate(approx 1.5 m/day).	Villegas (1982)
Waghad	India	Apr 1884	Homog	0,0,0	c-vb	CH/MH	Emb	unk	1881	240 (g)	32	1270	39.7	3H to 1V	2H to 1V	Reconstruction of gorge section in 1884 following overtop in 1883.	Penman (1986) Nagarkar et al (1978) Nagarkar et al (1981)
Lake Shelbyville	USA, Illanois	17-Sep-70	Homog	1,1,1	c-vb	CL	Emb	Sedimentary - shale, sandstone, coal, limestone	1966	100 (closure section)	33	1034	31.3	2.5 to 4H to 1V (with berm)	3 to 4H to 1V (with berm)	Failure within closure section on upstream slope. Observed when construction complete.	Humphrey & Leonard (1986, 1988) Crooks & Becker (1988)
Scout Reservation Dam	USA, Ohio	Sep-84	Homog	1,0,1	c-vb	CL	Emb	Sedimentary - shale, claystone and sandstone	1983	30 (but suspect much quicker)	13.7	245	17.9	2H to 1V	3H to 1V	Instability of upstream slope. Only observed when construction completed.	Mann and Snow (1992)
Muirhead	UK, Scotland	Sep-41	Puddle core earthfill	8,0,1	-	CL/CH	Emb	Volcanic, overlain by Boulder Clay	1940	25 increasing to 85 (85 at failure)	21.3 (at failure)	631	29.6	2.5H to 1V	3H to 1V	From May 1941 construction rate increased to approx 85 mm/day (4 fold increase in volume). 5 m below design height at failure.	Banks (1948) Skempton (1990) Penman (1986)
Dam FC10		Jan-37	Zoned Earth and rockfill	4,0,0	c-vb	CH	Emb	unk	1935	60 (g)	19.5	290	14.9	2 to 4H to 1V	3 to 4H to 1V	Most of construction in 1935, completed Dec 1936. Failure shortly after completion.	
Acu Dam	Brazil	15-Dec-81	Zoned Earth and rockfill	4,1,1	c-tk	CH (?)	Emb	unk	1980 (?)	unk	34.8 (at failure)	unk	-	2.5H to 1V	2.5H to 1V	Failed during construction when 5.2 m below design crest level.	Penman (1985)

Table D1.1: Case studies of slope instability of embankment dams – slides during construction (Sheet 2 of 10)

Name	EMBANKMENT MATERIALS																	
	Material 1 (Core)									Material 2 (Shoulder fill)								
	Source	ASCS Class[n]	% fines	CF (%)	PI (%)	Density Ratio	Moisture Content	Compaction	Comments	Source	ASCS Class[n]	% fines	CF (%)	PI (%)	Density Ratio	Moisture Content	Compaction	Comments
Otter Brook Dam	Glacial till	SC - clayey fine sand	45	12	15	100.5%	0.6% dry (20% > 1% wet)	Rolled, well compacted. 200 mm layers, 6 passes of sheepsfoot roller (16 tonne)	Large variation in moisture content at placement.	-	-	-	-	-	-	-	-	-
Truscott Dam	Sedimentary, clay shales	CH (?)	unk	unk	unk	unk	Variable, some wet zones	Suspect rolled, well compacted	Investigation indicates fill of stiff to very stiff strength consistency (Su ~ 55 to 190 kPa). Stiff zones associated with wetter zones.	-	-	-	-	-	-	-	-	-
Skiatook Dam	unk	CL/CH (?)	unk	unk	unk	unk	16 to 20%	Suspect rolled, well compacted	Investigation indicates fill of stiff to very stiff strength consistency. Lower strength zones (Su ~ 65 to 70 kPa) associated with wetter zones in fill.	-	-	-	-	-	-	-	-	-
Troneras Dam	Residual and saprolitic soils	ML	60 to 80	5 to 15	8 to 12	14.4 kN/cu.m. (dry density)	4% wet (avg), up to 10% wet	Rolled, well compacted. Pad foot rollers	Very rapid rate of construction. Placed well wet OMC, low undrained shear strength.	-	-	-	-	-	-	-	-	-
Punchina Cofferdam	Residual and saprolitic soils	SM	43	6	10.2	95.4%	4.1% wet (avg)	Rolled, well compacted. Pad foot rollers	Very rapid rate of construction. Placed well wet OMC. Material had low undrained shear strength, firm to stiff (Su ~ 50 kPa).	-	-	-	-	-	-	-	-	-
Waghad	Alluvial (black cotton soil)	CH/MH	63 to 93	-	35	80 to 85%	6% wet	No formal compaction. (By animal ?)	Normally consolidated (low preconsolidation pressure)	-	-	-	-	-	-	-	-	-
Lake Shelbyville	Glacial, till	CL - sandy clay	67	unk	16 (3 to 35)	100.2% (S Dev = 3.7%)	0.1% wet (S Dev = 1.1%)	Suspect rolled, well compacted	Broad variation in relative compaction (89 to 117%) and moisture content (2.5% dry to 4.5% wet)	-	-	-	-	-	-	-	-	-
Scout Reservation Dam	residual sedimentary soils	CL - silty clays	70 to 90	unk	8 to 21	17.3 kN/m^3 (dry unit weight)	16 to 20%	Suspect rolled, well compacted (given period of construction)	Post construction investigation indicated fill of stiff to very stiff strength consistency and generally unsaturated (with some zones close to saturation)	-	-	-	-	-	-	-	-	-
Muirhead	Glacial - Boulder Clay.	CL/CH	unk	unk	25	unk	wet OMC	puddled	Narrow puddle core placed well wet of OMC. Low undrained strength (Su ~ 20 kPa)	Glacial - Boulder Clay.	CL/SC/GC	45	20	25	< 95% (lower), 97% (upper)	up to 4% wet (lower), 1% wet (upper)	No formal compaction. Spread and compacted by bulldozers.	Poorer compaction of lower section, the upper portion of which was well wet of OMC and of firm consistency (Su ~ 35 kPa).
Dam FC10	Alluvial	CH	84	35	25	94.3%	4.5% wet (4 to 8%)	Rolled, well compacted. sheepsfoot roller in 150 mm layers	Core compacted well wet of OMC	Sandstone and Weathered shale	SC/SM	25	6	unk	unk	unk	Suspect poor compaction	Softened significantly when wetted, suspect poorly compacted.
Acu Dam	Alluvial	CH (?)	unk	unk	unk	unk	Initially wet, then close to OMC	Suspect involved formal compaction	Broad zone of core material upstream of centreline, also as a blanket under upstream shoulder.	Alluvial	SC/GC	unk	unk	unk	unk	unk	Suspect placed with formal compaction.	Formed zone in upstream shoulder and also downstream of centreline.

Table D1.1: Case studies of slope instability of embankment dams – slides during construction (Sheet 3 of 10)

Name	General Comments on Design and Compaction	PROPERTIES OF FOUNDATION										SLIDE LOCATION AND GEOMETRY			
		Foundation (General)		Foundation (if Foundation involved in Slide)								Slide Classification (Hutchinson, 1988)	Slope Failure Geometry	Slide Location	State
		Soil / Rock	Description	Description	ASCS Class[n]	% fines	CF (%)	PI (%)	Density	Moisture Content	Comments				
Otter Brook Dam	3 m thick outer sheet of gravel and rockfill.	Soil	Glacial till (SM/SC with gravel and boulders) over bedrock	-	-	-	-	-	-	-	-	Lateral bulging, not a failure.	Type 1	Bulging of upstream slope, some settlement of crest.	Lateral bulging
Truscott Dam	Section shows zoned earthfill embankment, however, same materials used in core and outer shell. Chimney drain downstream of core zone.	Rock (?), weathered.	unk	-	-	-	-	-	-	-	-	Lateral bulging, not a failure.	Type 1	Bulging of downstream slope. Confined to region of closure section.	Lateral bulging
Skiatook Dam	Section shows zoned earthfill embankment, however, same materials used in core and outer shell. Chimney drain downstream of core zone.	Soil (valley floor)	normally consolidated clay, 12 m thick. This was removed to bedrock in closure section with compacted fill.	-	-	-	-	-	-	-	-	Lateral bulging, not a failure.	Type 1	Bulging of downstream slope. Confined to region of closure section. Suspected lateral movement within softer fill zone near base of closure section.	Lateral bulging
Troneras Dam	Homogeneous embankment with upstream cutoff to residual soil. High rate of construction to complete construction in dry season.	Soil	Shallow layer of stream bed alluvium overlying deep residual soil profile.	-	-	-	-	-	-	-	-	Rotational (?), possibly only lateral bulging.	Type 1	Lateral bulging of downstream (and upstream ?) slope incorporating crest.	first time
Punchina Cofferdam	Homogeneous embankment with upstream rockfill toe. In narrow gully region embankment on bedrock, slopes on deep residual soil profile. High rate of construction to complete construction in dry season.	Rock	Bedrock in gully region. Deep residual soil profile on abutment slopes.	-	-	-	-	-	-	-	-	Rotational (?)	Type 1	Downstream slope, extended several metres back into crest level at time that movement occurred.	first time
Waghad	Homogeneous embankment constructed of CH/MH material. Placed wet without any formal compaction.	Soil	Murum over weathered bedrock	-	-	-	-	-	-	-	-	Rotational (possibly part translational)	Type 2 (?)	Failure of downstream slope within zone under remediation.	first time
Lake Shelbyville	Homogeneous earthfill embankment with embankment filter zone. Closure section of 150 m width placed from Nov 1969 to June 1970 with winter shutdown.	Soil	Alluvial - outwash sand of 3 m depth over bedrock.	-	-	-	-	-	-	-	Recent alluvials stripped off to outwash sand layer. Central cutoff to bedrock.	Compound - translational basal component	Type 1	Failure in upstream slope. Extended back to upstream side of crest centreline. Deep seated. Basal plane on more plastic layer. Confined to closure section.	first time
Scout Reservation Dam	Homogeneous embankment with cut-off upstream of centreline. Constructed using low plasticity silty clays. Contains zones of relatively low undrained shear strength (as low as 50 kPa).	Soil / Rock	Residual soils and weathered bedrock.	-	-	-	-	-	-	-	-	Compound - translational basal zone close to base of embankment.	Type 2	Relatively deep-seated slide in the upstream slope, extended back to the downstream edge of crest. Translational in lower portion of embankment close to foundation. Movement across 75% of the embankment length.	first time
Muirhead	Change in contractor in April 1941 with view to increase rate of construction. Four fold increase in rate of volume placed. Rockfill zone at upstream and downstream toe.	Soil	Boulder clays are glacial deposits formed by glacial crushing of parent rock. Medium plasticity, very stiff to hard strength consistency.	-	-	-	-	-	-	-	-	Compound - translational basal component in firm earthfill zone.	Type 1	Lateral bulging of upstream slope incorporating crest and upstream slope. Occurred during construction when approx. 5 m below design crest level.	first time
Dam FC10	Broad core zone (1.5H to 1V upstream) of CH clays with poorly placed random fill zone and thin outer rock shell.	Soil (valley floor)	Alluvial clays, sands and gravels over bedrock. Significant plastic clay layer of 12 m thickness.	-	-	-	-	-	-	-	-	Rotational (?), surface of rupture not determined.	Type 1	Failure of upstream slope over significant width of the central portion of the embankment. Occurred shortly after end of construction.	first time
Acu Dam	Upstream - zoned earthfill with silty clay placed as blanket under upstream shoulder. Downstream - zoned earth and rockfill with embankment and foundation filters.	Soil	Alluvial sands.	-	-	-	-	-	-	-	-	Compound - translational basal component in clay zone under upstream shoulder.	Type 2	Deep-seated failure of upstream slope during construction, extended back to the mid to downstream portion of the crest. Basal translational sliding plane on CH fill layer under the upstream shoulder.	first time

Table D1.1: Case studies of slope instability of embankment dams – slides during construction (Sheet 4 of 10)

Name	AT AND POST-FAILURE														Hydrogeology
	Slide Dimensions								Post-Failure Deformation Behaviour				Degree of Break-up of the Slide Mass	Comments	
	Width, W (m)	Length, L (m)	Depth, D (m)	Height (m)	Slope (deg)	Volume (cu.m.)	W/L	W/D	Displacement (m)	Velocity (mm/day)	Velocity Category	Comments			
Otter Brook Dam	unk	-	23 (no bulging of lower slope)	-	21.8	-	-	-	0.88 m monitored movement of upstream face (will be greater than this)	40	slow	Movement only occurred when construction in progress. Once placement suspended movement stopped within 1 to 2 days.	Intact	Lateral bulging of upstream slope. Suspect bulging is occurring within a wetter zone of fill.	Excess pore pressures in fill during construction. Piezometers indicate r_u up to 0.65 to 0.8 in some zones of fill. Suspect this is in the wetter zones of fill.
Truscott Dam	400	-	-	-	18.4	-	-	-	0.84 m monitored movement of downstream slope.	20	slow	Significant crack in lower region of embankment (3 m above foundation). Displacement at toe of slide over-rode lower section of embankment by 150 mm. At completion of construction further cracking observed.	Intact	Lateral bulging of downstream slope within closure section. Suspect bulging occurred within a wetter zone of the fill. Shear zone at toe of slide coincided with the elevation where the filling was left exposed for several months.	No information. Suspect potentially high excess pore pressures developed within wetter fill zones.
Skiatook Dam	50 to 60	85	22	22	16	-	0.65	2.50	0.79 m, lower downstream slope	23	slow	Significant crack in lower region of downstream slope, commensurate with identified softer and wetter zone of filling. Monitored movement of 655 mm in 29 days during which rate of construction = 0.23 m/day.	Intact	Lateral bulging of downstream slope within closure section. Bulging occurred within a wetter, softer zone of the fill.	Piezometer in core indicates r_u in the range 0.8 to 1.0. This is indicative of placement wet of optimum of low permeability material.
Troneras Dam	60	-	-	-	18.4	-	-	-	no information	600 (suspect high)	slow to moderate	Only quantitative reference to movement is that at one point the crest level could not be raised due to the bulging and one night the crest settled more than height of fill placed. Suspect that this rate may be a bit high.	Intact	Later part of embankment construction at a very rapid rate and during the start of the wet season. Fill placed very wet (had to use tractors to compact due to bogging of rollers). After placement of 1.8 m of top 9.1 m (in wet season) the fill did not rise further it merely bulged. The design was changed, but further bulging and cracking occurred. Construction suspended when 2 m from crest.	Very high excess pore pressures developed within the sandy silt fill, r_u from 0.4 to 1 (avg of 0.75 to 0.8). Very high annual rainfall (2 to 5.35 m) with only 3 month dry season during which construction can proceed.
Punchina Cofferdam	60	65	12	35	26.6	25000	0.92	5.00	1.57 m (max) on mid to lower downstream slope, 0.72 m at crest.	250 to 350	slow	SMPs established once movement observed. First sign was cracking on lower downstream slope and mis-alignment of surface drains. Embankment construction continued and further movements were observed. Movement stopped shortly after embankment completed (1 to 2 days after).	Virtually intact	Very rapid rate of construction of downstream stage of cofferdam in order to complete construction before start of wet season. Continued construction after first signs of movement resulted in relatively high velocities of movement of downstream slope (250 to 350 mm/day). Design altered to complete construction.	High excess pore pressures developed within the silty sand fill, r_u from 0.43 to 0.7, particularly during high construction rate period. Very high annual rainfall (3.1 m) with only 3 month dry season during which construction can proceed.
Waghad	61	60	18	29.5	26.5	35000	1.02	3.39	15.2 m toe, 6.4 m crest	-	Moderate (poss. Rapid)	Suspect moderate (potentially rapid) velocity of movement given distance travelled	Minor (?)	Limited information. Sections indicate movement incorporated upper part of upstream slope.	Excess pore pressures in fill during construction. Suspect pore pressures quite high given earthfill placed well wet of OMC.
Lake Shelbyville	165	46	18	15.5	21.8	75000	3.59	9.17	392 mm upper part upstream slope	24 (max), 0.5 to 2 (avg)	slow to very slow	Very slow movements (0.4 to 2 mm/day) from Oct 1970 to Dec 1971. Virtually stopped in Dec to Feb 1972. Acceleration in movement in Feb to March of 1972, suspect due to drawdown prior to remedial works.	Intact	Rate of movement appears to have been affected by reservoir level operation. Suspect a drawdown in Feb to March 1972, in preparation for repairs, caused the observed acceleration in movement. Looks like lower and mid portion of slip moving before upper portion.	Limited information on reservoir level operation. Maximium stored water level in July 1971 (inundated lower half of slide). Drawdown for remedial works must have started late Jan or early Feb 1972 (reservoir at 15 m below crest on 10 Feb 1972). Construction induced pore pressures ranged from r_u of 0.26 to 0.64 (avg 0.4 in slide area) and showed slow dissipation.
Scout Reservation Dam	180	42	10	13.7	26.6	30000	4.29	18.00	1.8 m, scarp height at crest.	10 reducing to <1	slow decreasing to very slow	First sign of movement was cracking at the end of construction. Slide scarp developed slowly over a period of 2 years (late 1984 to mid 1986). From late 1986 to 1988 movements increased during/following periods of heavy rainfall. Suspect cracks filled with water.	Virtually intact	No water stored in impoundment up to 1988 when repairs undertaken. Surface of rupture determined by inclinometer and wet layers of fill. Suspect movements from 1986 onward only occurred following rainfall with no movement during relatively dry periods.	Piezometers indicate variable phreatic surface within fill. Suspect that observations are a reflection of construction induced pore pressures and are variable due to moisture variation at fill placement.
Muirhead	100	62	15	15	21.8	60000	1.61	6.67	Up to 2.1 m on upstream slope.	40 to 115	Slow	Movements first observed on 16 Sept 1941. Survey on 19/9/41 indicated 1.45 m lateral bulge in upstream face. Movement renewed on re-commencement of filling operations (and continued for about a week after suspension of construction).	Virtually intact	Surface of rupture fully developed, passed through core and weaker zone of shoulder earthfill.	High pore pressures developed in filling placed well wet of OMC. No information on pore pressures, but suspect r_u greater than 0.5 as indicated from Knockendon Dam. Likely slow dissipation of pore pressures in low permeability material.
Dam FC10	120	66	14	19	18.4	60000	1.82	8.57	1.8 m crest, 2.1 to 2.8 m upstream slope.	-	Slow to Moderate	Significant movements of upstream face observed during construction. Slide mass accelerated after the end of construction (Jan 1937) when cracking was observed. The movement continued for many days.	Virtually intact	Movement within the embankment only (no movement at upstream toe). The largest movements occurred shortly after construction and suspect were related to reservoir operation. Preceeded by 'abnormal' movements during construction.	Likely high pore pressures in core due to compaction well wet of optimum. Stored reservoir level was relatively high from early November 1936 to mid January 1937. Possiblility that drawdown may have induced failure.
Acu Dam	600	107	26	34.8	21.8	1200000	5.61	23.08	15 m movement at crest (near vertical), 25 m displacement at upstream toe	1.2E+06	Rapid	Slide preceeded by cracking in the crest at the downstream edge of the core zone. This was followed by outward deformation of upstream slope, for distance of 25 m, on the CH clay fill layer placed under the upstream shoulder. Movement occurred within about 30 minutes.	Minor	Failure incorporated the central part of the crest and the upstream slope. Earlier failures occurred in the cofferdam (constructed of wet placed CH materials).	High pore pressures developed in silty clay filling placed wet of OMC.

Table D1.1: Case studies of slope instability of embankment dams – slides during construction (Sheet 5 of 10)

Name	MECHANICS OF FAILURE				General Comments
	Cause/s of Landsliding	Trigger of Landsliding	Failure Mechanism	Comments on Failure Mechanics	
Otter Brook Dam	Construction. High rate of construction led to development of high pore pressures in wet filling zones.	Construction	Not actually failure, only lateral bulging. Low modulus and undrained shear strength of wetter fill zones.	High excess pore pressures in some piezometers reflects wetter zones of fill. These zones likely to have relatively low undrained shear strength and modulus. Displacements preferentially occur within the lower strength wetter soil zones. High construction rate contributed to velocity of movement. Suspect FOS close to 1 even though authors think otherwise.	Case of lateral bulging. Authors report that factor of safety was greater than one during construction. US Corp Dam.
Truscott Dam	Construction. High rate of construction within closure section.	Construction.	Not actually failure, only lateral bulging. Low modulus and undrained shear strength of wetter fill zones.	Suspect high excess pore pressures developed in wetter zones of fill. These zones likely to have relatively low undrained shear strength and modulus. Displacements preferentially occur within the lower strength wetter soil zones. High construction rate contributed to movement.	Similar case to Otter Brook Dam. Lateral bulging during construction. US Corp Dam.
Skiatook Dam	Construction. High rate of construction (within closure section) and high pore pressure development.	Construction	Not actually failure, only lateral bulging. Low modulus and undrained shear strength of wetter fill zones.	High excess pore pressures developed in wetter zones of fill. These zones likely to have relatively low undrained shear strength and modulus. Displacements preferentially occur within the lower strength wetter soil zones. High construction rate contributed to movement.	Similar case to Otter Brook Dam and Truscott Dam. Lateral bulging during construction. US Corp Dam.
Troneras Dam	Construction. High excess pore pressures in fill placed well wet of OMC.	Construction.	Lateral bulging of wet placed sandy silts with low undrained shear strength. Suspect material is dilative and strain hardening on undrained shearing.	Sandy silt placed very wet in latter part of construction. Wet placed fill of low undrained shear strength and modulus. Lateral bulging occurred once factor of safety approached one. Suspect material is dilative and strain hardening in undrained loading (at low confining pressures) and therefore expect movement to stop once construction stops. Factor of safety continually at one while construction in progress; i.e., the bulging keeps it at one.	Late start to construction required very rapid rates of construction to complete embankment before start of wet season. Lateral bulging during period of very high construction rate. The design was altered when cracking occurred the day following significant lateral bulging.
Punchina Cofferdam	Construction at very rapid rates of fills well wet of OMC. High excess pore pressures developed in fill.	Construction.	Deformation indicates formation of failure (rather than just lateral bulging) in relatively steep downstream slope (2H to 1V). Undrained failure of near normally consolidated silty sand fill having low undrained shear strength.	Silty sand placed well wet of optimum moisture content. Very rapid rate of construction resulted in maintaining high pore pressures in fill. Suspect material is dilative and strain hardening in undrained loading and therefore expect movement to stop once construction stops. Suspect relatively steep embankment slope influenced high rate of movement observed. Limit equilibrium analysis indicates factor of safety of 0.97 to 1.	Late start to construction required very rapid rates of construction to complete cofferdam before start of wet season. Movements occurred during period of very high construction rate. The design was altered when relatively high rates of movement measured on downstream slope.
Waghad	Construction. Development of high pore pressures.	Construction	Undrained failure in near normally consolidated CH/MH fill placed well wet of OMC. Low undrained shear strength and likely strain weakening in undrained loading.	Suspect strain weakening in undrained loading due to strength loss associated with orientation of clay particles and reduction from fully softened to residual strength on shearing. Low pre-consolidation pressures due to wet placement.	During monsoon season of 1883 embankment was overtopped. Slide in 1884 was within section under re-construction following over-top. Suspect high rates of construction may have contributed to the failure.
Lake Shelbyville	Construction and high pore pressures (initial movements may have occurred during construction but not observed). Drawdown triggered acceleration in movement.	Suspect initial failure due to undrained instability. Suspect reservoir operation affected the velocity of movement, but limited information.	Undrained failure. Surface of rupture passed through the weaker fill layers (which controlled the slide). Back-scarp through partially saturated that would be dilative and strain weakening. Suspect movement observed at the end of construction was post-failure movement (i.e., surface of rupture had fully formed). Reduction in rate of movement suggests stabilisation possibly due to reduction in pore pressures (dissipation). But slope still of marginal stability as indicated by accelerations possibly associated with drawdown.	Partially saturated fills are likely to be strain hardening in undrained loading and strain weakening in drained loading due to dilative behaviour on shearing. Suspect reduced undrained strength of wetter and more plastic fill layers may be controlling the slide movement. Wetting up of the filling from infiltration (from inundation) would result in a reduction in the strength of unsaturated soils. This may potentially be a factor in the acceleration in movement observed on drawdown in Feb 1972. Initiation of movements in lower portion of the slide suggest the toe region is controlling the slide.	Slow to very slow movement of slide, but significant difference observable in the deformation behaviour between a point on the slide area and a point off it. Slow movement could be due to restraint on the lateral margins (from keying in of the closure section to the main fill) and from shear induced dilation of unsaturated soils in the backscarp. US Corp dam.
Scout Reservation Dam	Construction. Development of localised high pore pressure zones in wetter embankment zones.	Construction. Latter movements triggered by rainfall.	Suspect initial instability driven by weaker, wetter layers within fill near the upstream toe; therefore undrained instability. Variability of strength of filling would indicate shear plane probably passes through dilative soils.	The width of the slide possibly indicates the basal sliding plane may be laterally very extensive. It may have been wetted by rainfall or placed during a wet weather period. Lab tests indicate fill is strain weakening in undrained loading at low confining pressures. Reactivation of movement from 1986 suggests the slope is of marginal stability triggered by water infilled cracks.	Slow to very slow failure starting at end of construction and movement continuing for 4 years. Likely undrained instability initially, but later movements must be drained instability.
Muirhead	Construction. High rate of construction led to development of high pore pressures in wet and firm filling zones.	Construction.	Undrained instability of firm to stiff (and wet) filling. Core zone possibly strain weakening in undrained loading, but outer zone unlikely to be.	The monitoring results would indicate that, overall, the earthfill materials are not strain weakening in undrained loading as indicated by the reduction in velocity of the slide onceconstruction is suspended.	Case of lateral bulging due to limiting undrained stability condition in firm to stiff medium plasticity sandy and gravelly clay fill materials placed wet of optimum moisture content.
Dam FC10	Construction. Development of high pore pressures in broad core.	Not clear, combination of construction and possibly drawdown induced. Strength loss on saturation of the random fill zone may have had a significant influence on stability.	Undrained failure. Likely low undrained strength of CH core and near normally consolidated. CH core likely to be strain weakening in undrained loading.	Suspect CH core is strain weakening in undrained loading due to orintation of clay particles and strength reduction from fully softened to residual strength. Likely low undrained shear strength and low pre-consolidation pressure of core due to wet placement. Suspect drawdown may have triggered slide due to loss of support from water on upstream face and loss of strength in random fill layer once saturated.	During construction, movements indicated significant deformations of upstream slope compared with downstream slope. Core geometry flatter upstream (1.5H to 1V) than downstream (1H to 1V). Continued movements were observed for many days after initial failure observed indicating likely slow rate of movement.
Acu Dam	Construction. Development of high pore pressures in lower wet silty clay zones.	Construction	Undrained instability of wet placed silty clay filling. Suspect slide brittleness possibly associated with development of the surface of rupture through the outer clayey sand zone at the toe and/or through the partly saturated earthfill in the upper part of the core.	The lower portion of the CH core, including the section under the upstream slope, were placed wet of optimum. Therefore, lower undrained strengths likely in this material with instability initiated from this zone of the embankment. High shear stresses then transferred onto clayey sand zone at toe and also higher reaches of core. Once the failure initiated a significant reduction in shear strength within the clayey sand at the slide toe and upper core zones may have contributed to the slide brittleness and the rapid and relatively large run-out distance.	Unusual embankment design with upstream cutoff to bedrock and upstream shoulder underlain by silty clay material. Wet placement of core material significant in failure.

Table D1.1: Case studies of slope instability of embankment dams – slides during construction (Sheet 6 of 10)

Name	Location	Date of Failure	Embankment Zoning and Classification				Slide Location	Geology	CONSTRUCTION								References
									Construction		Embankment Dimensions						
			Type	Class[n]	Core Width	Core Type			Year Started	Rate (mm/day)	Height, H_e (m)	Length, L_e (m)	Ratio L_e/H_e	Upstream Slope	Downstream Slope	Comments	
Waco Dam	USA, Texas	Sep-61	Homog	1,1,1	c-vb	CL (?)	Emb & Fndn	Sedimentary - clay shales. Faulting.	1960	48	43 (25.9 at failure section)	5500	127.9	3 to 4.5H to 1V	2.5 to 3H to 1V	Failure during construction of downstream slope when 4 m below design level. Confined between faults in foundation.	Beene (1967) Stroman et al (1984) West (1962) Stroman and Karbs (1985)
West Branch Dam	USA, Ohio	20-Oct-64	Homog	1,0,1	c-vb	CL (?)	Emb & Fndn	Sedimentary - shale and sandstone, glacial	1963	600	22.5 (21.5 at failure)	3020	134.2	3 to 4.5H to 1V	3 to 4.5H to 1V	Failure of upstream slope when constructing closure section (400 m width). At 4 m below design crest level when abnormal movement observed.	Fetzer (1967)
North Ridge Dam	Canada	Sep-53	Homog	1,1,1	c-vb	CL	Emb & Fndn	Glacial soils (lacustrine)	1953	260	18.3 (at failure)	unk	-	4H to 1V	4.5H to 1V	Failure of downstream slope during construction when approx. 3 m below design level.	Peterson et al (1957)
Marshall Creek Dam	USA, Kansas	20-Sep-30	Homog	2,0,0	c-vb	CL (?)	Emb & Fndn	Sedimentary - limestone and shale	Mid 1930's	unk	24.4 (at failure)	480	17.5	3H to 1V	2.7H to 1V	Rapid failure of downstream slope during construction. 3 m below design level when failed.	Sherard et al (1963) ENR (1937a, 1937c, 1938a, 1938b)
Chingford	UK, Essex	30-Jul-37	Puddle core earthfill	8,0,1	-	CH	Emb & Fndn	Sedimentary marine. London Clay	1936	100	13	5600	430.8	3H to 1V	2.5H to 1V	Downstream shoulder failed during construction when 2.4 m below design level.	Cooling & Golder (1942) Skempton (1990) Penman (1986) Dounias et al (1988) Charles and Boden (1985)
Hollowell	UK, Northampton	Sept to Nov 1937	Puddle core earthfill	8,1,1	-	CH	Emb & Fndn	Sedimentary - mudstones (Upper Lias)	1936	21 (avg incl. shutdown periods)	11.4 (at failure)	427	37.5	3 to 5H to 1V	2.5 to 4H to 1V	Failure in downstream slope during construction when 1.7 m below design crest level. Limited movement.	Kennard (1955)
Carsington	UK	04-Jun-84	Zoned Earthfill	3,0,1	c-tn	CH	Emb & Fndn	Sedimentary, mudstone and sandstone	1982	110 (50 incl. seasonal shutdown)	36	1250	34.7	3H to 1V	2.3H to 1V	Failure in upstream slope during construction when very close to finished level.	Skempton and Vaughan (1993) Rocke (1993) Byrd and Middleboe (1984) Penman (1986) Potts et al (1990)
Lafayette Dam	USA, California	17-Sep-28	Zoned Earthfill	3,0,0	c-tm	CL/CH (?)	Emb & Fndn	Sedimentary - conglomerate, sandstone and clay	1927	85	35.5 (at failure)	380	10.7	3H to 1V	2.5 to 3H to 1V	Failure of downstream slope during construction when approx. 6 m below design level.	Bowers (1928) ENR (1929a, 1929b, 1929c)
Galisteo Dam	USA, New Mexico	26-Jan-70	Zoned Earthfill	3,1,1	c-vb	CL	Emb & Fndn	Sedimentary - sandstone and shale (Mancos Shale)	1967	50 to 100 (staged)	48.2	860	17.8	3.17H to 1V	2.5 to 3H to 1V	Failure of upstream slope during construction (9.4 m below design crest level when movement started).	Catanach and McDaniel (1972)
Dam FC21		15-Oct-69	Zoned Earthfill	3,1,1	c-tk	SC/GC	Emb & Fndn	Sedimentary - clay-shales and siltstone, glacial activity.	1966	50 to 60 (winter shutdown)	53 (43 when movement observed)	1005	19.0	3.3H to 1V	2.25H to 1V	Lateral spreading of foundation. Only aware when displacement in outlet conduit observed, no surface expression.	
Park Reservoir	USA, Wyoming	Oct-81	Zoned Earthfill	3,1,1	c-tk	CL (?)	Emb & Fndn	Lacustrine	1980's	unk	21.5 (at failure)	366	15.0	2.8H to 1V	2.5H to 1V	Failure in upstream slope during construction when 3 m below design crest level.	USCOLD (1988)

Table D1.1: Case studies of slope instability of embankment dams – slides during construction (Sheet 7 of 10)

Name	EMBANKMENT MATERIALS																	
	Material 1 (Core)									Material 2 (Shoulder fill)								
	Source	ASCS Class[n]	% fines	CF (%)	PI (%)	Density Ratio	Moisture Content	Compaction	Comments	Source	ASCS Class[n]	% fines	CF (%)	PI (%)	Density Ratio	Moisture Content	Compaction	Comments
Waco Dam	Sedimentary, shales	CL (?) - sandy clays and shaley clays	unk	unk	unk	unk	unk	Rolled, suspect well compacted	Limited information on materials. Comprised sandy clays and broken up shale.	-	-	-	-	-	-	-	-	-
West Branch Dam	No information. Glacial deposits or shales.	CL (?)	unk	unk	unk	bulk density = 20.4 kN/cu.m.	unk	Rolled, suspect well compacted	No information on materials. Sections only indicate "impervious fill" and very stiff.	-	-	-	-	-	-	-	-	-
North Ridge Dam	Glacial clays	CL	unk	unk	10 to 18	96.9%	0.1% dry	Rolled, suspect well compacted	Low plasticity clays of stiff to very stiff strength consistency.	-	-	-	-	-	-	-	-	-
Marshall Creek Dam	unk	CL (?)	unk	unk	unk	unk	14 to 16%	Rolled, well compacted. Placed in 200 mm layers and compacted by 12 to 14 passes of sheepsfoot roller.	Limited information on fill materials, refered to as "impervious fill".	-	-	-	-	-	-	-	-	-
Chingford	Marine sedimentary (London Clay)	CH	100 (close to it)	high	53	unk	well wet of OMC	No formal compaction. Tracked by wagon	Placement of puddle core. Very soft (Su ~ 10 kPa).	Alluvial (select and bank material)	CH	very high	very high	up to 100	unk	suspect wet of optimum	No formal compaction. tracked by wagon, bank material spread and tracked by dozer.	Select zone adjacent to core and outer bank fill. Outer bank fill comprised a mix of CH alluvial clay and ballast.
Hollowell	Sedimentary, Upper Lias clay (marine clay)	CH	Very high	45	32	unk	wet OMC	puddle, presume placed in thin layers.	Puddle core and select zones adjacent to core using Upper Lias clay (high plasticity). Placed wet of OMC. Suspect of low undrained shear strength.	unk	Sand and sand-rock material.	unk	unk	unk	unk	unk	unk	-
Carsington	Periglacial and residual	CH	unk	56	38	93.2%	8% wet	Rolled, well compacted. 200 to 250 mm layers with 28 tonne padfoot rollers.	Stiff consistency of core fill (Su ~ 60 to 65 kPa). Strain weakening in undrained loading with Sur of 30 kPa. Pre-consolidation pressure of 140 to 150 kPa.	Weathered mudstone	SC/CL	unk	34	22	101.10%	close to OMC	Rolled, well compacted. 300 mm layers compacted with 7 tonne grid rollers.	Heavily over-consolidated after compaction.
Lafayette Dam	Weathered and argillaceous sedimentary bedrock.	CL/CH (?)	high	50 (70% finer than 5 micron)	unk	unk	dry of OMC	Rolled, well compacted. Placed in 200 mm layers and heavily rolled.	Materials from Orinda formation, relatively young (Pliocene) deposit. Core slopes 0.5H to 1V.	Sandstone and conglomerate (conglom. only for d/stream shoulder).	GC (?)	low	< 15% (20% less than 5 micron)	unk	19.5 kN/m^3 (bulk density)	unk	Rolled, well compacted. Placed in 200 mm (upstream) to 300 mm (d/str) layers and heavily rolled	Materials also from Orinda formation.
Galisteo Dam	Alluvial and/or residual	CL - clays and sandy clays	high (?)	unk	unk (low to medium plasticity)	17.1 kN/m^3 (dry), Spec. > 95%	9.3 to 26.1% (Spec. OMC to 2% wet)	Rolled, suspect well compacted	Limited information. Undrained strength tests indicate firm to very stiff.	Alluvial and/or residual	CL (?)	unk	unk	unk (low to medium plasticity)	15.2 to 19.6 kN/m^3 (dry), Spec. > 95%	unk (Spec. 3% dry to OMC)	Rolled, suspect well compacted.	Similar materials used for outer earthfill as for core. Stiff to very stiff strength consistency.
Dam FC21	Glacial soils	SC/GC	low	low	unk	99.8%	0.2% dry (avg)	Rolled, well compacted. Placed in 150 mm layers and compacted by tamping rollers.	Limited information. Suspect dilative. Flat upstream slope (1.75H to 1V) and steep d/str slope (0.5H to 1V).	Glacial soils	sand, gravel and cobbles (cohesionless)	unk	unk	non plastic	unk	unk	Rolled, limited compacted. Placed in 300 mm layer and compacted by crawler tractors.	Downstream shoulder comprised outer zone of dumped cobbles and boulders.
Park Reservoir	lacustrine (?)	CL (?)	unk	unk	unk	unk	unk	unk	Limited information on fill materials, refered to as "impervious fill".	Glacial (?)	sand (?)	unk	unk	unk	unk	unk	unk	Only referred to as "sand shell"

Table D1.1: Case studies of slope instability of embankment dams – slides during construction (Sheet 8 of 10)

Name	General Comments on Design and Compaction	PROPERTIES OF FOUNDATION										SLIDE LOCATION AND GEOMETRY			
		Foundation (General)		Foundation (if Foundation involved in Slide)								Slide Classification (Hutchinson, 1988)	Slope Failure Geometry	Slide Location	State
		Soil / Rock	Description	Description	ASCS Class[n]	% fines	CF (%)	PI (%)	Density	Moisture Content	Comments				
Waco Dam	Homogeneous earthfill embankment with embankment and foundation filter zone. Central cut-off to bedrock foundation.	Soil	Alluvial - 2.5 to 5 m of clays and gravels over shale bedrock.	Surface of rupture along pre-sheared bentonitic clay shale bedding defect.	CH (?)	high (?)	high (?)	high (?)	unk	unk	Clay shales very stiff to hard, horizontally bedded. Extensive pre-sheared bedding plane in Pepper Shale between near vertical faults. Limited lateral resistance along faults.	Compound - translational basal component.	Type 5	Deep-seated slide in downstream slope. The slide back-scarp extended back to the upstream slope and the slide toe was 140 m beyond the downstream toe of embankment.	first time
West Branch Dam	Homogeneous embankment with downstream drainage blanket. Central cut-off to clay foundation. Closure section about 400 m width.	Soil	Glacial lake deposits overlain by alluvial silty sands. Soft to stiff clay stratum (15 to 18 m thickness) at 5 to 8 m depth below silty sands. Underlain by dense silty sands and very stiff clays.	Soft to stiff clay stratum, laminated (Su > 19 kPa)	CL - silty clay	high	unk	9 to 28	14.8 kN/cu.m. (dry density)	21 to 40% (several % below liquid limit)	Low to medium plasticity silty clay, soft to stiff.	Compound - translational basal component in clay foundation.	Type 5	Slide in upstream slope of embankment extending back to mid to upper level of foundation. Limited to zone of closure section. Basal surface 4 to 8 m below ground surface.	first time
North Ridge Dam	Homogeneous embankment with central cut-off to clay foundation. Embankment filter in downstream shoulder and filter on foundation. Constructed using low plasticity clays.	Soil	3 to 6 m of silty fine sand overlying firm to stiff high plasticity clays. Assume clays are lacustrine glacial deposits.	High plasticity clays	CH	high (?)	high (?)	51	15.3 kN/cu.m. (dry density)	36.50%	Of firm to stiff strength consistency. Undrained creep tests indicate Su ~ 40 kPa (compared with 55 kPa from quick triaxial tests)	Compound (?) - with translational basal component in foundation clays.	Type 5	Slide in downstream slope during construction. Cracks observed on upper portion of upstream slope. Deep seated.	first time
Marshall Creek Dam	Earthfill embankment with well compacted central and upstream clay zones. Downstream section comprises "loose rock and earth" rolled in 450 mm layers. Rockfill zone at toe.	Soil	15 m thickness of alluvium (clay, sandy clays silts and sands) over shale and limestone bedrock	Silty clay layer, 3 to 6 m thickness, soft to firm (not sure how extensive layer is)	CL/CH (?)	very high	30 to 60% (40 to 80% finer than 5 micron)	unk	unk	unk	Alluvial foundation comprises a mix of soil types. Not sure how extensive this layer is. References also indicate presence of loessic soils.	Compound (?) - with translational basal component in foundation.	Type 5	Deep-seated slide in the downstream slope. Slide crest at the upstream edge of the crest.	first time
Chingford	Suspect select and bank material placed relatively wet given low undrained strengths presribed to these materials (15 to 28 kPa). Ballast filter and rockfill toe downstream of puddle core.	Soil	Alluvial deposits comprising soft peaty clays and clays overlying river gravels. Up to 9 m depth the London Clay.	Clay (up to 4 m thick), soft to very soft (Su ~ 14 kPa)	CH	very high	very high	up to 100	14.9 kN/m^3 (bulk ?)	90%	Upper clay zone very soft to soft, very high plasticity and high moisture content.	Compound - translational basal component in soft clay foundation.	Type 2	Deep-seated slide in downstream shoulder during construction. Back-scarp at embankment crest, on the upstream side of the select fill.	first time
Hollowell	Puddle core earthfill dam. Drains installed in lower downstream zone comprising vertical rubble drains (perpendicular to centreline) and rockfill toe.	Soil	Alluvial or peri-glacial (?), layer of soft to very soft clay 1.5 m depth below foundation strip level.	Soft to very soft clay	unk	unk	unk	unk	unk	unk	No details on clay except that of soft to very soft undrained strength.	Compound - translational basal component rotational backscarp.	Type 5	Deep-seated slide in downstream shoulder. Back-scarp extended back to upstream side of select zone (on the crest).	first time
Carsington	Unusual boot design to upstream side of core. Core of CH clay placed well wet of OMC. Drainage layers placed in outer embankment zones. Small berm constructed at upstream toe over deepect section of embankment.	Soil (rock in gully section)	Periglacial high plasticity clay overlying residual soils and weathered bedrock profile.	Peri-glacial high plasticity clay with solifluction shears (reduced strength on shears).	CH	unk	62	43	unk	38%	Heavily over-consolidated (preconsolidation pressure > 600 kPa). Significantly reduced peak strength on solifluction shears (oriented parallel to ground surface) and small strain required to residual strength. Strain weakening in drained loading.	Compound - translational basal component in foundation, rotational through core.	Type 2	Failure in upstream shoulder, extended back to downstream side of core. Initial failure confined to 110 m width but spread to about 500 m. Suspect initiated in zone around boot where FEA indicated high shear stresses.	first time
Lafayette Dam	Zoned earthfill embankment with thin core (0.5H to 1V slopes) and broad sandy and gravelly (GC) outer earthfill zones. Shallow central cut-off then sheet piling to bedrock.	Soil	Alluvial (clays, sands and gravels) in broad valley section (2 - 3 m uo tp 20 m thick). Bedrock on abutment slopes.	Sandy clay alluvium (fine sand).	CH - fine sandy clay	high	high (?)	high (?)	unk	unk (but saturated)	Thick, near horizontal sandy clay stratum overlain by up to 5 m of surficial soils. Confined to deeper alluvial profile in broad gully region. No indication of shear strength but suspect relatively low.	Compound - translational basal component in clay (alluvium) foundation.	Type 5	Deep-seated slide in downstream slope, 12 to 15 m depth below ground surface. Back-scarp at upper edge of upstream slope.	first time
Galisteo Dam	Zoned earthfill embankment with thick core (2H to 1V upstream and 1H to 1V downstream). Thin outer earthfill zone on upstream side. Similar materials used for all zones, but wetter moisture spec. for core.	Soil	Alluvium (clay, sand, gravel and silty clay) up to 24 m thickness in broad gully. Abutments on bedrock.	Clay stratum in alluvial foundation. Up to 5 m thick and of firm to stiff strength consistency.	CL/CH (?)	unk	unk	unk	15.6 kN/m^3 (dry density)	24%	Laboratory testing indicates of firm to stiff strength consistency (Su ~ 50 kPa), with very stiff layers (?).	Compound - basal translational component on weak clay foundation layer.	Type 5	Deep-seated slide in upstream slope, limited to broad gully region of embankment. Slide back-scarp at upstream side of crest. Basal zone about 8 to 10 m below ground surface level.	first time
Dam FC21	Zoned earthfill embankment. Core has relatively flat upstream slope with relatively thin outer upstream zone. Central cutoff to bedrock.	Soil	Glacial soils of shallow depth in gully region overlying shale bedrock. Upper zone of shale glacially disturbed and contains bentonitic clay layers.	Glacially disturbed upper bedrock zone. Contains slickensided bentonitic shear zones.	CH	high	high	high	unk	unk	Upper glacially disturbed bedrock zone of 0.5 to 3 m thickness comprising CH clay with some cobbles and slickensided shear surfaces.	Compound - basal translational movement on pre-sheared bentonitic clays.	Type 5	Lateral spreading, both upstream and downstream, in central section of embankment. Greater upstream movement.	Lateral spreading
Park Reservoir	Zoned earthfill embankment with thick central core (1H to 1V slopes) and outer sand shells. Chimney filter on downstream side of core.	Soil	Lacustrine varved clays and silts under upstream shoulder, Glacial morraine under central and downstream shoulder.	Lacustrine varved clays and silts	CL (?)	high (?)	unk	unk	unk	unk	Limited information on properties of lacustrine deposits.	Compound - translational basal component in lacustrine foundation.	Type 2 (?)	Slide in upstream slope with back-scarp at the upstream edge of the crest. Translational within foundation.	first time

Table D1.1: Case studies of slope instability of embankment dams – slides during construction (Sheet 9 of 10)

Name	AT AND POST-FAILURE														Hydrogeology
	Slide Dimensions								Post-Failure Deformation Behaviour				Degree of Break-up of the Slide Mass	Comments	
	Width, W (m)	Length, L (m)	Depth, D (m)	Height (m)	Slope (deg)	Volume (cu.m.)	W/L	W/D	Displacement (m)	Velocity (mm/day)	Velocity Category	Comments			
Waco Dam	210	260	40	26	19.7	1.0E+06	0.81	5.25	7.9 m (max), downstream shoulder. 7.1 m crest settlement.	1600 to 1700 (max)	moderate	Slide first noted when cracks observed on the upper part of the downstream slope on 4/10/1961. Initial signs of movement dated back to 17/9/61. Movement accelerated slowly over many days (at least 30 days) then accelerated rapidly to 1700 mm/day by 25/10/61 before slowing.	Relatively minor, mostly in rear portion of slide and at toe.	Zone of bulging (toe of slide) located 140 m downstream of the embankment toe. Suspect slow acceleration of movement over more than 30 days associated with restraint on lateral margins through the embankment. Once a shear surface fully developed then the slide accelerated. Also passive restraint in toe region of slide a factor.	Very high excess pore pressures (r_u of 0.7 to 1) developed on the pre-sheared bentonitic seams and faults in the foundation. Excess construction pore pressures were measured as far as 800 from the dam on the pre-sheared surfaces.
West Branch Dam	200	150	27	21.5	14	300000	1.33	7.41	0.76 m (separation of conduit joints, 220 mm between 15 and 16)	21	slow	Joint separation (outlet conduit) between sections 15 and 16 first noted on 20/10/64. Filling continued whilst movement in outlet conduit monitored. Velocity of movement increased during fill placement. When filling was suspended deformation continued at a near constant rate. The crest was cut back to stp the movement.	Virtually intact	Only indication of movement was spreading of outlet conduit (i.e. no cracking observed on embankment). Fill placement stopped on 14/11/64. Cracking was observed on the embankment slopes on 19/11/64. The crest was then cut back and the movement stopped.	High pore pressures in soft clay stratum in the foundation, r_u of 0.8 to 0.85. Maybe less than this given suspected artesian pressures in underlying sands and gravels of 60 kPa. Excess pore pressures very slow to dissipate.
North Ridge Dam	unk	110	18	18.3	12.5	-	-	-	1.37 m, mid downstream slope, 0.9 m overthrust beyond toe.	unk	slow to moderate	No indication of velocity of movement. Cracking was observed on the upper upstream slope and mid height on downstream slope (no vertical displacement). The downstream toe and for 20 m beyond heaved and moved outward 0.9 m.	Virtually intact	Limited information on movement. Suspect driven by weak foundation and therefore movements most apparent in toe region. Amount of movement and relatively flat slopes would suggest movement probably occurred at a sloe to moderate velocity.	High excess pore pressures developed within the clay foundation, particularly in the upper layers (r_u approx. 0.7 to 0.85).
Marshall Creek Dam	240	80	26	24.4	20.5	300000	3.00	9.23	15 m at crest and on mid downstream slope.	1.5E+06	rapid	Crack initially observed near crest of embankment and then observed to increase in width. Movements accelerated, with the major portion of the movement occurring in 15 to 20 minutes (avg rate of 1 m/min). Heave movements (up to 4.3 m) for distance of 40 m beyond toe.	Some break up	Secondary crack observed on upper part of downstream slope typical of compound type slides with basal translational component.	No information. Suspect potentially high excess pore pressures developed within lower strength, low permeability clay zones in foundation.
Chingford	90	33	8.4	7.9	21.8	13000	2.73	10.71	0.6 m at crest, 4.3 m at downstream toe.	-	Moderate	Movement evident several days prior to slide (broken water pipe at toe, repaired then broke again). Suspect failure movement was at moderate rate ("after a while movement ceased").	Virtually intact	Deep seated compound failure with translational basal component through soft foundation and rear rotational backscarp through select and puddle core zones.	Suspect high pore pressures in soft clay foundation and embankment. Materials would be of very low permeability due to their high plasticity and high fines content.
Hollowell	200	50	11	11.4	14	80000 (main portion 12500)	4.00	18.18	490 mm at crest, 445 mm at toe	-	slow	Suspect slow given short distance of displacement.	Intact	Limited information on movement. Translational within soft to very soft foundation, rotational backscarp within select and core of embankment. Suspect significant lateral restraint due to limited persistence of the weak foundation.	Week of wet weather followed 33 day period of dry weather, during which a significant amount of fill was placed. Suspect high pore pressures in core and select fill, and possibly in clay foundation.
Carsington	500	105	22	28	18.4	550000	4.76	22.73	11.1 m at crest, 18.1 m at upstream toe.	17000 to 24000	Moderate	IVM in core indicated shear movements developing in October 1983. Disproportionate amount of lateral movement of upstream slope in late May 1984. Major slide started on 2nd to 3rd June and took place over 5 to 6 days. Initially at slow rate (< 5 mm/hr) and slowly increased over several days. Peak rate over-night on 5 June.	Limited	Upstream slide considered to have initiated in boot region where high shear stresses present. Significant restraint on lateral margins resulted in slowly accelerating movements over several days before major movement on night of 6 June.	Heavy rain on weekend that slide initiated. High pore pressures in core (r_u ~ 0.85) once pre-consolidation pressure exceeded (140 to 150 kPa). No excess pore pressures in foundation or Zone 2 outer fill (some in Zone 1 outer fill adjacent to core). Slow dissipation of pore pressures in core.
Lafayette Dam	160	155	50	35.5	20	700000	1.03	3.20	7 to 10 m at crest, 9 m at downstream toe.	2000 (avg over 3 days)	Moderate	Cracks observed at crest and along downstream toe (17/9/28 ?) followed by major movement of embankment (about 6 m) over 3 days. Bulging at toe preceeded major movement of embankment. Movement continued at a decreasing rate for a further 8 days after major movement.	Toe virtually intact, moderate to large degree of break up of backscarps.	No monitoring. Suspect movement similar to Carsington and Waco in that restraint on lateral margins resulted in a slow initial phase of acceleration before the slide was released at relatively high velocity. Significant period of continuing movement. Numerous deep cracks observed in crest region.	Water table at 6 to 9 m depth below ground surface. High pore pressures only encountered in clay stratum in foundation (r_u approx. 0.53 to 0.65). Reservoir level very low when failure occurred.
Galisteo Dam	400	150	38	38.5	17.5	1.2E+06	2.67	10.53	1.4 to 2 m (max) on mid to lower upstream slope.	50 (max)	slow	Movement first observed on 26/1/70 when cracks observed on mid upstream slope. Survey indicated up to 0.9 m movement on lower slopes. Placement suspended and toe berms added but movement continued when construction continued. Series of berm additions and stoppages to completion. Total displacement up to 2 m.	Virtually intact	A significant amount of movement had occurred before the slide was detected, and is indicative of initiation of the slide in the foundation. Movements stopped once construction completed. Movement of the upstream slope was significantly greater than that recorded for downstream slope (9 times greater).	Query over piezometer results. Excess pore pressures in core up to r_u values of 0.65 to 0.74. No piezometers in foundation, but suspect high pore pressures in weak clay foundation stratum.
Dam FC21	unk	170	42	43	18.4	unk	-	-	0.9 m lateral displacement (upstream) of conduit.	less than 1 (1970 construction period)	slow (?)	Unaware of movement until joint movements observed in outlet conduit on 14/10/69 (max 835 mm). Inclinometers installed after this recorded 50 mm displacement during 1970 construction period at rates < 1 mm/day. Rate of movement likely to have been much quicker during earlier un-recorded stage of movement.	Intact	No surface expression of movement. This may have been obscured by construction, but suspect would have observed cracking over shutdown period.	Very high pore pressures recorded at till shale interface during construction (r_u of 0.9 to 1). Very slow dissipation of pressures.
Park Reservoir	unk	80	17	21.3	19.7	-	-	-	0.9 m	unk	slow to moderate	Slide occurred overnight at suspected slow to moderate velocity given limited deformation. No reference to residual movements over subsequent days.	Virtually intact	Limited information. Section indicates movement in upstream zone of core and translational within foundation.	Excess pore pressures within varved clays and silts.

Table D1.1: Case studies of slope instability of embankment dams – slides during construction (Sheet 10 of 10)

Name	MECHANICS OF FAILURE				General Comments
	Cause/s of Landsliding	Trigger of Landsliding	Failure Mechanism	Comments on Failure Mechanics	
Waco Dam	Construction. High excess pore pressures on pre-sheared bedding surface and faults in foundation.	Construction.	Undrained failure at residual strength along pre-sheared bedding plane in foundation. Brittleness of slide mechanism associated with shearing through dilative, partially saturated embankment materials in backscarp and lateral margins, and also passive resistance at the toe of the slide.	Approximately 1 m of deformation occurred before slide accelerated at a rapid rate. Likely limited lateral restraint on near vertical faults. Interesting that toe of slide located 140 m downstream from dam, indicating this was the nearest positively oriented weakness in the foundation.	Translational movement on pre-sheared bentonitic bedding plane in Pepper Shale foundation. Slide limited to region between fault zones where Pepper Shale exposed at ground surface. Either side of faults no movement and much lower foundation pore pressures were observed.
West Branch Dam	Construction. High excess pore pressures developed in soft clay foundation.	Construction.	Undrained failure along soft clay foundation.	Possible strain weakening of the overall slide mass due to restraint on lateral margins and backscarp through the partially saturated embankment fill. Suspect the low plasticity, soft clay foundation is not strain weakening in undrained loading. Overall, the velocity of movement was slow and indicative of limited strain weakening to that point.	Case of lateral spreading of foundation during construction. Total movements relatively small, but continued movements (at near constant rate) once construction suspended indicate likely strain weakening of the slide mass. Movement only stopped when crest level cut back some 4 m. US Corp dam.
North Ridge Dam	Construction. Development of high pore pressures in low strength clay foundation.	Construction.	Undrained failure in low strength (firm), high plasticity clay foundation. Undrained strain weakening in CH clay foundation would contribute to distance of movement. Suspect brittleness of slide mechanism associated with development of shear surface through stiff to very stiff partially saturated embankment fill.	Failure controlled by low undrained strength clay stratum in foundation, along which translational movements took place. Suspect some degree of strain weakening of both the foundation (in undrained loading) and within the embankment fill.	Not clear if foundation is lacustrine deposits, but suspect so. High rate of construction contributed to failure as pore pressures in foundation had no time to dissipate and therefore strengthen the foundation.
Marshall Creek Dam	Construction. Likely development of high pore pressures in low strength clay foundation layers.	Construction. Trigger for rapid movement may have been collapse and flow liquefaction of loessic soils.	Suspect initial movements may have been associated with undrained instability of low strength clay layers in the foundation. However, this would not account for the rapid rate of movement of such a large volume. Suspect flow liquefaction of loessic soils.	Consider flow liquefaction of contractant loessic soils to be a possible cause for the rapid movement of the embankment. Liquefaction may have been triggered by movements associated with undrained instability of low strength clay layers.	Interesting failure given the large volume involved and the rapid rate of failure. Suspect flow liquefaction within loessic soils in the foundation may be a possible reason for the rapid movement.
Chingford	Construction. Development of high pore pressures. Relatively rapid rate of construction for puddle core earthfill dam.	Construction.	Undrained failure. Near normally consolidated CH earthfill and foundation. Both materials likely to be strain weakening in undrained loading, hence contributing to the distance and likely velocity of this small volume slide.	Strain weakening in undrained loading associated with orientation of clay particles and reduction in strength from fully softened to residual undrained strength on shearing. Normally consolidated.	Finite element analysis by Dounias et al (1988) was able to reasonably replicate the failure by total stress modelling. Very high shear stresses at the embankment toe and in the puddle core.
Hollowell	Construction and pore pressure development. Rainfall possible led to increased bulk density of the permeable shoulder fill.	Construction	Likely undrained failure through foundation and core zone.	Likely low undrained shear strength of foundation clay and embankment core and select fill. All likely near normally consolidated at relatively low confining pressures. Potential undrained strain weakening of CH core and possibly foundation. Suspect significant lateral restraint on the margins, due to the limited persistence of the weak foundation, limited the amount of movement.	Further movements observed after re-commenced construction (with new toe berm in place). Suspect lateral restrain significantly limited rate and amount of movement.
Carsington	Construction. High pore pressures in core. Solifluction shears in foundation.	Construction.	Progressive failure. Undrained failure through wet CH core, which lab tests indicate is strain weakening in undrained loading. Drained failure through foundation. Solifluction shears in foundation contributed significantly to progressive failure mechanism.	Finite element analyses by Potts et al (1990) indicates concentration of shear stresses and strains in core and boot region. Suspect undrained strength of core exceeded in boot region resulting in plastic straining and transfer of load onto foundation and other areas. Shear capacity of solifluction shears also exceeded which transferred load to ends of shears. Further straining resulted in strain weakening of core (undrained) and foundation (drained). Eventually factor of safety at or less than 1 resulting in acceleration of slide mass.	Classic case of progressive failure. CH core is strain weakening in undrained loading and foundation is strain weakening in drained loading. Presence of solifluction shears significantly contributed to progressive failure mechanism.
Lafayette Dam	Construction. High pore pressures developed in low strength alluvial clay stratum in foundation.	Construction.	Undrained failure within clay foundation. Back-scarp through high undrained strength and partially saturated embankment materials. Suspect slide brittleness associated with development of back-scarp through partially saturated soils and significant restraint on the lateral margins (limited persistence of weak foundation).	Significant restraint on the lateral margins due to extension of the slide beyond the possible extent of weak clay alluvium in the foundation. This would have given brittleness to the slide in addition to that associated with shearing through the dilative embankment materials. Bulging in downstream toe region prior to movement of embankment indicating that the foundation was driving the slide.	No monitoring. Slide occurred at a relatively "rapid" velocity. Suspect early warning signs of the slide were not detected until it was too late.
Galisteo Dam	Construction. Development of high excess pore pressures in clay foundation and undrained strength (of this layer) exceeded.	Construction.	Undrained failure along weak, low undrained strength clay layer in the foundation. Further movements after berm additions indicates strain weakening of slide mechanism. Strain weakening possibly associated with backscarp development through partially saturated earthfill and/or restraint on the lateral margins.	Suspect weak foundation layer is near normally consolidated under the embankment load. Relatively high pore pressures in core possibly suggest undrained failure through core (but of variable strength so potentially some dilation and strain weakening associated with shearing through core). Suspect significant restraint on the lateral margins due to tapering out of clay stratum at abutments and lateral shearing through embankment.	Would appear that the toe of the slide did not move in unison over a width of 400m. The initial 0.9 m displacement at the toe was limited to a width of about 60 m. Also latter movements varied significantly across the width of the embankment within the broad gully region.
Dam FC21	Construction. Pre-sheared bentonitic clay zones at residual strength.	Construction.	Lateral spreading (translational movement) along pre-sheared bentonitic clay seams at residual strength. Shear stress on basal shear plane exceeded, particularly in region close to embankment centreline. Consider that a slide surface had not fully developed through the embankment.	Suspect that a surface of rupture through the embankment had not fully developed. The slide initiated in the pre-sheared foundation (exceeded shear capacity) but the shear stress capacity of of the earthfill had not yet been exceeded. Possible passive resistance to sliding on shear plane in toe region. Also, restraint on the lateral margins (much greater glacial soil cover over bedrock on abutments).	Case of lateral spreading due to translational movements along pre-sheared bentonitic clays in the foundation. No surface expression of movement (cracking) observed.
Park Reservoir	Construction. Likely development of high pore pressures in foundation, not sure about core (no information).	Construction.	Delay in failure suggests progressive, strain weakening failure. Possibly undrained failure within foundation. Strain weakening maybe associated with development of shear surface through core.	Possible undrained strain weakening within foundation. No indication of width, but possible restraint on lateral margins may have delayed the failure.	Very limited information on failure and also embankment and foundation properties.

Table D1.2: Case studies of slope instability of embankment dams – slides in the upstream slope during drawdown.

Name	Location	Date of Failure	Years Since End of Construction	Embankment Zoning and Classification				Slide Location	Geology	Embankment Dimensions						EMBANKMENT MATERIALS								
																Material 1 (Core)								
				Zoning	Class[n]	Core Width	Core Type			Height, H_e (m)	Length, L_e (m)	Ratio L_e/H_e	Upstream Slope	Downstream Slope	Comments	Source	ASCS Class[n]	% fines	CF (%)	PI (%)	Density Ratio	Moisture Content	Compaction	Comments
Waghad	India	1919	34	Homog	2,0,0	c-vb	CH/MH	Emb	unk	26.9	1270	47.2	3H to 1V	4H to 1V	Embankment height reduced and downstream slope flattened after 1884 failure.	Alluvial (black cotton soil)	CH/MH	63 to 93	-	35	80 to 85%	6% wet	(By animal ?). Not formally compacted.	Near normally consolidated (low preconsolidation pressure)
Dam FD2		1993	32	Homog	0,0,0	c-vb	CL	Emb	Sedimentary - shales and sandstone	42 (28.7 failure section)	609	14.5	2.5H to 1V (upper 25 m), 10H to 1V below this.	2 to 4H to 1V	Zoned earthfill embankment in main section. In region of the failure (left abutment) the embankment is homogeneous with a 2H to 1V upstream slope, and constructed on an upstream sloping hillslope (7 to 13 degrees).	Alluvium	CL (some ML) - low plasticity sandy clay	81	28	15	100.5% (S Dev = 2.3%)	1% dry OMC (S Dev = 1%)	Rolled, well compacted. Placed in 225 mm layers and compacted by 12 passes of a sheepsfoot roller.	Well compacted, low plasticity, sandy clay. Likely high undrained shear strength and low permeability (2 x 10^{-10} m/sec). Variability of material plasticity and grading.
Dam FD3		2-Aug-31	20	Homog	2,0,0	c-vb	CL/CH	Emb	Sedimentary - shale	27.4	1980	72.3	2H to 1V (5H to 1V lower slope)	2.1H to 1V	Homogeneous earthfill embankment with drain and small rockfill zone at downstream toe. Upstream faced with concrete panels.	Alluvial / Colluvial	CL/CH - silty clay	85 to 100	30 to 45	14 to 34	15.2 kN/m^3 (dry) 95 to 100%	(Spec 3% dry to 3% wet). In 1933 - 17 to 24% (avg 1.5% wet)	Rolled, well compacted. Placed in 150 mm layers, compacted 12 to 21 tonne tamping rollers	Described after 1980's investigation as "moist and firm with some wet and soft zones"
Mondely Dam	France	Oct-81	1	Homog	1,1,1	c-vb	CL	Emb	unk	24	unk	-	3H to 1V	2.5H to 1V	Homogeneous earthfill embankment with central chimney filter and foundation filter.	Residual / Weathered argillaceous	CL	80	high (?)	10 to 30	98%	Placed wet of OMC	Rolled, well compacted. Cat 825 padfoot rollers	Lino (1997) considers filling to have been over-compacted. Compacted with heavy rollers at moisture contents wet of optimum. Low undrained shear strength, firm to stiff (Su ~ 40 to 80 kPa)
Sampna Tank	India	April 1961 and 1964	4 and 7	Zoned Earthfill	3,0,0	c-tk	CH	Emb	unk	21.3 (17.8 failure section)	unk	-	2H to 1V	2 to 3H to 1V	Zoned earthfill embankment with central cut-off and rockfill downstream toe.	Alluvium (black cotton soils)	CH	high	high	high	unk	unk	unk	No information.
Pilarcitos Dam	USA, California	1969	103	Puddle core earthfill	8,0,0	-	CL (?)	Emb	Sedimentary - sandstone (?)	29	158	5.4	2.5H to 1V	2H to 1V	Puddle core earthfill dam constructed in 1866. Downstream raise in 1874 (6 m raise) with puddle clay extending up the upstream face.	Colluvial	CL (?)	> 50	unk	> 11	unk	unk	Place in 75 mm layers, moistened then tracked by hauling wagons and carts	Finer material from colluvial borrow area. Presume placed wet of OMC, has low shear strength and low preconsolidation pressure.
Charmes Dam	France	20-Oct-09	3	Homog	0,0,0	c-vb	CL	Emb	Sedimentary	16.8	365	21.7	1.5H to 1V	1.9H to 1V	Homogeneous embankment with very steep upstream and downstream slopes. Concrete slab facing upstream slope. Constructed 1902-06.	fluvial and/or residual	CL - sandy silty clay	80	10	18	unk	unk	Rolled, reasonably compacted. Placed in thin layers and rolled with rollers.	Medium plasticity, slightly sandy, silty clay. Some formal compaction, but suspect limited given period of construction.
Enista Dam	Bulgaria	1982	13	Homog	1,0,1	c-vb	CL/CH (?)	Emb	unk	32.2	1370	42.5	3H to 1V	2.75 to 3H to 1V	Homogeneous embankment with foundation filter under downstream shoulder.	alluvial (?)	CL/CH (?) - silty clays	unk	unk	unk	unk	unk	Suspect rolled, well compacted (given period of construction)	Limited information. Permeability of 10^{-8} m/sec.
Telish Dam	Bulgaria	1982	14	Homog	0,0,0	c-vb	CL (?)	Emb	unk	29.5	1960	66.4	3H to 1V	2.5 to 3H to 1V	Homogeneous embankment with no filters. Constructed on an alluvial foundation.	alluvial (?)	CL (?)	unk	unk	unk	unk	unk	Suspect rolled, well compacted (given period of construction)	Limited information. Permeability of 1.5 x 10^{-9} m/sec.
Drenovets Dam	Bulgaria	1984	16	Homog	2,0,0	c-vb	CL (?)	Emb	unk	29	unk	-	3H to 1V	2 to 2.5H to 1V	Homogeneous embankment with rockfill zone at downstream toe.	alluvial (?)	CL (?) - silty clays	unk	unk	unk	unk	unk	Suspect rolled, well compacted (given period of construction)	Limited information. Silty clay of low permeability, 2 x 10^{-9} m/sec.
Mechka Dam	Bulgaria	1981	11	Homog	unk	c-vb	CL (?)	Emb	unk	32	unk	-	unk (suspect 3H to 1V)	unk	Homogeneous embankment. Little information available.	alluvial (?)	CL (?) - sandy silty clays	unk	unk	unk	unk	unk	Suspect rolled, well compacted (given period of construction)	No information. Constructed of sandy silty clays, suspect of low permeability, 2 x 10^{-9} m/sec.
Sushitsa Dam	Bulgaria	1981	11	Homog	unk	c-vb	CL (?)	Emb	unk	32.5	unk	-	unk (suspect 3H to 1V)	unk	Homogeneous embankment. Little information available.	alluvial (?)	CL (?) - sandy silty clays	unk	unk	unk	unk	unk	Suspect rolled, well compacted (given period of construction)	No information. Constructed of sandy silty clays, suspect of low permeability, 2 x 10^{-9} m/sec.
Malko Sharkovo Dam	Bulgaria	unk	1	Zoned Earthfill	3,0,1	unk	CL (?)	Emb	unk	41	1050	25.6	unk	unk	Zoned earthfill embankment. Very limited information and no section.	unk	unk	unk	unk	unk	unk	unk	Suspect rolled, well compacted (given period of construction)	No information.
Wassy Dam	France	1883	1	Homog	0,0,0	c-vb	CL	Emb	unk	16.5	unk	-	1.5H to 1V	1.9H to 1V	Homogeneous earthfill embankment with steep upstream and downstream slope. Constructed 1881 to 1883. Brick facing of upstream slope.	unk	CL - silty clay	85	< 10	18	unk	unk	unk	Medium plasticity silty clays. Possibly formal compaction, but suspect limited given period of construction. Calcareous material in some samples.
Mount Pisgah Dam	USA, Colorado	5-Sep-28	18	Homog	0,0,0	c-vb	ML	Emb	unk (possibly granitic)	23.2	195	8.4	1.5H to 1V	2H to 1V	Homogeneous earthfill embankment with steep upstream and downstream slopes.	Decomposed granite	ML - sandy silt	55	10 to 15	10	unk	unk	No formal compaction. Probable very poor construction practice.	Probable very poor compaction of low plasticity sandy silt earthfill
Forsythe Dam	USA, Utah	1921	1	Homog	0,0,0	c-vb	ML/SM	Emb	Igneous.	19.8	95	4.8	2H to 1V	1.5H to 1V	Homogeneous earthfill embankment with steep upstream and downstream slopes. Constructed 1915 to 1920.	Alluvial / Colluvial	SM/ML	35 to 55	< 10	3 to 8	unk	unk	No formal compaction. Spread in thin layers, moistened, then compacted by horses and wagons.	Likely limited level of compaction with high degree of variability. Lower portion of fill probably comprised clayey alluvium with a high organic content. Upper portion from colluvial/fluvial silty sands.
San Luis Dam	USA, California	04-Sep-81	14	Zoned Earth and Rockfill	4,2,2	c-vb	CL	Emb & Fndn	Sedimentary - marine deposits. Shales, sandstone and conglomerate.	56 (slide area), 116 dam	5650	48.7	3H to 1V (8H to 1V from 44 m below crest)	2 to 2.5H to 1V (6H to 1V from 44 m below crest)	Zoned earth and rockfill dam with very broad core section (2H to 1V upstream and 1H to 1V downstream) and thin outer earth and rockfill zones. Constructed early to mid 1960's.	Alluvial and Colluvial	CL (some SC) - sandy clay	66 (35 to 78)	unk	23 (8 to 36) medium plasticity	102.0%	1.2% dry	Rolled, well compacted. Placed in 150 mm layers and compacted by tamping rollers.	Well compacted, medium plasticity, sandy clay with high undrained shear strength and low permeability (10^{-9} m/sec). Placed dry of OMC.
Bear Gulch	USA, California	Oct 1936, Nov 1942, Nov 1944.	6 to 14 years after dam raising. (40 to 48 years after initial construction).	Homog	0,0,0 or 1,1,1	c-vb	CL	Emb & Fndn	Sedimentary - sandstone and shale.	19.4	220	11.3	3H to 1V	2H to 1V	Homogeneous earthfill embankment. Initially constructed in 1896 (to 13.7 m). Raised on downstream side in 1929/30 to 19.4 m. Rockfill drains in downstream slope, but no details.	Alluvial	CL - sandy clay	65	20 to 25	25 (medium plasticity)	unk	unk	No formal compaction. 1896 fill compacted by stock. 1929/30 fill - rolled in thin layers with sheepsfoot roller.	1896 fill poorly compacted. 1929/30 fill rolled (downstream raise). Sandy clay of medium plasticity with some gravel.
Old Eildon Dam	Australia	1927 and April 1929	2 to 4	Concrete corewall, rockfill	10,0,0	-	-	Emb & Fndn	Sedimentary - shale	42 (29 at failure section)	995	23.7	1.3 to 1.4H to 1V	1.5H to 1V (including two benches)	Concrete corewall rockfill embankment with zone of puddle clay on upstream side of corewall. Virtually completed by end of 1925.	Alluvial (puddle clay)	CL (?) - silty clay, some CH clays	high	70 to 80	unk	16.2 kN/m^3 (dry)	wet OMC	No formal compaction. Wetted and then trafficked with horse and dray	Puddle clay zone on upstream side of core-wall, 8 to 11 wide at base. Silty clay (of medium plasticity) placed well wet of OMC. Of soft strength consistency (Su as low as 20 kPa), stiff in upper 5 m. May have softened significantly on wetting.

Table D1.2 Case studies of slope instability of embankment dams – slides in the upstream slope during drawdown (Sheet 2 of 5).

Name	EMBANKMENT MATERIALS									General Comments on Design and Compaction	FOUNDATION MATERIAL PROPERTIES									
	Material 2 (Shoulder fill)										Foundation (General)		Foundation (If foundation Involved in Slide)							
	Source	ASCS Class[n]	% fines	CF (%)	PI (%)	Density Ratio	Moisture Content	Compaction	Comments		Soil / Rock	Description	Description	ASCS Class[n]	% fines	CF (%)	PI (%)	Density	Moisture Content	Comments
Waghad	-	-	-	-	-	-	-	-	-	Homogeneous embankment constructed of CH/MH earthfill. Placed wet without any formal compaction.	Soil	Murum over weathered bedrock	-	-	-	-	-	-	-	-
Dam FD2	-	-	-	-	-	-	-	-	-	Failure occurred in homogeneous section constructed on steep left abutment. Natural slope is 7 to 13 degrees in upstream direction.	Rock	Interbedded sandstones and shales.	-	-	-	-	-	-	-	-
Dam FD3	-	-	-	-	-	-	-	-	-	Homogeneous embankment constructed of medium to high plasticity sandy clays.	Soil	Alluvial - CL/CH clay "Adobe Clay", stiff to hard, friable, 2 to 12 m thickness. Underlain by Alluvial sand and gravel, then weathered shale.	-	-	-	-	-	-	-	-
Mondely Dam	-	-	-	-	-	-	-	-	-	Homogeneous embankment constructed of low to medium plasticity clays compacted wet of OMC.	unk	unk	-	-	-	-	-	-	-	-
Sampna Tank	unk	CL/CH	> 50	> 50	unk	unk	36%	unk	Limited information. Shoulder fill described as not free draining.	Zoned earthfill embankment with thick central core (1H to 1V slopes). Outer earthfill of high clay content and low permeability.	unk	unk	-	-	-	-	-	-	-	-
Pilarcitos Dam	colluvial	GC - clayey sandy gravel, low plasticity	23	< 10	11	94%	unk	Rolled, limited compaction. Placed in 300 mm layers, compacted by carts and hauling wagons then rolled with 3 ton roller.	Colluvial material derived from limited transport of local sandstone hillslopes. Fine to coarse gravel size. Layers sloping toward core.	Narrow puddle core of low plasticity sandy clay and shoulder fill of clayey sandy gravel.	Soil	Alluvial (sand, gravel and clay) of 14 m thickness overlying bedrock.	-	-	-	-	-	-	-	-
Charmes Dam	-	-	-	-	-	-	-	-	-	Homogeneous earthfill embankment constructed of medium plasticity sandy silty clays.	Soil	"Blue clay", not sure of origin. No information on properties.	-	-	-	-	-	-	-	-
Enista Dam	-	-	-	-	-	-	-	-	-	Homogeneous embankment constructed of silty clays.	Soil	Alluvial (?) - silty clay of 2 m thickness overlying clayey gravels.	-	-	-	-	-	-	-	-
Telish Dam	-	-	-	-	-	-	-	-	-	Homogeneous embankment constructed of low permeability materials. Suspect filling dominantly clayey.	Soil	Alluvial. Suspect relatively sandy or gravelly given permeability of 10^{-6} m/sec. Query over whether or not upper silt layer was adequately removed prior to construction.	-	-	-	-	-	-	-	-
Drenovets Dam	-	-	-	-	-	-	-	-	-	Homogeneous embankment constructed of silty clays. Rockfill zone at downstream toe.	Soil	Alluvial (?). Permeability of 2 x 10^{-7} m/sec.	-	-	-	-	-	-	-	-
Mechka Dam	-	-	-	-	-	-	-	-	-	Homogeneous embankment constructed of sandy silty clays.	unk	unk	-	-	-	-	-	-	-	-
Sushitsa Dam	-	-	-	-	-	-	-	-	-	Homogeneous embankment constructed of sandy silty clays.	unk	unk	-	-	-	-	-	-	-	-
Malko Sharkovo Dam	unk	Cl (?) - sandy clay	unk	unk	unk	unk	Likely wet of OMC.	Suspect rolled, well compacted (given period of construction)	Limited information. Reference to being dense, low permeability and having excess pore pressures post constructions.	Zoned earthfill embankment construction using a sandy clay of low permeability for the upstream shoulder.	unk	unk	-	-	-	-	-	-	-	-
Wassy Dam	-	-	-	-	-	-	-	-	-	Homogeneous embankment constructed of medium plasticity silty clays.	Soil	Section indicates the foundation is clay. No further information than this.	-	-	-	-	-	-	-	-
Mount Pisgah Dam	-	-	-	-	-	-	-	-	-	Homogeneous embankment constructed of sandy silts. Report that the work was not well done and was carried out with disregard of good dam engineering practice.	Soil	Shallow thickness (up to 3 m) of clayey sand overlying bedrock.	-	-	-	-	-	-	-	-
Forsythe Dam	-	-	-	-	-	-	-	-	-	Homogeneous embankment constructed of low plasticity sandy silts and silty sands.	Soil	Shallow thickness (3 m) of clay over bedrock.	-	-	-	-	-	-	-	-
San Luis Dam	Zone 3 - weathered sedimentary and alluvial earthfill, Zones 4 & 5 - crushed/blasted basalt rockfill.	CL/GC/SC - mixture of materials (Zone 3)	variable	variable	variable	99%	1.4% dry	Rolled, reasonable to well compaction of Zone 3 (300 mm layers rolled with tamping roller). Zones 4 & 5 - up to 900 mm, limited rolling	Zone 3 material comprises a mixture of weathered rock and alluvium, reasonably well compacted. Rockfill zones are loose placed.	Very broad core zone of medium plasticity sandy clays with thin outer rockfill zones on upstream slope.	Soil	Colluvial slopewash and residual soils of shallow depth overlying weathered bedrock.	Colluvial slopewash on hillslope.	CH (CL and GC in places) - slightly sandy clay	83	55	40 to 55	unk	dry (when placed)	Highly plastic slightly sandy clay slopewash of shallow thickness. Some variability with low plasticity and gravelly zones. Dry and hard when embankment constructed, fissured. Softened significantly on saturation. Low permeability (10^{-9} to 10^{-10} m/sec).
Bear Gulch	-	-	-	-	-	-	-	-	-	Homogeneous embankment constructed of medium plasticity sandy clays with no formal compaction. Raise in 1929/30, on downstream side, using rolled medium plasticity sandy clays.	Rock	Interbedded soft sandstone and clay shale. 1936 investigation encountered soft "mushy" clay stratum below upstream shoulder (0.9 to 1.2 m below foundation level).	-	-	-	-	-	-	-	Limited information. 1936 investigation (in upstream slope) encountered a "wet mushy clay stratum" immediately underlain by a permeable zone. Hole remained dry until this permeable stratum was encountered. Water level rose to that of the reservoir.
Old Eildon Dam	Sedimentary - soft shales and sandstones, and Metamorphic - hard slate	gravel to cobble size	very low	very low	unk	14 kN/m^3 (dry density)	unk	No compaction. Hand loaded onto wagons then dumped.	Rockfill dumped at its angle of repose (38 degrees). Shale prone weathering and breakdown, sandstone not so prone.	Zone of medium plasticity puddle clay placed upstream of core-wall. Rockfill dumped at its angle of repose.	Soil (in slide area)	Alluvium soils (clays overlying sandy gravels) of 6 to 20 m depth overlying bedrock.	Alluvial clays	CL to CH (?)	high	high (?)	unk	unk	unk	Alluvial clay of "firm" to stiff strength consistency.

Table D1.2 Case studies of slope instability of embankment dams – slides in the upstream slope during drawdown (Sheet 3 of 5).

Name	AT AND POST-FAILURE														
					Slide Dimensions								Post-Failure Deformation Behaviour			
	Slide Classification (Hutchinson, 1988)	Slope Failure Geometry	Slide Location	State	Width, W (m)	Length, L (m)	Depth, D (m)	Height (m)	Slope (deg)	Volume (cu.m.)	W/L	W/D	Displacement (m)	Velocity (mm/day)	Velocity Category	Comments
Waghad	Rotational (possibly part translational)	Type 2 (?)	Failure of upstream slope. Deep seated failure that extended back to downstream edge of crest.	first time	330 (?)	90	11	29	14	200000	3.67	30.00	4.8 m crest settlement, 10 m displacement on lower slope.	-	(Moderate to Rapid)	Suspect moderate to rapid velocity of movement given relatively large distance travelled. No indication of velity or time period of movement.
Dam FD2	Compound - possibly two translational planes on which sliding occurred.	Type 2	Failure in upstream slope. Crest of back-scarp 6.5 m below crest level.	reactivation	85	55	5.5	23	26.6	18000	1.55	15.45	0.423 m	27	slow	Reactivation of movement of existing slide monitored during 1994 drawdown. Movement did not start until reservoir drawn down 5.6 m. Slide moved as intact mass.
Dam FD3	Rotational	Type 1	Failure in upstream slope. Crest of back-scarp 7.9 m below crest level.	first time	100	23	5	12.1	26.6	7000	4.35	20.00	1.7 m at head of scarp, 6 to 12 m at toe.	unk	suspect rapid	Cracking at crest observed during 1928 drawdown. Slide occurred during 1931 drawdown. Large and likely rapid movement at the slide toe where it ran out onto the 2H to 1V upstream slope.
Mondely Dam	Rotational	Type 2 (?)	Failure in upstream slope. Extends back to near the centreline of the crest.	first time	unk	30	7	8.7	18.4	-	-	-	0.4 m on first drawdown (1981), 0.2 m on second drawdown.	3 (up to 30 ?)	very slow to slow	Failure developed slowly. Longitudinal cracks observed on crest followed by development of the failure surface. Similar slow movements occurred on the second drawdown.
Sampna Tank	Rotational (?)	Type 1 (?)	Failures in upstream slope. Both 1961 and 1964 slides extended back to the upstream edge of the crest.	first time (1964 slide)	100	30 (g)	5 to 8 (guess)	15	26.6	10000	3.33	15.38	11.9 m	-	rapid	1964 slide described as having "suddenly collapsed". Initial width 60 m, spread to 90 m in a couple of hours. Suspect rate of movement was in the rapid category.
Pilarcitos Dam	Rotational (?)	Type 1 (?)	Failure in upstream slope on rapid drawdown. Top of back scarp about 3 to 4 m below crest. Several backscarps on upper upstream slope.	first time	unk	unk	unk	unk	21.8	unk	-	-	1 m at backscarp, only rough estimate.	-	suspect slow	Upstream slope failure on very rapid drawdown (7.6 m in 2 weeks, 0.54 m/day). No information on velocity or timing of movement. Suspect slow given limited amount of deformation.
Charmes Dam	Rotational	Type 2	Failure in upstream slope. Extended back to the centreline of the crest. Possibly reasonably deep seated within embankment, but this is not confirmed.	first time	unk	25	8	17	33.7	unk	-	-	unk.	-	slow	No information on amount and velocity of movement. Sherard (1954) indicates movement occurred over a period of 6 weeks, therefore categorised as slow.
Enista Dam	Rotational (?)	Type 2 (?)	Failure in upstream slope. Top of backscarp 10 to 12 m below crest on upstream slope. Possibly an incipient failure.	first time	200	60	unk	20	18.4	unk	3.33	-	0.4 m (width of cracks on upstream slope)	unk	suspect slow	On large drawdown cracking was observed to have occurred over a width of 200 m on the mid to upper upstream slope. Only report on amount of deformation is 400 mm width of cracks.
Telish Dam	Rotational (?)	Type 2 (?)	Failure in upstream slope. Top of backscarp 8 m below crest on upstream slope.	first time	> 100	< 60	unk	20 (maximum likely)	18.4	unk	> 1.7	-	1.0 m.	unk	suspect slow	In 1977, on a routine drawdown, longitudinal cracks of 0.2 to 0.3 m width were observed on the upstream slope, at 10 m below crest level. The cracks were repaired. In 1980, on drawdown, wider and longer cracks were observed at 8 m below crest (also repaired). In 1982, still wider cracks and slide movements up to 1 m were observed.
Drenovets Dam	Rotational (?)	-	Failure in upstream slope. No indication of location or size of failure.	first time	unk	unk	unk	unk	18.4	unk	-	-	unk.	unk	suspect slow	No information on slide. Suspect that it occurred during a relatively routine drawdown.
Mechka Dam	unk	-	Failure in upstream slope. No indication of location or size of failure.	first time	unk	unk	unk	unk	18.4 (?)	unk	-	-	unk.	unk	suspect slow	No information on failure. Occurred during a routine drawdown.
Sushitsa Dam	unk	-	Failure in upstream slope. No indication of location or size of failure.	first time	unk	unk	unk	unk	18.4 (?)	unk	-	-	unk.	unk	suspect slow	No information on failure. Occurred during a routine drawdown.
Malko Sharkovo Dam	unk	-	Failure in upstream slope. No indication of location or size of failure.	first time	unk	unk	unk	unk	unk	unk	-	-	unk.	unk	unk	No information on amount of movement or velocity.
Wassy Dam	Rotational	Type 2	Failure of upstream slope on rapid drawdown (first drawdown). Top of back-scarp at upstream edge of crest.	first time	unk	25	6.5	16.5	33.7	-	-	-	unk.	unk	unk	No indication of velocity or amount of movement.
Mount Pisgah Dam	Rotational	Type 2 (?)	Failure of upstream slope following rapid drawdown. Top of back-scarp at downstream edge of crest.	first time	60	40	11	23.2	33.7	11000	1.50	5.45	7 m at crest, up to 9 m at toe.	unk	suspect moderate to rapid	No information on velocity of movement or comment on observations prior to or leading up to failure.
Forsythe Dam	Rotational (?)	Type 1 (?)	Failure of upstream slope following very rapid drawdown. Top of back-scarp shown at centre of the crest.	first time	unk	28	8	14.5	26.6	unk	-	-	4 m at crest. Possibly 22 m at toe.	-	suspect rapid	Limited information. Section showing post-failure profile is very approximate. Possible that the slide material that evacuated from the failure bowl moved rapidly on the 2H to 1V slope accumulating at the upstream toe of the slope.
San Luis Dam	Compound - translational basal component rotational backscarp through core material.	Type 2	Failure in upstream slope following rapid drawdown. Top of back-scarp located 4.5 m below crest on upstream slope.	first time	360	155	25	56	15.8 (upper slope 18.4)	1.0E+06	2.32	14.40	17 m crest to toe region.	~ 1000 to 2000	Moderate	Slide first observed on 14 September 1981. Photos showed scarp evident on 4 Sept. Suspect movement started much earlier (early August ?). Movement likely to have initiated at a slow rate and gradually increased to a peak (about 1 to 2 m/day) over a period of 30 to 50 days before decreasing in rate and eventually coming to rest some 100 to 130 days after movement began.
Bear Gulch	Compound - translational basal component in foundation. Steep backscarp through embankment.	Type 2	Failures in upstream slope following drawdowns in 1936, 1942 and 1944. Top of back-scarp located 3 to 6 m below crest on upstream slope. Movement vector at top of backscarp relatively flat (15 to 18 degrees).	first time	30	50	11.5	16.5	18.4	8000	0.60	2.61	1936 - 0.29 m; 1942 - 0.32 m at crest backscarp.	unk	suspect slow	Small slide in upstream slope in 1914 on very rapid drawdown (reservoir emptied in 3 days). In 1936 a large crack was observed in upstream slope extending down the upstream slope to the toe. Similar movement occurred in 1942, with the crack at a higher elevation. In 1944 - identical crack to 1942. Movement vector at backscarp 15 to 18 degrees to horizontal.
Old Eildon Dam	Compound - translational basal component on clay (alluvium) foundation or layer immediately above.	Type 2	Deep seated failure in upstream slope on drawdown. Top of backscarp is upstream side of corewall (centreline of crest). Slide located over alluvial clay foundation between bedrock foundation area and lower hillslope of the left abutment.	first time (1927), reactivated in 1929.	220 (widened to 365 m)	50	26	29	36	300000	4.40	8.46	9.1 m crest settlement up to Dec 1928. Apr to May 1929 - 14 m crest settlement, 17 m displacement at upstream toe.	> 5000 (max)	Moderate	Crest subsidence occurred prior to slide in 1929, and totaled 9.1 m. Suspect triggered by 1927 drawdown. Movements, at a moderate velocity, occurred in late April 1929 following drawdown and continued for several months at a relatively slow rate.

Table D1.2 Case studies of slope instability of embankment dams – slides in the upstream slope during drawdown (Sheet 4 of 5).

Name	POST FAILURE		HYDROGEOLOGY						
	Degree of Break-up of the Slide Mass	Comments	Reservoir Operation		Drawdown Causing Failure	Pore Pressures			Comments
			Steady / Fluctuating	Comment		Upstream	Core	Comments	
Waghad	minor to partial	Limited information. Section indicates relatively large movement and partial degree of break up.	unk	Maximum stored level at 24 m.	Water level at end of drawdown at 10 m (possible 14 m drawdown)	suspect limited response to reservoir (low permeability fill)	limited change (low permeability fill)	Standpipes indicate embankment is relatively permeable. Query this given CH/MH material classification. Possible that outer zones are permeable due to shrink/swell related cracking.	-
Dam FD2	Virtually intact	First time slide suspected of occurring in 1993 (fastest drawdown). Movement slowed once rate of drawdown decreased.	Fluctuating	Typical yearly drawdown of 4 to 6 m from full supply level. Significantly larger drawdowns in 1976/77, 1988/89, 1992, 1993 and 1994.	1993 drawdown was largest and fastest (up to 3 times the rate previously) and suspect that slide occurred during this event. 1977 and 1989 events were to about the same base level as in 1993. 1994 - 10.6 m @ 270 to 300 mm/day; 1993 - 16.7 m @ 335 to 400 mm/day; 1976/77/88/89/92 - 9 to 14.5 m at 100 to 130 mm/day.	Some response, but delayed compared to reservoir level. For 1977, 1988/89 and 1993 drawdowns piezometric head in outer fill greater than reservoir level.	Small response to reservoir fluctuation.	Permeable bedrock on downstream side of dam section. Zone 1 (or core) filling of low permeability.	-
Dam FD3	Significant, particularly at toe.	Slide material travelled down 2H to 1V slope onto flat berm and then onto 5H to 1V slope. Note that different plans show differing amounts of movement at the toe.	Fluctuating	Typical yearly drawdown of 4 to 6 m, mostly from near full supply level. Large drawdowns (> 10 m) in 1928, 1930 and 1931.	1931 - 10.3 m at 110 mm/day (max) to base water level (19.4 m below crest). 1928 - > 11 m at max 130 mm/day; 1930 - > 10 m at max 95 mm/day (Note: max is average over 2 month period)	Negligible change. Standpipe and piezometer records indicate negligible response to reservoir change.	Negligible response to reservoir drawdown.	Embankment is of very low permeability as indicated by negligible change in piezometer and standpipe levels to reservoir fluctuations.	Rainfall was not a contributing factor to instability (i.e. through water filled cracks). Limited rainfall for 12 months prior to failure and no significant heavy rain days leading up to slide.
Mondely Dam	Virtually intact	Drawdown failure in upstream slope that occurred very slowly. Stabilisation works in early 1982 did not stop additional movements occuring on the drawdown later that year.	Fluctuating	no information	First drawdown in history of embankment. Occurred 1 year after the end of construction.	Negligible change. Piezometers in upstream slope show little change to fluctuations in reservoir level.	Negligible response to reservoir drawdown.	Embankment materials of very low permeability ($k = 2 \times 10^{-11}$ m/sec).	Very high pore pressures within embankment fill developed during construction ($r_u \sim 0.8$). Very slow dissipation and still quite high at time of drawdown failure.
Sampna Tank	Virtually intact	1964 drawdown was the lowest drawdown in embankment history.	Suspect fluctuating	no information	No information on 1961 drawdown. 1964 - 9.1 m drawdown to 0.6 m above low water level (11.4 m below crest, 9.6 m below maximum level) over 8 months at rate of 30 to 60 mm/day.	Suspect limited change given low permeability of outer earthfill.	Suspect negligible.	Low permeability of outer zoned fill. High phreatic surface in upstream shoulder on drawdown.	-
Pilarcitos Dam	Virtually intact	Limited information.	unk	no information	Reservoir drawn down very rapidly in 1969; 7.6 m in 2 weeks (540 mm/day). Suspect most severe drawdown in history of dam.	Likely to follow reservoir level under normal drawdown conditions.	Suspect limited.	Expect shoulder fill to have relatively high permeability given grading. Likely to have lower vertical permeability than horizontal due to layering during construction. Also, sloping of layers toward core likely to result in perched water tables on very rapid drawdown.	Suspect most rapid drawdown in embankment history. This drawdown was undertaken at the start of the rainy season. May also have permeability restriction on upstream face due to siltation effects over the previous 100 + years.
Charmes Dam	unk	Limited information. Likely slow velocity of movement.	unk	no information	Deepest drawdown in history of embankment.	Suspect limited response to reservoir change given embankment constructed of medium plasticity sandy silty clay.	Suspect limited to negligible.	Likely low permeability of embankment fill.	Slide occurred at time of the deepest drawdown in embankment history.
Enista Dam	Intact	Possibly an incipient failure. No indication that movements occurred as shearing on a defined surface of rupture (i.e., no report on vertical displacement at back-scarp).	Suspect fluctuating	Lowest reservoir level prior to slide occurring was to 11.2 m below crest (or 8.9 m below max. level).	Deepest drawdown in 13 year history of embankment. Reservoir drawn down to 24.3 m below crest (22 m below maximum storage level).	Limited reduction in phreatic surface to reservoir drawdown. Phreatic surface in embankment only dropped 0.5 to 1 m from level prior to drawdown.	Likely negligible.	Low permeability of embankment fill. Very limited response of phreatic surface in upstream shoulder to drawdown.	-
Telish Dam	Intact (?)	1977 and 1980 cracking are indicative of an incipient failure and were a precursor to the slide movements that occurred in 1982.	Fluctuating	Reservoir undergoes seasonal drawdown. No indication of typical height or rate of drawdowns.	1977 - routine drawdown. Suspect 1980 and 1982 drawdowns were also relatively routine.	Negligible response to drawdown. 1983 drawdown - over 3 to 4 months phreatic surface only dropped 0.2 to 0.3 m.	Likely negligible.	Low permeability of embankment fill. Negligible response of phreatic surface in upstream shoulder to drawdown.	-
Drenovets Dam	Intact (?)	Suspect it is much like the failure at Telish Dam. No information given on the slide.	Suspect fluctuating	no information	No quantitative information, but suspect the 1984 drawdown was routine.	Suspect limited to negligible response to reservoir fluctuations.	Likely negligible.	Low permeability of embankment fill, therefore likely limited to negligible response of phreatic surface in upstream shoulder to drawdown.	-
Mechka Dam	Intact (?)	Suspect it is much like the slide at Telish Dam. No information given on the slide.	Suspect fluctuating	no information	No quantitative information, but reference to 1981 drawdown as being routine.	Suspect limited to negligible response to reservoir fluctuations.	Likely negligible.		-
Sushitsa Dam	Intact (?)	Suspect it is much like the slide at Telish Dam. No information given on the slide.	Suspect fluctuating	no information	No quantitative information, but reference to 1981 drawdown as being routine.	Suspect limited to negligible response to reservoir fluctuations.	Likely negligible.		-
Malko Sharkovo Dam	unk	Failure of the upstream slope occurred during the first drawdown. Construction pore pressures still present.	Failure on first drawdown	Failure on first drawdown	Failure on first drawdown. No quantitative information on the drawdown.	Limited to negligible response to reservoir fluctuations as indicated by slow dissipation of construction pore pressures.	Likely negligible.	Low permeability of upstream shoulder fill as indicated by presence of construction pore pressures 1 year after construction had been completed.	-
Wassy Dam	unk	Slide occurred on first drawdown, which was very rapid.	Failure on first drawdown	Failure on first drawdown	Was the first drawdown and was undertaken within a year of completion of construction. Very rapid drawdown of 10 m within 20 to 25 days (400 to 500 mm/day) from full supply level.	Little time for infiltration of stored water into the medium plasticity sandy clay embankment fill.	No opportunity for a response given short impoundment period.	Likely low permeability of embankment filling. If placed wet of optimum may have high excess pore pressures associated with construction.	Failure occurred at time of very rapid drawdown. Reservoir had only reached full supply level in early August 1883 before it was drawn down.
Mount Pisgah Dam	Some break up	Slide occurred following a rapid drawdown of the reservoir. Suspect of moderate to rapid velocity given the amount of movement that occurred.	unk	no information	Reservoir full in early summer months (June to July). Drawdown of 13.4 m over about two months initially at a steady rate and then at a very rapid rate for several days prior to the failure. Average rate for drawdown is 220 mm/day.	Some but likely limited reduction in phreatic surface to reservoir drawdown, particularly at high drawdown rates.	Suspect some response but likely delayed.	Likely that embankment fill is of moderate permeability and would respond with reservoir under slow drawdown conditions (contains 70% coarse silt to sand size and low clay content). Suspect delayed response under rapid drawdown.	Failure occurred following very rapid drawdown over a period of several days on the back of a steady drawdown over several months.
Forsythe Dam	Possibly significant break up.	Failure triggered by extremely rapid, but short, drawdown. Suspect failure confined to the mid to upper portion of the upstream slope and the run-out from the failure travelled down the steep upstream slope.	slide occurred on first drawdown	Erosion through spillway occurred shortly after reaching full supply level.	Once reservoir level reached full supply level erosion in the spillway region washed out a 4.6 m deep channel. The reservoir level was drawn down 4.6 m in several hours; i.e., at an extremely rapid rate (2.3 m/hour).	Negligible response likely under the extremely rapid drawdown.	Negligible response likely under the extremely rapid drawdown.	No time for drainage to occur in the short time (2 hours) it took for the reservoir level to fall 4.6 m.	Reservoir impounded some water during construction.
San Luis Dam	Virtually intact	Monitoring only picked up the latter part of movement, the slow down phase after the peak velocity. Peak velocity likely on or slightly before the 14 Sept 1981 (some 30 to 50 days after movement likely to have started). Movements show similar velocity on different parts of the slide surface.	Fluctuating	Typically, seasonal drawdown of 10 to 25 m (years preceeding slide). Larger events in 1975 (30 m at 350 mm/day), 1976 (43 m at 560 mm/day) and 1977 (36.5 m at 450 mm/day).	1981 - Drawdown from full supply level to EL 110.5 m (55 m) in 119 days at a maximum average 50 day rate of 625 mm/day. Largest drawdown in embankment history. Only 1977 drawdown was to a lower base water level (EL 107.5 m).	Zone 3 - responds with reservoir (some piezos show a delay). Zone 1 - upstream portion shows some to limited and delayed response. Slopewash - variable response, some piezos show lag with some response.	Zone 1 - delayed, very limited to negligible response to reservoir fluctuations.	The slopewash (or portions of it) and the upstream portion of the Zone 1 fill show a delayed and generally some to limited response to reservoir fluctuations. On large and rapid drawdowns therefore, the core and slopewash show a piezometric level above that of the reservoir. (Note that reference to the slopewash is in the vicinity of the slide area).	Failure occurred following the most rapid and largest drawdown in the history of the embankment. The reservoir had been subjected to several previous large and rapid drawdowns.
Bear Gulch	suspect virtually intact.	Small amount of movement would suggest slow velocity of movement. Small amount of "mushy" material material in crack (backscarp), but otherwise "sound and dense" material either side of crack. Movement suggests strongly translational with formation of tension crack at backscarp.	Fluctuating	Typical drawdown rate of about 90 mm/day.	1936 - 8.2 m drawdown at average of 90 mm/day, but occurred early in the season. 1942 - similar drawdown rate and to similar level as in 1936. 1944 drawdown similar again.	Unknown, suspect limited response given fill is medium plasticity sandy clay. Permeable zone in foundation follows reservoir.	Suspect limited to negligible.	No information on piezometric levels. Suspect some but delayed response to drawdown given embankment fill is a medium plasticity sandy clay.	-
Old Eildon Dam	Minor break up	Suspect large drawdown in 1927 initiated the slide, and that much of the crest subsidence prior to 1929 occurred during this event (reference to continued dumping of rockfill at crest to maintain elevation). In 1929 the movement was reactivated on drawdown. Widening of the crest (post the 1927 drawdown) attributed to decreasing the overall stability of the slope.	Fluctuating	Reservoir in operation whilst embankment under construction. Water impounded from 1922 and subject to seasonal drawdown. Reached full supply level in August 1927.	1927 - 32.5 m at average rate of 190 mm/day. Rate up to 500 mm/day in latter weeks of drawdown. 1929 - 15.5 m at average rate of 100 mm/day. Increased rate of 230 mm/day in 2 weeks prior to slide.	Rockfill permeable. Foundation - variable response, typically delayed response of lesser magnitude.	Puddle Clay - limited response to reservoir level fluctuations. Trend follows reservoir level but delayed.	Pore pressures from records covering 1944 to 1948. Elevated pore pressures in foundation and puddle core on large and rapid drawdowns.	Suspect initial failure occurred following the very large and rapid drawdown of 1927. Significant movement occurred on the much smaller 1929 drawdown. In between drawdowns the crest of the upstream slope was significantly widened.

Table D1.2 Case studies of slope instability of embankment dams – slides in the upstream slope during drawdown (Sheet 5 of 5).

Name	MECHANICS OF FAILURE				Other Comments	References
	Cause/s Landsliding	Trigger	Failure Mechanism	Comments on Failure Mechanics		
Waghad	Drawdown	Drawdown	Initiated as drained failure. Large movement of relatively flat upstream slope suggests embankment materials are significantly strain weakening.	Embankment materials are poorly compacted CH/MH placed well wet of OMC. Suspect that the earthfill is strain weakening on shearing from fully softened to residual strength.	No indication of previous movement during earlier drawdowns. Only limited information available.	Penman (1986) Nagarkar et al (1978) Nagarkar et al (1981)
Dam FD2	Drawdown, large and relatively rapid. 1993 event largest drawdown and fastest rate (~ 3 times previous rates).	Drawdown, 1993 likely event during which failure occurred.	Initiated in drained loading. Possible progressive undrained weakening under high shear stress conditions from large drawdowns prior to 1993. Initial slide may have occurred in 1993 following progressive weakening from 1977 and 1988/89 drawdowns.	Piezometers in outer zone of Zone 1 filling (core material in zoned section and material used in homogeneous section) indicated slow response to reservoir drawdown. Suspect instability associated with high piezometric levels in earthfill on large drawdown. Zone 1 material is dilative under low confining pressures and undrained strain weakening of dilative earthfill may have occurred under low confining pressures. Mechanism could incorporate progressive failure due to strain weakening on previous large drawdowns.	Drawdown induced failure occurred on left abutment (constructed on upstream sloping (7 to 13 degree slopes) hillside). Embankment design on left abutment is homogeneous earthfill at 2H to 1V slope.	
Dam FD3	1931 Drawdown, large and rapid. Relatively steep upstream slope (2H to 1V) for embankment constructed of medium plasticity clays.	Drawdown of 1931.	Slide initiated as drained failure. Potential for progressive undrained strain weakening of fill under high shear stress conditions from previous of large and rapid drawdowns of 1928 and 1930. Concrete facing and piling contributed to brittleness of slide.	Embankment fill is of very low permeability and shows little response to reservoir drawdown. Under drained conditions the fill would be dilative and strain weakening at low confining pressures. Previous large drawdowns possibly resulted in strain weakening, as indicated by cracking that occurred following 1928 slide. Restraint from concrete facing and piling contributed to brittleness of slide mechanism and rapid post failure velocity of the slide.	Rapid failure of upstream slope on drawdown. Cracking in 1928 indicative of marginal stability of slope to rapid and large drawdown. More recent large drawdowns have resulted in cracking of the embankment.	
Mondely Dam	Drawdown. High construction pore pressures in fill (placed wet of OMC and over-compacted).	First drawdown.	Suspect undrained failure through homogeneous fill triggered by drawdown. Suspect that embankment in limiting stability condition at the end of construction. Construction pore pressures were a significicant factor in the failure.	Alonso et al (1997) comment that they obtained a factor of safety of close to 1 for drained analysis (using pore pressure recorded from piezometers) but greater than one for undrained analysis. Their analysis would indicate the embankment was in a limiting stability condition at the end of construction.	This failure may be similar in some respects to that of Lake Shelbyville. Similarites are timing, velocity of movement and involvement of first drawdown. Very slow to slow failure in upstream slope on first drawdown.	Alonso et al (1997) Lino (1997)
Sampna Tank	Drawdown, low permeability of upstream shoulder fill (high phreatic surface).	Drawdown	Initiated as a drained failure. Large and rapid movement suggests embankment materials are significantly strain weakening on shearing. Brittleness possibly associated with surface of rupture passing through partially saturated soils. Possible progressive weakening from earlier drawdowns.	Relatively steep upstream slope would have contributed to rapid rate of movement as material evacuating failure bowl would break up and move relatively quickly on the 2H to 1V upstream slope, therefore having continued loss of toe support. Dominant influences on failure is the low permeability of shoulder fill and steep upstream slope. Suspect filling (if reasonably well compacted) would be dilative and strain weakening in drained and undrained loading at low to moderate levels of confining pressure.	Rapid failure of upstream slope on drawdown. Possible progressive strain weakening from previous drawdowns. Slope too steep for low permeability fill used in upstream shoulder.	Sinha (1968)
Pilarcitos Dam	Very rapid drawdown. Possible perched water tables due to layering sloping toward core. Rainfall during drawdown may also have had an effect.	Very rapid drawdown.	Drained failure in dilative outer shell of embankment (clayey sandy gravel). Suspect pore pressure within shoulder could not drain at same rate as reservoir leading therefore to slope failure.	Upstream shoulder fill would be dilative on shearing at low confining pressures. Likely that this dilative behaviour limited the amount of shear movement. Downstream sloping layering toward core likely to have restricted drainage and maintained phreatic surface at relatively high levels during very rapid drawdown.	Failure in upstream slope of clayey sandy gravel during very rapid drawdown. Limited details, but likely low rate of movement, possibly in slow category.	Sherard (1953) USCOLD (1975)
Charmes Dam	Drawdown, low permeability of upstream shoulder fill therefore likely high phreatic surface retained in embankment.	Drawdown	Initiated as a drained failure. Slow movements suggest embankment materials are not significantly strain weakening on shearing.	Suspect fill to have limited dilatancy on shearing at low confining pressures (due to likely limited strain weakening). Possible progressive undrained weakening occurred as a result of high shear stress levels associated with previous drawdowns. Would expect high shear stress to be present in upstream slope on drawdown due to steepness of upstream slope (1.5H to 1V).	Slow failure on deepest drawdown in embankment history in steep upstream slope (1.5H to 1V) of medium plasticity sandy silty clay.	Sherard (1953)
Enista Dam	Drawdown. Low permeability of fill resulting in limited reduction in phreatic surface in upstream shoulder of the embankment.	Drawdown (largest by some 13 m in embankment history)	Drained instability in upstream slope on large drawdown due to retention of high phreatic surface in upstream shoulder. Likely dilation on shearing resulted in limited and likely slow velocity of movement.	Further cracking occurred under drawdowns after 1982 (when stabilising berms had been added). This may indicate that the failure in 1982 was in the initial stages of failure and the dilative tendancy of the fill on shearing and its low permeability limited the amount of deformation. The later movements may have occurred at a lower undrained strength due to strain weakening and dilation after the 1982 event.	Possible incipient failure that occurred during a large drawdown (by far the biggest event in the embankments history). Limited movement on a upstream slope of 3H to 1V.	Abidjiev (1994)
Telish Dam	Drawdown. Low permeability of fill resulting in negligible reduction in the phreatic surface within the upstream shoulder of the embankment.	Drawdown (likely that was only a routine drawdown)	Initiated as a drained instability, but development of negative pore pressures on shearing in dilative fill may have limited the movement. Further movements under later drawdowns suggest progressive strain weakening of fill under the high shear stress conditions associated with seasonal drawdown.	Cracking in 1977 and again in 1980 were an indication of the progressive strain weakening of the embankment fill. The filling is likely to be dilative and strain weakening at low confining pressures.	Drawdown failure in 1982 under routine drawdown operation. Preceeded by cracking in 1977 and 1980, also under routine drawdowns. Failure indicative of progressive undrained strain weakening under routine (but large) operational drawdowns.	Abidjiev (1994)
Drenovets Dam	Drawdown. Low permeability of fill resulting in limited reduction in phreatic surface in upstream shoulder of the embankment.	Drawdown, possibly routine.	Suspect that given the similarities in the period of construction, embankment design, material type, embankment height, upstream slope and seasonal operation of the reservoirs, that the failures of Telish, Drenovets, Mechka and Sushitsa are all of similar mechanism.	-	Limited information. Failure in upstream slope (3H to 1V), possibly during routine drawdown.	Abidjiev (1994)
Mechka Dam		Drawdown, possibly routine.			Limited information. Failure in upstream slope during routine drawdown.	
Sushitsa Dam		Drawdown, possibly routine.			Limited information. Failure in upstream slope during routine drawdown.	
Malko Sharkovo Dam	Drawdown. Presence of residual excess pore pressures from construction in upstream shoulder fill.	First drawdown.	Possible undrained failure through cohesive upstream shoulder fill triggered by drawdown. Likely that the embankment was in a limiting stability condition at the end of construction.	Pore pressures developed during construction indicate placement on the wet side of optimum and therefore potentially relatively low undrained strength (depending on placement water content). It is possible that the embankment was in a limiting stability condition at the end of construction.	Very limited information. Upstream failure during first drawdown in zoned earthfill embankment with upstream shoulder of low permeability sandy clay. Construction pore pressures were still present in the upstream slope at the time of failure (1 year after construction).	Abidjiev (1994)
Wassy Dam	Drawdown, very rapid and first. Possibility of residual pore pressures associated with construction.	Drawdown, first drawdown and very rapid.	Several possibilities. Possible undrained failure triggered by drawdown. Possibly initiated as a drained failure if filling poorly placed and softened on wetting.	If an undrained failure, would require placement of filling wet of optimum and limiting stability condition at the end of construction (similar to Mondely). Another possibility is that filling was poorly placed (with no moisture control and/or in thick layers) resulting in relatively high horizontal permeability so that on reservoir filling water could readily penetrate the filling and cause softening.	Interesting failure. Suspect either undrained failure of wet compacted filling of low undrained shear strength or drained failure of poorly compacted filling that softened significantly on wetting.	Sherard (1953)
Mount Pisgah Dam	Rapid drawdown. Delayed response of phreatic surface on very rapid drawdown.	Rapid drawdown.	Suspect initiated as a drained failure. Large movement suggests likely rapid velocity of the slide mass, possibly indicating significant brittleness of the slide mass. Contributing factors to the brittleness would be the reinforced concrete upstream facing. The steep upstream slope is also a contributing factor to the large movements.	The steep upstream slope is likely to have had a significant influence on the likely rapid velocity of movement. Once the slide had initiated and the concrete facing was no longer supporting the steep upstream face, the slide occurred relatively quickly and travelled a large distance.	Likely rapid failure of upstream slope on very rapid drawdown. Embankment constructed of sandy silt with steep upstream face (1.5H to 1V). Poor quality of workmanship.	Sherard et al (1963) Sherard (1953)
Forsythe Dam	Extremely rapid drawdown.	Drawdown, extremely rapid.	Initiated as a drained failure, under extremely rapid drawdown conditions, of relatively steep (2H to 1V) upstream slope.	Possible that failure may have occurred as a series of thin sloughing type failures to give post-failure profile of slide shown by Sherard (1954).	Limited information. Likely rapid failure of mid to upper portion of the upstream slope on an extremely rapid drawdown.	Sherard (1953)
San Luis Dam	Drawdown of 1981. Elevated piezometric levels in slopewash and core. Strain weakening of both slopewash and core.	Drawdown of 1981, quickest and largest in embankment history.	Initiated as a drained failure and progressed under undrained conditions. It is likely that progressive strain weakening of the core and slopewash occurred under the 1981 and previous large drawdowns under the high shear stress conditions imposed under drawdown. The slopewash also softened significantly on saturation, and in the failure area is likely to have resulted in shear straining under the stress levels imposed. Further shear straining is likely to have occurred under the higher stress conditions imposed from previous large drawdowns. Likely significant lateral restraint on margins. Favourable orientation of the natural hillslope also a contributing factor.	The core material was rolled and well-compacted and would therefore have a high undrained shear strength at compaction. At relatively low confining pressures softening would occur due to swelling and saturation, however, it would still be dilative on shearing under these conditions. Further strain weakening (in undrained loading) potentially occurred under high stress conditions. Suspect that at failure that the strength of the core material was somewhere between peak and fully softened. For the slopewash it is possible that the strength at failure was somewhere between fully softened and residual (depending on the amount of shearing and degree of localisation). Restraint on the lateral margins is a significant factor. The slide was hinged about the southern end and the width of the slide gradually increased over time in the southern direction. Changes in the natural topography contributed to the restraint on the southern lateral margin.	Well documented and analysed case study of failure during drawdown. Failure occurred on the largest and most rapid drawdown in the embankments history. Progressive weakening from previous large drawdowns could have been a significant factor in the mechanics of failure.	Stark and Duncan (1987, 1991) Von Thun (1988)
Bear Gulch	Drawdown.	Drawdown.	Suspect possible progressive weakening within a layer in the foundation under drawdown. Movement vector at backscarp suggests strongly translational movement of slide. Movements occurred when the reservoir level was quite low suggesting possible high uplift pressures in toe region.	-	Surface of rupture is not confirmed through foundation, but is likely to have been located on wet, soft clay seam.	Sherard (1953)
Old Eildon Dam	Rapid drawdown (1927 and 1929). Construction (widening of upstream side of crest).	Rapid drawdown. Likely initiation following 1927 drawdown and reactivation following 1929 drawdown.	Several possibilities. In 1927 it is possible that construction pore pressures were still present in the puddle core and possibly the foundation. Therefore, the failure may have initiated as an undrained failure triggered by the drawdown in 1927. The movement in 1929 was a reactivation of the existing slide. Significant restraint on the lateral margins.	The chain of events are difficult to follow in the paper by Knight (1938) and the monitoring records indicate the crest settled up to 14 m (or 50% of its height) in about 20 to 25 days. For an additional 6 m of movement to occur following an initial 8 m in late April 1929 would suggest that rockfill was being dumped in the crest region of the failure, effectively reducing the stability of the slide. Restraint on the lateral margins is evidenced by the widening of the slide from 215 to 365 m. Therefore, spreading of load onto the margins of the slide occurred extending the width of the slide, as opposed to shearing through rockfill.	Slide in upstream slope on drawdown. Initiated in 1927 and reactivated on the 1929 drawdown. Impoundment during construction is considered to have had an effect on stability under drawdown (possible that failure may have occurred during construction if water not impounded).	Knight (1938) Speedie (1948)

Table D1.3: Case studies of slope instability of embankment dams – post-construction slides in the downstream slope.

Name	Location	Date of Failure	Years Since End of Construction	Embankment Zoning and Classification				Slide Location	Slope Failure Geometry	Geology	Embankment Dimensions						MATERIALS								
																	Material 1 (Core)								
				Zoning	Class[n]	Core Width	Core Type				Height, H_e (m)	Length, L_e (m)	Ratio L_e/H_e	Upstream Slope	Downstream Slope	Comments	Source	ASCS Class[n]	% fines	CF (%)	PI (%)	Density Ratio	Moisture Content	Compaction	Compaction Rating	Comments
Park Reservoir Dam	USA, Wyoming	May-69	60	Homog	2,0,0	c-vb	SC	Emb	Type 1	Glacial - moraine and lacustrine deposits.	24.4	366	15.0	3H to 1V	1.5H to 1V	Homogeneous earthfill embankment with rockfill toe, completed in 1909.	Glacial (?)	SC - silty and clayey sand.	unk	unk	unk	unk	unk	unk	unk	No information.
Arroyito Dam	Argentina	Jan-84	6	Homog	1,0,2	c-vb	GP/GW	Emb	Type 2	Sedimentary - sandstones and claystones.	20	3400	170.0	2.5 to 5H to 1V	2.5H to 1V	Homogeneous earthfill embankment constructed 1974 to 1978.	Alluvial - sandy gravels	GP/GW	10 (max)	unk	non plastic	D_R = 100%	unk	Compacted with heavy rollers	Rolled, well compacted	Well compacted sandy gravel with low content fines (maximum 10 % fines). Stratification in embankment with $k_h > k_v$.
Barton Dam	USA, Idaho	Jun-22	12	Homog	0,0,0	c-vb	CH	Emb	Type 1/2 (?)	Lacustrine	12.2	300	24.6	2.5H to 1V	1.5H to 1V	Homogeneous earthfill embankment, constructed in 1910. Relatively steep downstream slope, no filters.	Glacial	CH - silty clays	100	60	38	unk	unk	Probable thin moistened layers, and compacted by travel of teams and wagons.	No formal compaction	High plasticity silty clay. Potentially poor compaction if hard clays not broken up adequately prior to compaction. Possible stratification ($k_h > k_v$) in embankment.
Harrogate Dam	UK	18-Dec-51	81	Puddle core earthfill	8,0,0	-	CH	Emb (possibly Fndn also)	Type 2	Glacial - Boulder clay	8.8	unk	-	1.9H to 1V	1.9H to 1V	Puddle core earthfill embankment with narrow core and no filters. Constructed 1870.	Glacial - Boulder Clay	CH	high	high (?)	unk	unk	unk	Refered to as well compacted for period.	No formal compaction	High plasticity clay of soft to firm strength consistency (Su ~ 28 kPa). Narrow, steep sided central core zone.
Woodrat Knot Dam	USA, Oregon	May-61	5	Homog	0,0,0 (?)	c-vb	unk	Emb (possibly Fndn also)	unk	Tuff	26	230	8.8	2.5H to 1V	1.75H to 1V	Homogeneous earthfill embankment, completed in 1956.	unk	unk	unk	unk	unk	unk	unk	unk	unk	No information on earthfill. Suspect clayey and of relatively low permeability given slow time for dampness to be observed on the downstream slope. Likely stratification with $k_h > k_v$.
Fruitgrowers Dam	USA, Colorado	12-Jun-37	2 (after raise to 11 m), 39 (after initial construction)	Homog	0,0,0	c-vb	CL	Emb (possibly Fndn also)	Type 1/2 (?)	Sedimentary - shale	11	280	25.5	3H to 1V	2H to 1V	Homogeneous earthfill dam. Initial construction in 1898 (to 3 m) then raised in 1905 (to 6.7 m), 1910 (to 9.8 m) and 1935 (to 11 m). All raises on upstream slope.	Residual - soft shale	CL	98	30 to 40	17 - medium plasticity.	unk	unk	Placed in layers and compacted with teams. Reference to placement in dry condition.	No formal compaction	Medium plasticity silty clay. No formal compaction and possibly placed dry of OMC. For 1935 raise reference to moistening of fill.
Santa Ana Acaxochitlan Dam	Mexico	Dec-52	21	Homog	0,0,0	c-vb	CH	Emb & Fndn	Type 2	unk	12	unk	-	2.5H to 1V	2H to 1V	Homogeneous earthfill embankment. Initial embankment failed in 1925. Completely reconstructed, completed 1931.	unk	CH - silty clays	85	50	unk (high plasticity)	unk	unk	unk	Likely limited formal compaction given period of construction.	High plasticity silty clays. Limited information. Not sure of borrow source, possibly alluvial.
Siburua Dam	Venezuela	15-Jul-64	7	Homog	1,0,1	c-vb	CL	Emb & Fndn	Type 5	Sedimentary - marine shales.	14.4	900	62.5	2.5H to 1V	2H to 1V	Homogeneous embankment (in failed section) with foundation filter under downstream shoulder. Constructed 1956 to 1957.	residual - weathered shales and shaly clay	CL	unk	unk	21 - medium plasticity	2.03 t/m^3 (bulk density)	24 to 38 (in slide area), 21 to 25% (outside slide area)	unk	Rolled, well compacted	Limited information. Swelling of embankment post construction an indication of high compaction. Medium plasticity shaly clays. Low permeability, 10^{-10} m/sec.
Seven Sisters Dike	Canada	1949 to 1956 (13 failures)	0.3 to 7	Zoned Earth and Rockfill	4,0,1	c-vb	CH	Emb & Fndn	Type 5	unk	7.3	5600	767.1	3.5H to 1V	2.5H to 1V	Zoned earth and rockfill embankment with broad clay core (1.5H to 1V downstream and 2H to 1V upstream) and thin outer rockfill zones.	not known (alluvial or lacustrine)	CH	unk	unk	35	> 90% SMDD (1.97 t/m^3 bulk density)	5 to 10% wet OMC	unk	Suspect rolled, but relatively poor.	High plasticity clay of stiff strength consistency (Suv = 50 to 145 kPa, avg = 100 kPa). Variable plasticity (liquid limit range from 19 to 114).
Great Western	USA, Colorado	15-Jun-58	1 (after dam raise), 51 (since original construction)	Homog	0,0,0 (?)	c-vb	CL (?)	Emb & Fndn	Type 2	unk	18.6	580	31.2	unk	unk	Homogeneous earthfill embankment. No information on cross section geometry. Combined upstream and downstream slope = 4.5H to 1V.	alluvial (?)	CL (?)	unk	unk	unk	unk	unk	unk	unk	Referred to only as rolled earthfill.
Aran Dam	India	Apr-78	1	Zoned Earthfill	3,0,0	c-tk	CH	Emb & Fndn	Type 2/5 (?)	Sedimentary - conglomerate and other sedimentary rocks.	30.3	750	24.8	2 to 3H to 1V	2 to 2.5H to 1V	Zoned earthfill embankment with broad clay core (1H to 1V upstream and downstream). Central cut-off through to below the conglomerate layer. Constructed 1975 to 1977.	alluvial - black cotton soils	CH	very high	high	high	1.44 t/m^3 (dry density)	unk	Rolled earthfill	Suspect rolled, well compacted (given period of construction)	Limited information. Suspect reasonable well compacted given the age at construction (1975 to 1977). High plasticity.
Lake Yosemite Dam	USA, California	1943	60	Homog	0,0,0	c-vb	CL/SC	Emb & Fndn (?)	Type 2	unk	16.2	1500	92.6	2H to 1V	2H to 1V	Homogeneous earthfill embankment constructed in 1883 to 1884.	Alluvial / Colluvial	CL/SC - gravelly	50	10	11 - low plasticity	unk	unk	Placed in thin layers with scraper teams and compacted by travel of the teams.	No formal compaction	Constructed of slightly gravelly sandy clays and clayey sands of low plasticity. Limited compaction.
Yuba Dam	USA, California	Jan-51	2 (after raise of 0.9 m), 41 (after initial construction)	Homog	0,0,0	c-vb	CL	Emb & Fndn	Type 2	unk	7.6	270	35.5	2.5H to 1V	1.75H to 1V	Homogeneous earthfill embankment. Originally constructed in 1910 to 6.7 m. In 1949 raised (on downstream side) by 0.9 m height. Relatively steep downstream slope (1.75H to 1V).	Colluvial and Residual	CL - sandy clay	78	25	15 - medium plasticity	unk	unk	unk	Suspect no formal compaction (given period of construction)	Constructed of medium plasticity sandy clays with limited compaction (for original construction). Downstream raised section of better compaction and lower permeability.

Table D1.3: Case studies of slope instability of embankment dams – post-construction slides in the downstream slope (Sheet 2 of 4).

Name	MATERIALS											FOUNDATION MATERIAL PROPERTIES								
	Material 2 (Shoulder fill)										General Comments on Design and Compaction	Foundation (General)		Foundation (If foundation Involved in Slide)						
	Source	ASCS Class[n]	% fines	CF (%)	PI (%)	Density Ratio	Moisture Content	Compaction	Compaction Rating	Comments		Soil / Rock	Description	Description	ASCS Class[n]	% fines	CF (%)	PI (%)	Density	Moisture Content	Comments
Park Reservoir Dam	-	-	-	-	-	-	-	-	-	-	Homogeneous embankment constructed of silty and clayey sands. No information on construction methods.	Soil	Glacial moraine or lucustrine deposits.	-	-	-	-	-	-	-	-
Arroyito Dam	-	-	-	-	-	-	-	-	-	-	Homogeneous embankment constructed of well compacted sandy gravels of low fines content (maximum 10%). Stratification in embankment.	Soil	Sandy gravels to 10 m depth overlying bedrock.	-	-	-	-	-	-	-	-
Barton Dam	-	-	-	-	-	-	-	-	-	-	Homogeneous embankment constructed of CH lacustrine clays.	Soil	Lacustrine clays, high plasticity, heavily over-consolidated and very stiff to hard strength consistency.	-	-	-	-	-	-	-	-
Harrogate Dam	Glacial (?) - Boulder Clay (?)	CL	unk	unk	22 to 25 (medium plasticity)	19 kN/m^3 (bulk density)	22 to 38% (post failure)	unk	No formal compaction.	Medium plasticity clay of soft to firm strength consistency (Su ~ 18 to 35 kPa). No formal compaction.	Narrow puddle core of CH clay and shoulder zones of medium plasticity clays. No formal compaction.	Soil	Deep clay profile. Surface soil not removed. Clay of stiff to very stiff strength consistency (?).	-	-	-	-	-	-	-	-
Woodrat Knot Dam	-	-	-	-	-	-	-	-	-	-	Homogeneous earthfill embankment. Very limited data. Suspect clayey earthfill.	unk	unk	-	-	-	-	-	-	-	-
Fruitgrowers Dam	-	-	-	-	-	-	-	-	-	-	Homogeneous earthfill embankment of poorly compacted, medium plasticity silty clays.	Soil	Alluvial (?) - clayey sand. No details other than this.	-	-	-	-	-	-	-	-
Santa Ana Acaxochitlan Dam	-	-	-	-	-	-	-	-	-	-	Homogeneous earthfill embankment constructed of high plasticity silty clays.	Soil	Alluvial (?). No cleaning of foundation. Layer of high plasticity organic clay (0.5 m thick) overlying "soft" clay. Below this, "compact" clayey silt.	Organic clay layer	OH	80	high	22 to 32 (liquid limit = 70 to 114)	unk	unk (likely that saturated)	No foundation clean up. Embankment founded on a layer of high plasticity organic clay underlain by a "soft" clay.
Siburua Dam	-	-	-	-	-	-	-	-	-	-	Homogeneous embankment constructed of medium plasticity shaly clays. In slide area, foundation slopes in downstream direction at 7 to 11 degrees.	Soil	Residual Soil - Shaly clay of 3 to 4 m thickness overlying weathered shale. Bedding in shaledips in N to NW direction at 17 degrees (favourable oriented to slide location).	Shaly Clay	CL	unk	unk	21 - medium plasticity	unk	23 to 25% inside slip area, ~ 21% outside.	Medium plasticity shaly clays. Permeable layers through the foundation, more so in the weathered zone below the residual soil. Likely relict bedding in residual soil profile oriented favourably in slide location.
Seven Sisters Dike	unk	rockfill - gravel to boulder size (?)	unk	unk	unk	unk	unk	unk	unk	No information, referred to only as rockfill.	Zoned earth and rockfill embankment with broad CH clay core and thin outer rockfill shells.	Soil	Alluvial (?) - high plasticity clay of 3 to 6 m thickness underlain by low plasticity clay and/or bedrock.	High plasticity clay	CH	unk	unk	59	16.3 kN/m^3 bulk unit weight	up to 45%	High plasticity, firm to stiff (Su = 28 to 180 kPa, avg 88 kPa) clay. Upper 1 m cracked and fissured. Fissuring continues to 2.1 m. Stratified.
Great Western	-	-	-	-	-	-	-	-	-	-	Homogeneous earthfill embankment. Very limited data. Suspect clayey earthfill.	Soil	Alluvial - clay. No further information than this.	-	-	-	-	-	-	-	-
Aran Dam	Alluvial and Residual (murum and conglomerate)	suspect GC to GM	unk	unk	unk	1.76 t/m^3 (dry density)	unk	Rolled	Suspect rolled, well compacted (given period of construction)	Limited information. Suspect reasonable well compacted given the age at construction (1975 to 1977). High gravel content and likely low fines content. Phreatic surface shown through the downstream shoulder would indicate this material has a relatively low permeability.	Zoned earthfill embankment with broad CH clay core and gravelly earthfill shoulders.	Soil	Alluvial - fissured high plasticity clay of 5 m thickness overlying thin murum layer then conglomerate bedrock.	Fissured, high plasticity clay.	CH	high (?)	high (?)	high (?)	1.33 t/m^3 (dry density)	unk	High plasticity, highly fissured clay foundation. Reference to having alow undrained shear strength when saturated.
Lake Yosemite Dam	-	-	-	-	-	-	-	-	-	-	Homogeneous earthfill embankment constructed of slightly gravelly sandy clays and clayey sands. Limited compaction.	Soil	Alluvial (?) - referred to as cemented gravels, but similar to material of which embankment constructed (slightly gravelly sandy clays and clayey sands.	-	-	-	-	-	-	-	Limited information.
Yuba Dam	-	-	-	-	-	-	-	-	-	-	Homogeneous earthfill embankment constructed of medium plasticity sandy clays of likely no formal compaction. Raised zone on downstream side) of improved construction practice, but lower permeability.	Soil	Alluvial (?) - clay, no further information.	-	-	-	-	-	-	-	Very limited information.

Table D1.3: Case studies of slope instability of embankment dams – post-construction slides in the downstream slope (Sheet 3 of 4).

Name	AT AND POST-FAILURE																
	Slide Classification (Hutchinson 1988)	Slide Location	Slope Failure Geometry	State	Slide Dimensions								Post-Failure Deformation Behaviour				Degree of Break-up of the Slide Mass	Comments
					Width, W (m)	Length, L (m)	Depth, D (m)	Height (m)	Slope (deg)	Volume (cu.m.)	W/L	W/D	Displacement (m)	Velocity (mm/day)	Velocity Category	Comments		
Park Reservoir Dam	Rotational (?)	Shallow slide in upper section of downstream slope (above rockfill toe). Back-scarp at centre of crest.	Type 1	first time	12	21	5	11.5	33.7	750	0.57	2.40	Limited.	-	likely slow velocity	Limited movement, cracking at crest and bulging on mid downstream slope. Velocity of movement likely to be slow category.	Virtually intact	Limited information.
Arroyito Dam	Rotational	Shallow slide in mid downstream slope. Crest of back-scarp 7.5 m below crest on downstream slope. Very small failure, possibly classify as a slough.	Type 2	first time	30	15	3	6	21.8	1000	2.00	10.00	No information.	-	unk	No information on movement behaviour.	unk	-
Barton Dam	Rotational (?)	Slide in downstream slope with crest of back-scarp at downstream edge of crest. Cracking in upstream side of crest. No information on slide depth.	Type 1 or 2 (?)	first time	30	18	4 to 5 (estimate)	12.2	33.7	1000 to 1500 (estimate)	1.67	6.67	2.1 m at crest of backscarp.	unk	suspect moderate	No information on movement behaviour. Suspect potentially moderate velocity given steepness of downstream slope and potential for strain weakening of CH clay on shearing.	suspect virtually intact.	Limited information.
Harrogate Dam	Rotational (?)	Slide in downstream slope with crest of back-scarp at downstream edge of crest. No information on depth to surface of rupture.	Type 2	first time	24.5	16.2	4 to 6 (?)	8.8	27.8	1000 (estimate)	1.51	4.90	> 0.3 m at crest and > 0.23 m at toe.	Estimate up to 1000 (max.). 300 next morning.	slow, possibly up to the low end of moderate	Slide observed on morning of 18 Dec. 1951. Crest had moved 300 mm and toe 230 mm. The slide was still on the move at 12 to 13 mm/hour. Nearby slide developed as bulging on lower slope followed by cracking at crest.	Virtually intact	Toe of slide sand bagged and reservoir drawn down to stabilise the slope. Triggered by heavy and prolonged rainfall.
Woodrat Knot Dam	Rotational (?)	Slide in downstream slope. No further details beyond this.	unk	first time	90	unk	unk	unk	29.7	unk	-	-	9 m	1920	moderate	Movement occurred over a 3 month period. Started at a rate of 80 mm/hr (1920 mm/day) and slowed gradually.	unk	Limited information.
Fruitgrowers Dam	Rotational (?)	Slide in downstream slope when reservoir at highest historical level. Crest of back scarp at centre of crest. No indication that the failure incorporated the foundation.	Type 1 or 2 (?)	first time	18	25	10	11	26.6	2000 to 2500	0.72	1.80	2.7 m at crest, 7.6 m at toe.	-	suspect moderate to rapid	Suspect likely rapid velocity of movement given amount of movement and indication that movement had ceased. Further movements were then observed (as well as water pouring through cracks in back-scarp onto the slide mass) prior to intentional breaching of the embankment at the abutment.	Suspect reasonable amount of break up at toe.	Slide coincident with highest stored water level in reservoir. Likely rapid velocity of initial failure due to distance travelled. No indication that the failure incorporated the foundation.
Santa Ana Acaxochitlan Dam	Compound (?) - possible translational base in foundation.	Deep-seated slide in downstream slope. Crest of back-scarp intersected the upper portion of the upstream slope. Reservoir at close to spillway level when failure occurred. Resulted in total breach of embankment.	Type 2	first time	20	35	11	12	26.6	3000 (estimate)	0.57	1.82	not known. Must be greater than about 1.5 to 2 m for breach to occur.	-	suspect rapid	Cracks in crest and along upstream slope to below stored water level observed in early November when reservoir at 0.18 m below spillway. Failure occurred (in December) several minutes after inspection by a watchman indicating velocity of movement was likely to be in the rapid category.	unk	Limited information given that total breach of embankment followed the downslope failure. Occurred when reservoir at close to spillway level. This is close to the highest stored water level as the spillway had neven spilled before.
Siburua Dam	Compound (?) - Possible translational component in foundation and rotational backscarp according to vectors.	Deep seated (for slope height) slide in downstream slope. Back-scarp at 1.6 m below crest level in downstream slope and toe of slide beyond toe of embankment. . Reservoir at full supply level when slide initiated.	Type 5	first time	24	14	3.5	6.5	26.6	600	1.71	6.86	1.9 m at backscarp, 1.7 m at toe.	1000 (avg max. over 24 hours), likely max rate of 2000 to 5000.	moderate	Longitudinal crack observed on downstream face on 15/7/64 when reservoir at full supply level. Monitoring shows a slow increase in the velocity of movement for 28 days before a very large increase in velocity and large movement of the slide occurred (on 12/8/64). Movement continued (at a much slower rate) for the next 50 + days.	Minor break up.	Toe and head of slide moved at a similar rate leading up to and at the time of the large movement on the 12/8/64. The monitoring shows a gradual increase in the rate of movement leading up the large movement on the 12/8/64. The reservoir was at full supply when the slide initiated and was in the process of being drawn down when the failure occurred.
Seven Sisters Dike	Rotational (?)	Deep seated (for slope height) slide in downstream slope that passed through the foundation. Slide in section shows back-scarp of slide close to upstream edge of crest.	Type 5	first time	30 to 120	20 to 25	5 to 10	5 to 7.3	21.8	3000 to 15000	> 1.2	> 3	0.3 to 1.8 m at crest, heave at toe.	-	slow	13 failures occurred in 7 years. First indication is cracking on upstream side of crest (no vertical displacement). As movement progresses settlement occurs and cracks up to 0.3 m wide develop over widths of 30 to 120 m. Over several weeks scarps of 0.3 to 1.8 m high develop with heave in toe region.	Virtually intact	Failures occur where the field moisture content of the foundation is greater than 45% in the upper 2.4 m (thus areas of lower undrained shear strength).
Great Western	Compound (?), possibly rotational.	Deep-seated slide in downstream slope that passed through the foundation. Slide back-scarp was below the reservoir level on the upstream slope.	Type 2	first time	180	unk	~ 18 m	18.6	unk (but likely to be about 26)	60000 to 80000 (rough estimate)	> 3	10.00	3.35 m settlement, 4.3 m displacement	> 300	slow to moderate (high end of slow to low end of moderate)	Total movements reported as 3.35 m settlement (presumably of the crest) and 4.3 m displacement (presumably in the toe region). 4 days after slide started rate was 300 mm/day. Initial rate was likely to be higher than this, but not significantly greater. Lesser movement on margins (3.05 m compared with 4.3 m). Several scarps developed.	Virtually intact	Movement occurred 2 weeks after the reservoir had reached the new maximum storage level. Potential risk of complete breach. Sandbagging on crest only accelerated movement. Drawdown narrowly averted breach (only 0.9 m of freeboard remained). Placement of fill at downstream toe assisted in slowing slide movement.
Aran Dam	Compound (?) - likely basal translational component through foundation.	Deep-seated slide in downstream slope that passed through the foundation. Slide back-scarp was at the downstream edge of the crest.	Type 5 or 2 (?)	first time	150	75	17	21	23	80000 to 100000 (rough estimate)	2.00	8.82	10 m at crest, 9 to 11 m (maybe greater) at toe.	unk	likely rapid	Failure occurred one morning in April 1978. "Slipped with a rumbling noise". Suspect movement occurred at a rapid velocity.	Likely significant	Likely rapid failure. Occurred 10 months after completion of construction. Reservoir had been at full supply level for some 8 months. Rumbling noise suggests internal shearing, possibly on lateral margins.
Lake Yosemite Dam	Rotational (?), maybe compound (?)	Slide in downstream slope in section of embankment where the height was about 4.6 m. Top of back-scarp was on the upper downstream slope, 1.5 m below crest level. Sherard (1954) refers to the slide surface passing through the upper 0.5 m of the foundation.	Type 2	first time	45	6	2	3.1	26.6	300	7.50	22.50	0.6 m at crest of backscarp.	unk	slow to moderate	Only reference to movement is the total movement at the top of the backscarp. No indication of time period of movement. Suspect slow to moderate given limited amount of movement.	Intact (?)	Limited information.
Yuba Dam	Compound - basal translational component in foundation.	Slide in downstream slope that passed through the upper (less than 0.5 m) portion of the foundation.. Top of back-scarp at the centre of the crest.	Type 2	first time	23	16	4.5	7.6	29.7	1000	1.44	5.11	1.5 m at crest, 11 m at toe (from section)	unk	rapid to very rapid	Indications that slide occurred within minutes according to reports, therefore very likely at rapid to very rapid velocity.	Significant	Triggered by earthquake. Slide mass reported as "completely fissured and loose" indicating a significant degree of break up during failure.

Table D1.3: Case studies of slope instability of embankment dams – post-construction slides in the downstream slope (Sheet 4 of 4).

Name	HYDROGEOLOGY			MECHANICS OF FAILURE				Other Comments	References
	Rainfall	Seepage	Comments	Cause/s Landsliding	Trigger	Failure Mechanism	Comments on Mechanism		
Park Reservoir Dam	No information.	No information	Possible seepage on downstream face associated with layering in earthfill ($k_h >> k_v$), but no information.	Likely seepage or rainfall.	Likely seepage or rainfall.	Possible drained failure through dilative silty and clayey sand earthfill. Shallow failure (therefore low confining pressures). Limited movement on steep slope (1.5H to 1V).	Very limited information available on slide.	Small volume slide through the embankment only. Embankment constructed of silty and clayey sands. Very limited information.	USCOLD (1975)
Arroyito Dam	No information.	Perched water tables above phreatic surface due to stratification. Seepage observed on downstream face.	Reservoir level raised to operating level in 1982. Seepage observed on downstream face. Top of backscarp is below reservoir operating level.	Saturation of fill, perched water table/s in embankment and seepage.	High localised phreatic surface and seepage. Saturation of fill.	Drained failure in sandy dilative sandy gravel fill with low (< 10%) fines content. Possibly a sloughing type failure due to seepage pressures in cohesionless fill. Small volume and shallow depth.	-	Small volume slide through the embankment only. Embankment constructed of well-compacted sandy gravels. Very limited information.	Giuliani and Pujol (1985)
Barton Dam	No information.	Seepage appeared on downstream slope directly after construction. Increased in area with time until slope saturated to mid-height. May 1922 - considerable moisture on downstream slope.	Reservoir close to full supply level when slide occurred (had been for at least several months, possibly a lot longer). Likely stratification in embankment ($k_h > k_v$) and high phreatic surface.	Seepage. Gradual saturation of downstream slope.	Seepage and saturation of downstream slope.	Initiated as a drained failure. Likely progressive weakening of fill due to gradual saturation and reduction of matrix suction. Possible strain weakening on shearing in CH clays to residual strength.	Eventually reached a state of limiting stability, at which point failure occurred. Steepness of downstream slope contributed to amount of movement.	Small volume, likely shallow slide, through embankment. Embankment constructed of CH lacustrine clays (without filters) with no formal compaction. Steep downstream slope.	Sherard (1953)
Harrogate Dam	Annual average = 359 mm. 1951 - 656 mm for year and 210 mm in Nov, highest yearly and monthly (Nov) rainfall since embankment constructed.	No information	Failure occurred in the winter of a very wet year and was preceeded by a very wet November (wettest month on record). Water infilled shrinkage cracks and wetting up of downstream shoulder from rainfall.	Rainfall. Filling of deep shrinkage cracks and softening of fill in downstream shoulder.	Rainfall.	Initiated as a drained failure in a water softened and saturated downstream slope (softened and saturated by water infiltration and exaserbated by deep shrinkage cracks). Likely high phreatic surface or perched water table/s (due to rainfall). Slope at limiting stability under these conditions. Possibly some strain weakening on shearing to residual strength.	Surface of rupture on major slip plane was about 12 mm thick and had the consistency of "porridge" (soft to very soft ?) clay. Limiting stability condition in drained loading for relatively steep slope in medium plasticity clays.	Small volume failure in relatively steep downstream embankment slope of medium plasticity clays. Triggered by period of heavy and prolonged rainfall. Numerous shrinkage cracks in embankment contributed to saturation of slope and instability.	Davies (1953)
Woodrat Knot Dam	No information.	After 3 years operation dampness observed on downstream slope, about 11 m above the toe. Over the next 2 years the extent of the dampness increased.	Gradual saturation of downstream slope with time leading up to failure. No information on reservoir operation.	Seepage. Gradual saturation of downstream slope.	Seepage and saturation of downstream slope.	Likely progressive weakening of fill due to gradual saturation and reduction of matrix suction. Initiated as a drained failure once a limiting stability condition was reached in the relatively steep downstream slope. Likely strain weakening on shearing resulted in large movements at moderate velocity.	Eventually reached a state of limiting stability, at which point failure occurred. Steepness of downstream slope contributed to amount of movement. Large movements indicate strain weakening on shearing.	Suspect failure through embankment only. Limited information on material properties but reasonable information on slide movement.	ICOLD (1974)
Fruitgrowers Dam	No information.	Sloughing prior to 1930's indicative of seepage through the embankment. Stream of water poured from slide area about 4.3 m below crest level (coincident with crest level prior to 1905 raise).	Reservoir reached highest level in embankment history (2.1 m below crest level) 6 days prior to failure. Observations indicate a high phreatic surface through the embankment. Possible shrinkage cracking associated with staged construction may have contributed to formation of seepage paths.	High phreatic surface. Wetting up and softening of the downstream slope. Seepage pressures.	Rise of the reservoir level to the within 2.1 m of crest level, highest level in embankment history.	Initiated as a drained failure due to limiting stability of the downstream slope. Wetting up and softening of the embankment filling, a high phreatic surface and increased seepage pressures (all associated with highest water level) all contributed to the failure. Large amount and likely rapid velocity of movement in indicative of strain weakening on shearing. Possibly due to dilation of slide mass on shearing and availability of water to further soften the slide mass.	No definite indication that the failure occurred through the foundation. It is possible that the slide occurred in the embankment only and travelled a sufficient distance in the toe region to take out the outlet works.	Failure in downstream slope of embankment. Occurred 6 days after reservoir reached highest stored level. Likely rapid failure.	Sherard (1953) ENR (1937b, 1939b)
Santa Ana Acaxochitlan Dam	No information.	Moisture observed on downstream slope in early to mid November 1952 (shortly after cracking observed).	Slide coincident with high stored water level in embankment. Cracking in early November resulted in a change in the seepage path conditions through the embankment and moisture observation on the downstream slope.	High reservoir level. Cracking and adverse change in seepage path conditions.	Adverse change in seepage path conditions resulting in a higher phreatic surface, and wetting up and softening of the downstream shoulder.	Initiated as a drained failure. An increase in the phreatic surface, wetting up and softening of the downstream slope and increased seepage pressures all contributed to the failure. Potential rapid velocity of movement suggests brittleness in the failure mechanism.	Slide brittleness potentially due to a number of factors including: restraint on the lateral margins of a relatively narrow slide (W/L = 0.6); strain weakening on shearing of the high plasticity embankment materials and foundation; and entry of water into the dilating slide mass as failure is occurring resulting in further softening.	Downstream slope failure that extended back to the upstream slope and resulted in the breach of the embankment. Likely rapid failure within the embankment and foundation.	Marsal and Tamez (1955)
Siburua Dam	Relatively low rainfall area.	Significant increase in flow rate in drain at toe of slope (in the area of the slide) when reservoir at full supply level. Indicative of likely seepage through the foundation given piezometric levels.	Likely low phreatic surface in embankment fill. Piezometers in foundation show phreatic surface maintained within the foundation. High swelling movement in the vicinity of the slide may indicate seepage occurred through the fill and resulted in the wetting up and swelling of the embankment. Lower, weathered foundation responds with reservoir level. Upper foundation piezometer indicates a very limited response to reservoir level.	Gradual wetting up and softening of downstream embankment and foundation. Initial cracking occurred when reservoir at full supply level.	Gradual wetting up and softening of downstream embankment and foundation. Initial cracking occurred when reservoir at full supply level.	Initiated as a drained failure whena reaching a limiting stability condition reached in the downstream slope. Possible progressive failure in potentially dilative embankment materials (at low confining pressures and non saturated) and heavily over-consolidated foundation. Rapid velocity of movement suggests strain weakening on shearing of medium plasticity shaly clays and/or restraint on the lateral margins.	Suspect the failure may be driven by the foundation, along a possible relict bedding joint (bedding favourable oriented in region of slide). High moisture contents in the slide area indicate preferential wetting up in this area, possibly due to localised seepage path in the embankment (?). Filter material decribed as poor quality and containing 40% fines, but still flowed at high reservoir level. The foundation slope (7 to 11 degrees downstream) may also be a factor in the failure. Possible progressive failure, within the foundation, of a slope under relatively high shear stress conditions. Back analysis gives drained failure at less than peak strength (assuming embankment near saturated).	Small failure through homogeneous embankment and foundation of medium plasticity shaly clays. Slow increase in rate of movement up to failure (over 28 days) and then continued movement once failure occurred for some 50 days.	Wolfskill and Lambe (1967)
Seven Sisters Dike	No information.	No information	No information. Suspect development of phreatic surface in foundation and/or embankment enough to trigger failure. Potential seepage path along cracked and fissured zone of foundation.	Possible rise in phreatic surface in embankment or foundation.	Rise in phreatic surface in embankment or foundation.	Undrained failures through low undrained strength foundation and wet placed, low undrained strength CH earthfill. For failures more than 6 to 12 months after end of construction suspect the development of the phreatic surface had an influence on stability (i.e., enough to trigger slide in slope of limiting stability in undrained conditions).	Would consider CH foundation and wet placed CH earthfill are potentially strain weakening in undrained loading.	Numerous failures in downstream slope after construction. Typical of slow failures of embankments on soft ground.	Peterson et al (1957)
Great Western	No information.	No indication.	Movement started some 2 weeks after reservoir level raised to new maximum storage level. Suspact increase in phreatic surface enough to initiate failure.	Raising of embankment, high reservoir water level and increasing phreatic surface through the embankment.	High water level in reservoir and associated change in the phreatic surface or pore pressures in zones of the embankment or foundation.	Initiated as a drained failure due to limiting stability of the downstream slope under an increasing phreatic surface, pore pressures and/or seepage pressures associated with the new high reservoir level. Occurred 9 months after raising embankment some 4 m and 2 weeks after reservoir reached new maximum storage level. Suspect initiated in the alluvial clay foundation (referred to a "unstable" and "weak"). Possible strain weakening on shearing and possible restraint on lateral margins.	Very limited information on material properties. If the foundation is driving the slide then suspect that spreading of the slide width occurred due to restraint on the lateral margins where shearing through the embankment was required. In addition, the lateral persistence of the clay foundation may have been a factor in the slow velocity of movement. Other factors could also have contributed to the slide such as permeability differential between the new and old fill, and the presence of shrinkage cracks in the old embankment that were inundated when the embankment was raised.	Downstream slope failure that extended back to below the reservoir level on the upstream slope. Very close to a breach condition of the embankment, which may have only been averted because of the relatively low velocity of movement. Failure occurred within the embankment and foundation.	Sherard et al (1963) ENR (1958) ICOLD (1974)
Aran Dam	No information.	No information	Reservoir at full supply level since August 1977 (some 8 months prior to failure). Phreatic surface (shown by Dighe et al, 1985) shows relatively high level in downstream shoulder fill. This would suggest the downstream shoulder fill is of relatively low permeability.	A number of possibilities. Rising pore pressures in foundation and downstream shoulder, softening of foundation on wetting.	Not sure.	Suspect initiated as drained instability (in foundation) and possibly driven by gradual strength reduction of foundation on wetting (i.e., reduction of suction in the foundation had a significant effect on stability). Rapid movement suggests brittleness of failure mechanism, possibly on the lateral margins but maybe internally as well. Suspect the foundation may also strain weakening on shearing, but that this is not the dominant cause of brittleness.	Very limited information from which to draw any firm conclusions as to the mechanism of failure. If restraint on the lateral margins was significant it would be expected that pre-failure signs would have been clearly evident for a slide of 150 m width. Possible graben type failure that moved rapidly once internal shearing through the downstream shoulder fill (rumbling noise) occurred and released the slide.	Limited information. Relatively large failure in downstream slope that occurred 9 months after end of construction and some 8 months after reservoir at full supply level. Within embankment and foundation.	Dighe et al (1985)
Lake Yosemite Dam	No information.	Limited seepage had always occurred under the embankment and had formed marshy areas at the downstream toe. On occasion the bottom metre of the embankment slope had been reported as moist.	Seepage observations indicate the foundation is likely to be of greater permeability than the embankment. Likely relatively high phreatic surface in the embankment. For such a localised failure to occur so long after construction may suggest heavy rainfall preceeded the slide.	Not known.	Not known. Possibly localised change in seepage conditions through the foundation or embankment. Possibly triggered by rainfall.	Drained instability in downstream slope. Not a sloughing type failure. Reports during repair indicate the surface of rupture passed through the foundation.	Limited information. Possible change in seepage conditions resulted in localised instability of downstream slope or heavy rainfall triggered the slide. Dilation on shearing and availability of water may have resulted in further softening.	Localised small volume failure in low height section of the embankment that occurred some 60 years after initial construction. Incorporated the foundation.	Sherard (1953)
Yuba Dam	No information.	Prior to raise in 1949, considerable moisture was observed on the downstream slope. After the raise no moisture was noted indicating new fill material of lower permeability than original material.	High phreatic surface developed within the embankment due to the presence of the low permeability layer capping the downstream slope and crest. Likely increased pore pressures within the foundation.	Earthquake. High phreatic surface due to permeability differential.	Earthquake.	Earthquake was sufficient to trigger the slide. Likely that the slope was of limiting stability prior to earthquake given the high phreatic surface and relatively steep slope in medium plasticity sandy clays.	Limiting stability condition of the downstream slope prior to the earthquake and landslide. Likely that earthquake sufficient to reduce the factor of safety to less than one. The relatively large movement suggest strain weakening on shearing. Possible strain weakening in the outer downstream zone and foundation.	Relatively small volume failure triggered by earthquake. Rapid to very rapid failure within the embankment and foundation. Went close to breaching the embankment (backscarp at centre of the crest).	Sherard (1953)

2.0 FAILURES IN CUT SLOPES IN HEAVILY OVER-CONSOLIDATED HIGH PLASTICITY CLAYS

2.1 CUT SLOPES IN LONDON CLAY

The analysis of the post-failure deformation behaviour of cut slopes in the heavily over-consolidated high plasticity London clay comprises twenty-five case studies, the details for which are summarised in Table D2.3. The table provides details for each case study on; timing of the failure, slope type, slope geometry, material properties, slide geometry, post-failure deformation behaviour, hydro-geological conditions and references.

The London clay formation (Skempton et al 1969) is a marine clay of Eocene (early Tertiary) age. Following uplifting it has been subjected to erosion in the late Tertiary and Pleistocene periods, with estimated erosion depths of 150 to 300 m (Skempton et al 1969). The formation is heavily over-consolidated as a result of the significant depth of erosion and importantly, in terms of the assessment of cut slope instability, it is of uniform lithology in the London area (Skempton et al 1969).

The typical profile of the London clay formation (Skempton et al 1969; Skempton 1977) comprises a weathered and oxidised upper zone of 5 to 15 m depth, termed "brown" London clay by virtue of its colour, underlain by a thin transition zone inturn underlain by the unweathered "blue" London clay. The typical properties of the London clay (both brown and blue) are summarised in Table D2.1. It is a high plasticity fissured clay of low permeability and typically of stiff to very stiff undrained strength consistency.

The discontinuities and defects within the upper part of the London clay formation (Skempton et al 1969) are summarised as follows:

- Bedding – near horizontal and typically observed as a gently undulating surface. Not easily discernable as there is generally no lithological change.
- Jointing – typically a near vertical set of orthogonal joints with a thin layer of gouge clay on a plane surface. Sheeting joints are also observed with dips of between 5 and 15 degrees.
- Fissuring – In the upper 10 to 15 m the fissures are typically less than 150 mm in size with no preferred orientation, but with a tendency to concentrate in the sub-horizontal direction parallel to the bedding. The number of fissures increases and

the size decreases as the ground surface is approached. Typically, no appreciable relative movements have occurred along the fissures and the fissure surface has a matt texture. However, about 5% of the fissure surfaces are slickensided and have polished and striated surfaces.

- Faulting – limited.

The strength properties of London clay indicate that it is strain weakening in both drained (Figure D2.1) and undrained loading (Figure D2.2). The typical drained strength properties (Table D2.1) show the strength on defects is less than that of the intact soil.

Table D2.1: Summary of material properties of London clay*[1]

Material Property	**"Brown" London Clay**	**"Blue" London Clay**
Unit Weight (kN/m^3)	-	18.9
Plasticity		
Liquid Limit (%)	82 (62 to 95)	
Plastic Limit (%)	30	
Grading		
Clay fraction (%)*[2]	55 to 60	
Drained Strength		
Peak	$c' = 31$ kPa, $\phi' = 20°$	$c' = 18$ (15 to 23) kPa , $\phi' = 20°$ (19 to 21)
Fully softened	$c' = 0$ to 1.5 kPa, $\phi' = 20°$	$c' = 0$ to 1.5 kPa , $\phi' = 20°$
Residual	$c' = 0$ to 1.5 kPa, $\phi' = 16°$	$c' = 0$ to 1.5 kPa , $\phi' = 13°$ to 16°
Joints and Fissures	$c' = 7$ kPa , $\phi' = 18.5°$	-
Undrained Strength*[3]	Stiff increasing to very stiff with depth	Very stiff
Permeability	-	2 to 4 x 10^{-9} m/sec

*[1] Referenced from Skempton (1964, 1977), Skempton and La Rochelle (1965), Skempton et al (1969).

*[2] The clay fraction is as that fraction less than 2 micron.

*[3] Undrained strength terminology to Australian Standard AS 1726-1993 "Geotechnical Site Investigations". Stiff, S_u = >50 and ≤ 100 kPa; Very Stiff, S_u = >100 and ≤ 200 kPa, where S_u = undrained shear strength.

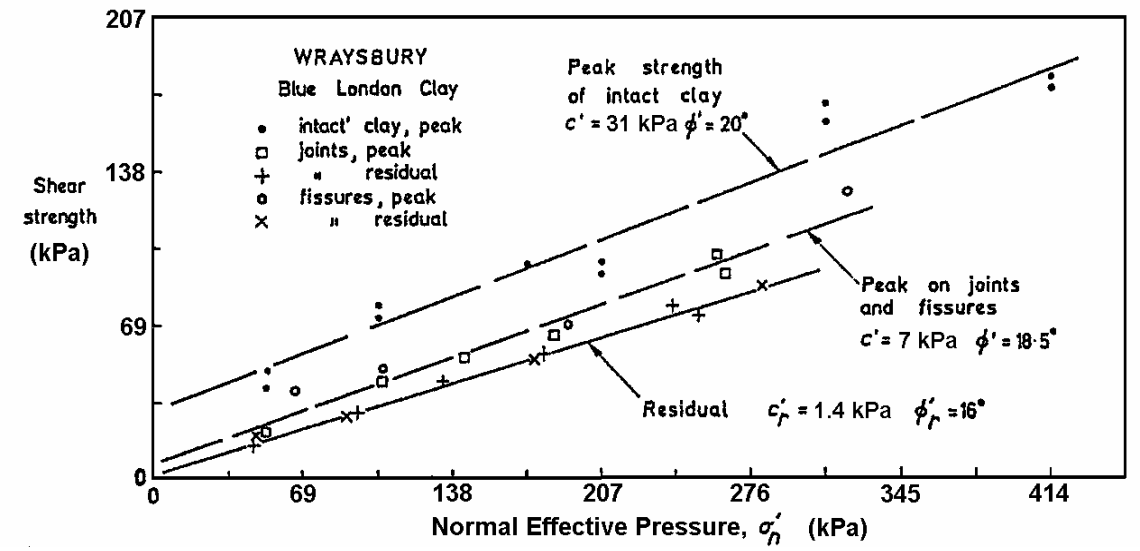

Figure D2.1: Drained strength properties of 'blue' London clay at Wraysbury (Skempton et al 1969)

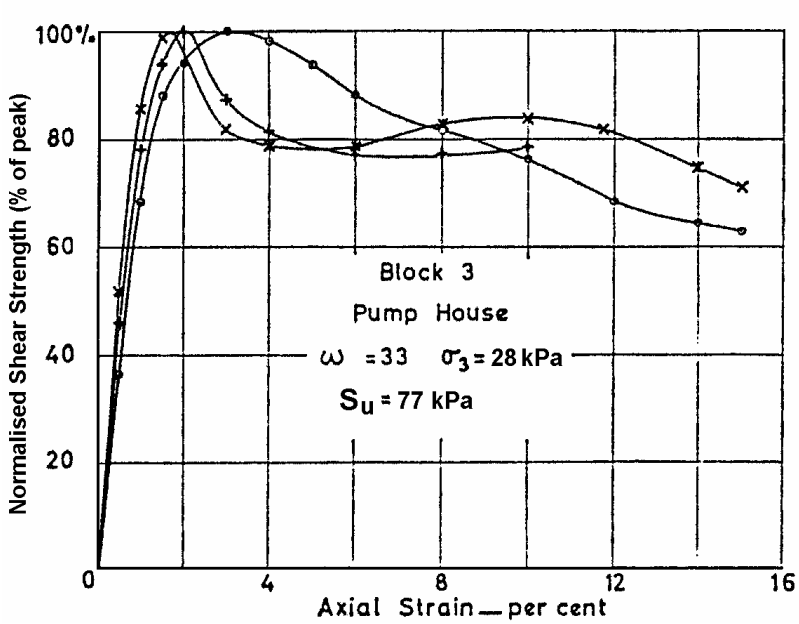

Figure D2.2: Undrained strength properties of London clay, Bradwell (Skempton and La Rochelle 1965)

2.2 CUT SLOPES IN WEATHERED UPPER LIAS CLAY

The analysis of the post-failure deformation behaviour of cut slopes in the heavily over-consolidated, weathered Upper Lias clay comprised 12 case studies, the details for which are summarised in Table D2.4. The table provides details for each case study on;

timing of the failure, slope type, slope geometry, material properties, slide geometry, post-failure deformation behaviour, hydro-geological conditions and references.

The Upper Lias clay formation (Chandler 1972) is a marine clay-shale of Jurassic age. Following uplifting the formation has been subjected to erosion, estimated at depths of up to 600 m (Chandler 1972), resulting in its present heavily over-consolidated condition. Chandler (1984a) indicates that the formation presently outcrops across the UK from the north eastern coast (south of the English – Scottish border) to the central region of the southern coast. The case studies of cut slope failures are located in the midlands region where extensive outcrops of the Upper Lias occur (Chandler 1972).

The Upper Lias clay is of relatively uniform lithology, although two different upper surface profiles have been identified by Chandler (1972) that are dependent on the development history of the slope during the Quaternary age. Chandler indicates that during the Pleistocene age the upper profile was significantly disturbed from permafrost conditions. He describes the disturbed, or brecciated, zone as *"small stratified lumps or lithorelicts in a matrix of softer clay"* and indicates the depth of brecciation at the time of disturbance was up to 10 to 11 m. Chandler (1972) found this brecciated profile to still be evident at some outcrop locations of the Upper Lias clay, and termed this the 'brecciated' profile. At other outcrops he identified that the zone of brecciation had been eroded and termed this the 'fissured' profile.

The material properties of the brecciated and the fissured weathered Upper Lias clay are summarised in Table D2.2. The weathered formation is of high plasticity and high clay fines content, and typically of stiff to very stiff undrained strength consistency. Chandler (1972) comments that the brecciated profile is typified by a lack of fissuring and a permeability one to two orders of magnitude greater than for the fissured profile. For the fissured profile he indicates that the fissuring is typically limited to the upper weathered zone and does not extend into the underlying un-weathered clay-shale profile. Other defects within the soil mass include near horizontal bedding. Slickensiding is observed on fissures in the more weathered materials.

The strength properties of the weathered Upper Lias clay are similar to London clay in that the soils are strain weakening in both drained and undrained loading. It is also suspected that the drained strength properties on fissures and other defects are likely to be less than that of the intact soil, and have a significant effect on the strength of the overall soil mass.

Table D2.2: Summary of material properties of weathered Upper Lias clay*[1]

Material Property	**'brecciated' clay**	**'fissured' clay**
Unit Weight (kN/m^3)	19.0	19.2
Plasticity - Liquid Limit (%) - Plastic Limit (%) - Plasticity Index (%)	60 28 32	
Grading Clay fraction	45	
Drained Strength - Peak - Fully softened - Residual *[2]	 $c' = 17$ kPa, $\phi' = 23°$ $c' = 1$ kPa, $\phi' = 23°$ $c' = 0$ kPa , $\phi' = 10$ to $17.5°$	 - $c' = 1$ to 2 kPa , $\phi' = 25°$ $c' = 0$ kPa , $\phi' = 10$ to $17.5°$
Undrained Strength*[3]	Stiff to very stiff increasing to hard with depth	Stiff to very stiff, increasing with depth
Permeability	10^{-9} to 10^{-10} m/sec	Less than 10^{-10} to as low as 10^{-12} m/sec

*[1] – Referenced from Chandler (1972, 1974, 1976)

*[2] – Dependency of residual strength on effective normal stress (refer Figure D2.3).

*[3] Undrained strength terminology to Australian Standard AS 1726-1993 "Geotechnical Site Investigations". Stiff, S_u = >50 and ≤ 100 kPa; Very Stiff, S_u = >100 and ≤ 200 kPa; Hard, S_u = >200 kPa, where S_u = undrained shear strength.

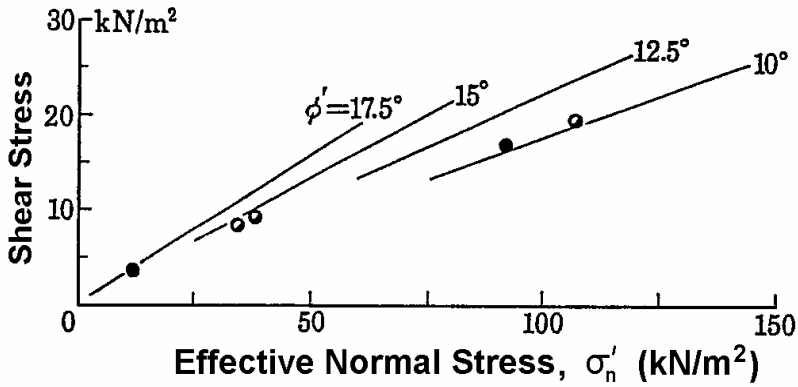

Figure D2.3: Effect of the normal effective stress on the residual strength of weathered Upper Lias clay (Chandler 1976).

2.3 TERMINOLOGY USED IN TABLES

An explanation of some of the terminology used in Table D2.3 and Table D2.4 is as follows:

- Some general terms or symbols used and their meaning are:

  - (?) = unsure of detail, but thought to be likely
  - unk = unknown
  - "-" = not required, not appropriate or not given
  - est = estimate
  - H to V refers to horizontal to vertical slope angle; i.e. 2H to 1V.
  - S_u = undrained shear strength
  - Soil classification symbols, where used, are in accordance with the Australian soil classification system (Australian Standard AS 1726-1993 "Geotechnical Site Investigations").
- Under the section on slope geometry;
  - For slope type, "Cut" = cut slope, "Cut-R" = retained cut slope. Only those failures in retained slopes where the surface of rupture passed below the retaining wall are classified "Cut-R".
  - The slope angle given for the partially retained cuts is the slope angle of the unsupported section of the cut, i.e. the slope angle above the retaining wall.
- For the material properties:
  - Undrained shear strength terms used are in accordance with the Australian soil classification system. Very Soft ≤ 12 kPa; Soft > 12 and ≤ 25 kPa; Firm > 25 and ≤ 50 kPa; Stiff > 50 and ≤ 100 kPa; Very Stiff > 100 and ≤ 200 kPa; Hard > 200 kPa.
- "Slide classification" refers to the classification of the shape of the surface of rupture (e.g., translational, rotational or compound) using the landslide classification system of Hutchinson (1988).
- "Slope Failure Geometry" refers to the location of the slide within the slope. Details are given in Section 1.3.2 of Chapter 1 and in Appendix A.
- For the slide dimensions, the slope angle allows for benching or partial retainment of the slope and it will, in some cases, be slightly different from the cut slope angle reported under the section under slope geometry. Only a small number of the case studies are affected by this, mainly partly retained cuts, otherwise the slope angle is equivalent to the cut slope angle.
- The limit equilibrium analysis refers to the drained strength parameters from back-analysis by others at failure (i.e. a factor of safety of 1). For the London clay case studies $f¢$ has been held constant at 20° for first time failures but is reported at less

than 20° for reactivated slides. The same principle has been applied to the cut slopes in Upper Lias clay with f' held constant at 25° for the 'fissured' profile and 23° for the 'brecciated' profile.

- For the post-failure deformation behaviour:
  - For the deformation column, "head" and "toe" refer to the head and toe regions of the slide.
  - Velocity category refers to the IUGS (1995) velocity categories.
  - The degree of break-up is a somewhat subjective assessment of the post-failure break up of the slide mass.

Table D2.3: Case studies of failures in cut slopes in London clay

Name	Date of Failure	Age of Slope at Failure (years)	Slope Geometry					Material Properties			Pre-Failure Deformation	Slide Details							
			Slope Type	Height, H_s (m)	Slope Angle (Degrees)	% of Slope Height Retained	Comments	Liq Limit (%)	Plastic Limit (%)	Undrained Strength		Slide Classification	State of Sliding	Slope Failure Geometry	Slide Dimensions				
															Width (m)	Height, H_f (m)	Depth, D (m)	Slope (°)	Volume (cu.m.)
Kensal Green	1941	29	Cut-R	6.1	15	61%	Large retaining wall at toe of cut. Cut slope above retaining wall at 15 degrees.	-	-	-	6 to 6.5 mm/year in 1929. Increase in rate after 1936 to 1937 up to failure in 1941.	Compound	first time	Type 5	unk	8.2	5.8	29.7	unk
Upper Holloway	1951	81	Cut-R	5.3	22.2	20%	Cut retained at toe of slope. Cut slope above retaining wall at 22.2 degrees. Flat slope at top of cut.	86	28	-	tension cracks observed prior to failure	Compound - translational base, rotational toe and back-scarp	first time	Type 5	unk	6.25	5.2	25	unk
Fareham	1961	59	Cut	9.5	19.5	-	Capped by layer of sand and gravel. Flat slope above cut.	-	-	-	na	rotational	reactivated	Type 2	> 60	12	6.5	19.5	8 to 10,000
West Acton - A	1966	44	Cut	4.7	18.4	-	Flat slope above cut.	-	-	-	na	rotational (?)	first time	Type 1	unk	4.1	2.4	18.4	unk
West Acton - B	1966	44	Cut	4.8	18.4	-	Flat slope above cut.	-	-	-	na	rotational (?)	first time	Type 2	unk	4.6	2.2	18.4	unk
Grove Park	1962	98	Cut	9.4	22.5	-	Flat slope above cut. Drain at toe of slope	-	-	-	na	Compound - translational base, rotational back-scarp	first time	Type 1	unk	4.8	3	22.5	unk
Dedham	1952	112	Cut	10.2	22	-	Capped by layer of sand and gravel. Flat slope above cut.	-	-	-	na	rotational (?)	First time	Type 2	15	8.5	3.6	22	600
Kingbury - S1	1947	16	Cut	6.2	23.5	-	Drain at crest of slope. Flat slope above cut.	-	-	-	na	rotational	first time	Type 2	unk	6	2.3	23.5	unk
St. Helier	1952	22	Cut	7.3	25.3	-	Counterfort drains at 45 m spacings. Capped by layer of sand.	-	-	-	Movement noted during periods of wet weather in years prior to slide in 1952.	Compound - translational toe, rotational back-scarp	first time (possible reactivation)	Type 2	< 45	7.6	4.7	25.3	600 to 1500
Crews Hill	1956	47	Cut	5.3	16.2	-	Capped by layer of gravel and sand.	-	-	-	na	Translational (shallow)	first time	Type 2	unk	5.3	1.1	16.2	unk
Althorne	1957, October	60	Cut	8.8	20.5	-	Flat slope at crest.	-	-	stiff (very soft on surface of rupture)	na	Compound - translational basal component, rotational back-scarp	reactivated	Type 2	unk	9	4	20.5	unk
Cuffley	1951 (winter)	38	Cut	12	20.7	-	Flat slope at crest.	-	-	softened zone defining surface of rupture	na	Translational (shallow at toe)	first time	Type 2	unk	12	4	20.7	unk
Hadley Wood	1951	70	Cut	13.6	13.5	-	1947 - slope trimmed back from 3.5H:1V to 4H:1V.	-	-	stiff, disturbed is soft (and soggy)	na	Compound - significant translational component	first time (possible reactivation)	Type 1	unk	10.4	2.2	13.5	unk
Whitstable	1959	99	Cut	11.4	18.4	13%	Small retaining wall at toe (not involved in slip). Flat slope above cut.	-	-	-	na	Compound - translational on brown/blue clay interface.	first time	Type 2	unk	9.9	4.4	18.4	unk
Grange Hill	1950	50 (?)	Cut	17.4	17.8	14%	Small retaining wall at toe (not involved in slip).	-	-	-	na	Rotational / Compound (?)	first time	Type 1	unk	13	6	17.8	unk
Isle of Sheppey - A	na	6	Cut	12	38	-	Steep cut.	-	-	soft to firm (?)	na	rotational (?)	first time	Type 2	unk	12	4.5	38	unk
Isle of Sheppey - B	na	8	Cut	10	41	-	Steep cut.	-	-	soft to firm (?)	na	rotational (?)	first time	Type 2	unk	10.1	3.5	41	unk
Bradwell	24-Apr-1957	0.014	Cut	14.8	63	-	Steep cut in London clay. Flatter benched slope in upper region of slope (average 29 degrees) in filling and Marsh Clay.	95	30	firm to very stiff	Bulging and cracking of clay face in toe region.	Rotational, retrogressive	first time	Type 2	27	14.8	9	56	2500
Wood Green	1948, November	55	Cut-R	11.3	18.4	43%	Large retaining wall at toe of cut. Cut slope above retaining wall at 18.4 degrees.	78	30	stiff to very stiff (slip surface - firm).	na	rotational (?)	first time	Type 5	73	14.4	8	28	7 to 10000
Sudbury Hill	1949	46	Cut	7	18.4	-	Flat slope above crest of cut.	82	28	-	na	Compound - translational toe, rotational back-scarp	first time	Type 2	unk	7	4	18.4	unk
New Cross	2-Nov-1841	3	Cut	23	33.7	-	Steep cut.	-	-	-	Initial slow creep type movements observed on day of slide.	Compound - translational toe, rotational back-scarp	first time	Type 1	110	17	13	33.7	40000
Northolt	1955, January	19	Cut	10.1	21.8	7%	Small retaining wall at toe (not involved in slip).	78	28	stiff to very stiff (slip surface - soft).	Tension cracks at crest of slope	Compound - translational toe, rotational back-scarp	first time	Type 1	83	6.8	4.4	21.8	3000
Wembley Hill	1918, February	13	Cut-R	17	18.5	41%	Large retaining wall at toe of cut. Slope above retaining wall cut at 18.5 degrees.	-	-	-	Movement observed several days prior to failure.	Compound	first time	Type 5	260	19.5	10.5	26	70000
Uxbridge - 1954	1954, November	54	Cut-R	10.2	18	77%	Large retaining wall at toe of cut. Slope cut at 18 degrees above the retaining wall.	86	24	stiff to very stiff (slip zone soft to firm)	Observations of cracking and movement at crest and toe of slope from Sept 1954.	Compound (?) - rotational behind retaining wall	first time	Type 5	85	13.3	12	32	8 to 10000
Uxbridge - 1937	1937	37	Cut	9	26	-	5 m wide excavation for new retaining wall behind existing retaining wall. Vertical cut, slope above = 26 degrees.	86	24	stiff to very stiff (slip zone soft to firm)	na	Rotational	first time	Type 2	32	9	4.6	43	2500

Table D2.3: Case studies of failures in cut slopes in London clay (Sheet 2 of 2)

Name	At And Post-Failure							Hydrology		Cause/s of Sliding	Trigger	Comments	References
	Limit Equilibrium Analysis (from references)		Post-Failure Deformation Behaviour					Hydro-geological Features	Rainfall / Snowmelt				
	c' (kPa)	phi ' (deg)	Deformation (m)	Peak Velocity (mm/day)	Velocity Category	Degree of Break-up	Comment						
Kensal Green	4	20	0.3	20 to 100	slow	Intact	Tension crack observed 6 m behind wall and thw wall had slid forward by 300 mm. Continued movement of 100 mm over following 8 months.	Phreatic surface assumed	unk	Excavation	High seasonal pore pressures (?)	Initial excavation in 1836. Widened and retained in 1912. Earlier failure in 1927. This section was first time failure.	Skempton (1964)
Upper Holloway	0.5	20	1.3 (crest), 0.2 to 0.7 (toe).	50 to 200 (est.)	suspect slow	Intact	Initial movements observed in 1951. New wall built in 1953 also failed (>300 mm movement between July 1953 and Apr 1955).	Piezos installed in 1956 and records used to estimate phreatic surface.	unk	Excavation	High seasonal pore pressures (?)	Continued movement after initial slip in 1951. Failure at fully softened strength. Suspect slow to moderate initial rate.	James (1970) Lo and Lee (1973)
Fareham	0	18 to 19.5	1.5 (crest), 2 to 4 (toe)	200 to 400 (est.)	suspect slow	partly broken up	Initial slip in winter of 1961/62 with approx. 0.5 to 1 m movemetn at toe (possible reactivation). Further movements in winter of 1967, up to 2.5 to 3 m at toe (definite reactivation).	Phreatic surface estimated from observations	unk	Excavation	High seasonal pore pressures (?)	Several large failures during construction therefore slopes cut back and drains installed. Suspect reactivated slide, therefore slow seasonal creep movement.	James (1970)
West Acton - A	0.5	20	0.36 (crest), 0.9 to 1.5 (toe)	200 to 400 (est.)	suspect slow	virtually intact	No details on timing of movement, but suspect slow given limited movement of slide.	Phreatic surface assumed	unk	Excavation	High seasonal pore pressures	First time failure.	James (1970)
West Acton - B	1	20	0.41 (crest), 1.5 to 2.5 (toe)	200 to 400 (est.)	suspect slow	virtually intact	No details on timing of movement, but suspect slow given limited movement of slide.	Phreatic surface assumed	unk	Excavation	High seasonal pore pressures	First time failure.	James (1970)
Grove Park	0.5	20	3.3 (crest), 10.8 (toe)	50000 to 400000 (est.)	rapid (toe)	broken up	Slide occurred in 1962. No indication of time over which movement occurred. Suspect moderate at crest and rapid at toe. Type 1 failure with 10.8 m movement beyond toe on 2H to 1V slope.	Piezos indicate slip surface above phreatic surface. Possibly high phreatic surface at time of slip ?	unk	Excavation	High seasonal pore pressures (?)	Failure in upper section of cut (Type 1). Translational component on bedding plane. Travel on 22.5 deg. cut slope angle, at likely rapid velocity.	James (1970)
Dedham	2.5	20	2.1 (crest), 3.5 to 5 (toe)	500 to 1500 (est)	moderate	partially broken up	Initial slip in 1910/11 (no details). Further slip in 1952, moved up to 3.5 to 4 m at toe. When toe cut back movement continued for up to 6 weeks.	Phreatic surface from water levels in standpipes after failure.	unk	Excavation	High seasonal pore pressures (?)	Large slip in winter of 1910/11, stabilised by drainage trenches. 1952 slip located near to the 1910 slip. Continued movement for weeks after initial slide suggests initially slow movement.	James (1970)
Kingbury - S1	3.5	20	0.5 (crest), 0.5 to 1 (toe)	50 to 200 (est.)	slow	virtually intact	No details on timing of movement. Suspect slow given small deformation.	Phreatic surface assumed	unk	Excavation	High seasonal pore pressures (?)	After slip slope was trimmed back to 2.5 - 3H to 1V and conterfort drainage was installed.	James (1970)
St. Helier	4.5	20	2.3 (crest), 2.5 (toe).	200 to 600 (est.)	slow to moderate	Minor break up	Initial failure prior to 1948 when slope trimmed back and drains installed. From 1948 movement observed between counterfort drains. Suspect 1952 movement is a reactivation.	Phreatic surface from water levels in standpipes. Movement occurred during wet weather.	Wet weather	Excavation	High seasonal pore pressures (?)	Slope trimmed and drains installed in 1948 (possible previous sliding). 1952 slip between to counterfort drains. Movement noted prior to 1952 during wet weather. Slipped material described as soggy with moisture content close to liquid limit.	James (1970)
Crews Hill	1	20	0.5 to 1.2 (crest), 1 to 1.5 (toe)	100 to 400 (est.)	suspect slow	partially broken up	Suspect possible prior movement of slip, and therefore 1956 movement is a reactivation.	Phreatic surface assumed	unk	Excavation	High seasonal pore pressures (?)	Shallow translational slip possibly on discontinuity. Movement prior to 1956 had been noted. Slipped clay described as soft and soggy. Suspect possible reactivation and r_u is greater than 0.3.	James (1970)
Althorne	0	16.5	1.5 to 2 (crest), 3 m (toe)	200 to 400 (est.)	suspect slow	partially broken up	Suspected reactivation of previous slip. Still active at time of investigation.	Phreatic surface assumed, suspected of being high.	unk	Excavation	High seasonal pore pressures (?)	Date of initial slide not known. Reactivated slide.	James (1970)
Cuffley	0	20	2.5 to 2.8 (crest), 3.5 m (toe)	50 to 100 (est.)	suspect slow	partially broken up	Seasonal movements in winter seasons over a period of 6 years (1951 to 1957).	Phreatic surface assumed	Wet weather	Excavation	High seasonal pore pressures	Suspect translational along reasonably continuous discontiuity.	James (1970)
Hadley Wood	0	19	0.7 to 0.9 (crest), 1.8 (toe)	50 to 200 (est.)	suspect slow	minor break up	No indication of time over which slide occurred during the winter of 1951/52. Possible reactivation given soft and wet nature of material and flatness of slope.	Phreatic surface assumed, failure in winter	unk	Excavation	High seasonal pore pressures (?)	First recorded slip in 1947. Slopes trimmed back to 4H:1V. Failed again in winter of 1951/52. Confined to brown London Clay. Original cut in 1850, widened in 1882.	James (1970)
Whitstable	1.5	20	1.5 (crest), 2 (toe)	50 to 200 (est.)	suspect slow	minor break up in toe region.	Slide occurred during the winter of 1958/59. Indication that movement occurred over a period of at least several weeks to months.	Phreatic surface assumed, failure in winter	unk	Excavation	High seasonal pore pressures (?)	Not clear if shallow translational failure or not. Possible shallow creep movements induced by freeze / thaw action.	James (1970)
Grange Hill	2	20	2 (crest and toe)	100 to 400 (est.)	suspect slow	virtually intact	Failure occurred in winter of 1950/51. Suspect slow.	Phreatic surface assumed, failure in winter (?). Shallow counterfort drains.	unk	Excavation	High seasonal pore pressures (?)	Whole of cut described as unstable. Definite slips occurred in 1950 / 51. Shallow counterforts, but not effective.	James (1970)
Isle of Sheppey - A	16	20	12.5 (toe)	100000 to 300000 (est)	suspect rapid	Broken up	Only information on movement is degraded profile indicating a total movement of 12.5 m at the toe. Suspect the initial failure occurred at a rapid velocity.	Phreatic surface assumed	unk	Excavation	Excavation (Possibly undrained failure)	Travel angle = 21.8 degrees. Average Su on slide surface 25 kPa (for undrained failure).	James (1970)
Isle of Sheppey - B	11.5	20	9 (toe)	100000 to 300000 (est)	suspect rapid	Broken up	Only information on movement is degraded profile indicating a total movement of 9 m at the toe. Suspect the initial failure occurred at a rapid velocity.	Phreatic surface assumed	unk	Excavation	Excavation (Possibly undrained failure)	Travel angle = 24.4 degrees. Average Su on slide surface 20 kPa (for undrained failure).	James (1970)
Bradwell	17.5	20	5 to 15 (unk)	100000 to 500000 (est.)	suspect rapid	Suspect high degree of break up	Failure occurred as a series of three retrogressive slips over a 24 hour period.	Prior to excavation groundwater levels 0.9 ro 1.2 m depth. Drained analysis using assumed r_u value.	no rainfall during excavation	Excavation	Excavation	No section showing post-failure profile. Likely very rapid, undrained failure of steep cut in fissured clay.	Skempton and La Rochelle (1965)
Wood Green	5.5	20	0.9 (toe)	100 to 200 (est.)	slow	Intact	Nov 1948 - heaving of track below retaining wall and crack in pavement above cut. Top of wall had moved forward ~ 0.9 m.	Phreatic surface from water levels in standpipes after failure.	unk	Excavation	High seasonal pore pressures (?)	Heaving of railway track in front of wall and crack in road pavement at crest of slope.	Henkel (1957)
Sudbury Hill	1	20	2.0 to 2.2 m (crest), 1.6 m (toe)	200 to 500 (est.)	slow	Intact	Section shows 2.05 m crest movement and 1.5 m movement at toe. Further slip movements in succeeding winters from 1949 to 1956. Suspect slow.	Assumed phreatic surface. Piezometers not installed until 7 years after failure.	unk	Excavation	High seasonal pore pressures (?)	Back analysis of failed slope indicates further movements at about residual strength.	Skempton (1977) Skempton (1964) Lo and Lee (1973).
New Cross	na	na	10 (crest) to 31 (toe)	60000 to 180000 (avg.)	rapid	broken up	Movement occurred over a period of 4 hours. Described as "in motion from top to bottom". Continued failures throughout winter of 1841/42.	Failed in winter. Possibly triggered by high groundwater table following heavy rainfall.	heavy seasonal rain	Excavation	Excavation (Possibly undrained failure) and high seasonal pore pressures (?)	Type 1 cut. Failure moved large distance. Travel angle = 14.6 degrees. Basal surface of rupture described as "glassy like surface". Suspect undrained failure.	Skempton (1977) Gregory (1844)
Northolt	4	20	1.2 m (crest), 0.8 m (toe).	200 to 1200 (est)	Slow to moderate	Virtually intact	Series of tension cracks observed at the top of the slope. Slide mass did not break up at the toe and travel down the 22 degree cut slope.	Failed in winter. Possibly triggered by high groundwater table.	unk	Excavation	High seasonal pore pressures (?)	Type 1 cut. Failure moved a relatively large distance due to break up at toe on 22 degree slope. Travel angle = 20.6 degrees. Material within failure bowl remained intact.	Skempton (1964) Henkel (1957).
Wembley Hill	9	20	6 m	290000	rapid	Virtually intact, bulging at toe.	Relatively rapid movement, slid forward 6 m in less than 0.5 hour. Bulging in front of retaining wall. Only slight movement after main slide. Loud report as cracks developed in retaining wall.	Failed in winter. Possibly triggered by high groundwater table. Phreatic surface assumed.	unk	Excavation	High seasonal pore pressures (?)	Large failure for London Clay. Moved large distance in short time (6 m in 0.5 hrs). Suspect brittleness of slide associated with failure through the retaining wall on the margins.	Skempton (1977) Anon (1918)
Uxbridge - 1954	6.2	20	More than 0.4 m (~ 0.6 to 0.8 m ?)	140	slow	Intact	In late Sept 1954 cracks observed in road and footpath above cut. Further evidence of movement in mid November prior to major movement from 23 Nov 1954. Movement occurred over several days whilst remedial measures in progress.	Failed in winter. Possibly triggered by high groundwater table. Phreatic surface from piezometers.	unk	Excavation	High seasonal pore pressures (?)	History of failures. 1937 failure was in the vicinity of this failure.	Watson (1956) Henkel (1956).
Uxbridge - 1937	na	na	5 m	240000 to 500000	rapid	partially broken up	Failure occurred during construction works for new retaining wall. Temporary support of excavation failed resulting in rapid failure.	Failed during excavatrion for new retaining wall	unk	Excavation for new retaining wall	Excavation for new retaining wall	Section indicates that failure occurred once excavation had reached shear band associated with original excavation, i.e., strain weakened zone.	Watson (1956)

Table D2.4: Case studies of failures in cut slopes in weathered Upper Lias clay

Name	Date of Failure	Age of Slope at Failure (years)	Slope Geometry						Material Properties			Slide Details		
			Slope Type	Fissured" or "Brecciated" Profile	Height, H_s (m)	Cut Slope (^{o})	% of Height Retained	Comments	Liq Limit (%)	Plastic Limit (%)	Undrained Strength	Slide Classification	State of Sliding	Slope Failure Geometry
Stowehill - A	1901	66	Cut	fissured	10.2	24.8	-	Original cut in 1832 to 1835. Slope above cut = 5 degrees. Cut-off trench at crest of cut.	58	27	stiff to hard (surface of rupture - soft)	Compound - significant mid slope translational component	first time	Type 2
Stowehill - B	1957	122	Cut	fissured	8.2	23	-	Original cut in 1832 to 1835. Slope above cut = 5 degrees.	58	27	stiff to hard (surface of rupture - soft)	Compound	first time	Type 2
Culworth - A	1957, November	61	Cut	fissured	8	26.5	-	Original cut in 1896. Flat slope above cut.	65	24	stiff to very stiff (surface of rupture - firm)	Compound	first time	Type 2
Culworth - B	1957, November	61	Cut	fissured	8	26.5	-	Original cut in 1896. Flat slope above cut.	65	24	stiff to very stiff (surface of rupture - firm)	Rotational	first time	Type 2
Heyford	1961, January	125	Cut	fissured	9.1	24	-	Original cut in 1835. Slope above cut = 8.5 degrees.	57	29	unk	Compound - significant translational component	first time	Type 2
Ardley	1960, August	52	Cut	fissured	15	22	24%	Original cut in 1908. Low height retaining wall at toe of slope (not involved in the failure), 6.5 degree slope above cut. Capped by sand layer.	59	28	unk	Rotational	first time	Type 1
Hunsbury Hill Tunnel -1920	1920	44	Cut	fissured	16.4	24.5	-	Original cut in 1877. Capped by layer of sand. Slope above at 4.5 degrees.	60	28	stiff to very stiff	Rotational	first time	Type 2
Hunsbury Hill Tunnel - 1954	1954	77	Cut	fissured	16.4	24.5	-	Original cut in 1877. Capped by layer of sand. Slope above at 4.5 degrees.	60	28	stiff to very stiff, soft on surface of rupture.	Rotational / Compound	reactivation of 1920 slide	Type 2
Charwelton	19-Apr-1955	40	Cut	fissured	9.6	27.2	-	Cut widened in 1939/40, 16 years prior to slip. slope above cut approx. 6.5 degrees.	59	26	unk	Rotational / Compound	first time	Type 2
Seaton	1963	67	Cut	brecciated	9.3	20.8	-	Original cut in 1896. Capped by layer of relatively permeable head. Slope above cut = 4 degrees.	58	29	unk	Compound	first time	Type 2
Wellingborough Station	1961, May	105	Cut	brecciated	10	31	-	Original cut in 1855. Partly benched slope from section provided. Capped by layer of sand, slope above = 4 degrees.	61	30	unk	Compound - sigificant mid-slope translational component	first time	Type 2
Wothorpe - B	1964-65, winter	5	Cut	brecciated	6.1	18.5	-	Original cut in 1959. Original cut at 1.5H to 1V but failed during construction, then cut back to 3H to 1V. Capped by layer of soliflucti on material. Slope above cut = 4 degrees.	68	27	stiff to very stiff	Translational	first time	Type 2
Barrowden	1961	83	Cut	brecciated	4.3	28.8	-	Original cut in 1878. Capped by layer of relatively permeable head. Slope above cut = 3.5 degrees.	62	31	unk	Rotational	first time	Type 2

Table D2.4: Case studies of failures in cut slopes in weathered Upper Lias (Sheet 2 of 3)

Name	Slide Dimensions					At And Post-Failure						
						Limit Equilibrium Analysis (from James,1970)		Post-Failure Deformation Behaviour				
	Width (m)	Height, H_f (m)	Depth, D (m)	Slope (^{o})	Volume (cu.m.)	c' (kPa)	phi ' (deg)	Movement (m)	Peak Velocity (mm/day)	Velocity Category	Degree of Break-up	Comment
Stowehill - A	unk	10.2	3.9	24.8	unk	2.5	25	2 (crest), 0.5 to 1 (toe)	unk	unk	minor break up	Suspect slow movement given age at failure. Possible series of retrogressive slips.
Stowehill - B	unk	7.6	3.8	23	unk	0.5	25	0.6 (crest), 1.4 (toe)	unk	unk	minor break up	Suspect slow movement given age at failure.
Culworth - A	unk	7.4	4.2	26.5	unk	1.9	25	2 (crest), 1.5 to 2 (toe)	unk	unk	virtually intact	suspect slow movement given age of cut and low cohesion.
Culworth - B	unk	9	4.8	26.5	unk	0.7	25	2 (crest), 0.5 to 1.6 (toe)	unk	unk	virtually intact	suspect slow movement given age of cut and low cohesion.
Heyford	unk	9.7	3.2	24	unk	2.5	25	2.0 (crest), 1.5 to 2.3 (toe)	unk	unk	virtually intact	suspect slow movement given age of cut.
Ardley	unk	4.9	3.1	22	unk	0	25	0.5 (crest), 0.8 (toe)	unk	unk	virtually intact	suspect slow due to limited deformation.
Hunsbury Hill Tunnel -1920	unk	15.8	6.1	24.5	unk	4	25	na	unk	unk	unk	Limited information available
Hunsbury Hill Tunnel - 1954	unk	15.8	6.1	24.5	unk	0	18	7.6 (crest), 0.8 to 1 (toe)	unk	suspect slow to moderate	minor break up.	Numerous failures over period from 1900 to 1954. Crest movement totalled 7.6 m. Suspect cutting back at toe for removal of slide debris affected stability of slope for failure in 1954.
Charwelton	46	9.6	5.4	27.2	2500 to 3000	2.4	25	1.4 (crest), 1.3 (toe)	200 to 400	suspect slow	virtually intact	Slide active for more than 1 week, therefore suspect slow.
Seaton	unk	9.8	3	20.8	unk	2.5	23	0.3 to 2.0 (crest), 0.7 to 2.2 (toe)	unk	unk	virtually intact	Limited information.
Wellingborough Station	unk	11	4	31	unk	0	23	unk	unk	unk	unk	Limited information available. Initial failure in 1961. Reactication of movement during 1964 remedial works.
Wothorpe - B	unk	6.1	1.6	18.5	unk	1	23	3.5 (crest), 1.5 to 2 (toe)	20 to 100 (reactivation)	suspect slow (initial slide)	virtually intact	Movement initiated in 1964-65 winter and continued to move thereafter. 1.5 m after 3 years.
Barrowden	unk	4.95	4.7	28.8	unk	0	23	0.55 (crest), 0.5 (toe)	unk	suspect slow	virtually intact	Suspect slow due to limited amount of movement.

Table D2.4: Case studies of failures in cut slopes in weathered Upper Lias (Sheet 3of 3)

Name	Hydrology		Cause/s of Sliding	Trigger of Slide	Comments	References (Author/Year)
	Hydro-geological Features	Rainfall / Snowmelt				
Stowehill - A	No information, phreatic surface assumed for stability analysis.	unk	Excavation	High seasonal pore pressures (?)	Original cut in 1832 to 1835. First failure in 1901 followed by subsequent larger failure (Stowehill - B) in 1957.	Chandler (1972) Chandler (1974)
Stowehill - B	No information, phreatic surface assumed for stability analysis. Counterfort drains on slope.	unk	Excavation	High seasonal pore pressures (?)	Original cut in 1832 to 1835. This failure partly encompasses 1901 failure, but is more extensive.	Chandler (1972) Chandler (1974)
Culworth - A	Previous summer had been very wet, possibly high piezometric surface.	very wet summer	Excavation	High seasonal pore pressures (?)	Original cut in 1896. Failures A and B were only 80 m apart. High water content observed on surface of rupture.	Chandler (1972) Chandler (1974)
Culworth - B	Previous summer had been very wet, possibly high piezometric surface.	very wet summer	Excavation	High seasonal pore pressures (?)	Original cut in 1896. Failures A and B were only 80 m apart. High water content observed on surface of rupture.	Chandler (1972) Chandler (1974)
Heyford	Limited information on water levels.	Very high Dec 1960 rainfall	Excavation	High seasonal pore pressures (?)	Original cut in 1835. Possible slip prior to 1961.	Chandler (1974)
Ardley	Piezometric levels from piezometers installed in 1969.	Heavy storms in August 1960 (76 mm on 7/8/60)	Excavation	High seasonal pore pressures (?)	Original cut in 1908.Type 1 cut slope failure in slope above retaining wall. Capped by sand layer.	Chandler (1974)
Hunsbury Hill Tunnel - 1920	no information. Piezometric levels for stability analysis assumed.	unk	Excavation	High seasonal pore pressures (?)	Original cut in 1877. History of slope failures with failures in 1900, 1920, 1921, 1928, 1935, 1945 and 1954. Slope then trimmed back.	Chandler (1974)
Hunsbury Hill Tunnel - 1954	no information. Piezometric levels for stability analysis assumed.	unk	Excavation	High seasonal pore pressures (?)	Original cut in 1877. History of slope failures. This failure reactivation at residual strength.	Chandler (1974)
Charwelton	Phreatic surface for stability analysis assumed.	unk	Excavation	High seasonal pore pressures (?)	Cut widened in 1939/40, 16 years prior to slip. Slip active for at least one week. Possibly deeper than indicated in figure because movement of railway tracks observed.	James (1970)
Seaton	Piezometers installed in 1969, maximum levels used for stability analysis.	unk	Excavation	High seasonal pore pressures (?)	Original cut in 1896.Translational failure in brecciated clay.	Chandler (1974)
Wellingborough Station	no information. Piezometric levels for stability analysis assumed.	no exceptional rainfallprior to slip	Excavation	High seasonal pore pressures (?)	Original cut in 1855. Reactivation in 1964 after remedial works.	Chandler (1974)
Wothorpe - B	Piezometric levels from piezometers.	unk	Excavation	High seasonal pore pressures (?)	Original cut in 1959. Failures occurred during construction in slopes at 1.5H to 1V. One of these failures continued to degrade even after trimming back to 3H to 1V.	Chandler (1972) Chandler (1974)
Barrowden	Piezometers installed in 1969, maximum levels used for stability analysis.	unk	Excavation	High seasonal pore pressures (?)	Original cut in 1878. Large seasonal variation in piezometric levels near to ground surface (virtually no change at depth).	Chandler (1974)

APPENDIX E

Case Studies of Concrete Face Rockfill Dams

1.0 CASE STUDY INFORMATION ON CONCRETE FACE ROCKFILL DAMS

Information on the individual case studies used for the analysis of rockfill deformation behaviour in embankment dams is presented in Table E1.1. The data set comprises thirty-five concrete faced rockfill dams and one central core earth and rockfill dam (El Infiernillo dam).

An explanation of some of the terminology used in Table E1.1 is as follows:

- General terms or symbols used and their meaning are:
  - "-" or "na" = not required, not appropriate or not known
  - "( )" in strength class, C_u, dry density and void ratio columns indicates the value has been estimated.
  - H to V refers to horizontal to vertical slope angle; i.e. 2H to 1V.
  - SMP = surface monitoring point.
  - HSG = hydro-static settlement gauge
  - IN = inclinometer
  - EOC = end of construction
  - FF = first filling
- The system for classification of the various rockfill zones used for the main rockfill is described in Section 6.2.4 of Chapter 6. The zoning classification used by the author/s of the referenced paper is given separately.
- Under the section construction:
  - Height, H = maximum embankment height
  - Length, L = crest length
  - Slab face area = the area of the upstream face in the plane measured normal to the upstream face.
- In the design section:
  - Main rockfill refers to the rockfill forming the main body of the embankment; i.e. Zone 3 for dumped rockfill, Zones 3A and 3B for compacted rockfill (refer Section 6.2.4 of Chapter 6 for details).
  - Facing details refers to the embankment zone between the facing slab and the main rockfill (refer to Section 6.2.4 of Chapter 6).
- In the section on rockfill material parameters and properties:

- Terms FR and SW, used in rockfill source column, refer to the rock weathering classification (fresh and slightly weathered respectively) used by the referenced author/s.
- Classification of the unconfined compressive strength (UCS) of the intact rock used in the rockfill is in accordance with Australian Standard AS 1726-1993 (refer Table 1.2 in Section 1.3.3 of Chapter 1).
- Particle size distribution parameters have been determined from the average grading curve for the rockfill where available or as reported by the referenced author/s.
- C_u = Grading uniformity coefficient of the rockfill particle size distribution (= D_{60}/D_{10}).
- C_c = Grading curvature coefficient of the rockfill particle size distribution (= $(D_{30}{}^2)/(D_{60} \cdot D_{10})$).
- D_{10}, D_{30}, etc., refer to the particle size (from the average grading curve) related to 10, 30, etc. percent passing.
- The dry density, void ratio and porosity are average values reported by the referenced author/s or calculated from the available data.
- The classification terms used to describe the "level of compaction" are defined in Section 1.3.3 of Chapter 1. "Good" refers to well-compacted, "poor" refers to dumped and well sluiced or poorly compacted, and "very poor" refers to dry dumped or dumped and poorly sluiced rockfill.
- 4p 10t SDVR = 4 passes of a 10 tonne (dead-weight) smooth drum vibrating roller.

- Definitions of and methods for calculation of the rockfill secant moduli during construction (E_{rc}) and the modulus on first filling (E_{rf}) are discussed in Chapter 6 (Sections 6.2.3 and 6.4.2). The rockfill secant modulus during construction (Erc) has generally been determined from deformation records in the lower 60% and central half of the embankment. In Table E1.1:
  - The "average [secant modulus] over the construction period" has determined by averaging the modulus estimates throughout the construction period. It includes values estimated when the embankment was in the early stages of construction right through to the end of construction; and

  - The "average at EOC (end of construction)" only considers those secant moduli estimates calculated at the end of the main rockfill construction, the calculation for which takes into consideration the effect of valley shape on the vertical stress. The "average" is a representative value of the modulus obtained by averaging where more than one estimate has been made (i.e. from or between different HSGs).

- Leakage. The time period of the long-term leakage rate is generally given in years after the end of first filling. For several cases, such as Dix River, it is given in terms of years after the end of main rockfill construction because the period of first filling was not known. For several embankments where first filling was not completed in the reported period and where a significant reduction in leakage rate occurred, such as due to repair, a long-term leakage rate is given (e.g. Khao Laem).
- Deformation monitoring:
  - The settlements during construction are generally based on the monitoring records from hydrostatic settlement gauges (HSG) installed as construction proceeded;
  - Post construction crest settlements are from after the end of main rockfill construction. "0.5 to 5 years" indicates the period of monitoring after the end of main rockfill construction;
  - Post construction crest settlements are given in millimetres and as a percentage of the embankment height;
  - For the deformation normal to the face slab, the references to percent of dam height or distance below the crest ("bc" = vertical distance below the crest) refer to the location on the face slab representative of the location of the deformation measurement.
  - The long-term deformation rates are in units of crest settlement (as a percentage of the embankment height) per log cycle of time, where time is measured in years after the end of main rockfill construction.

Table E1.1: Case studies information on concrete face rockfill dams

Name	GENERAL DETAILS		CONSTRUCTION								DESIGN				References
			Construction Timing		Dimensions							Facing Details (Support Zone for Face Slab)			
	Location / Owner	Geology	Year Completed	Time (years)	Height, H (m)	Length, L (m)	L/H	Slab Face Area (m^2)	Upstream Slope	Downstream Slope	Foundation (Soil/Rock)	Main Rockfill (Comments)	Thickness (normal to face slab), m	Material Type / Compaction	Comments	
Aguamilpa (Zone 3A)	CFE, Mexico	Tertiary volcanics - ignimbrites	1993	3 ?	185.5	475	2.6	130000	1.5 to 1	1.4 to 1	Rock - gravels in part of river section	Zone 3A upstream half. Zone 3T dowmstream central 1/3. Zone 3B - downstream outer 2/3. Zone 3B coaser than 3T.	-	River gravels (sandy gravel), rounded, well compacted.	-	Macedo et al (2000), Macedo (1999) Montanez et al (1993), Mori (1999) Gonzales & Mena (1997) Marulanda & Pinto (2000)
Aguamilpa (Zone 3T)																
Aguamilpa (Zone 3B)																
Alto Anchicaya	Columbia	metamorphic sediments, schists & chert	1974	1.5	140	260	1.9	31000	1.4 to 1	1.4 to 1	Gravels in river section	Zone 3A upstream half of main rockfill, Zone 3B downstream half of main rockfill.	1.75 to 7	finer well graded rockfill, well compacted	-	Materon (1985a), Regalado et al (1982) Amaya & Marulanda (2000)
Bastyan	Hydro Tasmania	Rhyolite	1983	1.5	75	430	5.7	19000	1.3 to 1	1.3 to 1	Rock	Zone 3A - 90% of main rockfill, Zone 3B in lower part of outer downstream shoulder. Slight influence from arching in lower gully.	3.7	finer well graded rockfill, well compacted	higher densities than main rockfill	HEC (1991a), Bowling (1981-82) Knoop and Lack (1985)
Cethana	Hydro Tasmania	Quartzite & quartzite conglomerate	1971	2.5	110	213	1.9	30000	1.3 to 1	1.3 to 1	Rock	Zone 3A - 75% of main rockfill, Zone 3B in outer downstream shoulder. Likely arching in lower gully.	3.7	finer well graded rockfill, well compacted	-	Forza & Hancock (1995a), Liggins (1971), Fitzpatrick et al (1973), Wilkins et al (1973), Fitzpatrick et al (1982), Pinto et al (1982), Giudici et al (2000)
Chengbing	China	Tuff lava	1989	2 to 2.5	74.6	325	4.4	15800	1.3 to 1	1.3 to 1	Rock	Zones 3B and 3C (Zone 3A) similar in rockfill type and compaction	2.4	crushed rockfill, finer than 3A and well compacted	Higher densities than main rockfill	Wu & Cao (1993) Wu et al (2000c)
Cogswell	LACFCD	Granitic Gneiss ?	1935	3.3	85.3	176.8	2.1	-	1.3 to 1	1.5 to 1	Rock	Laminated gunite facing damaged early in embankment life. Replaced in 1935 with timber facing and in 1947 with reinforced concrete facing.	1.8 to 5.5	derrick placed rockfill	Lean concrete facing placed on derrick rockfill	Baumann (1939, 1958, 1964)
Courtright	Pacific Gas & Electricity Co. San Francisco	granite	1959	2	97	274	2.8	20440	1.15 to 1	1.4 to 1	Rock	-	2.4 to 3.5	derrick placed rockfill, voids chinked	-	Cooke (1958) Regan (1997)
Crotty	Hydro Tasmania	sandstone, phyllite, conglomerate	1991	2	83	240	2.9	14500	1.3 to 1	1.5 to 1	Rock	Facing rockfill (Zones 2A and 2B) likely to have a lower modulus than the gravels used in the main fill (Zone 3A).	7.3	rockfill used, well compacted	tunnel spoil, rockfill from sedimentary geology units.	Davies (1993), Quinlan (1993) Li et al (1993), Cribben (1990) Giudici et al (2000)
Dix River	Kentucky Utilities Company	limestone & shale	1925	2	84	311	3.7	-	1.1 to 1	1.4 to 1	Rock	Suspect rockfill likely to be relatively coarse. Some rockfill placed directly from fired shots in abutments.	1.4 to 4.1	derrick placed rockfill, 2.7 to 9 tonne rocks used, voids chinked	-	Schmidt (1958) Howson (1939)
El-Infiernillo (Zone 3B)	CFE, Mexico	silicified conglomerate	1963	1.3	148	344	2.3	-	1.75 to 1	1.75 to 1	Soil/Rock	Central core earth and rockfill embankment. Included to give an estimate of moduli during construction for dry dumped rockfill.	na	na	na	Marsal & Ramirez de Arellano (1967)
El-Infiernillo (Zone 3C)																
Foz Do Areia (Zone 3A)	Brazil	Basalt & Basaltic Breccia	1979	2.5	160	828	5.2	139000	1.4 to 1	1.4 to 1	Rock	Complex design. Zone 3A on roughly upstream 1/3, Zones 3B (1C and 1D) in downstream 2/3 of main rockfill.	2.3 to 7.6	finer graded sound basalt (very high strength), well compacted		Pinto et al (1985a), Materon (1985b) Pinto et al (1982), Pinto et al (1993) Sobrinho et al (2000), Cooke (1999)
Foz Do Areia (Zone 3B)																
Golillas	Columbia	interbedded shale and sandstone	1978	1.75	125	107	0.9	17000	1.6 to 1	1.6 to 1	Rock	Clean gravels placed as chimney filter and in central section of main fill.	4.0	processed dirty gravels, finer graded, well compacted	slightly higher density than main rockfill	Amaya & Marulanda (1985) Amaya & Marulanda (2000)
Ita (Zone 3A)	Brazil	Basalt	1999	3	125	880	7.0	110000	1.3 to 1	1.3 to 1	Rock	Zone 3A - upstream 1/3; Zone 3B - downstream 2/3. Dumped rockfill placed in river section. Zone 3A incorporates dense basalt zone closest to upstream face and zone of lesser quality behind this.	3.5 to 5	crushed dense basalt, fine sized, well compacted	high densities than main rockfill	Sobrinho et al (2000) Sobrinho et al (1999) Silveira & Sardinha (1999)
Ita (Zone 3B)																
Kangaroo Creek	SA Water, South Australia	schist and gneiss	1969	1.75	60	178	3.0	-	1.3 to 1	1.4 to 1	Rock, some gravels	Zone 3A is main body of rockfill. Zone 3B is a basal layer of very high strength rockfill for drainage purposes.	8.0	Finer graded H to VH strength granitic gniess, well compacted	Zone 2 placed in 915 mm layers.	Good et al (1985), Good (1976, 1981) E&WSD (1981), SKM (1995) SA Water (1995)
Khao Laem (Zone 3A)	Thailand	limestone, shale, sandstone & siltstone	1984	2	130	1000	7.7	-	1.4 to 1	1.55 to 1	Rock, karstic	Zone 3A - 75% of main rockfill in section, Zone 3B in outer downstream shoulder (25% of main rockfill).	4.1	finer graded rockfill, 0.5 m layers, well compacted	D_{50} = 24 to 40 mm	Watakeekul et al (1985) Mahasandana & Mahatharadol (1985) Aphaiphuminart et al (1988)
Khao Laem (Zone 3B)																
Kotmale	Sri Lanka	foliated gneiss	1984	3	90	560	6.2	-	1.4 to 1	1.45 to 1	Rock	Limited information on rockfill properties. HSGs in higher elevations indicate higher modulus.	3.5	finer graded rockfill, well compacted	-	Gosschalk & Kulasinghe (1985, 1987) Casinader (1987) Kulasinghe & Tandon (1993)
Little Para	SA Water, South Australia	interbedded quartzite, slaty dolomite & slate	1977	2.5	53	225	4.2	-	1.3 to 1	1.4 to 1	Rock	No water available to add to rockfill for construction to 24 m height.	8.5	High strength (UCS = 36 to 45 MPa) quartzite rockfill, well compacted	Better quality rockfill used for facing layers.	Good et al (1985), Good (1981) Boucaut & Beal (1979)
Lower Bear No. 1	Pacific Gas & Electricity Co. San Francisco	granite	1952	1.5	75	293	3.9	17650	1.3 to 1	1.35 to 1	Rock	Coarse rockfill	3 to 6.4	derrick placed rockfill, 1.15 to 2.7 m^3 volume, voids chinked	-	Steele & Cooke (1958)
Lower Bear No. 2		granite	1952	<1.5	46	264	5.7	8400	1 to 1	1.3 to 1	Rock	Coarse rockfill	3 to 5.2			

Table E1.1: Case studies information on concrete face rockfill dams (Sheet 2 of 8)

Name	Material Parameters / Properties of Rockfill																		Material Parameters / Properties of Rockfill											
	Rockfill Zone		Rockfill Source	Particle Shape	Intact Rock Strength				Particle Size Distribution Parameters (from average grading curve)										Particle Size Distribution Parameters (from average grading curve)											
	Class[n]	Authors Class[n]			Strength Classification	UCS (MPa)	Wet/Dry Strength (%)	Absorption (%)	C_u	C_c	D_{10} (mm)	D_{30} (mm)	D_{50} (mm)	D_{60} (mm)	D_{80} (mm)	D_{90} (mm)	D_{max} (mm)	% finer 75 micron	% finer 19 mm	Clean / Dirty	C_u	C_c	D_{10} (mm)	D_{30} (mm)	D_{50} (mm)	D_{60} (mm)	D_{80} (mm)	D_{90} (mm)	D_{max} (mm)	% finer 75 micron	% finer 19 mm	Clean / Dirty
Aguamilpa (Zone 3A)	3A	3B	dredged alluvium	rounded	(Very High)	-	-	-	85	5.8	0.75	16.4	45	62	124	230	600	2	34	clean to dirty	85	5.8	0.75	16.4	45	62	124	230	600	2	34	clean to dirty
Aguamilpa (Zone 3T)	3T	T	ignimbrite	angular	Very High	180	-	-	30	2.4	2.9	24.5	61	88	204	290	500	2	28	clean	30	2.4	2.9	24.5	61	88	204	290	500	2	28	clean
Aguamilpa (Zone 3B)	3B	3C	ignimbrite	angular	Very High	180	-	-	22	1.4	9	-	150	-	-	-	700	-	-	clean	22	1.4	9	-	150	-	-	-	700	-	-	clean
Alto Anchicaya	3A	D	hornfels	angular	(Very High)	-	-	-	18	2.5	5.5	31	71	100	205	280	600	<2	22	clean	18	2.5	5.5	31	71	100	205	280	600	<2	22	clean
Bastyan	3A	3A	Rhyolite (SW to FR)	angular	(Very High)	-	-	-	42	3.3	2.4	28	69	100	190	300	600	3.3	25	clean (?)	42	3.3	2.4	28	69	100	190	300	600	3.3	25	clean (?)
Cethana	3A	3A	Quartzite, quarried	angular	(Very High)	-	-	-	23	2.0	4.8	32	75	108	250	440	900	2	21	clean	23	2.0	4.8	32	75	108	250	440	900	2	21	clean
Chengbing	3A	3B/3C	Tuff lava, quarried	angular	Very High	80	-	-	10.4	-	-	-	-	-	-	-	1000	-	-	clean (?)	10.4	-	-	-	-	-	-	-	1000	-	-	clean (?)
Cogswell	3A	3A	Granitic Gneiss	angular	High	45	-	-	7	2.3	100	-	650	-	-	-	1300	3	5	clean	7	2.3	100	-	650	-	-	-	1300	3	5	clean
Courtright	3A	3A	granite, blasted	angular	(Very High)	-	-	-	(<7)	-	-	-	550 to 1500	-	-	-	1750	-	-	clean ?	(<7)	-	-	-	550 to 1500	-	-	-	1750	-	-	clean ?
Crotty	3A	3A	Gravels (Pleitocene)	rounded	(Very High)	-	-	-	70	5.6	0.34	7.3	20	28	60	86	200	3.5	48	dirty	70	5.6	0.34	7.3	20	28	60	86	200	3.5	48	dirty
Dix River	3A	3A	Limestone & Shale (?), spillway excav	angular ?	(Very High)	-	-	-	low	-	-	-	-	-	-	-	-	-	-	-	low	-	-	-	-	-	-	-	-	-	-	-
El-Infiernillo (Zone 3B)	3B	3B	diorite & silicified conglomerate	angular	Very High	125	-	-	13	1.6	6.5	-	62	-	-	-	600	1	22	clean ?	13	1.6	6.5	-	62	-	-	-	600	1	22	clean ?
El-Infiernillo (Zone 3C)	3C	3C	diorite & silicified conglomerate	angular	Very High	Diorite = 125	-	-	<13	1.6 ?	> 7	-	-	-	-	-	>600	-	-	clean ?	<13	1.6 ?	> 7	-	-	-	-	-	>600	-	-	clean ?
Foz Do Areia (Zone 3A)	3A	1B	basalt (max 25% basaltic breccia)	angular	High to Very High	Basalt = 235 Breccia = 37	-	1.0	6	2.1	20	60	105	145	300	440	600	<1	10	clean	6	2.1	20	60	105	145	300	440	600	<1	10	clean
Foz Do Areia (Zone 3B)	3B	1C & 1D	mix basalt & basaltic breccia	angular	High to Very High	Basalt = 235 Breccia = 37	-	1.0	14.2	2.2	-	-	-	-	-	-	-	-	-	clean ?	14.2	2.2	-	-	-	-	-	-	-	-	-	clean ?
Golillas	3A	2	gravels, unprocessed	rounded	(Very High)	-	-	-	125	2.5	0.65	11.5	31	80	185	225	350	6	40	dirty	125	2.5	0.65	11.5	31	80	185	225	350	6	40	dirty
Ita (Zone 3A)	3A	E1/E3'	basalt (dense)	angular	(Very High)	-	-	-	11	1.6	13.4	57	113	152	275	425	700	1	12	clean	11	1.6	13.4	57	113	152	275	425	700	1	12	clean
Ita (Zone 3B)	3B	E3	Breccia and Basalt	angular	Basalt - VH Breccia - H (?)	-	-	-	13.3	1.6	10	46	100	133	250	385	750	1	15	clean	13.3	1.6	10	46	100	133	250	385	750	1	15	clean
Kangaroo Creek	3A	3	schist	angular to subangular	Medium to High	25	63	3.0	310	6.4	0.14	6.2	26	44	105	180	600	8.5	44	dirty	310	6.4	0.14	6.2	26	44	105	180	600	8.5	44	dirty
Khao Laem (Zone 3A)	3A	3A	limestone, quarried	angular	Very High	< 190	100	low	-	-	-	-	-	-	-	-	900	-	-	-	-	-	-	-	-	-	-	-	900	-	-	-
Khao Laem (Zone 3B)	3B	3B	limestone, quarried	angular	Very High	< 190	100	low	-	-	-	-	-	-	-	-	1500	-	-	-	-	-	-	-	-	-	-	-	1500	-	-	-
Kotmale	3A	3A	charnockitic / gneissic	angular	(High to Very High)	-	-	-	-	-	>2	-	-	-	-	-	700	-	-	-	-	-	>2	-	-	-	-	-	700	-	-	-
Little Para	3A	3A	dolomitic siltstone	angular, elongated ?	Medium	8 to 14	close to 100%	-	120	4.0	0.6	13	40	70	255	390	1000	5	35	dirty (soft rock)	120	4.0	0.6	13	40	70	255	390	1000	5	35	dirty (soft rock)
Lower Bear No. 1	3A	3A	granodiorite	angular	Very High	100 to 140	-	-	8 to 10	-	>100	-	700 to 800	-	-	-	2000 to 3000	low	low	clean	8 to 10	-	>100	-	700 to 800	-	-	-	2000 to 3000	low	low	clean
Lower Bear No. 2	3A	3A	granodiorite	angular	Very High	100 to 140	-	-																								

Table E1.1: Case studies information on concrete face rockfill dams (Sheet 3 of 8)

Name	SECANT MODULI VALUES				HYDROGEOLOGY			LEAKAGE		
	Modulus During, E_{tc} (MPa)		Modulus on First Filling, E_{rf}		Time for First Filling (from end of main rockfill construction)	Reservoir Level / Comments	Rainfall, average annual (mm)	Maximum Rate (l/sec)	Long-term (l/sec)	Comment
	Average over construction period	Average at EOC (adjusted for valley shape)	E_{rf} (MPa)	Comments						
Aguamilpa (Zone 3A)	305 (250 to 330)	305	770	Reduced modulus where Zone 3C has an influence on the deformation of the face slab.	0.48 to 1.83 years	-	-	200, at first filling	150 to 170 (4 years post ff)	Large increase in leakage rate when reservoir raised above certain level (due to cracking in upper part of face slab)
Aguamilpa (Zone 3T)	104	104								
Aguamilpa (Zone 3B)	36 (25 to 45)	36								
Alto Anchicaya	138 (100 to 170)	110	375 (@ 30 to 40% height)	-	0.18 to 0.2 (Oct 74) years.	-	-	1800	-	High rate of leakage on first filling, through the perimeter joint on the right abutment and open joints on left abutment. Repaired.
Bastyan	130 (120 to 140)	102	290	Maximum face deflection at about mid height.	0.86 to 1.05 years.	Steady	2100	10	5 (8 years post ff)	Approximately 10 l/sec on first filling. Gradual reduction with time to base flow of 5 l/sec.
Cethana	160 (120 to 210) in lower 25% 105 (85 to 120) in mid to lower 25%	103	300	-	0.26 to 0.48 years (1971).	Steady	2030	65 to 70	5 to 10 (4 years post ff)	-
Chengbing	43	43	110	Approx 2.5 times E during	-0.5 to 4 years (12/88 to 1993).	First filling started before embankment completed. Fluctuating, drawdowns up to 50 m.	-	75	-	Max leakage during construction when reservoir level rose above level of face slab. After completion leakage = 60 l/sec.
Cogswell	-	-	44	From measured face slab deformation.	Started filling 2.6 years after EOC. Filled in 71 hours in March 1938.	-	-	3600	-	Maximum in 1938 on first filling. Large crack in floater slab.
Courtright	-	-	-	-	0 to 9 years (from 1959).	Fluctuating	-	1275	-	Lower perimetric joints moved soon after completion affecting waterstops. Joints on abutments opened (~ 1968) and upper perimetric joint opened tearing waterstops in 1989.
Crotty	375 (113 to 636)	360	470	Relatively low modulus (compared with modulus during construction) may be associated with lower modulus of facing rockfill.	0.87 to 2.0 years.	Steady	2900	45	30 to 35 (2 years post ff)	Peak leakage rate of 45 l/sec. Thought to be seepage through the foundation on the abutments where the grouting failed.
Dix River	-	-	-	-	Started in 1925	-	-	2700 (1937, 12 yrs after EOC)	2000 (30 years post EOC)	Leakage near intake tower, through cracks and opened joints in slabs and through the foundation. Various methods to try and treat problem.
El-Infiernillo (Zone 3B)	39 (27 to 48)	35.5	-	-	0.33 yrs (June to Oct 1964)	Fluctuating	-	-	-	-
El-Infiernillo (Zone 3C)	22 (17 to 27)	20								
Foz Do Areia (Zone 3A)	47 (38 to 56)	47	80 (65 to 92)	Relatively large deformations in toe region compared with other CFRDs. Therefore lower moduli toward toe region (15% height above toe)	0.5 to 0.9 years (Apr to Aug 80).	Relatively steady, typical 5 m fluctuation	-	240	70 (5 years post ff)	Maximum leakage on first filling. Gradual reduction with time.
Foz Do Areia (Zone 3B)	32 (29 to 38)	32								
Golillas	155 (145 to 165) excludes those points thought to be affected by arching	107	250	Estimated by hydrostatic settlement cells for section below reservoir level.	4 to 5.17 years (June 82 to Aug 83).	Fluctuating. First filling interupted due to excessive seepage.	-	1080	270 to 500 (15 years post EOC)	Leakage through the foundation during first filling and some segregation of Zone 1 noted. Repaired and leakage reduced.
Ita (Zone 3A)	48	48	87 (83 to 91)	Relatively low because incorporates low modulus dumped rockfill in river gully (E during = 17 MPa).	0.7 to 0.9 years.	-	-	1700	-	Reached 1700 l/sec 4 months after first filling, due to cracking in slab. Reduced to 380 l/sec by dumping sand and silty sand on face.
Ita (Zone 3B)	24 (14 to 46)	24								
Kangaroo Creek	-	-	140	Reported (no data to confirm)	0 to 1.95 yrs (Sept 69 to Aug 71).	Fluctuating, seasonal drawdown of up to 42 m	600 to 800	11	2.5	On initial filling seepage heard through within the embankment. Possible seepage along horizontal layers in weak rockfill.
Khao Laem (Zone 3A)	59 (43 to 79)	43	130 to 240	High reading possibly affected by arching in deepest section of embankment, low reading possibly affected by "plum pudding" foundation.	0.6 to 1.9 years (June 84 to Nov 85).	Steady (?)	-	53	1.1 (after repair of face slab cracks)	Feb 1986 (3 months post first filling) leakage increased from 9 to 53 l/sec as a result of cracks in the face slab. Cracks repaired and leakage reduced.
Khao Laem (Zone 3B)	30	30								
Kotmale	61 (47 to 87)	52	145 (135 to 155)	Estimated from HSGs near to upstream face.	0.54 to 1.04 years (Nov 84 to Aug 85).	Fluctuating, seasonal drawdown up to 60 m	-	< 10	-	At close to end of first filling.
Little Para	21.5 (19.5 to 23.5)	20.5	-	No data for calculation	0.58 to 2.83 years (Aug 77 to Nov 79).	Seasonal fluctuation of about 5 m.	-	19.2	-	Maximum leakage measured just prior to first overflow in August 1981. Wet spots and seepage on downstream slope on right abutment.
Lower Bear No. 1	-	-	21	At end of 2 yrs and 42 m below crest (39% dam height). Likely under-estimate	0.07 to 0.58 years (Dec 52 to June 53).	Fluctuating, seasonal drawdown typically 35 m	-	113	43 (4 years post ff)	Maximum at FSL on first filling. Gradual reduction thereafter.
Lower Bear No. 2	-	-	40	At end of 1 year and 29 m below crest (39% dam height).	0.07 to 0.58 years (Dec 52 to June 53).	Fluctuating, seasonal drawdown typically 35 m	-	no leakage	-	Suspect relatively small in comparison to Lower Bear No. 1 and other CFRDs constructed in the 1950s.

Table E1.1: Case studies information on concrete face rockfill dams (Sheet 4 of 8)

Name	MONITORING									Other Comments
	Settlement During Construction (mm)	Post Construction Crest Deformation					Deformation Normal to Face Slab (mm)	Long Term Crest Settlement Rate (% per log time cycle) (t_o at EOC)	Comments	
		Settlement, total (mm)	Settlement, total (%)	Settlement on FF (mm)	Settlement on FF (%)	Lateral Displacement (mm)				
Aguamilpa (Zone 3A)	-	307 (0.4 to 5.7 yrs)	0.185	222	0.133	-	320 from ff to 6 years	0.090	Decreasing velocity of deformation with time. Face slab deformation greatest at crest (due to much lower modulus of Zone 3C rockfill). Limited time for estimation of long term creep rate.	Moduli during construction from literature.
Aguamilpa (Zone 3T)										
Aguamilpa (Zone 3B)										
Alto Anchicaya	-	153 mm (0.11 to 10.3 yrs)	0.109	15	0.011	-	160 mm to 5/77 (130 mm ff)	0.037	Decreasing rate of deformation with time. At 10 yrs < 2 mm/yr crest settlement. Crest points on top of concrete plinth.	Moduli during construction from literature.
Bastyan	> 219	50 mm (0.2 to 7.5 years, SC3)	0.066	15	0.02	16 mm (SC3), 7 mm ff	68 mm @ 34 m below crest	0.028	Decreasing rate of deformation post first filling (also decreasing on log scale).	
Cethana	> 560	137 mm (0 to 28.6 yrs)	0.124	46	0.043	83 mm to 7/92 (27 ff)	170 mm to 10/93 (114 ff 37m bc)	0.042	Decreasing rate of deformation post first filling (linear on log scale). Upper 12 m of rockfill placed 1 year after main body had been completed.	
Chengbing	-	-	-	-	-	-	154 mm after 10 years (?)	-	Insufficient information on deformation.	In 1989, during construction, the impounded water level exceeded the top level of the constructed face slab resulting in leakage through the embankment above the slab.
Cogswell	Estimated at 15.7 m.	271 mm (0 to 3 years, to 4/38)	0.317	< 271	< 0.317	-	403 mm vertical settlement to 4/38 (first filling)	-	In late 1933 a very hevy rain storm resulted in crest settlements of to a maximum of 3.41 m (due to collapse settlement). Artificial sluicing resulted in an additional 1.71 m.	
Courtright	-	1237 mm (0 to 38 yrs)	1.282	844	0.875	-	-	0.70 (from 5 year to 20+ years)	Relatively steady rate of crest settlement on log scale, but only limited number of data points.	No data to calculate modulus during construction or on first filling
Crotty	> 179	55 mm (0 to 8.5 years, SC4)	0.066	16	0.019	9 mm (SC3 - ff)	46 mm @ 49 m bc	0.045	Gradual reduction in rate of deformation after first filling, relatively steady on log scale.	
Dix River	-	1281 mm (Stn 16.9, to 1957, 32 yrs)	1.525	-	-	970 mm to 1957 (Stn 16.9)	-	0.58 to 1.44 (increasing with time)	Decreasing rate of deformation with time. At 30 yrs approximately 20 to 25 mm/year settlement, and 15 to 17 mm/yr displacement.	No data to calculate modulus during construction or on first filling
El-Infiernillo (Zone 3B)	1095 (1.9%) in IN3, and 2425 mm (2.2%) in IND1.	-	-	-	-	-	-	na	-	Central core earth and rockfill dam. Data used for analysis of rockfill deformation during construction.
El-Infiernillo (Zone 3C)										
Foz Do Areia (Zone 3A)	-	328 mm (0 to 11 years)	0.205	73	0.046	248mm to 1984 (180 ff), d/stream slope	780 mm @ 49% dam height (620 mm ff)	0.099	Log scale deformation plot shows sharp reduction in rate of deformation after 3 years and then acceleration in rate beyond 7 years (to that similar from 1 to 3 years).	
Foz Do Areia (Zone 3B)										
Golillas	-	52 mm (0.46 to 6.4 years, to 10/84)	0.042	20	0.016	7 mm to 10/84 (2 yrs)	160 mm @ 46% dam height by 3/84 (first filling)	0.033	Acceleration in crest settlement and face deflection toward end of first filling. Thereafter, significant reduction in rate of deformation, but limited data. Crest SMPs on parapet. Upstream face slab deformation estimated by HSGs and SMPs.	
Ita (Zone 3A)	-	-	-	-	-	-	461 mm (during ff)	-	Limited data.	Relatively complex cross section. Face slab cracked resulting in relatively high leakage rates.
Ita (Zone 3B)										
Kangaroo Creek	-	116 mm (0 to 26 yrs)	0.193	26	0.043	50 mm to 1979 (8yrs), 32 mm ff	-	0.126	Not sure when monitoring first started, possibly shortly after start of first filling or could have missed most of first filling entirely. Decreasing rate of movement with time post first filling. Crest SMPs on rockfill and face slab.	Initial monitoring possibly missed first filling to EL 220 (26 m below crest, 22 m below FSL), but cannot be sure. Dam raised approx. 3.4 m in 1983 for additional flood storage.
Khao Laem (Zone 3A)	> 550 (of embankment)	-	-	-	-	-	-	-	Significant settlement of foundation during construction.	Calculation of moduli during construction takes into consideration foundation settlement. Erf adjusted for filling to full supply level.
Khao Laem (Zone 3B)										
Kotmale	> 1020	255 mm (0 to 2.46 yrs)	0.283	96	0.107	62 mm to 10/86 (0 to 2 yrs)	98 mm to ff (estimated from HSG)	0.258 (limited data, possibly hasn't steadied as yet)	Initial reading very close to time of completion of rockfill. Last available readings approx 12 months after first filling, rate has not settled down as yet.	Modulus on first filling determined from deformation of HSGs adjacent to face slab.
Little Para	-	152 mm (0 to 22.6 yrs)	0.288	22	0.042	-	-	0.21	Monitoring appears to have started about June 1978, most likely when first filling started.	Wet spots and seepage observed on downstream slope (on right abutment). Indicative of high permeability variation between horizontal and vertical directions.
Lower Bear No. 1	-	375 mm (0.07 to 4.05 years, to 11/56)	0.56	< 335	< 0.50	305 mm to 11/56 (4 yrs), ff 270 mm	625 mm to 10/54 (2 yrs) @ 42 m bc	0.103	Rapid deformation on first filling with significant reduction in rate thereafter. Crest SMPs on upstream edge of crest.	
Lower Bear No. 2	-	116 mm (0.07 to 4.07 years, to 11/56)	0.271	73	0.171	116 mm to 11/56 (4 yrs), ff 88 mm	165 mm to 11/56 (4 yrs) @ 15 m bc, ff 137 mm	0.128	Rapid deformation on first filling with significant reduction in rate thereafter. Crest SMPs on upstream edge of crest.	

Table E1.1: Case studies information on concrete face rockfill dams (Sheet 5 of 8)

Name	GENERAL DETAILS		CONSTRUCTION								DESIGN				References
	Location / Owner	Geology	Construction Timing		Dimensions					Foundation (Soil/Rock)	Main Rockfill (Comments)	Facing Details (Support Zone for Face Slab)			
			Year Completed	Time (years)	Height, H (m)	Length, L (m)	L/H	Slab Face Area (m^2)	Upstream Slope	Downstream Slope		Thickness (normal to face slab), m	Material Type / Compaction	Comments	
Mackintosh	Hydro Tasmania	Greywacke, slate & phyllite	1981	2.75	75	465	6.2	27500	1.3 to 1	1.3 to 1	Rock	Zone 3B not used.	3.7	finer graded greywacke rockfill, well compacted	high densities achieved (higher than main rockfill)	Knoop & Lack (1985), Knoop (1982b) HEC (1991b), Bowling (1978) Giudici et al (2000)
Mangrove Creek (Zone 3A) Mangrove Creek (Zone 3B)	Sydney Water, NSW	Interbedded sandstones, siltstones and claystones	1981	2	80	380	4.8	-	1.5 to 1	1.6 to 1	Weathered Rock	Zone 3A - upstream facing (20 to 30%). Random fill (Zone 3B) makes up most of rockfill. Drainage layer below random fill.	1.5 to 2	finer graded siltstone rockfill, well compacted	-	Mackenzie & McDonald (1985) PWSD NSW (1998) Heinrichs (1996)
Murchison	Hydro Tasmania	Rhoylite	1982	2.25	94	200	2.1	17000	1.3 to 1	1.3 to 1	Rock	Zone 3A - 70% of main rockfill, Zone 3B in outer downstream shoulder.	3.7	finer crushed rockfill, watered and well compacted	Vey high strength rhyolite	Knoop & Lack (1985), Knoop (1982a) Gerke et al (1995), Robinson (1979) Giudici et al (2000)
Reece	Hydro Tasmania	laminated quartzite & amphibolite	1986	3	122	374	3.1	37800	1.3 to 1	1.4 to 1	Gravels in river section	Zone 3A - 75% of main rockfill, Zone 3B in outer downstream shoulder. River gravels left in place (except near upstream face).	3.7	crushed dolerite, finer grading, well compacted	-	Knoop & Lack (1985), Li (1991) Li et al (1991), Davies et al (1995) Partyka & Bowling (1984) Giudici et al (2000)
Salt Springs	Pacific Gas & Electricity Co. San Francisco	granite	1931	3	100	396	4.0	35300	1.3 to 1	1.4 to 1	Rock	Very coarse rockfill, "lot of large rocks with few fines". Likely low C_u.	4.6	Derrick placed rockfill with flat face in the plane of the face slab.	some rock pieces were observed to crush during construction.	Steele & Dreyer (1939) Steele & Cooke (1958), Regan (1997) Cooke & Strassburger (1988)
Salvajina (Zone 3A) Salvajina (Zone 3B)	Columbia	Tertiary sedimentary - siltstone and sandstone	1984	1.5 to 2	148	362	2.4	57500	1.5 to 1	1.4 to 1	Rock and soil, gravels in river section	Alluvials in gully were in dense state (moduli approx 320 MPa). Zone 3A - upstream 2/3, Zone 3B - downstream 1/3.	2.8	gravels, thin layers, well compacted.		Amaya & Marulanda (2000) Hacelas et al (1985), Sierra et al (1985)
Scotts Peak	Hydro Tasmania	interbedded argillite & sandstone	1972	1	43	1067	24.8	-	1.7 to 1	1.3 to 1	Rock	No Zone 3B. Bituminous concrete facing. Zone 2B (well-compacted gravels) placed at upstream toe to 13 m above foundation.	0.3	sound crushed rockfill, dolomite, well compacted.	-	Gerke et al (1993), Cole (1974) Baker (1972), Cole & Fone (1979)
Segredo (Zone 3A) Segredo (Zone 3B)	COPEL, Brazil	Basalt & Basaltic Breccia	1992	2.5	145	720	5.0	86000	1.3 to 1	1.4 to 1	Rock	Zone 3A - upstream 1/3. Zone 3B (1C and 1D) downstream 2/3. Dumped basalt rockfill in river section in downstream 2/3.	3.1	fine graded sound crushed basalt, well compacted	high densities, higher than main rockfill	Pinto et al (1985b), Pinto et al (1993) Sobrinho et al (2000), Blinder et al (1992)
Serpentine	Hydro Tasmania	quartzite and schists	1971	2	38	134	3.5	8000	1.5 to 1	1.5 to 1	Rock, gravels in river section	No Zone 3B used. Grading of 3A indicates significant breakdown on compaction.	0.3	150 mm minus rockfill	-	Forza & Hancock (1993) Giudici et al (2000)
Shiroro	Nigeria	Granite	1983	-	125	560	4.5	-	1.3 to 1	1.4 to 1	Rock	Similar rockfill for entire embankment. Localised enlargement of Zone 2A below EL 290 (bottom 30 m).	6.1	finer graded rockfill, well compacted	heavily compacted in thin layers.	Bodtman & Wyatt (1985)
Tianshengqiao - 1 (Zone 3A) Tianshengqiao - 1 (Zone 3B)	China	Sedimentary - limestone, sandstone and mudstone	1999	3.3	178	1168	6.6	173000	1.4 to 1	1.3 to 1	Rock	Zone 3A - upstream half. Zone 3B (mudstone) surrounded by coarse limestone rockfill (Zone 3D).	4.6	crushed limestone (SW to FR), relatively fine, well compacted.	high densities, wetted.	Wu et al (2000a, 2000b) Yang (1993) Jiyuan et al (2000)
Tullabardine	Hydro Tasmania	Greywacke & slate	1979	0.33	25	214	8.6	5500	1.3 to 1	1.3 to 1	Rock	No Zone 3B used.	3.7	finer crushed greywacke rockfill, well compacted	high densities achieved	Knoop & Lack (1985) Forza & Hancock (1995b) Bowling (1979)
White Spur	Hydro Tasmania	Volcanics - Tuff	1989	1.5 to 2 (?)	43	146	3.4	4300	1.3 to 1	1.3 to 1	Rock	No Zone 3B used.	3.7	fine crushed rock, thin layers, well compacted	Tuff and conglomerate.	HEC (1987), Morse (1995) Morse & Ward (1989)
Winneke	Melbourne Water	siltstone with interbedded sandstone	1978	1.4	85	1050	12.4	-	1.5 to 1	2.5 to 1	Rock	Zone 3A - upstream 1/3. Rockfill drainage layer below random fill (Zone 3B) in downstream 2/3.	2.8	finer crushed rockfill, watered and well compacted	High densities in Zone 2B	Regan (1980) Casinader & Watt (1985) MMBW (1975, 1981, 1995)
Wishon	Pacific Gas & Electricity Co. San Francisco	Glaciated granite	1958	1.75	90	1015	11.3	60400	1.15 to 1	1.4 to 1	Rock	Thinner rockfill lifts placed adjacent to upstream face.	2.4 to 3.5	derrick placed rockfill, 0.7 to 2 m size, voids chinked	Irregular surface finish	Cooke (1958) Regan (1997)
Xibeikou	China	Sedimentary - limestone	1989	3	95	222	2.3	23000	1.4 to 1	1.4 to 1	Rock, gravels in lower river bed.	Zone 3A - upstream half, Zone 3B - downstream half.	4.1	Fresh crushed limestone, finer graded than Zone 1, well compacted	high densities achieved.	Peng (2000), Wang et al (1988) Huang et al (1993) Wang et al (1993)
Xingo (Zone 3A) Xingo (Zone 3B)	CHESF, Brazil	Metamorphic - granitic gneiss, Precambrian	1993	6	140	850	6.1	135000	1.4 to 1	1.3 to 1	Rock, gravels in lower river bed.	Zone 3A - upstream 1/2; Zone 3B - downstream 1/2 Dumped rockfill at downstream toe.	4.5 to 5.8	fine crushed rockfill placed in thin layers, well compacted.	high densities and low void ratios.	Sobrinho et al (2000), Souza et al (1999) Eigenheer & Souza (1999) Saboya et al (2000) Vasconcelas & Eigenheer (1985)

Table E1.1: Case studies information on concrete face rockfill dams (Sheet 6 of 8)

Name	Material Parameters / Properties of Rockfill																										
	Rockfill Zone		Rockfill Source	Particle Shape	Intact Rock Strength				Particle Size Distribution Parameters (from average grading curve)													Density			Placement Methods			
	Class[n]	Authors Class[n]			Strength Classification	UCS (MPa)	Wet/Dry Strength (%)	Absorption (%)	C_u	C_c	D_{10} (mm)	D_{30} (mm)	D_{50} (mm)	D_{60} (mm)	D_{80} (mm)	D_{90} (mm)	D_{max} (mm)	% finer 75 micron	% finer 19 mm	Clean / Dirty	Dry Density (t/m^3)	Void Ratio, e	Porosity, n (%)	Layer Thickness (m)	Water Added	Plant	Level of Compaction
Mackintosh	3A	3A	Greywacke, some slate	angular, elongated	Medium to High	45	-	-	52	3.3	1	13	34	52	130	230	1000	3.5	38	dirty	2.20	0.24	19.4	1.0	10% by volume	8p 10t SDVR	Good
Mangrove Creek (Zone 3A)	3A	1B	fresh siltstone & sandstone	angular to subangular ?	High	45 to 64	40 - 60%	3.0 - 6.7%	310	9.9	0.45	25	88	140	225	280	400	4	27	dirty ?	2.24	0.18	15.5	0.45 to 0.6	5 to 7.5% by volume	4p 10t SDVR	Good
Mangrove Creek (Zone 3B)	3B	4	weathered to fresh siltstone & sandstone	angular to subangular ?	High	26 to 64	40 - 60%	3.0 - 6.7%	330	7.5	0.3	15	60	100	200	275	450	3	32	dirty (soft rock)	2.06 t/m3	0.26	21	0.45	Placed slightly dry of optimum	4p 10t SDVR	Good
Murchison	3A	3A	Rhyolite (SW to FR)	angular	Very High	148	-	-	19	2.1	5.3	33	75	100	180	290	600	1.5	22	clean (?)	2.27	0.234	19.6	1.0	20% by volume	8p 10t SDVR	Good
Reece	3A	3A	Dolerite	angular	Very High	171 (80 to 370)	-	-	10	1.6	16	63	120	160	330	475	1000	1	11	clean	2.287	0.29	22.7	1.0	5 to 10% by volume	4p 10t SDVR	Good
Salt Springs	3A	3A	granite, Mesozoic	angular, blocky	Very High	100 to 130	-	-	low (<10)	-	-	-	1000 (approx)	-	-	-	2000 to 3000	low	low	clean	(1.88)	0.41	29	5 to 52	sluiced, but poor quality	dumped and poorly sluiced	Poor to Very Poor
Salvajina (Zone 3A)	3A	2	natural gravels	rounded	(Very High)	-	-	-	9.2	1.2	5.2	17	34	48	80	110	400	0 to 13	32	dirty	2.24	0.25	20	0.6	Yes, water added	4p 10t SDVR	Good
Salvajina (Zone 3B)	3B	4	weak sandstone and siltstone	angular ?	Medium (?)	-	-	-	45	3.4	1.2	15	41	58	115	190	600	0 to 16	32	dirty	2.26	0.21	17.4	0.9	Yes, water added	6p 10t SDVR	Good
Scotts Peak	3A	3A	argillite - quarried	angular ?	Medium	22 dry, 13 wet	60%	-	380	6.6	0.21	10.5	44	80	205	370	914	7	38	dirty	2.095	0.266	21	0.915	no water added	4-6p 10t SDVR	Good
Segredo (Zone 3A)	3A	1B	basalt (<5% basaltic breccia)	angular	Very High	Basalt = 235 Breccia = 37	-	-	7.4	1.4	-	-	177	-	-	-	-	-	-	clean	2.13	0.37	27	0.8	25% by volume	6p 9t SDVR	Good
Segredo (Zone 3B)	3B	1C & 1D	basalt (<5% basaltic breccia)	angular	High to Very High	Basalt = 235 Breccia = 37	-	-	10.2	1.4	-	-	-	-	-	-	-	-	-	clean	2.01 t/m3	0.43	31	1D - 0.8 1C - 1.6	no water added	4p 9t SDVR	Reasonable
Serpentine	3A	3A	Ripped quartz schist	angular to subangular	(Medium to High)	-	-	-	210	0.11	0.025	0.12	1.5	5.3	43	76	152	24	69	dirty	2.10	0.262	21	0.6 to 0.9	Not sure, suspect likely	4p 9t SDVR	Good
Shiroro	3A	2	granite	angular	(Very High)	-	-	-	32	2.1	4	33	95	128	260	380	500	-	22	clean	2.226	0.20	17	1.0	15% by volume	6p 15t SDVR	Good
Tianshengqiao - 1 (Zone 3A)	3A	3B	Limestone, SW to FR - spillway excav.	angular	Very High	70 to 90 (wet)	-	-	15 to 20	-	-	-	90 to 120	-	-	-	800	-		clean	2.19	0.23	19	0.8	20% by volume	6p 16t SDVR	Good
Tianshengqiao - 1 (Zone 3B)	3B	3C	Mudstone	angular	Medium	16 to 20	-	-	40	-	-	-	-	-	-	-	600	-	20 to 35	dirty	2.23	0.21	17.5	0.8	20% by volume	6p 16t SDVR	Good
Tullabardine	3A	3A	Greywacke, some slate	angular, elongated	High	45	-	-	28	1.7	2.8	19	50	78	155	240	400	2.5	30.5	dirty	2.22	0.23	19	0.9 to 1.0	> 10% by volume	4p 10t SDVR	Good
White Spur	3A	3A	Quarried Tuff - SW to FR	angular	(Very High)	-	-	-	-	-	-	-	37 to 200	-	-	-	1000	-	-	-	2.30	0.18 to 0.25	15 to 20	1.0	> 10% by volume	SDVR (4p, 10t ?)	Good
Winneke	3A	3	SW to FR Siltstone, Quarried	angular	High	66	-	1.5 - 2.3%	33	1.7	2.8	21	58	91	200	310	800	4	28	suspect dirty	2.07	0.302	23	0.9	15% by volume	4 - 6p 10t SDVR	Good
Wishon	3A	3A	granite, blasted	angular	Very High	-	-	-	(<7)	-	-	-	550 to 750	-	-	-	1500 to 2000	-	-	clean ?	1.80	0.47	32	8 to 52 (variable)	Sluiced with high pressure jets, 300% by volume	dumped and sluiced	Poor
Xibeikou	3A	1	Limestone - Fresh	angular	Very High	240	28	-	-	-	-	-	90	-	-	-	600	-	-	clean ?	2.18	0.284	22.1	0.8	25 to 50% by volume	8p 12t SDVR	Good
Xingo (Zone 3A)	3A	3	granite gneiss	angular	High to Very High (?)	-	-	-	18	1.6	10	54	150	180	400	500	650	< 3	4 to 33	clean to dirty	2.15	0.28	21.8	1.0	15% by volume	4p 10t SDVR	Good
Xingo (Zone 3B)	3B	4	Sound and weathered granite gneiss	angular	Medium to Very High (?)	-	-	-	80	-	0.3 to 1	-	190	-	-	-	750	2 to 7	15 to 60	dirty	2.1	0.31	23.6	2	no water added	6p 10t SDVR	Reasonable

Table E1.1: Case studies information on concrete face rockfill dams (Sheet 7 of 8)

Name	SECANT MODULI VALUES				HYDROGEOLOGY			LEAKAGE		
	Modulus During, E_{rc} (MPa)		Modulus on First Filling, E_{rf}		Time for First Filling (from end of main rockfill construction)	Reservoir Level / Comments	Rainfall, average annual (mm)	Maximum Rate (l/sec)	Long-term (l/sec)	Comment
	Average over construction period	Average at EOC (adjusted for valley shape)	E_{rf} (MPa)	Comments						
Mackintosh	45 (35 to 60)	39	63	Face slab profile shows peak deformation is 24% above toe, this is quite low.	1.92 to 2.93 years.	Fluctuating (FSL to -10 m)	2135	21	8 to 10 (10 years post ff)	Max. at end of first filling. Gradual reduction with time.
Mangrove Creek (Zone 3A)	55 to 60	57.5	-	Not reached FSL.	0.6 to > 15 years (had not reached FSL by 1996).	First Filling - Oct 81 to …..	-	5.6	2.5 (15 years post EOC)	Max. leakage when storage level was at its highest (1991)
Mangrove Creek (Zone 3B)	46 (36 to 56)	46								
Murchison	190 (170 to 205)	154	560 (485 to 640)	-	1.04 to 1.09 yrs.	Large fluctuations on daily/weekly basis, up to 20 to 22 m.	-	3.5	2 (1995/96, 13 years after ff)	3.5 l/sec on first filling.
Reece	86 (57 to 115)	72	190 (175 to 205)	-	1.32 to 1.46 yrs (Apr to June 1986).	Fluctuating on daily/weekly basis, up to 8 m.	-	8 to 12	0.5 to 1.5 (8 to 9 years post ff)	Initial leakage virtually all from right abutment.
Salt Springs	-	-	20	Calculated from face slab displacements measured after 2 years	0 to 1.48 years (1931/32).	Fluctuating	1145	565	-	Leakage mostly through the upper part of the face slab (upper 35 m) through cracks in face slab, honeycombe pockets in concrete and open joints.
Salvajina (Zone 3A)	205 (175 to 260) (likely affected by arching)	130	500	By He (2000). GJH estimate is 615 MPa when reservoir at 14 m below FSL.	0.33 to >0.75 years (1985).	no details after first filling	-	74	-	Approx. 14 l/sec through abutments and 60 l/sec through face slab.
Salvajina (Zone 3B)	62 (likely affected by arching)	53								
Scotts Peak	20.5 (18.5 to 23.5)	20.5	59 (Zone 3A) 420 (Zone 2B)	Estimated from HSGs near to upstream face. Significantly higher modulus for gravels in lower section compared with argillite rockfill.	0.42 to 2.58 years (June 72 to Aug 74).	Steady	2130	100	2 to 4 (1994, 20 years post ff)	At close to FSL on first filling leakage increased from 5 to 100 l/sec due to cracking in face slab. Gravel blanket placed.
Segredo (Zone 3A)	55 (excludes points thought to be affected by arching)	55	175	-	Approx. 0.6 years.	-	-	390	45 (1.5 to 2 years post ff)	Max leakage on first filling when at FSL. Leakage reduced by dumping fill on lower portion of face slab.
Segredo (Zone 3B)	28 (25 to 33)	28								
Serpentine	92 (46 to 142)	92	97 (94 to 100)	Assumption that the river gravels have a significantly greater modulus (than rockfill) and have negligible contribution to deformation on first filling.	0.24 to 2.94 years (Dec 71 to Aug 74).	Steady	-	-	-	No estimates possible due to inundation of the downstream toe of the embankment
Shiroro	66 (61 to 71)	58	-	No deformation quoted for upstream face slab on first filling.	1.44 to >1.8 years (from 5/84).	By Oct 1984 not a FSL (10 m short)	-	1800	100 (0.5 years after max.)	When close to FSL. Cracking in face slab near junction with plinth.
Tianshengqiao - 1 (Zone 3A)	49 (40 to 57)	49	-	Not yet filled to FSL. Stored water during construction to within 40 m of FSL.	-1.5 to >0.8 years.	First filling started 1.3 years before end of construction.	-	53	-	Max at end Dec 1999 when reservoir at highest level. March 2000 ~ 30 l/sec. Repairs to cracks in face slab.
Tianshengqiao - 1 (Zone 3B)	37 (32 to 42)	37								
Tullabardine	74	74	170	-	2.05 to 2.35 years (5/81 to 8/81).	Fluctuating (FSL to -10 m)	-	1.5 to 2	0.5 to 1 (10 -12 yrs post ff)	Current base flow less than 1 l/sec.
White Spur	180 (160 to 200)	139	340	On virtually date of reaching FSL. 1 year later E = 200 to 240 MPa.	0.18 to 0.24 years (June to July 1989).	Fluctuating	3150	7	2 (6 years post ff)	Limited leakage. &l/sec shortly after first filling. Gradual reduction to approx. 2 l/sec.
Winneke	55 (50 to 59)	55	104	Determined from HSGs close to upstream face.	1.62 to 5.04 years (6/80 to 11/83).	Fluctuating - seasonal (no catchment, off stream storage)	700 to 1200	58	13 (10 to 12 years post ff)	Max. leakage when reservoir at FSL on first filling. Gradual decrease in leakage rate since.
Wishon	-	-	-	-	0.4 to 0.45 years (May 1958).	-	-	3120	850	Maximum within 2 months of first filling. Due to cracking in face slab, mainly at the perimeter joint. Series of repais to face slab over the years.
Xibeikou	80 (60 to 100)	80	260	Query on deflected shape of face slab after September 1993	-1.5 to 6 years (June 1995).	Impounded water during construction. Overtopped in 1987. Other problems during construction.	1150	-	-	-
Xingo (Zone 3A)	34 (30 to 39)	34	76 (73 to 80)	Calculated for measurements taken on the left abutment.	1.02 to 1.46 (mid to late 1994) years.	Steady. Springs observed on downstream slope of left abutment (associated with seepage through the face slab)	-	200	140 (4.5 years post ff)	Leakage increased post ff from 100 to 200 l/sec. Due to cracks in slab. Dumping soils on face reduced leakage to 140 l/sec.
Xingo (Zone 3B)	13 (12 to 14)	13								

Table E1.1: Case studies information on concrete face rockfill dams (Sheet 8 of 8)

Name	MONITORING									Other Comments
	Settlement During Construction (mm)	Post Construction Crest Deformation					Deformation Normal to Face Slab (mm)	Long Term Crest Settlement Rate (% per log time cycle) (t_o at EOC)	Comments	
		Settlement, total (mm)	Settlement, total (%)	Settlement on FF (mm)	Settlement on FF (%)	Lateral Displacement (mm)				
Mackintosh	> 780	333 mm (0 to 20.6 years)	0.444	99	0.132	130 mm (75 ff)	228 mm (173 ff)	0.184	Decreasing rates of deformation with time, approximately 5 mm/yr settlement and 5 to 6 mm/yr displacement at 10 yrs.	
Mangrove Creek (Zone 3A)	> 610	287 mm (0.67 to 15 yrs, 12/81 to 5/96)	0.359	> 287	> 0.359	196 mm (from 12/81 to 5/96)	-	0.251 (after 5 years, but still not reached full supply level)	First monitoring of crest SMPs 0.67 years after end of rockfill construction. Settlement rates with time still high to 1990 (highest water level) then reduced from 1990 to 1996.	Moduli during construction calculated from HSG deformation during construction and also taken from published values.
Mangrove Creek (Zone 3B)										
Murchison	> 255	104 mm (0.08 to 17.6 yrs, to 1999)	0.111	9	0.01	22 mm to 4/93 (8 ff)	77 mm to 4/93 (28 ff 67m bc)	0.056	Decreasing rates of movement with time, approximately 3mm/yr at 10 yrs	
Reece	> 820	221 mm (0.12 to 15 yrs, to end 1999)	0.181	85	0.07	68 mm (5/86 to 11/93), all post ff	264 mm to 8/94 (215 ff 66m bc (45%))	0.063	Decreasing rates of movement with time, approximately 4 mm/yr crest settlement at 5 yrs	
Salt Springs	-	1276 mm to 1996 (0.26 to 65 yrs)	1.276	380	0.38	550 mm to 1958 (27 yrs), ff 230 mm	1755 mm to 1958 (67 m bc), ff 1317 mm	0.29 to 0.77	Rapid deformation on first filling with significant reduction in rate thereafter. Acceleration at about 20 years when the full supply level was raised by 3 m. Crest SMPs on upstream edge of crest.	
Salvajina (Zone 3A)	-	90 mm (0.33 to 0.75 years)	0.061	> 90	> 0.061	-	55 mm to 14 m short of FSL	-	Limited data.	Constructed of dirty gravels with rockfill used in the downstream 1/3. High stiffness as indicated by high moduli. Limited deformation data in published literature.
Salvajina (Zone 3B)										
Scotts Peak	-	445 mm (0 to 18 years, to 12/89)	1.036	203	0.472	190 mm to 12/89 (17 yrs), ff 96 mm	178 mm to 12/89, 78 mm ff	0.178 (after 5 years)	High rate of deformation post first filling due to leakage through dam and wetting up of argillite rockfill. Long term rates approximately 2.5 mm/yr.	Cracking occurred as a result of tensile stresses in face slab due to very large differential stiffness in rockfill.
Segredo (Zone 3A)	-	229 mm (to 0.4 yrs post ff, 1992)	0.158	Approx. 200	0.138	-	340 mm (to 4 months post ff)	-	Limited information on deformation. Estimation of crest settlement from HSG device below crest.	
Segredo (Zone 3B)										
Serpentine	-	77 mm (0.24 to 25.5 yrs, to 1/97)	0.203	35	0.092	38 mm (12/71 to 1/92), ff 23 mm	-	0.109	-	
Shiroro	-	166 mm (0 to 1.8 years) to 12/84	0.133	> 66	> 0.053	27 mm to 12/84 (1 yr)	90 mm (when 32 m below FSL)	-	Limited deformation information. Could find nothing on deformation behaviour after 1984.	Modulus during construction taken from Bodtman and Wyatt (1985), however they may not have allowed for reduction in the vertical stress due to embankment shape. Therefore, the values are likely to over-estimate the modulus.
Tianshengqiao - 1 (Zone 3A)	-	926 mm (0.05 to 0.8 years, to Dec 1999)	0.52	> 926	> 0.52	670 mm to Dec 1999 (0.75 years), ff not completed.	-	-	First filling not completed.	During the early stages of construction the embankment (~40 m high) was overtopped 4 times during floods. Cracks noted in slab cushion zone during construction. Face slab cracking on first filling. Separation between face slab and cushion zone was noted during staged construction of the face slab, up to 100 mm gap.
Tianshengqiao - 1 (Zone 3B)										
Tullabardine	-	19 mm (0.2 to 12.8 years)	0.076	2	0.01	-	-	0.023	Negligible post construction settlement	
White Spur	> 65	58 mm (0.04 to 5.9 yrs, 4/89 to 2/95)	0.135	7	0.016	-	38 mm (@ 6 years), 15 mm ff	0.08	Rate of settlement reduced after completion of wave wall in January 1990. At 5yrs crest settlement rate approx. 1.25 mm/yr.	
Winneke	-	207 mm (0.17 to 16.2 yrs, Jan 79 to Jan 95)	0.244	105	0.124	-	M7 - 160 mm (3/80 to 2/94), 145 mm ff (all settlements)	0.107	Monitoring started shortly after end of rockfill construction (SMP 13 on upstream face used until crest SMP installed). Deceleration of settlement after first filling.	
Wishon	-	954 mm (0 to 38 yrs)	1.136	189	0.233	-	-	0.25 to 0.33	Monitoring started shortly after end of rockfill construction. Rapid movement on first filling with significant reduction in rate thereafter.	No data to calculate modulus during construction or on first filling
Xibeikou	-	-	-	-	-	-	75 mm (6.5 years), all ff	-	Query on results. Discrepancies between SMPs and HSGs in published literature.	Limited data available. Monitoring shows discrepancies in face slab deformation, and between surface monitoring points and hydrostatic settlement gauges.
Xingo (Zone 3A)	-	526 (1.0 to 6.2 yrs)	0.376	302	0.216	320 mm (1.0 to 6.2 yrs), 210 mm ff	510 mm (@ 6 years), 290 mm on ff.	0.25	SMPs base survey approx. 1 year after the end of rockfill construction. Cracking of face slab on left abutment and subsequent leakage resulted in acceleration of deformation of face slab and crest (i.e. wetting of rockfill).	Wetting of rockfill in left abutment resulted in acceleration in the rate of deformation (in this area). Springs observed high above river level on downstream slope of embankment (on the left abutment) indicative of wetting of Zone 3B rockfill.
Xingo (Zone 3B)										

APPENDIX F

Summary Tables and Plots for Embankment Dam Analysis

TABLE OF CONTENTS

1.0 SUMMARY TABLES FOR CASE STUDIES F1

2.0 SUMMARY PLOTS OF POST CONSTRUCTION DEFORMATION BEHAVIOUR F61

2.1 Post Construction Deformation of the Downstream Slope F61

2.2 Post Construction Deformation of the Upper Upstream Slope to Upstream Crest Region F76

LIST OF TABLES

Table F1.1: Central core earth and rockfill embankments case study information.....F5

Table F1.2: Zoned earth and rockfill embankments case study information.....F35

Table F1.3: Zoned earthfill embankments case study information.....F45

Table F1.4: Earthfill embankments (homogeneous earthfill, earthfill with filters and earthfill with rock toe) case study information.....F55

Table F1.5: Summary of embankment properties of puddle core earthfill embankments.....F58

1.0 SUMMARY TABLES FOR CASE STUDIES

Table F1. to Table F1.5 present a summary of aspects of the design, construction, embankments materials, reservoir operation, performance and references for most of the earthfill, zoned earth and earth-rockfill and puddle core earthfill embankment case studies within the database. The five tables are:

- Table F1. (of 30 pages) – central core earth and rockfill embankments;
- Table F1.2 (of 10 pages) – zoned earth and rockfill embankments, that are not of central core earth and rockfill design;
- Table F1.3 (of 10 pages) – zoned earthfill embankments;
- Table F1.4 (of 3 pages) – earthfill embankments including homogeneous, earthfill with filters and earthfill with rock toe embankment types; and
- Table F1.5 (of 3 pages) - puddle core earthfill dams.

For embankments with rolled earthfill zones (i.e. earthfill, zoned earthfill and zoned earth and rockfill embankments), the embankment performance aspects include a summary of the deformation behaviour of the core during construction, post construction deformation of SMPs (surface monitoring points) on the crest and shoulders (mainly from close to the maximum section), the positive pore water pressure response in the main earthfill zone (both during and post construction) and comments on observed cracking and overall observed performance.

For the puddle core earthfill embankments, the hydrogeology is an assessment of the response of the various embankment zones (upstream shoulder, puddle core and downstream shoulder) to changes in the reservoir level. Where possible the comments have been based on actual piezometer and standpipe records, however, for a number of embankments the response has been assumed based on assessment of the earthfill type and the presence or otherwise of a select earthfill zone in the upstream shoulder. The deformation monitoring records for the puddle core earthfill dams are fairly limited given the age of most of the dams in the data set. For most dams the monitoring records are from SMPs typically established in the 1970's to 1980's, many 10's of years after completion of construction. Some monitoring data and anecdotal information is available on the early performance of several embankments for estimation of the settlement from the end of construction.

Explanations and definitions of the terminology used in the tables (mainly for Tables F1.1 to F1.4, but also applicable to Table F1.5) is:

- General terminology and acronyms used throughout:
  - The earthfill materials have been classified in accordance with the Australian soil classification system (Australian Standard AS 1726-1993 Geotechnical Site Investigations).
  - The strength and weathering terms used to describe the rock used as rockfill are from the case study references. The acronyms FR = fresh, SW = slightly weathered, MW = moderately weathered, HW = highly weathered.
  - EOC = end of construction
  - FF = first filling
  - FSL = full supply level
  - Fndn = foundation
  - PWP = pore water pressure
  - UCS = unconfined compressive strength
  - SMDD = Standard (or Standard Proctor) Maximum Dry Density
  - MMDD = Modified Maximum Dry Density
  - OMC = Optimum moisture content for the laboratory compaction test method used. In most cases it is Standard or Standard Proctor optimum, but in several instances modified compaction or an adjusted compaction test type have been used.
  - Unk or nk = unknown. In most cases a "–" has been used, which indicates either the data is not known or is not appropriate.
- Instrumentation terminology is:
  - SMP = surface monitoring point
  - IVM or ES = internal vertical settlement gauge
  - IHM = internal horizontal monitoring gauge
  - IN = inclinometer
  - HSG = hydrostatic settlement gauge
- Terminology used for the owner / authority is:
  - USBR = United States Department of the Interior, Bureau of Reclamation
  - SMHEA = Snowy Mountains Hydro Electric Authority
  - State Water DLWC = Department of Land and Water Conservation

  - ACTEW = Australian Capitol Territory Electricity and Water Corporation
- For the construction / design section:
  - The embankment zoning classification system used is defined in Section 1.3.3 of Chapter 1.
  - Length, L = embankment crest length.
  - The embankment slopes are defined in terms of horizontal (H) to vertical (V).
- For the embankment materials section:
  - ASCS = Australian soil classification system
  - For placement methods, 6p 18t roller = 6 passes of an 18 tonne roller. SDVR = smooth drum vibrating roller.
  - D_R = relative density.
  - The "level of compaction" is a qualitative rating system of the degree of compaction. Details for the rockfill classification are given in Section 1.3.3 of Chapter 1.
  - The "Clean / Dirty" classification for rockfills is also a qualitative rating system. "Dirty" rockfills refer to those with a high fraction less than 19 to 25 mm. Generally, 25% has been used to delineate between clean and dirty rockfills, but if the references indicate the rockfill to be "dirty" then it is classified as such.
- For the hydrogeology section:
  - "Fluctuating" is where the reservoir is subject to a seasonal (usually annual) or regular (more than once per year) drawdown that is typically greater than about 0.1 to 0.2 times the height of the embankment at its maximum section.
  - "Fluctuating slow" is where the reservoir is subject to fluctuations that occur slowly over time (i.e. slow drawdown over several years).
  - "Steady" is where the reservoir remains steady over time (i.e. where the fluctuation is less than 0.1 to 0.15 times the height of the embankment at its maximum section).
  - r_u = pore water pressure coefficient (refer Equation 7.4 in Section 7.4.1.4 of Chapter 7)
- For monitoring during construction (Table F1. to Table F1.4):
  - The core settlement refers to the total settlement of the core during the period of construction and is given in units of millimetres and as a percentage of the embankment height, H, at the point of measurement.

  - If no information is given in the section "Other Types of Internal Monitoring Equipment" is does not necessarily mean no other deformation monitoring instrumentation was installed for that embankment.
- For monitoring post construction (Table F1. to Table F1.5):
  - The zero time reading is at the end of construction. Time readings given in this section are in terms of years after the end of construction (e.g. 1.3 years = 1.3 years after end of construction).
  - Settlements and displacements are generally from SMPs on or close to the main section. Values of settlement in % are settlement as a percentage of the height from the SMP to foundation level.
  - S_{LT} = long-term crest settlement rate in units of settlement (as a percentage of the height from the SMP to foundation level) per log cycle of time.

Comments specific to the puddle core earthfill embankment case studies (Table F1.5) are:

- In the classification of the puddle core, the terms "low", "medium" and "high" refer to the soil plasticity.
- For the post construction deformation:
  - The total crest settlements since end of construction are given in terms of millimetres and as a percentage of the embankment height, *H*.
  - The long-term settlement rates are, in most cases, specific to the crest settlement unless otherwise stated. The quoted values are for periods of normal reservoir operating conditions.

Table F1.1: Central core earth and rockfill embankments case study information

Name	GENERAL DETAILS				CONSTRUCTION / DESIGN											References
					Construction Timing		Embankment Classification			Dimensions						
	Location	Owner/ Authority	Geology	Foundation	Year Completed	Time (years)	Dam Zoning Class[n]	Core Width / Slope	Core Type	Height, H (m)	Length, L (m)	Ratio L/H	Upstream Slope (H to V)	Downstream Slope (H to V)	Comments on Design	
Agigawa	Japan	Water Resources Development Public Corp.	Welded tuffaceous rhyolite with granitic porphry intrusions, highly fractured.	Rock	1990's	-	5,1,1	c-tn	CL	102	460	4.5	2.6H to 1V	2H to 1V	Thin central clay core supported by compacted rockfill shoulders. Single filter zones up and downstream of core and drainage layer on downstream foundation.	Karasawa et al (1994) Yamazumi et al (1991)
Ajuare	Sweden	-	Glacial activity.	River section of embankment on bedrock. Abutments on glacial till.	1966, Oct	2	5,2,2	c-tn	SM	46	525	11.4	1.8H to 1V	1.7H to 1V	Very narrow central core with near vertical downstream edge supported by poorly compacted rockfill shoulders. Foundation filters used due to high fines content of rockfill.	Nilsson & Norstedt (1991)
Ataturk	Turkey	-	Limestone	Rock - karst limestone	1990, Aug	3.6	5,2,0	c-tm	CH	184	1664	9.0	2.15H to 1V	2.2H to 1V	Central clay core aligned slightly to upstream supported by rockfill shoulders of weathered to fresh rock types. Deep grout curtain (>180 m) in karst limestone. Cofferdam incorporated into the upstream toe of the embankment. The dam axis is arched to upstream.	Cetin et al (2000) Cetin (2002) Oziz et al (1990) Lask & Reinhardt (1986)
Bath County Upper Dam	USA, Virginia	-	Sedimentary - sandstones and siltstones	Rock	1984, Dec	3	5,2,0	c-tn	SC (?)	134	670	5.0	2.4H to 1V	2.5H to 1V	Thin central core with rockfill sourced from weathered to fresh rock types. A zone of fresh rockfill is used immediately downstream of the filters and on the downstream foundation for leakage control purposes.	Wong et al (1992)
Beliche	Portugal	-	Schists	Core and filters on MW schists, rockfill on alluvial sands and gravels of medium density.	1985, Mar	3	5,2,2	c-tn	GC	55	527	9.6	2H to 1V	1.95H to 1V	Narrow central core with weathered (Zone 3A) to fresh (Zone 3B) poorly compacted rockfill shoulders. Cofferdam upstream of the main dam.	Naylor et al (1997) Maranha Das Neves et al (1994) Naylor et al (1986) Pagano et al (1998)
Bellfield	Australia, Victoria	Wimmera Mallee Water	Sedimentary, mainly sandstones; granite intrusions.	Variable. At maximum section core and upstream shoulder on sandstone, downstream shoulder on alluvium.	1966, Apr	2.25	5,2,0	c-tm	CL/SC	40	823	20.6	1.6H to 1V	1.42H to 1V	Medium width central core with dry dumped rockfill shoulders. Embankment design changes associated with changes in foundation conditions. Slopes a series of steep benches at 1.2 - 1.33H to 1V (angle of repose).	Currey et al (1968) SMEC (1998a)
Bjelke Peterson	Australia, Queensland	QDNR (now Sun Water)	Complex geology, mix of sedimentary, metamorphic and volcanic	Excavation to bedrock for core and rockfill shoulders.	1988, Sept	1.7	5,2,1	c-tn	CL	41.5	650	15.7	1.7H to 1V	1.7H to 1V	Very narrow central core (0.1H to 1V up and downstream) with compacted rockfill shoulders.	QWRC (1986a, 1986b) Eadie (1988) QDNR (1997) Hadgraft (1984)
Blowering	Australia, New South Wales	State Water DLWC	Slightly metamorphosed sedimentary - interbedded phyllite, siltstone & quartzite	Excavation to bedrock for core and rockfill shoulders.	1968, Apr	2	5,2,0	c-tm	SC - CL	112	808	7.2	1.9H to 1V	1.9H to 1V	Central core (slopes of 0.5H to 1V up and 0.4H to 1V downstream) supported by compacted rockfill shoulders.	SMHEA (1964) Svenson (1964) Olsauskas et al (1966, 1967a, 1967b, 1968) Hunter & Bacon (1970) Bacon (1969, 1999)
Chaffey	Australia, New South Wales	State Water DLWC	Sedimentary - Jasper & Siltstone	Core and most of downstream shoulder on bedrock (MW to FR). Upstream shoulder on dense alluvial gravels (~ 12 thick).	1979, Mar	1	5,2,0	c-tm	CH/GC	54	530	9.8	1.75H to 1V	1.75H to 1V	Central clay core supported by compacted rockfill shoulders. Cofferdam at upstream toe. Large bench on upstream slope at 24 m depth below crest level. Disposal area at downstream toe.	DWR NSW (1989) WRC NSW (1979) Newland & Davidson (1979)
Cherry Valley	USA, San Francisco	Hetch Hetchy Water Supply	Granite, glacially scoured valley	Rock. Strip to weathered rock, cutoff to fresh granite.	1955, Oct	2	5,2,0	c-tk	SM/ML	100	793	7.9	1.85-2H to 1V	1.85-2H to 1V	Broad central core (0.7-0.75H to 1V) with thin filters zones and dumped and sluiced rockfill shoulders. Outer slopes in a series of benches sloped at 1.33H to 1V.	Lloyd et al (1958) Cooke & Strassburger (1988)
Chicoasen	Mexico	-	Limestone, some clay shales	Core on bedrock. Shoulders in river section on up to 60 m depth of granular alluvial deposits containing large boulders.	1980, May	-	5,2,0	c-tn	GC	261	463	1.8	2.35H to 1V	2H to 1V	Narrow central core with wide filter zones supported by well compacted rockfill shoulders. Constructed in 125 m wide gully with near vertical abutment slopes.	Alberro & Moreno (1982) Moreno & Alberro (1982)

Table F1.1: Central core earth and rockfill embankments case study information (Sheet 2 of 30)

Name	MATERIALS														
	Earthfill Core							Filters / Transition Zone							
	Zone	Source	ASCS Class[n]	Density Ratio or Dry Density (t/m^3)	Placement Methods	Moisture Content	Comment	Zone	Source	ASCS Class[n]	Relative Density or Dry Density (t/m^3)	Layer Thickness (mm)	Plant	Level of Compaction	Comment
Agigawa	1	-	CL (?)	(bulk density = 2.10 t/m^3)	Well compacted (?) - heavy rollers (?)	-	Likely well-compacted, typical practice in Japan is for heavy rolling of core.	2A (filter)	likely from crushed rock	-	2.12 t/m^3	-	-	-	Limited information, suspect well compacted. Very high moduli (Karasawa et al 1994). Single filter up and downstream of the core.
Ajuare	1	glacial till	SM	(bulk density = 2.24 t/m^3)	Reasonably to well compacted (?) - heavy crawler type tractors	4 to 6% wet of OMC	Silty morraine core placed well wet of OMC using Swedish method.	2A & 2B (filters)	river alluvium	-	(bulk density = 2.14 t/m^3)	500	4.5t SDVR, no indication of number of passes of rollers.	reasonable to good	Dual filters used up and downstream, combined width of 8 to 13 m.
Ataturk	1	-	CH - sandy clays	94.4% SMDD 1.52 t/m^3	reasonably to well compacted 300 mm layers, 6p sheepsfoot roller	average 1.5% dry of OMC	Reasonably to well compacted sandy clays of medium to high plasticity. Cetin et al (2000) query layer thickness used, they indicate it may have been up to 1m at times.	2A & 2B (filters)	river alluvium	SP/SW (2A) GP/GW (2B)	88 to 91% SMDD 1.84 - 1.97 t/m^3	-	compacted by vibratory rollers, no indication if water added.	reasonable to good (?)	Low fines content, less than 1.5%. Dual filters used up and downstream of the core.
Bath County Upper Dam	1	soil and weathered rock	SC/GC (?)	-	no information	-	Core of stiff to very stiff strength consistency, suggesting it is possibly well compacted and placed at close to OMC.	2A & 2B (filters)	crushed limestone	-	-	-	-	-	limited information. Dual filters downstream of the core. Upstream of the core, dual filters in the upper section and a single filter in the mid to lower section.
Beliche	1	-	GC - clayey sandy gravels, 20 to 36% fines	-	no information	close to OMC (Spec)	Suspect reasonably to well compacted given period of construction. Clayey sandy Gravels with low plasticity fines.	2A & 2B (filters)	gravels (2B)	GW/GP (2B)	-	-	-	-	limited information. Suspect at least reasonably compacted. Dual filter used up and downstream of the core.
Bellfield	1	alluvial (?)	CL/SC - sandy clays to clayey sands	-	Reasonably to well compacted - 380 mm layers, 12p 4t sheepsfoot roller	Spec 1.5% dry to 1.5% wet of OMC	Layer thickness on the large size for roller size (in todays standards). Sandy clays to clayey sands.	2A & 2B (filters)	quartzose sandstone (some sand and gravel)	GM (2A) GP (3A)	-	-	Compacted using SDVR, no indication if water added.	-	Limited information. Narrow width dual filters up and downstream of the core. Zone 2A contained 5 to 15% fines.
Bjelki-Peterson	1	colluvial, alluvial ?	CL, SC (some CH)	100% SMDD 1.72 - 1.88 t/m^3	Well compacted - 150 mm layers, pad foot rollers	(Spec. 1% dry to 1% wet of OMC)	Sandy clays to clayey sands of medium plasticity, some high plasticity sandy clays.	2A & 2B (filters)	alluvial sands & crushed rock	SM/SP (2A) GP/GW (2B)	Spec >95% SMDD (2A) and >70% D_R (2B)	350	10t SDVR, moist at compaction	Good	Fines content less than 15% (2A), less than 2% (2B). Dual filters downstream of core and single (Zone 2A) filter upstream.
Blowering	1	Colluvial, alluvial, residual	SC/CL - clayey sands to sandy clays, avg 46% fines (30 to 80%)	101.5% SMDD	Well compacted - 150 mm layers, 8p sheepsfoot roller	average 0.2% wet of OMC	Clayey sands and sandy clays of medium plasticity. Changes in moisture specification as construction proceeded. Bottom 34 to 37m 0.3% dry of OMC; mid region 0.3% wet of OMC; upper 40m 0.1% wet of OMC.	2A & 2B (filters)	Alluvial	2A - SW to GW 2B - GW/GP	2.14 t/m^3	450	4p 7.5t SDVR	Good	Well compacted filter zones. Zones 2A and 2B used up and downstream of the central core. Combined width of approx. 6 m.
Chaffey	1	colluvial	CH/GC - gravelly sandy clays to clayey gravels, average of 49% fines	102.4% SMDD 1.86 t/m^3	Well compacted - 150 mm layers, 3 to 4p, tamping rollers	1.5% dry of OMC	Gravelly sandy clays of medium to high plasticity. 0.6 m CH contact layer. Core centreline aligned slightly to upstream.	2, 2A & 2B (filters)	river gravels	GP to GW	D_R = 88% 2.10 t/m^3	400	minimum 1p 8t SDVR	Good	Well compacted filters. Dual filters downstream of the core (5m width), single filter upstream (2.5 m width).
Cherry Valley	1	decomposed granite	SM/ML - silty sands to sandy silts, 10 to 82% fines	91% MMDD 1.70 t/m^3	Well compacted - 225 mm (loose) layers, 12p 31t sheepsfoot roller	-	Well compacted silty sand to sandy silt core. Fines of low plasticity (PI = 1 to 5%). Likely placed wet due to wet field condition (5 to 15% wet of OMC).	2A & 2B (filters)	alluvial sands and gravels	GP/GW (sand to cobble size)	1.76 t/m^3	300 (compacted)	1p crawler tractor.	Reasonable	Thin (6 m wide) dual filters used up and downstream of the core.
Chicoasen	1	residual soils (weathered lutite)	GC - clayey gravels, 12 to 30% fines	-	Well compacted - 250 mm layers, 6p 7t padfoot vibratory roller.	close to OMC	Clayey gravels with medium plasticity fines. Higher clay content material used in lower portion. Placed 2 - 3% wet of OMC in the zone against the steep abutment slopes.	2A & 2B (filters)	alluvial (?)	GP/GW - sandy gravel (2A) to gravel (2B)	-	400	2p 10t SDVR	Good	Dual filters up and downstream of the core. Filters zone moderately wide in the lower half of the embankment.

Table F1.1: Central core earth and rockfill embankments case study information (Sheet 3 of 30)

Name	MATERIALS																	
	Rockfill Zone									Rockfill Zone (in some cases earthfill stabilising berm)								
	Zone	Source	Grading Description	Clean / Dirty	Dry Density (t/m^3)	Layer Thickness (m)	Placement Method	Level of Comp-action	Comment	Zone	Source	Grading Description	Clean / Dirty	Dry Density (t/m^3)	Layer Thickness (m)	Placement Method	Level of Comp-action	Comments
Agigawa	3A & 3B	-	-	-	2.00 t/m^3	-	SDVR	-	Suspect well compacted given typical procedures used in Japan at this time. Moduli = 130 MPa (Karasawa et al 1994).	-	-	-	-	-	-	-	-	-
Ajuare	3	schists and gneisses	high fines content	dirty	(bulk density = 2.04 t/m^3)	-	Spread by D8 dozer then sluiced after placing.	Poor	Poorly compacted rockfill, and suspect relatively poor quality rock given propensity to breakdown.	-	-	-	-	-	-	-	-	-
Ataturk	3A	weathered basalt (upstream), limestone (downstream)	high fines content for rockfill	dirty	2.03 - 2.06 t/m^3	0.6 to 1.5 (?)	compacted by vibratory rollers, water added if moisture content < 2%.	Reasonable (?)	Both rock types of medium to high UCS. Weathered basalt used as inner upstream rockfill zone and pliacated limestone used as inner downstream rockfill.	3B	basalt, sound	-	clean ?	2.26 t/m^3	0.6 to 1.5 (?)	compacted by vibratory rollers, water added if moisture content < 2%.	reasonable (?)	Suspect sound basalt of very high UCS. Limited information on placement methods. Zone 3B predoninantly used in the outer up and downstream shoulders.
Bath County Upper Dam	3B	Siltstone and sandstone - weathered to FR.	max 760 mm 10 to 25% fines	dirty	-	-	-	-	Limited information, suspect well-compacted. Zone 3B is the predominant rockfill type used.	3A, 3C	siltstone and sandstone, SW to FR (3C sandstone only)	max 760 mm, < 10% fines (3A) <10% passing 5 mm (3C)	3A - dirty 3C - clean ?	-	-	-	-	Limited information, suspect well-compacted. Zones 3A used as filter zone in the downstream shoulder and Zone 3C used in the upper upstream shoulder.
Beliche	3A	schists and greywacke, HW	significant fines	dirty	-	1.0	Light compaction, no indication if water added.	Poor to reasonable (?)	Lightly compacted. Zone 3A used as inner rockfill zone up and downstream of the core. Poor quality weathered rock used (Wet UCS = 9 to 12 Mpa, Moduli approx. 5 to 27 Mpa).	3B	Greywacke, high strength	max 600 mm <20% < 19 mm no fines	clean ?	-	1.0	Lightly compacted, no indication if water added.	Poor to reasonable	Lightly compacted. Zone 3B used as outer rockfill zone up and downstream. Greywacke of high strength (UCS = 30 to 45 MPa).
Bellfield	3A	quartzose sandstones (some siltstone and mudstone)	-	-	-	1.2 to 9.1	Dumped in 1.2 to 9.1 lifts, no water added. 5 m width next to filters - 1.2m layers 6p 4.5t SDVR.	poor	Lift thickess typically 1.2 to 2.4 m. Susceptible to significant collapse compression given dry placement.	4 (random)	alluvium and decomposed rock	-	-	-	-	-	-	Limited information. At main section, Zone 4 used as berm on the downstream shoulder.
Bjelki-Peterson	3A	Phyllite (MW or better)	max 300 mm 4 to 12% fines	dirty	Spec > 2 t/m^3	0.7	4p 10t SDVR, 20% by volume water added	Good	Well-compacted rockfill. Rock of medium to high UCS.	-	-	-	-	-	-	-	-	-
Blowering	3A	Quartzite	max < 900 mm 18 to 28% < 25mm	clean to dirty	2.06 t/m^3	900 (450 for 6m zone adjacent to filters)	Sluiced (0.9 to 1 ratio by volume) when tipped, then spread by dozer and compacted by 4p 7.5t SDVR	Good	Quartzite of high to very high strength when dry, large reduction (approx 30%) on saturation. Zone 3A used as the inner rockfill zone up and downstream of the central core. Also used a more permeable layer below Zone 3B in the downstream shoulder.	3B	Quartzite & Phyllite	Max < 1800mm 17 to 50% < 25mm	dirty	2.07 t/m^3	1800	Sluiced (0.9 to 1 ratio by volume) on tipping, then spread by dozer and compacted by 4p 7.5t SDVR	reasonable	Rock of high to very high strength when fresh, with large reduction in UCS on wetting (35 to 60%), particularly in the phyllite. Possible usage of lesser quality rock in lower elevations. Significant breakdown on surface of layer and large density variation within layer. Zone 3B used in outer up and downstream shoulders.
Chaffey	3	Jasper (SW to FR)	26 to 57% < 19mm %fines = 1 to 4%.	dirty	2.02 t/m^3	1.2	Spread by dozer, 2 to 4p 8t SDVR, no indication if water added.	reasonable to good	Some siltstone in rockfill.	-	-	-	-	-	-	-	-	-
Cherry Valley	3	Granite and granodiorite, fresh	-	clean ?	-	9.1	dumped and sluiced	poor	Rockfill adjacent to the filters was of lesser quality and was not sluiced.	-	-	-	-	-	-	-	-	-
Chicoasen	3A	limestone	max 500 to 600mm 5 to 50% < 19 mm 0 to 10% fines	dirty	-	0.6	4p 12t SDVR, water added	Good	Heavily compacted rockfill. Zone 3A formed most of rockfill in shoulders.	3B	limestone	-	-	-	-	Dumped	Poor	Zone 3B formed outer 10 to 25% of the rockfill zone of both the upstream and downstream shoulders.

Table F1.1: Central core earth and rockfill embankments case study information (Sheet 4 of 30)

Name	HYDROGEOLOGY						MONITORING - DURING CONSTRUCTION						
	First Filling		Reservoir Operation		Pore Pressures in Core	Rainfall (Average mm/year)	Core				Rockfill and/or Filters	Comment	Other Types of Internal Monitoring Equipment
	Timing (from end of embankment construction)	Comments	Steady / Fluctuating	Comment			Instrument Type/No.	Settlement		Comment			
								mm	% of H				
Agigawa	-	Filled in 5 months, but not sure of timing with respect to end of construction.	-	-	During construction - high PWP in core, r_u approx 0.5 (or greater).	-	IVM	2745	2.71%	vertical strain profile normal, 0 to 1% near crest increasing to 3 to 4% near base.	IVMs in rockfill, upstream = 1150 mm settlement or 1.35% and downstream = 905 mm or 1.48%.	IVMs indicate deformation of rockfill less than that of core.	-
Ajuare	not known	no information	Fluctuating	Seasonal drawdown of 9 m (?). Only limited data.	-	-	-	-	-	-	-	-	-
Ataturk	-0.6 to 3.5 ?	Started Jan 1990. No indication of operation. Close to FSL by March 1994.	-	No indication of operation.	-	-	IVM	-	-	no information	-	Large internal deformations of the core during latter stages of construction / early FF as indicated by loss of gauges at lower elevations.	-
Bath County Upper Dam	0.67 to 1.08 years	Aug 1985 to Dec 1985	Fluctuating	Rapid daily drawdowns of up to 32 m (for power generation)	During construction - PWP up to 70% of applied load. Slow dissipation post construction. PWP shows about 20% amplitude response to reservoir level on rapid drawdown.	-	-	-	-	-	-	-	-
Beliche	-0.2 to 4.1 years	Partial impounding to within 23 m of FSL following heavy rain in early 1985, overtopping the cofferdam and saturating the upstream rockfill. Virtually full by Jan 1988.	Steady	Steady for 5 years at FSL, then 17m drawdown.	Relatively high PWP in core during construction, estimate r_u = 0.3 to 0.6 at EOC.	-	IVM	2585	4.9 (1.5 to 7.4%)	Large plastic deformations in some zones of the core.	IVMs indicate large deformation of rockfill during construction. Estimated moduli for Zone 3A rockfill = 5 to 27 MPa.	Deformation distorted IN tubes so no readings possible, indicating large internal lateral displacements of the core.	IN, IVM in rockfill
Bellfield	no information	only have records after 1984 (18 years after EOC)	Steady	Generally steady at close to FSL. Drawdowns up to 3 to 5m, but not every year.	-	927	IVM	-	-	Only have post construction records after 1987	-	-	-
Bjelki-Peterson	0.3 to 1.6 years	Late 1988 to Mid 1990	Steady	Generally within 3 to 4 m of FSL. One drawdown of 12 m over several years.	During construction - positive PWP up to 35 to 130 kPa, r_u up to 0.2 (but will be higher because this does not allow for arching).	804	-	-	-	-	-	-	-
Blowering	0.07 to 1.7 years	Started May 1968, reached FSL in Nov-Dec 1969.	Fluctuating	Annual drawdown, typically of 10 to 30 m. Larger drawdowns in 1979/80 of 40m, 1982/83 of 58m, 1987/88 of 35m, and 1997/98 of 54m.	During construction - varied PWP response due to moisture variation. High PWP in the wetter placed earthfills (r_u up to about 0.7), lower positive PWP in lower and upper drier placed core (r_u up to 0.3 to 0.4). Slow dissipation of high PWP over more than 20 yrs. During operation - decreasing amplitude to reservoir fluctuations with increasing distance to downstream.	-	IVM, 1 (4.5m upstream of dam axis)	5875	5.63	High vertical strains in wet placed region of the core (up to 10 to 12%), lower strains in the dry placed lower region of the core (3 to 6%). Possible shear development in the core during the latter stages of construction at about 65 to 70 m depth.	-	HSGs indicate rockfill moduli is highest in the inner Zone 3A region (60 to 100 MPa) and least in the Zone 3B rockfill (10 to 20 MPa). Therefore, large differential between core and filters / inner Zone 3A.	HSGs and IHMs in downstream rockfill.
Chaffey	0.17 to 4.9 years.	May 1979 to Feb 1984. Fluctuated within this period before reaching FSL.	Steady	Typically at FSL except for low period from 1994 to 1996 (15 to 17 years).	During construction - negligible positive PWP in core. During operation - slow rise in PWP in core with time over 5 to 15 yrs.	800	1 IVM, 5 m u/str of axis.	911	1.51	Considered as "normal" behaviour. Strains range from 0.5% near crest to 3% near base (4.75% at contact).	-	-	-
Cherry Valley	0 to 1.72 years	May 1956 to July 1957. To within 15 m of FSL in 1956.	Fluctuating	Seasonal drawdown, 20 to 35 m in first two drawdowns.	-	precipitation mostly as snow.	-	-	-	-	-	-	-
Chicoasen	0 to 0.22	Started just prior to the end of construction.	Steady	Records only for first year post construction.	-	-	IVM	6650	0.03	Relatively large vertical strains (6 to 7%) in region 85 to 105 m below crest, likely plastic deformation.	-	-	-

Table F1.1: Central core earth and rockfill embankments case study information (Sheet 5 of 30)

Name	SURFACE MONITORING - POST CONSTRUCTION										Comments
	Time of Initial Readings (years after EOC)	Crest			Upstream Slope		Downstream Slope		Comments	Comments on Deformation and Observations.	
		Settlement (mm)	S_{LT} (% per log cycle of time)	Displacement (mm)	Settlement (mm)	Displace-ment (mm)	Settlement (mm)	Displace-ment (mm)			
Agigawa	no indication	-	-	47 mm (on first filling)	-	-	-	-	Only post construction information is 47mm downstream displacement of the crest on first filling.	-	Only have deformation during construction. IVM indicates deformation of core shows normal vertical strain profile. High moduli of filters (285 MPa) and rockfill (130 MPa).
Ajuare	0.25	138 mm or 0.30% (25 years)	0.085	310 mm (25 years)	-	-	-	-	Some but limited data. Not sure if monitoring captures the period of first filling. Relatively large downstream displacement for a dam of this height.	No indication of problems with embankment behaviour. Difficult to evaluate given limited amount of data.	Relatively large downstream movement for embankment of this height.
Ataturk	0 (crest) 0 to 1.5 (d/stream)	7225 or 4.0% (6.8 yrs)	3.05	-	-	-	924 mm or 0.86% (5.8 yrs)	1380 mm (5.8 yrs)	Very large magnitude of settlement of the crest during first filling. Latter period of monitoring indicates the settlement rate is very high. Much lower magnitudes of settlement of the downstream shoulder. Large magnitude displacements to downstream of the downstream shoulder.	Longitudinal cracks and scarps formed on the crest and slickensided surfaces found in the core near to its downstream interface. Together with the large differential settlement between the crest and downstream shoulder, a shear is likely to have developed in the core. Collapse compression of the upstream rockfill being a significant factor.	Case of 'abnormal' deformation behaviour. The magnitude of post construction crest settlement and settlement rate are clear outliers to similar embankment types. Suspect it is very likely that a shear has developed in the core.
Bath County Upper Dam	0.17	546 mm or 0.41% (6.3 yrs)	0.37	190 mm (6.3 yrs)	-	-	-	-	Limited data. Crest settlement indicates 'normal' behaviour. Most of downstream displacement occurred on first filling.	Consider deformation as 'normal'. The deformation behaviour and embankment performance would indicate the rockfills were possibly well compacted.	The purpose of the dam is for power generation and it is subject to rapid daily drawdowns. Embankment constructed of weathered to fresh siltstones and sandstones.
Beliche	0	1038 or 1.89% (9 yrs)	0.26	445 mm (9 yrs)	340 mm or 0.74% (3 years)	-	484 mm or 1.2% (9 yrs)	300 mm (9 yrs)	Large settlements on first filling, during the heavy rainfall in 1989 and on drawdown in 1993. Internal deformations post construction indicate large vertical strains in upper earth and rockfill zones. Large displacements to downstream on FF. On drawdown, the core displaced upstream whilst downstream shoulder remained steady.	A number of aspects of the deformation behaviour are considered 'abnormal' including the large magnitude settlement of the crest, and acceleration of the settlement rate during heavy rainfall and on drawdown. The large internal strains in upper core and upstream rockfill indicate plastic deformation or possible shearing.	The rockfill was poorly placed, both upstream and downstream, and of poor quality adjacent to the core. It was susceptible to large deformations on collapse compression as the monitoring records indicate. Suspect the deformation behaviour is 'abnormal'.
Bellfield	0 to 0.3 (?) (assumed, no indication of date of installation)	496 mm or 0.95% (31 yrs)	0.50	298 mm (31 yrs)	-	-	285 mm or 0.72% (31 yrs)	457 mm (31 yrs)	Missing period of SMPs records from base survey to 1987 (0/0.3 to 20 years after EOC). Long-term crest settlement rate on the high side for steady reservoir condition. Displacement rate is also on the high side.	Cracking on crest observed in 1985, but no details. Internal core settlements indicate the presence of localised concentrated zones of vertical strain post construction. Those that developed after 1987 are relatively minor and are not associated with drawdown.	Overall, SMPs indicate 'normal' behaviour, although the long-term rates are on the high side.
Bjelki-Peterson	0.41 years (started 10 Feb 1989)	40 mm or 0.10% (10 yrs)	0.045	7 mm (10 yrs)	38 mm or 0.12% (10 yrs)	15 mm (10 yrs)	20 mm or 0.07% (10 yrs)	11 mm (10 yrs)	Small magnitude deformations post construction. Very low long-term settlement rate.	Small magnitude deformations probably associated with low embankment height and well compacted condition of all embankment zones. Embankment in a very good condition, no cracking or settlement of crest.	Consider deformation behaviour as "normal".
Blowering	0.24 years (0 for IVM at crest)	785 mm or 0.73% (30 yrs) 1180 mm or 1.12% from IVM (28 yrs)	0.42	-85 mm (30 yrs)	895 mm or 0.84% (30 yrs)	-430 mm (30 yrs)	378 mm or 0.43% (30 yrs)	180 mm (30 yrs)	Relatively large magnitude settlement of the crest and upstream shoulder on first filling. Accelerations in settlement rate of the crest and upstream shoulder on large drawdown in 1982/83. Displacements show the d/str shoulder displaced d/str on and after FF; limited displacement of the crest on FF and then a slight upstream trend thereafter; and the upstream shoulder shows upstream displacement at an accelerating rate (in log time) and acceleration on large drawdown.	The deformation behaviour shows several 'abnormal' trends. The post construction IVM records show further shear type displacements at 65 to 70 m depth below crest level on first filling and possibly on large drawdown. On drawdown, the acceleration in settlement and non-recovered upstream displacements are indicative of shear deformation to upstream within the core. The increasing rate of displacement (in log time) of the upstream slope is potentially "abnormal"	Monitoring records indicates likely shear development in the core that initially developed during the latter stages of construction and re-occurred during first filling and on subsequent large drawdown. The very large crest settlement on first filling required the crest to be raised February 1969.
Chaffey	0.23 years	149 mm or 0.25% (17.5 yrs)	0.19	-19 mm (17.5 yrs), u/str edge 28 mm (17.5 yrs), d/str edge	113 mm or 0.22% (17.5 yrs)	-38 mm (17.5 yrs)	115 mm or 0.23% (17.5 yrs)	27 mm (17.5 yrs)	Small magnitude of displacements; upstream crest and slope displaced upstream, downstream crest and slope displaced downstream. Large proportion of settlement occurred on first filling.	Up to 50 mm crest spreading over monitored period. Small displacements possibly due to low FSL (15 m below crest level of 58 m high embankment). Internal settlement profile in core is normal.	Consider as normal deformation behaviour.
Cherry Valley	0.08 years after EOC	135 mm or 0.14% (2.5 years)	0.03	106 mm (2.5 yrs)	-	-	-	-	Limited settlement of central region of the crest, most of which occurred on first filling. Much greater settlement on FF of the upstream rockfill. A large proportion of the crest displacement on a filling cycle is recovered on drawdown.	Differential settlement between core and rockfill resulted in cracking along the junction of the core and transition on both the upstream and downstream edges of the crest. Collapse compression on wetting contributed to settlement of the rockfill.	Limited settlement of the broad SM/ML core indicative of its high moduli in comparison to the dumped and sluiced rockfill. Deformation behaviour considered "normal".
Chicoasen	0.1	849 mm or 0.33% (0.75 yrs)	-	-43 mm (0.33 yrs)	682 mm or 0.27% (0.75 yrs)	-43 mm (0.3 yrs)	-	-	On first filling concentrated zones of deformation in the upstream rockfill and filters in the upper half of the embankment.	Indication of possible shear type movements in the upstream filter on first filling, but not in the core. Localised zones of high deformation in rockfill possibly indicates localised zone of collapse compression.	Dam constructed in a narrow steep sided valley. Significant arching in the narrow core, particularly in the deep cut-off trench.

Table F1.1: Central core earth and rockfill embankments case study information (Sheet 6 of 30)

Name	GENERAL DETAILS				CONSTRUCTION / DESIGN										References
					Construction Timing		Embankment Classification			Dimensions					
	Location	Owner/ Authority	Geology	Foundation	Year Completed	Time (years)	Dam Zoning Class[n]	Core Width / Slope	Core Type	Height, H (m)	Length, L (m)	Ratio L/H	Upstream Slope (H to V)	Downstream Slope (H to V)	Comments on Design
Copeton	Australia, New South Wales	State Water DLWC	porpyritic biotite granite	Rock	1973, June	1.75	5,2,0	c-tm	SC	113	1484	13.1	1.7H to 1V	1.8H to 1V	Central clayey sand core supported by reasonably to well compacted rockfill (outer zone poorly compacted). Cofferdam incorporated into the upstream toe. Embankment slopes of 1.6H to 1V on the mid to upper slopes and 2H to 1V on lower slopes.	LWC NSW (1995a) PWD NSW (19XX)
Corin	Australia, ACT	ACTEW	folded quartzite, silicified sandstone & siltstone.	Rock	1968, Jan	1	5,2,0	c-tm	SM	74	282	3.8	1.8H to 1V	1.8H to 1V	Central core supported by compacted rockfill shoulders. Filters / transition 10.6 m wide downstream and 9 m wide upstream of the core.	CDW (1970) ACTEW (1994)
Cougar	USA, Oregon	US Corp of Engineers	tuffaceous sediments - tuff and mudstone Basalt on abutments	Rock - abutments and valley stripped to bedrock	1963, Oct	3 (seasonal)	5,2,0	c-tn (u)	GM	159	488	3.1	1.8H to 1V	1.6H to 1V	Very narrow core with slight upstream slope. Dual filters downstream and single filter upstream of core. Dam axis arched to upstream.	Pope (1967) Cooke & Strassburger (1988)
Dalesice	Checkoslovakia	-	-	Rock	1977, Nov	6	5,2,0	c-tn (u)	CL	90	330	3.7	1.65H to 1V	1.5H to 1V	Narrow core sloped slightly upstream of centreline supported by shoulders of compacted rockfill. Broad transition zone downstream of the core. The outlet conduits fill the width of the narrow gully.	Dolezalova & Leitner (1981) Brousek (1976) Vanicek (1982) Holomek (1994)
Dartmouth	Australia, Victoria	Goulburn Murray Water	granitic gneiss	Rock	1978, Nov	2.75	5,2,0	c-tm	SC/SM	180	670	3.7	1.75H to 1V	1.75H to 1V	Central core of clayey and silty sands supported by shoulders of dry placed and compacted rockfill. Dam located in a valley with narrow river section and moderately steep abutment slopes.	SMEC (1975, 1997a) GMW (1999) Cole & Cummins (1981) Murley & Cummins (1982)
Djatiluhur	Indonesia	Djatiluhur Authority	Sandstone and claystone, andesite on abutments.	Rock	1965	3 (?)	5,2,0	c-tn (u)	CH	105	1200	11.4	1.65H to 1	3.75H to 1	Thin slightly upstream sloping clay core supported by compacted to poorly compacted rockfill shoulders. Stability berm of random fill on the downstream slope due to slickensided surfaces in foundation. Upstream cofferdam incorporated into the upstream toe of the embankment.	Sowers et al (1993) Farhi & Hamon (1967) Bister et al (1994) Sherard (1973)
Eildon	Australia, Victoria	Goulburn Murray Water	Sedimentary - sandstone, siltstone, mudstone and shale	Core on bedrock. Shoulders on either bedrock or sandy gravels (1.5 to 3 m depth).	1955, June	2 to 2.5	5,1,0	c-tk	CL	79	937	11.9	2.5H to 1V	2H to 1V (2.5H to 1V on lower slopes)	Broad central core supported by poorly compacted rockfill shoulders of varying quality rockfill. Zoned core; inner zone (Zone 1) of clays and outer zone (Zone 1A) of clayey sands. Core built up ahead of filters and rockfill during construction (up to 18 m) .	SMEC (1999a) Shaw (1953) Speedie (1948)
El Infiernillo	Mexico	CFE (Federal Electricity Commission)	Metamorhic - silicified conglomerate, basaltic dykes.	Abutments on weathered bedrock. In narrow river section core, filters and inner downstream rockfill on bedrock; upstream shoulder and outer downstream shoulder on river bed deposits (boulders with fine sand).	1963, Dec	1.4	5,2,0	c-tn	CL-CH	148	344	2.3	1.75H to 1V	1.75H to 1V	Very narrow central clay core (0.09H to 1V up and downstream slopes) supported by shoulders of poorly compacted rockfill. Cofferdams incorporated into up and downstream shoulders. Constructed in narrow gorge with steep abutment slopes.	Marsal & Ramirez de Arellano (1964, 1967, 1972) Alberro (1972)
Eppalock	Australia, Victoria	Goulburn Murray Water	Sedimentary - sandstones and mudstones, dyke in lower river section.	Rock	1962, Mar	1.5	5,2,0	c-tk	CL	47	700	14.9	1.9H to 1V	1.65H to 1V	Central clay core (0.5H to 1V downstream and 0.75H to 1V upstream) supported by dry placed and poorly compacted rockfill shoulders. Steep benched outer slopes; 1.3H to 1V slopes with 4.3 to 7.5m bench widths. Stabilising fill at lower upstream toe and cofferdam incorporated into upstream rockfill toe.	Heitlinger et al (1965) Woodward Clyde (1999) SMEC (1998d)

Table F1.1: Central core earth and rockfill embankments case study information (Sheet 7 of 30)

Name	MATERIALS														
	Earthfill Core							Filters / Transition Zone							
	Zone	Source	ASCS Class[n]	Density Ratio or Dry Density (t/m^3)	Placement Methods	Moisture Content	Comment	Zone	Source	ASCS Class[n]	Relative Density or Dry Density (t/m^3)	Layer Thickness (mm)	Plant	Level of Compaction	Comment
Copeton	1	residual granite	SC (some SM and CL) - clayey sand, 19 to 60% fines	100.1% SMDD 1.76 t/m^3	Well compacted - 150 mm layers, sheepsfoot rollers	(Spec. 1% dry to 1% wet)	Clayey sand with medium plasticity fines. 1 m thick contact zone of CH/MH clays.	2A & 2B (filters)	blend crushed granite & washed sand	2A - SW/SP 2B - GW/GP	(Spec. >70% D_R), 1.85 (2A) & 2.08 (2B) t/m^3	375 to 450	minimum 1p 10t SDVR	Good	Dual filters used up and downstream of core. Combined width of 5 m downstream and 2.5 m upstream.
Corin	1	slopewash & weathered granite	SM (SC) - gravelly silty to clayey sands, avg of 46% fines	99.4% SMDD 1.75 t/m^3	Well compacted - 100 to 150 mm layers, 12p (minimum) sheepsfoot rollers	0.3% dry of OMC	Gravelly silty and clayey sands. Fines of medium plasticity. Downstream core slope of 0.3H to 1V and upstream of 0.4H to 1V.	2A, 2B & 3A (filters)	river sand & gravels (2A, 2B) rockfill (3A)	GW/GP	(Spec. D_R >70%)	450	10t SDVR, 4p for Zone 3A	Good	Dual filters up (2A & 3A) and downstream (2B and 3A). Zone 3A is rockfill transition of 6 m width. Combined width of 10.6 m downstream and 9 m upstream.
Cougar	1	weathered rock, talus and silt fines	GM - silty sandy gravel, 10 to 30% fines	100% SMDD 1.89 t/m^3	Well compacted - 300 mm (loose) layers, 4p 45t pneumatic roller	1% wet	Well-compacted silty sandy gravel core.	2A & 2B (filters)	alluvial/colluvial gravels and spalls	GP/GM	1.91 t/m^3	300	45t pneumatic roller (2A) or 4p 10t SDVR (2B)	Good	Well-compacted filters. Slightly silty (3 to 20% fines).
Dalesice	1	colluvium	CL	(bulk density = 2.09 t/m^3)	no information	Initially wet of OMC, then at OMC	Suspect well compacted given period of construction.	2A & 2B (filter / transition)	-	Gravelly Sand (2A) & Sandy Gravel (2B)	D_R = 72%	-	no information	-	Dual filter / transition zones up and downstream of the core. The downstream Zone 2B transition is very broad (approx 36m base width).
Dartmouth	1	residual granite	SC/SM - clayey to silty sands, avg 24% fines (15 to 50% range)	(Spec. >98% SMDD) 1.82 to 1.91 t/m^3	Well compacted - 150 mm layers, 8p sheepsfoot roller	(1.0 dry to 2% wet)	Clayey and silty sands. Fines of medium plasticity. Moisture spec. varied during construction - initially wet of OMC, then dry of OMC for mid section, upper part wet of OMC.	2A & 2B (filters)	processed granitic gneiss	GW/GP	2.2 t/m^3	500	1 to 4p 14t SDVR. Started at 4p, reduced due to high moduli of filters.	Good	Well compacted filters of high moduli (as indicated by low deformation). Dual filters downstream (width increasing from 5 - 6 m to 12 13 m). Single 2A filter upstream of core (dual in crest region).
Djatiluhur	1	weathered claystone	CH - sandy clays and clays	1.58 t/m^3, or 97% SMDD	no information	average of 2.2% wet of OMC	High plasticity clays and sandy clays placed wet of OMC. Investigation in 1986 (Sowers er al 1993) found the mid to upper region of the core (above EL 65m) was much wetter and softer than anticipated.	2A & 2B (filters)	-	-	-	-	water added during placement	-	limited information. Dual filters used up and downstream of the core.
Eildon	1 and 1A	alluvial and colluvial	1 - CL 1A - SC/SM/GM	Spec. > 100% Adjusted Proct Test (3 layers, 40 blows per layer)	Well compacted - 150 mm layers, 10p (minimum) sheepsfoot rollers	Spec 2% dry to 1% wet of OMC (OMC for adjusted test)	Very high compaction specification. Zone 1 (clays of low to medium plasticity) used in central region of the core. Zone 1A (clayey sands with low to medium plasticity fines) used in the outer core region.	2 (filter / transition)	alluvial	GP	-	-	end dumped, no compaction.	poor	Zone 2 material dumped over edge of Zone 1. Width of 4.5 to 6 m. Fines content = 7% average, but varies.
El Infiernillo	1	residual and alluvial (?)	CL/CH - sandy clays	1.59 t/m^3 93.7% SMDD	Reasonably to well compacted - 150 mm layers, 13.5t sheepsfoot rollers	3.7% wet of OMC	Core of medium to high plasticity sandy clays (54 to 70% fines) placed well wet of OMC. Likely arching across very narrow wet placed core.	2A & 2B (filters)	2A - alluvial sands 2B - processed gravels (?)	2A - SP 2B - GP	Spec. D_R >70% 1.87 (2A) to 2.00 (2B) t/m^3	300	4p 2t SDVR	reasonable to good	Dual filters placed up and downstream of core. Width of filter zone increasing with depth from approx. 2-5m near crest to 15-18m at base of core.
Eppalock	1	alluvial	CL - sandy clays, 50 to 85% fines	98.8% SMDD 1.73 t/m^3	Reasonably compacted - 380 mm (loose) layers, 12p sheepsfoot rollers	0.8% dry of OMC	Sandy clays of medium plasticity. Broad central core zone of relatively large width at crest (approx. 8.5m).	2A & 2B (filter / transition)	2A - screened river gravel 2B - crushed basalt	2A - GW/GC 2B - GP	(2a - bulk density = 1.94 t/m^3)	2A - 450 2B - ?	2A - spread using spreader box and compacted by light track rolling 2B - end dumped in high lifts	2A - reasonable 2B - poor	Zone 2A and 2B used both up and downstream of the central core, width of 4.5 to approx. 7m. High clay fines content in upper part of Zone 2A filter. Zone 2B is a rockfill transition zone.

Table F1.1: Central core earth and rockfill embankments case study information (Sheet 8 of 30)

Name	MATERIALS																
	Rockfill Zone									Rockfill Zone (in some cases earthfill stabilising berm)							
	Zone	Source	Grading Description	Clean / Dirty	Dry Density (t/m^3)	Layer Thickness (m)	Placement Method	Level of Comp-action	Comment	Zone	Source	Grading Description	Clean / Dirty	Dry Density (t/m^3)	Layer Thickness (m)	Placement Method	Level of Comp-action	Comments
Copeton	3A	Granite	-	clean ?	1.99 t/m^3	1.2	4p 10t SDVR, no water added	reasonable to good	Very high strength rock. Zone 3A used adjacent to central core, both upstream and downstream.	3B	Granite	-	clean ?	1.87 t/m^3	3.7	2p 10t SDVR, no water added. Also dumped in high lifts.	poor	Very high strength rock. Zone 3B used as outer rockfill zone and also in bulk of the upstream cofferdam. It is located immediately up and downstream of the filters in the upper 25 to 28 m.
Corin	3B	quartzite, sandstone & siltstone	-	clean	-	0.9	4p 10t SDVR	Good	Well-compacted rockfill. Zone 3B is inner rockfill shoulder zone adjacent to filters and transition.	3C	quartzite, sandstone & siltstone	-	clean	-	1.8	4p 10t SDVR	Reasonable	Reasonable compaction of rockfill. Zone 3C is outer rockfill shoulder zone.
Cougar	3A	Sound basalt and andesite (H to VH)	300 mm max no fines Cu ~ 10	clean	1.82 t/m^3	0.45 to 0.6	2p 45t pneumatic or 4p 10t SDVR	Good	Well compacted Zone 3A rockfill used in the in the inner downstream shoulder. Moduli approx. 40 to 60 MPa.	3B & 3C	sound (3B) to weathered (3C) basalt and andesite	3B - max 600 mm 3C - up to 25% < 4.75 mm	3B - clean 3C - dirty	-	3B - 0.9 m 3C - 0.6 m	3B & 3C - 2p D8 dozer, no indication if water added	Poor to reasonable	Poor to reasonably compacted rockfill used in the upstream shoulder and outer d/str shoulder. Lesser quality Zone 3C used in the inner upstream shoulder.
Dalesice	3	-	-	-	(bulk density = 2.40 t/m^3)	1.0 to 1.5	6p 8.3t & 13t SDVR	Good	Rockfill indicated as being of poor quality. Well compacted.	-	-	-	-	-	-	-	-	-
Dartmouth	3A	granitic gneiss (SW to Fr)	max 600 mm. 15% pass 19 mm.	clean	2.1 t/m^3	1.0 (0.5 m within 6 m of filters)	4p 14t SDVR, no water added	Good	Well compacted rockfill, placed without water addition. Zone 3A used upstream and downstream as inner shoulder rockfill adjacent to the central core.	3B	granitic gneiss (SW to Fr)	max 1.5 m (coarser than 3A)	clean ?	2.1 t/m^3	2.0	4p 14t SDVR, no warer added	reasonable	Zone 3B used in outer rockfill shoulders, both upstream and downstream. Placed without water addition.
Djatiluhur	3	andesite	-	-	-	0.5 to 2.0	Not precisely known. Roller compacted and no formal compaction (trafficked by trucks and bulldozers). Water added, from 30 % to 300% by volume.	poor (?)	Limited details. Farhi and Hamon (1967) indicate that the rockfill was not formally compacted in the upper elevations.	4	Random - all types of materials used	-	-	-	-	compacted, no details on methods.	-	Random fill zone acting as stabilising berm on downstream slope due to presence of slickensides in foundation.
Eildon	3A	quartzitic sandstone	gap graded	clean ?	-	2.0	Tipped over advancing face and spread by dozers. No indication that water was added.	Poor	Zone 3A is 'first' quality rockfill described on sections. It was used in the outer rockfill zone of the upstream shoulder and inner rockfill zone of the downstream shoulder.	3B & 3C	sedimentary rock types	-	dirty (prone to breakdown, high fines content)	-	2.0	Tipped (over advancing face) and spread by dozers. No indication that water was added.	Poor	Zone 3B is poorest quality rockfill (random rockfill) and was used in the outer downstream shoulder. Zone 3C descibed as medium quality rock and was used in the inner upstream shoulder, and contained gravel drainage layers.
El Infiernillo	3A	Diorite and silicified conglomerate, sound	Max size 600mm 23% < 20mm 2% fines	clean to dirty	1.85 t/m^3 32% voids ratio	0.6 to 1.0	4p D8 dozer, no water added	poor	Rock of very high strength (UCS = 125 MPa) not susceptible to strength loss on wetting. Zone 3A used as inner rockfill shoulder zones up and downstream of the central core. Moduli estimated at 30 to 50 MPa.	3B	Diorite and silicified conglomerate, sound	Max size > 600 mm	-	1.76 t/m^3 35% voids ratio	2.0 to 2.5	No formal compaction and no water added.	poor	Rock of very high strength (UCS = 125 MPa) not susceptible to strength loss on wetting. Zone 3B used as outer rockfill zones in up and downstream shoulder. Moduli estimated at 15 to 30 MPa.
Eppalock	3	basalt	Max size ~ 1.0m 20 to 25% < 25mm.	dirty	bulk density = 2.05 t/m^3	2.0 to 4.0, one 10m dumped layer	Spread by tractor, no water added	poor	High to very high strength basalt rock. Zone 3 used in up and downstream shoulders.	4 (stabilising fill)	sandstone and shale (HW to MW)	-	dirty	-	-	spread by dozer and compacted by construction traffic	Poor	Limited information available. Used in the stability berm on the upstream slope.

Table F1.1: Central core earth and rockfill embankments case study information (Sheet 9 of 30)

Name	HYDROGEOLOGY						MONITORING - DURING CONSTRUCTION						
	First Filling		Reservoir Operation		Pore Pressures in Core	Rainfall (Average mm/year)	Core				Rockfill and/or Filters	Comment	Other Types of Internal Monitoring Equipment
	Timing (from end of embankment construction)	Comments	Steady / Fluctuating	Comment			Instrument Type/No.	Settlement		Comment			
								mm	% of H				
Copeton	-0.8 to 5.2 years	Impounded water before EOC, reached within 45m of FSL before EOC. Reached FSL in August 1978.	Fluctuating	Variable water level, but not annual drawdown and generally not a rapid drawdown; extended low periods followed by rapid rise.	During construction - positive PWP in contact clay only (r_u approx 0.5), dissipating over 15 to 20 yrs. During operation - core responds to reservoir fluctuation, but with reducing amplitude and greater delay with increasing distance from the upstream face.	-	IVM, 4 in core	655 to 3575 mm	1.27% to 3.34%	Strain profile look normal (increasing strain with increasing depth). High strains near base in contact zone.	-	Some differential settlement during construction between core and rockfill (greater settlement of core). Possibly some arching, but core relatively broad (0.4H to 1V slopes).	HSGs in d/stream filter & rockfill. IHMs - 3 rows in main section.
Corin	0.31 to ?	Started in May 1968. Not sure when FSL reached.	Steady	seasonal drawdown of less than 10 m from 1984 to 1988, since then has been steady	-	-	-	-	-	-	-	-	-
Cougar	0 to 0.67 years (Nov 1963 to July 1964)	Reservoir at 57 m below FSL when monitoring started.	Fluctuating	seasonal drawdown of 40 to 70m	During construction - positive PWP, r_u > 0.2 to 0.5. Rapid dissipation of construction PWP after EOC. PWP respond to reservoir level, but at reduced amplitude.	-	-	-	-	-	Zone 3A rockfill - 2718 mm (up to 3%)	Deformation of Zone 3A indicates moduli = 40 to 60 MPa at EOC.	-
Dalesice	-1.3 to 2.2 years	July 76 to Jan 80. First filling started prior to EOC. Within 9 m of FSL at EOC.	-	no information	During construction - high PWP in lower, wetter placed region of the core (r_u ~ 0.96). Of lesser magnitude in the mid to upper region (r_u = 0.3 to 0.67). EPWP still present after 15 years post construction.	-	-	-	-	-	-	-	-
Dartmouth	-1 to 11 years	Started Nov 1977, 1 year prior to EOC. Reached within 70 m of FSL prior to EOC. Reached FSL in Nov 1989 (within 20 m at 3.7 years).	Fluctuating	Not an annual drawdown. Significant drawdowns in 1983 (of 70m), 1994 (of 20m) and 1997/98 (of 50m).	During construction - High PWP in lower region of core due to placement wet of OMC (r_u up to 0.85). Reduced moisture spec for mid sections (r_u = 0.45 to 0.65). Post construction slow dissipation of construction PWP.	-	IVM, 2 in core	3220 (ES2 H=104m) 7070 (ES1 H=179m)	3.10% (ES2) and 3.95% (ES1)	Variable strain profile (0.5% to 6 - 7%). Suspect due to continued adjustment of moisture spec. during construction.	-	HSGs indicate filters and transition (Zone 3A) of high moduli. Large differential deformation between core and filters, and filters and rockfill.	HSGs in core, filter & downstream rockfill; IHMs in downstream shoulder.
Djatiluhur	-0.75 to between 2 - 2.5 years	Water impounded during construction (to EL 80m or 31 m below FSL)	Fluctuating	Annual seasonal drawdown of 10 to 18 m. Largest drawdowns in 1972 (27m to EL 78m) and 1982 (30m to EL 77m).	1986 investigation indicated high pore pressures still present in core (20 years after construction), possibly affected by drilling and installation.	-	-	-	-	-	-	Large deformations of the crest and upstream slope during latter stages of construction. Crest cracking (longitudinal) near the downstream core interface observed during a shutdown period toward the EOC.	SMPs
Eildon	-0.85 to 1.2 years	Impounding began prior to the end of construction and reached to within approx 30 m of FSL at EOC. Reached FSL in July 1956.	Fluctuating	Annual drawdown, typically 5 to 15 m. Larger drawdown events of 18 to 28 m in 1967/68, 1981-83 (28 m), 1994/95, and 1997/98 (27m).	During construction - only minor PWP developed due to dry placement of core (dry of Standard optimum). During operation - upstream Zone 1A responds with reservoir fluctuation. Large drop in head across inner core (Zone 1).	-	-	-	-	-	-	IVMs installed in core, but no results during construction available.	-
El Infiernillo	0.5 to 0.85 years	June to October 1964	Fluctuating	Annual drawdown of 10 to 30m	-	-	IVM, I1	3815	3.00%	Records indicate 'normal' vertical strain profile, 0 to 1% in top 20m increasing to 4 to 6% below 80m. Likely affected by arching across narrow core.	IVM D1 (Zone 3A) vertical strains of < 1% in top 30m increasing to 4 to 6% below 80m depth. Higher vertical strains in Zone 3B (IVM I3).	Vertical strain profile in Zone 3A rockfill similar to core. Vertical strains in outer dumped rockfill (Zone 3B) higher than core and Zone 3A.	INs, IVMs in core, filters and rockfill.
Eppalock	0.18 to 1.65 years	Started May 1962, reached FSL Nov/Dec 1963.	Fluctuating	Annual drawdown, typically 3 - 5m. Larger drawdown events of 7 to 9.5 m in - 1967/68, 1976/78, 1982/83 (8.5m), 1994/95 (9.5m) and 1997/98 (8.5m).	During construction - positive PWP only observed in some piezometers in the core, maximum r_u of 0.22 (DCP1). Slow dissipation of PWP. During operation - delayed and reduced amplitude of response relative to the reservoir level.	-	IVM, 1	1015	2.28%	Vertical strain profile at EOC shows normal behaviour; 0 to 0.5% in upper 20m decreasing to 1.6 to 1.8% at depth (35 to 45m).	-	-	inclinometers installed 1997 to 1999

Table F1.1: Central core earth and rockfill embankments case study information (Sheet 10 of 30)

Name	SURFACE MONITORING - POST CONSTRUCTION										Comments
	Time of Initial Readings (years after EOC)	Crest			Upstream Slope		Downstream Slope		Comments	Comments on Deformation and Observations.	
		Settlement (mm)	S_{LT} (% per log cycle of time)	Displacement (mm)	Settlement (mm)	Displace-ment (mm)	Settlement (mm)	Displace-ment (mm)			
Copeton	0	781 mm or 0.72% (25 yrs), 185 mm differential to upstream	0.35	-8 mm (25 yrs), u/str edge 70 mm (25 yrs), d/str edge	817 mm or 0.79% (25 yrs)	61 mm (25 yrs)	501 mm or 0.53% (25 yrs)	238 mm (25 yrs)	Displacement of all SMPs initially downstream on FF. Post FF crest and upstream slope trend to upstream, whilst downstream slope continues downstream. Greater settlements of upstream crest and slope. Internal settlement profiles in core indicate large strains at 20 m depth in IVM C and 25 m depth in IVM A, both on upstream slide of dam axis.	Greater settlement of the upstream side of the crest is visually evident, and transverse and longitudunal cracks were observed in the bitumen surfacing on the crest. Suspect it is partly due to collapse settlement of the outer dumped rockfill. Large strains measured in upstream IVM indicate possible shearing in the upper core near to its upstream interface.	Possible shear development and continued deformation in this zone is possibly indicate of "abnormal" deformation behaviour. Timing of shear deformation is on first filling and thereafter during rising reservoir conditions. Acceleration in settlement of the upstream slope and upstream crest during these periods suggest differential movements triggering shear displacement. Otherwise trends in SMPs appear to be normal.
Corin	0.29 years	83 or 0.11% (26 years)	0.04	59 mm (26 years)	189 or 0.27% (26 years)	39 mm (26 years)	145 or 0.21% (26 years)	106 mm (26 years)	Gap of 7 years from base survey to second reading. Very low long-term settlement rate. Displacement is initially downstream for the upper slopes and crest, and then shows a slow upstream trend.	Consider as 'normal' deformation behaviour. Query the base survey of some SMPs (i.e. base date is possibly before EOC for SMPs on the shoulders).	Consider as 'normal' deformation behaviour. Well compacted central core of gravelly silty sand supported by compacted rockfill shoulders.
Cougar	0.12 years after EOC (started 9/12/63)	806 or 0.59% (3.1 years)	0.13	292 to 547 mm (3.1 years), upstream and downstream edge	-	-	-	-	Acceleration in upstream crest settlement on first filling and during both first and second drawdowns. Displacement records indicate crest spreading. Long-term settlement rate is normal.	Upstream crest deformation suggests collapse compression of upstream rockfill on FF. Cracking on crest at both the up and downstream core interface, both with vertical differential settlement across the crest to upstream. Possible shear development in the core on drawdown.	Upstream rockfill adjacent to filters comprised reasonable to poorly compacted weathered rockfill. Suspect this material was prone to collapse settlement as well as outer Zone 3B to some degree. Deformation of upstream crest and cracking indicative of "abnormal" deformation on and shortly after first filling.
Dalesice	no indication (assume close to EOC)	389 or 0.46% (15 years)	-	-	324 or 0.39% (15 years)	43 mm (15 years)	131 or 0.18% (15 years)	125 mm (15 years)	Limited data records. Upper slope and crest regions all moved downstream on and after first filling.	First filling to within 9 m of FSL prior to end of construction will have affected the magnitude of the post construction displacements measured from SMPs.	Limited deformation records. Unusual design in that outlet conduits fill the width of the river gully. Embankment then constructed above this.
Dartmouth	0.05 years	1189 mm or 0.67% (20 yrs)	0.37	29 mm (20 yrs)	1262 mm or 0.88% (20 yrs)	138 mm (20 yrs)	844 mm or 0.59% (20 yrs)	282 mm (20 yrs)	Large settlements during early stages of FF. Greater settlement of upstream shoulder, probably due to collapse compression in the dry placed upstream rockfill on wetting. Acceleration in the settlement rate of the crest and upstream slope during drawdown in 1983 and again on drawdown in 1997. Large fluctuations in crest displacement with fluctuations in reservoir.	Acceleration in settlement on drawdown indicates potentially 'abnormal' deformation behaviour. On drawdown in 1983 the crest and upstream shoulder settled 100 to 150 mm, and in 1997 settled 30 to 40 mm. Difficult to evaluate IVM data due to the moisture content variation of the core, but possible plastic deformations in the wetter placed core regions.	Well instrumented dam. Increase in the rate of settlement of the crest and upstream slope on large drawdown in 1983.
Djatiluhur	0 years (at EOC on 1 Sept 1965).	2480 or 2.36% (in 27 yrs) in centre.	1.17	-	509 (0.6 yrs)	- 104 (1.2 yrs), moved upstream	312 (1.2 yrs)	476 mm (1.2 yrs)	Large magnitude settlements on first filling. Long-term settlement rate for the crest is very high. Acceleration in crest settlement on large drawdown in 1972 and 1982, similar to increasing magnitudes of settlement on each drawdown. Large downstream displacement of the crest and downstream shoulder on FF.	Longitudinal cracking in crest observed during construction. Further longitudinal cracking soon after EOC. Pits in the core encountered horizontal cracks in the downstream region (Sherard 1973). Consider the deformation behaviour as "abnormal". In particular the acceleration in settlement on drawdown and high long-term settlement rate.	Sowers et al (1993) indicate limiting stability of the upstream shoulder above EL 65m (upper 50 m), presumably under a drawn down condition. Drawdown limitations involked. Similar to increasing magnitudes of crest settlement on similar magnitude large drawdowns is an unusual observation and potentially indicative of the limiting stability condition of the upstream shoulder.
Eildon	0.19 years - SMPs on slopes. 2.5 yrs - crest sett, 13.4 yrs - crest displ.	525 mm or 0.66% (in 43 yrs). Does not include first 2.5 yrs.	0.52	-35 mm (13.4 to 43 yrs). Does not include first 13.4 yrs.	1175 mm or 1.69% (in 43 yrs).	217 mm (43 yrs).	1475 mm or 2.18% (in 43 yrs).	1328 mm (43 yrs).	Large magnitude settlements of the up and downstream shoulders. Suspect it is largely due to collapse compression on wetting of the dry placed and poorly compacted rockfill. Large downstream displacement of downstream shoulder over first 5 years after EOC. Acceleration in settlement of the upstream crest and shoulder on large drawdown in 1968 and 1981/83.	Several aspects indicative of potentially "abnormal" behaviour including acceleration in settlement on drawdown. IVM records indicate localised zones of high vertical strain in the core post construction, with deformation in these zones on large drawdown. This indicates possible shear development within the core.	Potentially "abnormal" aspects of the post construction deformation behaviour. Possible shear development in the core as indicated from IVM records.
El Infiernillo	0.18 yrs (sett SMPs) 0.45 to 0.54 yrs (displ SMPs)	1190 mm or 0.81% (in 17 yrs).	0.09	348 mm (17 yrs).	930 mm or 0.83% (in 8 yrs).	-	580 mm or 0.52% (in 8 yrs), greater for SMPs over Zone 3B (0.66% in 8yrs)	405 mm (8 yrs).	Large magnitude of settlement of the crest and upstream slope on FF. Displacement of the crest is upstream in early stages of FF and then downstream in latter stages, thereafter it is downstream. From late 1966 to 1970 (all SMPs), sustained period of acceleration in settlement and downstream displacement occurred. Acceleration in crest settlement on earthquake (7.6 mag.) in 1979.	Overall, the deformation behaviour is considered "normal", but it does show several "abnormal" trends. Collapse settlement of the rockfill on wetting contributed to the large settlements of the shoulders. The post FF acceleration of the settlement and displacement was coincident with periods of heavy rainfall and tail-water inundation of the downstream toe. IVM data indicates possible shear development in the core.	Well instrumented embankment. Transverse cracking observed on the upper abutments, first noticed 3 days after the start of reservoir impounding. Possible shear development in the core post first filling, possibly drawdown related, but not sure.
Eppalock	0.26 years	510 mm or 1.11% (37yrs)	0.91	195 mm (CS2, 37yrs), -22 mm (CS1)	570 mm or 1.60% (37yrs)	-240 mm (37yrs)	840 mm or 2.38% (37yrs)	750 mm (37yrs)	Large settlements of upstream shoulders on FF and downstream shoulder in first 4 years, indicative of collapse settlement on wetting. Acceleration in settlement rate of SMPs on the crest and upstream shoulder on large drawdowns from 1982/83 on, with similar to increasing magnitudes at CS1 for subsequent drawdowns. Crest displacement shows change in trend from downstream to upstream, and also non-recovered upstream displacement on the 1994/95 drawdown.	Consider as case of "abnormal" deformation behaviour. Shear development in the core confirmed from inclinometers and observation during remedial works. Collapse compression of the rockfill is a significant factors contributing to the shear development due to the limited lateral support afforded to the core from the shoulders. Longitudinal cracking in the crest was first observed about 1973 and has since been persistent.	Case study of "abnormal" deformation behaviour. Woodward Clyde (1999) indicated the factor of safety of the upper region of the upstream shoulder was approaching a marginal condition. The similar magnitude of crest settlement on large drawdowns of similar magnitude in unusual. Remedial works were undertaken in 1999 to address the dam safety issues.

Table F1.1: Central core earth and rockfill embankments case study information (Sheet 11 of 30)

Name	GENERAL DETAILS				CONSTRUCTION / DESIGN										References
					Construction Timing		Embankment Classification			Dimensions					
	Location	Owner/ Authority	Geology	Foundation	Year Completed	Time (years)	Dam Zoning Class[n]	Core Width / Slope	Core Type	Height, H (m)	Length, L (m)	Ratio L/H	Upstream Slope (H to V)	Downstream Slope (H to V)	Comments on Design
Frauenau	Germany	-	Gneiss	Core on unweathered gneiss, shoulders on weathered gneiss.	1981, Aug ?	5	5,2,0	c-tn	SM	80	670	8.4	1.5H to 1V	1.5H to 1V	Narrow central core with central diaphragm wall. Dual filters up to 10 m wide up and downstream of the core. Dam axis arched upstream.	List & Beier (1985)
Fukada	Japan	-	Sedimentary - sandstone and mudstone	Rock	1976, Oct	1.1	4,1,2	c-tm	GC (?)	55.5	340	6.1	2.75H to 1V	2.75H to 1V	Central core with shoulders of weathered rockfill. Relatively flat shoulders for embankment of this type and height.	Yasunaka et al (1985)
Geehi	Australia, New South Wales	SMHEA	foiliated granodiorite and diorite (partly metamorphosed)	Rock	1966, Jan	2.5 (seasonal)	5,2,0	c-tn	SM	91	265	2.9	1.75H to 1V (2H to 1V from 45m below crest level)	1.75H to 1V	Central narrow core with inner shoulders of compacted rockfill and outer shoulders of dumped rockfill. Dual filters up and downstream.	Pinkerton & Paton (1968) Hilton et al (1974) Grimston (1989) GHD (1995a)
Gepatsch	Austria	TIWAG	Foliated gneiss, glacial activity	Core on bedrock. Shoulders on over-consolidated alluvium and colluvium up to 50 m deep.	1964, Nov	3.5 (seasonal)	5,2,0	c-tn	GM/GC	153	605	4.0	1.5H to 1V	1.5H to 1V	Narrow central core with broad filter/transition zones and shoulders of reasonably compacted rockfills placed without water addition. Slight upstream curvature to dam axis.	Lauffer & Schober (1964) Schober (1967) Schwab (1979)
Glenbawn, Saddle Dam A	Australia, New South Wales	State Water DLWC	Sedimentary - mudstones with igneous dyke (diorite) intrusions.	Rock	1986, Aug	0.5	5,2,0	c-tm	-	35	585	16.7	1.5H to 1V	1.5H to 1V	Central core supported by narrow width filters and rockfill shoulders. Former spillway to main dam at upstream toe. Saddle dam constructed as part of the works associated with raising of the main embankment.	Volk (1987) LWC NSW (1995b)
Glenbawn - main dam (prior to raising)	Australia, New South Wales	State Water DLWC	Sedimentary - sandstone, propylites, breccia & tuff; igneous dykes and sills.	Rock - 'soft and weak'	1957, Sept	3.5	5,1,0	c-tk	CL	76.5	823	10.8	3.4H to 1V (3H to 1V upper slope reducing to 4H to 1V)	3H to 1V (2.5H to 1V upper slope reducing to 5H to 1V)	Broad central zoned core supported by broad transition zone (up to 40 m width near base of dam) and poorly compacted rockfill shoulders. Cofferdam at upstream toe.	Stafford & Weatherburn (1958) Wilson & Scott (1957) WCIC (1982) Volk (1987) LWC NSW (1995b)
Googong	Australia, ACT	ACTEW	dacite and meta-sediment intruded by granite.	Rock	1977, Apr	1	5,2,0	c-tm	SC	62 (before raising)	423	6.8	1.8H to 1V	1.7H to 1V	Central core supported by compacted rockfill shoulders.	Goldsmith (1977) ACTEW (1993)
Kisenyama	Japan	Kansai Electric Power Co.	Sedimentary / Mertamorphic - slate, sandstone & chert	Rock	1963	unk	5,2,0	c-tm	unk	88	255	2.9	2.5H to 1V	2.2H to 1V	Medium width central core (0.28H to 1V slopes) supported by rockfill shoulders. Filters increasing in width with depth. Relatively flat upstream slope.	Kisa & Fukuroi (1994) Nose (1969)
Kurokawa	Japan	-	Tuff and breccia	Rock	1973, Nov	2.5	5,2,0	c-tn	-	98	325	3.3	2.5H to 1V	1.85H to 1V	The narrow core is aligned slightly to upstream (downstream slope of core is near vertical). Filters increasing in width with depth. Relatively flat upstream slope.	Kisa & Fukuroi (1994) JNCOLD (1976)
La Grande 2 (LG2)	Canada, James Bay	Hydro Quebec	Granite. Over-burden of glacial origin.	mainly on bedrock.	1978, Oct	-	5,2,0	c-tn (u)	SM	160	2900	18.1	1.8H to 1V	1.6H to 1V	Narrow core aligned slightly to upstream. Supported by compacted rockfill shoulders, with dual filter zones up and downstream of the core. Cofferdam incorporated into the upstream shoulder.	Pare et al (1982) Pare (1984) ICOLD (1989) Dascal (1987)
Maroon	Australia, Queensland	QDNR (now Sun Water)	Sedimentary - clay shales, siltstones, sandstones. Basalt sills intruded along bedding seams.	Rock. Overburden and weathered shale removed.	1973, June	1.7	5,2,2	c-tk	SC/CL	52	460	8.8	1.5H to 1V	1.5H to 1V	Weighting berms added both upstream and downstream during construction due to presence of pre-sheared clays seams in foundation.	Nutt (1975) QWRC (19XXa) Sbeghen (1990) Coffey & Hollingsworth (1971)
Matahina	New Zealand	Trust Power	Volcanic (ignimbrite) over tertiary sediments	Abutments on ignimbrite. In broad valley, core on heavily over-consolidated Tertiary sediments (clays, gravels and sands) and shoulders on alluvial gravels	1966, Oct (?)	2	5,1,0	c-tm	CL/ML	85	400	4.7	2.5H to 1V	2.6H to 1V	Central (zoned) core aligned slightly to upstream (slopes of vertical downstream and 0.6H to 1V upstream) supported by poorly compacted rockfill shoulders. Constructed in a wide valley with steep abutment slopes (approx. 50 degrees).	Penman (1988) Galloway (1970) WGL (1994)

Table F1.1: Central core earth and rockfill embankments case study information (Sheet 12 of 30)

Name	MATERIALS														
	Earthfill Core							Filters / Transition Zone							
	Zone	Source	ASCS Class[n]	Density Ratio or Dry Density (t/m^3)	Placement Methods	Moisture Content	Comment	Zone	Source	ASCS Class[n]	Relative Density or Dry Density (t/m^3)	Layer Thickness (mm)	Plant	Level of Compaction	Comment
Frauenau	1	residual soil	SM - silty sands	-	no information	-	Silty sands with low fines content and small clay fraction.	2A & 2B (filters)	-	-	-	-	-	-	no information. Dual filters of narrow width up and downstream of the core.
Fukada	1	weathered sandstone and granite	GC (?) - mix clay, sand & gravels	-	no information	-	Limited information. Suspect reasonably to well compacted given practices used in Japan at this time.	2 (filter)	-	-	-	-	-	-	No information. Single filter up and d/stream of the core. Dual horizontal filter in the lower region of the d/stream shoulder.
Geehi	1	completely weathered gniess	SM - silty sands, avg 43% fines	100.6% SMDD	Well compacted - 150 mm layers, 12p 3.5t sheepsfoot rollers.	0.5% wet of OMC	Silty sand with fines (43% average fines content) of low plasticity. Difficulty with moisture content due to breakdown of earthfill on compaction.	2A & 2B (filters)	crushed rockfill	2A - SP/SW 2B - GP/GW	(Spec. D_R >70%) easily met	300	2p 8t SDVR & 1p 20t crawler tractor	Good	Well compacted filter zones up and downstream of the central core, of thin width (combined width = 7.3 m).
Gepatsch	1 & 1A	talus (colluvium) and morraine	GM/GC - silty to clayey fravels, 17 to 42% fines	96 - 99% SMDD 2.18 t/m^3	Well compacted - 300 mm layers, 6p 40 t rubber tyred roller	2% wet (0.5 - 1% wet from 5/63)	GM/GC core placed wet of OMC. Upstream Zone 1A region of core had 1% bentonite added. After May 1663 improved compaction due to lower moisture content.	2 & 2A (filter / transition)	river deposits	GP	2.25 t/m^3 (n = 15.2%, e = 0.18)	600	2 - trafficked only 2A - 4p 40t rubber tyred roller or 4p 8.5t SDVR	2A - well compacted, 2 - reasonable	Reasonable to good compaction as indicated by the low compressibility of these layers. Zone 2 used up and downstream of the core, Zone 2A mainly in downstream shoulder.
Glenbawn, Saddle Dam A	1	-	-	-	no information	-	Limited information. Suspect reasonably to well compacted. Sloped at 0.45H to 1V upstream and 0.15H to 1V downstream.	2A & 2B (filters)	crushed rock (2B)	-	-	-	-	-	Limited information. Dual filters used up and downstream of the core.
Glenbawn - main dam (prior to raising)	1A & 1	alluvial / colluvial ?	1A - CL some CH 1 - SC	> 100% SMDD	Well compacted - 200 mm (loose) layers, ballasted tamping rollers	2.0% dry of OMC	Zone 1A, medium to high plasticity sandy clays, is the inner core region. Zone 1, clayey sands with low plasticity fines, is the outer core region up and downstream of Zone 1A.	2 (filter / transition)	river gravel & shingles	GC/GP (?)	D_R ~ 82%	300	trafficking by dozers and trucks	reasonable to good	Zone 2 transition up and downstream of the core. Of high relative density achieved by track rolling. Contains up to 20% fines. Of broad width, from several metres wide at the crest to about 35 m wide near the base.
Googong	1	colluvial	SC (some CL and SM)	(Spec. >98% SMDD)	Well compacted - 165 mm layers, padfoot rollers (Cat 835)	(Spec. 1% dry to 1% wet)	Clayey and silty sands to sandy clays, low plasticity. Fines content = 44% avg (30 to 55%). Core aligned slightly to upstream.	2 & 3A (filters / transition)	river gravels & crushed rock	-	2.10 t/m^3 (2)	500	2p 10t SDVR (2) 4p 10t SDVR (3A)	Good	Zone 2 & 3A used up and downstream of the central core. Zone 3A rockfill is a transition of ~ 6 m width.
Kisenyama	1	-	unk	-	no information	-	No information.	2A and 2B (filters)	-	unk	-	-	-	-	No information. Dual filters used up and downstream of the central core.
Kurokawa	1	-	unk	-	no information	-	No information.	2A and 2B (filters)	-	unk	-	-	-	-	No information. Dual filters used up and downstream of the central core.
La Grande 2 (LG2)	1	glacial till	SM - gravelly silty sands, avg 29% fines (non-plastic)	2.07 to 2.11 t/m^3	Well compacted - 450 mm layers, 4p 45t pneumatic rollers.	Spec. 1% dry to 2% wet of OMC	Well compacted gravelly silty sands (max size 250 mm, non-plastic fines). Core aligned slightly upstream (upstream slope of 0.44H to 1V and downstream of -0.09H to 1V).	2A & 2B (filters)	2A - gravels 2B - crushed stone	2A - SP/SW	(Spec. 90% results >70% D_R)	450	3-4p 3-5t SDVR, water added if necessary	Good	Well compacted filters. Dual filters used up and downstream of the central core. Width increasing with depth, up to 20m width upstream and 25 to 30m width downstream of core.
Maroon	1	alluvial / colluvial	SC/CL - sandy clays and clayey sands	(Spec. >98% SMDD)	Well compacted - 150 mm layers, tamping rollers	Spec. 1% dry to 2% wet of OMC	Well compacted sandy clays and clayey sands of medium plasticity.	2A, 2B (filters)	sands and gravels	sands to gravels	(Spec. >70% D_R)	300	4p 4.5t (min) SDVR, wetted prior to compaction	Good	Filter / transition zones used up and downstream of the core, and on the foundation under the up and downstream shoulders.
Matahina	1	greywacke, extremely weathered	CL - gravelly clay	97% SMDD (?)	Well compacted - 150 mm layers, 16p grid rollers (?)	dry of OMC, lower section 1% to 1.5% dry.	Lower region of the core placed well dry of OMC; this region was of very stiff consistency and brittle. Zone 1 is the narrow central region of the core encased in Zone 1A.	2 (transition)	Ignimbrite, weathered	GW/GM - sandy to silty gravels	-	-	-	-	Limited information. Considerable grading variation. Used up and downstream of central core (Zones 1 and 1A). Of broad width in lower section.

Table F1.1: Central core earth and rockfill embankments case study information (Sheet 13 of 30)

Name	MATERIALS																	
	Rockfill Zone									Rockfill Zone (in some cases earthfill stabilising berm)								
	Zone	Source	Grading Description	Clean / Dirty	Dry Density (t/m^3)	Layer Thickness (m)	Placement Method	Level of Comp-action	Comment	Zone	Source	Grading Description	Clean / Dirty	Dry Density (t/m^3)	Layer Thickness (m)	Placement Method	Level of Comp-action	Comments
Frauenau	3	-	-	-	-	-	-	-	No information	-	-	-	-	-	-	-	-	-
Fukada	3	Weathered sandstone and granite.	-	presume dirty	-	-	-	-	No information, but suspect compacted given E_{rc} estimated at 42 MPa from IVM data.	-	-	-	-	-	-	-	-	-
Geehi	3A	granitic gneiss	Max. 600 mm 6.3% finer than 19 mm.	clean	2.00 t/m^3	0.9	2p 8t SDVR & 2p 20t crawler tractor, sluiced	reasonable to good	Rock described as 'hard, durable and massive". Zone 3A is the inner rockfill zone located up and downstream of the central core (outer slope = 0.75H to 1V).	3B	granitic gneiss	Max size of 2.7 m (coarse rockfill)	clean	-	1.8 to 30 (30 m in lower sections)	Dumped & sluiced	Poor	Rock described as 'hard, durable and massive". Zone 3B is outer rockfill zone up and downstream. 3 m layer thickness in upper region.
Gepatsch	3	gneiss and oversize (> 200 mm) from Zone 1.	Coarse (max 1.7 m) 8 - 45% < 20 mm < 8% fines.	clean to dirty (variable)	1.89 t/m^3 (n = 28.8%, e = 0.41)	2.0	4p 8.5t SDVR, no water added	Reasonable	Finer material placed toward central section, coarser toward outer slopes. Described as "firm" haer eye gneiss. Thin Zone 3A transition between filters and rockfill.	-	-	-	-	-	-	-	-	-
Glenbawn, Saddle Dam A	3	limestone and sandstone	-	-	2.12 t/m^3	-	limited information	-	Suspect compacted given high density. Rock of very high strength. Zone 3 used in up and downstream shoulder.	-	-	-	-	-	-	-	-	-
Glenbawn - main dam (prior to raising)	3	limestone	suspect coarse sized and gap graded.	clean ?, brokedown on trafficking	-	1.8	Spread and levelled by tractors with rakes. Watered in early stages but discontinued.	poor	Zone 3 used as up and downstream shoulder fill. Indication of breakdown at top of each layer on trafficking. Drp placed and poorly compacted in mid to upper regions.	-	-	-	-	-	-	-	-	-
Googong	3B & 3C	dacite & granite	-	clean	-	3B = 1.0 3C = 2.0	4p 10t SDVR, compacted dry	reasonable (3C) to good (3B)	MW to FR rock, of very high UCS (except MW dacite - high UCS). Zone 3B is the predominant rockfill zone, 3C only used in the outer upstream slope.	-	-	-	-	-	-	-	-	-
Kisenyama	3	slate, chert and sandstone	-	-	-	-	-	-	No information, suspect reasonably to well compacted given procedures used in Japan at the time. Rock described as 'hard'.	-	-	-	-	-	-	-	-	-
Kurokawa	3	-	-	-	-	-	-	-	No information, suspect reasonably to well compacted given procedures used in Japan at the time.	-	-	-	-	-	-	-	-	-
La Grande 2 (LG2)	3	granite ?	Max size 1.0m 8 to 19% < 19mm < 3% fines.	clean	-	0.9 to 1.8	4p 9t SDVR, no water added	reasonable to good	Zone 3 used in up and downstream shoulders. Not sure if rock type is granite (assumed from geology).	-	-	-	-	-	-	-	-	-
Maroon	3A, 3B	Porphery	max 0.45 m (3A), 0.9 m (3B)	-	-	0.9 to 1.2 (3A) up to 1.5 (3B)	10t SDVR, water added	reasonable to good	Zone 3A used as rockfill transition in downstream shoulder. The coarser Zone 3B is the main rockfill zone. Rock described as 'very hard'.	4	materials from excavation	-	-	Spec. > 95% SMDD	0.3	rollers or general traffic	reasonable to good	Limited information. Various materials from excavation used, CH/MH clays excluded.
Matahina	3	Ignimbrite ('hard')	large portion from 150 to 900 mm size. Very few fines.	clean	-	1.0	Spread and rolled by tractor, no water added.	Poor.	Used for both up and downstream shoulders.	1A (part of central core zone)	Ignimbrite, highly weathered	SM/ML - sandy silts to silty sands, 34% fines.	-	-	0.15 m	Grid rollers (?), placed dry of OMC.	Good	Zone 1A used up and downstream of the central clay core (Zone 1). Sandy silts to silty sands, max. size 40 mm, 34% fines.

Table F1.1: Central core earth and rockfill embankments case study information (Sheet 14 of 30)

Name	HYDROGEOLOGY						MONITORING - DURING CONSTRUCTION						
	First Filling		Reservoir Operation		Pore Pressures in Core	Rainfall (Average mm/year)	Core				Rockfill and/or Filters	Comment	Other Types of Internal Monitoring Equipment
	Timing (from end of embankment construction)	Comments	Steady / Fluctuating	Comment			Instrument Type/No.	Settlement		Comment			
								mm	% of H				
Frauenau	no information	First filling occurred within the 3 year monitored period	-	not known	Negligible to limited positive PWP in core during construction.	-	IVM	1254	1.69 (0.7 to 3.6%)	Consider as normal, vertical strains increasing with increasing depth below the crest.	-	-	-
Fukada	4.8 to 5.8 years	Aug 1981 to Aug 1982. Delay between EOC and start of first filling.	Steady	close to FSL	-	-	IVM (H2)	755	1.45%	0 to 1% in upper part of core increasing to 3.0% in lower part. Normal.	800 mm or 1.6% (H1 upstream), 595 mm or 1.3% (H3 downstream)	H1 - 0 to 2.4% in rockfill, 2 to 4% in core near base. H3 - 0 to 2% (all in rockfill).	IHM in downstream rockfill.
Geehi	0 to 0.1 years.	Rapid filling in 5 weeks (Jan to Feb 1966).	Fluctuating	Subject to very rapid daily drawdowns, up to 30 to 40 m over several days.	During construction - high PWP developed in the core, but dissipated quickly. Negligible by the end of construction.	-	IVM	-	-	X-arm blocked with soil during construction, tube filled with concrete.	-	Moduli of Zone 3A rockfill ~ 110 MPa at EOC (from HSG 1 & 2).	HSGs and IHM in rockfill.
Gepatsch	-0.3 to 1.92 years	First filling started prior to end of construction, reached within 48 m of FSL at EOC. FF completed by Oct 1966.	Fluctuating	Annual seasonal drawdown. 1965 and 1966 drawdowns were 54 and 80 m respectively.	Construction - pwp up to 70 to 100% in core, but rapid dissipation (reduced to 30% within 3 to 12 months).	Most of stored water is from snowmelt.	IVM - 9 in total (5 in core)	-	-	limited information	limited information	Relatively large settlements of shoulders during construction. Arching across core confirmed by pressure cells. A number of the vertical tubes were lost due to considerable bending.	IHM, IN.
Glenbawn, Saddle Dam A	0 to 4.1 years	Started in August 1986 and reached FSL in Oct 1990. FSL is 11 m below crest level due to storage capacity for flood mitigation purposes.	Fluctuating	Not a annual drawdown. Significant drawdown in 1994-98 of 19m.	-	625	IVM	508	1.44%	'normal' behaviour. Strains increasing with depth from 0 to 1% in upper 15 m to 4 to 5% near the base of the core.	-	-	-
Glenbawn - main dam (prior to raising)	0.9 to 4.7 years	Started in August 1958 and reached FSL in May 1962. FSL is 15 m below crest level due to storage capacity for flood mitigation purposes.	Fluctuating	Not an annual drawdown. Significant drawdowns in 1964-66 of 23m, and 1979-81 of 26m.	During construction - positive PWP in core, r_u up to 0.4 in Zone 1A and 0.2 in Zone 1.	625	IVM	2425	3.21%	'normal' behaviour. Strains increasing with depth from 0.0 to 0.5% in upper to 10 to 15 m to 5 to 7% in lower 50 to 75 m.	-	-	-
Googong	-0.1 to 1.21 years	Started just prior to EOC in early March 1977. To FSL by Aug 1978.	steady	Maintained within ~ 3 m of FSL.	-	-	HSGs in core	1180	1.90%	Likely to under-estimate the settlement due to the 15 to 16 m spacing between HSGs.	-	Greater settlements in core than in filters and rockfill.	HSGs in core, filters and rockfill
Kisenyama	0 to 0.5	Filled within 0.5 years from EOC	Fluctuating	Subject to very rapid drawdowns (daily ?), typically 5m, but up to 36 m.	-	-	-	-	-	-	-	-	-
Kurokawa	0 to 1.75	Steady rise in reservoir to FSL over period of FF.	Fluctuating	Subject to rapid drawdowns (daily ?), typically 3 m but up to 20 m.	-	-	-	-	-	-	-	-	-
La Grande 2 (LG2)	0.12 to 1.2 years	Started late Nov 1978 and reached FSL in late Dec 1979.	-	No information beyond first filling	-	-	-	-	-	-	-	-	-
Maroon	0 to 1.23	Steady rise to FSL from June 1973 to mid 1974	Fluctuating	Not an annual drawdown, but reservoir level does fluctuate. Drawdowns slow and gradual. Lowest elevation = 18.3 m below FSL.	High PWP in core during construction (r_u = 0.3 to 0.75). Slow dissipation of excess PWP over 20 to 25 years.	-	IVM, 3	490 (H = 36) to 1120 (H = 51)	1.4 to 2.2%	Vertical strain increases with increasing fill depth from 0% near crest to 4 - 6% at depth.	-	-	-
Matahina	0.11 to 0.24 years	Nov 1966 to Jan 1967.	Steady	Close to FSL. Two large drawdowns to undertake repairs, 1988 (18m) and 1996-98 (18 m).	Negligible construction pore pressures.	-	-	-	-	-	-	Greater settlement of rockfill shoulders than the core. Foundation in valley settled approx 180 mm during construction. Differential settlement problems at abutments.	HSGs and foundation plates.

Table F1.1: Central core earth and rockfill embankments case study information (Sheet 15 of 30)

Name	SURFACE MONITORING - POST CONSTRUCTION										Comments
	Time of Initial Readings (years after EOC)	Crest			Upstream Slope		Downstream Slope		Comments	Comments on Deformation and Observations.	
		Settlement (mm)	S_{LT} (% per log cycle of time)	Displacement (mm)	Settlement (mm)	Displace-ment (mm)	Settlement (mm)	Displace-ment (mm)			
Frauenau	close to 0 (?)	150 mm or 0.18% (3 years)	-	250 mm (3 yrs)	-	-	-	-	Limited information. Displacement of the crest is downstream on first filling, and accelerated in last 10 m of first filling. Crest spreading on first filling of 60 mm.	Consider as normal in terms of magnitudes. IVM profile post construction indicates uniform strain profile in core.	Limited information. The core incorporates a central diaphragm wall.
Fukada	0	130 mm or 0.25% (7 years)	0.16	38 mm (7 years)	-	-	-	-	Displaced downstream on first filling (4.8 to 5.8 years). Low long-term settlement rate.	Limited data, but consider as 'normal'. Similar magnitude settlements between the core and weathered rockfill shoulders.	Consider as 'normal'. Very flat slopes for embankment height of 52 m. Rockfill is weathered sandstone and granite.
Geehi	0.07 years	236 mm or 0.27% u/str edge. 142 mm or 0.16%, d/str edge (33 yrs)	0.12	88 mm u/str edge (33 yrs). 118 mm d/str edge (33 yrs)	163 mm or 0.21% (33 yrs)	32 mm (33 yrs)	154 mm or 0.25% (33 yrs)	153 mm (33 yrs)	Settlement of upstream crest and shoulder on FF of greater magnitude than the downstream crest. Low long-term settlement rate. Displacement is downstream for all SMPs (upstream slope to downstream slope), fluctuating with reservoir level.	Consider as "normal" behaviour. Acceleration in rate of upstream crest and slope settlement in 1989 to 1991 (23 to 25 yrs) is when reservoir at low level and rising. Greater settlements on mid to lower d/str slope possibly due to greater thickness of dumped rockfill below SMP.	Consider as "normal" behaviour. Reservior Level subject to numerous large and rapid drawdowns.
Gepatsch	0 years (EOC on 6 Nov 1964).	1650 mm or 1.08% (13 yrs)	0.83	upstream moved upstream (500 mm, 13 yrs) and d/str moved d/str (~ 200 mm)	732 mm or 1.0% (22 yrs)	-665 mm (upstream) (22 yrs)	1087 mm or 1.41% (22 yrs)	886 mm (22 yrs)	Crest spreading of 600 to 750 mm at 2 yrs after EOC (upstream crest and slope moved upstream and downstream crest and slope moved downstream). Acceleration in deformation of upstream slope on first filling and first drawdown. Foundation under the shoulders contributed to the observed settlements.	Cracking in crest occurred as a result of the crest spreading and differential settlement. Collapse settlement of the dry placed and reasonably compacted rockfill on wetting contributed to the large magnitude deformations of the upstream shoulder on first filling.	Settlement during construction indicates broad filters of significantly higher moduli than the rockfill and core, resulting in arching of core and high stresses in filter zones.
Glenbawn, Saddle Dam A	0 (crest sett) 0.47 (slopes and crest displ)	225 mm or 0.70% (12 yrs)	0.16	-13 mm (12 yrs)	171 mm or 0.80% (12 yrs)	-172 mm (12 yrs)	66 mm or 0.31% (12 yrs)	46 mm (27 yrs)	On FF the crest and downstream slope displaced downstream, and the upstream slope displaced upstream. Post FF, the rate of settlement and displacement (to upstream) of the upstream shoulder is greater than the crest and downstream shoulder. Other SMPs on the upstream shoulder show similar trends.	Displacement of the upstream shoulder is potentially "abnormal", the displacement rate to upstream continues at a steady to increasing rate (in log time). The deformation behaviour of the crest and downstream are considered "normal". Embankment in good condition (LWC 1995).	Consider deformation behaviour of the upstream shoulder as potentially 'abnormal'. The deformation behaviour of the crest, downstream shoulder and internal core are considered "normal".
Glenbawn - main dam (prior to raising)	0 years	760 mm or 0.99% (27 yrs)	0.26	upstream edge moved upstream (315 mm) and d/str moved d/str (330 mm), 27 yrs	695 mm or 1.09% (27 yrs)	-260 mm (27 yrs)	450 mm or 0.71% (27 yrs)	260 mm (27 yrs)	Large settlements and displacements on first filling. The upstream crest and slope displaced upstream and the downstream crest and slope displaced downstream. Records indicate crest spreading of more than 500 mm.	The magnitude of crest spreading on FF is large. IVMs A and B indicate large vertical strains at close to the interface between the core and filters (both up and downstream), due to differential settlement as a result of collapse settlement of the dry placed and poorly compacted rockfill.	Embankment raised by almost 24 m to 100 m in 1985-87. Only the deformation of the original embankment has been considered here.
Googong	0 (settlement) 0.94 (displ)	233 mm or 0.37% (13 yrs)	0.20	79 mm (13 yrs)	-	-	-	-	Limited records. Crest displacement is downstream on first filling and remained virtually steady from 1980 to 1990.	1993 inspection descibed the embankment as having good alignment with no visible abnormalities. Consider deformation behaviour as 'normal', but have limited records.	Embankment raised by 4.5 m in 1991/92 to accomodate PMF analysis. Only the deformation behaviour prior to raising has been analysed. The embankment was also over-topped during construction.
Kisenyama	no information, suspect close to EOC	369 mm or 0.42% (16.5 years)	0.29	421 mm (16.5 yrs)	-	-	-	87 mm (3 yrs)	Large downstream displacement of the crest on FF (180 mm), most of which occurred when the reservoir was raised above 80% of the embankment height. Acceleration in crest displacement (to downstream) at 1 year, but not related to reservoir fluctuation.	Acceleration in downstream displacement at 1 year was possibly rainfall related. Displacement pattern follows reservoir level with general trend toward downstream.	Constructed in narrow river gully with 26 to 38 degree abutment slopes. Consider deformation behaviour as "normal", although downstream displacement is relatively large.
Kurokawa	no information, suspect close to EOC	323 mm or 0.33% (13 years)	0.17	258 mm (13 yrs)	-	-	-	-	Crest settlement and displacement profiles show normal behaviour.	Crest deformation considered normal	Constructed in broad river gully with steep (33 to 47 degree) abutment slopes.
La Grande 2 (LG2)	0.13 years (sett) 0.22 yrs (displ)	840 mm or 0.56% (5.7 yrs) 500 mm differential at main section.	0.135	675 mm (5.7 yrs)	-	-	-	-	Settlement of the upstream crest and both the up and downstream shoulders was relatively large on first filling, thereafter the long-term rate of settlement was normal cf similar materials. Large differential settlement at crest at the main section of 500mm. Large downstream crest displacement on FF, limited displacement thereafter.	Significant longitudinal cracking occurred during the latter stages of FF. Cracking located on upstream side of the crest and at the centre (mid 1979, length = 350m, width = 50mm). Late Sept 79 - 300mm differential settlement across crack in central crest region (width = 150mm). Sharp tilt in inclinometer on u/str edge of crest at 20m depth indicative of shear.	Consider as a case of 'abnormal' deformation during and shortly after the period of FF. Monitoring data indicates likely shear development in core that developed during first filling, which is probably associated with collapse compression on wetting of dry placed rockfill.
Maroon	0 for all except crest displacement (0.44 yrs)	269 mm or 0.56% (20 years)	0.46	-15 mm (20 yrs)	94 mm or 0.28% (20 years)	-22 mm (20 yrs)	114 mm or 0.34% (20 years)	-18 mm (20 yrs)	Settlement shows normal trend. Displacements are small (< 25 mm) and all displace to upstream. Long-term the rate of the displacement trend is virtually zero. The post construction internal settlement profile shows the settlement is distributed relatively uniformly over the full depth of the core.	Deformation behaviour considered 'normal'.	Weighting berms added during construction to upstream and downstream shoulders due to pre-sheared surfaces encountered in foundation along basalt sills.
Matahina	0.1 years	206 mm or 0.26% (20 yrs, to 1987 prior to earthquake)	0.11	484 mm (20 yrs, to 1987 prior to earthquake)	-	-	243 mm or 0.52% (20 yrs, to 1987 prior to earthquake)	-	Deformation records used were those prior to the earthquake in 1987. Large downstream displacement of the crest on first filling (212 mm). Greater post construction settlements of rockfill shoulders than core. Limited data records.	Limited post construction data records.	Deformation records used for Matahina dam were up to the time of the earthquake in 1987. During the earthquake the downstream shoulder settled some 100 mm, the core (at crest level) settled approx. 50 to 100 mm and the upper upstream shoulder settled 800 mm (Penman 1988). Matahina also had problems with piping adjacent to the abutments.

Table F1.1: Central core earth and rockfill embankments case study information (Sheet 16 of 30)

Name	GENERAL DETAILS				CONSTRUCTION / DESIGN											References
					Construction Timing		Embankment Classification			Dimensions					Comments on Design	
	Location	Owner/ Authority	Geology	Foundation	Year Completed	Time (years)	Dam Zoning Class[n]	Core Width / Slope	Core Type	Height, H (m)	Length, L (m)	Ratio L/H	Upstream Slope (H to V)	Downstream Slope (H to V)		
Mud Mountain	USA, Washington	US Corp of Engineers	Igneous and Volcanic - andesite, volcanic breccia, tuff	Rock.	1941, Dec	0.75	5,1,0	c-tm	SM/GM	128	213	1.7	2H to 1V	1.9H to 1V	Medium sized central core with thin filter zones and dumped rockfill shoulders. Outer slopes ranged from 1.75 to 2.25 H to 1V. Constructed in narrow, steep sided gully.	Cary (1958) Cooke & Strassburger (1988)
Naramata	Japan	Water Resources Development Public Corp.	Granite with liparite and dolerite intrusions.	Rock (?)	1987	3 (seasonal)	5,1,0	c-tn	GM/GC	158	520	3.3	2.7H to 1V	2.05H to 1V	Narrow central core supported by compacted rockfill shoulders. Single filter zones up and downstream of core. Relatively flat upstream slope.	Karasawa et al (1994) Okubo et al (1988) Oikawa et al (1997)
Netzahualcoyotl	Mexico	-	Sedimentary - cemented conglomerates and dense sandstones, folded	Core and downstream shoulder on bedrock. Upstream shoulder on dense river alluvium.	1964, Nov	1.5	5,2,0	c-tn	MH	132	480	3.6	2H to 1V	2H to 1V	Thin central core supported bypoorly compacted rockfill shoulders. Upper slopes at 1.75 H to 1V. Dam axis arched to upstream. Built in a valley with narrow river section and moderately steep abutment slopes.	Gamboa & Benassini (1967) Marsal & Alberro (1976) Casales (1976) Wilson (1973)
Nillahcootie	Australia, Victoria	Goulburn Murray Water	granite	Rock	1967, May	-	5,2,0	c-tm	CL	35	791	22.6	1.5H to 1V	1.55H to 1V	Central core supported by poorly compacted rockfill shoulders. Downstream slope is a series of benches at 1.33H to 1V. Upper 9 m of upstream slope at 1.33H to 1V. Cofferdam at upstream toe.	Jacobsen (1965) SMEC (1996a)
Nottely	USA, Tennessee	Tennessee Valley Authority	-	Rock - upstream half of core and rockfill zones. In-situ soils left in place under the downstream section of core.	1942, Jan	0.8 to 1.0	5,1,1	c-tk	CL	56	592	10.6	1.75H to 1V	1.75H to 1V	Broad central clay core (1H to 1V upstream, 1.2H to 1V downstream) with thin filters and dumped and sluiced rockfill shoulders. Outer slopes in series of benches sloped at 1.4H to 1V.	Leonard and Raine (1958) Blee and Meyer (1955)
Parangana	Australia, Tasmania	Hydro Electric Commission	Metamorphic - quartzite and schist. Glaciated valley.	River section and left abutment - core and shoulders mainly on gravels (talus & glacial drift) with cut-off to periglacial deposits. Right abutment on bedrock.	1968, June	1.5	5,2,2	c-tm	SM	53	189	3.6	1.33H to 1V	1.33H to 1V (upper 20m), then 2.5H to 1V	Medium width central core supported by shoulders of compacted rockfill. Weathered rockfill used in downstream shoulder underlain by a filter. Central cut-off (5 to 15m depth) to periglacial deposits. Cofferdam incorporated into the upstream toe.	Mitchell et al (1968) Paterson (1971) Gerke and Hancock (1995)
Peter Faust	Australia, Queensland	QDNR (now Sun Water)	Volcanic (andesitic) and Igneous (Dioritic)	Rock	1990, Oct	-	5,2,0	c-tn	CL	51	530	10.4	1.6H to 1V	1.6H to 1V	Thin central clay core with well compacted rockfill shoulders.	QDPI (1994) QDNR (1998)
Round Butte	USA, Oregon	Portland General Electric Co.	Basalt interbedded with stratified siltsones and sandstones	Core, transitions and downstream rockfill on bedrock. Upstream rockfill on shallow river bed deposits.	1964, July	2	5,2,0	c-tn (u)	SM	134	440	3.3	1.8H to 1V	1.7H to 1V	Thin core aligned very slightly to upstream. Dam axis has upstream curvature. Outer slopes steeper in upper 15 m.	Patrick (1967)
Rowallan	Australia, Tasmania	Hydro Electric Commission	Metamorphic - quartzites and schists. Glaciated valley.	Variable, from bedrock to 40m of fluvio-glacial deposits, due to ridge of bedrock in floor and abutments. Mostly on fluvio glacial gravels.	1967, Jan	2	5,1,0	c-tn	GM	43	579	13.5	1.33H to 1V	1.45H to 1V	Thin central core aligned slightly to upstream (slopes of 0.44H to 1V upstream and vertical downstream) supported by shoulders of compacted rockfill.	Mitchell et al (1968) Mitchell & Fitzpatrick (1979) Forza et al (1993)
Sagae	Japan		Diorite and Granite	Rock	1990	unk	5,2,0	c-tn	-	112	510	4.6	2.6H to 1V	2.3H to1V	Narrow central core (0.15H to 1V up and downstream) with dual filters up and downstream. Relatively flat upstream and downstream slopes.	Sakamoto et al (1994) Nose (1982)
Seto	Japan	-	-	Rock	1977	unk	5,1,0	c-tn	-	102	343	3.4	2.5H to 1V	2H to 1V	Narrow central core aligned slightly to upstream with single filter zones up and downstream of the core. Relatively flat upstream slope.	Kisa & Fukuroi (1994)
Shimokotori	Japan	Kansai Electric Power Co.	-	Rock	1972	unk	5,1,0	c-tn	-	119	289	2.4	2.4H to 1V	1.85H to 1V	Narrow central core with single filter up and downstream. Relatively flat upstream slope.	Kisa & Fukuroi (1994) Matsui (1976)

Table F1.1: Central core earth and rockfill embankments case study information (Sheet 17 of 30)

Name	MATERIALS														
	Earthfill Core							Filters / Transition Zone							
	Zone	Source	ASCS Class[n]	Density Ratio or Dry Density (t/m^3)	Placement Methods	Moisture Content	Comment	Zone	Source	ASCS Class[n]	Relative Density or Dry Density (t/m^3)	Layer Thickness (mm)	Plant	Level of Compaction	Comment
Mud Mountain	1	-	SM/GM	-	Well compacted - 150 mm layers, sheepsfoot rollers	-	Silty sandy gravels, max. size 150 mm, 20% fines.	2 (filter)	diorite, crushed	Gravelly (?) - max. size 100 mm.	-	300	compacted by caterpillar tractor	reasonable to good	Thin filter zone used up and downstream of the central core.
Naramata	1	breccia	GM/GC (?)	101% SMDD 2.02 t/m^3	Well compacted - 300 mm layers, 8p 18t vibrating tamping rollers	0.8% dry of OMC (9.6%)	Well compacted core of processed rockfill.	2A (filter)	weathered rhyolite and HW granite	-	2.12 t/m^3	300	4p 16t vibrating rollers	Good	Well compacted filter zone of high moduli, used up and downstream of the central core. Width approx. 10 - 13 m upstream and 12 increasing to 25m downstream.
Netzahualcoyotl	1	residual soil (weathered conglomerate)	MH - sandy silts/clays of high plasticity	92.5 - 94.5% SMDD 1.6 - 1.7 t/m^3	Reasonably to well compacted - 200 mm (loose) layers, 6p 3.5t SDVR	7 to 8% wet of OMC	High plasticity sandy silts/clays placed well wet of OMC. Of stiff strength consistency (S_u ~ 50 kPa).	2A & 2B (filter / transition)	river alluvium (2A), & rockfill (2B)	SP (2A) GW/GP (2B)	-	250 (2A) to 500 (2B)	4p 3.5t SDVR, wetted. 2B also used as haulage path.	Good	Well-compacted filters. Fines content < 2 to 3%. Dual filter used downstream of the core and single filter (Zone 2B) used upstream of the core. Width increasing with depth, up to 10 to 14 m at the base.
Nillahcootie	1	alluvial / colluvial	CL - silty and sandy clays	100% SMDD 1.85 t/m^3	Reasonably to well compacted (?)	~0.3% dry OMC	Silty and sandy clays. Suspect reasonably to well compacted (practice at the time).	2A, 2B, 3B (filters / transition)	washed sand & gravel (2A) and crushed rock (2B)	GP/GW (2A)	-	450 (2A) 900 (2B)	compacted	-	Suspect reasonably to well compacted. Single filters zones up and downstream of the core. Zone 3B is a "compacted" rockfill transition zone.
Nottely	1	-	CL - sandy clays	-	Well compacted (?) - 150 to 200 mm layers, sheepsfoot rollers	placed at close to OMC	Sandy clays. Foundation filter used under downstream 1/3 of core along the full embankment length.	2A & 2B (filters)	quarried rock ?	-	-	-	-	-	limited information. Dual filters used upstream and single filter used downstream of core. Filter extended under the downstream third of the core.
Parangana	1B & 1A	1B - decomposed granodiorite 1A - doleritic clay (debris)	1B - SM, silty sand (24% fines) 1A - CL, sandy gravelly clay	Spec. > 98% SMDD	Well compacted - 225 mm (loose) layers, 36t rubber tyred rollers	Spec. 1B - 1% dry to 1% wet of OMC; 1A - 1.5% dry to 1.5% wet.	Zone 1B used as main core material - silty sand with low plasticity fines. Zone 1A used in cut-off trench - medium to high plasticity clay.	2A & 2B (filters)	crushed dolerite river gravels	2A - GP 2B - GW	-	450 to 900	10t SDVR 450mm layers - 2p 900mm layers - 4p	reasonable to good	Single filter used upstream of central core (2.5 to 6m wide) and dual filter used downstream of core (7 to 10m width) and on the foundation of the downstream shoulder.
Peter Faust	1	alluvium	CL - sandy clays	Spec > 97% SMDD	Well compacted - 150 mm layers, pad foot rollers	Spec. 1% dry to 1% wet of OMC	Gravelly sandy clays of medium plasticity.	2A, 2B & 2C (filters)	alluvial sands & gravels, & crushed rock (2C)	SP/SW (2A&2B) GP (2C)	D_R = 60 to 70%	375	1p 10t SDVR (2A & 2B) 2p 10t SDVR (2C) moisture conditioned	Good	Dual filters / transitions up and downstream of the core.
Round Butte	1	alluvium	SM -silty gravelly sands	-	Well compacted - 305 mm layers, 45t pneumatic roller	-	Silty gravelly sands / sandy gravels. Average 30% non-plastic fines.	2A, 2B, 2C (filters)	processed sands and crushed rock	-	-	305	9t SDVR, no moisture conditioning	Good	Triple filter / transition zone used up and downstream of the core, of moderately thin width.
Rowallan	1	glacial till (doloritic)	GM - silty sandy gravel	Spec. > 98% SMDD 2.32 t/m^3	Well compacted - 450 mm layers, 8-12p 10t SDVR	Spec. OMC to 3% wet of OMC	Silty sandy gravels (23% fines, 62% gravel) with low plasticity fines. Contact zone with foundation is a high plasticity sandy clay.	2 & 2A (filters)	2 - fine rockfill 2A - fluvio-glacial gravels	2A - GW (< 5% fines, max. size 300mm)	2A - 2.0 t/m^3	2A - 450 2 - 1350 (?)	2p 10t SDVR	reasonable (2) and good (2A)	Single filter used upstream (Zone 2) and downstream (Zone 2A) of central core. Downstream filter of 2m minimum width.
Sagae	1	-	-	-	no information	-	No information. Suspect well compacted given typical practices used in Japan at this time.	2 (filter)	-	-	-	-	-	-	No information. Suspect well compacted. Dual filters used up and downstream of the core.
Seto	1	-	unk	-	no information	-	No information. Suspect well compacted given typical practices used in Japan at this time.	2 (filter)	-	-	-	-	-	-	No information. Suspect well compacted given typical practices used in Japan at this time. Filters up and downstream of the core.
Shimokotori	1	-	unk	-	no information	-	No information. Suspect well compacted given typical practices used in Japan at this time.	2 (filter)	-	-	-	-	-	-	No information. Suspect well compacted given typical practices used in Japan at this time.

Table F1.1: Central core earth and rockfill embankments case study information (Sheet 18 of 30)

Name	MATERIALS																	
	Rockfill Zone									Rockfill Zone (in some cases earthfill stabilising berm)								
	Zone	Source	Grading Description	Clean / Dirty	Dry Density (t/m^3)	Layer Thickness (m)	Placement Method	Level of Comp-action	Comment	Zone	Source	Grading Description	Clean / Dirty	Dry Density (t/m^3)	Layer Thickness (m)	Placement Method	Level of Comp-action	Comments
Mud Mountain	3	Andesite and tuff	Coarse, max 1.2m 45 - 55% < 550 mm	clean ?	-	1.2	dumped and sluiced, 100 to 150% by volume water to rock	poor	Very high strength rock.	-	-	-	-	-	-	-	-	-
Naramata	3A & 3B	rhyolite and granite	-	-	2.05 t/m^3	1.0	4p 16t SDVR	Good	Well-compacted rockfill. Karasawa et al (1994) indicate moduli is high for rockfill, 190 MPa.	-	-	-	-	-	-	-	-	-
Netzahualcoyotl	3	conglomerate, low strength	max = 100 mm 55% < 19 mm 4% fines	dirty	-	0.5 to 1.0	Spread by D8 and trafficked. Water addition specified and heavy rains during construction.	poor to reasonable.	Low strength conglomerate used as rockfill.	-	-	-	-	-	-	-	-	-
Nillahcootie	3A	metamorphosed sandstone and mudstone	-	-	-	-	dumped ?, no indication of lift thickness or if water added during placement.	poor (?)	No information on placement methods, suspect placed without formal compaction.	-	-	-	-	-	-	-	-	-
Nottely	3	quartzite with 20% mica schist	-	-	-	9.1	dumped and sluiced	poor	Rock described as "sound, durable rock of 'good' compressive strength".	-	-	-	-	-	-	-	-	-
Parangana	3A	quartzite, sound	max size ~0.9m <20% < 12.5mm	clean ?	-	1.35	4p 10t SDVR, no water addition required in specification.	reasonable to good	Quartzite described as 'extremely hard'. Zone 3A used in upstream shoulder as well as on the outer downstream shoulder.	3B	schist (HW to MW), and gravelly talus	high degree of variability max ~ 900 mm 0 to 90% < 19mm < 5% fines.	dirty	-	0.9	4p 10t SDVR, no water addition required in specification.	reasonable to good	Zone 3B used in downstream shoulder. Lesser quality rockfill than Zone 3A.
Peter Faust	3	hornfelsed andesite & andesitic tuff	-	clean ?	-	1.5 (0.75 within 3 m of filter)	6p 10t SDVR, 20% by volume water added.	reasonable to good	Rock of very high UCS. Well compacted.	-	-	-	-	-	-	-	-	-
Round Butte	3	basalt	-	-	-	0.61	4p 9t SDVR, no water added	good	Suspect relatively small sized rockfill given placed in 0.6 m lifts. Dry placed.	-	-	-	-	-	-	-	-	-
Rowallan	3A	quartzite, sound	max size 915mm <25% pass 20mm very low fines content	clean	1.93 to 2.08 t/m^3	1.35	4p 10t SDVR, no water addition required in specification.	reasonable to good	Zone 3A used in up and downstream shoulder. Grading, and relative density variation between lower and upper halves of layer.	-	-	-	-	-	-	-	-	-
Sagae	3	-	-	-	-	-	-	-	No information. Suspect well compacted given typical practices used in Japan at this time.	-	-	-	-	-	-	-	-	-
Seto	3	-	-	-	-	-	-	-	No information. Suspect well compacted given typical practices used in Japan at this time.	-	-	-	-	-	-	-	-	-
Shimokotori	3	-	-	-	-	-	-	-	No information. Suspect well compacted given typical practices used in Japan at this time.	-	-	-	-	-	-	-	-	-

Table F1.1: Central core earth and rockfill embankments case study information (Sheet 19 of 30)

Name	HYDROGEOLOGY						MONITORING - DURING CONSTRUCTION						
	First Filling		Reservoir Operation		Pore Pressures in Core	Rainfall (Average mm/year)	Core				Rockfill and/or Filters	Comment	Other Types of Internal Monitoring Equipment
	Timing (from end of embankment construction)	Comments	Steady / Fluctuating	Comment			Instrument Type/No.	Settlement		Comment			
								mm	% of H				
Mud Mountain	0 to >17 years	By 1958 had not yet reached FSL, still 30 m below FSL.	Fluctuating	Annual drawdown, 20 to 35 m in first two drawdowns.	-	precipitation mostly as snow.	-	-	-	-	-	-	-
Naramata	1 to 1.75 years (not sure of timing)	Started Oct 1988 and reached FSL in May 1989, but not sure of timing with respect to end of construction.	-	not known	-	heavy snow falls	IVM	2920	1.85%	Small strains for dam of this height, 0 to 0.5% near crest increasing to 2 to 2.5% near base.	-	Likely high moduli of dry, well compacted core.	-
Netzahualcoyotl	1.5 to > 4.8 years	Started late May 1966. Within 15 m of FSL in Jan 1967. Upstream rockfill flooded during construction when reservoir level rose above the crest of the cofferdam in Sept 63.	-	-	During construction - high PWP in core. r_u approx 0.45 based on estimated superimposed load, but will be higher when arching effects are considered.	2500	IVM	2970	2.72%	normal, vertical strain increasing with depth. Up to 1.5% in upper 20 m increasing to 4% at 90 m deth below crest.	IVM in rockfill. Vertical strains in rockfill greater magnitude than in the core at similar depths.	-	-
Nillahcootie	0 to 1.3 years, possibly less.	At FSL in August 1968 (1.3 years), which was start of records.	Fluctuating	Annual drawdown, typically between 4 and 8 m. Larger drawdowns in 1983 (10 m), and in 1991 (11.5 m).	-	985	-	-	-	-	-	-	-
Nottely	0 to 0.6 years	Jan 1942 to July 1942 (vitually at FSL).	Fluctuating	Annual drawdown. Lowest level is virtually empty.	-	-	-	-	-	-	-	No monitoring during construction	-
Parangana	0.6 to 0.74 years	First filling from Jan to Feb 1969	Steady	Generally remains close to FSL. One drawdown event in late 1969 of 26m.	-	1250	IVM, 4 (all close to centreline)	351mm (H=36.5m) to 733mm (H=52m)	0.96% to 1.41% (greater strains for increasing height)	Vertical strains of 0 to 1% in the upper 10 to 20m increasing to 2.5 to 3.5% at about 40 to 50m depth. Some variability.	-	-	-
Peter Faust	-0.85 to 0.42 years	Stored water during construction to within 22 m of FSL. Filled very quickly in mid to late Dec 1990.	Fluctuating (slow)	Slow reduction in reservoir level since reached FSL (10 m in 6 years).	During construction - high PWP in the contact zone, otherwise limited to negligible positive PWP (r_u approx 0 to 0.1).	-	-	-	-	-	-	-	-
Round Butte	-0.6 to 0.6 (Jan 1964 to Jan 1965)	Filling started before end of construction. Within 20 m of FSL at EOC.	Steady	Relatively steady once first filling completed	-	-	-	-	-	-	-	Monitoring of SMPs on slopes started before EOC.	-
Rowallan	0.38 to 0.7 years	First filling from April to Oct 1967	Fluctuating	Not an annual drawdown, but drawdowns are relatively rapid and typically range from 8 to 30m, largest in 1979 of 36 to 38m.	-	1780	-	-	-	-	-	-	-
Sagae	-	not known	-	not known	-	4000 (mostly as snowfall)	IVM	2430	2.2 (1.0 to 5.4%)	Increasing strain with depth. Considered normal.	-	-	-
Seto	0 to 0.45 years	-	Fluctuating	rapid daily drawdowns up to 34 m.	-	-	-	-	-	-	-	-	-
Shimokotori	0 to 1.25 years	-	Fluctuating	large annual drawdown of 30 to 40 m.	-	-	IVM	3850	3.25 (2 to 4.8%)	-	-	-	-

Table F1.1: Central core earth and rockfill embankments case study information (Sheet 20 of 30)

Name	SURFACE MONITORING - POST CONSTRUCTION										
	Time of Initial Readings (years after EOC)	Crest			Upstream Slope		Downstream Slope		Comments	Comments on Deformation and Observations.	Comments
		Settlement (mm)	S_{LT} (% per log cycle of time)	Displacement (mm)	Settlement (mm)	Displace-ment (mm)	Settlement (mm)	Displace-ment (mm)			
Mud Mountain	0	823 mm or 0.66% (8.5 yrs)	-	274 mm (8.5 yrs)	-	-	-	-	Significantly greater magnitude settlement of the rockfill shoulders (both up and downstream) than the crest above the core, approx. 450 mm greater.	Differential settlement between core and rockfill resulted in cracking along junction of the core and transition on both upstream and downstream sides. No measurable differential settlement since 1948.	Main embankment constructed from March to December 1941. Outlet works not completed until 1948 due to war interruption. Likely collapse settlement of dumped and sluiced rockfill shoulders.
Naramata	not known	-	-	177 mm (on first filling)	-	-	-	-	Only information is 177mm downstream displacement of crest on first filling. Most of displacement occurs when reservoir level above 85% of FSL.	-	Only have deformation during construction. IVM indicates vertical deformation of core is normal.
Netzahualcoyotl	0.08 (crest) 0.2 (d/stream) 0.36 (upstream)	596 mm or 0.45% (5.6 yrs), I3 (u/str edge) = 760mm or 0.70% (2.75 yrs)	0.23	-	471 mm or 0.41% (5.6 yrs)	-	303mm or 0.24% (5.6 yrs)	73 mm (2.2 years)	Large magnitude settlement of the crest and upstream slope prior to and on FF. The IVM at the crest indicates a large vertical differential at the upstream core/filter interface of 300 mm (greater shoulder settlement), and is reflected in the SMP data. The crest initially displaced upstream in the early to mid stages of FF then to downstream in the later stages when within 15m of FSL (similar pattern for the upper downstream shoulder).	Consider as 'normal' deformation behaviour. IVMs indicate shear type deformation at the upstream interface between the filter and core. No observation of crest cracking reported. It was likely that some collapse settlement of the upstream rockfill occurred during FF.	Consider as case of 'normal' deformation. IVM data indicate shear deformation at the upstream core / filter interface during first filling.
Nillahcootie	1.3 years.	66 mm or 0.19% (16 years)	0.21	34 mm (16 years)	171 mm or 0.50% (31 years)	-42 mm (31 years)	103 mm or 0.39% (31 years)	104 mm (31 years)	1.3 year delay to monitoring, which missed the period of FF. Displacements indicate post FF crest spreading (~ 120 mm), with upstream slope moving upstream. Acceleration in settlement and non-recoverable upstream displacement of the upper upstream shoulder on large drawdown.	Likely that rockfill was susceptible to collapse compression on wetting, which is likely to have affect the lateral support afforded to the central core. Potentially 'abnormal' behaviour on drawdowns of more than 9 m.	Potentially 'abnormal' behaviour on drawdowns of more than 9 m.
Nottely	0.33 (4 month after EOC)	310 mm or 0.56% (10.3 years)	0.47	62 mm (3 years)	-	-	-	-	SMPs in centre of crest. Up to 1955 (13 years after EOC) the upstream edge of the crest had settlement more than 250 mm more than the centre of the crest. Increase in settlement rate (rate in terms of log time) from 5 years after EOC. Crest displaced downstream on first filling.	Up to 1955, "severe" longitudinal cracking on crest coincident with the upstream edge of core. In 1955 longitudinal cracking more toward the centre of the crest. Initial cracking probably attributable to collapse settlement on wetting of the dumped and sluiced upstream rockfill. The increased settlement rate may be related to softening and cracking of the core due to poor lateral support from the rockfill.	Suspect deformation behaviour of upstream crest and shoulder is potentially "abnormal". The embankment is subject to very large drawdowns.
Parangana	0 yrs (sett) 0.5 yrs (displ)	111mm or 0.21% (26.5 yrs)	0.05	32mm (26.5 yrs)	-	-	-	-	SMPs only on the crest of the embankment. Magnitude of settlement is small and the long-term rate low. Acceleration of settlement rate during large drawdown in late 1969. Crest displacement is downstream on FF (very low rate long-term).	Surveillance review in 1995 commented that the embankment was in a satisfactory condition. Deformation is considered as 'normal'. On the large drawdown in 1969 the crest settled 15 to 20 mm.	Reservoir level is steady at close to FSL. The embankment has a relatively steep mid to upper upstream slope.
Peter Faust	0.34 years (close to FSL when started)	51 mm or 0.10 % (6.5 yrs)	0.12	-9 mm (6.5 yrs)	-	-	18 mm or 0.05 % (6.5 yrs)	2 mm (6.5 yrs)	Small post construction deformations. Deformation monitoring virtually missed first filling. Displacements less than 10 mm in 6.5 years. Low long-term settlement rate.	Consider deformation behaviour as 'normal'. Delay of 0.34 years before the start of monitoring, during which time first filling virtually completed.	Consider as 'normal' deformation. Post construction deformations of small magnitude.
Round Butte	0 for settlements 0.32 for displ of u/str crest	161 mm or 0.12% (1.3 yrs)	0.075	569 mm (1.3 yrs)	-	-	331 mm or 0.33% (1.3 yrs)	367 mm (1.3 yrs)	Greater settlement of rockfill shoulders than core. Crest spreading occurred on FF (> 130 mm). Large downstream displacement of crest during the latter stages of FF.	Longitudinal cracking on the crest observed as reservoir level approached FSL, gradually widened to 15 mm (filled by sluicing sand into crack). Crack located in area of transition on the downstream side of the core. Suspected differential settlement and cracking at upstream core interface.	Collapse settlement of upstream rockfill on first filling due to dry placement (even though reasonably to well compacted) contributed to the differential settlement and cracking. Tailwater impounds the lower part of downstream slope.
Rowallan	0.22 yrs	107mm or 0.27% (23 yrs)	0.095	60mm (23 yrs)	-	-	-	-	Data for SMPs on crest only. Settlements show small magnitude and low long-term rate. Crest displacement at main section is downstream on FF, with continued downstream trend post FF at a gradually reducing rate.	Surveillance review in 1995 commented that the embankment was in a satisfactory condition. Deformation behaviour is considered as 'normal'.	Consider deformation behaviour as 'normal'. Piping incident occurred shortly after first filling in 1968.
Sagae	-	-	-	-	-	-	-	-	No post construction deformation data.	Only have IVM data during construction. Deformation profile considered normal.	Dam used for flood control, municipal water supply and power generation. Only has internal settlement records for the core during construction.
Seto	no information, suspect close to EOC	359 mm or 0.35% (9 years)	0.22	201 mm (9 years)	-	-	-	-	Relatively large settlement on and shortly after FF (150 mm). Downstream displacement on FF of 120 mm, occurred when reservoir raised above 80% of embankment height.	Limited information. Settlement and displacement behaviour considered "normal" .	Constructed in narrow river gully with 39 degree abutment slopes. Deformation behaviour considered normal.
Shimokotori	no information, suspect close to EOC	542 mm or 0.46% (13 years)	0.25	139 mm (13 years)	-	-	-	-	Relatively large settlement on FF (300 mm), most of this occurred in the upper 40 m (from IVM). Downstream displacement on FF of 95mm occurred when reservoir raised above 80 to 85% of embankment height.	Acceleration in crest settlement on first 3 drawdowns and on several later drawdowns. Magnitude of settlement on drawdown of 10 to 50 mm. Possible plastic deformation of the core on large drawdowns, possibly within the upper 40m.	Constructed in narrow river gully with steep (40 to 47 degree) abutment slopes. Possibly "abnormal" deformation post construction given continued acceleration in crest settlement on drawdown.

Table F1.1: Central core earth and rockfill embankments case study information (Sheet 21 of 30)

Name	GENERAL DETAILS				CONSTRUCTION / DESIGN											References
					Construction Timing		Embankment Classification			Dimensions						
	Location	Owner/ Authority	Geology	Foundation	Year Completed	Time (years)	Dam Zoning Class[n]	Core Width / Slope	Core Type	Height, H (m)	Length, L (m)	Ratio L/H	Upstream Slope (H to V)	Downstream Slope (H to V)	Comments on Design	
Split Yard Creek	Australia, Queensland	QDNR (now Sun Water)	Interbedded quartzites & metavolcanics	Rock	1980, Feb	2	5,2,1	c-tm	CL	76	1141	15.0	1.75H to 1V	1.8H to 1V	Central clay core supported by well-compacted rockfill shoulders. Large step in upstream slope at about mid-height. Zone of weathered rockfill used in the lower downstream shoulder.	QWRC (1987, 19XXb) Rogers & Pearce (1991) QDPI (1995, 1996)
South Holson	USA, Tennessee	Tennessee Valley Authority	Sedimentary - shale and sandstone	Rock	1950, Oct	2 (seasonal)	5,2,1	c-tk	CL	87	487	5.6	1.9H to 1V	1.8H to 1V	Broad central clay core (0.75H to 1V up and downstream) with thin filters and dumped and sluiced rockfill shoulders.	Leonard and Raine (1958) Blee and Meyer (1955)
Srinagarind	Thailand	-	Sedimentary - limestone, sandstones, quartzites, shales	Core and filters on sound rock. Shoulders on at least weathered rock.	1978, May	2.3	5,2,0	c-tn	GC/SC	140	610	4.4	2H to 1V	1.9H to 1V	Narrow central core with broad transition zones (up to 28 m wide) and compacted limestone rockfill shoulders.	Champa & Mahatharadol (1982)
Svartevann	Norway	-	Granitic gneiss	Rock	1976, Oct	3 (seasonal)	5,2,0	c-tn (u)	GM	129	420	3.3	1.6H to 1V	1.43H to 1V	Very narrow central core, slightly upstream sloping with dual filters up and downstream. Embankment has a slight arch to upstream. Downstream slope is series of benches at 1.35H to 1V.	Kjaernsli et al (1982) Dibiagio et al (1982)
Taisetsu	Japan, Hokkaido	-	Metamorphic - clay slate	Rock	1975, Oct	7.5	5,1,0	c-tn	-	86.5	440	5.1	2.65H to 1V	2H to 1V	Narrow central core with single filter up and downstream. Relatively flat upstream slope.	JNCOLD (1976) Sakamoto et al (1994)
Talbingo	Australia, New South Wales	SMHEA	Volcanics - rhyolite lavas	Rock	1970, Oct	2.1	5,2,0	c-tm (u)	CL	162	701	4.3	2H to 1V	2H to 1V	Central clay core with slight upstream slope (0.9H to 1V up and -0.2H to 1V downstream) supported by compacted rockfill shoulders. Moisture of core material adjusted due to high pore pressures observed in early stages of construction.	Howard et al (1978) SMHEA (1998c)
Tedorigawa	Japan, Honshu Island	Electric Power Development Corporation	Gneiss and conglomerate with numerous porphyritic dyke intrusions.	Rock	1978, Nov	1.5 (seasonal)	5,2,0	c-tn	GM/GC	153	420	2.7	2.6H to 1V	1.85H to 1V	Central narrow core supported by broad filter/transition zones and compacted rockfill shoulders. Cofferdam at upstream toe. Upstream slope is relatively flat.	JNCOLD (1976) Kawashima & Kanazawa (1982) Sakamoto et al (1994) Nakagawa et al (1985)
Terauchi	Japan, Fukuada	-	Sedimentary (argillaceous) and metamorphic (schist)	Rock - of lesser quality under rockfill shoulders than core.	1977, Feb	4.25	5,2,0	c-tm	SC/SM	83	420	5.1	2.7H to 1V	2.1H to 1V	Medium width core aligned slightly to upstream. Dual filters up and downstream of the core. Relatively flat slopes.	Kanabayashi et al (1979)
Thomson	Australia, Victoria	Melbourne Water Corp.	Sedimentary - sandstone & siltstone.	Rock	1983, July	2.5	5,2,0	c-tm	SC	166	590	3.6	1.65H to 1V	1.75H to 1V	Central core (slopes of 0.3H to 1V up and 0.2H to 1V downstream) supported by compacted rockfill shoulders. Fill berm at upstream toe of right abutment.	SMEC (unpublished) MMBW (1987b) Connell Wagner (1998c)
Tokachi	Japan, Hokkaido	-	Sedimentary, some metamorphism - keratophyre, clay slate, sandstone	Rock ?	1983, August	4	5,1,0	c-tm	GC	84.3	406	4.8	2.6H to 1V	2H to 1V	Thin central core with narrow, single filter zone (6 m wide) up and downstream. Relatively flat slopes.	Shiraiwa & Takahashi (1985) Sakamoto et al (1994)
Upper Dam	Korea	-	Volcanics - tuff and rhyolite ashy tuff	Bedrock ?	1984, Sept	1.5	5,2,0	c-tn	GC	88.5	269	3.0	2.1H to 1V	1.8H to 1V	Narrow central core with dual filter / transition zones up and downstream and rockfill shoulders. No indication of degree of compaction of rockfill. Cofferdam incorporated into the upstream toe of the embankment.	Hong et al (1994)

Table F1.1: Central core earth and rockfill embankments case study information (Sheet 22 of 30)

Name	MATERIALS														
	Earthfill Core							Filters / Transition Zone							
	Zone	Source	ASCS Class[n]	Density Ratio or Dry Density (t/m^3)	Placement Methods	Moisture Content	Comment	Zone	Source	ASCS Class[n]	Relative Density or Dry Density (t/m^3)	Layer Thickness (mm)	Plant	Level of Compaction	Comment
Split Yard Creek	1	alluvial	CL, CL-SC - sandy clays to clayey sands	1.6 to 1.82 t/m^3 (Spec > 98% SMDD)	Well compacted (?) - 150 to 200 mm layers, padfoot rollers (Cat 815 & 825)	(Spec. 1% dry to 1% wet of OMC)	Sandy clay to clayey sands of medium plasticity, well-compacted. 0.6 m thick contact zone of wet placed medium to high plasticity clays.	2A & 2B (filters)	alluvial	2A < 8% fines	(Spec > 70% D_R)	300	2p 10t SDVR, watered prior to rolling	Good	Limited information. Dual filters downstream of core (width = 4.75 m), single filter upstream (Zone 2B). Zone 2B filter under the downstream shoulder.
South Holson	1	-	CL	-	Well compacted (?) - 150 to 200 mm layers, sheepsfoot rollers	possibly close to or wet of OMC	Sandy or silty clays of medium plasticity. Upper 3 m compacted by trucks and tractor.	2A & 2B (filters)	quarried rock ?	-	-	-	-	-	limited information. Dual filters of thin width (6.1 m wide) up and downstream of the core.
Srinagarind	1	colluvial, lateritic	GC/SC, but variable	100% SMDD 1.85 t/m^3	Well compacted - 400 mm (loose) layers, 4p SDVR	0.2% wet of OMC	Mainly clayey sandy gravels, with 26 to 42% medium plasticity fines (max. size 150 mm).	2A & 2B (filter / transition)	limestone (2A) & quartzite (2B)	GW	2.1 - 2.2 t/m^3 (Spec > 70% D_R)	400	3p SDVR (2A), 4p SDVR (2B)	Good	Well compacted filter / transition zones. Dual system used up and downstream of core and of moderate combined width. Fines content < 7%.
Svartevann	1	morraine	GM - silty sandy gravel, 20% fines	100.4% SMDD 2.15 t/m^3	Well compacted - 500 mm layers, 8p 8-10t SDVR	0.4% wet of OMC	Well compacted silty sandy gravel, max. size 170 mm.	2A & 2B (filters)	fluvial gravels (2A) & crushed rock (2B)	GW/GP	-	500 (2A) and 1000 (2B)	2p 8t SDVR (2A), 4p 13t SDVR (2B). Wetted prior to compaction.	Good	Well compacted filters of moderate width (8 to 13 m wide) up and downstream of the core. Fines content < 5%.
Taisetsu	1	-	unk	-	no information	-	No information. Suspect well compacted given typical practices used in Japan at this time.	2 (filter)	-	unk	-	-	-	-	No information. Suspect well compacted given typical practices used in Japan at this time.
Talbingo	1	CW to HW andesitic basalt, colluvium	CL (some CH, SC & GC) - mainly gravelly clays	101.6% SMDD 1.84 t/m^3	Well compacted - 150 mm layers, sheepsfoot rollers	Overall average is at OMC. Lower region wet of OMC, and upper region slightly dry of OMC.	Gravelly clays to clayey gravels of medium plasticity. Fines content 18 to 70%. Contact CL/CH clay placed slightly wet of OMC.	2A & 2B (filter / transition)	crushed rock, fresh	2A - SW/GW 2B - GW/GP	-	450	4p 10t SDVR. Zone 2B was sluiced.	Good	Zone 2A was of narrow width and placed only downstream of core. Broad Zone 2B transition up and downstream of the core; narrow width at crest increasing to ~ 60 m (d/str) and 30 m (upstr) at the base.
Tedorigawa	1	blended and processed talus or rock	GM/GC (max 150 mm)	1.9 t/m^3	Well compacted (?) - heavy rollers	Slightly wet of OMC	Limited information, but typical practice is for heavy rolling of materials processed or blended from talus and weathered rock.	2A & 2B (filters)	from crushed rock (?)	unk	2.04 t/m^3	-	-	-	Limited information, but suspect well compacted. Dual filters up and downstream of central core. Increasing width with depth, up to 60m wide at the base.
Terauchi	1	residual soil & weathered schist	SC/SM - gravelly silty sands	-	Well compacted - 200 mm layers, 12p Cat 825B pad foot roller	Spec. OMC to 2% wet of OMC	Well compacted gravelly silty sand core, 20 to 33% fines.	2A & 2B (filters)	-	GP/GW - gravels and cobbles	2.15 t/m^3	-	-	-	limited information, suspect well compacted. Slightly sandy gravels and cobbles.
Thomson	1	residual granite	SC - clayey sands, 44% avg fines content	99.9% SMDD 1.79 t/m^3	Well compacted - 150 mm layers, 12p 19t sheepsfoot rollers	2% wet of OMC	Clayey sands with fines of medium plasticity. Fines content = 44% and clay fraction = 15%. High pore pressures due to wet placement.	2A & 2B (filters)	sandstone, indurated	-	-	500	1p 10t SDVR, without vibration	reasonable	Light compaction to reduce potential acrhing effects in core. Estimated width of 6m downstream of core (2A and 2B combined) and 3m upstream (2A).
Tokachi	1	weathered clay slate and colluvium	GC - clayey sandy gravel (15% fines)	> 95% SMDD 2.07 t/m^3	Well compacted - 200 mm layers, 8p 33t compacting dozer (?)	Spec. 1% dry to 1% wet of OMC	Clayey sandy gravel core, max. size 50 mm. Blended mixture to control fines content.	2 (filter)	river alluvium	GP (slightly sandy gravel)	2.13 t/m^3 (n = 21%, e = 0.27)	400	-	-	limited information. Max size = 200 mm. 6.5% moisture content at placement. Suspect well compacted.
Upper Dam	1	colluvium and alluvium	GC - clayey sandy gravels, max size 150mm (well graded)	1.72 t/m^3	no information	17.3%	Limited information on materials and placement methods of the core.	2A & 2B (filters)	river alluvium	2A - SC (fine sand and clay ?) 2B - coarse sand	1.9 t/m^3	-	-	-	No information on placement methods of filters.

Table F1.1: Central core earth and rockfill embankments case study information (Sheet 23 of 30)

Name	MATERIALS																	
	Rockfill Zone									Rockfill Zone (in some cases earthfill stabilising berm)								
	Zone	Source	Grading Description	Clean / Dirty	Dry Density (t/m^3)	Layer Thickness (m)	Placement Method	Level of Comp-action	Comment	Zone	Source	Grading Description	Clean / Dirty	Dry Density (t/m^3)	Layer Thickness (m)	Placement Method	Level of Comp-action	Comments
Split Yard Creek	3A & 3B	brecciated quartzites and greenstone	max 1.0 m <19 mm = <15% (3A) & <30% (3B)	-	-	1.5 to 3.0	spread by dozer, 5p 10t SDVR, 5% by volume water added	reasonable	Rock of high to very high UCS. Zone 3A (fresh rock) used in upper region of the upstream shoulder, Zone 3B used in lower upstream shoulder and upper downstream shoulder.	3C	brecciated quartzites and greenstone	max 0.5 m <50% pass 9.5mm <10% fines	dirty (broke down on compaction)	1.84 to 2.25 t/m^3	0.75 to 1.5	spread by dozer, 5p 10t SDVR, 5% by volume water added	reasonable	MW to FR rock. Zone 3C used in the lower downstream section. Susceptible to breakdown on placement. Foundation filters used to control downstream seepage.
South Holson	3	sandstone, some shale	-	-	-	9.1	dumped and sluiced	poor	Sound, high to very high strength rock used in downstream shoulder and poorer quality used in upstream shoulder.	-	-	-	-	-	-	-	-	-
Srinagarind	3A & 3B	Limestone - hard and durable	Max 0.7 m (3A), 1.5 m (3B). 5 to 25% < 19 mm	clean ?	(n = 22%)	1.0 (3A), 2.0 (3B)	Spread by D8, then 4p 13.5t SDVR.	3A - good 3B - reasonable	Zone 3B forms the outer 20% of the rockfill zone.	-	-	-	-	-	-	-	-	-
Svartevann	3	granitic gneiss	-	-	-	2.0	8p 13t SDVR, no water added	Reasonable	Rockfill placed without addition of water, only reasonably compacted. No indication of grading.	-	-	-	-	-	-	-	-	-
Taisetsu	3	-	-	-	-	-	-	-	No information. Suspect well compacted given typical practices used in Japan at this time.	-	-	-	-	-	-	-	-	-
Talbingo	3A	rhyolite & porphyry (SW to FR)	-	clean	1.92 t/m^3	0.9	4p 10t SDVR, sluiced.	Good	Good quality rockfill. Zone 3A used as inner rockfill zone on downstream side of core.	3B & 3C	rhyolite & porphyry (3B - MW to FR, 3C - SW to FR)	-	3C - clean? 3B - dirty ?	3B - 2.07 t/m^3 3C - 2.01 t/m^3	3B - 0.9 m 3C - 1.8 m	4p 10t SDVR, Zone 3B was sluiced.	good (3B), reasonable (3C)	Zone 3B of lesser quality than 3A and 3C, possibly 'dirty'. Zone 3B used as outer rockfill in downstream shoulder. Zone 3C used in upstream shoulder.
Tedorigawa	3A & 3B	-	-	-	1.98 t/m^3	-	SDVR	-	Suspect well compacted given typical procedures used in Japan at this time.	-	-	-	-	-	-	-	-	-
Terauchi	3	lutaceous schist	max size 1.5m 2% fines Cu ~ 20	clean	2.1 t/m^3	0.5 to 1.5	4p 22t SDVR	good	Well compacted rockfill. Rock refered to as 'hard'.	-	-	-	-	-	-	-	-	-
Thomson	3A	Sandstone and siltstone, SW to FR	-	clean ?	(bulk density = 2.13 t/m^3)	1.0	4p 10.5t SDVR, no indication if water added.	good	Sandstone rock of very high strength and siltstone of high to very high strength. Zone 3A used in upstream shoulder and most of downstream shoulder.	3C	Sandstone and siltstone, MW to FR	-	dirty	-	1.0	4p 10.5t SDVR, no indication if water added.	reasonable to good	Zone 3C of lesser quality than Zone 3A rockfill. Zone 3C used in outer downstream shoulder.
Tokachi	3	keratophyre (VH strength), 30% slate	max 200 mm 25% < 19 mm Cu ~ 22	clean ?	2.1 t/m^3	1.0	-	-	Suspect well compacted given typical practices used in Japan at this time.	-	-	-	-	-	-	-	-	-
Upper Dam	3A & 3B	tuff and rhyolite	-	-	1.8 t/m^3	-	-	-	No information on placement methods of rockfill. Referred to as free draining.	-	-	-	-	-	-	-	-	-

Table F1.1: Central core earth and rockfill embankments case study information (Sheet 24 of 30)

Name	HYDROGEOLOGY						MONITORING - DURING CONSTRUCTION						
	First Filling		Reservoir Operation		Pore Pressures in Core	Rainfall (Average mm/year)	Core				Rockfill and/or Filters	Comment	Other Types of Internal Monitoring Equipment
	Timing (from end of embankment construction)	Comments	Steady / Fluctuating	Comment			Instrument Type/No.	Settlement		Comment			
								mm	% of H				
Split Yard Creek	3.8 to 5.7 years	Not commenced until July 1983 (3.8 yrs after EOC).	Fluctuating	Rapid daily drawdowns of typically 5 to 10 m. Largest drawdown (1995) of 50 m.	PWP levels in core remain fairly constant. Insufficient time to respond to rapid daily drawdowns.	-	IVM - (ES1 - on upstream side of core)	1320	1.76 (1 to 6%)	Normal vertical strain profile, close to 0% in upper 20 m increasing to 4 to 6% at 50 to 70 m depth.	-	-	3 INs to monitor horizontal movements
South Holson	0 to 1.62 years	Nov 1950 to mid 1952. By June 1951 reached within 9 m of FSL	Fluctuating	annual drawdown of 6 to 27 m (1951 to 1957).	-	-	-	-	-	-	-	No monitoring during construction	-
Srinagarind	-0.55 to > 2.9 years	First filling started prior to end of construction (to within 70 m of FSL before EOC). Not completed by April 1981	-	-	PWP in core during construction, maximum approx 45% of applied load.	-	-	-	-	-	-	-	-
Svartevann	-0.9 to 2.23 years	Late 1975 to end of 1978. Water stored during construction, to within 37 m of FSL at EOC.	Fluctuating	Annual drawdown of 15 to 20 m (?).	No EPWP in core during construction. Post construction - PWP in core fluctuates with reservoir level but at lower and reducing amplitude across the core.	-	-	-	-	-	-	-	-
Taisetsu	-	not known	-	not known	-	-	-	-	-	-	-	-	-
Talbingo	0.6 to 1.3 years	Started in May 1971 and reached FSL by Jan 1972.	steady	Typically within 5 m of FSL.	During construction - PWP in lower, wet placed region of the core were high (r_u up to 0.81), slow dissipation with time.	-	2 (both in core)	2410 (ES 2) & 5202 (ES 1)	2.46% (ES 2) & 3.40% (ES 1)	ES1 at main section (H = 154m), H = 98 m at ES2. Some variability but consider normal. Low strains in lower region possibly due to arching influence.	-	HSGs indicate Zone 2B is of high moduli compared with core and rockfill shoulders (3A to 3C).	HSGs and IHMs in rockfill zones.
Tedorigawa	0.6 to 1.5 years	Started June 1979, reached FSL in March 1980	-	not known	During construction - PWP up to 60 to 70% of applied load. Relatively rapid dissipation during winter shutdown and after construction.	-	HSGs in core	5860	3.96%	Large vertical strains in mid to lower region of core (up to 7 to 8%). Possible plastic deformation of core.	-	-	-
Terauchi	0 to 0.66 years	completed Oct 1977	Fluctuating (?)	Suspect fluctuating, only limited data post first filling showing one 15 m drawdown cycle.	-	-	-	-	-	-	-	-	-
Thomson	0 to 7.3 years	Started July 1983. Reached FSL at start of 1991.	Steady	Steady at FSL from 1991 to 1997 (7 to 14 yrs), then slow drawdown of 27 m from 1997 to mid 1998.	During construction - reasonably high PWP during construction, r_u values up to about 0.5. Dissipated by 1986 (3 years after EOC). During operation piezometers show large drop in PWP across the core.	-	-	-	-	IVMs installed in core but became blocked during construction, and were abandoned.	-	HSGs indicate limited diffferential settlement between the core, filters and rockfill during construction.	HSGs, IHMs and INs - mostly in rockfill, but also filters and core.
Tokachi	-	no information	-	No information	-	1000	-	-	-	-	-	-	-
Upper Dam	0.75 to 1.2 years	Started mid 1985, reached FSL by Nov 1985.	Fluctuating	Rapid daily drawdowns of up to 20m.	During construction - PWP in the core were measured at up to 70% of the applied embankment load. Slow dissipation post construction (still dissipating more than 8 yrs later). Limited response of core to reservoir fluctuation.	-	-	-	-	-	-	-	-

Table F1.1: Central core earth and rockfill embankments case study information (Sheet 25 of 30)

Name	SURFACE MONITORING - POST CONSTRUCTION										Comments
	Time of Initial Readings (years after EOC)	Crest			Upstream Slope		Downstream Slope		Comments	Comments on Deformation and Observations.	
		Settlement (mm)	S_{LT} (% per log cycle of time)	Displacement (mm)	Settlement (mm)	Displace-ment (mm)	Settlement (mm)	Displace-ment (mm)			
Split Yard Creek	0.1 (upstream edge of crest) 3.93 all other SMPs.	329 or 0.44% (19 yrs)	0.10	31 mm (19 yrs)	-	-	68 or 0.12% (19 yrs)	127 mm (19 yrs)	The majority of the post construction settlement and displacement occurred during FF. Very low long-term settlement rate for the crest. IVM indicates uniform post construction settlement profile with depth.	Consider deformation behaviour as "normal".	Embankment used as pumped storage for peak power generation. Subject to rapid daily reservoir fluctuations.
South Holson	0.08 to 0.13	874 or 1.01% (6.6 years)	0.47	-73 (6.6 years)	-	-	-	-	Large magnitude crest settlement on FF then steady long-term rate. Greater settlement of upstream rockfill on FF. Displacement of crest is upstream on FF, then trend is virtually steady (with fluctuations due to reservoir fluctuation).	Longitudinal cracking on crest observed due to greater magnitude of settlement of upstream rockfill than core, most likely due to collapse settlement of poor quality, dumped and sluiced rockfill. Acceleration in crest settlement on draw-down at 3 and 4 yrs, but not on large drawdown at 5 yrs.	Upstream crest displacement on first filling is unusual and potentially "abnormal". Accelerations of crest settlementon large drawdown in first four years, but not observed after this.
Srinagarind	0.04	857 mm or 0.61% (2.9 yrs)	-	-	-	-	800 mm or 0.8% (2.5 yrs)	-	Limited data records. First filling not complete in mid 1981. Crest settlement shows acceleration on rising reservoir level. Large settlement of downstream shoulder.	Limited information. Not sure of the reason for the large magnitude settlement of the downstream shoulder, maybe it is due to collapse compression in the outer reasonably compacted rockfill zone.	First filling not completed within period of collected records, still more than 20 m below FSL. The upstream rockfill zone between the cofferdam (crest 70 m below main dam crest) and main dam core was flooded prior to the end of construction to reduce the deformation on first filling.
Svartevann	0	799 mm or 0.62% (4 yrs)	0.87	1200 mm (4 yrs)	-	-	961 mm or 1.01% (4 yrs)	901 mm (4 years)	Large downstream displacement and settlement of crest and upper slopes during latter stages of first filling (from 1.8 to 2.2 years). Long-term crest settlement rate is also high.	Large downstream displacement likely to be associated with collapse compression in the downstream shoulder (post construction strains in the shoulder are high). Consider deformation behaviour as potentially "abnormal".	Stored water prior to end of construction, to within 40 m of FSL, but not likely to have greatly affected the post-construction deformation behaviour. Consider deformation behaviour as potentially 'abnormal' on first filling.
Taisetsu	no indication, suspect close to EOC	331 mm or 0.38% (13.6 years)	0.22	-	-	-	-	-	Several periods of acceleration in crest settlement in first 4 years, thereafter near contant settlement rate (rate per log time).	Limited information.	Constructed in broad river gully with 25 to 38 degree abutment slopes. Crest settlement considered normal.
Talbingo	-0.2 for SMPs on upper slopes, 0 for crest.	540 mm or 0.35% (28 yrs)	0.22	220 mm (28 yrs)	714 mm or 0.49% (28 yrs)	184 mm (28 yrs)	512 mm or 0.35% (28 yrs)	305 mm (28 yrs)	Displacement of SMPs on the upper slopes and crest is downstream. Long-term displacement rate is near zero for the crest and upstream shoulder, and very low for the downstream shoulder. Settlements show normal trend. Greater settlements of the upstream shoulder may be due to some collapse settlement in the upstream (Zone 3C) rockfill.	Consider post construction deformation behaviour as 'normal'. ES1 (IVM) shows greater settlements in lower core, which is probably due to consolidation on dissipation of construction PWP in the wet placed core material.	Consider deformation behaviour as 'normal'. Reservoir has remained close to FSL since first filled.
Tedorigawa	no indication, suspect close to EOC	675 mm or 0.44% (9 yrs)	0.27	-	-	-	-	-	Only have crest settlement data which indicates typical settlement behaviour. Several periods of acceleration during the period of FF. The long-term rate is steady (in log time).	Stress distribution indicates significant arching across the core. HSGs in core during construction indicate possible zones of plastic deformation of the wet placed core in mid to lower regions of core, with strains as high as 7 to 8%.	Consider post construction deformation behaviour as 'normal', although only have limited data. Possible development of plastic deformations in core during construction.
Terauchi	0.16 years after EOC	263 mm or 0.32% (13 years)	0.17	-	-	-	-	-	Relatively large settlement on first filling (185 mm), long-term rate is near constant (in log time).	Limited information.	Constructed in broad river gully with 30 to 35 degree abutment slopes. Crest settlement considered normal. Relatively flat slopes used in design.
Thomson	0 - SMPs on slopes 0.48 - crest	1060 mm or 0.64% (15 yrs)	0.21	155 mm (15 yrs)	1010 mm or 0.75% (15 yrs)	310 mm (15 yrs)	735 mm or 0.54% (15 yrs)	540 mm (15 yrs)	Acceleration in settlement rate during periods of rising reservoir level on FF. Net displacement on FF of the upper slopes and crest is downstream, but the initial displacement of crest and upstream slope was upstream. Relatively large magnitude of displacement of the crest and downstream shoulder on FF.	Consider as 'normal' deformation. Settlement plots indicate an acceleration of the crest settlement on drawdown in 1997-98, but the magnitude of settlement on drawdown is small (less than 30 to 40 mm).	Consider as case of 'normal' deformation behaviour. Well compacted core and rockfill shoulders. 300 mm greater settlement of upstream slope than downstream slope for SMPs at similar elevations. Difference likely due to some collapse settlement of the upstream sedimentary rockfill on wetting.
Tokachi	no indication, suspect close to EOC	160 mm or 0.19% (6 yrs)	0.17	-	-	-	-	-	Relatively small magnitude crest settlement. No indication of start of initial monitoring.	Limited information.	Constructed in broad river gully with 41 to 54 degree abutment slopes. Crest settlement considered normal. Relatively flat slopes used in design.
Upper Dam	0.17 years	830 mm or 0.94% (d/str edge at 8 yrs), greater sett of upstream edge.	0.75	-	-	-	-	-	Settlement of the downstream edge of the crest shows a normal trend, except that the long-term settlement rate is high. On FF greater settlements of the upstream edge of the crest (cf downstream edge) were measured and crest spreading.	Longitudinal cracking on the crest (up to 130m length and 50 mm width) first observed in Jan 1987. Filled with slurry grout. Further cracking in Feb 1989, Feb 1991, Aug 1992 and 1993/94. Cracks located on the up and downstream side of core, possibly due to differential settlement as a result of collapse settlement of the rockfill.	Differential crest settlements and crest spreading resulted in cracking which has persisted for a period of 8 years. The persistence of the cracking is a possible indicator of "abnormal" behaviour. Limited available information.

Table F1.1: Central core earth and rockfill embankments case study information (Sheet 26 of 30)

Name	GENERAL DETAILS				CONSTRUCTION / DESIGN											References
					Construction Timing		Embankment Classification			Dimensions						
	Location	Owner/ Authority	Geology	Foundation	Year Completed	Time (years)	Dam Zoning Class[n]	Core Width / Slope	Core Type	Height, H (m)	Length, L (m)	Ratio L/H	Upstream Slope (H to V)	Downstream Slope (H to V)	Comments on Design	
Upper Yarra	Australia, Victoria	Melbourne Water Corp.	Sedimentary - sandstone, siltstone	Rock	1957, Mar	3	5,0,0	c-tk	CL	90	610	6.8	2.4H to 1V	2.4H to 1V	Broad central core supported by poorly compacted rockfill shoulders. Core zone comprises inner central core of medium plasticity clays and outer core zones of clayey sands and gravels. Outer slopes flatten out from 2H to 1V in the upper section to 3.5H to 1V in the toe regions.	SMEC (1998b) MMBW (1986) Connell Wagner (1998d)
Vatnedalsvatn	Norway	-	-	Rock	1983, Sept	3.9	5,2,0	c-tn	SM	121	482	4.0	1.5H to 1V	1.5H to 1V	Narrow central core supported by dry placed and reasonably compacted rockfill shoulders. Dual filters up and downstream of the core. Dam has a slight arch to upstream. For hydro-electric purposes.	Myrvoll et al (1985)
Waipapa	New Zealand	Mighty River Power	Volcanic - ignimbrites.	Core on bedrock, shoulders on alluvials (ignimbrite silts and gravels)	1960, May	0.8	5,1,1	c-tk	CH/SC	36	183	5.1	3H to 1V	2.5H to 1V	Broad central high plasticity clay core supported by poorly compacted (?) rockfill shoulders. Random fill zone on downstream shoulder.	Wood (1960) Bialostocki (1961) Downer ES (1998)
Watuaga	USA, Tennessee	Tennessee Valley Authority	Sedimentary - shale	Rock	1948, Dec	1.1 (seasonal)	5,2,1	c-tk	CL/SC	94	274	2.9	2H to 1V	2H to 1V	Broad central clay core (0.85H to 1V up and downstream) with thin filters and dumped and sluiced rockfill shoulders. Outer slopes in series of benches sloped at 1.4H to 1V.	Leonard and Raine (1958) Blee and Meyer (1955) Blee and Riegel (1951)
William Hovell	Australia, Victoria	Goulburn Murray Water	Volcanics - rhyodacite	Rock	1971, Apr	1.5	5,2,0	c-tm	ML	34	357	10.5	1.33H to 1V	1.43H to 1V	Central core supported by compacted rockfill shoulders. Steep slopes. Downstream slope 1.33H to 1V with a single bench.	SMEC (1996b) Howley (1971) Cox (1972)
Windemere	Australia, New South Wales	State Water DLWC	Sedimentary - grit, sandstone and shale	Rock	1984, Apr	1.5	5,2,1	c-tm	CL	67	825	12.3	1.65H to 1V	1.55H to 1V	Central clay core supported by compacted rockfill shoulders. Small cofferdam at upstream toe and random fill zone at downstream toe. Core centreline slightly upstream of axis (0.6H to 1V upstream, 0.2H to 1V downstream).	Straw et al (1985) LWC NSW (1997)
Wivenhoe	Australia, Queensland	QDNR (now Sun Water)	Sedimentary - sandstone	Core on bedrock. Shoulders on alluvial sands and gravels (no indication of strength or density)	1982, Mar	6 (staged)	5,2,1	c-tn	CL	59	1200	20.3	1.75H to 1V	1.75H to 1V	Narrow central clay core with well compacted rockfill shoulders. Gravels used in upper upstream shoulder. Upper slopes at 1.5H to 1V and lower slopes at 2H to 1V.	QIWSC (1976) QWRC (1979a, 1979b)
Wyangala	Australia, New South Wales	State Water DLWC	porphyritic gneiss	Rock	1968, June	2.5 to 3	5,2,0	c-tm	SC-SM	86	1510	17.6	1.5H to 1V	1.6H to 1V	Central core supported by compacted rockfill shoulders. Existing concrete gravity dams forms the upstream toe of the embankment. Steep upper embankment slopes (1.3H to 1V for upper 6 m). Dual filter zones up and downstream of the core.	PWD NSW (1992b) LWC NSW (1994)

Table F1.1: Central core earth and rockfill embankments case study information (Sheet 27 of 30)

Name	MATERIALS														
	Earthfill Core							Filters / Transition Zone							
	Zone	Source	ASCS Class[n]	Density Ratio or Dry Density (t/m^3)	Placement Methods	Moisture Content	Comment	Zone	Source	ASCS Class[n]	Relative Density or Dry Density (t/m^3)	Layer Thickness (mm)	Plant	Level of Compaction	Comment
Upper Yarra	1 (inner clay core)	alluvial, colluvial	CL (CH in upper third) - sandy clays	Spec. 95 - 105% SMDD (bulk density = 2.05 t/m^3)	Well compacted - 200 mm (loose) layers, 12p sheepsfoot and grooved drum rollers	placed dry of OMC (Spec. 2% dry of OMC to OMC)	Sandy clays of medium plasticity for the most part. High plasticity clays used in the upper third of the core. Zone 1 is the inner core zone and its geometry varies with depth.	-	-	-	-	-	-	-	No specific filters used. Fine rockfill used at some locations, either up or downstream of coarse rolled fill sections.
Vatnedalsvatn	1	morraine	SM - gravelly silty sands	102.5% SMDD 2.09 t/m^3	Well compacted - 500 mm layers, 6p 11t SDVR	0.5% wet of OMC	Gravelly silty sands, max. size 150 mm, 31% fines.	2A & 2B (filters)	alluvium (2A) & crushed rock (2B)	GW/GP	-	1000	2p 11t SDVR, no water added	reasonable to good	Sandy gravels with < 2% non-plastic fines. Dual filters of thin width up and downstream of the core.
Waipapa	1	Ignimbrite ('soft')	CH/SC	98.5% SMDD 1.0 t/m^3	Well compacted - 200 mm (loose) layers, 12p sheepsfoot rollers	1.4% dry of OMC	Broad core, 1H to 1V upstream and 0.5H to 1V downstream. Some weaving problems when wet.	2 & 2A (filters)	Ignimbrite rockfill	GW/GP - sandy gravels	D_R = 70%	450	4-9p sheepsfoot rollers	reasonable to good	Well compacted filter zones. Zone 2 upstream of core (3 m width) and Zone 2A downstream of core (3m width). Relatively coarse (max. > 150mm), 6% fines.
Watuaga	1	-	CL/SC	-	Well compacted (?) - 150 to 200 mm layers, sheepsfoot rollers	possibly placed close to or wet of OMC	Low plasticity sandy clays to clayey sands.	2A & 2B (filters)	quarried rock ?	-	-	-	-		limited information. Dual filters of thin width (6.1 m wide) up and downstream of the core.
William Hovell	1	colluvial	ML (MH/CL) - sandy silts/clays	99.4% SMDD	Well compacted - 150 mm layers	0.4% wet of OMC	Medium to high plasticity sandy silts/clays.	2A & 2B (filters)	alluvial sands and gravels	SP (2A) GP (2B)	Spec > 70% D_R	< 450	SDVR	(good)	Dual filters up and downstream of the core, 2.7 to 4.2 m combined width.
Windemere	1	residual andesite & colluvium	CL (SC, CH, GC) - gravelly sandy clays	101.5% SMDD	Well compacted - 150 mm layers, Cat 825 padfoot roller	0.6% dry of OMC	Medium plasticity (but varies from low to high) gravelly sandy clays. Average of 60% fines. 0.6 m contact layer placed slightly wet of OMC.	2, 2A & 2B (filters)	alluvial sands and gravels	2A - SP 2, 2B - GP	D_R=85%	400	track rolled by dozers.	Good	High density ratio indicates the filters are well compacted. Dual filter (2A & 2B) downstream of core of 5 m width, single filer (Zone 2) of 2.5 m width upstream of the core.
Wivenhoe	1	alluvial	CL - sandy clays, 83% average fines content	101.1% SMDD	Well compacted - 150 mm layers, padfoot rollers	0.2% wet	Low to medium plasticity sandy clays. 0.6 m thickness wet placed contact layer.	2A, 2B & 2C (filters)	alluvial (washed)	2A - SW 2B -GP 2C - GP to SC/SM	D_R ~ 90% (85 to 156%)	300	SDVR, water added.	Good	Very high relative densities achieved in filters. Dual filters used up and downstream of the core. Combined width of about 3 m. Filters under downstream shoulder.
Wyangala	1	Residual granite	SC/SM - silty to clayey sands	102% SMDD 2.02 t/m^3	Well compacted - 150 mm layers, 8p sheepsfoot roller	1% dry of OMC	Well compacted central core of clayey to silty sands.	2A & 2B (filters)	alluvial sands (2A) & crushed rock (2B)	SW/GW (2A) GW (2B)	Spec. >70% D_R 1.87 to 2.02 t/m^3	300	8.5t SDVR	Good	Well-compacted filter zones. Combined width of 5 to 6.7m. Additional rockfill transition zone (Zone 3A) of 3.4 m width used on downstream side of core.

Table F1.1: Central core earth and rockfill embankments case study information (Sheet 28 of 30)

Name	MATERIALS																	
	Rockfill Zone									Rockfill Zone (in some cases earthfill stabilising berm)								
	Zone	Source	Grading Description	Clean / Dirty	Dry Density (t/m^3)	Layer Thickness (m)	Placement Method	Level of Comp-action	Comment	Zone	Source	Grading Description	Clean / Dirty	Dry Density (t/m^3)	Layer Thickness (m)	Placement Method	Level of Comp-action	Comments
Upper Yarra	3	sandstone & siltstone, HW to MW	indication of high fines content for some rockfill	dirty (?)	-	1.5	Spread in 1.5 m layers, no indication if water added.	poor	Poor compaction of weathered rockfill. Suspect breakdown under trafficking likely.	1A (outer core zone)	decomposed sandstone and siltstone	GC/SC - clayey sands to clayey gravels.	-	(bulk density = 2.08 t/m^3)	0.2 m	12p sheepsfoot and grooved drum rollers, moisture specification is from 2% dry of OMC to OMC	good	Well compacted clayey sands to clayey gravels with low plasticity fines. Zone 1A used up and downstream of the central clay core. Of variable geometry. Outer slopes of Zone 1A are approx 1H to 1V. Average fines = 29% (14% clay fraction).
Vatnedalsvatn	3	quartz, granite and gneiss	-	-	-	1.5	6p 11t SDVR, no water added	Reasonable	Placed without addition of water. No indication of grading.	-	-	-	-	-	-	-	-	-
Waipapa	3A & 3B	ignimbrite ('hard')	max up to 1.2m (?), variable.	-	-	1.8 (3A) 0.9 (3B)	Not formally compacted. No indication that water added.	Poor	Not formally compacted and placed without water addition. Some breakdown on handling. Zone 3A used in the downstream shoulder and Zone 3B used in the upstream shoulder.	4	sands and gravels, and ignimbrite	-	-	-	6m (rockfill) 0.2m sands & gravels	Rockfill dumped, Sands & gravels 10-12p 32t pneumatic tyred rollers.	very poor (rockfill), good (sands & gravels)	Random fill zone on downstream slope. Underlain by foundation drain.
Watuaga	3	quartzite	-	-	-	9.1	dumped and sluiced	poor	Sound, durable rock of at least high unconfined compressive strength.	-	-	-	-	-	-	-	-	-
William Hovell	3	rhyodacite	max 1.2 to 1.5m 13% < 19 mm 2 - 4% fines	clean (some dirty zones)	1.93 t/m^3 D_R = 75%	1.5	8p 4.5t SDVR	reasonable	Rockfill mostly of 'hard' fresh Rhyodacite, but some softer rock. Breakdown of surface of layer (upper 150 mm) on placement.	-	-	-	-	-	-	-	-	-
Windemere	3A	andesite (very high strength, FR)	-	clean	(2.15 t/m^3 - bulk density)	1.2	4p 10t SDVR, no indication if water added.	reasonable to good	Very high strength rock. Used as the inner rockfill zone upstream and downstream of the core. Narrow rockfill transition downstream of filters.	3B & 3C	andesite (very high strength, FR)	-	clean	(2.15 t/m^3 - bulk density)	2.0	2p 10t SDVR (3B) 6p 10t SDVR (3C) no indication if water added.	reasonable	Very high strength rock. Zone 3B used predominantly as outer rockfill zone. Zone 3C used as outer rockfill in downstream shoulder below about mid height.
Wivenhoe	3B & 3C	sandstone (ripped & blasted)	3B up to 1m max. 3C up to 0.3 m max.	dirty (3B definitely)	1.98 t/m^3 98% SMDD for weathered rockfill	3B - 1.0 3C - 0.5	4p 10t SDVR, water added (slightly dry of OMC for weathered rockfill)	Good	MW to FR rock used. FR is high strength, MW to SW is medium to high strength. Zone 3B is the main rockfill. Zone 3C used for up and downstream cofferdams.	3A (gravels)	alluvial (?)	GP/GW - sandy gravel	clean	2.20 t/m^3 D_R = 110%	< 1.0	2p (?) 10t SDVR, water added	Good	Well-compacted gravels as indicated by very high relative densities achieved. Zone 3A used in upper upstream shoulder.
Wyangala	3B	porphyritic gneiss	-	Clean	2.00 to 2.24 t/m^3	1.2	minimum 3p 8.5t SDVR, no water added	Reasonable to good	High to very high strength porphyritic gneiss (UCS = 55 to 160 MPa). Zone 3B used in the inner shoulder regions up and downstream.	3C	porphyritic gneiss	-	Clean	2.00 to 2.24 t/m^3	2.4	6p 8.5t SDVR, no water added	Reasonable to poor	High to very high strength porphyritic gneiss (UCS = 55 to 160 MPa). Zone 3C used in the outer shoulder regions up and downstream.

Table F1.1: Central core earth and rockfill embankments case study information (Sheet 29 of 30)

Name	HYDROGEOLOGY						MONITORING - DURING CONSTRUCTION						
	First Filling		Reservoir Operation		Pore Pressures in Core	Rainfall (Average mm/year)	Core				Rockfill and/or Filters	Comment	Other Types of Internal Monitoring Equipment
	Timing (from end of embankment construction)	Comments	Steady / Fluctuating	Comment			Instrument Type/No.	Settlement		Comment			
								mm	% of H				
Upper Yarra	0.41 to 1.78 years	July 1957 to Dec 1958	Fluctuating	Annual seasonal drawdown from 5 to 30 m. Large events of 27 to 33 m in 1966/68 (33 m), 1976, 1979, 1981/83 (33m), 1990 to 93 (23 to 30m annually).	During operation - steep phreatic surface across core. Upstream Zone 1A fluctuates with reservoir the level but at a reduced amplitude. Some to negligible response in central clay core and downstream Zone 1A.	-	IVM, 2 (in central Zone 1 core)	2380 (ES1) & 2190 (ES2)	2.69% (ES1), 2.64% (ES2)	Strain profile shows normal trend. Strains increase with depth below the crest, 0 to 1% in upper 10 m increasing to 3.5 to 4.5% near base. Their is some variability.	-	-	-
Vatnedalsvatn	-2.75 to 0.17 years	Jan 1981 to Dec 1983. Water stored during construction, to within 10 m of FSL before EOC.	Fluctuating	Seasonal drawdown of 40 to 60m.	Negligible positive pwp during construction. PWP fluctuates with reservoir level but a lower amplitude.	-	-	-	-	-	-	-	-
Waipapa	-	Unknown. Possibly in 1963.	Steady	Steady at FSL.	-	-	-	-	-	-	-	-	-
Watuaga	0 to 0.83 years	Dec 1948 to Sept 1949 (within 3 m of FSL)	Fluctuating	annual drawdown, to lowest level of 24 m below FSL (to 1957).	-	-	-	-	-	-	-	No monitoring during construction	-
William Hovell	0 to 0.6 years	April to Sept 1971	Fluctuating	Annual drawdown of 6 to 18 m. Largest drawdowns (to 18 m) in 1991 and 1998 (20 and 27 after EOC).	-	-	-	-	-	-	-	-	-
Windemere	0 to 6 years	slow rise in reservoir level to FSL from 1984 to 1990.	Steady	-	During construction - limited positive PWP in core, max r_u of about 0.1. During operation - steady.	-	IVM, 1 (7 m upstream of dam axis)	2134	3.2%.	Plot of vertical strain versus depth shows some variability. Vertical strain range from 2 to 6%.	-	-	-
Wivenhoe	0 to 6.4 years	1983 to 1988. Possibly completed earlier, but have no records between 3.6 and 5.6 years.	Fluctuating (slow)	Not annual drawdown. Subject to slow fluctuation, no rapid drawdown events.	During construction - some piezos in core showed positive PWPs (r_u up to 0.2, possibly higher) with slow dissipation post construction. Others in core showed negligible to limited positive PWP.	-	IVM - 2 in core	1085 (ES1) 840 (ES4)	1.55 to 1.85%	Vertical strain increases with increasing fill depth from 0% near crest to 4 - 5% at depth.	Rockfill - 255 mm or 1.4% (0.8 to 2.0%). Does not include deformation in alluvial foundation.	IVM results indicate significant settlements occurred within the foundation under the shoulders (415 mm to Dec 1989).	INs in core and shoulders.
Wyangala	-1.5 to 5.7 years.	Existing concrete gravity dam at upstream toe, stored water during construction. Reached FSL by Feb 1974.	Fluctuating (slow)	Generally within 5 - 10 m of FSL. Low period 1979 to 1984 (11 to 15 yrs after EOC) when the reservoir was gradually drawn down some 45 m.	-	-	IVM - 3 in core	1530 (A) 1550 (B) 572 (C.)	1.83% (A) 1.87% (B) 1.61% (C.)	Vertical strain profiles indicate normal behaviour. Strains range from 0.5 to 3% for the most part, and 4 to 4.5% in the base of the core.	-	HSGs & IVMs indicate settlements of similar magnitude in the core and filters zones, and slightly greater in the rockfill during construction.	IHMs and HSGs in downstream section (at main section).

Table F1.1: Central core earth and rockfill embankments case study information (Sheet 30 of 30)

Name	SURFACE MONITORING - POST CONSTRUCTION										Comments
	Time of Initial Readings (years after EOC)	Crest			Upstream Slope		Downstream Slope		Comments	Comments on Deformation and Observations.	
		Settlement (mm)	S_{LT} (% per log cycle of time)	Displacement (mm)	Settlement (mm)	Displace-ment (mm)	Settlement (mm)	Displace-ment (mm)			
Upper Yarra	0.38 years (prior to start of ff)	533 mm or 0.60% (41yrs)	0.57	140 mm (41yrs)	425 mm or 0.58% (41yrs)	37mm (34yrs)	398 mm or 0.53% (41yrs)	390 mm (41yrs)	Initial downstream displacement on FF of the crest and upper slope regions. The crest displacement shows a trend to upstream at 9 years, then a steady to slightly downstream displacement after about 27 years. Acceleration in the crest settlement rate during the large drawdown events of 1966-68, 1979 and 1993.	Deformation indicates 'abnormal' behaviour during large drawdown. During the 1966-68 drawdown the crest settled up to 100 mm at the main section and IVM ES1 (installed in the core) shows that most of this (about 75 mm) was concentrated at depths below crest level of 11.2 to 14.3 m. On subsequent large drawdowns, the magnitude of crest settlement decreased; 30 to 35 mm in 1979/80 and 22 mm in 1993.	"Abnormal" deformation behaviour during large drawdown events, in particular on the first large drawdown in 1966/68.
Vatnedalsvatn	0	400 mm or 0.33% (0.75 yrs)	-	200 mm (0.75 yrs)	400 mm or 0.37% (0.75 yrs)	400 mm (0.75 yrs), questionable reading ?	180 mm or 0.17% (0.75 yrs)	250 mm	Large downstream displacement of crest and upper slopes during last 10 m of filling to FSL. Records only until 0.75 years after end of construction.	Storage of water prior to EOC likely to have affected monitored post construction deformation due to the susceptibility of the dry placed and reasonably compacted rockfill to collapse compression on wetting.	Stored water to close to FSL before end of construction (within 10 m of FSL). Likely to have affected the post-construction deformation behaviour. Downstream displacements during the latter stages of first filling (I.e. last 10 m to FSL) were of large magnitude.
Waipapa	0.79 years (before start of ff)	36 mm or 0.10% (38 yrs)	0.075	41 mm (38 yrs)	-	-	39 mm or 0.13% (38 yrs)	23 mm (38 yrs)	Limited records for early years of operation. Very low long-term settlement rate. Displacements of the crest and downstream shoulder are downstream, and the rate is virtually zero long-term (from 25 to 38 yrs).	Consider as 'normal' deformation behaviour. Suspect that even though water was not added to the rockfill during placement, the wet climate provided sufficient wetting such that collapse compression on first filling was not an issue.	Consider as 'normal' deformation. Relatively small embankment (H = 36m) and deformations are relatively small.
Watuaga	0.08 (1 month after EOC)	970 or 1.03% (8.2 years)	0.44	-	-	-	-	-	SMPs in the centre of the crest. Greater magnitude settlement of the up and downstream shoulders than the core, 150 to 200 mm greater. No significant displacement on first filling.	Longitudinal cracking on crest, coincident with the up and downstream edges of the core. Due to greater settlement of the rockfill shoulders from collapse compression ?.	Suspect "normal" behaviour for this type of embankment. Possibly some collapse settlement of the upstream rockfill on first filling.
William Hovell	0.39 years	86 mm or 0.24% (28 yrs)	0.15	38 mm (28 yrs)	131 mm or 0.47% (28 yrs)	-	77 mm or 0.33% (28 yrs)	67 mm (28 yrs)	Crest settlement (in centre) shows acceleration in the settlement rate on the first 2 drawdowns greater than 9 m, thereafter the settlement rate is steady. Increased settlement rate for upstream shoulder after 5 years. Crest displacement shows upstream deformation during first 3 drawdowns then gradual, very slow downstream displacement.	Consider as 'normal' for the most part. Acceleration in crest settlement on the first 2 to 3 drawdowns and the relatively high long-term settlement rate of the upstream shoulder are indications of potentially "abnormal" deformation behaviour.	Overall, consider the deformation behaviour as 'normal'. Potential abnormalities possibly associated with steep slopes and "highly stressed conditions", and some collapse compression in the rockfill on wetting and reduced lateral support for the core.
Windemere	0.13 years	405 mm or 0.60% (14 yrs)	0.36	90 mm (14 yrs)	252 mm or 0.43% (14 yrs)	45 mm (14 yrs)	231 mm or 0.40% (14 yrs)	212 mm (14 yrs)	Settlement profiles show normal trend. Displacement of the crest and shoulders is downstream. IVM shows zone of high strain post construction from 10 to 30 m depth below the crest.	Consider as 'normal' deformation behaviour. The zone of relatively high vertical strain in the core is close to the upstream core / filter interface and it occurred on FF. It is probably associated with greater settlement of the upstream shoulder on FF, partly due to collapse compression.	Consider as 'normal' deformation. Possible broad shear zone in core at close to its upstream interface in the upper region of the core. In this upper region, Zone 3B is directly upstream of the filters and is considered more susceptible to collapse compression than the reasonably to well compacted Zone 3A.
Wivenhoe	0 yrs (crest sett) 1.94 yrs (slopes & crest displ)	181 mm or 0.32% (16 yrs)	0.20	65 mm (16 yrs)	38 mm or 0.08% (16 yrs)	59 mm (16 yrs)	75 mm or 0.32% (16 yrs)	69 mm (16 yrs)	Settlement show normal trends. Interrnal post construction settlement in the core shows uniform profile. Displacement of the crest and upper shoulders (both down and upstream) is downstream on and post FF.	No indication of any problems with embankment behaviour from surveillance reports. Consider deformation behavioour as "normal".	Consider deformation behaviour as 'normal'.
Wyangala	0.39 - crest sett 0.64 - slope sett 3.8 - displ	376 mm or 0.44% (31 yrs)	0.18	-186 mm (31 yrs) - u/str edge 30 mm (31 yrs) - d/str edge	419 mm or 0.53% (31 yrs)	-71 mm (31 yrs)	339 mm or 0.43% (31 yrs)	125 mm (31 yrs)	Displacement monitoring only captured the last 10 m of FF. The downstream crest and slope displace to downstream, and the upstream crest and slope displace to upstream. Crest spreading = 80 to 90 mm on FF, and reached close to 200 mm by 1999 (31 yrs). Acceleration in settlement of the crest and upstream slope on drawdown from 1979 to 1981, and again in 1994/95 (although of much lower magnitude).	Fine cracks (transverse and longitudinal) observed in crest prior to 1994. Reference to sink holes and settlements in crest (LWC NSW 1994) but no details. IVM B (upstream of axis and in core) indicates large strains localised to 22 to 30 m depth in the core close to its upstream interface. Possibly indicates a zone of plastic deformation or a broad shear zone within which deformations were initially triggered on first filling, but later on drawdown of the reservoir.	Deformation behaviour 'normal' except for broad "shear zone" in the core near to its upstream interface caused by differential settlement between the core and upstream shoulder. Acceleration in settlement of the crest and upper slopes on first drawdown.

Table F1.2: Zoned earth and rockfill embankments case study information

Name	GENERAL DETAILS				CONSTRUCTION / DESIGN											References
					Construction Timing		Embankment Classification			Dimensions					Comments on Design	
	Location	Owner/ Authority	Geology	Foundation	Year Completed	Time (years)	Dam Zoning Class[n]	Core Width	Core Type	Height, H (m)	Length, L (m)	Ratio L/H	Upstream Slope (H to V)	Downstream Slope (H to V)		
Andong	Korea	-	Granite (?)	Core and downstream shoulder on bedrock, upstream shoulder on decomposed granite.	1976, June	4	4,1,1	c-tn	SM	83	542	6.5	2H to 1V	1.7H to 1V	Narrow central core with shoulders of decomposed granite and rockfill. Cofferdam forms upstream embankment toe. Filters encase downstream decomposed granite zone.	Kim (1979) Sonu (1985) ADCO (1976)
Bradbury	USA, California	USBR	Sedimentary - siltstone & shale	In the floodplain, most of core and shoulders are founded on alluvial sands and gravels (up to 20 - 22 m depth). Cut-off trench to bedrock.	1953, Feb	1.5	4,1,1	c-tk	SC/GC	85	1022	12.0	3.25H to 1V	2.25H to 1V	Broad central core (1.7H to 1V upstream slope and 0.5H to 1V downstream) supported by outer earth and rockfill zones. Broad cut-off trench to bedrock, located upstream of dam axis.	USBR (1959) Stateler (1983)
Burrendong	Australia, New South Wales	State Water DLWC	Sedimentary (low grade metamorphism) - sandstone & greywacke	Core and abutments on bedrock. Rockfill shoulders in river section on gravels.	1963, Oct	2.25	4,2,1	c-tk	CL	76	1130	14.9	2.5H to 1V	2.25H to 1V	Broad central core with filters and outer dumped rockfill shoulders. Cofferdam incorporated into upstream toe. Core comprises central clay core with up and downstream zones of sandy silts and clayey sands and gravels.	Douglas (1965) WCIC NSW (1964) PWD NSW (1992a) WRC NSW (1992)
Canales	Spain	-	Sedimentary - sandstones of Tertiary age. Strongly tectonized.	Core and broad transition zones on sandstone bedrock. Steep abutments on bedrock. Shoulders in river section on gravels.	1986, Sept	7 (staged) 1979-81 to 100m 1985-86 to 156m	4,1,0	c-tn	CH	156	378	2.4	1.75H to 1V	1.7H to 1V	Narrow central clay core with broad transition zones and shoulders of limestone rockfill. Cofferdam at upstream toe. Constructed in broad river gully (100m wide) with near vertical abutment slopes.	Alvarez & Bravo (1976) Bravo (1979) Giron (1997) Bravo et al (1994)
Cardinia	Australia, Victoria	Melbourne Water Corporation	granodiorite	Rock	1973, May	1.7	4,2,1	c-tk	SC/CL	86	1542	17.9	1.85H to 1V	2H to 1V	Core zone comprises an inner Zone 1 zone (SC/CL) supported by broad silty sand zones (Zone 1A). Outer downstream earthfill shoulder and upstream rockfill shoulder.	SMEC (1971) MMBW (1987a) Connell Wagner (1998a)
Dixon Canyon	USA, Colorado	USBR	Sedimentary - sandstone & shale	Soil foundation. Low plasticity sandy clays, clayey sands, clayey gravels and sandy silts. Up to 10 m depth in valley and up to 5 m depth on abutments. Cut-off to bedrock.	1948, late (?)	1 (approx)	4,1,0	c-vb	CL	74	387	5.2	2.5H to 1V	2.5H to 1V	Very broad central clay core. Thin outer shoulder zones of rock fines and rockfill. Broad (55 m width) cut-off to bedrock, aligned upstream of dam axis.	USBR (1946, 1997)
Eucembene	Australia, New South Wales	SMHEA	Meta-sediments, low grade - quartzite & hornfels; with andesitic dyke intrusions.	Rock	1958, May	2.5	4,1,0	c-vb	SC	116	579	5.0	2.5 - 3.5H to 1V	2.0 - 3.5H to1V	Very broad central core (1.6H to 1V up and 1H to 1V downstream) of clayey sands with outer shoulders of sands and gravels, and rockfill. Slopes flatten toward toe.	SMHEA (1998a) SMEC (1990) USBR (1953) DPW NSW (1955)
Greenvale	Australia, Victoria	Melbourne Water Corporation	Basalt overlying granodiorite. Layer of sediments between geological units.	Variable - basalt and completely to highly weathered granodiorite.	1970, Aug	1.5	4,2,2	c-tk	SM	52	2500	48.1	1.8H to 1V	3H to 1V	Broad central core with downstream earthfill zone and upstream rockfill zone. Bench on upstream slope at 18 m below crest, below this the slope is 5H to 1V.	MMBW (1972, 1988) Reinhold (1969) Connell Wagner (1998b)
La Angostura	Mexico	CFE (Federal Electricity Commission)	Sedimentary - limestone with shale seams	Moderately karstic foundation. Core on bedrock. Outer shoulders on alluvium in river section (~ 15 to 20 m).	1973, Nov	2.5	4,0,0	c-tn	CL	146	295	2.0	2H to 1V	1.8H to 1V	Complex design. Very narrow central clay core with shoulders of sands and gravels, and rockfill. Cofferdam forms upstream toe of embankment.	Ramirez de Arellano & Gomez (1972) Benassini et al (1976)
La Grande 4 (LG4)	Canada	Hydro Quebec (James Bay Project)	Granite and gneiss	Rock.	1981, Nov	2.5 (seasonal)	4,1,0	c-tm	SM	125	3800	30.4	1.7H to 1V	1.7H to 1V	Narrow central core with shoulders of compacted sandy gravels and rockfill. Rockfill used in the outer slopes and at the downstream toe. Cofferdam at upstream toe. Constructed in broad glaciated valley.	Verma et al (1985) Pare et al (1984) McConnell et al (1982)
Nurek	Russia	-	Sedimentary - sandstones and siltstones	Core on bedrock. Shoulders on alluvium in gully (approx 7 m depth	1980 (?)	2	4,2,0	c-tn	GC/GM	289	700	2.4	2.25H to 1V	2.1H to 1V	Narrow central core with shoulders of sand to boulders. Rockfill on outer face of slopes and downstream toe. Cofferdam at upstream toe. Constructed in narrow, steep sided valley.	Borovoi et al (1982) Sokolov et al (1985) Borovoi & Mikhailov (1978)

Table F1.2: Zoned earth and rockfill embankments case study information (Sheet 2 of 10)

Name	MATERIALS												
	Earthfill Core (Zone 1)							Filter or Transition Zones					
	Zone	Source	ASCS Class[n]	Dry Density (t/m^3) or Density Ratio (% SMDD)	Placement Method	Moisture Content at Placement	Comments	Zone	Source	ASCS Class[n]	Relative Density or Dry Density (t/m^3)	Layer Thickness (mm)	Placement Method	Comment
Andong	1	decomposed granite	SM	99.7% SMDD 1.95 t/m^3	Well compacted - 200 mm layers, 8p 25t tamping roller	0.4% dry of OMC	Silty sandy gravel with non-plastic fines. Max size 10 mm, 18% fines. Difficulties with breakdown during compaction.	2	alluvial sandy gravels	GW	D_R = 82% 1.87 t/m^3	300	4p 10t SDVR, in moist condition	Well-compacted filters. Located upstream and downstream of central earthfill and encase downstream decomposed granite (Zone 3)
Bradbury	1	alluvial	SC/GC	98.9% SMDD 1.81 t/m^3	Well compacted - 150 mm layers, 12p (minimum) sheepsfoot roller	0.9% dry of OMC (12.6 to 14.6%)	Clayey sands and gravels of low fines content and low plasticity. Broad core zone with relatively flat upstream slope (1.7H to 1V).	2 (transition)	alluvial	GW/GP - sandy gravel with cobbles, < 5% fines	D_R = 89% 2.09 t/m^3	300 to 450	4p 20t crawler tractors.	Well compacted. Zone 2 used as upstream shoulder earthfill and also transition zone downstream of the core.
Burrendong	1A	alluvial	CL	(Spec. >98% SMDD)	Well compacted - 230 mm layers (loose), 12p sheepsfoot rollers	(Spec. 3% dry of OMC to OMC)	Low to medium plasticity gravelly sandy clays. Zone 1A is the narrow, central region of the core (0.25H to 1V slopes up and downstream).	2 & 2A	river gravels	2A - GC/GW 2 - GW/GP	(Spec. D_R >70%)	2A - 225 2 - 300 to 600	4p tamping rollers (2A) 2-4p 4.5t SDVR (2), watered as required	Good compaction of filters. Used up and downstream of broad central earthfill zone (Zones 1A, 1B & 1C). Width narrow at crest and broad at base (> 30 m).
Canales	1	residual	CH	-	-	Spec. OMC to 2% wet of OMC.	Likely that core was reasonably to well compacted. Silty clays of high plasticity.	2 (transition)	Kalkirita (limestone reduced to sand by tectonic action)	SC/SM (?)	-	-	-	Limited information. Very broad transition zones of clayey or silty gravelly sands. Increasing width with depth, up to 25m wide upstream and 60m wide downstream.
Cardinia	1 & 1A	1 - colluvial & residual 1A - residual granodiorite	1 - SC/CL (?) 1A - SM	(Spec. >98% SMDD)	Well compacted - 150 mm layers, 8p sheepsfoot rollers	1 - (OMC to 2% wet) 1A - (1.5% dry to 0.5% wet)	Central core (Zone 1) of clayey sands to sandy clays of medium plasticity. Outer core zone (Zone 1A) of silty sands. 0.6 m contact of CH clay placed wet of OMC.	2B (filter)	-	GP/GW (?)	(Spec. D_R >70%)	450	2p 8t SDVR	limited information. Filter zone of thin width used up and downstream of the central earthfill zone (Zones 1 and 1A).
Dixon Canyon	1	alluvial	CL	98.5% SMDD 1.78 t/m^3[a]	Well compacted - 150 mm layers, 12p tamping rollers	Avg 2.8% dry of OMC	Mainly sandy clays of low plasticity, placed well dry of Standard Proctor OMC.	2 & 2A (transitions)	2 - rockfill (rock fines) 2A - sand and gravel	GW/GP - 150mm max 2 - 17% < 6.75 mm, 2A - 39% < 6.75 mm	-	300	10p tamping rollers, wetted for compacteion	Well compacted. Zone 2 located downstream of central core. Zone 2A located upstream (upper 43 m) of central core. Width of Zone 2 increasing with depth (up to 30 m wide at base of dam).
Eucembene	1	decomposed granite	SC	(Spec. >95% MMDD)	Well compacted - 150 mm layers, 12p (minimum) 18t sheepsfoot roller.	Spec. OMC to 2% dry of OMC.	Clayey sand with low plasticity fines. Well compacted, placed on the dry side of OMC. Up to 20% of results outside the moisture spec.	2 and 4 (transition)	river sand & gravel (4) and crushed rock (2)	GP/GW, high gravel content (> 70%)	-	305	Spread by dozer, 4p 18t crawler tractors, watered	Likely reasonable level of compaction. Used as transition (together with Zone 1A) from core to outer rockfill both up and downstream of central core.
Greenvale	1	residual granodiorite	SM (SC/ML/MH)	100.2% SMDD	Well compacted - 150 mm layers (225 mm loose), 4p Cat 834 padfoot and 4p groove roller	0.3% wet of OMC	Well compacted clayey silty sands to sandy silts with medium to high plasticity fines. Fines content = 30 to 60%.	2A & 2B (filters)	crushed rock	SP/SW (2A) GP/GW (2B)	Spec. > 70% D_R	300 to 450 loose	4p 10t SDVR	Well-compacted filters. Located upstream and downstream of central earthfill and on downstream foundation.
La Angostura	1	-	CL	-	Well compacted - 250 mm layers, 8p 25t sheepsfoot	Spec. OMC to 2% wet of OMC.	Well-compacted silty clay of medium plasticity. High plasticity clays used in upper 20 m of core.	-	-	-	-	-	-	No filters used.
La Grande 4 (LG4)	1	morraine	SM	Spec. > 97% SMDD	Well compacted - 450 mm (loose) layers, 4p 45t pneumatic tyred rollers.	Spec. 1% dry to 2% wet of OMC	Well compacted gravelly silty sand. 25 to 35% non-plastic fines. High modulus (approx. 250 MPa).	2A (filter)	select sand and gravel	GP/GW	D_R = 85%	450 (loose)	3p 5.5t SDVR	Well compacted sandy gravels, < 5% fines. High moduli. Zone 2A used up and downstream of core, width narrow at crest increasing to 12 to 15 m at depth.
Nurek	1	colluvium and weathered rock	GC/GM	-	Well compacted - 250 to 300 mm layers, 70t rollers (pneumatic ?)	moisture conditioned prior to placement.	Well compacted sandy clayey gravel. Max size of 200 mm.	2A & 2B (filters)	alluvium and colluvium (screened and crushed)	SP/SW (2A) GP/GW (2B)	-	250 to 300	70t rollers (pneumatic ?)	Well-compacted filters. Located upstream and downstream of central core. 10 to 16 m width.

Table F1.2: Zoned earth and rockfill embankments case study information (Sheet 3 of 10)

Name	MATERIALS													
	Either Earthfill or Rockfill Zone							Either Earthfill or Rockfill						
	Zone	Source	Grading Description	Dry Density (t/m^3)	Layer Thickness (mm)	Placement Method	Comments	Zone	Source	Grading Description	Dry Density (t/m^3)	Layer Thickness (mm)	Placement Method	Comments
Andong	3 (earthfill)	decomposed granite	SM - silty gravelly sand. Max size 10 to 15 mm, 13 - 15% fines.	97.9% SMDD 1.93 t/m^3	300	8p 25t tamping roller, 0.6% dry of OMC	Well-compacted silty gravelly sands. Used up and downstream of the central core. Similar to central core material.	4 (rockfill)	rockfill	-	-	1000	4p tractor, no indication if water added, but moisture content of 1% would suggest water was not added.	Poor compaction. Limited information. Placed in outer downstream and upstream shoulders.
Bradbury	3 (rockfill)	shales, weathered	Max 0.3 to 0.45m size, 70% > 4.75 mm, some silt fines (medium plasticity)	-	450	12p sheepsfoot rollers, water added during placement.	Well-compacted. Placed in the mid-section of the downstream shoulder. Broke down under trafficking by haul trucks and on spreading.	4 (gravels)	alluvial	cobbles and boulders (> 75 mm)	-	900	Dumped and levelled off by dozers.	Oversize from Zone 1 screening. Used in downstream toe of embankment.
Burrendong	3 (rockfill)	Greywacke	-	(2.05 t/m^3 bulk density)	1800	Placed, spread and watered. High water volume used but not high pressure sluiced.	Refered to as 'good quality' rock. Used as outer rockfill zone up and downstream and in main body of upstream cofferdam.	1B & 1C (earthfill)	alluvial	1B - GC/SC, 15 to 40% fines 1C - ML, 50 to 90% silt fines.	(Spec. > 96 to 98% SMDD)	230 (loose)	16p sheepsfoot rollers (1B), pneumatic rollers also used.	Well compacted. Zone 1C located downstream and Zone 1B upstream of of central Zone 1A . Together, 1A, 1B and 1C formed central earthfill.
Canales	3B (rockfill)	limestone	-	-	-	-	Zone 3B used in the outer up and downstream shoulders. Reference to rock being hard and durable. Suspect either poorly compacted and/or dry placed due to large deformations on FF.	3A (rockfill)	limestone or coarse kalkirite	-	-	-	-	Thin (3m width) inner rockfill transition zone placed up and downstream of sandy transition zone.
Cardinia	3A & 3C (rockfill)	Granodiorite, SW to FR	-	-	3A - 1800 mm 3C - 900 mm	4p 8t SDVR, no indication if water added	Zone 3A (reasonably compacted) used in upstream outer shoulder. Zone 3C (well compacted) foundation drainage layer downstream of central core zone.	4 (rockfill)	granodiorite, residual soil to fresh rock	variable	-	600	4p 8t SDVR, no indication if moisture added.	Used in downstream shoulder. Underlain by drainage layer of Zone 3C.
Dixon Canyon	3 (rockfill)	Sedimentary - not specific on which type	gravel to boulder size	-	900	placed and spread, no water added.	Not formally compacted. No indication of rock type or strength. Zone 3 used as the outer fill zone in the up and downstream shoulders.	-	-	-	-	-	-	-
Eucembene	3 (rockfill)	quartzite	max 0.9 m	-	900	Spread by dozers and sluiced (2 to 1 by volume water added).	Very high strength rock. Zone 3 rockfill used as outer shoulder fill both up and downstream.	1A (earthfill)	weathered granite and decomposed quartzite.	GM/SM - variable gravel content, sometimes very 'rocky'.	(Spec. >95% MMDD).	150	12p (minimum) 18t sheepsfoot roller. Spec. OMC to 2% dry of OMC.	Difficulty meeting compaction (partic. when gravelly) and moisture specification. Zone 1A used up and downstream of central core.
Greenvale	1A (earthfill)	residual granodiorite	SM (SC/ML/MH) - Clayey silty sands to sandy silts / clays.	100.3% SMDD	150 (225 loose)	4p Cat 834 padfoot and 4p groove roller, 0.3% wet of OMC	Well-compacted clayey silty sands / sandy silts/clays with medium to high plasticity fines. Fines content = 30 to 55%. Used in downstream shoulder.	3 (rockfill)	Granodiorite, FR to MW	max < 0.7 m, 10 to 25% finer than 19 mm	-	1200 to 1800	4p 10t SDVR, placed dry (?)	Reasonably compacted. Early rockfill was dirty (10 to 25% finer than 19 mm leaving quarry). Used in upstream shoulder.
La Angostura	2 (gravels)	river alluvium	GW - sandy gravel, max size 100 mm, <3% fines (60 to 75% gravel)	-	300	4p 10t SDVR	Well-compacted. Formed the bulk of the downstream shoulder fill and 30 - 40% of the upstream shoulder fill. Used up and downstream of the central core.	4 (& 5) (rockfill)	Limestone (poor quality)	Max size 0.5 m.	-	Zone 4 - 0.6m Zone 5 ?	4 - 4p 10t SDVR 5 - dumped	Rockfill of high compressibility and relatively high fines content. Zone 4 used adjacent to Zone 2 (up and downstream) and Zone 5 in the outer shoulder regions.
La Grande 4 (LG4)	2B (transition)	select sand and gravel	GP/GW to SP/SW - Sandy gravel to gravelly sand, < 5% fines.	D_R = 85%	450 (loose)	4p 9t SDVR, moisture added if required.	Well-compacted broad transition zone in the up and downstream shoulders (outer slopes of 1H to 1V). Of high moduli .	3 (rockfill)	granite and gneiss	Zone 3A - Max 1.0m, 10% < 19 mm, C_u ~ 5. Zone 3B - max. size of 2.0 m.	-	1.0 (3A) to 2.0 (3B), 3B toward outer slope	4p 9t SDVR, no water added.	Reasonable (outer rockfill) to good (inner rockfill) compaction. Zone 3 used in the outer upstream and downstream shoulders.
Nurek	3 (gravels)	alluvium ?	sand to boulder sized	-	1000	70t rollers (pneumatic)	Reasonably to well compacted. No indication if water added. Formed bulk of fill in embankment shoulders.	4 (rockfill)	-	rock pices up to 1 m in size.	-	3000 to 6000	70t rollers (pneumatic ?)	Essentially a broad riprap zone on the outer shoulders and at the downstream toe.

Table F1.2: Zoned earth and rockfill embankments case study information (Sheet 4 of 10)

Name	HYDROGEOLOGY						MONITORING - DURING CONSTRUCTION						
	First Filling		Reservoir Operation		Pore Water Pressures in Earthfill Core	Rainfall (Average mm/year)	Core				Shoulders and/or Filters	Comment	Other Types of Internal Monitoring Equipment
	Timing (from end of embankment construction)	Comments	Steady / Fluctuating	Comment			Instrument Type / No. of	Settlement		Comment			
								mm	% of H				
Andong	-1.0 to 3.95 years	Mid 1975 to Mid 1981. First filling started before EOC and reached within 13 m of FSL before EOC.	Fluctuating	Annual drawdown of 10 to 15 m. Largest drawdown of 16 m in 1981/82 (4 - 5 years post EOC).	Excess PWP in core at end of construction. Slowly dissipated with time over 6 to 8 years.	-	IVM	1040	1.25%	Vertical strain profile varied from 0.5 - 1.0% in the upper section to 2.2% the near base (3.8% in contact zone).	-	HSGs indicated relatively uniform settlements between core and outer earth and rockfill zones.	HSGs and IHMs.
Bradbury	-0.3 to 5.1 years	Filling started prior to end of construction. Reached FSL in April 1958.	Fluctuating (small) / Steady	Annual drawdown, typically less than 5m. Larger drawdowns of 8 to 12m in 1970/72, 1975/77 and 1984/86. Largest drawdown of 26m from 1986 to 1991 (33 to 38 yrs).	During operation core & foundation respond to reservoir level fluctuation; amplitude decays as move downstream. Minimal lag to reservoir.	460	IVM, 1 in core	720	1.21%	Considered as "normal" behaviour. Vertical strain increases with depth from 0 to 1% near crest to 3 to 4% near base.	IVM B in Zone 3 - 143mm or 0.38%.	Relatively small deformations indicate relatively high moduli of compacted rockfill.	-
Burrendong	-0.6 to 6.2 years	Started in Feb 1966. Reached FSL in Dec 1969.	Fluctuating (slow)	Initially steady (1969 to 1979). Fluctuating after 1979, but not an annual drawdown. Large drawdown events (18 to 25 m) in 1979/81, 1981/83, 1993/95 and 1997/98.	During construction, PWP only recorded in the contact zone of Zone 1A (r_u ~ 0.3), dissipated in 2 years. Otherwise no postive PWP in core during construction.	-	IVM	1795 (IVM B)	2.46%	Considered as "normal" behaviour. Vertical strain increases with depth from 0 to 1% near crest to 5% near base.	Zone 1C (IVM A) - 2.60% Zone 1B (IVM C) - 2.46%	Similar strain profiles in Zones 1B and 1C.	-
Canales	0.4 to 10 years	Started in 1987, reached FSL in early 1996. Within 28m of FSL in early 1990 (3.7 yrs).	Fluctuating	Annual drawdown, typically of 20 to 40m. Maximum reservoir level varies from year to year. Rapid rise of 90m over 5 months to FSL in 1996.	-	-	-	-	-	-	-	-	-
Cardinia	unk	Only have records since 1980 (6.5 yrs), filled prior to this.	Fluctuating (small)	Annual drawdown, typically 2 to 7 m. Larger drawdown of 17 m in1982/83 (8.5 to 10 yrs).	During construction, high pwp in Zone 1 (r_u up to 0.7). Slow dissipation over more than 26 years.	1090	-	-	-	-	-	-	-
Dixon Canyon	2.25 to 4.45 years	Started in Mar 1951. Reached FSL in May 1953.	Fluctuating	Annual drawdown, typically up to 20 m, but several larger events up to 30 m in 1954, 1955, 1958 and 1976. 1954 drawdown largest (30 m) and to lowest elevation.	USBR (1997) refer to piezometric levels still rising within the dam.	-	-	-	-	-	-	-	-
Eucembene	-1 to ?	Possibly stored water during construction, but not sure to what level. Unknown when reached FSL.	Steady	No annual drawdown. Maintained within 10 m of FSL.	Line of equi-potentials indicates uniform head loss across the core zone.	710	-	-	-	-	-	-	IVMs installed in core, but insufficient results to analyse.
Greenvale	0.96 to 3.04 years	1971 to mid 1973. Delay whilst embankment completed.	Steady (after 1983) / Fluctuating	Annual drawdown of 2 to 8 m, reduced to 2 to 5 m after 1983. Largest drawdown in 1982 (12 - 13 yrs) of 12 m.	On reservoir fluctuation, ~ 60% of response recorded in upstream region of the core, but virtually no response in the central region.	-	-	-	-	-	-	-	-
La Angostura	0.4 to >1.1	Filling started in May 1974. Within 15 m of FSL by Dec 1974.	-	no information.	-	-	IVM	-	-	-	-	Significant differential settlement and therefore arching across core.	IVM, HSGs, IHMs.
La Grande 4 (LG4)	1.3 to 1.75 years.	March 1983 to Dec 1983	-	-	During construction - low PWP in core (r_u ~ 0.1 to 0.2 max). Almost complete dissipation during winter shutdown.	700 (30 to 40% as snow)	IVM	-	-	Limited settlement of core during construction.	-	-	-
Nurek	not known	First filling occurred as construction proceeded. Near FSL at EOC.	-	no information.	During construction - positive PWP not recorded until 15 to 25 m of fill above piezometer. Thereafter PWP increased in proportion with increasing embankment height (r_u up to 0.93).	-	IVM	13700	4.80%	no indication of profile of internal settlements.	Internal settlement of gravel shoulders, Upstream - 11.9 m Downstream 4 to 6.5 m	Greater settlement of upstream shoulder due to collapse settlement on saturation.	-

Table F1.2: Zoned earth and rockfill embankments case study information (Sheet 5 of 10)

Name	SURFACE MONITORING - POST CONSTRUCTION										General Comments
	Time of Initial Readings (years after EOC)	Crest			Upstream Shoulder		Downstream Shoulder		Comments	Comments on Deformation and Observations.	
		Settlement (mm)	S_{LT} (% per log cycle of time)	Displacement (mm)	Settlement (mm)	Displacement (mm)	Settlement (mm)	Displacement (mm)			
Andong	0 (shoulders) 0.13 (crest)	276 mm or 0.33% (7.5 yrs)	0.39	-	232 mm or 0.34% (7.5 yrs)	-	127 mm or 0.22% (1.7 yrs)	10 mm (1.7 yrs)	Crest settlement shows an increase in rate (on log scale) after 6 years, which is at odds to the behaviour of the upstream slope. Displacement records are limited, but indicates downstream displacement of downstream shoulder in early years.	Internal core settlement behaviour is considered normal. Would consider as normal except for acceleration in crest settlement after 6 years. Not sure of cause of observed crest settlement behaviour, does not appear to be due to reservoir operation.	The cause of the acceleration in the crest settlement rate after 6 years is not known. S_{LT} is high in comparison to dams with SM/GM cores.
Bradbury	0.23 years	215 mm or 0.33% (44 yrs)	0.06	61 mm (44 yrs)	205 mm or 0.32% (44 yrs)	43 mm (44 yrs)	160 mm or 0.37% (44 yrs)	67 mm (44 yrs)	Settlement shows large reduction in rate after first filling. Acceleration in rate of settlement (all SMPs on main section) between 36 and 41 years, possibly due to historically large drawdown. Displacement results are erratic but indicate downstream displacement.	Consider as "normal" deformation behaviour for main section of dam. The acceleration in settlement rate appears to have also occurred in the foundation (IVM B). SMPs indicated approx. 50 mm settlement over this period whilst IVM B indicates approx. 43 mm. Possibly due to a change in effective stress conditions in the foundation.	Deformation behaviour of main section of embankment is considered "normal". Greater settlements (as a percentage of the embankment height) on the left abutment between Stations 26 and 28. Settlement of the foundation at IVM B about 30 to 40% of the post construction crest settlement at main section.
Burrendong	0 - slopes and crest sett 0.33 - crest displ	330 mm or 0.43% (34 yrs)	0.16	-11 mm (34 yrs)	191 mm or 0.33% (34 yrs)	-131 mm (34 yrs)	113 mm or 0.20% (34 yrs)	67 mm (34 yrs)	Settlement is considered normal. Displacement of shoulders is upstream for upstream slope and downstream for downstream slope. Displacement of the crest is limited.	Consider as "normal" deformation behaviour. Several SMPs show large deformations, but these were indicated as being "loose" or "undermined". Greater settlement (as % of H) of SMPs on the poorly compacted shoulders than the core. Settlement rate increase of the upstream shoulder on rapid drawdown in 1997/98.	Consider as "normal" deformation case. Note increase in settlement rate (to ~20 mm/yr) of upstream slope on 1997/98 drawdown (the most rapid event in dam history).
Canales	0.29 years	1009 mm or 0.65% (10.3 yrs). Much less for downstream edge.	-	-	-	-	-	-	Centre of crest settled some 400 mm during the rapid filling in 1996 to FSL. Data records to 1992 show large differential settlement (approx. 500mm) between downstream edge of crest and centre of crest.	Longitudinal cracking on crest located a the downstream edge of the clay core, first observed in 1989. Differential settlement across the crack of up to 600 mm. Indicates collapse settlement of upstream rockfill and either large plastic deformation or shear development in the wet placed CH clay core.	Case of abnormal deformation behaviour. Vertical scarp developed at downstream edge of core of up to 600 mm. Possible development of shear in core. Rockfill susceptible to collapse settlement on wetting, indicating likely poor placement methods of rockfill.
Cardinia	0.14 on slopes, 0.43 on crest.	288 mm or 0.34% (25 yrs)	0.19	-65 mm (25 yrs)	70 mm or 0.11% (2.5 yrs)	-55 mm (2.5 yrs)	114 mm or 0.18% (25 yrs)	134 mm (25 yrs)	Gradual reduction in rate of settlement with time (normal time). Displacements - crest and upstream slope displaced upstream, downstream slope displaced downstream. Crest displacement responds to reservoir fluctuation.	Consider as "normal". Crest displacement is upstream, but this occurred during the first 2 years (presumably on first filling), and thereafter the trend has been virtually constant, with some fluctuation following the fluctuation in reservoir level. No observation of cracking.	Consider as "normal" deformation behaviour.
Dixon Canyon	0.36 years	1150 mm or 1.80% (39 yrs)	1.38	82 mm (39 yrs)	1320 mm or 1.97% (47 yrs)	-158 mm (47 yrs)	590 mm or 1.14% (47 yrs)	296 mm (47 yrs)	Large magnitude and high long-term rate of settlement. Trend shows a gradual increase in settlement rate for the crest and upper downstream slope. Displacement is upstream for u/str slope, then shift to downstream after 30 yrs. Crest and d/stream slope displace d/str with continuing d/str trend.	Suspect some influence but limited of foundation on settlement, but not possible to quantify. Suspect increase in rate of settlement (on log time scale) is possibly due to gradual wetting up of earthfill as indicated by increasing piezometric heads for more than 40 years. Possible that the dry placed earthfill is susceptible to collapse compression on wetting.	Consider as possibly 'abnormal' deformation behaviour given the large magnitude and on going high rate of settlement. Embankment raised in 1988 due to large magnitude of crest settlement and to provide storage for the maximum probable flood.
Eucembene	0.42 vertical 6.6 horiz.	160 mm or 0.14% (40 yrs)	0.08	96 mm (40 yrs)	-	-	104 mm or 0.14% (40 yrs)	44 mm (40 yrs)	Limited records during early years of operation. Displacement is downstream for crest and downstream slope (base reading is 6.6 yrs after EOC). Settlements are small in magnitude.	Consider as 'normal' deformation behaviour. Displacement show continuing downstream deformation and settlements show slow rate of settlement.	Consider as a case of "normal" deformation behaviour. The reservoir is maintained at a steady level.
Greenvale	0.21 to 0.31 (well before start of first filling)	70 mm or 0.13% (28 yrs)	0.0 (when reservoir steady)	58 mm (28 yrs)	-	-	8 mm or 0.02% (28 yrs)	54 mm (28 yrs)	Downstream displacement of the crest and d/str slope on first filling, continuing at decreasing rate with normal time. Settlement pattern similar.	Consider as normal deformation behaviour. IVM at 25 m high section shows initial settlement and then a gradual heave post construction. Downstream SMP at main section shows initial heave followed by small settlement.	Consider as "normal" case
La Angostura	0.4 (from start of ff)	127 mm or 0.09% (0.6 yrs)	-	107 mm (0.6 yrs)	515 mm or 0.38% (0.6 yrs)	-230 mm (0.6 yrs)	158 mm or 0.14% (0.6 yrs)	121 mm (0.6 yrs)	Most of the post construction deformation occurred within the rockfill, with limited deformation in the gravels (Zone 2). The downstream crest and shoulder displaced downstream on first filling, and the upstream crest and slope displaced upstream.	Displacement on first filling indicates crest spreading of 180 to 190 mm. Cracking may have occurred as a result. Larger settlement of upstream slope possibly associated with collapse compression in the rockfill on wetting.	Limited deformation data, only 6 months during the period of first filling. Deformation indicates crest spreading and greater settlement of upstream slope (than core and downstream slope). Likely arching between the narrow, wet placed clay core ansd the well compacted inner gravel shoulders.
La Grande 4 (LG4)	unknown (before first filling, < 1.3 yrs)	-	-	60 mm (2.6 yrs)	-	-	-	63 mm (2.6 yrs)	Limited data. Relatively small downstream displacement on and post first filling.	Limited data. Very high moduli of core and Zones 2A and 2B likely reason for small magnitude displacement on first filling.	Limited data.
Nurek	-	-	-	-	-	-	-	-	No data.	No information	Reservoir filling occurred as construction proceeded. Records indicate collapse compression of the upstream sand-boulder fill was a significant factor in the large magnitude of settlement during construction.

Table F1.2: Zoned earth and rockfill embankments case study information (Sheet 6 of 10)

Name	GENERAL DETAILS				CONSTRUCTION / DESIGN										References
					Construction Timing		Embankment Classification			Dimensions				Comments on Design	
	Location	Owner/ Authority	Geology	Foundation	Year Completed	Time (years)	Dam Zoning Class[n]	Core Width	Core Type	Height, H (m)	Length, L (m)	Ratio L/H	Upstream Slope (H to V)	Downstream Slope (H to V)	
Pueblo (right abutment embankment)	USA, Colorado	USBR	Sedimentary - sandstone and shale (with bentonite seams)	Central cut-off to bedrock, up to 20m depth. Shoulders founded on low plasticity clays and weathered shales.	1974, Oct (?)	2	4,0,1	c-vb	CL	51	1480	29.0	3H to 1V	2.5H to 1V	Very broad earthfill zone with downstream shoulder of compacted weathered rockfill and gravels. Rockfill zone under upstream shoulder and foundation drain under downstream shoulder.	Kinney & Bartholomew (1987) Wright (1987) USBR (1972)
Rector Creek	USA, California	-	-	Broad central cut-off (max. 15m depth and 45m base width) to bedrock with shoulders on 15m depth of pervious soils (sands and gravels ?). Abutments on bedrock or shallow soil profile.	1946, late	-	4,0,0 (close to homog 0,0,0)	c-vb	SC/SM	61	271	4.4	2.5H to 1V	2.25H to 1V	Very broad zoned central earthfill core with thin shoulder zones of gravels (upstream) and rockfill (downstream). Broad central cut-off of max 15m depth.	Sherard et al (1963) Sherard (1973) ICOLD (1974)
San Justo	USA, California	USBR	Pliocene-Pleistocene age non-marine sediments. Over-consolidated clays, silty sands and clayey sands.	Over-consolidated clays of low to high plasticity, clayey sands and silty sands of 100's of metres depth.	1986, Jan	0.5	4,2,2	c-tk	CL	41	340	8.3	2.5H to 1V	2H to 1V	Broad central clay core supported by compacted earth and rockfill shoulders. Waste berm at upstream toe.	USBR (1995)
San Luis - Main Dam	USA, California	USBR	Sedimentary, marine - shales, sandstones & conglomerates	Soil - deep alluvials in floodplain area. Bedrock and shallow soil profile on hillslopes.	1967, June	6	4,2,1	c-vb	CL	116	5650	48.7	3H to 1V (upper 44m), 8H to 1V below this	2.25H to 1V (upper 44m), 6H to 1V below this.	Very broad central core (2H to 1V upstream and 1H to 1V downstream) supported by shoulder zones of compacted earth and rockfill.	USBR (1974) Hickox & Murray (1984) Morfitt (1984) Von Thun (1988)
San Luis - Slide Area	USA, California	USBR	Sedimentary, marine - shales, sandstones & conglomerates	Bedrock and shallow soil profile. Colluvial (slope-wash) and residual soil profile.	1967, June	6	4,1,1	c-vb	CL	30 to 45	-	-	3H to 1V (upper 44m), 8H to 1V below this	2.25H to 1V	Very broad central core (2H to 1V upstream and 1H to 1V downstream) supported by shoulder zones of compacted earth and rockfill. Constructed on upstream sloping hill-slope.	USBR (1974) Ballard et al (1981) Morfitt (1984) Von Thun (1982, 1988) Stark & Duncan (1987, 1991)
Soyang	Korea	-	-	Bedrock (?)	1972, Dec	5	4,1,0	c-tm	GC	123	530	4.3	2H to 1V	2H to 1V	Central core with shoulders of sand & gravel, and rockfill. Cofferdam forms upstream toe. Filters on upstream and downstream side of core.	Kim (1979) Sonu (1985)
Spring Canyon	USA, Colorado	USBR	Sedimentary - sandstone & shale	Soil foundation. Low plasticity sandy clays, clayey sands, clayey gravels and sandy silts. Up to 15 m depth in valley and 3 m depth on abutments. Cut-off to bedrock.	1948, late (?)	1 (approx)	4,1,0	c-vb	CL	68	347	5.1	2.5H to 1V	2.5H to 1V	Very broad central core with outer shoulders of rock fines and rockfill. Broad (50 m wide) cut-off to bedrock, aligned upstream of dam axis.	USBR (1946, 1997)
Tooma	Australia, New South Wales	SMHEA	granitic gniess & biotite granite	Core on sound rock (except in upper abutments), Shoulders on weathered / decomposed to sound rock.	1961, March	1.5 (seasonal)	4,1,2	c-tk	SM	67	305	4.6	2.5H to 1V	2.25H to 1V	Broad central core with 0.25H to 1V upstream and 1H to 1V downstream slope. Supported by compacted earthfill downstream and poorly compacted rockfill upstream. Filters either side of central core and on downstream foundation.	Hunter et al (1974) SMEC (1986) GHD (1995b)
Tullaroop	Australia, Victoria	Goulburn Murray Water	Sedimentary (Ordivician) - mudstones siltstones and sandstones, overlain by tertiary basalts.	Removal of alluvium in valley floor to expose HW sedimentary rocks. Abutments on tertiary alluvials and basalt.	1959, Apr	0.8	4,1,0 (close to 2,1,0)	c-vb	CL	41	427	10.4	2.35H to 1V	2.5H to 1V	Very broad central clay core with small rockfill zones upstream and downstream	SMEC (1996c) HECEC Aust. (1999)

Table F1.2: Zoned earth and rockfill embankments case study information (Sheet 7 of 10)

Name	MATERIALS													
	Earthfill Core (Zone 1)							Filter or Transition Zones						
	Zone	Source	ASCS Class[n]	Dry Density (t/m^3) or Density Ratio (% SMDD)	Placement Method	Moisture Content at Placement	Comments	Zone	Source	ASCS Class[n]	Relative Density or Dry Density (t/m^3)	Layer Thickness (mm)	Placement Method	Comment
Pueblo (right abutment embankment)	1	alluvial	CL (SC & GC)	(Spec. >100% SMDD)	Well compacted - 150 mm layers, 12p tamping rollers	(Spec. 0.5% dry to 1.5% dry of OMC)	Zone 1 makes up approx. 90% of materials used. Clay to gravel size materials. Max size 125 mm.	-	-	-	-	-	-	No filters used.
Rector Creek	1	Residual / weathered igneous rock	SC/SM	-	Well compacted - 150 mm layers, 10p sheepsfoot rollers	2 to 4% dry of OMC	Well compacted clayey sands to silty sands of low plasticity placed well dry of OMC. Fines content approx. 45%. Zone 1 used in central lower core section and cut-off.	-	-	-	-	-	-	No filters used.
San Justo	1 & 1A	pleistocene sediments	CL (CH,SC, SM,ML)	100% SMDD	Well compacted Zone 1 - 150 mm layers by tamping rollers	-	Zone 1 is central core with 0.5H to 1V up and downstream slopes. Zone 1A earthfill zone in downstream shoulder.	2A & 2B (filters)	-	2A - SP 2B - GP	D_R = 90%	2A - 300 2B - 600	vibratory rollers	Well compacted filter zones. Dual filter on downstream side of central core (combined width of 8m) and on downstream foundation. Single filter (Zone 2A) used upstream of core.
San Luis - Main Dam	1	alluvial & colluvial	CL (SC)	102% SMDD	Well compacted - 150 mm layers, tamping rollers	1.2% dry of OMC	Well-compacted sandy clays of low to medium plasticity (66% avg fines content) . Very broad central earthfill zone.	2 (transition)	alluvium	sand, gravel & cobbles	-	300	crawler tractors	Likely well compacted. Zone 2 located downstream of core over lower half of core height. Only used in main sections.
San Luis - Slide Area	1	alluvial & colluvial	CL (SC)	102% SMDD	Well compacted - 150 mm layers, tamping rollers	1.2% dry of OMC	Well-compacted broad central core zone. Sandy clay (66% avg fines content) of low to medium plasticity.	-	-	-	-	-	-	Zone 2 not used in embankment section in slide area.
Soyang	1	-	GC	99.5% SMDD 1.81 t/m^3	Reasonably to well compacted - 350 mm layers, 8p 25t tamping roller	1.2% wet of OMC	Clayey sandy gravel, no indication of plasticity. 20 to 36% fines.	2 (filter)	alluvial (?)	GW - sandy gravel	2.16 t/m^3 D_R = 70%	400	7p 18t pneumatic roller, in moist condition	Well-compacted filters. Located upstream and downstream of central earthfill core.
Spring Canyon	1	alluvial	CL	98.8% SMDD 1.78 t/m^3	Well compacted - 150 mm layers, 12p tamping rollers	Avg 2.9% dry of OMC	Mainly sandy clays of low plasticity, placed well dry of Standard Proctor OMC.	2 (transition)	rockfill (rock fines)	GM - 125 mm max, 43% pass 6.75 mm, 13.3% fines	2.08 t/m^3	300	10p tamping rollers, wetted for compaction	Well compacted. Located downstream of central core over the full dam height and upstream over the upper 43 m. Width increasing with depth (up to 30 m wide at base of dam).
Tooma	1	completely weathered granite	SM	98.7% SMDD 1.72 t/m^3	Well compacted - 150 mm layers, 12p (minimum) sheepsfoot roller	1.0% wet of OMC	Well-compacted silty gravelly sand. Fines (31%) of low plasticity. Particle breakdown during compaction shifted fines content and OMC.	2 (filter)	crushed rock (& sand blend)	2 - GW/GP (max size 40 mm, avg 8% fines)	-	150 to 305	4 passes of crawler type tractor	Problems with achieving grading specification, particularly early on due to high fines content. Filters located on up and downstream side of core and on downstream foundation.
Tullaroop	1	-	CL	1.76 t/m^3	Known to be rolled	-	limited information.	2 (filter)	-	gravels	-	-	-	Limited information. Located between clay core and rockfill toe, up and downstream .

Table F1.2: Zoned earth and rockfill embankments case study information (Sheet 8 of 10)

Name	MATERIALS													
	Either Earthfill or Rockfill Zone							Either Earthfill or Rockfill						
	Zone	Source	Grading Description	Dry Density (t/m^3)	Layer Thickness (mm)	Placement Method	Comments	Zone	Source	Grading Description	Dry Density (t/m^3)	Layer Thickness (mm)	Placement Method	Comments
Pueblo (right abutment embankment)	2 (gravels)	alluvial	sand, gravel & cobbles, max size 300 mm	Spec D_R >75%	300	4p 18t crawler tractors, watered	Well compacted. Zone 2 used in outer downstream shoulder (inner slope 2H to 1V, outer slope 2.5H to 1V)	3 and 4 (rockfill)	3 - sandstone 4 - limestone, shale and sandstone (weathered ?)	3 - coarse 4 - ?	-	3 - 900mm 4 - 300 mm	3 - spread, no formal compaction 4 - 12p tamping rollers, placed close to OMC	Poorly compacted Zone 3 used under upstream shoulder. Well compacted Zone 4 used the in inner downstream shoulder zone
Rector Creek	2 (earthfill)	Residual / weathered igneous rock	SC/SM ?	-	150	10p sheepsfoot rollers, 2 to 4% dry of OMC	Same source to Zone 1 but coarser grading. Zone 2 used as broad fill zone in upper portion of embankment and up and downstream of Zone 1.	3 (gravels), 4 (rockfill)	-	-	-	-	-	Limited information. Zone 3 (gravels) used in outer upstream shoulder, and Zone 4 (rockfill) used in outer downstream shoulder. Both relatively thin shoulder zones.
San Justo	3 (rockfill)	limestone	-	-	1000	vibratory rollers	Zone 3 used in upper and outer upstream shoulder. Suspect well-compacted.	4 1A (both earthfill)	4 - decomposed granite 1A - pleistocene sediments	4 - ? 1A - CL	4 - ? 1A - 100% SMDD	300	pneumatic tyred rollers	Reasonably to well compacted. Zone 4 used in upstream shoulder (upstream of central core). In the downstream shoulder, Zone 4 encapsulates Zone 1A.
San Luis - Main Dam	4 & 5 (rockfill)	basalt	clean ?	-	4 - 300 mm 5 - 900 mm	crawler tractor	No formal compaction of rockfill zones. Zones 4 and 5 used in the mid to upper region of the upstream shoulder. Zone 4 used downstream of central core and along downstream foundation as a filter zone.	3 (earth and rockfill)	alluvial, colluvial & weathered rock (mix)	variable	99% SMDD	300	tamping rollers, placed 1.4% dry of OMC	Reasonably to well compacted. Miscellaneous fill zone used in lower upstream shoulder and in outer downstream shoulder.
San Luis - Slide Area	4 & 5 (rockfill)	basalt	clean ?	-	4 - 300 mm 5 - 900 mm	crawler tractor	No formal compaction of rockfill zones. Zones 4 and 5 used in the mid to upper region of the upstream shoulder. Zone 4 used downstream of central core and along downstream foundation as a filter zone.	3 (earth and rockfill)	alluvial, colluvial & weathered rock (mix)	variable	99% SMDD	300	tamping rollers, placed 1.4% dry of OMC	Reasonably to well compacted. Miscellaneous fill zone used in lower upstream shoulder and in outer downstream shoulder.
Soyang	3 (gravels)	alluvial (?)	GW - sandy gravel with 1 to 4% fines (80% gravel)	2.16 t/m^3 D_R = 70%	600	5p 10t SDVR. In moist condition.	Well-compacted. Inner earthfill zone upstream and downstream of the central core.	4 (rockfill)	-	-	-	1000	Trafficked by dump truck	Poor compaction. Limited information. Placed in outer downstream and upstream shoulders.
Spring Canyon	3 (rockfill)	Sedimentary - not specific on which type	gravel to boulder size	-	900	no formal compaction, no water added.	No indication of rock type or strength. Zone 3 used as outer fill zone in up and downstream shoulders.	-	-	-	-	-	-	-
Tooma	3 (rockfill)	granite ?	-	-	3000 upstream 900 to 3000 downstream	spread and sluiced	Poorly compaction. Zone 3 used in upstream shoulder. Rockfill also used in lower and very outer slope of downstream shoulder.	1A (earthfill)	weathered granite (?) - CW to HW	variable	92.6% to >98% SMDD	150	12p sheepsfoot rollers, average 1% dry of OMC	Reasonable compaction of highly variable material. Zone 1A used in downstream shoulder.
Tullaroop	3 (rockfill)	basalt	-	-	-	-	Limited information. Located at upstream and downstream toe regions.	-	-	-	-	-	-	-

Table F1.2: Zoned earth and rockfill embankments case study information (Sheet 9 of 10)

Name	HYDROGEOLOGY						MONITORING - DURING CONSTRUCTION						
	First Filling		Reservoir Operation		Pore Water Pressures in Earthfill Core	Rainfall (Average mm/year)	Core				Shoulders and/or Filters	Comment	Other Types of Internal Monitoring Equipment
	Timing (from end of embankment construction)	Comments	Steady / Fluctuating	Comment			Instrument Type / No. of	Settlement		Comment			
								mm	% of H				
Pueblo (right abutment embankment)	-0.75 to 11 years	Started Jan 1974, reached FSL in Sept 1985 (close to FSL in 1983 & 1984).	Fluctuating	Annual drawdown, typically less than 10 to 15 m	-	-	-	-	-	-	-	Foundation settlement under upstream shoulder of 370 to 460mm.	Base plates under upstream shoulder.
Rector Creek	Approx. 0 to 2.5 years	Jan 1947 to May 1949	Fluctuating	Seasonal drawdown of 15 to 20 m. Limited data, only first 3.5 years of operation.	Suspect negligible pore pressures in core during construction due to placement well dry of OMC.	-	-	-	-	-	-	-	-
San Justo	0.1 to 2.1 years	Started February 1986, reached FSL Feb 1988.	Fluctuating	annual drawdown of up to 20m	During construction- No positive PWPs indicating likely placement of the core on the dry side of OMC. During operation - piezometric levels continued to rise (1986-1998) and have not reached steady conditions. Core shows some but limited response to reservoir fluctuation.	-	-	-	-	-	-	Base plates indicate fndn settled 76 mm during construction.	1 base plate, 1 inclinometer
San Luis - Main Dam	0.25 to 2 years	Started Sept 1967, reached FSL June 1969	Fluctuating	Annual seasonal drawdown typically up to 40 m, larger events - 1981 of 65 m, 1994 of 50+m & 1997 of 50 m.	No records from during construction. During operation - response (timing and amplitude) to reservoir fluctuation dependent on the piezometer location. Negligible response in centre of Zone 1.	-	IVM, 2 (B & D)	2120 (B) 3060 (D)	2.44% (B) 3.14% (D)	Increasing strain with increasing depth below crest.	-	Large foundation settlements for embankment section over alluvial floodplain deposits.	base plates, IHMs, IVMs (upstream shoulder)
San Luis - Slide Area	0.25 to 2 years	Started Sept 1967, reached FSL June 1969	Fluctuating	Annual seasonal drawdown typically up to 40 m, larger events - 1981 of 65 m, 1994 of 50+m & 1997 of 50 m.	No records from during construction. During operation - response (timing and amplitude) to reservoir fluctuation dependent on piezometer location. Negligible response in centre of Zone 1. Elevated pore pressures in Zone 1 and soil foundation on large and rapid drawdown.	-	-	-	-	-	-	-	-
Soyang	-0.3 to 2.85 years	Sept 1972 to Oct 1975. First filling started shortly before end of construction. 85 m below FSL at EOC.	Fluctuating	Annual drawdown of 15 to 25m.	High PWP in core at end of construction (r_u up to 0.7). Dissipated within 1 to 2 years. Limited response to reservoir level post construction.	-	IVM	3800	3.10%	Vertical strain profile varied from 1.0% in the upper section to 4.5 to 6% the near base.	Significantly lower magnitude of settlement in the sandy gravels.	Likely arching in narrow clayey gravel core. Relatively Large plastic deformations in the mid section of core.	IHMs.
Spring Canyon	2.4 to 4.6 years	Started in Apr 1951. Reached FSL in May 1953.	Fluctuating	Annual drawdown, typically up to 20 m, but several larger events up to 30 m in 1954, 1955, 1958 and 1976. 1954 drawdown largest (30 m) and to lowest elevation.	USBR (1997) refer to piezometric levels still rising within the dam.	-	-	-	-	-	-	-	-
Tooma	0 to 0.2 years	Approximate estimation of time of first filling.	Fluctuating	Subject to rapid drawdowns of up to 30 m. Daily fluctuation is up to 3 m/day.	During operation - gradual loss of head and reduced respose to reservoir level across core.	-	1 (core)	1527	2.24%	Vertical strain profile varied from 0.5 to 1.0% in the upper section to 3.5 to 4.5% the near base (6.3% at contact). Considered normal.	-	IVM in core located slightly upstream of dam axis.	-
Tullaroop	0 to ?	No records of reservoir operation in first 9 years. Suspect FF by late 1960 to mid 1961 (1.5 to 2 yrs).	Fluctuating	Annual drawdown of 5 to 8 m. Larger drawdowns of 10 to 11.5 m in 1983, 1995, and 1998.	Limited response of piezometers within the core to changes in reservoir level.	490	-	-	-	Data from IVMs not available for construction period.	-	-	-

Table F1.2: Zoned earth and rockfill embankments case study information (Sheet 10 of 10)

Name	SURFACE MONITORING - POST CONSTRUCTION										General Comments
	Time of Initial Readings (years after EOC)	Crest			Upstream Shoulder		Downstream Shoulder		Comments	Comments on Deformation and Observations.	
		Settlement (mm)	S_{LT} (% per log cycle of time)	Displacement (mm)	Settlement (mm)	Displacement (mm)	Settlement (mm)	Displacement (mm)			
Pueblo (right abutment embankment)	0.88 years (reservoir 36m below FSL)	455 mm or 0.80% (22.5 yrs)	0.61	58 mm (22.5 yrs), readings erratic	295 mm or 0.76% (22.5 yrs)	-35 mm (22.5 yrs), erratic readings	340 mm or 0.99% (22.5 yrs)	160 mm (22.5 yrs), erratic readings	Settlements show decreasing rate with time (normal time). Displacement records are erratic, general trends are upstream slope deforms upstream, crest and downstream shoulder deform downstream.	Consider as 'normal' deformation. Displacement readings are erratic. There is some consistency with fluctuating reservoir level, but limited consistency between the crest and downstream shoulder.	Central concrete buttress flanked by two earthfill embankments. Deformation post construction is considered 'normal'.
Rector Creek	0.1 to 0.2 years	855 mm or 1.74% (10 yrs)	1.65	140mm (10 yrs)	-	-	-	-	Large magnitude crest settlements and high settlement rate post FF. Displacements initially upstream (approx. 240mm max.) for most of first filling and then sharp change to downstream at 2 to 2.2 years.	Cracking first observed in Feb 1947, 18mm wide diagonal crack across crest persistent for depths > 7m. New cracks in Dec 1949 (end of 16m drawdown) at each end of embankment, also diagonal across crest, 12mm width. Cracking and displacement behaviour (ICOLD 1974) due to gradual wetting up of dry placed earthfill. Large settlements likely a result of collapse compression on wetting of the dry placed earthfill. Possible fndn influence also.	Consider as a case of 'abnormal' deformation in terms of settlement and displacement trends. Collapse compression of the dry placed earthfill is a likely significant factor in the deformation behaviour observed. Likely brittleness of the dry placed earthfill was probably a significant factor contributing to the cracking.
San Justo	0.25 yrs	48 mm or 0.11% (10 yrs)	0.125	2 mm (10 yrs)	40 mm or 0.15% (8.5 yrs)	-22 mm (8.5 yrs)	35 mm or 0.09% (10 yrs)	11 mm (10 yrs)	Deformations of small magnitude. Settlement shows 'normal' trend. Displacements < 10mm on first filling. Long-term, crest shows very slow d/stream trend as does d/stream slope, upstream shows u/str trend. Deformations affected by Loma Prieta earthquake in 1989.	Relatively small post construction deformations. Base plate shows fndn heave of 45 mm since EOC, most of which occurred during FF, which has probably reduced the amount of settlement measured by the SMPs. Following the earthquake in Oct 1989, SMPs on shoulders settled some 15 mm (crest negligible) and SMPs displaced upstream some 10 to 20 mm. Some crest cracking, but not sure if this is related to the earthquake.	Consider embankment deformation behaviour as 'normal'. Slide in left abutment away from dam.
San Luis - Main Dam	0 to 0.08 years	415 mm or 0.38% (Stn 110, 30 yrs)	0.26	165 mm (Stn 100, 30 yrs)	415 mm or 0.43% (Stn 110, 30 yrs)	-55 mm (Stn 100, 30 yrs)	195 mm or 0.34% (Stn 110, 30 yrs)	185 mm (Stn 100, 30 yrs)	SMPs taken at Stn 110 where fndn is bedrock or a shallow soil depth. SMPs show relatively large settlement on FF, thereafter behaviour is 'normal' . Upstream slope displaces u/str on first filling then gradual d/str trend. Crest and d/str slope displace downstream on FF with gradual downstream trend, more so for the d/str slope.	Differential displacements on first filling indicate crest spreading of 225 mm at Stn 110. Crest spreading observed for SMPs along a large portion of the embankment length. Longitudinal cracking on the crest observed (as a result of crest spreading) along large portions of the crest. Larger deformations (both settlement and displacements) were observed for the embankment section over the soft alluvium.	Consider deformation behaviour at main section as 'normal'. Crest spreading and cracking was observed along large portions of the embankment, and was not confined to the area of the upstream slide in 1981. Suspect wetting of the dry placed earthfill as well as the foundation and hill-slope topography were influences on the crest cracking.
San Luis - Slide Area	1 to 0.08 years	130 mm or 0.41% (Stn 138, 30 yrs)	0.35	-65 mm (Stn 138, 30 yrs)	158 mm or 0.53% (Stn 136, 14 yrs, prior to slide)	-183 (Stn 136, 14 yrs, prior to slide)	-	-	Significant difference in settlement between the upstream and downstream sides of the crest. Displacement is upstream for SMPs on crest and upstream slope, and shows crest spreading. SMPs on upstream slope (13m upstream) show acceleration in settlement during the large drawdowns at years 8 and 10. This is exaserbated at Stn 136 when the settlement is plotted as % of embankment height.	Settlement behaviour on large drawdowns (prior to slide) shows acceleration in settlement of SMPs 13m upstream. Plotting settlement as % of dam height highlights the deformation at SMP 136 as abnormal (in the slide vicinity). This may be an indicator of the impending failure, although the natural slope topography is likely to have an influence. The SMP at 13m upstream at Stn 136 was located just above the backscarp of the slide.	Slide in upstream slope occurred during the large drawdown in 1981. Consider the deformation behaviour of the SMPs on the upstream slope in the vicinity of the slide as 'abnormal'.
Soyang	0	360 mm or 0.29% (5 yrs) from IVM.	0.095	-	-	-	62 mm or 0.08% (5 yrs)	-	Relatively small magnitude settlements post construction as measured by SMPs. IVM indicates greater settlement of core.	Consider as normal deformation. IVM indicates post construction settlements in core of up to 360 mm after 5 years, with most of the settlement (70%) within the lower third of the embankment. Possibly related to consolidation as the high construction pore water pressures dissipated.	Consider as 'normal' deformation behaviour.
Spring Canyon	0.25 years (approx.)	900 mm or 1.50% (39 yrs)	1.31	-18 mm (39 yrs)	955 mm or 1.54% (47 yrs)	-45 mm (47 yrs)	420 mm or 1.13% (47 yrs)	160 mm (47 yrs)	Large magnitude and long-term rate of settlement, particularly the crest and upstream shoulder. Settlement rate (in log time) trend shows an increase with time for crest the and upper d/stream slope. Displacement is u/str for crest and u/str slope, then shift to downstream after 20 to 30 yrs. D/stream shoulder displaces d/str with continuing d/str trend.	Suspect some but limited influence of the foundation on settlement, but cannot quantify. The increase in settlement rate (on log time scale) is possibly due to gradual wetting up of earthfill as indicated by increasing piezometric heads for more than 40 years. The dry placed earthfill may be susceptible to collapse compression.	Consider as possibly 'abnormal' deformation behaviour given magnitude and long-term rate of settlement. Embankment raised in 1988 due to large magnitude of crest settlement and to provide storage for the maximum probable flood.
Tooma	0.10 years	121 mm or 0.20% (38 yrs)	0.12	-32 mm (38 yrs)	142 mm or 0.21% (38 yrs)	-41 mm (38 yrs)	47 mm or 0.09% (38 yrs)	8 mm (38 yrs)	Settlement trends look normal, apart from acceleration of upstream slope from 13 to 16 years. Displacement of crest and upstream shoulder is upstream on first filling with continued upstream deformation post first filling. Downstream slope displaces downstream on FF then steady to upstream trend.	Consider as 'normal' deformation behaviour. Unlikely that the acceleration in settlement of the upstream slope is drawdown related as the embankment had been subject to several rapid 30 m drawdowns previously. Not sure of cause, but effect it not evident in internal core settlement profile.	Consider as "normal" deformation behaviour. Zoned earth and rockfill embankment with upstream shoulder of poorly compacted and sluiced rockfill. Subject to rapid fluctuations in reservoir level (up to 3 m/day).
Tullaroop	1.32 years	138 mm or 0.33% (40 yrs)	0.23	86 mm (40 yrs)	88 mm or 0.29% (40 yrs)	-68 mm (40 yrs)	171 mm or 0.51% (40 yrs)	84 mm (40 yrs)	Displacement of upstream shoulder was downstream for the first 20 years, then deformed upstream. The rest of embankment deformed downstream.	Consider as 'normal' deformation behaviour. Internal core settlement profile (from 1979 to 1998) shows no indication of plastic of shear zones. Change in displacement of upstream shoulder may indicate cracking that has developed under the cyclic operation of the reservoir.	Consider as "normal" deformation behaviour. Embankment could be classified as earthfill with rock toe (2,1,0).

Table F1.3: Zoned earthfill embankments case study information

Name	GENERAL DETAILS				CONSTRUCTION / DESIGN											References
					Construction Timing		Embankment Classification			Dimensions						
	Location	Owner/ Authority	Geology	Foundation	Year Completed	Time (years)	Dam Zoning Class[n]	Core Width	Core Type	Height, H (m)	Length, L (m)	Ratio L/H	Upstream Slope (H to V)	Downstream Slope (H to V)	Comments on Design	
Benmore	New Zealand	Meridian Energy	Sedimentary - argillite & greywacke	Core on bedrock. Shoulders on recent alluvial gravels in the river section (20 to 22 m depth and medium dense to dense, $D_R > 65\%$)	1964, May	4	3,2,1	c-tk	GM/GC	110	823	7.5	2.5H to 1V	2.2H to 1V	Broad central gravelly core supported by compacted gravelly shoulders. Some rockfill used in the downstream shoulder.	Boyle (1965) Jones (1965) Tait (1965) Opus (1998a) WCS (1996a)
Cairn Curran	Australia, Victoria	Goulburn Murray Water	Granodiorite, meta-sediments in upper left abutment	Bedrock.	1956, Apr	9 (shutdown for ~ 3yrs)	3,0,0	c-vb	CL/ML	44	656	14.9	2.75H to 1V	2.7H to 1V	Very broad central clay/silt earthfill core with sands and gravels in the outer shoulders.	State Rivers (1983) Hydro Technology (1995)
Cobb	New Zealand	Trans Alta	Igneous - magnesite and serpentine. Glaciated valley.	Rock.	1955, Mar - Apr	2.3	3,0,1	c-tk	GM/GP	35	213	6.1	3H to 1V	2.75H to 1V	Broad central core with relatively flat shoulders of sandy gravels (upstream) and talus downstream. No embankment filters.	Jones (1955) Oborn (1985)
Hirakud	India	-	-	Foundation stripped to bedrock	1956	4 (seasonal)	3,0,1	c-vb	SC-GC	59	24300	412	3H to 1V	2.25H to 1V	Very broad central earthfill zone with up and downstream zones of compacted earthfill. Rockfill at downstream toe and an upstream facing of riprap.	Rao (1957) Rao & Wadhwa (1958)
Horsetooth	USA, Colorado	USBR	Sedimentary - sandstone & shale	Soil foundation. Low plasticity sandy clays, clayey sands, clayey gravels and sandy silts. Up to 10 to 20m depth in valley, thin mantle on abutments. Cut-off to bedrock.	1948, Dec	0.6	3,0,0	c-vb	CL	48	567	11.8	3H to 1V	2.5H to 1V	Very broad central clay core with outer shoulders of compacted sands and gravels, and weathered rockfill. Transition of rock fines on upstream side of core. Broad (30 m width) cut-off to bedrock upstream of dam axis.	USBR (1946, 1997)
Kastraki	Greece	Public Power Corp. of Greece	-	Core on bedrock. Shoulders on alluvium in gully (approx 8 m depth)	1969, May	1.75	3,1,0	c-tn	CL	95	450	4.7	2.25H to 1V	1.75H to 1V	Narrow central core with shoulders of well-compacted gravelly sands.	Katzias & Stamatopoulos (1975) Coumoulos & Koryalos (1979) Pagano et al (1998)
Khancoban	Australia, New South Wales	SMHEA	Alluvial deposits overlying metamorphic bedrock	Core and shoulders (at main section) on gravels.	1965	1.3	3,0,2	c-vb	SM	18	1067	59.3	3.25H to 1V	2.25H to 1V	Central & downstream zone of silty sand earthfill with gravels in upstream shoulder. Transition zone on upstream of core and filters on foundation. Cut-off slightly upstream of axis.	SMHEA (1998b) Howard et al (1974) P.J. Burgess & Assoc. (1991)
Kremasta	Greece	Public Power Corp. of Greece	Sedimentary - limestone, karstic foundation	Karstic foundation.	1965, Sept	-	3,1,0	c-tn	CL	165	-	-	2.5H to 1V	2H to 1V	Narrow central core with shoulders of well-compacted sands and gravels	Coumoulos (1979) Breznik (1979)
Mammoth Pool	USA, California	Southern California Edison Co.	Granite	Abutments on granite bedrock. In narrow river section part of core on bedrock (cut-off), shoulders on river sands and gravels (up to 30m depth)	1959, Oct	1	3,2,2	c-tk	SM	113	250	2.2	3.5H to 1V	2H to 1V	Broad core (1.1H to 1V upstream and near vertical downstream slopes) supported by shoulders of compacted earthfill. Rockfill toe.	ENR (1960) Wilson (1973)
Meeks Cabin	USA, Wyoming	USBR	Glacial activity - morraine deposits overlying Tertiary aged clay shales with pre-sheared bentonitic seams.	Over-consolidated glacial deposits, some alluvial deposits. Cut-off to bedrock where glacial deposits relatively shallow (maximum section and right abutment). Pre-sheared bentonitic seams in shale.	1970, Aug	4 (seasonal)	3,1,1	c-tk	CL	57.5	1005	17.5	3H to 1V	2.25H to 1V	Broad central core (1.75H to 1V upstream slope and 0.5H to 1V downstream) supported by outer gravel shoulder zones. Broad (30m wide) cut-off trench to bedrock located upstream of dam axis.	USBR (1998)

Table F1.3: Zoned earthfill embankments case study information (Sheet 2 of 10)

Name	MATERIALS												
	Earthfill Core							Filters / Transition Zone					
	Zone	Source	ASCS Class[n]	Density Ratio, or Dry Density (t/m^3)	Placement Method	Moisture Content	Comments	Zone	Source	ASCS Class[n]	Relative Density, or Dry Density (t/m^3)	Placement Method	Comment
Benmore	1	alluvial	GM/GC	102.7% SMDD 2.04 t/m^3	Well compacted - 380 mm (loose) layers, 8-10p 45t pneumatic tyred rollers	0.5% dry of OMC	Silty to clayey gravels, averages fines content = 12%. Sub-zones used for materials assessed as outside specification. Cracking and weaving occured when placed close to or wet of OMC.	2A & 3A (filters)	alluvial	3A - gravelly	D_R = 95% (2A), 81% (3A)	900 mm (?) layers, 4-6p 3.7t SDVR, watered when required	Reasonably to well compacted (given high density ratio). Dual filters used downstream of central core, no filters upstream. Zone 3A also used as a thick drainage blanket on downstream foundation.
Cairn Curran	1	alluvial, colluvial	CL/ML	(Spec. 100% SMDD) 1.63 to 1.73 t/m^3	Reasonably to well compacted - 250 mm layers, 15p 15t tapered foot rollers	dry of OMC (Spec. 1.5% dry to 1.5% wet)	Silty sandy clays of medium plasticity. The embankment design includes zoning within the central core, but materials used and placement methods were virtually the same.	-	-	-	-	-	No filters used.
Cobb	1	morraine	GM/GP	100.3% SMDD 1.99 t/m^3	Well compacted - 150 mm layers, 16-20p sheepsfoot rollers	Slightly above OMC (weaving under traffic)	Well-compacted slightly silty sandy gravels (8 to 16% fines). Core slopes 0.9H to 1V up and downstream.	-	-	-	-	-	No filters used.
Hirakud	1	Various	SC to GC, some CL	2.01 to 2.09 t/m^3	Reasonably to well compacted - 230 mm layers, sheepsfoot rollers	Spec. 1 to 3% dry of OMC	High degree of variability of materials used for Zone 1. Dominant classification is SC to GC. Fines of variable plasticity, low to high.	-	-	-	-	-	No filters used, but outer earthfill zones (Zone 2) are effectively transition zones.
Horsetooth	1	alluvial	CL	98.0% SMDD 1.80 t/m^3	Well compacted - 150 mm layers, 12p tamping rollers	Average of 2.2 to 2.5% dry of OMC	Mainly sandy clays of low plasticity placed well dry of Standard Proctor OMC. Selective zoning of earthfill within the broad core, the more gravelly and sandy soils used in the outer regions of the core.	2 (transition)	rockfill (rock fines)	-	-	300 mm layers, compacted by tamping rollers.	Well compacted (?). Zone 2 used upstream of the core and only in the mid to upper region.
Kastraki	1	-	CL	99.8% SMDD 1.78 t/m^3	Well compacted (?)	0.14% dry of OMC	High density ratio indicates well compacted. The sandy clays are of low to medium plasticity.	2 (filters)	alluvial	SP - gravelly sands	2.03 t/m^3	300 mm layers, 12p SDVR or pneumatic tyred roller	Well-compacted filter. Used upstream and downstream of the central clay core.
Khancoban	1	completely weathered granite	SM	-	Well compacted (?) - 150 mm layers, compacted by rollers	-	Suspect earthfill well compacted. Slightly gravelly silty sands, fines of low plasticity.	2 and 1A (filters)	weathered granite	GM/SM	-	1A - 150 mm layers 2 - 300 mm layers (details not known)	Zone 1A used upstream of Zone 1. Zone 2 used on downstream foundation.
Kremasta	1	-	CL	98.7% SMDD 2.04 t/m^3	Well compacted (?)	(Spec. 3% dry to 3% wet of OMC)	Sandy clays of low plasticity. High density ratio indicates well compacted.	2 (filters)	alluvial	Sands and gravels	-	-	Suspect well compacted (similar to Kastraki ?)
Mammoth Pool	1	completely weathered granite	SM	-	Well compacted (?) - 10p sheepsfoot rollers	(Spec. 1% dry to 1% wet of OMC) OMC = 10 to 15%	Gravelly silty sand. 20% non-plastic fines. Likely high moduli.	2A & 2B (filters)	2A - alluvial 2B - rockfill	2A - sand 2B - gravel (6 to 40mm size)	-	vibratory rollers	Suspect well compacted. Dual filter (of 6m combined width) on downstream side of core and on downstream foundation. No filters upstream of core.
Meeks Cabin	1	morraine	GC/GM	99.8% SMDD 2.02 t/m^3	Well compacted - 150 mm layers, 12p tamping rollers	0.2% dry of OMC. Avg = 9.6%	Silty to clayey sandy gravels. Fines of low plasticity (average 22% fines content). Broad core zone with relatively flat upstream slope (1.75H to 1V).	2 (transition)	morraine	sand, gravel & cobbles (max size 300 mm)	-	305 mm layers, 4p 18t crawler tractors	Reasonable compaction. Zone 2 is a broad tranition zone used in the upstream shoulder and inner downstream shoulder.

Table F1.3: Zoned earthfill embankments case study information (Sheet 3 of 10)

Name	MATERIALS													
	Earthfill in the Shoulder							Earthfill in the Shoulder						
	Zone	Source	Grading Description	Dry Density (t/m^3)	Layer Thickness (mm)	Plant	Comments	Zone	Source	Grading Description	Dry Density (t/m^3)	Layer Thickness (mm)	Plant	Comments
Benmore	3C (gravels)	alluvial	Max size 150 to 300 mm, 1% fines (3C).	D_R = 85% > 2.24 t/m^3	900	4-6p 3.7t SDVR, watered if required.	Well-compacted gravels. Zone 3C used in the upstream shoulder.	3B (gravels, some rockfill)	alluvial (gravels) and rockfill (argillite)	Max size 150 to 300 mm, 1% fines (gravel). Rockfill high fines content ('dirty').	D_R = 82% (gravels) R'fill - D_R<65% (initially), >70% (later)	900 to 1200	4-6p 3.7t SDVR, watered if required. Rockfill in early stages spread by dozer in 1.2 m layers with no formal compaction.	Reasonably to well compacted gravels with interlayers of poorly compacted rockfill. Zone 3B used in the downstream shoulder. Rockfill of poor quality and prone to breakdown under trafficking, only used in the lower shoulder region.
Cairn Curran	3 (gravels)	alluvial (?)	SP/GP to SM/GM - silty sandy gravels & gravelly sands.	1.76 to 1.99 t/m^3	-	trafficked by plant	Used in outer shoulder zones, up and downstream of the very broad earthfill core.	-	-	-	-	-	-	-
Cobb	3A (gravels)	alluvial , outwash	GP/GW - sandy gravels, 2 to 8% fines, max size 150 mm.	1.94 t/m^3 98.4% SMDD	200	16-20p sheepsfoot rollers	Well compacted gravels. Used in upstream shoulder and lower downstream shoulder.	3B	talus	Gravelly, max size 300 mm, variable grading	1.85 t/m^3 96.2% SMDD	305	12-20p sheepsfoot rollers	Well compacted. Used in downstream shoulder. Poorly graded angular material.
Hirakud	2	Various	SC to GP/GW - Clayey sands to sandy gravels.	2.09 to 2.25 t/m^3	225	sheepsfoot rollers	Reasonable compaction. Used in upstream and downstream shoulders.	-	-	-	-	-	-	-
Horsetooth	3 (gravels)	alluvial	sand, gravel & cobbles (max size 200 mm)	-	305	compacted	Zone 3 used on the outer upstream and downstream shoulders.	-	-	-	-	-	-	-
Kastraki	3 (gravels)	alluvial	SP - gravelly sands	2.34 t/m^3	300	12p SDVR or pneumatic tyred roller	Well compacted gravelly sands. Used in the upstream shoulder and downstream shoulder.	-	-	-	-	-	-	-
Khancoban	3 (gravels)	alluvial ?	gravels, up to 0.9 m size (but likely to be much less than this)	-	900	Spread and sluiced.	Zone 3 gravels used in the upstream shoulder.	-	-	-	-	-	-	-
Kremasta	3 (gravels)	alluvial	sands and gravels	-	-	-	Suspect well compacted (similar to Kastraki ?). Used in the upstream shoulder and downstream shoulder.	-	-	-	-	-	-	-
Mammoth Pool	3 (earthfill)	weathered granite	GM (?)	-	-	45p pneumatic tyred rollers, moisture within 1% of OMC	Suspect well compacted and likely high moduli. Zone 3 used in up and downstream shoulders.	-	-	-	-	-	-	-
Meeks Cabin	4 (gravels)	Morraine	cobbles & boulders	-	915	spread, no formal compaction	Not formally compacted. Zone 4 used in outer downstream shoulder.	3	morraine	-	-	305	4p 18t crawler tractors	Miscellaneous material used at the upstream toe.

Table F1.3: Zoned earthfill embankments case study information (Sheet 4 of 10)

Name	HYDROGEOLOGY						MONITORING - DURING CONSTRUCTION						
	First Filling		Reservoir Operation		Pore Pressures in Core	Rainfall (Average mm/year)	Core				Shoulders and/or Filters	Comment	Other Types of Internal Monitoring Equipment
	Timing (from end of embankment construction)	Comments	Steady / Fluctuating	Comment			Instrument Type/No.	Settlement		Comment			
								mm	% of H				
Benmore	0.42 to 0.67 years	Oct 1964 to Jan 1965	Steady	Steady at FSL.	During construction - positive PWP up to 30 to 60% of applied load. Post Construction - slow dissipation. Piezometers indicate steady fall in pore pressure across the core.	380	-	-	-	-	-	-	-
Cairn Curran	not known	Data records start at Apr 1968, 12 years after EOC.	Fluctuating	Annual drawdown of 2 to 8 m. Larger drawdowns in 1983 (10 m), 1991 (14.5 m) and 1995 (11 m).	Post Construction - upstream region of the central earthfill zone responds to reservoir level (delayed response at lesser amplitude). Limited response in the central and no response in the downstream region where the phreatic surface is at a low water.	-	-	-	-	IVMs, but no data prior to 1980.	-	-	-
Cobb	-	-	-	-	-	2210	IVM	235	0.67%	Normal profile, 0% near crest increasing to 1.15% near base.	-	-	-
Hirakud	0.3 to 1.4 years	August 1956 to Sept 1957. Within 5m of FSL in Nov 1956.	-	Water impounded during construction. During the monsoon season of 1952 water was impounded both sides of embankment in the deep gully section.	Negligible during construction. During first filling slow rise of phreatic surface within Zone 1.	-	IVM, C	2170	4.45%	Vertical strains less than 0.5% in upper 15m increasing to 10 to 14% at 40 to 50m depth. Very high strains in lower portions of earthfill.	-	-	-
Horsetooth	2.25 to 4.45 years	Started in Apr 1951. Reached FSL in May 1953.	Fluctuating	Seasonal drawdown, typically up to 20 m, but several larger events up to 30 m in 1954, 1955, 1958 and 1976. 1954 drawdown largest (30 m) and to lowest elevation.	Increasing piezometric levels in central & downstream section of the core since construction (for 40+ years). Only upstream face responds to reservoir.	-	IVM, 2	479 (A) 415 (B)	1.37% (A) 1.21% (B)	Vertical strain profiles show increasing strain with increasing depth.	-	Very large foundation settlement during construction, 960 mm at IVM A and 465 mm at IVM B.	-
Kastraki	-	no information.	-	no information.	Positive PWP developed during construction, r_u up to 0.4 to 0.55	-	IVM, S1 & S2	2560 (S1) 1885 (S2)	3.0% (S1), 2.7% (S2)	S1 at main section. Vertical strain profile varied from 0.5 to 1.0% in the upper section to 7 to 8% near the base.	-	Consider normal. High strain at base possibly in contact zone.	-
Khancoban	unk	No indication of timing of first filling, suspect filled prior to 1968 (< 2 to 2.5 years after EOC)	Fluctuating	Subject to rapid fluctuation. Maximum drawdown rate of 3m/day and maximum drawdow is 10.7 m.	-	-	-	-	-	-	-	-	-
Kremasta	-	no information.	-	no information.	-	-	IVM, S1 & S2	5135 (S1) 3800 (S2)	3.47% (S1), 3.42% (S2)	S1 at main section. Vertical strain profile varied from 0.5 to 1.0% in the upper section to 6 to 8% near the base.	-	Consider normal. High strain at base possibly in contact zone.	-
Mammoth Pool	0.15 to 0.35 years (approx)	First filling in winter of 1959/60 (Dec 59 to Feb 60)	-	no information.	-	-	IVM, C4	1615	1.6%	Vertical strain profile varied from 0 to 1.0% in the upper 20 to 30m to 2.5 to 3.5% at 80 to 100m depth.	IVM C5 in upstream Zone 3.	Vertical strain profile in C5 indicates slightly higher moduli of Zone 3 shoulder fill.	-
Meeks Cabin	-0.22 to 1.85 years	Started May 1970, reached FSL in June 1972. Close to FSL in May-June 1971.	Fluctuating	Limited details, possibly annual drawdown of typically 20 to 30 m.	High PWP in glacially disturbed shale foundation during construction (r_u up to 0.9 to 1.0). Very slow dissipation of foundation PWP post construction.	864	-	-	-	-	-	Spreading of foundation on pre-sheared bentonitic clay seams during construction.	-

Table F1.3: Zoned earthfill embankments case study information (Sheet 5 of 10)

Name	SURFACE MONITORING - POST CONSTRUCTION										General Comments
	Time of Initial Readings (years after EOC)	Crest			Upstream Slope		Downstream Slope		Comments	Comments on Deformation and Observations.	
		Settlement (mm)	S_{LT} (% per log cycle of time)	Displacement (mm)	Settlement (mm)	Displacement (mm)	Settlement (mm)	Displacement (mm)			
Benmore	0.5 years	134 mm or 0.12% (34 yrs)	0.055	45 mm (32 yrs)	-	-	84 mm or 0.12% (32 yrs)	73 mm (32 yrs)	Base survey was prior to first filling. Small magnitude and long-term rate of settlements post construction. Crest and downstream shoulder displaced downstream on first filling, with continuing downstream deformation of downstream shoulder.	Consider as 'normal' deformation behaviour. Small magnitude of settlement post contruction, typical of reasonably to well compacted gravels.	Consider as "normal" deformation behaviour.
Cairn Curran	2.1 years	120 mm or 0.32% (48 yrs)	0.32	-2 mm (48 yrs)	76 mm or 0.23% (48 yrs)	-6 mm (48 yrs)	115 mm or 0.35% (48 yrs)	83 mm (48 yrs)	IVM ES2 indicates the crest settlement in the first 2.1 years after EOC is approx. 40 mm. Displacement trend of u/str crest and slope is downstream then upstream. Trend of d/str slope is for steady d/str displacement.	Consider as 'normal' deformation behaviour. Internal core settlement profile (from 1980 to 1998) is normal. Change in displacement of upstream crest and slope may indicate development of tensile stresses. No crest cracking observed.	Consider as 'normal' deformation behaviour. The change in direction of displacement trend of the upstream crest and shoulder is not coincident with a large drawdown. It is possibly associated with the cyclic operation of the reservoir.
Cobb	-	-	-	-	-	-	-	-	Limited information post construction. Base readings not until 20 years after construction, therefore data not used.	-	Small magnitude of total core settlement during construction.
Hirakud	-	-	-	-	-	-	-	-	No records post construction.	-	"Abnormally" high vertical strains measured in the lower region of the core during construction (in the embankment section within the deep gully). Due to collapse compression of the earthfill following wetting during the 1952 monsoon season. High compressibility of the wetted earthfill.
Horsetooth	0.63	685 mm or 1.9% (39 yrs)	0.62 to 0.7	255 mm (39 yrs)	545 mm or 1.36% (47 yrs)	162 mm (47 yrs)	710 mm or 3.95% (47 yrs)	247 mm (47 yrs)	Very large settlements on first filling. Large post construction settlements in the foundation, up to 30 to 50% of the measured crest settlement. Large downstream displacement on first filling of upper u/str slope, crest and downstream slope, then steady downstream trend.	The foundation had a significant influence on the post construction deformation behaviour, particularly during first filling. The large downstream displacements on first filling are likely affected by the foundation settlement and upstream location of the cut-off trench. Apart from this, the deformation is considered "normal". The downstream shoulder shows an increase in the displacement rate (rate in log time) after 25 to 30 years, which is possibly associated with continued advancement of phreatic surface.	Embankment deformations considered "normal". Foundation influence is significant. Embankment raised in 1988 due to large magnitude of crest settlement and to provide storage for the maximum probable flood.
Kastraki	-	-	-	-	-	-	-	-	No data on post construction deformation.	-	Narrow central clay core with shoulders of well compacted sandy gravels (of suspected high moduli). Arching likely across the core.
Khancoban	0 (or very close to it)	31 mm or 0.17% (33 yrs)	0.09	16 mm (33 yrs)	-	-	15 mm or 0.17% (33 yrs)	11 mm (33 yrs)	Settlement behaviour is normal. Crest displacement is initially upstream (presumably on and shortly after first filling) and then downstream.	Consider as 'normal'. No problems observed with performance. Possible foundation settlement on first filling may have resulted in the initial upstream deformation of the crest.	Consider deformation behaviour as 'normal'. Relatively small embankment (18 m maximum) with 6 m cut-off trench, founded on gravels at main section.
Kremasta	-	-	-	-	-	-	-	-	No data on post construction deformation.	-	Narrow central clay core with shoulders of well compacted sandy gravels (of suspected high moduli). Arching likely across the core.
Mammoth Pool	0.05 years	222mm or 0.23% (8.8 yrs)	0.16	0 to 24mm (8.8 yrs)	-	-	-	-	Crest settlement behaviour is normal. Crest displacements are relatively small (15 to 45mm), showing a small upstream displacement on first filling (approx. 20 mm) and then a slow downstream displacement thereafter.	No cracking observed. Consider deformation behaviour of crest as 'normal'.	Embankment constructed in narrow gorge with river section of about 30 m width and abutment slopes on average of 40 to 60 degrees. Relatively flat upstream slope (3.5H to 1V). Earthfill materials well compacted and of high moduli.
Meeks Cabin	0.25 years	220 mm or 0.39% (25 yrs)	0.24	-9 mm (25 yrs), results erratic	185 mm or 0.36% (25 yrs)	-12 mm (25 yrs), results erratic	120 mm or 0.34% (25 yrs)	-40 mm (25 yrs), results erratic	Settlement shows typical behaviour. Displacements are limited, typically less than 20 to 25mm, but somewhat erratic.	Embankment in good condition, no cracking observed. Small magnitude of settlements and particularly the displacements. No observation of continuance of foundation spreading post construction.	Lateral spreading of the foundation (up to 1m) was observed during construction, with shear displacements likely along clay seams in the glacially disturbed upper shale zone. Post construction deformation behaviour considered 'normal'. Embankment has significant upstream curvature.

Table F1.3: Zoned earthfill embankments case study information (Sheet 6 of 10)

Name	GENERAL DETAILS				CONSTRUCTION / DESIGN											References
					Construction Timing		Embankment Classification			Dimensions					Comments on Design	
	Location	Owner/ Authority	Geology	Foundation	Year Completed	Time (years)	Dam Zoning Class[n]	Core Width	Core Type	Height, H (m)	Length, L (m)	Ratio L/H	Upstream Slope (H to V)	Downstream Slope (H to V)		
Navajo	USA, New Mexico	USBR	Sedimentary - interbedded sandstones (predominant) & shales	Central core founded on bedrock. Inner shoulders founded on gravel deposits and outer shoulders on silty sands and gravels. At the maximum section gravels of shallow depth (4 m thickness), but deeper on the right abutment.	1962, Aug	3	3,1,1	c-tk	CL	123	1113	9.0	2.75H to 1V	2.4H to 1V	Broad central clay core supported by compacted gravels and earthfill shoulders. The upstream portion of the embankment acted as cofferdam during the early stages of construction.	USBR (1963a, 1966a) Davis & Kisselman (1963)
Pukaki	New Zealand	Meridian Energy	Glacial and lacustrine deposits.	Core and shoulders on "contorted silts" (over-consolidated lacustrine deposits of silty sands to sandy silts).	1976, Oct	2.5	3,2,1	c-tk	GM	76	610	8.0	2.9H to 1V	2.3H to 1V	Broad central silty gravel core supported by compacted gravel shoulders. Core zone extends under the upstream shoulder and is used as an upstream blanket to control seepage.	Bryson (1980) Convery (1977) Read (1976) WCS (1996b), Opus (1998b)
Rosshaupten	Germany	-	Sedimentary - sandstones and clay marls	Bedrock	1953, Sept	1.3	3,1,1	c-tm	GM	41	-	-	2H to 1V	1.75H to 1V	Central earthfill core supported by shoulders of compacted gravels. Blanket of Zone 1 underlies upstream shoulder. Concrete cut-off upstream from dam axis.	Treiber (1958a, 1958b)
Ruataniwha	New Zealand	Meridian Energy	Sedimentary - greywacke	Rock	1982, Jan	1	3,2,1	c-tk	GM	50	210	4.2	2.5H to 1V	2.2H to 1V	Central gravelly core supported by well-compacted gravelly shoulders. Filter zones up and downstream of the core.	MWD (1987) Opus (1999)
Soldier Canyon	USA, Colorado	USBR	Sedimentary - sandstone & shale	Soil foundation. Low plasticity sandy clays, clayey sands, clayey gravels and sandy silts. Up to 10 m depth in valley, thin mantle on abutments. Cut off to bedrock.	1948, late (?)	1 (approx.)	3,0,0	c-vb	CL	70	440	6.3	2.5H to 1V	2.5H to 1V	Very broad central core with thin outer shoulders of compacted sands and gravels, and transition of rock fines on the upstream side of core. Broad (55 m width) cut-off to bedrock, aligned slightly upstream of the dam axis.	USBR (1946, 1997)
Steinaker	USA, Utah	USBR	Sedimentary - interbedded sandstones & shales	In the broad valley region - loose fine sands and soft to firm clays up to 28m thickness. Bedrock on the abutments.	1960, Nov	1.5 (seasonal)	3,0,0	c-vb	CL	49	609	12.4	2.5H to 1V	2H to 1V	Very broad central earthfill core (slopes 1.5H to 1V up and downstream) supported by compacted earthfill and gravel shoulders. No filter zones. Flatter slopes in toe regions (4H to 1V downstream toe). Disposal zone at the upstream toe.	USBR (1963b) Cyganiewicz and Dise (1997)
Trinity	USA, California	USBR	Metamorphic - greenstone, low grade metamorphism of basaltic and andesitic lavas	Bedrock - decomposed under outer slopes	1960, Sept	3 (seasonal)	3,0,0	c-tk	SM/GM	164	750	4.6	2.5H to 1V	2.5H to 1V	Broad central core (slopes 0.75-1.0H to 1V) of weathered greenstone supported by transition zone and shoulders of gravels. Flattening of upstream slope at toe.	USBR (1965, 1966b) Walker and Harber (1961) Gray (1972)

Table F1.3: Zoned earthfill embankments case study information (Sheet 7 of 10)

Name	MATERIALS												
	Earthfill Core							Filters / Transition Zone					
	Zone	Source	ASCS Class[n]	Density Ratio, or Dry Density (t/m^3)	Placement Method	Moisture Content	Comments	Zone	Source	ASCS Class[n]	Relative Density, or Dry Density (t/m^3)	Placement Method	Comment
Navajo	1	alluvial	CL	100.6% SMDD 1.78 t/m^3	Well compacted - 150 mm layers, 39t tamping rollers	0.8% dry of OMC	Sandy clays of low plasticity. Fines content variable, from 26 to 94%, average 67%. Some wetter layers within the earthfill as indicated by the high pore water pressures measured in isolated piezometers.	-	-	-	-	-	No filters specifically used, but the broad Zone 2 is effectively a transition zone up and downstream of central core.
Pukaki	1	morraine	GM	approx. 98% SMDD 2.04 - 2.25 t/m^3	Well compacted - 200 to 450 mm (loose) layers, 4-6p 9t SDVR	0.2 to 1.0% dry of OMC	Very broad core of well compacted silty sandy gravels (max size 200 mm, 20 to 40% fines). Weaving under heavy plant.	2, 2A & 2B (filters)	sand (2A & 2?), 2B - gravel	2A - SW/SP (gravelly sands) 2B - GW/GP (sandy gravels)	D_R = 86 to 87% (avg) 2.03 (2A) to 2.27 (2B) t/m^3	450 mm layers, 10p 9t SDVR, wetted prior to rolling	Well compacted filters. 2A and 2B used downstream of core (9m combined width) and Zone 2 upstream (2 to 2.5m width).
Rosshaupten	1	Boulder clay	GM (?)	2.04 t/m^3	Well compacted - 200 mm layers, 8p 16t tamping rollers, 43t pneumatic tyred rollers also used.	7% (close to OMC ?)	Well compacted silty to clayey gravels. Fines content = 35 to 55%, and likely to be of low plasticity given that OMC is close to 7%.	2 (filters)	gravels, screened	GW/GP - sandy gravels	-	-	Filter of thin width (1.2 m horizontal width) used up and downstream of the central core. Sandstone rockfill used for downstream foundation drainage layer.
Ruataniwha	1 & 1A	alluvial	GM	99.1% SMDD 2.24 t/m^3	Well compacted - 300 to 450 mm (loose) layers, 10-15t SDVR	0.3% dry of OMC	Well compacted silty sandy gravels. Average fines content of 27% and fines are of low plasticity. Weaving of core during construction.	2A & 2B (filters)	alluvial	SW (2A) GW (2B)	D_R = 83% (2A), 95% (2B) 2.11 to 2.39 t/m^3	300 to 500 mm layers (2A), 900 mm (2B) 6p 10t SDVR, watered prior to rolling	Well-compacted filters. Zone 2A used upstream and Zones 2A & 2B used downstream of the central core.
Soldier Canyon	1	alluvial	CL	98.2% SMDD 1.80 t/m^3	Well compacted - 150 mm layers, 12p tamping rollers	Avg 2.6% dry of OMC	Mainly sandy clays of low plasticity, placed well dry of Standard Proctor OMC.	2 (transition)	rockfill (rock fines)	-	-	300 mm layers, compacted by tamping rollers.	Well compacted (?). Zone 2 used upstream of the core and only in the mid to upper region.
Steinaker	1	alluvial	CL (ML)	100.5% SMDD	Well compacted - 150 mm layers, 12p sheepsfoot rollers	1% dry of OMC	Well compacted. Mainly sandy clays of low plasticity with fines content = 81% (65 to 97%).	-	-	-	-	-	no filters
Trinity	1	weathered greenstone	SM/GM	98.7% SMDD 1.88 t/m^3	Well compacted - 150 mm layers, 12p sheepsfoot rollers (8.3 tonne per lineal metre)	1.2% dry of OMC	Well compacted silty gravelly sands. Average of 25% fines and fines of low plasticity.	2 (transition)	weathered shale	Silty sandy gravel (GM) - 45% gravel, < 50% fines.	94.2% SMDD 1.87 t/m^3	300 mm layers, 12p tamping or sheepsfoot rollers (as per Zone 1 ?)	Reasonably to well compacted transition zone of weathered shale. Zone 2 used up and downstream of the central core. Width increases with depth (0.5H to 1V width).

Table F1.3: Zoned earthfill embankments case study information (Sheet 8 of 10)

Name	MATERIALS													
	Earthfill in the Shoulder							Earthfill in the Shoulder						
	Zone	Source	Grading Description	Dry Density (t/m^3)	Layer Thickness (mm)	Plant	Comments	Zone	Source	Grading Description	Dry Density (t/m^3)	Layer Thickness (mm)	Plant	Comments
Navajo	2 (gravels)	alluvial, river deposits	sandy gravels & cobbles. Max size ~ 200mm, 15% > 75 mm, 5% fines	D_R = 87% 2.21 t/m^3	450	3p vibrating rollers and crawler tractors	Well-compacted. Zone 2 comprised most of the upstream shoulder and encased Zone 3 in downstream shoulder.	3 (earthfill)	alluvial	varaible - clays to gravels & cobbles (mix of Zones 1 and 2)	97.1% SMDD 1.85 t/m^3	300	3p vibrating rollers and crawler tractors, avg moisture content 0.4% dry of OMC	Reasonably to well compacted. Zone 3 comprised the bulk of the downstream shoulder fill (encased in Zone 2) and was used at the upstream toe.
Pukaki	3A & 3B (gravels)	Alluvial and glacial, outwash gravels.	GW - slightly sandy gravel, avg 2% fines.	D_R = 80 to 85% (avg) 2.31 t/m^3	900	4-6p 9-14t SDVR, minimal water added	Well compacted. Mainly clean river gravels used. Used in up and downstream shoulders.	-	-	-	-	-	-	-
Rosshaupten	3 (gravels)	Morraine	GW - sandy gravels, max size 100mm, < 10% fines.	D_R approx. 70 to 75% (n = 18%)	1000	7.3t vibrating grates, water added.	Reasonably to well compacted. Zone 3 used up and downstream of the central core.	-	-	-	-	-	-	-
Ruataniwha	3A & 3B (gravels)	alluvial - outwash gravels.	Max size 150 to 200 mm, 3 - 4% fines (3A). 3B same as 2B.	D_R = 85% 2.34 t/m^3	450 to 900	6p 10t SDVR, watered prior to rolling	Well-compacted gravels. Zone 3A main shoulder fill. Zone 3B used in upper upstream shoulder. Of likely high moduli.	-	-	-	-	-	-	-
Soldier Canyon	3 (gravels)	alluvial	sand, gravel & cobbles (max size 200 mm)	-	305	compacted	Zone 3 used on the outer upstream and downstream shoulders.	-	-	-	-	-	-	-
Steinaker	3 (gravels)	alluvial	sand, gravel & cobbles, 9% fines, 35% < 4.75 mm.	D_R = 73%	305	4p crawler tractor tracks, initially wetted	Reasonable compaction. Zone 3 used in the outer downstream shoulder and upper portion of the outer upstream shoulder.	2 (earthfill)	alluvial	Variable - mix of clays, gravels and cobbles	90.1% SMDD	300	sheepsfoot rollers, placed 1.3% dry of OMC	The low density ratio indicates poor compaction. Zone 2 used in the lower region of the outer upstream shoulder.
Trinity	3 (gravels)	alluvial	75% gravel, 4.5% fines	D_R = 87%	300 to 450	4p crawler tractor, wetted when required	High density ratio indicates well compacted. Zone 3 forms the bulk of the up and downstream shoulder. Rockfill used in toe regions as a thin layer on the outer slopes.	-	-	-	-	-	-	-

Table F1.3: Zoned earthfill embankments case study information (Sheet 9 of 10)

Name	HYDROGEOLOGY						MONITORING - DURING CONSTRUCTION						
	First Filling		Reservoir Operation		Pore Pressures in Core	Rainfall (Average mm/year)	Core				Shoulders and/or Filters	Comment	Other Types of Internal Monitoring Equipment
	Timing (from end of embankment construction)	Comments	Steady / Fluctuating	Comment			Instrument Type/No.	Settlement		Comment			
								mm	% of H				
Navajo	-0.15 to 1 year (?)	Stop logs placed in late June 1962. Records don't start mid 1965 and indicate reached FSL in July 1973. Suspect first filling (or close to it) in first year.	Fluctuating / Steady (small fluctuation cf dam height)	Annual drawdown of typically 10 m or less, with several larger events. Largest from records was 35 m drawdown in 1965 (3 yrs after EOC).	During construction - positive PWP in lower core region were low to negligible. Isolated regions of high PWP in the mid to upper region (up to 60% of the applied load). During operation - PWPs reached steady condition by early 1980s (20 yrs after EOC). Show little response to reservoir fluctuation.	200 to 430	IVM, 1 in core	4075 (A)	3.34% (A)	IVM A located 7m upstream of axis at main section. Vertical strain profile varied from 0.5 to 1.0% in the upper section to 4 to 6% near the base (100m depth).	IVM B in downstream shoulder 1190 mm or 1.98% during construction.	Higher strains in clay core than gravel shoulders.	IHMs in downstream shoulder
Pukaki	-0.8 to 2.6 years	Started Jan 1976 and reached FSL in May 1979. Within 30 m of FSL before EOC.	Fluctuating	Annual drawdown of 5 to 12m.	Weaving under roller during construction suggests high pore water pressures at compaction.	-	-	-	-	-	-	-	-
Rosshaupten	-0.8 to 0.8 years	Stored water to EL 760m (21m below FSL) during construction. Filled by July 1954.	Fluctuating	Annual drawdown up to 16m.	At EOC pore pressures = 36 to 65% of superimposed load. Construction pore water pressures still dissipating 4 years after EOC.	-	Concrete ringed shaft.	700	1.71%	No indication of vertical strain profile.	-	Likely high moduli of compacted gravel shoulders.	-
Ruataniwha	0.1 to 0.2 years	March to April 1982.	Steady	Steady at close to FSL.	During construction - high PWP up to 50 to 70% of applied fill load. Slow dissipation post construction (20 to 30 kPa per year).	-	-	-	-	-	-	-	-
Soldier Canyon	2.25 to 4.45 years	Started in Apr 1951. Reached FSL in May 1953.	Fluctuating	Annual seasonal drawdown, typically up to 20 m, but several larger events up to 30 m in 1954, 1955, 1958 and 1976. 1954 drawdown largest (30 m) and to lowest elevation.	USBR (1997) refer to piezometric levels still rising within the dam.	-	-	-	-	-	-	-	-
Steinaker	1.25 to 5.75 years	Started early 1962, reached FSL in June 1965. Within 10m of FSL in June 1962 and 4m in May 1963.	Fluctuating	Annual seasonal drawdown, typically 5 to 10 m. Larger drawdowns of 15 to 17 m in 1977, 1989 and 1993. 1993 drawdown was the largest and most rapid.	Post construction - the central to downstream region of the core is slow to respond to reservoir change and the amplitude of response is small.	205	IVM A	925	2.05%	The strain profile is quite variable, but shows a general trend of increasing strain with increasing depth.	-	Large foundation settlement during construction; 830 mm at IVM A.	-
Trinity	0.13 to 2.5 years	Started Nov 1960, reached FSL in April 1963.	Fluctuating	Annual drawdown, typically 10 to 15m. Largest drawdown event in 1976-77 of 65m. Gradual drawdown of 55m from 1986 to 1992.	During construction - positive PWP up to 10 to 15% of applied load in lower section of embankment. Post construction - upstream region of the core responds with reservoir, and central to downstream region shows some to very limited response.	1015	IVM B	1560	3.36%	Normal strain profile. Large strain at base (7.4%) where wetter placed fill used.	-	-	IHMs - limited deformation.

Table F1.3: Zoned earthfill embankments case study information (Sheet 10 of 10)

Name	SURFACE MONITORING - POST CONSTRUCTION										General Comments
	Time of Initial Readings (years after EOC)	Crest			Upstream Slope		Downstream Slope		Comments	Comments on Deformation and Observations.	
		Settlement (mm)	S_{LT} (% per log cycle of time)	Displacement (mm)	Settlement (mm)	Displacement (mm)	Settlement (mm)	Displacement (mm)			
Navajo	0.73 (u/str slope) 0.05 to 0.23 (crest & d/str slope)	665 mm or 0.55% (34 yrs)	0.22	237 mm (34 yrs)	520 mm or 0.45% (34 yrs)	-21 mm (34 yrs)	150 mm or 0.19% (34 yrs)	110 mm (34 yrs)	Suspect reservoir reached close to FSL in first year after EOC due to large settlement and displacement from IVMs and IHMs. Suspect SMPs starting at 0.73 years after EOC may have missed first filling. The early records for the crest and downstream slope include the IVM & IHM records for this period. For the upstream slope the records are likely to be post FF.	Large downstream displacement on first filling of crest and downstream slope. Suspect similar deformation for upstream slope. Relatively large settlement of the crest on first filling. Deformation of SMPs and IVMs post construction indicate 'normal' behaviour.	Consider deformation behaviour as "normal". Seepage problems with the abutment foundations; seepage causing loss of material due to solutioning of gypsum. Modification works in 1986 addressed the seepage problem.
Pukaki	0 yrs (sett readings) 3.9 yrs (displ)	108 mm or 0.15% (22 yrs)	0.06	-8 mm (4 to 22 yrs)	-	-	72 mm or 0.12% (22 yrs)	2 mm (22 yrs)	Majority of the post construction settlement occurred on first filling; the long-term crest settlement rate is very low. Displacement records start post first filling and indicate small displacements of less than 10 mm.	Consider as 'normal' deformation behaviour.	Consider as 'normal' deformation. Foundation is lacustrine silty sands to sandy silts, consolidated by glacial activity.
Rosshaupten	0	195 mm or 0.48% (3.5 yrs)	0.07	10 mm (3.5 yrs)	-	-	-	-	A large proportion of the crest settlement occurred within 0.5 yrs of EOC whilst the reservoir was at a low level. The displacement of the crest was initially upstream (18 mm) then downstream in latter stages of FF (net 0 mm at end of FF). Post FF, crest displacement is downstream at small magnitude.	Consider as case of 'normal' deformation from available records. Post construction, the large settlements shortly after EOC may be related to consolidation. The internal deformation records indicate the core has a slight bulge to downstream that developed on first filling. The crest displacements are very small.	Consider as case of 'normal' deformation from available records.
Ruataniwha	0.1 years	-	-	-	-	-	20 mm or 0.05% (17 yrs)	-29 mm (17 yrs)	Base survey prior to first filling. Small settlements due to well-compacted state of fill materials. Gradual upstream displacement of SMPs on the upper downstream slope.	Consider as 'normal' deformation behaviour. MWD (1987) consider the upstream displacement of the downstream shoulder to be due to consolidation of the core on dissipation of pore pressures.	Consider as "normal" deformation behaviour. Very limited settlements. The gravelly fill materials were well-compacted and are therefore likely to be of very high moduli.
Soldier Canyon	0.36 years (approx.)	535 mm or 0.81% (39 yrs)	0.61	-40 mm (39 yrs)	560 mm or 0.88% (47 yrs)	-64 mm (47 yrs)	230 mm or 0.51% (47 yrs)	100 mm (47 yrs)	Settlements much less than for other Horsetooth reservoir dams. Displacement is upstream for the crest and upstream slope, and downstream for the downstream shoulder.	Consider as 'normal' deformation behaviour. The magnitude and long-term rate of settlement are much lower than at other dams in the Horsetooth Reservoir series.	Consider as 'normal' deformation behaviour. Embankment raised in 1988 due to large magnitude of crest settlement and to provide storage for the maximum probable flood.
Steinaker	0 to 0.08 years	631 mm or 1.40% (37 yrs) (dam only = 330 mm or 0.73%)	0.19	76 mm (37 yrs)	480 mm or 1.06% (37 yrs)	76 mm (37 yrs)	160 mm or 0.65% (37 yrs)	73 mm (37 yrs)	Large magnitude of settlement post construction, but large contribution from the foundation (approx 50%). A large proportion of the settlement occurred on first filling. Displacements are erratic, but indicate a downstream displacement of the crest and downstream shoulder.	Consider the deformation behaviour of the main section as 'normal'. A large component of the settlement is within the alluvial foundation.	In 1993 a stabilising berm was added to downstream slope due to concerns over potential for liquefaction of the foundation under earthquake. A slide occurred in the left abutment during the large and rapid drawdown in 1993.
Trinity	0.28 to 0.33 years	-	0.21	-	588 mm or 0.40% (37 yrs)	149 mm (37 yrs)	143 mm or 0.13% (37 yrs)	37 mm (37 yrs)	Acceleration in settlement of upstream slope during 1976-77 large drawdown. Displacements of the upper upstream shoulder and downstream shoulder are downstream approach very low rates (rate per log time) long-term.	Consider deformation behaviour of main section as 'normal'. Acceleration in settlement rate in 1976-77 possibly due to high effective stress conditions in saturated Zone 1 in dam history (Zone 1 placed partially saturated). Limited deformation of foundation.	Consider as "normal" deformation behaviour.

Table F1.4: Earthfill embankments (homogeneous earthfill, earthfill with filters and earthfill with rock toe) case study information

Name	GENERAL DETAILS						CONSTRUCTION / DESIGN								Main Earthfill Zone				
							Construction		Embankment Dimensions										
	Location	Owner/ Authority	Dam Type	Dam Zoning Class[n]	Geology	Foundation	Year Completed	Time (years)	Height, H (m)	Length, L (m)	Ratio L/H	Upstream Slope	Downstream Slope	Comments on Design	Source	ASCS Class[n]	Dry Density (t/m^3) or Density Ratio (% SMDD)	Placement Method	Comments
Belle Fourche	USA, South Dakota	USBR	Homogeneous Earthfill	0,0,0	Sedimentary - bentonitic shale.	Alluvial clays (Holocene age) overlying weathered shales. Alluvium comprises over-consolidated clays of medium to high plasticity of stiff to hard strength consistency.	1911	6 (seasonal)	35	1860	53.1	2H to 1V (steeper near crest region)	2.1H to 1V (steeper near crest region)	Homogeneous earthfill embankment with central cut-off trench of 2 to 6m depth. Relatively steep slopes (1.5 - 2H to 1V upstream and 1.6 - 2H to 1V downstream). Upper 21m of upstream slope faced with concrete panels on gravel bedding layer. Drainage at downstream toe.	alluvial / colluvial	CL - CH	95 - 100% SMDD, 1.55 t/m^3	Well compacted - 150 mm layers, compacted by 11 to 19 tonne rollers with lugs, moist when placed.	Medium to high plasticity clays (fines content = 85 to 100%). Investigations in the 1980s decribed Zone 1 as "moist and firm with some wet and soft zones".
Biet Netufa	Israel	-	Earthfill with rock toe	2,0,0	-	High plasticity clays, fissured and slickensided	1952, Dec	0.3	11	-	-	3H to 1V	3H to 1V	Earthfill embankment with rockfill toe and upstream facing of riprap underlain by filters.	alluvial / colluvial ?	CH	97% SMDD, 1.27 to 1.40 t/m^3	Well compacted - 200 mm loose layers, 10 to 12 passes sheepsfoot rollers, moisture conditioned	High plasticity clays. Likely placed at or slightly dry of OMC given no PWP during construction.
Enders	USA, Nebraska	USBR	Earthfill with thin rockfill shell	2,0,0	Sedimentary - Tertiary aged cemented and uncemented sands, some gravels, silts and clays.	Abutments on Tertiary aged sedimentary deposits. In river section, embankment on alluvial sands and gravels, cut-off to tertiary sediments.	1949, Nov	2.5 (seasonal)	31.5	794	25.2	2.5 to 3H to 1V	2.65H to 1V	Virtually homogeneous embankment. Zone 1 enclosed by thin shell of pervious earthfill and dumped rockfill. Cut-off (located upstream of axis) up to 13m deep in river section.	loess	SM/ML	100% SMDD, 1.77 t/m^3	Well compacted - 150 mm layers, 12 passes tamping rollers, avg 1.3% dry of OMC	Silty sands to sandy silts of low plasticity. 50% fines, max. 75 mm.
Fresno	USA, Montana	USBR	Earthfill with rock toe	2,0,0	Sedimentary - sandstones and shales. Glacial activity.	Abutments on bedrock. Broad river section on alluvial deposits (compressible silty sands, sands and clays up to 9m depth) overlying glacial outwash soils (firm to hard clayey sands and sandy clays).	1939, Sept	1.3	24	575	24.0	3H to 1V	2.75H to 1V	Earthfill embankment with rockfill toe. Upstream facing of riprap underlain by sands and gravels. Broad cut-off trench (upstream of dam axis) to glacial deposits. Berm of waste material and rockfill at downstream toe.	glacial outwash and alluvium	ML-CL	99.8% SMDD 1.91 t/m^3	Well compacted - 150 mm layers, 12 passes sheepsfoot rollers, avg 0.2% dry of OMC	Sandy silts and sandy clays of low plasticity (avg of 54% fines). Of very low permeability.
Mita Hills	Africa, Zambia	Zambia Broken Hill Dev. Co.	Earthfill with filters	1,2,1	Metamorphics - quartzite and mica schist	Bedrock. Right abutment quartzite, left abutment weathered mica schist.	1957, Dec	0.5	49	366	7.5	2.5H to 1V	2.1H to 1V	Earthfill embankment with upstream sloping dual chimney filter. Rockfill blanket on upstream slope.	-	CL-ML (?)	-	Well compacted - 150 mm layers, compacted by sheepsfoot rollers, moisture spec. 2% dry of OMC to OMC	No indication of source of earthfill, possibly decomposed metamorphics.
Pueblo (left abutment embankment)	USA, Colorado	USBR	Earthfill, rockfill toe	1,0,1 (or 3,0,1)	Sedimentary - sandstone and shale (with bentonite seams)	Central cut-off to bedrock, up to 7m depth. Shoulders founded on low plasticity clays and weathered shales.	1974, Oct (?)	2	37	1090	29.5	3H to 1V	2.5H to 1V	Earthfill embankment with thin outer zone of gravels on the downstream shoulder. Rockfill zone under upstream shoulder and foundation drain under downstream shoulder. Stability berm on downstream shoulder, placed in 1981.	alluvial	CL (SC & GC)	Spec. >100% SMDD	Well compacted - 150 mm layers, 12 passes tamping rollers, moisture spec. 0.5% dry to 1.5% dry of OMC	Zone 1 makes up approx. 90% of embankment. Clay to gravel size materials. Max size 125 mm.
Roxo	Portugal	-	Earthfill, rockfill toe	2,0,0	Schist and porphyry	Weathered schist under most of earthfill embankment	1968	3 to 4	34	847	24.9	3H to 1V	2.5H to 1V	Part earthfill part concrete gravity & buttress dam. Earthfill section (max. 27m height) is earthfill dam with rockfill toe, hand placed rock facing on up and downstream slopes.	weathered schist	CL/SC	Spec > 95% SMDD	Details not known. Moisture spec. 2% dry of OMC to OMC	No indication of placement method. Sandy clays to clayey sands of medium plasticity.
Sasumua	Kenya	-	Earthfill with filters	1,2,0	Volcanics - lavas and pyroclastic sediments, basic	Decomposed lavas	1955, Sept	1.75	35	335	9.6	4H to 1V (2H to 1V rockfill toe section)	2H to 1V	Earthfill embankment with central chimney filter (dual filters) and large rockfill zones at up and downstream toe. Upstream slope faced with rock blanket. Significant arch to upstream.	residual lavas	MH	101.1% SMDD 1.13 t/m^3	Well compacted - 150 mm loose layers, 7p each of 18t sheepsfoot rollers, 41t and 18t pneumatic rollers, avg 0.8% dry of OMC	Heavy compaction of core. Halloysite clays of high plasticity (classify as MH).

Table F1.4: Earthfill embankment (homogeneous earthfill, earthfill with filters and earthfill with rock toe) case study information (Sheet 2 of 3)

Name	Description of Other Embankment Zones (e.g. Filters, Rockfill Toe)	HYDROGEOLOGY						MONITORING - DURING CONSTRUCTION					
		First Filling		Reservoir Operation		Pore Water Pressure Development	Rainfall (Average mm/year)	Earthfill Zone				Other Types of Internal Monitoring Equipment	Comment
		Timing (from end of embankment construction)	Comments	Steady / Fluctuating	Comment			Instrument Type/No. of	Settlement		Comment		
									mm	% of H			
Belle Fourche	-	-1 to 4 years	Started May 1910, reached within 1m of FSL in Aug 1915.	Fluctuating	Annual seasonal drawdown of typically 4 to 10m, less than 5m since 1993. Larger events (> 9m) in 1928, 1930, 1931, 1985, 1988 & 1989 (no records for 1936 to 1982).	During operation, steep phreatic surface in earthfill. Standpipe readings indicate steady phreatic surface reached more than 20 years after construction. (High phreatic surface in foundation.)	-	-	-	-	-	-	-
Biet Netufa	-	0 to 1.3 years	Dec 1952 to March 1954	Fluctuating	Not a annual drawdown, reservoir level varies.	No PWP during construction. During operation - slow development of phreatic surface in earthfill. High phreatic surface in foundation, above ground surface at downstream toe (springs and swampy conditions).	-	IVM	49	0.54%	Low vertical strains during construction in low height embankment.	-	-
Enders	Thin (3 to 6 m width) outer zones of sandy alluvium and rockfill ("dirty" sandstone rockfill) on the outer upstream and downstream face of the embankment. Sandy alluvium well-compacted using tamping rollers, rockfill placed and spread in 0.9 m lifts.	0.9 to 2.2 years	Oct 1950 to Feb 1952 (to normal operating level).	Fluctuating	Annual seasonal drawdown, typically of 3 to 6 m.	-	-	2 IVMs (C & D)	235 (D) 400 (C)	0.81 to 1.15%	Data not available to assess vertical strain profile. Relatively low strains indicative of high moduli of earthfill.	-	-
Fresno	-	-0.5 to 2.75 years	Started May 1939, reached within 5.5 m of FSL by June 1943. This is close to maximum level reached from EOC to 1953.	Fluctuating	Not annual drawdown. Fluctuations of up to 12m.	During construction - PWP to a maximum pore pressure coefficient, r_u, of 0.5. During operation - reached close to steady state conditions after 14 years. Slow response of piezometers to reservoir fluctuations.	-	2 IVMs (B & D), 4m upstream of crest centre.	270 (B) 300 (D)	1.17 to 1.28%	Only cumulative settlement and strain given, no vertical strain profile	-	Large foundation settlements during construction (1330 to 1445 mm under dam axis)
Mita Hills	Dual chimney filters, Zones 2A fine filter and Zone 2B coarse filter. No indication of material source or placement method.	0.85 to 4.1 years	FF to within 6m of FSL from Oct 1958 to Feb 1959. Filling to FSL in Jan 1962	Fluctuating	Drawdowns of up to 15m	-	1000	-	-	-	-	-	-
Pueblo (left abutment embankment)	Zone of well-compacted sand to cobble sized earthfill (alluvial origin) in outer downstream shoulder. Zone of sandstone rockfill (placed in 0.9 m layers and spread) in the lower upstream shoulder.	-0.75 to 11 years	Started Jan 1974, reached FSL in Sept 1985 (close to FSL in 1983 & 1984). Not yet reached flood capacity.	Fluctuating	Annual seasonal drawdown, typically less than 10 to 15 m	-	-	-	-	-	-	Inclinometers installed in embankment shoulders.	Inclinometers indicated possible shear movements on bentonitic seams in foundation of downstream shoulder.
Roxo		-	No information on reservoir operation	-	No information on reservoir operation	-	-	-	-	-	-	-	-
Sasumua	Rockfill in toe sections sourced from clayey lavas (SW to FR). Placed in 600 mm layers, heavily watered and rolled by vibratory rollers (well compacted).	-	No information on timing of reservoir filling	-	No information on reservoir operation	Limited pore pressures developed during construction. Net average close to 0% at EOC. Several piezometers showed initial positive pore pressure that decreased to negative.	1400	IVM	130	0.76%	Vertical strain profile shows increase with depth below crest from 0.3% to 1.21% at 15m depth.	-	-

Table F1.4: Earthfill embankments (homogeneous earthfill, earthfill with filters and earthfill with rock toe) case study information (Sheet 3 of 3)

Name	SURFACE MONITORING - POST CONSTRUCTION										General Comments	References
	Time of Initial Readings (years after EOC)	Crest			Upstream Slope		Downstream Slope		Comments	Comments on Deformation and Observations.		
		Settlement (mm)	S_{LT} (% per log cycle of time)	Displacement (mm)	Settlement (mm)	Displacement (mm)	Settlement (mm)	Displacement (mm)				
Belle Fourche	0.1 to 0.6 years (not sure of time of EOC)	525 mm or 2.01% (17 yrs, Stn 34)	1.8 (10 - 12 yrs), 4.5 (80 yrs)	-	-	-	-	-	SMPs initially on crest only and settlement records for 17 yrs (1911 to 1928). Show settlement of large magnitude (1.5 to 2.3% after 17 yrs) , but at decreasing rate with time. In 1984 to 1989 additional SMPs established on crest and slopes. "Abnormal" deformation of upstream slope in closure section (between Stn 40 and 43).	In 1928 longitudinal cracking observed on crest following first large drawdown. Slide in upstream slope on large drawdown in 1931. Further cracking in crest following large drawdowns in 1985, 1988 and 1989. Monitoring since 1984 indicates relatively high deformation rates in the closure section (8 to 15 mm/yr sett and 6 to 10 mm/yr displ). Upstream slope (MP5) shows acceleration in settlement and upstream displacement on large drawdown. In the 1990's SMPs on the crest and d/stream slope show increased rates of settlement and d/stream displacement, possibly due to the high reservoir levels and potentially rising phreatic surface.	Consider as case of "abnormal" deformation behaviour with respect to deformation of the upstream slope and crest on large drawdown. The cracking and slide in the upstream slope following large drawdown are indicative of highly stresses conditions in the steep upstream slope. The slide area was excavated and reconstructed. Remedial works on the upstream slope were undertaken in 1939 and again in 1977 to improve its stability under drawdown. In the early 1990's a maximum drawdown rate was enforced. Since then reservoir levels have remained relatively high and have potentially resulted in a rising phreatic surface within the embankment, possibly explaining the increased rate of settlement and downstream displacement of the crest and downstream slope.	Ready (1910) USGS (190X) USBR (1996) Sherard (1953) Savage (1931)
Biet Netufa	0 years	18mm or 0.20% (2.5 years), excludes fndn settlement	0.09	-	-	-	-	-	Upper 3m shows swelling of CH clay, affected by seasonal influence. All of post construction settlement occurred in lower 3m.	Limited records. Low rate settlement with time. Fluctuations about general trend due to seasonal shrink-swell influence.	Consider as case of 'normal' deformation behaviour. Shrink-swell of CH clay influences settlement behaviour.	Bar-Shany et al (1957)
Enders	Approx. 0.1 years	79mm or 0.25% (41 years)	0.44	-	-	-	24mm or 0.10% (41 years)	-	Small settlements. Heave in early years of operation of some SMPs, particularly on the downstream slope. From about 2 years after construction, increased rate of settlement in log time.	Embankment in satisfactory condition. Initial heave deformations possibly associated with wetting up of dry placed earthfill. Cause of increased log rate of settlement possibly related to increased magnitude of drawdown.	Consider, from available deformation records, as 'normal' deformation behaviour. Overall, settlements are small. Problems with foundation seepage.	USBR (1951, 19xx) Gould (1954)
Fresno	0 yrs (IVM) 0.17 yrs (SMPs)	803 mm (14 yrs), dam only 88 mm or 0.37% (14 yrs)	1.8 (fndn influence)	-	625 mm (14 yrs)	-	544 mm (14 yrs)	-	Large foundation settlements post construction (630 to 1030 mm under crest). Embankment only settlements only a fraction of foundation settlement (88 mm at IVM B after 14 yrs).	Crest re-capped twice (1943 and 1950) due to large foundation settlements. Embankment settlements on the dam axis are small.	Embankment constructed on compressible foundation. Foundation settlements are a very large proportion of the total settlements (85% during construction and 90 to 95% post construction).	Daehn (1955) Esmiol (1955)
Mita Hills	0.44 years	680 mm or 1.39% (10.5 yrs)	0.21	170mm (10.5 yrs)	-	-	92 mm or 0.27% (10.5 yrs)	90mm (10.5 yrs)	Large settlement of crest, most of which occurred in first 3.5 to 4 years of operation. As a percentage of dam height, the crest settlement is much greater than that measured on the downstream berm. Displacement of crest and downstream slope is downstream at a gradually decreasing rate.	Embankment in good condition. Reasons for high crest settlements in early post construction preiod possibly due to collapse compression, but the marginal stability of the upstream slope could be a factor. Otherwise, deformation behaviour is considered 'normal'.	Hydro power dam constructed for mine site. Consider long-term deformation behaviour to be 'normal', although early crest settlements were of large magnitude. Seepage problems through both the left and right abutments during operation.	Legge (1970)
Pueblo (left abutment embankment)	0.88 years (reservoir 36m below FSL)	315 mm or 0.75% (22.5 yrs)	0.68	79 mm (22.5 yrs)	240 mm or 0.95% (22.5 yrs)	-130 mm (22.5 yrs)	340 mm or 1.78% (22.5 yrs)	21 mm (22.5 yrs)	Settlements show decreasing rate with time. Relatively large settlement of downstream shoulder (in comparison to crest and upstream shoulder). Displacement records are erratic, but indicate upstream slope deforms upstream, and limited deformation of the crest and downstream shoulder.	Consider as 'normal' deformation. Not clear what is cause of relatively large settlement of downstream shoulder. Displacement is limited (21mm at 22 yrs) so stability is not considered an issue.	Central concrete buttress flanked by two earthfill embankments. Monitoring during construction indicated possible shear development within bentonitic clay seams in the foundation under the downstream shoulder. This was identified as a possible mechanism prior to construction, hence inclinometers were installed in the outer slope regions. The post construction deformation behaviour is considered "normal".	Kinney & Bartholomew (1987) Wright (1987) USBR (1972)
Roxo	0 years (?)	< 47 mm to 600 mm; 0.23 to 1.87% (8 yrs)	2.4 (20 m from CG section) 0.22 (90 m from CG section)	-	-	-	-	-	"Abnormally" high magnitude of crest settlements in earthfill embankment adjacent to concrete section (up to 1.87% within 0 to 50m on the interface with the concrete section). More than 90m from the interface settlements are much smaller at 0.23% of dam height.	The zone of large crest settlement is confined to the closure zone adjacent to the concrete embankment section. Findings were not conclusive as to cause. Investigations indicated earthfill had been well compacted, but had saturated and soft layers. Suspect possible collapse compression on wetting.	Consider as case of 'abnormal' deformation behaviour due to high magnitude settlements in earthfill section adjacent to concrete section. Displacements were limited.	de Melo & Direito (1982)
Sasumua	-	-	-	-	-	-	-	-	Post construction crest settlements described as 'too small to be measured'.	-	Only have deformation during construction. Relatively small settlements measured in IVM during construction.	Terzaghi (1958) Dixon (1958)

Table F1.5: Summary of embankment properties of puddle core earthfill embankments

Name	Owner / Authority	Year Completed	Height, H (m)	Length, L (m)	Upstream Slope (H to V)	Downstream Slope (H to V)	Core Dimensions		Geology	EMBANKMENT MATERIALS				
										Puddle Core		Select Zone Adjacent to Core		
							Top Width (m)	Core Slope (H to V)		Source	Class[n]	Yes/No	Material Description	Placement Method
Burnhope, UK	-	1935	41	nk	nk	nk	nk	nk	Carboniferous shale and limestone	Boulder Clay	CL (medium)	Yes	Boulder Clay - medium plasticity Sandy CLAY (CL)	450 mm layers, compacted by benzol rammers and 17t steam rollers
Challacombe, UK	-	1944	15	nk	3 to 1	2.5 to 1	1.2 m	1 to 15	nk	nk	ML (medium)	Yes	-	nk
Cwnwernderi, UK	-	1901	22	nk	3 to 1	2.75 to 1	1.5	1 to 10	nk	nk	CL (medium)	No ?	Not sure if design incorporates a select zone	-
Dean Head, UK	-	1840	19	nk	nk	nk	nk	nk	nk	nk	nk	nk	-	-
Happy Valley, Australia	South Australian Water Corp.	1896	25	806	3 to 1	2 to 1	2.44	1 to 8.25	Alluvial/tertiary sediments over sedimentary Cambrian bedrock	residual	CL	Yes	Silty and Sandy CLAYS (CL) - finer grained than outer shoulder earthfill.	150 mm layers compacted by wagons, carts and grooved rollers
Hollowell, UK	-	1937	13.1	427	3-5 to 1	2.5-4 to 1	2	1 to 10	Upper Lias Clays (marine clay-shale of Jurassic age)	Upper Lias - blue clay	CH	Yes	Lias clay from cut-off trench, CLAY (CH)	nk
Holmestyes, UK	Yorkshire Water	1840	25	158	3 to 1	2 to 1	2	1 to 20	Millstone Grit Series	Boulder Clay	CL ? (medium)	No	-	-
Hope Valley, Australia	South Australian Water Corp.	1870	21	765	3 to 1	2 to 1	1.8	1 to 12	Alluvial/tertiary sediments	alluvial / fluvial sandy clays and clays	CH	Yes	Sandy CLAYS and CLAYS (CL/CH)	300 mm layers compacted by 3.5t sheepsfoot roller (~ 90% SMDD)
Ladybower, UK	-	1945	43	nk	nk	nk	nk	nk	nk	nk	nk	nk	nk	nk
Langsett, UK	-	1904	33	nk	3 to 1	~3.5 to 1	nk	nk	shale, Millstone Grit series	clay	nk	Yes	nk	placed in thin layers
Ogden, UK	Yorkshire Water	1858	25	180 (approx)	3 to 1	2 to 1	2	1 to 10	Millstone Grit Series	Boulder Clay	CH	No	-	-
Ramsden, UK	Yorkshire Water	1883	25	120	3 to 1	2 to 1	3	1 to 12	Millstone Grit Series	Boulder Clay	ML/MH (medium to high)	Yes	Boulder Clay / weathered rock - sandy CLAYS with gravel and sandstone fragments	nk
Selset, UK	Cleveland Water Board	1959	39	930	4 to 1	>4 to 1	1.5	1 to 20	glacial drift deposits over sedimentary	Boulder Clay	CL (low)	Yes	Boulder Clay - Sandy CLAYS (CL) of low plasticity	placed in 225 mm layers, compacted by dozers and 13.6 t rollers (98.7% SMDD)
Walshaw Dean (Lower), UK	Yorkshire Water	1907	22	200 (approx)	3 to 1	2 to 1	2.6	1 to 12	Millstone Grit Series	Boulder Clay	CL (medium)	No	-	-
Widdop, UK	-	1878	20	nk	nk	nk	nk	nk	nk	nk	nk	No	-	-
Yan Yean, Australia	Melbourne Water Corp.	1857	9.6	962	3 to 1	2 to 1	3.05	1 to 3.3	Deep alluvial deposits, upper layer fissured	alluvium	CL/CH (medium to high)	No	-	-
Yateholme, UK	Yorkshire Water	1872	17	600	3 to 1	2 to 1	nk	nk	Millstone Grit Series	Boulder Clay	CL (medium)	No	-	-

Table F1.5: Summary of embankment properties of puddle core earthfill embankments (Sheet 2 of 3)

Name	EMBANKMENT MATERIALS			HYDROGEOLOGY				
	General Earthfill in Shoulders		Other Zones / Features	Reservoir		Pore Water Pressure Response to Reservoir Fluctuations		
	Material Description	Placement Method		Steady / Fluctuating	Comment	Upstream	Core	Downstream
Burnhope	Mudstone - hard	placed in 450 mm layers and compacted by 10t and 13t steam rollers	Rock from cut-off trench used to form embankment toes	nk	nk	assume delayed response in select zone	assume delayed response due to presence of select sandy clay zone	assume negligible response
Challacombe	nk	nk	-	Steady	normally full	assume delayed response in select zone	assume delayed response due to presence of select sandy clay zone	assume negligible response
Cwnwernderi	nk	nk	-	Steady	normally full, empty 9/77 to 1/81	nk	delayed response to re-filling	assume negligible response
Dean Head	nk	nk	-	nk	nk	nk	nk	nk
Happy Valley	Silty and Sandy CLAYS (CL) with pockets of sands and gravels	150 mm layers compacted by wagons, carts and grooved rollers (avg 88% MMDD)	-	Fluctuating	seasonal drawdown typically 4m, but as much as 6 to 7 m	outer face responds to reservoir level, limited response in select zone	assumed limited response	no change
Hollowell	Sand and sand-rock	placed in thin layers by dozer	stone filled trenches in downstream shoulder for drainage	nk	nk	assume delayed response in select zone	assume delayed response due to presence of select sandy clay zone	assume negligible response
Holmestyes	Weathered mudstones & sandstones, mix sandy silty clays with gravel to boulder size fragments	nk	puddle blanket placed on upstream face	nk	10 m drawdown in 1990	no change	no change	no change
Hope Valley	Outer downstream shoulder of silty to clayey sands and gravels (SC/SM/GC)	placed in 1.2 m layers and compacted by 3.5t sheepsfoot roller	Stabilising fill at downstream toe	Fluctuating	seasonal drawdown typically 3 to 4 m, up to 5 m	variable response to reservoir level adjacent to core	assume limited response	Not likely, but little information, possible perched water.
Ladybower	nk	nk	-	nk	nk	nk	nk	nk
Langsett	Not sure, possibly weathered shale	placed in 900 mm lifts and compacted by haulage traffic.	-	nk	nk	nk	assumed limited response	Assume little response
Ogden	Weathered mudstones & sandstones, mix sandy silty clay with gravel to boulder size fragments.	Likely placed in thick given the period of construction.	puddle blanket placed on upstream face, but not effective	Fluctuating	Full drawdown in 1990/91 and 10 m drawdown in 1992/93	responds with reservoir level	likely some response	no change
Ramsden	Weathered mudstones & sandstones, mix sandy silty clay with gravel to boulder size fragments	Likely placed in thick given the period of construction.	-	Fluctuating	Emptied in 1988, 6 m drawdown in 1989	responds with reservoir level	some response	no change, affected by tailwater level
Selset	Boulder Clay - Sandy CLAYS (CL) of low plasticity	placed in 225 mm layers, compacted by dozers and 13.6 t rollers (98.7% SMDD)	drains installed in embankment slopes and foundation	nk	nk	Likely response given presence of drains	assume limited response due to presence of select zone	assume negligible response
Walshaw Dean (Lower)	Weathered mudstones & sandstones, mix sandy silty clay with gravel to boulder size fragments	nk	-	Fluctuating	Large drawdowns, typically 10 to 15 m	responds with reservoir	partial response to reservoir	assume negligible response
Widdop	nk	nk	-	nk	nk	nk	nk	nk
Yan Yean	alluvial clays (CL/CH) of medium to high plasticity in upstream shoulder and sandy silts to silty clays (ML/CL) in downstream shoulder	placed in 600 to 1200 mm lifts	-	Fluctuating	Seasonal drawdown up to 2.5 m	little to no response adjacent to core	little to no response	negligible response
Yateholme	Weathered mudstones & sandstones, mix sandy silty clay with gravel to boulder size fragments	nk	-	Fluctuating	Seasonal 4 to 7 m drawdown	responds with reservoir	likely partial response to reservoir	assume negligible response

Table F1.5: Summary of embankment properties of puddle core earthfill embankments (Sheet 3 of 3)

Name	POST CONSTRUCTION DEFORMATION					Comments	References
	Timing	Total Settlement Since End of Construction		S_{LT} (% settlement per log cycle time)	Summary of Monitoring		
		mm	% of H				
Burnhope	EOC to 1957	702	1.71	0.80	Settlement of upstream slope and crest from EOC.	Greater post construction settlement of the crest relative to the upstream shoulder.	Skempton (1990)
Challacombe	from const to 1981	520	3.48	0.80	Settlement of crest only	520 mm crest settlement to 1989. Rate slightly greater than 1 mm/year from 1981 to 1989 (37 to 45 years after construction).	Charles and Watt (1987) Charles and Tedd (1991)
Cwnwernderi	1977 to 1989	-	-	0.90 (at steady reservoir)	Settlement of crest only	Reservoir emptied from 1977 to 1981. Long-term rate is for settlements after this period to 1989.	Charles and Watt (1987) Charles and Tedd (1991)
Dean Head	1977 to 1984	-	-	7.4	Settlement of crest only	Major drawdown caused large settlement, but this period of monitoring has been excluded from the long-term settlement rate, S_{LT}.	Charles and Tedd (1991)
Happy Valley	1897 to 1973 1982 to 1998	772 mm to 1973	3.10	1.0 (crest and d/stream slope) 1.5 (upstream slope)	Early monitoring from EOC is crest settlement. Later monitoring from 1982 is settlement and displacement of the upper slope regions and the downstream toe	Piezometric levels in outer adge of the upstream shoulder respond to drawdown. The response decreases the further the distance into the upstream shoulder. It has been assumed that the select upstream zone acts as water barrier in addition to core.	EWSD SA (1981a) Pinkerton (1984) Collingham and Newman (1977)
Hollowell	from EOC to 1954	817	6.24	0.70 (1948 to 1954)	Settlement of crest only	Slide in downstream slope occurred during construction. Large early crest settlements are possibly influenced by deformations due to the limited stability of downstream slope.	Kennard (1955)
Holmestyes	1990 to 1991	-	-	2.3 (but only on 18 mnths data)	Settlement and displacement of crest for 18 month period	Initial muddy leakage problem. In 1857 upstream slope blanketed with puddle clay. Very limited response of piezometers in upstream fill, core and downstream fill on 10 m drawdown in 1990 indicating the upstream clay layer is an effective water barrier.	Tedd et al (1997b) Tedd et al (1993)
Hope Valley	1870 to 1994 1988 on	1820	8.7	2.6	From 1870 - settlement of crest; From 1988 - settlement and displacement of downstream slope	Large settlements in early years of embankment operation. Foundation seepage problem on first filling and clay blanket placed in impoundment area. Piezometers in the upstream shoulder show a variable response to reservoir fluctuation, ranging from 25 to 100% of the change due to the reservoir.	EWSD SA (1981b) Collingham (1997) SMEC (1995, 1999b)
Ladybower	1950 to 1984	-	-	2.0	Settlement of crest only	Limited information available for Ladybower dam.	Charles and Tedd (1991)
Langsett	1904 to 1907	124 (first 3 years)	0.38	0.20	Settlement of crest only	No information on reservoir fluctuation, or even if the reservoir was filled during the period of monitoring.	Skempton (1990)
Ogden	1989 to 1993	-	-	10 (on 10 m drawdown)	Settlement of crest, upstream and downstream shoulders from 1989. IVM installed in core in 1980's.	Pore water pressure response in upstream slope on drawdown indicates possible perched water tables due to sloping of earthfill layers toward the core. The upstream blanket is not effective as a water barrier. Very high long-term settlement rate based on the permanent settlement on 10 m drawdown. Suspect the rate during normal operation is much less than this.	Tedd et al (1997b)
Ramsden	1949 - 85 1988 - 90	-	-	6.6 (1977 to 1985) 9.5 (1949 to 1986)	Settlement and displacement of crest and slopes. IVM installed in core in 1980's.	IVM results on large drawdown indicate possible shear in core at 10 - 11 m depth. Note that CPTs show soft zone at 9 - 10 m. Large settlement on full drawdown in 1988/89. Lower downstream slope inundated by Brownhill reservoir.	Holton (1992) Tedd et al (1990) Tedd and Holton (1987) Tedd et al (1997b)
Selset	from EOC to 1970	313 (first 10 years)	0.80	0.40	Settlement of crest only	Large differential settlement between core and shoulders during construction due to lateral yielding of the puddle core. Crains in foundation and shoulder earthfill to dissipate pore water pressures during construction.	Bishop and Vaughan (1962) Kennard and Kennard (1962) Charles and Tedd (1991)
Walshaw Dean (Lower)	some early data, 1990 to 1995	-	-	6.7 (poss 4.5 early)	Settlement and displacement of crest. IVM installed in core in 1980's.	leakage and erosion problems early on, possibly through the cut-off trench.	Tedd et al (1997b) Charles and Watt (1987)
Widdop	1988 to 1990	-	-	nk	Crest settlement during large drawdown.	Large permanent settlement of crest during large drawdown (virtually emptied the reservoir).	Tedd et al (1997a)
Yan Yean	1986 to 1999	1200 (approx)	12.5% (approx)	0.5 (upstream edge of crest) 5.0 (downstream edge of crest)	Settlement and displacement of crest (up and downstream edges), and downstream slope and toe.	Very limited change in pore water pressure in the upstream shoulder on drawdown. Deformation of the downstream slope is indicative of a tertiary creep phase of movement. Stability berm added to downstream slope due to stability and internal erosion concerns.	MMBW (1985) SMEC (1996d, 1997b, 1998c) Connell Wagner (1999)
Yateholme	1989 to 1992	-	-	5.4	Settlement of crest only	Long-term settlement rate determined from only a short period of monitoring during which the measured settlement was only 3 to 4 mm. The rate may be on the high side.	Tedd et al (1997b)

2.0 SUMMARY PLOTS OF POST CONSTRUCTION DEFORMATION BEHAVIOUR

In the following sections data from the case study analysis of embankment dams is presented for the post construction surface deformation of the downstream (Section 2.1) and upstream (Section 2.2) slope regions. The data is from surface measurement points (SMP).

Zero time, t_0, is established at the end of embankment construction to provide a consistent basis point for comparison. If the SMP was installed and measurements taken prior to the end of construction, then those measurements from prior to end of construction have been excluded and the base survey re-established on or slightly after the end of construction. The unit of time used for all plots is years.

Where possible the deformation records used are the actual records. This has been possible for a large number of the Australian dams and most of the United States Bureau of Reclamation (USBR) dams. For a number of case studies however, the data has been digitised from published plots in the literature. For these cases the digitised points are and any change in slope shown in the plotted figures will be only a representation of the actual data points.

2.1 *POST CONSTRUCTION DEFORMATION OF THE DOWNSTREAM SLOPE*

For the post construction surface deformation of the downstream slope region, SMPs for each case study have been preferentially selected from the mid to upper region of the downstream slope, in the range 0.6 to 0.8 times the embankment height. But embankments were not excluded if the only SMPs on the downstream slope were outside this region.

The layout of the data presented is as follows:

- Section 2.1.1 – Total post construction settlement plots at 3, 10 and 20 to 25 years after the end of embankment construction;
- Section 2.1.2 – Settlement versus time plots; and
- Section 2.1.3 – Lateral displacement (normal to the dam axis) versus time plots.

2.1.1 Post Construction Total Settlement of the Downstream Slope

The total post construction surface settlement for the mid to upper region of the downstream slope is presented as plots of settlement versus dam height at selected times after the end of construction; at 3, 10 and 20 to 25 years after the end of embankment construction (Figure F2.1 to Figure F2.3).

Base readings for the data are generally in the range from 0 to 0.5 years after the end of construction, with several slightly outside this range. The data are mainly for embankments on rock foundations. Several embankments on soil/rock or soil foundations have been included where the foundation is considered to have a limited influence on the dam settlement, or where it can be excluded by deducting foundation settlement from base plate or base cross-arm readings from IVM gauges.

For the mid to upper downstream slope region, the data has been sorted based on material type of the downstream shoulder fill. The embankments with rockfill shoulders have been further divided into compaction rating of the rockfill. Embankments with dry placed and poorly compacted rockfills have been highlighted.

The height designated for each case study is the height from the SMP to foundation level. For several cases the height is from the SMP to bedrock level, but this has only be undertaken for cases studies where the foundation has some but not an overly significant influence on the deformation and its thickness is less than about 20 % of the height of the embankment at the SMP location.

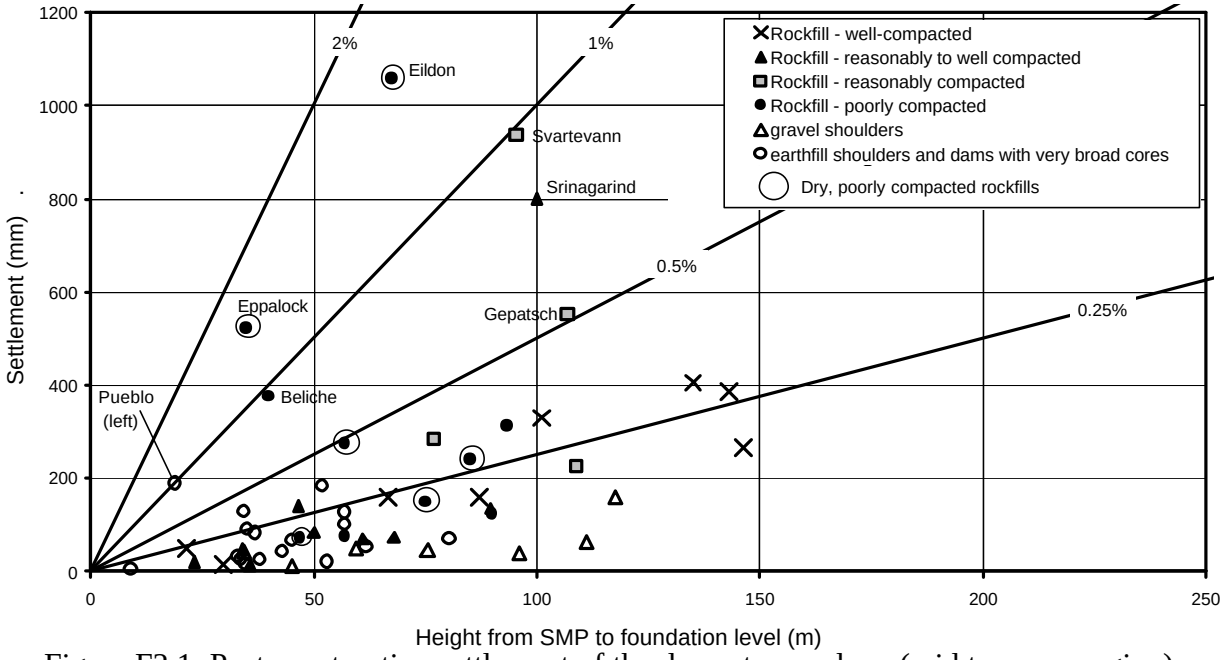

Figure F2.1: Post construction settlement of the downstream slope (mid to upper region) at 3 years after end of construction.

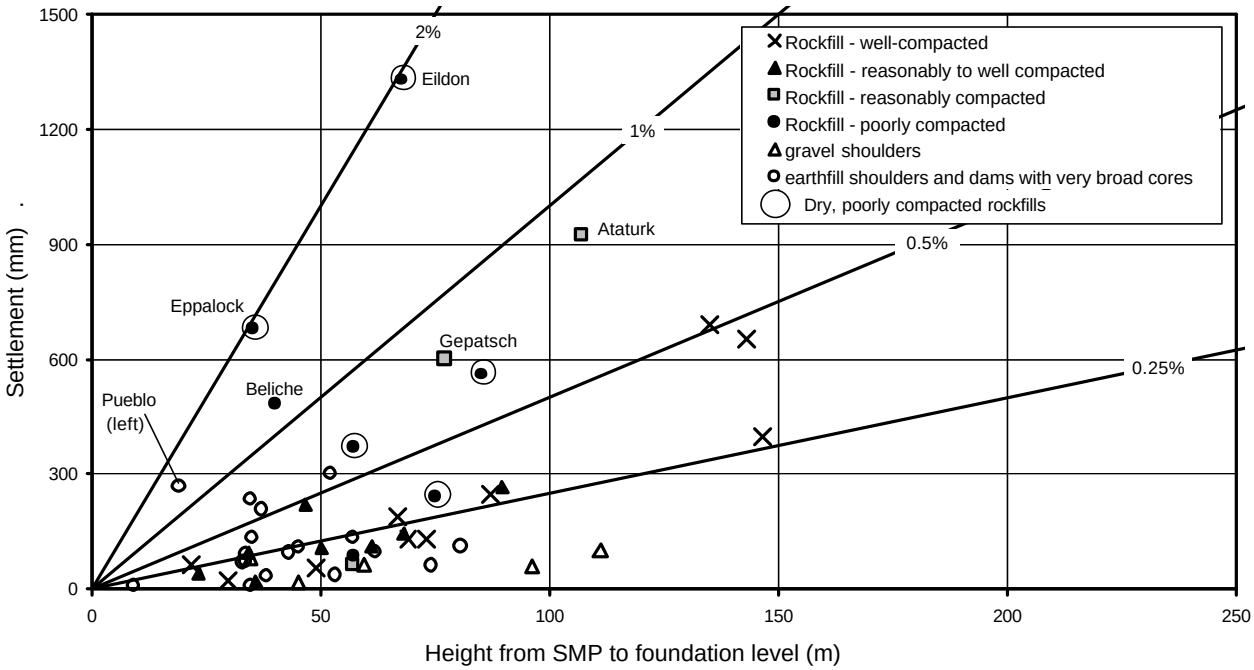

Figure F2.2: Post construction settlement of the downstream slope (mid to upper region) at 10 years after end of construction.

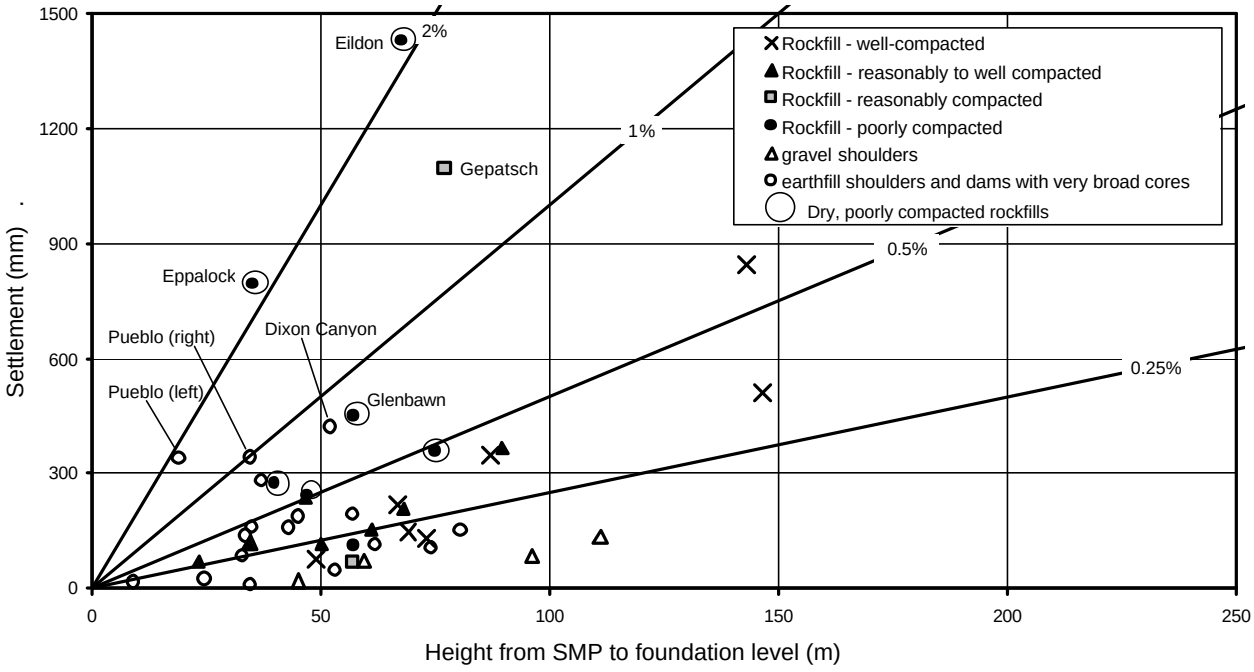

Figure F2.3: Post construction settlement of the downstream slope (mid to upper region) at 20 to 25 years after end of construction.

2.1.2 Post Construction Settlement Versus Time of the Mid to Upper Region of the Downstream Slope.

The post construction settlement versus time records of the mid to upper region of the downstream slope are presented in Figure F2.4 to Figure F2.11 in the form of settlement, as a percentage of the height from the SMP to foundation level, versus time (in years since end of construction) on a log scale.

The case studies have been sorted based on material type forming the downstream shoulder. For embankments with rockfill in the downstream shoulder, further sorting based on compaction rating (refer Section 1.3.3 of Chapter 1 for definitions of the terms used). The data is presented in the following figures:

- Figure F2.4 – zoned earth and rockfill embankments with well-compacted rockfill in the downstream shoulder;
- Figure F2.5 – zoned earth and rockfill embankments with reasonably to well compacted rockfill in the downstream shoulder;
- Figure F2.6 – zoned earth and rockfill embankments with reasonably compacted rockfill in the downstream shoulder;
- Figure F2.7 – zoned earth and rockfill embankments with poorly compacted rockfill;
- Figure F2.8 – zoned earth and rockfill embankments with compacted gravels in the downstream shoulder;
- Figure F2.9 – zoned earth and rockfill embankments with compacted earthfills in the downstream shoulder;
- Figure F2.10 - embankments with very broad central earthfill zones, and limited foundation influence; and
- Figure F2.11 – embankments with very broad central earthfill zones, and potentially significant foundation influence. For this figure settlement is plotted in millimetres.

No limitations on inclusion or exclusion of case studies have been placed on the timing of the base survey reading for the data presented. In most cases the base survey reading was within 0.5 years of end of embankment construction, but for a number of cases it was after this time.

The size of each figure has been set to the same margins for each plot area and the time interval standardised to cover from 0.1 to 100 years to allow for visual comparison between the figures. In most cases a standard vertical axis of 0 to 1.2% settlement has

been used, but for several plots where settlements were larger a broader vertical axis has been adopted. On occasion a secondary plot with the standard vertical axis of 0 to 1.2% settlement is presented as figure b if a broader axis has been used.

Several other points to note from the figures are:

- Where the data does not extend to the y-axis it is because the base reading is or has assumed to be at the end of construction; i.e. at zero time.
- The end of first filling has been indicated in the figures by an arrow for each case study. There are several reasons why first filling is not indicated for a number of cases studies:
  - First filling was not completed in the period of deformation shown;
  - First filling was completed prior to the base survey reading; and
  - For cases with the base reading at zero time first filling occurred in the time period from 0 to the time of the first reading point shown.

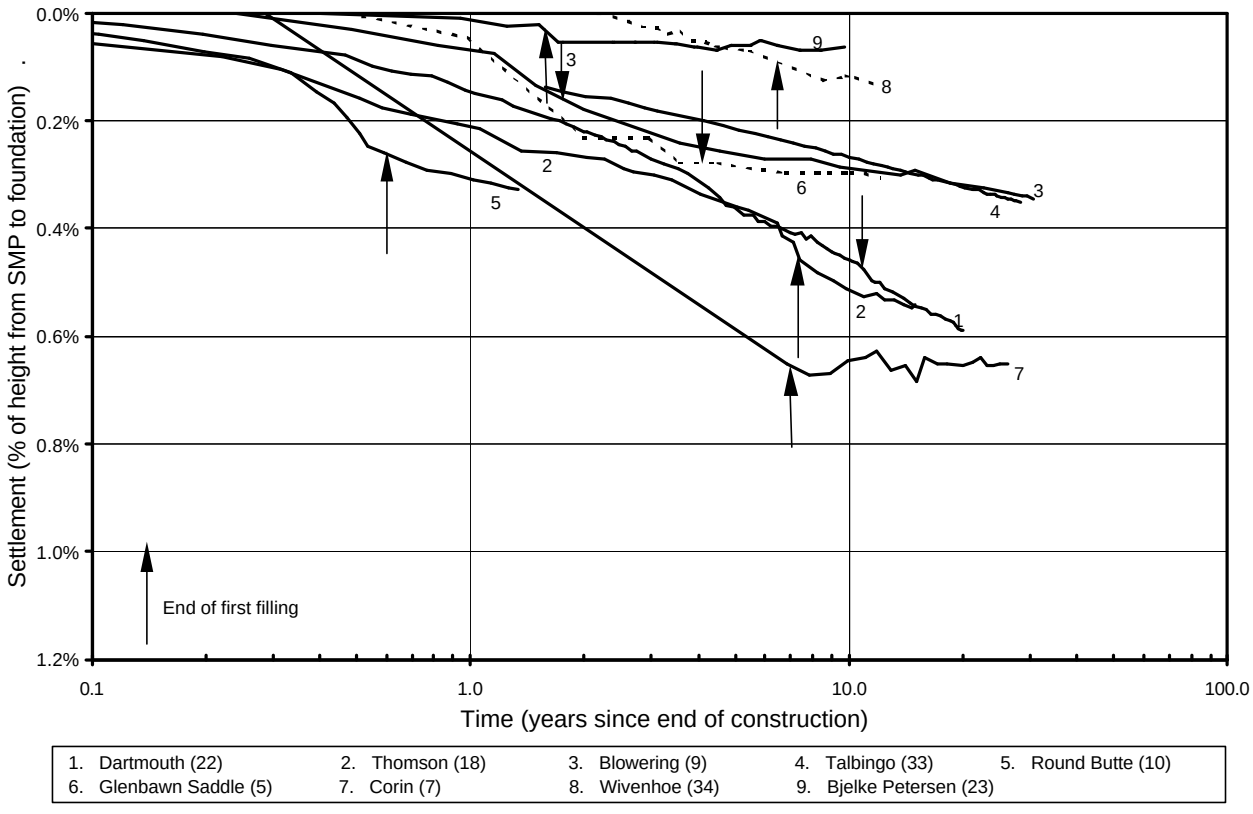

Figure F2.4: Post construction settlement of the downstream slope (mid to upper region) for central core earth and rockfill embankments with well-compacted rockfill in the downstream shoulder.

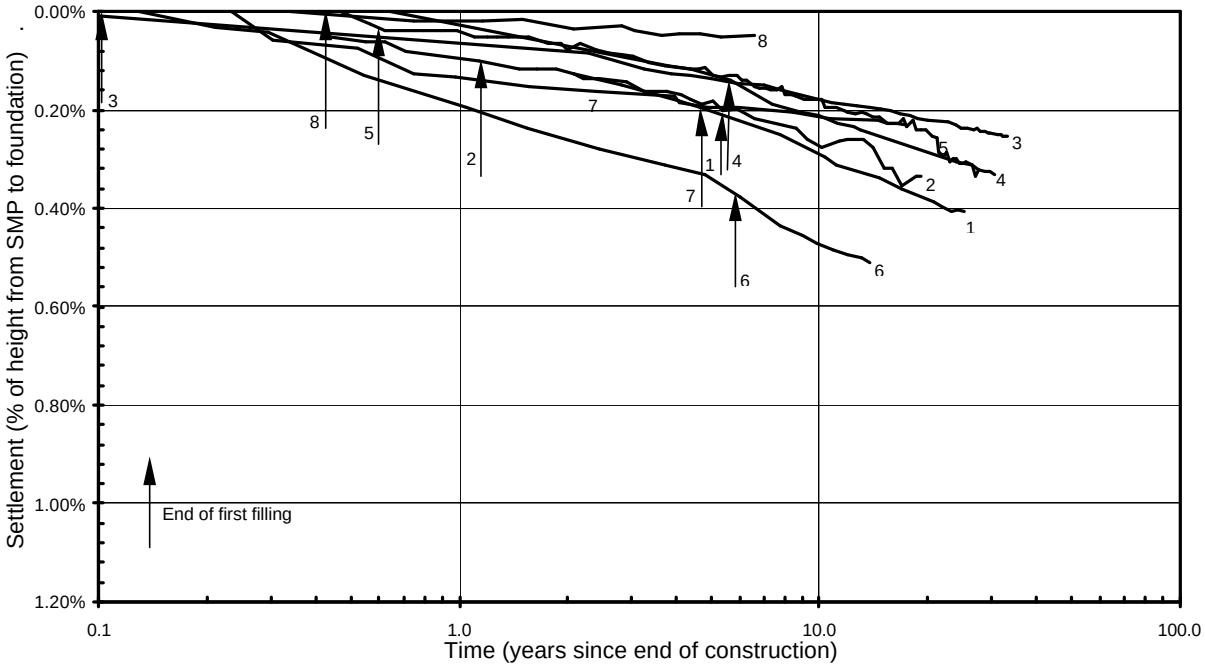

1. Copeton (101) 2. Maroon (31) 3. Geehi (18) 4. Wyangala (17) 5. William Hovell (Ch 503)
6. Windemere (13) 7. Chaffey (9) 8. Peter Faust (SS08)

Figure F2.5: Post construction settlement of the downstream shoulder (mid to upper region) for zoned earth and rockfill embankments with reasonably to well compacted rockfill in the downstream shoulder.

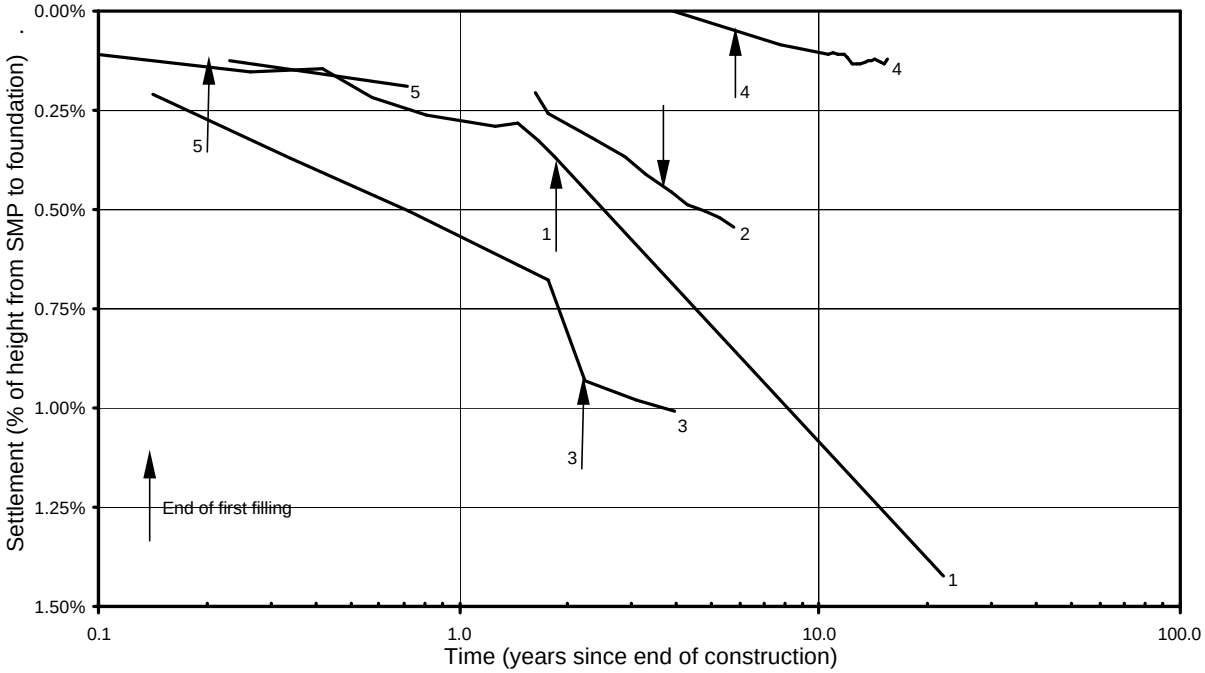

1. Gepatsch (4) 2. Ataturk (133) 3. Svartevann (EL 870) 4. Split Yard Creek (SS28) 5. Vatnedalsvatn

Figure F2.6: Post construction settlement of the downstream shoulder (mid to upper region) for zoned earth and rockfill embankments with reasonably compacted rockfill in the downstream shoulder.

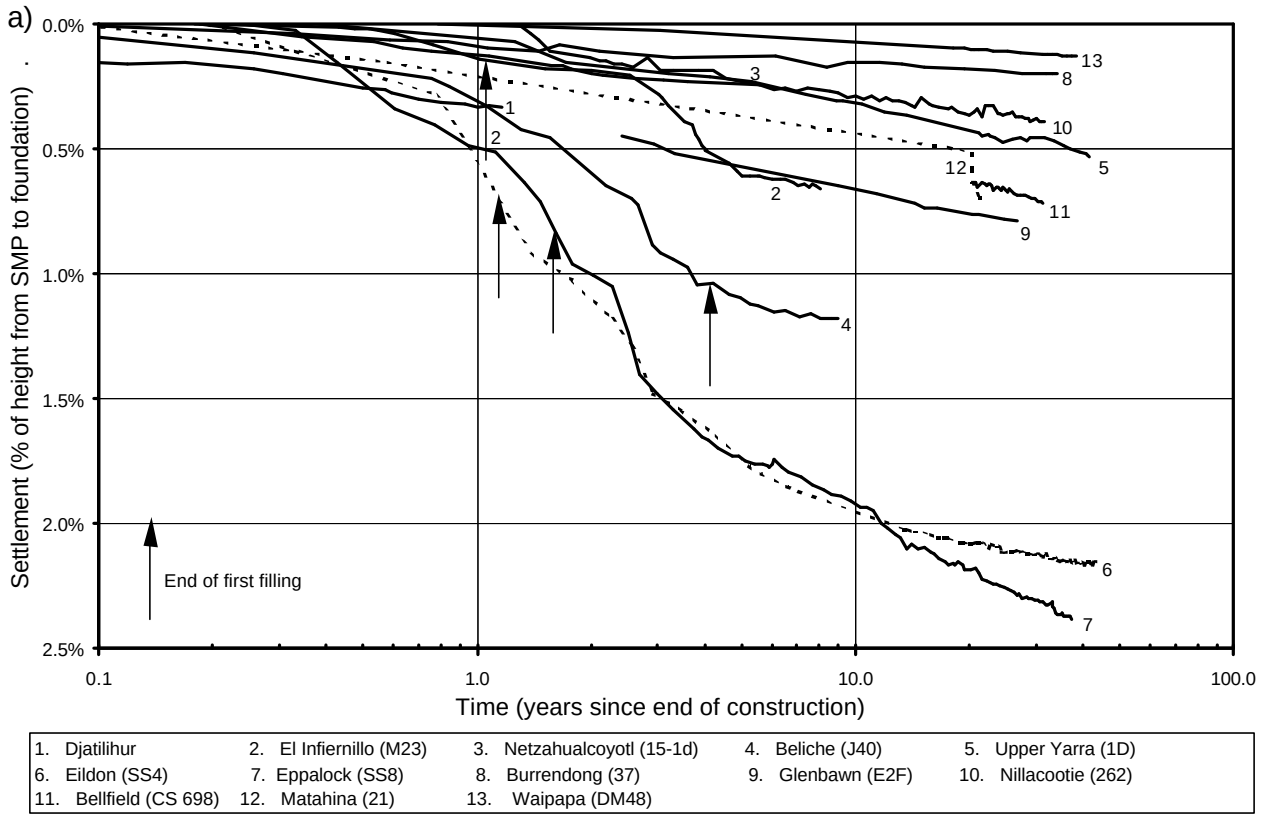

1. Djatilihur 2. El Infiernillo (M23) 3. Netzahualcoyotl (15-1d) 4. Beliche (J40) 5. Upper Yarra (1D)
6. Eildon (SS4) 7. Eppalock (SS8) 8. Burrendong (37) 9. Glenbawn (E2F) 10. Nillacootie (262)
11. Bellfield (CS 698) 12. Matahina (21) 13. Waipapa (DM48)

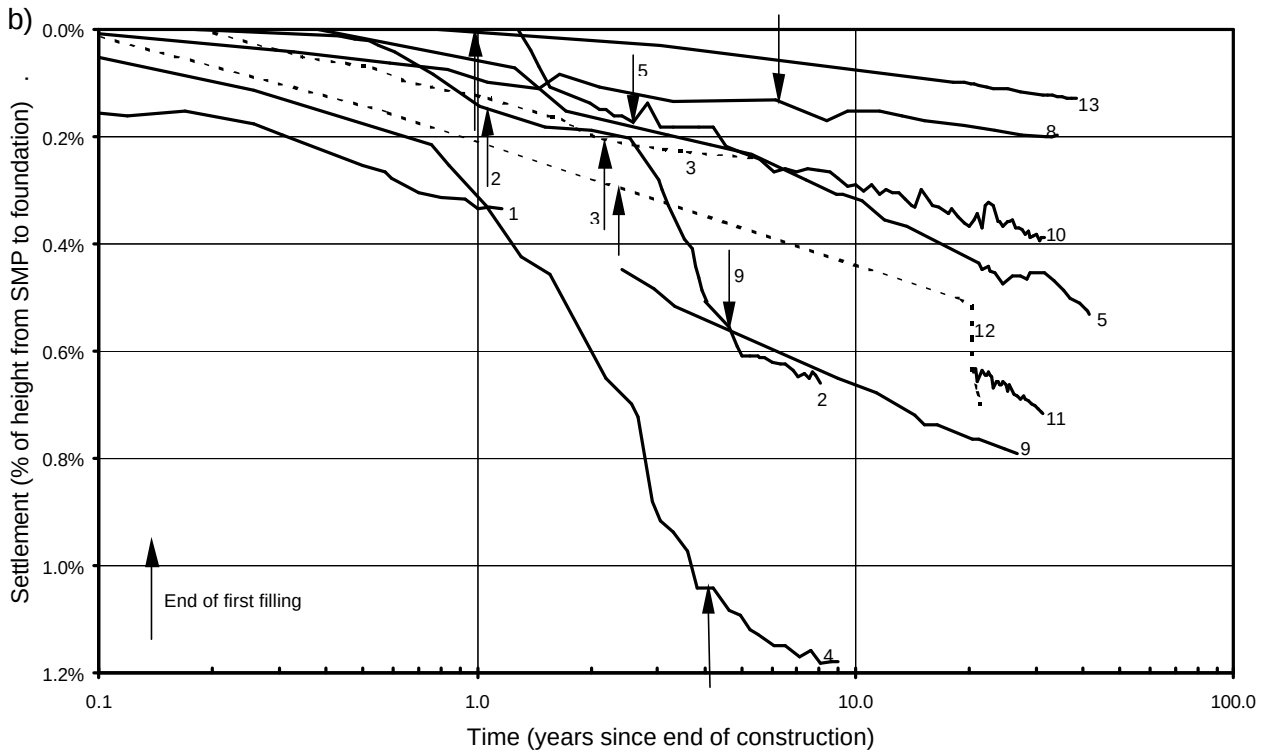

1. Djatilihur 2. El Infiernillo (M23) 3. Netzahualcoyotl (15-1d) 4. Beliche (J40) 5. Upper Yarra (1D) 8. Burrendong (37)
9. Glenbawn (E2F) 10. Nillacootie (262) 11. Bellfield (CS 698) 12. Matahina (21) 13. Waipapa (DM48)

Figure F2.7: Post construction settlement of the downstream slope (mid to upper region) for zoned earth and rockfill embankments with poorly compacted rockfill in the downstream shoulder.

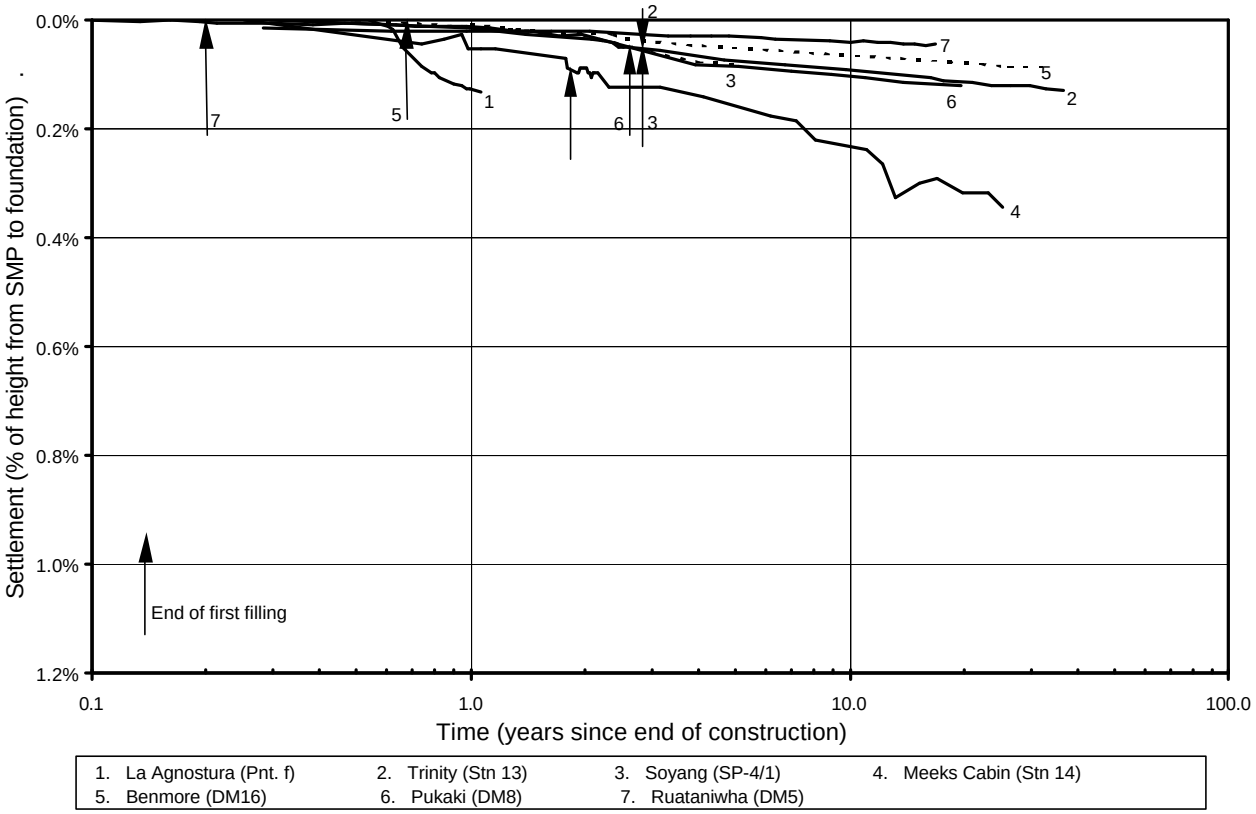

Figure F2.8: Post construction settlement of the downstream slope (mid to upper region) for zoned embankments with compacted gravels in the downstream shoulder.

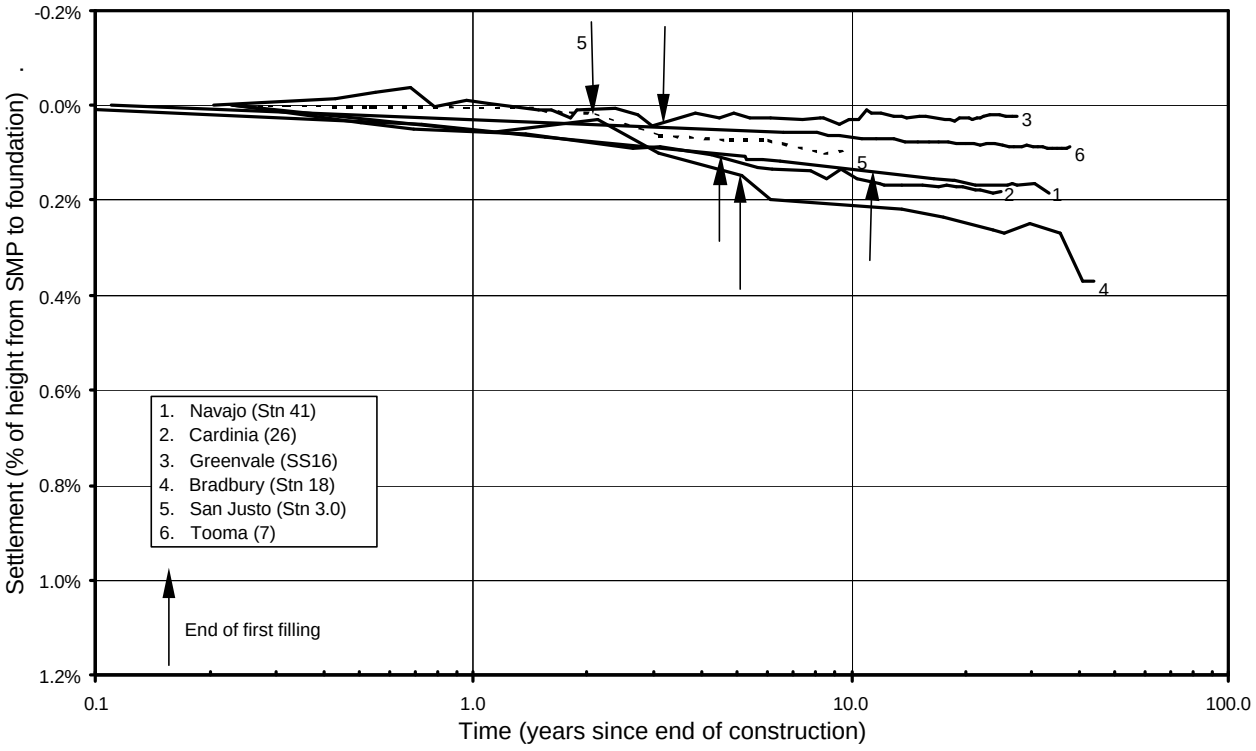

Figure F2.9: Post construction settlement of the downstream slope (mid to upper region) for zoned embankments with compacted earthfills in the downstream shoulder.

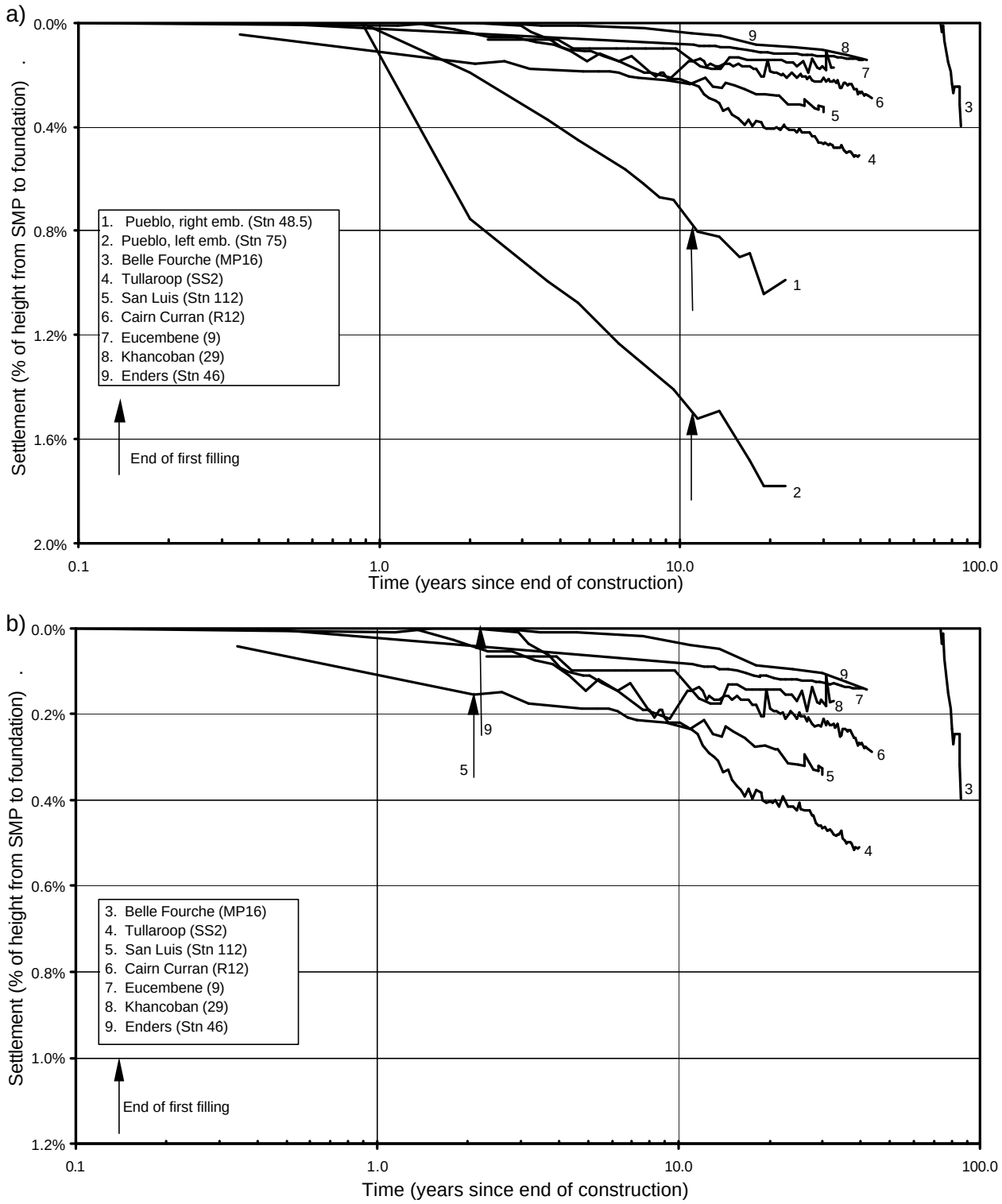

Figure F2.10: Post construction settlement of the downstream slope (mid to upper region) for embankments with very broad central earthfill zones, and limited foundation influence.

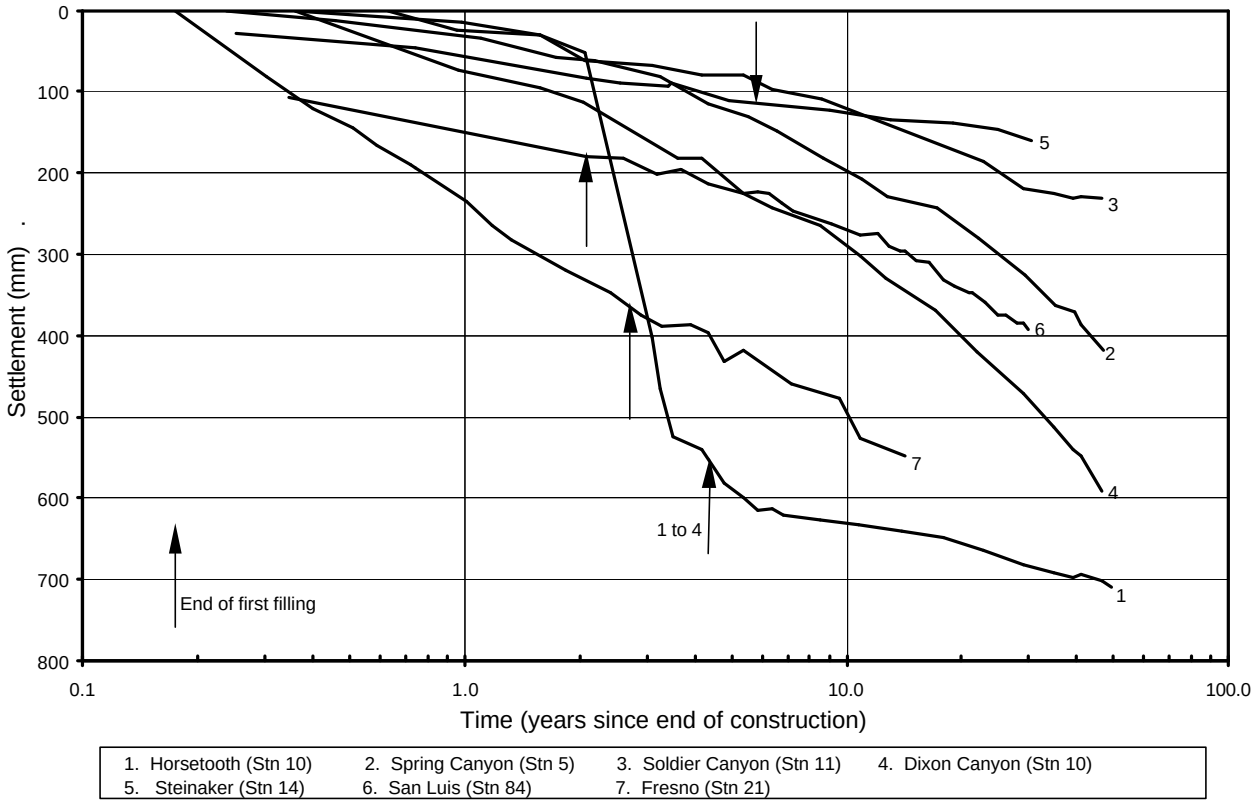

Figure F2.11: Post construction settlement of downstream slope (mid to upper region) for embankments with very broad central earthfill zones, and potentially significant foundation influence.

2.1.3 Post Construction Displacement of the Mid to Upper Region of the Downstream Slope.

The case study data of the post construction displacement normal to the dam axis versus time for the mid to upper region of the downstream slope is presented in Figure F2.12 to Figure F2.19 in the form of displacement, in millimetres, versus time (in years since the end of construction) on a log scale. Displacement in a downstream direction is positive and in an upstream direction is negative.

As for the settlement versus time plots, the case studies have been sorted based on material type forming the downstream shoulder and the embankments with rockfill further sorting based on compaction rating.

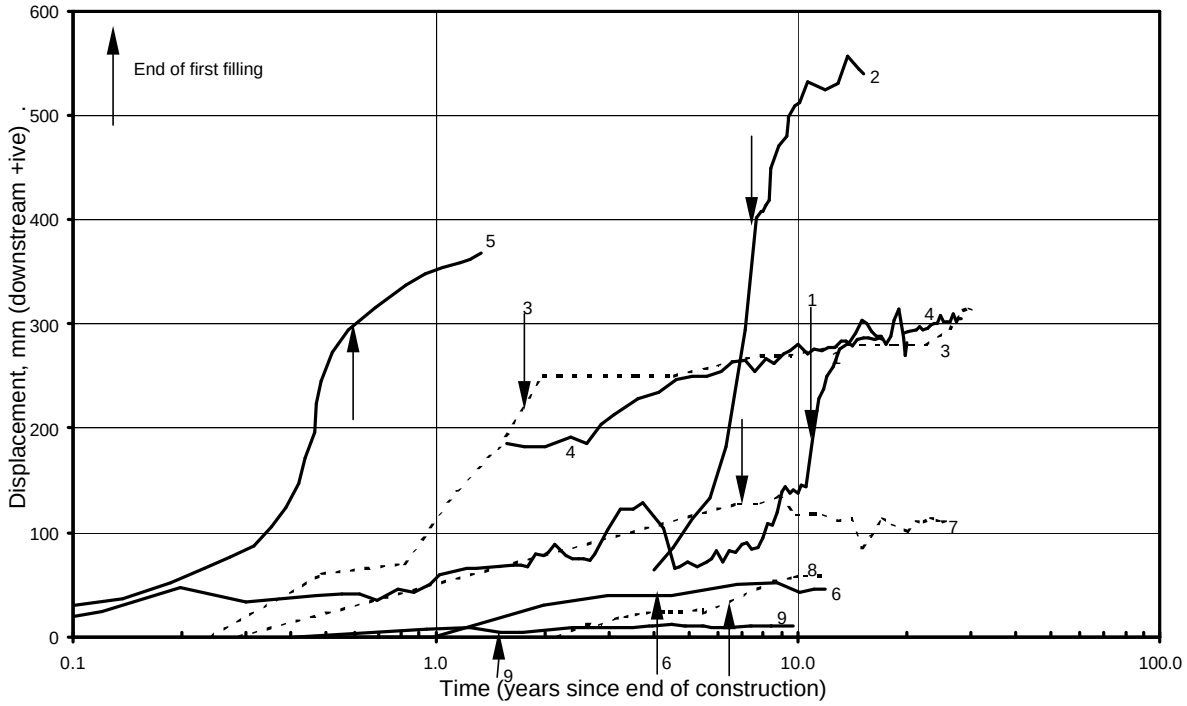

Figure F2.12: Post construction displacement of the downstream slope (mid to upper region) for central core earth and rockfill embankments with well-compacted rockfill in the downstream shoulder.

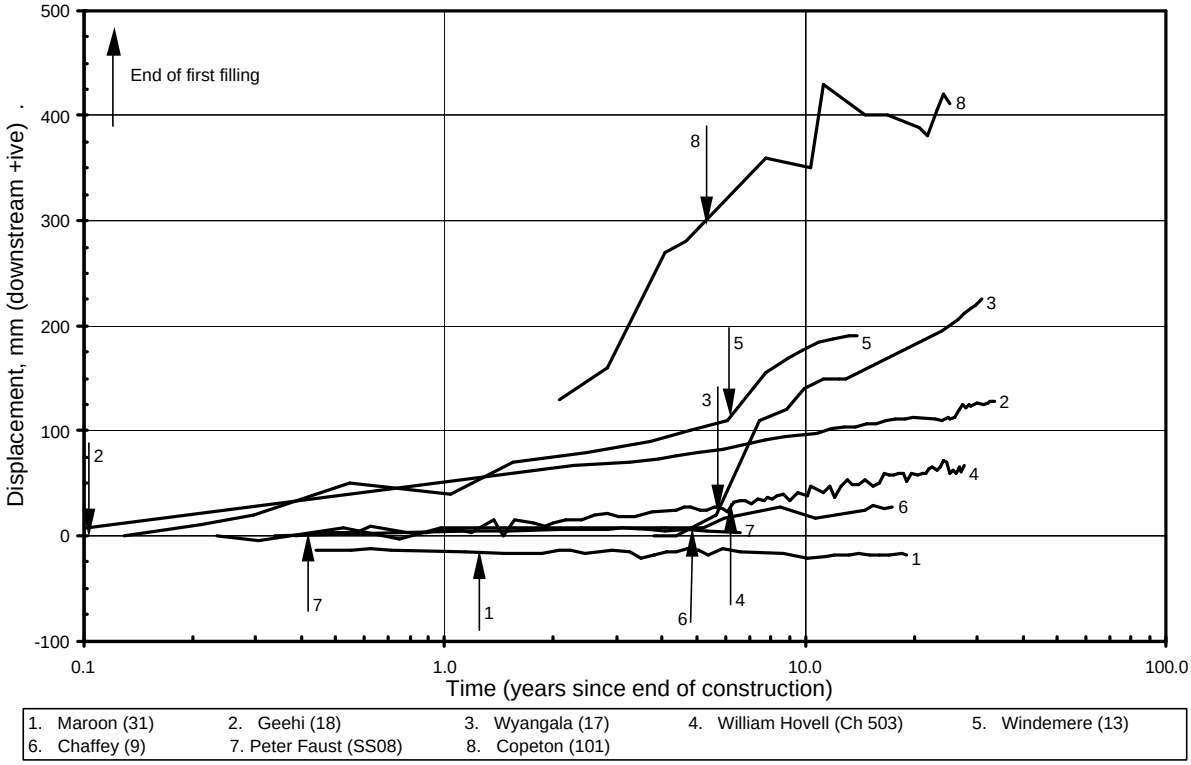

Figure F2.13: Post construction displacement of the downstream slope (mid to upper region) for central core earth and rockfill embankments with reasonably to well compacted rockfill in the downstream shoulder.

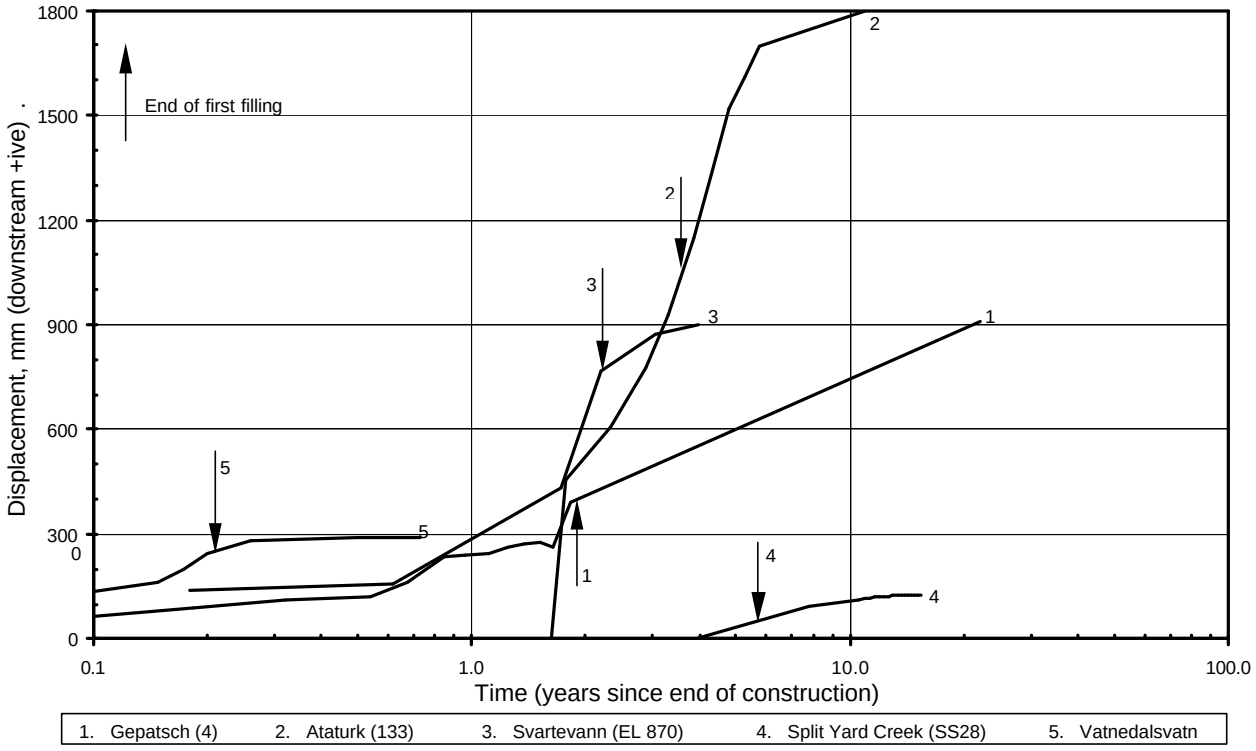

Figure F2.14: Post construction displacement of the downstream slope (mid to upper region) for central core earth and rockfill embankments with reasonably compacted rockfill in the downstream shoulder.

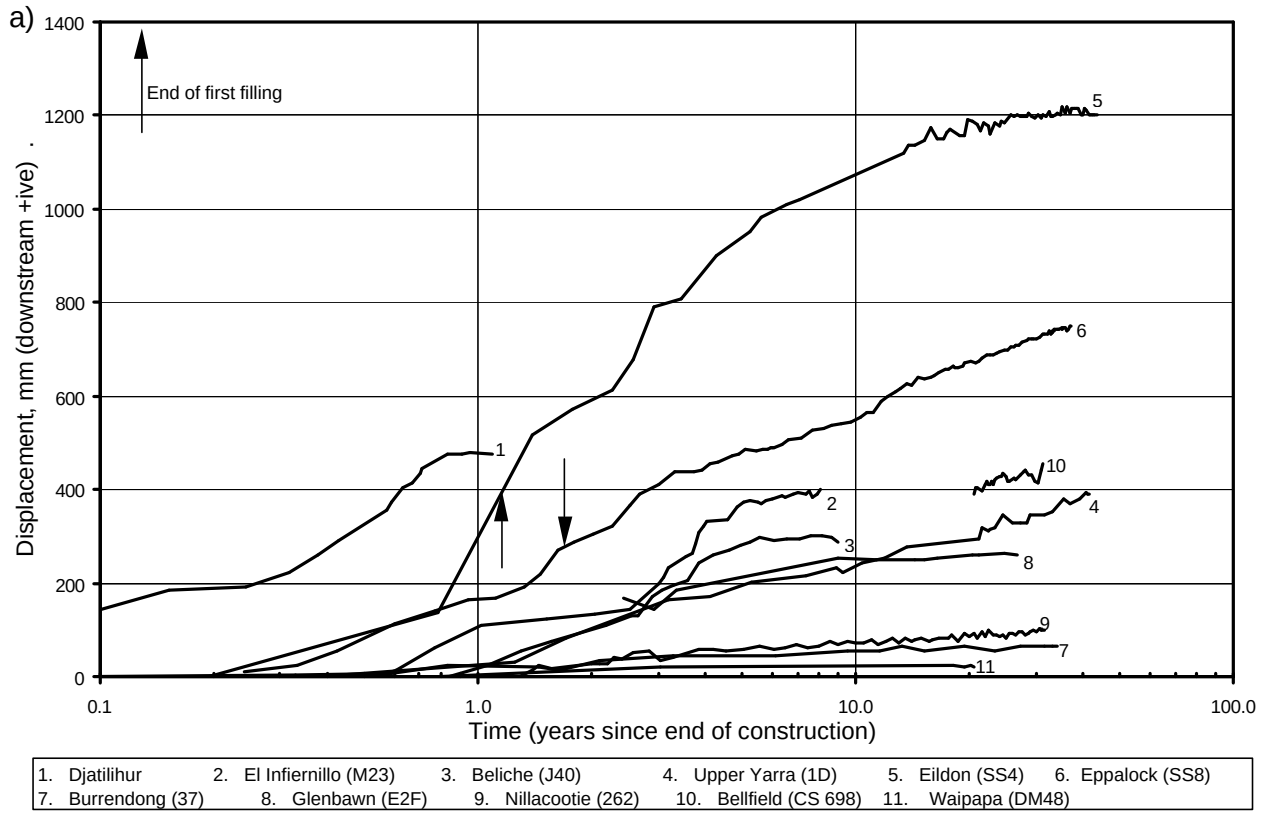

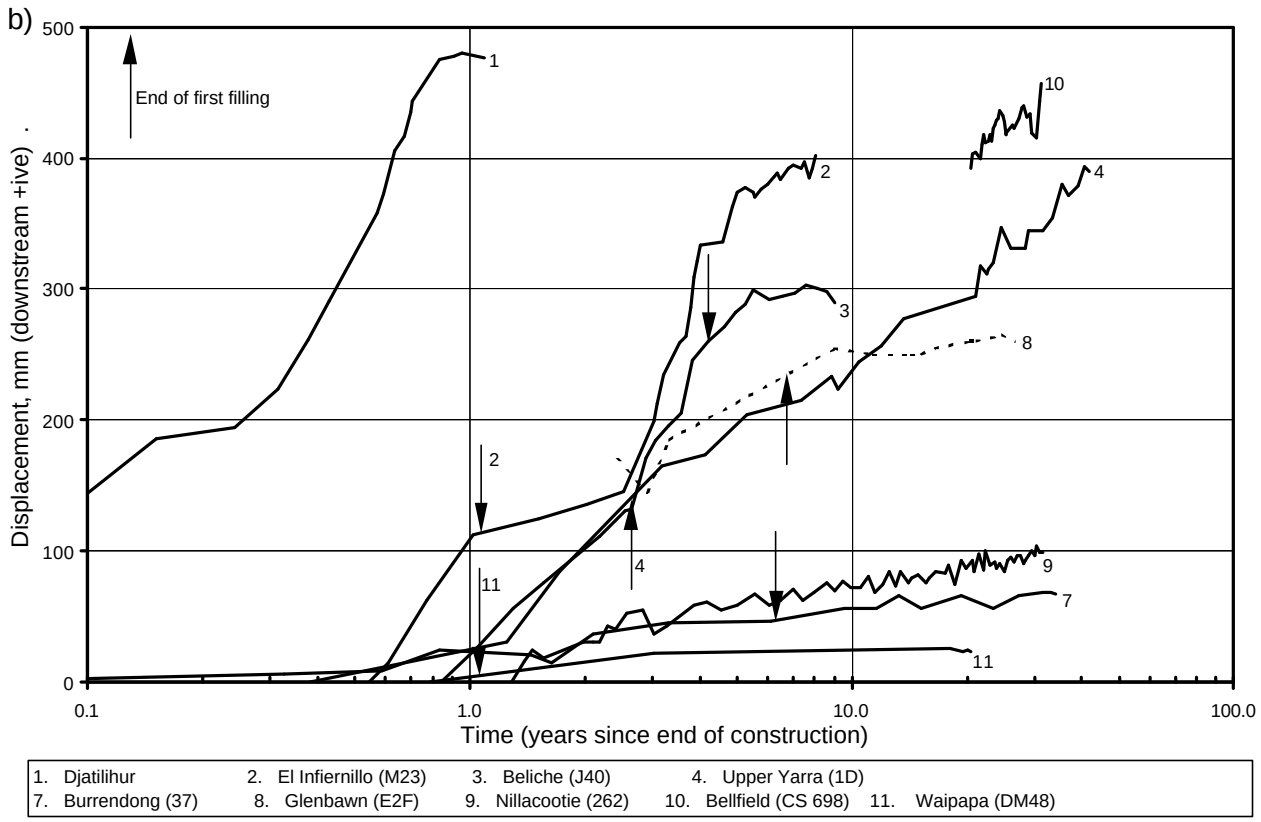

Figure F2.15: Post construction displacement of the downstream slope (mid to upper region) for zoned earth and rockfill embankments with poorly compacted rockfill in the downstream shoulder.

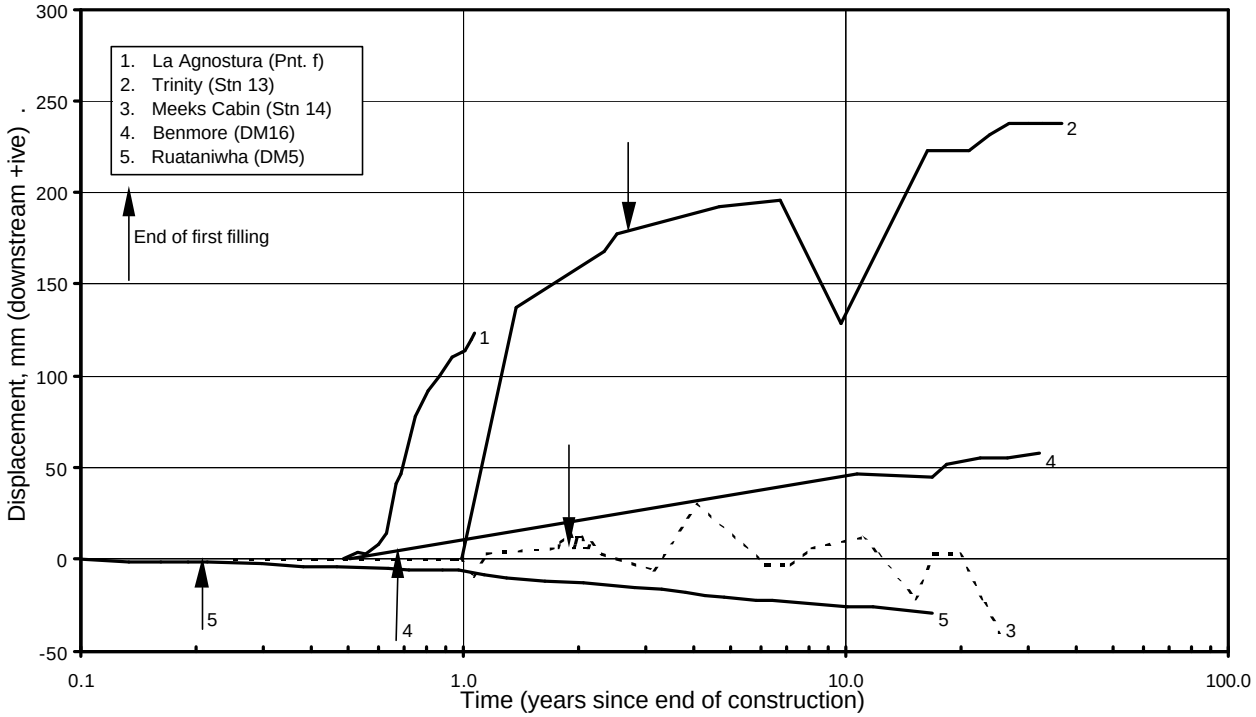

Figure F2.16: Post construction displacement of the downstream slope (mid to upper region) for zoned embankments with compacted gravels in the downstream shoulder.

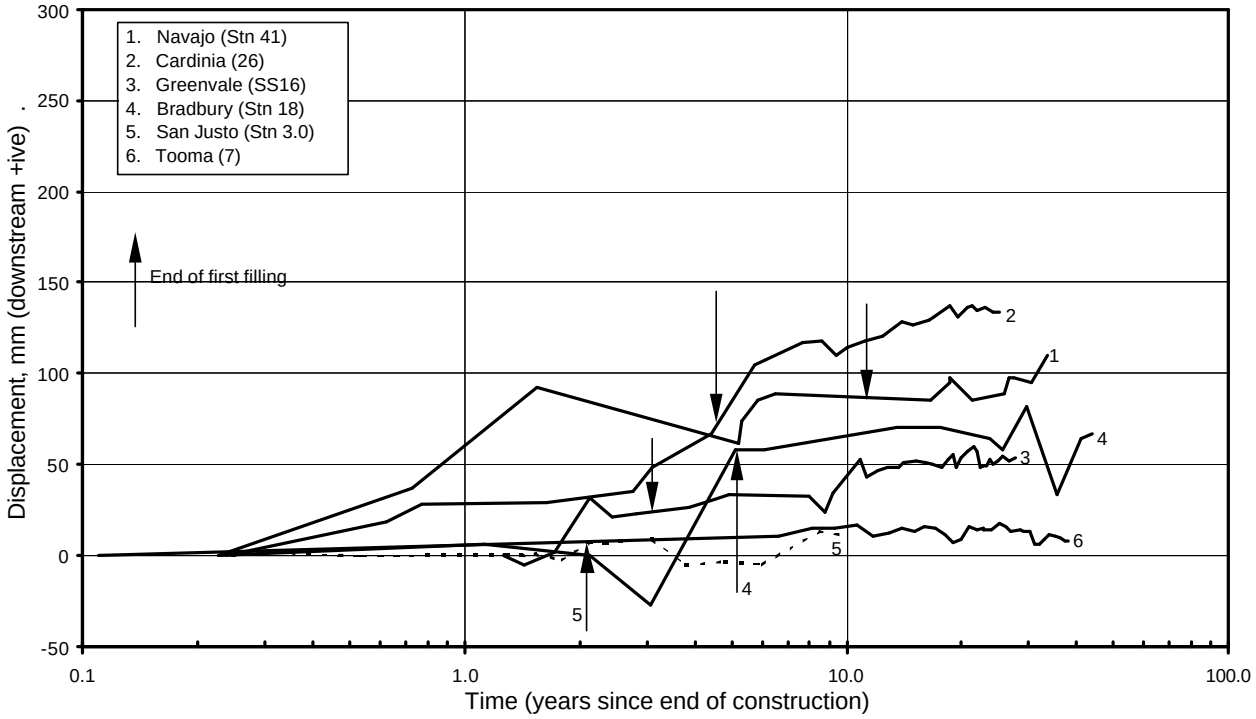

Figure F2.17: Post construction displacement of the downstream slope (mid to upper region) for zoned embankments with compacted earthfills in the downstream shoulder.

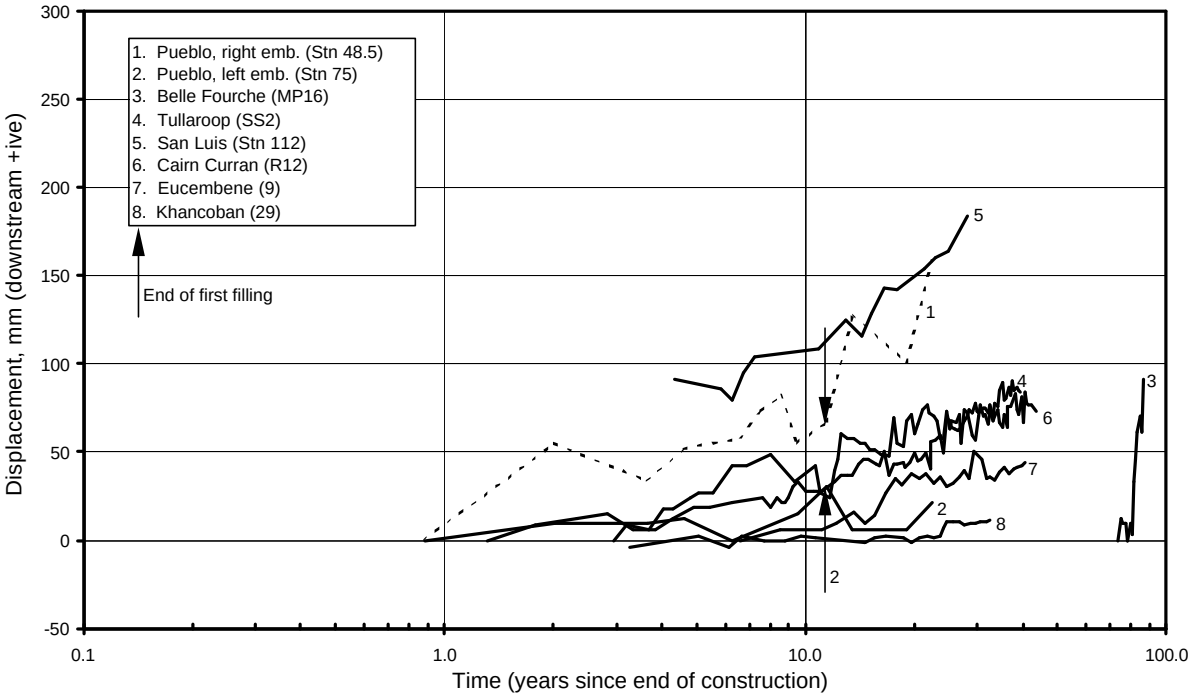

Figure F2.18: Post construction displacement of the downstream slope (mid to upper region) for embankments with very broad central core regions and limited foundation influence.

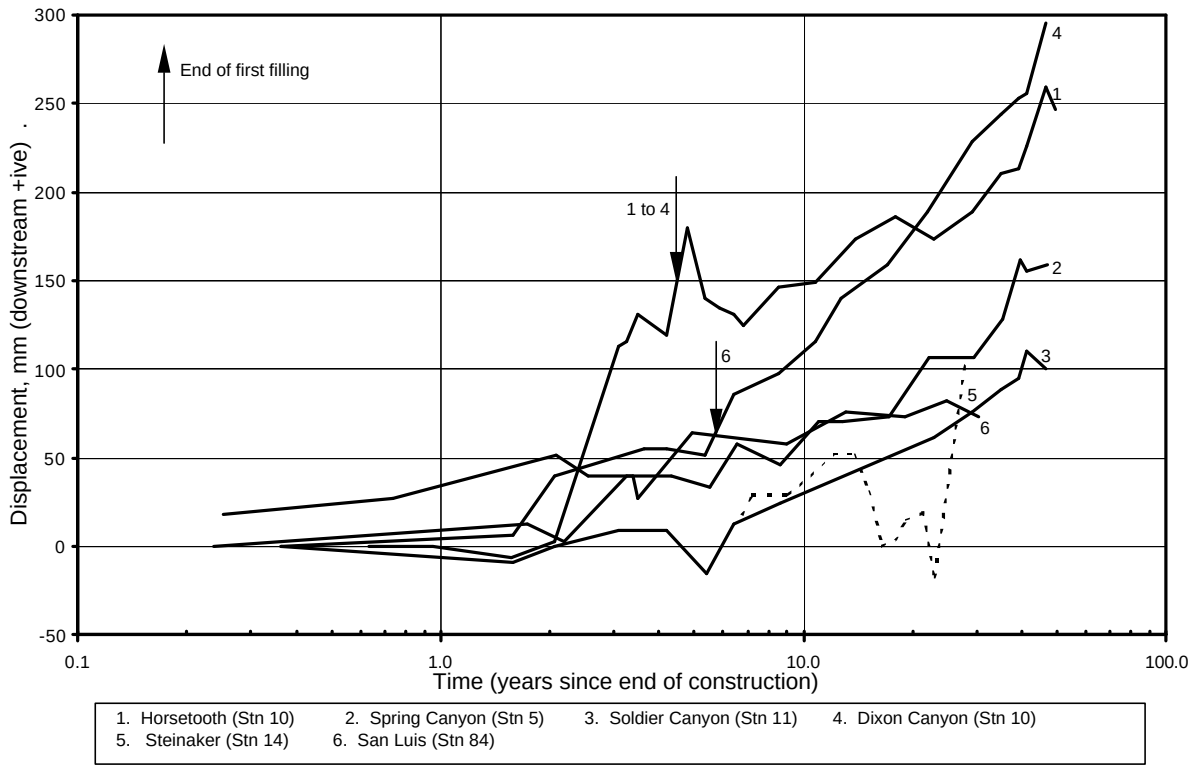

Figure F2.19: Post construction displacement of the downstream slope (mid to upper region) for embankments with very broad central core regions and possibly significant foundation influence.

2.2 *POST CONSTRUCTION DEFORMATION OF THE UPPER UPSTREAM SLOPE TO UPSTREAM CREST REGION*

For the post construction surface deformation of the upstream slope, SMPs for each case study have been preferentially selected from the upper upstream slope to upstream crest region. For embankments with thick or very broad central earthfill zones the SMP from the upper upstream slope region has been used.

The layout of the data presented is as follows:

- Section 2.2.1 – Total post construction settlement plots at 3, 10 and 20 to 25 years after the end of embankment construction;
- Section 2.2.2 – Settlement versus time plots; and
- Section 2.2.3 – Lateral displacement (normal to the dam axis) versus time plots.

2.2.1 Post Construction Total Settlement of the Upper Upstream Slope to Upstream Crest Region

The total post construction surface settlement for the upper upstream slope to upstream crest region is presented as plots of settlement versus dam height at selected times after the end of construction; at 3, 10 and 20 to 25 years after the end of embankment construction (Figure F2.20 to Figure F2.22). Base readings for the data are generally in the range from 0 to 0.5 years after the end of construction, with several case studies slightly outside this range.

The data are mainly for embankments on rock foundations. Several embankments on soil/rock or soil foundations have been included where the foundation is considered to have a limited influence on the dam settlement, or where it can be excluded by deducting foundation settlement from base plate or base cross-arm readings from IVM gauges.

For the upper upstream slope to upstream crest region, the data has been sorted based on material type of the upstream shoulder fill. The embankments with rockfill shoulders have been further divided into compaction rating of the rockfill. Embankments with dry placed and poorly compacted rockfills have been highlighted.

The height designated for each case study is the height from the SMP to foundation level. For several cases the height is from the SMP to bedrock level, but this has only be undertaken for cases studies where the foundation has some but not an overly

significant influence on the deformation and its thickness is less than about 20 % of the height of the embankment at the SMP location.

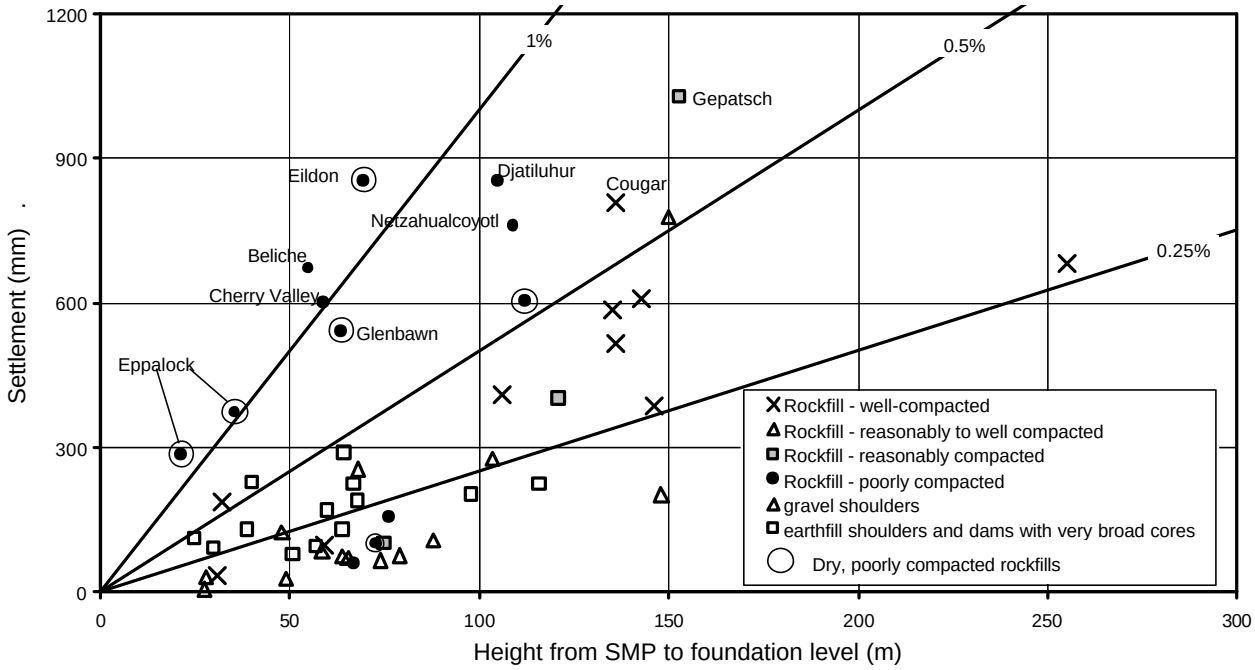

Figure F2.20: Post construction settlement of the upper upstream slope and upstream crest region at 3 years after end of construction.

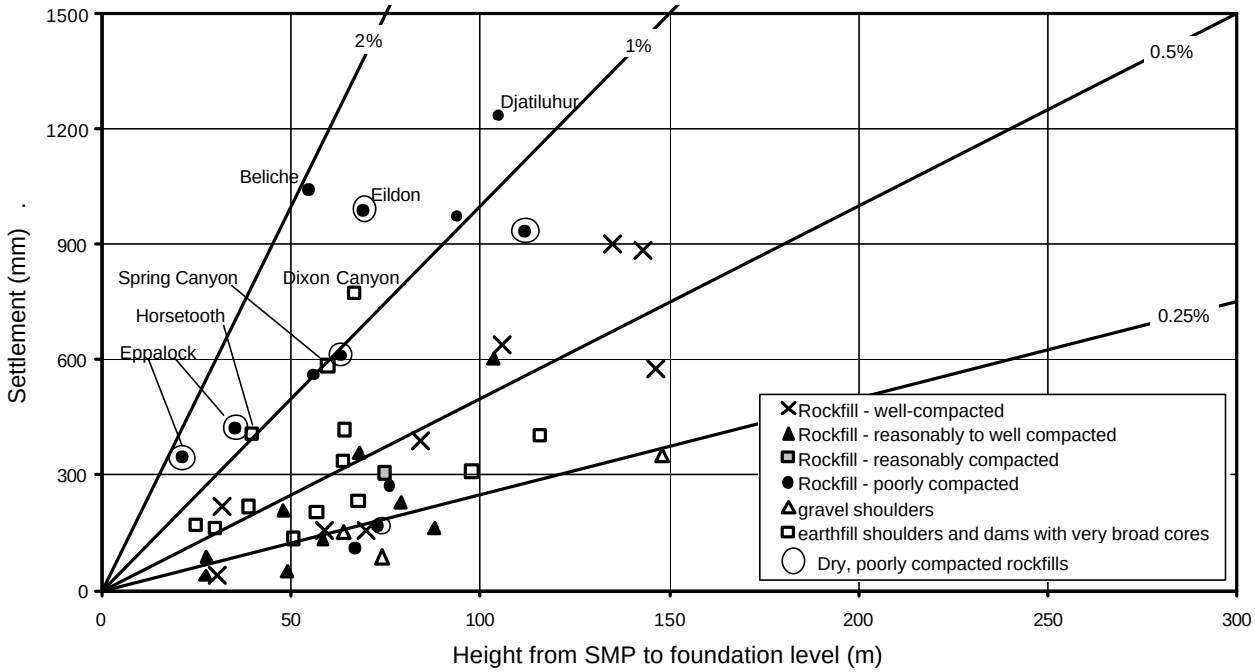

Figure F2.21: Post construction settlement of the upper upstream slope and upstream crest region at 10 years after end of construction.

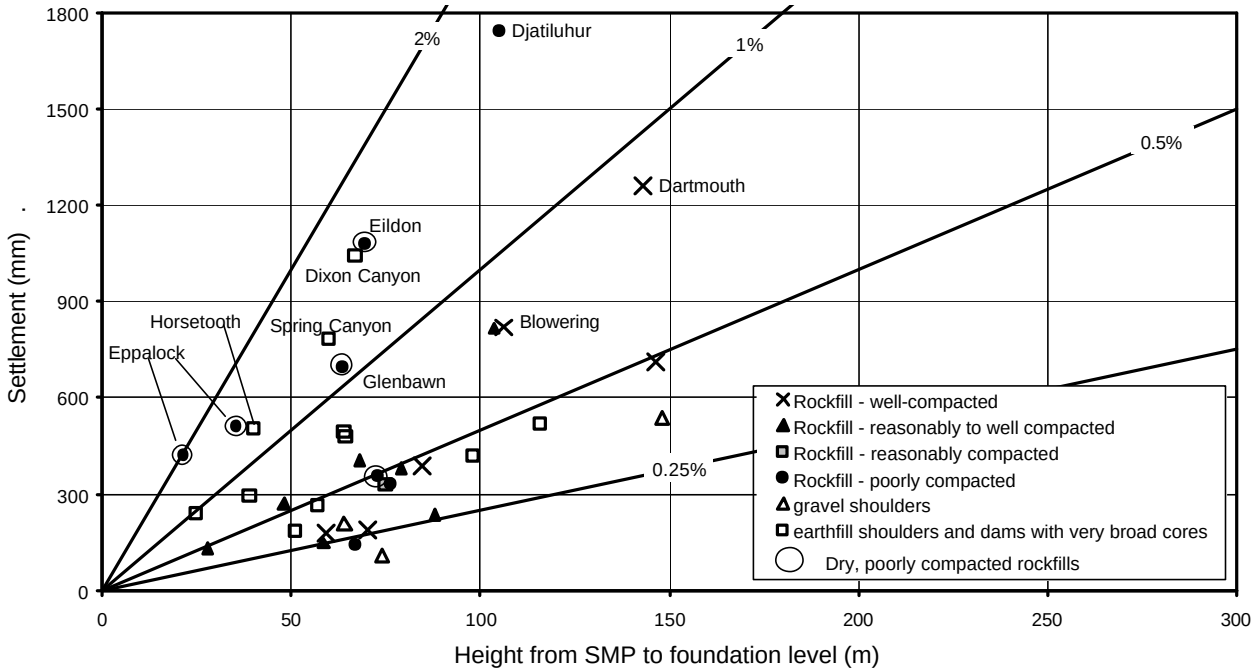

Figure F2.22: Post construction settlement of the upper upstream slope and upstream crest region at 20 to 25 years after end of construction.

2.2.2 Post Construction Settlement Versus Time of the Upper Upstream Slope to Upstream Crest Region.

The post construction settlement versus time records of the upper upstream slope to upstream crest region are presented in Figure F2.23 to Figure F2.29 in the form of settlement, as a percentage of the height from the SMP to foundation level, versus time (in years since end of construction) on a log scale.

The case studies have been sorted based on material type forming the upstream shoulder and the embankments with rockfill in the upstream shoulder have been further sorted based on compaction rating. The data is presented in the following figures:

- Figure F2.23 – zoned earth and rockfill embankments with well-compacted rockfill in the upstream shoulder;
- Figure F2.24 – zoned earth and rockfill embankments with reasonably or reasonably to well compacted rockfill in the upstream shoulder;
- Figure F2.25 - zoned earth and rockfill embankments with reasonably compacted rockfill;
- Figure F2.26 – zoned earth and rockfill embankments with poorly compacted rockfill;

- Figure F2.27 – zoned earth and rockfill embankments with compacted gravels or earthfills in the upstream shoulder;
- Figure F2.28 – embankments with very broad central earthfill zones, and limited foundation influence; and
- Figure F2.29 - embankments with very broad central earthfill zones, and potentially significant foundation influence. For this figure settlement is plotted in millimetres.

No limitations on inclusion or exclusion of case studies have been placed on the timing of the base survey reading for the data presented. In most cases the base survey reading was within 0.5 years of end of embankment construction, but for a number of cases it was after this time.

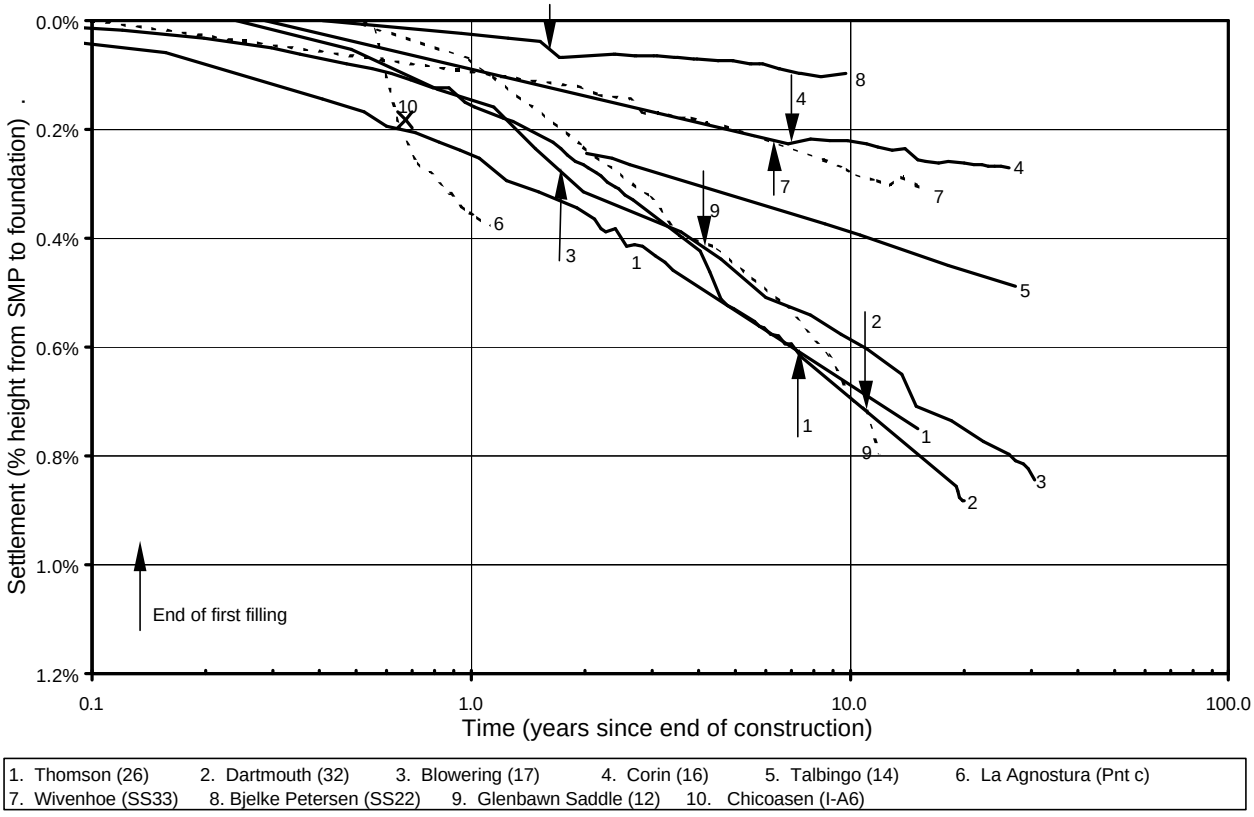

Figure F2.23: Post construction settlement of the upper upstream slope to upstream crest region of zoned earth and rockfill embankments with well-compacted rockfill in the upstream shoulder.

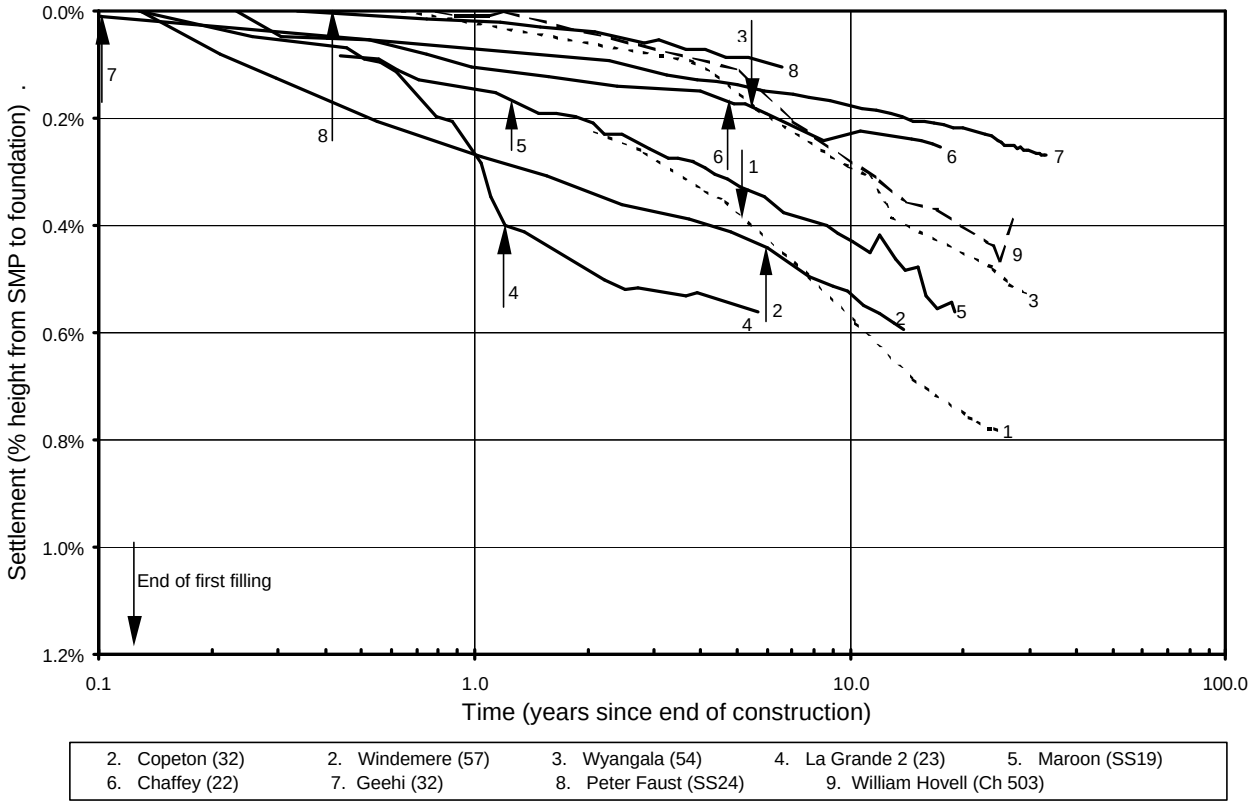

Figure F2.24: Post construction settlement of the upper upstream slope to upstream crest region of zoned earth and rockfill embankments with reasonably to well compacted rockfill in the upstream shoulder.

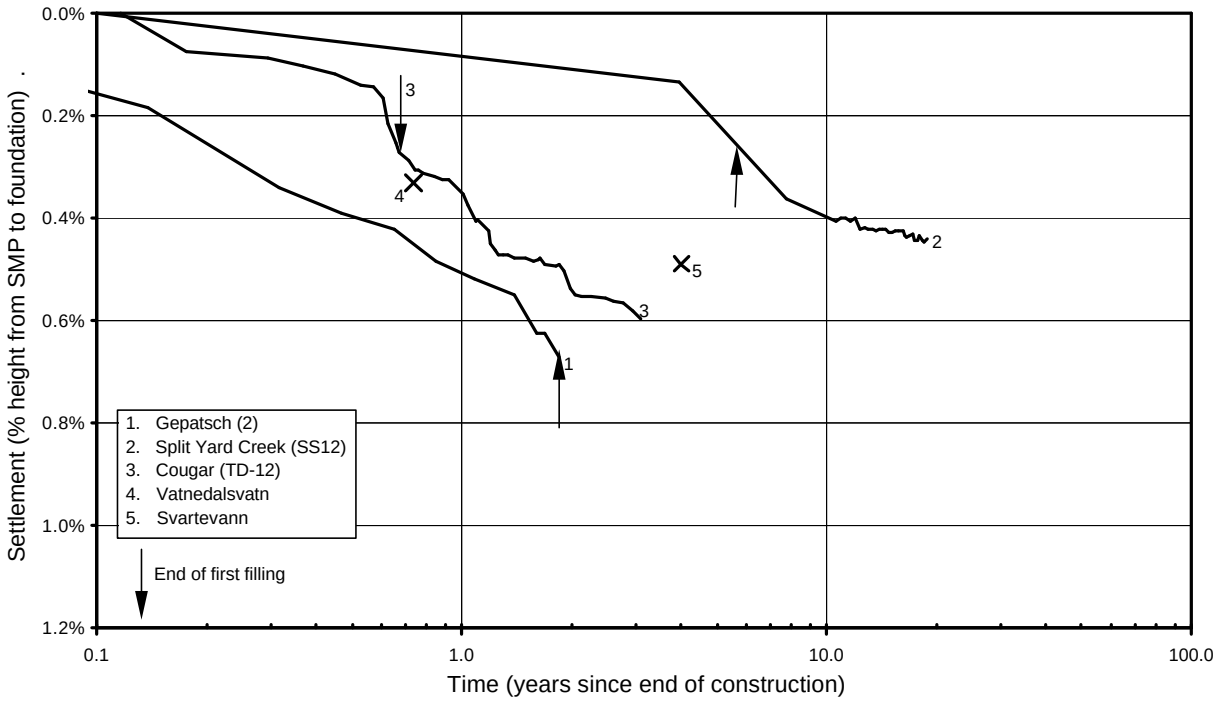

Figure F2.25: Post construction settlement of the upper upstream slope to upstream crest region of zoned earth and rockfill embankments with reasonably compacted rockfill in the upstream shoulder.

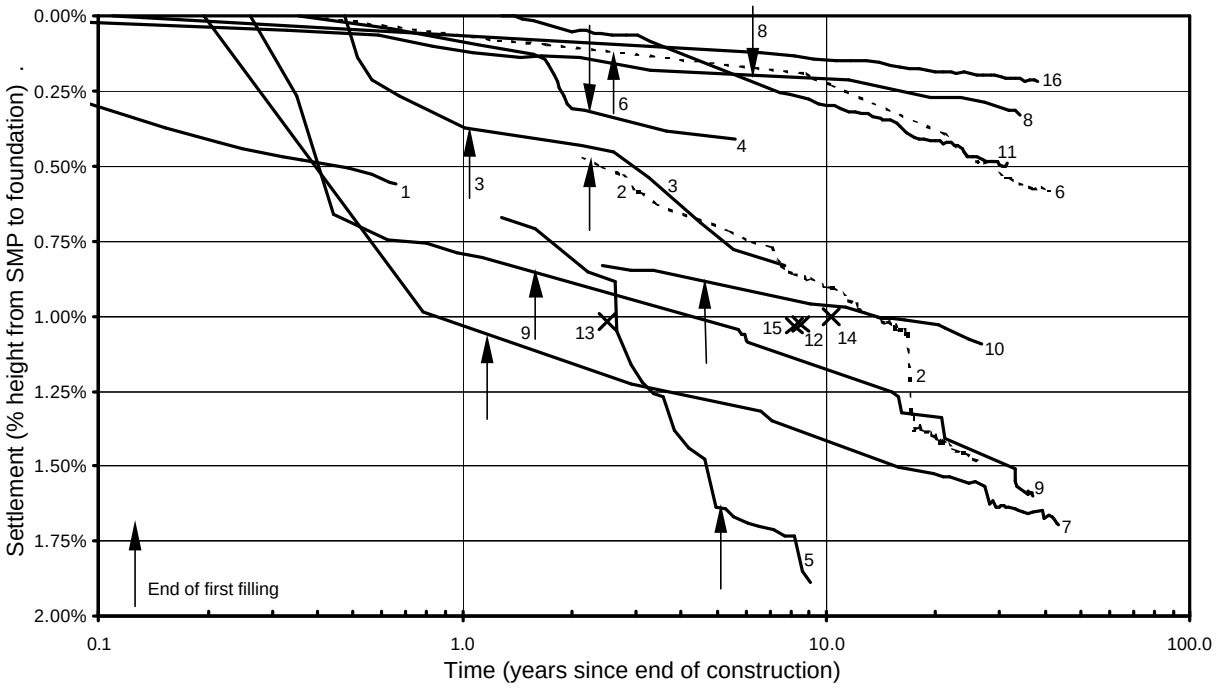

1. Djatilihur 2. Djatilihur (C9) 3. El Infiernillo (IVM D1) 4. Netzahualcoyotl (14-2u) 5. Beliche (M54) 6. Upper Yarra (1U)
7. Eildon (SS10) 8. Burrendong (103) 9. Eppalock (SS2) 10. Glenbawn (L3M) 11. Nillacootie (6U) 12. Mud Mountain
13. Cherry Valley 14. Nottely 15. Watuaga 16. Tooma (25)

Figure F2.26: Post construction settlement of the upper upstream slope to upstream crest region of zoned earth and rockfill embankments with poorly compacted rockfill in the upstream shoulder.

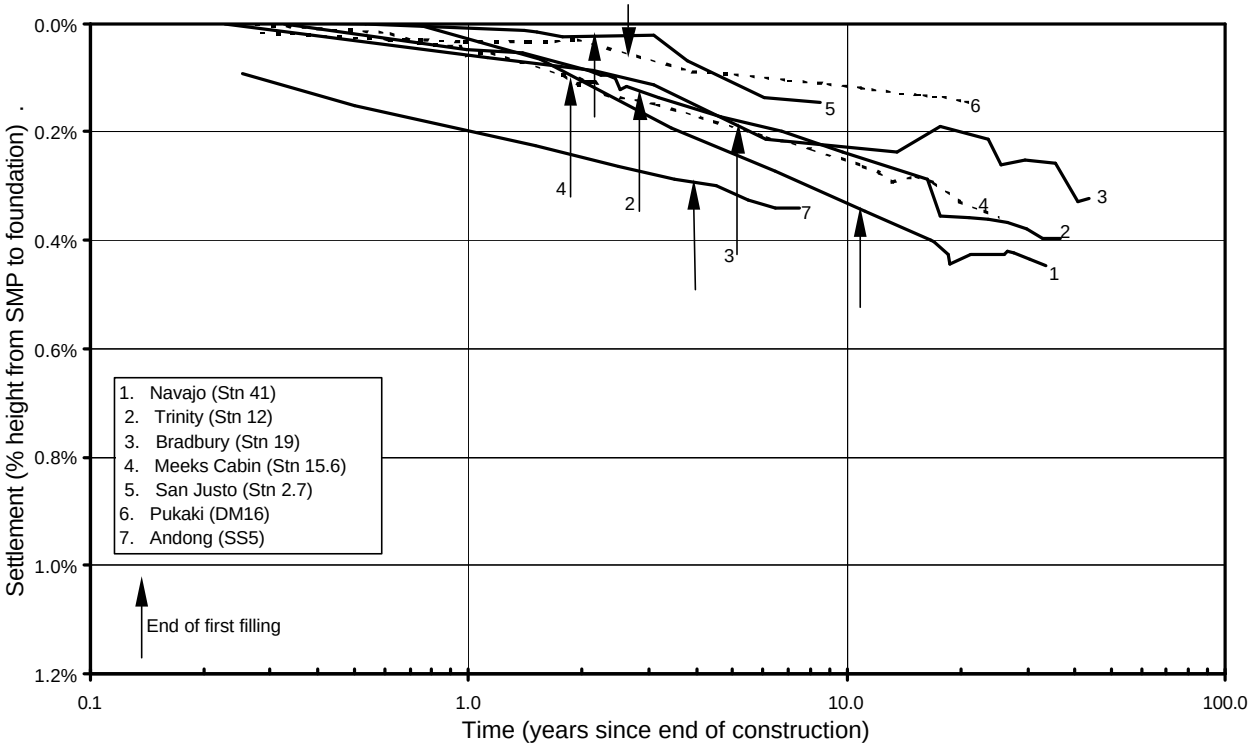

Figure F2.27: Post construction settlement of the upper upstream slope to upstream crest region of zoned embankments with earthfills and gravels in the upstream shoulder.

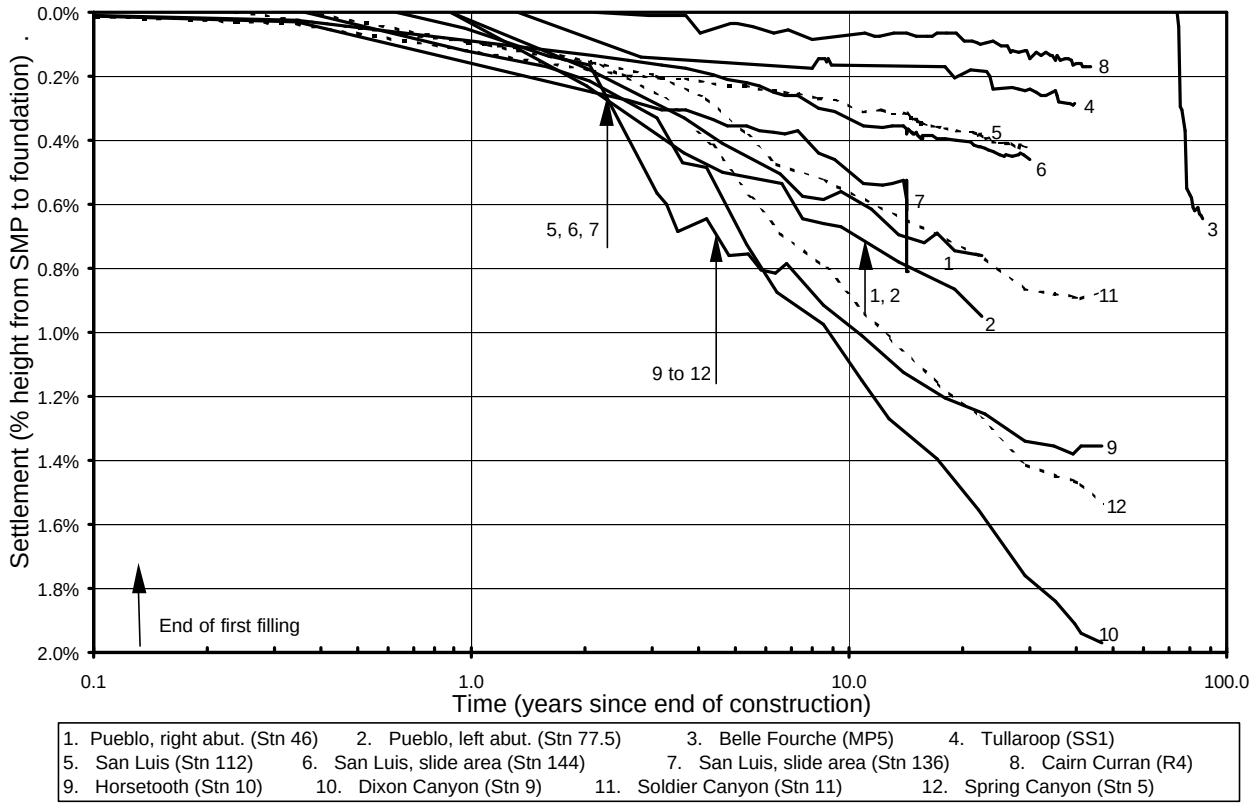

Figure F2.28: Post construction settlement of the upper upstream slope region of zoned embankments with very broad central earthfill zones, and limited foundation influence.

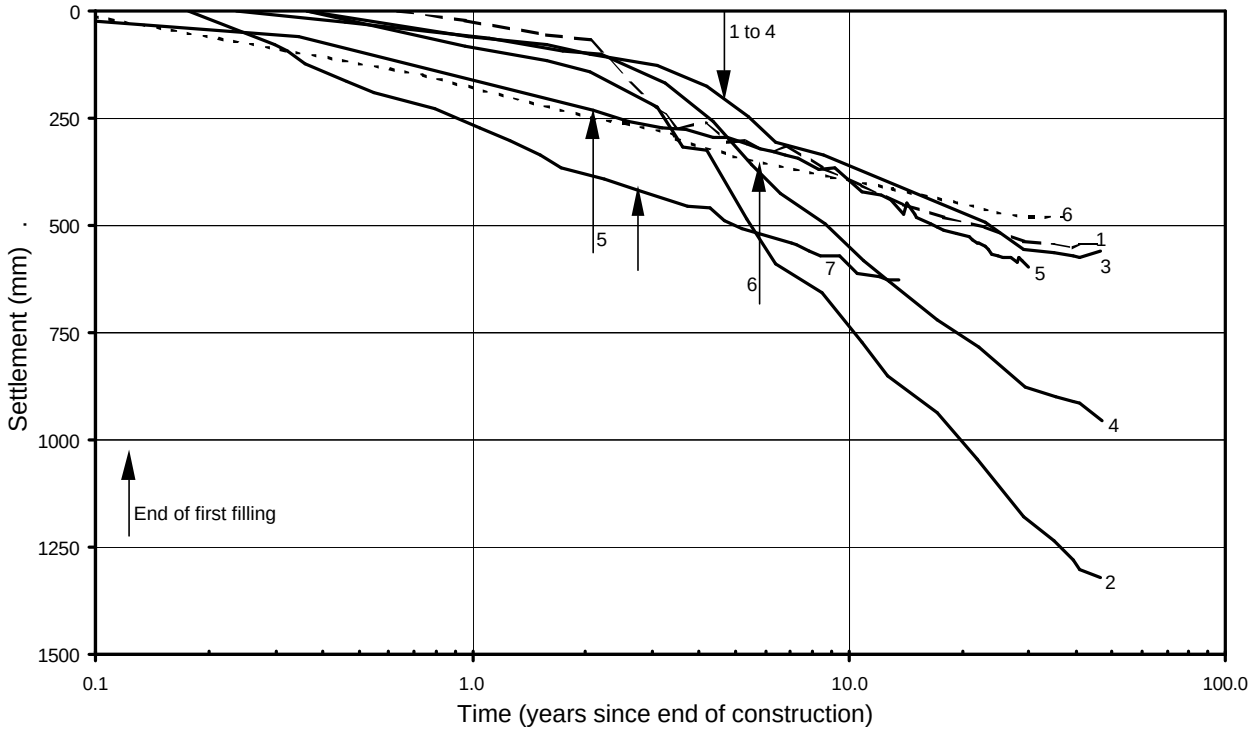

Figure F2.29: Post construction settlement of the upper upstream slope region of zoned embankments with very broad central earthfill zones, and potentially significant foundation influence.

2.2.3 Post Construction Displacement of the Upper Upstream Slope and Upstream Crest Region.

The case study data of the post construction displacement normal to the dam axis versus time for the upper upstream slope to upstream crest region is presented in Figure F2.30 to Figure F2.36 in the form of displacement, in millimetres, versus time (in years since the end of construction) on a log scale. Displacement in a downstream direction is positive and in an upstream direction is negative.

As for the settlement versus time plots, the case studies have been sorted based on material type forming the upstream shoulder and the embankments with rockfill in the upstream shoulder have been further sorted based on compaction rating.

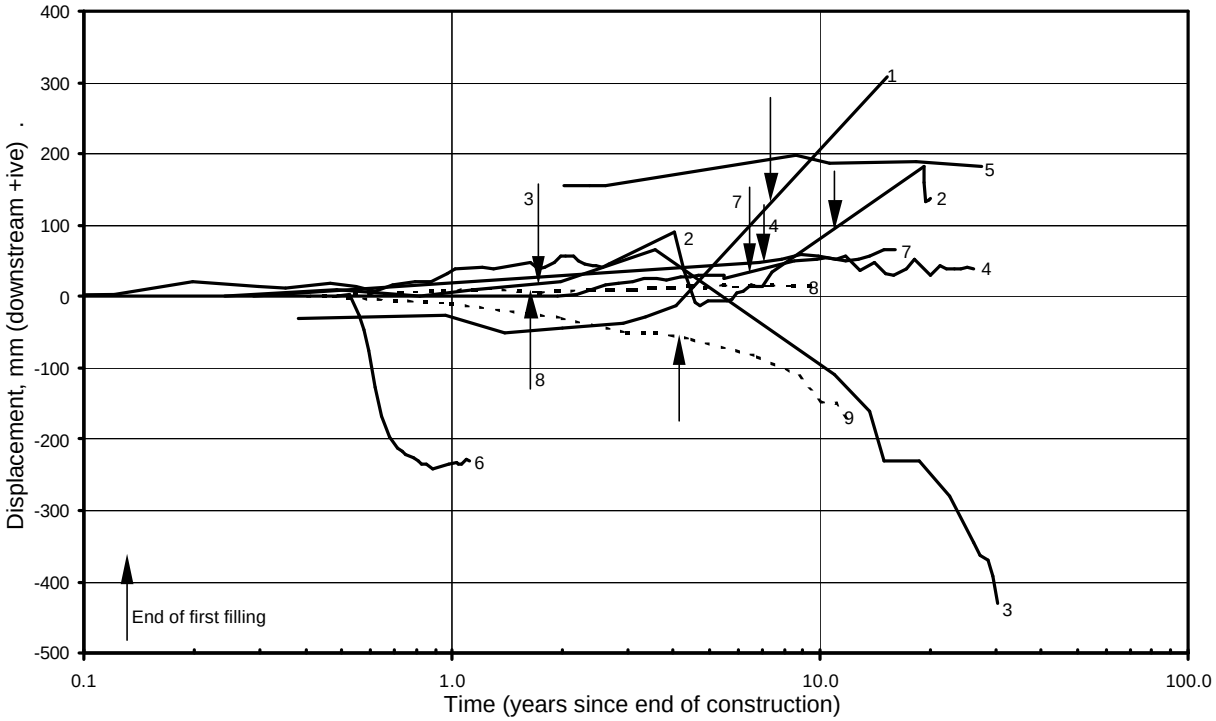

Figure F2.30: Post construction displacement of the upper upstream slope to upstream crest region of zoned earth and rockfill embankments with well-compacted rockfill in the upstream shoulder.

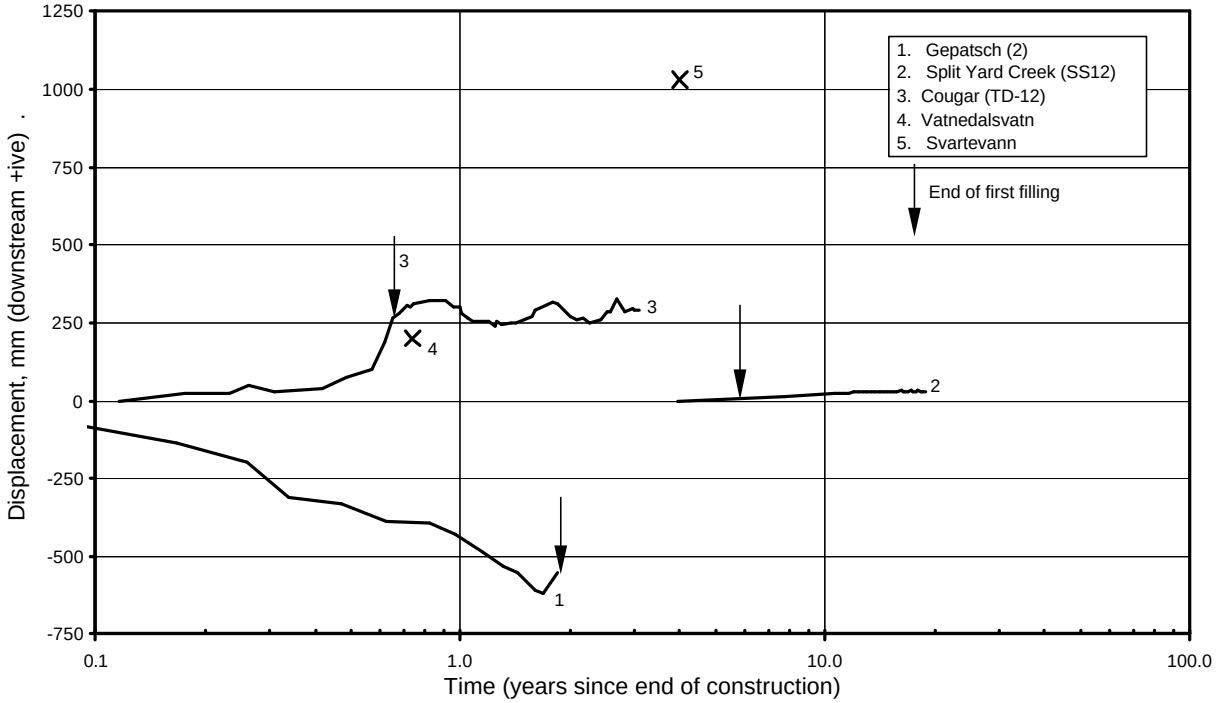

Figure F2.31: Post construction displacement of the upper upstream slope to upstream crest region of zoned earth and rockfill embankments with reasonably compacted rockfill in the upstream shoulder.

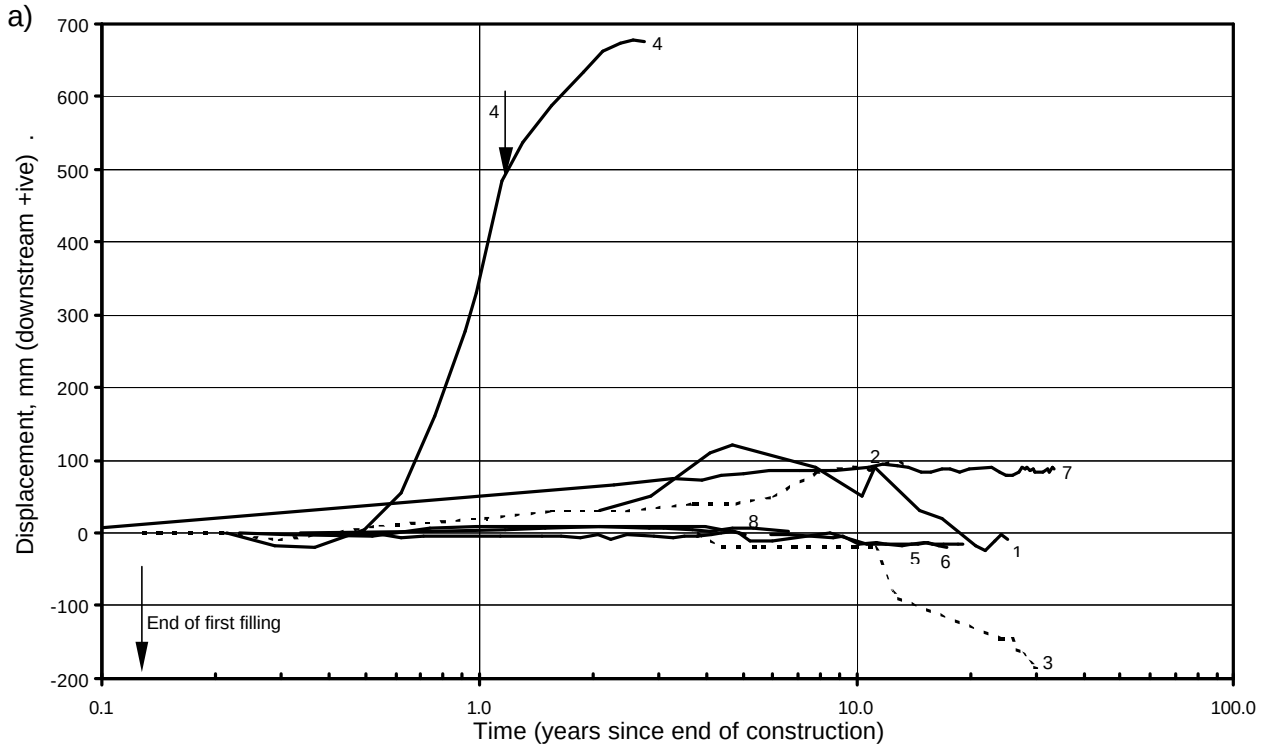

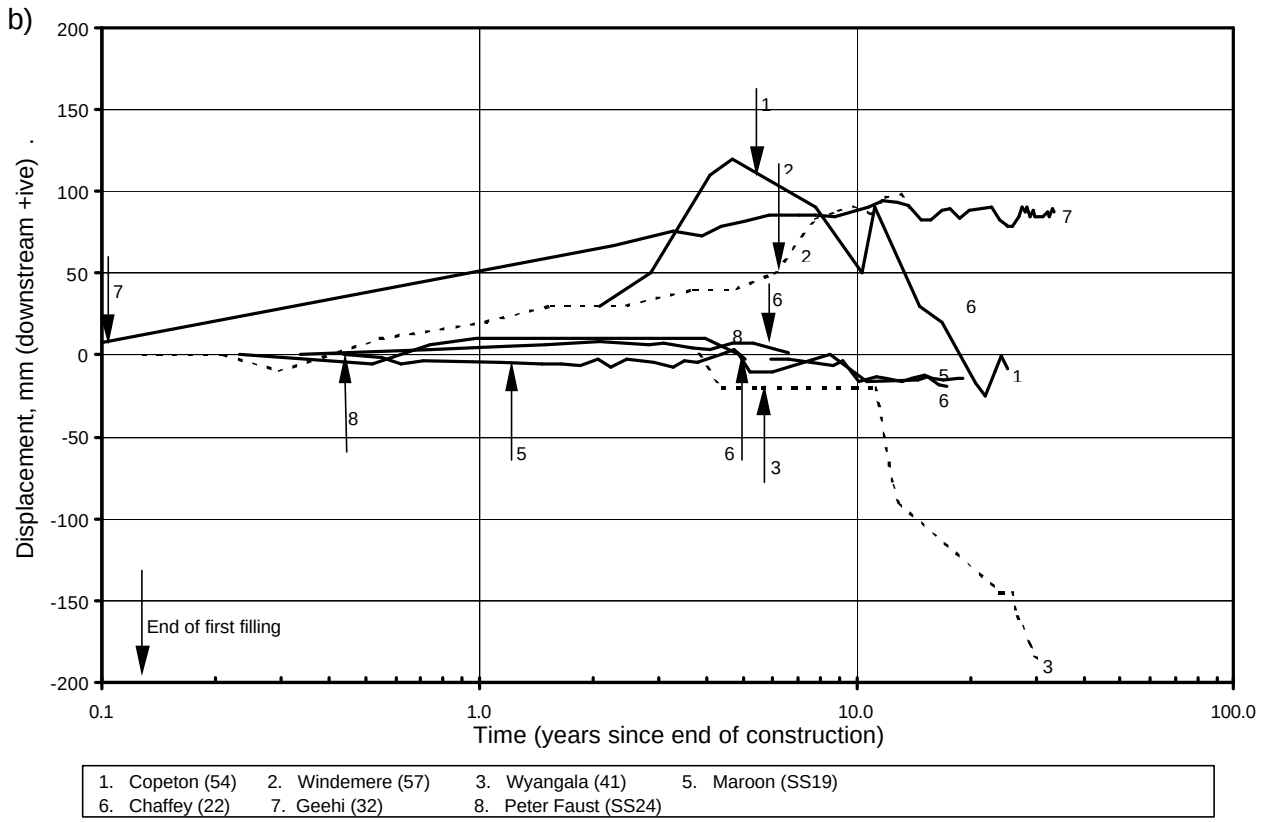

Figure F2.32: Post construction displacement of the upper upstream slope to upstream crest region of zoned earth and rockfill embankments with reasonably to well compacted rockfill in the upstream shoulder.

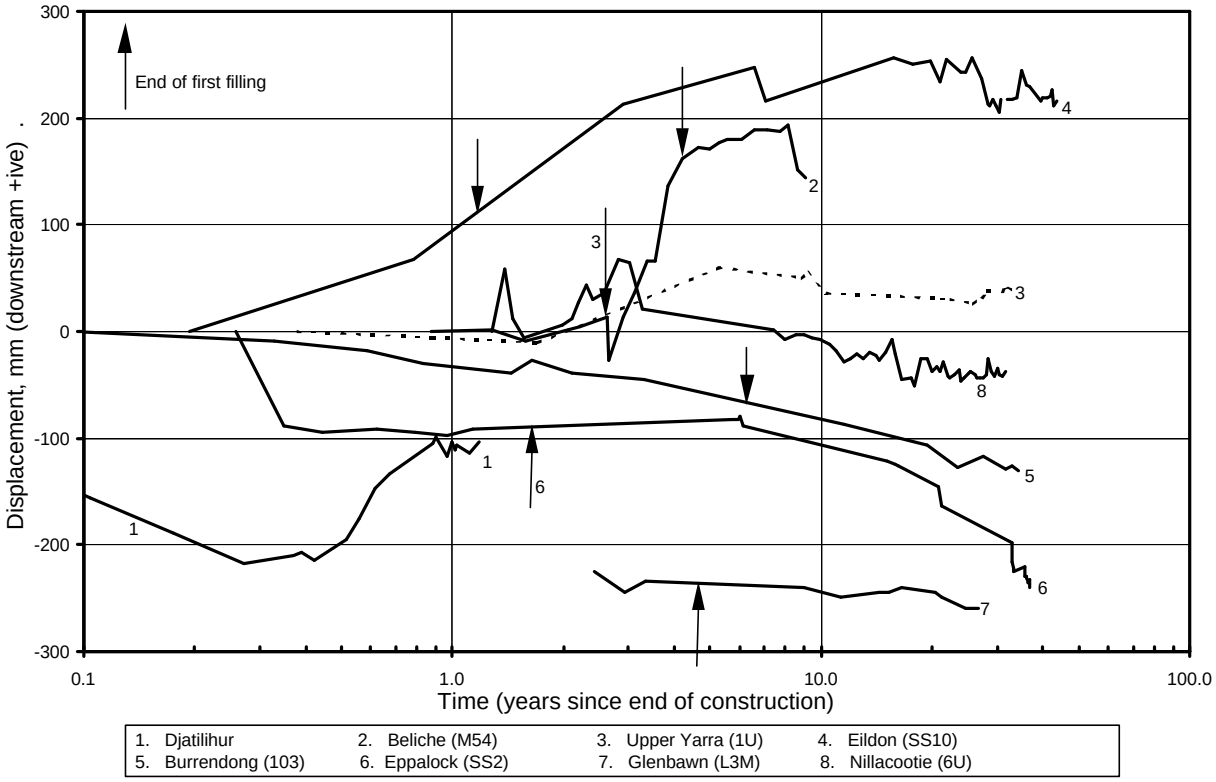

Figure F2.33: Post construction displacement of the upper upstream slope to upstream crest region of zoned earth and rockfill embankments with poorly compacted rockfill in the upstream shoulder.

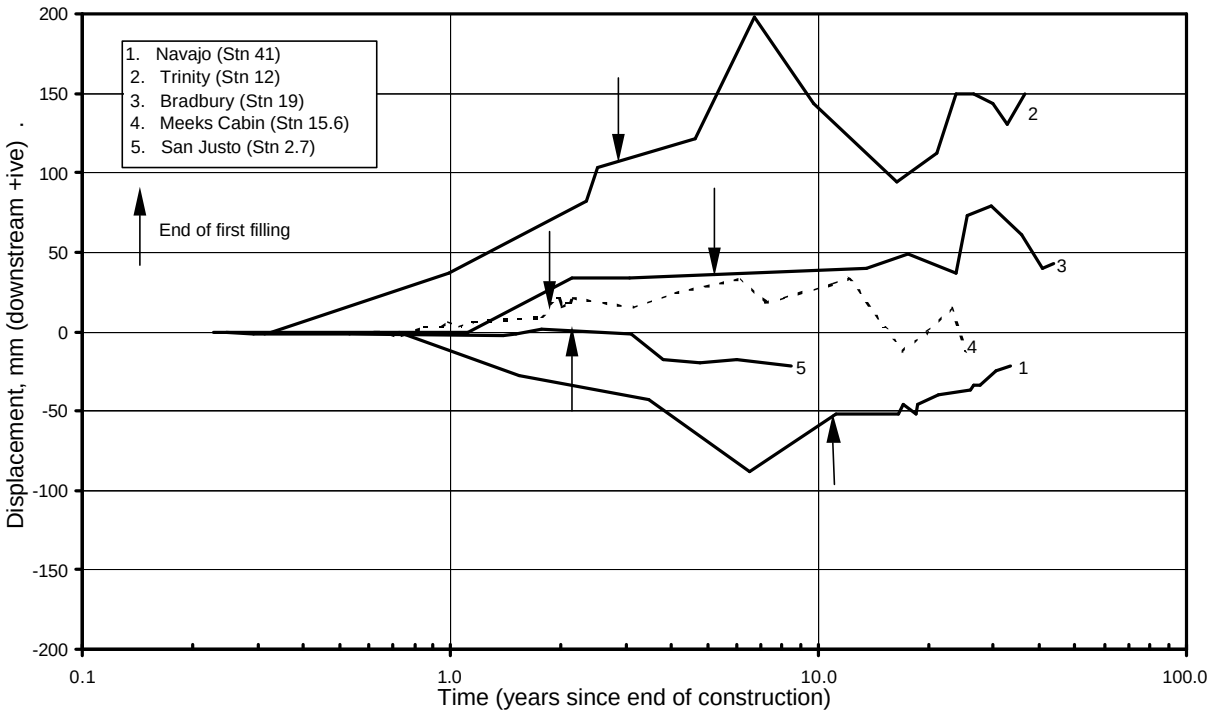

Figure F2.34: Post construction displacement of the upper upstream slope to upstream crest region of zoned embankments with earthfills and gravels in the upstream shoulder.

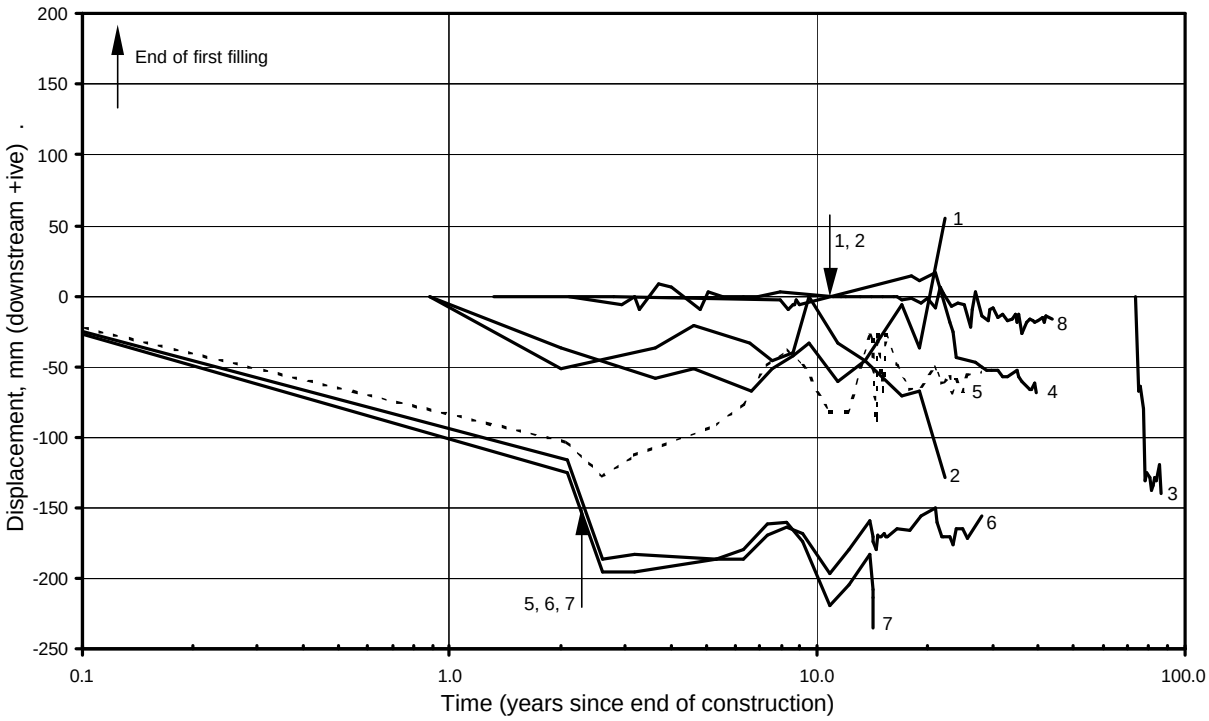

1. Pueblo, right emb. (Stn 46) 2. Pueblo, left emb. (Stn 77.5) 3. Belle Fourche (MP5) 4. Tullaroop (SS1)
5. San Luis (Stn 112) 6. San Luis, slide area (Stn 144) 7. San Luis, slide area (Stn 136) 8. Cairn Curran (R4)

Figure F2.35: Post construction displacement of the upper upstream slope region of embankments with very broad central core regions and limited foundation influence.

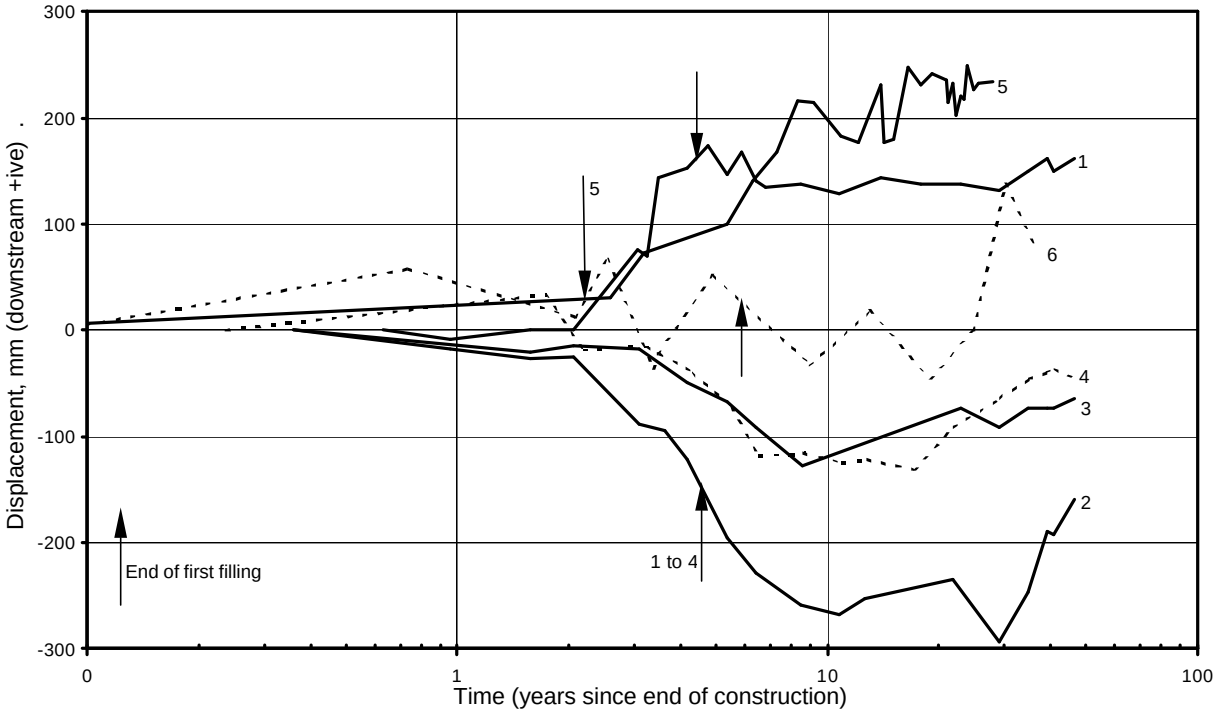

1. Horsetooth (Stn 10) 2. Dixon Canyon (Stn 9) 3. Soldier Canyon (Stn 11) 4. Spring Canyon (Stn 5)
5. San Luis (Stn 80) 6. Steinaker (Stn 14)

Figure F2.36: Post construction displacement of the upper upstream slope region of embankments with very broad central core regions and possibly significant foundation influence.

APPENDIX G

Deformation Behaviour of Selected Case Studies of Embankment Dams

TABLE OF CONTENTS

1.0 CENTRAL CORE EARTH AND ROCKFILL DAMS..... G1

1.1 Ataturk Dam..... G1
1.2 Bellfield Dam..... G6
1.3 Beliche Dam..... G11
1.4 Chicoasen Dam..... G19
1.5 Copeton Dam..... G25
1.6 Cougar Dam..... G36
1.7 Djatiluhur Dam..... G41
1.8 Eildon Dam..... G49
1.9 El Infiernillo Dam..... G58
1.10 Eppalock Dam..... G66
1.11 Gepatsch Dam..... G76
1.12 La Grande No. 2 (LG-2) Dam..... G82
1.13 Svartevann Dam..... G86
1.14 Talbingo Dam..... G92
1.15 Upper Yarra Dam..... G100
1.16 Wyangala Dam..... G108

2.0 ZONED EARTH AND ROCKFILL EMBANKMENTS G116

2.1 Canales Dam..... G116
2.2 San Luis Dam..... G119

3.0 ZONED EARTHFILL EMBANKMENTS G127

3.1 Carsington Dam..... G127
3.2 Hirakud Dam..... G130
3.3 Horsetooth Reservoir Dams G132
3.4 Pueblo Dam..... G149
3.5 Rector Creek Dam..... G156

4.0 EARTHFILL AND HOMOGENEOUS EARTHFILL EMBANKMENTS G159

4.1 Belle Fourche Dam..... G159

4.2 Mita Hills Dam G167
4.3 Roxo Dam G170

5.0 PUDDLE CORE EARTHFILL EMBANKMENTS G174
5.1 Happy Valley Dam G174
5.2 Yan Yean Dam G179
5.3 Hope Valley Dam G185
5.4 Ramsden Dam G192
5.5 Walshaw Dean (Lower) Dam G199
5.6 Selset Dam G203

6.0 BLOWERING DAM G207
6.1 Introduction G207
6.2 Background on Blowering Dam G207
6.3 Monitored Performance of Blowering dam G216
6.4 Summary of Numerical and Limit Equilibrium Analysis G236

LIST OF TABLES

LIST OF FIGURES

1.0 CENTRAL CORE EARTH AND ROCKFILL DAMS

1.1 ATATURK DAM

Ataturk dam (Figure G1.1 and Figure G1.2), located on the Euphrates River in Turkey, is a central core earth and rockfill embankment of 184 m height (Cetin et al 2000). Embankment construction took nearly 4 years and was completed in August 1990. In summary, the materials and construction methods (Cetin et al 2000; Cetin 2002) consisted of:

- A thin central core (Zone 1) of high plasticity clays to sandy clays placed in 300 mm layers and compacted by sheepsfoot roller. The average moisture content of the earthfill was 1.5% dry of Standard optimum.
- Filters (Zones 2a and 2b) of gravelly sands to sandy gravels, sourced from river alluvium, compacted by vibratory rollers.
- Rockfill placed in 0.6 m to 1.5 m layers and compacted by vibratory rollers. Moisture contents at placement were in the range 2 to 6%. The rockfill zones (Figure G1.1) comprised:
  - Inner upstream zone of weathered, vesicular basalt. Unconfined compressive strength tests indicate the weathered rock to be of medium strength.
  - Inner downstream zone of pliacated limestone. The placed material had such a high fraction of sand sized or less (50% finer than 2 mm) that it is probably best described by soil terminology or as a very "dirty" rockfill.
  - Outer upstream and downstream shoulders of sound basalt of very high unconfined compressive strength.

Details on the layer thickness, roller type and number of passes for the various rockfill zones are not precisely known. But, for the layer thickness used, and assuming roller size and number of passes in accordance with generally adopted procedures, the compaction rating is likely to be between reasonable compaction and well-compacted. What is evident is that the materials used within the inner rockfill zones up and downstream are from weathered rock types and potentially of relatively high compressibility for rockfill.

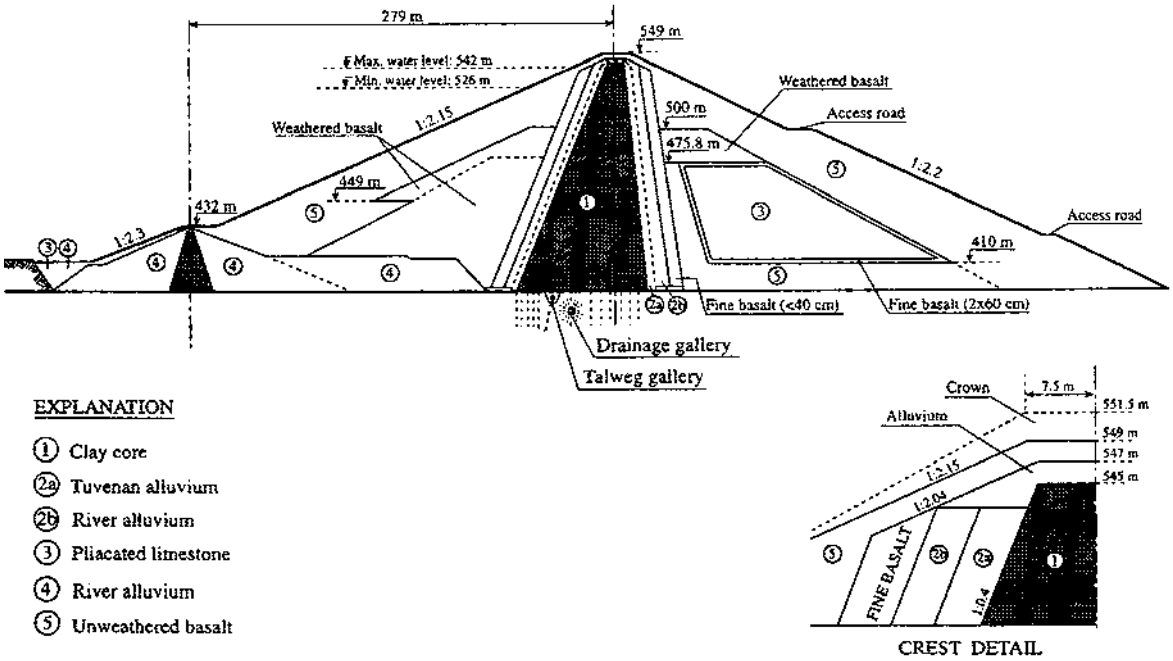

Figure G1.1: Ataturk dam; cross section of the embankment (Cetin et al 2000)

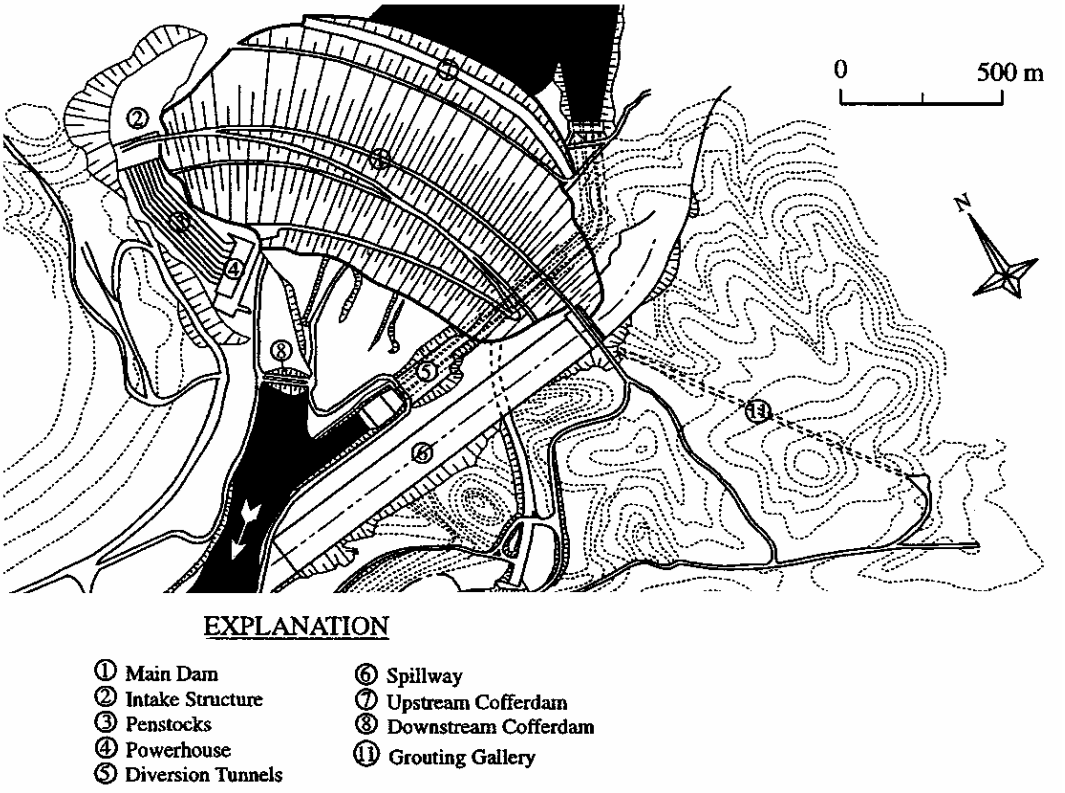

Figure G1.2: Ataturk dam; plan and general layout of the dam (Cetin et al 2000).

Details on the actual reservoir operation are sketchy. Ozis et al (1990) comments that first filling started in January 1990, some 7 to 8 months prior to end of construction, and Cetin (2002) indicates that the reservoir was within 7 m of full supply level in March

1994 (3.6 years post construction). Between these times periods of rapid rise in reservoir level to new high levels occurred following winter and spring rains, particularly in 1990 and 1992, and after May 1992 to March 1994 the rise in reservoir level has been very slow (Cetin 2002).

The post construction settlement and displacement records for Ataturk dam at about the main section are presented in Figure G1.3 and Figure G1.4. In summary, the figures and comparison to other embankments shows, and significant comments by Cetin et al (2000), are:

- The very large magnitude of the post construction crest settlement at Ataturk dam of more than 7 metres in less than 7 years (close to 4% of the dam height), which clearly stands out as an outlier in comparison to similar type embankments (Figures 7.46a and 7.53a in Section 7.6 of Chapter 7). Cetin et al (2000) indicate that large settlements occurred in June to December 1990 and again in early 1992 (1.5 to 2 years post construction) during periods of relatively rapid rise in reservoir level to new high levels.
- The magnitude of settlement of the crest is very much larger than that of the downstream shoulder (Figure G1.3). Most of the differential occurred in the first 1.5 years after construction, but has continued in the latter 4 to 5 years.
- The average crest settlement rate over the period from 3 to 7 years after construction is about 3% per log cycle of time. In comparison to similar embankments the crest settlement rate at Ataturk dam is a clear outlier (Figures 7.62 in Section 7.6 of Chapter 7).
- The settlement and displacement of the downstream slope, whilst still of relatively large magnitude, is more in line with "normal" type deformation behaviour when compared to similar type embankments (Figures 7.39 in Section 7.5 and 7.50 in Section 7.6 of Chapter 7).
- In June 1990, several months before the end of construction, a number of internal monitoring gauges in the lower elevations were lost. Cetin et al (2000) comment that this coincided with the beginning of reservoir filling.
- Cetin et al (2000) refer to "*landslides*" occurring in the upstream slope in May 1992. It is possible that they are referring to the surface expression of differential settlement between the upstream shoulder and core.

- During reconstruction of the upper 6 to 7 m of the crest in 1997 slickensided surfaces were observed in the core at close to the interface between the core and downstream filters.

Cetin et al (2000) considered slaking of the vesicular basalt in the upstream shoulder and possible poor placement of the core (suspected that the core was placed in layers up to 1 m thickness) as potential factors in the very large settlement of the crest post construction. Degradation of the basalt has since been discounted as a possible cause of the large deformation (Riemer 2001).

It is difficult to surmise the potential cause/s and mechanics controlling the deformation behaviour of the embankment given the limited information available. Notwithstanding this, it is suspected that collapse settlement of the upstream rockfill on wetting is likely to be a significant factor, particularly within the inner upstream weathered basalt rockfill zone. Observations and the SMP records indicate differential settlement between the upstream shoulder and core, and the core and downstream shoulder. Two mechanisms are considered possible:

- Development of a shear surface and shear deformations in the core toward upstream. The anecdotal information would suggest that the shear surface formed during a rising reservoir condition in the early stages of first filling and prior to the end of construction, with further shear type deformations significant during the early part of 1992 on a rising reservoir. It is possible that localised instability developed in the core due to stress transfer from the upstream rockfill onto the core following collapse settlement of the upstream rockfill.
- Plastic deformation of the core as a result of collapse settlement of the rockfill. As shown by generic numerical modelling (refer Section 7.5.2 of Chapter 7), earthfill cores of low undrained shear strength will deform with the upstream shoulder as it collapse settles and large shear strains develop at the downstream interface of the core.

The former is considered the more likely scenario because of the reported dry placement of the core and therefore likely high undrained shear strength of the core. The presence of slickensided surfaces in the dry placed earthfill core near to the downstream core / filter interface, exposed during crest reconstruction works, indicate the likely formation of a shear surface in the core. How extensive the surface of rupture

might be is not known, but the loss of internal instruments in the lower elevations of the embankment may have occurred due to shear type displacements.

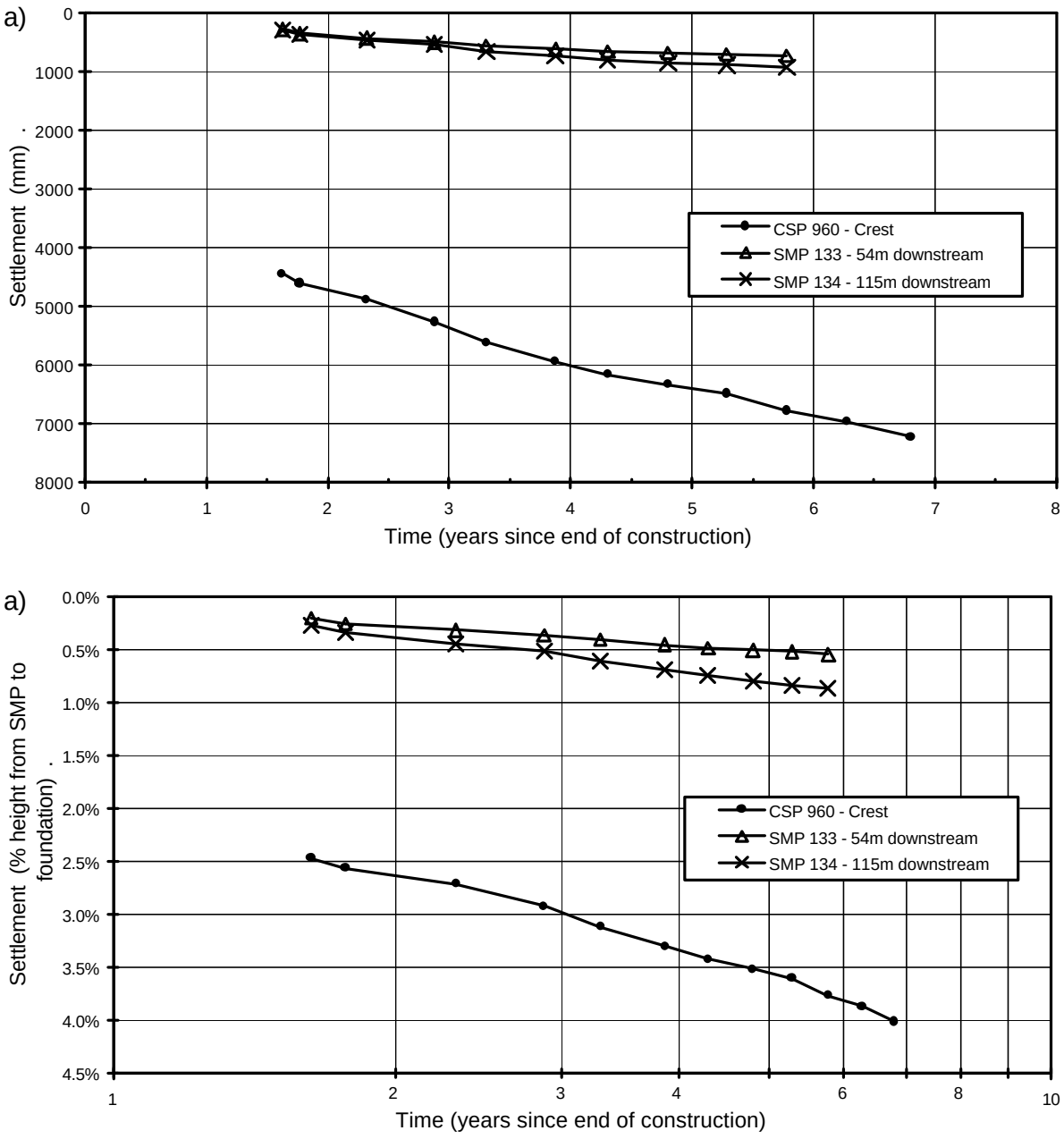

Figure G1.3: Ataturk dam, post construction settlement of SMPs at the main section.

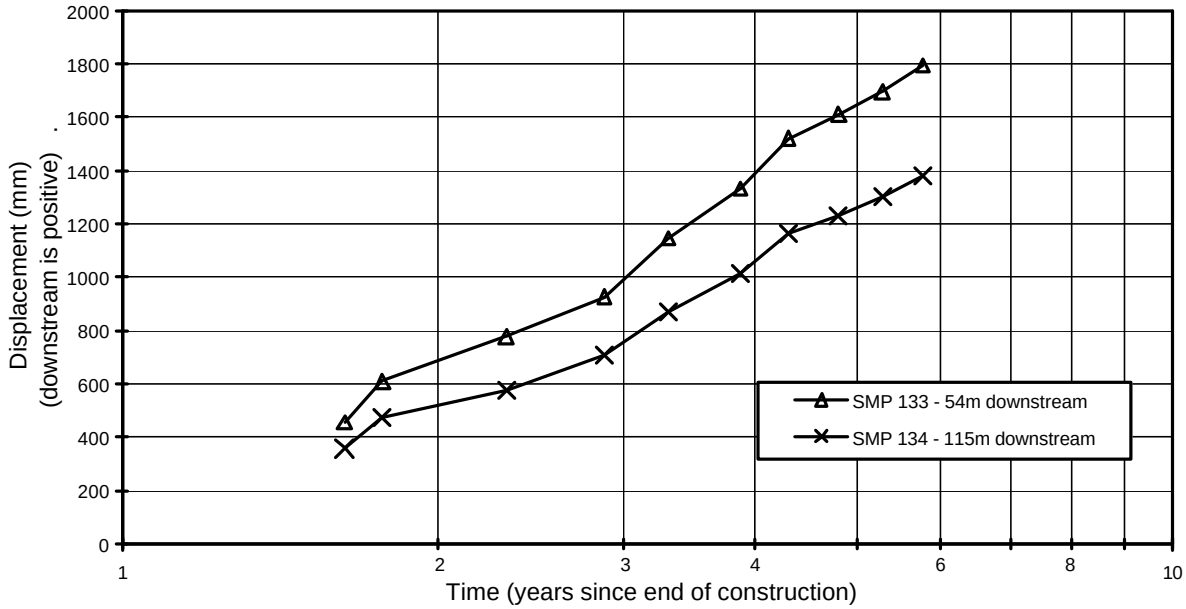

Figure G1.4: Ataturk dam, post construction displacement normal to the dam axis of SMPs on the downstream slope.

1.2 BELLFIELD DAM

Bellfield dam (Figure G1.5 and Figure G1.6) is a central core earth and rockfill embankment of 50 m maximum height located on Fyans Creek nears Halls Gap in north-western Victoria, Australia. The embankment was constructed from 1963 to 1966 (completed in about April of 1966). At the main section (Figure G1.5) the embankment consists of:

- A medium width central earthfill core (Zone 1) of sandy clays to clayey sands placed in 380 mm thick layers and compacted by 12 passes of sheepsfoot rollers. The specified moisture content range was 1.5% dry to 1.5% wet of Standard optimum moisture content.
- Filter / transition zones of alluvial sands and gravels (Zone 2A) and crushed sandstone (Zones 3A and 3C) compacted using flat drum rollers.
- Rockfill shoulders (Zone 3B) sourced mainly from quarried sandstone but with some siltstone and mudstone, dumped/placed in 1.2 m to 9.1 m lifts without the addition of water or formal compaction.
- Downstream stability berm (Zone 4) of waste material from excavations.

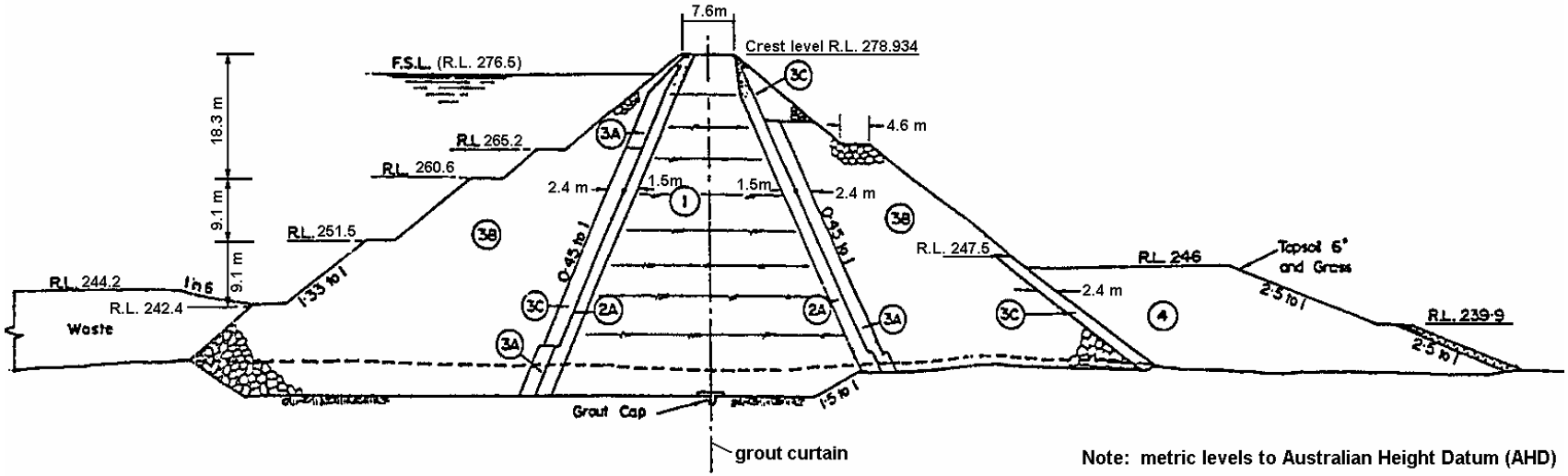

Figure G1.5: Bellfield dam, main section at chainage 701 m (courtesy of Wimmera Mallee Water)

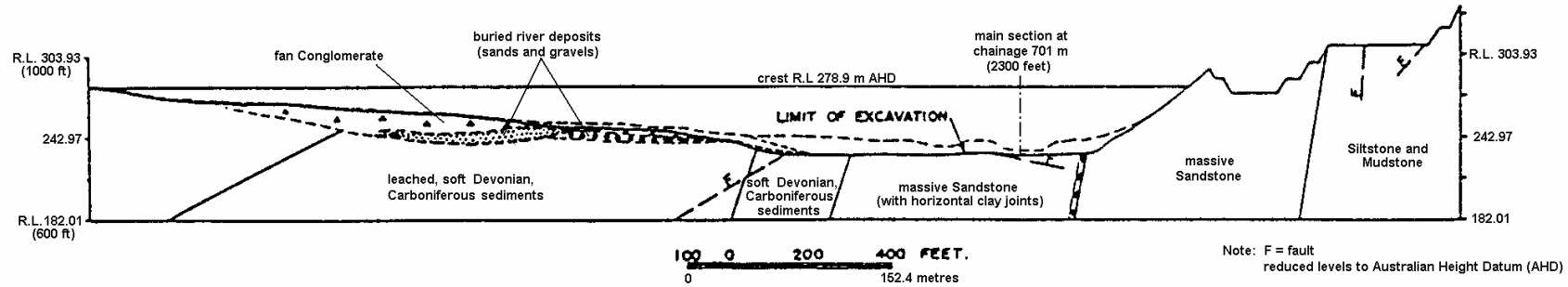

Figure G1.6: Bellfield dam, geological section on embankment centreline (adapted from Currey et al 1968).

Instrumentation (Figure G1.7) consisted of an internal vertical settlement gauge installed in the central core and surface measurement points (SMP) on the crest and slopes.

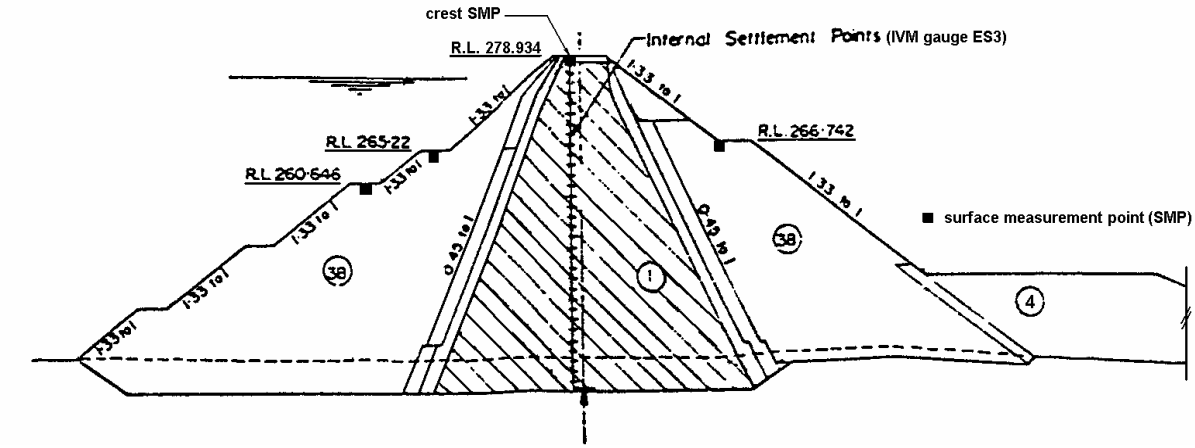

Figure G1.7: Bellfield dam, instrumentation layout at main section (courtesy of Wimmera Mallee Water).

The date of the base survey of the original SMPs in not known. Additional SMPs were installed on the crest and slopes in the late 1970's to early 1980's. Data records of the IVM and SMPs were obtained from the SMEC (1998a) surveillance report and only cover the post construction period from 1987 to 1997 (21 to 31 years after construction). The IVM records for this period are presented in Figure G1.8 and the SMP records at the main section in Figure G1.9 and Figure G1.10. Only the records from the original SMPs have been used in the plots. The figures show:

- Concentrated zones of internal core settlement at 14 to 15 m and 35 m depth below crest level (Figure G1.8a) developed at some time during the first 21 years after construction. The timing and cause of the concentrated settlement is not known, however, it could possibly be related to localised shear type deformations in the core.
- Limited internal settlement occurred in the core over the period 20.5 to 31 years post construction (Figure G1.8b). A large proportion of what settlement did occur over this period was concentrated between 28 and 30 m depth below crest level (28 mm or 50% of the total recorded settlement). Deformation versus time plots show this localised concentration in settlement to have occurred gradually over the period 21 to 32 years (i.e. it was not related to drawdown).

- The settlement versus time plots for the SMPs (Figure G1.10) show a steady long-term settlement rate (rate in log time). In comparison to similar type embankments the long-term crest settlement rate is on the high side for embankments with steady reservoir operation (Figure 7.62b in Section 7.6 of Chapter 7). The long-term settlement rate of the downstream slope is also on the high side (Figure 7.78b in Chapter 7), but neither is considered to be "abnormal".
- The displacement versus time plots for the SMPs (Figure G1.9) show a steady downstream rate of displacement (rate in log time) for the crest and downstream shoulder. In normal time, the average long-term displacement rate is 6.5 mm/year. In comparison to similar type embankments the magnitude and long-term rate of the crest displacement (Figure 7.68 in Section 7.6 of Chapter 7) are on the high side.
- The additional SMP installations indicate that in the last 15 to 20 years (since their installation) differential settlement across the crest is 30 mm, with greater settlement on the upstream side, and crest spreading is 20 to 30 mm.

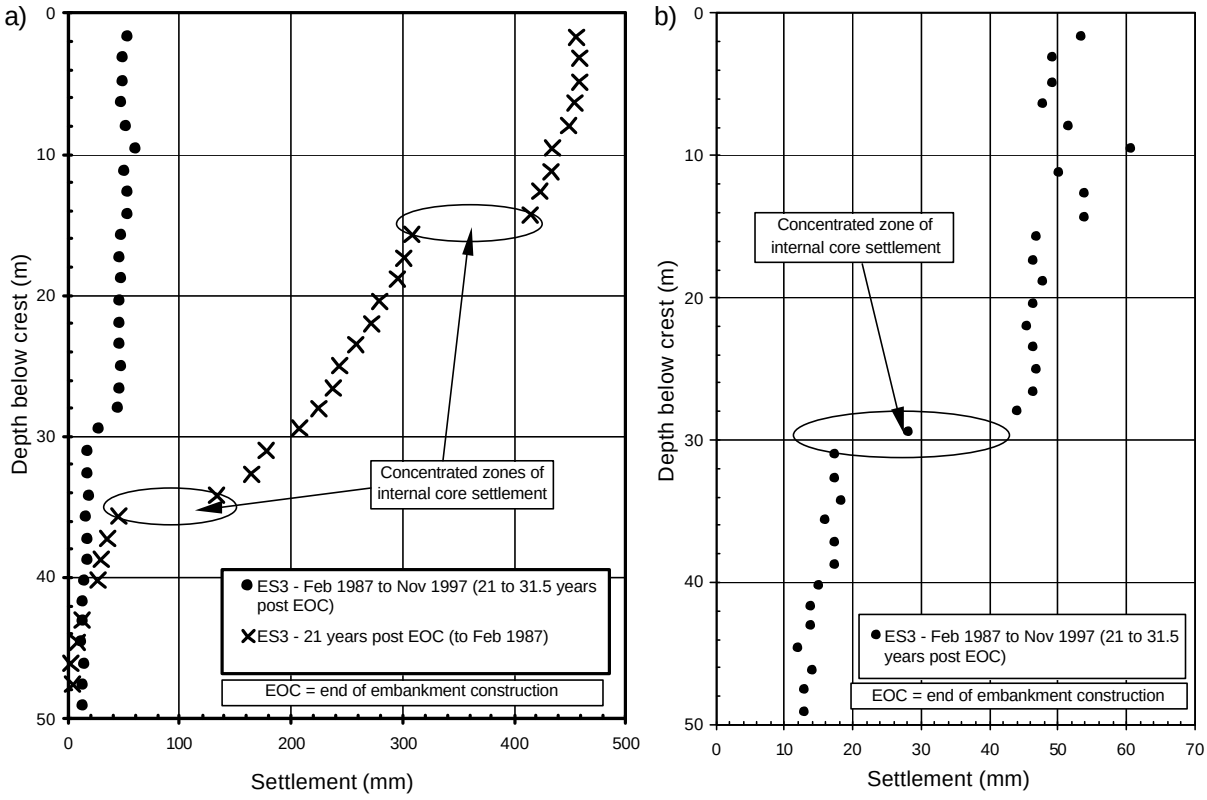

Figure G1.8: Bellfield dam, post construction internal settlement of the core.

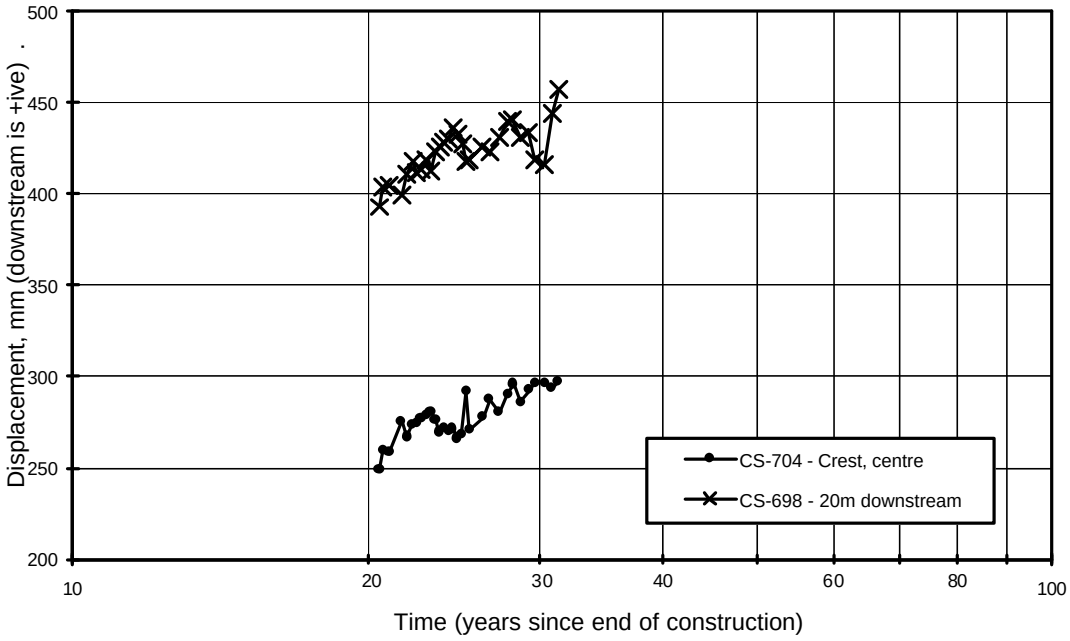

Figure G1.9: Bellfield dam, post construction displacement normal to dam axis versus time of SMPs at the main section.

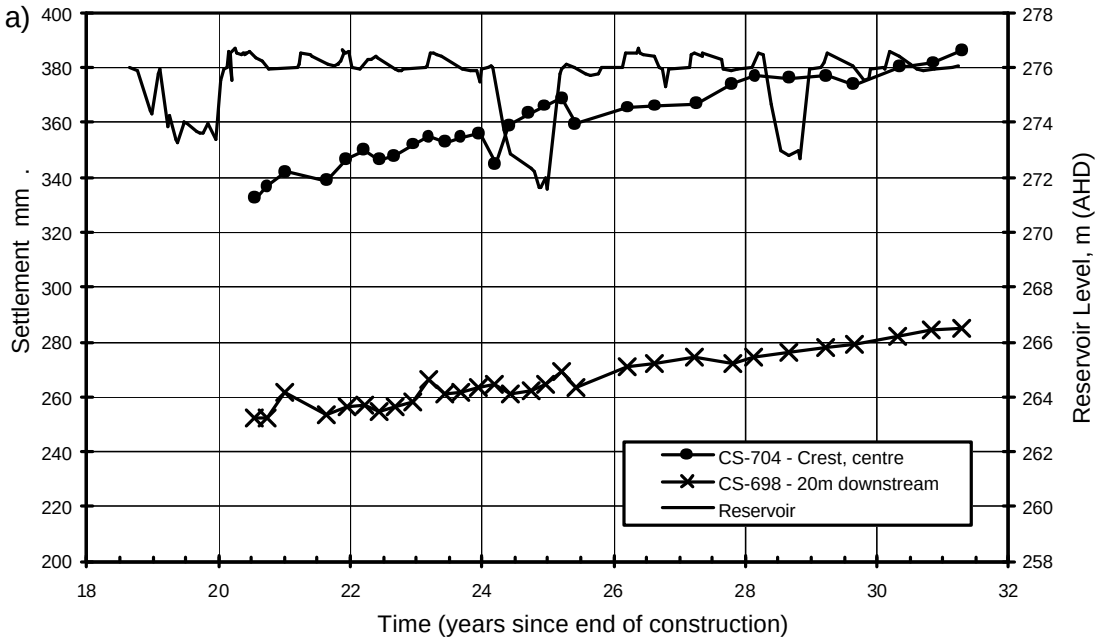

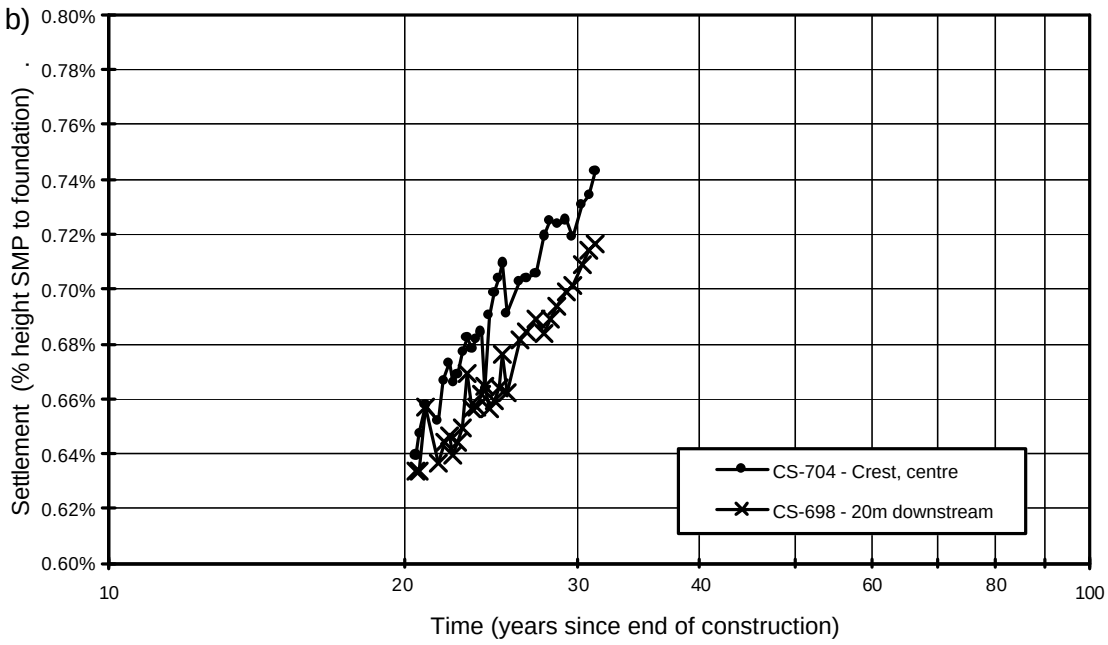

Figure G1.10: Bellfield dam, post construction settlement versus time of SMPs at the main section.

In comparison to similar type embankments under steady reservoir operation, the long-term rate and magnitude of the settlement and displacement of the crest and downstream slope at Bellfield dam are relatively high, although they are not considered "abnormally" high. The deformations possibly reflect the relatively higher shear stress conditions present in an embankment with such steep embankment slopes.

The cause of the localised internal settlement regions prior to 1987 is not known. It is possible that they may represent shear surfaces in the core that have developed post construction in much the same way as they are thought to have developed at Eppalock dam (refer Section 1.10 of this Appendix), a similar dam in terms of design and construction.

The localised zone of concentrated settlement that has developed over the period 1987 to 1997 has done so gradually, and is not related to drawdown. This may be reflective of gradual softening with time under near constant effective stress conditions.

1.3 BELICHE DAM

Beliche dam (Figure G1.11), located in southern Portugal, is a central core earth and rockfill embankment. The embankment has a crest length of 527 m and maximum height of 55 m. Construction of the embankment was completed in 1986. In summary,

the materials and placement methods (Maranha das Neves et al 1994; Naylor et al 1997) comprised:

- Thin earthfill core (Zone 1) of clayey sandy gravels with low plasticity fines, placed at moisture contents close to Standard optimum moisture content (specification ± OMC).
- Dual filters up and downstream of the central core. The outer filter (Zone 2B) consisted of gravels. No indication is given of the layer thickness or placement method.
- Inner rockfill zone (Zone 3A) of highly weathered and fractured schists and greywackes of medium strength (wet unconfined compressive strength of 9 to 12 MPa) placed in 1.0 m lift thickness and "*relatively lightly compacted*". Naylor et al (1997) commented that the 3A rockfill comprised a "*significant proportion*" of fines.
- Outer rockfill zone (Zone 3B) of "*good quality*" greywackes also placed in 1.0 m lift thickness and "*relatively lightly compacted*".
- Water is indicated as being added to the rockfill, but in what proportion or to which zones is not clear.

The purpose of the light compaction of the rockfill was to increase the margin of safety against internal erosion by reducing as far as practicable the potential for arching in the core during construction and on first filling.

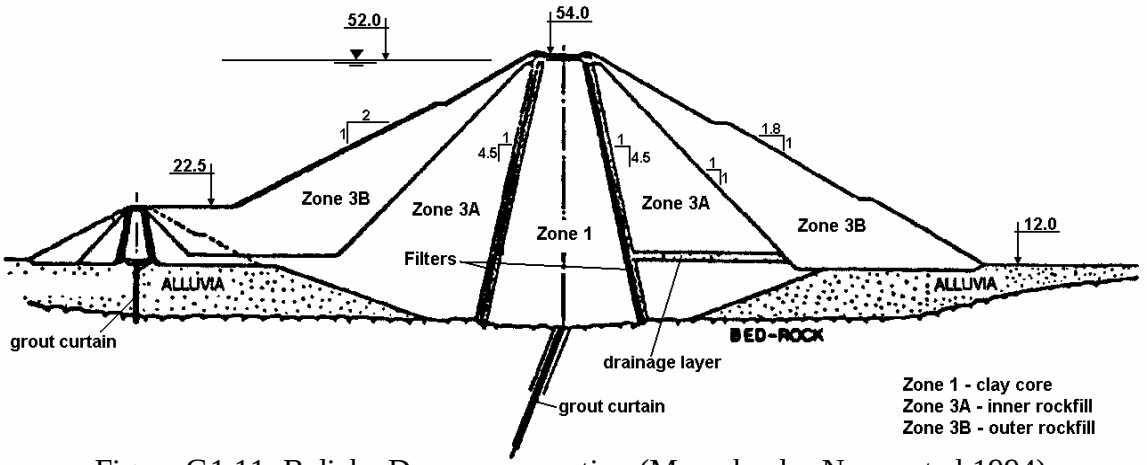

Figure G1.11: Beliche Dam, cross section (Maranha das Neves et al 1994)

Deformation monitoring instrumentation (Figure G1.12) comprised inclinometers, installed as construction proceeded, capable of measuring both vertical and horizontal

deformations and SMPs on the crest and slopes. Pressure cells and piezometers were also installed during construction.

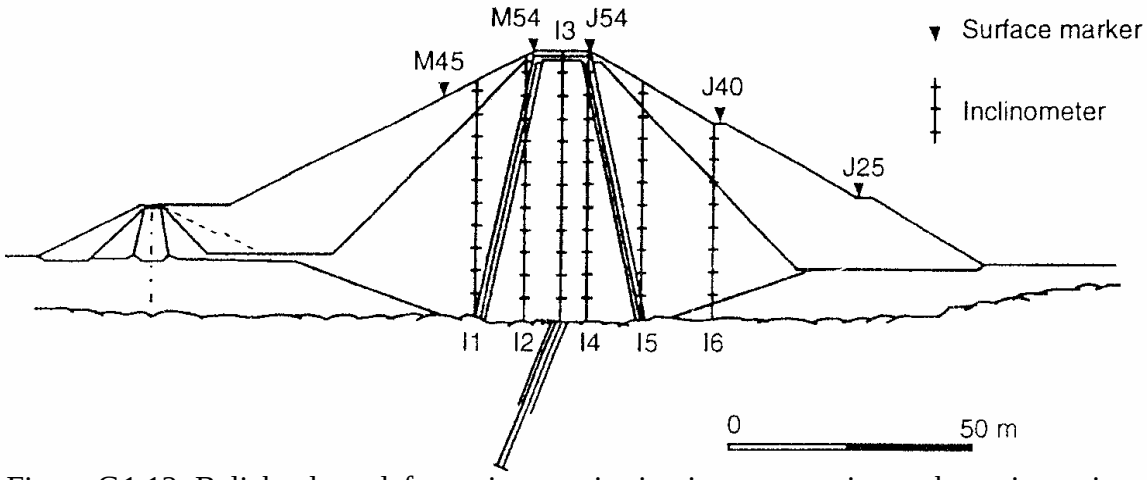

Figure G1.12: Beliche dam, deformation monitoring instrumentation at the main section (Naylor et al 1997).

1.3.1 Embankment Performance During Construction

Naylor et al (1997) undertook finite element analysis (FEA) of the construction and first filling stages for Beliche dam. Their results and the measured embankment performance during construction (Naylor et al 1997; Pagano et al 1998) are summarised as follows:

- The pressure cells and FEA indicated very high stresses were developed in the filter zones, much greater than over-burden pressures. The total vertical stresses measured in the core indicated arching across the core, and were over-predicted by the FEA. The results indicate stress transfer occurred from the core to the filters and possibly also from the rockfill to the filters, most likely due to relatively high moduli of the filters.
- Large deformations during construction distorted the inclinometer tubes such that horizontal deformations could not be monitored.
- Heavy rains in early 1985, prior to embankment completion, resulted in the over-topping of the upstream cofferdam (the reservoir reached elevation 29 m) resulting in saturation and collapse settlement of the upstream rockfill to this elevation.

- Pore pressures in the core were relatively high during construction reaching values in the order of 400 to 500 kPa in the lower quarter of the earthfill core at end of construction, equivalent to r_u values up to about 0.6.

The total settlement of the core to end of construction was "abnormally" large in comparison to similar type embankments (Figure 7.23 in Section 7.4 of Chapter 7). The internal vertical strains at end of construction (Figure G1.13) were in the order of 4 to 8% in the mid to lower region of the core and, in comparison to similar embankments (Figure 7.21a in Chapter 7), are very high. The vertical strain versus fill height at selected cross-arms from the lower region of the core (Figure 7.20a in Chapter 7) showed that the vertical strains increased almost linearly with increasing fill height.

The large vertical strains, and hence large total core settlement, during construction are considered to be a result of plastic type deformation of the wet placed core, which are evident from the large region of the core over which high vertical strains were measured and the large lateral deformation of the core (as indicated the distortion of the inclinometer tubes). The large lateral deformation of the core would have been a significant contributor to the large vertical strains measured to maintain volumetric uniformity in undrained loading. The likely high compressibility of the weathered and poorly compacted inner rockfill zone is considered to be a significant factor to the likely large lateral displacements.

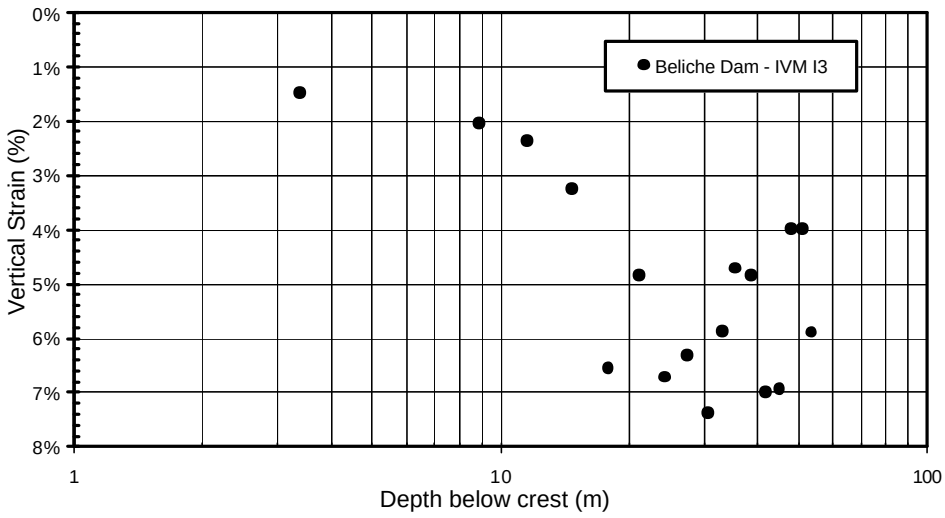

Figure G1.13: Beliche dam, vertical strain profile in the core at end of construction.

It is possible that collapse settlement on saturation of the upstream rockfill during construction (when the upstream cofferdam was over-topped) contributed to the lateral displacement of the core. However, no significant acceleration in vertical strain rate was observed at the time of inundation for the selected cross-arms represented in Figure 7.20b in Chapter 7 (Section 7.4).

1.3.2 Embankment Performance Post Construction

The post construction deformation at Beliche dam is presented in the following figures:

- Figure G1.14 - Internal vertical settlements of the core, and upstream and downstream rockfill zones. Locations of the IVM gauges are shown in Figure G1.12.
- Figure G1.15 - Settlement of SMPs on the crest and slopes of the embankment at the main section.
- Figure G1.16 - Displacement of SMPs on the crest and slopes of the embankment at the main section.

First filling was started prior to end of construction and reached within 6.5 m of full supply level 2.7 years after end of construction and within 1.5 m at 4.1 years (Figure G1.15a). Thereafter the reservoir remained steady until being drawn down to elevation 32 m starting at 7.9 years (from February 1993).

Notable aspects of the post construction deformation behaviour include:

- Very large vertical strains (average of 3.2%) were recorded in the upper 10 to 12 m of the core in the period of first filling (Figure G1.14). Large vertical strains (average of 2.1%) were also recorded in the upstream rockfill (IVM I1) between elevations 27 and 38 m.
- Post construction vertical strains in the mid to lower section of the core are, on average, much lower than in the upper 10 to 12 m during the period of first filling (average of 0.7%).
- Acceleration in the rate of settlement of the upstream and downstream crest SMPs is coincident with the latter stages of first filling. To a lesser degree SMP J40 (on the downstream slope) also shows acceleration, but the settlement over this period is of lesser magnitude (65 mm compared to 110 to 150 mm for the crest).

- Post first filling, acceleration in settlement rate is observed for SMPs on the up and downstream edge of the crest. Both SMPs show an increase in settlement rate on drawdown at 8 years, with settlements over the drawdown period in the order of 90 mm. SMP M54 (upstream edge of the crest) also shows an increase in settlement rate at 4.8 years, which is coincident with a period of high rainfall (more than 1000 mm in 2 months), the highest in the post construction embankment history.
- Displacement of the SMPs is downstream (Figure G1.16) and:
  - An increase in displacement rate of all SMPs occurred at 3.6 years. This is approximately coincident with the period when the reservoir level was raised from elevation 47 m to 50.5 m.
  - Lateral spreading of the crest reached 260 mm at 8 years after end of construction.

During first filling the region of high vertical strain in the upstream rockfill between elevations 27 and 38 m is largely due to collapse type settlement on initial wetting. It is concentrated above about elevation 29 m due to earlier saturation to this level prior to the end of construction. The region of high vertical strain in the core on first filling is above about elevation 26 m and coincident with that of the upstream rockfill. The core deformation is considered to be largely due to plastic type deformation of the wet placed earthfill core of low undrained shear strength and controlled by the collapse settlement of the upstream rockfill (refer to Figure 4.35 and the discussion in Section 7.5.2 of Chapter 7). The earthfill core deforms with the upstream shoulder because it is reliant on the upstream shoulder for support as it cannot support itself. Hence, the post construction vertical strain profile in the thin core is similar to that in the upstream rockfill. Large shear strains potentially developed in the core near to its downstream interface due to the differential settlement between the core and downstream shoulder (refer Figure 7.35c in Chapter 7). Further discussion on this mechanism is given in Section 7.10 in Chapter 7.

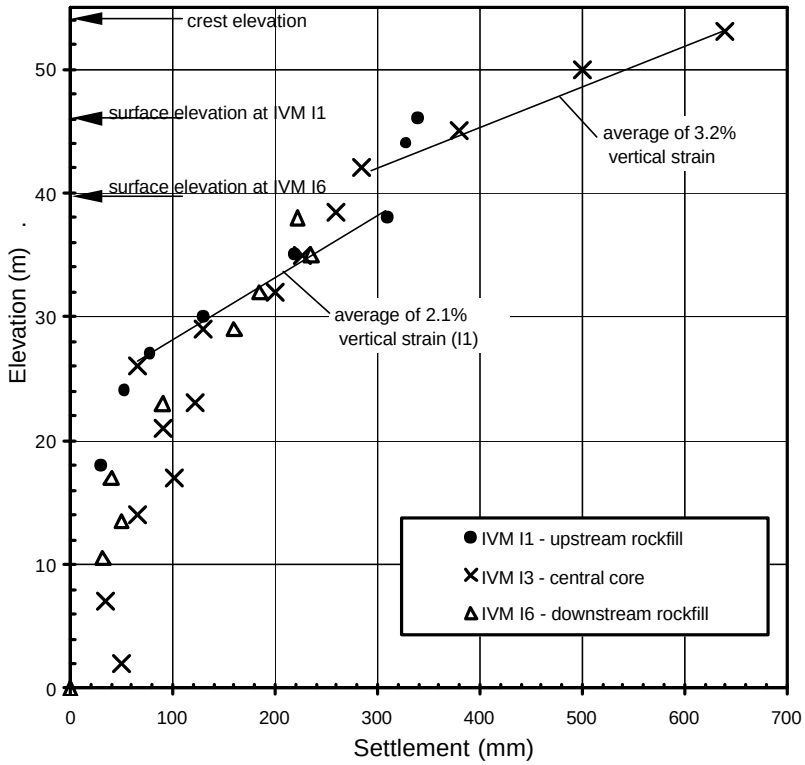

Figure G1.14: Beliche dam, post construction internal vertical settlement profile within the core, and upstream and downstream rockfill zones for the period from end of construction to 2.75 years post construction.

Post first filling, accelerations in settlement of crest SMPs occur on first drawdown and following heavy rainfall. This acceleration of SMP 54, located on the upstream edge of the crest, following heavy rainfall is possibly due to collapse settlement on wetting of the upper 3 to 4 m of rockfill. The acceleration on first large drawdown is a relatively common observation and thought to be associated with the decrease in water load acting on the upstream face of the core and lateral spreading of the core as lateral stresses increase in the upstream shoulder. This mechanism is discussed in Section 7.10 of Chapter 7.

Overall, the post construction settlement at Beliche dam is relatively high in comparison to similar embankment types. A large portion of the crest settlement is attributable to deformation in the upper 10 to 12 m of the core that occurred on first filling, for which the vertical strains are very high in comparison to those observed in other embankments.

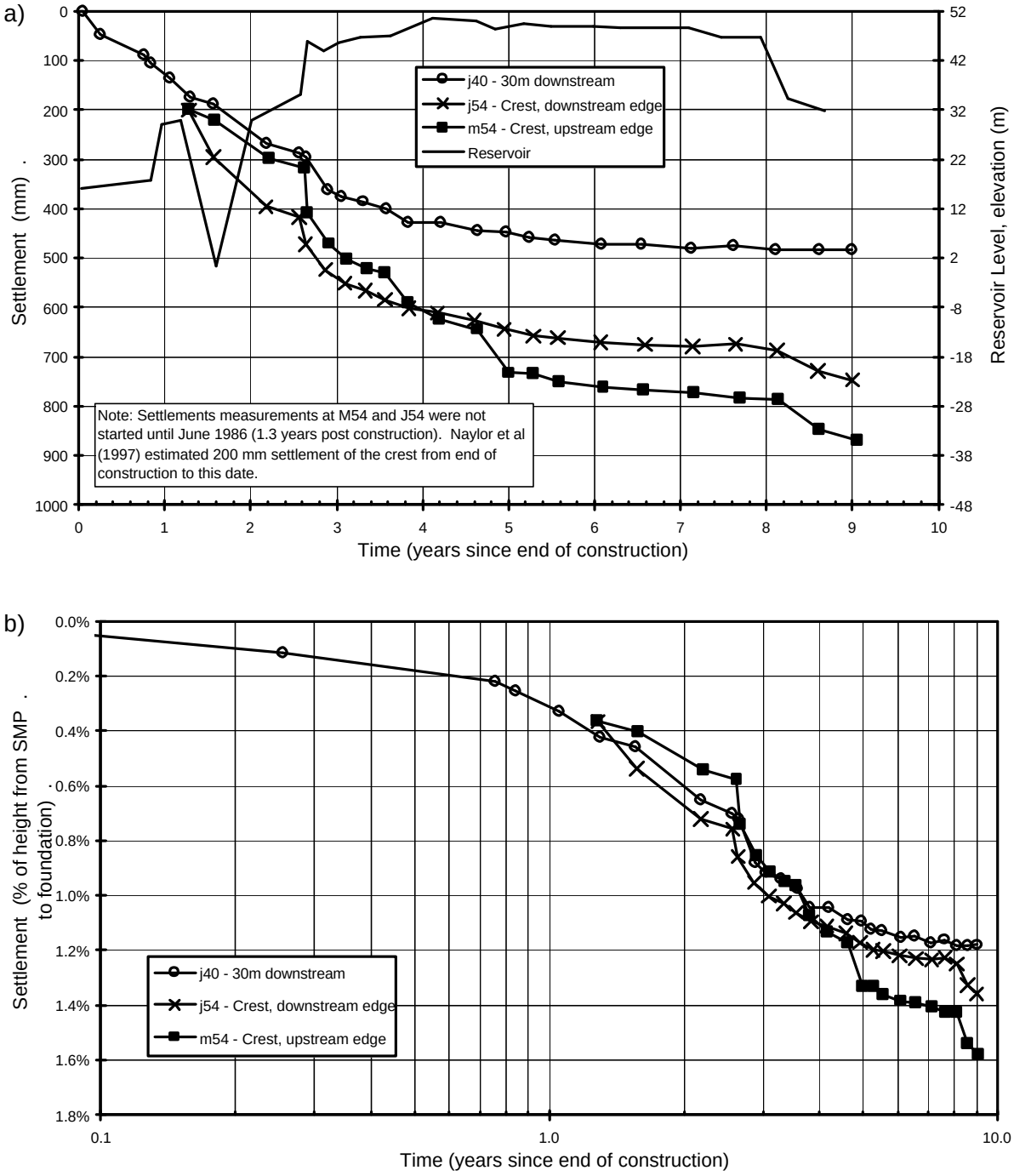

Figure G1.15: Beliche dam, post construction settlement versus time for SMPs at the main section.

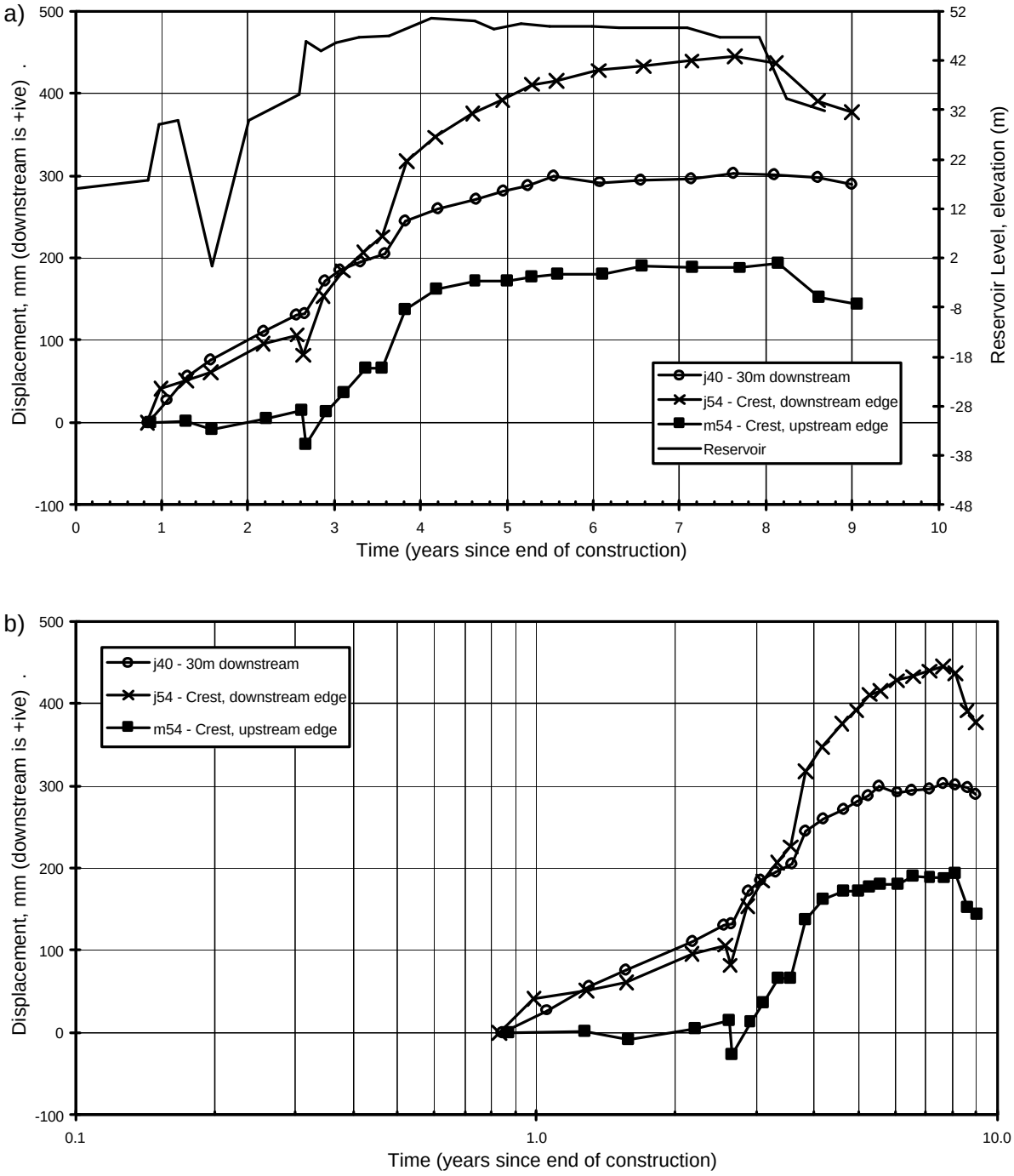

Figure G1.16: Beliche dam, post construction displacement normal to the dam axis of SMPs at the main section.

1.4 CHICOASEN DAM

Chicoasen dam (Figure G1.17), located on the Grijalva River in south-eastern Mexico, is a central core earth and rockfill embankment of 261 m maximum height for which embankment construction was completed in May 1980. The embankment is located within a narrow gorge with near vertical slopes (Figure G1.18) cut through limestone.

In summary, the materials and placement methods (Moreno and Alberro 1982) comprised:

- Core (Zone 1) – clayey gravel core with low plasticity fines derived from residual lutite for the most part, placed in 250 mm layers and compacted by vibrating padfoot rollers. Moisture contents were on average 0.8% dry of Standard optimum for the bulk of the earthfill. More plastic earthfills, placed on the wet side of Standard optimum, were used in the lower region of the core and adjacent to the steep abutment slopes.
- Filters / transitions (Zones 2A and 2B) of sandy gravels and gravels placed in 400 mm layers and compacted with 2 passes of a 10 tonne smooth drum vibrating roller.
- Zone 3A, the main rockfill zone, comprised quarried limestone placed in 600 mm layers and compacted with 4 passes of a 12 tonne smooth drum vibrating roller.
- Zone 3B, the outer rockfill zone, of dumped quarried limestone.

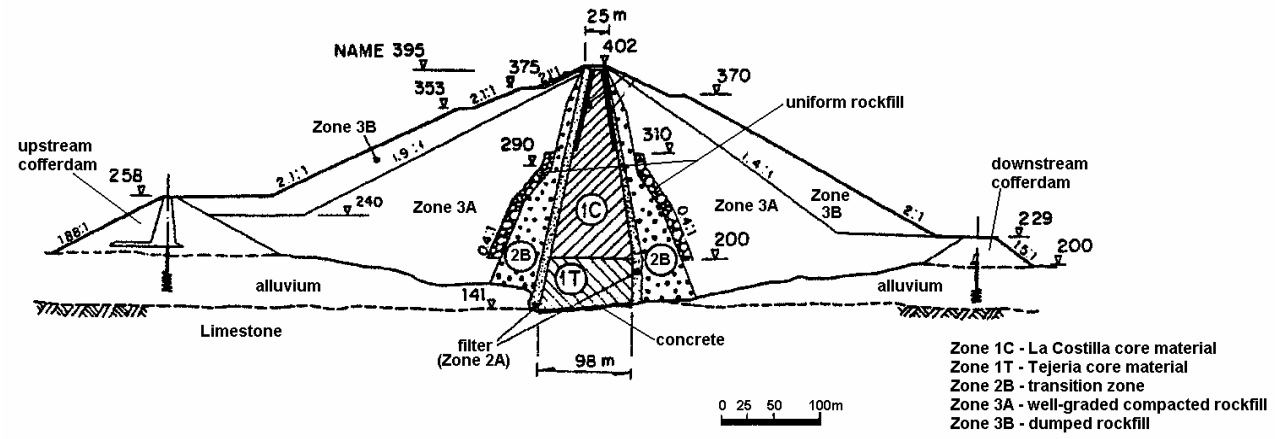

Figure G1.17: Chicoasen dam, main section (Moreno and Alberro 1982).

First filling was started on 1 May 1980, about one month prior to the end of construction when the embankment was about 12 m short of design crest level. The reservoir was filled to elevation 387 m, 8 m below the extraordinary maximum water level, over a period of about 3 months (by late July 1980) and thereafter remained steady through to March 1981, the end of published deformation monitoring records.

The embankment was well instrumented (Moreno and Alberro 1982). At the main section the instrumentation (Figure G1.19) included inclinometers (that measure both vertical and horizontal deformations) and cross-arm gauges within the rockfill, filter/transition and core zones. Moreno and Alberro (1982) only present a selection of

the instrumented deformation behaviour during construction and on first filling, and only some of this is presented in the following figures:

- Internal vertical strain profile in the core versus depth below crest level at end of construction from IVM I-B4 (Figure G1.20), located in the centre of the core but toward the left abutment.
- Internal vertical settlement (Figure G1.21) and displacement normal to the dam axis (Figure G1.22) during the period of first filling. Note that the initial and final monitoring dates shown are different between some of the instruments plotted in these figures.

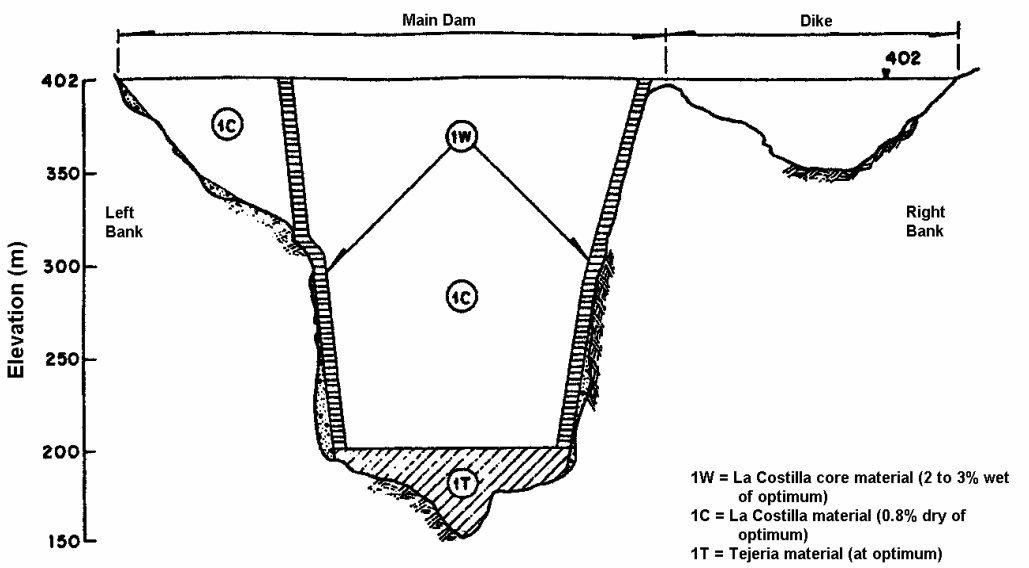

Figure G1.18: Chicoasen dam, longitudinal section (Moreno and Alberro 1982).

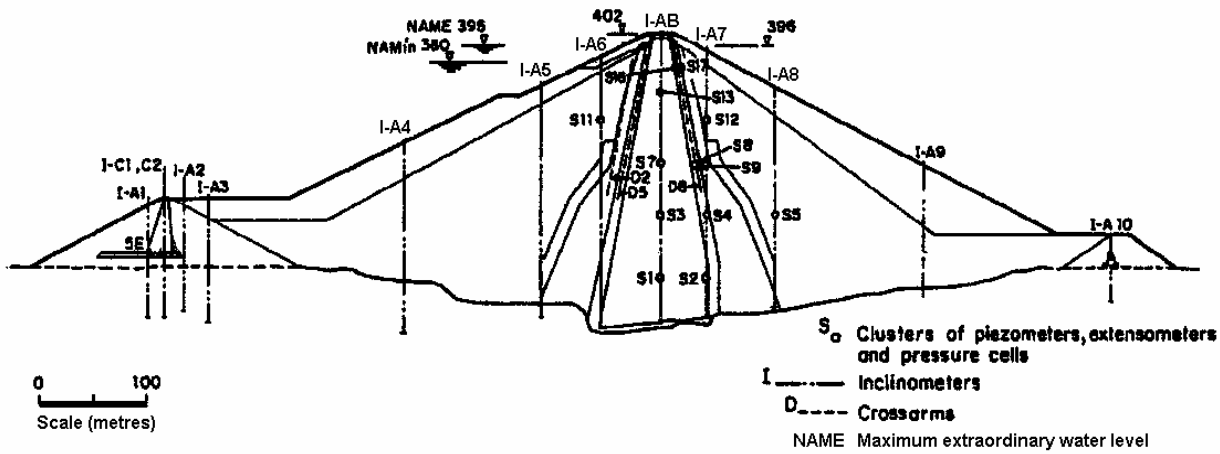

Figure G1.19: Chicoasen dam, inclinometer, cross-arm and pressure cell locations at the main section (Moreno and Alberro 1982).

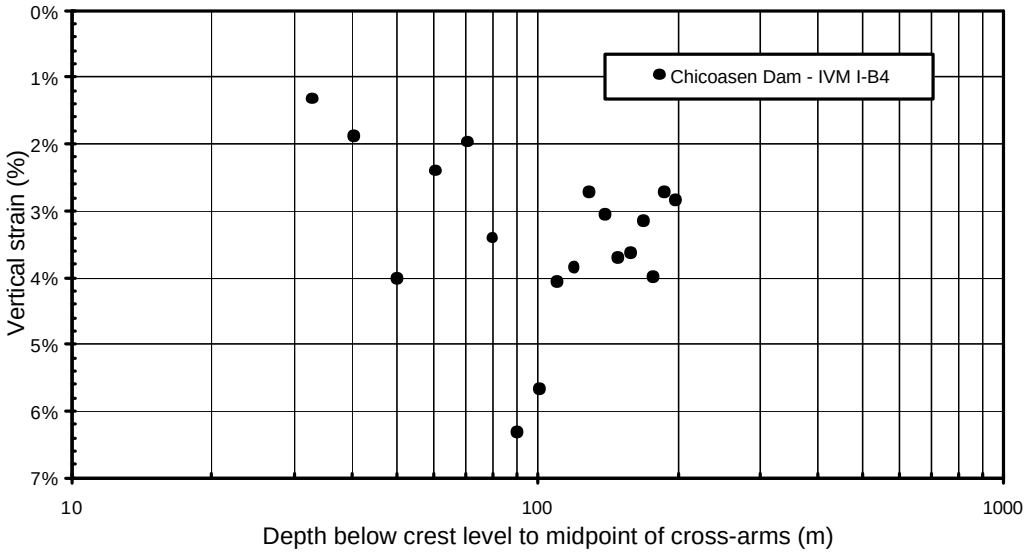

Figure G1.20: Chicoasen dam, vertical strain profile in the core at end of construction

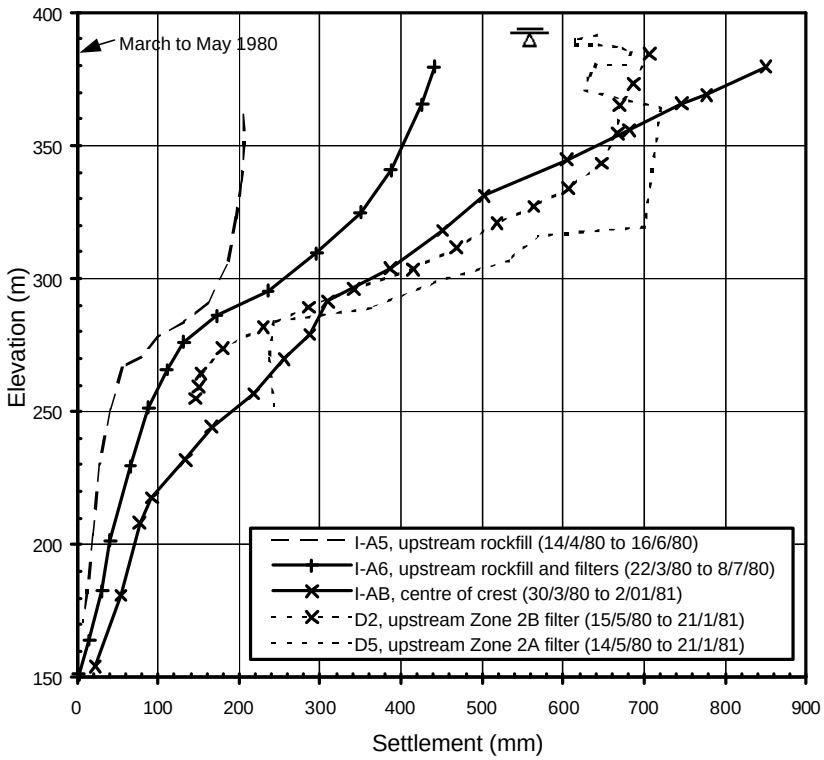

Figure G1.21: Chicoasen dam, internal settlement profiles during first filling (adapted from Moreno and Alberro 1982).

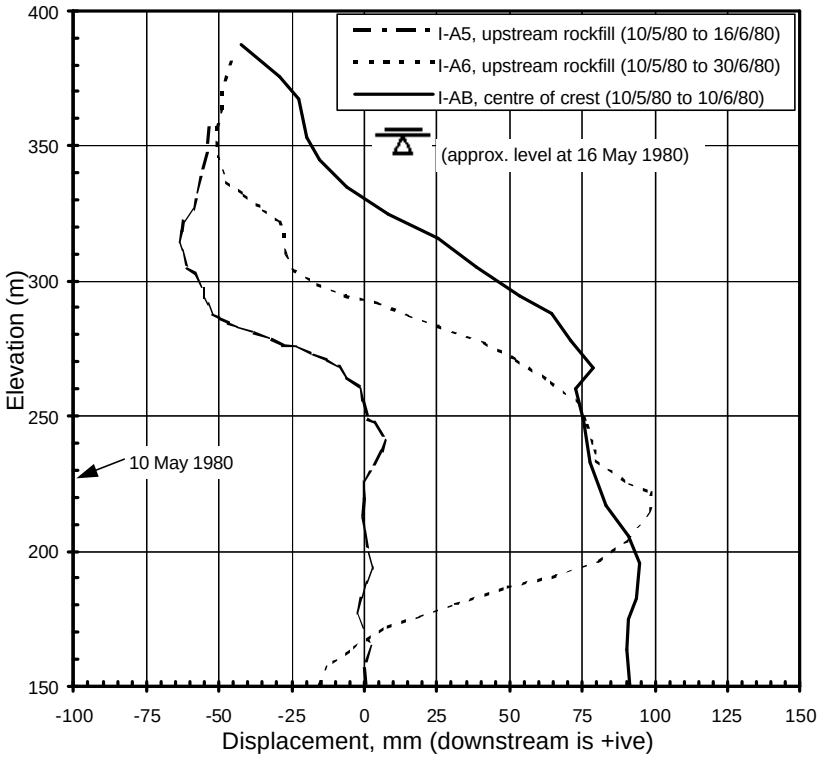

Figure G1.22: Chicoasen dam, internal lateral displacement profiles normal to the dam axis during first filling (adapted from Moreno and Alberro 1982).

The vertical strain profile in the core at the end of construction (Figure G1.20) shows a small region of high vertical strain of 5.5 to 6.5% over the depth range 85 to 105 m depth below crest level (from elevation 295 to 315 m). In comparison to similar embankments (Figure 7.21a in Section 7.4 of Chapter 7) vertical strains of this magnitude at this depth range are outside of the indicative bounds, but are not overly high. This possibly reflects the influence of the well-compacted, moderately wide to wide gravelly filter / transition zones and well-compacted inner rockfill shoulders on limiting the lateral deformation of the core and therefore the vertical plastic strain. This region of high vertical strain at IVM I-B4 is at an elevation that is coincident with the upper portion of the plastic region of the core identified by Moreno and Alberro (1982) from numerical analysis. It is also notable that this region of high vertical strain is coincident with the base of the core region where the filter / transition width is relatively thin (Figure G1.17).

Other notable observations during construction by Moreno and Alberro (1982) and Alberro and Moreno (1982) were:

- The pressures cells in the core indicated arching between the filters and the thin core occurred during construction. Differential settlements between the core, filter and

transition zones were reported to be less than 300 mm. Figure 7.7 (in Section 7.4 of Chapter 7) is further evidence that arching occurred in the narrow core during construction.

- Differential settlements between the core and very steep abutments were concentrated in the wet placed earthfill zones at the abutment interface.

The deformation records during first filling (Figure G1.21 and Figure G1.22) show:

- Regions of high vertical and lateral deformation in the upstream rockfill (IVM I-A5 and I-A6) concentrated between elevation 260 m and 300 m. Vertical strains in this region are in the order of 0.4 to 0.5%.
- Moreno and Alberro (1982) comment that no concentration of deformation was measured in the downstream rockfill.
- In the core, vertical strains during first filling are much greater above about elevation 290 m, in the order of 0.5% to 0.75%, than below elevation 290 m (average 0.3% vertical strain). Corresponding lateral deformation of the core is toward upstream above about elevation 290 m.
- In the upstream filter zones vertical strains are concentrated between elevations intermediate to those in the upstream rockfill and core. In the Zone 2A filter (IVM D5) the vertical strain profile shows localised concentrated zones of vertical deformation at elevations 285 m and 317 m, possibly indicative of shear type deformations.

The internal settlement profiles during first filling possibly reflect collapse type settlement in the upstream well-compacted rockfill on wetting, localised between elevations 260 m and 300 m. It is not clear why the settlement and displacement is localised in this region. Moreno and Alberro (1982) comment that it may be due to plastic type behaviour resulting from the reduction in effective horizontal stresses. However, it could also be that at the stress levels in the rockfill at this elevation the limestone rockfill is susceptible to collapse type deformation on saturation. Similar high vertical strains may not have occurred below elevation 260 m due to saturation of the rockfill between the cofferdam and main embankment during construction (crest of cofferdam at elevation 258 m), a practice that was used at El Infiernillo dam to reduce as far as practicable collapse type settlement on first filling.

In a similar fashion to El Infiernillo dam, the region of high vertical strain in the core on first filling at Chicoasen dam is at elevations above that where high strains were measured in the upstream rockfill and the region of high strain in the filters is at elevations intermediate to the rockfill and core. This behaviour suggests that the collapse type deformation of the upstream rockfill has a controlling influence on the deformation in the upstream filter / transition zones and core. The localised shear zones in the upstream Zone 2A filter at elevations 285 m and 317 m are most likely the result of high shear stresses developed due to the down drag effect of the upstream rockfill following collapse settlement. The deformation behaviour of the core during first filling suggests that the region of greater vertical strain above elevation 290 m on first filling is largely plastic type deformation as the core responds to the deformation of the upstream shoulder. This type of mechanism of deformation during first filling is discussed in Sections 7.5.2 (Figure 7.35) and 7.11 of Chapter 7.

1.5 COPETON DAM

Copeton dam (Figure G1.23), located in central New South Wales, Australia, is a central core earth and rockfill dam of 113 m maximum height and 1480 m length. The upstream cofferdam was completed by April 1971 and the main embankment constructed from late 1971 to mid 1973. Foundations for the embankment were excavated to bedrock. In summary, the materials and placement methods at Copeton dam were:

- Core (Zone 1) of clayey sands of medium plasticity, sourced from residual granite, placed in 150 mm layers and compacted by sheepsfoot roller. The specified moisture content range was 1% dry to 1% wet of Standard optimum. The low to negligible positive pore water pressures that developed during construction suggest likely placement on the dry side of Standard optimum.
- Filters (Zones 2, 2A and 2B) of blended washed sand and crushed granite placed in 375 mm to 450 mm layers and compacted by 9 tonne vibrating roller.
- Rockfill sourced from quarried fine to coarse grained granite of very high compressive strength, comprising:
  - Zone 3B – inner rockfill zone placed in 1.2 m lifts and compacted by 4 passes of a 9 tonne vibrating roller.

- Zone 3C – outer rockfill zone placed in 3.7 m lifts and compacted by 4 passes of a 9 tonne vibrating roller.
- Rockfill dumped in high lifts was used for the bulk of the cofferdam forming the upstream toe of the embankment.
- No water was added during placement or compaction of the rockfill.

The embankment was well instrumented. Monitoring equipment included:

- Piezometers in the core and foundation.
- Four internal vertical settlement gauges (IVM) in the core (IVMs A to D). Cross-arms were at about 5 foot (1.5 m) spacing.
- Hydrostatic settlement gauges (HSG) and internal horizontal and vertical displacement measurement gauges (IHM) in the filter and rockfill zones downstream of the core.
- Surface measurement points (SMP) on the crest and slopes.

The approximate locations of the deformation monitoring equipment at the maximum section are shown in Figure G1.24.

The reservoir impounded water for several years prior to the end of construction and reached a maximum elevation of 527.5 m (within 45 m of full supply level), therefore over-topping the upstream cofferdam. First filling was virtually completed in August 1978, 5.2 years after the end of construction, when the reservoir reached within 1 m of full supply level. Since first filling the reservoir has fluctuated within about 60 m of full supply level (Figure G1.28).

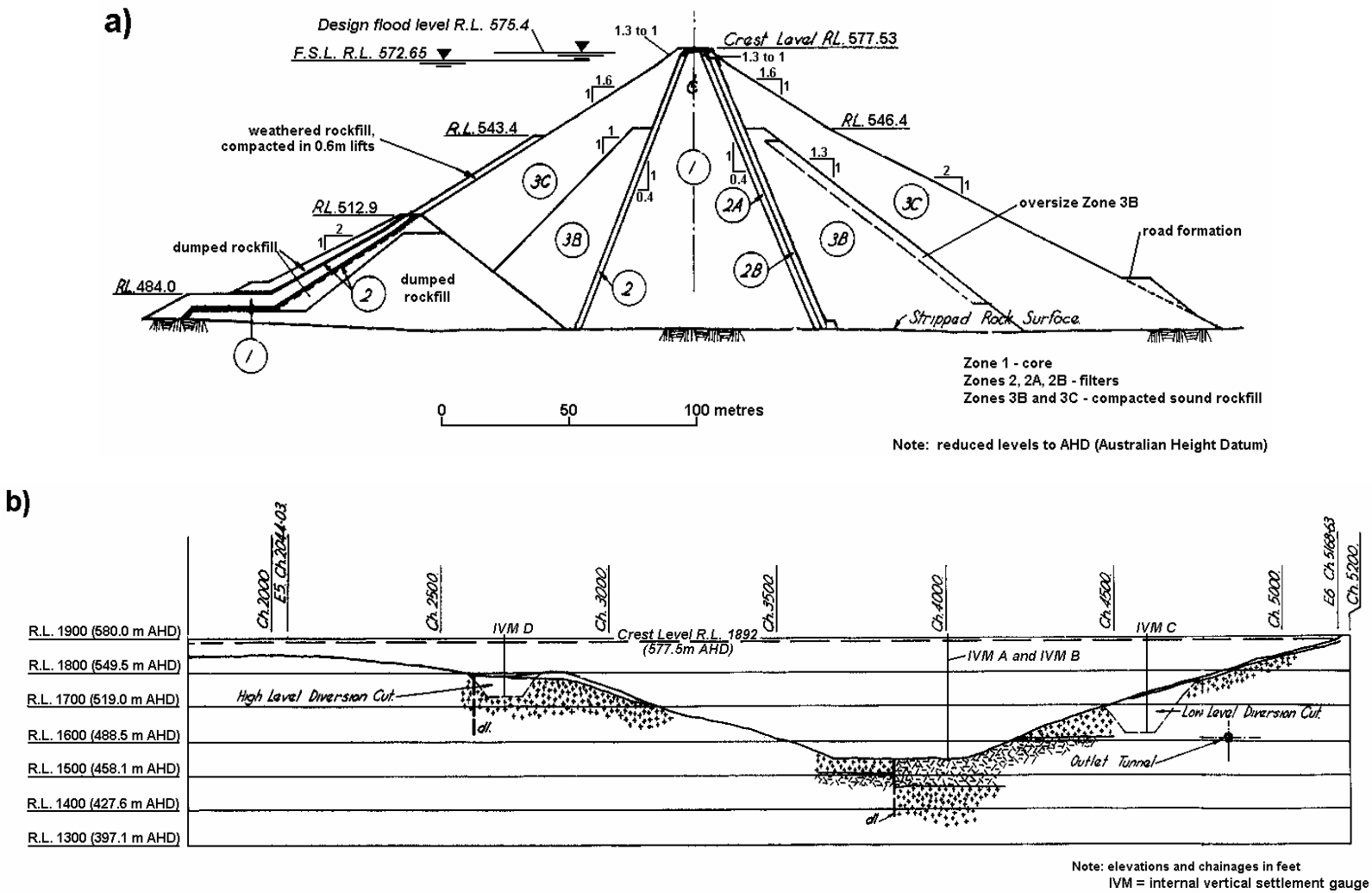

Figure G1.23: Copeton dam; *(a)* maximum section and *(b)* long section on the embankment centreline (courtesy of New South Wales Department of Land and Water Conservation).

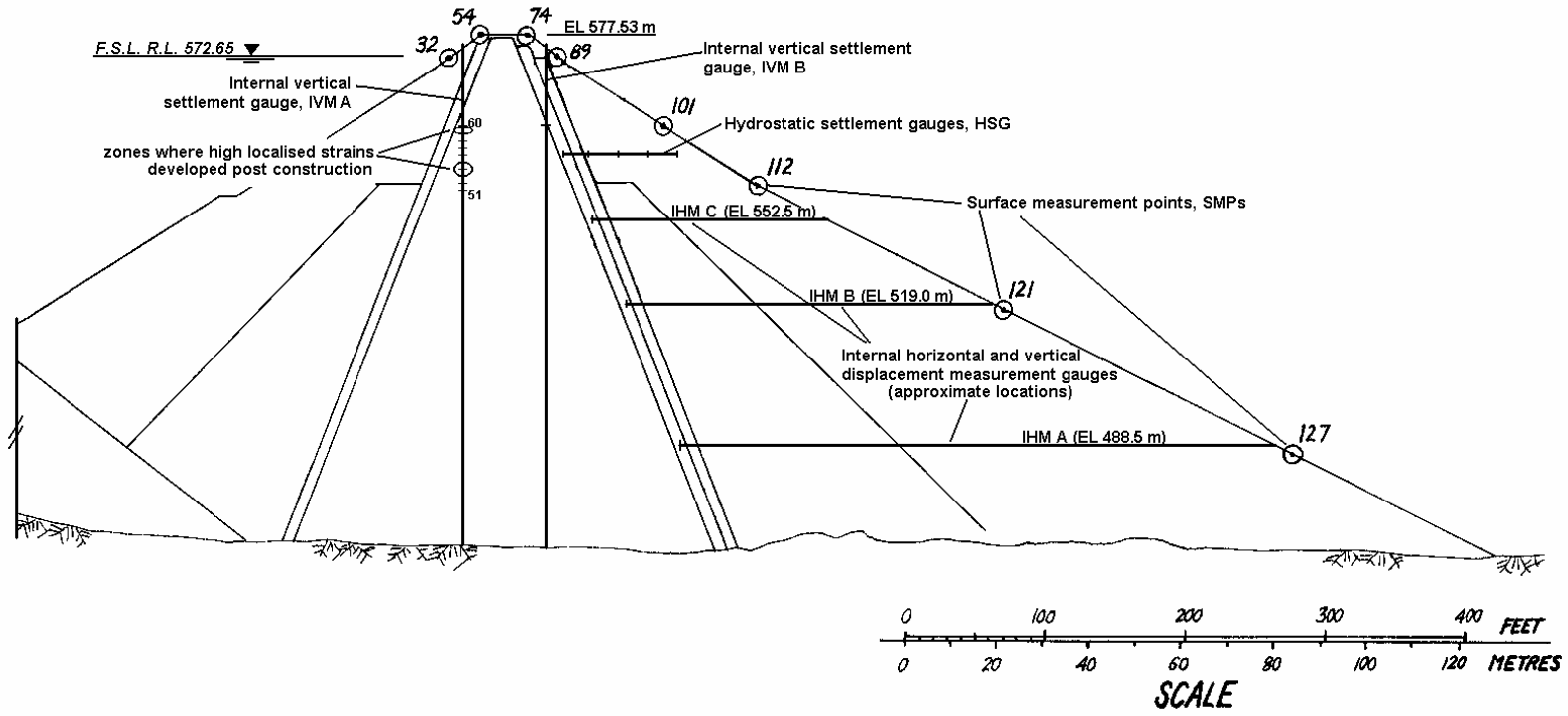

Figure G1.24: Copeton dam; deformation instrumentation at the maximum section (courtesy of New South Wales Department of Land and Water Conservation).

1.5.1 Deformation During Construction at Copeton Dam

The deformation behaviour of Copeton dam during construction in comparison to other similar dams was considered "normal". The internal vertical strain profiles within the core at end of construction (Figure G1.25) show vertical strains increasing with increasing depth below crest and reaching maximum strains of 5 to 6%. The high vertical strain at the base of IVM B is within the contact zone of high plastic clay placed on the wet side of Standard optimum. Calculated "confined" secant moduli within the core were in the order of 20 to 35 MPa.

The estimated lateral displacement ratio of the core (Figure 7.12 in Section 7.4 of Chapter 7) from the IHM data records was less than 1%, which is low in comparison to other central core earth and rockfill dams.

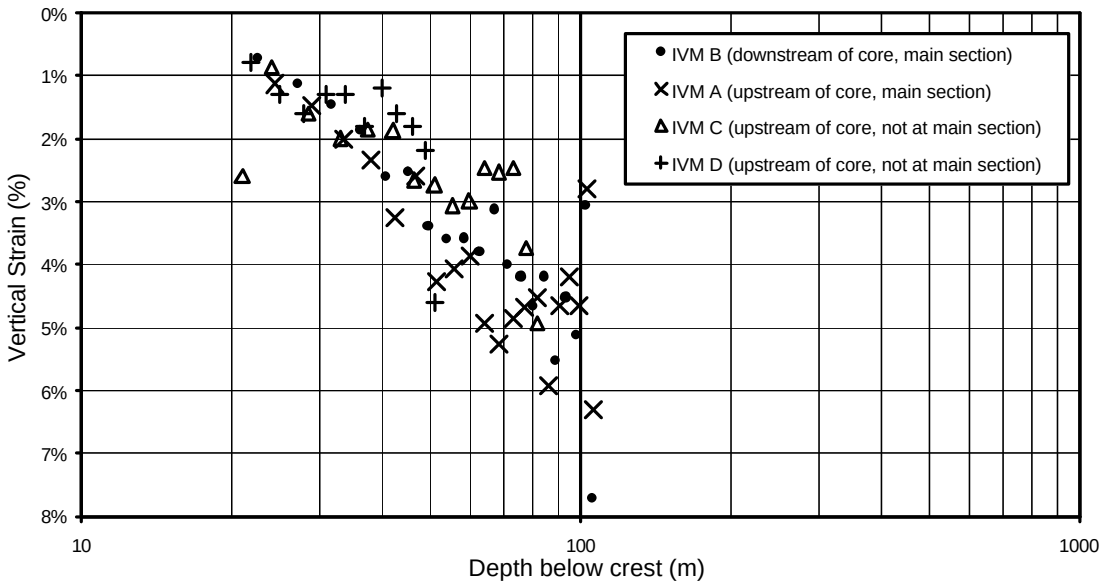

Figure G1.25: Copeton dam; vertical strain profiles in the core at end of construction from IVM gauges.

1.5.2 Post Construction Deformation Behaviour at Copeton Dam

Post construction, the deformation behaviour of the SMPs on the crest and slopes of Copeton dam at the main section is considered "normal" in comparison to similar type embankments. However, several interesting deformation trends are evident from the IVM results post construction.

The post construction internal vertical settlement profiles from end of construction (June 1973) to March 1999 are shown in:

- Figure G1.26a for IVM A at the main section, located about 9 m upstream of the dam axis (Figure G1.24).
- Figure G1.26b for IVM B at the main section, located about 9 m downstream of the dam axis.
- Figure G1.27 for IVM C on the right abutment, located about 9 m upstream of the dam axis.

The plots show the development of localised zones of high strain in IVMs A and C, located upstream of the dam axis, at depths of 20 to 30 m below crest level (at an elevation above RL 545 m AHD). In both IVMs the highest region of strain is between the two top cross-arms and close to the upstream interface of the core with the upstream filter. A secondary localised zone of high strain in IVM A is located about 9 m below the upper zone of high strain. For IVM A, the locations of these zones of high vertical strain are shown on Figure G1.24. It is notable that the regions of high strain in IVMs A and C are at elevations above where the Zone 3C rockfill (dry placed in 3.7 m lifts) is located on the upstream side of the Zone 2 filter (refer Figure G1.24), i.e. there in no Zone 3B rockfill zone between the filter and Zone 3C rockfill. By March 1999 post construction vertical strains between the upper cross-arms was 6.3% in IVM A (cross-arms 59 to 60) and 8.5% in IVM C (cross-arms 43 to 44), or 95 and 129 mm respectively. In the lower region of high strain in IVM A (cross-arms 53 to 55) the post construction settlement was 76 mm, equivalent to a vertical strain of 2.5%.

In contrast the settlement profile at IVM B, located downstream of the dam axis, shows no localised regions of high strain. This type of deformation behaviour is considered “normal”.

The high strains at the base of IVMs A and B are due to consolidation type settlements within the wet placed lower region of the core. Pore water pressures within this lower region were high at end of construction and dissipation of about 450 kPa occurred over a period of many years after construction.

The settlement versus time for the regions of high vertical strain in IVMs A and C (Figure G1.28) show that increases in the settlement between the cross-arms occur at similar times; during first filling, sometime between 9 and 13 years, and sometime between 20 and 26 years.

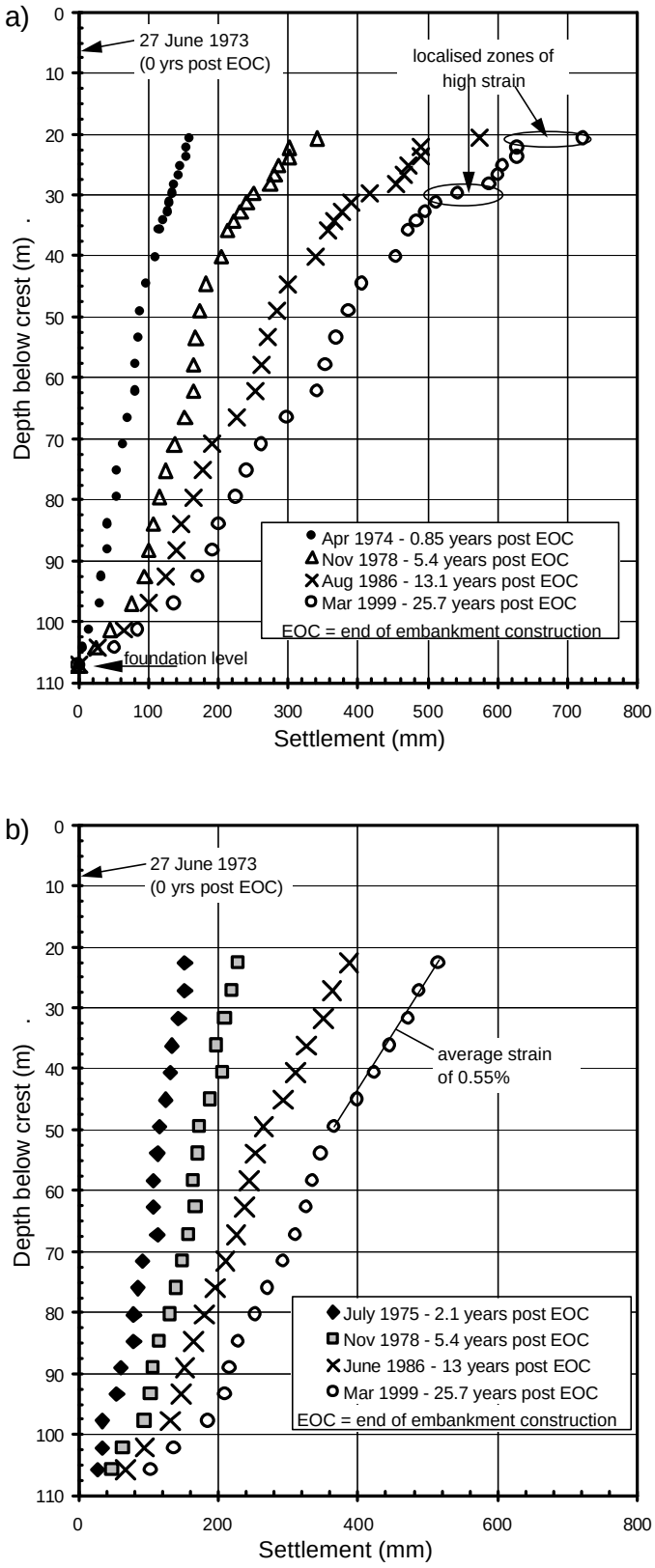

Figure G1.26: Copeton dam, post construction internal settlement profiles in the core at the main section, *(a)* IVM A at 9 m upstream of the dam axis and *(b)* IVM B at 9 m downstream of the dam axis.

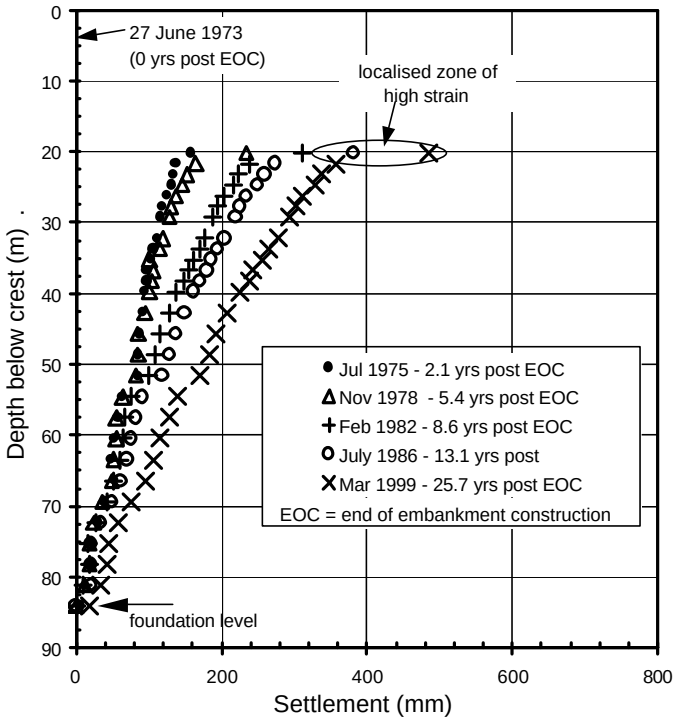

Figure G1.27: Copeton dam, post construction internal settlement profiles in the core at IVM C.

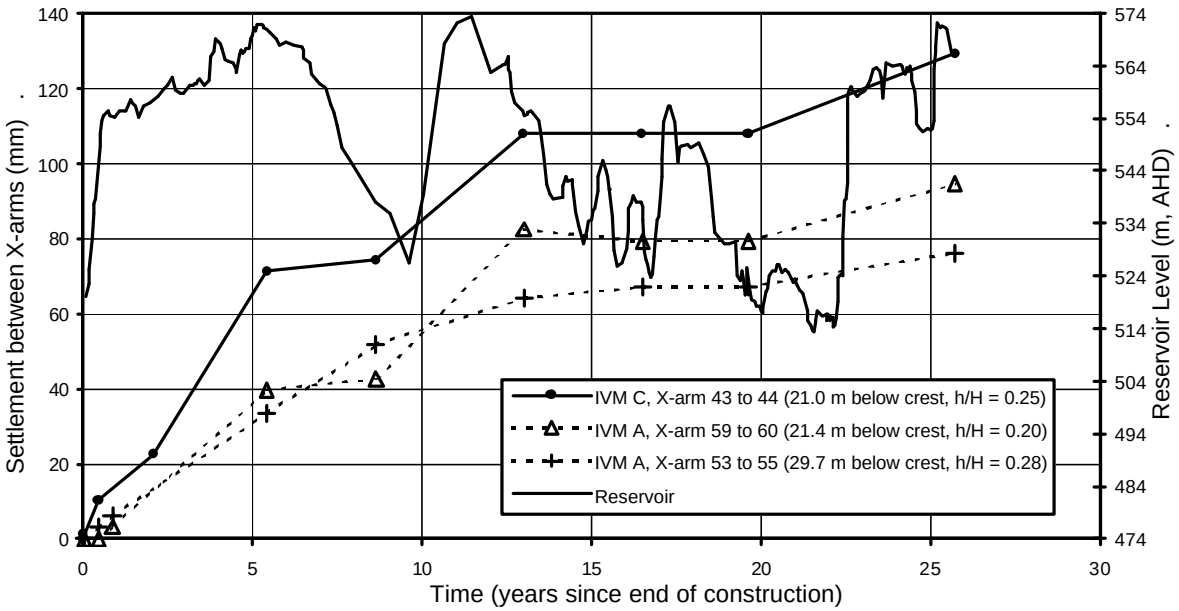

Figure G1.28: Copeton dam; post construction vertical strain versus time

The post construction surface measurement point (SMP) deformations of the crest and slopes of the main section at Copeton dam are shown in Figure G1.29 (settlement) and Figure G1.30 (horizontal displacement). The settlement of the surface markers at IVMs

A and B are included in Figure G1.29. Overall, the plots are indicative of "normal" type deformation behaviour. The settlement plots show a steady to decreasing rate of settlement (rate in terms of log time, Figure G1.29b). The displacement of the downstream slope shows a steady long-term trend after about 10 years, and the crest and upstream slope show a gradual upstream trend after 5 years, with fluctuations about the general trend due to fluctuations in the reservoir level. It is notable that for SMP 74, on the downstream edge of the crest, the magnitude of settlement (Figure G1.29b) is similar to that of the downstream slope, yet the displacement trend is similar to that of the upstream slope to crest region (Figure G1.30).

The SMPs on the right abutment near IVM C show similar patterns of deformation behaviour to those at the main section.

The settlement records (Figure G1.29) for SMP 54 on the upstream edge of the crest show a small but perceptible increase in the rate of settlement between 10.35 to 11.2 years post construction, which is coincident in time with the rise in reservoir level to full supply level. A similar increase in settlement rate is shown for IVM A, although the data is relatively erratic after 10 years. Comparing the settlement at IVM A and B large differences in settlement occur during first filling (160 mm) and on rising reservoir level at 10.35 to 11.2 years (50 mm); at other periods the settlement difference develops more gradually. Displacements during this period (Figure G1.30) show a sharp downstream movement of 50 to 90 mm, which is not unexpected given the large rise in reservoir level.

The possible cause and mechanism associated with the development of the localised regions of high strain can only be surmised from the data. It is reasonable to conclude that localised straining between the upper cross-arms in IVMs A and C is concentrated during periods of rising reservoir level, most likely above the elevation of these regions of high strain at 545 to 560 m. A possible mechanism to explain the deformation behaviour is the development of shear type displacements within the core. The cause of the shear displacements is greater settlement of the upstream rockfill than that of the core as indicated by the SMP data. The mechanism is likely to involve collapse type settlements of the upstream rockfill resulting in development of high shear stresses at the upstream interface between the Zone 2 filter and Zone 3C rockfill, and between the core and filter.

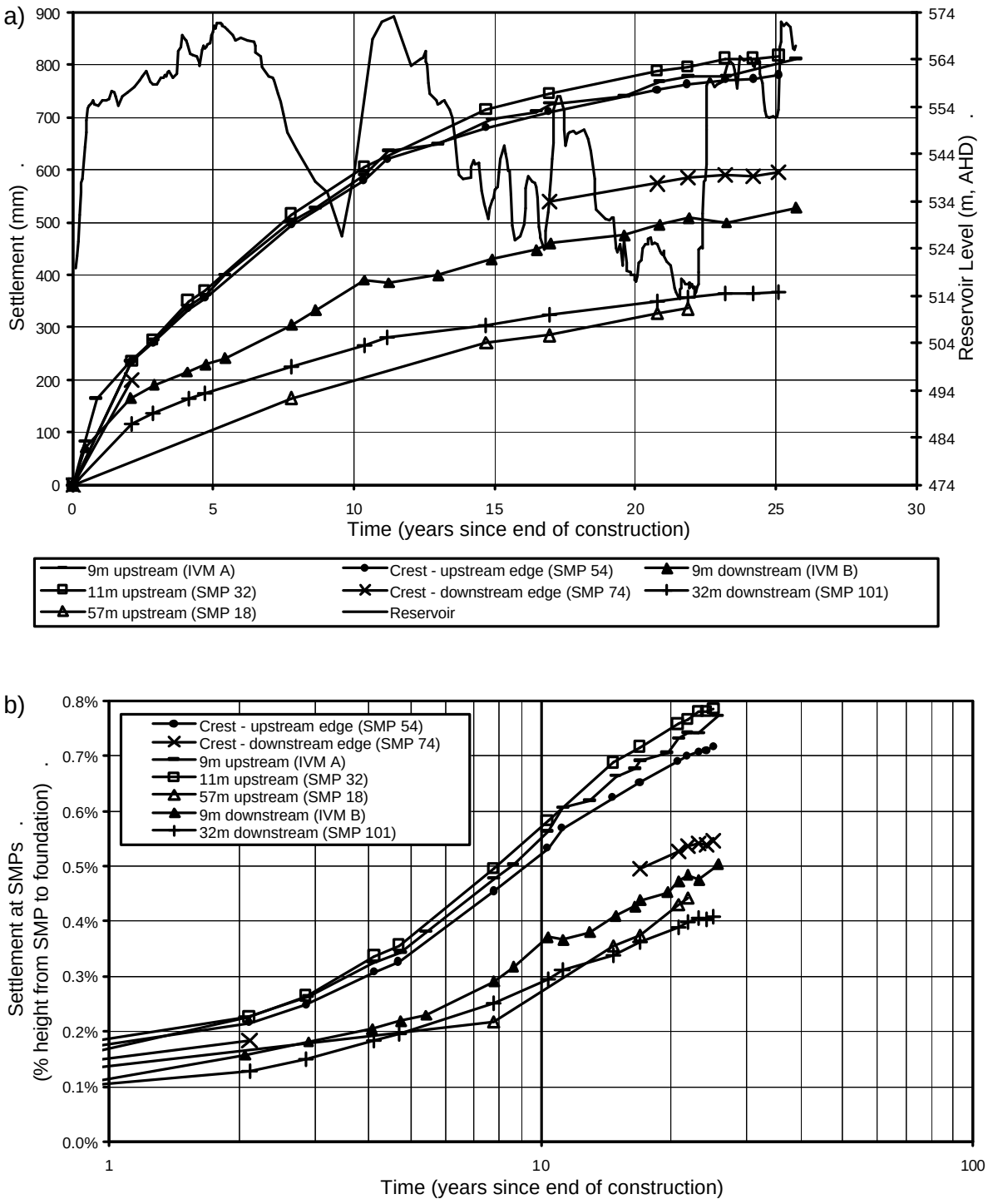

Figure G1.29: Copeton dam, post construction settlement of SMPs at the main section.

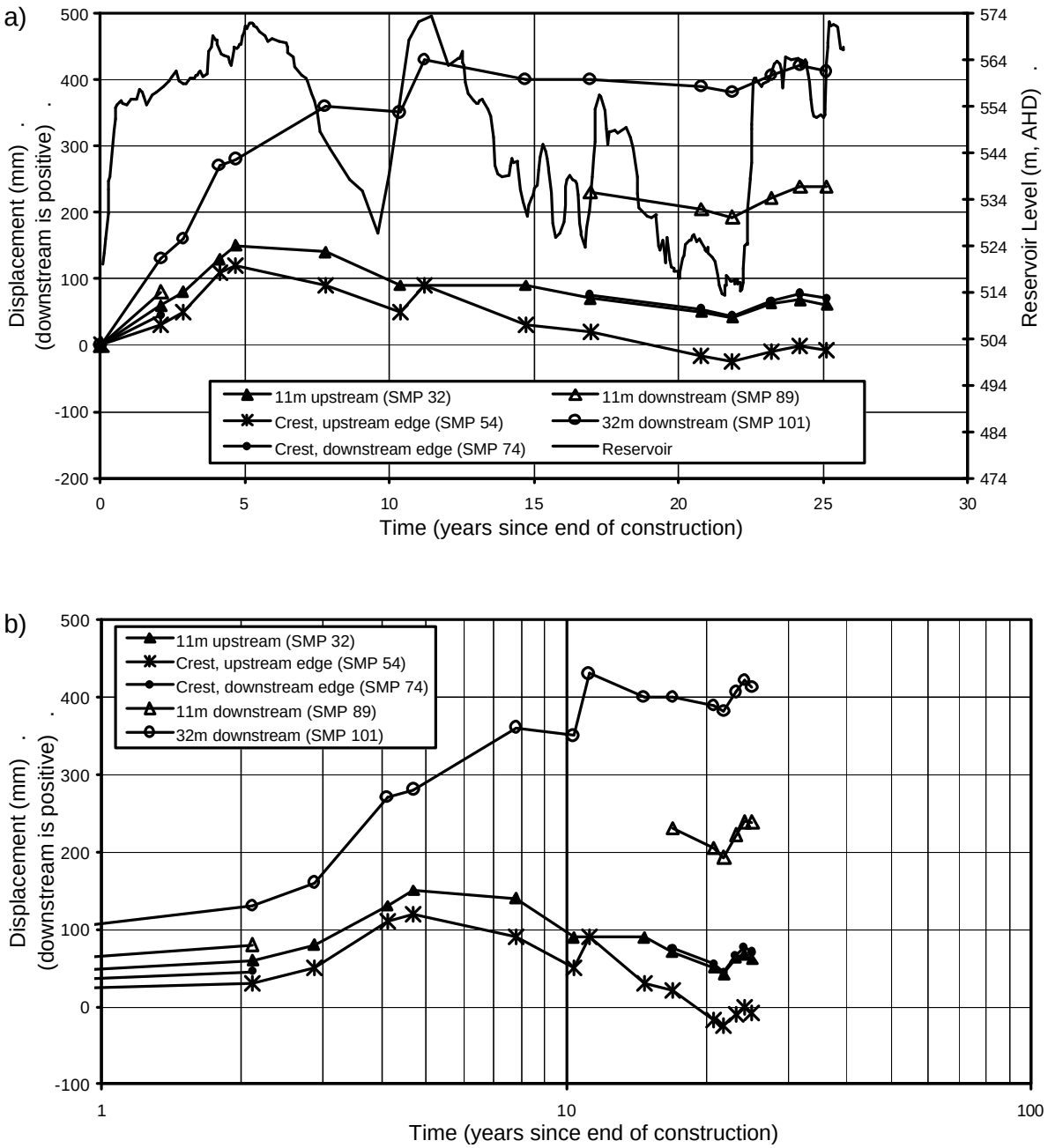

Figure G1.30: Copeton dam, displacement normal to the dam axis of SMPs at the main section.

This mechanism of shear development during the period of first filling is explainable by collapse type settlement of the dry placed, poorly compacted Zone 3C limestone rockfill (placed in 3.7 m lifts). As previously discussed the elevations of the regions of high vertical strain in the core are located above the elevation at which the Zone 3C rockfill was placed directly upstream of the Zone 2 filter (Figure G1.23a and Figure G1.24). The subsequent shear displacements during rising reservoir at about 10.5 to 11 years, and then again at 22 or 25 years, are most likely due to further differential settlement of

the upstream shoulder as indicated by the SMP and IVM data records. A possible explanation for the differential settlement post first filling is softening or degradation of the upstream rockfill over time.

The post construction surveillance reports (WRC NSW (1978) and LWC NSW (1995a)) refer to the presence of transverse and longitudinal cracking in the bitumen seal of the road on the crest. WRC NSW (1978) comment that longitudinal cracking over the deepest section of the embankment was first observed in June 1977 (4 years after construction), and by mid 1978 the cracks covered a length of 330 m and were a maximum of 10 mm in width. LWC NSW (1995a) refer to fine transverse cracks on the left and right abutment above the deepest section of the embankment, and to longitudinal cracks in the bitumen seal on the crest. They also indicate that the greater settlement of the upstream side of crest is "*visually evident*". These observations support the deformation monitoring records.

It is not clear if the road was re-surfaced between 1978 and 1995. If it had been re-surfaced, which is possible given the elapsed period of time, then the cracking observation in 1995 would be in response to differential deformations between the upstream shoulder and core post first filling as the monitoring data indicates.

1.6 COUGAR DAM

Cougar dam (Figure G1.31), located in north-western Oregon, USA, is a 159 m high central core earth and rockfill embankment constructed in the early 1960's for flood control and power generation purposes (Pope 1967). Most of the embankment foundation was stripped to bedrock. In summary, the materials and placement methods (Pope 1967) comprised:

- Core (Zone 1) – slightly upstream sloping thin central core of silty gravels sourced from weathered rock and talus. The fines content (minus 75 micron) of the earthfill averaged 15% and the fines were of medium plasticity. The earthfill was placed in 300 mm loose thickness layers and compacted with heavy pneumatic rollers at an average moisture content of 1% wet of Standard optimum.
- Filter / transition zones of gravelly alluvium (Zone 2A) and minus 150 mm sound rock spalls (Zone 2B) placed in 300 mm layers and compacted by heavy pneumatic rollers and smooth drum vibrating rollers.
- Rockfill of quarried basalt and andesite in the following embankment zones:

- Zone 3A, located downstream of the core, was of sound rock placed in 450 to 600 mm layers and compacted using 4 passes of a 10 tonne smooth drum vibrating roller. The secant moduli of the Zone 3A rockfill during construction was estimated at 60 to 80 MPa from the internal settlement records.
- Zone 3B, located in the outer up and downstream shoulders, was of sound rock placed in 900 mm layers and tracked by 2 passes of a D8 bulldozer.
- Zone 3C, located upstream of the core, was of lesser quality rock comprising up to 25% weathered rock. It was placed in 600 mm layers and tracked by D8 bulldozer.
- There was no indication if water was added to the rockfill at placement.

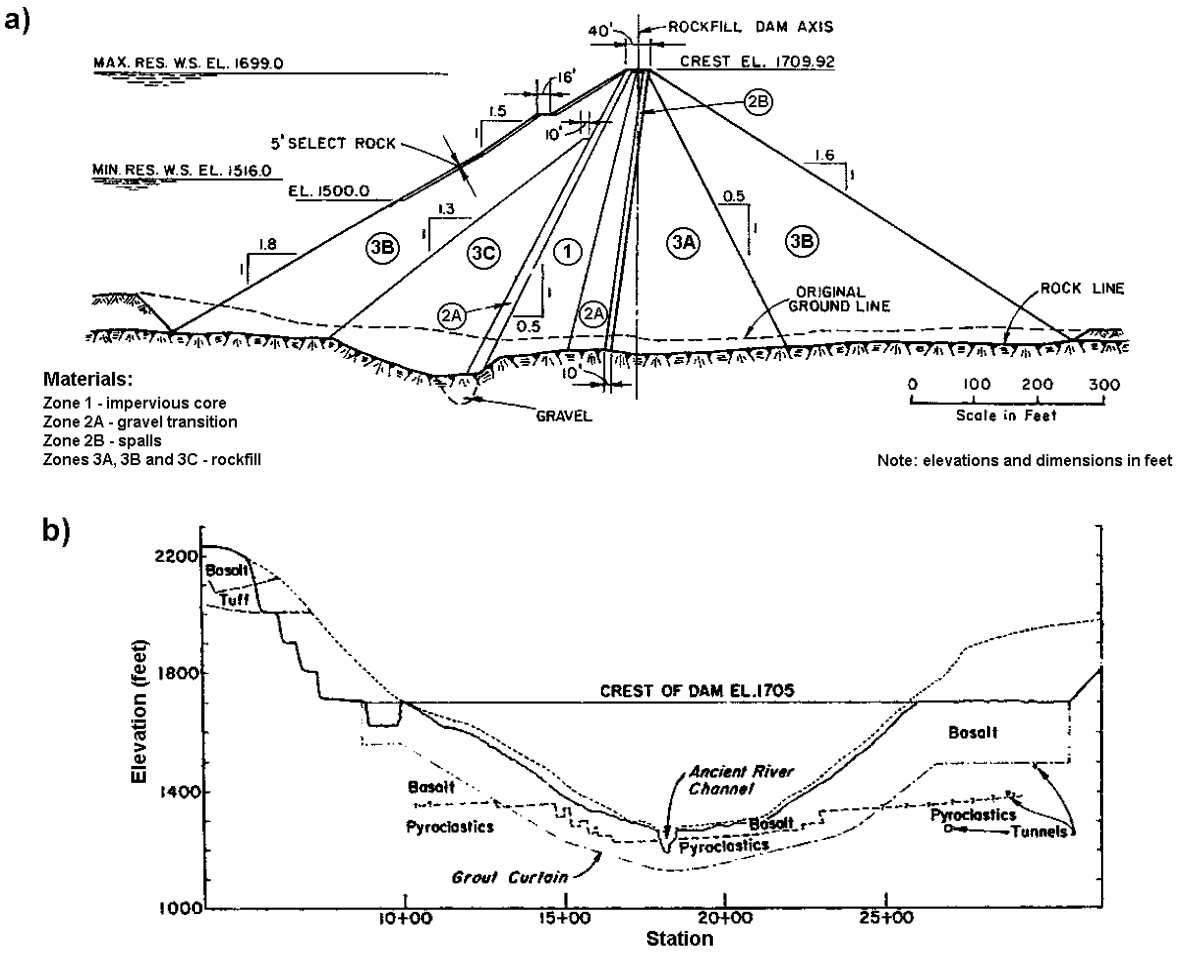

Figure G1.31: Cougar dam, *(a)* cross section (Cooke and Strassburger 1988), and *(b)* long section showing geology (Pope 1967).

Instrumentation installed in Cougar dam (Pope 1967) consisted of piezometers in the core, an internal settlement gauge in the Zone 3A rockfill and SMPs on the upstream

and downstream edge of the crest. Pore water pressures measured in the core during construction (Pope 1967) were equivalent to 20 to 50% of the fill pressure calculated as the depth below crest times the bulk density. The actual pore water pressures were likely to have been a much higher percentage of the total vertical stress at the depth of the piezometer tips when the effect of embankment shape and the potential for arching in the thin core on the total vertical stress are taken into consideration.

Post construction, the reservoir was filled rapidly to full supply level within about 7 months after the end of construction and in the following two years was subject to a seasonal drawdown of 40 to 70 m (Figure G1.33).

On first filling the post construction crest deformations (at the upstream and downstream edge of the crest) at about the maximum section were small and relatively uniform (Figure G1.33) during the early stages of filling. However, during the last 20 m to full supply level the settlement and downstream displacement increased significantly in magnitude and were not uniform. Settlements were greater at the upstream edge of the crest (about 125 mm greater) and displacements greater at the downstream edge of the crest (about 120 mm greater). In comparison to similar type embankments the crest displacement on first filling at Cougar dam was quite large (Figure 7.38 and 7.40 in Section 7.5 of Chapter 7), but not "abnormally" so.

Post first filling:

- The displacement of the downstream edge of the crest shows a gradual downstream trend and the upstream edge of the crest a steady trend, with fluctuations about the trend due to reservoir operation. This type of displacement behaviour is considered "normal", although the lateral spreading of the crest continued to increase reaching 250 mm at 3 years after construction.
- The settlement of the downstream edge of the crest continued at a steady rate. The post first filling settlement rate of 0.13 to 0.16 % per log cycle of time is typical of similar type embankments (Table 7.21 in Section 7.6 of Chapter 7).
- The settlement of the upstream edge of the crest, however, increased in settlement rate during periods of drawdown, the magnitude of settlement on drawdown decreasing with subsequent drawdowns. In comparison to similar embankments this ongoing acceleration post first filling is indicative of "abnormal" behaviour (Figure 7.85 in Section 7.6 of Chapter 7). At 3 years after construction the differential settlement of the crest had increased to about 400 mm.

Cracking of the embankment was a consequence of the differential deformation between the upstream and downstream edges of the crest. Observations of cracking at the crest, mainly from Pope (1967), are:

- A diagonal to transverse crack across the crest 12 m from the left abutment was observed on 19 June 1964, at about the end of first filling. The crack was 25 to 40 mm wide at the downstream edge of the crest (decreasing in width to hairline size at 1.5 m depth) and closed at the upstream edge. Pope (1967) thought the cause of the transverse crack was due to differential deformation as a result of construction of the left abutment on a ridge oriented perpendicular to the river.
- Longitudinal cracking of the crest, first observed on 22nd June 1964 at the end of first filling. Within several days the crack had extended and was near continuous over a length of almost 300 metres. The cracking was mostly near the downstream core / transition interface. Crack widths were in the order of 6 to 13 mm. The greater settlement of the upstream shoulder was visibly noticeable. Re-grading of the crest obliterated the cracks.
- The cracking re-appeared in January 1965, shortly after the end of the first drawdown to elevation 472 m. As shown in Figure G1.32 cracking occurred at the up and downstream core / filter interfaces and the downstream Zone 2A / Zone 2B interface. Cracks widths were up to 150 mm. Differential vertical displacement (to upstream) across the crack occurred at the up and downstream edges of the core of 300 mm and 150 mm respectively.
- In 1967 the crest was regarded, shoulders raised and roadway paved and Pope (1969) commented that no further cracking had since occurred.
- Cooke and Strassburger (1988) refer to repair of a transverse crack in 1980. It is not clear if this was a new crack or repair of the earlier crack that had re-opened since paving of the roadway.

Pope (1967) considered collapse type settlement of the upstream rockfill on wetting, particularly within the lesser quality track rolled Zone 3C rockfill, to be a significant factor in the observed deformation behaviour and cracking. Squier (1968) commented that the locations of the cracking and vertical differential in settlement indicate stress transfer occurred during first filling from the upstream shoulder to the core as a result of the collapse settlement, and then from the core to the downstream shoulder.

What is interesting with the deformation at Cougar dam is that a large proportion of the differential deformation at the crest occurred during drawdown and not on first filling. This would suggest that collapse settlement of the upstream rockfill on initial saturation, whilst significant, is not the major cause of the differential deformation. A possible reason for this large differential settlements post first filling is that the lesser quality Zone 3C rockfill lost additional strength whilst saturated, and then under the increasing effective stress conditions on drawdown further settlement of the upstream rockfill occurred. The second drawdown was to a lower level than the first resulting in higher effective stress conditions in the upstream rockfill than at the end of the first drawdown, which may explain the further increase in settlement on the second drawdown.

The writer agrees in principle with the stress transfer mechanism described by Squier (1968), but several observations are worth noting:

- The vertical offset at the downstream core / filter interface could indicate a potential shear development in the silty gravel core caused largely as a result of the high shear stresses at the upstream core / filter interface.
- The fact that no cracking was observed at the upstream filter / rockfill interface is interesting because these materials probably have the greatest difference in compressibility properties. It is possible that a shear surface has developed in the upstream gravel filter at some point (and extends along the core / gravel interface) and as a result the upper part of the gravel filter deforms with the upstream rockfill.

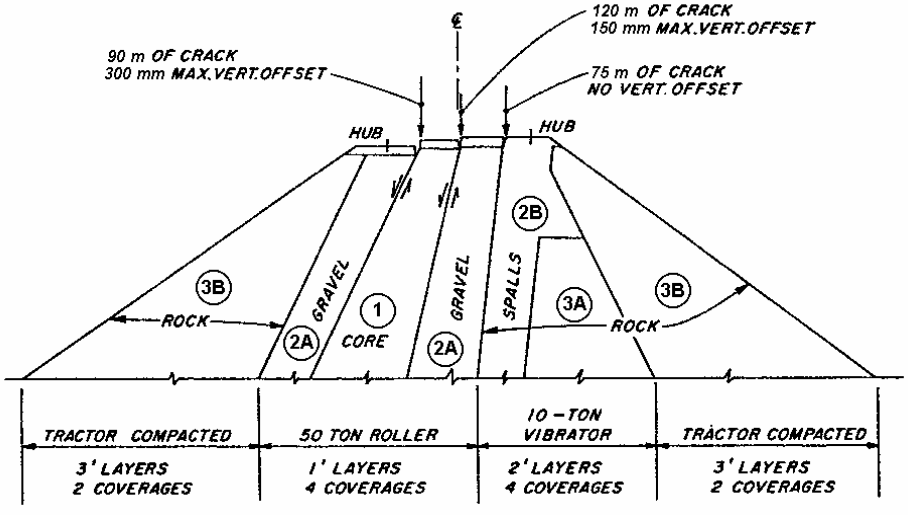

Figure G1.32: Cougar dam; differential settlement and cracks on crest (Pope 1967)

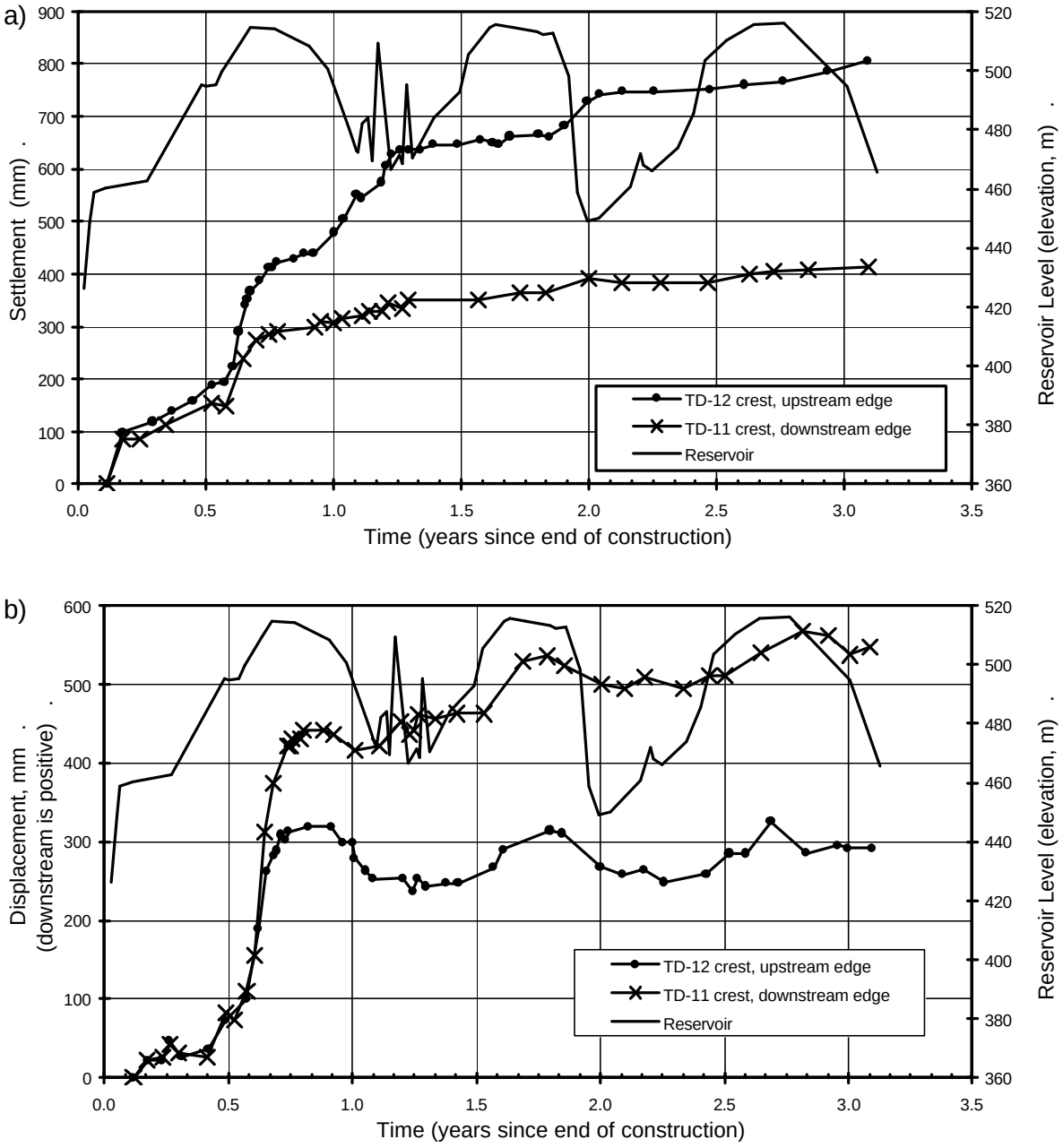

Figure G1.33: Cougar dam; post construction *(a)* settlement and *(b)* displacement normal to dam axis of the crest at the maximum section (adapted from Pope 1967).

1.7 DJATILUHUR DAM

Djatiluhur dam (Figure G1.34 and Figure G1.35), located in west Java, Indonesia, is a central core earth and rockfill dam of 105 m maximum height constructed in the early to mid 1960's. In summary, the materials and placement methods (Sowers et al 1993; Farhi and Hamon 1967) comprised:

- Thin, slightly upstream sloping, core (Zone 1) of high plasticity clay derived from weathered claystone, placed at moisture contents on the wet side of Standard optimum.
- Rockfill (Zones 3A and 3B) derived from quarried andesite. Details on the placement methods are not precisely known, but thought to include both roller compacted and dumped methods with layer thickness ranging from 0.5 m up to 2 m. Farhi and Hamon (1967) comment that most of the rockfill in the mid to lower elevation was well sluiced (300% water by volume added), and in the upper section the rockfill was placed in 1 to 2 m lifts with 30% by volume water added and trafficked by trucks and bulldozer.
- Downstream stabilising berm (Zone 4) of compacted earth and rockfill materials ranging from weathered andesite to gravels, silts and clays.

By early January 1965 the embankment had reached elevation 103 m, 11.5 m below the design crest level, when construction was halted. As described by Sherard (1973), shortly after construction was stopped a longitudinal crack appeared at the boundary between the core and downstream filter (Figure G1.36a), reaching a total length of some 500 m. Monitoring points were then established at elevation 103 m, and the measured deformation records (Figure G1.36 and Figure G1.37) show:

- During the period of no construction:
  - Greater settlements were recorded for the core (Figure G1.36b) than the shoulders. The lowest settlements were on the downstream shoulder.
  - Spreading of the top of the embankment (at elevation 103 m) of some 400 mm over the period January to July 1965. During this period the downstream stabilising berm was constructed, which would have affected the deformation behaviour of the downstream shoulder and probably the core as well.
- On raising the embankment to design level in August 1965 the core settlement at elevation 103 m totalled some 800 mm, well in excess of that measured on the downstream slope at a similar elevation. Relatively large settlements of about 400 mm were also recorded on the upstream slope at elevation 100 m over this period.

During this time the impounded reservoir level fluctuated between elevation 70 and 80 m, which is above the level of the upstream cofferdam.

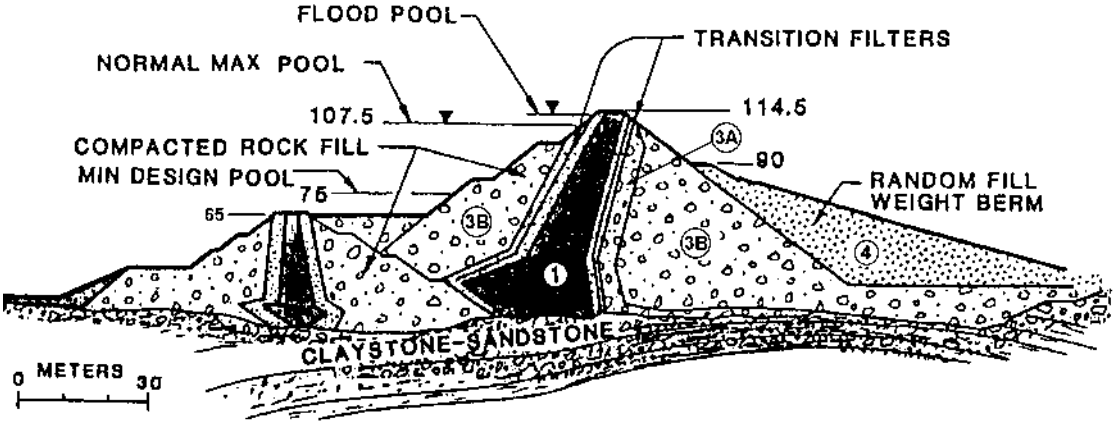

Figure G1.34: Djatiluhur dam, main section (Sowers et al 1993)

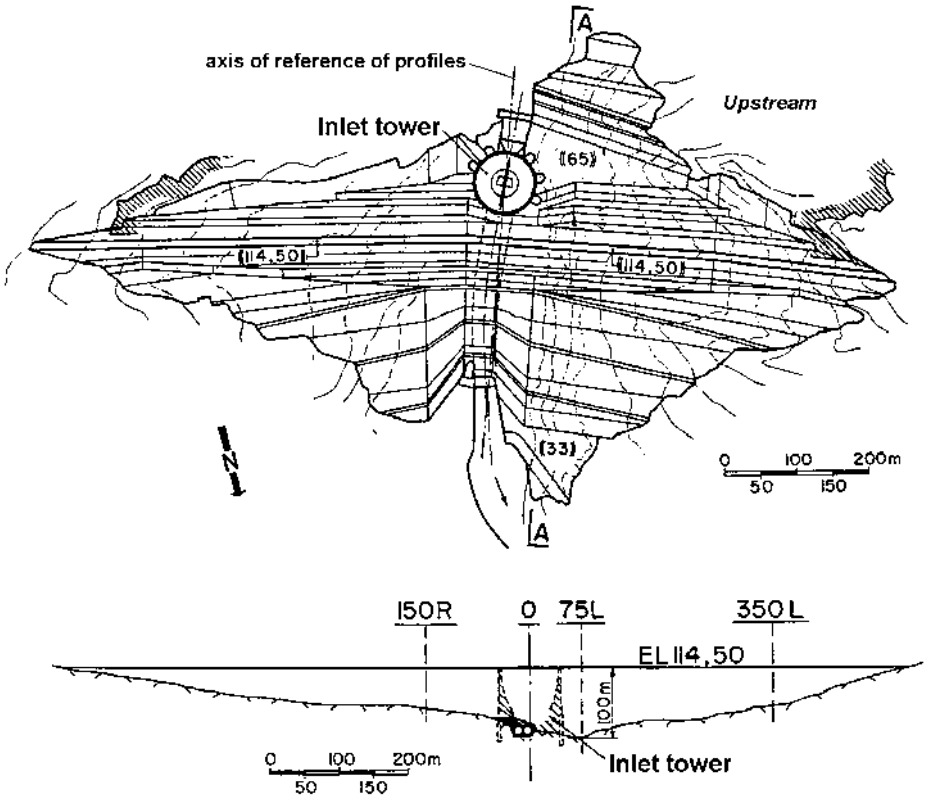

Figure G1.35: Djatiluhur dam, plan and longitudinal section (Farhi and Hamon 1967)

A significant portion of the very large measured settlement of the core on raising the embankment to design level is most likely attributable to undrained plastic type deformations due largely to lateral spreading of the core. The large differential displacement between the upstream and downstream shoulder of about 530 mm during this construction period (Figure G1.37b) is indicative of the likely large lateral displacement of the core. In addition, the differential settlement and lateral spreading would lead to arching or stress transfer from the core to the shoulders. Consolidation

type settlements in the wet placed, high plasticity clay core are likely to have been limited.

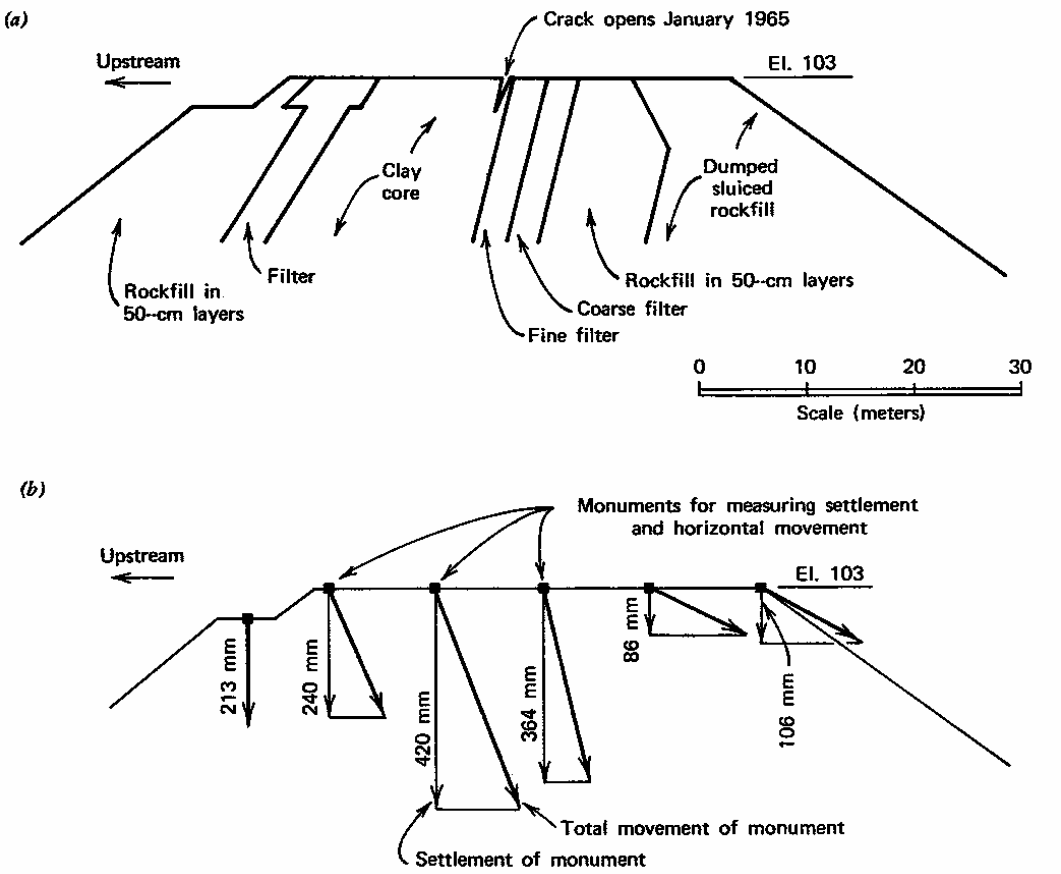

Figure G1.36: Djatiluhur dam; *(a)* location of crack observed during construction, January 1965; and *(b)* deformation of monuments at elevation 103 m, January to April 1965 (Sherard 1973).

Soon after embankment construction was completed a longitudinal crack (300 m in length and 25 to 40 mm in width) developed on the crest (Sherard 1973). Several deep test pits were excavated within the core to investigate the cracking. The pit excavated in the crest near the maximum section exposed a number of horizontal cracks up to 10 to 60 mm width (Sherard 1973), some of which extended around the full circumference of the pit. No cracks in the core were observed in the pit excavated in the upper upstream slope. Further investigation and testing (Sherard 1973) showed that under relatively low water pressures the cracks in the upper region of the core would open up and leakage occur at a high rate.

The low water pressures to cause "jacking" of the existing horizontal cracks is indicative of the low total stress conditions in the core due by arching between the core

and shoulders. The greater number of horizontal cracks observed in the downstream portion of the core (as exposed in the test pits) indicates that a greater amount of differential settlement has occurred at the downstream interface of the core. This is probably largely attributable to the embankment zoning geometry with the core oriented slightly upstream and the downstream shoulder having an upstream sloping upstream face (Figure G1.34), and to the low undrained shear strength of the wet placed core.

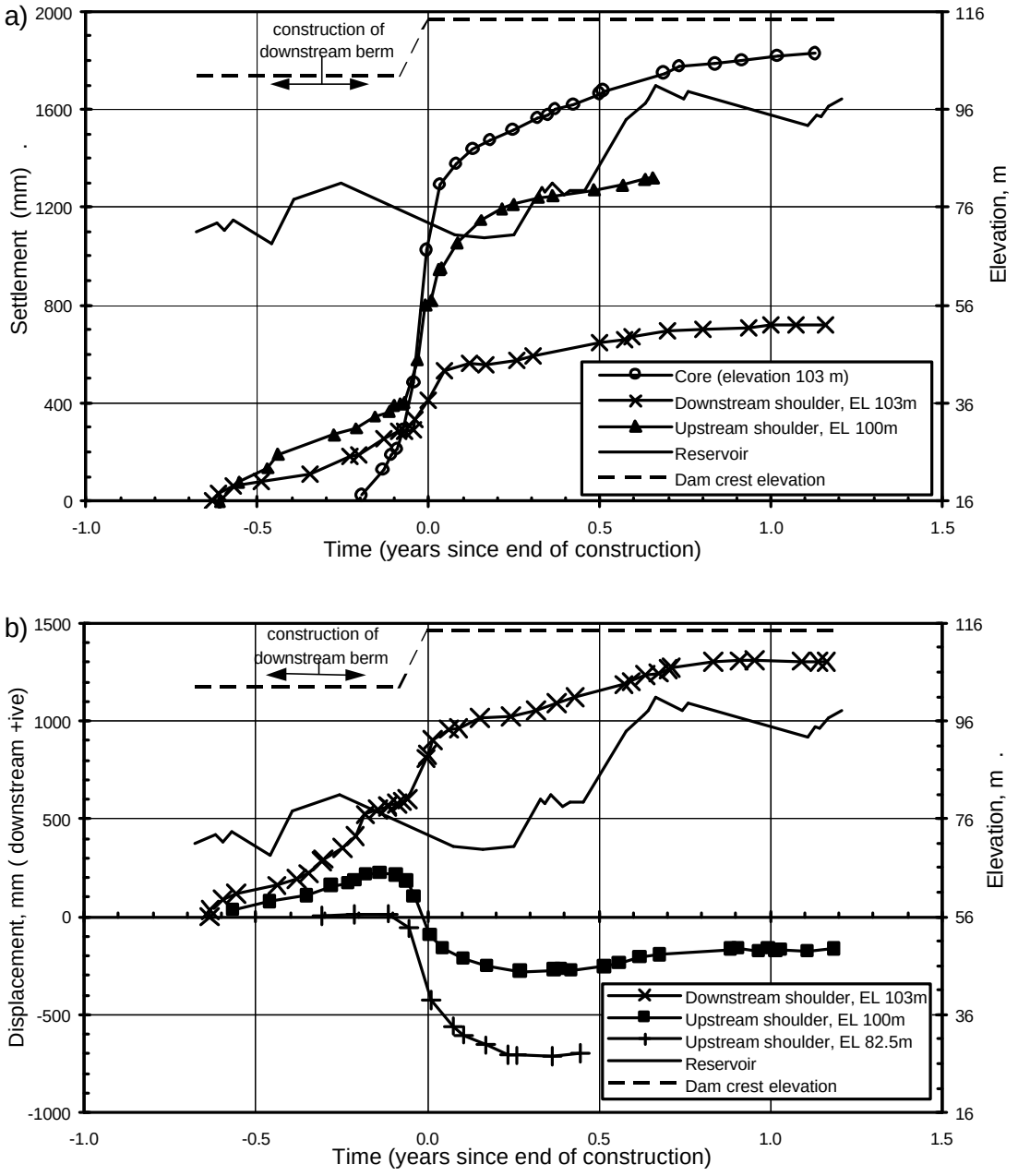

Figure G1.37: Djatiluhur dam, SMP deformation versus time in the period prior to and shortly after end of construction; *(a)* settlement, *(b)* displacement normal to dam axis (adapted from Farhi and Hamon 1967).

The post construction deformation at Djatiluhur dam is presented in Figure G1.38 (settlement) and Figure G1.39 (displacement normal to the dam axis). For these figures the base deformation reading has been established at the end of embankment construction.

The post construction deformation behaviour at Djatiluhur dam, in comparison to similar type embankments and as shown in the plots, shows:

- The settlement of the core is much greater than that of the upstream crest and upper upstream shoulder. In comparison to similar embankments, the magnitude of settlement of the crest is "abnormally" large (Figures 7.46 to 7.48 and 7.54 in Section 7.6 of Chapter 7).
- Sowers et al (1993) comment that the settlement of the downstream shoulder was less than 100 mm since 1967 (from about 1.5 years or post first filling), which is much smaller than for the upstream shoulder and core.
- Accelerations in the settlement rate of the core and upstream edge of the crest occur post first filling on large drawdown to below about elevation 80 m. This type of behaviour is considered "abnormal".
- The post first filling settlement rate (rate per log of time) for the periods between large drawdown, in comparison to other embankments, is high for the crest (Figure 7.62b in Section 7.6 of Chapter 7), possibly "abnormally" so, and is on the high side for the upstream edge of the crest (Figure 7.83 in Chapter 7).
- The displacement plot shows a large differential displacement (almost 600 mm) between the up and downstream slopes at about elevation 100 m during first filling. More than half of this occurred during the first 0.1 years after end of construction whilst the reservoir level was steady, and is probably therefore a time dependent deformation related to the large deformations during the latter part of construction as was observed when construction was halted at elevation 103 m.
- The crest displacement, in comparison to similar type embankments, is of large magnitude (Figure 7.69 in Chapter 7) both during first filling (Figure 7.38 in Chapter 7) and post first filling (Figure 7.77 in Chapter 7), possibly "abnormally" so.

An important aspect of the post construction deformation behaviour at Djatiluhur dam is the behaviour during large drawdown. In comparison to other embankments that show acceleration in the settlement rate on large drawdown, the magnitude of settlement

during drawdown at Djatiluhur dam is large (in the order of 120 to more than 300 mm) and the magnitude of settlement of the core between the drawdowns in 1972 and 1982 is similar. This latter point is important because similar magnitude settlements during drawdowns of similar magnitude is an unusual observation, the general trend is for either negligible or reduced magnitude settlement on a second large drawdown of similar magnitude, or a larger magnitude second drawdown is required to observe an increase in the settlement rate. Sowers et al (1993) comment that the continuing deformation of the central and upstream region of the crest is reflective of the "highly" stressed state of the upstream slope as indicated by its marginal factor of safety under static loading. They add that the accelerations in settlement on large drawdown are potentially indicative of shear type displacements.

The writer agrees with Sowers et al (1993) but add that the settlement data on drawdown also indicates a softening in the material strength properties over time. This would suggest that the development of a shear surface and strength loss due to shearing on this surface of rupture, at least in the core, is likely.

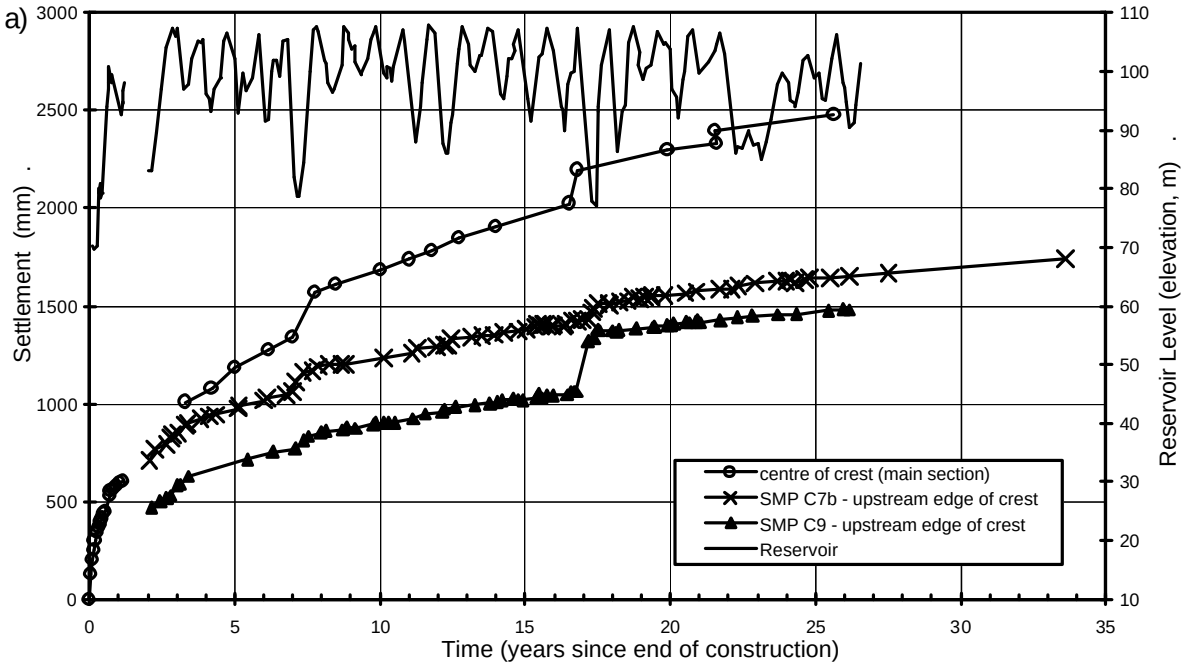

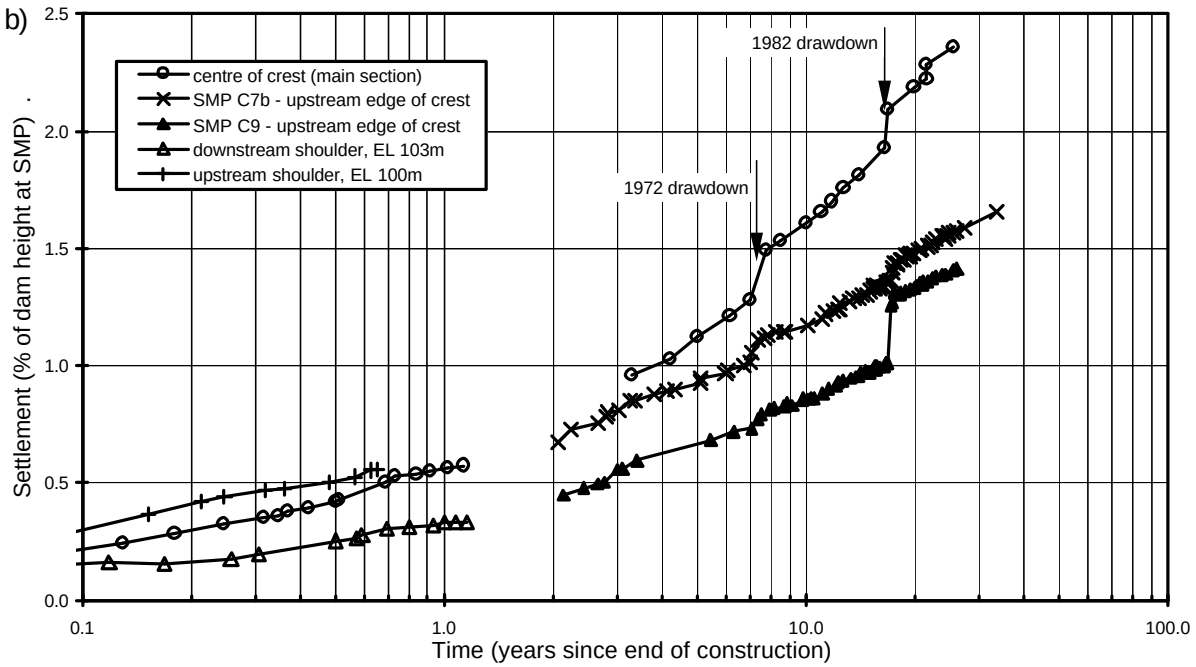

Figure G1.38: Djatiluhur dam, post construction settlement of SMPs on the embankment crest and slopes.

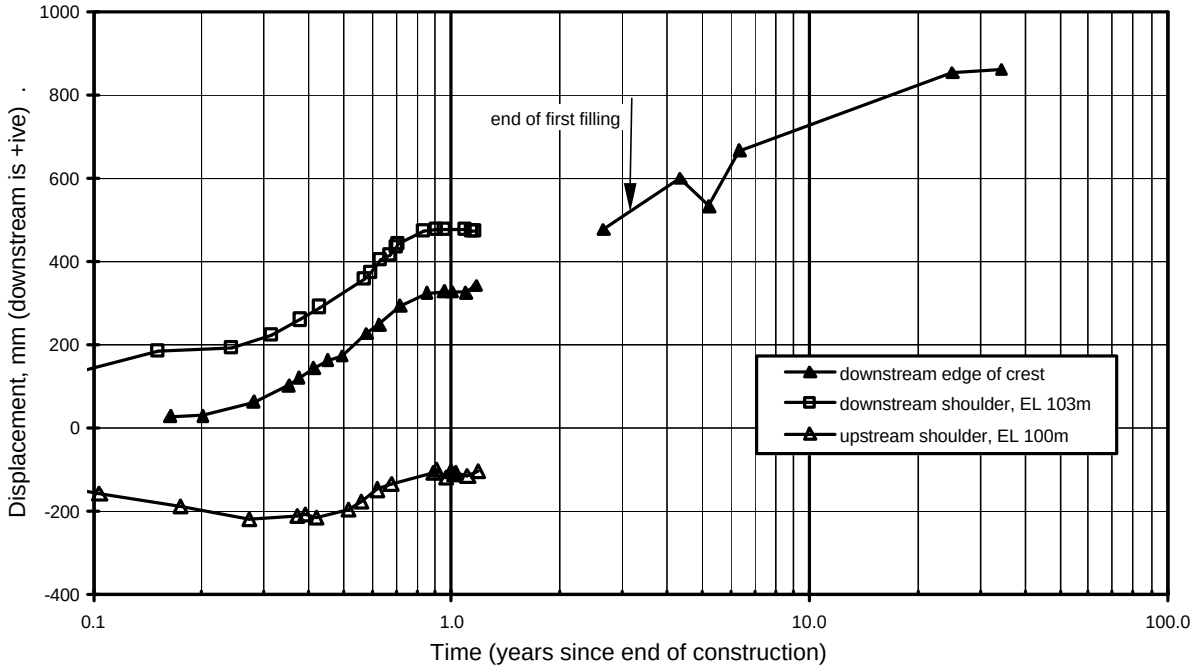

Figure G1.39: Djatiluhur dam, post construction displacement normal to the dam axis versus log time.

1.8 EILDON DAM

Eildon dam (Figure G1.40), located on the Goulburn River in central Victoria, Australia, is a central core earth and rockfill embankment of 80 m maximum height and 985 m length. The embankment was constructed in the early to mid 1950's (completed in June 1955) and replaced the old concrete core-wall embankment located upstream of this dam. In the broad valley section the foundation was stripped to bedrock under the wide central core, and to gravels under most of the shoulder region (Figure G1.40a). In summary (Shaw 1953; SMEC 1999a), the materials, placement methods and other features of the design and construction are:

- Core – zoned central core consisting of a central inner zone (Zone 1A) of medium plasticity silty to sandy and gravelly clays sourced from alluvium and colluvium, and outer zone (Zone 1B) of clayey sands to silty sands. These materials were placed in 150 mm layers and compacted by sheepsfoot rollers to high density ratios. The specified moisture content range was 2% dry to 1% wet of optimum moisture from a 3 layer, 40-blows/layer compaction test. In comparison to Standard optimum moisture content the earthfills are likely to have been placed on the dry side.
- Filter / transition zone (Zone 2) of alluvial sandy gravels mostly placed by end dumping without compaction, although in the upper part test pits showed it was well compacted.
- Rockfill in the embankment shoulders comprised:
  - Zone 3A – sourced from quartzitic sandstone and referred to as *"first quality rock*", placed in 2 m thick layers and not formally compacted. Used in the inner downstream and outer upstream shoulders.
  - Zone 3B – alternate layers of "*medium quality rock*" and gravels placed in 2 m thick layers and not formally compacted. Used in the inner upstream shoulder.
  - Zone 3C – random rockfill zone in the outer downstream shoulder comprising unsuitable rock that was poorly graded and contained a high fraction of finer sized rockfill.
  - There is no indication if water was added during construction. The large post construction settlement of the shoulders suggests that water was probably not added during rockfill placement.

- The core was constructed well ahead of the rockfill shoulders at various stages during construction. Vertical height differences between the core and shoulders were up to 18 to 25 m for a large period of the construction.
- Only minor pore water pressures were developed in the core during construction, confirming placement on the dry side of Standard optimum.

Instrumentation installed in the embankment consisted of piezometers and internal vertical settlement gauges (IVM) in the core, and surface measurement points (SMP) on the crest and slopes. Locations of the IVM and SMP are shown in Figure G1.41 and Figure G1.40a, the IVMs being located about 5 m upstream of the dam axis. Base survey readings of the SMPs were 0.19 years after the end of construction on the slopes, 2.5 years for the crest settlement and 13.4 years for the crest displacement.

Impounding of the reservoir began in mid 1954 prior to the end of construction, and reached within 33 m of full supply level (elevation 256.6 m AHD) before the end of construction. Full supply level was reached in July 1956, 1.2 years after the end of construction. Since filling, the reservoir is subjected to an annual drawdown of typically 5 to 15 m, but larger drawdowns of up to 28 m have occurred during drought periods (Figure G1.42a).

No details of the internal deformation of the core from the IVM records are available for the period of construction or for the first 26 years after construction. Analysis of the deformation behaviour of Eildon dam is therefore only for the post construction period.

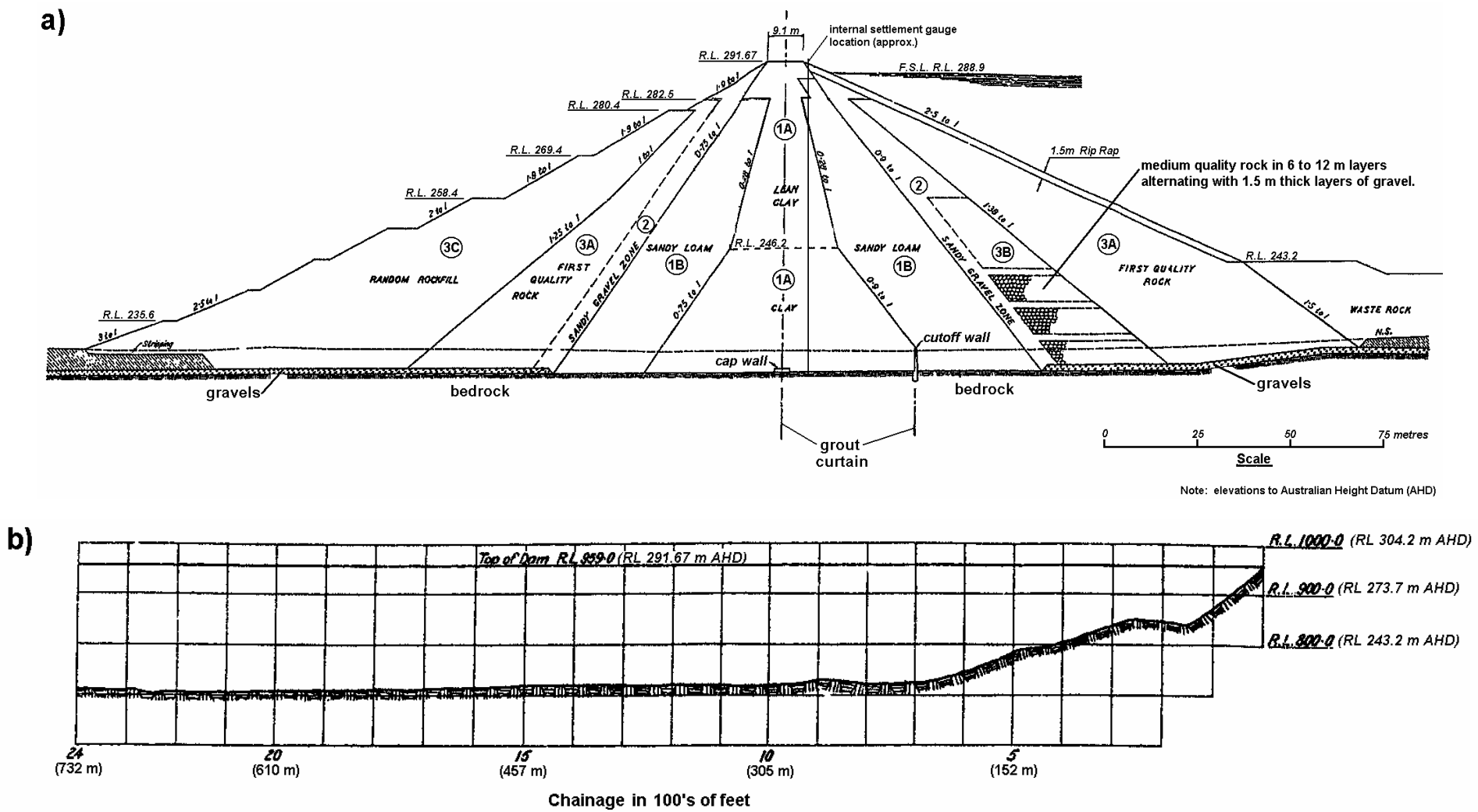

Figure G1.40: Eildon dam, *(a)* main section and *(b)* longitudinal section (courtesy of Goulburn Murray Water).

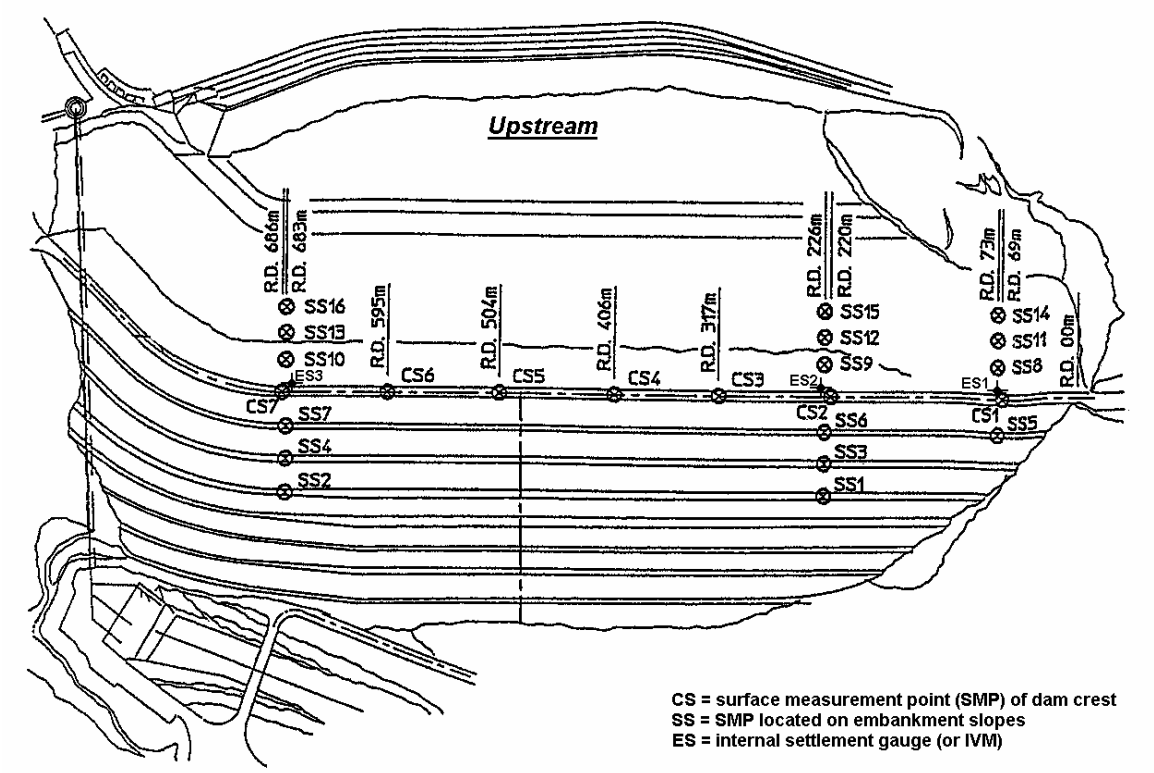

Figure G1.41: Eildon dam; plan showing surface point and IVM gauge locations (SMEC 1999a)

The post construction settlement and horizontal displacement normal to the dam axis of the SMPs at chainage 685 m is shown in Figure G1.42 and Figure G1.43 respectively. As the figures show and in comparison to other similar embankments, the post construction deformation behaviour of Eildon dam displays several notable features:

- The magnitude of settlement of the upstream and downstream shoulders of the embankment is large. In comparison to similar embankments (Figures 7.50, 7.52, 7.79 and 7.84 in Section 7.6 of Chapter 7, and Figure F2.7 in Appendix F) it is large, but not necessarily "abnormally" large given the poor compaction and likely dry placement of the rockfill. A high proportion of the settlement of both the up and downstream shoulders occurred on and shortly after first filling.
- The long-term settlement rate (per log time cycle) of the crest and slopes, excluding the periods of acceleration during large drawdown, is in the "normal" range of similar embankments.
- The magnitude of displacement of the downstream slope is large in comparison to similar embankments (Figure 7.81 in Chapter 7 and Figure F2.15a in Appendix F). Most of the displacement occurred in the first 5 years after the end of construction and then decreased to much lower rates thereafter.

- Post first filling, SMPs on the crest and upstream slope show an increase in settlement rate on large drawdown at 13 years (1968) and 27 years (1982/83), and also show a non-recoverable upstream displacement at 27 years. Most of the other SMPs on the crest and upstream slope (SMEC 1999a) displayed a similar increase in settlement rate and non-recovered upstream displacement during the year 13 (1968) and year 27 (1982/83) drawdowns. These deformation trends are indicative of "abnormal" type behaviour.

Available records from the IVMs in the core start in 1981 some 26 years after the end of construction. Figure G1.44 shows the settlement profiles in the core for the period from 1981 to 1998 and Figure G1.45 the settlement versus time for selected cross-arm intervals. The internal settlement records of the core show:

- For IVM ES3 measurements post 1981 are limited to the upper 12 cross-arms (or 20 m) of the IVM gauge out of a total 49 cross-arms installed. The cause or timing of this blockage or constriction in the tube is not known. The cross-arms have subsequently been numbered 1 to 12.
- Localised zones of high vertical strain are observed in IVM ES2 and ES3 at 17 to 20 m depth below crest level (cross-arms 37 to 39 in ES2 and below cross-arm 3 in ES3). Cross sections show that these zones are located in Zone 1A within 1 to 2 m of the upstream interface with Zone 1B.
- A large portion of the settlement measured in the upper regions of IVMs ES2 and ES3, and the localised settlement between cross-arms 36 and 39 in ES2, occurred during the latter stages of the large drawdown in 1982/83 at 27 years (Figure G1.45).
- An increased rate of settlement is observed for ES2 and ES3 after 38 to 39 years (Figure G1.45). This is possibly due to the larger magnitude of drawdown after this date.

The very large settlements of the upstream shoulder during first filling are considered to be largely due to collapse type settlements on wetting in the poorly compacted, likely dry placed upstream rockfill shoulder. The large settlements of the downstream shoulder in the first five years after construction are also likely to be largely related to collapse type settlements possibly due to wetting from rainfall. The poorer quality rockfills used in the inner upstream shoulder and outer downstream

shoulder are potentially more susceptible to larger collapse type settlements. The downstream shoulder displacement on and after first filling was downstream due to the influence of the embankment zoning geometry as the shoulder settled relative to the core as well as the influence of application of the water load. The post construction differential displacement between the upstream and downstream shoulder at about elevation 280 m (about 12 m below crest level) was 680 mm at 3 years after construction increasing to 890 mm by 6.5 years. This is also probably largely due to the effect of embankment zoning geometry and the greater settlement of the shoulders relative to the core.

The core itself was placed on the dry side of Standard optimum and well compacted. It will therefore be of high undrained strength and relatively low compressibility. It is likely that the settlement of the core was less than the shoulders during and shortly after first filling, and the differential deformation is likely to have resulted in the development of high shear stresses at the interface region between the rockfill shoulders, filters and core.

The "abnormal" deformation behaviour on large drawdown post first filling is potentially indicative of shear type deformations in the core. This is supported by the localised concentration in vertical settlement observed within the inner core during drawdown in 1982/83 and well as the acceleration in settlement and non-recovered upstream displacement of SMPs on the crest. The constriction in ES3 below 20 m depth is possibly also shear related. Plastic type deformations of the core are not considered a likely explanation of the deformation behaviour due to the dry placement and high density ratio of the well-compacted core.

The timing of the initial shear development is not known. It may have initially occurred on first filling due to the likely high stresses at the upstream interface between the core and shoulder resulting from the large differential settlements following collapse settlement of the poorly compacted rockfill.

The internal settlement records in the core indicate that deformations on the shear surface were triggered by the large drawdown in 1982/83. Shear type deformations probably occurred prior to this drawdown as indicated by the acceleration in crest settlement on large drawdown in 1968 and the existing constriction in IVM ES3 prior to 1981. The mechanism for shear deformation on large drawdown is associated with the changes in effective stress conditions in the upstream shoulder on drawdown and the reduction in lateral stresses acting on the core. It is possibly that the reduction in lateral

stress on the upstream side of the core on drawdown triggers further shear deformation in the core and the upstream part of the upper core region deforms upstream until the sufficient lateral stress is developed in the upstream shoulder to support the core. Other factors such the differential deformation between material zones, high shear stresses at the interface region and softening of the strength properties could also influence the deformation behaviour. It is notable that the 1982/83 drawdown was historically the largest and deepest, and that a similar magnitude drawdown in 1997/98 did not appear to have triggered further shear deformation in the core. It is emphasised that the shear development in the core does not indicate that the overall stability of the embankment on large drawdown is questionable; in fact it is quite acceptable reflecting the relatively flat slopes adopted.

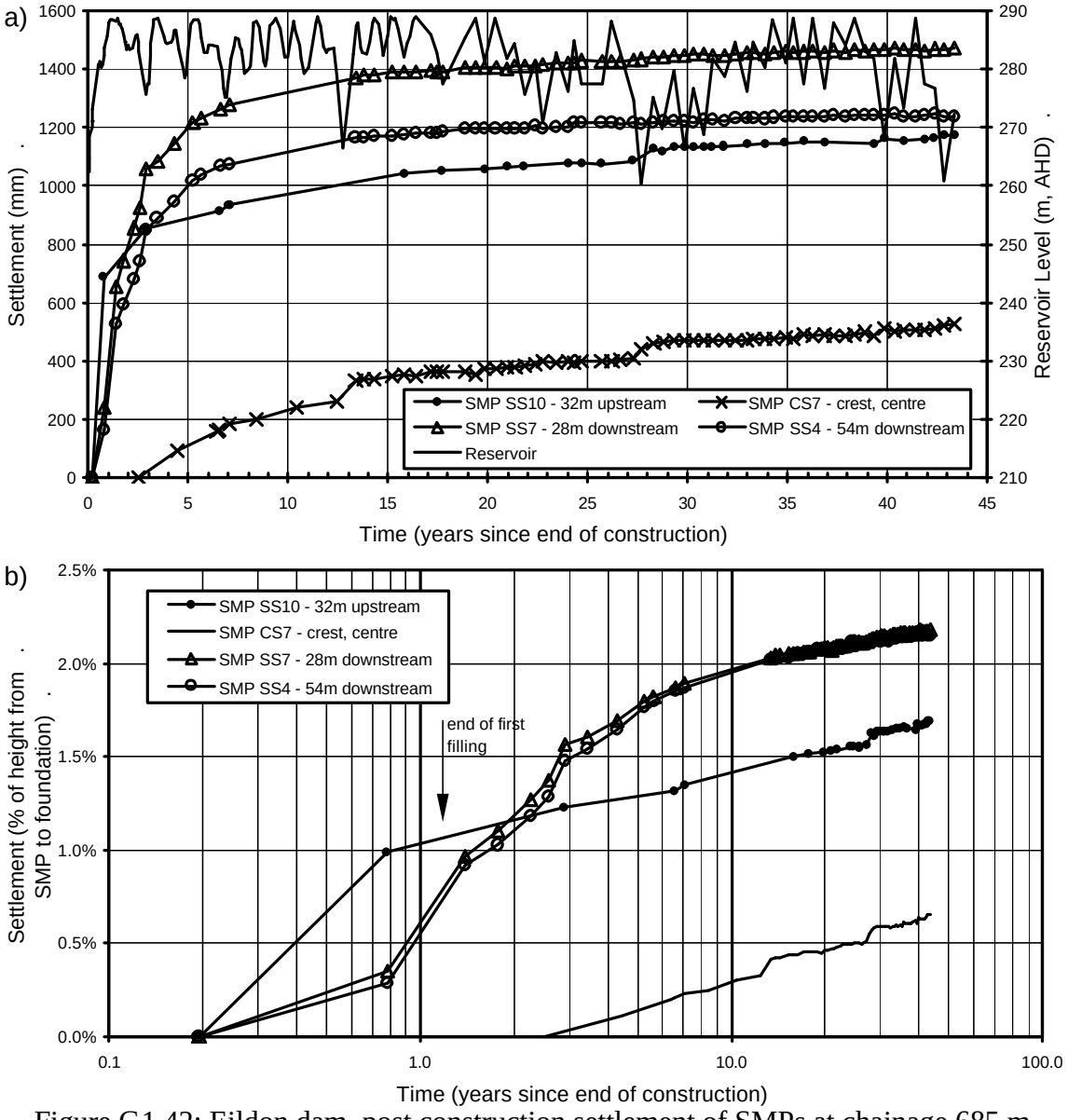

Figure G1.42: Eildon dam, post construction settlement of SMPs at chainage 685 m.

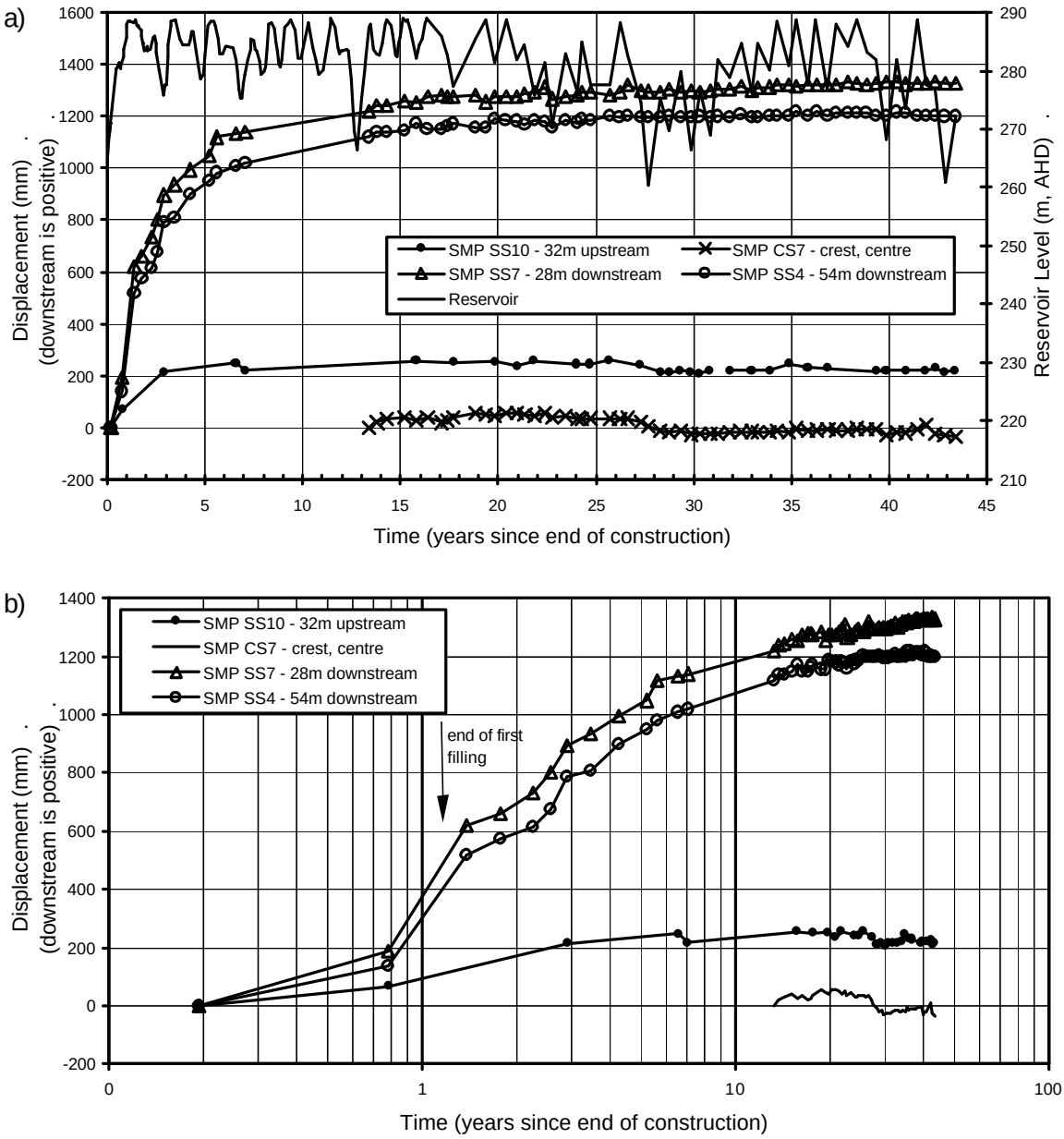

Figure G1.43: Eildon dam, post construction displacement normal to the dam axis of SMPs at chainage 685 m.

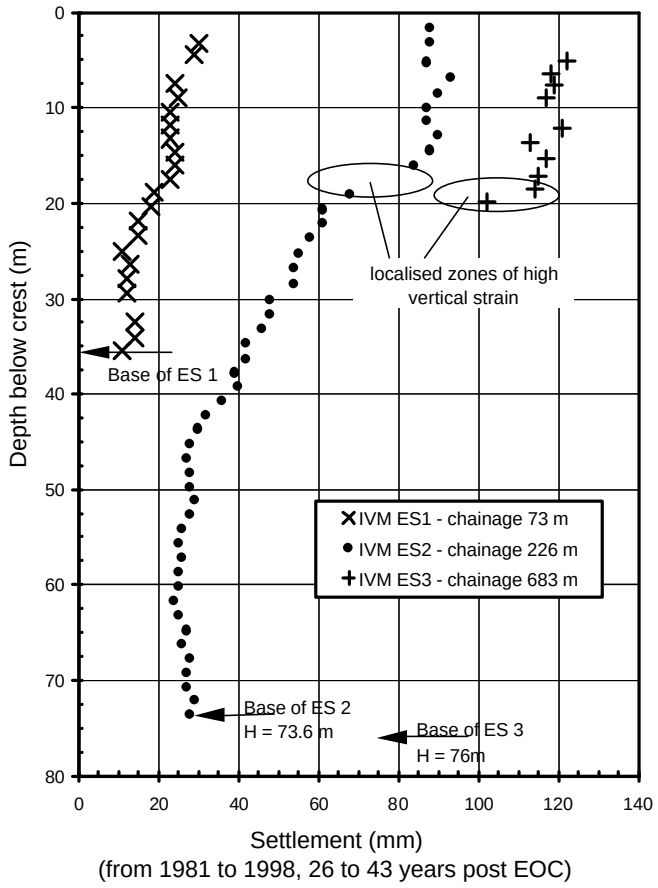

Figure G1.44: Eildon dam, internal settlement profiles in core from IVM records for the period 1981 to 1998 (26 to 43 years after end of construction).

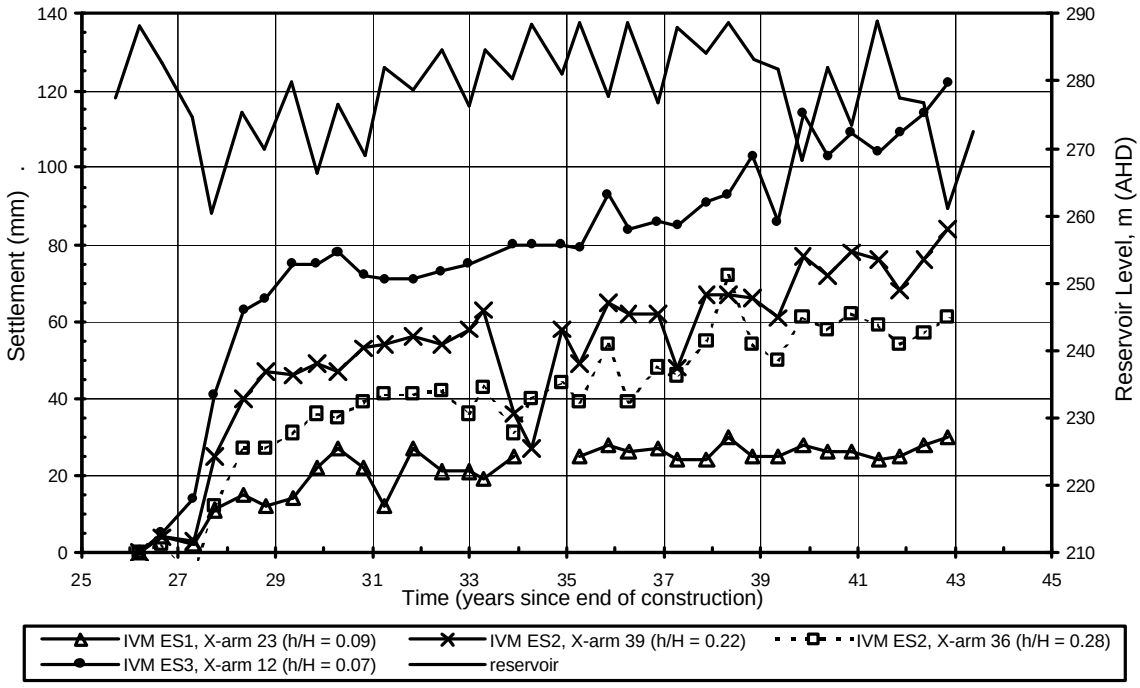

Figure G1.45: Eildon dam, post construction settlement of selected cross-arms from the IVM gauges.

1.9 EL INFIERNILLO DAM

El Infiernillo dam (Figure G1.46), located on the Balsas River in south-western Mexico, is a central core earth and rockfill dam of 148 m maximum height (Marsal and Ramirez de Arellano 1967). It is located within a narrow valley with average abutment slopes of 40 to 45 degrees and 50 m wide river section. The embankment was constructed in the early 1960's and completed December 1963. In the valley section the core, filters and downstream inner rockfill zone were founded on bedrock, and the remainder on sand to boulder size riverbed deposits. The abutments were on a bedrock foundation. In summary, the materials and placement methods (Marsal and Ramirez de Arellano 1964, 1967) were:

- Zone 1 – central, very thin core of medium to high plasticity sandy clays placed in 150 mm loose thickness layers and compacted by heavy sheepsfoot rollers. The average moisture content at placement was 3.7% wet of Standard optimum.
- Filter / transition zones of washed alluvial sands (Zone 2A) and processed sandy gravels (Zone 2B) placed in 300 mm layers and compacted by 2 ton vibrating roller.
- Rockfill of quarried diorites and silicified conglomerates of very high unconfined compressive strength placed as:
  - Zone 3A, inner rockfill zone, placed in 0.6 to 1.0 m thick layers and trafficked by D8 bulldozer. No water was added during placement.
  - Zone 3B, outer rockfill zone, placed in 2.0 to 2.5 m thick layers and trafficked by D8 bulldozer. No water was added during placement.

a)

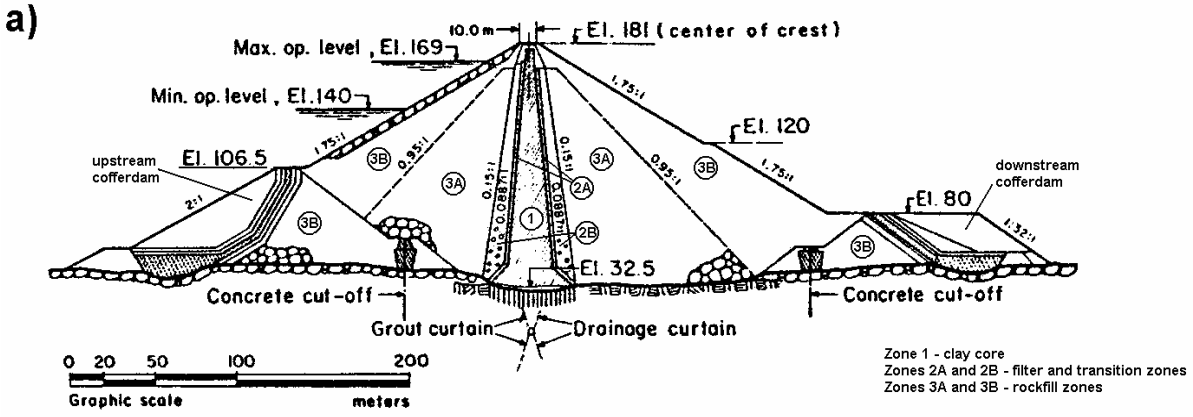

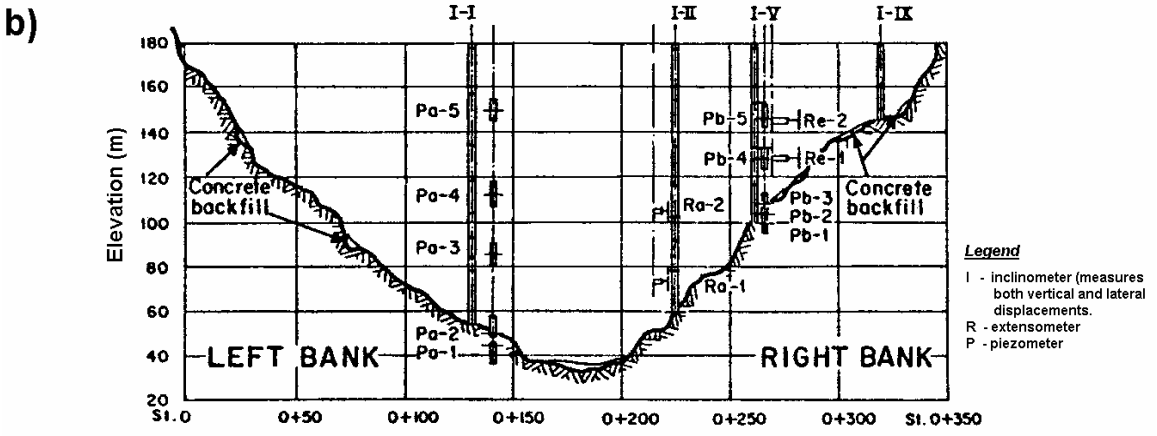

Figure G1.46: El Infiernillo dam, *(a)* maximum cross section and *(b)* long section (Marsal and Ramirez de Arellano 1967)

Collapse type settlements of the upstream rockfill on wetting were foreseen as a potential problem. To reduce the impact of these type of settlements post construction the upstream rockfill zone was flooded to the height of the upstream cofferdam during construction.

Reservoir filling began in June 1964, about 0.5 years post construction, and reached within 1 m of maximum operating level by January 1965, approximately 1.05 years post construction.

El Infiernillo dam was well instrumented. Marsal and Ramirez de Arellano (1967) give details. In summary, the deformation instrumentation included monitoring of internal vertical and horizontal deformations in the core, filters and rockfill using inclinometers and internal settlement gauges (IVM), and surface measurement points (SMP) on the crest and downstream shoulder (Figure G1.46b on the dam axis and Figure G1.47 at Station 0+135). Piezometers were installed in the core, and extensometers for strain measurement were installed in the core and downstream rockfill.

Marsal and Ramirez de Arellano (1964; 1967; 1972), Marsal (1982), Squier (1970), Nobari and Duncan (1972b), and others present aspects of the deformation behaviour of El Infiernillo dam during construction, on first filling and post first filling. Only a summary of several aspects of the post construction deformation behaviour are discussed here.

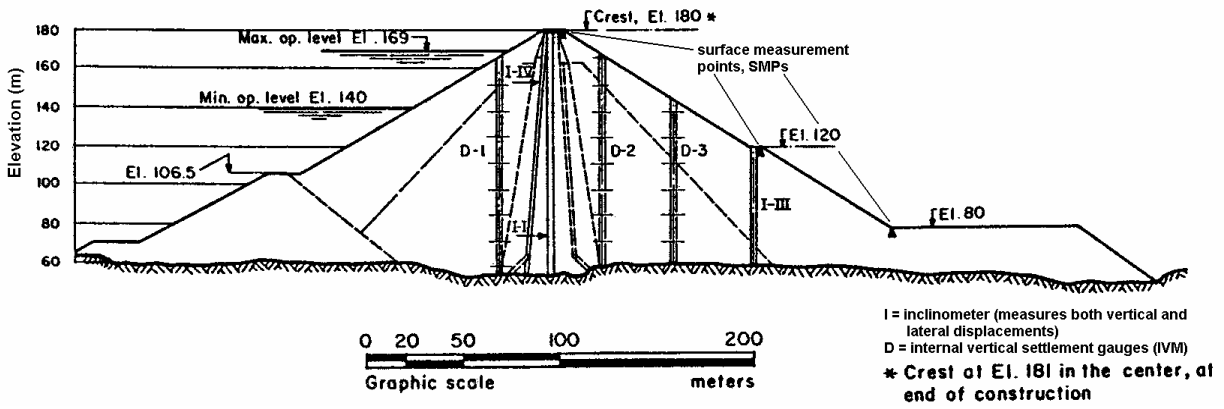

Figure G1.47: El Infiernillo dam, deformation instrumentation on station 0+135 at the lower left abutment (Marsal and Ramirez de Arellano 1967).

The post construction settlement and displacement normal to the dam axis of SMPs at the main section and the surface of inclinometer and IVM gauges are shown in Figure G1.48. Notable aspects are:

- The initial upstream then downstream crest displacement during first filling. Nobari and Duncan (1972b) consider that the upstream displacement, which occurred in the early stages of first filling, was due to collapse settlement of the upstream rockfill and the subsequent downstream displacement was due to the influence of water load on the upstream face of the core in the latter stages of first filling. This type of behaviour is discussed further in Sections 7.5.2 and 7.10 of Chapter 7.
- The increased rate of settlement and downstream displacement of the crest and slopes post first filling over a prolonged period of time from about 3 to 6 years after construction. In comparison to similar embankments this deformation behaviour is "abnormal". Marsal and Ramirez de Arellano (1972) comment that the increased rate of deformation was coincident with the flooding of the lower portion of the downstream rockfill due to high tail water levels in October 1966 (2.8 years), January 1967 (3.1 years) and September 1967 (3.8 years).
- The acceleration in crest settlement rate that occurred as a result of a magnitude 7.6 earthquake on 14 March 1979 (15.2 years after construction) at a distance of about 100 km from the dam site (Marsal 1982). Significant cracking of the embankment due to the earthquake was observed.

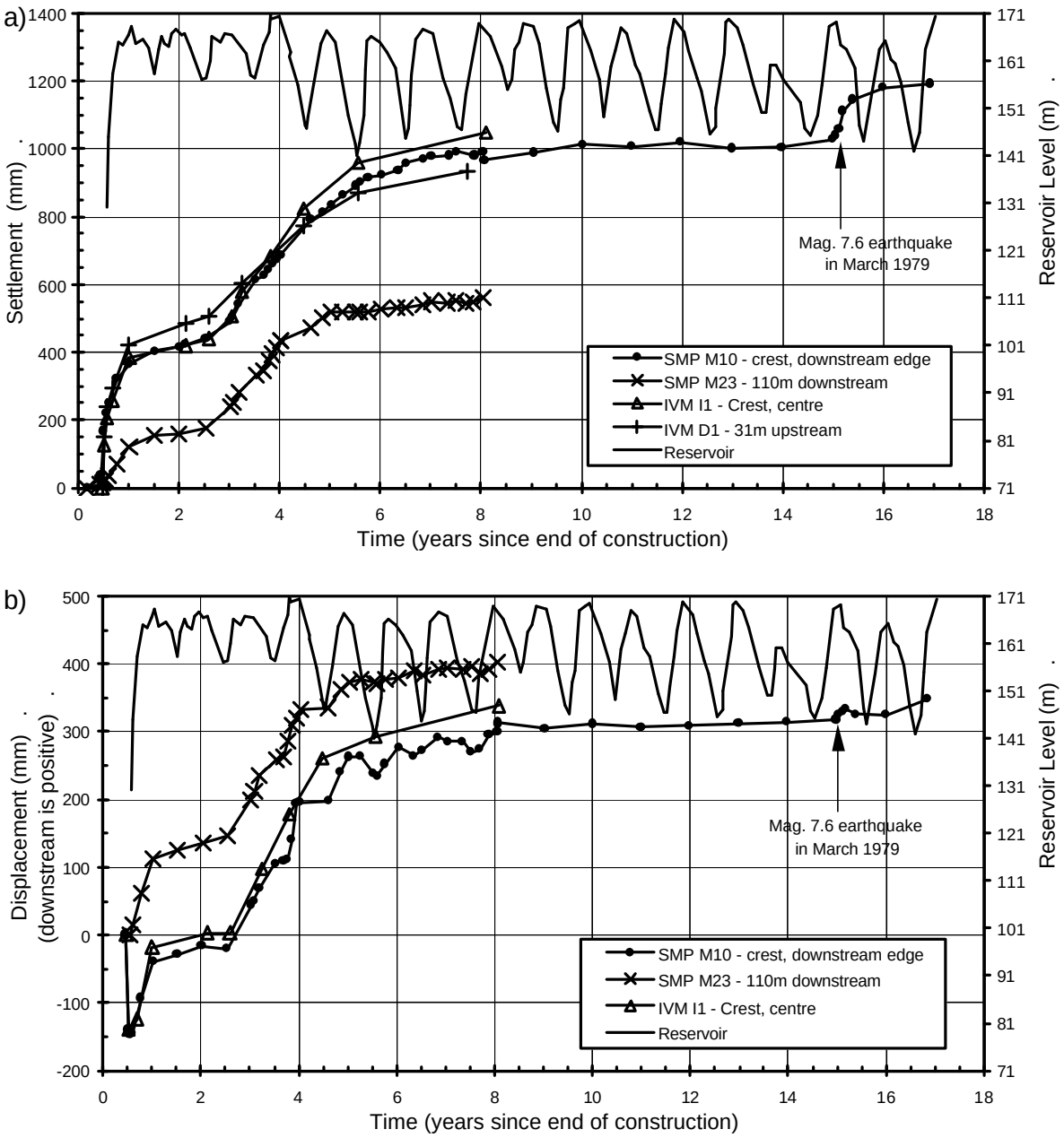

Figure G1.48: El Infiernillo dam, post construction *(a)* settlement and *(b)* displacement of surface markers.

The post construction internal deformation at Station 0+135 (refer Figure G1.47 for instrument layout) is presented in Figure G1.49 and Figure G1.50 for the period during and shortly after first filling, and Figure G1.51 for the post first filling period from 1966 to 1972 (2.6 to 8.1 years after construction). The plots highlight a number of interesting features:

- During first filling:
  - The settlement profiles of the core, upstream filter and upstream rockfill are similar, and different to that of the downstream rockfill.

  - At end of first filling, large and uniform strains are observed in the upstream rockfill between elevations 85 and 125 to 130 m. Similarly large strains are observed in the core, but at higher elevations, from 105 to 145 m.
  - In the upstream filter (IVM I4) localised zones of high vertical strain are observed at about elevations 102 m and of lesser magnitude at 132 m.
  - The upstream then downstream displacement of the mid to upper core region on first filling and the bow shaped profile of the core at end of first filling (Figure G1.50).
- Post first filling, from mid 1966 (2.6 years after construction) to 1972:
  - Settlements in the downstream rockfill are confined to below about elevation 125 m and displacements are largely downstream.
  - A localised zone of high vertical strain has developed in the core at about elevation 135 m. It is evident in October 1967 and has continued to progressively develop into the early 1970s. The core displacement (Figure G1.51b) shows a block type deformation above about elevation 130 m and a linear downstream displacement below this elevation.

The internal deformation records, in conjunction with the surface deformation records, provide an interesting picture of the post construction deformation behaviour of El Infiernillo dam during and post first filling. Important aspects highlighted by Marsal and Ramirez de Arellano (1972) are the incompatibility of the stress-strain characteristics between the materials used in the embankment, the susceptibility of the structure to post construction collapse type deformations of the rockfill on wetting and the very sensitive nature of the core to interactions with the surrounding granular mass.

The deformation during first filling is largely controlled by the collapse settlement of the upstream rockfill in addition to the water load acting on the upstream face of the core as discussed by Nobari and Duncan (1972b). The lower portion of the upstream rockfill (below about elevation 80 m) is not susceptible to collapse settlement due to pre-saturation of the rockfill between the core and upstream cofferdam prior to end of construction. Differential settlement at the upstream rockfill / filter interface, due to the collapse settlement of the upstream rockfill, will result in stress transfer from the rockfill to the filter (Squier 1970; Nobari and Duncan 1972b). The localised regions of high vertical strains that develop in the upstream filter during first filling (Figure G1.49) occur at elevations of 102 m and 132 m, which are above the base elevation of collapse

settlement in the upstream rockfill (about elevation 80 m). The regions of localised high strain are likely shear type deformations that have developed due to the high shear stresses at the interface with the upstream rockfill. A similar pattern of shear deformation was observed in the upstream filters at Chicoasen dam.

The deformation during first filling of the wet placed core is largely controlled by the deformation of the upstream filter and upstream rockfill shoulder because of its likely low undrained strength and therefore limited capacity to support additional stresses. This is demonstrated by the horizontal deformation behaviour of the core (Figure G1.50) as well as its vertical deformation behaviour, which is similar in shape to that of the upstream filter and rockfill shoulder but very different to that of the downstream rockfill. Deformations of the core are considered to be largely undrained plastic type deformations.

Accelerations in settlement and displacement of SMPs on the crest and downstream slope in the post first filling period from late 1966 to 1968 (3 to 5 years after construction) coincided with periods of flooding of the downstream rockfill and possibly periods of very heavy rainfall events (Marsal and Ramirez de Arellano 1972). The mechanism of deformation in the downstream rockfill shoulder, however, is not clear. Collapse type deformations on wetting are suspected, but the region of settlement in the downstream rockfill extends to elevation 120 m, well above that of the tail water inundation level, which only reached a maximum elevation of 68 m. This would suggest other factors have contributed to the rockfill deformation.

The deformation behaviour of the core over the period from late 1966 and into the early 1970's (2.6 to 8 years after construction) indicates that at about elevation 135 m in IVM I1 a near vertical shear zone has developed with a vertical shear component of 130 to 140 mm by January 1972. The shear zone is possibly oriented to upstream with a dip of about 80 degrees based on the horizontal deformation in IVM I1. Interpretation of the deformation behaviour and mechanism leading to development of this potential shear zone is not clear. If it is a shear zone and is oriented to upstream it could be related to drawdown.

It is important to confirm that the overall stability of the embankment is not in question and that, as Marsal and Ramirez de Arellano (1972) indicate, the "abnormalities" in the post construction deformation behaviour are largely controlled by collapse type deformations of dry and poorly placed rockfill, and due to incompatibility of the stress-strain characteristics between the materials used in the embankment.

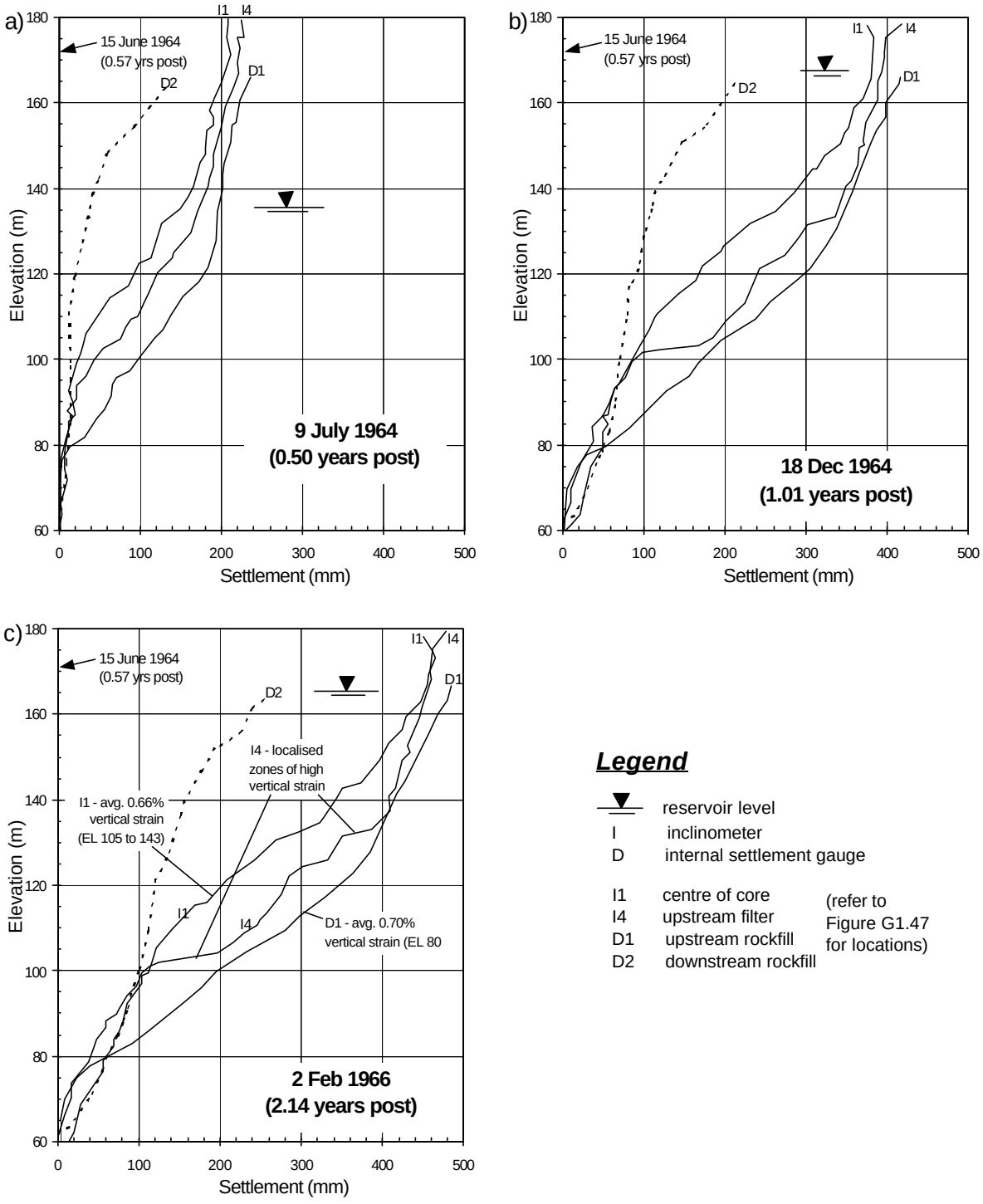

Figure G1.49: El Infiernillo dam, internal settlements during first filling.

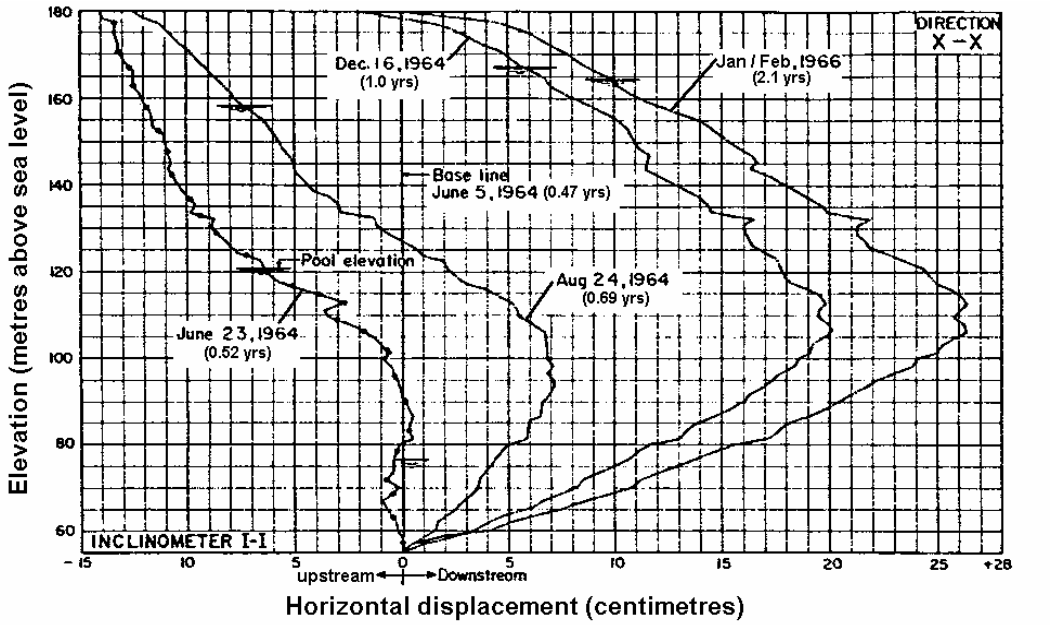

Figure G1.50: El Infiernillo dam, internal displacement normal to the dam axis of the core during first filling (Marsal and Ramirez de Arellano 1967).

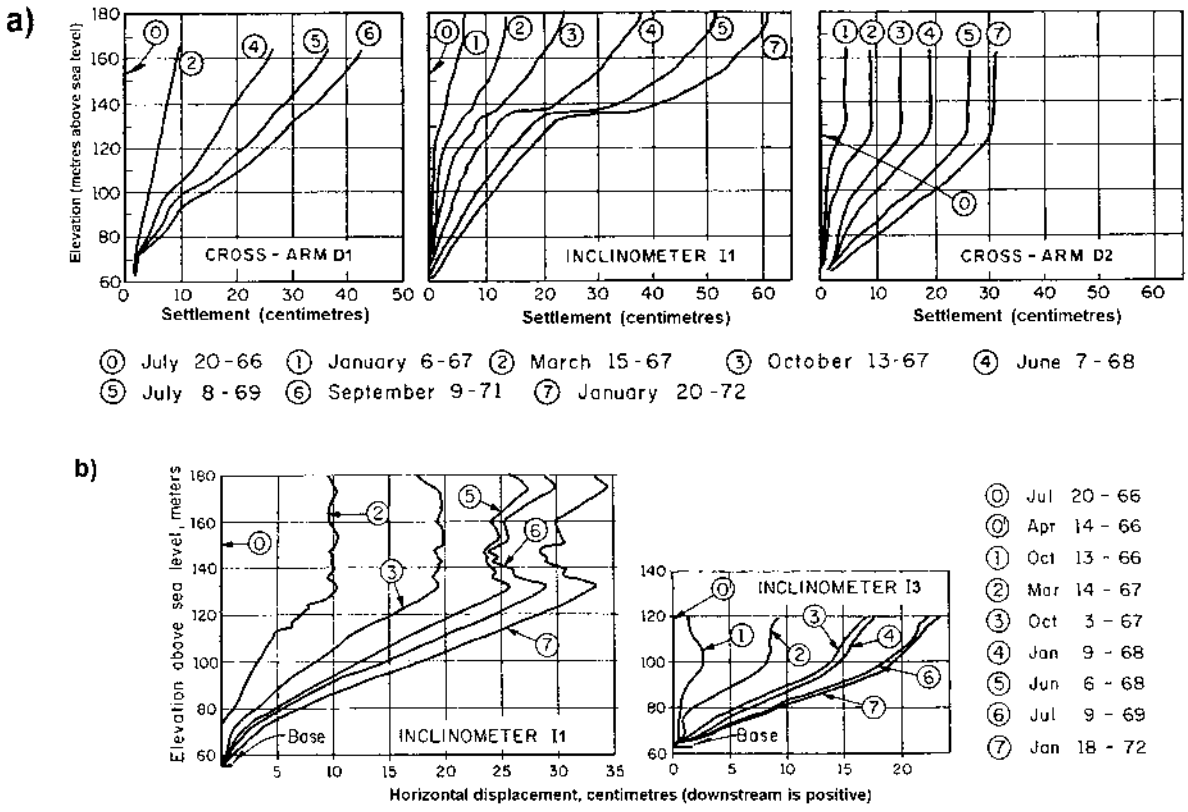

Figure G1.51: El Infiernillo dam, internal *(a)* settlement and *(b)* displacements normal to the dam axis from 1966 to 1972 (2.6 to 8.1 years after construction) (Marsal and Ramirez de Arellano 1972).

1.10 EPPALOCK DAM

Eppalock dam (Figure G1.52 and Figure G1.53), located on the Campaspe River in central Victoria, Australia, is a central core earth and rockfill embankment of 47 m maximum height and 700 m crest length. The embankment was constructed in the early 1960's, completed in March of 1962. Foundations were excavated to bedrock under the core and rockfill shoulders. In summary, the materials and placement methods (Heitlinger et al 1965; SMEC 1998d; Woodward Clyde 1999) are:

- Zone 1 – central core of medium plasticity sandy clays of alluvial origin placed in 380 mm loose thickness layers and compacted by sheepsfoot rollers. Moisture contents were on average 0.8% dry of Standard optimum.
- Filter zones of screened alluvial gravels (Zone 2A) and crushed basalt rock (Zone 2B). Zone 2A materials were placed in 450 mm layers and compacted by light rolling. Zone 2B materials were end dumped in high lifts.
- Zone 3A - rockfill sourced from quarried basalt of high to very high unconfined compressive strength. Placed in 2.0 to 4.0 m lifts (and one 10 m lift) and spread by tractor. No water was added during placement.
- Zone 4 – upstream stabilising fill of highly to moderately weathered sandstones and shales, spread by dozer and trafficked by construction equipment.

Instrumentation consisted of piezometers and one internal settlement gauge (IVM 1) within the core and surface measurement points (SMP) on the crest and slopes. Base readings of the SMPs were taken 0.26 years after the end of construction. Locations of the SMPs and IVM are shown in Figure G1.52 and Figure G1.53.

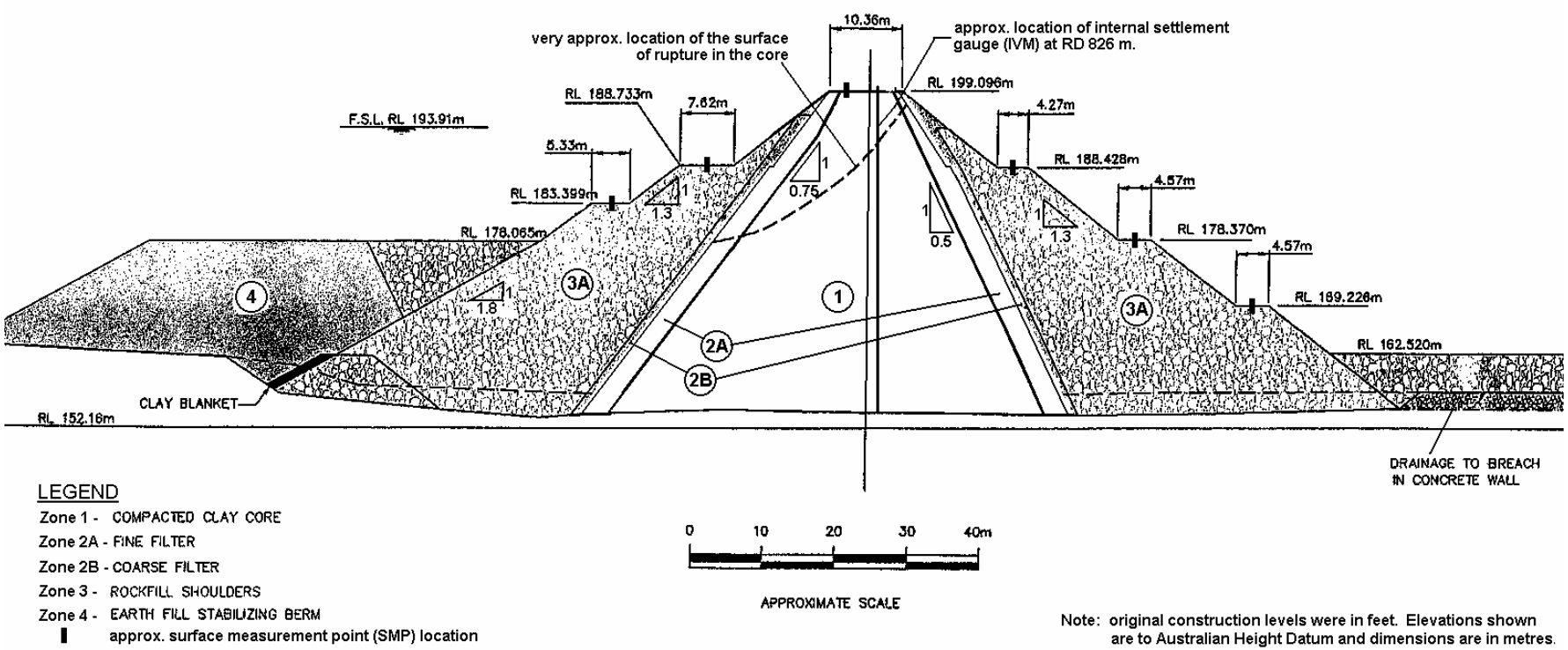

Figure G1.52: Eppalock dam, original design at maximum section (Woodward Clyde 1999)

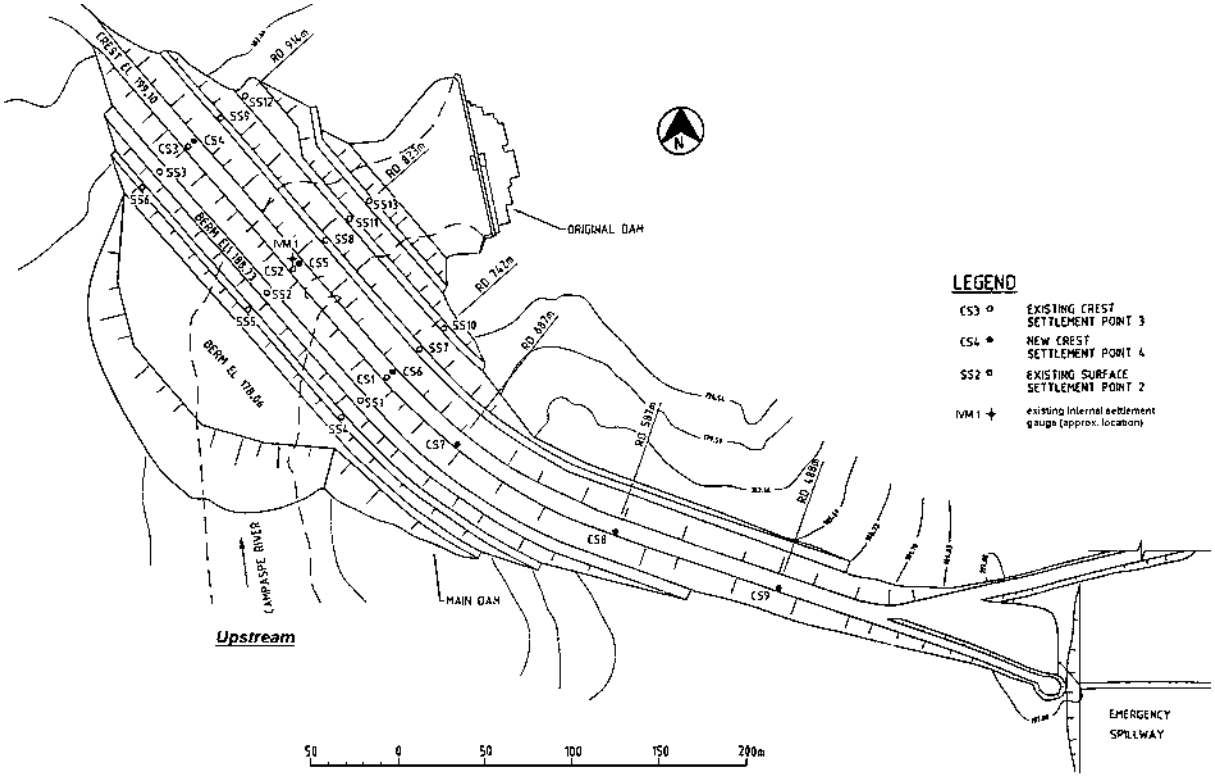

Figure G1.53: Eppalock dam, plan showing SMP and IVM locations (SMEC 1998d).

1.10.1 Instrumentation Records During Construction at Eppalock Dam

Pore water pressures during construction (Heitlinger et al 1965) were only registered in piezometers installed in the lower 5 m of the earthfill core (elevation 158.3 m AHD) and reached values in the range 50 to 200 kPa at the end of construction, which are equivalent to a pore pressure coefficient in the range 0.05 to 0.3. No positive pore water pressures were registered in piezometers installed in the mid to upper region of the core.

Vertical strains in the core at end of construction (Figure G1.54), determined from the IVM records, indicate "normal" type deformation behaviour. Vertical strains reached almost 2% at depths of 35 to 45 m below crest level.

1.10.2 Instrumentation Records Post Construction at Eppalock Dam

The reservoir was first filled over the period from May 1962 to November 1963, 0.2 to 1.65 years after construction. Thereafter, the reservoir is subjected to a seasonal drawdown of typically 3 to 5 m. Larger drawdowns of 7 to 10 m occurred at 5 to 6

years (1967/68), 14 to 16 years (1976/78), 20 to 21 years (1982/83), 32 to 33 years (1994/95) and 36 to 38 years (1997/99) as shown in Figure G1.56.

Deformation records for the IVM gauge are only available until March 1964 or for 3 years after construction (Heitlinger et al 1965). The post construction internal settlement profile (Figure G1.55) to this date shows a smooth curve indicative of "normal" type deformation behaviour at this location.

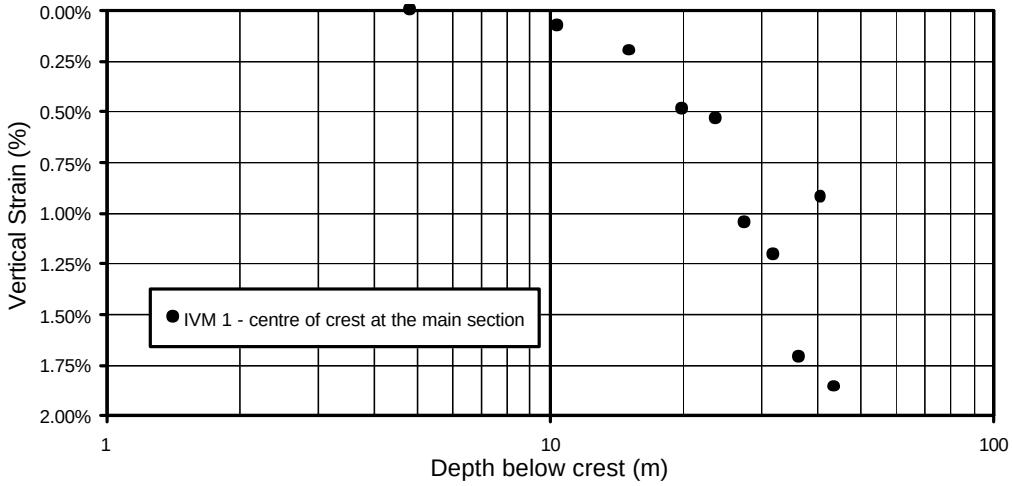

Figure G1.54: Eppalock dam, vertical strain profile in the core at end of construction (adapted from Heitlinger et al 1965).

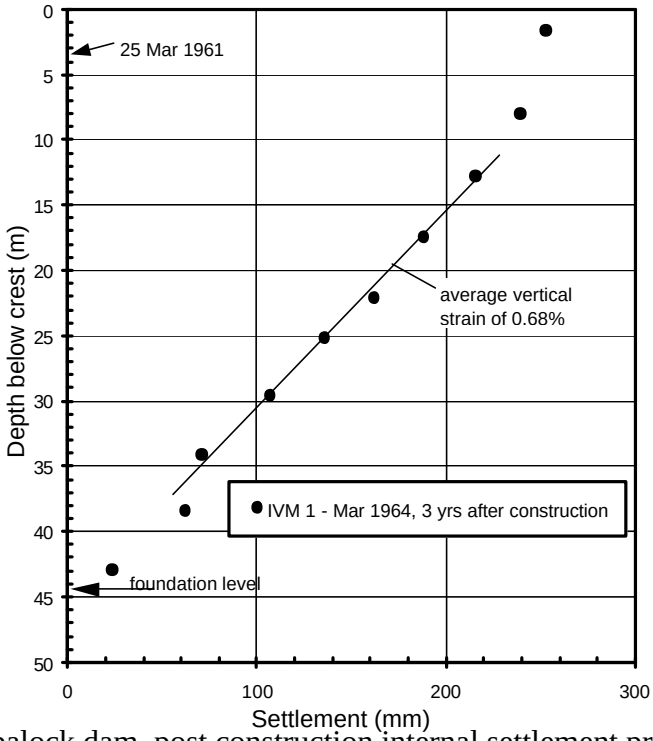

Figure G1.55: Eppalock dam, post construction internal settlement profile (in IVM 1) 3 years after construction.

The post construction settlement and displacement normal to the dam axis of SMPs at the main section and at SMP CS1 (settlement only) are shown in Figure G1.56 and Figure G1.57 respectively. In comparison to similar type embankments several aspects of the post construction deformation behaviour at Eppalock dam are notable, they are:

- The large settlement of the upstream shoulder during first filling, which is due to collapse type settlement on wetting. Settlements of this magnitude are not "abnormal" for dry placed poorly compacted rockfill.
- The large magnitude of settlement of the downstream shoulder, most of which occurred in the first 3 to 4 years after construction. The log time settlement plot (Figure G1.56b) shows a significant reduction in settlement rate after 3 to 4 years.
- The "abnormal" deformation trends on larger drawdown, including:
  - Accelerations in the settlement rate of SMPs on the crest during the larger drawdowns, in particular the drawdowns at 20 to 21 years (SMP CS1 only), 32 to 33 years and 35 to 38 years. It is notable that the crest settlement on large drawdown in 1967/68 (5 to 6 years) was limited, and then of much larger magnitude during the lesser magnitude drawdown at 20 to 21 years and on later drawdowns. This deformation pattern suggests softening of material strength parameters with time.
  - The non-recoverable upstream crest displacement on large drawdown at 32 to 33 years and 38 years.
  - Acceleration of settlement and non-recoverable upstream displacement of SMP SS2 on the upstream shoulder. The change in deformation over the drawdown period is small, in the order of 10 to 25 mm, but is considered indicative of "abnormal" type behaviour.
- The relatively high long-term crest settlement rate in the periods between large drawdown. In comparison to other dry placed clay cores subjected to fluctuating reservoir (Figure 7.62 in Section 7.6 of Chapter 7) the high settlement rate at Eppalock dam is potentially "abnormal".
- The change in crest displacement behaviour at SMP CS2. Up to 1975/76 (about 13 years after construction) the displacement was downstream and of similar trend to that of the downstream shoulder. After about 13 years the displacement trend differed from the downstream slope, it was steady from 13 to 33 years, and then displaced to upstream after 33 years. A similar trend is observed at SMP CS1. The

vector representation of the post construction deformation at the main section (Figure G1.58) highlights the change in displacement behaviour at SMP CS2.

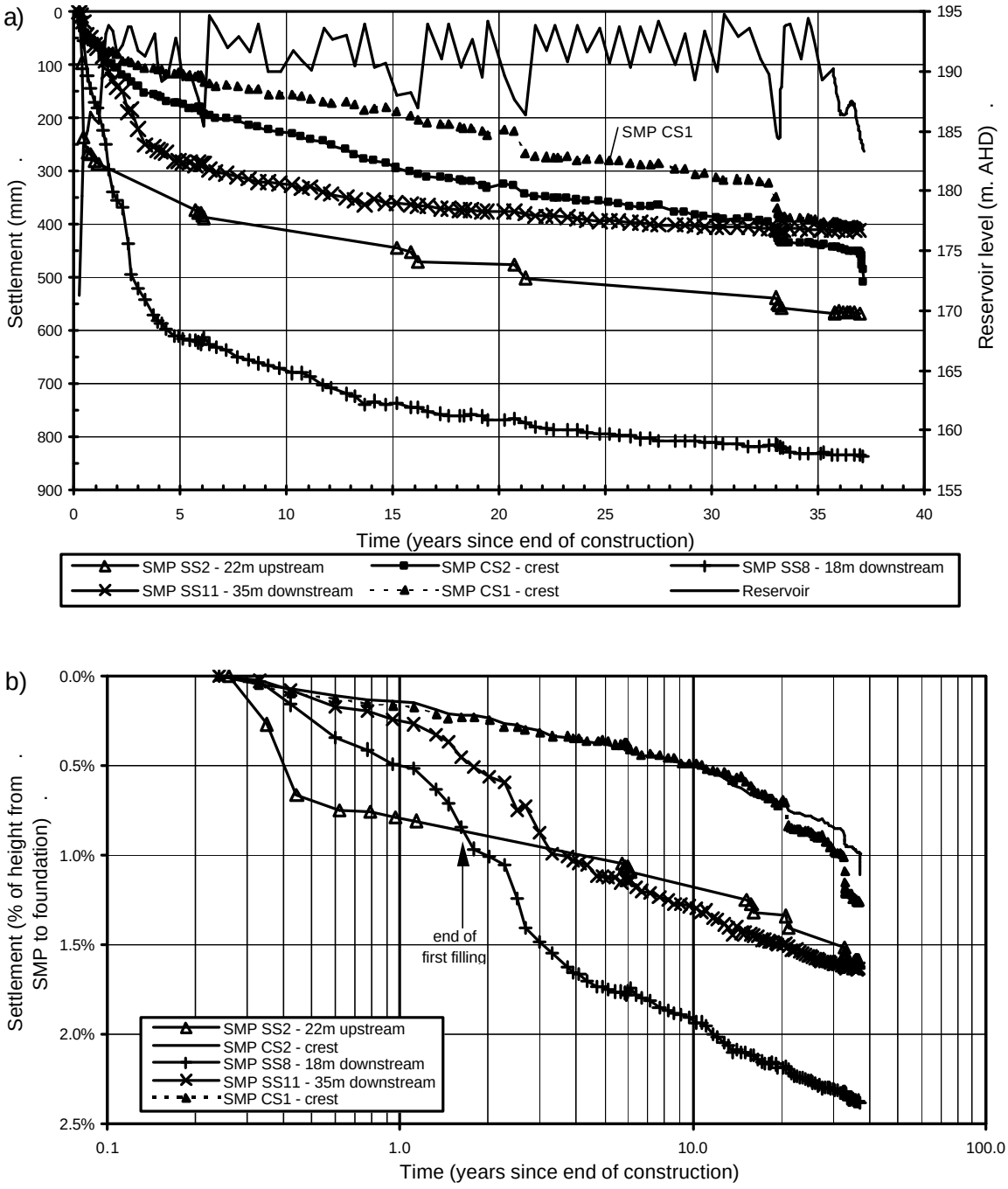

Figure G1.56: Eppalock dam, post construction settlement at main section and CS2.

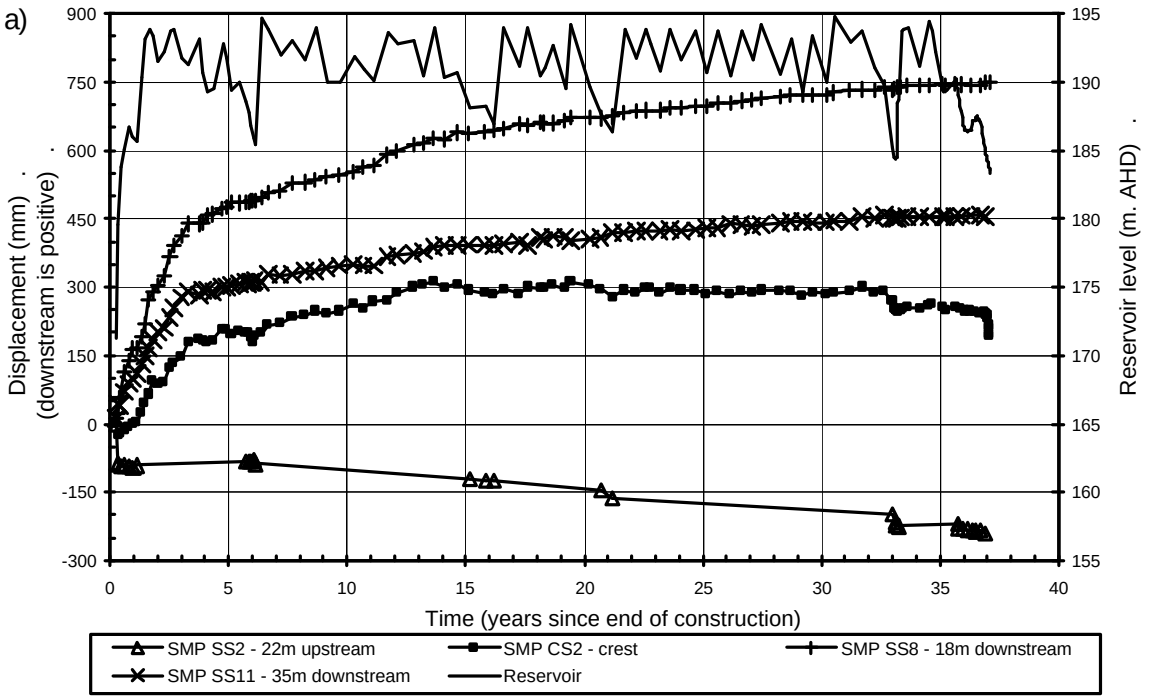

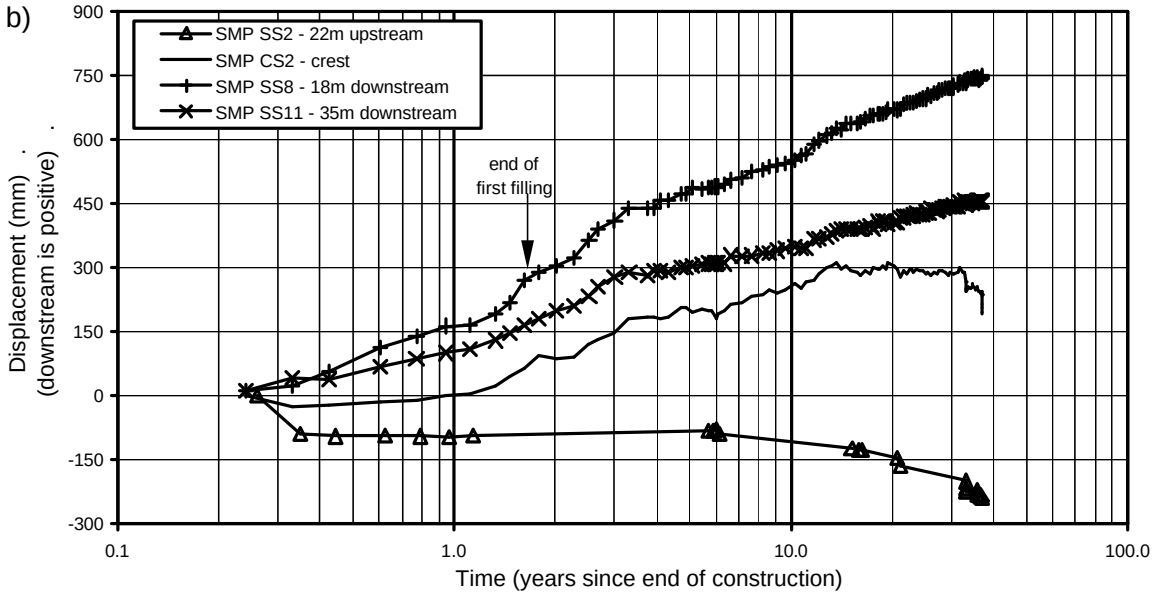

Figure G1.57: Eppalock dam, post construction displacement normal to dam axis at main section.

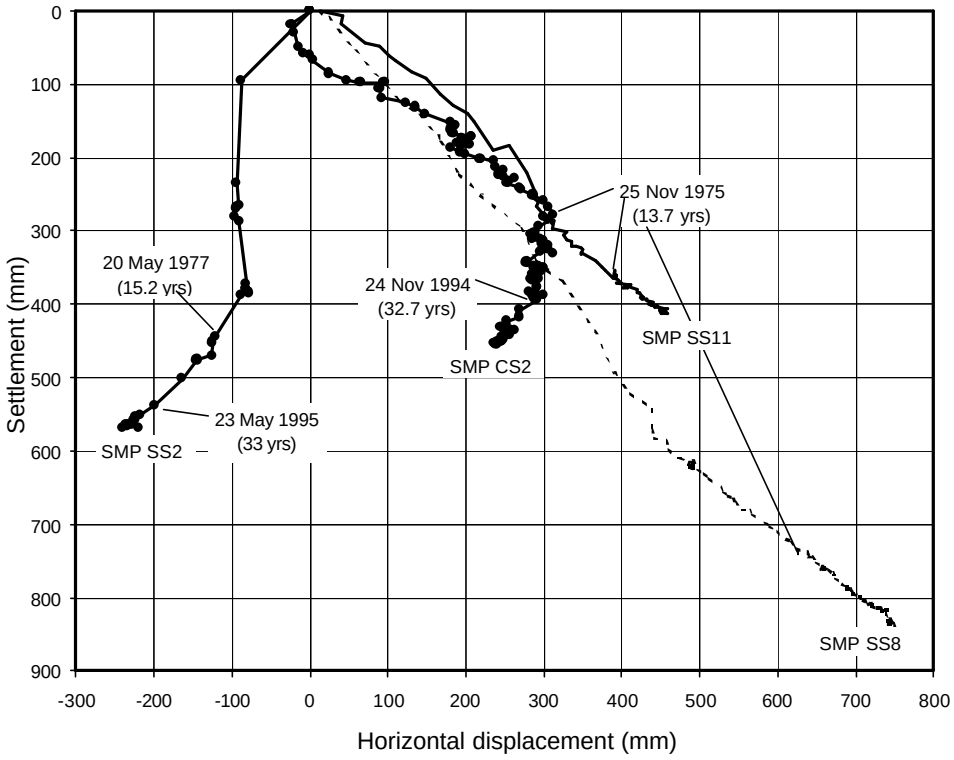

Figure G1.58: Eppalock dam, vector representation of the post construction deformations at the main section.

A number of other notable findings, detailed by Woodward Clyde (1999), relating to the deformation behaviour at Eppalock dam are:

- Longitudinal cracking on the crest of the embankment. Cracking was initially observed as early as 1973 and since then has continued to persist. In 1985 the crest was repaired on account of the cracking, but cracking was again observed in 1986. Test pitting in the late 1990's indicated the longitudinal cracks were open (5 to 10 mm width) to about 1.2 m depth with softening around the crack. Below 1.2 m the crack persisted as a softened zone up to 100 mm in width to depths in excess of 3.8 m. The dip of the discontinuity was 80 to 90 degrees to upstream. Woodward Clyde (1999) comment that roadbase levels either side of a crack showed a vertical differential to upstream, but that it is not conclusive if it is due to a shear type displacement, because it could be a result of the crest works in 1985.
- A series of softened zones at angles of 45 to 70 degrees to the horizontal were observed in the upper 4 m of the core in tube samples recovered from boreholes drilled in the 1990's. The moisture content in the softened zones was about 3% greater than the "normal" moisture content in the embankment.

- Piezocone testing (in the 1990's) indicated softening in the upper 5 to 6 m of the core. This depth of softening was also confirmed from tube sampling and pressuremeter testing in boreholes.
- Test pitting in the rockfill indicated it was "dirty", containing up to 20 to 25% finer than 25 mm. The finer fractions predominantly filled the voids of the larger basalt rock pieces.
- Inclinometers were installed in the crest in 1997. On drawdown in 1998 (35 to 36 years) a localised shear type displacement of 1 to 2 mm was observed at 11 m depth below crest level in IN2, located next to SMP CS1. The localised displacement occurred between mid March and mid April 1998 when the reservoir was drawn down below 186.8 m AHD to a low at 186.4 m AHD. Further localised shear type displacement at this depth and also at 4 m depth were detected during (and following) placement of additional rockfill on the upper berm of the upstream slope at the time of the remedial works in 1999.

Woodward Clyde (1999) concluded from their analysis that two mechanisms were occurring:

- A down drag on the clay core and resultant tensile cracking caused by the significantly greater settlement of the rockfill shoulders post construction.
- Conditions approaching limiting equilibrium of the upper portion of the upstream slope. Limit equilibrium analysis showed that under a reservoir drawdown condition, rainwater penetrating the existing cracks and softening of the undrained strength of the clay core, the factor of safety of the upstream slope was approaching 1. They envisaged that under a drawn down reservoir, heavy rainfall could trigger shear type deformation.

For the deeper slide surface, as indicated by the shear type displacements at 11 m depth in IN2, the factor of safety against sliding is around 1.3.

Remedial works were undertaken in 1999 to improve dam safety of the embankment, including improvement of the stability of both the upstream and downstream slopes and placement of a new multi-zone filter in the upper part of the downstream filter. Design and construction of the remedial works are summarised by Davidson et al (2001) and Fox and Fyfe (2001). During the construction works shear type deformations (Davidson et al 2001) were observed along existing longitudinal

cracks in the core. The most significant surface expression of the shear type deformation was on the downstream batter of the exposed core. Shear type deformations were also observed in inclinometers as described above.

Several issues relating to the post construction deformation behaviour and its mechanics are worth discussing further. These include the differential deformation between the rockfill shells and the core, and the potential timing for development of cracking and the shear surface/s in the embankment core.

Collapse type settlements of the dry and poorly placed rockfill in the upstream and downstream shoulders are a significant factor in very large settlements measured. The large settlement of the upstream rockfill zone occurred during wetting on first filling and for the downstream shoulder occurred in the first 4 to 5 years after construction, probably partly due to wetting from rainfall. During the first 3 years after construction the settlement of the rockfill shoulders was much greater than that of the core and, as indicated by Woodward Clyde (1999), stress transfer from the shoulders to the core would result in localised shear or down-drag at the core / shoulder interface. Given that the fine filter was compacted it is likely that localised shears developed in this zone as have been observed at El Infiernillo and Chicoasen dams (refer Sections 1.9 and 1.4 of this Appendix).

From about 3 to 4 years after construction, the settlement of the core has been of similar magnitude to that of the rockfill shoulders, and it is unlikely that beyond this point in time any further increase in shear stress developed at the interface. It is suspected therefore, that the longitudinal cracking observed from 1973 (11 years after construction) is unlikely to be caused by the differential settlement between the shoulders and core alone, although it is a contributing factor that led to the initial crack development. The ongoing cracking is considered to be reflective of differential deformation between the upstream and downstream portions of the core, and not just as shear type deformations, but the monitoring records are not available to confirm such behaviour. The change in displacement trend of SMP CS2 on the crest provides some indication of the differential deformation behaviour of the core, as does the markedly different deformation shown by the new SMPs installed on the downstream side of the crest in early 1998 (locations of CS4 to CS6 are shown in Figure G1.53) compared to that of the original SMPs on the upstream side of the crest (Woodward Clyde 1999).

It is notable from the vector representation of the SMP deformation (Figure G1.58) that the deformation vector of SMP CS2 changes in about November 1975 (13.65 years)

from being similar to that of the downstream shoulder to being similar to that of the upstream shoulder. The timing of the change is shortly after the initial observation of longitudinal cracking in 1973 (11 to 12 years after construction). These observations suggest that development of significant cracking in the core initially occurred at about this period from 1973 to late 1975.

The initial cause of the cracking is not precisely known, but is likely to be a combination of factors highlighted by Woodward Clyde (1999) including:

- Poor lateral confinement of the upper portion of the core from the poorly compacted and thin rockfill shoulders.
- Differential settlement between the rockfill shoulders and core leading to stress transfer and development of high shear stresses at the core / shoulder interfaces.
- Softening of the strength properties of the core due to wetting and reduction of matric suction, as well as softening due to deformation.

Accelerations in deformation of SMPs on the crest during large drawdown are not clearly evident until the drawdown at 20 years (1982/83), and then it is only clearly evident in SMP CS1. This deformation behaviour is probably indicative of the initial development of shear type deformations in the core. Significant shear type deformations are unlikely to have occurred before this because they are not evident in the larger drawdown at 5 to 6 years (1967/68) and nor are they evident in the internal deformation of the core (IVM 1) during construction and the first three years after construction. Therefore, it is likely that cracking initially developed due to tensile stresses in the core and then this may have later developed in to shear type deformation incorporating the earlier formed discontinuities. The continued shear type deformations are indicative of a gradual deterioration in the strength properties of the embankment materials, as are the observations of softening in the upper 5 to 6 m.

1.11 GEPATSCH DAM

Gepatsch dam (Figure G1.59), located in the Kauner Valley in Austria, is a central core earth and rockfill dam of 153 m maximum height and 605 m crest length that was constructed over the period 1961 to 1964. Glacial activity resulted in the deepening and over-steepening of slopes in the valley. The sub-surface conditions at the dam site are characterised by deep overburden deposits of talus, boulder clay and river deposits, up

to 25 to 50 m thickness, on the lower slopes and river section overlying gneissic bedrock. Foundation preparation consisted of excavation to bedrock under the core region whilst the over-burden soils were left in place under the embankment shoulders. The material properties and placement methods (Lauffer and Schober 1964) are summarised as follows:

- Thin central core (Zones 1 and 1A) of silty to clayey sandy gravels derived from screened talus and moraine. 1% bentonite was added to the upstream part, or Zone 1A, of the core. The earthfill was placed in 150 to 300 mm layers and compacted using 20 to 40 tonne rubber tyred rollers. Average moisture contents ranged from 0.5% to 2% wet of Standard optimum.
- Filter/ transition zones (Zones 2 and 2A) of sandy gravels, sourced from river deposits, placed in 600 mm thickness layers and compacted.
- Rockfill shoulders (Zone 3) sourced from quarried gneiss and oversize Zone 1 screenings placed in 2.0 metre thick layers and compacted by 4 passes of 8.5 tonne vibrating rollers. No water was added during placement and compaction. Gradations indicate the rockfill to be quite coarse. Density tests indicate the compacted rockfill to be of relatively low density (1.9 t/m^3) and high porosity (29%).

Filling of the reservoir commenced approximately 3 months prior to the end of construction. By the end of construction the reservoir level was within 48 m of full supply level. By October 1966 (1.9 years after construction) the reservoir was close to full supply level.

The embankment was well instrumented; Lauffer and Schober (1964) give details. Instrumentation included piezometers, pressure cells, internal horizontal and vertical deformation devices in the core and rockfill shoulders, and surface monitoring points (SMP) on the crest and slopes. Locations of instrumentation in the core are shown in Figure G1.59.

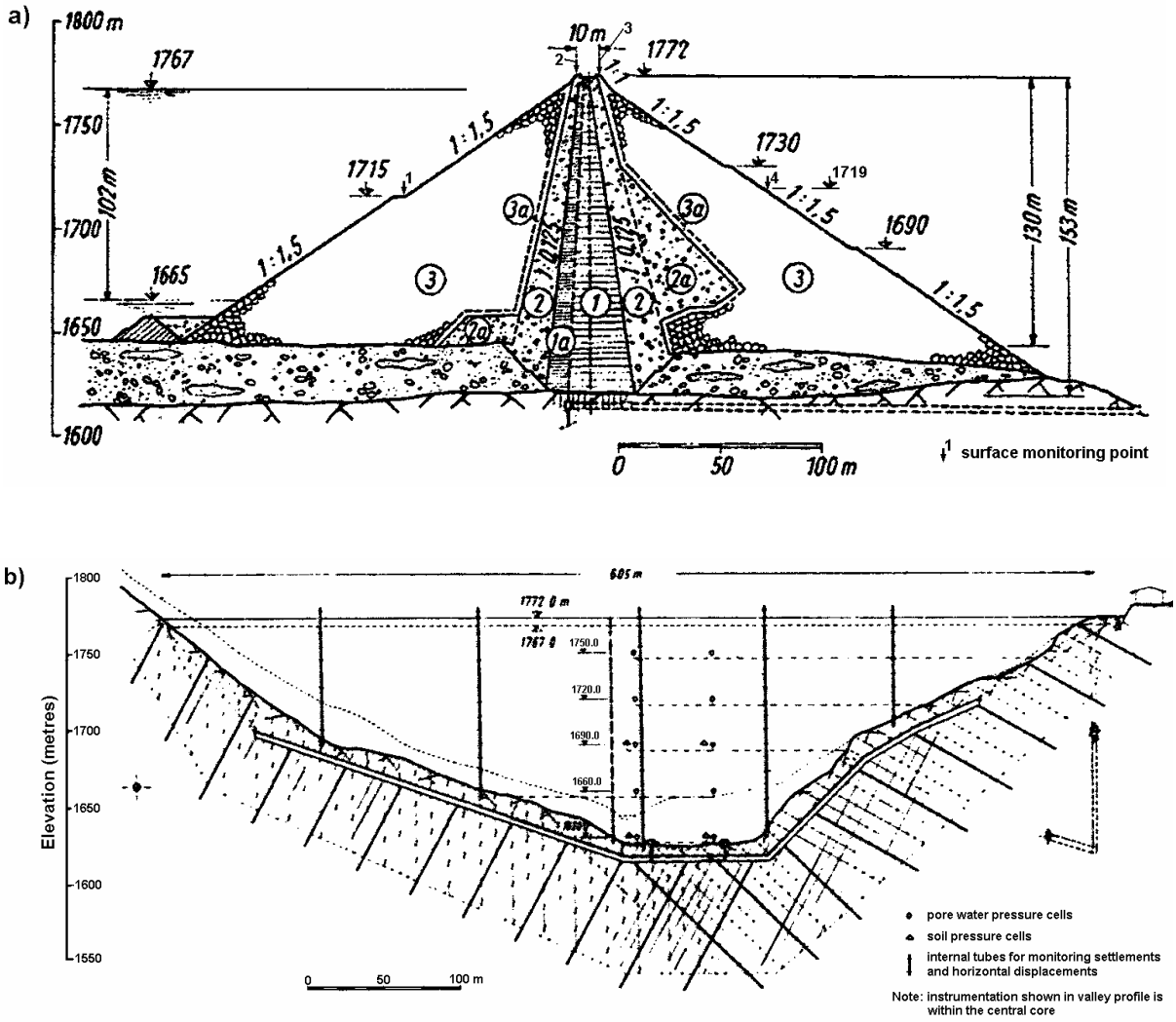

Figure G1.59: Gepatsch dam, *(a)* main section (Schober 1967), *(b)* longitudinal section along dam axis (Lauffer and Schober 1964).

Schober (1967, 1970) and Schwab (1979) discuss the measurement records and embankment performance at Gepatsch dam. The post construction deformation at four SMPs installed at the main section (locations shown in Figure G1.59a) is shown in Figure G1.60 and Figure G1.61. Notable aspects of the embankment performance as discussed by Schober (1967) are summarised as follows:

- Pore water pressures in the core were very high immediately after placement, in some cases reaching r_u values close to 1.0. Under these conditions significant weaving under trafficking occurred. Relatively rapid dissipation occurred in the months following placement with r_u values reducing to about 0.3 after 3 months and to less than about 0.2 at the end of construction.
- Pressures cells indicated arching occurred across the thin core. High vertical stress levels were recorded in the filter / transition zones.

- Very large settlements during construction were observed in the rockfill, much greater than for the core and the filter / transition zones.
- The soil foundation contributed to the large settlements in the shoulders. Data presented by Schwab (1979) shows settlements in the deep soil foundation at the main section of up to 2.2 metres upstream of the core 14 years after end of construction (equates to almost 10% vertical strain within the soil foundation) and 0.8 to 1.2 m downstream of the core (4.5% to 6% vertical strain within the soil foundation).
- Large collapse type settlements occurred in the upstream rockfill on saturation during first filling. This is shown in Figure G1.60a by the much greater settlement of SMP 1 on the upstream slope compared to SMP 4 on the downstream slope at a similar elevation.
- The increase in rate of settlement of the upstream slope on drawdown at 0.2 to 0.45 years is notable. Schober (1967) attributes this behaviour to increased vertical effective stresses in the upstream rockfill on drawdown due to completion of embankment construction under high reservoir level.
- In the latter stages of construction the internal monitoring records showed that the upper portion of the upstream transition displaced to upstream whilst only a slight displacement (to downstream) occurred in the downstream transition, indicating relatively large lateral spreading of the core in this region. Schober (1967) attributed the lateral spreading to the influence of collapse settlement in the upstream rockfill as well as the thinner width of the filter / transition zones upstream of the core.
- Lateral spreading of the crest, amounting to some 600 to 700 mm, occurred during the period of first filling after the end of construction (Figure G1.61b). The upstream edge displaced to upstream in the order of 500 to 600 mm and the downstream edge displaced downstream up to 200 mm, fluctuating with reservoir level. The longitudinal crack that occurred in the crest was attributed to the differential deformation of the crest.

Collapse settlement of the upstream rockfill, as discussed by Schober (1967), contributed significantly to the deformation behaviour of the embankment during the period of first filling, which included the latter stages of construction. The rockfill at Gepatsch dam was particularly susceptible to collapse type deformation due to its

placement in 2 metre thick layers without the addition of water. In comparison to other embankments:

- The large upstream displacement of the upstream edge of the crest on first filling stands out as an outlier both in terms of magnitude and direction (Figures 7.40 in Section 7.5 and 7.86 in Section 7.6 of Chapter 7).
- The magnitude of settlement of the upstream slope and upstream crest is large, but not "abnormally" so for dry placed rockfill susceptible to large collapse type settlements (Figures 7.51, 7.52 and 7.85 in Section 7.6 of Chapter 7, and Figure F2.25 in Appendix F).
- The settlement of the crest is at the upper range of magnitude for wet placed clayey sand to clayey gravel cores (Table 7.19 and Figures 7.46, 7.47 and 7.56 in of Chapter 7). The post first filling settlement rate is on the high side (Figure 7.62 in Chapter 7), but not necessarily "abnormally" so.
- The crest displacement is comparable to similar core types (Figure 7.71 in of Chapter 7).
- For the downstream slope, the magnitude and rate of settlement and displacement are on the high side, but not "abnormally" so (Figures Table 7.22 and Figure 7.78, 7.79 and 7.81 in Section 7.6 of Chapter 7, and Figures F2.1 to F2.3, F2.6 and F2.14 of Appendix F).

Overall, the magnitude and ongoing rate of settlement and displacement of the SMPs on the crest and slopes of Gepatsch dam are on the high side in comparison to similar type embankments. This is largely attributable to placement of the rockfill in 2 metre thick layers without the addition of water, and its susceptibility to collapse type deformations. Deformations of the upstream shoulder were much greater than the downstream shoulder during the period of first filling, but post first filling the magnitude of deformation of the downstream shoulder is much greater. This is probably due to the greater potential for deformation of the downstream rockfill on wetting following heavy rainfall.

The long term settlement rates of the crest and slopes at Gepatsch dam are possibly over-stated in the tables and figures in Chapter 7. This is because the monitoring records post first filling found in the literature were limited, and therefore the quoted rates have been estimated from the dashed lines shown in Figure G1.61. It is likely, particularly for the downstream slope, that the deformation rates (per log cycle of time)

were higher in the period shortly after first filling but have since decreased, as has been observed for other case studies with rockfills placed dry and in thick layers (e.g. Eildon, Eppalock and El Infiernillo dams).

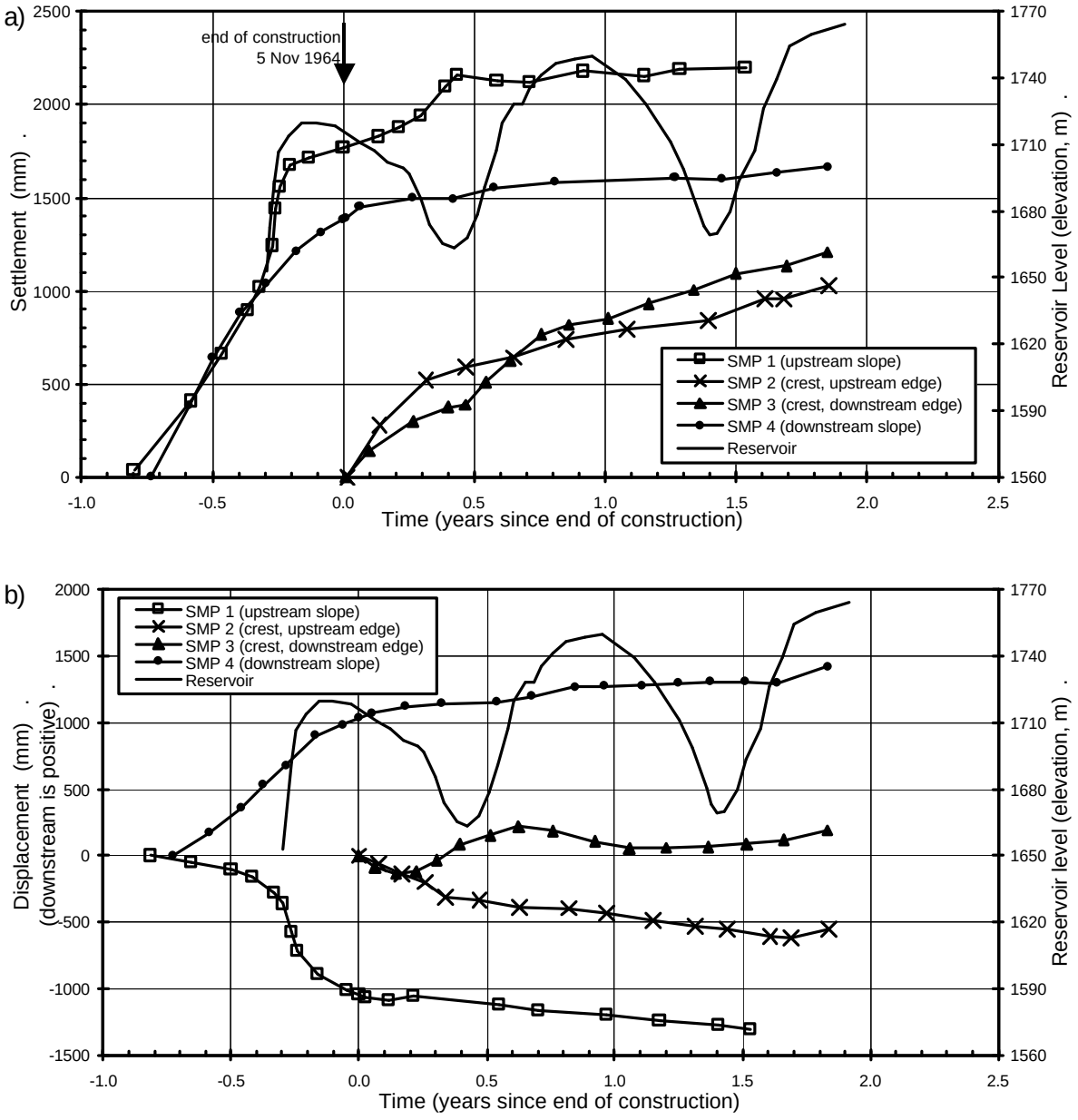

Figure G1.60: Gepatsch dam; *(a)* settlement and *(b)* displacement normal to the dam axis versus time for period prior to and for 2 years after the end of construction.

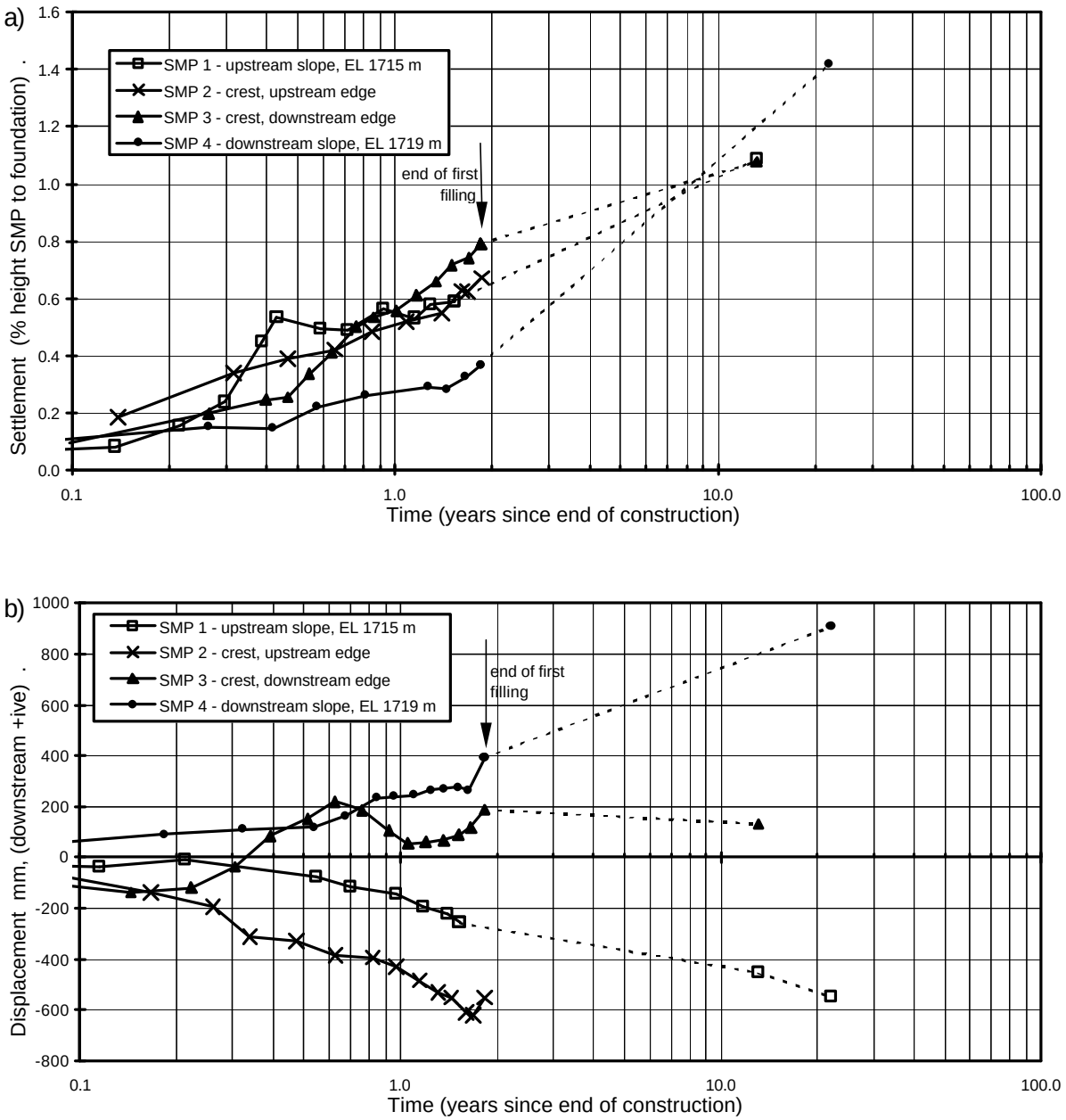

Figure G1.61: Gepatsch dam; *(a)* settlement and *(b)* displacement normal to dam axis versus log time. Deformations set to zero at end of construction.

1.12 LA GRANDE NO. 2 (LG-2) DAM

LG-2 dam is part of the James Bay hydroelectric complex located in Quebec, Canada. The main embankment (Figure G1.62), completed in October 1978, is a 160 m high central core earth and rockfill dam, with the core slightly inclined to upstream, constructed on a bedrock foundation. In summary, the materials and placement methods (Paré et al 1982; Dascal 1987) comprised:

- Thin core (Zone 1) of non-plastic gravelly silty sands, sourced from moraine deposits, placed in 450 mm layers and compacted by heavy pneumatic rollers. The specified moisture content range was 1% dry to 2% wet of Standard optimum.
- Moderately wide filter / transition zones (Zones 2A, 2B and 2C) of gravelly sands to sandy gravels sourced from alluvium and crushed stone. Materials were placed in 450 mm layers, wetted if necessary, and compacted with 3 to 4 passes of a 3 to 5 tonne smooth drum vibratory roller.
- Rockfill shoulders (Zones 3A, 3B and 3C) of quarried granitic gneiss placed in 0.9 to 1.8 m thick layers and compacted with 4 passes of a 9 tonne smooth drum vibratory roller. No water was added during placement.

The reservoir was filled to close to maximum water level over the period October 1978 to December 1979 (0.1 to 1.2 years after construction). The reservoir operation after first filling is not known.

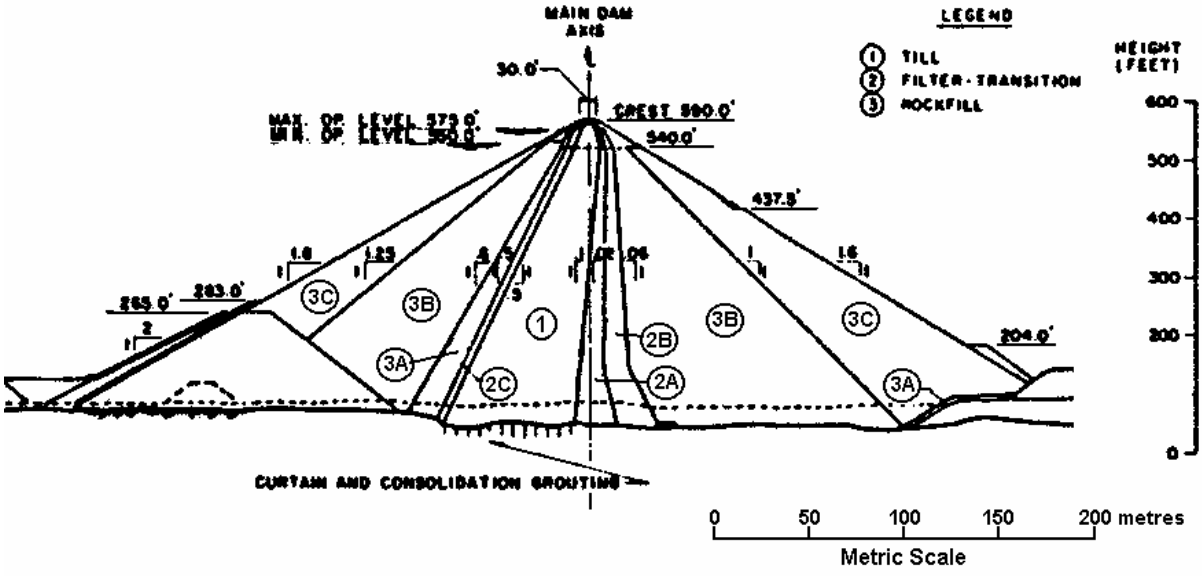

Figure G1.62: LG-2 dam, typical cross section (Dascal 1987)

The post construction settlement and displacement of SMP 23, located on the upstream edge of the crest (Figure G1.64), is shown in Figure G1.63. The data shows the large magnitude of settlement and downstream displacement on first filling at SMP 23, and the significant decrease in deformation rates that occurred shortly after first filling. In comparison to similar embankments:

- The crest displacement on first filling is unusually high (Figure 7.38 in Section 7.5 of Chapter 7).
- The magnitude of settlement is large compared to other embankments with moraine cores (Dascal 1987), but is not overly large in comparison to that for reasonably to well compacted rockfills (Figure F2.24 of Appendix F).

Extensive cracking of the crest, described by Paré (1984), occurred during the latter stages of first filling. Longitudinal cracking was observed at the upstream edge of the crest as well as close to the centreline of the crest. Investigation undertaken after first filling found that the near vertical crack in the central region of the crest was in the order of 150 to 200 mm wide, decreasing to 50 mm wide at 3.5 m depth, and differential settlement to upstream across the crack was about 500 mm (Figure G1.64). Paré (1984) also refers to a "s*harp tilt*" that developed in September 1980 within an inclinometer located in the upstream portion of the core (Figure G1.64) and became blocked at about 18 m depth in November 1980. The timing of these observations is 1.9 to 2.2 years after end of construction, almost 1 year after completion of first filling.

Paré (1984) considered the localised straining in the inclinometer was indicative of the development of a shear plane in the core. He attributes the longitudinal cracking and shear formation to a combination of the large downstream displacement of the core on first filling (due to the water load) and collapse settlement of the upstream rockfill on wetting.

An interesting aspect of the deformation behaviour is the timing of the "*sharp tilt*" and blockage in the inclinometer. Paré (1984) indicates that this occurred almost 1 year after completion of first filling. The shear surface in the core developed during the latter stages of first filling as indicated by the timing of the crack and it would have been expected that some indication of the shear formation would have been identified in the deformation of the inclinometer. However, there is no indication from Paré (1984) that any tilt was recorded during first filling; maybe the inclinometer was not installed until after first filling when a potential slip surface was identified. The observation of shear deformation from September to November 1980 is possibly drawdown related and due to the reduction in lateral support on the upstream face of the core as the reservoir level was lowered. This reduction in lateral support possibly led to a locally unstable condition of the upstream wedge of the core, which then deformed to upstream until adequate lateral support was provided by the upstream shoulder.

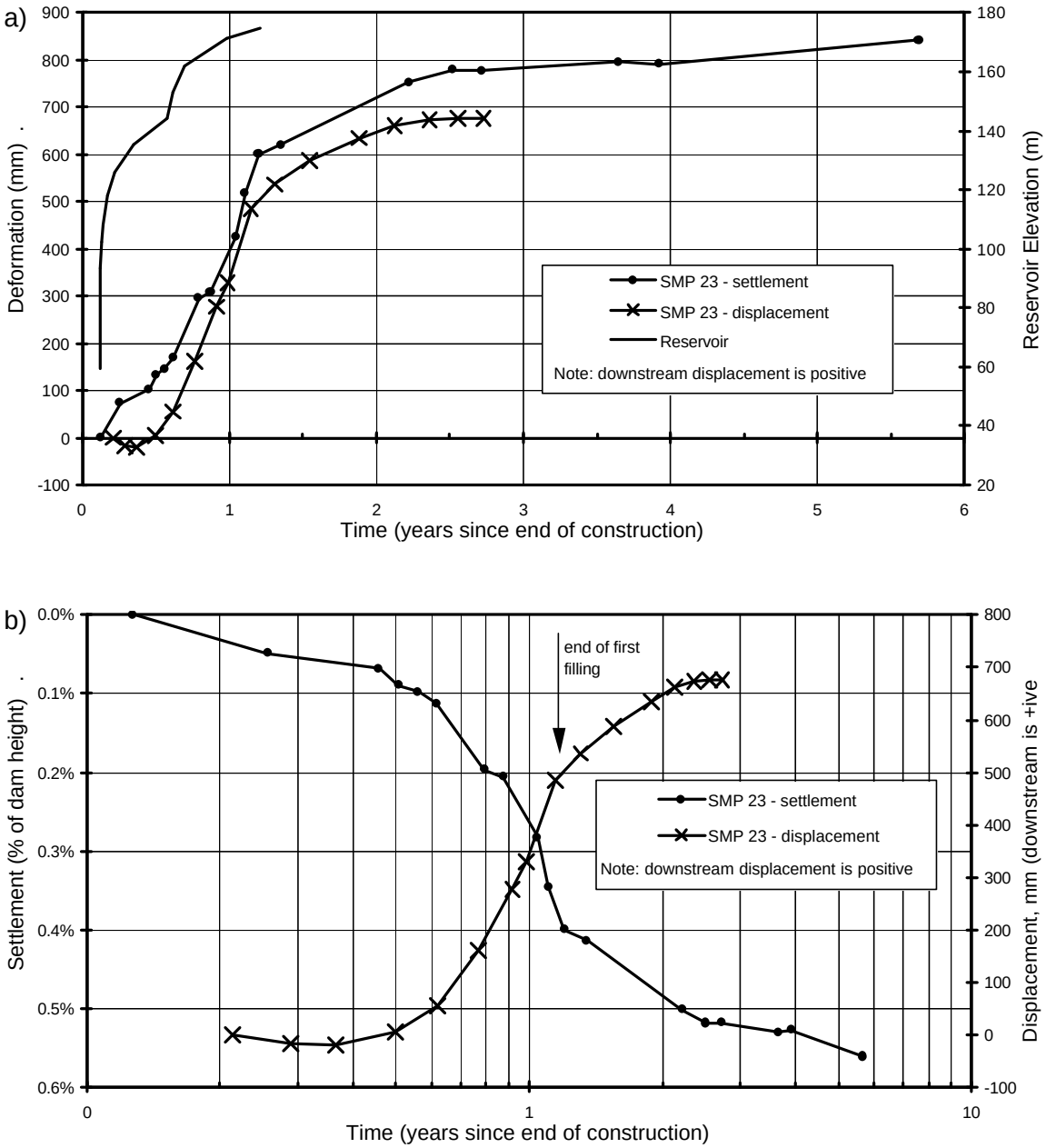

Figure G1.63: LG-2 dam, post construction settlement and displacement for SMP 23 located on the upstream edge of the crest (data from Paré (1984) and Dascal (1987)).

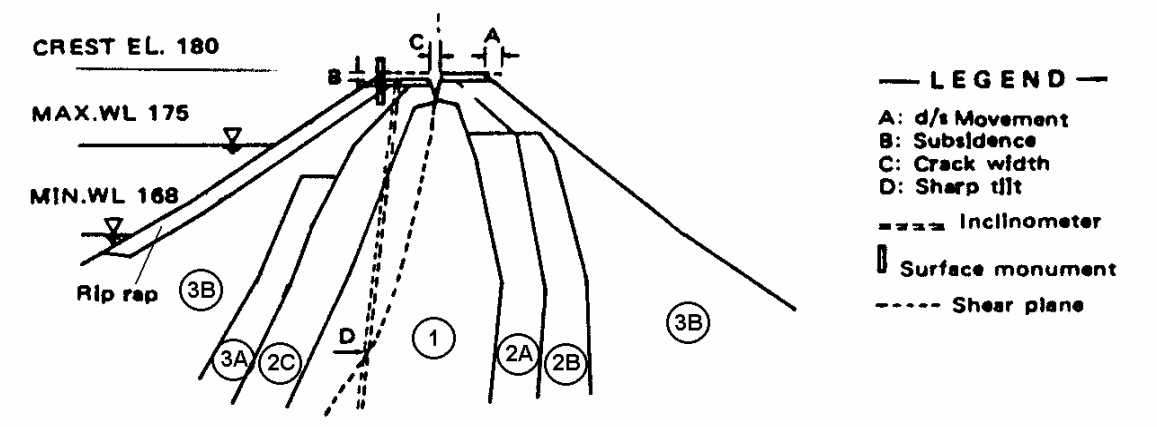

Figure G1.64: LG-2 dam; post construction deformation at crest and possible shear plane in core (Paré 1984)

1.13 SVARTEVANN DAM

Svartevann dam (Figure G1.65), located in western Norway, is a central core earth and rockfill dam with a thin, slightly upstream sloping core. The embankment is 129 m in height and of 420 m crest length, and founded entirely on sound granitic gneiss. It was constructed in the seasonally warmer months between 1973 and 1976. Water was stored during construction, reaching within 37 m of full supply level prior to the end of construction. In summary, the materials and placement methods (Kjœrnsli et al 1982) comprised:

- Core (Zone 1) of silty sands to silty gravels, sourced from moraine deposits, compacted in 500 mm layers by heavy vibrating rollers. The average moisture content at placement was 0.4% wet of Standard optimum.
- Filters (Zone 2A) of fluvial sandy gravels compacted in 500 mm layers by vibrating rollers. Water was added prior to compaction.
- Transition (Zone 2B) of quarry run crushed sound rock placed in 1.0 m layers, sluiced and compacted by heavy vibrating rollers (4 passes of a 13 tonne roller).
- Rockfill (Zone 3A), sourced from quarried granitic gneiss, placed in 2 metre layers and compacted with 8 passes of a 13 tonne smooth drum vibrating roller. No water was added during placement and compaction. The porosity of the placed rockfill was 26.5%.

Svartevann dam is part of a hydroelectric scheme. It is used as a pumped storage for the dry season and is subjected to seasonal drawdown. The reservoir reached within

about 1.5 m of full supply level in late November early December 1978, approximately 2.3 years after the end of construction (Figure G1.69a).

Dibiagio et al (1982) indicate that the embankment was well instrumented with internal settlement and displacement gauges, extensometers, pressure cells and piezometers, and numerous SMPs on the crest and slopes. Only a limited amount of the monitored data was located in the published literature (Dibiagio et al 1982; Kjœrnsli et al 1982), and only for the period up to 4 years after construction (to 1980).

Piezometers in the core showed that during construction pore water pressures at placement were initially relatively high, but then dissipated rapidly in the construction period. This behaviour is typical of that for wet placed silty sand to silty gravel earthfills (refer Section 7.4.1.4 of Chapter 7). Post construction, the piezometric pressures in the core fluctuated with reservoir level, those closest to the upstream face at a similar amplitude to the reservoir and at a reduced amplitude for those closest to the downstream face.

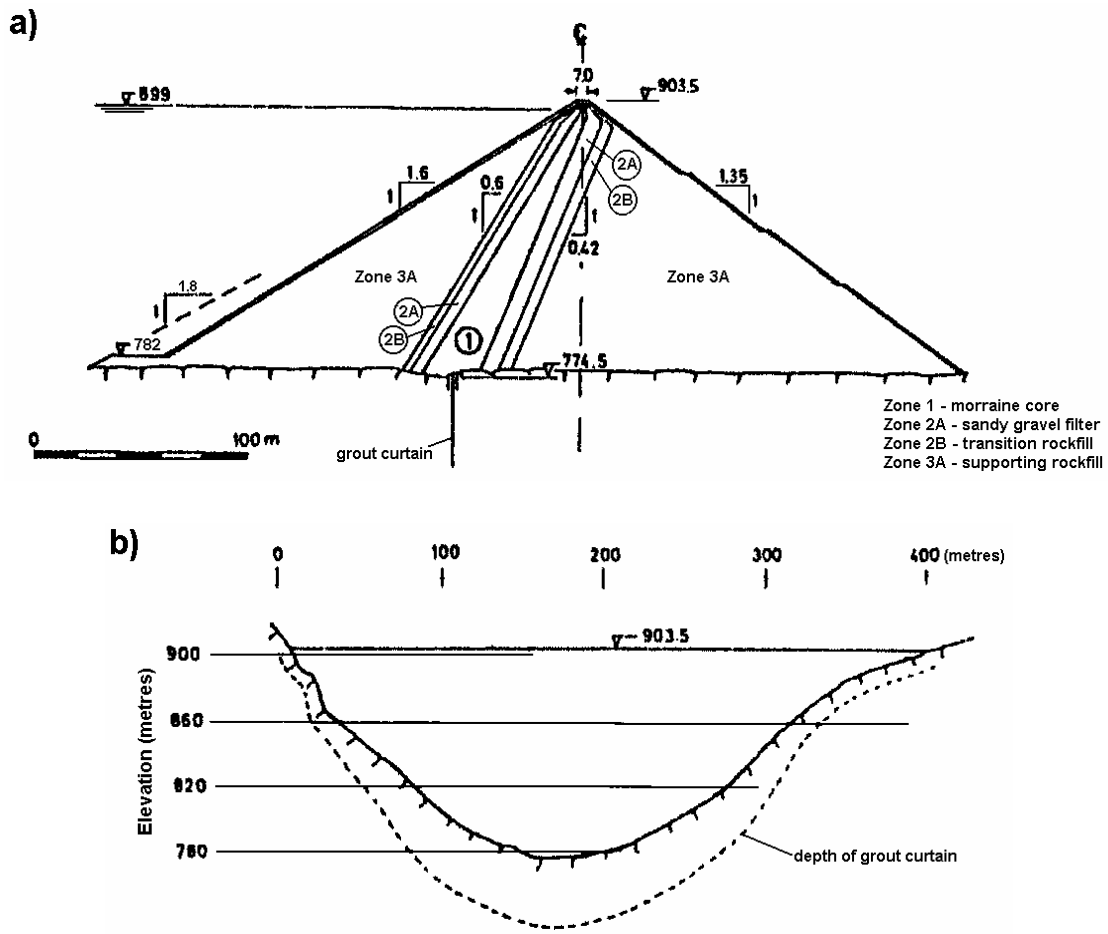

Figure G1.65: Svartevann dam; *(a)* main section and *(b)* cross valley profile (Kjœrnsli et al 1982)

The post construction deformations at Svartevann dam, particularly during the period of first filling, were relatively high (Figure G1.66 to Figure G1.68). Compared to the case study data for zoned earth and rockfill dams with moraine cores (Dascal 1987) the crest deformation at Svartevann is clearly very large. In comparison to similar type embankments for the case studies analysed, notable aspects of the deformation behaviour at Svartevann dam are:

- Very high downstream displacement of the crest during first filling of about 1100 mm. This magnitude of displacement was a clear outlier to other case studies (Figure 7.38 in Section 7.5 and 7.72 in Section 7.6 of Chapter 7). The downstream displacement of the downstream slope was also of large magnitude (up to almost 800 mm) on first filling, and was comparatively high, but not "abnormally" so, compared to other case studies (Figure 7.39 in Section 7.5 of Chapter 7, and Figure F2.6 in Appendix F).
- The magnitude of crest settlement on the left abutment was "abnormally" large (Figure 7.46 and 7.57 in Section 7.6 of Chapter 7) whilst at the main section was large, but not "abnormally" so.
- The magnitude of settlement of the downstream shoulder is also large at close to 1% at 4 years after construction, and is possibly an outlier for reasonably compacted rockfills (Figure 7.49 in Chapter 7and Figure F2.14 of Appendix F).
- Post first filling the settlement rate for the crest at the left abutment is relatively high at 0.87 % per log cycle of time (Figure 7.62 in Chapter 7); however, it is representative of only 1.5 years post first filling and may have since reduced.

The post first filling settlement rate of the downstream slope at 0.1 to 0.3% per log cycle of time (Figure G1.69) is "normal" in comparison to other embankments.

Dibiagio et al (1982) comment that very high lateral extension strains (greater than 8%) normal to the dam axis were measured in the core over the abutment slopes. A large proportion of the extension was measured during the post construction first filling period.

The deformation records at Svartevann dam indicate the embankment underwent very large, in some cases "abnormally" large, settlements and displacements of the crest and downstream slope during the period of first filling. As shown in Figure G1.68 and Figure G1.69, a large portion of the surface deformation occurred during the final 20 m raising of the reservoir to full supply level, although significant settlements were also

measured for the upper downstream slope shortly after the end of construction. Finite element analysis of the construction and first filling of Svartevann dam by Dibiagio et al (1982) was unable to accurately model the deformation behaviour within the downstream shoulder, it significantly over-predicted the horizontal displacements and significantly under-predicted the settlements.

For the downstream shoulder of the embankment, the post construction internal deformations (Figure G1.67) show that large settlements and displacements occurred in the mid to upper region of the slope in the first 4 years after end of construction. Vertical strains were estimated (from Figure G1.67) at 1.4 to 2.2% in the mid to upper region of the downstream rockfill for this post construction period, with much lower vertical strains, 0.5 to 1.0%, estimated for the lower 45 to 50 m (below elevation 820 m). In addition, the deformation time plots of SMPs on the downstream shoulder (Figure G1.68 and Figure G1.69) show that very large settlements and downstream displacements of the mid to upper slopes occurred during the latter stages of first filling, but not on the lower downstream slope. The finite element analysis by Dibiagio et al (1982) was unable to model the large settlement of the downstream slope during first filling.

The large crest deformations on first filling observed at Svartevann dam appear to be related to the deformation of the downstream shoulder. In effect, the core deforms with the downstream shoulder. It is shown that large settlements and deformations were mainly confined to the mid to upper region of the downstream shoulder, a significant proportion of which occurred during the latter stages of first filling. The inability of the finite element analysis (Dibiagio et al 1982) to model the deformation behaviour on first filling, particularly the vertical component, suggests that the application of the water load and the associated changes in stress conditions on its own does not account for the actual deformation behaviour. In addition, time dependent or creep related deformations would not account for the vertical deformation because the magnitudes are too large. The slower rates post first filling are more typical of creep or time dependent settlement rates for compacted rockfill. It is considered that the large deformations of the mid to upper region of the downstream shoulder are due to collapse type settlements in the rockfill placed in thick layers and without the addition of water. The trigger for the collapse type settlement must be moisture related, so possibly either heavy rainfall or snowmelt is the source of water, and the timing during the latter stages of first filling is somewhat coincidental.

Another notable aspect of the settlement behaviour of SMPs on the mid to upper downstream slope (Figure G1.69a) is that accelerations in settlement rate (in terms of normal time) in the first 2 years post construction occur at the same time period each year, from 0.8 to 1.2 and 1.8 to 2.2 years corresponding to the period from June to September, or summer. This is the seasonally wettest and warmest period for the western coast of Norway. Therefore, heavy rainfall together with snowmelt may sufficiently wet the downstream rockfill for collapse settlement to occur, and possibly 1978 was a relatively wet summer or the winter one of high snowfall.

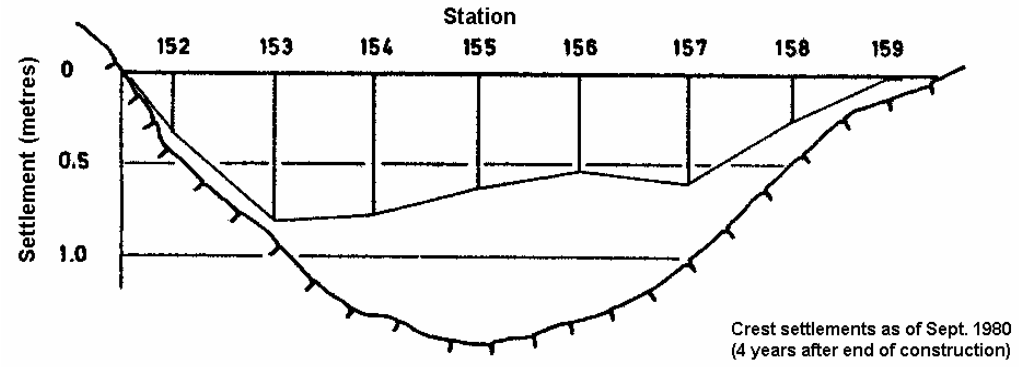

Figure G1.66: Svartevann dam; post construction settlement of crest (Kjœrnsli et al 1982)

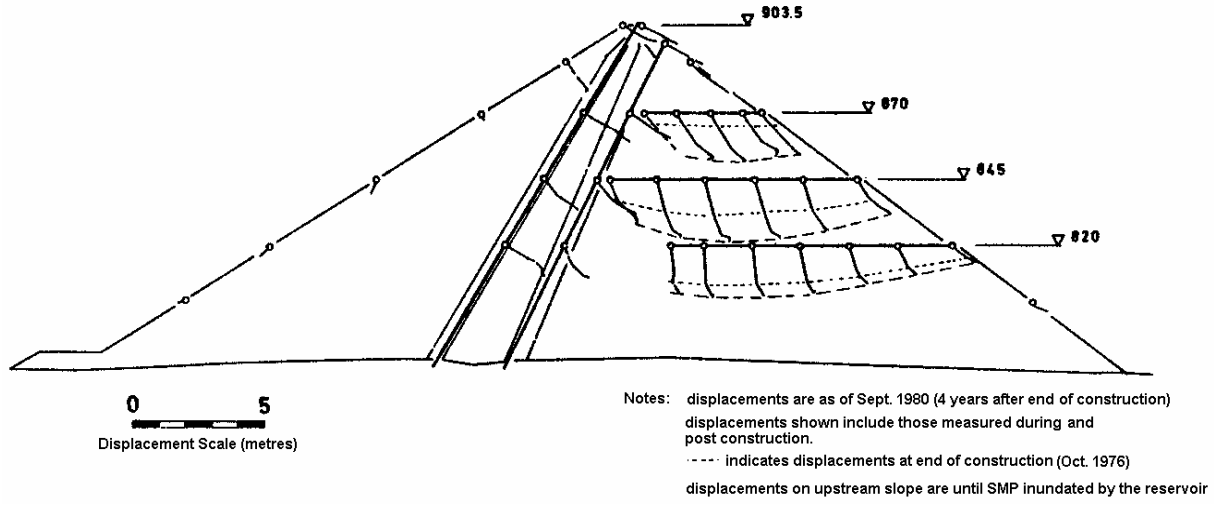

Figure G1.67: Svartevann dam; internal and surface deformations during and post construction at the main section (Kjœrnsli et al 1982).

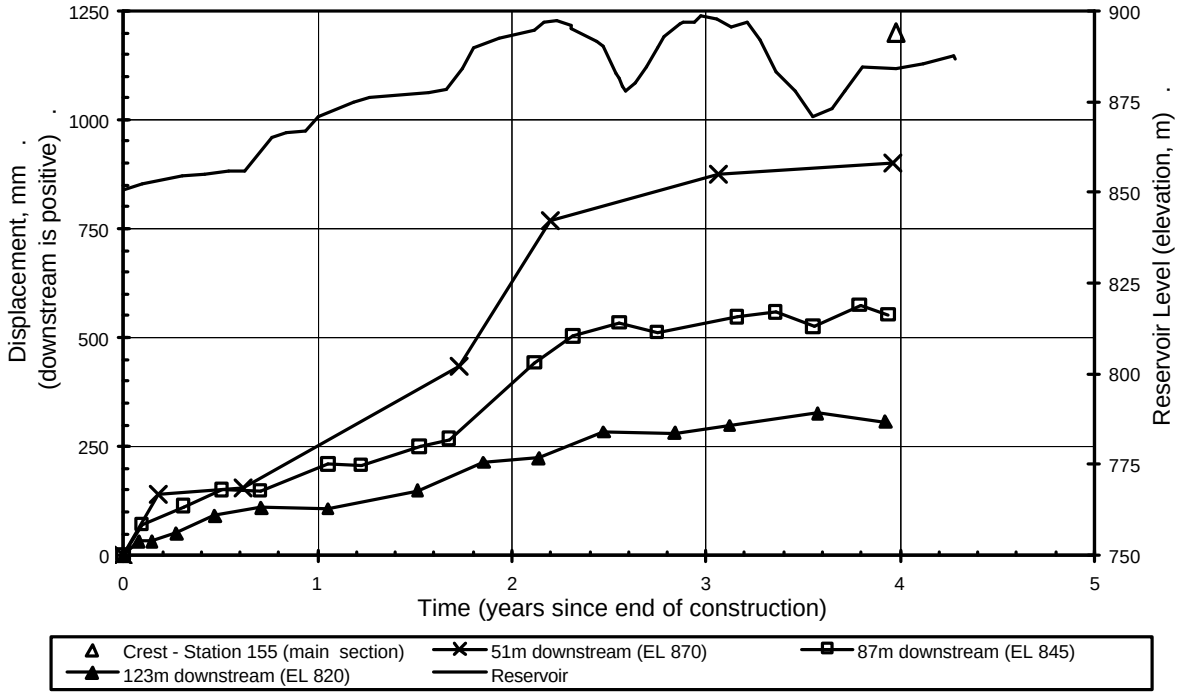

Figure G1.68: Svartevann dam, post construction displacement normal to the dam axis of the downstream slope.

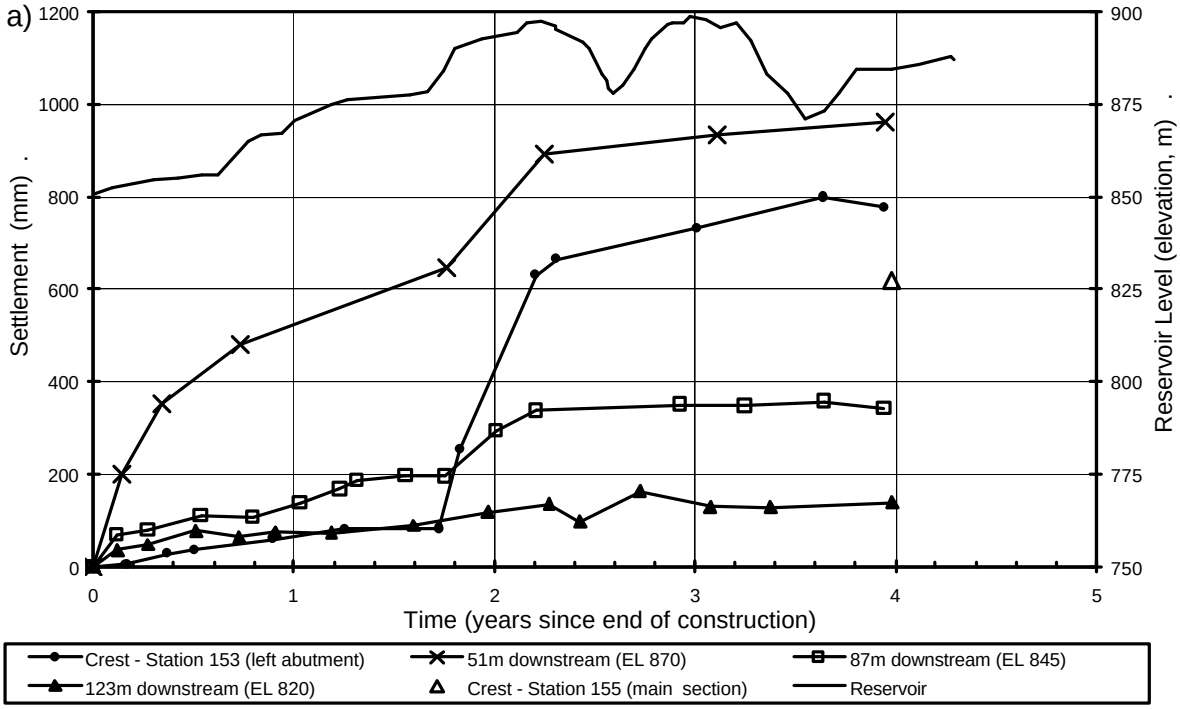

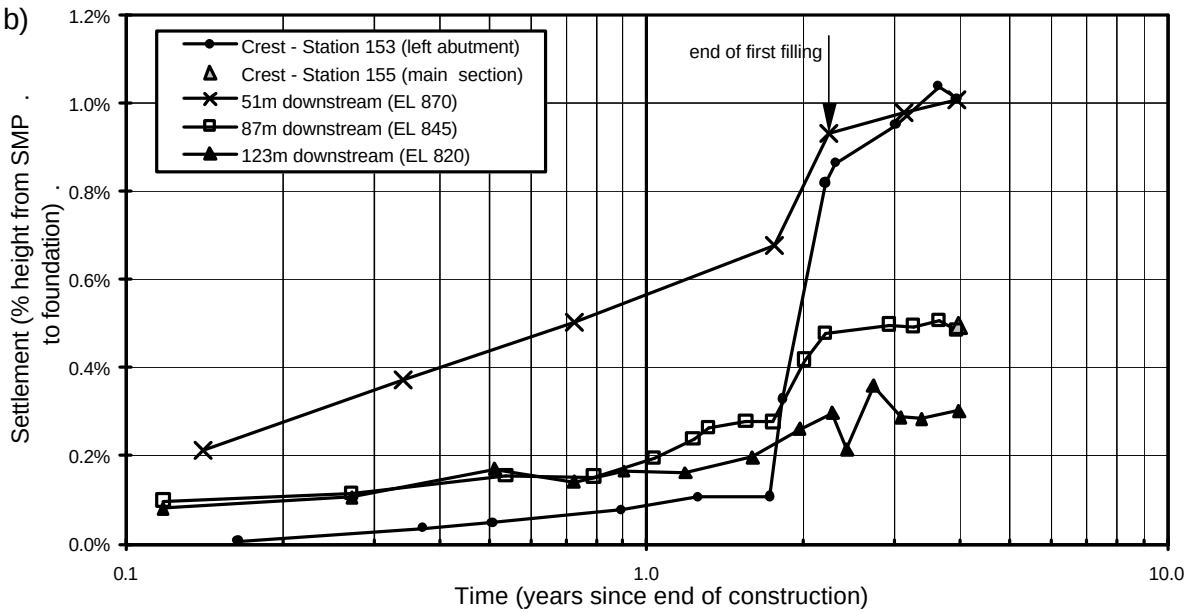

Figure G1.69: Svartevann dam, post construction settlement versus time of the crest and downstream slope.

1.14 TALBINGO DAM

Talbingo dam (Figure G1.70 and Figure G1.71b), located in the Snowy Mountains in southern New South Wales, Australia, is a central core earth and rockfill embankment, with slightly upstream sloping core, of 162 m height and 700 m crest length. The embankment was constructed in the late 1960's, and completed in October 1970. Foundations were stripped to bedrock for all embankment zones. In summary, the materials and placement methods comprised:

- Core (Zone 1) of medium plasticity gravelly clayey sands to sandy clays, sourced from landslide debris comprising slopewash and completely to highly weathered andesite, placed in 150 mm layers and compacted by sheepsfoot rollers. The specified moisture content range was initially from OMC to 2% wet of OMC, but was lowered by 0.8% above about elevation 1430 feet (upper 115 m), presumably due to the very high pore water pressures measured in the lower region of the core. Overall, the average moisture content was equal to Standard optimum, slightly wet in the lower region and slightly dry in the mid to upper region.
- Filters / transition zones (Zones 2A and 2B) of crushed fresh rock placed in 450 mm layers, sluiced and compacted by 4 passes of a 10 tonne smooth drum vibratory roller.

- Rockfill shoulders (Zones 3A, 3B and 3C) of quarried rhyolite and porphyry, placed in 0.9 m (Zones 3A and 3B) to 1.8 m (Zone 3C) layers, sluiced and compacted by 4 passes of a 10 tonne smooth drum vibratory roller. Slightly weathered to fresh rock was used for most of the placed rockfill. The specification allowed for moderately weathered to fresh rock for Zone 3B in the outer downstream shoulder.

A comprehensive range of instrumentation was installed within and on the embankment (Figure G1.71) including internal vertical and horizontal movement gauges (IVM and IHM), hydrostatic settlement cells (HSG), extensometers, surface measurement points (SMP), piezometers and pressure cells.

The reservoir was first filled from May 1971 to January 1972, 0.6 to 1.3 years after construction. Since filling the reservoir has remained steady at close to full supply level.

1.14.1 Embankment Performance During Construction

During the early stages of embankment construction the clay core of Talbingo dam was placed on the wet side of Standard optimum (Howard et al 1978) and very high pore water pressures, 70 to 80% of the total vertical stress measured by pressure cells, were developed in this region of the core (HP8 and HP16 in Figure G1.72). Drier placement of the core above about elevation 1430 feet (upper 115 m), following reduction of the moisture specification by 0.8%, significantly reduced the magnitude of positive pore water pressure as shown for Piezometer HP23 in Figure G1.72.

The pressure cells within the core also showed a change in response associated with the reduction in moisture content specification (Howard et al 1978). In the lower, wet placed region of the core high total horizontal stresses, equivalent to 80 to 100% of the measured total vertical stress, were measured and maintained during the period of construction and for many years after. Reduced horizontal stresses were measured in the mid to upper drier placed region of the core, ranging from 15 to 60% of the measured total vertical stress.

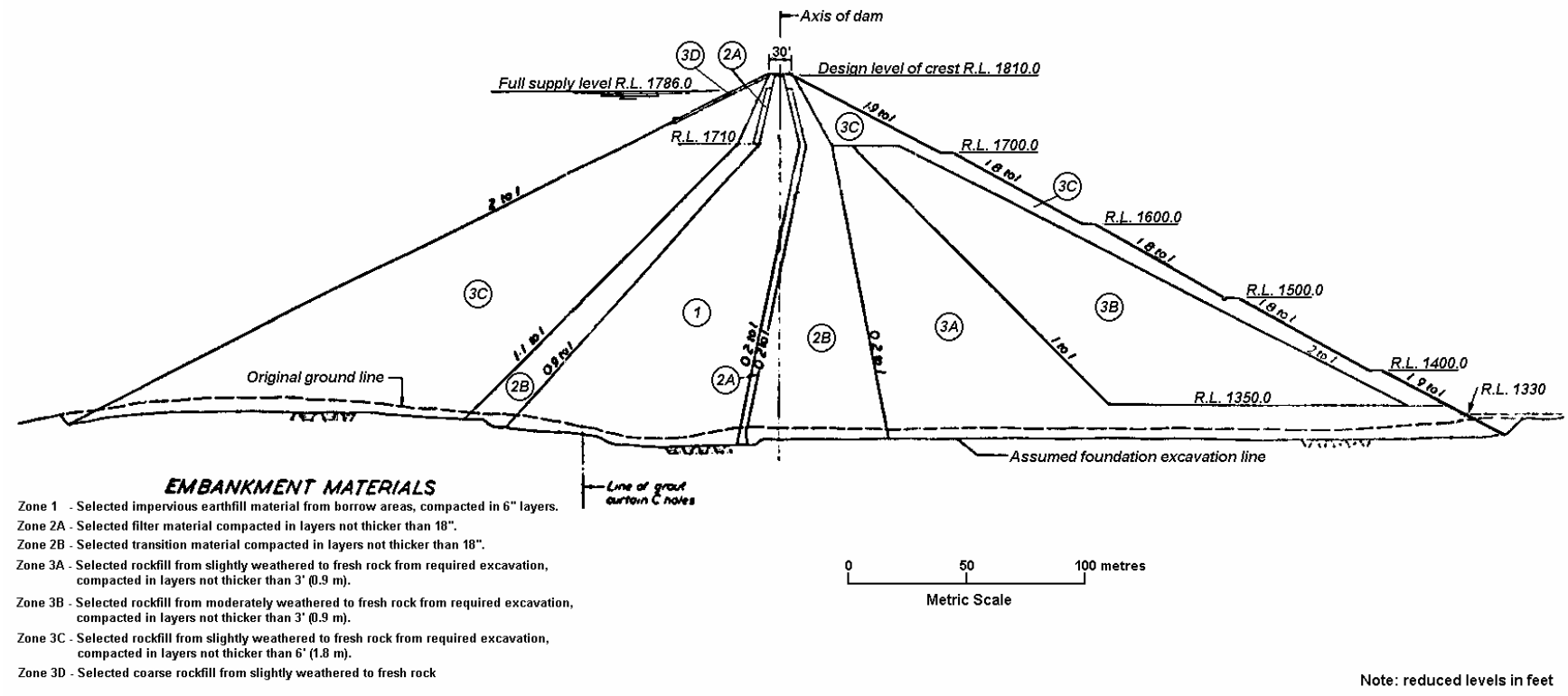

Figure G1.70: Talbingo dam, main section at Station 22+00 (courtesy of Snowy Mountains Hydro Electric Authority).

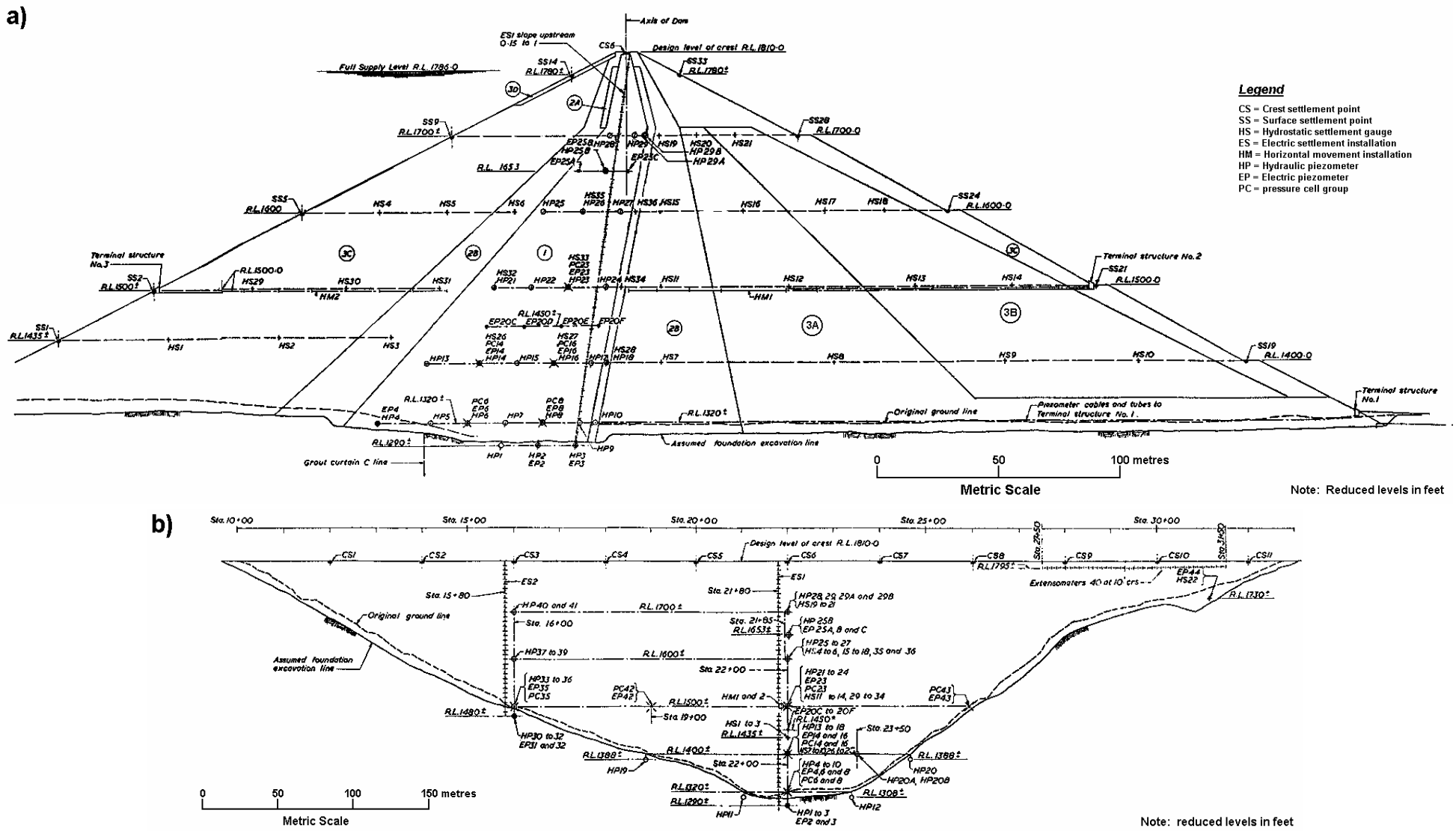

Figure G1.71: Talbingo dam, instrumentation *(a)* main section and *(b)* longitudinal section (courtesy Snowy Mountains Hydro Electric Authority)

The measured total vertical stresses in the lower central region of the core (Figure 7.7 in Section 7.4 of Chapter 7) closely approximated those estimated for a homogeneous embankment condition indicating arching had a negligible influence on the total stresses in the central region of the core. However, the internal settlements (Figure G1.73) and pore water pressure response suggests that arching of the core occurred in the vicinity of the near vertical downstream filter / transition, but not in the upstream region of the core near to the sloping core / filter interface. Pore water pressures measured in the upstream region of the core were similar in magnitude to those in the central region of the core; however, in the downstream region pore water pressures were much lower. Measured internal settlements at elevation 1500 feet (Figure G1.73) show a similar response, with similar magnitude settlements in the central to upstream part of the core but much lower settlements in the downstream part of the core. Settlements in the filter and transition zones, both up and downstream of the core, were much smaller and are indicative of the high modulus of these materials, estimated at greater than 100 to 120 MPa.

For the Zone 3A rockfill the settlement during construction was intermediate to that of the core and filter zones. Secant moduli for the Zone 3A rockfill were estimated, from the monitored settlement records, to be in the range 40 to 100 MPa. Lower moduli were estimated for the Zone 3A rockfill below about elevation 1400 feet and higher moduli above this elevation.

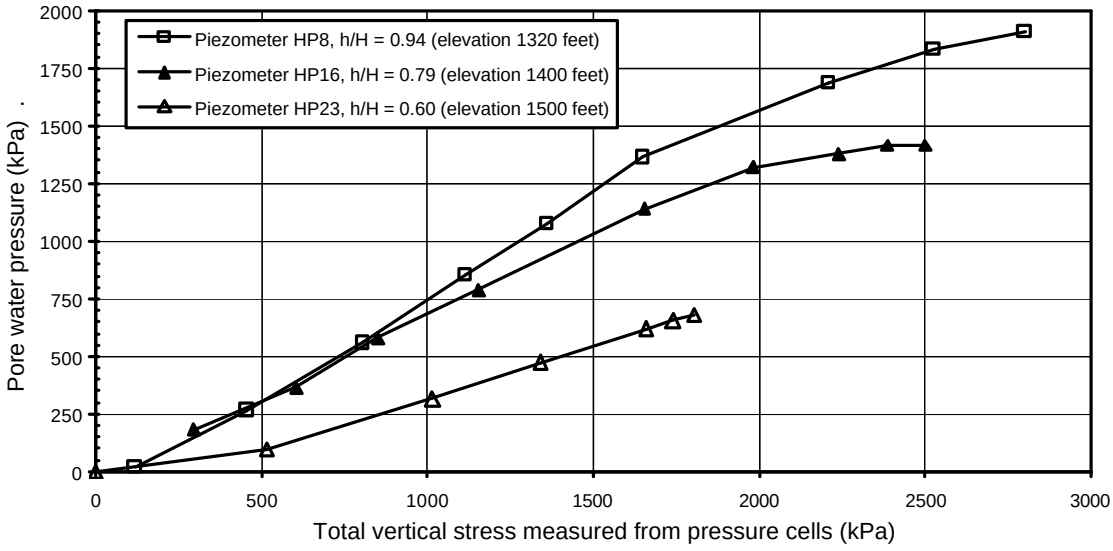

Figure G1.72: Talbingo dam; pore water pressure development in the core during construction.

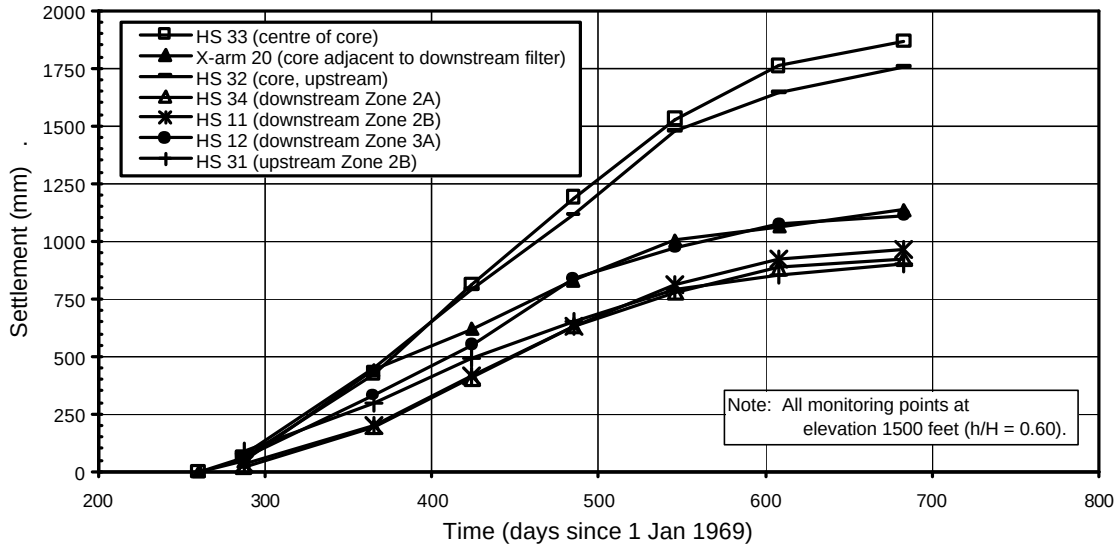

Figure G1.73: Talbingo dam; monitored internal settlements during construction in the core, filters, transition and rockfill zones at elevation 1500 feet (h/H = 0.60).

The internal vertical strain profile in the core at end of construction (Figure G1.74) is comparable to that observed in similar embankments with wet placed cores (Figure 7.22 in Section 7.4 of Chapter 7). The lower strains recorded below about 100 m depth at the main section (below about elevation 1500 feet) are most probably due to arching between the core and downstream filter, affected by the close proximity of IVM ES1 to the downstream filter at these elevations (Figure G1.71a).

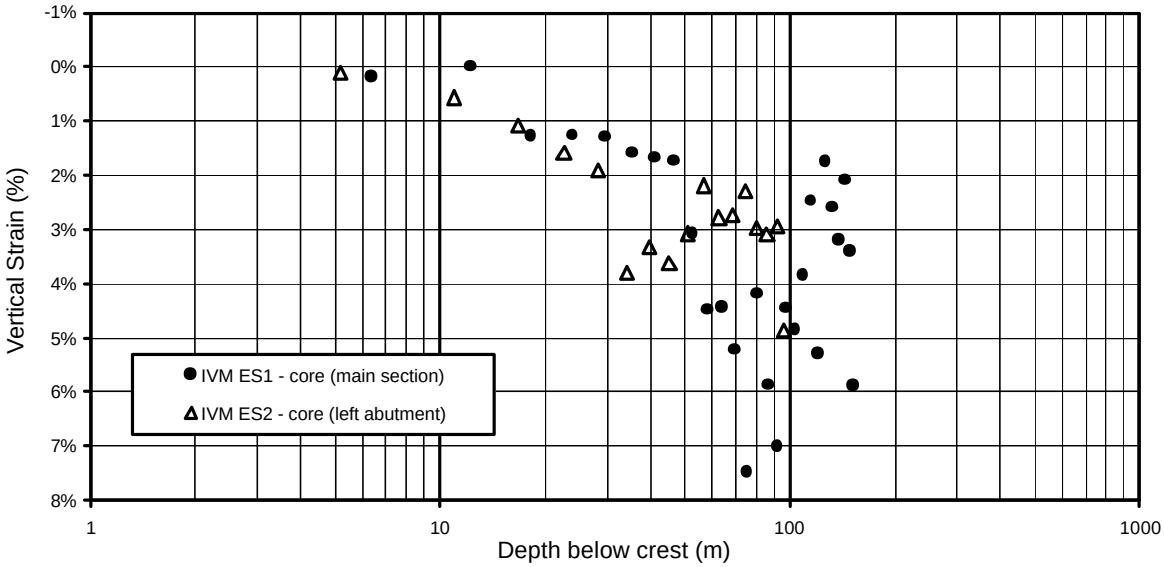

Figure G1.74: Talbingo dam; internal vertical strain profiles in the core at end of construction.

1.14.2 Embankment Performance Post Construction

The cumulative post construction settlement plot of IVM ES1 at Talbingo dam (Figure G1.75), located in the core at the main section, is considered representative of "normal" type deformation behaviour. The greater post construction vertical strains in the lower 40 to 50 m (average of 0.7% at 24 years post construction) are within the wetter placed region of the core below about elevation 1430 feet. The larger vertical strains in this region are considered to be due to consolidation type settlements as indicated by the large dissipation of pore water pressure of as much as 600 to 1100 kPa over a 20 plus year period post first filling. Construction pore water pressures were very high in this region of the core (Figure G1.72) and on first filling increased by some 200 to 400 kPa before slowly dissipating. In the mid region of the core the magnitude of the reduction in pore water pressures due to dissipation post first filling was much less and is reflected in the lower vertical strains in this region (average of 0.3% at 24 years post construction).

The localised zone of high settlement between 55 and 58 m depth below crest level is considered to most probably be a systematic error in the IVM readings. The large localised settlement occurred in the period between 0 and 0.15 years post construction, prior to first filling, and since then the differential settlement between these cross-arm gauges has increased only marginally. In addition, the vertical strain during construction at this location was not unusually high in comparison to the adjacent regions. Therefore, the localised settlement is not likely to be due to localised plastic deformation of a wet placed layer and nor is it likely to be a shear type displacement.

The post construction settlement and displacement normal to the dam axis of SMPs on the crest and slopes are shown in Figure G1.76. The base survey of SMPs used was just prior to the end of construction and the next survey was at 1.6 to 2 years, after the period of first filling. The monitored records show:

- Greater settlement of the upstream slope than the crest and downstream slope over the period of first filling.
- Uniform settlement rates (per log cycle of time) over the monitored period for each SMP as well uniform rates between the SMPs.
- Downstream displacement of all SMPs post construction, most of which occurred during first filling. Post first filling the downstream displacement of the crest and upstream slope approach a near zero rate and for the downstream slope approaches a low steady downstream rate (per log cycle of time).

The post construction trend and magnitude of the deformation behaviour of Talbingo dam, in comparison to similar type embankments, is considered to be "normal". The steady level of the reservoir, which has remained at close to full supply level since first filling, is considered largely responsible for the uniform rate and very little fluctuation of the deformation post first filling.

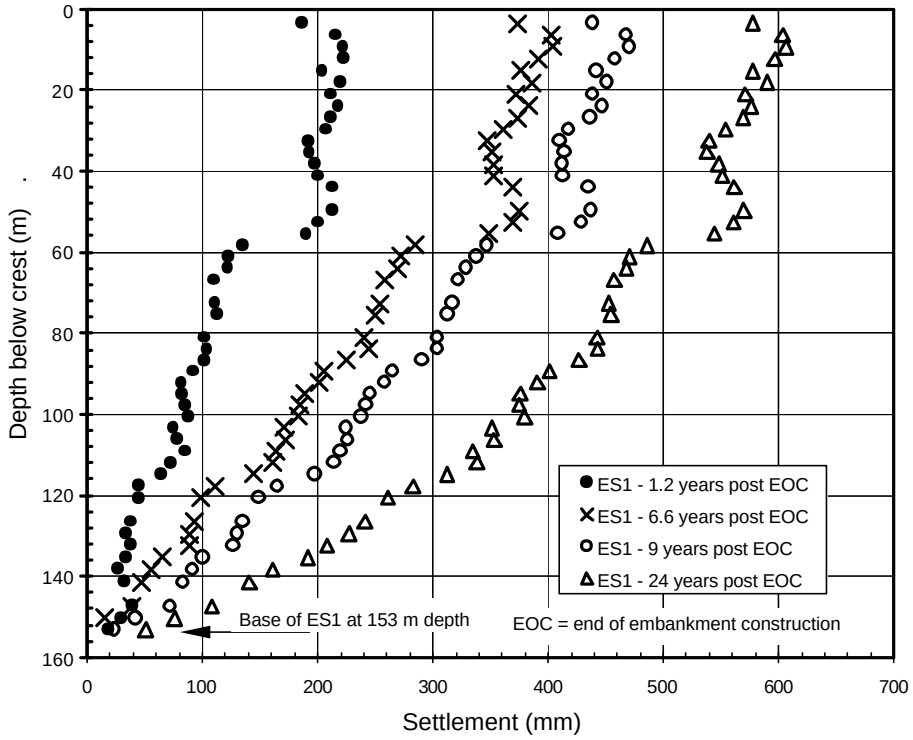

Figure G1.75: Talbingo dam, post construction internal settlement in the core at the main section (IVM ES1).

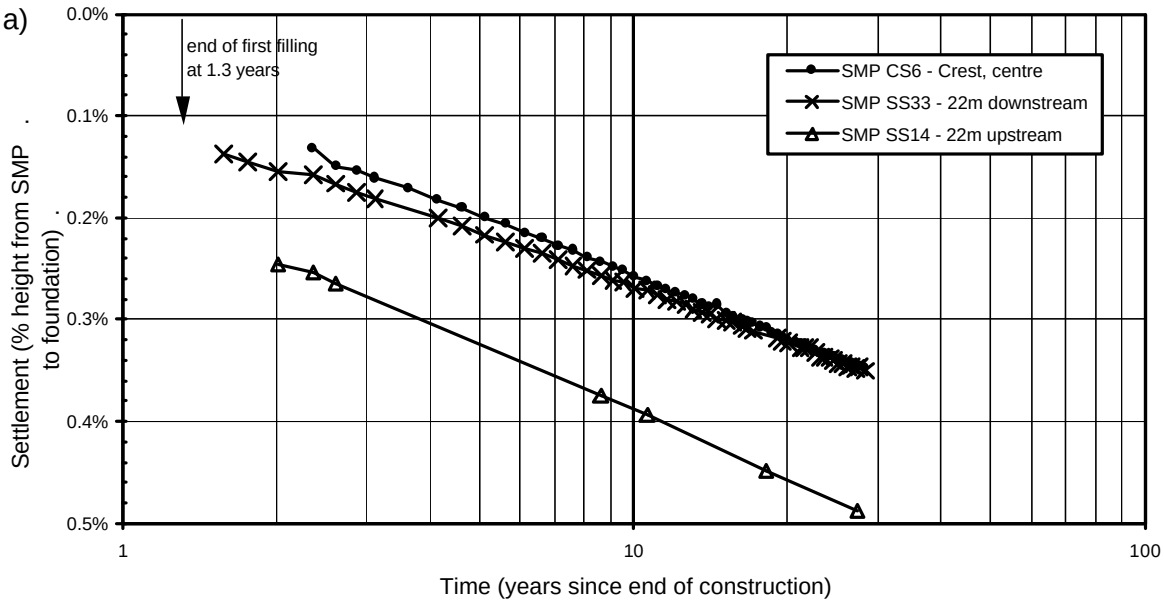

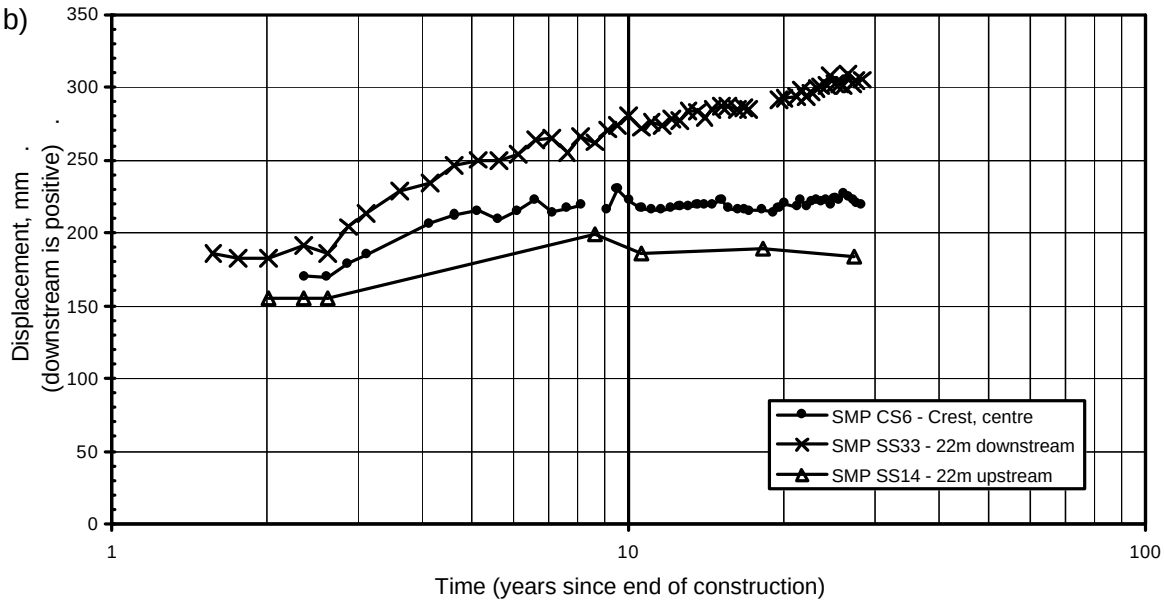

Figure G1.76: Talbingo dam; post construction *(a)* settlement and *(b)* displacement normal to the dam axis for SMPs on the crest and slopes.

1.15 UPPER YARRA DAM

Upper Yarra dam (Figure G1.77 and Figure G1.78), located in southern Victoria, Australia, is a central core earth and rockfill dam of 90 m maximum height and 610 m crest length. As shown in Figure G1.77 the embankment has an unusual core geometry that changes in width and slopes at various elevations. Embankment construction was started in early 1954 and completed in about March 1957. Foundations for all embankment zones were stripped to bedrock. In summary, the materials and placement methods (SMEC 1998b) comprised:

- Central core of low to high plasticity sandy clays, sourced from alluvial and colluvial deposits, placed in 200 mm layers and compacted by sheepsfoot and grooved drum rollers. The moisture specification was for placement between 2% dry of OMC and OMC (OMC = Standard optimum moisture content).
- Broad transition zones upstream and downstream of the core of decomposed or "soft" sandstone and siltstone placed and compacted to the same specification as the core. The compacted "soft" rock classified as a clayey sand to clayey gravel with low plasticity fines. Recent investigations found that for at least the upper 6 m of the embankment the transition zone earthfill was of very similar material type to the core.

- Rockfill shoulders of "*firm to hard* [quarried] *sandstones and siltstones*" placed in 1.5 m lifts without formal compaction. There was no indication that water was added during placement. SMEC (1998b) state that the "*main body of rockfill has been described as being generally moderately to highly weathered material, with up to 50% fines (although no grading records are available)*". Presumably by fines they mean minus 20 to 25 mm sized rock fragments. To generate such a high percentage of fines it is likely that the weathered rock in the rockfill was susceptible to mechanical breakdown on handling and placement.

The reservoir was filled from July 1957 to December 1958, 0.4 to 1.8 years after the end of construction. Post first filling the reservoir is subjected to a seasonal drawdown varying in magnitude from 5 to 35 m (Figure G1.80a).

Instrumentation (Figure G1.78) consisted of two internal settlement gauges (IVM) in the core, piezometers in the core and transition zones, and SMPs on the crest and slopes. The base survey for the SMPs was August 1957, 0.4 years after the end of construction.

1.15.1 Deformation During Construction

Comparison of the vertical strain profiles in the core at end of construction from the IVM gauges (Figure G1.79) to similar type embankments (Figure 7.18a in Section 7.4 of Chapter 7) indicates "normal" type deformation behaviour. Vertical strains at end of construction increase with increasing depth below the crest (or increasing effective vertical stress), reaching maximum strains in the order of 4 to 4.5% near the base of the core.

In calculation of effective vertical stresses for Figure 7.18a (Chapter 7), pore water pressures and suctions were assumed to be negligible. Even though piezometers were installed during construction, no records were available prior to 1959 and the assumption of negligible pore water pressure is based on placement of the core on the dry side of Standard optimum.

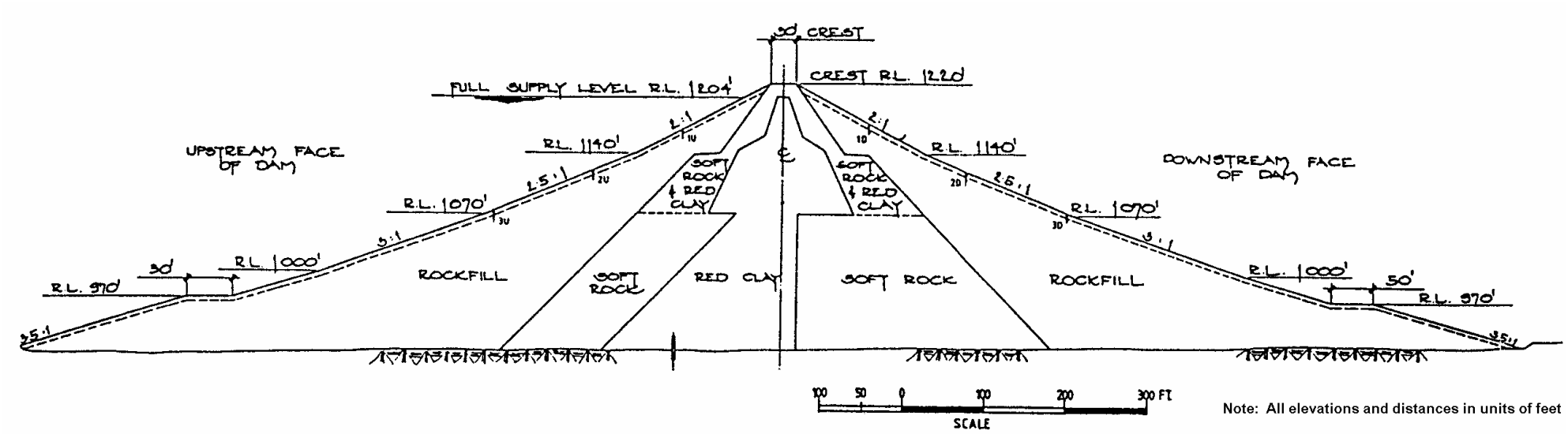

Figure G1.77: Upper Yarra dam; main cross section at chainage 2000 feet (courtesy of Melbourne Water Corporation).

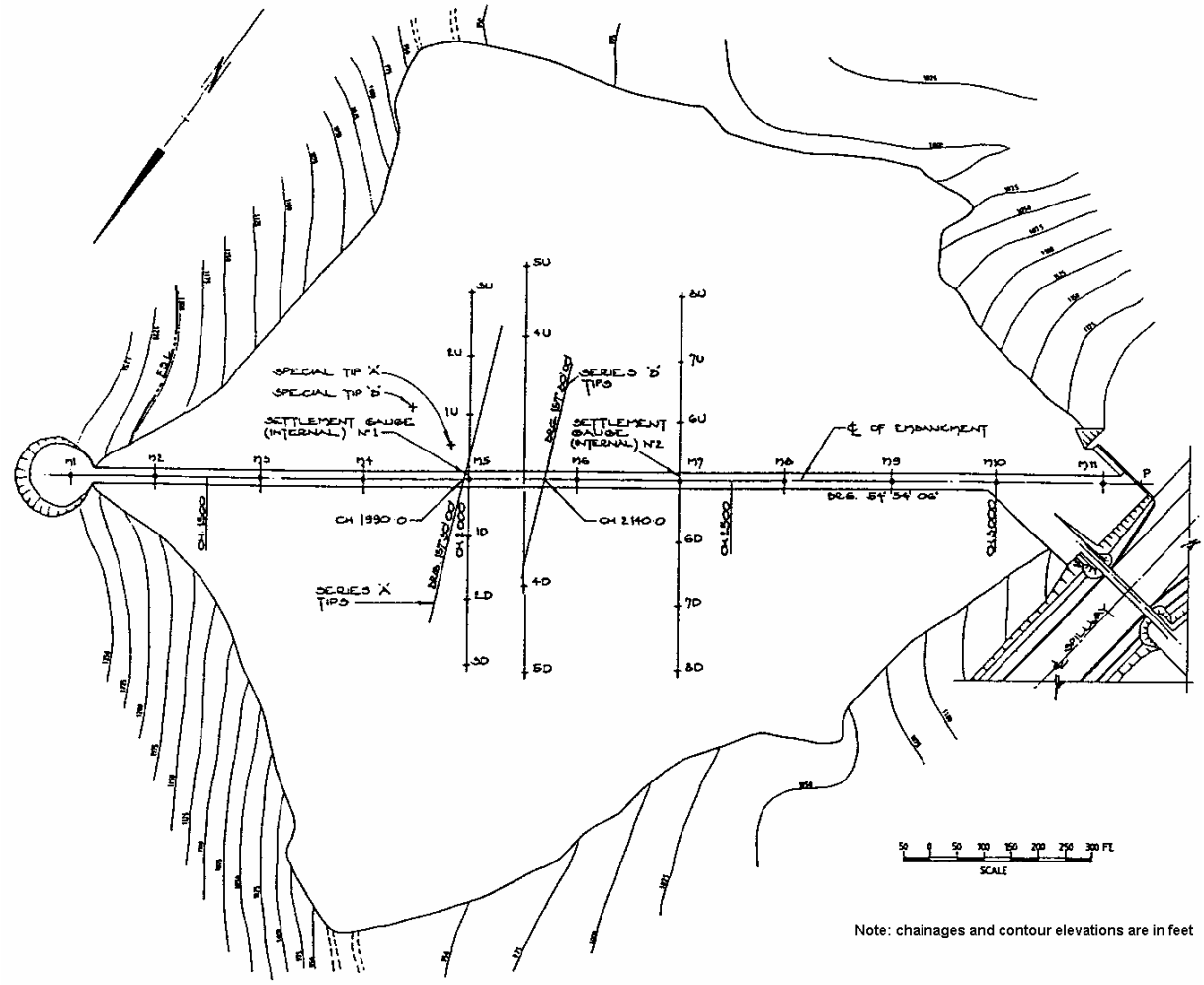

Figure G1.78: Upper Yarra dam; plan showing locations of SMPs and cross-arm (IVM) gauges (courtesy of Melbourne Water Corporation).

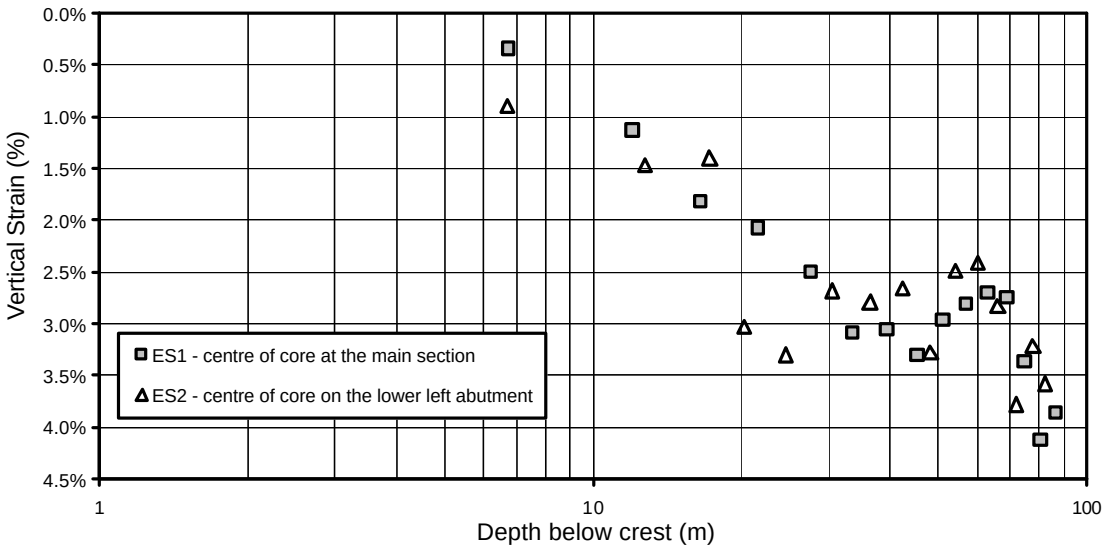

Figure G1.79: Upper Yarra dam; vertical strain profiles in the core at end of construction.

1.15.2 Deformation Post Construction

The post construction settlement and displacement of SMPs on the crest and upper shoulders at the main section of Upper Yarra dam are shown in Figure G1.80 and Figure G1.81 respectively. In comparison to similar embankments, the post construction deformation behaviour of the SMPs at Upper Yarra dam shows some trends that are somewhat anomalous to the general behaviour of most dams; these include:

- Periods of sharp increase in the crest settlement rate on large drawdown post first filling (Figure 7.58 in Section 7.6 of Chapter 7). At SMP M5 acceleration of the settlement occurred during large drawdown in 1967/68 (5 to 6 years), 1979/80 (23 years) and 1993 (36 years); settling approximately 95 mm on the 33.5 m drawdown of 1967/68, approximately 30 to 35 mm on the 30 m drawdown of 1979, and approximately 22 mm on the 30 m drawdown of 1993.
- The change in direction of the trend of crest displacement from initially downstream to upstream some 6 to 7 years after first filling (Figure 7.73 in Chapter 7). Long-term (after about 27 years), the crest displacement trend is steady to slightly downstream.
- The long-term settlement rates of the upstream and downstream slopes are on the high side (Figures 7.78 and 7.83 in Section 7.6 of Chapter 7), but they are not excessively high as to be considered “abnormal”.

The acceleration in crest settlement on large drawdown in 1967/68, 1979/80 and 1993 was observed for the crest SMPs between the mid abutment slopes (i.e. all but the crest SMPs on the higher abutment slopes) covering a crest length of about 400 to 425 m. It is notable that the magnitude of settlement on drawdown decreases with each subsequent large drawdown event. The acceleration in settlement was triggered when the reservoir level was drawn down below about RL 345 to 350 m (reservoir gauge level of 36 to 42 m) during the 1967/68 drawdown and below this level on later large drawdowns (about RL 341 m or reservoir gauge level of about 33 to 35 m). The acceleration is not observed on all large drawdowns (Figure G1.80a).

The internal settlement gauges in the core (IVM ES1 and ES2) were monitored for the post construction period up to late 1972 (to 15.6 years after the end of construction). The post construction settlement profile of the core at IVM ES1 at various stages after construction is shown in Figure G1.82. During the 1967/68 drawdown the records show a concentration in vertical strain occurred between 11.2 and 14.3 m depth below crest

level (between cross-arms 52 and 54). The development with time of the differential vertical settlement between cross-arms 52 and 54 is shown (Figure G1.83) to largely occur during the latter part of the drawdown at 10 to 12 years, then ceasing at the end of drawdown. This figure also shows that of the 110 mm crest settlement at SMP MP5 over the period from 9 to 12 years after construction, 75 mm (or 70%) occurred between this cross-arm interval. Similarly at IVM ES2, vertical strains in the core on drawdown in 1967/68 were concentrated within the zone from 17.3 to 20.2 m depth below crest level (cross arms 45 to 47). The IVMs were not monitored after 1972, so no data on internal vertical strains in the core is available for the later large drawdowns.

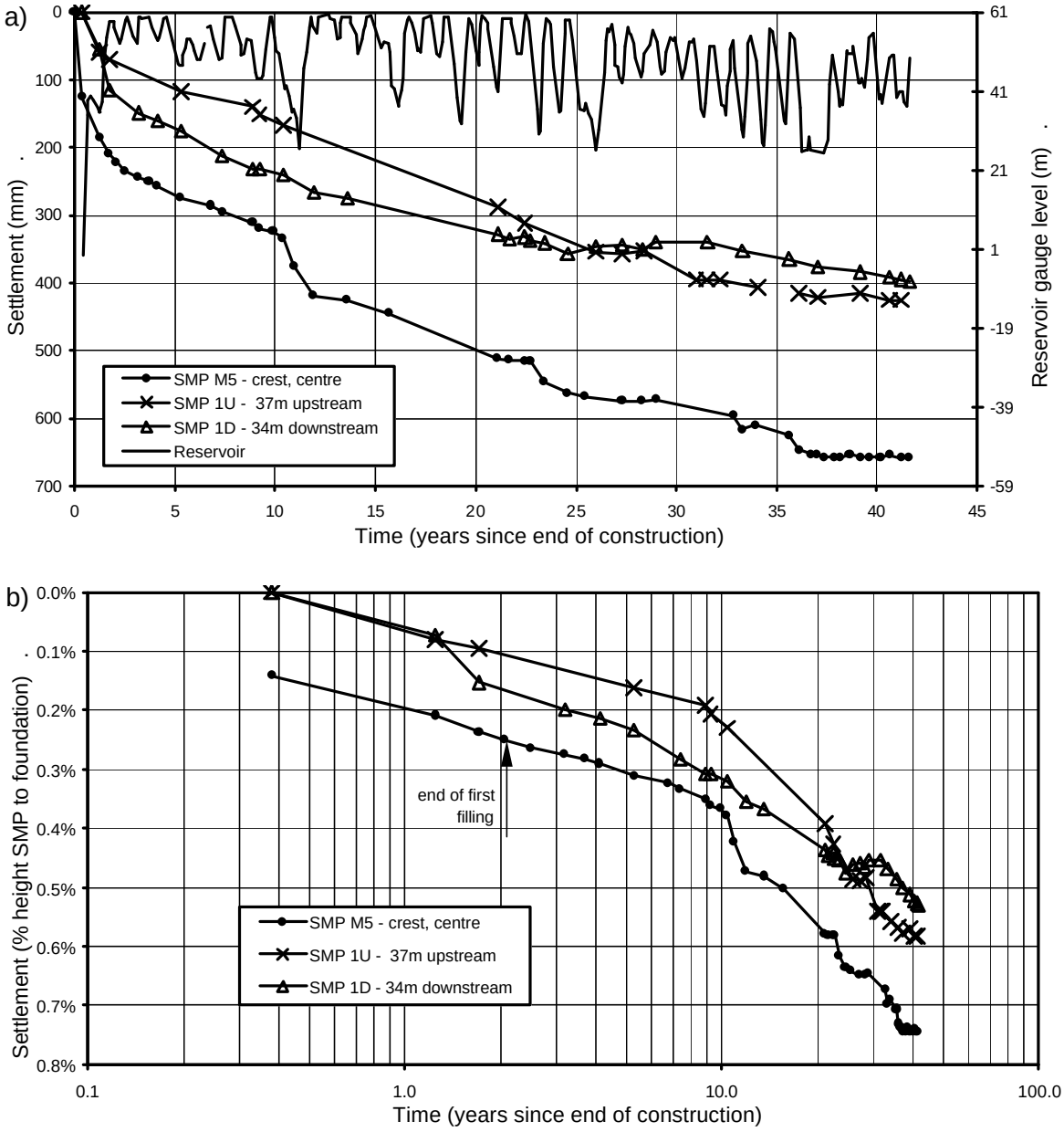

Figure G1.80: Upper Yarra dam, post construction settlement of SMPs versus time.

Investigation of the potentially "abnormal" deformation behaviour of Upper Yarra dam is still under investigation by the owners consultants. Investigation by test pit and cone penetration testing has been undertaken in recent years, and inclinometers have been installed in the core to monitor lateral displacements. The consultants have confirmed that stability of the upstream slope is adequate under drawdown and that the piping potential is of negligible concern.

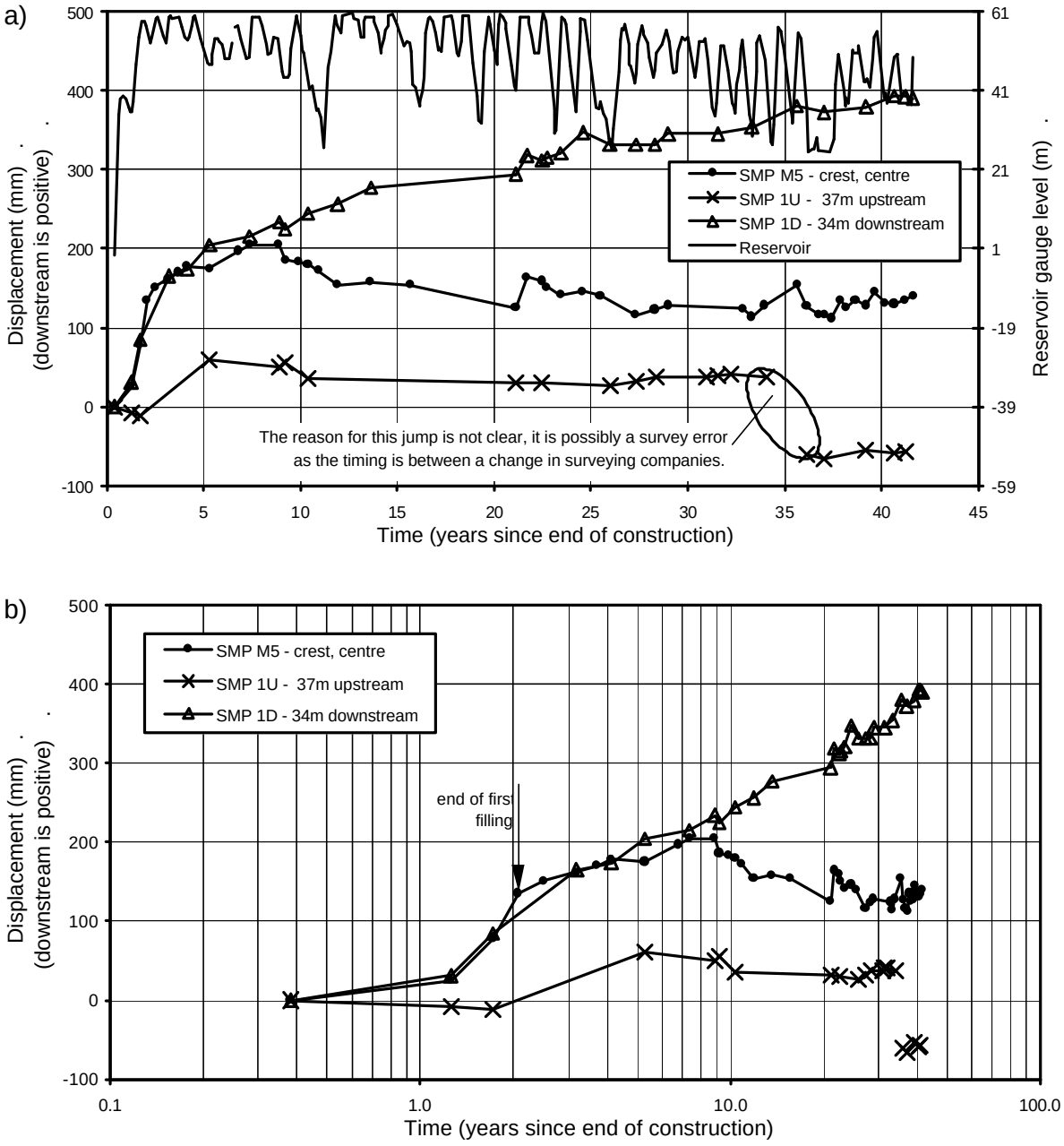

Figure G1.81: Upper Yarra dam, post construction displacement normal to the dam axis versus time.

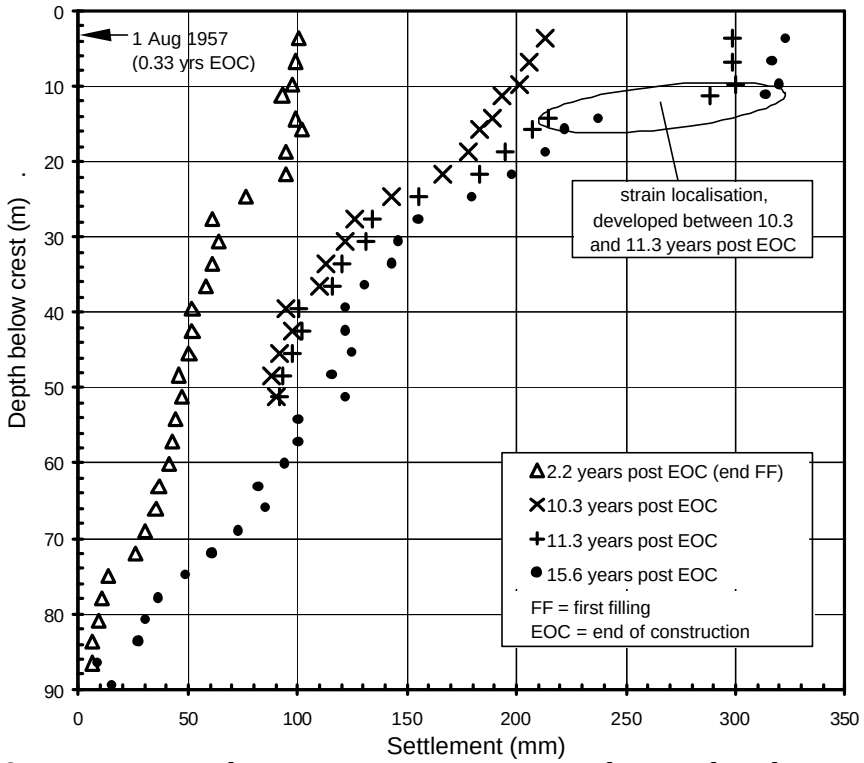

Figure G1.82: Upper Yarra dam, post construction internal vertical settlement profiles at IVM ES1.

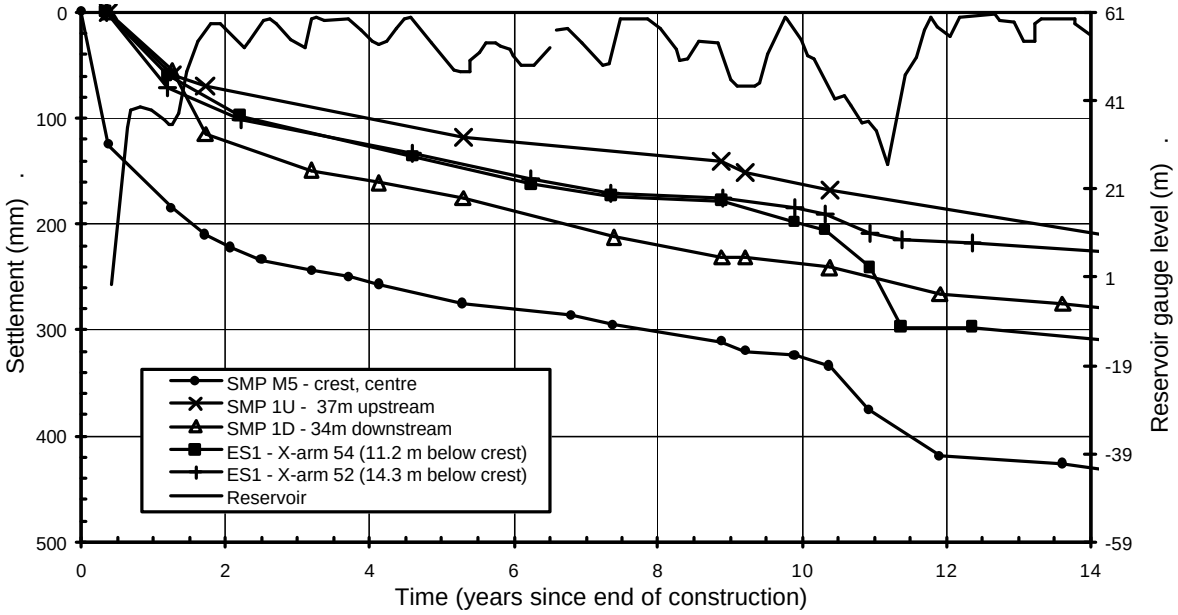

Figure G1.83: Upper Yarra dam; localised settlement at 11.2 to 14.3 m depth in IVM ES1 on first large drawdown.

1.16 WYANGALA DAM

Wyangala dam (Figure G1.84), located on the Lachlan River in central New South Wales, Australia, is a central core earth and rockfill dam of 85 m maximum height and 1510 m crest length. In the deeper valley section the old concrete dam forms the upstream toe of the earth and rockfill dam. Foundations for the embankment were stripped to bedrock. The embankment was constructed in the 1960's, and completed in May 1968. The materials and placement methods for the earth and rockfill embankment are summarised as follows:

- Central core (Zone 1) of silty to clayey sands, sourced from residual granite, placed in 150 mm layers and compacted using sheepsfoot rollers achieving a high density ratio (average of 102% of Standard maximum dry density). The average moisture content was 1% dry of Standard optimum.
- Filters of river sands and gravels (Zone 2A) and crushed rock (Zone 2B) placed in 300 mm layers and compacted by vibratory rollers.
- Rockfill of mostly quarried porphyritic gneiss of high to very high compressive strength when fresh, forming the following zones:
  - Zone 3A – transition zone of rockfill downstream of the core placed in 0.9 m layers and compacted with 3 passes of an 8.5 tonne vibratory roller.
  - Zone 3B – inner rockfill zone placed in 1.2 m layers and compacted with 3 passes of an 8.5 tonne vibratory roller.
  - Zone 3C – outer rockfill zone placed in 2.4 m layers and compacted with 6 passes of an 8.5 tonne vibratory roller.
  - No water was added to Zones 3B and 3C during placement and compaction.

First filling took almost 6 years from May 1968 to February 1974. Post first filling the reservoir level has fluctuated between full supply level and 45 to 50 m below this level, but is not subjected to an annual drawdown.

The embankment was instrumented with piezometers and vertical settlement gauges (IVM) in the core; hydrostatic settlement gauges, horizontal and vertical deformation gauges in the downstream shoulder, and SMPs on the crest and slopes of the embankment. The locations of SMPs and IVMs in the core at the main section are shown in Figure G1.85.

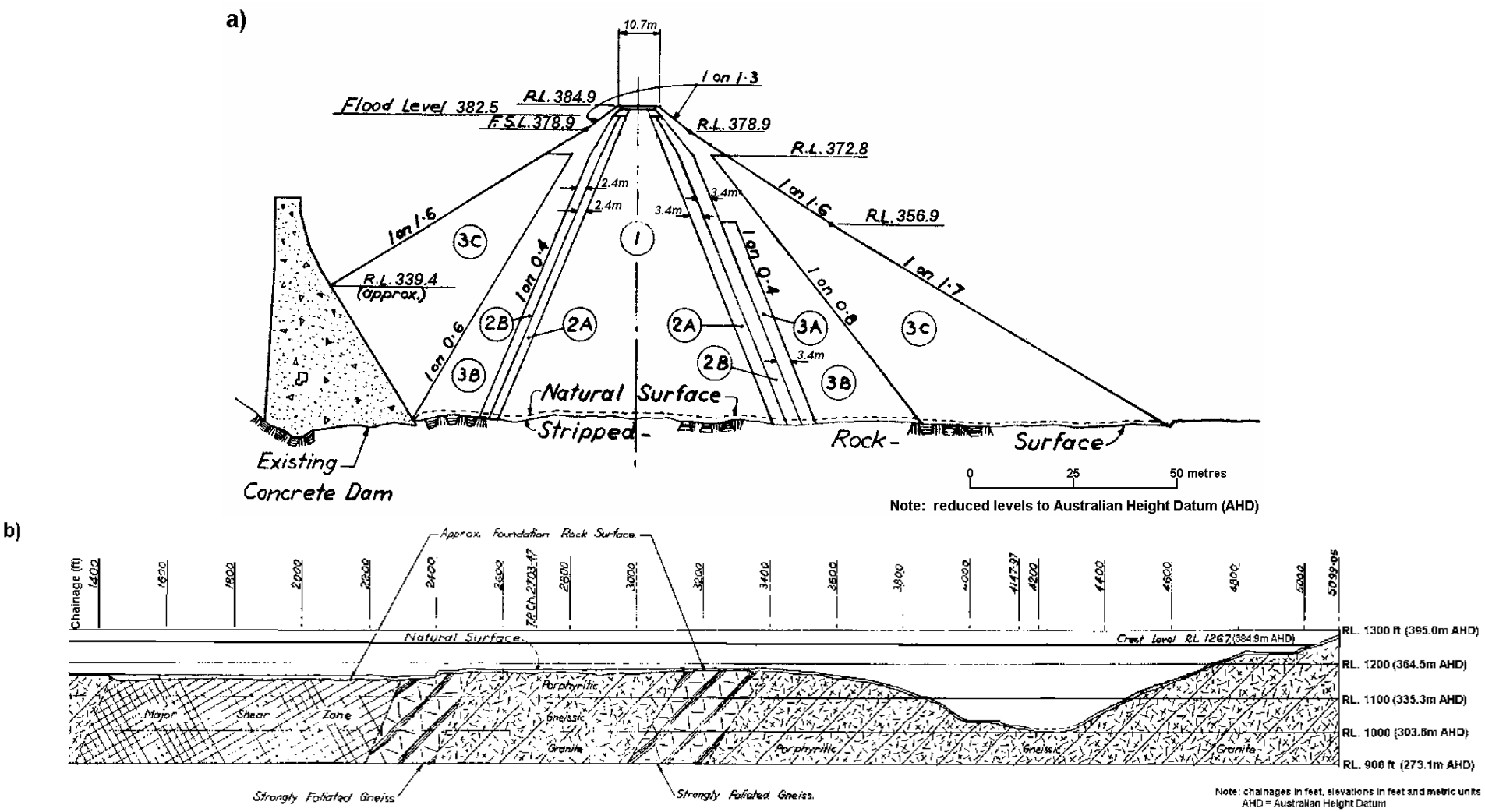

Figure G1.84: Wyangala dam, *(a)* main section and *(b)* longitudinal section (courtesy of New South Wales Department of Land and Water Conservation).

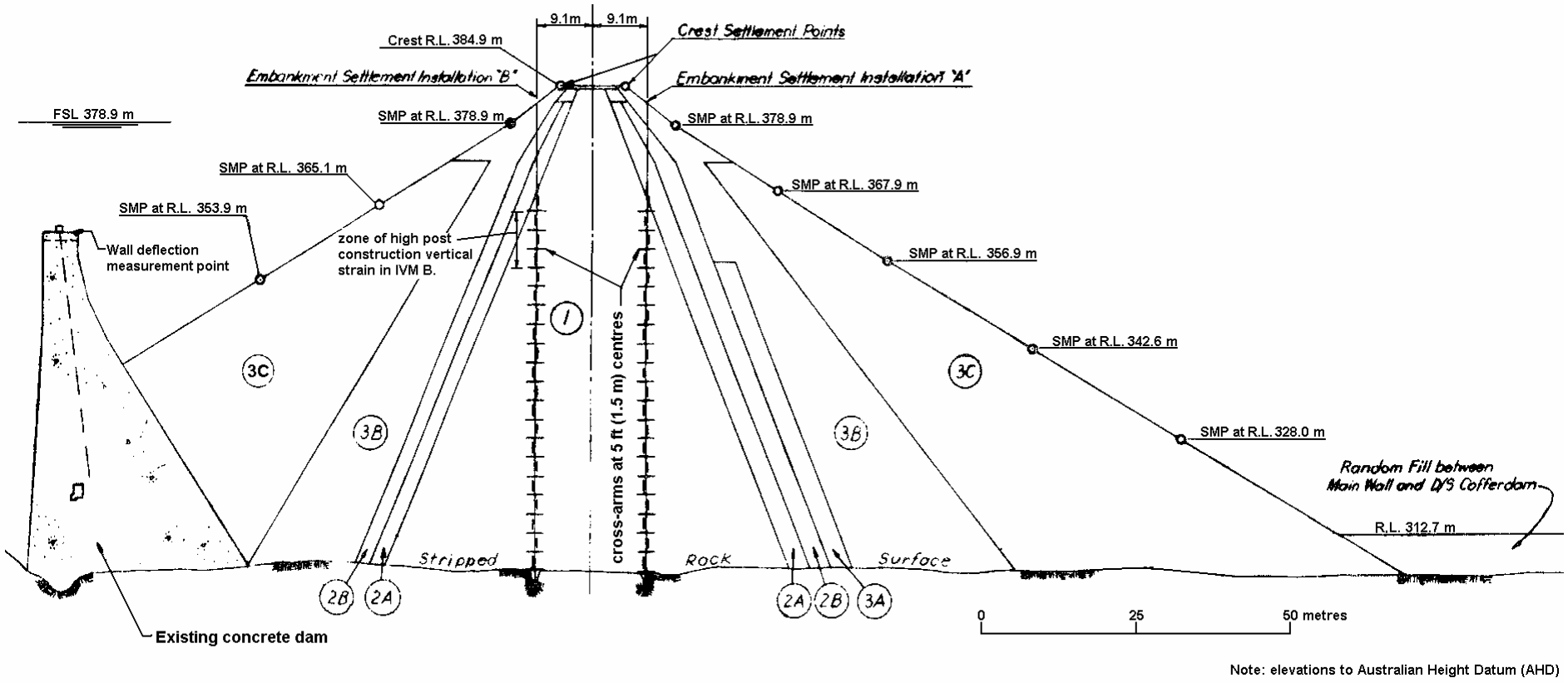

Figure G1.85: Wyangala dam; SMP and IVM locations at main section (courtesy of New South Wales Department of Land and Water Conservation).

During construction, the deformation behaviour of Wyangala dam was considered "normal" in comparison to other similar dams. Vertical strains in the core were relatively low and estimated secant moduli relatively high, in the order of 40 to 65 MPa (Figures 7.16 and 7.19 in Section 7.4 of Chapter 7). The estimated lateral displacement ratio of the core (Figure 7.12 in Chapter 7) was low in comparison to other central core earth and rockfill dams.

Post construction, the deformation behaviour of Wyangala dam was, for the most part, considered "normal". But, several unusual or potentially "abnormal" aspects were evident in comparison to similar type embankments, these and other notable aspects of the deformation behaviour are:

- During first filling, the settlement of all SMPs is similar for the first 4 to 4.5 years. It is not until the reservoir level was raised the last 10 m to full supply level that greater settlements were observed for the upstream crest to upstream slope region, probably due to collapse type settlements of the upstream rockfill.
- The surface settlement at the main section (Figure G1.86) shows an increase in the rate of settlement of the crest (both upstream and downstream edges) and upstream slope on large drawdown over the period 10.5 to 13 years (1979 to 1981). A very slight increase in settlement rate is perceptible at year 26 during a 20 m drawdown.

- The displacement normal to the dam axis (Figure G1.87) shows:
  - A possible non-recoverable upstream displacement of the upstream edge of the crest and upstream slope during the large drawdown from 10.5 to 13 years. It is also possibly that this also occurred for SMP 32 on the downstream edge of the crest.
  - Sometime after the large drawdown, but before 24 years, the displacement of SMP 41 at the upstream edge of the crest developed a displacement trend to upstream. In comparison to similar embankments (Figure F2.32 of Appendix F) this displacement trend is possibly "abnormal". The SMPs on the upstream shoulder and downstream edge of the crest do not display this trend; they are more in line with "normal" type behaviour.
  - The downstream slope displaces independently of the remainder of the embankment, showing a downstream displacement on and post first filling. The rate of displacement post first filling is on the high side compared to similar type embankments (Figure F2.11 of Appendix F).

- The post construction internal settlement profile in IVM B (Figure G1.88), located 9 m upstream of the dam axis, shows very high vertical strains developed in the core between 23 and 32 m depth below crest level (1.85% at 21 years after end of construction). This is very much higher than the average vertical strain of 0.48% in IVM A at a similar depth (Figure G1.89) and the low vertical strain (less than 0.15%) in the mid to lower region of the core at IVM B. The localised high strains at 23 to 32 m depth below crest level in IVM B developed steadily over the first 11.5 years (1.2% vertical strain at 11.5 years), but increased in rate in the period from 11.5 to 17 years (0.5% vertical strain over this period for a total of 1.7% to 17 years).

The magnitude of the post construction settlements of the embankment shoulders and crest are comparable with those measured for similar type embankments. Collapse type settlements of the dry placed porphyritic gneiss rockfill are evident from the difference in settlement between the up and downstream edges of the crest, but the influence is small.

Of more significance is the high post construction strains observed in the core at IVM B between 23 and 32 m depth and the acceleration in settlement and possible non-recovered upstream displacement of the crest and upstream slope on large drawdown over 10.5 to 13 years. As shown in Figure G1.85, the region of high strain in the core is located at close to the upstream core interface with the filters. The magnitude of settlement between the cross-arms (over the region of high strain) totals 155 mm in 17 years, which is approximately equivalent to the differential settlement between the up and downstream edges of the crest (about 100 to 120 mm) plus the settlement in IVM A over the same depth range (20 to 30 mm). The deformation data would indicate the region of high strain relates to differential movement between the core and upstream shoulder. Whilst this is a shear type movement in itself, a single distinct shear surface does not appear to have been developed as indicated by the broad width of the region of high strain. It is possible that a series of shears may have developed or that general softening of the earthfill may be a factor within the zone of high strain.

The increase in rate of settlement on drawdown and possible (but not definite) non-recovered upstream displacement of the full width of the crest and upstream slope would suggest that the shear zone may extend across the full width of the core. The acceleration in deformation rate on drawdown is possibly due to the reduction in the

hydrostatic pressures acting on the upstream face of the core and deformation between the core and upstream shoulders in re-establishing equilibrium lateral stress conditions.

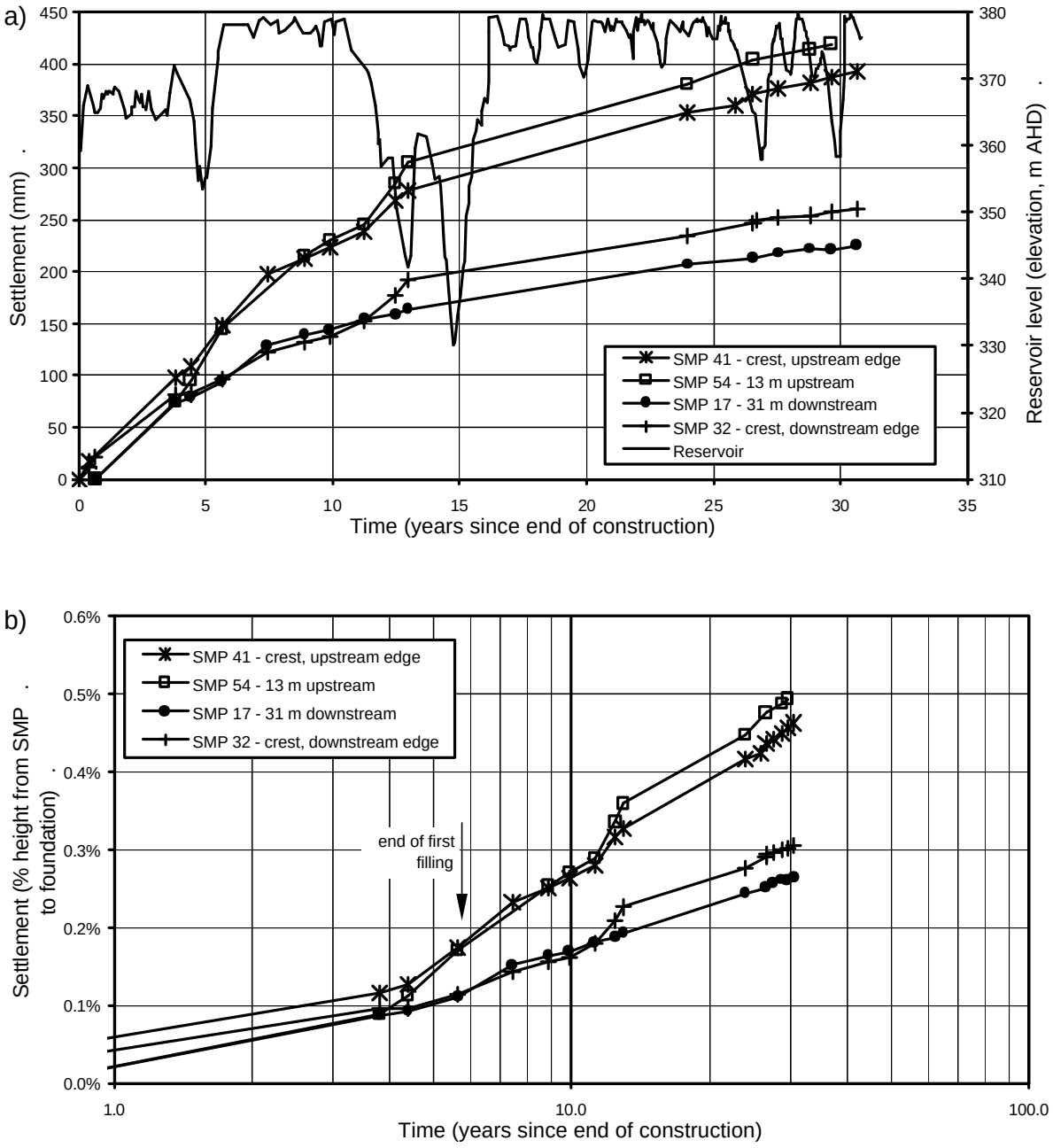

Figure G1.86: Wyangala dam, post construction settlement of SMPs on the crest and slopes at the main section.

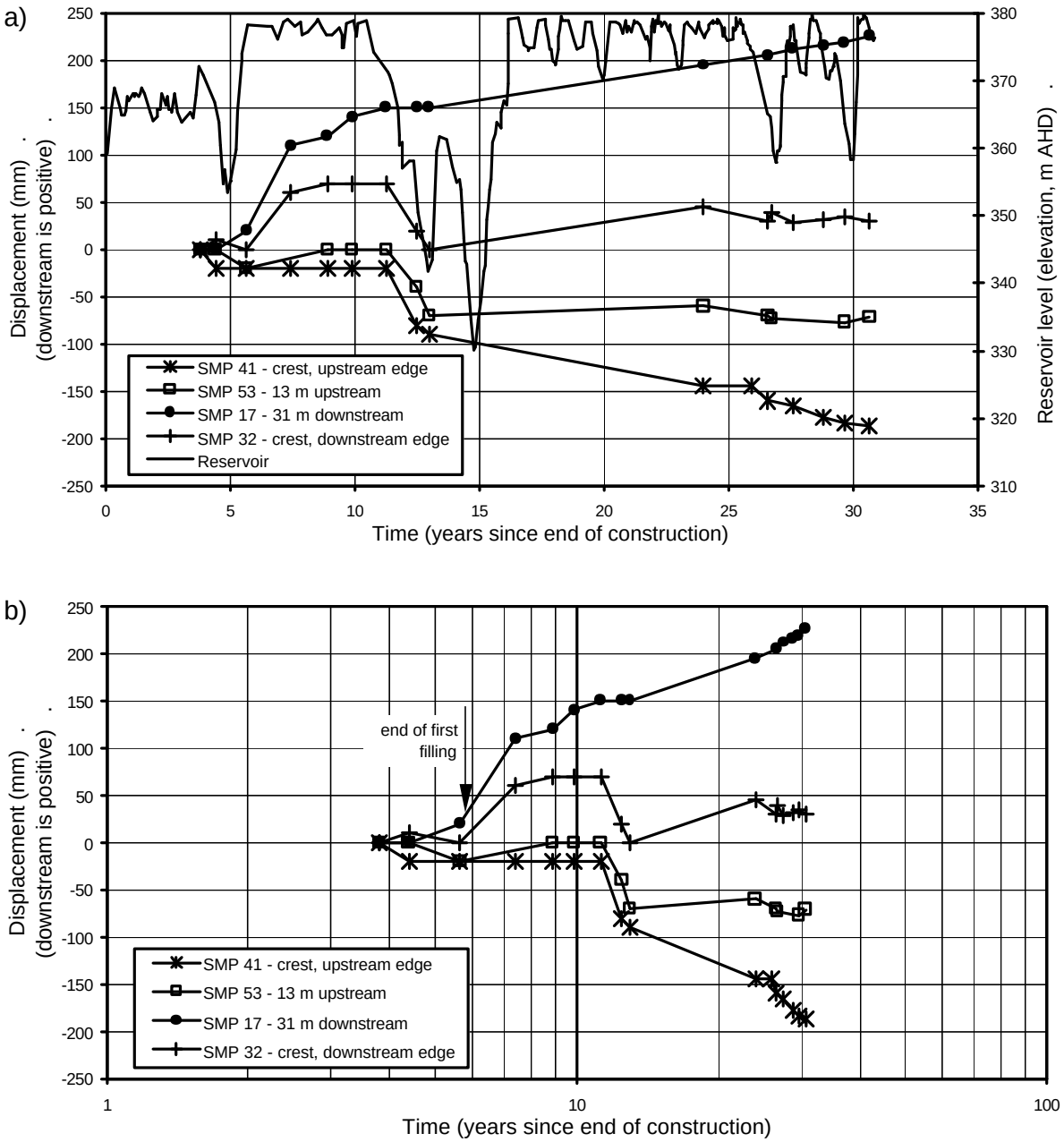

Figure G1.87: Wyangala dam, post construction displacement normal to dam axis of SMPs on the crest and slopes at the main section.

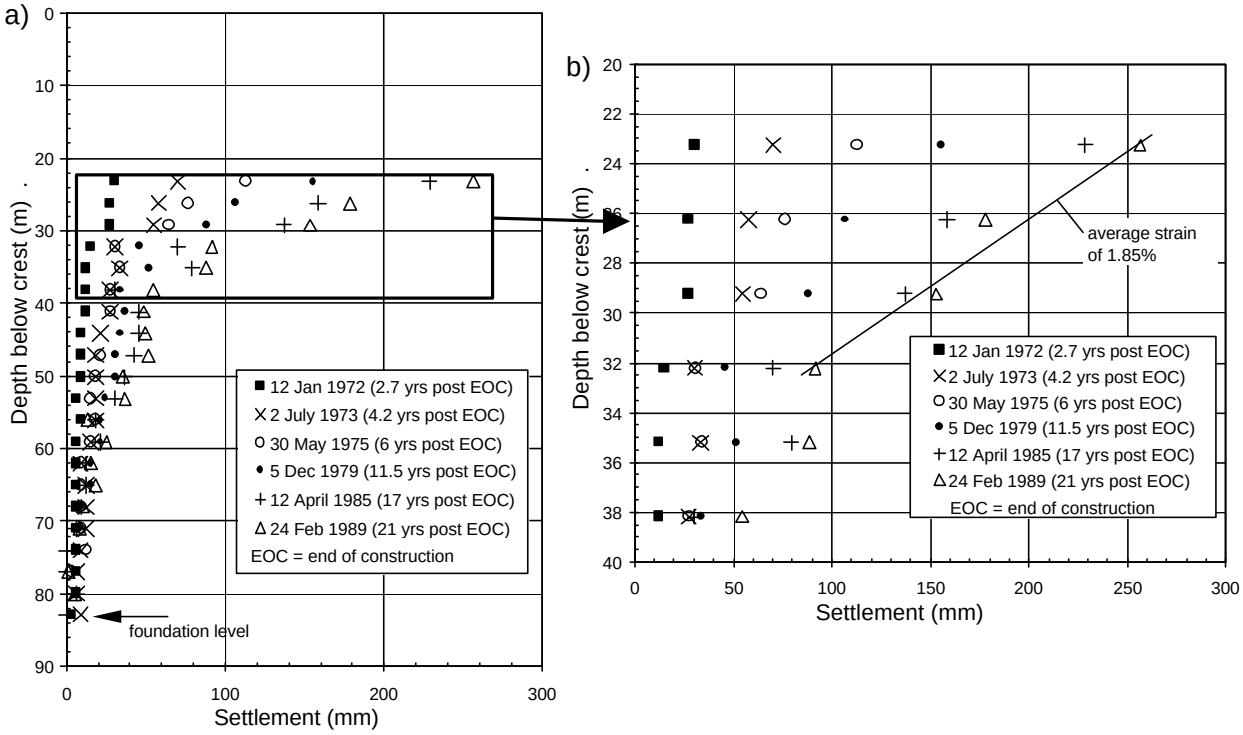

Figure G1.88: Wyangala dam, post construction internal settlement in IVM B located 9 m upstream of dam axis.

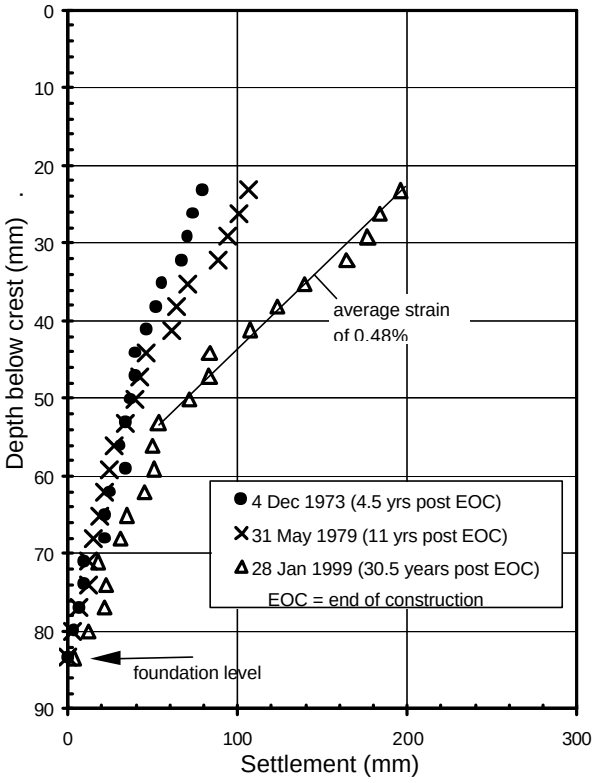

Figure G1.89: Wyangala dam, post construction internal settlement in IVM A located 9 m downstream of dam axis.

2.0 ZONED EARTH AND ROCKFILL EMBANKMENTS

2.1 CANALES DAM

Canales dam (Figure G2.1), located on the Genil River in southern Spain, is a zoned earth and rockfill embankment with narrow central core constructed in a narrow, steep sided valley. The embankment is of 156 m maximum height and 380 m crest length. It was constructed in two stages; the first stage of 100 m (to elevation 910 m) from 1979 to 1981, and the second stage to crest level from 1985 to 1986. According to Bravo (1979) the staged construction was part of the measures to avoid fissuring due to the abrupt change in abutment slopes, and the second stage was delayed until the first stage had "*registered the majority of the settlement*".

In summary, the materials and construction methods (Bravo 1979) consisted of a central core (Zone 1) of high plasticity silty clays placed at moisture contents on the wet side of Standard optimum (from OMC to 2% wet of OMC). The very broad transition zone (Zone 2) was of clayey to silty gravelly sands derived from limestone (kalkirita), which had been reduced to sand size by tectonic action. The rockfill shoulders (Zone 3A) were of quarried limestone. Bravo (1979) refers to the embankments materials as being compacted to "*the highest possible density*".

First filling began in 1987 and the reservoir level rose rapidly to about elevation 870 m in a period of 5 months following heavy rainfall. Thereafter, the reservoir did not reach full supply level until almost 10 years after the end of embankment construction (Figure G2.3).

During the period of first filling a substantial longitudinal crack developed in the crest between the core and downstream transition (Figure G2.2). Giron (1997) provides the following sequence of events on development of the crack:

- The first sign of crack development was observed in 1989 (2 years after end of construction) when the recorded differential settlement of the crest was about 200 mm.
- On reservoir raising to elevation 930 m (3.8 years post construction) a vertical slump had clearly developed with differential settlement across the slump of 405 mm.

- Towards the end of 1995 (9.5 to 9.6 years post) the reservoir quickly rose back to elevation 930 m, but no increase in the rate of settlement was observed (Figure G2.3).
- On reservoir raising to full supply level (elevation 958 m) for the first time, the rate of settlement of the mid to upstream portion of the crest increased significantly and differential settlement across the crack increased to about 1000 mm. The high rate of settlement continued, at a gradually reducing velocity, for some months after full supply level had been reached.
- By late 1996 settlement rates had reduced to less than 0.5 mm/day and remained at about this rate into 1997.

Giron (1997) and Bravo et al (1994) attribute the crest settlement behaviour to collapse settlement of the upstream shoulder fill on saturation.

An interesting aspect of the deformation behaviour is the relatively uniform settlement of the upstream crest and central core, and concentration of the differential settlement at the downstream interface of the core and transition, as shown in Figure G2.2. Bravo et al (1994) indicate that they were able to numerically model the deformation behaviour reasonably well, but do not comment on the reason for the concentration of the differential settlement at this point. Several possible explanations are considered:

- The wet placed, high plasticity clay core has a low undrained strength and consequently must deform with the upstream shoulder as it collapse settles because it relies on the shoulders for support. In this case the deformation of the core would be predominantly undrained plastic type deformation and largely due to lateral spreading of the core.
- The deformation occurs as a shear type movement in the core, along a defined plane of shearing with backscarp at the downstream core / transition interface.
- A combination of the above.

The first explanation is considered more feasible than the second mainly because the period of rapid crest settlement (after 9.6 years) occurs when the collapse settlement of the upstream rockfill is localised to the upper 20 to 30 m of the upstream shoulder, and when the reservoir level is close to full supply level at a level where it would provide a high level of support to the upstream face of the core. For this reason shear type

movements on a pre-existing shear surface in the core seem less likely than plastic deformation of a wet placed high plasticity clay core. However, a combination of both is considered possible.

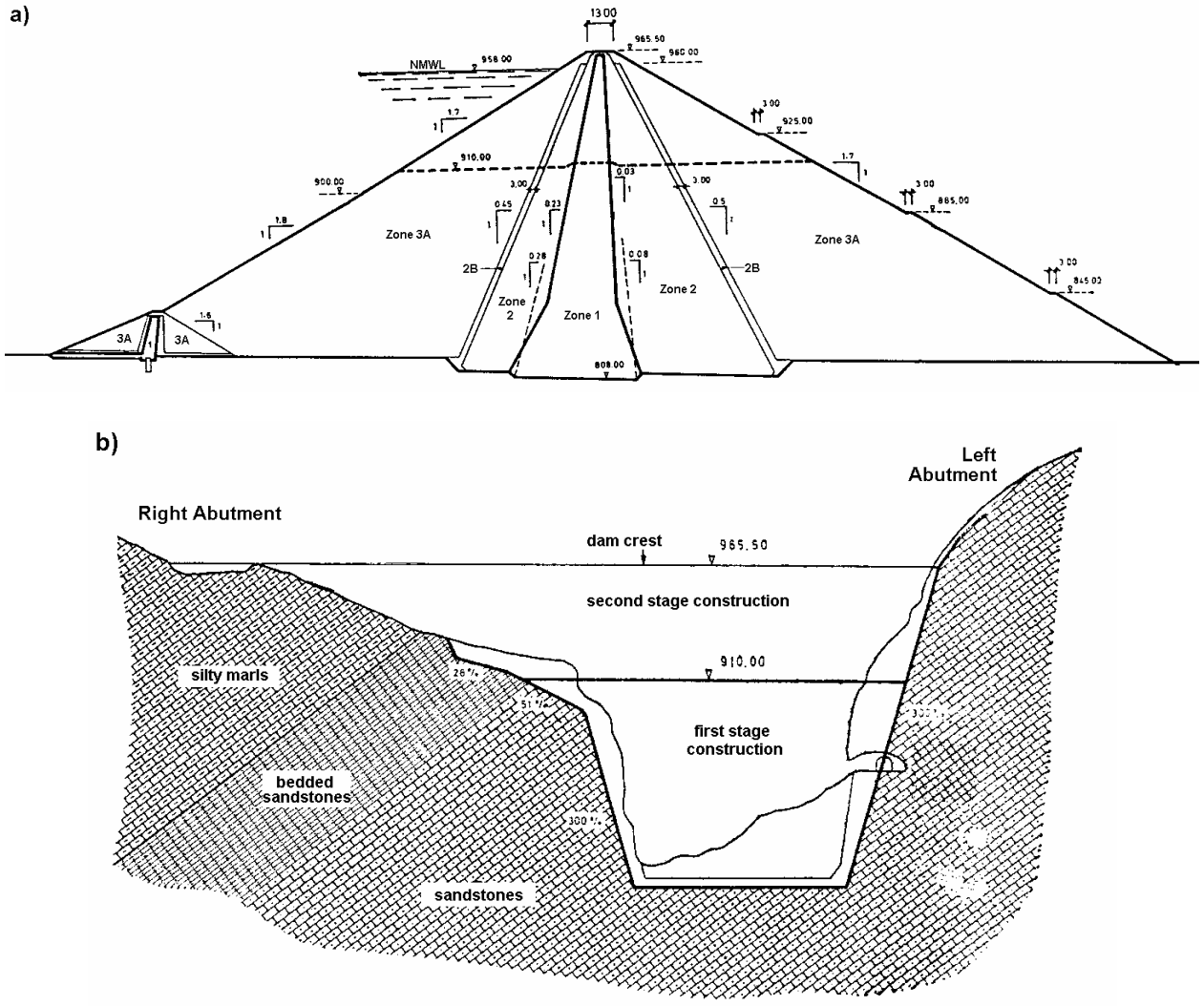

Figure G2.1: Canales dam, *(a)* typical section, and *(b)* longitudinal section (Bravo 1979).

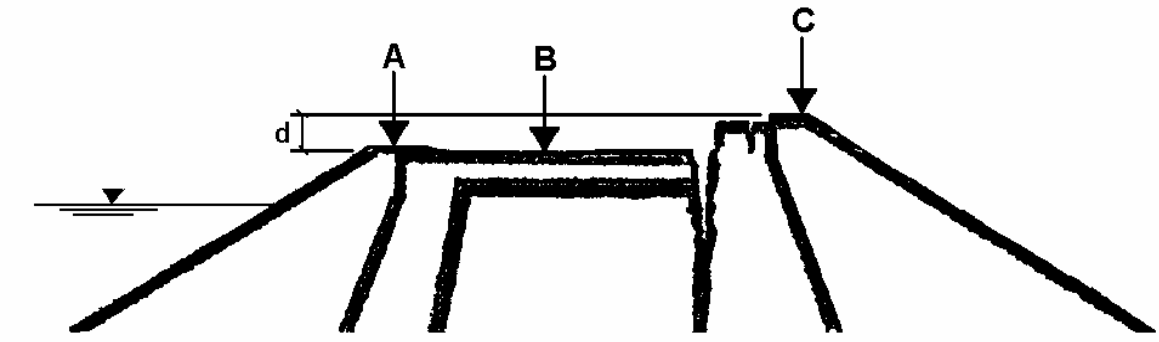

Figure G2.2: Canales dam, cracking and differential settlement at the crest (Giron 1997)

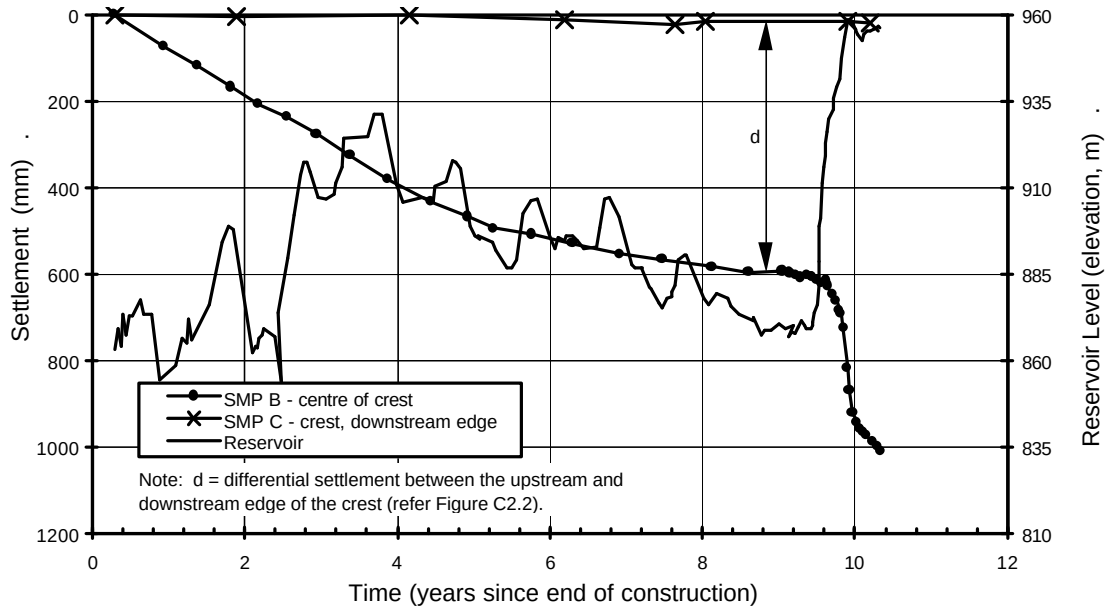

Figure G2.3: Canales dam, post construction settlement at the crest (adapted from Giron 1997)

2.2 SAN LUIS DAM

San Luis dam, located in California USA, is a zoned earth and rockfill embankment with very broad central earthfill zone. The embankment is of 116 m maximum height and 5650 m crest length. Foundation conditions vary along the length of the embankment, from deep alluvial deposits in the floodplain area to bedrock at shallow depth on hill slopes. Changes to the embankment design were made according to the foundation conditions and typical sections are shown in Figure G2.4. The embankment in plan section is shown in Figure G2.5. Embankment construction was completed in June 1967. In summary, the materials and placement methods comprised:

- Very broad central earthfill core (Zone 1) of mainly low to medium plasticity sandy clays, sourced from alluvial terrace and floodplain deposits, compacted by tamping rollers in 150 mm layers to high density ratio (average 102.0% of Standard maximum dry density). Moisture contents were on average 1.2% dry of Standard Proctor optimum.
- Filter / transition zones of sand to cobble sized river alluvium (Zone 2) and rock fragments (Zone 4) compacted in 300 mm layers by crawler tractor.

- Miscellaneous fill zone (Zone 3) in the outer downstream shoulder and upstream toe regions. Materials ranged from Zone 1 type earthfills to weathered rock, and were placed and compacted in 300 mm layers.
- Thin rockfill zone (Zone 5) of quarried basalt placed in the outer upstream shoulder above elevation 400 feet.

First filling started in November 1966, about 0.7 years before the end of construction, and reached within about 65 m of full supply level prior to the end of construction. Full supply level was reached in July 1969, 2.1 years after construction. Post first filling, the reservoir has been subjected to a seasonal drawdown ranging in magnitude from 5 m to about 65 m (Figure G2.8).

In September 1981, some 14 years after construction, a slide occurred in the upstream slope during large drawdown (Von Thun 1988; Stark and Duncan 1987, 1991). The deep-seated slide (Figure G2.6) was approximately 460 metres in width (from Station 122 to 137), 1 million cubic metres in volume, and slid a distance of about 20 m. The slide was located on the left abutment in a region where the original ground surface under the embankment sloped in an upstream direction at about 10 to 15 degrees.

Von Thun (1988) considered that the persistent, but minor, longitudinal crest cracking over the 14 years up to the slide and settlement behaviour of SMPs on the upstream shoulder at Stations 136 and 138 as indicators of "abnormal" deformation behaviour prior to the slide and precursory warning signs of potential instability. Although, he added that the actual prediction of the timing of the slide was not possible from the monitored deformation.

Evaluating these potential indicators of "abnormal" deformation behaviour leading up to the slide, it is evident that the longitudinal crest cracking at San Luis dam was not confined to the region of the slide; it was more of a general occurrence along the length of the embankment. Comparison of displacements along the line of SMPs 42 feet (or 13 metres) upstream of the dam axis with those 21 feet (6.5 metres) downstream of the dam axis (Figure G2.7b) shows lateral spreading of 50 to 150 mm occurred along most of the embankment length. In the region of the slide most of the differential displacement between the SMPs up and downstream of the crest occurred during first filling (Figure G2.8). However, there is some query on the original zero and the accuracy of the lateral displacement measurements in the 1960's and 1970's.

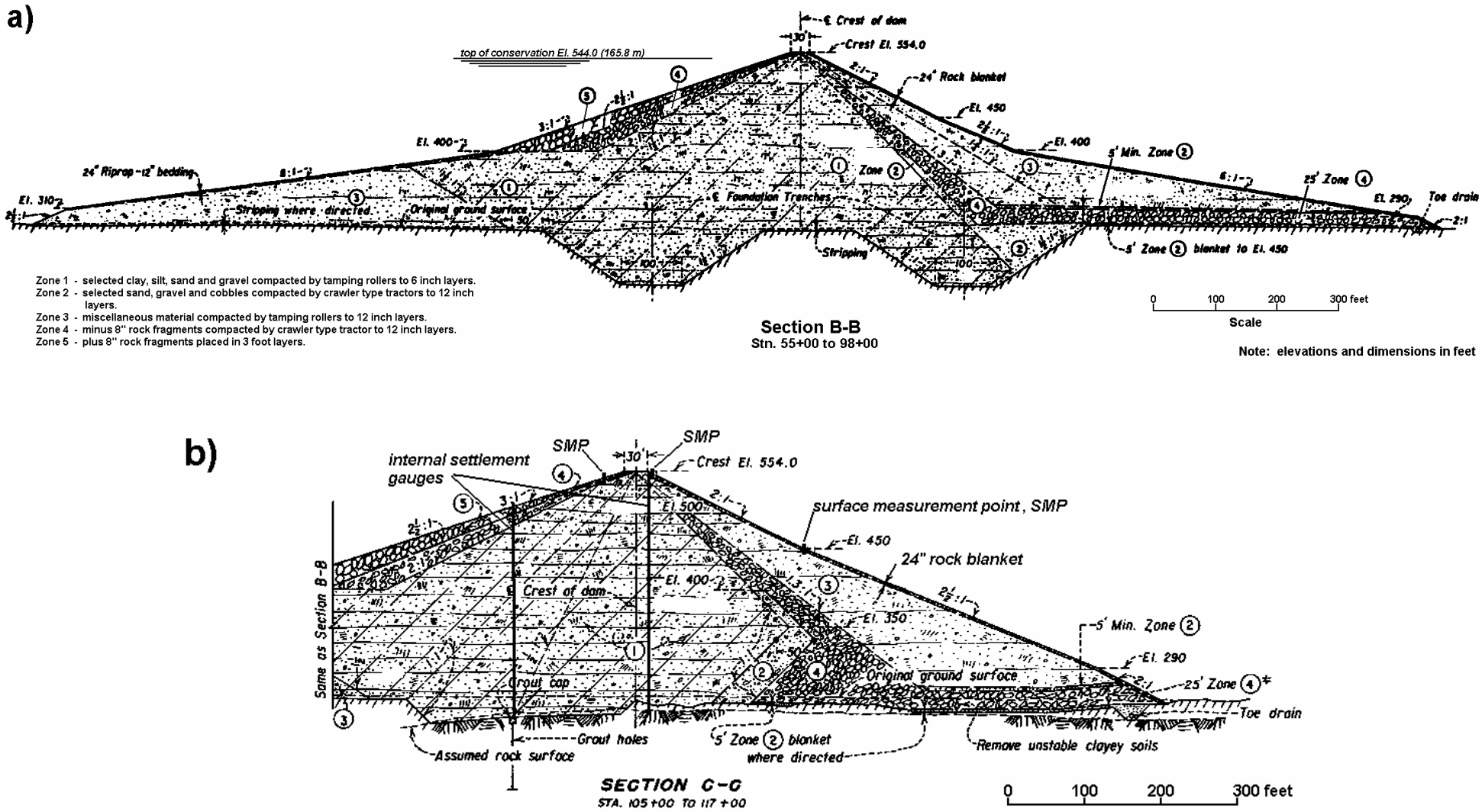

Figure G2.4: San Luis dam; sections in the vicinity of the maximum embankment height (courtesy of United States Bureau of Reclamation).

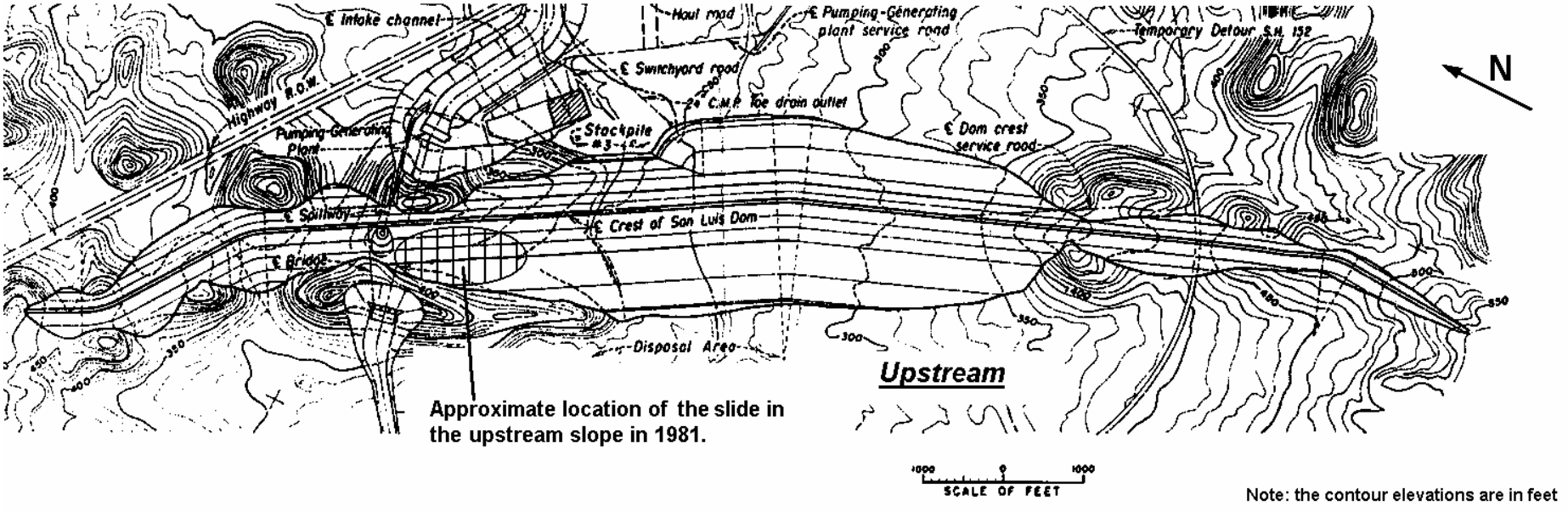

Figure G2.5: San Luis dam, plan section (courtesy of United States Bureau of Reclamation).

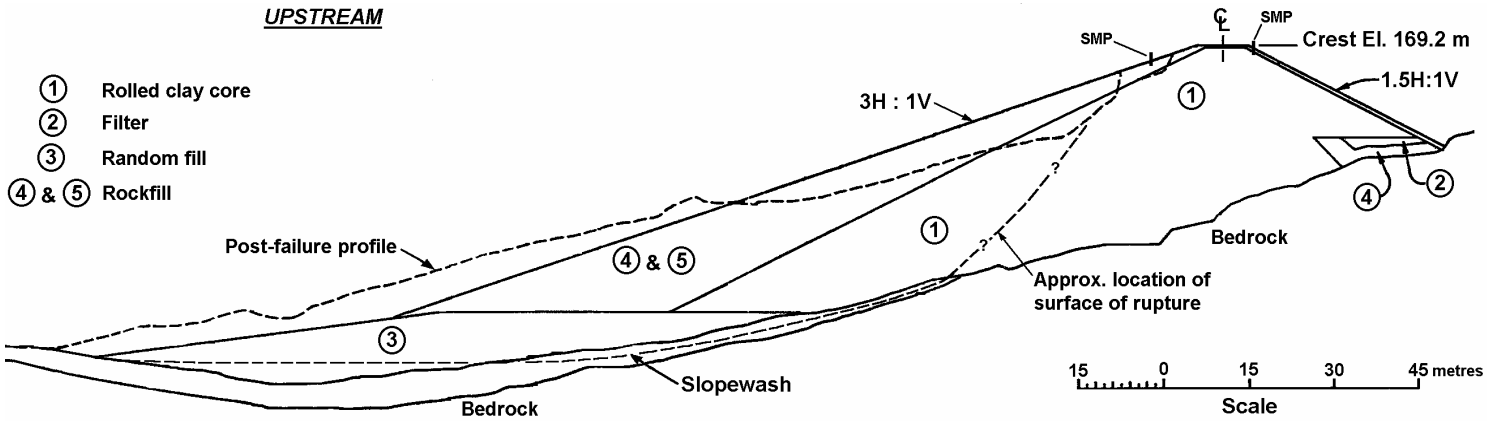

Figure G2.6: San Luis dam, section of the slide in the upstream slope in 1981 at Station 135+00 (courtesy of USBR).

Von Thun (1988) suggests that in the area of the slide the crest cracking "*was associated with the saturation and progressive straining of the slopewash on the hillsides*". But, for the embankment overall, the longitudinal crest cracking will more typically be associated with differential deformations due to progressive development of the phreatic surface in the dry placed and brittle earthfill, and the stress conditions developed in the earthfill. Therefore, it is difficult to consider the crest cracking as an indicator of "abnormal" deformation behaviour and precursor to slope instability unless persistence of the cracking was confined to the vicinity of the slide area.

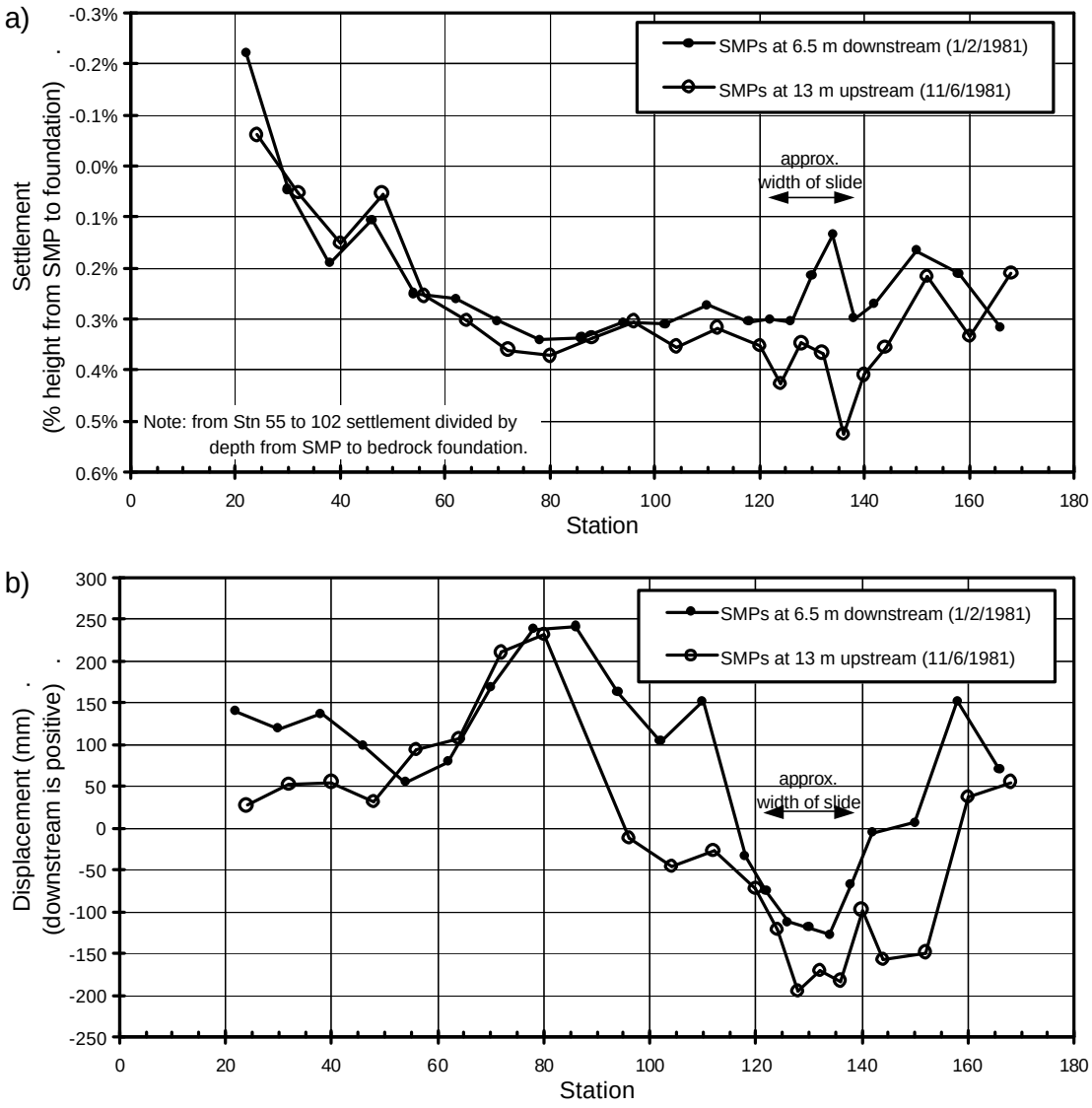

Figure G2.7: San Luis dam, comparison of *(a)* settlement and *(b)* displacement between SMPs at 13 m upstream of dam axis and SMPs at 6.5 m downstream.

With respect to the settlement behaviour of SMPs on the upstream slope, Von Thun (1988) comments that the very large differential between the actual and predicted post construction settlements at Stations 136 and 138 (Figure G2.9) was a clear indicator of the "*anomalous*" behaviour in the region of the slide prior to the failure. It should be noted that these SMPs on the upstream slope are several metres above and therefore outside of the initial slide area as shown on Figure G2.6. Figure G2.7a presents the actual post construction settlements measured to the date of the last reading prior to the slide (some months prior to the slide) for SMPs at 13 m upstream and those at 6.5 downstream of the dam axis. The figure shows that at most locations the measured settlements up and downstream of the crest are similar, however, a large differential is notable for the SMPs from Station 130 to 140, in particular at about Station 136 where the slide initiated.

The settlement versus time of SMPs in the region of the slide (Figure G2.10) shows:

- The larger magnitude of settlement (as a percentage of the height from the SMP to foundation level) of the upstream shoulder at Station 136. In comparison to similar type embankments though, the magnitude of settlement at this SMP is quite "normal" (Figure 7.52 in Section 7.6 of Chapter 7).
- The acceleration in normalised settlement of the SMP at Station 136 on the upstream slope during the first large drawdown period from 8 to 10 years after construction (Figure G2.10b) might be considered "abnormal" in comparison to other SMPs on the upstream slope in the slide vicinity.

In comparison to the settlement behaviour at SMPs on the upstream slope of San Luis dam well away from the slide area (Figure G2.11), the acceleration in settlement at Station 136 during the drawdown at 8 to 10 years also appears to be "abnormal".

In summary, the settlement behaviour of the SMP on the upstream slope at Station 136, located in the region of but not within the slide area, during the first large drawdown appears "abnormal" compared to the deformation behaviour at similar embankments and more importantly to other SMPs on the upstream shoulder at San Luis dam. During the next large drawdown in 1981, at 14 years after construction, the slide in the upstream slope occurred. In hindsight, the settlement behaviour of this SMP could be considered as a precursory sign of the failure, although, it would be almost impossible to predict the occurrence of the slide based on the deformation records as concluded by Von Thun (1988).

The longitudinal crest cracking at San Luis dam is not considered as a reliable indicator of “abnormal” deformation behaviour and precursory sign of slope instability in this case, because of its widespread occurrence along the embankment.

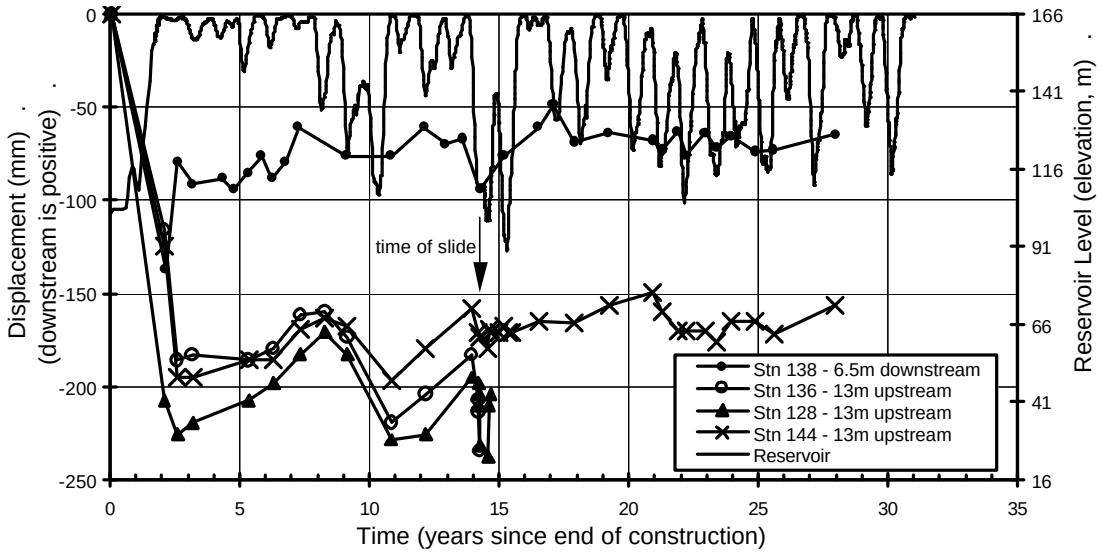

Figure G2.8: San Luis dam, post construction displacement normal to the dam axis of SMPs in the vicinity of the slide area.

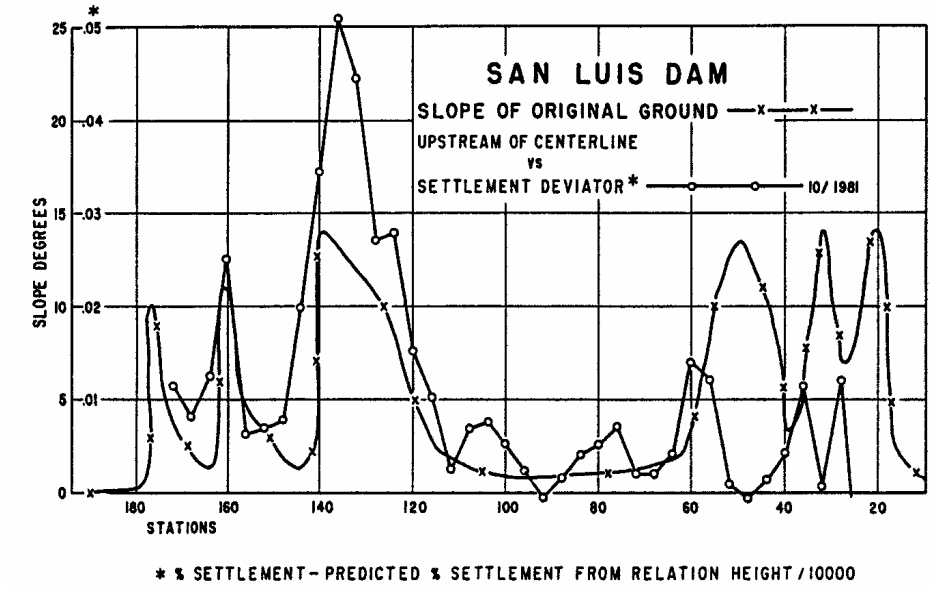

Figure G2.9: San Luis dam, difference between actual and predicted settlement (Von Thun 1988)

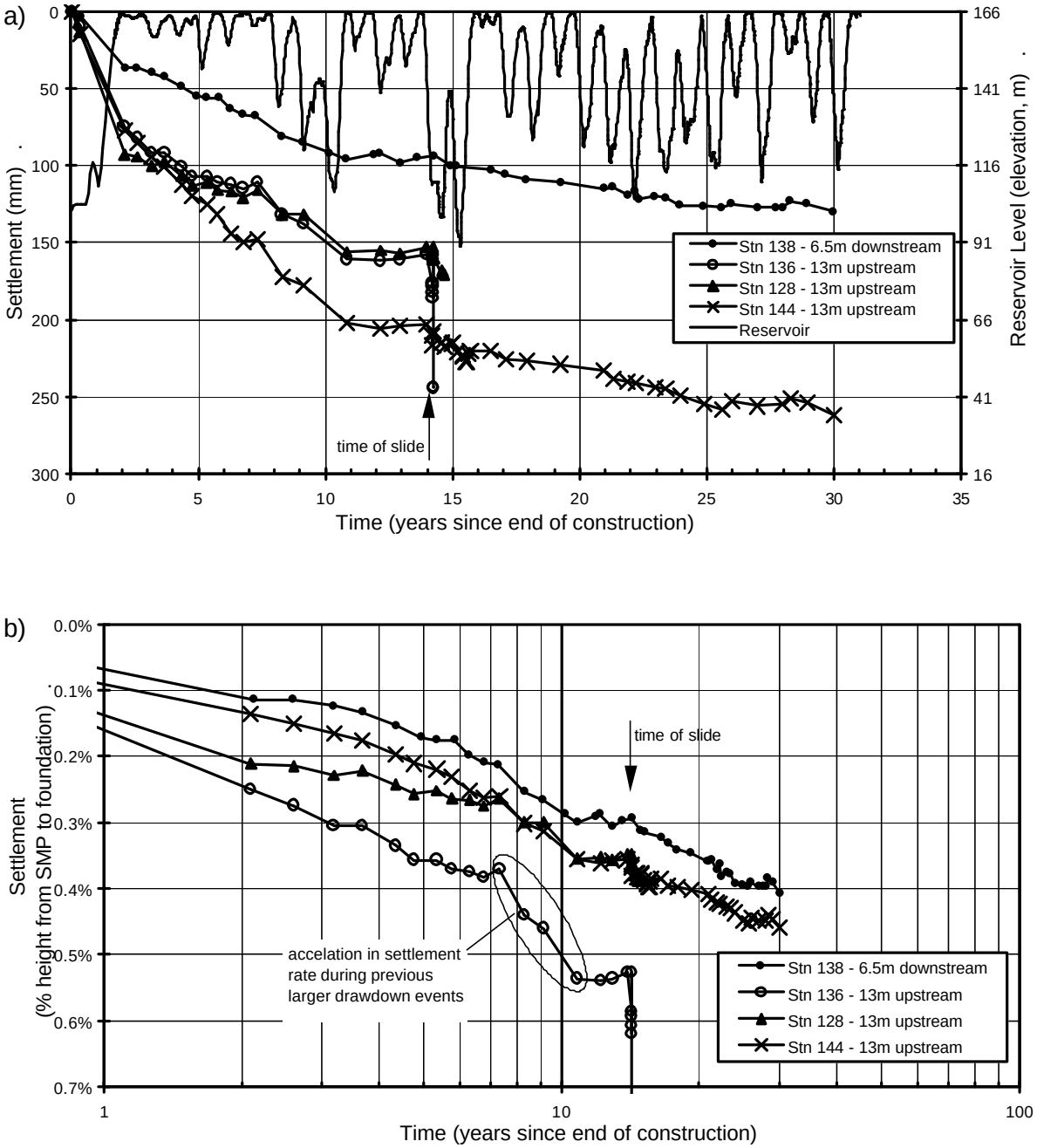

Figure G2.10: San Luis dam, post construction settlement of SMPs in the vicinity of the slide area.

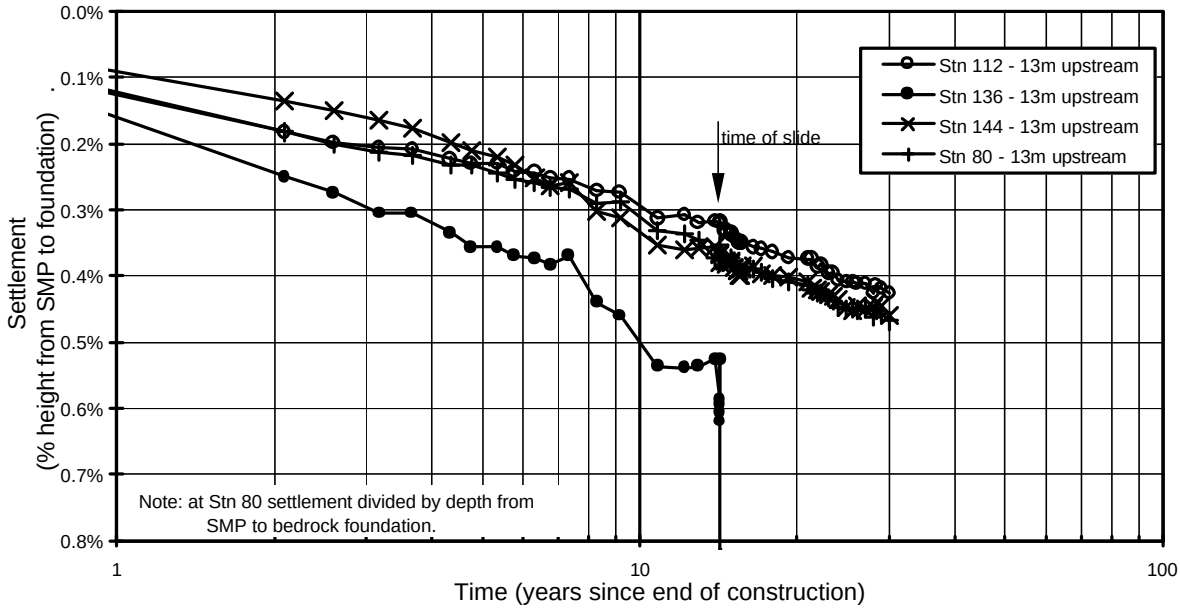

Figure G2.11: San Luis dam, post construction settlement of SMPs located 13 metres (42 feet) upstream of dam axis.

3.0 ZONED EARTHFILL EMBANKMENTS

3.1 CARSINGTON DAM

Carsington dam (Figure G3.1) is a zoned earthfill embankment of 36 m maximum height that failed during construction in early June of 1984. Skempton and Vaughan (1993), amongst others, describe the failure. IVM records from within the central core show the development of regions of high localised vertical strain prior to failure, which is potentially indicative of a shear development in the core. The IVM records from Carsington dam are presented and discussed to highlight the deformation behaviour that is potentially indicative of shear surface development in a wet placed clay core.

The central core of Carsington dam, including its unusual "boot" structure on the upstream side, consisted of high plasticity clays that were placed on average 8% wet of Standard optimum moisture content and heavily rolled. Peak undrained shear strengths (Potts et al 1990) were in the order of 42 kPa. The outer earthfill zones were of weathered mudstone placed in thin layers and well compacted.

During construction high positive pore water pressures were developed in the core. Initially the pore water pressure response was zero to negative at fill heights less than about 8 m above the piezometer gauge, equivalent to total vertical stresses in the range

140 to 150 kPa. Above this height positive pore water pressures were developed that were equivalent to about 80 to 90% of the incremental increase in total vertical stress.

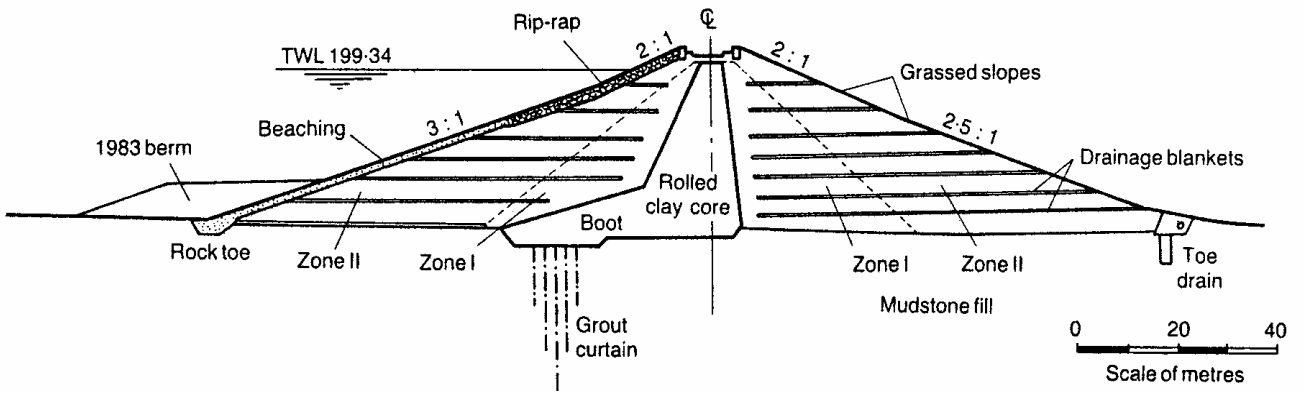

Figure G3.1: Carsington dam, typical section (Skempton and Vaughan 1993)

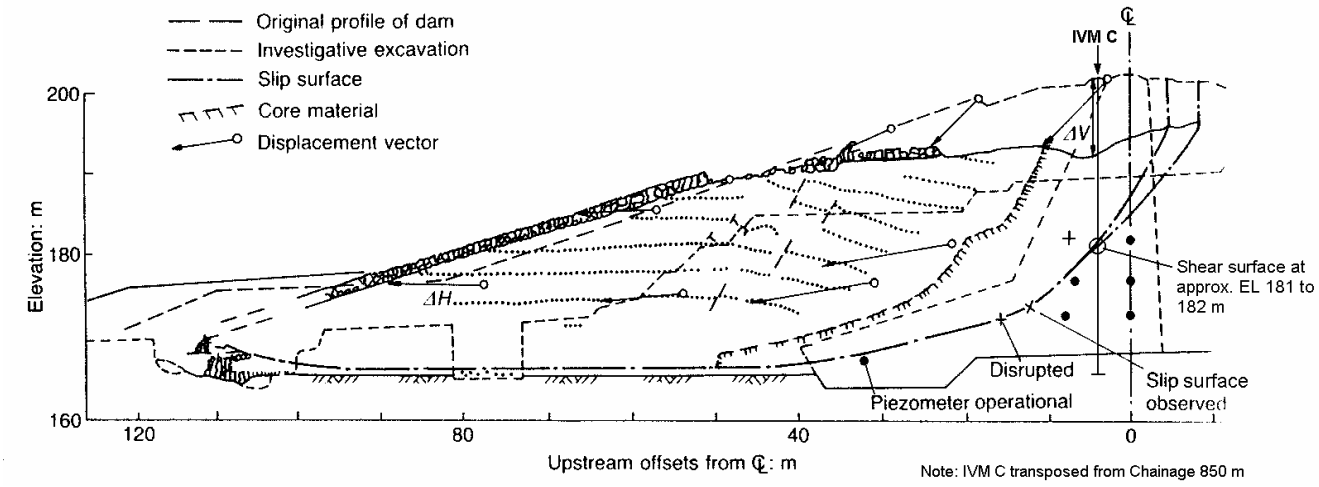

Figure G3.2: Carsington dam, section after failure at chainage 825 m (adapted from Skempton and Vaughan 1993).

The IVM records (Figure G3.3 and Figure G3.4) highlight several interesting aspects with respect to the vertical strain in the core:

- At IVM C, located 4 m upstream of the dam axis at chainage 850 m (Figure G3.2), shear strains in the range 4 to 7% were recorded at fill depths greater than 8 m at the end of the shutdown period in late September 1983 when the embankment was about 5 m below the final design level. In comparison to other embankments with wet placed, thin to medium width clay earthfill cores (Figure 7.22 in Section 7.4 of Chapter 7) vertical strains of this magnitude at these depths are very high, well

outside the approximate bounds shown. However, the vertical strains are comparable to those recorded in other IVMs at Carsington dam.

- During the first month of the shutdown period in late 1983 the vertical strain in IVM C at about elevation 180 m increased from 7% to 9% (Figure G3.3a). After this date, and during the shutdown period, the IVM tube became constricted and then blocked at this elevation. The location of the blockage is coincident with the surface of rupture determined after the failure (Figure G3.2). Note that IVM C, located at chainage 850 m, has been transposed from onto this section at chainage 825 m.
- At IVM B (Figure G3.3b) a large increase in vertical strain is recorded between elevations 185 to 192 m from late May to early June 1984, in the days immediately prior to and during the development of the failure.

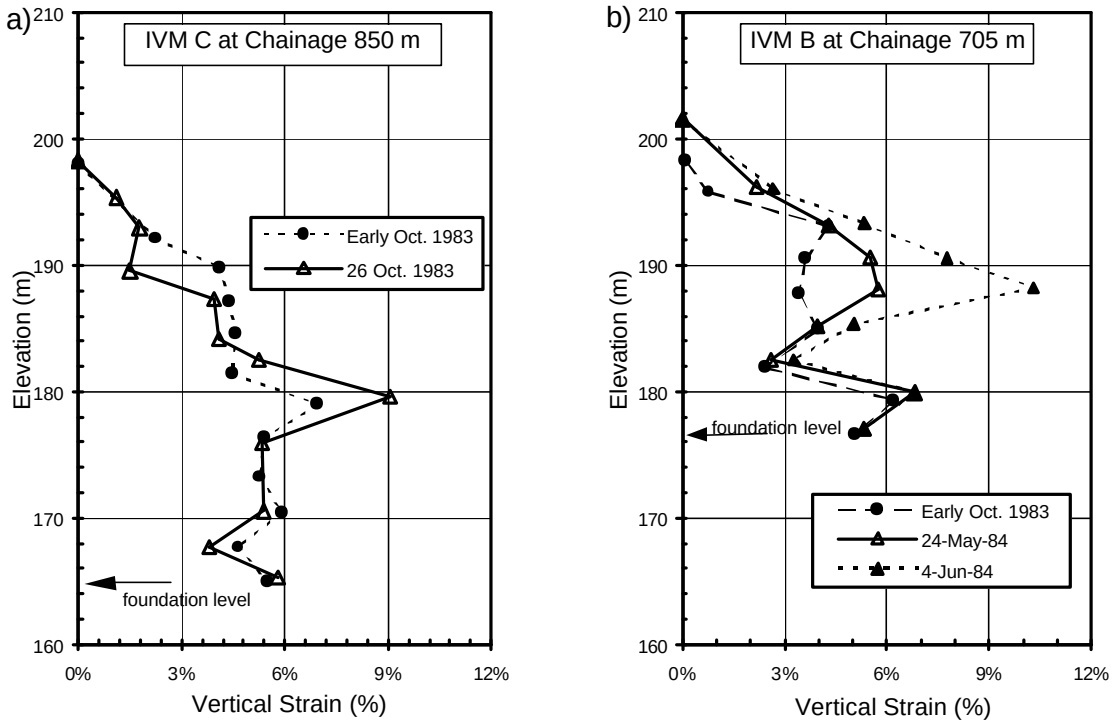

Figure G3.3: Carsington dam, vertical strain profiles from IVM during construction, *(a)* IVM C at chainage 850 m, and *(b)* IVM B at chainage 705 m (adapted from Rowe 1991).

Figure G3.4, from Rowe (1991), highlights the large magnitude of localised vertical strains that developed in IVMs B and C during non-construction periods leading up to the failure. Comparable plots for wet placed clay cores of selected cross-arm intervals (Figure 7.20 in Section 7.4 of Chapter 7) show a constant to decreasing rate of vertical

strain versus increasing fill height above the cross-arm interval. The contrasting deformation behaviour in the core at Carsington is considered "abnormal" and indicative of shear type deformation. In IVM C this shear deformation was concentrated at elevation 179 to 180 m, which was coincident with the elevation of the surface of rupture at this location, and was evident in the winter shutdown period prior to the failure.

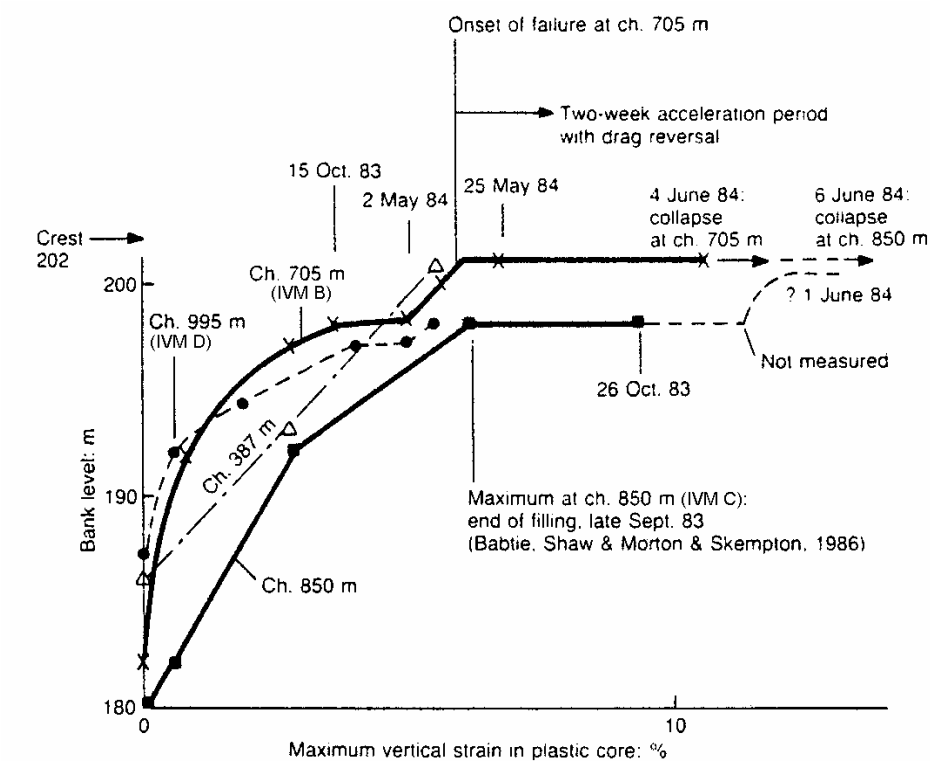

Figure G3.4: Carsington dam, variation of the maximum vertical strain in the core with bank level (Rowe 1991).

3.2 HIRAKUD DAM

Hirakud dam (Figure G3.5), located in India, is a 59 m high zoned earthfill embankment with a very broad central earthfill core and downstream rockfill toe. The core was constructed of mostly low to medium plasticity clayey gravels to clayey sands placed in 225 mm layers and compacted by sheepsfoot rollers at moisture contents in the range 1% to 3% dry of Standard optimum.

The vertical deformation during construction in IVM C (Figure G3.6), located in the deeper gully section, is presented in Figure G3.7. At the end of construction (Figure G3.7a) vertical strains reached values in the range 7.5% to 13.5% in the lower 15 m of

the core (35 to 49 m). These values are well in excess of and clear outliers to the typical vertical strains recorded at end of construction for similar dry placed earthfills (Figure 7.18b in Section 7.4 of Chapter 7).

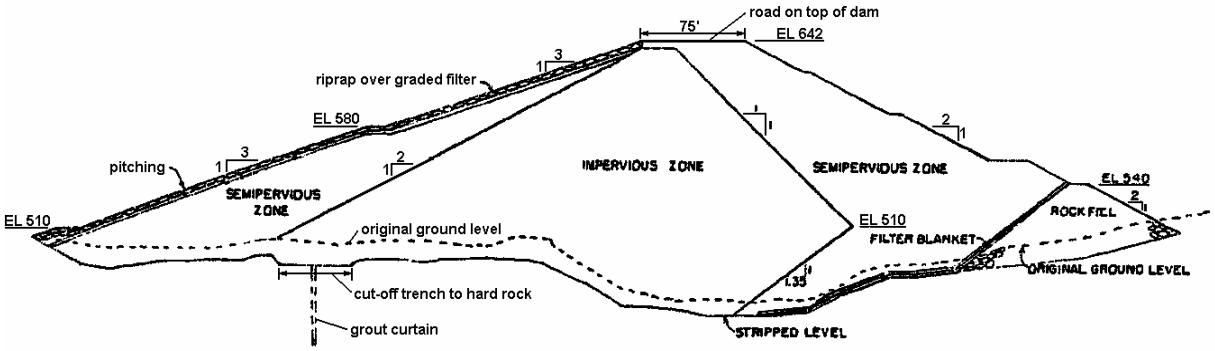

Figure G3.5: Cross section within the deeper gully section at Hirakud dam (Rao and Wadhwa 1958)

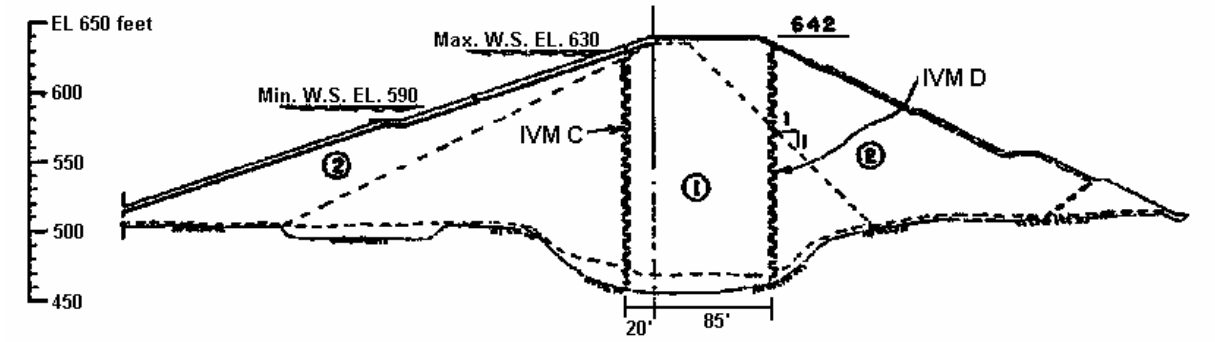

Figure G3.6: IVM locations in deeper gully section, Station 71 + 90 (Rao and Wadhwa 1958)

Rao (1957) attributes the large vertical strains to wetting of the earthfill during the shutdown period of the 1952 monsoon season when high water levels were impounded in the reservoir and backwaters engulfed the embankment section within the gully region from July to December 1952. At this time the embankment height at mid section was about 12 to 13 m based on the number of cross-arms installed. The cumulative settlement during construction at IVM C (Figure G3.7b) shows the settlement that occurred during the 1952 monsoon season shutdown period and subsequent large settlements during the following two construction periods in 1953 and 1954. Investigations at end of construction (Rao 1957) encountered "*soft soil patches*" in the lower 21 m where moisture contents were as high as 10% above Standard optimum, well in excess of the placement moisture content on the dry side of Standard optimum.

It is considered that the large settlement during the 1952 shutdown period were due to collapse settlement on wetting of the dry placed earthfill core. The subsequent large settlements in 1953 and 1954 were largely concentrated within the lower section of the core and reflect the likely low modulus of the saturated earthfill. By end of construction 1430 mm of a total of 2170 mm settlement (66%) in IVM C was measured within the lower 15 m, or lower 30%, of the core.

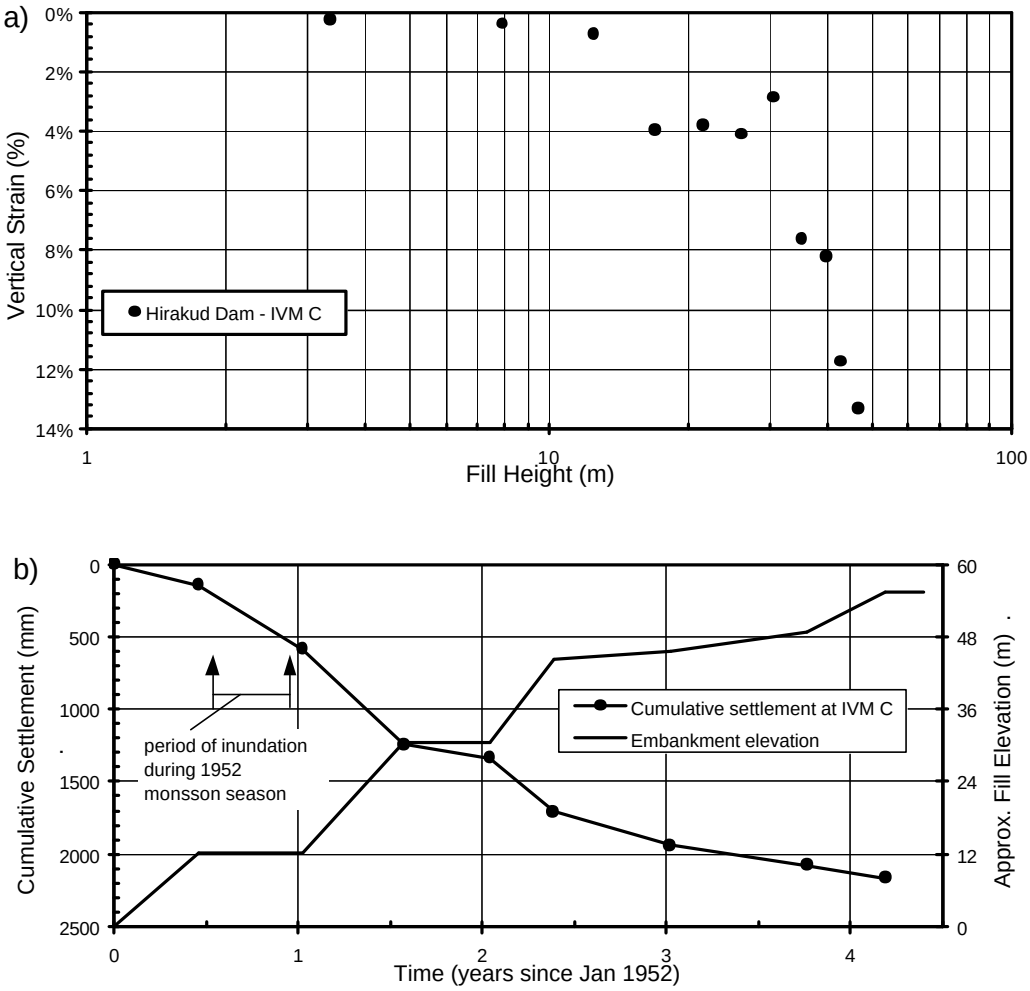

Figure G3.7: IVM C at Hirakud dam, *(a)* vertical strain at end of construction, and *(b)* cumulative settlement during construction (adapted from Rao 1957).

3.3 HORSETOOTH RESERVOIR DAMS

The Horsetooth Reservoir development, located in northern Colorado, USA, consists of four embankments (Table G3.1) and at least one dyke constructed to impound the reservoir. The embankments were constructed in the late 1940's. All four

embankments are of similar design having a very broad earthfill zone and thin shoulder zones of pervious gravels or rockfill. The cross section and long section for Horsetooth and Dixon Canyon dams are shown in Figure G3.8 and Figure G3.9 respectively.

For the embankment section constructed across the alluvial plain, most of the embankment was founded on the alluvial soils with a cut-off section to bedrock. For Dixon Canyon, Spring Canyon and Soldier Canyon dams the cut-off trench was very broad at bedrock level (about 55 m width) and centrally located, as shown for Dixon Canyon dam in Figure G3.9. At Horsetooth dam (Figure G3.8) the cut-off was of narrower width and located upstream of the dam centreline. The depth of alluvium in the broad gully regions was up to 10 to 20 m depth. Approximate depths of overburden at the maximum section ranged from 5 to 11 m (Table G3.1). On the hill-slopes over-burden soils consisted of a thin mantle of colluvium and residual soils.

The broad earthfill zone was constructed using mainly low plasticity sandy clays to clayey sands and clayey gravels of alluvial origin, the finer materials placed in the central region of the core and the coarser materials toward the outer slopes. The earthfill was placed in 150 mm layers and compacted by tamping rollers. Moisture contents were well dry of Standard Proctor optimum; they averaged from 2.2% to 2.9% dry at the four embankments.

First filling started in April 1951, some 2.4 years after end of construction for most embankments, and reached close to full supply level in May 1953 (4.5 years after end of construction). The reservoir is subjected to a seasonal drawdown of typically 5 to 15 m (Figure G3.12a). The maximum drawdown was to 28.5 m below maximum water level in 1976 (27 years after construction).

Table G3.1: Horsetooth Reservoir main embankments.

Dam Name	**Dam Type**	**Height (m) *[1]**	**Length (m)**	**Approx. Depth of Over-burden at Maximum Section**	**Figure References**
Horsetooth	Zoned earthfill	48	567	7 to 11 m	Figure G3.8
Soldier Canyon	Zoned earthfill	70	440	5 to 7 m	
Spring Canyon	Zoned earth and rockfill	68	347	10 m	
Dixon Canyon		74	387	4 to 6 m	Figure G3.9

Note: *[1] maximum height from crest to base of cut-off trench.

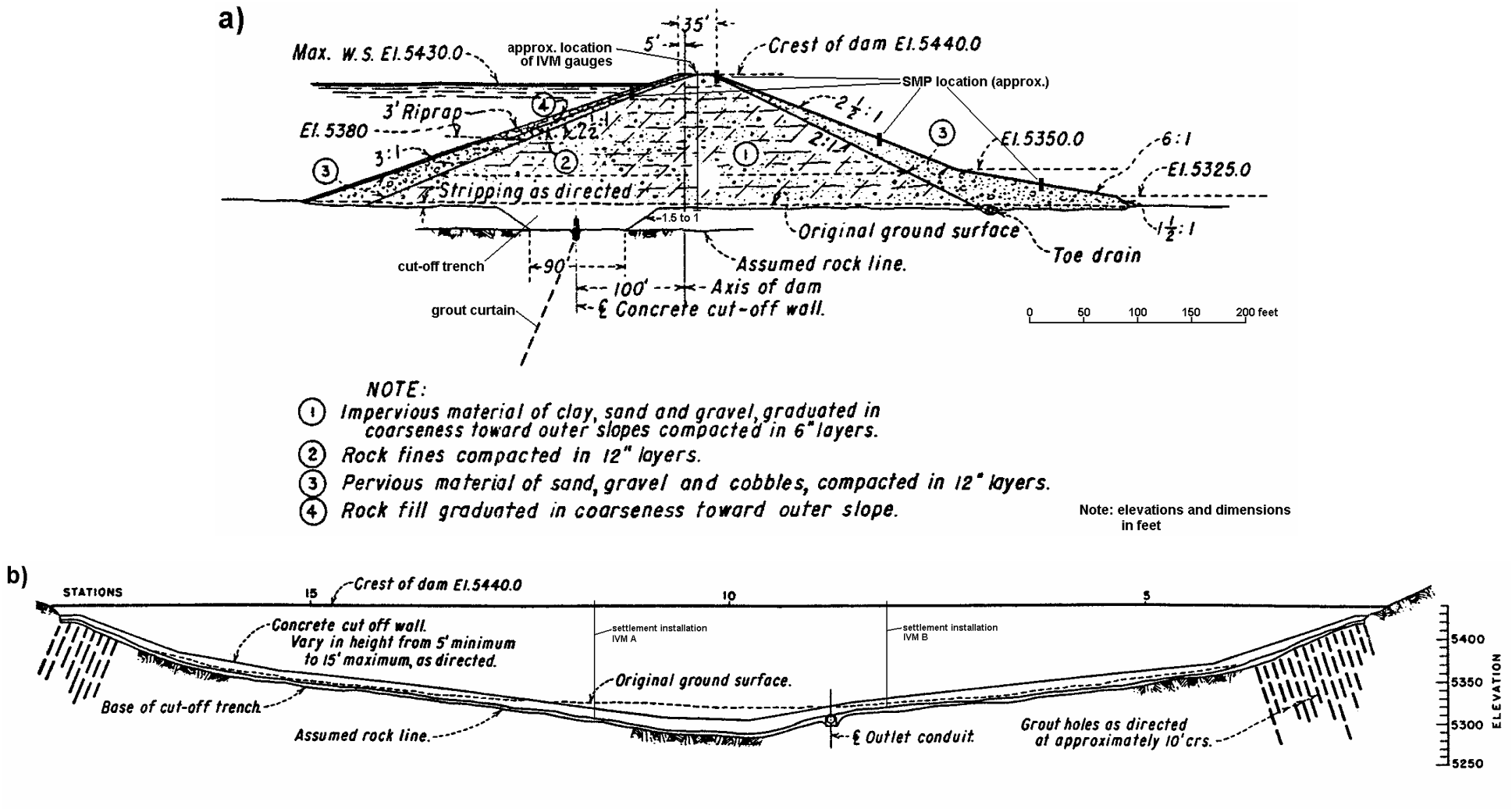

Figure G3.8: Horsetooth dam; *(a)* maximum section and *(b)* long section (courtesy of U.S. Bureau of Reclamation).

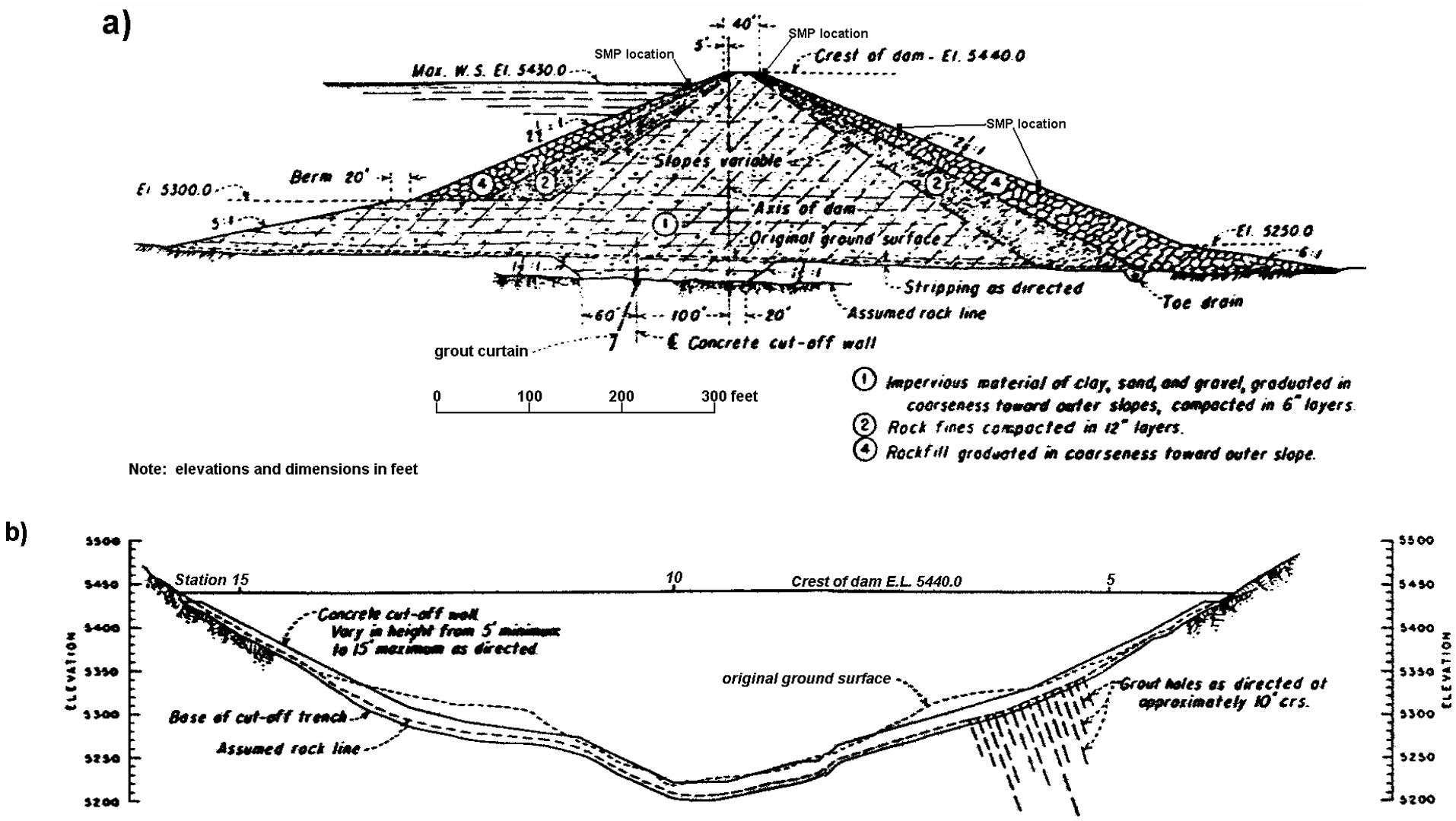

Figure G3.9: Dixon Canyon dam; *(a)* maximum section and *(b)* long section (courtesy of U.S. Bureau of Reclamation).

Instrumentation at most embankments consisted of piezometers in the main earthfill zone and surface measurement points on the crest and slopes. Two internal vertical settlement gauges (IVM) were installed in Horsetooth dam, both located close to the dam centreline at 3 m downstream of the dam axis (Figure G3.8).

In 1988, some 40 years after end of construction, crest modification works were undertaken at all four embankments to raise the crest levels by 1.5 to 2.5 metres. This was partly due to the large post construction settlements experienced at most of the embankments (discussed below) as well a requirement to raise the embankments to provide storage for the maximum probable flood.

3.3.1 Deformation Behaviour at Horsetooth Dam

3.3.1.1 Internal Settlement of Earthfill from IVM Gauges

The internal vertical strain profiles in the core of Horsetooth dam at end of construction are shown in Figure G3.10. In comparison to the vertical strain profile in the core of embankments with dry placed clay earthfills (Figure 7.18a in Section 7.4 of Chapter 7) the profiles at Horsetooth dam are "normal". The larger vertical strains of 3 to 5% near the base of IVM A may reflect placement of the earthfill at higher moisture content at the contact zone.

The settlement during construction of the foundation at Horsetooth dam, estimated from the settlement of the lowest cross-arm, was 955 mm at IVM A and 465 mm at IVM B. These values equate to vertical strains of almost 15% in the over-burden, assuming that all the foundation settlement was confined to the over-burden soil. Percentage wise these strains are very large, much larger than those within the embankment, and indicate the foundation soils to be highly compressible.

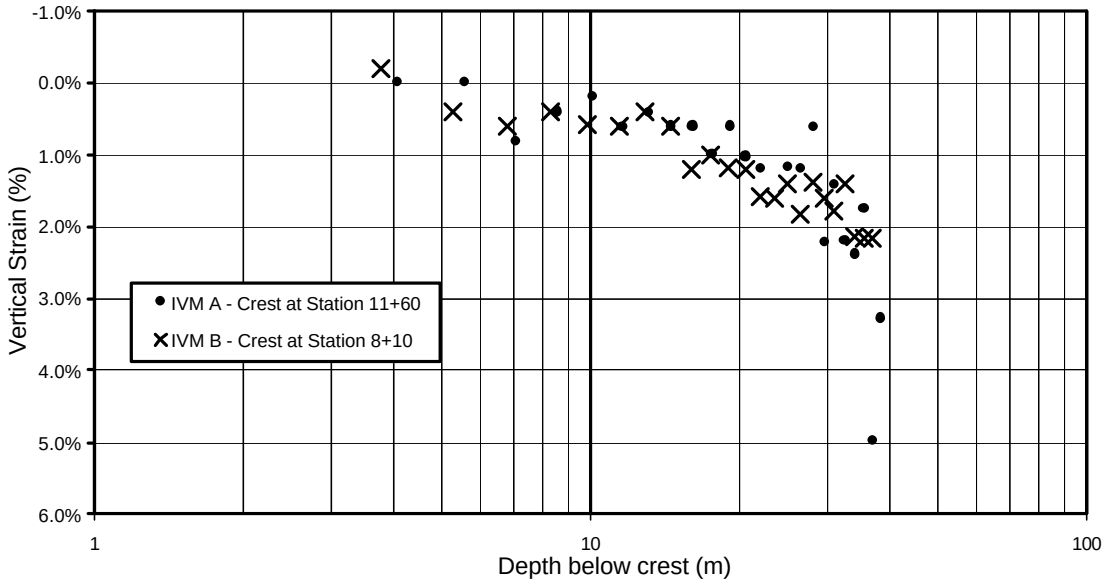

Figure G3.10: Horsetooth dam; internal vertical strain profiles at end of construction.

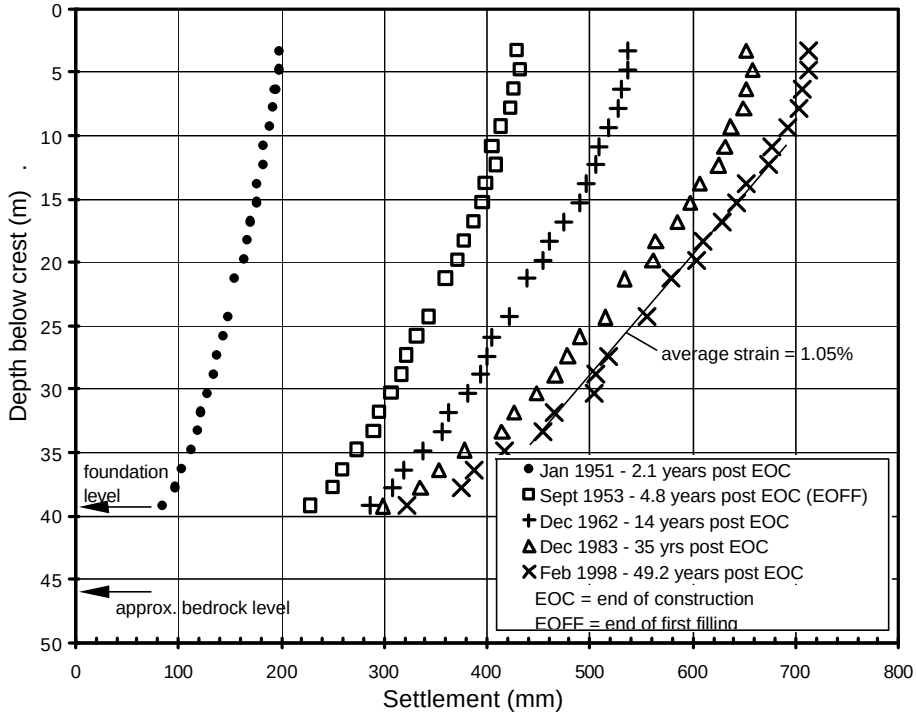

Figure G3.11: Horsetooth dam, post construction internal settlement profiles at IVM A.

The post construction internal settlement profile at IVM A (Figure G3.11) shows that:

- The settlement profile within the core of the embankment is “normal” as indicated by the smooth shape of the profiles.

- At 45 years after end of construction the vertical strains in most of the earthfill was on average 1.05%, with lower strains in the upper 8 m (average of 0.2%) and higher strains in the lower 6 m (average of 2.2%).
- A large portion of the post construction settlement at IVM A was within the foundation. 323 mm or 45% of the total post construction settlement was within the foundation. This equates to a post construction vertical strain of about 5% in the foundation soils, assuming all the settlement was within the over-burden soils.
- Most of the foundation settlement (about 70%) occurred within the first 5 years after construction, or during the period of first filling.
- About 50% of the post construction settlement in the earthfill core occurred during first filling. Very little settlement of the core has occurred since 1983, or more than 35 years after construction.

3.3.1.2 *Post Construction Surface Deformation at Horsetooth Dam*

The post construction settlement and displacement normal to the dam axis of SMPs on the crest and slopes of Horsetooth dam are shown in Figure G3.12 and Figure G3.13 respectively. The approximate SMP locations are shown in Figure G3.8a. Evaluation of the deformation data is complicated by the significant foundation influence and positioning of the cut-off trench in relation to the dam axis.

Notable aspects of the post construction settlement behaviour (Figure G3.12) are:

- Large settlements of the crest and downstream slope occurred on first filling, a large portion of which was within the foundation as indicated by the IVM records.
- In comparison, the magnitude of settlement on first filling of the upstream slope is much less. This is to be expected because the upstream SMP overlies the cut-off trench excavated to bedrock (Figure G3.8a).
- The long-term settlement rate (per log cycle of time) of the crest and upstream shoulder are relatively high in comparison to the rate prior to first filling and to that of the downstream shoulder. The settlement rate of the upstream slope does reduce after 30 years; suggesting it may be affected by the magnitude and depth of reservoir drawdown. The slight acceleration in the crest settlement rate at 23 to 29 years may possibly have occurred at the time of the large drawdown at year 27.
- In comparison to similar embankments:

- The long-term crest settlement rate of the embankment only (calculated from the IVM records) is on the high side, but is not "abnormally" high (Figure 7.63 in Section 7.6 of Chapter 7).
- The settlement of the downstream shoulder, particularly during drawdown, is large compared to similar embankments (Figure F2.11 in Appendix F). It is not considered "abnormal" because of the significant influence of the foundation settlement.
- The magnitude of settlement of the upstream shoulder (Figure 7.52 in Chapter 7, and Figures F2.28 and F2.22 in Appendix F) is large, possibly "abnormally" so.
- The settlement rate of the upstream slope from 8 to 30 years after construction at 0.8% per log cycle of time is high compared to similar embankments with very broad earthfill zones (Figure 7.83 and Table 7.23 in Section 7.6 of Chapter 7). After 30 years the rate has decreased significantly.

The post construction displacement normal to the dam axis at Horsetooth dam (Figure G3.13) shows:

- The period of negligible displacement in the first 2 years is prior to the start of reservoir filling.
- Large downstream displacement occurs on first filling. Displacements of this magnitude are unusual when compared with similar embankments (Figures 7.38 in Section 7.5 and 4.76 in Section 7.6 of Chapter 7, and Figures F2.19 and F2.36 in Appendix F), but the large settlement of the foundation downstream of the cut-off trench and the upstream location of the cut-off trench would have resulted in a downstream rotation of the embankment and therefore contributed significantly to the measured downstream displacement.
- Post first filling the displacement remained relatively steady and, for the most part, is considered "normal". The increase in displacement rate (per log cycle of time) after about 30 years, particularly evident for the downstream slope, is potentially indicative of "abnormal" behaviour.

USBR (1997) refer to the long-term trend of rising piezometric levels in a number of piezometers and comment that the earthfill is still saturating and is possibly yet to reach equilibrium conditions. This continued increase in pore water pressures in the earthfill

and therefore change in effective stress conditions may be a factor that is affecting the displacement behaviour.

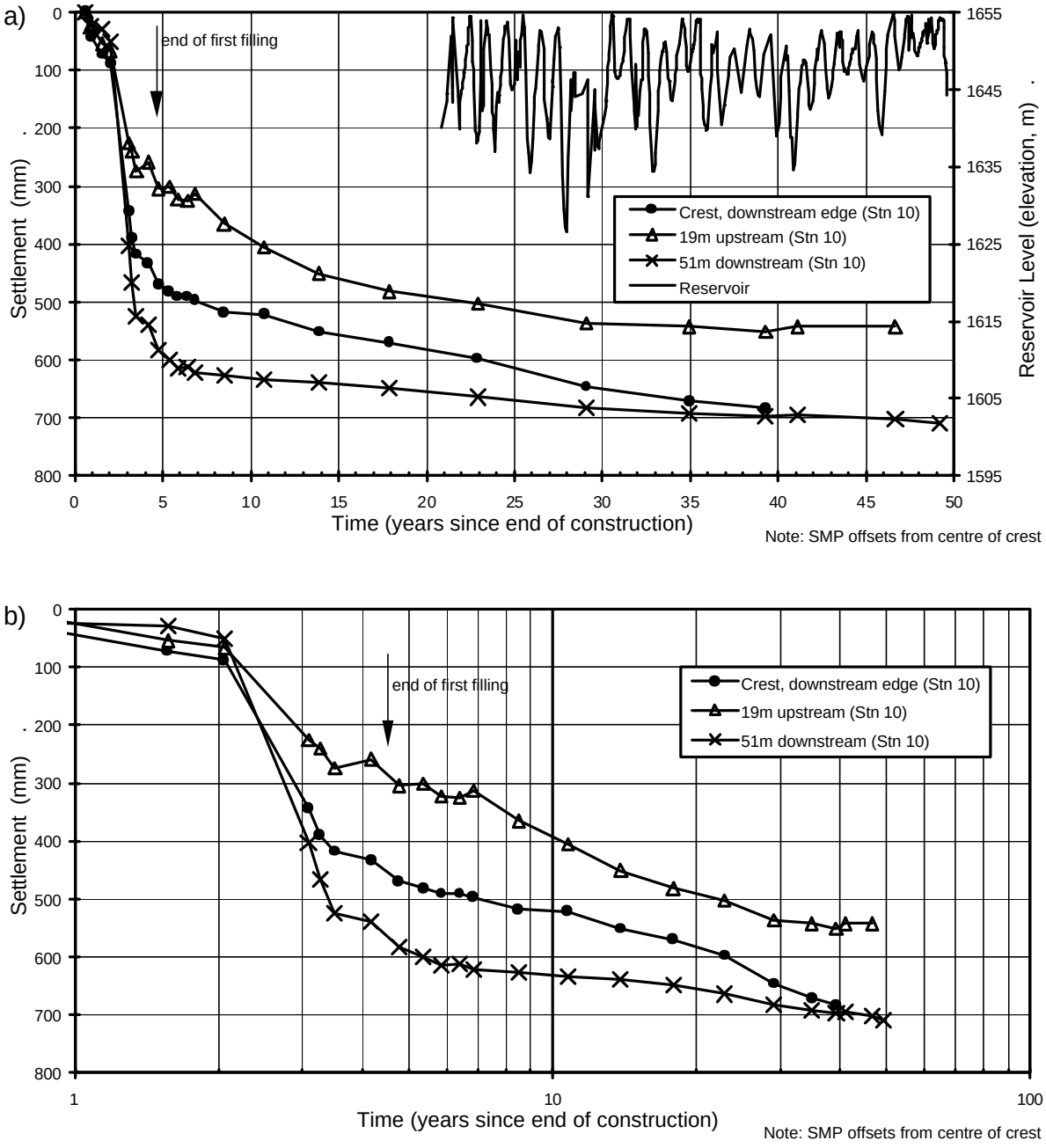

Figure G3.12: Horsetooth dam, post construction settlement of SMPs near to the main section.

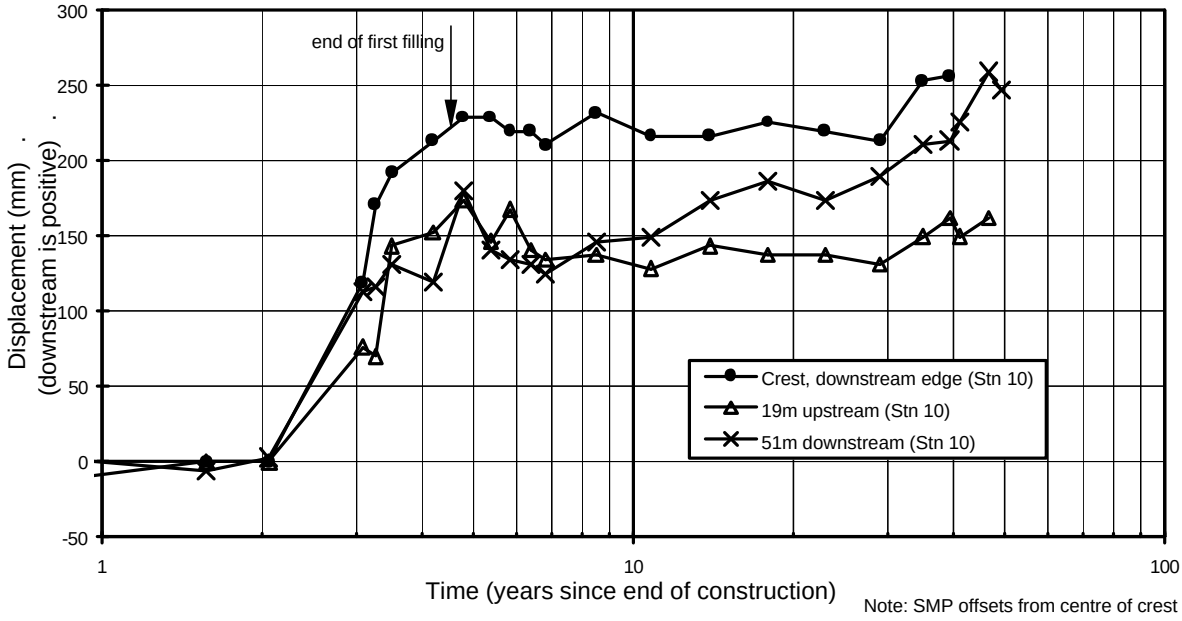

Figure G3.13: Horsetooth dam, post construction displacement of SMPs near to the main section.

3.3.2 Deformation Behaviour at Dixon Canyon Dam

The post construction deformation behaviour of Dixon Canyon dam is identified, from comparison with similar type embankments, as having several potentially "abnormal" aspects. However, it is difficult to evaluate the post construction deformation behaviour because it is not clear what influence the foundation has had. It is likely to have had some influence, and this is discussed below. The depth of the foundation soils at Dixon Canyon dam are much less than at Horsetooth dam, where the foundation had a significant influence, so the foundation influence would be expected to be less than that at Horsetooth dam.

Figure G3.14 presents the settlement and displacement behaviour of SMPs near to the main section. The SMP locations are shown on Figure G3.9a. Potentially "abnormal" aspects of the deformation behaviour at Dixon Canyon dam identified from comparison with similar type embankments are:

- Crest settlement – magnitude of 1.8% at 39 years and long-term settlement rate of 1.38% per log cycle of time. The magnitude of settlement (Figures 7.48 and 7.61 in Section 7.6 of Chapter 7) and the long-term crest settlement rate (Figure 7.63 in Chapter 7) are high, potentially "abnormally" so, for embankments with very broad

earthfill zones. The foundation is likely to have some, but possibly limited influence as the SMP is located over the downstream slope of the cut-off trench.

- Settlement of the upstream slope - "abnormally" large magnitude of settlement (Figures 7.52 in Chapter 7, and Figures F2.22 and F2.28 in Appendix F) and "abnormally" high long-term settlement rate (Figure 7.83 in Chapter 7). At 47 years the settlement is 1.97% of the height from the SMP to foundation and the long-term settlement rate is 1.38% per log cycle of time. The foundation is likely to have a limited influence, as the SMP is located over the cut-off trench.
- Displacement of the upstream slope – large upstream displacement on first filling and for several years thereafter, and change to downstream displacement from about 30 years. Compared to similar embankments the displacement of the upstream slope (Figure F2.36 in Appendix F) is potentially "abnormal". But, it may not be appropriate to label the displacement as "abnormal" because it is not known what influence the differential settlement of the foundation has on the displacement of the upstream slope. A large settlement of the foundation upstream of the cut-off trench on first filling may have had a significant influence on the upstream displacement of the upstream slope, which is quite different to that of the crest and downstream slope. Collapse type deformations on wetting of the dry placed earthfill could also explain the displacement behaviour.
- Settlement of the downstream slope – large magnitude of settlement (Figures F2.3 and F2.11 in Appendix F) and high long-term settlement rate (Figure 7.78 in Section 7.6 of Chapter 7). The foundation may potentially have a significant influence.
- Displacement of the downstream slope – "normal" during first filling, but the continuing downstream displacement at a near constant rate per log cycle of time is potentially "abnormal" (Figure F2.19 in Appendix F).

Collapse type settlement on wetting of the dry placed earthfill could possibly explain the large post construction settlements of the crest and upstream slope as well as the upstream then downstream displacement trend for the upstream slope, which is not that dissimilar to the behaviour at Rector Creek. USBR (1997) indicates that the piezometric levels at Dixon Canyon dam show a long-term rising trend. This continued increase in pore water pressures and change in effective stress conditions in the very broad earthfill zone, as well as progressive saturation, may be influencing the deformation behaviour at Dixon Canyon dam.

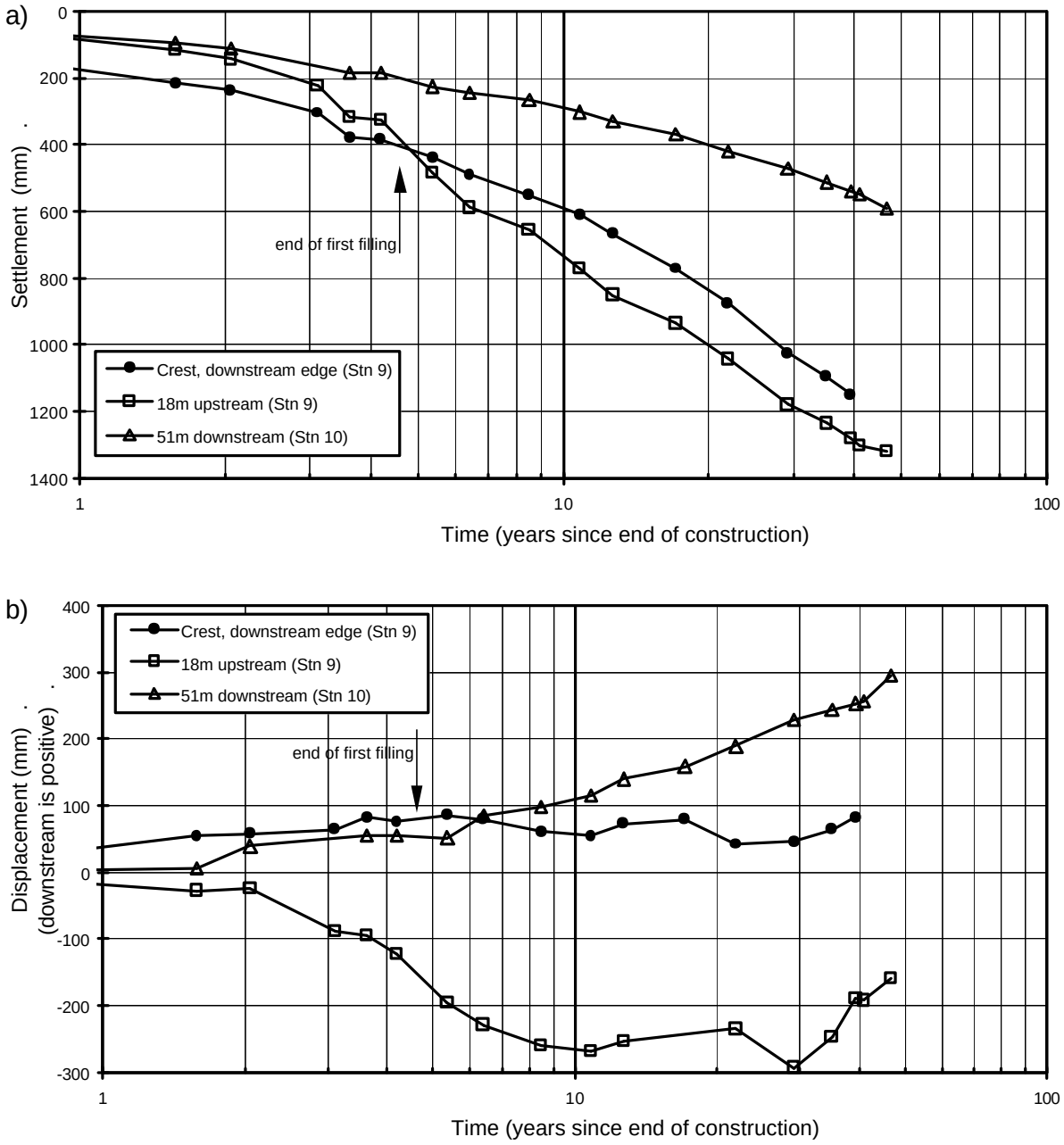

Figure G3.14: Dixon Canyon dam; post construction *(a)* settlement and *(b)* displacement normal to the dam axis of SMPs near to the main section.

3.3.3 Deformation Behaviour at Spring Canyon Dam

The post construction deformation behaviour of Spring Canyon dam is similar to that at Dixon Canyon dam and shows, in comparison with similar type embankments, similar potentially "abnormal" aspects. As for Dixon Canyon dam, it is difficult to evaluate the deformation behaviour at Spring Canyon dam because the extent of the influence of the foundation is not known.

Figure G3.15 presents the post construction settlement and displacement normal to the dam axis of SMPs at Spring Canyon dam near to the main section. The SMP locations are very similar to those at Dixon Canyon dam (Figure G3.9a). Potentially "abnormal" aspects of the deformation behaviour at Spring Canyon dam identified from comparison with similar type embankments and other aspects from Figure G3.15 are:

- Crest settlement – large magnitude of settlement (Figures 7.48 and 7.61 in Section 7.6 of Chapter 7), 1.5% at 39 years, and potentially "abnormally" high long-term crest settlement rate of 1.3% per log cycle of time (Figure 7.63 in Chapter 7). The foundation is likely to have some, but possibly limited influence as the SMP is located over the downstream slope of the cut-off trench.
- Settlement of the upstream slope - "abnormally" large magnitude of settlement (Figures 7.52 in Chapter 7, and Figures F2.22 and F2.28 in Appendix F), 1.54% at 47 years. High, but not "abnormally" so, long-term settlement rate (Figure 7.83 in Chapter 7). The long-term settlement rate was relatively high in the period from post first filling to 30 years after construction, but has since reduced in the last 15 years. The foundation is likely to have a limited influence, as the SMP is located over the cut-off trench.
- Displacement of the upstream slope – upstream displacement on first filling and for several years thereafter, and change to downstream displacement from about 18 years. The magnitude of displacement of the upstream slope at Spring Canyon dam is considered to be within the range of similar embankments (Figure F2.36 in Appendix F).
- Settlement of the downstream slope – large magnitude of settlement (Figure F2.3 and F2.11 in Appendix F) and high long-term settlement rate (Figure 7.78 in of Chapter 7). The foundation may potentially have a significant influence.
- Displacement of the downstream slope – "normal" during first filling, but continuing downstream displacement at a near constant rate per log cycle of time is potentially "abnormal" (Figure F2.19 in Appendix F).

The influence of the foundation on the embankment deformation behaviour at Spring Canyon dam is not well known. Its influence on the settlement of SMPs on the crest and upper upstream slope will be limited because this region of the embankment overlays the cut-off trench founded on bedrock, but it has probably influenced the deformation of SMPs on the downstream shoulder. Differential settlements between the

foundation and cut-off trench earthfill may cause some upstream rotation of the upstream slope of the embankment and similarly some downstream rotation of the downstream slope. Collapse type settlements on wetting of the dry placed earthfill could be a significant factor influencing the deformation behaviour at Spring Canyon dam.

As for the other Horsetooth Reservoir embankments, the piezometric levels at Spring Canyon dam show a long-term rising trend. As previously discussed, this could influence the deformation behaviour due to changes in effective stress conditions and softening of material strength properties.

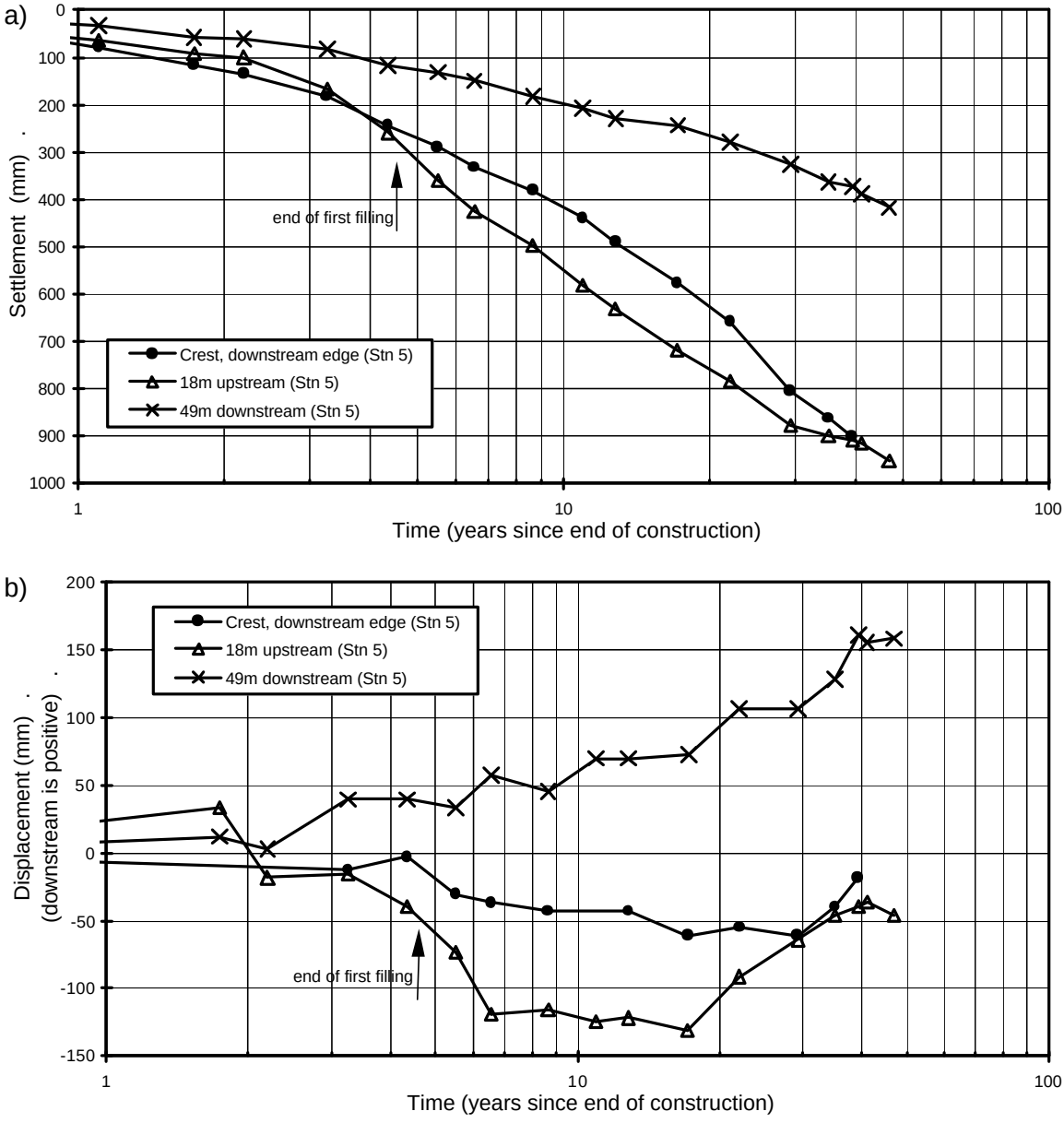

Figure G3.15: Spring Canyon dam; post construction *(a)* settlement and *(b)* displacement normal to the dam axis of SMPs near to the main section.

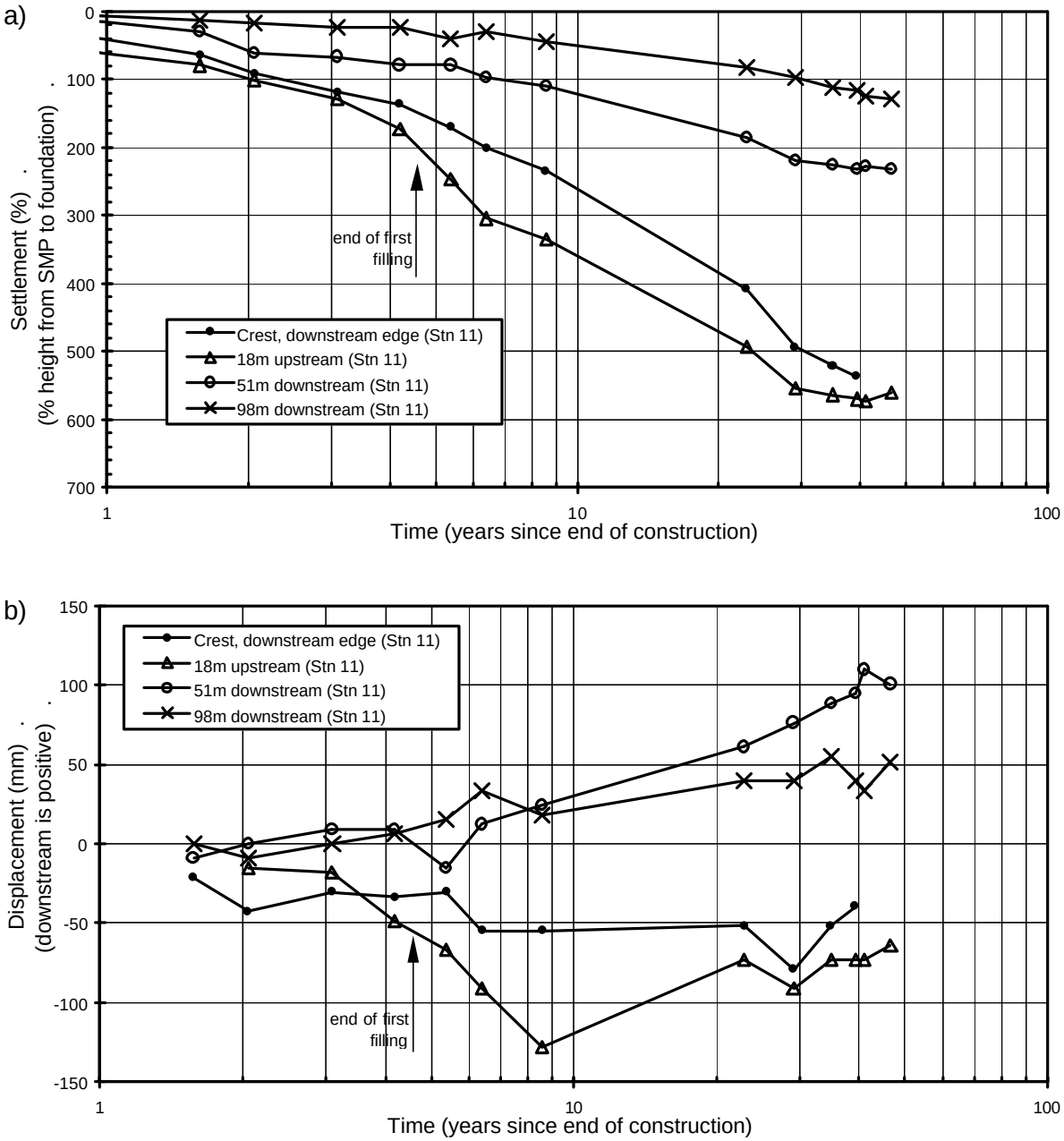

Figure G3.16: Soldier Canyon dam; post construction *(a)* settlement and *(b)* displacement normal to the dam axis of SMPs near to the main section.

3.3.4 Deformation Behaviour at Soldier Canyon Dam

Figure G3.16 presents the post construction settlement and displacement normal to the dam axis of SMPs near to the main section for Soldier Canyon dam. The SMP locations are very similar to those at Horsetooth dam shown in Figure G3.8a, and those on the upper upstream slope and downstream edge of the crest overlay the cut-off trench excavated to bedrock.

In comparison to similar type embankments with a very broad earthfill zone, the post construction deformation behaviour at Soldier Canyon is, for the most part, considered "normal" and therefore contrasts some aspects of the deformation behaviour at Spring and Dixon Canyon dams. The magnitude of settlement and long-term rate of settlement of the crest and slopes are within the typical range of similar embankments. The displacement behaviour shows similar trends to that observed at the other Horsetooth Reservoir embankments, but the magnitude of displacement is generally lower.

3.3.5 Summary of Post Construction Deformation of the Horsetooth Reservoir Embankments

From the previous discussions for the Horsetooth Reservoir embankments it is evident that there are similarities in the post construction deformation behaviour of SMPs on the crest and slopes for several of the embankments, as well as differences and several potentially "abnormal" aspects. This section presents a summary of the possible factors affecting the embankment deformation behaviour. Table G3.2 presents a summary of selected post construction measurement indices for each of the embankments.

The deformation of the foundation was shown to significantly affect aspects of the deformation behaviour at Horsetooth dam, most notably the displacement of the embankment and settlement of SMPs not vertically aligned over the region of the cut-off trench, i.e. those SMPs on the crest and downstream slope. The foundation influence was very significant during the period of first filling, but not greatly significant thereafter. For the other Horsetooth Reservoir embankments the influence of the foundation cannot be quantified, but is thought to be of much lesser significance based on the deformation trends. In particular, the settlement and displacement of SMPs on the downstream slope during first filling show the behaviour at Horsetooth dam to be vastly different from that at the other embankments.

Apart from the influence of the foundation at Horsetooth dam, several potentially "abnormal" aspects of deformation behaviour are evident. In summary, these are:

(i) The large magnitude of settlement of the crest and/or upper upstream slope region at Horsetooth, Dixon Canyon and Spring Canyon dams.

(ii) The high long-term settlement rate of the crest and/or upper upstream slope region at Dixon Canyon and Spring Canyon dams.

(iii) The increase in displacement rate to downstream many years after the end of first filling or high long-term displacement rate of SMPs on the upper upstream slope, crest and downstream slope observed for all embankments.

Table G3.2: Summary of measured post construction deformations at the Horsetooth Reservoir dams.

Measurement	**Typical Range (*[1], *[2])**	**Horsetooth**	**Dixon Canyon**	**Spring Canyon**	**Soldier Canyon**
Crest Settlement: - Magnitude at 20 to 25 yrs - LTSR *[3]	 0.05 to 0.76% 0.07 to 0.70 % (most < 0.35%)	 0.97 0.62	 1.37 1.38	 1.06 1.31	 0.61 0.61
Crest Displacement: - first filling - post first filling	 -50 to 200 mm -20 to 120 mm	 229*[4] 27	 88 6	 -30 -15	 -30 -6
Downstream Slope, Settlement: - Magnitude at 20 to 25 yrs - LTSR	 < 0.50% < 0.40%	 3.7 *[4] 0.88	 0.81 1.08	 0.76 0.85	 0.41 0.33
Downstream Slope, Displacement: - first filling - post first filling to 47 years	 0 to 110 mm na	 180 *[4] 67	 52 244	 34 124	 9 92
Upstream Slope, Settlement: - Magnitude at 20 to 25 yrs - LTSR	 0.40 to 0.80% 0.10 to 0.60%	 1.26 0.80, 0.23 *[5]	 1.56 1.38	 1.31 0.61	 0.77 0.56
Upstream Slope, Displacement: - first filling - post first filling to 47 years	 -125 to 50 mm na	 174 *[4] -12	 -195 37	 -73 27	 -67 3

*[1] Typical range for embankments with very broad central earthfill zones

*[2] For displacements, -ive values indicate upstream and +ive values downstream displacement

*[3] LTSR = long-term settlement rate in % per log cycle of time

*[4] For Horsetooth dam settlement of the foundation had a significant influence on the deformation

*[5] 0.80% is the average for the period 7 to 30 years after construction, and 0.23% the average after 30 years.

For most of these points the magnitude and rate of deformation is greatest at Dixon Canyon dam.

For (i) and (ii) collapse type settlements on wetting of the initially dry placed earthfill is considered a possible factor affecting the settlement behaviour. Related to this would be the effect of softening due to wetting on the strength and compressibility properties of the earthfill. At Spring Canyon and Horsetooth dams (and Soldier Canyon dam) the settlement rate (per log cycle of time) of SMPs on the upstream slope decreases after 30 years. This may be related to a general reduction in the magnitude of

drawdown at about this point in time, but this is not clear as available reservoir records start at 21 years.

For (iii) the higher average reservoir level after 35 years and the continued increase in pore water pressure within the earthfill zone (USBR 1997) are considered to have influence the observed downstream displacement trend of the SMPs. The increase in pore water pressures would affect the effective stress conditions within the embankment and it also suggests that equilibrium conditions are yet to be reached, indicating that progressive saturation is still occurring.

An interesting aspect of the deformation behaviour is the lesser magnitude and lower rates of deformation at Soldier Canyon dam, which are more in line with "normal" type deformation behaviour (Table G3.2). The reason for this is not known.

3.4 PUEBLO DAM

Pueblo dam, located on the Arkansas River just upstream of Pueblo, Colorado USA, was constructed in the early to mid 1970's and comprises a central concrete buttress section of 63 m maximum height in the river section flanked by zoned earthfill embankments on the abutments (Figure G3.17). The right abutment embankment (Figure G3.18) is of 51 m maximum height and about 1400 m length and the left abutment embankment (Figure G3.19) is of 37 m maximum height and about 1100 m length. The embankment designs for the right and left abutment embankments are similar and both comprise a very broad main earthfill zone.

Both embankments are founded predominantly on over-burden soils, up to 20 m and 7 m depth for the right and left embankments respectively, with a central cut-off trench to bedrock. Kinney and Bartholomew (1987) refer to the presence of loess deposits in the foundation of a portion of the right abutment embankment that were susceptible to collapse settlement on saturation and loading. They indicate that these regions of the foundation were wetted prior to embankment construction to assist with consolidation settlement during construction. Settlements in the foundation under the upstream shoulder of the right abutment embankment were measured at 350 to 450 mm during construction.

For both embankments, the main earthfill zone (Zone 1) consisted of clay to gravel size alluvium placed in 150 mm layers and compacted by tamping rollers. The moisture specification required the mean moisture content to be in the range 0.5% dry to 1.5%

dry of Standard Proctor optimum. Coarser and more permeable alluvial soils were used in the outer up and downstream regions. In the downstream shoulder of the right abutment embankment Zone 4 comprised limestone, sandstone and shale fragments placed in 300 mm layers, moisture conditioned and compacted. In addition, a relatively small zone of sandstone rockfill was placed in the lower upstream shoulder (Figure G3.18); placed in 0.9 m layers without formal compaction.

Shear type deformations along weak bentonitic clay seams in the shale foundation (of the Graneros Formation) were identified as a potential mechanism of deformation during embankment construction. Inclinometers were therefore installed in the toe regions of the embankments prior to construction to monitor for these potential deformations. When the embankment was within about 7 m of crest level shear type deformations were measured in the downstream toe region of the left abutment embankment. Additional inclinometers were installed in this region and showed shear type deformations along the weak bentonitic clay seams in the foundation at depths of 3 to 11 m below foundation level. By end of construction total shear type displacements were estimated at more than 150 mm at the downstream toe of the left abutment embankment (USBR 1996). The shear deformations virtually ceased shortly after the end of construction. A stability berm (Figure G3.19) was constructed in the early 1980's (about 5 years after end of construction) along the downstream toe of the left abutment embankment due to concerns over the potential limiting stability of the downstream slope.

3.4.1 Post Construction Deformation of the Right Abutment Embankment

The post construction settlement and displacement normal to the dam axis of SMP on the crest and slopes of the right abutment embankment are shown in Figure G3.20 and Figure G3.21 respectively (data courtesy of the U.S. Bureau of Reclamation). Settlements are plotted in millimetres rather than as a percentage of the embankment height due to the possible influence of the foundation on the deformation behaviour. The trend of the post construction deformation behaviour is considered to be "normal", although, the displacements are difficult to evaluate due to their erratic behaviour.

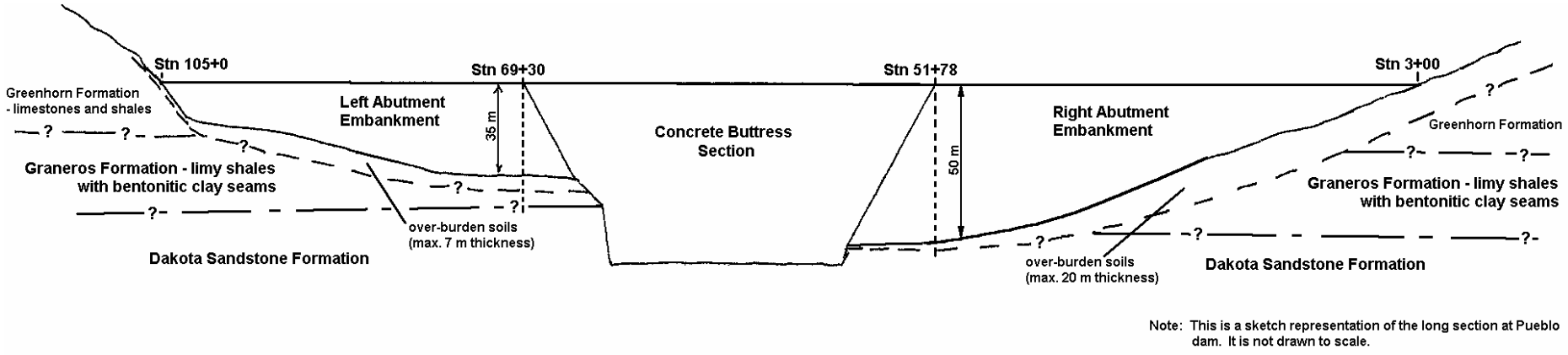

Figure G3.17: Pueblo dam, sketch representation of the long section showing the geological units of the foundation.

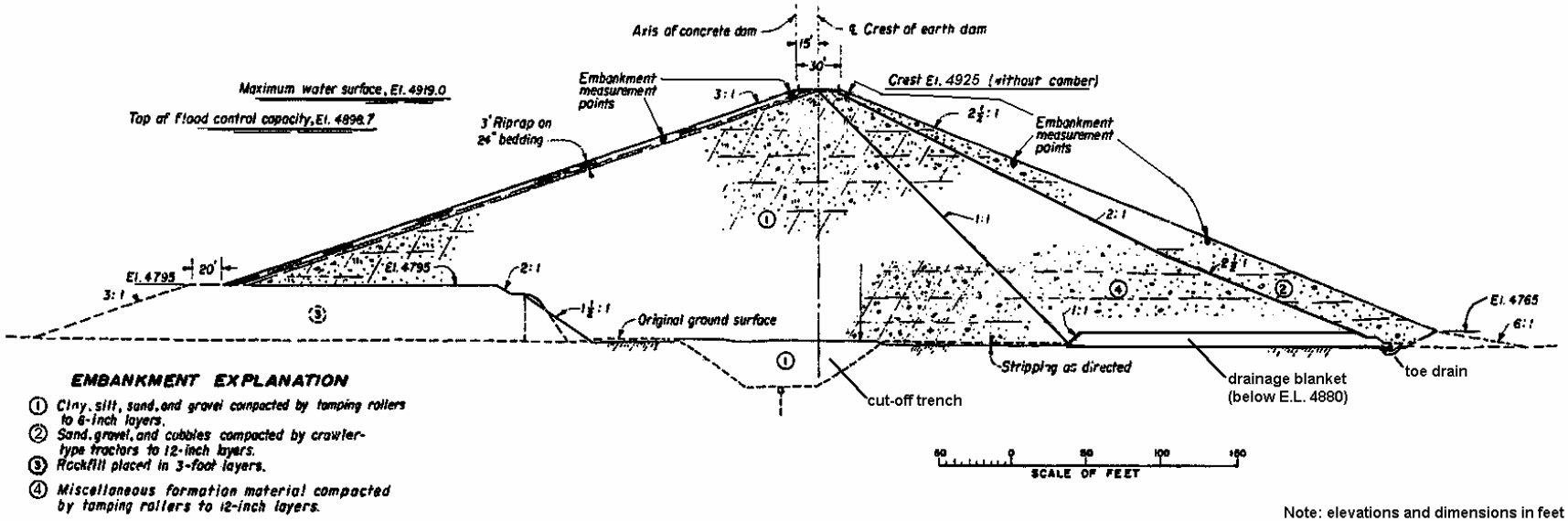

Figure G3.18: Pueblo dam; typical section of the right abutment embankment (courtesy of U.S. Bureau of Reclamation).

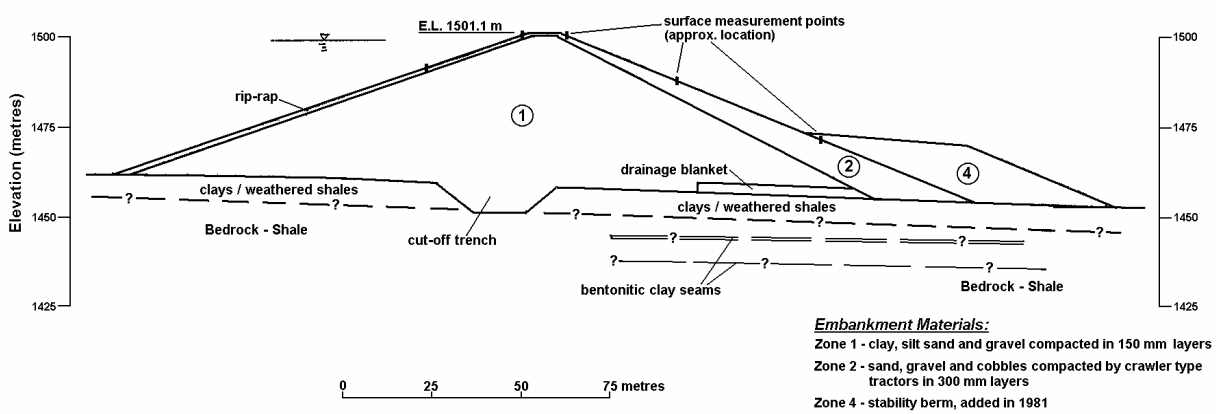

Figure G3.19: Pueblo dam; cross section of the left abutment embankment at Station 75.

The deformation behaviour of the downstream shoulder of the right embankment compared to similar type embankments shows that the magnitude of settlement in on the large side (Figure F2.10 in Appendix F) and long-term settlement rate on the high side (Figure 7.78 in Section 7.6 of Chapter 7). In comparison to the SMPs in the crest region, which are located over the cut-off trench excavation, the trend of the settlement of the downstream slope is similar (Figure G3.20). This suggests that the foundation under the downstream slope contributes to the measured post construction settlement and would account for the relatively large magnitude and high long-term settlement rate in comparison to other embankments.

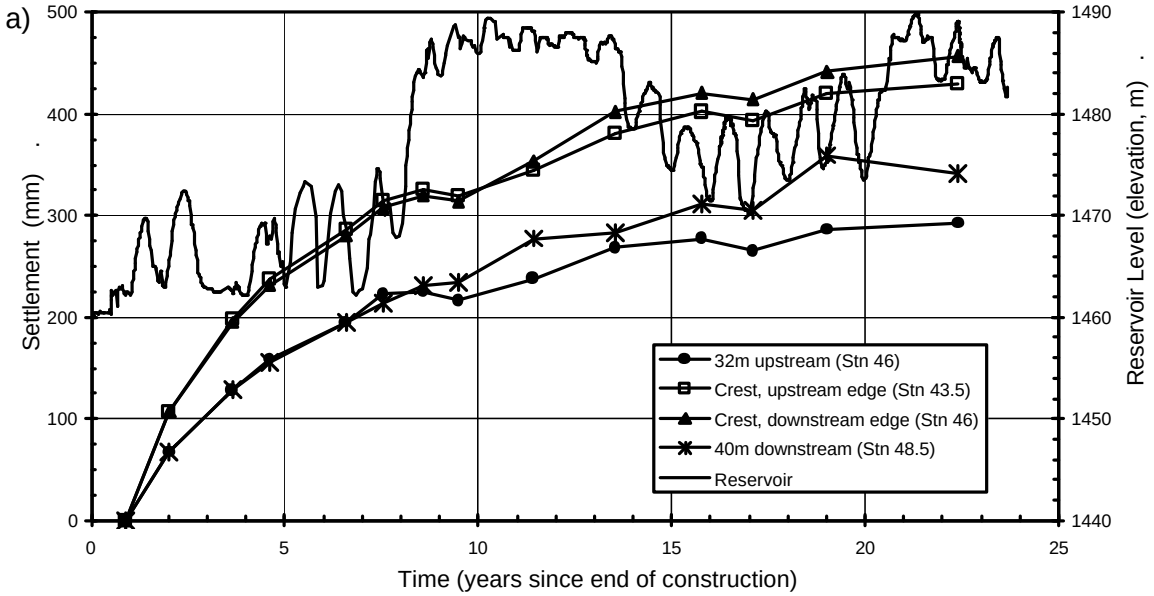

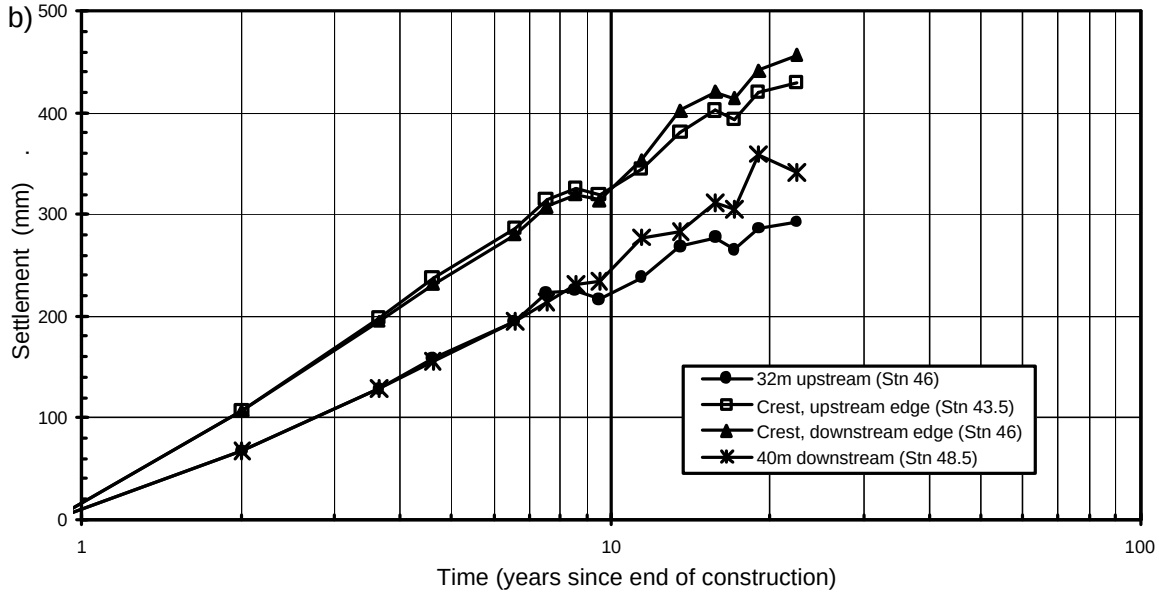

Figure G3.20: Pueblo dam; post construction surface settlement near maximum section of right abutment embankment.

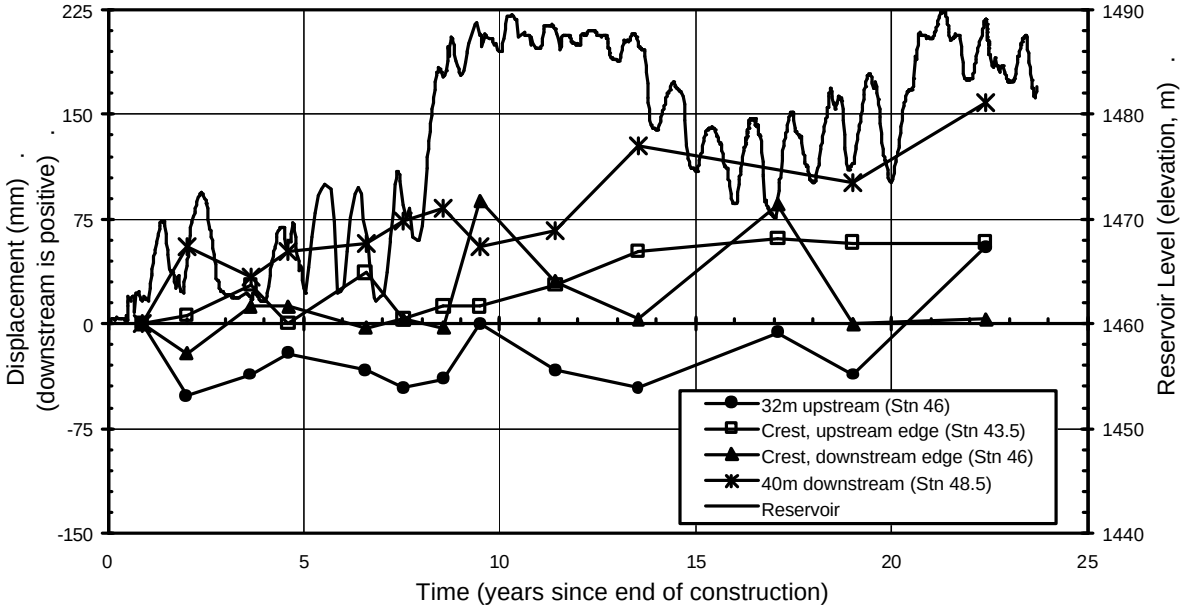

Figure G3.21: Pueblo dam, post construction displacement normal to the dam axis of the right abutment embankment.

3.4.2 Post Construction Deformation of the Left Abutment Embankment

The post construction settlement and displacement normal to the dam of SMPs on the crest and slopes of the left abutment embankment near Station 75 are shown in Figure G3.22 and Figure G3.23 respectively.

The depth of over-burden under the embankment shoulders of the left abutment embankment is much less than that of the right embankment. In the vicinity of Station

75, borehole records indicate the soils are mainly weathered shales, for which the post construction deformation is likely to be limited and therefore not greatly influence the deformation behaviour of the embankment. In addition, the shear type deformations observed in the foundation during construction had virtually ceased at the end of construction, and therefore would not influence the post construction deformation behaviour of the downstream shoulder with the stability berm added.

The deformation records show that large settlements were measured for the downstream shoulder, which are particularly evident when the settlement is plotted as a percentage of the height from the SMP to foundation level (Figure G3.22b). The displacement data, whilst erratic, appears to be "normal" for the most part. The last reading at 22.5 years after construction shows a large downstream displacement of the downstream crest and large upstream displacement of the upstream slope (but not the crest). These readings are unusual when compared to the previous readings and those at the other SMPs, and may be due to survey inaccuracy or error.

In comparison to similar type embankments with very broad earthfill zones:

- The settlement behaviour of the crest and upstream slope are "normal", although the long-term crest settlement rate is on the high side (Figure 7.63 in Section 7.6 of Chapter 7).
- The displacement of the crest and slopes, although erratic, is considered "normal".
- The total settlement of the downstream slope (Figure F2.10 in Appendix F) is "abnormally" high in comparison to similar type embankments. The long-term settlement rate of this SMP is on the high side, but not "abnormally" so (Figure 7.78 in Chapter 7).

As Figure G3.22 shows, the first settlement reading after the base survey of the SMP on the downstream shoulder is very high, almost 150 mm, and contributes significantly to the large post construction settlement (0.75% of a total of 1.78% over 23 years, or 42% of the measured post construction settlement). After this first reading the settlement behaviour is similar in magnitude to other SMPs on the embankment crest and upstream slope, although the settlement rate (per log cycle of time) is slightly higher. Other SMPs along the downstream slope of the left embankment abutment in the vicinity of Station 75 show similar settlement behaviour.

It is not clear what the cause of this observed settlement behaviour for the downstream shoulder is. It is not due to shear type deformations involving the

foundation and nor is it due to construction of the stability berm, which started in 1980 some 5 to 5.5 years after end of construction.

Apart from this, the post construction deformation behaviour at the left abutment embankment of Pueblo dam is considered “normal”.

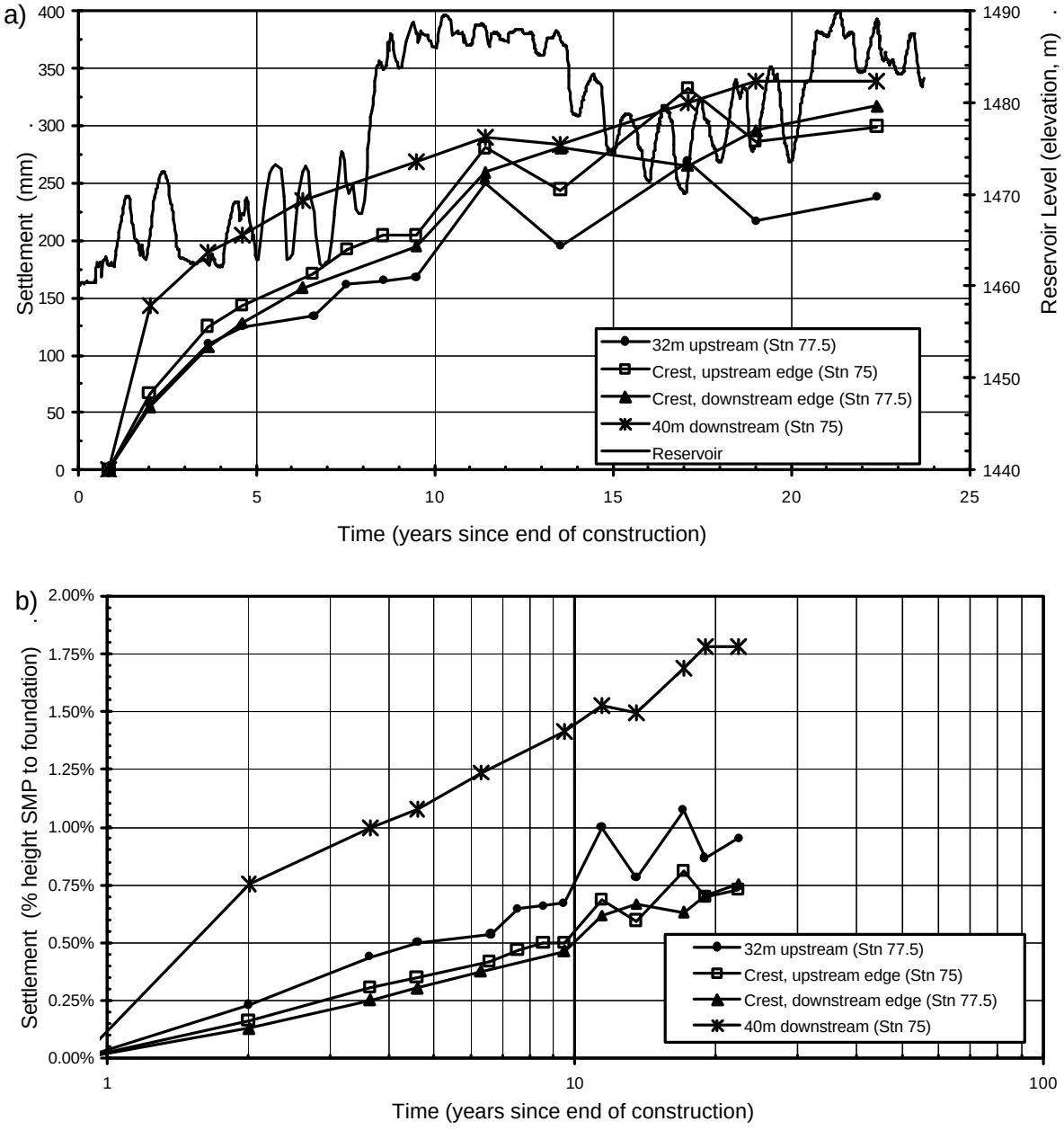

Figure G3.22: Pueblo dam, post construction settlement of the left abutment embankment near Station 75.

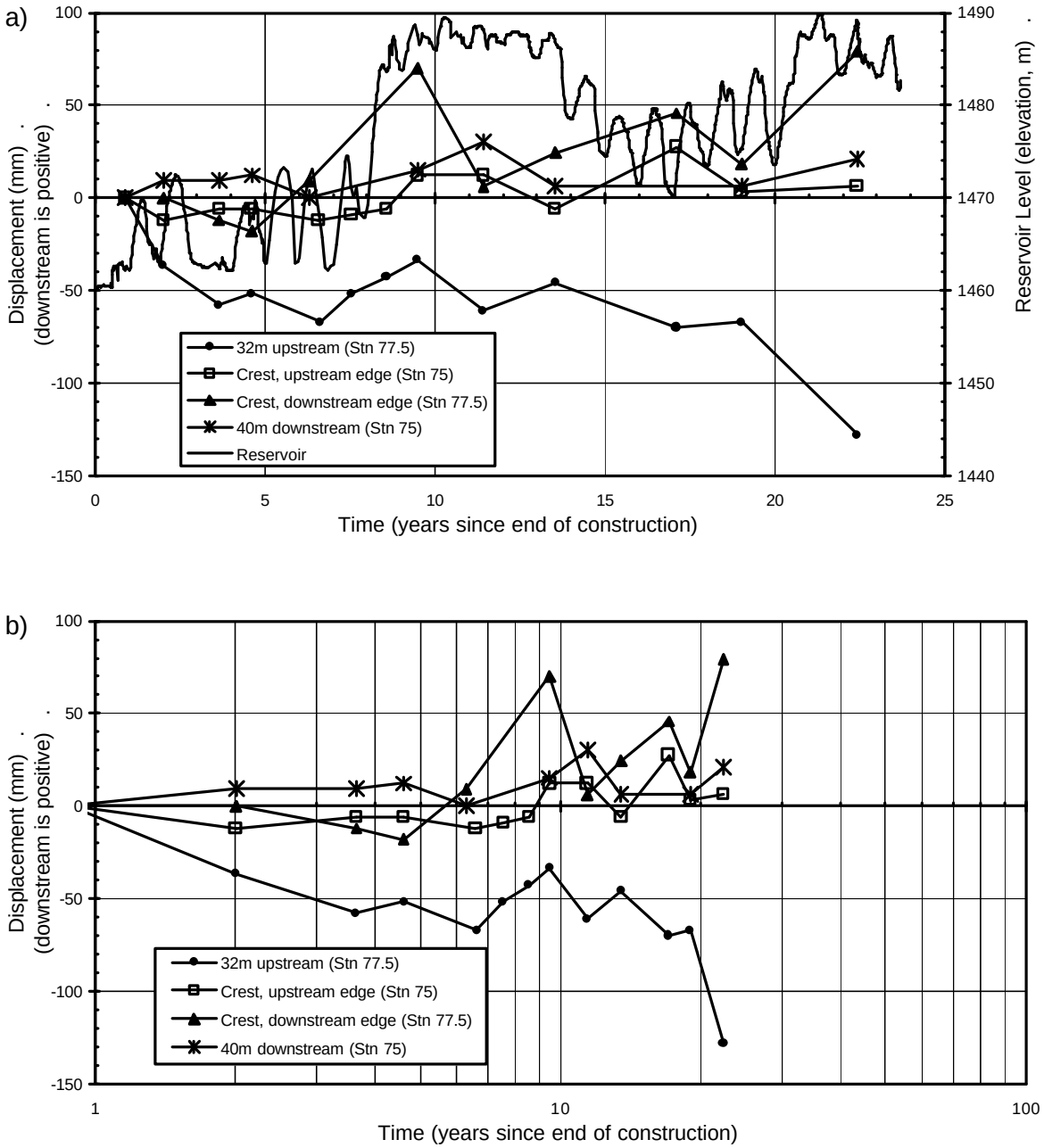

Figure G3.23: Pueblo dam, post construction displacement (normal to the dam axis) of the left abutment embankment near Station 75.

3.5 RECTOR CREEK DAM

Rector Creek dam (Sherard et al 1963; Sherard 1973; ICOLD 1974), located in California USA, is a 61 m high zoned earthfill embankment (Figure G3.24). A broad central cut-off was excavated to bedrock and the shoulder regions were founded on pervious soils of up to 15 m depth. Embankment construction was completed in January 1947. The central earthfill region (Zones 1 and 2) was of silty to clayey sands

with low plasticity fines sourced from residual, partially metamorphosed igneous rock. Finer grained earthfills were used in the central core region (Zone 1) and the coarser earthfills in the outer Zone 2 region. Compaction was in 150 mm layers by heavy sheepsfoot roller. ICOLD (1974) indicates that, although wetted in the borrow area, the earthfills in Zones 1 and 2 were placed at moisture contents in the range 2 to 4% dry of optimum.

The post construction deformation of SMPs on the crest near to the main section (Figure G3.25) shows the large magnitude of crest settlement, close to 1.8% at 10 years after construction, and the large upstream then downstream displacement. In comparison to similar embankments a number of aspects of the post construction crest deformation of Rector Creek dam are "abnormal" to the general trend, they include:

- The large magnitude of crest settlement (Figures 7.46, 7.47 and 7.60 in Section 7.6 of Chapter 7).
- The "abnormally" high long-term crest settlement rate of 1.65% per log cycle of time (refer Figure 7.63 in Chapter 7).
- The large upstream displacement of the crest on first filling of almost 300 mm (Figure 7.38 in Section 7.5 and Figure 7.75 in Section 7.6 of Chapter 7). This is clearly an outlier to the generally observed behaviour.
- The large downstream displacement post first filling of almost 350 mm, and the continued high downstream displacement rate (rate in log time) from 2.3 to 10 years after construction (Figures 7.75 and 7.77 in Section 7.6 of Chapter 7).

ICOLD (1974) consider that collapse settlement on wetting of the dry placed earthfill and the gradual development of the phreatic surface within the embankment contributed to the observed crest settlement and displacement behaviour, and to the observed cracking (see below). Initial wetting and collapse settlement of the upstream shoulder resulted in the upstream displacement of the crest, and subsequent wetting and collapse settlement in the central to downstream portion of the embankment resulted in the change in direction of displacement to downstream some 2 to 2.3 years after construction. Notably, the large fluctuations in reservoir level have a limited influence on the crest displacement.

Cracking of the embankment (Sherard et al 1963; Sherard 1973; ICOLD 1974) was observed in February 1947 shortly after completion of construction and shortly after the start of first filling. A diagonal crack across the crest was observed on the left abutment

about 30 m from the end of the dam. The width of the crack was about 20 mm at crest level and of 12 to 13 mm width at 8 m depth below crest. Further cracking on both abutments occurred near each end of the dam in December 1949 (almost 3 years after end of construction), but these cracks self healed. The cracking was located in areas where longitudinal extension of the crest in the direction of the dam axis was recorded.

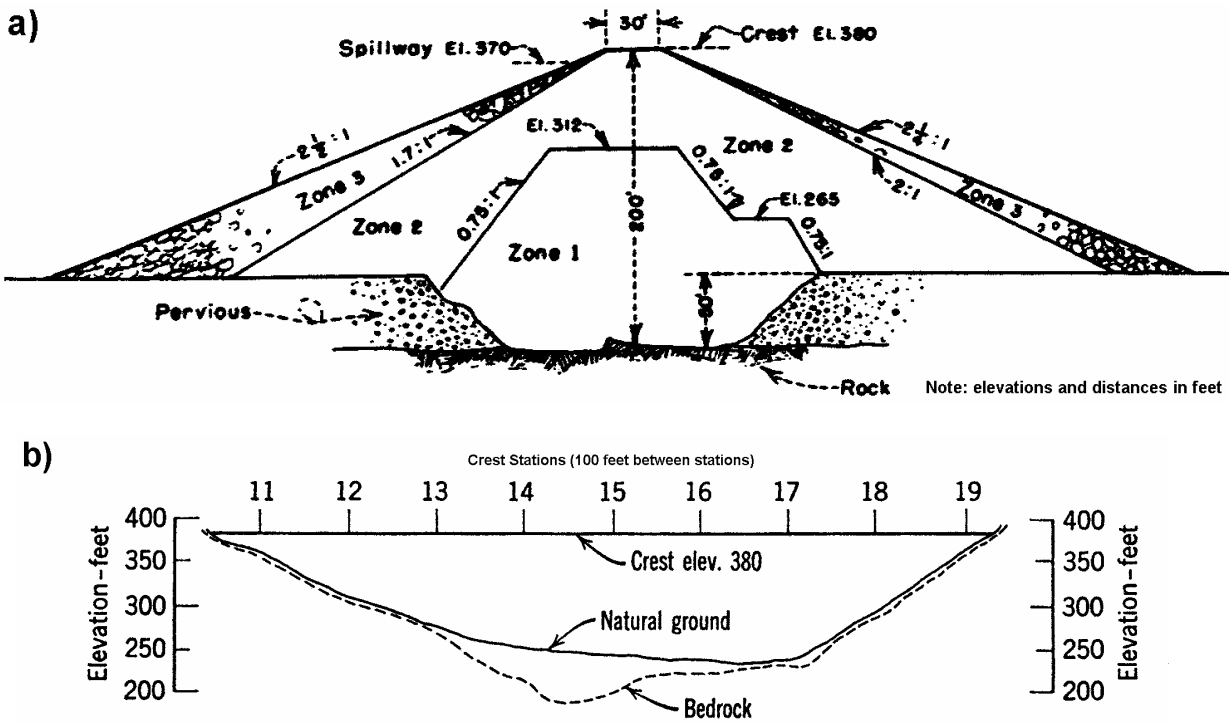

Figure G3.24: Rector Creek dam; *(a)* main section (Sherard 1953), and *(b)* long section (Sherard et al 1963)

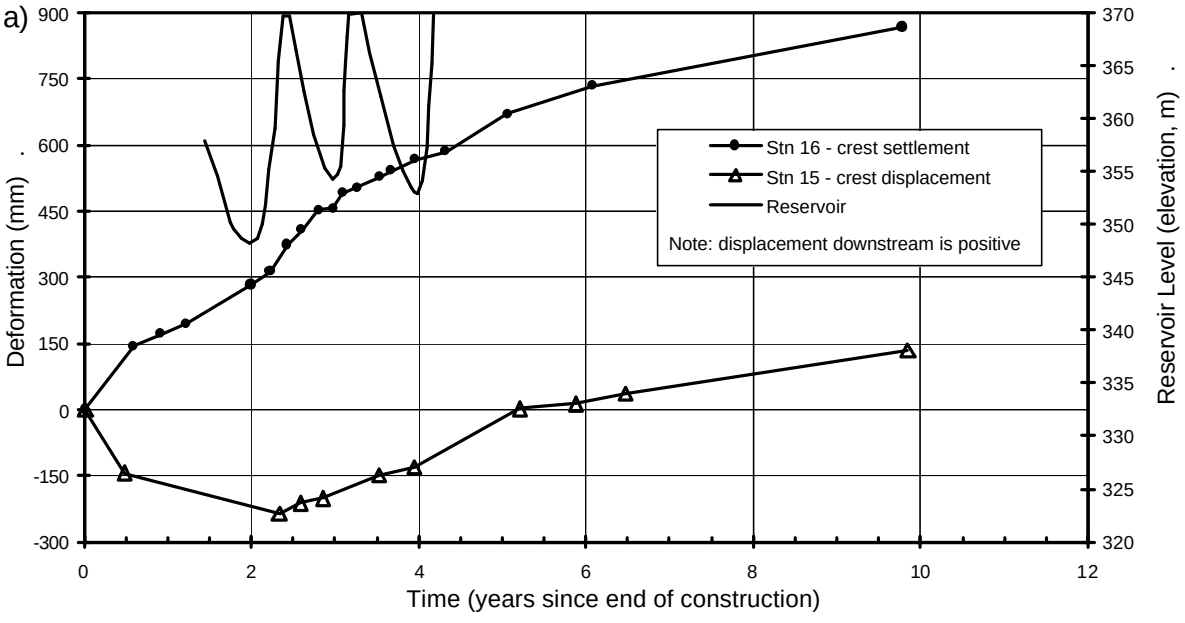

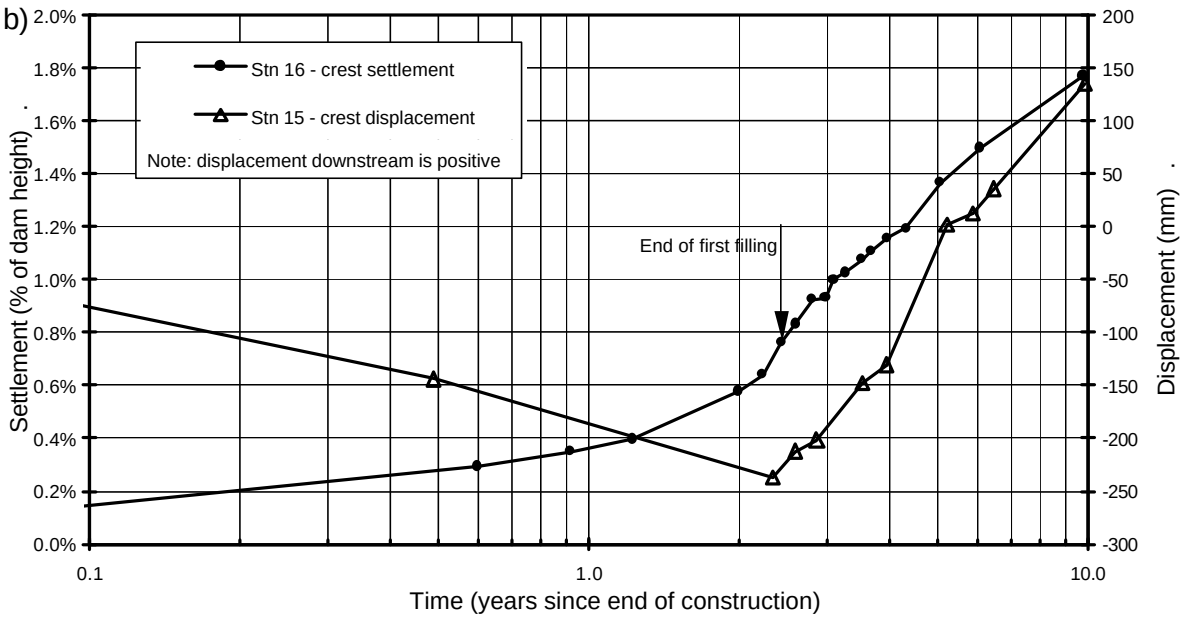

Figure G3.25: Rector Creek dam; post construction settlement and displacement versus *(a)* time on normal scale, and *(b)* log time (adapted from Sherard et al 1963).

4.0 EARTHFILL AND HOMOGENEOUS EARTHFILL EMBANKMENTS

4.1 BELLE FOURCHE DAM

Belle Fourche dam (Figure G4.1 and Figure G4.3), located in South Dakota, USA, is an earthfill embankment with small downstream rockfill toe. The embankment is of 35 m maximum height and about 1850 m crest length, and was constructed over the period 1905 to 1911. Foundations for the embankment consist of medium plasticity alluvial adobe clay of 2 to 12 m thickness overlying thin sand and gravel layer and in-turn shale bedrock. In summary, features of the embankment design, construction materials and placement methods include:

- The embankment has steep upstream and downstream slopes for the type of construction materials used.
- The steep portion of the upstream slope was faced with concrete slabs placed on a 0.6 m layer of gravel and supported at the toe (elevation 2920 feet) on a concrete footing and driven wooden piles.

- The earthfill for embankment construction was sourced from the medium plasticity adobe clays. It was placed in 150 mm layers, "sprinkled" with water and compacted using heavy rollers (11 to 19 tonne) with diagonal lugs.
- The closure section at Owl Creek (Figure G4.3), between stations 40+50 and 42+50, was constructed last and was built very rapidly.
- The toe drain, trench, drainage wells and an earthfill berm were constructed at the downstream toe after the observation of seepage (in 1910) from the partially filled reservoir appeared downstream of the dam.

Filling of the reservoir at Belle Fourche dam started in March 1911 and reached within 1.5 m of the active conservation capacity in September 1915 (4.2 years after construction). The reservoir is subjected to a seasonal drawdown, usually over the late spring to early autumn period, generally in the range of 4 to 8 metres (Figure G4.4a and Figure G4.5a). Larger drawdown events, of greater than 9 m, occurred in 1928 (17 years), 1930 (19 years), 1931 (20 years), 1985 (74 years), 1988 (77 years) and 1989 (78 years), and possibly several more between 1936 and 1984.

Remedial works of the steep upstream slope were undertaken in 1939 (following the failure in the upstream slope on rapid drawdown in 1931, see below) and 1977 to address concerns over embankment stability under drawdown. In 1939 a gravel stabilising berm was added to the lower upstream slope below elevation 2950 feet, flattening the upstream slope to 3H to 1V below this elevation. In 1977 (Figure G4.2) the upper portion of the upstream slope was flattened to a slope of 2.33H to 1V, the crest widened 1.4 m to upstream and the crest re-surfaced.

The embankment has performed relatively poorly during the larger drawdown events (Sherard 1953; USBR 1996), summarised as follows:

- 1928 (17 years after construction) – longitudinal cracking on the downstream edge of the crest (Sherard 1953). 5 cracks, each 5 to 50 m in length, 12 to 50 mm in width and 1 to 3.5 m deep, were observed between Stations 27 and 42, including the Owl Creek closure section. The cracking was observed on 10th November and therefore is likely to have occurred after the drawdown had been completed.

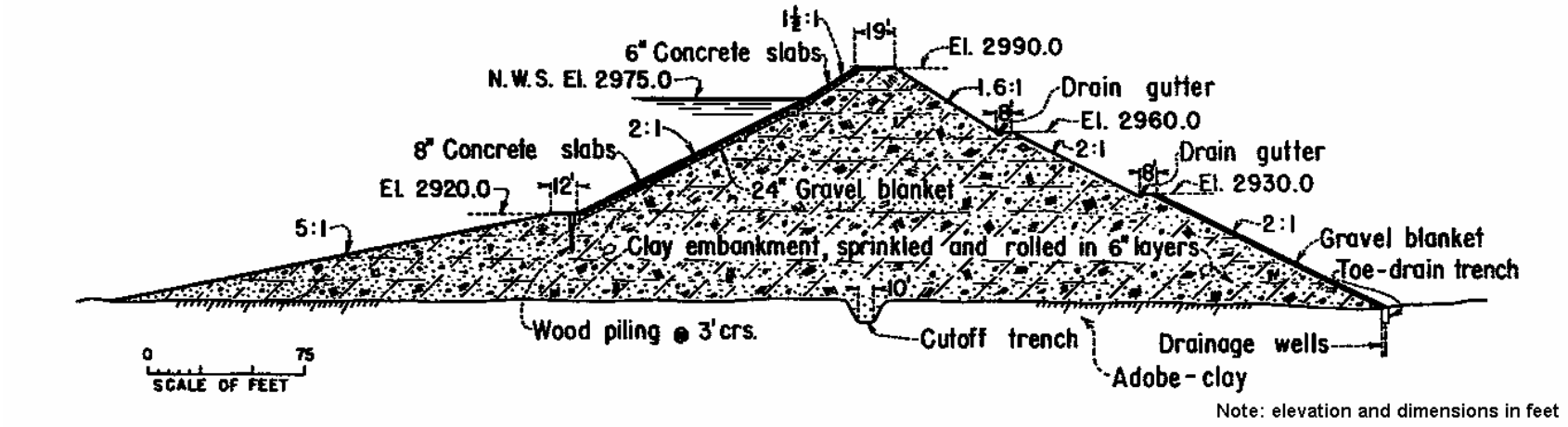

Figure G4.1: Belle Fourche dam; main section as constructed in 1911 (courtesy of U.S. Bureau of Reclamation).

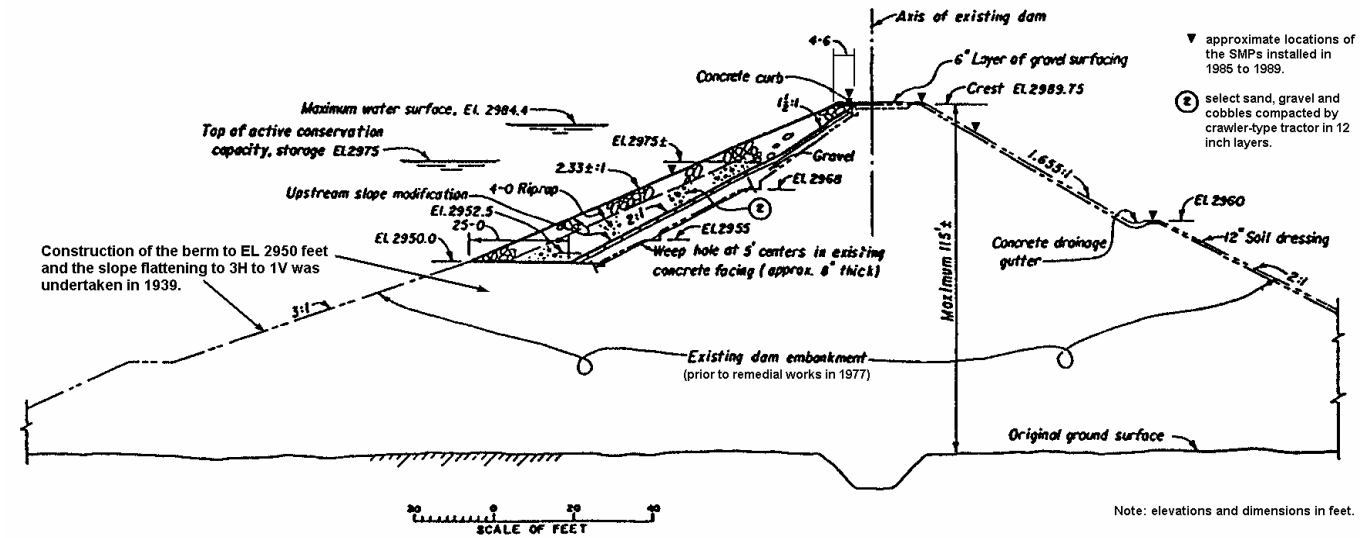

Figure G4.2: Belle Fourche dam; typical section after remedial works in 1939 and 1977 (courtesy of U.S. Bureau of Reclamation).

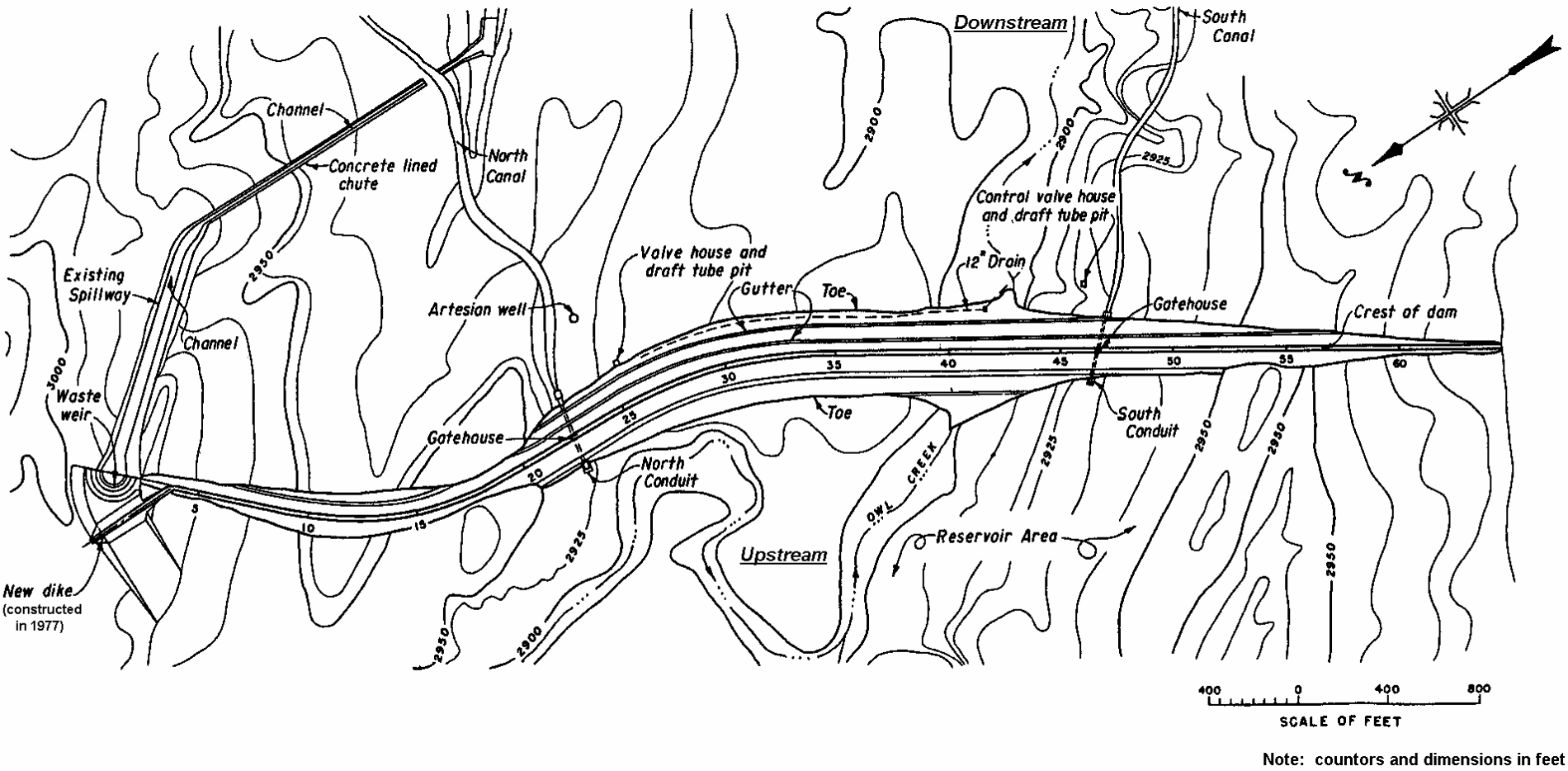

Figure G4.3: Belle Fourche dam; general plan (courtesy of U.S. Bureau of Reclamation).

- 1931 (19 years after construction) – slide in upstream slope on 2nd August during drawdown. The slide was approximately 110 m in width and 3 to 5 m in depth located within the steeper upstream slope between Stations 43 and 46+50. The head of the backscarp was about 7 m below crest level. In 1931 the slide mass was excavated and the upstream slope rebuilt to its original configuration.
- 1985 (74 years after construction) – longitudinal cracking on the crest, between Stations 39 and 46, located 1.2 m from the upstream edge of the crest. The crack, which was centred on the Owl Creek closure section, was about 200 m in length and up to 75 to 100 mm width. A vertical displacement to upstream of 50 mm was measured across the crack. Investigation found that the crack was coincident with the upstream edge of the original structure, located directly above the buried concrete kerb.
- 1988 and 1989 (77 and 78 years after construction) – opening of 1985 crack and a greater vertical differential across the crack.

In 1992 a hairline crack was observed on the crest (USBR 1996) parallel to the 1985 crack but offset about 1 m toward downstream.

Instrumentation for monitoring the deformation behaviour at Belle Fourche dam is by surface measurement points (SMP). At end of construction a series of SMPs were installed along the crest in 1911 and were monitored for vertical deformation over a period of about 17 years. The measured settlement of several of these markers is shown in Figure G4.4. In 1985, some 74 years after construction, SMPs were installed on the crest and slopes between Stations 26 and 46 (Figure G4.2). The settlement and displacement normal to the dam axis of the SMPs installed at Station 40 to 42 (within the Owl Creek closure section) are shown in Figure G4.5.

Notable observations from the post construction deformation behaviour at Belle Fourche dam from the figures and in comparison to similar type embankments are:

- In the first 17 years after end of construction the magnitude of crest settlements were very large, reaching more than 2% of the embankment height. In comparison to similar embankments the magnitude of crest settlement at Belle Fourche is “abnormally” large (Figures 7.48 and 7.60 in Section 7.6 of Chapter 7).
- The long-term crest settlement rate (rate in log time) is “abnormally” high in comparison to similar embankments (Figure 7.63 and Table 7.21 in Section 7.6 of Chapter 7). At 10 to 12 years after construction the rate was about 1.8% per log

cycle of time, and increased to about 4.5% per log cycle of time at 75 to 85 years after construction.

- Of the SMPs installed on the crest and slopes of the embankment after 1985, the deformations between Stations 40 and 42 (i.e. within the Owl Creek closure section) were up to 1.5 to 2 times greater than those measured elsewhere on the embankment, and were very much larger at MP5 (located at station 42+00) on the upstream slope.
- Acceleration in settlement and non-recoverable upstream displacement at MP5 (located at station 42+00) on the upstream slope during large drawdown at 74 years (1985) and again at 77 years (1988). During both these drawdowns cracking was observed and the greater settlement of the upstream edge of the crest visibly evident. At 86 years further non-recoverable upstream displacement was observed for MP5. This deformation behaviour is considered "abnormal".
- The deformation records after 75 years show relatively similar behaviour for the crest and downstream slope, with average settlement rates of 6 to 10 mm/year and displacement rates of 6 to 13 mm/year downstream. An increase in displacement rate of the SMPs on the crest and downstream slope is observed after 82 years, and is approximately coincident with a period of higher average reservoir level. An increase in settlement rate of the downstream edge of the crest and downstream slope occurs after year 85 (1996). The increased deformation rates may reflect a change in effective stress conditions due to a rising phreatic surface under the high average reservoir level.

During piezometer installations in 1982 softened and very wet zones were encountered within the earthfill and foundation (Hickox and Murray 1983).

The embankment performance during large drawdown is indicative of the marginal stability of the upstream slope on drawdown, as evidenced by the failure in the upstream slope during the 1931 drawdown.

USBR (1996) attributes the observed cracking and monitored "abnormal" deformation behaviour of the upstream slope to upstream crest region during the drawdowns in 1985, 1988 and 1989 to settlement / consolidation of the original earthfill under the added weight of the granular filling in the upstream shoulder berm placed in 1977. However, they do not discount the potential for deep-seated movements. A notable aspect of the deformation behaviour of the upstream slope during large

drawdown is that only at MP5 (located within the Owl Creek closure section) is the acceleration in settlement and displacement observed, no such behaviour is observed at other SMPs on the upstream slope, also located on the newly placed granular filling.

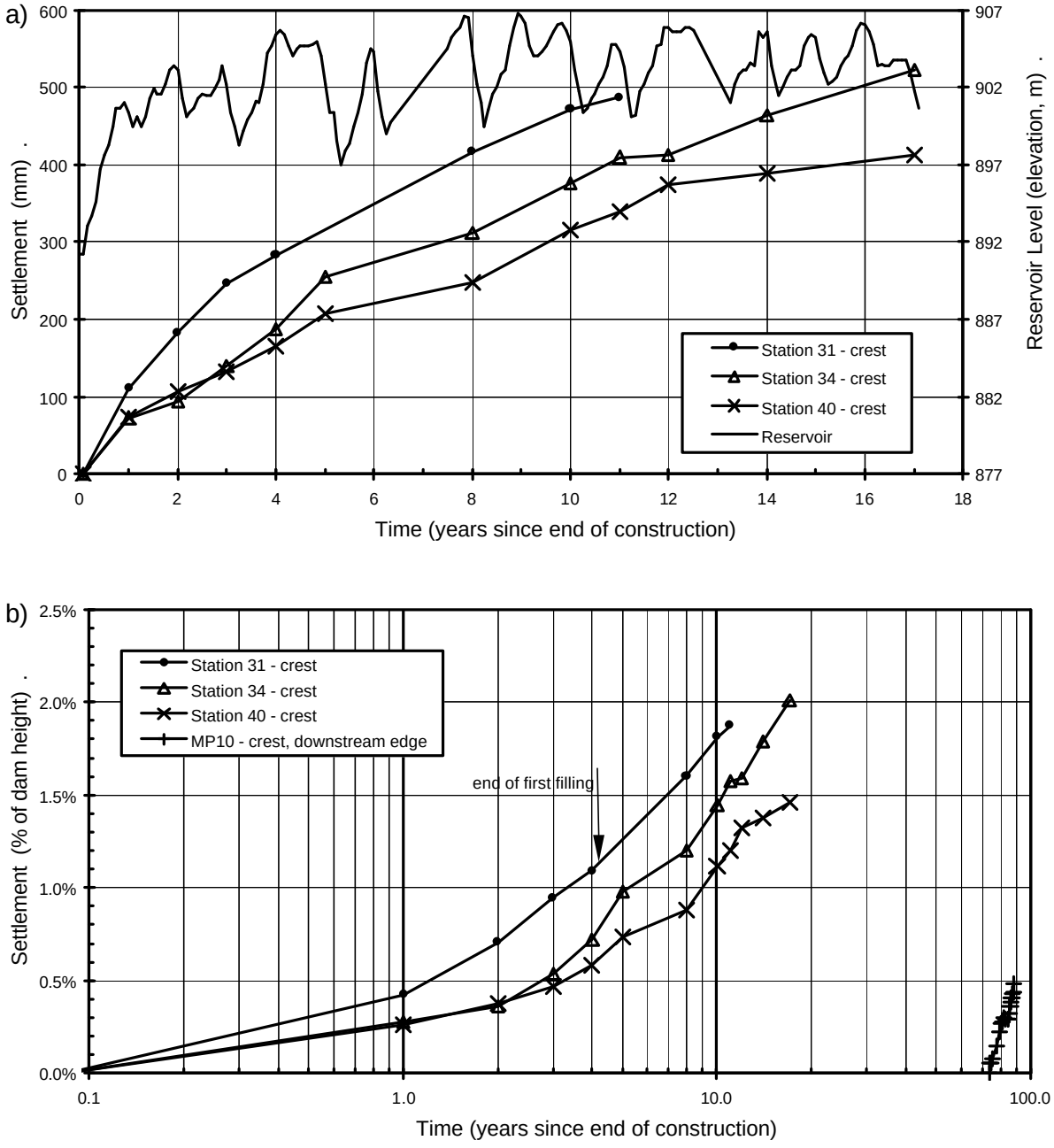

Figure G4.4: Belle Fourche dam; post construction crest settlement over the period 1911 to 1928 (to 17 years post construction).

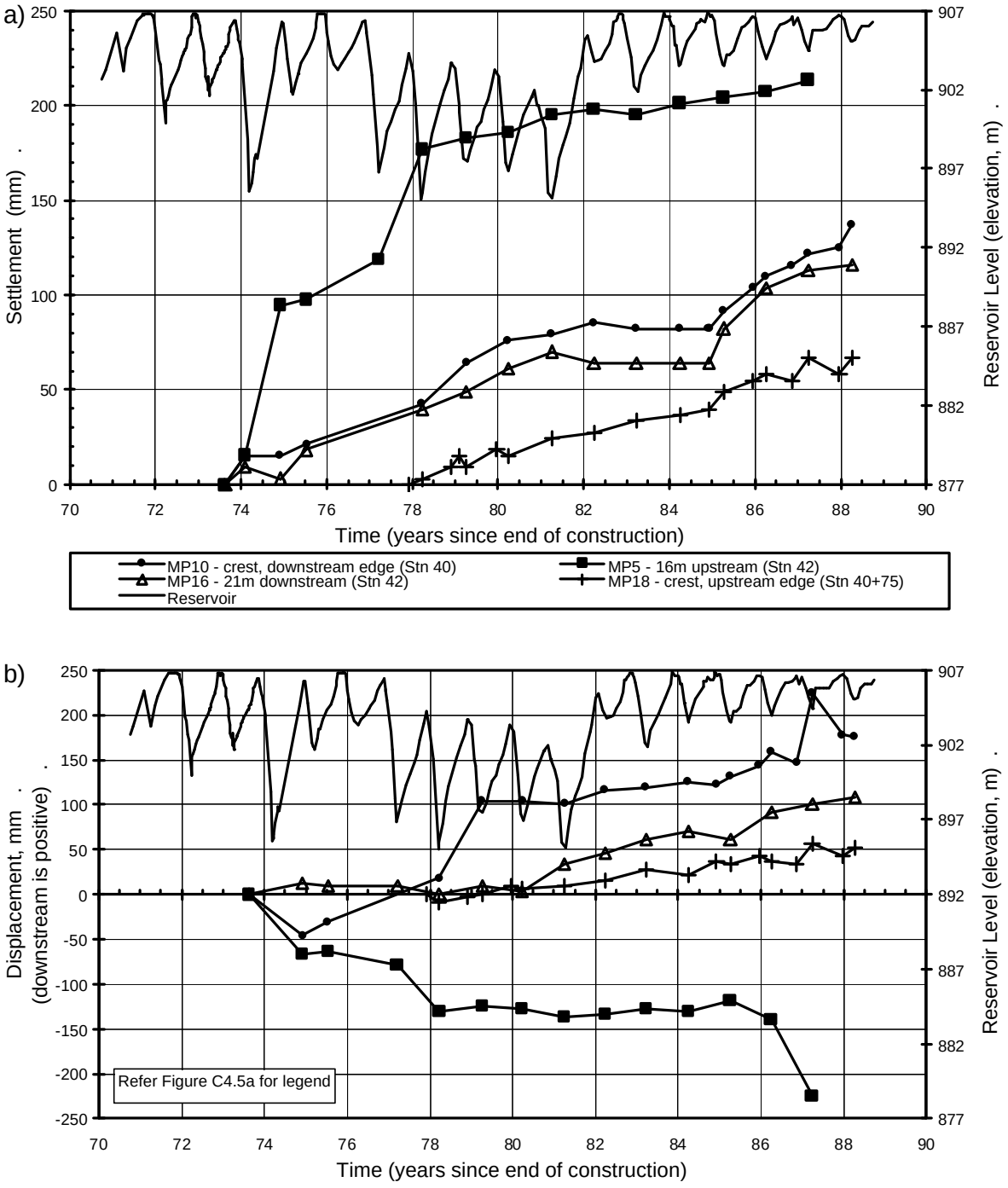

Figure G4.5: Belle Fourche dam; post construction *(a)* settlement and *(b)* displacement normal to dam axis of the crest and slopes over the period 1985 to 2000 (73 to 89 years post construction).

Overall, the long-term deformation behaviour at Belle Fourche dam is considered as "abnormal" in comparison to similar embankments. The "abnormal" deformation of the crest and slopes, particularly in the vicinity of the Owl Creek closure section (Stations 40 to 42), possibly reflects the "highly stressed" conditions within this embankment due

to the steepness of the embankment slopes for an earthfill embankment constructed of medium plasticity clays. An important aspect of the deformation behaviour is the much higher crest settlement rates (per log cycle of time) from recent monitoring compared to those at 10 to 12 years after construction. This possibly reflects softening of the undrained strength properties of the earthfill due to wetting of the earthfill, strain weakening under the high stress conditions imposed during large drawdown, lateral spreading in the crest region and cracking in the upper portion of the embankment.

The USBR comment that the Owl Creek closure section, which was constructed very rapidly, is a definite discontinuity along the dam embankment and that the deformation behaviour within this closure section is somewhat unique to the rest of the embankment. This is indicated by the greater magnitudes of deformation measured for the SMPs on the crest and slopes of the embankment installed more than 75 years after the end of construction.

4.2 MITA HILLS DAM

Mita Hills dam (Figure G4.6) is a water supply dam for hydropower serving a mine site in Zambia (Legge 1970). The embankment, of 49 m maximum height and 365 m crest length, is a rolled earthfill embankment with chimney filters and was constructed on a bedrock foundation. It was constructed in the mid to late 1950's. Legge (1970) refers to the earthfill as being placed in 150 mm layers and compacted by heavy sheepsfoot rollers. The specified range in moisture content was 2% dry to 1% wet of Standard optimum, with dry placement specified for the bulk of the earthfill and placement at close to Standard optimum for Zone 2.

The post construction crest settlement and displacement of SMP A4 (located at close to maximum section, Figure G4.6b) are shown in Figure G4.7. The actual direction of the horizontal crest displacement normal to the axis is not clear from Legge (1970). In graphical presentations Legge (1970) shows the displacement to be upstream, but in the text indicates the direction is downstream. Where presented in this thesis the displacement has been assumed as upstream.

In comparison to other similar embankments, aspects of the post construction crest deformation at Mita Hills are potentially "abnormal", these include:

- The high magnitude of crest settlement of more than 1% (Figures 7.46, 7.47 and 7.60 in Section 7.6 of Chapter 7), most of which occurred on first filling.

- The magnitude and upstream direction of the crest displacement normal to the dam axis (Figures 7.38 in Section 7.5 and Figure 7.75 in Section 7.6 of Chapter 7).

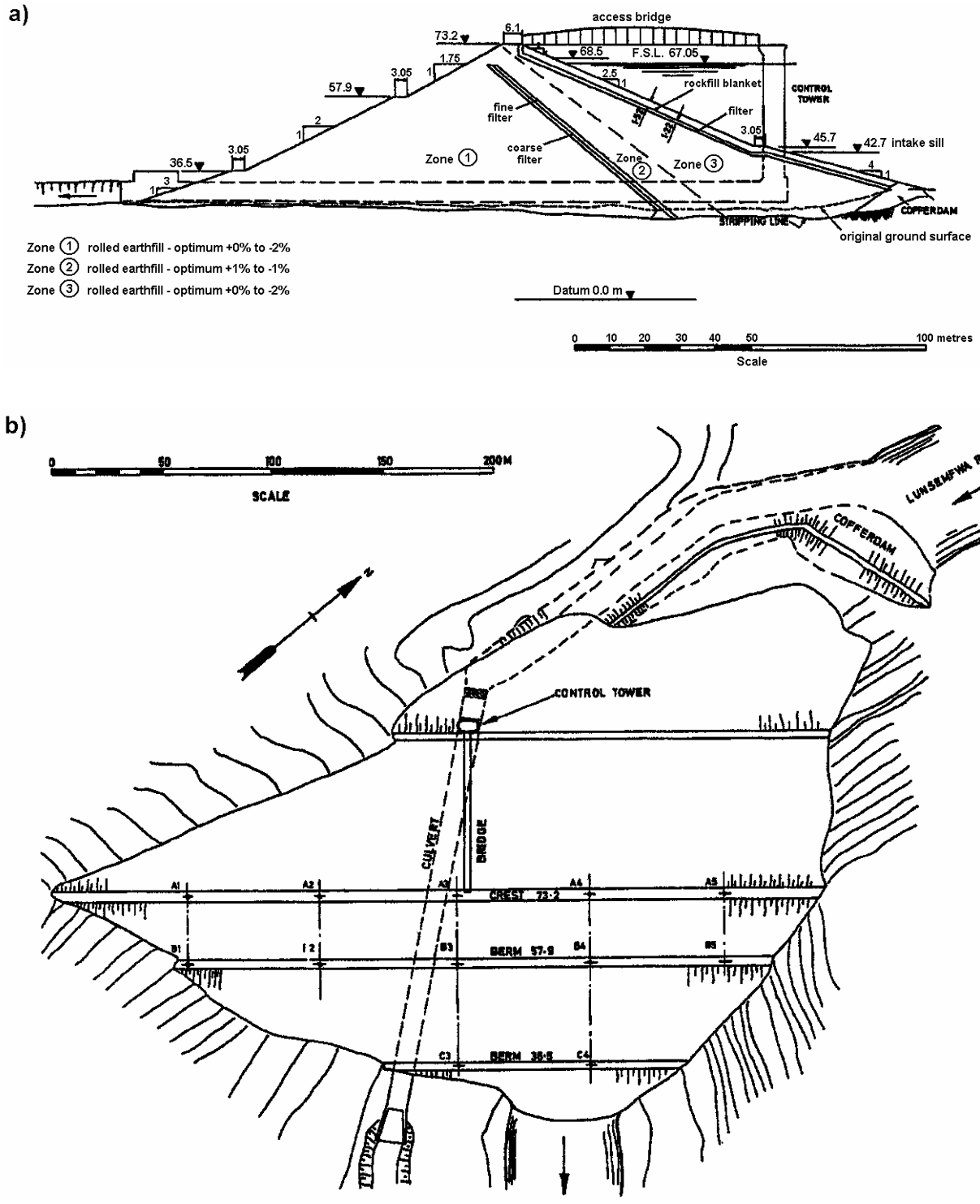

Figure G4.6: Mita Hills dam, *(a)* cross section, and *(b)* plan showing SMP locations (Legge 1970).

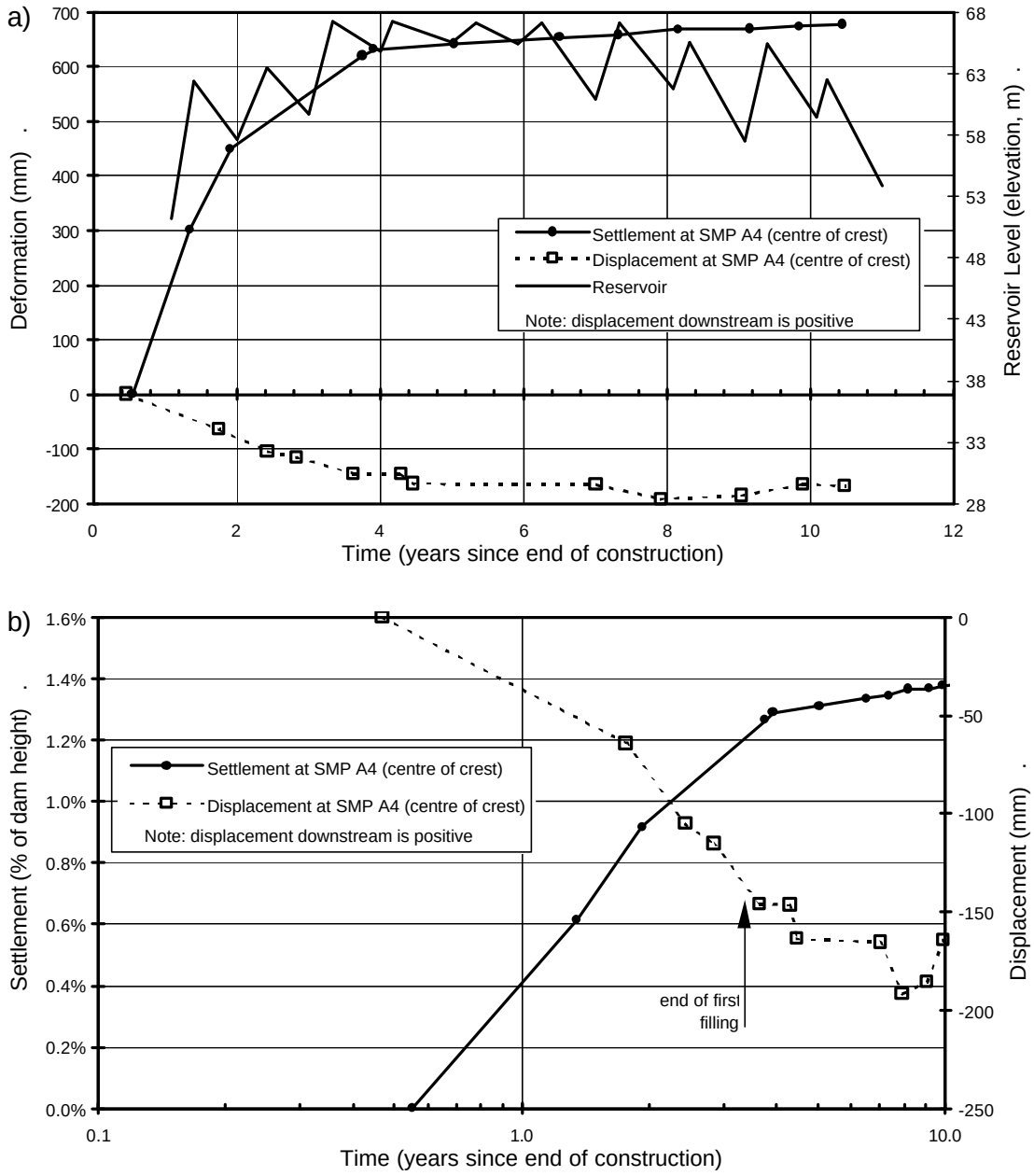

Figure G4.7: Mita Hills; post construction crest settlement and displacement normal to the dam axis versus *(a)* time on normal scale and *(b)* log time.

As shown in Figure G4.7, most of the settlement and upstream displacement occurred during first filling. Post first filling the deformation behaviour has been "normal" in comparison with that of other embankments.

Other crest SMPs, except for SMP A1, showed similar settlement and displacement behaviour to SMP A4 (Legge 1970). After more than 10 years measured crest settlements have ranged from 1.4% to 2.3% of the embankment height at the SMP

location, the greatest magnitude settlements as a percentage of the embankment height being on the mid abutment slopes at SMPs A2 and A5.

Post construction settlements and displacements on the downstream berm were less than 92 mm (Legge 1970), which equates to a settlement of 0.27% of the height from SMP to foundation level at the main section. This is markedly less than the settlement at the crest.

Reasons for the large and potentially "abnormal" crest deformations are difficult to evaluate, more so due to the lack of clarity on the direction of the horizontal deformation. Assuming the displacement to be upstream, it is possible that collapse settlement on saturation of the dry placed earthfill upstream of the filters (i.e. within Zone 3) has influenced the deformation behaviour. This would explain the marked difference in behaviour between the crest and downstream slope and the upstream displacement vector could be a result of the embankment zoning geometry. Marginal stability of the upstream slope could also be a factor. However, an instability mechanism seems unlikely as no acceleration in settlement rate or further upstream displacement is observed on drawdown. The influence of the foundation, comprising quartzite and decomposed mica-schist, is assumed to be insignificant.

4.3 ROXO DAM

Roxo dam, in Portugal, is part concrete (gravity and buttress) and part earthfill embankment (De Melo and Direito 1982), and was constructed in the mid to late 1960's. The earthfill embankment section forms the right abutment and is of earthfill with downstream rockfill toe embankment type. It is of 27 to 32 m maximum height and of 650 m crest length, with slopes of 3H to 1V upstream and 2.5H to 1V downstream. The earthfill is of medium plasticity clayey sands to sandy clays derived from weathered schists. The specified moisture content range at placement was from 2% dry of OMC to OMC (OMC = Standard optimum moisture content).

Large post construction crest settlements of the earthfill embankment were measured near to its interface with the concrete embankment (discussed below). Figure G4.8 shows the interface in elevation view and Figure G4.9 the crest settlement monitoring records for up to 8 years after the end of construction.

Several important aspects of the embankment construction and post construction performance raised by De Melo and Direito (1982) are summarised as follows:

- Construction staging was such that the 80 to 100 metre long section of the earthfill embankment at the interface between the structures was the final stage of construction.
- Poor foundation conditions for a concrete gravity structure were encountered near the interface between the embankment types and as a consequence the length of the concrete section was reduced. Faults, schist veins and highly fractured, highly permeable quartz veins intersected the porphyry formation of the foundation.
- Post construction and post first filling; high pore water pressures were measured in the earthfill near the interface between the structures and close to foundation level.
- Investigations and excavation found that:
  - Water reached the base of the earthfill, near the interface, with little loss of head.
  - The circulation of water at the interface was substantial.
  - The earthfill was generally of "*high quality*". Moisture contents were variable, ranging from close to the as placed moisture content to well above the placed values in wet and softened layers. Wetted and softened layers were located close to those in the as placed condition.
- Post construction horizontal displacements, from inclinometers and surface points, were not significant.

The crest settlements at 20 m, 55m and 95 m offset from the interface are presented versus time in Figure G4.10. As shown, large post construction settlements, up to almost 2% of the embankment height at 8 years, were observed close to the interface between the embankment sections. In comparison to similar embankments, the post construction crest settlement of the embankment section near to the interface is shown to be "abnormal" in terms of magnitude (Figures 7.46, 7.47 and 7.60 in Section 7.6 of Chapter 7) and in terms of long-term settlement rate (Figure 4.63 in Chapter 7). At 95 metres from the interface the post construction crest settlement is more typical of "normal" type behaviour.

De Melo and Direito (1982) discount the possibility of slope instability due to the insignificant lateral displacements recorded. They also discount consolidation type settlements due to the dry placement of the earthfill. De Melo and Direito (1982) consider the problems to be a combination of factors including:

- Low vertical stresses in the central lower earthfill region developed due to arching across changes in foundation geometry near to the abutment (from Figure G4.8 this

change in geometry occurs within 15 to 20 m of the interface, beyond this the foundation slope is relatively flat).

- Formation of horizontal cracks within the earthfill at the interface with the concrete section, formed as a result of differential settlement and stress transfer between the earthfill and concrete.

But these are not likely to be the only factors. Both of these factors would influence the deformation in the vicinity of the interface. However, the settlement records indicate that excessive settlements at "abnormally" high long-term rates (> 1.4 %/log time cycle at 55 m from the interface) are observed for more than 50 to 60 metres from the interface. Poor compaction of dry placed layers of earthfill in the closure section could be a factor. If present, these poorly compacted layers would be susceptible to collapse settlement on wetting as well significant softening in strength and compressibility properties on wetting, which could explain the large settlements measured beyond the zone of influence of the interface with the concrete embankment. But, there are not sufficient details to draw any firm conclusions.

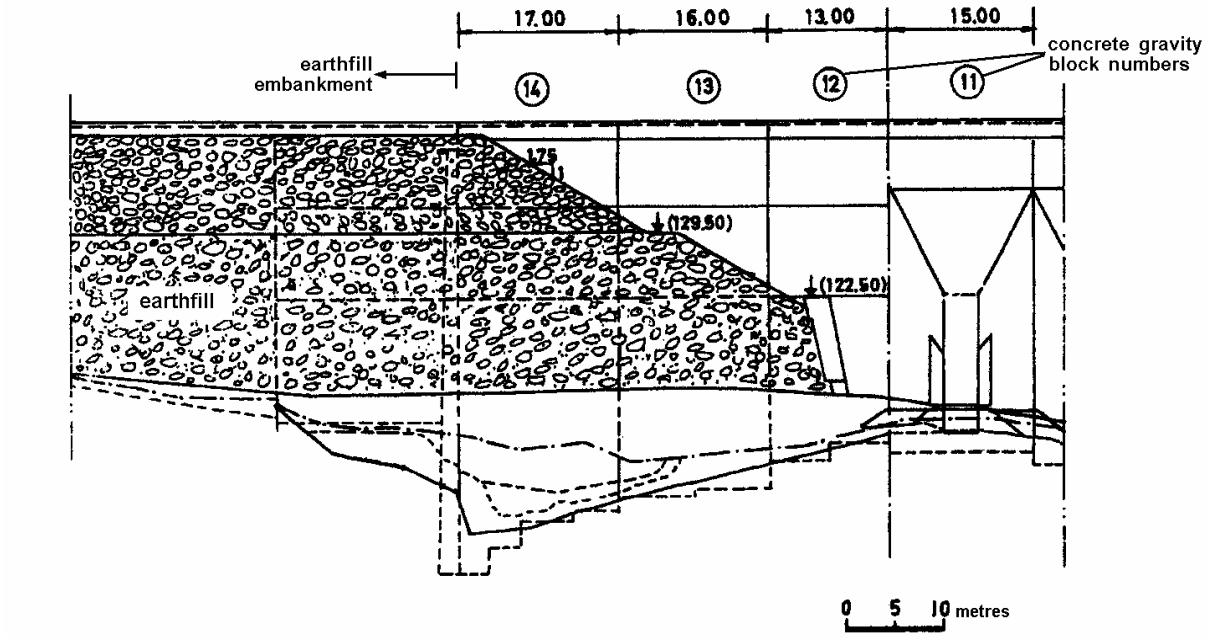

Figure G4.8: Roxo dam, junction between earthfill and concrete gravity embankment sections on the right abutment (De Melo and Direito 1982).

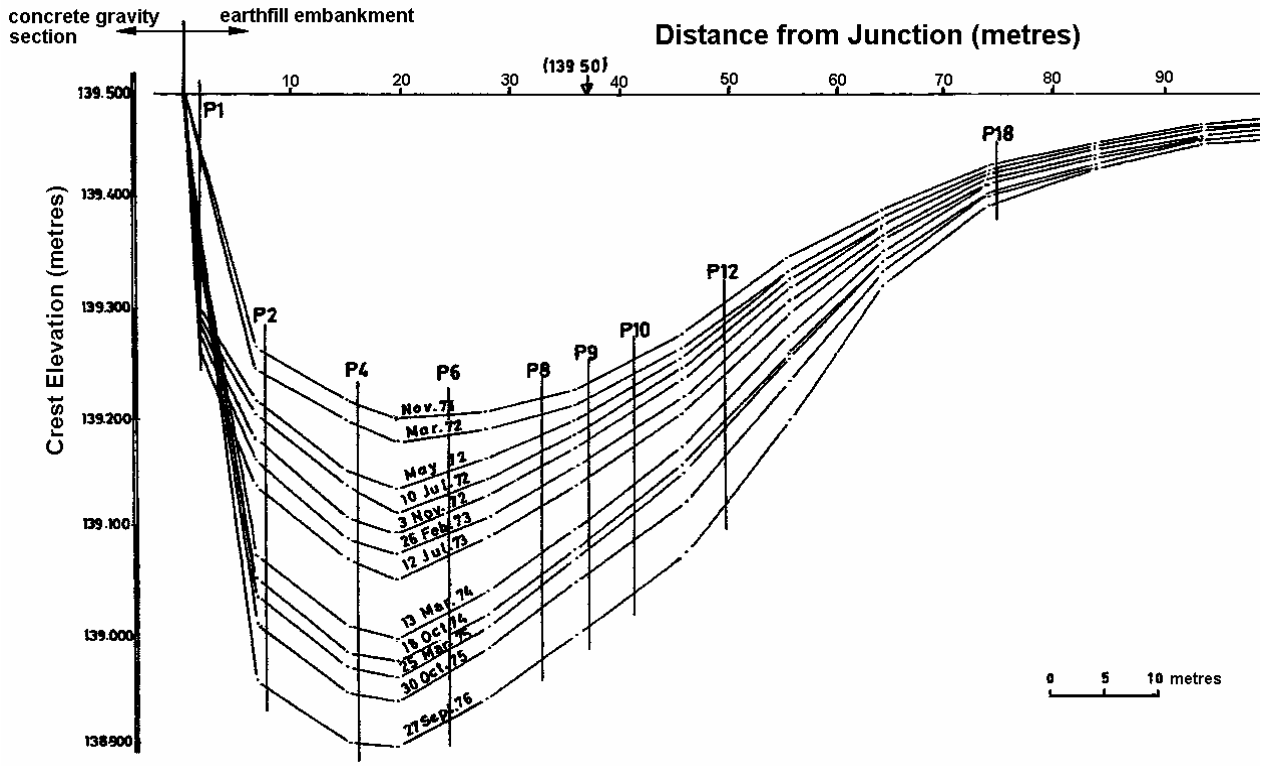

Figure G4.9: Roxo dam, crest settlement of left abutment earthfill embankment (De Melo and Direito 1982).

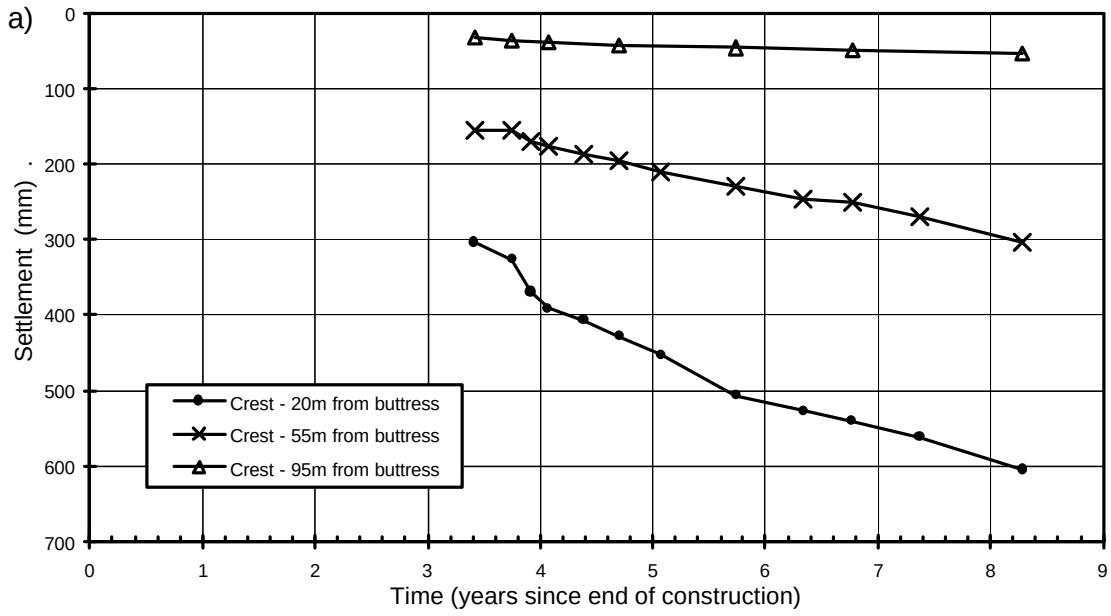

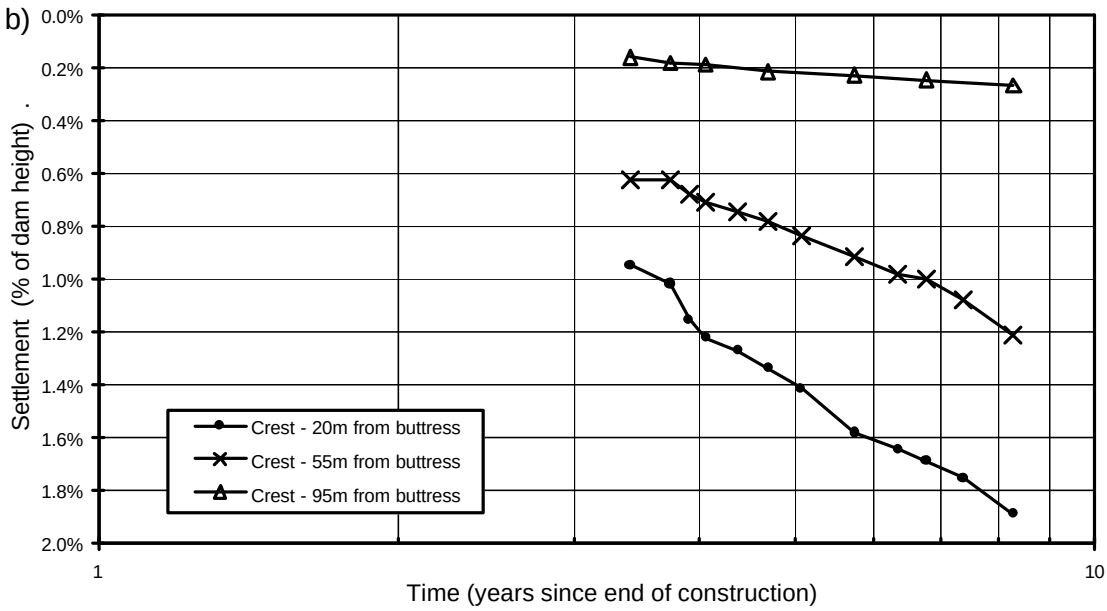

Figure G4.10: Roxo dam; settlement versus *(a)* normal time and *(b)* log time (adapted from De Melo and Direito 1982).

5.0 PUDDLE CORE EARTHFILL EMBANKMENTS

5.1 HAPPY VALLEY DAM

Happy Valley dam (Figure G5.1) is the main reservoir of the metropolitan water supply system to the city of Adelaide, South Australia. It is a puddle core earthfill embankment of 25 m maximum height and 806 m crest length for which construction was completed in late 1896. The narrow puddle core is supported by shoulders sloped at 3H to 1V (horizontal to vertical) upstream and 2H to 1V downstream. At the main section the dam foundation comprises clays of shallow depth overlying Cambrian aged limestones, siltstones and slates. The puddle clay cut-off (maximum depth of 11 m) is founded through the surface clays and weathered bedrock.

The central puddle core has a top width of 2.44 m and slopes of 1H to 8.25V, and was constructed of low plasticity silty clays placed wet in 150 mm layers and compacted by bullocks. Recent investigations indicate the core to be in a near saturated condition (average degree of saturation of 95%) and of firm undrained strength consistency. Density estimates from tube samples indicated an average density ratio of 81% of Modified Maximum Dry Density and the moisture content is consistently close to 30%.

The embankment slopes are constructed of predominantly silty and sandy clays with pockets of sands, gravels, rock fragments and organic matter placed in 150 mm lifts and compacted by wagons, carts and grooved rollers. Better quality filling (finer material) was used adjacent to the puddle core. Density estimates from tube samples reported an average density ratio of 88% of Modified Maximum Dry Density in the shoulder fill, indicating a reasonable level of compaction was achieved. In the upstream slope the degree of saturation is in the range 85 to 100% (average 90%), although the moisture content profile varies, probably due to material variation. In the downstream slope the moisture content and degree of saturation is lower in the upper 10 m, and below 10 m the degree of saturation is generally greater than 90%. Observations of free water in the downstream slope were recorded at depths below about 8 m in the more permeable filling.

Drainage in the downstream slope comprised a system of French drains.

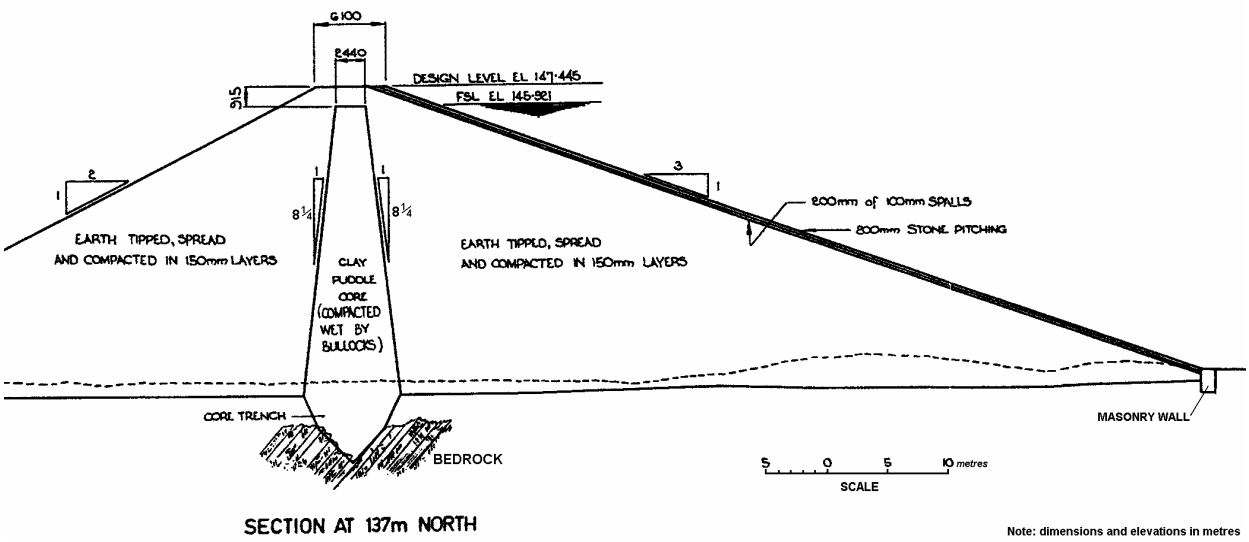

Figure G5.1: Cross section of Happy Valley dam (courtesy of South Australian Water Corporation)

A drawdown test was undertaken in the upstream shoulder earthfill in the early 1980's and indicated the earthfill was of sufficiently low permeability such that only a small fraction of the depth of reservoir drawdown reservoir was recorded in the piezometers within the select filling on the upstream side of the puddle core.

Other observations of piezometric levels within the embankment are summarised as follows:

- The phreatic surface in the outer upstream filling responded with reservoir level.

- The further the distance into the upstream slope the lower the piezometric response relative to the change in reservoir level.
- No change was recorded in the downstream slope.

The recorded settlement and lateral displacement of selected surface measurement points (SMP) on the upper upstream slope, upper downstream slope and downstream toe for the period from 1982 to 1998 (85 to 102 years after construction) are shown in Figure G5.2 and Figure G5.3 respectively. Comments on the recorded movements are as follows:

- All SMP show a general trend of settlement and downstream displacement with time.
- All SMP show an oscillation of the settlement and displacement about the general trend that, from the available records, largely responds with reservoir level.
- The rate of deformation of the upstream slope was significantly greater in the period 85 to 91 years after construction, during which time the reservoir fluctuations were larger than those more than 91 years after construction.
- The average long-term crest settlement rate for the period of monitoring was 1.5 % per log cycle of time for the upstream slope and 1.0% per log cycle of time for the upper downstream slope. In comparison to other puddle embankments these values are considered typical for embankments where the puddle core experiences only a relatively minor change in effective stress due to reservoir level fluctuations.
- The fluctuations in displacement of the downstream toe and downstream slope are considered relatively large given that the water level monitoring in the downstream slope indicated no response to changes in reservoir level. Also, at about 101 years after construction, displacements of 4 to 6 mm were recorded for negligible change in reservoir level. It is considered that the possible mechanism of this movement may be due to infiltration from rainfall and/or shrink swell related movements.

Some records of crest settlement were available from the end of construction and indicate a total post construction settlement of about 720 mm (2.9% of dam height) in 76 years (plotted in Figure 7.92 in Section 7.7 of Chapter 7). This correlates to a long-term crest settlement rate (S_{LT}) of 1.0 % per log cycle of time, and is similar to the S_{LT} values estimated from the recent monitoring records.

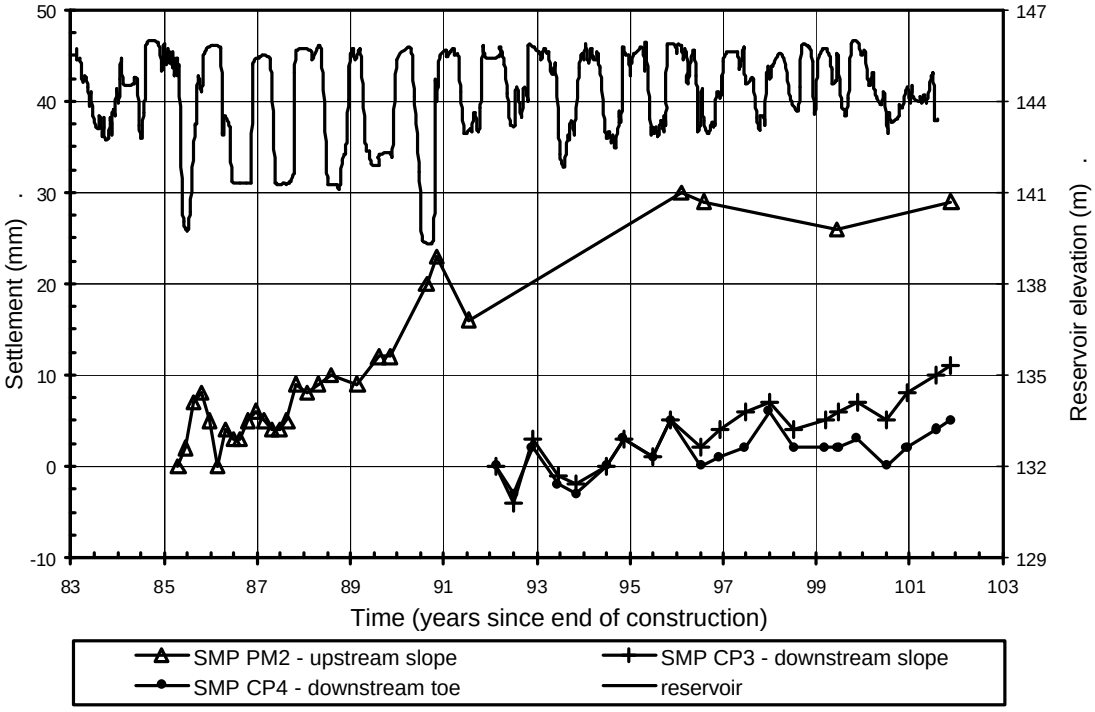

Figure G5.2: Happy Valley dam, long-term post construction settlement versus time

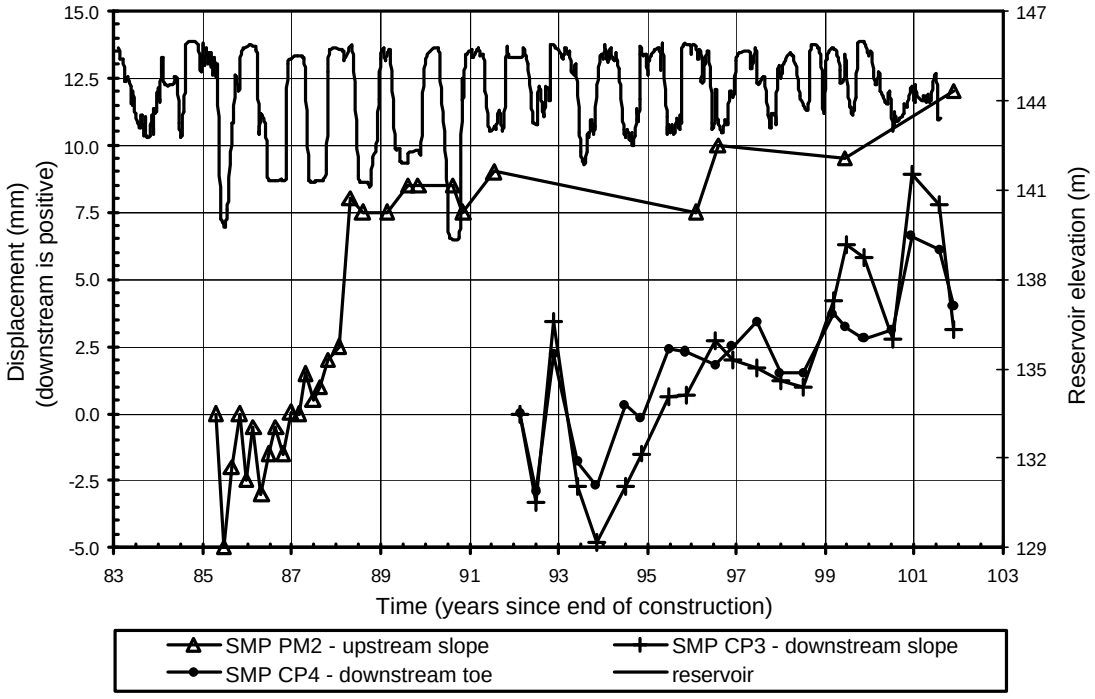

Figure G5.3: Happy Valley dam, long-term post construction horizontal displacement with time

Dam inspection reports of Happy Valley dam (EWSD SA 1981a; Pinkerton 1984) note a depression on the upstream slope near to the crest. It is understood that the depression

was first observed in the early 1970's at the time of the first reported inspection, but it is not known when it occurred. The depression extends across most of the length of the embankment and is greatest at the maximum section. A two metre deep wet seam was observed in the face of a test pit dug through the depression, but it is not clear of the orientation of the wet seam in relation to the embankment section. Monitoring since 1982 (SMPs on upstream face) indicated little movement of the depression.

A low factor of safety of the upstream shoulder on reservoir drawdown is not considered to be the cause of the depression. Stability analysis (Nadilo 1983) indicates a factor of safety of greater than 1.3 for the upstream shoulder on full rapid drawdown. In addition, if localised instability on drawdown were a factor then it would be anticipated that the depression would be localised, which is not the case.

SMEC (2002) were able to model the formation of the depression on the upstream slope using the computer program FLAC. Their results indicated that the post construction consolidation of the core (in the first few years after construction) resulted in the formation of a shear band from the upstream face through to the core. The location and depth of the modelled depression were similar to the observed depression. The depression in the upper upstream shoulder could also be explained by downstream displacement of the core and downstream shoulder under the applied water load on first filling (and exacerbated by deformations due to collapse compression in the downstream shoulder fill from wetting from seepage or rainfall infiltration), with a narrow wedge of the upper upstream shoulder adjacent to the core dropping to form a "reverse" scarp.

Other influences on the deformation behaviour of Happy Valley dam on and subsequent to first filling would include collapse compression of the upstream shoulder on wetting, and deformations due to yielding on drawdown of the water softened shoulder fill (refer Section 7.7.2.1 of Chapter 7).

Overall, it is considered that the deformation behaviour of the embankment indicates normal embankment performance. In relation to the recorded deformations at other puddle embankments (refer Table F1.5 in Appendix F) the deformation rates at Happy Valley dam are relatively low.

5.2 YAN YEAN DAM

Yan Yean dam is an off-river water storage dam for the city of Melbourne, Australia. The puddle core embankment (Figure G5.4) is of 9.6 m maximum height and 960 m length constructed over the period 1853 to 1857. Local steepening at the crest is possibly due to raising of the embankment to regain freeboard following crest settlement. The dam foundation comprises a deep profile of medium to high plasticity alluvial clays of stiff to very stiff strength consistency with random desiccation fissuring in the upper clay layer. A relatively wide puddle clay cut-off of 3 m depth is located below the central puddle core.

The central puddle core has a top width of 3.05 m and slopes of 1H to 3V and was constructed of medium to high plasticity silty clays in 225 mm layers compacted by heeling in (by feet). Recent investigations indicate the core to be of firm strength consistency with undrained strengths in the range 30 to 50 kPa.

The upstream shoulder comprises medium to high plasticity clays placed in 600 to 1200 mm layers without any formal compaction. The downstream shoulder comprises a mixture of sandy silts and silty clays generally of low plasticity with some rocky zones, also placed in 600 to 1200 mm layers without any formal compaction. No drainage was provided in the downstream slope.

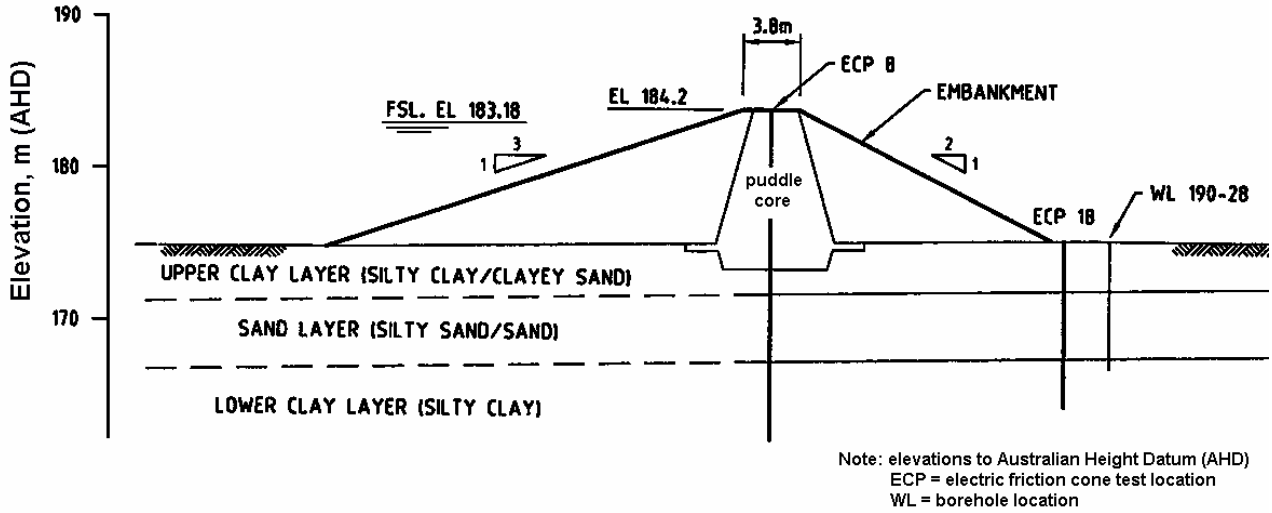

Figure G5.4: Cross section Yan Yean dam (courtesy of Melbourne Water)

Monitoring of pore water pressures since 1989 (from 132 years after the end of construction) indicates the phreatic surface is close to reservoir level in the upstream slope and falls rapidly across the relatively wide puddle core to low levels in the

downstream shoulder, but still saturates the lower portion of the downstream shoulder. On drawdown the piezometers in the embankment show virtually no response to the seasonal fluctuations in reservoir level, but do show a very slow general response to the average reservoir level. The foundation also shows a slow general response to the average reservoir level.

Available information indicates the embankment was raised by about 0.9 m, but there is no indication of when the raising was undertaken. It is also not clear what the original level of the crest was. Indications are that it was 5 feet (1.5 m) above top water level with a requirement in the design for 3.25 feet (1.0 m) of freeboard. Based on the current crest levels (0.22 m above the nominal design crest level allowing for 1.0 m of freeboard), total post construction settlement could be as much as 1.2 m or 12.5% of the maximum dam height (refer Figure 7.92 in Section 7.7 of Chapter 7). Given the stiff to very stiff strength consistency of the soils in the foundation, settlement of the foundation post construction would be expected to contribute only a small percentage of this.

The results of recent monitoring from late 1985 to early 1999 (128 to 142 years after construction) of settlement and horizontal displacement of SMPs on the crest (upstream and downstream edge), upstream slope, downstream slope and downstream toe are presented in Figure G5.5 and Figure G5.6. Figure G5.5 is for SMPs at about chainage 600 m and Figure G5.6 for SMPs at about chainage 150 m including the SMP on the downstream edge of the crest at chainage 750 m. The deformation behaviour from the recent monitoring shows:

- Negligible settlement and displacement of the upstream slope (SMP 6005) and upstream edge of the crest (SMPs 6001 and 1501). The long-term settlement rate, S_{LT}, for this region is estimated at 0.5% per log cycle of time. The plots of these SMPs show a fluctuation about the general trend that generally follows the reservoir level fluctuation. The low long-term rate of settlement is expected and is typical of similar puddle dams given that the changes in effective stress conditions in the core due to reservoir level fluctuation are minimal.
- SMPs on the downstream edge of the crest (SMPs 1502, 6002 and 7502) show an increasing rate of settlement for SMPs 1502 and 7502 (reaching a maximum rate of 4 mm/year) and steady rate of downstream displacement, up to 4.5 to 5.5 mm/year. The plots clearly show the differential deformation between the upstream and downstream edge of the crest with a maximum differential settlement of 40 mm

(SMP 1502) and differential displacement 75 mm (SMP 7502) over the monitored period. The long-term settlement rate, S_{LT}, of the downstream edge of the crest is estimated at a maximum of 11%, well in excess of that of the upstream edge of the crest.

- SMPs on the mid downstream slope (SMPs 1503 and 6003) show an increasing rate of settlement (up to 10 mm/year) and steady rate of downstream displacement of 2 to 3 mm/year.

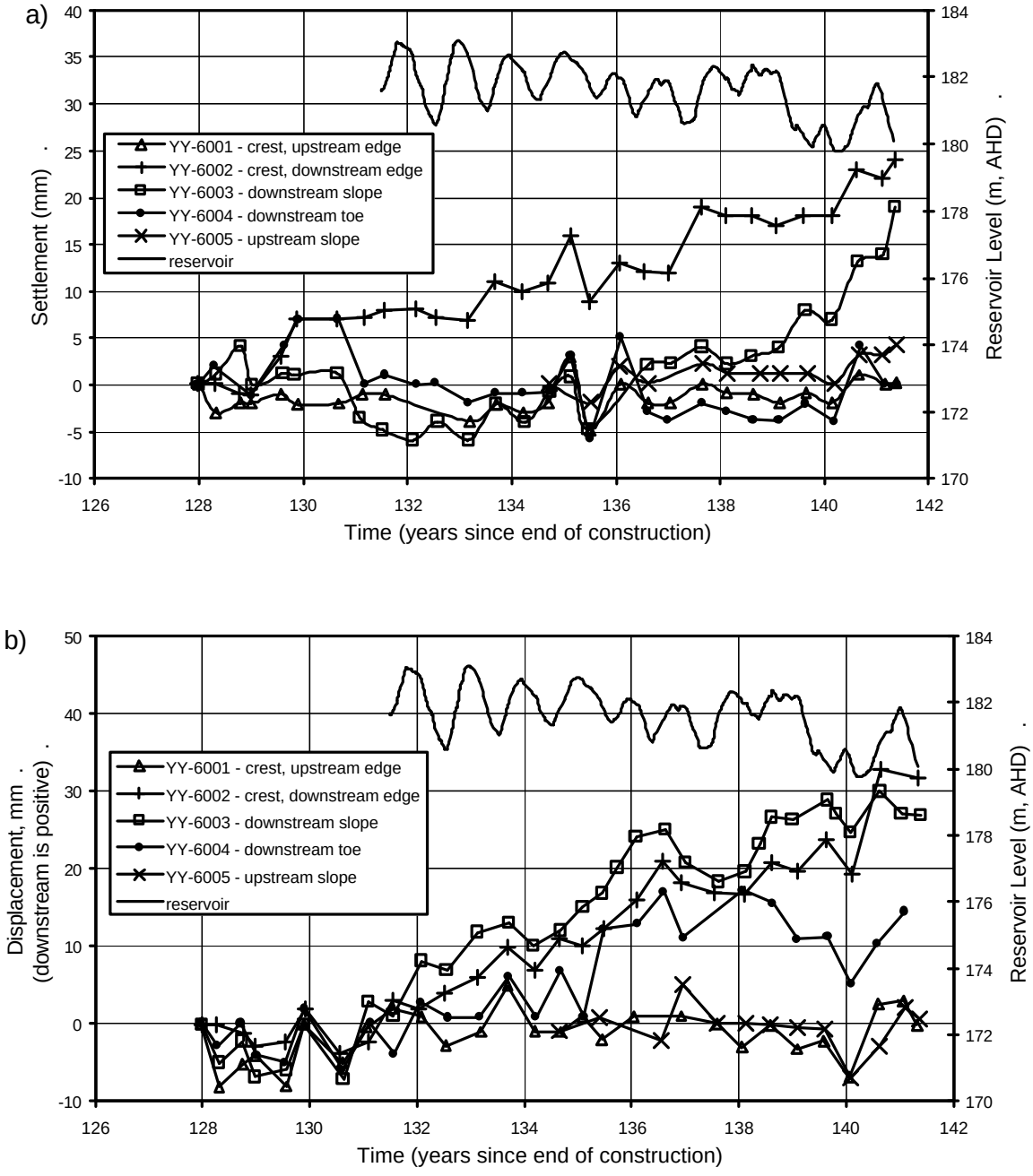

Figure G5.5: Yan Yean dam, *(a)* settlement and *(b)* horizontal displacement for SMPs at Chainage 600 m.

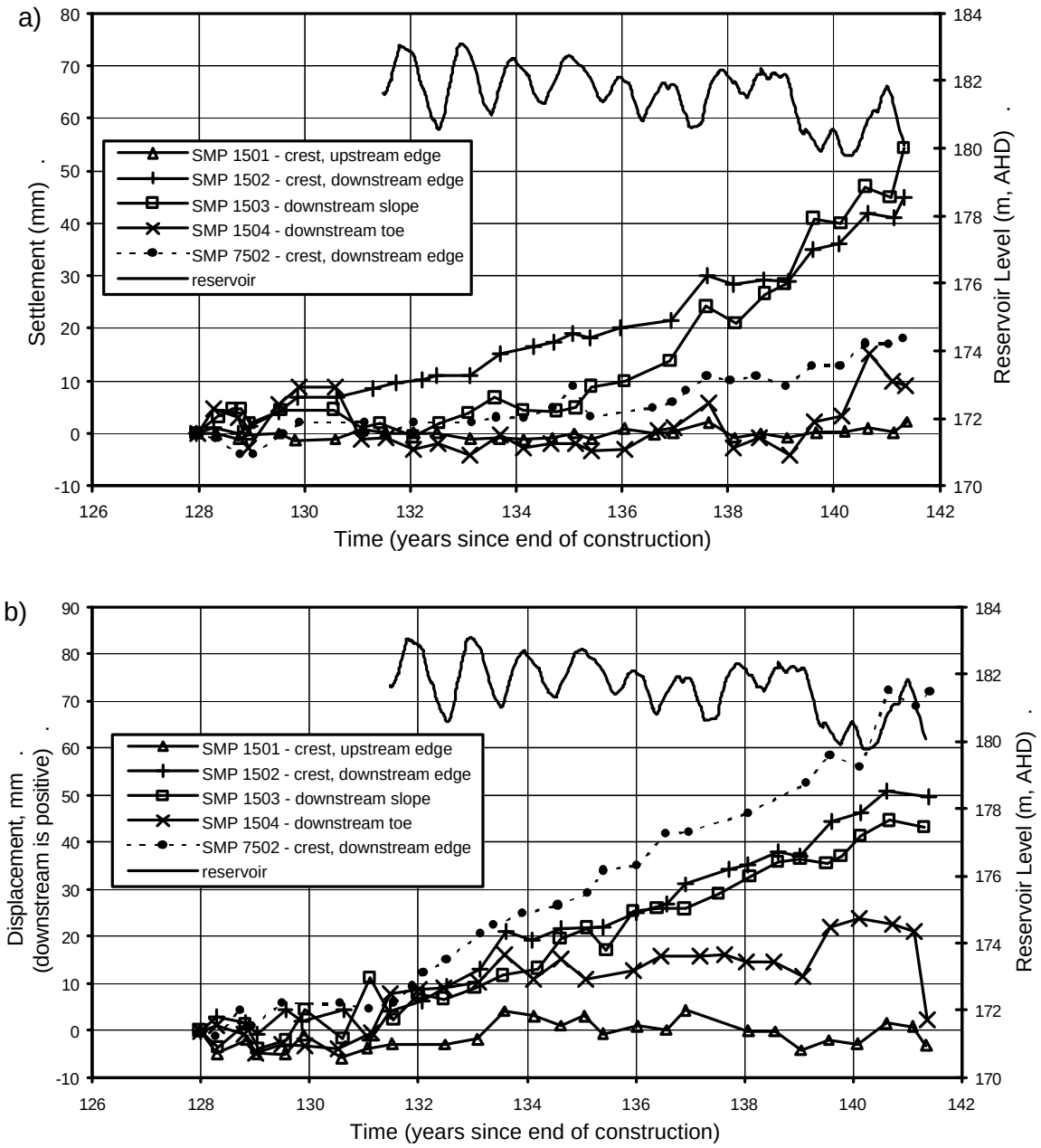

Figure G5.6: Yan Yean dam, *(a)* settlement and *(b)* horizontal displacement for SMPs at Chainage 150 m and 750 m.

- SMPs at the downstream toe (SMPs 1504 and 6004) show negligible settlement (except for 10 mm settlement at SMP 1504 in the last 18 months) and stick-slip type downstream displacement. SMP 6004 shows a 10 mm jump in displacement at about 135 years and SMP 1504 shows two jumps of about 10 mm displacement, one at 131 years and the other at 139.5 years.

Longitudinal cracking was observed on the crest of Yan Yean dam (MMBW 1985; SMEC 1996d). Following the hot, dry summer of 1985 (with the reservoir at 3.5 m below full supply level) longitudinal cracks of 5 to 6 mm width were observed to be randomly distributed along 40% of the crest length and extended down to at least the top of the puddle core. There is also reference to longitudinal cracking having been observed prior to 1985 and the cracks in-filled with granular material. During rainfall, therefore, water could enter the cracks and the applied pressures would act to reduce the factor of safety.

The possible mechanisms associated with the deformation behaviour of Yan Yean dam are:

- Initial dam operation (note that these comments are speculative as there are no deformation records of the early embankment performance):
  - Collapse compression of the upstream filling on first filling due to the poor compaction and high lift thicknesses of the likely dry placed clayey earthfill.
  - On the first few drawdown events significant settlement of the upstream filling would have occurred due to yielding as a result of increases in effective stress conditions of the now softened upstream shoulder earthfill.
  - Large settlements of the puddle core, predominantly as undrained plastic deformations, are likely to have occurred following deformation of the upstream shoulder as the puddle core deformed with the upstream shoulder, and from lateral deformations of the core due to the greater compressibility of the upstream earthfill once softened from wetting.
  - For the downstream shoulder, initial settlement rates would be expected to be relatively high due to the poor compaction of the earthfill. Some collapse compression may have occurred following wetting from seepage or due to rainfall.
  - The net deformation behaviour during the initial 10 to 20 years of operation would be for large deformations mainly as a result of collapse compression and also from changes in stress conditions during drawdown.
- Recent monitoring, more than 130 years after construction:
  - The deformation of the upstream slope and upstream edge of the crest indicates a general trend (following reservoir cycling) of negligible settlement and displacement. This behaviour is to be expected given the minor response in

piezometers levels in the core and inner upstream shoulder earthfill to fluctuations in reservoir level.

- The deformation behaviour of the downstream crest and slope is considered to be independent of the fluctuation in reservoir level. The general trend of several SMPs on the downstream slope shows an increasing rate of deformation, potentially indicating the onset of a tertiary creep, or a creep to failure condition. Figure G5.7 shows the acceleration in settlement rate (i.e. possible tertiary creep phase of deformation) of SMPs on the downstream edge of the crest and downstream slope at Chainage 150 and 750 m. Each data point represents the average settlement rate over three data readings, which was undertaken to reduce the scatter in the data.
- The possible mechanisms involved in the deformation behaviour of the downstream slope are considered to possibly be a combination of stress changes at the top of the slope due to moisture infiltration into cracks when the reservoir is in a drawn down condition and to progressive failure of the foundation or base of the saturated embankment. It would appear that stick-slip type deformation behaviour of the downstream toe at several locations indicates that the movements are being driven from the top of the slope resulting in build up of stresses in the foundation. Continued movements of this type of the over-consolidated foundation would gradually result in strain weakening and progressive failure within the fissured clay foundation.
- Stability analyses of the downstream slope (SMEC 1996d) indicate the factor of safety to be greatly dependent on the strength of the foundation (which is fissured) and the pore water pressure profile. SMEC obtained a factor of safety of close to 1.0 for the downstream shoulder adopting residual strength for the foundation (assumed as $f\ell$ of 16°) and residual undrained strength for the saturated base of the downstream shoulder. Therefore, allowing for water filled tension cracks at the top of the downstream slope; the factor of safety may drop below 1.0.

It is considered that there is still some brittleness in the slip mechanism given that several SMPs are showing continued increases in the rate of movement. Therefore, the

expected future movement trends would be for further increases in the rate of movement.

The monitoring records presented are up until remedial works were undertaken incorporating construction of a stabilising berm on the downstream slope of the embankment to address the marginal stability condition.

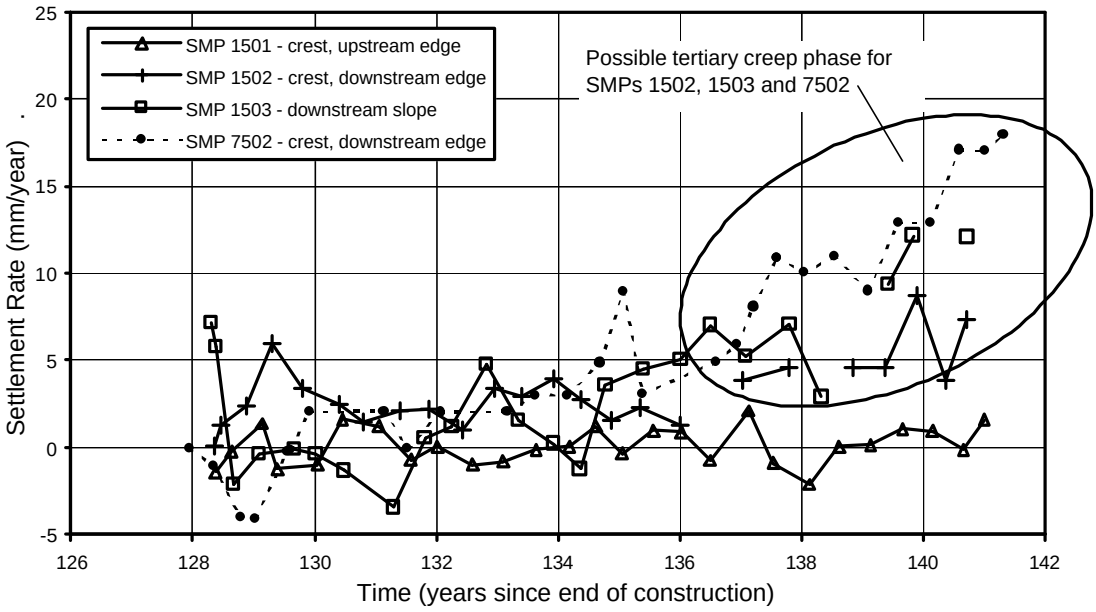

Figure G5.7: Yan Yean dam; settlement rate versus time for SMPs at Chainage 150 and 750 m.

5.3 HOPE VALLEY DAM

Hope Valley dam is an off-stream water supply storage for the city of Adelaide, South Australia. The puddle core earthfill embankment (Figure G5.8) was completed in 1870. It is of 21 m maximum height and 765 m length with embankment slopes of 3H to 1V (horizontal to vertical) for the upstream shoulder and 2H to 1V for the downstream shoulder. A stabilising berm was constructed at the downstream toe approximately 6 years after completion due to excessive seepage through the foundation. The embankment was also raised approximately 12 years after embankment construction due to excessive settlements of the crest. The dam foundation comprises a thin layer of medium to high plasticity fissured alluvial clays overlying Tertiary aged fluvial deposits to depth. The fluvial deposits comprise a thin layer of calcareously cemented, very stiff

to hard sandy clays overlying very dense, partially cemented sands to depth. A puddle clay cut-off of 1 to 2.7 m depth extends down to the very stiff to hard sandy clays.

The central, narrow puddle core has a top width of 1.8 m and slopes of 1H to 12V and was constructed of high plasticity sandy clays in 225 mm layers compacted by heeling in by feet and hand ramming. The shoulder filling was placed in layers sloping toward the central core, which was common practise at the time. The upstream shoulder and inner downstream shoulder comprise medium to high plasticity sandy clays placed in 300 mm layers and compacted by hand ramming and a 3.5 tonne horse-drawn sheepsfoot roller. The outer downstream shoulder comprises a mixture of clayey sands and silty sands with some gravel placed in 1200 mm layers and compacted by construction traffic and the 3.5 tonne sheepsfoot roller. Recent test pits exposed thin layers of high plasticity clays at about 1.2 m depths suggesting each layer of fill was capped with the plastic clay. The stabilising fill comprises materials similar to the outer downstream fill.

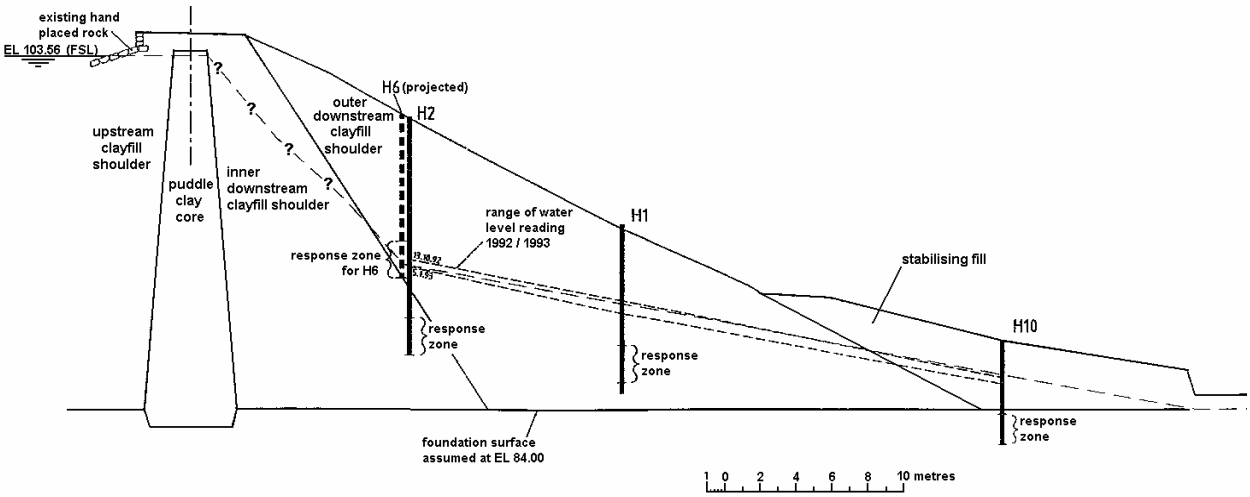

Figure G5.8: Cross section of Hope Valley dam (courtesy of South Australian Water Corporation).

Monitoring of pore water pressures since 1981 indicates the phreatic surface and its response to fluctuations in reservoir level within the upstream shoulder is variable. Close to outer slope of the upstream face and at one location near to the core, the phreatic surface is close to the reservoir level. However, at two other locations within the upstream shoulder the phreatic surface is below the reservoir level, up to 8.5 m at one location. On drawdown the response of piezometers in the embankment is as follows:

- Close to the outer face of the upstream shoulder the piezometric levels closely follow the reservoir level.
- Within the upstream shoulder the piezometric response to changes in reservoir level is variable, ranging from 25% to 100% of the change in reservoir level.
- There is not sufficient information on piezometric response downstream of the core to comment on changes due to changes in reservoir level, however, it is suspected that the change would be minor.

The records of the pore pressure monitoring indicate that the permeability of the upstream filling is highly variable. Sections of the upstream filling act as an effective water barrier, with piezometric levels well below the reservoir level and showing minor response to changes in the reservoir level. At other locations within the upstream filling, the material is quite permeable with piezometric pressures responding to the reservoir level. Therefore, at any point on the upstream side of the core, the piezometric response to change in reservoir level ranges from about 25% to 100% of the actual reservoir level change.

During the early stages of operation of the embankment problems with foundation seepage were encountered. On initial filling of the reservoir in June of 1872 seepage was observed emanating from downstream of the embankment. When the reservoir level reached about 12 m height above the base elevation, the rate of seepage was observed to increase and as a result the reservoir level was lowered to 8 m height in September of 1872. It was thought that the seepage was passing through the foundation. To combat the foundation seepage problem:

- A layer of puddle clay was placed below the 8 m level over the impoundment area of the reservoir from July 1873 to 1878, although this was never fully completed.
- A drainage system was installed at the downstream toe in about 1878 and the stabilising berm constructed. The downstream toe of the dam was referred to as "quite sodden".

After 1878 it is assumed that the reservoir operated as designed.

Early records of the crest settlement start from shortly after the end of embankment construction in late 1870 and the settlement versus time at the maximum section is plotted in Figure 7.92 in Section 7.7 of Chapter 7. The settlement records show the following features:

- An initial period of settlement at a relatively low settlement rate for the first 5 to 6 years after construction. This equates relatively closely with the period during which the puddle lining was being constructed and a time when the reservoir level would have remained at a low level.
- A period of rapid settlement from 6 to 11 years after construction (1877 to 1882). This period is probably coincident with the period of initial filling to full supply level and the first few cycles of reservoir drawdown.
- After 1882, the rate of settlement is significantly reduced. The long-term rate of crest settlement, S_{LT}, is calculated at 2.5% per log cycle of time. This is within the lower range of settlement rates for embankments where the change in piezometric level on the upstream side of the core closely follows that of the reservoir level.

In 1884 the embankment crest was raised as a result of excessive settlement to this date, estimated at more than 1200 mm (or 5.4% of the embankment height). The settlement was in proportion to the height of the dam, with the maximum settlement coincident with the maximum height.

The results of recent monitoring for the period 1988 to 1998 (118 to 128 years after construction) of settlement and lateral displacement of SMPs on the upper and mid to lower downstream slope are presented in Figure G5.9 and Figure G5.10 respectively. The deformation behaviour from the recent monitoring shows:

- The settlement behaviour shows a general trend for settlement of the upper section of the downstream slope at a rate of about 2 mm/year, which equates to an average long-term settlement rate of 2.6 % per log cycle of time, which is similar to that of the crest post 1882. The fluctuations about the general trend are somewhat erratic in that they do not correspond with the reservoir level; however they may correspond with fluctuating levels in the downstream slope that lag behind the reservoir level. Another possible explanation for the fluctuation is the effect of rainfall and development of perched water tables in the outer downstream fill. The overall settlement of the lower downstream slope is negligible.
- The horizontal displacement of the downstream slope is in a downstream direction at a steady rate of 4.5 to 5 mm/year on the upper slope and negligible on the lower slope. The rate oscillates about the general trend with fluctuations in reservoir level (negligible or upstream movement on drawdown and downstream movement on rising reservoir level).

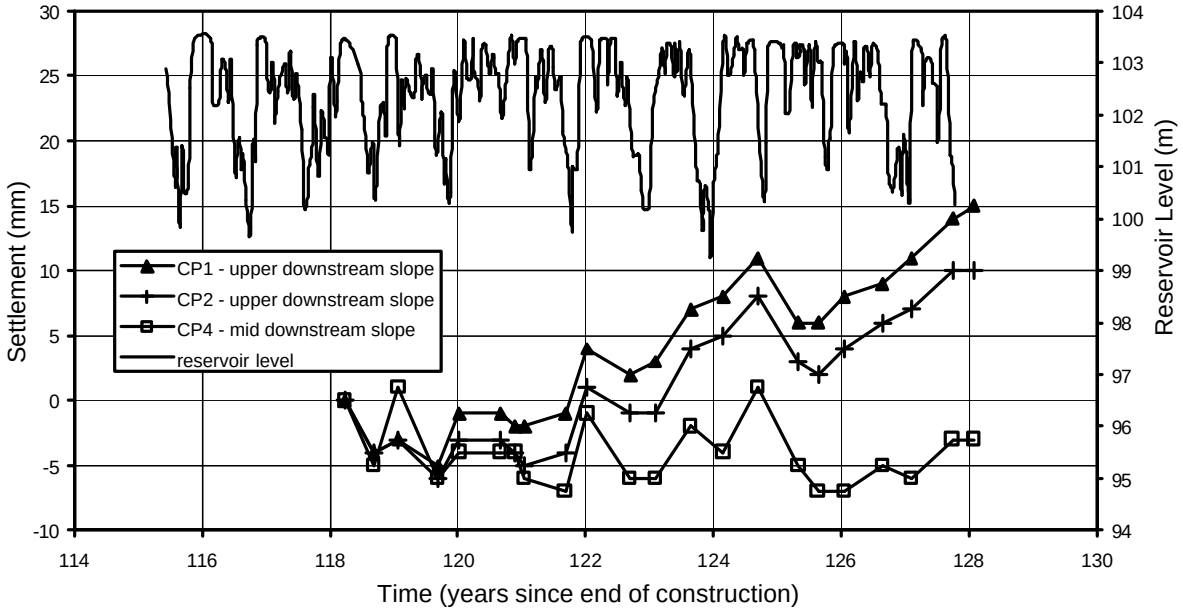

Figure G5.9: Hope Valley dam, settlement versus time (1982 to 1998).

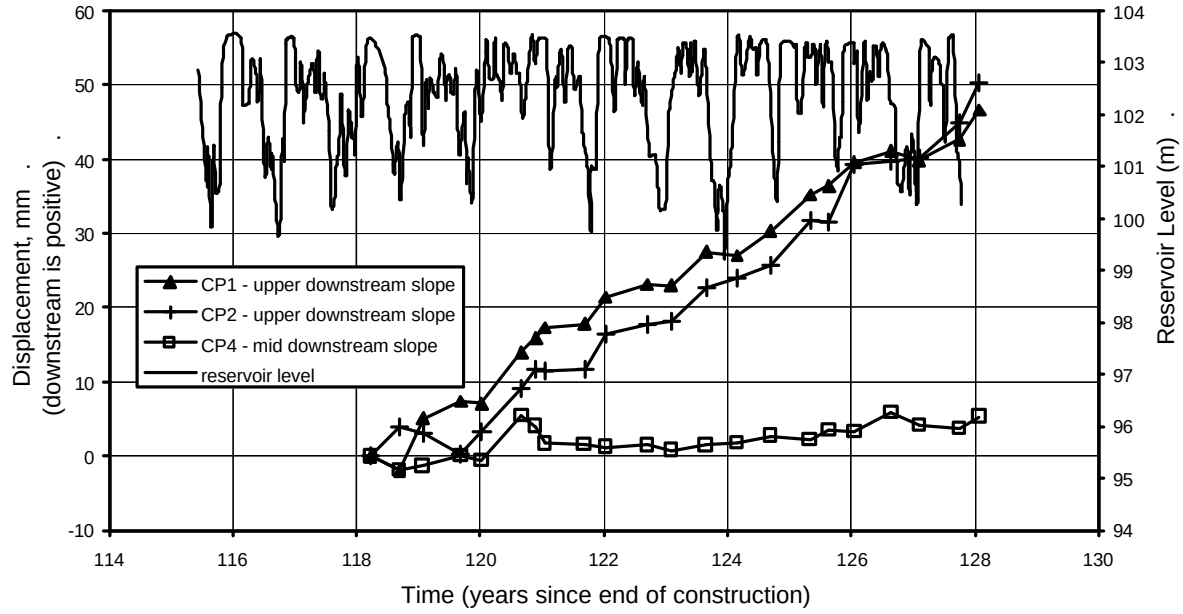

Figure G5.10: Hope Valley dam, horizontal displacement versus time (1982 to 1998).

The possible mechanisms associated with the deformation behaviour of Hope Valley dam are:

- Initial dam operation:
  - Collapse compression on first filling of the poorly compacted earthfill in the upstream shoulder.

- On the first few drawdown events, significant settlement of the upstream filling would have occurred due to yielding as the effective stresses increased in the now softened upstream filling, although instability of the upstream slope in the early life of the embankment should be considered.
- Large settlements of the puddle core, predominantly as undrained plastic deformations, are likely to have occurred as the puddle core deformed with the upstream shoulder (because of its low undrained strength and necessary support from the shoulders), and from lateral deformations of the core under the stress changes associated with fluctuations in the reservoir level due to the greater compressibility of the wetted and softened upstream shoulder earthfill. Deformations would also occur due to consolidation on dissipation of construction pore water pressures to "steady state" conditions.
- For the downstream shoulder, initial settlement rates would be expected to be relatively high due to poor compaction of the filling and collapse compression of wetted material. The "sodden" condition of the downstream toe of the embankment at the time of construction of the stabilizing berm in 1878 indicates that part of the downstream shoulder earthfill has been wetted. The most likely seepage path was from upward seepage pressures associated with seepage through the foundation, but leakage through hydraulic fracture in the core is a possibility. The potential for hydraulic fracture has not been investigated; however, it is possible it could have occurred due to the variability of permeability of the upstream fill. On first filling, the water pressures acting on the upstream face of the puddle core are likely to have varied from possibly as low as zero (regions of low permeability in the upstream earthfill shoulder) to 100% of the reservoir level (high permeability regions). In this context, and considering the low effective stresses likely to be present in the relatively narrow core due to arching during construction, hydraulic fracture could have occurred.
- The net effect during the initial 10 to 12 years of operation would therefore be expected to result in large deformations mainly as a result of collapse compression in the upstream shoulder on wetting and from changes in stresses during drawdown events, but also potentially from collapse compression of the downstream earthfill shoulder due to wetting from upward seepage pressures at the toe and potentially from leakage through hydraulic fracture.

- Recent monitoring, 118 to 128 years after construction:
  - The deformation of the upper downstream slope indicates a general trend (following reservoir cycling) of steady settlement and downstream displacement. On the mid to lower downstream slope there are minor long-term deformations although there is some cyclic fluctuation.
  - It is possible the settlement trend of the upper downstream slope is due to the cyclic stress changes associated with fluctuations in the reservoir level, as the long-term settlement rate is comparable to the estimate for the crest from earlier monitoring. In comparison to the behaviour of the upper downstream slope of Happy Valley dam, the long-term settlement rate is higher; however, it would be expected to be higher because the stress changes associated with changes in reservoir level would be greater at Hope Valley dam given the piezometric response in the upstream earthfill shoulder adjacent to the puddle core.
  - The displacement rate of the upper downstream slope, in comparison to other puddle dams, is considered relatively high. The rate is similar to that of Yan Yean dam (considered to possibly be in a tertiary creep phase of movement), although the rate at Hope Valley dam is virtually constant. In comparison to the crest of Lower Walshaw Dean dam, which also shows a steady downstream displacement rate, the rate is higher at Hope Valley dam. This may be due to type of material used as shoulder filling and potentially lower factor of safety of the downstream slope at Hope Valley dam.
  - Based on the available deformation records and in comparison with other puddle dams, it is considered that a significant proportion of the movement of the downstream slope can be attributed to long-term creep and cyclic stress changes associated with reservoir level fluctuations. However, it is not possible to conclude that these are solely the explanation for the movement without considering the possibility of localised slope instability. The discerning factor is the rate of downstream displacement, possibly indicating a marginal factor of safety. This was shown to be the case and a second berm has since been constructed on the downstream slope (Gosden et al 2002).

5.4 RAMSDEN DAM

Ramsden Dam is a puddle core earthfill embankment, located in Yorkshire, England, for which construction was completed in 1883 (Holton 1992). The embankment (Figure G5.11) is of 25 m maximum height and 120 m length with embankment slopes of 3H to 1V (horizontal to vertical) upstream and 2H to 1V downstream. The dam foundation comprises bedrock of the sedimentary Millstone Grit series. A central, concrete filled cut-off of 2 m width and 22 m maximum depth extended down through permeable bedrock strata. The lower 6 m of the downstream shoulder is submerged by the Brownhill reservoir.

The narrow central puddle core (Holton 1992) has an estimated top width of 3 m and slopes of 1H to 12V. It was constructed of medium to high plasticity sandy silts and sandy clays of Boulder clay. Investigations in the 1980's (Tedd and Holton 1987) indicate the condition of the puddle core to range from "*good quality*" to extremely soft. Undrained triaxial compression tests on undisturbed samples of the puddle core (Charles and Watt 1987) indicate undrained strengths to be generally in the range 25 to 40 kPa, with several results below 20 kPa in the upper 10 m and one result as low as 4 kPa (at 9.5 m below crest level).

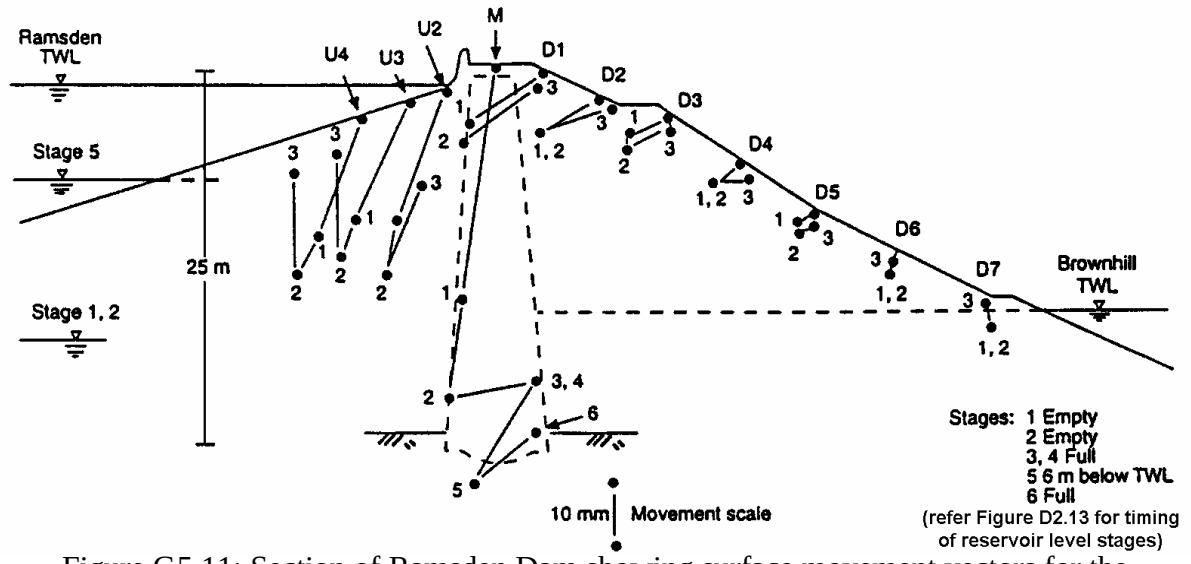

Figure G5.11: Section of Ramsden Dam showing surface movement vectors for the period 1988 to 1990 (Tedd et al 1997b).

The shoulder filling comprises variably weathered bedrock of the Millstone Grit series (Tedd et al 1997b), having the consistency of silty to sandy clays with gravel to boulder size mudstone, siltstone and sandstone rock fragments. Tedd and Holton (1987)

indicate the consistency of the downstream shoulder filling to be highly variable, ranging from layers of sandy clay to layers of predominantly rock fragments, reflecting the range in permeability from constant head tests of 2.0×10^{-5} to 10^{-7} m/sec. The construction drawings (Tedd et al 1990) indicate that selected fill was placed either side of core, presumably comprising more cohesive and less granular material. Given the age of the embankment, it is assumed that compaction of the shoulder filling was relatively poor in terms of today's standards.

The hydrogeology of Ramsden Dam is summarised as follows:

- Kovacevic et al (1997) describe the shoulder filling as free draining. The phreatic surface in the upstream shoulder is therefore assumed to closely follow the reservoir level.
- Pore water pressures in the downstream shoulder earthfill correspond to the water level in Brownhill reservoir, which inundates the lower portion of the downstream slope of Ramsden Dam. Pore water pressures measurements in the mid to upper levels of the downstream fill indicated the presence of several perched water tables (Tedd and Holton 1987), with water levels typically 0.5 to 2 m above the tip of the piezometer. Tedd and Holton indicate the perched water table is probably due to the layering of the shoulder fill, which slopes toward the central puddle core, and the variation in material type and vertical permeability of the layers of earthfill.
- Pore water pressures measured in the centre of the puddle core (Charles and Watt 1987) show a pore water pressure profile below hydrostatic, decreasing from about 85% in the upper part of the core to 65% at 18 m depth below crest level.

The observations indicate the puddle core is acting as an effective water barrier. On drawdown it is presumed from the available information that the phreatic surface in the upstream filling follows that of the reservoir level and therefore, the upstream side of the puddle core feels the full effect of the drawdown. Some changes in pore water pressure in the puddle core are therefore likely to occur on reservoir fluctuation, but no change is considered likely in the downstream filling.

Tedd et al (1997b) estimate the post construction crest settlement to be in excess of 1 m since end of construction in 1883. The embankment is known to have been raised at least 3 times, including in 1949 and more recently in 1990. Charles and Watt (1987) estimate the crest settlement from 1949 to 1983 at 430 mm (or 1.7% of the dam height) based on survey levels. For the period 1949 to 1990 the long-term crest settlement rate

of nearly 10% per log cycle of time for Ramsden dam is relatively high in comparison to other puddle core earthfill dams (refer Figure 7.92 in Section7.7 of Chapter 7), but this includes the abnormally large drawdown of 1988. During normal reservoir operating conditions Tedd and Holton (1987) indicate the long-term crest settlement rate is slightly lower at 6.6% per log cycle of time (for the period from 1977 to 1986).

In the late 1980s SMPs were established on the crest and slopes of the embankment and an internal gauge was installed in the puddle core to monitor settlements and horizontal displacements. Tedd et al (1990) report the monitoring results for the period from 1988 to early 1990 (from 105 to 107 years after the end of embankment construction) and are shown in Figure G5.12 to Figure G5.15. Figure G5.12 and Figure G5.13 present the settlement and displacement of SMPs on the crest and slopes of the embankment. Figure G5.14 is the internal vertical strain and Figure G5.15 the internal horizontal displacement measured within the puddle core. The monitoring period includes two reservoir cycles, the abnormally large drawdown cycle in 1988 when the reservoir was virtually emptied and the 6 m drawdown in 1989, which is more typical of normal operating conditions. The monitoring records show:

- For the abnormally large drawdown cycle in 1988:
  - A large permanent crest settlement of 51 mm (Figure G5.12). The internal settlement records (Figure G5.14) show most of the settlement in the core was within the mid to lower region where permanent vertical strains were in the range 0.25% to 0.4%. Much smaller strains were measured in the upper region of the puddle core (approximately 0.1%).
  - The settlement of the upstream slope was also relatively large on drawdown (30 mm), but most of this was recovered on re-filling. The net permanent settlement for the drawdown cycle was 8 to 10 mm, which is still relatively large.
  - Settlements of the downstream shoulder were smaller at less than 10 mm on drawdown, and permanent settlements less than 5 mm.
  - Displacement of SMPs on the crest and upper slopes showed a displacement to upstream on drawdown followed by a displacement to downstream on re-filling. The net displacement of the slopes was negligible, but for the crest was 7 mm downstream.
  - Internal displacements of the puddle core show a similar upstream then downstream pattern on drawdown and re-filling over the full depth of the core.

Notably, the mid to lower region of the core shows a net upstream displacement. The displacement between 10 to 15 m depth below crest level is somewhat unusual and is discussed further below.

- For the more typical 6 m drawdown cycle in 1989 a similar pattern of deformation behaviour is observed as on the large drawdown in 1988 except that the magnitude of deformations (both maximum and permanent) are generally much smaller. Notable observations are:
  - The relatively large net permanent crest settlement of 10 mm. The internal settlement records show the settlement in the core to be localised to 0 to 6.5 m and possibly 9.1 to 12.6 m depth below crest level.
  - The displacements of SMPs on the crest and upper slopes are of similar magnitude to the larger drawdown.
  - The internal core displacement profile shows an upstream displacement over the full depth of the core on drawdown that is much smaller in magnitude over the mid to lower region of the core.

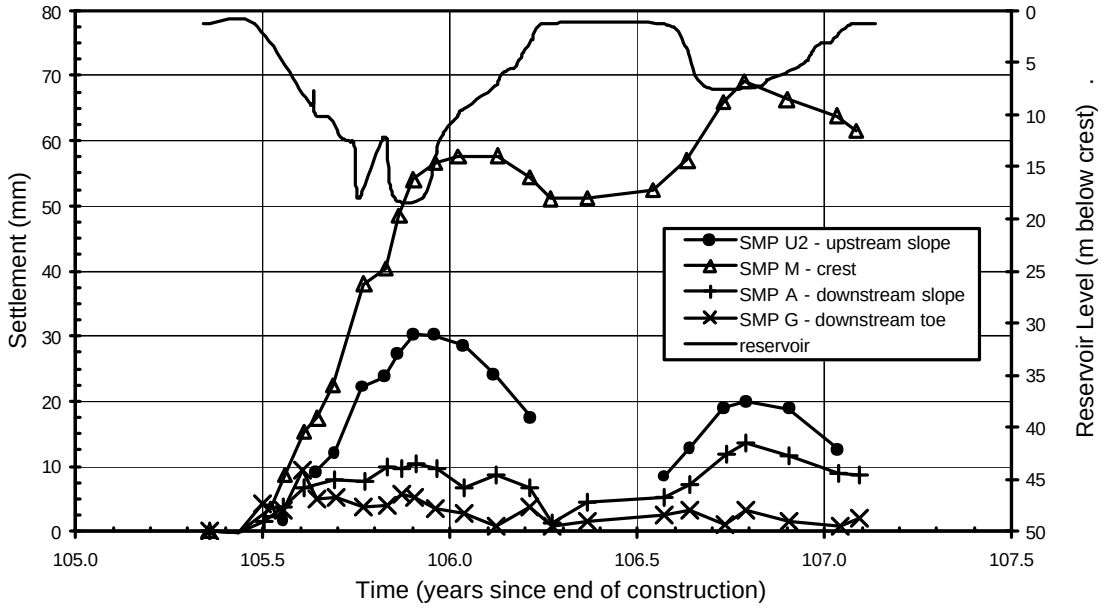

Figure G5.12: Ramsden Dam, settlement versus time of SMPs from 1988 to 1990.

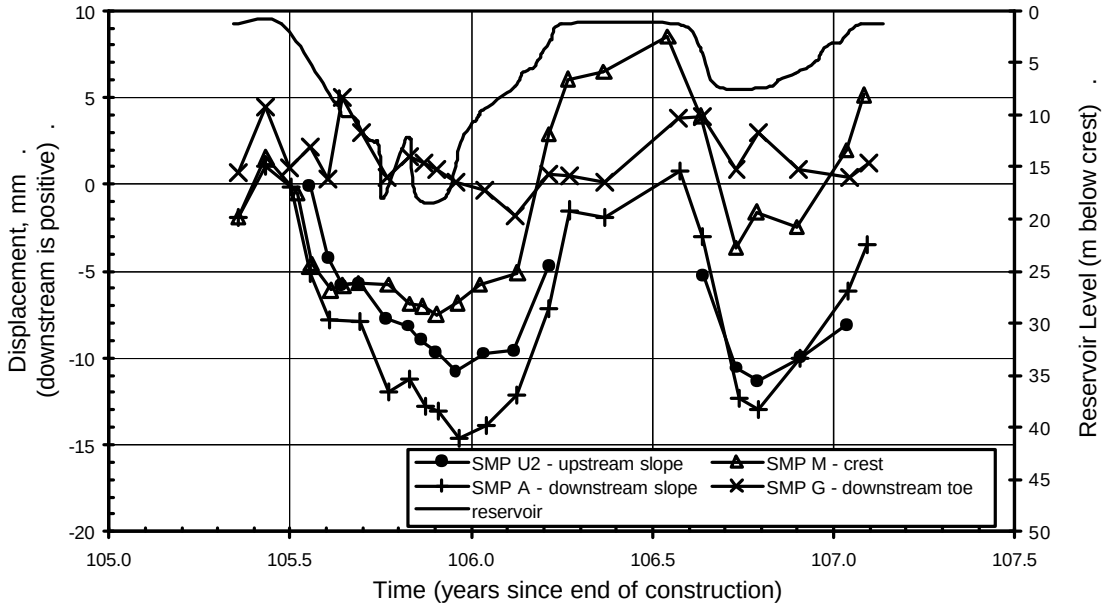

Figure G5.13: Ramsden Dam, displacement versus time of SMPs from 1988 to 1990

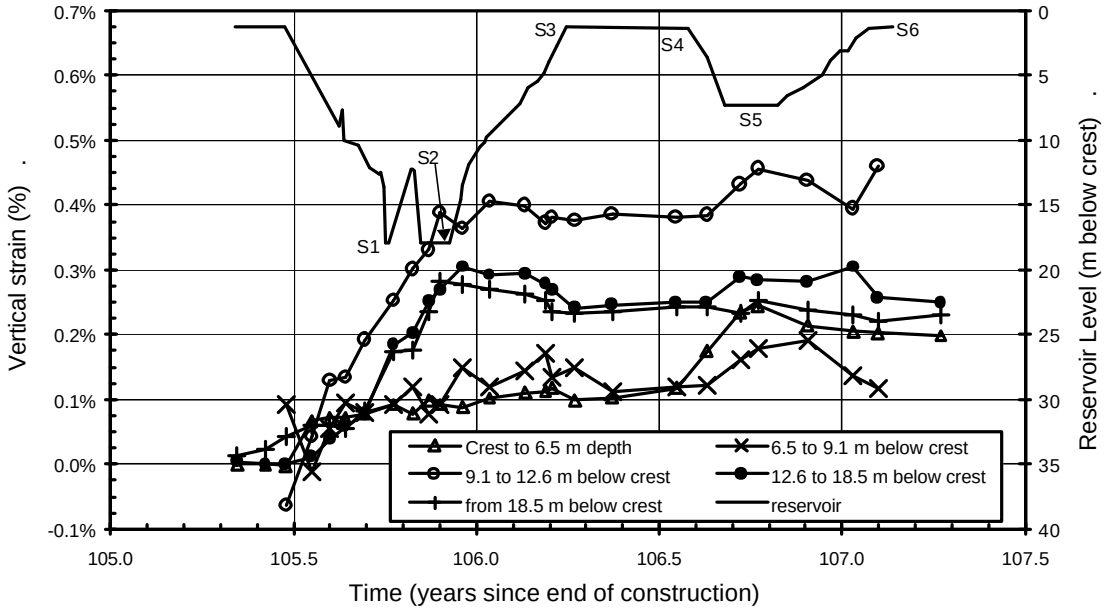

Figure G5.14: Ramsden Dam, post construction internal vertical strains in the puddle core from 1988 to 1990 (data from Tedd et al 1997b; Kovacevic et al 1997).

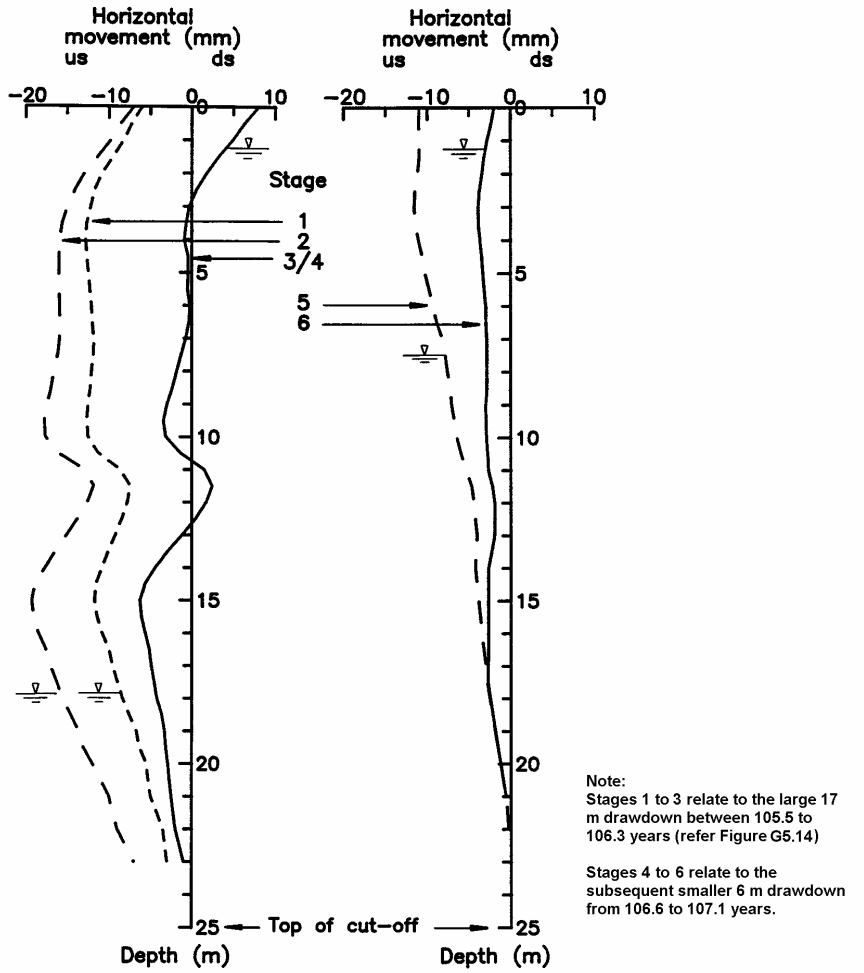

Figure G5.15: Ramsden Dam, internal horizontal deformation of puddle core during drawdown cycles from 1988 to 1990 (Holton 1992).

Tedd et al (1997b), and the finite element analysis by Kovacevic et al (1997) shows, that the mechanism controlling the deformation behaviour under normal operating conditions of reservoir fluctuation relates to the difference in material compressibility properties between loading and unloading (refer Section 7.7.3.4 of Chapter 7). The general trend of crest deformation is for settlement at a rate of about 6.5 to 7 % per log cycle of time. Whilst quite high compared to a number of the puddle core earthfill dams, it is considered to be representative of normal behaviour for a puddle dam with permeable upstream filling and fluctuating reservoir level. The internal displacement behaviour of the puddle core of upstream than downstream displacement over the full depth of the core is expected, and is due to the reduction then increase in horizontal water pressure acting over the full depth of the upstream side of the core as the reservoir is lowered then raised.

The possible mechanism/s associated with the deformation behaviour of Ramsden Dam during abnormally large drawdown are:

- For the upstream shoulder, the permanent settlement is primarily due to yielding associated with the increase in effective vertical stress within the shoulder on drawdown. If this were the largest historical drawdown the effective stresses in the upstream shoulder would be the highest experienced by the wetted and softened upstream earthfill (i.e. since first filling). The net permanent settlement is about 10 mm, which is relatively large given the age and height of the embankment.
- For the low undrained strength puddle core the permanent settlement is considered to be primarily due to yielding, mainly as plastic type deformations largely as a result of lateral spreading in the mid to lower region of the core. The lateral spreading is considered to be due to the very large reduction in horizontal water load acting on the upstream face of the core, and the transfer of stress onto to the upstream shoulder to maintain equilibrium lateral stress conditions between the puddle core and upstream shoulder. A permanent lateral displacement occurs as a result of this stress transfer and is reflected in the net displacement profile (Figure G5.15). The abnormally large drawdown has a significant influence on the amount of permanent displacement because of the unusually high horizontal stresses imposed on the water softened upstream shoulder. The monitored records show most of the permanent deformation occurs at depth in the embankment.
- The continued deformation once the initial full drawdown has occurred could be due to time lag in pore pressure dissipation in the upstream shoulder and also pore pressure dissipation in the puddle core itself, resulting in consolidation.
- The possibility that shear type deformation in the core has contributed to the observed deformation behaviour cannot be discounted. The internal displacement records indicate a possible localised shear type deformation at 10 to 12 m depth below the crest, which has resulted in a slight rotation of the upper part of the core and is evident on comparison of the net displacement profiles between the drawdown cycles of 1988 and 1989 (Figure G5.15). Other evidence supporting a possible shear type deformation in the core is that the region of highest vertical strain in the puddle core is between 9.1 m and 12.6 m depth below crest, and the very low undrained strength zone at about 9.5 m depth. It is considered possible that undrained shear movements have occurred on a weak plane though the core during the first stage of the full drawdown.

The finite element analysis of Ramsden dam by Kovacevic et al (1997) was able to model the deformations on the smaller drawdown in late 1989 quite well, but could not model the deformation during the abnormally large drawdown. A probable reason for this is the difficulty in modelling the variation in compressibility properties of the upstream shoulder earthfill over the stress range involved with the larger drawdown.

5.5 WALSHAW DEAN (LOWER) DAM

Walshaw Dean dam is a puddle core earthfill embankment, located in Yorkshire, England, for which construction was completed in 1907. The embankment (Figure G5.16) is of 22 m maximum height and about 200 m crest length with embankment slopes of 3H to 1V (horizontal to vertical) upstream and 2H to 1V downstream (Tedd et al 1997b; Charles and Watt 1987). The dam foundation comprises sandstones and mudstones of the sedimentary Millstone Grit series. The narrow (3 m wide) central cut-off has been constructed with puddle clay and extends down through highly fissured sandstone to a maximum depth of about 40 m below crest level.

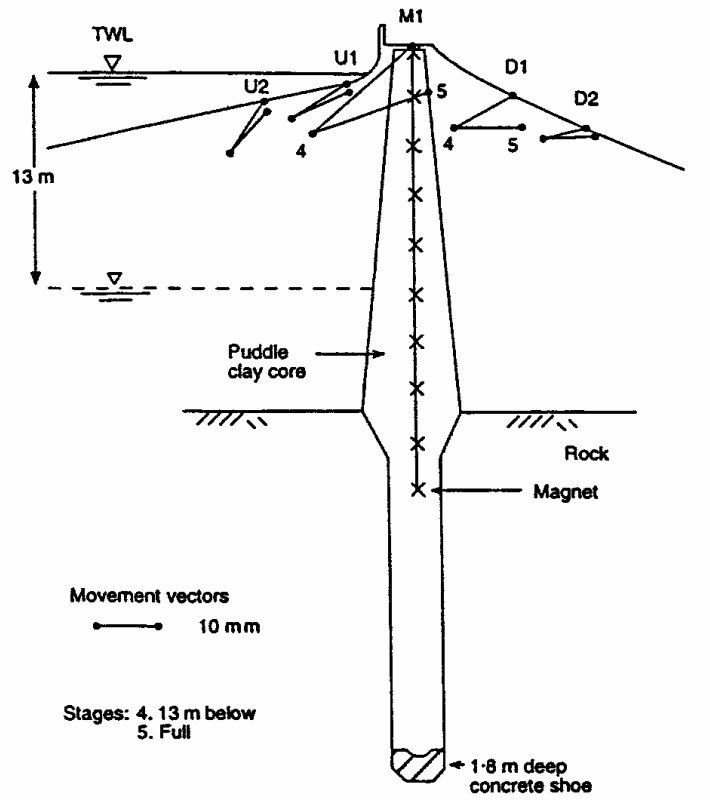

Figure G5.16: Section of Walshaw Dean Lower dam showing SMP locations and deformation vectors during drawdown cycle at 87 years (Tedd et al 1997b)

The central puddle core has an estimated top width of 2.6 m and slopes of 1H to 12V. It was constructed of medium to high plasticity sandy clays, sourced from Boulder Clay, by conventional puddling methods at the time. Tedd et al (1997b) indicate the shoulder filling comprises variably weathered bedrock of the Millstone Grit series, having the consistency of silty to sandy clays with gravel to boulder size mudstone, siltstone and sandstone rock fragments. Given the age of the embankment, it is assumed that compaction of the shoulder filling was relatively poor in terms of today's standards.

The hydro-geology of Walshaw Dean dam, as inferred from Tedd et al (1997b), is assumed to be similar to that of Ramsden dam (refer Section 5.4). The permeability of the embankment shoulders is assumed to be variable, but relatively high, due to material variation and layering effects on placement, and the puddle core acts as an effective water barrier. On reservoir fluctuation the pore water pressures within the upstream shoulder are assumed to closely follow the reservoir level, with the upstream face of the core experiencing the full effect of the fluctuation. The phreatic surface is assumed to be at a fairly low level in the downstream shoulder and is not affected by reservoir fluctuation. The reservoir operation (Figure G5.17) consists of large seasonal drawdowns in the range 12 to 18 m (reservoir empty) depth below crest level.

Tedd et al (1997b) estimate the post construction crest settlement since end of construction in 1907 to be about 1 m, although it could be significantly greater than this given that the crest settlement rate in the early to mid 1990's is approximately 10 mm/year. The embankment is known to have been raised at least once in its history, in about 1943.

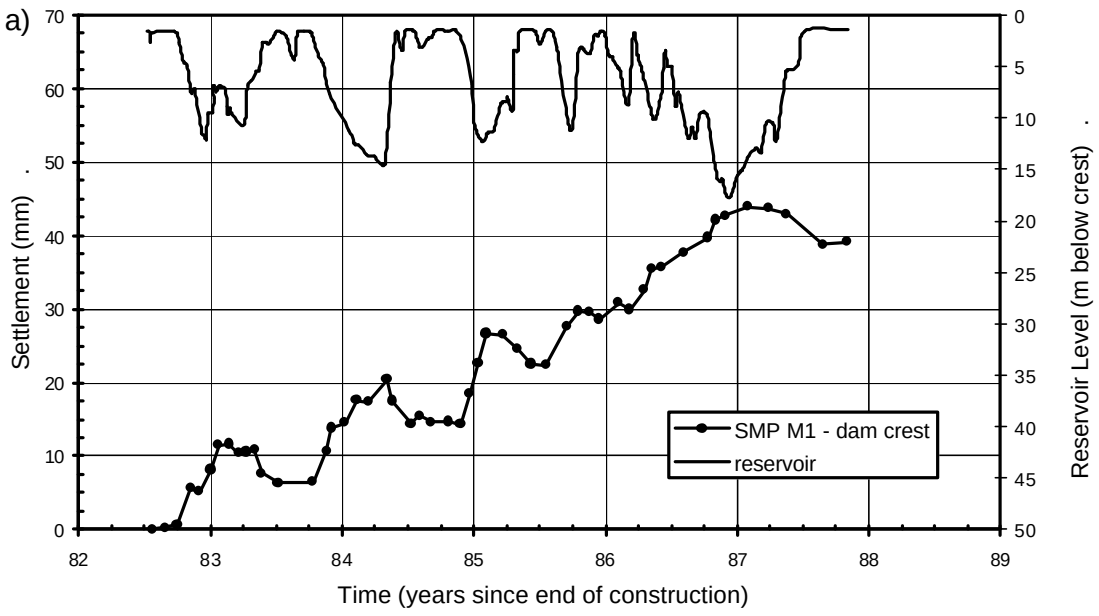

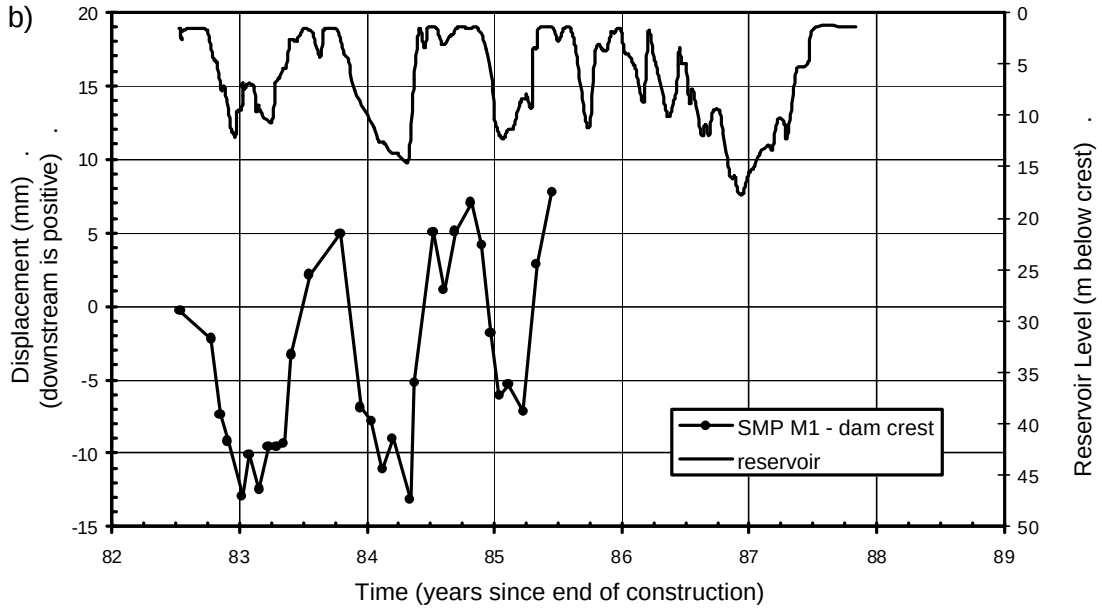

Figure G5.17: Walshaw Dean Lower dam, long-term *(a)* crest settlement and *(b)* horizontal displacement versus time from 1990 to 1995 (data from Tedd et al 1997a).

The monitored crest settlement and displacement records for the period 1990 to 1995 (82 to 88 years after construction) are shown in Figure G5.17. Figure G5.18 is a plot of the internal vertical strain within the puddle core over the period 1990 to 1992. The monitoring records show:

- A steady general trend of crest settlement of about 7.5 mm/year with variation about the general trend due to fluctuations in reservoir level. The period of crest settlement shown equates to a long-term settlement rate (S_{LT}) of 6.6% per log cycle of time.
- A steady general trend of downstream crest displacement of about 3 mm/year with large fluctuations about the general trend due to the fluctuating reservoir level. Crest displacements are upstream on drawdown and downstream on re-filling.
- The deformation pattern of the upstream and downstream slope in comparison to the crest during one cycle of reservoir drawdown and re-filling (Figure G5.16) shows a similar pattern of displacement and generally a smaller magnitude of settlement. The exception is SMP on the upper downstream slope, which shows a settlement of similar magnitude to that of the crest.
- The internal vertical strain in the puddle core (Figure G5.18) ranges from 0.05% to 0.19% over the monitored period and shows a similar fluctuation to the crest settlement. The greatest magnitude of permanent vertical strain is for the depth

range 6.2 to 12.1 m below crest level, where the vertical strain is approximately 3 to 4 times greater than in the other regions of the core.

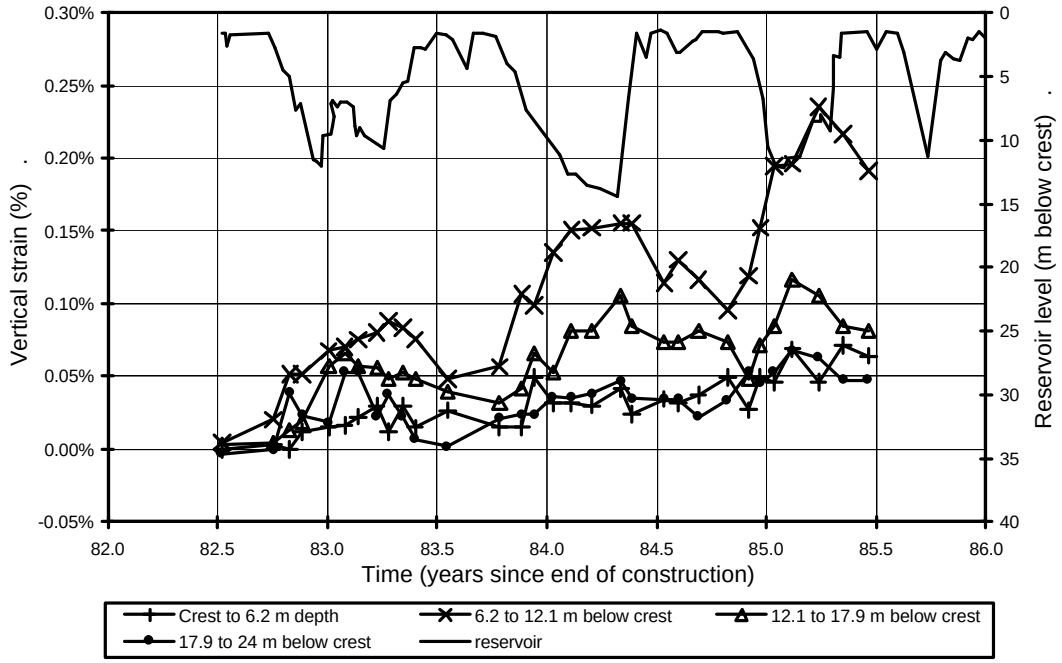

Figure G5.18: Walshaw Dean Lower dam, internal vertical strains in the puddle core from 1990 to 1992 (data from Tedd et al 1997b).

Tedd et al (1997b) comments and the finite element analysis by Kovacevic et al (1997) shows that the mechanism associated with the deformation behaviour of Walshaw Dean dam under normal operating conditions (a large annual drawdown is normal operation) is related to the cyclic stress conditions within the upstream shoulder earthfill and the difference in material compressibility properties between drawdown and refilling. Deformations of the puddle core are considered to be largely undrained type plastic deformation due to lateral spreading of the core under the fluctuation in lateral stress conditions acting on the upstream side of the core and within the upstream shoulder with fluctuations in reservoir level. The general trend of long-term crest deformation is for settlement at a rate of approximately 6.6% per log cycle of time and downstream displacement at a rate of about 3 mm/year. These rates are comparable with those at Ramsden dam during normal reservoir operation. The rate of settlement, whilst quite high, is considered to be representative of normal behaviour for a puddle dam with permeable upstream filling and fluctuating reservoir level.

The finite element analysis of Walshaw Dean dam by Kovacevic et al (1997) was able to model the deformations on drawdown and re-filling reasonable well. The ratio

of modulus during unloading (re-filling) to loading (drawdown) was 1.5 and was based on the laboratory oedometer test results by BRE (Tedd et al 1997b).

5.6 SELSET DAM

Selset Dam (Figure G5.19), located in northern England (owned by the Cleveland Water Board, UK), is a puddle core earthfill embankment of 39 m maximum height and 930 m crest length that was constructed in the late 1950's (Kennard and Kennard 1962; Bishop and Vaughan 1962). The embankment foundation was Boulder clay deposits comprising saturated sandy clays of firm strength consistency. Embankment construction materials were sourced from the Boulder clay deposits and comprised low plasticity sandy clays. The stability of the embankment during construction was of concern to the designers due to potential development of high pore pressures, both in the saturated, firm clay foundation and the embankment shoulders where the wet borrow sources necessitated placement on the wet side of Standard Optimum moisture content. As a consequence, extensive drainage was installed in the foundation and embankment shoulders to dissipate pore pressures, and relatively flat embankment slopes were adopted. The embankment shoulders were compacted in 225 mm lifts by trafficking with construction equipment and 2 to 3 passes of a 13.6 tonne smooth drum roller, achieving an average density ratio of 98.7 % of Standard Maximum Dry Density and average moisture content of 1% wet of Standard Optimum.

Monitoring during construction comprised settlement gauges at foundation level, within the core and within the downstream shoulder. Numerous piezometers were installed to monitor pore water pressures. The results of internal settlement monitoring (Figure G5.20) indicated the settlement of the core was significantly greater than the shoulders. Bishop and Vaughan (1962) commented that the larger part of the settlement within the core occurred during the period of construction and not in the period of winter shut down. They concluded that the deformation of the core was not significantly due to consolidation, but to lateral yield (i.e. plastic deformation) of the saturated, virtually incompressible core during periods of construction, and that the large settlements can be accounted for by relatively small lateral deformation (or spreading) of the narrow core.

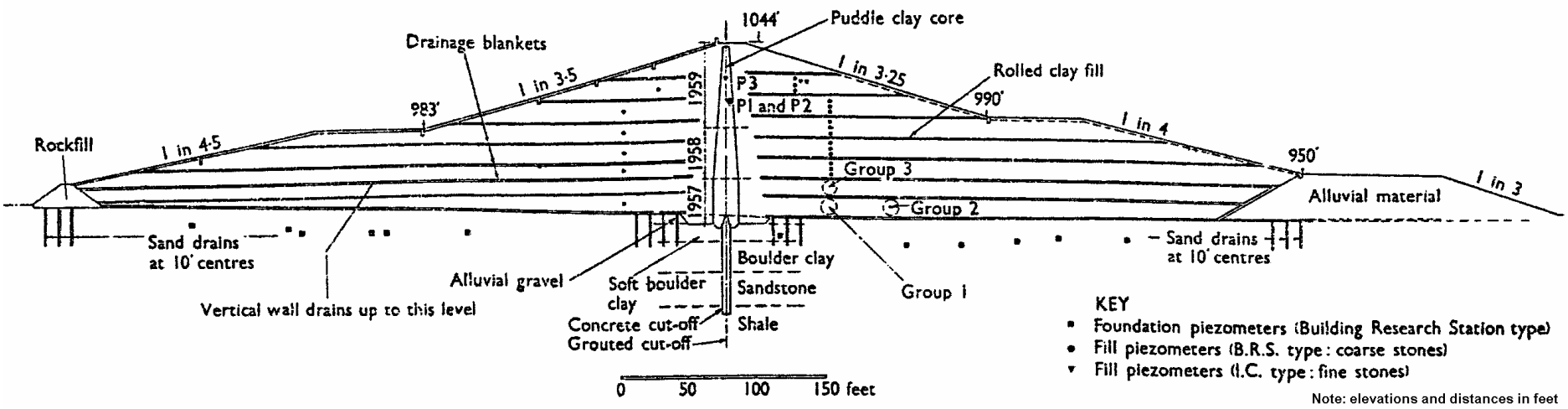

Figure G5.19: Selset Dam cross section (Bishop and Vaughan 1962)

Bishop and Vaughan (1962) commented on the development of arching across the core due to the significant differential settlement between the core and shoulders and the consequent reduction in vertical stress and lateral thrust of the core. Figure G5.21 shows the development of pore pressures in the upper region of the puddle core, and the effect of side shear on the development of pore pressures and vertical stress in the core. Equation 5 referred to on Figure G5.21 is a simple vertical stress equilibrium equation corresponding to plastic equilibrium of the core. Figure G5.21 shows that the pore water pressures in the core are still relatively high at the completion of construction and that limited dissipation of pore water pressures in the puddle core occurred during the period of construction.

The post construction crest settlement at Selset dam is plotted with other puddle core earthfill embankments in Figure 7.92 in Section 7.7 of Chapter 7. Up to 1970, some 10 years after end of construction, the total post construction crest settlement was 313 mm (Charles and Tedd 1991), or 0.80% of the embankment height. The long-term post construction settlement rate is estimated at 0.4% per log cycle of time. The normal operating conditions of the reservoir are not known.

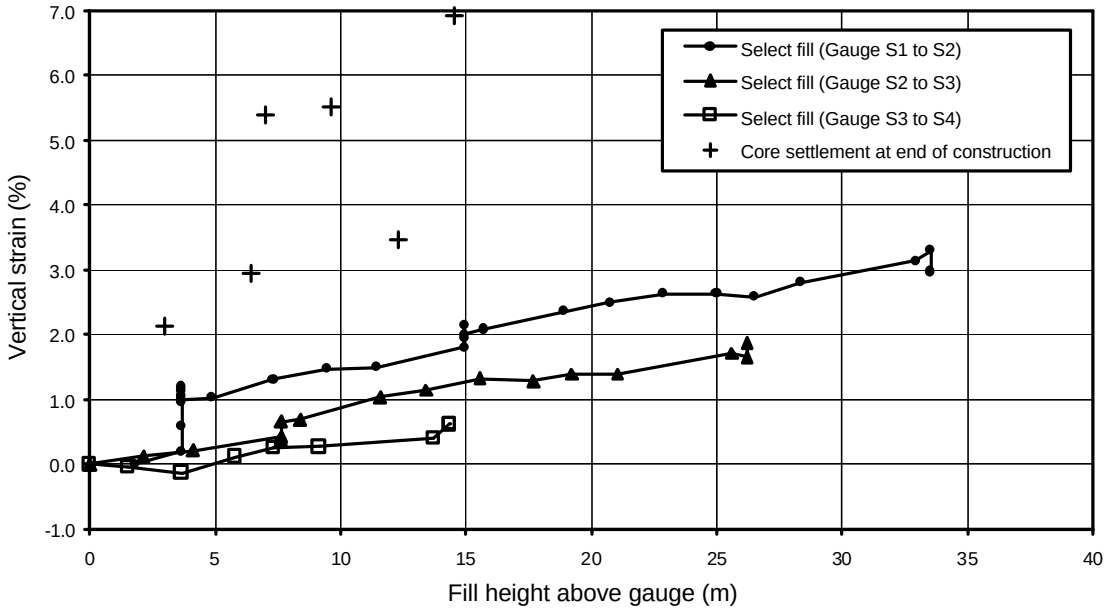

Figure G5.20: Selset Dam internal settlements during construction (data from Bishop and Vaughan 1962).

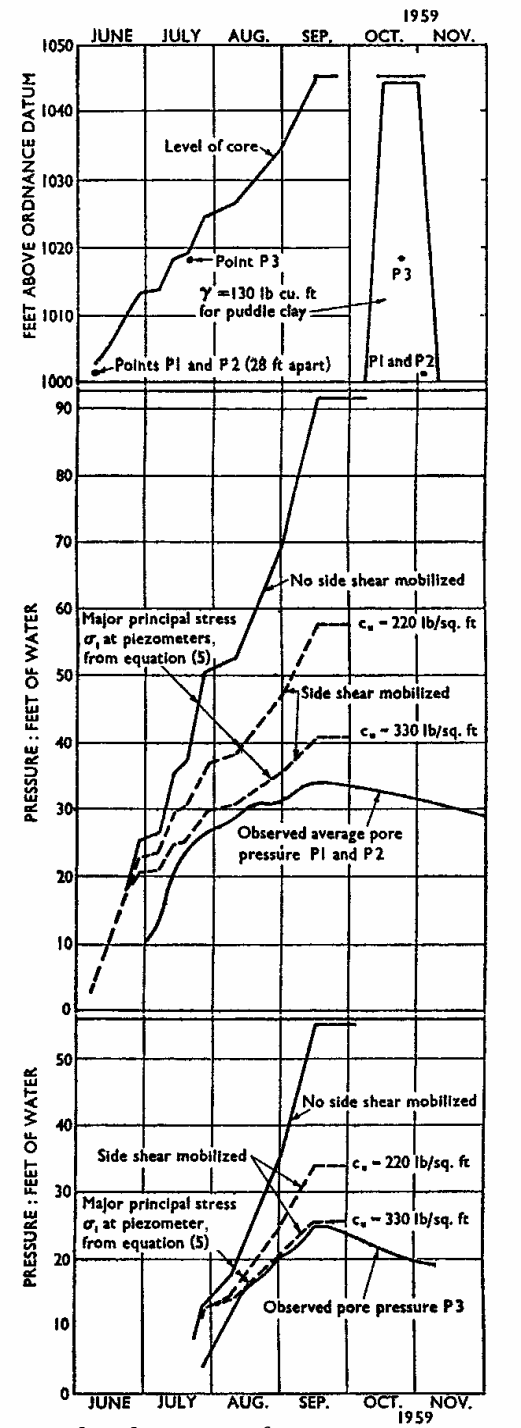

Figure G5.21: Selset Dam development of pore pressure in puddle clay core during construction (Bishop and Vaughan 1962).

6.0 BLOWERING DAM

6.1 INTRODUCTION

From analysis of the deformation behaviour of zoned earth and rockfill dams aspects of the deformation behaviour of Blowering Dam during construction, on first filling and post construction have been identified as potentially "abnormal". Review of the deformation behaviour indicates that a shear surface may have developed in the core during construction and may have, in addition to large plastic type deformations, contributed to the "abnormally" large total settlement of the core during construction. Further deformations along this shear surface may have occurred during first filling and on large drawdown.

It is important to note that whilst aspects of the deformation behaviour of the embankment may be "abnormal" the overall stability, as limit equilibrium analysis shows, is sufficiently stable and not approaching a marginal condition.

In the following sections the monitored performance and deformation behaviour of Blowering dam during construction, on first filling and post first filling is presented, the main purpose being to highlight some of the potentially "abnormal" aspects of the deformation behaviour. Section 6.2 provides the background information on embankment construction, materials used and placement methods. Section 6.3 summarises the instrumentation records during and post construction, mainly the deformation data but also the pore water pressure and pressure cell response in the core. Section 6.4.1 presents the results of a simplified finite difference analysis modelling the deformation behaviour during construction, and Section 6.4.2 the results of limit equilibrium analysis of the embankment.

6.2 BACKGROUND ON BLOWERING DAM

Blowering Dam, constructed over the period 1964 to 1968, is located on the Tumut River in the southern region of New South Wales on the lower western slopes of the Snowy Mountains. The State of New South Wales owns the dam. Snowy Mountains Hydro Electric Authority (SMHEA) undertook design and construction supervision and Dams and Civil Section of the NSW Department of Public Works and Services (DPWS) carry out surveillance.

Blowering dam (Figure G6.1, Figure G6.2) is a central core earth and rockfill dam 112 m high and 808 m in length with embankment slopes of 1.75 - 2H to 1V (horizontal to vertical). The foundation comprises Silurian aged interbedded phyllite, meta-siltstone and quartzite derived from low-grade metamorphism of shale, siltstone and sandstone.

Sources of information on materials, construction, testing and instrumentation records have been obtained from:

- Construction materials report by SMHEA (Svenson et al 1964);
- Construction progress reports by SMHEA issued at 6 monthly time intervals (Olsauskas et al 1966, 1967a, 1967b and 1968);
- The contract document specification (SMHEA 1964);
- Surveillance records courtesy of the NSW Department of Public Works and Services, Dams and Civil Section;
- Published papers on Blowering dam including Hunter and Bacon (1970) and Bacon (1969); and
- Discussion with Mr. Alec Bacon who was associated with the construction of Blowering dam (Bacon 1999).

6.2.1 Foundation Preparation

Excavation for the foundation of all embankment zones was to a "*secure foundation on sound or partially weathered rock of sufficient strength*". Treatment of open seams and defects, and grouting are not discussed here. The deformation records show the foundation settlement (maximum of about 200 mm) to be negligible in comparison to the embankment and it has been ignored in the analysis.

6.2.2 Embankment Construction

Placement of embankment materials started about March 1966 and continued, virtually without stoppage, to completion in April 1968. End of construction, for post deformation analysis purposes, was assumed to be 7 April 1968.

During the early stages of construction, whilst the foundation for the core was being prepared, the Zone 3B rockfill was constructed in advance of the rest of the embankment, reaching a maximum difference in elevation of about 20 m. By February

1967 a consistent elevation across all zones of the embankment was reached and was maintained for the remainder of construction. At this time the embankment was at about elevation RL 316 m AHD, equivalent to a maximum height of about 35 to 38 metres.

The embankment was constructed with a 0.6 m camber to allow for post construction settlement. Hunter and Bacon (1970) indicate that by January 1969, after the end of first filling, crest settlements had reached a maximum of 0.55 m virtually using up the camber. As a consequence the crest was reconstructed in February 1969.

6.2.3 Earthfill Core - Zone 1

Materials for construction of the clay core were sourced mainly from colluvial slopewash soils (derived predominantly from phyllite and porphyry) located on the lower hill slopes in close proximity to the embankment. The borrow materials used also included weathered river gravels and weathered porphyry bedrock, if suitable for use, that underlay the slopewash.

The dominant classification types of the earthfill (Figure G6.3) were clayey sands (SC) and sandy clays (CL) with gravel contents ranging from 10% to 40% and fines of medium plasticity (average Liquid Limit in the low 40's and Plasticity Index in the range 10 to 20%). Permeability of the compacted earthfill was low, averaging about $2x10^{-10}$ m/sec from laboratory testing. The specification called for the more pervious materials from the borrow to be placed to the outside of the core.

The earthfill core was placed in 150 mm thick layers (compacted thickness) and compacted by a minimum 8 passes of a sheepsfoot roller. The specification required compaction to a minimum dry density of 98% relative to Standard maximum dry density (SMDD). Placement moisture content were initially specified within the range 2% dry of OMC to 2% wet of OMC (Standard optimum moisture content), but this was adjusted during placement (see below). The foundation contact zone was specified at 0.6 m thickness of selected finer, more plastic materials compacted at a moisture content within the range 1 to 3% wet of OMC. The results of control testing are summarised in Table G6.1 and indicate the core was well compacted.

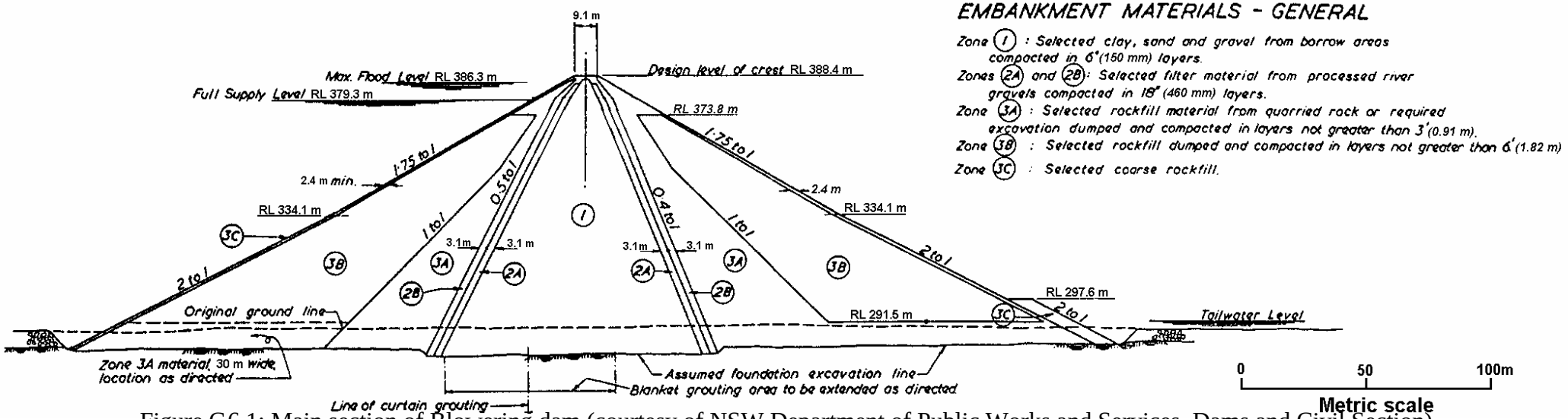

Figure G6.1: Main section of Blowering dam (courtesy of NSW Department of Public Works and Services, Dams and Civil Section).

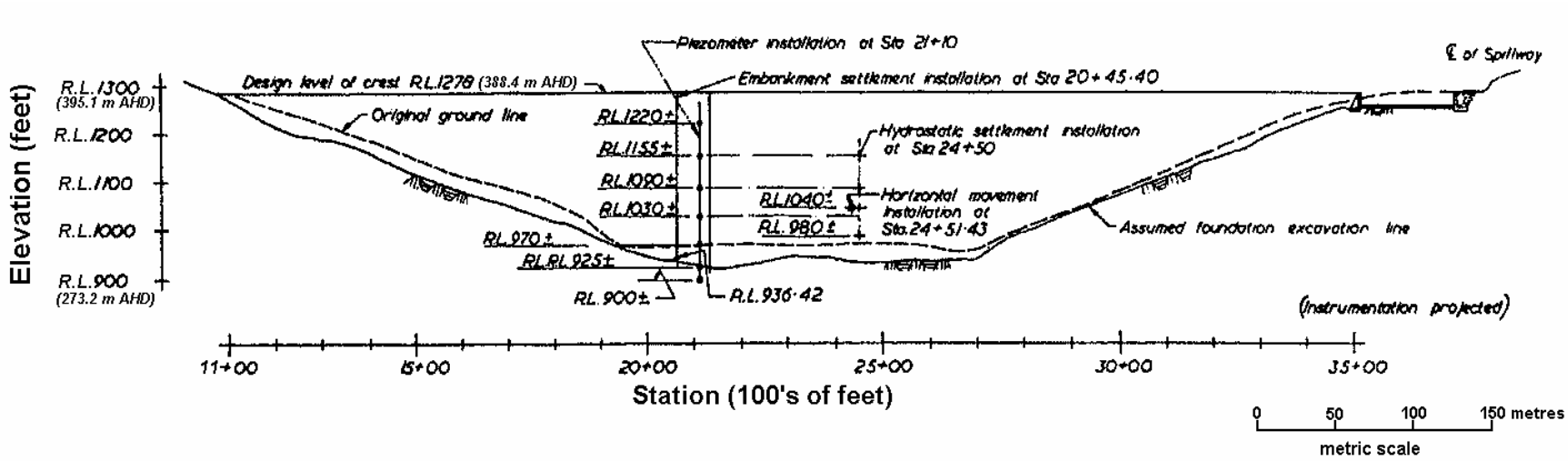

Figure G6.2: Long section profile of Blowering dam (courtesy of NSW Department of Public Works and Services, Dams and Civil Section).

During the course of construction several changes were made to the moisture specification, which are reflected in the variation of field moisture content relative to OMC (Figure G6.4). The moisture specification was initially set at 1.3% dry to 0.7% wet of OMC for 80% of results and the average from July 1966 to February 1967 was 0.3% dry. In February to March 1967 the moisture specification was adjusted toward the wet side of OMC (0.7% dry to 1.3% wet of OMC for 80% of results) because "*a certain amount of brittleness and cracking of the material was evident*" during installation of piezometers at elevation RL 312 m (Olsauskas et al 1967a). This elevation of the Zone 1 earthfill was slightly higher than the piezometer elevation at this time and equivalent to a maximum embankment height of about 34 to 37 m. This adjustment in moisture content is clearly evident in Figure G6.4, with the average monthly moisture content increasing to about 0.3% wet of OMC.

In about October 1967 the moisture specification was again adjusted "*due to difficulties experienced by placing equipment on the wet fill, and to the development of high pore water pressures*" (Olsauskas et al 1967b). It was adjusted to 1.0% dry to 1.0% wet for 80% of results. The fill elevation at this time was in the range RL 346 to 353 m (maximum embankment height of 67 to 74 m), and once again the change is evident in the variation of field to optimum moisture content (Figure G6.4).

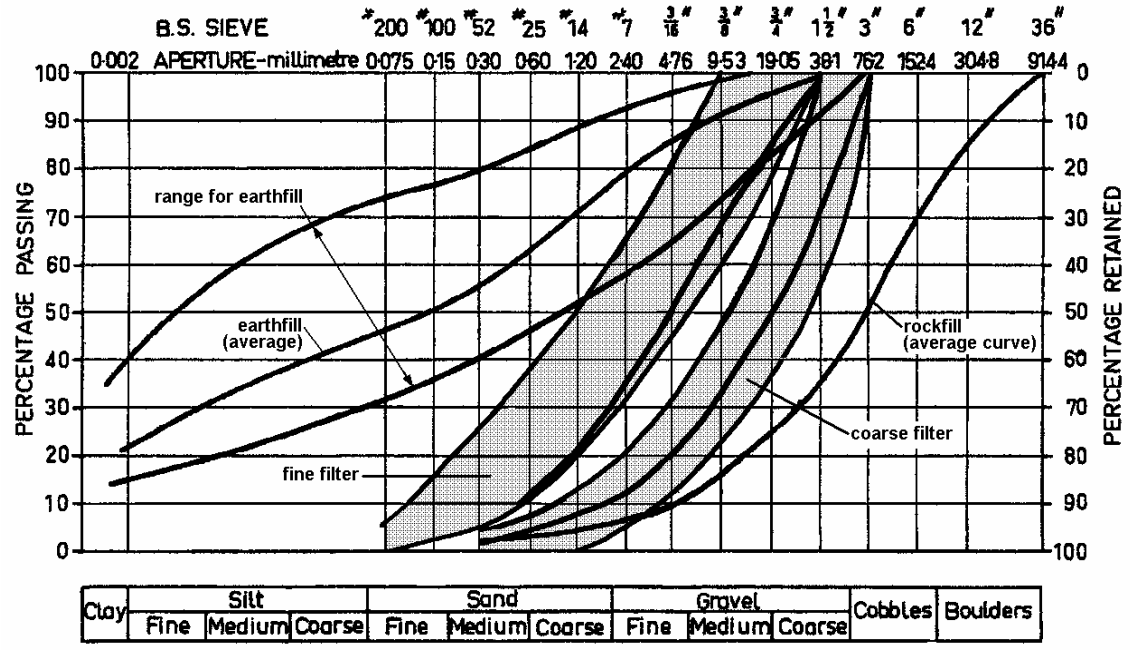

Figure G6.3: Particle size distributions of materials used in construction (Hunter and Bacon 1970).

Table G6.1: Summary of compaction control test results on the core (excludes contact zone).

Time Period	Fill Height (RL and height)	Dry Density (t/m^3)	Density Ratio *[1] (% SMDD)	Moisture Content	
				FMC to OMC *[2]	FMC *[2] (%)
July to Dec 1966	RL 279 to 305 (0 to 26 m)	1.79	101.8%	0.3% dry	16.5
Jan to June 1967	RL 305 to 331 (26 to 52 m)	1.75	101.4%	0.37% wet	16.9
July to Dec 1967	RL 331 to 366 (52 to 87 m)	1.76	101.5%	0.26% wet	-
Jan to Apr 1968	RL 366 to 389 (87 to 112 m)	1.78	101.3%	0.22% wet	16.4
Full Construction Period					
- median		1.78	101.5%	0.2% wet	16.5
- mean		1.78	101.9%	0.15% dry	16.8
- std dev *[3]		0.064	1.9%	0.6%	1.92

Note: median values are quoted for the individual time periods.

*[1] SMDD = Standard maximum dry density

*[2] OMC = Standard optimum moisture content and FMC = field moisture content.

*[3] Std Dev = standard deviation

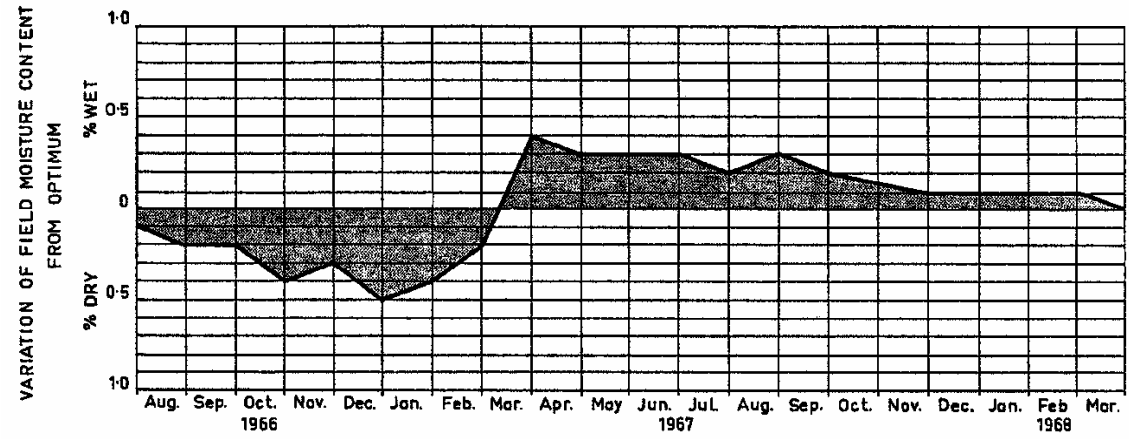

Figure G6.4: Variation of field moisture content from optimum moisture content (Hunter and Bacon 1970).

Hunter and Bacon (1970) comment that the material used for earthfill also varied, being predominantly quartzite and phyllite slopewash below about elevation RL 316 m and predominantly porphyry slopewash, a finer-grained material, above this level. This change is in elevation is close to that of the change in moisture content specification,

and Hunter and Bacon (1970) comment that it may also have influenced the material properties of the earthfill and its deformation behaviour.

6.2.4 Transition Filters, Zones 2A and 2B

The embankment design (Figure G6.1) incorporated dual transition filters (Zones 2A and 2B), each of 3.1 m width and total combined width of 6.2 m, up and downstream of the earthfill core. During construction the width of the filter zones was reduced to a combined width of 3.7 m upstream and 4.3 m downstream (Olsauskas et al 1967b). But, Olsauskas et al (1968) indicates that due to the method of placement the actual width was wider than specified.

Zones 2A and 2B consisted of processed sandy gravels sourced from alluvial river deposits adjacent to the Tumut River. The specified ranges and average particle size distributions for the filters are shown in Figure G6.3. Both filter zones were placed in 450 mm layers (after compaction), wetted and compacted with 4 passes of an 8.1 tonne smooth drum vibrating roller. Reported results of field testing indicate high values of relatively density (average of 86 to 90%) and an average dry density of 2.16 t/m^3, porosity of 19% and void ratio of 0.24. Given the material type and well-compacted condition of the filters it is likely that they would have a relatively high modulus in comparison to the earthfill core and rockfill shoulders.

6.2.5 Rockfill - Zones 3A and 3B

Rockfill was sourced from a nearby quarry in the Silurian aged Brandy Mary Beds. Rock types comprised slightly weathered to fresh phyllite, meta-siltstone and quartzite derived from low-grade metamorphism of shale, siltstone and sandstone. The specification limited placement of the weaker phyllites to the outer Zone 3B. The construction progress reports indicate that after about April 1967 the rockfill was mainly quartzite and meta-siltstone. Therefore, only limited quantities of phyllite would have been used in the Zone 3B rockfill above about elevation RL 325 m (the upper 65 m of construction).

The engineering properties of the rockfill types from laboratory testing (Svenson et al 1964) are summarised in Table G6.2. Of note is the large difference in unconfined compressive strength between the wet and dry states (35 to 62% reduction) and high

sodium sulphate soundness loss for moderately to slightly weathered phyllite and meta-siltstone. Hunter and Bacon (1970) describe the phyllite as "*a soft but tough rock*" and Bacon (1969) refers to the Blowering rockfill as "*much finer and weaker*" in comparison to the hard and fresh granites used at other Snowy embankments.

Table G6.2: Summary of the properties of the rock types used as rockfill.

Laboratory Test / Material Property	**Quartzite**	**Phyllite**	**Meta-Siltstone**
Unconfined compressive strength (UCS)	200 MPa (dry) 130 MPa (saturated) both on fresh rock	123 MPa (dry and fresh) 47 MPa (saturated)	52 MPa
Moh's hardness scale	3.5 to 6	3 to 5	2.5 to 4
Friction angle, f' (from large scale triaxial tests on dense compacted, graded rockfills)	50° to 55° (cp < 250 kPa) 40° to 41° (cp 1500 to 2000 kPa)	42° to 50° (cp <250 kPa) 39° (cp = 1500 kPa)	
Specific gravity	2.71 to 2.81 t/m^3		
Sodium sulphate soundness	2.5% loss (fresh)	21.6% to 34.3% loss (MW to SW)	
Accelerated weathering	weather resistant	weather resistant	weather resistant
Aggregate crushing value	12.7 to 15.3% (dry) 17.7 to 21.7% (saturated)	20.5% (dry) 26.4 to 32.2% (saturated)	16.7 to 18.4% (dry) 21.8 to 24.4% (saturated)
Absorption (from aggregate crushing tests)	1.0%	1.6 to 2.2%	0.7 to 1.0%

Note: cp = confining pressure, MW = moderately weathered, SW = slightly weathered.

Procedures for placement of the rockfill were:

- Zone 3A – placed in 900 mm lift thicknesses, watered (at a ratio of 0.9 to 1 by volume), levelled by bulldozer and compacted with 4 passes of the 8.1 tonne smooth drum vibrating roller (SDVR). Over a width of about 6 to 7 metres adjacent to Zone 2B, the Zone 3A rockfill was placed in 450 mm layers with 4 passes of the roller on each layer. Olsauskas et al (1966) indicates the contractor was allowed to place the Zone 3A rockfill in 1.8 m lifts in the downstream section of the embankment, but it is not clear to what extent this practice was allowed or adopted. Bacon (1999) does not believe this practice was ever adopted.
- Zone 3B – placed in 1.8 m lift thicknesses, watered (at a ratio of 0.9 to 1 by volume), levelled by bulldozer and compacted with 4 passes of the 8.1 tonne SDVR. Olsauskas et al (1967a) indicates the contractor was given the option of placing the Zone 3B rockfill in 900 mm lifts (same as Zone 3A) with either 2 passes of the roller per 900 mm lift or 4 passes every second lift. Olsauskas et al (1967b, 1968)

indicate the contractor did not make much use of the practice to place Zone 3B in 900 mm lifts from July 1967. Bacon (1999) comments that the adoption of this practice during the first half of 1967 (900 mm lift and 2 passes of the SDVR) was a consequence of a visit by J Barry Cooke during which it was observed that in a density test that rock particles could be removed by hand from the base of a compacted layer.

The high volumes of water used during placement of the rockfill were specified as a consequence of the large reduction in compressive strength between the dry and wetted states of the rock. The designers were attempting to offset as far as practicable the potential for collapse type settlements in the rockfill post construction. During construction water was ponded between the upstream cofferdam and dam to about elevation 305 to 308 m, therefore saturating the lower region of the upstream rockfill.

Control testing of the rockfill during construction consisted of density and particle size determination. The results of the testing are summarised in Table G6.3 and average grading of the rockfill shown in Figure G6.3. The results show:

- Significant variation in density, and therefore porosity, with depth in Zone 3B for the first construction period. Based on the test results for Zone 3B in the first period and assuming a specific gravity of 2.71 t/m^3, the porosity is calculated to vary throughout the layer from 15% (top 0.4 m) to 32% (mid section of layer) to 42% (bottom 0.6 m).
- The average dry density in both the Zone 3A and 3B increased in consecutive construction period. Between the first and third construction periods the average results show a 10% to 15% increase.
- The average percent less than 25 mm size (over the full layer depth) is 23% for Zone 3A and 28% for Zone 3B. The initial specification called for a maximum of 15% passing 25 mm, but it was recognised early on that this would have resulted in a very high proportion of wastage from the quarry. Hunter and Bacon (1970) comment that a higher percentage of minus 25 mm was accepted provided "*the fines were granular and the material reasonably free-draining*".
- The higher percent minus 25 mm in the upper 380 mm of Zone 3B compared to the full layer depth indicate significant breakdown of the rockfill occurred during compaction.

Table G6.3: Summary of test results on rockfill during construction

Time Period	Zone	Average Dry Density (t/m^3)	Average % finer than 25 mm	Comments
4/7/66 to 31/12/66	3A	1.94	18 – 23%	3 tests to full depth
	3B	1.99	23 – 24%	2 tests to 1.2 m depth
	3B	1.85	25%	1 test to full depth (1.8 m)
	3B	2.29	35 & 42%	2 tests to 380 mm depth
4/7/66 to 30/6/67	3B	2.06	17 & 50%	2 tests to full depth
1/7/67 to 31/12/67	3A	2.235	28.5%	2 tests to full depth
	3B	2.155	26%	2 tests to full depth
1/1/68 to 30/6/68	-	-	-	No testing in this period
Total Period (4/7/66 to 30/6/68)	3A	2.055	23%	5 tests to full depth
	3B	2.070	28%	6 tests to full depth

The variation in density with depth within a layer and breakdown would be expected to occur on compaction and the degree of density variation is likely to be strongly dependent on layer thickness. The estimated low density (1.57 t/m^3) and high porosity (42%) in the base of a 1.8 m thick Zone 3B rockfill layer during the first construction period is indicative of loosely compacted rockfill and is highlighted by the ability to remove by hand rockfill pieces from the base of the layer. The results and observations indicate that the layer thickness of 1.8 m for the Zone 3B may not have been compatible with the roller mass and number of passes to achieve a well-compacted material.

During the early stages of development of the rockfill quarry Olsauskas et al (1966) comment on the high percentage of wastage of 24%, mainly in weathered phyllite and meta-siltstone, for the period from July to December 1966. It is possible that as a result, a lesser quality of rockfill was used in the lower sections of the embankment. The improving quality of rockfill as construction progressed and the placement of Zone 3B in 0.9 m lifts in the early 1967 construction period are possible reasons for the increased layer density observed in the test results.

6.3 MONITORED PERFORMANCE OF BLOWERING DAM

From comparison with similar type embankments it is evident that aspects of deformation behaviour of Blowering dam were potentially "abnormal", including:

- Large settlement of the core during the period of construction. The total settlement of the core during the construction period at Blowering exceeded 5% (Figure 7.23 in

Section 7.4 of Chapter 7), well in excess of the 3 to 3.5% settlement typical for embankments with clay cores of 100 to 120 m height;

- Very high vertical strains (in the range 6 to 12%) in the wet placed portion of the earthfill core at end of construction (Figure 7.22 in Section 7.4 of Chapter 7);
- Accelerations in the rate of settlement and/or displacement of SMPs on the upstream shoulder and crest on large drawdown post first filling (Figures 7.54, 7.69, 7.85 and 7.86 in Section 7.6 of Chapter 7);
- The non-recoverable lateral displacement of the upstream shoulder during large drawdown events post first filling (Figure 7.86 in Section 7.4 of Chapter 7); and
- The continuing higher than usual rate (on log scale) of post construction horizontal displacement in the upstream direction of the upstream shoulder (Figure 7.86 in Chapter 7) and to some extent the crest (Figure 7.69 in Chapter 7).

The monitored results of instrumentation at Blowering dam are presented in the following sub-sections, highlighting the potentially "abnormal" aspects of the deformation behaviour.

6.3.1 Monitoring Equipment

Instrumentation installed at Blowering Dam (Figure G6.5) comprised:

- 37 hydraulic piezometers, 4 in the foundation and 33 (HP5 to HP37) in the core, installed at Station 21 + 10;
- 10 hydrostatic settlement gauges (HSG) installed in the downstream rockfill at Station 24 + 50;
- 1 internal horizontal movement gauge (IHM) with 13 cross-arms installed at approximately elevation RL 316 m in downstream rockfill at Station 24 + 50;
- 1 internal vertical movement gauge (IVM) with 33 cross-arms installed in central core at Station 20 + 50. The gauge is located slightly upstream of the dam axis; and
- 50 surface monitoring points (SMP) installed on the crest and slopes of the embankment. SMPs on the embankment slopes were located at four levels and were installed as construction progressed. The base survey after end of construction was on 4 July 1968, 0.24 years after construction, for most SMPs. Only the base survey of the displacement of SMPs on the crest was after this in October 1968.

- 5 pressure cells installed in the core near to Station 24 + 10 at elevation RL 285.4 m. The locations are not shown in Figure G6.5, but are approximately coincident with piezometers 5, 7 and 9, and similarly numbered (i.e. Cells 5A, 7A, 9A, 9B, 9C where A, B and C refer to the orientation of the gauge).

6.3.2 Embankment Performance During Construction

The plots of monitoring records during construction are, in most cases, presented against total vertical stress estimated from finite difference analysis of a total stress model of the zoned embankment (refer Section 6.4.1 of this Appendix for details of the model). The model was relatively simple and used a linear elastic perfectly plastic Mohr Coulomb failure criteria for the earthfill core (based on estimated total stress parameters), filters and rockfill zones. The earthfill core was divided into three main regions reflecting the changes in moisture content specification. Some iteration of material parameters was used to approximate the measured deformations at end of construction.

6.3.2.1 *Pressure Cells in the Earthfill Core*

The measured results from the pressure cells as construction proceeds are shown in Figure G6.6. Also shown are the total vertical stress versus height relationships at Cell 9 from the numerical models for the simple zoned analysis and a homogeneous embankment model. The results indicate that arching or stress transfer from the core to the filters occurred during construction and affected the vertical stress distribution in the central region of the core (Cell 9). The effect of arching was more significant for Cells 5A and 7A located closer to the filter, as expected.

The simple zoned model is shown to reasonably represent the measured total vertical stress versus embankment height relationship at Cell 9A under the embankment centreline. On this basis, as well as the ability to model the lower vertical stresses toward the filter zones, the model was used to estimate the vertical stresses at piezometers and cross-arms in the central region of the core. Further details on the stress distributions from the finite difference modelling are presented in Section 6.4.1 (of this Appendix).

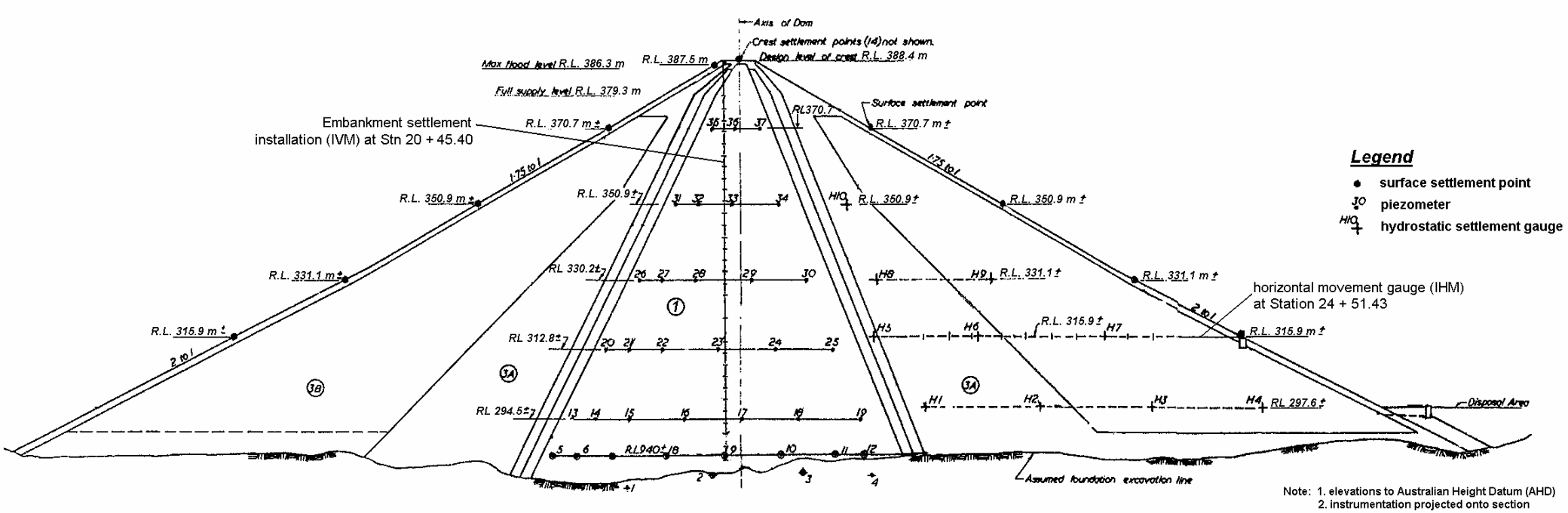

Figure G6.5: Location of monitoring equipment, projected onto section at Station 21 + 10 (courtesy of NSW Department of Public Works and Services, Dams and Civil Section).

The measured pressure cell records at Cell 9 during construction also showed:

- Similar horizontal stresses were measured in the directions perpendicular (Cell 9C) and parallel to (Cell 9B) the dam axis;
- The effective stress ratio of vertical to horizontal stress (s'_v/s'_h) at Cell 9 remained constant during construction at a ratio of 2. Effective stresses were estimated by deducting the pore water pressure measured at HP9 from the total stress (suction effects and negative pore water pressures were not considered); and
- The total stress ratio (s_v/s_h) at Cell 9 decreased from an initial value of 2 to 1.4 - 1.45 at end of construction.

Assuming confined conditions at Cell 9 (i.e. zero lateral strain), which is not unreasonable given the proximity of the pressure cell to the foundation level, it is possible from elastic theory to estimate Poisson's ratio from the effective and total stress ratio. The estimates are:

- Effective Poisson's ratio, *?´*, is constant at 0.33.
- Total Poisson's ratio, $?_u$, increases with increasing total vertical or mean normal stress from 0.33 at placement to 0.41 at end of construction (Figure G6.7).

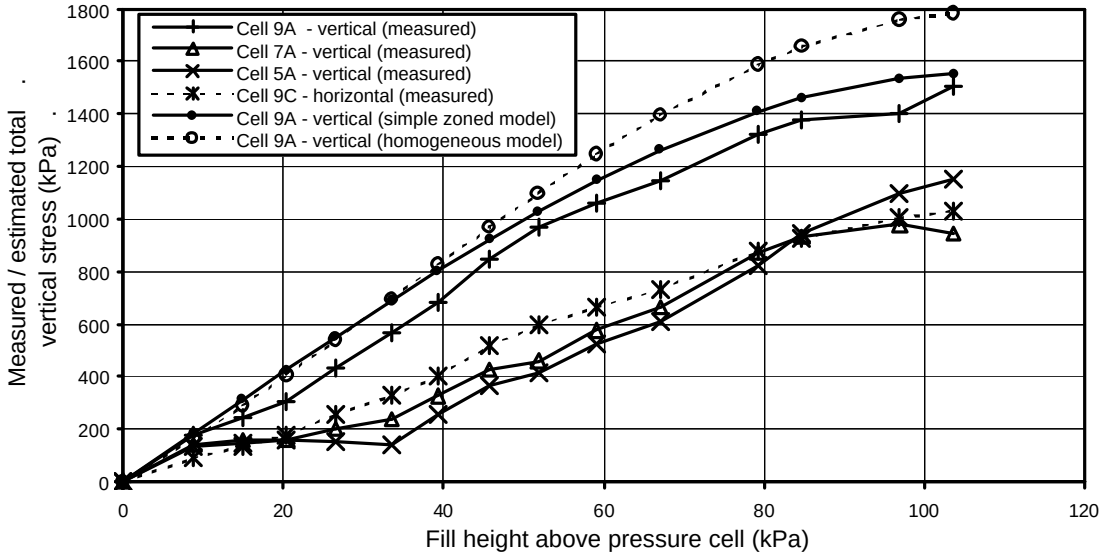

Figure G6.6: Measured and modelled stresses in the core as construction proceeds.

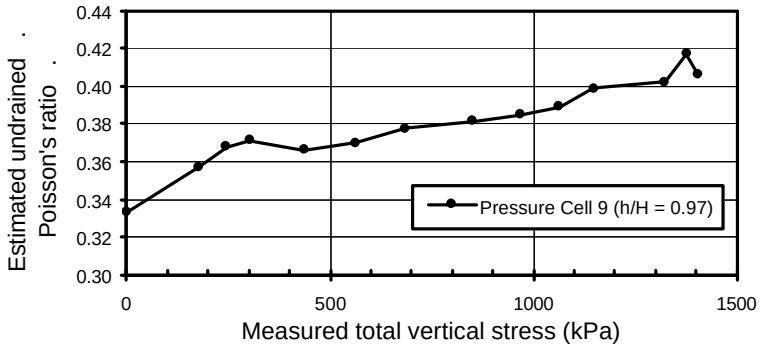

Figure G6.7: Estimated undrained Poisson's ratio versus total vertical stress at Cell 9.

6.3.2.2 *Piezometers in the Earthfill Core*

Figure G6.8 presents the measured pore water pressures from piezometers located close to centreline of the core versus total vertical stress estimated from the simple zoned numerical analysis. The pore water pressure response reflects the changing moisture content conditions within the core. Piezometers 9 and 16, located in the deepest section of the core, show a period of low or negative pore water pressure prior to the development of positive pore pressures. This behaviour is considered to be associated with initial development of negative pore pressures due to placement of the material on the dry side of Standard optimum. Piezometers 29, 33 and 36, located in the mid to upper region of the core, all registered an immediate positive pore water pressure response and were all in regions placed on the wet side of Standard optimum. The immediate positive pore water pressure response is indicative of a high degree of saturation at placement. Piezometer 23 is intermediary between the two types of response. It is located at elevation RL 312.8 m, the region of the change in moisture content placement from dry to wet of Standard optimum.

The shape of the curves for Piezometers 9 and 23 is typical of that predicted using the Hilf method (1948) assuming undrained conditions and matric suction equals zero, although the Hilf method predicts the pore water pressures approaching 100% of the total vertical stress. Even though the assumption of undrained conditions is considered reasonably valid for the central region of the very low permeability earthfill core at Blowering dam, the results the pore water pressure response levels reaches an equilibrium response equivalent to about 70 to 80% of the estimated total vertical stress.

As discussed in Section 7.4.1.4 of Chapter 7, for partially saturated soils of very low permeability the rate of pore pressure increase in confined compression will in most

cases be less than the rate of vertical stress increase due to the presence of a small volume of air voids that remain under the magnitude of effective stresses likely in embankment dams. Other factors likely to affect the pore water pressure response include:

- Over prediction of total vertical stress from the numerical modelling;
- Some dissipation of pore water pressure due to drainage during construction; and
- The invalid assumption that the total lateral stress increment equals the total vertical stress increment for a saturated soil in undrained loading conditions in the latter stages of embankment construction. As discussed in Section 7.4.1.4 of Chapter 7, the total stress ratio in Skempton's equation for pore water pressure decreases as the constructed layer width decreases in the latter stages of construction, which invalidates this assumption.

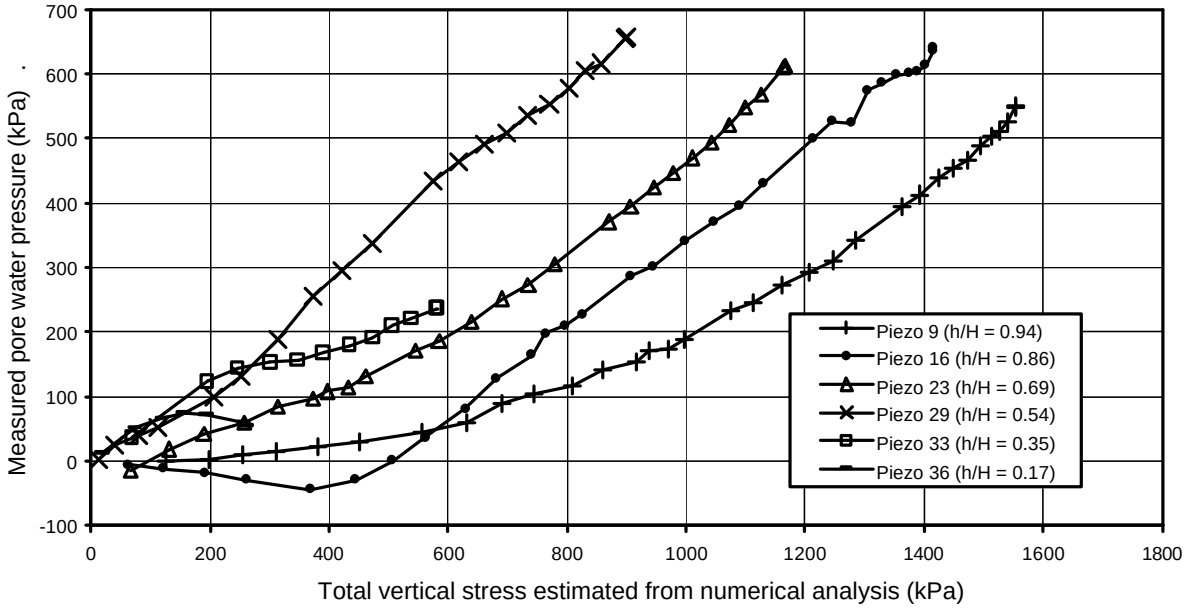

Figure G6.8: Measured pore water pressures during construction in the central region of the earthfill core.

6.3.2.3 Internal Settlement of the Earthfill Core

The total settlement of the core during construction, as measured by the internal settlement gauge (IVM), equated to some 5.8 metres, or an overall average of about 5.5% of the dam height. When compared to other dams of similar construction (Figure 7.23 in Section 7.4 of Chapter 7), Blowering Dam stands out as an outlier to the general trend. Comparison of the vertical strain at end of construction (Figure 7.22 in Chapter

7) highlights the very high strain within regions of the wet placed core at Blowering dam as outliers to the general trend.

Figure G6.9 presents the vertical strain profile in the core at end of construction. The large difference in vertical strain between the region of dry placed earthfill in the lower 30 to 35 metres and the region of wet placed earthfill is clearly evident. Within the wet placed region the high vertical strains, which reached as high as 10 to 12%, could not be explained by elastic type settlements on loading or consolidation. Settlements due to consolidation would be relatively small because little pore water pressure dissipation occurred during construction as shown by the piezometer response (Figure G6.8).

The increase in vertical strain as construction proceeds for selected cross-arm intervals in the IVM are shown in Figure G6.10 plotted against the total vertical stress estimated from numerical analysis. Settlements have been adjusted such that zero strain is equivalent to zero vertical stress at the midpoint between cross-arms. Several notable aspects of the deformation behaviour are:

- At a given vertical stress, vertical strains in the lower dry placed region of the core (below cross-arm 11 to 12) are lower than in the wet placed region of the core;
- For most cross-arms, the vertical strain increases almost linearly with total vertical stress or shows a slight increase in the rate of strain; and
- The deformation behaviour between cross-arms 13 and 14 is markedly different to that at other cross-arms, showing a very large increase in strain rate at total vertical stresses greater than about 850 to 900 kPa.

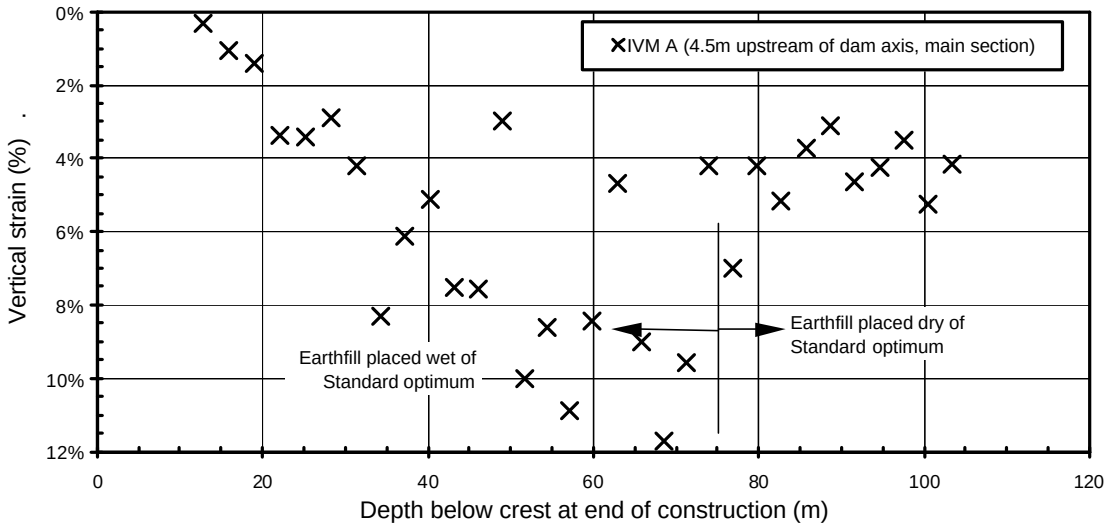

Figure G6.9: Vertical strain profile in the earthfill core of Blowering dam at end of construction.

The plot of vertical strain versus effective vertical stress (Figure G6.11) for selected cross-arms provides a clearer picture of the deformation behaviour of the core during construction. The stress-strain relationship in the dry placed, lower region of the core is near linear, and is considered to approximate deformation in the elastic region of the Mohr Coulomb model. The effective stress path estimated from the pressure cells and piezometer response in the centre of the core at elevation RL 285.4 m (h/H = 0.97) confirms this. The effective stress ratio of 2 indicates the effective stress path is below the critical state line defined by an effective angle of internal friction for the earthfill of 31 degrees. The near linear response between vertical stress and vertical strain would indicate the effective secant modulus in this lower region of the core is near constant as shown in Figure G6.12.

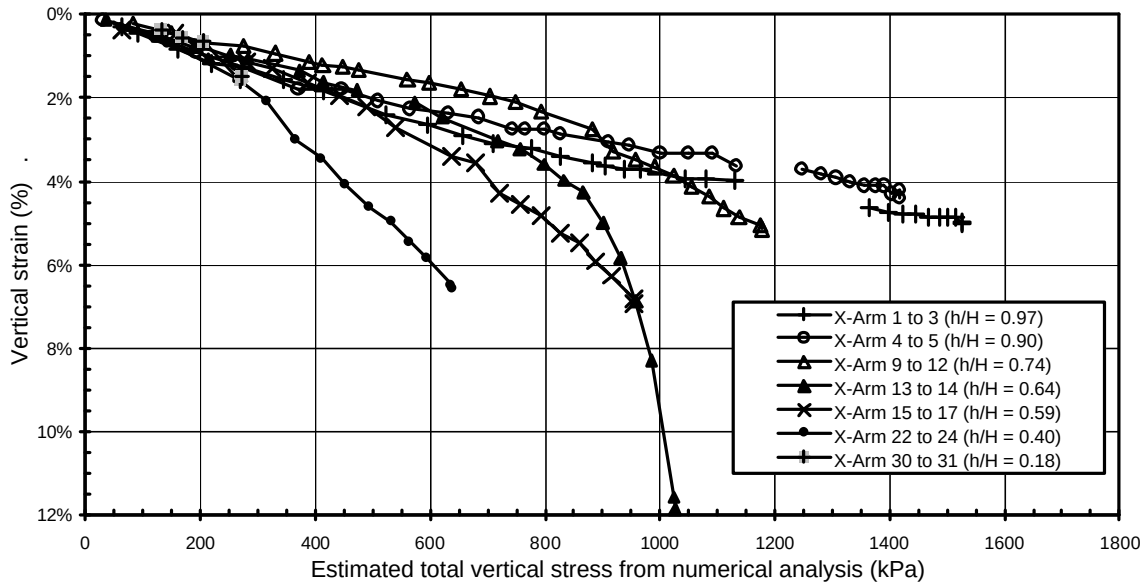

Figure G6.10: Vertical strain as construction proceeds for selected IVM cross-arms.

In the wet placed region of the core the effective stress-strain response at low stress levels is similar to that of the drier placed earthfills, possibly indicating an elastic type response. But, at effective vertical stresses in excess of 100 to 200 kPa the measured strains exceed those of the elastic type response in the drier placed earthfill. This is thought to be due to plastic type deformation of the core. This change in the stress-strain behaviour is reflected as a large increase in the incremental strain per unit increase in effective vertical stress (Figure G6.11). At this point, the vertical effective secant modulus values (Figure G6.12) are meaningless for the wet placed core because its deformation occurs largely as plastic type deformations in undrained conditions.

The total vertical stress versus vertical strain response measured between cross-arms 13 and 14 is very different to that measured in other parts of the wet placed region of the core, such as between cross-arms 15 and 17 located immediately above this zone (Figure G6.10). It is at total vertical stresses greater than 850 kPa that the vertical strains become very large and are considered to be potentially indicative of shear type deformation in the core.

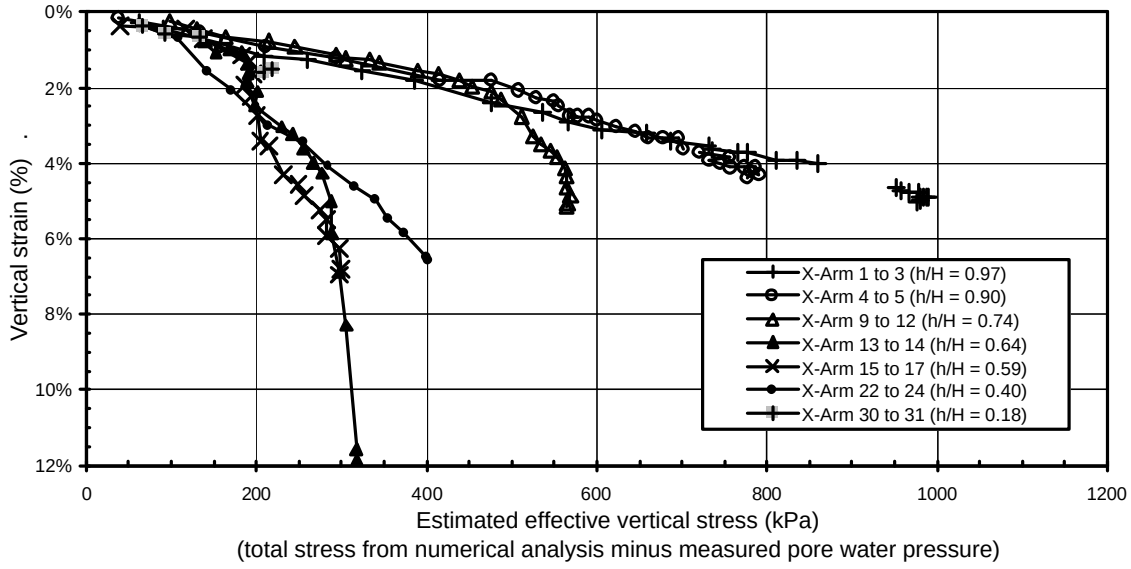

Figure G6.11: Vertical strain versus estimated effective vertical in the core for selected cross-arms.

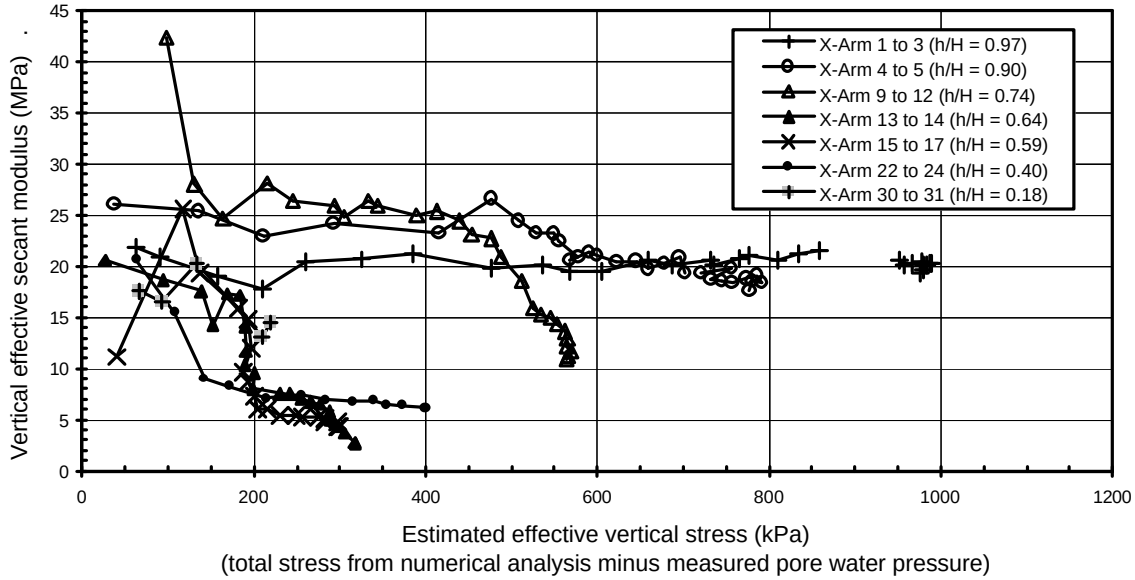

Figure G6.12: Estimated effective secant modulus versus estimated effective vertical stress in the core.

6.3.2.4 Internal Vertical Deformation of the Downstream Rockfill Shoulder

The vertical deformation in the downstream shoulder during construction from the hydrostatic gauges (HSG) is presented in Figure G6.13. Estimated secant moduli versus estimated vertical stress are shown in Figure G6.14. In both plots, vertical settlements have been corrected so that zero strain equates to zero vertical stress or zero fill height above the mid point between the HSG gauges. Vertical stresses at the mid point have been estimated from finite difference analysis of the simple zoned embankment model (Section 6.4.1 of this Appendix).

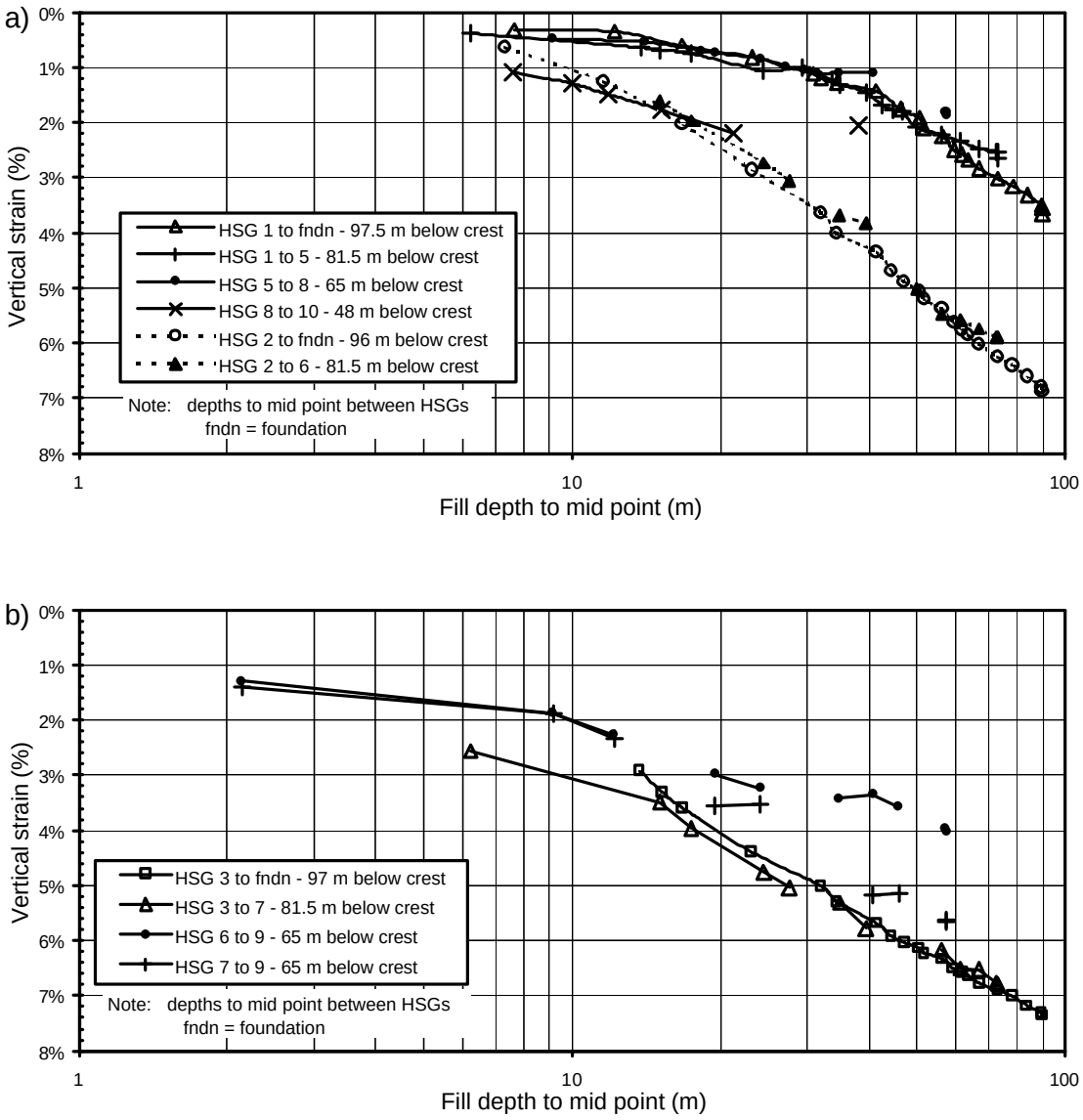

Figure G6.13: Vertical strain in rockfill during construction, *(a)* Zone 3A rockfill, and *(b)* Zone 3B rockfill.

The deformation records show that the region of lowest compressibility in the rockfill is closest to the filter where the rockfill was placed in 450 mm lift thicknesses and compacted by four passes of the roller (HSGs 1 to foundation, 1 to 5, 5 to 8 and 8 to 10). Estimated secant moduli for this region range from 90 to 110 MPa at low vertical stress levels decreasing to 60 to 90 MPa at vertical stress levels in excess of 2000 kPa (Figure G6.14a). The estimated secant moduli between HSGs 8 and 10 is lower than for the other HSGs in this region. It is possible that, with the reduction in the width of the filters, HSG 10 is located in the region of Zone 3A placed in 900 mm lifts and therefore representative of the outer Zone 3A.

The rockfill zone with the highest compressibility is the Zone 3B rockfill (HSGs 3 to foundation, 3 to 7 and 7 to 9). Secant moduli for the Zone 3B range from 9 to 18 MPa and show a decrease in secant moduli with increasing total vertical stress (Figure G6.14b). The compressibility of the outer Zone 3A rockfill (HSGs 2 to foundation and 2 to 6) is intermediary between the inner Zone 3A region and Zone 3B, with secant moduli estimated at 20 to 40 MPa (Figure G6.14a).

The deformation behaviour of the rockfill during construction is "normal". The secant moduli values are comparable to those from rockfill placed in concrete faced rockfill dams (refer Section 6.4.2 of Chapter 6) assuming the intact rock strength to be of high unconfined compressive strength. The outer well-compacted Zone 3A rockfill is classified as well-compacted and the Zone 3B rockfill as reasonably compacted. The trend of decreasing modulus with increasing vertical stress is generally typical of rockfill.

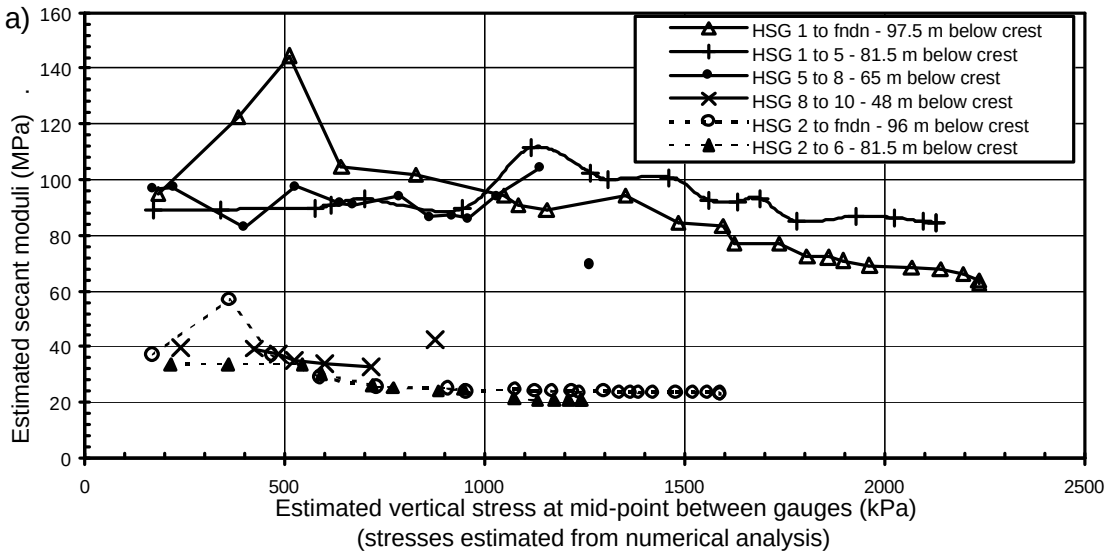

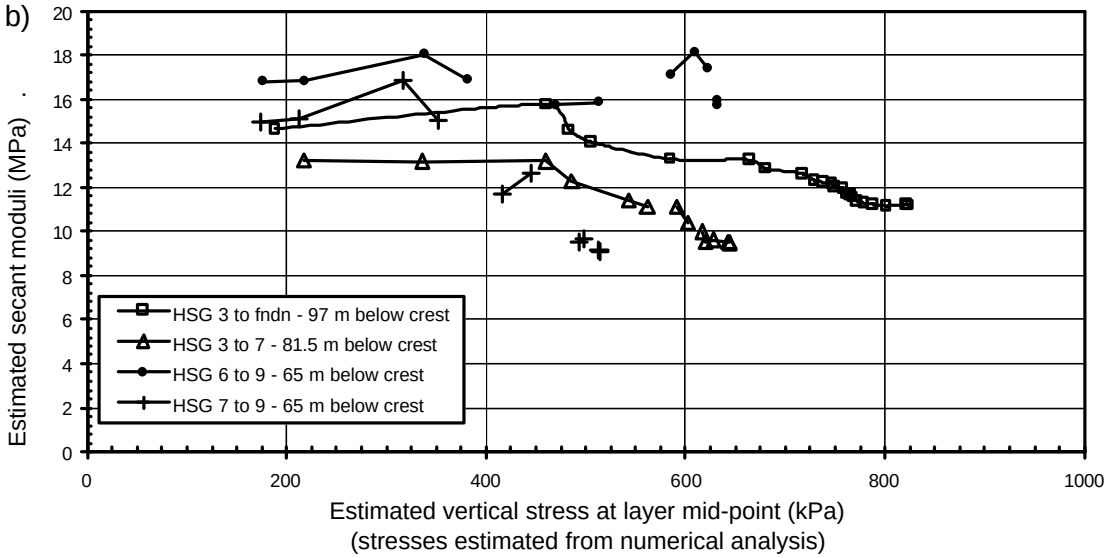

Figure G6.14: Estimated secant modulus versus vertical stress in rockfill during construction, *(a)* Zone 3A rockfill, and *(b)* Zone 3B rockfill.

6.3.2.5 Internal Lateral Displacements of the Downstream Shoulder

The internal lateral displacements measured in the horizontal movement gauge (IHM) installed in the downstream shoulder at elevation RL 316 m (h/H = 0.70) are shown in Figure G6.15. At end of construction the lateral deformation was about 730 mm at gauge 1 in the filter zone and a maximum of about 780 mm at gauge 3.

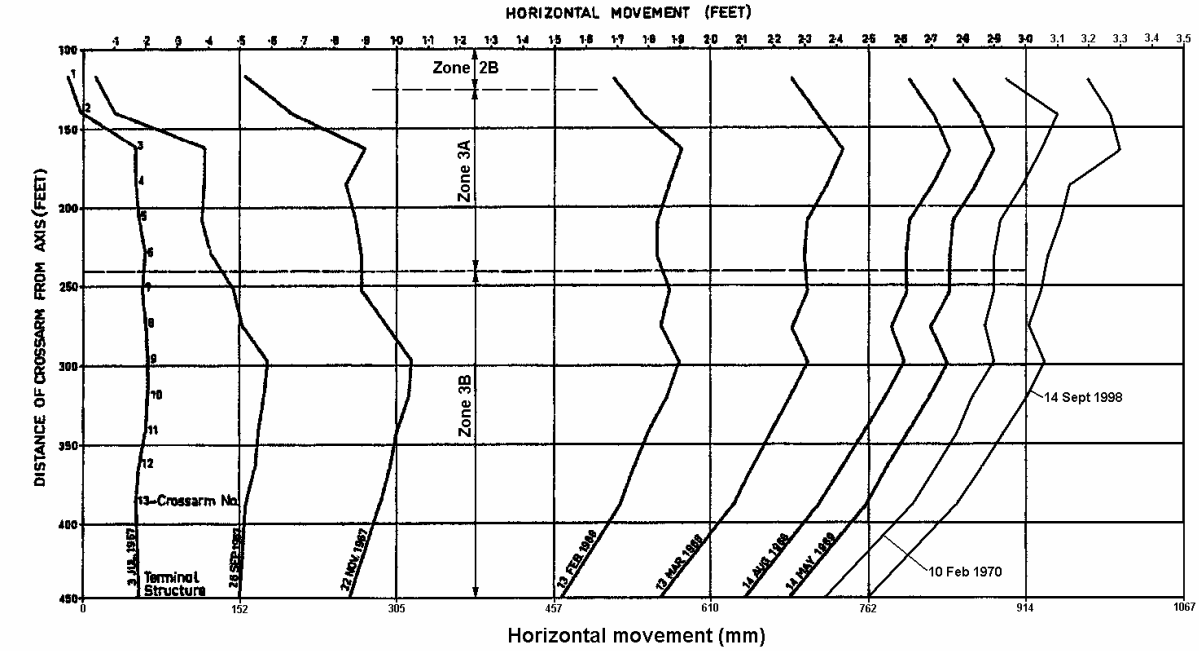

Figure G6.15: Horizontal deformation measured in the downstream shoulder at elevation RL 316 m (adapted from Hunter and Bacon 1970).

The lateral deformation at Blowering dam is compared against that measured at other embankments in Section 7.4.2 of Chapter 7. Comparisons are based on what is termed the lateral displacement ratio of the core calculated by dividing the measured lateral displacement from the IHM gauge nearest the core by the core width. The deformation is assumed to be symmetrical where records are only available from one side of the core. The lateral displacement ratio of the core at elevation RL 316 m (h/H = 0.70) at Blowering dam was relatively high in comparison to other dams, but not "abnormally" so (refer Figures 7.12 and 7.13 in Section 7.4 of Chapter 7).

6.3.3 Embankment Performance Post Construction

6.3.3.1 Reservoir Operation and Pore Water Pressure Response

Blowering Dam was first filled over the period May 1968 to October 1969 (from 0.1 to 1.6 years after construction), being filled rapidly to within 20 m of full supply by January 1969. The reservoir is subject to seasonal drawdown (Figure G6.16a) of typically 5 to 35 m and has been subjected to two large drawdown events, 1982/83 (14.5 to 15 years) and 1997/98 (29.5 to 30 years). In 1982/83 the reservoir level was drawn down 57 m from RL 364 m to RL 307 m over the period 1 August 1982 to 18 February 1983. This is the largest drawdown and to the lowest reservoir level in its history. In 1997/98 the reservoir level was drawn down 53 m from RL 372 m to RL 319 m in a period of 6.5 to 7 months.

On first filling no significant increase in pore water pressure was recorded in the piezometers installed in the core. Post first filling the trend of pore water pressure response varied within the core. In the lower elevations where the core was placed slightly dry of Standard optimum, pore water pressures post first filling increased over time. In the wetter placed mid to upper region of the core the change in pore water pressure over time was generally limited. Only in the piezometers at elevation RL 330 m did pore water pressures show any substantial decrease over time, decreasing some 300 kPa over 8 to 10 years. The contribution of consolidation to the post construction settlement of the core would therefore have been limited.

The response of the piezometers to reservoir drawdown is typical for earthfill cores of low permeability. Those closest to the upstream face of the core respond relatively quickly to drawdown and the further the distance into the core from the upstream face

the slower and the lesser the magnitude of the response. The downstream section of the core showed minimal to negligible response. On large drawdown in 1982/83 and 1997/98 the slow and limited response of the mid the downstream region of the core meant the pore water pressure in these regions were elevated above that of the reservoir. An indication of the pore water pressure profile in the core many years after construction is shown in the plots as part of the limit equilibrium analysis (refer Section 6.4.2 of this Appendix).

6.3.3.2 *Post Construction Deformation of Surface Measurement Points*

The post construction settlement and horizontal displacement of SMPs on the crest and slopes of Blowering Dam for the period 1968 to 1998 is shown in Figure G6.16 and Figure G6.17 respectively. The SMP plotted are close to the maximum section.

For the most part, the post construction settlement and displacement of SMPs on the crest and slopes is considered "normal", except for several potentially "abnormal" aspects. These include the large crest settlement in the early stages of first filling, the increased rate of settlement of SMPs on the upstream slope and crest on large drawdown and the long-term trend of the horizontal displacement of the upstream slope and crest.

During the early stages of first filling the magnitude of settlement of the crest measured at IVM A was very large, almost 500 mm or 0.47% at 0.65 years after construction. Whilst this is large in comparison to similar type embankments (Figure 7.54 in Section 7.6 of Chapter 7), on its own it may not necessarily be "abnormal". But, the internal settlement of the core (refer Section 6.3.3.3 of this Appendix) showed that very high vertical strains were localised to a small region of the core, indicating likely shear type movements on the existing surface of rupture in the core. This is discussed further in Section 6.3.3.3 (of this Appendix).

The SMPs on the crest and slopes missed a large portion of this early settlement because the base survey was at 0.24 years after construction. It is possible that the settlement of the upstream slope may also have been large during this period due to collapse compression on saturation of the rockfill as the reservoir was filled to within 47 m of full supply level.

On large drawdown in 1982/83 (14 to 15 years after construction) acceleration in the rate of settlement of SMPs on the crest and upstream shoulder was observed. The crest

settlement for the drawdown period was 45 mm. The displacement records show the upstream slope, crest and upper downstream slope to displace upstream on drawdown as expected. But, it is possible, although difficult to establish due to the time spacing of readings, if a component of the displacement of the upstream slope and possibly the crest is non-recoverable. Together with the internal settlement records (refer Section 6.3.3.3 of this Appendix) it is likely that the deformation was associated with a reactivation of movement along the existing shear surface in the core, possibly triggered by the reduction in water load acting on the upstream face of the core.

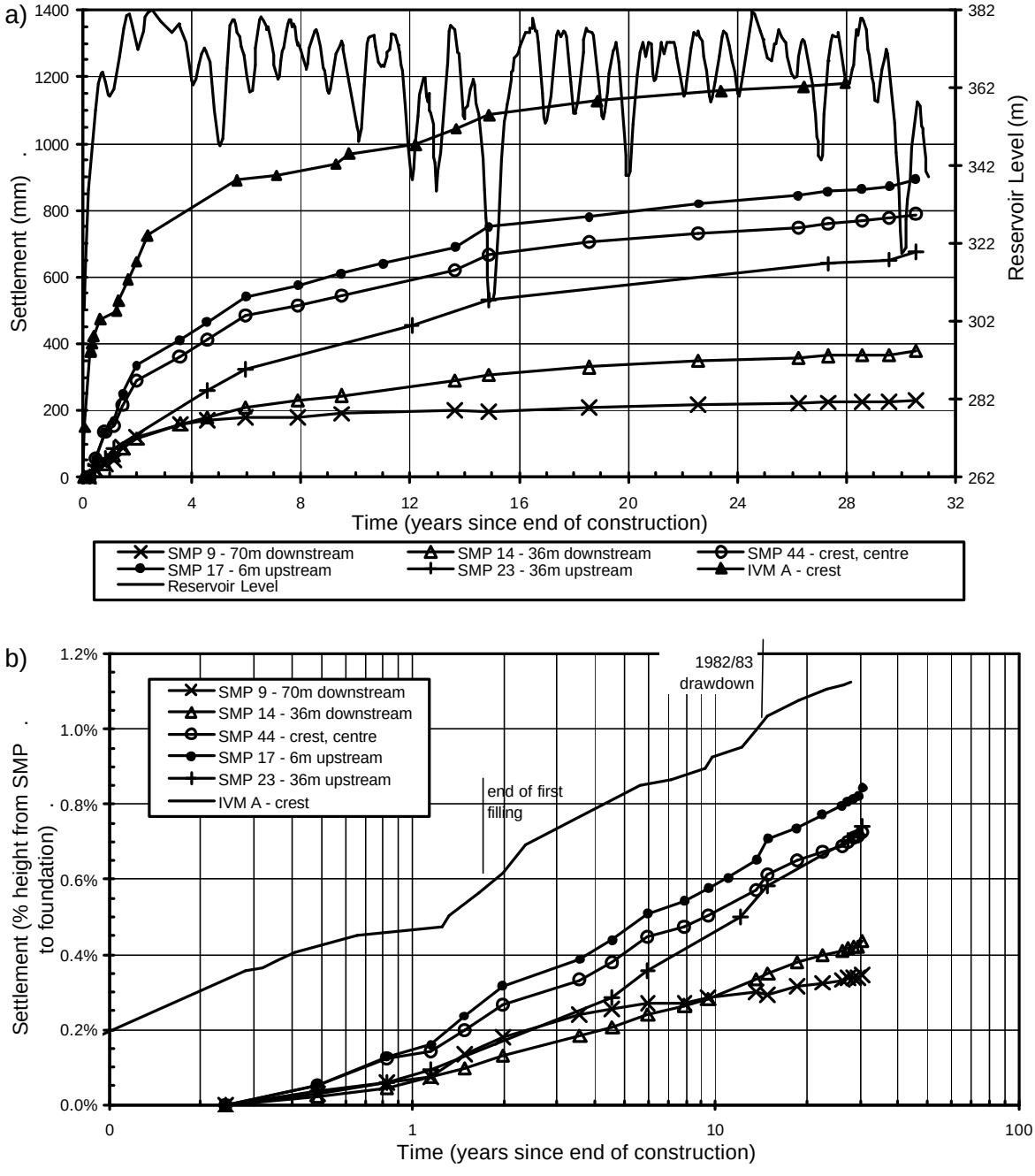

Figure G6.16: Post construction vertical deformation of SMPs at the main section.

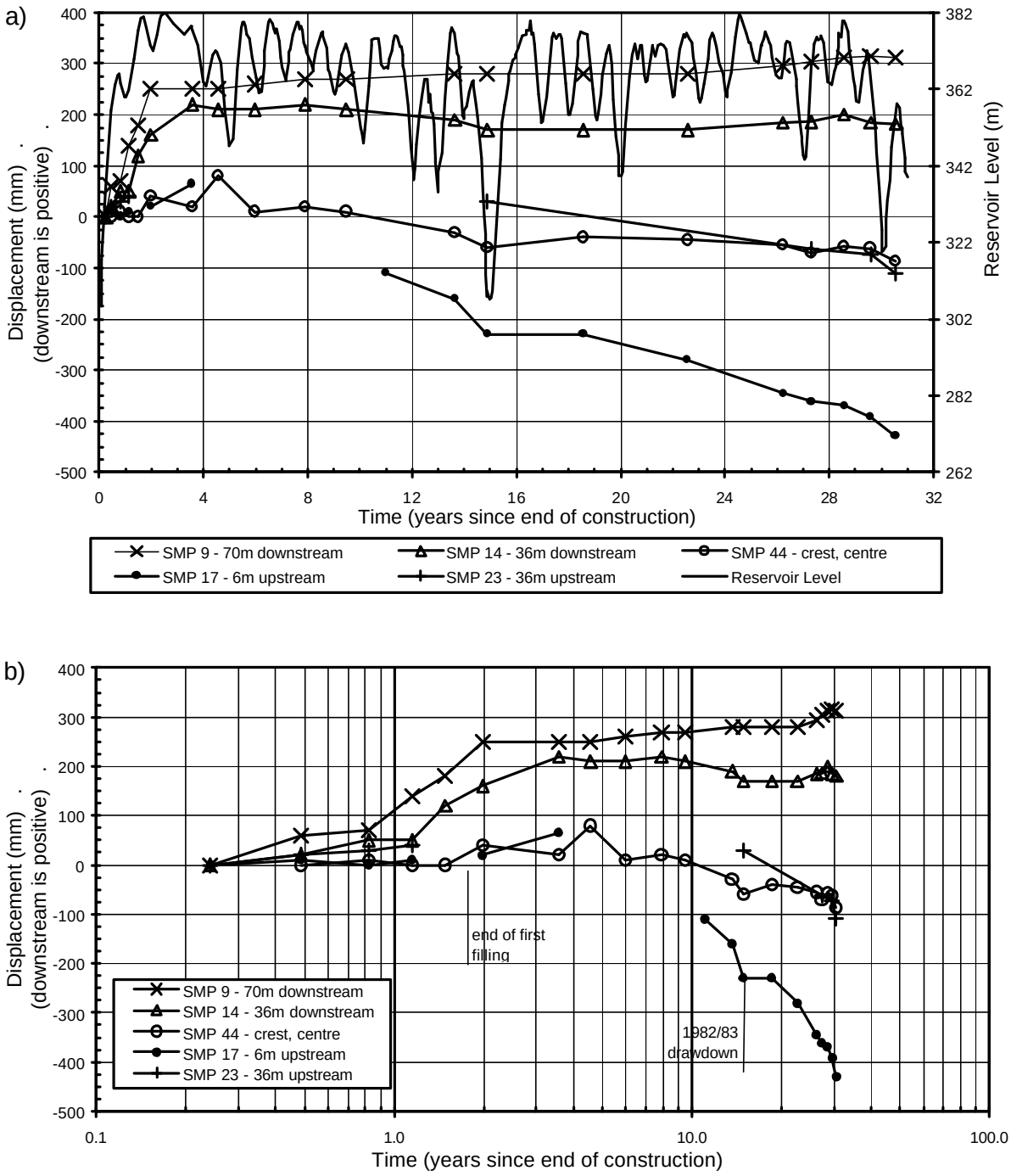

Figure G6.17: Post construction displacement normal to the dam axis of SMPs at the main section.

Further acceleration in the rate of settlement of SMPs on the upstream slope occurred during the next large drawdown of 53 m in 1997/98 (29 to 30 years after construction). A similar mechanism of movement as for the 1982/83 drawdown is possible.

The horizontal displacement of the upstream slope shows a general trend of constant to increasing rate of displacement well after the end of first filling. This behaviour is considered “abnormal” in comparison to that at similar embankments (Figure 7.86 in

Section 7.6 of Chapter 7). The long term rate and magnitude of upstream displacement post first filling of the crest is also potentially "abnormal" in comparison to similar embankments (Figures 7.69 and 7.77 in Chapter 7). The potentially "abnormal" crest displacement behaviour is possibly related to non-recoverable upstream displacement associated with shear deformation of the core on large drawdown. However, for the upstream shoulder the reason for the "abnormal" deformation behaviour is not known.

6.3.3.3 *Post Construction Internal Deformation of the Core*

The post construction internal settlement profiles within the core at Blowering dam for the period of first filling and post first filling are shown in Figure G6.18. For the early period of first filling high localised vertical strains were measured between cross-arms 13 and 15 (64.5 to 70 m below crest level) and possibly between cross-arms 17 and 18 (55.9 to 58.5 m below crest level). As shown in Figure G6.19, the vertical strain between cross-arms 13 and 15 averaged 1.57% for the short time period to 0.36 years after construction. The vertical strain in this region was very much higher than that measured in the lower region of the core where the earthfill was placed slightly dry of Standard optimum and in the upper 64.5 m of the embankment over the same period. In addition, a constriction or blockage developed within the IVM tube between cross-arms 13 and 14. For the period just after completion of construction to early August it was not possible to pass the torpedo beyond cross-arm 14 at 67 m below crest level. On 15 August a full set of readings were obtained, but in late August 1968 the torpedo became blocked on its withdrawal between cross-arms 13 and 14.

It is considered that the deformation behaviour is indicative of shear type deformation within the core along a surface of rupture that probably developed toward the end of construction, as previously discussed. The region of very high localised vertical strain post construction, between cross-arms 13 and 15, is the same region where "abnormally" large vertical strains developed at the end of construction. The large deformations are likely to have eventually resulted in the constriction or kink in the IVM tube at this location. The monitored deformations for the upper part of the IVM for the remainder of the first filling period (Figure G6.18a) after the 15 August 1968 would suggest that further shear type movements occurred, possibly a further 100 to 140 mm (or 1.8 to 2.5% vertical strain).

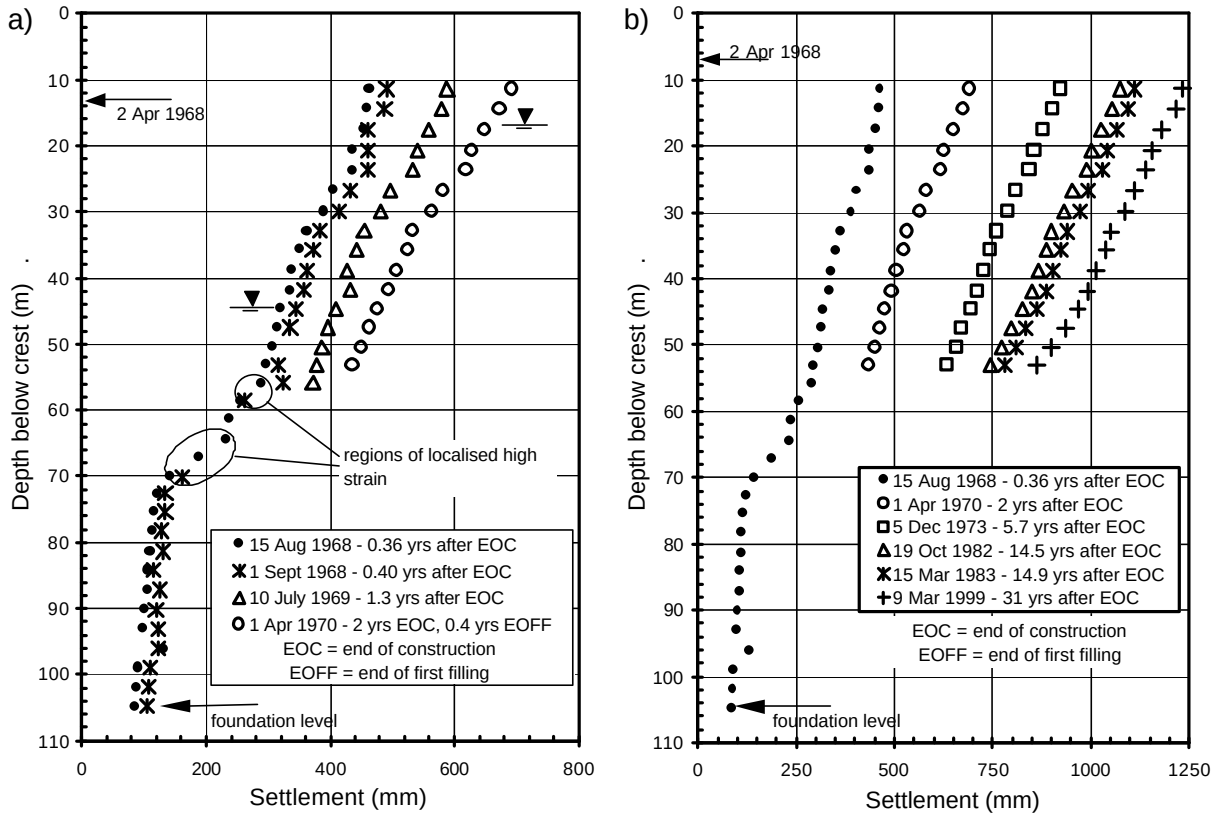

Figure G6.18: Post construction internal settlement of the core from IVM A, *(a)* during first filling, and *(b)* post first filling.

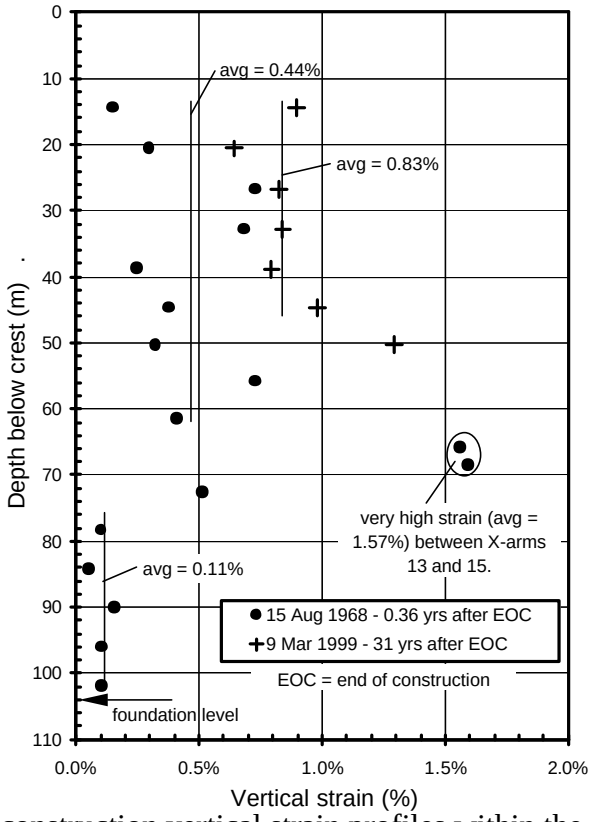

Figure G6.19: Post construction vertical strain profiles within the core from IVM A.

During the 1982/83 drawdown the centre of the crest settled somewhere between 45 and 80 mm and the upstream shoulder more than 60 to 80 mm. The IVM measurements indicated a block type settlement of the upper 55 m of the core during drawdown (i.e. a very limited amount of the settlement on drawdown occurred within the upper 55 m), with most of the settlement occurring below cross-arm 19 in the lower 50 m of the core. It is possible that this settlement represents further shear type deformation in the shear zone within the core reactivated by the large drawdown. The trigger for the movement was possibly associated with the reduction in lateral stress acting on the upstream face of the core on drawdown.

Figure G6.20 shows that the greater magnitude of settlement over the drawdown period was in the lower 50 m of the core. Given that most of the settlement in the lower region is likely to occur between 35 and 50 m, the wetter placed region of the core, Figure G6.20 suggests that the increased magnitude of settlement during the drawdowns at 5, 10 and 12/13 years may also have been due to reactivations of shear type deformation. But, there are no internal records in the lower region of the core to confirm if this is the case.

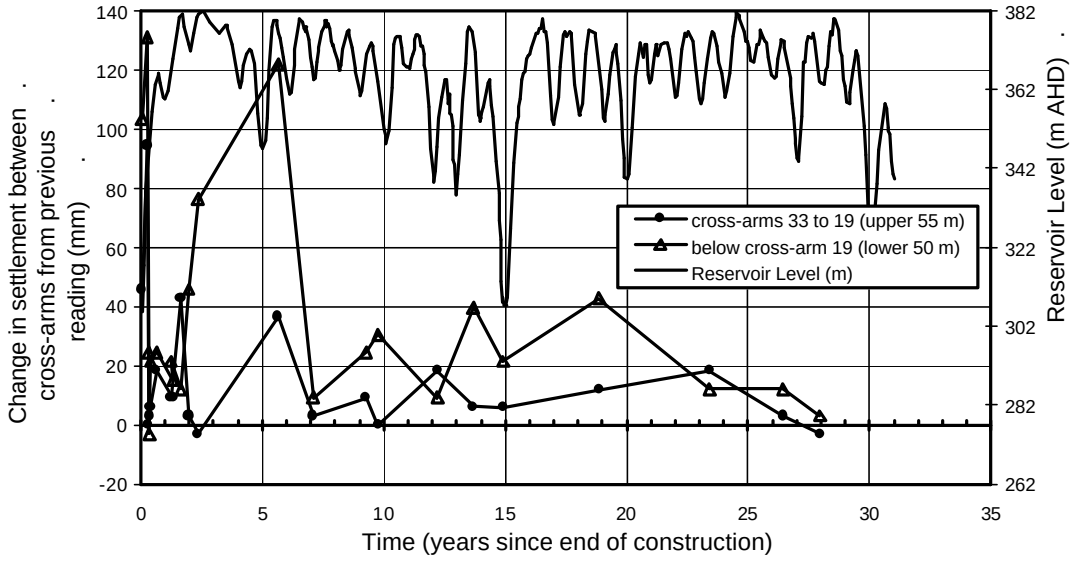

Figure G6.20: Change in internal settlement in upper and lower regions of the core.

The internal horizontal deformation gauge in the downstream shoulder shows that the downstream shoulder displaced downstream post first filling, with most of the deformation occurring on first filling (Figure G6.15). Of the approximately 158 mm downstream displacement of the gauge nearest the core on first filling, 42 mm was

taken up as compressive strain in the downstream rockfill and 116 mm downstream displacement of the terminal well. Post first filling, the measured displacements are less than about 80 to 85 mm.

6.4 SUMMARY OF NUMERICAL AND LIMIT EQUILIBRIUM ANALYSIS

6.4.1 Numerical Modelling of Embankment Construction

The numerical analysis of the construction of Blowering dam was undertaken using the computer program FLAC, an explicit finite difference code specifically developed for modelling soil and rock structures. The analysis was undertaken to model the total stresses within the embankment and the trend of the deformation behaviour of the core.

The modelled embankment is shown in Figure G6.21. Construction of the embankment (107 m high at the modelled section) was modelled in 14 stages, ranging in thickness from 4 to 10 m. A Mohr Coulomb linear elastic perfectly plastic model was used for the rockfill, filters and earthfill core, and the core modelled using total stress parameters (see below). The limitations of using such a simplistic model are recognised, but the main purpose of the analysis was to evaluate the stress conditions within the embankment to then use the stresses in the analysis and interpretation of the monitored deformation records (refer Sections 6.3.2 and 6.3.3 in this Appendix for the analysis).

The strength and compressibility properties of the embankment material zones were derived as far as practicable from the monitored records. This involved an iterative procedure for the modulus parameters because of the dependency on the stresses from the modelling. The material properties are summarised in Table G6.4.

The embankment regions are summarised as follows:

- The core is modelled as three main regions; the lower "dry" placed zone (Core Region 1), the mid "wet" placed region (Core Region 2) and the upper region placed at close to Standard optimum (Core Region 3). An intermediate zone was modelled between regions 1 and 2 where the first change in moisture specification occurred over a period of about a month (and is reflected in the pore water pressure monitoring). Core Regions 2 and 3 were modelled with a high undrained Poisson's ratio.
- The well compacted filters were modelled with low compressibility.

- The rockfill shoulders were modelled in several zones according to the placement methods, which were reflected in the monitored deformation records:
  - Inner Zone 3A of well compacted finer sized rockfill placed in 450 mm layers. This zone was of low compressibility;
  - Outer Zone 3A of well compacted rockfill placed in 0.9 m thick layers. The compressibility of this zone was greater than that of the inner Zone 3A;
  - Zone 3B of reasonably compacted rockfill (1.8 m lift thicknesses) and high compressibility;
  - Hybrid Zone 3 in the upper regions of the embankment. This zone was not critical to the model.

Table G6.4: Material properties for numerical modelling of Blowering dam

Material Property	**Earthfill Core *[1]**			
	Region 1	Region 1/2	Region 2	Region 3
Bulk unit weight (kN/m^3)	20.1	20.1	19.7	20.1
Strength properties:				
- cohesion, c_u (kPa)	200	100	50	65
- friction angle, f_u (deg)	4.9	6.2	4	6
Compressibility props:				
- Young's Modulus, E (MPa)	16	15	25 to 30	35
- Poisson's ratio (n_u)	0.33 to 0.41	0.33 to 0.41	0.45	0.45
- Bulk Modulus, K (MPa)	28	24	27	31
- Shear Modulus, G (MPa)	5.7	5.7	2.8	3.2
Material Property	**Filter and Rockfill Zones *[1]**			
	Filter	Rockfill 3A-1	Rockfill 3A-2	Rockfill 3B
Bulk unit weight (kN/m^3)	21.5	20.9	20.6	20.6
Strength properties:				
- cohesion, $c\ell$ (kPa)	0	0	0	10*[2]
- friction angle, $f\ell$ (deg)	40	43	40	38
Compressibility properties:				
- Young's Modulus, E (MPa)	150 to 200	75	30	10
- Poisson's ratio (ν)	0.2 to 0.25	0.25	0.25	0.25
- Bulk Modulus, K (MPa)	100	50	20	6.7
- Shear Modulus, G (MPa)	60	30	12	4

Notes: *[1] Refer to Figure G6.21 for the material zones

*[2] A small cohesion is used to offset potentially large strains being developed on the outer slopes.

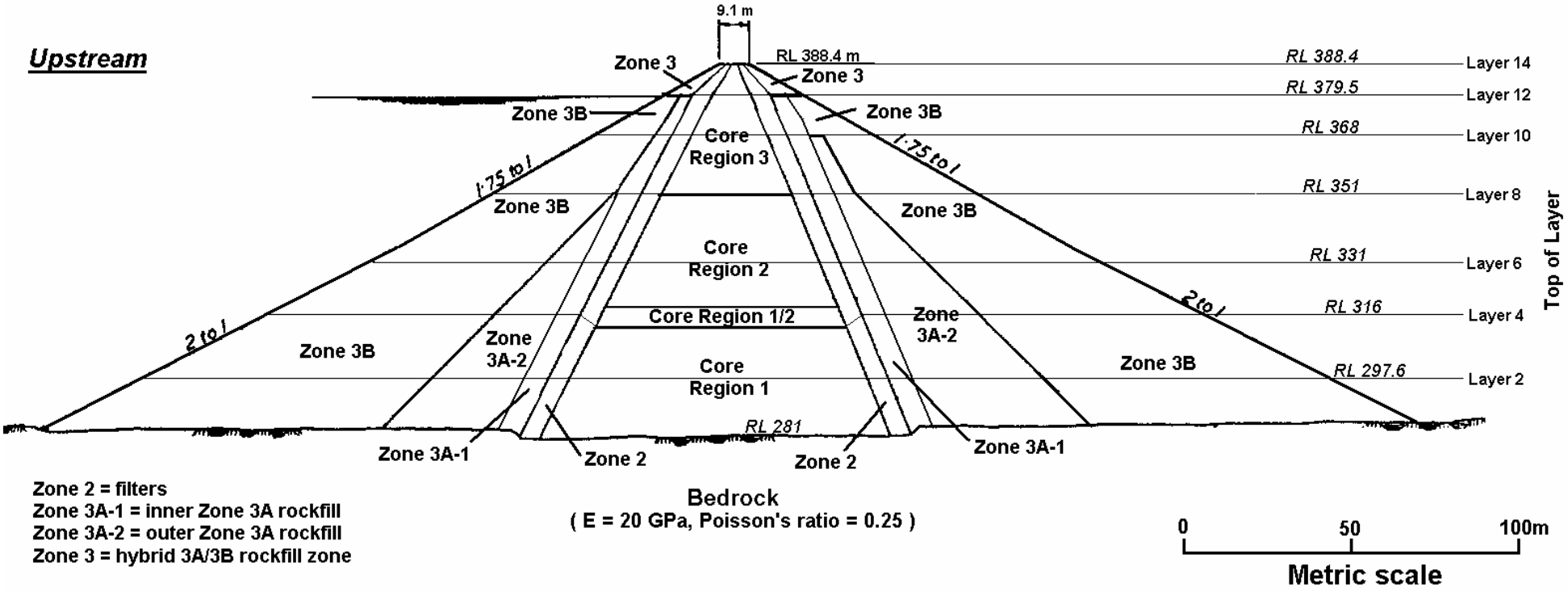

Figure G6.21: FLAC model for simple numerical model of Blowering dam

The results of the analysis with respect to the vertical stress comparison at Pressure Cell 9 are presented in Figure G6.6. The total vertical stress profile in section is shown in Figure 6.22. As shown, very high vertical stresses are developed in filters and inner Zone 3A rockfill, the zones of low compressibility. Arching occurs in the medium width core.

The comparison of vertical deformations in the core is presented in Figure 6.23 and Figure 6.24. As shown, the deformation trends from the FLAC model reasonably model the actual deformations. This is to be expected given that part of the iterative procedure was to model these trends. What the simplistic numerical model has not been able to model is the incremental increase in vertical strain between cross-arms 13 and 14.

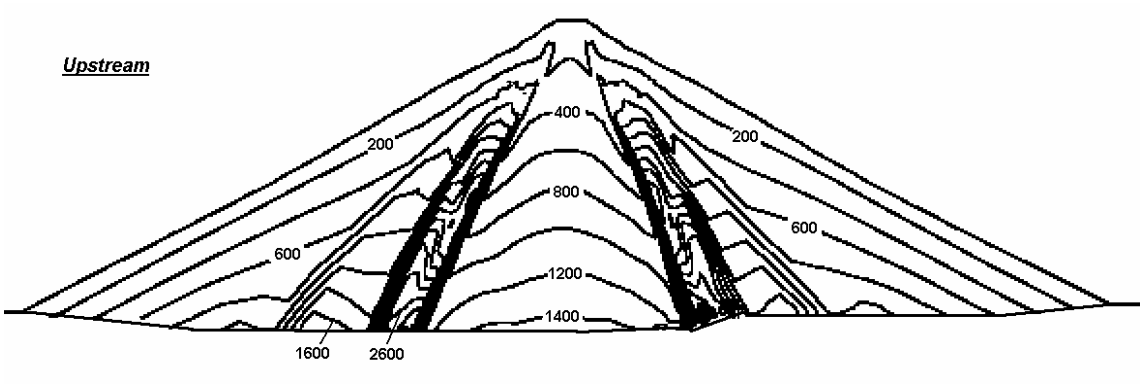

Figure 6.22: Total vertical stress profile at end of construction

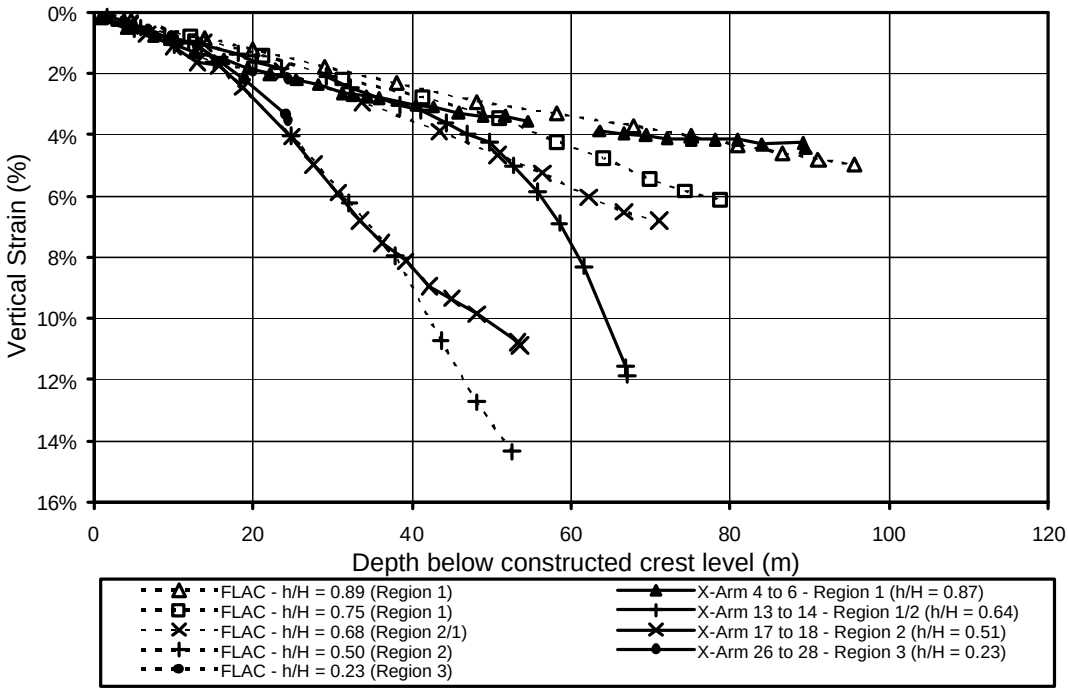

Figure 6.23: Deformation of the core during construction – comparison of monitored and FLAC model.

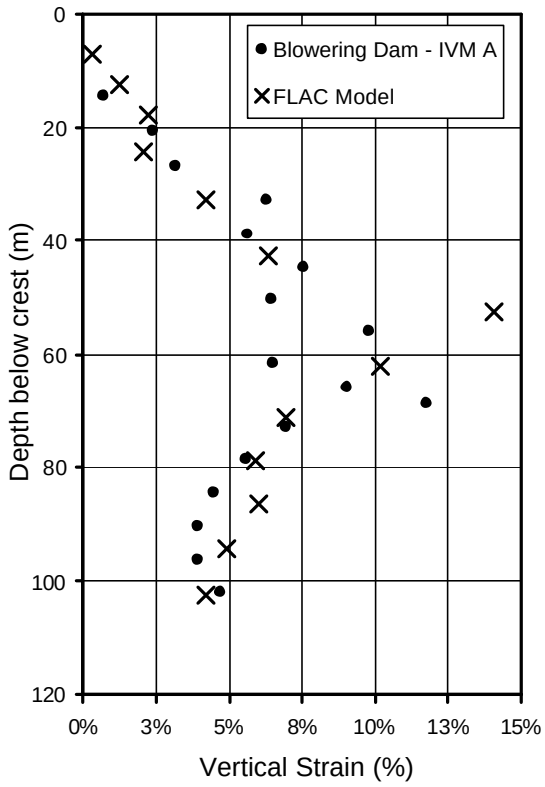

Figure 6.24: Comparison of vertical strain profiles in the core at end of construction – FLAC model to measured strains.

6.4.2 Limit Equilibrium Analysis

Limit equilibrium analysis was undertaken on the main section at Blowering dam at the end of construction condition, and post construction under a full reservoir condition and the drawdown condition as at 18 February 1983. The results are presented in Hunter and Fell (2003) and only summarised here. Both total and effective stress analyses were undertaken, the effective stress analyses using pore water pressure profiles in the core evaluated from assessment of the piezometer records.

In summary, the results indicated:

- An overall minimum factor of safety for a deep seated failure surface of greater than 1.3 immediately on completion of construction;
- Variation in the strength of the earthfill has a relatively minor effect on the minimum factor of safety. Reducing the strength in the core to the residual undrained strength of the earthfill, resulted in a reduction in factor of safety from 1.39 to 1.33;

- The factor of safety post construction is slightly higher (minimum 1.40) than at completion of construction. This was expected given that the highest pore water pressures in the earthfill are at completion of construction;
- The drawdown has virtually no impact on the factor of the deep seated slip surface in the upstream shoulder; and
- Reducing the shear strength of the rockfill in the upstream shoulder (due to saturation) has a significant effect on the factor of safety as expected. Reducing the friction angles to values as low as 34° to 36° in the Zone 3B and higher stressed regions of the Zone 3A rockfill reduced the factor of safety to as low as 1.24 to 1.27.

TABLE OF CONTENTS

9.0 REFERENCES R1

9.0 REFERENCES

Aas, G. (1981) Stability of natural slopes in quick clays. *Proceedings of the Tenth International Conference on Soil Mechanics and Foundation Engineering*, San Francisco, Balkema, Rotterdam, Vol. 3, pp. 333-338.

Aas, G., Lacasse, S., Lunne, T. and Höeg, K. (1986) Use of in situ tests for foundation design in clay. *Proceedings of the ASCE Conference on Use of In Situ Tests in Geotechnical Engineering*, (Clemence ed.) Blacksburg, Virginia, ASCE, New York. pp. 1-30.

Abadjiev, C.B. (1994) Safety assessment and stability improvements of the upstream slope of earth dams. *Proceedings of the 18th International Congress on Large Dams*, Durban, ICOLD. pp. 261-273 (Q.68 R.20).

Abele, G. (1974) Bergsturze in den Alpen (in German). *Wissenschaftliche Alpenvereinshefte*, No. 25, Munich.

Alberro, J. (1972) Stress-strain analysis of El Infiernillo dam. *Proceedings, ASCE Speciality Conference on Performance of Earth and Earth Retaining Structures*, Purdue University, Indianna, ASCE, New York. Vol. 1 (Part I) pp. 837-852.

Alberro, J.A. and Moreno, E. (1982) Interaction phenomena in the Chicoasen dam: construction and first filling. *Proceedings of the 14th International Congress on Large Dams*, Rio de Janiero, ICOLD. pp. 183-202 (Q.52 R.10).

Almeida, M.S.S. (1982) *The undrained behaviour of the Rio de Janiero clay in the light of critical state theories.* Report No. TR 119 ISSN 0309 - 7439, Cambridge University Engineering Department (CUED/D-Soils).

Almeida, M.S.S. and Ramalho-Ortigao, J.A. (1982) Performance of finite element analyses of a trial embankment on soft clay. *Proceedings, International Symposium on Numerical Models in Geomechanics*, (Dungar, Pande & Studer ed.) Zurich, Balkema, Rotterdam. pp. 548-556.

Alonso, E., Fry, J.J. and Isambert, F. (1997) Rupture et confortment du barrage en argile humide de Mondely et retour d'experience. *Nineteenth International Congress on Large Dams*, Florence, ICOLD. Vol. 4, pp. 711-733 (Q75 R49).

Alonso, E.E. and Oldecop, L.A. (2000) Fundamentals of rockfill collapse. *Proceedings of the Asian Conference on Unsaturated Soils (Unsat-Asia 2000)*, (Rahardjo, Toll and Leong ed.) Singapore, Balkema, Rotterdam. pp. 3-13.

Alvarez, A. and Bravo, G. (1976) A composed-core rockfill dam: the Canales dam. *Proceedings of the 12th International Congress on Large Dams*, Mexico City, ICOLD. Vol. 4, pp. 1077-1097 (C.20).

Amaya, F. and Marulanda, A. (1985) Golillas dam - design, construction and performance. *Proceedings of the Symposium on Concrete Face Rockfill Dams - Design, Construction and Performance*, (Cooke and Sherard ed.) Detroit, Michigan, ASCE New York. pp. 98-120.

Amaya, F. and Marulanda, A. (2000) Columbian experience in the design and construction of concrete face rockfill dams. In Concrete Face Rockfill Dams, J. Barry Cooke Volume (Mori, Sobrinho, Dijkstra, Guocheng and Borgatti ed.), Beijing, pp. 89-115.

Andong Dam Construction Office (1976) Development of new core material in zone fill dam, use of decomposed granite in Andong dam. *Proceedings of the 12th International Congress on Large Dams*, Mexico, ICOLD. pp. 731-748 (Q.44 R.38).

Andrus, R.D. and Stokoe, K.H. (1997) Liquefaction resistance based on shear wave velocity. *Proceedings of the NCEER Workshop on Evaluation of Liquefaction Resistance of Soils*, (Youd and Idriss ed.) Salt Lake City, Utah, National Centre for Earthquake Engineering Research. pp. 89-128.

Anon (1918) Reconstruction of a retaining wall on the Great Central Railway. *The Engineer*, Vol. 126, pp. 536-537.

Aphaiphuminart, S., Chanpayom, O., Mahasandana, T., Bhucharoen, V. and Pinrode, J. (1988) Design, construction and performance - Khao Laem dam. *Proceedings of the 16th International Congress on Large Dams*, San Francisco, ICOLD. pp. 95-114 (Q.61 R.6).

Aulitzky, H. (1989) The debris flows in Austria. *Bulletin of the International Association of Engineering Geology*, Bulletin No. 40, pp. 5-13.

Australian Capital Territory Electricity and Water (1993) *ACT dam safety: Googong dam surveillance report.* Report No. DSU 93/04, Dam Safety Unit.

Australian Capital Territory Electricity and Water (1994) *ACT dam safety: Corin dam surveillance report.* Report No. DSU 94/08, Dam Safety Unit.

Ayotte, D. and Hungr, O. (1998) *Runout analysis of debris flows and debris avalanches in Hong Kong, Final Report.* Geotechnical Engineering Office, Hong Kong.

Ayoubian, A. and Robertson, P.K. (1998) Void ratio redistribution in undrained triaxial extension tests on Ottawa sand. *Canadian Geotechnical Journal*, Vol 35, pp. 351-359.

Bacon, G.A. (1969) Observed behaviour of dam embankments instrumented by the Snowy Mountains Authority. *ANCOLD Bulletin*, Vol. 29 (October), pp. 40-54.

Bacon, G.A. (1999) *Personal communication with Mr. G. Bacon on the construction of Blowering dam*.

Baker, R. (1972) *Report of inspections and tests for Scotts Peak dam.* Laboratory Report 4164-1, Hydro-Electric Commission Tasmania, Civil Engineering Laboratories.

Ballard, R., Smith, B. and Von Thun, L. (1981) *Back analysis of the upstream slide near Station 135 at San Luis dam (unpublished report).* Interim Report No. 1, United States Bureau of Reclamation, Division of Design, Embankment Dams Section.

Banks, D., Strohm, W.E., De Angulo, M. and Lutton, R.J. (1975) *Study of clay shale along the Panama Canal. Report 3: Engineering analysis of slides and strength properties of clay shales along the Gaillard Cut.* Report 5-70-9, U.S. Army Eng. Waterways Experiment Station, Vicksburg.

Banks, D.C. and Strohm, W.E. (1974) Calculations of rock slide velocities. *Proceedings, Congress ISRM*, Denver, Vol. 2, pp. 839-847.

Banks, J.A. (1948) Construction of Muirhead reservoir, Scotland. *Proceedings of the 2nd International Conference on Soil Mechanics and Foundation Engineering*, Rotterdam, Vol. 2, pp. 24-31.

Bar-Shany, M., Korlath, G. and Zeitlae, J.G. (1957) The use of fat clay in dam construction in Israel. *Proceedings of the 4th International Conference on Soil Mechanics and Foundation Engineering*, London, Butterworths Scientific Publications, London. Vol. 2, pp. 273-277.

Baumann, P. (1939) Discussion on Galloway paper: The design of rock-fill dams. *Transactions, ASCE*, Vol. 104, pp. 39-40.

Baumann, P. (1958) Rockfill dams: Cogswell and San Gabriel dams. *A.S.C.E., Journal of the Power Division*, Vol. 84 (PO3), pp. 1687-1 to 33.

Baumann, P. (1964) Limit height criteria for loose-dumped rockfill dams. *Proceedings of the 8th International Congress on Large Dams*, Edinburgh, ICOLD. Vol. 3, pp. 781- (Q.31 R.13).

Baziar, M.H. and Dobry, R. (1995) Residual strength and large deformation potential of loose silty sands. *A.S.C.E., Journal of Geotechnical Engineering*, Vol 121 (12), pp. 896-906.

Becker, D., Crooks, J.H.A., Jeffries, M.G. and McKenzie, K. (1984) Yield behaviour and consolidation, II: Strength gain. *Proceedings of the ASCE Symposium on Sedimentation Consolidation Models, Prediction and Validation*, (Yong & Townsend ed.) San Francisco, ASCE, New York. pp. 382-398.

Been, K. and Jefferies, M.G. (1985) A state parameter for sands. *Geotechnique*, Vol 35 (2), pp. 99-112.

Been, K., Jefferies, M.G. and Hachey, J. (1991) The critical state of sands. *Geotechnique*, Vol 41, (3), pp. 365-381.

Beene, R.R.W. (1967) Waco dam slide. *Journal of the Soil Mechanics and Foundations Division, ASCE*, Vol. 93 (SM4), pp. 35-44.

Benassini, A., Casales, V., Hungsberg, U., Canales, R. and Esquivel, R. (1976) Mexican National Committee on Large Dams; General paper. *Proceedings of the 12th International Congress on Large Dams*, Mexico, ICOLD. Vol. 4, pp. 609-660 (G.P.9).

Bentley, S.P. and Smalley, I.J. (1984) Landslips in sensitive clays. In Slope Instability (Brunsden and Prior ed.), John Wiley & Sons, pp. 457-490.

Bernell, L. (1958) Water content and its effects on settlements in earth dams. *Proceedings of the 6th International Congress on Large Dams*, New York, ICOLD. pp. 373-384 (Q.22 R.117).

Bernell, L. (1982) Experiences of wet compacted dams in Sweden. *Proceedings of the 14th International Congress on Large Dams*, Rio de Janiero, ICOLD. pp. 421-431 (Q.55 R.24).

Berti, G., Villa, F., Dovera, D., Genevois, R. and Brauns, J. (1988) The disaster of Stava/Northern Italy. *Hydraulic Fill Structures, ASCE Speciality Conference, Geotechnical Special Publication No. 21*, (Van Zyl and Vick ed.) Colorado, ASCE, New York. pp. 492-510.

Bertuccioli, P., D'Elia, B. and Esu, F. (1996) Instrumental prediction of a high cut stability in a jointed o.c. clay. *Proceedings of the Seventh International Symposium on Landslides*, (Senneset ed.) Trondheim, Norway, Balkema. Vol. 3, pp. 1509-1514.

Bialostocki, R.J. (1961) *Waipapa Power Project: Inspection report on field control testing of earth dam materials.* New Zealand Ministry of Works.

Binnie, G.M. (1978) The collapse of Dale Dyke dam in retrospect. *Quarterly Journal of Engineering Geology*, Vol. 11, pp. 305-324.

Bishop, A.W. (1952) *The stability of earth dams*. Ph.D. Thesis, University of London.

Bishop, A.W. (1957) Some factors controlling the pore pressure set up during the construction of earth dams. *Proceedings of the 4th International Conference on Soil Mechanics and Foundation Engineering*, London, Butterworths Scientific Publications, London. Vol. 2, pp. 294-300.

Bishop, A.W. (1967) Progressive failure - with special reference to the mechanism causing it. *Proceedings of the Geotechnical Conference on Shear Strength Properties of Natural Soils and Rocks*, Oslo, Vol. 2, pp. 142-150.

Bishop, A.W. (1973) The stability of spoil heaps. *Quarterly Journal of Engineering Geology*, Vol 6, pp. 335-376.

Bishop, A.W., Hutchinson, J.N., Penman, A.D.M. and Evans, H.E. (1969) Geotechnical investigation into the causes and circumstances of the disaster of 21 October 1966. In A selection of technical reports submitted to the Aberfan Tribunal H.M.S.O., London, Welsh Office, pp. 1-80, (Item 1).

Bishop, A.W. and Vaughan, P.R. (1962) Selset Reservoir: design and performance of the embankment. *Proceedings of the Institution of Civil Engineers*, Vol. 21 (Feb.), pp. 305-345.

Bister, D., Fry, J.J., Costaz, J., Houis, J., Dupas, J.M., Degoutte, G., Lino, M. and Rizzoli, J.L. (1994) Reassessment of earthfill and rockfill dams safety - case histories. *Proceedings of the 18th International Congress on Large Dams*, Durban, ICOLD. Vol. 1, pp. 645-670 (Q.68 R.43).

Bjerrum, L. (1967) Progressive failure in slopes of overconsolidated plastic clay and clay shales (Terzaghi Lecture). *A.S.C.E., Journal of the Soil Mechanics and Foundations Division*, Vol. 93 (SM5), pp. 2-49.

Bjerrum, L. (1972) Embankments on soft ground. *Proceedings, ASCE Speciality Conference on Performance of Earth and Earth Retaining Structures*, Purdue University, Lafayette, Vol. 2, pp. 1-54.

Bjerrum, L. (1973) Problems of soil mechanics and construction on soft clays and structurally unstable soils (collapsible, expansive and others). *Proceedings, Eighth International Conference on Soil Mechanics and Foundation Engineering*, Moscow, Vol. 3, pp. 111-159.

Bjerrum, L., Loken, T., Heiberg, S. and Foster, R. (1969) A field study of factors responsible for quick clay slides. *Seventh International Congress on Soil Mechanics & Foundation Engineering*, Mexico, Vol. 1, pp. 531-540.

Bleasdale, A. (1969) Meteorological conditions relating to the Aberfan inquiry. In A selection of technical reports submitted to the Aberfan Tribunal H.M.S.O., London, Welsh Office, pp. 207-218 (Item 7).

Blee, C.E. and Meyer, A.A. (1955) Measurement of settlements at certain dams on the TVA system and assumptions for earthquake loadings for dams in the TVA area. *Proceedings of the 5th International Congress on Large Dams*, Paris, ICOLD. pp. 141-157 (Q.18 R.5).

Blee, C.E. and Reigel, R.M. (1951) Rock fill dams. *Proceedings of the 4th International Congress on Large Dams*, New Delhi, ICOLD. pp. 189-208 (Q.13 R.22).

Blight, G. (1997) Destructive mudflows as a consequence of tailings dyke failures. *Geotechnical Engineering, Proc. Institution of Civil Engineers*, Vol 125 (Jan), pp. 9-18.

Blight, G.E., Robinson, M.J. and Diering, J.A.C. (1981) The flow of slurry from a breached tailings dam. *Jnl of the South African Inst. of Mining and Metallurgy*, Vol 81 (1), pp. 1-8.

Blinder, S., Toniatti, N.B. and Ribeiro, M.S. (1992) Construction progress and behavioural monitoring of Segredo dam. *Water Power & Dam Construction* (April), pp. 18-21.

Blondeau, F., Queyroi, D., Peignaud, M., Mieussens, C., Levillian, J.P. and Vogien, M. (1977) Instrumentation du remblai experimental. *Proceedings, International Symposium on Soft Clay*, (Brenner & Brand ed.) Bangkok, Asian Institute of Technology. pp. 419-435.

Bodtman, W.L. and Wyatt, J.D. (1985) Design and performance of Shiroro rockfill dam. *Proceedings of the Symposium on Concrete Face Rockfill Dams - Design, Construction and Performance,* (Cooke and Sherard ed.) Detroit, Michigan, ASCE New York. pp. 231-251.

Borovoi, A.A. and Mikhailov, L.P. (1978) The Nurek multipurpose development. *Water Power & Dam Construction*, Vol. 30 (9), pp. 53-55.

Borovoi, A.A., Mikhailov, L.P., Moiseev, I.S. and Radchenko, V.G. (1982) Soils for and methods of embankment dam construction. *Proceedings of the 14th International Congress on Large Dams*, Rio de Janiero, ICOLD. Vol. 4, pp. 503-515 (Q.55 R.29).

Boucaut, W.R.P. and Beal, J.C. (1979) *The engineering geology of the Little Para dam site*. Report Bk. 79/2, Department of Mines and Energy, South Australia.

Bowers, N.A. (1928) Uncompleted Lafayette rolled-fill earth dam damaged by movement. *Engineering News Record* (27 Sept.), pp. 483-485.

Bowling, A.J. (1978) *Mackintosh dam rockfill control testing.* Report 4301-18, Hydro-Electric Commission Tasmania, Civil Engineering Laboratories.

Bowling, A.J. (1979) *Tullabardine dam rockfill control testing.* Report 4333-1 and -2, Hydro-Electric Commission Tasmania, Civil Engineering Laboratories.

Bowling, A.J. (1981) Laboratory investigations into the suitability of rockfill for concrete faced rockfill dams. *ANCOLD Bulletin*, Vol. 59, pp. 21-29.

Bowling, A.J. (1981-82) *Bastyan dam - rockfill control testing.* Report 4395-1 to -6, Hydro-Electric Commission Tasmania, Civil Engineering Laboratories.

Boyle, R.J. (1965) *Benmore power station. Earth dam. Report on testing and inspection.* New Zealand Ministry of Works.

Brand, E.W. (1985a) Discussion: Embankment failure on clay near Rio de Janiero. *A.S.C.E., Journal of Geotechnical Engineering*, Vol 11 (2), pp. 257-259.

Brand, E.W. (1985b) Predicting the failure of residual soil slopes. *Proceedings of the 11th International Conference on Soil Mechanics and Foundation Engineering*, San Francisco, Vol. 5, pp. 2541-2578.

Brand, E.W. (1989) Correlation between rainfall and landslides. *Proceedings 12th International Conference on Soil Mechanics and Foundation Engineering*, Rio, Vol. 5, pp. 3091-3093.

Brand, E.W. (1995) Keynote paper: Slope instability in tropical areas. *Proceedings of the Sixth International Symposium on Landslides*, (Bell ed.) Christchurch, Balkema, Rotterdam. Vol. 3, pp. 2031-2051.

Brand, E.W. and Premchitt, J. (1989) Comparison of the predicted and observed performance of the Muar test embankment. *Proceedings, International Symposium on Trial Embankments on Malaysian Marine Clays*, (Hudson, Toh & Chan ed.) Kuala Lumpur, Malaysian Highway Authority. Vol. 2, pp. 10.1-10.29.

Brand, E.W., Premchitt, J. and Phillipson, H.B. (1984) Relationship between rainfall and landslides in Hong Kong. *Proceedings of the Fourth International Symposium on Landslides*, Toronto, Canada, Balkema. Vol. 1, pp. 377-384.

Bravo, G. (1979) The excavation to support the core of Canales dam. *Proceedings of the 13th International Congress on Large Dams*, New Delhi, ICOLD. Vol. 1, pp. 1221-1232 (Q.48 R.69).

Bravo, G., Giron, F. and Olalla, C. (1994) Behaviour models and actual behaviour of Canales dam. *Proceedings of the 18th International Congress on Large Dams*, Durban, ICOLD. Vol. 3, pp. 293-306 (Q.70 R.20).

Breznik, M. (1979) The reliability of and damage to underground dams and other cut-off structures in karst regions. *Proceedings of the 13th International Congress on Large Dams*, New Delhi, ICOLD. Vol. 4, pp. 57-79 (C.04).

Brousek, M. (1976) Technology of placing the rock material at the rockfill dam of Dalesice as to the exploitation of aggregates of worse quality. *Proceedings of the 12th International Congress on Large Dams*, Mexico, ICOLD. Vol. 1, pp. 697-707 (Q.44 R.36).

Bryson, V.R. (1980) *Lake Pukaki dam - Earth dam construction.* Ministry of Works and Development, New Zealand.

Burland, J.B., Longworth, T.I. and Moore, J.F.A. (1977) A study of ground movement and progressive failure caused by a deep excavation in Oxford Clay. *Geotechnique*, Vol. 27 (4), pp. 557-591.

Byrd, T. and Middleboe, S. (1984) Weak ground cited as Carsington fails. *New Civil Engineer* (14 June).

Byrne, P.M. and Beaty, M. (1998) "Post-liquefaction" theoretical/conceptual issues. *National Science Foundation Workshop on Shear Strength of Liquefied Soils*, (Stark Olson Kramer and Youd ed.) Urbana, Illinois, National Science Foundation. pp. 10-39.

Caine, N. (1980) The rainfall intensity - duration control of shallow landslides and debris flows. *Geografiska Annaler*, Vol 62 A (1-2), pp. 23-27.

Campbell, D.B. and Shaw, W.H. (1978) Performance of a waste rock dump on moderately to steeply sloping foundations. *Proceedings of the First International Symposium on Stability in Coal Mining*, (Brawner and Dorling ed.) Vancouver, Miller Freeman. pp. 395-405.

Cannon, S.H. and Ellen, S.D. (1988) Chapter 3. Rainfall that resulted in abundant debris-flow activity during the storm. In Landslides, floods, and marine effects of the storm of January 3-5, 1982, in the San Francisco Bay region, California. U.S. Geological Survey Professional Paper 1434 (Ellen & Wieczorek ed.), U.S. Geological Survey, pp. 27-33.

Cary, A.S. (1958) Rockfill dams: Performance of Mud Mountain dam. *A.S.C.E., Journal of the Power Division*, Vol. 84 (PO4), pp. 1745-1 to 3.

Casagrande, A. (1965) Role of the "calculated risk" in earthwork and foundation engineering (Terzaghi lecture). *A.S.C.E., Journal of the Soil Mechanics and Foundations Division*, Vol 91 (SM4), pp. 1-40.

Casales, V.L. (1976) Discussion during technical session of Question 47. *Proceedings of the 12th International Congress on Large Dams*, Mexico City, ICOLD. Vol. 5, pp. 495-500.

Casinader, R. (1987) Discussion on paper: Kotmale dam and observations on CFRD. *A.S.C.E., Journal of Geotechnical Engineering*, 113 (10), pp. 1198-1200.

Casinader, R. and Watt, R.E. (1985) Concrete face rockfill dams of the Winneke project. *Proceedings of the Symposium on Concrete Face Rockfill Dams - Design, Construction and Performance*, (Cooke and Sherard ed.) Detroit, Michigan, ASCE New York. pp. 140-162.

Castro, G. (1998) "Post-liquefaction" shear strength from case histories. *National Science Foundation Workshop on Shear Strength of Liquefied Soils*, (Stark, Olson, Kramer and Youd ed.) Urbana, Illinois, National Science Foundation. pp. 53-57.

Castro, G., Poulos, S.J. and Leathers, F.D. (1985) Re-examination of the slide of Lower San Fernando Dam. *A.S.C.E., Journal of Geotechnical Engineering*, Vol 111 (9), pp. 1093-1106.

Castro, G., Seed, R.B., Keller, T.O. and Seed, H.B. (1992) Steady-state strength analysis of Lower San Fernando Dam slide. *A.S.C.E., Journal of Geotechnical Engineering*, Vol 118 (3), pp. 406-427.

Catanach, R. and McDaniel, T.N. (1972) Lateral deformation of a dam embankment. *Performance of Earth and Earth Retaining Structures*, Vol. 1 (Part 1), pp. 867-883.

Cavounidis, S. and Höeg, K. (1977) Consolidation during construction of earth dams. *A.S.C.E., Journal of the Geotechnical Engineering Division*, Vol 103 (GT10), pp. 1055-1067.

Cetin, H. (2002) *Personal communication with Mr. H. Cetin of Cukurova University, Turkey*.

Cetin, H., Laman, M. and Ertunc, A. (2000) Settlement and slaking problems in the world's fourth largest rock-fill dam, the Ataturk dam in Turkey. *Engineering Geology*, Vol. 56, pp. 225-242.

Champa, S. and Mahatharadol, B. (1982) Construction of Srinagarind dam. *Proceedings of the 14th International Congress on Large Dams*, Rio de Janiero, ICOLD. pp. 255-278 (Q.55 R.15).

Chan, Y.C., Pun, W.K., Wong, H.N., Li, A.C.O. and Yeo, K.C. (1996) *Investigation of some major slope failures between 1992 and 1995.* GEO Report 52, Geotechnical Engineering Office, Civil Engineering Department, Hong Kong.

Chandler, R.J. (1972) Lias clay: weathering processes and their effect on shear strength. *Geotechnique*, Vol. 22 (3), pp. 403-431.

Chandler, R.J. (1974) Lias clay: the long-term stability of cutting slopes. *Geotechnique*, Vol. 24 (1), pp. 21-38.

Chandler, R.J. (1976) The history and stability of two Lias clay slopes in the upper Gwash valley, Rutland. *Phil. Trans. R. Soc. Lond. A.*, 283, pp. 463-491.

Chandler, R.J. (1984a) Delayed failure and observed strengths of first time failures in stiff clays: a review. *Proceedings of the Fourth International Symposium on Landslides*, Toronto, Vol. 2, pp. 19-25.

Chandler, R.J. (1984b) Recent European experience of landslides in over-consolidated clays and soft rocks. *Proceedings of the Fourth International Symposium on Landslides*, Toronto, Vol. 2, pp. 61-81.

Chandler, R.J. and Tosatti, G. (1995) The Stava tailings dam failure, Italy, July 1985. *Proc. Institution of Civil Engineers: Geotechnical Engineering*, Vol 113 (1), pp. 67-79.

Charles, J.A. (1976) The use of one-dimensional compression tests and elastic theory in predicting deformations of rockfill embankments. *Canadian Geotechnical Journal*, Vol. 13 (3), pp. 189-200.

Charles, J.A. (1986) The significance of problems and remedial works at British earth dams. *Proceedings of the BNCOLD-IWES Conference on Reservoirs*, pp. 123-141.

Charles, J.A. (1997) Special problems associated with earthfill dams. *Proceedings of the 19th International Congress on Large Dams*, Florence, ICOLD. Vol. 2, pp. 1083-1196 (GR. Q73).

Charles, J.A. (1998) Lives of embankment dams: construction to old age. *Dams and Reservoirs*, Vol 8 (Dec.), pp. 11-23.

Charles, J.A. and Boden, J.B. (1985) The failure of embankment dams in the United Kingdom. *Proceedings of the Symposium on Failures in earthworks*, London, Thomas Telford. pp. 181-202.

Charles, J.A. and Tedd, P. (1991) Long term performance and ageing of old embankment dams in the United Kingdom. *Proceedings of the 17th International Congress on Large Dams*, Vienna, ICOLD. pp. 461-473 (Q.65 R.25).

Charles, J.A. and Watts, K.S. (1987) The measurement and significance of horizontal earth pressures in the puddle clay cores of old earth dams. *Proceedings of the Institution of Civil Engineers*, Vol 82 (Feb), pp. 123-152.

Church, M. and Miles, M.J. (1987) Meteorological antecedents to debris flow in southwestern British Columbia; some case studies. *Reviews in Engineering Geology, Geological Society of America*, Vol 7, pp. 63-79.

Clausen, C.J.F. (1972) *Measurement of pore water pressures, settlements and lateral deformations at a test fill on soft clay brought to failure at Mastemyr, Oslo.* Technical Report 11, Norwegian Geotechnical Institute, Oslo.

Clements, R.P. (1984) Post-construction deformation of rockfill dams. *A.S.C.E., Journal of Geotechnical Engineering*, Vol. 110 (7), pp. 821-840.

Clough, R.W. and Woodward, R.J. (1967) Analysis of embankment stresses and deformations. *A.S.C.E., Journal of the Soil Mechanics and Foundations Division*, Vol. 93 (SM4), pp. 529-549.

Coffey & Hollingsworth (1971) *Study of weak clays within the foundation. Maroon dam.* Project No. 4260B/2, for Queensland Irrigation and Water Supply Commission.

Cole, B.A. (1974) *Gordon River power development - Stage 1, Scotts Peak Dam, design report.* Report CDR 264, Hydro-Electric Commission Tasmania, Civil Design Division.

Cole, B.A. and Fone, P.J.E. (1979) Repair of Scotts Peak dam, Tasmania. *Proceedings of the 13th International Congress on Large Dams*, New Delhi, ICOLD. pp. 211-231 (Q.49 R.15).

Cole, B.R. and Cummins, P.J. (1981) Behaviour of Dartmouth dam during construction. *Proceedings of the 10th International Conference on Soil Mechanics and Foundation Engineering*, Stockholm, Balkema, Rotterdam. Vol. 1, pp. 81-85.

Collingham, E. (1997) *Hope Valley dam safety evaluation: Preliminary pitting investigation.* Report Ref. SA Water: 4810/96, South Australian Water Corporation.

Collingham, E.B. and Newman, R.J. (1977) *A report on the field work and laboratory testing for the Design Branch study of the Happy Valley dam.* South Australian Government, Engineering and Water Supply Department, Design Branch, Soils and Foundations Section.

Commonwealth Department of Works (1970) *Corin dam: Design and construction report.* CDW, Canberra Branch.

Connell Wagner (1998a) *Cardinia Reservoir: Surveillance graphs 26-27/05/98.* for Melbourne Water Corporation.

Connell Wagner (1998b) *Greenvale Reservoir: Surveillance graphs 31/3/98 to 1/4/98.* for Melbourne Water Corporation.

Connell Wagner (1998c) *Thomson reservoir: Surveillance graphs.* Ref. V018.01, for Melbourne Water Corporation.

Connell Wagner (1998d) *Upper Yarra reservoir, main dam: Surveillance graphs.* for Melbourne Water Corporation.

Connell Wagner (1999) *Yan Yean reservoir: Surveillance graphs.* for Melbourne Water Corporation.

Convery, D.J. (1977) *Upper Waitaka power development. Pukaki earth dam. Earth dam materials report.* New Zealand Ministry of Works and Development.

Cooke, J.B. (1958) Rockfill dams: Wishon and Courtright concrete face dams. *A.S.C.E., Journal of the Power Division*, Vol. 84 (PO3), pp. 1746-1 to 33.

Cooke, J.B. (1984) Progress in rockfill dams (18th Terzaghi lecture). *ASCE, Journal of Geotechnical Engineering*, Vol 110 (10), pp. 1383-1414.

Cooke, J.B. (1993) Rockfill and the rockfill dam. *Proceedings of the International Symposium on High Earth-Rockfill Dams*, (Jiang, Zhang & Qin ed.) Beijing,

Cooke, J.B. (1997) The concrete face rockfill dam. *Non-Soil Water Barriers for Embankment Dams, 17th Annual USCOLD Lecture Series*, San Diego, California, USCOLD. pp. 117-132.

Cooke, J.B. (1999) The development of today's CFRD dam. *Proceedings of the Second Symposium on Concrete Face Rockfill Dams*, Florianopolis, Brazil, Brazilian Committee on Dams. pp. 3-11.

Cooke, J.B. and Sherard, J.L. (1987) Concrete-face rockfill dam: II. Design. *ASCE, Journal of Geotechnical Engineering*, Vol 113 (10), pp. 1113-1133.

Cooke, J.B. and Strassburger, A.G. (1988) Section 6: Rockfill Dams. In Development of Dam Engineering in the United States (Kollgaard & Chadwick ed.), Permagon Press, pp. 885-1030.

Cooling, L.F. and Golder, H.Q. (1942) The analysis of the failure of an earth dam during construction. *Journal of the Institution of Civil Engineers* (No. 1 (1942-43), Nov.), pp. 38-55.

Cooper, B., Khalili, N. and Fell, R. (1997) Large deformations due to undrained strain weakening slope instability at Hume Dam No. 1 embankment. *Proceedings of the*

19th International Congress on Large Dams, Florence, ICOLD. Vol. 2, pp. 797-818 (Q.73 R.46).

Cooper, M.R., Bromhead, E.N., Petley, D.J. and Grant, D.I. (1998b) The Selborne cutting stability experiment. *Geotechnique*, Vol. 48 (1), pp. 83-101.

Cornforth, D.H., Worth, E.G. and Wright, W.L. (1974) Observations and analysis of a flow slide in sand fill. *Proc. of the Symposium on Field Instrumentation in Geotechnical Engineering*, (British Geotechnical Society ed.) England, Butterworths, London. pp. 136-151.

Corominas, J. (1996a) The angle of reach as a mobility index for small and large landslides. *Canadian Geotechnical Journal*, Vol 33, pp. 260-271.

Corominas, J. (1996b) Debris slide. In Landslide Recognition: Identification, Movement and Causes (Dikau, Brunsden, Schrott and Ibsen ed.), John Wiley, pp. 97-102.

Corominas, J., Remondo, J., Farias, P., Estevao, M., Zezere, J., Diaz de Teran, J., Dikau, R., Schrott, L., Moya, J. and Gonzales, A. (1996) Debris flow. In Landslide Recognition: Identification, Movement and Causes (Dikau, Brunsden, Schrott and Ibsen ed.), John Wiley, pp. 161-180.

Costa-Filho, L.M., Werneck, M.L.G. and Collet, H.B. (1977) The undrained strength of a very soft clay. *Proceedings, Ninth International Symposium on Soil Mechanics and Foundation Engineering*, Tokyo, Vol. 1, pp. 69-72.

Coumoulos, D.G. (1979) Discussion: Engineering properties and performance of clay fills. *Proceedings ICE Conference on Clay Fills*, London, The Institution of Civil Engineers, London. pp. 221-224.

Coumoulos, D.G. and Koryalos, T.P. (1979) Performance of the clay core of a large embankment dam during construction. *Proceedings ICE Conference on Clay Fills*, London, The Institution of Civil Engineers, London. pp. 73-78.

Cox, F. (1972) *The geology of the Lake William Hovell dam: First Stage.* State Rivers and Water Supply Commission Victoria.

Cribben, N.E. (1990) *K.R.P.D., Crotty Dam, Field dry density testing on Zone 3A material.* Report 4652-1, Hydro-Electric Commission Tasmania, Engineering and Scientific Services Department.

Crooks, J.H.A. (1987) Some observations on the stability of structures founded on soft clays. *Proceedings, International Symposium on Prediction and Performance in Geotechnical Engineering*, (Joshi & Griffiths ed.) Calgary, Balkema, Rotterdam. pp. 27-38.

Crooks, J.H.A. and Becker, D.E. (1988) Discussion: Slide in the upstream slope of Lake Shelbyville Dam by Humphreys and Leonards. *Journal of Geotechnical Engineering, ASCE,* Vol. 114 (4), pp. 506-508.

Crooks, J.H.A., Becker, D.E., Jefferies, M.G. and McKenzie, K. (1984) Yield behaviour and consolidation. I: Pore pressure response. pp. 356-381.

Cubrinovski, M. and Ishihara, K. (2000) Flow potential of sandy soils with different grain compositions. *Soils and Foundations*, Vol 40 (4), pp. 103-119.

Currey, D.T., Michels, V. and Little, D.J. (1968) Bellfield dam, Victoria. *Institution of Engineers, Australia: Annual Engineering Conference Papers*, IEAust, Sydney. pp. 33-49.

Cyganiewicz, J.M. and Dise, K.M. (1997) Case history of a rapid drawdown failure at Steinaker Dam. *Proceedings of the 19th International Congress on Large Dams*, Florence, ICOLD. Vol. 4, pp. 481-497 (Q75 R36).

D'Appolonia, D.J., Lambe, T.W. and Poulos, H.G. (1971a) Evaluation of pore pressures beneath an embankment. *A.S.C.E., Journal of the Soil Mechanics and Foundations Division*, Vol 97 (SM6), pp. 881-897.

D'Elia, B., Picarelli, L., Leroueil, S. and Vaunet, J. (1998) Geotechnical characterisation of slope movements in structurally complex clay soils and stiff jointed clays. *Italian Geotechnical Engineer*, Anno XXXII (No. 3), pp. 5-32.

Daehn, W.W. (1955) Behaviour of a rolled earth dam constructed on a compressible foundation. *Proceedings of the 5th International Congress on Large Dams*, Paris, ICOLD. pp. 171-191 (Q.18 R.7).

Dascal, O. (1987) Postconstruction deformations of rockfill dams. *A.S.C.E., Journal of Geotechnical Engineering*, Vol. 113 (1), pp. 46-59.

Dascal, O. and Tournier, J.P. (1975) Embankments on soft and sensitive clay foundation. *A.S.C.E., Journal of the Geotechnical Engineering Division*, Vol 101 (GT3), pp. 297-314.

Davidson, R.R., Vreugdenhil, R. and Foster, M. (2001) The dam safety upgrade at Lake Eppalock. *ANCOLD Bulletin*, Issue 118 (August), pp. 59-70.

Davies, D.G. (1953) The Harrogate Dam failure. *Journal of the Institution of Water Engineers*, Vol. 7 (1), pp. 57-79.

Davies, T.J.G. (1993) *King River power development, Crotty Dam, Record Design Report.* Report CDR 614, Hydro-Electric Commission Tasmania, Consulting Business Unit.

Davies, T.J.G., Smith, O. and Hancock, D.J. (1995) *Reece dam, Surveillance Report No. 2 (1988 - 1995).* Report ENE-0010-SF-007, Hydro-Electric Commission Tasmania, Civil and Water Resources Engineering Group.

Davis, F.J. and Kisselman, H.E. (1963) *Summary of earthworks control for Navajo dam. Upper Colorado River Storage Project.* United States Department of the Interior Bureau of Reclamation, Office of Chief Engineer.

Dawson, R.F. (1994) *Mine waste geotechnics*. Doctor of Philosophy, Department of Civil Engineering, University of Alberta, Edmonton.

Dawson, R.F., Morgenstern, N.R. and Stokes, A.W. (1998) Liquefaction flowslides in Rocky Mountain coal mine waste dumps. *Canadian Geotechnical Journal*, Vol 35, pp. 328-343.

de Alba, P. (1998) Written statement: Shear strength of liquefied soils from laboratory and field tests. Discussion. *National Science Foundation Workshop on Shear Strength of Liquefied Soils*, (Stark Olson Kramer and Youd ed.) Urbana, Illinois, National Science Foundation. pp. 113-115.

de Groot, M.B. and Stoutjesdijk, T.P. (1997) Undrained stress path of loose sand predicted from dry tests. *Canadian Geotechnical Journal*, Vol 34, pp. 131-138.

de Melo, F.G. and Direito, F.T. (1982) The behaviour of Roxo dam. *Proceedings of the 14th International Congress on Large Dams*, Rio de Janiero, ICOLD. pp. 387-400 (Q.52 R.23).

Department of Public Works New South Wales (1955) *Schedule of rate contract for construction of embankment, intake structure, stilling basin and certain other works at Adaminaby dam.* Contract No. 17-55/56.

Department of Water Resources New South Wales (1989) *Chaffey dam - design report.* Public Works Department, Dams Section.

Dibiagio, E., Myrvoll, F., Valstad, T. and Hansteen, H. (1982) Field instrumentation, observations and performance of Svartevann dam. *Proceedings of the 14th International Congress on Large Dams*, Rio de Janiero, ICOLD. pp. 789-826 (Q.52 R.49).

Dighe, M.R., Gaikwad, R.S., Nemade, V.D. and Jawalge, M.M. (1985) Failure analysis of Aran Dam. *Fifteenth International Congress on Large Dams*, Lausanne, ICOLD. pp. 1117-1124 (Q.57 C.4).

Dixon, H.H. (1958) Moisture control and compaction methods used during construction of the Sasumua dam, Kenya. *Proceedings of the 6th International Congress on Large Dams*, New York, ICOLD. pp. 139-152 (Q.22 R.10).

Dobry, R. and Alvarez, L. (1967) Seismic failure of Chilean tailings dams. *A.S.C.E., Journal of the Soil Mechanics and Foundations Division*, Vol 93 (SM6), pp. 237-260.

Dolezalova, M. and Leitner, F. (1981) Prediction of Dalesice dam performance. *Proceedings of the 10th International Conference on Soil Mechanics and Foundation Engineering*, Stockholm, Balkema, Rotterdam. Vol. 1, pp. 111-114.

Douglas, A.W. (1965) Burrendong dam construction. *I.E. Aust., Civil Engineering Transactions* (October), pp. 49-62.

Dounias, G.T., Potts, D.M. and Vaughan, P.R. (1988) Finite element analysis of progressive failure: two case studies. *Computers and Geotechnics. Special issue on Embankment Dams*, Vol. 6 (2), pp. 155-175.

Dounias, G.T., Potts, D.M. and Vaughan, P.R. (1996) Analysis of progressive failure and cracking in old British dams. *Geotechnique*, Vol 46 (4), pp. 621-640.

Downer Energy Services Ltd (1998) *Waipapa dam: Report on the Type B deformations survey*. for Electricity Corporation of New Zealand, Northern Generation Group.

Duncan, J.M. (1996) State of the art: Limit equilibrium and finite-element analysis of slopes. *A.S.C.E., Journal of Geotechnical Engineering*, Vol 122 (7), pp. 577-595.

Duncan, J.M. and Dunlop, P. (1969) Slopes in stiff fissured clays and shales. *A.S.C.E., Journal of the Soil Mechanics and Foundations Division*, Vol. 95 (SM2), pp. 467-492.

Duncan, J.M., Lefebvre, G. and Lade, P. (1980) *The landslide at Tuve, near Goteborg, Sweden, on November 30, 1977*. Committee on Natural Disasters, Commission on Sociotechnical Systems, National Research Council.

Duncan, J.M., Wright, S.G. and Wong, K.S. (1990) Slope stability during rapid drawdown. *Proceedings, H. Bolton Seed Memorial Symposium*, (Duncan ed.) BiTech, Vancouver. Vol. 2, pp. 253-272.

Eadie, A. (1988) *Geological investigations for construction of The Bjelke-Petersen dam.* Ref. No. PP 1700, Queensland Water Resources Commission, Planning Division, Engineering Geology Section.

Eckersley, J.D. (1985) Flowslides in stockpile coal. *Engineering Geology*, Vol 22, pp. 13-22.

Eckersley, J.D. (1986) *The initiation and development of slope failures with particular reference to flowslides*. Doctor of Philosophy, James Cook University of North Queensland, Department of Civil & Systems Engineering.

Eckersley, J.D. (1990) Instrumented laboratory flowslides. *Geotechnique*, Vol 40 (3), pp. 489-502.

Eden, W.J. (1977) Evidence of creep in steep natural slopes of Champlain sea clay. *Canadian Geotechnical Journal*, Vol 14, pp. 620-627.

Eden, W.J., Fletcher, E.B. and Mitchell, R.J. (1971) South Nation River landslide, 16 May 1971. *Canadian Geotechnical Journal*, Vol 8, pp. 446-451.

Edgars, L. and Karlsrud, K. (1983) Soil flows generated by submarine slides - Case studies and consequences. *Proc. of the Third International Conference on the Behaviour of Off-shore Structures*, (Connor and Chryssostomos ed.) MIT, Hemisphere Pub. Corp., pp. 425-437.

Eide, O. and Bjerrum, L. (1956) The slide at Bekkelaget. *Geotechnique*, Vol 6, pp. 88-100.

Eigenheer, L.P.Q.T. and Souza, R.J.B. (1999) Xingo concrete face rockfill dam. *Proceedings of the Second Symposium on Concrete Face Rockfill Dams*, Florianopolis, Brazil, Brazilian Committee on Dams. pp. 271-284.

Eisenstein, Z. and Law, S.T.C. (1977) Analysis of consolidation behaviour of Mica dam. *A.S.C.E., Journal of the Geotechnical Engineering Division*, Vol. 103 (GT8), pp. 879-895.

El-Ramley, H. (2001) *Probabilistic analysis of landslides hazards and risks: Bridging theory and practice*. Ph.D. Thesis, Department of Civil and Environmental Engineering, University of Alberta, Edmonton.

Ellen, S.D., Algus, M.A., Cannon, S.H., Fleming, R.W., Lahr, P.C., Peterson, D.M. and Reneau, S.L. (1988) Chapter 6. Description and mechanics of soil slip/debris flows in the storm. In Landslides, floods, and marine effects of the storm of January 3-5, 1982, in the San Francisco Bay region, California. U.S. Geological Survey Professional Paper 1434 (Ellen & Wieczorek ed.), U.S. Geological Survey, pp. 63-111.

Ellen, S.D. and Fleming, R.W. (1987) Mobilisation of debris flows from soil slips, San Francisco Bay region, California. *Reviews in Engineering Geology, Geological Society of America*, Vol 7, pp. 31-40.

Engineering and Water Supply Department (1981) *Kangaroo Creek dam. Historical account of Construction and Operations.* Ref. 81/41, South Australian Government.

Engineering and Water Supply Department South Australia (1981a) *Happy Valley dam: Historical account of construction and operations.* Ref. No. 81/11, Design Services Branch.

Engineering and Water Supply Department South Australia (1981b) *Hope Valley dam: Historical account of construction and operations.* Ref. No. 81/10, Design Services Branch.

ENR (1929a) Modified completion Lafayette Dam recommended. *Engineering News Record* (17 Jan.), pp. 116.

ENR (1929b) Plastic foundations. *Engineering News Record* (31 January), pp. 167.

ENR (1929c) Reconstruction of Lafayette Dam advised. *Engineering News Record* (31 Jan.), pp. 190-192.

ENR (1937a) Foundation of earth dam fails. *Engineering News Record* (30 Sept.), pp. 532 & 535.

ENR (1937b) Small earthfill dam fails. *Engineering News Record* (24 June), pp. 932.

ENR (1937c) WPA dam fails at Kansas City. *Engineering News Record* (23 Sept.), pp. 495.

ENR (1938a) Foundation caused dam failure. *Engineering News Record* (24 Feb.), pp. 281-282.

ENR (1938b) Why Marshall dam failed. *Engineering News Record* (24 Mar.), pp. 431-432.

ENR (1939a) Large slide in Fort Peck Dam caused by foundation failure. *Engineering News Record* (11 May) pp. 55-58.

ENR (1939b) Small earthfill dam typical of modern practice. *Engineering News Record* (26 Oct.), pp. 47.

ENR (1958) Near Denver, a 60 ft earth dam sunk 11 ft. *Engineering News Record* (26 June), pp. 23.

ENR (1960) High earth dam plugs narrow canyon for power. *Engineering News Record* (7 Apr.), pp. 44-51.

Esmiol, E.E. (1955) Foundation consolidation beneath four Bureau of Reclamation rolled earth dams as determined from field observations. *Proceedings of the 5th International Congress on Large Dams*, Paris, ICOLD. pp. 123-139 (Q.18 R.3).

Evans, M.D. and Zhou, S. (1995) Liquefaction behavior of sand-gravel composites. *A.S.C.E., Journal of Geotechnical Engineering*, Vol 121 (3), pp. 287-298.

Evans, N.C., Huang, S.W. and King, J.P. (1997) *The natural terrain landslide study, Phases I and II.* Special Project Report SPR 5/97, Geotechnical Engineering Office, Civil Engineering Department, Hong Kong.

Fannin, R.J. and Rollerson, T.P. (1992) Debris flows: some physical characteristics and behaviour. *Canadian Geotechnical Journal*, Vol 30, pp. 71-81.

Fannin, R.J., Wise, M.P., Wilkinson, J.M. and Rollerson, T.P. (1996) Landslide initiation and runout on clearcut hillslopes. *Proceedings of the Seventh International Symposium on Landslides*, (Senneset ed.) Trondheim, Norway, Balkema. Vol. 1, pp. 195-199.

Farhi, F.J. and Hamon, M. (1967) Djatiluhur dam. Fill deformations and core cracking (in French). *Proceedings of the 9th International Congress on Large Dams*, Istanbul, ICOLD. pp. 457-478 (C.10).

Fear, C.E. and McRoberts, E.C. (1995) Reconsideration of initiation of liquefaction in sandy soils. *A.S.C.E., Journal of Geotechnical Engineering*, Vol 121 (3), pp. 249-261.

Fell, R. (2002) *Personnel communication with Prof. Fell of University of New South Wales, Australia*.

Fell, R., Hungr, O., Leroueil, S. and Riemer, W. (2000) Keynote lecture - Geotechnical engineering of the stability of natural slopes, and cuts and fills in soil. *Proceedings of the International Conference on Geotechnical and Geological Engineering (GeoEng2000)*, Melbourne, Technomic, Lancaster. Vol. 1, pp. 21-120.

Fell, R., MacGregor, J.P. and Stapleton, D. (1992) *Geotechnical Engineering of Embankment Dams*. Balkema, Rotterdam, pp. 675.

Fell, R., MacGregor, J.P. and Stapleton, D. (in press) *Geotechnical Engineering of Embankment Dams*.

Fell, R., Wong, P. and Stone, P. (1987) Slope instability in soft ground. *Soil Slope Instability and Stabilisation*, (Walker & Fell ed.) Balkema, Rotterdam. pp. 231-278.

Ferkh, Z. and Fell, R. (1994) Design of embankments on soft clay. *Proceedings, 13th International Conference on Soil Mechanics and Foundation Engineering*, New Delhi, Balkema, Rotterdam. pp. 733-738.

Fetzer, C.A. (1967) Electro-osmotic stabilisation of West Branch Dam. *A.S.C.E., Journal of the Soil Mechanics and Foundations Division*, Vol. 93 (SM4), pp. 85-106.

Finlay, P.J., Fell, R. and Maguire, P.K. (1997) Relationship between the probability of landslide occurrence and rainfall. *Canadian Geotechnical Journal*, Vol. 34 (6), pp. 811-824.

Finlay, P.J., Mostyn, G.R. and Fell, R. (1999) Landslide risk assessment: prediction of travel distance. *Canadian Geotechnical Journal*, Vol. 36, pp. 556-562.

Fitzpatrick, M.D., Cole, B.A., Kinstler, F.L. and Knoop, B.P. (1985) Design of concrete-faced rockfill dams. *Proceedings of the Symposium on Concrete Face Rockfill Dams - Design, Construction and Performance*, (Cooke and Sherard ed.) Detroit, Michigan, ASCE New York. pp. 410-434.

Fitzpatrick, M.D., Liggins, T.B. and Barnett, R.H.W. (1982) Ten years of surveillance of Cethana dam. *Proceedings of the 14th International Congress on Large Dams*, Rio de Janiero, ICOLD. pp. 847-866 (Q.52 R.51).

Fitzpatrick, M.D., Liggins, T.B., Lack, L.J. and Knoop, B.P. (1973) Instrumentation and performance of Cethana dam. *Proceedings of the 11th International Congress on Large Dams*, Madrid, ICOLD. pp. 145-164 (Q.42 R.9).

Fleming, R.W., Ellen, S.D. and Algus, M.A. (1989) Transformation of dilative and contractive landslide debris into debris flows - An example from Marin County, California. *Engineering Geology*, Vol 27, pp. 201-223.

Folkes, D.J. and Crooks, J.H.A. (1985) Effective stress paths and yielding in soft clays below embankments. *Canadian Geotechnical Journal*, Vol 22, pp. 357-374.

Folkes, D.J. and Crooks, J.H.A. (1986) Reply: Effective stress paths and yielding in soft clays below embankments. *Canadian Geotechnical Journal*, Vol 23, pp. 413.

Forza, S.J. and Hancock, D.J. (1995a) *Cethana dam, Surveillance Report No. 2 (1982 - 1995).* Report ENE-0010-SF-004, Hydro-Electric Commission Tasmania, Civil and Water Resources Engineering Group.

Forza, S. and Hancock, D. (1995b) *Tullabardine dam, Surveillance Report No. 2 (1986 - 1994).* Report ENE-0010-SF-002, Hydro-Electric Commission Tasmania, Civil and Water Resources Engineering.

Forza, S., Hancock, D. and Young, A.J.A. (1993) *Rowallan dam: Surveillance Report No. 2 (1985 - 1993).* Report No. CDR 590, Hydro-Electric Commission, Tasmania.

Forza, S.J. and Hancock, D.J. (1993) *Serpentine dam, Surveillance Report No. 2 (1980 - 1993).* Report CDR 602, Hydro-Electric Commission Tasmania, Consulting Business Unit.

Foster, M.A. (1999) *The probability of failure of embankment dams by internal erosion and piping*. Ph.D. Thesis, The University of New South Wales, School of Civil and Environmental Engineering.

Foster, M.A., Fell, R. and Spannagle, M. (2000) The statistics of embankment dam failures and accidents. *Canadian Geotechnical Journal*, Vol. 37, pp. 1000-1024.

Fourie, A.B. (2000) Static liquefaction as the mechanism for flow failures of tailings dams under non-seismic conditions. *Proceedings of the International Conference on Geotechnical and Geological Engineering (GeoEng2000)*, Melbourne, Vol. 1, pp. 1263-1269.

Fox, S.D. and Fyfe, G.E. (2001) It's more fun when you do it yourself - constructing the Lake Eppalock main embankment remedial works project. *ANCOLD Bulletin*, Issue 118 (August), pp. 71-79.

Franks, C.A.M. (1995) *Engineering Geological Assessment of landslide at Milestone 14.5 on the Castle Peak Road.* Geological Report GR 1/95, Geotechnical Engineering Office, Civil Engineering Department, Hong Kong.

Franks, C.A.M. (1996) *Study of rainfall induced landslides on natural slopes in the vicinity of Tung Chung New Town, Lantau Island.* Special Project Report SPR 4/96, Geotechnical Engineering Office, Civil Engineering Department, Hong Kong.

Fredlund, D.G. and Rahardjo, H. (1993) *Soil mechanics for unsaturated soils*. John Wiley & Sons, New York, pp. 517.

Fugro Scott Wilson Joint Venture (1999a) *Detailed study of the landslide at Fung Wong Reservoir on 9 June 1998.* LSR 5/99, Geotechnical Engineering Office, Civil Engineering Department, Government of Hong Kong.

Fugro Scott Wilson Joint Venture (1999b) *Detailed study of the landslide below Au Tau Village Road, Tseung Kwan O on 9 June 1998.* LSR 6/99, Geotechnical Engineering Office, Civil Engineering Department, Government of Hong Kong.

Fugro Scott Wilson Joint Venture (1999c) *Detailed study of the landslide The Outward Bound School on 9 June 1998.* LSR 7/99, Geotechnical Engineering Office, Civil Engineering Department, Government of Hong Kong.

Fugro Scott Wilson Joint Venture (1999d) *Detailed study of the landslides at Yue Sun Garden, Wo Mei on 9 June 1998.* LSR 8/99, Geotechnical Engineering Office, Civil Engineering Department, Government of Hong Kong.

Galloway, J.D. (1939) The design of rock-fill dams. *ASCE, Transactions*, Vol. 104, pp. 1-24.

Galloway, J.H.H. (1970) *Matahina Power Project: Earth dam design report.* Report No. 92/12/75/4/1, Ministry of Works New Zealand, Power Design Office.

Gamboa, J. and Benassini, A. (1967) Behavior of Netzahualcoyotl dam during construction. *A.S.C.E., Journal of the Soil Mechanics and Foundations Division*, Vol. 93 (SM4), pp. 211-229.

Geotechnical Engineering Office (1994) *Report on the Kwun Lung Lau landslide of 23 July 1994.* Volume 2, Civil Engineering Department, Hong Kong Government.

Geotechnical Engineering Office (1996a) *Report on the Fei Tsui Road landslide of 13 August 1995.* Volume 2, Civil Engineering Department, Hong Kong Government.

Geotechnical Engineering Office (1996b) *Report on the Shum Wan Road landslide of 13 August 1995.* Volume 2, Civil Engineering Department, Hong Kong Government.

Gerke, D., Forza, S.J. and Hancock, D.J. (1995) *Murchison dam, Surveillance Report No. 2 (1985 - 1995).* Report ENE-0010-SF-005, Hydro-Electric Commission Tasmania, Civil and Water Resources Engineering Group.

Gerke, D. and Hancock, D. (1995) *Parangana dam: Surveillance Report No. 2 (1986 - 1994).* Report No. ENE-0010-SF-001, Hydro-Electric Commission Tasmania, Civil and Water Resources Engineering.

Gerke, D., Quinlan, P. and Hancock, D.J. (1993) *Scotts Peak dam, Surveillance Report No. 2 (1985 - 1993).* Report CDR 570, Hydro-Electric Commission Tasmania, Consulting Business Unit.

Giron, F.C. (1997) Collapse settlement in the Canales dam. *Proceedings of the 19th International Congress on Large Dams*, Florence, ICOLD. pp. 197-203 (Q73, Contribution 2).

Giudici, S., Herweynen, R. and Quinlan, P. (2000) Hydro-Electric Commission experience in concrete faced rockfill dams - past, present and future. *Proceedings of the International Symposium on Concrete Faced Rockfill Dams*, Beijing, ICOLD. pp. 29-46.

Giuliani, F.L. and Pujol, A. (1985) Seepage and slide downstream slope Arroyito Dam, Argentina remedial measures. *Fifteenth International Congress on Large Dams*, Lausanne, ICOLD. pp. 43-50 (Q.59 R.4).

Glastonbury, J. and Fell, R. (2000) *Report on the analysis of "rapid" natural rock slope failures.* UNICIV Report R-390, The University of New South Wales, School of Civil and Environmental Engineering.

Glastonbury, J., Fell, R. and Mostyn, G. (2002) *Report on the post-collapse behaviour of debris from rock slope failures.* UNICIV Report No. R-406, The University of New South Wales, School of Civil and Environmental Engineering.

Golder Associates Limited (1994) *Failure run-out characteristics of mine waste dumps in mountainous terrain.* Unpublished report to the Canadian Centre for Mineral and Energy Technology, Edmonton. Prepared in association with O. Hungr Geotechnical Research Ltd.

Golder Associates Limited (1995) *Mined rock and overburden piles: Runout characteristics of debris from dump failures in mountainous terrain. Stage 2: Analysis, modelling and prediction.* Interim Report British Columbia Mine Waste Rock Pile Research Committee and CANMET, In conjunction with O. Hungr Geotechnical Research Ltd.

Goldsmith, R.C.M. (1977) *Geological report on construction of the Googong dam, Queanbeyan River, New South Wales, 1975-1977.* Report No. GOG.51, Department of National Development, Bureau of Mineral Resources, Geology and Geophysics.

Gonzales, F.V. and Mena, E.S. (1997) Aguamilpa dam behaviour. *Non-Soil Water Barriers for Embankment Dams, 17th Annual USCOLD Lecture Series*, San Diego, California, USCOLD. pp. 133-147.

Good, R.J. (1976) Kangaroo Creek dam. Use of a weak schist as rockfill for a concrete faced rockfill dam. *Proceedings of the 12th International Congress on Large Dams*, Mexico, ICOLD. pp. 645-665 (Q.44 R.33).

Good, R.J. (1981) Behaviour of concrete faced rolled rockfill dams in South Australia. *ANCOLD Bulletin*, Vol 59, pp. 45-56.

Good, R.J., Bain, D.L.W. and Parsons, A.M. (1985) Weak rock in two rockfill dams. *Proceedings of the Symposium on Concrete Face Rockfill Dams - Design, Construction and Performance*, (Cooke and Sherard ed.) Detroit, Michigan, ASCE New York. pp. 40-72.

Gosden, G.D., Belland, G.J. and Parsons, A.M. (2002) Hope Valley dam safety investigation and remedial works. *ANCOLD Bulletin*, Issue 120 (April), pp. 89-99.

Gosschalk, E.M. and Kulasinghe, A.N.S. (1985) Kotmale dam and observations on CFRD. *Proceedings of the Symposium on Concrete Face Rockfill Dams - Design, Construction and Performance*, (Cooke and Sherard ed.) Detroit, Michigan, ASCE New York. pp. 379-395.

Gosschalk, E.M. and Kulasinghe, A.N.S. (1987) Closure to discussion on paper: Kotmale dam and observations on CFRD. *A.S.C.E., Journal of Geotechnical Engineering*, 113 (10), pp. 1202-1208.

Goulburn-Murray Water (1999) *Lake Dartmouth: Report on dam safety surveillance and behaviour (June 1998 to September 1998).*

Gould, J.P. (1953) The compressibility of rolled fill materials determined from field observations. *Proceedings of the Third International Conference on Soil Mechanics and Foundation Engineering*, Switzerland, Vol. 2, pp. 239-244.

Gould, J.P. (1954) *Compression characteristics of rolled fill materials in earth dams.* Technical Memorandum No. 648, United States Department of the Interior, Bureau of Reclamation.

Government of Hong Kong (1977) *Report on the slope failures at Sau Mau Ping August 1976.* Report 67675-7K-1/77.

Graham, J., Crooks, J.H.A. and Bell, A.L. (1983) Time effects on the stress-strain behaviour of natural soft clays. *Geotechnique*, Vol 33 (3), pp. 327-340.

Gray, E.W. (1972) Construction pore pressure dissipation in earth dams. *Proceedings of the Speciality Conference on Performance of Earth and Earth Retaining Structures*, Purdue University, Indianna, ASCE, New York. Vol. III, pp. 295-314.

Gregersen, O. (1981) The quick clay slide at Rissa, Norway. *Proceedings of the 10th International Conference on Soil Mechanics and Foundation Engineering*, Stockholm, Balkema, Rotterdam. Vol. 3, pp. 421-426.

Gregersen, O. and Loken, T. (1979) The quick-clay slide at Baastad, Norway, 1974. *Engineering Geology*, Vol 14, pp. 183-196.

Gregory, C.H. (1844) On railway cuttings and embankments; with an account of some slips in the London clay; on the line of the London and Croydon Railway. *Minutes of the Proceedings of Civil Engineers*, Vol. 3 (March 26), pp. 135-173.

Grimston, J.O. (1989) *Surveillance report: Geehi dam 1966 - 1989.* Snowy Mountains Hydro-Electric Authority, Civil Group.

Gu, W.H., Morgenstern, N.R. and Robertson, P.K. (1993) Progressive failure of Lower San Fernando Dam. *A.S.C.E., Journal of Geotechnical Engineering*, Vol 119 (2), pp. 333-349.

Guadagno, F.M. (1991) Debris flows in the Campanian volcaniclastic soils. *Proceedings of the International Conference on Slope Stability*, Isle of Wight, Thomas Telford. pp. 125-130.

Gutierrez, M. (1998) Written statement: Theoretical/Conceptual Issues. Discussion. *National Science Foundation Workshop on Shear Strength of Liquefied Soils*, (Stark Olson Kramer and Youd ed.) Urbana, Illinois, National Science Foundation. pp. 88-89.

Gutteridge Haskins and Davey Pty Ltd (1995a) *Surveillance review report for Geehi dam.* for Snowy Mountains Hydro-Electric Authority.

Gutteridge Haskins and Davey Pty Ltd (1995b) *Surveillance review report for Tooma dam.* for Snowy Mountains Hydro-Electric Authority.

H.M.S.O. (1967) *Report of the Tribunal appointed to inquire into the disaster at Aberfan on October 21st, 1966.* Her Majesty's Stationery Office, London.

Hacelas, J.E., Ramirez, C.A. and Regalado, G. (1985) Construction and performance of Salvajina dam. *Proceedings of the Symposium on Concrete Face Rockfill Dams - Design, Construction and Performance*, (Cooke and Sherard ed.) Detroit, Michigan, ASCE New York. pp. 286-315.

Hadgraft, R.G. (1984) *Design report for main dam: Bjelke-Petersen dam.* (Internal report) Queensland Water Resources Commission.

Halcrow Asia Partnership Ltd. (1998a) *Report on the Ching Cheung Road landslide of 3 August 1997.* Geotechnical Engineering Office, Civil Engineering Department, Government of Hong Kong.

Halcrow Asia Partnership Ltd. (1998b) *Report on the landslide at Ten Thousand Buddhas' Monastery on 2 July 1997.* Geotechnical Engineering Office, Civil Engineering Department, Government of Hong Kong.

Halcrow Asia Partnership Ltd. (1998c) *Report on the landslides at Hut No. 26 Kau Wa Keng Upper Village on 4 June 1997.* Geotechnical Engineering Office, Civil Engineering Department, Government of Hong Kong.

Halcrow Asia Partnership Ltd. (1999a) *Investigation of some selected landslide incidents in 1997 (Volume 2).* GEO Report 88, Geotechnical Engineering Office, Civil Engineering Department, Government of Hong Kong.

Halcrow Asia Partnership Ltd. (1999b) *Investigation of some selected landslide incidents in 1997 (Volume 3).* GEO Report 89, Geotechnical Engineering Office, Civil Engineering Department, Government of Hong Kong.

Halcrow Asia Partnership Ltd. (1999c) *Investigation of some selected landslide incidents in 1997 (Volume 4).* GEO Report 90, Geotechnical Engineering Office, Civil Engineering Department, Government of Hong Kong.

Halcrow Asia Partnership Ltd. (1999d) *Investigation of some selected landslide incidents in 1997 (Volume 5).* GEO Report 91, Geotechnical Engineering Office, Civil Engineering Department, Government of Hong Kong.

Halcrow Asia Partnership Ltd. (1999e) *Investigation of some selected landslide incidents in 1997 (Volume 6).* GEO Report 92, Geotechnical Engineering Office, Civil Engineering Department, Government of Hong Kong.

Harder, L.F. (1997) Application of the Becker penetration test for evaluating the liquefaction potential of gravelly soils. *Proceedings of the NCEER Workshop on Evaluation of Liquefaction Resistance of Soils,* (Youd and Idriss ed.) Salt Lake City, Utah, National Centre for Earthquake Engineering Research. pp. 129-148.

Hazen, A. (1918) A study of the slip in the Calaveras Dam. *Engineering News Record*, Vol 81, (26 (Dec 26)), pp. 1158-1164.

Hazen, A. and Metcalf, L. (1918) Middle section of upstream slide of Calaveras Dam slips into reservoir. *Engineering News Record*, Vol 80, (14 (April 4)), pp. 679-681.

He, G. (2000) Technical study on crest overflow of concrete face rockfill dams. *Proceedings of the International Symposium on Concrete Faced Rockfill Dams*, Beijing, ICOLD. pp. 283-291.

HECEC Australia Pty Ltd (1999) *Tullaroop dam. Report on comprehensive dam inspection March 1999.* for Goulburn-Murray Water.

Heim, A. (1932) *Landslides and human lives (Bergsturz and Menchen leben). N. Skermer, translator*. Bi-Tech Publishers, Vancouver, pp. 196.

Heinrichs, P.W. (1996) Mangrove Creek dam embankment behaviour and surveillance. *ANCOLD Bulletin*, No. 102 (April), pp. 22-34.

Heitlinger, D., Moffatt, T.S. and Little, D.J. (1965) Design and construction of Eppalock earth and rockfill dam, and turbine-pumping station, on the Campaspe River, Victoria. *The Journal of the Institution of Engineers, Australia* (Oct-Nov), pp. 325-356.

Henkel, D.J. (1956) Discussion on paper by Watson: Earth movement affecting L.T.E. railway in deep cutting east of Uxbridge. *Proceedings of the Institution of Civil Engineers*, Vol. 5, Part 2 (27 March), pp. 320-323.

Henkel, D.J. (1957) Investigations of two long-term failures in London clay slopes at Wood Green and Northolt. *Proceedings of the Fourth International Conference on Soil Mechanics and Foundation Engineering*, London, Vol. 2, pp. 315-320.

Henkel, D.J. (1961) The shear strength of saturated remoulded clays. *Proceedings of the ASCE Research Conference on Shear Strength of Cohesive Soils*, Boulder, Colorado, pp. 533-554.

Hickox, R.W. and Murray, B.C. (1983) *Structural behavior report: Belle Fourche Dam.* United States Bureau of Reclamation, Division of Dam Safety, Structural Behavior Branch.

Hickox, R.W. and Murray, B.C. (1984) *Structural behavior report: San Luis dam, Central Valley Project, California, Mid-Pacific Region.* United States Bureau of Reclamation, Division of Dam Safety, Structural Behavior Branch, Embankment Dam Instrumentation Section.

Hilf, J.W. (1948) Estimating construction pore pressures in rolled earth dams. *Proceedings, 2nd International Conference on Soil Mechanics and Foundation Engineering*, Rotterdam, Vol. 3, pp. 234-240.

Hilton, J.R., Gibson, E.J.R. and Pinkerton, I.L. (1974) *Geehi dam project. Geehi dam: Final design report.* Technical Memorandum No. C.D. 226, Snowy Mountains Hydro-Electric Authority, Civil Engineering Design Division.

HKIE Geotechnical Division (1998) *Soil nails in loose fill. A preliminary study.* Draft Report Hong Kong Institution of Engineers, Geotechnical Division.

Höeg, K., Andersland, O.B. and Rolfsen, E.N. (1969) Undrained behaviour of quick clay under load tests as Asrum. *Geotechnique*, Vol 19 (1), pp. 101-115.

Holomek, S. (1994) Safety evaluation methods of Dalesice dam. *Proceedings of the 18th International Congress on Large Dams*, Durban, ICOLD. Vol. 1, pp. 19-28 (Q.68 R.03).

Holton, I.R. (1992) In-service deformation of a puddle clay core dam. *Dams and Reservoirs*, Vol 2 (1), pp. 12-18.

Holtz, R.D. and Holm, G. (1979) Test embankment on an organic silty clay. *Proceedings, Seventh European Conference on Soil Mechanics and Foundation Engineering*, Brighton, England, British Geotechnical Society. Vol. 3, pp. 79-86.

Holtz, R.D. and Kovac, W.D. (1981) *An Introduction to Geotechnical Engineering*. (N. M. Newmark and W. J. Hall ed.), Prentice Hall, New Jersey, pp. 733.

Hong, S.W., Sohn, J.I., Bae, G.J., Ahn, S.R., Um, Y.S. and Park, E.Y. (1994) A case study of rockfill dam: Stability evaluation and remedial treatment. *Proceedings of the 13th International Conference on Soil Mechanics and Foundation Engineering*, New Delhi, Balkema, Rotterdam. pp. 967-970.

Howard, S.R., Gardner, P.E.J., McConnel, A.D., Gibson, E.J.R. and Pinkerton, I.L. (1974) *Khancoban and Murray 2 projects. Khancoban dam and excavation for Murray 2 power station. Final design report.* Technical Memorandum No. C.D. 277, Snowy Mountains Hydro-Electric Authority, Civil Engineering Design Division.

Howard, S.R., Hilton, J.I., Bell, G.J., Gibson, E.J.R. and Pinkerton, I.L. (1978) *Tumut 3 project. Talbingo dam, spillway, headrace channel & pipeline inlet structure. Final design report.* Technical Memorandum No. C.D. 285, Snowy Mountains Hydro-Electric Authority, Civil Engineering Design Division.

Howard, T.R., Baldwin, J.E. and Donley, H.F. (1988) Chapter 9. Landslides in Pacifica, California, caused by the storm. In Landslides, floods, and marine effects of the storm of January 3-5, 1982, in the San Francisco Bay region, California. U.S. Geological Survey Professional Paper 1434 (Ellen & Wieczorek ed.), U.S. Geological Survey, pp. 163-183.

Howley, I.A. (1971) *King River Project: Report on rockfill in the main embankment.* State Rivers and Water Supply Commission Victoria.

Howson, G.W. (1939) Discussion on paper by Galloway: The design of rock-fill dams. *ASCE, Transactions*, Vol. 104, pp. 42-45.

Hsü, K.J. (1975) Catastrophic debris streams (sturzstroms) generated by rockfalls. *Geological Society of America Bulletin*, Vol 86, pp. 129-140.

Huang, Y., Peng, Z., Si, H. and Li, G. (1993) Monitoring and performance of Xibeikou CFRD. *Proceedings of the International Symposium on High Earth-Rockfill Dams*, (Jiang, Zhang & Qin ed.) Beijing, Vol. 1, pp. 475-482.

Humphrey, D.N. and Leonards, G.A. (1986) Slide in the upstream slope of Lake Shelbyville Dam. *Journal of Geotechnical Engineering, ASCE*, Vol. 112 (5), pp. 564-577.

Humphrey, D.N. and Leonards, G.A. (1988) Closure: Slide in the upstream slope of Lake Shelbyville Dam. *Journal of Geotechnical Engineering, ASCE*, Vol. 114 (4), pp. 510-513.

Hungr Geotechnical Research Inc. (1998) *Mobility of landslide debris in Hong Kong: Pilot back analyses using a numerical model.* Geotechnical Engineering Office, Hong Kong.

Hungr, O. (1990) Mobility of Rock Avalanches. *Report of the National Research Institute for Earth Science and Diaster Prevention, Tsukuba, Japan*, No. 46, pp. 11-20.

Hungr, O. (1995) A model for the runout analysis of rapid flow slides, debris flows, and avalanches. *Canadian Geotechnical Journal*, Vol 32, pp. 610-623.

Hungr, O., Dawson, R.F., Kent, A., Campbell, D. and Morgenstern, N.R. (1998) Rapid flow slides of coal mine waste in British Columbia, Canada. *Submitted for Publication to Canadian Geotechnical Journal*.

Hungr, O. and Kent, A. (1995) Coal mine waste dump failures in British Columbia, Canada. *Landslide News*, No. 9 (Dec.), pp. 26-28.

Hunter, G. and Fell, R. (2001) *"Rapid" failure of soil slopes.* UNICIV Report No. R-400, The University of New South Wales, School of Civil and Environmental Engineering.

Hunter, G. and Fell, R. (2002a) *The deformation behaviour of rockfill.* UNICIV Report No. R-405, The University of New South Wales, School of Civil and Environmental Engineering.

Hunter, G. and Fell, R. (2002b) *Post failure deformation of slides in embankment dams and cut slopes in over-consolidated high plastic clays.* UNICIV Report No. R-411, The University of New South Wales, School of Civil and Environmental Engineering.

Hunter, G. and Fell, R. (2003) *The deformation behaviour of embankment dams*. UNICIV Report No. R-416, The University of New South Wales, School of Civil and Environmental Engineering.

Hunter, G., Fell, R. and Khalili, N. (2000) *The deformation behaviour of embankments on soft ground.* UNICIV Report No. R-391, The University of New South Wales, School of Civil and Environmental Engineering.

Hunter, J.R. and Bacon, G.A. (1970) Behaviour of Blowering dam embankment. *Proceedings of 10th the International Congress on Large Dams*, Montreal, ICOLD. pp. 217-242 (Q.38 R.15).

Hunter, J.R., Gibson, E.J.R. and Pinkerton, I.L. (1974) *Tooma - Tumut project. Tooma dam: Final design report.* Technical Memorandum No. C.D. 227, Snowy Mountains Hydro-Electric Authority, Civil Engineering Design Division.

Hutchinson, J.N. (1961) A landslide on a thin layer of quick clay at Furre, central Norway. *Geotechnique*, Vol 11 (2), pp. 69-94.

Hutchinson, J.N. (1965) *The landslide of February, 1959, at Vibstad in Namdalen.* Publication 61, Norwegian Geotechnical Institute.

Hutchinson, J.N. (1986) A sliding-consolidation model for flow slides. *Canadian Geotechnical Journal*, Vol 23, pp. 115-126.

Hutchinson, J.N. (1988) General Report: Morphological and geotechnical parameters of landslides in relation to geology and hydrogeology. *Proceedings of the Fifth International Symposium on Landslides*, (Bonnard ed.) Lausanne, Switzerland, Balkema. Vol. 1, pp. 3-35.

Hydro Electric Commission (1991a) *Dams Surveillance Report, Bastyan Dam, 1986 - 1991 (No. 2).* Report CDR 560, HEC Tasmania, Safety of Dams Unit.

Hydro Electric Commission (1991b) *Dams Surveillance Report, Mackintosh Dam, 1985 - 1991 (No. 2).* Report CDR 559, HEC Tasmania, Safety of Dams Unit.

Hydro Electric Commission Tasmania (1987) *Anthony power development, specification for excavation and rockfill for White Spur dam.* Specification C.E. 2023.

Hydro Technology (1995) *Cairn Curran Reservoir: Safety Surveillance 1994 and Formal Dam Safety Inspection 17 November 1994.* Report No. 90/10351, Rural Water Corporation, Victoria.

ICOLD (1974) *Lessons from Dam Incidents*. In (Committee on Failures and Accidents to Large Dams ed.), ICOLD, pp. 1069.

ICOLD (1989a) *Moraine as embankment and foundation material.* Bulletin No. 69, International Commission on Large Dams.

ICOLD (1989b) *Rockfill dams with concrete facing. State of the art.* Bulletin 70, International Commission on Large dams.

ICOLD (1993) *Rock materials for rockfill dams.* Bulletin No. 92, International Commission on Large Dams.

Ikeya, H. (1989) Debris flows and its countermeasures in Japan. *Bulletin of the International Association of Engineering Geology,* Bulletin No. 40, pp. 15-33.

Imam, S.M.R., Morgenstern, N.R., Robertson, P.K. and Chan, D.H. (2002) Yielding and flow liquefaction of loose sand. *Soils and Foundations*, Vol 42 (3), pp. 19-31.

Indraratna, B., Balasubramanian, A.S. and Balachandran, S. (1992) Performance of test embankment constructed to failure to failure on soft marine clay. *A.S.C.E., Journal of Geotechnical Engineering*, Vol 118 (1), pp. 12-33.

Irfan, T.Y. (1997) Occurrence investigation and analysis of structurally controlled landslides in weathered rock. *Submitted for Publication to Quarterly Journal Engineering Geology*.

Irfan, T.Y. and Woods, N.W. (1998) Discontinuity controlled landslides in weathered rocks in Hong Kong. *Submitted for Publication to Transactions, Hong Kong Institution of Engineers*.

Ishihara, K. (1985) Stability of natural deposits during earthquakes. *Proceedings of the 11th International Conference on Soil Mechanics and Foundation Engineering*, San Francisco, Vol. 1 pp. 321-376.

Ishihara, K. (1993) Liquefaction and flow failure during earthquakes. *Geotechnique*, Vol 43 (3), pp. 351-415.

IUGS Working Group on Landslides (1995) *A suggested method for describing the rate of movement of a landslides.* Bulletin 52, pp 75-78, International Association of Engineering Geology.

Iverson, R.M., Reid, M.E. and LaHusen, R.G. (1997) Debris flow mobilisation from landslides. *Annual Review of Earth and Planetary Sciences*, Vol. 25, pp. 85-138.

Jacobson, G. (1965) *Nillahcootie damsite: Geology.* Progress Report No. 1, State Rivers and Water Supply Commission, Victoria.

James, P.M. (1970) *Time effects and progressive failure in clay slopes*. Ph.D. Thesis, London University.

Japanese National Committee on Large Dams (1976) *Dams in Japan*. JNCOLD.

Jardine, R.J. and Hight, D.W. (1987) The behaviour and analysis of embankments on soft clay. In Embankments on Soft Ground Public Works Research Centre, Greece, pp. 195-244.

Jefferies, M. (1998) Written statement: Theoretical/Conceptual Issues. Discussion. *National Science Foundation Workshop on Shear Strength of Liquefied Soils*, (Stark Olson Kramer and Youd ed.) Urbana, Illinois, National Science Foundation. pp. 93-97.

Jennings, J.E. (1979) The failure of a slimes dam at Bafokeng, mechanism of failure and associated design considerations. *The Civil Engineer in South Africa*, Vol 21 (6), pp. 135-141.

Jeyapalan, J.K., Duncan, J.M. and Seed, H.B. (1983a) Analyses of flow failures of mine tailings dams. *A.S.C.E., Journal of the Geotechnical Engineering Division*, Vol 109 (2), pp. 150-171.

Jeyapalan, J.K., Duncan, J.M. and Seed, H.B. (1983b) Investigation of flow failures of tailings dams. *A.S.C.E., Journal of the Geotechnical Engineering Division*, Vol 109 (2), pp. 172-189.

Jiyuan, S., Zhu, B. and Liang, C. (2000) Characteristic and experience of the design, construction and performance of TSQ-1 concrete faced rockfill dam. *Proceedings of the International Symposium on Concrete Faced Rockfill Dams*, Beijing, ICOLD. pp. 97-105.

Johnson, A.M. (1980) *Disasters at Aberfan, South Wales and at Buffalo Creek, West Virginia*. National Academy of Sciences, Committee on Excess Spoils from Coal Mining.

Johnson, A.M. and Rodine, J.R. (1984) Debris flow. In Slope Instability (Brunsden and Prior ed.), John Wiley, pp. 257-361.

Jones, O.T. (1955) Construction of the Cobb earthfill dam. *New Zealand Engineering* (15th November), pp. 353-360.

Jones, O.T. (1965) Design of Benmore earth dam. *New Zealand Engineering* (January), pp. 13-23.

Josseaume, H., Blondeau, F. and Pilot, G. (1977) Etude du comportment non draine de trios argyles molles application au calcul de remblais. *Proceedings, International Symposium on Soft Clay*, (Brenner & Brand ed.) Bangkok, Asian Institute of Technology. pp. 487-504.

Justo, J.L. (1991) Collapse: Its importance, fundamentals and modelling. In Advances in Rockfill Structures (Maranha das Neves ed.), Kluwer Academic Publishers, Netherlands, pp. 97-152.

Kanbayashi, Y., Maeoka, M. and Harita, K. (1979) Deformation at the interface between embankment and foundation of Terauchi dam. *Proceedings of the 13th International Congress on Large Dams*, New Delhi, ICOLD. pp. 459-479 (Q.48 R.26).

Karasawa, S., Shimazu, Y., Shirakawa, N. and Kuwashima, T. (1994) A consideration of the behaviour of zoned rockfill dams. *Proceedings of the 18th International Congress on Large Dams*, Durban, ICOLD. pp. 851-882 (Q.68 R.52).

Karlsrud, K. and Edgars, L. (1982) Some aspects of submarine slope stability. *Proc. NATO Workshop on Marine Slides and Other Mass Movements*, (Nieuwenhuis, Saxov and Svend ed.) Algarve, Portugal, Plenum Press. pp. 61-81.

Kawashima, T. and Kanazawa, K. (1982) Design of rockfill dams on weathered foundation with large scale faults. *Proceedings of the 14th International Congress on Large Dams*, Rio de Janiero, ICOLD. Vol. 2, pp. 75-99 (Q.53 R.5).

Kennard, J. (1955) Difficulty experienced in the construction of the Hollowell dam, Northampton. *Proceedings of the 5th International Congress on Large Dams*, Paris, ICOLD. pp. 467-474 (Q.18 R.58).

Kennard, J. and Kennard, M.F. (1962) Selset Reservoir: design and construction. *Proceedings of the Institution of Civil Engineers*, Vol. 21 (Feb.), pp. 277-304.

Khalili, N. (2002) *Personnel communication with Dr. Khalili of University of New South Wales, Australia*.

Khalili, N., Fell, R. and Tai, K.S. (1996) A simplified method for estimating failure induced deformation in embankments. *Proceedings, Seventh International Symposium on Landslides*, (Senneset ed.) Trondheim, Norway, Balkema, Rotterdam. Vol. 2, pp. 1263-1268.

Kim, S.K., Hong, W.P. and Kim, Y.M. (1991) Prediction of rainfall triggered landslides in Korea. *Proceedings of the Sixth International Symposium on Landslides*, (Bell ed.) Christchurch, Balkema, Rotterdam. Vol. 2 pp. 989-994.

Kim, Y.I. (1979) Dam behaviour measured by embedded instruments. *Proceedings of the 13th International Congress on Large Dams*, New Delhi, ICOLD. pp. 419-438 (Q.49 R.28).

King, J.P. (1996) *The Tsing Shan debris flow.* Special Project Report SPR 6/96 (Volumes 1, 2 and 3), Geotechnical Engineering Office, Civil Engineering Department, Hong Kong.

King, J.P. (1997) *Natural terrain landslide study, Damage to Lui Pok School by a natural terrain landslide.* Discussion Note DN 2/97, Geotechnical Engineering Office, Civil Engineering Department, Hong Kong.

Kinney, J.L. and Bartholomew, C.L. (1987) *Structural behaviour report: Pueblo dam.* United States Bureau of Reclamation, Division of Dam Safety, Structural Behavior Branch, Concrete Dam Instrumentation Section.

Kisa, H. and Fukuroi, H. (1994) Safety evaluation of the deformation behaviour of rockfill dams based on the long-term observation. *Proceedings of the 18th International Congress on Large Dams*, Durban, ICOLD. pp. 829-850 (Q.68 R.51).

Kjœrnsli, B., Kvale, G., Lunde, J. and Mathiesen, J.B. (1982) Design, construction control and perfermance of Svartevann earth-rockfill dam. *Proceedings of the 14th International Congress on Large Dams*, Rio de Janiero, ICOLD. pp. 319-337 (Q.55 R.19).

Kleiner, D.E. (1976) Design and construction of an embankment dam to impound gypsum wastes. *12th International Congress on Large Dams*, Mexico City, ICOLD. Vol. 1, pp. 235-249 (Q44 R12).

Knight, R.G. (1938) The subsidence of a rockfill dam and the remedial measures employed at Eildon Reservoir, Australia. *Journal of the Institution of Civil Engineers Australia* (March), pp. 111-208.

Knill, J. (1996a) *Report on the Fei Tsui Road landslide of 13 August 1995.* Volume 1, for Geotechnical Engineering Office, Civil Engineering Department, Hong Kong Government.

Knill, J. (1996b) *Report on the Shum Wan Road landslide of 13 August 1995.* Volume 1, for Geotechnical Engineering Office, Civil Engineering Department, Hong Kong Government.

Knoop, B.P. (1982a) *Performance design report on Murchison dam.* Report CDR 433, Hydro-Electric Commission Tasmania, Civil Design Section.

Knoop, B.P. (1982b) *Report on the performance of Mackintosh Dam.* Report CDR 421, Hydro-Electric Commission Tasmania.

Knoop, B.P. and Lack, L.J. (1985) Instrumentation and performance of concrete faced rockfill dams in the Pieman River power development. *Proceedings of the 15th International Congress on Large Dams*, Lausanne, ICOLD. pp. 1103-1120 (Q.56 R.58).

Knox, G. (1927) Landslides in South Wales valleys. *Proceedings of the South Wales Institute of Engineers*, Vol 43, pp. 161-247, 257-290.

Koerner, H.J. (1977) Flow mechanisms and resistances in the debris streams of rock slides. *Bulletin of the International Association of Engineering Geology*, Vol. 16, pp. 101-104.

Koppejan, A.W., Wamelan, B.M. and Weinberg, L.J.H. (1948) Coastal flow slides in the Dutch province of Zeeland. *Proceedings of the 2nd International Conference on Soil Mechanics and Foundation Engineering*, Rotterdam, Vol. 5, pp. 89-96.

Kotzias, P.C. and Stamatopoulos, A.C. (1975) Statistical quality control at Kastraki earth dam. *A.S.C.E., Journal of the Geotechnical Engineering Division*, Vol. 101 (GT9), pp. 837-853.

Kovacevic, N. (1994) *Numerical analyses of rockfill dams, cut slopes and road embankments*. Doctor of Philosophy, London University (Imperial College of Science, Technology and Medicine), Faculty of Engineering.

Kovacevic, N., Potts, D.M., Vaughan, P.R., Charles, J.A. and Tedd, P. (1997) Assessing the safety of old embankment dams by observing and analysing movement during reservoir operation. *Proceedings of the 19th International Congress on Large Dams*, Florence, ICOLD. Vol. 2, pp. 551-566 (Q73 R35).

Kramer, S.L. (1988) Triggering of liquefaction flow slides in coastal soil deposits. *Engineering Geology*, Vol 26, pp. 17-31.

Kramer, S.L. (1998) Written statement: Theoretical/Conceptual Issues. Discussion. *National Science Foundation Workshop on Shear Strength of Liquefied Soils*, (Stark, Olson, Kramer and Youd ed.) Urbana, Illinois, National Science Foundation. pp. 104-105.

Kuerbis, R., Negussey, D. and Vaid, Y.P. (1988) Effect of gradation and fines content on the undrained response of sand. *ASCE Speciality Conference on Hydraulic Fill Structures, Geotechnical Special Publication No. 21*, (Van Zyl and Vick ed.) Fort Collins, Colorado, ASCE, New York. pp. 330-345.

Kulasinghe, A.N.S. and Tandon, G., N, (1993) Technical and behavioural aspects of Kotmale dam. *Proceedings of the International Symposium on High Earth-Rockfill Dams*, (Jiang, Zhang & Qin ed.) Beijing, pp. 233-244.

La Rochelle, P., Trak, B., Tavenas, F. and Roy, M. (1974) Failure of a test embankment on a sensitive Champlain clay deposit. *Canadian Geotechnical Journal*, Vol 11, pp. 142-164.

Ladd, C.C. (1972) Test embankment on sensitive clay. *Proceedings, ASCE Speciality Conference on Performance of Earth and Earth Retaining Structures*, Purdue University, Lafayette, Vol. 1 (1), pp. 101-128.

Ladd, C.C. (1991) Stability evaluation during staged construction (The 22nd Karl Terzaghi Lecture). *ASCE, Journal of Geotechnical Engineering*, Vol 117 (4), pp. 538-615.

Lade, P.V. (1992) Static instability and liquefaction of loose fine sandy slopes. *A.S.C.E., Journal of Geotechnical Engineering*, Vol 118 (1), pp. 51-71.

Lade, P.V. and Yamamuro, J.A. (1997) Effect of nonplastic fines on static liquefaction of sands. *Canadian Geotechnical Journal*, Vol 34, pp. 918-928.

Lambe, T.W. (1973) Predictions in soil engineering. *Geotechnique*, Vol. 23 (2), pp. 149-202.

Lambe, T.W. and Whitman, R.V. (1979) *Soil Mechanics*. Wiley & Sons, New York, pp. 553.

Land and Water Conservation NSW (1994) *Wyangala dam surveillance report.*

Land and Water Conservation NSW (1995a) *Copeton dam surveillance report.*

Land and Water Conservation NSW (1995b) *Glenbawn dam surveillance report.*

Land and Water Conservation NSW (1996) *Blowering dam: Notes for Dam Safety Committee Inspection.*

Land and Water Conservation NSW (1997) *Windemere dam surveillance report.*

Lask, E. and Reinhardt, W.G. (1986) Turks building a rock mountain. *Engineering News Record*, Vol. 217 (6), pp. 40-42.

Lauffer, H. and Schober, W. (1964) The Gepatsch rockfill dam in the Kauner Valley. *Proceedings of the 8th International Congress on Large Dams*, Edinburgh, ICOLD. pp. 635-660 (Q.34 R.39).

Lavallée, J.G., St-Arnaud, G., Gervais, R. and Hammamji, Y. (1992) Stability of the Olga C test embankment. *ASCE Geotechnical Special Publication No. 31, Stability and Performance of Slopes and Embankments II*, (Seed & Boulanger ed.) Berkeley, California, ASCE, New York. Vol. 2, pp. 1006-1021.

Lawrence, D.E., Aylsworth, J.M. and Morey, C.R. (1996) Sensitive clay flows along the South Nation River, Ontario, Canada. *Proceedings of the Seventh International Symposium on Landslides*, (Senneset ed.) Trondheim, Norway, Balkema, Rotterdam. Vol. 1, pp. 479-484.

Lefebvre, G. (1996) Soft sensitive clays. In Landslides - Investigation and Mitigation, Transportation Research Board Special Report No. 247 (Turner and Schuster ed.), National Academy Press, pp. 607-619.

Lefebvre, G., Rosenberg, P., Paquette, J. and Lavallee, J.G. (1991) The September 5, 1987, landslide on the La Grande River, James Bay, Quebec, Canada. *Canadian Geotechnical Journal*, Vol 28 (2), pp. 263-275.

Legge, G.H.H. (1970) Mulungushi and Mita Hills dams - Operation and performance. *Proceedings of the 10th International Congress on Large Dams*, Montreal, ICOLD. pp. 71-90 (Q.38 R.6).

Leonard, G.K. and Raine, O.H. (1958) Rockfill dams: Performance of TVA central core dams. *A.S.C.E., Journal of the Power Division*, Vol. 84 (PO4), pp. 1736-1 to 16.

Leroueil, S. (1996) Compressibility of clays: fundamental and practical aspects. *A.S.C.E., Journal of Geotechnical Engineering*, Vol 122 (7), pp. 534-543.

Leroueil, S. (2001) Natural slopes and cuts: movement and failure mechanisms (Thirty-ninth Rankine Lecture). *Geotechnique*, Vol. 51 (3), pp. 197-243.

Leroueil, S., Locat, J., Vaunat, J., Picarelli, L., Lee, H. and Faure, R. (1996) Geotechnical characterisation of slope movements. *Proceedings of the Seventh International Symposium on Landslides*, (Senneset ed.) Trondheim, Norway, Balkema, Rotterdam. Vol. 1, pp. 53-74.

Leroueil, S. and Marques, M.E.S. (1996) Importance of strain rate and temperature effects in geotechnical engineering. *ASCE Geotechnical Special Publication No.*

61, Measuring and Modeling Time Dependent Soil Behavior, (Sheahan & Kaliakin ed.) Washington, D.C., ASCE, New York. pp. 1-60.

Leroueil, S. and Tavenas, F. (1986) Discussion: Effective stress paths and yielding in soft clays below embankments. *Canadian Geotechnical Journal*, Vol 23, pp. 410-413.

Leroueil, S., Tavenas, F. and Le Bihan, J.-P. (1983) Proprietes caracteristiques des argiles de l'est du Canada. *Canadian Geotechnical Journal*, Vol. 20 (4), pp. 681-705.

Leroueil, S., Tavenas, F., Mieussens, C. and Peignaud, M. (1978a) Construction pore pressures in clay foundations under embankments. Part II: generalised behaviour. *Canadian Geotechnical Journal*, Vol 16, pp. 66-82.

Leroueil, S., Tavenas, F., Trak, B., La Rochelle, P. and Roy, M. (1978b) Construction pore pressures in clay foundations under embankments. Part I: the Saint-Alban test fills. *Canadian Geotechnical Journal*, Vol 16, pp. 54-65.

Li, C.Y. (1963) Placing earthfill for Columbia's Troneras dam. *Civil Engineering*, Vol. 33 (February), pp. 37-39.

Li, C.Y. (1967) Construction pore pressures in three earth dams. *A.S.C.E., Journal of the Soil Mechanics and Foundations Division*, Vol. 93 (SM2), pp. 1-26.

Li, S. (1991) *Pieman power development, Reece dam, civil design report (record).* Report CDR 551, Hydro-Electric Commission Tasmania, Civil Design Section.

Li, S.S.Y., Giudici, S. and Tindall, W.F. (1993) Design of Crotty dam and spillway. *Proceedings of the International Symposium on High Earth-Rockfill Dams*, Vol. 1, pp. 263-271.

Li, S.S.Y., Paterson, S.J. and Kinstler, F.L. (1991) A concrete faced rockfill dam constructed on a deeply weathered foundation. *Proceedings of the 17th International Congress on Large Dams*, Vienna, ICOLD. pp. 1601-1612 (Q.66 R.85).

Li-Tianchi, C. (1983) A mathematical model for predicting the extent of a major rockfall. *Zietschrift fur Geomorphologie*, Vol. 27 (4), pp. 473-482.

Liggins, T. (1971) *Mersey-Forth power development, Cethana dam, design report.* Report CDR 218, Hydro-Electric Commission Tasmania, Civil Design Division.

Linell, K.A. and Shea, H.F. (1960) Strength and deformation characteristics of various glacial tills in New England. *ASCE, Research Conference on Shear Strength of Cohesive Soils*, University of Colorado, ASCE. pp. 275-314.

Lino, M. (1997) Le glissment dans le talus amont du barrages homogene en argile humide de Mondely. *Nineteenth International Congress on Large Dams*, Florence, ICOLD. Vol. 5, pp. 617-622 (Q.75-19).

List, F. and Beier, H. (1985) The Frauenau dam monitoring and observations. *Proceedings of the 15th International Congress on Large Dams*, Lausanne, ICOLD. pp. 335-351 (Q.56 R.17).

Lloyd, H.E., Moore, O.L. and Getts, W.F. (1958) Rockfill dams: Cherry Valley central core dam. *A.S.C.E., Journal of the Power Division*, Vol. 84 (PO4), pp. 1733-1 to 24.

Lo, K.Y. and Lee, C.F. (1973) Analysis of progressive failure in clay slopes. *Proceedings of the Eighth International Conference on Soil Mechanics and Foundation Engineering*, Moscow, Vol. 1.1, pp. 251-258.

Locat, J. and Leroueil, S. (1997) Landslide stages and risk assessment issues in sensitive clays and other soft sediments. *Proc. International Workshop on Landslide Risk Assessment*, (Cruden and Fell ed.) Hawaii, Balkema, Rotterdam. pp. 261-270.

Macedo, G.G. (1999) Concrete face behaviour of Aguamilpa dam. *Proceedings of the Second Symposium on Concrete Face Rockfill Dams*, Florianopolis, Brazil, Brazilian Committee on Dams. pp. 211-222.

Macedo, G.G., Castro, A.J. and Montanez, C.L. (2000) Behaviour of Aguamilpa dam. In Concrete Face Rockfill Dams, J. Barry Cooke Volume (Mori, Sobrinho, Dijkstra, Guocheng and Borgatti ed.), Beijing, pp. 117-151.

Mackenzie, P.R. and McDonald, L.A. (1985) Mangrove Creek dam: Use of soft rock for rockfill. *Proceedings of the Symposium on Concrete Face Rockfill Dams - Design, Construction and Performance*, (Cooke and Sherard ed.) Detroit, Michigan, ASCE New York. pp. 208-230.

Magnan, J.P., Humbert, P. and Mouratidis, A. (1982) Finite element analysis of soil deformations with time under an experimental embankment at failure. *Proceedings, International Symposium on Numerical Models in Geomechanics*, (Dungar, Pande & Studer ed.) Zurich, Balkema, Rotterdam. pp. 601-609.

Mahasandana, T. and Mahatraradol, B. (1985) Monitoring systems of Khao Laem dam. *Proceedings of the 15th International Congress on Large Dams*, Lausanne, ICOLD. pp. 1- (Q.56 R.1).

Malaysian Highway Authority (1989a) Factual report on the performance of the 13 trial embankments. *Proceedings, International Symposium on Trial Embankments on*

Malaysian Marine Clays, (Hudson, Toh & Chan ed.) Kuala Lumpur, Malaysian Highway Authority. Vol. 1.

Malaysian Highway Authority (1989b) 3 m high control embankment on untreated soft ground. *Proceedings, International Symposium on Trial Embankments on Malaysian Marine Clays*, (Hudson, Toh & Chan ed.) Kuala Lumpur, Malaysian Highway Authority. Vol. 2, pp. 2.1-2.30.

Mann, M.J. and Snow, R.E. (1992) Analysis of slope failure and remedial design of an earth dam. *ASCE Geotechnical Special Publication No. 31*, (Seed and Boulanger ed.) Berkeley, California, ASCE. Vol. 2, pp. 923-939.

Marachi, N.D., Chan, C.K., Seed, H.B. and Duncan, J.M. (1969) *Strength and deformation characteristics of rockfill materials.* Report No. TE-69-5, University of California, Department of Civil Engineering.

Maranha das Neves, E., Ramos, C.M., Veiga Pinto, A. and Direito, M.T. (1994) Safety improvement of Beliche dam. *Proceedings of the 18th International Congress on Large Dams*, Durban, ICOLD. pp. 1167-1179 (Q.68 R.67).

Marche, R. and Chapuis, R. (1974) Controle de la stabilite des remblais par la mesure des deplacements horizontaux. *Canadian Geotechnical Journal*, Vol 11, pp. 182-201.

Marcuson, W.F., Ballard, R.F. and Ledbetter, R.H. (1979) Liquefaction failure of tailings dams resulting from the near Izu Oshima earthquake, 14 and 15 January 1978. *6th Pan American Conference on Soil Mechanics & Foundation Engineering*, Lima, Bitech Publishing. Vol. 2, pp. 69-80.

Marsal, R.J. (1982) Monitoring of embankment dam behaviour. *Proceedings of the 14th International Congress on Large Dams*, Rio de Janiero, ICOLD. pp. 1441-1467 (Q.52 R.84).

Marsal, R.J. and Alberro, J.A. (1976) Performance of dams built in Mexico. *Proceedings of the 12th International Congress on Large Dams*, Mexico City, ICOLD. pp. 791-798 (C.2).

Marsal, R.J. and Ramirez de Arellano, L. (1964) El Infiernillo rockfill dam. *Proceedings of the 8th International Congress on Large Dams*, Edinburgh, ICOLD. Vol. 3 pp. 855-877 (Q.31 R.18).

Marsal, R.J. and Ramirez de Arellano, L. (1967) Performance of El Infiernillo dam 1963-1966. *A.S.C.E., Journal of the Soil Mechanics and Foundations Division*, Vol. 93 (SM4), pp. 265-298.

Marsal, R.J. and Ramirez de Arellano, L. (1972) Eight years of observations at El Infiernillo dam. *Proceedings, ASCE Speciality Conference on Performance of Earth and Earth Retaining Structures*, Purdue University, Lafayette, ASCE, New York. Vol. 1 (Part I), pp. 703-722.

Marsal, R.J. and Tamez, G. (1955) Earth dams in Mexico. Design construction and performance. *Proceedings of the 5th International Congress on Large Dams*, Paris, ICOLD. pp. 1123-1178 (C.30).

Marsal, R.L. (1973) Mechanical properties of rockfill. In Embankment Dam Engineering (Casagrande Volume) (Hirschfeld and Poulos ed.), John Wiley and Sons, New York, pp. 109-200.

Marsland, A. and Powell, J.J.M. (1977) The behaviour of a trial bank constructed to failure on soft alluvium of the River Thames. *Proceedings, International Symposium on Soft Clay*, (Brenner & Brand ed.) Bangkok, Asian Institute of Technology. pp. 505-525.

Martin, G.R. (1998) "Post-liquefaction" shear strength from laboratory and field tests. *National Science Foundation Workshop on Shear Strength of Liquefied Soils*, (Stark, Olson, Kramer and Youd ed.) Urbana, Illinois, National Science Foundation. pp. 40-52.

Marulanda, A. and Pinto, N.L. (2000) Recent experience on design, construction, and performance of CFRD dams. In Concrete Face Rockfill Dams, J. Barry Cooke Volume (Mori, Sobrinho, Dijkstra, Guocheng and Borgatti ed.), Beijing, pp. 279-315.

Materon, B. (1985a) Alto Anchicaya dam - ten years performance. *Proceedings of the Symposium on Concrete Face Rockfill Dams - Design, Construction and Performance*, (Cooke and Sherard ed.) Detroit, Michigan, ASCE New York. pp. 73-87.

Materon, B. (1985b) Construction of Foz do Areia dam. *Proceedings of the Symposium on Concrete Face Rockfill Dams - Design, Construction and Performance*, (Cooke and Sherard ed.) Detroit, Michigan, ASCE New York. pp. 192-207.

Matsui, I. (1976) Measurement on relative displacement between different materials at boundary zones and a consideration on a proposed analysis for fill dams taking into account the measurement. *Proceedings of the 12th International Congress on Large Dams*, Mexico City, ICOLD. Vol. 4, pp. 895-917 (C.8).

McConnell, A.D., Paré, J.J., Verma, N.S. and Rattue, A.B. (1982) Materials for construction methods for the dam and dyke embankments of the LG-4 project.

Proceedings of the 14th International Congress on Large Dams, Rio de Janiero, ICOLD. pp. 123-144 (Q.55 R.8).

Melbourne and Metropolitan Board of Works (1972) *Greenvale Reservoir construction report.*

Melbourne and Metropolitan Board of Works (1975) *Sugarloaf reservoir project, design report.* Water Supply Division.

Melbourne and Metropolitan Board of Works (1981) Notes on rock materials used at Winneke dam. *ANCOLD Bulletin*, Vol 59, pp. 57-61.

Melbourne and Metropolitan Board of Works (1985) *Toorourrong - Yan Yean system description and data and notes for inspection report.* File No. 505/002/0502, Structural Surveillance Section, Water Supply Division.

Melbourne and Metropolitan Board of Works (1986) *Upper Yarra reservoir: Surveillance report.* MMBW, Water Supply Division, Surveillance Group.

Melbourne and Metropolitan Board of Works (1987a) *Cardinia reservoir surveillance report.* Report No. 505/008/0502, MMBW, Structural Surveillance Section, Systems Planning Division.

Melbourne and Metropolitan Board of Works (1987b) *Thomson reservoir: Surveillance report.* Report No. 505/012/0502, MMBW, Structural Surveillance Section, System Planning Division.

Melbourne and Metropolitan Board of Works (1988) *Greenvale Reservoir surveillance report.* Water Supply Division.

Melbourne and Metropolitan Board of Works (1995) *Sugarloaf reservoir, monitoring report (7 June 1995).* Water Assets Section.

Mesri, G. and Choi, Y.K. (1979) Excess pore water pressures during consolidation. *Proceedings, Sixth Asian Conference on Soil Mechanics and Foundation Engineering*, Singapore, Vol. 1, pp. 151-154.

Middlebrooks, T.A. (1940) Fort Peck slide. *A.S.C.E. Transactions* (December), pp. 723-742.

Midgley, D.C. (1979) The failure of a slimes dam at Bafokeng; hydrological aspects and a barrier to further escape of slimes. *The Civil Engineer in South Africa*, Vol 21 (6), pp. 151-154.

Ministry of Works and Development New Zealand (1987) *Ohau B Power Project: Earthworks construction report.*

Mitchell, J.K. (1964) Shearing resistance of soils as a rate process. *A.S.C.E., Journal of the Soil Mechanics and Foundations Division*, Vol 90 (SM1), pp. 29-61.

Mitchell, J.K. (1986) Practical problems from surprising soil behaviour, 20th Terzaghi Lecture. *A.S.C.E., Journal of the Geotechnical Division*, Vol 112 (3), pp. 255-289.

Mitchell, J.K. (1993) *Fundamentals of Soil Behavior*. John Wiley & Sons, Inc.

Mitchell, R.J. and Eden, W.J. (1972) Measured movements of clay slopes in the Ottawa area. *Canadian Journal of Earth Sciences*, Vol 9, pp. 1001-1013.

Mitchell, R.J. and Markell, A.R. (1974) Flowsliding in sensitive soils. *Canadian Geotechnical Journal*, Vol 11, pp. 11-31.

Mitchell, R.J. and Williams, D.R. (1981) Induced failure of an instrumented clay slope. *Proceedings of the 10th International Conference on Soil Mechanics and Foundation Engineering*, Stockholm, Balkema, Rotterdam. Vol. 3, pp. 479-484.

Mitchell, W.R., Fidler, J. and Fitzpatrick, M.D. (1968) Rowallan and Parangana rockfill dams. *The Journal of The Institution of Engineers, Australia* (Oct-Nov), pp. 239-251.

Mitchell, W.R. and Fitzpatrick, M.D. (1979) An incident at Rowallan dam. *Proceedings of the 13th International Congress on Large Dams*, New Delhi, ICOLD. pp. 195-210 (Q.49 R.14).

Montanez, L.E., Hacelas, J.E. and Castro, A.J. (1993) Design of Aguamilpa dam. *Proceedings of the International Symposium on of High Earth Rockfill Dams*, Beijing, ICOLD. pp. 337-363.

Moreno, E. and Alberro, J.A. (1982) Behaviour of the Chicoasen dam: construction and first filling. *Proceedings of the 14th International Congress on Large Dams*, Rio de Janiero, ICOLD. pp. 155-182 (Q.52 R.9).

Morfitt, B.J. (1984) *Preliminary analysis of static stability of San Luis dam abutments.* Technical Memorandum No. SL-III-222-1, United States Bureau of Reclamation, Division of Design, Embankment Dams Section.

Morgenstern, N.R. (1994) *Report on the Kwun Lung Lau landslide of 23 July 1994.* Volume 1, for Geotechnical Engineering Office, Civil Engineering Department, Hong Kong Government.

Morgenstern, N.R. (2000) Performance in geotechnical practice. The first Lumb lecture. pp. 1-58.

Mori, R.T. (1999) Deformation and cracks in concrete face rockfill dams. *Proceedings of the Second Symposium on Concrete Face Rockfill Dams*, Florianopolis, Brazil, Brazilian Committee on Dams. pp. 49-61.

Mori, R.T. and Pinto, N.L.S. (1988) Analysis of deformations in concrete face rockfill dams to improve face movement prediction. *Proceedings of the 16th International Congress on Large Dams*, San Francisco, ICOLD. pp. 27-34 (Q.61 R.2).

Morris, S.B. (1939) Discussion on Galloway paper: The design of rock-fill dams. *Transactions, ASCE*, Vol. 104, pp. 35-38.

Morse, A.R. (1995) *White Spur dam, Surveillance Report No. 1 (1986 - 1995).* Report ENE-0010-SF-013, Hydro-Electric Commission Tasmania, Civil and Water Resources Engineering Group.

Morse, A.R. and Ward, M.J. (1989) *Anthony power development, White Spur Dam, Civil Design Report (record).* Report CDR 523, Hydro-Electric Commission Tasmania, Civil Design Section.

Muir Wood, D. (1990) *Soil Behaviour and Critical State Soil Mechanics.* Cambridge University Press, Cambridge, pp. 462.

Murley, K.A. and Cummins, P.J. (1982) Design considerations of materials during construction of Dartmouth dam, Australia. *Proceedings of the 14th International Congress on Large Dams*, Rio de Janiero, ICOLD. pp. 627-641 (Q.55 R.37).

Myrvoll, F., Larsen, S., Sande, A. and Romslo, N.B. (1985) Field instrumentation and performance observations for the Vatnedalsvatn dams. *Proceedings of the 15th International Congress on Large Dams*, Lausanne, ICOLD. pp. 1039-1069 (Q.56 R.56).

Nadilo, J.P. (1983) *Happy Valley dam. Report on stability of embankment.* Ref. No. 83/27, South Australian Government, Engineering and Water Supply Department, Design Services Branch.

Nagarkar, P.K., Kulkarni, R.P. and Kulkarni, M.V. (1978) Case histories of two dams in Maharshtra. *Proceedings of Geocon Conference on Geotechnical Engineering*, New Delhi, Vol. 1, pp. 64-69.

Nagarkar, P.K., Kulkarni, R.P., Kulkarni, M.V. and Kulkarni, D.G. (1981) Failures of a monozone earth dam of expansive clay. *Proceedings of the 10th International Conference on Soil Mechanics and Foundation Engineering*, Stockholm, Vol. 3, pp. 491-494.

Nakagawa, K., Komada, H. and Kanazawa, K. (1985) Application of improved analysis on the pore pressure behaviour within the impervious zone to a prototype rockfill dam. *Proceedings of the 15th International Congress on Large Dams*, Lausanne, ICOLD. Vol. 1, pp. 537-578 (Q.56 R.26).

National Science Foundation (1998) Shear strength of liquefied soils. *National Science Foundation Workshop on Shear Strength of Liquefied Soils*, (Stark, Olson, Kramer and Youd ed.) Urbana, Illinois, National Science Foundation.

Naylor, D.J., Maranha das Neves, E., Mattar, D. and Veiga Pinto, A.A. (1986) Prediction of construction performance of Beliche dam. *Geotechnique*, Vol. 36 (3), pp. 359-376.

Naylor, D.J., Maranha, J.R., Maranha das Neves, E. and Veiga Pinto, A.A. (1997) A back-analysis of Beliche dam. *Geotechnique*, Vol. 47 (2), pp. 221-233.

Naylor, D.J., Tong, S.L. and Shahkarami, A.A. (1989) Numerical modelling of saturation shrinkage. *Proc. Numerical models in Geomechanics NUMOG III*, (Pietruszczak & Pande ed.) Amsterdam, Elsevier. pp. 636-648.

Newland, J.R. and Davidson, J.S. (1979) *Chaffey dam: Construction report 1975 - 1979.* Water Resources Commission, New South Wales.

Nichols, R.S. (1982) Waste dump stability at Fording Coal Limited in B.C. *Proceedings of the Third International Symposium on Stability in Surface Mining*, pp. 795-813.

Nilsson, A. and Norstedt, U. (1991) Evaluation of aging processes in two Swedish dams. *Proceedings of the 17th International Congress on Large Dams*, Vienna, ICOLD. pp. 23-47 (Q.65 R.2).

Nobari, E.S. and Duncan, J.M. (1972a) *Effect of reservoir filling on stresses and movements in earth and rockfill dams.* Report TE-72-1, University of California, Department of Civil Engineering.

Nobari, E.S. and Duncan, J.M. (1972b) Movements in dams due to reservoir filling. *Proceedings, ASCE Speciality Conference on Performance of Earth and Earth Retaining Structures*, Purdue University, Indianna, ASEC, New York. Vol. 1 (Part 1), pp. 797-815.

Nonveiller, E. and Anagnosti, P. (1961) Stresses and deformations in cores of rockfill dams. *Proceedings, 5th International Conference on Soil Mechanics and Foundation Engineering*, Paris, Vol. 2, pp. 673-680.

Norem, H., Locat, J. and Schieldrop, B. (1990) An approach to the physics and the modelling of submarine flowslide. *Marine Geotechnology*, Vol. 9, pp. 93-111.

Nose, M. (1969) Kisenyama pumped storage project. *Water Power*, Vol. 21 (11), pp. 411-420.

Nose, M. (1982) Present trends in construction and operation of dams in Japan. *Proceedings of the 14th International Congress on Large Dams*, Rio de Janiero, ICOLD. pp. 693-728 (GP/RS.1).

Nutt, K.D. (1975) Maroon dam embankment and foundation. *Proceedings of the 2nd Australia New Zealand Conference on Geomechanics*, Brisbane, IEAust, Sydney. pp. 129-133.

Oborn, L.E. (1985) *Cobb Power Station SEED Examination: Report on Engineering Geology.* for Electricity Corporation of New Zealand Limited (Electricorp).

Oikawa, T., Harita, K. and Mizuno, M. (1997) Sealing works for an old river bed gravel stratum on a reservoir bank. *Proceedings of the 19th International Congress on Large Dams*, Florence, ICOLD. Vol. 3, pp. 449-487 (Q.74 R.28).

Okubo, R., Nakahira, E. and Miyagawa, T. (1988) Automated embankment management for the construction of rockfill dam. *Proceedings of the 16th International Congress on Large Dams*, San Francisco, ICOLD. Vol. 3, pp. 1003-1025 (C.5).

Olsauskas, A.A., Kotowicz, M. and Paton, R.J. (1967a) *Blowering dam and appurtenant works, Contract No. 20,094. Construction progress report: 30th June 1967.* Snowy Mountains Hydro Electric Authority.

Olsauskas, A.A., Lawrence, A.I. and Paton, R.J. (1967b) *Blowering dam and appurtenant works, Contract No. 20,094. Construction progress report: 31st December 1967.* Snowy Mountains Hydro Electric Authority.

Olsauskas, A.A., Lawrence, A.I. and Paton, R.J. (1968) *Blowering dam and appurtenant works, Contract No. 20,094. Construction progress report: Final Report.* Snowy Mountains Hydro Electric Authority.

Olsauskas, A.A., Perkins, R.W., Macoun, K. and Paton, R.J. (1966) *Blowering dam and appurtenant works, Contract No. 20,094. Construction progress report: 31st December 1966.* Snowy Mountains Hydro Electric Authority.

Olsen, R.S. (1997) Cyclic liquefaction based on the cone penetrometer test. *Proceedings of the NCEER Workshop on Evaluation of Liquefaction Resistance of Soils*, (Youd and Idriss ed.) Salt Lake City, Utah, National Centre for Earthquake Engineering Research. pp. 225-276.

Olson, S.M., Stark, T.D. and Castro, G. (2000) 1907 static liquefaction and flow failure of the north dike of Wachusett Dam. *A.S.C.E., Journal of Geotechnical and Geoenvironmental Engineering*, Vol 126 (12), pp. 1184-1193.

Opus International Consultants Ltd (1998a) *Benmore power station: Deformation Survey No. 22B.* Contract No. EC95002 Report No. 236, for Electricity Corporation of New Zealand, Southern Generation.

Opus International Consultants Ltd (1998b) *Pukaki Lake control: Deformation Survey No. 17B.* Contract No. EC95002, Report No. 243, for Electricity Corporation New Zealand, Southern Generation.

Opus International Consultants Ltd (1999) *Ruataniwha dam & spillway: Deformation Survey No. 26.* Contract No. EC95002 Report No. 272, for Electricity Corporation of New Zealand.

Oziz, U., Basmaci, E. and Harmancioglu, N. (1990) Ataturk nears completion. *Water Power & Dam Construction*, September, pp. 12-16.

Pagano, L., Desideri, A. and Vinale, F. (1998) Interpreting settlement profiles of earth dams. *A.S.C.E., Journal of Geotechnical and Geoenvironmental Engineering*, Vol. 124 (10), pp. 923-932.

Paré, J.J. (1984) Earth dam behaviour on the La Grande project. *Proceedings of the International Conference on Safety of Dams*, (Serafim ed.) Coimbra, Portugal, Balkema, Boston. pp. 153-160.

Paré, J.J., Boncompain, B., Konrad, J.M. and Verma, N.S. (1982) Embankment compaction and quality control at James Bay hydroelectric development. *Transportation Research Record 897* pp. 8-15.

Paré, J.J., Verma, N.S., Keira, H.M.S. and McConnell, D. (1984) Stress-deformation predictions for the LG-4 main dam. *Canadian Geotechnical Journal*, Vol. 21, pp. 213-222.

Parkin, A.K. (1971) Application of rate analysis to settlement problems involving creep. *Proceedings of the First Australia New Zealand Conference on Geomechanics*, Melbourne, Vol. 1, pp. 138-143.

Parkin, A.K. (1977) The compression of rockfill. *Australian Geomechanics Journal*, Vol. G7, pp. 33-39.

Partyka, G. and Bowling, A.J. (1984) *P.R.P.D., Lower Pieman dam, Rockfill and filter material control testing.* Report 4413-9, Hydro-Electric Commission Tasmania, Civil Engineering Laboratories.

Paterson, S.J. (1971) Engineering geology of the Lemonthyme hydro-electric scheme, Tasmania. *I.E. Aust., Civil Engineering Transactions* (April), pp. 17-24.

Patrick, J.G. (1967) Post-construction behavior of Round Butte dam. *A.S.C.E., Journal of the Soil Mechanics and Foundations Division*, Vol. 93 (SM4), pp. 251-263.

Peng, Z. (2000) Analysis of the deformation of Xibeikou CFRD in eight years of operation. *Proceedings of the International Symposium on Concrete Faced Rockfill Dams*, Beijing, ICOLD. pp. 555-564.

Penman, A.D.M. (1985) The failure of Acu Dam (Technical Note 6). *Proceedings of the Symposium on Failures in Earthworks, ICE*, London, Thomas Telford, London. pp. 414-416.

Penman, A.D.M. (1986) On the embankment dam. *Geotechnique*, Vol 36 (3), pp. 303-348.

Penman, A.D.M. (1988) *Remedial measures at Matahina dam following the Edgecumbe earthquake of 2 March 1987.* for Electricity Corporation of New Zealand (Electricorp).

Penman, A.D.M., Burland, J.B. and Charles, J.A. (1971) Observed and predicted deformations in a large embankment dam during construction. *Proceedings of the Institution of Civil Engineers*, Vol 49 (May), pp. 1-21.

Peter J. Burgess & Associates Pty Ltd (1991) *Khancoban dam safety review.* for Snowy Mountains Hydro-Electric Authority.

Peterson, O.W. (1939) Discussion on Galloway paper: The design of rock-fill dams. *Transactions, ASCE*, Vol. 104, pp. 40-41.

Peterson, R., Iverson, N.L. and Rivard, P.J. (1957) Studies of several dam failures on clay foundations. *Proceedings of the Fourth International Conference on Soil Mechanics and Foundation Engineering*, London, Vol. 2, pp. 348-352.

Picarelli, L. (2000) Mechanisms and rates of slope movements in fine grained soils. *Proceedings of the International Conference on Geotechnical and Geological Engineering (GeoEng2000)*, Melbourne, Technomic, Lancaster. Vol. 1, pp. 1618-1670.

Picarelli, L., Urciuoli, G. and Russo, C. (2000) Mechanics of slope deformation and failure in stiff clays and clay shales as a consequence of pore pressure fluctuation. *Proceedings of the 8th International Symposium on Landslides*, Cardiff, Wales, Balkema.

Pierson, T.C. and Costa, J.E. (1987) A rheologic classification of subaerial sediment-water flows. *Geological Society of America, Reviews in Engineering Geology*, Vol 7, pp. 1-12.

Pilot, G. (1972) Study of five embankment failures on soft soils. *Proceedings, ASCE Speciality Conference on Performance of Earth and Earth Retaining Structures*, Purdue University, Lafayette, Vol. 1 (1), pp. 81-100.

Pinkerton, I.L. (1984) *Review of Happy Valley dam to assess structural adequacy and safety.* For the Engineering and Water Supply Department of the South Australian Government.

Pinkerton, I.L. and Paton, R.J. (1968) Design and construction of Geehi dam. *The Journal of the Institution of Engineers, Australia,* Vol. 40 (March), pp. 33-48.

Pinto, N.L.d.S., Blinder, S. and Toniatti, N.B. (1993) Foz do Areia and Segredo CFRD dams - 12 years evolution. *Proceedings of the International Symposium on High Earth-Rockfill Dams*, (Jiang, Zhang & Qin ed.) Beijing, Vol. 1, pp. 381-398.

Pinto, N.L.d.S. and Marques Filho, P.L. (1998) Estimating the maximum face slab deflection in CFRDs. *Hydropower & Dams*, No. 6.

Pinto, N.L.d.S., Marques Filho, P.L. and Maurer, E. (1985a) Foz do Areia dam - design, construction and behaviour. *Proceedings of the Symposium on Concrete Face Rockfill Dams - Design, Construction and Performance*, (Cooke and Sherard ed.) Detroit, Michigan, ASCE New York. pp. 173-191.

Pinto, N.L.d.S., Marques Filho, P.L. and Maurer, E. (1985b) Segredo dam - basic design aspects. *Proceedings of the Symposium on Concrete Face Rockfill Dams - Design, Construction and Performance*, (Cooke and Sherard ed.) Detroit, Michigan, ASCE New York. pp. 587-593.

Pinto, N.L.d.S., Materon, B. and Marques Filho, P.L. (1982) Design and performance of Foz do Areia concrete membrane as related to basalt properties. *Proceedings of the 14th International Congress on Large dams*, Rio de Janiero, ICOLD. pp. 873-906 (Q.55 R.51).

Pinto, N.L.S. and Marques Filho, P.L. (1985) Discussion of Clements paper: Post-construction deformation of rockfill dams. *A.S.C.E., Journal of Geotechnical Engineering*, Vol. 111 (12), pp. 1472-1475.

Pitman, T.D., Robertson, P.K. and Sego, D.C. (1994) Influence of fines on the collapse surface of loose sands. *Canadian Geotechnical Journal,* Vol 31, pp. 728-739.

Pope, R.J. (1967) Evaluation of Cougar dam embankment performance. *A.S.C.E., Journal of the Soil Mechanics and Foundations Division*, Vol. 93 (SM4), pp. 231-250.

Pope, R.J. (1969) Closure: Evaluation of Cougar dam embankment performance. *A.S.C.E., Journal of the Soil Mechanics and Foundations Division*, Vol. 95 (SM4), pp. 1116.

Potts, D.M., Dounias, G.T. and Vaughan, P.R. (1990) Finite element analysis of progressive failure of Carsington embankment. *Geotechnique*, Vol. 40 (1), pp. 79-101.

Potts, D.M., Kovacevic, N. and Vaughan, P.R. (1997) Delayed collapse of cut slopes in stiff clay. *Geotechnique,* Vol. 47 (5), pp. 953-982.

Poulos, H.G., Booker, J.R. and Ring, G.J. (1972) Simplified calculations of embankment deformations. *Soils and Foundations, Tokyo*, Vol 12 (4), pp. 1-17.

Poulos, H.G. and Davis, E.A. (1974) *Elastic Solutions for Soil and Rock Mechanics*. Wiley, New York.

Poulos, H.G., Lee, C.Y. and Small, J.C. (1990) *Predicted and observed behaviour of a test embankment on Malaysian soft clays.* Research Report R620, The University of Sydney, NSW, Australia.

Poulos, S.J. (1998) Written statement: Shear strength of liquefied soils from laboratory and field tests. Discussion. *National Science Foundation Workshop on Shear Strength of Liquefied Soils,* (Stark, Olson, Kramer and Youd ed.) Urbana, Illinois, National Science Foundation. pp. 152-156.

Public Works and Services Department NSW (1998) *Mangrove Creek dam - Post construction embankment behaviour.* Report DC98072, DPWS NSW, Dams and Civil Section.

Public Works Department N.S.W. (1990) *Gosford Wyong water supply, Mangrove Creek dam monitoring survey (unpublished).*

Public Works Department NSW (1992a) *Burrendong dam design report.* PWD NSW, Dams and Civil Section (for Department of Water Resources).

Public Works Department NSW (1992b) *Wyangala dam design report.* PWD NSW, Dams and Civil Section (for Department of Water Resources).

Public Works Department NSW (19XX) *Copeton dam design report.* PWD NSW, Dams Branch (for Department of Water Resources).

Pun, W.K. and Yeo, K.C. (1995) *Report on the investigation of the 23 July and 7 August 1994 landslides at Milestone 14.5 Castle Peak Road.* Advisory Report ADR 1/95, Geotechnical Engineering Office, Civil Engineering Department, Hong Kong.

Queensland Department of Natural Resources (1997) *Bjelke-Petersen dam: Five yearly safety inspection, 10th to 12th June 1997.* QDNR, State Waters Projects.

Queensland Department of Natural Resources (1998) *Peter Faust dam: Five yearly safety inspection.* QDNR, State Waters Projects.

Queensland Department of Primary Industries (1994) *Design of Peter Faust dam.* Report No. 69/R13, QDPI, Water Resources, Water Production Division.

Queensland Department of Primary Industries (1995) *Split-Yard Creek dam - Data book.*

Queensland Department of Primary Industries (1996) *Split-Yard Creek dam safety review*. QDPI, Water Resources (report for Austa Electric).

Queensland Irrigation and Water Supply Commission (1976) *The geology of Wivenhoe dam site: Part 1*.

Queensland Water Resources Commission (1979a) *A report on the construction of Wivenhoe dam Stage II.* Draft Report.

Queensland Water Resources Commission (1979b) *Schedule of rate contract for third stage construction of Wivenhoe dam.* Contract No. 2120 (Volumes II & III), QWRC, Design and Construction.

Queensland Water Resources Commission (1986a) *Barker-Barambah Irrigation Project. Schedule of rates contract. Construction of Bjelke-Petersen dam and appurtenant works.* Contract No. 2580 (Volumes II & IV).

Queensland Water Resources Commission (1986b) *Sources of construction materials for construction of Bjelke-Petersen dam.*

Queensland Water Resources Commission (1987) *Post-construction report on Split-Yard Creek dam (Wivenhoe dam and pumped storage hydro-electric project).* Ref. No. CD/1, QWRC, Construction Division.

Queensland Water Resources Commission (19XXa) *Maroon Dam Safety Evaluation Data Book.*

Queensland Water Resources Commission (19XXb) *Split-Yard Creek dam - Draft design report.*

Quinlan, P. (1993) *King River power development, Crotty Dam, Performance Report.* Report CDR 610, Hydro-Electric Commission Tasmania, Consulting Business Unit.

Ramalho-Ortigao, J.A., Lacerda, W.A. and Werneck, M.L.G. (1983a) The behaviour of the instrumentation of an embankment on soft clay. *Proceedings, International Symposium on Field Measurements in Geomechanics*, (Kovari ed.) Zurich, Vol. 1, pp. 703-717.

Ramalho-Ortigao, J.A., Werneck, M.L.G. and Lacerda, W.A. (1983b) Embankment failure on clay near Rio de Janiero. *A.S.C.E., Journal of Geotechnical Engineering*, Vol 109 (11), pp. 1460-1479.

Ramirez de Arellano, L. and Gomez, E.M. (1972) Field measurements at La Angostura cofferdams. *Proceedings, ASCE Speciality Conference on Performance of Earth and Earth Retaining Structures*, Purdue University, Indianna, ASCE, New York. Vol. 1 (Part 1), pp. 779-796.

Rao, K.L. (1957) Behaviour of recent earth dams and levees in India. *Proceedings of the 4th International Conference on Soil Mechanics and Foundation Engineering*, London, Butterworths Scientific Publications, London. Vol. 2, pp. 361-367.

Rao, K.L. and Wadhwa, H.L. (1958) Observation at Hirakud earth dam. *Proceedings of the 6th International Congress on Large Dams*, London, ICOLD. pp. 471-482 (Q.21 R.53).

Read, S.A.L. (1976) *Upper Waitaka power development scheme. Pukaki Lake control. Engineering geological completion report.* Report No. EG268, New Zealand Geological Survey, Dept Scientific and Industrial Research, Engineering Geology Section.

Ready, O.T. (1910) Construction of the Belle Fourche dam. *Engineering Record*, Vol. 61 (14), pp. 466-469.

Regalado, G., Materon, B., Ortega, J.W. and Vargas, J. (1982) Alto Anchicaya concrete face rockfill dam behaviour of the concrete face membrane. *Proceedings of the 14th International Congress on Large Dams*, Rio de Janiero, ICOLD. Vol. 4, pp. 517-535 (Q.55 R.30).

Regan, P.J. (1997) Performance of concrete-faced rockfill dams of the Pacific Gas & Electric Company. *Non-Soil Water Barriers for Embankment Dams, Proceedings of the 17th Annual USCOLD Lecture Series*, San Diego, California, USCOLD. pp. 149-162.

Regan, W.M. (1980) *Winneke Reservoir, main dam geological report on construction.* Engineering Geology Section Report 81/489, Melbourne and Metropolitan Board of Works.

Reinhold, J.J. (1969) *The geology of the western area: Greenvale Reservoir site.* Report No. 3, Melbourne and Metropolitan Board of Works, Civil Engineering Laboratories.

Resendiz, D. and Romo, M.P. (1972) Analysis of embankment deformations. *Proceedings, ASCE Speciality Conference on Performance of Earth and Earth Retaining Structures*, Purdue University, Indianna, ASCE, New York. Vol. 1 (Part I), pp. 817-836.

Riemer, M.F. (1998) Written statement: Shear strength of liquefied soils from laboratory and field tests. Discussion. *National Science Foundation Workshop on Shear Strength of Liquefied Soils*, (Stark, Olson, Kramer and Youd ed.) Urbana, Illinois, National Science Foundation. pp. 232-237.

Riemer, W. (2001) *Personnel communication with Dr. W. Riemer (Geological Consultant)*.

Robertson, P.K., Woeller, D.J. and Finn, W.D.L. (1992) Seismic cone penetration test for evaluating liquefaction potential under cyclic loading. *Canadian Geotechnical Journal*, Vol. 29 (3), pp. 686-695.

Robertson, P.K. and Wride, C.E. (1997) Cyclic liquefaction and its evaluation based on the SPT and CPT. *Proceedings of the NCEER Workshop on Evaluation of Liquefaction Resistance of Soils*, (Youd and Idriss ed.) Salt Lake City, Utah, National Centre for Earthquake Engineering Research. pp. 41-87.

Robinson, P. (1979) *Murchison dam - Control testing of rockfill placing.* Report 4352-1, Hydro-Electric Commission Tasmania, Civil Engineering Laboratories.

Rocke, G. (1993) Technical Note: Investigation of the failure of Carsington Dam. *Geotechnique*, Vol. 43 (1), pp. 175-180.

Rodine, J.D. (1974) *Analysis of the mobilisation of debris flows*. Ph.D. dissertation, Stanford University, California.

Rogers, B.T., Been, K., Hardy, M.D., Johnson, G.J. and Hachey, J.E. (1990) Re-analysis of Nerlerk B-67 berm failures. *Proceedings of the Canadian Geotechnical Engineering Conference*, Laval University, Quebec, Vol. I pp. 227-237.

Rogers, R.L. and Pearce, K.G. (1991) Effect of the foundation on design, construction and filling of Split-Yard Creek dam. *Proceedings of the 17th International Congress on Large Dams*, Vienna, ICOLD. pp. 1577-1599 (Q.66 R.84).

Rowe, P.W. (1991) A reassessment of the causes of the Carsington embankment failure. *Geotechnique*, 41 (3), pp. 395-421.

Rowe, R.K., Gnanendran, C.T., Landva, A.O. and Valsangkar, A.J. (1995) Construction and performance of a full-scale geotextile reinforced test embankment, Sackville, New Brunswick. *Canadian Geotechnical Journal*, Vol 32, pp. 514-534.

Rowe, R.K., Gnanendran, C.T., Landva, A.O. and Valsangkar, A.J. (1996) Calculated and observed behaviour of a reinforced embankment over soft compressible soil. *Canadian Geotechnical Journal*, Vol 33, pp. 324-338.

Rudd, R.T. (1979) The failure of a slimes dam at Bafokeng; the Bafokeng disaster and its legal implications. *The Civil Engineer in South Africa*, Vol 21 (6), pp. 146-150.

Saboya, F., Barbosa, R. and Vasconcelos, A. (2000) The influence of the left abutment geometry on the behaviour of Xingo rockfill dam. *Proceedings of the International Symposium on Concrete Faced Rockfill Dams*, Beijing, ICOLD. pp. 565-572.

Saboya, F.J. and Byrne, P.M. (1993) Parameters for stress and deformation analysis of rockfill dams. *Canadian Geotechnical Journal*, Vol. 30, pp. 690-701.

Saito, M. (1965) Forecasting the time of occurrence of a slope failure. *Proceedings of the 6th International Conference on Soil Mechanics and Foundation Engineering*, Montreal, Vol. 2, pp. 537-541.

Sakamoto, T., Takebayashi, S., Nakamura, A. and Yasuda, N. (1994) Safety assessment based on the observed behaviour of zoned rockfill dams. *Proceedings of the 18th International Congress on Large Dams*, Durban, ICOLD. pp. 925-953 (Q.68 R.55).

Sassa, K. (1988) Special lecture: Geotechnical model for the motion of landslides. *Proceedings of the Fifth International Symposium on Landslides*, (Bonnard ed.) Lausanne, Switzerland, Balkema. Vol. 1, pp. 37-55.

Savage, J.L. (1931) *Report on repairs to Belle Fourche dam, Belle Fourche Project.* United States Department of the Interior, Bureau of Reclamation.

Sbeghen, B. (1990) *Geological investigations for Maroon dam safety evaluation.* Ref. No. PP2351, Queensland Water Resources, Planning Division, Engineering Geology Section.

Scheidegger, A.E. (1973) On the prediction of the reach and velocity of catastrophic landslides. *Rock Mechanics*, Vol 5, pp. 231-236.

Schiffman, R.L., Pane, V. and Gibson, R.E. (1984) The theory of one-dimensional consolidation of saturated clays, IV: An overview on non-linear finite strain sedimentation and consolidation. *Proceedings of the ASCE Symposium on Sedimentation Consolidation Models, Prediction and Validation*, (Yong & Townsend ed.) San Francisco, ASCE, New York. pp. 1-29.

Schmidt, L.A.J. (1958) Rockfill dams: Performance and maintenance of Dix River dam. *A.S.C.E., Journal of the Power Division*, Vol. 84 (PO3), pp. 1683-1 to 29.

Schober, W. (1967) Behaviour of the Gepatsch rockfill dam. *Proceedings of the 9th International Congress on Large Dams*, Istanbul, ICOLD. pp. 677-699 (Q.34 R.39).

Schober, W. (1970) Behaviour interior stress distribution of the Gepatsch rockfill dam. *Proceedings of the 10th International Congress on Large Dams*, Montreal, ICOLD. Vol. 1, pp. 169-187 (Q.36 R.10).

Schuyler, J.D. (1912) *Reservoirs for Irrigation, Water-Power and Domestic Water Supply*. John Wiley and Sons, New York.

Schwab, H.H. (1979) The Gepatsch rockfill dam - Analysis relating to long-term behaviour (1962 to 1978) (in German). *Osterreichische Wasserwirtschaft*, Vol. 31 (5/6), pp. 202-210.

Seed, H.B. (1979) Soil liquefaction and cyclic mobility evaluation for level ground during earthquakes. *A.S.C.E., Journal of the Geotechnical Engineering Division*, Vol 105 (GT2), pp. 210-255.

Seed, H.B. (1987) Design problems in soil liquefaction. *A.S.C.E., Journal of Geotechnical Engineering*, Vol 113 (8), pp. 827-845.

Seed, H.B., Idriss, I.M. and Arango, I. (1983) Evaluation of liquefaction potential using field performance data. *A.S.C.E., Journal of Geotechnical Engineering*, Vol 109 (3), pp. 458-482.

Seed, H.B., Lee, K.L. and Idriss, I.M. (1969) Analysis of Sheffield Dam failure. *A.S.C.E., Journal of the Soil Mechanics and Foundations Division*, Vol 95 (SM6), pp. 1453-1490.

Seed, H.B., Lee, K.L., Idriss, I.M. and Makdisi, F.I. (1975) The slides in the San Fernando dams during the earthquake of February 9, 1971. *A.S.C.E., Journal of the Geotechnical Engineering Division*, Vol 101 (GT7), pp. 651-688.

Seed, H.B., Tokimatsu, K., Harder, L.F. and Chung, R. (1985) Influence of SPT procedures in soil liquefaction resistance evaluations. *A.S.C.E., Journal of Geotechnical Engineering*, Vol 115 (12), pp. 1425-1445.

Seed, R.B. and Harder, L.F. (1990) SPT-based analysis of cyclic pore pressure generation and undrained residual strength. *Proceedings, H. Bolton Seed Memorial Symposium*, (Duncan ed.) BiTech Publishers. Vol. 2, pp. 351-376.

Shaw, E.D. (1953) Construction of the Eildon project. *Unpublished paper (?).*

Sherard, J.L. (1953) *Influence of soil properties and construction methods on the performance of homogeneous earth dams*. Ph.D. Thesis, Harvard University.

Sherard, J.L. (1973) Embankment dam cracking. In Embankment Dam Engineering (Casagrande Volume) (Hirschfeld and Poulos ed.), John Wiley and Sons, New York, pp. 271-353.

Sherard, J.L. and Cooke, J.B. (1987) Concrete-face rockfill dam: I. Assessment. *Journal of Geotechnical Engineering, ASCE,* Vol 113 (10), pp. 1096-1112.

Sherard, J.L., Woodward, R.J., Gizienski, S.F. and Clevenger, W.A. (1963) *Earth and Earth-Rock Dams*. John Wiley and Sons, New York, pp. 725.

Shiraiwa, K. and Takahashi, Y. (1985) Construction of Tokachi dam on the Tokachi River. *Civil Engineering in Japan*, Vol. 24, pp. 133-148.

Siddle, H.J., Wright, M.D. and Hutchinson, J.N. (1996) Rapid failures of colliery spoil heaps in the South Wales coalfield. *Quarterly Journal of Engineering Geology*, Vol 29, pp. 103-132.

Sierra, J.M., Ramirez, C.A. and Hacelas, J.E. (1985) Design features of Salvajina dam. *Proceedings of the Symposium on Concrete Face Rockfill Dams - Design, Construction and Performance*, (Cooke and Sherard ed.) Detroit, Michigan, ASCE New York. pp. 266-285.

Silvas, F. and de Groot, M.B. (1995) Flow slides in the Netherlands: experience and engineering practice. *Canadian Geotechnical Journal*, Vol 32, pp. 1086-1092.

Silveira, J.F. and Sardinha, A.E. (1999) Behaviour of Ita CFRD at the end of the construction period. *Proceedings of the Second Symposium on Concrete Face Rockfill Dams*, Florianopolis, Brazil, Brazilian Committee on Dams. pp. 37-48.

Sinclair Knight Merz (1995) *Kangaroo Creek dam - Report on 1st stage of safety evaluation.* For Engineering and Water Supply Department of South Australia.

Singh, A. and Mitchell, J.K. (1968) General stress-strain-time function for soil. *ASCE, Journal of the Soil Mechanics and Foundations Division*, Vol 94 (SM1), pp. 21-46.

Sinha, D.S. (1968) Dams in distress. *Irrigation and Power*, Vol. 25 (3), pp. 301-320.

Sivathayalan, S. and Vaid, Y.P. (1998) Truly undrained response of granular soils with no membrane-penetration effects. *Canadian Geotechnical Journal*, Vol 35, pp. 730-739.

Skempton, A.W. (1948) The rate of softening of stiff, fissured clays. *Proceedings of the Second International Conference on Soil Mechanics and Foundation Engineering*, Rotterdam, Vol. 2, pp. 50-53.

Skempton, A.W. (1954) The pore pressure coefficients A and B. *Geotechnique*, Vol. 4 (4), pp. 143-147.

Skempton, A.W. (1964) Long-term stability of clay slopes. *Geotechnique*, Vol. 14 (2), pp. 77-101.

Skempton, A.W. (1977) Slope stability of cuttings in brown London Clay. *Proceedings of the Ninth International Conference on Soil Mechanics and Foundation Engineering*, Tokyo, Vol. 3, pp. 261-270.

Skempton, A.W. (1985) Residual strength of clays in landslides, folded strata and the laboratory. *Geotechnique*, Vol. 35 (1), pp. 3-18.

Skempton, A.W. (1986) Standard penetration test procedures and the effects in sands of overburden pressure, relative density, particle size, aging and overconsolidation. *Geotechnique*, Vol. 36 (3), pp. 425-447.

Skempton, A.W. (1990) Historical development of British embankment dams to 1960. *Clay Barriers for Embankment Dams*, London, Thomas Telford, London. pp. 15-52.

Skempton, A.W. and La Rochelle, P. (1965) The Bradwell slip: A short-term failure in London clay. *Geotechnique*, Vol. 15 (3), pp. 221-242.

Skempton, A.W., Schuster, R.L. and Petley, D.J. (1969) Joints and fissures in the London clay at Wraysbury and Edgeware. *Geotechnique*, Vol. 19 (2), pp. 205-217.

Skempton, A.W. and Vaughan, P.R. (1993) The failure of Carsington Dam. *Geotechnique*, Vol. 43 (1), pp. 151-173.

Sladen, J.A., D'Hollander, R.D. and Krahn, J. (1985a) The liquefaction of sands, a collapse surface approach. *Canadian Geotechnical Journal*, Vol 22, pp. 564-578.

Sladen, J.A., D'Hollander, R.D., Krahn, J. and Mitchell, D.E. (1985b) Back analysis of the Nerlerk berm liquefaction slides. *Canadian Geotechnical Journal*, Vol 22, pp. 579-588.

Sladen, J.A. and Hewitt, K.J. (1989) Influence of placement method on the in situ density of hydraulic sand fills. *Canadian Geotechnical Journal*, Vol 26, pp. 453-466.

Smith, D. and Hungr, O. (1992) *Failure behaviour of large rockslides.* Report No. 16-11-6, Thurber Engineering Ltd., Report to the Geological Survey of Canada and BC Hydro and Power Authority.

Snowy Mountains Engineering Corporation (1971) *Cardinia Creek dam and appurtenant works: Design report.* for Melbourne and Metropolitan Board of Works.

Snowy Mountains Engineering Corporation (1975) *Dartmouth dam project: Interim design report.* for State Rivers and Water Supply Commission, Victoria.

Snowy Mountains Engineering Corporation (1986) *Tooma dam: Report on safety review*. for Snowy Mountains Hydro-Electric Authority.

Snowy Mountains Engineering Corporation (1990) *Island Bend, Tantangara, Guthega and Eucumbene dams: Review of instrumentation results and records.* for Snowy Mountains Hydro-Electric Authority.

Snowy Mountains Engineering Corporation (1995) *Hope Valley dam safety evaluation report.* Document No. 35501.001, for Engineering and Water Supply Department of South Australia.

Snowy Mountains Engineering Corporation (1996a) *Lake Nillahcootie: Safety Surveillance 1995 and formal Dam Safety Inspection 18 April 1996.* Document No. 44519.200, for Goulburn-Murray Water.

Snowy Mountains Engineering Corporation (1996b) *Lake William Hovell: Report on Safety Surveillance and Behaviour 1995.* Document No. 44519.130, for Goulburn Murray Water.

Snowy Mountains Engineering Corporation (1996c) *Tullaroop Reservoir: Report on Safety Surveillance and Behaviour 1995.* Document No. 44519.300, for Goulburn-Murray Water.

Snowy Mountains Engineering Corporation (1996d) *Yan Yean dam: Safety review of dam and outlets.* Document No. 34509.01, for Melbourne Water Corporation.

Snowy Mountains Engineering Corporation (1997a) *Lake Dartmouth: Report on safety surveillance and behaviour 1996.* for Goulburn-Murray Water.

Snowy Mountains Engineering Corporation (1997b) *Yan Yean dam stability review: further investigation and analysis.* Document No. 44615.400, for Melbourne Water Corporation.

Snowy Mountains Engineering Corporation (1998a) *Lake Bellfield: Report on Safety Surveillance and Behaviour 1997 and formal Dam Safety Inspection 26 February 1998.* Document No. 44812.100, for Wimmera Mallee Water.

Snowy Mountains Engineering Corporation (1998b) *Upper Yarra dam embankment safety review*. Document No. 44818.200, for Melbourne Water Corporation.

Snowy Mountains Engineering Corporation (1998c) *Yan Yean dam: Embankment rehabilitation design report.* Document No. 44823.200, for Melbourne Water Corporation.

Snowy Mountains Engineering Corporation (1998d) *Lake Eppalock Geotechnical Investigation - Phase 2.* Document No. 44821.110 CDB11JK8, for Goulburn Murray Water.

Snowy Mountains Engineering Corporation (1999a) *Eildon design review - stage 1.* Document No. 44930, for Goulburn-Murray Water.

Snowy Mountains Engineering Corporation (1999b) *Hope Valley dam study.* Document No. 35901.001, for South Australian Water Corporation.

Snowy Mountains Engineering Corporation (2002) *Happy Valley dam: Interim report on the numerical modelling.* Document No. 35001.002.02, for South Australian Water Corporation.

Snowy Mountains Engineering Corporation (unpublished) *Thomson dam: Draft design report.*

Snowy Mountains Hydro-Electric Authority (1964) *Schedule of rates contract for Blowering dam and appurtenant works: Contract No. 20,094.*

Snowy Mountains Hydro-Electric Authority (1998a) *Eucumbene dam and saddle dam: 1998 annual report.* SMHEA, Operations Dam Safety Section.

Snowy Mountains Hydro-Electric Authority (1998b) *Khancoban dam 1998 annual report.* SMHEA, Operations Dam Safety Section.

Snowy Mountains Hydro-Electric Authority (1998c) *Talbingo dam 1998 annual report.* SMHEA, Operations Dam Safety Section.

Sobrinho, J.A., Sadinha, A.E., Albertoni, S.C. and Dijkstra, H.H. (2000) Development aspects of CFRD in Brazil. In Concrete Face Rockfill Dams, J. Barry Cooke Volume (Mori, Sobrinho, Dijkstra, Guocheng and Borgatti ed.), Beijing, pp. 153-175.

Sobrinho, J.A., Sardinha, A.E. and Fernandes, A.M. (1999) Ita dam - design and construction. *Proceedings of the Second Symposium on Concrete Face Rockfill Dams*, Florianopolis, Brazil, Brazilian Committee on Dams. pp. 377-390.

Soga, K. and Mitchell, J.K. (1996) Rate dependent deformation of structured natural clays. *ASCE Geotechnical Special Publication No. 61, Measuring and Modeling Time Dependent Soil Behavior*, (Sheahan & Kaliakin ed.) Washington, D.C., ASCE, New York. pp. 243-257.

Sokolov, I.B., Marchuk, A.N., Kuznetsov, V.S., Aleksandrovskaya, E.A., Kuzmin, K.K., Pavlov, V.L., Tsaryov, A.I. and Alipov, V.V. (1985) Analysis and interpretation of measurement data illustrated by the construction and staged commissioning of the Sayano-Shushenskaya and Nurek hydro power plants. *Proceedings of the 15th International Congress on Large Dams*, Lausanne, ICOLD. pp. 1471-1482 (Q.56 R.75).

Sonu, J. (1985) Performance of instrument in rockfill dams in Korea. *Proceedings of the 15th International Congress on Large Dams*, Lausanne, ICOLD. pp. 855-868 (Q.56 R.46).

South Australian Water Corporation (1995) *Dam Safety Committee inspection of Kangaroo Creek dam.*

Souza, R.J.B., Cavalcanti, A.J.C.T., Silva, S.A. and Silveira, J.F. (1999) Xingo concrete face rockfill dam behaviour of the dam on the left abutment. *Proceedings of the*

Second Symposium on Concrete Face Rockfill Dams, Florianopolis, Brazil, Brazilian Committee on Dams. pp. 143-157.

Sowers, G.F., Davie, J., Soenarno and Mansoer, M.N. (1993) Jatiluhur Dam: problems and rehabilitation. *Proc. of the Conference on Geotechnical Practice in Dam Rehabilitation*, (Anderson ed.) ASCE, New York. pp. 17-34.

Sowers, G.F., Williams, R.C. and Wallace, T.S. (1965) Compressibility of broken rock and the settlement of rockfills. *Proceedings of the 6th International Conference on Soil Mechanics and Foundation Engineering*, Montreal, University of Toronto Press. Vol. 2, pp. 561-565.

Soydemir, C. and Kjœrnsli, B. (1975) *A treatise on the performance of rockfill dams with unyielding foundations in relation to the design of Storvass dam.* Report No. 53203, Norwegian Geotechnical Institute.

Soydemir, C. and Kjœrnsli, B. (1979) Deformations of membrane-faced rockfill dams. *Proceedings, 7th European Conference on Soil Mechanics and Foundation Engineering*, Brighton, England, Vol. 3, pp. 281-284.

Speedie, M.G. (1948) Investigations and designs for Eildon Dam enlargement. *Journal of the Institution of Engineers, Australia*, Vol. 20 (7-8), pp. 81-91.

Squier, L.R. (1968) Discussion: Evaluation of Cougar dam embankment performance (by Pope 1967). *A.S.C.E., Journal of the Soil Mechanics and Foundations Division*, Vol. 94 (SM3), pp. 780-783.

Squier, L.R. (1970) Load transfer in earth and rockfill dams. *A.S.C.E., Journal of the Soil Mechanics and Foundations Division*, Vol. 96 (SM1), pp. 213-233.

Stafford, C.T. and Weatherburn, D.C. (1958) Glenbawn dam: construction. *The Journal of The Institution of Engineers, Australia*, Vol. 30 (12), pp. 333-351.

Stark, T.D. and Duncan, J.M. (1987) *Mechanisms of strength loss in stiff clays.* Virginia Polytechnic Institute and State University, Dept. of Civil Engineering, Geotechnical Engineering.

Stark, T.D. and Duncan, J.M. (1991) Mechanisms of strength loss in stiff clays. *A.S.C.E., Journal of Geotechnical Engineering*, Vol. 117 (1), pp. 139-155.

Stark, T.D. and Mesri, G. (1992) Undrained shear strength of liquefied sands for stability analysis. *A.S.C.E., Journal of Geotechnical Engineering*, Vol 118, (11), pp. 1727-1747.

State Rivers and Water Supply Commission Victoria (1983) *Cairn Curran Dam: Preliminary design review report.* Major Projects Design Division.

Stateler, J.N. (1983) *Structural behaviour report: Bradbury dam, Cachuma Project, California (Mid-Pacific Region).* United States Department of the Interior Bureau of Reclamation, Division of Dam Safety, Structural Behaviour Branch.

Steele, I.C. and Cooke, J.B. (1958) Rockfill dams: Salt Springs and Lower Bear River concrete face dams. *A.S.C.E., Journal of the Power Division*, Vol. 84 (PO4), pp. 1737-1 to 43.

Steele, I.C. and Dreyer, W. (1939) Discussion on Galloway paper: The design of rock-fill dams. *Transactions, ASCE*, Vol. 104, pp. 53-63.

Stille, H., Fredriksson, A. and Broms, B.B. (1976) Analysis of a test embankment considering the anisotropy of the soil. *Proceedings, Second International Conference on Numerical Methods in Geomechanics*, (Desai ed.) Virginia, ASCE, New York. Vol. 2, pp. 611-622.

Stoutjesdijk, T.P., de Groot, M.B. and Lindenberg, J. (1998) Flow slide prediction method: influence of slope geometry. *Canadian Geotechnical Journal*, Vol 35, pp. 43-54.

Straw, A.J., Bennett, C.A., Reid, G.B., Druce, M.J. and Chenhall, G.A. (1985) *Windemere dam main embankment: Construction report 1980 - 1985.* Department of Water Resources, New South Wales.

Stroman, W.R., Beene, R.R.W. and Hull, A.M. (1984) Clay shale foundation slide at Waco dam, Texas. *Proceedings of the International Conference on Case Histories in Geotechnical Engineering*, (Prakash ed.) Rolla, USA, Vol. 2, pp. 579-586.

Stroman, W.R. and Karbs, H.E. (1985) Monitoring and analyses of pore pressures; clay shale foundation, Waco Dam, Texas. *15th International Congress on Large Dams*, Lausanne, ICOLD. pp. 599-620 (Q.56 R.29).

Su, W.X. and Miller, H.D.S. (1995) Waste pile stability and debris flow formation. *Rock Mechanics*, (Daemen & Schultz ed.) Balkema. pp. 831-836.

Sun, H.W. (1999) *Review of fill slope failures in Hong Kong.* GEO Report 96, Geotechnical Engineering Office, Civil Engineering Department, Government of Hong Kong.

Svenson, D., Burgess, J.B. and Hosking, A.D. (1964) *Report on sources of construction materials for Blowering dam and appurtenant works.* Snowy Mountains Hydro Electric Authority.

Tait, G.A. (1963) Some construction aspects of the Benmore earth dam. *Proceedings of the 4th Australia-New Zealand Conference on Soil Mechanics and Foundation Engineering*, Adelaide, IEAust, Sydney. pp. 76-80.

Takahashi, M. and Nakayama, K. (1973) The effect of regional conditions in Japan on design and construction of impervious elements of rockfill dams. *Proceedings of the 11th International Congress on Large Dams*, Madrid, ICOLD. pp. 501-524 (Q.42 R.29).

Tavenas, F. (1984) Landslides in Canadian sensitive clays - A state-of-the-art. *Proceedings of the Fourth International Symposium on Landslides*, Toronto, Vol. 1, pp. 141-153.

Tavenas, F., Changnon, J.Y. and La Rochelle, P. (1971) The Saint-Jean-Vianney landslide: Observations and eyewitnesses accounts. *Canadian Geotechnical Journal*, Vol 8, pp. 463-478.

Tavenas, F. and Leroueil, S. (1977) Effects of stresses and time on yielding of clays. *Proceedings, Ninth International Conference on Soil Mechanics and Foundation Engineering*, Tokyo, Vol. 1, pp. 319-326.

Tavenas, F. and Leroueil, S. (1980) The behaviour of embankments on clay foundations. *Canadian Geotechnical Journal*, Vol 17, pp. 236-260.

Tavenas, F. and Leroueil, S. (1981a) Creep and failure of slopes in clay. *Canadian Geotechnical Journal*, Vol 18, pp. 106-120.

Tavenas, F. and Leroueil, S. (1981b) Reply: The behaviour of embankments on clay foundations. *Canadian Geotechnical Journal*, Vol 18, pp. 462-466.

Tavenas, F., Leroueil, S., La Rochelle, P. and Roy, M. (1978) Creep behaviour of an undisturbed lightly overconsolidated clay. *Canadian Geotechnical Journal*, Vol 15, pp. 402-423.

Tavenas, F., Mieussens, C. and Bourges, F. (1979) Lateral displacements in clay foundations under embankments. *Canadian Geotechnical Journal*, Vol 16, pp. 532-550.

Taylor, R.K. (1984) *Composition and engineering properties of British colliery discard.* National Coal Board, Mining Department.

Tedd, P., Charles, J.A. and Holton, I.R. (1997a) Settlement of old embankment dams: a guide to measurement and interpretation. *Dams and Reservoirs*, Vol 7 (March), pp. 18-23.

Tedd, P., Charles, J.A., Holton, I.R. and Robertshaw, A.C. (1994) Deformation of embankment dams due to changes in reservoir level. *Proceedings of the 13th International Conference on Soil Mechanics and Foundation Engineering*, New Delhi, Vol. 3, pp. 951-954.

Tedd, P., Charles, J.A., Holton, I.R. and Robertshaw, A.C. (1997b) The effect of reservoir drawdown and long-term consolidation on the deformation of old embankment dams. *Geotechnique*, Vol 47 (1), pp. 33-48.

Tedd, P., Claydon, J.R. and Charles, J.A. (1990) Deformation of Ramsden dam during reservoir drawdown and refilling. *Proceedings of the 6th Conference of the British Dams Society (BNCOLD). The Embankment Dam.*, Nottingham, Thomas Telford, London. pp. 171-176.

Tedd, P. and Holton, I.R. (1987) *Ramsden dam: interim report on the investigation of the downstream fill and crest settlements.* Note N28/87, Building Research Establishment.

Tedd, P., Robertshaw, A.C. and Holton, I.R. (1993) Investigation of an old embankment dam with an upstream clay blanket and central clay core. *Dams and Reservoirs*, Vol 3 (1), pp. 6-9.

Terzaghi, K. (1950) Mechanism of landslides. *Engineering Geology (Berkley) Volume, The Geological Society of America* (November), pp. 83-123.

Terzaghi, K. (1956) Varieties of submarine slope failures. *Proceedings of the Eighth Texas Conference on Soil Mechanics and Foundation Engineering*, University of Texas, Austin, pp. 1-41.

Terzaghi, K. (1958) Design and performance of the Sasumua dam. *Proceedings of The Institution of Civil Engineers*, Vol. 9 (April), pp. 369-394.

Terzaghi, K. (1960) Discussion on 1958 paper by Steele & Cooke: Rockfill dams: Salt Springs and Lower Bear River concrete face dams. *ASCE, Transactions*, Vol. 125 (Part II), pp. 139-148.

Terzaghi, K. and Peck, R.B. (1948) *Soil mechanics in engineering practice*. John Wiley and Sons, New York.

Torrence, J.K. (1996) On the development of high sensitivity: Mineralogical requirements and constraints. *Proc. 7th International Symposium on Landslides*, (Senneset ed.) Trondheim, Norway, Balkema, Rotterdam. Vol. 1, pp. 491-496.

Trak, B. and Lacasse, S. (1996) Soils susceptible to flow slides and associated failure mechanisms. *Proceedings of the Seventh International Symposium on Landslides*, (Senneset ed.) Trondheim, Norway, Balkema, Rotterdam. Vol. 1, pp. 497-506.

Treiber, I.F. (1958a) Compaction methods adopted for the construction of Rosshaupten dam, their effectiveness, and the behaviour of the impervious loam core. *Proceedings of the 6th International Congress on Large Dams*, London, ICOLD. pp. 123-137 (Q.22 R.8).

Treiber, I.F. (1958b) Measurement and observations on Rosshaupten dam. *Proceedings of the 6th International Congress on Large Dams*, London, ICOLD. pp. 215-231 (Q.21 R.5).

Troncoso, J.H. (1988) Evaluation of seismic behavior of hydraulic fill structures. *Hydraulic Fill Structures, ASCE Speciality Conference, Geotechnical Special Publication No. 21,* (Van Zyl and Vick ed.) Colorado, ASCE, New York. pp. 475-491.

Troncoso, J.H. (2000) Failure mechanisms and shear failures of tailings dams under earthquake loadings. *Proceedings of the International Conference on Geotechnical and Geological Engineering (GeoEng2000)*, Melbourne, Vol. 1, pp. 1254-1262.

Troncoso, J.H., Vergara, A. and Avendano, A. (1993) The seismic failure of Barahona tailings dam. *Proc. Third International Conference on Case Histories in Geotechnical Engineering*, St. Louis, Missouri, Vol. 3, pp. 1473-1479.

United States Department of the Interior Bureau of Reclamation (1946) *Schedules, specifications and drawings. Horsetooth Reservoir, Colorado-Big Thompson Project, Colorado.* Specification No. 1275.

United States Department of the Interior Bureau of Reclamation (1951) *Enders dam: Final embankment report.*

United States Department of the Interior Bureau of Reclamation (1953) *Adaminaby dam: Report on design of earth embankment.* Earth Dams Section, Dams Branch, Design and Construction Division (for Snowy Mountains Hydro-Electric Authority and Department of Public Works New South Wales).

United States Department of the Interior Bureau of Reclamation (1959) *Cachuma dam: Technical record of design and construction.*

United States Department of the Interior Bureau of Reclamation (1963a) *Final construction report: Navajo dam. Colorado River Storage Project.* Navajo Unit Project Office.

United States Department of the Interior Bureau of Reclamation (1963b) *Steinaker dam: Technical record of design and construction.*

United States Department of the Interior Bureau of Reclamation (1965) *Technical record of design and construction. Trinity River division features of the Central Valley Project, California. Volumes I - Design.*

United States Department of the Interior Bureau of Reclamation (1966a) *Navajo dam and reservoir: Technical record of design and construction.*

United States Department of the Interior Bureau of Reclamation (1966b) *Technical record of design and construction. Trinity River division features of the Central Valley Project, California. Volumes II - Construction.*

United States Department of the Interior Bureau of Reclamation (1972) *Design considerations for construction of Pueblo dam, Fryingpan-Arkansas Project, Colorado.*

United States Department of the Interior Bureau of Reclamation (1974) *San Luis dam: Technical record of design and construction.*

United States Department of the Interior Bureau of Reclamation (1995) *Performance parameters for San Justo dam.* Technical Memorandum No. JU-8311-1.

United States Department of the Interior Bureau of Reclamation (1996) *Performance parameters for Belle Fourche dam.* Technical Memorandum No. BF-8311-1.

United States Department of the Interior Bureau of Reclamation (1997) *Performance parameters for the Horsetooth Reservoir dams.* Technical Memorandum No. JT-8312-1.

United States Department of the Interior Bureau of Reclamation (1998) *Performance parameters for Meeks Cabin dam (draft report).* Technical Memorandum (Draft) No. MS-8312-2.

United States Department of the Interior Bureau of Reclamation (19xx) *Enders dam: Technical record of design and construction.*

United States Geological Survey (190X) *Advertisement, proposal and specifications. Belle Fourche project, South Dakota. Dam and distribution canals, third contract.* Specification No. 56, Department of the Interior, Reclamation Service.

USCOLD (1975) *Lessons from Dam Incidents USA.* United States Committee on Large Dams, Committee on Failures and Accidents to Large Dams, ASCE, New York, pp. 387.

USCOLD (1988) *Lessons from Dam Incidents USA-II*. United States Committee on Large Dams, Subcommittee on Dam Incidents and Accidents of the Committee on Dam Safety, ASCE, New York, pp. 222.

Uthayakumar, M. and Vaid, Y.P. (1998) Static liquefaction of sands under multiaxial loading. *Canadian Geotechnical Journal,* Vol 35, pp. 273-283.

Vaid, Y.P. and Campanella, R.G. (1977) Time dependent behavior of undisturbed clay. *A.S.C.E., Journal of the Geotechnical Engineering Division,* Vol 103 (GT7), pp. 693-709.

Vaid, Y.P. and Eliadorani, A. (1998) Instability and liquefaction of granular soils under undrained and partially drained tests. *Canadian Geotechnical Journal*, Vol 35, pp. 1053-1062.

Vail, A.J. (1972) *A Report on the Po Shan Road landslide.* The Commission of Enquiry into the Rainstorm Disasters of June 1972, The Public Works Department, Government of Hong Kong.

Van Gassen, W. and Cruden, D.M. (1989) Momentum transfer and friction in the debris of rock avalanches. *Canadian Geotechnical Journal*, Vol 26, pp. 623-628.

Vanicek, I. (1982) Simple non-standard laboratory tests before and during construction of Dalesice dam. *Proceedings of the 14th International Congress on Large Dams*, Rio de Janiero, ICOLD. Vol. 1, pp. 605-610 (Q.52 R.38).

Varnes, D.J. (1978) Slope movement types and processes. In Landslides: analysis and control, Special Report No. 176, Transportation Research Board. (Schuster & Krizek ed.), National Academy of Sciences, Washington D.C., pp. 11-33.

Varnes, D.J. (1982) Time-deformation relations in creep to failure of earth materials. *Proceedings of the Seventh Southeast Asian Geotechnical Conference*, (McFeat-Smith and Lumb ed.) Hong Kong, Vol. 2, pp. 107-130.

Vasconcelos, A.A. and Eigenheer, L.P. (1985) The Xingo rockfill dam. *Proceedings of the Symposium on Concrete Face Rockfill Dams - Design, Construction and Performance*, (Cooke and Sherard ed.) Detroit, Michigan, ASCE New York. pp. 559-565.

Vaunet, J., Leroueil, S. and Faure, R. (1994) Slope movements: a geotechnical perspective. *Proceedings of the 7th International Congress of the International Association of Engineering Geology*, Lisbon, pp. 1637-1646.

Verdugo, R., Castillo, P. and Briceno, L. (1995) Initial soil structure and steady state strength. *Proceedings of the Conference on Earthquake Geotechnical Engineering*, (Ishihara ed.) Balkema. pp. 209-214.

Verma, N.S., Paré, J.J., Boncompain, B., Garneau, R. and Rattue, A.B. (1985) Behaviour of the LG-4 main dam. *Proceedings of the 11th International Conference on Soil Mechanics and Foundation Engineering*, San Francisco, Balkema, Brookfield. Vol. 4, pp. 2049-2054.

Villegas, F. (1982) Difficulties during construction of the Punchina cofferdam. *Fourteenth International Congress on Large Dams*, Rio de Janeiro, ICOLD. pp. 1081-1101 (Q.55 R.60).

Villegas, F. (1984) Incipient failures of dams built with tropical residual soils and their behavior during seismic events. *Proceedings of the International Conference on Safety of Dams*, Coimbra, pp. 39-43.

Volk, P.L. (1987) *Glenbawn dam enlargement: Geological construction report.* Water Conservation and Irrigation Commission NSW.

Von Thun, J.L. (1988) San Luis Dam upstream slide. *Proceedings of the 11th International Conference on Soil Mechanics and Foundation Engineering*, San Francisco, Balkema, Brookfield. Vol. 5, pp. 2593-2598.

Von Thun, L. (1982) *Back analysis of the San Luis slide with additional attention to the Qs surface and the deformed section.* Draft Report, Technical Memorandum No. SL-II-222-2, United States Bureau of Reclamation, Division of Design, Embankment Dams Section.

W.A. Wahler & Associates (1973) *Analysis of coal refuse dam failure, Middle Fork Buffalo Creek, Saunders, West Virginia.* USBM Contract S0122084, for U.S. Dept. of the Interior, Bureau of Mines.

Wagener, F.M., Craig, H.J., Blight, G., McPhail, G., Williams, A.A.B. and Strydom, J.H. (1998) The Merriespruit tailings dam failure - A review. *Proc. Tailings and Mine Waste '98*, Fort Collins, pp. 925-952.

Walker, F.C. and Harber, W.G. (1961) Design of the Trinity dam, an earthfill structure 537 feet high. *Proceedings of the 5th International Conference on Soil Mechanics and Foundation Engineering*, Paris, Vol. 2, pp. 743-748.

Walker, W.L. and Duncan, J.M. (1984) Lateral bulging of earth dams. *A.S.C.E., Journal of Geotechnical Engineering*, Vol. 110 (7), pp. 923-937.

Wang, P., Shen, Y. and Wang, Y. (1993) Design and construction of Xibeikou concrete-faced rockfill dam. *Proceedings of the International Symposium on High Earth-Rockfill Dams*, (Jiang, Zhang & Qin ed.) Beijing, Vol. 1, pp. 418-429.

Wang, Y., Chen, J. and Shen, Y. (1988) Xibeikou concrete face rockfill dam. *Proceedings of the 16th International Congress on Large Dams*, San Francisco, ICOLD. pp. 1075-1090 (Q.61 R.57).

Watakeekul, S., Roberts, G.J. and Coles, A.J. (1985) Khao Laem - a concrete face rockfill dam on karst. *Proceedings of the Symposium on Concrete Face Rockfill Dams - Design, Construction and Performance*, (Cooke and Sherard ed.) Detroit, Michigan, ASCE New York. pp. 336-361.

Water Conservation and Irrigation Commission NSW (1964) *Burrendong dam: Report on main wall construction.*

Water Conservation and Irrigation Commission NSW (1982) *Glenbawn dam enlargement. Core material for embankments: Existing embankment material.*

Water Resources Commission NSW (1978) *Copeton dam: Surveillance report.*

Water Resources Commission NSW (1979) *Chaffey dam: Construction control, Design summary to 4-1-79.*

Water Resources Commission NSW (1992) *Burrendong dam surveillance report.* Report No. TS No. 93.055.

Watson, J.D. (1956) Earth movement affecting L.T.E. railway in deep cutting east of Uxbridge. *Proceedings of the Institution of Civil Engineers*, Vol. 5, Part 2 (27 March), pp. 302-331.

West, R.P. (1962) Waco Dam slide: Its cause and correction. *Engineering News Record* (2 August), pp. 34-36.

Wieczorek, G.F. (1987) Effect of rainfall intensity and duration on debris flows in central Santa Cruz mountains, California. *Reviews in Engineering Geology, Geological Society of America*, Vol. VII, pp. 93-104.

Wieczorek, G.F., Harp, E.L. and Mark, R.K. (1988) Chapter 8. Debris flows and other landslides in San Mateo, Santa Cruz, Contra Costa, Alameda, Napa, Solano, Sonoma Lake and Yolo Counties, and other factors influencing debris-flow distribution. In Landslides, floods, and marine effects of the storm of January 3-5, 1982, in the San Francisco Bay region, California. U.S. Geological Survey Professional Paper 1434 (Ellen & Wieczorek ed.), U.S. Geological Survey, pp. 163-183.

Wilkes, P.F. (1972) An induced failure at a trial embankment at King's Lynn, Norfolk, England. *Proceedings, ASCE Speciality Conference on Performance of Earth and Earth Retaining Structures*, Purdue University, Lafayette, Vol. 1 (1), pp. 29-63.

Wilkins, J.K., Mitchell, W.R., Fitzpatrick, M.D. and Liggins, T. (1973) The design of Cethana concrete face rockfill dam. *Proceedings of the 11th International Congress on Large Dams*, Rio de Janiero, ICOLD. pp. 25-43 (Q.42 R.3).

Wilson, N.A. and Scott, H.S. (1957) The design of Glenbawn dam. *The Journal of The Institution of Engineers, Australia*, Vol. 29 (Dec), pp. 333-343.

Wilson, S.D. (1973) Deformation of earth and rockfill dams. In Embankment Dam Engineering (Casagrande Volume) (Hirschfeld and Poulos ed.), John Wiley and Sons, New York, pp. 365-417.

Wilson, S.D. and Squier, R. (1969) Earth and rockfill dams. *Proceedings, 7th International Conference on Soil Mechanics and Foundation Engineering*, Mexico,

Sociodad Mexicana de Mecanica de Suelos, A.C. State of the Art Volume pp. 137-223.

Wolfskill, L.A. and Lambe, T.W. (1967) Slide in Siburua Dam. *Journal of the Soil Mechanics and Foundations Division, ASCE*, Vol. 93 (SM4), pp. 107-133.

Wong, H.N., Chen, Y.M. and Lam, K.C. (1996) *Factual report on the November 1993 natural terrain landslides in three study areas on Lantau Island.* Special Project Report SPR 10/96 (Volumes 1, 2 and 3), Geotechnical Engineering Office, Civil Engineering Department, Hong Kong.

Wong, H.N. and Ho, K.K.S. (1996) Travel distance of landslide debris. *Proceedings of the Seventh International Symposium on Landslides*, (Senneset ed.) Trondheim, Norway, Balkema, Rotterdam. Vol. 1, pp. 417-422.

Wong, H.N., Ho, K.K.S. and Chan, Y.C. (1997) Assessment of the consequences of landslides. *Landslide Risk Assessment*, (Cruden & Fell ed.) Honolulu, Hawaii, Balkema. pp. 111-149.

Wong, K.L., Kleiner, D.E., Wood, A.M., Geary, M.C. and Oechsel, R.G. (1992) Design and performance of Bath County Upper Dam and reservoir slopes. *Proceeding of the Conference on Stability and Performance of Slopes and Embankment - II. Geotechnical Special Publication No. 31*, (Seed & Boulanger ed.) Berkeley, California, ASCE, New York. Vol. 1, pp. 371-386.

Wood, J.J. (1960) *Waipapa Power Project: Earth dam construction report.* New Zealand Ministry of Works.

Woodland, A.W. (1969) Geological report on the Aberfan tip disaster of October 21st, 1966. In A selection of technical reports submitted to the Aberfan Tribunal H.M.S.O., London, Welsh Office, pp. 119-145, (Item 4).

Woodward Clyde (1999) *Lake Eppalock main embankment remedial works, design report.* for Goulburn Murray Water.

Works Consultancy Services Ltd (1996a) *Benmore power station: Deformation Survey No. 22, April 1996.* WCS Report No. 138, for Electricity Corporation New Zealand, Southern Generation.

Works Consultancy Services Ltd (1996b) *Pukaki Lake control: Deformation Survey No. 17.* for Electricity Corporation New Zealand, Southern Generation.

Works Geothermal Ltd (1994) *Report on the Type B deformation survey of Matahina dam.* for Electricity Corporation of New Zealand, report prepared for the Waikato Hydro Group.

Wright, E.L. (1987) *Final construction geology report for Pueblo dam.* United States Department of the Interior Bureau of Reclamation, Missouri Basin Regional Office.

Wroth, C.P. and Simpson, B. (1972) An induced failure at a trial embankment. Part II finite element computations. *Proceedings, ASCE Speciality Conference on Performance of Earth and Earth Retaining Structures*, Purdue University, Lafayette, Vol. 1 (1), pp. 65-79.

Wu, G., Freitas, M.S., Araya, J.A.M. and Huang, Z.Y. (2000a) Planning and construction of Tianshengqiao 1 CFRD (China). *Proceedings of the International Symposium on Concrete Faced Rockfill Dams*, Beijing, ICOLD. pp. 481-496.

Wu, G., Freitas, M.S., Araya, J.A.M., Huang, Z.Y. and Mori, R.T. (2000b) Tianshengqiao-1 CFRD - monitoring and performance - lessons and new trends for future CFRDs (China). *Proceedings of the International Symposium on Concrete Faced Rockfill Dams*, Beijing, ICOLD. pp. 573-586.

Wu, H., Wujie, Wang, S., Wu, Q. and Cao, K. (2000c) Ten years surveillance of Chengbing concrete face rockfill dam. *Proceedings of the International Symposium on Concrete Faced Rockfill Dams*, Beijing, ICOLD. pp. 595-605.

Wu, Q. and Cao, K. (1993) Concrete faced rockfill dam of Chengbing project. *Proceedings of the International Symposium on High Earth-Rockfill Dams*, (Jiang, Zhang & Qin ed.) Beijing, Vol. 1, pp. 440-447.

Yamamuro, J.A. and Lade, P.V. (1997) Static liquefaction of very loose sands. *Canadian Geotechnical Journal*, Vol 34, pp. 905-917.

Yamamuro, J.A. and Lade, P.V. (1998) Steady state concepts and static liquefaction of silty sands. *A.S.C.E., Journal of Geotechnical and Geoenvironmental Engineering*, Vol 124 (9), pp. 868-877.

Yamazumi, A., Hara, N. and Harita, K. (1991) Foundation treatment for Agigawa rockfill dam constructed on fissured rock. *Proceedings of the 17th International Congress on Large Dams*, Vienna, ICOLD. Vol. 3, pp. 831-852 (Q.66 R.47).

Yang, S. (1993) Design of TSQ-1 concrete face rockfill dam. *Proceedings of the International Symposium on High Earth-Rockfill Dams*, (Jiang, Zhang & Qin ed.) Beijing, Vol. 1, pp. 448-543.

Yasunaka, M., Tanaka, T. and Nakano, R. (1985) The behaviour of Fukada earthfill dam during construction and impounding of the reservoir. *Proceedings of the 15th International Congress on Large Dams*, Lausanne, ICOLD. pp. 499-518 (Q.56 R.24).

Yoshimi, Y., Tokimatsu, K. and Hosaka, Y. (1989) Evaluation of liquefaction resistance of clean sands based on high-quality undisturbed samples. *Soils and Foundations*, Vol. 29 (1), pp. 868-877.

Yoshimi, Y., Tokimatsu, K. and Ohara, J. (1994) In situ liquefaction resistance of clean sands over a wide density range. *Geotechnique*, Vol. 44 (3), pp. 479-494.

Youd, T.L., Idriss, I.M., Arango, R.D., Castro, G., Christian, J.T., Dobry, R., Finn, W.D.L., Harder, L.F., Hynes, M.E., Ishihara, K., Koester, J.P., Liao, S.S.C., Marcuson, W.F., Martin, G.R., Mitchell, J.K., Moriwaki, Y., Power, M.S., Robertson, P.K., Seed, R.B. and Stokoe, K.H. (1997) Summary Report. *Proceedings of the NCEER Workshop on Evaluation of Liquefaction Resistance of Soils*, (Youd and Idriss ed.) Salt Lake City, Utah, National Centre for Earthquake Engineering Research. pp. 1-40.